WILEY-VCH

Edited by Graeme Moad and Ezio Rizzardo

RAFT Polymerization

Methods, Synthesis and Applications

Volume 1

RAFT Polymerization

RAFT Polymerization

Methods, Synthesis and Applications

Volume 1

Edited by

Graeme Moad
Ezio Rizzardo

WILEY-VCH

RAFT Polymerization

Methods, Synthesis and Applications

Volume 2

Edited by

Graeme Moad
Ezio Rizzardo

WILEY-VCH

Editors

Prof. Dr. Graeme Moad
CSIRO Manufacturing
Research Way
Clayton, Victoria 3168
Australia

Dr. Ezio Rizzardo
CSIRO Manufacturing
Research Way
Clayton, Victoria 3168
Australia

Library of Congress Card No.:
applied for

British Library Cataloguing-in-Publication Data
A catalogue record for this book is available from the British Library.

Bibliographic information published by the Deutsche Nationalbibliothek
The Deutsche Nationalbibliothek lists this publication in the Deutsche Nationalbibliografie; detailed bibliographic data are available on the Internet at <http://dnb.d-nb.de>.

Print ISBN: 978-3-527-34495-6
ePDF ISBN: 978-3-527-82134-1
ePub ISBN: 978-3-527-82136-5
oBook ISBN: 978-3-527-82135-8

Cover Design Formgeber, Mannheim, Germany
Typesetting Straive, Chennai, India

Printed on acid-free paper

10 9 8 7 6 5 4 3 2 1

Contents

Contents

Preface

This volume is intended to provide a detailed synopsis of the current state of RAFT (reversible addition fragmentation chain transfer) polymerization. It is an update of the 2008 Handbook of RAFT Polymerization and of the review series 'Living Radical Polymerization by the RAFT Process' published over the period 2005–2012 in the *Australian Journal of Chemistry*.

RAFT polymerization has been a success, there are now more than 10 000 publications that relate to the understanding, development, and/or application of the technique, and the rate of publication shows no signs of waning. Commercial success is more difficult to judge. A search reveals over 1000 patent families. On the other hand, there are few examples of actual RAFT products. Maybe commercial implementation will increase now that the first RAFT patents have reached the end of their enforceable life.

Although some might argue that RAFT is now a mature technique, there are still significant efforts striving for a more complete understanding of the mechanism and scope of the process. It is our hope that by compiling this work and by highlighting recent achievements in RAFT chemistry, we will inspire further research and further drive the ever-increasing range of applications.

Clayton, Victoria, Australia
September 2021

Graeme Moad and Ezio Rizzardo

Acknowledgements

The editors are extremely grateful to Caroline Bray, Guoxin Li, Catherine Moad, and Lisa Strover for proofreading the various chapters and to CSIRO for allowing substantial time to be spent on this exercise.

1

Overview of RAFT Polymerization

Graeme Moad and Ezio Rizzardo

CSIRO Manufacturing, Research Way, Clayton, VIC 3168, Australia

The first announcement of RAFT (reversible addition–fragmentation chain transfer), polymerization making use of thiocarbonylthio transfer agents as a means of controlling the outcome of radical polymerization was made at the IUPAC Word Polymer Congress Macro 98 by Dr Ezio Rizzardo just over 21 years ago in July 1998. The first publication on RAFT polymerization detailing the work at CSIRO was published shortly thereafter [1]. The paper in Macromolecules [1] that announced the RAFT process, is currently the most highly cited paper in that journal.

RAFT polymerization had been disclosed in a CSIRO/DuPont patent that was published in January 1998 [2]. A patent describing the parallel development of MADIX (MAcromolecule Design by Interchange of Xanthates – RAFT with xanthate transfer agents) at Rhodia was published in December 1998 [3]. That first RAFT patent [2] was, by 2005, one of the most highly cited patents in the field of chemistry and related science, and the patent literature now abounds with a still-increasing number of RAFT-related inventions (Figure 1.1). However, commercial success stories associated with RAFT polymerization and other reversible-deactivation radical polymerization (RDRP) are few [4]. With the first RAFT patents having reached the end of their enforceable life, we might now envisage an upsurge in commercial applications.

The further development of RAFT was chronicled in a series of reviews that appeared in the Australian Journal of Chemistry in 2005 [5], 2006 [6], 2009 [7], and 2012 [8]. Since that time reviews of RAFT polymerization have targeted specific application areas or have been otherwise limited in scope. A number of perspectives have recently appeared to mark the 20th anniversary of the discovery of RAFT polymerization [9–11].

The year 2008 saw the publication of the Handbook of RAFT Polymerization that comprised 12 chapters from major players in the field at the time [12]. The 10 years leading up to the handbook had seen a revolution in the field of radical polymerization, which can, in large part, be attributed to the invention of RAFT and other RDRP methods. Many of the same authors who contributed to that handbook have also provided chapters for the present work.

RAFT Polymerization: Methods, Synthesis and Applications, First Edition.
Edited by Graeme Moad and Ezio Rizzardo.

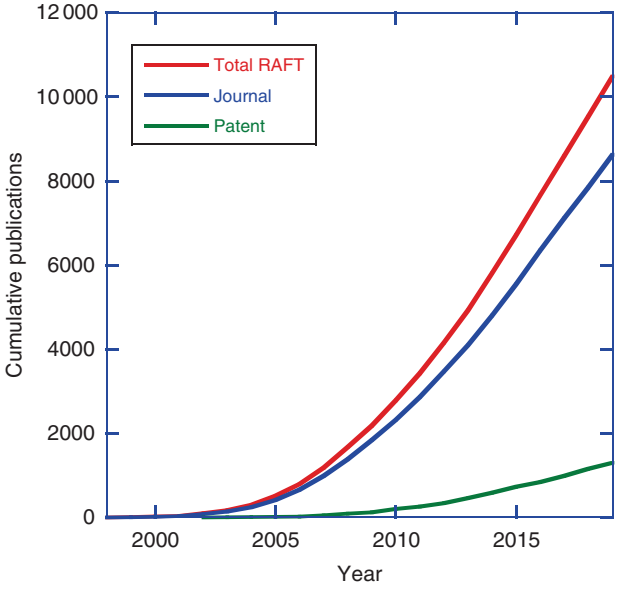

Figure 1.1 Cumulative publications relating to RAFT polymerization for the period 1998–2019 based on a Scifinder™ substructure search on the major classes of RAFT agent carried out in February 2020 on the RAFT agent structures and the terms 'RAFT' and 'MADIX' (in the case of xanthates).

Publications relating to RAFT polymerization show no signs of abating. The present work is intended as a survey of developments in RAFT polymerization focusing on the last 10 years.

RAFT polymerization is a form of RDRP and can impart living characteristics (low molar mass dispersity, high-end group fidelity, ability to synthesize complex architectures) to radical polymerization. The technique owes its success to the wide range of tolerated functionality and polymerization conditions, and to the vast range of monomers whose (co)polymerization can be successfully controlled.

In 2008, at the time the RAFT Handbook was published, one factor seen as significant in holding back the exploitation of RAFT polymerization was that RAFT agents were not commercially available [13]. This situation has now been redressed [14].

It has often been pointed out that to achieve the highest level of control over polymerization, one needs to select the RAFT agent for the monomer(s) being polymerized. A dizzying array of RAFT agents, Z—C(=S)S—R, varying in the activating (Z) and reinitiating (R) substituents, are now available commercially or are able to be synthesized [15]. However, with just two RAFT agents, e.g. a trithiocarbonate, for more activated monomers such as styrenes and (meth)acrylates, and a xanthate or a dithiocarbamate, for less activated monomers such as vinyl esters or vinyl amides, one can achieve acceptable control over the full monomer spectrum [16]. Moreover, by using a switchable RAFT agent or a RAFT agent with balanced activity, e.g. a 1*H-pyrazole*-1-carbodithioate [17, 18], one can achieve only slightly compromised control with just one RAFT agent.

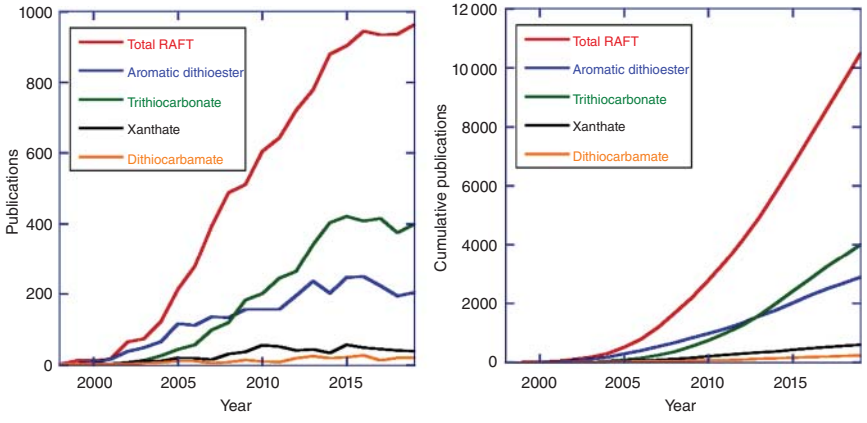

Figure 1.2 Publication rate for RAFT polymerization using different classes of RAFT agent for the period 1998–2019. Includes both patent and open literature publications. Based on a Scifinder™ substructure search carried out in February 2020 on the RAFT agent structures and the terms 'RAFT' and 'MADIX' (in the case of xanthates). The total RAFT number relates to a search on the terms 'RAFT polymerization' or 'reversible addition fragmentation chain transfer'.

In the following text we mention the chapters of this work by topic and refer to chapters of the 2008 Handbook of RAFT Polymerization on similar topics.

We commence with a chapter on terminology in RDRP and RAFT polymerization [19]. Then we go back to the basics and provide a beginner's guide on *How to Do a RAFT polymerization* [14].

There are four chapters concerning the detailed kinetics and mechanism of the RAFT process: *Kinetics and Mechanism of RAFT Polymerizations* [20], *RAFT Polymerization, Mechanistic Considerations* [21], *Mechanisms, Quantum Studies of RAFT Polymerization* [22], and *Mathematical Modelling of RAFT Polymerization* [23]; these concern the detailed kinetics and mechanism of the RAFT process and the ongoing efforts to enhance our understanding of the process (2008 chapters [24, 25]).

The next four chapters provide a critical survey of the four major classes of RAFT agents, namely, dithioesters [26], trithiocarbonates [27], xanthates [28], and dithiocarbamates [29] as regards activity as RAFT agents, polymerization mechanisms, and their application in polymer synthesis (2008 chapters [16, 30, 31]). The year 2008 marked the point in time at which trithiocarbonates became the most popular RAFT agents (Figure 1.2).

There are two chapters concerning the more recent developments in processes for initiating RAFT polymerization. *Overview of Photoregulated Reversible Addition–Fragmentation Chain Transfer (RAFT) Polymerization* [32], *Redox-Initiated RAFT Polymerization, and (Electro)Chemical Activation of RAFT Agents* [33].

Further two chapters relate specifically to RAFT polymerization in aqueous solution or in heterogeneous medium and to polymerization-induced self-assembly: *Considerations for and Applications of Aqueous RAFT Polymerization* [34], *RAFT-Mediated Polymerization-Induced Self-Assembly (PISA)* (2008 chapters [35, 36]) [37].

Three chapters concern the synthesis of functional polymers, sequence-defined polymers, and RAFT end-group transformation. *RAFT Functional End Groups: Installation and Transformation* [38], *Sequence-Encoded RAFT Oligomers and Polymers* [39], *Synthesis and Application of Reactive Polymers via RAFT Polymerization* (2008 chapter [40]) [41].

We then go into detail on the other aspects of polymer architecture with chapters on *RAFT Crosslinking Polymerization* [42], *Complex Polymeric Architectures Synthesized Through RAFT Polymerization* [43], *Star Polymers by RAFT Polymerization* [44], *Surface and Particle Modification via RAFT Polymerization: An update* (2008 chapters [45–47]).

Two chapters relate to application areas. *An Industrial History of RAFT Polymerization* [48] describes the development of RAFT by reference to the patent literature and points to where RAFT is being applied in industry (2008 chapters [49, 50]). The application of high throughput robotic platforms to RAFT polymerization as an aid to shortcut the process of selecting reaction conditions and to create polymer libraries for screening purposes is discussed in *High Throughput/High Output Experimentation in RAFT Polymer Synthesis* [51].

A final chapter demonstrates that the RAFT process is not applicable only to radical polymerization and details the recent work on *Cationic RAFT Polymerization* [52].

It is our hope that by compiling and highlighting recent achievements in RAFT chemistry, we will inspire further research and further drive the ever-increasing range of applications.

It should be stated that there is no lack of recent review material relating to RAFT polymerization and its application. At least 30 reviews have been published since 2017 specifically on RAFT polymerization (non-English language reviews are not included in this list). These include overviews and perspectives [9–11, 53, 54], polymerization-induced self-assembly (PISA) [55*, 56–58], monomers from renewable resources [59], polymer brushes [60], therapeutics and bioapplications [61–63], star polymers for bioapplications [64], hydrogels for drug delivery [65], organic/inorganic nanohybrids for bioapplications [66], gold nanoparticles [67], 3D-printing [68], stimuli-responsive polymers [69], conjugated diene monomers [70], single-unit monomer insertion (RAFT-SUMI) [71], redox initiation [72], hydroxyl radical initiation [73], photoRAFT [74], externally regulated polymerization [75], initiation with ionizing radiation [76], dithiocarbamate RAFT agents [77]*, optoelectronic applications [78], and graft copolymers by transfer-to [79]. An asterisk (*) indicates that an update to the review appears in this volume. Earlier reviews on RAFT polymerization have been summarized previously [5–8, 69].

There are additionally many reviews on radical or RDRP methods more generally that contain substantial content on RAFT polymerization or RAFT applications. The more than 50 reviews published since 2017 include reviews on ultrahigh molar mass polymers [80, 81], self-condensing vinyl polymerization [82], complex architectures by copolymerization of multi-vinyl monomers [83], nanoparticles by surface-initiated polymerization [84], synthesis of multi-block copolymers

[85], PISA [86–89], biosensors [90, 91], hydrogels [92], biopolymer conjugates [93–95], glycopolymers for bioapplications [96, 97], phosphonium polymers for bioapplications [98], stimuli-responsive polymers in bioapplications [99–101], oligonucleotide-based nanomaterials [102], star polymers for bioapplications [103, 104], biocatalytic initiation [105, 106], alkylborane initiators [107], the use of Fenton chemistry for initiation [108], dialkyldiazene initiation [109], influence of external fields on radical polymerization [110], polymerization of alkyl 2-cyanoacrylates [111], semi-fluorinated (meth)acrylates [112], terpenes [113], rosin-derived monomers [114], polymers with pedant fatty acid chains [115], lignin-derived polymers [116], chitosan-derived polymers [117], graphene-derived polymers [118], functionalization of carbon nanotubes [119], cyclopolymerization for sequence-defined polymers [120], PhotoRDRP [121–124], thermoresponsive polymer ionic liquids [125], polyhedral oligomeric silsesquioxane (POSS)-hybrids [126], 3D-printing [127], porous polymers [128], combination or RAFT or atom-transfer-radical polymrerization (ATRP) with ring-opening polymerization [129], metal-free RDRP [130], cyclic polymers [131], end-group modification [132], and metallopolymers [133].

References

1 Chiefari, J., Chong, Y.K., Ercole, F. et al. (1998). *Macromolecules* 31: 5559–5562. https://doi.org/10.1021/ma9804951.

2 Le, T.P., Moad, G., Rizzardo, E., and Thang, S.H. (1998). Polymerization with living characteristics (DuPont/CSIRO). WO9801478A1.

3 Corpart, P., Charmot, D., Biadatti, T., Zard, S., and Michelet, D. (1998). Block polymer synthesis by controlled radical polymerization (Rhodia Chimie). WO9858974A1.

4 Destarac, M. (2018). *Polym. Chem.* 9: 4947–4967. https://doi.org/10.1039/C8PY00970H.

5 Moad, G., Rizzardo, E., and Thang, S.H. (2005). *Aust. J. Chem.* 58: 379–410. https://doi.org/10.1071/CH05072.

6 Moad, G., Rizzardo, E., and Thang, S.H. (2006). *Aust. J. Chem.* 59: 669–692. https://doi.org/10.1071/CH06250.

7 Moad, G., Rizzardo, E., and Thang, S.H. (2009). *Aust. J. Chem.* 62: 1402–1472. https://doi.org/10.1071/CH09311.

8 Moad, G., Rizzardo, E., and Thang, S.H. (2012). *Aust. J. Chem.* 65: 985–1076. https://doi.org/10.1071/CH12295.

9 Matyjaszewski, K. (2020). *Macromolecules* 53: 495–497. https://doi.org/10.1021/acs.macromol.9b02054.

10 Moad, G. and Rizzardo, E. (2020). *Polym. Int.* 69: 658–661. https://doi.org/10.1002/pi.5944.

11 Perrier, S. (2017). *Macromolecules* 50: 7433–7447. https://doi.org/10.1021/acs.macromol.7b00767.

12 Barner-Kowollik, C. (ed.) (2008). *Handbook of RAFT Polymerization*. Weinheim: Wiley-VCH. https://doi.org/10.1002/9783527622757.

13 Barner-Kowollik, C. (2008). Introduction. In: *Handbook of RAFT Polymerization* (ed. C. Barner-Kowollik), 1–4. Weinheim: Wiley-VCH. https://doi.org/10.1002/9783527622757.ch1.

14 Postma, A. and Skidmore, M. (2022). How to do a RAFT polymerisation. In: *RAFT Polymerization: Materials, Synthesis and Applications* (eds. G. Moad and E. Rizzardo), 25–58. Weinheim: Wiley-VCH.

15 Keddie, D.J., Moad, G., Rizzardo, E., and Thang, S.H. (2012). *Macromolecules* 45: 5321–5342. https://doi.org/10.1021/ma300410v.

16 Rizzardo, E., Moad, G., and Thang, S.H. (2008). RAFT polymerization in bulk monomer or in (organic) solution. In: *Handbook of RAFT Polymerization* (ed. C. Barner-Kowollik), 189–234. Weinheim: Wiley-VCH. https://doi.org/10.1002/9783527622757.ch6.

17 Gardiner, J., Martinez-Botella, I., Kohl, T.M. et al. (2017). *Polym. Int.* 66: 1438–1447. https://doi.org/10.1002/pi.5423.

18 Gardiner, J., Martinez-Botella, I., Tsanaktsidis, J., and Moad, G. (2016). *Polym. Chem.* 7: 481–492. https://doi.org/10.1039/C5PY01382H.

19 Moad, G. (2022). Terminology in reversible deactivation radical polymerization (RDRP) and reversible addition-fragmentation chain transfer (RAFT) polymerization. In: *RAFT Polymerization: Materials, Synthesis and Applications* (eds. G. Moad and E. Rizzardo), 15–24. Weinheim: Wiley-VCH.

20 Buback, M. (2022). Kinetics and mechanism of RAFT polymerizations. In: *RAFT Polymerization: Materials, Synthesis and Applications* (eds. G. Moad and E. Rizzardo), 59–94. Weinheim: Wiley-VCH.

21 Quinn, J.F., Moad, G., and Barner-Kowollik, C. (2022). RAFT polymerization: mechanistic considerations. In: *RAFT Polymerization: Materials, Synthesis and Applications* (eds. G. Moad and E. Rizzardo), 95–138. Weinheim: Wiley-VCH.

22 Coote, M.L. (2022). Quantum-chemical studies of RAFT polymerization. In: *RAFT Polymerization: Materials, Synthesis and Applications* (eds. G. Moad and E. Rizzardo), 139–186. Weinheim: Wiley-VCH.

23 López-Domínguez, P., Zapata-González, I., Saldívar-Guerra, E., and Vivaldo-Lima, E. (2022). Mathematical modeling of RAFT polymerization. In: *RAFT Polymerization: Materials, Synthesis and Applications* (eds. G. Moad and E. Rizzardo), 187–222. Weinheim: Wiley-VCH.

24 Moad, G. and Barner-Kowollik, C. (2008). The mechanism and kinetics of the RAFT process: overview, rates, stabilities, side reactions, product spectrum and outstanding challenges. In: *Handbook of RAFT Polymerization* (ed. C. Barner-Kowollik), 51–104. Weinheim: Wiley-VCH. https://doi.org/10.1002/9783527622757.ch3.

25 Coote, M.L., Krenske, E.H., and Izgorodina, E.I. (2008). Quantum-chemical studies of RAFT polymerization: methodology, structure-reactivity correlations and kinetic implications. In: *Handbook of RAFT Polymerization* (ed. C. Barner-Kowollik), 5–49. Weinheim: Wiley-VCH. https://doi.org/10.1002/9783527622757.ch2.

26 Moad, G. (2022). Dithioesters in RAFT polymerization. In: *RAFT Polymerization: Materials, Synthesis and Applications* (eds. G. Moad and E. Rizzardo), 223–370. Weinheim: Wiley-VCH.

27 Moad, G. (2022). Trithiocarbonates in RAFT polymerization. In: *RAFT Polymerization: Materials, Synthesis and Applications* (eds. G. Moad and E. Rizzardo), 371–494. Weinheim: Wiley-VCH.

28 Wang, M., Marty, J.-D., and Destarac, M. (2022). Xanthates in RAFT polymerization. In: *RAFT Polymerization: Materials, Synthesis and Applications* (eds. G. Moad and E. Rizzardo), 495–550. Weinheim: Wiley-VCH.

29 Moad, G. (2022). Dithicarbamates in RAFT polymerization. In: *RAFT Polymerization: Materials, Synthesis and Applications* (eds. G. Moad and E. Rizzardo), 551–610. Weinheim: Wiley-VCH.

30 Zard, S.Z. (2008). The radical chemistry of thiocarbonylthio compounds: an overview. In: *Handbook of RAFT Polymerization* (ed. C. Barner-Kowollik), 151–187. Weinheim: Wiley-VCH. https://doi.org/10.1002/9783527622757.ch5.

31 Taton, D., Destarac, M., and Zard, S.Z. (2008). Macromolecular design by interchange of xanthates: background, design, scope and applications. In: *Handbook of RAFT Polymerization* (ed. C. Barner-Kowollik), 373–421. Weinheim: Wiley-VCH. https://doi.org/10.1002/9783527622757.ch10.

32 Chapman, R., Jungb, K., and Boyer, C. (2022). Overview of photoregulated reversible addition-fragmentation chain transfer (RAFT) polymerization. In: *RAFT Polymerization: Materials, Synthesis and Applications* (eds. G. Moad and E. Rizzardo), 611–646. Weinheim: Wiley-VCH.

33 Lorandi, F., Fantin, M., and Matyjaszewski, K. (2022). Redox initiated RAFT polymerization and (electro)chemical activation of RAFT agents. In: *RAFT Polymerization: Materials, Synthesis and Applications* (eds. G. Moad and E. Rizzardo), 647–678. Weinheim: Wiley-VCH.

34 Fortenberry, A.W., McCormick, C.L., and Smith, A.E. (2022). Considerations for and Applications of Aqueous RAFT Polymerization. In: *RAFT Polymerization: Materials, Synthesis and Applications* (eds. G. Moad and E. Rizzardo), 679–706. Weinheim: Wiley-VCH.

35 Lowe, A.B. and McCormick, C.L. (2008). RAFT polymerization in homogeneous aqueous media: initiation systems, RAFT agent stability, monomers and polymer structures. In: *Handbook of RAFT Polymerization* (ed. C. Barner-Kowollik), 235–284. Weinheim: Wiley-VCH. https://doi.org/10.1002/9783527622757.ch7.

36 Urbani, C.N. and Monteiro, M.J. (2008). RAFT-mediated polymerization in heterogeneous systems. In: *Handbook of RAFT Polymerization* (ed. C. Barner-Kowollik), 285–314. Weinheim: Wiley-VCH. https://doi.org/10.1002/9783527622757.ch8.

37 D'Agosto, F., Lansalot, M., and Rieger, J. (2022). RAFT-mediated polymerization-induced self-assembly (PISA). In: *RAFT Polymerization: Materials, Synthesis and Applications* (eds. G. Moad and E. Rizzardo), 707–752. Weinheim: Wiley-VCH.

38 Lowe, A.B. and Dallerba, E. (2022). RAFT functional end-groups: installation and transformation. In: *RAFT Polymerization: Materials, Synthesis and Applications* (eds. G. Moad and E. Rizzardo), 753–804. Weinheim: Wiley-VCH.

39 Haven, J.J., Neve, J.D., and Junkers, T. (2022). Sequence-encoded RAFT oligomers and polymers. In: *RAFT Polymerization: Materials, Synthesis and Applications* (eds. G. Moad and E. Rizzardo), 805–828. Weinheim: Wiley-VCH.

40 Barner, L. and Perrier, S. (2008). Polymers with well-defined end groups via RAFT – synthesis, applications and postmodifications. In: *Handbook of RAFT Polymerization* (ed. C. Barner-Kowollik), 455–482. Weinheim: Wiley-VCH. https://doi.org/10.1002/9783527622757.ch12.

41 Gauthier-Jaques, M., Mutlu, H., Gaballa, H., and Theato, P. (2022). Synthesis and application of reactive polymers via RAFT polymerization. In: *RAFT Polymerization: Materials, Synthesis and Applications* (eds. G. Moad and E. Rizzardo), 829–872. Weinheim: Wiley-VCH.

42 Pérez-Salinas, P., López-Domínguez, P., Rosas-Aburto, A. et al. (2022). RAFT crosslinking polymerization. In: *RAFT Polymerization: Materials, Synthesis and Applications* (eds. G. Moad and E. Rizzardo), 873–932. Weinheim: Wiley-VCH.

43 Floyd, T.G., Häkkinen, S., Hartlie, M. et al. (2022). Complex polymeric architectures synthesised through RAFT polymerization. In: *RAFT Polymerization: Materials, Synthesis and Applications* (eds. G. Moad and E. Rizzardo), 933–982. Weinheim: Wiley-VCH.

44 Allison-Logan, S., Karimi, F., Nothling, M.D., and Qiao, G.G. (2022). Star polymers by RAFT polymerization. In: *RAFT Polymerization: Materials, Synthesis and Applications* (eds. G. Moad and E. Rizzardo), 983–1016. Weinheim: Wiley-VCH.

45 Stenzel, M.H. (2008). Complex architecture design via the RAFT process: scope, strengths and limitations. In: *Handbook of RAFT Polymerization* (ed. C. Barner-Kowollik), 315–372. Weinheim: Wiley-VCH. https://doi.org/10.1002/9783527622757.ch9.

46 Li, Y., Schadler, L.S., and Benicewicz, B.C. (2008). Surface and particle modification via the RAFT process: approach and properties. In: *Handbook of RAFT Polymerization* (ed. C. Barner-Kowollik), 423–453. Weinheim: Wiley-VCH. https://doi.org/10.1002/9783527622757.ch11.

47 Pribyl, J. and Benicewicz, B.C. (2022). Surface and particle modification via RAFT polymerization: an update. In: *RAFT Polymerization: Materials, Synthesis and Applications* (eds. G. Moad and E. Rizzardo), 1017–1050. Weinheim: Wiley-VCH.

48 Moad, G. (2022). An industrial history of RAFT polymerization. In: *RAFT Polymerization: Materials, Synthesis and Applications* (eds. G. Moad and E. Rizzardo), 1077–1158. Weinheim: Wiley-VCH.

49 Junkers, T., Lovestead, T.M., and Barner-Kowollik, C. (2008). The RAFT process as a kinetic tool: accessing fundamental parameters of free radical polymerization. In: *Handbook of RAFT Polymerization* (ed. C. Barner-Kowollik), 105–149. Weinheim: Wiley-VCH. https://doi.org/10.1002/9783527622757.ch4.

50 Favier, A., de Lambert, B., and Charreyre, M.-T. (2008). Toward new materials prepared via the RAFT process: from drug delivery to optoelectronics? In: *Handbook of RAFT Polymerization* (ed. C. Barner-Kowollik), 483–535. Weinheim: Wiley-VCH. https://doi.org/10.1002/9783527622757.ch13.

51 Guerrero-Sanchez, C., Yañez-Macias, R., Rosales-Guzmán, M. et al. (2022). High throughput / high output experimentation in RAFT polymer synthesis. In: *RAFT Polymerization: Materials, Synthesis and Applications* (eds. G. Moad and E. Rizzardo), 1051–1076. Weinheim: Wiley-VCH.

52 Uchiyama, M. and Kamigaito, M. (2022). Cationic RAFT polymerization. In: *RAFT Polymerization: Materials, Synthesis and Applications* (eds. G. Moad and E. Rizzardo), 1077–1158. Weinheim: Wiley-VCH.

53 Haven, J.J., Hendrikx, M., Junkers, T. et al. (2018). Elements of RAFT navigation. RAFT 20 years later. RAFT-synthesis of uniform, sequence-defined (co)polymers. In: *Reversible Deactivation Radical Polymerization: Mechanisms and Synthetic Methodologies*, ACS Symposium Series 1284 (eds. K. Matyjaszewski, H. Gao, B.S. Sumerlin and N.V. Tsarevsky), 77–103. Washington, DC: American Chemical Society. https://doi.org/10.1021/bk-2018-1284.ch004.

54 McCombie, S.W., Quiclet-Sire, B., and Zard, S.Z. (2018). *Tetrahedron* 74: 4969–4979. https://doi.org/10.1016/j.tet.2018.03.042.

55 D'Agosto, F., Rieger, J., and Lansalot, M. (2020). *Angew. Chem. Int. Ed.* 59: 8368–8392. https://doi.org/10.1002/anie.201911758.

56 Wang, X. and An, Z. (2019). *Macromol. Rapid Commun.* 40: 1800325. https://doi.org/10.1002/marc.201800325.

57 Palmiero, U.C., Singh, J., and Moscatelli, D. (2018). *Curr. Org. Chem.* 22: 1285–1296. https://doi.org/10.2174/1385272822666180322123124.

58 Zhou, J., Yao, H., and Ma, J. (2018). *Polym. Chem.* 9: 2532–2561. https://doi.org/10.1039/C8PY00065D.

59 Hatton, F.L. (2020). *Polym. Chem.* https://doi.org/10.1039/C9PY01128E.

60 Caykara, T. (2018). Polymer brushes by surface-mediated RAFT polymerization for biological functions. In: *Polymer and Biopolymer Brushes*, vol. 1 (eds. O. Azzaroni and I. Szleifer), 97–121. Hoboken, NJ: Wiley. https://doi.org/10.1002/9781119455042.ch3.

61 Daniselson, A.P., Dougherty, M.L., Falatach, R. et al. (2018). Biocatalytic polymerization, bioinspired surfactants, and bioconjugates using RAFT polymerization. In: *Reversible Deactivation Radical Polymerization: Materials and Applications*, ACS Symposium Series 1285 (eds. K. Matyjaszewski, H. Gao, B.S. Sumerlin and N.V. Tsarevsky), 219–232. American Chemical Society. https://doi.org/10.1021/bk-2018-1285.ch012.

62 Xin, X. and John, J.R. (2018). *Curr. Drug Deliv.* 15: 1084–1086. https://doi.org/10.2174/1567201815666180220100733.

63 Delaittre, G., Beloqui, A., Gil Alvaradejo, G. et al. (2018). *Chem. Ing. Tech.* 90: 1331–1331. https://doi.org/10.1002/cite.201855430.

64 Hu, J., Qiao, R., Whittaker, M.R. et al. (2017). *Aust. J. Chem.* 70: 1161–1170. https://doi.org/10.1071/CH17391.

65 Xian, C., Yuan, Q., Bao, Z. et al. (2020). *Chin. Chem. Lett.* 31: 19–27. https://doi.org/10.1016/j.cclet.2019.03.052.

66 Huang, X., Hu, J., Li, Y. et al. (2019). *Biomacromolecules* 20: 4243–4257. https://doi.org/10.1021/acs.biomac.9b01158.

67 Pereira, S., Barros-Timmons, A., and Trindade, T. (2018). *Polymers* 10: 189. https://doi.org/10.3390/polym10020189.

68 Zhang, Z., Corrigan, N., Bagheri, A. et al. (2019). *Angew. Chem. Int. Ed.* 58: 17954–17963. https://doi.org/10.1002/anie.201912608.

69 Moad, G. (2017). *Polym. Chem.* 8: 177–219. https://doi.org/10.1039/C6PY01849A.

70 Moad, G. (2017). *Polym. Int.* 66: 26–41. https://doi.org/10.1002/pi.5173.

71 Xu, J. (2019). *Macromolecules* 52: 9068–9093. https://doi.org/10.1021/acs.macromol.9b01365.

72 Reyhani, A., McKenzie, T.G., Fu, Q., and Qiao, G.G. (2019). *Aust. J. Chem.* 72: 479–489. https://doi.org/10.1071/CH19109.

73 McKenzie, T.G., Reyhani, A., Nothling, M.D., and Qiao, G.G. (2018). Hydroxyl radical activated RAFT polymerization. In: *Reversible Deactivation Radical Polymerization: Mechanisms and Synthetic Methodologies*, ACS Symposium Series 1284 (eds. K. Matyjaszewski, H. Gao, B.S. Sumerlin and N.V. Tsarevsky), 307–321. American Chemical Society. https://doi.org/10.1021/bk-2018-1284.ch014.

74 Figg, C.A. and Sumerlin, B.S. (2018). Aqueous visible-light RAFT polymerizations and applications. In: *Reversible Deactivation Radical Polymerization: Materials and Applications*, ACS Symposium Series 1285 (eds. K. Matyjaszewski, H. Gao, B.S. Sumerlin and N.V. Tsarevsky), 43–56. American Chemical Society. https://doi.org/10.1021/bk-2018-1285.ch003.

75 Shanmugam, S., Boyer, C., and Matyjaszewski, K. (2018). Recent developments in external regulation of reversible addition fragmentation chain transfer (RAFT) polymerization. In: *Reversible Deactivation Radical Polymerization: Mechanisms and Synthetic Methodologies*, ACS Symposium Series 1284 (eds. K. Matyjaszewski, H. Gao, B.S. Sumerlin and N.V. Tsarevsky), 273–290. American Chemical Society. https://doi.org/10.1021/bk-2018-1284.ch012.

76 Barsbay, M. and Güven, O. (2020). *Radiat. Phys. Chem.* 169: 107816. https://doi.org/10.1016/j.radphyschem.2018.04.009.

77 Moad, G. (2019). *J. Polym. Sci., Part A: Polym. Chem.* 57: 216–227. https://doi.org/10.1002/pola.29199.

78 Tian, X., Ding, J., Zhang, B. et al. (2018). *Polymers* 10: 318. https://doi.org/10.3390/polym10030318.

79 Foster, J.C., Radzinski, S.C., and Matson, J.B. (2017). *J. Polym. Sci., Part A: Polym. Chem.* 55: 2865–2876. https://doi.org/10.1002/pola.28621.

80 An, Z. (2020). *ACS Macro Lett.* 9: 350–357. https://doi.org/10.1021/acsmacrolett.0c00043.

81 Fang, J., Yan, K., and Luo, Y. (2018). Synthesis of well-defined polystyrene with molar mass exceeding 500 kg/mol by RAFT emulsion polymerization. In: *Reversible Deactivation Radical Polymerization: Materials and Applications*, ACS

Symposium Series 1285 (eds. K. Matyjaszewski, H. Gao, B.S. Sumerlin and N.V. Tsarevsky), 81–106. Washington, DC: American Chemical Society. https://doi.org/10.1021/bk-2018-1285.ch005.

82 Wang, X. and Gao, H. (2017). *Polymers* 9: 188. https://doi.org/10.3390/polym9060188.

83 Gao, Y., Zhou, D., Lyu, J. et al. (2020). *Nat. Rev. Chem.* 4: 194–212. https://doi.org/10.1038/s41570-020-0170-7.

84 Mocny, P. and Klok, H.-A. (2020). *Prog. Polym. Sci.* 100: 101185. https://doi.org/10.1016/j.progpolymsci.2019.101185.

85 Beyer, V.P., Kim, J., and Becer, C.R. (2020). *Polym. Chem.* 11: 1271–1291. https://doi.org/10.1039/C9PY01571J.

86 Mane, S.R. (2020). *New J. Chem.* 44: 6690–6698. https://doi.org/10.1039/C9NJ05638F.

87 Penfold, N.J.W., Yeow, J., Boyer, C., and Armes, S.P. (2019). *ACS Macro Lett.* 8: 1029–1054. https://doi.org/10.1021/acsmacrolett.9b00464.

88 Chen, S.-l., Shi, P.-f., and Zhang, W.-q. (2017). *Chin. J. Polym. Sci.* 35: 455–479. https://doi.org/10.1007/s10118-017-1907-8.

89 Gurnani, P. and Perrier, S. (2020). *Prog. Polym. Sci.* 102: 101209. https://doi.org/10.1016/j.progpolymsci.2020.101209.

90 Hu, Q., Gan, S., Bao, Y. et al. (2020). *J. Mater. Chem. B* 8: 3327–3340. https://doi.org/10.1039/C9TB02419K.

91 Kim, S. and Sikes, H.D. (2020). *Polym. Chem.* 11: 1424–1444. https://doi.org/10.1039/C9PY01801H.

92 Ida, S. (2019). *Polym. J.* 51: 803–812. https://doi.org/10.1038/s41428-019-0204-5.

93 Messina, M.S., Messina, K.M.M., Bhattacharya, A. et al. (2020). *Prog. Polym. Sci.* 100: 101186. https://doi.org/10.1016/j.progpolymsci.2019.101186.

94 Wang, Y. and Wu, C. (2018). *Biomacromolecules* 19: 1804–1825. https://doi.org/10.1021/acs.biomac.8b00248.

95 Sui, B., Cheng, C., and Xu, P. (2019). *Adv. Ther.* 2: 1900062. https://doi.org/10.1002/adtp.201900062.

96 Van Bruggen, C., Hexum, J.K., Tan, Z. et al. (2019). *Acc. Chem. Res.* 52: 1347–1358. https://doi.org/10.1021/acs.accounts.8b00665.

97 Pramudya, I. and Chung, H. (2019). *Biomater. Sci.* 7: 4848–4872. https://doi.org/10.1039/C9BM01385G.

98 Loczenski Rose, V., Mastrotto, F., and Mantovani, G. (2017). *Polym. Chem.* 8: 353–360. https://doi.org/10.1039/C6PY01855F.

99 Sponchioni, M., Palmiero, U.C., and Moscatelli, D. (2019). *Mater. Sci. Eng., C* 102: 589–605. https://doi.org/10.1016/j.msec.2019.04.069.

100 Nagase, K. and Okano, T. (2018). Thermoresponsive polymer brushes for thermally modulated cell adhesion and detachment. In: *Polymer and Biopolymer Brushes*, vol. 1 (eds. O. Azzaroni and I. Szleifer), 361–375. Hoboken, NJ: Wiley. https://doi.org/10.1002/9781119455042.ch12.

101 Taylor, M.J., Tomlins, P., and Sahota, T.S. (2017). *Gels* 3: 4. https://doi.org/10.3390/gels3010004.

102 Sun, H., Yang, L., Thompson, M.P. et al. (2019). *Bioconjugate Chem.* https://doi.org/10.1021/acs.bioconjchem.9b00166.

103 Yang, D.-P., Oo, M.N.N.L., Deen, G.R. et al. (2017). *Macromol. Rapid Commun.* 38: 1700410. https://doi.org/10.1002/marc.201700410.

104 Khor, S.Y., Quinn, J.F., Whittaker, M.R. et al. (2019). *Macromol. Rapid Commun.* 40: 1800438. https://doi.org/10.1002/marc.201800438.

105 Pollard, J. and Bruns, N. (2018). Biocatalytic ATRP. In: *Reversible Deactivation Radical Polymerization: Mechanisms and Synthetic Methodologies*, ACS Symposium Series 1284 (eds. K. Matyjaszewski, H. Gao, B.S. Sumerlin and N.V. Tsarevsky), 379–393. American Chemical Society. https://doi.org/10.1021/bk-2018-1284.ch019.

106 Rodriguez, K.J., Gajewska, B., Pollard, J. et al. (2018). *ACS Macro Lett.* 7: 1111–1119. https://doi.org/10.1021/acsmacrolett.8b00561.

107 Lv, C., Du, Y., and Pan, X. (2020). *J. Polym. Sci.* 58: 14–19. https://doi.org/10.1002/pola.29477.

108 Reyhani, A., McKenzie, T.G., Fu, Q., and Qiao, G.G. (2019). *Macromol. Rapid Commun.* 40: 1900220. https://doi.org/10.1002/marc.201900220.

109 Moad, G. (2019). *Prog. Polym. Sci.* 88: 130–188. https://doi.org/10.1016/j.progpolymsci.2018.08.003.

110 Zhou, Y.-N., Li, J.-J., Wu, Y.-Y., and Luo, Z.-H. (2020). *Chem. Rev.* 120: 2950–3048. https://doi.org/10.1021/acs.chemrev.9b00744.

111 Duffy, C., Zetterlund, P.B., and Aldabbagh, F. (2018). *Molecules* 23: 465. https://doi.org/10.3390/molecules23020465.

112 Gong, H., Gu, Y., and Chen, M. (2018). *Synlett* 29: 1543–1551 (1543 pp). https://doi.org/10.1055/s-0036-1591974.

113 Kamigaito, M. and Satoh, K. (2017). Sustainable vinyl polymers via controlled polymerization of terpenes. In: *Sustainable Polymers from Biomass* (eds. C. Tang and C.Y. Ryu), 55–90. Weinheim: Wiley-VCH. https://doi.org/10.1002/9783527340200.ch4.

114 Wang, J., Liu, S., Yu, J. et al. (2017). Rosin-derived monomers and their progress in polymer application. In: *Sustainable Polymers from Biomass* (eds. C. Tang and C.Y. Ryu), 103–149. Weinheim: Wiley-VCH. https://doi.org/10.1002/9783527340200.ch6.

115 Yuan, L., Wang, Z., Trenor, N.M., and Tang, C. (2017). Preparation and applications of polymers with pendant fatty chains from plant oils. In: *Sustainable Polymers from Biomass* (eds. C. Tang and C.Y. Ryu), 181–207. Weinheim: Wiley-VCH. https://doi.org/10.1002/9783527340200.ch8.

116 Ganewatta, M.S., Lokupitiya, H.N., and Tang, C. (2019). *Polymers* 11: 1176. https://doi.org/10.3390/polym11071176.

117 Cheaburu-Yilmaz, C.N., Karavana, S.Y., and Yilmaz, O. (2017). *Curr. Org. Synth.* 14: 785–797. https://doi.org/10.2174/1570179414666161115150818.

118 Eskandari, P., Abousalman-Rezvani, Z., Roghani-Mamaqani, H. et al. (2019). *Adv. Colloid Interface Sci.* 273: 102021. https://doi.org/10.1016/j.cis.2019.102021.

119 Abousalman-Rezvani, Z., Eskandari, P., Roghani-Mamaqani, H., and Salami-Kalajahi, M. (2020). *Adv. Colloid Interface Sci.* 278: 102126. https://doi.org/10.1016/j.cis.2020.102126.

120 Pasini, D. and Nitti, A. (2020). *Eur. Polym. J.* 122: 109378. https://doi.org/10.1016/j.eurpolymj.2019.109378.

121 Junkers, T. and Laun, J. (2018). Controlled reversible deactivation radical photopolymerization. In: *Photopolymerisation Initiating Systems* (eds. J. Lalevée and J.-P. Fouassier), 244–273. Cambridge: The Royal Society of Chemistry. https://doi.org/10.1039/9781788013307-00244.

122 Buss, B.L. and Miyake, G.M. (2018). *Chem. Mater.* 30: 3931–3942. https://doi.org/10.1021/acs.chemmater.8b01359.

123 Burridge, K.M., Wright, T.A., Page, R.C., and Konkolewicz, D. (2018). *Macromol. Rapid Commun.* 39: 1800093. https://doi.org/10.1002/marc.201800093.

124 Shanmugam, S., Xu, J., and Boyer, C. (2017). *Macromol. Rapid Commun.* 38: 1700143. https://doi.org/10.1002/marc.201700143.

125 Yu, J.R., Zuo, Y., and Xiong, Y.B. (2018). Thermo-responsive poly(ionic liquid) nanogels prepared via one-step cross-linking copolymerization. In: *Polymerized Ionic Liquids* (ed. A. Eftekhari), 202–224. Cambridge: The Royal Society of Chemistry. https://doi.org/10.1039/9781788010535-00202.

126 Chen, F., Lin, F., Zhang, Q. et al. (2019). *Macromol. Rapid Commun.* 40: 1900101. https://doi.org/10.1002/marc.201900101.

127 Bagheri, A. and Jin, J. (2019). *ACS Appl. Polym. Mater.* 1: 593–611. https://doi.org/10.1021/acsapm.8b00165.

128 Zhu, J., Yang, C., Lu, C. et al. (2018). *Acc. Chem. Res.* 51: 3191–3202. https://doi.org/10.1021/acs.accounts.8b00444.

129 Palmiero, U.C., Sponchioni, M., Manfredini, N. et al. (2018). *Polym. Chem.* 9: 4084–4099. https://doi.org/10.1039/C8PY00649K.

130 Kreutzer, J. and Yagci, Y. (2018). *Polymers* 10: 35. https://doi.org/10.3390/polym10010035.

131 Chang, Y.A. and Waymouth, R.M. (2017). *J. Polym. Sci., Part A: Polym. Chem.* 55: 2892–2902. https://doi.org/10.1002/pola.28635.

132 Lunn, D.J., Discekici, E.H., Read de Alaniz, J. et al. (2017). *J. Polym. Sci., Part A: Polym. Chem.* 55: 2903–2914. https://doi.org/10.1002/pola.28575.

133 Zhao, L., Liu, X., Zhang, L. et al. (2017). *Coord. Chem. Rev.* 337: 34–79. https://doi.org/10.1016/j.ccr.2017.02.009.

2

Terminology in Reversible Deactivation Radical Polymerization (RDRP) and Reversible Addition–Fragmentation Chain Transfer (RAFT) Polymerization

Graeme Moad

CSIRO Manufacturing, Research Way, Clayton, VIC 3168, Australia

2.1 Terminology for Reversible Deactivation Radical Polymerization (RDRP)

In this chapter, we consider the terminology used to describe reversible deactivation radical polymerization (RDRP) and reversible addition–fragmentation chain transfer (RAFT) polymerization. RDRP [1] is a recently introduced term to describe what, until 2010, had been known under various terms that include living radical polymerization, controlled radical polymerization, controlled/living radical polymerization, quasi-living radical polymerization, pseudo-living polymerization, mediated polymerization, and some others.

The decade prior to 2010 had seen controversy over the use of the terms 'living' and 'controlled' for describing radical polymerizations that show some living characteristics [2–7]. The IUPAC recommendation that a living polymerization is 'a chain polymerization from which irreversible chain transfer and irreversible chain termination (deactivation) are absent' precluded the use of the term 'living' when describing any form of radical process [8]. In any polymerization that involves radicals as the propagating species, some termination is inevitable even if the products are not always readily detected. With respect to other forms of polymerization, it is acceptable to use the term that describes a dominant reaction mechanism and characteristics of the process, even if side reactions occur or are possible.

The use of the adjective 'controlled' by itself, without some explanation, to designate these polymerizations is also contrary to IUPAC recommendations. The term, controlled polymerization, should only be used when the particular aspect of polymerization that is being controlled has been specified. The word should not be used in an exclusive sense to mean a particular form of polymerization since it has an established, much broader usage. The construct 'controlled living polymerization' would seem acceptable when used to refer to those living polymerizations whose outcomes are defined by controlling the reaction conditions or other features, but the adjective 'controlled' must not be used to specify systems as having a lesser degree of livingness. Terms such as 'pseudo-living' and 'quasi-living'

RAFT Polymerization: Methods, Synthesis and Applications, First Edition.
Edited by Graeme Moad and Ezio Rizzardo.

Table 2.1 IUPAC recommendations on terminology for reversible deactivation radical polymerization (RDRP).

Term	Definition	Notes	References
controlled polymerization	Term indicating control of a certain kinetic feature of a polymerization or structural aspect of the polymer molecules formed, or both.	*Note 1*: The expression "controlled polymerization" is sometimes used to describe a *radical* or *ionic polymerization* in which *reversible deactivation* of the *chain carriers* is an essential component of the mechanism, interrupting the propagation to secure control of one or more kinetic features of the *polymerization* or one or more structural aspects of the macromolecules formed, or both. *Note 2*: The expression *controlled radical polymerization* is sometimes used to describe a radical polymerization conducted in the presence of reagents that lead to, e.g., *atom-transfer radical polymerization* (ATRP), *nitroxide-[aminoxyl] mediated polymerization* (NMP), or *reversible-addition-fragmentation chain transfer* (RAFT) polymerization. *Note 3*: Generally, the adjective "controlled" should not be used without specifying the particular kinetic or structural feature that is subject to control.	[1, 8]
living polymerization	*Chain polymerization* in which *chain termination* and irreversible *chain transfer* are absent.	*Note 1*: In many cases, the rate of *chain initiation* is fast compared with the rate of *chain propagation*, so that the number of *kinetic-chain carriers* is essentially constant throughout the reaction. This is not a necessary condition for living polymerization. *Note 2*: In a living polymerization, the reversible (temporary) deactivation of *active sites* can take place (see *reversible chain deactivation*). *Note 3*: In a living polymerization, all the macromolecules formed possess the potential for further growth. *Note 4*: Use of the adjectives "pseudo-living", "quasi-living", and "immortal" is discouraged.	[1, 8]

reversible-deactivation radical polymerization, RDRP **controlled reversible-deactivation radical polymerization**	*Chain polymerization*, propagated by radicals that are deactivated reversibly, bringing them into active-dormant equilibria of which there might be more than one.	*Note 1:* The abbreviated term "controlled radical polymerization" shall be permitted, provided that its context (i.e., the nature of the control) is specified at the first occurrence. *Note 2:* Names containing the word "living" are discouraged. Definition 84 in the Kinetics document [8] stipulates that chain termination and irreversible chain transfer must be absent if a polymerization is to be regarded as living. Examples of discouraged terms include "living radical polymerization", "controlled/living polymerization" and "quasi-living polymerization". *Note 3:* Atom-transfer radical polymerization, reversible-addition-fragmentation chain-transfer polymerization, and polymerization mediated by an aminoxyl (or similarly acting substance) all fall into this polymerization category. *Note 4:* When the equilibria are established rapidly compared to the rate of propagation, the process may show many of the observable characteristics associated with living polymerization. One consequence of rapid equilibration is that it may become possible to exert control over the shape of the chain-length distribution, prepare polymers of low dispersity (i.e., polymers with a high degree of uniformity), and extend chains to form block copolymers, the block lengths of which are of low dispersity, by the sequential addition of monomers. Although some termination is inevitably taking place, the equilibrium between the remaining propagating radicals and dormant species is maintained.	[1]

are also discouraged by IUPAC [1, 8]. It has been stated that the definition of living polymerization 'tolerates no restrictive adjectives implying something close to but not strictly living' [5] (Table 2.1).

2.2 Terminology in Reversible Addition–Fragmentation Chain Transfer (RAFT) Polymerization

Much of the terminology used to describe RAFT polymerization is illustrated in the simplified mechanism shown in Scheme 2.1. Initiation, propagation, and termination are the same as in radical polymerization (Table 2.2).

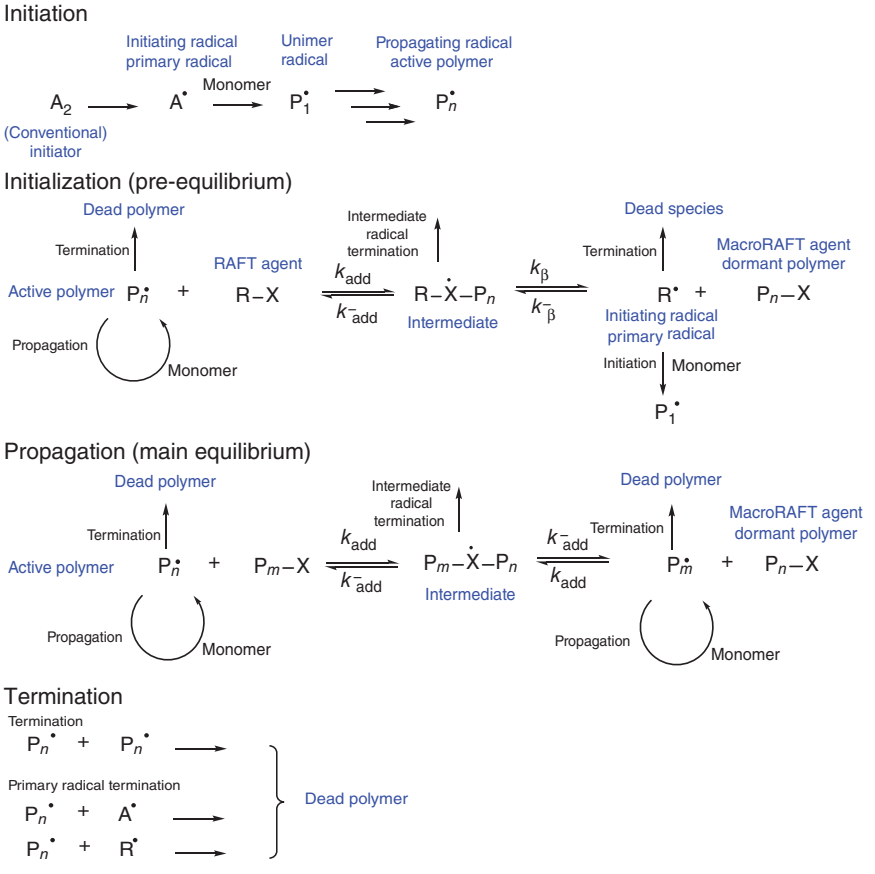

Scheme 2.1 Simplified mechanism for reversible addition–fragmentation chain transfer (RAFT) polymerization with initiation by a conventional initiator (A_2), e.g. a dialkyldiazene. Source: Figure adapted from Moad, Chemistry of Radical Polymerization, © Elsevier 2021.

Table 2.2 IUPAC recommendations on terminology for reversible addition–fragmentation chain transfer (RAFT) polymerization.

Term	Definition	Notes	References
chain deactivation	Conversion of a *chain carrier* into an inactive species.	*Note 1:* Chain deactivation, unlike chain termination, may be reversible; see reversible chain deactivation. *Note 2:* The reverse of chain deactivation is *chain reactivation*.	[8]
chain initiation (in a chain polymerization) **initiation**	Chemical reaction in which *initiating species* add to monomer to form *chain carriers*.	*Note*: The recommended symbol for the rate constant for chain initiation in a *polymerization* is k_i.	[8]
chain propagation (in a chain polymerization) **propagation**	Chemical reaction between a *chain carrier* and a monomer that results in the growth of a polymer chain and the regeneration of at least one chain carrier.	*Note 1*: The recommended symbol for the rate constant for chain propagation in a *homopolymerization* is k_p. *Note 2:* For chain propagation in copolymerization, see cross-propagation.	[8]
chain reactivation **chain activation**	Conversion of an inactive chain into a *chain carrier*.		[8]
chain termination (in a chain polymerization) **irreversible chain deactivation, termination**	Chemical reaction in which a *chain carrier* is converted irreversibly into a non-propagating species without the formation of a new chain carrier.	*Note 1*: The recommended symbol for the rate constant or coefficient for chain termination in a *homopolymerization* is k_t. *Note 2*: The term "chain deactivation" is often used to stress that, in contrast to chain termination, the formation of non-propagating species may be reversible; see *chain deactivation* and *reversible chain deactivation*. Note 3: See also combination, cross-termination, disproportionation, and spontaneous termination.	[8]
chain transfer (in a chain polymerization) **transfer**	Chemical reaction occurring during a *chain polymerization* in which an *active center* is transferred from a growing macromolecule or oligomer molecule to another molecule or to another site on the same molecule.	*Note 1*: See also intermolecular chain transfer, intramolecular chain transfer, and backbiting. Note 2: The recommended symbol for the rate constant of chain transfer in a *homopolymerization* is k_{tr}.	[8]

(*continued*)

Table 2.2 (Continued)

Term	Definition	Notes	References
chain-transfer agent **transfer agent**	Substance able to react with a chain carrier by a reaction in which the original *chain carrier* is deactivated and a new *chain carrier* is generated.	*Note:* In a *polymerization*, the common occurrence is that a new *chain carrier* of lower molar mass is generated.	[8]
chain-transfer constant, C_{tr}	In a *homopolymerization*, rate constant for chain transfer, k_{tr}, divided by the rate constant for *chain propagation, k_p, i.e.,* $C_{tr} = k_{tr}/k_p$.		[8]
degenerative chain transfer **degenerate chain transfer**	Chain transfer reaction that generates a new *chain carrier* and a new *chain-transfer agent* with the same reactivity as the original *chain carrier* and *chain-transfer agent*.		[8]
degradative chain transfer	*Chain-transfer* reaction that generates a new *chain carrier* of much lower reactivity than that of the original chain carrier.		[8]
degenerate-transfer radical polymerization, DTRP	*Controlled reversible-deactivation radical polymerization* in which the deactivation of the radicals involves degenerative transfer (DT) of a group (or atom).	*Note*: Examples of DT-active groups include those mentioned below under *reversible-addition-fragmentation chain-transfer polymerization*, iodine (iodine transfer polymerization, ITP) and certain derivatives of Te, As, Sb, or Bi.	[1]
dormant polymer chain	Temporarily deactivated *chain carrier*.		[1]

initiating species	Species to which monomer adds to start *chain polymerization*.	*Note 1*: An initiating species may be formed from an *initiator* or be the initiator itself. *Note 2*: In radical polymerization, initiating species formed directly from an initiator are called *primary radicals*.	[8]
initiator	Substance introduced into a reaction system in order to cause *chain initiation*.	*Note*: In contrast to a catalyst, an initiator is consumed in the reaction.	[8]
initiator efficiency, *f*	Number of growing chains initiated divided by the number of *active centers* generated from *initiator* molecules.	*Note 1*: In a *radical polymerization*, the rate of radical production from an initiator that provides two similar radicals is $2k_d f$, where k_d is the rate constant for initiator decomposition. *Note 2*: In some texts, the initiator efficiency is defined as the fraction of radicals that escapes the cage (see *cage effect*).	[8]
primary radical (in a chain polymerization)	*Radical* that is formed from an *initiator* or monomer molecule and that is capable of initiating *polymerization*.	*Note 1*: A primary *radical* may be formed by the action of heat, irradiation or electrode charge transfer. *Note 2*: The recombination of primary radicals and their reactions with other species may lead to reduced *initiator efficiency*. *Note 3*: The term "primary radical" is also used to designate a radical centered on a primary carbon atom, for example, an ethyl radical. See secondary radical.	[8]
secondary radical (in a chain polymerization)	*Radical* formed by the rearrangement or fragmentation of a *primary radical* that is capable of initiating a *polymerization*.	*Note*: The term "secondary radical" is also used to designate a radical centered on a secondary carbon atom, e.g., a 2-propyl radical. See *primary radical*.	[8]

(*continued*)

Table 2.2 (Continued)

Term	Definition	Notes	References
reversible-addition-fragmentation chain-transfer polymerization **RAFT polymerization, RAFT**	*Degenerate-transfer radical polymerization* in which chain activation and chain deactivation involve a degenerative chain-transfer process which occurs by a two-step addition-fragmentation mechanism.	*Note 1*: Examples of RAFT agents include certain dithioesters, trithiocarbonates, xanthates (dithiocarbonates), and dithiocarbamates. *Note 2*: RAFT with xanthates is also known as MADIX (macromolecular design by interchange of xanthate).	[1]
reversible chain deactivation	Deactivation of a *chain carrier* in a *chain polymerization*, reversibly converting an *active center* into an inactive one and then, within the average lifetime of a growing macromolecule, regenerating an active center on the same *original carrier*.	*Note 1*: The temporarily deactivated species created in this process are often described as dormant. *Note 2*: Reversible deactivation often involves reversible *combination* or reversible *chain transfer*.	[1]

Table 2.3 Additional terminology for reversible addition–fragmentation chain transfer (RAFT) polymerization.

Term	Definition	Notes
blocking efficiency (in RAFT polymerization)	Fraction of an initial macroRAFT agent converted to a block copolymer in the course of RAFT polymerization.	
initialization (in RAFT polymerization)	Process for conversion of an initial RAFT agent to a macroRAFT agent	
initialization efficiency (in RAFT polymerization)	Fraction of an initial RAFT agent converted to a macroRAFT agent in the course of RAFT polymerization.	*Note:* when the initial RAFT agent is a macroRAFT agent the term blocking efficiency may be used.
intermediate (in RAFT polymerization)	Transient intermediate formed by radical addition to a RAFT agent or macroRAFT agent	
intermediate radical termination	Termination reaction where one reactant is the intermediate formed by radical addition to a RAFT agent or macroRAFT agent.	
reversible addition-fragmentation chain transfer agent **RAFT agent**	(a) A transfer agent that provides chain transfer by a reversible addition-fragmentation mechanism (b) Reagent that reacts by addition to give an intermediate that fragments to provide a product which is in itself a RAFT agent.	
macroRAFT agent	(a) RAFT agent formed during RAFT polymerization comprising one or more monomer units. (b) RAFT agent formed by end-functionalization of a preformed polymer or oligomer.	
SUMI-RAFT agent **unimer RAFT agent**	A *macroRAFT* agent that comprises only one unit of monomer.	
thiocarbonylthio RAFT agent	RAFT agent where the reactive double bond is a thiocarbonyl double bond.	
macromonomer RAFT agent	RAFT agent where the reactive double bond is a carbon-carbon double bond	
unimer	Species derived from a single monomer unit	

2.3 Terminology That Is Not Ratified by IUPAC

The terms below are commonly encountered in describing RAFT polymerization but are not defined in the current IUPAC document. These terms may form part of a proposed IUPAC document *Terminology for Chain Polymerization* currently in preparation [9] (Table 2.3).

References

1 Jenkins, A.D., Jones, R.I., and Moad, G. (2010). *Pure Appl. Chem.* 82: 483–491. https://doi.org/10.1351/PAC-REP-08-04-03.

2 Matyjaszewski, K. and Mueller, A.H.E. (1997). *Polym. Prepr. (Am. Chem. Soc., Div. Polym. Chem.)* 38 (1): 6–9.

3 Ivan, B. (2000). *Polym. Prepr. (Am. Chem. Soc., Div. Polym. Chem.)* 41 (2): 6a–12a.

4 Howell, B.A. (2000). *Polym. Mater. Sci. Eng.* 83: 578.

5 Quirk, R.P. and Lee, B. (1992). *Polym. Int.* 27: 359–367. https://doi.org/10.1002/pi.4990270412.

6 Darling, T.R., Davis, T.P., Fryd, M. et al. (2000). *J. Polym. Sci., Part A: Polym. Chem.* 38: 1706–1708. https://doi.org/10.1002/(SICI)1099-0518(20000515)38:10<1706::AID-POLA20>3.0.CO;2-5.

7 Darling, T.R., Davis, T.P., Fryd, M. et al. (2000). *J. Polym. Sci., Part A: Polym. Chem.* 38: 1709. https://doi.org/10.1002/(SICI)1099-0518(20000515)38:10<1709::AID-POLA30>3.0.CO;2-W.

8 Penczek, S. and Moad, G. (2008). *Pure Appl. Chem.* 80: 2163–2193. https://doi.org/10.1351/pac200880102163.

9 Anon. (2014). *Chemistry International* 32 (4): 24–24. https://doi.org/10.1515/ci.2010.32.4.24.

3

How to Do a RAFT Polymerization

Almar Postma and Melissa Skidmore

CSIRO Manufacturing, Bayview Avenue, Clayton, VIC 3168, Australia

3.1 Introduction

Reversible addition–fragmentation chain transfer (RAFT) polymerization is one of the most versatile methods for providing living characteristics to radical polymerization. RAFT polymerization provides the ability to control polymerization of most monomers polymerizable by radical polymerization.

In an ideal living polymerization, all chains are initiated at the beginning of the process, grow at a similar rate, and survive the polymerization (there is no irreversible chain transfer or termination). If initiation is rapid with respect to propagation the molecular weight distribution is very narrow, and chains can be extended by the provision of further monomer. In a radical polymerization all chains cannot be simultaneously active. In RAFT polymerization, the majority of living chains are maintained in a dormant form. A rapid equilibrium between active (propagating radicals) and dormant chains (macroRAFT agents) ensures that all chains grow at a similar rate. Under these conditions, molecular weights can increase linearly with conversion and molecular weight distributions can be very narrow.

The reactions associated with RAFT equilibria (Scheme 3.1) are in addition to those that occur during conventional radical polymerization (i.e. initiation, propagation, and termination). The RAFT agent is a transfer agent and does not suppress termination. Retention of the thiocarbonylthio groups in the polymeric product is responsible for the living character of RAFT polymerization. RAFT polymerization can be used in the synthesis of well-defined homo-, gradient, diblock, triblock, and star polymers and more complex architectures including microgels and polymer brushes (Figure 3.1).

The best way to understand the power of RAFT polymerization is to simply perform a conventional radical polymerization and then perform the same polymerization and add an appropriately selected RAFT agent (see Table 3.1, Figure 3.2) to it. Nearly all conventional radical polymerizations and, in particular,

RAFT Polymerization: Methods, Synthesis and Applications, First Edition.
Edited by Graeme Moad and Ezio Rizzardo.

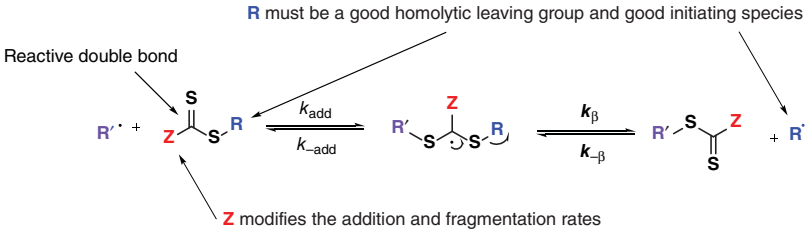

Scheme 3.1 Mechanism for reversible addition–fragmentation chain transfer (RAFT).

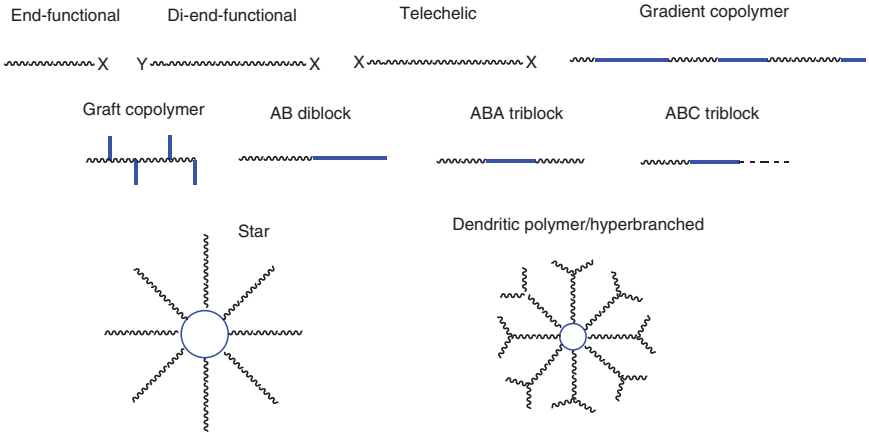

Figure 3.1 Polymer architectures amenable to RAFT polymerization.

solvent-based radical polymerizations, can easily become RAFT polymerizations; the same solvents, initiators, and reaction temperatures can be used. It should be noted that for optimal control of the RAFT process, it is important to pay attention to factors such as initiator concentration and RAFT agent selection. Standard ratios of reagents are [initiator]/RAFT/[monomer] = [1]/[4–10]/[2000–5000]. One starting point may be to choose the conditions such that the target molecular weight is ~10% of that which would have been obtained in the absence of the RAFT agent. The molecular weight can be predicted using Eq. (3.1) or, if initiator-derived chains are significant, Eq. (3.2); $M_{n(calc)}$ is the predicted molecular weight, X is the monomer conversion, mM and mRAFT are molecular weights of the monomer and the RAFT agent respectively, and [M] and [RAFT] are the initial concentrations of the monomer and RAFT agent respectively. In Eq. (3.2), $M_{n(calc)}$ is the predicted molecular weight, mM and mRAFT are the molecular weights of the monomer and the RAFT agent respectively, $[M]_0$ and $[M]_f$ are the concentrations of the monomer at the start and end of the reaction respectively, $[RAFT]_0$ is the concentration of the RAFT agent at the start of the reaction, $[I]_0$ and $[I]_f$ are the concentrations of the initiator at the start and end of the reaction respectively, mRAFT is the molecular

Table 3.1 A list of selected commonly used RAFT agents with their suitability for various monomer types: **A** excellent control of molecular weight with low dispersities (<1.1); **B** excellent control of molecular weight with moderate dispersities; **C** good control of molecular weight with high dispersities (>1.3); **X** not suitable.

	Styrenes	Acrylate	Methacrylates	Acrylamides	Methacrylamides	Vinyl esters	Vinyl amides
	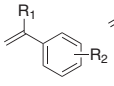	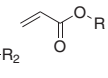					
RAFT agent							
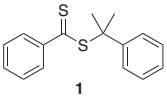 1	**A**	**A**	**A**	**A**	**A**	**X**	**X**
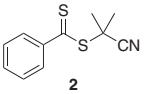 2	**A**	**A**	**A**	**A**	**A**	**X**	**X**
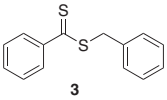 3	**B**	**B**	**X**	**B**	**X**	**X**	**X**
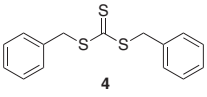 4	**B**	**B**	**X**	**B**	**X**	**X**	**X**
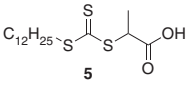 5	**B**	**B**	**X**	**B**	**X**	**X**	**X**
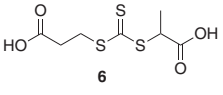 6	**B**	**B**	**X**	**B**	**X**	**X**	**X**
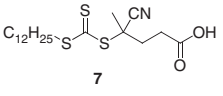 7	**A**	**A**	**A**	**A**	**A**	**X**	**X**
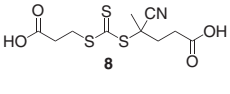 8	**A**	**A**	**A**	**A**	**A**	**X**	**X**
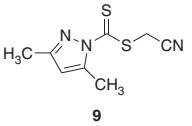 9	**A**	**A**	**X**	**A**	**X**	**B**	**B**

Table 3.1 (Continued)

	Styrenes	Acrylate	Methacrylates	Acrylamides	Methacrylamides	Vinyl esters	Vinyl amides
	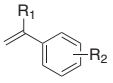						
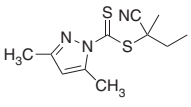 10	A	A	C	C	C	B	B
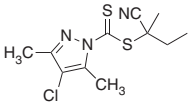 11	A	A	B	B	B	B	B
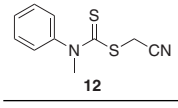 12	X	X	X	X	X	A	A

Source: Table adapted Rizzardo et al. [1]. © John Wiley and Sons.

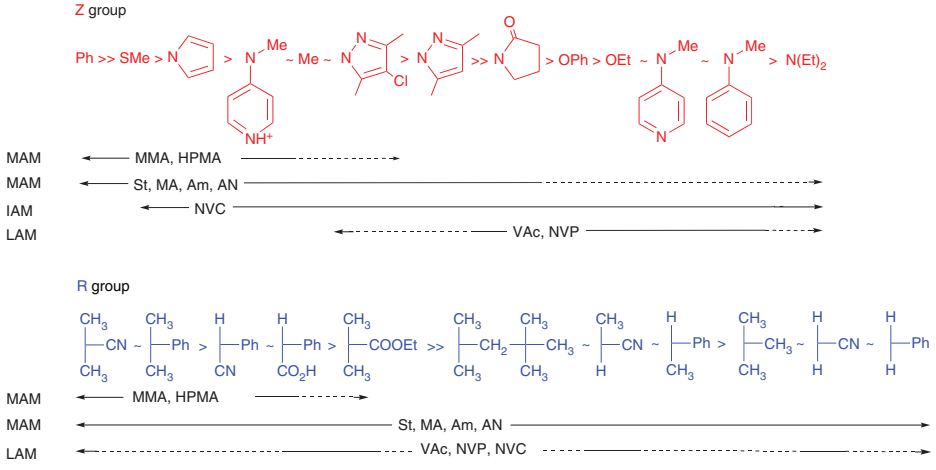

Figure 3.2 Guidelines for the selection of RAFT agents for various polymerizations. For Z, addition rates decrease and fragmentation rates increase from left to right. For R, fragmentation rates decrease from left to right. Dashed line indicates partial control (i.e. control of molar mass but poor control over dispersity or substantial retardation in the case of VAc, NVC, or NVP). AN - acrylonitrile, HPMA - *N*-(2-hydroxypropyl)methacrylamide, Am - acrylamide. Source: Figure adapted from Moad et al. [2]. © CSIRO and Gardiner et al. [3]. © Society of Chemical Industry.

weight of the RAFT agent, d is the number of chains produced from radical–radical termination, and f is the initiator efficiency [2].

$$M_n\,(\text{calc}) = \left(X\frac{[\text{M}]_0}{[\text{RAFT}]_0}m\text{M}\right) + m\text{RAFT} \tag{3.1}$$

$$M_n\,(\text{calc}) = \frac{[\text{M}]_0 - [\text{M}]_f}{[\text{RAFT}]_0 + df([\text{I}]_0 - [\text{I}]_t)}m\text{M} + m\text{RAFT} \tag{3.2}$$

3.2 IP Landscape

There is now no barrier to scale up RAFT polymerization procedures as RAFT agents are now commercially available in gram to ton quantities through Boron Molecular, http://www.boronmolecular.com/raftmonotable, in smaller quantities from chemical suppliers such as STREM, Merck (Sigma-Aldrich), and FUJIFILM Wako Pure Chemical Corporation, and due to the expiration of a number of the foundation patents there is increased freedom to utilize RAFT technology. At the time of printing, if a user is polymerizing a monomer using traditional RAFT agents such as **1**–**7** or **12**, using traditional manufacturing methods described in WO/98/01478 or WO/99/31144, then the user may, after making their own assessment, make RAFT-based polymers without seeking a licence from CSIRO, and in any field. If the user is polymerizing a monomer using any new and improved RAFT agents such as **8**–**11** protected by CSIRO-held patents, such as those stemming from the published applications (WO/2010/083569, WO/2016/197187, WO/2016/054689, and WO/2017/035570) then they will need to seek a licence directly from CSIRO, or by buying the RAFT agents from a licenced commercial supplier subject to a label licence. A summary of the current field restrictions and patent coverage of commonly used RAFT agents is provided in Table 3.2. The label licence sets out the conditions for use of the RAFT agents **8**–**11** and allows the end user to use the RAFT agents for applications outside specifically listed electronics fields. This is because DuPont still holds commercial interest in a few electronic fields and thus users will require pre-approval from DuPont in those fields. Purchasing of RAFT agents from a research supplier may still require a licence from CSIRO, depending on the RAFT agents and the polymerization method adopted and the functionality or end use that is anticipated.

3.3 General Experimental Conditions

In the laboratory, solvents are generally of analytical reagent grade and distilled before use. To remove inhibitors and for further purification, monomers are filtered through neutral or basic alumina (70–230 mesh), fractionally distilled under reduced pressure, and redistilled under reduced pressure immediately prior to use. Initiators such as azobisisobutyronitrile VAZO-64® (AIBN) and 1,1′-azobis(cyclohexanenitrile) VAZO-88® (ACHN) are purified by crystallization

Table 3.2 Summary of field restrictions for commonly used RAFT agents.

RAFT agent	Patent	Electronic field restriction
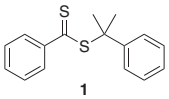 1	WO/98/01478	Expired
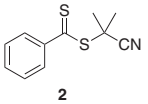 2	WO/98/01478	Expired
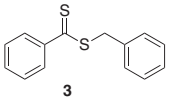 3	WO/98/01478	Expired
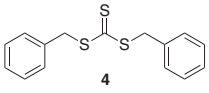 4	WO/98/01478	Expired
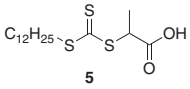 5	WO/98/01478	Expired
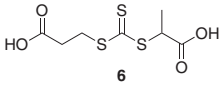 6	WO/98/01478	Expired
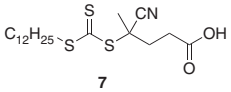 7	WO/98/01478	Expired
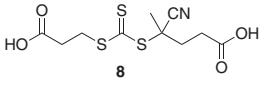 8	WO/2017/035570	Yes
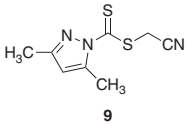 9	WO/2016/197187	Yes
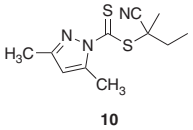 10	WO/2016/197187	Yes
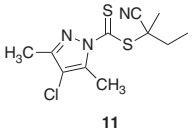 11	WO/2016/054689	Yes
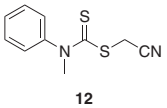 12	WO/99/31144	Expired

Table 3.3 Bulk RAFT polymerization of un-purified commercial MMA with 4-cyano-4-(((dodecylthio) carbonothioyl)thio)pentanoic acid **7** under various degassing methods (10 g MMA, 20 mg **7**, 5 mg AIBN at 80 °C for time specified) [2].

Atmosphere	Time (h)	Conversion (%)	M_n [a)]	$Đ$
Freeze–evacuate	1.5	93	100 000	1.25
N_2 flush	1.5	87	90 000	1.25
In air[b)]	1.5	26	38 000	1.38
In air[b)]	3.0	88	112 000	1.26

a) GPC molecular weight in PSt equivalents.
b) No degassing.
Source: Moad et al. [2]. © CSIRO.

from chloroform/methanol. These precautions allow for reproducibility in a laboratory setting, but are not necessary for successful RAFT polymerization; un-purified monomers and initiators will work effectively, and small adjustments to the amount of initiator may be needed to account for impurities or incomplete degassing. The effects of these factors are exemplified for methyl methacrylate (MMA) with the bulk RAFT polymerization of un-purified commercial MMA with the RAFT agent 4-cyano-4-(((dodecylthio)carbonothioyl)thio)pentanoic acid **7** under various degassing methods; it is seen that all polymerizations provide narrow molecular weight distributions and molecular weight control. However, polymerizations with no degassing give substantial retardation. All polymerizations yield a lower-than-expected molecular weight, which is attributed to the use of un-purified monomer (and molecular weights are in polystyrene equivalents); see Table 3.3, [2]. In the laboratory, freeze–evacuate–thaw cycles are often used to degas polymerization solutions; bubbling or flushing with nitrogen produces very similar results, as exemplified in Table 3.3. Different monomer systems or experimental setups could provide considerably different outcomes to these results for MMA RAFT polymerization.

RAFT polymerization provides the ability to control the polymerization of most monomers polymerizable by conventional radical polymerization. These include (meth)acrylates, (meth)acrylamides, acrylonitrile, styrenes, dienes, and vinyl monomers. It is tolerant of unprotected functionality in the monomer and the solvent (e.g. OH, NR_2, COOH, $CONR_2$, SO_3H). The process is compatible with a wide range of reaction conditions (e.g. bulk, organic or aqueous solution, emulsion, miniemulsion, suspension).

The polymerization conditions for RAFT polymerization (bulk or solution) are generally the same as for conventional radical polymerization. Sections 3.3.1–3.3.4 describe the generic requirements for RAFT polymerization, outside of conventional radical polymerization, that are helpful in achieving favourable outcomes.

3.3.1 Initiator

For polymerizations under RAFT control, careful attention must be paid to the selection and concentration of radical initiators, with the initiator concentration or radical generation chosen such that there is an acceptable rate of polymerization and a low level of radical–radical termination (dead chains). Prolonged polymerization times should be avoided; once full monomer conversion is achieved further exposure to the generated radical can result in dead chains and unwanted radical side reactions.

Conventionally, thermal initiators are used as a radical source (e.g. AIBN, azobis(4-cyanopentanoic acid) [ACPA], dibenzoyl peroxide, potassium peroxydisulfate). However, polymerizations can be initiated with any source of radicals – redox [4, 5], UV and visible [6–9], and γ sources [10–15].

Styrene can self-initiate above 100 °C without the need for an external source of radicals [16].

It should be noted that some initiators (e.g. peroxides and peroxydisulfates) may oxidize RAFT agents and RAFT end-groups [17].

3.3.2 Solvent

The RAFT process is compatible with a wide range of solvents, functional groups, and reaction media, mirroring conventional radical polymerization conditions. These include common organic solvents, protic solvents (alcohols, water [18–21], ionic liquids [22]), and supercritical carbon dioxide [23, 24]. Functional groups to be avoided include primary amines. Care should also be taken in polar media, increasing pH, and when using Lewis acids as RAFT agents can show hydrolytic sensitivity [25–27]. From this, we can infer a trend indicating that the sensitivity is highest with dithiobenzoates, lower with trithiocarbonates or aliphatic dithioesters, and the lowest with dithiocarbamates [25–28].

3.3.3 Temperature

RAFT polymerizations have been performed from below ambient up to 140 °C. Higher temperatures provide higher propagation rates, allowing a higher conversion to be achieved in a shorter period of time. Greater RAFT agent transfer constants and fragmentation rate constants of the intermediates can also be achieved at higher temperatures. In line with this, there is some data to show that narrower molecular weight distributions and reduction in retardation with dithiobenzoates can be obtained at higher temperatures [29].

RAFT agents and RAFT polymer end-groups are known to be unstable at high temperatures for prolonged times [30–35]. In some cases, the RAFT agent is less stable than the resulting polymer end-group, at elevated temperatures. Under those conditions it is best to tailor the polymerization to have fast RAFT agent consumption to the more stable RAFT polymer.

3.3.4 Pressure

High pressure conditions (1–5 kbar) reduce radical–radical termination and increase propagation, allowing for the formation of higher molecular weight polymers at higher polymerization rates [36–39].

The following sections will outline how RAFT polymerization of styrenes (Section 3.4), (meth)acrylates (Section 3.5), (meth)acrylamides (Section 3.6), and vinyl monomers (Section 3.7) can be achieved under various conditions and detail the appropriate experimental methodology for the construction of block copolymers (Section 3.8) using RAFT polymerization.

3.4 RAFT Polymerization of Styrene

Styrene was one of the first monomers used to demonstrate the RAFT process [40]. We demonstrated the effect on molecular weight and dispersity with the addition of 2-phenyl-2-propyl benzodithioate **1** to a conventional radical polymerization. It was shown that thermal polymerization of styrene at 110 °C for 16 hours resulted in a 72% conversion to polystyrene of M_n = 323 700 and $Đ$ = 1.74, whereas in the presence of 1.47×10^{-2} M **1**, polystyrene of M_n = 30 900 and $Đ$ = 1.05 was obtained in 53% yield (Figure 3.3). The lower conversion in the presence of the dithio compound is most likely due to a reduction in the gel effect brought about by the formation of a lower molecular weight polymer. Since this initial work, it has been shown that with lower concentrations of RAFT agents such as **1** or 2-cyano-2-propyl benzodithioate **2** (<0.03 M) the rates of polymerization for styrene and MMA do not vary greatly from that expected in the absence of RAFT agent and appear independent of the particular dithiobenzoate [41–43].

Styrene is a secondary more activated monomer (2° MAM). Good control over RAFT polymerization of styrene and styrenic derivatives requires a RAFT agent suitable for 2° MAMs (see Table 3.1). RAFT agents that are suitable for the

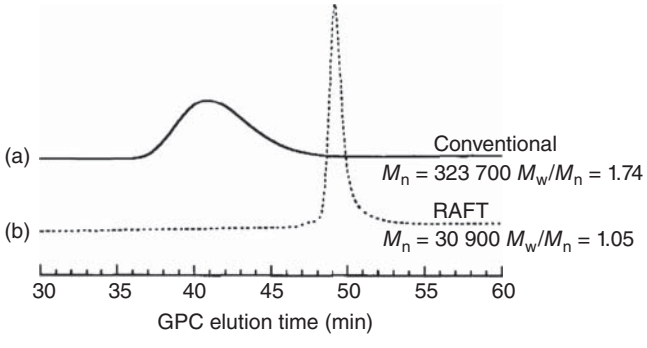

Figure 3.3 Comparison of conventional and RAFT polymerization. (a) Thermal polymerization of styrene at 110 °C. (b) Thermal polymerization of styrene at 110 °C in the presence of 1.47×10^{-2} M of 2-phenyl-2-propyl benzodithioate **1**. Source: Rizzardo et al. [40]. © John Wiley and Sons.

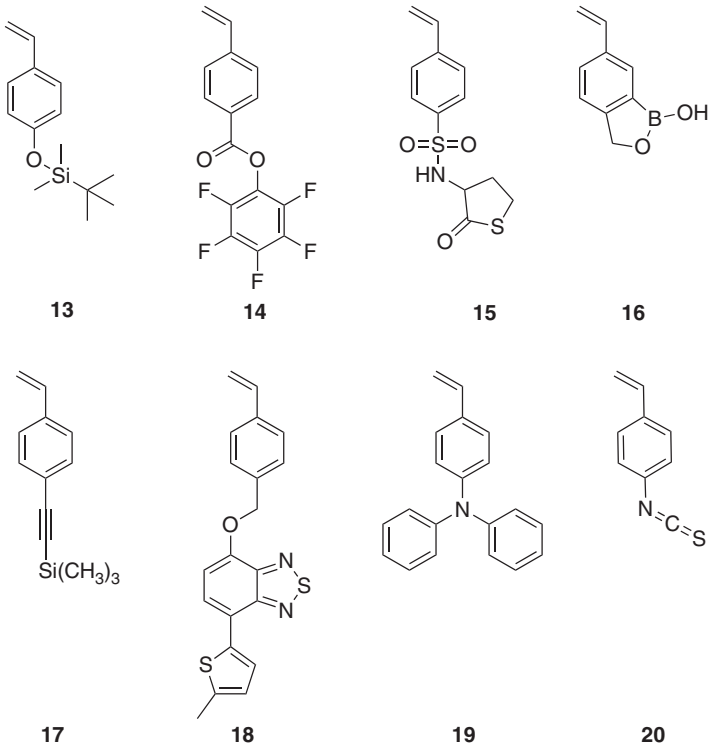

Figure 3.4 Examples of functional styrenic monomers amenable to RAFT polymerization.

polymerization of styrene are primary, secondary, and tertiary dithiobenzoates (Z = Ph), trithiocarbonates (Z = S-R′), and pyrazole dithiocarbamates (Z = N-R′N). RAFT agents that are ineffective for the controlled polymerization of styrene are dithiocarbamates (Z = N-R′$_2$) and xanthates (Z = O-R′). The RAFT polymerization of styrene can be done in bulk, solution, emulsion, or dispersion. RAFT polymerization has been carried out successfully on a number of functional styrenes as depicted in Figure 3.4. These include monomers that contain bulky pendant groups **13** [44], active ester or similar functionality (**14**, **15**) [45, 46], boroxole functionality **16** [47], or alkyne **17** [48] functionality. Many of the functional styrenes have been used to prepare polymers for optoelectronic use (**18**, **19**) [49, 50]. Isocyanate or isothiocyanate functionality **20** [48] is compatible with RAFT polymerization; however, some care must be taken in the selection of the RAFT agent and other components of the polymerization medium such that they do not also contain other functionalities that are inherently reactive (such as carboxy) [51].

3.4.1 Experimental Procedures for the RAFT Polymerization of Styrene

*Bulk polymerization of styrene in the presence of 2-phenyl-2-propyl benzodithioate **1** at 100 °C*. A stock solution of styrene 25 ml and **1** (200 mg) was prepared and 5 ml was transferred to four separate ampoules; the ampoules were degassed with three

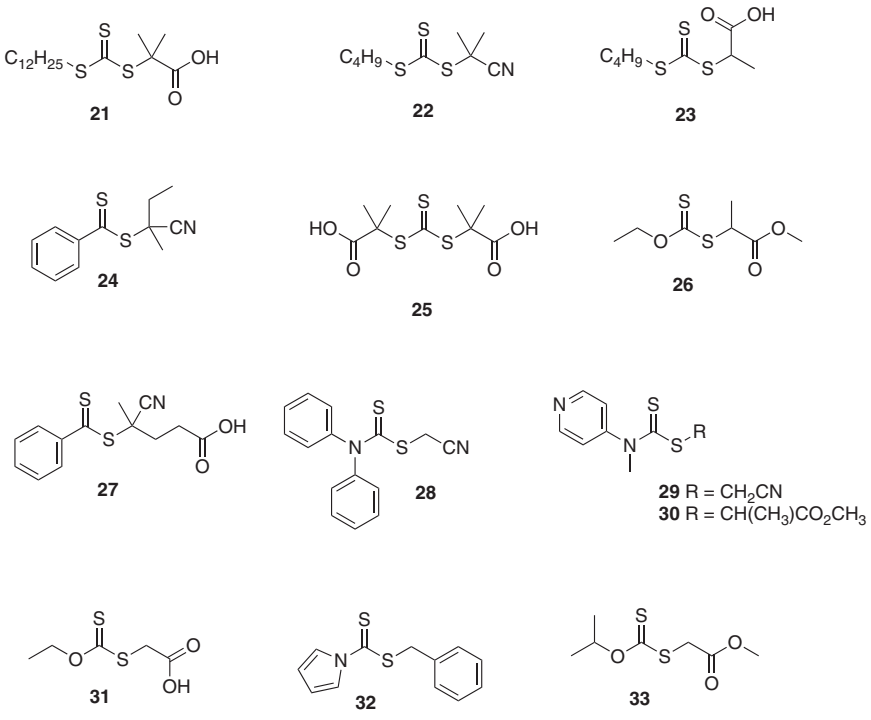

Figure 3.5 Selection of RAFT agents described in experimental procedures. RAFT agents also appear in Tables 3.1 and 3.2.

Table 3.4 Molecular weight/conversion data for the bulk thermal polymerization of styrene at 100 °C in the presence **1** (0.029 M).

Time (h)	Conversion (%)	M_n [a]	$M_{n(Calc)}$ (g mol^{-1}) [b]	$Đ$
2	4.3	1 500	1 300	1.12
6	14.3	5 700	4 500	1.08
20	40.0	13 800	12 500	1.08
64	81.0	25 200	25 300	1.12

a) GPC molecular weight in PSt equivalents.
b) Calculated molecular weight using Eq. (3.1), (g mol^{-1}).
Source: Rizzardo et al. [40]. © John Wiley and Sons.

freeze–evacuate–thaw cycles, sealed, and heated at 100 ± 1 °C for the periods of time indicated in Table 3.4. The excess monomer and solvent were removed by evaporation at ambient temperature under vacuum and the residues analyzed directly by GPC; see Table 3.4 [40].

Initial work into RAFT-mediated styrene emulsion polymerization demonstrated a major limitation of the RAFT process, due to the lack of colloidal stability,

suggesting that RAFT agent transportation was problematic. The success in all RAFT emulsion polymerization depends strongly on the choice of RAFT agent and polymerization conditions. This is attributed in part to the slow transportation of the RAFT agent between the droplet phase and the particle phase and in part to the way in which molecular weight distributions evolve during RAFT polymerization. Successful heterogeneous RAFT experiments rely on rapid co-localizing of the RAFT agent with the particulate phase. In the past, these emulsion polymerizations have been successfully achieved through starve-feeding of the emulsion, seeded particle approach, and later via an amphiphilic macroRAFT approach. These can be performed via multistep processes, use amphiphilic macroRAFT agents, and/or make use of miniemulsion or seeded emulsion techniques (a summary of the development of RAFT emulsion polymerization [52] and discussion on emulsion polymerization are captured in chapter 15 on this book [53] and its corresponding publication [54]).

*Emulsion polymerization of styrene in the presence of RAFT agent **3** at 80 °C*. A five-neck reaction vessel equipped with a condenser, thermocouple, and mechanical stirrer was charged with water (75 g) and sodium dodecyl sulfate (3 g of 10% aqueous solution). The solution was heated at 80 °C for 40 minutes while purging with nitrogen. ACPA (211 mg) and benzyl dithiobenzoate (**3**) (228 mg) in styrene (4.7 g) were then added. Further styrene (39.2 g, 0.2 ml min^{-1}) and initiator (211 mg in 24 g of 1% [w/w] aqueous sodium dodecyl sulfate, 0.089 ml min^{-1}) were added by syringe pumps. After completion of the feeds, the reaction was held at 80 °C for 90 minutes. The polymerization was sampled periodically to establish conversion and for GPC analysis. Final polymerization results (>99%, $M_n = 53\,200$; $Đ = 1.37$) [41].

Surfactant-free emulsion polymerization of styrene in the presence of poly(N,N-dimethylacrylamide PDMAm-macroRAFT agent at 80 °C: PDMAm-macroRAFT agent. Polymerization of 4.0 g of *N*,*N*-dimethylacrylamide DMAm (2.0 mol l^{-1}) was carried out in 16 ml of 1,4-dioxane with ACPA (5.7 mg, 1.0×10^{-3} mol l^{-1}) and *S*,*S*′-bis(α,α′-dimethyl-α″-acetic acid)-trithiocarbonate **25** (74 mg, 1.0×10^{-2} mol l^{-1}); a small amount (242 mg, 0.13 mol l^{-1}) of 1,3,5-trioxane was added as an internal reference for determination of the monomer consumption by ^{1}H NMR spectroscopy. The solution was poured in a septum-sealed flask, purged for 30 minutes with nitrogen in an ice bath, and heated to 80 °C in a thermostatted oil bath under stirring, for 13 minutes. The polymerization was quenched by immersion of the flask in iced water. The polymer was recovered by two precipitations in petroleum ether and dried under reduced pressure (47%, $M_n = 10\,700$, $Đ = 1.09$).

Emulsion polymerization of styrene. The aqueous emulsion polymerization of styrene was performed at 80 °C at a stirring speed of 375 rpm, using an initial monomer concentration of 1.1 mol l^{-1}_{latex} (11 wt% with respect to the total latex) and a macroRAFT/initiator molar ratio of 5 : 1. In a typical experiment, 323 mg of poly(*N*,*N*-dimethylacrylamide) macroRAFT agent ($M_n = 10\,700$; 3.8×10^{-3} mol l^{-1}) was dissolved in 7.39 ml of deionized water. Then, 0.5 ml of a stock solution of ACPA in water (concentration of 4.4 g l^{-1} neutralized by

3.5 M equivalent of sodium bicarbonate ($NaHCO_3$)) and 1.01 g (9.7×10^{-3} mol) of styrene was added. After deoxygenation by bubbling with nitrogen for 30 minutes, the septum-sealed flask containing the reaction mixture was immersed in an oil bath thermostatted at 80 °C for four hours. The polymerizations were quenched by immersion of the sample vials in iced water and conversion was determined by gravimetry (83%, $M_n = 39\,600$; $Đ = 1.73$) [55].

Surfactant-free emulsion polymerization of styrene in the presence of poly(ethylene oxide) (PEO) macroRAFT agent. *PEO-MacroRAFT Agent* – A solution of 2-(dodecylthiocarbonothioylthio)-2-methylpropionic acid **21** (1.82 g, 5×10^{-3} mol), *N*,*N*′-dicyclohexylcarbodiimide (DCC) (1.03 g, 5×10^{-3} mol), and 4-(dimethylamino)pyridine (DMAP) (0.06 g, 5×10^{-4} mol) in 40 ml of anhydrous tetrahydrofuran (THF) was introduced under nitrogen atmosphere in a flask containing 5 g of dried α-methoxy ω-hydroxy poly(ethylene oxide) (MPEO) (2.5×10^{-3} mol). The esterification reaction proceeded under stirring at room temperature for 120 hours. The polymer was recovered by precipitation of the mixture in cold diethyl ether. After filtration, the product was dried under vacuum at 40 °C and stored at 5–8 °C (90%, $M_n = 2420$ g mol^{-1} [NMR]; end-functionality: >95%). The macroRAFT agent can also be obtained commercially at several molecular weights, as a trithiocarbonate or dithiobenzoate, and with two different R leaving groups from suppliers such as Merck/Sigma Aldrich.

Emulsion polymerization of styrene. Surfactant-free batch emulsion polymerization of styrene was conducted in the presence of PEO-TTC $[styrene]_0/[PEO\text{-}TTC]_0 = 145$. In a typical experiment, 0.18 g PEO-TTC (0.073 mmol) was dissolved in 7.63 g of deionized water. Then, 1.04 g of styrene (10.0 mmol) was added to the solution in a 25 ml septum-sealed flask. An aqueous stock solution of ACPA was prepared (10 mg ml^{-1}) and neutralized by $NaHCO_3$ (3.5 M equivalents with respect to ACPA). Finally, 0.48 ml of this solution (ACPA: 0.017 mmol) was added to the reaction mixture, deoxygenated by bubbling with nitrogen for 30 minutes at 3 °C, and then immersed in an oil bath thermostatted at 80 °C for 23 hours (67%, $M_n = 12\,200$; $Đ = 1.16$, $D_z = 260$ nm (0.16) dispersity, $N_p = 9.7 \times 10^{12}$ (g_{latex}^{-1})) [56].

3.5 RAFT Polymerization of Methacrylates and Acrylates

The choice of RAFT agent is critical in the success of the polymerization; this is particularly important in relation to methacrylates. Figure 3.1 provides a general summary of how to select the appropriate RAFT agent for particular monomers. Note should be made of the dashed lines in the chart, particularly in relation to the choice of R group for methacrylate polymerization. Although some control might be achieved with these monomer/RAFT agent combinations, the molecular weight distribution may be broad or there may be substantial retardation or prolonged inhibition. Aromatic dithioesters such as **1** and **2** are among the most active RAFT agents and have general utility in the polymerization of methacrylates and acrylates. However, these RAFT agents may give retardation particularly when used in high

concentrations and are more sensitive to hydrolysis and decomposition induced by Lewis acids [57]. The RAFT polymerization of acrylates and methacrylates can be carried out in bulk, solution, emulsion, or dispersion polymerization. RAFT agents that are ineffective for the controlled polymerization of acrylates and methacrylates are dithiocarbamates and xanthates.

3.5.1 Methacrylates

Methacrylates are tertiary more activated monomers (3° MAMs). Good control over RAFT polymerization of methacrylates requires a RAFT agent suitable for 3° MAMs (Table 3.1, Figure 3.5). Methacrylates can only be homopolymerized in the presence of 3° dithiobenzoates (Z = Ph), trithiocarbonates (Z = S-R′), and some pyrazole dithiocarbamates (Z = N-R′N). RAFT agents that are ineffective for the controlled polymerization of methacrylates are 2° dithiobenzoates (Z = Ph), trithiocarbonates (Z = S-R′), pyrazole dithiocarbamates (Z = N-R′N), dithiocarbamates (Z = N-R′$_2$), and xanthates (Z = O-R′).

A wide range of methacrylate monomers have been successfully polymerized under RAFT reaction conditions to produce polymers of controlled molecular weight and low dispersity. These include 2-(acetoacetoxy)ethyl methacrylate, 2-aminoethyl methacrylate (hydrochloride), allyl methacrylate, cholesteryl methacrylate, butyl methacrylate, *t*-butyldimethylsilyl methacrylate, (diethylene glycol monomethyl ether)methacrylate, 2-(diethylamino)ethyl methacrylate, (ethylene glycol monomethyl ether)methacrylate, 2-hydroxyethyl methacrylate, hexyl methacrylate, isobutyl methacrylate, dodecyl methacrylate, methyl methacrylate, methacryloyloxyethyl phosphorylcholine, (poly(ethylene glycol)monomethyl ether)methacrylate, pentafluorophenyl methacrylate, and 2-(trimethylammonium)ethyl methacrylate, as well as a variety of less common functional acrylate and methacrylate monomers (depicted in Figure 3.3), demonstrating that steric bulk **34** [58], a variety of functional groups including glycomonomers **35** [59], protected thiol **36** [60, 61], ferrocenyl **37** [62], isocyanate **38** [63], ketal **39** [64], and oleyl-based monomers **40** [44] are compatible with the RAFT polymerization process.

3.5.2 Acrylates

Acrylates are 2° MAMs. Good control over RAFT polymerization of acrylates requires a RAFT agent suitable for more activated monomers (MAMs) (see Table 3.1, Figure 3.5). Acrylates can be polymerized in the presence of the following classes of primary, secondary, and tertiary RAFT agents: dithiobenzoates (Z = Ph), trithiocarbonates (Z = S-R′), and pyrazole dithiocarbamates (Z = N-R′N). RAFT agents that are ineffective for the controlled polymerization of acrylates are dithiocarbamates (Z = N-R′$_2$) and xanthates (Z = O-R′). The best control is with the use of trithiocarbonates, aliphatic dithioester, or activated dithiocarbamates. Dithiobenzoates can impart good control under conditions where low reaction temperatures or high RAFT agent concentrations are avoided, or retardation and inhibition will be observed.

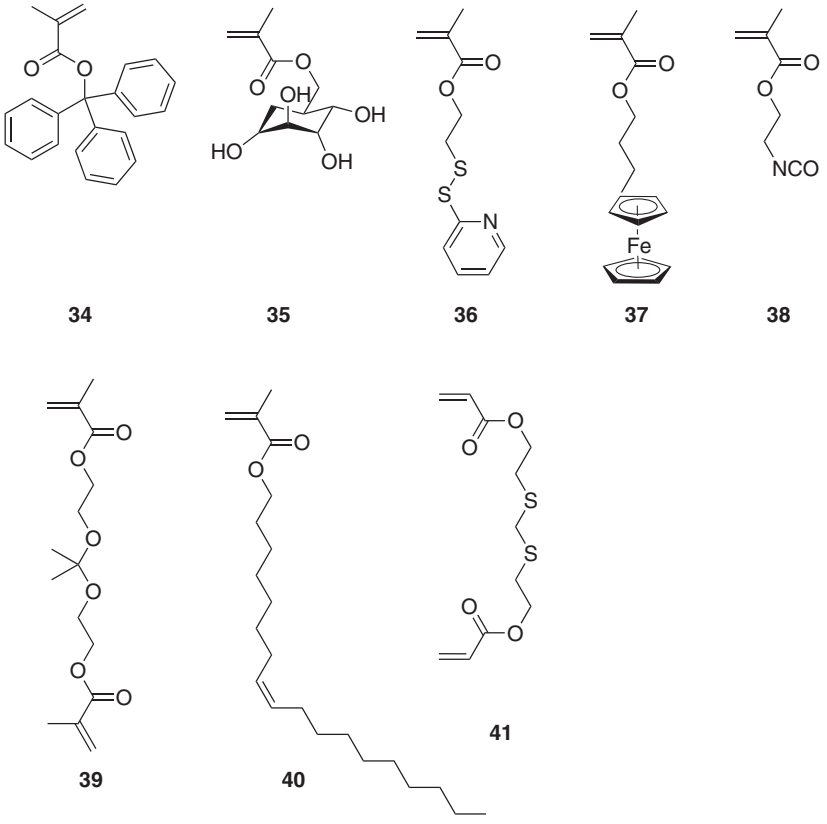

Figure 3.6 Examples of functional methacrylate and acrylate monomers amenable to RAFT polymerization.

A wide range of acrylate monomers with a variety of functional groups and steric bulk have been successfully polymerized under RAFT control to produce polymers of controlled molecular weight and low dispersity. These include 2-(acryloyloxy)ethyl phosphate, butyl acrylate (BA), 3-chloropropyl acrylate, dodecyl acrylate, di(ethylene glycol) 2-ethylhexyl ether acrylate, 2-(dimethylamino)ethyl acrylate, ethyl acrylate, ethoxyethyl acrylate, ethyl α-acetoxyacrylate, 2-ethylhexyl acrylate, isobornyl acrylate, methyl acrylate, propargyl acrylate, (poly(ethylene glycol) monomethyl ether)acrylate, *t*-butyl acrylate (*t*BA), and disulfide linker **41** [65] to list but a few (Figure 3.6).

3.5.3 Experimental Procedures for the RAFT Polymerization of Methacrylates

*Solution polymerization of MMA at 90 °C in the presence of 4-cyano-4-(((dodecylthio) carbonothioyl)thio)pentanoic acid **7***. An aliquot (2 ml) of a stock solution composed of MMA (14 ml), ACHN (9.8 mg), and benzene (6 ml) was added to each of a series of ampoules containing weighed amounts of **7**. The contents were degassed,

Table 3.5 Molecular weights and molar mass dispersities for PMMA formed by polymerization of MMA (6.55 M) with ACHN (0.0018 M) as initiator and RAFT agent **7** for six hours at 90 °C [66].

$[RAFT]_0$ ($M \times 10^2$)	M_n [a)]	$M_{n(Calc)}$ ($g\,mol^{-1}$) [b)]	$Đ$	Conversion (%)
19.92	2 870	3 000	1.18	80
9.96	5 040	5 600	1.14	80
4.95	9 940	10 400	1.12	79
2.48	21 800	22 600	1.13	91
1.24	41 100	45 300	1.14	>99
0.61	80 900	80 100	1.13	>99
0.32	126 000	125 000	1.15	>99

a) Calculated from Eq. (3.2) ($d = 1.67$ for PMMA with ACHN) [42] and f is the initiator efficiency (taken as 0.5). It was calculated from the known value of k_d ($k_d = 2.53 \times 10^{-5}\ M^{-1}\ s^{-1}$ at 90 °C for ACHN) [67, 68].

b) GPC molecular weight: PMMA molecular weights are based on use of a Universal calibration and Mark–Houwink–Sakaruda parameters of $K = 11.4 \times 10^8\ g\,l^{-1}$, $\alpha = 0.716$ (PMMA) and $K = 9.44 \times 10^8\ g\,l^{-1}$, $\alpha = 0.719$ (polystyrene) [69].

Source: Moad et al. [66]. © Elsevier.

the ampoules sealed, and heated at 90 °C for six hours. The polymer was isolated by exhaustive evaporation of monomer or precipitation in methanol and conversions were determined gravimetrically. Molecular weight and conversion data are shown in Table 3.5 [66].

Solution polymerization of methyl methacrylate at 100 °C in the presence of 2-cyanobutan-2-yl 4-chloro-3,5-dimethyl-1H-pyrazole-1-carbodithioate **11**. A solution containing MMA (0.64 mL, 3.5 M), 1,1′-azobis(cyclohexanenitrile) (ACHN) (2.58 mg, 0.005 M), **11** (14.2 mg, 0.03 M), trioxane (10 mg; internal standard) and acetonitrile (1.36 mL) was prepared in a 5 mL microwave vial. The resulting mixture was degassed, sealed and heated at 100 °C by microwave irradiation for 4 h. The volatiles were removed in vacuo to give poly(MMA) (72%, $M_n = 8{,}400$; $Đ = 1.34$) [3].

*Solution polymerization of 6-O-methacryloyl mannose (MAMan) glycomonomer **35** in the presence of 2-phenyl-2-propyl benzodithioate **1** at 70 °C*. In a round-bottom flask 1.0 g (4.028 mmol) MAMan, 5.59 mg (0.020 mmol) **1**, and 0.66 mg (0.004 mmol) AIBN were dissolved in 10 ml *N*,*N*-dimethylacetamide (DMAc), sealed with a septum, and degassed by bubbling with nitrogen for several minutes. The flask was heated at 70 °C in an oil bath for 180 minutes. Polymer purification was performed by precipitating the polymer in methanol, followed by freeze-drying from water (73%, $M_n = 42\,500$; $Đ = 1.23$) [70].

*Solution polymerization of MMA with 2-cyano-2-propyl benzodithioate **2** at 60 °C*. AIBN (4.4 mg, 2.67×10^{-5} mol) and **2** (11.8 mg, 5.342×10^{-5} mol) were weighed

into a 25 ml Schlenk tube inside a glove box. Nitrogen-purged MMA (2 ml, 18.69 mmol) and dry toluene (0.7 ml) were then added to the Schlenk tube and immediately frozen on a liquid N_2 bath. The solution was degassed with three freeze–pump–thaw cycles using N_2 and warmed to room temperature and then heated at 60 °C for 20 hours. The polymer sample was collected on precipitation from excess hexane, which was dried in a vacuum oven (93%, M_n = 25 900; $M_{n(calc)} = 32\,700\ g\ mol^{-1}$; $Đ = 1.20$) [71].

*Solution polymerization MMA in the presence of 2-cyano-2-propyl benzodithioate **2** at 70 °C*. MMA (5.00 ml, 4.67×10^{-2} mol) was placed in a Schlenk tube along with **2** (1.03×10^{-1} g, 4.68×10^{-4} mol) and AIBN (7.68×10^{-3} g, 4.68×10^{-5} mol) with a ratio of [MMA]:[**2**]:[AIBN] = 1000 : 10 : 1. The reagents were dissolved in acetonitrile (9.36 ml) and the Schlenk tube was sealed and subjected to four freeze–pump–thaw cycles. After the last cycle the tube was refilled with dry nitrogen and the Schlenk tube was placed in a preheated oil bath (70 °C) for 16 hours. The polymer was collected by precipitation into a cold mixture of methanol and water (75 : 25) and dried under vacuum. The traces of monomers were removed by Soxhlet extraction for four hours in methanol to obtain a pink solid of poly(methyl methacrylate) (PMMA) (conversion = 70%, M_n(NMR) = 7230; M_n(GPC) = 7600; $Đ = 1.09$) [72].

*Solution polymerization of benzyl methacrylate (BnMA) in the presence of 2-phenyl-2-propyl benzodithioate **1** at 70 °C*. **1** (81.6 mg, 0.30 mmol), AIBN (9.8 mg, 0.06 mmol), and benzyl methacrylate BnMA (3.172 g, 18.00 mmol) were dissolved in 7 ml of anisole in a Schlenk tube. The solution was degassed with N_2 for 30 minutes. The tube was sealed with a rubber septum and immersed in a water bath that was preheated at 70 °C for the times specified in Table 3.6. Aliquots were withdrawn at determined time intervals and analyzed by ^{1}H NMR spectroscopy and GPC with *N*,*N*-dimethylformamide (DMF) as a mobile phase for monitoring the degree of polymerization of BnMA. After six hours, the polymerization was quenched by immersing the tube into liquid nitrogen and opening to the air. The reaction mixture was diluted with THF and precipitated three times with hexane before being vacuum dried to obtain a pink powder of the PBnMA homopolymer [73].

3.5.4 Experimental Procedures for the RAFT Polymerization of Acrylates

*Solution polymerization of n-butyl acrylate in the presence of 2-cyano-2-propyl benzodithioate **2** at 60 °C*. A solution containing butyl acrylate (2.0 g), **2** (17.3 mg), and AIBN (0.5 mg) was placed in an ampoule, degassed with three freeze–evacuate–thaw cycles, sealed, and heated at 60 °C for 16 hours. Removal of the volatiles under reduced pressure provided a pink polymer (0.5 g, 25% conversion, M_n = 6200, $Đ$ = 1.07). A similar procedure can be used in the presence of 2-cyano-propan-2-yl butyl trithiocarbonate **22**: butyl acrylate (2.0 g), **22** (72.8 mg), and AIBN (5.1 mg) were degassed and heated at 60 °C for 16 hours, with 95% conversion, M_n = 6800; $Đ = 1.07$ [74].

Table 3.6 RAFT polymerization of BnMA using **1** as a chain transfer agent.

Time (min)	Conversion (%)[a)]	$M_{n(GPC)}$[b)]	$Đ$
90	40	3000	1.16
180	68	3800	1.21
270	83	4300	1.22
360	89	4800	1.17

a) NMR.
b) Poly(ethylene oxide) (PEO) equivalents.
Source: Data from Wei et al. [73].

S*urfactant-free batch emulsion polymerization of n-butyl acrylate at 70 °C in the presence of PEO-TTC*. 0.1670 g PEO-TTC (0.069 mmol) (see Section 3.4.1) was dissolved in 7.63 g of deionized water, and 1.28 g of *n*-butyl acrylate (10.0 mmol) was added to the solution in a 25 ml septum-sealed flask. An aqueous stock solution of ACPA was prepared (10 mg ml^{-1}) and neutralized by $NaHCO_3$ (3.5 M equivalents with respect to ACPA). Finally, 0.48 ml of this solution (ACPA: 0.017 mmol) was added to the reaction mixture, deoxygenated by bubbling with nitrogen for 30 minutes at 3 °C, and then immersed in an thermostatted oil bath at 70 °C for seven hours (M_n = 22 200; $Đ$ = 1.26; 96%; D_z = 200 nm (0.16) dispersity; $N_p = 3.3 \times 10^{13}$ (g_{latex}^{-1})) [56].

*Solution polymerization of 3,5-dibromobenzyl acrylate in the presence of S,S-dibenzyl trithiocarbonate **4** at 70 °C*. 3,5-Dibromobenzyl acrylate (2.8 g; 0.0087 mol), **4** (0.1626 g; 5.6×10^{-4} mol), and AIBN (0.0184 g; 1.12×10^{-4} mol) in THF (5 ml) were degassed with argon for 15 minutes. The reaction flask was sealed under high vacuum pressure and then immersed into an oil bath preheated to 70 °C. After five hours, the reaction was quenched by placing the flask in liquid nitrogen, and the reaction mixture was diluted with THF and precipitated into acetone (300 ml). The polymer was collected by filtration to give a yellow powder (1.68 g; 60.0%; M_n = 2200; $Đ$ = 1.3) [75].

*Solution polymerization of 2-ethylhexyl acrylate in the presence of S,S-dibenzyl trithiocarbonate **4** at 70 °C*. 2-Ethylhexyl acrylate (10.07 g; 0.054 mol), **4** (0.58 g; 2.0×10^{-3} mol), and AIBN (0.065 g; 4.0×10^{-4} mol) in THF (10 ml) were purged with argon for 30 minutes and immersed into an oil bath preheated to 70 °C. After six hours, the reaction was quenched in liquid nitrogen, and the mixture was diluted with acetone and precipitated into cold methanol/water (50 : 50; 300 ml). The polymer was collected by decantation and dried, to give a viscous yellow oil (yield = 6.54 g; 65%; M_n = 3700; $Đ$ = 1.2) [74].

*Solution polymerization of octadecyl acrylate in the presence of S,S-dibenzyl trithiocarbonate **4** at 70 °C*. Octadecyl acrylate (10 g; 0.0308 mol), **4** (0.580 g; 2.0×10^{-3} mol), and AIBN (0.0656 g; 4.0×10^{-4} mol) in THF (10 ml) were purged with argon for 20 minutes and immersed into an oil bath preheated to 70 °C. After five hours,

the reaction was quenched in liquid nitrogen, and the mixture was diluted with THF and precipitated into methanol (300 ml). The polymer was filtered off to give a yellow powder (yield = 5.9 g; 59%, M_n = 9100, $Đ$ = 1.3) [75].

*Solution polymerization of oligo(ethylene glycol) acrylate (M_n = 480 g mol^{-1}) (OEGA-480) in the presence of 2-(butylthiocarbonothioylthio)propanoic acid **23** at 70 °C*. A mixture of 480 mg of OEGA480 (1 mmol), 29.8 mg of **23** (0.125 mmol), and 2 mg of AIBN (0.013 mmol) were dissolved in 2 ml absolute ethanol in a capped vial leading to a final monomer concentration of 0.5 mol l^{-1}. The reaction mixture was bubbled with argon for half an hour. The reaction solution was placed in a preheated oil bath at 70 °C. After five hours, the mixture was cooled to ambient temperature. The solution was precipitated into cold diethyl ether (92%; M_n = 3600; $Đ$ = 1.15) [76].

*Solution polymerization of acrylic acid (AA) in the presence of 2-dodecylsulfanyl-thiocarbonylsulfanyl-2-methylpropionic acid **21** at 80 °C*. Acrylic acid (AA) (7.20 g, 0.1 mol), **24** (364 mg, 1 mmol), THF (8.0 ml), and AIBN (16.4 mg, 0.1 mmol) with the molar ratio of AA/**24**/AIBN 1000 : 10 : 1 were added to a 25 ml polymerization vial with a magnetic stirring bar. After three freeze–evacuate–thaw cycles, the vial was sealed under high vacuum and placed in an oil bath at 80 °C while stirring. After two hours, the vial was cooled to room temperature by placing in an ice/water bath and opened. Poly(acrylic acid) (PAA) was obtained by the precipitation of polymerization mixture into excess diethyl ether under filtration and vacuum drying at room temperature overnight (61%; M_n = 4400; $Đ$ = 1.13) [77].

*Redox-initiated solution polymerization of t-butyl acrylate (tBA) in the presence of 2-dodecylsulfanyl-thiocarbonylsulfanyl-2-methylpropionic acid **21** at −5 °C*. *t*BA (0.64 g, 5 mmol), **24** (18.2 mg, 0.05 mmol), ascorbic acid (17.6 mg, 0.1 mmol), and dioxane (5.0 ml) were added into a 25 m, round-bottom flask equipped with a magnetic stirring bar. Another portion of dioxane was added until the total solution volume was 9.0 ml. The flask was sealed with a rubber septum, and the mixture was purged with nitrogen for 30 minutes at 10 °C. A dioxane solution of cumene hydroperoxide (1.0 ml, 50 mM) was injected into the reaction mixture. The flask was subsequently kept in the chamber of a cryoreactor (DHJF-4002, Greatwall Scientific Industry & Trade Co. Lt., China) at −5 °C for 32 hours. The polymerization was stopped by rapid cooling in liquid nitrogen for a fixed duration. After the polymerization was stopped, the reaction mixture was precipitated in a large excess of methanol/H_2O (2/1, v/v) at −20 °C, followed by purification by further precipitation and drying under vacuum at room temperature (94%; M_n = 10 900; $Đ$ = 1.05) [78].

3.6 RAFT Polymerization of Acrylamides and Methacrylamides

Acrylamides and methacrylamides are MAMs. RAFT polymerization of acrylamides and methacrylamides requires a RAFT agent suitable for MAMs (see

Table 3.1, Figure 3.5); these include dithiobenzoates (Z = Ph), trithiocarbonates (Z = S-R′), and pyrazole dithiocarbamates (Z = N-R′N). RAFT agents that are ineffective for the controlled polymerization of acrylamides are dithiocarbamates (Z = N-R′$_2$) and xanthates (Z = O-R′). The RAFT polymerization of acrylamides and methacryamides can be carried out in bulk, solution, or by emulsion polymerization. RAFT homo- and copolymerization resulting in controlled molecular weight and low dispersity have been achieved for a variety of acrylamides and methacrylamides.

3.6.1 Methacrylamides

The choice of RAFT agent for polymerization of methacrylamides is subject to similar constraints as mentioned for the methacrylates. In particular, the 'R' group should be selected so as to be a good leaving group with respect to the propagating radical. Methacrylamides are 3° MAMs. Good control over RAFT polymerization of methacrylamides requires a RAFT agent suitable for 3° MAMs (Table 3.1, Figure 3.5). Methacrylamides can only be homopolymerized in the presence of 3° dithiobenzoates (Z = Ph), trithiocarbonates (Z = S-R′), and some pyrazole dithiocarbamates (Z = N-R′N). RAFT agents that are ineffective for the controlled polymerization of methacrylamides are 2° dithiobenzoates (Z = Ph), trithiocarbonates (Z = S-R′), pyrazole dithiocarbamates (Z = N-R′N), dithiocarbamates (Z = N-R′$_2$), and xanthates (Z = O-R′). Polymerization of commercially sourced methacrylamides including *N*-(2-aminoethyl)methacrylamide (hydrochloride), *N*-(3-aminopropyl) methacrylamide (hydrochloride), *N*-(2-hydroxypropylmethacrylamide), and many functionalized methacrylamides such as zwitterionic monomer, carboxybetaine methacrylamide **42** [65], and hydrazide **43** [79] have been successfully reported.

3.6.2 Acrylamides

The attributes for RAFT polymerization of acrylates that we have previously discussed generally also apply to acrylamides polymerizations and thus require RAFT agents suitable for MAMs (see Table 3.1, Figure 3.5). Enhanced rates of polymerization are achieved under aqueous conditions and in the presence of Lewis acids. Polymerization of commercially sourced acrylamides including acrylamide, *N*,*N*-dimethylacrylamide, 2-acrylamido-2-methylpropane-1-sulfonic acid sodium salt, *N*-benzylacrylamide, *N*-cyclohexylacrylamide, diacetone acrylamide, *N*,*N*-diethylacrylamide, *N*-(2-(dimethylamino)ethyl)acrylamide, *N*-isopropylacrylamide, *N*-octylacrylamide, and many functionalized acrylamides such as anionic bisphosphonate monomers **44** [80], 3[2-(*N*-methyl acrylamido)ethyldimethylammonio]propanesulfonate **45** [81], or amino functionality **46** [82] have been successfully reported (Figure 3.7).

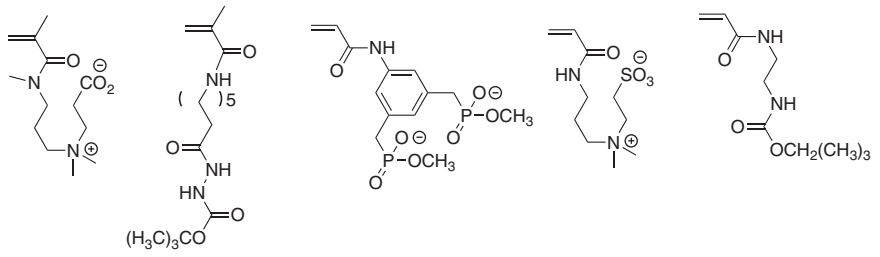

Figure 3.7 Examples of functional methacrylamide and acrylamide monomers amenable to RAFT polymerization.

3.6.3 Experimental Procedures for the RAFT Polymerization of Acrylamides and Methacrylamides

*Solution polymerization of N-(2-hydroxypropyl)methacrylamide HPMA in the presence of 4-cyano-4-(phenylcarbonothioylthio)pentanoic acid **27** at 70 °C.* Polymerization was performed directly in an acetic acid buffer at pH 5.2, (0.27 nmol l^{-1} acetic acid and 0.73 mol l^{-1} sodium acetate), initial monomer concentration ($[M]_0$) of 1 M, and feed ratio of $[HPMA]_0/[CTA]_0/[AIBN]_0 = 40/1/0.2$. HPMA (0.716 g, 0.005 mol), **27** (34.5 mg, 1.23×10^{-4} mol), ACPA (6.9 mg, 2.46×10^{-5} mol), and acetic buffer (5 ml) were mixed. The reaction mixture was purged with nitrogen in an ice bath for 30 minutes. It was then placed in an oil bath at 70 °C for six hours. The polymerization solution was dialyzed against water for three hours to remove salt (water was changed hourly) and then freeze-dried. The solid was dissolved in ethanol and the polymer was precipitated in diethyl ether. The precipitation was repeated twice. The product was dried in vacuo to yield a pink powder (70%; $M_n = 8200$; $Đ = 1.04$) [83].

*Aqueous solution polymerization of N-[3-aminopropyl]methacrylamide (APMA) in the presence of 4-cyano-4-(phenylcarbonothioylthio)pentanoic acid **27** at 70 °C.* The polymerization was performed directly in acetate buffer (pH = 5, 0.27 mol l^{-1} acetic acid and 0.73 mol l^{-1} sodium acetate) with an initial monomer concentration $[M]_0 = 1.8$ M. (Note that the buffer system was used to maintain the hydrochloride salt form of the monomer during polymerization.) The initial $[M]_0/[CTA]_0$ was 200, while the CTA to initiator ratio was 5 : 1. The homopolymerization was conducted by dissolving APMA (0.97 g, 5.4 mmol), **27** (7.6 mg, 0.027 mmol), and V-501 (1.51 mg, 0.0054 mmol) in a 25 ml round-bottom flask and diluting the resulting mixture to a final volume of 3 ml with the acetate buffer. The reaction solution was purged with nitrogen for 45 minutes and subsequently placed in a water bath at 70 °C. The polymerization was allowed to proceed for 60 minutes before being quenched by rapid cooling in liquid nitrogen. The poly(*N*-[3-aminopropyl]methacrylamide (PAPMA)

was then purified by dialysis against deionized water followed by lyophilization (31%; $M_n = 15\,000$; $Đ = 1.08$) [84].

*Solution polymerization of N,N-dimethylacrylamide (DMAm) in the presence of cyanomethyl 3,5-dimethyl-1H pyrazole-1-carbodithioate **6** at 100 °C.* A solution containing DMA (0.618 ml, 3 M), ACHN (2.93 mg, 0.006 M), **6** (12.68 mg, 0.03 M), trioxane (10 mg; internal standard), and acetonitrile (1.4 ml) was prepared in a 5 ml microwave vial. The resulting mixture was degassed, sealed, and heated at 100 °C by microwave irradiation for one hour. The volatiles were removed in vacuo to give poly(DMA) (99%; $M_n = 12\,100$; $Đ = 1.07$) [70].

*Solution polymerization of NIPAm in the presence of cyanomethyl 4-cyano-4-(dodecylsulfanylthiocarbonyl) sulfanyl pentanoic acid **7** at 60 °C.* Into a flask were placed 2 g (17.7 mmol) of NIPAm, 54 mg (0.134 mmol) of **7**, and 2.2 mg (13.4 μmol) of AIBN in 4 g *p*-dioxane. The flask was purged with N_2 for 30 minutes and heated at 60 °C for 12 hours, followed by precipitation into pentane. The product was dried under vacuum, dialyzed against DI water at 4 °C, and freeze-dried ($M_n = 15\,700$; $Đ = 1.01$; dn/dc of 0.074) [85].

*Solution polymerization of acrylamide in the presence of 2-(1-carboxy-1-methylethylsulfanylthio carbonylsulfanyl)-2-methylpropionic acid **25** at 70 °C.* Acrylamide (15.4 g, 0.217 mol), **25** (76.6 mg, 0.271 mmol), and V-501 (15.2 mg, 0.0542 mmol) were added to a 250 ml round-bottom flask equipped with a magnetic stirring bar. Dimethyl sulfoxide was added until the total solution volume was 108.5 ml. The flask was sealed with a rubber septum, and the contents were purged with nitrogen for 60 minutes. The flask was subsequently immersed in a water bath preheated to 70 °C, and the polymerization proceeded for four hours before being quenched by rapid cooling with liquid nitrogen. The polymer was then purified by direct precipitation into 20 times excess of acetone ($M_n = 36\,200$ g mol^{-1}; $Đ = 1.25$) [86].

*Solution polymerization of N,N-diethylacrylamide in the presence of 2-cyano-2-propyl benzodithioate **2** at 80 °C.* *N*,*N*-Diethylacrylamide (13.3 g, 104 mmol), **2** (0.582 g, 2.66 mmol), and AIBN (76 mg, 0.463 mmol) were mixed in a round-bottom flask equipped with a magnetic stir bar. The resulting homogeneous solution was stirred at room temperature while being purged with N_2 for a period of one hour. The flask was then immersed in a preheated oil bath at 80 °C for 2.5 hours. The polymerization was quenched by exposure to air while cooling the flask with ice. THF (8.0 ml) was then added to the flask to dilute the monomer/polymer mixture. The polymer was isolated by precipitation (×2) into hexane (600 ml) followed by Buchner filtration and drying in vacuo, yielding 8.7 g of poly(*N*,*N*-diethylacrylamide) (65%; $M_n = 1790$; $Đ = 1.06$) [87].

3.7 RAFT Polymerization of Vinyl Esters and Vinyl Amides

Most vinyl ester and vinyl amide monomers are secondary less activated monomers (LAMs) with the exception of 2-vinyl-4,4-dimethylazlactone (VDMA), which

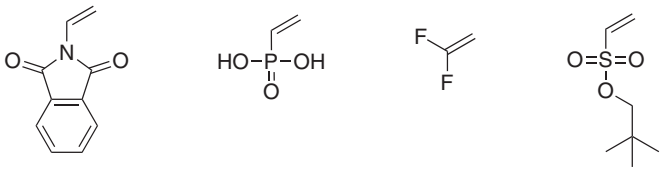

47 48 49 50

Figure 3.8 Examples of functional vinylic monomers amenable to RAFT polymerization.

behaves as a 2° MAM. Good control over RAFT polymerization of vinyl esters and vinyl amides requires a RAFT agent suitable for 2° LAMs. Primary, secondary, and tertiary pyrazole dithiocarbamates (Z = N-R′N), dithiocarbamates (Z = N-R′$_2$), and xanthates (Z = O-R′) RAFT agents give good control over the homopolymerization of vinyl ester and vinyl amide (see Table 3.1, Figure 3.5). RAFT agents that are not suitable for the polymerization of vinyl ester and vinyl amide are dithiobenzoates (Z = Ph) and trithiocarbonates (Z = S-R′). Vinyl ester and vinyl amide polymerizations are generally carried out in solution. RAFT homo- and copolymerization resulting in controlled molecular weight and low dispersity have been achieved for a variety of vinyl esters including vinyl acetate, vinyl butyrate, and vinyl benzoate (VAc, VB, VBz), *N*-vinyl amides and imides such as *N*-vinylcaprolactam and *N*-vinylpyrrolidone, *N*-vinyl heteroaromatics such as 4-vinylimidazole, vinylsulfonates such as 1-butyl ethenesulfonate and neopentyl ethenesulfonate, vinylphosphonic acid, protected amino functionality **47** [88], phosphonic acid functionality **48** [89], haloolefins **49** [90] and sulfonic acid-containing monomers **50** [91]. The polymerization of *N*-vinylpyrrolidone (NVP) in aqueous media was reported as problematic due to the sensitivity of the macroRAFT agent with a terminal NVP unit to hydrolysis. It has recently been shown that this problem can be overcome by conducting the polymerization at ambient temperature with redox initiation [92] (Figure 3.8).

3.7.1 Experimental Procedures for the RAFT Polymerization of Vinyl Esters and Vinyl Amides

*Solution polymerization of N-vinylcarbazole (NVC) in the presence of cyanomethyl phenyl(pyridin-4-yl)carbamodithioate **29** at 60 °C*. A stock solution containing **29** (24.3 mg), NVC (2.12 g), AIBN (8.3 mg), and 1,4-dioxane to a volume of 5 ml was prepared in a volumetric flask. The reaction mixture was transferred to an ampoule, degassed by three repeated freeze–evacuate–thaw cycles, and sealed. The ampoule was heated at 60 °C for 20 hours (95%; $M_n = 16\,900$; $Đ = 1.19$) [93].

*Solution polymerization of vinyl acetate in the presence of O-ethyl S-(1-methoxycarbonylethyl) dithiocarbonate (Rhodixan A1) **26** at 60 °C*. A mixture of vinyl acetate (2.8 g, 3.2×10^{-2} mol), AIBN (8 mg, 0.049 mmol), and **26** (97 mg, 0.47 mmol) in ethyl acetate (2.9 g) was degassed by four freeze–pump–thaw cycles, backfilled with argon, sealed, and placed in an oil bath at 60 °C. After 15 hours, the reaction was stopped by cooling in liquid nitrogen. The polymer was dried in vacuo ($M_n = 6050$ g mol^{-1}; $Đ = 1.61$) [94].

Solution polymerization of vinyl benzoate in the presence of ethylxanthogenacetic acid (EXGA) ***31*** *at 70 °C*. A stock solution was prepared of vinyl benzoate (1.90 g, 12.8 mmol), **31** (23.1 mg, 0.128 mmol), AIBN (4.2 mg, 0.026 mmol), and anisole (0.45 ml). An aliquot (1 ml) was sealed in a 10 ml microwave vial equipped with a magnetic stir bar. The resulting solution was purged with nitrogen for 20 minutes. The reaction vial was placed in the cavity of the microwave instrument, and the temperature was programmed to 70 °C. After 48 minutes, the polymerization was quenched by ceasing the microwave irradiation, removing the vial from the instrument, rapidly cooling the vial in an ice water bath, and exposing the reaction solution to air (41%; $M_n = 7300\ \mathrm{g\ mol^{-1}}$; $Đ = 1.26$) [95].

Solution polymerization of N-vinylphthalimide (NVPI) ***47*** *in the presence of benzyl 1H-pyrrole-1-carbodithioate* ***32*** *at 60 °C*. **47** (0.174 g, 1.0 mmol), **32** (4.7 mg, 0.020 mmol), AIBN (1.6 mg, 0.010 mmol), and DMF (0.5 ml) were placed in a dry glass ampoule equipped with a magnetic stirring bar; the solution was degassed by three freeze–evacuate–thaw cycles. After the ampoule was flame-sealed under vacuum, it was stirred at 60 °C for 24 hours. The characteristic yellow colour remained during the polymerization. The reaction was stopped by rapid cooling with liquid nitrogen. The polymer obtained was purified by precipitation from a DMF solution into a large excess of diethyl ether, and the resulting product was dried at room temperature under vacuum to yield poly(NVPI) as a white powder (84%; $M_n = 7300$; $Đ = 1.29$) [88].

Redox initiated solution polymerization of N-vinylpyrrolidone (NVP) in the presence of O-ethyl-S-(1-methoxycarbonyl)ethyldithiocarbonate (Rhodixan A1) ***26*** *at room temperature*. **26** (122 mg, 5.8×10^{-4} mol), NVP (5 g, 4.5×10^{-2} mol), distilled water (2.5 ml), and *tert*-butyl hydroperoxide (85 mg, 6.6×10^{-4} mol) were placed in a 15 ml Schlenk flask. The polymerization mixture was degassed by purging with ultrahigh-purity argon for 20 minutes. Ascorbic acid (115 mg, 6.5×10^{-4} mol) was added under a stream of argon. The reaction was stopped after 24 hours at room temperature (97%; $M_n = 14\,600\ \mathrm{g\ mol^{-1}}$; $Đ = 1.30$) [92].

3.8 Copolymers

Copolymerization under RAFT control allows for the polymer chains to all have a similar composition. As polymer chains grow throughout the copolymerization, the compositional drift of the monomers are captured within the chain structure, unlike with conventional radical copolymerizations, where the polymers are generally not homogeneous in composition.

Gradient, alternating, statistical, and pseudo-block copolymers can be synthesized in a batch type polymerization by choosing the appropriate reactivity ratio of monomer pairs.

The choice of RAFT agent for a successful copolymerization is not based on the requirement for all monomers to be amenable to its control. Examples of good control over molecular weight and narrow molecular weight distributions for vinylic monomers copolymerized with acrylates using trithiocarbonates exist provided the

monomer that is amenable to homopolymerization with the chosen RAFT agent, in the monomer pair, does not deplete during the copolymerization. Alternatively, a RAFT agent that can control both monomer pairs, such as the pyrazole carbodithioate class chain transfer agents **9–11**, can be used.

3.8.1 Experimental Procedures for RAFT Copolymers

*Preparation of poly(N,N-dimethylacrylamide-covinyl acetate) using cyanomethyl 3,5-dimethyl-1H-pyrazole-1-carbodithioate **9** at 100 °C*. A solution containing DMA (0.010 ml, 0.048 M), VAc (0.553 ml, 3 M), ACHN (5.86 mg, 0.012 M), **9** (20.28 mg, 0.048 M), and ethyl acetate (1.437 ml) was prepared in a 5 ml microwave vial. The resulting mixture was degassed, sealed, and heated at 100 °C via microwave irradiation for 12 hours. The volatiles were removed in vacuo to give poly(DMA-*co*-VAc) at 55% conversion (>99% of DMA and 54% VAc), with $M_n = 4700$; $Đ = 1.23$ [70].

*Preparation of poly(methyl methacrylate-co-trimethylsilyl methacrylate-co-4-(tert-butyldimethylsilyloxy)styrene **13**) p(MMA-co-TMS-MA-co-TBDMS-OS) with 2-cyano-2-propyl benzodithioate **2** at 60 °C*. Polymerizations were carried out in a Schlenk tube. MMA (1.90 g, 19 mmol), TMS-MA (1.58 g, 11 mmol), **13** (0.6 g, 2.6 mmol), **2** (0.015 g, 0.07 mmol), and AIBN (0.9 mg, 0.006 mmol) were dissolved in anisole (4 ml) and the reaction mixture was degassed by three freeze–pump–thaw cycles. The polymerizations were conducted under argon atmosphere for 20.5 hours at a constant temperature of 70 °C. The reaction was stopped by freezing the Schlenk tube in liquid nitrogen. The reaction mixture was then slowly precipitated in *n*-hexane, the polymer was filtered off, and dried under vacuum. GPC (eluent: THF, RI, polystyrene [PSt]-standards): $M_n = 30\,700$; $Đ = 1.13$ [96].

*Preparation of poly(triphenylmethyl methacrylate **34**-co-methacrylic acid) with 2-phenyl-2-propyl benzodithioate **1** at 60 °C*. In a 50 ml round-bottom flask were placed toluene (5.40 ml), **34** (4.41 ml of 1.36 M solution in toluene), MAA (0.51 ml, 6.01 mmol), 1,2,3,4-tetrahydronaphthalene (0.48 ml) as an internal standard, and toluene solutions of AIBN (0.60 ml of 100 mM solution in toluene) and **1** (0.60 ml of 200 mM solution in toluene) at room temperature. The total volume of the reaction mixture was 12.0 ml. Immediately after mixing, the solution was evenly charged in six glass tubes and the tubes were sealed by flame under nitrogen atmosphere. The tubes were immersed in a thermostatic oil bath at 60 °C. In predetermined intervals, the polymerization was terminated by cooling the reaction mixtures in liquid N_2. Monomer conversion was determined from the concentration of residual monomer measured by ^{1}H NMR spectroscopy against the internal standard. The quenched reaction solutions were evaporated to dry to give poly(MAA-*grad*-TrMA). Details of the polymerization results are given in Table 3.7; [58].

*Preparation of poly(methacrylic acid)-co-(oleyl methacrylate **40**) (PMAoa 8.0 mol%) with 4-cyano-4-(((dodecylthio)carbonothioyl)thio)pentanoic acid **7** at 60 °C*. RAFT agent **7** (26.30 mg, 11.7 mmol), Vazo 68 (3.60 mg, 13.0 mmol), MMA (1.01 g, 12.0 mmol), and **40** (0.44 g, 1.29 mmol) were combined with 1,4-dioxane (3.0 ml)

Table 3.7 RAFT copolymerization of triphenylmethyl methacrylate **34** and methacrylic acid using **1** as a chain transfer agent.

Time (h)	Conversion (34/MAA%)[a]	$M_{n(GPC)}$[b]	$Đ$
3	3/18	5 300	1.16
10	41/81	7 100	1.21
150	88/100	10 100	1.22

a) NMR.
b) PMMA equivalents.
Source: Data from Ishitake et al. [58].

in an ampoule. The solution was degassed with four freeze–pump–thaw cycles, flame-sealed, and transferred to a temperature-controlled oil bath at 60 °C for seven hours. The polymerization was then quenched by rapid cooling in liquid nitrogen. The monomer/polymer mixture was twice precipitated from a workable dioxane/THF mixture into diethyl ether/hexane (3 : 1). The polymer was recovered by filtration and dried under suction (1.24 g; 85%; M_n = 25 200; $Đ$ = 1.19 [Molecular weight of methylated polymer obtained using THF, GPC calibrated with PMMA standards]) [44].

*Preparation of poly(N-isopropylacrylamide (80%)-co-sodium methacrylate (10%)-co-N-cyclohexylacrylamide (10%)) p(NIPAm-co-NaMA-co-CA) with S,S′-bis(α,α′-dimethyl-α″-acetic acid)-trithiocarbonate **25** at 60 °C*. NIPAm (1.488 g, 13.1 mmol), sodium methacrylate (0.142 g, 1.3 mmol), and *N*-cyclohexylacrylamide (0.209 g, 1.3 mmol) were dissolved in methanol (20 ml) in a polymerization tube fitted with a septum cap. The mixture was degassed by bubbling nitrogen through it for 30 minutes. **25** (74.4 mg, 0.26 mmol) and 2,2′-Azobis(2-methylpropionamidine)dihydrochloride V-50 (23.8 mg, 0.08 mmol) were then added and the mixture was heated to 60 °C for 48 hours. The solvent was evaporated, the residue dissolved in THF, and precipitated into pentane, and then left to dry to give a pale yellow powder (M_n = 3800; $Đ$ = 1.31) [80].

3.9 Block Copolymers

The order of constructing the blocks of a block copolymer is very important. The propagating radical for the first formed block must be a good homolytic leaving group with respect to that of the second block. For example, in the synthesis of a methacrylate–acrylate or methacrylate–styrene diblock, the methacrylate block must be prepared first. The styrene or acrylate propagating radicals are very poor leaving groups with respect to methacrylate propagating radicals. For the construction of polyMAM-*block*-polyLAM, the block comprising MAM needed to be synthesized first. This sequence is necessary because polyLAM propagating radicals are poor radical leaving groups with respect to polyMAM propagating radicals, and

consequently, polyLAM macroRAFT agents can have very low transfer constants in MAM polymerization.

Attempts to synthesize PSt-*block*-PVAc or other PSt-*block*-polyLAM starting from a PSt macroRAFT may require a different strategy to other polyMAM-*block*-polyLAM synthesis. It has been shown that attempts to synthesize PSt-*block*-PVAc or other PSt-*block*-polyLAM starting from a PSt macroRAFT agent (prepared with methyl 2-[methyl(4-pyridinyl)carbamothioylthio]propionate **30**) using the RAFT polymerization conditions (initiator:RAFT agent ~ 1 : 10) that had proved successful for other polyMAM-*block*-polyLAM or PSt-*block*-polyMAM gave no significant yield of polymer after an extended reaction period (>four hours) [97]. As it has been observed that it is possible to synthesize low molecular weight PSt-*block*-poly(methyl acrylate) (PMA) and PMA-*block*-PVAc, [98] the copolymerization of a mixture of MA and VAc in the presence of the PSt macroRAFT in its deprotonated form allows for the synthesis of PSt-MA-VAc (PSt-*block*-P(MA-*grad*-VAc)-*block*-PVAc) [99].

3.9.1 Experimental Procedures for RAFT Block Copolymers

*Preparation of poly(methyl methacrylate)-b-poly(n-butyl acrylate) using 2-cyano-2-propyl benzodithioate **2** at 70 °C*. MMA (15 g, 150 mmol), 2-cyano-2-propyl benzodithioate **2** (0.0664 g, 0.300 mmol), AIBN (0.0123 g, 0.075 mmol), and toluene (6.46 g, 30 wt%) were mixed together, degassed, and heated at 70 °C under N_2 for six hours and the reaction quenched in ice (55%, M_n = 28 800 g mol^{-1}, $Đ$ = 1.09). PMMA homopolymer (M_n = 28 800 g mol^{-1}, $Đ$ = 1.09, 0.3370 g, 0.0117 mmol), BA (1.4998 g, 11.7 mmol), AIBN (0.0004 g, 0.0023 mmol), and 30 wt% toluene (0.78 g) were mixed together, degassed, and heated at 70 °C for 90 minutes, and the reaction quenched in ice after precipitation in cold methanol to give PMMA-PBA block copolymer (44% [BA]; M_n = 77 300 g mol^{-1}; $Đ$ = 1.37) [100].

*Preparation of poly(methyl acrylate)-b-poly(N-vinylcarbazole) using methyl 2-(methyl (pyridin-4-yl)carbamothioylthio)propanoate **30** at 60 °C*. A stock solution (I) of AIBN (8.5 mg) in acetonitrile (25 ml) was prepared. A stock solution (II) of **30** (47.6 mg, 0.0353 M) and *p*-toluenesulfonic acid (38.0 mg, 0.04 M) in acetonitrile (5.0 ml) was prepared. Aliquots of stock solution (I) (1.0 ml), stock solution (II) (2.0 ml), and methyl acrylate (2.0 ml) were transferred to ampoules that were degassed by three repeated freeze–evacuate–thaw cycles and sealed. The ampoule was heated at 60 °C for seven hours. The volatiles were removed in vacuo to give poly(methyl acrylate) (87.3%; M_n = 31 100; $Đ$ = 1.08). A stock solution (I) consisting of the poly(methyl acrylate) (prepared as above) (1.67 g; M_n = 31 100; $Đ$ = 1.08) and *N*,*N*-dimethylaminopyridine (10.0 mg) in acetonitrile (10 ml) was prepared. A stock solution (II) of AIBN (10 mg) in acetonitrile (5 ml) was prepared. NVC (0.5 g), stock solution (I) (2.0 ml), stock solution (II) (1.0 ml), and acetonitrile (1.0 ml) were transferred into a test tube ampoule, which was degassed by three repeated freeze–evacuate–thaw cycles, and sealed. The ampoule was heated at 60 °C for 16 hours. The volatiles were removed in vacuo to give poly(methyl acrylate)-*b*-poly(*N*-vinylcarbazole) (almost complete

conversion of *N*-vinylcarbazole based on ^{1}H-NMR spectroscopy) with GPC result $M_n = 48\,000$; $Đ = 1.33$ [98].

*Preparation of poly(N,N-dimethylacrylamide)-b-poly(vinyl acetate) using cyanomethyl 3,5-dimethyl-1H-pyrazole-1-carbodithioate **9** at 100 °C*. A solution containing DMA (0.309 ml, 1.5 M), ACHN (1.47 mg, 0.003 M), and cyanomethyl 3,5-dimethyl-1*H*-pyrazole-1-carbodithioate **9** (12.68 mg, 0.03 M) in acetonitrile was prepared in a 5 ml microwave vial. The resulting mixture was degassed, sealed, and heated at 100 °C via microwave irradiation for one hour (98%, M_n = 5800, $Đ$ = 1.05). The vial cap was removed and VAc (0.553 ml) and ACHN (1.47 mg) were added. The vial was again sealed, degassed, and heated at 100 °C via microwave irradiation for 24 hours. The volatiles were removed in vacuo to give poly(DMA)-*block*-poly(VAc) at >99% conversion of DMA and 55% conversion of VAc, with $M_n = 8500$; $Đ = 1.24$ [70].

*Preparation of poly(vinyl pivalate)-b-poly(vinyl acetate) (PVPv-b-PVAc) using methyl (isopropoxycarbonothioyl)sulfanyl acetate **33** at 100 °C*. **33** (46.1 mg, 0.21 mmol, 9.9 mM) and AIBN (3.8 mg, 0.023 mmol, 1.1 mM) were dissolved in freshly distilled vinyl pivalate (VPv) (21.2 ml, 143 mmol). The reaction was sealed, degassed by freeze–pump–thaw cycles (×3), and heated to 60 °C for three hours. The reaction was removed from the heating bath and cooled under running water to terminate the polymerization. Excess vinyl pivalate monomer was removed under reduced pressure, and the resulting solids were freeze-dried from benzene in vacuo (22.5%, M_n = 14 800 g mol^{-1} (GPC-LS), $Đ$ = 1.28 (PSt Standards)). The PVPv-macroRAFT agent (0.5 g, 0.034 mmol) was dissolved in VAc (6.3 ml, 68.3 mmol); residual AIBN present in the macro-chain transfer agent was used as the sole source of initiator. The reaction was degassed by freeze–pump–thaw cycles (×3), sealed, and heated to 60 °C for 3.5 hours. The reaction was removed from the heating bath and cooled under running water to terminate the reaction. Excess vinyl acetate monomer was removed by rotary evaporation. The resulting solid polymer was freeze-dried from benzene in vacuo (6.8%; $M_{n(NMR)} = 24\,800$; 50.4 mol% VAc; $Đ = 1.33$ [PSt standards]) [101].

*Preparation of polystyrene-b-poly(vinyl acetate) (PSt-b-PVAc) using methyl 2-((methyl (pyridin-4-yl)carbamothioyl)thio)propanoate **30** at 70 °C*. A solution comprising ACHN (12.2 mg), **30** (94.5 mg), *p*-toluenesulfonic acid (TsOH) (60.2 mg), and styrene (5 ml) was transferred to an ampoule that was degassed by three freeze–evacuate–thaw cycles, sealed, and then heated at 90 °C for six hours. To avoid unwanted cationic polymerization of styrene, it is important that TsOH is not added directly to the styrene monomer. The ampoule was cooled, opened, and the polymerization mixture evaporated to dryness in vacuo. The residue was taken up in chlorobenzene and evaporated under vacuum several times until no styrene signals were detectable by ^{1}H NMR spectroscopy. The residue (2-PSt-H$^+$) was dissolved in dichloromethane and percolated through a carefully crushed and dried sodium carbonate bed. The colour of the solution changed from yellow to colourless. Removal of the solvent gave the PSt macroRAFT (18%, $M_n = 1850$, $Đ = 1.22$). A solution of PSt macroRAFT agent (18%; $M_n = 1850$; $Đ = 1.22$; 0.030 g; 0.01 M), AIBN (1.4 mg, 0.005 M), and VAc (1.4 g) was transferred to an ampoule

Table 3.8 Preparation of poly(*N*-(2-hydroxypropyl) methacrylamide)-*b*-poly(benzyl methacrylate) using a PBnMA macro-RAFT agent.

Time (h)	Conversion (%)[a)]	$M_{n(GPC)}$[b)]	$Đ$
9	20	7 700	1.22
14	30	9 000	1.23
17	36	10 800	1.22
30	61	19 200	1.26

a) NMR.
b) M_n in poly(ethylene oxide) (PEO) equivalents.
Source: Data from Wei et al. [73]

that was degassed by three freeze–evacuate–thaw cycles and sealed. The ampoule was heated at 70 °C for eight hours, and the volatiles were removed in vacuo (100%; $M_n = 73\,600$; $Đ = 1.95$) [97].

Synthesis of poly(N-(2-hydroxypropyl)methacrylamide)-b-poly(benzyl methacrylate) PHPMA-b-PBnMA in the presence of PBnMA macro-CTA at 70 °C. PBnMA (see Section 3.5.3) was used as the macro chain transfer agent (macro-CTA). PBnMA macro-CTA ($M_n = 4800$; $Đ = 1.17$) (500 mg, 0.05 mmol), AIBN (1.6 mg, 0.01 mmol), and HPMA (1.432 g, 10 mmol) were dissolved in 4.0 ml of DMAc. The solution was degassed with N_2 for 30 minutes, and the polymerization was carried out at 70 °C for the times specified in Table 3.8. Aliquots were withdrawn at determined time intervals and analyzed by ^{1}H NMR spectroscopy and GPC with DMF as a mobile phase for monitoring the degree of polymerization (DP) of HPMA. The reaction mixture was diluted with DMF and precipitated three times from DMF/diethyl ether before being dried in vacuum [73].

3.10 Conclusion

Since its first report in 1998 [18], RAFT polymerization has become a tool adopted by the broader scientific community and it is utilized by not only polymer chemists but also synthetic chemists, material engineers, bioengineers, medicinal chemists, and nanotechnologists, generating a plethora of materials with enormous structural complexity and variation in areas ranging from microelectronics, batteries, plastic solar cells, lubricants, surface modifiers, emulsion stabilizers, paints, adhesives, cosmetics, polymer therapeutics, biosensors, and more. With the lapsing of the foundation patents, a range of versatile RAFT agents now being commercially available in a variety of quantities, and industry having shown that scaling up of RAFT agents and polymers is feasible, [102] the time is ripe for scientists to explore the RAFT polymerization technology as a simple tool for the production of complex and functional materials.

References

1 Rizzardo, E., Moad, G., and Thang, S.H. (2009). *Encyclopedia of Polymer Science and Technology*. Wiley. https://doi.org/10.1002/0471440264.pst564.

2 Moad, G., Rizzardo, E., and Thang, S.H. (2005). *Aust. J. Chem.* 58: 379–410. https://doi.org/10.1071/CH05072.

3 Gardiner, J., Martinez-Botella, I., Kohl, T.M. et al. (2017). *Polym. Int.* 66: 1438–1447. https://doi.org/10.1002/pi.5423.

4 Carmean, R.N., Becker, T.E., Sims, M.B., and Sumerlin, B.S. (2017). *Chem* 2: 93–101. https://doi.org/10.1016/j.chempr.2016.12.007.

5 Martin, L., Gody, G., and Perrier, S. (2018). *Reversible Deactivation Radical Polymerization: Materials and Applications*, ACS Symposium Series 1285, 57–79. American Chemical Society. https://doi.org/10.1021/bk-2018-1285.ch004.

6 Quinn, J.F., Barner, L., Barner-Kowollik, C. et al. (2002). *Macromolecules* 35: 7620–7627. https://doi.org/10.1021/ma0204296.

7 Lewis, R.W., Evans, R.A., Malic, N. et al. (2018). *Polym. Chem.* 9: 60–68. https://doi.org/10.1039/C7PY01752A.

8 You, Y.-Z., Hong, C.-Y., Bai, R.-K. et al. (2002). *Macromol. Chem. Phys.* 203: 477–483. https://doi.org/10.1002/1521-3935(20020201)203:3<477::Aid-macp477>3.0.Co;2-m.

9 Lu, L., Zhang, H., Yang, N., and Cai, Y. (2006). *Macromolecules* 39: 3770–3776. https://doi.org/10.1021/ma060157x.

10 Bai, R.-K., You, Y.-Z., and Pan, C.-Y. (2001). *Macromol. Rapid Commun.* 22: 315–319. https://doi.org/10.1002/1521-3927(20010301)22:5<315::Aid-marc315>3.0.Co;2-o.

11 Bai, R.-K., You, Y.-Z., Zhong, P., and Pan, C.-Y. (2001). *Macromol. Chem. Phys.* 202: 1970–1973. https://doi.org/10.1002/1521-3935(20010601)202:9<1970::Aid-macp1970>3.0.Co;2-q.

12 Quinn, J.F., Barner, L., Davis, T.P. et al. (2002). *Macromol. Rapid Commun.* 23: 717–721. https://doi.org/10.1002/1521-3927(20020801)23:12<717::Aid-marc717>3.0.Co;2-i.

13 Barner, L., Quinn, J.F., Barner-Kowollik, C. et al. (2003). *Eur. Polym. J.* 39: 449–459. https://doi.org/10.1016/S0014-3057(02)00247-1.

14 Zhou, Y., Zhu, J., Zhu, X., and Cheng, Z. (2006). *Radiat. Phys. Chem.* 75: 485–492. https://doi.org/10.1016/j.radphyschem.2005.10.012.

15 Millard, P.-E., Barner, L., Stenzel, M.H. et al. (2006). *Macromol. Rapid Commun.* 27: 821–828. https://doi.org/10.1002/marc.200600115.

16 Chiefari, J., Mayadunne, R.T.A., Moad, C.L. et al. (2003). *Macromolecules* 36: 2273–2283. https://doi.org/10.1021/ma020883+.

17 Vana, P., Albertin, L., Barner, L. et al. (2002). *J. Polym. Sci., Part A: Polym. Chem.* 40: 4032–4037. https://doi.org/10.1002/pola.10500.

18 Chiefari, J., Chong, Y.K., Ercole, F. et al. (1998). *Macromolecules* 31: 5559–5562. https://doi.org/10.1021/ma9804951.

19 McCormick, C.L. and Lowe, A.B. (2004). *Acc. Chem. Res.* 37: 312–325. https://doi.org/10.1021/ar0302484.

20 Lowe, A.B. and McCormick, C.L. (2002). *Aust. J. Chem.* 55: 367–379. https://doi.org/10.1071/CH02053.

21 Fortenberry, A.W., McCormick, C.L., and Smith, A.E. (2022). *RAFT Polymerization: Materials, Synthesis and Applications* (eds. G. Moad, S.H. Thang and E. Rizzardo). Weinheim: Wiley-VCH. https://doi.org/10.1000/000000000.chxx.

22 Perrier, S., Davis, T.P., Carmichael, A.J., and Haddleton, D.M. (2002). *Chem. Commun.*: 2226–2227. https://doi.org/10.1039/B206534G.

23 Arita, T., Beuermann, S., Buback, M., and Vana, P. (2005). *Macromol. Mater. Eng.* 290: 283–293. https://doi.org/10.1002/mame.200400274.

24 Arita, T., Beuermann, S., Buback, M., and Vana, P. (2004). *e-Polymers* 003 https://doi.org/10.1515/epoly.2004.4.1.20.

25 Thomas, D.B., Convertine, A.J., Hester, R.D. et al. (2004). *Macromolecules* 37: 1735–1741. https://doi.org/10.1021/ma035572t.

26 Albertin, L., Stenzel, M.H., Barner-Kowollik, C., and Davis, T.P. (2006). *Polymer* 47: 1011–1019. https://doi.org/10.1016/j.polymer.2005.12.069.

27 Mertoglu, M., Laschewsky, A., Skrabania, K., and Wieland, C. (2005). *Macromolecules* 38: 3601–3614. https://doi.org/10.1021/ma048268o.

28 Moad, G., Rizzardo, E., and Thang, S.H. (2016). *Reference Module in Materials Science and Materials Engineering*. Elsevier. https://doi.org/10.1016/B978-0-12-803581-8.01349-7.

29 Chiefari, J. and Rizzardo, E. (2002). *Handbook of Radical Polymerization* (eds. K. Matyjaszewski and T.P. Davis), 629–690. https://doi.org/10.1002/0471220450.ch12.

30 Liu, Y., He, J., Xu, J. et al. (2005). *Macromolecules* 38: 10332–10335. https://doi.org/10.1021/ma0513970.

31 Xu, J., He, J., Fan, D. et al. (2006). *Macromolecules* 39: 3753–3759. https://doi.org/10.1021/ma060184n.

32 Postma, A., Davis, T.P., Moad, G., and O'Shea, M.S. (2005). *Macromolecules* 38: 5371–5374. https://doi.org/10.1021/ma050402x.

33 Chong, B., Moad, G., Rizzardo, E. et al. (2006). *Aust. J. Chem.* 59: 755–762. https://doi.org/10.1071/CH06229.

34 Postma, A., Davis, T.P., Li, G. et al. (2006). *Macromolecules* 39: 5307–5318. doi: 10.1021/ma0604338.

35 Postma, A., Davis, T.P., Evans, R.A. et al. (2006). *Macromolecules* 39: 5293–5306. https://doi.org/10.1021/ma060245h.

36 Monteiro, M.J., Bussels, R., Beuermann, S., and Buback, M. (2002). *Aust. J. Chem.* 55: 433–437. https://doi.org/10.1071/CH02079.

37 Rzayev, J. and Penelle, J. (2004). *Angew. Chem. Int. Ed.* 43: 1691–1694. https://doi.org/10.1002/anie.200353025.

38 Arita, T., Buback, M., and Vana, P. (2005). *Macromolecules* 38: 7935–7943. https://doi.org/10.1021/ma051012d.

39 Arita, T., Buback, M., Janssen, O., and Vana, P. (2004). *Macromol. Rapid Commun.* 25: 1376–1381. https://doi.org/10.1002/marc.200400204.

40 Rizzardo, E., Chiefari, J., Chong, B.Y.K. et al. (1999). *Macromol. Symp.* 143: 291–307. https://doi.org/10.1002/masy.19991430122.

41 Moad, G., Chiefari, J., Chong, Y.K. et al. (2000). *Polym. Int.* 49: 993–1001. https://doi.org/10.1002/1097-0126(200009)49:9<993::Aid-pi506>3.0.Co;2-6.

42 Chong, Y.K., Krstina, J., Le, T.P.T. et al. (2003). *Macromolecules* 36: 2256–2272. https://doi.org/10.1021/ma020882h.

43 Moad, G., Chiefari, J., Mayadunne, R.T.A. et al. (2002). *Macromol. Symp.* 182: 65–80. https://doi.org/10.1002/1521-3900(200206)182:1<65::Aid-masy65>3.0.Co;2-e.

44 Hosta-Rigau, L., Chandrawati, R., Saveriades, E. et al. (2010). *Biomacromolecules* 11: 3548–3555. https://doi.org/10.1021/bm101020e.

45 Nilles, K. and Theato, P. (2011). *Polym. Chem.* 2: 376–384. https://doi.org/10.1039/C0PY00261E.

46 Espeel, P., Goethals, F., Stamenović, M.M. et al. (2012). *Polym. Chem.* 3: 1007–1015. https://doi.org/10.1039/C2PY00565D.

47 Kim, H., Kang, Y.J., Kang, S., and Kim, K.T. (2012). *J. Am. Chem. Soc.* 134: 4030–4033. https://doi.org/10.1021/ja211728x.

48 Roth, P.J. and Theato, P. (2011). *Non-Conventional Functional Block Copolymers*, ACS Symposium Series 1066, 23–37. American Chemical Society. https://doi.org/10.1021/bk-2011-1066.ch003.

49 Häussler, M., Lok, Y.P., Chen, M. et al. (2010). *Macromolecules* 43: 7101–7110. https://doi.org/10.1021/ma1008572.

50 Chen, M., Häussler, M., Moad, G., and Rizzardo, E. (2011). *Org. Biomol. Chem.* 9: 6111–6119. https://doi.org/10.1039/C1OB05276D.

51 Flores, J.D., Shin, J., Hoyle, C.E., and McCormick, C.L. (2010). *Polym. Chem.* 1: 213–220. https://doi.org/10.1039/B9PY00294D.

52 Stace, S.J., Vanderspikken, J., Howard, S.C. et al. (2019). *Polym. Chem.* 10: 5044–5051. https://doi.org/10.1039/C9PY00893D.

53 D'Agosto, F., Lansalot, M., and Rieger, J. (2022). *RAFT Polymerization: Materials, Synthesis and Applications* (Chapter 15) (eds. G. Moad, S.H. Thang and E. Rizzardo). Weinheim: Wiley-VCH. https://doi.org/10.1000/000000000.chxx.

54 D'Agosto, F., Rieger, J., and Lansalot, M. (2020). *Angew. Chem. Int. Ed.* 59: 8368–8392. https://doi.org/10.1002/anie.201911758.

55 Rieger, J., Zhang, W., Stoffelbach, F., and Charleux, B. (2010). *Macromolecules* 43: 6302–6310. https://doi.org/10.1021/ma1009269.

56 Rieger, J., Stoffelbach, F., Bui, C. et al. (2008). *Macromolecules* 41: 4065–4068. https://doi.org/10.1021/ma800544v.

57 Chong, Y.K., Moad, G., Rizzardo, E. et al. (2007). *Macromolecules* 40: 9262–9271. https://doi.org/10.1021/ma071100t.

58 Ishitake, K., Satoh, K., Kamigaito, M., and Okamoto, Y. (2012). *Polym. Chem.* 3: 1750–1757. https://doi.org/10.1039/C1PY00401H.

59 Pfaff, A., Barner, L., Müller, A.H.E., and Granville, A.M. (2011). *Eur. Polym. J.* 47: 805–815. https://doi.org/10.1016/j.eurpolymj.2010.09.020.

60 Wong, L., Kavallaris, M., and Bulmus, V. (2011). *Polym. Chem.* 2: 385–393. https://doi.org/10.1039/C0PY00256A.

61 Jia, Z., Liu, J., Boyer, C. et al. (2009). *Biomacromolecules* 10: 3253–3258. https://doi.org/10.1021/bm900817a.

62 Herfurth, C., Voll, D., Buller, J. et al. (2012). *J. Polym. Sci., Part A: Polym. Chem.* 50: 108–118. https://doi.org/10.1002/pola.24994.

63 Moraes, J., Maschmeyer, T., and Perrier, S. (2011). *J. Polym. Sci., Part A: Polym. Chem.* 49: 2771–2782. https://doi.org/10.1002/pola.24710.

64 Syrett, J.A., Haddleton, D.M., Whittaker, M.R. et al. (2011). *Chem. Commun.* 47: 1449–1451. https://doi.org/10.1039/C0CC04532B.

65 Ting, S.R.S., Min, E.H., Zetterlund, P.B., and Stenzel, M.H. (2010). *Macromolecules* 43: 5211–5221. https://doi.org/10.1021/ma1004937.

66 Moad, G., Chong, Y.K., Postma, A. et al. (2005). *Polymer* 46: 8458–8468. https://doi.org/10.1016/j.polymer.2004.12.061.

67 Overberger, C.G., Biletch, H., Finestone, A.B. et al. (1953). *J. Am. Chem. Soc.* 75: 2078–2082. https://doi.org/10.1021/ja01105a017.

68 Moad, G. and Solomon, D.H. (2005). *The Chemistry of Radical Polymerization*, 2e (eds. G. Moad and D.H. Solomon), 49–166. Amsterdam: Elsevier Science Ltd. https://doi.org/10.1016/B978-008044288-4/50022-4.

69 Hutchinson, R.A., McMinn, J.H., Paquet, D.A. et al. (1997). *Ind. Eng. Chem. Res.* 36: 1103–1113. https://doi.org/10.1021/ie9604031.

70 Gardiner, J., Martinez-Botella, I., Tsanaktsidis, J., and Moad, G. (2016). *Polym. Chem.* 7: 481–492. https://doi.org/10.1039/C5PY01382H.

71 Jana, S., Parthiban, A., and Chai, C.L.L. (2011). *J. Polym. Sci., Part A: Polym. Chem.* 49: 1494–1502. https://doi.org/10.1002/pola.24572.

72 Yhaya, F., Binauld, S., Callari, M., and Stenzel, M.H. (2012). *Aust. J. Chem.* 65: 1095–1103. https://doi.org/10.1071/CH12158.

73 Wei, C., Wu, K., Li, J. et al. (2012). *Macromol. Chem. Phys.* 213: 557–565. https://doi.org/10.1002/macp.201100607.

74 Chen, M., Moad, G., and Rizzardo, E. (2009). *J. Polym. Sci., Part A: Polym. Chem.* 47: 6704–6714. https://doi.org/10.1002/pola.23711.

75 Bivigou-Koumba, A.M., Görnitz, E., Laschewsky, A. et al. (2010). *Colloid. Polym. Sci.* 288: 499–517. https://doi.org/10.1007/s00396-009-2179-9.

76 Krieg, A., Pietsch, C., Baumgaertel, A. et al. (2010). *Polym. Chem.* 1: 1669–1676. https://doi.org/10.1039/C0PY00156B.

77 He, W.-D., Sun, X.-L., Wan, W.-M., and Pan, C.-Y. (2011). *Macromolecules* 44: 3358–3365. https://doi.org/10.1021/ma2000674.

78 Sun, X.-L., He, W.-D., Pan, T.-T. et al. (2010). *Polymer* 51: 110–114. https://doi.org/10.1016/j.polymer.2009.11.014.

79 Chytil, P., Etrych, T., Kříž, J. et al. (2010). *Eur. J. Pharm. Sci.* 41: 473–482. https://doi.org/10.1016/j.ejps.2010.08.003.

80 Tominey, A.F., Liese, J., Wei, S. et al. (2010). *Beilstein J. Org. Chem.* 6: 66. https://doi.org/10.3762/bjoc.6.66.

81 Flores, J.D., Xu, X., Treat, N.J., and McCormick, C.L. (2009). *Macromolecules* 42: 4941–4945. https://doi.org/10.1021/ma900517w.

82 Liang, M., Lin, I.C., Whittaker, M.R. et al. (2010). *ACS Nano* 4: 403–413. https://doi.org/10.1021/nn9011237.

83 Boyer, C., Granville, A., Davis, T.P., and Bulmus, V. (2009). *J. Polym. Sci., Part A: Polym. Chem.* 47: 3773–3794. https://doi.org/10.1002/pola.23433.

84 Alidedeoglu, A.H., York, A.W., Rosado, D.A. et al. (2010). *J. Polym. Sci., Part A: Polym. Chem.* 48: 3052–3061. https://doi.org/10.1002/pola.24083.

85 Nash, M.A., Yager, P., Hoffman, A.S., and Stayton, P.S. (2010). *Bioconjugate Chem.* 21: 2197–2204. https://doi.org/10.1021/bc100180q.

86 Thomas, D.B., Convertine, A.J., Myrick, L.J. et al. (2004). *Macromolecules* 37: 8941–8950. https://doi.org/10.1021/ma048199d.

87 Harvison, M.A., Davis, T.P., and Lowe, A.B. (2011). *Polym. Chem.* 2: 1347–1354. https://doi.org/10.1039/C1PY00046B.

88 Maki, Y., Mori, H., and Endo, T. (2007). *Macromol. Chem. Phys.* 208: 2589–2599. https://doi.org/10.1002/macp.200700330.

89 Blidi, I., Geagea, R., Coutelier, O. et al. (2012). *Polym. Chem.* 3: 609–612. https://doi.org/10.1039/C2PY00541G.

90 Girard, E., Marty, J.-D., Ameduri, B., and Destarac, M. (2012). *ACS Macro Lett.* 1: 270–274. https://doi.org/10.1021/mz2001143.

91 Mori, H., Kudo, E., Saito, Y. et al. (2010). *Macromolecules* 43: 7021–7032. https://doi.org/10.1021/ma100905w.

92 Guinaudeau, A., Mazières, S., Wilson, D.J., and Destarac, M. (2012). *Polym. Chem.* 3: 81–84. https://doi.org/10.1039/C1PY00373A.

93 Keddie, D.J., Guerrero-Sanchez, C., Moad, G. et al. (2012). *Macromolecules* 45: 4205–4215. https://doi.org/10.1021/ma300616g.

94 Girard, E., Tassaing, T., Marty, J.-D., and Destarac, M. (2011). *Polym. Chem.* 2: 2222–2230. https://doi.org/10.1039/C1PY00209K.

95 Roy, D. and Sumerlin, B.S. (2011). *Polymer* 52: 3038–3045. https://doi.org/10.1016/j.polymer.2011.04.051.

96 Riedel, M., Stadermann, J., Komber, H. et al. (2011). *Eur. Polym. J.* 47: 675–684. https://doi.org/10.1016/j.eurpolymj.2010.10.010.

97 Benaglia, M., Chen, M., Chong, Y.K. et al. (2009). *Macromolecules* 42: 9384–9386. https://doi.org/10.1021/ma9021086.

98 Benaglia, M., Chiefari, J., Chong, Y.K. et al. (2009). *J. Am. Chem. Soc.* 131: 6914–6915. https://doi.org/10.1021/ja901955n.

99 Moad, G., Benaglia, M., Chen, M. et al. (2011). *Non-conventional Functional Block Copolymers*, ACS Symposium Series 1066, 81–102. American Chemical Society. https://doi.org/10.1021/bk-2011-1066.ch007.

100 Sriprom, W., James, M., Perrier, S., and Neto, C. (2009). *Macromolecules* 42: 3138–3146. https://doi.org/10.1021/ma9004428.

101 Lipscomb, C.E. and Mahanthappa, M.K. (2009). *Macromolecules* 42: 4571–4579. https://doi.org/10.1021/ma900477d.

102 Perrier, S. (2017). *Macromolecules* 50: 7433–7447. https://doi.org/10.1021/acs.macromol.7b00767.

4

Kinetics and Mechanism of RAFT Polymerizations

Michael Buback

Georg-August-University Goettingen, Faculty of Chemistry, Institute of Physical Chemistry, Tammannstrasse 6, 37077 Goettingen, Germany

4.1 Introduction

Reversible addition–fragmentation chain transfer (RAFT) polymerization is one of the leading methods for producing polymers of controlled size and architecture. To take full advantage of this powerful strategy, the RAFT mechanism needs to be understood and the relevant rate coefficients should be accurately known to enable simulation of polymerization kinetics and product properties and to adequately select RAFT agents for specific monomer systems and reaction conditions. Because of its chain transfer nature, the concentration of radicals during RAFT polymerization under ideal conditions is not affected by the superimposed RAFT equilibrium. As a consequence, monitoring of polymerization rate as well as analysis of polymer size provides no clear mechanistic picture. In particular, such problems occur with RAFT polymerizations mediated by dithiobenzoates (DTBs). These systems exhibit strong anomalies, such as induction periods with virtually no polymerization taking place, and significant rate retardation over the entire course of the reaction as compared to conventional radical polymerization, i.e. reactions without RAFT agent under otherwise identical conditions.

Two completely different mechanisms have been used to interpret rate retardation during DTB-mediated polymerizations [1]. One model, which traces back to Monteiro and de Brouwer [2], assumes intermediate radical termination (IRT), i.e. reaction of the intermediate radical species, produced by addition of a propagating radical to the RAFT agent, with another radical species including the possibility of self-termination of intermediate radicals. The other model adopts slow fragmentation (SF) of the intermediate radical as the cause for retardation [3].

Monomer conversion vs. time data for DTB-mediated RAFT polymerizations may be fitted by these two limiting mechanisms. The fragmentation rate coefficients of the intermediate radical associated with the two models, however, may differ by more than 6 orders of magnitude [4], which is a nightmare for kineticists.

Objections against the SF model result from electron paramagnetic resonance (EPR) evidence on the measured intermediate radical concentrations, which are

RAFT Polymerization: Methods, Synthesis and Applications, First Edition.
Edited by Graeme Moad and Ezio Rizzardo.

orders of magnitude below the values predicted using the SF model [5]. The IRT model can account for the experimentally observed low intermediate radical concentration, but was unable to explain the absence of significant amounts of products from irreversible termination, i.e. three-arm star species, among the products of acrylate polymerizations [6, 7]. Investigations into styrenic systems demonstrated that such three-arm stars are stable at typical polymerization temperatures [8].

The controversial situation with DTB-mediated RAFT polymerizations has been addressed by a task group of IUPAC Polymer Division in 2006 [4]. More recent investigations are contained in Moad's thorough review [1], in which he concludes that the evidence for IRT being the primary cause for retardation in DTB-mediated RAFT polymerizations appears overwhelming. The SF model should thus not be applied towards the analysis of polymerizations mediated by DTBs. Recent *ab initio* studies [9] have demonstrated that the earlier quantum chemical calculations, which appeared to provide support for the SF model, need revision in the case of DTB systems. The present study addresses the application of the single pulse-pulse laser polymerization-electron paramagnetic resonance (SP-PLP-EPR) method towards the analysis of RAFT kinetics and mechanism. Pulsed-laser polymerization (PLP) is almost instantaneously induced by a laser single pulse (SP), which decomposes a photoinitiator. The subsequent time evolution of intermediate and of propagating radicals is measured by online EPR spectroscopy with a time resolution of microseconds. As radical species are directly monitored, the method is perfectly suited for detailed analysis of conventional and reversible deactivation (controlled) radical polymerizations [10]. Moreover, products from the reaction of DTB model systems have been analysed to clarify the mechanism.

In Section 4.2, aspects of ideal RAFT polymerization kinetics are outlined. Section 4.3 illustrates the SP-PLP-EPR technique. Section 4.4 briefly addresses the recently applied quantum chemical procedure [9]. Section 4.5 deals with RAFT polymerizations mediated by one xanthate, two trithiocarbonates, and one dithiobenzoate as well as with RAFT-related model systems with a focus on the anomalies seen in the case of dithiobenzoate RAFT agents.

4.2 Ideal RAFT Polymerization Kinetics

The RAFT kinetic scheme encompasses the well-known steps of conventional radical polymerization, i.e. initiation, propagation, termination, and transfer processes [1], onto which the reactions associated with the RAFT equilibrium are superimposed. As can be seen from Scheme 4.1, two such RAFT equilibria may be distinguished. One refers to the pre-equilibrium period, where a small radical species (P_m^*) adds with rate coefficient $k_{ad,1}$ to the RAFT agent **1**, R—S—C(=S)—Z, to yield the intermediate radical **2**. Species **2** may either fragment back, with rate coefficient $k_{\beta,1}$, or may fragment with rate coefficient $k_{\beta,2}$ to produce a macroRAFT agent **3**, with the leaving group P_m being specific for the polymerizing monomer. After consumption of **1**, rapid exchange of radicals P_m^* and P_n^* occurs via the polymeric intermediate radical **4**, which, in what follows, will be referred to as INT^*. The chain lengths of

the radicals P_m^* and P_n^* should be close to each other and should gradually increase during the course of polymerization. Upon ignoring the early RAFT polymerization period and a potential chain length dependence of the addition and fragmentation rate coefficients, the main equilibrium, with rate coefficients k_{ad} and k_β, may provide an adequate representation of the RAFT process. The main equilibrium is characterized by the equilibrium constant $K_{eq} = k_{ad}/k_\beta$, which is a measure of the stability of the intermediate radical.

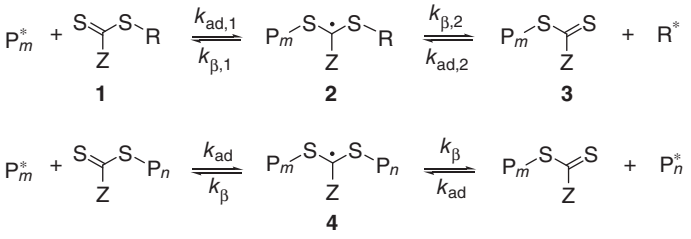

Scheme 4.1 Pre-equilibrium and main equilibrium RAFT processes.

More detailed studies take primary addition steps into account by which initiator-derived radicals R^* add to the monomer producing the growing monomer-specific radicals P_m^*. Moreover, termination reactions, by combination or disproportionation, may occur between R^*, P_m^*, P_n^*, and the intermediate radicals **2** and **4**. A further process, the so-called 'missing step' [11], that refers to the reaction of the product from cross-combination of **4** and P_m^* with a radical P*, will be presented below, as this reaction is not part of the ideal RAFT polymerization kinetics.

4.3 Pulsed Laser Experiments in Conjunction with EPR Detection

As rate measurements and studies into polymer molar mass distributions are not diagnostic with respect to the RAFT mechanism, PLP techniques in conjunction with online EPR spectroscopy are particularly helpful for elucidating mechanistic details [10]. In addition to the analysis of RAFT kinetics [12, 13], the SP-PLP-EPR method has been successfully applied towards the analysis of chain-length-dependent termination [14] and of backbiting processes [15] as well as towards the detailed analysis of atom transfer radical polymerization (ATRP) [16] and of organometallic-mediated radical polymerization (OMRP) [17].

An important advantage of photoinitiation by laser pulses relates to externally triggering the amount of photoinitiator-derived primary radicals. Within the SP-PLP-EPR experiment an intense burst of such primary radicals is almost instantaneously produced, and the type and concentration of radicals is subsequently measured by quantitative EPR spectroscopy. The beauty of the method consists of the combination of instantaneous production of a high radical concentration, mostly up to 10^{-5} mol l^{-1}, with the sensitive time-resolved EPR spectroscopic

detection of the decay of radical concentrations to values as low as 10^{-8} mol l^{-1}, in both organic and aqueous solutions. Moreover, as a consequence of the extremely short laser pulse used for initiation, no further primary radicals are produced during the period of time-resolved EPR detection of radicals after firing the laser pulse at $t = 0$.

In the situation where the leaving radical of the RAFT agent is identical in chemical reactivity to the monomer radical, a particularly simple EPR spectroscopic situation is created with only two types of radicals being present, INT* and P_m^*. Most of the SP-PLP-EPR investigations reported here take advantage of this strategy. The primary photoinitiator-derived radicals are not seen in most cases, as they add too rapidly to the monomer or to the RAFT agent.

The components of the SP-PLP-EPR setup are illustrated in Figure 4.1. More details are given in Ref. [18]. The sample contained in a quartz tube of 5 mm outer and 4 mm inner diameter is placed into the EPR cavity and is irradiated by UV laser pulses through a grid. The EPR signal intensity is measured as a function of time t after applying the laser pulse. The spectrometer and the laser are synchronized by a pulse generator. Signal intensity is calibrated for absolute radical concentration against a 2,2,6,6-tetramethylpiperidine-1-yl-oxyl (TEMPO) solution at conditions as close as possible to the ones of the actual polymerization, e.g. in butyl acrylate (BA)/toluene solution. First, the double integral of the EPR spectrum is calibrated against the TEMPO solution. Secondly, the peak signal intensity at a fixed magnetic field is calibrated against the double integral of the full EPR spectrum, as detailed, e.g. in Ref. [19]. It should be noted that all components of the setup in Figure 4.1 are commercially available.

In an early SP-PLP-EPR study into RAFT kinetics, the concentration of INT* was measured for *S*,*S*′-bis(methyl-2-propionate)trithiocarbonate (BMPT,

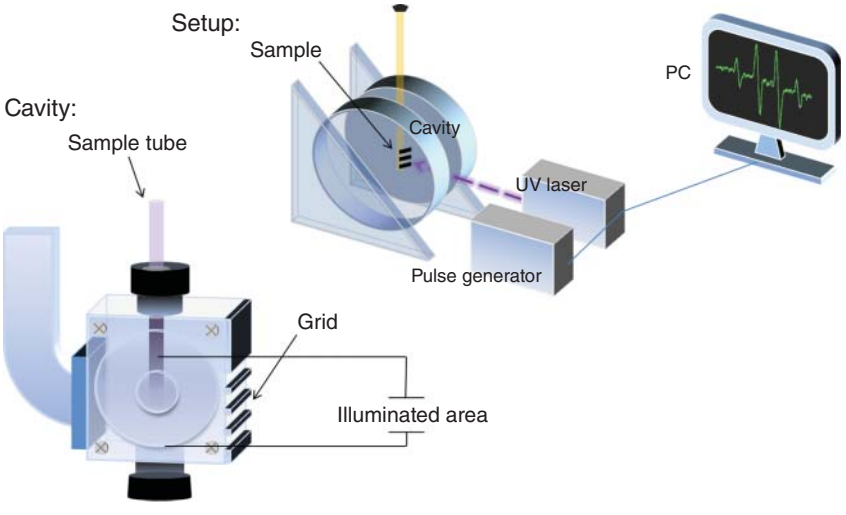

Figure 4.1 SP–PLP–EPR setup entirely consisting of commercially available instrumentation; for more details see Ref. [18].

Scheme 4.2)-mediated butyl acrylate (2 mol l^{-1} BA in toluene) polymerization at −30 °C [12]. The left-hand part of Figure 4.2 shows normalized EPR peak intensities measured at the field position of maximum intensity, H_{fix}, of INT* with a microsecond time resolution after firing the laser pulse. This data illustrates that, after applying the intense laser pulse of nanosecond width onto the system consisting of a photoinitiator, a monomer, and a RAFT agent, the addition of primary radicals R* (or $R-(BA)_n^*$) to the RAFT agent occurs at a very fast rate. Crude kinetic analysis of the initial reaction period reveals that k_{ad} is above 10^5 l mol^{-1} s^{-1} [12, 19]. The extended millisecond time range of the experiment is depicted in the right-hand part of Figure 4.2. As with most other experiments, 2-methyl-1-[4-(methylthio)phenyl]-2-morpholin-4-ylpropan-1-one (MMMP, Scheme 4.2) was used as the photoinitiator. The early SP-PLP-EPR-type study in Figure 4.2 demonstrates that this RAFT intermediate radical, INT*, is very rapidly formed, but is not long-lived and decays quickly.

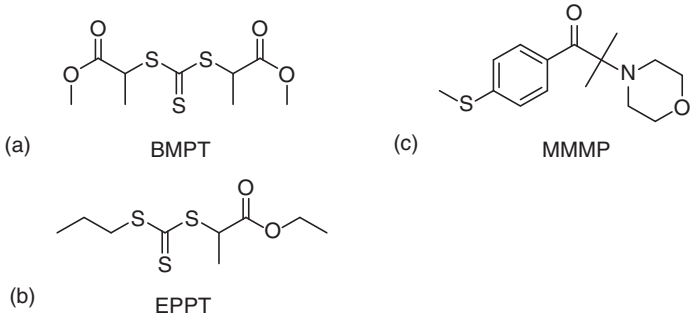

Scheme 4.2 (a) *S*,*S*′-Bis(methyl 2-propionate) trithiocarbonate (BMPT), (b) *S*-(methyl 2-propionate) *S*′-propyl trithiocarbonate (EPPT), and (c) 2-methyl-1-[4-(methylthio)phenyl]-2-morpholin-4-ylpropan-1-one (MMMP) [20].

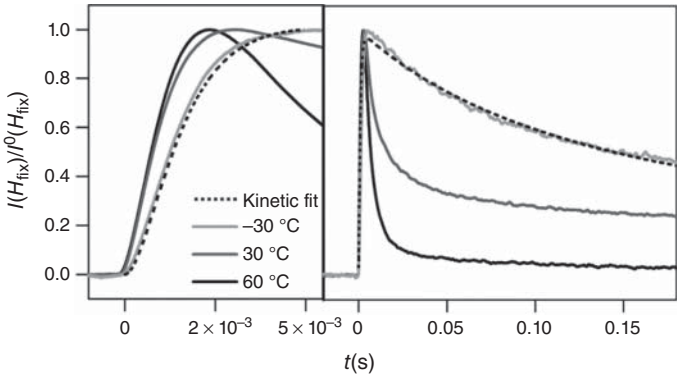

Figure 4.2 Time evolution, after applying a single laser pulse at $t = 0$, of the normalized EPR signal at the field position H_{fix} of the EPR peak maximum for INT* in BMPT-mediated BA polymerizations ($C_{BMPT} = 4.1 \times 10^{-3}$ mol l^{-1}, $C_{BA} = 2.0$ mol l^{-1} in toluene) [12].

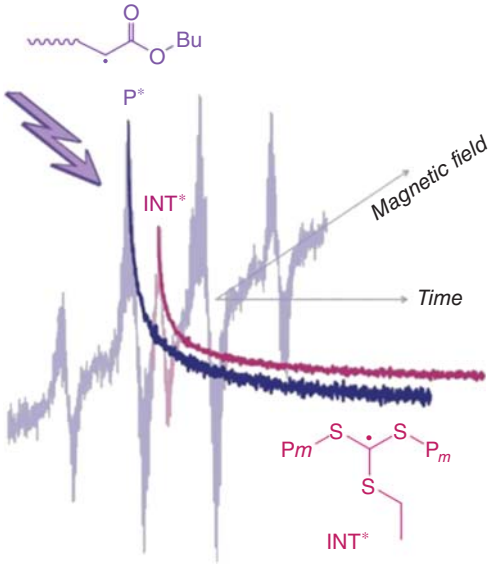

Figure 4.3 SP-PLP-EPR traces of INT* and P* species after applying a laser single pulse, at $t = 0$, during a trithiocarbonate-mediated BA polymerization (1.5 M in toluene solution) at −40 °C [20].

Within the SP-PLP-EPR experiments described below, absolute concentrations are monitored for both propagating and intermediate radicals. As representative results, data for a trithiocarbonate-mediated BA RAFT polymerization at −40 °C are illustrated in Figure 4.3 [20]. The EPR spectrum, which consists of the four-line spectrum of secondary BA radicals and of the EPR singlet component associated with INT*, is displayed along the magnetic field axis. The time evolution of both species is monitored at the magnetic field position of the maxima of the BA radical, P*, and of the INT* component, respectively. PREDICI® fitting of the experimental radical concentration vs. time traces using literature data for the rates of propagation and of chain-length-dependent termination provides the rate coefficients k_{ad} and k_β with an assumption only being required for the size of the cross-termination rate coefficient, $k_{t,cross}$, i.e. for the reaction rate of the INT* species with a propagating radical.

The SP-PLP-EPR method is laborious in that calibration of the individual radicals is required under conditions as close as possible to the ones of the RAFT polymerization experiment. Thus, within a second EPR-based experiment, the ratio of the double integrals of the deconvoluted individual EPR spectra is measured. This ratio is identical to the ratio of INT* to P* concentrations, C_{INT^*}/C_{P^*}. Thus, no EPR calibration is required for accessing the ratio C_{INT^*}/C_{P^*} which has been determined for several initial RAFT agent concentrations under quasi-stationary conditions during continuous laser pulsing, typically at a repetition rate of 20 Hz. The slope of the plot of the ratio of the two double integrals, i.e. of the two radical concentrations, vs. the initial RAFT agent concentration, C^0_{RAFT}, yields $K_{eq} = k_{ad}/k_\beta$ according to Eq. (4.1):

$$C_{INT^*}/C_{P^*} = k_{ad}/k_\beta \cdot C_{RAFT} = K_{eq} \cdot C_{RAFT} \tag{4.1}$$

As pointed out by Kwak et al. [5], Eq. (4.1) is valid when cross-termination and INT* self-termination rates are negligible compared to the addition and fragmentation rates. This requirement is fulfilled in most cases but needs to be checked for each

system. The method via Eq. (4.1) is applied within kinetic studies into monomer-free model systems, where growing radicals P_m^* are absent. The SP-PLP-EPR experiment, on the other hand, is used during RAFT polymerizations, i.e. in the presence of the monomer. As BA was the monomer under investigation, the polymerizations (1.5 M BA in toluene) were carried out at −40 °C to avoid mid-chain radical formation, which would result in unnecessary complications due to the occurrence of a second type of growing radicals, such as mid-chain radicals produced from secondary radicals by backbiting [21]. With the xanthate, trithiocarbonate, and dithiobenzoate RAFT agents under investigation, the leaving group has been selected such as to be chemically identical to an acrylate radical. Predici treatment of these systems is enormously simplified, as only P_m^* and INT* need to be considered.

The RAFT agent should weakly absorb at the laser wavelength, $\lambda = 351$ nm, and should be stable towards laser irradiation. By exposing the RAFT agents dissolved in toluene to UV irradiation, it was confirmed that the RAFT concentration decreases by no more than 1% even upon applying sequences of laser pulses as used within the quasi-stationary experiments. That these laser sequences do not affect RAFT agent performance has been demonstrated for trithiocarbonate-mediated bulk BA polymerizations, in which the number average molar mass has been found to linearly increase with the degree of monomer conversion, at least up to 40% conversion, while dispersity remains below 1.3 [19, 22].

4.4 Quantum Chemical Calculations of the RAFT Equilibrium

Only a brief account of the method will be given, as the strategy used by the Mata group in carrying out the recent RAFT-related quantum chemical calculations is presented in more detail elsewhere [9].

Local pair natural coupled cluster (DLPNO-CCSD(T)) calculations have been applied in a tailored conjugate method, including basis set extrapolation and solvation effects. Thus, molecular systems of sizes that otherwise would be beyond reach can be treated. Use is made of the close-range character of dynamic electronic correlation, constructing a smaller set of configurations on the basis of local occupied and virtual orbital spaces. This allows for the inclusion of higher order correlation effects, as canonical wave function methods scale with system size.

The structures were optimized in solution at the B3LYP-D3/def2-TZVP (with Becke-Jones damping of the D3 correction) level of theory [23, 24]. The zero-point vibrational energy corrections, and thermal corrections to enthalpy and entropy, were computed at the same level. Solvent effects of toluene were included via a continuum solvation model, i.e. the *Conductor-like Polarizable Continuum Model* (CPCM) [25]. The electronic energies for each species were refined through a conjugate expression, summarized as

$$E_{\mathrm{el}} = E\left[\mathrm{CC/TZ}\right] + \Delta\mathrm{CBS} + \Delta\mathrm{Solv} \tag{4.2}$$

The electronic energy at the DLPNO-CCSD(T)/cc-pVTZ level of theory [26], E[CC/TZ], has thus been adjusted by two terms: ΔCBS includes a complete basis set extrapolation using the cc-pVDZ and cc-pVTZ basis sets [27]. Solvent effects are taken into account by ΔSolv, which refers to the difference in an MP2/cc-pVTZ calculation with and without the CPCM solvation model.

The calculations were carried out with the ORCA 4.0 program package [9]. The equilibrium constant K_{eq} of the RAFT reaction was calculated from the reaction free energy, ΔG_r:

$$K_{eq}(T) = \left(C^0\right)^{\Delta n} e^{-\Delta G_r/RT} \tag{4.3}$$

where T is the absolute temperature, C^0 is the standard unit of concentration, which is 1 mol l^{-1} for the solution phase, Δn is the change in moles upon reaction, and R is the universal gas constant.

4.5 Xanthate-, Trithiocarbonate- and Dithiobenzoate-Mediated Polymerizations

4.5.1 General Aspects of Actual RAFT Polymerizations

According to ideal kinetics, the RAFT polymerization rate is identical to that of a conventional radical polymerization carried out under otherwise same conditions. Minor differences may occur, as the chain length distribution of radicals in conventional radical polymerization and in RAFT polymerization will mostly be different, which affects the rate of chain-length-dependent termination [28]. Clear rate reductions with RAFT polymerizations are assigned to inhibition in the early reaction period and to retardation in the subsequent range up to high degrees of monomer conversion. In addition, several avoidable causes of retardation may occur, such as the presence of air, impurities, instability of the RAFT agent, and a poor choice of the initiator [1]. The latter effect is part of the initialization process, which has been thoroughly investigated by Klumperman and colleagues [29, 30]. Initialization refers to the period during which the initial RAFT agent is consumed. Within this time interval several addition steps need to be considered, i.e. the addition of initiator fragments I*, of leaving radicals R*, and of propagating radicals P* to the RAFT agent and to the monomer, followed by fragmentation reactions of the so-obtained products. The very low rate of monomer consumption during initialization is primarily determined by slow addition of the leaving group R*. Moreover, termination reactions of the multitude of radical species may play a role. The rather complex kinetic situation has been carefully analysed by Klumperman and his group [29]. The complexity of the initial period may be reduced by selecting the leaving radical R* such as to be identical to the primary radical from initiator decomposition. A significant simplification is reached by selecting R* such that it is chemically equivalent to the monomer-specific propagating radical P*. Moreover, using macroRAFT agents such that R* is an oligomeric radical based on the monomer under investigation leads to further simplification in that no initialization period occurs and the

system immediately enters the main equilibrium situation (unless avoidable causes of retardation come into play).

The initialization period is determined by the type of initiator and of the RAFT agent, in particular, the competition of the I* and R* addition rates to the monomer and to the primary RAFT agent, the fragmentation rates of the products from these early addition reactions, and the termination reactions of the different kinds of small radicals formed in the initial period of the RAFT reaction. The initialization period is over as soon as the primary RAFT agent R—S—C(=S)—Z is consumed and has been converted at least into single monomer RAFT adduct species, I—M—S—C(=S)—Z or R—M—S—C(=S)—Z without producing polymers with the degree of polymerization exceeding unity. While initialization may be largely modified and even completely avoided, retardation occurs up to high degrees of monomer conversion.

Both initialization and retardation effects may be very pronounced in the case of dithiobenzoate RAFT agents. During initialization, the polymerization rate may be very low or even negligible. In the subsequent time range, polymerization is retarded and remains at a reduced level. The situation is illustrated in Figure 4.4 for BA polymerizations at 70 °C mediated by cumyl dithiobenzoate (CDB), cyano-*iso*-propyl dithiobenzoate (CPDB), and ethyl-*S*-thiobenzoyl-2-thiopropionate (ETTP, see Scheme 4.3a) at two RAFT agent concentrations: 1.5×10^{-3} mol l^{-1} (open symbols) and 2.0×10^{-2} mol l^{-1} (half-filled symbols) [13].

The dotted line in Figure 4.4 represents monomer conversion vs. time data for conventional radical polymerization, i.e. without RAFT agent. At the lower RAFT agent concentration (1.5×10^{-3} mol l^{-1}), no inhibition occurs, but some retardation does. As can be seen from the slope of the conversion vs. time data, this retardation is almost the same for the three dithiobenzoates but depends on the RAFT agent concentration. At 2.0×10^{-2} mol l^{-1} (full symbols in Figure 4.4), extended inhibition occurs for CDB-mediated polymerization. This strong effect is assigned to the low addition rate to the monomer of the resonance-stabilized cumyl radical produced by the fragmentation of **2** (Scheme 4.1). This pre-equilibrium effect is considerably smaller with the two other dithiobenzoates, where ethyl acrylate

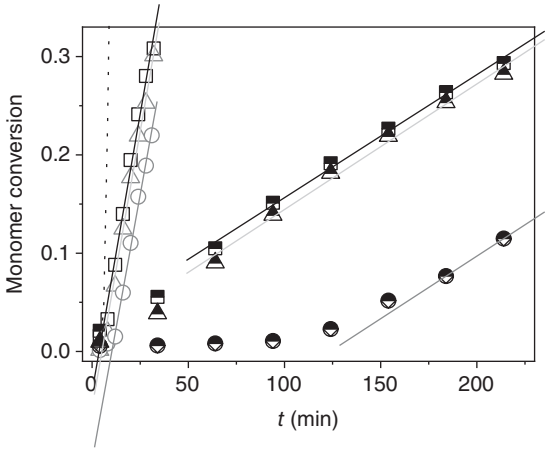

Figure 4.4 Inhibition as well as rate retardation during RAFT polymerizations of BA at 70 °C mediated by ETTP (squares), CPDB (triangles) and CDB (circles) as well as without RAFT agent (dotted line); AIBN (1.5×10^{-3} mol l^{-1}) was the initiator; the RAFT agent concentrations were 1.5×10^{-3} mol l^{-1} (open symbols) and 2.0×10^{-2} mol l^{-1} (half-filled symbols) [13].

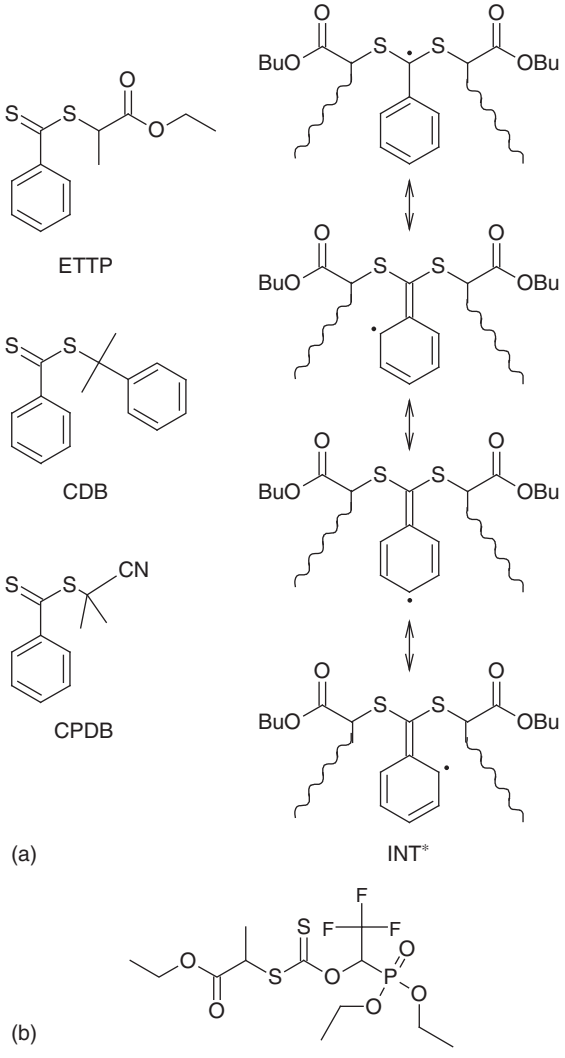

Scheme 4.3 (a) Dithiobenzoate RAFT agents under investigation (left) and resonance structures (right) of the common INT* species under main equilibrium conditions of BA polymerization. (b) EDTCP (ethyl 2-[1-diethoxyphosphoryl-2,2,2-trifluoroethoxythio carbonylsulfanyl] propionate).

and cyano-isopropyl radicals, respectively, are released from **2**. The addition of a cumyl radical to BA, under otherwise identical conditions, is by about a factor of 700 slower than the addition of a butyl acrylate propagating radical to BA (i.e. during homopropagation) [31, 32]. This factor reduces to about 10 for the addition of the cyano-isopropyl radical to BA [33].

In the case of ETTP, the reinitiation efficiency of ethyl acrylate radicals is supposed to be very fast. As a consequence, no inhibition occurs. In the initial stage of RAFT polymerizations, the rate is essentially determined by the addition of the

leaving radical R* to the monomer [34]. Along these lines, Moad [1] concluded that retardation in the initial period is associated with the R group, whereas retardation after consumption of the initial RAFT agent is determined by the Z group. In order to avoid inhibition, it appears recommendable to use RAFT agents with R* being a good leaving group and also a good (re)initiating radical. In the case of poorly initiating R*, termination reactions come into play, which may heavily reduce the polymerization rate.

As can be seen from the RHS of Scheme 4.3a, the resonance-stabilized INT* species for BA polymerizations mediated by the three dithiobenzoates ETTP, CDB, and CPDB are identical. Thus it comes as no surprise that, after passing the initial stage, the slopes of the monomer conversion vs. time correlations in Figure 4.4 are more or less identical under main equilibrium conditions.

The main equilibrium rates, given by the slope of the straight lines in Figure 4.4, are lower than those for the associated conventional BA polymerizations by a factor of 10 for $C_{\mathrm{RAFT}} = 1.5 \times 10^{-3}$ mol l^{-1} and by a factor of 140 for $C_{\mathrm{RAFT}} = 2.0 \times 10^{-2}$ mol l^{-1}. The subsequent text exclusively refers to the main equilibrium situation, which is associated with pronounced and unavoidable retardation in most dithiobenzoate-mediated RAFT polymerizations. Initial inhibition may be shortened or even avoided by sensibly selecting the RAFT agent, whereas retardation is observed throughout the course of the polymerization [1]. Initialization will not be further addressed, as excellent reviews are available on this topic [1, 29, 30].

Retardation is weak or even negligible with xanthate and trithiocarbonate RAFT polymerizations, but may be strong with dithiobenzoate-mediated BA polymerizations. These large effects will be used to illustrate and unravel the mechanism behind this kinetic behaviour, which has been under debate for a long time.

4.5.2 Xanthates

The SP-PLP-EPR technique has been applied towards BA polymerizations in a solution of toluene at −40 °C with EDTCP being the xanthate/MADIX agent [35]. MADIX is the acronym for *Macromolecular Design via the Interchange of Xanthates*. RAFT and MADIX processes are identical with MADIX referring to the specific case of the Z moiety in Z—C(=S)—S—R being OR.

EDTCP was selected, because phosphor and/or fluorine atoms disfavour conjugation between the C=S double bond and the electron pair on the oxygen atom and thus enhance reactivity. Moreover, EDTCP carries a leaving group that is chemically close to the propagating radical in BA polymerization. Thus the addition rate coefficients to monomer have been assumed to be identical for the EDTCP-derived radical and for the propagating radical. The reverse reaction, i.e. the fragmentation step, is also assumed to be identical for species produced by the two addition reactions. Fragmentation of intermediate radicals may occur via two pathways: In addition to normal β-scission, the alkoxy group may be split. The latter reaction may however be ignored at −40 °C [35], as confirmed by subjecting product samples to end-group

analysis by mass spectrometry [36]. These experiments provided no indication of the polymer (oligomer) from re-initiation by the Z-group.

The concentrations of INT* and P* were measured at the magnetic field positions of the characteristic peak maxima via time-resolved EPR after firing an intense laser pulse at time $t = 0$ [35]. For deducing absolute radical concentrations, calibration of the setup with the stable radical TEMPO has been carried out. The entire three-step calibration procedure is detailed elsewhere [37].

To enhance signal-to-noise quality, up to 20 radical concentration vs. time traces were co-added in the case of INT* and up to 200 for P*. Illustrated in Figure 4.5 is the so-obtained time evolution of P* and INT* concentrations. The data on the RHS of Figure 4.5 demonstrates that INT* exhibits maximum concentration immediately after firing the laser pulse, which indicates rapid addition of the primary MMMP-derived radical to EDTCP. The experimental traces were fitted to a simple kinetic scheme via the parameter estimation module of the program package PREDICI version 6.4.6 on an Intel Core Duo, 1.87 GHz computer [35]. The scheme encompasses initiation, propagation, chain-length-dependent termination, the individual RAFT pre- and main equilibrium steps as well as cross-termination of the intermediate radical. As radical chain length i increases linearly with time t after firing the laser pulse at $t = 0$, this variation has been included into the PREDICI simulation using the independently determined chain-length-dependent termination rate coefficients $k_t(i,i)$ for reaction of two BA radicals, both of chain length i [15]. The primary radical concentration, C_R^0, which is instantaneously produced at $t = 0$, and the rate coefficient for addition of the initiator-derived radical to the RAFT agent $k_{ad,1}$ (Scheme 4.1), were obtained by fitting the early maximum of the experimental C_{INT^*} and C_{P^*} traces. The rate coefficient for addition of the first monomer molecule to the radical fragment from initiator decomposition was assumed to be $k_i = 10 \times k_p$. The selection of the parameters C_R^0, k_i as well as $k_{ad,1}$ does not significantly affect the fitting of k_{ad} and k_β, as the importance of these parameters is restricted to the very initial part of the radical concentration vs. time traces (see Figure 4.2).

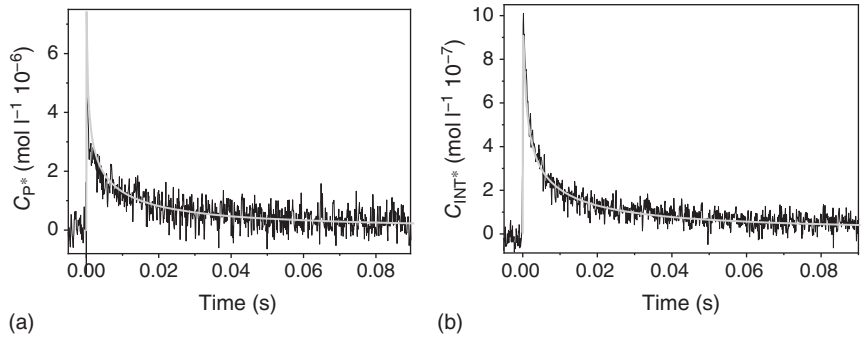

Figure 4.5 Comparison of simulated and experimental concentration vs. time traces for the propagating (LHS) and the intermediate (RHS) radicals in a BA polymerization (1.5 mol l^{-1} in toluene) at −40 °C with EDTCP being the RAFT agent (2.1×10^{-2} mol l^{-1}) and MMMP the photoinitiator (1.0×10^{-2} mol l^{-1}) [35].

With the exception of the rate coefficient for the reaction of INT* with P*, $k_{t,\mathrm{cross}}$, the parameters required for PREDICI simulation of the measured radical concentration vs. time traces are known from separate experiments. Simulations under extensive variation of $k_{t,\mathrm{cross}}$ between 0 (SF model) and k_t revealed that $k_{t,\mathrm{cross}}$ has no significant impact on the $C_{\mathrm{INT*}}$ and $C_{\mathrm{P*}}$ vs. time traces with EDTCP-mediated BA polymerization. The associated change of k_β is by less than a factor of 2. This weak impact of $k_{t,\mathrm{cross}}$ is not surprising in view of the low INT* concentration, which decays with a half-life of about 1 ms.

The excellent PREDICI fit of the experimental curves in Figure 4.5 is achieved with $k_{t,\mathrm{cross}} \approx 0.5 \cdot k_t(i,i)$. From experiments at −40 °C and two EDTCP concentrations, the following mean values are obtained: $k_{\mathrm{ad}} = (2.5 \pm 0.1) \times 10^4$ l mol^{-1} s^{-1} and $k_\beta = (2.3 \pm 0.3) \times 10^3$ s^{-1}, corresponding to an equilibrium constant of $K_{\mathrm{eq}} = (11.1 \pm 1.2)$ l mol^{-1}.

The second EPR-based method, via Eq. (4.1), where pulse-periodic initiation is used to create quasi-stationary radical concentrations for various initial RAFT agent concentrations, has also been applied. Shown in Figure 4.6 is an EPR spectrum measured during an EDTCP-mediated BA polymerization at −40 °C. The individual EPR bands for INT* and P* were fitted to the overall band [35].

From $C_{\mathrm{INT*}}/C_{\mathrm{P*}}$ measured at different initial EDTCP concentrations, the RAFT equilibrium constant is obtained as $K_{\mathrm{eq}} = (12.0 \pm 0.2)$ l mol^{-1}, i.e. in almost perfect agreement with the value from the SP-PLP-EPR experiment. The low K_{eq} value is consistent with the poor control observed in xanthate-mediated acrylate polymerizations. The value refers to main equilibrium conditions, which has been checked by SEC analysis of polymer samples after pulse-periodic irradiation.

The kinetic studies were not carried out under conditions of effective polymerization control, but were directed towards the determination of rate coefficients. Thus, it was of primary importance to select xanthate concentrations such that accurate rate coefficients are obtained. The stationary method via Eq. (4.1) does not require calibration for absolute radical concentration. On the other hand, the SP-PLP-EPR method, which needs such calibration, is far more powerful, as individual k_{ad} and

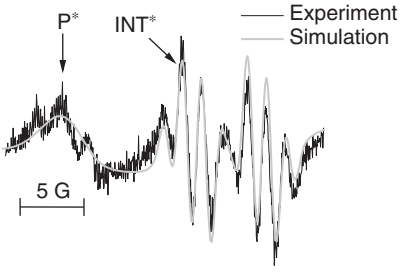

Figure 4.6 Section of the EPR spectrum used for $C_{\mathrm{INT*}}/C_{\mathrm{P*}}$ determination; *black line*: EPR spectrum recorded during laser-induced polymerization of BA (1.5 mol l^{-1} in toluene) in the presence of EDTCP (2.1×10^{-2} mol l^{-1}) at −40 °C; pulse repetition rate: 20 Hz; sweep time: 42 seconds; *grey line*: simulated EPR spectrum on the basis of the separately measured hyperfine coupling constants of INT* and P* species. The field positions used for monitoring INT* and P* concentrations during the SP-PLP-EPR experiment are indicated by the arrows.

Table 4.1 Summary of the addition rate coefficients k_{ad} and fragmentation rate coefficients k_β deduced from SP-PLP-EPR experiments on BA polymerized in toluene solution at −40 °C.

RAFT agent/ monomer in toluene	k_{ad} (l mol^{-1} s^{-1}) SP-PLP-EPR	k_β (s^{-1}) SP-PLP-EPR	K_{eq} (l mol^{-1}) SP-PLP-EPR	K_{eq} (l mol^{-1}) via Eq. (4.1)
EDTCP/BA	$(2.5 \pm 0.1) \times 10^4$	2300 ± 300	11.1 ± 1.2	12.0 ± 0.2
BMPT/BA	$(4.1 \pm 0.9) \times 10^6$	45 ± 5	$(9.0 \pm 3.0) \times 10^4$	$(7.0 \pm 0.2) \times 10^4$
EPPT/BA	$(3.4 \pm 0.3) \times 10^6$	140 ± 40	$(2.6 \pm 0.8) \times 10^4$	$(2.6 \pm 0.1) \times 10^4$
ETTP/BA	$(1.4 \pm 0.4) \times 10^6$	4.7 ± 1.5	$(3.4 \pm 0.6) \times 10^5$	$(2.3 \pm 0.6) \times 10^5$

Also listed in the Table 4.1 are the equilibrium constants K_{eq}, from SP-PLP-EPR and from EPR experiments according to the procedure via Eq. (4.1).

k_β values are accessible. Moreover, the model assumption $r_t^{cross} \ll r_{ad}, r_\beta$ underlying Eq. (4.1) does not need to be made, but the applicability of Eq. (4.1) may be checked on the basis of individual rate coefficients from the SP-PLP-EPR studies.

RAFT-related rate coefficients and RAFT equilibrium constants for several xanthates have been estimated by Coote et al. [38], although not for the special EDTCP agent. Quantum chemical calculations indicate that the addition of propagating radicals to xanthates is much slower than to dithioesters. This is indeed what the SP-PLP-EPR studies say: The addition rate coefficient of BA-type radicals to xanthates is approximately 2 orders of magnitude smaller than the associated numbers for addition to trithiocarbonates and to dithiobenzoates (see Section 4.6 and Table 4.1).

4.5.3 Trithiocarbonates

Rate coefficients k_{ad} and k_β have been measured via the SP-PLP-EPR method for BA polymerizations mediated by *S*-(methyl 2-propionate) *S*′-propyl trithiocarbonate EPPT, see Scheme 4.2) and by *S*,*S*′-bis(methyl 2-propionate) trithiocarbonate (BMPT, see Scheme 4.2) [20].

Intermediate and propagating radical concentrations, C_{INT*} and C_{P*}, measured during EPPT-mediated BA polymerizations at −40 °C, are shown in Figure 4.7. As compared to the situation with EDTCP, the INT* lifetime is extended from about 1 ms (Figure 4.5) to around 50–100 ms (Figure 4.7), but is approximately 1 order of magnitude smaller than the INT* lifetime with dithiobenzoate-mediated BA polymerizations at −40 °C [13]. The radical concentration vs. time profiles were fitted to the kinetic scheme presented in the Supporting Information associated with Ref. [20], which has also been used for simulating EDTCP-mediated BA polymerization. It is again assumed that $k_p^{rein} = k_p$ and $k_i = 10 \times k_p$, that $k_{t,cross}$ exhibits the same chain length dependence as $k_t^{i,i}$ (see Section 4.5.2), and that k_{ad} as well as k_β are identical for the leaving group R* and for the propagating radical P*. The propagation rate coefficient k_p and the chain-length-dependent termination rate coefficient for BA $k_t^{i,i}$ were again taken from the literature.

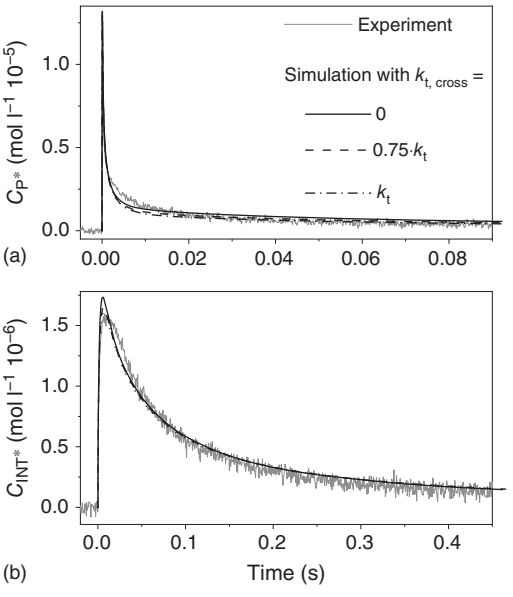

Figure 4.7 Comparison of simulated and experimental concentration vs. time profiles for propagating and for intermediate radicals during BA polymerization (1.5 mol l^{-1} in toluene) at −40 °C with EPPT being the RAFT agent (5.0×10^{-5} mol l^{-1}) and MMMP being the photoinitiator (1.0×10^{-2} mol l^{-1}). The simulations were carried out adopting different values for the cross-termination coefficient $k_{t,\mathrm{cross}}$, which was implemented as a chain-length-dependent quantity [20].

Figure 4.7 compares the experimental and simulated radical concentration vs. time traces for an EPPT-mediated BA polymerization at −40 °C. To check for the impact of cross-termination, $k_{t,\mathrm{cross}}$ has been varied between 0 and $k_t^{i,i}$. The fits of C_{P^*} and C_{INT^*} vs. time obtained for these very different cross-termination coefficients sit upon each other, indicating that $k_{t,\mathrm{cross}}$ has only negligible influence on the time evolution of the intermediate and propagating radical concentrations after laser pulsing at $t = 0$.

PREDICI simulation of the SP-PLP-EPR traces in Figure 4.7 yields the mean values of addition and fragmentation rate coefficients at −40 °C as $(3.4 \pm 0.3) \times 10^6$ l mol^{-1} s^{-1} and $(1.4 \pm 0.4) \times 10^2$ s^{-1}, respectively, which results in $K_{\mathrm{eq}} = (2.6 \pm 0.8) \times 10^4$ l mol^{-1} for a solution in toluene. In view of the low temperature, k_{ad} and k_β are both large and they are almost insensitive towards the size of $k_{t,\mathrm{cross}}$, as is presented in more detail in Ref. [20].

SP-PLP-EPR traces of C_{INT^*} and C_{P^*} measured during BMPT-mediated BA polymerization at −40 °C are shown in Figure 4.8. Adequate fits are obtained adopting $k_{t,\mathrm{cross}}$ to be between 0 and $0.2 \times k_t^{i,i}$. Towards higher $k_{t,\mathrm{cross}}$, the C_{INT^*} vs. time curve can still be well fitted, but the decay of C_{P^*} becomes faster than is experimentally observed. A slower cross-termination with three-armed INT*s, as compared to two-armed INT*s, is assigned to steric hindrance. The half-life of INT* for BMPT is about three times larger than that with the '2-arm' intermediate radical occurring in EPPT-mediated polymerization (Figure 4.7). Since the BMPT-derived INT* carries three arms (chains), a 3D treatment should, in principle, be used. To avoid the associated extensive numerical effort, the reactions involving a three-arm intermediate radical were translated into a one-dimensional problem. The implementation of the associated kinetic scheme into PREDICI is detailed in the Supporting Information associated with Ref. [20].

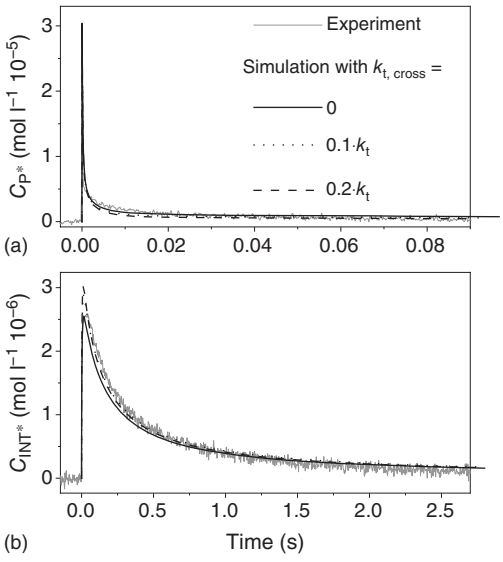

Figure 4.8 Comparison of simulated and experimental concentration vs. time profiles for propagating and intermediate radicals in BA polymerization (1.5 mol l^{-1} in toluene) at −40 °C with BMPT being the RAFT agent at 3.5×10^{-5} mol l^{-1} and MMMP at 1.0×10^{-2} mol l^{-1} the photoinitiator. The simulations were carried out for different sizes of the (chain-length-dependent) cross-termination rate coefficient, $k_{t,\,cross}$ [20].

The RAFT-related rate coefficients deduced from the SP-PLP-EPR data for BMPT-mediated BA polymerization at −40 °C are $k_{ad} = (4.1 \pm 0.9) \times 10^6$ l mol^{-1} s^{-1} and $k_\beta = (45 \pm 5)$ s^{-1}. These numbers result in $K_{eq} = (9.0 \pm 3.0) \times 10^4$ l mol^{-1}. The addition of a growing radical to BMPT is thus close to the one for addition of a BA radical to EPPT, whereas fragmentation is slower, by about a factor of 3. This reduction is assigned to delocalization of the radical functionality over three sulfur atoms with BMPT rather than over two sulfur atoms with EPPT.

In addition, the procedure according to Eq. (4.1) has been used for deducing K_{eq} via the C_{INT^*}/C_{P^*} ratios obtained from the EPR spectra [20]. The ratios obtained for BMPT are plotted vs. RAFT agent concentration in Figure 4.9. The slope of the straight line passing through the origin yields $K_{eq} = (7.0 \pm 0.2) \times 10^4$ l mol^{-1} at −40 °C, which is remarkably close to the number from the SP-PLP-EPR technique.

To check for a potential chain length dependence of K_{eq}, the stationary EPR experiments for EPPT were carried out for the monomeric RAFT agent of chain length $i = 1$ as well as for two pre-polymerized EPPT-type RAFT agents of initial mean chain

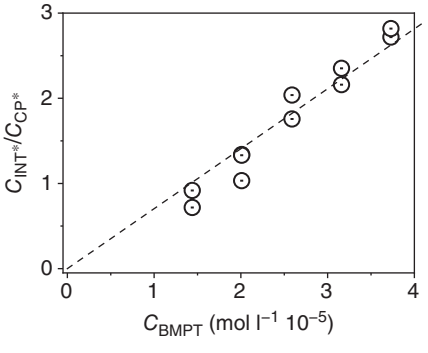

Figure 4.9 Ratio of intermediate radical and propagating radical concentrations, C_{INT^*}/C_{P^*}, plotted vs. BMPT concentration for BA polymerizations (1.5 mol l^{-1} in toluene) at −40 °C using MMMP (1.0×10^{-2} mol l^{-1}) as the photoinitiator [20].

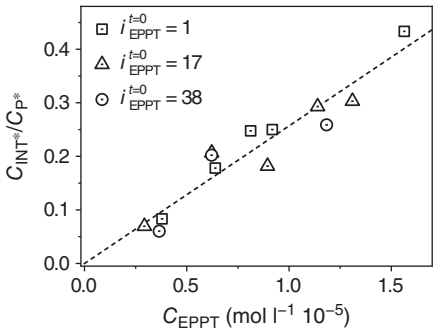

Figure 4.10 Ratio of intermediate radical and propagating radical concentrations, C_{INT^*}/C_{P^*}, plotted vs. EPPT concentration for BA polymerizations (1.5 mol l^{-1} in toluene) at −40 °C using MMMP (1.0×10^{-2} mol l^{-1}) as the photoinitiator. The EPR experiments under stationary conditions were carried out with monomeric ($i_{EPPT} = 1$ at $t = 0$) and macroRAFT agents ($i_{EPPT} = 17$ at $t = 0$ and $i_{EPPT} = 38$ at $t = 0$). The slope of the straight-line fit corresponds to $K_{eq} = (2.6 \pm 0.1) \times 10^4$ l mol^{-1} [20].

lengths 17 and 38, respectively. The measured C_{INT^*}/C_{P^*} ratios for the monomeric and macroRAFT agents are plotted vs. RAFT agent concentration in Figure 4.10. The resulting equilibrium constant, $K_{eq} = (2.6 \pm 0.1) \times 10^4$ l mol^{-1}, applies to the three EPPT-type RAFT agents that differ considerably in size. This finding indicates that either K_{eq} is not chain length dependent or the main equilibrium situation is very rapidly reached with monomeric EPPT. The K_{eq} value of EPPT-mediated BA polymerization at −40 °C obtained via the stationary approach (Eq. (4.1)) is in perfect agreement with the value deduced by the SP-PLP-EPR technique. For BMPT, the K_{eq} values from the two EPR-based techniques are slightly apart, $(7.0 \pm 0.2) \times 10^4$ l mol^{-1} (via Eq. (4.1)) and $(9.0 \pm 3.0) \times 10^4$ l mol^{-1} (from SP-PLP-EPR), but agree within the limits of experimental accuracy, suggesting that the kinetic scheme underlying the PREDICI simulation of the time-resolved traces adequately represents BA polymerizations mediated by these trithiocarbonates.

K_{eq} of BMPT is slightly above K_{eq} for EPPT, which may be due to the reduced fragmentation rate of the 'three-arm' intermediate radical. The K_{eq} values for the two trithiobenzoates are about 3 orders of magnitude larger than the xanthate K_{eq}.

Within the limits of experimental accuracy, the rate coefficients for addition of propagating BA radicals to trithiocarbonates at −40 °C are the same: $(4.1 \pm 0.9) \times 10^6$ l mol^{-1} s^{-1} for BMPT and $(3.4 \pm 0.3) \times 10^6$ l mol^{-1} s^{-1} for EPPT. This result fits the *ab initio* estimate provided by Coote et al. of k_{ad} being typically in the range 10^5 to 10^7 l mol^{-1} s^{-1} [38]. The fragmentation rate coefficients k_β of the INT* species are (140 ± 40) s^{-1} for EPPT and (45 ± 5) s^{-1} for BMPT. These values for −40 °C indicate fast fragmentation.

Fragmentation rate coefficients from *ab initio* estimates are not available so far. However, the *ab initio* value of $K_{eq} = 1.4 \times 10^4$ l mol^{-1} reported by the Coote group for BMPT-mediated methyl acrylate polymerization in toluene at −30 °C, which is close to the numbers from the EPR methods, suggests that also the k_β values from SP-PLP-EPR should be consistent with the earlier *ab initio* data [39]. In view of the

minor differences in monomer type and temperature, the agreement of K_{eq} from SP-PLP-EPR with the equilibrium constant deduced from the earlier *ab initio* calculations appears very satisfactory.

The recent *ab initio* estimates carried out for conditions as used within the SP-PLP-EPR experiments yield $K_{eq} = 3.1 \times 10^5$ and 3.9×10^3 l mol^{-1} for BA polymerizations at −40 °C mediated by BMPT and EPPT, respectively [9]. Within an accuracy of about 1 order of magnitude, these *ab initio* data agree with the experimental values and are relatively close to the number from the earlier K_{eq} estimates for BMPT-mediated methyl acrylate polymerization in toluene at −30 °C as provided by the Coote group [39]. It is gratifying to note that the earlier *ab initio* procedure allows for estimating adequate numbers of K_{eq} in the case of trithiocarbonates and probably also with xanthates. The same is not true for dithiobenzoate-mediated polymerizations, where the early predictions yield K_{eq} data, which are several orders of magnitude larger than the data measured via the EPR-based techniques.

4.5.4 Dithiobenzoates

The mechanism of RAFT polymerizations mediated by DTBs, $C_6H_5C(=S)—SR$, has been controversially discussed for a long time. The observed retardation has been assigned to either SF of the INT* species or to IRT, i.e. cross-termination of INT* with propagating radicals P*. Retardation due to these two limiting mechanisms may be illustrated by Scheme 4.4, which refers to main equilibrium conditions. Both reaction of INT* with P* and slow fragmentation of INT* reduce P* concentration and thus may give rise to retardation.

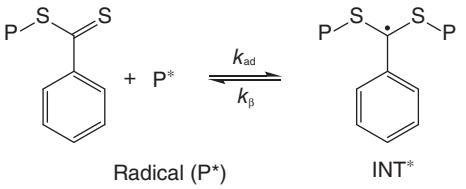

Scheme 4.4 Main equilibrium situation with dithiobenzoate-mediated RAFT polymerizations.

Both models can account for the observed retardation, but at the expense of the associated fragmentation rate coefficient k_β differing by several orders of magnitude. Adopting $k_{t,cross}$ to be either zero (SF model) or to occur at a comparable rate to conventional termination via IRT has enormous consequences for k_β, as has been illustrated in the IUPAC dilemma paper on DTB-mediated RAFT kinetics and mechanisms [4]. Upon using the SF model with $k_{t,cross} = 0$, styrene polymerizations at 60 °C mediated by CDB result in a k_β value of about 3×10^{-2} s^{-1} and in K_{eq} being around 1.6×10^7 l mol^{-1}. Applying the IRT model with $k_{t,cross} = k_t$ to the experimental styrene RAFT data results in a k_β value of about 1×10^5 s^{-1} and in K_{eq} around 80. Early *ab initio* studies into this system provided high K_{eq}, e.g. 7.3×10^6 l mol^{-1}, for

the cumyl radical —S=C(Ph)SCH_3 system at 30 °C, which was used as an argument in favour of the slow fragmentation model. The SF mechanism is however unable to explain the measured low INT* concentrations, whereas the IRT mechanism can provide this explanation but, with acrylates being polymerized, is in conflict with the observed extremely low yield of the three-arm star product.

In an attempt to stay with part of the SF picture, Konkolewicz et al. assumed that termination may occur by fast cross-termination of INT* with propagating radicals of chain lengths up to $i = 3$, whereas cross-termination with larger propagating radicals is extremely slow [40]. Short radicals undergoing termination would not significantly affect the overall molecular mass and thus could account for the absence of three-arm star material. However, as pointed out by Moad [1], this model extension is not consistent with experimental findings. Termination of intermediate radicals exclusively with very short propagating radicals is in conflict with *Monte Carlo* simulations of the contact probability between radical chain ends and various positions on star-branched chains with up to six arms [41]. In addition, the termination rate being fast for very small radicals and being negligible at radical chain lengths above $i = 3$ would be associated with a highly unusual chain length dependence of the termination rate coefficient. Thus, even with the modification of IRT exclusively occurring with very small radicals, the SF picture provides no adequate explanation of retardation with DTB-mediated acrylate polymerization. As a consequence, the IRT model must be considered as the preferred one, in particular, as Geleen and Klumperman have found that small amounts of three-arm star and four-arm star species were produced even during DTB-mediated BA polymerization [42].

4.5.5 The 'Missing Step' Reaction

To resolve the mechanistic puzzle of three-arm star material being more or less absent in dithiobenzoate-mediated acrylate polymerizations despite IRT taking place, the 'missing step' reaction has been introduced as a follow-up reaction of a propagating radical with the star-shaped product P_k–Int from irreversible cross-termination of INT* and P* (Scheme 4.5) [11].

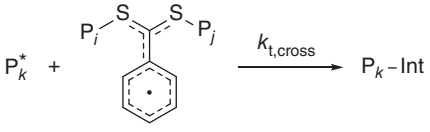

Scheme 4.5 Cross-termination reaction [11].

Under main equilibrium conditions, the macroINT* (or polyINT*) species **4** controls polymerization. Resonance structures of **4** are depicted in Scheme 4.6 [11].

Extended delocalization of radical functionality is associated with enhanced stability compared to the situation with xanthate and trithiocarbonate RAFT agents. Another consequence of delocalization is the occurrence of a plethora of isomeric

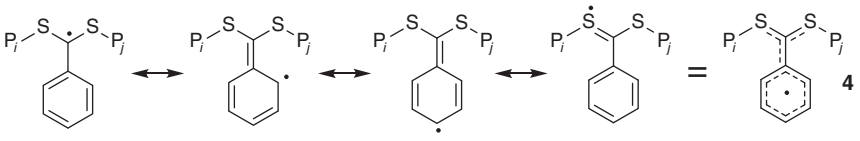

Scheme 4.6 Resonance structures of the macroINT* species **4** [11].

products P_k–Int (Scheme 4.7), as P_k^* may add at different sites of **4** (see Scheme 4.6). The chain lengths *i* and *j* are close to each other in the case of well-controlled RAFT polymerization. Delocalization of the radical functionality, in particular into the para position of the phenyl ring, reduces problems associated with steric hindrance for radical–radical reactions between macroINT* and P_k^*.

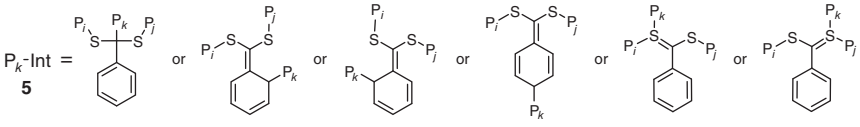

Scheme 4.7 Examples of the P_k–Int species **5** produced by reaction of **4** with propagating radicals P_k^* [11].

The 'missing step' reaction, as introduced in Ref. [11], is illustrated in Scheme 4.8 for one out of the multitude of cross-termination products **5**. The propagating radical P_l reacts with **5** to yield the combination product, P_l–P_k, as in conventional termination. Basically, a growing radical picks up a radical moiety from P–Int. The reaction may occur by combination, as illustrated in Scheme 4.8, but also by disproportionation. The basic signature of the 'missing step' in acrylate polymerizations consists of the transformation of a highly reactive growing radical, P*, and a labile cross-combination product **5** into a stable termination product, by combination or disproportionation, and a resonance-stabilized macroRAFT intermediate radical **4**. Because of the multitude of potential P–Int species, a variety of 'missing step' reactions may occur, although with different rate coefficients $k_{tr,Int}$.

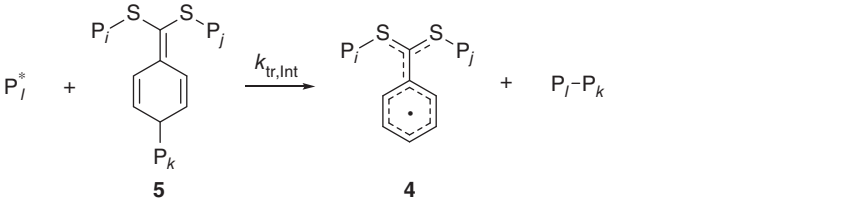

Scheme 4.8 'Missing step' reaction illustrated for one out of a multitude of P_i–Int cross-termination products **5**.

The occurrence of the 'missing step' reaction may be verified by NMR product analysis. In addition, by-products of benzyl dithiobenzoate-mediated styrene polymerization have provided support for such a process [43]. The mechanism of the

'missing step' has not yet been studied in detail. Potential pathways are illustrated in Scheme 4.9. According to the upper option, P_l picks up the P_k moiety from the six-membered ring. The pathway in the lower part of Scheme 4.9 suggests that P_l first adds to a double bond of the six-membered ring prior to the release of P_l–P_k and the formation of INT* by bond rearrangement.

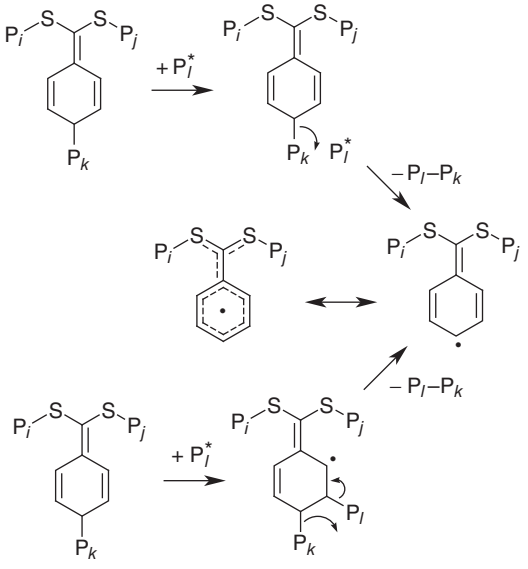

Scheme 4.9 Two examples of potential 'missing step' pathways [44].

Within a third pathway (not shown in Scheme 4.9), the radical P_l^* may abstract the H atom at the para position of the phenyl ring producing a radical species with extended delocalization of radical functionality. Subsequent fragmentation yields a macroRAFT species with the P_k moiety at the para position. The observation of such ring-substituted RAFT components serves as a safe criterion for the occurrence of 'missing step' processes (see Section 4.5.5).

The enormous driving force behind the 'missing step' reaction (Scheme 4.8) has been demonstrated by quantum chemical calculations [44]. This step may be very fast, with $k_{tr,Int}$ even approaching k_{ad} [11]. With the 'missing step' being included into the kinetic scheme, the absence of three-arm star products in dithiobenzoate-mediated acrylate polymerizations is adequately understood. The impact of the 'missing step' reaction depends on the specific monomer and thus on the type of propagating radicals. At typical polymerization temperatures, the three-arm star combination product, P_k–Int, has been reported to be stable with styrenic systems [8]. The styrene radical may be resonance-stabilized to such an extent that no significant reaction with P–Int occurs. In acrylate polymerizations mediated by dithiobenzoates, the 'missing step' however is fully in action and will result in the production of dead polymer $P_i - P_k$ (or $P_i + P_k$).

As detailed in Ref. [11], including the 'missing step' into the ideal RAFT kinetic scheme allows for adequately simulating the time evolution of monomer conversion, as well as of INT* and P–Int concentrations. The kinetic scheme subjected to the PREDICI simulation is presented in Scheme 4.10 with a 'missing step' (MS) being added in bold.

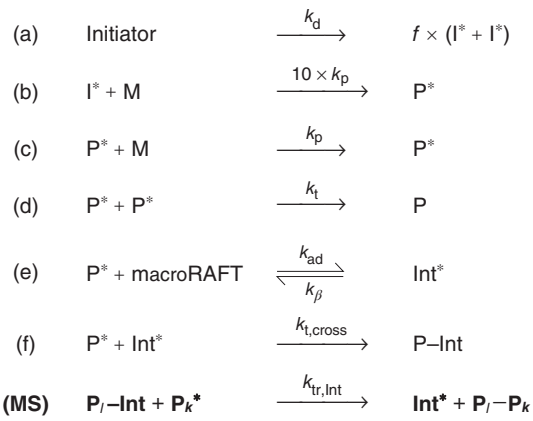

Scheme 4.10 Kinetic scheme underlying the PREDICI simulations with the 'missing step' (MS) being included; (a) initiator decomposition with efficiency f, (b) monomer addition to the initiator fragment, I^*, (c) propagation, (d) termination, (e) reversible reaction of a growing radical with **3** to produce species **4**, and (f) cross-termination to yield **5**.

The 'missing step' neither affects the conversion vs. time profile nor the time evolution of the concentration of the macroRAFT intermediate **4**. The latter finding ensures effective RAFT control during the course of the polymerization. With the rate coefficient of the 'missing step' $k_{tr,Int}$ approaching the addition rate coefficient k_{ad} the amount of (normal) termination product P_i–P_k largely exceeds that of P–Int, i.e. of the primary product from IRT.

In Figure 4.11, the overall impact of the 'missing step' is illustrated [11]. The intermediate radical **4** undergoes two successive irreversible reactions, one with rate coefficient $k_{t,cross}$, to yield the cross-termination product **5**, and a second one, with rate coefficient $k_{tr,Int}$, which produces **4** back. The overall process resembles a catalytic cycle by which two propagating radicals P* react to a conventional termination product with the concentration of the intermediate macroRAFT radical remaining unchanged.

With acrylates, the strong driving force of the 'missing step' may give rise to hydrogen abstraction from the cross-termination product P–Int. Star–star coupling reactions of two intermediate macroRAFT radicals may occur as well [11]. Perhaps follow-up processes of products from such reactions need to be additionally considered, as should the chain-length-dependent and conversion-dependent rate coefficients be. Examination of these effects requires very detailed and accurate studies into DTB-mediated RAFT kinetics. The extended scheme, including the 'missing step', should be applied towards all systems for which the macroRAFT

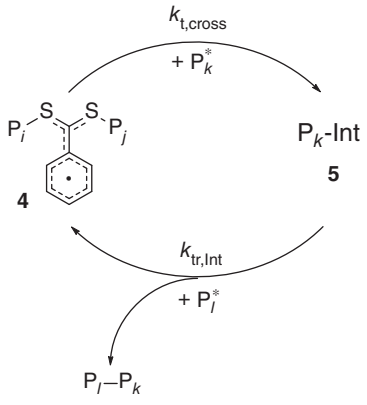

Figure 4.11 Catalytic cycle of radical termination mediated by a dithiobenzoate intermediate radical [11].

intermediate is relatively stable, i.e. also with substituted dithiobenzoates and with dithionaphthoate-type RAFT agents. It appears advisable to use the expanded kinetic scheme even for RAFT polymerizations, where INT* is high in energy and fragmentation rate is very fast. Under such conditions, the 'missing step' will however be of minor relevance.

Clear evidence for 'missing step' reactions has been deduced from NMR analysis of products from reactions of the model system phenylethyl radical (PE*)–phenylethyl dithiobenzoate (PEDB) [45], which contains only two relevant types of radicals, PE* and INT*, with PE* resembling a styrenic radical. The initiator *meso*-1,2-bis(1-phenylethyl)diazene (PEDA) serves as the source of PE*, but is not a suitable photoinitiator. Only at and above 110 °C, PEDA reacts (in toluene solution) with two 2,3-butane-2,3-diyldibenzenes (BDDBs), i.e. with the diastereomers produced by PE* dimerization. Towards lower temperatures a side product occurs, which most likely is *tris*(1-phenylethyl)amine [45]. The product mixture from the reaction at 110 °C of PEDA and PEDB in toluene was analysed on the basis of the comprehensive set of reactions depicted in Scheme 4.11, including cross-termination (IV) and 'missing step' reactions (V). Products from other cross-termination reactions at 110 °C have not been found. Steps (I) through (III) in Scheme 4.11 refer to initiator decomposition, to dimerization of the PE*, and to the RAFT equilibrium, respectively.

The solid product from the PEDA–PEDB reaction at 110 °C contains 23% CT1, 44% PEDB, 3% $PEDB^{MS}$, and 30% BDDB [45]. The occurrence of the 'missing step' reaction is demonstrated by the product 1-phenylethyl-4-(1-phenylethyl)benzodithioate ($PEDB^{MS}$) that has been identified by ^{1}H and ^{13}C NMR spectroscopy. The high concentration of CT1 suggests that this cross-termination product is relatively stable against attack of resonance-stabilized PE*. The latter finding is consistent with the observation of the Fukuda group that three-arm star material may occur in dithiobenzoate-mediated styrene polymerization [8].

Moreover, the ratio of radical concentrations, C_{INT*}/C_{PE*}, was EPR-spectroscopically measured during the reaction of PEDA and PEDB in toluene at 110 °C. The overlapping EPR bands were deconvoluted via the separately measured EPR spectra of the individual components [45]. Analysis via Eq. (4.1) of the C_{INT*}/C_{PE*} data,

which were back-extrapolated towards $t = 0$, yields $K_{eq} = (30.7 \pm 3.0)\,l\,mol^{-1}$. Adopting a typical size for k_{ad} of around $1 \times 10^6\,l\,mol^{-1}\,s^{-1}$ results in a fragmentation rate coefficient of about $k_\beta = 3.2 \times 10^4\,s^{-1}$, which demonstrates fast fragmentation. Goto et al. reported a value of $k_\beta \approx 6.5 \times 10^4\,s^{-1}$ for polystyryl dithiobenzoate-mediated styrene polymerization at 40 °C [46]. This number is close to $k_\beta = 1.8 \times 10^4\,s^{-1}$ determined for polystyryl dithiobenzoate-mediated styrene polymerization at 60 °C by the same group [8].

The occurrence of 'missing step' reactions has also been shown for the cyano-*iso*-propyl radical (CIP*)–CPDB system [47, 48]. Azobis-*iso*-butyronitrile was the source of CIP*. The initiation process, the mutual reactions of the CIP radicals, and the RAFT equilibrium steps are listed as reactions I–IV in Ref. [48]. Scheme 4.12 just contains the mechanistically relevant cross-termination (Va and Vb), H-shift (VI), and 'missing step' (VIIa and VIIb) reactions. The numbering of the equations in Scheme 4.12 does not fit to the numbers in Scheme 4.11, but refers to the notations I to IV of Scheme 1 in [48].

The reaction of CPDB and azobis-*iso*-butyronitrile (AIBN) in toluene solution at 80 °C yields 71% CPDB and 15% tetramethyl succinonitrile (from CIP* dimerization) together with the cross-termination products CT1 (3%) and CT3 (8%) as well as 3% of the 'missing step' product CPDB^{MS}. The components CT1, CT3, and CPDB^{MS}

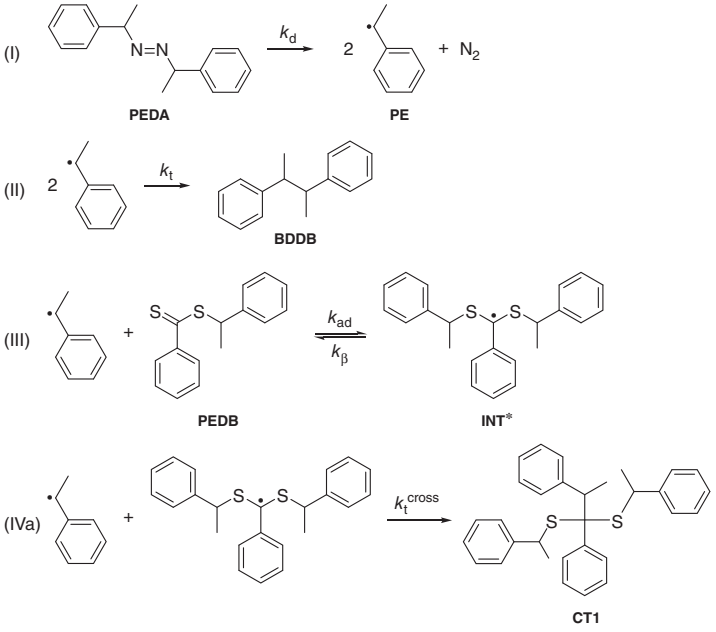

Scheme 4.11 Kinetic scheme for the model system PE*–PEDB reacting in toluene at 110 °C; PEDA: *meso*-1,2-bis(1-phenylethyl)diazene; PE*: phenylethyl radical; BDDB: 2,3-butane-2,3-diyldibenzene; PEDB: 1-phenylethyl dithiobenzoate; INT*: RAFT intermediate radical; CT1: cross-termination product 1; CT2: cross-termination product 2; INT2*: ring-substituted intermediate radical; PEDB^{MS}: ring-substituted PEDB.

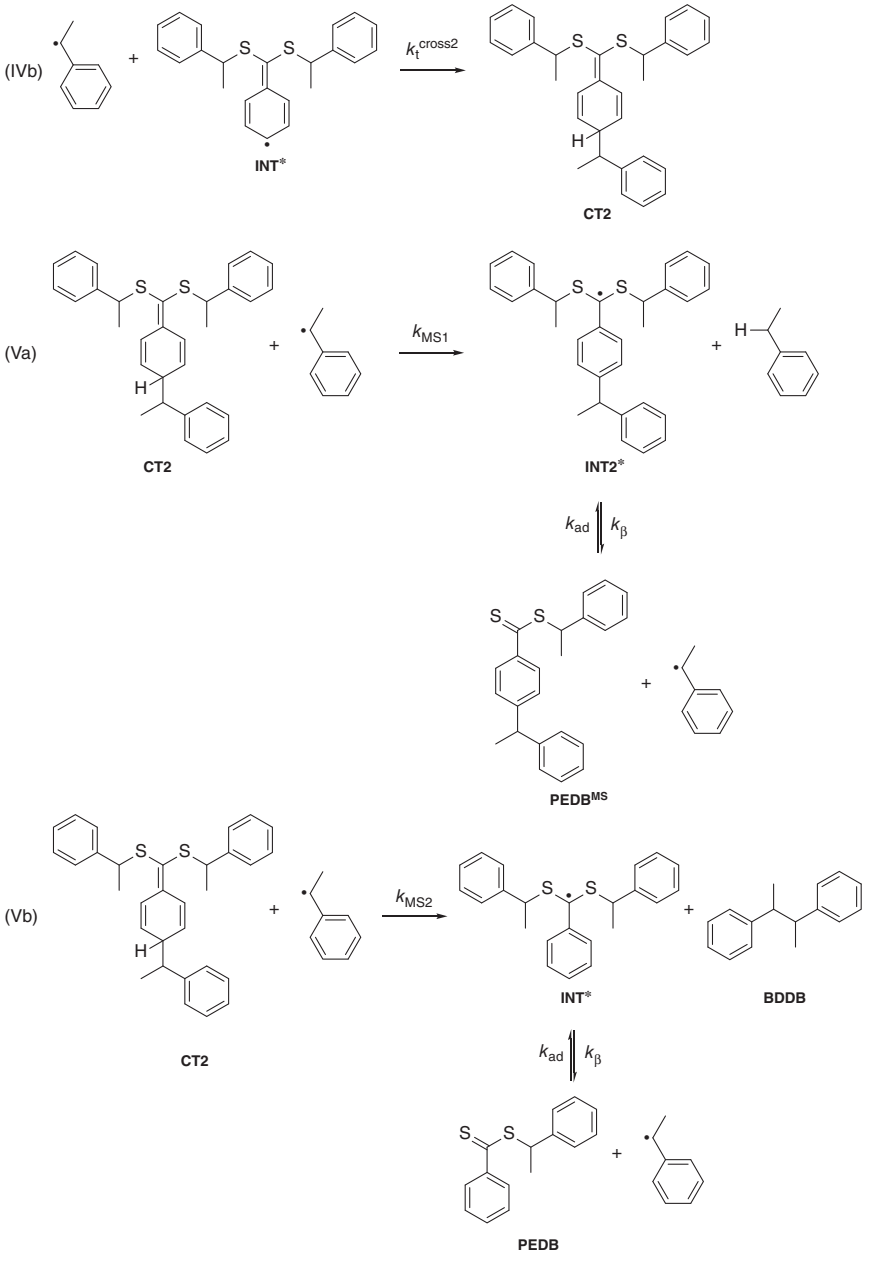

Scheme 4.11 (*Continued*)

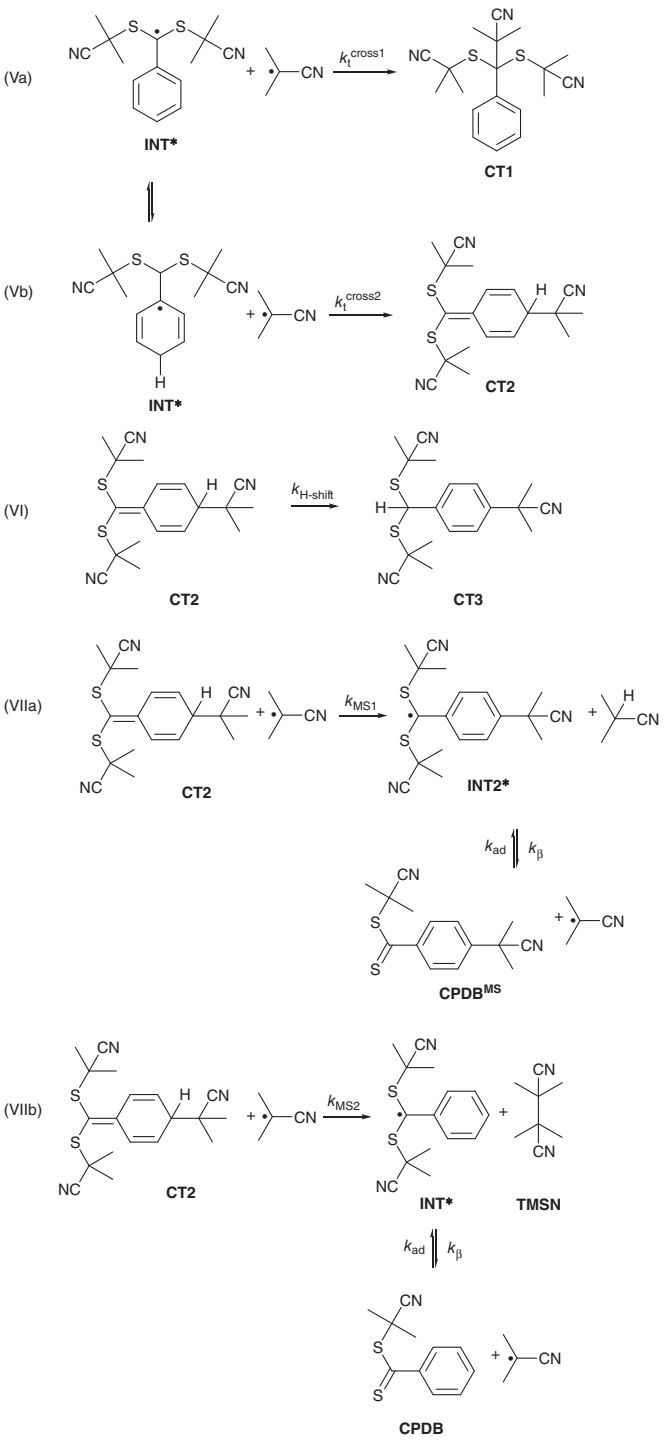

Scheme 4.12 Kinetic scheme for the model system CIP*–CPDB; CT1: cross-termination product 1; CT2: cross-termination product 2; $CPDB^{MS}$; 'missing step' product.

have been confirmed by ^{1}H and ^{13}C NMR spectroscopy [48]. The cross-termination product CT2 is absent, most likely due to the lower stability of this compound, which exhibits no delocalization of the radical functionality over the cyclic moiety. Aromaticity may be reached by the H-shift reaction of CT2 to yield CT3. CT2 may undergo a 'missing step' reaction (MS1) to form INT2*, which fragments to the observed product $CPDB^{MS}$. A second 'missing step' process (MS2, Eq. (VIIb)) produces CPDB back; see Eq. (VIIb).

4.5.6 Kinetic Analysis of Dithiobenzoate-Mediated BA Polymerizations

SP-PLP-EPR experiments have been carried out on ETTP-mediated BA polymerizations (1.5 M in toluene) at −40 °C and ETTP concentrations between 7.4×10^{-6} and 2.6×10^{-5} mol l^{-1} [13]. For the stationary experiments a sweep time of 1.3 seconds was selected, during which less than 1% ETTP was consumed by the UV irradiation. Since ETTP bears an acrylate-type leaving group, again only two kinds of radicals need to be considered.

From the EPR band for the INT* and P* signals measured at different initial ETTP concentrations, the RAFT equilibrium constant has been estimated via Eq. (4.1) to be $K_{eq} = (2.3 \pm 0.6) \times 10^5$ l mol^{-1} at −40 °C [13]. The experimental number averages of molar mass, $M_n > 700$ g mol^{-1}, indicate that main equilibrium conditions apply. The K_{eq} value is about 1 order of magnitude larger than the one for BA polymerization mediated by trithiocarbonates [49] and is about 4 orders of magnitude larger than K_{eq} for BA polymerized in the presence of xanthates [35].

The individual rate coefficients, k_{ad} and k_{β}, were determined via SP-PLP-EPR monitoring of C_{INT^*} and of C_{P^*}. In Figure 4.12, the measured time dependences of INT* and P* concentration are shown.

The data on the RHS of Figure 4.12 demonstrate that the resonance-stabilized BA-ETTP* intermediate decays on a time scale of a few seconds with a half-life of about one second. The decay of INT* suggested by the SF model, which is illustrated

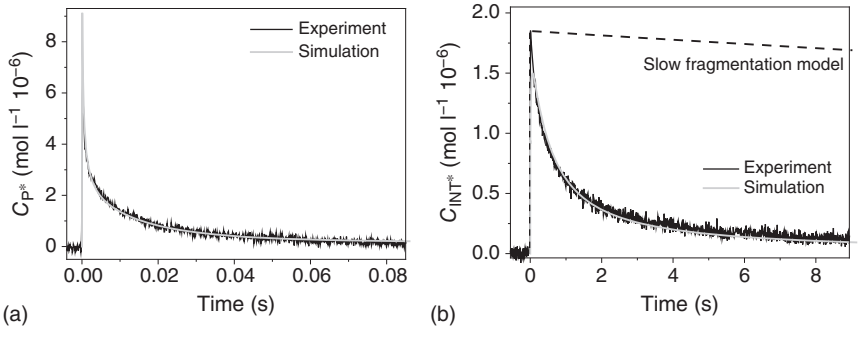

Figure 4.12 Experimental and simulated concentration vs. time traces for propagating and intermediate radicals during a butyl acrylate polymerization (1.5 mol l^{-1} in toluene) at −40 °C. The initial ETTP and MMMP concentrations were 2.0×10^{-5} and 1.0×10^{-2} mol l^{-1}, respectively. The full grey lines represent the PREDICI simulations, which are based on the kinetic parameters and the kinetic scheme detailed in Ref. [13].

by the dashed line, would be far too slow to be consistent with experiment. Thus, slow fragmentation is additionally demonstrated to be an unlikely explanation for retardation in DTB-mediated acrylate polymerizations. The SF model would predict a half-life of more than 10 seconds at 60 °C [50], which corresponds to a half-life of several hours at −40 °C. The analysis of the experimental radical concentration vs. time traces has been carried out via PREDICI (version 6.4.6 on an Intel Core Duo, 1.87 GHz computer) applying the rather simple kinetic scheme mentioned above and detailed in Ref. [35]. The scheme encompasses initiation, propagation, chain-length-dependent termination as well as chain-length-dependent cross-termination of INT*. It is again assumed that the addition and the fragmentation rate coefficients of the ETTP-derived radical species are identical to the associated rate coefficients of BA radicals. Moreover, the leaving group is assumed to add to a monomer molecule, and thus to re-initiate, as does a propagating radical, i.e. $k_p^{\text{rein}} = k_p$. The propagation rate coefficient k_p and the chain-length-dependent termination rate coefficient $k_t(i,i)$ are known from the literature [37]. The initiation rate coefficient was again assumed to be $k_i = 10 \times k_p$. The primary free-radical concentration C_R^0 has been obtained by fitting the maxima of the experimental $C_{\text{INT*}}/C_{\text{P*}}$ traces. The selection of the parameters C_R^0, k_i and of the addition rate coefficient of P* to the primary RAFT agent $k_{\text{ad,1}}$ (Scheme 4.1) does not significantly affect the k_{ad} and k_β values from PREDICI fitting of the SP-PLP-EPR data.

No independently measured number is currently available for the cross-termination rate coefficient. Kwak et al. estimated $k_{t,\text{cross}}$ to be around $0.5 \times k_t$ [8]. To check for the impact of cross-termination, parameter estimates have again been carried out for various sizes of relative cross-termination rate, $C_{\text{cross}} = k_{t,\text{cross}}/k_t$, with C_{cross} being varied from zero to unity [13]. Other than with the xanthate and trithiocarbonate RAFT agents, very low values of $k_{t,\text{cross}}$, i.e. of C_{cross} approaching zero, which would correspond to the SF model, do not allow for adequate fit of the radical concentration vs. time traces in Figure 4.12.

Best fits of the $C_{\text{INT*}}$ and $C_{\text{P*}}$ vs. time traces were obtained for $0.2 \times k_t < k_{t,\text{cross}} < 0.3 \times k_t$. Thus $k_{t,\text{cross}} = 0.25 \times k_t$ was used within the simulations. This number indicates fast cross-termination. Fitting of the $C_{\text{INT*}}$ and $C_{\text{P*}}$ vs. time traces in Figure 4.12 results in $k_{\text{ad}} = (1.4 \pm 0.4) \times 10^6$ l mol^{-1} s^{-1} and $k_\beta = (4.7 \pm 1.5)$ s^{-1}, respectively. These coefficients yield $K_{\text{eq}} = k_{\text{ad}}/k_\beta = (3.4 \pm 0.6) \times 10^5$ l mol^{-1} in close agreement with $K_{\text{eq}} = (2.3 \pm 0.6) \times 10^5$ l mol^{-1}, as obtained from the measured ratios of INT* to P* concentrations (see above). The two EPR-based equilibrium constants are several orders of magnitude smaller than the K_{eq} value obtained via the earlier *ab initio* methods for radical–dithiobenzoate systems extrapolated to −40 °C [38, 51].

The k_{ad} and k_β values from SP-PLP-EPR may also be used to check whether the reaction conditions of the stationary experiments allow for reasonable estimates of K_{eq} via Eq. (4.1). This procedure results in $r_{t,\text{cross}}$, the rate of cross-termination, being indeed negligible compared to the addition and fragmentation rates, r_{ad} and r_β.

Both pulsed laser experiments demonstrate that the SF model cannot account for the experimental results of ETTP-mediated BA polymerization. With this system as well as with CDB- and CPDB-mediated BA polymerization, IRT occurs in conjunction with subsequent 'missing step' reactions. As the major support for the SF model

with DTB-mediated RAFT polymerizations has emerged from the early quantum chemical calculations, it appears mandatory to have a look at such estimates by applying advanced quantum chemical methods [9].

4.5.7 Quantum Chemical Calculations for the CIP* – CPDB Model System

The earlier and the actual quantum chemical estimates of K_{eq} for DTB RAFT agents are compared with the example of the CIP* + CPDB system in equilibrium with the associated CIP–CPDB* species. The actual quantum chemical calculations for the CIP*–CPDB system yield $K_{eq} = 1.0\ \mathrm{l\ mol^{-1}}$ in an environment of toluene at 70 °C [9]. This number is affected by the quality of estimating the entropy penalty upon formation of the intermediate radical. Although the impact of the applied approximations is still heavily disputed, K_{eq} in a solution of toluene is expected to be accurate within at least 1–2 orders of magnitude. The value of $K_{eq} = 1.0\ \mathrm{l\ mol^{-1}}$ is far below the gas-phase value for 70 °C obtained by the earlier calculations: $K_{eq} = 2.35 \times 10^5\ \mathrm{l\ mol^{-1}}$ [52]. After correction for the experimental solution conditions, by using COSMO-RS solvation energies, the resulting literature $K_{eq} = 2.31 \times 10^4\ \mathrm{l\ mol^{-1}}$ is still significantly above K_{eq} of the recent *ab initio* estimate and of the EPR-based experiment. A discrepancy of about 2 orders of magnitude remains even after an additional correction for solvation effects [53].

The ratio of the radical concentrations, C_{CPDB*}/C_{CIP*}, measured via EPR with CIP* being produced by thermal decomposition of AIBN yields $K_{eq} = (9 \pm 1)\ \mathrm{l\ mol^{-1}}$ for a toluene environment at 70 °C [47]. This value agrees within the limits of accuracy with $K_{eq} = 1.0\ \mathrm{l\ mol^{-1}}$ as obtained from the actual quantum chemical estimates. The experimental reaction enthalpy and entropy are however not in close agreement with the associated data from the recent *ab initio* calculations. This discrepancy may be due to side reactions that are not adequately taken into account within the experiments carried out over a wide temperature range.

Of particular relevance is the mismatch between the earlier and the recent *ab initio* calculations, because strong support for the SF model has evolved on the basis of the earlier *ab initio* data [50]. As the correction for the molecular environment is not trivial, it appears recommendable to directly compare K_{eq} for identical conditions, i.e. for the gas phase at 70 °C. These numbers are estimated from the earlier [52] and from the recent [9] quantum chemical calculations to be $K_{eq} = 2.35 \times 10^5$ and $0.29\ \mathrm{l\ mol^{-1}}$, respectively. The earlier quantum chemical method thus yields an equilibrium constant for the same dithiobenzoate system, which is about 6 orders of magnitude larger than both the experimental value and the number from the actual *ab initio* calculations. The level of theory used for describing the highly delocalized radicals appears to be the prime reason for the large mismatch in K_{eq}. In the earlier quantum chemical approach, the system has been divided into parts that were treated at different levels of theory, i.e. the delocalized species has been subjected to the G3(MP2)-RAD level. Within the recent calculations, the entire system has been treated at the higher level of DLPNO-CCSD(T). Another factor to be considered is the lack of dispersion corrections in the earlier studies. The results indicate that

higher level calculations than used for the earlier studies are required in case of the dithiobenzoate RAFT systems with extended delocalization of radical functionality.

4.5.8 Dithiobenzoate-Mediated MMA Polymerizations and Model Systems

That dithiobenzoate RAFT agents do not necessarily induce retardation [1] can be seen from CPDB-mediated methyl methacrylate (MMA) bulk polymerizations studied at 60 °C and pressures of up to 2000 bar. Upon varying CPDB concentration up to 2.0×10^{-2} mol l^{-1}, only minor retardation is observed. As polymers of lower molar mass are produced towards higher C_{RAFT}, this retardation may be assigned to the chain length dependence of the termination rate coefficient [54]. High pressure increases polymerization rate but has no effect on dispersity. Irrespective of the applied pressure, the molar mass dispersity ($Đ$) of the poly(MMA) samples generated by the CPDB-mediated reaction lie on a single line, with $Đ$ decreasing towards higher degrees of monomer conversion.

In addition, RAFT polymerizations of MMA mediated by 2-methyl methacryl dithiobenzoate (MMADB) have been studied via stationary EPR experiments using MMMP as the photoinitiator [55]. The ratio of INT* to MMA* concentrations was measured at different initial MMADB concentrations using the same deconvolution strategy as applied towards the PE*–PEDB and CIP*–CPDB systems. The ratio C_{INT*}/C_{MMA*} decreases with polymerization time t, which indicates considerable cross-termination. The C_{INT*}/C_{MMA*} data were thus back-extrapolated to $t = 0$, i.e. to the situation of the accurately known initial RAFT agent concentration. Analysis via Eq. (4.1) yields $K_{eq} = (4.4 \pm 0.4) \times 10^3$ l mol^{-1} as the mean value for −40 °C. This number is by about 2 orders of magnitude below K_{eq} of dithiobenzoate-mediated BA polymerization.

Owing to the strong overlap of the EPR signals for INT* and P*, the SP-PLP-EPR method cannot be applied towards the measurement of individual k_{ad} and k_β for dithiobenzoate-mediated MMA polymerization. Thus Sidoruk et al. used literature data for k_{ad} and $E_a(k_{ad})$ to estimate 2.5×10^4 and 6.4×10^4 l mol^{-1} s^{-1} as the lower and upper values, respectively, of k_{ad} at −40 °C [55]. From the above K_{eq}, the fragmentation rate coefficient k_β is obtained via these k_{ad} values to be $5.2\ s^{-1} < k_\beta < 13.5\ s^{-1}$, which is close to $k_\beta = 6\ s^{-1}$ for DTB-mediated BA polymerization [13]. Thus, fragmentation rate provides no conclusive argument as to whether retardation occurs, as retardation is absent with DTB-mediated MMA polymerization, but is strong with acrylate polymerizations. The low addition rate, however, appears to significantly contribute to the absence of retardation with DTB-mediated MMA polymerizations. It is known that MMA radicals add at a lower rate to the C=S double bond [56]. Relatively low k_{ad} reduces K_{eq} and results in a lower C_{INT*}, which is similar to the situation with xanthate-mediated BA polymerization.

Further studies have been carried out on the model system MMA*–MMADB. Large concentrations of MMA* were produced by thermal decomposition of the initiator dimethyl-2,2′-azobis-(2-methylpropionate) (AIBME) [55]. Among the products of the AIBME plus MMADB reaction in toluene at 66 °C is 27% of the 'missing

step' product MMADB^{MS} (2-methylmethacryl-4-[2-methylmethacryl]benzodithioate). This fraction reduces to 13% at 127 °C. Such amounts of 'missing step' product are far above the ones observed with the CIP*–CPDB and PE*–PEDB systems.

The amount of MMADB^{MS} (Scheme 4.13) also largely exceeds that of the cross-termination product CT1 (2% at 66 °C and 3% at 127 °C, Scheme 4.14), which indicates that cross-termination of MMA* with INT* at the para position of the phenyl group is favoured over MMA* attack at the carbon atom between the two sulfur atoms.

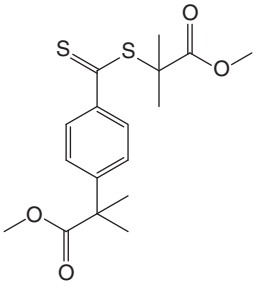

Scheme 4.13 Structure of the 'missing step' product MMADB^{MS} from reaction of AIBME with MMADB.

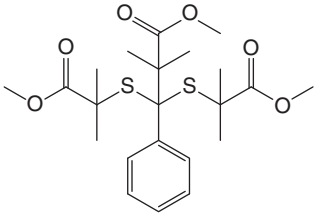

Scheme 4.14 Structure of the cross-termination product CT1 (dimethyl 2,2′-(3methoxy-2,2-dimethyl-3-oxo-1-phenylpropane-1,1-diyl)bis(sulfanediyl)bis(2-methylpropanoate)).

The analysis of the products from the MMA*–PEDB reaction thus provides additional evidence for the occurrence of 'missing step' processes with dithiobenzoate-mediated polymerizations.

4.6 Summary of Results and Concluding Remarks

Pulsed laser experiments carried out in conjunction with the highly time-resolved quantitative monitoring of radical concentrations via EPR spectroscopy allow for detailed investigations into the kinetics of radical polymerizations. The two EPR-based methods illustrated above are perfectly suited for the in-depth understanding of the RAFT polymerization mechanism.

Data obtained for butyl acrylate polymerizations mediated by one xanthate (EDTCP), two trithiocarbonates (BMPT and EPPT), and one dithiobenzoate (ETTP) in toluene solution at −40 °C are summarized in Table 4.1. Given in the first three columns are the addition rate coefficient k_{ad}, the fragmentation rate coefficient k_β, both from SP-PLP-EPR, and the resulting equilibrium constant K_{eq}. Listed in column 4 is K_{eq} deduced via the EPR-based method according to Eq. (4.1).

The rate coefficients for addition of propagating BA radicals to trithiocarbonate and to dithiobenzoate RAFT agents, at −40 °C, are close to each other: $(4.1 \pm 0.9) \times 10^6$ l mol^{-1} s^{-1} for BMPT, $(3.4 \pm 0.3) \times 10^6$ l mol^{-1} s^{-1} for EPPT, and $(1.4 \pm 0.4) \times 10^6$ l mol^{-1} s^{-1} for ETTP, in agreement with the result from early *ab initio* calculations that predict the k_{ad} of most RAFT agents to be in the range 10^5–10^7 l mol^{-1} s^{-1} [38]. Xanthate k_{ad} differs from this behaviour, as the reactivity of the thiocarbonyl bond is reduced due to interaction with the oxygen lone pair, which significantly lowers k_{ad}, e.g. to $(2.5 \pm 0.1) \times 10^4$ l mol^{-1} s^{-1} for EDTCP at −40 °C. Associated with the lower xanthate k_{ad} is the higher fragmentation rate coefficient: $k_\beta = 2300 \pm 300$ (Table 4.1). The two rate coefficients and the resulting low equilibrium constant indicate low INT* concentrations, which account for the absence of significant cross-termination reactions and thus of retardation.

With all four RAFT-mediated BA polymerizations, the two types of experimental K_{eq} values are close to each other (Table 4.1). The earlier quantum chemical calculations provide good estimates for trithiocarbonate-mediated polymerizations and probably also for xanthate systems, but need revision in the case of DTB-mediated polymerizations, where the radical functionality is delocalized over the phenyl moiety. The failure is demonstrated by comparison of the earlier and most recent quantum chemical calculations for the CIP*–CPDB system. Under ostensibly the same conditions, i.e. for the gas phase at 70 °C, the K_{eq} values from the earlier calculations are about 6 orders of magnitude larger than the actual quantum chemical calculations (and above the experimental value).

The values in column 2 of Table 4.1 demonstrate that it is essentially k_β that causes the differences between K_{eq} of the trithiocarbonate and dithiobenzoate RAFT agents. Adopting a typical activation energy for $E_A(k_\beta)$ of 50 kJ mol^{-1}, the experimental rate coefficients for −40 °C result in k_β values, which are about 4 orders of magnitude larger at a polymerization temperature of 60 °C. The entire set of k_β values in Table 4.1 thus is clearly indicative of fast fragmentation. The numbers that have been reported on the basis of the SF model for dithiobenzoate-mediated polymerizations at 60 °C [4, 50] are in the range of about 10^{-2} s^{-1}, which is not consistent with the EPR results deduced from quantitative online monitoring of the relevant radical species.

As k_{ad} is associated with a weak temperature dependence, i.e. with an activation energy $E_A(k_{ad})$ probably even below 10 kJ mol^{-1}, the equilibrium constants for the trithiocarbonates and the dithiobenzoate in Table 4.1 correspond to K_{eq} values in the range 1–100 l mol^{-1} at around 60 °C.

The SP-PLP-EPR method unambiguously demonstrates that the IRT model, in conjunction with 'missing step' reactions, provides an adequate representation of the entire body of experimental observations for dithiobenzoate-mediated RAFT

polymerizations. It should also be noted that Suzuki et al. measured rates of dithiobenzoate-mediated styrene polymerization in bulk and in miniemulsion and found significantly higher rates with the miniemulsion polymerization [57]. The authors conclude that the experimental observation cannot be simulated with the SF model, but may be adequately understood via the IRT model assuming relatively high k_β and high $k_{t,\mathrm{cross}}$. This result is in full agreement with the EPR-based data. Mechanisms of radical polymerization processes that are in conflict with EPR evidence should be considered with extreme care or, even better, should be discarded.

The K_{eq} value for ETTP-mediated BA polymerization from SP-PLP-EPR, $K_{\mathrm{eq}} = 3.4 \times 10^5\,\mathrm{l\,mol^{-1}}$ at $-40\,^\circ\mathrm{C}$, is above K_{eq} of trithiocarbonates. This difference mainly results from $k_{\beta,}$ which, for ETTP, is 1 order of magnitude smaller than the number for BMPT and a factor of 30 smaller than the EPPT value (Table 4.1). Under conditions of similar k_{ad}, slower fragmentation thus appears to be the essential reason behind the significant rate retardation observed in the case of dithiobenzoate-mediated polymerizations.

To summarize, via SP-PLP-EPR experiments the debate on the RAFT mechanism with dithiobenzoate-mediated polymerizations, SF vs. IRT, can be safely decided in favour of the IRT model. The argument raised against IRT that three-arm star material is absent in the product mixture from RAFT polymerization is invalidated by introducing the 'missing step'. This reaction has been overlooked for a long time, but has now been confirmed by observation of reaction products that are unambiguously due to this 'missing step'. However, even after solving the main controversy with DTB-mediated polymerizations, further work remains to be done: The SP-PLP-EPR technique should be applied towards the measurement of addition and fragmentation rate coefficients for a variety of RAFT agents and monomers and within a wider range of temperatures.

References

1 Moad, G. (2014). *Macromol. Chem. Phys.* 215: 9–26.
2 Monteiro, M.J. and de Brouwer, H. (2001). *Macromolecules* 34: 349–352.
3 Barner-Kowollik, C., Quinn, J.F., Morsley, D.R., and Davis, T.P. (2001). *J. Polym. Sci. Part A Polym. Chem.* 39: 1353–1365.
4 Barner-Kowollik, C., Buback, M., Charleux, B. et al. (2006). *J. Polym. Sci. Part A Polym. Chem.* 44: 5809–5831.
5 Kwak, Y., Goto, A., Tsujii, Y. et al. (2002). *Macromolecules* 35: 3026–3029.
6 Ah Toy, A., Vana, P., Davis, T.P., and Barner-Kowollik, C. (2004). *Macromolecules* 37: 744–751.
7 Feldermann, A., Ah Toy, A., Davis, T.P. et al. (2005). *Polymer* 46: 8448–8457.
8 Kwak, Y., Goto, A., and Fukuda, T. (2004). *Macromolecules* 37: 1219–1225.
9 Werner, M., Oliveira, J.C.A., Meiser, W. et al. (2020). *Macromol. Theory Simul.* 29: 2000022. https://doi.org/10.1002/mats.202000022.
10 Buback, M., Kattner, H., and Schroeder, H. (2016). *Macromolecules* 49: 3193–3213.

11 Buback, M. and Vana, P. (2006). *Macromol. Rapid Commun.* 27: 1299–1305.
12 Buback, M., Hesse, P., Junkers, T., and Vana, P. (2006). *Macromol. Rapid Commun.* 27: 182–187.
13 Meiser, W., Barth, J., Buback, M. et al. (2011). *Macromolecules* 44: 2474–2480.
14 Buback, M., Egorov, M., Junkers, T., and Panchenko, E. (2004). *Macromol. Rapid Commun.* 25: 1004–1009.
15 Barth, J., Buback, M., Hesse, P., and Sergeeva, T. (2010). *Macromolecules* 43: 4023–4031.
16 Soerensen, N., Barth, J., Buback, M. et al. (2012). *Macromolecules* 45: 3797–3801.
17 Schroeder, H. and Buback, M. (2015). *Macromolecules* 48: 6108–6113.
18 Kattner, H. (2016). Radical polymerization kinetics of non-ionized and fully-ionized monomers studied by pulsed-laser EPR. Doctoral Thesis, University of Goettingen.
19 Buback, M., Junkers, T., and Vana, P. (2006). Pulsed-laser initiated RAFT polymerization. In: *Controlled/Living Radical Polymerization*, *ACS Symposium Series. 944* (ed. K. Matyjaszewski), 455–472.
20 Meiser, W., Buback, M., and Sidoruk, A. (2013). *Macromol. Chem. Phys.* 214: 2108–2114.
21 Willemse, R.X.E., van Herk, A.M., Panchenko, E. et al. (2005). *Macromolecules* 38: 5098–5103.
22 Meiser, W. (2012). Investigation of the kinetics and mechanism of RAFT polymerization via EPR spectroscopy. Doctoral Thesis, University of Goettingen.
23 Weigend, F. and Ahlrichs, R. (2005). *Phys. Chem. Chem. Phys.* 7: 3297–3305.
24 Grimme, S., Antony, J., Ehrlich, S., and Krieg, H. (2010). *J. Chem. Phys.* 132: 154104.
25 Takano, Y. and Houk, K.N. (2005). *J. Chem. Theory Comput.* 1: 70–77.
26 Woon, D.E. and Dunning, T.H. (1993). *J. Chem. Phys.* 98: 1358–1371.
27 Saitow, M., Becker, U., Riplinger, C. et al. (2017). *J. Chem. Phys.* 146: 164105.
28 Barner-Kowollik, C. and Russell, G.T. (2009). *Prog. Polym. Sci.* 34: 1211–1259.
29 McLeary, J.B., Tonge, M.P., and Klumperman, B. (2006). *Macromol. Rapid Commun.* 27: 1233–1240.
30 McLeary, J.B., Calitz, F.M., McKenzie, J.M. et al. (2006). *Macromolecules* 37: 2383–2394.
31 McManus, N.T., Penlidis, A., and Dube, M.A. (2002). *Polymer* 43: 1607–1614.
32 Coote, M.L. and Davis, T.P. (1999). *Macromolecules* 32: 4290–4298.
33 Fischer, H. and Radom, L. (2001). *Angew. Chem. Int. Ed.* 40: 1340–1371.
34 Klumperman, B., van den Dungen, E.T.A., Heuts, J.P.A., and Monteiro, M.J. (2010). *Macromol. Rapid Commun.* 31: 1846–1862.
35 Meiser, W., Buback, M., Barth, J., and Vana, P. (2010). *Polymer* 51: 5977–5982.
36 Buback, M., Frauendorf, H., Guenzler, F., and Vana, P. (2007). *Polymer* 48: 5590–5598.
37 Barth, J., Buback, M., Hesse, P., and Sergeeva, T. (2009). *Macromol. Rapid Commun.* 30: 1969–1974.
38 Coote, M.L., Krenske, E.H., and Izgorodina, E.I. (2006). *Macromol. Rapid Commun.* 27: 473–497.

39 Lin, C.Y. and Coote, M.L. (2009). *Aust. J. Chem.* 62: 1479–1483.

40 Konkolewicz, D., Hawkett, B.S., Gray-Weale, A., and Perrier, S. (2008). *Macromolecules* 41: 6400–6412.

41 Froehlich, M.G., Vana, P., and Zifferer, G. (2007). *J. Chem. Phys.* 127: 1649061–1649067.

42 Geleen, P. and Klumperman, B. (2007). *Macromolecules* 40: 3914–3920.

43 Moad, G., Chong, Y.K., Mulder, R. et al. (2009). New features of the mechanism of raft polymerization. In: *Controlled/Living Radical Polymerization: Progress in RAFT, DT, NMP & OMRP*, ACS Symposium Series, vol. 1024 (ed. K. Matyjaszewski), 3. Washington: American Chemical Society.

44 Buback, M., Janssen, O., Oswald, R. et al. (2007). *Macromol. Symp.* 248: 158–167.

45 Meiser, W., Buback, M., Ries, O. et al. (2013). *Macromol. Chem. Phys.* 214: 924–933.

46 Goto, A., Sato, K., Tsujii, Y. et al. (2001). *Macromolecules* 34: 402–408.

47 Meiser, W. and Buback, M. (2011). *Macromol. Rapid Commun.* 32: 1490–1494.

48 Meiser, W. and Buback, M. (2012). *Macromol. Rapid Commun.* 33: 1273–1279.

49 Barth, J., Buback, M., Meiser, W., and Vana, P. (2010). *Macromolecules* 43: 51–54.

50 Feldermann, A., Coote, M.L., Stenzel, M.H. et al. (2004). *J. Am. Chem. Soc.* 126: 15915–15923.

51 Coote, M.L. (2005). *J. Phys. Chem. A* 109: 1230–1239.

52 Coote, M.L., Izgorodina, E.I., Krenske, E.H. et al. (2006). *Macromol. Rapid Commun.* 27: 1015–1022.

53 Junkers, T., Barner-Kowollik, C., and Coote, M.L. (2011). *Macromol. Rapid Commun.* 32: 1891–1898.

54 Buback, M., Meiser, W., and Vana, P. (2009). *Aust. J. Chem.* 62: 1484–1487.

55 Sidoruk, A., Buback, M., and Meiser, W. (2013). *Macromol. Chem. Phys.* 214: 1738–1748.

56 Chong, Y.K., Krstina, J., Le, T.P. et al. (2003). *Macromolecules* 36: 2256–2272.

57 Suzuki, K., Nishimura, Y., Kanematsu, Y. et al. (2012). *Macromol. React. Eng.* 6: 17–23.

5

RAFT Polymerization: Mechanistic Considerations

John F. Quinn[1,2], Graeme Moad[3], and Christopher Barner-Kowollik[4]

[1] *Monash University (Parkville Campus), Monash Institute of Pharmaceutical Sciences, Faculty of Pharmacy and Pharmaceutical Sciences, 381 Royal Parade, Parkville Victoria 3052, Australia*
[2] *Monash University (Clayton Campus), Department of Chemical Engineering, Faculty of Engineering, Wellington Road, Clayton, Victoria 3800, Australia*
[3] *CSIRO Manufacturing, Research Way, Clayton, VIC 3168, Australia*
[4] *Queensland University of Technology, School of Chemistry and Physics, Faculty of Science, Gardens Point Campus, Brisbane, QLD 4001, Australia*

5.1 Introduction

The development of polymerization with reversible addition–fragmentation transfer (RAFT) [1] has enabled the synthesis of an extraordinary array of polymers with well-defined molecular weight and readily functionalizable end-groups [2–5]. For any given monomer, the utility of RAFT as a tool for controlling polymer properties is highly dependent on the choice of RAFT agent, which in turn requires understanding the mechanism by which RAFT polymerization proceeds. In its simplest form, the mechanism involves processes that are inherent to any radical polymerization: initiation, propagation, chain transfer, and termination. However, in the case of RAFT, the chain transfer step proceeds via a reversible addition–fragmentation process [6], and the polymeric product formed is itself a RAFT agent (see Scheme 5.1).

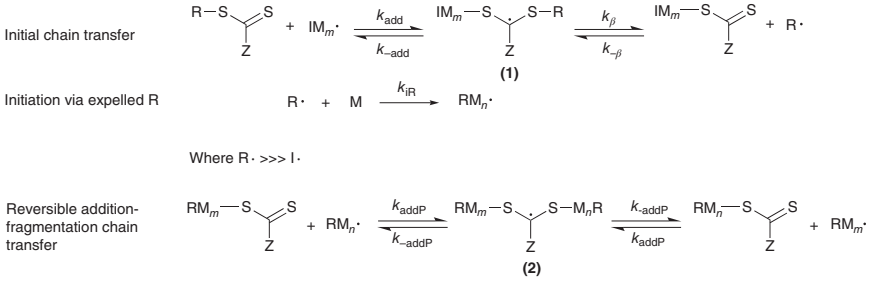

Scheme 5.1 Processes unique to RAFT polymerization: initial chain transfer of a small molecule 'RAFT agent'; initiation of new polymer chains via the expelled group R; and reversible addition–fragmentation chain transfer of the macromolecular transfer agent formed. The majority of chains are initiated via the R group where $R^{\cdot} >> I$.

RAFT Polymerization: Methods, Synthesis and Applications, First Edition.
Edited by Graeme Moad and Ezio Rizzardo.

The first reported RAFT polymerization involved the use of methacrylate macromonomers [7, 8]. However, in the vast majority of reports the employed chain transfer agent is a thiocarbonylthio compound, although other species such as selenocarbonylseleno compounds [9–11] are also used. Importantly, not every thiocarbonylthio compound is compatible with every monomer, and, as such, there is an imperative to understand the attributes of the chain transfer agent that render it applicable for a particular monomer. Copolymerization introduces further complications to the mechanism [12].

One of the simplest forms of a chain transfer agent that reacts by RAFT (i.e. a so-called RAFT agent) is depicted below:

Depending on the identity of Z, the RAFT agent may be a dithioester, trithiocarbonate, xanthate, or dithiocarbamate. Each of these categories of RAFT agents has been the subject of extensive research, and specific chapters in this text are dedicated to each [13–16]. There are also more exotic examples wherein dithiobenzoic acid [17] and bis(thionaphthoyl)disulfide [18] have been employed to yield RAFT agents in situ, although these are typically accompanied by long induction times and reduced rates of polymerization for reasons that will become evident. Both the groups R and Z impact on the suitability of the RAFT agent for application in RAFT polymerization with a particular monomer. The roles of R and Z are considered in more detail below.

5.2 Role of the R Group

5.2.1 Chain Transfer and Leaving Group Ability

The R group in the general structure R—S—(C=S)Z is – at its most basic level – a good homolytic leaving group relative to the propagating radical that is itself capable of efficiently initiating polymerization. The leaving group ability of R can be characterized via the transfer constant (C_{tr}):

$$C_{tr} = \frac{k_{tr}}{k_p} \tag{5.1}$$

i.e. the ratio of the rate coefficient for chain transfer (k_{tr}) to the propagation rate coefficient (k_p).

In actuality, the efficiency of a RAFT agent is determined by the values of two transfer constants, C_{tr} ($=k_{tr}/k_p$) and C_{-tr} ($=k_{-tr}/k_i$). The rate coefficient for chain transfer (k_{tr}) for a RAFT agent is given by Eq. (5.2), with the value of k_{tr} depending on the rate of addition of the propagating radical ($P_n\cdot$) to the RAFT agent and a partition coefficient (ϕ), which describes the partitioning of intermediate radical (**1**) between the starting materials and the products – see Scheme 5.1.

$$k_{tr} = k_{add}\phi = k_{add}\left[\frac{k_\beta}{k_{-add} + k_\beta}\right] \tag{5.2}$$

The radical ($R^{\cdot}$) expelled from the transfer agent is also partitioned between adding to the monomer and reacting with the macromolecular RAFT agent. The rate coefficient associated with this reaction ($k_{-\mathrm{tr}}$) is thus defined as shown in Eq. (5.3).

$$k_{-\mathrm{tr}} = k_{-\beta}(1-\phi) = k_{-\beta}\left[\frac{k_{-\mathrm{add}}}{k_{-\mathrm{add}}+k_{\beta}}\right] \tag{5.3}$$

A high chain transfer constant is associated with good leaving group ability and, provided that the R group can efficiently initiate further polymer chains, polymers with narrow molecular weight distribution are formed. In cases where the transfer constant is low, the RAFT agent is consumed more slowly and as a result the bulk of the chains are not initiated at the same time. In such situations it is possible to apply the methods used for measuring transfer coefficients for conventional chain transfer agents. As such, it is prudent at this point to include some description of the various methods for determining these constants.

5.2.2 Measurement of the Chain Transfer Constant

Mayo reported the first equation for determination of the chain transfer constant in 1943 [19]. This initial report was associated with the specific scenario of chain transfer to solvent. By observing that the degree of polymerization (X_n) in the polymerization of styrene could be determined by dividing the rate of chain growth by the total rate of chain termination (including chain transfer to solvent, termination by disproportionation, and chain transfer to monomer) at low conversion (i.e. where the relative concentrations of monomer and solvent remain constant), Mayo developed the following expression:

$$X_{\mathrm{n}} = \frac{k_{\mathrm{p}}\left[\mathrm{P}_n^{\cdot}\right][\mathrm{M}]}{k_{\mathrm{tr}}\left[\mathrm{P}_n^{\cdot}\right][\mathrm{S}] + k_{\mathrm{t}}\left[\mathrm{P}_n^{\cdot}\right]^2 + k_{\mathrm{tr(M)}}\left[\mathrm{P}_n^{\cdot}\right][\mathrm{M}]} \tag{5.4}$$

After taking the reciprocal and using steady-state approximation to remove the term $[\mathrm{P}_n^{\cdot}]$ from the equation, this reduces to

$$\frac{1}{X_{\mathrm{n}}} = \frac{k_{\mathrm{tr}}[S]}{k_{\mathrm{p}}[M]} + \frac{\sqrt{k_{\mathrm{i}}k_{\mathrm{t}}} + k_{\mathrm{tr}(M)}}{k_{\mathrm{p}}} \tag{5.5}$$

With no added chain transfer agent (i.e. in this case solvent), the first term on the RHS reduces to zero, and therefore the second term represents the inverse of degree of polymerization in the absence of added chain transfer agent. Thus, the equation can be recast as

$$\frac{1}{X_{\mathrm{n}}} = C_{\mathrm{tr}}\frac{[\mathrm{S}]}{[\mathrm{M}]} + \frac{1}{\mathrm{X_{n0}}} \tag{5.6}$$

where X_{n0} is the degree of polymerization achieved in the absence of chain transfer agent and C_{tr} is the chain transfer constant, as defined above in Eq. (5.1). Provided that the value for k_{p} is known, k_{tr} can also be accessed via this method. Although initially derived to describe chain transfer to the solvent, this equation is also used to describe the chain transfer constant for added chain transfer agents. One of the key limitations of the Mayo method for determining the chain transfer constant

is that the degree of polymerization must be known to a high degree of accuracy, and therefore the method is susceptible to error associated with size exclusion chromatography (SEC) measurements. Specifically, determination of X_n via SEC is often relative, and the computed value for X_n is sensitive to small variations in the baseline. To overcome this limitation, Gilbert and Clay proposed an alternative approach [20], wherein the chain transfer constant is determined via the gradient of a plot of the natural logarithm of the number chain length distribution (CLD) in the high chain length region against the ratio of the chain transfer agent (CTA) and monomer concentrations (Eq. (5.7)).

$$\frac{d \ln y_n}{dn} = C_{\mathrm{tr}} \frac{[\mathrm{CTA}]}{[\mathrm{M}]} + \frac{\langle k_{\mathrm{t}} \rangle [\mathrm{P}_n^{\cdot}]}{k_{\mathrm{p}} [\mathrm{M}]} \tag{5.7}$$

where in y_n is the number fraction of dead polymer molecules with chain length n. This approach has the advantage of being much less susceptible to variations in the baseline of the measured CLD. Subsequent work by G. Moad and C. L. Moad [21] has shown that applying this equation to those chain lengths having the highest signal to noise ratio for the number CLD (i.e. the top 80% of the number CLD) enables determination of C_{tr} values to a high degree of accuracy.

It is important to note that both the Mayo method and the ln(CLD) method require data for low monomer and transfer agent conversions, and as such rapid consumption of the transfer agent and efficient re-initiation renders these approaches unsuitable for estimating the C_{tr} for the most effective RAFT agents. Further, since the original method of Mayo does not contemplate the polymeric product of chain transfer also behaving as a chain transfer agent, there are limitations in applying these methods to RAFT systems (e.g. $C_{-\mathrm{tr}}$ is assumed to be zero, which is unlikely for reactive RAFT agents such as trithiocarbonates and dithiobenzoates). Nevertheless, these methods have been applied to estimate the chain transfer constant in RAFT polymerizations where the rate of chain transfer is sufficiently low (e.g. where $C_{\mathrm{tr}} < 2$). In situations where the chain transfer constant is higher, other approaches need to be employed.

In early publications on polymerization with RAFT mediated by thiocarbonylthio compounds, Moad and coworkers [22] proposed the application of another classical method, known as the Walling method [23] or the O'Brien method [24], (but which could also be attributed to Mayo and coworkers [25]) for evaluating the transfer coefficient. This approach involves evaluating the relative consumption of the transfer agent and monomer and enables estimation of the chain transfer constant via Eq. (5.8):

$$\frac{d [\mathrm{CTA}]}{d [\mathrm{M}]} = C_{\mathrm{tr}} \frac{[\mathrm{CTA}]}{[\mathrm{M}] + C_{\mathrm{tr}} [\mathrm{CTA}] + C_{-\mathrm{tr}} [\mathrm{macroCTA}]} \tag{5.8}$$

where [CTA] is the concentration of the chain transfer agent and [macroCTA] is the concentration of the polymeric RAFT agent formed, $C_{\mathrm{tr}} = k_{\mathrm{tr}}/k_{\mathrm{p}}$ and $C_{-\mathrm{tr}} = k_{-\mathrm{tr}}/k_{\mathrm{i}}$. This expression takes into account the consumption of the transfer agent due to the reactivity of both propagating radicals and the expelled radical formed by homolytic cleavage of the intermediate radical ($\mathrm{R}^{\cdot}$). Provided that the rate of reaction of the

group R· to the transfer agent is negligible (not always a fair assumption, see Section 5.2.4) and the chains are sufficiently long, this equation reduces to

$$\frac{d[\mathrm{CTA}]}{d[\mathrm{M}]} \approx C_{\mathrm{tr}} \frac{[\mathrm{CTA}]}{[\mathrm{M}]} \tag{5.9}$$

By rearranging and integrating

$$\int_{[\mathrm{CTA}]_0}^{[\mathrm{CTA}]} \frac{d[\mathrm{CTA}]}{[\mathrm{CTA}]} \approx C_{\mathrm{tr}} \int_{[\mathrm{M}]_0}^{[\mathrm{M}]} \frac{d[\mathrm{M}]}{[\mathrm{M}]} \tag{5.10}$$

$$\ln[\mathrm{CTA}] - \ln[\mathrm{CTA}]_0 \approx C_{\mathrm{tr}} \ln[\mathrm{M}] - \ln[\mathrm{M}]_0 \tag{5.11}$$

$$\ln[\mathrm{CTA}] \approx C_{\mathrm{tr}} \ln[\mathrm{M}] + \text{constant} \tag{5.12}$$

As such, a plot of ln[CTA] and ln[M] will yield the chain transfer constant as the gradient, i.e.

$$C_{\mathrm{tr}} \approx \frac{d(\ln[\mathrm{CTA}])}{d(\ln[\mathrm{M}])} \tag{5.13}$$

An example of the use of Eq. (5.2) with parameter estimation by kinetic simulation is given in Figure 5.1. The C_{tr} and $C_{-\mathrm{tr}}$ for PhC(=S)SC(CH_3)$_2$Ph in methyl methacrylate (MMA) polymerization were estimated as 25 and 450, respectively.

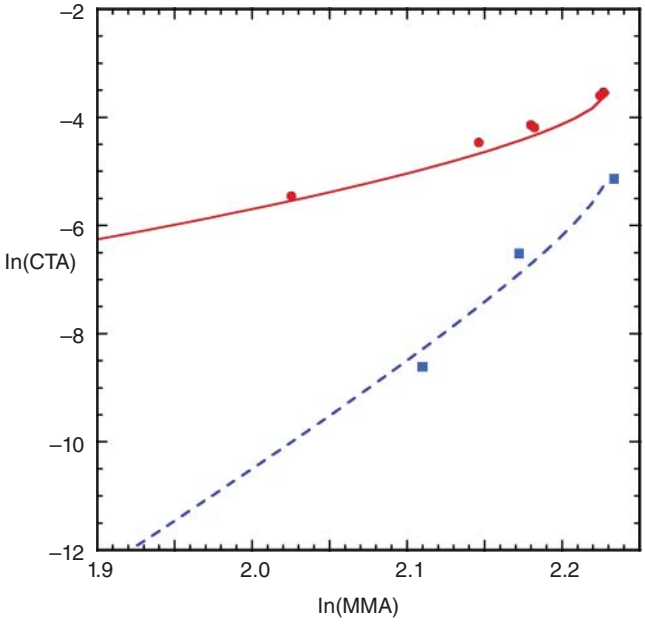

Figure 5.1 Double log plot of chain transfer agent concentration against monomer concentration for polymerization of methyl methacrylate in the presence of PhC(=S)SC(CH_3)$_2$Ph (CTA). Data are for bulk MMA polymerization at 60 °C with azobisisobutyronitrile as the initiator in the concentration range 0.0005–0.04 M and with 0.0058 M (●) or 0.029 M (■) PhC(=S)SC(CH_3)$_2$Ph as RAFT agent. Lines are those predicted by Eq. (5.1) with $C_{\mathrm{tr}} = 25$ and $C_{-\mathrm{tr}} = 450$. Source: Adapted with permission from Chong et al. [22]. © 2003, American Chemical Society.

Note that use of the simplified expression (5.6) gives an apparent transfer constant of 5.9. Equation (5.6) is recommended only for giving an approximate ranking in the case of more active RAFT agents where a series of experiments are conducted under similar conditions (of $[\text{RAFT agent}]_0$ and $[\text{M}]_0$).

One of the challenges of this approach is employing a method to simply determine the conversion of the chain transfer agent, as these are typically present in low concentrations. Moad has also proposed an elegant method for determining the amount of residual chain transfer by comparing the calculated and experimental molecular weights via the relationship:

$$\text{Conv}\,(\text{CTA}) = \frac{[\text{CTA}]_0 - [\text{CTA}]_t}{[\text{CTA}]_0} = \frac{\frac{[\text{M}]_0 - [\text{M}]_t}{[\text{CTA}]_0}}{\frac{[\text{M}]_0 - [\text{M}]_t}{[\text{CTA}]_0 - [\text{CTA}]_t}} = \frac{X_\text{n}\,(\text{calcd})}{X_\text{n}\,(\text{found})} \tag{5.14}$$

where X_n(calcd) is the expected number-average degree of polymerization assuming complete conversion of the chain transfer agent and X_n(found) is the number-average degree of polymerization determined experimentally. It may be beneficial to correct X_n(calcd) by considering those radicals derived from the initiator in addition to those from the R group of the transfer agent. This may be achieved using the expression

$$X_\text{n}\,(\text{calcd}) = \frac{[\text{M}]_0 - [\text{M}]_t}{[\text{CTA}]_0 - df\left([\text{I}]_0 - [\text{I}]_t\right)} \tag{5.15}$$

wherein d is the number of chains produced from radical–radical reaction, f is the initiator efficiency, and $[\text{I}]_0 - [\text{I}]_t$ can be calculated via the exponential decay of the initiator using k_d, the rate constant for initiator decomposition:

$$[\text{I}]_0 - [\text{I}]_t = [\text{I}]_0\left(1 - e^{-k_\text{d}t}\right) \tag{5.16}$$

In cases where the initiator concentration and radical flux are low such that the number of initiator-derived chains is negligible, this term may be ignored.

It is implicit in the derivation of the Mayo, lnCLD, and Walling methods that the value $C_{-\text{tr}}$ is zero. However, in the case of more active RAFT agents it is well understood that this is not the case. Nevertheless, the Walling method applied to data obtained under a consistent set of reaction conditions may still be employed to obtain a qualitative ranking of RAFT agent activity via apparent transfer constants. However, the values of C_tr may be underestimated by several orders of magnitude.

As an example, the Walling approach, or conventional Mayo analysis, has been applied to a series of dithioesters with systematic variation of the R group structure (see Table 5.1). The value of the chain transfer constant broadly correlates with the homolytic leaving group ability of the R group with respect to propagating methacrylyl radicals. Based on these and other observations, it can be considered that steric factors, polar effects, and the stability of the radical $\text{R}^\cdot$, all contribute to the transfer constant and therefore the effectiveness of the RAFT agents. Significantly, the R group is shown to have little impact on the rate of addition to the thiocarbonyl group.

In a number of examples, such as the polymerization of styrene using benzyl dithiobenzoate as a chain transfer agent, a significant narrowing of molecular

Table 5.1 Transfer constants of various dithiobenzoates in MMA polymerization at 60 °C.

R group	C_s
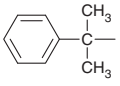	5.9
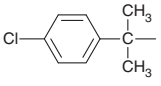	6.6
	6.8
	1.7
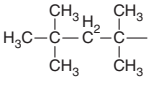	0.4
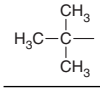	0.03

Source: Data are taken from Walling [23].

weight distribution occurs as the polymerization progresses. This behaviour is caused by the initial transfer agent being consumed relatively slowly. While this enables estimation of the chain transfer constant, to get a low dispersity at low conversions the initial RAFT agent must be quickly consumed. This illustrates the difficulty associated with the estimation of chain transfer constants for highly efficient RAFT agents.

The value of the chain transfer constant for the initial transfer step may also be estimated by other methods. For instance, in cases where the polymerization proceeds with the so-called 'hybrid RAFT polymerization behaviour' (i.e. a rapid initial increase in the degree of polymerization followed by a linear evolution of molecular weight with conversion), Barner-Kowollik and coworkers proposed a method to determine C_{tr} via SEC measurements. This approach relies on the expression

$$k_{\mathrm{add},0} = \frac{k_{\mathrm{p}}[\mathrm{M}]_0}{\left(X_{\mathrm{n}}^{\mathrm{inst}} - 1\right)[\mathrm{CTA}]_0 \phi} \tag{5.17}$$

wherein $k_{\mathrm{add},0}$ is the rate coefficient for the addition of the propagating polymer radical to the chain transfer agent, k_{p} is the propagation rate coefficient, X_n^{inst} is the initial degree of polymerization, and ϕ is the probability of fragmentation in favour of the products [26]. In the case of the initial chain transfer step with an agent that primarily fragments to expel the radical R$^{\cdot}$, the value of $\phi = 1$ and therefore $k_{\mathrm{add},0} = k_{\mathrm{tr},0}$,

and the expression can be rearranged to give [27]

$$X_n^{inst} = \frac{[M]_0}{C_{tr,0}[CTA]_0} + 1 \tag{5.18}$$

As such, a plot of the degree of polymerization of the initially formed polymer vs. $[M]_0/[CTA]_0$ can be used to deduce C_{tr} as the reciprocal of the gradient. While the afore-mentioned methods for determining the C_{tr} are readily applicable to the initial transfer step, their application to the main RAFT equilibrium is difficult for practical reasons (such as the difficulty in accurately determining concentration changes for the macroCTA). As a result, approaches for determining C_{tr} for the main RAFT equilibrium have also been developed, many of which have been derived from treatment of degenerative chain transfer. For example, Goto, Fukuda and coworkers proposed a method that employs very low concentrations of macroCTA relative to the monomer [28]. Under these conditions, the larger number of monomer units added per activation–deactivation cycle enables resolution of the chain extended polymer from the macroCTA in the SEC chromatograms. By using the relative peak areas corresponding to the macroCTA and chain extended polymer, it is possible to estimate a value for the activation rate coefficient k_{act} via the expression

$$\ln \frac{S_0}{S} = k_{act} t \tag{5.19}$$

where S_0 and S are the concentrations for macroCTA and chain extended polymer respectively. As such plotting the natural logarithm of the ratio of the SEC peak areas for the macroCTA and the polymer at various times vs. time will yield k_{act} as the gradient. This can in turn be used to determine k_{tr} via the expression

$$k_{act} = k_{ex}[P^{\cdot}] \tag{5.20}$$

wherein $k_{ex} = k_{tr}/2$ (since $C_{tr} = C_{-tr}$). As such, by plotting k_{act} against $R_p/[M]$, C_{tr} can be extracted via the gradient.

Goto and Fukuda have also proposed determination of the chain transfer constant in degenerative chain transfer via analysis of the dispersity. In this case, the dispersity factor Y (i.e. $Y = Đ - 1$) is related to the chain transfer constant via the following expression: [29]

$$\left[Y - \left(\frac{1}{X_n}\right)\right]^{-1} = C_{tr}\left(\frac{x}{2-x}\right) \tag{5.21}$$

where x is the fractional conversion. This expression has been further extended to account for conventional initiation and termination reactions [30]. Nevertheless, Eq. (5.21) (and its extended version) does not consider possible transfer reactions with the initial chain transfer agent, and as such it is only valid in situations where the RAFT agent is consumed relatively quickly (i.e. monomer conversions below a small percentage). Moreover, the method is strictly only applicable to macroCTA where the C_{tr} values for the initial and product RAFT agents are the same (because they differ only in chain length). As such, the application of this method to provide a transfer constant for an initial RAFT agent in a polymerization is at best debatable. However, the method has proved useful when used to rank the activity of RAFT

agents in a series of polymerizations conducted under similar conditions. A further issue with this methodology is the accuracy of experimentally determined dispersity measurements.

Values of transfer coefficients can also be estimated via kinetic simulation using either numerical integration [31] or Monte Carlo methods [32]. In these cases, the values are chosen in order to fit the experimental data. For a range of values of $C_{-\mathrm{tr}}$ that may cover orders of magnitude, it is often possible to choose a value of $C_{-\mathrm{tr}}$ such that a satisfactory fit is obtained. This may account for the wide range of values that appear in the literature for certain systems (e.g. for the 2-phenylprop-2-yl dithiobenzoate mediated polymerization of styrene) [33] and serves to emphasize that these values should be treated with caution.

While methods for describing degenerative chain transfer can be applied to determine the chain transfer coefficients in RAFT polymerization, such approaches do not provide values for the isolated addition and fragmentation rate coefficients. To address this, Buback and coworkers have recently proposed an approach for determination of the addition–fragmentation equilibrium coefficient K_{eq} using electron paramagnetic resonance (EPR) spectroscopy [34]. Specifically, these researchers proposed determination of the ratio of the propagating macroradicals and intermediate radical species, which could then be combined to estimate K_{eq} via the expression

$$K_{\mathrm{eq}} = \frac{k_{\mathrm{add}}}{k_{\mathrm{frag}}} = \frac{[\mathrm{Int}]_{\mathrm{eq}}}{[\mathrm{P}^{\cdot}]_{\mathrm{eq}}[\mathrm{P}]_{\mathrm{eq}}} = \frac{[\mathrm{Int}]}{[\mathrm{P}^{\cdot}]\,[\mathrm{P}]} \tag{5.22}$$

wherein k_{add} is the rate constant for addition, k_{frag} is the rate constant for fragmentation, and [Int] is the intermediate radical concentration; $[P^{\cdot}]$ is the total concentration of macroradicals, $[P]$ is the total concentration of deactivated chains, and the suffix 'eq' denotes equilibrium. By combining this EPR approach with pulsed laser initiation the decay of [Int] and $[P^{\cdot}]$ with time can be determined, provided that the EPR is suitably calibrated to determine both radical populations [35]. Subsequent fitting of the resulting decay curves using a modelling package such as Predici® enables the values for k_{add} and k_{frag} to be estimated. This approach is described in some detail in the chapter by Buback [36].

For a comprehensive treatment of methods available to estimate the chain transfer constants in RAFT polymerization (including others not described here), the reader is referred to the recent review on the topic by Barner-Kowollik, D'hooge, and coworkers [27].

5.2.3 Mechanistic Implications for Block Copolymer Synthesis

The need for the R group to be an effective homolytic leaving group has important implications for block copolymer synthesis. In general, there is a requirement that the first synthesized block yields a superior homolytic polymeric leaving group; this is essential to enable radical addition of the second monomer to the first block. In situations where the first synthesized block is a poor leaving group with respect to the radical derived from the second monomer, block formation will be minimal, and

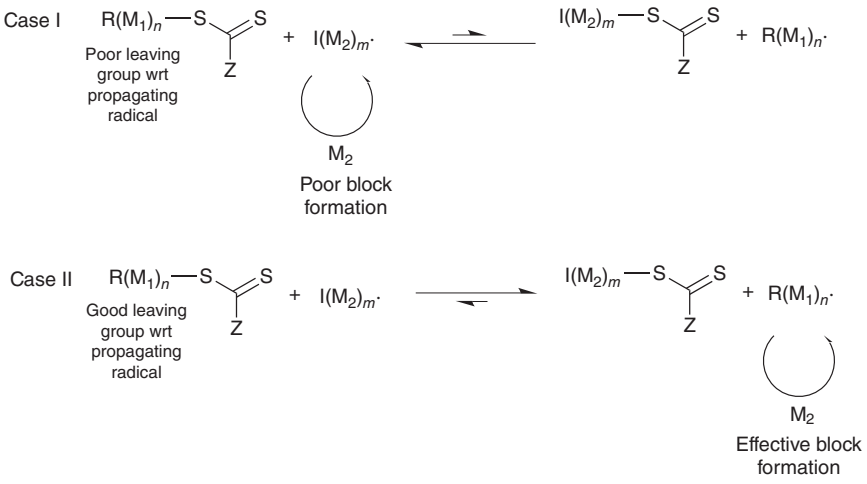

Scheme 5.2 Formation of block copolymers via RAFT. Where the polymeric radical from the first formed block is an inferior leaving group to those radicals formed from the second monomer, fragmentation occurs principally in the direction of the starting reactants, leading to minimal block formation (case 1). When the polymeric radical from the first formed block is a good leaving group relative to radicals formed from the second monomer, blocks can readily form via addition of the second monomer to the expelled polymer radical (case 2).

a significant proportion of the macromolecular chain transfer agent will be present in the product (Scheme 5.2).

It is also important that the R· radical is a very good initiating radical. If addition to the monomer is slow, poor blocking efficiencies may be observed, along with by-products from the self-reaction of R· (see Section 5.2.4).

Despite the general requirement for high transfer constants of the initially formed macromolecular chain transfer agent to enable block formation via RAFT, there are a small number of exceptions to this rule in the literature. Moad et al. demonstrated the successful synthesis of poly(styrene-*block*-methyl methacrylate) (P[Sty-*block*-MMA]) wherein the polystyrene block was synthesized first by employing starved-feed emulsion polymerization [37]. They applied the same approach to prepare polystyrene by RAFT emulsion polymerization with a xanthate RAFT agent [37]. These authors had previously shown that starved-feed conditions could be employed to make low dispersity polymers and block copolymers from macromonomer RAFT agents [8]. As such, an initial block of polystyrene was prepared by RAFT emulsion using benzyl dithioacetate as the RAFT agent to reach a conversion >99%; MMA was then added by slow addition at a rate commensurate with the rate of polymerization, thereby maintaining the very low concentration of monomer relative to the chain transfer agent. This approach overcame the limitation imposed on the monomer order of addition by the low C_{tr} of the polystyryl macromolecular chain transfer agent. The methodology takes advantage of compartmentalization effects to limit the extent of termination. This approach has also recently been exploited by Haddleton and coworkers [38] to prepare multiblock polymers using unsaturated methacrylate oligomers as non-sulfurous

reversible addition–fragmentation chain transfer agents. It has also been used to prepare low-dispersity poly(methyl methacrylate) (PMMA) with xanthate RAFT agents [39]. In principle, other agents with low transfer constants could also be potentially applied in this manner. The observations made in these experiments also provided the basis for the use of RAFT polymerization in the rapid synthesis of multiblock copolymers by the 'nanoreactor concept' [40–42].

Barner-Kowollik and coworkers have also previously reported on a system where the chain transfer kinetics of the initial agent differs substantially from that of the formed macromolecular transfer agent [43] (Figure 5.2a) and this example illuminates the potential implications of inappropriately chosen conditions/reagents for RAFT polymerization. Cumyl phenyldithioacetate (CPDA) functions effectively as a RAFT agent for the bulk polymerization of styrene initiated by azobisisobutyronitrile (AIBN) at 60 °C, with the formation of polymers having controlled molecular weight and linear evolution of molecular weight with conversion. However, application of the same agent with MMA yields remarkably different behaviour. Specifically, the initial chain transfer reaction is sufficiently slow with respect to propagation that at low conversions (i.e. low yields of polymeric transfer agent), behaviour approximating classical chain transfer is observed. However, as the CPDA is consumed, the emergence of a second 'living' distribution becomes evident (Figure 5.2b), with the distribution returning to being unimodal and shifting clearly to higher molecular weight at higher conversions (Figure 5.2c). Significantly, the excess of CPDA at low conversions enables the chain transfer constant to be determined via the Mayo method. In this case, C_s values of 4.1, 3.8, and 3.9 (corresponding to k_{tr} of 1324, 1645, and 2219 l mol^{-1} s^{-1}) were determined at 25 °C, 35 °C, and 45 °C, respectively, enabling calculation of the activation energy for the transfer reaction as 26 kJ mol^{-1}. This approach, based on chromatographic analysis, is similar to that used by Fukuda and coworkers [28] to estimate C_{tr} for macroRAFT agents (macroCTA).

5.2.4 Re-Initiation and Initialization

The choice of transfer agent for a particular monomer is also influenced by the suitability of R for reinitiating polymerization. In general, the rate of addition of R to the monomer should be greater than the propagation rate (i.e. the rate constant for addition of the group R to monomer should exceed the propagation rate coefficient [$k_{iR} > k_p$]). Importantly, the factors that tend to make R a suitable homolytic leaving group (and thus provide an adequate rate of chain transfer) also tend to reduce the rate of addition of R to the monomer. As such, a balance needs to be found between the leaving group ability of the R group and its propensity to add to the monomer. Helpful data for the rate of addition of several R group candidates are readily available in the literature [44, 45]. A selection of these data is included in Table 5.2 [46].

For the polymerization of styrenic and methacrylate monomers R groups such as 2-cyanoprop-2-yl and 2-phenylprop-2-yl are generally suitable, as the rate of addition of these radicals to the corresponding monomers is sufficiently fast. However, for polymerization of monomers such as *N*-vinylpyrrolidone and vinyl acetate the rate of addition of 2-cyanoprop-2-yl and 2-phenylprop-2-yl groups is

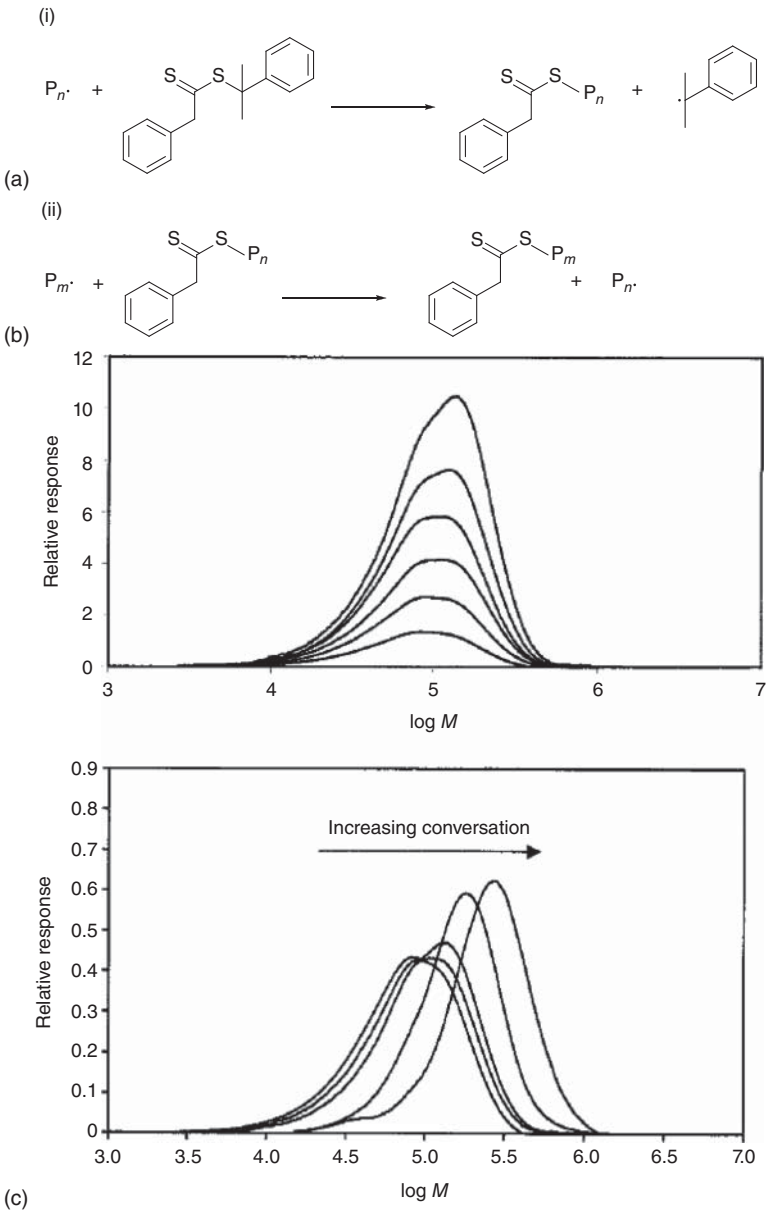

Figure 5.2 (a) Chain transfer reactions for (i) cumyl phenyldithioacetate and (ii) poly (methyl methacrylyl) phenyldithioacetate. (b) Evolution of molecular weight distributions in a cumyl phenyldithioacetate mediated (bulk) polymerization of MMA at 60 °C. The initial RAFT agent concentration was close to 3.7×10^{-3} mol l^{-1} and the initiator (AIBN) concentration was 2.6×10^{-3} mol l^{-1}. The area under each distribution is scaled relative to monomer conversions of 3.1%, 6.2%, 9.6%, 13.3%, 16.7%, and 22.3%, respectively. (c) Evolution of molecular weight distributions in a cumyl phenyldithioacetate mediated (bulk) polymerization of MMA at 60 °C. The initial RAFT agent and initiator (AIBN) concentrations are as above. The areas under the individual curves are all normalized. The additional two distributions correspond to overall monomer conversions of 57% and 82%, respectively. Source: Taken from Barner-Kowollik et al. [43]. © 2001, American Chemical Society.

Table 5.2 Estimated monomer addition rate coefficients for initiator-derived radicals (k_i) at 60 °C.

	Rate coefficient[a] (10^3 M^{-1} s^{-1})							
	CH_2CN	$(CH_3)_2$ CCN	CH_2 (CO_2R)	$(CH_3)_2$ C(COR)	$(CH_3)_3C$	$PhCH_2$	$(CH_3)_2$ CPh	k_p[b]
MMA	790	3.3	2600	9.7	950	8.3	7.8	1.2
Styrene	1160	4.9	4000[c]	13.5	220	4.7	3.8	0.34
MA	410	0.87	1130	3.4	1500	2.0	2.6	28
AN	410	4.1	1220	7.0	6330	8.7	6.5	3[d]
VAc[c]	70	0.086	1700	0.092	12.0	0.10	[e]	8.3

a) Addition rate coefficient based on the activation parameters suggested by Fischer and Radom [44] and their recommended log (A/M^1s^1) of 8.5 for primary radicals and 7.5 for tertiary radicals [46].
b) IUPAC recommended values of propagation rate coefficients in bulk monomer [47]. Value indicated is based on the absolute rate constants reported by Fischer and Radom [44] and the literature cited therein.
c) Note that for VAc the reported activation energies are not consistent with the rate constants from which they were derived.
d) Polymer Handbook [48] – value typical for organic solvents.
e) No data available.
Source: Moad [46]. © Wiley-VCH.

slower, leading to long inhibition times. Instead, for these monomers R groups such as cyanomethyl are preferable. Importantly, suitability of a R group for styrene and methacrylates does not immediately translate to suitability for acrylates and acrylamides, and this is certainly the case for 2-cyanoprop-2-yl and 2-phenylprop-2-yl radicals. These add relatively slowly to acrylamides and acrylates, and as such there are better candidates for the R group in the polymerization of these monomers (e.g. leaving groups that approximate the structure of acrylates). It is worth noting that R groups that have lower re-initiation efficiency may also preferentially add to the thiocarbonylthio group, giving a symmetrical intermediate radical. For monomers for which the thiocarbonyl is highly activated to radical addition (e.g. dithiobenzoates or trithiocarbonates), this preferential addition of the R group to the RAFT agent may occur to a significant extent, exacerbating rate retardation and in some cases leading to complete inhibition of polymerization (e.g. for the polymerization of vinyl acetate in the presence of 2-phenylprop-2-yl dithiobenzoate). This demonstrates that the choice of R group for a given monomer cannot be made completely in isolation: the Z group will also influence the extent to which R will efficiently re-initiate polymerization or preferentially add to the CTA. If the latter reaction is sufficiently dominant then no polymerization at all may be observed.

Further, in the RAFT oligomerization of acrylamides (e.g. *N,N*-dimethylacrylamide [DMAm]) mediated by tertiary cyanoalkyl trithiocarbonates it is possible to detect the product from combination of R radicals in amounts predicted by kinetic simulation, indicating that this is a cause of retardation [49].

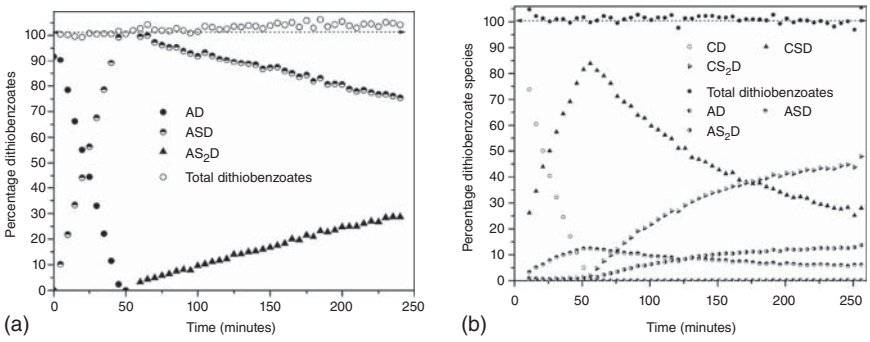

Figure 5.3 (a) Relative concentrations of methyl protons of dithiobenzoate species vs. time in the radical polymerization of styrene in the presence of cyanoisopropyl dithiobenzoate using AIBN as an initiator at 70 °C. The reaction mixture includes 3.56×10^{-3} mol of C_6D_6, 6.75×10^{-5} mol of AIBN, 2.40×10^{-3} mol of styrene, 4.84×10^{-4} mol of 2-cyanoprop-2-yl dithiobenzoate. Source: Taken from McLeary et al. [50]. © 2004, Royal Society of Chemistry. (b) Relative concentrations of the methyl protons of the dithiobenzoate species vs. time in the radical polymerization of styrene in the presence of 2-phenylprop-2-yl dithiobenzoate using azobis(isobutyronitrile) as an initiator at 84 °C. The reaction mixture includes 2.99×10^{-3} mol of C_6D_6, 6.30×10^{-5} mol of azobis(isobutyronitrile), 2.46×10^{-3} mol of styrene, and 3.68×10^{-4} mol of cumyl dithiobenzoate. Source: Taken from McLeary et al. [51]. © 2005, American Chemical Society.

In cases where the R group (and the adduct of the R group with a single added monomer group) undergoes rapid reaction with the thiocarbonyl preferentially to propagation, the result is an 'initialization' period in which the predominant species formed is the single monomer unit adduct (Figure 5.3a) [50]. Only after the complete consumption of the initial chain transfer agent will chains with higher degree of polymerization start to form. Initial studies in this area focused on the polymerization of styrene using 2-cyanoprop-2-yl dithiobenzoate as a transfer agent and AIBN as the initiator: in this case, the initiator-derived radicals and expelled radical R are identical ($(CH_3)_2(CN)C\cdot$) [52]. Subsequent work has investigated more complex situations in which the radical R and initiator fragments are distinct (Figure 5.3b) [51]. The same phenomenon, which was called selective initialization, is observed with most monomers when effective RAFT agents are used. Importantly, these phenomena can impact the reaction kinetics, with the process of initialization proposed as an explanation for the inhibition periods observed in certain RAFT polymerizations.

Selective initialization is also observed in the case of both thermally initiated and photo-induced electron/energy transfer (PET)–RAFT of *N,N*-dimethylacrylamide with tertiary cyanoalkyl RAFT agents [53, 54]. In this case, (i) the rate of addition of $R^{\cdot}$ to monomer is rate determining; (ii) $R^{\cdot}$ is a much better homolytic leaving group than the propagating species; and (iii) the transfer constant is such that on average less than one monomer is added per activation cycle. Thus, $R^{\cdot}$ adds to the monomer, but the resulting species $RM^{\cdot}$ immediately reacts with the initial RAFT agent to expel $R^{\cdot}$. As soon as the initial RAFT agent is consumed, polymerization accelerates dramatically.

5.2.5 R Group Stability and Implications for Chain Transfer Kinetics

Changes to the R group that occur on storage may alter the chemical identity of the agent and therefore the C_{tr}, and thus lead to significantly poorer performance in mediating polymerization. Fuchs and Thurecht recently observed that RAFT agents in which the R group includes both a nitrile moiety and carboxylic acid may hydrolyse on storage, resulting in conversion of the nitrile to an amide moiety (Scheme 5.3) [55]. This alteration was accompanied by a significant decrease in C_{tr} (from 16.7 to 2.5 for the dodecyl trithiocarbonate) for polymerization of MMA. This decrease in C_{tr} was accompanied by a concomitant decrease in suitability for controlling MMA polymerization, with the molecular weight distribution (MWD) shown to broaden significantly. As the 4-cyanopentanoic acid R group is frequently employed in RAFT polymerization the potential impact of these reactions cannot be ignored. That being said, the chemistry requires water and our own observations show that the problem of decomposition in storage can be largely avoided by ensuring that the RAFT agent is maintained in a dry state. Additionally, the pathway seems to be less of an issue with the corresponding dithiobenzoate.

5.2.6 Differential Leaving Group Ability and Mechanistic Discrimination

RAFT polymerization can be achieved using a variety of different initiation sources, including thermal autoinitiation of the monomer (e.g. polymerization of styrene at >100 °C) [56], addition of a thermally labile initiator such as an azo-initiator or organic peroxide [28], redox initiation [57], or by applying ionizing radiation either with [58] or without [59] an added photoinitiator. Interestingly, early reports on the application of thiocarbonylthio compounds to control polymerization under ionizing radiation (e.g. γ radiation or ultraviolet radiation) attributed the observed behaviour to differing mechanisms. Specifically, the observed behaviour was attributed to either (i) a photoiniferter mechanism in which the radiation causes homolytic cleavage of the C—S bond, liberating the thiocarbonylthiyl radical, which reversibly terminates the propagating polymer chains [60, 61]; or (ii) a RAFT mechanism analogous to that operative with thermal initiation [62]. In order to discriminate between the two mechanisms, Quinn et al. applied a methodology that exploited the differing leaving group ability of 1-phenylethyl and 2-cyanoprop-2-yl groups with respect to polymethacrylyl radicals [63]. Under a photoiniferter mechanism, both 1-phenylethyl and 2-cyanoprop-2-yl dithiobenzoates ought to show living radical behaviour, as both the 1-phenylethyl and 2-cyanoprop-2-yl groups would initiate the polymerization of MMA upon cleavage of the C—S bond, thus yielding propagating polymer chains that could be reversibly terminated by the thiocarbonylthiyl radicals. On the other hand, where a RAFT mechanism is operative only the 2-cyanoprop-2-yl dithiobenzoate ought to show living behaviour with MMA, as the 1-phenylethyl dithiobenzoate would not undergo sufficient chain transfer to have all chains initiated concurrently (see Figure 5.4a). This methodology was applied to both γ-initiated and UV-initiated polymerization and, in both cases,

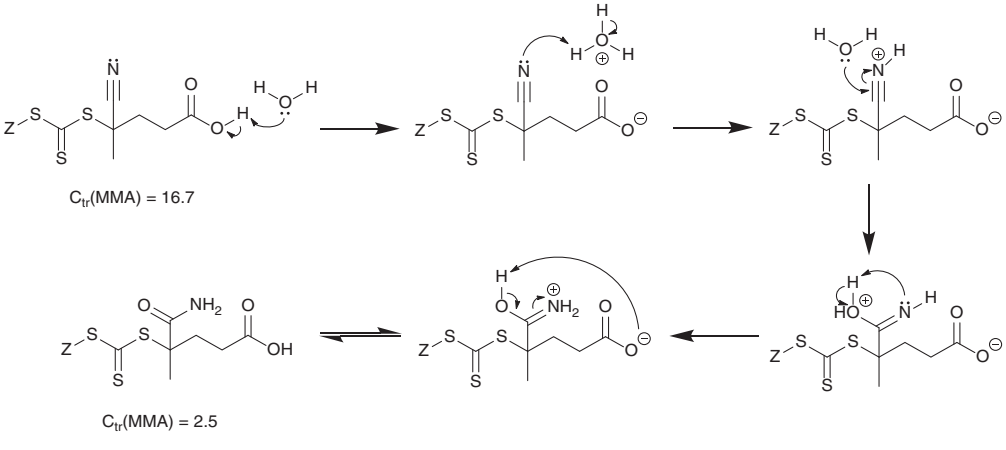

Scheme 5.3 Proposed acid-catalysed cyano-hydrolysis mechanism for 4-cyanopentanoic acid dodecyltrithiocarbonate. Source: Adapted from Fuchs et al. [55]. © American Chemical Society.

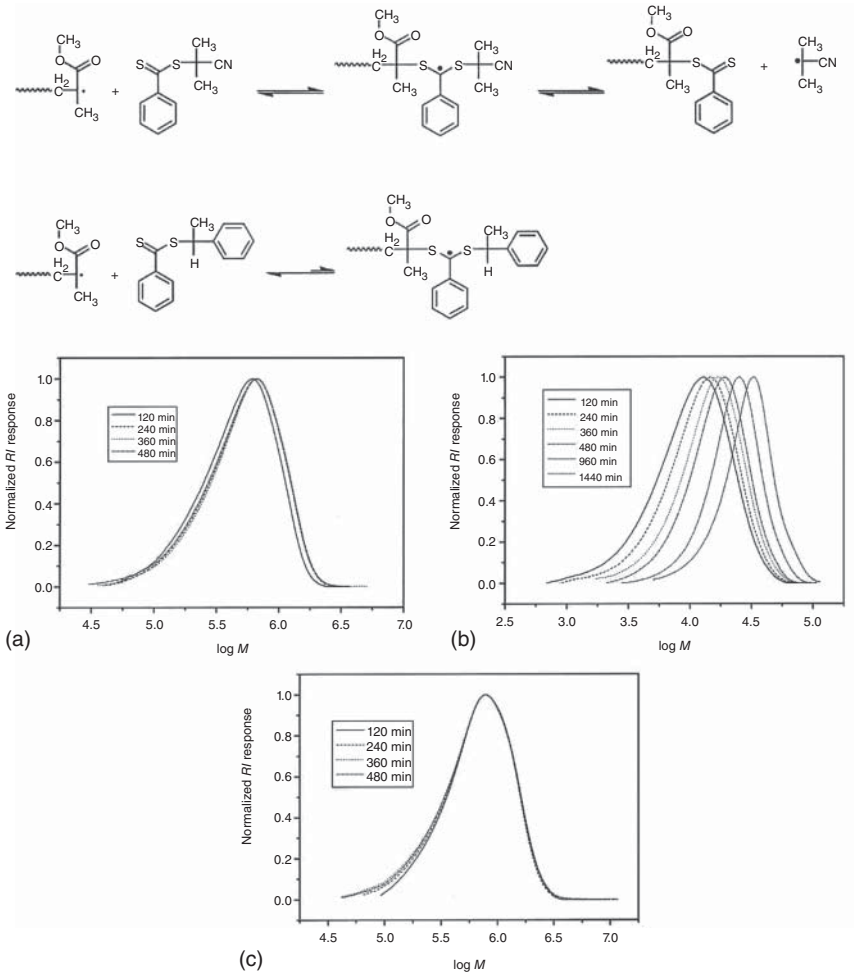

Figure 5.4 (a) Initial chain transfer reaction for RAFT polymerization of MMA using dithiobenzoates with either 2-cyanoprop-2-yl or 1-phenylethyl groups, showing the impact of leaving group ability on the initial chain transfer step. (b) Evolution of molecular weight distribution with time for the polymerization of methyl methacrylate at $T = 23\,^{\circ}C$ mediated with a 1-phenylethyl dithiobenzoate ([PEDB] = 8.2 mmol l^{-1}), (b) 2-cyanoprop-2-yl dithiobenzoate ([CPDB] = 8.1 mmol l^{-1}), and (c) dibenzyl trithiocarbonate ([DBTC] = 7.6 mmol l^{-1}). Source: Adapted from Quinn et al. [63]. © Wiley Periodicals, Inc.

it was demonstrated that the principal mechanism behind the observed living behaviour was RAFT rather than reversible termination (see Figure 5.4b for an example of gamma-initiated living polymerization). These studies demonstrate that by exploiting the inherent consequences of an operative RAFT mechanism, it is possible to discriminate between conflicting explanations of living behaviour under ionizing radiation.

5.3 Role of the Z Group

5.3.1 The Z Group and Radical Addition to the Thiocarbonyl

The principal role of the Z group in RAFT polymerization is to dictate the reactivity of the thiocarbonyl group toward propagating polymer radicals. As such, it is essential that the Z group is properly chosen for the particular monomer being polymerized. Representative Z-groups, and some of the classes of monomer for which they are suitable, are given in Table 5.3.

Early research by Moad and coworkers examined the suitability of a series of thiocarbonylthio compounds for mediating the polymerization of styrene thermally initiated at 110 °C [88]. The series in question (Scheme 5.4) employed benzyl R groups, which were previously shown to be a satisfactory homolytic leaving group for mediating the polymerization of styrene. It was demonstrated that those agents

Table 5.3 Main classes of transfer agents suitable for RAFT polymerization and example monomers.

Class	General structure	Examples	Suitable monomers
Dithioester		Z_1 = Ph, naphthyl, phenanthryl, CH_3, CH_2Ph, substituted Ph	Styrene [64] Acrylates [65] Methacrylates [66] Acrylamides [67] Methacrylamides [68] Acrylonitrile [69] Vinylpyridine [70]
Trithiocarbonates		Z_1 = CH_3, $(CH_2)_nCH_3$ CH_2Ph, $(CH_2)_nCOOH$	Styrenics [71] Acrylates [72] Methacrylates [73] Acrylamides [74] Methacrylamides [75] Acrylonitrile [76]
Dithiocarbamates		Z_1 = Z_2 = CH_2CH_3, Ph, Z_1–Z_2 = pyrrolo, phthalimido, pyrrolidono	Styrenics [77] Acrylates [78] Methacrylates [79] Acrylamides [80] Vinyl esters [81] *N*-vinyl pyrrolidone [82]
Xanthates		Z_1 = CH_2CH_3, Ph	Styrene [83] Acrylates [84] Acrylamides [85] Vinyl esters [86] *N*-vinyl pyrrolidone [87]

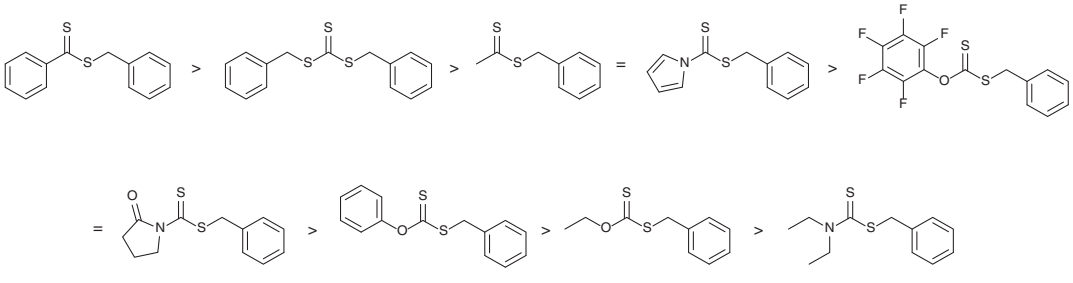

Scheme 5.4 Order of chain transfer efficiency for various thiocarbonylthio compounds with benzylic leaving groups. The presented order reflects the C_{tr} measured in polymerization of styrene at 110 °C. Source: Data from Chiefari et al. [88]. © American Chemical Society.

for which zwitterionic canonical forms were possible (i.e. alkyl xanthates and *N,N*-dialkyldithiocarbamates; see Scheme 5.5) demonstrated the least favourable chain transfer kinetics in styrene polymerization. This was attributed to the interaction of the lone pair on the N or O with the thiocarbonyl, reducing the double bond character of the C=S and increasing the lowest unoccupied molecular orbital (LUMO) (and highest occupied molecular orbital [HOMO]). These factors were considered to reduce the reactivity of the thiocarbonyl toward radical addition. Importantly, the introduction of substituents that can delocalize the electrons on the N (and therefore restore the double bond character to the thiocarbonyl) can result in effective RAFT agents for styrene polymerization. Examples include dithiocarbamates incorporating pyrrolo, pyrridinolo, and phenyl substituents.

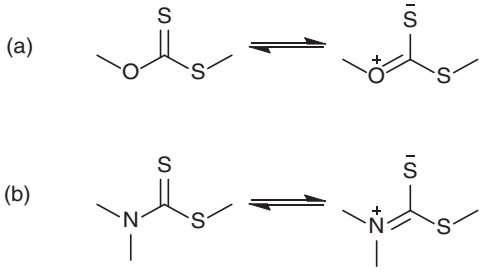

Scheme 5.5 Zwitterionic canonical forms of (a) xanthates and (b) *N,N*-dialkyldithiocarbamates. Source: Adapted from Chiefari et al. [88]. © American Chemical Society.

5.3.2 The Z-Group and Side Reactions

Although not effective as RAFT agents for the polymerization of styrene and other more activated monomers (MAMs) (such as methacrylates), *O*-alkyl xanthates and *N*,*N*-dialkylcarbamates have been shown to be highly effective at mediating the polymerization of vinyl acetate. This is because the reactivity of the thiocarbonyl is suitable for the highly reactive propagating poly(vinyl acetate) radical, and the requisite fragmentation reaction is also suitably facile. In a recent innovation, Monteil and coworkers have demonstrated the application of certain *O*-alkyl xanthates in the polymerization of ethylene via a RAFT process [89]. By employing a suitable combination of solvent (dimethyl carbonate, DMC) and pressure (200 bar), these authors were able to prepare polyethylene with defined molecular weight and end-groups from which chain extension was possible. In this case, so-called side fragmentation was possible. Specifically, a proportion of the fragmentation occurs at the O–CH_2 yielding a polymer that incorporates a mid-chain backbone carbonyl (Scheme 5.6). Of course, these carbonyls are not active to radical addition and as such the chains formed via side fragmentation are no longer able to propagate, resulting in the so-called dead chains.

Importantly, the level of side fragmentation can be significantly reduced by employing an aromatic xanthate (methyl 2-(phenoxycarbonothioylthio)acetate) instead of an alkyl xanthate (Figure 5.5a) [90]. However, these agents induced

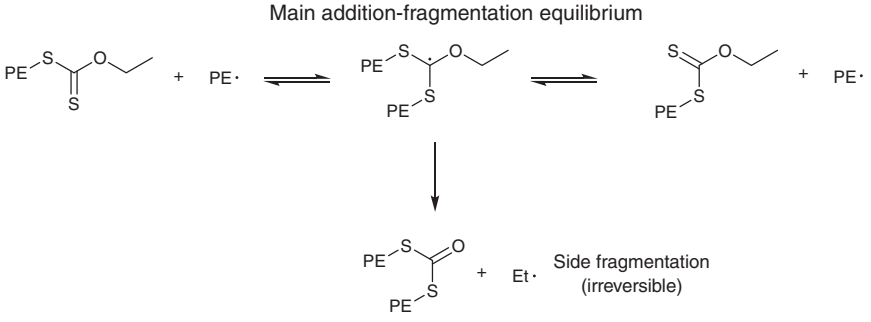

Scheme 5.6 Side fragmentation in the RAFT-mediated polymerization of ethylene using *O*-alkyl xanthates. Source: Adapted from Dommanget et al. [89]. © Wiley Periodicals, Inc.

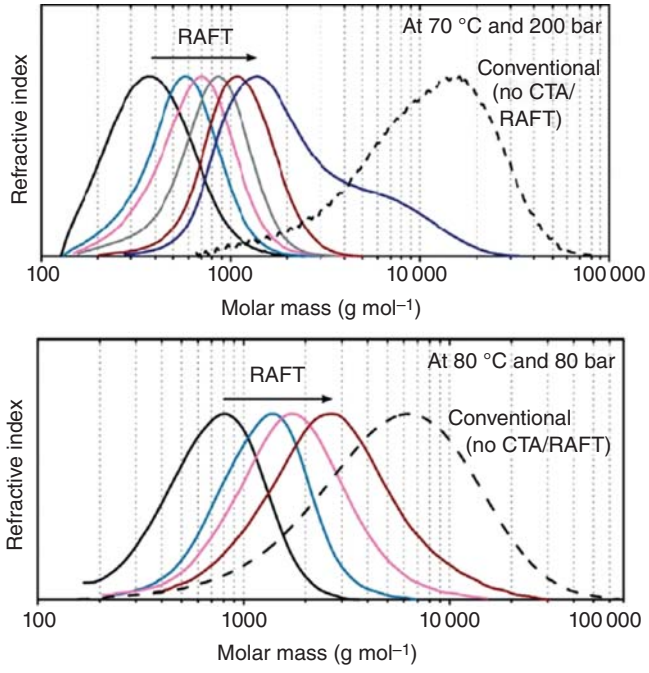

Figure 5.5 (a) Molecular weight distributions of polyethylene produced in a conventional system (no CTA/RAFT) after one hour and in the presence of methyl 2-(phenoxycarbonothioylthio)acetate after one, two, three, four, five, and six hours. At six hours, the appearance of a high molecular weight species can be observed. (b) Molecular weight distributions of polyethylene produced in a conventional system (no CTA/RAFT) after four hours and in the presence of methyl 2-(4-methoxyphenoxycarbonothioylthio)acetate after 2, 4, 7, and 16 hours. Source: Taken from Wolpers et al. [90]. © Wiley Periodicals, Inc.

significant retardation to the polymerization, attributed to cross-termination of the intermediate radical with a propagating polyethyl radical. Moreover, there is a significant proportion of material formed with high molecular weight, which the authors attributed to the occurrence of conventional radical (i.e. non-RAFT) polymerization. This was postulated to occur as a result of the dispersion behaviour of the formed polymer in supercritical DMC. As a result, the formation of dead polymer is not avoided by this structural adjustment. Interestingly, the authors were able to significantly reduce the proportion of high molecular weight material by lowering the pressure at which the polymerization was conducted from 200 to 80 bar (Figure 5.5b). Moreover, RAFT polymerization of polyethylene could also be achieved with a high degree of livingness by employing various dithiocarbamates as the chain transfer agent. Although the molecular weight distributions achieved were relatively broad ($Đ > 1.5$), the preservation of chain end functionality for polyethylene (PE) synthesized using the dithiocarbamates was superior to both alkyl and aromatic xanthates. These results demonstrate that the quest for low dispersity does not necessarily lead to the best outcome: in this case, the higher dispersity PE with higher chain end fidelity will be more useful for the preparation of subsequent block copolymers than lower dispersity PE with compromised chain end fidelity.

5.3.3 Manipulating Z to Dictate Reactivity: 'Switchable' RAFT Agents

The need to employ different RAFT agents for less activated monomers (LAMs) and more activated monomers (MAMs) has motivated the development of the so-called switchable RAFT agents that can be used to prepare block copolymers incorporating segments of polymerized LAM and MAM (polyMAM-*block*-polyLAM). As noted above, the zwitterionic canonical forms of *N,N*-dialkyldithiocarbamates have been associated with the unsuitability of those RAFT agents for the polymerization of MAMs. In order to abolish the zwitterionic character of the canonical form and hence retain the double bond character of the thiocarbonyl, Benaglia et al. proposed the preparation of a series of *N*-(4-pyridinyl)-*N*-methyldithiocarbamates that can be protonated via the pyridinyl group (Scheme 5.7) [91]. Protonation via a stoichiometric amount of a strong acid (such as trifluoromethanesulfonic acid or 4-toluenesulfonic acid) leads to a non-zwitterionic canonical form and hence suitability of the agent for polymerization of MAMs such as styrene, MMA, and MA (depending on the nature of the R group employed). By adding a stoichiometric amount of a base such as *N,N*-dimethylaminopyridine the protonation is reversed, restoring the zwitterionic character of the canonical form and rendering the agent suitable for polymerization of LAMs. By using this methodology, poly(MMA)-*block*-poly(VAc) and poly(methyl acrylate [MA])-*block*-(*N*-vinyl carbazole [NVC]) were successfully synthesized. Subsequent investigations have extended this approach to include poly(MAM)-*block*-poly(LAM) examples such as polystyrene (PS)-*block*-poly(VAc) [92], poly(DMAm)-*block*-poly(NVC) [93], poly (DMAm)-*block*-poly(VAc), poly(DMAm)-*block*-poly(*N*-vinyl pyrrolidone [NVP]), and more sophisticated structures such as PS-*block*-poly(MA)-*block*-poly(VAc) and

PS-*block*-poly(MA-*grad*-VAc)-*block*-poly(VAc). Importantly, the reactivity of these agents to radical addition can be modulated via variation of the non-pyridinyl N substituent, thereby enabling application of these agents with a wide variety of different monomers.

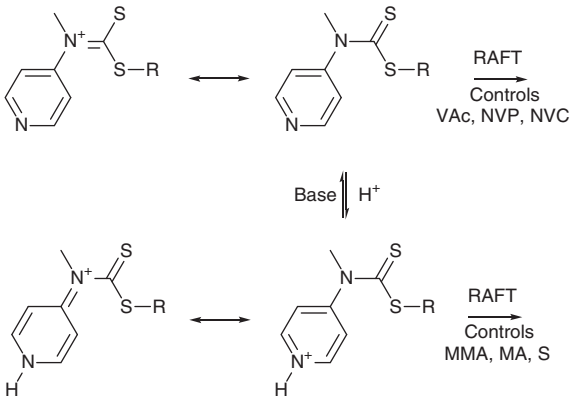

Scheme 5.7 Application of *N*-(4-pyridinyl)-*N*-methyldithiocarbamates for RAFT polymerization of LAMs and MAMs. Source: Adapted from Benaglia et al. [91]. © American Chemical Society.

Gardiner and coworkers have reported an alternative family of dithiocarbamates wherein the reactivity is broadly similar to that of protonated *N*-(4-pyridinyl)-*N*-methyldithiocarbamates (Scheme 5.8) [94]. Specifically, 3,5-dimethyl-1*H*-pyrazole-1-carbodithioates were applied successfully in the polymerization of *N,N*-dimethylacrylamide, methyl acrylate, methyl methacrylate, styrene, and vinyl acetate. Except for MMA, $Đ < 1.2$ was attainable provided that the R group was chosen appropriately for the monomer under study. In comparison to *N*-(4-pyridinyl)-*N*-methyldithiocarbamates, 3,5-dimethyl-1*H*-pyrazole-1-carbodithioates gave greater retardation in the polymerization of vinyl acetate, which was attributed to the stability of the intermediate formed by addition to the RAFT agent, and the consequent effect on side reactions involving that radical. The higher dispersities observed in the polymerization of MMA ($Đ > 1.4$) were indicative of a relatively low value of C_{tr} for the tertiary 3,5-dimethyl-1*H*-pyrazole-1-carbodithioates employed at 100 °C ($C_{tr} \approx 3.7$). As noted earlier, low dispersities (e.g. $Đ < 1.1$ with X_n of 150 at 75% conversion) would require a C_{tr} of >20. 3,5-Dimethyl-1*H*-pyrazole-1-carbodithioates were also deployed in the copolymerization of MMA with styrene and DMA. Provided there was sufficient comonomer present in the system the dispersities achieved were lower than the corresponding homopolymerizations using MMA. While *N*-(4-pyridinyl)-*N*-methyldithiocarbamates require protonation or deprotonation of the pyridyl group in order to facilitate preparations of block copolymers of LAMs and MAMs, 3,5-dimethyl-1*H*-pyrazole-1-carbodithioates could be used successfully without the need to alter the solution pH. Specifically, poly(DMA) macromolecular chain transfer agent was successfully employed to prepared a block copolymer

with VAc, with relatively low dispersities observed where the ratio of VAc to DMA units in the macroCTA was 1 : 1 ($Đ < 1.3$: higher dispersity was observed when the amount of VAc was increased). Importantly, in this series of experiments the blocks prepared are more appropriately described as quasi-blocks, as the initial macroCTA was not purified before chain extension. As such, the second block is strictly a copolymer. Nevertheless, the resulting MWDs are essentially monomodal with limited evidence of terminated product or high molecular weight PVAc (Figure 5.6). Importantly, whether by the use of 3,5-dimethyl-1*H*-pyrazole-1-carbodithioates or *N*-(4-pyridinyl)-*N*-methyldithiocarbamates, the use of RAFT enables the preparation of sophisticated block structures that are not readily accessible via other reversible deactivation radical polymerization (RDRP) techniques such as nitroxide-mediated polymerization or atom transfer radical polymerization, highlighting the utility of RAFT polymerization. Moreover, the development of these agents highlights how mechanistic insights can drive judicious design of transfer agent structure.

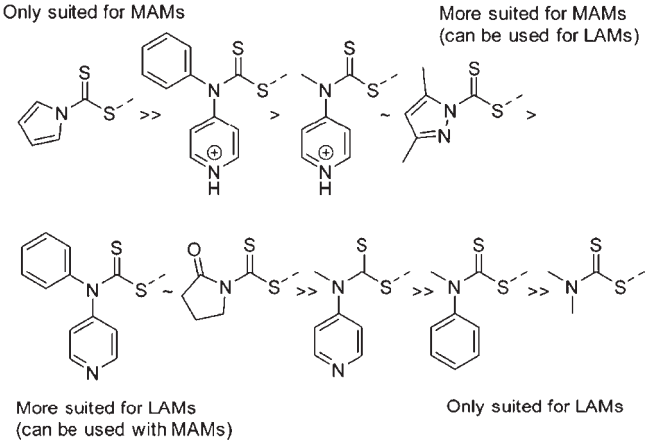

Scheme 5.8 Relative activity of dithiocarbamate 'ZC(=S)S−' groups in RAFT polymerization. MAM − more activated monomer, LAM − less activated monomer. Source: Taken from Gardiner et al. [94]. © Royal Society of Chemistry.

5.3.4 The Z-Group and Reaction Kinetics

RAFT agents in which the Z-group is phenyl (i.e. dithiobenzoates) have been associated with significant kinetic effects. For example, such agents have been observed to cause significant inhibition of polymerization [95], particularly at lower temperatures [96]. Moreover, the polymerization of styrene has been shown to proceed with a rather reduced rate relative to the homopolymerization of styrene under equivalent conditions in the absence of a RAFT agent. Such rate retardation has also been observed in the polymerization of (meth)acrylates [97] and (meth)acrylamides [98]. Based on initial investigations into the polymerization of styrene in the presence of various dithiobenzoates, Monteiro and de Brouwer [99] and Barner-Kowollik

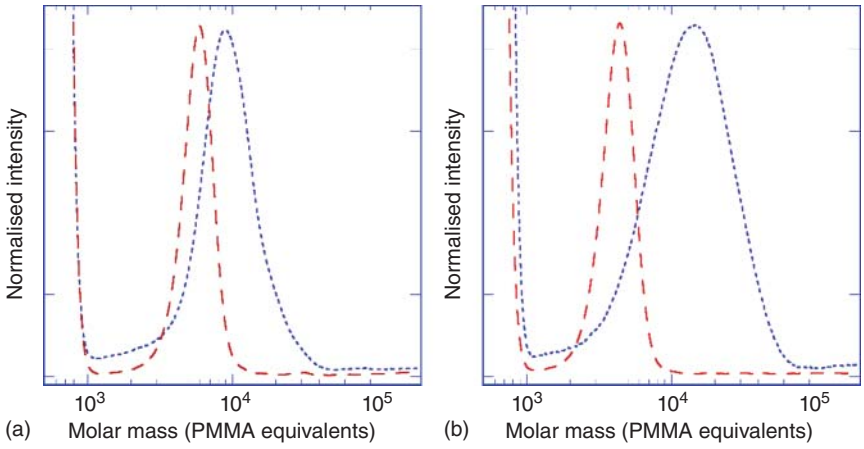

Figure 5.6 Molecular weight distributions for poly(*N,N*-dimethylacrylamide) macro-RAFT agent prepared with (a) 2-cyanobutanyl-2-yl 3,5-dimethyl-1*H*-pyrazole-1-carbodithioate or (b) cyanomethyl (3,5-dimethyl-1*H*-pyrazole)-carbodithioate (— —) and the derived poly(*N,N*-dimethylacrylamide)-*block*-poly(vinyl acetate) (- - - -). The large peak with apparent molar mass < 10^3 poly(MMA) equivalents is a 'salt peak' associated with the LiBr/DMAc SEC eluent. Source: Taken from Gardiner et al. [94]. © Royal Society of Chemistry.

et al. [100] postulated explanations for these observed phenomena, both employing simulations to support the observed evolution of conversion with time. Specifically, Monteiro and de Brouwer postulated that rate retardation could be attributed to termination of the intermediate radical formed during chain equilibration, while Barner-Kowollik et al. suggested that slow fragmentation of the intermediate radical was a suitable explanation. These initial studies on the topic precipitated a substantial subsequent work aimed at elucidating not only the origins of rate retardation observed in the dithiobenzoate-mediated polymerization of styrene, but also the phenomenon of rate retardation in RAFT polymerization more generally. Given that dithiobenzoates are important agents for mediating the polymerization of various monomers and typically give rise to very low dispersities, there was substantial motivation for understanding the origin of these effects, leading to the establishment of an IUPAC working group in 2005 'Towards a Holistic Mechanistic Model for RAFT Polymerizations: Dithiobenzoates as Mediating Agents', which published a situation paper in 2006 [101] and an update in 2014 [102]. Although retardation has primarily been associated with the Z group, it is important to remember that – as noted above – improper choice of the R group may also lead to significant kinetic effects including inhibition. Moreover, such R group originating kinetic effects can be potentially exacerbated by the use of dithiobenzoates (i.e. Z = Ph).

5.3.5 Intermediate Radical Termination

In their initial report, Monteiro and de Brouwer observed a concentration-dependent decrease in the overall rate of reaction when methyl 2-methyl-2-((phenylcarbonothioyl)thio)propanoate was added to mediate the polymerization of styrene

initiated by AIBN at 80 °C. They postulated that the loss of intermediate radicals via termination with another radical species (Scheme 5.9) was a possible reason for the observed retardation.

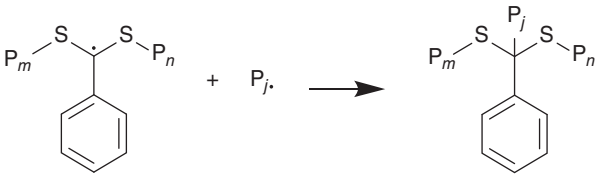

Scheme 5.9 Intermediate radical termination as proposed by Monteiro and de Brouwer [99]. Source: Modified from Monteiro and de Brouwer [99].

Application of the intermediate radical termination model enabled simulation of experimental conversion–time data for styrene polymerization in toluene at 80 °C initiated using AIBN. Good agreement was obtained between the simulated and experimental data, and the simulated intermediate radical concentrations for this system are consistent with those measured previously by the CSIRO group, once allowance is made for the different reaction conditions and temperature [103]. Previous work from Monteiro's laboratory demonstrated that irradiation of a dithiobenzoate-terminated polymer with ultraviolet radiation could lead to a proportion of the sample trebling in molecular weight, an observation consistent with possible reaction of the intermediate radical with another polymeric radical [104]. The general feasibility of such a reaction was firmly established in a model system using polystyryl bromide and polystyryl dithiobenzoate, wherein the polystyryl radical was produced from PSt–Br by the catalytic reaction of a CuBr/Me_6TREN complex [105]. Subsequent studies by Kwak et al. examined the reaction between 1-phenylethyl dithiobenzoate and 1-phenylethyl bromide and demonstrated that, in addition to bimolecular coupling at the bis-thiosubstituted benzylic carbon, reaction was also possible at the ortho and para positions on the phenyl ring (Scheme 5.10) [106]. Moreover, the structures formed were shown to be stable at both 60 and 100 °C for 24 hours, indicating that the reaction is likely to be essentially irreversible at polymerization temperatures.

Despite these findings, attempts to identify the three-armed star formed by bimolecular intermediate radical termination *in a polymerizing system* either spectroscopically or chromatographically have generally been unsuccessful [107, 108]. If intermediate termination is potentially operational, the quantity of the generated star polymer should exceed the amount of conventionally terminated polymer by at least 1 order of magnitude, as the intermediate radical concentration exceeds the propagating species concentration under both the fast and slow fragmentation scenarios substantially [107]. Such quantities of three-armed star polymers have never been identified. To address this, a number of solutions have been proposed to demonstrate why the terminated intermediate radical may not necessarily be identified.

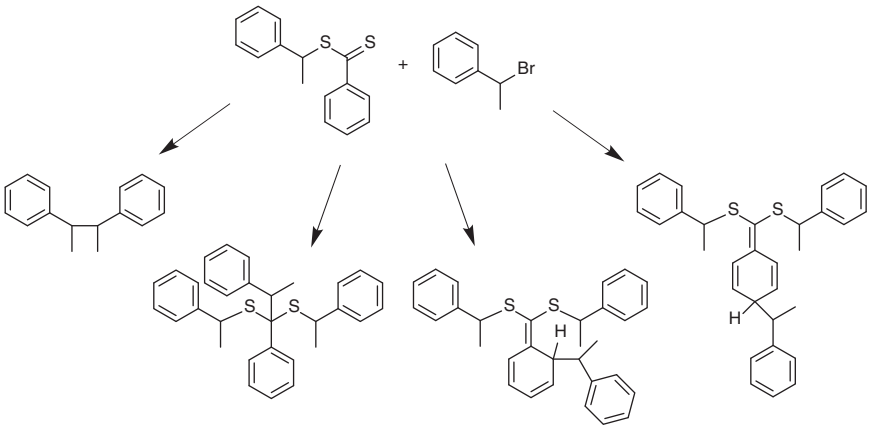

Scheme 5.10 Model compounds prepared in the study of Kwak et al. [106] demonstrating that radical reactions with the RAFT intermediate can potentially occur at the ortho and para positions of the phenyl ring of the dithiobenzoate. Source: Modified from Kwak et al. [106].

Vana and Buback proposed that the three-armed star formed via intermediate radical termination might itself be reactive, resulting in re-liberation of the intermediate radical and dead polymer, which is essentially analogous to that formed via termination of propagating chains (Scheme 5.11) [109]. Inclusion of this so-called 'missing step' enables simulation of conversion–time profiles that

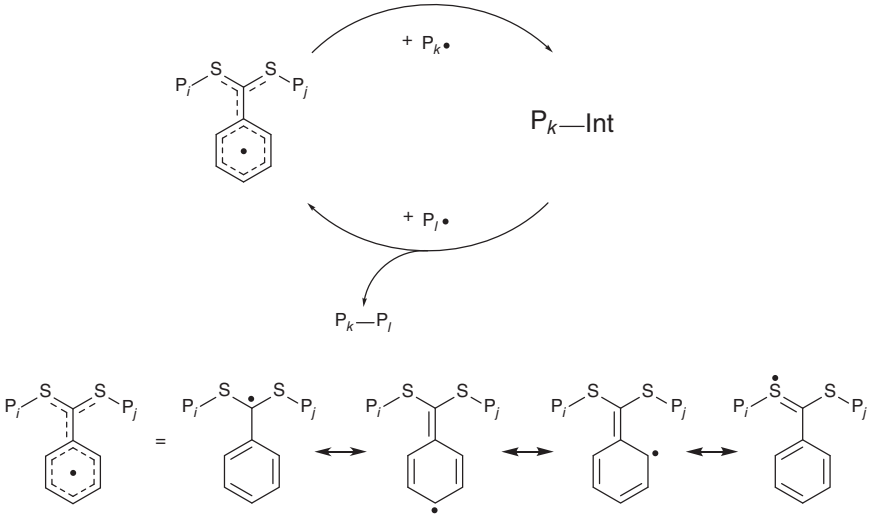

Scheme 5.11 (a) Reaction of the three-armed star formed via intermediate radical termination with a propagating radical: the so-called 'missing step' of the RAFT mechanism. (b) Resonance structures of the intermediate radical formed when polymerization is mediated with a dithiobenzoate. Source: Adapted from Buback and Vana [109]. © Wiley Periodicals, Inc.

show concentration-dependent rate retardation, but which also give intermediate radical concentrations consistent with those observed experimentally. Subsequent investigations using (i) 1-phenylethyl dithiobenzoate and a source of 1-phenylethyl radicals [110] and (ii) 2-cyanoprop-2-yl dithiobenzoate and AIBN [111] have demonstrated the experimental feasibility of these reactions.

An alternative explanation for the absence of obvious three-armed star fractions in systems where there is significant retardation was proposed by Konkolewicz et al. [112]. This proposal suggests that to the extent that intermediate radical termination

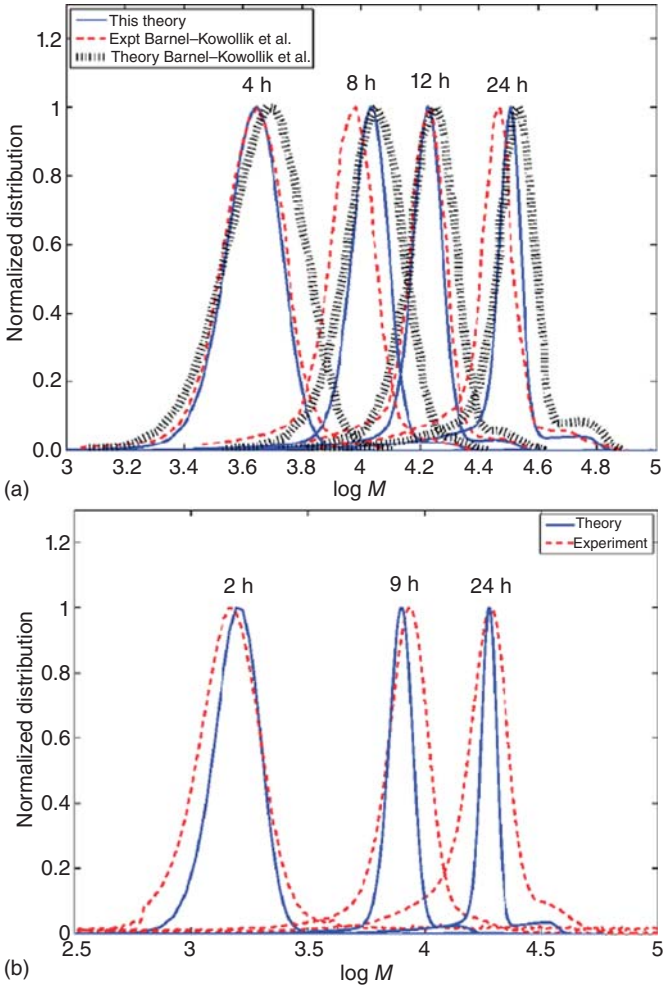

Figure 5.7 (a) Comparison between the molecular weight distributions suggested by the theory of Konkolewicz et al. and the experimental molecular weight distribution of Barner-Kowollik et al. for 2-phenylprop-2-yl dithiobenzoate. (b) Comparison between the theoretical and experimental molecular weight distributions for [CPDB] = 1.42×10^{-2} mol/l with samples taken at 2, 9, and 24 hours. Source: Taken from Konkolewicz et al. [112].

occurs, it does so primarily via termination with short radicals (i.e. with initiator fragments or oligomeric chains wherein the number of added monomer units is two or less) [113]. Implementation of this model enabled accurate prediction of the conversion, molecular weight, and dispersity as a function of time (Figure 5.7). Moreover, the low molecular weight of the species reacting with the intermediate radical means that there was no appreciable formation of polymer with triple the molecular weight of the main population, and hence the model was able to rationalize the failure to identify and isolate appreciable quantities of the three-armed star expected via intermediate radical termination.

Subsequently, Ting et al. tested the hypothesis of Konkolewicz et al. by employing a macromolecular initiator and macromolecular chain transfer agent (polystyryl dithiobenzoate) in the polymerization of styrene [114]. In this system there were no short radicals present, and hence if there is validity to the explanation of Konkolewicz et al. then a wholly macromolecular system should exhibit diminished retardation compared to one in which short chains are introduced (e.g. via a conventional azo-initiator). This was indeed the case, at least up to approximately 40% conversion, after which there was minimal difference in the rate of polymerization between the macromolecular and small molecule initiators (Figure 5.8). As such these experiments provide a level of confirmation for Konkolewicz's model, although the discrepancy at higher conversions indicates that there is still more to learn in order to develop a complete understanding of rate retardation in dithiobenzoate-mediated polymerization.

5.3.6 Slow Fragmentation of the Intermediate Radical

Slow fragmentation of the intermediate radical has also been proposed as the origin of rate retardation in dithiobenzoate-mediated polymerization [100, 115]. Under this explanation, β-scission of the intermediate is sufficiently slow as to effectively provide a radical sink, reducing the propagating radical concentration and thus leading to a reduced rate of polymerization. While a slow fragmentation model was successfully employed to model the evolution of conversion, molecular weight, and

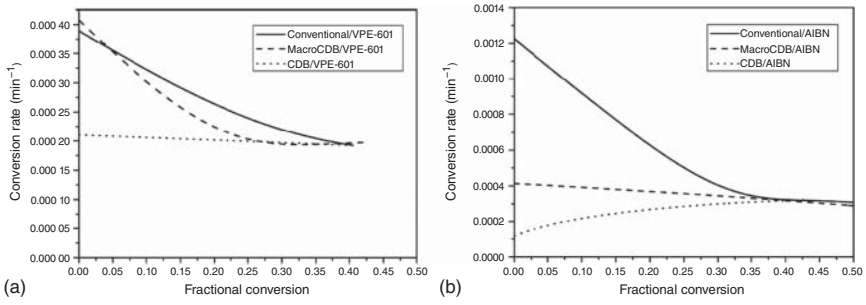

Figure 5.8 Styrene conversion rates (min^{-1}) vs. fractional conversion for the systems (a) VPE-601, macroCDB/VPE-601, and CDB/VPE-601 and (b) AIBN, macroCDB/AIBN, and CDB/AIBN at [St]/[RAFT agent] = 1226 (except when RAFT agent is not present). Source: Taken from Ting et al. [114]. © 2011, American Chemical Society.

dispersity as a function of time, the predicted concentrations of the intermediate radical greatly exceed those that have been measured via EPR [97, 116]. Nevertheless, despite these differences in the observed intermediate radical concentrations, there have been a number of experiments and calculations that support the slow fragmentation hypothesis. For example, Coote et al. have computed equilibrium coefficients ($K = k_{\mathrm{addR}}/k_{-\mathrm{addR}}$) for 2-cyanoprop-2-yl dithiobenzoate-mediated polymerization that were consistent with potential rate retardation via slow fragmentation [117], although these values were substantially higher than those determined previously by McLeary et al. [118] Klumperman and coworkers found a similar value of K as Coote et al. within 1 order of magnitude (i.e. 10^4 vs. 10^5) and suggested that perhaps the slow fragmentation and intermediate radical termination explanations were not as irreconcilable as had been previously claimed. Nevertheless, these high values of K are still in contrast to EPR determinations by Meiser and Buback, and as such the need for further mechanistic elucidation remains [119, 120].

In addition to the theoretical calculations in support of slow fragmentation, Davis and coworkers conducted an interesting 'radical storage' experiment to demonstrate the existence of a long-lived radical sink in the 2-phenylprop-2-yl dithiobenzoate-mediated polymerization of styrene (Figure 5.9a) [121]. In this case, a solution of the transfer agent in styrene was irradiated at ambient temperature with γ-radiation for 18 hours, and then isolated from the γ-source for a predetermined 'waiting' period of 10–60 minutes. The solution was then heated to 60 °C for 22 hours. In contrast to control samples that were not irradiated, all irradiated samples (regardless of the waiting time) polymerized when heated to 60 °C to conversions between 5% and 6%. Moreover, a sample of pure styrene (i.e. without any added chain transfer agent) polymerized to less than 2%. Taken together, these results are highly suggestive of a hidden radical sink in the dithiobenzoate/styrene system. Moreover, kinetic simulation using the commercial Predici® simulation package indicated that by using the intermediate radical termination model as the exclusive source of rate retardation there should be no radical sink in the system (unless one of the formed species is in fact reversible) (Figure 5.9b): this stands in contrast to the slow fragmentation model where the radical concentration decreases more slowly (Figure 5.9c). These results cannot be reconciled with the work of Kwak et al. (see Section 5.3.5), who demonstrated that model low molecular weight stars formed via 1-phenylethyl dithiobenzoate are chemically inert at 60 °C. As such, there are clearly peculiarities of the 2-phenylprop-2-yl system that remain unelucidated.

The experimental evidence thus shows that intermediate radical termination can, in principle, be operational and is favoured by slow fragmentation. Undoubtedly, fragmentation of dithiobenzoate-derived intermediates is slow compared to other RAFT intermediate radicals – with equilibrium constants up to 10^4–10^5 depending on the type of equilibrium, with possibly lower equilibrium constants for the main equilibrium driven by the fact that the fragmentation rate of polymer chains with defined cleave points is strongly entropic and thus chain length dependent, as established by Barner-Kowollik et al. [122] Further, it is this sluggish fragmentation that enhances the chances of intermediate radical termination reactions [99].

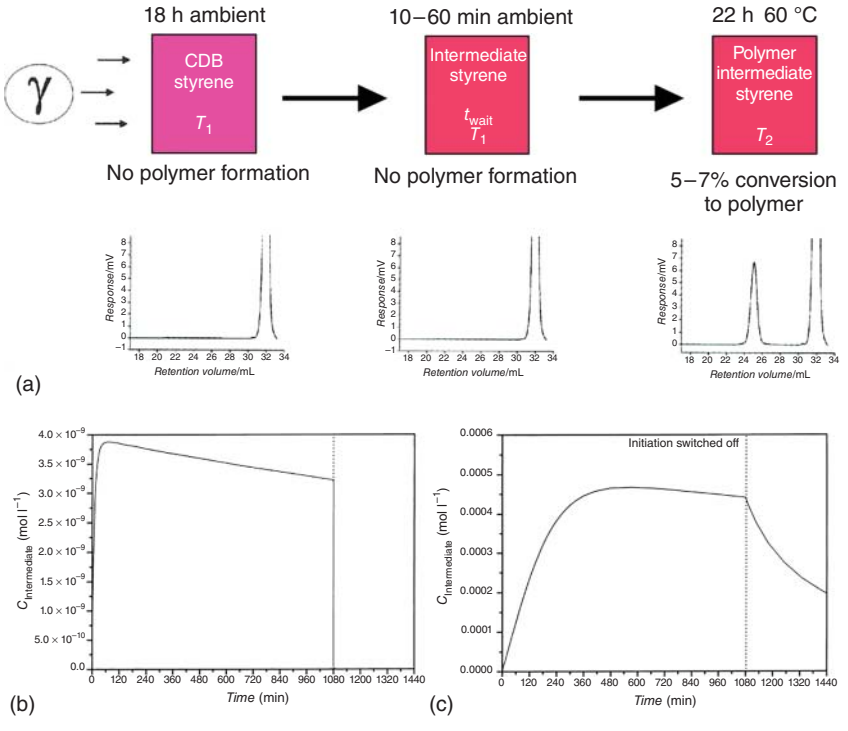

Figure 5.9 (a) Experimental procedure used to probe 2-phenylprop-2-yl dithiobenzoate-mediated styrene polymerizations for the formation of intermediate species. The lower part of the scheme gives examples of molecular weight distributions typical for each sequence step (the large peak at 32 minutes is due to monomer in the reaction mixture). These clearly demonstrate the absence or presence of a polymer peak. (b) Simulated intermediate macroRAFT radical concentration vs. time profile for a CDB-mediated styrene bulk polymerization at 60 °C using the RAFT mechanism with irreversible intermediate macroRAFT radical termination. The following set of rate coefficients was used: $k_{tr} = 5 \times 10^5$ l mol^{-1} s^{-1}, $k_t = 1 \times 10^8$ l mol^{-1} s^{-1}, $k_p = 340$ l mol^{-1} s^{-1}, $k_{add} = 4 \times 10^6$ l mol^{-1} s^{-1}, $k_{frag} = 1 \times 10^5$ s^{-1}, and $k_{t,\,intermediate} = 1 \times 10^8$ l mol^{-1} s^{-1}. Initiation by γ-radiation was simulated using decomposition of an initiator with a decomposition rate coefficient of 5.2×10^{-6} s^{-1} and an initial concentration of 3.5×10^{-3} mol l^{-1}. At $t = 18$ hours, this concentration was set to zero to represent removal of the γ-source. (c) Simulated intermediate macroRAFT radical concentration vs. time profile for a CDB-mediated styrene bulk polymerization at 60 °C using the RAFT mechanism without intermediate radical termination and the following set of rate coefficients: $k_{tr} = 3.5 \times 10^5$ l mol^{-1} s^{-1}, $k_t = 4 \times 10^8$ l mol^{-1} s^{-1}, $k_p = 340$ l mol^{-1} s^{-1}, $k_{add} = 5.4 \times 10^5$ l mol^{-1} s^{-1}, and $k_{frag} = 3.3 \times 10^{-2}$ s^{-1}. The dotted line indicates the point in time where the initiation was switched off. Initiation by γ-radiation was simulated by decomposition of an initiator with a decomposition rate coefficient of 5.2×10^{-6} s^{-1} and an initial concentration of 3.5×10^{-3} mol l^{-1}. At $t = 18$ hours, this concentration was set to zero to simulate removal of the γ-source. Source: Adapted from Barner-Kowollik et al. [121]. © Wiley Periodicals, Inc.

As noted above, numerous approaches have been applied to reconcile the slow fragmentation and intermediate radical termination models, including the postulation of reversible intermediate radical termination occurring on the phenyl moiety [109] and termination exclusively via short radicals [112, 113]. While such reactions might support both the observed conversion–time profiles and radical concentrations, observation of the postulated structures spectroscopically or chromatographically remains challenging. It is worth noting that significant rate retardation during RAFT polymerization is principally observed in a limited set of circumstances: the application of relatively slow-propagating monomers with RAFT agents having thiocarbonyl groups that are highly activated to radical addition. In this respect, rate retardation can generally be overcome by selecting a more suitable RAFT agent such as a trithiocarbonate, for which rate retardation is less of an issue.

5.3.7 Stability of the Z Group During Reaction

One of the issues noted in the course of investigating the observed rate retardation in 2-phenylprop-2-yl dithiobenzoate-mediated polymerization of styrene was the potential instability of the RAFT agent, and the resulting presence of degradation products capable of inhibiting and/or retarding polymerization [123]. Specifically, the use of RAFT agent purified via column chromatography was shown to give noticeably different kinetics than that purified via high performance liquid chromatography (HPLC), with the former leading to significantly longer inhibition periods and slower overall rate of polymerization for both styrene and 2-hydroxyethyl methacrylate. Importantly, it was observed that storage of 2-phenylprop-2-yl dithiobenzoate at −20 °C for three months led to a substantial reduction in the rate of polymerization of styrene compared to polymerizations using a RAFT agent that was stored for only one week. These results are significant in that they highlight the sensitivity of RAFT reactions to potential impurities in the chain transfer agent.

In light of these observations regarding the stability of 2-phenylprop-2-yl dithiobenzoate, it is worth considering the potential for degradation of the thiocarbonylthio moiety in the course of a polymerization reaction. Clearly, in order to retain control of the polymerization throughout the duration of the reaction, it is important that the macromolecular chain transfer agent formed is suitably stable in the polymerization medium. This becomes particularly important in the scenario that the polymerization is conducted in a protic solvent such as water, ethanol, or methanol, or wherein the monomer can potentially react with the thiocarbonylthio moiety (e.g. monomers containing a nucleophile). McCormick and coworkers demonstrated the successful polymerization of a number of monomers in water using dithiobenzoates [124–126], illustrating that hydrolysis of these CTAs is sufficiently slow under polymerization conditions to avoid obvious impacts on the molecular weight distribution. One notable exception occurs in the case of acrylamide, which has been demonstrated to be rather pH sensitive [127]. Specifically, these authors observed that when the polymerization was conducted at pH = 7.0 there was a total loss of control, with high molecular weights observed

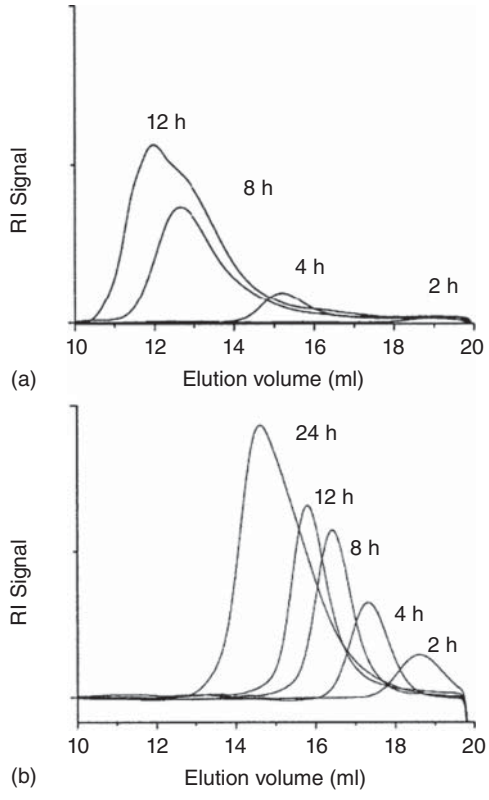

Figure 5.10 (a) Aqueous size exclusion chromatograms (refractive index [RI] detection) for the polymerization of acrylamide at pH = 7 in the presence of sodium 2-(2-thiobenzoyl-sulfonylpropionylamino)ethanesulfonate (STPE). Two hours: no polymer observed; four hours: all colour bleached from reaction medium, M_n = 24 900 g mol^{-1}, $Đ$ = 1.09, conversion = 6%; 8 hours: M_n = 114 000 g mol^{-1}, $Đ$ = 1.87, conversion = 32%; 12 hours: M_n = 239 000 g mol^{-1}, $Đ$ = 2.98, conversion = 70%. (b) Successful RAFT polymerization of acrylamide with STPE in an acetic acid/sodium acetate buffer showing the evolution of molecular weight with time (2 hours: M_n = 5300 g mol^{-1}, $Đ$ = 1.15, conversion = 3%; 4 h: M_n = 9790 g mol^{-1}, $Đ$ = 1.05, conversion = 9%; 8 hours: M_n = 13 700 g mol^{-1}, $Đ$ = 1.04, conversion = 11%; 12 hours: M_n = 18 600 g mol^{-1}, $Đ$ = 1.06, conversion = 18%; 24 hours: M_n = 28 900 g mol^{-1}, $Đ$ = 1.26, conversion = 28%). Source: Adapted with permission from Thomas et al. [127]. © 2003, American Chemical Society.

at polymerization times beyond four hours (Figure 5.10a). This was accompanied by loss of the CTA's characteristic colour, consistent with degradation of the RAFT agent. In contrast, by conducting the polymerization in acetate buffer at pH = 5.0 it was possible to achieve much lower molecular weights, which increased linearly with conversion (Figure 5.10b). The inability to control the polymerization at pH = 7.0 was attributed to hydrolysis of acrylamide under these conditions, liberating ammonia as a by-product. Reaction of the liberated ammonia with the thiocarbonylthio moiety yielded (i) low molecular weight thioamide and (ii) thiol-terminated polymer. The loss of thiocarbonylthio groups abolished

the RAFT equilibrium, leading to high molecular weight polyacrylamide. These results illustrate the possibility of reactions between the solvent and/or monomer interfering with the RAFT process and compromising the observed control over the polymerization. This is particularly important in aqueous systems, although the impact of other protic solvents such as methanol and ethanol cannot be discounted.

In an extension of this study, Thomas et al. predicted the rates of dithiobenzoate end-group hydrolysis for the synthesis of polyacrylamide and poly(sodium 2-acrylamido-2-methylpropanesulfonate) (AMPS), and determined the impact of these reactions on the proportion of living and dead chains across the duration of the polymerization [128]. In the case of acrylamide, hydrolysis of the monomer yielding aqueous ammonia required the additional consideration of aminolysis on the thiocarbonylthio end-group. The proportion of living and dead chains for acrylamide and AMPS are given in Figure 5.11a,b, respectively. The number of

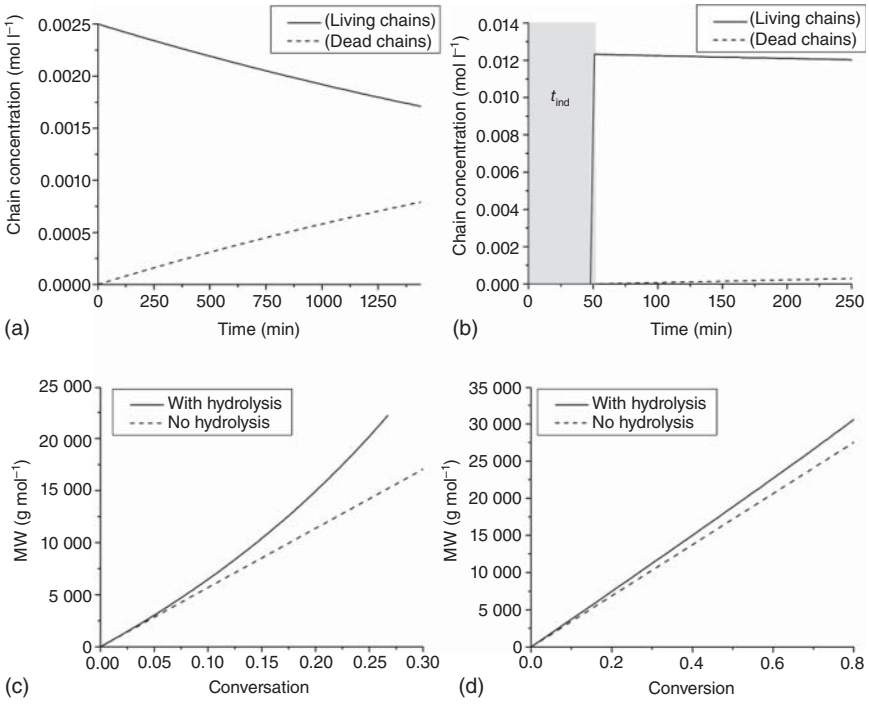

Figure 5.11 Theoretically predicted concentrations of living and dead chain ends for (a) acrylamide polymerization at pH = 5.5, 70 °C, and (b) AMPS polymerization at pH = 7, 70 °C. Molecular weights as a function of conversion for (c) acrylamide polymerization at pH = 5.5, 70 °C, and (d) AMPS polymerization at pH = 7, 70 °C. Molecular weights with and without hydrolysis were calculated utilizing Eqs. (5.10) and (5.8) from D. B. Thomas et al., Macromolecules 2004, respectively. (For acrylamide polymerizations $t_{ind} = 0$ min, $k_p^* = 0.36 \times 10^{-5}$ s^{-1}, $k_{a,macro} = 0$, $[NH_3] = 0.02$ M, $k_{hyd,CTP} = 1.8 \times 10^{-5}$ s^{-1}, and $k_{hyd,macro} = 0.44 \times 10^{-5}$ s^{-1}; for AMPS polymerizations $t_{ind} = 51$ min, $k_p^* = 12 \times 10^{-5}$ s^{-1}, $k_{a,macro} = 0.6$, $[NH_3] = 0$, $k_{hyd,CTP} = 2.5 \times 10^{-5}$ s^{-1}, and $k_{hyd,macro} = 0.2 \times 10{-}5$ s^{-1}.) Source: Taken from Thomas et al. [128]. © 2004, American Chemical Society.

dead chains is noticeably higher in the case of acrylamide polymerization for two principle reasons: (i) the RAFT polymerization of acrylamide under these conditions is sufficiently slow as to allow more extensive hydrolysis before the polymerization is completed; and (ii) the added impact of aminolysis serves to accentuate the loss of thiocarbonylthio end-group during the polymerization. The loss of RAFT end-group during the reaction leads to an increase in the ratio of [M]/[CTA], thereby leading to higher molecular weights than would be observed if all CTA moieties remained intact. This manifests as an increasing departure from theoretical molecular weight as higher conversions are reached (Figure 5.11c,d). Again, the impact is most noticeable for acrylamide polymerization where the slower rate of polymerization and more significant loss of thiocarbonylthio end-group due to hydrolysis and aminolysis lead to substantial departures from theoretical molecular weight at higher conversions. Altogether, these results demonstrate the importance of solvent choice for RAFT polymerization. The use of solvents that lead to any loss of thiocarbonylthio end-group during polymerization can, in turn, result in substantial departures from the theoretical molecular weight. This will be exacerbated by long polymerization times, and, as such, adjustment of conditions to maximize the rate of polymerization relative to the rate of hydrolysis will generally be an effective strategy for overcoming this issue.

The polymerization of monomers that incorporate a nucleophile represent a further challenge. Nucleophiles such as amines and hydroxide are well known to react with thiocarbonylthio groups and have been extensively used in the quantitative removal of the end-groups formed during RAFT polymerization. As such, polymerizing monomers that incorporate such groups is difficult, and frequently involves the use of protecting groups such as *tert*-butoxycarbonyl (BOC). Nevertheless, there have been examples in which primary amine-containing monomers such as 2-aminoethyl methacrylate (AEMA) have been successfully polymerized by controlling the pH and temperature of the reaction medium, thereby minimizing the potential for aminolysis of the RAFT end-group (or various other side reactions of the monomer and polymer chains, for that matter). Specifically, Morgan and coworkers have demonstrated that by maintaining the pH at 5.2 and polymerizing at 50 °C using VA-044 as the initiator it was possible to prepare poly(AEMA) with good control over molecular weight and relatively narrow molecular weight distribution (Figure 5.12)

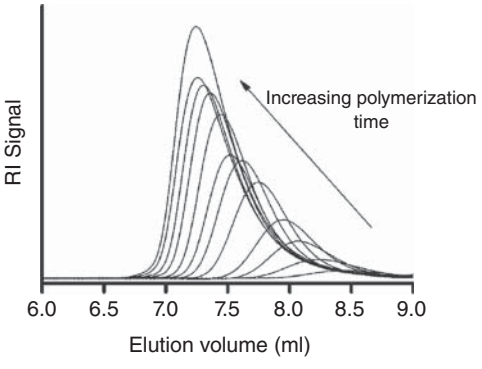

Figure 5.12 Aqueous size exclusion chromatograms (with RI detection) for the homopolymerization of 2-aminoethyl methacrylate (AEMA) at 50 °C showing the detector response as a function of elution volume. Source: Taken from Alidedeoglu et al. [129]. © Wiley Periodicals, Inc.

[129]. This has been achieved with sufficient efficiency as to enable the synthesis of block copolymers with *N*-(2-hydroxypropyl)methacrylamide (HPMAm).

5.4 Light Effects on the Rate of Polymerization

Several groups [130] have observed that trithiocarbonate and other RAFT agents can be used to mediate the polymerization of acrylates and acrylamides under visible light (e.g. $\lambda = 460\,\text{nm}$) [131] without the addition of a photoinitiator or catalyst. A lower yield of by-products was attributed to selective excitation of the forbidden $n \rightarrow \pi^*$ electronic transition. In photoinitiated RAFT, once radicals are generated the normal RAFT mechanism becomes operative and is responsible for the control. The observations of higher selectivity with blue light photoinitiation motivated a subsequent study of the effect of visible light on the stability of several trithiocarbonates [132]. Notably, trithiocarbonates with tertiary cyanoalkyl R groups, such as 2-cyanoprop-2-yl, were shown to degrade faster under visible light than those with secondary R groups. Moreover, these agents were shown to lead to faster initiation of polymerization for MA under blue light, with no discernible inhibition or initialization period observed under these conditions. In contrast, those trithiocarbonates secondary leaving groups were far more stable under blue light (as assessed using UV–visible spectrophotometry) and gave significant inhibition periods (c. 4–6 hours). However, despite these long inhibition periods, the resulting polymers displayed excellent end-group fidelity, which was attributed to the superior stability of the secondary thiocarbonylthio group under the blue light source. The results indicate that in the case of trithiocarbonate-mediated polymerization initiated under blue light, lengthy inhibition periods do not necessarily compromise the end-group fidelity of the resulting polymer. Even so, despite the inherent instability of the tertiary leaving group under blue light, low-dispersity polymers were still successfully obtained due to the rapid polymerization of the monomer relative to the rate of loss of the end-group under these conditions.

The inhibition periods observed in these experiments are most likely related to trace amounts of air or impurities in the RAFT agents. These cause inhibition until they are consumed, with the length of inhibition period dependent on the rate of radical photogeneration and the level of impurities. Because the radical concentrations are very low, it does not require much impurity to cause a substantial inhibition period. With tertiary trithiocarbonates the rate of photogeneration of radicals is significantly higher than that with secondary trithiocarbonates. This means that inhibition periods will be shorter. Also, because of the higher radical concentrations generated, cross-termination reactions (between $R^{\cdot}$ or ZCS_2^{-}) are more likely both in the presence and absence of monomer.

A further interesting consequence of trithiocarbonate activation via the forbidden $n \rightarrow \pi^*$ electronic transition under visible light is that trithiocarbonate-mediated RAFT polymerizations tend to be accelerated under fluorescent laboratory lighting (see Figure 5.13) [133]. This phenomenon has been observed for both methyl methacrylate and methyl acrylate where a chain transfer agent incorporating a

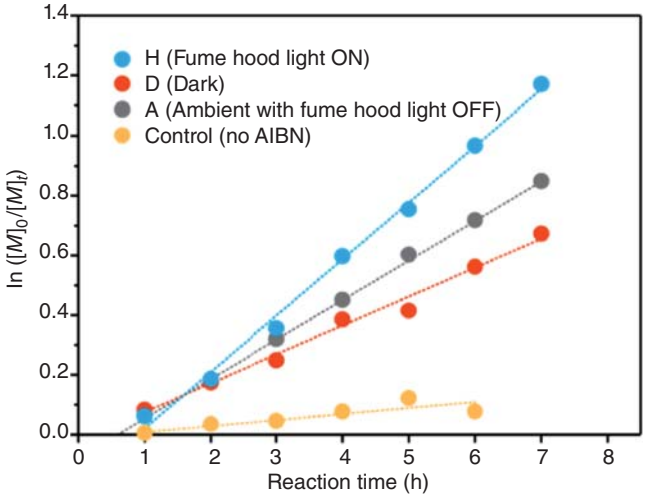

Figure 5.13 RAFT reaction of MMA with 4-cyano-4-((dodecylthio)carbonothio)pentanoic acid and 0.05 equiv of AIBN under various lighting conditions at 70 °C. Source: Taken from da M. Costa et al. [133]. © American Chemical Society.

4-cyanopentanoic acid leaving group is employed. Notably, the effect of lighting is quite dramatic in these experiments. Moreover, R groups incorporating a pendant nitrile on the α-carbon are extremely commonly used in RAFT polymerization, and as such caution should be exercised where such R groups are combined with a trithiocarbonate Z group. This insight highlights the need for tightly controlling all reaction variables in order to ensure that results can be readily reproduced and are not compromised by variations in laboratory lighting, either with time or between sites.

Further examples and details of visible light photoinititated RAFT polymerization can be found in the chapter of Chapman et al. [130] and in the chapters relating to specific RAFT agents.

5.5 Conclusion

While there are certain elements of the RAFT mechanism that have been discussed in the literature, overall the mechanism of RAFT polymerization is well understood. Those areas where there has been significant debate have generally been related to a very narrow class of chain transfer agents (dithiobenzoates) that – although highly useful – are by no means the only choice for conducting the RAFT polymerization of most monomers. In the choice of chain transfer agent there is, of course, a necessity to ensure that R and Z groups are appropriate for the monomer being polymerized, and that the solvent, temperature, and initiation source are suitable. As such, a basic mechanistic understanding of RAFT is essential for good experimental planning. Within the last decade, there have been some important advances that have exploited the mechanistic understanding of RAFT to design new, more versatile chain transfer

agents. In particular, the development of the so-called switchable RAFT agents that are suitable for both LAMs and MAMs is a significant advance. These agents have enabled the synthesis of new and interesting materials that are substantially more complicated to make via other techniques. Moreover, the advance in understanding of side reactions such as side fragmentation in the case of xanthates, and the development of approaches that can minimize these reactions have enabled RAFT to be applied to the simplest yet most challenging of monomers, ethylene [89, 90, 134]. Further exploration into the intricacies of the RAFT mechanism will undoubtedly yield new insights – insights that will likely unlock even more opportunities for applying the most versatile, widely applicable, and robust of the RDRP techniques: The RAFT process.

References

1 Chiefari, J., Chong, Y.K., Ercole, F. et al. (1998). *Macromolecules* 31: 5559–5562.
2 Moad, G., Rizzardo, E., and Thang, S.H. (2005). *Aust. J. Chem.* 58: 379–410.
3 Moad, G., Rizzardo, E., and Thang, S.H. (2006). *Aust. J. Chem.* 59: 669–692.
4 Moad, G., Rizzardo, E., and Thang, S.H. (2009). *Aust. J. Chem.* 62: 1402–1472.
5 Moad, G., Rizzardo, E., and Thang, S.H. (2012). *Aust. J. Chem.* 65: 985–1076.
6 Moad, C.L., Moad, G., Rizzardo, E., and Thang, S.H. (1996). *Macromolecules* 29: 7717–7726.
7 Krstina, J., Moad, C.L., Moad, G. et al. (1996). *Macromol. Symp.* 111: 13–23.
8 Krstina, J., Moad, G., Rizzardo, E. et al. (1995). *Macromolecules* 28: 5381–5385.
9 Zhang, Z., Zhu, J., Zhou, N. et al. (2013). *J. Polym. Sci., Part A: Polym. Chem.* 51: 2606.
10 Zhu, J., Zhang, Z., Pan, X. et al. (2013). *J. Polym. Sci., Part A: Polym. Chem.* 51: 3159.
11 Matioszek, D., Brusylovets, O., Wilson, D.J. et al. (2013). *J. Polym. Sci., Part A: Polym. Chem.* 51: 4361–4368.
12 Feldermann, A., Ah Toy, A., Phan, H. et al. (2004). *Polymer* 45: 3997.
13 Moad, G. (2022). Dithioesters in RAFT polymerization. In: *RAFT Polymerization: Materials, Synthesis and Applications* (eds. G. Moad and E. Rizzardo). Weinheim: Wiley-VCH. 223–370.
14 Moad, G. (2022). Trithiocarbonates in RAFT polymerization. In: *RAFT Polymerization: Materials, Synthesis and Applications* (eds. G. Moad and E. Rizzardo). Weinheim: Wiley-VCH. 371–494.
15 Wang, M., Marty, J.-D., and Destarac, M. (2022). Xanthates in RAFT polymerization. In: *RAFT Polymerization: Materials, Synthesis and Applications* (eds. G. Moad and E. Rizzardo). Weinheim: Wiley-VCH. 495–550.
16 Moad, G. (2022). Dithiocarbamates in RAFT polymerization. In: *RAFT Polymerization: Materials, Synthesis and Applications* (eds. G. Moad and E. Rizzardo). Weinheim: Wiley-VCH. 551–610.
17 Nguyen, D.H. and Vana, P. (2006). *Aust. J. Chem.* 59: 549.

18 Zhu, J., Zhu, X., and Zhou, D. (2004). *J. Macromol. Sci. Part A: Pure Appl. Chem.* 41: 827.

19 Mayo, F.R. (1943). *J. Am. Chem. Soc.* 65: 2324–2329.

20 Clay, P.A. and Gilbert, R.G. (1995). *Macromolecules* 28: 552–569.

21 Moad, G. and Moad, C.L. (1996). *Macromolecules* 29: 7727–7733.

22 Chong, Y.K., Krstina, J., Le, T.P.T. et al. (2003). *Macromolecules* 36: 2256–2272.

23 Walling, C. (1948). *J. Am. Chem. Soc.* 70: 2561–2564.

24 O'Brien, J.L. and Gornick, F. (1955). *J. Am. Chem. Soc.* 77: 4757–4763.

25 Gregg, R.A., Alderman, D.M., and Mayo, F.R. (1948). *J. Am. Chem. Soc.* 70: 3740–3743.

26 Theis, A., Feldermann, A., Charton, N. et al. (2005). *Macromolecules* 38: 2595.

27 Derboven, P., Van Steenberge, P.H.M., Reyniers, M.F. et al. (2016). *Macromol. Theory Simul.* 25: 104–115.

28 Goto, A., Sato, K., Tsujii, Y. et al. (2001). *Macromolecules* 34: 402–408.

29 Goto, A. and Fukuda, T. (2004). *Prog. Polym. Sci.* 29: 329–385.

30 Gao, X. and Zhu, S. (2011). *J. Appl. Polym. Sci.* 122: 497.

31 Vana, P., Davis, T.P., and Barner-Kowollik, C. (2002). *Macromol. Theory Simul.* 11: 823–835.

32 Drache, M., Schmidt-Naake, G., Buback, M., and Vana, P. (2005). *Polymer* 46: 8483–8493.

33 Barner-Kowollik, C., Coote, M.L., Davis, T.P. et al. (2003). *J. Polym. Sci. Part A Chem.* 41: 2828–2832.

34 Barth, J., Buback, M., Meiser, W., and Vana, P. (2010). *Macromolecules* 43: 51–54.

35 Meiser, W., Barth, J., Buback, M. et al. (2011). *Macromolecules* 44: 2474–2480.

36 Buback, M. (2022). Kinetics and mechanism of RAFT polymerizations. In: *RAFT Polymerization: Materials, Synthesis and Applications* (eds. G. Moad and E. Rizzardo). Weinheim: Wiley-VCH.

37 Moad, G., Chiefari, J., Chong, Y.K. et al. (2000). *Polym. Int.* 49: 993.

38 Engelis, N.G., Anastasaki, A., Nurumbetov, G. et al. (2017). *Nat. Chem.* 9: 171–178.

39 Destarac, M., Matioszek, D., Vila, X. et al. (2018). How can xanthates control the RAFT polymerization of methacrylates? In: *ACS Symposium Series 1284* (eds. K. Matyjaszewski, H. Gao, B.S. Sumerlin and N.V. Tsarevsky), 291–305. Washington, DC: American Chemical Society.

40 Khan, M., Guimarães, T.R., Zhou, D. et al. (2019). *J. Polym. Sci., Part A, Polym. Chem.* 57 (18): 1938–1946.

41 Guimaraes, T.R., Khan, M., Morrow, I.C. et al. (2019). *Macromolecules* 52 (8): 2965–2974.

42 Clothier, G.K.K., Guimarães, T.R., Khan, M. et al. (2019). *ACS Macro Lett.* 8 (8): 989–995.

43 Barner-Kowollik, C., Quinn, J.F., Nguyen, T.L.U. et al. (2001). *Macromolecules* 34: 7849.

44 Fischer, H. and Radom, L. (2001). *Angew. Chem. Int. Ed.* 40: 1340.

45 Moad, G. and Solomon, D.H. (2006). *The Chemistry of Radical Polymerization*, 2e. Oxford, UK: Elsevier.

46 Moad, G. (2017). *Macromol. Chem. Phys.* 218 (19): 1700381.

47 (a) Beuermann, S., Buback, M., Davis, T.P. et al. (1997). *Macromol. Chem. Phys.* 198: 1545–1560.(b) Buback, M., Gilbert, R.G., Hutchinson, R.A. et al. (1995). *Macromol. Chem. Phys.* 196: 3267–3280.(c) Buback, M., Kurz, C.H., and Schmaltz, C. (1998). *Macromol. Chem. Phys.* 199: 1721–1727.(d) Hutchinson, R.A., Paquet, D.A. Jr., and McMinn, J.H. (1995). *DECHEMA Monogr.* 131: 467–492.

48 Kamachi, M. and Yamada, B. (1999). Elements of RAFT navigation. In: *Polymer Handbook*, 4e (eds. J.I. Brandrup, H. Edmund, A. Grulke, Eric, et al.). Wiley.

49 Zhou, Y., Zhang, Z., Reese, C. et al. (2020). *Macromol. Rapid Commun.* 41 (1): 1900478.

50 McLeary, J.B., McKenzie, J.M., Tonge, M.P. et al. (2004). *Chem. Commun.* (17): 1950–1951.

51 McLeary, J.B., Calitz, F.M., McKenzie, J.M. et al. (2005). *Macromolecules* 38: 3151–3161.

52 McLeary, J.B., Calitz, F.M., McKenzie, J.M. et al. (2004). *Macromolecules* 37: 2383–2394.

53 Haven, J.J., Hendrikx, M., Junkers, T. et al. (2018). Reversible deactivation radical polymerization: mechanisms and synthetic methodologies. In: *ACS Symposium Series* 1284 (eds. K. Matyjaszewski, H. Gao, B.S. Sumerlin and N.V. Tsarevsky), 77–103. Washington, DC: American Chemical Society.

54 Aerts, A., Lewis, R.W., Zhou, Y. et al. (2018). *Macromol. Rapid Commun.* 39: 1800240. https://doi.org/10.1002/marc.201800240.

55 Fuchs, A.V. and Thurecht, K.J. (2017). *ACS Macro Lett.* 6: 287–291.

56 Liu, C.H. and Pan, C.Y. (2007). *Polymer* 48: 3679.

57 Reyhani, A., McKenzie, T.G., Ranji-Burachaloo, H. et al. (2017). *Chem. Eur. J.* 23: 7221.

58 Zhao, J.C., Lalevee, J., Lu, H.X. et al. (2015). *Polym. Chem.* 6: 5053.

59 Quinn, J.F., Barner, L., Barner-Kowollik, C. et al. (2002). *Macromolecules* 35: 7620.

60 You, Y.Z., Hong, C.Y., Bai, R.K. et al. (2002). *Macromol. Chem. Phys.* 20: 477.

61 Bai, R.K., You, Y.Z., and Pan, C.Y. (2001). *Macromol. Rapid Commun.* 22: 315.

62 Quinn, J.F., Barner, L., Rizzardo, E., and Davis, T.P. (2002). *J. Polym. Sci., Part A: Polym. Chem.* 40: 19.

63 Quinn, J.F., Barner, L., Davis, T.P. et al. (2002). *Macromol. Rapid Commun.* 23: 717.

64 Whittaker, M.R., Goh, Y.K., Gemici, H. et al. (2006). *Macromolecules* 39: 9028.

65 Grover, G.N., Alconcel, S.N.S., Matsumoto, N.M., and Maynard, H.D. (2009). *Macromolecules* 42: 7657.

66 Lima, V., Jiang, X.L., Brokken-Zijp, J. et al. (2005). *J. Polym. Sci., Part A: Polym. Chem.* 43: 959.

67 Favier, A., Charreyre, M.T., Chaumont, P., and Pichot, C. (2002). *Macromolecules* 35: 8271.

68 York, A.W., Scales, C.W., Huang, F.Q., and McCormick, C.L. (2007). *Biomacromolecules* 8: 2337.

69 Tang, C.B., Kowalewski, T., and Matyjaszewski, K. (2003). *Macromolecules* 36: 8587.

70 Zheng, G.H. and Pan, C.Y. (2006). *Macromolecules* 39: 95.

71 Mayadunne, R.T.A., Rizzardo, E., Chiefari, J. et al. (2000). *Macromolecules* 33: 243.

72 Wood, M.R., Duncalf, D.J., Findlay, P. et al. (2007). *Aust. J. Chem.* 60: 772.

73 Zhang, W.J., D'Agosto, F., Dugas, P.Y. et al. (2013). *Polymer* 54: 2011.

74 Convertine, A.J., Ayres, N., Scales, C.W. et al. (2004). *Biomacromolecules* 5: 1177.

75 Hong, C.Y. and Pan, C.Y. (2006). *Macromolecules* 39: 3517.

76 Spoerl, J.M., Ota, A., Beyer, R. et al. (2014). *J. Polym. Sci., Part A: Polym. Chem.* 52: 1322.

77 Mayadunne, R.T.A., Rizzardo, E., Chiefari, J. et al. (1999). *Macromolecules* 32: 6977–6980.

78 Zhou, Y., Zhu, X., Cheng, Z., and Zhu, J. (2007). *J. Appl. Polym. Sci.* 103: 1769.

79 Chong, Y.K., Moad, G., Rizzardo, E. et al. (2007). *Macromolecules* 40: 9262.

80 Sun, X.L., He, W.D., Li, J. et al. (2008). *J. Polym. Sci., Part A: Polym. Chem.* 46: 6950.

81 Hornung, C.H., Guerrero-Sanchez, C., Brasholz, M. et al. (2011). *Org. Process. Res. Dev.* 15: 593.

82 Jana, S. and Parthiban, A. (2011). *Macromol. Chem. Phys.* 212: 790.

83 Destarac, M., Bzducha, W., Taton, D. et al. (2002). *Macromol. Rapid Commun.* 23: 1049.

84 Wood, M.R., Duncalf, D.J., Rannard, S.P., and Perrier, S. (2006). *Org. Lett.* 8: 553.

85 Taton, D., Wilczewska, A.Z., and Destarac, M. (2001). *Macromol. Rapid Commun.* 22: 1497.

86 Postma, A., Davis, T.P., Li, G. et al. (2006). *Macromolecules* 39: 5307.

87 Wan, D.C., Satoh, K., Kamigaito, M., and Okamoto, Y. (2005). *Macromolecules* 38: 10397.

88 Chiefari, J., Mayadunne, R.T.A., Moad, C.L. et al. (2003). *Macromolecules* 36: 2273–2283.

89 Dommanget, C., D'Agosto, F., and Monteil, V. (2014). *Angew. Chem. Int. Ed.* 53: 6683.

90 Wolpers, A., Bergerbit, C., Ebeling, B. et al. (2019). *Angew. Chem. Int. Ed.* 58: 14295.

91 Benaglia, M., Chiefari, J., Chong, Y.K. et al. (2009). *J. Am. Chem. Soc.* 131: 6914.

92 Moad, G., Benaglia, M., Chen, M. et al. (2011). Block copolymer synthesis through the use of switchable RAFT agents. In: *Non-conventional functional block copolymers*, *ACS Symposium Series*, vol. 1066 (eds. P. Theato, A.F.M. Kilbinger and E.B. Coughlin), 81. Washington, D.C.: American Chemical Society.

93 Keddie, D.J., Guerrero-Sanchez, C., Moad, G. et al. (2011). *Macromolecules* 44: 6738.

94 Gardiner, J., Martinez-Botella, I., Tsanaktsidis, J., and Moad, G. (2016). *Polym. Chem.* 7: 481.

95 Perrier, S., Barner-Kowollik, C., Quinn, J.F. et al. (2002). *Macromolecules* 35: 8300.

96 Quinn, J.F., Rizzardo, E., and Davis, T.P. (2001). *Chem. Commun.*: 1044.

97 Chernikova, E.V., Tarasenko, A.V., Garina, E.S., and Golubev, V.B. (2008). *Polym. Sci., Ser. A* 50: 353.

98 Scales, C.W., Vasilieva, Y.A., Convertine, A.J. et al. (2005). *Biomacromolecules* 6: 1846.

99 Monteiro, M.J. and de Brouwer, H. (2001). *Macromolecules* 34: 349–352.

100 Barner-Kowollik, C., Quinn, J.F., Morsley, D.R., and Davis, T.P. (2001). *J. Polym. Sci., Part A: Polym. Chem.* 39: 1353.

101 Barner-Kowollik, C., Buback, M., Charleux, B. et al. (2006). *J. Polym. Sci. Part A: Polym. Chem.* 44: 5809.

102 Moad, G. (2014). *Macromol. Chem. Phys.* 215: 9–26.

103 Hawthorne, D.G., Moad, G., Rizzardo, E., and Thang, S.H. (1999). *Macromolecules* 32: 5457.

104 de Brouwer, H., Schellekens, M.A.J., Klumperman, B. et al. (2000). *J. Polym. Sci., Part A: Polym. Chem.* 19: 3596.

105 Kwak, Y., Goto, A., and Fukuda, T. (2004). *Macromolecules* 37: 1219.

106 Kwak, Y., Goto, A., Komatsu, K. et al. (2004). *Macromolecules* 37: 4434.

107 Feldermann, A., Ah Toy, A., Davis, T.P. et al. (2005). *Polymer* 46: 8448–8457.

108 Ah Toy, A., Vana, P., Davis, T.P., and Barner-Kowollik, C. (2004). *Macromolecules* 37: 744–751.

109 Buback, M. and Vana, P. (2006). *Macromol. Rapid Commun.* 27: 1299.

110 Meiser, W., Buback, M., Ries, O. et al. (2013). *Macromol. Chem. Phys.* 214: 924.

111 Meiser, W. and Buback, M. (2012). *Macromol. Rapid Commun.* 33: 1273.

112 Konkolewicz, D., Hawkett, B.S., Gray-Weale, A., and Perrier, S. (2008). *Macromolecules* 41: 6400.

113 Konkolewicz, D., Hawkett, B.S., Gray-Weale, A., and Perrier, S. (2009). *J. Polym. Sci., Part A: Polym. Chem.* 47: 3455.

114 Ting, S.R.S., Davis, T.P., and Zetterlund, P. (2011). *Macromolecules* 44: 4187.

115 Feldermann, A., Coote, M.L., Davis, T.P. et al. (2004). *J. Am. Chem. Soc.* 126: 15915–15923.

116 Tonge, M.P., Calitz, F.M., and Sanderson, R.D. (2006). *Macromol. Chem. Phys.* 207: 1852.

117 Coote, M.L., Krenske, E.H., and Izgorodina, E.I. (2006). *Macromol. Rapid Commun.* 27: 473.

118 McLeary, J.B., Tonge, M.P., and Klumperman, B. (2006). *Macromol. Rapid Commun.* 27: 1233.

119 Sidoruk, A., Buback, M., and Meiser, W. (2013). *Macromol. Chem. Phys.* 214: 1738.

120 Meiser, W. and Buback, M. (2011). *Macromol. Rapid Commun.* 32: 1490.

121 Barner-Kowollik, C., Vana, P., Quinn, J.F., and Davis, T.P.J. (2002). *Polym. Sci. Part A: Chem.* 40: 1058–1063.
122 Pahnke, K., Brandt, J., Gryńova, G. et al. (2016). *Angew. Chem. Int. Ed.* 55: 1514–1518.
123 Plummer, R., Goh, Y.K., Whittaker, A.K., and Monteiro, M.J. (2005). *Macromolecules* 38: 5352–5355.
124 Sumerlin, B.S., Donovan, M.S., Mitsukami, Y. et al. (2001). *Macromolecules* 34: 6561–6564.
125 Donovan, M.S., Lowe, A.B., Sumerlin, B.S., and McCormick, C.L. (2002). *Macromolecules* 35: 4123–4132.
126 Donovan, M.S., Sumerlin, B.S., Lowe, A.B., and McCormick, C.L. (2002). *Macromolecules* 35: 8663–8666.
127 Thomas, D.B., Sumerlin, B.S., Lowe, A.B., and McCormick, C.L. (2003). *Macromolecules* 36: 1436–1439.
128 Thomas, D.B., Convertine, A.J., Hester, R.D. et al. (2004). *Macromolecules* 37: 1735–1741.
129 Alidedeoglu, A.H., York, A.W., McCormick, C.L., and Morgan, S.E. (2009). *J. Polym. Sci. Part A. Chem.* 47: 5405–5415.
130 Chapman, R., Jung, K., and Boyer, C. (2022). Overview of photoregulated Reversible Addition-Fragmentation Chain Transfer (RAFT) polymerization. In: *RAFT Polymerization: Materials, Synthesis and Applications* (eds. G. Moad and E. Rizzardo). Weinheim: Wiley-VCH.
131 McKenzie, T.G., Fu, Q., Wong, E.H.H. et al. (2015). *Macromolecules* 48: 3864–3872.
132 McKenzie, T.G., da M. Costa, L.P., Fu, Q. et al. (2016). *Polym. Chem.* 7: 4246–4253.
133 da M. Costa, L.P., McKenzie, T.G., Schwarz, K.N. et al. (2016). *ACS Macro Lett.* 5: 1287–1292.
134 Busch, M., Roth, M., Davis, T.P. et al. (2007). *Aust. J. Chem.* 60: 788–793.

6

Quantum Chemical Studies of RAFT Polymerization

Michelle L. Coote

Australian National University, ARC Centre of Excellence in Electromaterials Science, Research School of Chemistry, Canberra 2601, Australia

6.1 Introduction

Quantum chemistry allows one to predict, from first principles, the energetics of chemical reactions. One can also use the calculations to visualize the electron density and how the atoms rearrange along a reaction path. This information can be used to elucidate reaction mechanisms, make first principles predictions of kinetics and thermodynamics, and provide insights into the origin of structure–reactivity trends. Quantum chemistry is particularly useful for complicated multi-step processes such as reversible addition–fragmentation chain transfer (RAFT) polymerization [1] because, on the one hand, information about the kinetics and structure–reactivity trends are essential in choosing optimal RAFT agents and reaction conditions, and because, on the other hand, there is no experimental method for directly measuring the individual rate coefficients.

Unsurprisingly then there have been several quantum chemical studies of the RAFT process, addressing mechanistic issues, structure–reactivity analysis, reagent design, and first principles predictions of rate coefficients. Chapter 2 in the first edition of this book reviewed the early studies of this process [2], which were also summarized in Ref. [3]. Herein, we recap these early studies, while also providing an update on more recent work. We begin with a description of the types of methods that are used and discuss their accuracy and their outstanding problems. We then show how computational chemistry can be used to clarify and improve models for reaction kinetics, and indeed how computational calculations can be used directly in kinetic simulations to predict the macroscopic outcome of a process. Finally, we examine the RAFT process at a deeper mechanistic level, using computational data to model and explain structure–reactivity trends and show how these insights can be applied to the practical problem of RAFT agent design.

RAFT Polymerization: Methods, Synthesis and Applications, First Edition.
Edited by Graeme Moad and Ezio Rizzardo.

6.2 Methodology

In order to select reliable yet cost-effective theoretical procedures, assessment studies are performed. In essence, one takes a small prototypical example of the class of chemical reaction under study and calculates the geometries, frequencies, barriers, enthalpies, rate coefficients, and other properties at a variety of levels of theory, ranging from the extremely accurate but highly computationally intensive to those that are computationally inexpensive but potentially subject to very large errors. For each type of property, one compares the results at the lower levels of theory with the highest level results and (where possible) also with reliable gas-phase experimental data. For the case of addition–fragmentation processes, assessment studies have been performed for the prototypical reactions $\cdot CH_3 + S{=}C(R)R' \rightarrow CH_3SC\cdot(R)R'$ (R, R′ = H, CH_3) [4] and also the more RAFT-related systems, $R'SC(Z){=}S + \cdot R \rightarrow R'SC\cdot(Z)SR$ (various combinations of R, R′ = CH_3, CH_2CH_3, CH_2CN, $C(CH_3)_2CN$, CH_2COOCH_3, $CH(CH_3)COOCH_3$, CH_2OCOCH_3, CH_2Ph, $CH(CH_3)Ph$, and Z = CH_3, H, Cl, CN, CF_3, NH_2, Ph, CH_2Ph, OCH_3, OCH_2CH_3, $OCH(CH_3)_2$, $OC(CH_3)_3$, F) [5]. In addition, the accuracy of the harmonic oscillator approximation [6, 7] and the applicability of standard (rather than variational) transition state theory have been explored [6]. Finally, solution-phase calculations on small-molecule models have been compared directly with the corresponding experimental data for the same systems [8]. On the basis of these studies, the following guidelines for performing theoretical calculations are suggested.

6.2.1 Electronic Structure Calculations

For simple systems, it is possible to conduct reliable geometry optimizations and frequency calculations for the stationary species (i.e. the reactants and products) in the RAFT process at relatively low levels of theory, such as B3-LYP/6-31G(d) or HF/6-31G(d) [4]. For example, provided the energies are calculated at a consistent level of theory, the reaction enthalpies for $\cdot CH_3 + S{=}CRR'$ (R, R′ = H, CH_3) vary by less than 1 kJ mol^{-1}, regardless of whether low levels such as B3-LYP/6-31G(d) or HF/6-31G(d) or higher levels such as CCSD(T)/6-311+G(d,p) are used for the geometry optimizations [4]. Likewise, provided the recommended scale factors are used [9], the zero-point vibrational energy (and hence the frequency calculations) at these lower levels of theory agrees to within 1–2 kJ mol^{-1} of the CCSD(T)/6-311+G(d,p) calculations [4]. These earlier studies were performed on simple systems that do not involve significant non-covalent interactions and at a time when dispersion-corrected density functional theory (DFT) methods were not readily available. It is now well recognized that if intra- or inter-molecular hydrogen bonding and/or other non-covalent interactions are important, DFT methods that take account of dispersion either through corrections or parameterization should be used in place of Hartree–Fock (HF) or non-dispersion-corrected DFT methods such as B3-LYP [10].

Regardless of whether dispersion is included, for transition structures extra precautions are required. In particular, DFT methods significantly flatten the potential energy surface and overestimate the length of the forming bond in the transition state, finding transition structures that are too early. HF fares somewhat better, but does underestimate the forming bond length, finding transition structures that are too late. To address this problem, the transition structures should be corrected to higher levels of theory via IRCmax [4]. In the IRCmax method [11, 12], one calculates the minimum energy path of the chemical reaction at a low level of theory, and then calculates single-point energies along this reaction path at a higher level of theory, such as RMP2/6-311+G(3df,2p). The IRCmax transition structure is then identified as that species corresponding to the maximum point of the minimum energy path, as calculated at the *higher* level of theory. In essence, one optimizes the most sensitive part of the geometry optimization (i.e. the reaction coordinate) at the higher level of theory, at a fraction of the cost of a full geometry optimization at that level. For the case of radical addition to C=S bonds, the IRCmax transition structures have forming bond lengths within less than 0.05 Å, and provide reaction barriers within 1 kJ mol^{-1} of those obtained using full geometry optimizations at the CCSD(T)/6-311+G(d,p) level [4].

In contrast to geometries and frequencies, accurate calculations of the energetics of these types of chemical reactions require very high levels of theory. Ideally, such calculations should be performed using W1 theory or better. W1 aims to approximate coupled cluster energies [URCCSD(T)] with an infinite basis set via extrapolation, and includes corrections for core correlation and relativistic effects [13]. It has been shown to deliver 'kJ accuracy' when assessed against a large test set of gas-phase experimental data [13] and has performed well in assessment studies for the prototypical system $\cdot CH_3 + S{=}CH_2$ [4] as well as other types of radical reactions such as radical addition to C=C bonds [14] and hydrogen atom abstraction [15]. Unfortunately, such calculations are computationally very intensive and currently only practicable for up to approximately six to eight non-hydrogen atoms. The G3 and G4 families of methods provide a lower cost alternative to W1. Like W1, they attempt to approximate coupled cluster energies with a large basis set, but achieve this via additivity approximations at the MP2 and/or MP4 levels of theory. As a result, they are less expensive than W1 but also less reliable. They have been shown to deliver 'kcal accuracy' when assessed against a large test set of experimental thermochemical data [16, 17] and to provide good agreement with W1 for a variety of radical reactions [14, 15]. For the specific problem of radical addition to C=S double bonds, G3-methods provide excellent agreement with W1 for the forward reaction barriers; for reaction enthalpies, the errors are slightly larger (c. 10 kJ mol^{-1}) but are likely to be reasonably systematic for a class of reactions and therefore suitable for studying substituent effects [4]. Nonetheless, they are also currently too computationally intensive for all but the simplest RAFT systems, being currently only feasible for systems of up to approximately 17 non-hydrogen atoms.

For practical RAFT systems, lower cost procedures are necessary and unfortunately these procedures can be subject to large errors. In particular, most DFT

methods comprehensively fail, even when modelling the qualitative trends let alone quantitative kinetics and thermodynamics of addition–fragmentation processes [5]. Moreover, this failing has also been observed for other radical reactions such as R—X bond dissociation reactions (R = Me, Et, *i*-Pr, *t*-Bu; X = H, CH_3, OCH_3, OH, F) [18], propagation rate coefficients [19], and even simple closed-shell systems such as the cyclization energies of alkenes [20] and alkane isomerization energies [21, 22]. Restricted open-shell second order Møller–Plesset perturbation theory (RMP2), which is slightly more expensive than DFT but can still be practically applied to relatively large systems, has been shown to fare much better than DFT. It generally provides reasonable absolute values (within 10 kJ mol^{-1}) and excellent relative values (within 4 kJ mol^{-1} or better) for the barriers and enthalpies of the addition–fragmentation processes [4, 5] as well as a variety of other radical reactions [14, 15, 18, 19]. However, it breaks down when the attacking radical is substituted with a group (such as phenyl or CN) that delocalizes the unpaired electron, with errors of over 15 kJ mol^{-1} being reported in some cases [5, 6]. Since such radicals are common in practical RAFT systems, this severely compromises the utility of RMP2.

Given these problems, we have designed an alternative approach that is based on our own N-layered integrated molecular orbital + molecular mechanic (ONIOM) procedure of Morokuma and coworkers [23]. In the ONIOM method, one first defines a 'core' section of the reaction that, in the very least, contains all forming and breaking bonds and would preferably include the principal substituents attached to them. In forming the core system, deleted substituents are replaced with 'link atoms' (typically hydrogens), chosen so that the core system provides a good chemical model of the reaction centre. One then calculates the core system at both a high level of theory and a lower level; the 'full system' is calculated at only the lower level. The full system at the high level of theory is then approximated as the sum of (i) the core system at the high level and (ii) the substituent effect measured at the low level of theory. The approximation is valid if the low level of theory measures the substituent effect accurately; this in turn depends upon the level of theory chosen, and the way in which the core system is defined.

For the RAFT systems, we know from above that W1 provides accurate absolute values of barriers and enthalpies, and G3(MP2)-RAD provides excellent relative values. For small systems, such as reaction (6.1), the W1 enthalpy could thus be approximated as the sum of the W1 enthalpy for the core reaction (6.2), and the difference in the G3(MP2)-RAD enthalpies for (6.1) and (6.2).

$$^{\cdot}CH_2Ph + S{=}C(CH_3)SCH_3 \rightarrow PhCH_2SC^{\cdot}(CH_3)SCH_3 \quad (6.1)$$

$$^{\cdot}CH_3 + S{=}CH_2 \rightarrow CH_3SCH_2^{\cdot} \quad (6.2)$$

For larger systems, where G3(MP2)-RAD calculations are not currently feasible, we add an additional 'ONIOM-layer' in which the full system is calculated using RMP2/6-311+G(3df,2p), the core system is calculated using G3(MP2)-RAD, and the 'inner core' is studied at W1. For example, one could approximate the W1 enthalpy for reaction (6.3) as the sum of the W1 value for the inner core (6.2), the G3(MP2)-RAD difference for the core (6.1), and the inner core (6.2), and the

RMP2/6-311+G(3df,2p) difference for the full (6.3) and core (6.1) systems.

$$\cdot CH(Ph)CH_2C(CH_3)_2CN + S{=}C(CH_2)SC(CH_3)_2Ph \rightarrow (CH_3)_2C(CN)CH_2CH(Ph)SC^{\cdot}(CH_2Ph)SC(CH_3)_2Ph \quad (6.3)$$

The ONIOM procedure provides an accurate alternative to high-level calculations on the full system, provided that the lower level of theory measures the substituent effects accurately. While the RMP2/6-311+G(3df,2p) method normally provides excellent relative values of barriers and enthalpies, it does break down in situations where the unpaired electron is highly delocalized. It is therefore extremely important to partition the full and core systems carefully, such that the delocalized radical is treated at the G3(MP2)-RAD level of theory and the RMP2/6-311+G(3df,2p) method is used only to measure remote substituent effects. Based on a careful assessment study, the following general guidelines are suggested [5] for partitioning the core and full systems: in the addition–fragmentation reaction (6.4), a suitable core system should include all α-substituents on the attacking radical R· but could replace the R′ group with a methyl substituent and, if necessary, also replace the Z group with a methyl substituent.

$$\cdot R + S{=}C(Z)SR' \rightarrow RSC^{\cdot}(Z)SR' \quad (6.4)$$

Even when the Z group is itself a substituent capable of delocalizing the unpaired electron in the RAFT-adduct radical, its replacement with CH_3 in the core system does not introduce substantial error [5]. This is presumably because the radical is already highly delocalized by the thiyl groups (which are of course included in both the core and inner core systems), and the additional delocalization by the Z substituent is not as significant as in an ordinary carbon-centred radical [24]. This ONIOM-based procedure allows one to study quite large RAFT systems (c. 30–40 non-hydrogen atoms) with kcal accuracy [5]. Similar performance has also been demonstrated for a range of other radical reactions including the bond dissociation energy (BDEs) of a range of organic compounds, propagation, hydrogen and halogen atom transfer reactions, and radical ring opening [25].

6.2.2 Kinetics and Thermodynamics

Having obtained the geometries, energies, and frequencies of the reactants, products, and transition structures, it is possible to calculate the rates $k(T)$ and equilibrium constants $K(T)$ of chemical reactions, using the standard textbook formulae [26, 27].

$$k(T) = \kappa(T)\frac{k_B T}{h}\left(c^{\circ}\right)^{1-m} e^{\left(-\Delta G^{\ddagger}/RT\right)} = \kappa(T)\frac{k_B T}{h}\left(c^{\circ}\right)^{1-m}\frac{Q_{\ddagger}}{\underset{\text{reactants}}{\Pi Q_i}} e^{\left(-\Delta E^{\ddagger}/RT\right)} \quad (6.5)$$

$$K(T) = \left(c^{\circ}\right)^{\Delta n} e^{\left(-\Delta G/RT\right)} = \left(c^{\circ}\right)^{\Delta n}\left(\frac{\underset{\text{products}}{\Pi Q_j}}{\underset{\text{reactants}}{\Pi Q_i}}\right) e^{\left(-\Delta E/RT\right)} \quad (6.6)$$

In these formulae, $\kappa(T)$ is the tunnelling correction factor, T is the temperature (K), k_B is Boltzmann's constant (1.380658×10^{-23} J mol^{-1} K^{-1}), h is Planck's constant ($6.6260755 \times 10^{-34}$ J s), c° is the standard unit of concentration (mol l^{-1}), R is the universal gas constant (8.3142 J mol^{-1} K^{-1}), m is the molecularity of the reaction and Δn the change in moles upon reaction, $Q_{\ddagger}$, Q_i, and Q_j are the molecular partition functions of the transition structure, reactant *I,* and product *j* respectively, $\Delta G^{\ddagger}$ is the Gibbs free energy of activation, ΔG is the Gibbs free energy of reaction, $\Delta E^{\ddagger}$ the 0 K, zero-point energy corrected energy barrier for the reaction, and ΔE is the 0 K, zero-point energy corrected energy change for the reaction. The value of c° depends on the standard-state concentration assumed in calculating the thermodynamic quantities (and translational partition function). For example, if these quantities were calculated for 1 mol of an ideal gas at 333.15 K and 1 atm, then $c^\circ = P/RT = 0.0365971$ mol l^{-1}. The tunnelling coefficient $\kappa(T)$ corrects for quantum effects in motion along the reaction path [28–31]. Whilst tunnelling is important in certain chemical reactions such as hydrogen abstraction, it is negligible (i.e. $\kappa \approx 1$) for the addition of carbon-centred radicals to thiocarbonyl compounds at typical polymerization temperatures (such as 333.15 K) because the masses of the rearranging atoms are large and the barriers for the reactions are relatively broad [6].

The molecular partition functions and their associated thermodynamic functions (i.e. enthalpy, H and entropy, S) can be calculated using the standard textbook formulae [26, 27], based on the statistical thermodynamics of an ideal gas under the harmonic oscillator/rigid rotor approximation. These formulae require knowledge of the point group, multiplicity, geometry, and vibrational frequencies of each species; the accuracy of the results depends upon both the accuracy of the calculated geometries and frequencies and the validity of the harmonic oscillator/rigid rotor approximation. As noted above, the geometries and frequencies are well described with dispersion-corrected DFT methods, provided that transition structures are corrected via IRCmax and frequencies are scaled by appropriate scale factors. However, the use of the harmonic oscillator/rigid rotor approximation can lead to errors of 1–2 orders of magnitude in both the kinetics and thermodynamics of the addition–fragmentation equilibrium [6, 7]. To address this problem, the partition functions for the low-frequency torsional modes (<300 cm^{-1}) should instead be treated as hindered internal rotations. Full details of these calculations are published elsewhere [6, 32], but a short description is provided below.

For each low-frequency torsional mode, one first calculates the full rotational potential $V(\theta)$. This can be calculated at a relatively low level of theory, such as B3-LYP/6-31G(d), and is performed as a relaxed (rather than frozen) scan in steps of 10° through 360°. The potential is then fitted with a Fourier series of up to 18 terms, so that it can be interpolated to a finer numerical grid (typically 300 points instead of 36). The corresponding energy levels are found by numerically solving the one-dimensional Schrödinger equation (6.7) for a rigid rotor [33–35].

$$-\frac{h^2}{8\pi l_r}\frac{\partial^2 \Psi}{\partial \theta^2} + V(\theta)\,\Psi = \varepsilon \Psi \tag{6.7}$$

The reduced moment of inertia (I_r) is calculated using the equation for $I^{2,3}$, as defined by East et al. [36]. The resulting energy levels ε_i are then summed to obtain the partition function at the specified temperature, as follows:

$$Q_{\text{int rot}} = \frac{1}{\sigma_{\text{int}}} \sum_i \exp\left(-\frac{\varepsilon_i}{k_B T}\right) \tag{6.8}$$

where σ_{int} is the symmetry number associated with that rotation. It should be noted that, in this method, the low-frequency torsional modes have been approximated as one-dimensional rigid rotors, while in practice these modes can be coupled with another. However, a study of coupled internal rotations in another radical addition reaction (ethyl benzyl radical addition to ethene) indicated that the errors incurred in using a one-dimensional treatment are relatively minor, particularly when compared with the errors incurred under the harmonic oscillator approximation [37].

By treating low-frequency torsional modes as 1D-hindered internal rotations, one is effectively averaging contributions from conformations that are within a single bond rotation of the starting geometry. Provided that this starting geometry is the global minimum conformation for that species, this normally captures all of the energetically relevant conformers and no further Boltzmann averaging is needed. To find the global minimum, one needs to perform a conformational search because procedures for optimizing geometries only find the nearest local minimum structure. The best way to do this is to start with an optimized geometry, and generate starting structures by rotating bonds in increments of 120° (or 180° if cis–trans isomerization is being considered). All combinations of such bond rotations should in principle be considered, which means that the number of structures to be optimized increases rapidly with system size. Even a simple radical adduct of methacrylate dimer with $S{=}C(SCH_2CH_3)SC(CH_3)C(O)OCH_3$ has over 1.4 million different conformers and, even if one assumes all esters to be cis, there are still well over 150 000 structures to optimize in a complete conformational search. Given this bottleneck, many different types of conformational searching algorithms have been designed –ranging from fully stochastic methods to semi-systematic methods and genetic algorithms. The semi-systematic algorithm energy-directed tree search (EDTS) [38] was designed and benchmarked specifically for tackling this problem for oligomeric polymerization reactions, including RAFT polymerization. The algorithm reduces the scaling from 3^n to 2^n (where n is the number of rotatable bonds) in the worst-case scenario, making it suitable for systems that are too big for complete conformational searches but still small enough for chemically accurate electronic structure calculations. Benchmarking on large systems (e.g. containing as many as 80 000 conformers) showed that the algorithm consistently found the global minimum, or a structure with an energy within 1 kcal mol^{-1} of it, with the calculation of a manageable number of species (a few hundreds at most, usually less) [38].

The other key aspect to conformational searching is the choice of quantity upon which to base the search. Early studies used the electronic energies from gas-phase geometry optimizations [3]. However, follow-up studies of radical propagation kinetics showed that this could give incorrect results in systems displaying intramolecular non-covalent interactions such as hydrogen bonding [39]. On the one hand, such

interactions lead to lower electronic energies in the gas phase and hence searches that are based on gas-phase electronic energies tend to find hydrogen-bonded conformations. However, these interactions also lead to lower entropy, which raises the Gibbs free energies at relevant reaction temperatures. Moreover, the energetic importance of hydrogen bonding is also reduced in solution compared with the gas phase, and solvation also tends to favour non-hydrogen-bonded conformations. The net effect of these two factors is that the lowest solution-phase Gibbs free energy conformations tend to be more open and differ from the hydrogen-bonded conformations obtained when electronic energies are used. Indeed, several studies have shown that the inclusion of solvent effects is crucial in conformational searching when non-covalent interactions such as hydrogen bonding are important [40, 41]. Methods for modelling solvent effects are discussed in Section 6.2.3.

In evaluating the rate coefficients, the method for identifying the transition structure is also important. Standard geometry optimization algorithms identify the transition structure as a first order saddle point in the potential energy surface, that is, as the structure having the maximum internal energy (E) along the minimum energy path. However, ideally the rate calculations should be performed using the structure having the maximum Gibbs free energy (G). At non-zero temperatures, E and G are non-equal and thus the geometries corresponding to their maximum values are not necessarily equivalent. The corresponding methods for calculating the rate coefficients are known as standard transition state theory and variational transition state theory, respectively [31]. Variational transition state theory is more accurate but also more expensive, as it entails the calculation of the energies and partition functions not just at the transition structure but at several points along the minimum energy path. In practice, for reactions with significant energy barriers, the differences between transition state theory and variational transition state theory are relatively minor, and the lower cost standard method can be used. However, for barrierless reactions (and also for some low-barrier reactions), variational effects can become important.

Radical addition to the sulfur atom of a C=S double bond is typically a fast reaction, having a low or even negative barrier ($\Delta E^{\ddagger}$) in most cases. The positive Gibbs free energy barrier results from opposing enthalpic and entropic effects [6]. In other words, both ΔE and ΔH decrease along the reaction coordinate but $-T\Delta S$ increases and its opposing interaction leads to the maximum in ΔG. Under these circumstances, one might have expected variational effects to be very important for these systems. However, in an assessment study for the prototypical RAFT systems $R\cdot + S{=}C(Z)SCH_3$ (R = CH_3, CH_2Ph, CH_2COOCH_3, $C(CH_3)_2CN$; Z = CH_3, Ph, CH_2Ph), it was found that provided the transition structures were corrected via IRCmax, the use of variational transition state theory had little or no effect on the reaction barriers [6]. The effects on the entropies and hence reaction rates were somewhat larger (up to a factor of 16) in the case of the $\cdot CH_3$ addition reactions, but for the reaction of the substituted radicals (which are more indicative of real polymerization systems), they remained relatively small (c. a factor of 2). Thus, while variational transition state theory should always be used when possible for

these systems, standard transition state theory may be adopted for large systems without incurring significant additional error.

6.2.3 Solvent Effects

The methodology described thus far is designed to reproduce chemically accurate values of the rate and equilibrium constants for gas-phase systems; however, the majority of RAFT polymerizations occur in solution. The development of cost-effective methods for treating the solvent in chemical reactions is an ongoing area of research [42, 43]. The simplest and most computationally efficient methods are continuum models, in which each solute molecule is embedded in a cavity surrounded by a dielectric continuum of permittivity ε [43]. Some of the more sophisticated continuum models, such as the *ab initio* conductor-like solvation model (COSMO) [44] and the polarizable continuum model (PCM) [45], also include terms for the non-electrostatic contributions of the solvent, such as dispersion, repulsion, and cavitation. Continuum models are designed to reproduce bulk or macroscopic behaviour, and can fare extremely well in certain applications such as the calculation of the solvation free energies [46], redox potentials [47], and pK_a values [48] of various organic molecules. However, the results obtained using continuum models are highly sensitive to the choice of cavities (which are typically parameterized to reproduce the free energies of solvation for a set of small organic molecules), and the choice of appropriate cavities for weakly bound species such as transition structures can be problematic [46]. Moreover, their accuracy can suffer if there are explicit solute–solvent interactions such as complex formation and hydrogen bonding [49]. Although this problem can be overcome by including a small number of explicit solvent molecules in the *ab initio* calculation, as in a cluster-continuum model [50], this adds significantly to the cost of the calculation. Such explicit solute–solvent interactions might be expected to be particularly important when studying aqueous-phase polymerizations of monomers capable of undergoing strong hydrogen-bonding interactions (such as acrylic acid).

The impact of solvent effects on both the quantitative results and the qualitative trends is clear in Figure 6.1, which compares the effect of chain length (n) on the equilibrium constant (K; $\mathrm{l\,mol^{-1}}$) at 298.15 K for a model trithiocarbonate-mediated polymerization of acrylamide and a model dithiobenzoate-mediated polymerization of methyl methacrylate in the gas phase and bulk solution. [40] In both cases, but particularly the acrylamide, the inclusion of solvent affects the trends and quantitative results by as much as 7 orders of magnitude. Nonetheless, while this shows that solvent effects are crucial, they can to a large extent be captured accurately with continuum solvation models, as evident in a range of benchmarking studies for small molecule and polymeric systems [8, 51, 52].

6.2.4 Accuracy and Outstanding Challenges

Normally, one might establish the accuracy of *ab initio* calculations through comparison with reliable experimental data. However, in the case of the RAFT process this

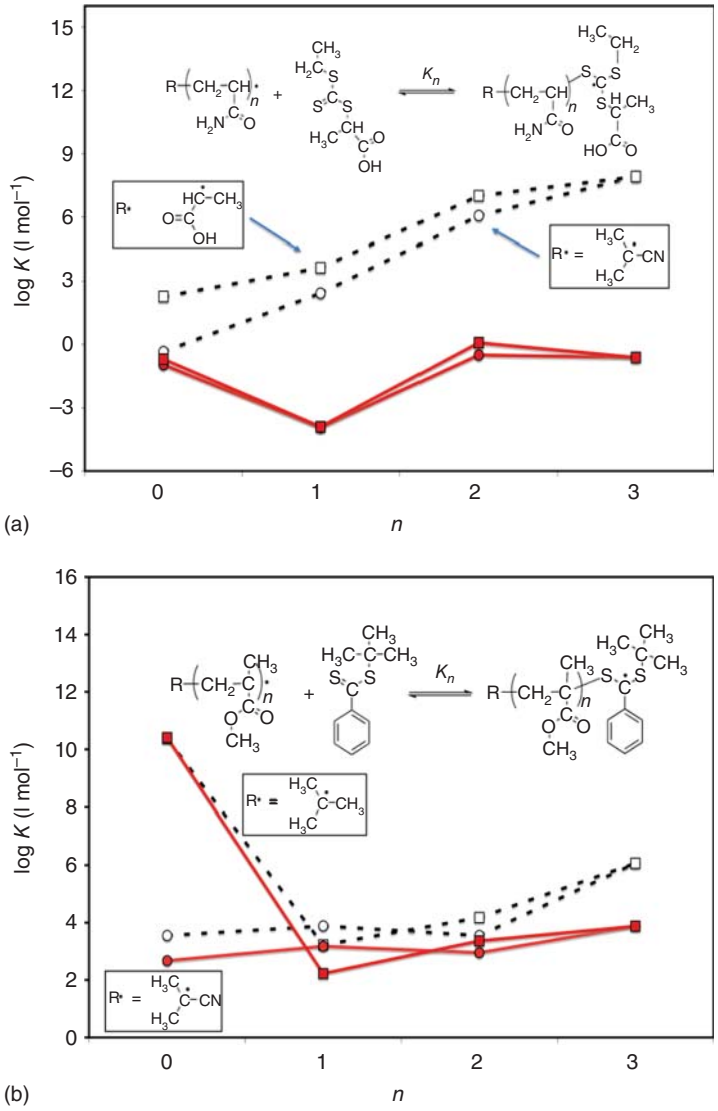

Figure 6.1 The effect of chain length (*n*) on the equilibrium constant (*K*; l mol^{-1}) at 298.15 K for (a) a model trithiocarbonate-mediated polymerization of acrylamide and (b) a model dithiobenzoate-mediated polymerization of methyl methacrylate. In each case, solid lines are in bulk solution, dashed lines in the gas phase, circles indicate reactions where R is the initiator fragment (i.e. $C(CH_3)_2CN$), and square points indicate reactions where R is the leaving group of the RAFT agent (i.e. $CH(CH_3)COOH$ and $C(CH_3)_3$ and respectively) [40].

is difficult as there is no model-free manner in which to measure experimentally the rates and equilibrium constants of the individual addition–fragmentation processes. Even if one makes the assumption that addition and fragmentation are chain length independent beyond the dimer stage, a complete kinetic model would be needed to contain in excess of 100 adjustable parameters (see Scheme 6.1 [53]). As a result, various simplifications and approximations are made in obtaining experimental measurements, and these are a potential source of error. Alternative experimental measurements for ostensibly the same system can differ by several orders of magnitude, and choosing the 'correct' experimental value for comparison with the theoretical data is problematic. For example, although there is excellent agreement between the calculated equilibrium constant of 4.2×10^6 l mol^{-1} (the originally reported value of 7.3×10^6 l mol^{-1} [54] corrected to W1-theory) for cumyl dithiobenzoate (CDB)-mediated polymerization of styrene at 303.15 K and the experimental values (1.06×10^7 l mol^{-1}) obtained from model-fitting to low-conversion kinetic data [54], both the experimental and theoretical values are in conflict with those estimated from electron paramagnetic resonance (EPR) data (8×10^1 l mol^{-1}) albeit under different polymerization conditions [55].

Nonetheless, there is greater consensus amongst the various experimental groups with regard to measurements of the rate constant for addition to the RAFT agent, and the values obtained thus far (c. 10^6 l mol^{-1} s^{-1}) also appear to be relatively insensitive to the nature of the dithioester and attacking radical (see for example Table 3.2 of Chapter 3 of Ref. [56]). These experimental values are in excellent agreement with the theoretical calculations for related small radicals; for example, the calculated values for addition of R· to S=C(CH_3)SCH_3 are 1.2×10^6 and 3.8×10^6 l mol^{-1} s^{-1} for the typical R groups C(CH_3)$_2$CN and CH(Ph)CH_3, although slightly faster values are obtained (c. 10^7–10^8) for more reactive small radical species (such as CH_2COOCH_3 and CH(CH_3)OCOCH_3) [3].

Support for the accuracy of the computational predictions was also provided in a kinetic modelling study of the initialization period in cyanoisopropyl dithiobenzoate-mediated polymerization of styrene [57]. In this work, *ab initio* predictions of the equilibrium constants for the first eight addition–fragmentation reactions of the RAFT process were combined with reliable experimental values of the rate coefficient for radical addition to the RAFT agent and the rate coefficients for initiation, propagation, and termination in styrene homopolymerization. These parameters were then used to predict, without any additional model fitting, the overall monomer conversion and individual concentration profiles of the low molecular weight thiocarbonyl compounds formed during the early stages of the process. These *ab initio* predictions showed excellent agreement with previously measured experimental data (obtained under the same reaction conditions used in the kinetic simulation), despite the fact that no adjustable fit parameters were used (see Figure 6.2 [57]). This work will be discussed in more detail in Section 6.3.4.

Other strategies have also been used for testing the accuracy of the theoretical calculations. To begin with, we recall that the levels of theory have been selected on the basis of assessment studies, and their accuracy established through comparison with high levels of theory, which in turn have been benchmarked against gas-phase

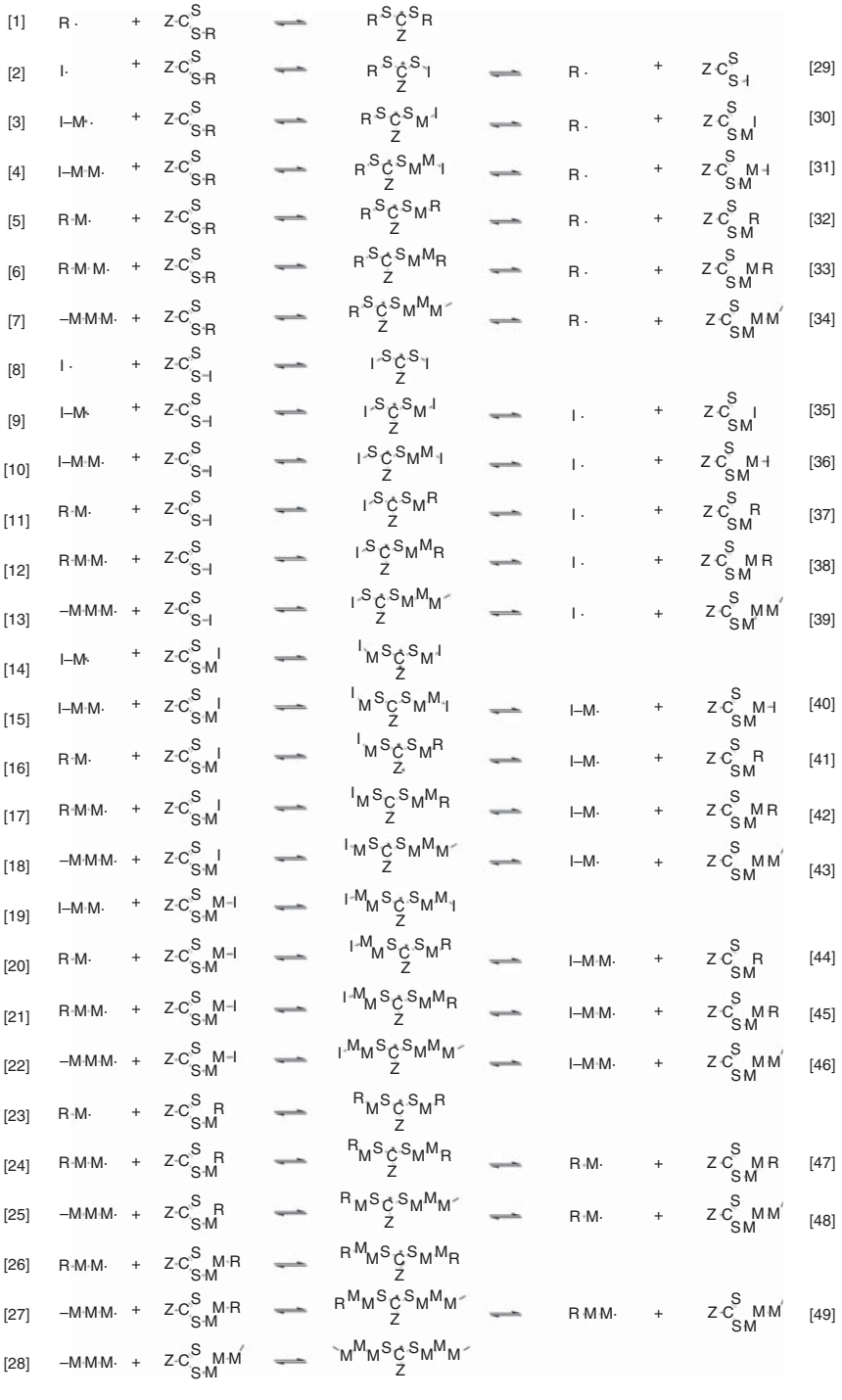

Scheme 6.1 Set of addition–fragmentation reactions to be included in a complete RAFT reaction scheme if chain length effects extend to the trimer stage [53].

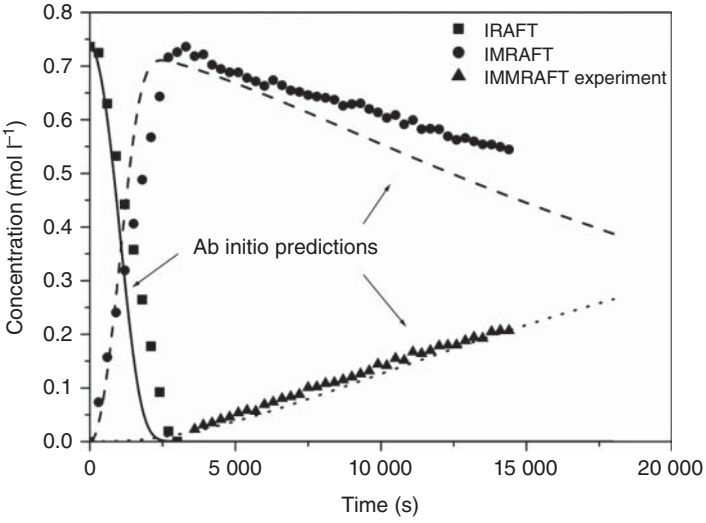

Figure 6.2 Experimental (McCleary et al. [58], symbols) and simulated (Coote et al. [57], lines) evolutions of the initial RAFT agent (cyanoisopropyl dithiobenzoate, IRAFT, full line), and the RAFT agents having one monomer unit (IMRAFT, dashed line) and two monomer units (IMMRAFT, dotted line) inserted. The concentrations of the reagents were $C^0_{\text{IRAFT}} = 0.736\,\text{mol}\,\text{l}^{-1}$, $C^0_{\text{AIBN}} = 0.10\,\text{mol}\,\text{l}^{-1}$, $C^0_{\text{Styrene}} = 3.65\,\text{mol}\,\text{l}^{-1}$, and $C^0_{\text{C6D6}} = 5.4\,\text{mol}\,\text{l}^{-1}$ and the temperature was 70 °C.

thermochemical data [4–6]. On the basis of these assessment studies, it is concluded that the selected procedures can model the absolute barriers and enthalpies for radical addition C=S double bonds to within approximately 4 kJ mol^{-1}. It is also possible to benchmark the calculations against (relatively model-free) solution-phase experimental data for related small systems. For example, Scaiano and Ingold [59] have studied the addition of *tert*-butyl radicals to di-*tert*-butyl thioketone via laser flash photolysis, obtaining an equilibrium constant of 1.2×10^6 $\text{l}\,\text{mol}^{-1}$ at 25 °C. This is in very good agreement with the corresponding theoretical value (7.9×10^5 $\text{l}\,\text{mol}^{-1}$) [60], the latter being slightly lower due to the neglect of the solvent in the calculations. Moreover, more recent benchmarking studies in which the solvent is taken into account do reproduce the experiment very well for addition reactions to dithioesters [8, 51, 52].

The computational methodology can also be benchmarked against experimental data for polymeric systems for the case of the propagation rate coefficients. Although not chemically identical to an addition–fragmentation reaction, a propagation reaction is still a radical addition reaction and has the advantage that reliable experimental data can be obtained using pulsed laser polymerization (PLP) [61]. A computational study of the propagation of vinyl chloride and acrylonitrile yielded values within a factor of 2 of the experimental polymeric values, and demonstrated that the rate coefficient for the polymeric propagating species was adequately modelled using the corresponding rate coefficient for the dimer [19]. Further studies of a wider range of monomers are currently underway, but it does seem that 'chemical accuracy' is now attainable.

Despite this success, a number of challenges remain. In particular, as noted above, the treatment of solvent effects is not yet satisfactory, and larger errors might be expected for solvent-sensitive systems such as acrylic acids. It should also be stressed that the above methodology is not suitable for studying the diffusion-controlled termination processes. In principle, one could calculate the chemically controlled component of the termination reaction using computational chemistry, and this could be extremely helpful in some situations. For example, there is currently a debate about whether the RAFT-adduct radical is capable of undergoing termination [54, 55, 62–70]; establishing whether the chemically controlled component is fast or slow would be an important contribution to this debate. However, the above methodology, which makes use of methods with single-reference wavefunctions, is not likely to be suitable for studying the transition structure of a radical–radical process. Unfortunately, multireference methods are considerably more computationally intensive and further work is needed to identify reliable low-cost alternatives for such systems.

Even in the case of the addition–fragmentation reaction, the computational cost of the calculations remains an issue. Although the ONIOM-based approach facilitates the calculation of accurate energetics for relatively large systems, other computational bottlenecks are now emerging. Larger systems (such as the reactions of dimer radicals with RAFT agents) have a high degree of conformational complexity, and finding the minimum energy conformations of these species can be computationally very demanding. We currently identify these via a complete conformational search; that is, we optimize geometries for every (non-unique) conformation about every bond (or forming bond) in the molecule (or transition structure). For example, in a relatively simple species such as $(CH_3)_2C(Ph)–CH_2–CH(Ph)–S–C\cdot(Ph)–S–C(CH_3)_2Ph$, we might need to consider 324 possible conformations. Inserting just one extra styryl unit increases the number of possible conformers to 2916 and the calculations rapidly become impractical. To address this problem, as noted above we have developed a more efficient algorithm for exploring conformational space called the *Energy-Directed Tree Search* [38]. Preliminary indications are that it is possible to find the global minimum reliably at a cost of approximately 10% of a full search for typical RAFT systems, but further savings would be desirable. A related computational bottleneck stems from the need to treat the low-frequency torsional modes as hindered internal rotations. As explained above, this entails the calculation of full rotational potentials (typically 36 geometry optimizations) for each mode considered. This too can rapidly become computationally infeasible, and strategies for reducing this computational expense are currently being investigated. Nonetheless, despite these problems, it is now possible to perform accurate calculations on systems that are large enough (c. 30–40 non-hydrogen atoms) to be of relevance to practical polymerization systems.

6.3 Computational Modelling of RAFT Kinetics

One of the main advantages of a computational approach to studying RAFT polymerization kinetics is the ability to determine the rate and equilibrium constants of

individual reactions directly, without having to fit a kinetic model to data. This is particularly useful for complex processes such as RAFT because the kinetic models for these processes potentially can contain more adjustable parameters than can practically be estimated from the available experimental data. For example, as noted above, even if we make the assumption that the addition–fragmentation equilibrium becomes chain length independent beyond the dimer stage, a 'complete' kinetic model for the process would need to contain 49 addition rate coefficients and 49 fragmentation rate coefficients (see Scheme 6.1 [53]), in addition to various re-initiation rate coefficients, and the usual initiation, propagation, termination, and transfer coefficients. Since this is impractical, experimental studies typically make simplifying assumptions – such as replacing all 98 rate coefficients by just 2 or 4 – and these assumptions are a potential source of error. In particular, such simplifications are likely to affect the description of subtle yet important effects such as the concentration profiles of the various species during the early stages of the process [58, 71].

Computational chemistry can assist the kinetic modelling of RAFT in a number of ways. Firstly, it is possible to study the effects of chain length and other remote substituents on the addition–fragmentation equilibria. This information can be used to identify which simplifying assumptions are justifiable in a kinetic model, and thereby assist experimental studies. The same information can also be used to assist the computational studies by identifying which remote substituents can be replaced with smaller groups without affecting the calculated results. Secondly, it is possible to use computational chemistry to establish whether side reactions (such as alternative fragmentation pathways) are likely to be operative in particular systems, and thus whether they need to be taken into account in the kinetic modelling schemes. Finally, it is possible to calculate the rate and equilibrium constants for many of the early reactions in the RAFT process, and thereby help minimize the number of adjustable parameters that need to be measured experimentally. Indeed, provided suitable small models for the polymeric reactions can be designed, it is possible in principle to calculate all chemically controlled rate coefficients for a RAFT process, so as to evaluate the performance of new RAFT agents prior to experimental studies.[1] These aspects are now examined in turn.

6.3.1 Simplified Models for Theory and Experiment

Both theoretical and experimental studies of radical polymerization processes rely heavily on the fact that in a chemically controlled reaction, the effects of substituents diminish rapidly with their distance from the reaction centre. From an experimental perspective, it allows one to treat the reactions of species differing only in their remote substituents as identical, thereby reducing the number of adjustable parameters in kinetic models. From a theoretical perspective, it allows one to replace these unimportant remote substituents with smaller chemical groups,

1 One would need to use experimental data for the diffusion controlled termination rate coefficients but these could be obtained from a single homopolymerization polymerization of the specified monomer in the absence of RAFT agent.

thereby reducing the computational cost of the calculations. For example, in free radical copolymerization, the reactivity of the propagating radical is determined solely by the nature of its terminal and penultimate units, and is independent of the chemical composition of the remainder of the polymer chain [72]. As a result, kinetic models for copolymerization need only to consider the propagation reactions of four types of propagating radicals instead of thousands, while computational studies can determine the radical and monomer reactivity ratios using dimers as chemical models of the propagating species. This has been confirmed in both experimental [73, 74] and theoretical [19] studies of the homopropagation rate coefficients, which indicate that the rate coefficients have largely converged to their long chain limit at the dimer radical stage and completely converged well before the decamer stage.

In the RAFT process, there are two key areas where simplifications to kinetic and theoretical studies are desirable. In the generic addition–fragmentation process R· + S=C(Z)SR′, it is important to discover whether the kinetics and thermodynamics are affected by the nature of the 'attacking group' (R·) and the 'non-participating group' (R′) and, if so, at what point the remote substituent effects become negligible. Recent experimental [1, 75, 76] and theoretical [6, 7, 24, 53, 77, 78] studies of the effects of substituents on the RAFT process indicate that the kinetics and thermodynamics are extremely sensitive to the nature of the attacking radical and the Z group of the RAFT agent (S=C(Z)SR′). For example, the equilibrium constant (at 333.15 K) for $\cdot CH_3$ addition to $S{=}C(CH_3)SCH_3$ increases by approximately 6 orders of magnitude when the CH_3 Z group is replaced with a phenyl substituent, and decreases by 7 orders of magnitude when the methyl attacking group is replaced with the initiating radical derived from 2,2′-azobis(isobutyronitrile) (AIBN), $\cdot C(CH_3)_2CN$ [7]. It is therefore essential that reactions differing in the nature of their Z groups and/or the primary substituents of their R groups are treated as being kinetically distinct. The influence of the R′ is less significant and some simplifications are possible. For example, the calculated equilibrium constants for $\cdot CH_3$ addition to $S = C(CH_3)SR'$ for R′ = CH_2X, $CH(CH_3)X$, and $C(CH_3)_2X$ and X = H, CH_3, CN, Ph, $COOCH_3$, $OCOCH_3$ range over 3 orders of magnitude (see Table 6.1) [53]. However, this effect is mainly steric in origin, with the bulky R′-groups destabilizing the thiocarbonyl compound to a greater extent than the more flexible RAFT-adduct radical. As a result, the *K* values for individual classes of monosubstituted, disubstituted, and trisubstituted R′ groups fall into much smaller ranges and, depending on the nature of the monomer and initial R′ group, it may be possible to ignore the effect of R′ in some kinetic models.

Given that the R, Z and, to some extent, the R′ groups all affect the addition–fragmentation equilibrium, it is not surprising that the addition–fragmentation equilibrium is also affected by the chain length of the R and R′ groups. Figure 6.1 above shows the effects of chain length (n) on the equilibrium constant (K; l mol^{-1}) at 298.15 K for a model trithiocarbonate-mediated polymerization of acrylamide and a model dithiobenzoate-mediated polymerization of methyl methacrylate [40]. Figure 6.3 below shows the effects of chain length (n) on the equilibrium constants for addition of styryl radicals of varying chain lengths, $(NC)C(CH_3)_2{-}(CH_2CHPh)_n\cdot$

Table 6.1 Effect of R′ on the calculated enthalpies (ΔH), entropies (ΔS), and equilibrium constants (K)[a] at 333.15 K for the model RAFT reaction, $\cdot CH_3 + S{=}C(CH_3)SR' \rightarrow CH_3SC\cdot(CH_3)SR'$.

X	R′ = CH_2X			R′ = $CH(CH_3)X$			R′ = $C(CH_3)_2X$		
	$-\Delta H$	$-\Delta S$	K	$-\Delta H$	$-\Delta S$	K	$-\Delta H$	$-\Delta S$	K
H	76.0	149.0	3.8×10^{7}						
CH_3	79.9	138.6	1.8×10^{7}	81.8	146.2	1.7×10^{7}	94.3	145.3	1.7×10^{9}
CN	92.9	161.5	1.8×10^{8}	93.2	163.2	1.5×10^{8}	102.4	146.4	2.9×10^{10}
Ph	87.8	166.4	1.5×10^{7}	89.9	151.0	1.8×10^{8}	104.5	153.3	2.9×10^{10}
$COOCH_3$	90.0	168.1	3.3×10^{7}	97.1	175.4	1.8×10^{8}	97.5	158.6	1.4×10^{9}
$OCOCH_3$	92.0	166.3	8.1×10^{7}	99.5	167.2	1.1×10^{9}	106.3	153.1	6.1×10^{10}

a) ΔH (kJ mol^{-1}), ΔS (J mol^{-1} K^{-1}) and K (l mol^{-1}). The original data reported in Ref. [53] was re-calculated at the W1-ONIOM//B3-LYP/6-31G(d) level of theory in conjunction with the harmonic oscillator approximation and taken from Ref. [3].

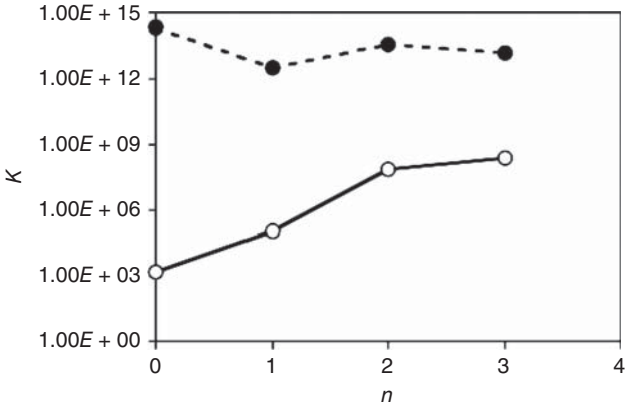

Figure 6.3 The effect of chain length (n) on the equilibrium constant (K; l mol^{-1}) at 333.15 K for the addition of $(NC)C(CH_3)_2{-}(CH_2CHPh)_n\cdot$ to $S{=}C(Ph)SCH_3$ (○) and addition of $CH_3\cdot$ to $S{=}C(Ph)S{-}(CH(Ph)CH_2)_n{-}C(CH_3)_2CN$ (●) [3].

($n = 0$, 1, 2, 3), to $S{=}C(Ph)SCH_3$, and the addition of $\cdot CH_3$ radicals to the corresponding macroRAFT agents, $S{=}C(Ph)S{-}(CHPhCH_2)_n{-}C(CH_3)_2CN$ [53].

From Figures 6.1 and 6.3 it is clear that chain length effects in the early stages of the RAFT process, and chain length effects on the attacking radical R· (in $R\cdot + S{=}C(Z)SR'$) are significant and variable. In general, however, they appear to have converged by the $n = 3$ trimer species. In the case of the RAFT agent substituent R′ chain length effects appear to be much less significant and converge after $n = 1$. In other words, in the early stages of the reaction, chain length effects in the attacking radical, and to a lesser extent the RAFT agent substituent, are significant and neglecting them leads a serious over-simplification of the initialization kinetics. Based on the currently available computational results, it seems reasonable to

suppose that reactions of the various primary species (R· and I·), unimeric radicals (I–M· and R–M·), dimeric radicals (R–M–M· and I–M–M·), and the remaining longer chain species do need to be treated as being kinetically distinct.

Beyond the trimer, chain length effects on the reaction energies appear to have converged; however, entropic chain length effects cannot be ruled out. Such chain length effects are known to converge rapidly in reactions such as propagation, which involve a polymeric species adding to a small molecule to produce a polymeric species of similar size. However, RAFT reactions can involve a polymeric species adding to a polymeric RAFT agent to produce a species that is significantly larger than either. In those situations, entropic effects converge much more slowly and this could account for the few orders of magnitude discrepancy between small-molecule RAFT equilibrium constants (by theory or experiment) [79] and the corresponding experimental equilibrium constants for the addition of polymeric species to polymeric RAFT constants [80]. Regardless, a 'complete' kinetic model of the addition–fragmentation kinetics would thus resemble at least that provided in Scheme 6.1, and would contain far too many unknown parameters for fitting to experimental data alone. As will be seen below, computational chemistry offers the prospect of reducing the number of unknown parameters by providing direct calculations of the relevant values for the early small-molecule reactions of the RAFT process, leaving the estimation of a smaller number of parameters corresponding to the longer chain radicals to experiment.

6.3.2 Side Reactions

In designing an appropriate kinetic model for RAFT polymerization, it is also necessary to determine whether additional side reactions need to be incorporated into the kinetic scheme. In principle, one could use computational chemistry to *find* all possible side reactions of a process from first principles. However, this would entail the calculation of a complete multi-dimensional potential energy surface for the chemical system, followed by molecular dynamics simulations for a wide variety of possible trajectories. Unfortunately, this is currently too computationally intensive for practical RAFT systems. However, it is possible to study specific postulated side reactions and test whether they are likely to occur. For example, if hydrogen abstraction reactions involving the RAFT-adduct radical were suspected to be a problem in certain polymerization systems, one could calculate rate coefficients for the various possible reactions (i.e. abstraction of the different hydrogen atoms on the monomer, polymer, RAFT agent, and so forth). By comparing their rates with the normal β-scission reaction, one could thereby establish which (if any) of the possible abstraction reactions were likely to be competitive.

For example, computational chemistry was used to show that competitive β-scission of the C—O bond of the alkoxy group in xanthate-mediated polymerization of vinyl acetate was important [81]. Rate coefficients (333.15 K) for both the normal β-scission of the vinyl acetate radical and the side reaction were calculated for a series of model RAFT-adduct radicals, $CH_3SC{\cdot}(OZ')SCH_2OCOCH_3$ for Z′ = Me, Et, *i*-Pr, and *t*-Bu (see Scheme 6.2) [3]. It was shown that for the

Z′ = Me, Et, and *i*-Pr systems, the normal β-scission reaction is favoured and this is consistent with the experimental observation that these systems display normal RAFT behaviour. In contrast, for the *t*-Bu case, the side reaction is preferred, and this provided a suitable explanation for the experimentally observed inhibition in this system. In general, it would be worth considering this side reaction when the Z′ substituent of the xanthate is a good radical leaving group (such as *t*-Bu) and/or the propagating radical is a poor leaving group (as in vinyl acetate or ethylene polymerization).

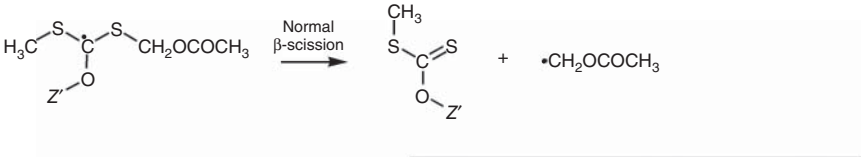

Z′	k_β Alkoxy	k_β Normal	Ratio
Me	3.2×10^4	2.3×10^5	1.4×10^{-1}
Et	3.5	1.7×10^5	1.2×10^{-5}
i-Pr	1.6×10^2	6.8×10^2	2.4×10^{-1}
t-Bu	2.1×10^5	1.7×10^2	1.2×10^3

Scheme 6.2 Competitive β-scission processes in xanthate-mediated polymerization of vinyl acetate [3].

Other side reactions might also be conceivable under certain circumstances, although their feasibility is yet to be confirmed computationally. As noted above, there is some debate as to whether the RAFT-adduct radical is capable of undergoing irreversible and/or reversible termination reactions (see Scheme 6.3) to any significant extent in normal polymerizing RAFT systems [54, 55, 62–70, 82]. Recently Buback and coworkers used DFT calculations to study the thermodynamics of several of these steps, showing that they are thermodynamically feasible [82]. However, calculations of the corresponding rate coefficients would be required to identify which, if any, of the reactions in Scheme 6.3 are capable of out-competing the β-scission reaction of the intermediate radical under normal polymerization conditions. Although computational quantum chemistry is not currently capable of predicting diffusion-controlled rate coefficients, computational calculations could nonetheless be used to calculate the chemically controlled component of the termination rate and establish a lower bound to the termination rate coefficient. To this end, work is currently underway to identify cost-effective multireference methods for studying such systems.

Another side reaction that is worth considering is the attack of the propagating radical at the carbon centre (rather than the sulfur centre) of the C=S bond to produce a sulfur-centred radical. Studies of radical addition to simple thiocarbonyl compounds indicate that this side reaction is actually thermodynamically preferred, though it is kinetically less favourable by 1–2 orders of magnitude [4, 83]. This is

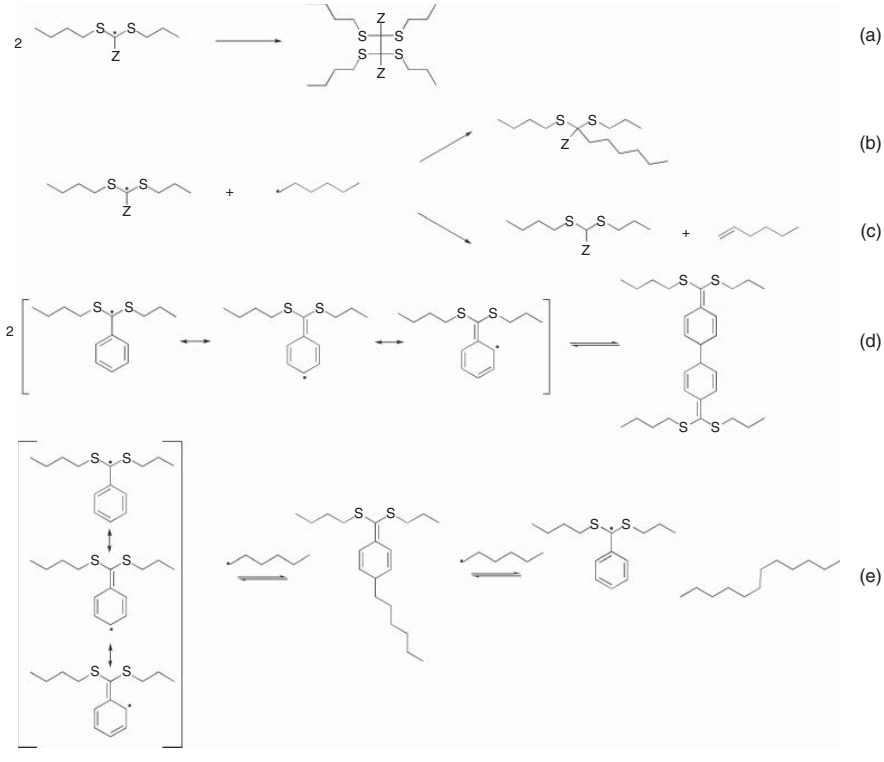

Scheme 6.3 Possible reversible and irreversible termination reactions of the RAFT-adduct radical.

due in part to the greater steric hindrance at the carbon centre and in part to the stronger early bonding interaction when attack occurs at sulfur (see below) [83]. In RAFT systems, the steric hindrance at the carbon centre is yet greater, and the kinetic preference for addition at carbon should normally be very small. Nonetheless, given that addition to the RAFT agent occurs many thousands of times during the lifetime of the propagating radical, even a low relative rate of addition at carbon might be sufficient to affect the polymerization kinetics in certain systems. Other side reactions that have been suggested include reaction of the RAFT-adduct radical with the monomer (i.e. copolymerization), the *syn*-elimination of tertiary R-groups (as the corresponding alkenes) at elevated temperatures, and reactions with oxygen impurities [1, 84]. Computational studies of these and other pathways could help establish their feasibility and clarify their mechanism. Finally, while it is unlikely in the context of normal RAFT conditions, decomposition of RAFT-based polymers has also been studied both experimentally and computationally [85, 86].

6.3.3 Computational Model Predictions

Provided calculations are performed at an appropriately high level of theory, computational chemistry can be used to determine the rates and equilibrium constants for the individual reactions in a RAFT polymerization. The resulting values can then be used to study structure–reactivity trends, reduce the number of adjustable parameters in a kinetic analysis of experimental data, or, ultimately, predict the kinetic behaviour of a RAFT polymerization system from first principles. Table 6.2 shows a compilation of the main equilibrium constants that have been reported to date [3]. Owing to their greater computational expense, the reaction rates for RAFT systems have been less widely studied. However, the rate coefficients have been reported for a number of small model systems and these are provided in Table 6.3 [3]. Owing to the significant errors that occur at low levels of theory, only high-level *ab initio* values are included in these tables. However, where possible, the original calculations were improved to the W1-ONIOM level of theory and re-calculated at a consistent temperature (333.15 K) [3]. Values obtained under the harmonic oscillator approximation are reported for all systems and where possible the more accurate hindered rotor values are also reported.

The data confirm that the equilibrium constants (and thus the addition–fragmentation kinetics) are dependent upon the nature of the attacking radical and the RAFT agent. In a practical RAFT system it is not valid to treat all of the possible reactions as having the same rates. Thus, for example, when calculated at a uniform level of theory, the equilibrium constant for addition of a styryl radical to RAFT agents of the form S=C(Ph)SCH$(CH_3)_2$ vary from 2.9×10^5 to 3.6×10^9, depending on whether styryl is modelled as a unimer with an H end-group, a $C(CH_3)_2CN$ end-group, a $C(CH_3)_2Ph$ end-group, or as a dimer with an H end-group. This explains why simplified models do not appear to be capable of describing the initialization period in RAFT systems; indeed, as will be shown below, once these effects are taken into account excellent agreement between the experimental data and model predictions is obtained [57, 91]. Chain length effects may also

Table 6.2 Effect of R, Z, and R′ on the calculated equilibrium constants (K)[a] at 333.15 K for the model RAFT reaction, $\cdot R + S{=}C(Z)SR' \rightarrow RSC\cdot(Z)SR'$.

R·		K(HO)	K(HR)	R·		K(HO)	K(HR)
$CH(CH_3)CN$	$Z = CH_3$ $R' = CH_3$	2.9×10^{0}		CH_2COOCH_3	$Z = CH_3$ $R' = CH_3$	6.0×10^{3}	6.7×10^{4}
$C(CH_3)_2CN$ (AIBN)	$Z = CH_3$ $R' = CH_3$	1.2×10^{-1}	9.6×10^{-1}		$Z = Ph$ $R' = CH_3$	4.1×10^{7}	
	$Z = Ph$ $R' = CH_3$	1.5×10^{3}	2.6×10^{4}		$Z = CH_2Ph$ $R' = CH_3$	1.1×10^{4}	
	$Z = CH_2Ph$ $R' = CH_3$	1.3×10^{0}			$Z = CH_3$ $R' = CH_2COOCH_3$	8.6×10^{4}	
	$Z = Ph$ $R' = CH(CH_3)_2$	1.1×10^{5}	7.4×10^{4}		$Z = F$ $R' = CH_3$	2.1×10^{1}	
	$Z = F$ $R' = CH_3$	9.4×10^{-4}		$CH(CH_3)COOCH_3$ (MA)	$Z = CH_3$ $R' = CH_3$	3.5×10^{2}	
	$Z = CN$ $R' = CH_3$	1.4×10^{7}			$Z = CH_3$ $R' = CH_2CN$	1.5×10^{3}	
	$Z = OCH_3$ $R' = CH_3$	3.8×10^{-6}			$Z = Ph$ $R' = CH_3$	1.0×10^{6}	5.6×10^{6}
	$Z = Ph$ $R' = C(CH_3)_2CN$	1.1×10^{5}			$Z = Ph$ $R' = CH(CH_3)_2$	5.9×10^{6}	3.6×10^{7}
CH_2CH_3	$Z = CH_3$ $R' = CH_3$	1.8×10^{6}		$C(CH_3)_2COOCH_3$	$Z = CH_3$ $R' = CH_3$	4.3×10^{0}	
$CH(CH_3)_2$	$Z = CH_3$ $R' = CH_3$	4.7×10^{5}		CH_2OCOCH_3	$Z = CH_3$ $R' = CH_3$	1.3×10^{6}	

$C(CH_3)_3$	$Z = CH_3$ $R' = CH_3$	1.5×10^5			$Z = F$ $R' = CH_3$	2.3×10^3	
	$Z = F$ $R' = CH_3$	4.1×10^3			$Z = CN$ $R' = CH_3$	4.5×10^{14}	
CH_2Ph	$Z = CH_3$ $R' = CH_3$	2.7×10^0	2.8×10^2		$Z = OCH_3$ $R' = CH_3$	5.6×10^0	
	$Z = Ph$ $R' = CH_3$	2.8×10^5			$Z = OCH_2CH_3$ $R' = CH_3$	1.7×10^1	
	$Z = CH_2Ph$ $R' = CH_3$	4.1×10^1			$Z = OCH(CH_3)_2$ $R' = CH_3$	7.8×10^1	
	$Z = F$ $R' = CH_3$	2.9×10^{-3}			$Z = OC(CH_3)_3$ $R' = CH_3$	3.7×10^2	
	$Z = CN$ $R' = CH_3$	1.5×10^9		$CH(CH_3)OCOCH_3$ (VA)	$Z = CH_3$ $R' = CH_3$	9.6×10^5	5.0×10^7
	$Z = OCH_3$ $R' = CH_3$	5.3×10^{-5}			$Z = OCH_3$ $R' = CH_3$	1.3×10^0	1.5×10^1
$CH(CH_3)Ph$ (STY)	$Z = CH_3$ $R' = CH_3$	1.1×10^0	5.1×10^1		$Z = F$ $R' = CH_3$	2.0×10^3	3.4×10^4
	$Z = Ph$ $R' = CH_3$	1.5×10^5	3.4×10^6	$C(CH_3)_2OCOCH_3$	$Z = CH_3$ $R' = CH_3$	6.6×10^4	
	$Z = Ph$ $R' = CH(CH_3)_2$	2.9×10^5	6.6×10^5	$CH(CH_3)COOH$ (AA)	$Z = CH_3$ $R' = CH_3$	2.0×10^1	
	$Z = Ph$ $R' = C(CH_3)_2CN$	6.5×10^7			$Z = F$ $R' = CH_3$	2.1×10^{-1}	1.9×10^0
	$Z = F$ $R' = CH_3$	1.0×10^{-3}	8.8×10^{-3}		$Z = N$-Pyrrole $R' = CH_3$	1.2×10^2	

(*continued*)

Table 6.2 (Continued)

R·		*K*(HO)	*K*(HR)	R·		*K*(HO)	*K*(HR)
	$Z = OCH_3$ $R' = CH_3$	1.1×10^{-5}	1.8×10^{-4}	$CH(CH_3)CONH_2$ (AM)	$Z = CH_3$ $R' = CH_3$	8.0×10^{2}	
$C(CH_3)_2Ph$ (Cumyl)	$Z = CH_3$ $R' = CH_3$	6.9×10^{-2}			Z = F $R' = CH_3$	1.2×10^{0}	7.9×10^{0}
	Z = Ph $R' = CH_3$	2.4×10^{3}	4.6×10^{4}		Z = *N*-Pyrrole $R' = CH_3$	4.1×10^{3}	
	Z = Ph $R' = CH(CH_3)_2$	1.3×10^{5}	2.5×10^{5}	AIBN-STY	Z = Ph $R' = CH_3$	1.1×10^{5}	
Cumyl-STY	Z = Ph $R' = CH_3$	1.3×10^{7}			Z = Ph $R' = CH(CH_3)_2$	1.2×10^{6}	
	Z = Ph $R' = CH(CH_3)_2$	8.7×10^{7}			Z = Ph $R' = C(CH_3)_2CN$	2.3×10^{9}	
Cumyl-STY-STY	Z = Ph $R' = CH_3$	2.8×10^{8}		AIBN-STY-STY	Z = Ph $R' = CH_3$	7.4×10^{7}	
STY-STY	Z = Ph $R' = CH_3$	2.2×10^{8}			Z = Ph $R' = C(CH_3)_2CN$	1.8×10^{11}	
	Z = Ph $R' = CH(CH_3)_2$	3.6×10^{9}		STY-STY-STY	Z = Ph $R' = CH_3$	2.5×10^{8}	

a) Equilibrium constants K ($l\,mol^{-1}$) calculated at the W1-ONIOM//B3-LYP/6-31G(d) level of theory in conjunction with the harmonic oscillator (HO) approximation and, where data were available, also the hindered rotor (HR) model. The original electronic structure data were taken from previous studies [5, 7, 24, 53, 54, 78, 81, 87–89] and corrected to the W1-ONIOM level in Ref. [3] using W1 calculations [4] for the core reaction. For most systems, a two-layer ONIOM approach was possible in which the inner core was calculated at W1 and the rest of the system at G3(MP2)-RAD. For a limited number of larger systems (such as reactions in which Z = Ph and reactions of dimer radicals with various substrates), a three-layer ONIOM approach was used in which the outer layer was calculated at RMP2/6-311+G(3df,2p).

Table 6.3 Calculated addition (k_{add}), fragmentation (k_{frag}), and equilibrium (K) constants[a] at 333.15 K for the Model RAFT reaction, $\cdot R + S{=}C(Z)SCH_3 \rightarrow RSC\cdot(Z)SCH_3$.

R·	Z	k_{add} (HO)	k_{add} (HR)	k_{frag}(HO)	k_{frag}(HO)	K (HO)	K (HR)
CH_3	CH_3	9.6×10^{5}	1.7×10^{6}	9.6×10^{-2}	3.4×10^{-2}	1.0×10^{7}	4.9×10^{7}
	Ph	4.2×10^{7}	7.7×10^{7}	2.5×10^{-4}	7.2×10^{-6}	1.7×10^{11}	1.1×10^{13}
	CH_2Ph	2.6×10^{6}	1.2×10^{7}	1.4×10^{-2}	1.7×10^{-3}	1.9×10^{8}	7.3×10^{9}
	OCH_3	1.2×10^{4}		1.4×10^{3}		8.2×10^{0}	
	OCH_2CH_3	3.1×10^{4}		8.2×10^{2}		3.8×10^{1}	
	$OCH(CH_3)_2$	3.4×10^{4}		5.6×10^{2}		6.1×10^{1}	
	$OC(CH_3)_3$	3.2×10^{4}		1.8×10^{2}		1.8×10^{2}	
CH_2Ph	CH_3	6.6×10^{5}	3.9×10^{6}	1.2×10^{5}	1.4×10^{4}	5.6×10^{0}	2.8×10^{2}
$CH(CH_3)Ph$	CH_3	7.5×10^{5}	3.8×10^{6}	6.8×10^{5}	7.5×10^{4}	1.1×10^{0}	5.1×10^{1}
	F	2.3×10^{5}	1.8×10^{6}	2.3×10^{8}	2.1×10^{8}	1.0×10^{-3}	8.8×10^{-3}
	OCH_3	6.2×10^{3}	4.4×10^{4}	5.8×10^{8}	2.5×10^{8}	1.1×10^{-5}	1.8×10^{-4}
CH_2COOCH_3	CH_3	5.7×10^{7}	1.7×10^{8}	1.1×10^{4}	2.5×10^{3}	5.2×10^{3}	6.8×10^{4}
$C(CH_3)_2CN$	CH_3	4.5×10^{5}	1.2×10^{6}	3.7×10^{6}	1.2×10^{6}	1.2×10^{-1}	9.6×10^{-1}
CH_2OCOCH_3	OCH_3	1.3×10^{6}		2.3×10^{5}		5.6×10^{0}	
	OCH_2CH_3	2.8×10^{6}		1.7×10^{5}		1.7×10^{1}	
	$OCH(CH_3)_2$	5.2×10^{4}		6.8×10^{2}		7.8×10^{1}	
	$OC(CH_3)_3$	6.2×10^{4}		1.7×10^{2}		3.7×10^{2}	
$CH(CH_3)OCOCH_3$	CH_3	6.3×10^{7}	4.2×10^{8}	6.7×10^{1}	8.4×10^{0}	9.6×10^{5}	5.0×10^{7}
	F	1.5×10^{8}	5.6×10^{8}	7.5×10^{4}	1.7×10^{4}	2.0×10^{3}	3.4×10^{4}
	OCH_3	3.9×10^{6}	5.0×10^{7}	3.0×10^{6}	3.3×10^{6}	1.3×10^{0}	1.5×10^{1}

a) Rate coefficients for addition ($l\,mol^{-1}\,s^{-1}$) and fragmentation (s^{-1}) and equilibrium constants ($l\,mol^{-1}$) calculated at the W1-ONIOM//B3-LYP/6-31G(d) level of theory in conjunction with the harmonic oscillator approximation (HO) and, where data were available, also the hindered rotor model (HR). The original electronic structure data were taken from previous studies [6, 81, 89, 90] and corrected to the W1-ONIOM level in Ref. [58] using W1 calculations [4] for the core reaction. Reactions of $\cdot CH_3$ radical and $\cdot CH_2OCOCH_3$ radical with the xanthates were studied via standard transition state theory; all other reactions were studied via variational transition state theory.

help explain the large discrepancies in the experimental values for the rates and equilibrium constants in CDB-mediated polymerization that are obtained by fitting simplified models to experimental data, though it seems likely that additional factors (such as missing side reactions) may be required to resolve the problem fully [80].

Secondly, although the equilibrium constants vary considerably, this variability arises mainly in the fragmentation reaction. For most substituents, the addition rate coefficients fall into a relatively narrow range (10^5–10^7 l mol^{-1} s^{-1}). In these cases, it may be reasonable to treat all (or most) of the possible addition reactions in a specific process as having the same rate coefficients, provided the rates of their reverse fragmentation reactions are allowed to vary. However, there are a few important exceptions. In particular, the addition of propagating radicals to xanthates is typically much slower than to dithioesters (Z = alkyl, aryl) unless the propagating radical is highly reactive (as in vinyl acetate polymerization). As a result of their slow addition rate, monomers with stable propagating radicals (such as styrene) are not normally well controlled by xanthates. Moreover, within the xanthate reactions themselves, there is a large variation in the addition rate coefficient depending on whether the propagating radical is capable of undergoing H-bonding interactions with the alkoxy group of xanthate in the transition structure (see Section 6.4.1). Indeed, this H-bonding interaction may be partially responsible for the success of xanthates in controlling vinyl acetate. In this regard, it is worth noting that the xanthates have been less successful in controlling ethylene polymerization, another system in which the propagating radical is relatively unstable but for which the H-bonding interaction is absent. From Table 6.3, it is seen that even for the methyl radical, which might reasonably be expected to be more reactive than the ethyl propagating species, the addition rate coefficient for the xanthate agent is relatively low (c. 10^4 l mol^{-1} s^{-1}).

Finally, the data indicate that slow fragmentation of the RAFT-adduct radical can help explain the experimentally observed inhibition periods in cumyl dithiobenzoate-mediated polymerizations [54]. Kinetic studies indicate that rate retardation is likely to be significant when K is greater than or equal to approximately 10^6 l mol^{-1} [92]. The equilibrium constants for addition of unimers of methyl acrylate (3.6×10^7) and dimers (3.6×10^9) of styrene satisfy this condition, while that for addition of cumyl (2.5×10^5) and the styrene unimer (6.6×10^5) lie within the level of possible error. In contrast, fragmentation of $\cdot C(CH_3)_2CN$ from the RAFT-adduct radical is not predicted to be retarded (7.4×10^4), consistent with the experimental observation [93] that cyanoisopropyl dithiobenzoate does not display a significant inhibition period. On the basis of Table 6.2, other retarded processes would include the fragmentation reactions of the RAFT-adduct radicals bearing a cyano Z group, and the fragmentation of ethyl radicals and vinyl acetate radicals from the adduct radicals of dithioesters. Table 6.2 also correctly predicts that in the case of vinyl acetate this rate retardation is relieved when xanthates are used instead. They also indicate that similar success is likely with fluorodithioformates (Z = F), the new computationally designed class of RAFT agents [87]. In this way, such simple calculations can be used to evaluate quickly whether a polymerization is likely to be successful.

6.3.4 *Ab initio* Kinetic Modelling

It is clear from both computational and experimental studies of RAFT kinetics that simplified kinetic models in which side reactions and chain length effects are ignored are not capable of providing an adequate description of all aspects of the RAFT process [80]. However, kinetic models in which these effects are properly taken into account would contain too many unknown adjustable parameters for fitting to experimental data. As noted above, computational chemistry offers a potential solution to this problem by allowing for the rates and equilibrium constants of the individual steps to be calculated independently. The calculated values could be used to reduce the number of fit parameters in the kinetic model to more manageable levels or, ultimately, replace the fit parameters altogether. In the latter case, one would have a truly *ab initio* kinetic modelling tool that could allow for predictions of the macroscopic properties of the polymerization process without recourse to experimental fit parameters.[1] Such predictions could be compared directly with experimental data so as to provide a sensitive test of a kinetic model's validity. Moreover, having identified a suitable kinetic model, *ab initio* kinetic modelling could then be used to test new RAFT agents and optimize reaction conditions prior to experiment.

Proof of principle for *ab initio* kinetic modelling was provided for cyanoisopropyl dithiobenzoate-mediated polymerization of styrene at 70 °C in the presence of the initiator AIBN [57]. Based on computational studies of the chain length dependence of the addition–fragmentation reaction, a kinetic model that included a chain-length-dependent fragmentation reaction was constructed using modelling software PREDICI® [94]. In this model, chain length effects in the attacking radical were included up to the trimer stage and chain length effects in the macroRAFT agent, which were found to be considerably smaller, were considered only up to the unimer stage (see Scheme 6.4). Equilibrium constants (at 70 °C) were then calculated for the eight kinetically distinct addition–fragmentation reactions and used in conjunction with the chain-length-independent experimental value for the addition rate coefficient so as to obtain the corresponding chain-length-dependent fragmentation rate coefficients. These were combined with reliable experimental data for the initiation, propagation, and termination reactions, as taken from styrene homopolymerization experiments. A kinetic simulation of the process was then performed using identical reaction conditions to those in an earlier experiment on the same system [58]. The concentration profiles obtained for the low molecular weight thiocarbonyl compounds formed during the early stages of the reaction, together with the corresponding experimental data, are shown in Figure 6.2 [57]. The predicted and measured rates of overall monomer conversion were also compared [57]. As noted above, there is excellent agreement between the *ab initio* kinetic simulation and the experimental data despite the fact that no model fitting of any kind was performed, and hence the model and calculations are sufficiently accurate for predictive purposes. Further confirmation of this accuracy was recently provided in an *ab initio* kinetic modelling study of 2-cyano-2-propyl dodecyl trithiocarbonate-mediated polymerization of styrene [95]. *Ab initio* kinetic

I. Initiation

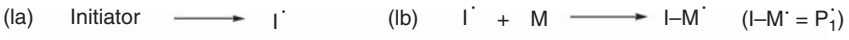

II. RAFT equilibria

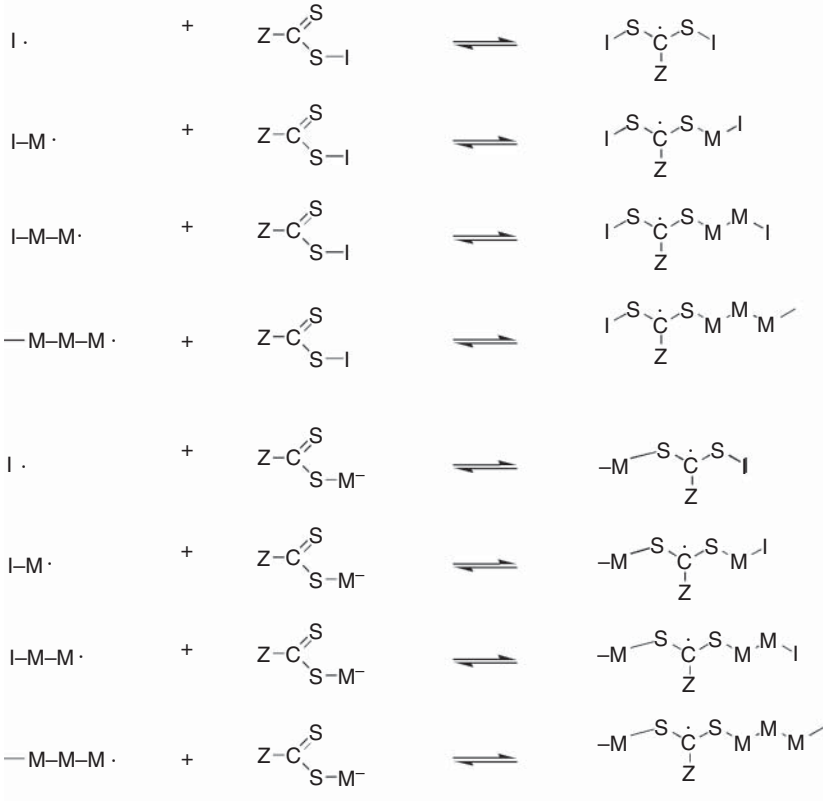

III. Propagation

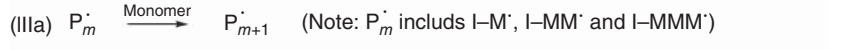

V. Termination

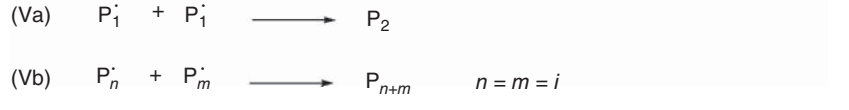

Scheme 6.4 Reaction scheme for *ab initio* kinetic modelling of cyanoisopropyl dithiobenzoate-mediated polymerization of styrene in the presence of AIBN.

modelling is now a practical possibility for studying RAFT polymerization and the scope of its potential applications can be expected to expand further with increasing computer power.

6.4 Structure–Reactivity Studies

Computational quantum chemistry also has an important role to play in providing an underlying understanding of the reaction mechanism and structure–reactivity trends. At one level, computational chemistry can be used as a tool for determining the rate or equilibrium constants of the individual addition–fragmentation processes for a variety of RAFT agent and monomer combinations. In this regard, it offers a complementary approach to experimental techniques, which are better suited to measuring more practical quantities, such as the extent of control or the apparent chain transfer constant. At a deeper level, computational chemistry can also offer convenient access to additional mechanistic information, such as the geometries, charges, and spin densities, and to other relevant energetic quantities, such as radical stabilization energies of the adduct radical. This information can greatly assist in the interpretation of the structure–reactivity trends. Based on both *ab initio* calculations and experimental approaches, there is now a very good understanding of why C=S double bonds are so effective at addition–fragmentation reactions, and how the RAFT agent substituents affect this process. In what follows, these fundamental and practical aspects are summarized in turn, and we then show how this information can be used to design optimal RAFT agents.

6.4.1 Fundamental Aspects

A key aspect to controlling free radical polymerization by RAFT is the establishment of an addition–fragmentation equilibrium in which there is rapid exchange between the propagating species and the dormant macroRAFT agent. This in turn entails that *both* the addition of the propagating radical to the RAFT agent and the fragmentation of the resulting RAFT-adduct radical (which is effectively the reverse reaction) are sufficiently fast. In radical addition to C=C bonds this is normally quite difficult to achieve. Typically, if addition is fast, the reaction is highly exothermic and fragmentation is too slow. If instead the addition reaction is not very exothermic, then fragmentation becomes relatively facile but addition is then too slow. Although some success has been achieved with macromonomers [96], alkenes are not generally suitable as practical RAFT agents. The question then arises: why are compounds containing C=S bonds so much more effective, and are there any other types of double bond that would serve the same purpose?

To understand the high reactivity of thiocarbonyl RAFT agents, it is helpful to examine a simple curve-crossing model analysis of prototypical radical additions to C=S and C=C bonds [83]. The curve-crossing model was developed by Pross and Shaik [97–99] as a theoretical framework for explaining barrier formation in chemical reactions. The basic idea is to think of a chemical reaction as comprising

a rearrangement of electrons, accompanied by a rearrangement of nuclei (i.e. a geometric rearrangement). We can then imagine holding the arrangement of electrons constant in its initial configuration (which we call the reactant configuration), and examining how the energy changes as a function of the geometry. Likewise, we could hold the electronic configuration constant in its final form (the product configuration), and again examine the variation in energy as a function of the geometry. If these two curves (energy vs. geometry) are plotted, we form a 'state correlation diagram'. The overall energy profile for the reaction, which is also plotted, is formed by the resonance interaction between the reactant and product configurations (and any other low-lying configurations). State correlation diagrams allow for a qualitative explanation for how the overall energy profile of the reaction arises and can then be used to provide a graphical illustration of how variations in the relative energies of the alternative valence bond (VB) configurations affect the barrier height.

In radical addition to double bonds (X=Y), the principal VB configurations that may contribute to the ground-state wavefunction are the four lowest doublet configurations of the three-electron three-centre system formed by the initially unpaired electron at the radical carbon (R) and the electron pair of the π bond in X=Y (A) [100].

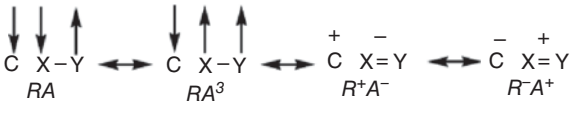

(6.9)

The first configuration (*RA*) corresponds to the arrangement of electrons in the reactants, the second to that of the products (RA^3), and the latter two (R^+A^- and R^-A^+) to possible charge transfer configurations. The state correlation diagram showing (qualitatively) how the energies of these configurations should vary as a function of the reaction coordinate is provided in Figure 6.4 [3]. In plotting this figure we have arbitrarily designated the R^+A^- configuration to be lower in energy than the R^-A^+ configuration.

In the early stages of the reaction, the reactant configuration (*RA*) is the lowest energy configuration and dominates the reaction profile. This is due to the stabilizing influence of the bonding interaction in the π bond of the *RA* configuration, which is an anti-bonding interaction in the RA^3 configuration. However, as the reaction proceeds, the C···X=Y distance decreases and the unpaired electron on the radical is able to interact with the X=Y species. This growing interaction destabilizes the *RA* configuration but stabilizes the RA^3 configuration due to the increasing bonding interaction in the forming C···X bond (which is an anti-bonding interaction in the RA configuration). As the relative energies of the *RA* and RA^3 configurations converge, the increasing interaction between the alternative configurations stabilizes the ground-state wavefunction, with the strength of the stabilizing interaction increasing as the energy difference between the alternate configurations decreases. It is this mixing of the reactant and product configurations that leads to the avoided crossing, and accounts for barrier formation. Beyond the transition

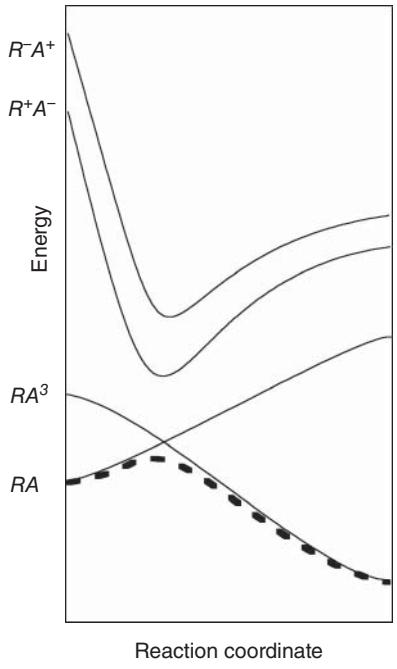

Figure 6.4 State correlation diagram for radical addition to double bonds [3].

structure, the product configuration is lower in energy and dominates the wavefunction. The charge transfer configurations of the isolated reactants and the isolated products are high in energy, but in the vicinity of the transition structure they are stabilized via favourable Coulombic interactions and can sometimes be sufficiently low in energy to interact with the ground-state wavefunction. In those cases, the transition structure is further stabilized, and (if one of the charge transfer configurations is lower than the other) the mixing is reflected in the degree of partial charge transfer between the reactants.

Using this state correlation diagram, in conjunction with simple VB arguments, the curve-crossing model can be used to predict the qualitative influence of various energy parameters on the reaction barrier [97–99]. In particular, the barrier is lowered by an increase in the reaction exothermicity (see Figure 6.5a), a decrease in the RA–RA^3 separation in the reactants and/or products (see Figure 6.5b), and/or a

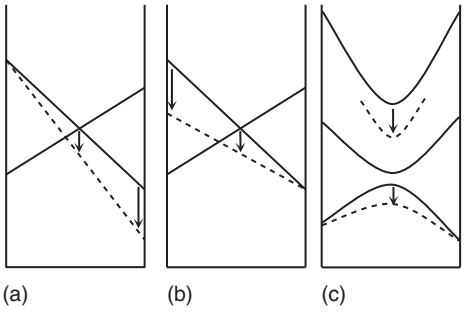

Figure 6.5 State correlation diagrams showing the qualitative effect on the barrier height of (a) increasing the exothermicity; (b) decreasing the singlet–triplet excitation gap; and (c) decreasing the relative energy of one of the charge transfer configurations [3].

decrease in the relative energies of one or both of the charge transfer configurations, provided that these are sufficiently low in energy to contribute to the ground-state wavefunction (see Figure 6.5c). Of these parameters, the reaction exothermicity is of course directly accessible from *ab initio* molecular orbital calculations. For the radical addition reactions, the RA–RA^3 separation is related to the singlet–triplet excitation gap of the alkene or thiocarbonyl species. The relative importance of the charge transfer configurations can be assessed on the basis of the energy for charge transfer between the isolated reactants, and can be further assessed by examining the actual extent of charge transfer in the transition structures.

With these simple principles in hand, it then becomes obvious why thiocarbonyls make much more effective RAFT agents than alkenes. As is well known, the π bond of a thiocarbonyl is much weaker than that of an alkene, due to the poorer overlap between the p–π orbitals of the (third row) S atom and the (second row) C atom [101]. This reduced π bond strength is reflected in a greatly reduced singlet–triplet gap for the thiocarbonyl species, and hence in lower barriers and earlier transition structures for radical addition [83]. Indeed, unless there is substantial stabilization of the C=S bond (via, for example, resonance with lone pair donor substituents at carbon), radical addition to C=S bonds is typically barrierless (i.e. $\Delta H^{\ddagger} \approx 0$), the free energy barrier (i.e. $\Delta G^{\ddagger} > 0$) arising merely due to the opposing enthalpic and entropic effects [6]. Conversely, in the reverse direction, the transition state is very late and almost completely dominated by the reaction exothermicity (i.e. $\Delta H^{\ddagger} \approx \Delta H$).

The low singlet–triplet gap explains not only why dithioesters are generally very reactive to radical addition but also how it is possible to manipulate the RAFT agent substituents so as to ensure that fragmentation is also sufficiently fast. The curve-crossing model predicts that the barrier is affected by the reaction enthalpy: the less exothermic the reaction, the greater the barrier. Indeed, in the absence of any additional factors (such as steric or polar effects), the well-known Evans–Polanyi rule [102] ($\Delta H^{\ddagger} = \alpha \Delta H$) will hold. In radical addition to C=C bonds, this raises a problem. If one wishes to promote the fragmentation reaction, one needs to make the addition reaction less exothermic but, in doing so, this raises the barrier to radical addition. In radical addition to C=S bonds this is also the case, but there is an important difference. Owing to the early transition structures, the influence of the exothermicity on the addition reaction is greatly reduced (i.e. the proportionality constant α is much smaller), and there is much greater scope for manipulating the reverse fragmentation reaction without compromising the addition rate.

The dominant influence of the triplet configuration of the π bond also helps to explain the regioselectivity of the radical addition reaction. As explained above, radical addition to the carbon centre of the C=S bond is actually the thermodynamically preferred reaction, although in practice addition occurs at S due to kinetic factors [4, 83]. The spin density is considerably greater on S than on C in the triplet configuration of the thiocarbonyl, and there is thus a much stronger early bonding interaction when addition occurs at this site. Although the preference for attack at sulfur is countered by the reduced exothermicity, the early transition structure ensures that influence of the triplet configuration dominates.

Finally, it is worth exploring whether compounds containing other types of double bonds would be suitable in RAFT processes. In particular, dithiophosphinate esters have been proposed as possible alternative RAFT agents [103]. In such systems, the propagating radical would add to the sulfur centre of the P=S bond, generating a phosphoranyl radical (instead of a carbon-centred radical) as the intermediate.

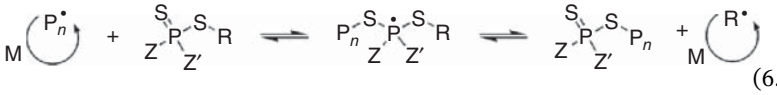

(6.10)

Although there is some experimental indication that styrene polymerization can be controlled using $S{=}P(SCH(CH_3)Ph)_3$ and $S{=}P(Ph)_2SCH(CH_3)Ph$ [103], the observed control was by no means perfect and there was clear evidence of hybrid behaviour. Computationally, it was shown that radical addition to the P=S bonds of dithiophosphinate esters was considerably less reactive and less exothermic than addition to the corresponding C=S compounds [104]. This is due in part to the lower inherent stabilization energy of its phosphoranyl radical product and in part to its stronger double bond [104]. Indeed, unlike the C=S double bond of dithioesters, the P=S bond has a significant ionic character (i.e. a large resonance contribution from $P^+–S^-$), which generally renders it less susceptible to radical addition (unless the attacking radical is highly electrophilic). On this basis, it was concluded that dithiophosphinate esters are likely to have only limited applicability as RAFT agents, and would be most suited to the control of electrophilic monomers [104].

More recent studies have also explored the potential of Se-based RAFT agents [105]. Theoretical studies suggest that identically substituted dithio- and diselenocarbamate RAFT agents will have similar reactivity but that diselenocarbamate RAFT agents are more likely to undergo intermediate radical termination as a result of the enhanced stability of the intermediate radical. These results have been backed by experimental studies on the same systems [105]. The suitability of other types of compounds has yet to be explored computationally; however, studies of prototypical systems have revealed that C=C, C=O, and C≡C bonds all have significantly larger singlet–triplet gaps than the corresponding C=S bonds [83, 106]. As a result, they are less reactive to radical addition than C=S bonds, and less likely to function as effective RAFT agents.

6.4.2 Structure–Reactivity in Practical RAFT Systems

Notwithstanding the high reactivity of C=S bonds, the precise nature of the other substituents (R and Z) in a RAFT agent S=C(Z)SR is critical to a controlled polymerization. The degree of control that can be achieved is reliant on the propensity for addition of the propagating radical $P_n\cdot$ to the C=S bond, and the subsequent ability of $P_n\cdot$ to be released from the RAFT-adduct radical. Both of these depend on the steric and electronic properties of R and Z. As a result of numerous experimental studies [1], there now exists a broad understanding of how effective a given R or Z group is for a certain class of polymerization. For example, polymerizations of styrene, acrylates, or methacrylates are well controlled by dithioester RAFT agents having

simple alkyl or aryl Z groups, whereas the polymerization of vinyl acetate is not. For vinyl acetate, control can be achieved with xanthates (Z = OR) or dithiocarbamates ($Z = NR_2$). Equally, it is known [75] that a RAFT agent having R = benzyl would be suitable for polymerization of methyl acrylate, but not for polymerization of methyl methacrylate: the tertiary R group $C(CH_3)_2Ph$ is necessary in the latter case.

Building on the wealth of structure–reactivity data now available from experimental studies, computational chemistry adds a powerful tool that allows these trends to be explained, and this in turn has predictive power. Our computational investigations have been founded on the observation that despite the mechanistic complexity of RAFT polymerization, the effects of R and Z can in large part be understood by considering simplified versions of the chain transfer reaction (Eq. (6.11)).

(6.11)

To begin with, it is clear from Table 6.3 that as expected on the basis of the considerations detailed in Section 6.4.1, the fragmentation rate constants generally follow the same order as the fragmentation enthalpies. A useful analysis of structure–reactivity relationships can therefore be carried out on the basis of the thermodynamic parameters. Moreover, the analysis can be further simplified through the use of isodesmic reactions to separate and rank the effects of R and Z [78]. First of all, the fragmentation efficiency associated with a particular Z group is measured by the enthalpy change (ΔH_{frag}) for the reaction $CH_3SC{\cdot}(Z)SCH_3 + S{=}C(H)SCH_3 \rightarrow CH_3SC{\cdot}(H)SCH_3 + S{=}C(Z)SCH_3$. Next, the chain transfer efficiency for a given R group is measured by the enthalpy change (ΔH_{CT}) for the reaction $CH_3{\cdot} + S{=}C(CH_3)SR \rightarrow S{=}C(CH_3)SCH_3 + R{\cdot}$. The stabilities of RAFT agents with different Z groups are compared by considering the enthalpies of the reactions $S{=}C(Z)SCH_3 + CH_4 \rightarrow S{=}C(H)SCH_3 + CH_3Z$, while the stabilities of RAFT agents with different R groups are compared by the reactions $S{=}C(CH_3)SR + CH_3SH \rightarrow S{=}C(CH_3)SCH_3 + RSH$. The well-known quantity, radical stabilization energy (RSE) [24, 107], is used to estimate the stabilities of the radical species.

In the overall chain transfer reaction (Eq. (6.11)), the effect of Z involves both the RAFT agent (and the polyRAFT agent) and the intermediate RAFT-adduct radical. One must therefore consider each addition–fragmentation step separately. In Figure 6.6, a variety of Z groups are ranked in the order of increasing fragmentation efficiency $-\Delta H_{frag}$. Shown on the same graph are the stabilities of the two relevant Z-containing species: the RAFT agent and the RAFT-adduct radical. The fragmentation efficiencies span a range of 100 kJ mol^{-1}, making it clear that the choice of Z is critical. We have suggested [78] that in considering the effects of Z, RAFT agents may be divided into three broad classes based on their values of ΔH_{frag}. In one class are the agents with Z groups favouring fragmentation ($Z = OR$ or NR_2), in the second are those with low fragmentation efficiencies (Z = CN, Ph, or CF_3), and in the third are those with moderate efficiencies (Z = SR, and modified OR or NR_2). As will be discussed below, the different classes are of varying utility depending on the monomer of interest.

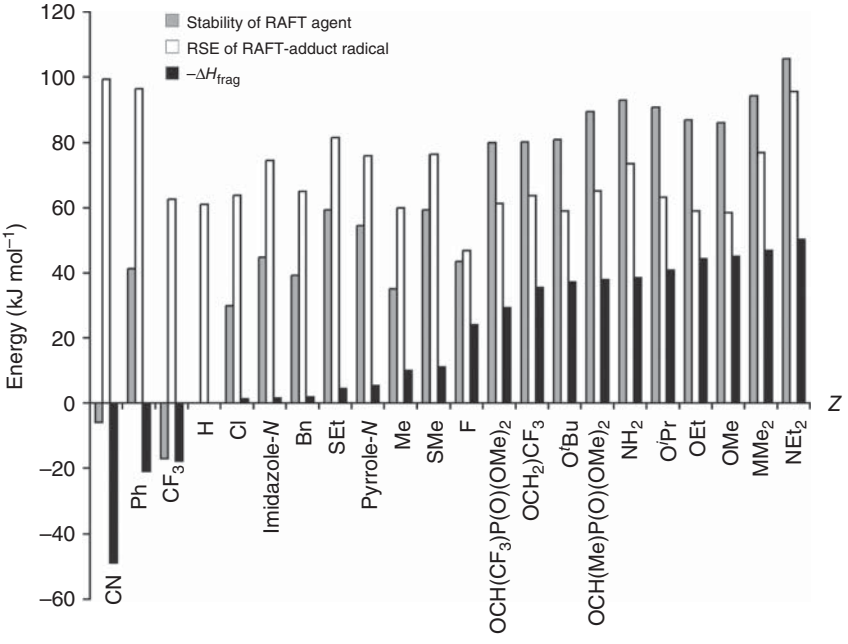

Figure 6.6 Effect of Z group on fragmentation efficiency, RAFT agent stability, and RAFT-adduct radical stability [3].

For the RAFT agents (and polyRAFT agents), there are two main ways in which Z affects stability. First, lone pair donor Z groups such as OR, NR_2, and SR enhance stability through delocalization of electron density into the C=S bond as shown in Eq. (6.12).

(6.12)

Second, RAFT agents are destabilized by σ-withdrawal. This property can be clearly seen with the RAFT agents that have Z = CN or CF_3. Within this stability scheme, the positions of several Z groups are worthy of note. For example, the groups Z = pyrrole and Z = imidazole confer much less stabilization on a RAFT agent than do aliphatic amino groups such as NMe_2. This is consistent with the notion that incorporating the nitrogen lone pair into an aromatic system reduces the capacity for electron delocalization according to Eq. (6.12) [108].

For RAFT-adduct radicals, the effects of Z are somewhat more complicated. Here, a major increase in stability is gained if Z is a π-acceptor group such as CN or Ph. Stabilization by π-acceptor groups is common for carbon-centred radicals, and in RAFT-adduct radicals the effect can be enhanced because the lone pair donor SR groups can engage in captodative effects. In principle, the presence of a lone pair donor Z group should be an alternative stabilizing feature (as in other carbon-centred radicals), but in RAFT-adduct radicals this is not always borne

out. We have shown [24] that the delocalization of electron density from an SR group onto a carbon radical centre places the unpaired electron into a higher energy orbital, making further delocalization onto a second SR group much less favourable. A RAFT-adduct radical has two lone pair donor SR groups even before Z is considered, and the capacity for a third interaction involving a lone pair donor Z group is therefore small. Only when Z is a stronger lone pair donor than SR will there be enhanced stabilization. Making the situation more complicated, RAFT-adduct radicals are strongly destabilized by σ-withdrawal (as demonstrated when Z = F), which means that only those Z groups for which lone pair donation is stronger than σ-withdrawal (and stronger than the lone pair donation by a SR group) will confer enhanced stabilization. In Figure 6.6, the only Z groups that satisfy both criteria are the simple amino groups NR_2 (R = H, Me, Et). The alkoxy groups, although being strong lone pair donors, are unable to enhance stability because of their strong σ-withdrawing character.

Considering next the effects of R, we have found that it is usually sufficient to consider the overall chain transfer equilibrium without giving separate attention to the individual steps. Several earlier computational studies have also adopted this approach. For example, semi-empirical methods have been used to show that the chain transfer efficiency of dithiobenzoate RAFT agents varied with R in the order $CH_2COOEt < CH_2COOH < CH(Me)COOEt$ [109]. A related study [77] on a wide range of R groups using DFT reached similar conclusions, suggesting that chain transfer is affected by both steric and polar effects. The overall chain transfer equilibrium is, of course, a competition between the radicals R· and P_n· for adding to the C=S bond. In most cases, the position of the equilibrium is determined mainly by the relative stabilities of the radicals R· and P_n·: the group whose release from the RAFT-adduct radical is favoured is the one whose RSE is greatest. The values of ΔH_{CT} for a range of common R groups are shown in order of increasing chain transfer propensity in Figure 6.7, together with the stabilities of the relevant RAFT agents and radicals R·.

Considering first the R· radicals, the RSEs can be largely explained on the basis of factors normally associated with stability in carbon-centred radicals [110]. Thus, the presence of π-acceptor groups (such as CN or Ph) as α-substituents within R leads to enhanced stability, as does the capacity for hyperconjugative interactions provided by α-CH_3 substituents. On the other hand, in the RAFT agents, the presence of α-CH_3 groups or π-acceptor α-substituents in R results in destabilization. Here, methylation primarily induces unfavourable steric interactions. The π-acceptor groups destabilize the RAFT agents by reducing the capacity for delocalization of the sulfur lone pair onto the double bond (Eq. (6.13)).

(6.13)

The steric and electronic properties of R therefore influence chain transfer in two reinforcing ways – one effect on the RAFT agent and the opposite effect on the R· radical. These combined effects render the commonly used R groups $CH(CH_3)Ph$,

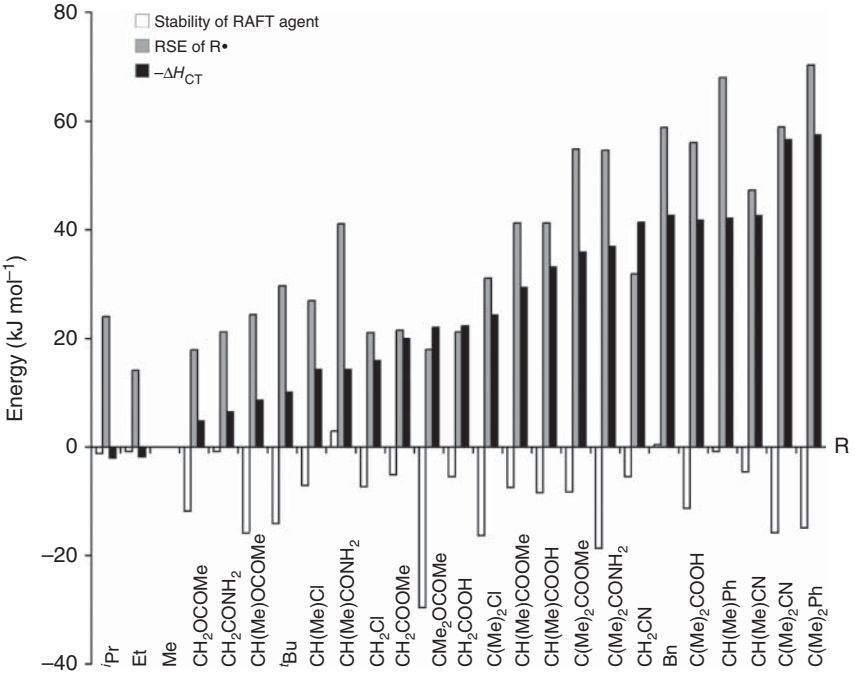

Figure 6.7 Effect of R on RAFT agent stability, R· stability, and chain transfer efficiency [3].

$C(CH_3)_2CN$, and $C(CH_3)_2Ph$ very good leaving group radicals. However, it is not correct to assume that a well-controlled polymerization will result if one simply chooses the best leaving group R = $C(CH_3)_2Ph$. If R· is *too* stable compared with the monomer, then the subsequent re-initiation step is disfavoured, and polymerization will not proceed past the stage of the unimeric RAFT agent. When faced with a new polymerization, a sensible initial approach would therefore be first to take into account the stability of the propagating radical (which is roughly measured by the stability of the monomeric radicals shown in Figure 6.7, and could be better measured using calculations on the dimers), and then to choose an R group for which R· is only slightly more or less stable than M·.

The simplifications involved in deriving the structure–reactivity relationships just described are accompanied, of course, by a number of exceptional cases. One important case is where a system does not obey the usual correlation between kinetics and thermodynamics. For example, by using computational investigations, we have found [81] that in the xanthate-mediated polymerization of vinyl acetate, the rate constant for fragmentation of the RAFT-adduct radical $CH_3SC{\cdot}(Z)SCH_2OCOCH_3$ (Z = OCH_3) is 3 orders of magnitude larger than that for the radical where Z = O^{t}Bu. This result cannot solely be due to the steric effect of Z, however, because for the related RAFT-adduct radicals $CH_3SC{\cdot}(Z)SCH_3$ the rate constants for Z = OCH_3 and Z = O^{t}Bu are nearly identical. The source of the discrepancy lies instead in a hydrogen-bonding interaction in the transition state for the fragmentation of

$CH_3SC{\cdot}(OCH_3)SCH_2OCOCH_3$. A close contact takes place between the carbonyl oxygen and an OCH_3 hydrogen, leading to significant stabilization, whereas no analogous interactions take place for the other three species.

A breakdown of the structure–reactivity trends can also occur if there are synergistic interactions between the groups R, Z, and P_n. For example, we have shown [24] that fragmentation of electron-withdrawing R groups is enhanced by a homoanomeric effect in which the withdrawal of electron density from sulfur towards the R group reduces the ability of sulfur to donate electron density to the radical centre. If the R group contains a π-acceptor substituent, this induces an altered CS–R conformation in which the unpaired electron is delocalized into a CS–R anti-bonding orbital. This not only weakens the S—R bond but is accompanied by a strengthening of the S—P_n bond in compensation. As a result, altered chain transfer efficiencies arise that would not have been predicted on the basis of R· stabilities alone. Moreover, the homoanomeric interaction is further modulated by the nature of Z: for example, a fluorine substituent in the Z position can inhibit the effect of a π-acceptor-containing R group [88]. This example and the vinyl acetate example given above emphasize the importance of conducting specific computational or experimental investigations once one has selected a range of candidate RAFT agents for a particular application.

Going beyond structure–reactivity trends within the RAFT itself, computational studies have also aimed at developing linear free energy relationships for multiple families of controlled radical polymerization processes, including RAFT, atom transfer radical polymerization (ATRP), and nitroxide-mediated polymerization (NMP) [111]. This work employed the ionization energy (IE) of the attacking radical and the electron affinity (EA) of the control agent as polar descriptors, Tolman's cone angle of the attacking radical as a steric descriptor, and the RSE of the attacking radical and the highest occupied molecular orbital–lowest unoccupied molecular orbital (HOMO–LUMO) gap of the control agent as resonance descriptors. Apart from providing a predictive relationship for the R—X bond energy of any control agent, the linear free energy relationship also allows for general observations about the relative role of polar, steric, and resonance effects in the various processes. Specifically, it was shown that RAFT is equally dominated by resonance, steric, and polar effects, while ATRP is dominated by steric and polar effects and NMP by resonance and steric effects. Other studies have analysed trends in RAFT agent reactivity in terms of HOMO–LUMO gaps [112, 113] (Figure 6.8).

6.4.3 RAFT Agent Design

The ultimate goal of computational studies of RAFT polymerization is to design new and improved RAFT agents to tackle any specific control problem. One could envisage a two-stage approach in which one first utilizes the structure–reactivity relationships to select promising combinations of substituents, and then tests the candidate RAFT agents with direct calculations using model propagating radicals. Having established computationally that a certain RAFT agent was likely to be successful, one could then pursue experimental testing.

BDFE [R–X] = – 20.8 θ[R] – 9.73 IP[R] – 1.10 RSE[R] + 192 θ[X] + 57.4 EA[X] – 62.0 resonance[X] + 250

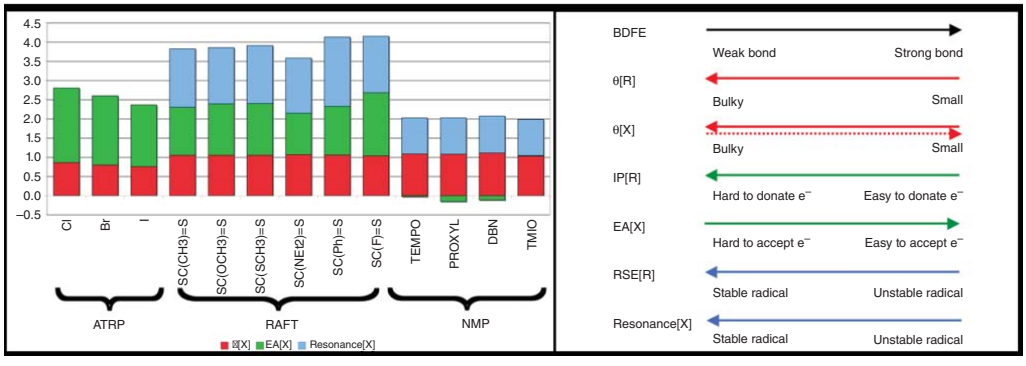

Figure 6.8 Steric (θ), polar (ionization potential [IP], EA), and resonance contributions to the various R–X BDFEs (bond dissociation free energy) in model RAFT, NMP, and ATRP reactions [111].

The kinetic requirements of a successful RAFT agent are now fairly well understood: it should have a reactive C=S bond (k_{add} high) but the intermediate radical should undergo fragmentation at a reasonable rate (typically $K = k_{add}/k_{\beta} < 10^6$ l mol^{-1}); the R group should fragment preferentially from the intermediate radical in the pre-equilibrium but also be capable of re-initiating polymerization; and there should be no side reactions [1, 92]. Computational data shown in Tables 6.2 and 6.3 and in Figures 6.5 and 6.6 can assist in choosing RAFT agents that satisfy these criteria. For example, if one predicted that a propagating radical was relatively stable, then in order to provide good control, its addition to the C=S bond would need to be fast enough to compete with addition to monomer. One could then select a Z group that destabilized the C=S bond, promoting addition (i.e. ΔH_{frag} in Figure 6.6 is large). In contrast, if one predicted that the propagating radical was relatively unstable, then it would be necessary to ensure that the propagating radical did not become trapped for too long as the RAFT-adduct radical. In this case, one would choose a Z group that destabilized the RAFT-adduct radical relative to the C=S compound (i.e. ΔH_{frag} is small). Amongst substituents displaying acceptable ΔH_{frag} values, one could further optimize control by choosing the Z-group that gave the lowest RAFT agent stability, and hence the fastest addition rates. Likewise, one could use ΔH_{CT} values (as in Figure 6.7) to choose the R group – an optimal group usually having a ΔH_{CT} value marginally lower than that of the model propagating radical. Having selected candidate RAFT agents on the basis of the simplified isodesmic measures, they could then be tested computationally through direct calculation of the addition–fragmentation kinetics in more realistic model systems.

There is a growing interest in using computational calculations as a basis for RAFT agent design. Matyjaszewski and Poli [77] and Patten and coworkers [109] have advocated the use of calculated chain transfer energies (Eq. (6.11)) as a basis for choosing appropriate R groups for specified monomers; Matyjaszewski et al. [77, 114, 115] and Tordo and coworkers [116] have applied similar strategies to atom transfer radical polymerization and NMP, respectively. Building on this work, the first computationally designed class of RAFT agents, the fluorodithioformates (S=C(F)SR or 'F-RAFT'), was proposed [87]. These were designed as multi-purpose RAFT agents capable of controlling monomers with stable propagating radicals and also those with unstable propagating radicals. Other current RAFT agents for unstable monomers promote fragmentation of the propagating radicals by stabilizing the thiocarbonyl product of fragmentation (i.e. the RAFT agent). As a result, they are not sufficiently reactive for controlling monomers with stable propagating radicals. In contrast, F-RAFT promotes fragmentation by destabilizing the RAFT-adduct radical without deactivating the C=S bond of the RAFT agent. The fluorine Z-group achieves this through its strong σ-withdrawing capacity, which contributes a destabilizing influence to both the radical and the C=S bond, and helps to counterbalance the stabilizing influence of its lone pair donor capacity. It can be seen in Figure 6.6 that the stability of the fluorinated RAFT agent is comparable to other dithioesters, and much lower than that of the xanthates. On this basis, it is predicted that the RAFT agent is sufficiently reactive for

controlling stable propagating radicals, and the calculated addition rate coefficients (1.8×10^6 l mol^{-1} s^{-1} for a styrene unimer adding to $CH_3SC(F)=S$ at 333.15 K) seem to confirm this [89]. Although the reduced stability renders fragmentation less facile, this is counterbalanced to some extent by the reduced stability of the RAFT-adduct radical. As a result, the equilibrium constant for fragmentation of a model vinyl acetate radical (3.4×10^4 l mol^{-1} at 333.15 K) [89], though higher than that for xanthates, is still considerably lower than the threshold above which rate retardation occurs (c. 10^6 l mol^{-1} [92]). The computational calculations thus predict that F-RAFT should function as a multi-purpose RAFT agent.

Experimental testing has already indicated that benzyl fluorodithioformate is capable of controlling styrene polymerization, although testing of vinyl acetate (and indeed other 'unstable' monomers such as ethylene) is still under way [88]. For these monomers, RAFT agents with alternative leaving groups are required; benzyl fluorodithioformate is not likely to be suitable for controlling vinyl acetate polymerization, due to the slow rate of re-initiation by the benzyl leaving group. Instead, based on further computational calculations [89], we predict that a RAFT agent with a CH_2CN leaving group would be more suitable. With successful practical applications such as this, it is clear that computational quantum chemistry is showing promise as a kinetic tool for studying complicated radical polymerization processes such as RAFT.

More recent RAFT agent design endeavours include the design of a metal-free Dissociative Electron Transfer Reversible Addition–Fragmentation Chain Transfer Polymerization (DET–RAFT) method, which avoids both conventional radical initiators and photo-redox processes, for the polymerization of different monomer families near room temperature. It is based on the use of inorganic sulfites in combination with common RAFT agents and was shown to be successful for a wide range of monomers [117]. In another work, a joint experimental–theoretical study showed that cyanomethyl methyl(phenyl)carbamodithioate (CMPCD) was found to be an efficient RAFT agent enabling the controlled/living polymerization of vinyl chloride [118], while another showed that 2-(2-cyanopropanyl dithiobenzoate) is suitable for 2-acetamidoacrylic acid [119]. More generally, a theoretical study showed that the sulfonyl radical would be effective as a universal leaving group for RAFT polymerization [120], while a joint theory–experiment study showed that strongly electron-deficient sulfonyldithioformate-based RAFT agents could function as building blocks for hetero Diels–Alder reactions [121]. Another theoretical–experimental study used theory and experiment to demonstrate that 4-halogeno-3,5-dimethyl-1*H*-pyrazole-1-carbodithioates have broad applicability [122] while others examined the synthesis of block copolymers based on 2-vinyl-4,4-dimethyl-5-oxazolone [123], or poly(vinylidine fluoride) (PVDF)-*b*-PVAc [124]. Finally, recent theoretical work has explained the mechanism by which sequence-controlled and stereospecific oligomers are synthesized via alternating radical chain growth and sequential photoinduced RAFT single unit monomer insertion [125].

6.5 Outlook

While the key methodological guidelines for studying RAFT processes were established over a decade ago, improvements in computer power have made these methods more widely accessible and applicable to a broad range of systems. At the same time, the crucial role of entropy in polymeric RAFT equilibria and solvent effects has been revealed, further improving the accuracy and applicability of computational studies. This maturing of the methodology has been accompanied by developments in structure–reactivity studies to the extent that it is now possible to select RAFT agents for a given process on the basis of simple computational descriptors, and several successful examples of RAFT agent have been published as a result. While challenges remain, the use of computational chemistry as a useful complementary tool in RAFT agent design is now well established.

Abbreviations

AIBN	α,α′-azobis(isobutyronitrile)
ATRP	atom transfer radical polymerization
BDE	bond dissociation energy
B3-LYP	A DFT method with the Becke's B3 exchange and the correlation functional of Lee, Yang, and Parr
CDB	cumyl dithiobenzoate
COSMO	*ab initio* conductor-like solvation model
DFT	density functional theory
EPR	electron paramagnetic resonance spectroscopy
G3	Gaussian-3; a family of high-level composite methods, e.g. G3, G3B3, G3(MP2)
G3-RAD	a family of G3 methods designed for radical chemistry, e.g. G3(MP2)-RAD
HF	Hartree–Fock
HOMO	highest occupied molecular orbital
LUMO	lowest unoccupied molecular orbital
MP2	second order Møller–Plesset perturbation theory
NMP	nitroxide-mediated polymerization
ONIOM	our own N-layered integrated molecular orbital + molecular mechanic
PCM	polarizable continuum model; a method for incorporating solvent effects
PLP	pulsed laser polymerization
RAFT	reversible addition–fragmentation chain transfer
VB	valence bond (theory)
W1	Wiezmann-1; a high-level composite method

References

1 Moad, G., Rizzardo, E., and Thang, S.H. (2005). *Aust. J. Chem.* 58: 379–410.
2 Coote, M.L., Krenske, E.H., and Izgorodina, E.I. (2008). Quantum-chemical studies of raft polymerization: methodology, structure-reactivity correlations and kinetic implications. In: *Handbook of Raft Polymerization* (ed. C. Barner-Kowollik), 5–49. Weinheim, Germany: Wiley-VCH.
3 Coote, M.L., Krenske, E.H., and Izgorodina, E.I. (2006). *Macromol. Rapid Commun.* 27: 473–497.
4 Coote, M.L., Wood, G.P.F., and Radom, L. (2002). *J. Phys. Chem. A* 106: 12124–12138.
5 Izgorodina, E.I. and Coote, M.L. (2006). *J. Phys. Chem. A* 110: 2486–2492.
6 Coote, M.L. (2005). *J. Phys. Chem. A* 109: 1230–1239.
7 Coote, M.L. (2004). *Macromolecules* 37: 5023–5031.
8 Chernikova, E., Golubev, V., Filippov, A. et al. (2010). *Polym. Chem.* 1: 1437–1440.
9 Scott, A.P. and Radom, L. (1996). *J. Phys. Chem.* 100: 16502–16513.
10 Grimme, S., Hansen, A., Brandenburg, J.G., and Bannwarth, C. (2016). *Chem. Rev.* (9): 5105–5154.
11 Malick, D.K., Petersson, G.A., and Montgomery, J.A. (1998). *J. Chem. Phys.* 108: 5704–5713.
12 Schwartz, M., Marshall, P., Berry, R.J. et al. (1998). *J. Phys. Chem. A* 102: 10074–10081.
13 Martin, J.M.L. and Parthiban, S. (2001). W1 and W2 theories and their variants: thermochemistry in the kJ/mol accuracy range. In: *Quantum Mechanical Prediction of Thermochemical Data* (ed. J. Cioslowski), 31–65. Dordrecht, The Netherlands: Kluwer-Academic.
14 Gómez-Balderas, R., Coote, M.L., Henry, D.J., and Radom, L. (2004). *J. Phys. Chem. A* 108: 2874–2883.
15 Coote, M.L. (2004). *J. Phys. Chem. A* 108: 3865–3872.
16 Henry, D.J., Parkinson, C.J., and Radom, L. (2002). *J. Phys. Chem. A* 106: 7927–7936.
17 Henry, D.J., Sullivan, M.B., and Radom, L. (2003). *J. Chem. Phys.* 118: 4849–4860.
18 Izgorodina, E.I., Coote, M.L., and Radom, L. (2005). *J. Phys. Chem. A* 109: 7558–7566.
19 Izgorodina, E.I. and Coote, M.L. (2006). *Chem. Phys.* 324: 96–110.
20 Check, C.E. and Gilbert, T.M. (2005). *J. Org. Chem.* 70: 9828–9834.
21 Grimme, S. (2006). *Angew. Chem. Int. Ed.* 45: 4460–4464.
22 Wodrich, M.D., Corminboeuf, C., and Schleyer, P.v.R. (2006). *Org. Lett.* 8: 3631–3634.
23 Vreven, T. and Morokuma, K. (2003). *Theor. Chem. Acc.* 109: 125–132.
24 Coote, M.L. and Henry, D.J. (2005). *Macromolecules* 38: 1415–1433.

25 Izgorodina, E.I., Brittain, D.R.B., Hodgson, J.L. et al. (2007). *J. Phys. Chem. A* 111: 10754–10768.

26 Atkins, P.W. (1990). *Physical Chemistry*, 4e. Oxford: Oxford University Press.

27 These formulae are described in full inCoote, M.L. (2004). *Encyclopedia of Polymer Science and Technology* (ed. J.I. Kroschwitz), 319–371. New York, NY: Wiley.

28 Bell, R.P. (1980). *The Tunnel Effect in Chemistry*, 276. London and New York: Chapman and Hall.

29 Truhlar, D.G., Isaacson, A.D., Skodje, R.T., and Garrett, B.C. (1982). *J. Phys. Chem.* 86: 2252–2261.

30 Truhlar, D.G. and Garrett, B.C. (1989). *J. Am. Chem. Soc.* 111: 1232–1236.

31 See for example: Truhlar, D.G., Garrett, B.C., and Klippenstein, S.J. (1996). *J. Phys. Chem.* 100: 12771–12800.

32 Lin, C.Y., Izgorodina, E.I., and Coote, M.L. (2008). *J. Phys. Chem. A* 112: 1956–1964.

33 Nordholm, S. and Bacskay, G.B. (1976). *Chem. Phys. Lett.* 42: 253–258.

34 Heuts, J.P.A., Gilbert, R.G., and Radom, L. (1996). *J. Phys. Chem.* 100: 18997–19006.

35 Heuts, J.P.A., Gilbert, R.G., and Radom, L. (1995). *Macromolecules* 28: 8771–8781.

36 East, A.L.L. and Radom, L. (1997). *J. Chem. Phys.* 106: 6655.

37 Van Speybroeck, V., Van Neck, D., and Waroquier, M. (2002). *J. Phys. Chem. A* 106: 8945–8950.

38 Izgorodina, E.I., Lin, C.Y., and Coote, M.L. (2007). *Phys. Chem. Chem. Phys.* 9: 2507–2516.

39 Lin, C.Y., Izgorodina, E.I., and Coote, M.L. (2010). *Macromolecules* 43: 553–560.

40 Lin, C.Y. and Coote, M.L. (2011). *Aust. J. Chem.* 64: 747–756.

41 Haworth, N.L., Wang, Q., and Coote, M.L. (2017). *J. Phys. Chem. A* 121: 5217–5225.

42 Voth, G.A. and Hochstrasser, R.M. (1996). *J. Phys. Chem.* 100: 13034–13049.

43 Tomasi, J. (2004). *Theor. Chem. Acc.* 112: 184–203.

44 Barone, V. and Cossi, M. (1998). *J. Phys. Chem. A* 102: 1995–2001.

45 Miertus, S., Scrocco, E., and Tomasi, J. (1981). *J. Chem. Phys.* 55: 117.

46 Takano, Y. and Houk, K.N. (2005). *J. Chem. Theory Comput.* 1: 70–77.

47 Marenich, A.V., Ho, J., Coote, M.L. et al. (2014). *Phys. Chem. Chem. Phys.* 16: 15068–15106.

48 Magill, A.M., Cavell, K.J., and Yates, B.F. (2004). *J. Am. Chem. Soc.* 126: 8717–8724.

49 Ho, J. and Coote, M.L. (2009). *J. Chem. Theory Comput.* 5: 295–306.

50 Pliego, J.R. Jr., and Riveros, J.M. (2001). *J. Phys. Chem. A* 105: 7241–7247.

51 Lin, C.Y. and Coote, M.L. (2009). *Aust. J. Chem.* 62: 1479–1483.

52 Junkers, T., Barner-Kowollik, C., and Coote, M.L. (2011). *Macromol. Rapid Commun.* 32: 1891–1898.

53 Izgorodina, E.I. and Coote, M.L. (2006). *Macromol. Theory Simul.* 15: 394–403.

54 Feldermann, A., Coote, M.L., Stenzel, M.H. et al. (2004). *J. Am. Chem. Soc.* 126: 15915–15923.

55 Kwak, Y., Goto, A., and Fukuda, T. (2004). *Macromolecules* 37: 1219–1225.

56 Moad, G. and Barner-Kowollik, C. (2008). The mechanism and kinetics of the raft process: overview rates stabilities side reactions product spectrum and outstanding challenges. In: *Handbook of Raft Polymerization* (ed. C. Barner-Kowollik), 51–104. Weinheim Germany: Wiley-VCH.

57 Coote, M.L., Izgorodina, E.I., Krenske, E.H. et al. (2006). *Macromol. Rapid Commun.* 27: 1015–1022.

58 McLeary, J.B., Calitz, F.M., McKenzie, J.M. et al. (2004). *Macromolecules* 37: 2382–2394.

59 Scaiano, J.C. and Ingold, K.U. (1976). *J. Am. Chem. Soc.* 98: 4727–4732.

60 Ah Toy, A., Chaffey-Millar, H., Davis, T.P. et al. (2006). *Chem. Commun.*: 835–837.

61 Olaj, O.F., Bitai, I., and Hinkelmann, F. (1987). *Makromol. Chem.* 188: 1689.

62 Wang, A.R., Zhu, S., Kwak, Y. et al. (2003). *J. Polym. Sci. A* 41: 2833–2839.

63 Barner-Kowollik, C., Coote, M.L., Davis, T.P. et al. (2003). *J. Polym. Sci., Part A: Polym. Chem.* 41: 2828–2832.

64 Calitz, F.M., McLeary, J.B., McKenzie, J.M. et al. (2003). *Macromolecules* 36: 9687–9690.

65 de Brouwer, J.A.M., Schellekens, M.A.J., Klumperman, B. et al. (2000). *J. Polym. Sci. A* 19: 3596.

66 Kwak, Y., Goto, A., Komatsu, K. et al. (2004). *Macromolecules* 37: 4434–4440.

67 Ah Toy, A., Vana, P., Davis, T.P., and Barner-Kowollik, C. (2004). *Macromolecules* 37: 744–751.

68 Prescott, S.W., Ballard, M.J., Rizzardo, E., and Gilbert, R.G. (2005). *Macromolecules* 38: 4901–4912.

69 Feldermann, A., Ah Toy, A., Stenzel, M.H. et al. (2005). *Polymer* 46: 8448–8457.

70 Venkatesh, R., Staal, B.B.P., Klumperman, B., and Monteiro, M.J. (2004). *Macromolecules* 37: 7906–7917.

71 McLeary, J.B., Calitz, F.M., McKenzie, J.M. et al. (2005). *Macromolecules* 38: 3151–3161.

72 Coote, M.L. and Davis, T.P. (1999). *Prog. Polym. Sci.* 24: 1217–1251.

73 Zetterlund, P., Busfield, W., and Jenkins, I. (1999). *Macromolecules* 32: 8041–8045.

74 Deady, M., Mau, A.W.H., Moad, G., and Spurling, T.H. (1993). *Makromol. Chem.* 194: 1691.

75 Chong, Y.K., Krstina, J., Le, T.P.T. et al. (2003). *Macromolecules* 36: 2256–2272.

76 Chiefari, J., Mayadunne, R.T.A., Moad, C.L. et al. (2003). *Macromolecules* 36: 2273–2283.

77 Matyjaszewski, K. and Poli, R. (2005). *Macromolecules* 38: 8093–8100.

78 Krenske, E.H., Izgorodina, E.I., and Coote, M.L. (2006). An ab initio guide to structure-reactivity trends in reversible addition fragmentation chain transfer (RAFT) polymerization. In: *Controlled/Living Radical Polymerization: From*

Synthesis to Materials, ACS Symposium Series, vol. 944 (ed. K. Matyjaszewski), 406–420. Washington, DC: American Chemical Society.

79 Pahnke, K., Brandt, J., Gryn'ova, G. et al. (2016). *Angew. Chem. Int. Ed.* 55: 1514–1518.

80 Barner-Kowollik, C., Buback, M., Charleux, B. et al. (2006). *J. Polym. Sci. A* 44: 5809–5831.

81 Coote, M.L. and Radom, L. (2004). *Macromolecules* 37: 590–596.

82 Buback, M., Janssen, O., Oswald, R. et al. (2007). *Macromol. Symp.* 248: 158–167.

83 Henry, D.J., Coote, M.L., Gómez-Balderas, R., and Radom, L. (2004). *J. Am. Chem. Soc.* 126: 1732–1740.

84 Zard, S.Z. (2006). *Aust. J. Chem.* 59: 663–668.

85 Altintas, O., Riazi, K., Lee, R. et al. (2013). *Macromolecules* 46: 8079–8091.

86 Desmet, G.B., D'hooge, D.R., Sabbe, M.K. et al. (2016). *J. Org. Chem.* 81: 11626–11634.

87 Coote, M.L. and Henry, D.J. (2005). *Macromolecules* 38: 5774–5779.

88 Theis, A., Stenzel, M.H., Davis, T.P. et al. (2005). *Aust. J. Chem.* 58: 437–441.

89 Coote, M.L., Izgorodina, E.I., Cavigliasso, G.E. et al. (2006). *Macromolecules* 39: 4585–4591.

90 Coote, M.L. and Radom, L. (2003). *J. Am. Chem. Soc.* 125: 1490–1491.

91 McLeary, J.B., Tonge, M.P., and Klumperman, B. (2006). *Macromol. Rapid Commun.* 27: 1233–1240.

92 Vana, P., Davis, T.P., and Barner-Kowollik, C. (2002). *Macromol. Theory Simul.* 11: 823–835.

93 Perrier, S., Barner-Kowollik, C., Quinn, J.F. et al. (2002). *Macromolecules* 35: 8300–8306.

94 Wulkow, M. (1996). *Macromol. Theory Simul.* 5: 393–416.

95 Desmet, G.B., Rybel, N.D., Steenberge, P.H.M.V. et al. (2018). *Macromol. Rapid Commun.* 38: 1700403.

96 Krstina, J., Moad, G., Rizzardo, E. et al. (1995). *Macromolecules* 28: 5381–5385.

97 Pross, A. and Shaik, S.S. (1983). *Acc. Chem. Res.* 16: 363.

98 Pross, A. (1985). *Adv. Phys. Org. Chem.* 21: 99–196.

99 Shaik, S.S. (1985). *Prog. Phys. Org. Chem.* 15: 197–337.

100 Fischer, H. and Radom, L. (2001). *Angew. Chem. Int. Ed.* 40: 1340–1371.

101 Schmidt, M.W., Truong, P.H., and Gordon, M.S. (1987). *J. Am. Chem. Soc.* 109: 5217–5227.

102 Evans, M.G. (1947). *Disc. Faraday Soc.* 2: 271–279.

103 Gigmes, D., Bertin, D., Marque, S. et al. (2003). *Tetrahedron Lett.* 44: 1227–1229.

104 Hodgson, J.L., Green, K.A., and Coote, M.L. (2005). *Org. Lett.* 7: 4581–4584.

105 Matioszek, D., Mazières, S., Brusylovets, O. et al. (2019). *Macromolecules* 52: 3376–3386.

106 Gómez-Balderas, R., Coote, M.L., Henry, D.J. et al. (2003). *J. Phys. Chem. A* 107: 6082–6090.

107 The use of radical stabilization energies (RSEs) to compare the stabilities of two radicals R· and R′· is only meaningful if the discrepancy between the R–H

and R′–H bond strengths is negligible. In the case of carbon-centered radicals this assumption is normally reasonable but minor discrepancies can arise due to non-canceling steric or polar interactions in the closed shell compounds. More generally, in other types of radical, such as phosphoranyl radicals, this assumption can break down altogether. For a more detailed discussion of this problem, see for example:Hodgson, J.L. and Coote, M.L. (2005). *J. Phys. Chem. A* 109: 10013–10021, and references cited therein.

108 Mayadunne, R.T.A., Rizzardo, E., Chiefari, J. et al. (1999). *Macromolecules* 32: 6977–6980.

109 Farmer, S.C. and Patten, T.E. (2002). *J. Polym. Sci., Part A: Polym. Chem.* A40: 555–563.

110 Coote, M.L., Lin, C.Y., Beckwith, A.L.J., and Zavitsas, A.A. (2010). *Phys. Chem. Chem. Phys.* 12: 9597–9610.

111 Lin, C.Y., Marque, S.R.A., Matyjaszewski, K., and Coote, M.L. (2011). *Macromolecules* 44: 7568–7583.

112 Rodríguez-Sanchez, I., Zaragoza-Contreras, E.A., and Glossman-Mitnik, D. (2010). *J. Mol. Model.* 16: 95–105.

113 Rodríguez-Sanchez, I., Zaragoza-Contreras, E.A., and Glossman-Mitnik, D. (2009). *J. Mol. Model.* 15: 1133–1143.

114 Gillies, M.B., Matyjaszewski, K., Norrby, P.-O. et al. (2003). *Macromolecules* 36: 8551–8559.

115 Singleton, D.A., Nowlan, D.T. III, Jahed, N., and Matyjaszewski, K. (2003). *Macromolecules* 26: 8609–8616.

116 Marsal, P., Roche, M., Tordo, P., and de Sainte Claire, P. (1999). *J. Phys. Chem. A* 103: 2899–2905.

117 Maximiano, P., Mendonça, P.V., Costa, J.R.C. et al. (2016). *Macromolecules* 49: 1597–1604.

118 Abreu, C.M.R., Mendonca, P.V., Serra, A.C. et al. (2012). *Macromolecules* 45: 2200–2208.

119 Dedeoglu, B., Ugur, I., Degirmenci, I. et al. (2013). *Polymer* 54: 5122–5132.

120 Gryn'ova, G., Guliashvili, T., Matyjaszewski, K., and Coote, M.L. (2013). *Aust. J. Chem.* 66: 308–313.

121 Nebhani, L., Sinnwell, S., Lin, C.Y. et al. (2009). *J. Polym. Sci. A Polym. Chem.* 47: 6053–6071.

122 Gardiner, J., Martinez-Botella, I., Kohl, T.M. et al. (2017). *Polym. Int.* 66: 1438–1447.

123 Pascual, S., Blin, T., Saikia, P.J. et al. (2010). *J. Polym. Sci., Part A: Polym. Chem.* 48: 5053–5062.

124 Guerre, M., Rahaman, S.M.W., Améduri, B. et al. (2016). *Polym. Chem.* 7: 6918–6933.

125 Huang, Z., Noble, B.B., Corrigan, N. et al. (2018). *J. Am. Chem. Soc.* 140: 13392–13406.

7

Mathematical Modelling of RAFT Polymerization

Porfirio López-Domínguez[1], Iván Zapata-González[2], Enrique Saldívar-Guerra[3], and Eduardo Vivaldo-Lima[1]

[1] Universidad Nacional Autónoma de México, Facultad de Química, Departamento de Ingeniería Química, Circuito Exterior S/N, Ciudad Universitaria, Coyoacán, Ciudad de México, CP 04510, México
[2] Cátedras CONACYT-Tecnológico Nacional de México/Instituto Tecnológico de Tijuana, Centro de Graduados e Investigación Química, CONACYT, AP 1166, Tijuana 22430, Baja California, México
[3] Centro de Investigación en Química Aplicada, CIQA, Boulevard Enrique Reyna 140, Saltillo, Coahuila 25100, México

7.1 Introduction

The first reports on modelling of reversible addition–fragmentation chain transfer (RAFT) polymerization appeared soon after the process was disclosed in the open literature [1–11]. Modelling and simulation of reversible deactivation radical polymerization (RDRP) processes, including RAFT polymerization, have been achieved by using several numerical approaches. The method of moments (MMs), kinetic Monte Carlo (kMC) simulations, and the software Predici® have been used in many literature reports [11–14]. Application of these numerical techniques to RAFT polymerization includes mainly (i) the synthesis of homopolymers with narrow molar mass distributions (MMDs) or molecular weight distributions (MWDs) [2–5], (ii) the synthesis of polymer networks by crosslinking/branching reactions of vinyl/divinyl monomers [15–19], (iii) microwave-assisted radical polymerization (RP) [20, 21], (iv) copolymers with controlled chain composition distributions via semibatch reactor operation [22, 23], (v) dispersion polymerizations in supercritical carbon dioxide ($scCO_2$) [24], (vi) continuous stirred tank reactors [2, 25], and (vii) miniemulsion polymerization [26–28].

When some RAFT agents, such as dithiobenzoates, are used in radical polymerizations, the so-called retardation effect (reduced polymerization rate) is important [29, 30]. The 'slow fragmentation' (SF) [3] and the 'intermediate radical termination' (IRT) [31] models have been proposed to account for the retardation effect. Both models can satisfactorily describe the available experimental data on polymerization rate (R_p) and evolution of molecular weights (MWs) by fitting their corresponding kinetic rate constants representing addition ($k_{\text{add}} = k_a$), fragmentation ($k_{\text{bd}} = k_b$), and cross-termination (k_{tir}, only in IRT model) reactions. As a consequence, there is a difference of six orders of magnitude between the estimated kinetic

RAFT Polymerization: Methods, Synthesis and Applications, First Edition.
Edited by Graeme Moad and Ezio Rizzardo.

rate constants for the fragmentation reaction, $k_b \approx 10^{-2} - 10^{-1}$ s^{-1} for the SF model and $k_b \approx 10^{3} - 10^{5}$ l mol^{-1} s^{-1} for the IRT model [29, 32]. Other kinetic models for RAFT polymerization consider some additional reactions between the participating species [29, 33–36].

7.2 Deterministic Modelling Techniques (DMTs)

Deterministic modelling techniques (DMTs) are based on first principles: kinetic laws and initial conditions. The model comprises the solution of a system of equations describing mass balances derived from the polymerization scheme and kinetic hypotheses for a given reactor type, in which the full information is available throughout the solution trajectory. In this type of models, random variations must be excluded from the calculations. The most popular modelling approach in this category is the method of moments, but recently new DMTs have been developed with the purpose of providing calculation of the full MWD with relatively low computer processing time, involving chain-length (CL)-dependent kinetic rate constants and multidimensional approaches for non-linear polymer molecules produced in common steps, such as addition–fragmentation, cross-termination, branching, or crosslinking.

7.2.1 Method of Moments (MM)

The MM in the context of polymerization kinetic modelling has been used for over 65 years [37, 38]. This statistical-kinetic technique has become a fundamental and powerful tool in the modelling of polymerization processes. Specifically, in RAFT polymerization, this versatile deterministic method has been continuously used in the development of mathematical models for the analysis of kinetic theories, such as the so-called IRT [4, 31, 39], missing step theory (MST) [36], intermediate radical termination with oligomers (IRTO) [40, 41], and SF [32, 41], for estimation of kinetic rate coefficients [42, 43], design of polymers with well-defined microstructures [44], and design of monomer feeding policies [45]. The polymerization processes addressed include homogenous and heterogeneous media, different reactor operating configurations (batch [46], semibatch [22, 47], and continuous [25]), homo- and copolymerization systems [48], as well as linear and non-linear chain polymer product architectures (crosslinking [15, 17] and branching [18, 49]). The main advantages of the MM are simplicity and important dimensional reduction of the mathematical system, resulting in reliable predictions of average characteristics, such as number (M_n), weight (M_w), and z-(M_z) average molecular weights, molar mass dispersity ($Đ$), end-group functionality (EGF), and selectivity (S).

The first step in the application of the technique is the derivation of the population balance equations (PBEs) for each type and length of polymer molecule species involved in the polymerization scheme, as shown in Table 7.1 for RAFT homopolymerization of vinyl monomers, where M is the monomer, I is the initiator, AB is

Table 7.1 Polymerization scheme for RAFT polymerization.

Step	Equation
Initiation	$I \xrightarrow{(f)k_d} 2\mathrm{R}^{\bullet}_{\mathrm{in}}$
	$\mathrm{R}^{\bullet}_{\mathrm{in}} + \mathrm{M} \xrightarrow{k_i} \mathrm{R}^{\bullet}_1$
Re-initiation	$\mathrm{B}^{\bullet} + \mathrm{M} \xrightarrow{k_i} \mathrm{R}^{\bullet}_1$
Propagation	$\mathrm{R}^{\bullet}_m + \mathrm{M} \xrightarrow{k_p} \mathrm{R}^{\bullet}_{m+1}$
Reversible chain transfer to the RAFT agent (pre-equilibrium)	$\mathrm{R}^{\bullet}_m + \mathrm{AB} \underset{k_{-\mathrm{add}}}{\overset{k_{\mathrm{add}}}{\rightleftarrows}} \mathrm{R}_m\mathrm{A}^{\bullet}\mathrm{B} \underset{k_{-bd}}{\overset{k_{bd}}{\rightleftarrows}} \mathrm{R}_m\mathrm{A} + \mathrm{B}^{\bullet}$
Chain equilibration (main equilibrium)	$\mathrm{R}^{\bullet}_m + \mathrm{R}_n\mathrm{A} \underset{k_{-a}}{\overset{k_a}{\rightleftarrows}} \mathrm{R}_m\mathrm{A}^{\bullet}\mathrm{R}_n \underset{k_{-b}}{\overset{k_b}{\rightleftarrows}} \mathrm{R}_m\mathrm{A} + \mathrm{R}^{\bullet}_n$
Intermediate radical termination	$\mathrm{R}_p\mathrm{A}^{\bullet}\mathrm{R}_q + \mathrm{R}^{\bullet}_r \xrightarrow{k_{\mathrm{tir}}} \mathrm{R}_p\mathrm{R}_q\mathrm{R}_r$
Termination by combination	$\mathrm{R}^{\bullet}_m + \mathrm{R}^{\bullet}_n \xrightarrow{k_{\mathrm{tc}}} \mathrm{P}_{m+n}$
Termination by disproportionation	$\mathrm{R}^{\bullet}_m + \mathrm{R}^{\bullet}_n \xrightarrow{k_{\mathrm{td}}} \mathrm{P}_m + \mathrm{P}_n$

the RAFT agent, and $\mathrm{R}^{\bullet}_{\mathrm{in}}$ is a primary radical. Then, the PBEs are transformed into moment equations by multiplying them by the summation of chain length to the given moment order power, for all chain sizes. This results in a finite system of 'i' ordinary differential equations (ODEs) for each polymer species, where i is the moment order.

For illustration purposes, let us consider a simple representation of RAFT polymerization. For simplicity, only four types of polymer molecules are considered: (i) living polymer radicals ($\mathrm{R}^{\bullet}_m$), (ii) intermediate polymer radicals (1 and 2 arms: $\mathrm{R}_m\mathrm{A}^{\bullet}\mathrm{B}$ and $\mathrm{R}_m\mathrm{A}^{\bullet}\mathrm{R}_n$, respectively), (iii) dormant polymer molecules ($\mathrm{R}_m\mathrm{A}$), and (iv) dead polymer molecules (P_m or $\mathrm{P}_m\mathrm{P}_n\mathrm{P}_t$). Definitions for the i-th moment of polymer radicals, intermediate polymer radicals, and dormant and dead polymer molecules are provided in Eqs. (7.1)–(7.4), respectively:

$$Y_{\mathrm{i}} = \sum_{m=1}^{\infty} m^i \left[\mathrm{R}^{\bullet}_m\right]; m = 0, 1, 2, \ldots \tag{7.1}$$

$$F_{i,j} = \sum_{m=1}^{\infty}\sum_{n=1}^{\infty} m^i n^j \left[\mathrm{R}_m\mathrm{A}{\cdot}\mathrm{R}_n\right]; n, m = 0, 1, 2, \ldots \tag{7.2}$$

$$Z_i = \sum_{m=1}^{\infty} m^i \left[\mathrm{R}_m\mathrm{A}\right]; m = 0, 1, 2, \ldots \tag{7.3}$$

$$Q_i = \sum_{m=1}^{\infty} m^i \left[\mathrm{P}_m\right]; m = 0, 1, 2, \ldots \tag{7.4}$$

The following step is to transform the PBEs into moment equations by multiplying them by chain length raised to the order moment being considered and then applying the summation operator over all chain lengths. This is equivalent to applying the operators defined by Eqs. (7.1)–(7.4) to the PBEs. This procedure leads to

Eqs. (7.5)–(7.8) for the zeroth, first, and second order moments for each polymer species.[1]

$$\frac{dY_i}{dt} = 2fk_d[\mathrm{I}] + \beta_i + \left(k_{-a} + k_b\right)F_{i,0} - \left(k_a + k_{-b}\right)Y_0Z_i - \left(k_{\mathrm{td}} + k_{\mathrm{tc}}\right)Y_0Y_i - k_{\mathrm{tir}}Y_iF_{0,0} \tag{7.5}$$

$$\frac{dF_{i,j}}{dt} = \left(k_a + k_{-b}\right)Y_0Z_i - \left(k_{-a} + k_b\right)F_{i,0} - k_{\mathrm{tir}}Y_iF_{0,0} \tag{7.6}$$

$$\frac{dZ_i}{dt} = -\left(k_a + k_{-b}\right)Y_0Z_i + \left(k_{-a} + k_b\right)F_{i,0} \tag{7.7}$$

$$\frac{dQ_i}{dt} = k_{\mathrm{td}}Y_0Y_i + \varepsilon_{\mathrm{tc}} + k_{\mathrm{tir}}Y_iF_{0,0} \tag{7.8}$$

$i = 0, 1, 2$.

Average properties are related to moments through the expressions given by Eqs. (7.9)–(7.13)[1]:

$$X_n = \left(\frac{\mathcal{B}_1}{\mathcal{B}_0}\right) \tag{7.9}$$

$$X_w = \left(\frac{\mathcal{B}_2}{\mathcal{B}_1}\right) \tag{7.10}$$

$$X_z = \left(\frac{\mathcal{B}_3}{\mathcal{B}_2}\right) \tag{7.11}$$

$$Đ = \frac{X_w}{X_n} \tag{7.12}$$

$$\mathrm{EGF} = \frac{Y_0 + \frac{1}{2}F_{0,0} + Z_0}{\mathcal{B}_0} \tag{7.13}$$

where $\mathcal{B}_i$ denotes the i-th bulk moment, as defined in Eq. (7.14).[2]

$$\mathcal{B}_i = Y_i + \boldsymbol{F}_i + Z_i + Q_i \tag{7.14}$$

$\mathcal{B}_0$, $\mathcal{B}_1$, and $\mathcal{B}_2$ are total polymer concentration, total monomer units incorporated into polymer molecules, and total second order moment, respectively. X_n (also denoted as DP_n) and X_w are number- and weight- average degree of polymerization or chain length. If these averages are multiplied by monomer MW, M_n and M_w are obtained. A detailed description of the general methodology and its application to RAFT polymerization can be found in the literature [13, 50, 51].

7.2.1.1 Homogeneous Systems

The MM has been used in a good number of contributions on RAFT polymerization of vinyl monomers carried out in bulk and solution [31–64]. As is well known, kinetic theories aimed at describing the RAFT mechanism, to account mainly for the strong retardation effect observed in dithiobenzoate-mediated polymerizations,

1 β_i and $\varepsilon_{\mathrm{tc}}$ (termination by combination term) are defined in Ref. [11].
2 $\boldsymbol{F_i}$ is a defined by the i-th moment; $\boldsymbol{F}_0 = 0.5F_{0,0}$, $\boldsymbol{F}_1 = F_{1,0}$, $\boldsymbol{F}_2 = F_{2,0} + F_{1,1}$.

have been debated intensely in the literature [30, 33, 52]. The MM has been essential to gain a first overall understanding of the kinetic mechanism involved in RAFT polymerization. By using this method, it is possible to compare predictions of the four theories: IRT, SF, IRTO, and MST. MM models can in principle be used to discriminate among the existent theories available to explain controversial phenomena in RAFT polymerization, such as the retardation effect, if adequate model discrimination techniques are used [43].

A summary of the kinetic behaviour and selectivity between growing and intermediate chains predicted by each theory is shown in Figure 7.1. Although all the aforementioned theories result in similar predictions of polymer species concentrations, polymerization rate, and average molecular weight properties, the selectivity of growing radicals displays strong discrepancies, by orders of magnitude, between SF and the other theories (see Figure 7.1d).

The IRT theory postulated by Monteiro and de Brouwer [31] introduced the so-called three-arm star polymer molecule ($P_mP_nP_t$) into the kinetic scheme. This theory was studied by Wang and Zhu [4]. They proposed that the addition–fragmentation step (main equilibrium reaction in Table 7.1) can be simplified to what is shown in Eq. (7.15), resulting in a reduction of the number of rate coefficients.

$$R^{\bullet}_m + R_nA \xrightarrow{k_a} R_mA^{\bullet}R_n \xrightarrow{k_b} R_mA + R^{\bullet}_m \tag{7.15}$$

The model of Wang and Zhu allowed capturing low levels in the concentration of intermediate radicals, F_0, close to those exhibited by polymer radicals, and the build-up of dead polymer (Q_0) in the system, as observed in Figure 7.1c. The model was adapted to include SF theory ($k_b = 10^{-2}$ s^{-1} and $k_{\text{tir}} = 0$), in which a low value of k_b generated high concentration levels of intermediate radicals [32], as observed in Figure 7.1c.

A comprehensive comparative study between IRT, SF, and a simple model based on direct reversible chain transfer (absence of the intermediate radical species), using a self-developed code for the MM equations and the Predici™ software, was carried out by Pallares et al. [11]. They observed that simulations based on the complete polymerization scheme proposed by CSIRO for RAFT polymerization and calculations carried out using Eq. (7.14) produced the same results. However, calculations based on the simpler third model were qualitatively correct, but quantitatively deviated from experimental data. Using the MM, Monteiro simulated all the possible reaction events [39], including those involving primary radicals produced by the initiator and chain transfer agent (AB), and the formation of four-arm star polymers through intermediate–IRT, as described in Eq. (7.16). The scenarios considered in their parametric analysis included the presence of poor leaving groups, slow re-initiation of primary radicals (B$^{\bullet}$), inhibition, and kinetic characteristics of IRT and SF. However, the introduction of Eq. (7.16) did not improve the performance behaviour of the model.

$$\begin{gathered} R_mA^{\bullet}R_n + R_sA^{\bullet}R_t \xrightarrow{k_{\text{iRR}}} R_mR_nA - AR_sR_t \\ m = 1, 2, \ldots; n = 1, 2, \ldots; s = 1, 2, \ldots; t = 1, 2, \ldots \end{gathered} \tag{7.16}$$

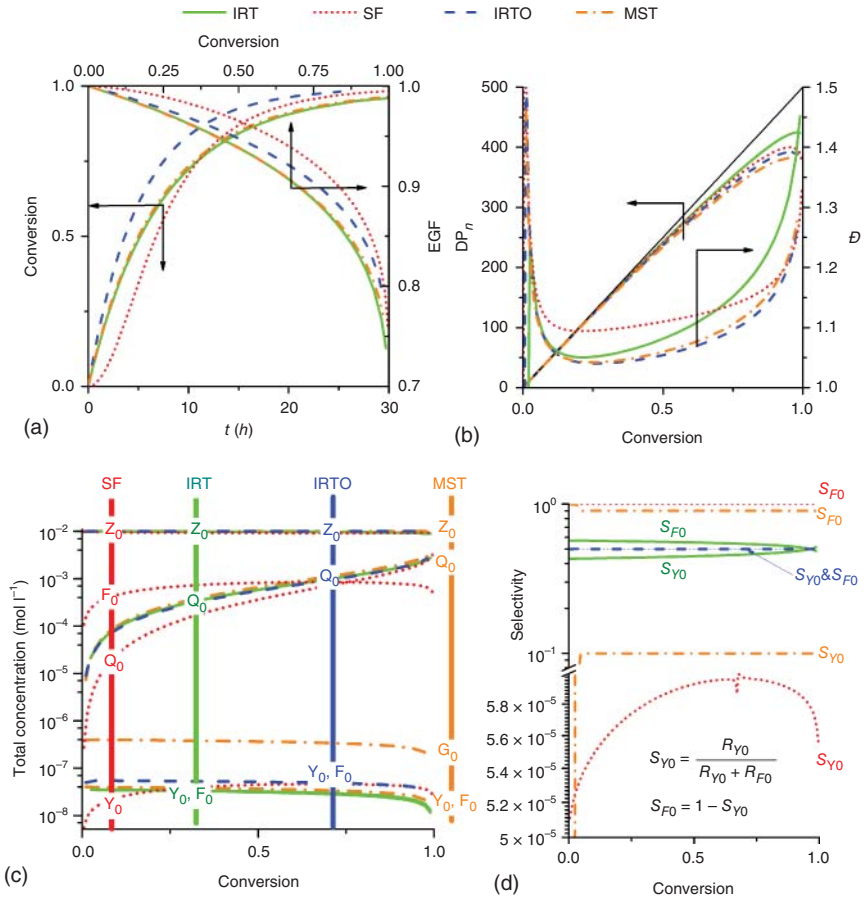

Figure 7.1 Evolution of average characteristics using different kinetic theories: (a) conversion and EGF vs. time; (b) X_n and $Đ$ vs. conversion; (c) total polymer concentration (zeroth moment) vs. conversion; and (d) selectivity of growing (Y_0) and intermediate (F_0) polymer radicals vs. conversion. Kinetic rate constants: for IRT, $k_b = 1 \times 10^4\ s^{-1}$, $k_{tir} = 1 \times 10^7\ s^{-1}$; SF: $k_b = 5 \times 10^{-1}\ s^{-1}$, and $k_{tir} = 0$; for IRTO, $k_b = 1 \times 10^4\ s^{-1}$, $k_{tir} = 1 \times 10^7$; and for MST, $k_b = 1 \times 10^4\ s^{-1}$, $k_{tir} = 1 \times 10^7\ s^{-1}$; $k_{tMS} = 1 \times 10^7\ s^{-1}$. Other kinetic rate constants are considered as in Ref. [41], or [53] for MST. $[M]_0 : [AB]_0 : [I]_0 = 500 : 1 : 05$.

Konkolewicz et al. proposed the IRTO theory [34], where radicals involved in cross-termination are limited to small sizes, as shown in Eq. (7.17), thus resulting in the elimination of three-arm star products without affecting the general kinetic behaviour. This is illustrated in Figure 7.1.

$$R_m A^{\cdot} R_n + R_t^{\cdot} \xrightarrow{k_{tir}} R_m R_n R_t \quad m = 1, 2, \ldots; n = 1, 2, \ldots; t = 1, 2, \ldots \tag{7.17}$$

Zapata-González et al. reported another comparative study between IRT, SF, and IRTO by using the MM and also carried out calculations of full MWDs [41]. They analysed the validity of the quasi steady-state approximation (QSSA) for polymer

radicals ($R^{\cdot}_m$) and intermediate polymer radicals ($R_mA^{\cdot}R_n$). They found that the QSSA hypothesis is adequate for both types of polymer radicals in IRT and IRTO. However, it turned out that the QSSA was invalid in SF for $R_mA^{\cdot}R_n$, due to the high stability and accumulation of these species. They also observed that the standard one-dimensional implementation of the RAFT polymerization scheme in Predici™ does not generate adequate predictions of second and higher order moments [46].

Buback and Vanna introduced an additional step into the RAFT polymerization scheme shown in Eq. (7.18), under MST [33]. This step consists of the regeneration of two-arm intermediate polymer radicals through a chain transfer reaction between three-arm polymer stars and living polymer radicals. Zapata-González et al. [36] modelled this modified version of MST, using the MM and experimental data of styrene (Sty) and butyl acrylate (BA) RAFT polymerizations reported in the literature. They found that the model provides adequate descriptions of both systems.

$$R_mR_nR_t + R^{\cdot}_s \xrightarrow{k_{tMS}} R_mA^{\cdot}R_n + R_sR_t$$
$$m = 1, 2, \ldots; n = 1, 2, \ldots; s = 1, 2, \ldots; t = 1, 2, \ldots \tag{7.18}$$

Recently, Masoumi et al. developed a sequential Bayesian Monte Carlo model discrimination technique applied to the case of RAFT polymerization [43]. Two rival models based on the MM (chain equilibration step as represented in Table 7.1 vs. the reduced expression shown in Eq. (7.15)) were compared. It was found that M_n seems to be the best output for model discrimination purposes. The Bayesian technique proved to be capable of discriminating rival RAFT models. However, the limited experimental data usually available (e.g. conversion, M_n and $Đ$ as shown in Figure 7.1a,b) does not allow to fully analyse the zones where rival models differ, and no definite answer as to which theory is best has yet been obtained [43].

A kinetic approach known as degenerative chain transfer model [54, 55] greatly reduces the complexity of the mathematical representation of RAFT polymerization. The model neglects the contribution of intermediate species in the kinetic scheme and the addition–fragmentation step is substituted by a degenerative chain transfer step, given by Eq. (7.19). A mathematical model based on that approach allowed calculations of X_n, $Đ$, and the transfer coefficient C_{tr} [56]. One of the three models studied by Pallares et al., the simplest one, had the same structure but it was reversible [11].

$$R^{\cdot}_m + R_nA \xrightarrow{k_{tr(main)}} R_mA + R^{\cdot}_n \tag{7.19}$$

Monteiro [9] carried out a parametric sensitivity analysis of a RAFT copolymerization system using a general model where the retardation effect was negligible. He used a degenerative chain transfer model and a semibatch process. He found that the effect of C_{trs} on X_n was negligible but it strongly affected $Đ$.

Targeting tailored-designed products and microstructure control can be achieved through semibatch and continuous processes. A comprehensive modelling study focused on the RAFT polymerization of methyl methacrylate (MMA) in different reactor configurations (batch, semibatch, single continuous stirred tank reactor (CSTR), and a series of CSTRs) was reported by Zhang and Ray [2, 57]. The model

that they developed was generated from a general polymerization scheme using 2-cyanopropan-2-yl 1*H*-pyrrole-1-carbodithioate as RAFT agent. They included diffusion-controlled effects by using the so-called Ross–Laurence gel effect factor correlation [58]. They found that as the number of CSTR reactors was increased, both monomer conversion and X_n increased but $Đ$ decreased. Higher values of $Đ$ than those generated in the analogous batch mode were observed. Although semibatch polymerization turned out to be quite robust, exhibiting the best characteristics to produce polymer with controlled microstructures and high productivity levels, proper selection of thermal initiator and RAFT agent for optimal operation were required. Wang et al. [59] carried out a comprehensive study on semibatch RAFT copolymerization of vinyl monomers. They modelled a generic system with kinetic parameters corresponding to dithiobenzoate RAFT agents. They focused on optimizing feed policies for control of copolymer composition distributions (CCDs). Their model was based on an IRT polymerization scheme. Constant copolymer composition throughout the polymerization was obtained, in contrast to batch processes, but reduced polymerization rate and higher $Đ$ were obtained as a consequence of the use of a semicontinuous process. These results were more pronounced in systems with larger differences between reactivity ratios. Ye et al. [60] developed mathematical models for calculation of chain length, chain length sequences, and their distributions. They included the Ross–Laurence gel effect correlation in their model. They validated their model by comparison against experimental data of RAFT polymerization of MMA. Jiang et al. [45] synthesized copolymers of Sty/BA with uniform CCDs and narrow MWDs by semibatch RAFT copolymerization using model-based optimized monomer feeding policies. Other studies on the effect of reactor configuration and operation on polymerization rate and molecular weight development in RAFT polymerization include the use of plug flow tubular reactors (PFTR) [61] and series of CSTR and PFTR reactors, both with backmixing [25].

Although most modelling studies on RAFT polymerization use dithiobenzoates as RAFT agents, other controllers have also been studied. Zhou et al. [62] presented a modelling study on RAFT polymerization using xanthates. Jiang et al. [18] modelled the copolymerization of Sty and BA using a trithiocarbonate RAFT agent. Ulitin et al. [63–65] also considered trithiocarbonate RAFT agents in the modelling of RAFT homopolymerizations of Sty and BA. All these models assumed an IRT scheme to account for the retardation effect.

7.2.1.2 Heterogeneous Systems

Polymerizations carried out as heterogeneous processes are advantageous since they provide high polymerization rates, easy of separation, and good temperature control. In these systems, two phases are usually present, due to the low or null solubility of the polymers produced: solvent-rich (continuous) and polymer-rich (dispersed) phases. The kinetic study of heterogeneous polymerization processes is rather complex since mass transport of the involved species between continuous and dispersed phases must be considered in addition to polymerization kinetics.

Emulsion Polymerization In conventional emulsion polymerization (EP), the recipe includes water, monomers, surfactant, and a water-soluble initiator. Recently, several alternatives to surfactants have been proposed. In polymerization-induced self-assembly (PISA), a water-soluble macroRDRP agent is used to produce block copolymers [66].

The copolymerization of Sty and BA using 3-benzyltrithiocarbonyl propionic acid (BCPA) and potassium persulfate (KPS) has been conducted as miniemulsion polymerization in batch and semibatch processes [67]. The method of moments and the pseudo-kinetic rate constants method were employed to calculate X_n and $Đ$. The experimental data corresponding to RAFT batch copolymerization were used to estimate the RAFT kinetic constants. The model captured well the effect of comonomer content on total monomer conversion, copolymer composition, diameter of unswollen particles, and the number of particles per volume.

Dispersion Polymerization Dispersion polymerizations carried out in supercritical carbon dioxide ($scCO_2$) are important since $scCO_2$ is a good solvent for polar/non-polar compounds and has a relatively low critical point. Block copolymers can be produced in $scCO_2$. A one-pot synthesis can be implemented: monomer A is first polymerized to full conversion in the presence of a RAFT agent; monomer *B* is then fed using a high-performance liquid chromatography (HPLC) pump [68].

The RAFT polymerization of Sty using *S*-thiobenzoyl thioglycolic acid (TBTGA) and 2,2′-azobis(2-methylpropionitrile) (AIBN) in $scCO_2$ at 80 °C and 300 bar was studied using two modelling approaches [69]. In the first approach (Model A), the 'complete' model for RAFT polymerization [11] was used to describe the polymerization kinetics in the continuous and dispersed phases. Three stages were considered in this approach. Monomer and solvent concentrations in each phase were approximated by using semi-empirical partition equations. The second modelling approach (Model B) was developed in the Predici™ software [24] using the 'Q-type' approach for each phase (see Section 7.2.3.3 in this chapter). Mass transfer between the continuous and dispersed phases for the components included in the reaction mixture was modelled using Predici's 'phase exchange' step. Migration of radicals from the continuous to the dispersed phase was modelled using Predici's '$k(s)$-termination' step. Four cases were addressed by Jaramillo et al. [70]. Case 1 represented a conventional case (no RAFT agent included in the reacting mixture) while Cases 2–4 contained increasing amounts of a RAFT agent. Both approaches described well the experimental data of monomer conversion vs. time, as well as M_n and $Đ$ vs. conversion for Case 1. A linear relationship between M_n and conversion was obtained, as observed in Figure 7.2. However, both models predicted wider differences in M_n and higher values of $Đ$ for Cases 2–4.

Suspension Polymerization Although suspension polymerization has not been used as a common operation mode for RAFT polymerizations, a few studies have been reported [71–76]. However, no reports on modelling of polymerization kinetics or particle size distribution calculations for RAFT polymerizations carried out in suspension are available to the best of our knowledge.

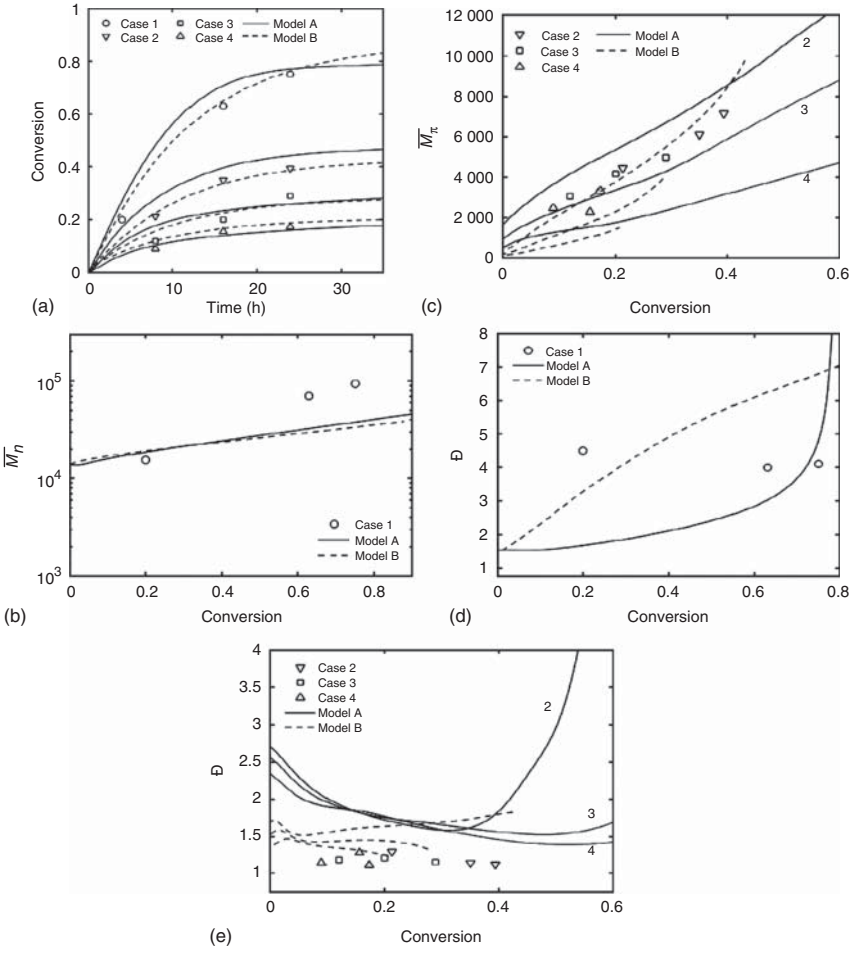

Figure 7.2 Comparison of Models A and B (see text) against experimental data of (a) monomer conversion against time, (b) M_n against conversion (Case 1), (c) M_n against conversion (Cases 2–4), (d) $Đ$ against conversion (Case 1), and (e) $Đ$ against conversion (Cases 2–4). Source: Reproduced with permission from López-Domínguez et al. [69]. © 2018, John Wiley & Sons.

7.2.2 Diffusion-Controlled or CL-Dependent Coefficients

It is well established that termination and, to a lesser extent, propagation reactions in conventional RP are diffusion controlled [77, 78]. The intensity of the effect varies with conversion and the average molecular weight of the polymer being produced. It was suggested in early studies on RDRP that some reactions in these systems could also become diffusion controlled at certain reaction conditions, especially at moderate to high conversions, including the activation and deactivation reactions [79, 80]. Diffusional limitations in RDRP in general have been reviewed by D'hooge et al. [81]. Additionally, it is known that the termination coefficient in RP is chain length dependent [78] and it has been reported that the propagation kinetic rate

coefficient (k_p) is CL dependent for the first 10 propagation steps [77, 81]. Since the first mathematical models on RAFT polymerization were published, some authors introduced expressions for diffusion control effects (DCE) on kinetic rate constants in some of the reaction steps. As mentioned in Section 7.2.1.1, Zhang and Ray [2] used the Ross–Laurence correlation [58] in their modelling of RAFT polymerization of MMA, using MM, to take into account DCE in the termination and propagation reactions. They justified the use of the same DCE correlations applicable to RP by assuming that the onset of the auto-acceleration effect (inflexion point in a conversion vs. time plot) would occur at a conversion at which the average chain length of the polymer being produced would be sufficiently long, above the entanglement chain length of poly(MMA) (around 100). No DCE were considered in the kinetic rate constants for reactions involving RAFT agents or macroRAFT dormant polymer molecules, based on the argument that those kinetic rate constants (e.g. $\sim 10^4\,\mathrm{l\,mol^{-1}\,s^{-1}}$ for the forward addition reaction) are much lower than typical termination rate constants ($\sim 10^7\,\mathrm{l\,mol^{-1}\,s^{-1}}$).

Wang and Zhu [5] were apparently the first to introduce the concept of DCE for the addition step in RAFT polymerization (equivalent to the deactivation step in systems exhibiting the persistent radical effect). They argued that in RDRP systems the deactivation kinetic coefficient is usually orders of magnitude higher than the corresponding one for activation and, therefore, the deactivation reaction was more prone to show DCE. They used free-volume theory to incorporate DCE. They found that DCE in termination tends to improve molecular weight control, while the opposite occurs for DCE in the addition step. Jiang et al. [48] studied the effects of chain transfer to monomer and solvent reactions on the RAFT copolymerization of Sty and BA. They found that these reactions can have significant effects on M_n and $Đ$. They used the MM with free volume theory-based semi-empirical expressions for diffusion-controlled termination. De Rybel et al. [14] introduced DCE expressions for the initiation, termination, addition, fragmentation, and cross-termination steps in an MM-based model for RAFT polymerization of Sty using 2-cyanopropan-2-yl dodecyl carbonotrithioate and AIBN at 80 °C.

Other approaches for modelling of DCE are available. For instance, Johnston-Hall and Monteiro [55] used an expression previously developed by them [82, 83] for chain-length- (l) and conversion (x)-dependent termination kinetic rate constants ($k_t^{l,l}(x)$) for the modelling of RAFT and RP of MMA using 2-cyanopropan-2-yl dithiobenzoate and AIBN) at 80 °C. The addition step of the RAFT polymerization scheme was also conversion and CL dependent while propagation kinetic rate constants were only CL dependent. They used two modelling approaches, MM and solution of the full MWD, obtaining good agreement with experimental data. Konkolewicz et al. [34, 40] used an IRTO model where DCE were considered by using a chain-length (l)-dependent termination kinetic rate constant. The effect of chain length on k_t depended on the size regime. Two size regimes were considered; in the regime of relatively short chains, $k_{tX_n} = k_{t1} X_n^{-\alpha}$, where X_n is number average chain length and α is a power-law exponent; a similar expression was used for longer chains. The modelling approach that they used is described in more detail in Section 7.4. Lovestead et al. [84] developed a RAFT model designed to estimate the

termination kinetic rate constant between two chains of disparate (short-long, *s, l*) lengths, $k_t^{s,l}$. Their model was applied to a theoretical study on RAFT polymerization of Sty at 80 °C. Peklak et al. [10, 85] modelled the RAFT polymerization of MMA including DCE in bimolecular reactions of the RAFT polymerization scheme. The kinetic rate constants depended on conversion and chain length, and contained two contributions, chemical and diffusional. The diffusional portion was based on free volume theory. In one case [85], they favourably compared their model predictions against experimental data of RAFT polymerization of MMA using cumyl dithiobenzoate (C-DB) and AIBN at 70 °C. In a second paper [10], they compared two models with different levels of detail: one taking into account diffusional limitations based on average chain lengths, and the other using the complete MWD and accounting individually for each pair of interacting chains of different lengths. In spite of their initial expectations, significant differences in their calculations (conversion, MWD dispersity) were obtained. More recently, Devlaminck et al. [42] modelled the macromolecular design by interchange of xanthates (MADIX) polymerization of Sty and Sty/BA using (*O*-ethyl xanthate)-2-ethyl propionate as RAFT agent. They used a hybrid modelling approach (see Section 7.4 for details). The termination kinetic rate constant was assumed to be CL dependent. DCE in the other kinetic rate coefficients were neglected. Recently, De Rybel et al. [44] used a deterministic approach to test the validity of the quasi-steady-state approximation for polymer radicals in a RAFT polymerization scheme where the termination kinetic rate constant considered DCE. Model predictions were compared against experimental data of RAFT polymerization of Sty using 2-cyano-2-propyl dodecyl trithiocarbonate and 2,2-azobis(2-methylpropionitrile). DCE on all the reactions involving polymer molecules in the RAFT copolymerization of hydroxyethyl methacrylate (HEMA) and ethylene glycol dimethacrylate (EGDMA) were required in order to adequately describe experimental data of polymerization rate, molecular weight development, gel fraction, and swelling index evolution with a model based on MM and a multifunctional approach [16, 17] (see Chapter 19 of this handbook for further details).

7.2.3 Calculation of Full Molecular Weight Distributions

It is well known that the end-use properties of polymers are directly correlated to their MWDs [86]. It is therefore important to calculate full MWDs and not only averages. The solution of the mathematical system of kinetic equations derived from a given polymerization scheme is a challenge. A few models based on analytical solutions of the full MWD in RAFT polymerization systems that reduce such difficult task have been developed [34, 55, 87, 88]. De Rybel et al. [44] compared calculations of full MWDs carried out using the so-called extended model (based on assumed Flory-Schulz and Poisson distributions) against calculations obtained using a rigorous solution of the full MWD for a RAFT polymerization system. The resulting distribution of macroradicals calculated with both methods differed strongly, but the average properties had good agreement, depending on the gel regime. Devlaminck et al. [42] analysed the MADIX polymerization of Sty. The MWD obtained for

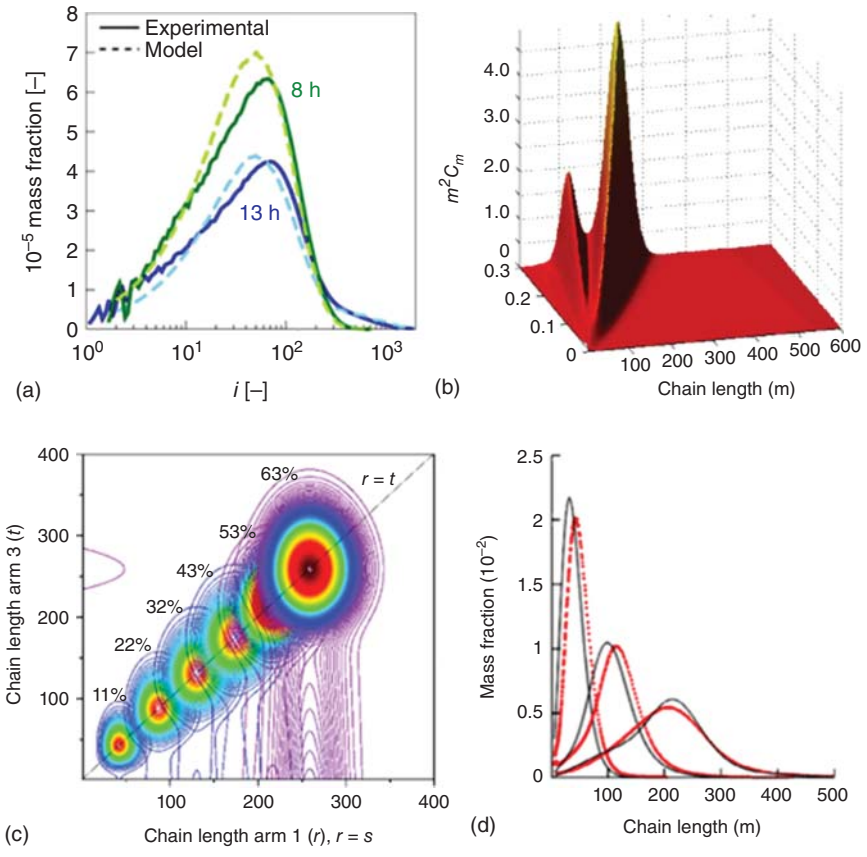

Figure 7.3 (a) Comparison between experimental (solid lines) and simulated (dashed lines) mass chain-length distributions (CLDs) at eight hours of reaction in the MADIX polymerization of Sty. Source: Reproduced with permission from Devlaminck et al. [42]. © 2017, Royal Society of Chemistry. (b) 3-D plot of the total MWD in dithiobenzoate-mediated polymerization for the SF model where C_m is concentration of polymer with total chain length m. Source: Reproduced with permission from Zapata-González et al. [41]. © 2011, John Wiley & Sons. (c) Contour plot of evolution of the bivariate population of three-arm star species in MST; the labels denote conversion (mol%). Source: Reproduced with permission from Zapata-Gonzalez et al. [36]. © 2018, Elsevier. (d) Comparison of experimental (red dotted line) and simulated (black solid line) number mass chain length distribution of trithiocarbonate-mediated polymerization of Sty; conversions: 0.1, 0.3, and 0.6, left to right. Source: Reproduced with permission from De Rybel et al. [44]. © 2018, Elsevier.

this process was a Flory–Schulz distribution, which can be considered as a special case of RAFT polymerizations, as shown in Figure 7.3a.

7.2.3.1 Explicit Integration Methods

PBEs derived from RAFT polymerization schemes, such as that shown in Table 7.1, result in very large systems of ODEs (10^6–10^8 equations), which are usually stiff [89]. Numerical implicit integration methods (which require the inversion of the Jacobian matrix of the system) are often required to integrate stiff ODE systems

[90]. Derboven et al. [91] used this technique to describe a RAFT polymerization scheme based on a degenerative chain transfer model. The use of this technique for larger systems, such as the entire RAFT system, may become computationally prohibitive. On the other hand, it is possible to take advantage of the different dynamics exhibited by the polymer species present in this type of system. The QSSA can be used for the subset of ODEs describing the fast dynamic species (growing and intermediate radicals). These ODEs can then be transformed into algebraic equations. In this way, the remaining ODEs with reduced stiffness can be easily solved by using an inexpensive explicit integration numerical method (such as Euler, Heun, Runge–Kutta, etc.), which does not require the Jacobian matrix inversion. The coupled algebraic equations system for the fast species is solved in a sequential, explicit, and computationally inexpensive way. Two methodologies for calculation of full MWDs using these concepts have been reported: the so-called reduced stiffness by QSSA (RSQSSA) [92], and the extended RSQSSA method [44].

RSQSSA has been used for comparison of calculations of full MWDs in RAFT polymerization systems using dithiobenzoate RAFT agents, considering IRT, SF, and IRTO RAFT models [41]. Unimodal MWDs were predicted for IRT and IRTO RAFT models. The dormant species was the most abundant, as expected. Two-arm polymer intermediates ($R_m A^{\cdot} R_n$) were modelled as polymer molecules with 2-D distributions. Average chain lengths about twice the length of dormant polymer molecules, but of very low concentrations, were predicted by the model. In contrast, bimodal MWDs were predicted for RAFT polymerizations based on the SF model (see Figure 7.3b). These bimodal MWDs result from combination of populations of low molecular weight dormant polymer and high molecular weight two-arm intermediate polymer. The calculations obtained by using the RSQSSA technique were compared against calculations obtained using Predici™ [44]. MWDs calculated using both techniques for growing, dormant, and dead polymer species (1-D species) completely overlapped. However, calculations of MWDs for two-arm intermediates (2-D species) differed significantly. The RSQSSA technique uses a full 2-D treatment of the polymer two-arm adduct population. It contains complete information about interconnectivity of all length combinations for the two arms. In the Predici™ implementation, the introduction of two 1-D distributions serves as chain length memory for two polymer molecules tethered to the two-arm polymer intermediates. The interconnectivity information seems to be lost in the Predici™ model.

In another research contribution, a kinetic analysis of the MST using the RSQSSA method was carried out [36]. The MST involves 2- and 3-D polymer species (two-arm intermediates and three-arm star polymers [Eq. 7.17]), giving rise to a very large system of ODEs (2.7×10^7 equations). The model predictions agreed well with the average molecular weight reported in the literature for polymerizations of Sty and MA, and with concentrations of two-arm intermediate polymer molecules measured by electron paramagnetic resonance (EPR) spectroscopy. Unimodal MWDs predicted by the model corresponded to dormant polymer molecules and two-arm intermediate polymer molecules with symmetrical chain lengths in both arms. The maximum concentration of three-arm star polymers corresponded to symmetrical structures, namely molecules with equal chain lengths ($m = n = t$), as observed in Figure 7.3c.

However, as also observed in Figure 7.3c, unexpected polymer star molecules with broad arm MWDs were also produced by cross-termination. The extended RSQSSA model used for MWD calculations considered diffusion-controlled termination. It is observed in Figure 7.3d that good agreement between calculated and experimental MWDs is obtained for the RAFT polymerization of Sty using 2-cyano-2-propyl dodecyl trithiocarbonate as RAFT agent [44].

7.2.3.2 Probability-Generating Function

The probability-generating function (PGF) of a discrete distribution R_j, which for the purposes of this chapter represents the concentration of polymer species of length j, is defined by the transformation indicated in Eq. (7.20), where s is a number in the unit circle of the complex domain.

$$\mathrm{PGF}(s,t) = \sum_{j=1}^{\infty} s^j R_j(t) \tag{7.20}$$

It is possible to calculate full MWDs in polymerization processes by using the PGF. The technique consists of transforming the system of equations representing mass balances of the polymer species into the generating function domain. This transformation results in a system of ODEs. These equations are then numerically solved and discrete points of the full MWD are transformed back to the chain length domain by numerical inversion of the PGF. In some simple cases, an analytical inversion is also possible. Although the technique has been applied to a good number of polymerization systems [93] since its first use in this field back in 1955 [94], only a couple of contributions from the same group have used it for calculation of full MWDs in RAFT polymerization [95, 96]. In one of these contributions [95], three RAFT kinetic models (SF, IRT, and IRTO) were evaluated by using the PGF technique. In the case of intermediate two-arm adduct, a 2-D distribution is obtained. The method favourably compares in computation time with direct integration of the full set of ODEs [41]. However, a drawback of the technique is that spurious numerical oscillations appear at the tail of the distribution, at large molecular weights, due to the inversion procedure (see Figure 7.4).

7.2.3.3 Calculations Using the Predici® Software

The Predici® software of CiT has been used to model RAFT polymerization processes. The basic steps used for modelling of RAFT polymerization are listed in Table 7.2. The main equilibrium between active and dormant polymers is described by introducing two polymer populations, $Q_1(m)$ and $Q_2(n)$ (Q-type approach), which keep track of the size of the two-arm adduct [97, 98].

A model implementation in Predici™, based on the SF model, was used to study the RAFT polymerization of tert-butyldimethylsilyl methacrylate using 2-cyanopropan-2-yl dithiobenzoate and AIBN, in toluene, at 70 °C [99]. The propagation kinetic rate constant k_p for this system was estimated by pulsed laser polymerization (PLP)–size exclusion chromatography (SEC) experiments. The bimolecular termination kinetic rate constant k_t was fitted from experimental data of conversion vs. time without RAFT agent. The cases with RAFT agent

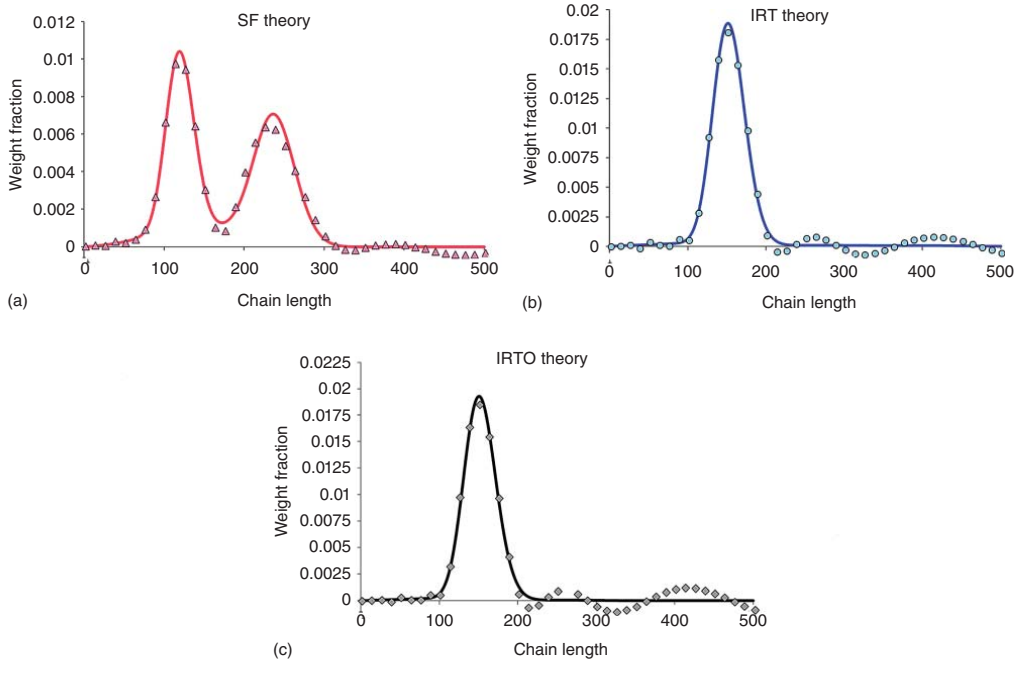

Figure 7.4 MWDs for the RAFT polymerization of Sty obtained by the PGF (symbols) and by direct integration (solid lines). Initial molar concentrations of [AB] : [I] : [M] = 0.01 : 0.005 : 5. (a) SF theory, (b) IRT theory, and (c) IRTO theory. Source: Reproduced with permission from Fortunatti et al. [95]. © 2018, John Wiley & Sons.

Table 7.2 Steps used in Predici™ for kinetic modelling of RAFT polymerization.

Reaction	Step name	Step pattern	Kinetic coefficient
Initiation and first propagation	Initiation (rad)	$I \rightarrow 2\mathrm{R}_{\mathrm{in}}^{\bullet}$	f, k_d
		$\mathrm{R}_{\mathrm{in}}^{\bullet} + M \rightarrow \mathrm{R}^{\bullet}(1)$	
First propagation of leaving group	Initiation (anion)	$\mathrm{B}^{\bullet} + \mathrm{M} \rightarrow \mathrm{R}^{\bullet}(1)$	k_{i}
Propagation	Propagation	$\mathrm{R}^{\bullet}(m) + \mathrm{M} \rightarrow \mathrm{R}^{\bullet}(m+1)$	k_p
RAFT pre-equilibrium	Elemental	$\mathrm{R}_{\mathrm{in}}^{\bullet} + \mathrm{AB} \rightarrow \mathrm{R}_{\mathrm{in}}\mathrm{A}^{\bullet}\mathrm{B}$	k_{add}
	Elemental	$\mathrm{R}_{\mathrm{in}}\mathrm{A}^{\bullet}\mathrm{B} \rightarrow \mathrm{R}_{\mathrm{in}}^{\bullet} + \mathrm{AB}$	k_{bd}
	Change	$\mathrm{R}^{\bullet}(m) + \mathrm{AB} \rightarrow \mathrm{RA}^{\bullet}\mathrm{B}(m)$	k_{add}
	Change	$\mathrm{RA}^{\bullet}\mathrm{B}(m) \rightarrow \mathrm{R}^{\bullet}(m) + \mathrm{AB}$	k_{bd}
	Change	$\mathrm{RA}^{\bullet}\mathrm{B}(m) \rightarrow \mathrm{RA}(m) + \mathrm{B}^{\bullet}$	k_{bd}
	Change	$\mathrm{RA}(m) + \mathrm{B}^{\bullet} \rightarrow \mathrm{RA}^{\bullet}\mathrm{B}(m)$	k_{add}
Addition	D-termination	$\mathrm{R}^{\bullet}(m) + \mathrm{RA}(n) \rightarrow \mathrm{Q}_1(m) + \mathrm{Q}_2(n)$	k_a
Fragmentation	Change	$\mathrm{Q}_1(m) \rightarrow \mathrm{RA}(m)$	k_b
	Change	$\mathrm{Q}_1(m) \rightarrow \mathrm{R}^{\bullet}(m)$	k_b
	Change	$\mathrm{Q}_2(n) \rightarrow \mathrm{RA}(n)$	k_b
	Change	$\mathrm{Q}_2(n) \rightarrow \mathrm{R}^{\bullet}(n)$	k_b
Intermediate radical termination	Condensation	$\mathrm{R}^{\bullet}(r) + \mathrm{Q}_1(q) \rightarrow \mathrm{T}(r+q)$	k_{tir}
	Condensation	$\mathrm{R}^{\bullet}(r) + \mathrm{Q}_2(q) \rightarrow \mathrm{T}(r+q)$	k_{tir}
Termination	Termination by combination/ disproportionation	$\mathrm{R}^{\bullet}(n) + \mathrm{R}^{\bullet}(m) \rightarrow \mathrm{P}(n+m)$	k_{tc}
		$\mathrm{R}^{\bullet}(n) + \mathrm{R}^{\bullet}(m) \rightarrow \mathrm{P}(n) + \mathrm{P}(m)$	k_{td}
Termination of small radicals	Change	$\mathrm{R}_{\mathrm{in}}^{\bullet} + \mathrm{R}^{\bullet}(n) \rightarrow \mathrm{P}(n)$	k_t
	Change	$\mathrm{B}^{\bullet} + \mathrm{R}^{\bullet}(n) \rightarrow \mathrm{P}(n)$	k_t
	Elemental	$\mathrm{B}^{\bullet} + \mathrm{B}^{\bullet} \rightarrow \mathrm{BB}$	k_t

were used to estimate all the addition and fragmentation kinetic rate constants ($k_{\mathrm{add}} = k_a = 1.80 \times 10^4$ l mol^{-1}s^{-1} and $k_{\mathrm{bd}} = k_b = 2.0 \times 10^{-2}$ s^{-1}). Very good agreement between experimental data and calculated profiles of monomer conversion vs. time, RAFT agent consumption, as well as M_w and $Đ$ vs. conversion, was obtained. The model used also described well the effect of initiator concentration. A short induction period, probably induced by slow fragmentation of the one-arm adduct in the pre-equilibrium, was observed.

The RAFT polymerization of Sty using 1,1′-azobis(cyclohexanecarbonitrile) as initiator and 2-[(phenylthioxomethyl)thio]-acetic acid as RAFT agent (RAFT agent with relatively poor leaving group), conducted in batch and discrete semibatch modes under bulk and solution (toluene) conditions, at 90 °C, was studied by Hlalele et al. [100]. The *Q*-type Predici™ modelling approach was used to model RAFT polymerizations in batch and semibatch modes. In the case of semibatch

operating mode, a fraction of the total monomer (~14% w/w) was polymerized at the early stages of polymerization, yielding low-dispersity RAFT oligomers; thereafter, the remaining monomer was added in a single shot to complete the reaction. As a result, narrower molar mass distributions, with reduced amounts of low molar mass oligomers, were obtained. Lower $Đ$ values were obtained as monomer feed time of the remaining monomer was delayed. Also, it was shown that the fraction of polymer molecules retaining EGF reached similar values to the fraction of polymer molecules obtained when using a RAFT agent with a good living group after 30% monomer conversion.

The polymerization kinetics of BA, using *S*-thiobenzoyl-2-thiopropionate and α-methyl-4(methylmercapto)-α-morpholinopropiophenone, was studied in toluene at −40 °C [101]. Two experimental methods were used to estimate the equilibrium constant $\left(K_{eq} = \frac{k_a}{k_b}\right)$: single fast EPR scanning, during (pseudo)stationary photopolymerization, which results in $K_{eq} = (2.3 \pm 0.6) \times 10^5$ l mol^{-1}; and microsecond time-resolved EPR, which leads to $K_{eq} = (3.4 \pm 0.6) \times 10^5$ l mol^{-1}. In the second method, the propagating ($R^{\cdot}_m$) and intermediate ($R_m A^{\cdot} R_n$) radical concentrations were monitored after applying the laser pulse. The experimental profiles were subsequently used to estimate the fragmentation kinetic rate constant, leading to $k_b = 3.1 \times 10^4$ s^{-1}. The addition–fragmentation equilibrium constant was estimated using a kinetic model developed in Predici™ that considered the occurrence of intermediated radical termination. The best fit was attained with $C_{cross} = \frac{k_{tir}}{k_t} = 0.25$.

7.3 Stochastic Modelling Techniques (SMTs)

Stochastic or random processes are based on the theory of probability. They are a collection of random variables indexed by time. Contrary to DMTs, in which there is a unique solution for the analysed system, in SMTs some degree of uncertainty is present even if the initial conditions are known. The process can evolve in multiple ways (often infinite) and, therefore, there are multiple solutions of the system. One event is selected between the whole range of possibilities depending on the type of SMT used. The most popular SMT in polymer reaction engineering (PRE) is kMC.

7.3.1 Monte Carlo

In this algorithm, initially proposed by Ulam and von Neumann during the Manhattan Project and later modified by Gillespie [102, 103] (in the so-called kMC), *the events are selected according to probabilities calculated from macroscopic or microscopic parameters* [104]. Comprehensive reviews on kMC have been published in the literature [104, 105]. In addition, both aspects, computation time and solution precision, are determined by the initial number of molecules in the analysed system. One of the advantages of kMC, compared to DMTs, is the more detailed microstructural information of the polymer chains provided by kMC.

7.3.1.1 Homogeneous Systems

Drache et al. [7] carried out the RAFT polymerization of methyl acrylate using C-DB as RAFT agent, at 80 °C. They also simulated the system using a kMC model based on IRT theory. Good agreement between model predictions and experimental data was obtained. Pre-equilibrium and main equilibrium steps were included in the RAFT polymerization scheme. The MWDs calculated with the model showed good agreement with SEC measurements. They also modelled the RAFT polymerization of Sty using benzyl dithiobenzoate (Bz-DB), 1-phenylethyl dithiobenzoate (PhEt-DB), and C-DB, at 120 °C, via Monte Carlo simulations [106, 107]. Drache et al. [108] presented a software program based on a kMC algorithm (mcPolymer) capable of modelling RAFT polymerizations, even in parallel programming environments. In fact, parallel programing has been demonstrated to be a remarkable strategy to decrease computation time in kMC models, presenting the same level of performance (running times) as the Predici™ software for versions not including kMC [109].

Prescott et al. [110] described the influence of CL-dependent kinetic rate constants related to reactions that involve radicals, dormant and dead polymer molecules in both homogeneous and heterogeneous systems. They used a kMC modelling technique with pseudo-random number generators. Their results showed that the presence of dormant species of large chain lengths led to increased lifetimes for polymer radicals since reduced termination kinetic rate constants and zero–one kinetic behaviour were inapplicable to RAFT emulsion polymerization. They also studied the radical loss observed in the RAFT emulsion polymerization of Sty using 2-phenylpropan-2-yl phenyldithioacetate (PPPDTA) as RAFT agent [111]. The system did not show a retardation effect. Nuclear magnetic resonance (NMR) analyses did not show the presence of three-arm star polymer molecules, or build-up of intermediate polymer radicals. Monte Carlo simulations suggested that radical loss is mainly due to termination between two large polymer radical molecules. Other contributions on the use of kMC method for modelling of homogeneous RAFT polymerizations include a discussion on discrimination between IRT and SF theories by the addition of an alkoxyamine [112]; analysis of theories for RAFT polymerization using the Julia programming language [113]; fitting of kinetic rate constants by using IRT including Eq. (7.15) and all possible reactions with primary radicals [114]; and modelling of the RAFT polymerization Sty at 110 °C, including self-initiation in the polymerization Scheme [1].

7.3.1.2 Heterogeneous Systems

Tobita has modelled miniemulsion RAFT polymerizations using a kMC technique based on the 'competition technique', which resulted in a faster execution code [27, 115–117]. In his first contribution, he compared IRT and SF theories. In the former theory polymerization rate significantly increased when particle size (D_p) decreased. In contrast, an almost negligible increase in polymerization rate was observed as D_p decreased, when the second model was used [27]. However, calculated MWDs were inaccurate due to an improper account of the repetition of active periods. In a subsequent publication, he considered the overall connection probability to account for the 'repetition of active periods' effect in a proper manner [115]. He derived

expressions for D_p in RAFT miniemulsion polymerization [116]. Additionally, based on previous RAFT model discrimination proposals using the Monte Carlo approach [117], a series of poly(styryl dithiobenzoate)-mediated RAFT miniemulsion polymerizations of Sty were carried out at 60 °C. The experimental results agreed well with calculated profiles using IRT theory, in which polymerization rate increased when D_p decreased [118]. Another contribution on RAFT miniemulsion polymerization included the study of droplet nucleation [119].

7.4 Hybrid Methods

Modelling methods that combine deterministic and stochastic or probabilistic techniques are explored and discussed in this section. Several Monte Carlo simulation studies that obtain information from deterministic models expressed as systems of ODEs have been used to model radical polymerization processes (see for instance [120, 121]). However, very few of such studies have focused on the modelling of RAFT polymerization. The use of these combined techniques is intended to reduce the computation time of standard Monte Carlo algorithms.

The modelling technique used by Konkolewicz et al. [34, 40] in the development of their IRTO model can be considered a hybrid one. They used a basic deterministic model to describe the evolution of conversion, average molecular weights, and dispersity, resulting in a low dimensionality system of ODEs; however, the full MWD was described by using a probabilistic approach. Each of the polymer distributions (dormant, living, and dead polymer) was described by using probabilistic derivations, arguably to avoid direct integration of a large set of ODEs (one equation for each chain size). However, one of the individual polymer populations, the dead polymer distribution, was obtained by accumulating the previous distribution to that of the newly formed dead polymer molecule in a discrete time interval, which is equivalent to a numerical integration of the corresponding equations. Probabilities for the full MWD were updated at each time interval by taking updated kinetic information from the solution of the system of ODEs representing the basic model.

In the modelling work of Devlaminck et al. [42] for the MADIX polymerization of Sty and copolymerization of Sty/BA, two approaches were used. A simple deterministic model employing a variation of the MM was applied for the calculation of conversion and average polymer properties (averages of the MWD and average chain end-functionality). On the other hand, a modified version of Gillespie's kMC method was used to describe detailed copolymer composition microstructure.

7.5 Specific or Novel Polymerization Processes

7.5.1 Semibatch Polymerization

Polymerization rate in batch radical copolymerization depends on (co)monomers and polymer radical current concentrations. Their concentration profiles are governed by the initial quantities charged to the reactor. In semibatch reactors, on the

other hand, the addition to the reactor of one or more reactants is dosified, in order to modify/improve product quality, according to the reactants feeding policy.

Mole balances for the components present in semibatch copolymerization reactors are given by Eq. (7.21), where C_m, R_m, Q_m, MW_m, ρ_m, and V are the concentration, consumption rate, molar feeding flow rate, molar mass and density for component m, and volume, respectively. The change in volume for the reacting mixture contained in the reactor is given by the sum of solvent feeding flow rate, F_s, feeding flow rate for component m, and the term related to the difference in densities between comonomers ρ_m and polymer ρ_p, as shown in Eq. (7.22).

$$\frac{d\left(C_m V\right)}{dt} = R_m V + \frac{Q_m \mathrm{MW}_m}{\rho_m} \tag{7.21}$$

$$\frac{dV}{dt} = F_s + \sum\nolimits_m \frac{Q_m \mathrm{MW}_m}{\rho_m} + \sum\nolimits_m V R_m \mathrm{MW}_m \left(\frac{1}{\rho_m} - \frac{1}{\rho_p}\right) \tag{7.22}$$

Total monomer conversion and cumulative copolymer composition (CF_m) are calculated using Eqs. (7.23) and (7.24), respectively.

$$x = \frac{\sum_m \left(V_o C_{m0} + \int Q_m dt - V C_m\right)}{\sum_m \left(V_o C_{m0} + \int Q_m dt\right)} \text{ for } m = \text{A and B} \tag{7.23}$$

$$\mathrm{CF}_m = \frac{V_o C_{m0} + \int Q_m dt - V C_m}{\sum_m \left(V_0 C_{m0} + \int Q_m dt - V C_m\right)} \text{ for } m = \text{A and B} \tag{7.24}$$

Semibatch reactors are often used to control cumulative copolymer composition, CF_m, and/or component m number average sequence length, $\mathrm{SL}_{n,m}$ [122–124]. In binary copolymerization of comonomers A and B, the monomer that reacts faster, say B, is usually fed following a semibatch feeding policy. The initial amount of comonomer B charged to the reactor can be calculated from the Mayo–Lewis equation, Eq. (7.25) and (7.26), where f_A and f_B are the unreacted molar fractions of monomer A and monomer B, respectively. F_A and F_B are the instantaneous copolymer compositions of monomer A and monomer B, respectively.

$$F_\mathrm{A} = \frac{r_1 f_\mathrm{A}^2 + f_\mathrm{A} f_\mathrm{B}}{r_1 f_\mathrm{A}^2 + 2 f_\mathrm{A} f_\mathrm{B} + r_2 f_\mathrm{B}^2} \tag{7.25}$$

$$F_\mathrm{B} = 1 - F_\mathrm{A} \tag{7.26}$$

The addition of comonomer B, Q_B, in a time interval Δt should satisfy a given relationship between instantaneous copolymer composition and the number average chain length (X_n), given by $F_m = f(X_n)$, for m = A or B, in order to obtain the desired CF_m vs. conversion profile. Different composition profiles can be designed; for instance, uniform, linear gradient or tanh gradient, as defined in Eq. (7.27)–(7.30), where $R_{p,m}$ is the monomer m consumption rate and $X_{n,\,\mathrm{targeted}}$ is the targeted number average chain length.

$$F_A = \frac{R_{p,A}}{R_{p,A} + R_{p,B}}, F_B = 1 - F_A \tag{7.27}$$

$$\text{Uniform}: F_m = 0.5 \tag{7.28}$$

$$\text{Linear gradient} : F_m = \frac{X_n}{X_{n,\text{targeted}}} \tag{7.29}$$

$$\tan\, h \text{ gradient} : F_m = \frac{1}{2} + \frac{1}{2}\tan h\lambda \left(\frac{X_n}{X_{n,\text{targeted}}} - \frac{1}{2} \right) \tag{7.30}$$

Wang et al. theoretically demonstrated that the synthesis of copolymers with controlled copolymer compositions (uniform and gradient) is possible through semibatch operation during the copolymerization [59]. They carried out their calculations using the terminal model and the MM [59]. They compared the composition performance of two cases, namely batch and semibatch RAFT copolymerization of two monomers (A and B), assuming hypothetical values for the kinetic rate constants, and addressed two sets of reactivity ratios ($r_A = 2$, (10) and $r_B = 10$, (0.1), respectively). In a subsequent publication [22], they studied the semibatch copolymerization of Sty and BA using benzyl dithioisobutyrate (BDIB) and AIBN, at 70 °C. The feeding flow rate of comonomer B was controlled by a metering pump programmed with the optimal profile. Their experimental data agreed well with the predicted profiles (an implicit penultimate model was used) of monomer conversion, CF_m, M_n, and $Đ$ for a targeted uniform composition of $CF_A = 0.25$ and a linear gradient semibatch policy. This group also studied the semibatch copolymerization of St/BA using BDIB and 1,1′-azobis(cyclohexane carbonitrile) (ACC) at 88 °C, yielding uniform, linear gradient, and tan h gradient copolymers, as well as triblock copolymers with linear gradient mid-block composition profiles [23].

Constant and linear gradient copolymer composition, CF_m, and constant number average sequence length, SL_n, profiles for the copolymerization of MMA (monomer A) with a hypothetical monomer (denoted as B) of higher propagation rate, using AIBN and 2-cyanopropan-2-yl 1H-pyrrole-1-carbodithioate at 60 °C, were obtained by using a chain model coupled to a sequence model, both derived by Ye and Schork [60]. The proposed models were based on the MM for calculation of average properties. The presence of intermediate radicals was neglected. Two sets of reactivity ratios were investigated, $r_A = 0.5$ (0.1) and $r_B = 2$ (10), respectively. Copolymers with constant composition, $F_A = 0.5$, linear gradient, $F_B = \frac{X_n}{1000}$, and constant number average sequence length, $SL_{n,A} = 3$ or $SL_{n,B} = 3$, were attained by adjusting the feeding flow rate of monomer B.

7.5.2 Polymerizations in CSTRs/PFR

The effect of backmixing on the RAFT polymerization of a hypothetical monomer carried out in a tubular reactor was addressed using two modelling approaches: a train of CSTR-in-series (train of 1, 3, 5, and 10 reactors), and a recycle model (1–99% recycling) [25]. A hypothetical ratio of [M] : [AB] : [I] = 1000 : 2 : 1 and a space–time of 30 hours were assumed. The increase of backmixing (lower number of CSTR-in-series or higher recycling percentage) resulted in a decrease of monomer conversion, shorter chain lengths, and broader molar mass distributions. It was found that M_n of dead polymer molecules was independent of backmixing, but the concentration of dead polymer molecules decreased due to lower bimolecular

termination rates. Simulations generated with both models were similar in terms of monomer conversion. However, monomer conversion was predicted to be higher at the beginning of the polymerization when the recycle model was used. Polymerization rate decreased afterwards.

The copolymerization of two hypothetical monomers, identified as A and B in continuous reactors, with assumed reactivity ratios of $r_A = 2$ and $r_B = 0.5$, was studied using the MM [125]. Three reactor configurations were addressed: single CSTR, CSTR-PFR-CSTR trains, and PFR-CSTR-PFR trains, with a residence time of $\tau = 20\,000$ s for each reactor. Lower conversions, lower X_n, and higher $Đ$ were attained in the CSTRs. In contrast, the use of plug flow reactors (PFRs) resulted in higher conversions, higher X_n, and lower $Đ$. Copolymer compositions and sequence length averages were calculated for each case. Compositional drift was observed only in PFRs.

7.5.3 Branched Copolymerizations

The RAFT emulsion copolymerization of 1,3-butadiene and acrylonitrile (AN) using KPS and 2-(((dodecylsulfanyl)carbonothioyl)sulfanyl)propanoic acid (DoPAT) in water at 45–55 °C was modelled using Predici™ [126]. A high ratio of $[AB]_0 : [I]_0$ was required to produce copolymers with low $Đ$ values. Although branching was neglected in the model, polymerization rate, expressed as conversion vs. time, was adequately described. Since the predictions of molecular weight development were underestimated with the model, a correction to account for branching, using an additional exponent to the theoretical $M_{n,\mathrm{th}}$, was implemented, as shown in Eq. (7.31).

$$M_n = M_{n,\mathrm{th}}^{1+x_b} + M_{\mathrm{RAFT}} \tag{7.31}$$

A value of $x_\mathrm{b} = 0.065$ fitted M_n, the experimental data, well at different RAFT agent concentrations. A two-stage temperature operation was also considered in order to reduce the observed inhibition periods. The first polymerization stage proceeded at 55 °C and lasted four hours; the temperature was then lowered to 45 °C.

Hyperbranched polymers with narrow MWDs can be synthesized using RAFT agents with single double bonds, as observed in Figure 7.5.

The modelling of hyperbranching polymerization has been achieved with application of the segment model, modified for inclusion of branch trackers [127]. Three copolymerizations using 4-vinylbenzyl 1*H*-imidazole-4-carbodithioate (RAFT agent) and AIBN were addressed: acrylamide/acrylic acid, acrylonitrile/methacrylic acid, and ethylene/Sty. The system acrylamide/acrylic acid yielded

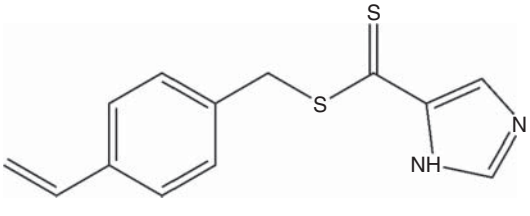

Figure 7.5 4-vinylbenzyl 1*H*-imidazole-4-carbodithioate.

hyperbranched polymers with low dispersities ($X_n \approx 15\ 000$, $Đ \approx 1$) whereas the other cases produced low X_n, indicating that hyperbranched structures were not obtained.

The MM has been applied to the synthesis of hyperbranched polymers from *N*-isopropylacrylamide (NIPAm) using 4-vinylbenzyl 1*H*-imidazole-4-carbodithioate and AIBN at 65 °C, in dioxane [128]. A mathematical model considering inhibition and retardation was developed. Three experimental cases were addressed: [M] : [AB] : [I] = 100, 150, 200 : 1 : 0.5. Calculated $Đ$ values of 1.2–1.4 and branch points of 0.4–0.6 were obtained, indicating the formation of well-defined hyperbranched copolymers.

The Predici™ software of CiT was used to calculate R group molar mass distributions of star polymerizations [129]. The RAFT equilibrium was modelled using the *Q*-approach while star chain lengths were calculated as the addition of their arms.

7.5.4 Microwave-Assisted (MA) RAFT Polymerization

Organic chemistry syntheses carried out in the presence of microwave irradiation (MI) offer faster heating and polymerization rates, compared to conventional heating [130]. The phenomena observed in microwave-activated radical polymerizations can be explained by what are known as 'thermal effects' (TE) or 'microwave effects' (ME) conceptual approaches. The former accounts for temperature gradients reached within the reaction mixture due to lack of optimal temperature monitoring and control. The resulting elevated temperatures directly affect polymerization rate and molar mass development. In the case of ME, one or more reactions are affected; these reactions reach unusually high kinetic rate constant values. Alternatively, ME may be caused by side reactions that greatly affect the evolution of the reaction. It is recommended to use optic fibre sensors to accurately measure reactor temperature profiles and to help assess what causes the increases in polymerization rate [131, 132].

Mathematical models for different microwave-assisted polymerization situations, including microwave-assisted reversible addition–fragmentation chain transfer (MA-RAFT) polymerization of vinyl monomers, based on ME, TE, or combinations of both, have been proposed by Vivaldo-Lima's group [20, 21, 133–137]. Three main models have been used: (i) microwave-induced generation of radicals from monomer (a ME approach, identified as Model 1); (ii) non-isothermal polymerization (TE approach, identified as Model 2); and (iii) a specific reaction or a small set of reactions that proceed much faster (a type of ME, identified here as Model 3). An example of Model 1, where monomeric radicals ($M_r^{\bullet}$) are generated from monomer (M) due to microwave irradiation, is shown in Table 7.3. This approach was first proposed by Aldana-García et al. to describe the emulsion polymerization of Sty in water with sodium dodecyl sulphate as surfactant and KPS as initiator at 50 and 70 °C [133]. The model was tested with several experimental cases under conductive heating (CH) and MI obtaining fairly good predictions. This approach has also been used in the study of RDRP systems [20, 21, 134–137].

Table 7.3 Implementation of Model 1 in Predici.

Reaction	Step in Predici	Pattern	Kinetic coefficient
Microwave-induced generation of radicals	Elemental	$M \rightarrow 2M_r^{\bullet}$	k_{ir}
First propagation	Initiation (anion)	$M + M_r^{\bullet} \rightarrow P(1)$	k_i
Propagation	Propagation	$M + P(s) \rightarrow P(s+1)$	k_p

In Model 2 all the kinetic rate constants depend on temperature, $k_j(T)$. If actual temperature profiles are not known, predefined profiles, $T(t)$, can be assumed. This approach has been explored in the modelling of other RDRP cases [134–137].

Hernández-Ortiz et al. reported the first study on MA-RAFT polymerization of Sty by application of the MM [20]. They addressed eight cases with and without initiator (AIBN) under conventional and microwave heating at 60, 72, and 98 °C, using 2-cyanopropan-2-yl naphthalene-1-carbodithioate (CPDN) as RAFT agent. The cases under conventional heating were used to fit the kinetic rate constants associated to the addition–fragmentation reactions. They used Model 1 for the cases under MI. It was found that their approach described reasonably well the experimental data, although M_n was overestimated at low conversions and $Đ$ was overestimated in all cases. The model captured well the faster polymerization rate in MA RAFT polymerizations.

Zetterlund et al. modelled the MA-RAFT polymerization of Sty by implementing Models 1–3 in the Predici software. They used 2-cyanopropan-2-yl dithiobenzoate (CPDB) as the RAFT agent and AIBN as the initiator at 60 °C [21]. Regarding the implementation of Model 2, they assumed that the system reached temperatures of 80 and 100 °C. The propagation and first addition to RAFT agent reactions were assumed to be enhanced by MI in Model 3. The best results were obtained with Model 3 where kinetic rate coefficients k_p and k_{add} were increased by one order of magnitude.

7.6 Closing Remarks

The modelling and simulation of RAFT polymerization of vinyl monomers has been achieved by using several numerical approaches. A large number of research reports are based on the method of moments, kMC simulations, and the software Predici. The cases modelled include synthesis of homopolymers with narrow molar mass distributions, synthesis of polymer networks by crosslinking/branching reactions of vinyl/divinyl monomers, microwave-assisted polymerizations, synthesis of copolymers with controlled chain composition distributions via semibatch operation modes, dispersion polymerizations carried out in supercritical carbon dioxide, continuous stirred tank reactors, and miniemulsion polymerizations.

The use of modelling tools has been useful in the design of materials and processes based on RAFT polymerization. There are still issues to be addressed, but research efforts are already targeted at them.

Acknowledgments

Financial support from the following sources is gratefully acknowledged: (i) Consejo Nacional de Ciencia y Tecnología (CONACYT, México), Project CB 239364 granted to E.V.-L., Project CB 256358 granted to E.S.-G., Project 'Cátedras' 707 granted to I.Z-G., and a PhD scholarship granted to P.L.-D.; (ii) DGAPA-UNAM, Projects PAPIIT IG100718, IV100119 and sabbatical PASPA support to E.V.-L.; and (iii) Facultad de Química-UNAM, research funds granted to E. V.-L. (PAIP 5000-9078).

References

1 Li, L., He, J., and Yang, Y. (2000). Monte Carlo simulation on living radical polymerization with RAFT process. *Chem. J. Chinese U.* 21 (7): 1146–1148.
2 Zhang, M. and Ray, W.H. (2001). Modeling of "living" free-radical polymerization with RAFT chemistry. *Ind. Eng. Chem. Res.* 40 (20): 4336–4352.
3 Barner-Kowollik, C., Quinn, J.F., Morsley, D.R. et al. (2001). Modeling the reversible addition – fragmentation chain transfer process in cumyl dithiobenzoate-mediated styrene homopolymerizations: assessing rate coefficients for the addition – fragmentation equilibrium. *J. Polym. Sci., Part A: Polym. Chem.* 39 (9): 1353–1365.
4 Wang, A.R. and Zhu, S. (2003). Modeling the reversible addition – fragmentation transfer polymerization process. *J. Polym. Sci., Part A: Polym. Chem.* 41 (11): 1553–1566.
5 Wang, A.R. and Zhu, S. (2003). Effects of diffusion-controlled radical reactions on RAFT polymerization. *Macromol. Theory Simul.* 12 (2–3): 196–208.
6 Luo, Y.W. (2003). Monte Carlo simulations for the very beginning of RAFT seeded emulsion polymerization. *Chem. J. Chinese U.* 24 (10): 1926–1928.
7 Drache, M., Schmidt-Naake, G., Buback, M. et al. (2005). Modeling RAFT polymerization kinetics via Monte Carlo methods: Cumyl dithiobenzoate mediated methyl acrylate polymerization. *Polymer* 46 (19): 8483–8493.
8 Theis, A., Feldermann, A., Charton, N. et al. (2005). Living free radical polymerization (RAFT) of dodecyl acrylate: chain length dependent termination, mid-chain radicals and monomer reaction order. *Polymer* 46 (18): 6797–6809.
9 Monteiro, M.J. (2005). Modeling the molecular weight distribution of block copolymer formation in a reversible addition – fragmentation chain transfer mediated living radical polymerization. *J. Polym. Sci., Part A: Polym. Chem.* 43 (22): 5643–5651.

10 Peklak, A.D. and Butte, A. (2006). Modeling of diffusion limitations in bulk RAFT polymerization. *Macromol. Theory Simul.* 15 (7): 546–562.

11 Pallares, J., Jaramillo-Soto, G., Flores Cataño, C. et al. (2006). A comparison of reaction mechanisms for reversible addition – fragmentation chain transfer polymerization using modeling tools. *J. Macromol. Sci. Part A Pure Appl. Chem.* 43 (9): 1293–1322.

12 Mastan, E., Li, X., and Zhu, S. (2015). Modeling and theoretical development in controlled radical polymerization. *Prog. Polym. Sci.* 45: 71–101.

13 Zhou, Y.-N. and Luo, Z.-H. (2016). State-of-the-art and progress in method of moments for the model-based reversible- deactivation radical polymerization. *Macromol. React. Eng.* 10 (6): 516–534.

14 De Rybel, N., Van Steenberge, P.H.M., Reyniers, M.-F. et al. (2017). An update on the pivotal role of kinetic modeling for the mechanistic understanding and design of bulk and solution RAFT polymerization. *Macromol. Theory Simul.* 26 (1): 1600048.

15 Hernández-Ortiz, J.C., Vivaldo-Lima, E., Dubé, M.A. et al. (2014). Modeling of network formation in reversible addition-fragmentation transfer (RAFT) copolymerization of vinyl/divinyl monomers using a multifunctional polymer molecule approach. *Macromol. Theory Simul.* 23 (3): 147–169.

16 Espinosa-Pérez, L., Hernández-Ortiz, J.C., López-Domínguez, P. et al. (2014). Modeling of the production of hydrogels from hydroxyethyl methacrylate and (Di)ethylene glycol dimethacrylate in the presence of RAFT agents. *Macromol. React. Eng.* 8 (8): 564–579.

17 López-Domínguez, P., Hernández-Ortiz, J.C., Barlow, K.J. et al. (2014). Modeling the kinetics of monolith formation by RAFT copolymerization of styrene and divinylbenzene. *Macromol. React. Eng.* 8 (10): 706–722.

18 Jiang, J., Wang, W., Li, B., and Zhu, S. (2017). Modeling and experimentation of RAFT solution copolymerization of styrene and butyl acrylate, effect of chain transfer reactions on polymer molecular weight distribution. *Macromol. React. Eng.* 11: 1700029. doi:https://doi.org/10.1002/mren.201700029.

19 Oliveira, D., Dias, R.C.S., and Costa, M.R.P.F.N. (2016). Modeling RAFT gelation and grafting of polymer brushes for the production of molecularly imprinted functional particles. *Macromol. Symp.* 370 (1): 52–65.

20 Hernández-Ortiz, J.C., Jaramillo-Soto, G., Palacios-Alquisira, J. et al. (2010). Modeling of polymerization kinetics and molecular weight development in the microwave-activated RAFT polymerization of styrene. *Macromol. React. Eng.* 4 (3–4): 210–221.

21 Zetterlund, P.B. and Perrier, S. (2011). RAFT polymerization under microwave irradiation: toward mechanistic understanding. *Macromolecules* 44 (6): 1340–1346.

22 Sun, X., Luo, Y., Wang, R. et al. (2007). Programmed synthesis of copolymer with controlled chain composition distribution via Semibatch RAFT copolymerization. *Macromolecules* 40 (4): 849–859.

23 Sun, X., Luo, Y., Wang, R. et al. (2008). Semibatch RAFT polymerization for producing ST/BA copolymers with controlled gradient composition profiles. *AlChE J.* 54 (4): 1073–1087.

24 Jaramillo-Soto, G., Castellanos-Cárdenas, M.L., García-Morán, P.R. et al. (2008). Simulation of RAFT dispersion polymerization in supercritical carbon dioxide. *Macromol. Theory Simul.* 17 (6): 280–289.

25 Bitsch, B., Barner-Kowollik, C., and Zhu, S. (2011). Modeling the effects of reactor backmixing on RAFT polymerization. *Macromol. React. Eng.* 5 (1): 55–68.

26 Butté, A., Storti, G., and Morbidelli, M. (2001). Miniemulsion living free radical polymerization by RAFT. *Macromolecules* 34 (17): 5885–5896.

27 Tobita, H. and Yanase, F. (2007). Monte Carlo simulation of controlled/living radical polymerization in emulsified systems. *Macromol. Theory Simul.* 16 (4): 476–488.

28 Altarawneh, I.S., Gomes, V.G., and Srour, M.S. (2008). The influence of xanthate-based transfer agents on styrene emulsion polymerization: mathematical Modeling and model validation. *Macromol. React. Eng.* 2 (1): 58–79.

29 Barner-Kowollik, C., Buback, M., Charleux, B. et al. (2006). Mechanism and kinetics of dithiobenzoate-mediated RAFT polymerization. I. The current situation. *J. Polym. Sci., Part A: Polym. Chem.* 44 (20): 5809–5831.

30 Moad, G. (2014). Mechanism and kinetics of dithiobenzoate-mediated RAFT polymerization - status of the dilemma. *Macromol. Chem. Phys.* 215 (1): 9–26.

31 Monteiro, M.J. and De Brouwer, H. (2001). Intermediate radical termination as the mechanism for retardation in reversible addition-fragmentation chain transfer polymerization. *Macromolecules* 34 (3): 349–352.

32 Wang, A.R., Zhu, S., Kwak, Y. et al. (2003). A difference of six orders of magnitude: a reply to "the magnitude of the fragmentation rate coefficient". *J. Polym. Sci., Part A: Polym. Chem.* 41 (18): 2833–2839.

33 Buback, M. and Vana, P. (2006). Mechanism of dithiobenzoate-mediated RAFT polymerization: a missing reaction step. *Macromol. Rapid Commun.* 27 (16): 1299–1305.

34 Konkolewicz, D., Hawkett, B.S., Gray-Weale, A. et al. (2008). RAFT polymerization kinetics: combination of apparently conflicting models. *Macromolecules* 41 (17): 6400–6412.

35 Li, C., He, J., Liu, Y. et al. (2012). Probing the RAFT process using a model reaction between alkoxyamine and dithioester. *Aust. J. Chem.* 65 (8): 1077–1089.

36 Zapata-Gonzalez, I., Saldivar-Guerra, E., and Licea-Claverie, A. (2017). Kinetic modeling of RAFT polymerization via dithiobenzoate agents considering the missing step theory. *Chem. Eng. J.* 326: 1242–1254.

37 Bamford, C.H. and Tompa, H. (1953). On the calculation of molecular weight distributions from kinetic schemes. *J. Polym. Sci.* 10 (3): 345–350.

38 Bamford, C.H. and Tompa, H. (1954). The calculation of molecular weight distributions from kinetic schemes. *Trans. Faraday Soc.* 50: 1097–1115.

39 Monteiro, M.J. (2005). Design strategies for controlling the molecular weight and rate using reversible addition-fragmentation chain transfer mediated living radical polymerization. *J. Polym. Sci., Part A: Polym. Chem.* 43 (15): 3189–3204.

40 Konkolewicz, D., Hawkett, B.S., Gray-Weale, A. et al. (2009). RAFT polymerization kinetics: how long are the cross-terminating oligomers? *J. Polym. Sci., Part A: Polym. Chem.* 47 (14): 3455–3466.

41 Zapata-González, I., Saldívar-Guerra, E., and Ortiz-Cisneros, J. (2011). Full molecular weight distribution in RAFT polymerization. New mechanistic insight by direct integration of the equations. *Macromol. Theory Simul.* 20 (6): 370–388.

42 Devlaminck, D.J.G., Van Steenberge, P.H.M., De Keer, L. et al. (2017). A detailed mechanistic study of bulk MADIX of styrene and its chain extension. *Polym. Chem.* 8 (45): 6948–6963.

43 Masoumi, S., Duever, T.A., Penlidis, A. et al. (2018). Model discrimination between RAFT polymerization models using sequential Bayesian methodology. *Macromol. Theory Simul.* 27 (5): 1800016.

44 De Rybel, N., Van Steenberge, P.H.M., Reyniers, M.-F. et al. (2018). How chain length dependencies interfere with the bulk RAFT polymerization rate and microstructural control. *Chem. Eng. Sci.* 177: 163–179.

45 Jiang, J., Wang, W.-J., Li, B.-G. et al. (2018). Tailoring uniform copolymer composition distribution via policy II RAFT solution copolymerization of styrene and butyl acrylate. *Macromol. React. Eng.* 12 (4): 1800014.

46 Zapata-González, I., Saldívar-Guerra, E., Flores-Tlacuahuac, A. et al. (2012). Efficient numerical integration of stiff differential equations in polymerisation reaction engineering: computational aspects and applications. *Can. J. Chem. Eng.* 90 (4): 804–823.

47 Wang, D., Li, X., Wang, W.-J. et al. (2012). Kinetics and Modeling of semi-batch RAFT copolymerization with hyperbranching. *Macromolecules* 45 (1): 28–38.

48 Jiang, J., Wang, W.-J., Li, B.-G. et al. (2017). Modeling and experimentation of RAFT solution copolymerization of styrene and butyl acrylate, effect of chain transfer reactions on polymer molecular weight distribution. *Macromol. React. Eng.* 11 (6): 1700029.

49 Pinto, M.A., Li, R., Immanuel, C.D. et al. (2008). Effects of reversible addition fragmentation transfer (RAFT) on branching in vinyl acetate bulk polymerization. *Ind. Eng. Chem. Res.* 47 (3): 509–523.

50 Hutchinson, R.A. (2005). Free-radical polymerization: homogeneous. In: *Handbook of Polymer Reaction Engineering* (eds. T. Meyer and J. Keurentjes), 153–212. Weinheim: Wiley-VCH.

51 Mastan, E. and Zhu, S. (2015). Method of moments: a versatile tool for deterministic modeling of polymerization kinetics. *Eur. Polym. J.* 68: 139–160.

52 Klumperman, B., van den Dungen, E.T.A., Heuts, J.P.A. et al. (2010). RAFT-mediated polymerization-a story of incompatible data? *Macromol. Rapid Commun.* 31 (21): 1846–1862.

53 Magallanes, A.R. (2019). Computational study of RAFT polymerization, exploring the effect of retardation. Instituto Tecnologico de Tijuana. Bachelor Thesis, filed 26 November 2019 and issued 26 November 2019.

54 Goh, Y.-K. and Monteiro, M.J. (2006). Novel approach to tailoring molecular weight distribution and structure with a difunctional RAFT agent. *Macromolecules* 39 (6): 4966–4974.

55 Johnston-Hall, G. and Monteiro, M.J. (2007). Kinetic Modeling of "living" and conventional free radical polymerizations of methyl methacrylate in dilute and gel regimes. *Macromolecules* 40 (20): 7171–7179.

56 Gao, X. and Zhu, S. (2011). Modeling analysis of chain transfer in reversible addition-fragmentation chain transfer polymerization. *J. Polym. Sci., Part A: Polym. Chem.* 112 (1): 497–508.

57 Zhang, M. and Ray, W.H. (2002). Modeling of "living" free-radical polymerization processes. I. Batch, semibatch, and continuous tank reactors. *J. Appl. Polym. Sci.* 86 (7): 1630–1662.

58 Ross, R.T. and Laurence, R.L. (1976). Gel effect and free volume in the bulk polymerization of methyl methacrylate. *AlChE Symp. Ser.* 160: 1974–1974.

59 Wang, R., Luo, Y., Li, B. et al. (2006). Design and control of copolymer composition distribution in living radical polymerization using semi-batch feeding policies: a model simulation. *Macromol. Theory Simul.* 15 (4): 356–368.

60 Ye, Y. and Schork, F.J. (2009). Modeling and control of sequence length distribution for controlled radical (RAFT) copolymerization. *Ind. Eng. Chem. Res.* 48 (24): 10827–10839.

61 Zhang, M. and Ray, W.H. (2002). Modeling of "living" free-radical polymerization processes. II. Tubular reactors. *J. Appl. Polym. Sci.* 86 (5): 1047–1056.

62 Zhou, Y.-N., Guan, C.-M., and Luo, Z.-H. (2010). Kinetic modeling of two-step RAFT process for the production of novel fluorosilicone triblock copolymers. *Eur. Polym. J.* 46 (11): 2164–2173.

63 Ulitin, N.V., Nasyrov, I.I., Deberdeev, T.R. et al. (2012). Kinetic approach to modeling the radical polymerization of styrene in the presence dibenzyl trithiocarbonate. *Russ. J. Phys. Chem. B* 6 (6): 752–760.

64 Ulitin, N.V. and Oparkin, A.V. (2014). Kinetic modeling of Pseudoliving free radical styrene polymerization occurring via reversible addition – fragmentation chain transfer. *Theor. Found. Chem. Eng.* 48 (4): 434–443.

65 Ulitin, N.V., Tereshenko, K.A., Deberdeev, T.R. et al. (2015). Pseudolive radical polymerization of butyl acrylate in the presence of trithiocarbonates: modeling the kinetics and regulation of the molecular mass characteristics of the polymer. *Theor. Found. Chem. Eng.* 49 (1): 79–87.

66 Velasquez, E., Rieger, J., Stoffelbach, F. et al. (2016). Surfactant-free poly(vinylidene chloride) latexes via one-pot RAFT-mediated aqueous polymerization. *Polymer* 106: 275–284.

67 Li, X., Wang, W.-J., Weng, F. et al. (2014). Targeting copolymer composition distribution via model-based monomer feeding policy in semibatch RAFT mini-emulsion copolymerization of styrene and butyl acrylate. *Ind. Eng. Chem. Res.* 53 (18): 7321–7332.

68 Jennings, J., Beija, M., Kennon, J.T. et al. (2013). Advantages of block copolymer synthesis by RAFT-controlled dispersion polymerization in supercritical carbon dioxide. *Macromolecules* 46 (17): 6843–6851.

69 López-Domínguez, P., Jaramillo-Soto, G., and Vivaldo-Lima, E. (2018). A modeling study on the RAFT polymerization of vinyl monomers in supercritical carbon dioxide. *Macromol. React. Eng.* 12 (4): 1800011.

70 Jaramillo-Soto, G., García-Morán, P.R., Enríquez-Medrano, F.J. et al. (2009). Effect of stabilizer concentration and controller structure and composition on polymerization rate and molecular weight development in RAFT polymerization of styrene in supercritical carbon dioxide. *Polymer* 50 (21): 5024–5030.

71 Biasutti, J.D., Davis, T.P., Lucien, F.P. et al. (2005). Reversible addition–fragmentation chain transfer polymerization of methyl methacrylate in suspension. *J. Polym. Sci., Part A: Polym. Chem.* 43 (10): 2001–2012.

72 Nguyen, T.L.U., Farrugia, B., Davis, T.P. et al. (2007). Core-shell microspheres with surface grafted poly(vinyl alcohol) as drug carriers for the treatment of hepatocellular carcinoma. *J. Polym. Sci., Part A: Polym. Chem.* 45 (15): 3256–3272.

73 Cunningham, M.F. (2008). Controlled/living radical polymerization in aqueous dispersed systems. *Prog. Polym. Sci.* 33 (4): 365–398.

74 Zhang, Y., Ding, J., and Gong, S. (2013). Preparation of molecularly imprinted polymers for vanillin via reversible addition-fragmentation chain transfer suspension polymerization. *J. Appl. Polym. Sci.* 128 (5): 2927–2932.

75 Gonçalves, M.A.D., Pinto, V.D., Costa, R.A.S. et al. (2013). Stimuli-responsive hydrogels synthesis using free radical and RAFT polymerization. *Macromol. Symp.* 333 (1): 41–54.

76 Oliveira, M., Barbosa, B.S., Nele, M. et al. (2014). Reversible addition–fragmentation chain transfer polymerization of vinyl acetate in bulk and suspension systems. *Macromol. React. Eng.* 8 (6): 493–502.

77 Odian, G. (2004). *Principles of Polymerization*, 4e. Hoboken, NJ, N: Wiley.

78 Moad, G. and Solomon, D.H. (2006). *The Chemistry of Radical Polymerization*, 2e. San Diego, CA: Elsevier.

79 Shipp, D.A. and Matyjaszewski, K. (1999). Kinetic analysis of controlled/"living" radical polymerizations by simulations. 1. The importance of diffusion-controlled reactions. *Macromolecules* 32 (9): 2948–2955.

80 Delgadillo-Velazquez, O., Vivaldo-Lima, E., Quintero-Ortega, I.A. et al. (2002). Effects of diffusion-controlled reactions on atom-transfer radical polymerization. *AlChE J.* 48 (11): 2597–2608.

81 D'hooge, D.R., Reyniers, M.-F., and Marin, G.B. (2013). The crucial role of diffusional limitations in controlled radical polymerization. *Macromol. React. Eng.* 7 (8): 362–379.

82 Johnston-Hall, G., Stenzel, M.H., Davis, T.P. et al. (2007). Chain length dependent termination rate coefficients of methyl methacrylate (MMA) in the gel regime: accessing ktii using reversible addition-fragmentation chain transfer (RAFT) polymerization. *Macromolecules* 40 (8): 2730–2736.

83 Vana, P., Davis, T.P., and Barner-Kowollik, C. (2002). Easy access to chain-length-dependent termination rate coefficients using RAFT polymerization. *Macromol. Rapid Commun.* 23 (16): 952–956.

84 Lovestead, T.M., Theis, A., Davis, T.P. et al. (2006). Accessing the chain length dependence of the termination rate coefficient for disparate length radicals via reversible addition fragmentation chain transfer chemistry: a theoretical study. *Macromolecules* 39 (15): 4975–4982.

85 Peklak, A.D., Butte, A., Storti, G. et al. (2005). Gel effect in the bulk reversible addition – fragmentation chain transfer polymerization of methyl methacrylate: modeling and experiments. *J. Polym. Sci., Part A: Polym. Chem.* 44 (3): 1071–1085.

86 Read, D.J., Auhl, D., Das, C. et al. (2011). Linking models of polymerization and dynamics to predict branched polymer structure and flow. *Science* 333 (6051): 1871–1874.

87 Tobita, H. (2006). Fundamental molecular weight distribution of RAFT polymers. *Macromol. React. Eng.* 2 (5): 371–381.

88 Harrisson, S. (2018). Distribution of an ideal deactivation radical radical polymerization deactivation polymerization. *Polymers* 10 (8): 887–887.

89 Enright, W.H., Hull, T.E., and Lindberg, B. (1975). Comparing numerical methods for stiff systems of O.D.E.s. *BIT* 15: 10–48.

90 Byrne, D. and Hindmarsh, A.C. (1987). Siff ODE solvers: a review of corning attractions. *J. Comput. Phys.* 70 (1): 1–62.

91 Derboven, P., Van Steenberge, P.H.M., Vandenbergh, J. et al. (2015). Improved livingness and control over branching in RAFT polymerization of acrylates: could microflow synthesis make the difference? *Macromol. Rapid Commun.* 36 (24): 2149–2155.

92 Saldívar-Guerra, E., Infante-Martínez, R., Vivaldo-Lima, E. et al. (2010). Returning to basics: direct integration of the full molecular-weight distribution equations in addition polymerization. *Macromol. Theory Simul.* 19 (6): 151–157.

93 Dotson, N.A., Galván, R., Laurence, L.R. et al. (1996). *Polymerization Process Modeling*. New York, NY: Wiley-VCH.

94 Howe, J.P. (2004). Method of integrating the rate equations for free radical initiated. *J. Chem. Phys.* 23 (5): 899–902.

95 Fortunatti, C., Sarmoria, C., and Brandolin, A. (2014). Modeling of RAFT polymerization using probability generating functions. Detailed prediction of full molecular weight distributions and sensitivity analysis. *Macromol. React. Eng.* 8 (12): 781–795.

96 Fortunatti, C., Sarmoria, C., Brandolin, A. et al. (2014). Prediction of the full molecular weight distribution in RAFT polymerization using probability generating functions. *Comput. Chem. Eng.* 66: 214–220.

97 Vana, P., Davis, T.P., and Barner-Kowollik, C. (2002). Kinetic analysis of reversible addition fragmentation chain transfer (RAFT) polymerizations: conditions for inhibition, retardation, and optimum living polymerization. *Macromol. Theory Simul.* 11 (8): 823–835.

98 Wulkow, M., Busch, M., Davis, T.P. et al. (2004). Implementing the reversible addition–fragmentation chain transfer process in PREDICI. *J. Polym. Sci., Part A: Polym. Chem.* 42 (6): 1441–1448.

99 Nguyen, N.M., Margaillan, A., Pham, T.Q. et al. (2018). RAFT polymerization of tert-butyldimethylsilyl methacrylate: kinetic study and determination of rate coefficients. *Polymers* 10 (2): 224.

100 Hlalele, L., Pfukwa, R., and Klumperman, B. (2017). Simulation studies of the discrete semi-batch RAFT–mediated polymerization of styrene using a RAFT agent with relatively poor leaving group. *Eur. Polym. J.* 95: 596–605.

101 Meiser, W., Barth, J., Buback, M. et al. (2011). EPR measurement of fragmentation kinetics in dithiobenzoate-mediated RAFT polymerization. *Macromolecules* 44 (8): 2474–2480.

102 Gillespie, D.T. (1977). Exact stochastic simulation of coupled chemical reactions. *J. Phys. Chem.* 81 (25): 2340–2361.

103 Gillespie, D.T. (2001). Approximate accelerated stochastic simulation of chemically reacting systems approximate accelerated stochastic simulation of chemically reacting systems. *J. Chem. Phys.* 115 (4): 1716–1733.

104 Brandão, A.L.T., Soares, J.B.P., Pinto, C. et al. (2015). When polymer reaction engineers play dice: applications of Monte Carlo models in PRE. *Macromol. Theory Simul.* 9 (3): 141–185.

105 Meimaroglou, D. and Kiparissides, C. (2014). Review of Monte Carlo methods for the prediction of distributed molecular and morphological polymer properties. *Ind. Eng. Chem. Res.* 53 (22): 8963–8979.

106 Drache, M. and Schmidt-Naake, G. (2007). RAFT polymerization – investigation of the initialization period and determination of the transfer coefficients. *Macromol. Symp.* 259 (1): 397–405.

107 Drache, M. and Schmidt-Naake, G. (2008). Initialization of RAFT agents with different leaving groups – determination of the transfer coefficients. *Macromol. Symp.* 271 (1): 129–136.

108 Drache, M. and Drache, G. (2012). Simulating controlled radical polymerizations with mcPolymer – A Monte Carlo approach. *Polymers* 4 (3): 1416–1442.

109 Chaffey-Millar, H., Stewart, D., Chakravarty, M.M.T. et al. (2007). A parallelised high performance Monte Carlo simulation approach for complex polymerisation kinetics. *Macromol. Theory Simul.* 16 (6): 575–592.

110 Prescott, S.W. (2003). Chain-length dependence in living/controlled free-radical polymerizations: physical manifestation and Monte Carlo simulation of reversible transfer agents. *Macromolecules* 36 (25): 9608–9621.

111 Prescott, S.W., Ballard, M.J., Rizzardo, E. et al. (2005). Radical loss in RAFT-mediated emulsion polymerizations. *Macromolecules* 38 (11): 4901–4912.

112 Ao, Y., He, J., Han, X. et al. (2007). Kinetic analysis of the cross reaction between dithioester and alkoxyamine by a Monte Carlo simulation. *J. Polym. Sci., Part A: Polym. Chem.* 45 (3): 374–387.

113 Pintos, E., Sarmoria, C., Brandolin, A. et al. (2016). Modeling of RAFT polymerization processes using an efficient Monte Carlo algorithm in Julia. *Ind. Eng. Chem. Res.* 55 (31): 8534–8547.

114 Ganjeh-Anzabi, P., Hadadi-Asl, V., Salami-Kaljahi, M. et al. (2012). A new approach for Monte Carlo simulation of RAFT polymerization. *Iran. J. Chem. Chem. Eng.* 31 (3): 75–84.

115 Tobita, H. (2010). Modeling controlled/living radical polymerization kinetics: bulk and miniemulsion. *Macromol. React. Eng.* 4 (11–12): 643–662.

116 Tobita, H. (2011). Threshold particle diameters in miniemulsion reversible-deactivation radical polymerization. *Polymers* 3 (4): 1944–1971.

117 Tobita, H. (2013). On the discrimination of RAFT models using miniemulsion polymerization. *Macromol. Theory Simul.* 22 (8): 399–409.

118 Suzuki, K., Kanematsu, Y., Miura, T. et al. (2014). Experimental method to discriminate RAFT models between intermediate termination and slow fragmentation via comparison of rates of miniemulsion and bulk polymerization. *Macromol. Theory Simul.* 23: 136–146.

119 Luo, Y. and Yu, B. (2005). Monte Carlo simulation of droplet nucleation in RAFT free radical miniemulsion polymerization. *Polym. Plast. Technol. Eng.* 43 (5): 1299–1321.

120 Paper, F., Tripathi, A.K., and Sundberg, D.C. (2015). A hybrid algorithm for accurate and efficient Monte Carlo simulations of free-radical polymerization reactions. *Macromol. Theory Simul.* 24 (1): 52–64.

121 Neuhaus, E., Herrmann, T., Vittorias, I. et al. (2014). Modeling the polymeric microstructure of LDPE in tubular and autoclave reactors with a coupled deterministic and stochastic simulation approach. *Macromol. Theory Simul.* 23 (7): 415–428.

122 Kozub, D.J. and MacGregor, J.F. (1992). Feedback control of polymer quality in semi-batch copolymerization reactors. *Chem. Eng. Sci.* 47 (4): 929–942.

123 Arzamendi, G. and Asua, J.M. (1989). Monomer addition policies for copolymer composition control in semicontinuous emulsion copolymerization. *J. Appl. Polym. Sci.* 38: 2019–2036.

124 Saldívar, E. and Ray, W.H. (1997). Control of semicontinuous emulsion copolymerization reactors. *AlChE J.* 43 (8): 2021–2033.

125 Zargar, A. and Schork, F.J. (2009). Design of copolymer molecular architecture via design of continuous reactor systems for controlled radical polymerization. *Ind. Eng. Chem. Res.* 48 (9): 4245–4253.

126 Hlalele, L., D'hooge, D.R., Dürr, C.J. et al. (2014). RAFT-mediated ab initio emulsion copolymerization of 1,3-butadiene with acrylonitrile. *Macromolecules* 47 (9): 2820–2829.

127 Zargar, A., Chang, K., Taite, L.J. et al. (2011). Mathematical modeling of hyperbranched water-soluble polymers with applications in drug delivery. *Macromol. React. Eng.* 5 (9–10): 373–384.

128 Kim, S.Y., Van Dyke, R., Chang, K. et al. (2015). Modeling of highly branched water-soluble polymers with applications to drug delivery model extensions and validation. *Macromol. React. Eng.* 9 (6): 545–555.

129 Chaffey-Millar, H., Busch, M., Davis, T.P. et al. (2005). Advanced computational strategies for modelling the evolution of full molecular weight distributions formed during multiarmed (star) polymerisations. *Macromol. Theory Simul.* 14 (3): 143–157.

130 De la Hoz, A. and Loupy, A. (2012). *Microwaves in Organic Synthesis*, 3e. Weinheim: Wiley-VCH.

131 Herrero, M.A., Kremsner, J.M., and Kappe, C.O. (2008). Nonthermal microwave effects revisited: on the importance of internal temperature monitoring and agitation in microwave chemistry. *J. Organomet. Chem.* 73 (1): 36–47.

132 Kappe, C.O. (2013). How to measure reaction temperature in microwave-heated transformations. *Chem. Soc. Rev.* 42 (12): 4977–4990.

133 Aldana-García, M.A., Palacios, J., and Vivaldo-Lima, E. (2005). Modeling of the microwave initiated emulsion polymerization of styrene. *J. Macromol. Sci. Part A Pure Appl. Chem.* 42 (9): 1207–1225.

134 López-Domínguez, P. and Vivaldo-Lima, E. (2013). Analysis of the microwave activated atom transfer radical polymerization of methyl methacrylate and styrene using modeling tools. *Macromol. React. Eng.* 7 (9): 463–476.

135 López-Domínguez, P., Olvera-Mancilla, J., Palacios-Alquisira, J. et al. (2018). Kinetic modeling of vinyl acetate telomerization catalyzed by metal transition complexes under thermal and microwave heating. *J. Macromol. Sci. Part A Pure Appl. Chem.* 55 (3): 231–242.

136 Hernández-Meza, J.J., Jaramillo-Soto, G., García-Morán, P.R. et al. (2009). Modeling of polymerization kinetics and molecular weight development in the microwave-activated nitroxide-mediated radical polymerization of styrene. *Macromol. React. Eng.* 3 (2–3): 101–107.

137 Xie, Z.-K., Guo, J.-K., and Luo, Z.-H. (2018). Assessment of microwave effect on polymerization conducted under ARGET ATRP conditions. *Macromol. React. Eng.* 12 (1): 1700032.

8

Dithioesters in RAFT Polymerization

Graeme Moad

CSIRO Manufacturing, Research Way, Clayton, VIC 3168, Australia

8.1 Introduction

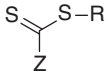

1a Z = Aryl
1b Z = Alkyl

Aromatic dithioesters **1a**, which include the dithiobenzoates, are one of the most widely reported classes of RAFT agents with close to 3000 Scifinder™ entries relating to papers or patents showing structure **1a** in the context of RAFT polymerization between 1998 and 2020 (Figure 8.1). They are the most used RAFT agents for mediating the polymerization of methacrylates and methacrylamides where they can offer better control over molar mass and molar mass distribution, and higher end-group fidelity than other classes of RAFT agents (i.e. trithiocarbonates, xanthates, and dithiocarbamates). Consistent with their high activity as RAFT agents, they also tend to be more reactive in other contexts. This means that the dithioester end-groups are more readily removed or transformed. This can be advantageous, or even essential, in some biomedical [1, 2] and optoelectronic applications [3] where the presence of the dithioester end-groups can present issues. However, poor end-group stability can be detrimental to polymerization kinetics and can impact adversely on some polymer properties. Methods for RAFT end-group transformation are discussed in the chapter by Lowe and Dallerba [4]. For further specific information on dithioesters, see Section 8.17.

Even though aliphatic dithioesters (**1b**) are also described in the first papers and patents concerning RAFT polymerization, they have been seldom exploited, with there being less than 250 Scifinder reports of structure **1b** in the context of RAFT polymerization (Figure 8.1). They (**1b**) have significantly lower activity as RAFT agents than the aromatic dithioesters (**1a**), but they are also less prone to side reactions and cause less retardation than the aromatic dithioesters.

RAFT Polymerization: Methods, Synthesis and Applications, First Edition.
Edited by Graeme Moad and Ezio Rizzardo.

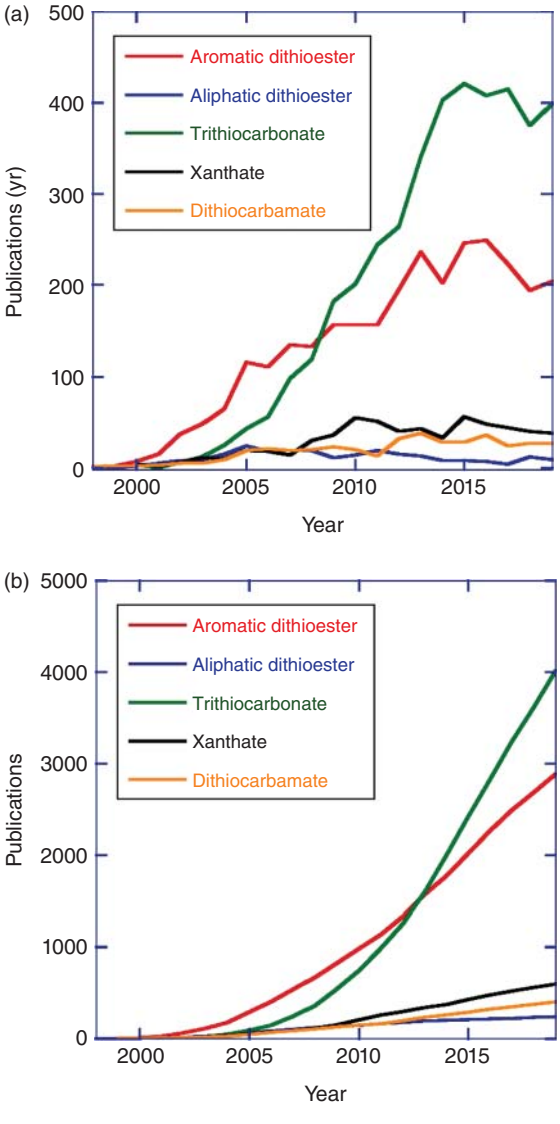

Figure 8.1 Publication rate of papers on RAFT polymerization using various classes of RAFT agents provided as (a) publications per year and (b) cumulative publications for the period 1998–2019. The data includes both patent and open literature publications and is based on Scifinder™ substructure searches carried out in February 2020 on the indicated structures refined with the terms 'RAFT' and 'MADIX' (in the case of xanthates).

8.2 Mechanism of RAFT Polymerization with Dithioester Mediators

The sequence of addition–fragmentation equilibria that comprise RAFT polymerization [5] is shown in Scheme 8.1. This scheme shows the RAFT agent as an ideal transfer agent. In these circumstances, as in any radical polymerization with an ideal chain transfer agent, the kinetics of RAFT polymerization should not be affected by the presence of the RAFT agent, notwithstanding effects attributable to the different molar mass of the reacting species (e.g. chain length dependent termination).

Termination occurs at a rate dictated by the radical concentration and, when an exogenous initiator is used, the number of chains that undergo termination must ultimately match the number of chains generated by initiation processes. It follows that living characteristics will only be imparted when the molar mass of the polymer formed is substantially lower than that which would be formed under similar conditions in the absence of a RAFT agent. Thus, for good control, the number of polymer molecules formed with RAFT agent-derived ends should far exceed the number of dead chains formed by termination.

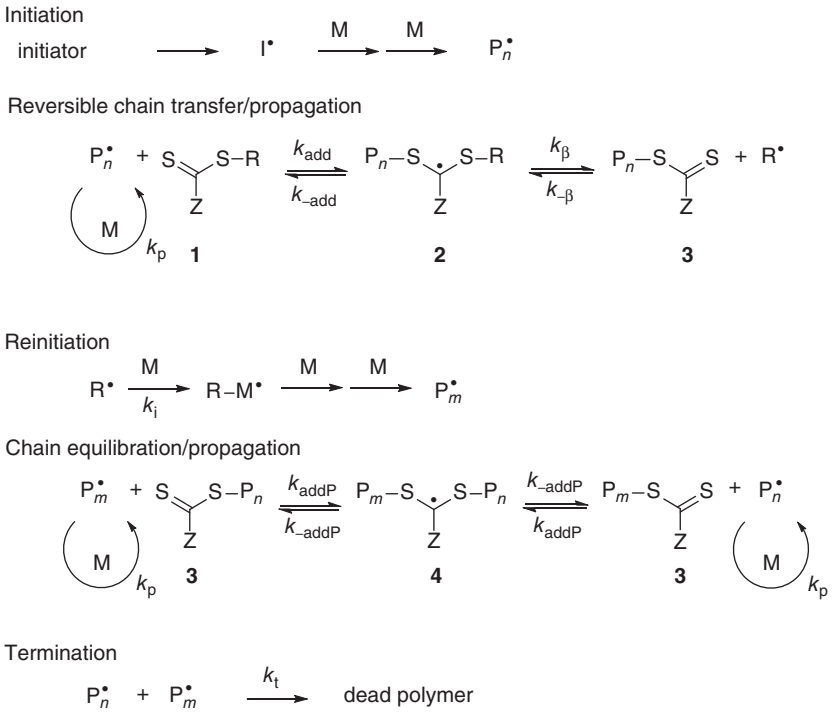

Scheme 8.1 Mechanism of RAFT polymerization with exogenous initiator.

While the basics of the mechanism have not changed from that described in the first paper [5] and patent [143], the finer details of the mechanism of RAFT polymerization mediated by dithiobenzoates have been the subject of intense study over the past 20 years. Of concern have been the factors that cause retardation, the stability of the various intermediates, and the extent to which those intermediates might undergo side reactions such as intermediate radical termination. In 2006 an IUPAC task group, 'Towards a Holistic Mechanistic Model for RAFT Polymerizations: Dithiobenzoates as Mediating Agents', published a 'dilemma paper' [7] that surveyed the then literature on polymerization with dithiobenzoate RAFT agents and summarized the evidence for and against the various mechanisms for retardation.

There were four major views expressed:

(a) That intermediate radical fragmentation (of species **2** and/or **4** in Scheme 8.1) was slow such that this process, by itself, was responsible for retardation.
(b) That intermediate radical fragmentation would not by itself cause retardation but was nonetheless sufficiently slow such that side reactions, such as intermediate radical termination by self-reaction or cross-reaction with other radical species, competed with fragmentation, consumed active chains, and thereby caused retardation.
(c) That reinitiation by the expelled radical R· was rate determining, causing initialization to be slow. For example, there is clear evidence for this when R· is 2-cyano-2-propyl and the monomer is an acrylate or an acrylamide [8].
(d) That apparent retardation was caused by extraneous factors not directly related to the RAFT process, such as mitigation of auto-acceleration caused by the gel or Trommsdorff effect, ineffective degassing, or impurities in the RAFT agent(s) and other components of the polymerization medium.

Combinations of the above were also canvassed.

In 2014, the 'dilemma paper' [7] was followed by a paper summarizing developments in the mechanistic understanding that had occurred during the period 2006–2013 [9]. That period had seen the original paper [7] being well cited and a doubling of the publication rate of papers concerning dithiobenzoate RAFT agents (Figure 8.1). The period also saw publications on the use of dithiobenzoates in controlling polymerization of acrylates, acrylamides, and styrenes significantly diminish as a fraction of the total RAFT papers, mainly in favour of trithiocarbonate RAFT agents [10–13]. The latter are generally more readily synthesized [14], are less sensitive to hydrolysis and many other forms of degradation, and significantly, polymerizations with these reagents generally display much less or (often) no discernible retardation.

The 2014 review [9] came to the conclusion that, once the extraneous factors, i.e. explanations (c) and (d) above, were eliminated, the experimental evidence was overwhelmingly in favour of intermediate radical termination as the most likely cause of retardation in polymerizations of more activated monomers (MAMs). Nonetheless, debate on the importance of intermediate radical termination and intermediate stability in dithiobenzoate-mediated RAFT polymerization continues [15–20]. Further discussion on kinetics and retardation mechanisms in RAFT polymerization will be found in the chapters by Buback [21] and Quinn et al. [22].

8.2.1 Transfer Coefficients of Dithioesters

The activity of a RAFT agent is determined by the values of two transfer coefficients, C_{tr} ($=k_{tr}/k_p$) and C_{tr} ($=k_{-tr}/k_{-\beta}$). The chain transfer rate coefficient (k_{tr}) for a RAFT agent is given by Eq. (8.1). The value of k_{tr} depends on the rate of addition of the propagating radical ($P_n\cdot$) to the RAFT agent and a partition coefficient (ϕ), which

describes the partitioning of the intermediate radical (**2**) between the starting materials and products – refer to Scheme 8.1:

$$k_{tr} = k_{add}\phi = k_{add}\left[\frac{k_\beta}{k_{-add} + k_\beta}\right] \tag{8.1}$$

The transfer agent-derived radical (R˙) is also partitioned between adding to the monomer and reacting with the macroRAFT agent (**3**). The rate coefficient associated with this reaction (k_{-tr}) is defined in Eq. (8.2).

$$k_{-tr} = k_{-\beta}\phi_\beta = k_{-\beta}\left[\frac{k_{-add}}{k_{-add} + k_\beta}\right] \tag{8.2}$$

Methods used for measuring the transfer coefficients for conventional (irreversible) transfer agents can be used to estimate C_{tr} when the value of C_{tr} is low (e.g. <1). However, these methods, which include an assumption that C_{-tr} is zero, will underestimate C_{tr} (Table 8.1). It is recommended that these values should be called apparent transfer coefficients C_{tr}^{app}. For dithiobenzoates, actual values of C_{tr} may be higher than C_{tr}^{app} by *several orders of magnitude* [23, 34]. A dependence of C_{tr}^{app} on the RAFT agent concentration and/or on monomer conversion provides an indication that the reverse reaction is important.

The situation is simplified for macroRAFT agents in homopolymerization, where, notwithstanding the effects of chain length, the forward and reverse reactions are the same ($C_{tr} = C_{-tr}$) and the partition coefficient ϕ is 0.5 (Table 8.2).

Methods for determining transfer coefficients of RAFT agents (C_{tr}^{app}, C_{tr}, or C_{-tr}) are described elsewhere in this volume [22]. However, one method of transfer constant estimation requires special mention. The expression for dispersity for polymerization with degenerative chain transfer (Eq. (8.3)) [39] can be rearranged to provide a qualitative estimate of the transfer constant (C_{tr}) (Eq. (8.4)).

$$Đ = 1 + \frac{1}{X_n} + \left(\frac{2-x}{x}\right)\frac{1}{C_{tr}} \tag{8.3}$$

where X_n is the number average degree of polymerization and x is the monomer conversion.

$$C_{tr} = \left(\frac{2-x}{x}\right) \Big/ \left(Đ - 1 - \frac{1}{X_n}\right) \tag{8.4}$$

Strictly, the Dispersity method is only applicable to macroRAFT agents where the C_{tr} values for the initial and product RAFT agent are the same (because they differ only in chain length). Nonetheless, we have applied Eq. (8.4) to provide a ranking of C_{tr} values for aromatic dithioesters [ZC(=S)—C$(CH_3)_2$CN] in MMA polymerization. The estimates will be lower than the actual values. The data of Benaglia et al. [40] for low (5–10%) monomer conversion was used to generate Figure 8.2. The presence of ortho-substituents (**b**, **c**, **e**, **g**; blue shading in Figure 8.2) significantly reduces the activity of dithiobenzoate RAFT agents. The presence of para substituents (**d**, **f**, **I**, **n**; magenta shading) has little effect on activity. Perfluoro- (**l**) and bis-meta electron-withdrawing substituents (**j**, **k**; red shading) enhance activity. The pyridyl analogues (**h**, **m**; green shading) show significantly enhanced activity, substantially

Table 8.1 Transfer coefficients of dithioester RAFT agents Z−C(=S)S−R in RAFT polymerization.

RAFT agent[a)]	Z	R	Monomer	T (°C)	C_{tr}^{app} [b)]	C_{tr}	C_{-tr}	Method[c)]	References
5	Ph	$C(CH_3)_2(Ph)$	MMA	60	6.6	56	2500	W/K	[23]
6	Ph	$C(CH_3)_2(CN)$	MMA	60	6.8	25	450	W/K	[23]
11a	Ph	$C(CH_3)_2(CO_2Et)$	MMA	60	1.7	—	—	W	[23]
11a	Ph	$C(CH_3)_2C(CH_3)_3$	MMA	60	0.4	—	—	W	[23]
12	Ph	$C(CH_3)_3$	MMA	60	0.03	—	—	W	[23]
5	Ph	$CH(CH_3)(Ph)$	MMA	60	0.15	—	—	W	[23]
21	Ph	CH_2Ph	MMA	60	< 0.03	—	—	W	[23]
5	Ph	$C(CH_3)_2(Ph)$	St	60	—	2000	10000	K	[23]
21	Ph	CH_2Ph	MA	60	105	—	—	W	[23]
70	$PhCH_2$	$C(CH_3)_2(CO_2Et)$	MA	60	70	—	—	K	[24]
6	Ph	$C(CH_3)_2(CN)$	MMA	80	40	—	—	W	[25]
6	Ph	$C(CH_3)_2(CN)$	*t*BDMSMA	70	9.3	—	—	K	[26]
9	Ph	$C(CH_3)(CN)CH_2CH_2CO_2H$	MMA	80	> 50	—	—	W	[25]
12	Ph	$C(CH_3)_3$	MMA	80	0.7	—	—	M	[25]
17	Ph	$CH(Ph)(CH_3)$	MMA	60	—	40-280	9900	W	[27]
21	Ph	CH_2Ph	MMA	80	0.2	—	—	M	[25]
6	Ph	$C(CH_3)_2(CN)$	MPEGMA	65	9.1	—	—	W	[28]
7	Ph	$C(CH_3)(C_2H_5)(CN)$	DEGMA	70	0.5	—	—	W	[29]
7	Ph	$C(CH_3)(C_2H_5)(CN)$	MPEGMA	70	0.5	—	—	W	[29]
5	Ph	$C(CH_3)_2(Ph)$	St	120	—	2037	34	K	[30]

17	Ph	$CH(CH_3)(Ph)$	St	120	—	3331	4173	K	[30]
21	Ph	CH_2Ph	St	120	—	92	1057	K	[30, 31]
21	Ph	CH_2Ph	St	60	190	—	—	W	[32]
24	Ph	CH_2CO_2H	St	90	6	—	—	M	[33]
—	Ph	$C(CH_3)_2(CONH_2)$	VAc	95	4	—	—	B	[33]

a) Initial RAFT agent used in polymerization.
b) Published values of transfer coefficients that are based on a model that does not allow for partitioning of the intermediate radicals and/or the reversibility of chain transfer are considered as apparent transfer coefficients (see text).
c) Method used: M – Mayo method, W – Walling method, K – kinetic simulation, B – $M_n(0)$ method. Refer to the chapter by Quinn et al. [22] and to the cited papers for a detailed of the description of the methods.

For a full list of abbreviations, see the Abbreviations section.

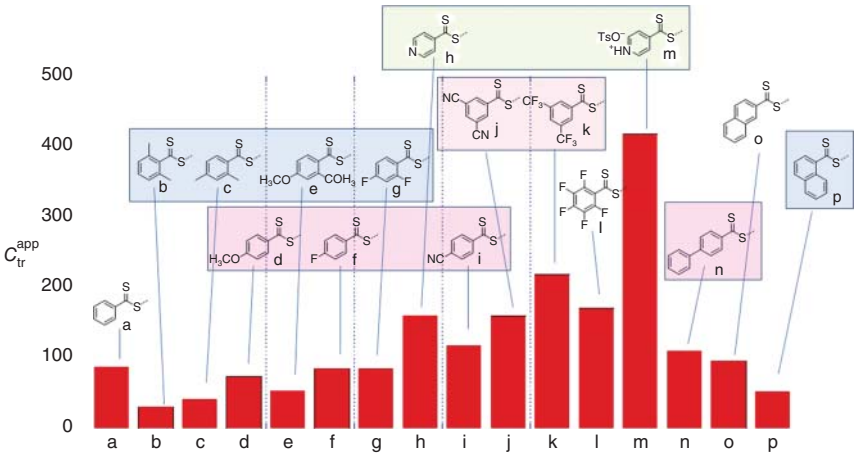

Figure 8.2 Values of apparent transfer coefficients (C_{tr}^{app}) for aromatic dithioesters [ZC(=S)S−C(CH$_3$)$_2$CN] in MMA polymerization estimated by the Dispersity method.

more so if protonated. The finding that para-substituents have relatively little effect on the activity of dithiobenzoates is supported by other studies [41].

8.2.2 RAFT Equilibrium Coefficients with Dithioesters

The properties of RAFT agents are often discussed in terms of the values of the equilibrium coefficients ($K = k_{add}/k_{-add}$) associated with radical addition to a thiocarbonylthio compound [21, 42]. Rate coefficients (k_{add}) for addition reported for aromatic dithioesters **1b** are ~10^6 M^{-1} s^{-1} (Table 8.3). A high equilibrium coefficient implies a low fragmentation rate for the radical adduct and an increased likelihood for retardation and/or side reaction involving this species.

Methods for evaluating the equilibrium coefficients and implications concerning retardation in RAFT processes are described elsewhere in this volume [21, 47].

8.3 Choice of RAFT Agents

The criteria for an effective RAFT polymerization can be summarized as follows (Scheme 8.1, Figure 8.3): [6]

- The initial RAFT agents (**1**) and the macroRAFT agent (**3**) should have a reactive C=S double bond (high k_{add}).
- The intermediate radicals (**2**) and (**4**) should fragment rapidly (high k_β, weak S—R bond in the intermediate) and give no side reactions.
- The intermediate (**2**) should partition in favour of products ($k_\beta \geq k_{-add}$).
- The expelled radicals (R$^\bullet$) must efficiently reinitiate polymerization ($k_i > k_p$).

Table 8.2 Transfer coefficients of dithioester macroRAFT agents Z−C(=S)S−P_n in RAFT polymerization.

Z	P_n	Monomer	T (°C)	C_{tr}^{app} a)	C_{tr}	Method[b]	References
Ph	PMMA	MMA	60	140	140	C	[35, 36]
Ph	PMMA	BA	60	482	—	C	[36]
Ph	PBA	MMA	60	5	—	C	[36]
Ph	PBA	BA	60	~248	~248	C	[36]
Ph	PMMA	MMA	80	>500	—	W	[25]
Ph	PSt	St	40	—	~6000	C	[35]
Ph	PSt	St	60	$>10^3$	—	W	[32]
Ph	PAA	AA	70	8.3	—	K	[37]
$PhCH_2$	PMMA	MMA	60	11	11	W	[36]
$PhCH_2$	PMMA	BA	60	205	—	W	[36]
$PhCH_2$	PBA	MMA	60	2.6	—	W	[36]
$PhCH_2$	PBA	BA	60	116	116	W	[36]
$(CH_3)_2CH$	PSt	St	60	42	42	W	[36]
$(CH_3)_2CH$	PSt	BA	60	54	—	W	[36]
$(CH_3)_2CH$	PBA	St	60	50	—	W	[36]
$(CH_3)_2CH$	PBA	BA	60	59	59	W	[36]
CH_3	PSt	St	60	—	180	C	[35]
CH_3	PSt	St	40	—	220	C	[38]
CH_3	PSt	MMA	40	—	0.83	C	[38]
CH_3	PMMA	St	40	—	420	C	[38]
CH_3	PMMA	MMA	40	—	40	C	[38]

a) For macroRAFT agents in homopolymerization, it is assumed that $C_{tr}^{app} = C_{tr} = C_{-tr}$.
b) Method used: W – Walling method, K – kinetic simulation, C – chromatography. Refer to the chapter by Quinn et al. [22] and the cited papers for further details.
For a full list of abbreviations, see the Abbreviations section.

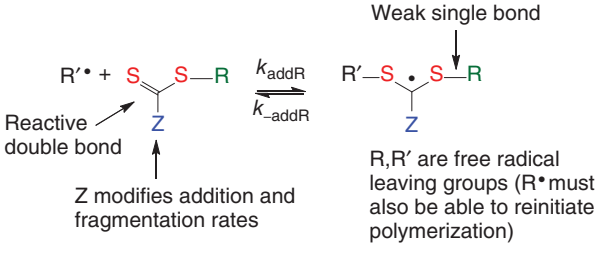

Figure 8.3 Structural features of thiocarbonylthio RAFT agent and the intermediate formed on radical addition. Source: Moad et al. [6]. Copyright 2005, CSIRO.

Table 8.3 Values of the RAFT equilibrium coefficients with dithioesters.

RAFT agent[a)]	Z	R	Monomer/radical	T (°C)	k_{add} (M^{-1} s^{-1})	k_{-add} (s^{-1})	K_{eq} (M^{-1})	Method[b)]	References
20	Ph---	PBA	BA	−40	1.4×10^{6}	4.7	3.4×10^{5}	EPR2	[43]
20	Ph---	PBA	BA	−40	—	—	2.3×10^{5}	EPR1	[43]
				70	—	—	75		
6	Ph---			60	—	—	13	EPR1	[44]
				70	—	—	9		
				90	—	—	5.1		
				100	—	—	4.6		
11b	Ph---			70	—	—	10.8	EPR1	[45]
				90	—	—	7.1		
				100	—	—	5.6		
				110	—	—	2.6		
12	Ph---			20	5×10^{6}	8×10^{-3}	$6(\pm4)\times10^{8}$	EPR3	[46]
12	Ph---			20	—	—	4.5×10^{8}	Theory	[46]

a) Initial RAFT agent used.

b) EPR1 – direct determination of radical concentrations by electron paramagnetic resonance spectroscopy; EPR2 – measurement of radical concentrations vs. time in SP-PLP-EPR (single pule-pulsed laser photolysis-electron paramagnetic resonance) experiments and Predeci™ simulation of experimental data; EPR3 – spin trapping experiments; theory – *ab initio* calculations.

For a full list of abbreviations, see the Abbreviations section.

8.3.1 Aromatic Dithioesters (Z = Aryl or Heteroaryl)

RAFT polymerizations making use of the more common (most used or commercially available) aromatic dithioesters and a few others chosen for their relevance to the text are shown in Table 8.4. We consider functional dithioesters and bis-dithioesters separately below.

The tertiary aralkyl or cyanoalkyl dithiobenzoates, e.g. **5**–**9** (Table 8.4) are much used (Figure 8.4) for synthesizing polymers based on 1,1-disubsituted monomers, namely, methacrylates (e.g. MMA) or methacrylamides (e.g. HPMAm). This can be understood in terms of these RAFT agents offering the highest transfer coefficients in polymerizations of these monomers and thence the lowest dispersities and highest end-group fidelity (cf. Figure 8.5). Retardation when preparing such polymers with $X_n > 50$ appears minimal. Auto-acceleration is also minimal [23].

However, the aromatic dithioesters are more sensitive to nucleophilic attack and more prone to hydrolysis, for example, when employed in aqueous media [557, 558]. Issues of RAFT agent stability can give rise to a conversion plateau, for example, in the polymerization of HPMAm in aqueous solution. An advantage of the aromatic dithioesters is that they are more reactive in end-group transformation/removal reactions post-RAFT polymerization (Section 8.17).

The tertiary alkoxycarbonylalkyl dithiobenzoates, e.g. **11**, are considerably less active than **5**–**9** and offer, at best, poor control over polymerization of 1,1-disubsituted monomers. Primary, secondary and unsubstituted tertiary alkyl dithiobenzoates do not provide significant control polymerization of 1,1-disubsituted monomers in a batch process. These dithiobenzoates are those preferred for mediating polymerization of monosubstituted monomers.

Dithiobenzoates typically give some retardation in polymerizations of acrylates and acrylamides and this can be pronounced particularly when targeting low molar

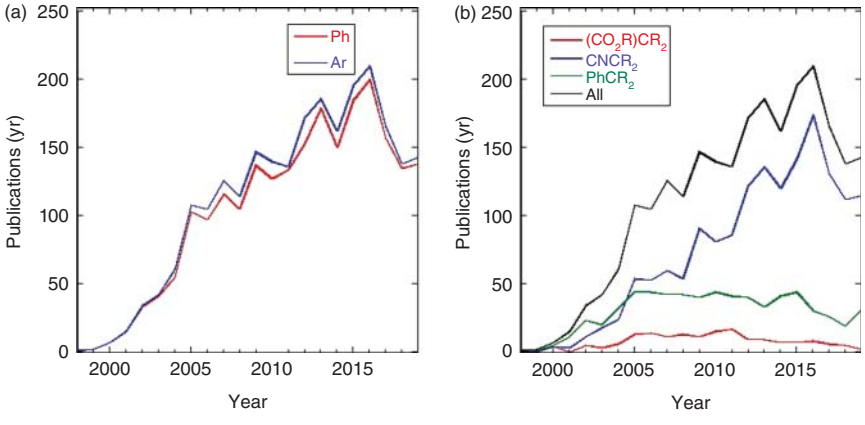

Figure 8.4 Rate of journal publication on aryl dithioesters **1a** in the period 1998–2019 based on a Scifinder™ search carried out in January 2020. The key word 'RAFT' was used to exclude references that do not relate to RAFT polymerization. For the situation (a) where Z is phenyl or aryl and R is any alkyl, and (b) where Z is aryl and R is carboxyalkyl, cyanoalkyl, aralkyl, or any alkyl.

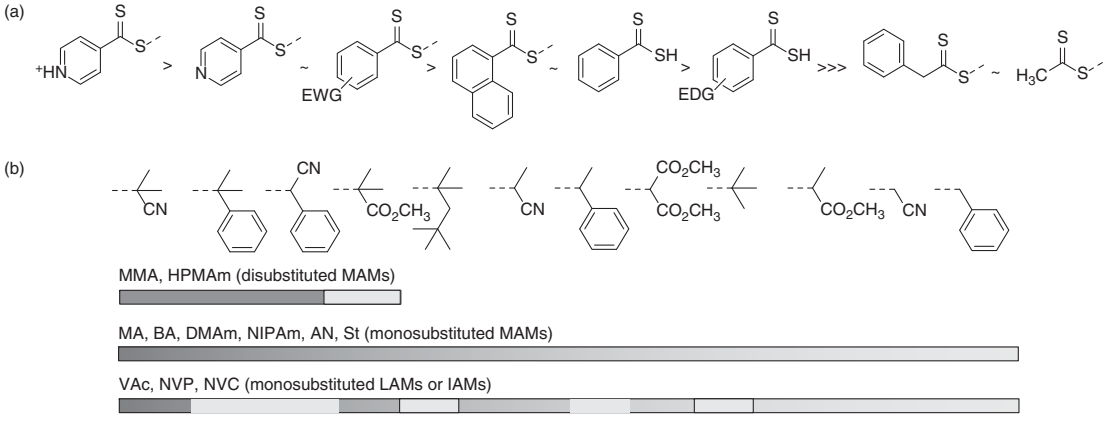

Figure 8.5 (a) Effect of ZC(=S)– group and (b) R group on the activity of dithioesters ZC(=S)SR in RAFT polymerization. Activity increases from right to left. Source: Figure 8.5b is adapted with permission from Moad [757]. Copyright 2019, John Wiley & Sons. Note that dithioesters are not generally useful in mediating polymerization of LAMs. MAM, more activated monomer; LAM, less activated monomer; IAM, intermediate activated monomer; AN, acrylonitrile; BA, butyl acrylate; DMAm, *N*,*N*-dimethylacrylamide; HPMAm, *N*-(2-hydroxypropyl)methacrylamide; MA, methyl acrylate; MMA, methyl methacrylate; NIPAm, *N*-isopropylacrylamide; NVC, *N*-vinylcarbazole; NVP, *N*-vinylpyrrolidone; St, styrene; VAc, vinyl acetate; EDG, electron-donating group; EWG, electron-withdrawing group.

mass polymers. Note, however, that dithiobenzoates are, nonetheless, suitable for RAFT single unit monomer insertion (SUMI), where higher transfer coefficients are desirable and propagation is not desirable [172].

The tertiary aralkyl or cyanoalkyl dithiobenzoates are not the preferred RAFT agents for use when preparing low molar mass polymers based on acrylates and acrylamides because reinitiation by 'R' is rate determining. This is likely to be an additional cause of retardation.

8.3.2 Functional Aromatic Dithioesters (Z = Aryl or Heteroaryl)

A wide variety of functional RAFT agents have been reported. Many of these are listed in Table 8.5 (p 251), however, this list should not be considered as comprehensive. Carboxy-functional RAFT agents (**9**, **15**, **19**, **24**) are included in Table 8.4. RAFT monomers (or dithioester inimers) are shown in Table 8.22. Many of the listed RAFT agents were used as precursor to other functional RAFT agents, macroRAFT agents, or to RAFT functional surfaces. Surface-initiated RAFT polymerization to prepare modified surfaces and particles is covered in detail in the chapter by Pribyl and Benicewicz [646].

The lists can be considered as indicative of tolerated functionality. Unfortunately, in many papers the quantitative characterization that would enable a rigorous evaluation of the effectiveness of the various chemistries is sometimes lacking. The alkyne functionality present in RAFT agents such as **37**, **38**, **40**, or **41** is potentially reactive under the conditions used for RAFT polymerization and it is desirable to protect with a trimethylsilyl group as in **39** [587]. The synthesis of reactive polymers by RAFT polymerization is described in the Chapter by Gauthier-Jaques et al. [647].

Another application of functional RAFT agents is in mechanism-transformation processes (Section 8.11). Thus, hydroxyl-functional RAFT agents (e.g. **25** or **27**) can be used in ROP-*T*-RAFT (Section 8.11.1), while those with appropriate alkene functionality (e.g. **45** or **46**) can be used in ROMP-*T*-RAFT (Section 8.11.2).

8.3.3 Bis-aromatic Dithioesters (Z = Aryl or Heteroaryl)

Some bis-dithioesters are shown in Table 8.6. These bis-RAFT agents are precursors to telechelics and to symmetric triblock (and potentially higher order block) copolymers. Multi-dithioesters, which are precursors to star polymers, are not directly considered in this document. Star polymer synthesis is dealt with in the chapter by Allison-Logan et al. [673].

'R-connected' bis-dithioesters can be used to form BAB triblocks by sequential monomer addition (Scheme 8.2). The dithioester groups are retained at the chain ends. The product is telechelic. 'Z-connected' bis-dithioesters can be used to form ABA triblocks by sequential monomer addition (Scheme 8.3). The dithioester groups are retained with the structure. If the dithioester groups are cleaved AB blocks are formed. This form of bis-dithioester is, in this context, analogous to a trithiocarbonate.

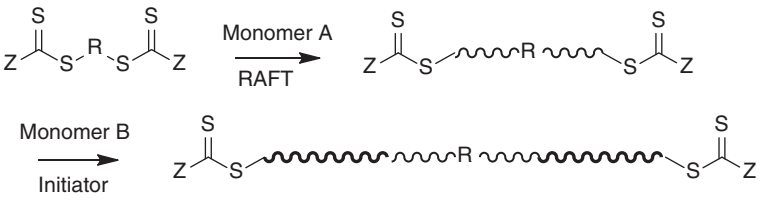

Scheme 8.2 RAFT polymerization mediated by a 'R-connected' bis-dithioester to form a BAB triblock.

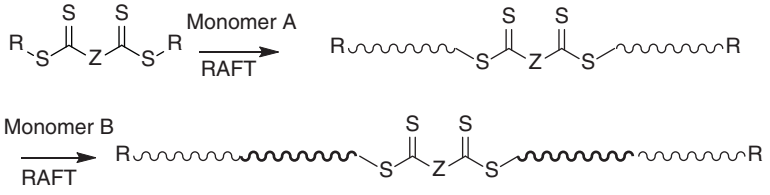

Scheme 8.3 RAFT polymerization mediated by a 'Z-connected' bis-dithioester to form an ABA triblock.

8.3.4 Aliphatic Dithioesters (Z = Alkyl or Aralkyl)

For aliphatic dithioesters, the most common Z groups are methyl and phenylmethyl (Figure 8.6a), while the most common R group is benzyl or substituted benzyl. A few papers relate to dithioesters where R is cyanomethyl or carboxymethyl (Figure 8.6b).

Aliphatic dithioesters **1b** have transfer coefficients approximately an order of magnitude lower than those of similar aromatic dithioesters **1a** (Table 8.2). As such, they

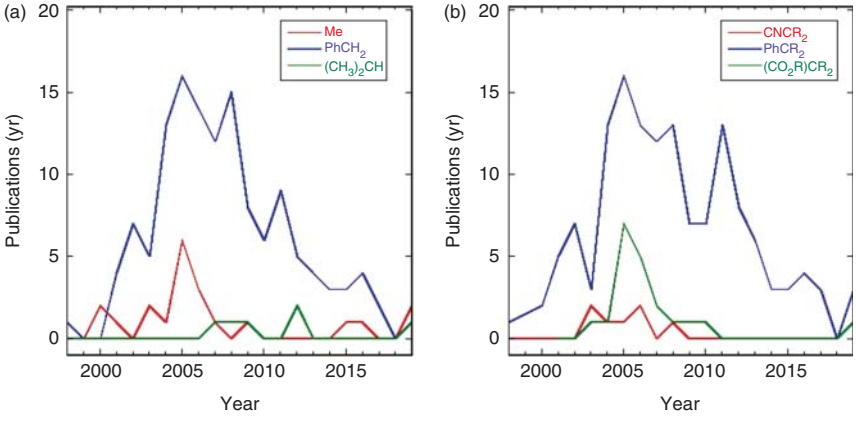

Figure 8.6 Rate of journal publication on aliphatic dithioesters **1b** in the period 1998–2019 based on a Scifinder™ search carried out in January 2020. The key word 'RAFT' was used to exclude references that do not relate to RAFT polymerization. For the situation (a) where Z is phenylmethyl, isopropyl or methyl and R is any alkyl, and (b) where Z is any alkyl and R is carboxyalkyl, cyanoalkyl, or aralkyl.

are not generally suitable for forming low-dispersity polymers in polymerizations of 1,1-disubstituted monomers, such as methacrylates, in batch RAFT polymerization. Thus, they are little used for such monomers (Table 8.7, p 260). The issue of low transfer coefficients has been addressed through the use of a starved-feed addition protocol [48].

With appropriate choice of R, the transfer coefficients of aliphatic dithioesters **1b** are, nonetheless, suitable for producing low-dispersity polymers from monosubstituted MAMs (e.g. styrenes, acrylates). There was early interest (2000–2010) in aliphatic dithioesters **1b** in circumstances where a RAFT agent with lower activity than an aromatic dithioester was advantageous. For example, in polymerizations of monosubstituted MAMs, aliphatic dithioesters **1b** give no or substantially less retardation than the corresponding aromatic dithioesters **1a** with the same R [48]. Another example is RAFT emulsion or miniemulsion polymerization, where the use of a less active RAFT agent avoids retardation [48, 698, 723] and issues associated with colloidal instability caused by the formation of a large population of very short chains (the phenomenon known as superswelling) [699].

More recently, these issues have also been addressed with the use of trithiocarbonate RAFT agents [13], which can have similar properties and are more readily available or more easily synthesized.

8.3.5 Bis-aliphatic Dithioesters (Z = Alkyl or Aralkyl)

Examples of bis-aliphatic dithioesters are shown in Table 8.8.

8.4 Synthesis of Dithioester RAFT Agents

The methods most commonly exploited for the synthesis of (low molar mass) dithioester RAFT agents are listed below. The method of choice is dependent on the structure of the specific RAFT agent, the amount required, the toxicity and ease of handling of reagents, and a variety of other factors. A critical review of synthetic methods for RAFT agent synthesis was published in 2012 [14] and the major methods are summarized in Scheme 8.4. Within this chapter further details are provided only for the few methods that require further comment or have seen development since that time. For examples of the methods, refer to The RAFT agent synthesis column in Tables 8.4–8.8.

A. Reaction of a carbodithioate salt with an alkylating agent.
   This is the most popular method of synthesizing dithioesters with primary and secondary R (e.g. **13**–**21** and **23**) [14].
B. Addition of a dithioacid across an olefinic double bond.
   The reaction between a dithioacid and an olefinic double bond that leads to Markovnikov adducts with electron-rich alkenes and to Michael adducts with electron-poor alkenes was reported in 1972 [727]. Only the former are generally useful as RAFT agents. The reaction has been widely used for the synthesis of dithioester RAFT agents from styrene derivatives and simple alkenes. The

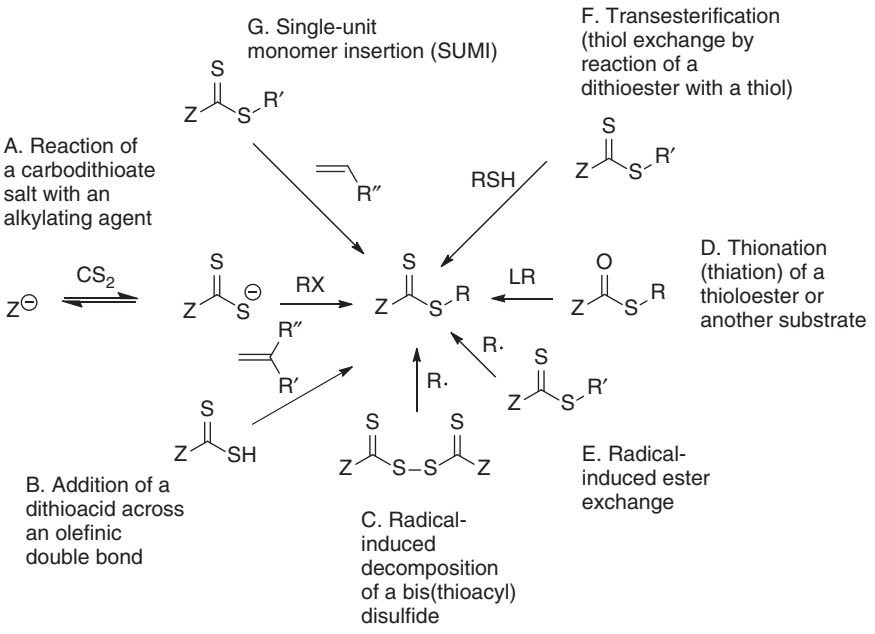

Scheme 8.4 Major methods for dithioester RAFT agent synthesis. RX, alkylating agent; LR, Lawesson's reagent. For details on individual processes, refer to Ref. [14].

reaction, which is considered an ene reaction, has been studied using molecular orbital calculations [728].

C. Radical-induced decomposition of a bis(thioacyl) disulfide.
This is the most popular method of synthesizing dithioesters with tertiary R-containing electron-withdrawing substituents (e.g. **6**–**11**) [14].

D. Thionation (Thiation) of a thioloester or another substrate.
A recent paper shows that dithioesters can be prepared in good to excellent yields by reaction of a thiol, RSH, with the desired acid chloride, Z(C=O)Cl, in the presence of triethylamine followed by thionation with Lawesson's reagent [505].

E. Radical-induced ester exchange.

F. Transesterification (thiol exchange by reaction of a dithioester with a thiol).

G. SUMI, see Section 8.10.

H. Esterification or amidation (carbodiimide)
A common method of dithioester macroRAFT agent synthesis involves esterification (Steglich esterification) or amidation of a carboxy-functional RAFT agent with a hydroxy- or amino-functional polymer. An example is the formation of a poly(3-hexylthiophene) (P3HT) macroRAFT agent by amidation of a carboxy-functional RAFT agent with an amino-functional polymer (Scheme 8.5) [729]. The reaction with amines is usually rapid and proceeds in high yield. The reaction of the amine with the carbodiimide adduct is very much faster than any reaction between the amine and the dithioester. The reaction of an alcohol with a DCC adduct is slower, requires a catalyst, and can give variable yields. It is important that each of the substrates is rigorously dried.

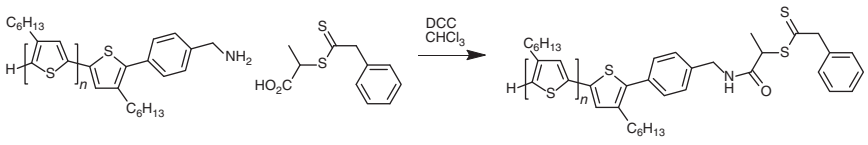

Scheme 8.5 Formation of a P3HT macroRAFT agent by *N*,*N*′-dicyclohexylcarbodiimide (DCC)-mediated amidation of a carboxy-functional RAFT agent.

I. Esterification (acid chloride).
J. Esterification (Mitsunobu reaction).
K. Esterification (other).
L. Active ester–amine reaction or active ester–thiol reaction.
M. Other methods.
N. Commercial availability
The indicated RAFT agents were commercially available at the time of writing [43, 44].

8.5 Monomers for Dithioester-Mediated RAFT Polymerization

Polymer syntheses by RAFT polymerization mediated by the more common dithioesters are surveyed in Tables 8.4–8.6 (aromatic dithioesters) and Tables 8.7 and 8.8 (aliphatic dithioesters). Some of the more exotic monomers mentioned in these tables are also included in the tables that follow. They include 1,1-disubsituted MAMs in Section 8.5.1, which include methacrylates (Table 8.9, Section 8.5.1.1), methacrylamides (Table 8.10, Section 8.5.1.2), and other 1,1-disubstituted monomers (Table 8.11, Section 8.5.1.3); monosubstituted MAMs in Section 8.5.2, which include acrylates (Table 8.12, Section 8.5.2.1), acrylamides (Table 8.13, Section 8.5.2.2), styrene derivatives (Table 8.14, Section 8.5.2.3), and diene monomers (Section 8.5.2.4); 1,2-disubsituted MAMs in Section 8.5.3; and monosubstituted less activated monomers (LAMs) in Section 8.5.4 (Table 8.15). Monomers from all of these classes that additionally contain other reactive functionality appear in Section 8.5.5 (Table 8.16, p 281).

There is substantial interest in RAFT polymerization of various bio-related or sustainably sourced monomers, which include those derived from amino acids [750], such as acrylamides **217**–**224** and glycomonomers, such as methacrylates **130**–**139**, acrylates **189**–**190**, methacrylamides **170**–**174** and **176**–**177**, acrylamides **213**–**216**, and styrenes **236**–**237**.

8.5.1 1,1-Disubsituted Monomers

8.5.1.1 Methacrylates

Dithiobenzoates are the most used RAFT agents for mediating RAFT polymerization of methacrylates. The achievement of low dispersities requires that the dithiobenzoate R group is a good leaving group with respect to the methacrylate

propagating radical. Methacrylates mentioned in Tables 8.2–8.4 include AAEMA, AEMA, AMA, CMA, BMA, BDSMA, DEGMA, DMAEMA, EOEMA, HEMA, HMA, *i*BMA, LMA, MAEP, MMA, MOEMA, MPC, MPEGMA, PFPMA (**262**), TMAEMA, TMAPMA, and TPMMA (see Abbreviations), those in Table 8.9 (p 263), and those in Table 8.16 (see Section 8.5.5, p 279). The monomers in Table 8.9 are grouped by application.

8.5.1.2 Methacrylamides

Many examples are appearing on RAFT (co)polymerization of HPMAm, particularly with respect to various bioapplications [1]. Other examples of methacrylamide monomers recently used in RAFT polymerization are the primary amino-functional monomers, AEMAm and APMAm, the tertiary amino-functional monomers DEAPMAm and DMAPMAm, those shown in Table 8.10, and the functional methacrylamides included in Table 8.16 (see Section 8.5.5, p 279). The choice of RAFT agent for polymerization of methacrylamides is subject to similar constraints as mentioned for the methacrylates. In particular, the 'R' group of the initial RAFT agent should be selected so as to be a good leaving group with respect to the propagating radical. The RAFT agents preferred include dithiobenzoate **9**, and derivatives **32** and **33**, which are chosen for their solubility in aqueous media under the conditions used.

8.5.1.3 Other 1,1-Disubsituted Monomers

Other 1,1-disubstituted monomers that have been used in dithioester-mediated RAFT (co)polymerization include itaconates (DBI, DEHI and **287**, Table 8.16(f), see Section 8.5.5, p 279), the methylenebutyrolactones (**182**–**184**), and the itaconimide derivative (**185**, Table 8.11).

8.5.2 Monosubstituted MAMs

Attaining low molar mass dispersities in RAFT polymerization of monosubstituted MAMs requires a RAFT agent suitable for MAMs. Dithioesters are generally suitable in this context. It is also important that the homolytic leaving group R of the dithioester is a good initiating radical such that addition of the R radical is not rate determining (i.e. k_i should be greater than k_p – refer Scheme 8.1). For example, the rate of addition of 2-cyano-2-propyl radical is rate determining in polymerization of acrylates and acrylamides. This can cause retardation or an inhibition period, especially in circumstances where low mass is targeted.

8.5.2.1 Acrylates

Acrylates mentioned in this survey include AEP, BA, CPA, DA, DEHEA, DMAEA, EA, EAA, EEA, EHA, *i*BoA, MA, PA, (poly(ethylene glycol)monomethyl ether) acrylate (PEGA), *t*BA, those in Table 8.12, and those in Table 8.16 (see Section 8.5.5, p 279).

(*continued on page 273*)

Table 8.4 RAFT polymerizations with popular or commercially available aromatic dithioesters.

RAFT agent	Synthesis[a)]	Polymerizations [b)]
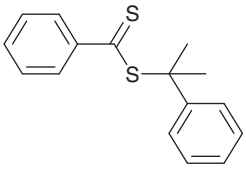 2-Phenylpropan-2-yl benzodithioate **5**	B [48, 49] N [50, 51]	*Methacrylates*: AAEMA [52] AEMA [53] *BMA* [5] BzMA [54, 55] DMAEMA [5, 56–58] HEMA [58] GMA [59] GMA [60] LMA [61] *MAA* [62, 63] MMA [5, 23, 54, 64–74] *MMA* [75] MMA [60] MMA [76–78] MPEGMA [79–81] MAEP [52] PFPMA [82] POSSMA [83] *t*BMA [84] *t*BDMSMA [85] TFPMA [86] (TPMMA) [85, 87, 88] TPSiMA [85] **82** [89, 90] **88** [91] **91** [92] **96** [93] **97** [93] **297** [85] **299** [85] **301** [85] **302** [85] **303** [85] **109** [94] **112** [95] **113** [96] **114** [97, 98] **115** [97] **120** [99] **120** [100] **130** [101] **132** [102] **251** [103] **282** [104] *Other 1,1-disubstituted MAMs*: (DBI) [105, 106] **185** [106] **313** [107] **326** [108] *Acrylates*: (MA) [109] MA [23, 110–114] MA [114] BA [43, 48] (BA) [60] *Acrylamides*: Am [115] DMAm [56, 80, 116] NIPAm [56, 117, 118] **205** [119] **206** [120] **205** [121] **223** [80] *Styrenes*: CMS [122] St [5, 23, 35, 48, 56, 70, 71, 122–130] (*St*) [75, 131–136] St [76, 78] PFPVB [137] PVS [137] *t*BDMSOS [138] 2VP [139] 4VP [139] **228** [140] **225** [141] **226** [141] **268** [142] **269** [90] **271** [142] **272** [142] **273** [142] **274** [142] **325** [143] **330** [144] *Vinyls*: (NVP) [145] *Copolymers*: MMA/HEMA [5] MMA/BDSMA [146] MMA/EGDMA [147] MMA/4VP [148] (MAA/TPMMA) [88] (MAA/**104**) [88] DEGMA/MPEGMA [149] DMAEMA/POSSMA/**150a** [150] MMA/LMA [79] *t*BMA/DMAEMA/**80** [151] St/AcS [152] St/CMS [122] St/AN [5, 58] 4VP/EGDMA [153] *BA/**327*** [154] St/MAH [58, 155] St/DVB [156] BMA/TMSEMA [157] DMAEMA/**96** [93] DMAEMA/**323** [158] *Blocks*: AEMA-*b*-**166** [53] BzMA-*b*-MAA [54] BzMA-*b*-DMAEMA [54] BzMA-*b*-HPMAm [55] MMA-*b*-St [54] MMA-b-DMAEMA [73] (St-*b*-DMAEMA) [129] MMA-*b*-St [23] (St-*b*-MMA) [23] St-*b*-MeS [23] St-*b*-DMAm [23] DEGMA/MPEGMA-*b*-DMAPMAm [149] LMA-*b*-*BzMA/**339*** [61] MMA-*b*-AN [72]

(*continued*)

Table 8.4 (Continued)

RAFT agent	Synthesis[a)]	Polymerizations[b)]
		MMA-*b*-St [74] MMA-*b*-St [76] MMA-*b*-BMA [77] MPEGMA-*b*-MMA [79] MPEGMA-*b*-**241** [81] LMA/MMA-*b*-MPEGMA [79] **114**-*b*-**95** [98] **251**-*b*-MPEGMA [103] **282**-*b*-BzMA [104] AAEMA-*b*-AEP [52] AAEMA-*b*-MAEP [52] MAEP-*b*-AAEMA [52] TFPMA-*b*-*t*BA [86] St-*b*-CMS [122] St-*b*-NIPAm [127] St-*b*-HEMA/DMAEMA [49] **225**-*b*-**265** [141] **226**-*b*-**265** [141] **269**-*b*-**82** [89] **120**-*b*-St [99] DMAm-*b*-**223** [80] MPEGMA-*b*-**223** [80] **88**-*b*-MPEGMA [91] POSSMA-*b*-4VP [83] POSSMA-*b*-St [83] POSSMA-*b*-St-*b*-4VP [83] 2VP-*b*-4VP [139] St-*b*-MAH [71] **326**-*b*-BA [108]**328** [159] **96**-*b*-St [93] **97**-*b*-St [93] GMA-*b*-POSSMA [59]
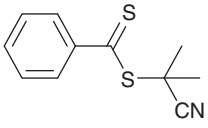 2-Cyanopropan-2-yl benzodithioate **6**	A [48] C [160–162] E [23] N	*Methacrylates*: BMA [163] *BMA* [164] DMAEMA [165] EOEMA [166] GMA [167, 168] HFBMA [169] (iBMA) [170] LMA [171] (MMA) [172] MMA [11, 23, 25, 68, 160, 173–187] *MMA* [188] MMA [189] MPEGMA [28, 190–192] PDFOMA [193] *t*BDMSMA [26, 187, 194] TPSiMA [194] **79** [168, 195–198] **301** [194] **100** [199] **101** [200] **108** [201] **109** [94] **117** [202] (**119**) [203] **122** [204] **123** [205] **124** [205] **128** [206] **141** [207] **144** [208] **145** [209–211] **146b** [212] **149** [213] **151** [214] **153** [186] **158** [215] **163** [216] **164** [216] **165** [216] **182** [217] **184** [217] **252** [218] **253** [218] **257** [219] **258** [220] **319** [221] **324** [194] *Acrylates*: BA [36, 43, 183, 222] *HFBA* [223] MA [23, 113, 183] iBoA [183] **190** [224] **197** [224] **192** [208] **193** [225] *Acrylamides*: DEAm [226, 227] NIPAm [228, 229] NIPAm [172] *Styrenes*: *t*BOS [230] St [128, 174, 181, 222, 227, 231] (*St*) [132] St [172] **242** [232] 231 [233] 240 [234] 348 [235] *Dienes*: Cp [236, 237] *Cp* [236] (Ip) [238] Ip [239] *Vinyls*: VBz [5] *Others*: AN [240, 241] iPOx [242]

(*continued*)

Table 8.4 (Continued)

RAFT agent	Synthesis[a)]	Polymerizations[b)]
		Copolymers: AMA/MMA [243] DMAEMA/**118** [244] DMAEMA/DEAEMA [245] IPhMA/MMA [246] LMA/**258** [220] MMA/**92** [246] MMA/**90** [246] (MMA/**254**) [243] MAA/MPEGMA [28] HEMAm/MPEGMA/MPEGMAm [247] MMA/**149**b [248] MMA/**282** [249–251] MMA/BA/*t*BDMSMA [187] BzMA/**282** [251] *t*BA/**283** [250] MMA/TMSMA [252] MMA/TMSMA/*t*BDMSOS [252] MMA/**110** [253] MMA/**111** [253] MMA/**146a**/**252** [254] MMA/**146b**/**252** [254] MMA/**146c**/**252** [254] AA/**287** [255] DMAm/**287** [255] **288**/**287** [255]NMS/HPMAm [256] iPOx/NIPAm [242] HMA/**163** [216] LMA/**163** [216] HMA/**165** [216] LMA/**165** [216] MMA/**199** [257] MA/**199** [257] MA/**200** [257] MA/**202** [257] St/MAH [155, 210, 258] St/**230** [259] MMA/BA [36] MMA/**119** [203] HEMAm/PEGMA/TEGMAm [247] **107**/NAS *Blocks*: BMA-*b*-**162** [260] BMA-*b*-**243** [163] *BMA-b-DFHMA* [164] MMA-*b*-BA/**199** [261] MMA-*b*-**153** [186] DMAEMA/DEAEMA-*b*-DMAEMA [245] EOEMA-*b*-*DMAm* [166] EOEMA-*b*-*NAM* [166] LMA-*b*-EGDMA [171] LMA-*b*-EGDMA-*b*-DMAEMA [171] MMA-*b*-**162** [262] MMA-*b*-BA/*t*BDMSMA [187] MPEGMA-*b*-NMS [191] MPEGMA-*b*-NMS-*b*-**94** [191]/*t*BDMSMA-*b*-BA/MMA [187] **79**-*b*-*HPMA* [168, 195] **79**-*b*-*BzMA* [198] **79**-*b*-*HPMA* [168, 195] **79**-*b*-*MOEMA* [196] **79**-*b*-***80*** [197] **101**-*b*-HEMA [200] **128**-*b*-**129** [206] **146b**-*b*-**152** [212] **151**-*b*-**146b** [214] **190**-*b*-**197** [224] **197**-*b*-**190** [224] MMA/TMSMA-*b*-PFS [252] MMA/TMSMA/tBDMSOS-*b*-PFS [252] PDFOMA-b-THPOS [193] **141**-*b*-**152** [207] **145**-*b*-St/MAH [210] **145**-*b*-**227** [211] St-*b*-St/**307** [231] GMA-*b*-PFS [167] MMA-*b*-S [174] *HFBMA-b-BMA* [169] MMA-*b*-BA [175] NIPAm-*b*-DEAm [228] *t*BOS-*b*-St [230] St-*b*-MAH [172] St-*b*-(NIPAm) [172] 231-*b*-**240**-*b*-AA [233] **122**-*b*-**93** [204] **123**-*b*-**93** [205] **124**-*b*-**93** [205]

(*continued*)

Table 8.4 (Continued)

RAFT agent	Synthesis[a)]	Polymerizations[b)]
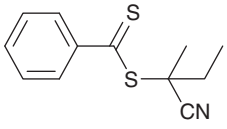 2-Cyanobutan-2-yl benzodithioate **7**	C [263] N [50]	*Methacrylates*: MAA [264, 265] BMA [266] BzMA [266] DEGMA [264, 267] DMAEMA [266] EOEMA [264] MMA [266, 268, 269] MPEGMA [264] **167** [270] **147** [271] **81** [272] **253** [273] 317 [274] *Acrylates*: BzA [266] EEA [275] EHA [266] MA [266] *t*BA [266] *Copolymers*: MAA/AA [265] **95**/MMA [276] DMAEMA/MPEGMA [277] DEGMA/MPEGMA [29] DEGMA/**150b** [278] DEGMA/MPEGMA/**150b** [278] MMA/**253** [273] MAA/MPEGMA [264] MMA/DMAEMA [279] *Blocks*: MAA-*b*-AA [265] DEGMA-*b*-DMAEMA [267] MMA-*b*-DMAEMA [279] MMA-*b*-**253** [273]
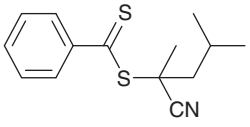 2-Cyano-4-methylpentan-2-yl benzodithioate **8**	C [40] N	*Methacrylates*: MMA [40]
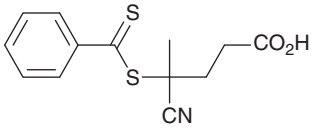 4-Cyano-4-((phenylcarbonothioyl)thio)pentanoic acid **9**	C [2, 161, 263, 280–282] N	*Methacrylates*: AEMA [53, 283–285] BMA [286] BMA [287] DEAEMA [288–290] DEGMA [291] DMAEMA [5, 292–295] DMAEMA [296] DPAEMA [297] GMA [296] LMA [61, 294] MAA [25, 291, 298–303] MMA [287, 304–315] MMA [296] MPC [316, 317] MPEGMA [295, 297, 318–323] MPEGMA [309] *PFBEMA* [324] *PFHEMA* [324] *PFOEMA* [324] PFPMA [325–329] POSSMA [330] TFEMA [287] TPSiMA [331] VBTAC [282, 332–336] **79** [337, 338] **83** [339] **84** [340] **100** [199] **114** [341] **131** [289, 342] **132** [102] **133** [101, 343] **134** [344] **135** [345] **137** [344, 346] **139** [347] **140** [348] **143** [349] **157** [350] **158** [351] **160** [298] **161** [298] **162** [352] **169** [353] **277** [354–356] **284** [357] **281** [358] **285** [357] **315** [359, 360]

(*continued*)

Table 8.4 (Continued)

RAFT agent	Synthesis[a)]	Polymerizations[b)]
		Acrylates: DMAEA [361] HFBA [362] NAS [363] HA [364] MA [365, 366] **MA** [367] PFPA [329] **190** [368] **284** [357] **285** [357]
		Methacrylamides: APMAm [284, 369, 370] DMAPAm [369] HPMAm [302, 371, 372] HPMAm [308] **170** [373] **173** [373] **174** [347] **175** [374] **176** [375] **177** [375] **179** [298] **293** [376, 377] **294** [377]
		Acrylamides: AEMAm [370, 377] Am [378] AMPS [379, 380] DMAm [381] **DMAm** [367] NIPAm [365, 382–384] **NIPAm** [367] **178** [385] **211** [386] **217** [387]
		Styrenes: St [137, 348, 388] **St** [367] (PFPVS) [137] SSO_3Na [5, 389] **273** [142] (**274**) [142] (**304**) [390]
		Other MAM: AN [391] *AN* [392]
		Vinyls: (NVP) [393]
		Copolymers: MAA/MPEGMA [28] MAA/**142** [394] MMA/**257** [395] PFPMA/LMA [326] PFPMA/PFPA [329] MMA/PFPMA [396] MPEGMA/PFPMA [396] MPEGMA/**251** [397] MPC/**138** [316] MPC/**170** [316] MPC/**171** [316] **158**/**157** [351] **159**/[2]**278** [398] AEMAm/**172** [370] APMAm/**172** [370] HPMAm/**284** [399] HPMAm/APMAm [400] EOEMA/**186** [401] MPEGMA/**207** [401] HPMAm/APMAm [402] HPMAm/**181** [403] *t*BMA/**280** [404] BMA/**308**/PEGDMA [405] **309**/EGDA [406] PEGA/MAH [407]
		Blocks: ***79***-*b*-*HPMA* [337] **140**-*b*-DEAm [348] **143**-*b*-MMA [349] **158**-*b*-**157** [351] AMPS-*b*-**217** [379, 380] AEMA-*b*-HPMAm [284, 285] **131**-*b*-HEMA-*b*NIPAm [342] DEAEMA-*b*-**131** [289] DMAEMA-*b*-HEMA [292] DMAEMA/MPEGMA [321] DMAEMA-*b*-*BzMA*/***239*** [290] DMAEMA-b-*BzMA-b-PFHEMA* [408] (DMAEMA+MPEGMA)-*b*-DMAEA/**346** [295] DMAEMA-*b*-**168** [293] DMAEMA-*b*-**148** [294] LMA-*b*-**148** [294] LMA-*b*-*BzMA*/***339*** [61] LMA-*b*-*BzMA*/***340*** [61] MMA-*b*-**162** [409–411] MPEGMA-*b*-**148** [412] MPEGMA-*b*-DMAEMA [321] MPEGMA-*b*-VBTAC [334] MPEGMA-*b*-**276** [413] PFPMA-*b*-TEGMA [328] TEGMA-*b*-PFPMA [328] AEMAm-*b*-**172** [370] APMAm-*b*-**172** [370] HPMAm-*b*-DMAPMAm [371] **178**-*b*-HPMAm [385] St-*b*-PFPVS [137] St-*b*-DEAm [348]

(*continued*)

Table 8.4 (Continued)

RAFT agent	Synthesis[a)]	Polymerizations[b)]
		APMAM-*b*-NIPAm [69, 376] *MAA-b-DFHMA* [299] BMA-*b*-MPC [286] P DEGMA-*b*-**265** [291] MAA-*b*-*MMA* [303] MMA-*b*-MAA [54] MMA-*b*-St [54] MMA-*b*-**265** [291] DMAm-*b*-**211** [386] DMAEMA-*b*-NIPAm [288] DPAEMA-*b*-MPEGMA MPEGMA/AMPS [319, 320] MPEGMA-*b*-AMPS [319, 320] MPEGMA-*b*-**252** [318] **84**-*b*-**286** [340] **262**-*b*-LMA [325] **294**-*b*-293 [377] **134**-*b*-BMA [344] **137**-*b*-DMAEMA [344] **137**-*b*-BA [344] **139**-*b*-**174** [347] **160**-*b*-MAA [298] MAA-*b*-**160** [298] MAA-*b*-**161** [298] MMA-*b*-**160** [298] MMA-*b*-**161** [298] DMAm-*b*-NIPAm/**260** [381] NIPAm-*b*-**295** [384] NIPAm/**293** [377] MPC/**294** [377] **277**-*b*-HPMAm [354] HPMAm/APMAm-*b*-DMAPMAm [402] HPMAm/**181**-*b*-**280** [403] St-*b*-**265** [388] **156**-*b*-DEAm [317] **156**-*b*-VBA [317] **156**-*b*-**157** [317] **156**-*b*-**234** [317] **157**-*b*-HPMA [350] **170**-*b*-AEMAm [373] **170**-*b*-MPC [373] **173**-*b*-AEMAm [373] **173**-*b*-APMAm [373] APMAm-*b*-**173** [373] **179**-*b*-Am [298] VBTAC-*b*-**233** [335] NAS-*b*-Am [363] POSSMA-*b*-PFOEMA [330] **162**-*b*-NIPAm [352] PEGA/MAc-*b*-St [407]
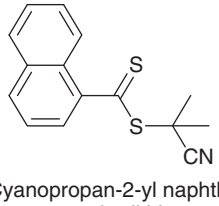 2-Cyanopropan-2-yl naphthalene-1-carbodithioate **10**	C [414]	*Methacrylates*: BMA [415] DMAEMA [415] GMA [416] GMA [415] MMA [366, 414, 417–421] MMA [422] MMA [415, 423] MPEGMA [424] MPEGMA [415, 425] PEMA [426] **105** [427] **106** [427] **116** [428] **121** [429] *Others*: (AN) [430] AN [431, 432] *Styrenes*: St [129, 433, 434] 4VP [415] *Copolymers*: MMA/**102** [435] St/NMMI [436] St/NPrMI [436] *Blocks*: MMA-*b*-S [414] GMA-*b*-St [437] **116**-*b*-MMA [428] **116**-*b*-St [428] (St-*b*-DMAEMA) [129]

(*continued*)

Table 8.4 (Continued)

RAFT agent	Synthesis[a)]	Polymerizations[b)]
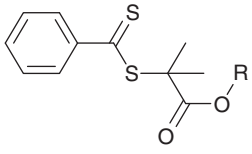 Alkyl 2-methyl-2-((phenylcarbonothioyl)thio)propanoate **11a** R = C_2H_5 **b** R = CH_3	A [23] C [438] N	*Methacrylates*: MMA [23, 45, 68, 74] *Acrylates*: **312** [439] *Styrenes*: St [23, 438, 440] (St) [133] *Dienes*: Cp [441] *Copolymers*: PEGMA/**95** [442] (AA/MMA) [443] 4VP/BA [444] *Blocks*: MMA-*b*-St [74] St-*b*-Cp [441]
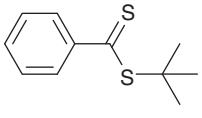 *tert*-Butyl benzodithioate **12**	D [23, 445, 446] F [446–448] N	*Methacrylates*: (MMA) [23, 25, 449, 450] *Acrylates*: AA [451] BA [449] EHA [448] *Acrylamides*: DEAm [452] *t*BAm [453] DEAm [449] DMAm [449, 454] NAM [447, 453] NIPAm [449, 450] *Styrenes*: St [23] *St* [455, 456] AcS [457] *Vinyls*: (VAc) [458] (NVP) [393] *Copolymers*: BA/S [459] VCl2/MA [446, 460] DMA/NAS [454] NAM/NAS [447, 461, 462] *Blocks*: *EHA-b-MA* [448, 463] DMA-*b*-(DMA/NAS) [454] *t*BAm-*b*-NAM [453] DMAm/NAS [464] NAM-*b*-*t*BAm [453] NAM/NAS-*b*-NAM [461]
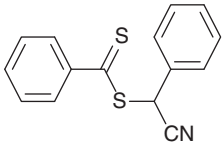 Cyano(phenyl)methyl benzodithioate **13**	A [41]	*Methacrylates*: MMA [41] *MMA* [188] *Acrylates*: BA [41] *t*BA [41] *Styrenes*: AcS [41] St [41]
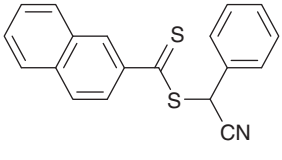 Cyano(phenyl)methyl naphthalene-2-carbodithioate **14**	A [41]	*Methacrylates*: *MMA* [188] **256** [465] *Acrylates*: BA [41] *Styrenes*: St [41] *Blocks*: **256**-*b*-MMA [465]

(*continued*)

Table 8.4 (Continued)

RAFT agent	Synthesis[a)]	Polymerizations[b)]
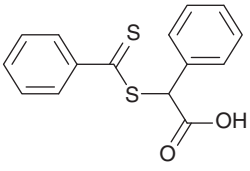 2-Phenyl-2-((phenylcarbonothioyl)thio)acetic acid **15**	A [466] N	HA [364]
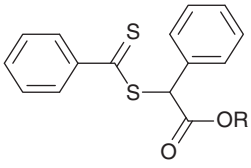 Alkyl 2-phenyl-2-((phenylcarbonothioyl)thio)acetate **16a** R = CH_3 **b** R = C_2H_5	A [467] C [438] N	*Methacrylates*: MMA [438, 450, 467] *Acrylates*: BA [468] HA [364] MA [467] *t*BA [469–471] **194** [472] *Acrylamides*: NIPAm [450, 473] *Styrenes*: St [438, 467] 4VP [474] *Copolymers*: DMAEMA/**331** [475] DMAEMA/**332** [475] DMAEMA/**332** [475] DMAEMA/**335** [475] HEMA/**331** [475] HEMA/**332** [475] HEMA/**332** [475] HEMA/**335** [475] MAA/MPEGMA [476] MMA/**154** [477] MMA/**155** [477] MMA/**331** [475] MMA/**332** [475] MMA/**333** [475] MMA/**334** [475] MMA/**335** [475] St/CMS [478] St/2VP [479] St/**228** [480] *Blocks*: MMA-*b*-NIPAm [450] THPA-*b*-S [481] THPA-*b*-St/**255** [482] *t*BA-*b*-**194** [469–471] **194**-*b*-SSO_3Na [472] NIPAm-*b*-**194** [473] 4VP-*b*-**194** [474]
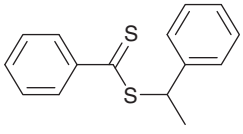 1-Phenylethyl benzodithioate **17**	A [483] B [23] D [445] N	*Methacrylates*: (MMA) [23] *Acrylates*: AA [5] BA [23, 54] MA [54] PEGA [483, 484] *Styrenes*: St [129, 485, 486] (*St*) [131] **237** [487] **232** [488] *Copolymers*: St/EVE [489] (St/MAH) [489] BP/MAH [490] St/Bd [143] (St/Bd) [491] *Blocks*: BA-*b*-AA [54] MA-*b*-EA [54] (St-*b*-DMAEMA) [129] St-*b*-MAH [486]
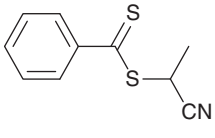 1-Cyanoethyl benzodithioate **18**	A [492] C [438]	*Others*: AN [492] *Copolymers*: AN/BP [493]

(*continued*)

Table 8.4 (Continued)

RAFT agent	Synthesis[a)]	Polymerizations [b)]
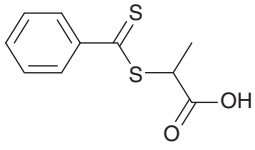 2-((Phenylcarbonothioyl)thio)propanoic acid **19**	A [494, 495] N	*Acrylates*: AA [37] DEGA [496] *Acrylamides*: NAA [495] NAM [494, 495] NAPi [495] NIPAm [497] *Styrenes*: St [497] *Blocks*: NAM-*b*-NAPi [495] NAM-*b*-NAA [495] St-*b*-NIPAm [497] (used to prepare other functional RAFT agents) [495, 498]
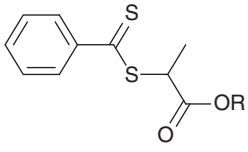 Alkyl 2-((Phenylcarbonothioyl)thio)propanoate **20a** R = C_2H_5 **b** R = CH_3	A [43, 497, 499] C [438] F [446] N	*Acrylates*: BA [43, 500] PEGA [484] *Acrylamides*: NIPAm [499] *Styrenes*: St [500, 501] VBPDE [502] *Copolymers*: MA/BP [503] SSO_3Na/MPEGMA [504] VCl_2/MA [446] *Blocks*: VBPDE-THPFDA [502]
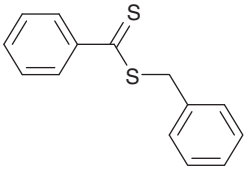 Benzyl benzodithioate **21**	A [23] D [445, 505] F [446] N	*Methacrylates*: (MMA) [23, 25] *Acrylates*: AA [506, 507] BA [5, 23, 508] *BA* [509] HEA [510] MA [23] (MA) [511] PEGA [512] **219** [513] *Acrylamides*: DEAm [514] DMAm [515] NIPAm [516] **218** [517] **219** [518, 519] **221** [519, 520] **220** [80, 517] **222** [519] **223** [80, 521] **224** [522] **236** [523] *Others*: (NVPI) [524] *Styrenes*: St [23, 31, 32, 54, 69, 128, 507, 508, 515, 525, 526] PFPVS [137] PVS [137] **236** [523] **337** [527–529] (**338**) [527] **267** [530] **306** [531] *Vinyls*: (VAc) [458] (NVP) [393] (NES) [532] (BES) [532] *Copolymers*: MAA/EGDMA [533] MAA/MA [534] MMA/**337** [528] AA/St [506, 507] BA/**337** [528] *t*BA/St [506] AN/**337** [528] (St/Bd) [491] St/MAH [535, 536] St/**337** [528] 4VP/**337** [528] MAH/**329** [537] VCl2/MA [446] (DVE/MAH) [538] *Blocks*: HEA-*b*-**336** [510] PEGA-*b*-NIPAm [512] (PFPVS-*b*-PSt) [137] (**255**-*b*-EA) [531] **219**-*b*-**229** [513] **220**-*b*-**223** [80] St-*b*-MeS [54] St-*b*-DMAm [54] (St-*b*-DMAm) [515] St-*b*-4VP [525]

(*continued*)

Table 8.4 (Continued)

RAFT agent	Synthesis[a)]	Polymerizations[b)]
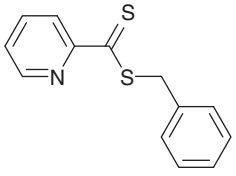 Benzyl pyridine-2-carbodithioate **22**	M [539]	*Acrylates*: iBoA [540] *t*BA [541, 542] **135** [543] *Styrenes*: St [540, 544, 545] (*St*) [131] **268** [142] **272** [142] **273** [142] *Copolymers*: AN/Bd [546] St/AN [546]
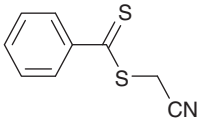 Cyanomethyl benzodithioate **23**	A [547] N	*Acrylates*: DEGMA [548] (MA) [549] *Vinyls*: (NVC) [550]
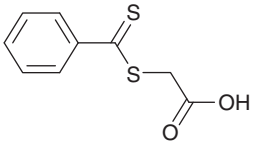 2-((Phenylcarbonothioyl)thio)acetic acid **24**	N	*Methacrylates*: (MAA) [551] (MMA) [449] *Acrylates*: BA [449] HA [364] *Styrenes*: (*St*) [33] *Acrylamides*: Am [552] (DEAm) [449] (DMAm) [449] (NIPAm) [449, 551, 553] **215** [552] *Dienes*: (Cp [237]) *Copolymers*: St/DVB [443, 554, 555] m/**215** [552] Am/**214** [552] *Blocks*: (NIPAm-*b*-NAS) [553] (NIPAm-*b*-MAA) [551]

a) Details of RAFT agent synthesis. The letter (A–N) indicates the synthetic method used – see Section 8.4.

b) Monomers used. Polymerizations leading to block copolymers are designated as A-*b*-B. The first mentioned monomer (A) was polymerized first, and the polymer formed was used as a macroRAFT agent in polymerization of the second mentioned monomer (B), etc. Those leading to gradient or statistical copolymers are designated as A/B. The following apply: Purple – crosslinking polymerization. Block copolymers prepared by crosslinking polymerization will be arm-first stars. Red – photoinitiated polymerization. Orange – SUMI. **Bold Orange** – PhotoSUMI. Green – redox RAFT. *Blue Italics* – heterogeneous polymerization (emulsion, miniemulsion, dispersion). If the monomer(s) appear in parentheses, a relatively broad molar mass distribution ($Đ > 1.4$), significant retardation/inhibition, and/or other issues were encountered.

For a full list of abbreviations, see the Abbreviations section.

Table 8.5 Functional dithioester RAFT agents.

Hydroxyl	Synthesis[a)]	Polymerizations[b)]
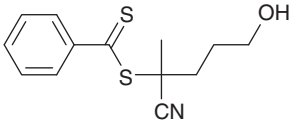 **25**	C [23, 161] N	*Methacrylates*: BMA [559] DMAEMA [560, 561] MMA [5, 23, 559, 560] *MMA* [188] *Acrylates*: HA [364] *Acrylamides*: NIPAm [382] *Styrenes*: St [562, 563] *Blocks*: RAFT-*T*-ROP: MMA-*b*-CL [564] BMA-*b*-CL [564] *t*BMA-*b*-CL [564] MMA-*b*-VL [564] BMA-*b*-VL [564] *t*BMA-*b*-VL [564]
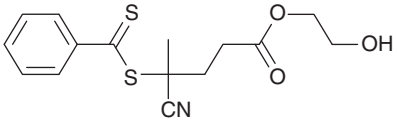 **26**	H [102]	*Methacrylates*: **132** [102] *Blocks*: **132**-*b*-BA [102]
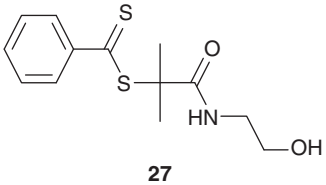 **27**	C [23, 565]	*Methacrylates*: (MMA) [23] *Copolymers*: NIPAm/DMAm [566–569] ROP-*T*-RAFT: NIPAm/DMAm-*b*-CL [566, 569] NIPAm/DMAm-*b*-LA [566, 568]
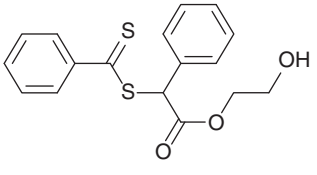 **28**	A [364]	*Acrylates*: HA [364]
Protected primary amine 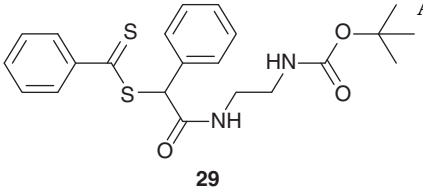 **29**	A [364]	*Acrylates*: HA [364]

(*continued*)

Table 8.5 (Continued)

Hydroxyl	Synthesis[a)]	Polymerizations[b)]
Active ester		
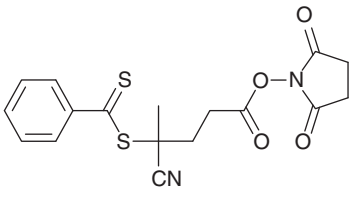 **30**	C [570] C/H [571–573] H [574–578] N	*Styrenes*: **270** [572]
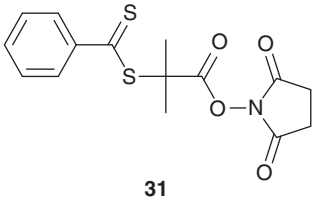 **31**	D [579]	
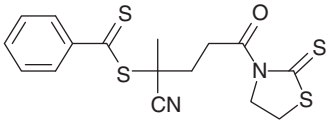 **32**	H [580]	*Methacrylamides*: HPMAm [372] (used to prepare other functional RAFT agents) [365, 580–583]
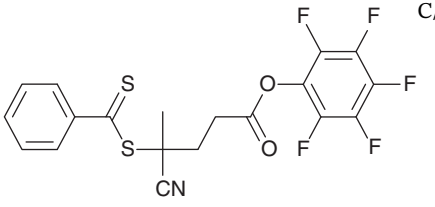 **33**	C/H [584]	*Methacrylates*: *t*BMA [585] DEGMA [584, 585] LMA [69, 584] MMA [584] MPEGMA [69, 584] *Methacrylamides*: NIPMAm [584]
Azide		
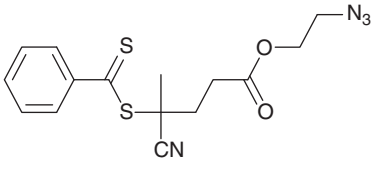 **34**	H [586]	*Methacrylates*: MMA [586]

(*continued*)

Table 8.5 (Continued)

Hydroxyl	Synthesis[a)]	Polymerizations[b)]
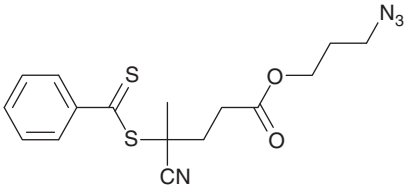 **35**	H [587–589]	*Methacrylates*: APMA [589] DMAEMA [590, 591] MMA [591] *Acrylamides*: DMAm [588] NIPAm [592] *Styrenes*: St [587, 588, 591–593] 2VP [594] 4VP [591] *Blocks*: DMAm-*b*-St [588] St-*b*-DMAm [588] St-*b*-MAH [592]
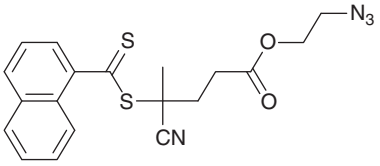 **36**	C,H [595]	*Styrenes*: St [595]
Alkyne		
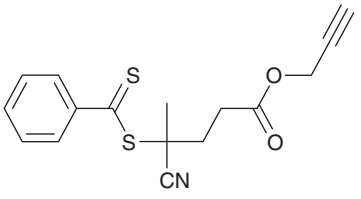 **37**	H [586, 589, 594, 596–598]	*Methacrylates*: AEMA [599] APMA [589] BMA [586] TESPMA [594] **98** [598] **140** [597, 600] *Blocks*: PEGA-*b*-TMSPA/191 [601] **140**-*b*-MPEGMA [600]
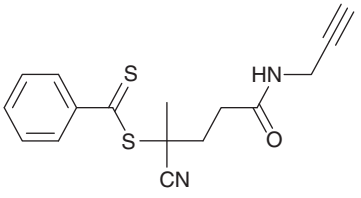 **38**	L [585]	*Methacrylates*: *t*BMA [585] MMA [585] DEGMA [585]
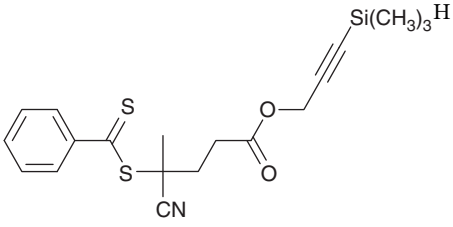 **39**	H [587]	*Methacrylates*: **133** [602] *Styrenes*: St [587]

(*continued*)

Table 8.5 (Continued)

Hydroxyl	Synthesis[a)]	Polymerizations[b)]
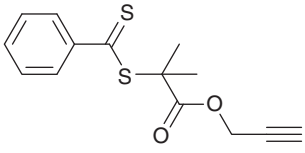 **40**	A [592]	*Styrenes*: St [592] *Blocks*: St-*b*-MAH-*b*-NIPAm [592]
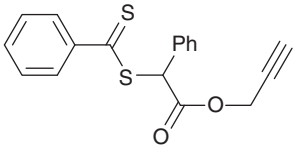 **41**	-	*Blocks*: THPA-*b*-S [481]
Alkene		
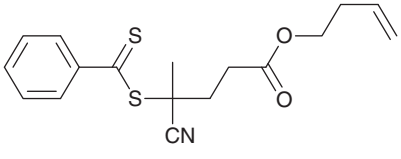 **42**	H [603]	*Copolymers*: DEGMA/HEMA [603]
Dibromomaleimide		
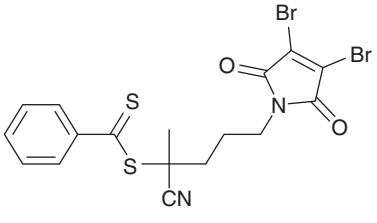 **43**	M [604, 605]	*Acrylamides*: DMAm [604] NIPAm [604, 605]
Thiolactone		
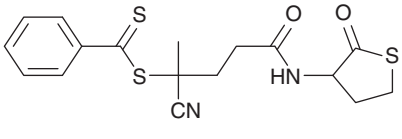 **44**	C [606]	*Styrenes*: St [606]

(*continued*)

Table 8.5 (Continued)

Hydroxyl	Synthesis[a)]	Polymerizations[b)]
ROMP monomer		
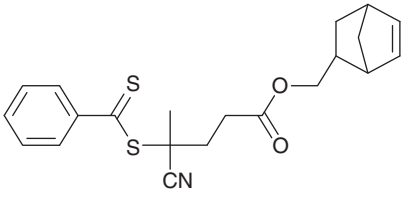 **45**	H [607, 608]	*Methacrylates*: MMA [607, 608] *Acrylates*: MA [608] *Styrenes*: St [608] *Copolymers*: 4HS/NPMI [609] RAFT-*T*-ROMP [607–609]
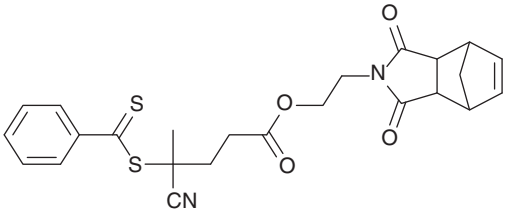 **46**	H [610]	ROMP-*T*-RAFT [610, 611]
Protected maleimide		
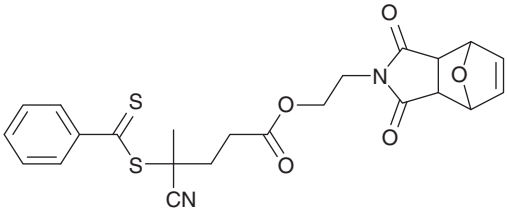 **47**	H [612–614]	*Methacrylates*: MMA [612–616]NMA [615]
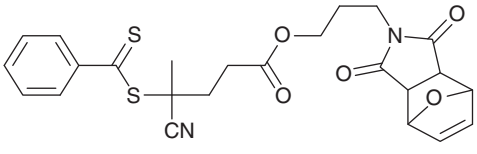 **48**	H [603, 617]	*Methacrylates*: MPC [617] *Copolymers*: DEGMA/HEMA [603]
Poly(dimethylsiloxane)		
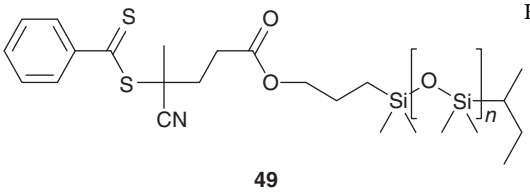 **49**	H [618]	*Copolymers*: MMA/**150b** [618] BMA/**150b** [618] HMA/**150b** [618]

(*continued*)

Table 8.5 (Continued)

Hydroxyl	Synthesis[a)]	Polymerizations[b)]
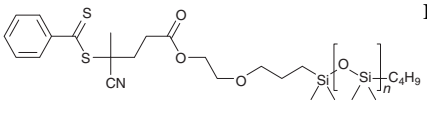 **50**	H [619]	*Methacrylates*: DMAEMA [619] *Blocks*: DMAEMA-*b*-HEMA [619]
Poly(ethylene glycol)		
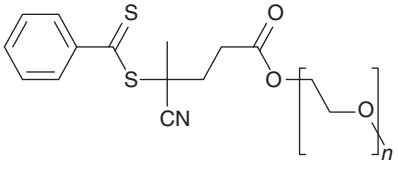 **51**	H [620]	*Methacrylates*: BzMA [54] DMAEMA [321, 621] HEMA [622] TMAEMA [623] **126** [624] *Acrylates*: *BA* [620] *Styrenes*: St [54] *St* [621, 625] 2VP [626] *Copolymers*: St/DVB [627] *Blocks*: DMAEMA-*b*-*St* [621] 2VP-*b*-St [626]
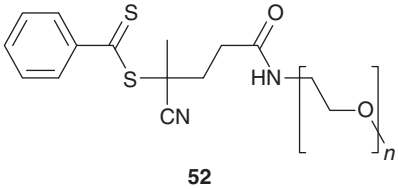 **52**	L [54]	*Styrenes*: St [54]
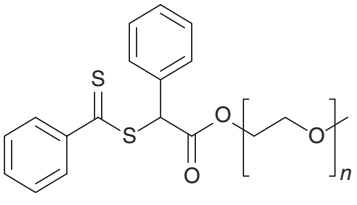 **53**	H [628]	*Methacrylates*: MMA [628] *Blocks*: MMA-*b*-St [628]
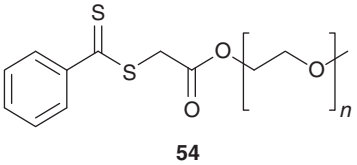 **54**	K [449]	*Methacrylates*: (MMA) [449] *Acrylates*: BA [449] *Acrylamides*: (DMAm) [449] (NIPAm) [449]

(*continued*)

Table 8.5 (Continued)

Hydroxyl	Synthesis[a)]	Polymerizations[b)]
Lipid 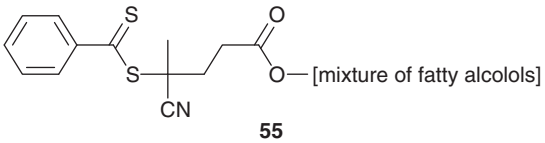 **55**	H [629]	*Methacrylates*: DMAEMA [629]

a) Details of RAFT agent synthesis. The letter (A–N) indicates the method(s) used – see Section 8.4.
b) See footnote 'b' of Table 8.4. In the case of bis-RAFT agents, sequential polymerization of two monomers will yield a triblock copolymer.
For a full list of abbreviations, see the Abbreviations section.

Table 8.6 Bis-dithioester RAFT agents.

RAFT agent	Synthesis[a)]	Polymerizations[b)]
'R'-connected		
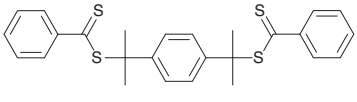 **56** 1,4-Phenylenebis(propane-2,2-diyl) dibenzodithioate	B [49, 648–651]	*Methacrylates*: BMA [54, 652] DMA [648] DMAEMA [649–654] TFEMA [654] MMA [54, 648, 655] **80** [656] *Acrylates*: AA [649] BA [652] *Acrylamides*: NAM [447] *Styrenes*: S [649, 652] *Copolymers*: HEMA/DMAEMA [49] *Blocks*: BMA-*b*-MMA [54] BMA-*b*-St [54] DMAEMA-*b*-BMA [652] DMAEMA-*b*-BA [652] DMAEMA-*b*-S [652] HEMA/DMAEMA-*b*-St [49] MMA-*b*-HEMA [54]MMA-*b*-**154** [655] MMA-*b*-**154**/MMA [655] **80**-*b*-**85** [656]
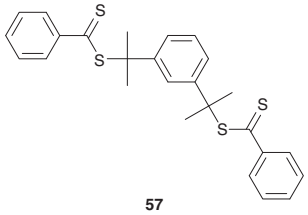 **57** 1,3-Phenylenebis(propane-2,2-diyl) dibenzodithioate	B [49, 657]	*Methacrylates*: MPC [657] *Acrylamides*: NAM [447] *Copolymers*: DMAEMA/HEMA [49] *Blocks*: DMAEMA/HEMA-*b*-St [49]

(*continued*)

Table 8.6 (Continued)

RAFT agent	Synthesis[a)]	Polymerizations[b)]
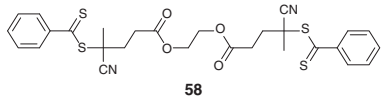 **58** Ethane-1,2-diyl bis(4-cyano-4-((phenylcarbonothioyl)thio)pentanoate)	H [106]	*Methacrylates*: PEGMA [658] TEGMA [659] *Other*: (DEHI) [106] DBI [106] *Blocks*: PEGMA-*b*-Am/AN [658] DBI-*b*-**185** [106]
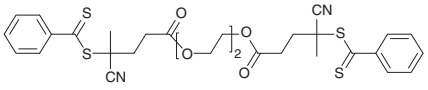 **59**	H [398]	*Acrylamides*: **212** [398]
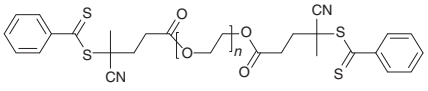 **60**	H [660–662]	*Methacrylates*: MMA [660, 661] **169** [663] *Acrylates*: BA [660] *Styrenes*: St [660, 661] SSO_3Na [301, 662] 2VP [661] *Blocks*: MMA-*b*-St [661] MMA-*b*-St-*b*-2VP [661] MMA-*b*-2VP [661] MMA-*b*-2VP-*b*-St [661] MMA-*b*-EGDMA [660] BA-*b*-EGDA [660] St-*b*-DVB [660] St-*b*-2VP [661] 2VP-*b*-St [661]
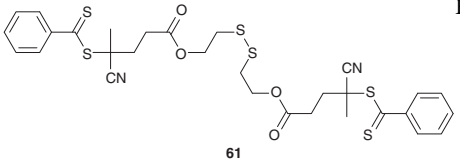 **61**	H [664]	*Blocks*: **125**/**290**-*b*-**87**-*b*-MPC [664]
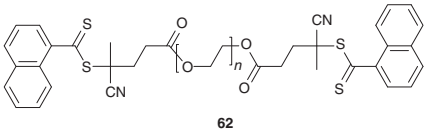 **62**	H [665]	*Methacrylates*: DMAEMA [665]

(*continued*)

Table 8.6 (Continued)

RAFT agent	Synthesis[a)]	Polymerizations[b)]
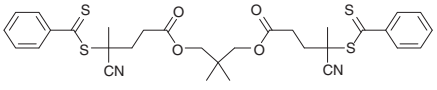 **63**	H [666]	*Methacrylates*: TMSEMA [666] *Blocks*: TMSEMA-*b*-**86** [666]
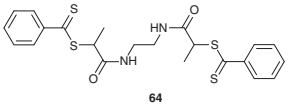 **64**	A [386]	*Acrylamides*: DMAm [386] *Blocks*: DMAm-*b*-**211** [386]
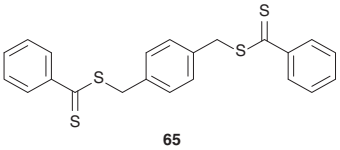 **65**	A [555, 648]	*Acrylates*: *t*BA [667] *Acrylamides*: NIPAm [653] *Styrenes*: St [648, 668] SSO_3Na [669] CMS [670] *Copolymers*: DA/ODA [555] *Blocks*: *t*BA-*b*-St [667] SSO_3Na-*b*-NIPAm/MBAm [669] CMS-*b*-St [670] ODA/DA-*b*-St [555]
'Z'-connected		
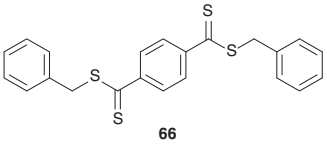 **66**	A [671]	*Styrenes*: St [143]
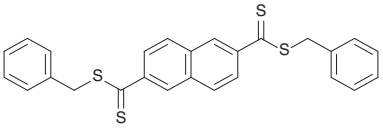 **67**	D [672]	*Acrylates*: *t*BA [672] *Blocks*: *t*BA-*b*-St [672]

a) Details of RAFT agent synthesis. The letter (A–N) indicates the synthetic method used – see Section 8.4.

b) See footnote 'b' of Table 8.4. In the case of bis-RAFT agents, sequential polymerization of two monomers will yield a triblock copolymer.

For a full list of abbreviations, see the Abbreviations section.

Table 8.7 RAFT agents and RAFT polymerizations – aliphatic dithioester RAFT agents (Z = alkyl or aralkyl).

RAFT agent	Synthesis[a)]	Polymerizations[b)]
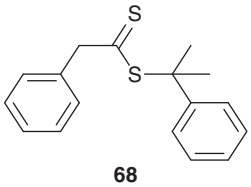 **68** 2-Phenylpropan-2-yl 2-phenylethanedithioate	B [674, 675]	*Methacrylates*: (MMA) [675, 676] *Acrylates*: AA [677] *BA* [678] MA [113, 183, 679] BA [183, 677, 679] HPA [677] **187** [680] (**204**) [681] *Styrenes*: St [682–684] *St* [685–687] MeS [677] *Copolymers*: Bd/AN [688] BP/NPMI [689] St/**307** [690] *Blocks*: MMA-*b*-AA [675] MMA-*b*-AA-*b*-*MMA/BA* [675]
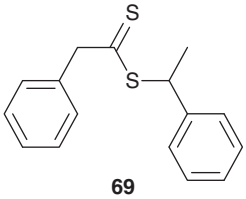 **69** 1-Phenylethyl 2-phenylethanedithioate	B [691]	*Acrylates*: AEP [52] MA [691] BA [36, 509] (*BA*) [509] TFPA [86] *Acrylamides*: DEAm [692] NIPAm [693–695] *Styrenes*: AcS [696] St [697] *St* [698–702] PFS [86] *Blocks*: *St-b-St/Bd* [700] *St-b-Bd-b-St* [700] *Copolymers*: St/MAH [703] BP/MAH [490] DMAm/**180** [704]
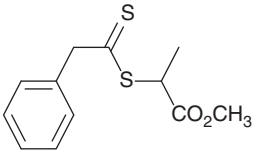 **70** Methyl 2-((2-phenylethane-thioyl)thio)propanoate	A [24]	*Acrylates*: MA [24, 705, 706] BA [705] DA [705] *Copolymers*: MA/BP [503]
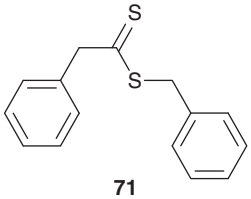 **71** Benzyl 2-phenylethanedithioate	A [683]	*Acrylamides*: NIPAm [693, 707–711] *Styrenes*: St [712–714] *St* [701, 715] *Dienes*: Bd [715] Cp [441] *Other MAM*: *MMBL* [716] *Copolymers*: St/MAH [713] *St/MMBL* [716] MMA/BA [36] BP/NPMI [689] BP/NMMI [689] BP/NEMI [689] St/Bd [715] *Blocks*: *St-b-*(St/*Bd*) [714, 715, 717] St-*b*-(St/MAH) [713] *St-b-Bd-b-St* [718] (St/MAH)-*b*-St [713] *St/MAH-b-St/Bd* [719, 720] NIPAm-*b*-MAA [711] TFPA-*b*-*t*BA [86] PFS-*b*-*t*BA [86]

(*continued*)

Table 8.7 (Continued)

RAFT agent	Synthesis[a)]	Polymerizations[b)]
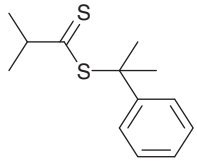 **72** 2-Phenylpropan-2-yl 2-methylpropanedithioate	B [509]	*Acrylates*: BA [509] (*BA*) [509]
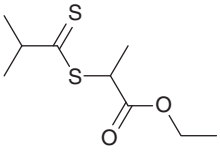 **73** Ethyl 2-((2-methylpropane-thioyl)thio)propanoate	—	*Acrylates*: BA [500]
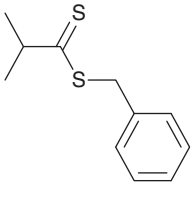 **74** Benzyl 2-methylpropanedithioate	A [721] D [505]	*Acrylates*: BA [36, 509, 721] *BA* [509] *Styrenes*: St [721] *Copolymers*: St/BA [721, 722] MAA/EGDMA [533]
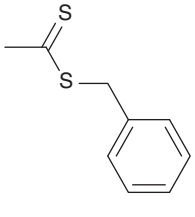 **75** Benzyl ethanedithioate	D [505]	*Acrylates*: BA [5, 48] *Styrenes*: *St* [48, 723] *Blocks*: *St-b-MMA* [48]

a) Details of RAFT agent synthesis. The letter (A–N) indicates the method(s) used – see Section 8.4.

b) See footnote 'b' of Table 8.4. If the monomer(s) appear in parentheses, a relatively broad molar mass distribution ($Đ > 1.4$), significant retardation/inhibition, and/or other issues were encountered.

For a full list of abbreviations, see the Abbreviations section.

Table 8.8 RAFT agents and RAFT polymerizations – bis-dithioester RAFT agents (Z = alkyl or aralkyl).

RAFT agent	Synthesis[a)]	Polymerizations[b)]
'R'-connected		
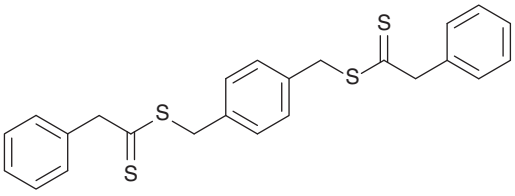 **76**	A [724]	*Styrenes*: St [724]
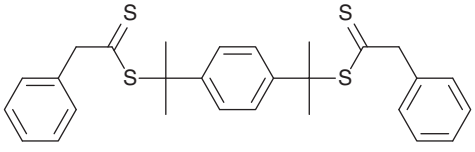 **77**	B [712]	*Styrenes*: St [712]
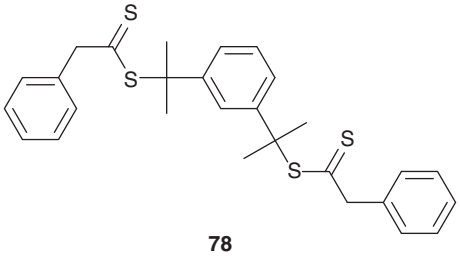 **78**	B [712, 725]	*Styrenes*: St [712, 725, 726]

a) Details of RAFT agent synthesis. The letter (A–N) indicates the method(s) used – see Section 8.4 *Synthesis of RAFT Agents*.

b) See footnote 'b' of Table 8.4. In the case of bis-RAFT agents, sequential polymerization of two monomers will yield a triblock copolymer.

For a full list of abbreviations, see the Abbreviations section.

Table 8.9 Methacrylate monomers subjected to RAFT polymerization.

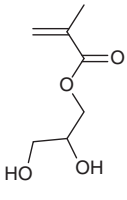

79 GMMA

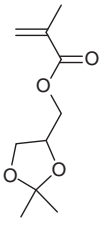

80 SKMA

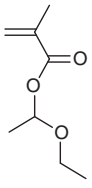

81 [272]

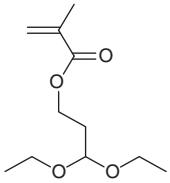

82 [89, 90]

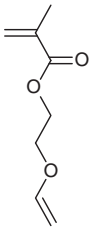

83 [339]

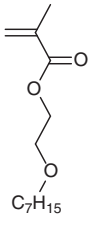

84

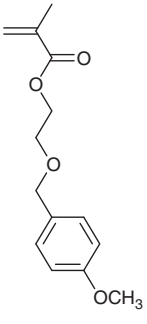

85 [656]

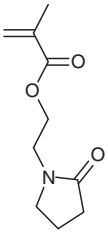

86

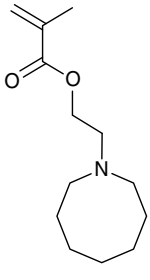

87

Metallo-monomers

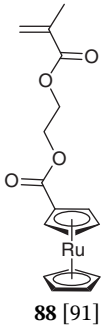

88 [91]

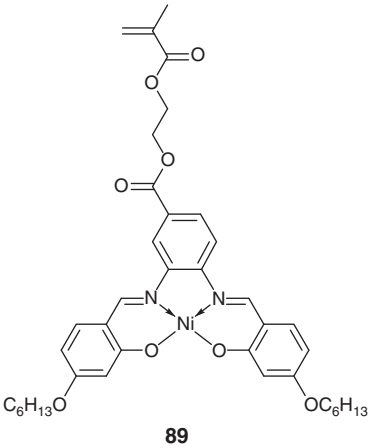

89

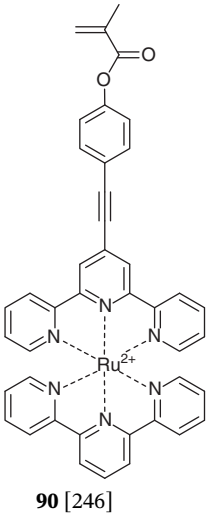

90 [246]

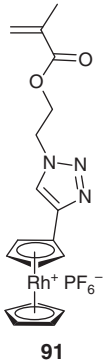

91

(*continued*)

Table 8.9 (Continued)

Ligating monomers

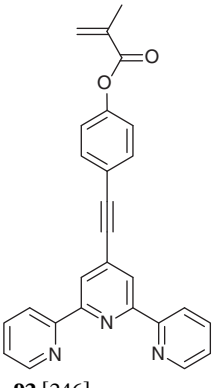

92 [246]

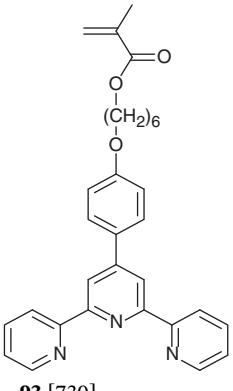

93 [730]

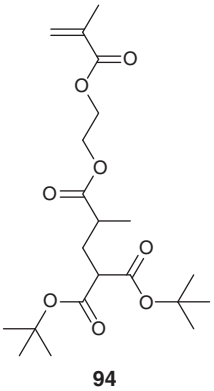

94

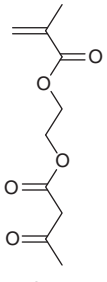

95

Boron, sulfonate, phosphonate, and phosphate-containing monomers

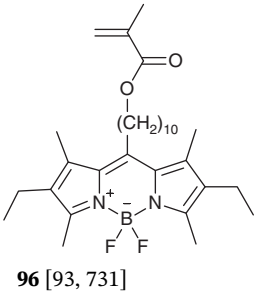

96 [93, 731]

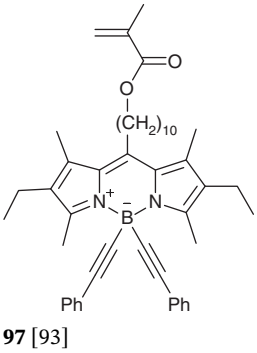

97 [93]

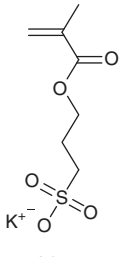

98

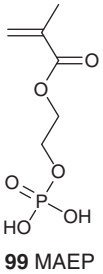

99 MAEP

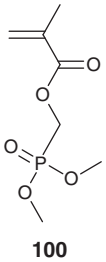

100

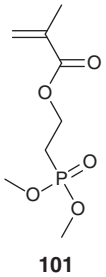

101

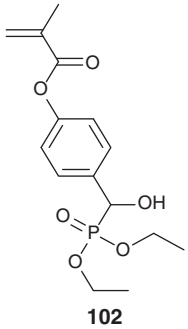

102

(*continued*)

Table 8.9 (Continued)

Bulky monomers

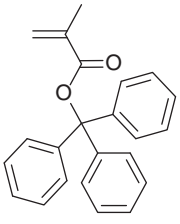

TPMMA
103 [87]

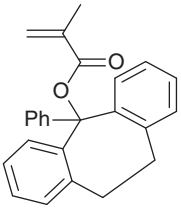

104 [88]

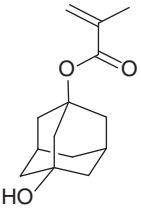

105 [427]

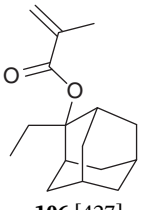

106 [427]

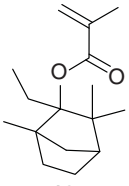

107

Monomers containing aziridine or thiirane functionality

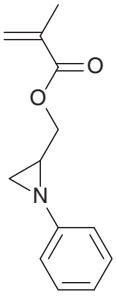

108 [201]

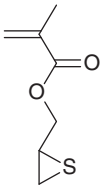

109 [94]

Dye monomers

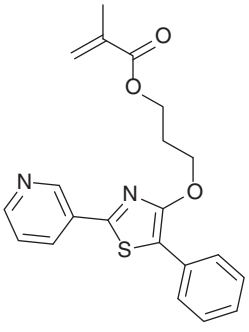

110 [253]

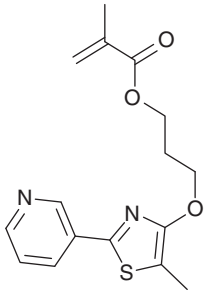

111 [253]

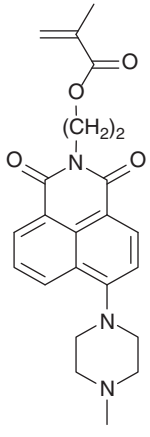

112 [95]

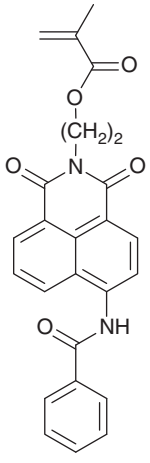

113 [96]

(*continued*)

Table 8.9 (Continued)

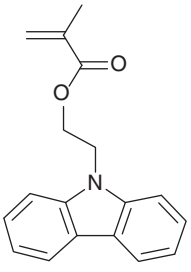

114

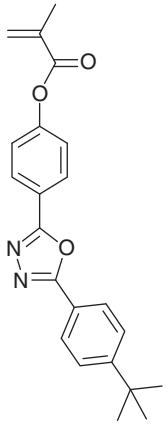

115 [97]

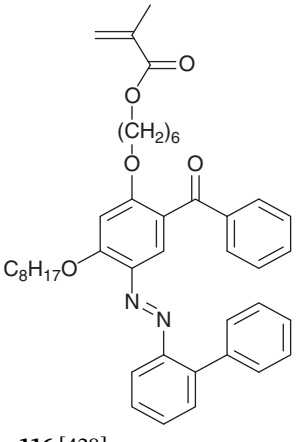

116 [428]

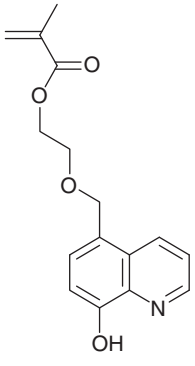

117 [202]

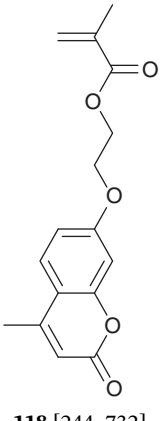

118 [244, 732]

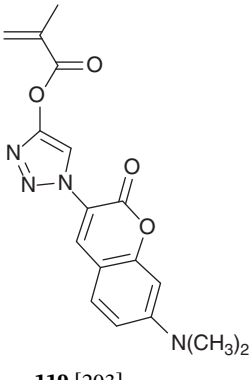

119 [203]

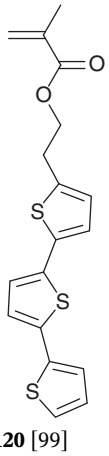

120 [99]

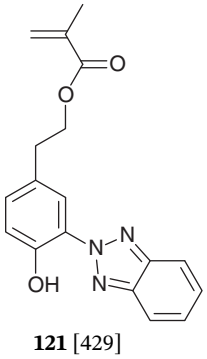

121 [429]

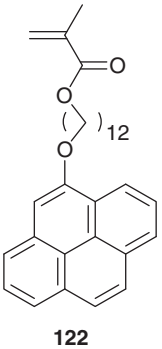

122

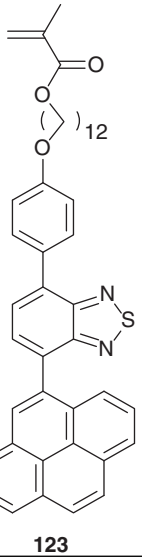

123

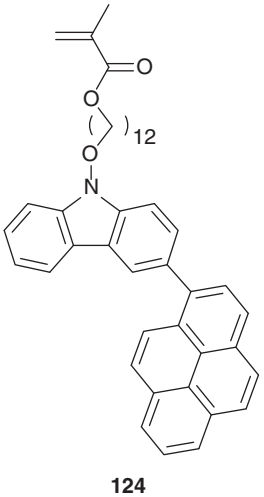

124

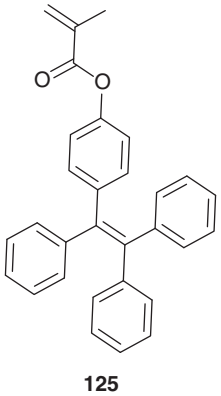

125

(*continued*)

Table 8.9 (Continued)

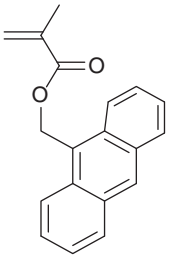

126

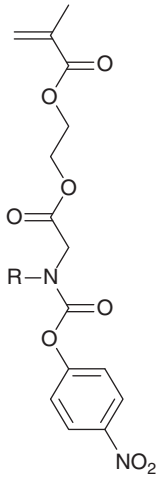

127 R = benzyl, isopropyl

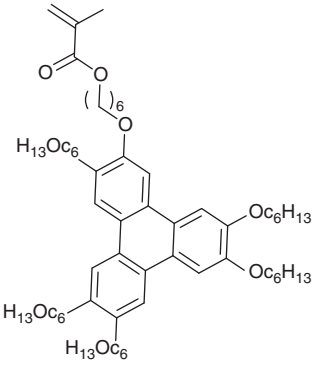

129

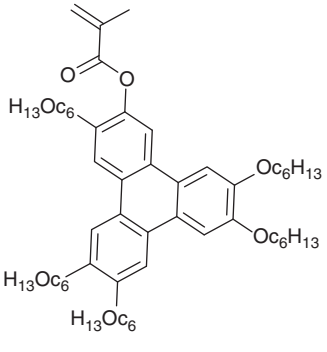

128

Glycomonomers

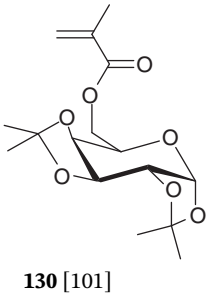

130 [101]

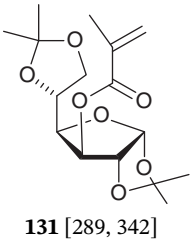

131 [289, 342]

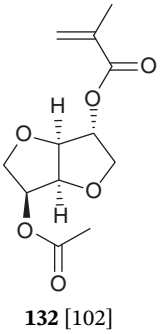

132 [102]

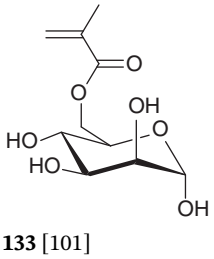

133 [101]

(*continued*)

Table 8.9 (Continued)

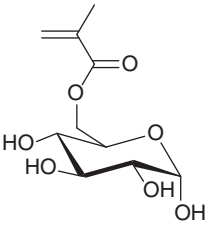

134 [344]

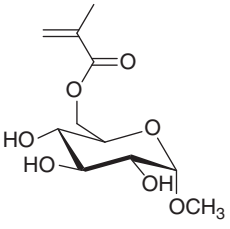

135 [345]

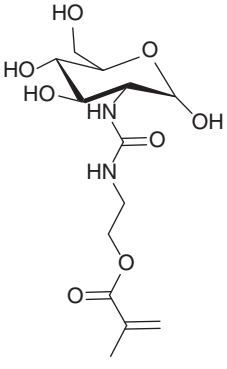

136 [343]

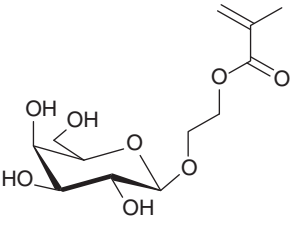

137 [344]

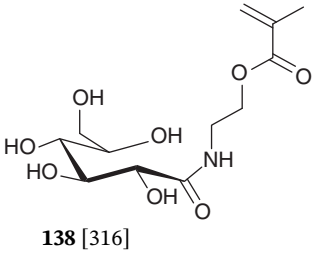

138 [316]

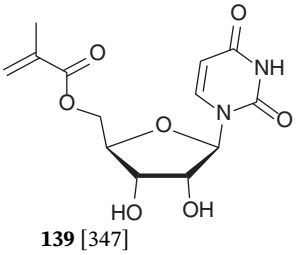

139 [347]

Liquid crystalline monomers

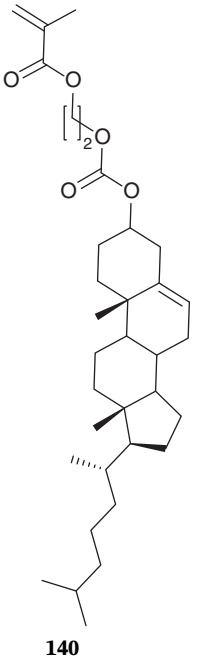

140

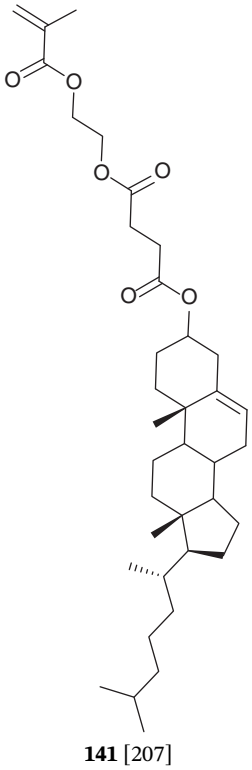

141 [207]

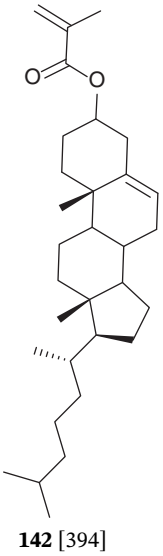

142 [394]

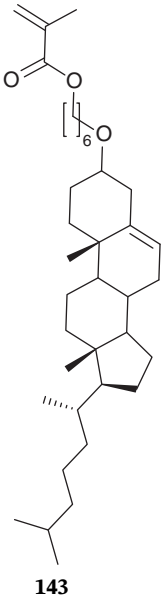

143

(*continued*)

Table 8.9 (Continued)

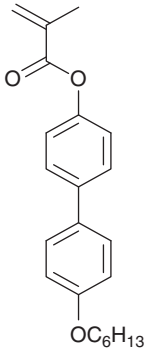

144

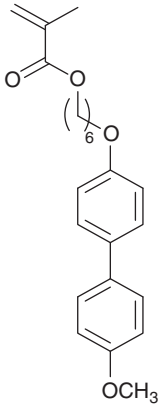

145

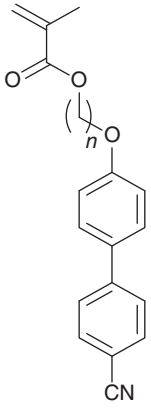

146a $n = 2$
146b $n = 6$
146c $n = 8$

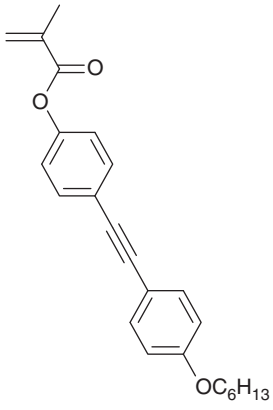

147 [271]

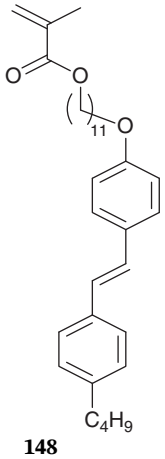

148

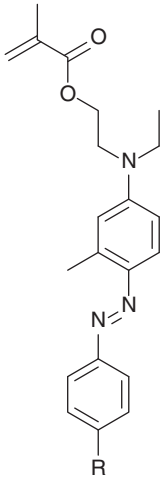

149
R = CN, OCH_3

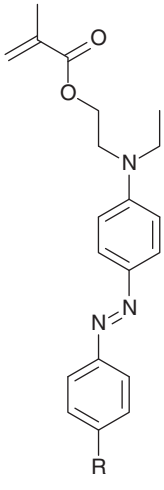

150a R = H
150b R = NO_2

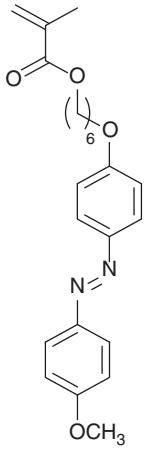

151

(*continued*)

Table 8.9 (Continued)

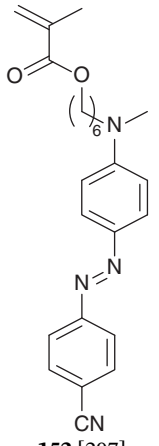

152 [207]

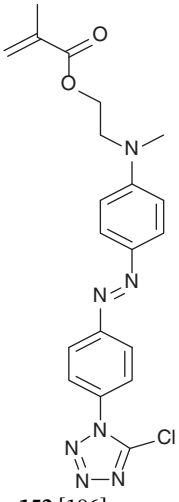

153 [186]

Dendrons

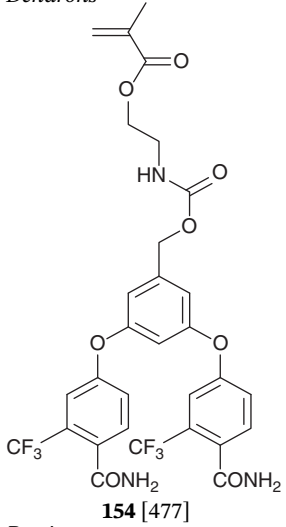

154 [477]

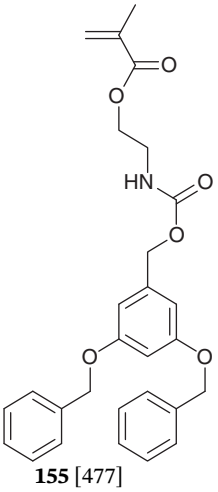

155 [477]

Betaines

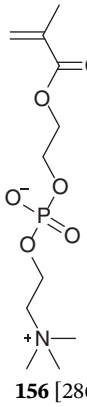

156 [286, 317]
MPC

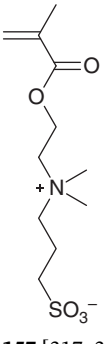

157 [317, 350]
DMAPS

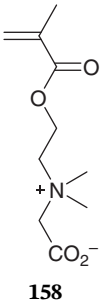

158

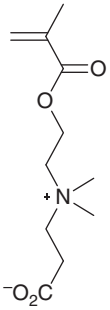

159

(*continued*)

Table 8.9 (Continued)

Ionic liquid monomers

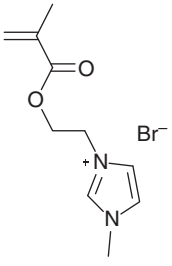

160 [298]

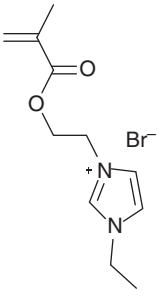

161 [298]

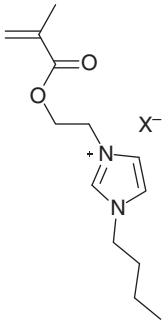

162

Amine/ammonium functional

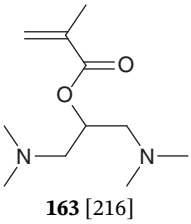

163 [216]

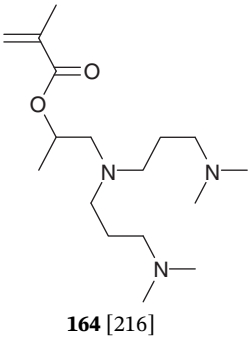

164 [216]

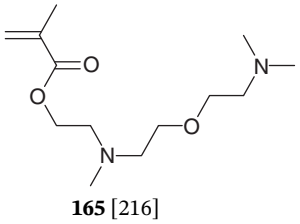

165 [216]

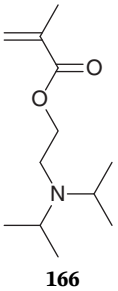

166

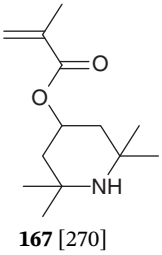

167 [270]

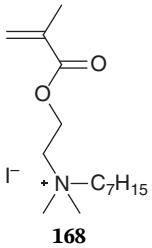

168

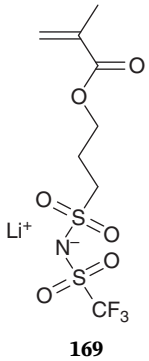

169

Table 8.10 Methacrylamide derivatives subjected to RAFT polymerization.

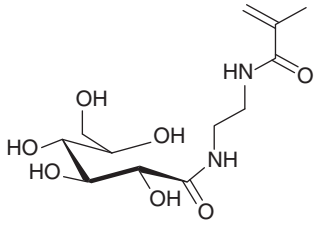

170 [316]

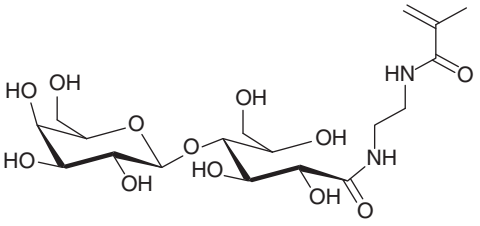

171 [316]

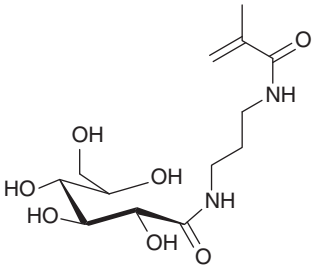

172 [370]

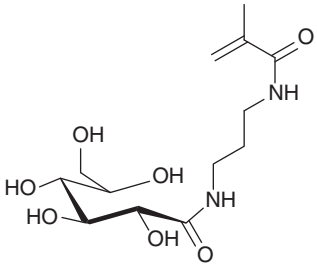

173 [373]

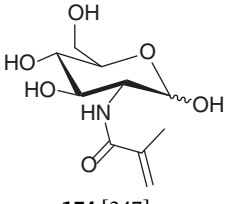

174 [347]

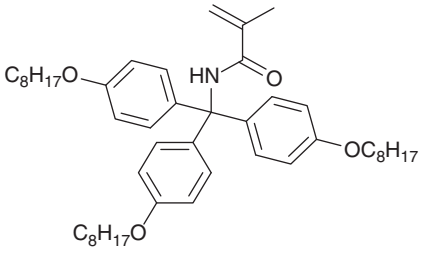

175

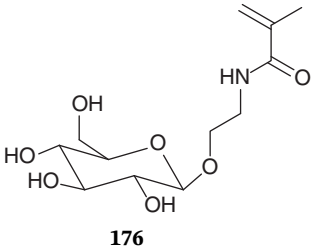

176

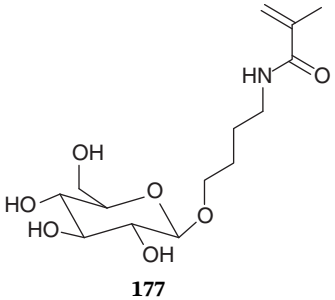

177

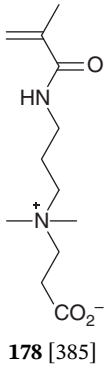

178 [385]

(*continued*)

Table 8.10 (Continued)

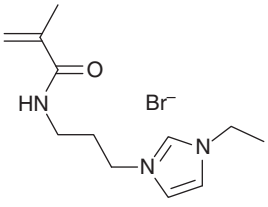

179 [298]

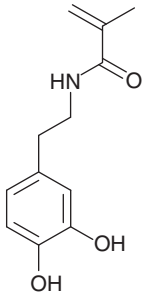

180

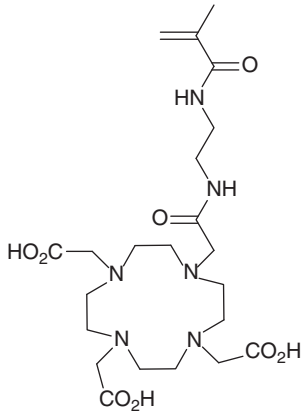

181

Table 8.11 Other 1,1-disubsituted monomers subjected to RAFT polymerization.

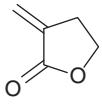

182

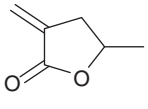

183 MMBL

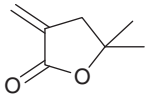

184

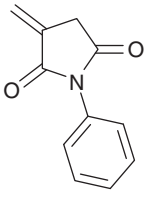

185

(*continued from page 240*)

Many acrylate esters commonly undergo chain transfer to polymers during polymerization, leading to branched and even gelled polymers. It has been reported that the extent of branching is higher for conventional radical polymerization than for RDRP (ATRP, RAFT, NMP) [751, 752]. Explanation for this has been proposed in terms of the differences in the concentrations of short-chain radicals between RDRP and conventional radical polymerization and in terms of radical life times (the time between chain activation and deactivation) being of the same order of magnitude or shorter than the time required for the conformational change required for intermolecular hydrogen atom transfer [753]. On this basis, the process might be anticipated to be less prevalent with dithiobenzoates than with less active RAFT agents. However, this hypothesis has not been tested.

8.5.2.2 Acrylamides

Attaining low dispersities with RAFT polymerization of acrylamides requires a RAFT agent suitable for MAMs. Acrylamides include Am, DEAm, DMAm, NIPAm,

Table 8.12 Acrylate monomers subjected to RAFT polymerization.

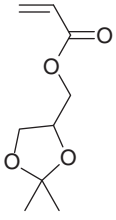

186 [733]
Solketal acrylate

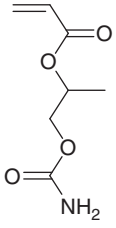

187 [680]

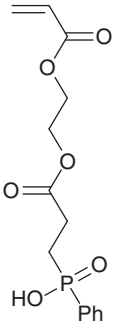

188 [734]

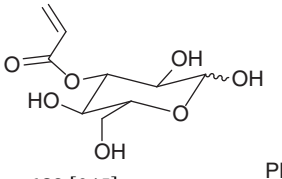

189 [345]

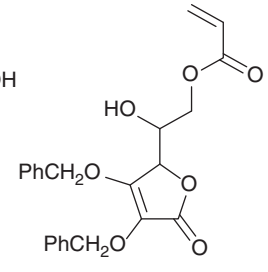

190 [224]

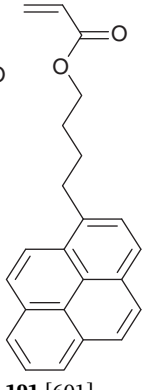

191 [601]

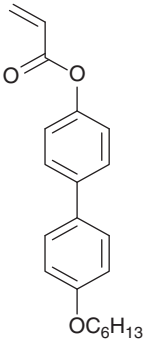

192

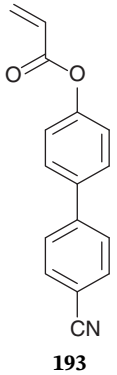

193

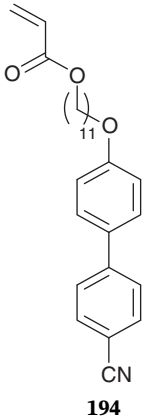

194

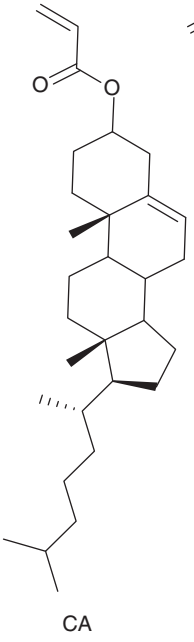

195 [735]

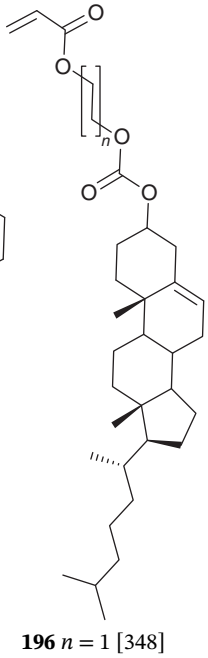

196 $n = 1$ [348]
197 $n = 2$ [224]
198 $n = 4$ [736]

(*continued*)

Table 8.12 (Continued)

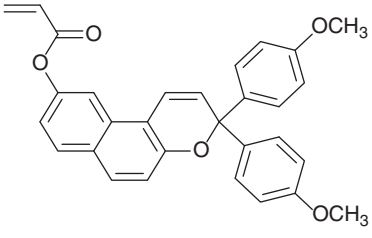

199 [261]

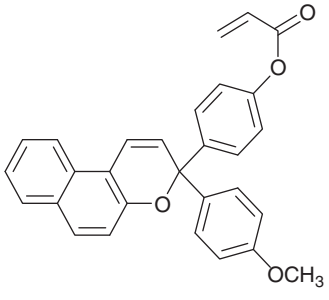

200 [257]

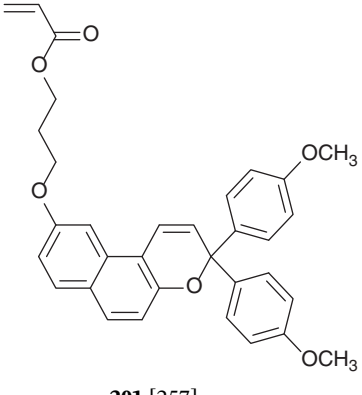

201 [257]

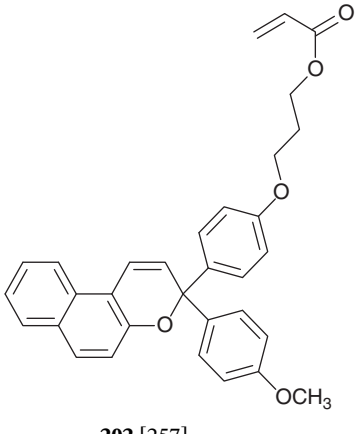

202 [257]

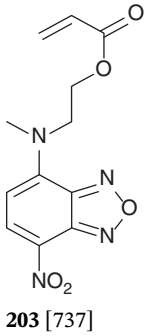

203 [737]

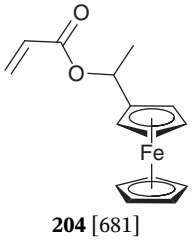

204 [681]

NAM (see Abbreviations), those listed in Table 8.13, and those in Table 8.16 (see Section 8.5.5, p 279).

8.5.2.3 Styrenics

Styrenic monomers subjected to dithiobenzoate-mediated RAFT polymerization include AcS, AMS, CMS, HMS, 4HS, MeS, PFS, SSO_3Na, St, *t*BDMSOS, *t*BOS,

Table 8.13 Acrylamide derivatives subjected to RAFT polymerization.

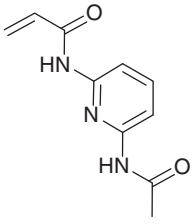

205 [119]

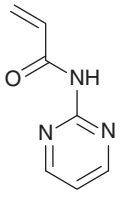

206 [120]

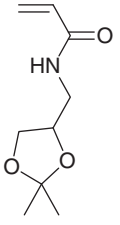

207 [401]

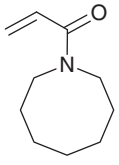

208 NAA

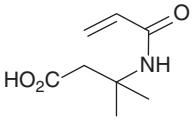

209 [738]

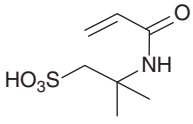

210
AMPS

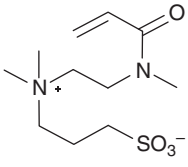

211

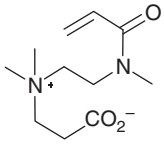

212

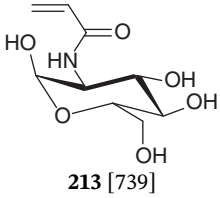

213 [739]

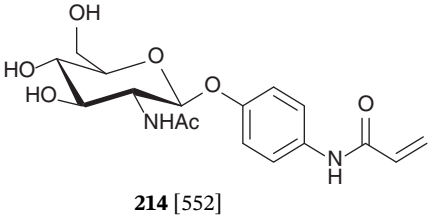

214 [552]

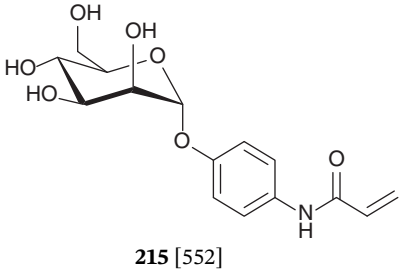

215 [552]

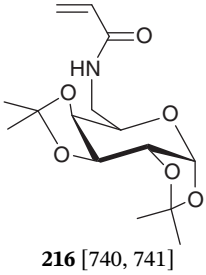

216 [740, 741]

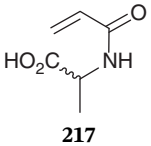

217

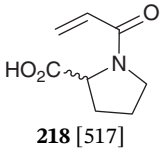

218 [517]

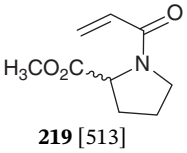

219 [513]

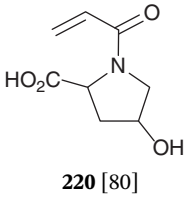

220 [80]

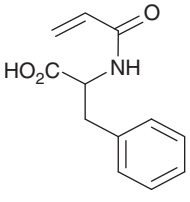

221 [519, 742]

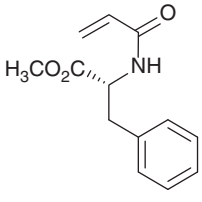

222

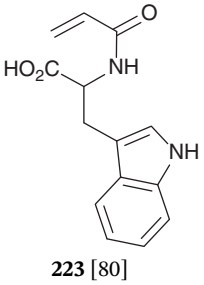

223 [80]

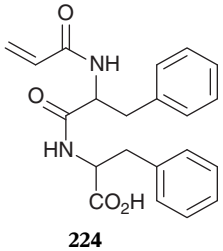

224

Table 8.14 Styrene derivatives subjected to RAFT polymerization.

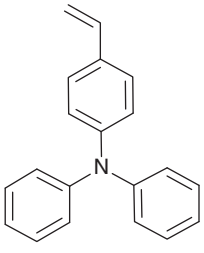

225 [141]

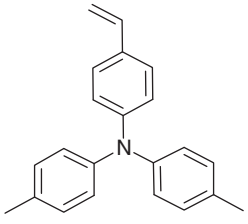

226 [141]

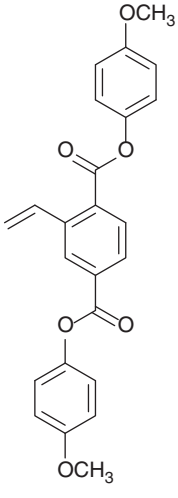

227

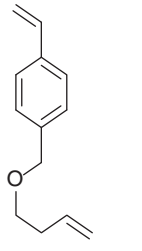

228 [140, 480]

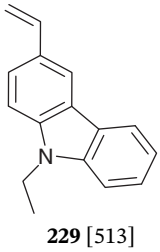

229 [513]

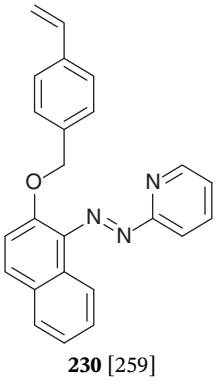

230 [259]

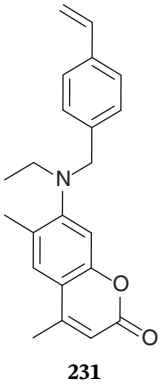

231

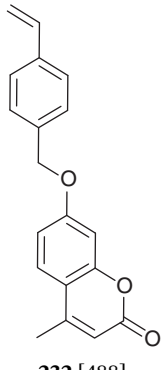

232 [488]

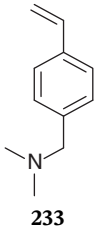

233

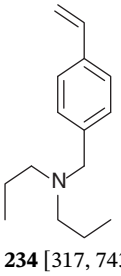

234 [317, 743]

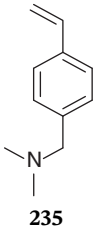

235

(*continued*)

Table 8.14 (Continued)

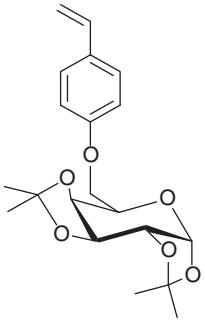

236 [523]

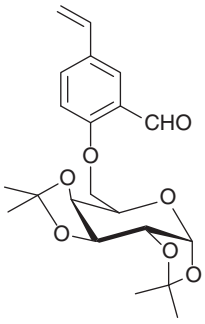

237 [487]

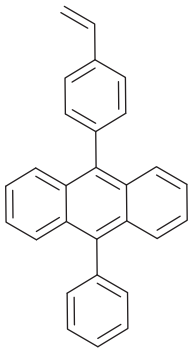

238 [235]

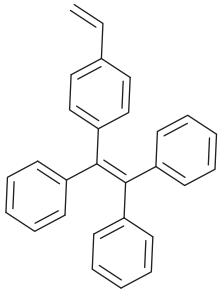

239

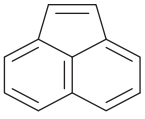

240 [235]
acenapthylene

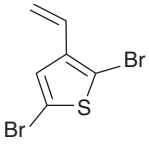

241

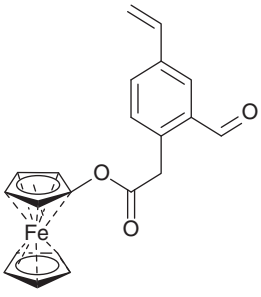

242 [232]

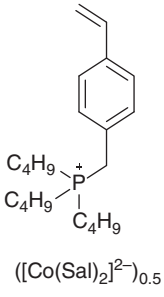

243 [163]

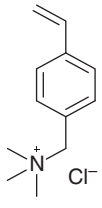

VBTAC
244

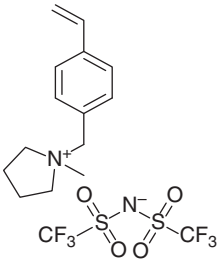

245 [744]

THPOS (see Abbreviations), those listed in Table 8.14, and those included in Table 8.16 (see Section 8.5.5, p 279). Rates of RAFT polymerization of styrenes are relatively slow and may be slower when mediated by aromatic dithioesters. Much has been written on the potential retardation mechanisms [7, 9, 22, 754].

8.5.2.4 Diene Monomers

RAFT polymerization of diene monomers generally requires a more active RAFT agent and the use of higher reaction temperatures to obtain good control and a reasonable rate of polymerization (e.g. 125 °C). RAFT homopolymerizations of Bd and Ip in solution are slow [755].

Table 8.15 Monosubstituted LAMs and IAMs (vinyl monomers).

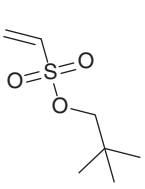

246 NES [532]

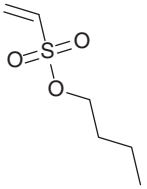

247 BES [532]

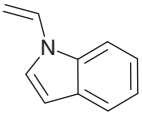

248 [745]

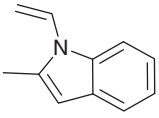

249 [745]

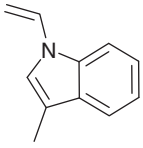

250 [745]

There are conflicting results for RAFT polymerization of Ip mediated by **6** at 120 °C, with one report indicating that the dithiobenzoate was unstable [238], and the other indicating reasonable control [239]. It was noted that low molar mass was targeted in the latter experiment. Another difference was the use of DCP vs. AIBN as initiator respectively.

8.5.3 1,2-Disubstituted MAMs

1,2-Disubsituted MAMs used in dithioester-mediated RAFT polymerization include MAH and the maleimide derivatives, NPMI, NEMI, NMMI, and NPrMI. These monomers are not used in homopolymerization but are used in RAFT copolymerization and in RAFT-SUMI (Section 8.10) to form end-functional polymers.

8.5.4 Monosubstituted IAMs and LAMs

The monosubstituted LAMs and intermediate activated monomers (IAMs), such as the vinyl esters (e.g. VAc), the *N*-vinyl amides and imides (e.g. NVP), the *N*-vinyl heteroaromatics (e.g. NVC, **248–250**), and the halo-olefins (e.g. VC) generally require the use of a RAFT agent more suited for those classes of monomers (usually a xanthate [756] or an appropriate dithiocarbamate [556, 757]).

Thus, substantial retardation is seen with the dithiobenzoates in the polymerization of VAc [458], BES, and NES [532], and the vinyl aromatics NVC [550] and **248**–**250** [745]. Intermediate radical termination is a likely cause of the retardation with these systems. However, poor R group selection may also be an issue. For example, benzyl radical is slow to add to LAMs (e.g. VAc, NVP) [758].

8.5.5 Monomers with Reactive Functionality

There is a need for processes for polymer modification after RAFT polymerization (the so-called polymer analogous reactions) that ideally proceed with quantitative yield under mild reaction conditions. The reactive functionality may be present on the Z or R groups of the RAFT agent (Section 8.3.2) or in the monomers. Monomers used in this context can be incorporated in blocks to serve as a precursor to a polymer brush, or they may be copolymerized to provide sites for the attachment

of functionality or for crosslinking. Examples of functional monomers used in dithiobenzoate-mediated RAFT polymerization are shown in Table 8.16, p 279.

Many papers are concerned with the combination of RAFT and azide–alkyne 1,3-dipolar cycloaddition. There are some issues with the use of azides and alkynes in radical polymerization, which extend to RAFT polymerization. Alkynes are not completely unreactive towards radicals. Thus, alkyne-functional monomers (Table 8.16(a)) are often protected as the silyl ether and used in that form. The azido group of azido-functional monomers (Table 8.16(b)) may undergo cycloaddition reaction with electron-deficient monomers (e.g. (meth)acrylates, acrylamides) and this may occur during polymerization [759]. The extent of this side reaction can be mitigated by the use of lower reaction temperatures and shorter reaction times.

Active ester monomers that have been subject to RAFT polymerization are shown in Table 8.16(c). Thialactones and azlactones, which are used similarly, are shown in Table 8.16(d). The active ester groups undergo facile reaction with primary or secondary amines. They may also react with alcohols, thiols, and other nucleophiles. A potential issue is that nucleophilic reagents may also react with dithioester groups. The rate of reaction of primary amines with active esters is generally more facile than that with a dithioester group to the extent that end-group removal is only observed when an excess of the amine is used.

Methacrylate ester **282** and acrylate **283** (Table 8.16(e)) also contain xanthate functionality. The xanthate functionality with 'R' = primary alkyl appears essentially inert as a RAFT agent during copolymerizations of MMA and *t*BA, respectively, mediated by **6**. The monomers were used as precursor to thiol functionality following transformation of the xanthate groups in the product copolymers.

Primary or secondary amine (or hydrazine) functionality is reactive towards dithioester functionality and must be protected during RAFT polymerization (Table 8.16(f)). Commonly the *tert*-butyloxycarbonyl (BOC) protecting group is used. However, simple protonation is also effective as a protection strategy.

Several papers have explored polymerization of monomers containing isocyanate functionality; see Table 8.16(h) [231, 390, 531]. RAFT polymerization and the thiocarbonylthio group are compatible with isocyanate functionality. However, some care must be taken in the selection of the RAFT agent to ensure that it does not contain any other functionality that is inherently reactive towards isocyanates (such as carboxy) [390].

It is possible to use monomers that contain initiator functionality for other forms of RDRP such as ATRP (Table 8.16(i)) or NMP (Table 8.16(j)) – refer also Section 8.11.

8.5.6 Macromonomers

RAFT polymerization of macromonomers provides a route to comb polymers and a method for including arms in stars. References to the use of the macromonomers shown in Table 8.17 in RAFT polymerization with dithioesters can be found in Table 8.4. The end-groups of macromonomers remote from the double bond

(*continued on page 287*)

Table 8.16 Monomers with reactive functionality.

(a) *Alkyne*

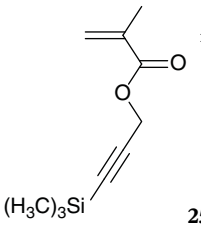

251 [103]

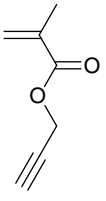

252 [218, 318]

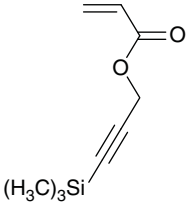

253 [746]

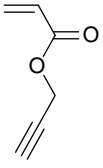

254
PA

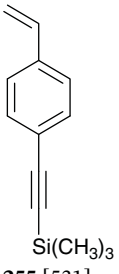

255 [531]

(b) *Azide*

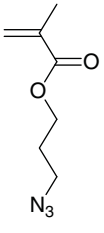

256 [465]

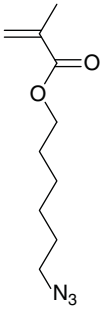

257 [219]

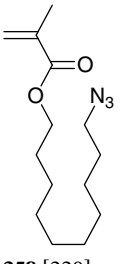

258 [220]

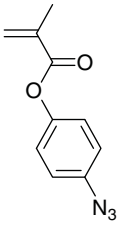

259 [747]

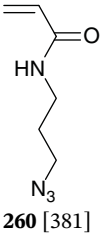

260 [381]

(c) *Active ester*

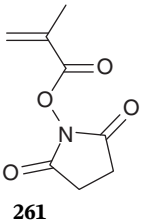

261
NMS

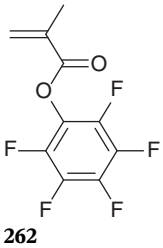

262
PFPMA [326–329]

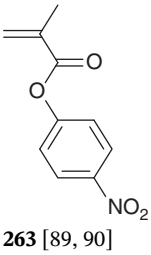

263 [89, 90]

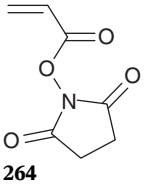

264
NAS [583]

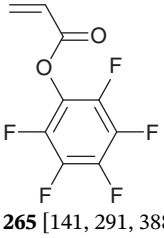

265 [141, 291, 388]
PFPA [329, 748]

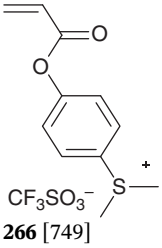

266 [749]

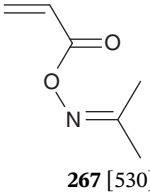

267 [530]

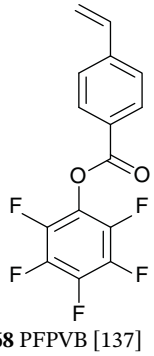

268 PFPVB [137]

(*continued*)

Table 8.16 (Continued)

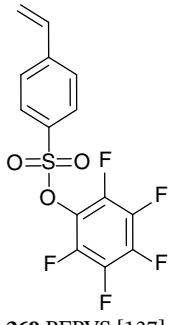

269 PFPVS [137]

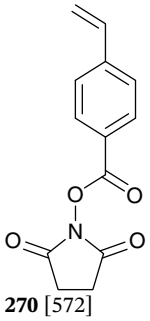

270 [572]

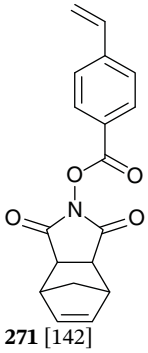

271 [142]

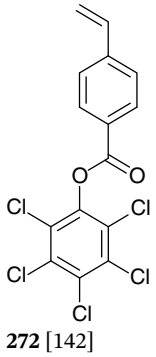

272 [142]

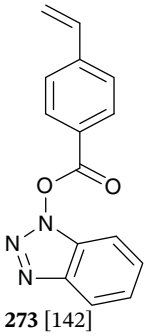

273 [142]

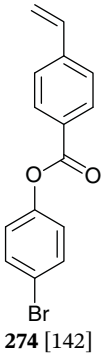

274 [142]

(d) *Thialactone, azlactone*

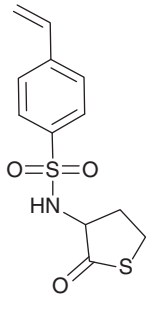

275

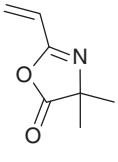

276

(*continued*)

(e) *Protected thiol (2-pyridyldisulfide, thioacetyl, xanthate)*

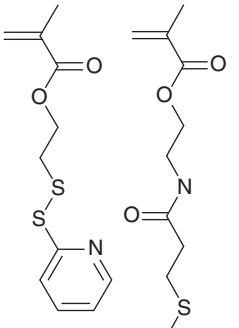

277

278

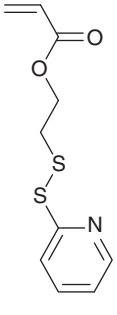

279

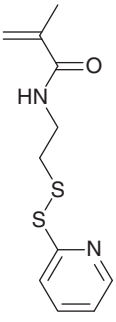

280

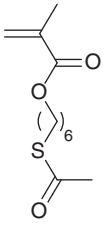

281

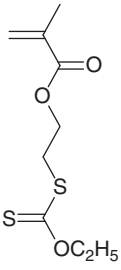

282

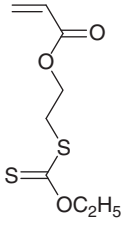

283

(f) *Protected amine or hydrazide*

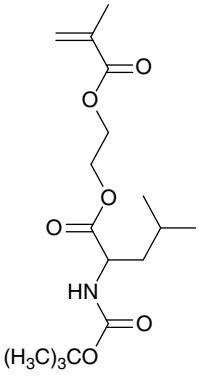

284

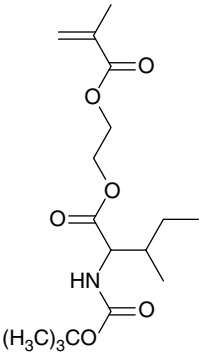

285

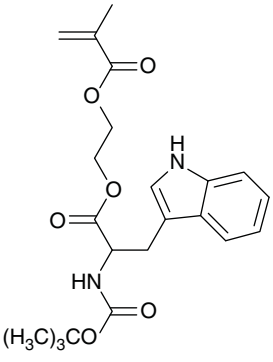

286

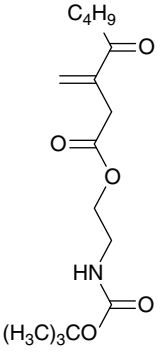

287a R = C_3H_7
287b R = C_4H_9

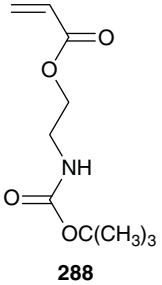

288

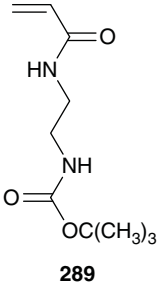

289

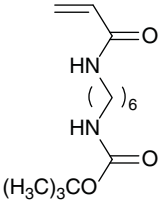

290

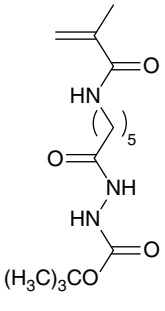

291

(*continued*)

Table 8.16 (Continued)

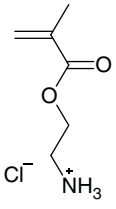

292 AEMA

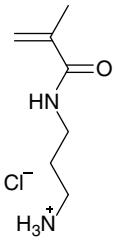

293 APMAm

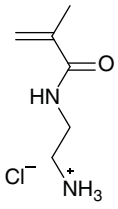

294 AEMAm

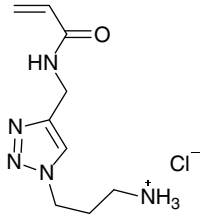

295 [384]

(g) *Silyl ether*

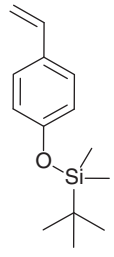

296 *t*BDMSOS

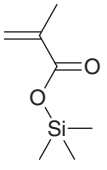

297

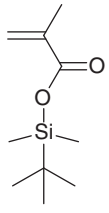

298 *t*BDMSMA

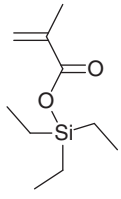

299

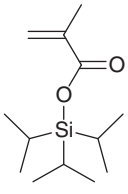

300 TPSiMA

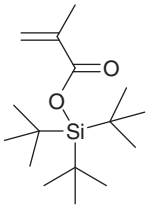

301

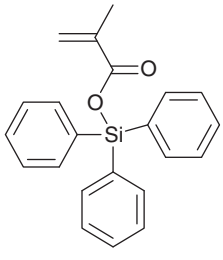

302

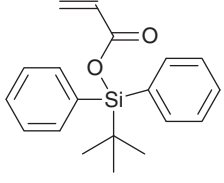

303

(h) *Isocyanate or isothiocyanate*

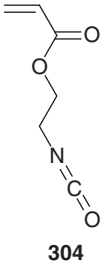

304

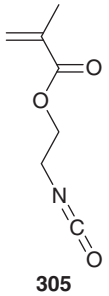

305

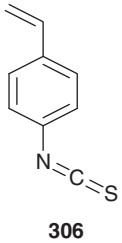

306

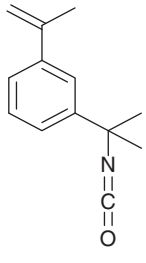

307

(*continued*)

Table 8.16 (Continued)

(i) *ATRP initiator*

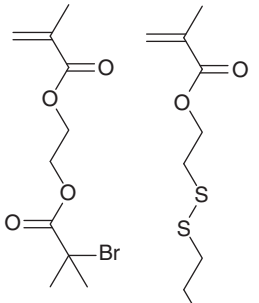

308

309

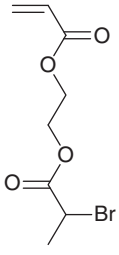

310

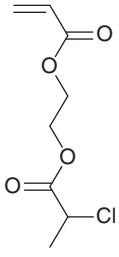

311

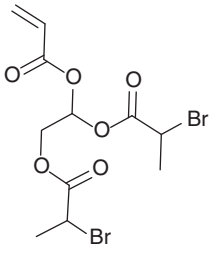

312

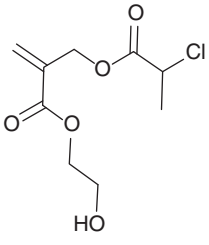

313

(j) *NMP initiator*

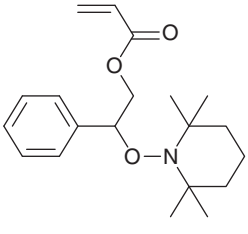

314

Table 8.17 Macromonomers subjected to RAFT polymerization.

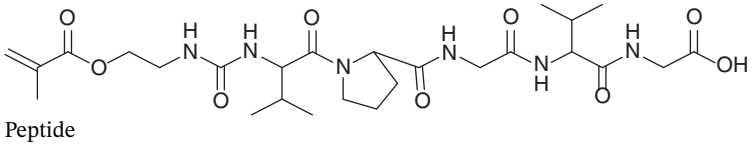

Peptide macromonomer
315

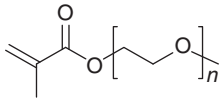

PEGMA (MPEGMA)
316

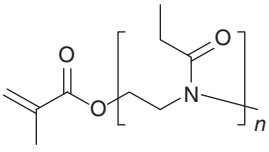

Poly(2-ethyl-2-oxazoline) macromonomer [274]
317

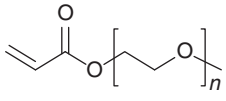

PEGA (MPEGA)
318

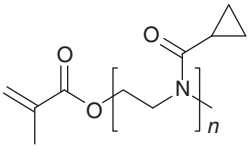

Poly(2-cyclopropyl-2-oxazoline) macromonomer [221]
319

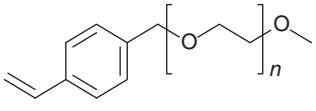

PEG macromonomer
320

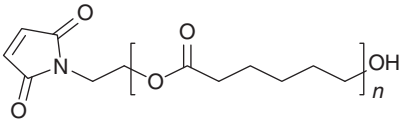

PCL macromonomer
321

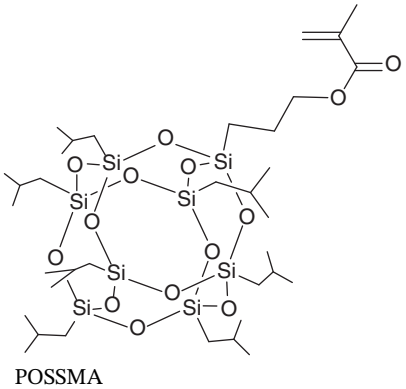

POSSMA
322

(*continued*)

Table 8.17 (Continued)

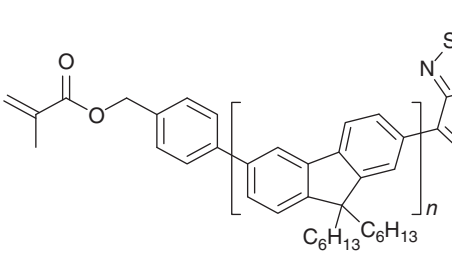	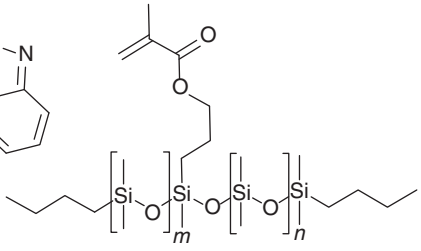
Polyfluorene macromonomer [158] **323**	PDMS macromonomer **324**

(*continued from page 280*)

are often not explicitly specified. Those based on poly(ethylene glycol) (PEG) (e.g. **316**-**320**) are almost invariably the monomethyl ether but in a few cases, may be the monoethyl ether or simply hydroxy.

8.6 Cyclopolymerization

Examples of monomers used in dithioester-mediated RAFT cyclopolymerization or cyclocopolymerization are provided in Table 8.18 (p 288). Details of the RAFT agents used will be found in Table 8.4. There appear to be no specific constraints on cyclopolymerization imposed by the RAFT process.

Dithiobenzoates are not generally suitable for mediating the polymerization of ketene acetals, which are LAMs. However, RAFT copolymerizations of **339** and BMDO (**340**) with methacrylates are controlled [61].

Monomers such as DEGMA or DSDMA (**344**) do not undergo efficient cyclopolymerization. However, RAFT crosslinking copolymerizations with DEGMA or DSDMA (**344**) have been explored to ascertain the extent of the intermolecular branching and intramolecular cyclization (cyclopolymerization) that occur [283, 760].

8.7 Ring-Opening Polymerization

RAFT ring-opening polymerization provides a simple method of forming polymers with readily cleavable linkages, i.e. esters, thioesters, and/or disulfides, into the carbon–carbon backbone of a polymer chain (Table 8.19) [475]. The monomers **331**–**335** were copolymerized with MMA, DMAm, and HEMA.

Dithiobenzoates are not generally suitable for mediating the polymerization of ketene acetals, which are LAMs. However, RAFT copolymerizations of **339** and BMDO (**340**) with methacrylates are controlled [61].

Table 8.18 Monomers used in experiments on dithioester-mediated RAFT cyclopolymerization.

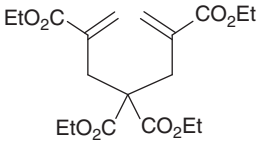

325 [143]

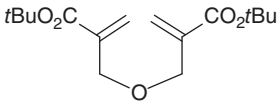

326 [108]

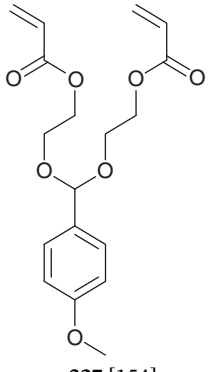

327 [154]

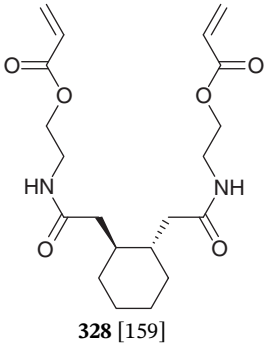

328 [159]

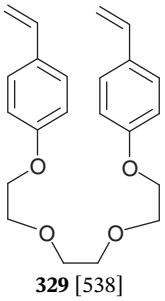

329 [538]

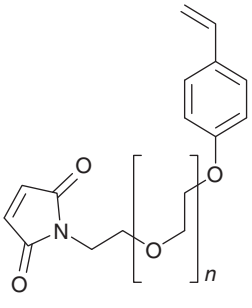

330 [144]

8.8 RAFT Crosslinking Polymerization

Crosslinking monomers are used both in the synthesis of hyperbranched polymers (sometimes called microgels) and polymer networks. Crosslinking monomers include DEGDMA, EGDMA, TEGDMA, EGDA, HDDA, TEGDA, MBAm, and DVB and the multiolefinic monomers in Table 8.20. Use of monomers such as **343**, with an acetal linkage, or **344**–**346**, with disulfide linkages, results in the formation of degradable crosslinks, which can be important in controlled release applications. The crosslinks can also be cleaved to allow for polymer analysis.

Use of a macroRAFT agent to mediate RAFT crosslinking polymerization provides a mechanism for forming arm-first stars. The use of the hyperbranched polymers formed by RAFT crosslinking polymerization to mediate further RAFT polymerization provides core-first stars. Details of these processes are provided in the Chapters by Floyd et al. [767] and Allison-Logan et al. [673] Examples of both processes are included in Table 8.4 and are indicated by purple highlighting.

Model co-networks, so called because the distance between crosslinks is relatively well defined, can be formed by RAFT crosslinking polymerizations mediated by a

Table 8.19 Monomers used in experiments on dithioester-mediated RAFT ring opening polymerization.

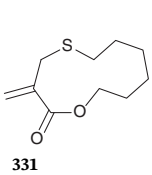

331

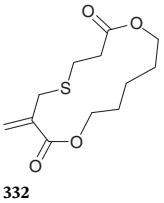

332

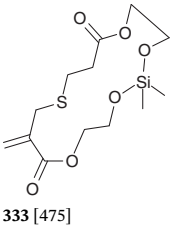

333 [475]

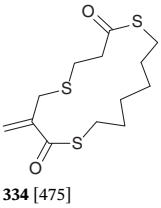

334 [475]

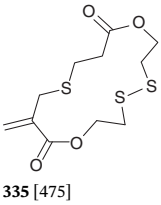

335 [475]

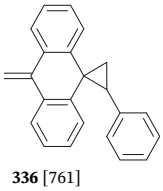

336 [761]

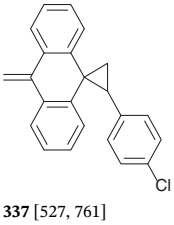

337 [527, 761]

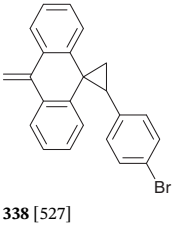

338 [527]

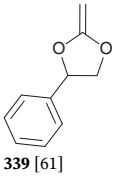

339 [61]

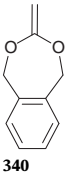

340
BMDO

Table 8.20 Crosslinking monomers.

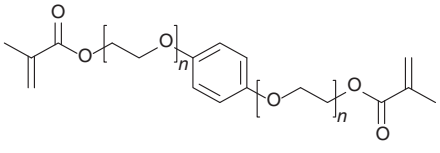

341 [762]

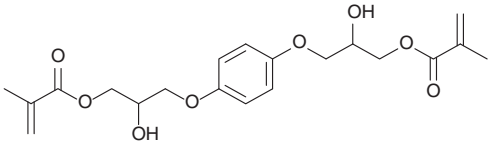

342 [762]

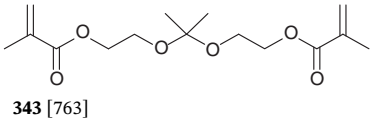

343 [763]

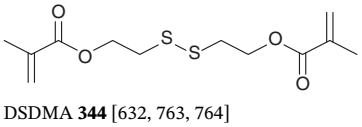

DSDMA **344** [632, 763, 764]

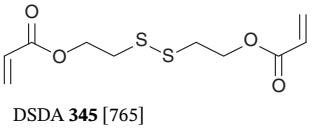

DSDA **345** [765]

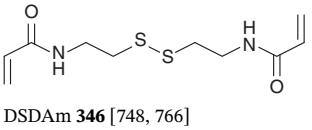

DSDAm **346** [748, 766]

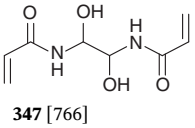

347 [766]

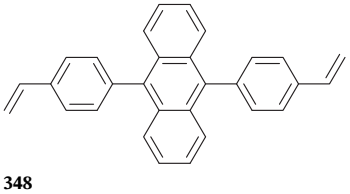

348

Table 8.21 Preparation of model co-networks by RAFT polymerization with 'R'-connected bis-macroRAFT agents.

Initial RAFT Agent	Monomers	X-linker[a)]	Comment	Application	References
56	BMA DMAEMA	EGDMA	bis-MacroRAFT agent prepared in first step	Model co-networks	[768]
56	BA BMA DMAEMA St	EGDMA	bis-MacroRAFT agent prepared in first step	Model (co)networks	[652]
56	TFEMA DMAEMA	EGDMA	bis-MacroRAFT agent prepared in first step	Model (co)networks	[654]
56	DMAEMA MAA	EGDMA	bis-MacroRAFT agent prepared in first step	Model (co)networks	[769]
60	MMA BA St	EGDMA EGDA	bis-MacroRAFT agent prepared in first step	Model (co)networks	[660]
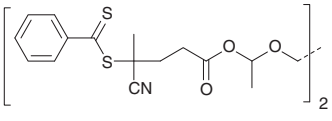	DMAEMA MMA	EGDMA	bis-MacroRAFT agent prepared in first step	Model (co)networks with hydrolytically degradable crosslinks	[644]

a) Crosslinker.

bis-macroRAFT agent [644, 652, 654, 660, 768, 769]. Examples of co-networks made using bis-dithiobenzoates are shown in Table 8.21.

8.9 RAFT Self-condensing Vinyl Polymerization

RAFT self-condensing vinyl polymerization provides a method of preparing dithioester-functional hyperbranched polymers that can be precursors to core-first star polymers. The topic has been reviewed [770, 771] and details of the process are covered in the Chapters by Floyd et al. [767] and Allison-Logan et al. [673] Examples of dithioester RAFT monomers (sometimes called inimers) are shown in Table 8.22 (p 293). These polymerizations comprise copolymerization of the RAFT monomer to form a hyperbranched structure. A second RAFT step or 'block synthesis' then results in adding arms to produce a core-crosslinked star.

There are two forms of hyperbranched core that can be formed depending on whether the double bond of the inimer RAFT agent is located on 'Z' or 'R'. Most inimer RAFT agents (**349–352**, Table 8.22) possess a double bond as part of the homolytic leaving group R. When the double bond is on 'Z' (as in **353**), dithioester group cleavage should provide a linear polymer [644]. The RAFT agents **350a** and **b** contain a cleavable disulfide linkage that also enables the hyperbranched core to be decomposed.

8.10 RAFT-Single-Unit Monomer Insertion (RAFT-SUMI) into Dithioesters

RAFT-SUMI into trithiocarbonates and dithiobenzoates was originally developed as a method of synthesizing functional RAFT agents or macroRAFT agents. The topic has been reviewed by Xu [772] and Haven et al. [773]. See also the chapter in the present volume on sequence-encoded RAFT oligomers and polymers [774].

Successful SUMI requires a RAFT agent with C_{tr} such that, on average, there is $\ll$1 monomer inserted per activation cycle (i.e. $k_p[M] \ll k_{tr}[\text{RAFT agent}]$) and is facilitated by $k_i \gg k_p$, by $k_\beta \gg k_{-add}$, (refer to Scheme 8.1), and by low relative monomer concentrations (i.e. stoichiometric with RAFT agent). These same factors are responsible for the selective initialization phenomenon first reported by McLeary, Klumperman, and coworkers and appear general for RAFT polymerization with more effective RAFT agents (those with high C_{tr}). They reported data for dithiobenzoates **5** and **6** with St [775, 776], St/MAH [155], and MA [113]. Similar findings were reported by Moad et al. [128], who found selective initialization in St polymerization with dithiobenzoates **5** and **6** (where R is cumyl or 2-cyanoprop-2-yl, respectively) but not with **22** (R is benzyl). The finding was attributed to the much lower C_{tr} of **22** in St polymerization that allows multiple additions of St in an activation cycle. It was also shown that selective initialization is, not unexpectedly, favoured by a high RAFT agent/monomer ratio [128].

Table 8.22 RAFT monomers for self-condensing vinyl polymerization.

RAFT monomer	Synthesis[a)]	Polymerizations[b)]
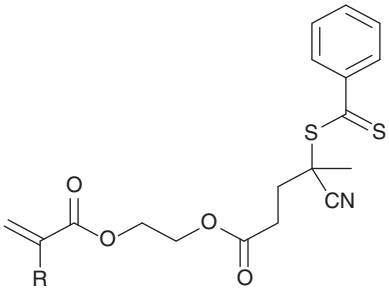 **349** a R = CH_3 b R = H	**a** [630, 631]	**349a**/St [630] **349a**/**130** [631]
	b [631]	**349b**/**216** [631]
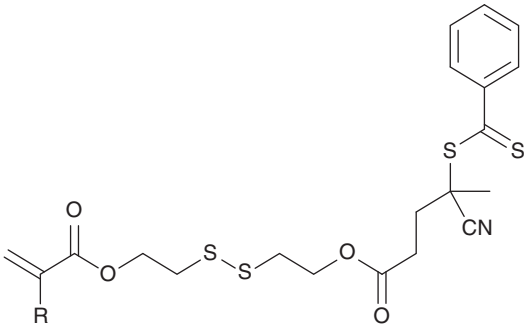 **350** a R = CH_3 b R = H	**a** [632]	**350**a/DMAEMA [632] **350**a/GMA/copolymer [633] **350**a/GMA/copolymer-*b*-GPMA/MPEGMA [633]
	b [634]	**350b**/GMA [635] **350b**/GMA/MPEGMA [636] **350b**/GMA/MPEGMA-*b*-MPEGMA [636] **350b**/**320**/**321** [634]
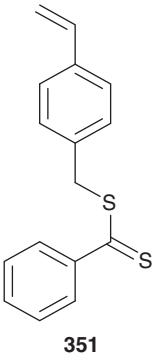 **351**	A [637]	**351**/AA [638] **351**/St [637, 639] **351**/DMAEA [640]

(*continued*)

Table 8.22 (Continued)

RAFT monomer	Synthesis[a)]	Polymerizations[b)]
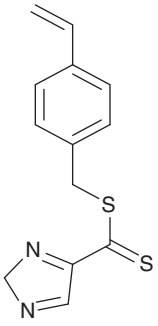 **352**	A [641]	**352**/NIPAm [641, 642] **352**/NIPAm/**79** [642, 643] **352**/NIPAm/**79**/**126** [643] **352**/NIPAm-*b*-**79** [642]
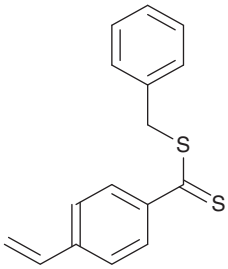 **353**	A [644, 645]	**353**/St [644, 645] **353**/4VP [644] **353**/2VP [644] **353**/St-*b*-4VP [644] **353**/St-*b*-2VP [644] **353**/4VP-*b*-St [644] **353**/2VP-*b*-St [644]

a) Refer Section 8.4.
b) Homopolymers and statistical copolymer will typically be hyperbranched. For A-*b*-B block copolymers, block A will be a hyperbranched core and block B will be the arms of core-first stars.

The SUMI process is simplified with the use of monomers that either do not propagate or are slow to propagate. The SUMI of MAH has been used for end-functionalization of PSt prepared with **17** [486], or PMMA-dithiobenzoate prepared with **5** [71], with a succinic anhydride unit (Scheme 8.6).

In 2004, Chen et al. [233] applied SUMI in the synthesis of light-harvesting polymers when they prepared new dithiobenzoate macroRAFT agents by selectively inserting a single unit of various styrene derivatives.

A complication in SUMI initiated with an added initiator is the formation of products from the reaction of the initiator-derived radicals with the monomer. One way of resolving this problem is to ensure that the initiator-derived radicals are identical to the RAFT agent 'R' group [172, 777]. This is the case for a first SUMI step when a dialkyldiazene of structure R—N=N—R is used as the initiator. The issue can also be resolved by the use of SUMI with direct photoinitiation or PET-RAFT-SUMI when radicals are generated directly from the precursor RAFT agent [367]. Xu et al. [367]

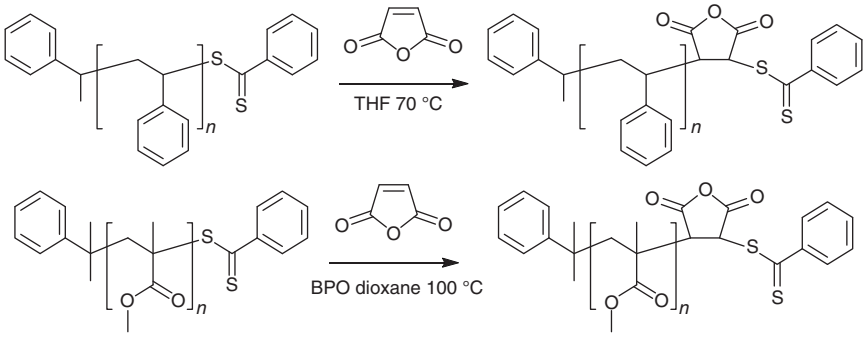

Scheme 8.6 Examples of chain-end functionalization by RAFT-SUMI of MAH into a dithiobenzoate macroRAFT agent.

have demonstrated selective PET-RAFT-SUMI for insertion of St, BA, MA, DMAm, and NIPAm into dithiobenzoate **9**.

8.11 Dithioesters in Mechanism-Transformation Processes

Block, star, or graft copolymers comprising segments formed by RAFT and other processes (other RDRP, RDP, living polymerizations) can be combined through the use of dual initiator-RAFT agents [778–780] and/or through the use of orthogonally reactive monomers, which enable such functionalities to be combined in situ. The term RAFT-*T*-'process' (RAFT first) or 'process'-*T*-RAFT (other process first) was coined [778] to describe such processes, where *T* is short for transformation. We do not focus on examples (of which there are many) of transformation of end-functional polymers to polymers with dithioester functionality by end-group modification or where RAFT-synthesized polymers are linked to other end-functional polymers in this section.

Dithioester-mediated RAFT polymerization can often be successfully conducted in the presence of the initiator functionality used in other RDRP methods (e.g. alkoxyamines for NMP, alkyl halides for ATRP). However, the high reactivity of dithiobenzoates in radical polymerization means that the converse is seldom true.

8.11.1 Ring-Opening Polymerization (ROP)

Hydroxy-functional dithioesters (e.g. **25–28**) allow sequential or, in a few cases, simultaneous hydroxy-initiated ring-opening polymerization (ROP) and dithioester-mediated RAFT polymerization. Examples of ROP-*T*-RAFT (ROP step first) and RAFT-*T*-ROP (RAFT first) are shown in Table 8.5 (p 251).

There are also many examples in the literature of the use of end functional polymers, which are converted to a macroRAFT agent to form a block copolymer by

RAFT polymerization. Examples include the PDMS macroRAFT agents **49** and **50** (Table 8.5), where the PMDS can be formed by ROP of a cyclic siloxane, and PEG macroRAFT agents, where the PEG might be formed by ROP of ethylene oxide but is most often obtained commercially.

8.11.2 Ring-Opening Metathesis Polymerization (ROMP)

Many of the 1,2-disubsituted olefins commonly used as monomers for ROMP appear inert under the conditions used for RAFT polymerization. Thus, dithiobenzoates can contain a norbornene group (**45**, Table 8.5), and the RAFT-synthesized polymers formed with these RAFT agents can be used as a precursor to brush polymers by ROMP in a RAFT-*T*-ROMP process [607–609]. ROMP-*T*-RAFT (ROMP first) making use of dithioester **46** has also been described [611].

8.11.3 Atom Transfer Radical Polymerization (ATRP)

Many RAFT agents have been used as pseudo-halides in ATRP. There are also examples of photo-redox processes or PET-RAFT involving dithioesters, which can be considered under the umbrella of RAFT-*T*-ATRP. Some of these are mentioned in Section 8.14.

ATRP initiators can be converted to RAFT agents by activation in the presence of a bis-dithioacyl disulfide. This process is an example of Method C (Section 8.4) [438, 781]. The process has been applied both in the synthesis of low molar mass RAFT agents and for the transformation of ATR-synthesized polymers into macroRAFT agents. The process has been called atom transfer radical addition–fragmentation (ATRAF). For dithioesters, the reported yields are generally high (82–92%) [438, 781], but lower yields were observed for dithiocarbamate (65%) and xanthates (43%) [438].

ATRP (alkyl halide) initiators (and ATRP conditions for activation) can also be used to initiate dithioester-mediated RAFT polymerization. In this, the RAFT agents or macroRAFT agents may also act as pseudo-halide ATRP initiators; the precise mechanism of the concurrent ATRP/RAFT process is not always clear [782].

In the absence of an ATRP activator or catalyst, ATRP alkyl halide initiators are typically inert. Thus, RAFT polymerization can be used to form polymeric architectures containing ATRP initiator functionality, which can subsequently be activated by addition of the ATRP activator. For example, graft (bottlebrush) and star polymers were prepared by RAFT-*T*-ATRP. The process involved RAFT polymerization to form a polymer based on the monomer bearing pendant ATRP initiator functionality, which was subsequently used in growing arms on the RAFT-synthesized core/backbone. Examples of monomers containing ATRP initiator functionality (sometimes known as ATRP inimers) are provided in Table 8.16(i) and examples of their use appear in Table 8.4. For clarity of mechanism and to ensure product purity, it may be desirable to remove the RAFT end-group before commencing the ATRP step.

8.11.4 Nitroxide-Mediated Polymerization (NMP)

Various processes for implementing RAFT-*T*-NMP have been described [778–780]. The ESARA process (Exchange of Substituents between [macro]Alkoxyamines and [macro]RAFT Agents) [579] allows exchange of homolytic leaving groups between alkoxyamines and (macro)RAFT agents; the pathways are illustrated in Scheme 8.7 for the case of formation of a PSt–SG1 macro-alkoxyamine from the macroRAFT agent PSt–DB. The radical derived from the initial alkoxyamine [$(CH_3)_2\dot{C}(CO_2H)$ – MAMA] must be able to displace the PSt R group of the macro-RAFT agent. The desired outcome is favoured by choosing a temperature such that the initial alkoxyamine (MAMA–SG1) is labile (i.e. undergoes reversible C—O bond homolysis) and the product alkoxyamine (PSt-SG1) is stable. The kinetics of the cross-reaction between alkoxyamines and dithioesters has been studied by He and coworkers [783, 784].

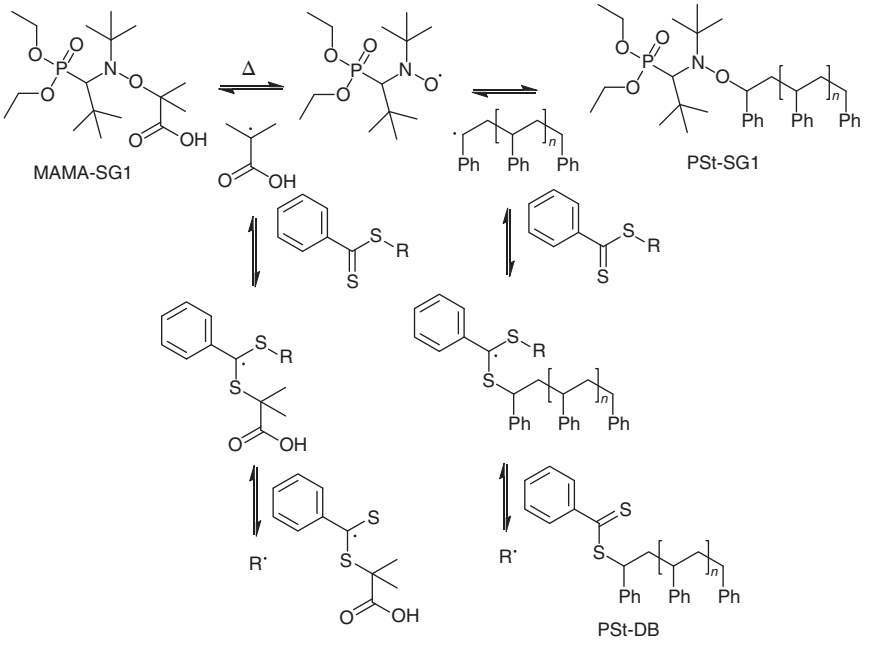

Scheme 8.7 Potential reaction pathways during an ESARA process used to form a macro alkoxyamine (PSt–SG1) from a macroRAFT agent (PSt–DB).

The one-way transformation of an alkoxyamine NMP initiator to a dithiobenzoate RAFT agent by heating the NMP initiator with dibenzoyl disulfide has been also been demonstrated [785].

Dual RAFT agent/NMP-initiators can be synthesized directly or formed in situ by RAFT copolymerization of an NMP inimer (e.g. **314**, Table 8.16(j)) [786, 787].

8.12 Thermally Initiated RAFT Polymerization with Dithioesters

RAFT polymerization requires a source of free radicals. Historically, this has taken the form of an added thermal initiator, most often a dialkyldiazene. The use of dialkyldiazenes in RAFT polymerization has been described in a recent review [8]. However, in principle, almost any radical source might be used. Thus, radicals might be generated thermally from an added initiator, the monomer, or the RAFT agent, by UV–visible irradiation, electrochemically, or by any other process.

Two important considerations to bear in mind in choosing a radical source are that (a) the initiator-derived radicals, when different from the RAFT agent 'R' radical, will limit the end group fidelity since there will be a mixture of initiator-derived and RAFT agent-derived chain-ends formed, and (b) for every radical generated by initiation, one must ultimately be consumed whether by termination, initiator inefficiency or some other process.

When using an added thermal initiator, it is possible to estimate the maximum fraction of living chains (L) using expression (8.5) or (8.6) [6].

$$L = \frac{[\mathrm{RAFT}]_0}{[\mathrm{RAFT}]_0 + df\left(\left[\mathrm{A_2}\right]_0 - \left[\mathrm{A_2}\right]_t\right)} \tag{8.5}$$

$$= \frac{[\mathrm{RAFT}]_0}{[\mathrm{RAFT}]_0 + df\left[\mathrm{A_2}\right]_0\left(1 - e^{-k_\mathrm{d}t}\right)} \tag{8.6}$$

where $[\mathrm{RAFT}]_0$ is the initial transfer agent concentration, $df\left(\left[\mathrm{A_2}\right]_0 - \left[\mathrm{A_2}\right]_t\right) = df\left[\mathrm{A_2}\right]_0\left(1 - e^{-k_\mathrm{d}t}\right)$ is the number of initiator derived chains, d is the number of chains produced in a radical–radical termination event ($1 < d < 2$, e.g. $d \sim 1.67$ in MMA and $d \sim 1.2$ in styrene polymerization [788]), f is the initiator efficiency ($0 < f < 1$), $[\mathrm{A_2}]_0$ is the initial initiator concentration, k_d is the rate coefficient of initiator disappearance, and t is the reaction time.

A guideline for achieving control proposed in the first RAFT patent [5, 143] was that conditions should be chosen such that the amount of initiator decomposed was <10 mol% of the amount of RAFT agent. This would ensure an end-group fidelity of >80% and most likely >90%, depending on the initiator efficiency and the mode of termination.

It is important that the initiator-derived radical is a good homolytic leaving group with reference to the R group of both the initial RAFT agent and the product macroRAFT agent; otherwise, the RAFT agent can be converted to a relatively stable 'by-product'. For example, AIBMe was found to be a poor initiator choice in MMA polymerization [64] mediated by dithioester **6** since the initiator-derived RAFT agent (**11b**) has a low transfer coefficient both with respect to **6** and the PMMA macroRAFT agent [64]. The initiator-derived RAFT agent **11b** was observed to accumulate during the experiment.

Most peroxide initiators can be successfully used in RAFT polymerization with dithioesters as long as conditions are such that the initiator-derived radicals react with monomer rather than with the RAFT agent. Rate coefficients k_i for

oxygen-centred radicals adding to monomer [758, 789] are typically substantially higher than those for tertiary alkyl radicals adding to monomer [790].

8.13 Photoinitiated RAFT with Dithioesters

RAFT photoinitiation was foreshadowed and claimed in the first RAFT patent in 1998 [143]. However, this document contained no examples of photoinitiation whether direct or with the use of photoinitiators. A process equivalent to photo-SUMI (into xanthates) was first reported by Delduc et al. [791] in 1988. For additional information on photoinitiated RAFT processes making use of dithioesters, the reader is referred to the chapter of Chapman et al. [792] and other recent reviews [793]. Examples of photoinitiated RAFT polymerization and photo-SUMI are indicated in Table 8.4 (entries in Red and **Bold Orange**, respectively).

Dithioesters have been used in photoinitiated RAFT polymerization. The $\pi \rightarrow \pi$ transition appears at ~295 nm ($\varepsilon \sim 15\,000$). The forbidden $n \rightarrow \pi$ transition for primary and secondary dithioesters appears at ~510 nm ($\varepsilon \sim 100$) and is red-shifted to ~530 nm for tertiary dithioesters [794]. The use of direct photoinitiation or PET-RAFT appears to give less by-products than conventionally initiated (with a thermal initiator) RAFT polymerization. Additionally, the use of visible light irradiation (excitation of the $n \rightarrow \pi$ transition) appears to result in fewer issues than does the use of UV light [66, 795–797]. This is attributed to a lower incidence of side reactions. However, the specific side reactions have not been defined and it is not clear whether the process is more selective for the desired C—S bond scission (Scheme 8.8) or whether higher selectivity is simply a consequence of lower radical concentrations. The occurrence of termination will lead to an excess of ZC(=S)S radicals, which may retard radical generation.

Initiation

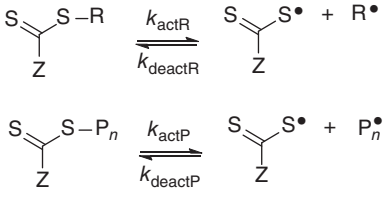

Scheme 8.8 Mechanism for initiation of RAFT polymerization without an exogenous initiator.

The mechanism for radical generation by direct photoinitiation is described by the two reactions shown in Scheme 8.8. As with systems with an exogenous initiator (Scheme 8.1), termination occurs at a rate dictated by the radical concentration. While it might be considered that reversible deactivation steps shown in Scheme 8.8 could, by themselves, provide a mechanism for control (one analogous to Otsu's iniferter process [798]), to achieve low dispersities at low conversions, the dominant

control mechanism must be RAFT. The use of photoinitiation does not turn off the activity of dithioesters as RAFT agents.

At least four forms of photoinitiated RAFT polymerization should be considered: (i) polymerizations conducted in the presence of an added photoinitiator; (ii) direct photoinitiation when the dithioester dissociates into radicals by photocleavage of the C—S single bond; and PET (photo-induced energy or electron transfer) RAFT that might involve either (iii) photosensitization or a (iv) photo-redox process. Examples of photoinitiated RAFT polymerization are highlighted in the Table 8.4. However, we do not distinguish the form of photoinitiation there. Catalysts used in PET-RAFT of MMA with dithiobenzoate **9** include $Ru(bpy)_3Cl_2$ [304], $Ir(ppy)_3$ [304], and Eosin-Y [305] with blue light, ZnTPP with yellow light [799], and TPP [306] and ZnTPP [306] with red light (refer Table 8.4).

8.14 Redox-Initiated RAFT with Dithioesters

In this section, we consider RAFT polymerization initiated by a redox process involving the RAFT agent. We do not consider RAFT polymerization initiated by redox initiators. The redox properties of dithioesters and redox/electrochemical initiation are detailed in the chapter by Lorandi et al. [800] and so a detailed discussion will not be given in this chapter. The electrochemical behaviour of dithioesters is described by Strover et al. [801].

Examples of redox-RAFT are identified in Table 8.4 (entries in Green). At least two forms of direct redox-initiated RAFT can be distinguished, (i) where the RAFT agent behaves as a pseudo-halide in an ATRP-type mechanism [76, 77, 423, 425, 802], and (ii) involving electron transfer to the RAFT agent with formation of a radical anion intermediate. The latter process has been called dissociative electron-transfer RAFT polymerization (DET-RAFT) [296, 803].

A report of 'ATRP' of MMA mediated by Cu(II) dithiobenzoate as activator, PMDETA as ligand, and with AIBN initiator at 100 °C should also be considered here [804]. In this and many other cases, the mechanism has not been fully established [415, 805].

8.15 Reaction Conditions and Side Reactions of Dithioesters

The mechanism of RAFT with dithioesters and other RAFT agents and complicating side reactions have been briefly mentioned above and are described in greater detail in the chapters by Buback [21] and Quinn et al. [22] Some specific situations have been discussed elsewhere in this chapter.

Low conversion initiator efficiencies in RAFT polymerization appear to be the same as in conventional radical polymerization [128]. Conversion plateaus, where the conversion of monomer to polymer reaches a limiting value, are sometimes observed in RAFT polymerization. These can have a number of causes, which

include decomposition of the RAFT agent (or other species) during polymerization to form compound(s) that inhibit polymerization (for dithioester examples see [9, 806, 807]), exhaustion of the initiator, and reduced initiator efficiencies at high monomer conversions.

It is known that initiator efficiencies for dialkyldiazenes reduce dramatically with conversion for higher monomer conversions [8]. This can cause rates of initiation drop to near zero at high monomer conversion. Polymerization cannot then be continued and cannot be simply restarted by addition of further initiator. Conversion plateaus in RAFT polymerization may, in part, be attributed to the fact that dialkyldiazenes are the most commonly used initiators.

Although many RAFT polymerizations can be carried out in the presence of air to still yield low-dispersity polymers, they, nonetheless, show sensitivity to air and it is clear that rigorous degassing is critical in any study of RAFT polymerization kinetics [6, 9]. Depending on the monomer and the particular RAFT agent, the presence of air can cause retardation, an inhibition period, and/or loss of RAFT agent, all of which can lead to the degree of control being reduced. RAFT polymerization mediated by aromatic dithioesters such as dithiobenzoates may be more air sensitive than that with most other RAFT agents (e.g. aliphatic dithioesters, trithiocarbonates) because of the longer lifetimes of the intermediate radicals.

8.16 RAFT Emulsion/Miniemulsion Polymerization Mediated by Dithioesters

Examples of heterogeneous polymerization are identified in Table 8.4 (entries in *Blue*). RAFT emulsion polymerizations commencing with low-molar mass dithioesters were first reported by CSIRO in the initial RAFT papers [5, 48] and patents [143]. The reported processes were starved-feed (also known as semi-batch) emulsion polymerizations and successfully provided low-dispersity polymers (e.g. $Đ_m < 1.2$). The conditions used were similar to those successfully used in forming low-dispersity block polymers with the so-called macromonomer RAFT agents [808, 809]. The starved-feed protocol was used because initial attempts to form low-dispersity polymers by *ab initio* batch emulsion RAFT polymerization with dithiobenzoates had failed [9].

Monteiro and coworkers studied RAFT emulsion polymerization in greater depth and found that the direct use of more active RAFT agents (in particular, cumyl dithiobenzoate, **5**) in a batch *ab initio* process was generally unsuccessful and the polymerizations were characterized by substantial retardation or inhibition, poor latex stability, and broad or multimodal molar mass distributions. Luo and Cui [810] proposed an explanation for the lack of success in RAFT emulsion polymerization with dithioesters in terms of 'super swelling' caused by the presence of the high concentrations of short oligomers that are formed early in the polymerization, which is characteristic of an efficient RDRP. They found that the problem could be mitigated, though not fully resolved, through the use of very high concentrations of conventional surfactants and/or by the use of non-ionic surfactants [701].

Several groups reported that less active (low transfer constant) RAFT agents such as the aliphatic dithioesters, **68**, **69**, or **75**, could be used to conduct a successful batch *ab initio* emulsion polymerization [698, 811]. This avoided the formation of high concentrations of short oligomers at low monomer conversions. However, the level of control achievable was then compromised in that polymers with low molar mass dispersity were not formed ($Đ_m$ usually >2).

Most recent studies on RAFT emulsion polymerization with dithioesters have been based on the use of amphiphilic macroRAFT agents usually in the context of polymerization-induced self-assembly (PISA). PISA is discussed in the Chapter of D'Agosto et al. [812].

8.17 Dithioester Group Removal/Transformation

The presence of a dithioester group in RAFT-synthesized polymers means that these polymers are likely to be coloured. The colour may range from violet through red (aromatic dithioesters including dithiobenzoates) to orange (aliphatic dithioesters). This may provide a reason for end-group removal.

Dithiobenzoate RAFT agents and macroRAFT agents have also been found to very effectively quench the fluorescence of coumarone derivatives and acenaphthylene units [235, 813, 814]. No such quenching was observed for polymers from which the dithioester end-group had been removed [235, 813]. Thus, the thiocarbonylthio groups are often removed from polymers used in optoelectronic applications.

In their review, Fairbanks et al. [2] reported that some toxicity can be observed for polymers formed with dithiobenzoate RAFT agents for high concentrations of polymers but also pointed out that most applications call for concentrations that are well below the toxicity threshold. Nonetheless, for many biomedical applications it is considered desirable to avoid any unforeseen issues by removing the thiocarbonylthio functionality. Fortunately, dithioester chain ends may be easily removed by a variety of techniques to leave the RAFT-synthesized polymer with no intrinsic toxicity attributable to the mechanism of polymerization.

There are also many other circumstances when it may be desirable to transform a dithioester group to achieve a desired functionality or for use in a subsequent process post-RAFT polymerization. Methods for end-group transformation are discussed in detail in the chapter by Lowe and Dallerba [4]. Earlier reviews on end-group transformation may also be consulted [815–817]. In this chapter, we focus on methods that are used for dithioester end-group transformation.

8.17.1 Dithioester Group Removal by Reaction with Nucleophiles

RAFT-synthesized polymers are an often-used source of polymers comprising thiol chain ends. The thiocarbonylthio group of RAFT-synthesized polymers reacts with nucleophiles to provide a thiol end [250, 818]. A theoretically estimated order of reactivity of thiocarbonylthio groups towards primary amine nucleophiles is dithioate ≥ dithiobenzoate > xanthate ≥ trithiocarbonate ≫ dithiocarbamates [818]

(this order can be modified by substituents). Nucleophilic reactants used in this context include primary and secondary amines, thiols, hydroxide, azide, and hydride reducing agents, borohydride (examples of most of these are provided in Table 8.23).

Various side reactions can complicate thiol formation. These include disulfide formation by oxidative coupling and intramolecular thiolactone formation. The side reactions depend strongly on reaction conditions and can be mitigated by trapping the thiol end-group in situ, for example, through a thio-Michael adduct [174, 229] or the methyl or other disulfide [822].

The reaction of dithioesters with thiols has been used as a method of RAFT agent synthesis by thiol exchange. (Method F, Section 8.4) [827]. The method was applied in the synthesis of **12**, **20**, and **21** (refer Table 8.4). Dithiobenzoates and polymers with dithionenzoate ends react with cysteine or homocystine to form a polymer with a thiol end-group and release hydrogen sulfide (Scheme 8.9) [505, 824].

8.17.2 Dithioester Group Removal by Radical-Induced Reactions

Various radical-induced processes for thiocarbonylthio group removal, which include radical-induced coupling, radical-induced disproportionation, and radical-induced reduction are described in the chapter on trithiocarbonates [13] and will not be described in detail here.

The processes involve generation of radicals, usually from an exogenous initiator, and conversion of the macroRAFT agent to propagating species by radical addition–fragmentation, which can then terminate by radical–radical reaction (giving radical-induced coupling or radical-induced disproportionation) or by irreversible chain transfer (to give radical-induced reduction) – refer to Scheme 8.10.

8.17.2.1 Radical-Induced Coupling/Disproportionation

Radical-induced coupling as a method of end-group removal was introduced by Perrier et al. [828] and involves heating a RAFT-synthesized polymer with a very large excess (typically ~20 molar equiv) of a radical initiator. The method has been successfully applied to many dithioesters and is most effective for polymers with a terminal methacrylate unit. Most often, the initiator used is a dialkyldiazene such as AIBN, although other initiators can be used. Some examples are provided in Table 8.24. Additional examples are reported in the Chapter by Lowe and Dallerba [4].

While dithiobenzoate end-group removal for polymers with a terminal methacrylate unit appears generally efficient when using 20 molar equiv of dialkyldiazene, variable results have been reported for polymers with a terminal St or acrylate unit, with removal efficiencies being as low as <30% even though reaction conditions appear generally similar (Table 8.24).

Undecyl radicals (from LPO) are poor radical leaving groups and their addition to the dithioester thiocarbonyl is irreversible. However, a pronounced bimodal molecular weight distribution was seen when using LPO alone, indicating that the undecyl

Table 8.23 Dithioester end-group transformation by reaction with nucleophiles.

Terminal monomer[a)]	Z[b)]	Reagent(s)[c)]	Trapping, etc.[d)]	Comment	References
St	Ph	$NaBH_4$	—	—	[485]
St	Ph	$NaBH_4/PBu_3$	Acrylates	In situ thiol-ene	[174]
BA	Npth	NaN_3	DTT	Sequential	[819]
St	Ph	Ethylamine	Zn/CH_3CO_2H	Sequential	[645]
St	Ph	Propylamine/ PBu_3	Acrylates	In situ thiol-ene	[174]
St	Ph	Propylamine	—	—	[485]
St	Ph	Hexylamine/ $NaHSO_3$	—	Subsequently used in disulfide formation	[649]
St	Ph	Hydrazine hydrate		No disulfide formation	[820]
St/StOAc	Ph	Hydrazine hydrate	—	Simultaneous ester cleavage	[152]
$StSO_3Na$	Ph	$NaBH_4$		In situ reaction with gold surface	[821]
St/2VP	Ph	Hexylamine/ $Na_2S_2O_4$	—	—	[479]
MMA	Ph	hexylamine/ $Na_2S_2O_4$	—	Subsequently used in thiol-ene	[559]
MMA	Ph	Hexylamine	—	Conditions to favour disulfide formation	[468]
MMA	Ph	Propylamine	MTS	In situ trapping	[822]
MMA	Ph	NaN_3	DTT	Sequential	[819]
LMA	Ph	Propylamine/ $Na_2S_2O_4$	—	—	[608]
DMAEMA	Ph	Hexylamine/ $NaHSO_3$	—	Subsequently used in disulfide formation	[649]
MAA	Ph	NaOH	—	e)	[823]
HPMA	Ph	Hydroxypropylamine	—	e)	[823]
MPEGMA	Ph	Hydrazine	—		[323]
MPEGMA	Ph	Cysteine		With release of H_2S	[824]
AA	Ph	Hexylamine/ $NaHSO_3$	—	Subsequently used in disulfide formation	[649]

(*continued*)

Table 8.23 (Continued)

Terminal monomer[a)]	Z[b)]	Reagent(s)[c)]	Trapping, etc.[d)]	Comment	References
BA	Npth	NaN_3	DTT	Sequential	[819]
MA	Ph	Hydrazine hydrate		No disulfide formation	[820]
MA	Ph	Hexylamine	Et_3N/MBP Et_3N/EBiB	Thio-bromo 'click'	[365]
PEGA	Ph	Butylamine		Subsequently used in thiol-ene	[484]
PEGMA	Ph	Cysteine		With release of H_2S	[2, 824]
NIPAm	Ph	$NaBH_4$	—	Gold nanoparticles	[416]
NIPAm	Ph	$LiB(C_2H_5)_3H$	—	Subsequently used in thiol-ene	[382]
NIPAm	Ph	Octylamine/ DMPP	AMA	In situ thiol-ene	[229]
NIPAm	Ph	Ictylamine/ DMPP	PA	In situ thiol-ene	[229]
NIPAm	Ph	Hexylamine	Et_3N/MBP Et_3N/EBiB	Thio-bromo 'click'	[365]
DEAm	Ph	Hexylamine/ DMPP	TMPTA	In situ thiol-ene	[226]
DMAm	Ph	Hydrazine			[116]
DMAm	Ph	$NaBH_4$		In situ reaction with gold surface	[821, 825]
AMPS	Ph	NH_3	—	Kinetic study	[558]
AN	Ph	Propylamine/ MTS	MTS	Thiol trapped as disulfide	[826]

a) Monomer unit adjacent to thiocarbonylthio group.
b) Z group of macroRAFT agent. Npth = 2-naphthyl.
c) Nucleophile/reducing agent: DMPP – dimethylphenylphosphine.
d) Reagent used to trap initially formed thiol: DTT, dithiothreitol; EBiB, ethyl 2-bromoisobutyrate; TMPTA, trimethylolpropane triacrylate; MBP, methyl 2-bromopropionate; MTS, methyl methanethiolsulfonate (*S*-methyl methanesulfonothioate).
e) During conversion of RAFT-synthesized poly(pentafluorophenyl methacrylate) to poly(methacrylic acid) (by reaction with NaOH) or a poly(*N*-alkylmethacrylamide) (by reaction with a primary amines; such as 2-hydroxypropylamine). Conversion efficiency to thiol end-group was determined as >80%.

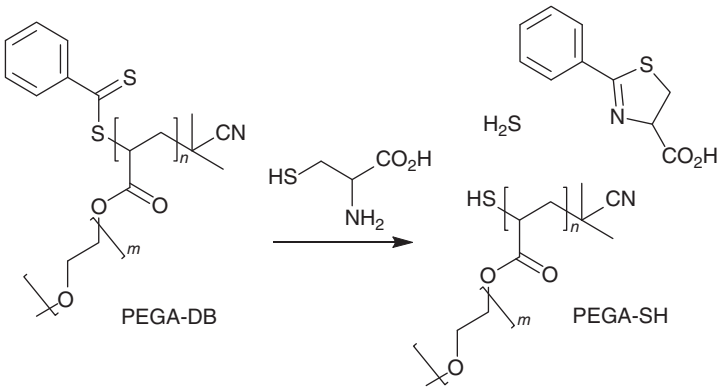

Scheme 8.9 Transformation of polymers with dithiobenzoate end-group (PEGA-DB) with cysteine to form polymer with a thiol end-group (PEGA-SH) and release hydrogen sulfide.

radical is unable to trap the propagating radicals efficiently. A combination of LPO and AIBN was found to completely remove the thiocarbonylthio end-groups of PSt and PBA without formation of a bimodal molecular weight distribution [222].

It is important to note, if using this process to prepare end-functional polymers, that reaction of (for example) 2-cyano-2-propyl radicals with propagating radicals may involve disproportionation as well as combination. For example, the combination/disproportionation ratio for 2-cyano-2-propyl reacting with PSt propagating radical is reported as 0.61.

8.17.2.2 Radical-Induced Reduction

Examples of radical-induced reduction of dithioesters are provided in Table 8.25. The comments on the process provided in the Chapter on trithiocarbonates [13] are relevant here and do not require elaboration.

8.17.3 Dithioester Group Removal by Oxidation

Examples of dithioester-group removal by oxidation are provided in Table 8.26. Li et al. [70] found that dithiobenzoates are slowly converted to thiobenzoates on heating with an initiator (usually AIBN) under air in an inert solvent (benzene), in some cases with replacement of 'R' with an initiator-derived radical. This process may complicate end-group removal by radical-induced coupling.

On the other hand, heating under air with initiator in THF solvent provides a polymer with hydroperoxide end-groups, which can be reduced to hydroxyl end-groups [159, 720].

RAFT end-groups can be readily removed by reaction with hydrogen peroxide [5, 833–836]. The process has been demonstrated for dithiobenzoates [834, 836], trithiocarbonates [834, 835], and xanthates [833]. The processes reportedly [833, 834] lead to the thiocarbonylthio group being replaced with a hydroxyl group though the exact mechanism has not yet been established or the end-group structure experimentally confirmed. It is known that low-molar mass dithiobenzoates (e.g. **21**) undergo reaction with alkaline hydrogen peroxide to form benzoic acid [837], with the benzyl group being converted (initially) to the thiolate anion.

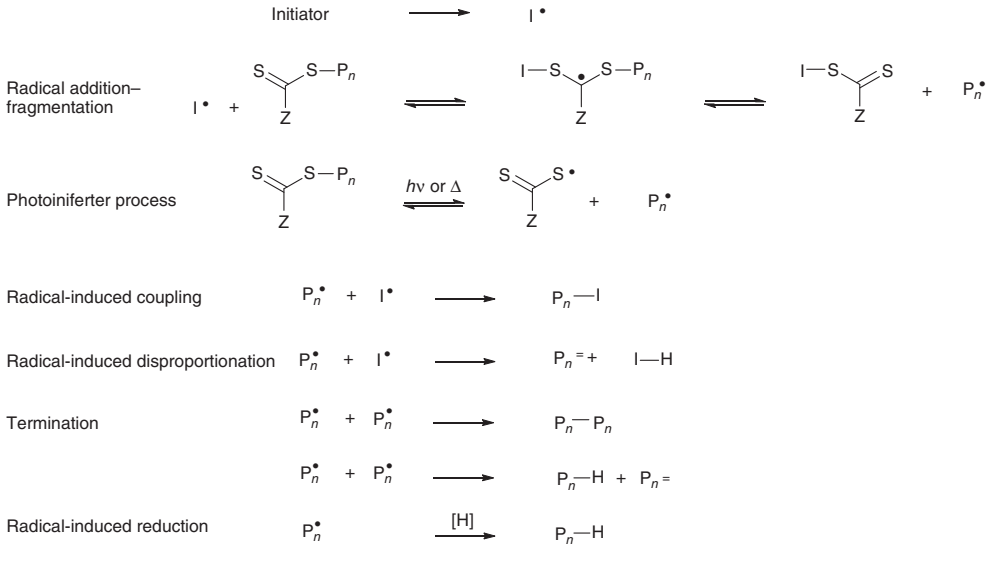

Scheme 8.10 Dithioester group (Z = aryl or alkyl) removal by radical-induced reaction pathways including radical-induced coupling, radical-induced disproportionation, and radical-induced reduction.

Table 8.24 Dithioester group removal by radical-induced reactions (coupling or disproportionation).

ZCS_2[a]	Terminal monomer unit	Initiator	[Initiator] [RAFT][b]	Temperature (°C/h)[c]	% ends removed[d]	References
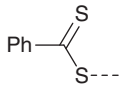	St	AIBN	20	80/2.5	100	[828]
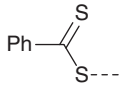	St	AIBN	20	80/4	28	[222]
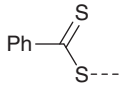	St	AIBN	100	80/4	80	[222]
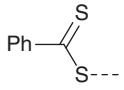	St	LPO[e]	2	80/4	100	[222]
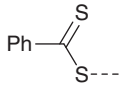	St	AIBN+LPO	20+2	80/4	100	[222]
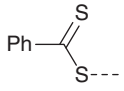	PEGA/ DMAEA	ACHN	20	80/2.5	100	[828]
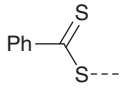	MA	ACPA	20	80/2.5	100	[828]
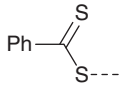	BA	AIBN	30	80/4	27	[222]
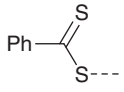	BA	AIBN + LPO	20 + 2	80/4	100	[222]
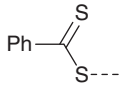	MMA	AIBN	20	80/2.5	100	[828]
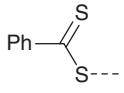	MMA/ PFPMA	AIBN	20	80/2.5	100	[396]
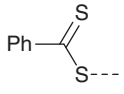	MMA	Et_3B/O_2	5	25/1 min	100	[829]
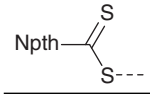	PEMA	AIBN		60/48	100	[426]

a) ZCS_2 group of macroRAFT agent. Npth = 2-naphthyl.
b) Mole ratio of initiator to RAFT synthesized polymer.
c) Temperature/reaction time.
d) Percentage of end-groups removed.
e) Bimodal molar mass distribution observed.

Table 8.25 Dithioester group removal by radical-induced reduction.

Dithioester group	Polymer	Initiator	Reagent[a)]	comment	References
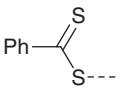	MMA	$h\nu$ (365 nm)	EPHP		[830]
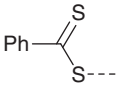	St	LPO, BPO	*i*PrOH	Bimodal MMD[b)]	[125]
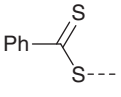	St	ACHN	EPHP		[125]
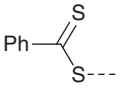	St	AIBN	$C_{12}H_{25}SH/Ph_3SiH$	Incomplete	[831]
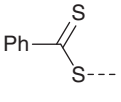	St	TPO/$h\nu$	$C_{12}H_{25}SH/Ph_3SiH$		[831]
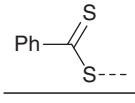	St	$h\nu$ (365 nm)	$C_{12}H_{25}SH/Ph_3SiH$		[831]

a) ZCS_2 group of macroRAFT agent.
b) *i*PrOH, isopropanol; EPHP, *N*-ethylpiperidine hypophosphate.
c) Bimodal molar mass distribution.

8.17.4 Dithioester Group Removal by Thermolysis

Legge et al. [838] examined the stability of a range of RAFT agents (including dithiobenzoates **9** and **15**) by thermogravimetric analysis and reported that dithiobenzoates are significantly more thermally stable than similar trithiocarbonates, xanthates, or dithiocarbamates.

Chong et al. [178] studied the use of thermolysis as a means of end-group removal for PMMA-dithiobenzoate and PMMA-trithiocarbonate. For the dithiobenzoate, end-group loss by a Chugaev mechanism occurred at 180–220 °C to leave a polymer with an unsaturated chain end that had little change in molecular weight from the precursor polymer. These findings were confirmed in general terms by Bressy et al. [839], Katsikas et al. [173], Bekanova et al. [840], and Bressy et al. [839] also examined the thermal stability of poly(*tert*-butyldimethylsilyl methacrylate)-dithiobenzoate. The PMMA 'macromonomer' formed is more stable to (further) weight loss than that formed by conventional radical polymerization, but noticeably less stable than the polymer formed from PMMA-dithiobenzoate

Table 8.26 Dithioester group removal by oxidation.

Polymer	Z	Reagent	Comment	Product end-group	References
MA	Ph	*t*BuOOH	sulfine intermediate	—(C=O)SPh	[110]
MMA, acrylates	Ph	Air	AIBN, THF solvent	–OOH	[183, 832]
MMA, St	Ph	Air	AIBN, benzene	—(C=O)SPh	[70]
MMA	$Ph(CH_3)_2$	Air	THF, acid	SH[a)]	[181]
St	Ph	H_2O_2	—	–OH	[833]

a) Presumed end-group [181].

after end-group removal by aminolysis (with thiol end-group) [648] or sequential aminolysis and thio-Michael reaction [559].

PMMA-dithiobenzoate is reported to be relatively unstable when heated in solution at ≥100 °C. Xu et al. [841] reported that PMMA with dithiobenzoate ends degrades at substantially lower temperature than found in the abovementioned work [178]. Factors that might lead to PMMA appearing less stable include the presence of residual initiator (left over from polymer synthesis), exposure to light during thermolysis, or metal contamination in the sample.

8.17.5 Electrocyclic Reactions of Dithioesters

The hetero-Diels–Alder reaction involving thiocarbonyl group as heterodienophile provides a route to dihydrothiopyrans [842, 843]. The cycloaddition is facilitated by α-electron-withdrawing substituents and is catalysed by Lewis and Brønsted acids. Barner-Kowollik and coworkers demonstrated this chemistry for RAFT agents and macroRAFT agents with electron-withdrawing 'Z' (2-pyridyl (e.g. **22**), phosphonate, and phenylsulfonyl) and suitable dienes (Scheme 8.11) [540, 544, 844–851]. The process has been used in the synthesis of block copolymers [540, 543, 546, 563, 844], star polymers [544, 546, 844, 847], graft copolymers [851], and modified surfaces [848, 849]. To achieve acceptable rates, the reaction is typically catalysed by trifluoroacetic acid [844].

Aliphatic diazo-compounds undergo a facile 1,3-dipolar cycloaddition with electron-deficient thiocarbonyl dipolarophiles [852, 853]. Low-molar mass RAFT-synthesized PMMA with dithiobenzoate ends undergoes facile reaction

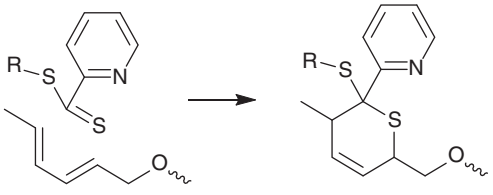

Scheme 8.11 Hetero-Diels–Alder process with 2-pyridyl dithioester as dienophile.

with diazomethane as indicated by immediate decolourization and a quantitative doubling of molar mass [182]. Higher molar mass PMMA-dithiobenzoates are also rapidly decolourized by diazomethane to provide a product with a bimodal molar mass distribution. The proposed mechanism is shown in Scheme 8.12. Historically, diazomethane has been widely used to methylate carboxylic acid functionality, e.g. in polymers containing acrylic or methacrylic acid units [854]. In another study, methylation of PAA-dithiobenzoate with trimethylsilyldiazomethane provided a PMA with ~30% thiol chain end plus other undefined chain ends [855]. Under similar conditions, trithiocarbonates were found to either not react with diazomethane (PMMA) [182] or to give complex mixtures (PAA or PMA) [855].

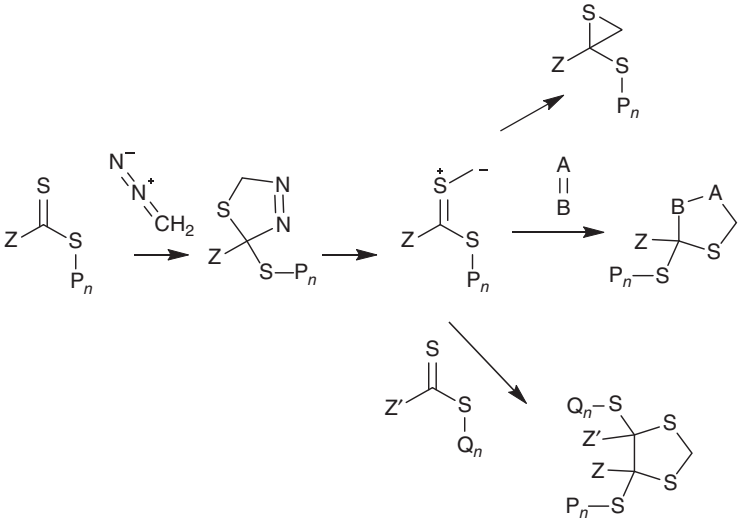

Scheme 8.12 Proposed pathways for reaction of a dithioester with diazomethane by 1,3-dipolar cycloaddition. A = B is another dipolarophile.

8.17.6 Boronic Acid Cross-Coupling

A copper-promoted cross-coupling reaction between thiocarbonylthio end-groups (of PSt-dithiobenzoate) and arylboronic acids has been reported [74]. The method was effective with styrenics (PSt-dithiobenzoate, PPFS-dithiobenzoate) but failed with PMMA-dithiobenzoate (prepared with **16b**). A strategy comprising SUMI of styrene into the PMMA-dithiobenzoate to introduce a terminal styrene unit as shown in Scheme 8.13 enabled successful cross-coupling and provided >95% end-group replacement [74].

8.17.7 Conclusions and Outlook

This chapter was intended as a critical survey of the synthesis, properties, and application of dithioester RAFT agents of general structure **Z**C(=S)SR. Aromatic

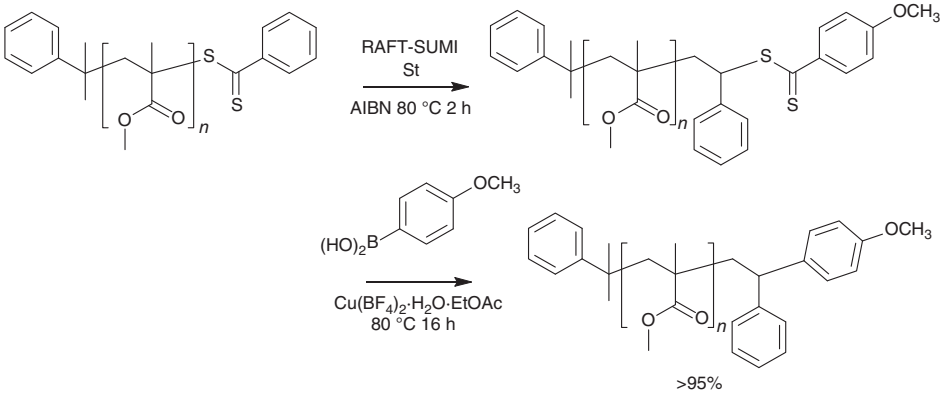

Scheme 8.13 Sequential SUMI of styrene (St) and copper-promoted cross-coupling for transformation of PMMA-dithiobenzoate by cross-coupling.

dithioesters (**Z** = aryl), specifically, dithiobenzoates, reported in the initial publications on RAFT polymerization, dominated the early literature and remain amongst the most popular RAFT agents. This can be attributed to the better control offered by the dithiobenzoates over molar mass, molar mass distribution, and end-group fidelity with respect to most other RAFT agents, in the polymerization of 1,1-disbustituted monomers. Aromatic dithioesters are less suited for mediating RAFT polymerization of monosubstituted monomers, where their use is often associated with significant retardation, side reactions, and other factors that limit control. Aliphatic dithioesters (**Z** = alkyl or substituted alkyl) were also described in the first patents and publications on RAFT but have seen relatively little use. They are substantially less active than the aromatic dithioesters but also tend to give less side reactions and less retardation.

Abbreviations

Abbreviations are listed alphabetically by the abbreviated term. In general abbreviations of methacrylates end with 'MA' methacrylamides end with 'MAm' acrylates end with 'A' acrylamides end with 'Am' or begin with 'NA' (for *N*-acryloyl). Except as indicated below the prefix 'P' is an abbreviation for 'poly()', thus PBA is an abbreviation for poly(butyl acrylate).

AA	acrylic acid
AAEMA	2-(acetoacetoxy)ethyl methacrylate
AcS	4-acetoxystyrene
AEMA	2-aminoethyl methacrylate (hydrochloride)
AEMAm	*N*-(2-aminoethyl)methacrylamide (hydrochloride)
AEP	2-(acryloyloxy)ethyl phosphate
AIBN	azobis(isobutyronitrile) [2,2′-azobis(2-methylpropionitrile)]
ACHN	1,1′-azobis(1-cyclohexanenitrile)
ACPA	4,4′-azobis(4-cyanopentanoic acid)
AIBMe	azobis(methyl isobutyrate) [dimethyl 2,2′-azobis(2-methylpropionate)]
Am	acrylamide
AMA	allyl methacrylate
AMPS	2-acrylamido-2-methylpropanesulfonic acid sodium salt (AMPS)
AMS	α-methylstyrene
AN	acrylonitrile
APMAm	*N*-(3-aminopropyl)methacrylamide (hydrochloride)
ATRP	atom-transfer radical polymerization
BA	butyl acrylate
BAm	*N*-butylacrylamide
Bd	butadiene
BES	1-butyl ethenesulfonate (**247**)
BMA	butyl methacrylate
BzAm	*N*-benzylacrylamide

BDSMA	*t*-butyldimethylsilyl methacrylate
BP	β-pinene
BzMA	benzyl methacrylate
ClPEA	2-chloropropionyloxyethyl acrylate
BPO	benzoyl peroxide
CHAm	*N*-cyclohexylacrylamide
CCT	catalytic chain transfer
CHMA	cyclohexyl methacrylate
CL	ε-caprolactone
CMS	4-(chloromethyl)styrene
CMA	cholesteryl methacrylate
Cp	chloroprene
CPA	3-chloropropyl acrylate
$Đ$ or $Đ_m$	molar mass dispersity = ratio of mass average to number average molar mass [856]
DA	dodecyl acrylate
DTT	dithiothreitol
DAAm	diacetone acrylamide (*N*-(1,1-dimethyl-3-oxobutyl)acrylamide)
DADMAC	diallyldimethylammonium chloride
Dc	1-decene
DBI	dibutyl itaconate
DCC	*N,N′*-dicyclohexylcarbodiimide
DEAm	*N,N*-diethylacrylamide
DEAEMA	2-(diethylamino)ethyl methacrylate
DEAPMAm	*N*-(3-(diethylamino)propyl)methacrylamide (hydrochloride)
DEGA	(diethylene glycol monomethyl ether) acrylate
DEGDMA	diethylene glycol dimethacrylate
DEGMA	(diethylene glycol monomethyl ether) methacrylate
DEHEA	di(ethylene glycol) 2-ethylhexyl ether acrylate
DEHI	di-2-ethylhexyl itaconate
DFHMA	dodecafluoroheptyl methacrylate
DFHMA	decafluoroheptyl methacrylate
DMA	dodecyl methacrylate
DMAm	*N,N*-dimethylacrylamide
DMAEA	2-(dimethylamino)ethyl acrylate
DMAEAm	*N*-(2-(dimethylamino)ethyl)acrylamide
DMAEMA	2-(dimethylamino)ethyl methacrylate
DMAPMAm	*N*-(3-(dimethylamino)propyl)methacrylamide (hydrochloride)
DPAEMA	2-(diisopropylamino)ethyl methacrylate
DSDMA	disulfide dimethacrylate (**344**)
DVB	divinylbenzene
DVE	divinyl ether
EA	ethyl acrylate
EAA	ethyl 2-acetoxyacrylate
E	ethene
EEA	ethoxyethyl acrylate

EGDA	ethylene glycol diacrylate
EGDMA	ethylene glycol dimethacrylate
EHA	2-ethylhexyl acrylate
EOEMA	2-ethoxyethyl methacrylate
EtOAc	ethyl acetate
EVC	*N*-ethyl-3-vinylcarbazole
EVE	ethyl vinyl ether
EWG	electron-withdrawing group
GMA	glycidyl methacrylate
GMMA	glycerol monomethacrylate (**79**)
GPMAm	*N*-3-guanidinopropyl)methacrylamide
HA	hexyl acrylate
HDDA	hexane-1,6-diol diacrylate
HEA	2-hydroxyethyl acrylate
HEMA	2-hydroxyethyl methacrylate
HEMAm	*N*-(2-hydroxyethyl)methacrylamide
HFBA	2,2,3,4,4,4-hexafluorobutyl acrylate
HFBMA	2,2,3,4,4,4-hexafluorobutyl methacrylate
HMA	hexylmethacrylate
HMS	4-(hydroxymethyl)styrene
HPA	hydroxypropyl acrylate (mixture of isomers)
HPMA	2-hydroxypropyl methacrylate
HPMAm	*N*-(2-hydroxypropyl)methacrylamide
4HS	4-hydroxystyrene
IAM	intermediate activated monomer (includes *N*-vinyl monomers such as NVC)
iBoA	isobornyl acrylate
iBMA	isobutyl methacrylate
Ip	isoprene
IPhMA	4-iodophenyl methacrylate
iPOx	2-Isopropenyl-2-oxazoline
LA	lactic acid
LAM	less activated monomer (includes vinyl monomers such as VAc and NVP)
LMA	dodecyl (lauryl) methacrylate
Lim	limonene
LPO	dodecanoyl peroxide (lauroyl peroxide)
LR	Lawesson's reagent
MA	methyl acrylate
MAA	methacrylic acid
MAc	maleic acid
MADIX	Macromolecular Design by Interchange of Xanthate
MAEP	2-(methacryloyloxy)ethyl phosphate (**99**)
MAH	maleic anhydride
MAM	more activated monomer (includes styrenes, acrylates, acrylamides)
MAN	methacrylonitrile

MBAm	methylene-bis-acrylamide
MeS	4-methylstyrene
MMA	methyl methacrylate
MMBL	γ-methyl-α-methylene-χ-butyrolactone (**183**)
MOEMA	2-methoxyethyl methacrylate
MPC	methacryloyloxyethyl phosphorylcholine (**156**)
MPEGMA	(poly(ethylene glycol) monomethyl ether) methacrylate
MPEGMAm	(poly(ethylene glycol) monomethyl ether) methacrylamide
MVK	methyl vinyl ketone
NAA	*N*-acryloylazocane (**208**)
NAM	*N*-acryloylmorpholine
NAPM	*N*-acryloyl-L-proline methyl ester
NAPAM	*N*-acryloyl-L-phenylalanine methyl ester
NAPi	*N*-acryloylpiperidine
NAP	*N*-acryloylpyrrolidine
NAS	*N*-acryloyloxysuccinimide (**264**)
NEMI	*N*-ethylmaleimide
NES	neopentyl ethenesulfonate (**246**)
NIPAm	*N*-isopropylacrylamide
NMA	2-(naphthalen-2-yloxy)ethyl methacrylate
NMMI	*N*-methylmaleimide
NMP	aminoxyl-(nitroxide-) mediated polymerization
NPMI	*N*-phenylmaleimide
NPrMI	*N*-propylmaleimide
NMS	*N*-methacryloyloxysuccinimide (**261**)
NVC	*N*-vinylcarbazole
NVP	*N*-vinylpyrrolidone
NVPI	N-vinylphthalimide
OAm	*N*-octylacrylamide
ODA	octadecyl acrylate
PAm	*N*-propylacrylamide
PA	propargyl acrylate
PAA	α-propylacrylic acid (2-methylenepentanoic acid)
PDFOMA	pentadecylfluorooctyl methacrylate
PDMS	poly(dimethylsiloxane)
PE	polyethylene
PEG	poly(ethylene glycol) monomethyl ether
PEGA	(poly(ethylene glycol) monomethyl ether) acrylate
PEGDMA	poly(ethylene glycol) dimethacrylate
PEGMA	poly(ethylene glycol) methacrylate
PEMA	2-phenylethyl methacrylate
PEO	poly(ethylene oxide)
PFPMA	pentafluorophenyl methacrylate
PET-RAFT	photo-induced electron or energy transfer-RAFT
PFBEMA	2-(perfluorobutyl)ethyl methacrylate

PFHEMA	2-(perfluorohexyl)ethyl methacrylate
PFPVB	pentafluorophenyl 4-vinylbenzoate
PFOEMA	2-(perfluorooctyl)ethyl methacrylate
PFPVS	pentafluorophenyl 4-vinylbenzenesulfonate
PFS	2,3,4,5,6-pentafluorostyrene
Ph	phenyl
PLA	poly(lactic acid)
PMA	propargyl methacrylate
PMVE	perfluoro(methyl vinyl ether)
POSSMA	isobutyl polyhedral oligomeric silsesquioxane methacrylate (**322**)
PVK	phenyl vinyl ketone
PVS	phenyl 4-vinylbenzenesulfonate
P3HT	poly(3-hexylthiophene)
RAFT	reversible addition–fragmentation chain transfer
RDRP	reversible deactivation radical polymerization
ROMP	ring-opening metathesis polymerization
ROP	ring-opening polymerization
SKMA	solketal methacrylate (**80**)
SSO_3Na	sodium styrene-4-sulfonate
St	styrene
SUMI	single unit monomer insertion
$\mathcal{T}$	transformation
*t*BAm	*N*-*tert*-butylacrylamide
*t*BA	*tert*-butyl acrylate
*t*BDMSOS	4-(*tert*-butyldimethylsilyloxy)styrene (**296**)
*t*BDMSMA	*tert*-butyldimethylsilyl methacrylate (**298**)
*t*BMA	*tert*-butyl methacrylate
*t*BOS	4-(*tert*-butoxy)styrene
TEGDA	triethylene glycol diacrylate
TEGMA	(triethylene glycol monomethyl ether) methacrylate
TEGDMA	triethylene glycol dimethacrylate
TEGMAm	triethylene glycol monomethyl ether methacrylamide [*N*-(2,5,8,11-tetraoxatridecan-13-yl)methacrylamide]
TESPMA	3-(triethoxysilyl)propyl methacrylate
TFEMA	2,2,2-trifluoroethyl methacrylate
TFPMA	2,2,3,3-tetrafluoropropyl methacrylate
TFPA	2,2,3,3-tetrafluoropropyl acrylate
THF	tetrahydrofuran
THPA	tetrahydropyran acrylate
THPFDA	1,1,2,2-tetrahydroperfluorodecyl acrylate
THPOS	3-(2-tetrahydropyranyloxy)styrene
TMAEMA	2-(trimethylammonium)ethyl methacrylate
TMAPMA	3-(trimethylamonium)propyl methacrylate
TMSEA	2-(trimethylsilyloxy)ethyl acrylate
TMSEMA	2-(trimethylsilyloxy)ethyl methacrylate

TMSMA	trimethylsilyl methacrylate
TMSPA	3-(trimethylsilyl)propyl acrylate
TPMMA	triphenylmethyl methacrylate (**103**)
TPO	diphenyl(2,4,6-trimethylbenzoyl)phosphine
TPSiMA	triisopropylsilyl methacrylate (**300**)
VAc	vinyl acetate
VB	vinyl butyrate
VBA	4-vinylbenzaldehyde
VBPDE	vinylbenzylphosphonic acid diethylester
VBSC	4-vinylbenzenesulfonyl chloride
VBDA	(4-vinylbenzyl)dimethylamine
VBTAC	(vinylbenzyl)trimethylammonium chloride
VBTPC	(4-vinylbenzyl)trimethylphosphonium chloride
VBz	vinyl benzoate
VCl2	vinylidene chloride
VF2	vinylidene fluoride
Vim	4-vinylimidazole
VL	γ-valerolactone
VPv	vinyl pivalate
2VP	2-vinylypyridine
4VP	4-vinylpyridine.

References

1 Boyer, C., Bulmus, V., Davis, T.P. et al. (2009). *Chem. Rev.* 109: 5402–5436. https://doi.org/10.1021/cr9001403.

2 Fairbanks, B.D., Gunatillake, P.A., and Meagher, L. (2015). *Adv. Drug Deliv. Rev.* 91: 141–152. https://doi.org/10.1016/j.addr.2015.05.016.

3 Moad, G., Chen, M., Häussler, M. et al. (2011). *Polym. Chem.* 2: 492–519. https://doi.org/10.1039/c0py00179a.

4 Lowe, A.B. and Dallerba, E. (2022). RAFT functional end-groups: installation and transformation. In: *RAFT Polymerization: Materials, Synthesis and Applications* (eds. G. Moad and E. Rizzardo), 753–804. Weinheim: Wiley-VCH.

5 Chiefari, J., Chong, Y.K., Ercole, F. et al. (1998). *Macromolecules* 31: 5559–5562. https://doi.org/10.1021/ma9804951.

6 Moad, G., Rizzardo, E., and Thang, S.H. (2005). *Aust. J. Chem.* 58: 379–410. https://doi.org/10.1071/CH05072.

7 Barner-Kowollik, C., Buback, M., Charleux, B. et al. (2006). *J. Polym. Sci., Part A: Polym. Chem.* 44: 5809–5831. https://doi.org/10.1002/pola.21589.

8 Moad, G. (2019). *Prog. Polym. Sci.* 88: 130–188. https://doi.org/10.1016/j.progpolymsci.2018.08.003.

9 Moad, G. (2014). *Macromol. Chem. Phys.* 215: 9–26. https://doi.org/10.1002/macp.201300562.

10 Mayadunne, R.T.A., Rizzardo, E., Chiefari, J. et al. (2000). *Macromolecules* 33: 243–245. https://doi.org/10.1021/ma991451a.

11 Rizzardo, E., Chen, M., Chong, B. et al. (2007). *Macromol. Symp.* 248: 104–116. https://doi.org/10.1002/masy.200750211.

12 Moad, G., Li, G., Pfaendner, R. et al. (2006). RAFT copolymerization and its application to the synthesis of novel dispersants/intercalants/exfoliants for polymer-clay nanocomposites. Some interesting results from RAFT (co)polymerization. In: *Controlled/Living Radical Polymerization. From Synthesis to Materials*, ACS Symposium Series, vol. 944 (ed. K. Matyjaszewski), 514–532. Washington, DC: American Chemical Society. https://doi.org/10.1021/bk-2006-0944.ch035.

13 Moad, G. (2022). Trithiocarbonates in RAFT polymerization. In: *RAFT Polymerization: Materials, Synthesis and Applications* (eds. G. Moad and E. Rizzardo), 223–370. Weinheim: Wiley-VCH.

14 Keddie, D.J., Moad, G., Rizzardo, E., and Thang, S.H. (2012). *Macromolecules* 45: 5321–5342. https://doi.org/10.1021/ma300410v.

15 Ranieri, K., Delaittre, G., Barner-Kowollik, C., and Junkers, T. (2014). *Macromol. Rapid Commun.* 35: 2023–2028. https://doi.org/10.1002/marc.201400518.

16 Fortunatti, C., Sarmoria, C., Brandolin, A., and Asteasuain, M. (2014). *Macromol. React. Eng.* 8: 781–795. https://doi.org/10.1002/mren.201400020.

17 Chernikova, E.V., Golubev, V.B., Filippov, A.N., and Garina, E.S. (2015). *Polym. Sci., Ser. C* 57: 94–109. https://doi.org/10.1134/S1811238215010026.

18 De Rybel, N., Van Steenberge, P.H.M., Reyniers, M.-F. et al. (2017). *Macromol. Theory Simul.* 26: 1600048. https://doi.org/10.1002/mats.201600048.

19 Devlaminck, D.J.G., Van Steenberge, P.H.M., Reyniers, M.-F., and D'hooge, D.R. (2019). *Polymers* 11: 320. https://doi.org/10.3390/polym11020320.

20 Zapata-Gonzalez, I., Saldivar-Guerra, E., and Licea-Claverie, A. (2017). *Chem. Eng. J.* 326: 1242–1254. https://doi.org/10.1016/j.cej.2017.06.051.

21 Buback, M. (2022). Kinetics and mechanism of RAFT polymerizations. In: *RAFT Polymerization: Materials, Synthesis and Applications* (eds. G. Moad and E. Rizzardo), 59–94. Weinheim: Wiley-VCH.

22 Quinn, J.F., Moad, G., and Barner-Kowollik, C. (2022). RAFT polymerization: mechanistic considerations. In: *RAFT Polymerization: Materials, Synthesis and Applications* (eds. G. Moad and E. Rizzardo), 95–138. Weinheim: Wiley-VCH.

23 Chong, Y.K., Krstina, J., Le, T.P.T. et al. (2003). *Macromolecules* 36: 2256–2272. https://doi.org/10.1021/ma020882h.

24 Theis, A., Feldermann, A., Charton, N. et al. (2005). *Macromolecules* 38: 2595–2605. https://doi.org/10.1021/ma047476d.

25 Chernikova, E.V., Tarasenko, A.V., Garina, E.S., and Golubev, V.B. (2008). *Polym. Sci., Ser. A* 50: 353–364. https://doi.org/10.1134/S0965545X08040019.

26 Nguyen, M.N., Margaillan, A., Pham, Q.T., and Bressy, C. (2018). *Polymers* 10: 224. https://doi.org/10.3390/polym10020224.

27 Han, X., Fan, J., He, J. et al. (2007). *Macromolecules* 40: 5618–5624. https://doi.org/10.1021/ma070220y.

28 Rinaldi, D., Hamaide, T., Graillat, C. et al. (2009). *J. Polym. Sci., Part A: Polym. Chem.* 47: 3045–3055. https://doi.org/10.1002/pola.23374.

29 Pietsch, C., Fijten, M.W.M., Lambermont-Thijs, H.M.L. et al. (2009). *J. Polym. Sci., Part A: Polym. Chem.* 47: 2811–2820. https://doi.org/10.1002/pola.23363.

30 Drache, M. and Schmidt-Naake, G. (2008). *Macromol. Symp.* 271: 129–136.

31 Drache, M. and Schmidt-Naake, G. (2007). *Macromol. Symp.* 259: 397–405. https://doi.org/10.1002/masy.200751345.

32 Chernikova, E.V., Tarasenko, A.V., Garina, E.S., and Golubev, V.B. (2006). *Polym. Sci., Ser. A* 48: 1046–1057. https://doi.org/10.1134/S0965545X06100051.

33 Uzulina, I., Kanagasabapathy, S., and Claverie, J. (2000). *Macromol. Symp.* 150: 33–38. https://doi.org/fp9hp3.

34 Chiefari, J., Mayadunne, R.T.A., Moad, C.L. et al. (2003). *Macromolecules* 36: 2273–2283. https://doi.org/10.1021/ma020883+.

35 Goto, A., Sato, K., Tsujii, Y. et al. (2001). *Macromolecules* 34: 402–408. https://doi.org/10.1021/ma0009451.

36 Gao, J., Luo, Y., Wang, R. et al. (2009). *Polymer* 50: 802–809. https://doi.org/10.1016/j.polymer.2008.12.014.

37 Konkolewicz, D., Siauw, M., Gray-Weale, A. et al. (2009). *J. Phys. Chem. B* 113: 7086–7094. https://doi.org/10.1021/jp900684t.

38 Kubo, K., Goto, A., Sato, K. et al. (2005). *Polymer* 46: 9762–9768. https://doi.org/10.1016/j.polymer.2005.08.045.

39 Goto, A. and Fukuda, T. (2004). *Prog. Polym. Sci.* 29: 329–385. https://doi.org/10.1016/j.progpolymsci.2004.01.002.

40 Benaglia, M., Rizzardo, E., Alberti, A., and Guerra, M. (2005). *Macromolecules* 38: 3129–3140. https://doi.org/10.1021/ma0480650.

41 Li, C.Z. and Benicewicz, B.C. (2005). *J. Polym. Sci., Part A: Polym. Chem.* 43: 1535–1543. https://doi.org/10.1002/pola.20658.

42 Klumperman, B., van den Dungen, E.T.A., Heuts, J.P.A., and Monteiro, M.J. (2010). *Macromol. Rapid Commun.* 31: 1846–1862. https://doi.org/10.1002/marc.200900907.

43 Meiser, W., Barth, J., Buback, M. et al. (2011). *Macromolecules* 44: 2474–2480. https://doi.org/10.1021/ma102491x.

44 Meiser, W. and Buback, M. (2011). *Macromol. Rapid Commun.* 32: 1490–1494. https://doi.org/10.1002/marc.201100228.

45 Sidoruk, A., Buback, M., and Meiser, W. (2013). *Macromol. Chem. Phys.* 214: 1738–1748. https://doi.org/10.1002/macp.201300247.

46 Chernikova, E., Golubev, V., Filippov, A. et al. (2010). *Polym. Chem.* 1: 1437–1440. https://doi.org/10.1039/C0PY00245C.

47 Coote, M.L. (2022). Quantum-chemical studies of RAFT polymerization. In: *RAFT Polymerization: Materials, Synthesis and Applications* (eds. G. Moad and E. Rizzardo), 139–186. Weinheim: Wiley-VCH.

48 Moad, G., Chiefari, J., Krstina, J. et al. (2000). *Polym. Int.* 49: 993–1001. https://doi.org/10.1002/1097-0126(200009)49:9<993::AID-PI506>3.0.CO;2-6.

49 Guice, K.B., Marrou, S.R., Gondi, S.R. et al. (2008). *Macromolecules* 41: 4390–4397. https://doi.org/10.1021/ma8003746.

50 Strem Chemicals. http://www.strem.com/uploads/resources/documents/raft.pdf (accessed 28 April 2009).

51 Grajales, S. (ed.) (2012). *Controlled Radical Polymerization Guide*. St. Louis, MO: Sigma-Aldrich.

52 Suzuki, S., Whittaker, M.R., Grondahl, L. et al. (2006). *Biomacromolecules* 7: 3178–3187. https://doi.org/10.1021/bm060583q.

53 He, L., Read, E.S., Armes, S.P., and Adams, D.J. (2007). *Macromolecules* 40: 4429–4438. https://doi.org/10.1021/ma070670q.

54 Chong, Y.K., Le, T.P.T., Moad, G. et al. (1999). *Macromolecules* 32: 2071–2074. https://doi.org/10.1021/ma981472p.

55 Wei, C., Wu, K., Li, J. et al. (2012). *Macromol. Chem. Phys.* 213: 557–565. https://doi.org/10.1002/macp.201100607.

56 Rizzardo, E., Chiefari, J., Mayadunne, R.T.A. et al. (2000). Synthesis of defined polymers by reversible addition fragmentation chain transfer. In: *Controlled/Living Radical Polymerization*, ACS Symposium Series, vol. 768 (ed. K. Matyjaszewski), 278–296. Washington, DC: American Chemical Society. https://doi.org/10.1021/bk-2000-0768.ch020.

57 Hotchkiss, J.W., Lowe, A.B., and Boyes, S.G. (2007). *Chem. Mater.* 19: 6–13. https://doi.org/10.1021/cm0622912.

58 Fan, D.Q., He, J.P., Xu, J.T. et al. (2006). *J. Polym. Sci., Part A: Polym. Chem.* 44: 2260–2269.

59 Xu, Y., Chen, J., Huang, J. et al. (2016). *High Perform. Polym.* 29: 1148–1157. https://doi.org/10.1177/0954008316671792.

60 Cao, H., Wang, G., Xue, Y. et al. (2019). *ACS Macro Lett.* 8: 616–622. https://doi.org/10.1021/acsmacrolett.9b00320.

61 Guégain, E., Zhu, C., Giovanardi, E., and Nicolas, J. (2019). *Macromolecules* 52: 3612–3624. https://doi.org/10.1021/acs.macromol.9b00161.

62 Zheng, C., Zhou, Y., Jiao, Y., and Zhang, H. (2019). *Macromolecules* 52: 143–156. https://doi.org/10.1021/acs.macromol.8b02031.

63 Zheng, C., Zhou, Y., and Zhang, H. (2020). *ACS Appl. Polym. Mater.* 2: 220–233. https://doi.org/10.1021/acsapm.9b00766.

64 Moad, G., Chiefari, J., Moad, C.L. et al. (2002). *Macromol. Symp.* 182: 65–80. https://doi.org/dnhr7s.

65 Johnston-Hall, G., Theis, A., Monteiro, M.J. et al. (2005). *Macromol. Chem. Phys.* 206: 2047–2053. https://doi.org/10.1002/macp.200500354.

66 Lu, L., Zhang, H., Yang, N., and Cai, Y. (2006). *Macromolecules* 39: 3770–3776. https://doi.org/10.1021/ma060157x.

67 Peklak, A.D., Butte, A., Storti, G., and Morbidelli, M. (2006). *J. Polym. Sci., Part A: Polym. Chem.* 44: 1071–1085. https://doi.org/10.1002/pola.21218.

68 Chong, Y.K., Moad, G., Rizzardo, E. et al. (2007). *Macromolecules* 40: 9262–9271. https://doi.org/10.1021/ma071100t.

69 Roth, P.J., Kessler, D., Zentel, R., and Theato, P. (2009). *J. Polym. Sci., Part A: Polym. Chem.* 47: 3118–3130. https://doi.org/10.1002/pola.23392.

70 Li, C., He, J., Zhou, Y. et al. (2011). *J. Polym. Sci., Part A: Polym. Chem.* 49: 1351–1360. https://doi.org/10.1002/pola.24554.

71 Sasso, B., Dobinson, M., Hodge, P., and Wear, T. (2010). *Macromolecules* 43: 7453–7464. https://doi.org/10.1021/ma1011683.

72 Serrano, J.M., Liu, T., Khan, A.U. et al. (2019). *Chem. Mater.* 31: 8898–8907. https://doi.org/10.1021/acs.chemmater.9b02918.

73 Hu, L., Wang, Y., Yin, Q. et al. (2019). *J. Appl. Polym. Sci.* 136: 47972. https://doi.org/10.1002/app.47972.

74 Golf, H., O'Shea, R., Braybrook, C. et al. (2018). *Chem. Sci.* 9: 7370–7375. https://doi.org/10.1039/C8SC01862F.

75 Apostolovic, B., Quattrini, F., Butté, A. et al. (2006). *Helv. Chim. Acta* 89: 1641–1659. https://doi.org/10.1002/hlca.200690163.

76 Kwak, Y., Nicolay, R., and Matyjaszewski, K. (2008). *Macromolecules* 41: 6602–6604. https://doi.org/10.1021/ma801502s.

77 Nicolaÿ, R., Kwak, Y., and Matyjaszewski, K. (2010). *Angew. Chem. Int. Ed.* 49: 541–544. https://doi.org/10.1002/anie.200905340.

78 Kwak, Y., Yamamura, Y., and Matyjaszewski, K. (2010). *Macromol. Chem. Phys.* 211: 493–500. https://doi.org/10.1002/macp.200900509.

79 Kim, Y., Pourgholami, M.H., Morris, D.L., and Stenzel, M.H. (2011). *Macromol. Biosci.* 11: 219–233. https://doi.org/10.1002/mabi.201000293.

80 Mori, H., Takahashi, E., Ishizuki, A., and Nakabayashi, K. (2013). *Macromolecules* 46: 6451–6465. https://doi.org/10.1021/ma400596r.

81 Lo, C.-T., Watanabe, Y., Murakami, D. et al. (2019). *Macromol. Rapid Commun.* 40: 1900115. https://doi.org/10.1002/marc.201900115.

82 Eberhardt, M. and Théato, P. (2005). *Macromol. Rapid Commun.* 26: 1488–1493.

83 Xu, Y., Chen, M., Xie, J. et al. (2013). *React. Funct. Polym.* 73: 1646–1655. https://doi.org/10.1016/j.reactfunctpolym.2013.09.008.

84 Cazares-Cortes, E., Baker, B.C., Nishimori, K. et al. (2019). *Macromolecules* 52: 5995–6004. https://doi.org/10.1021/acs.macromol.9b00412.

85 Ishitake, K., Satoh, K., Kamigaito, M., and Okamoto, Y. (2011). *Macromolecules* 44: 9108–9117. https://doi.org/10.1021/ma202155b.

86 Suzuki, S., Whittaker, M.R., Wentrup-Byrne, E. et al. (2008). *Langmuir* 24: 13075–13083. https://doi.org/10.1021/la802300q.

87 Ishitake, K., Satoh, K., Kamigaito, M., and Okamoto, Y. (2009). *Angew. Chem. Int. Ed.* 48: 1991–1994. https://doi.org/10.1002/anie.200805168.

88 Ishitake, K., Satoh, K., Kamigaito, M., and Okamoto, Y. (2012). *Polym. Chem.* 3: 1750–1757. https://doi.org/10.1039/C1PY00401H.

89 Li, R.C., Hwang, J., and Maynard, H.D. (2007). *Chem. Commun.*: 3631–3633. https://doi.org/10.1039/b709304g.

90 Hwang, J.Y., Li, R.C., and Maynard, H.D. (2007). *J. Controlled Release* 122: 279–286. https://doi.org/10.1016/j.jconrel.2007.04.010.

91 Yan, Y., Zhang, J., Qiao, Y. et al. (2013). *Macromolecules* 46: 8816–8823. https://doi.org/10.1021/ma402039u.

92 Yan, Y., Deaton, T.M., Zhang, J. et al. (2015). *Macromolecules* 48: 1644–1650. https://doi.org/10.1021/acs.macromol.5b00471.

93 Nagai, A., Kokado, K., Miyake, J., and Chujo, Y. (2009). *Macromolecules* 42: 5446–5452. https://doi.org/10.1021/ma900840y.

94 de Sordi, M.L.T., Ceschi, A., Petzhold, C.L., and Muller, A.H.E. (2007). *Macromol. Rapid Commun.* 28: 63–71. https://doi.org/10.1002/marc.200600641.

95 Jiang, J., Leng, B., Xiao, X. et al. (2009). *Polymer* 50: 5681–5684. https://doi.org/10.1016/j.polymer.2009.10.003.

96 Zhao, P., Jiang, J., Leng, B., and Tian, H. (2009). *Macromol. Rapid Commun.* 30: 1715–1718. https://doi.org/10.1002/marc.200900318.

97 Zhao, P., Ling, Q.D., Wang, W.Z. et al. (2007). *J. Polym. Sci., Part A: Polym. Chem.* 45: 242–252. https://doi.org/10.1002/pola.21771.

98 Papagiannouli, I., Demetriou, M., Krasia-Christoforou, T., and Couris, S. (2014). *RSC Adv.* 4: 8779–8788. https://doi.org/10.1039/C3RA46132G.

99 Islam, M.S., Qiao, Y., Tang, C., and Ploehn, H.J. (2015). *ACS Appl. Mater. Interfaces* 7: 1967–1977. https://doi.org/10.1021/am507751m.

100 Qiao, Y., Islam, M.S., Han, K. et al. (2013). *Adv. Funct. Mater.* 23: 5638–5646. https://doi.org/10.1002/adfm.201300736.

101 Pfaff, A., Barner, L., Müller, A.H.E., and Granville, A.M. (2011). *Eur. Polym. J.* 47: 805–815. https://doi.org/10.1016/j.eurpolymj.2010.09.020.

102 Gallagher, J.J., Hillmyer, M.A., and Reineke, T.M. (2015). *ACS Sustain. Chem. Eng.* 3: 662–667. https://doi.org/10.1021/sc5008362.

103 Withey, A.B.J., Chen, G., Nguyen, T.L.U., and Stenzel, M.H. (2009). *Biomacromolecules* 10: 3215–3226. https://doi.org/10.1021/bm901050x.

104 Teulère, C. and Nicolaÿ, R. (2017). *Polym. Chem.* 8: 5220–5227. https://doi.org/10.1039/C7PY00875A.

105 Szablan, Z., Toy, A.A., Terrenoire, A. et al. (2006). *J. Polym. Sci., Part A: Polym. Chem.* 44: 3692–3710. https://doi.org/10.1002/pola.21470.

106 Satoh, K., Lee, D.-H., Nagai, K., and Kamigaito, M. (2013). *Macromol. Rapid Commun.* https://doi.org/10.1002/marc.201300638.

107 Ding, A., Xu, J., Gu, G. et al. (2017). *Sci. Rep.* 7: 12601. https://doi.org/10.1038/s41598-017-12710-y.

108 Erkoc, S. and Acar, A.E. (2008). *Macromolecules* 41: 9019–9024. https://doi.org/10.1021/ma801492a.

109 Arita, T., Beuermann, S., Buback, M., and Vana, P. (2005). *Macromol. Mater. Eng.* 290: 283–293. https://doi.org/10.1002/mame.200400274.

110 Vana, P., Albertin, L., Barner, L. et al. (2002). *J. Polym. Sci., Part A: Polym. Chem.* 40: 4032–4037. https://doi.org/10.1002/pola.10500.

111 Toy, A.A., Vana, P., Davis, T.P., and Barner-Kowollik, C. (2004). *Macromolecules* 37: 744–751. https://doi.org/10.1021/ma035244t.

112 McLeary, J.B., McKenzie, J.M., Tonge, M.P. et al. (2004). *Chem. Commun.*: 1950–1951. https://doi.org/10.1039/b404857a.

113 van den Dungen, E.T.A., Matahwa, H., McLeary, J.B. et al. (2008). *J. Polym. Sci., Part A: Polym. Chem.* 46: 2500–2509. https://doi.org/10.1002/pola.22582.

114 Elsen, A.M., Nicolaÿ, R., and Matyjaszewski, K. (2011). *Macromolecules* 44: 1752–1754. https://doi.org/10.1021/ma200263w.

115 Thomas, D.B., Convertine, A.J., Myrick, L.J. et al. (2004). *Macromolecules* 37: 8941–8950. https://doi.org/10.1021/ma048199d.

116 Li, S., Nie, H., Gu, S. et al. (2019). *ACS Macro Lett.* 8: 783–788. https://doi.org/10.1021/acsmacrolett.9b00371.

117 Ganachaud, F., Monteiro, M.J., Gilbert, R.G. et al. (2000). *Macromolecules* 33: 6738–6745. https://doi.org/10.1021/ma0003102.

118 Mertoglu, M., Garnier, S., Laschewsky, A. et al. (2005). *Polymer* 46: 7726–7740. https://doi.org/10.1016/j.polymer.2005.03.101.

119 Tao, Y., Satoh, K., and Kamigaito, M. (2011). *Macromol. Rapid Commun.* 32: 226–232. https://doi.org/10.1002/marc.201000614.

120 Wan, D.C., Pu, H.T., and Yang, G.J. (2007). *Chin. Chem. Lett.* 18: 1141–1144. https://doi.org/10.1016/j.cclet.2007.07.037.

121 Wan, D.C., Satoh, K., and Kamigaito, M. (2006). *Macromolecules* 39: 6882–6886. https://doi.org/10.1021/Ma0615654.

122 Save, M., Manguian, M., Chassenieux, C., and Charleux, B. (2005). *Macromolecules* 38: 280–289. https://doi.org/10.1021/ma048487+.

123 Barner-Kowollik, C., Quinn, J.F., Morsley, D.R., and Davis, T.P. (2001). *J. Polym. Sci., Part A: Polym. Chem.* 39: 1353–1365. https://doi.org/10.1002/pola.1112.

124 Arita, T., Buback, M., and Vana, P. (2005). *Macromolecules* 38: 7935–7943. https://doi.org/10.1021/ma051012d.

125 Chong, Y.K., Moad, G., Rizzardo, E., and Thang, S.H. (2007). *Macromolecules* 40: 4446–4455. https://doi.org/10.1021/ma062919u.

126 Konkolewicz, D., Hawkett, B.S., Gray-Weale, A., and Perrier, S. (2008). *Macromolecules* 41: 6400–6412. https://doi.org/10.1021/ma800388c.

127 Yi, F. and Zheng, S. (2009). *Polymer* 50: 670–678. https://doi.org/10.1016/j.polymer.2008.11.038.

128 Moad, G., Chong, Y.K., Mulder, R. et al. (2009). New features of the mechanism of RAFT polymerization. In: *Controlled/Living Radical Polymerization. Progress in RAFT, NMP & OMRP*, ACS Symposium Series, vol. 1024 (ed. K. Matyjaszewski), 3–18. Washington, DC: American Chemical Society https://doi.org/10.1021/bk-2009-1024.ch001.

129 Bai, Y.X., Liu, Y.B., Li, Y.F., and Zhang, Q. (2012). *Polym. Adv. Technol.* 23: 581–587. https://doi.org/10.1002/pat.1928.

130 Monteiro, M.J. and de Brouwer, H. (2001). *Macromolecules* 34: 349–352. https://doi.org/10.1021/ma001484m.

131 Nozari, S. and Tauer, K. (2005). *Polymer* 46: 1033–1043. https://doi.org/10.1016/j.polymer.2004.11.039.

132 Tsavalas, J.G., Schork, F.J., de Brouwer, H., and Monteiro, M.J. (2001). *Macromolecules* 34: 3938–3946. https://doi.org/10.1021/ma001888e.

133 Monteiro, M.J., Hodgson, M., and De Brouwer, H. (2000). *J. Polym. Sci., Part A: Polym. Chem.* 38: 3864–3874. https://doi.org/10.1002/1099-0518(20001101)38:21<3864::aid-pola30>3.0.co;2-3.

134 Moad, G., Rizzardo, E., and Thang, S.H. (2006). *Aust. J. Chem.* 59: 669–692. https://doi.org/10.1071/CH06250.

135 Moad, G., Rizzardo, E., and Thang, S.H. (2009). *Aust. J. Chem.* 62: 1402–1472. https://doi.org/10.1071/CH09311.

136 Moad, G., Rizzardo, E., and Thang, S.H. (2012). *Aust. J. Chem.* 65: 985–1076. https://doi.org/10.1071/CH12295.

137 Nilles, K. and Theato, P. (2011). *Polym. Chem.* 2: 376–384. https://doi.org/10.1039/C0PY00261E.

138 Takeshima, H., Satoh, K., and Kamigaito, M. (2020). *J. Polym. Sci.* 58: 91–100. https://doi.org/10.1002/pola.29453.

139 Convertine, A.J., Sumerlin, B.S., Thomas, D.B. et al. (2003). *Macromolecules* 36: 4679–4681. https://doi.org/10.1021/ma034361l.

140 Dong, Z.M., Liu, X.H., Lin, Y., and Li, Y.S. (2008). *J. Polym. Sci., Part A: Polym. Chem.* 46: 6023–6034. https://doi.org/10.1002/pola.22913.

141 Zorn, M. and Zentel, R. (2008). *Macromol. Rapid Commun.* 29: 922–927. https://doi.org/10.1002/marc.200800165.

142 Nilles, K. and Theato, P. (2009). *J. Polym. Sci., Part A: Polym. Chem.* 47: 1696–1705. https://doi.org/10.1002/pola.23270.

143 Le, T.P., Moad, G., Rizzardo, E., and Thang, S.H. (1998). Polymerization with living characteristics (DuPont/CSIRO), WO9801478A1.

144 Zou, L., Liu, J.a., Zhang, K. et al. (2013). *J. Polym. Sci., Part A: Polym. Chem.* https://doi.org/10.1002/pola.27004.

145 Bilalis, P., Pitsikalis, M., and Hadjichristidis, N. (2006). *J. Polym. Sci., Part A: Polym. Chem.* 44: 659–665. https://doi.org/10.1002/pola.21198.

146 Bressy, C., Nguyen, M.N., Tanguy, B. et al. (2010). *Polym. Degrad. Stab.* 95: 1260–1268. https://doi.org/10.1016/j.polymdegradstab.2010.03.017.

147 Lin, F.-Y., Yan, M., and Cochran, E.W. (2019). *Macromolecules* 52: 7005–7015. https://doi.org/10.1021/acs.macromol.9b00707.

148 Jin, C., Zhang, T., Wang, L. et al. (2014). *RSC Adv.* 4: 45890–45894. https://doi.org/10.1039/C4RA09347J.

149 Tian, H.-Y., Yan, J.-J., Wang, D. et al. (2011). *Macromol. Rapid Commun.* 32: 660–664. https://doi.org/10.1002/marc.201000713.

150 Xu, Y., Cao, J., Li, Q. et al. (2018). *RSC Adv.* 8: 16103–16113. https://doi.org/10.1039/C8RA01660G.

151 Kaur, B., D'Souza, L., Slater, L.A. et al. (2011). *Macromolecules* 44: 3810–3816. https://doi.org/10.1021/ma200357u.

152 Lee, C.-U., Roy, D., Sumerlin, B.S., and Dadmun, M.D. (2010). *Polymer* 51: 1244–1251. https://doi.org/10.1016/j.polymer.2010.01.033.

153 Pan, G., Zu, B., Guo, X. et al. (2009). *Polymer* 50: 2819–2825. https://doi.org/10.1016/j.polymer.2009.04.053.

154 Chan, Y., Bulmus, V., Zareie, M.H. et al. (2006). *J. Controlled Release* 115: 197–207. https://doi.org/10.1016/j.jconrel.2006.07.025.

155 van den Dungen, E.T.A., Rinquest, J., Pretorius, N.O. et al. (2006). *Aust. J. Chem.* 59: 742–748. https://doi.org/10.1071/CH06238.

156 Norisuye, T., Morinaga, T., Tran-Cong-Miyata, Q. et al. (2005). *Polymer* 46: 1982–1994. https://doi.org/10.1016/j.polymer.2004.12.043.

157 Adelmann, R., Mela, P., Gallyamov, M.O. et al. (2009). *J. Polym. Sci., Part A: Polym. Chem.* 47: 1274–1283. https://doi.org/10.1002/pola.23230.

158 Deng, C. and Ling, J. (2016). *Macromol. Rapid Commun.* 37: 1352–1356. https://doi.org/10.1002/marc.201600188.

159 Ochiai, B., Ootani, Y., and Endo, T. (2008). *J. Am. Chem. Soc.* 130: 10832–10833. https://doi.org/10.1021/ja801491m.

160 Milovanovic, M.B., Avramovic, M., Katsikas, L., and Popovic, I.G. (2010). *J. Serb. Chem. Soc.* 75: 1711–1719. https://doi.org/10.2298/jsc100628082m.

161 Thang, S.H., Chong, Y.K., Mayadunne, R.T.A. et al. (1999). *Tetrahedron Lett.* 40: 2435–2438. https://doi.org/10.1016/S0040-4039(99)00177-X.

162 Bouhadir, G., Legrand, N., Quiclet-Sire, B., and Zard, S.Z. (1999). *Tetrahedron Lett.* 40: 277–280. https://doi.org/10.1016/S0040-4039(98)02380-6.

163 Shi, Z., May, A.W., Kohno, Y. et al. (2017). *J. Polym. Sci., Part A: Polym. Chem.* 55: 2961–2965. https://doi.org/10.1002/pola.28623.

164 Qinghua, Z., Xiaoli, Z., Fengqiu, C. et al. (2007). *J. Polym. Sci., Part A: Polym. Chem.* 45: 1585–1594. https://doi.org/10.1002/pola.21930.

165 Sahnoun, M., Charreyre, M.T., Veron, L. et al. (2005). *J. Polym. Sci., Part A: Polym. Chem.* 43: 3551–3565. https://doi.org/10.1002/pola.20813.

166 Hawkins, G., Zetterlund, P.B., and Aldabbagh, F. (2015). *J. Polym. Sci., Part A: Polym. Chem.* 53: 2351–2356. https://doi.org/10.1002/pola.27688.

167 Gudipati, C.S., Tan, M.B.H., Hussain, H. et al. (2008). *Macromol. Rapid Commun.* 29: 1902–1907. https://doi.org/10.1002/marc.200800515.

168 Blanazs, A., Madsen, J., Battaglia, G. et al. (2011). *J. Am. Chem. Soc.* 133: 16581–16587. https://doi.org/10.1021/ja206301a.

169 Zhou, X., Ni, P., Yu, Z., and Zhang, F. (2007). *J. Polym. Sci., Part A: Polym. Chem.* 45: 471–484. https://doi.org/10.1002/pola.21861.

170 Rojas, R., Harris, N.K., Piotrowska, K., and Kohn, J. (2009). *J. Polym. Sci., Part A: Polym. Chem.* 47: 49–58. https://doi.org/10.1002/pola.23119.

171 Kitiri, E.N., Varnava, C.K., Patrickios, C.S. et al. (2018). *J. Polym. Sci., Part A: Polym. Chem.* 56: 2161–2174. https://doi.org/10.1002/pola.29176.

172 Moad, G., Guerrero-Sanchez, C., Haven, J.J. et al. (2014). RAFT for the control of monomer sequence distribution – single unit monomer insertion (SUMI) into dithiobenzoate RAFT agents. In: *Sequence-Controlled Polymers: Synthesis, Self-assembly and Properties*, vol. 1170 (eds. J.-F. Lutz, M. Ouchi, M. Sawamoto and T. Meyer), 133–147. Washington, DC: ACS Symposium Series, American Chemical Society. https://doi.org/10.1021/bk-2014-1170.ch009.

173 Katsikas, L., Avramovic, M., Cortes, R.D.B. et al. (2008). *J. Serb. Chem. Soc.* 73: 915–921. https://doi.org/10.2298/JSC0809915K.

174 Spruell, J.M., Levy, B.A., Sutherland, A. et al. (2009). *J. Polym. Sci., Part A: Polym. Chem.* 47: 346–356. https://doi.org/10.1002/pola.23138.

175 Sriprom, W., James, M., Perrier, S.b., and Neto, C. (2009). *Macromolecules* 42: 3138–3146. https://doi.org/10.1021/ma9004428.

176 Johnston-Hall, G., Stenzel, M.H., Davis, T.P. et al. (2007). *Macromolecules* 40: 2730–2736. https://doi.org/10.1021/ma062405v.

177 Johnston-Hall, G. and Monteiro, M.J. (2007). *Macromolecules* 40: 7171–7179. https://doi.org/10.1021/ma070984d.

178 Chong, B., Moad, G., Rizzardo, E. et al. (2006). *Aust. J. Chem.* 59: 755–762. https://doi.org/10.1071/CH06229.

179 Puttick, S., Irvine, D.J., Licence, P., and Thurecht, K.J. (2009). *J. Mater. Chem.* 19: 2679–2682. https://doi.org/10.1039/b817181p.

180 Gerstel, P. and Barner-Kowollik, C. (2011). *Macromol. Rapid Commun.* 32: 444–450. https://doi.org/10.1002/marc.201000730.

181 Jana, S., Parthiban, A., and Chai, C.L.L. (2011). *J. Polym. Sci., Part A: Polym. Chem.* 49: 1494–1502. https://doi.org/10.1002/pola.24572.

182 Chen, M., Moad, G., and Rizzardo, E. (2011). *Aust. J. Chem.* 64: 433–437. https://doi.org/10.1071/CH10471.

183 Dietrich, M., Glassner, M., Gruendling, T. et al. (2010). *Polym. Chem.* 1: 634–644. https://doi.org/10.1039/b9py00273a.

184 Yhaya, F., Binauld, S., Callari, M., and Stenzel, M.H. (2012). *Aust. J. Chem.* 65: 1095–1103. https://doi.org/10.1071/CH12158.

185 Perevyazko, I.Y., Vollrath, A., Pietsch, C. et al. (2012). *J. Polym. Sci., Part A: Polym. Chem.* 50: 2906–2913. https://doi.org/10.1002/pola.26071.

186 Xue, X., Yang, J., Huang, W. et al. (2015). *React. Funct. Polym.* 96: 61–70. https://doi.org/10.1016/j.reactfunctpolym.2015.09.007.

187 Nguyen, M.N., Pham, Q.T., Le, V.D. et al. (2018). *Asian J. Chem.* 30: 1125–1130. https://doi.org/10.14233/ajchem.2018.21217.

188 Gregory, A.M., Thurecht, K.J., and Howdle, S.M. (2008). *Macromolecules* 41: 1215–1222. https://doi.org/10.1021/ma702017r.

189 Fu, Q., Ruan, Q., McKenzie, T.G. et al. (2017). *Macromolecules* 50: 7509–7516. https://doi.org/10.1021/acs.macromol.7b01651.

190 Ng, Y.-H., di Lena, F., and Chai, C.L.L. (2011). *Polym. Chem.* 2: 589–594. https://doi.org/10.1039/C0PY00139B.

191 Huynh, V.T., Binauld, S., de Souza, P.L., and Stenzel, M.H. (2012). *Chem. Mater.* 24: 3197–3211. https://doi.org/10.1021/cm301556b.

192 Bebis, K., Jones, M.W., Haddleton, D.M., and Gibson, M.I. (2011). *Polym. Chem.* 2: 975–982. https://doi.org/10.1039/C0PY00408A.

193 Wang, C., Li, X., and Deng, H. (2019). *ACS Macro Lett.* 8: 368–373. https://doi.org/10.1021/acsmacrolett.9b00178.

194 Pavlović, D., Lafond, S., Margaillan, A., and Bressy, C. (2016). *Polym. Chem.* 7: 2652–2664. https://doi.org/10.1039/C6PY00026F.

195 Blanazs, A., Ryan, A.J., and Armes, S.P. (2012). *Macromolecules* 45: 5099–5107. https://doi.org/10.1021/ma301059r.

196 Brotherton, E.E., Hatton, F.L., Cockram, A.A. et al. (2019). *J. Am. Chem. Soc.* 141: 13664–13675. https://doi.org/10.1021/jacs.9b06788.

197 Jesson, C.P., Cunningham, V.J., Smallridge, M.J., and Armes, S.P. (2018). *Macromolecules* 51: 3221–3232. https://doi.org/10.1021/acs.macromol.8b00294.

198 Cunningham, V.J., Alswieleh, A.M., Thompson, K.L. et al. (2014). *Macromolecules* 47: 5613–5623. https://doi.org/10.1021/ma501140h.

199 Canniccioni, B., Monge, S., David, G., and Robin, J.-J. (2013). *Polym. Chem.* 4: 3676–3685. https://doi.org/10.1039/C3PY00426K.

200 Solimando, X., Catel, Y., Moszner, N. et al. (2020). *Polym. Chem.* 11: 3237–3250. https://doi.org/10.1039/D0PY00337A.

201 de Sordi, M.L.T., de Oliveira da Silva, E., Ceschi, M.A., and Petzhold, C.L. (2011). *React. Funct. Polym.* 71: 648–654. https://doi.org/10.1016/j.reactfunctpolym.2011.02.005.

202 Li, S.J., Lin, M.N., Lu, J., and Liang, H. (2009). *Macromolecules* 42: 1258–1263. https://doi.org/10.1021/ma802236s.

203 Li, D., Zhu, J., Cheng, Z. et al. (2009). *React. Funct. Polym.* 69: 240–245. https://doi.org/10.1016/j.reactfunctpolym.2009.01.008.

204 Li, C.H., Ng, A.M.C., Mak, C.S.K. et al. (2012). *ACS Appl. Mater. Interfaces* 4: 74–80. https://doi.org/10.1021/am201561g.

205 Lo, K.C., Hau, K.I., and Chan, W.K. (2018). *Nanoscale* 10: 6474–6486. https://doi.org/10.1039/C7NR09670D.

206 Ban, J., Pan, L., Shi, B., and Zhang, H. (2018). *New J. Chem.* 42: 13581–13588. https://doi.org/10.1039/C8NJ02568A.

207 Zhu, Y., Zhou, Y., Chen, Z. et al. (2012). *Polymer* 53: 3566–3576. https://doi.org/10.1016/j.polymer.2012.05.063.

208 Bin, N., Yongbin, L., Yujie, L. et al. (2015). *New J. Chem.* 39: 6568–6577. https://doi.org/10.1039/C5NJ01315A.

209 Hao, X.J., Heuts, J.P.A., Barner-Kowollik, C. et al. (2003). *J. Polym. Sci., Part A: Polym. Chem.* 41: 2949–2963. https://doi.org/10.1002/pola.10894.

210 Hao, X., Stenzel, M.H., Barner-Kowollik, C. et al. (2004). *Polymer* 45: 7401–7415. https://doi.org/10.1016/j.polymer.2004.08.068.

211 Xie, H.-L., Liu, Y.-X., Zhong, G.-Q. et al. (2009). *Macromolecules* 42: 8774–8780. https://doi.org/10.1021/ma9017668.

212 Zhu, Y. and Wang, X. (2013). *Dyes and Pigments* 97: 222–229. https://doi.org/10.1016/j.dyepig.2012.12.014.

213 Cao, H.Z., Zhang, W., Zhu, J. et al. (2008). *Express Polym. Lett.* 2: 589–601. https://doi.org/10.3144/expresspolymlett.2008.71.

214 Zhao, Y., Qi, B., Tong, X., and Zhao, Y. (2008). *Macromolecules* 41: 3823–3831. https://doi.org/10.1021/ma8000302.

215 Shrivastava, S. and Matsuoka, H. (2016). *Colloid Polym. Sci.* 294: 879–887. https://doi.org/10.1007/s00396-016-3839-1.

216 Yu, B. and Lowe, A.B. (2009). *J. Polym. Sci., Part A: Polym. Chem.* 47: 1877–1890. https://doi.org/10.1002/pola.23281.

217 Trotta, J.T., Jin, M., Stawiasz, K.J. et al. (2017). *J. Polym. Sci., Part A: Polym. Chem.* 55: 2730–2737. https://doi.org/10.1002/pola.28654.

218 Quemener, D., Le Hellaye, M., Bissett, C. et al. (2008). *J. Polym. Sci., Part A: Polym. Chem.* 46: 155–173. https://doi.org/10.1002/pola.22367.

219 Li, Y. and Benicewicz, B.C. (2008). *Macromolecules* 41: 7986–7992. https://doi.org/10.1021/Ma801551z.

220 Rayeroux, D., Travelet, C., Lapinte, V. et al. (2017). *Polym. Chem.* 8: 4246–4263. https://doi.org/10.1039/C7PY00632B.

221 Bloksma, M.M., Weber, C., Perevyazko, I.Y. et al. (2011). *Macromolecules* 44: 4057–4064. https://doi.org/10.1021/ma200514n.

222 Chen, M., Moad, G., and Rizzardo, E. (2009). *J. Polym. Sci., Part A: Polym. Chem.* 47: 6704–6714. https://doi.org/10.1002/pola.23711.

223 Chakrabarty, A. and Singha, N.K. (2013). *J. Colloid Interface Sci.* 408: 66–74. https://doi.org/10.1016/j.jcis.2013.07.031.

224 Liu, Y., Wang, Y., Zhuang, D. et al. (2012). *J. Colloid Interface Sci.* 377: 197–206. https://doi.org/10.1016/j.jcis.2012.04.004.
225 Li, Y., Zhao, J., Chen, L. et al. (2019). *React. Funct. Polym.* 134: 112–120. https://doi.org/10.1016/j.reactfunctpolym.2018.10.013.
226 Chan, J.W., Yu, B., Hoyle, C.E., and Lowe, A.B. (2008). *Chem. Commun.*: 4959–4961. https://doi.org/10.1039/b813438c.
227 Harvison, M.A., Davis, T.P., and Lowe, A.B. (2011). *Polym. Chem.* 2: 1347–1354. https://doi.org/10.1039/C1PY00046B.
228 Ge, Z., Cai, Y., Yin, J. et al. (2007). *Langmuir* 23: 1114–1122. https://doi.org/10.1021/la062719b.
229 Yu, B., Chan, J.W., Hoyle, C.E., and Lowe, A.B. (2009). *J. Polym. Sci., Part A: Polym. Chem.* 47: 3544–3557. https://doi.org/10.1002/pola.23436.
230 Tanaka, S., Nishida, H., and Endo, T. (2009). *Macromolecules* 42: 293–298. https://doi.org/10.1021/ma801431a.
231 Moraes, J., Maschmeyer, T., and Perrier, S. (2011). *J. Polym. Sci., Part A: Polym. Chem.* 49: 2771–2782. https://doi.org/10.1002/pola.24710.
232 Shi, M., Li, A.-L., Liang, H., and Lu, J. (2007). *Macromolecules* 40: 1891–1896. https://doi.org/10.1021/ma062577s.
233 Chen, M., Ghiggino, K.P., Mau, A.W.H. et al. (2004). *Macromolecules* 37: 5479–5481. https://doi.org/10.1021/ma049037k.
234 Chen, M., Ghiggino, K.P., Thang, S.H. et al. (2005). *J. Org. Chem.* 70: 1844–1852. https://doi.org/10.1021/jo047899d.
235 Chen, M., Ghiggino, K.P., Rizzardo, E. et al. (2008). *Chem. Commun.*: 1112–1114. https://doi.org/10.1039/b716471h.
236 Ozoe, S. (2009). Chloroprene-based block copolymer, soapless polychloroprene latexes, and processes for producing same (Tosoh Corporation, Japan), US20090036608A1.
237 Pullan, N., Liu, M., and Topham, P.D. (2013). *Polym. Chem.* 4: 2272–2277. https://doi.org/10.1039/c3py21151g.
238 Jitchum, V. and Perrier, S. (2007). *Macromolecules* 40: 1408–1412. https://doi.org/10.1021/ma061889s.
239 Li, J., El harfi, J., Howdle, S.M. et al. (2012). *Polym. Chem.* 3: 1495–1501. https://doi.org/10.1039/C2PY20066J.
240 Liu, X.H., Li, Y.G., Lin, Y., and Li, Y.S. (2007). *J. Polym. Sci., Part A: Polym. Chem.* 45: 1272–1281. https://doi.org/10.1002/pola.21899.
241 An, Q., Qian, J., Yu, L. et al. (2005). *J. Polym. Sci., Part A: Polym. Chem.* 43: 1973–1977. https://doi.org/10.1002/pola.20622.
242 Weber, C., Neuwirth, T., Kempe, K. et al. (2011). *Macromolecules* 45: 20–27. https://doi.org/10.1021/ma2021387.
243 Perez-Baena, I., Asenjo-Sanz, I., Arbe, A. et al. (2014). *Macromolecules* 47: 8270–8280. https://doi.org/10.1021/ma5017133.
244 He, J., Tremblay, L., Lacelle, S., and Zhao, Y. (2011). *Soft Matter* 7: 2380–2386. https://doi.org/10.1039/C0SM01383H.
245 Wright, D.B., Patterson, J.P., Pitto-Barry, A. et al. (2015). *Polym. Chem.* 6: 2761–2768. https://doi.org/10.1039/C4PY01782J.

246 Breul, A.M., Schäfer, J., Friebe, C. et al. (2012). *Macromol. Chem. Phys.* 213: 808–819. https://doi.org/10.1002/macp.201100499.
247 Lossada, F., Jiao, D., Yao, X., and Walther, A. (2020). *ACS Macro Lett.* 9: 70–76. https://doi.org/10.1021/acsmacrolett.9b00997.
248 Cao, H., Zhu, J., Zhang, W. et al. (2010). *e-Polymers* https://doi.org/10.1515/epoly.2010.10.1.534.
249 Nicolaÿ, R. (2011). *Macromolecules* 45: 821–827. https://doi.org/10.1021/ma202344y.
250 Le Neindre, M., Magny, B., and Nicolay, R. (2013). *Polym. Chem.* 4: 5577–5584. https://doi.org/10.1039/C3PY00754E.
251 Kröger, A.P.P., Boonen, R.J.E.A., and Paulusse, J.M.J. (2017). *Polymer* 120: 119–128. https://doi.org/10.1016/j.polymer.2017.05.040.
252 Riedel, M., Stadermann, J., Komber, H. et al. (2011). *Eur. Polym. J.* 47: 675–684. https://doi.org/10.1016/j.eurpolymj.2010.10.010.
253 Menzel, R., Breul, A., Pietsch, C. et al. (2011). *Macromol. Chem. Phys.* 212: 840–848. https://doi.org/10.1002/macp.201000752.
254 Berndt, A., Pospiech, D., Jehnichen, D. et al. (2015). *ACS Appl. Mater. Interfaces* 7: 12339–12347. https://doi.org/10.1021/am5069479.
255 Himmelsbach, A., Schneider-Chaabane, A., and Lienkamp, K. (2019). *Macromol. Chem. Phys.* 220: 1900346. https://doi.org/10.1002/macp.201900346.
256 Yanjarappa, M.J., Gujraty, K.V., Joshi, A. et al. (2006). *Biomacromolecules* 7: 1665–1670. https://doi.org/10.1021/bm060098v.
257 Sriprom, W., Neel, M., Gabbutt, C.D. et al. (2007). *J. Mater. Chem.* 17: 1885–1893. https://doi.org/10.1039/b617865k.
258 Smith, A.A.A., Autzen, H.E., Laursen, T. et al. (2017). *Biomacromolecules* https://doi.org/10.1021/acs.biomac.7b01136.
259 Zhou, D., Zhu, X.L., Zhu, J., and Cheng, Z.P. (2008). *Polymer* 49: 3048–3053. https://doi.org/10.1016/j.polymer.2008.05.011.
260 Yamane, M., Fadil, Y., Tokuda, M. et al. (2020). *Macromol. Rapid Commun.*: 2000141. https://doi.org/10.1002/marc.202000141.
261 Sriprom, W., Neto, C., and Perrier, S. (2010). *Soft Matter* 6: 909–914. https://doi.org/10.1039/b920133e.
262 Tokuda, M., Yamane, M., Thickett, S.C. et al. (2016). *Soft Matter* 12: 3955–3962. https://doi.org/10.1039/C6SM00269B.
263 Rizzardo, E., Thang, S.H., and Moad, G. (1999). Synthesis of dithioester chain-transfer agents and use of bis(thioacyl) disulfides or dithioesters as chain-transfer agents in radical polymerization. (CSIRO), WO9905099.
264 Becer, C.R., Hahn, S., Fijten, M.W.M. et al. (2008). *J. Polym. Sci., Part A: Polym. Chem.* 46: 7138–7147. https://doi.org/10.1002/pola.23018.
265 Krieg, A., Pietsch, C., Baumgaertel, A. et al. (2010). *Polym. Chem.* 1: 1669–1676. https://doi.org/10.1039/C0PY00156B.
266 Fijten, M.W.M., Paulus, R.M., and Schubert, U.S. (2005). *J. Polym. Sci., Part A: Polym. Chem.* 43: 3831–3839. https://doi.org/10.1002/pola.20868.
267 Kostiainen, M.A., Pietsch, C., Hoogenboom, R. et al. (2011). *Adv. Funct. Mater.* 21: 2012–2019. https://doi.org/10.1002/adfm.201002597.

268 Fijten, M.W.M., Meier, M.A.R., Hoogenboom, R., and Schubert, U.S. (2004). *J. Polym. Sci., Part A: Polym. Chem.* 42: 5775–5783. https://doi.org/10.1002/pola.20346.

269 Paulus, R.M., Becer, C.R., Hoogenboom, R., and Schubert, U.S. (2009). *Aust. J. Chem.* 62: 254–259. https://doi.org/10.1071/CH09064.

270 Janoschka, T., Teichler, A., Krieg, A. et al. (2012). *J. Polym. Sci., Part A: Polym. Chem.* 50: 1394–1407. https://doi.org/10.1002/pola.25907.

271 Pavlov, G.M., Breul, A.M., Hager, M.D., and Schubert, U.S. (2012). *Macromol. Chem. Phys.* 213: 904–916. https://doi.org/10.1002/macp.201100653.

272 Van Camp, W. and Du Prez, F.E. (2006). *ACS Symp. Ser.* 944: 171–184. https://doi.org/10.1021/bk-2006-0944.ch013.

273 Krieg, A., Becer, C.R., Hoogenboom, R., and Schubert, U.S. (2009). *Macromol. Symp.* 275–276: 73–81. https://doi.org/10.1002/masy.200950109.

274 Weber, C., Becer, C.R., Hoogenboom, R., and Schubert, U.S. (2009). *Macromolecules* 42: 2965–2971. https://doi.org/10.1021/ma8028437.

275 Hoogenboom, R., Schubert, U.S., Van Camp, W., and Du Prez, F.E. (2005). *Macromolecules* 38: 7653–7659. https://doi.org/10.1021/ma050906v.

276 Ulbricht, C., Becer, C.R., Winter, A., and Schubert, U.S. (2010). *Macromol. Rapid Commun.* 31: 827–833. https://doi.org/10.1002/marc.200900787.

277 Fournier, D., Hoogenboom, R., Thijs, H.M.L. et al. (2007). *Macromolecules* 40: 915–920. https://doi.org/10.1021/ma062199r.

278 Pietsch, C., Hoogenboom, R., and Schubert, U.S. (2009). *Angew. Chem. Int. Ed.* 48: 5653–5656. https://doi.org/10.1002/anie.200901071.

279 Hoogenboom, R., Fijten, M.W.M., Paulus, R.M., and Schubert, U.S. (2006). *ACS Symp. Ser.* 944: 473–485. https://doi.org/10.1021/bk-2006-0944.ch032.

280 Grande, C.D., Tria, M.C., Jiang, G. et al. (2011). *React. Funct. Polym.* 71: 938–942. https://doi.org/10.1016/j.reactfunctpolym.2011.05.013.

281 Esteves, A.C.C., Hodge, P., Trindade, T., and Barros-Timmons, A.M.M.V. (2009). *J. Polym. Sci., Part A: Polym. Chem.* 47: 5367–5377. https://doi.org/10.1002/pola.23586.

282 Mitsukami, Y., Donovan, M.S., Lowe, A.B., and McCormick, C.L. (2001). *Macromolecules* 34: 2248–2256. https://doi.org/10.1021/ma0018087.

283 Li, Y.T. and Armes, S.P. (2009). *Macromolecules* 42: 939–945. https://doi.org/10.1021/ma802750x.

284 Alidedeoglu, A.H., York, A.W., Rosado, D.A. et al. (2010). *J. Polym. Sci., Part A: Polym. Chem.* 48: 3052–3061. https://doi.org/10.1002/pola.24083.

285 Alidedeoglu, A.H., York, A.W., McCormick, C.L., and Morgan, S.E. (2009). *J. Polym. Sci., Part A: Polym. Chem.* 47: 5405–5415. https://doi.org/10.1002/pola.23590.

286 Chu, H., Liu, N., Wang, X. et al. (2009). *Int. J. Pharm.* 371: 190–196. https://doi.org/10.1016/j.ijpharm.2008.12.033.

287 Zhu, Y. and Egap, E. (2020). *Polym. Chem.* 11: 1018–1024. https://doi.org/10.1039/C9PY01604J.

288 Smith, A.E., Xu, X., Abell, T.U. et al. (2009). *Macromolecules* 42: 2958–2964. https://doi.org/10.1021/ma802827p.

289 Liu, L., Zhang, J., Lv, W. et al. (2010). *J. Polym. Sci., Part A: Polym. Chem.* 48: 3350–3361. https://doi.org/10.1002/pola.24119.

290 Huo, M., Ye, Q., Che, H. et al. (2017). *Macromolecules* 50: 1126–1133. https://doi.org/10.1021/acs.macromol.6b02499.

291 Meuer, S., Oberle, P., Theato, P. et al. (2007). *Adv. Mater.* 19: 2073–2078. https://doi.org/10.1002/adma.200602516.

292 Samsonova, O., Pfeiffer, C., Hellmund, M. et al. (2011). *Polymers* 3: 693–718. https://doi.org/10.3390/polym3020693.

293 Lechuga-Islas, V.D., Festag, G., Rosales-Guzmán, M. et al. (2020). *Eur. Polym. J.* 124: 109457. https://doi.org/10.1016/j.eurpolymj.2019.109457.

294 Guan, S., Wen, W., Yang, Z., and Chen, A. (2020). *Macromolecules* 53: 465–472. https://doi.org/10.1021/acs.macromol.9b01757.

295 Teo, J., McCarroll, J.A., Boyer, C. et al. (2016). *Biomacromolecules* 17: 2337–2351. https://doi.org/10.1021/acs.biomac.6b00185.

296 Maximiano, P., Mendonça, P.V., Costa, J.R.C. et al. (2016). *Macromolecules* 49: 1597–1604. https://doi.org/10.1021/acs.macromol.5b02647.

297 Hu, Y.Q., Kim, M.S., Kim, B.S., and Lee, D.S. (2007). *Polymer* 48: 3437–3443. https://doi.org/10.1016/j.polymer.2007.04.011.

298 Vijayakrishna, K., Jewrajka, S.K., Ruiz, A. et al. (2008). *Macromolecules* 41: 6299–6308. https://doi.org/10.1021/ma800677h.

299 Xu, S. and Liu, W. (2008). *J. Fluorine Chem.* 129: 125–130. https://doi.org/10.1016/j.jfluchem.2007.09.008.

300 Pelet, J.M. and Putnam, D. (2009). *Macromolecules* 42: 1494–1499. https://doi.org/10.1021/ma801433g.

301 Yokoyama, Y. and Yusa, S.-i. (2013). *Polym. J.* 45: 985–992. https://doi.org/10.1038/pj.2013.2.

302 Boyer, C., Granville, A., Davis, T.P., and Bulmus, V. (2009). *J. Polym. Sci., Part A: Polym. Chem.* 47: 3773–3794. https://doi.org/10.1002/pola.23433.

303 Farooq, U., Upadhyaya, L., Shakeel, A. et al. (2020). *J. Membr. Sci.* 611: 118181. https://doi.org/10.1016/j.memsci.2020.118181.

304 Xu, J., Jung, K., and Boyer, C. (2014). *Macromolecules* 47: 4217–4229. https://doi.org/10.1021/ma500883y.

305 Xu, J., Shanmugam, S., Duong, H.T., and Boyer, C. (2015). *Polym. Chem.* 6: 5615–5624. https://doi.org/10.1039/C4PY01317D.

306 Shanmugam, S., Xu, J., and Boyer, C. (2015). *J. Am. Chem. Soc.* 137: 9174–9185. https://doi.org/10.1021/jacs.5b05274.

307 Cheng, B.-F., Wang, L.-H., and You, Y.-Z. (2016). *Macromol. Res.* 24: 811–815. https://doi.org/10.1007/s13233-016-4106-5.

308 Corrigan, N., Xu, J., and Boyer, C. (2016). *Macromolecules* 49: 3274–3285. https://doi.org/10.1021/acs.macromol.6b00542.

309 Wu, C., Chen, H., Corrigan, N. et al. (2019). *J. Am. Chem. Soc.* 141: 8207–8220. https://doi.org/10.1021/jacs.9b01096.

310 Jiang, J., Ye, G., Wang, Z. et al. (2018). *Angew. Chem. Int. Ed.* 57: 12037–12042. https://doi.org/10.1002/anie.201807385.

311 Theriot, J.C., Miyake, G.M., and Boyer, C.A. (2018). *ACS Macro Lett.* 7: 662–666. https://doi.org/10.1021/acsmacrolett.8b00281.

312 Wang, G.-X., Liu, M.-s., Liang, E., and He, B. (2018). *J. Polym. Res.* 25: 70. https://doi.org/10.1007/s10965-018-1459-9.

313 Hakobyan, K., Gegenhuber, T., McErlean, C.S.P., and Müllner, M. (2019). *Angew. Chem. Int. Ed.* 58: 1828–1832. https://doi.org/10.1002/anie.201811721.

314 Thum, M.D., Wolf, S., and Falvey, D.E. (2020). *J. Phys. Chem. A*. https://doi.org/10.1021/acs.jpca.0c02678.

315 Zhu, Y., Liu, Y., Miller, K.A. et al. (2020). *ACS Macro Lett.* 9: 725–730. https://doi.org/10.1021/acsmacrolett.0c00232.

316 Bhuchar, N., Deng, Z., Ishihara, K., and Narain, R. (2011). *Polym. Chem.* 2: 632–639. https://doi.org/10.1039/C0PY00300J.

317 Yu, B., Lowe, A.B., and Ishihara, K. (2009). *Biomacromolecules* 10: 950–958. https://doi.org/10.1021/bm8014945.

318 Zhang, X., Lian, X., Liu, L. et al. (2008). *Macromolecules* 41: 7863–7869. https://doi.org/10.1021/ma801405j.

319 Bouhamed, H., Boufi, S., and Magnin, A. (2007). *J. Colloid Interface Sci.* 312: 279–291. https://doi.org/10.1016/j.jcis.2007.03.060.

320 Bouhamed, H., Boufi, S., and Magnin, A. (2009). *J. Colloid Interface Sci.* 333: 209–220. https://doi.org/10.1016/j.jcis.2009.01.030.

321 Venkataraman, S., Ong, W.L., Ong, Z.Y. et al. (2011). *Biomaterials* 32: 2369–2378. https://doi.org/10.1016/j.biomaterials.2010.11.070.

322 Shen, W., Chang, Y., Liu, G. et al. (2011). *Macromolecules* 44: 2524–2530. https://doi.org/10.1021/ma200074n.

323 Tucker, B.S., Stewart, J.D., Aguirre, J.I. et al. (2015). *Biomacromolecules* 16: 2374–2381. https://doi.org/10.1021/acs.biomac.5b00623.

324 Huo, M., Li, D., Song, G. et al. (2018). *Macromol. Rapid Commun.* 39: 1700840. https://doi.org/10.1002/marc.201700840.

325 Barz, M., Tarantola, M., Fischer, K. et al. (2008). *Biomacromolecules* 9: 3114–3118. https://doi.org/10.1021/bm800684b.

326 Allmeroth, M., Moderegger, D., Biesalski, B. et al. (2011). *Biomacromolecules* 12: 2841–2849. https://doi.org/10.1021/bm2005774.

327 Gibson, M.I., Danial, M., and Klok, H.-A. (2011). *ACS Comb. Sci.* 13: 286–297. https://doi.org/10.1021/co100099r.

328 Nuhn, L., Hirsch, M., Krieg, B. et al. (2012). *ACS Nano* 6: 2198–2214. https://doi.org/10.1021/nn204116u.

329 Chua, G.B.H., Roth, P.J., Duong, H.T.T. et al. (2012). *Macromolecules* 45: 1362–1374. https://doi.org/10.1021/ma202700y.

330 Zhang, K., Li, X., Zhao, Y. et al. (2016). *Prog. Org. Coat.* 93: 87–96. https://doi.org/10.1016/j.porgcoat.2016.01.005.

331 Wald, S., Wurm, F.R., Landfester, K., and Crespy, D. (2016). *Polymers* 8: 303. https://doi.org/10.3390/polym8080303.

332 Meng, S., Liu, Y., Yeo, J. et al. (2020). *Colloid Polym. Sci.* https://doi.org/10.1007/s00396-020-04637-0.

333 Marras, A.E., Vieregg, J.R., Ting, J.M. et al. (2019). *Polymers* 11: 83. https://doi.org/10.3390/polym11010083.
334 Haladjova, E., Mountrichas, G., Pispas, S., and Rangelov, S. (2016). *J. Phys. Chem. B* 120: 2586–2595. https://doi.org/10.1021/acs.jpcb.5b12477.
335 Mitsukami, Y., Hashidzume, A., Yusa, S.-i. et al. (2006). *Polymer* 47: 4333–4340. https://doi.org/10.1016/j.polymer.2006.04.026.
336 Baussard, J.-F., Habib-Jiwan, J.-L., Laschewsky, A. et al. (2004). *Polymer* 45: 3615–3626. https://doi.org/10.1016/j.polymer.2004.03.081.
337 Li, Y. and Armes, S.P. (2010). *Angew. Chem. Int. Ed.* 49: 4042–4046. https://doi.org/10.1002/anie.201001461.
338 Sun, L., Hong, L., and Wang, C. (2016). *Macromol. Rapid Commun.* 37: 691–699. https://doi.org/10.1002/marc.201600003.
339 Jia, Z., Liu, J., Davis, T.P., and Bulmus, V. (2009). *Polymer* 50: 5928–5932. https://doi.org/10.1016/j.polymer.2009.10.030.
340 Datta, L.P., De, D., Ghosh, U., and Das, T.K. (2018). *Polymer* 138: 103–112. https://doi.org/10.1016/j.polymer.2018.01.044.
341 Grande, C.D., Tria, M.C., Jiang, G. et al. (2011). *Macromolecules* 44: 966–975. https://doi.org/10.1021/ma102065u.
342 Luo, Y., Liu, L., Wang, X. et al. (2012). *Soft Matter* 8: 1634–1642. https://doi.org/10.1039/C1SM06412F.
343 Kitano, H., Hayashi, A., Takakura, H. et al. (2009). *Langmuir* 25: 9361–9368. https://doi.org/10.1021/la9008625.
344 Cameron, N.R., Spain, S.G., Kingham, J.A. et al. (2008). *Faraday Discuss.* 139: 359–368. https://doi.org/10.1039/b717177c.
345 Albertin, L. and Cameron, N.R. (2007). *Macromolecules* 40: 6082–6093. https://doi.org/10.1021/ma070967o.
346 Spain, S.G. and Cameron, N.R. (2011). *Polym. Chem.* 2: 1552–1560. https://doi.org/10.1039/C1PY00030F.
347 Pearson, S., Allen, N., and Stenzel, M.H. (2009). *J. Polym. Sci., Part A: Polym. Chem.* 47: 1706–1723. https://doi.org/10.1002/pola.23275.
348 Boissé, S., Rieger, J., Di-Cicco, A. et al. (2009). *Macromolecules* 42: 8688–8696. https://doi.org/10.1021/ma9018137.
349 Krishnasamy, V., Qu, W., Chen, C. et al. (2020). *Macromolecules* https://doi.org/10.1021/acs.macromol.9b02264.
350 Doncom, K.E.B., Warren, N.J., and Armes, S.P. (2015). *Polym. Chem.* 6: 7264–7273. https://doi.org/10.1039/C5PY00396B.
351 Lim, J., Matsuoka, H., Yusa, S.-i., and Saruwatari, Y. (2019). *Langmuir* 35: 1571–1582. https://doi.org/10.1021/acs.langmuir.8b02952.
352 Karjalainen, E., Chenna, N., Laurinmäki, P. et al. (2013). *Polym. Chem.* 4: 1014–1024. https://doi.org/10.1039/C2PY20815F.
353 Olmedo-Martínez, J.L., Porcarelli, L., Alegría, Á. et al. (2020). *Macromolecules* https://doi.org/10.1021/acs.macromol.0c00703.
354 Jia, Z., Wong, L., Davis, T.P., and Bulmus, V. (2008). *Biomacromolecules* 9: 3106–3113. https://doi.org/10.1021/bm800657e.

355 Wong, L., Boyer, C., Jia, Z. et al. (2008). *Biomacromolecules* 9: 1934–1944. https://doi.org/10.1021/bm800197v.

356 Wong, L., Kavallaris, M., and Bulmus, V. (2011). *Polym. Chem.* 2: 385–393. https://doi.org/10.1039/C0PY00256A.

357 Bauri, K., Roy, S.G., Pant, S., and De, P. (2013). *Langmuir* 29: 2764–2774. https://doi.org/10.1021/la304918s.

358 Hrsic, E., Zografou, I., Schulte, B. et al. (2013). *Polymer* 54: 495–504. https://doi.org/10.1016/j.polymer.2012.11.059.

359 Fernandez-Trillo, F., Dureault, A., Bayley, J.P.M. et al. (2007). *Macromolecules* 40: 6094–6099. https://doi.org/10.1021/ma070527x.

360 Fernández-Trillo, F., Van Hest, J.C.M., Thies, J.C. et al. (2009). *Adv. Mater.* 21: 55–59. https://doi.org/10.1002/adma.200801986.

361 Li, Z., Serelis, A.K., Reed, W.F., and Alb, A.M. (2010). *Polymer* 51: 4726–4734. https://doi.org/10.1016/j.polymer.2010.08.015.

362 Koiry, B.P., Moukwa, M., and Singha, N.K. (2013). *J. Fluorine Chem.* 153: 137–142. https://doi.org/10.1016/j.jfluchem.2013.04.005.

363 Gujraty, K.V., Yanjarappa, M.J., Saraph, A. et al. (2008). *J. Polym. Sci., Part A: Polym. Chem.* 46: 7249–7257. https://doi.org/10.1002/pola.23031.

364 Cortez-Lemus, N.A., Salgado-Rodríguez, R., and Licea-Claveríe, A. (2010). *J. Polym. Sci., Part A: Polym. Chem.* 48: 3033–3051. https://doi.org/10.1002/pola.24082.

365 Xu, J., Tao, L., Boyer, C. et al. (2010). *Macromolecules* 43: 20–24. https://doi.org/10.1021/ma902154h.

366 Wang, J., Rivero, M., Muñoz Bonilla, A. et al. (2016). *ACS Macro Lett.* 5: 1278–1282. https://doi.org/10.1021/acsmacrolett.6b00818.

367 Xu, J., Shanmugam, S., Fu, C. et al. (2016). *J. Am. Chem. Soc.* 138: 3094–3106. https://doi.org/10.1021/jacs.5b12408.

368 Zhuang, D., Nie, J., and Yang, J. (2011). *J. Polym. Sci., Part A: Polym. Chem.* 49: 1999–2007. https://doi.org/10.1002/pola.24627.

369 Tran, J.D., Mikulec, S.N., Calzada, O.M. et al. (2020). *Macromol. Chem. Phys.* 221: 1900397. https://doi.org/10.1002/macp.201900397.

370 Ahmed, M. and Narain, R. (2011). *Biomaterials* 32: 5279–5290. https://doi.org/10.1016/j.biomaterials.2011.03.082.

371 Kirkland-York, S., Zhang, Y., Smith, A.E. et al. (2010). *Biomacromolecules* 11: 1052–1059. https://doi.org/10.1021/bm100020x.

372 Tao, L., Liu, J., Xu, J., and Davis, T.P. (2009). *Org. Biomol. Chem.* 7: 3481–3485. https://doi.org/10.1039/B907061C.

373 Deng, Z., Ahmed, M., and Narain, R. (2009). *J. Polym. Sci., Part A: Polym. Chem.* 47: 614–627.

374 Manning, K.B., Shtukenberg, A.G., Nichols, S.M. et al. (2015). *J. Polym. Sci., Part A: Polym. Chem.* 53: 2563–2568. https://doi.org/10.1002/pola.27774.

375 Adharis, A., Vesper, D., Koning, N., and Loos, K. (2018). *Green Chem.* 20: 476–484. https://doi.org/10.1039/C7GC03023A.

376 Li, Y., Lokitz, B.S., and McCormick, C.L. (2006). *Angew. Chem. Int. Ed.* 45: 5792–5795. https://doi.org/10.1002/anie.200602168.

377 Deng, Z.C., Bouchekif, H., Babooram, K. et al. (2008). *J. Polym. Sci., Part A: Polym. Chem.* 46: 4984–4996. https://doi.org/10.1002/pola.22826.
378 Kanayama, N., Shibata, H., Kimura, A. et al. (2009). *Biomacromolecules* 10: 805–813. https://doi.org/10.1021/bm801301b.
379 Kellum, M.G., Smith, A.E., York, S.K., and McCormick, C.L. (2010). *Macromolecules* 43: 7033–7040. https://doi.org/10.1021/ma100983p.
380 Kellum, M.G., Harris, C.A., McCormick, C.L., and Morgan, S.E. (2011). *J. Polym. Sci., Part A: Polym. Chem.* 49: 1104–1111. https://doi.org/10.1002/pola.24524.
381 Jiang, X.Z., Zhang, J.Y., Zhou, Y.M. et al. (2008). *J. Polym. Sci., Part A: Polym. Chem.* 46: 860–871. https://doi.org/10.1002/pola.22430.
382 Shan, J., Zhao, Y., Granqvist, N., and Tenhu, H. (2009). *Macromolecules* 42: 2696–2701. https://doi.org/10.1021/ma802482e.
383 Isoda, K., Kanayama, N., Miyamoto, D. et al. (2011). *React. Funct. Polym.* 71: 367–371. https://doi.org/10.1016/j.reactfunctpolym.2010.11.020.
384 Zhou, Y., Jiang, K., Chen, Y., and Liu, S. (2008). *J. Polym. Sci., Part A: Polym. Chem.* 46: 6518–6531. https://doi.org/10.1002/pola.22961.
385 Rodriguez-Emmenegger, C., Schmidt, B.V.K.J., Sedlakova, Z. et al. (2011). *Macromol. Rapid Commun.* 32: 958–965. https://doi.org/10.1002/marc.201100176.
386 Donovan, M.S., Lowe, A.B., Sanford, T.A., and McCormick, C.L. (2003). *J. Polym. Sci., Part A: Polym. Chem.* 41: 1262–1281. https://doi.org/10.1002/pola.10658.
387 Lokitz, B.S., Convertine, A.J., Ezell, R.G. et al. (2006). *Macromolecules* 39: 8594–8602. https://doi.org/10.1021/ma061672y.
388 Zorn, M., Meuer, S., Tahir, M.N. et al. (2008). *J. Mater. Chem.* 18: 3050–3058. https://doi.org/10.1039/b802666a.
389 Barsbay, M., Guven, O., Davis, T.P. et al. (2009). *Polymer* 50: 973–982. https://doi.org/10.1016/j.polymer.2008.12.027.
390 Flores, J.D., Shin, J., Hoyle, C.E., and McCormick, C.L. (2010). *Polym. Chem.* 1: 213–220. https://doi.org/10.1039/B9PY00294D.
391 Kopeć, M., Krys, P., Yuan, R., and Matyjaszewski, K. (2016). *Macromolecules* 49: 5877–5883. https://doi.org/10.1021/acs.macromol.6b01336.
392 He, J.-Y. and Lu, M. (2019). *J. Macromol. Sci., Part A: Pure Appl. Chem.* 56: 443–449. https://doi.org/10.1080/10601325.2019.1581575.
393 Chernikova, E., Terpugova, P., Filippov, A. et al. (2009). *Russ. J. Appl. Chem.* 82: 1882–1889. https://doi.org/10.1134/s1070427209100267.
394 Chandrawati, R., Städler, B., Postma, A. et al. (2009). *Biomaterials* 30: 5988–5998. https://doi.org/10.1016/j.biomaterials.2009.07.040.
395 Li, J. and Benicewicz, B.C. (2013). *J. Polym. Sci., Part A: Polym. Chem.* 51: 3572–3582. https://doi.org/10.1002/pola.26748.
396 Alex, J., González, K., Kindel, T. et al. (2020). *Biomacromolecules* https://doi.org/10.1021/acs.biomac.0c00096.
397 Stals, P.J.M., Cheng, C.-Y., van Beek, L. et al. (2016). *Chem. Sci.* 7: 2011–2015. https://doi.org/10.1039/C5SC02319J.

398 Chien, H.-W., Xu, X., Ella-Menye, J.-R. et al. (2012). *Langmuir* 28: 17778–17784. https://doi.org/10.1021/la303390j.
399 Chytil, P., Etrych, T., Kríz, J. et al. (2010). *Eur. J. Pharm. Sci.* 41: 473–482. https://doi.org/10.1016/j.ejps.2010.08.003.
400 York, A.W., Huang, F., and McCormick, C.L. (2010). *Biomacromolecules* 11: 505–514. https://doi.org/10.1021/bm901249n.
401 Rossi, N.A.A., Zou, Y., Scott, M.D., and Kizhakkedathu, J.N. (2008). *Macromolecules* 41: 5272–5282. https://doi.org/10.1021/ma800606k.
402 York, A.W., Zhang, Y., Holley, A.C. et al. (2009). *Biomacromolecules* 10: 936–943. https://doi.org/10.1021/bm8014768.
403 Luo, Q., Xiao, X., Dai, X. et al. (2018). *ACS Appl. Mater. Interfaces* 10: 1575–1588. https://doi.org/10.1021/acsami.7b16345.
404 Ju, Y., Xing, C., Wu, D. et al. (2017). *Chem. Eur. J.* 23: 3366–3374. https://doi.org/10.1002/chem.201604843.
405 Cuthbert, J., Zhang, T., Biswas, S. et al. (2018). *Macromolecules* 51: 9184–9191. https://doi.org/10.1021/acs.macromol.8b01880.
406 Liu, Y., Kang, G., Sun, L. et al. (2020). *ACS Appl. Polym. Mater.* 2: 263–272. https://doi.org/10.1021/acsapm.9b00786.
407 Ohshio, M., Mizoue, Y., Shiino, D. et al. (2020). *Polym. J.* 52: 189–197. https://doi.org/10.1038/s41428-019-0278-0.
408 Huo, M., Zeng, M., Li, D. et al. (2017). *Macromolecules* 50: 8212–8220. https://doi.org/10.1021/acs.macromol.7b01629.
409 Du, C., Ma, X., Li, J., and Wu, C. (2017). *J. Appl. Polym. Sci.*: 134. https://doi.org/10.1002/app.44751.
410 Meek, K.M., Sharick, S., Ye, Y. et al. (2015). *Macromolecules* 48: 4850–4862. https://doi.org/10.1021/acs.macromol.5b00926.
411 Ye, Y., Choi, J.-H., Winey, K.I., and Elabd, Y.A. (2012). *Macromolecules* 45: 7027–7035. https://doi.org/10.1021/ma301036b.
412 Guan, S. and Chen, A. (2020). *ACS Macro Lett.* 9: 14–19. https://doi.org/10.1021/acsmacrolett.9b00868.
413 Zhu, Y., Quek, J.Y., Lowe, A.B., and Roth, P.J. (2013). *Macromolecules* 46: 6475–6484. https://doi.org/10.1021/ma401096r.
414 Zhu, J., Zhu, X.L., Cheng, Z.P. et al. (2002). *Polymer* 43: 7037–7042. https://doi.org/10.1016/S0032-3861(02)00655-9.
415 Gu, Y., Zhao, J., Liu, Q. et al. (2015). *Polym. Chem.* 6: 359–363. https://doi.org/10.1039/C4PY01248H.
416 Zhu, M.-Q., Wang, L.-Q., Exarhos, G.J., and Li, A.D.Q. (2004). *J. Am. Chem. Soc.* 126: 2656–2657. https://doi.org/10.1021/ja038544z.
417 Zhou, Y., Zhu, J.A., Zhu, X.L., and Cheng, Z.P. (2006). *Radiat. Phys. Chem.* 75: 485–492. https://doi.org/10.1016/j.radphyschem.2005.10.012.
418 Zhang, Z.B., Zhu, X.L., Zhu, J. et al. (2006). *J. Polym. Sci., Part A: Polym. Chem.* 44: 3343–3354. https://doi.org/10.1002/pola.21438.
419 Zhang, Z., Wang, W., Cheng, Z. et al. (2010). *Macromolecules* 43: 7979–7984. https://doi.org/10.1021/ma101379r.

420 Zhang, Z., Wang, W., Xia, H. et al. (2009). *Macromolecules* 42: 7360–7366. https://doi.org/10.1021/ma901064h.
421 Wang, H., Chang, T., Li, X. et al. (2016). *Nanoscale* 8: 14950–14955. https://doi.org/10.1039/C6NR04459J.
422 Tu, K., Xu, T., Zhang, L. et al. (2017). *RSC Adv.* 7: 24040–24045. https://doi.org/10.1039/C7RA03103C.
423 Zhang, Z., Zhang, W., Zhu, X. et al. (2007). *J. Polym. Sci., Part A: Polym. Chem.* 45: 5722–5730. https://doi.org/10.1002/pola.22320.
424 Chen, L., Chen, B., Liu, X. et al. (2016). *J. Mater. Chem. B* 4: 3377–3386. https://doi.org/10.1039/C6TB00315J.
425 Pan, J., Miao, J., Zhang, L. et al. (2013). *Polym. Chem.* 4: 5664–5670. https://doi.org/10.1039/C3PY00671A.
426 Hirosawa, K., Fujii, K., Ueki, T. et al. (2016). *Macromolecules* 49: 8249–8253. https://doi.org/10.1021/acs.macromol.6b01987.
427 Sohn, H.-S., Cha, S.-H., Lee, W.-K. et al. (2011). *Macromol. Res.* 19: 722–728. https://doi.org/10.1007/s13233-011-0705-3.
428 Zhang, Y., Cheng, Z., Chen, X. et al. (2007). *Macromolecules* 40: 4809–4817. https://doi.org/10.1021/ma070257i.
429 Sun, B., Zhu, X.L., Zhu, H. et al. (2007). *Macromol. Chem. Phys.* 208: 1101–1109. https://doi.org/10.1002/macp.200700040.
430 Xu, Y., Sun, J., Chen, H. et al. (2015). *J. Polym. Sci., Part A: Polym. Chem.* 53: 1305–1309. https://doi.org/10.1002/pola.27600.
431 Huang, Z., Zhang, L., Cheng, Z., and Zhu, X. (2017). *Polymers* 9: 4. https://doi.org/10.3390/polym9010004.
432 Zhang, S., Yin, L., Wang, J. et al. (2017). *Polymers* 9: 26. https://doi.org/10.3390/polym9010026.
433 Zhu, J., Zhu, X.L., Zhou, D., and Chen, J.Y. (2003). *e-Polymers* 3: 576–586. https://doi.org/10.1515/epoly.2003.3.1.576.
434 Hernández-Ortiz, J.C., Jaramillo-Soto, G., Palacios-Alquisira, J., and Vivaldo-Lima, E. (2010). *Macromol. React. Eng.* 4: 210–221. https://doi.org/10.1002/mren.200900047.
435 Tian, C., Xu, T., Zhang, L. et al. (2016). *RSC Adv.* 6: 34659–34665. https://doi.org/10.1039/C6RA02809H.
436 Ji, Y., Zhang, L., Gu, X. et al. (2017). *Angew. Chem. Int. Ed.* 56: 2328–2333. https://doi.org/10.1002/anie.201610305.
437 Kim, S.-M., Han, S.S., Kim, A.Y. et al. (2015). *J. Nanosci. Nanotechnol.* 15: 7866–7870. https://doi.org/10.1166/jnn.2015.11216.
438 Kwak, Y., Nicolay, R., and Matyjaszewski, K. (2009). *Macromolecules* 42: 3738–3742. https://doi.org/10.1021/ma9005389.
439 Fu, Z., Tao, W., and Shi, Y. (2008). *J. Polym. Sci., Part A: Polym. Chem.* 46: 362–372. https://doi.org/10.1002/pola.22386.
440 Zheng, G.H. and Pan, C.Y. (2006). *Macromolecules* 39: 95–102. https://doi.org/10.1021/ma0517897.
441 Hui, J., Dong, Z., Shi, Y. et al. (2014). *RSC Adv.* 4: 55529–55538. https://doi.org/10.1039/c4ra08715a.

442 Li, Z., Li, D., Wang, L. et al. (2019). *Polymer* 168: 16–20. https://doi.org/10.1016/j.polymer.2019.02.004.

443 Sui, X., Fu, Z., and Shi, Y. (2011). *J. Appl. Polym. Sci.* 121: 1860–1865. https://doi.org/10.1002/app.33589.

444 Sievers, M., Namyslo, J.C., Lederle, F., and Hübner, E.G. (2018). *Express Polym. Lett.* 12: 556–568. https://doi.org/10.3144/expresspolymlett.2018.46.

445 Sudalai, A., Kanagasabapathy, S., and Benicewicz, B.C. (2000). *Org. Lett.* 2: 3213–3216. https://doi.org/10.1021/ol006407q.

446 Severac, R., Lacroix-Desmazes, P., and Boutevin, B. (2002). *Polym. Int.* 51: 1117–1122. https://doi.org/10.1002/pi.932.

447 Favier, A., Charreyre, M.T., Chaumont, P., and Pichot, C. (2002). *Macromolecules* 35: 8271–8280. https://doi.org/10.1021/ma020550c.

448 Houillot, L., Bui, C., Save, M. et al. (2007). *Macromolecules* 40: 6500–6509. https://doi.org/10.1021/ma0703249.

449 Seifert, D., Kipping, M., Adler, H.K.P., and Kuckling, D. (2007). *Macromol. Symp.* 254: 386–391. https://doi.org/10.1002/masy.200750856.

450 Tang, T., Castelletto, V., Parras, P. et al. (2006). *Macromol. Chem. Phys.* 207: 1718–1726.

451 Ladaviere, C., Dorr, N., and Claverie, J.P. (2001). *Macromolecules* 34: 5370–5372. https://doi.org/10.1021/ma010358v.

452 Zhang, X., Oddon, M., Giani, O. et al. (2010). *Macromolecules* 43: 2654–2656. https://doi.org/10.1021/ma9025916.

453 de Lambert, B., Charreyre, M.-T., Chaix, C., and Pichot, C. (2007). *Polymer* 48: 437–447. https://doi.org/10.1016/j.polymer.2006.11.059.

454 Marcelo, G., Martinho, J.M.G., and Farinha, J.P.S. (2013). *J. Phys. Chem. B* 117: 3416–3427. https://doi.org/10.1021/jp312198k.

455 Saikia, P.J., Lee, J.M., Lee, B.H., and Choe, S. (2007). *J. Polym. Sci., Part A: Polym. Chem.* 45: 348–360. https://doi.org/10.1002/pola.21834.

456 Butte, A., Storti, G., and Morbidelli, M. (2001). *Macromolecules* 34: 5885–5896. https://doi.org/10.1021/ma002130y.

457 Kanagasabapathy, S., Sudalai, A., and Benicewicz, B.C. (2001). *Macromol. Rapid Commun.* 22: 1076–1080. https://doi.org/10.1002/1521-3927(20010901)22:13<1076::AID-MARC1076>3.0.CO;2-K.

458 Chernikova, E., Yulusov, V., Mineeva, K. et al. (2011). *Polym. Sci., Ser. B* 53: 437–447. https://doi.org/10.1134/s1560090411070025.

459 Chernikova, E.V., Morozov, A.V., Kaziev, M.B. et al. (2007). *Polym. Sci., Ser. A* 49: 962–974. https://doi.org/10.1134/s0965545x07090027.

460 Lacroix-Desmazes, P., Severac, R., and Boutevin, B. (2002). *ACS Symp. Ser.* 854: 570–585. https://doi.org/10.1021/bk-2003-0854.ch039.

461 Favier, A., D'Agosto, F., Charreyre, M.-T., and Pichot, C. (2004). *Polymer* 45: 7821–7830. https://doi.org/10.1016/j.polymer.2004.09.042.

462 Relogio, P., Bathfield, M., Haftek-Terreau, Z. et al. (2013). *Polym. Chem.* 4: 2968–2981. https://doi.org/10.1039/C3PY00059A.

463 Raust, J.-A., Houillot, L., Save, M. et al. (2010). *Macromolecules* 43: 8755–8765. https://doi.org/10.1021/ma101627d.

464 Lou, X., Zhang, G., Herrera, I. et al. (2007). *Angew. Chem. Int. Ed.* 46: 6111–6114. https://doi.org/10.1002/anie.200700796.

465 Li, Y., Yang, J.W., and Benicewicz, B.C. (2007). *J. Polym. Sci., Part A: Polym. Chem.* 45: 4300–4308. https://doi.org/10.1002/pola.22172.

466 Legge, T.M., Slark, A.T., and Perrier, S. (2007). *Macromolecules* 40: 2318–2326. https://doi.org/10.1021/ma061372g.

467 Perrier, S., Takolpuckdee, P., Westwood, J., and Lewis, D.M. (2004). *Macromolecules* 37: 2709–2717. https://doi.org/10.1021/ma035468b.

468 Gemici, H., Legge, T.M., Whittaker, M. et al. (2007). *J. Polym. Sci., Part A: Polym. Chem.* 45: 2334–2340. https://doi.org/10.1002/pola.21985.

469 Lee, H.-G., Munir, S., and Park, S.-Y. (2016). *ACS Appl. Mater. Interfaces* 8: 26407–26417. https://doi.org/10.1021/acsami.6b09624.

470 Seo, J., Song, M., Jeong, J. et al. (2016). *ACS Appl. Mater. Interfaces* 8: 23862–23867. https://doi.org/10.1021/acsami.6b08257.

471 Lee, D.-Y., Seo, J.-M., Khan, W. et al. (2010). *Soft Matter* 6: 1964–1970. https://doi.org/10.1039/B926461B.

472 Omer, M., Islam, M.T., Khan, M. et al. (2014). *Macromol. Res.* 22: 888–894. https://doi.org/10.1007/s13233-014-2112-z.

473 Khan, W., Seo, J.-M., and Park, S.-Y. (2011). *Soft Matter* 7: 780–787. https://doi.org/10.1039/C0SM00758G.

474 Omer, M. and Park, S.-Y. (2014). *Anal. Bioanal. Chem.* 406: 5369–5378. https://doi.org/10.1007/s00216-014-7900-y.

475 Paulusse, J.M.J., Amir, R.J., Evans, R.A., and Hawker, C.J. (2009). *J. Am. Chem. Soc.* 131: 9805–9812. https://doi.org/10.1021/ja903245p.

476 Krivorotova, T., Vareikis, A., Gromadzki, D. et al. (2010). *Eur. Polym. J.* 46: 546–556. https://doi.org/10.1016/j.eurpolymj.2009.12.001.

477 Seo, M., Beck, B.J., Paulusse, J.M.J. et al. (2008). *Macromolecules* 41: 6413–6418. https://doi.org/10.1021/ma8009678.

478 Kim, S., Lee, B., Kim, S. et al. (2010). *Macromol. Chem. Phys.* 211: 1188–1195. https://doi.org/10.1002/macp.201000104.

479 Kim, B.J., Bang, J., Hawker, C.J. et al. (2007). *Langmuir* 23: 12693–12703. https://doi.org/10.1021/la701906n.

480 Campos, L.M., Killops, K.L., Sakai, R. et al. (2008). *Macromolecules* 41: 7063–7070. https://doi.org/10.1021/ma801630n.

481 O'Reilly, R.K., Joralemon, M.J., Hawker, C.J., and Wooley, K.L. (2006). *J. Polym. Sci., Part A: Polym. Chem.* 44: 5203–5217. https://doi.org/10.1002/pola.21602.

482 O'Reilly, R.K., Joralemon, M.J., Hawker, C.J., and Wooley, K.L. (2006). *Chem. Eur. J.* 12: 6776–6786. https://doi.org/10.1002/chem.200600467.

483 Grover, G.N., Alconcel, S.N.S., Matsumoto, N.M., and Maynard, H.D. (2009). *Macromolecules* 42: 7657–7663. https://doi.org/10.1021/ma901036x.

484 Chang, C.-W., Bays, E., Tao, L. et al. (2009). *Chem. Commun.*: 3580–3582. https://doi.org/10.1039/b904456f.

485 Nishi, H. and Kobatake, S. (2008). *Chem. Lett.* 37: 630–631. https://doi.org/10.1246/cl.2008.630.

486 Feng, X.S. and Pan, C.Y. (2002). *Macromolecules* 35: 4888–4893. https://doi.org/10.1021/ma020004j.
487 Xiao, N.-Y., Li, A.-L., Liang, H., and Lu, J. (2008). *Macromolecules* 41: 2374–2380. https://doi.org/10.1021/ma702510n.
488 Fu, Q., Cheng, L.L., Zhang, Y., and Shi, W.F. (2008). *Polymer* 49: 4981–4988. https://doi.org/10.1016/j.polymer.2008.09.017.
489 Tinsley, J.F., Jahnke, J.P., Adamson, D.H. et al. (2009). *Energy Fuels* 23: 2065–2074. https://doi.org/10.1021/ef800651d.
490 Wang, Y., Ai, Q., and Lu, J. (2015). *J. Polym. Sci., Part A: Polym. Chem.* 53: 1422–1429. https://doi.org/10.1002/pola.27601.
491 Senyek, M.L., Kulig, J.J., and Parker, D.K. (2002). Dibenzyltrithiocarbonate molecular weight regulator for emulsion polymerization of butadiene and styrene (Goodyear Tire & Rubber), US6369158B1.
492 Tang, C., Kowalewski, T., and Matyjaszewski, K. (2003). *Macromolecules* 36: 8587–8589. https://doi.org/10.1021/ma034942a.
493 Li, A.L., Wang, Y., Liang, H., and Lu, J. (2006). *J. Polym. Sci., Part A: Polym. Chem.* 44: 2376–2387. https://doi.org/10.1002/pola.21316.
494 D'Agosto, F., Hughes, R., Charreyre, M.-T. et al. (2003). *Macromolecules* 36: 621–629. https://doi.org/10.1021/ma025646l.
495 Jo, Y.S., van der Vlies, A.J., Gantz, J. et al. (2008). *Macromolecules* 41: 1140–1150. https://doi.org/10.1021/ma071710t.
496 Kumar, S., Deike, S., and Binder, W.H. (2018). *Macromol. Rapid Commun.* 39: 1700507. https://doi.org/10.1002/marc.201700507.
497 Liu, Y., Tu, W., and Cao, D. (2010). *Ind. Eng. Chem. Res.* 49: 2707–2715. https://doi.org/10.1021/ie901143p.
498 Dong, S., Sun, W., Wang, D. et al. (2019). *Macromol. Rapid Commun.* 40: 1900058. https://doi.org/10.1002/marc.201900058.
499 Seno, R. and Kobatake, S. (2015). *Dyes Pigm.* 114: 166–174. https://doi.org/10.1016/j.dyepig.2014.11.010.
500 Li, D., Luo, Y., Li, B.-G., and Zhu, S. (2008). *J. Polym. Sci., Part A: Polym. Chem.* 46: 970–978. https://doi.org/10.1002/pola.22440.
501 Ladaviere, C., Lacroix-Desmazes, P., and Delolme, F. (2009). *Macromolecules* 42: 70–84. https://doi.org/10.1021/ma8013788.
502 Ribaut, T., Oberdisse, J., Annighofer, B. et al. (2011). *J. Phys. Chem. B* 115: 836–843. https://doi.org/10.1021/jp108888x.
503 Wang, Y., Li, A.-L., Liang, H., and Lu, J. (2006). *Eur. Polym. J.* 42: 2695–2702. https://doi.org/10.1016/j.eurpolymj.2006.06.015.
504 Christman, K.L., Vazquez-Dorbatt, V., Schopf, E. et al. (2008). *J. Am. Chem. Soc.* 130: 16585–16591. https://doi.org/10.1021/ja803676r.
505 Cerda, M.M., Newton, T.D., Zhao, Y. et al. (2019). *Chem. Sci* 10: 1773–1779. https://doi.org/10.1039/C8SC04683B.
506 Vishnevetskii, D.V., Plutalova, A.V., Yulusov, V.V. et al. (2015). *Polym. Sci., Ser. B* 57: 197–206. https://doi.org/10.1134/S1560090415030094.
507 Chernikova, E.V., Zaitsev, S.D., Plutalova, A.V. et al. (2018). *RSC Adv.* 8: 14300–14310. https://doi.org/10.1039/C8RA00048D.

508 Chen, C.-L., Lo, Y.-H., Lee, C.-Y. et al. (2010). *Inorg. Chem. Commun.* 13: 603–605. https://doi.org/10.1016/j.inoche.2010.02.013.

509 Luo, Y.W., Liu, B., Wang, Z.H. et al. (2007). *J. Polym. Sci., Part A: Polym. Chem.* 45: 2304–2315. https://doi.org/10.1002/pola.21999.

510 Mori, H. and Tanaka, H. (2011). *Macromol. Chem. Phys.* 212: 2349–2359. https://doi.org/10.1002/macp.201100357.

511 Hua, D.B., Ge, X.P., Bai, R.K. et al. (2005). *Polymer* 46: 12696–12702. https://doi.org/10.1016/j.polymer.2005.10.111.

512 Han, D.-H. and Pan, C.-Y. (2008). *J. Polym. Sci., Part A: Polym. Chem.* 46: 341–352. https://doi.org/10.1002/pola.22384.

513 Mori, H. and Okabayashi, S. (2009). *React. Funct. Polym.* 69: 441–449. https://doi.org/10.1016/j.reactfunctpolym.2009.01.012.

514 Wu, M., Zhang, H., and Liu, H. (2019). *Polym. Bull.* 76: 825–848. https://doi.org/10.1007/s00289-018-2411-1.

515 Wong, K.H., Davis, T.P., Barner-Kowollik, C., and Stenzel, M.H. (2007). *Polymer* 48: 4950–4965. https://doi.org/10.1016/j.polymer.2007.06.048.

516 Roohi, F. and Titirici, M.M. (2008). *New J. Chem.* 32: 1409–1414. https://doi.org/10.1039/b800851e.

517 Mori, H., Kato, I., Matsuyama, M., and Endo, T. (2008). *Macromolecules* 41: 5604–5615. https://doi.org/10.1021/ma800181h.

518 Mori, H., Iwaya, H., Nagai, A., and Endo, T. (2005). *Chem. Commun.*: 4872–4874. https://doi.org/10.1039/b509212d.

519 Mori, H., Sutoh, K., Iwaya, H. et al. (2006). Controlled synthesis of amino acid-based polymers by reversible addition fragmentation chain transfer polymerization. In: *Controlled/Living Radical Polymerization. From Synthesis to Materials*, Controlled/Living Radical Polymerization, vol. 944 (ed. K. Matyjaszewski), 533–546. Washington, DC: American Chemical Society. https://doi.org/10.1021/bk-2006-0944.ch036.

520 Mori, H., Matsuyama, M., Sutoh, K., and Endo, T. (2006). *Macromolecules* 39: 4351–4360. https://doi.org/10.1021/ma052756u.

521 Singh, P., Srivastava, A., and Kumar, R. (2014). *Polym. Int.* 63: 633–645. https://doi.org/10.1002/pi.4549.

522 Yonenuma, R., Ishizuki, A., Nakabayashi, K., and Mori, H. *J. Polym. Sci., Part A: Polym. Chem.* https://doi.org/10.1002/pola.29531.

523 Wang, J., Zhu, X.L., Cheng, Z.P. et al. (2007). *J. Polym. Sci., Part A: Polym. Chem.* 45: 3788–3797. https://doi.org/10.1002/pola.22105.

524 Maki, Y., Mori, H., and Endo, T. (2007). *Macromol. Chem. Phys.* 208: 2589–2599. https://doi.org/10.1002/macp.200700330.

525 Li, H., Shen, H., Pei, C. et al. (2019). *ChemCatChem* 11: 3882–3891. https://doi.org/10.1002/cctc.201900626.

526 Mettry, M., Hess, A.E., Goetting, I. et al. (2019). *J. Vac. Sci. Technol., A* 37: 020923. https://doi.org/10.1116/1.5080119.

527 Mori, H., Tando, I., and Tanaka, H. (2010). *Macromolecules* 43: 7011–7020. https://doi.org/10.1021/ma100820z.

528 Mori, H., Masuda, S., and Endo, T. (2008). *Macromolecules* 41: 632–639. https://doi.org/10.1021/ma0714262.
529 Mori, H., Masuda, S., and Endo, T. (2006). *Macromolecules* 39: 5976–5978. https://doi.org/10.1021/ma0612879.
530 Metz, N. and Theato, P. (2007). *Eur. Polym. J.* 43: 1202–1209. https://doi.org/10.1016/j.eurpolymj.2007.01.009.
531 Roth, P.J. and Theato, P. (2011). *ACS Symp. Ser.* 1066: 23–37 (3 pp). https://doi.org/10.1021/bk-2011-1066.ch003.
532 Mori, H., Kudo, E., Saito, Y. et al. (2010). *Macromolecules* 43: 7021–7032. https://doi.org/10.1021/ma100905w.
533 Xu, S., Li, J., and Chen, L. (2011). *Talanta* 85: 282–289. https://doi.org/10.1016/j.talanta.2011.03.060.
534 Zamyshlyayeva, O.G., Ionychev, B.N., Frolova, A.I. et al. (2019). *Russ. J. Appl. Chem.* 92: 775–786. https://doi.org/10.1134/S1070427219060077.
535 Han, J., Silcock, P., McQuillan, A.J., and Bremer, P. (2008). *Colloid Polym. Sci.* 286: 1605–1612. https://doi.org/10.1007/s00396-008-1934-7.
536 Zhu, M.Q., Wei, L.H., Li, M. et al. (2001). *Chem. Commun.*: 365–366. https://doi.org/10.1039/B009815I.
537 Jia, Y.-g., Liu, L.-y., Lei, B. et al. (2011). *Macromolecules* 44: 6311–6317. https://doi.org/10.1021/ma201247d.
538 Serbin, A.V., Karaseva, E.N., Dunaeva, I.V. et al. (2011). *Polym. Sci., Ser. B* 53: 116–124. https://doi.org/10.1134/s1560090411030079.
539 Abrunhosa, I., Gulea, M., and Masson, S. (2004). *Synthesis* 2004: 928–934 (928 pp). https://doi.org/10.1055/s-2004-822311.
540 Inglis, A.J., Sinnwell, S., Stenzel, M.H., and Barner-Kowollik, C. (2009). *Angew. Chem. Int. Ed.* 48: 2411–2414. https://doi.org/10.1002/anie.200805993.
541 Goldmann, A.S., Tischer, T., Barner, L. et al. (2011). *Biomacromolecules* 12: 1137–1145. https://doi.org/10.1021/bm101461h.
542 Kumar, J., Bousquet, A., and Stenzel, M.H. (2011). *Macromol. Rapid Commun.* 32: 1620–1626. https://doi.org/10.1002/marc.201100331.
543 Glassner, M., Delaittre, G., Kaupp, M. et al. (2012). *J. Am. Chem. Soc.* 134: 7274–7277. https://doi.org/10.1021/ja301762y.
544 Inglis, A.J., Sinnwell, S., Davis, T.P. et al. (2008). *Macromolecules* 41: 4120–4126. https://doi.org/10.1021/ma8002328.
545 Alberti, A., Benaglia, M., Guerra, M. et al. (2005). *Macromolecules* 38: 7610–7618. https://doi.org/10.1021/ma050652d.
546 Dürr, C.J., Hlalele, L., Kaiser, A. et al. (2013). *Macromolecules* 46: 49–62. https://doi.org/10.1021/ma302017c.
547 Previero, A. and Pechere, J.-F. (1970). *Biochem. Biophys. Res. Commun.* 40: 549–556. https://doi.org/10.1016/0006-291X(70)90937-X.
548 Niu, X., Ran, F., Chen, L. et al. (2016). *Langmuir* 32: 4297–4304. https://doi.org/10.1021/acs.langmuir.6b00562.
549 Christmann, J., Ibrahim, A., Charlot, V. et al. (2016). *ChemPhysChem* 17: 2309–2314. https://doi.org/10.1002/cphc.201600034.

550 Keddie, D.J., Guerrero-Sanchez, C., and Moad, G. (2013). *Polym. Chem.* 4: 3591–3601. https://doi.org/10.1039/c3py00487b.

551 Yang, C. and Cheng, Y.L. (2006). *J. Appl. Polym. Sci.* 102: 1191–1201. https://doi.org/10.1002/app.24415.

552 Toyoshima, M. and Miura, Y. (2009). *J. Polym. Sci., Part A: Polym. Chem.* 47: 1412–1421. https://doi.org/10.1002/pola.23250.

553 Quan, C.-Y., Wu, D.-Q., Chang, C. et al. (2009). *J. Phys. Chem. C* 113: 11262–11267. https://doi.org/10.1021/jp902637n.

554 Jaramillo-Soto, G. and Vivaldo-Lima, E. (2012). *Aust. J. Chem.* 65: 1177–1185. https://doi.org/10.1071/CH12291.

555 Wang, S., Vajjala Kesava, S., Gomez, E.D., and Robertson, M.L. (2013). *Macromolecules* 46: 7202–7212. https://doi.org/10.1021/ma4011846.

556 Moad, G. (2022). Dithicarbamates in RAFT polymerization. In: *RAFT Polymerization: Materials, Synthesis and Applications* (eds. G. Moad and E. Rizzardo), 551–610. Weinheim: Wiley-VCH.

557 Fortenberry, A.W., McCormick, C.L., and Smith, A.E. (2022). Considerations for and applications of aqueous RAFT polymerization. In: *RAFT Polymerization: Materials, Synthesis and Applications* (eds. G. Moad and E. Rizzardo), 679–706. Weinheim: Wiley-VCH.

558 Thomas, D.B., Convertine, A.J., Hester, R.D. et al. (2004). *Macromolecules* 37: 1735–1741. https://doi.org/10.1021/ma035572t.

559 Lima, V., Jiang, X.L., Brokken-Zijp, J. et al. (2005). *J. Polym. Sci., Part A: Polym. Chem.* 43: 959–973. https://doi.org/10.1002/pola.20558.

560 Coulembier, O., Lohmeijer, B.G.G., Dove, A.P. et al. (2006). *Macromolecules* 39: 5617–5628. https://doi.org/10.1021/ma0611366.

561 Zheng, Y., Turner, W., Zong, M. et al. (2011). *Macromolecules* 44: 1347–1354. https://doi.org/10.1021/ma1027092.

562 Inglis, A.J., Pierrat, P., Muller, T. et al. (2010). *Soft Matter* 6: 82–84. https://doi.org/10.1039/B920806M.

563 Inglis, A.J., Stenzel, M.H., and Barner-Kowollik, C. (2009). *Macromol. Rapid Commun.* 30: 1792–1798. https://doi.org/10.1002/marc.200900363.

564 Yu, Y., Li, G., Kang, H., and Youk, J. (2012). *Colloid Polym. Sci.* 290: 1707–1712. https://doi.org/10.1007/s00396-012-2788-6.

565 Kinoshita, K., Takami, T., Mori, Y. et al. (2017). *J. Polym. Sci., Part A: Polym. Chem.* 55: 1356–1365. https://doi.org/10.1002/pola.28504.

566 Li, W., Li, J., Gao, J. et al. (2011). *Biomaterials* 32: 3832–3844. https://doi.org/10.1016/j.biomaterials.2011.01.075.

567 Akimoto, J., Nakayama, M., Sakai, K., and Okano, T. (2009). *Biomacromolecules* 10: 1331–1336. https://doi.org/10.1021/bm900032r.

568 Akimoto, J., Nakayama, M., Sakai, K., and Okano, T. (2008). *J. Polym. Sci., Part A: Polym. Chem.* 46: 7127–7137. https://doi.org/10.1002/pola.23017.

569 Akimoto, J., Nakayama, M., Sakai, K. et al. (2013). *Polym. J.* 45: 233–237. https://doi.org/10.1038/pj.2012.108.

570 Bathfield, M., D'Agosto, F., Spitz, R. et al. (2006). *J. Am. Chem. Soc.* 128: 2546–2547. https://doi.org/10.1021/ja057481c.

571 Zheng, Q. and Pan, C.Y. (2005). *Macromolecules* 38: 6841–6848. https://doi.org/10.1021/ma050455e.
572 Aamer, K.A. and Tew, G.N. (2007). *J. Polym. Sci., Part A: Polym. Chem.* 45: 5618–5625. https://doi.org/10.1002/pola.22309.
573 Yang, H., Liang, F., Wang, X. et al. (2013). *Macromolecules* 46: 2754–2759. https://doi.org/10.1021/ma400261y.
574 Yuan, K., Li, Z.F., Lu, L.L., and Shi, X.N. (2007). *Mater. Lett.* 61: 2033–2036. https://doi.org/10.1016/j.matlet.2006.08.010.
575 Yuan, K., Lu, L.-L., Li, Z.-F., and Shi, X.-N. (2008). *Chin. J. Chem.* 26: 1929–1934. https://doi.org/10.1002/cjoc.200890346.
576 Warren, N.J., Rosselgong, J., Madsen, J., and Armes, S.P. (2015). *Biomacromolecules* 16: 2514–2521. https://doi.org/10.1021/acs.biomac.5b00767.
577 Sun, P., Zhang, Y., Shi, L., and Gan, Z. (2010). *Macromol. Biosci.* 10: 621–631. https://doi.org/10.1002/mabi.200900434.
578 Gurbuz, N., Demirci, S., Yavuz, S., and Caykara, T. (2011). *J. Polym. Sci., Part A: Polym. Chem.* 49: 423–431. https://doi.org/10.1002/pola.24454.
579 Favier, A., Luneau, B., Vinas, J. et al. (2009). *Macromolecules* 42: 5953–5964. https://doi.org/10.1021/ma9006939.
580 Li, C., Han, J., Ryu, C.Y., and Benicewicz, B.C. (2006). *Macromolecules* 39: 3175–3183. https://doi.org/10.1021/ma051983t.
581 Liu, J., Yang, W., Zareie, H.M. et al. (2009). *Macromolecules* 42: 2931–2939. https://doi.org/10.1021/ma802256g.
582 Xu, J., Tao, L., Liu, J. et al. (2009). *Macromolecules* 42: 6893–6901. https://doi.org/10.1021/ma901290a.
583 Xu, J., Tao, L., Boyer, C. et al. (2011). *Macromolecules* 44: 299–312. https://doi.org/10.1021/ma102386j.
584 Roth, P.J., Wiss, K.T., Zentel, R., and Theato, P. (2008). *Macromolecules* 41: 8513–8519. https://doi.org/10.1021/ma801681b.
585 Wiss, K.T. and Theato, P. (2010). *J. Polym. Sci., Part A: Polym. Chem.* 48: 4758–4767. https://doi.org/10.1002/pola.24267.
586 Li, Y. and Benicewicz, B.C. (2007). *Polym. Prepr. (Am. Chem. Soc., Div. Polym. Chem.)* 48: 524–525.
587 Quemener, D., Davis, T.P., Barner-Kowollik, C., and Stenzel, M.H. (2006). *Chem. Commun.*: 5051–5053. https://doi.org/10.1039/b611224b.
588 Gondi, S.R., Vogt, A.P., and Sumerlin, B.S. (2007). *Macromolecules* 40: 474–481. https://doi.org/10.1021/ma061959v.
589 Mendonça, P.V., Serra, A.C., Popov, A.V. et al. (2014). *React. Funct. Polym.* 81: 1–7. https://doi.org/10.1016/j.reactfunctpolym.2014.04.001.
590 Hanisch, A., Schmalz, H., and Müller, A.H.E. (2012). *Macromolecules* 45: 8300–8309. https://doi.org/10.1021/ma3017579.
591 Ye, Y.-S., Chen, Y.-N., Wang, J.-S. et al. (2012). *Chem. Mater.* 24: 2987–2997. https://doi.org/10.1021/cm301345r.
592 Shi, G.Y., Tang, X.Z., and Pan, C.Y. (2008). *J. Polym. Sci., Part A: Polym. Chem.* 46: 2390–2401. https://doi.org/10.1002/pola.22573.

593 Goldmann, A.S., Quemener, D., Millard, P.E. et al. (2008). *Polymer* 49: 2274–2281. https://doi.org/10.1016/j.polymer.2008.03.017.

594 Zhang, K., Gao, L., and Chen, Y. (2010). *Polymer* 51: 2809–2817. https://doi.org/10.1016/j.polymer.2010.04.042.

595 Zhu, J., Zhu, X., Kang, E.T., and Neoh, K.G. (2007). *Polymer* 48: 6992–6999. {Goldmann, 2008 #1001}

596 Cha, Y., Jarrett-Wilkins, C., Rahman, M.A. et al. (2019). *ACS Macro Lett.* 8: 835–840. https://doi.org/10.1021/acsmacrolett.9b00335.

597 Zhou, F., Li, Y., Jiang, G. et al. (2015). *Polym. Chem.* 6: 6885–6893. https://doi.org/10.1039/C5PY01003A.

598 Lorenz, M., Vogg, S., Finkelstein, P. et al. (2019). *Macromol. Mater. Eng.* 304: 1900311. https://doi.org/10.1002/mame.201900311.

599 Alidedeoglu, A.H., Harris, C.A., Martinez-Castro, N. et al. (2010). *ACS Symp. Ser.* 1053: 113–129 (6 pp). https://doi.org/10.1021/bk-2010-1053.ch006.

600 Zhou, F., Zhang, Z., Jiang, G. et al. (2016). *Polym. Chem.* 7: 2785–2789. https://doi.org/10.1039/C6PY00545D.

601 Müllner, M., Schallon, A., Walther, A. et al. (2010). *Biomacromolecules* 11: 390–396. https://doi.org/10.1021/bm901099p.

602 Ting, S.R.S., Granville, A.M., Quemener, D. et al. (2007). *Aust. J. Chem.* 60: 405–409. https://doi.org/10.1071/CH07089.

603 Arslan, M., Aydin, D., Degirmenci, A. et al. (2017). *ACS Omega* 2: 6658–6667. https://doi.org/10.1021/acsomega.7b00787.

604 Long, S., Tang, Q., Wu, Y. et al. (2014). *React. Funct. Polym.* 80: 15–20. https://doi.org/10.1016/j.reactfunctpolym.2013.11.006.

605 Tang, Q. and Zhang, K. (2015). *Polym. Int.* 64: 1060–1065. https://doi.org/10.1002/pi.4906.

606 Stamenović, M.M., Espeel, P., Baba, E. et al. (2013). *Polym. Chem.* 4: 184–193. https://doi.org/10.1039/C2PY20751F.

607 Li, A., Ma, J., Sun, G. et al. (2012). *J. Polym. Sci., Part A: Polym. Chem.* 50: 1681–1688. https://doi.org/10.1002/pola.25954.

608 Patton, D.L. and Advincula, R.C. (2006). *Macromolecules* 39: 8674–8683. https://doi.org/10.1021/ma061382h.

609 Su, L., Heo, G.S., Lin, Y.-N. et al. (2017). *J. Polym. Sci., Part A: Polym. Chem.* 55: 2966–2970. https://doi.org/10.1002/pola.28647.

610 Zhang, J., Pellechia, P.J., Hayat, J. et al. (2013). *Macromolecules* 46: 1618–1624. https://doi.org/10.1021/ma4000013.

611 Qiao, Y., Islam, M.S., Yin, X. et al. (2015). *Polymer* 72: 428–435. https://doi.org/10.1016/j.polymer.2015.02.011.

612 Müller, R., Feuerstein, T.J., Trouillet, V. et al. (2018). *Chem. Eur. J.* 24: 18933–18943. https://doi.org/10.1002/chem.201803966.

613 Jiang, Y., Lu, H., Dag, A. et al. (2016). *J. Mater. Chem. B* 4: 2017–2027. https://doi.org/10.1039/C5TB02576A.

614 Jiang, Y., Liang, M., Svejkar, D. et al. (2014). *Chem. Commun.* 50: 6394–6397. https://doi.org/10.1039/C4CC00616J.

615 Zhao, J., Zhou, Y., Zhou, Y. et al. (2016). *Polym. Chem.* 7: 1782–1791. https://doi.org/10.1039/C5PY01861G.
616 Lederhose, P., Abt, D., Welle, A. et al. (2018). *Chem. Eur. J.* 24: 576–580. https://doi.org/10.1002/chem.201705393.
617 Chang, D. and Olsen, B.D. (2016). *Polym. Chem.* 7: 2410–2418. https://doi.org/10.1039/C5PY01894C.
618 Spiridon, M.C., Demazy, N., Brochon, C. et al. (2020). *Macromolecules* 53: 68–77. https://doi.org/10.1021/acs.macromol.9b01551.
619 Qin, X., Li, Y., Zhou, F. et al. (2015). *Appl. Surf. Sci.* 328: 183–192. https://doi.org/10.1016/j.apsusc.2014.12.019.
620 Guo, J., Poros-Tarcali, E., and Perez-Mercader, J. (2019). *Chem. Commun.* 55: 9383–9386. https://doi.org/10.1039/C9CC03486B.
621 dos Santos, A.M., Pohn, J., Lansalot, M., and D'Agosto, F. (2007). *Macromol. Rapid Commun.* 28: 1325–1332. https://doi.org/10.1002/marc.200700146.
622 Ma, Y., Zhao, Y., Bejjanki, N.K. et al. (2019). *ACS Nano* 13: 8890–8902. https://doi.org/10.1021/acsnano.9b02466.
623 Zhou, W., Wang, J., Ding, P. et al. (2019). *Angew. Chem. Int. Ed.* 58: 8494–8498. https://doi.org/10.1002/anie.201903513.
624 Hu, C., Dong, B., and Liu, L. (2019). *J. Polym. Sci., Part A: Polym. Chem.* 57: 1333–1343. https://doi.org/10.1002/pola.29394.
625 Martins dos Santos, A., Le Bris, T., Graillat, C. et al. (2009). *Macromolecules* 42: 946–956. https://doi.org/10.1021/ma802117h.
626 Bharatiya, B., Yusa, S.-I., Aswal, V. et al. (2011). *Bull. Soc. Chem. Soc. Jpn.* 84: 1227–1233. https://doi.org/10.1246/bcsj.20110184.
627 Zheng, Q., Zheng, G.-H., and Pan, C.-Y. (2006). *Polym. Int.* 55: 1114–1123. https://doi.org/10.1002/pi.2089.
628 Bang, J., Kim, S.H., Drockenmuller, E. et al. (2006). *J. Am. Chem. Soc.* 128: 7622–7629. https://doi.org/10.1021/ja0608141.
629 El Asmar, A., Morandi, G., and Burel, F. (2019). *Macromolecules* 52: 9160–9167. https://doi.org/10.1021/acs.macromol.9b01348.
630 Wei, Z., Hao, X., Kambouris, P.A. et al. (2012). *Polymer* 53: 1429–1436. https://doi.org/10.1016/j.polymer.2012.02.011.
631 Wei, Z., Hao, X., Gan, Z., and Hughes, T.C. (2012). *J. Polym. Sci., Part A: Polym. Chem.* 50: 2378–2388. https://doi.org/10.1002/pola.26012.
632 Tao, L., Liu, J., Tan, B.H., and Davis, T.P. (2009). *Macromolecules* 42: 4960–4962. https://doi.org/10.1021/ma900865c.
633 Hu, X., Liu, G., Li, Y. et al. (2015). *J. Am. Chem. Soc.* 137: 362–368. https://doi.org/10.1021/ja5105848.
634 Zhang, M., Liu, H., Shao, W. et al. (2013). *Macromolecules* 46: 1325–1336. https://doi.org/10.1021/ma3025283.
635 Li, C., Liu, H., Tang, D., and Zhao, Y. (2015). *Polym. Chem.* 6: 1474–1486. https://doi.org/10.1039/C4PY01495B.
636 Zheng, L., Wang, Y., Zhang, X. et al. (2018). *Bioconjugate Chem.* 29: 190–202. https://doi.org/10.1021/acs.bioconjchem.7b00699.

637 Heidenreich, A.J. and Puskas, J.E. (2008). *J. Polym. Sci., Part A: Polym. Chem.* 46: 7621–7627. https://doi.org/10.1002/pola.23062.
638 Shallcross, L., Roche, K., Wilcock, C.J. et al. (2017). *J. Mater. Chem. B* 5: 6027–6033. https://doi.org/10.1039/C7TB00144D.
639 Heidenreich, A.J., Puskas, J.E., Schappacher, M. et al. (2012). *J. Polym. Sci., Part A: Polym. Chem.* 50: 1238–1247. https://doi.org/10.1002/pola.25889.
640 Zhang, M., Liu, H., Shao, W. et al. (2012). *Macromolecules* 45: 9312–9325. https://doi.org/10.1021/ma301973v.
641 Carter, S., Hunt, B., and Rimmer, S. (2005). *Macromolecules* 38: 4595–4603. https://doi.org/10.1021/ma047742n.
642 Carter, S., Rimmer, S., Sturdy, A., and Webb, M. (2005). *Macromol. Biosci.* 5: 373–378. https://doi.org/10.1002/mabi.200400218.
643 Hopkins, S., Carter, S., Swanson, L. et al. (2007). *J. Mater. Chem.* 17: 4022–4027. https://doi.org/10.1039/B708415C.
644 Rikkou-Kalourkoti, M. and Patrickios, C.S. (2012). *Macromolecules* 45: 7890–7899. https://doi.org/10.1021/ma3012416.
645 Wang, Z.M., He, J.P., Tao, Y.F. et al. (2003). *Macromolecules* 36: 7446–7452. https://doi.org/10.1021/ma025673b.
646 Pribyl, J. and Benicewicz, B.C. (2022). Surface and particle modification via RAFT polymerization: an update. In: *RAFT Polymerization: Materials, Synthesis and Applications* (eds. G. Moad and E. Rizzardo), 1017–1050. Weinheim: Wiley-VCH.
647 Gauthier-Jaques, M., Mutlu, H., Gaballa, H., and Theato, P. (2022). Synthesis and application of reactive polymers via RAFT polymerization. In: *RAFT Polymerization: Materials, Synthesis and Applications* (eds. G. Moad and E. Rizzardo), 829–872. Weinheim: Wiley-VCH.
648 Patton, D.L., Mullings, M., Fulghum, T., and Advincula, R.C. (2005). *Macromolecules* 38: 8597–8602. https://doi.org/10.1021/ma051035s.
649 You, Y.-Z., Manickam, D.S., Zhou, Q.-H., and Oupicky, D. (2007). *Biomacromolecules* 8: 2038–2044. https://doi.org/10.1021/bm0702049.
650 You, Y.-Z., Manickam, D.S., Zhou, Q.-H., and Oupický, D. (2007). *J. Controlled Release* 122: 217–225. https://doi.org/10.1016/j.jconrel.2007.04.020.
651 You, J.-O., Guo, P., and Auguste, D.T. (2013). *Angew. Chem. Int. Ed.* 52: 4141–4146. https://doi.org/10.1002/anie.201209804.
652 Achilleos, M., Krasia-Christoforou, T., and Patrickios, C.S. (2007). *Macromolecules* 40: 5575–5581. https://doi.org/10.1021/ma070614p.
653 You, Y.-Z., Zhou, Q.-H., Manickam, D.S. et al. (2007). *Macromolecules* 40: 8617–8624. https://doi.org/10.1021/ma071176p.
654 Pafiti, K.S., Loizou, E., Patrickios, C.S., and Porcar, L. (2010). *Macromolecules* 43: 5195–5204. https://doi.org/10.1021/ma100552v.
655 Park, N., Seo, M., and Kim, S.Y. (2012). *J. Polym. Sci., Part A: Polym. Chem.* 50: 4408–4414. https://doi.org/10.1002/pola.26256.
656 Huang, K., Canterbury, D.P., and Rzayev, J. (2010). *Macromolecules* 43: 6632–6638. https://doi.org/10.1021/ma100971w.

657 Harvey, A.C., Madsen, J., Douglas, C.W.I. et al. (2016). *Biomacromolecules* 17: 2710–2718. https://doi.org/10.1021/acs.biomac.6b00760.

658 Fu, W. and Zhao, B. (2016). *Polym. Chem.* 7: 6980–6991. https://doi.org/10.1039/C6PY01517D.

659 Zhu, K., Zhu, Z., Zhou, H. et al. (2017). *Chin. Chem. Lett.* 28: 1276–1284. https://doi.org/10.1016/j.cclet.2017.03.020.

660 Achilleos, M., Legge, T.M., Perrier, S., and Patrickios, C.S. (2008). *J. Polym. Sci., Part A: Polym. Chem.* 46: 7556–7565. https://doi.org/10.1002/pola.23061.

661 Pafiti, K.S., Patrickios, C.S., Abetz, C., and Abetz, V. (2013). *J. Polym. Sci., Part A: Polym. Chem.* 51: 4957–4965. https://doi.org/10.1002/pola.26936.

662 Peng, Z., Wang, D., Liu, X., and Tong, Z. (2007). *J. Polym. Sci., Part A: Polym. Chem.* 45: 3698–3706. https://doi.org/10.1002/pola.22119.

663 Porcarelli, L., Aboudzadeh, M.A., Rubatat, L. et al. (2017). *J. Power Sources* 364: 191–199. https://doi.org/10.1016/j.jpowsour.2017.08.023.

664 Su, X., Ma, B., Hu, J. et al. (2018). *Bioconjugate Chem.* 29: 4050–4061. https://doi.org/10.1021/acs.bioconjchem.8b00671.

665 Zhu, C., Zheng, M., Meng, F. et al. (2012). *Biomacromolecules* 13: 769–778. https://doi.org/10.1021/bm201693j.

666 Shi, Y., Zhu, W., Yao, D. et al. (2014). *ACS Macro Lett.* 3: 70–73. https://doi.org/10.1021/mz400619g.

667 Banerjee, R., Maiti, C., Dutta, S., and Dhara, D. (2015). *Polymer* 59: 243–251. https://doi.org/10.1016/j.polymer.2015.01.004.

668 Samakande, A., Sanderson, R.D., and Hartmann, P.C. (2009). *Eur. Polym. J.* 45: 649–657. https://doi.org/10.1016/j.eurpolymj.2008.11.014.

669 Li, J., Cong, H., Li, L., and Zheng, S. (2014). *ACS Appl. Mater. Interfaces* 6: 13677–13687. https://doi.org/10.1021/am503148v.

670 Banerjee, R., Maiti, S., and Dhara, D. (2014). *Green Chem.* 16: 1365–1373. https://doi.org/10.1039/C3GC41722K.

671 Delfanne, I. and Levesque, G. (1989). *Macromolecules* 22: 2589–2592. https://doi.org/10.1021/ma00196a007.

672 Dureault, A., Taton, D., Destarac, M. et al. (2004). *Macromolecules* 37: 5513–5519. https://doi.org/10.1021/ma030420j.

673 Allison-Logan, S., Karimi, F., Nothling, M.D., and Qiao, G.G. (2022). Star polymers by RAFT polymerization. In: *RAFT Polymerization: Materials, Synthesis and Applications* (eds. G. Moad and E. Rizzardo), 983–1016. Weinheim: Wiley-VCH.

674 Barner-Kowollik, C., Quinn, J.F., Nguyen, T.L.U. et al. (2001). *Macromolecules* 34: 7849–7857. https://doi.org/10.1021/ma010349m.

675 Sontakke, T.K. and Jagtap, R.N. (2013). *J. Dispersion Sci. Technol.* 34: 1575–1584. https://doi.org/10.1080/01932691.2012.756377.

676 Yao, L., Rong, M.Z., Zhang, M.Q., and Yuan, Y.C. (2011). *J. Mater. Chem.* 21: 9060–9065. https://doi.org/10.1039/C1JM10655D.

677 Becer, C.R., Groth, A.M., Hoogenboom, R. et al. (2008). *QSAR Comb. Sci.* 27: 977–983. https://doi.org/10.1002/qsar.200720159.

678 Zhou, G.T. and Ma, Y. (2008). *Chem. Lett.* 37: 850–851. https://doi.org/10.1246/cl.2008.850.
679 Lovestead, T.M., Hart-Smith, G., Davis, T.P. et al. (2007). *Macromolecules* 40: 4142–4153. https://doi.org/10.1021/ma0701484.
680 Haehnel, A.P., Stach, M., Chovancova, A. et al. (2014). *Polym. Chem.* 5: 862–873. https://doi.org/10.1039/C3PY00948C.
681 Herfurth, C., Voll, D., Buller, J. et al. (2012). *J. Polym. Sci., Part A: Polym. Chem.* 50: 108–118. https://doi.org/10.1002/pola.24994.
682 Gruendling, T., Hart-Smith, G., Davis, T.P. et al. (2008). *Macromolecules* 41: 1966–1971. https://doi.org/10.1021/ma702163v.
683 Johnston-Hall, G., Harjani, J.R., Scammells, P.J., and Monteiro, M.J. (2009). *Macromolecules* 42: 1604–1609. https://doi.org/10.1021/ma802795j.
684 Johnston-Hall, G. and Monteiro, M.J. (2008). *Macromolecules* 41: 727–736. https://doi.org/10.1021/ma702569m.
685 Szkurhan, A.R., Kasahara, T., and Georges, M.K. (2006). *J. Polym. Sci., Part A: Polym. Chem.* 44: 5708–5718. https://doi.org/10.1002/pola.21635.
686 Prescott, S.W., Ballard, M.J., Rizzardo, E., and Gilbert, R.G. (2002). *Macromolecules* 35: 5417–5425. https://doi.org/10.1021/ma011840g.
687 Prescott, S.W., Ballard, M.J., Rizzardo, E., and Gilbert, R.G. (2005). *Macromolecules* 38: 4901–4912. https://doi.org/10.1021/ma047373v.
688 Kaiser, A., Brandau, S., Klimpel, M., and Barner-Kowollik, C. (2010). *Macromol. Rapid Commun.* 31: 1616–1621. https://doi.org/10.1002/marc.201000162.
689 Wang, Y., Chen, Q., Liang, H., and Lu, J. (2007). *Polym. Int.* 56: 1514–1520. https://doi.org/10.1002/pi.2294.
690 Barner, L., Pereira, S., Sandanayake, S., and Davis, T.P. (2006). *J. Polym. Sci., Part A: Polym. Chem.* 44: 857–864. https://doi.org/10.1002/pola.21216.
691 Quinn, J.F., Rizzardo, E., and Davis, T.P. (2001). *Chem. Commun.*: 1044–1045. https://doi.org/10.1039/B101794M.
692 Matsumoto, M., Wakabayashi, R., Tada, T. et al. (2016). *Macromol. Chem. Phys.* 217: 2576–2583. https://doi.org/10.1002/macp.201600239.
693 Biswas, C., Mitra, K., Singh, S. et al. (2015). *Colloid Polym. Sci.* 293: 1749–1757. https://doi.org/10.1007/s00396-015-3562-3.
694 Biswas, C.S., Mitra, K., Singh, S., and Ray, B. (2016). *J. Chem. Sci.* 128: 415–420. https://doi.org/10.1007/s12039-016-1033-0.
695 Biswas, C.S., Wu, Y., Wang, Q. et al. (2017). *J. Rheol.* 61: 1345–1357. https://doi.org/10.1122/1.5006807.
696 Chaffey-Millar, H., Hart-Smith, G., and Barner-Kowollik, C. (2008). *J. Polym. Sci., Part A: Polym. Chem.* 46: 1873–1892. https://doi.org/10.1002/pola.22562.
697 Fujii, S., Yokoyama, Y., Nakayama, S. et al. (2018). *Langmuir* 34: 933–942. https://doi.org/10.1021/acs.langmuir.7b02670.
698 Lansalot, M., Davis, T.P., and Heuts, J.P.A. (2002). *Macromolecules* 35: 7582–7591. https://doi.org/10.1021/ma012214m.
699 Luo, Y.W., Wang, R., Yang, L. et al. (2006). *Macromolecules* 39: 1328–1337.
700 Wang, Z., Zhang, Q., Zhan, X. et al. (2016). *J. Polym. Res.* 23: 253. https://doi.org/10.1007/s10965-016-1152-9.

701 Urbani, C.N., Nguyen, H.N., and Monteiro, M.J. (2006). *Aust. J. Chem.* 59: 728–732. https://doi.org/10.1071/CH06231.
702 Hartmann, J., Urbani, C., Whittaker, M.R., and Monteiro, M.J. (2006). *Macromolecules* 39: 904–907. https://doi.org/10.1021/ma052295c.
703 Sirohi, S., Singh, D., Nain, R. et al. (2015). *RSC Adv.* 5: 34377–34382. https://doi.org/10.1039/C4RA16988C.
704 García-Peñas, A., Biswas, C.S., Liang, W. et al. (2019). *Polymers* 11: 991. https://doi.org/10.3390/polym11060991.
705 Theis, A., Stenzel, M.H., Davis, T.P., and Barner-Kowollik, C. (2006). Obtaining chain length dependent termination rate coefficients via thermally initiated reversible addition fragmentation chain transfer experiments. In: *Controlled/Living Radical Polymerization*, ACS Symposium Series, vol. 944, 486–500. American Chemical Society. https://doi.org/10.1021/bk-2006-0944.ch033.
706 Lovestead, T.M., Davis, T.P., Stenzel, M.H., and Barner-Kowollik, C. (2007). *Macromol. Symp.* 248: 82–93. https://doi.org/10.1002/masy.200750209.
707 Katsumoto, Y. and Kubosaki, N. (2008). *Macromolecules* 41: 5955–5956. https://doi.org/10.1021/ma800881r.
708 Yusa, S.-i., Fukuda, K., Yamamoto, T. et al. (2007). *Langmuir* 23: 12842–12848. https://doi.org/10.1021/la702741q.
709 Biswas, C.S., Patel, V.K., Vishwakarma, N.K. et al. (2011). *Macromolecules* 44: 5822–5824. https://doi.org/10.1021/ma200735k.
710 Shimoaka, T., Rikiyama, K., Katsumoto, Y., and Hasegawa, T. (2013). *Anal. Bioanal. Chem.* 405: 9411–9418. https://doi.org/10.1007/s00216-013-7400-5.
711 Alam, M., Keiko, H., Yusa, S., and Nakashima, K. (2014). *Colloid Polym. Sci.* 292: 1611–1617. https://doi.org/10.1007/s00396-014-3205-0.
712 Whittaker, M.R., Goh, Y.-K., Gemici, H. et al. (2006). *Macromolecules* 39: 9028–9034. https://doi.org/10.1021/ma061070e.
713 Yao, Z., Zhang, J.-S., Chen, M.-L. et al. (2011). *J. Appl. Polym. Sci.* 121: 1740–1746. https://doi.org/10.1002/app.33816.
714 Wang, Z.X., Zhang, Q.H., Yu, Y.T. et al. (2010). *Chin. Chem. Lett.* 21: 1497–1500. https://doi.org/10.1016/j.cclet.2010.06.001.
715 Wei, R., Luo, Y., and Li, Z. (2010). *Polymer* 51: 3879–3886. https://doi.org/10.1016/j.polymer.2010.06.023.
716 Qi, G.G., Nolan, M., Schork, F.J., and Jones, C.W. (2008). *J. Polym. Sci., Part A: Polym. Chem.* 46: 5929–5944. https://doi.org/10.1002/pola.22909.
717 Wang, Z., Zhang, Q., Zhan, X. et al. (2013). *J. Polym. Res.* 20: 1–13. https://doi.org/10.1007/s10965-013-0288-0.
718 Wei, R., Luo, Y., Zeng, W. et al. (2012). *Ind. Eng. Chem. Res.* 51: 15530–15535. https://doi.org/10.1021/ie302067n.
719 Yu, Y., Zhang, Q., Wang, Z. et al. (2012). *J. Macromol. Sci., Part A: Pure Appl. Chem.* 49: 60–66. https://doi.org/10.1080/10601325.2012.630946.
720 Yu, Y., Zhang, Q., Zhan, X., and Chen, F. (2013). *J. Appl. Polym. Sci.* 127: 2557–2565. https://doi.org/10.1002/app.37785.
721 Sun, X.Y., Luo, Y.W., Wang, R. et al. (2007). *Macromolecules* 40: 849–859. https://doi.org/10.1021/ma061677v.

722 Sun, X., Luo, Y., Wang, R. et al. (2008). *AIChE J.* 54: 1073–1087. https://doi.org/10.1002/aic.11446.

723 Nozari, S., Tauer, K., and Ali, A.M.I. (2005). *Macromolecules* 38: 10449–10454. https://doi.org/10.1021/ma051531g.

724 Schmid, C., Weidner, S., Falkenhagen, J., and Barner-Kowollik, C. (2012). *Macromolecules* 45: 87–99. https://doi.org/10.1021/ma2022452.

725 Goh, Y.-K. and Monteiro, M.J. (2006). *Macromolecules* 39: 4966–4974. https://doi.org/10.1021/ma060395s.

726 Johnston-Hall, G. and Monteiro, M.J. (2009). Influence of molecular weight distribution (MWD) on k_t and the onset of the gel effect using the RAFT-CLD-T method. In: *Controlled/Living Radical Polymerization: Progress in RAFT, DT, NMP & OMRP*, ACS Symposium Series, vol. 1024, 19–35. American Chemical Society. https://doi.org/10.1021/bk-2009-1024.ch002.

727 Oae, S., Yagihara, T., and Okabe, T. (1972). *Tetrahedron* 28: 3203–3216. https://doi.org/10.1016/S0040-4020(01)93661-0.

728 Chiacchio, M.-A., Legnani, L., Caramella, P. et al. (2018). *Tetrahedron* 74: 5627–5634. https://doi.org/10.1016/j.tet.2018.07.056.

729 Rajaram, S., Armstrong, P.B., Kim, B.J., and Frechet, J.M.J. (2009). *Chem. Mater.* 1775–1777. https://doi.org/10.1021/cm900911x.

730 Tam, W.Y., Mak, C.S.K., Ng, A.M.C. et al. (2009). *Macromol. Rapid Commun.* 30: 622–626. https://doi.org/10.1002/marc.200800714.

731 Nagai, A., Kokado, K., Miyake, J., and Chujo, Y. (2009). *J. Polym. Sci., Part A: Polym. Chem.* 48: 627–634. https://doi.org/10.1002/pola.23813.

732 He, J., Yan, B., Tremblay, L., and Zhao, Y. (2010). *Langmuir* 27: 436–444. https://doi.org/10.1021/la1040322.

733 Huang, Y., Hou, T., Cao, X. et al. (2010). *Polym. Chem.* 1: 1615–1623. https://doi.org/10.1039/C0PY00165A.

734 Hua, D., Tang, J., Jiang, J., and Zhu, X. (2009). *Polymer* 50: 5701–5707. https://doi.org/10.1016/j.polymer.2009.09.074.

735 He, S.-J., Zhang, Y., Cui, Z.-H. et al. (2009). *Eur. Polym. J.* 45: 2395–2401. https://doi.org/10.1016/j.eurpolymj.2009.04.030.

736 Zhang, X., Boisse, S., Bui, C. et al. (2012). *Soft Matter* 8: 1130–1141. https://doi.org/10.1039/C1SM06598J.

737 Tao, L., Kaddis, C.S., Loo, R.R.O. et al. (2009). *Chem. Commun.*: 2148–2150. https://doi.org/10.1039/b822799c.

738 Flores, J.D., Xu, X., Treat, N.J., and McCormick, C.L. (2009). *Macromolecules* 42: 4941–4945. https://doi.org/10.1021/ma900517w.

739 Min, E.H., Ting, S.R.S., Billon, L., and Stenzel, M.H. (2010). *J. Polym. Sci., Part A: Polym. Chem.* 48: 3440–3455. https://doi.org/10.1002/pola.24129.

740 Gody, G., Boullanger, P., Ladaviere, C. et al. (2008). *Macromol. Rapid Commun.* 29: 511–519. https://doi.org/10.1002/marc.200700768.

741 Jiang, X., Ahmed, M., Deng, Z., and Narain, R. (2009). *Bioconjugate Chem.* 20: 994–1001. https://doi.org/10.1021/bc800566f.

742 Mori, H., Matsuyama, M., and Endo, T. (2009). *Macromol. Chem. Phys.* 210: 217–229. https://doi.org/10.1002/macp.200800446.

743 Zhang, H., Deng, J., Lu, L., and Cai, Y. (2007). *Macromolecules* 40: 9252–9261. https://doi.org/10.1021/ma071287o.

744 Maksym, P., Tarnacka, M., Bielas, R. et al. (2020). *Polymer* 192: 122262. https://doi.org/10.1016/j.polymer.2020.122262.

745 Maki, Y., Mori, H., and Endo, T. (2007). *Macromolecules* 40: 6119–6130. https://doi.org/10.1021/ma062839q.

746 Semsarilar, M., Ladmiral, V., and Perrier, S.b. (2010). *Macromolecules* 43: 1438–1443. https://doi.org/10.1021/ma902587r.

747 Li, G., Zheng, H., and Bai, R. (2009). *Macromol. Rapid Commun.* 30: 442–447. https://doi.org/10.1002/marc.200800666.

748 Boyer, C., Whittaker, M., and Davis, T.P. (2011). *J. Polym. Sci., Part A: Polym. Chem.* 49: 5245–5256. https://doi.org/10.1002/pola.25001.

749 Kakuchi, R. and Theato, P. (2012). *Macromolecules* 45: 1331–1338. https://doi.org/10.1021/ma202175z.

750 O'Reilly, R.K. (2010). *Polym. Int.* 59: 568–573. https://doi.org/10.1002/pi.2830.

751 Ahmad, N.M., Charleux, B., Farcet, C. et al. (2009). *Macromol. Rapid Commun.* 30: 2002–2021. https://doi.org/10.1002/marc.200900450.

752 Ballard, N. and Asua, J.M. (2018). *Prog. Polym. Sci.* 79: 40–60. https://doi.org/10.1016/j.progpolymsci.2017.11.002.

753 Reyes, Y. and Asua, J.M. (2011). *Macromol. Rapid Commun.* 32: 63–67. https://doi.org/10.1002/marc.201000375.

754 Moad, G. and Barner-Kowollik, C. (2008). The mechanism and kinetics of the RAFT process: overview, rates, stabilities, side reactions, product spectrum and outstanding challenges. In: *Handbook of RAFT Polymerization* (ed. C. Barner-Kowollik), 51–104. Weinheim: Wiley-VCH. https://doi.org/10.1002/9783527622757.ch3.

755 Bar-Nes, G., Hall, R., Sharma, V. et al. (2009). *Eur. Polym. J.* 45: 3149–3163. https://doi.org/10.1016/j.eurpolymj.2009.08.004.

756 Wang, M., Marty, J.-D., and Destarac, M. (2022). Xanthates in RAFT polymerization. In: *RAFT Polymerization: Materials, Synthesis and Applications* (eds. G. Moad and E. Rizzardo), 495–550. Weinheim: Wiley-VCH.

757 Moad, G. (2019). *J. Polym. Sci., Part A: Polym. Chem.* 57: 216–227. https://doi.org/10.1002/pola.29199.

758 Fischer, H. and Radom, L. (2001). *Angew. Chem. Int. Ed.* 40: 1340–1371. https://doi.org/10.1002/1521-3773(20010417)40:8<1340::AID-ANIE1340>3.0.CO;2-%23.

759 Ladmiral, V., Legge, T.M., Zhao, Y.L., and Perrier, S. (2008). *Macromolecules* 41: 6728–6732. https://doi.org/10.1021/ma8010262.

760 Rosselgong, J. and Armes, S.P. (2012). *Macromolecules* 45: 2731–2737. https://doi.org/10.1021/ma3002609.

761 Nakabayashi, K., Tsuda, A., Otani, H., and Mori, H. (2015). *React. Funct. Polym.* 86: 52–59. https://doi.org/10.1016/j.reactfunctpolym.2014.11.004.

762 Leung, D. and Bowman, C.N. (2012). *Macromol. Chem. Phys.* 213: 198–204. https://doi.org/10.1002/macp.201100402.

763 Syrett, J.A., Haddleton, D.M., Whittaker, M.R. et al. (2011). *Chem. Commun.* 47: 1449–1451. https://doi.org/10.1039/C0CC04532B.

764 Luzon, M., Boyer, C., Peinado, C. et al. (2010). *J. Polym. Sci., Part A: Polym. Chem.* 48: 2783–2792. https://doi.org/10.1002/pola.24027.

765 Ting, S.R.S., Min, E.H., Zetterlund, P.B., and Stenzel, M.H. (2010). *Macromolecules* 43: 5211–5221. https://doi.org/10.1021/ma1004937.

766 Ferreira, J., Syrett, J., Whittaker, M. et al. (2011). *Polym. Chem.* 2: 1671–1677. https://doi.org/10.1039/C1PY00102G.

767 Floyd, T.G., Häkkinen, S., Hartlie, M. et al. (2022). Complex polymeric architectures synthesised through RAFT polymerization. In: *RAFT Polymerization: Materials, Synthesis and Applications* (eds. G. Moad and E. Rizzardo), 933–982. Weinheim: Wiley-VCH.

768 Krasia, T.C. and Patrickios, C.S. (2006). *Macromolecules* 39: 2467–2473. https://doi.org/10.1021/ma051747i.

769 Pafiti, K.S., Philippou, Z., Loizou, E. et al. (2011). *Macromolecules* 44: 5352–5362. https://doi.org/10.1021/ma200668v.

770 Alfurhood, J.A., Bachler, P.R., and Sumerlin, B.S. (2016). *Polym. Chem.* 7: 3361–3369. https://doi.org/10.1039/C6PY00571C.

771 Wang, X. and Gao, H. (2017). *Polymers* 9: 188. https://doi.org/10.3390/polym9060188.

772 Xu, J. (2019). *Macromolecules* 52: 9068–9093. https://doi.org/10.1021/acs.macromol.9b01365.

773 Haven, J.J., Hendrikx, M., Junkers, T. et al. (2018). Elements of RAFT navigation. RAFT 20 years later. RAFT-synthesis of uniform, sequence-defined (co)polymers. In: *Reversible Deactivation Radical Polymerization: Mechanisms and Synthetic Methodologies*, ACS Symposium Series, vol. 1284 (eds. K. Matyjaszewski, H. Gao, B.S. Sumerlin and N.V. Tsarevsky), 77–103. Washington, DC: American Chemical Society. https://doi.org/10.1021/bk-2018-1284.ch004.

774 Haven, J.J., Neve, J.D., and Junkers, T. (2022). Sequence-encoded RAFT oligomers and polymers. In: *RAFT Polymerization: Materials, Synthesis and Applications* (eds. G. Moad and E. Rizzardo), 805–828. Weinheim: Wiley-VCH.

775 McLeary, J.B., Tonge, M.P., and Klumperman, B. (2006). *Macromol. Rapid Commun.* 27: 1233–1240. https://doi.org/10.1002/marc.200600238.

776 McLeary, J.B., Calitz, F.M., McKenzie, J.M. et al. (2004). *Macromolecules* 37: 2383–2394. https://doi.org/10.1021/ma035478c.

777 Houshyar, S., Keddie, D., Moad, G. et al. (2012). *Polym. Chem.* 3: 1879–1889. https://doi.org/10.1039/C2PY00529H.

778 Guo, X., Choi, B., Feng, A., and Thang, S.H. (2018). *Macromol. Rapid Commun.* 39: 1800479. https://doi.org/10.1002/marc.201800479.

779 Kermagoret, A. and Gigmes, D. (2016). *Tetrahedron* 72: 7672–7685. https://doi.org/10.1016/j.tet.2016.07.002.

780 Pearson, S., St. Thomas, C., Guerrero-Santos, R., and D'Agosto, F. (2017). *Polym. Chem.* 8: 4916–4946. https://doi.org/10.1039/C7PY00344G.

781 Wager, C.M., Haddleton, D.M., and Bon, S.A.F. (2004). *Eur. Polym. J.* 40: 641–645. https://doi.org/10.1016/j.eurpolymj.2003.10.025.
782 Kwak, Y., Nicolay, R., and Matyjaszewski, K. (2009). *Aust. J. Chem.* 62: 1384–1401.
783 Ao, Y., He, J., Han, X. et al. (2007). *J. Polym. Sci., Part A: Polym. Chem.* 45: 374–387. https://doi.org/10.1002/pola.21798.
784 Li, C., He, J., Liu, Y. et al. (2012). *Aust. J. Chem.* 65: 1077–1089. https://doi.org/10.1071/CH12152.
785 Petton, L., Ciolino, A.E., Stamenović, M.M. et al. (2012). *Macromol. Rapid Commun.* 33: 1310–1315. https://doi.org/10.1002/marc.201200207.
786 Zehm, D., Laschewsky, A., Liang, H., and Rabe, J.P. (2011). *Macromolecules* 44: 9635–9641. https://doi.org/10.1021/ma2015613.
787 St Thomas, C., Maldonado-Textle, H., Rockenbauer, A. et al. (2012). *J. Polym. Sci., Part A: Polym. Chem.* 50: 2944–2956. https://doi.org/10.1002/pola.26081.
788 Moad, G. and Solomon, D.H. (2006). Propagation. In: *The Chemistry of Radical Polymerization*, 167–232. Oxford: Elsevier. https://doi.org/10.1016/B978-008044288-4/50023-6.
789 Moad, G. (2017). *Macromol. Chem. Phys.* 218: 1700381. https://doi.org/10.1002/macp.201700381.
790 Moad, G. and Solomon, D.H. (2006). Initiation. In: *The Chemistry of Radical Polymerization*, 49–166. Oxford: Elsevier. https://doi.org/10.1016/B978-008044288-4/50022-4.
791 Delduc, P., Tailhan, C., and Zard, S.Z. (1988). *J. Chem. Soc., Chem. Commun.*: 308–310. https://doi.org/10.1039/C39880000308.
792 Chapman, R., Jungb, K., and Boyer, C. (2022). Overview of photoregulated reversible addition-fragmentation chain transfer (RAFT) polymerization. In: *RAFT Polymerization: Materials, Synthesis and Applications* (eds. G. Moad and E. Rizzardo), 611–646. Weinheim: Wiley-VCH.
793 Li, S., Han, G., and Zhang, W. (2020). *Polym. Chem.* 11: 1830–1844. https://doi.org/10.1039/D0PY00054J.
794 Skrabania, K., Miasnikova, A., Bivigou-Koumba, A.M. et al. (2011). *Polym. Chem.* 2: 2074–2083. https://doi.org/10.1039/C1PY00173F.
795 McKenzie, T.G., Fu, Q., Uchiyama, M. et al. (2016). *Adv. Sci.* 3: 1500394. https://doi.org/10.1002/advs.201500394.
796 Shanmugam, S., Xu, J., and Boyer, C. (2017). *Macromol. Rapid Commun.* 38: 1700143. https://doi.org/10.1002/marc.201700143.
797 Xu, J., Shanmugam, S., Corrigan, N.A., and Boyer, C. (2015). Catalyst-free visible light-induced RAFT photopolymerization. In: *Controlled Radical Polymerization: Mechanisms*, ACS Symposium Series, vol. 1187 (eds. K. Matyjaszewski, B.S. Sumerlin, N.V. Tsarevsky and J. Chiefari), 247–267. American Chemical Society. https://doi.org/10.1021/bk-2015-1187.ch013.
798 Otsu, T. (2000). *J. Polym. Sci., Part A: Polym. Chem.* 38: 2121–2136. https://doi.org/10.1002/(SICI)1099-0518(20000615)38:12<2121::AID-POLA10>3.0.CO;2-X.
799 Upadhya, R., Murthy, N.S., Hoop, C.L. et al. (2019). *Macromolecules* 52: 8295–8304. https://doi.org/10.1021/acs.macromol.9b01923.

800 Lorandi, F., Fantin, M., and Matyjaszewski, K. (2022). Redox initiated RAFT polymerization and (electro)chemical activation of RAFT agents. In: *RAFT Polymerization: Materials, Synthesis and Applications* (eds. G. Moad and E. Rizzardo), 647–678. Weinheim: Wiley-VCH.

801 Strover, L.T., Cantalice, A., Lam, J.Y.L. et al. (2019). *Macro Lett.* 8: 1316–1322. https://doi.org/10.1021/acsmacrolett.9b00598.

802 Nicolaÿ, R. and Kwak, Y. (2012). *Isr. J. Chem.* 52: 288–305. https://doi.org/10.1002/ijch.201100124.

803 Lorandi, F., Fantin, M., Shanmugam, S. et al. (2019). *Macromolecules* 52: 1479–1488. https://doi.org/10.1021/acs.macromol.9b00112.

804 Liu, X.-h., Li, H.-n., Zhang, F.-j. et al. (2016). *Polymer* 107: 170–176. https://doi.org/10.1016/j.polymer.2016.11.019.

805 Jiang, H., Pan, X., Li, N. et al. (2017). *React. Funct. Polym.* 111: 1–6. https://doi.org/10.1016/j.reactfunctpolym.2016.12.007.

806 Nejad, E.H., Castignolles, P., Gilbert, R.G., and Guillaneuf, Y. (2008). *J. Polym. Sci., Part A: Polym. Chem.* 46: 2277–2289. https://doi.org/10.1002/pola.22563.

807 David, G., Asri, Z.E., Rich, S. et al. (2009). *Macromol. Chem. Phys.* 210: 631–639. https://doi.org/10.1002/macp.200800540.

808 Krstina, J., Moad, G., Rizzardo, E. et al. (1995). *Macromolecules* 28: 5381–5385. https://doi.org/10.1021/ma00119a034.

809 Krstina, J., Moad, C.L., Moad, G. et al. (1996). *Macromol. Symp.* 111: 13–23. https://doi.org/10.1002/masy.19961110104.

810 Luo, Y.W. and Cui, X.F. (2006). *J. Polym. Sci., Part A: Polym. Chem.* 44: 2837–2847. https://doi.org/10.1002/pola.21407.

811 Monteiro, M.J., Sjöberg, M., van der Vlist, J., and Göttgens, C.M. (2000). *J. Polym. Sci., Part A: Polym. Chem.* 38: 4206–4217. https://doi.org/dwkfgw.

812 D'Agosto, F., Lansalot, M., and Rieger, J. (2022). RAFT-mediated polymerization-induced self-assembly (PISA). In: *RAFT Polymerization: Materials, Synthesis and Applications* (eds. G. Moad and E. Rizzardo), 707–752. Weinheim: Wiley-VCH.

813 Farinha, J.P.S., Relogio, P., Charreyre, M.-T. et al. (2007). *Macromolecules* 40: 4680–4690. https://doi.org/10.1021/ma070444g.

814 Kitchin, A.D., Velate, S., Chen, M. et al. (2007). *Photochem. Photobiol. Sci.* 6: 853–856. https://doi.org/10.1039/b702811c.

815 Harvison, M.A., Roth, P.J., Davis, T.P., and Lowe, A.B. (2011). *Aust. J. Chem.* 64: 992–1006. https://doi.org/10.1071/CH11152.

816 Moad, G., Rizzardo, E., and Thang, S.H. (2011). *Polym. Int.* 60: 9–25. https://doi.org/10.1002/pi.2988.

817 Willcock, H. and O'Reilly, R.K. (2010). *Polym. Chem.* 1: 149–157. https://doi.org/10.1039/b9py00340a.

818 Desmet, G.B., D'hooge, D.R., Sabbe, M.K. et al. (2016). *J. Org. Chem.* 81: 11626–11634. https://doi.org/10.1021/acs.joc.6b01844.

819 Wu, Y., Zhou, Y., Zhu, J. et al. (2014). *Polym. Chem.* 5: 5546–5550. https://doi.org/10.1039/c4py00732h.

820 Shen, W., Qiu, Q., Wang, Y. et al. (2010). *Macromol. Rapid Commun.* 31: 1444–1448. https://doi.org/10.1002/marc.201000154.

821 Sumerlin, B.S., Lowe, A.B., Stroud, P.A. et al. (2003). *Langmuir* 19: 5559–5562.
822 Roth, P.J., Kessler, D., Zentel, R., and Theato, P. (2008). *Macromolecules* 41: 8316–8319. https://doi.org/10.1021/ma801869z.
823 Gibson, M.I., Fröhlich, E., and Klok, H.-A. (2009). *J. Polym. Sci., Part A: Polym. Chem.* 47: 4332–4345. https://doi.org/10.1002/pola.23486.
824 Urquhart, M.C., Dao, N.V., Ercole, F. et al. (2020). *ACS Macro Lett.* 9: 553–557. https://doi.org/10.1021/acsmacrolett.0c00066.
825 Lowe, A.B., Sumerlin, B.S., Donovan, M.S., and McCormick, C.L. (2002). *J. Am. Chem. Soc.* 124: 11562–11563. https://doi.org/10.1021/ja020556h.
826 Carlson, J.S., Hill, M.R., Young, T., and Costanzo, P.J. (2010). *Polym. Chem.* 1: 1423–1426. https://doi.org/10.1039/C0PY00191K.
827 Leon, N.H. and Asquith, R.S. (1970). *Tetrahedron* 26: 1719–1725. https://doi.org/10.1016/s0040-4020(01)93022-4.
828 Perrier, S., Takolpuckdee, P., and Mars, C.A. (2005). *Macromolecules* 38: 2033–2036. https://doi.org/10.1021/ma047611m.
829 Alagi, P., Hadjichristidis, N., Gnanou, Y., and Feng, X. (2019). *ACS Macro Lett.* 8: 664–669. https://doi.org/10.1021/acsmacrolett.9b00357.
830 Carmean, R.N., Figg, C.A., Scheutz, G.M. et al. (2017). *ACS Macro Lett.* 6: 185–189. https://doi.org/10.1021/acsmacrolett.7b00038.
831 Uchiyama, M., Satoh, K., and Kamigaito, M. (2019). *Chem. Commun.* 55: 5327–5330. https://doi.org/10.1039/C9CC00900K.
832 Gruendling, T., Dietrich, M., and Barner-Kowollik, C. (2009). *Aust. J. Chem.* 62: 806–812. https://doi.org/10.1071/CH09080.
833 Pfukwa, R., Pound, G., and Klumperman, B. (2008). *Polym. Prepr. (Am. Chem. Soc., Div. Polym. Chem.)* 49: 117–118.
834 Jesson, C.P., Pearce, C.M., Simon, H. et al. (2017). *Macromolecules* 50: 182–191. https://doi.org/10.1021/acs.macromol.6b01963.
835 Zhang, T. and Palasz, P.D. (2017). Thiocarbonylthio-free RAFT polymers and the process of making the same (Henkel), WO2017027557A1.
836 Vega-Rios, A. and Licea-Claverie, A. (2011). *J. Mex. Chem. Soc.* 55: 21–32. https://doi.org/10.29356/jmcs.v55i1.848.
837 Grellepois, F. and Portella, C. (2008). *Synthesis* 2008: 3443–3446 (3443 pp). https://doi.org/10.1055/s-0028-1083190.
838 Legge, T.M., Slark, A.T., and Perrier, S. (2006). *J. Polym. Sci., Part A: Polym. Chem.* 44: 6980–6987. https://doi.org/10.1002/pola.21803.
839 Bressy, C., Ngo, V.G., and Margaillan, A. (2013). *Polym. Degrad. Stab.* 98: 115–121. https://doi.org/10.1016/j.polymdegradstab.2012.10.023.
840 Bekanova, M.Z., Neumolotov, N.K., Jablanović, A.D. et al. (2019). *Polym. Degrad. Stab.* 164: 18–27. https://doi.org/10.1016/j.polymdegradstab.2019.03.017.
841 Xu, J., He, J., Fan, D. et al. (2006). *Macromolecules* 39: 3753–3759. https://doi.org/10.1021/ma060184n.
842 Metzner, P. (1999). *Top. Curr. Chem.* 204: 127–181. https://doi.org/10.1007/3-540-48956-8_2.

843 Heuzé, B., Gasparova, R., Heras, M., and Masson, S. (2000). *Tetrahedron Lett.* 41: 7327–7331. https://doi.org/10.1016/S0040-4039(00)01221-1.

844 Sinnwell, S., Inglis, A.J., Davis, T.P. et al. (2008). *Chem. Commun.*: 2052–2054. https://doi.org/10.1039/b718180a.

845 Sinnwell, S., Synatschke, C.V., Junkers, T. et al. (2008). *Macromolecules* 41: 7904–7912. https://doi.org/10.1021/ma8013959.

846 Sinnwell, S., Lammens, M., Stenzel, M.H. et al. (2009). *J. Polym. Sci., Part A: Polym. Chem.* 47: 2207–2213. https://doi.org/10.1002/pola.23299.

847 Sinnwell, S., Inglis, A.J., Stenzel, M.H., and Barner-Kowollik, C. (2008). *Macromol. Rapid Commun.* 29: 1090–1096. https://doi.org/10.1002/marc.200800233.

848 Nebhani, L., Sinnwell, S., Inglis, A.J. et al. (2008). *Macromol. Rapid Commun.* 29: 1431–1437. https://doi.org/10.1002/marc.200800244.

849 Nebhani, L., Gerstel, P., Atanasova, P. et al. (2009). *J. Polym. Sci., Part A: Polym. Chem.* 47: 7090–7095. https://doi.org/10.1002/pola.23756.

850 Nebhani, L., Sinnwell, S., Lin, C.Y. et al. (2009). *J. Polym. Sci., Part A: Polym. Chem.* 47: 6053–6071. https://doi.org/10.1002/pola.23647.

851 Bousquet, A., Boyer, C., Davis, T.P., and Stenzel, M.H. (2010). *Polym. Chem.* 1: 1186–1195. https://doi.org/10.1039/C0PY00075B.

852 Huisgen, R., Kalvinsch, I., Li, X., and Mloston, G. (2000). *Eur. J. Org. Chem.* 2000: 1685–1694. https://doi.org/10.1002/(sici)1099-0690(200005)2000:9<1685::aid-ejoc1685>3.0.co;2-6.

853 Mlostoń, G., Urbaniak, K., Gulea, M. et al. (2005). *Helv. Chim. Acta* 88: 2582–2592. https://doi.org/10.1002/hlca.200590198.

854 Katchalsky, A. and Eisenberg, H. (1951). *J. Polym. Sci.* 6: 145–154. https://doi.org/10.1002/pol.1951.120060202.

855 López-Pérez, L., Maldonado-Textle, H., Elizalde-Herrera, L.E. et al. (2019). *Polymer* 168: 116–125. https://doi.org/10.1016/j.polymer.2019.02.025.

856 Gilbert, R.G., Hess, M., Jenkins, A.D. et al. (2009). *Pure Appl. Chem.* 81: 351–353. https://doi.org/10.1351/PAC-REC-08-05-02.

9

Trithiocarbonates in RAFT Polymerization

Graeme Moad

CSIRO Manufacturing, Research Way, Clayton, VIC 3168, Australia

9.1 Introduction

Since 2008, trithiocarbonates, R—S(C=S)SR″ (Figure 9.1), have been the most popular form of transfer agents employed in radical polymerization with reversible addition–fragmentation chain transfer (RAFT polymerization) (Figure 9.2). This can be attributed to their broad applicability in controlling the polymerization of, in particular, MAMs, and their ready commercial availability or ease of synthesis. Trithiocarbonates can provide a good balance between high activity, and low retardation and incidence of side reactions. The use of thiocarbonates as RAFT agents was described in 1998 in the first patents on RAFT polymerization [1, 2] and the first open-literature publications concerning their application in RAFT polymerization appeared in 2000 [3, 4].

With appropriate selection of the substituents, trithiocarbonates provide good control (i.e. low dispersity, predicted M_n, high end-group fidelity) over RAFT polymerization of most MAMs [5]. Retardation is generally very low or not observable when targeting $M_n > 3000$ [6]. Some retardation is observed when preparing lower molar mass polymers [7]. Good control can also be observed for the IAM, *N*-vinylcarbazole (NVC) [8]. However, trithiocarbonates are not well suited for polymerization where all the monomers are LAMs, such as vinyl esters or vinyl amides, where strong retardation or inhibition is usually observed [5].

9.2 Mechanism of RAFT Polymerization with Trithiocarbonate Mediators

In general terms, the mechanism or trithiocarbonate-mediated RAFT polymerization is analogous to that involving other thiocarbonylthio RAFT agents (dithioesters, xanthates, or dithiocarbamates). However, we need to distinguish two classes of trithiocarbonates, known as the non-symmetric and symmetric RAFT agents that comprise one or two good homolytic leaving groups, respectively.

RAFT Polymerization: Methods, Synthesis and Applications, First Edition.
Edited by Graeme Moad and Ezio Rizzardo.

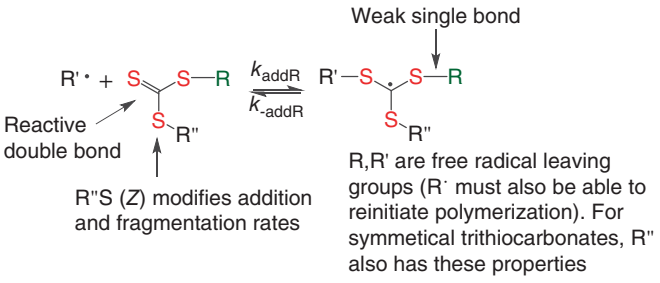

Figure 9.1 Structural features of trithiocarbonate RAFT agents and the intermediate formed on radical addition.

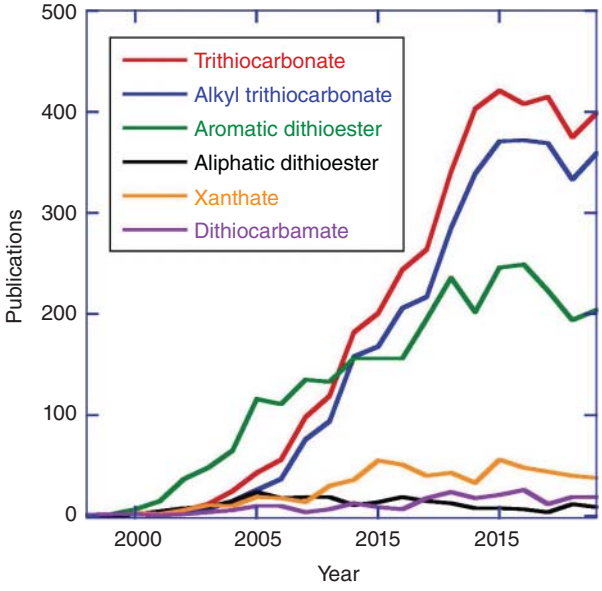

Figure 9.2 Publication rate for RAFT polymerization using different classes of RAFT agents. Includes both patent and open literature publications. Based on a Scifinder™ substructure search carried out in February 2020 on the RAFT agent structures and the terms 'RAFT' and 'MADIX' (in the case of xanthates). The term 'trithiocarbonate' includes all symmetric and non-symmetric trithiocarbonates. The term 'alkyl trithiocarbonate' embraces only non-symmetric trithiocarbonates where SR″ is a primary alkyl group of structure S-CH_3 or S-CH_2CH_2-alkyl.

The mechanism of RAFT polymerization with non-symmetric trithiocarbonate RAFT agents (R″SC(=S)SR, **1** in Scheme 9.1), where R· is a good homolytic leaving group and R″· is a poor homolytic leaving group with respect to the propagating species (P_n·), is described by the usual RAFT mechanism [9]. Examples of R″, which are poor homolytic leaving groups with respect to MAM propagating species, are primary alkyl (e.g. SR″ = $SC_{12}H_{25}$) and aryl. In the case of these RAFT agents, the trithiocarbonate functionality is always retained as the ω-chain-end.

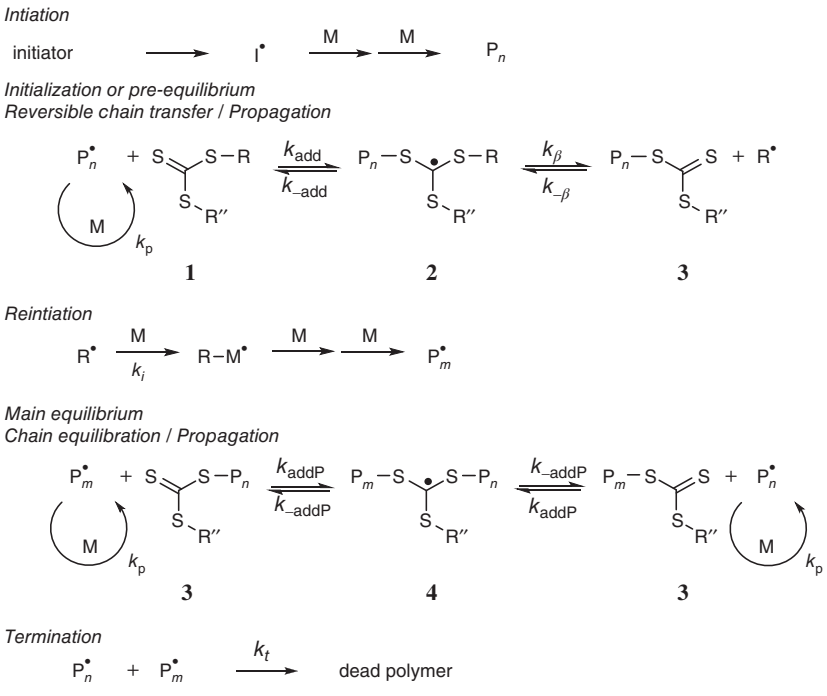

Scheme 9.1 Mechanism of RAFT polymerization with non-symmetric trithiocarbonates and R″ is a poor homolytic leaving group.

In the case of symmetric trithiocarbonates (RSC(=S)SR, **5** in Scheme 9.2), where both R substituents are good homolytic leaving groups, further reactions must be added as shown in Scheme 9.2. The product will usually retain the trithiocarbonate functionality located centrally within the polymer chain.

If the homolytic leaving group ability for the R substituent of the initial RAFT agent 5 is significantly lower than that of the propagating species P_n·, the trithiocarbonate functionality will not be centrally located at least for low monomer conversions [10–12]. In extreme cases, the mechanism, may be better represented by Scheme 9.1.

All radical species formed during RAFT polymerization, including I·, R·, and the various intermediates (e.g., **2**, **4**, **6**, **8** or **10**), may undergo termination by combination or disproportionation. However, rates of fragmentation for the intermediates formed by radical addition to the trithiocarbonates are usually sufficiently rapid that there is a low probability of intermediate radical termination in RAFT polymerization of MAMs.

The initiating species I· can also react by RAFT with any RAFT agent or macro-RAFT agent. This reaction assumes greater importance in polymerizations to give lower molar mass polymers and at high monomer conversions when the ratio of monomer to RAFT agent is low. The process is of particular importance or concern in single-unit monomer insertion (SUMI) experiments (Section 9.15) [13, 14]. Initiator-derived by-products can be largely avoided when the initiating radicals are generated directly from the RAFT agent, e.g. in PhotoRAFT, photoinduced electron

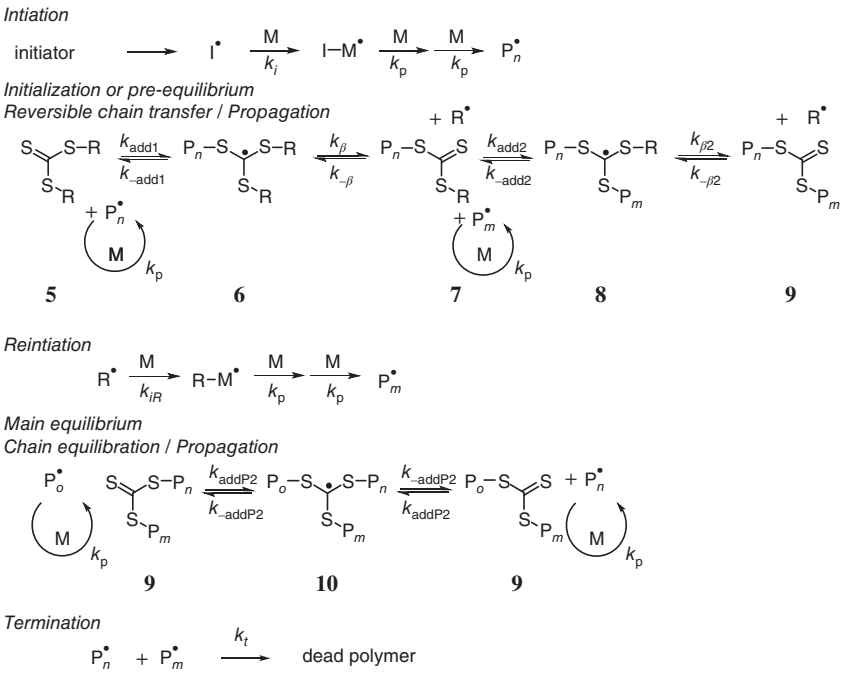

Scheme 9.2 Mechanism of RAFT polymerization with symmetric trithiocarbonates.

or energy transfer-RAFT (PET-RAFT, Section 9.17 and the Chapter 12 of Chapman et al. [15]), eRAFT or redox RAFT (Section 9.18 and the Chapter 13 of Lorandi et al. [16]).

9.2.1 Transfer Coefficients for Trithiocarbonates in RAFT Polymerization

The efficiency of an initial RAFT agent, such as the non-symmetric trithiocarbonate **1**, is determined by the values of two transfer coefficients, C_{tr} ($= k_{tr}/k_p$) and C_{-tr} ($= k_{-tr}/k_i$). The rate coefficient for chain transfer (k_{tr}) for a RAFT agent is then given by Eq (9.1), where the value of k_{tr} depends on the rate of addition of the propagating radical ($P_n\cdot$) to the RAFT agent and a partition coefficient (ϕ) that describes the partitioning of the intermediate radical (9.2) between the starting materials and products – refer to Scheme 9.1:

$$k_{tr} = k_{add}\phi = k_{add}\left[\frac{k_\beta}{k_{-add} + k_\beta}\right] \tag{9.1}$$

The transfer agent-derived radical (R·) is also partitioned between adding to the monomer and reacting with the macroRAFT agent (9.3). The rate coefficient associated with this reaction (k_{-tr}) is defined as shown in Eq. (9.2).

$$k_{-tr} = k_{-\beta}(1-\phi) = k_{-\beta}\left[\frac{k_{-add}}{k_{-add} + k_\beta}\right] \tag{9.2}$$

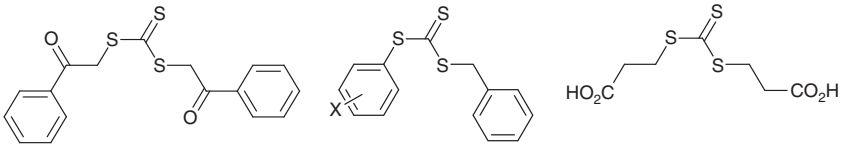

11 **12** **13**

Figure 9.3 Structures of some trithiocarbonates referred to in Table 9.1 (others appear in subsequent tables).

The high reactivity of trithiocarbonates towards radical addition means that $C_{-\mathrm{tr}}$ is unlikely to be zero.

For the case of symmetric RAFT agents we should consider a second set of transfer coefficients C_{tr2} ($= k_{\mathrm{tr2}}/k_{\mathrm{p}}$) and $C_{-\mathrm{tr2}}$ ($= k_{-\mathrm{tr2}}/k_{\mathrm{i}}$) relating to loss of the second R leaving group where the rate coefficients k_{tr2} and $k_{-\mathrm{tr2}}$ might be defined as shown in Eqs. (9.3) and (9.4) (assuming no dependence on P_n).

$$k_{\mathrm{tr2}} = k_{\mathrm{add2}}\phi_2 = k_{\mathrm{add2}}\left[\frac{k_{\beta 2}}{k_{-\mathrm{add2}} + k_{\beta 2}}\right] \tag{9.3}$$

$$k_{-\mathrm{tr2}} = k_{-\beta 2}\left(1 - \phi_2\right) = k_{-\beta 2}\left[\frac{k_{-\mathrm{add2}}}{k_{-\mathrm{add2}} + k_{\beta 2}}\right] \tag{9.4}$$

Little is known about values of C_{tr2} and $C_{-\mathrm{tr2}}$ and they are generally assumed to be the same as C_{tr} and $C_{-\mathrm{tr},}$ respectively, where R and R″ are the same. For RAFT homopolymerization, there should, in most circumstances, be no distinction between the propagating species attached to an intermediate.

Note that for macroRAFT agents in homopolymerization, or if the properties of R· are the same as those of $\mathrm{P}_n\cdot$, $k_{\beta} = k_{-\mathrm{add}}$ and $k_{\mathrm{tr}} = k_{-\mathrm{tr}} = k_{\mathrm{add}}/2$.

A listing of apparent transfer coefficients ($C_{\mathrm{tr}}{}^{\mathrm{app}}$) for trithiocarbonates is provided in Table 9.1 (see also Figure 9.3). The methods for determining apparent transfer coefficients ($C_{\mathrm{tr}}{}^{\mathrm{app}}$) of trithiocarbonates include the Mayo method (M in Table 9.1), the walling method (W) [20, 30–34], the dispersity method (D) [35, 36], and the $M_n(0)$ method [37] (B). Details of these methods are provided elsewhere in this volume [29]. It is implicit in the derivation of each of these methods that the value of $C_{-\mathrm{tr}}$ for the initial RAFT agent is zero. For the more active trithiocarbonates this assumption cannot be justified and the actual values of C_{tr} may be higher than $C_{\mathrm{tr}}{}^{\mathrm{app}}$ by as much as several orders of magnitude. Nonetheless, data obtained under a consistent set of polymerization conditions may still be relied on for a qualitative ranking of RAFT agent activity.

A method of evaluating transfer coefficients C_{tr} and $C_{-\mathrm{tr}}$, which is applicable when the transfer coefficients are high, involves an evaluation of the usage of transfer agent as a function of monomer conversion for several different initial RAFT agent concentrations (Method K in Table 9.1) [34, 38]. Values of transfer coefficients estimated by kinetic simulation are numbers chosen to fit the experimental data. For a range of values of $C_{-\mathrm{tr}}$ that may span orders of magnitude, it is often possible to choose a value of $C_{-\mathrm{tr}}$ such that a fit is obtained [13]. This may account for very different values that

Table 9.1 Transfer coefficients for initial trithiocarbonates in RAFT polymerization.

RAFT agent	Z (R′S)	R	Monomer[a)]	*T* (°C)	C_{tr}^{app}[b)]	C_{tr}	C_{-tr}	Method[c)]	References
14	$(CH_3)_2(CO_2H)CS$	$(CH_3)_2(CO_2H)C^{\cdot}$	St	70	25.2	—	—	M	[17]
11	$PhC(=O)CH_2S$	$PhC(=O)CH_2^{\cdot}$	St	70	19	—	—	M	[17]
13	$CH_2(CO_2H)CH_2S$	$CH_2(CO_2H)CH_2^{\cdot}$	St	70	4.3	—	—	M	[17]
63	$CH_2(CO_2H)CH_2S$	$CH_3\dot{C}H(CO_2H)$	St	70	13.9	—	—	M	[17]
48	$CH_2(CO_2H)CH_2S$	$(CH_3)_2(CO_2H)C^{\cdot}$	St	70	20.2	—	—	M	[17]
75	$C_{12}H_{25}S$	$PhCH_2^{\cdot}$	St	110	9.4	—	—	W	[18]
40	$C_{12}H_{25}S$	$(CH_3)_2\dot{C}(CN)$	St	70	—	1875	1.6	K	[13]
40	$C_{12}H_{25}S$	$(CH_3)_2\dot{C}(CN)$	St	80		128	0.23	K	[19]
40	$C_{12}H_{25}S$	$(CH_3)_2\dot{C}(CN)$	NIPAm	70	—	1850	10	K	[13]
22	$PhCH_2S$	$PhCH_2^{\cdot}$	St	110	18	—	—	W	[20]
12	4-(MeO)PhS	$PhCH_2^{\cdot}$	St	110	11.6	—	—	W	[18]
12	PhS	$PhCH_2^{\cdot}$	St	110	12.4	—	—	W	[18]
12	4-FPhS	$PhCH_2^{\cdot}$	St	110	18.5	—	—	W	[18]
12	3,4-F_2PhS	$PhCH_2^{\cdot}$	St	110	19.5	—	—	W	[18]
12	4-ClPhS	$PhCH_2^{\cdot}$	St	110	18.4	—	—	W	[18]
12	3,4-Cl_2PhS	$PhCH_2^{\cdot}$	St	110	17.4	—	—	W	[18]
12	2,3,4,5,6-Cl_5PhS	$PhCH_2^{\cdot}$	St	110	18.7	—	—	W	[18]
12	4-pyS	$PhCH_2^{\cdot}$	St	110	22.2	—	—	W	[18]
12	3,5-$(CF_3)_2$PhS	$PhCH_2^{\cdot}$	St	110	23.0	—	—	W	[18]
24	$PhCH(CN)C(S)S(CH_2)_4S$	$Ph\dot{C}H(CN)$	St	70	—	72	0	K	[21]
24	$PhCH(CN)C(S)S(CH_2)_4S$	$Ph\dot{C}H(CN)$	MMA	70	—	43	377	K	[21]

24	$PhCH(CN)C(S)S(CH_2)_4S$	$Ph\dot{C}H(CN)$	GMA	70	—	23	255	K	[21]
22	$PhCH_2S$	$PhCH_2^{\cdot}$	OFPA	80	14	—	—	W	[22]
—	$PHCH_2CH_2S$	$(CH_3)\dot{C}(CN)(C_2H_4CO_2H)$	MMA	75	21.1	—	—	D	[23]
44	$C_{12}H_{25}S$	$(CH_3)\dot{C}(CN)(C_2H_4CO_2H)$	MMA	75	16.7	—	—	D	[23]
40	$C_{12}H_{25}S$	$(CH_3)_2\dot{C}(CN)$	TFPMA	70	1.6	—	—	W	[24]
44	$C_{12}H_{25}S$	$(CH_3)\dot{C}(CN)(C_2H_4CO_2H)$	TFPMA	70	3.2	—	—	W	[24]
—	$PhCH_2CH_2S$	$(CH_3)\dot{C}(CONH_2)(C_2H_4CO_2H)$	MMA	75	4.3	—	—	D	[23]
—	$C_{12}H_{25}S$	$(CH_3)\dot{C}(CONH_2)(C_2H_4CO_2H)$	MMA	75	2.5	—	—	D	[23]
—	$CH(CH_3)(CO_2Et)S$	$(CH_3)\dot{C}H(CO_2Et)$	MA	60	112	—	—	B	[25, 26]
—	$CH(CH_3)(CO_2Et)S$	$(CH_3)\dot{C}H(CO_2Et)$	BA	60	98	—	—	B	[26, 27]
—	$CH(CH_3)(CO_2Et)S$	$(CH_3)\dot{C}H(CO_2Et)$	DA	60	98	—	—	B	[26, 28]

a) For a full list of monomer abbreviations see Abbreviations.

b) Published values of transfer coefficients that are based on a model that does not allow for partitioning of the intermediate radicals and/or the reversibility of chain transfer are considered as apparent transfer coefficients [29]. Caution should be used when comparing values obtained in different studies under different conditions.

c) Method used: M, Mayo method; W, Walling method; K, Kinetic simulation; D, Dispersity method; B, $M_n(0)$ method.

Table 9.2 Values of the RAFT equilibrium coefficient for trithiocarbonates.

RAFT agent[a]	*Z* (R′S)	R	Monomer/radical	*T* (°C)	k_{add} (M^{-1}/s)	k_{-add} (s^{-1})	K_{eq} (M^{-1})	Method[b]	References
19	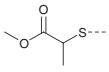	P(MA)	MA	−30	—	—	1.4×10^4	Theory	[41]
19	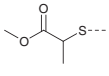	P(BA)	BA	−40	4×10^6	45	8×10^4	EPR	[42]
73		P(BA)	BA	−40	—	—	1.0×10^4	EPR	[43]
67		P(BA)	BA	−40	3.4×10^6	1.4×10^2	2.6×10^4	EPR	[42]
40	$C_{12}H_{25}S$---		St	70	1×10^7	2×10^4	500	Kinetics	[13]
40	$C_{12}H_{25}S$---		NIPAm	70	1×10^7	1×10^3	1×10^4	Kinetics	[13]
40	$C_{12}H_{25}S$---			70	1×10^4	4×10^3	2.5	Kinetics	[13]
40	$C_{12}H_{25}S$---			70	1×10^4	5×10^3	2	Kinetics	[13]
40	$C_{12}H_{25}S$---			70	1×10^4	2×10^4	0.5	Kinetics	[13]
40	$C_{12}H_{25}S$---			70	1×10^4	2×10^4	0.5	Kinetics	[13]
23				25	2.2×10^5	2×10^{-2}	1.1×10^7	EPR	[44]
23				20	—	—	5.3×10^4	Theory	[44]
22				20	—	—	1.1	Theory	[44]
23				20	—	—	4.34×10^3	Theory	[44]

a) Initial RAFT agent used.
b) EPR, determination of radical concentrations; Theory, *ab initio* calculations; Kinetics, kinetic simulation.

appear in the literature for the given systems (e.g. styrene with **40**) [13, 19] and serves to emphasize that all values of C_{tr} and C_{-tr} should be treated circumspectly.

9.2.2 RAFT Equilibrium Coefficients for Trithiocarbonates

The properties of RAFT agents are often discussed in terms of the value of the equilibrium coefficients ($K = k_{add}/k_{-add}$) associated with radical addition to a thiocarbonylthio compound [39, 40].

For all RAFT agents, including trithiocarbonates, addition rates decrease and fragmentation rates increase in the series where R is bulkier, where R becomes more electron withdrawing, and where R becomes more stable. It is found that addition rates decrease and fragmentation rates increase in the series where R is primary > secondary > tertiary, and where the alpha substituent on R is CN ~ Ph > CO_2alkyl > CONalkyl$_2$ > alkyl. Penultimate unit effects are significant such that a propagating species generally adds slower and fragments faster than a unimeric model.

Rates of addition reported for trithiocarbonates are high, in the range 10^4–10^7 M^{-1}/s (Table 9.2). However, the amount of experimental data is limited. A higher equilibrium coefficient implies a low fragmentation rate for the radical adduct and an increased likelihood for retardation and/or side reaction involving this species. It is generally believed that for trithiocarbonate-mediated polymerization of MAMs, fragmentation rates for R are sufficiently fast that side reactions involving the intermediate radicals are unlikely.

Methods for determining equilibrium coefficients for RAFT processes are described elsewhere in this volume [40, 45]. Rate coefficients for addition k_{add} and fragmentation k_{β} or k_{-add} (not distinguished) have been measured via the single pulse-pulsed laser photolysis-electron paramagnetic resonance (SP-PLP-EPR) method for butyl acrylate (BA) polymerizations mediated by the non-symmetric trithiocarbonate, ethyl 2-(((ethylthio)carbonothioyl)thio)propanoate (**67**), and the symmetric trithiocarbonate, dimethyl 2,2′-(thiocarbonylbis(sulfanediyl))dipropionate (**19**) [42].

Fitting the time evolution of products vs. time in SUMI experiments by numerical integration of the differential equations can allow estimation of values of the rate coefficients for addition and fragmentation [13]. However, the uncertainties inherent in this method are high. K values have also been estimated through the use of molecular orbital calculations [44].

9.3 Choice of Homolytic Leaving Group R for Trithiocarbonate RAFT Agents

The trithiocarbonate homolytic leaving groups R (and R′) need to be chosen for compatibility with the monomer(s) to be polymerized. The criteria for selection are mentioned in Chapter 3 in this volume [29] and guidelines to R group selection are provided in Figure 9.4b [5, 46]. These guidelines do not differ from those that apply in the cases of dithioesters [36], xanthates [47], or dithiocarbamates [36, 48, 878] with the main requirements ensuring control being as follows:

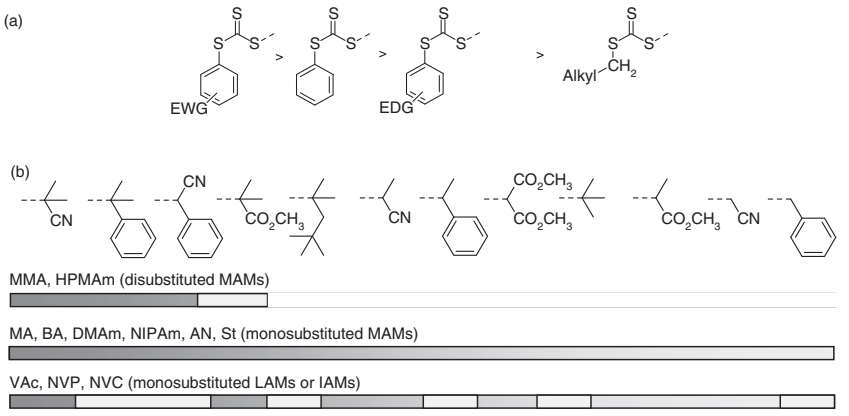

Figure 9.4 (a) Effect of R′SC(=S)– group on non-symmetric trithiocarbonates [R′SC(=S)SR] and (b) R group on activity of symmetric or non-symmetric trithiocarbonates (R′SC(=S)SR or RSC(=S)SR) in RAFT polymerization. Activity increases from right to left. Source: Figure 4b from [48]. © John Wiley and Sons. MAM, more activated monomer; LAM, less activated monomer; IAM, intermediate-activated monomer; AN, acrylonitrile; BA, butyl acrylate; DMAm, *N*,*N*-dimethylacrylamide; HPMAm, *N*-(2-hydroxypropyl)methacrylamide; MA, methyl acrylate; MMA, methyl methacrylate; NIPAm, *N*-isopropylacrylamide; NVC, *N*-vinylcarbazole; NVP, *N*-vinylpyrrolidone; St, styrene; VAc, vinyl acetate, EDG, electron-donating group; EWG, electron-withdrawing group.

- The radical R· should be a good homolytic leaving group relative to the propagating radicals generated (ideally $k_{\beta} \geq k_{-\mathrm{add}}$).
- The rate coefficient for reinitiation by R· (k_{iR}) should be greater than or equal to the propagation rate coefficient (k_{p}). Otherwise, there may be some retardation and there is a likelihood of by-products from self-reaction of R·. Values for R· adding to common monomers are known [29, 49–51].

Additional criteria may be the ease of synthesis or commercial availability, compatibility (e.g. stability, solubility) with the reaction conditions, and the presence or ease of transformation/removal of functionality.

9.3.1 Homolytic Leaving Group 'R' for 1,1-Disubsituted MAMs

Tertiary cyanoalkyl R (e.g. in trithiocarbonates **37**–**45**) are among the best homolytic leaving groups and are currently the preferred R groups for 1,1-disubsituted MAMs, such as methacrylates or methacrylamides, when low dispersities are required. Note, however, that the nitrile group of trithiocarbonates with a 4-cyanopentanoic acid R group may hydrolyse during storage under moist conditions to form a less active trithiocarbonate (see Section 9.20) [52].

Alternative R for 1,1-disubsituted MAMs are 1-aryl-1-cyanomethyl (R = –CHPh(CN), e.g. **24**, **53**) [53] or 1-aryl-1-carboxymethyl (R = –CHPh(CO_2X) with X = H or alkyl, e.g. **54**–**59**) [3]. These R substituents are good homolytic leaving groups. Rate coefficients for addition of these R· to the monomer may be sufficiently low to cause an inhibition period, particularly when low molar masses are targeted. An

advantage of these trithiocarbonates with a secondary R is that they are more readily synthesized by method A (refer Section 9.8).

2-Carboxyprop-2-yl radicals are relatively poor homolytic leaving groups with respect to propagating radicals derived from 1,1-disubsituted MAMs, such as methyl methacrylate (MMA). Use of trithiocarbonates comprising such R (i.e. R = $-C(CH_3)_2(CO_2X)$ with X = H or alkyl as in **14**–**17** or **47**–**51**) [54] provides molar mass control and allows block synthesis, but relatively high dispersities (typically > 1.3) are obtained with 1,1-disubsituted MAMs. Moreover, transfer coefficients are such that, in a batch polymerization, the initial RAFT agent may not be fully consumed until high monomer conversions.

9.3.2 Homolytic Leaving Group 'R' for Monosubstituted MAMs

Trithiocarbonates with R = tertiary cyanoalkyl (**54**-**59**) can be successfully used in polymerizations of monosubstituted MAMs. However, rates of addition to monomer may be rate determining during the initialization stage of polymerization with acrylates and acrylamides [55], which manifests as an inhibition period, or period of slow polymerization.

Trithiocarbonates with R = 2-carboxyprop-2-yl (R = $-C(CH_3)_2(CO_2X)$ with X = H or alkyl, e.g. **14**–**17**, **47**–**51**) [54] or 1-carboxyethyl (R = $-CH(CH_3)(CO_2X)$ with X = H or alkyl, e.g. **19**, **20**, **62**–**70**) are well suited for use with monosubstituted MAMs.

One of the most versatile R substituents, suited to most 1-substituted MAMs and LAMs, is the cyanomethyl group (e.g. **41**) [8, 56]. Cyanomethyl trithiocarbonates are not suitable for 1,1-disubsituted MAMs. The phthalimidomethyl trithiocarbonates (e.g. **21**, **25**, **70**) are suitable for 1-substituted MAMs and LAMs, but these RAFT agents have low solubility in many solvents [10, 57].

Trithiocarbonates with R = 1-phenylethyl (e.g. **20**, **60**, **61**), benzyl (e.g. **22**, **71**-**75**), or tertiary alkyl (e.g. **23**) are suitable for mediating RAFT polymerizations of most monosubstituted MAMs.

9.3.3 Homolytic Leaving Group 'R' for IAMs and LAMs

Trithiocarbonates are not generally suitable for IAMs or LAMs. When used, marked retardation or inhibition is typical. However, the cyanomethyl trithiocarbonate is suitable (even preferred) for NVC polymerization. It has been possible to conduct efficient PET-RAFT-SUMI of VAc or limonene into macro-trithiocarbonates with a terminal maleimide unit [58].

9.3.4 Macro-leaving Group 'R' for Block Copolymer Synthesis

The same factors used in selecting the trithiocarbonate 'R' suggest guidelines for the preferred order for incorporating monomers in the synthesis of a block copolymer by sequential monomer addition. Thus, 1,1-disubstituted monomers must generally be incorporated before monosubstituted monomers; MAMs before

IAMs before LAMs; monomers with electron-deficient double bonds before those with electron-rich double bonds.

In specific circumstances, the influence of these guidelines can be relaxed by using copolymerization, by implementing starved-feed monomer addition protocol [29], or through the use of PET-RAFT or direct photoinitiation [59].

9.4 Choice of Activating Group 'Z' for Trithiocarbonate RAFT Agents

The effectiveness of a RAFT agent depends on the monomer being polymerized and is determined by the properties of the radical leaving group R and the group Z, which can be chosen to activate or deactivate the thiocarbonyl double bond of the RAFT agent (**1**) and modify the stability of the various intermediate radicals **2**, **4** (Scheme 9.1) **6**, **8**, and **10** (Scheme 9.2).

Two main classes of trithiocarbonate RAFT agents are distinguished. The symmetrically substituted dialkyl trithiocarbonates (Tables 9.3, 9.4). and 9.7) have 2 equiv homolytic leaving groups. The non-symmetrically substituted trithiocarbonates (Tables 9.6 and 9.8) have one good homolytic leaving group (R) and a substituent (R″), which is not a leaving group under polymerization conditions and is almost always primary alkyl. Aryl trithiocarbonates (R″ is aryl) are also effective in this context and show higher transfer coefficients than similar RAFT agents where R″ is primary alkyl (Figure 9.4) [18]. However, they are not readily available.

9.5 Symmetric Trithiocarbonates

One of the attractions of symmetric trithiocarbonates is that they enable [2] the one-step synthesis of ABA triblock (or, more correctly, AB—SC(=S)S—BA triblock) copolymers as illustrated in Scheme 9.3 [3]. The same applies to Z-connected, bis-trithiocarbonates (Section 9.5.1). A potential disadvantage is that the trithiocarbonate group generally ends up near the centre of the chain (see Section 9.2) meaning that the chain is likely to be cleaved into two on trithiocarbonate group removal/transformation (Section 9.21).

9.5.1 Bis-trithiocarbonates

A wide variety of bis-trithiocarbonates have been described. Some examples are listed in Table 9.4 (connected by the Z substituent) and Table 9.5 (connected by the R substituent).

Z-connected bis-trithiocarbonates with two good homolytic leaving groups (R) are functionally equivalent to symmetric trithiocarbonates in that the trithiocarbonate groups are retained in the centre of the macromolecule (Scheme 9.3). For these

Table 9.3 RAFT polymerizations with symmetrically substituted trithiocarbonate RAFT agents.

RAFT agent	Synthesis[a)]	Polymerizations[b),c)]
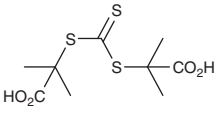 2,2′-(thiocarbonylbis(sulfanediyl))bis(2-methylpropanoic acid) **14**	F [60, 61] N	*Methacrylates*: BAMA [62] MMA [63] (MMA) [54] *MMA* [64] ODMA [65] (TFPMA) [24] **176** [66] *Acrylates*: AA [54, 67–70] AA [71, 72] BA [54, 73–76] EA [54] HEA [54, 77] MA [76, 78, 79] MEA [80, 81] *MMA* [82] *Acrylamides*: Am [83, 84] DMAm [77, 83, 85] (*DMAm*) [85] NIPAm [60, 67, 69, 86–90] NIPAm [91] **228** [92] **230** [79] MBAm [93, 94] PBAm [93] BBAm [93] *Styrenes*: St [17, 54, 95–97] 4VP [98] 2VP [99] 2VP [100] *Other MAM*: AN [101, 102] **356** [103] *Vinyls*: NVP [104] *Copolymers*: MAA/CHAm/NIPAm [105] MAA/BzAm/NIPAm [105] MAA/NIPAm/**239** [105] MAA/OAm/NIPAm [105] MAA/NIPAm/**234** [105] TEGDMA/**365** [61] HPMAm/**351** [106] NIPAm/**327** [107] TMAPMA/PEGMA/NIPAm [108] (PEGMA/**199**) [109] (PEGMA/**225**) [109] AEMA/**180**/**185** [110] (DMAm/MEA) [80, 81] AA/AN [111] AA/St [112] AN/Am [102] AEMA/**185**/**248** [110] HPMA copolymer [113] NIPAm/tBAm [114] NIPAm/**234** [105] NIPAm/**239** [105]

(*continued*)

Table 9.3 (Continued)

RAFT agent	Synthesis[a)]	Polymerizations[b),c)]
		Blocks: MMA-*b*-(PEGMA/NIPAm) [63] ODMA-*b*-NIPAm [65] **176**-*b*-GMA [66] (NVP-*b*-MMA) [115, 116] AA-*b*-EA [54] AA/St-*b*-NVP [112] EHA-*b*-EA [54] DMAm-*b*-**228** [92] DMAm-*b*-**228**-*b*-NIPAm [92] NIPAm-*b*-DMAm [87] NIPAm-*b*-Am [90] 2VP-*b*-EA [99] St-*b*-AA [54] St-*b*-tBA/TMSPMA [96] (MEA-*b*-DMAm) [80, 81] NIPAm/TBAm-*b*-DMAm/AA [114] NIPAm/TBAm-*b*-DMAm/NAS [114] NIPAm-*b*-ODA [89] St-*b*-NIPAm [97] St-*b*-4VP [98] **230**-*b*-MA [79]
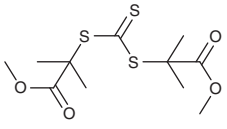 dimethyl 2,2′-(thiocarbonylbis(sulfanediyl))bis(2-methylpropanoate) **15**	A [11]	*Methacrylates*: MMA [11] *Acrylates*: BA [117] tBA [117] **206** [118] *Styrenes*: St [117] 4VP [117, 119] *Other*: AN [101, 120] *Blocks*: **206**-*b*-**214** [118, 121] 4VP-*b*-**214** [119, 122]
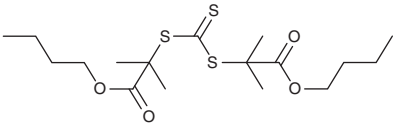 dimethyl 2,2′-(thiocarbonylbis(sulfanediyl))bis(2-methylpropanoate) **16**	F/J [123]	*Acrylates*: BA [123] *Styrenes*: St [123]
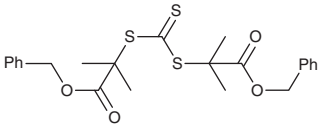 dibenzyl 2,2′-(thiocarbonylbis(sulfanediyl))bis(2-methylpropanoate) **17**	F [124]	*Methacrylates*: (MMA) [125] *Acrylates*: BA [91, 125] tBA [91, 124–126] MEA [91, 124, 126] HEA [91] MA [91, 125] *Aacrylamides*: Am [125] DMAm [91, 124, 126] (DMAm) [125] NIPAm [91, 124, 126] (NIPAm) [125]

(*continued*)

Table 9.3 (Continued)

RAFT agent	Synthesis[a)]	Polymerizations[b),c)]
		Blocks: *AA-b-BA* [72] *AA-b-EA* [72] *AA-b-TFEA* [72] *AA-b-HFBA* [72] DMAm-*b*-BA [91] DMAm-*b*-MEA [91] DMAm-*b*-NIPAm [91]
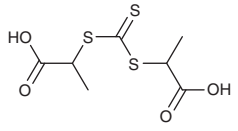 2,2′-(thiocarbonylbis(sulfanediyl))dipropionic acid **18**	A [127–129]	*Acrylates*: HEA [91] MA [91] *Acrylamides*: DMAm [91] NAM [129] NIPAm [130] NIPAm [91] *Vinyls*: (VAc) [91] *Copolymers*: AA/BA [128] St/MAH [127] *Blocks*: AA/BA-*b*-*MMA/BA* [128] DMAm-*b*-BA [91] NAM-*b*-**250** [129]
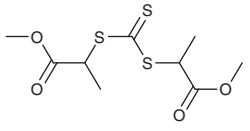 dimethyl 2,2′-(thiocarbonylbis(sulfanediyl))dipropionate **19**	A [101]	*Acrylates*: BA [42, 117] MA [41] tBA [117] **206** [118] *Styrenes*: St [117] 4VP [117] *Other*: **AN** [101, 102] *Copolymers*: AN/Am [102] *Blocks*: **206**-*b*-**214** [118]
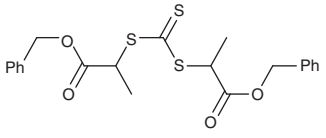 dibenzyl 2,2′-(thiocarbonylbis(sulfanediyl))dipropionate	H [91]	*Acrylates*: HEA [91] MA [91] *Acrylamides*: NIPAm [91]
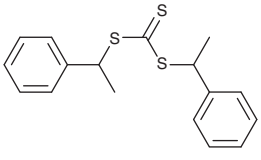 bis(1-phenylethyl) carbonotrithioate **20**	A [131–133]	*Acrylates*: AA [134] tBA [135] *Styrenes*: St [3, 132, 136] *Blocks*: St-*b*-BA [3] St-*b*-BEA [136] St-*b*-EA [132]
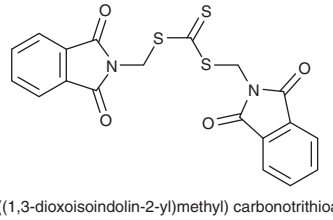 bis((1,3-dioxoisoindolin-2-yl)methyl) carbonotrithioate **21**	A [10]	*Styrenes*: St [10, 137]

(*continued*)

Table 9.3 (Continued)

RAFT agent	Synthesis[a)]	Polymerizations[b),c)]
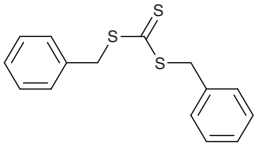 dibenzyl carbonotrithioate **22**	A [101, 131, 133, 138] B [139] M [140] N	*Acrylates*: AA [141–143] AdA [144] BA [117, 145–147] DMAEA [148] MA [139, 145] iBoA [145] ODA [149] 2EHA [149] PEGA [150] tBA [117, 145, 151] OFPA [22] **206** [118] *Acrylamides*: Am [83, 152] *Styrenes*: CMS [153] St [3, 117, 143, 145, 147, 149, 154–156] *St* [4] tBS [149] 4VP [117] *Other MAM*: AN [101, 102, 157] *Vinyls*: NVP [158] (VAc) [146] *Copolymers*: MAA/MA [159] AA/St [142, 143] tBA/St [142] Bd/AN [160] DVE/MAH [161, 162] *St/AA* [163] St/MAH/NVP [164, 165] AN/Am [102] (St/AA) [166] **186**/PEGA [167] **186**/AMPS [167] **186**/**329** [167] *Blocks*: PEGA-*b*-CIPEA [150] ODA-*b*-NIPAm [149] 2EHA-*b*-NIPAm [149] (BA-*b*-VAc) [146] St-*b*-NIPAm [149] tBS-*b*-NIPAm [149] OFPA-*b*-AA [22] OFPA-*b*-tBA [22] AdA-*b*-THFA [144] St-*b*-NIPAm [156] *St/AA-b-St* [163] DVE/MAH-*b*-St [161, 162] **206**-*b*-**214** [118] (St/AA-*b*-BA) [166]
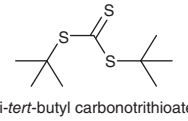 di-*tert*-butyl carbonotrithioate **23**	A M [140]	*Acrylates*: BA [117] tBA [117] **211** [168] **211**-*b*-**214** [168] *Styrenes*: St [117] (4VP) [117] *Vinyls*: VAc [146] (NVP) [158] *Blocks*: (VAc-*b*-BA) [146]

a) The letter A-N refers to the method of RAFT agent synthesis. Refer to Section 9.8.
b) Purple – crosslinking polymerization. Red – photoinitiated polymerization. *Italics* – heterogeneous polymerization. A-*b*-B blocks in most cases will be triblocks of structure AB—SC(=S)S—BA.
c) For a full list of monomer abbreviations, see Abbreviations section.

Table 9.4 RAFT polymerizations with symmetrically substituted, Z-connected, bis-trithiocarbonate RAFT agents.

RAFT agent	Synthesis[a)]	Polymerizations[b),c)]
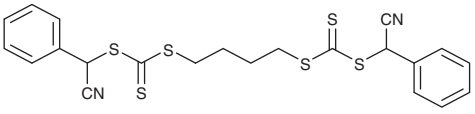 butane-1,4-diyl bis(cyano(phenyl)methyl) bis(carbonotrithioate) **24**	A [21]	*Methacrylates*: MMA [21] GMA [21] *Styrenes*: St [21] *Blocks*: MMA-*b*-GMA [21] GMA-*b*-MMA [21]
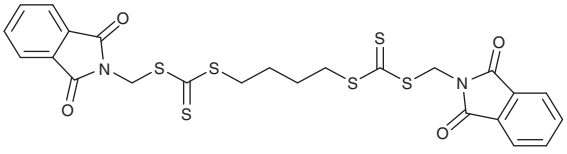 butane-1,4-diyl bis((1,3-dioxoisoindolin-2-yl)methyl) bis(carbonotrithioate) **25**	A [10]	*Styrenes*: St [10, 137]
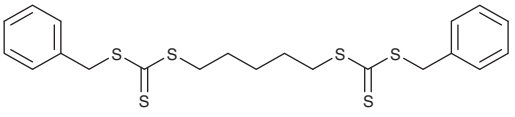 dibenzyl pentane-1,5-diyl bis(carbonotrithioate) **26**	A [169]	*Acrylates*: tBA [169] *Styrenes*: St [169]

a) The letter A-N refers to the method of RAFT agent synthesis. Refer to Section 9.8.
b) The A-*b*-B blocks will in most cases be ABA triblocks (Scheme 9.3).
c) For a full list of monomer abbreviations, see Abbreviations section.

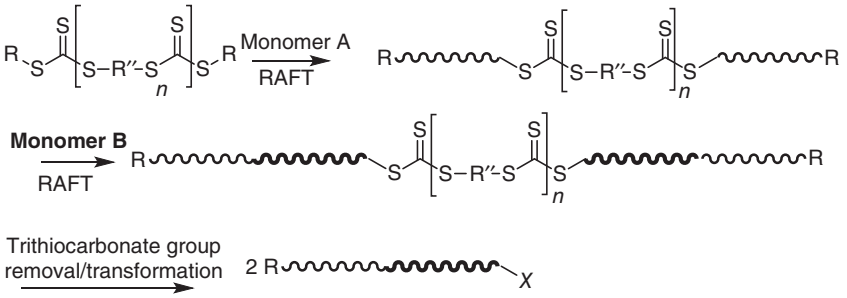

Scheme 9.3 Process of RAFT polymerization with symmetric trithiocarbonates ($n = 0$) or R″-connected bis-trithiocarbonates ($n = 1$) showing how the trithiocarbonate groups are retained in the centre of the product macromolecule (R is a homolytic leaving group, R″ is a poor homolytic leaving group). The process provides a route to ABA triblocks. The group X formed on trithiocarbonate group removal/transformation depends on the process used. Source: Adapted with permission from Moad et al. [46]. Copyright 2013, Royal Society of Chemistry.

Table 9.5 RAFT polymerizations with symmetrically substituted, R-connected, bis-trithiocarbonate RAFT agents.

RAFT agent	Synthesis[a)]	Polymerizations[b),c)]
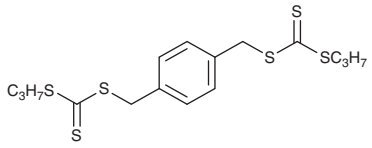 1,4-phenylenebis(methylene) dipropyl bis(carbonotrithioate) **27**	A [169]	*Acrylamides*: NIPAm [149]
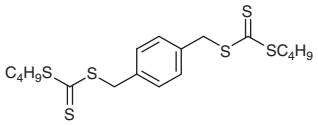 1,4-phenylenebis(methylene) dibutyl bis(carbonotrithioate) **28**	A [170]	*Acrylates*: BA [171] **216** [171] *Acrylamides*: DMAm [170] *Blocks*: DMAm-*b*-NIPAm [170]
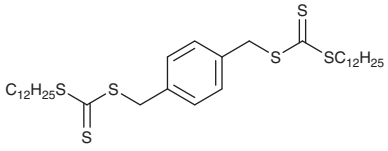 1,4-phenylenebis(methylene) didodecyl bis(carbonotrithioate) **27**	A	*Acrylates*: tBA [169] *Styrenes*: St [169, 172]
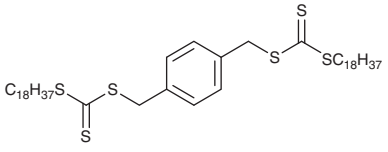 1,4-phenylenebis(methylene) dioctadecyl bis(carbonotrithioate) **30**	A [173]	
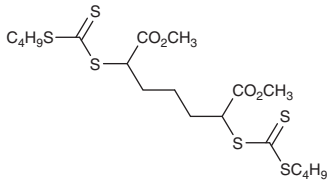 dimethyl 2,6-bis(((butylthio)carbonothioyl)thio)heptanedioate **31**	A [174]	*Acrylates*: tBA [174] CIPEA [150] *Blocks*: tBA-*b*-AA/tBA [174] CIPEA-*b*-PEGA [150]

Table 9.5 (Continued)

RAFT agent	Synthesis[a)]	Polymerizations[b),c)]
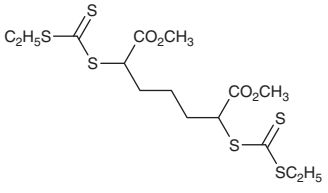 dimethyl 2,6-bis(((ethylthio)carbonothioyl)thio)heptanedioate **32**	A [174]	*Acrylates*: BA [175] *Blocks*: BA-*b*-**361** [175]
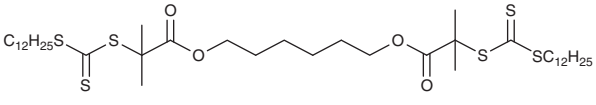 hexane-1,6-diyl bis(2-((((dodecylthio)carbonothioyl)thio)-2-methylpropanoate) **33**	177	*Styrenes*: St [176] *Blocks*: St-*b*-MA/ODA [176]
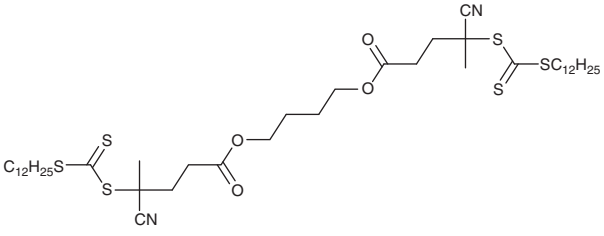 butane-1,4-diyl bis(4-cyano-4-(((dodecylthio)carbonothioyl)thio)pentanoate) **34**	H [177]	*Methacrylates*: DMAEMA [177] *Blocks*: DMAEMA-*b*-PEGMA [177]
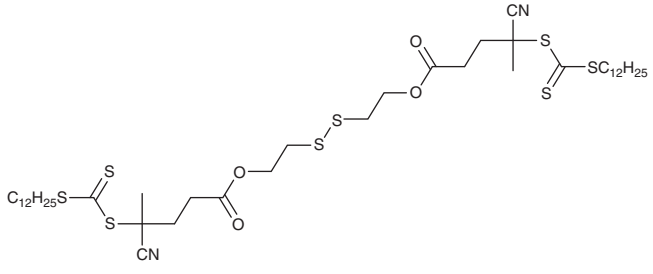 disulfanediylbis(ethane-2, 1-diyl) bis(4-cyano-4-(((dodecylthio)carbonothioyl)thio)pentanoate) **35**	H [178]	*Methacrylates*: DMAEMA [178] *Blocks*: DMAEMA-*b*-**292** [178] DMAEMA-*b*-**292**-*b*-HPMAm [178]

a) The letter A-N refers to the method of RAFT agent synthesis. Refer to Section 9.8.
b) The A-*b*-B blocks shown will in most cases be BAB triblocks (Scheme 9.4).
c) For a full list of abbreviations, see Abbreviations section.

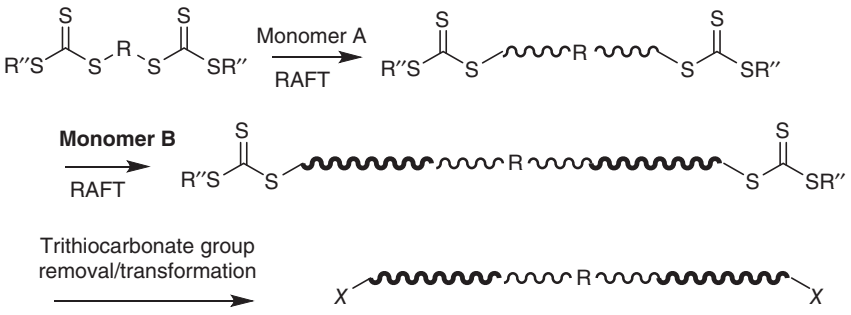

Scheme 9.4 Process of RAFT polymerization with R-connected bis-RAFT agents (R is a homolytic leaving group, R″ is a not a homolytic leaving group) to form telechelic BAB triblocks. The groups X formed on trithiocarbonate-group removal/transformation depend on the process used. Source: Adapted from [46]. Copyright 2013, Royal Society of Chemistry.

structures, the molar mass will be approximately halved on trithiocarbonate group removal/transformation.

With R-connected bis-trithiocarbonates, the trithiocarbonate groups are retained as end-groups (Scheme 9.4). As with non-symmetric trithiocarbonates, there will be little change of molar mass on trithiocarbonate group removal/transformation since the polymer chain is maintained intact.

9.6 Non-symmetric Trithiocarbonates

There is little data on the dependence of k_{add} values or transfer coefficients for non-symmetric trithiocarbonate RAFT agents **1** on the particular R″S (or Z) substituent. When R″ is primary alkyl, it is generally assumed that the activity is independent of chain length and the presence of remote functionality on R″. The frequently encountered R″ substituents are CH_3, C_2H_5, $CH_2CH_2CO_2H$, CH_2CH_2Ph, C_3H_7, C_4H_9, and $C_{12}H_{25}$ (Figure 9.5). The most common R″ substituent is $C_{12}H_{25}$. This can be attributed to the relatively low volatility of dodecylmercaptan and the consequent relatively low odour of the RAFT agent and the derived polymers. The trithiocarbonates where R″ is C_2H_5 or $CH_2CH_2CO_2H$ are commonly used where aqueous solubility is required.

For styrene polymerization with aryl benzyl trithiocarbonates **12**, there is a clear trend for RAFT agent activity to increase with the electron-withdrawing qualities of the aryl substituents (Table 9.1) [18]. This observation is in line with other observations of enhanced activity for RAFT agents with electron-withdrawing Z.

While the R″S substituent may have little effect on RAFT agent activity, it does influence the properties of the polymer formed. For example, despite making up only a very small fraction of the polymer ($M_n > 20$ K), the terminal groups (C_2H_5 vs. $C_{12}H_{25}$) have been shown to have a significant influence on both the conformation and assembly of PNIPAm and its analogues below the critical temperature (Table 9.6) [553].

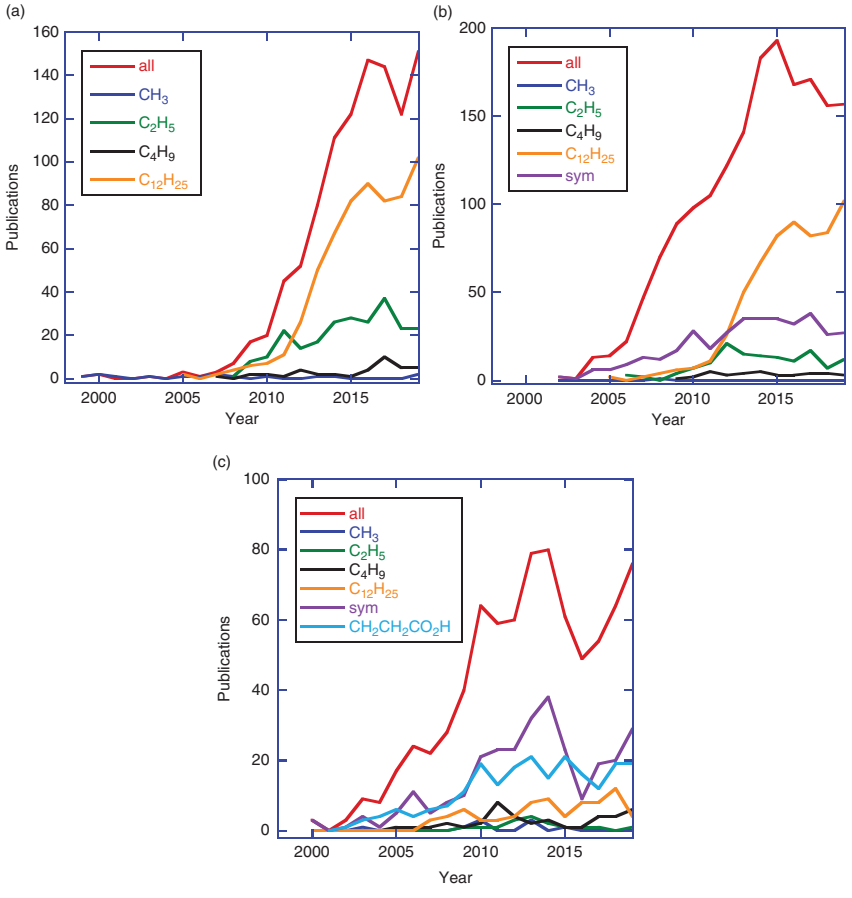

Figure 9.5 Publication rate for RAFT polymerization for the three most popular forms of trithiocarbonate where the homolytic leaving group is (a) *t*-cyanoalkyl (e.g. **36–45**), (b) *t*-carboxyalkyl (e.g. **47–51**), and (c) benzyl (e.g. **71–75**) with various S–R″ groups as indicated (sym = symmetrical trithiocarbonate). Includes both patent and open literature publications. Based on a Scifinder™ Search on the RAFT agent substructure and the term 'RAFT' conducted in June 2020.

9.7 Functional Trithiocarbonates

A wide variety of functional RAFT agents have been reported. Examples appear in Table 9.7 (based on symmetric trithiocarbonates) and Table 9.8 (non-symmetric trithiocarbonates). This list should not be considered as comprehensive. Carboxy-functional RAFT agents are included in Tables 9.5 and 9.6. Trithiocarbonates containing polymerizable double bonds (known as trithiocarbonate inimers) are shown in Table 9.21.

These RAFT agents are used in the synthesis of other RAFT agents and in preparing RAFT functional surfaces. Surface-initiated RAFT polymerization to prepare modified surfaces and particles is covered in detail in the Chapter 22 by Pribyl and Benicewicz [731].

Table 9.6 RAFT polymerizations with non-symmetric trithiocarbonate RAFT agents.

RAFT agent	Synthesis[a)]	Polymerizations[b),c)]
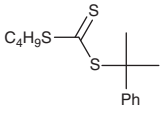 butyl (2-cyanopropan-2-yl) carbonotrithioate **36**	C	*Other*: **361** [175] *Copolymers*: BzMA/Lim/NPMI [179] **197**/NPMI [180]
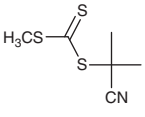 2-cyanopropan-2-yl methyl carbonotrithioate **37**	C	*Methacrylates*: MMA [3, 181–183] *Acrylates*: MA [3] tBA [184] *Styrenes*: St [3, 185] *Copolymers*: tBA/AcS [154] tBA/AcS/St [154] *Blocks*: tBA-*b*-AcS [154] tBA-*b*-AcS-*b*-St [154]
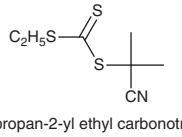 2-cyanopropan-2-yl ethyl carbonotrithioate **38**	C [186]	*Methacrylates*: DMAEMA [187] TrMA [186] *Acrylamides*: **222** [188] *Other*: **198** [189] **359** [190] **361** [175] *Copolymers*: HPMAm/**194** [191] BzMA/Lim/NPMI [179] *Blocks*: DMAEMA-*b*-BzMA [187]
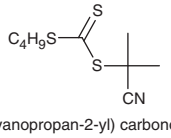 butyl (2-cyanopropan-2-yl) carbonotrithioate **39**	A [192] C [193]	*Methacrylates*: BMA [193] HxMA [193] HpMA [193] MMA [192] OMA [193] **159** [194] *Acrylates*: BA [195] *Methacrylamides*: **191** [196] *Styrenes*: St [195] **251** [197] **254** [197] **255** [197] *Copolymers*: BMA/HxMA [193] BMA/OMA [193] BMA/LMA [193] NPMI/Lim [198] **251**-*b*-**254** [197] **251**-*b*-**255** [197] **254**-*b*-**251** [197]
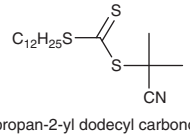 2-cyanopropan-2-yl dodecyl carbonotrithioate **40**	C [199, 200] N	*Methacrylates*: BMA [201] FMA [202] GMA [203] MMA [199, 204–206] MMA [207] ODMA [65] tBMA [208] TFPMA [24] **169** [209] **330** [210] *Acrylates*: HEA [211] BA [212] MA [213] MA [212, 214] **358** [215] *Methacrylamides*: BzMAm [216] PhMAm [216] *Acrylamides*: DMAm [217] LAm [218] MPAm [217] NAM [217] NIPAm [13] NIPAm [13, 217] *Styrenes*: St [13, 219, 220] St [13] **274** [221] **278** [222] **258** [223] **356** [224] *Vinyls*: NVC [8] **285** [225] **289** [226]

(*continued*)

Table 9.6 (Continued)

RAFT agent	Synthesis[a)]	Polymerizations[b),c)]
		Copolymers: MAA/MA [159] tBMA/NIPAm [227] tBMA/**343** [200] HPMAm/**297** [228] St/GMA [229] PEGA/DA/AMPS [230] St/DVB [231] DMAm/MBAm [217] NAM/MBAm [217] NAM/PIPBAm [217] MPAm/MBAm [217] NIPAm/PIPBAm [217] DMAm/NAM [217] DMAm/NIPAm [217] St/**277** [232] NIPAm/AN [233] CMS/**266** [217, 234]
		Blocks: BMA-*b*-MMA [201] GMA-*b*-**310** [203, 235] ODMA-*b*-NIPAm [65] tBMA/DMAEMA [208] TFPMA-*b*-MAA [24] TFPMA-*b*-MA [24] TFPMA-*b*-GMA [24] BA-*b*-**222** [236] St/DVB-*b*-VPBA [231] St/DVB-*b*-DVPP [231] St-*b*-NIPAm [13] **258**-*b*-**305** [223]
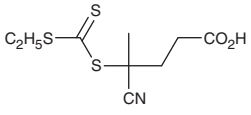 4-cyano-4-(((ethylthio)carbonothioyl)thio)pentanoic acid **41**	C [237–240]	*Methacrylates*: DEAEMA [239, 241] DMAEMA [238, 242, 243] PEGMA [244–247] **299** [248]
		Acrylates: (**339**) [249]
		Methacrylamides: HPMAm [250]
		Acrylamides: DMAm [85] *DMAm* [85] HPMAm [251, 252] **193** [251] **223** [253]
		Others: PAA [254] **288** [255]
		Copolymers: MAA/PEGMA [245] NIPAm/**223** [253] APMAm/DEAPMAm [256] APMAm/DMAPMAm [256] DEGMA/PEGMA/EGDMA [257] DMAEMA/DEGMA [243] HPMAm/APMAm [258] HPMAm/**350**/**352** [259]
		Blocks: DEAEMA-*b*-NIPAm [241] DMAEMA-*b*-NIPAm [260] DMAEMA-*b*-AA/BMA/DMAEMA [239] DMAEMA-*b*-PEGMA [243] DMAEMA/DEGMA-*b*-PEGMA [243] *PEGMA/MAA-b-St* [245, 261] *PEGMA/MAA-b-BzMA* [262] *PEGMA/MAA-b-**166*** [263] PAA-*b*-DMAm/**313** [254] DMAEMA-*b*-(PAA/BMA/DMAEMA) [238, 242] HPMAm/APMAm-*b*-HPMAm/DMAPMAm [258] HPMAm-*b*-**193** [251] PEGMA/**155** [264]

(*continued*)

Table 9.6 (Continued)

RAFT agent	Synthesis[a)]	Polymerizations[b),c)]
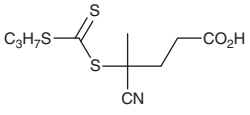 4-cyano-4-(((propylthio)carbonothioyl)thio)pentanoic acid **42**		*Methacrylamides*: DMAPMAm [265] *Acrylates*: AA [70] *Styrenes*: 4VP [266] *Copolymers*: AA/BA [267] *Blocks*: AA/BA-*b*-*MMA/BA* [267] AA/BA-*b*-*MA/BA* [267] AA/BA-*b*-*MMA/BA/EGDA* [267] 4VP-*b*-St [266] **279**-*b*-St-*b*-St/DEGDMA [266] DMAPMAm-*b*-*MMA* [265] DMAPMAm-*b*-*BA* [265] DMAPMAm-*b*-*MMA/BA* [265]
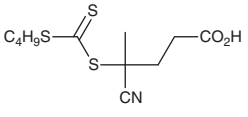 4-(((butylthio)carbonothioyl)thio)-4-cyanopentanoic acid **43**	C [268]	*Methacrylates*: HEMA [269] MAA [182] PEGMA [268–270] *Acrylates*: PEGA [270] *Methacrylamides*: **191** [196] *Copolymers*: PEGA/TFEA [271] *Blocks*: *PEGA-b-St* [270] *PEGMA-b-St* [270] *PEGA/TFEA-b-Sty/3VBA* [271]
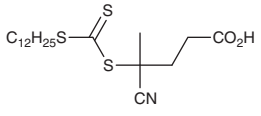 4-cyano-4-(((dodecylthio)carbonothioyl)thio)pentanoic acid **44**	C [272] N	*Methacrylates*: CMA [273] DMAEMA [274] GMA [275] GMMA [276] MAA [277] MMA [275, 278] MMA [279] PEGMA [280–282] PMA [283] TFPMA [24] **150** [171] **168** [284] **176** [285] **319** [286] **320** [286] PAA [277] *Acrylates*: AA [54] BA [287] BA [275] EAA [277] EA [54] HEA [288] MA [288] PEGA [282] **217** [171] **241** [289] *Acrylamides*: DMAm [287] DMAm [288] NAM [290] NIPAm [287, 291] NIPAm [288] tBAm [54] **222** [292] **309** [288] *Methacrylamides*: **181** [293] **191** [196] **192** [196] **187** [196] **188** [196] **348** [294] *Styrenes*: PFS [288] **276** [295] *Others*: Bd [296] Ip [297, 298]

(*continued*)

Table 9.6 (Continued)

RAFT agent	Synthesis[a)]	Polymerizations[b),c)]
		Copolymers: tBMA/**168** [284] BMA/**343**/PEGDMA [299] DMAEMA/PAA/DSDA [300] DMAEMA/PEGMA/**305** [301] GMA/Ip [297, 298] HPMA/**304** [302] IPMA/**304** [302] LMA/**304** [303] MAA/MMA [304] MAA/DFHA [305] MMA/**368** [306] MAA/**364** [307] MMA/**292** [308] OeMA/MMA [273] PEGMA/**366** [281] **149**/**172**/**174** [272] **149**/**171**/**172**/**174** [309] HDFDMA/**168** [284] HPMAm/**304** [302] NIPMAm/**304** [302] **189**/DEGDMA [310] AA/**370** [307] Am/**222** [311] DMAm/**305** [312] Bd/AN [296] MMA/PEGDMA/**384** [278] MMA/**383** [278] MMA/**383**/**384** [278] *Blocks*: MMA-*b*-BMA [279] MMA-*b*-BA [275] **319**-*b*-MMA [286] **320**-*b*-MMA [286] NIPAm-*b*-DMAEAm [291] DMAEMA-*b*-*BzMA*-*b*-**253** [274] *GMMA-b-HPMA/DMAEMA/AMA* [276] *PEGMA-b-GMA* [280] *PEGMA-b-HPMA* [282] *PEGA-b-HPMA* [282] *PEGMA-b-GMA* [280] **149**/**172**/**174**-*b*-PFOEMA [272] AA-*b*-EA [54] AA-*b*-*St* [54] **176**-*b*-VCL/MBAm [285] **348**-*b*-NIPAm [294] **348**-*b*-PEGMA [294] NAM-*b*-**305**/NAM [290, 313] *RAFT-T-ATRP*: BMA/**343**/PEGDMA-*g*-BA [299] BA/**345**/PEGDA-*g*-OFPA [299] BMA/**343**/PEGDMA-*g*-BA [299] BA/**345**/PEGDA-*g*-OFPA [299]
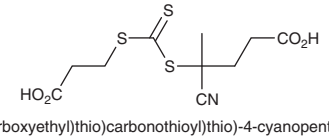 4-(((2-carboxyethyl)thio)carbonothioyl)thio)-4-cyanopentanoic acid **45**	N C	*Methacrylates*: PEGMA [314] *Acrylamides*: DMAm [315, 316] *Styrenes*: **St** [58] **CMS** [58] **tBS** [58]

(*continued*)

Table 9.6 (Continued)

RAFT agent	Synthesis[a)]	Polymerizations[b),c)]
		Copolymers: HEMA/PEGMA [317] MAA/DMAPMAm/tBMAm [318] *Blocks*: **St**-*b*-**NPMI** [58] **St**-*b*-**NPMI**-*b*-**VAc** [58] *HEMA/PEGMA-b-LMA* [317] *HEMA/PEGMA-b-**176*** [317]
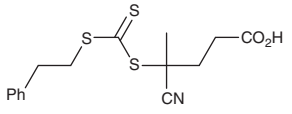 4-cyano-4-(((phenethylthio)carbonothioyl)thio)pentanoic acid **46**	C [319]	*Methacrylates*: DMAEMA [320, 321] GMMA [322, 323] LMA [324] MAA [325] ODMA [326] **335** [327] **338** [319] *Copolymers*: MMA/**353** [328] PEGMA/**158**/DSDM [329] *Blocks*: DMAEMA-b-*BzMA* [320, 321] GMMA-b-*HPMA* [323] GMMA-b-*MAA* [323] GMMA-*b*-*TFEMA* [322] LMA-*b*-*MMA* [324] MAA-*b*-*BMA* [325] MAA-*b*-*BzMA* [325] ODMA-*b*-*BzMA* [326] **335**-*b*-*BzMA* [327] **338**-*b*-*HPMA* [319] MMA/**353**-*b*-MMA [328] PEGMA/**158**/DSDM-*b*-PEGMA/TFEMA [329]
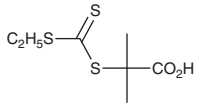 2-(((ethylthio)carbonothioyl)thio)-2-methylpropanoic acid **47**	F	*Arylates*: MA [240] *Styrenes*: St [240] (**339**) [249] *Acrylamides*: DMAm [85, 92, 240, 330] *DMAm* [85] NIPAm [240, 331] **227** [332] **228** [92, 332] **233** [333] **246** [330] *Other*: **355** [334] **359** [190] *Blocks*: DMAm-*b*-**228** [92] DMAm-*b*-**228**-*b*-NIPAm [92] DMAm-*b*-**235**-*b*-**224** [335] DMAm-*b*-NIPAm/**233** [333] **228**-*b*-**227** [332]
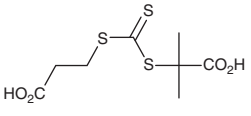 2-(((2-carboxyethyl)thio)carbonothioyl)thio)-2-methylpropanoic acid **48**	F [73]	*Acrylates*: BA [73] *Acrylamides*: DMAm [336, 337] BA [336] *Styrenes*: St [17] *Copolymers*: *AA/Am* [338] *Am-b-AA* [338] DMAm/**242** [339] DMAm/**243** [339] DMAm/**244** [339] HEAm/**245** [340]

(*continued*)

Table 9.6 (Continued)

RAFT agent	Synthesis[a)]	Polymerizations[b),c)]
		Blocks: DMAm-*b*-NIPAm [336] DMAm-*b*-MA [336] BA-*b*-MA [336]
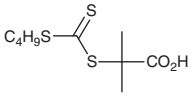 2-(((butylthio)carbonothioyl)thio)-2-methylpropanoic acid **49**	A [192, 341–343] F [344–346]	*Methacrylates*: CHMA [341] MMA [192] **159** [194] *Acrylamides*: AMPS [346, 347] *Vinyls*: NVC [194] *Copolymer*: AMPS/HEAm [346] *Blocks*: *AMPS-b-BA* [347] *AMPS-b-St* [347] AMPS-*b*-HEAm [346] $(AMPS\text{-}b\text{-}HEAm)_4$ [346] AMPS-*b*-NAM [346] $(AMPS\text{-}b\text{-}NAM)_2$ [346] AMPS-*b*-MBAm [346] AMPS-*b*-DVB [346] AMPS-*b*-DEGDA [346]
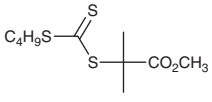 methyl 2-(((butylthio)carbonothioyl)thio)-2-methylpropanoate **50**	M [173]	
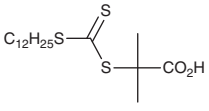 2-(((dodecylthio)carbonothioyl)thio)-2-methylpropanoate **51** (DDMAT, Lubrizol CTA-acid)	F [348]	*Methacrylates*: (BMA) [349] (*BMA*) [349] CMA [350] MMA [151, 351] (MMA) [351] ODMA [352] (TFPMA) [24] **154** [353] **296** [354, 355] **305** [356] **349** [357] *Acrylates*: AA [358, 359] BA [73] CA [360] tBA [361] tBA [91] MA [362] PFOEA [363] **200** [364] **203** [365] **218** [366] *Acrylamides*: BAm [367] DEAm [367, 368] DMAm [367, 368] DMAm [91] EMAm [367, 368] NIPAm [367–371] PAm [367, 371] DMAm [85, 372–374] (*DMAm*) [85] MPAm [375] NIPAm [291, 374, 376] **225** [377] **240** [378] **236** [379] *Others*: MVK [380] PVK [380] **195** [381]

(*continued*)

Table 9.6 (Continued)

RAFT agent	Synthesis[a)]	Polymerizations[b),c)]
		Styrenes: St [7, 349, 358, 382–385] *St* [386] (*St*) [349] St [387] CMS [387] HMS [387] PFS [388] tBS [99] **261** [387] **264** [389] **265** [390] **267** [391] **268** [392] **269** [392] **315** [393] 4VP [388, 394, 395] 2VP [100] *Dienes*: Ip [396–398] **280** [396] *Other MAM*: **310** [383, 399, 400] *Vinyls*: (NVP) [401] NVP [104] **285** [225] *Copolymers*: BMA/PEGMA/**311** [402] CEMA/**292**/NIPAm [403] PAA/NIPAm [404] AA/PEGA [405, 406] BA/**200** [364] (tBMA/DMAEMA/**147**) [407] HEA/PEGA [408] PA/PEGA [408] DMAm/**160** [372] DMAm/PFS [409] HADA/MADA/NLAA [410] DMAm/**314**/**323** [411] HADM/MADM/NLAM [410] **172**/tBA/St/AcS [412] (BMA/BA) [349] (*BMA/BA*) [349] (BMA/St) [349] (*BMA/St*) [349] MAH/Dc [413] MAH/Dc/VAc [413] MAH/Dc/MA [413] MAH/Dc/St [413] EHA/PFOEA [363] *St/DVB* [414] 4VP/**295** [415] St/**308** [416] BA/**167** [417] BA/**167**/EGDMA [417] St/**156** [418] St/**291** [418] St/**161** [419] St/**342** [420] tBA/St/AcS/**172** [412] *Blocks*: ODMA-*b*-*MMA* [352] AA-*b*-St [381, 386] AA-*b*-*St*-*b*-*MMBL/St* [381] St/**308** [416] HEMA/Ip [396] HEA/Ip [396]Ip/**280** [396] AA/PEGA-*b*-**209** [405] *AA/PEGA*-*b*-*St* [406] **203**-*b*-*BA* [365] **203**-*b*-*BA/St* [365] (**203**-*b*-*St*) [365] **349**-*b*-St [357] St/**342**-*b*-TEGA/**293** [420] *AA/PEGA*-*b*-***210*** [263] *AA*-*b*-*St* [359] DMAm-*b*-NIPAm [372] DMAm/**160**-*b*-NIPAm [372]

(*continued*)

Table 9.6 (Continued)

RAFT agent	Synthesis[a)]	Polymerizations[b),c)]
		DMAm-*b*-NIPAm/**160** [372] DMAm/**160**-*b*-NIPAm/**160** [372] NIPAm-*b*-DMAEAm [291] PFS-*b*-PFPVS [409] 4VP-*b*-PFS [388] *4VP-b-St* [394] DMAm-*b*-MA [374] DMAm-*b*-BA [374] DMAm-*b*-NIPAm [374] NIPAm-*b*-MA [374] NIPAm-*b*-BA [374] NIPAm-*b*-DMAm [374] **240**-*b*-NIPAm [378] (NVP-*b*-Ip) [401] **331**X-*b*-St [392] tBA-*b*-Ip [361] tBA-*b*-St [361] tBA-*b*-IP-*b*-tS [361] tBA-*b*-St-*b*-IP [361] MA-*b*-NAS/MAM [362] CMA-*b*-TMSEMA [350] St/MAH-*b*-Ip [421] St/MAH-*b*-X**332**X [392] Ip-*b*-St [398] Ip-*b*-St-*b*-DMAm [398] NVP-*b*-2VP [104] NIPAm/MAA [422] NIPAm/PAA [422] PAM-*b*-NIPAm [368, 371] PAm-*b*-NIPAm-*b*-EMAm [368, 371] NIPAm/NAS/X**279**X [423] X**320**X-*b*-NIPAm [378] St-*b*-CMS [387] St-b-**310** [383–385] CMS-*b*-HMS [387] 4VP-*b*-Ss [395] *4VP-b-St* [395] St-*b*-CA [360] Ip-*b*-St [397] MMBL/St [381] St-*b*-NIPAm [424] 4VP/**295**-*b*-St [415] PFOEA-*b*-HEA [363] **315**-*b*-St [393] St/**156**-*b*-NIPAm [418] St/**291**-*b*-NIPAm [418] St/**161**-*b*-NIPAm/**156**/**291** [419]
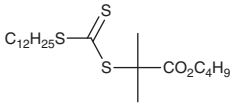 butyl 2-(((dodecylthio)carbonothioyl)thio)-2-methylpropanoate **52** (Lubrizol CTA-ester)	F [425]	*Styrenes*: St [426] *Other MAMs*: **281** [427] **282** [427] **283** [427] **284** [427] *Copolymers*: St/MAH [428] *Blocks*: St-*b*-MAH [426] St-*b*-St/MAH [428]
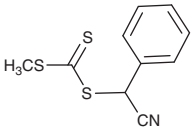 cyano(phenyl)methyl methyl carbonotrithioate **53**	A	*Methacrylates*: MMA [53]

(*continued*)

Table 9.6 (Continued)

RAFT agent	Synthesis[a)]	Polymerizations[b),c)]
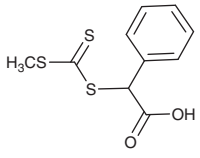 2-(((methylthio)carbonothioyl)thio)-2-phenylacetic acid **54**	A [429, 430]	*Methacrylates*: MPC [431] *Acrylates*: BA [432] MA [3] *Acrylamides*: NIPAm [433–437] *Styrenes*: St [3, 438] SSO3Na [439] *Blocks*: MPC-*b*-DMAEMA/NIPAm [431] NIPAm-*b*-DMAPMAm [434] NIPAm-*b*-AA [435, 436] NIPAm-*b*-SSO3Na [437] SSO3Na-*b*-AA [439] SSO3Na-*b*-NIPAm [439]
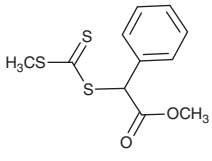 methyl 2-(((methylthio)carbonothioyl)thio)-2-phenylacetate **55**	A	*Methacrylates*: MMA [440]
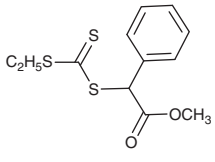 methyl 2-(((ethylthio)carbonothioyl)thio)-2-phenylacetate **56**	A	*Acrylates*: BA [175] MA [175] *Other*: **361** [175] *Blocks*: BA-*b*-**361** [175] MA-*b*-**361** [175]
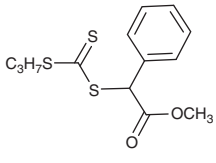 methyl 2-phenyl-2-(((propylthio)carbonothioyl)thio)acetate **57**	A [441]	*Methacrylates*: **(**MMA) [441] *Acrylates*: BA [441] MA [441] *Acrylamides*: DMAm [441] NIPAm [441] *Styrenes*: St [441]
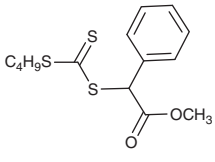 methyl 2-(((butylthio)carbonothioyl)thio)-2-phenylacetate **58**	A [442]	*Methacrylates*: MEMA [442] METAC [442] *Copolymers*: MEMA/METAC [442]

(*continued*)

Table 9.6 (Continued)

RAFT agent	Synthesis[a)]	Polymerizations[b),c)]
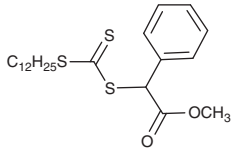 methyl 2-(((dodecylthio)carbonothioyl)thio)-2-phenylacetate **59**	A [443, 444]	*Acrylates*: **204** [444] *Methacrylamides*: **179** [443] *Styrenes*: St [444] *Copolymers*: (St/**204**) [444] *Blocks*: (**204**-*b*-St) [444] St-*b*-**204** [444]
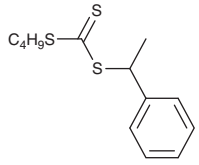 butyl (1-phenylethyl) carbonotrithioate **60**	A [445]	*Acrylates*: BA [445] ODA [445] *Copolymers*: ODA/DMAEA [445] ODA/NVP [445] ODA/PEGA [445] *Blocks*: ODA-*b*-DMAEA [445]
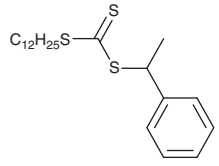 dodecyl (1-phenylethyl) carbonotrithioate **61**	A [445]	*Acrylates*: ODA [445] *Acrylamides*: **231** [356] *Copolymers*: ODA/DMAEA [445] ODA/AN [445] ODA/MAA [445] ODA/MEP [445] ODA/MAH [445] ODA/MAH/MMA [445] ODA/NVP [445] St/**263** [446] *Blocks*: St/**263**-*b*-NIPAm [446]
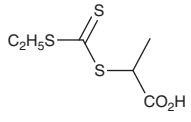 2-(((ethylthio)carbonothioyl)thio)propanoic acid **62**	A	*Acrylamides*: Am [447] *Other*: **355** [334] **359** [190]
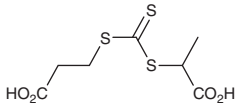 3-((((1-carboxyethyl)thio)carbonothioyl)thio)propanoic acid **63**	A [448, 449]	*Acrylates*: *AA* [450] BA [73] *Acrylamides*: Am [83] *Am* [451] DMAm [452] NAM [453] **225** [377] *Styrenes*: St [17] VBA [454] **275** [454] **276** [454] *Copolymers*: MAA/DMAm [455] AA/DMAm [455] *AA/Am* [338] Am/DAAm [448]

(*continued*)

Table 9.6 (Continued)

RAFT agent	Synthesis[a)]	Polymerizations[b),c)]
		Blocks: DMAm-*b*-DAAm [452] NAM-*b*-DMAm [453] NAM-*b*-DMAm-*b*-DEAm [453] NAM-*b*-DMAm-*b*-DEAm-*b*- NAM-*b*-DMAm-*b*-DEAm [453] NAM-*b*-HEAm-*b*-NIPAm-*b*- NAM-*b*-HEAm-*b*-NIPAm [453]
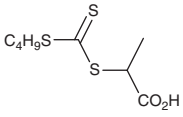 2-(((butylthio)carbonothioyl)thio)propanoic acid **64**	A [456, 457]	*Acrylates*: AA [456, 458, 459] HEA [77] HEA [314] MA [460] tBA [460] PEGA [461] PEGA [314] *Acrylamides*: DEAm [314, 462] DMAm [77, 457, 463] DMAm [314, 462] NIPAm [463, 464] NIPAm [460, 462] **246** [461] *Styrenes*: St [465, 466] *Copolymers*: AA/BA [68, 128] AA/PEGA [459] AA/**260** [467] EGDA/HEA [460] NIPAm/NVC [468] NIPAm/**182** [469] NIPAm/**183** [469] NIPAm/**184** [469] *Blocks*: AA-*b*-*BA* [456, 458, 470] AA-*b*-*MA* [456] AA-*b*-*BA*-*b*-*St* [456] AA-*b*-*St* [470] AA/BA-*b*-*MMA/BA* [128] AA-*b*-PEGA [459] DMAm [471] DMAm-*b*-St [471] MA-*b*-HEA [460] MA-*b*-PEGA [460] DMAm-*b*-NIPAm [314] St-*b*-St/**340** [465] St-*b*-tBDMSOS [466] DMAm-*b*-PEGA [462] PEGA-*b*-BA [461] PEGA-*b*-BA-*b*-*BA* [461] **246**-*b*-BA [461] **246**-*b*-BA-*b*-*BA* [461] DMAm-*b*-NIPAm/**310** [463] NIPAm-*b*-DMAm/**310** [463]
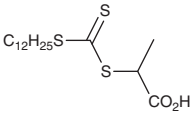 2-(((dodecylthio)carbonothioyl)thio)propanoic acid **65**	A [456, 472, 473]	*Methacrylamides*: APMAm [473] *Acrylates*: AA [456, 473, 474] BA [148, 475] HEA [476] MA [476–478] *Styrenes*: St [148] CMS [479] *Dienes*: (Bd) [480] (Ip) [480] 215 [171] (DMAEA) [148] *Others*: (DADMAC) [481] **152** [482] *Vinyls*: **290** [483] *Copolymers*: AA-*b*-*BA* [456] AN/Bd [160] (AN/BD) [484] St/MAH [472] tBA/**360** [485] AN/Bd/**296** [486]

(*continued*)

Table 9.6 (Continued)

RAFT agent	Synthesis[a)]	Polymerizations[b),c)]
		Blocks: (AA-*b*-TFEMA) [474] AA-*b*-St [480] (AA-*b*-St-*b*-BD) [480] (AA-*b*-St-*b*-Ip) [480] (AA-*b*-St-*b*-Ip) [480] (AA-*b*-BA-*b*-St-*b*-BD) [480] NIPAm/NVC-*b*-DMAEA [468] NIPAm/EGDMA [487] NIPAm/DVB [487] NIPAm/**369** [487] **152**-*b*-**151** [482]
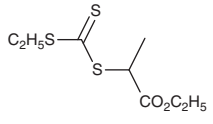 ethyl 2-(((ethylthio)carbonothioyl)thio)propanoate **66**	A [488]	*Acrylates*: BA [488] RAFT-*T-Cationic Polymerization*: (BA-*b*-IBVE) [488]
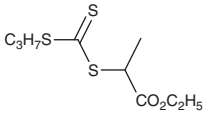 ethyl 2-(((propylthio)carbonothioyl)thio)propanoate **67**	A [42]	*Acrylates*: BA [42]
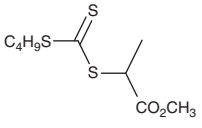 methyl 2-(((butylthio)carbonothioyl)thio)propanoate **68**	A [342, 489, 490] [343, 491]	*Acrylates*: MA [492] DEGA [492] DMAEA [491] PEGA [493] tBA [492, 494] *Acrylamides*: DEAm [492] DMAm [492] HEAm [492, 495] NAM [492] NIPAm [489, 490, 494] **225** [494] **324** [494] *Copolymers*: DMAEA/NIPAm [496] BA/DMAEA/NIPAm [496] DMAEA/NIPAm/St [496] TEGA/**199** [497] DMAm/NIPAm [343, 498] Am/**294** [499] NIPAm/St [343, 500] *Blocks*: PEGA-*b*-**310**/MBAm [493] DMA/NIPAm-*b*-*CS/St* [498] NIPAm-*b*-*St* [490] NIPAm/St-*b*-*St* [500]
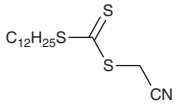 cyanomethyl dodecyl carbonotrithioate **69**	A [199] N	*Acrylates*: AA [277] BA [199, 204] HEA [501] PEGA [501] NAS [502] *Acrylamides*: DDAm [503] DEAm [476] DMAm [476] NIPAm [504, 505] NIPAm [476] *Styrenes*: St [199] CMS [479] DMOS [506] 4HS [309]

(*continued*)

Table 9.6 (Continued)

RAFT agent	Synthesis[a)]	Polymerizations[b),c)]
		Vinyls: NVC [8] *Other*: **355** [334] **196** [507] DADMAC [481] *Copolymers*: Am/AN [508] BA/**208** [509] MA/VAc [510] *St/DVB* [414] St/MAH [511] *Blocks*: NIPAm-*b*-VBA [505] DDAm-*b*-TPAm [503] DMOS-*b*-St [506] HEA-*b*-DMAEA/DEGDA [501] PEGA-*b*-DMAEA/DEGDA [501] NIPAm-*b*-St [489]
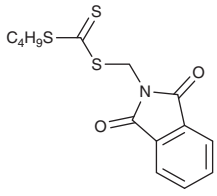 butyl ((1,3-dioxoisoindolin-2-yl)methyl) carbonotrithioate **70**	A [10, 512]	*Acrylates*: BA [57, 513] *Acrylamides*: DEAm [514] DMAm [515] NIPAm [57, 513, 516] *Styrenes*: St [10, 137, 513] *Vinyls*: (NVP) [57] **325** [517] *Copolymers*: AA/PA [512, 518]AA/CPA [512]
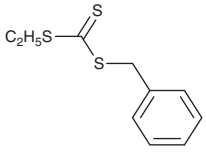 benzyl ethyl carbonotrithioate **71**	A	*Acrylates*: BA [519] *Acrylamides*: DMAm [246] *Copolymers*: PEGA/MEA [246] *Blocks*: PEGA/MEA-*b*-*NIPAm/MBAm* [246] BA-*b*-NVP [519] DMAm-*b*-*NIPAm/MBAm* [246]
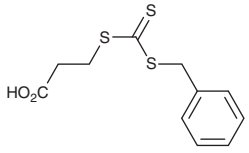 3-(((benzylthio)carbonothioyl)thio)propanoic acid **72**	A [151]	*Acrylates*: AA [520] PEGA [521] tBA [521] OBA [522] **213** [523] **207** [524] PEGA [525, 526] *Acrylamides*: MAm [527] NIPAm [521, 528, 529] **226** [530] **229** [530] **246** [531] *Styrenes*: St [151, 527, 532] (St) [533] (SSO3Na) [534] **257** [524] **262** [535] *Others*: DADMAC [536] NVC [524] NVPI [524] **238** [537] *Copolymers*: HEA/**202** [529] PEGA/DEGA [521] 257 [524] BA/**157** [538] NVC/**257** [524] St/CMS [532] PEGA/PFPA [539]

(*continued*)

Table 9.6 (Continued)

RAFT agent	Synthesis[a)]	Polymerizations[b),c)]
		Blocks: AA-*b*-SSO3Na [520] PEGA-*b*-NIPAm/**293** [525] OBA-*b*-MA-*b*-**293** [522] **213**-*b*-**247** [523] **238**-*b*-DMAm [537] (St-*b*-DMAm) [527] PEGA-*b*-373 [521] PEGA-*b*-**374** [521] PEGA-*b*-***371*** [521] PEGA-*b*-**373** [521] tBA-*b*-**374** [521] NIPAm-*b*-**374** [521] PEGA/DEGA-*b*-**374** [521] PEGA-*b*-MBAm/**310** [526] **257**-*b*-**207** [524] NIPAm-*b*-HEA/**292** [529] *RAFT-T-ATRP*: St/CMS-*g*-MMA [532]
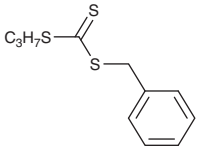 benzyl propyl carbonotrithioate **73**	A [540]	*Acrylates*: BA [43] *Acrylamides*: NiPAm [540] *Other MAM*: **310** [541–543] *Copolymers*: MA/**360** [544] PEGA/**360** [544] NIPAm/**360** [544] DMAm/**360** [544] NMMI/**360** [545] NPMI/**360** [545] NPFPMI/**360** [545] *Blocks*: **310**-*b*-DMAm [542] **310**-*b*-NIPAm [542]
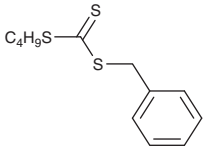 benzyl butyl carbonotrithioate **74**	A	*Styrenes*: **St** [546] 4VP [546] *Dienes*: *Cp* [547] *Other*: NPMI [548] *Blocks*: **NPMI**-*b*-**Ind** [548] **NPMI**-*b*-**Ind**-*b*-**NPMI** [548] **NPMI**-*b*-**Ind**-*b*-**NPMI**-*b*-**Ind** [548] **NPMI**-*b*-**Ind**-*b*-**NPMI**-*b*-**Ind**-*b*-**NPMI** [548] St-*b*-4VP [546]
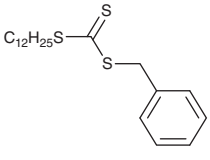 benzyl dodecyl carbonotrithioate **75**	A	*Acrylates*: MA [460] **205** [549] *Styrenes*: St [18] *St* [550] *Dienes*: *Cp* [547] *Other*: **310** [541] *Copolymers*: DEGA/PEGA/**201** [551] PEA/PEGA/**324** [552] PEA/PEGA/**323** [552]

a) The letter A-N refers to the method of RAFT agent synthesis. Refer to Section 9.8.
b) Purple – crosslinking polymerization. Block copolymers prepared by crosslinking polymerization will be arm-first stars. Red – photoinitiated polymerization. Orange – SUMI. **Bold Orange** – PhotoSUMI or photoinduced electron or energy transfer-single-unit monomer insertion (PET-SUMI). Green – redox RAFT. *Blue Italics* – heterogeneous polymerization (emulsion, miniemulsion, dispersion).
c) For a full list of monomer abbreviations, see Abbreviations section.

Table 9.7 RAFT polymerizations with functional trithiocarbonates derived from symmetric.

RAFT agent	Synthesis[a)]	Polymerizations[b)]
Hydroxyl 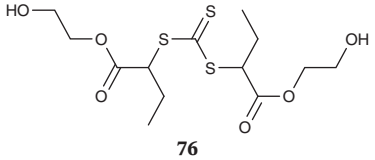 **76**	A [554]	*ROP-T-RAFT*: LA-*b*-NIPAm [554]
Active ester 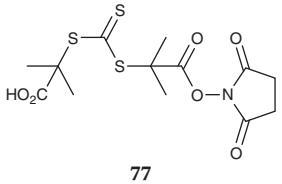 **77**	H [555]	RAFT agent synthesis [555, 556]
Protected maleimide 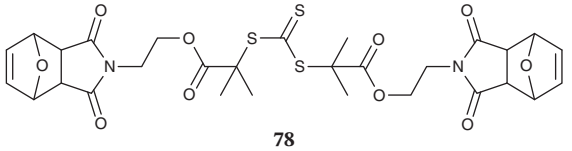 **78**	I [557] I/M [558]	*Methacrylates*: MMA [557]
Protected thiol 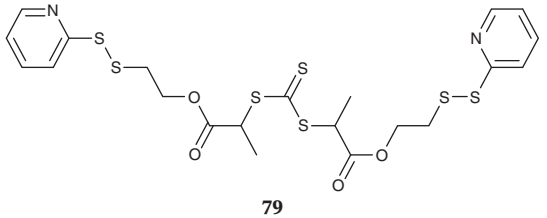 **79**	H [559]	*Acrylates*: PEGA [559]
protected aminoxy 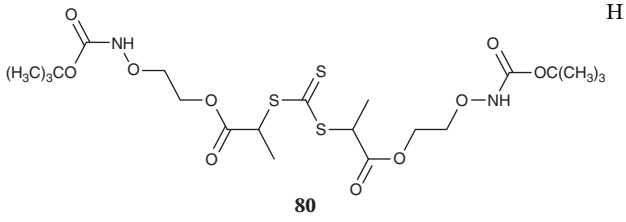 **80**	H [559]	*Acrylates*: PEGA [559]

(*continued*)

Table 9.7 (Continued)

RAFT agent	Synthesis[a)]	Polymerizations[b)]
Alkyne		
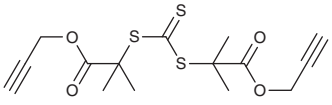 **81**	J [560, 561] H [562] F,H [563] F, I [560, 564, 565]	*Acrylamides*: NIPAm [563, 565] RAFT agent synthesis [560–562, 564, 566]
NMP initiator		
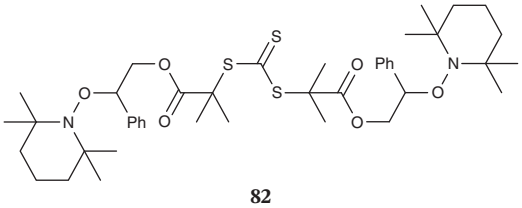 **82**	J [567]	*Acrylates*: AA [568] BA [567]
ROAMP initiator		
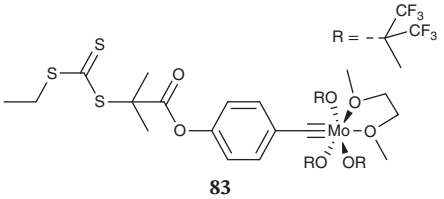 **83**	M [569]	*Acrylates*: MA [569]
ROMP monomer		
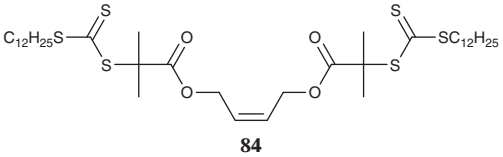 **84**	I [570]	ROMP-*T*-RAFT [570]

a) The letter A-N refers to the method of RAFT agent synthesis. Refer to Section 9.8.
b) For a full list of monomer abbreviations, see Abbreviations section.

Table 9.8 RAFT polymerizations with functional trithiocarbonates derived from non-symmetric trithiocarbonates.

RAFT Agent	Synthesis[a)]	Polymerizations[b)]
Hydroxyl		
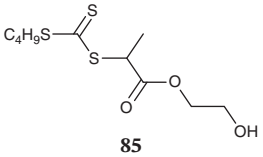 **85**	H [571]	*Acrylates*: MA [571] ROP-*T*-RAFT: CL [571] VL [572] CL-*b*-MA [571] VL-*b*-MA [572]
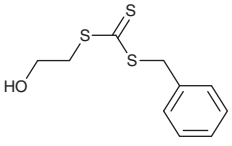 **86**	A [573, 574]	*Methacrylates*: (**318**) [574] *Acrylates*: **305** [575] *Acrylamides*: NIPAm [573] **301** [576] *Copolymers*: Am/**249** [577] *Blocks*: **305**-*b*-BA [575] Am/**249**-*b*-NIPAm [577] ROP-*T*-RAFT: CL [573, 578, 579] LA [580] CL-*b*-HEMA [581] CL-*b*-St [582] CL-*b*-DEGMA [579] CL-*b*-PEGMA [583] CL-*b*-NIPAm [579] CL-*b*-tBAm [579] CL-*b*-**179**/**362** [578] (GA/LA-*b*-PEGMA) [584] LA-*b*-NAM/NAS LA-*b*-Sty/DVB [585]
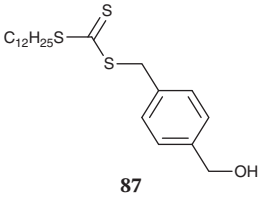 **87**	A [586]	ROP-*T*-RAFT: LA [586–589] PDL [590] LA-*b*-THPA [586–588] LA-*b*-**293** [589] PDL-*b*-EHA [590] PDL-*b*-MA [590] PDL-*b*-NIPAm [590]
Active ester		
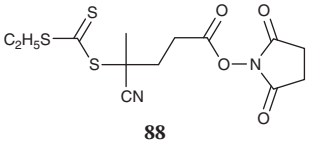 **88**	H [591, 592]	*Methacrylates*: MMA [593] PEGMA [591] RAFT agent synthesis [592, 594–598]
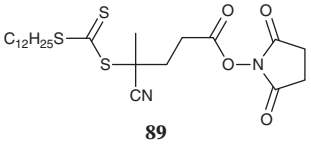 **89**	H [599, 600]	*Methacrylamides*: HPMAm [600] RAFT agent synthesis [599, 601–603]

(*continued*)

Table 9.8 (Continued)

RAFT Agent	Synthesis[a)]	Polymerizations[b)]
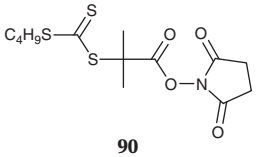 **90**	H [604]	RAFT agent synthesis [604]
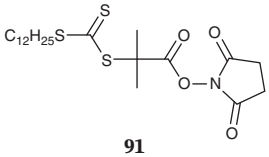 **91**	H [605–607]	*Methacrylates*: CMA [608] *Acrylates*: DMAEA [609] *Acrylamides*: NIPAm [610] *Styrenes*: [605] *Blocks*: CMA-*b*-DMAEMA [608] St-*b*-DVB [605] RAFT agent synthesis [601, 606, 607, 611–623]
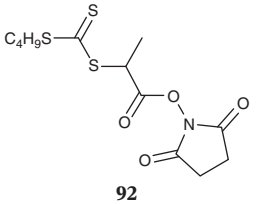 **92**	H [592, 624–626]	*Acrylates*: HEA [624] *Copolymers*: PEGMA/PFOEMA [627] RAFT agent synthesis [592, 625, 626]
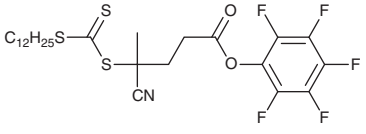	H [592]	RAFT agent synthesis [592]
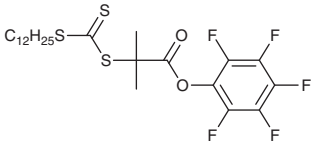	M [628]	*Methacrylamides*: HPMAm [629] *Acrylates*: OPA [628] *Acrylamides*: DMAm [630] HEAm [464, 629, 631–633] *Styrenes*: **252** [634]
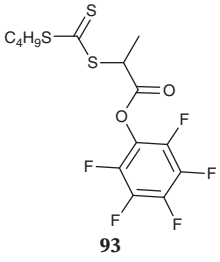 **93**	H [624, 625]	*Acrylates*: HEA [624] RAFT agent synthesis [625, 635]

(*continued*)

Table 9.8 (Continued)

RAFT Agent	Synthesis[a)]	Polymerizations[b)]
2-Mercaptothiazoline 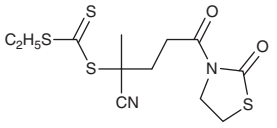 **94**	H [636]	*Acrylates*: PEGA [636] RAFT agent synthesis [637]
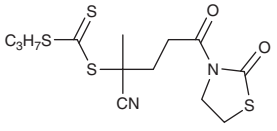 **95**	H [638]	RAFT agent synthesis [638]
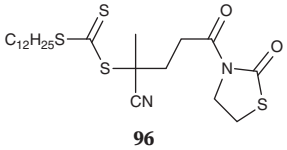 **96**	H [600]	*Methacrylamides*: HPMAm [600]
Azlactone 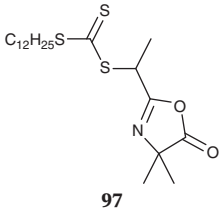 **97**	A [639]	*Acrylates*: EA [639] *Acrylamides*: NIPAm [639] *Styrenes*: St [639]
Trifluoroborate iminium 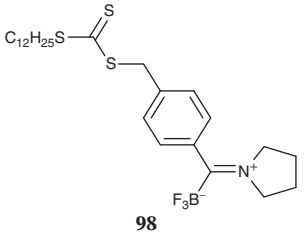 **98**	A [640]	*Acrylamides*: NIPAm [640]

(*continued*)

Table 9.8 (Continued)

RAFT Agent	Synthesis[a)]	Polymerizations[b)]
Protected thiol		
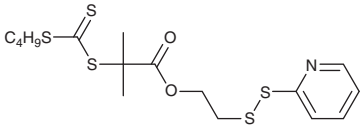 **99**	H [604]	*Acrylamides*: NIPAm [604] *Blocks*: NIPAm-*b*-*St* [604]
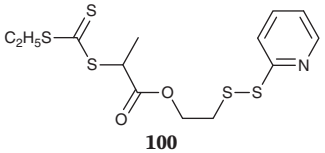 **100**	H [641]	*Styrenes*: **272** [641] *Copolymers*: PEGMA/PFOEMA [627]
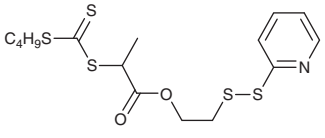 **101**	H [462, 624]	*Acrylates*: DEGA [642] HEA [624] PEGA [643] RAFT agent synthesis [462]
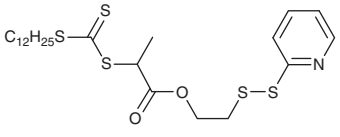 **102**	I	*Acrylates*: PEGA [526] *Blocks*: PEGA-*b*-MBAm/**310** [526]
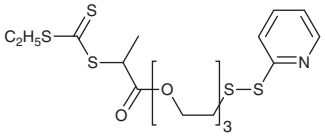 **103**	H [641]	*Styrenes*: **272** [641]
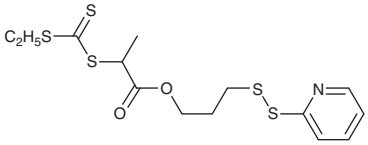 **104**	H [644]	*Acrylates*: PEGA [644]

(*continued*)

Table 9.8 (Continued)

RAFT Agent	Synthesis[a)]	Polymerizations[b)]
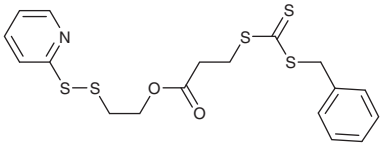 **105**	I [645]	*Acrylates*: PEGA [645] *Blocks*: PEGA-*b*-BA [645]
Thioketal 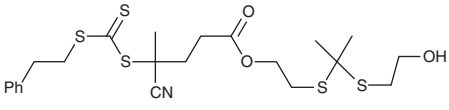 **106**	H [646]	*Acrylamides*: DMAm [646]
Protected amine 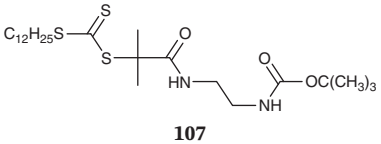 **107**	K [606]	*Acrylamides*: NIPAm [606] RAFT agent synthesis [606]
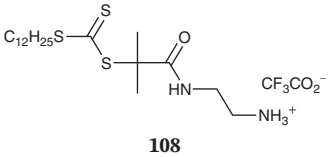 **108**	M [606]	RAFT agent synthesis [606]
Alkyne 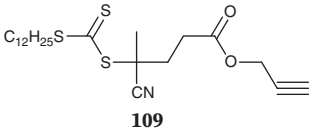 **109**	H [647, 648]	*Methacrylates*: PEGMA [648] *Copolymers*: PEGMA/**317**/dye/EGDMA [647] *Blocks*: PEGMA-*b*-DMAEMA/TFEMA-*b*-**368** [648]
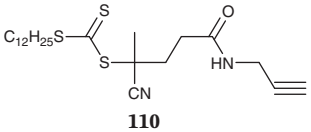 **110**	H [649]	*Acrylamides*: NIPAm [649]

(*continued*)

Table 9.8 (Continued)

RAFT Agent	Synthesis[a)]	Polymerizations[b)]
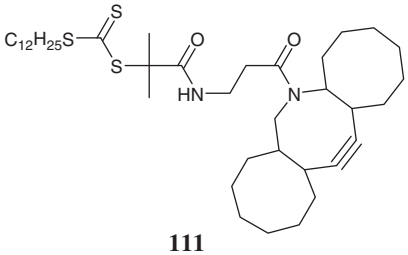 **111**	H [650]	*Methacrylates*: **178** [650] *Blocks*: **178**-*b*-**175** [650]
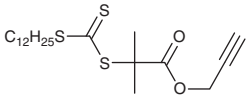 **112**	H [651–654]	*Methacrylates*: MMA [655] **321** [656] *Acrylates*: tBA [657] EHA [657] DA [657] PEGA [657] *Acrylamides*: NAM [658] NIPAm [654, 659–661] *Styrenes*: St [662, 663] tBOS [662] 4VP [348] RAFT agent synthesis [651–653, 664–669]
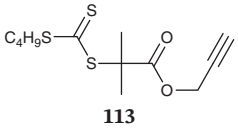 **113**	H [604]	*Acrylamides*: NIPAm [604] *Blocks*: NIPAm-*b*-*St* [604]
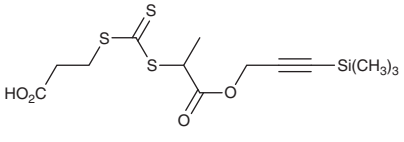	A [539]	*Acrylates*: PEGA [539, 670] *Other MAM*: **310** [671] *Copolymers*: PEGA/PFPA/DSDA [539] **310**/PFPA [671] *Blocks*: PEGA-*b*-PFPA/DSDAm [539] PEGA-*b*-**310**/MBAm **310**-*b*-PFPA [671]
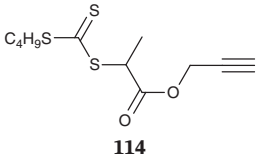 **114**	H [604]	*Acrylates*: HEA [672] tBA [471] *Acrylamides*: DMAm [471] *Styrenes*: CMS [673] *Blocks*: CMS-*b*-St [673] tBA-*b*-St [471] DMAm-*b*-St [471]
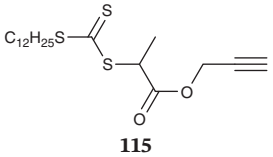 **115**	H [486]	*Copolymers*: AN/Bd [486]

(*continued*)

Table 9.8 (Continued)

RAFT Agent	Synthesis[a)]	Polymerizations[b)]
Azide		
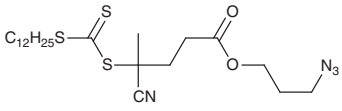 **116**	J [674]	*Methacrylates*: MMA [674, 675] *Vinyls*: **310** [675]
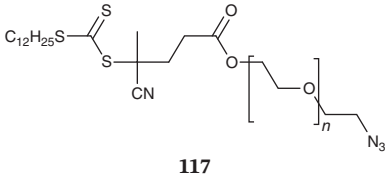 **117**	H [676]	*Styrenes*: St [676]
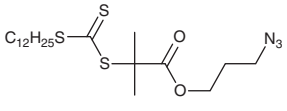 **118**	I [677] N	*Acrylates*: PFPA [678] *Acrylamides*: DMAm [677, 679] NEAm [679] NIPAm [680] (NIPAm) [681] *Styrenes*: St [677] 2VP [682] RAFT agent synthesis [683, 684]
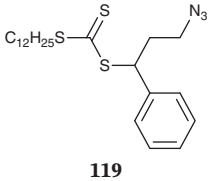 **119**	A [685]	**337** [685]
Dibromomaleimide		
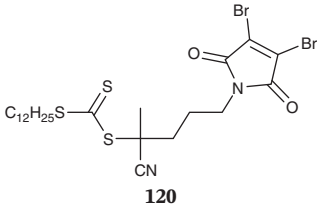 **120**	I [686]	*Acrylates*: PEGA [686] *Blocks*: PEGA-*b*-**219**
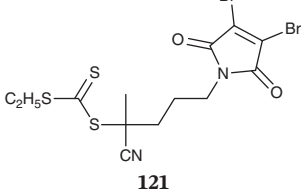 **121**	J [687]	RAFT agent synthesis [687]

(*continued*)

Table 9.8 (Continued)

RAFT Agent	Synthesis[a)]	Polymerizations[b)]
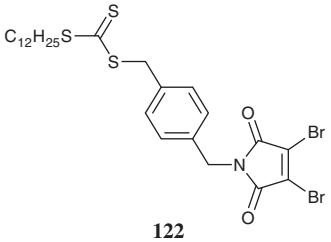 **122**	M [688]	*Acrylates*: BA [688] MA [688] TEGA [688] *Acrylamides*: NIPAm [688] *Styrenes*: St [688] RAFT agent synthesis [689]
Thiolactone 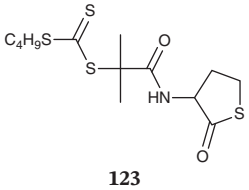 **123**	K [604]	*Acrylamides*: NIPAm [604] *Blocks*: NIPAm-*b*-*St* [604]
Carbonyl azide (transforms to isocyanate in situ) 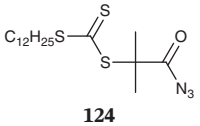 **124**	M [690]	*Methacrylates*: MMA [690] *Acrylates*: MA [690] *Acrylamides*: NIPAm [690] *Styrenes*: St [690]
Protected maleimide/ROMP monomer 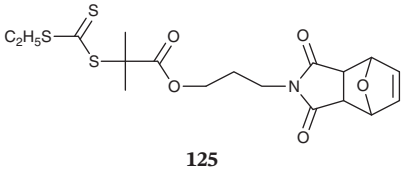 **125**	H [691]	*Methacrylates*: **176** [691] *Acrylates*: HPA [692] *Acrylamides*: NIPAm [691, 693, 694] *Copolymers*: MEA/DEGA [692]
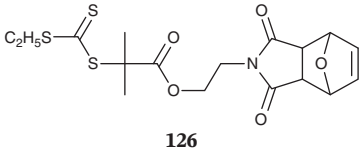 **126**	I [695]	*Acrylamides*: DEAm [695]

(*continued*)

Table 9.8 (Continued)

RAFT Agent	Synthesis[a)]	Polymerizations[b)]
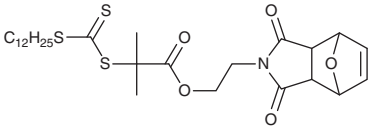 **127**	H [696, 697]	*Methacrylates*: MMA [698] *Acrylamides*: NIPAm [697, 699, 700] *Styrenes*: St [696, 698, 700–702] *Copolymers*: MMA/St [698] RAFT-*T*-ROMP [696, 701]
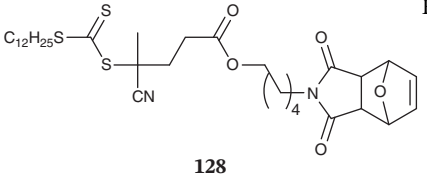 **128**	H [703]	*Methacrylates*: MMA [703] *Acrylates*: BA [703] *Styrenes*: St [703] RAFT-*T*-ROMP [703]
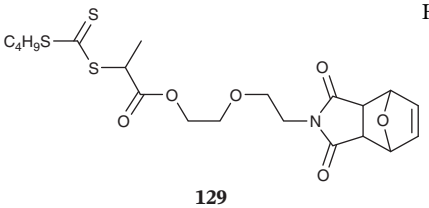 **129**	H [624]	*Acrylates*: (HEA) [624]
Urazole (1,2,4-triazoline-3,5-dione precursor)		
9 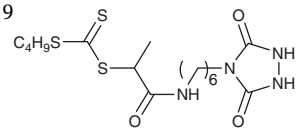 **130**	K [626]	*Acrylates*: BA [626]
Sulfonyl fluoride		
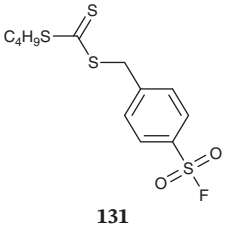 **131**	M [704]	*Methacrylates*: (MMA) [704] *Acrylates*: tBA [704] *Acrylamides*: NAM [704] *Styrenes*: St [704]

(*continued*)

Table 9.8 (Continued)

RAFT Agent	Synthesis[a)]	Polymerizations[b)]
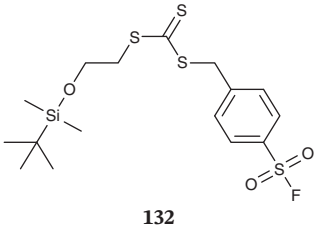 **132**	A [705]	*Methacrylates*: **177** [706] *Acrylamides*: NIPAm [705] *Vinyls*: NVP [705] *Blocks*: **177-b-186** [706]
ATRP initiator 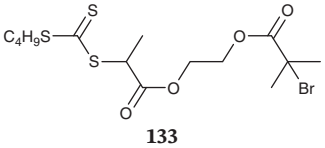 **133**	H [707]	*Acrylates*: MA [707] *RAFT-T-ATRP*: MA-*b*-MMA [707]
Norbornene (ROMP monomer) 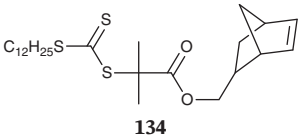 **134**	H [708–710]	*Acrylates*: tBA [708, 711, 712] *Acrylamides*: NAM [713] *Styrenes*: St [709–711, 714, 715] *Blocks*: St-*b*-MA [714] St-*b*-MA-*b*-tBA [714] RAFT-*T*-ROMP [708–715]
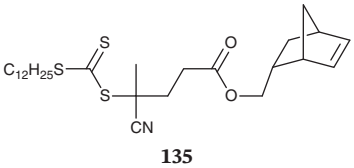 **135**	H [716]	*Methacrylates*: MMA [716] *Styrenes*: St [716]
Alkoxysilane 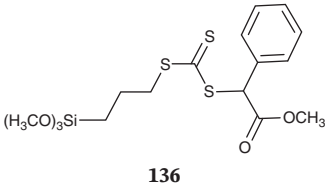 **136**	A [441, 717]	RAFT agent synthesis [441, 717]

(*continued*)

Table 9.8 (Continued)

RAFT Agent	Synthesis[a)]	Polymerizations[b)]
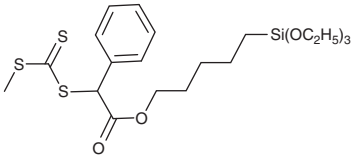 **137**	A [718]	RAFT agent synthesis [718, 719]
t-Butyldimethsilyl (see also **132**)		
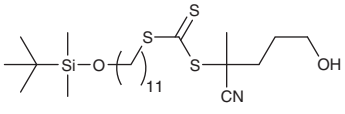 **138**	C [720]	*Styrenes*: St [720]
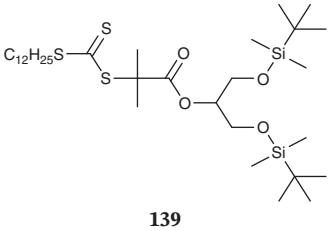 **139**	H [721]	*Acrylates*: **220** [721] **221** [721]
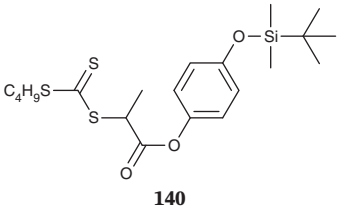 **140**	H [704]	*Acrylamides*: NAM [704]

Table 9.8 (Continued)

RAFT Agent	Synthesis[a)]	Polymerizations[b)]
Poly(dimethylsiloxane)		
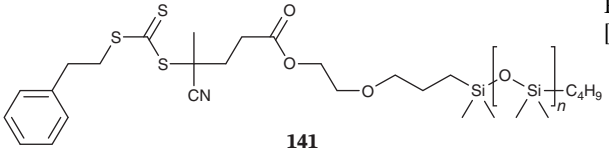 **141**	H [722, 723]	*Methacrylates*: *BzMA* [722, 723] *DMAEMA* [723] *GMMA* [723] *MMA* [723] *TFEMA* [723] tBDMSMA [724] *Copolymers*: BMA/ tBDMSMA [724] PEGMA/ TBSiMA [725] PEGMA/ TPSiMA [725]
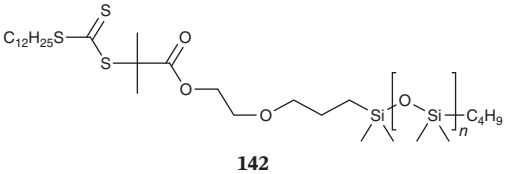 **142**	H [726]	*Styrenes*: St [726] MeS [726] tBS [726]
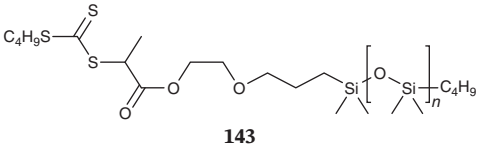 **143**	H [727]	*Acrylates*: DMAEA [727]
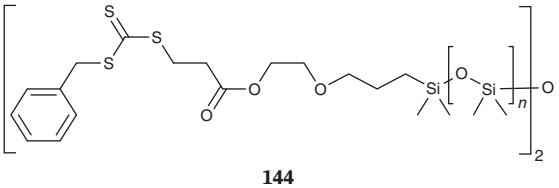 **144**	H [728]	*Vinyls*: NVP [728]
Peptide		
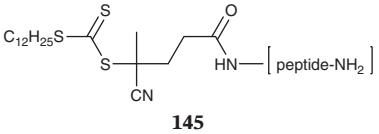 **145**	M [729, 730]	*Methacrylates*: BMA [730] DMAEMA [730] PEGMA [730] *Blocks*: PEGA-*b*-BA [729]

a) The letter A-N refers to the method of RAFT agent synthesis. Refer to Section 9.8.
b) *Blue italics* – heterogeneous polymerization (emulsion, miniemulsion, dispersion). Purple – crosslinking polymerization. Red – photoinduced polymerization.
For a full list of monomer abbreviations, see Abbreviations section.

Functional RAFT agents also facilitate the synthesis of conjugates post-RAFT polymerization. In this context, this summary can be used for guidance as to the functionalities tolerated by the RAFT process. Unfortunately, in many papers the quantitative characterization that would enable a rigorous evaluation of the effectiveness of the various chemistries is lacking.

Azide functionality is best installed post-RAFT polymerization. It has been found that azide functionality (e.g. from **118**) is not completely stable to the conditions used for RAFT polymerization [681]. The synthesis of reactive polymers by RAFT polymerization is detailed in the Chapter 18 by Gauthier-Jaques et al. [732].

9.8 Synthesis of Trithiocarbonates

The methods most commonly exploited for the synthesis of (low molar mass) trithiocarbonates are listed below. The method of choice is dependent on the specific structure, the amount required, the toxicity and ease of handling of reagents, and other factors. A critical review [5] of synthetic methods for RAFT agent synthesis provides further details of the various methods listed below and they will not be elaborated here. Two recent reviews on the synthesis of organic trithiocarbonates have appeared [733, 734].

Procedures for RAFT agent synthesis referred to in Tables 9.3–9.8 are as follows:

A. Reaction of a carbodithioate salt with an alkylating agent.
   A process for the synthesis of symmetrical trithiocarbonates from carbon disulfide and various alkyl halides in dimethyl sulfoxide (DMSO) with 1 equiv of $CsOH.H_2O$ at 50 °C [735]. The method has been used for **20** ($PhCH(CH_3)Br$, 60 minutes, 81%) and **22** ($PhCH_2Cl$, 45 minutes, 91%; $PhCH_2Br$, 30 minutes, 96%). No reaction was observed for the tertiary halides including $Ph(CH_3)_2Br$ or $C(CH_3)_3Br$.
B. Reaction of a dithiochloroformate or a thiocarbonyl-bis-imidazole with a nucleophile.
C. Radical-induced decomposition of a bis(thioacyl)disulfide.
D. Radical-induced ester exchange.
E. Transesterification (thiol exchange by reaction of a dithioester with a thiol).
F. Ketoform reaction (used for the synthesis of carboxy functional RAFT agents).
G. Single-unit monomer insertion (SUMI).
   RAFT-SUMI and PET-RAFT-SUMI are described in Section 9.15.
H. Esterification or amidation (carbodiimide)
I. Esterification (acid chloride)
J. Esterification (Mitsunobu reaction)
K. Active ester–amine reaction or active ester–thiol reaction
L. 1,3-Dipolar cycloaddition
M. Other methods
   An imidazole-mediated process for the synthesis of symmetrical trithiocarbonates from carbon disulfide and various alkyl halides in wet DMSO or

N,N-dimethylformamide (DMF) has been described [140]. The method was used for (**22** ($PhCH_2Cl$, 4.5 hours, 92%; $PhCH_2Br$, 3.5 hours, 91%)) and **23** [$C(CH_3)_3Br$, 14 hours, 65%].

N. Commercially available.

9.9 Polymer Syntheses with Trithiocarbonates

The more common monomers subjected to RAFT polymerization with trithiocarbonates are referred to using abbreviations (Section 9.23). The structures of more exotic monomers are included in the tables that follow. They include 1,1-disubsituted monomers, namely, methacrylates (Table 9.9), methacrylamides (Table 9.10), and others (Table 9.11), and monosubstituted monomers, namely, acrylates (Table 9.12), acrylamides (Table 9.13), styrene derivatives (Table 9.14), and vinyl monomers (Table 9.15). Monomers with reactive functionality appear in Table 9.16. To assist in finding the trithiocarbonate RAFT agents that might best be used for a specific monomer, some guidance is provided in the preamble section before each table. Example polymerizations can be found in Tables 9.3–9.8 by searching for the corresponding abbreviation or compound number. The monomer numbers in Tables 9.3–9.8 are hyperlinked to the monomer structures in the online version of this chapter.

There is substantial interest in RAFT polymerization of monomers derived from renewable resources [763]. More commonly encountered monomers in this category include those derived from amino acids [764], such as acrylamides (Table 9.12), and glycomonomers, such as acrylates **204** and **205**, methacrylamides **180–179**, acrylamide **247,** and styrene derivative **272**.

9.9.1 Methacrylates

RAFT polymerization with trithiocarbonates has been successfully applied to a very wide range of methacrylates. These include allyl methacrylate (AMA), cholesteryl methacrylate (CMA, **165**), butyl methacrylate (BMA), (diethylene glycol monomethyl ether) methacrylate (DEGMA), (2-dimethylamino)ethyl methacrylate (DMAEMA), 2-hydroxyethyl methacrylate (HEMA), lauryl methacrylate (LMA), methyl methacrylate (MMA), (methacryloyloxy)ethyl phosphorylcholine (MPC), (polyethylene glycol monomethyl ether) methacrylate (PEGMA), (3-trimethylaminonium)propyl methacrylate (TMAPMA) (for other examples see *Abbreviations*), and those listed in Tables 9.9 and 9.16 (functional methacrylates).

Low $Đ$ in RAFT polymerization of methacrylates requires the use of a RAFT agent with a suitably high transfer coefficient. This requires that the RAFT agent R group is a good leaving group with respect to the methacrylate propagating radical. Amongst the better RAFT agents for methacrylates are the tertiary cyanoalkyl trithiocarbonates **37–45**. Tertiary carboxy trithiocarbonates **47**–**51** provide control over molar mass but $Đ$ is typically > 1.3 even at high monomer conversions. The 1-phenyl-1-carboxy trithiocarbonates **54–59** can give good control, but often give some retardation due to slow reinitiation, which is most noticeable for high RAFT agent concentrations.

Table 9.9 Methacrylate monomers subjected to RAFT polymerization.

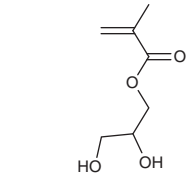

glycerol monomethacrylate (GMMA)
146

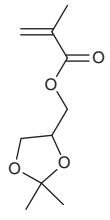

solketal methacrylate
147

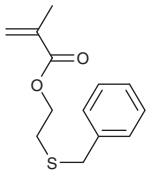

148 [736]

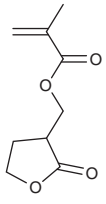

149

Metallomonomers

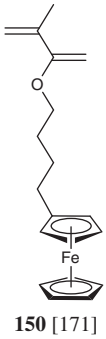

150 [171]
[171]

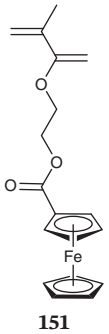

151

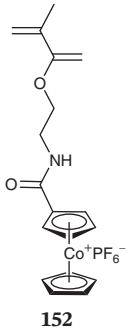

152

Ligating monomer

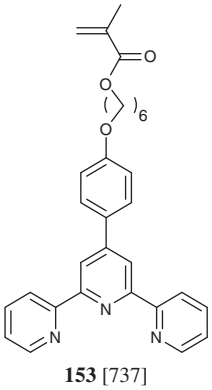

153 [737]

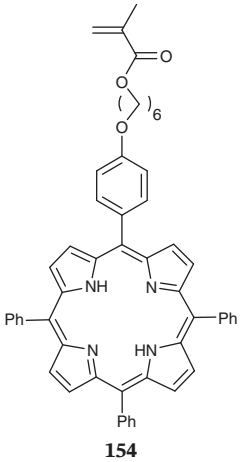

154

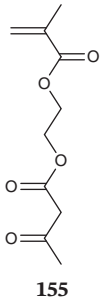

155

(*continued*)

Table 9.9 (Continued)

Dyes

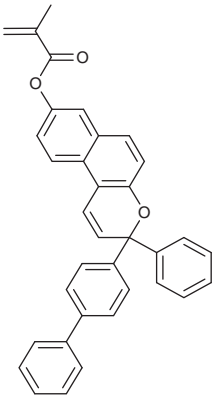

156

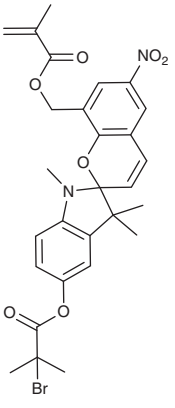

157

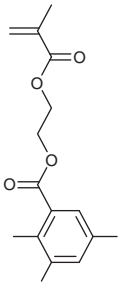

158

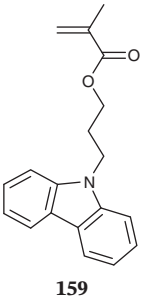

159

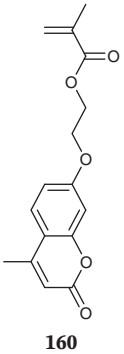

160

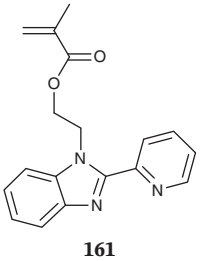

161

Liquid crystals

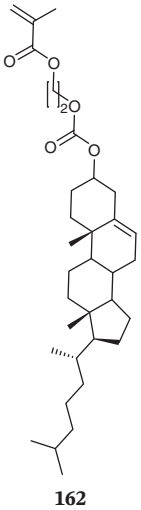

162

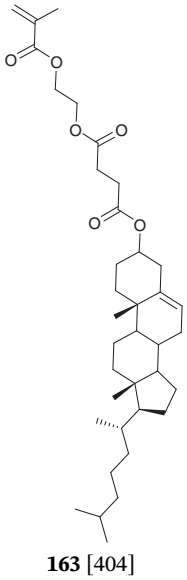

163 [404]

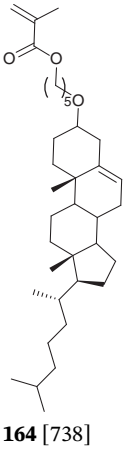

164 [738]

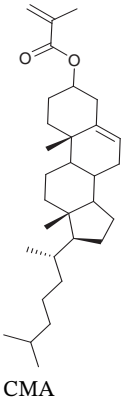

CMA
165 [739]

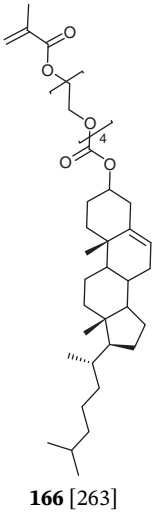

166 [263]

(*continued*)

Table 9.9 (Continued)

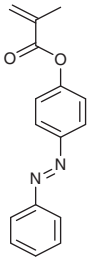

167

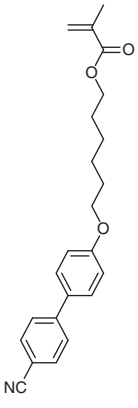

168

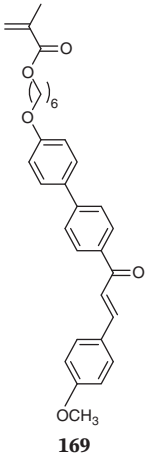

169

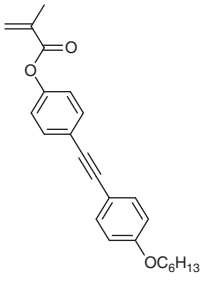

170 [740]

Bulky monomers

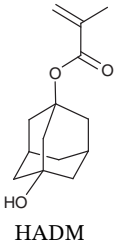

HADM
171 [741]

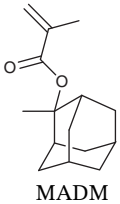

MADM
172

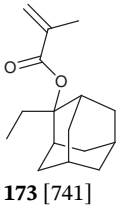

173 [741]

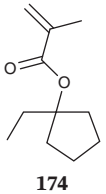

174

Betaines, ionic liquids

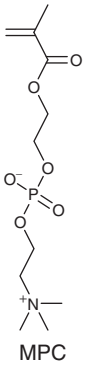

MPC
175

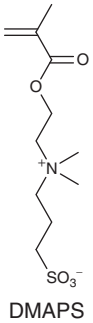

DMAPS
176

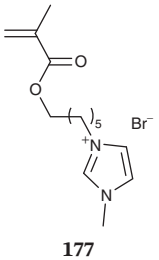

177

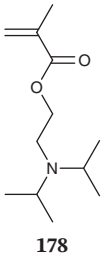

178

Table 9.10 Methacrylamide derivatives subjected to RAFT polymerization.

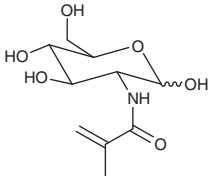

179

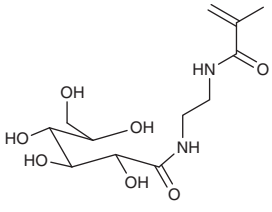

180

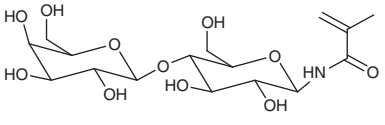

181

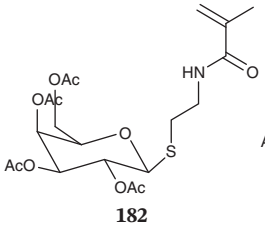

182

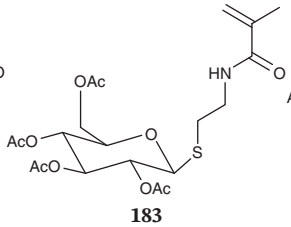

183

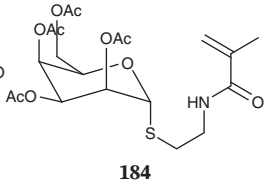

184

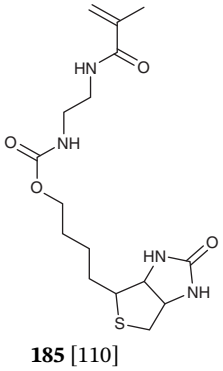

185 [110]

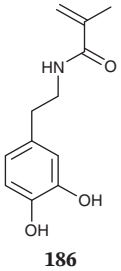

186

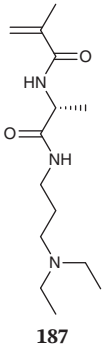

187

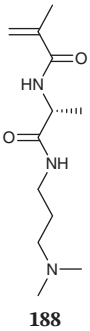

188

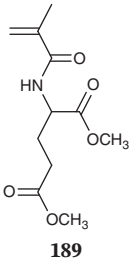

189

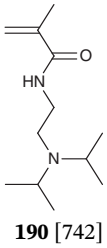

190 [742]

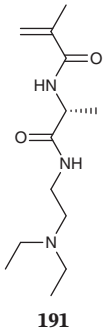

191

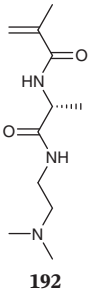

192

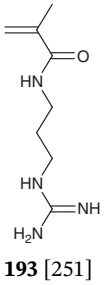

193 [251]

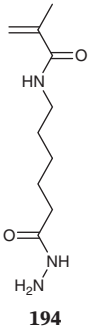

194

Table 9.11 Other 1,1-disubstituted monomers subjected to RAFT polymerization.

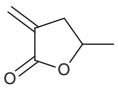
MMBL
195

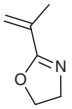
196

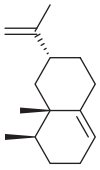
197

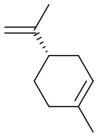
Lim

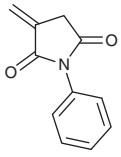
198

Table 9.12 Acrylate monomers subjected to RAFT polymerization.

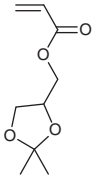
199

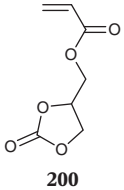
200

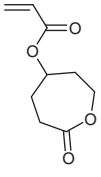
201

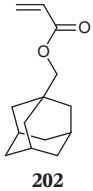
202

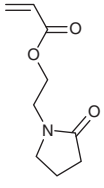
203

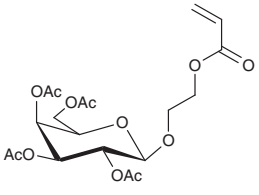
204 [444]

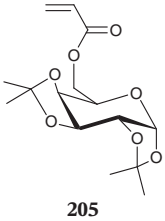
205

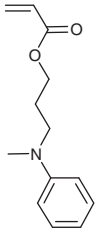
206

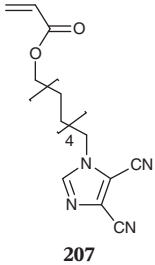
207

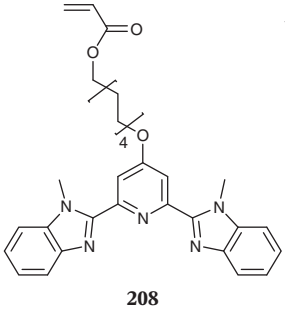
208

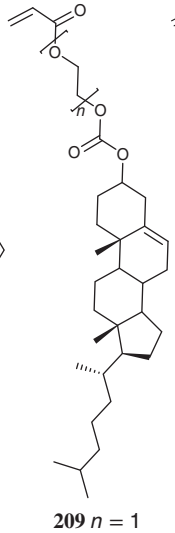
209 $n = 1$
210 $n = 4$

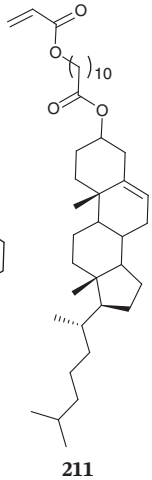
211

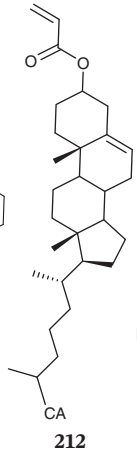
212

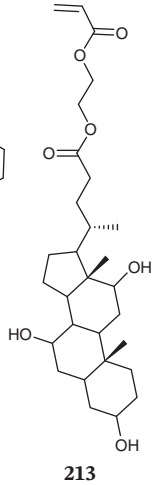
213

(*continued*)

Table 9.12 (Continued)

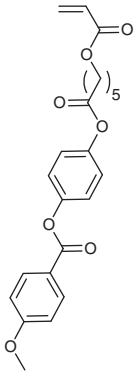
214

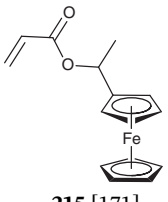
215 [171]

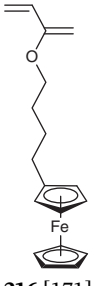
216 [171]

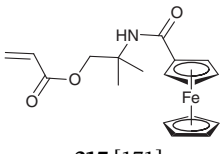
217 [171]

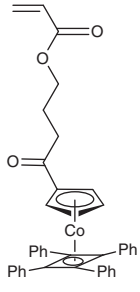
218 [171]

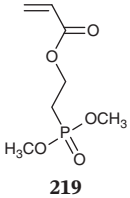
219

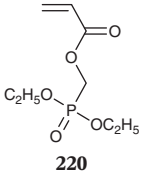
220

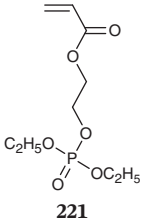
221

Table 9.13 Acrylamide derivatives subjected to RAFT polymerization.

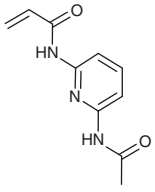
222 [188, 292]

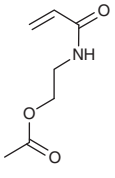
223

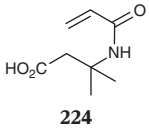
224

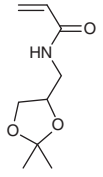
225

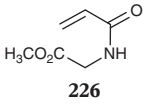
226

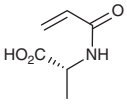
227

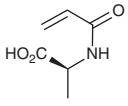
228

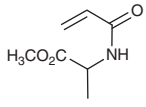
229

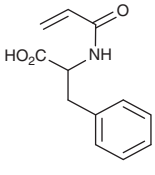
230

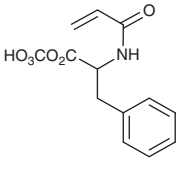
231

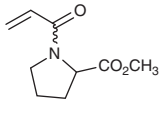
232

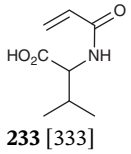
233 [333]

(*continued*)

Table 9.13 (Continued)

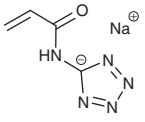

234 [105]

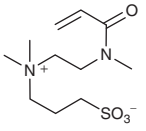

235

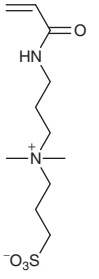

236

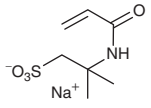

AMPS

237

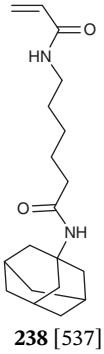

238 [537]

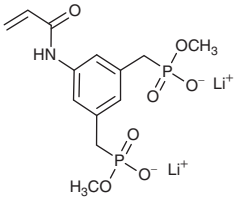

239 [105]

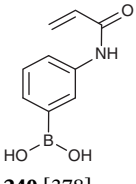

240 [378]

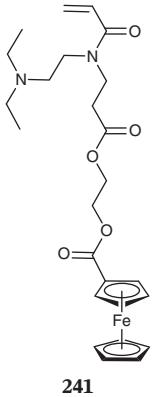

241

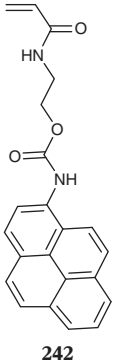

242

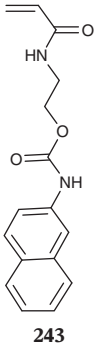

243

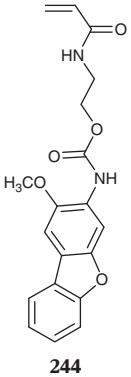

244

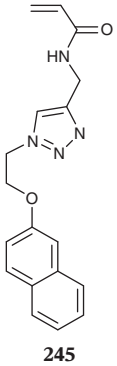

245

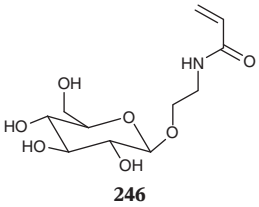

246

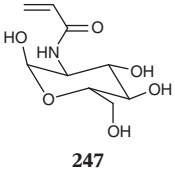

247

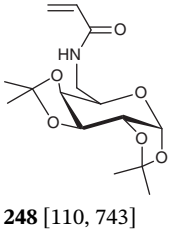

248 [110, 743]

Table 9.13 (Continued)

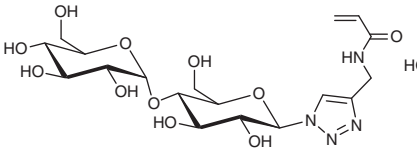

249

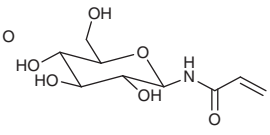

250

Table 9.14 Styrene derivatives subjected to RAFT polymerization.

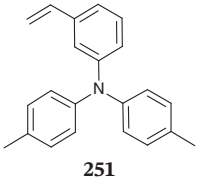

251

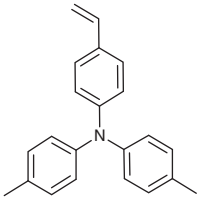

252 [744]

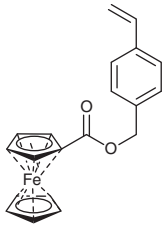

253

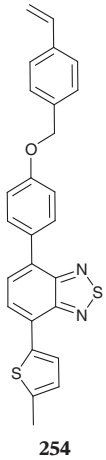

254

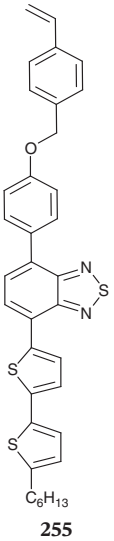

255

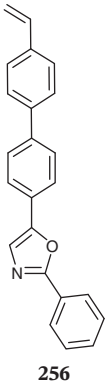

256

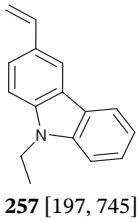

257 [197, 745]

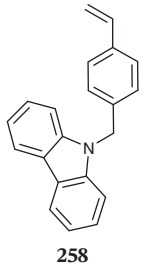

258

(*continued*)

Table 9.14 (Continued)

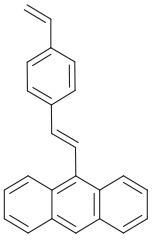

259 [746]

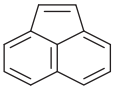

acenaphthylene
260

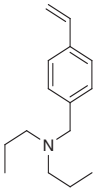

261 [387, 747]

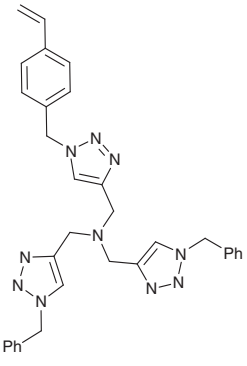

262 [535]

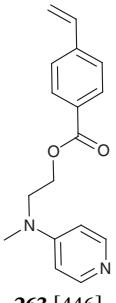

263 [446]

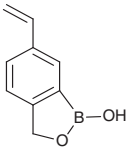

264 [389]

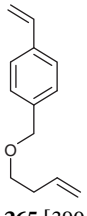

265 [390, 748]

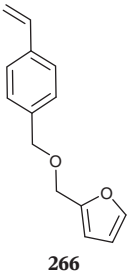

266

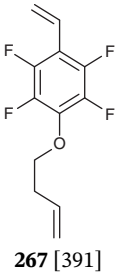

267 [391]

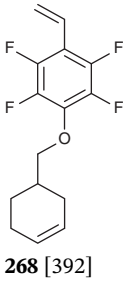

268 [392]

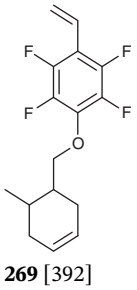

269 [392]

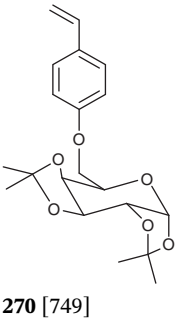

270 [749]

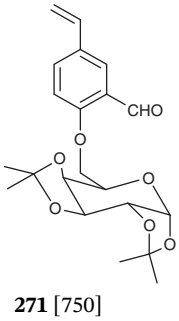

271 [750]

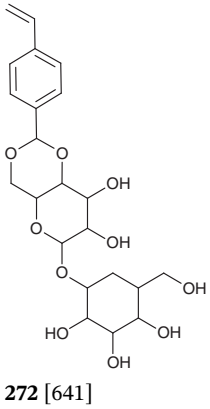

272 [641]

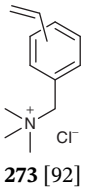

273 [92]

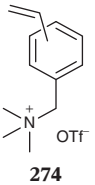

274

(*continued*)

Table 9.14 (Continued)

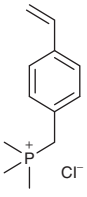

275

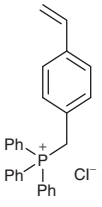

276

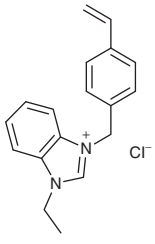

277

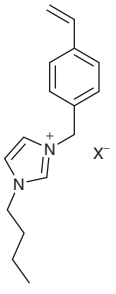

278

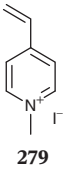

279

Table 9.15 Vinyl derivatives subjected to trithiocarbonate-mediated RAFT polymerization.

Thioacrylates

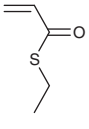

281

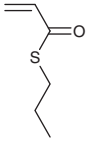

282

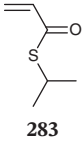

283

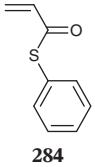

284

Vinylsulfides

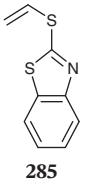

285

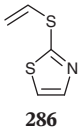

286

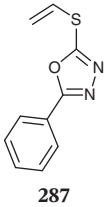

287

Others

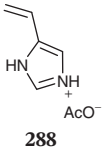

288

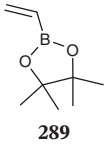

289

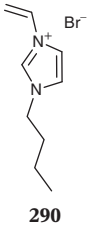

290

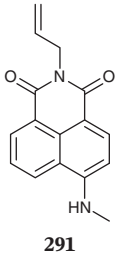

291

Table 9.16 Monomers with reactive functionality used in trithiocarbonate-mediated RAFT (co)polymerization.

(a) *Alkyne*

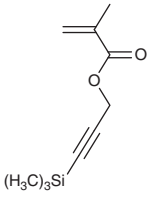

292

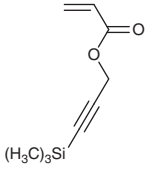

293

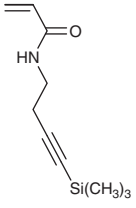

294

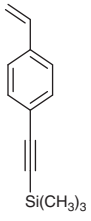

295

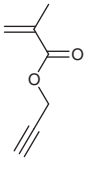

296 [751, 752]

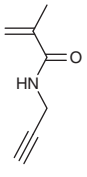

297

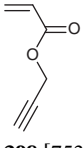

298 [753–755]

(b) *Azide*

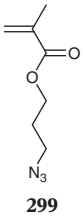

299

(c) *Active ester*

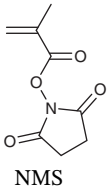

NMS
300 [756]

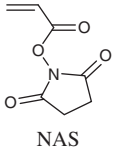

NAS
301

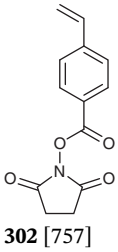

302 [757]

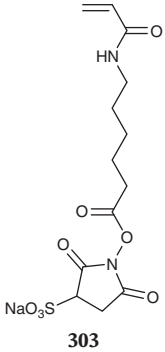

303

(*continued*)

Table 9.16 (Continued)

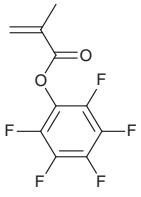
PFPMA
304

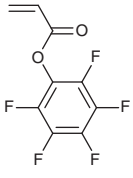
PFPA
305

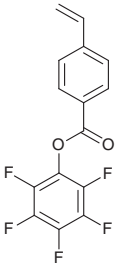
PFPVB
306 [409]

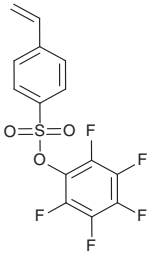
PFPVS
307 [409]

(d) *Thialactone, azlactone*

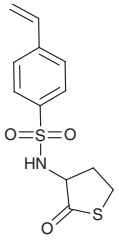
308 [416]

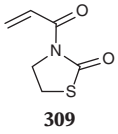
309

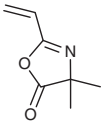
310

(e) *Protected thiol, hydrazide, or amino functionality*

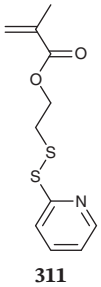
311

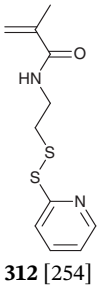
312 [254]

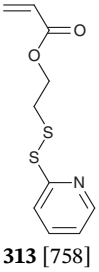
313 [758]

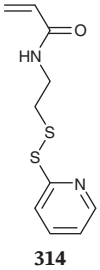
314

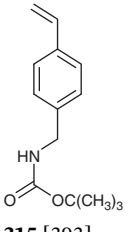
315 [393]

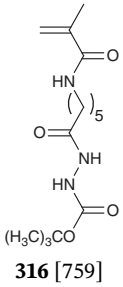
316 [759]

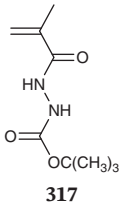
317

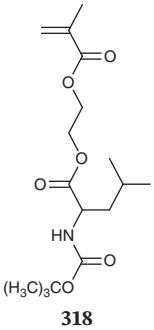
318

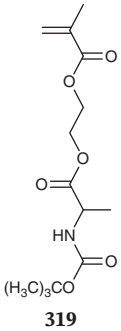
319

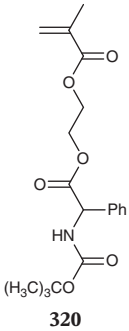
320

(*continued*)

Table 9.16 (Continued)

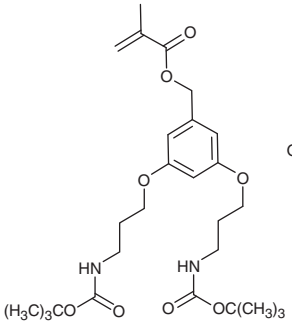

321 [656]

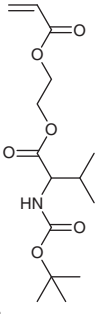

322

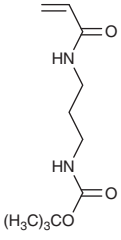

323

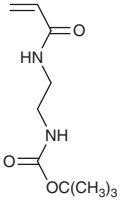

324

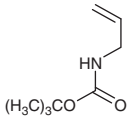

325

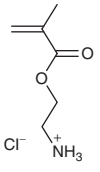

AEMA
326

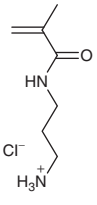

APMAm
327

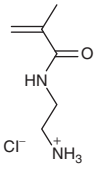

AEMAm
328

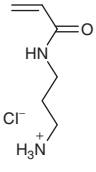

APAm
329

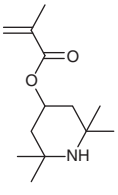

330

(f) *Silyl ether (see also TBSiMA, TPSiMA)*

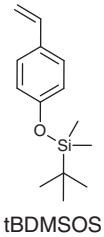

tBDMSOS
331
[760, 761]

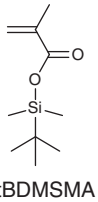

tBDMSMA
332

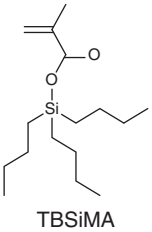

TBSiMA
333

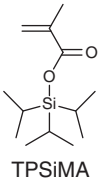

TPSiMA
334

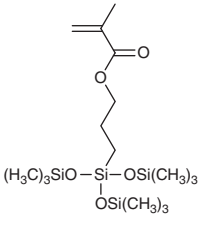

335

(g) *Protected aldehyde, protected sulfonate*

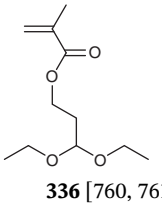

336 [760, 761]

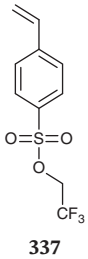

337

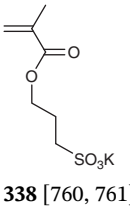

338 [760, 761]

(*continued*)

Table 9.16 (Continued)

(h) *Isocyanate functionality*

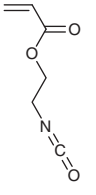

339 [249]

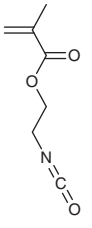

340 [465]

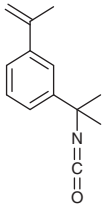

341 [465]

(i) *ROMP monomer*

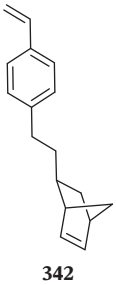

342

(j) *ATRP inimers*

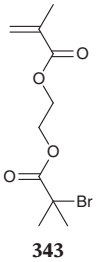

343

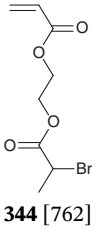

344 [762]

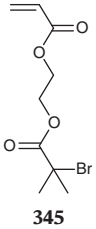

345

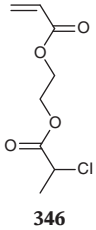

346

(k) *NMP inimers*

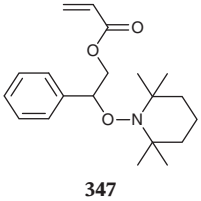

347

9.9.2 Methacrylamides

Many examples have appeared of RAFT (co)polymerization of HPMAm, particularly with respect to various bioapplications [765]. Other examples of methacrylamide monomers recently used in RAFT polymerization are the primary amino-functional monomers, AEMAm (**328**) and APMAm (**327**), and the tertiary amino-functional monomers, DEAPMAm, DMAPMAm, and those shown in Table 9.10. Various functional methacrylamides appear in Table 9.16.

The choice of RAFT agent for polymerization of methacrylamides is subject to similar constraints as mentioned for the methacrylates. In particular, the R group should be selected to be a good leaving group with respect to the propagating radical.

9.9.3 Other 1,1-Disubstituted Monomers

Other 1,1-disubsitueted monomers that have been used in trithiocarbonate-mediated RAFT (co)polymerization include derivatives of γ-butyrolactones (**195**) oxazoline (**196**), maleimide (**198**) (Table 9.11). The sesquiterpene **197** [181] and limonene (Lim) [180] are not readily homopolymerized but can be used as comonomers or in SUMI experiments (Section 9.15) [58].

9.9.4 Acrylates

Acrylates include 2-(acryloyloxy)ethyl phosphate (AEP), butyl acrylate (BA), 3-chloropropyl acrylate (CPA), dodecyl acrylate (DA), (2-dimethylamino)-ethyl acrylate (DMAEA), 2-ethylhexyl acrylate (EHA), isobornyl acrylate (iBoA), methyl acrylate (MA), propargyl acrylate (PA), (polyethylene glycol monomethyl ether) acrylate (PEGA), *tert*-butyl acrylate (*t*BA) (for other examples see *Abbreviations*), and those listed in Table 9.12.

Many acrylate esters have been shown to undergo intramolecular chain transfer to polymer (backbiting) during polymerization leading to branched structures. It has been reported that the extent of branching is higher for conventional radical polymerization than for RDRP (atom-transfer radical polymerization [ATRP], RAFT, NMP) [766, 767]. A qualitative explanation was proposed in terms of the differences in the concentrations of short-chain radicals between RDRP and conventional radical polymerization. Reys and Asua [768] have proposed an alternative explanation in terms of radical life times (the time between chain activation and deactivation) being of the same order of magnitude or shorter than the time required for the conformation change necessary for intermolecular hydrogen atom transfer. Conventional chain transfer agents (*n*-octanethiol) [769] and H-bonding solvents (*n*-butanol) [770] also appear to reduce the extent of branching in conventional radical polymerization.

9.9.5 Acrylamides

Attaining low dispersities with RAFT polymerization of acrylamides requires a RAFT agent suitable for MAMs. Acrylamides include acrylamide Am, 2-acrylamido-2-methylpropane-1-sulfonic acid sodium salt (AMPS, **237**), *N*-benzylacrylamide BzAm, *N*-cyclohexylacrylamide CHAm, diacetone acrylamide DAAm, *N*,*N*-diethyl-acrylamide DEAm, *N*,*N*-dimethylacrylamide DMAm, *N*-(2-(dimethylamino)ethyl)

acrylamide DMAEAm, *N*-isopropylacrylamide NIPAm, *N*-acryloylmorpholine NAM and *N*-octylacrylamide OAm (for other examples see *Abbreviations*), and those listed in Table 9.13.

9.9.6 Styrenics

Styrenic monomers used in RAFT polymerization include those listed in Table 9.14 plus, 4-acetoxystyrene (AcS), 4-chloromethylstyrene (CMS), 4-chlorostyrene (CS), 3,4-dimethoxystyrene (DMOS), 4-hydroxymethylstyrene (HMS), 4-methylstyrene (MeS), 2,3,4,5,6-pentafluorostyrene (PFS), sodium 4-styrenesulfonate (SSO3Na), 4-(*tert*-butyldimethylsilyloxy)styrene (tBDMSOS), 4-*tert*-butylstyrene (tBS), 4-*tert*-butoxystyrene (tBOS), 4-hydroxystyrene (4HS), **295**, **302**, **306**, **307**, **308**, **337**, **341**, **342** (see Section 9.9, Table 9.16). Good control over RAFT polymerization of styrene and derivatives requires a RAFT agent suitable for MAMs. Many of the styrenes in Table 9.14 have been used to prepare polymers for optoelectronic applications. The advantage of the styrenic monomers over acrylic monomers in this context is that the functionality is typically not attached through a potentially labile ester or amide linkage.

9.9.7 Diene Monomers

RAFT polymerization of diene monomers, like other MAMs, generally requires a more active RAFT agent. RAFT homopolymerizations of Bd and Ip in solution are slow and generally require the use of higher reaction temperatures to obtain good control and reasonable rate of polymerization (e.g. 125 °C) [480]. Emulsion (co)polymerization of the diene monomers (Bd, Ip, and Cp) mediated by trithiocarbonate RAFT agents is more facile even at low (near ambient) temperature and has been extensively reported in the patent literature (Table 9.15) [771].

The RAFT copolymerization of Ip with hydroxy-functional monomers, HEMA, HEA and **280**, with trithiocarbonate (**51**) has been explored [396]. Diels–Alder reaction of Ip with the (meth)acrylates was observed as a side reaction. The (meth) acrylates are consumed preferentially to Ip, and thus their copolymers with Ip have a gradient structure. The copolymer of Ip with diene **280** is a more random copolymer.

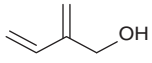

280 [398]

9.9.8 Other Monosubstituted Monomers (MAMs, IAMs, LAMs), Vinyl Monomers

Trithiocarbonates are not generally suited for mediating polymerization of LAMs. A study on the use of benzyl and *t*-butyl trithiocarbonate and dithiobenzoate RAFT agents for VAc polymerization has appeared [146]. Intermediate radical termination was proposed to be a significant cause of retardation with these systems.

Trithiocarbonates are suited for controlling polymerization of IAMs such as NVC [8] and *S*-vinylsulfides (**285–287**).

9.9.9 Monomers with Reactive Functionality

There is a need for processes that permit polymer modification post-RAFT polymerization. So-called polymer analogous reaction make use of reactive functionality that can be present on the Z or R groups of the RAFT agent or can be associated with the monomer(s) [772]. The functionality must be inert to the conditions of polymerization and yet polymerization must proceed on demand in quantitative yield under mild reaction conditions.

Many papers consider the combination of RAFT and azide–alkyne 1,3-dipolar cycloaddition. Some alkyne-functional monomers are listed in Table 9.16a; those with azide functionality appear in Table 9.16b. Alkynes with a terminal C–H may be reactive towards radicals and therefore are commonly protected as the silyl ether. Azides react with election-deficient monomers and are most often incorporated post-RAFT polymerization. Further detail can be found in the Chapter 18 *Synthesis and Application of Reactive Polymers via RAFT Polymerization* [732].

'Active ester' monomers that have been subjected to RAFT polymerization are shown in Table 9.16c. These active ester groups undergo facile reaction with substrates containing primary amine functionality.

Several recent papers have explored polymerization of monomers containing isocyanate functionality (Table 9.16h) [249, 465, 773]. RAFT polymerization and the thiocarbonylthio group are compatible with isocyanate functionality. However, some care must be taken in the selection of the RAFT agent and other components of the polymerization medium such that they do not also contain any other functionality that is inherently reactive (such as carboxy) [249].

ATRP inimers (Monomers with ATRP initiator functionality) include CMS and the monomers shown in Table 9.16i [762, 774]. NMP inimers are shown in Table 9.16j. Some applications of these inimers are described in Section 9.16.

9.10 Macromonomers

RAFT polymerization of macromonomers provides a route to comb polymers by a 'grafting through' process. RAFT-crosslinking copolymerization of macromonomers is another route to arm-first stars. RAFT-SUMI of macromonomers into RAFT agents is a route to macroRAFT agents. Some examples of macromonomers used in trithiocarbonate-mediated RAFT polymerization are provided in Table 9.17. Additionally, there are many examples of RAFT polymerization of PEG-based macromonomers, PEGA, PEGMA, polyethylene gycol diacrylate (PEGDA), and polyethylene gycol dimethacrylate (PEGDMA). The PVDF macromonomer (**353**) was prepared by xanthate-mediated RAFT polymerization and end-group modification [328].

9.11 Cyclopolymerization

Some of the monomers used in trithiocarbonate-mediated RAFT cyclopolymerization are listed in Table 9.18. Attempted RAFT cyclopolymerization of DADMAC with trithiocarbonate **69** has been reported [481]. While the polymerizations show some

Table 9.17 Macromonomers subjected to RAFT polymerization.

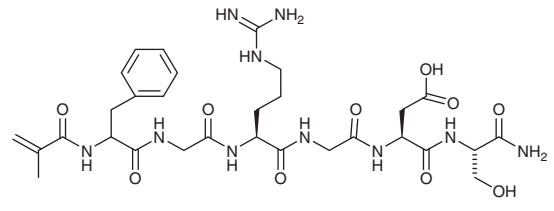

Peptide macromonomer
348

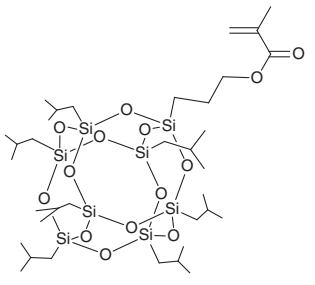

POSSMA
349

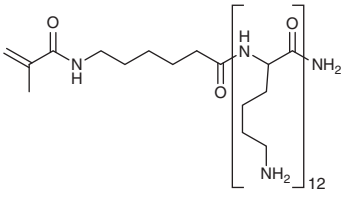

Peptide macromonomer
350

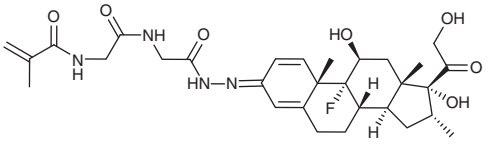

351

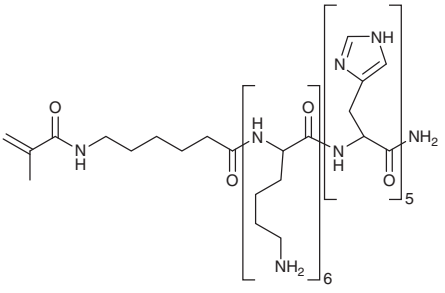

Peptide macromonomer
352

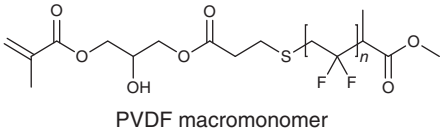

PVDF macromonomer
353

living character, conversions are generally low and dispersities are poor ($Đ > 1.5$). Trithiocarbonates are not ideal for DADMAC, which is a LAM. A xanthate is more appropriate for such monomers [775, 776].

Better results (high conversions, low $Đ$) were observed for RAFT cyclopolymerization of MAM **355** with trithiocarbonates **47**, **63**, or **69** [334]. RDRP cyclopolymerization has been proposed as a method for precision synthesis of periodic polymers [777, 778] in which monomer sequence, polymer molar mass, and dispersity are simultaneously controlled. An example involves cyclopolymerization of **358** mediated by **40** [215]. High dilution conditions were required to avoid crosslinking.

A 1 : 2 mixture of divinyl ether (DVE) and maleic anhydride (MAH) with dibenzyl trithiocarbonate was reported to undergo alternating RAFT cyclopolymerization mediated by dibenzyl trithiocarbonate (**22**) to provide the polymer **354** as shown in Scheme 9.5 [161, 162].

Table 9.18 Monomers subjected to RAFT cyclopolymerization.

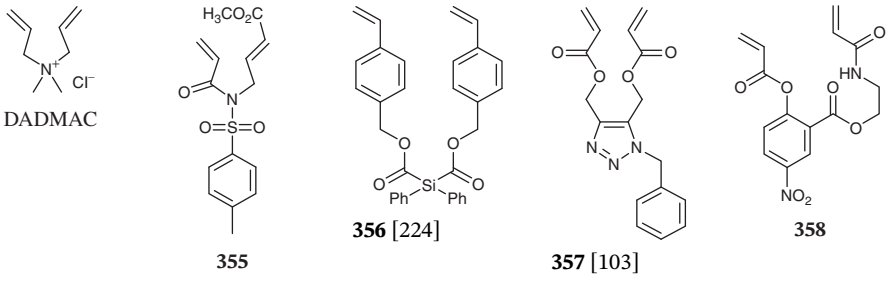

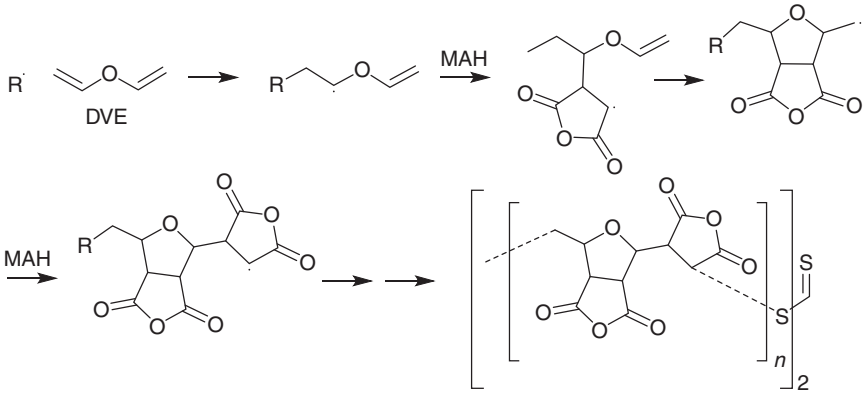

Scheme 9.5 RAFT cyclocopolymerization of DVE/MAH.

9.12 Radical Ring-Opening Polymerization

Radical ring-opening polymerization (ROP) provides a simple method of forming polymers with readily cleavable linkages, i.e. esters, thioesters, and/or disulfides, into the carbon–carbon backbone of a polymer chain by radical polymerization [779]. Several ring-opening MAMs (**359–361**) that have been used in trithiocarbonate-mediated RAFT (co)polymerization are listed in Table 9.19.

Trithiocarbonates are not generally suitable RAFT agents for mediating the copolymerization of LAMs, such as the ketene acetals. However, RAFT copolymerizations of monomers, such as BMDO (**362**) or **363** (Table 9.19) with acrylates [780] or methacrylates [545, 578, 781] are effectively controlled.

9.13 RAFT Crosslinking Polymerization

Star synthesis by RAFT crosslinking polymerization is described in the Chapter 21 by Allison-Logan et al. [782] and the process will not be detailed here. Examples making use of trithiocarbonates are highlighted in Tables 9.3 and 9.6 and examples of multiolefinic monomers used in this process are included in Table 9.20. Network

Table 9.19 Monomers used in trithiocarbonate-mediated RAFT ring-opening polymerization.

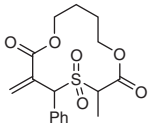
359

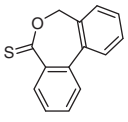
360

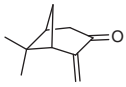
Pinocarvone
361

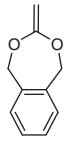
BMDO
362


363

Table 9.20 Examples of multiolefinic monomers used in RAFT Crosslinking polymerization mediated by trithiocarbonates.

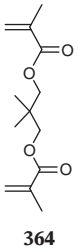
364

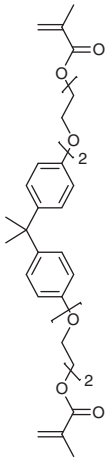
365

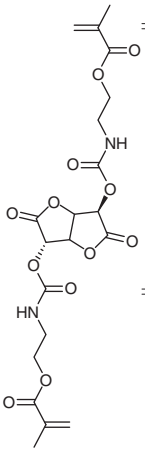
366

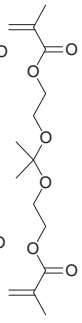
367

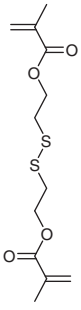
DSDM
368

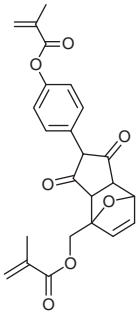
369


370

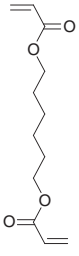
HDDA
371

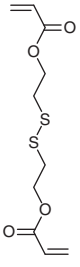
DSDA
372

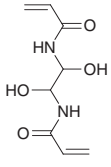
373

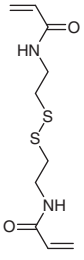
N,N-bis(acryloyl)cystamine (DSDAm)
374

For a full list of monomer abbreviations, see Abbreviations section.

formation by RAFT crosslinking polymerization has been reviewed by Moad [783] and is covered in the Chapter 19 by Pérez-Salinas et al. [784].

The kinetics of network formation in RAFT polymerization of various acrylamide monomers mediated by trithiocarbonate **40** was examined [217]. A process for gel point normalization was developed, which was proposed to enable the targeting of specific number and weight average molar masses in the synthesis of hyperbranched polymers using RDRP. Applications of RAFT-synthesized polymer networks that have made use of trithiocarbonate RAFT agents include networks for molecular imprinting [307], monolithic flow reactors [231, 785], dynamic-covalent networks, and self-healing materials [487].

Multiolefinic monomers used in the synthesis of microgels and polymer networks include (diethylene glycol)dimethacrylate (DEGDMA), TEGDMA, ethylene glycol dimethacrylate (EGDMA), HDDA, MBAm, PIPBAm, and DVB and compounds **365–374** (Table 9.20). Use of monomers such as **367**, with an acetal linkage, and **368** and **374**, with disulfide linkages, results in the formation of degradable crosslinks that can be important in controlled release applications. The crosslinks can also be cleaved to allow polymer analysis, for example, to determine arm length in star synthesis.

9.14 RAFT Self-condensing Vinyl Polymerization

Self-condensing vinyl polymerization provides a method of hyperbranched polymer synthesis. The first RAFT examples appear in the patent literature. The area has recently been reviewed [786, 787]. Examples of trithiocarbonate RAFT monomers (sometimes called inimers) are shown in Table 9.21. These polymerizations comprise copolymerization of the RAFT monomer to form a hyperbranched structure. A second RAFT step or 'block synthesis' can then result in adding arms to produce a core-crosslinked star. Star synthesis is dealt with in greater detail in the Chapter 21 by Allison-Logan et al. [782].

Examples of trithiocarbonate inimers in the synthesis of polymer networks are contained in Table 9.22. These networks have an inbuilt mechanism for stress relief and self-healing [800–804, 806].

9.15 RAFT-Single-Unit Monomer Insertion (RAFT-SUMI) into Trithiocarbonates

RAFT-SUMI into trithiocarbonates and dithiobenzoates was originally developed as a method of synthesizing functional RAFT agents or macroRAFT agents. Iterative SUMI has also been explored as a method for synthesizing sequence-defined oligomers. The area has recently been reviewed by Xu [807] and Haven et al. [14]. See also the Chapter 17 in the present volume on sequence-encoded RAFT oligomers and polymers [808]. Many of the more recent examples of RAFT-SUMI into MAMs have made use of trithiocarbonates [14, 58, 288, 315, 548, 809, 810].

Table 9.21 RAFT monomers for self-condensing vinyl polymerization.

RAFT monomer	Synthesis[a)]	Polymerizations[b)]
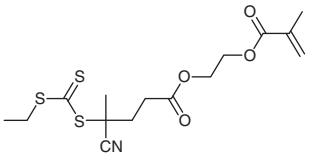 **375**	C/H [788]	**375**/BMA/DEAEMA, **375**/BMA/DEAEMA-*b*-**312**/DMAm [788]
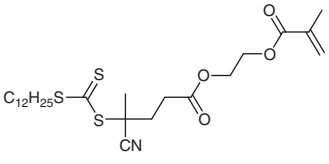 **376**	C/H [789]	**376**/PEGMA/TFEMA [789] **376**/PEGMA, PEGMA-*b*-St [790]
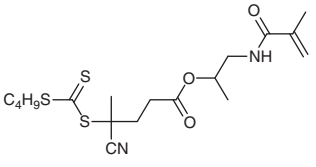 **377**	C/H [791]	**377**/HPMAm [791]
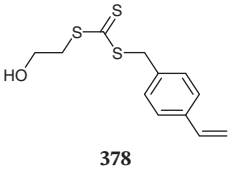 **378**	A [574]	**378**/**318** [574]
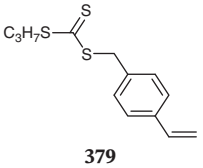 **379**	A [792]	**379**/MMA, **379**/MA, **379**/tBA, **379**/St, **379**/St-*b*-St, **379**/St-*b*-**379**/tBA [792] **379**/DMAEMA [793] **379**/St, **379**/CMS, **379**/St-*b*-**379**/CMS, **379**/CMS-*b*-Ip [794] **379**/St, **379**/St-*b*-tBA, **379**/St-*b*-NIPAm, **379**/St-*b*-DMAEA, **379**/St-*b*-AA-*b*-NIPAm, **379**/St-*b*-DMAEA-*b*-NIPAm [424] **379**/PEGMA [795, 796]
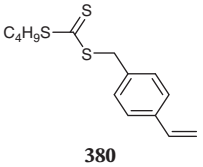 **380**	A [797, 798]	**380**/**322**, **380**/**322**-*b*-**380**/DEGA/PEGA [798] **380**/NIPAm [797]

(*continued*)

Table 9.21 (Continued)

RAFT monomer	Synthesis[a)]	Polymerizations[b)]
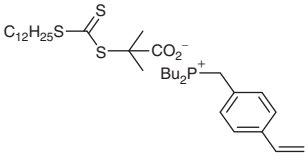 **381**	M [799]	**381**/NIPAm, **381**/NIPAm-*b*-**276** [799]

a) The letter in this column refers to the method of RAFT agent synthesis. Refer to Section 9.8.
b) Polymerizations comprise copolymerization of RAFT monomer to form a hyperbranched structure. A second RAFT step or 'block synthesis' results in adding arms to produce a core-crosslinked star.

Table 9.22 RAFT monomers for synthesis of combs and defined networks.

RAFT monomer	Synthesis[a)]	Polymerizations[b)]
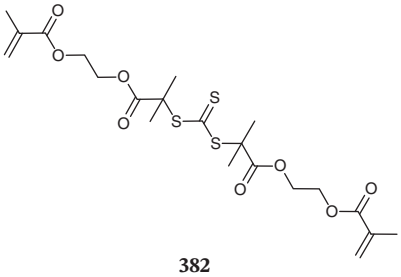 **382**	J [800, 801] I [802]	**382**/MMA [800, 802] **382**/BA [803] **382**/MMA-*b*-St [802] **382**/BisGMA/TEGDMA [804]
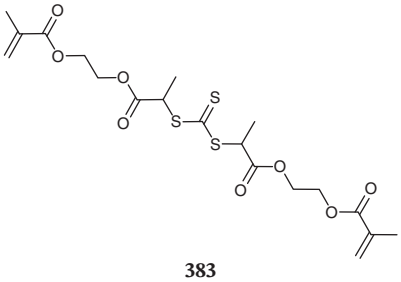 **383**	A/H [278]	For examples, see Table 9.6 trithiocarbonate **44**
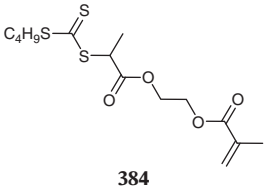 **384**	A/H [805]	**384**, **384**-*b*-DMAm, **384**/MMA, **384**/MMA-*b*-MA [805] See also under **Table** 9.6 trithiocarbonate **44**

a) The letter in this column refers to the method of RAFT agent synthesis. Refer to Section 9.8.
b) RAFT agent appears inert during polymerization of methacrylates. Red – photoinitiated polymerization.

Further examples of RAFT SUMI include end-functionalization of macroRAFT agents through SUMI of a functional monomer, such as MAH or a maleimide [811] or an allyl monomer **325** (Scheme 9.6) [812], and the synthesis of macroRAFT agents from macromonomers, for example, a P3HT macroRAFT agent as shown in Scheme 9.7 or the RAFT functionalization of pendant methacrylate double bonds, present in a molecular imprinted polymer formed by crosslinking copolymerization, by SUMI into trithiocarbonate **47** [813].

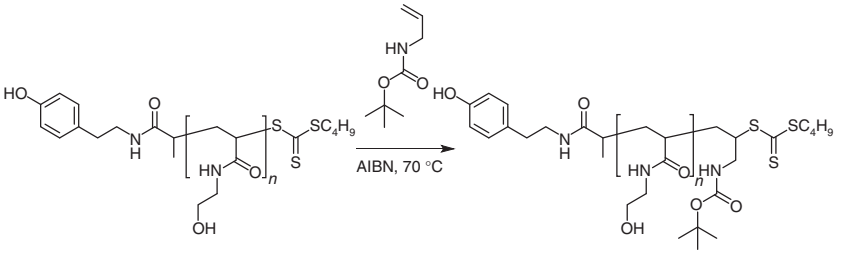

Scheme 9.6 Example of chain-end functionalization by RAFT-SUMI of allyl monomer **325** into a trithiocarbonate macro RAFT agent.

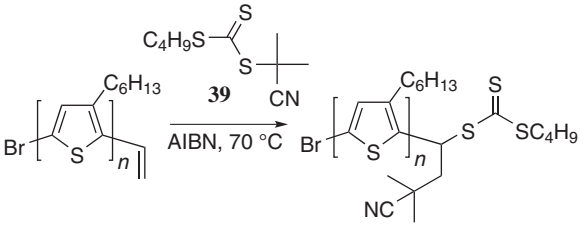

Scheme 9.7 Example of formation of macroRAFT agents by RAFT-SUMI of a macromonomer.

9.16 Trithiocarbonates in Mechanism Transformation Processes

Block, star, or graft copolymers comprising segments formed by different mechanisms can be combined using post-polymerization modification techniques or through the use of a dual initiator-RAFT agent [814, 815]. Of significance is the orthogonality of the various processes. Trithiocarbonate-mediated RAFT polymerization can often be successfully conducted in the presence of the initiator functionality used in other RDRP methods (e.g. alkoxyamines for NMP, alkyl halides for ATRP). However, the converse is seldom true.

We do not consider examples (of which there are many) of transformation of end-functional polymers to polymers with trithiocarbonate functionality by end-group modification in this section.

9.16.1 Ring-Opening Polymerization (ROP)

Hydroxy-functional trithiocarbonates (e.g. **76**, **86**, or **87**) allow sequential or, in some cases, one-pot ROP and RAFT polymerization, Examples of ROP-Ŧ-RAFT (ROP step first) are provided in Tables 9.7 and 9.8 (ROP of lactones, e.g. caprolactone [CL], lactic acid [LA], is compatible with retention of the trithiocarbonate functionality). Examples of RAFT-Ŧ-ROP (RAFT first) or simultaneous ROP and RAFT have also been demonstrated [571].

Amine or ammonium functional RAFT agents (e.g. **108**) might be used for ROP-Ŧ-RAFT of, for example, *N*-carboxyanhydrides to form block copolymers with peptides [606]. However, amine-functional RAFT agents may also cause aminolysis of the RAFT agent. RAFT-Ŧ-ROP has been carried out with RAFT agents containing protected amine functionality (e.g. **107**), which is deprotected post-RAFT polymerization to enable RAFT-Ŧ-ROP.

It is also possible to use thiol-functional polymers formed by end-group aminolysis directly for initiating ROP of *N*-carboxyanhydrides in RAFT-Ŧ-ROP [816]. The success of this strategy depends on the stability of the terminal thiol.

End-group transformation by sequential aminolysis and thio-Michael addition to APMAm can also be used to provide amine end-functionality for RAFT-Ŧ-ROP of *N*-carboxyanhydrides (Scheme 9.8) [252].

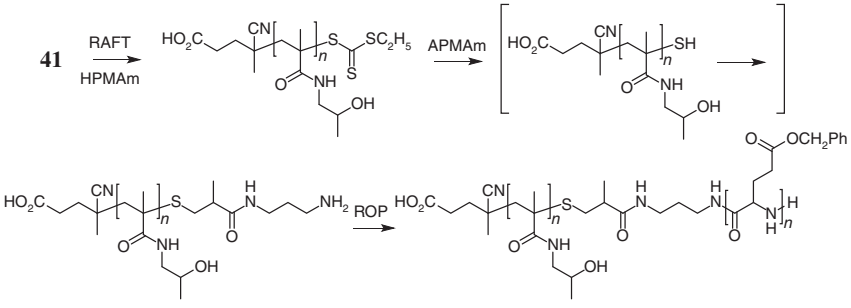

Scheme 9.8 Example of RAFT-Ŧ-ROP involving RAFT polymerization of HPMAm mediated by **41**, followed by end-group transformation, by one-pot aminolysis, and thio-Michael addition to APMAm, and amine-initiated ROP of an *N*-carboxyanhydride.

9.16.2 Ring-Opening Metathesis Polymerization (ROMP)

RAFT polymerization and ring-opening metathesis polymerization (ROMP) appear orthogonal such that RAFT polymerization can be carried out in the presence of some ROMP active monomers (1,2-disubstituted olefins) and ROMP can be conducted in the presence of trithiocarbonate functionality. RAFT polymerization mediated by a trithiocarbonate containing a norbornene group as a ROMP-active but RAFT-inert monomer functionality to form macromonomers can be used to form bottlebrush polymers in a ROMP 'grafting through' polymerization [708, 711]. A one-pot process for simultaneous ROMP and RAFT polymerization was also

described [817]. Examples of ROMP-*T*-RAFT (ROMP first) have also been reported for the synthesis of triblock [570] and graft copolymers [818].

Examples of trithiocarbonates also containing ROMP monomer functionality include **84** (*cis*-1,2-disubsituted double bond), **127** and **128** (furan protected maleimide), and **134** and **135** (norbornene).

9.16.3 Ring-Opening Opening Alkyne Metathesis Polymerization (ROAMP)

A reagent comprising both a molybdenum complex as initiator for ring-opening alkyne metathesis polymerization (ROAMP) and trithiocarbonate functionality (**83**) has been reported, which allowed sequential ROAMP and RAFT polymerization to provide a poly(*o*-phenylene ethynylene)-*block*-poly(methyl acrylate) [569].

9.16.4 Cationic Polymerization

RAFT agents can be used to mediate both cationic and RAFT polymerization and examples of cationic polymerization-*T*-RAFT can be found in the Chapter 25 by Uchiyama and Kamigaito [819].

9.16.5 Anionic Polymerization

Trithiocarbonates can act as an initiator for the anionic ROP of thiiranes with tetraphenylphosphonium chloride as catalyst [820, 821]. One-pot and sequential polymerization processes were developed for polymers containing PDMAm (by RAFT polymerization) and poly(methylthiarane) (by anionic ROP) segments [820].

9.16.6 Nitroxide Mediated Polymerization (NMP)

Processes for RAFT-*T*-NMP have been described in reviews on RDRP transformation processes [814, 815]. These include the ESARA process in which thiocarbonylthio and alkoxyamine groups are exchanged [822] and the use of species that contain both RAFT agent and alkoxyamine initiator functionality [568].

9.16.7 Atom Transfer Radical Polymerization (ATRP)

Many RAFT agents can be used as pseudohalides in ATRP though trithiocarbonates are seldom used in this context. There are also examples of what are believed to be photo-redox processes that go under the umbrella of PET-RAFT (see Section 9.17). The RAFT agent/ATRP initiator **133** was used first for PET-RAFT of MA, followed by organo-ATRP of MMA, to form a low-dispersity PMA-*b*-PMMA [707]. The pentyl methacrylate (PMA)–trithiocarbonate would not be expected to be an effective mediator of MMA polymerization under the conditions used. However, the complete orthogonality of the ATRP and RAFT steps is not fully established.

Graft (bottlebrush) and star polymers have been prepared by RAFT-Ŧ-ATRP. The process involves RAFT (co)polymerization of an ATRP inimer, a monomer containing ATRP initiator functionality (Table 9.16i) [150, 200, 299, 823–825], to form a polymer with pendant ATRP initiator moieties, which can then be used to grow arms on the core/backbone by ATRP. For example, ATRP was used to add arms to hyperbranched cores formed by RAFT crosslinking polymerization mediated by trithiocarbonate **44** and that incorporate monomer **345** or **343** [299]. The chloro- or bromo-compounds used as ATRP initiators are generally inert in RAFT polymerization in the absence of an activator.

9.17 Photoinitiated RAFT with Trithiocarbonates

RAFT photoinitiation was foreshadowed and claimed in the first RAFT patent in 1998 [1]. However, this document contained no examples of photoinitiation whether direct or with the use of photoinitiators. A process equivalent to photo-SUMI (into xanthates) was first reported by Delduc et al. [826] in 1988. Trithiocarbonates have been widely used in photoinitiated RAFT polymerization. The $n \rightarrow \pi$ transition for primary and secondary trithiocarbonates appears at ~430 nm and is red-shifted to ~440 nm for tertiary trithiocarbonates [173]. The use of direct photoinitiation or PET-RAFT appears to give fewer by-products than conventionally initiated (with a thermal initiator) RAFT polymerization. Additionally, the use of visible light irradiation appears to give rise to fewer issues than does UV light [827–829].

At least four forms of photoinitiated RAFT polymerization should be considered: (i) polymerizations conducted in the presence of an added photoinitiator; (ii) direct photoinitiation when the trithiocarbonate dissociates into radicals by photocleavage of the C—S single bond and PET (photo energy or electron transfer) RAFT, which might involve either a (iii) photosensitization or a (iv) photo-redox process. There is also a range of photo-redox processes [477]. Examples of photo-RAFT polymerization are highlighted in Tables 9.3 and 9.6 with entries in Red (polymerization) or **Bold Orange** (SUMI). However, we do not distinguish the form of photo-process there and the reader should refer to the references cited.

For additional information on photoinitiated RAFT processes making use of dithioesters the reader is referred to the Chapter 12 of Chapman et al. [15] and other recent reviews [830].

9.18 Redox-Initiated RAFT with Trithiocarbonates

RAFT polymerization can be initiated by a redox process involving the RAFT agent. The redox properties of various RAFT agents and their utility in redox/electrochemical initiation are detailed in the Chapter 18 by Lorandi et al. [16] and so a detailed discussion will not be given in this chapter.

The electrochemical behaviour of trithiocarbonates has been described by Strover et al. [831]. The major reduction peak moves to more cathodic potentials in the series dithiobenzoates > trithiocarbonates > heteroaromatic dithiocarbamates > xanthates ~ *N*-alkyl-*N*-aryldithiocarbamates generally paralleling the order of activity as RAFT agents. The reduction peak for trithiocarbonates makes it most suitable for direct or mediated eRAFT, in that it is suitably distant from that for redox active monomers or other components of the electrochemical reaction medium.

Examples of redox-RAFT are identified in Table 9.6 (entries in Green). At least two forms of direct redox-initiated RAFT can be distinguished, though not all have been demonstrated for trithiocarbonates: (i) where the RAFT agent behaves as a pseudo-halide in an ATRP-type mechanism [832–836], and (ii) involving electron transfer to the RAFT agent with formation of a radical anion intermediate. The latter process has been called dissociative electron-transfer RAFT (DET-RAFT) [837, 838].

9.19 RAFT Emulsion/Miniemulsion/Dispersion Polymerization Mediated by Trithiocarbonates

Examples of heterogeneous polymerization are identified in Tables 9.3 and 9.6 (entries in *blue italics*). In 2000, Moad et al. [4] provided a first report of trithiocarbonate-mediated RAFT emulsion polymerization. They compared the efficacy of a series of benzylic RAFT agents in semi-batch RAFT emulsion polymerization of St. Except for the example using cumyl dithiobenzoate as mediator, polymerization was rapid and little coagulum was observed. RAFT emulsion polymerization mediated by the trithiocarbonate and xanthate provided molar mass control but with $Đ \sim 2$ (Table 9.23).

A significant advance in RAFT emulsion polymerization came with the development of so-called 'surfactant-free' RAFT emulsion polymerization based on amphiphilic macroRAFT agents [456, 458]. A recent review has summarized the status of this method [839]. Most examples make use of trithiocarbonates.

Table 9.23 Molecular weight and conversion data obtained in semi-batch emulsion polymerizations of styrene at 80°C in the presence of various RAFT agents.

RAFT agent	M_n	$Đ$	% Conversion	RAFT agent	M_n [a)]	$Đ$	% Conversion
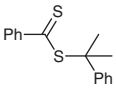	39900	7.09	96	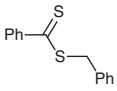	32400	1.98	>99
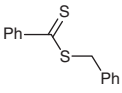	53200	1.37	>99	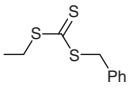	31300	2.04	>99
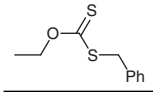	35600	1.38	>99	Control	132600	2.71	>99

a) Number average molar mass in polystyrene equivalents.

The process typically involves initial synthesis of a hydrophilic block, such as propacrylic acid (PAA) [163, 456, 458], poly(*N*-acryloylpyrrolidine) [840], PEG [841], poly(PEGA-*co*-HEAm) [842], or poly(DEGMA-*co*-HPMA-*co*-PEGMA) [843] by solution RAFT polymerization followed by formation of a hydrophobic block usually composed of the monomer being polymerized and which can be produced in situ. An issue with this methodology is that the product is always a block copolymer with the hydrophilic segment of the macroRAFT agent stoichiometrically incorporated into the final product. The hydrophilic block can be important to polymerization-induced self-assembly (PISA). In other cases, it comprises an impossible-to-remove 'impurity' in the product.

Most recent studies on RAFT emulsion polymerization with dithioesters have been based on the use of amphiphilic macroRAFT agents usual in the context of PISA. PISA during RAFT dispersion polymerization has been extensively studied by Armes and coworkers [844]. Many examples (for some examples see Table 9.6) involve solution polymerization mediated by trithiocarbonate **46** followed by dispersion polymerization. PISA is described in detail in the Chapter 15 by D'Agosto et al. [845].

9.20 Reaction Conditions and Side Reactions of Trithiocarbonates

One disadvantage of many trithiocarbonates is that thermal or hydrolytic decomposition yields thiols that may be odorous. This issue can be mitigated by using trithiocarbonates based on thiols with low volatility and provides a case for end-group removal post-RAFT polymerization.

Trithiocarbonates are less prone to hydrolysis and reaction with nucleophiles than dithioesters and they are probably the most used RAFT agents for polymerizations conducted in aqueous media [52]. Nonetheless, it is desirable to conduct aqueous polymerizations at lower temperatures (e.g. <50 °C) [846] to minimize hydrolysis (Scheme 9.9).

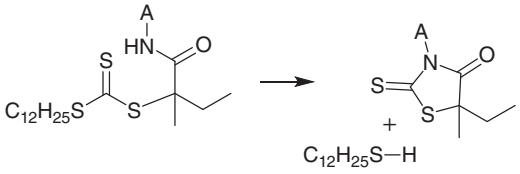

Scheme 9.9 Proposed mechanism for loss of trithiocarbonate functionality from methacrylamide macroRAFT agents.

Trithiocarbonates containing a 4-cyanopentanoic acid group as R (reported for R″ = C_2H_5 (**41**), C_4H_9 (**43**), $C_{12}H_{25}$ (**44**), or CH_2CH_2Ph) have been found to be subject to a side reaction in which the nitrile substituent is converted to a primary amide (Scheme 9.10) [23]. The process has not been reported for other tertiary

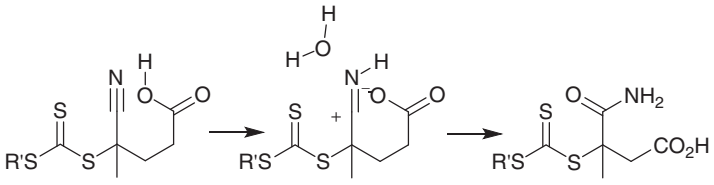

Scheme 9.10 Proposed mechanism for nitrile hydrolysis for trithiocarbonates with R = 4-cyanopentanoic acid.

cyanoalkyl trithiocarbonates and is therefore thought to involve intramolecular acid catalysis. This results in the nitrile being converted to an iminium salt that is then hydrolysed to the amide by reaction with the water present in the sample. The $-CN \rightarrow -CONH_2$ transformation has also been reported as a complication during the synthesis of peptide RAFT agents based on **44** [730]. The process has not (yet) been reported for other compounds containing the 4-cyanopentanoic acid group such as similar dithioester RAFT agents or the initiator 4,4′-azobis(2-cyanopentanoic acid) (ACPA).

The rate of RAFT polymerization is enhanced with the use of ionic liquids as the polymerization medium. Examples of such RAFT polymerizations mediated by trithiocarbonates include the solution polymerization of BMA [201] and FMA [202] and the dispersion polymerization of St [847].

Trithiocarbonate functionality in PAA has been shown to be unstable during methylation with trimethylsilyldiazomethane undergoing a side reaction that results in conversion of the trithiocarbonate to a thiol [70].

The sensitivity of RAFT polymerization to air or oxygen has long been a concern. In high throughput experimentation a range of methods have been applied to alleviate the issue, which include freeze-thaw degassing [848] and enzyme degassing [849, 850]. The PET-RAFT process with DMSO solvent has been found to be remarkably insensitive to air [476, 851–853]. The DMSO solvent imparts oxygen tolerance through its ability to quench singlet oxygen generated by photosensitization.

9.21 Trithiocarbonate Group Removal/Transformation

Most of the methods described for removal or transformation of thiocarbonylthio groups of RAFT-synthesized polymers [854–857] are applicable to polymers containing trithiocarbonate groups. For polymers formed from symmetrical trithiocarbonates, removal of the thiocarbonylthio group will usually result in cleavage of the polymer chain. A review of RAFT end-group transformation is provided in Chapter 16 by Lowe and Dallerba [856].

9.21.1 Trithiocarbonate Group Removal by Radical-Induced Coupling

Various radical-induced processes for trithiocarbonate group removal have been developed including radical-induced coupling, radical-induced disproportionation,

and radical-induced reduction (Scheme 9.11). They involve initial conversion of the macroRAFT agent to a propagating species either by radical addition–fragmentation or by photo-induced C—S bond scission through a photoiniferter-like process. The challenge in applying these methods is to find conditions that maximize the desired pathway(s), particularly with respect to radical–radical termination.

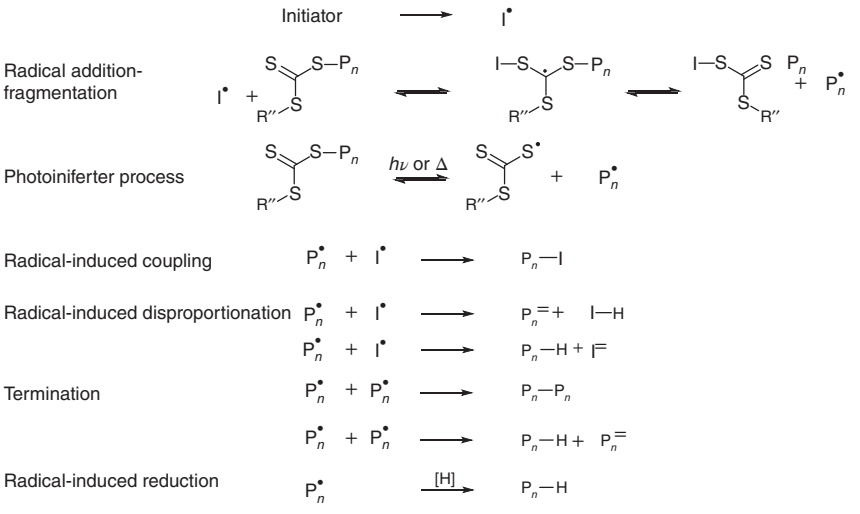

Scheme 9.11 Trithiocarbonate group removal by various radical-induced reaction pathways including radical-induced coupling, radical-induced disproportionation, and radical-induced reduction. The '=' in 'P_n=' or 'I=' indicates unsaturation.

A method developed by Perrier et al. [440] involves heating a RAFT-synthesized polymer with a large excess of a radical initiator (e.g. 20 molar equiv), most often a dialkyldiazene such as AIBN. The method has been successfully applied to many trithiocarbonates. For examples of trithiocarbonate group removal by radical-induced coupling, see Table 9.24.

Several studies have explored the conditions required for thiocarbonylthio group replacement by radical-induced coupling and how this depends on the macroRAFT agent and initiator used [195, 205]. Side reactions include the reaction of propagating species with other radicals (e.g. other propagating species, the RAFT intermediates). The reaction of propagating radicals with other radicals is usually shown as combination and this appears to be the dominant pathway for methacrylate propagating species and 2-cyano-2-propyl radicals. However, the process depends of the radical source and the propagating species and may also involve disproportionation (see Section 9.21.2).

End-group removal to produce a monomodal product from PMMA-trithiocarbonate ($C_{12}H_{25}S(C{=}S)$— end) was found to require milder conditions (20-fold excess AIBN, 80 °C, 2.5 hours) than [2] that from PMMA-dithiobenzoate (at least 100-fold excess AIBN for 80 °C, 2.5 hours) [205]. The relative ease of end-group removal from the trithiocarbonate by this method was associated with the shorter

Table 9.24 Trithiocarbonate group removal by radical-induced coupling.

ZCS2	Terminal monomer	Initiator	[Initiator] [RAFT][a]	Temperature (°C)[b]	% ends removed[c]	References
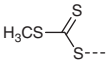	MMA	AIBN	20	80	100	[440]
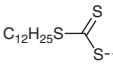	MMA	AIBN	20, 40	80	100	[205]
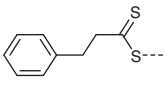	TFEMA[d]	LPO	7.5	70	100	[858]
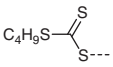	BA	AIBN	20	80	25	[195]
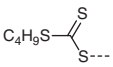	BA	AIBN+LPO	20+2	80	100	[195, 267]
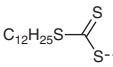	HEA	AIBN	20	70	100	[859]
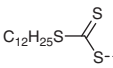	HPA	AIBN	10	80	(100)	[860]
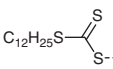	HPA	BPO	10	80	100	[860]
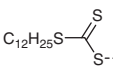	DAMEA/ TFEA	AIBN	20	65	100	[861]
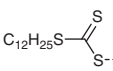	HADA/ MADA/ NLAA	AIBN	20	60	100	[410]
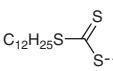	NIPAm	AIBN	(20)	(80)	(100)	[606]
	NIPAm	AIBN	(20)	80	(100)	[862]
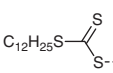	NAM/NAS	AIBN	400	80	(100)	[362]
	DMAm	AIBN	(20)	80	(100)	[862]

(*continued*)

Table 9.24 (Continued)

ZCS2	Terminal monomer	Initiator	[Initiator] [RAFT][a)]	Temperature (°C)[b)]	% ends removed[c)]	References
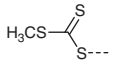	St	AIBN	20	80	(100)	[440]
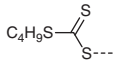	St	AIBN	20	80	24	[195]
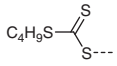	St	AIBN	100	80	64	[195]
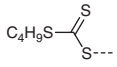	St	AIBN+LPO	20+2	80	100	[195]
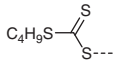	St	AIBN	20	80	~95	[10]
	St	AIBN	(20)	80	(100)	[862]

a) Mole ratio of initiator to RAFT-synthesized polymer.
b) Temperature.
c) Percentage of end-groups removed. Where details of polymer characterization are not provided the values appear in parentheses.
d) Nanoparticle dispersion.

lifetime of intermediate radicals formed by radical addition to the trithiocarbonate, which reduced the complications from intermediate radical termination.

For polymers based on monosubstituted monomers (BA, St) the efficiency of end-group removal by radical-induced coupling is significantly lower than for those based on 1,1-disubstituted monomers (MMA) [195]. The problem relates to the homolytic leaving group ability of the propagating species and is noticeable when a dialkyldiazene, such as AIBN, is used as a radical source. Use of a dialkyldiazene and a peroxide (lauroyl peroxide [LPO] or BPO) in combination is substantially more effective than the use of a dialkyldiazene alone [195]. The peroxide-derived radicals are poor homolytic leaving groups relative to the propagating radicals, while the dialkyldiazene-derived radicals are more effective in trapping the propagating species [195].

9.21.2 Trithiocarbonate Group Removal by Radical-Induced Disproportionation

A method for removing thiocarbonylthio groups by radical-induced disproportionation involves the use of a triakylborane (most often triethylborane) and oxygen to

Table 9.25 Trithiocarbonate-group removal by radical-induced disproportionation.

Trithiocarbonate group	Polymer	Initiator	Comment	References
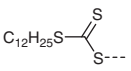	St	$B(C_2H_5)_3/O_2$	Product is PSt-H plus some PSt-PSt. Ethylene is also formed.	[863]
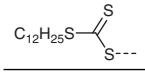	MA	$B(C_2H_5)_3/O_2$	Product is PMA-H plus minor products. Ethylene is also formed.	[863]

generate ethyl radicals that react with macroRAFT agents to produce a propagating species by irreversible addition–fragmentation [863]. These react with further ethyl radicals mainly by disproportionation by H-transfer to the propagating species. Smaller amounts of other chain ends may also be formed. The process appears to provide rapid and quantitative end-group removal. Examples of applying the method to remove trithiocarbonate ends are shown in Table 9.25.

9.21.3 Trithiocarbonate Group Removal by Radical-Induced Reduction

Radical-induced reduction allows the thiocarbonylthio group of RAFT-synthesized polymers to be replaced with a hydrogen atom (for example see Table 9.26) [199, 866, 867]. The process involves treating a polymer with a radical source in the presence of H-donor transfer agents, such as stannanes, silanes, or hypophosphites [199]. The efficiency of end-group removal depends on the polymer, the hydrogen atom donor, and the radical source. Peroxide initiators (LPO, BPO) appear generally more effective than dialkyldiazenes such as AIBN [199]. This is attributed to the peroxide-derived radicals being poor homolytic leaving groups and thus more effective in displacing the propagating radicals from the RAFT intermediate. However, the peroxide initiators are also prone to provide end-groups.

The effectiveness of hydrogen donors increases in the series toluene < 2-propanol < triethylsilane < triphenylsilane ~ tris(trimethylsilyl)silane < *N*-ethylpiperidine hypophosphite < tributylstannane. With poor H-donors such as toluene or 2-propanol radical–radical reaction between propagating radicals competes with reduction even when they are used in vast excess as the solvent for the reaction. This is manifest in the products as bimodal molar mass distributions (PBA, PSt) or unsaturated end-groups (PMMA) [199].

Photo-generation of radicals directly from the RAFT agent offers an alternative to using conventional initiators and also solves a potential issue associated with the formation of by-products derived from the initiator [78, 864, 865].

Cooperative reduction of trithiocarbonate groups making use of a thiol as a polarity reversal catalyst in conjunction with a hydrosilane as the apparent reducing agent is more effective. Thus a combination of $C_{12}H_{25}SH$ and Ph_3SiH has been used [78]. The use of either reagent alone was less successful.

Table 9.26 Trithiocarbonate group removal by radical-induced reduction.

Trithiocarbonate group	Polymer	Initiator	Reagent[a)]	References
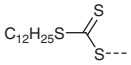	BA, St	BPO, LPO	Toluene	[199]
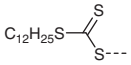	BA	BPO	Toluene/*i*PrOH	[199]
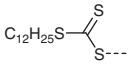	MMA	BPO	Toluene/PrOH	[199]
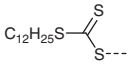	MMA	ACHN	EPHP	[199]
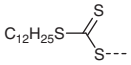	MA, DMAm	*hν*	Bu_3SnH	[864]
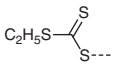	MA	AIBN or *hν*	$C_{12}H_{25}SH/Ph_3SiH$	[78]
	MA	AIBN or *hν*	$C_{12}H_{25}SH/Ph_3SiH$	[78]
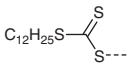	*t*BA	*hν*	PTH-NBu_3-HCOOH	[865]

a) EPHP, *N*-ethylpiperidine hypophosphate; PTH, 10-phenylphenothiazine.

9.21.4 Trithiocarbonate Group Removal by Reaction with Nucleophiles

The thiocarbonylthio end-group of RAFT-synthesized polymers can be removed by reaction with nucleophiles to replace the RAFT-end with a thiol-end [868, 869]. The theoretically estimated order of reactivity of RAFT end-groups towards primary amine nucleophiles is dithioacetate ≥ dithiobenzoate > xanthate ≥ trithiocarbonate ≫ dithiocarbamate [869]. For examples of removal of trithiocarbonate ends through reaction with nucleophiles, see Table 9.27.

Often conversion of a trithiocarbonate group to a thiol end-group is preliminary to use of the thiol end-group in a thio-Michael reaction or other chemistry [870].

9.21.5 Trithiocarbonate Group Removal by Thermolysis

Studies on the thermolysis of trithiocarbonates are summarized in Table 9.28. The trithiocarbonate group can be thermally labile at temperatures >100 °C when, depending on substituents, it becomes susceptible to C—S bond homolysis and direct (Chagaev-type) elimination (Schemes 9.12–9.14). Mechanisms for end-group loss by thermolysis are discussed in reviews on end-group transformation [855]. The onset temperature also depends on reaction conditions (e.g. the medium and the presence of radical sources).

Table 9.27 Trithiocarbonate group removal through reaction with nucleophiles.

Trithiocarbonate group	Polymer	Reagent (solvent)[a)]	Comment	References
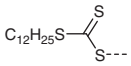	St	HA/TEA (DMF)	RT 12 h	[220]
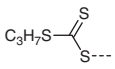	NIPAm	HA (CH_2Cl_2)	RT 24 h	[540]
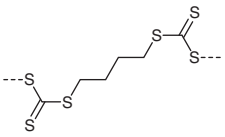	St	Pip (THF)	Reflux 1 h	[6]
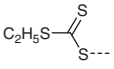	MA, DMAm, NIPAm, St	hydrazine hydrate (DMF)	RT 1–5 min no disulfide formation	[240]
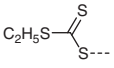	MA, DMAm, NIPAm, St	Butylamine (DMF)	RT 1–20 h	[240]

a) HA, hexylamine; Pip, piperidine; RT, room temperature; TEA, triethylamine; THF, tetrahydrofuran.

Table 9.28 End-group removal by thermolysis.

Trithiocarbonate group	Polymer	Temperature (°C)	Comment	References
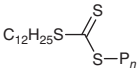	St, 4VP	165	In solution (DEG, nitrobenzene) with Cu(0) catalyst	[871]
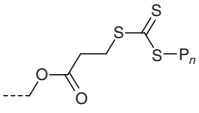	St	140	Z-attached stars	[872]
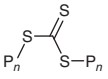	St, BA	100–200	Mid-chain trithiocarbonate	[873]
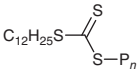	St, BA	100–200		[873]
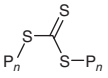	St, BA, St/BA			[12]
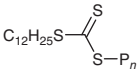	MA	220	End-group removal in flow	[185]
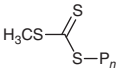	St	220	End-group removal in flow	[185]
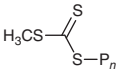	MMA	220		[183]
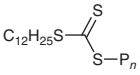	MMA		Comparison with dithiobenzoate	[206]

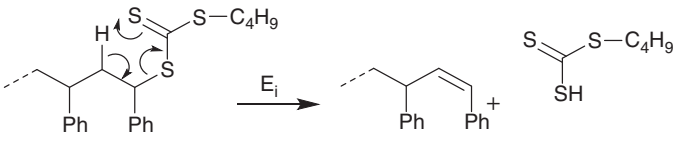

Scheme 9.12 Trithiocarbonate group loss by Chagaev elimination (e.g. PSt). E_i, electrocyclic intramolecular.

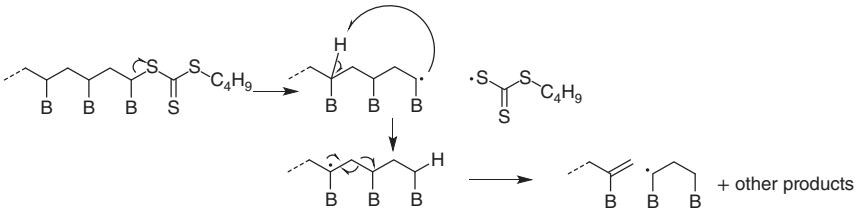

Scheme 9.13 Trithiocarbonate group loss by homolysis followed by backbiting and chain scission (e.g. PBA). Multiple backbiting reactions may occur in succession.

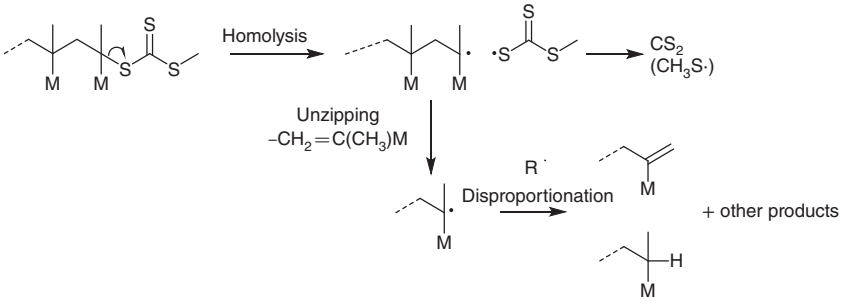

Scheme 9.14 Trithiocarbonate group loss by homolysis followed by unzipping (e.g. PMMA).

9.21.6 Trithiocarbonate Group Removal by Oxidation

Examples of trithiocarbonate group removal by oxidation are shown in Table 9.29. RAFT end-groups can be readily removed by reaction with hydrogen peroxide [9, 874–877]. The process has been demonstrated for dithiobenzoates [874, 877], trithiocarbonates [874, 875], and xanthates [876]. The processes reportedly [874, 876] lead to the thiocarbonylthio group being replaced with a hydroxyl group but the chemistry has not been established in most cases.

9.22 Conclusions and Outlook

This chapter provided a survey of the synthesis, reactions, and applications of trithiocarbonates RAFT agents. Only the more common agents were included in the detailed survey. Trithiocarbonates have some limitations. Dithioesters may offer lower dispersities with 1,1-disubsituted MAMs. Xanthates and dithiocarbamates

Table 9.29 Trithiocarbonate group removal by oxidation.

Trithiocarbonate group	Polymer	Reagent	References
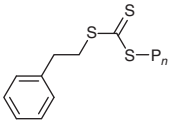	HPMA	H_2O_2	[874]
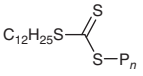	AA/MA/EHA	H_2O_2	[875]

may be more suited to mediating polymerization of LAMs. Nonetheless, trithiocarbonates are currently the most popular, and perhaps most versatile, form of RAFT agent for mediating radical polymerization. Trithiocarbonates are also effective as initiators in direct photoRAFT, in PET RAFT in redox RAFT, and in mediated eRAFT. The trithiocarbonate group is generally stable under the conditions usually used for radical polymerization yet is readily transformed post-RAFT polymerization. We anticipate that the use of trithiocarbonates as RAFT agents will continue to grow.

Abbreviations

Abbreviations are listed alphabetically by the abbreviated term. In general, abbreviations of methacrylates end with 'MA', methacrylamides end with 'MAm', acrylates end with 'A'. acrylamides end with 'Am' or begin with 'NA' (for *N*-acryloyl). Except as indicated below the suffix 'P' is an abbreviation for 'poly()'. Thus, poly(methyl methacrylate) is abbreviated as PMMA. The abbreviations often reflect common usage rather than IUPAC names. For some entries, alternative names are provided within parentheses, and IUPAC names are provided within brackets.

AA	acrylic acid
AcO^-	acetate
ACPA	4,4′-azobis(4-cyanopentanoic acid) [4,4′-(diazene-1,2-diyl)bis(4-cyanopentanoic acid)]
AcS	4-acetoxystyrene
AdA	1-adamantyl acrylate (**202**)
AEMA	2-aminoethyl methacrylate (or hydrochloride salt (**326**))
AEMAm	*N*-(2-aminoethyl)methacrylamide
AEP	2-(acryloyloxy)ethyl phosphate
AIBN	2,2′-azobis(2-methylpropionitrile) [2,2′-(diazene-1,2-diyl)bis(2-methylpropanenitrile)]
Am	acrylamide
AMA	allyl methacrylate
AMPS	2-acrylamido-2-methylpropane-1-sulfonic acid sodium salt (**237**)

AN	acrylonitrile
APAm	*N*-(2-aminopropyl)acrylamide
ATRP	atom-transfer radical polymerization
BA	butyl acrylate
BAm	*N*-butylacrylamide
Bd	butadiene
BisGMA	bisphenylglycidyl dimethacrylate [((propane-2,2-diylbis(4,1-phenylene))bis(oxy))bis(2-hydroxypropane-3,1-diyl) bis(2-methylacrylate)]
BMA	butyl methacrylate
BMDO	5,6-benzo-2-methylene-1,3-dioxepane (**362**)
BPO	benzoyl peroxide [benzoic peroxyanhydride]
BzAm	*N*-benzylacrylamide
BzMA	benzyl methacrylate
BzMAm	*N*-benzylmethacrylamide
CEMA	2-chloroethyl methacrylate
CHAm	*N*-cyclohexylacrylamide
CHMA	cyclohexyl methacrylate
CIPEA	2-chloropropionyloxyethyl acrylate
CL	caprolactone [oxepan-2-one]
CMA	cholesteryl methacrylate (**165**)
CMS	4-chloromethylstyrene
Cp	chloroprene
CPA	3-chloropropyl acrylate
CS	4-chlorostyrene
CTA	chain transfer agent
DA	dodecyl acrylate (lauryl acrylate)
DAAm	diacetone acrylamide [*N*-(2-methyl-4-oxopentan-2-yl)acrylamide]
DADMAC	diallyl dimethyl ammonium chloride (Table 9.18)
DDMAT	2-(Dodecylthiocarbonothioylthio)-2-methylpropanoic acid (*S*-Dodecyl-*S*′-(α,α′-dimethyl-α′′-acetic acid)trithiocarbonate) (**51**)
DEAm	*N,N*-diethylacrylamide
DEAEMA	(2-diethylamino)ethyl methacrylate
DEGA	(diethylene glycol monomethyl ether) acrylate
DEGDA	(diethylene glycol) diacrylate
DEGDMA	(diethylene glycol) dimethacrylate
DEGMA	(diethylene glycol monomethyl ether) methacrylate
DMAEA	(2-dimethylamino) ethyl acrylate
DMAEAm	*N*-(2-(dimethylamino)ethyl)acrylamide
DMAEMA	(2-dimethylamino)ethyl methacrylate
DMAm	*N,N*-dimethylacrylamide
DMAPMAm	*N*-[3-(Dimethylamino)propyl]methacrylamide
DMF	*N,N*-dimethylformamide
DMOS	3,4-dimethoxystyrene
DMSO	dimethyl sulfoxide
DSDM	disulfide dimethacrylate [bis(2-methacryloyloxy)ethyl disulfide (**368**)]

DSDAm	disulfide diacrylamide (*N*,*N*-bis(acryloyl)cystamine (**374**))
DSDA	disulfide diacrylate [bis(2-acryloyloxy)ethyl disulfide (**372**)]
DVB	divinylbenzene
DVE	divinyl ether
DVPP	diphenyl(4-vinylphenyl)phosphane
EGDA	ethylene glycol diacrylate
EGDMA	ethylene glycol dimethacrylate
EHA	2-ethylhexyl acrylate
EMAm	*N*-ethyl-*N*-methylacrylamide
ESARA	exchange of substituents between (macro)alkoxyamines and (macro)RAFT agents
FMA	furfuryl methacrylate
EPR	electron paramagnetic resonance spectroscopy
eRAFT	electrochemically initiated RAFT polymerization
GA	glycolic acid
GMMA	glycerol monomethacrylate (**146**) (2,3-dihydroxypropyl methacrylate)
GMA	glycidyl methacrylate
HADA	3-hydroxy-1-adamantyl acrylate
HADM	3-hydroxy-1-adamantyl methacrylate (**171**)
HDDA	hexanediol diacrylate (**371**)
HDFDMA	3,3,4,4,5,5,6,6,7,7,8,8,9,9,10,10,10-heptadecafluorodecyl methacrylate
HEA	2-hydroxyethyl acrylate
HEAm	*N*-(2-hydroxylethyl)acrylamide
HEMA	2-hydroxyethyl methacrylate
HMS	4-hydroxymethylstyrene
HPMA	2-hydroxypropyl methacrylate
HPMAm	*N*-(2-hydroxylpropyl)methacrylamide
iAA	isoamyl acrylate
iBoA	isobornyl acrylate
IBVE	isobutyl vinyl ether
Ind	indene
Ip	isoprene
IPMA	isopropyl methacrylate
LA	lactic acid (stereoisomers not distinguished)
LMA	lauryl methacrylate [dodecyl methacrylate]
LAm	*N*-laurylacrylamide [*N*-dodecylacrylamide]
LAM	less activated monomer
Lim	limonene
LPO	lauroyl peroxide (dodecanoyl peroxide) [dodecanoic peroxyanhydride]
MA	methyl acrylate
MAA	methacrylic acid
MADA	2-methyl-2-adamantyl acrylate
MADIX	macromolecular design by interchange of xanthates
MADM	2-methyl-2-adamantyl methacrylate (**172**)

MAM	more activated monomer
MAH	maleic anhydride
MBAm	methylene-bis-acrylamide
MEA	2-methoxyethyl acrylate
MEMA	2-methoxyethyl methacrylate
MEP	2-methacryloylethyl phosphate
MeS	4-methylstyrene
METAC	[2-(methacryloyloxy)ethyl]trimethylammonium chloride
MMA	methyl methacrylate
MMBL	γ-methyl-α-methylene-γ-butyrolactone [5-methyl-3-methylenedihydrofuran-2(3*H*)-one]
MPAm	*N*-(3-methoxypropyl)acrylamide
MPC	(methacryloyloxy)ethyl phosphorylcholine (**175**)
NAM	*N*-acryloylmorpholine
NAS	*N*-acryloylsuccinimide
NEAm	*N*-ethylacrylamide
NIPAm	*N*-isopropylacrylamide
NIPMAm	*N*-isopropylmethacrylamide
NMMI	*N*-methylmaleimide
NMP	nitroxide-mediated polymerization [aminoxyl-mediated radical polymerization]
NPMI	*N*-phenylmaleimide
NPFPMI	*N*-perfluorophenylmaleimide
NVC	*N*-vinylcarbazole
NVP	*N*-vinylpyrrolidone
NVPI	*N*-vinylphthalimide
OAm	*N*-octylacrylamide
OBA	3-oxobutyl acrylate
ODA	octadecyl acrylate
ODMA	octadecyl methacrylate
OeMA	oleyl methacrylate
OFPA	2,2,3,3,4,4,5,5-octafluoropentyl acrylate
OPA	2-oxopropyl acrylate (acetonyl acrylate)
OTf^-	triflate [trifluoromethanesulfonate]
PA	propargyl acrylate
PAA	propacrylic acid [2-methylenebutanoic acid]
PAm	*N*-propylacrylamide
PDL	ω-pentadecalactone [oxacyclohexadecan-2-one]
PEA	2-phenylethyl acrylate
PEG	poly(ethylene glycol)
PEGA	(polyethylene glycol monomethyl ether) acrylate [includes OEGA (oligoethylene glycol monomethyl ether) acrylate
PEGDA	polyethylene glycol diacrylate
PEGDMA	polyethylene glycol dimethacrylate

PEGMA	(polyethylene glycol monomethyl ether) methacrylate [also includes OEGMA (oligoethylene glycol monomethyl ether) methacrylate
PET-RAFT	photoinduced electron or energy transfer-RAFT
PET-SUMI	photoinduced electron or energy transfer-single-unit monomer insertion
PFOEA	2-(perfluorooctyl)ethyl acrylate [3,3,4,4,5,5,6,6,7,7,8,8,9,9,10,10,10-heptadecafluorodecyl acrylate]
PFOEMA	2-(perfluorooctyl)ethyl methacrylate [3,3,4,4,5,5,6,6,7,7,8,8,9,9,10,10, 10-heptadecafluorodecyl methacrylate]
PFPA	perfluorophenyl acrylate (**305**)
PFS	2,3,4,5,6-pentafluorostyrene
PhMAm	*N*-phenylmethacrylamide
PIPBAm	1,4-bis(acryloyl)piperazine
PLP	pulsed laser photolysis
PMA	pentyl methacrylate
RAFT	reversible addition–fragmentation chain transfer
RDRP	reversible-deactivation radical polymerization
SSO3Na	sodium 4-styrenesulfonate
St	styrene
SUMI	single-unit monomer insertion
tBA	*tert*-butyl acrylate
tBMA	*tert*-butyl methacrylate
tBAm	*N*-*tert*-butylacrylamide
tBDMSMA	*tert*-butyldimethylsilyl methacrylate (**332**)
tBDMSOS	4-(*tert*-butyldimethylsilyloxy)styrene (**331**)
tBOS	4-*tert*-butyloxystyrene
tBS	4-*tert*-butylstyrene
TBSiMA	tributylsilyl methacrylate (**333**)
TEGA	(tetraethylene glycol monomethyl ether) acrylate
TFEA	2,2,2-trifluoroethyl acrylate
TFEMA	2,2,2-trifluoroethyl methacrylate
TFPMA	2,2,3,3-tetrafluoropropyl methacrylate
THFA	tetrahydrofurfuryl acrylate [(tetrahydrofuran-2-yl)methyl acrylate]
THPA	tetrahydropyran-2-yl acrylate [tetrahydro-2*H*-pyran-2-yl acrylate]
TMAPMA	(3-trimethylaminonium)propyl methacrylate
TPSiMA	triisopropylsilyl methacrylate (**334**)
TrMA	trityl methacrylate
VAc	vinyl acetate
3VBA	3-vinylbenzaldehyde
VBA	4-vinylbenzoic acid
VPBA	(4-vinylphenyl)boronic acid
VL	γ-valerolactone [tetrahydro-2*H*-pyran-2-one]
4HS	4-hydroxystyrene
2VP	2-vinylpyridine
4VP	4-vinylpyridine

References

1 Le, T.P., Moad, G., Rizzardo, E., and Thang, S.H. (1998). Polymerization with living characteristics. (DuPont/CSIRO), WO9801478A1.

2 Corpart, P., Charmot, D., Biadatti, T., et al. (1998). Block polymer synthesis by controlled radical polymerization. (Rhodia Chimie), WO9858974A1.

3 Mayadunne, R.T.A., Rizzardo, E., Chiefari, J. et al. (2000). *Macromolecules* 33: 243–245. https://doi.org/10.1021/ma991451a.

4 Moad, G., Chiefari, J., Krstina, J. et al. (2000). *Polym. Int.* 49: 993–1001. https://doi.org/10.1002/1097-0126(200009)49:9<993::AID-PI506>3.0.CO;2-6.

5 Keddie, D.J., Moad, G., Rizzardo, E., and Thang, S.H. (2012). *Macromolecules* 45: 5321–5342. https://doi.org/10.1021/ma300410v.

6 Moad, G., Chong, Y.K., Rizzardo, E. et al. (2005). *Polymer* 46: 8458–8468. https://doi.org/10.1016/j.polymer.2004.12.061.

7 Gao, Y., Lv, L., Zou, G., and Zhang, Q. (2017). *Macromol. Res.* 25: 931–935. https://doi.org/10.1007/s13233-017-5099-4.

8 Keddie, D.J., Guerrero-Sanchez, C., and Moad, G. (2013). *Polym. Chem.* 4: 3591–3601. https://doi.org/10.1039/c3py00487b.

9 Chiefari, J., Chong, Y.K., Ercole, F. et al. (1998). *Macromolecules* 31: 5559–5562. https://doi.org/10.1021/ma9804951.

10 Postma, A., Davis, T.P., Evans, R.A. et al. (2006). *Macromolecules* 39: 5293–5306. https://doi.org/10.1021/ma060245h.

11 Chernikova, E.V., Terpugova, P.S., Baskakov, A.A. et al. (2010). *Polym. Sci., Ser. B* 52: 119–128. https://doi.org/10.1134/S1560090410030012.

12 Chernikova, E.V., Plutalova, A.V., Garina, E.S., and Vishnevetsky, D.V. (2016). *Polym. Chem.* 7: 3622–3632. https://doi.org/10.1039/C6PY00301J.

13 Houshyar, S., Keddie, D., Moad, G. et al. (2012). *Polym. Chem.* 3: 1879–1889. https://doi.org/10.1039/C2PY00529H.

14 Haven, J.J., Hendrikx, M., Junkers, T. et al. (2018). Elements of RAFT Navigation. RAFT 20 years later. RAFT-synthesis of uniform, sequence-defined (co)polymers. In: *Reversible Deactivation Radical Polymerization: Mechanisms and Synthetic Methodologies*, vol. 1284 (eds. K. Matyjaszewski, H. Gao, B.S. Sumerlin and N.V. Tsarevsky), 77–103. Washington, DC: ACS Symposium Series, American Chemical Society. https://doi.org/10.1021/bk-2018-1284.ch004.

15 Chapman, R., Jungb, K., and Boyer, C. (2022). Overview of photoregulated reversible addition-fragmentation chain transfer (RAFT) polymerization. In: *RAFT Polymerization: Materials, Synthesis and Applications* (eds. G. Moad and E. Rizzardo). Weinheim: Wiley-VCH, 611–646.

16 Lorandi, F., Fantin, M., and Matyjaszewski, K. (2022). Redox initiated RAFT polymerization and (electro)chemical activation of RAFT agents. In: *RAFT Polymerization: Materials, Synthesis and Applications* (eds. G. Moad and E. Rizzardo). Weinheim: Wiley-VCH, 647–678.

17 Ran, R., Chen, Z., and Wang, X.L. (2009). *J. Appl. Polym. Sci.* 111: 2011–2017. https://doi.org/10.1002/app.29262.

18 Bicciocchi, E., Chong, Y.K., Giorgini, L. et al. (2010). *Macromol. Chem. Phys.* 211: 529–538. https://doi.org/10.1002/macp.200900557.

19 De Rybel, N., Van Steenberge, P.H.M., Reyniers, M.-F. et al. (2018). *Chem. Eng. Sci.* 177: 163–179. https://doi.org/10.1016/j.ces.2017.11.043.

20 Chiefari, J., Mayadunne, R.T.A., Moad, C.L. et al. (2003). *Macromolecules* 36: 2273–2283. https://doi.org/10.1021/ma020883+.

21 Strube, O.I., Nothdurft, L., Drache, M., and Schmidt-Naake, G. (2011). *Macromol. Chem. Phys.* 212: 574–582. https://doi.org/10.1002/macp.201000572.

22 Grigoreva, A., Polozov, E., and Zaitsev, S. (2019). *Colloid Polym. Sci.* https://doi.org/10.1007/s00396-019-04559-6.

23 Fuchs, A.V. and Thurecht, K.J. (2017). *ACS Macro Lett.* 6: 287–291. https://doi.org/10.1021/acsmacrolett.7b00100.

24 Grigoreva, A., Polozov, E., and Zaitsev, S. (2020). *J. Fluorine Chem.* 232: 109484. https://doi.org/10.1016/j.jfluchem.2020.109484.

25 Theis, A., Feldermann, A., Charton, N. et al. (2005). *Macromolecules* 38: 2595–2605. https://doi.org/10.1021/ma047476d.

26 Moad, G. and Barner-Kowollik, C. (2008). The mechanism and kinetics of the RAFT process: overview, rates, stabilities, side reactions, product spectrum and outstanding challenges. In: *Handbook of RAFT Polymerization* (ed. C. Barner-Kowollik), 51–104. Weinheim: Wiley-VCH. https://doi.org/10.1002/9783527622757.ch3.

27 Theis, A., Feldermann, A., Charton, N. et al. (2005). *Polymer* 46: 6797–6809. https://doi.org/10.1016/j.polymer.2005.06.004.

28 Buback, M., Hesse, P., Junkers, T., and Vana, P. (2006). *Macromol. Rapid Commun.* 27: 182–187. https://doi.org/10.1002/marc.200500716.

29 Quinn, J.F., Moad, G., and Barner-Kowollik, C. (2022). RAFT polymerization: mechanistic considerations. In: *RAFT Polymerization: Materials, Synthesis and Applications* (eds. G. Moad and E. Rizzardo). Weinheim: Wiley-VCH, 95–138.

30 Walling, C. (1948). *J. Am. Chem. Soc.* 70: 2561–2564. https://doi.org/10.1021/ja01187a079.

31 O'Brien, J.L. and Gornick, F. (1955). *J. Am. Chem. Soc.* 77: 4757–4763. https://doi.org/10.1021/ja01623a019.

32 Smith, W.V. (1946). *J. Am. Chem. Soc.* 68: 2059–2064. https://doi.org/10.1021/ja01214a055.

33 Gregg, R.A., Alderman, D.M., and Mayo, F.R. (1948). *J. Am. Chem. Soc.* 70: 3740–3743. https://doi.org/10.1021/ja01191a058.

34 Chong, Y.K., Krstina, J., Le, T.P.T. et al. (2003). *Macromolecules* 36: 2256–2272. https://doi.org/10.1021/ma020882h.

35 Gardiner, J., Martinez-Botella, I., Tsanaktsidis, J., and Moad, G. (2016). *Polym. Chem.* 7: 481–492. https://doi.org/10.1039/C5PY01382H.

36 Moad, G. (2022). Dithioesters in RAFT polymerization. In: *RAFT Polymerization: Materials, Synthesis and Applications* (eds. G. Moad and E. Rizzardo). Weinheim: Wiley-VCH, 223–370.

37 Derboven, P., Van Steenberge, P.H.M., Reyniers, M.-F. et al. (2016). *Macromol. Theory Simul.* 25: 104–115. https://doi.org/10.1002/mats.201500076.

38 Drache, M. and Schmidt-Naake, G. (2007). *Macromol. Symp.* 259: 397–405. https://doi.org/10.1002/masy.200751345.

39 Klumperman, B., van den Dungen, E.T.A., Heuts, J.P.A., and Monteiro, M.J. (2010). *Macromol. Rapid Commun.* 31: 1846–1862. https://doi.org/10.1002/marc.200900907.

40 Buback, M. (2022). Kinetics and mechanism of RAFT polymerizations. In: *RAFT Polymerization: Materials, Synthesis and Applications* (eds. G. Moad and E. Rizzardo). Weinheim: Wiley-VCH, 59–94.

41 Lin, C.Y. and Coote, M.L. (2009). *Aust. J. Chem.* 62: 1479–1483. https://doi.org/10.1071/ch09269.

42 Meiser, W., Buback, M., and Sidoruk, A. (2013). *Macromol. Chem. Phys.* 214: 2108–2114. https://doi.org/10.1002/macp.201300304.

43 Barth, J., Buback, M., Meiser, W., and Vana, P. (2010). *Macromolecules* 43: 51–54. https://doi.org/10.1021/ma902111z.

44 Golubev, V.B., Filippov, A.N., Chernikova, E.V. et al. (2011). *Polym. Sci., Ser. C* 53: 14–26. https://doi.org/10.1134/s1811238211040023.

45 Coote, M.L. (2022). Quantum-chemical studies of RAFT polymerization. In: *RAFT Polymerization: Materials, Synthesis and Applications* (eds. G. Moad and E. Rizzardo). Weinheim: Wiley-VCH, 139–186.

46 Moad, G., Rizzardo, E., and Thang San, H. (2013). Fundamentals of RAFT polymerization. In: *Fundamentals of Controlled/Living Radical Polymerization*, RSC Polymer Chemistry Series No. 4 (eds. N.V. Tsarevsky and B.S. Sumerlin), 205–249. Cambridge: Royal Society of Chemistry. https://doi.org/10.1039/9781849737425-00205.

47 Wang, M., Marty, J.-D., and Destarac, M. (2022). Xanthates in RAFT polymerization. In: *RAFT Polymerization: Materials, Synthesis and Applications* (eds. G. Moad and E. Rizzardo). Weinheim: Wiley-VCH, 495–550.

48 Moad, G. (2019). *J. Polym. Sci., Part A: Polym. Chem.* 57: 216–227. https://doi.org/10.1002/pola.29199.

49 Fischer, H. and Radom, L. (2001). *Angew. Chem. Int. Ed.* 40: 1340–1371. https://doi.org/10.1002/1521-3773(20010417)40:8<1340::AID-ANIE1340>3.0.CO;2-%23.

50 Moad, G. (2017). *Macromol. Chem. Phys.* 218: 1700381. https://doi.org/10.1002/macp.201700381.

51 Moad, G. (2019). *Prog. Polym. Sci.* 88: 130–188. https://doi.org/10.1016/j.progpolymsci.2018.08.003.

52 Fortenberry, A.W., McCormick, C.L., and Smith, A.E. (2022). Considerations for and applications of aqueous RAFT polymerization. In: *RAFT Polymerization: Materials, Synthesis and Applications* (eds. G. Moad and E. Rizzardo). Weinheim: Wiley-VCH, 679–706.

53 Moad, G., Rizzardo, E., and Thang, S.H. (2006). *Aust. J. Chem.* 59: 669–692. https://doi.org/10.1071/CH06250.

54 Lai, J.T., Filla, D., and Shea, R. (2002). *Macromolecules* 35: 6754–6756. https://doi.org/10.1021/ma020362m.

55 Moad, G. (2014). *Macromol. Chem. Phys.* 215: 9–26. https://doi.org/10.1002/macp.201300562.

56 Moad, G., Keddie, D., Guerrero-Sanchez, C. et al. (2015). *Macromol. Symp.* 350: 34–42. https://doi.org/10.1002/masy.201400022.

57 Postma, A., Davis, T.P., Li, G. et al. (2006). *Macromolecules* 39: 5307–5318. https://doi.org/10.1021/ma0604338.

58 Xu, J., Fu, C., Shanmugam, S. et al. (2017). *Angew. Chem. Int. Ed.* 56: 8376–8383. https://doi.org/10.1002/anie.201610223.

59 Easterling, C.P., Xia, Y., Zhao, J. et al. (2019). *ACS Macro Lett.* 8: 1461–1466. https://doi.org/10.1021/acsmacrolett.9b00716.

60 Chang, K., Dicke, Z.T., and Taite, L.J. (2012). *J. Polym. Sci., Part A: Polym. Chem.* 50: 976–985. https://doi.org/10.1002/pola.25854.

61 Leung, D. and Bowman, C.N. (2012). *Macromol. Chem. Phys.* 213: 198–204. https://doi.org/10.1002/macp.201100402.

62 Lu, L., Zhang, H., Yang, N., and Cai, Y. (2006). *Macromolecules* 39: 3770–3776. https://doi.org/10.1021/ma060157x.

63 Qu, T., Wang, A., Yuan, J. et al. (2009). *Colloids Surf., B* 72: 94–100. https://doi.org/10.1016/j.colsurfb.2009.03.020.

64 Ma, J., Yang, C., Luo, J. et al. (2012). *J. Macromol. Sci., Part A* 49: 321–329. https://doi.org/10.1080/10601325.2012.662068.

65 Zhao, X. and Shan, G. (2019). *Colloid Polym. Sci.* 297: 1353–1363. https://doi.org/10.1007/s00396-019-04556-9.

66 Chou, Y.-N., Venault, A., Cho, C.-H. et al. (2017). *Langmuir* 33: 9822–9835. https://doi.org/10.1021/acs.langmuir.7b02164.

67 Millard, P.-E., Barner, L., Stenzel, M.H. et al. (2006). *Macromol. Rapid Commun.* 27: 821–828. https://doi.org/10.1002/marc.200600115.

68 Das, P., Zhong, W., and Claverie, J. (2011). *Colloid. Polym. Sci.*: 1–15. https://doi.org/10.1007/s00396-011-2466-0.

69 Hart-Smith, G., Lovestead, T.M., Davis, T.P. et al. (2007). *Biomacromolecules* 8: 2404–2415. https://doi.org/10.1021/bm700526j.

70 López-Pérez, L., Maldonado-Textle, H., Elizalde-Herrera, L.E. et al. (2019). *Polymer* 168: 116–125. https://doi.org/10.1016/j.polymer.2019.02.025.

71 Yu, L., Wei, Y., Tu, Y. et al. (2018). *J. Polym. Sci., Part A: Polym. Chem.* 56: 2437–2444. https://doi.org/10.1002/pola.29217.

72 Huang, Z., Qiu, T., Xu, H. et al. (2018). *Macromolecules* 51: 7329–7337. https://doi.org/10.1021/acs.macromol.8b01523.

73 Wang, R., McCormick, C.L., and Lowe, A.B. (2005). *Macromolecules* 38: 9518–9525. https://doi.org/10.1021/ma050669w.

74 Lima, V., Jiang, X.L., Brokken-Zijp, J. et al. (2005). *J. Polym. Sci., Part A: Polym. Chem.* 43: 959–973. https://doi.org/10.1002/pola.20558.

75 Jiang, X.L., Schoenmakers, P.J., van Dongen, J.L.J. et al. (2003). *Anal. Chem.* 75: 5517–5524. https://doi.org/10.1021/ac034556r.

76 Jiang, W., Lu, L., and Cai, Y. (2007). *Macromol. Rapid Commun.* 28: 725–728. https://doi.org/10.1002/marc.200600788.

77 Reyhani, A., Ranji-Burachaloo, H., McKenzie, T.G. et al. (2019). *Macromolecules* 52: 3278–3287. https://doi.org/10.1021/acs.macromol.9b00038.

78 Uchiyama, M., Satoh, K., and Kamigaito, M. (2019). *Chem. Commun.* 55: 5327–5330. https://doi.org/10.1039/C9CC00900K.
79 Hendrich, M., Lewerdomski, L., and Vana, P. (2015). *J. Polym. Sci., Part A: Polym. Chem.* https://doi.org/10.1002/pola.27753.
80 Haraguchi, K., Kubota, K., Takada, T., and Mahara, S. (2014). *Biomacromolecules* 15: 1992–2003. https://doi.org/10.1021/bm401914c.
81 Haraguchi, K., Takehisa, T., Mizuno, T., and Kubota, K. (2015). *ACS Biomater. Sci. Eng.* 1: 352–362. https://doi.org/10.1021/acsbiomaterials.5b00079.
82 Liu, Y., Hu, X., Meng, M. et al. (2016). *Chem. Eng. J.* 302: 609–618. https://doi.org/10.1016/j.cej.2016.05.097.
83 Lewis, R.W., Evans, R.A., Malic, N. et al. (2017). *Polym. Chem.* 8: 3702–3711. https://doi.org/10.1039/C7PY00682A.
84 Thomas, D.B., Convertine, A.J., Myrick, L.J. et al. (2004). *Macromolecules* 37: 8941–8950. https://doi.org/10.1021/ma048199d.
85 Sogabe, A., Flores, J.D., and McCormick, C.L. (2010). *Macromolecules* 43: 6599–6607. https://doi.org/10.1021/ma1008463.
86 Nuopponen, M., Kalliomaki, K., Laukkanen, A. et al. (2008). *J. Polym. Sci., Part A: Polym. Chem.* 46: 38–46. https://doi.org/10.1002/pola.22355.
87 Kirkland, S.E., Hensarling, R.M., McConaughy, S.D. et al. (2008). *Biomacromolecules* 9: 481–486. https://doi.org/10.1021/bm700968t.
88 Demirel, G., Rzaev, Z., Patir, S., and Piskin, E. (2009). *J. Nanosci. Nanotechnol.* 9: 1865–1871. https://doi.org/10.1166/jnn.2009.388.
89 Wu, J., Sun, X., Zhang, R. et al. (2016). *Colloid Polym. Sci.* 294: 1989–1995. https://doi.org/10.1007/s00396-016-3958-8.
90 Díaz-Silvestre, S.E., St Thomas, C., Maldonado-Textle, H. et al. (2018). *Colloid Polym. Sci.* 296: 1699–1710. https://doi.org/10.1007/s00396-018-4391-y.
91 Chen, M., Deng, S., Gu, Y. et al. (2017). *J. Am. Chem. Soc.* 139: 2257–2266. https://doi.org/10.1021/jacs.6b10345.
92 Lokitz, B.S., Convertine, A.J., Ezell, R.G. et al. (2006). *Macromolecules* 39: 8594–8602. https://doi.org/10.1021/ma061672y.
93 Zhou, S., Zhang, D., Bai, L. et al. (2016). *Polymers* 8: 135. https://doi.org/10.3390/polym8040135.
94 Zhang, Y., Wen, X., Shi, Y. et al. (2019). *Ind. Eng. Chem. Res.* 58: 1142–1149. https://doi.org/10.1021/acs.iecr.8b04913.
95 Ran, R., Wan, T., Gao, T. et al. (2008). *Polym. Int.* 57: 28–34. https://doi.org/10.1002/pi.2307.
96 Li, W., Thanneeru, S., Kanyo, I. et al. (2015). *ACS Macro Lett.* 4: 736–740. https://doi.org/10.1021/acsmacrolett.5b00321.
97 Cetintas, M. and Kamperman, M. (2016). *Polymer* 107: 387–397. https://doi.org/10.1016/j.polymer.2016.08.033.
98 Kajita, T., Tanaka, H., Noro, A. et al. (2019). *J. Mater. Chem. A* 7: 15585–15592. https://doi.org/10.1039/C9TA01890E.
99 Noro, A., Matsushita, Y., and Lodge, T.P. (2008). *Macromolecules* 41: 5839–5844. https://doi.org/10.1021/ma800739c.

100 Luo, J., Li, M., Xin, M. et al. (2016). *Macromol. Chem. Phys.* 217: 1777–1784. https://doi.org/10.1002/macp.201600141.

101 Chernikova, E., Poteryaeva, Z., Belyaev, S., and Sivtsov, E. (2011). *Russ. J. Appl. Chem.* 84: 1031–1039. https://doi.org/10.1134/s1070427211060231.

102 Chernikova, E.V., Kishilov, S.M., Plutalova, A.V. et al. (2014). *Polym. Sci., Ser. B* 56: 553–565. https://doi.org/10.1134/s1560090414050029.

103 Li, C., Liu, H., and Li, Y. (2011). *Macromol. Chem. Phys.* 212: 1050–1055. https://doi.org/10.1002/macp.201100104.

104 Bilalis, P., Pitsikalis, M., and Hadjichristidis, N. (2006). *J. Polym. Sci., Part A: Polym. Chem.* 44: 659–665. https://doi.org/10.1002/pola.21198.

105 Tominey, A.F., Liese, J., Wei, S. et al. (2010). *Beilstein J. Org. Chem.* 6: 66. https://doi.org/10.3762/bjoc.6.66.

106 Liu, X.-M., Quan, L.-D., Tian, J. et al. (2008). *Pharm. Res.* 25: 2910–2919. https://doi.org/10.1007/s11095-008-9683-3.

107 Deng, Z.C., Bouchekif, H., Babooram, K. et al. (2008). *J. Polym. Sci., Part A: Polym. Chem.* 46: 4984–4996. https://doi.org/10.1002/pola.22826.

108 Rossi, N.A.A., Jadhav, V., Lai, B.F.L. et al. (2008). *J. Polym. Sci., Part A: Polym. Chem.* 46: 4021–4029. https://doi.org/10.1002/pola.22743.

109 Rossi, N.A.A., Zou, Y., Scott, M.D., and Kizhakkedathu, J.N. (2008). *Macromolecules* 41: 5272–5282. https://doi.org/10.1021/ma800606k.

110 Jiang, X., Ahmed, M., Deng, Z., and Narain, R. (2009). *Bioconjugate Chem.* 20: 994–1001. https://doi.org/10.1021/bc800566f.

111 Zhao, C., Dolmans, L., and Zhu, X.X. (2019). *Macromolecules* 52: 4441–4446. https://doi.org/10.1021/acs.macromol.9b00794.

112 Ran, F., Nie, S., Li, J. et al. (2012). *Macromol. Biosci.* 12: 116–125. https://doi.org/10.1002/mabi.201100249.

113 Wei, X., Wu, J., Zhao, G. et al. (2018). *Mol. Pharm.* 15: 3456–3467. https://doi.org/10.1021/acs.molpharmaceut.8b00433.

114 Tamate, R., Takahashi, K., Ueki, T. et al. (2017). *Biomacromolecules* 18: 281–287. https://doi.org/10.1021/acs.biomac.6b01672.

115 Pang, D.-X., Liu, W.-D., Li, T. et al. (2011). *J. Appl. Polym. Sci.* 119: 2953–2960. https://doi.org/10.1002/app.33014.

116 Ran, F., Nie, S., Zhao, W. et al. (2011). *Acta Biomater.* 7: 3370–3381. https://doi.org/10.1016/j.actbio.2011.05.026.

117 Vishnevetskii, D.V., Chernikova, E.V., Garina, E.S., and Sivtsov, E.V. (2013). *Polym. Sci., Ser. B* 55: 515–525. https://doi.org/10.1134/s156009041308006x.

118 Bugakov, M.A., Boiko, N.I., Chernikova, E.V., and Shibaev, V.P. (2013). *Polym. Sci., Ser. B* 55: 294–303. https://doi.org/10.1134/s1560090413050011.

119 Bugakov, M.A., Boiko, N.I., Chernikova, E.V. et al. (2018). *Polym. Sci., Ser. C* 60: 3–13. https://doi.org/10.1134/S1811238218010022.

120 Chernikova, E., Poteryaeva, Z., Belyaev, S. et al. (2011). *Polym. Sci., Ser. B* 53: 391–403. https://doi.org/10.1134/s1560090411070013.

121 Boiko, N.I., Bugakov, M.A., Chernikova, E.V. et al. (2015). *Polym. Chem.* 6: 6358–6371. https://doi.org/10.1039/C5PY00555H.

122 Bugakov, M., Boiko, N., Abramchuk, S. et al. (2020). *J. Mater. Chem. C* 8: 1225–1230. https://doi.org/10.1039/C9TC06397H.
123 Bertrand, A., Chen, S., Souharce, G.g. et al. (2011). *Macromolecules* 44: 3694–3704. https://doi.org/10.1021/ma200540u.
124 Chen, M. and Johnson, J.A. (2015). *Chem. Commun.* 51: 6742–6745. https://doi.org/10.1039/C5CC01562F.
125 Lamb, J.R., Qin, K.P., and Johnson, J.A. (2019). *Polym. Chem.* 10: 1585–1590. https://doi.org/10.1039/C9PY00022D.
126 Chen, M., MacLeod, M.J., and Johnson, J.A. (2015). *ACS Macro Lett.* 4: 566–569. https://doi.org/10.1021/acsmacrolett.5b00241.
127 Harrisson, S. and Wooley, K.L. (2005). *Chem. Commun.*: 3259–3261. https://doi.org/10.1039/b504313a.
128 Nguyen, D., Zondanos, H.S., Farrugia, J.M. et al. (2008). *Langmuir* 24: 2140–2150. https://doi.org/10.1021/la7027466.
129 Albertin, L., Wolnik, A., Ghadban, A., and Dubreuil, F. (2012). *Macromol. Chem. Phys.* 213: 1768–1782. https://doi.org/10.1002/macp.201200256.
130 Lorenzo, M.M., Decker, C.G., Kahveci, M.U. et al. (2016). *Macromolecules* 49: 30–37. https://doi.org/10.1021/acs.macromol.5b02323.
131 Srivastava, N., Saxena, M., and Shukla, M. (2019). *Rasayan J. Chem.* 12: 333–337. https://doi.org/10.31788/rjc.2019.1215038.
132 Tang, B., White, S.P., Frisbie, C.D., and Lodge, T.P. (2015). *Macromolecules* 48: 4942–4950. https://doi.org/10.1021/acs.macromol.5b00882.
133 Chaturvedi, D., Mishra, N., Chaturvedi, A.K., and Mishra, V. (2008). *Monats. Chem.* 139: 1467–1470. https://doi.org/10.1007/s00706-008-0956-7.
134 Ladaviere, C., Dorr, N., and Claverie, J.P. (2001). *Macromolecules* 34: 5370–5372. https://doi.org/10.1021/ma010358v.
135 Majonis, D., Herrera, I., Ornatsky, O. et al. (2010). *Anal. Chem. (Washington, DC, US)* 82: 8961–8969. https://doi.org/10.1021/ac101901x.
136 Gu, Y. and Lodge, T.P. (2011). *Macromolecules* 44: 1732–1736. https://doi.org/10.1021/ma2001838.
137 Postma, A., Davis, T.P., Moad, G., and O'Shea, M.S. (2005). *Macromolecules* 38: 5371–5374. https://doi.org/10.1021/ma050402x.
138 Kiasat, A.R., Badri, R., and Sayyahi, S. (2008). *Chin. Chem. Lett.* 19: 1301–1304. https://doi.org/10.1016/j.cclet.2008.07.019.
139 Wood, M.R., Duncalf, D.J., Rannard, S.P., and Perrier, S. (2006). *Org. Lett.* 8: 553–556. https://doi.org/10.1021/ol0525617.
140 Soleiman-Beigi, M. and Taherinia, Z. (2014). *J. Sulfur Chem.* 35: 470–476. https://doi.org/10.1080/17415993.2014.919296.
141 Loiseau, J., Ladaviere, C., Suau, J.M., and Claverie, J. (2005). *Polymer* 46: 8565–8572. https://doi.org/10.1016/j.polymer.2005.04.083.
142 Vishnevetskii, D.V., Plutalova, A.V., Yulusov, V.V. et al. (2015). *Polym. Sci., Ser. B* 57: 197–206. https://doi.org/10.1134/S1560090415030094.
143 Chernikova, E.V., Zaitsev, S.D., Plutalova, A.V. et al. (2018). *RSC Adv.* 8: 14300–14310. https://doi.org/10.1039/C8RA00048D.

144 Lu, W., Wang, Y., Wang, W. et al. (2017). *Polym. Chem.* 8: 5741–5748. https://doi.org/10.1039/C7PY01225J.

145 Dietrich, M., Glassner, M., Gruendling, T. et al. (2010). *Polym. Chem.* 1: 634–644. https://doi.org/10.1039/b9py00273a.

146 Chernikova, E., Yulusov, V., Mineeva, K. et al. (2011). *Polym. Sci., Ser. B* 53: 437–447. https://doi.org/10.1134/s1560090411070025.

147 Chernikova, E.V., Terpugova, P.S., Garina, E.S., and Golubev, V.B. (2007). *Polym. Sci., Ser. A* 49: 108–119.

148 Li, Z., Serelis, A.K., Reed, W.F., and Alb, A.M. (2010). *Polymer* 51: 4726–4734. https://doi.org/10.1016/j.polymer.2010.08.015.

149 Bivigou-Koumba, A., Görnitz, E., Laschewsky, A. et al. (2010). *Colloid. Polym. Sci.* 288: 499–517. https://doi.org/10.1007/s00396-009-2179-9.

150 Zehm, D., Laschewsky, A., Heunemann, P. et al. (2011). *Polym. Chem.* 2: 137–147. https://doi.org/10.1039/C0PY00200C.

151 Skey, J. and O'Reilly, R.K. (2008). *Chem. Commun.*: 4183–4185. https://doi.org/10.1039/b804260h.

152 Su, X.L., Zhao, Z.G., Li, H. et al. (2008). *Eur. Polym. J.* 44: 1849–1856. https://doi.org/10.1016/j.eurpolymj.2008.03.012.

153 Couture, G. and Améduri, B. (2012). *Eur. Polym. J.* 48: 1348–1356. https://doi.org/10.1016/j.eurpolymj.2012.03.020.

154 Bae, S.-k., Lee, S.-Y., and Hong, S.C. (2011). *React. Funct. Polym.* 71: 187–194. https://doi.org/10.1016/j.reactfunctpolym.2010.12.002.

155 Lefay, C., Glé, D., Rollet, M. et al. (2011). *J. Polym. Sci., Part A: Polym. Chem.* 49: 803–813. https://doi.org/10.1002/pola.24496.

156 Bivigou-Koumba, A.M., Kristen, J., Laschewsky, A. et al. (2009). *Macromol. Chem. Phys.* 210: 565–578. https://doi.org/10.1002/macp.200800575.

157 Liu, X.H., Zhang, G.B., Lu, X.F. et al. (2006). *J. Polym. Sci., Part A: Polym. Chem.* 44: 490–498. https://doi.org/10.1002/pola.21169.

158 Chernikova, E., Terpugova, P., Filippov, A. et al. (2009). *Russ. J. Appl. Chem.* 82: 1882–1889. https://doi.org/10.1134/s1070427209100267.

159 Zamyshlyayeva, O.G., Ionychev, B.N., Frolova, A.I. et al. (2019). *Russ. J. Appl. Chem.* 92: 775–786. https://doi.org/10.1134/S1070427219060077.

160 Kaiser, A., Brandau, S., Klimpel, M., and Barner-Kowollik, C. (2010). *Macromol. Rapid Commun.* 31: 1616–1621. https://doi.org/10.1002/marc.201000162.

161 Serbin, A.V., Karaseva, E.N., Dunaeva, I.V. et al. (2011). *Polym. Sci., Ser. B* 53: 116–124. https://doi.org/10.1134/s1560090411030079.

162 Serbin, A., Karaseva, E., Chernikova, E. et al. (2010). *Macromol. Symp.* 296: 80–91. https://doi.org/10.1002/masy.201051013.

163 Freal-Saison, S., Save, M., Bui, C. et al. (2006). *Macromolecules* 39: 8632–8638. https://doi.org/10.1021/ma061572s.

164 Hu, Z.Q., Tao, M., and Zhang, Z.C. (2007). *Colloids Surf., A* 302: 307–311. https://doi.org/10.1016/j.colsurfa.2007.02.049.

165 Hu, Z.Q. and Zhang, Z.C. (2006). *Macromolecules* 39: 1384–1390.

166 Mogami, H. and Mori, H. (2020). *ACS Omega* 5: 3678–3688. https://doi.org/10.1021/acsomega.9b04282.

167 Na, H.-K., Kim, H., Son, J.G. et al. (2019). *Appl. Surf. Sci.* 483: 1069–1080. https://doi.org/10.1016/j.apsusc.2019.04.059.

168 Shibaev, V., Ivanov, M., Boiko, N., and Chernikova, E. (2009). *Dokl. Chem.* 427: 183–185. https://doi.org/10.1134/s0012500809080011.

169 O'Reilly, R. and Hansell, C. (2009). *Polymers* 1: 3–15. https://doi.org/10.3390/polym1010003.

170 Skrabania, K., Li, W., and Laschewsky, A. (2008). *Macromol. Chem. Phys.* 209: 1389–1403. https://doi.org/10.1002/macp.200800108.

171 Herfurth, C., Voll, D., Buller, J. et al. (2012). *J. Polym. Sci., Part A: Polym. Chem.* 50: 108–118. https://doi.org/10.1002/pola.24994.

172 Samakande, A., Sanderson, R.D., and Hartmann, P.C. (2009). *Eur. Polym. J.* 45: 649–657. https://doi.org/10.1016/j.eurpolymj.2008.11.014.

173 Skrabania, K., Miasnikova, A., Bivigou-Koumba, A.M. et al. (2011). *Polym. Chem.* 2: 2074–2083. https://doi.org/10.1039/C1PY00173F.

174 Schwabe, M., Rotzoll, R., Küchemann, S. et al. (2010). *Macromol. Chem. Phys.* 211: 1673–1677. https://doi.org/10.1002/macp.201000037.

175 Miyaji, H., Satoh, K., and Kamigaito, M. (2016). *Angew. Chem. Int. Ed.* 55: 1372–1376. https://doi.org/10.1002/anie.201509379.

176 Fei, P. and Cavicchi, K.A. (2010). *ACS Appl. Mater. Interfaces* 2: 2797–2803. https://doi.org/10.1021/am100481p.

177 Hinton, T.M., Guerrero-Sanchez, C., Graham, J.E. et al. (2012). *Biomaterials* 33: 7631–7642. https://doi.org/10.1016/j.biomaterials.2012.06.090.

178 Williams, E.G.L., Hutt, O.E., Hinton, T.M. et al. (2017). *Biomacromolecules* 18: 4099–4112. https://doi.org/10.1021/acs.biomac.7b01168.

179 Ojika, M., Satoh, K., and Kamigaito, M. (2017). *Angew. Chem. Int. Ed.* 56: 1789–1793. https://doi.org/10.1002/anie.201610768.

180 Hashimoto, H., Takeshima, H., Nagai, T. et al. (2019). *Polym. Degrad. Stab.* 161: 183–190. https://doi.org/10.1016/j.polymdegradstab.2019.01.025.

181 Chong, Y.K., Moad, G., Rizzardo, E. et al. (2007). *Macromolecules* 40: 9262–9271. https://doi.org/10.1021/ma071100t.

182 Rizzardo, E., Chen, M., Chong, B. et al. (2007). *Macromol. Symp.* 248: 104–116. https://doi.org/10.1002/masy.200750211.

183 Chong, B., Moad, G., Rizzardo, E. et al. (2006). *Aust. J. Chem.* 59: 755–762. https://doi.org/10.1071/CH06229.

184 Lee, T.-Y., Lin, Y.-J., Yu, C.-Y., and Chang, J.-F. (2010). *J. Appl. Polym. Sci.* 118: 3245–3254. https://doi.org/10.1002/app.32610.

185 Hornung, C.H., Postma, A., Saubern, S., and Chiefari, J. (2014). *Polymer* 55: 1427–1435. https://doi.org/10.1016/j.polymer.2014.01.023.

186 Ishitake, K., Satoh, K., Kamigaito, M., and Okamoto, Y. (2009). *Angew. Chem. Int. Ed.* 48: 1991–1994. https://doi.org/10.1002/anie.200805168.

187 Zhang, B., Lv, X., Zhu, A. et al. (2018). *Macromolecules* 51: 2776–2784. https://doi.org/10.1021/acs.macromol.8b00246.

188 Tao, Y., Satoh, K., and Kamigaito, M. (2011). *Macromol. Rapid Commun.* 32: 226–232. https://doi.org/10.1002/marc.201000614.

189 Satoh, K., Lee, D.-H., Nagai, K., and Kamigaito, M. (2013). *Macromol. Rapid Commun.* https://doi.org/10.1002/marc.201300638.

190 Huang, H., Sun, B., Huang, Y., and Niu, J. (2018). *J. Am. Chem. Soc.* 140: 10402–10406. https://doi.org/10.1021/jacs.8b05365.

191 Sivak, L., Subr, V., Tomala, J. et al. (2017). *Biomaterials* 115: 65–80. https://doi.org/10.1016/j.biomaterials.2016.11.013.

192 Haridharan, N., Bhandary, R., Ponnusamy, K., and Dhamodharan, R. (2012). *J. Polym. Sci., Part A: Polym. Chem.* 50: 1491–1502. https://doi.org/10.1002/pola.25890.

193 Fu, W., Bai, W., Jiang, S. et al. (2018). *Macromolecules* 51: 1674–1680. https://doi.org/10.1021/acs.macromol.7b02755.

194 Haridharan, N. and Dhamodharan, R. (2011). *J. Polym. Sci., Part A: Polym. Chem.* 49: 1021–1032. https://doi.org/10.1002/pola.24518.

195 Chen, M., Moad, G., and Rizzardo, E. (2009). *J. Polym. Sci., Part A: Polym. Chem.* 47: 6704–6714. https://doi.org/10.1002/pola.23711.

196 Luo, C., Fu, W., Li, Z., and Zhao, B. (2016). *Polymer* 101: 319–327. https://doi.org/10.1016/j.polymer.2016.08.091.

197 Häussler, M., Lok, P., Chen, M. et al. (2010). *Macromolecules* 43: 7101–7010. https://doi.org/10.1021/ma1008572.

198 Satoh, K., Matsuda, M., Nagai, K., and Kamigaito, M. (2010). *J. Am. Chem. Soc.* 132: 10003–10005. https://doi.org/10.1021/ja1042353.

199 Chong, Y.K., Moad, G., Rizzardo, E., and Thang, S.H. (2007). *Macromolecules* 40: 4446–4455. https://doi.org/10.1021/ma062919u.

200 He, S., Chen, L., Cui, J. et al. (2019). *J. Am. Chem. Soc.* 141: 19708–19714. https://doi.org/10.1021/jacs.9b08458.

201 Santha Kumar, A.R.S., Roy, M., and Singha, N.K. (2018). *Eur. Polym. J.* 107: 294–302. https://doi.org/10.1016/j.eurpolymj.2018.08.018.

202 Singha, N.K., Pramanik, N.B., Behera, P.K. et al. (2016). *Green Chem.* 18: 6115–6122. https://doi.org/10.1039/C6GC01677D.

203 Lokitz, B.S., Wei, J., Hinestrosa, J.P. et al. (2012). *Macromolecules* 45: 6438–6449. https://doi.org/10.1021/ma300991p.

204 Moad, G., Rizzardo, E., and Thang, S.H. (2011). *Strem Chem.* 25: 2–10.

205 Bekanova, M.Z., Neumolotov, N.K., Jablanovic, A.D. et al. (2019). *Polym. Sci., Ser. C* 61: 186–197. https://doi.org/10.1134/S1811238219010028.

206 Bekanova, M.Z., Neumolotov, N.K., Jablanović, A.D. et al. (2019). *Polym. Degrad. Stab.* 164: 18–27. https://doi.org/10.1016/j.polymdegradstab.2019.03.017.

207 Fu, Q., McKenzie, T.G., Tan, S. et al. (2015). *Polym. Chem.* 6: 5362–5368. https://doi.org/10.1039/C5PY00840A.

208 Shieh, Y.-T., Yeh, Y.-C., and Cheng, C.-C. (2019). *ACS Omega* 4: 15479–15487. https://doi.org/10.1021/acsomega.9b01728.

209 Kawatsuki, N., Shoji, H., Inada, Y. et al. (2014). *Polym. J.* 46: 85–88. https://doi.org/10.1038/pj.2013.59.

210 Janoschka, T., Teichler, A., Krieg, A. et al. (2012). *J. Polym. Sci., Part A: Polym. Chem.* 50: 1394–1407. https://doi.org/10.1002/pola.25907.

211 Cazares-Cortes, E., Baker, B.C., Nishimori, K. et al. (2019). *Macromolecules* 52: 5995–6004. https://doi.org/10.1021/acs.macromol.9b00412.
212 Zhu, Y. and Egap, E. (2020). *Polym. Chem.* 11: 1018–1024. https://doi.org/10.1039/C9PY01604J.
213 De Neve, J., Haven, J.J., Harrisson, S., and Junkers, T. (2019). *Angew. Chem. Int. Ed.* 58: 13869–13873. https://doi.org/10.1002/anie.201906842.
214 Fu, Q., Xie, K., McKenzie, T.G., and Qiao, G.G. (2017). *Polym. Chem.* 8: 1519–1526. https://doi.org/10.1039/C6PY01994C.
215 Kametani, Y., Tournilhac, F., Sawamoto, M., and Ouchi, M. (2020). *Angew. Chem. Int. Ed.* 59: 5193–5201. https://doi.org/10.1002/anie.201915075.
216 Abel, B.A. and McCormick, C.L. (2016). *Macromolecules* 49: 465–474. https://doi.org/10.1021/acs.macromol.5b02463.
217 Mann, J.L., Rossi, R.L., Smith, A.A.A., and Appel, E.A. (2019). *Macromolecules* 52: 9456–9465. https://doi.org/10.1021/acs.macromol.9b02109.
218 Ebata, K., Hashimoto, Y., Ebara, K. et al. (2019). *Polym. Chem.* 10: 835–842. https://doi.org/10.1039/C8PY01660G.
219 Moad, G., Chong, Y.K., Mulder, R. et al. (2009). New features of the mechanism of RAFT polymerization. In: *Controlled/Living Radical Polymerization. Progress in RAFT, NMP & OMRP*, ACS Symposium Series, vol. 1024 (ed. K. Matyjaszewski), 3–18. Washington, DC: American Chemical Society https://doi.org/10.1021/bk-2009-1024.ch001.
220 Pei, M., Ko, J.S., Shin, H. et al. (2018). *Macromol. Res.* 26: 942–949. https://doi.org/10.1007/s13233-018-6129-6.
221 Baddam, V., Aseyev, V., Hietala, S. et al. (2018). *Macromolecules* 51: 9681–9691. https://doi.org/10.1021/acs.macromol.8b01810.
222 Steinkoenig, J., Bloesser, F.R., Huber, B. et al. (2016). *Polym. Chem.* 7: 451–461. https://doi.org/10.1039/C5PY01320H.
223 Fokina, A., Lee, Y., Chang, J.H. et al. (2016). *Adv. Mater. Interfaces* 3: 1600279. https://doi.org/10.1002/admi.201600279.
224 Ferri, N., Ozaydin, G.B., Zeffiro, A. et al. (2018). *J. Polym. Sci., Part A: Polym. Chem.* 56: 1593–1599. https://doi.org/10.1002/pola.29044.
225 Nakabayashi, K., Matsumura, A., Abiko, Y., and Mori, H. (2016). *Macromolecules* 49: 1616–1629. https://doi.org/10.1021/acs.macromol.5b02573.
226 Nishikawa, T. and Ouchi, M. (2019). *Angew. Chem. Int. Ed.* 58: 12435–12439. https://doi.org/10.1002/anie.201905135.
227 Kametani, Y., Sawamoto, M., and Ouchi, M. (2018). *Angew. Chem. Int. Ed.* 57: 10905–10909. https://doi.org/10.1002/anie.201805049.
228 Yu, F., Wang, Y., Hang, Y. et al. (2019). *J. Polym. Sci., Part A: Polym. Chem.* 57: 2235–2242. https://doi.org/10.1002/pola.29512.
229 Benvenuta-Tapia, J.J., Tenorio-López, J.A., and Vivaldo-Lima, E. (2018). *Macromol. React. Eng.* 12: 1800003. https://doi.org/10.1002/mren.201800003.
230 Liu, R. and Lindsey, J.S. (2019). *ACS Macro Lett.* 8: 79–83. https://doi.org/10.1021/acsmacrolett.8b00907.
231 Barlow, K.J., Hao, X., Hughes, T.C. et al. (2014). *Polym. Chem.* 5: 722–732. https://doi.org/10.1039/c3py01015e.

232 Garmendia, S., Lawrenson, S.B., Arno, M.C. et al. (2019). *Macromol. Rapid Commun.* 40: 1900071. https://doi.org/10.1002/marc.201900071.

233 Sayyar, S., Moskowitz, J., Fox, B. et al. (2019). *J. Appl. Polym. Sci.* 136: 47932. https://doi.org/10.1002/app.47932.

234 Hou, J., Liu, Y., Liu, Y. et al. (2019). *Chem. Eng. Sci.* 201: 167–174. https://doi.org/10.1016/j.ces.2019.02.033.

235 Kumar, R., Lokitz, B.S., Sides, S.W. et al. (2015). *RSC Adv.* 5: 21336–21348. https://doi.org/10.1039/C5RA00974J.

236 Wang, S., Li, M., Zhang, H. et al. (2016). *J. Polym. Sci., Part A: Polym. Chem.* 54: 1633–1638. https://doi.org/10.1002/pola.28019.

237 Liu, J., Setijadi, E., Liu, Y. et al. (2010). *Aust. J. Chem.* 63: 1245–1250. https://doi.org/10.1071/ch1009110.1071/ch10.

238 Nelson, C.E., Gupta, M.K., Adolph, E.J. et al. (2012). *Biomaterials* 33: 1154–1161. https://doi.org/10.1016/j.biomaterials.2011.10.033.

239 Convertine, A.J., Benoit, D.S.W., Duvall, C.L. et al. (2009). *J. Controlled Release* 133: 221–229. https://doi.org/10.1016/j.jconrel.2008.10.004.

240 Shen, W., Qiu, Q., Wang, Y. et al. (2010). *Macromol. Rapid Commun.* 31: 1444–1448. https://doi.org/10.1002/marc.201000154.

241 Smith, A.E., Xu, X., Kirkland-York, S.E. et al. (2010). *Macromolecules* 43: 1210–1217. https://doi.org/10.1021/ma902378k.

242 Convertine, A.J., Diab, C., Prieve, M. et al. (2010). *Biomacromolecules* 11: 2904–2911. https://doi.org/10.1021/bm100652w.

243 Wais, U., Chennamaneni, L.R., Thoniyot, P. et al. (2018). *Polym. Chem.* 9: 4824–4839. https://doi.org/10.1039/C8PY01113C.

244 Liu, G., Qiu, Q., Shen, W., and An, Z. (2011). *Macromolecules* 44: 5237–5245. https://doi.org/10.1021/ma200984h.

245 Zhang, X., Boissé, S.p., Zhang, W. et al. (2011). *Macromolecules* 44: 4149–4158. https://doi.org/10.1021/ma2005926.

246 Qiu, Q., Liu, G., and An, Z. (2011). *Chem. Commun.* 47: 12685–12687. https://doi.org/10.1039/C1CC15679A.

247 Shen, W., Chang, Y., Liu, G. et al. (2011). *Macromolecules* 44: 2524–2530. https://doi.org/10.1021/ma200074n.

248 Crownover, E., Duvall, C.L., Convertine, A. et al. (2011). *J. Controlled Release* 155: 167–174. https://doi.org/10.1016/j.jconrel.2011.06.013.

249 Flores, J.D., Shin, J., Hoyle, C.E., and McCormick, C.L. (2010). *Polym. Chem.* 1: 213–220. https://doi.org/10.1039/B9PY00294D.

250 Pan, X., Zhang, F., Choi, B. et al. (2019). *Eur. Polym. J.* 115: 166–172. https://doi.org/10.1016/j.eurpolymj.2019.03.016.

251 Treat, N.J., Smith, D., Teng, C. et al. (2012). *ACS Macro Lett.* 1: 100–104. https://doi.org/10.1021/mz200012p.

252 Holley, A.C., Ray, J.G., Wan, W. et al. (2013). *Biomacromolecules* 14: 3793–3799. https://doi.org/10.1021/bm401205y.

253 Hou, Y., Guo, Y., Qian, S. et al. (2019). *Polymer* 167: 159–166. https://doi.org/10.1016/j.polymer.2019.02.008.

254 Crownover, E.F., Convertine, A.J., and Stayton, P.S. (2011). *Polym. Chem.* 2: 1499–1504. https://doi.org/10.1039/C0PY00071J.

255 Allen, M.H., Hemp, S.T., Smith, A.E., and Long, T.E. (2012). *Macromolecules* 45: 3669–3676. https://doi.org/10.1021/ma300543h.

256 Paslay, L.C., Abel, B.A., Brown, T.D. et al. (2012). *Biomacromolecules* https://doi.org/10.1021/bm3007083.

257 Luzon, M., Boyer, C., Peinado, C. et al. (2010). *J. Polym. Sci., Part A: Polym. Chem.* 48: 2783–2792. https://doi.org/10.1002/pola.24027.

258 Parsons, K.H., Holley, A.C., Munn, G.A. et al. (2016). *Polym. Chem.* 7: 6044–6054. https://doi.org/10.1039/C6PY01048B.

259 Johnson, R.N., Burke, R.S., Convertine, A.J. et al. (2010). *Biomacromolecules* 11: 3007–3013. https://doi.org/10.1021/bm100806h.

260 Smith, A.E., Xu, X., Savin, D.A., and McCormick, C.L. (2010). *Polym. Chem.* 1: 628–630.

261 Zhang, W., D'Agosto, F., Boyron, O. et al. (2011). *Macromolecules* 44: 7584–7593. https://doi.org/10.1021/ma201515n.

262 Zhang, X., Rieger, J., and Charleux, B. (2012). *Polym. Chem.* 3: 1502–1509. https://doi.org/10.1039/C1PY00060H.

263 Zhang, X., Boisse, S., Bui, C. et al. (2012). *Soft Matter* 8: 1130–1141. https://doi.org/10.1039/C1SM06598J.

264 Huang, Z., Wang, R., Chen, Y. et al. (2019). *J. Mater. Res.* 34: 3011–3019. https://doi.org/10.1557/jmr.2019.163.

265 Engström, J., Benselfelt, T., Wågberg, L. et al. (2019). *Nanoscale* 11: 4287–4302. https://doi.org/10.1039/C8NR08057G.

266 Wang, H., Vendrame, L., Fliedel, C. et al. (2020). *Macromolecules* https://doi.org/10.1021/acs.macromol.9b02582.

267 Pearson, S., Pavlovic, M., Augé, T. et al. (2018). *Macromolecules* 51: 3953–3966. https://doi.org/10.1021/acs.macromol.8b00541.

268 Klimkevicius, V. and Makuska, R. (2017). *Eur. Polym. J.* 86: 94–105. https://doi.org/10.1016/j.eurpolymj.2016.11.026.

269 Klimkevicius, V., Steponaviciute, M., and Makuska, R. (2019). *Eur. Polym. J.*: 109356. https://doi.org/10.1016/j.eurpolymj.2019.109356.

270 Zhao, W., Gody, G., Dong, S. et al. (2014). *Polym. Chem.* 5: 6990–7003. https://doi.org/10.1039/C4PY00855C.

271 Zhao, W., Ta, H.T., Zhang, C., and Whittaker, A.K. (2017). *Biomacromolecules* 18: 1145–1156. https://doi.org/10.1021/acs.biomac.6b01788.

272 Sheehan, M.T., Farnham, W.B., Okazaki, H. et al. (2008). *Proc. SPIE* 6923: 69232E/69231–69232E/69239. https://doi.org/10.1117/12.772115.

273 Hosta-Rigau, L., Chandrawati, R., Saveriades, E. et al. (2010). *Biomacromolecules* 11: 3548–3555. https://doi.org/10.1021/bm101020e.

274 Shi, P., Qu, Y., Liu, C. et al. (2016). *ACS Macro Lett.* 5: 88–93. https://doi.org/10.1021/acsmacrolett.5b00928.

275 Cao, H., Wang, G., Xue, Y. et al. (2019). *ACS Macro Lett.* 8: 616–622. https://doi.org/10.1021/acsmacrolett.9b00320.

276 Yu, L., Zhang, Y., Dai, X. et al. (2019). *Chem. Commun.* 55: 11920–11923. https://doi.org/10.1039/C9CC05812E.
277 Riber, C.F., Andersen, A.H.F., Rolskov, L.A. et al. (2017). *ACS Macro Lett.* 6: 935–940. https://doi.org/10.1021/acsmacrolett.7b00471.
278 Shanmugam, S., Cuthbert, J., Flum, J. et al. (2019). *Polym. Chem.* 10: 2477–2483. https://doi.org/10.1039/C9PY00213H.
279 Ma, Y. and Lodge, T.P. (2016). *Macromolecules* 49: 3639–3646. https://doi.org/10.1021/acs.macromol.6b00315.
280 Dai, X., Yu, L., Zhang, Y. et al. (2019). *Macromolecules* 52: 7468–7476. https://doi.org/10.1021/acs.macromol.9b01689.
281 Pal, S., Brooks, W.L.A., Dobbins, D.J., and Sumerlin, B.S. (2016). *Macromolecules* 49: 9396–9405. https://doi.org/10.1021/acs.macromol.6b02079.
282 Zhang, Y., Yu, L., Dai, X. et al. (2019). *ACS Macro Lett.* 8: 1102–1109. https://doi.org/10.1021/acsmacrolett.9b00509.
283 Nitschke, A., Riemann, L., Kollenbach, L. et al. *Macromol. Chem. Phys.*: 1900345. https://doi.org/10.1002/macp.201900345.
284 Concellón, A., Zentner, C.A., and Swager, T.M. (2019). *J. Am. Chem. Soc.* 141: 18246–18255. https://doi.org/10.1021/jacs.9b09216.
285 Saha, P., Kather, M., Banerjee, S.L. et al. (2019). *Eur. Polym. J.* 118: 195–204. https://doi.org/10.1016/j.eurpolymj.2019.05.063.
286 Kumar, S., Roy, S.G., and De, P. (2012). *Polym. Chem.* 3: 1239–1248. https://doi.org/10.1039/C2PY00607C.
287 Hornung, C.H., Guerrero-Sanchez, C., Brasholz, M. et al. (2011). *Org. Proc. Res. Dev.* 15: 593–601. https://doi.org/10.1021/op1003314.
288 Fu, C., Huang, Z., Hawker, C.J. et al. (2017). *Polym. Chem.* 8: 4637–4643. https://doi.org/10.1039/C7PY00713B.
289 Jiang, X., Li, R., Feng, C. et al. (2017). *Polym. Chem.* 8: 2773–2784. https://doi.org/10.1039/C7PY00091J.
290 Gaballa, H. and Theato, P. (2019). *Biomacromolecules* 20: 871–881. https://doi.org/10.1021/acs.biomac.8b01508.
291 Nash, M.A., Yager, P., Hoffman, A.S., and Stayton, P.S. (2010). *Bioconjugate Chem.* 21: 2197–2204. https://doi.org/10.1021/bc100180q.
292 Asadujjaman, A., Ahmadi, V., Yalcin, M. et al. (2017). *Polym. Chem.* 8: 3140–3153. https://doi.org/10.1039/C7PY00539C.
293 Rosencrantz, S., Tang, J.S.J., Schulte-Osseili, C. et al. (2019). *Macromol. Chem. Phys.* 220: 1900293. https://doi.org/10.1002/macp.201900293.
294 Chen, C. and Thang, S.H. (2018). *Polym. Chem.* 9: 1780–1786. https://doi.org/10.1039/C7PY01887H.
295 Biswas, Y., Maji, T., Dule, M., and Mandal, T.K. (2016). *Polym. Chem.* 7: 867–877. https://doi.org/10.1039/C5PY01574J.
296 Enriquez-Medrano, F.J., Soriano-Corral, F., Acuna-Vazquez, P. et al. (2014). *J. Mex. Chem. Soc.* 58: 194–201.
297 Rosales-Guzmán, M., Pérez-Camacho, O., Guerrero-Sánchez, C. et al. (2019). *ACS Comb. Sci.* https://doi.org/10.1021/acscombsci.9b00110.

298 Contreras-López, D., Fuentes-Ramírez, R., Albores-Velasco, M. et al. (2018). *J. Polym. Sci., Part A: Polym. Chem.* 56: 2463–2474. https://doi.org/10.1002/pola.29221.

299 Cuthbert, J., Martinez, M.R., Sun, M. et al. (2019). *Macromol. Rapid Commun.* 40: 1800876. https://doi.org/10.1002/marc.201800876.

300 Blackburn, C., Tai, H., Salerno, M. et al. (2019). *Eur. Polym. J.* 120: 109259. https://doi.org/10.1016/j.eurpolymj.2019.109259.

301 Li, L., Xu, Z., Sun, W. et al. (2020). *J. Membr. Sci.* 598: 117661. https://doi.org/10.1016/j.memsci.2019.117661.

302 Heraud, C., Basuki, J., Hughes, T.C., and Mueller, M. (2019). *Macromol. Rapid Commun.* 40: 1900278. https://doi.org/10.1002/marc.201900278.

303 Enke, M., Jehle, F., Bode, S. et al. (2017). *Macromol. Chem. Phys.* 218: 1600458. https://doi.org/10.1002/macp.201600458.

304 Sun, Z. and Luo, Y. (2011). *Soft Matter* 7: 871–875. https://doi.org/10.1039/C0SM00983K.

305 Chen, H. and Luo, Y. (2011). *Macromol. Chem. Phys.* 212: 737–743. https://doi.org/10.1002/macp.201000664.

306 Liang, S., Li, X., Wang, W.-J. et al. (2016). *Macromolecules* 49: 752–759. https://doi.org/10.1021/acs.macromol.5b02596.

307 Gonzato, C., Pasetto, P., Bedoui, F. et al. (2014). *Polym. Chem.* 5: 1313–1322. https://doi.org/10.1039/c3py01246h.

308 Prasher, A., Loynd, C.M., Tuten, B.T. et al. (2016). *J. Polym. Sci., Part A: Polym. Chem.* 54: 209–217. https://doi.org/10.1002/pola.27942.

309 Sheehan, M.T., Farnham, W.B., Chambers, C.R. et al. (2011). *Proc. SPIE* 7972 https://doi.org/10.1117/12.882960.

310 Sar, P., Roy, S.G., De, P., and Ghosh, S. *Macromol. Mater. Eng.*: 1900809. https://doi.org/10.1002/mame.201900809.

311 Asadujjaman, A., Ahmadi, V., Michel Claude Franc, A., and Bertin, A. (2019). *J. Polym. Sci., Part A: Polym. Chem.* 57: 2064–2073. https://doi.org/10.1002/pola.29474.

312 Lin, S., Das, A., and Theato, P. (2017). *Polym. Chem.* 8: 1206–1216. https://doi.org/10.1039/C6PY01996J.

313 Gaballa, H., Shang, J., Meier, S., and Theato, P. (2019). *J. Polym. Sci., Part A: Polym. Chem.* 57: 422–431. https://doi.org/10.1002/pola.29226.

314 Shanmugam, S., Xu, J., and Boyer, C. (2017). *Macromolecules* 50: 1832–1846. https://doi.org/10.1021/acs.macromol.7b00192.

315 Aerts, A., Lewis, R.W., Zhou, Y. et al. (2018). *Macromol. Rapid Commun.* 39: 1800240 (7 pp). https://doi.org/10.1002/marc.201800240.

316 Zhou, Y., Zhang, Z., Reese, C. et al. (2020). *Macromol. Rapid Commun.* 41: 1900478 (6 pp). https://doi.org/10.1002/marc.201900478.

317 Das, D., Gerboth, D., Postma, A. et al. (2016). *Polym. Chem.* 7: 6133–6143. https://doi.org/10.1039/C6PY01172A.

318 Weaver, L.G., Stockmann, R., Thang, S.H., and Postma, A. (2017). *RSC Adv.* 7: 31033–31041. https://doi.org/10.1039/C7RA04723A.

319 Semsarilar, M., Ladmiral, V., Blanazs, A., and Armes, S.P. (2011). *Langmuir* 28: 914–922. https://doi.org/10.1021/la203991y.
320 Farooq, U., Upadhyaya, L., Shakeel, A. et al. (2020). *J. Membr. Sci.* 611: 118181. https://doi.org/10.1016/j.memsci.2020.118181.
321 Rubio, A., Desnos, G., and Semsarilar, M. (2018). *Macromol. Chem. Phys.* 219: 1800351. https://doi.org/10.1002/macp.201800351.
322 Hunter, S.J., Penfold, N.J.W., Chan, D.H. et al. (2020). *Langmuir* 36: 769–780. https://doi.org/10.1021/acs.langmuir.9b03389.
323 Kim, Y.-Y., Fielding, L.A., Kulak, A.N. et al. (2018). *Chem. Mater.* 30: 7091–7099. https://doi.org/10.1021/acs.chemmater.8b02912.
324 Cornel, E.J., Smith, G.N., Rogers, S.E. et al. (2020). *Soft Matter* 16: 3657–3668. https://doi.org/10.1039/C9SM02425E.
325 Cockram, A.A., Bradley, R.D., Lynch, S.A. et al. (2018). *React. Chem. Eng.* 3: 645–657. https://doi.org/10.1039/C8RE00066B.
326 Parker, B.R., Derry, M.J., Ning, Y., and Armes, S.P. (2020). *Langmuir* 36: 3730–3736. https://doi.org/10.1021/acs.langmuir.0c00211.
327 Rymaruk, M.J., O'Brien, C.T., Brown, S.L. et al. (2020). *Macromolecules* 53: 1785–1794. https://doi.org/10.1021/acs.macromol.9b02697.
328 Guerre, M., Ameduri, B., and Ladmiral, V. (2016). *Polym. Chem.* 7: 441–450. https://doi.org/10.1039/C5PY01651G.
329 Wang, K., Peng, H., Thurecht, K.J. et al. (2016). *Polym. Chem.* 7: 1059–1069. https://doi.org/10.1039/C5PY01707F.
330 Das, P.K., Dean, D.N., Fogel, A.L. et al. (2017). *Biomacromolecules* 18: 3359–3366. https://doi.org/10.1021/acs.biomac.7b01007.
331 Golden, A.L., Battrell, C.F., Pennell, S. et al. (2010). *Bioconjugate Chem.* 21: 1820–1826. https://doi.org/10.1021/bc100169y.
332 Lokitz, B.S., Stempka, J.E., York, A.W. et al. (2006). *Aust. J. Chem.* 59: 749–754. https://doi.org/10.1071/CH06264.
333 Lokitz, B.S., York, A.W., Stempka, J.E. et al. (2007). *Macromolecules* 40: 6473–6480. https://doi.org/10.1021/ma070921v.
334 Huang, H., Wang, W., Zhou, Z. et al. (2019). *J. Am. Chem. Soc.* 141: 12493–12497. https://doi.org/10.1021/jacs.9b05568.
335 Flores, J.D., Xu, X., Treat, N.J., and McCormick, C.L. (2009). *Macromolecules* 42: 4941–4945. https://doi.org/10.1021/ma900517w.
336 Carmean, R.N., Figg, C.A., Becker, T.E., and Sumerlin, B.S. (2016). *Angew. Chem. Int. Ed.* 55: 8624–8629. https://doi.org/10.1002/anie.201603129.
337 Carmean, R.N., Becker, T.E., Sims, M.B., and Sumerlin, B.S. (2017). *Chem* 2: 93–101. https://doi.org/10.1016/j.chempr.2016.12.007.
338 Ouyang, L., Wang, L., and Schork, F.J. (2010). *Macromol. Chem. Phys.* 211: 1977–1983. https://doi.org/10.1002/macp.201000213.
339 Appel, E.A., Forster, R.A., Koutsioubas, A. et al. (2014). *Angew. Chem. Int. Ed.* 53: 10038–10043. https://doi.org/10.1002/anie.201403192.
340 Coulston, R.J., Jones, S.T., Lee, T.-C. et al. (2011). *Chem. Commun.* 47: 164–166. https://doi.org/10.1039/C0CC03250F.

341 Haridharan, N., Ponnusamy, K., and Dhamodharan, R. (2010). *J. Polym. Sci., Part A: Polym. Chem.* 48: 5329–5338. https://doi.org/10.1002/pola.24333.

342 Bobrin, V.A., Chen, S.-P.R., Jia, Z., and Monteiro, M.J. (2018). *Biomacromolecules* 19: 4703–4709. https://doi.org/10.1021/acs.biomac.8b01558.

343 Bobrin, V.A. and Monteiro, M.J. (2015). *J. Am. Chem. Soc.* 137: 15652–15655. https://doi.org/10.1021/jacs.5b11037.

344 Skrabania, K., Laschewsky, A., Berlepsch, H.v., and Böttcher, C. (2009). *Langmuir* 25: 7594–7601. https://doi.org/10.1021/la900253j.

345 Li, H., Bapat, A.P., Li, M., and Sumerlin, B.S. (2011). *Polym. Chem.* 2: 323–327. https://doi.org/10.1039/C0PY00178C.

346 Bray, C., Peltier, R., Kim, H. et al. (2017). *Polym. Chem.* 8: 5513–5524. https://doi.org/10.1039/C7PY01062A.

347 Gurnani, P., Bray, C.P., Richardson, R.A.E. et al. (2019). *Macromol. Rapid Commun.* 40: 1800314. https://doi.org/10.1002/marc.201800314.

348 Zhang, T., Wu, Y., Pan, X. et al. (2009). *Eur. Polym. J.* 45: 1625–1633. https://doi.org/10.1016/j.eurpolymj.2009.03.016.

349 Stoffelbach, F., Tibiletti, L., Rieger, J., and Charleux, B. (2008). *Macromolecules* 41: 7850–7856. https://doi.org/10.1021/ma800965r.

350 Zhou, Y. and Kasi, R.M. (2008). *J. Polym. Sci., Part A: Polym. Chem.* 46: 6801–6809. https://doi.org/10.1002/pola.22988.

351 Puttick, S., Irvine, D.J., Licence, P., and Thurecht, K.J. (2009). *J. Mater. Chem.* 19: 2679–2682. https://doi.org/10.1039/b817181p.

352 Chakrabarty, A. and Teramoto, Y. (2020). *ACS Sustain. Chem. Eng.* 8: 4623–4632. https://doi.org/10.1021/acssuschemeng.0c00687.

353 Cao, H., Qin, Y., Zhuo, C. et al. (2019). *ACS Catal.* 9: 8669–8676. https://doi.org/10.1021/acscatal.9b02741.

354 Zhang, Y., He, H., Gao, C., and Wu, J. (2009). *Langmuir* 25: 5814–5824. https://doi.org/10.1021/la803906s.

355 He, H., Zhang, Y., Gao, C., and Wu, J. (2009). *Chem. Commun.*: 1655–1657. https://doi.org/10.1039/B821280E.

356 Moore, B.L. and O'Reilly, R.K. (2012). *J. Polym. Sci., Part A: Polym. Chem.* 50: 3567–3574. https://doi.org/10.1002/pola.26141.

357 Mya, K.Y., Lin, E.M.J., Gudipati, C.S. et al. (2010). *J. Phys. Chem. B* 114: 9119–9127. https://doi.org/10.1021/jp102731e.

358 Hotchkiss, J.W., Lowe, A.B., and Boyes, S.G. (2007). *Chem. Mater.* 19: 6–13. https://doi.org/10.1021/cm0622912.

359 He, W.-D., Sun, X.-L., Wan, W.-M., and Pan, C.-Y. (2011). *Macromolecules* 44: 3358–3365. https://doi.org/10.1021/ma2000674.

360 He, S.-J., Zhang, Y., Cui, Z.-H. et al. (2009). *Eur. Polym. J.* 45: 2395–2401. https://doi.org/10.1016/j.eurpolymj.2009.04.030.

361 Germack, D.S. and Wooley, K.L. (2007). *Macromol. Chem. Phys.* 208: 2481–2491. https://doi.org/10.1002/macp.200700433.

362 Li, Y., Akiba, I., Harrisson, S., and Wooley, K.L. (2008). *Adv. Funct. Mater.* 18: 551–559. https://doi.org/10.1002/adfm.200700532.

363 Grignard, B., Jerome, C., Calberg, C. et al. (2007). *J. Polym. Sci., Part A: Polym. Chem.* 45: 1499–1506. https://doi.org/10.1002/pola.21920.
364 Boujioui, F., Damerow, H., Zhuge, F., and Gohy, J.-F. *Macromol. Chem. Phys.*: 1900556. https://doi.org/10.1002/macp.201900556.
365 Deane, O.J., Musa, O.M., Fernyhough, A., and Armes, S.P. (2020). *Macromolecules* 53: 1422–1434. https://doi.org/10.1021/acs.macromol.9b02394.
366 Hadadpour, M., Liu, Y., Chadha, P., and Ragogna, P.J. (2014). *Macromolecules* 47: 6207–6217. https://doi.org/10.1021/ma501323q.
367 Cao, Y., Zhu, X.X., Luo, J.T., and Liu, H.Y. (2007). *Macromolecules* 40: 6481–6488. https://doi.org/10.1021/ma0628230.
368 Cao, Y. and Zhu, X.X. (2007). *Can. J. Chem.* 85: 407–411. https://doi.org/10.1139/V07-043.
369 An, Z.S., Shi, Q.H., Tang, W. et al. (2007). *J. Am. Chem. Soc.* 129: 14493–14499. https://doi.org/10.1021/ja0756974.
370 Lai, J.J., Hoffman, J.M., Ebara, M. et al. (2007). *Langmuir* 23: 7385–7391. https://doi.org/10.1021/la062527g.
371 Cao, Y., Zhao, N., Wu, K., and Zhu, X.X. (2009). *Langmuir* 25: 1699–1704. https://doi.org/10.1021/la802971s.
372 He, J., Yan, B., Tremblay, L., and Zhao, Y. (2010). *Langmuir* 27: 436–444. https://doi.org/10.1021/la1040322.
373 Diehl, C., Laurino, P., Azzouz, N., and Seeberger, P.H. (2010). *Macromolecules* 43: 10311–10314. https://doi.org/10.1021/ma1025253.
374 Roy, D., Ullah, A., and Sumerlin, B.S. (2009). *Macromolecules* 42: 7701–7708. https://doi.org/10.1021/ma901471k.
375 Savelyeva, X., Li, L., and Marić, M. (2015). *J. Polym. Sci., Part A: Polym. Chem.* 53: 59–67. https://doi.org/10.1002/pola.27437.
376 Li, M., De, P., Li, H., and Sumerlin, B.S. (2010). *Polym. Chem.* 1: 854–859. https://doi.org/10.1039/C0PY00025F.
377 Sharma, N., Rajan, R., Makhaik, S., and Matsumura, K. (2019). *ACS Omega* 4: 12186–12193. https://doi.org/10.1021/acsomega.9b01409.
378 Roy, D., Cambre, J.N., and Sumerlin, B.S. (2009). *Chem. Commun.*: 2106–2108. https://doi.org/10.1039/b900374f.
379 Rajan, R. and Matsumura, K. (2017). *Macromol. Rapid Commun.* 38: 1700478. https://doi.org/10.1002/marc.201700478.
380 Cheng, C., Sun, G., Khoshdel, E., and Wooley, K.L. (2007). *J. Am. Chem. Soc.* 129: 10086–10087. doi: https://doi.org/10.1021/ja073541y.
381 Xu, S., Huang, J., Xu, S., and Luo, Y. (2013). *Polymer* 54: 1779–1785. https://doi.org/10.1016/j.polymer.2013.02.007.
382 Potzsch, R., Fleischmann, S., Tock, C. et al. (2011). *Macromolecules* 44: 3260–3269. https://doi.org/10.1021/ma2000724.
383 Choi, J.W., Carter, M.C.D., Wei, W. et al. (2016). *Macromolecules* 49: 8177–8186. https://doi.org/10.1021/acs.macromol.6b01734.
384 Carter, M.C.D., Jennings, J., Speetjens, F.W. et al. (2016). *Macromolecules* 49: 6268–6276. https://doi.org/10.1021/acs.macromol.6b01268.

385 Speetjens, F.W., Carter, M.C.D., Kim, M. et al. (2014). *ACS Macro Lett.* 3: 1178–1182. https://doi.org/10.1021/mz500654a.
386 Luo, Y., Wang, X., Li, B.-G., and Zhu, S. (2011). *Macromolecules* 44: 221–229. https://doi.org/10.1021/ma102378w.
387 Zhang, H., Deng, J., Lu, L., and Cai, Y. (2007). *Macromolecules* 40: 9252–9261. https://doi.org/10.1021/ma071287o.
388 Riedel, M., Stadermann, J., Komber, H. et al. (2011). *Eur. Polym. J.* 47: 675–684. https://doi.org/10.1016/j.eurpolymj.2010.10.010.
389 Kim, H., Kang, Y.J., Kang, S., and Kim, K.T. (2012). *J. Am. Chem. Soc.* 134: 4030–4033. https://doi.org/10.1021/ja211728x.
390 Dong, Z.M., Liu, X.H., Lin, Y., and Li, Y.S. (2008). *J. Polym. Sci., Part A: Polym. Chem.* 46: 6023–6034. https://doi.org/10.1002/pola.22913.
391 Ma, J., Cheng, C., Sun, G., and Wooley, K.L. (2008). *Macromolecules* 41: 9080–9089. https://doi.org/10.1021/ma802057u.
392 Ma, J., Cheng, C., and Wooley, K.L. (2009). *Macromolecules* 42: 1565–1573. https://doi.org/10.1021/ma8024255.
393 Stadermann, J., Fleischmann, S., Messerschmidt, M. et al. (2009). *Macromol. Symp.* 275–276: 35–42. https://doi.org/10.1002/masy.200950104.
394 Wan, W.-M. and Pan, C.-Y. (2010). *Polym. Chem.* 1: 1475–1484. https://doi.org/10.1039/C0PY00124D.
395 Bozovic-Vukic, J., Manon, H.T., Meuldijk, J. et al. (2007). *Macromolecules* 40: 7132–7139. https://doi.org/10.1021/ma070789z.
396 Gramlich, W.M., Theryo, G., and Hillmyer, M.A. (2012). *Polym. Chem.* 3: 1510–1516.
397 Germack, D.S. and Wooley, K.L. (2007). *J. Polym. Sci., Part A: Polym. Chem.* 45: 4100–4108. https://doi.org/10.1002/pola.22226.
398 Mulvenna, R.A., Prato, R.A., Phillip, W.A., and Boudouris, B.W. (2015). *Macromol. Chem. Phys.* 216: 1831–1840. https://doi.org/10.1002/macp.201500201.
399 Lokitz, B.S., Messman, J.M., Hinestrosa, J.P. et al. (2009). *Macromolecules* 42: 9018–9026. https://doi.org/10.1021/ma9015399.
400 Kim, J.S., Sirois, A.R., Vazquez Cegla, A.J. et al. (2019). *Bioconjugate Chem.* 30: 1220–1231. https://doi.org/10.1021/acs.bioconjchem.9b00155.
401 Bartels, J.W., Billings, P.L., Ghosh, B. et al. (2009). *Langmuir* 25: 9535–9544. https://doi.org/10.1021/la900753r.
402 Bickerton, S., Jiwpanich, S., and Thayumanavan, S. (2012). *Mol. Pharm.* 9: 3569–3578. https://doi.org/10.1021/mp3004226.
403 Ormategui, N., García, I., Padro, D. et al. (2012). *Soft Matter* 8: 734–740. https://doi.org/10.1039/C1SM06310C.
404 Zhu, Y., Zhou, Y., Chen, Z. et al. (2012). *Polymer* 53: 3566–3576. https://doi.org/10.1016/j.polymer.2012.05.063.
405 Boissé, S., Rieger, J., Di-Cicco, A. et al. (2009). *Macromolecules* 42: 8688–8696. https://doi.org/10.1021/ma9018137.
406 Boisse, S., Rieger, J., Belal, K. et al. (2010). *Chem. Commun.* 46: 1950–1952. https://doi.org/10.1039/B923667H.

407 Kaur, B., D'Souza, L., Slater, L.A. et al. (2011). *Macromolecules* 44: 3810–3816. https://doi.org/10.1021/ma200357u.

408 Grogna, M., Cloots, R., Luxen, A. et al. (2011). *Polym. Chem.* 2: 2316–2327. https://doi.org/10.1039/C1PY00198A.

409 Nilles, K. and Theato, P. (2011). *Polym. Chem.* 2: 376–384. https://doi.org/10.1039/C0PY00261E.

410 Lou, Q., Kishpaugh, M.A., and Shipp, D.A. (2010). *J. Polym. Sci., Part A: Polym. Chem.* 48: 943–951. https://doi.org/10.1002/pola.23850.

411 Jackson, A.W. and Fulton, D.A. (2012). *Macromolecules* 45: 2699–2708. https://doi.org/10.1021/ma202721s.

412 Li, H., Liu, J., Zheng, X. et al. (2016). *J. Polym. Res.* 23: 102. https://doi.org/10.1007/s10965-016-0996-3.

413 Ma, J., Cheng, C., Sun, G., and Wooley, K.L. (2008). *J. Polym. Sci., Part A: Polym. Chem.* 46: 3488–3498. https://doi.org/10.1002/pola.22682.

414 Gonçalves, M.A.D., Pinto, V.D., Dias, R.C.S. et al. (2013). *Macromol. Symp.* 333: 273–285. https://doi.org/10.1002/masy.201300046.

415 Stadermann, J., Riedel, M., and Voit, B. (2013). *Macromol. Chem. Phys.* 214: 263–271. https://doi.org/10.1002/macp.201200409.

416 Espeel, P., Goethals, F., Stamenovic, M.M. et al. (2012). *Polym. Chem.* 3: 1007–1015. https://doi.org/10.1039/C2PY00565D.

417 Ma, X., Lan, X., Wu, L. et al. (2020). *Eur. Polym. J.* 123: 109446. https://doi.org/10.1016/j.eurpolymj.2019.109446.

418 Li, D., Jiang, J., Huang, Q. et al. (2016). *Polym. Chem.* 7: 3444–3450. https://doi.org/10.1039/C6PY00490C.

419 Li, D., Munyentwali, A., Wang, G. et al. (2015). *Dyes Pigm.* 117: 92–99. https://doi.org/10.1016/j.dyepig.2015.02.009.

420 Hansell, C.F. and O'Reilly, R.K. (2012). *ACS Macro Lett.* 1: 896–901. https://doi.org/10.1021/mz300230c.

421 Germack, D.S., Harrisson, S., Brown, G.O., and Wooley, K.L. (2006). *J. Polym. Sci., Part A: Polym. Chem.* 44: 5218–5228. https://doi.org/10.1002/pola.21614.

422 Yin, X., Hoffman, A.S., and Stayton, P.S. (2006). *Biomacromolecules* 7: 1381–1385. https://doi.org/10.1021/bm0507812.

423 Rowe, M.D., Thamm, D.H., Kraft, S.L., and Boyes, S.G. (2009). *Biomacromolecules* 10: 983–993. https://doi.org/10.1021/bm900043e.

424 Sudo, Y., Kawai, R., Sakai, H. et al. (2018). *Langmuir* 34: 653–662. https://doi.org/10.1021/acs.langmuir.7b04213.

425 Yodice, R., Johnson, J.R., Beebe, R.L. et al. (2014). Process for making substituted trithiocarbonate derivatives. (The Lubrizol Corporation, USA), US8791286B2.

426 Moriceau, G., Gody, G., Hartlieb, M. et al. (2017). *Polym. Chem.* 8: 4152–4161. https://doi.org/10.1039/C7PY00787F.

427 Aksakal, S. and Remzi Becer, C. (2016). *Polym. Chem.* 7: 7011–7018. https://doi.org/10.1039/C6PY01721E.

428 Moriceau, G., Tanaka, J., Lester, D. et al. (2019). *Macromolecules* 52: 1469–1478. https://doi.org/10.1021/acs.macromol.8b02231.

429 Yusa, S.-I., Endo, T., and Ito, M. (2009). *J. Polym. Sci., Part A: Polym. Chem.* 47: 6827–6838. https://doi.org/10.1002/pola.23722.

430 Legge, T.M., Slark, A.T., and Perrier, S. (2006). *J. Polym. Sci., Part A: Polym. Chem.* 44: 6980–6987. https://doi.org/10.1002/pola.21803.

431 Goto, F., Ishihara, K., Iwasaki, Y. et al. (2011). *Polymer* 52: 2810–2818. https://doi.org/10.1016/j.polymer.2011.04.033.

432 Gemici, H., Legge, T.M., Whittaker, M. et al. (2007). *J. Polym. Sci., Part A: Polym. Chem.* 45: 2334–2340. https://doi.org/10.1002/pola.21985.

433 Iwasaki, Y., Sakiyama, M., Fujii, S., and Yusa, S.-i. (2013). *Chem. Commun.* 49: 7824–7826. https://doi.org/10.1039/C3CC44072A.

434 Khimani, M., Yusa, S., Nagae, A. et al. (2015). *Eur. Polym. J.* 69: 96–109. https://doi.org/10.1016/j.eurpolymj.2015.05.027.

435 Yee, M.M., Tsubone, M., Morita, T. et al. (2016). *J. Lumin.* 176: 318–323. https://doi.org/10.1016/j.jlumin.2016.02.043.

436 Khimani, M., Yusa, S.-i., Aswal, V.K., and Bahadur, P. (2019). *J. Mol. Liq.* 276: 47–56. https://doi.org/10.1016/j.molliq.2018.11.135.

437 Matsuoka, H., Moriya, S., and Yusa, S.-i. (2018). *Colloid Polym. Sci.* 296: 77–88. https://doi.org/10.1007/s00396-017-4217-3.

438 Rizzardo, E., Chiefari, J., Mayadunne, R.T.A. et al. (2000). Synthesis of defined polymers by reversible addition fragmentation chain transfer. In: *Controlled/Living Radical Polymerization*, ACS Symposium Series, vol. 768 (ed. K. Matyjaszewski), 278–296. Washington, DC: American Chemical Society. https://doi.org/10.1021/bk-2000-0768.ch020.

439 Mizusaki, M., Endo, T., Nakahata, R. et al. (2017). *Polymers* 9: 367. https://doi.org/10.3390/polym9080367.

440 Perrier, S., Takolpuckdee, P., and Mars, C.A. (2005). *Macromolecules* 38: 2033–2036. https://doi.org/10.1021/ma047611m.

441 Zhao, Y. and Perrier, S. (2007). *Macromolecules* 40: 9116–9124. https://doi.org/10.1021/ma0716783.

442 Klimkevicius, V., Graule, T., and Makuska, R. (2015). *Langmuir* 31: 2074–2083. https://doi.org/10.1021/la504213t.

443 Ting, S.R.S., Min, E.H., Zetterlund, P.B., and Stenzel, M.H. (2010). *Macromolecules* 43: 5211–5221. https://doi.org/10.1021/ma1004937.

444 Escalé, P., Ting, S.R.S., Khoukh, A. et al. (2011). *Macromolecules* 44: 5911–5919. https://doi.org/10.1021/ma201208u.

445 Moad, G., Li, G., Pfaendner, R. et al. (2006). RAFT copolymerization and its application to the synthesis of novel dispersants/intercalants/exfoliants for polymer-clay nanocomposites. Some interesting results from RAFT (co)polymerization. In: *Controlled/Living Radical Polymerization. From Synthesis to Materials*, ACS Symposium Series, vol. 944 (ed. K. Matyjaszewski), 514–532. Washington, DC: American Chemical Society. https://doi.org/10.1021/bk-2006-0944.ch035.

446 Cotanda, P., Lu, A., Patterson, J.P. et al. (2012). *Macromolecules* 45: 2377–2384. https://doi.org/10.1021/ma2027462.

447 Lucius, M., Falatach, R., McGlone, C. et al. (2016). *Biomacromolecules* 17: 1123–1134. https://doi.org/10.1021/acs.biomac.5b01743.
448 Ido, Y., Maçon, A.L.B., Iguchi, M. et al. (2017). *Polymer* 132: 342–352. https://doi.org/10.1016/j.polymer.2017.10.057.
449 Cimen, D., Yildirim, E., and Caykara, T. (2015). *J. Polym. Sci., Part A: Polym. Chem.* 53: 1696–1706. https://doi.org/10.1002/pola.27613.
450 Ouyang, L., Wang, L., and Schork, F.J. (2011). *Macromol. React. Eng.* 5: 163–169. https://doi.org/10.1002/mren.201000050.
451 Qi, G., Eleazer, B., Jones, C.W., and Schork, F.J. (2009). *Macromolecules* 42: 3906–3916. https://doi.org/10.1021/ma802741u.
452 Parkinson, S., Hondow, N.S., Conteh, J.S. et al. (2019). *React. Chem. Eng.* 4: 852–861. https://doi.org/10.1039/C8RE00211H.
453 Kuroki, A., Martinez-Botella, I., Hornung, C.H. et al. (2017). *Polym. Chem.* 8: 3249–3254. https://doi.org/10.1039/C7PY00630F.
454 Wang, R. and Lowe, A.B. (2007). *J. Polym. Sci., Part A: Polym. Chem.* 45: 2468–2483. https://doi.org/10.1002/pola.22009.
455 Saubern, S., Nguyen, X., Nguyen, V. et al. (2017). *Macromol. React. Eng.* 11: 1600065. https://doi.org/10.1002/mren.201600065.
456 Ferguson, C.J., Hughes, R.J., Nguyen, D. et al. (2005). *Macromolecules* 38: 2191–2204. https://doi.org/10.1021/ma048787r.
457 Nai, Y.H., Jones, R.C., and Breadmore, M.C. (2013). *Electrophoresis* 34: 3189–3197. https://doi.org/10.1002/elps.201300288.
458 Ferguson, C.J., Hughes, R.J., Pham, B.T.T. et al. (2002). *Macromolecules* 35: 9243–9245. https://doi.org/10.1021/ma025626j.
459 Krieg, A., Pietsch, C., Baumgaertel, A. et al. (2010). *Polym. Chem.* 1: 1669–1676. https://doi.org/10.1039/C0PY00156B.
460 McKenzie, T.G., Fu, Q., Wong, E.H.H. et al. (2015). *Macromolecules* 48: 3864–3872. https://doi.org/10.1021/acs.macromol.5b00965.
461 Gurnani, P., Lunn, A.M., and Perrier, S. (2016). *Polymer* 106: 229–237. https://doi.org/10.1016/j.polymer.2016.08.093.
462 Xu, J., Jung, K., Corrigan, N.A., and Boyer, C. (2014). *Chem. Sci.* 5: 3568–3575. https://doi.org/10.1039/C4SC01309C.
463 Levere, M.E., Ho, H.T., Pascual, S., and Fontaine, L. (2011). *Polym. Chem.* 2: 2878–2887. https://doi.org/10.1039/C1PY00320H.
464 Won, S., Hindmarsh, S., and Gibson, M.I. (2018). *ACS Macro Lett.* 7: 178–183. https://doi.org/10.1021/acsmacrolett.7b00891.
465 Moraes, J., Maschmeyer, T., and Perrier, S. (2011). *J. Polym. Sci., Part A: Polym. Chem.* 49: 2771–2782. https://doi.org/10.1002/pola.24710.
466 Hur, Y.H., Song, S.W., Mays, J. et al. (2017). *Mol. Syst. Des. Eng.* 2: 589–596. https://doi.org/10.1039/C7ME00085E.
467 Swift, T., Swanson, L., Geoghegan, M., and Rimmer, S. (2016). *Soft Matter* 12: 2542–2549. https://doi.org/10.1039/C5SM02693H.
468 Suchao-in, N., Chirachanchai, S., and Perrier, S. (2009). *Polymer* 50: 4151–4158. https://doi.org/10.1016/j.polymer.2009.06.047.

469 von der Ehe, C., Rinkenauer, A., Weber, C. et al. (2016). *Macromol. Biosci.* 16: 508–521. https://doi.org/10.1002/mabi.201500346.
470 Pham, B.T.T., Nguyen, D., Ferguson, C.J. et al. (2003). *Macromolecules* 36: 8907–8909. https://doi.org/10.1021/ma035175i.
471 Konkolewicz, D., Poon, C.K., Gray-Weale, A., and Perrier, S. (2011). *Chem. Commun.* 47: 239–241. https://doi.org/10.1039/C0CC02429E.
472 Zhang, L., Fang, K., Fu, S. et al. (2012). *J. Appl. Polym. Sci.* 125: 915–921. https://doi.org/10.1002/app.33606.
473 Gormley, A.J., Chapman, R., and Stevens, M.M. (2014). *Nano Lett.* 14: 6368–6373. https://doi.org/10.1021/nl502840h.
474 Chen, Y., Luo, W., Wang, Y. et al. (2012). *J. Colloid Interface Sci.* 369: 46–51. https://doi.org/10.1016/j.jcis.2011.12.005.
475 Alb, A.M., Drenski, M.F., and Reed, W.F. (2009). *J. Appl. Polym. Sci.* 113: 190–198. https://doi.org/10.1002/app.29501.
476 Corrigan, N., Rosli, D., Jones, J.W.J. et al. (2016). *Macromolecules* 49: 6779–6789. https://doi.org/10.1021/acs.macromol.6b01306.
477 Kuhn, L.R., Allegrezza, M.L., Dougher, N.J., and Konkolewicz, D. (2020). *J. Polym. Sci.* 58: 139–144. https://doi.org/10.1002/pol.20190343.
478 Hakobyan, K., Gegenhuber, T., McErlean, C.S.P., and Müllner, M. (2019). *Angew. Chem. Int. Ed.* 58: 1828–1832. https://doi.org/10.1002/anie.201811721.
479 Tilley, A.J., Chen, M., Danczak, S.M. et al. (2012). *Polym. Chem.* 3: 892–899. https://doi.org/10.1039/C2PY00580H.
480 Bar-Nes, G., Hall, R., Sharma, V. et al. (2009). *Eur. Polym. J.* 45: 3149–3163. https://doi.org/10.1016/j.eurpolymj.2009.08.004.
481 Blinco, J.P., Greiner, A., Barner-Kowollik, C., and Agarwal, S. (2011). *Eur. Polym. J.* 47: 111–114. https://doi.org/10.1016/j.eurpolymj.2010.10.025.
482 Yang, P., Pageni, P., Kabir, M.P. et al. (2016). *ACS Macro Lett.* 5: 1293–1300. https://doi.org/10.1021/acsmacrolett.6b00743.
483 Ke, Y., Zhang, J., Xie, Y. et al. *ChemSusChem* https://doi.org/10.1002/cssc.201902214.
484 Dürr, C.J., Emmerling, S.G.J., Kaiser, A. et al. (2012). *J. Polym. Sci., Part A: Polym. Chem.* 50: 174–180. https://doi.org/10.1002/pola.25033.
485 Smith, R.A., Fu, G., McAteer, O. et al. (2019). *J. Am. Chem. Soc.* 141: 1446–1451. https://doi.org/10.1021/jacs.8b12154.
486 Dürr, C.J., Emmerling, S.G.J., Lederhose, P. et al. (2012). *Polym. Chem.* 3: 1048–1060. https://doi.org/10.1039/C2PY00547F.
487 Wilborn, E.G., Gregory, C.M., Machado, C.A. et al. (2019). *Macromolecules* 52: 1308–1316. https://doi.org/10.1021/acs.macromol.8b01967.
488 Li, J., Kerr, A., Häkkinen, S. et al. (2020). *Polym. Chem.* https://doi.org/10.1039/C9PY01785B.
489 Kessel, S., Urbani, C.N., and Monteiro, M.J. (2011). *Angew. Chem.* 123: 8232–8235. https://doi.org/10.1002/ange.201102651.
490 Kessel, S., Thakar, N., Jia, Z. et al. (2019). *J. Polym. Sci., Part A: Polym. Chem.* 57: 1956–1963. https://doi.org/10.1002/pola.29342.

491 Truong, N.P., Jia, Z., Burges, M. et al. (2011). *Biomacromolecules* 12: 1876–1882. https://doi.org/10.1021/bm200219e.

492 Wu, C., Chen, H., Corrigan, N. et al. (2019). *J. Am. Chem. Soc.* 141: 8207–8220. https://doi.org/10.1021/jacs.9b01096.

493 Duong, H.T.T., Jung, K., Kutty, S.K. et al. (2014). *Biomacromolecules* 15: 2583–2589. https://doi.org/10.1021/bm500422v.

494 Liang, M., Lin, I.C., Whittaker, M.R. et al. (2009). *ACS Nano* 4: 403–413. https://doi.org/10.1021/nn9011237.

495 Kerr, A., Hartlieb, M., Sanchis, J. et al. (2017). *Chem. Commun.* 53: 11901–11904. https://doi.org/10.1039/C7CC07241D.

496 Tran, N.T.D., Jia, Z., and Monteiro, M.J. (2019). *Ind. Eng. Chem. Res.* 58: 21003–21013. https://doi.org/10.1021/acs.iecr.9b01991.

497 Zhang, Q., Vanparijs, N., Louage, B. et al. (2014). *Polym. Chem.* 5: 1140–1144. https://doi.org/10.1039/C3PY00971H.

498 Chen, S.-P.R., Jia, Z., Bobrin, V.A., and Monteiro, M.J. (2019). *Biomacromolecules* https://doi.org/10.1021/acs.biomac.9b01088.

499 Nagao, M., Fujiwara, Y., Matsubara, T. et al. (2017). *Biomacromolecules* 18: 4385–4392. https://doi.org/10.1021/acs.biomac.7b01426.

500 Holdsworth, C.I., Jia, Z., and Monteiro, M.J. (2016). *Polymer* 106: 200–207. https://doi.org/10.1016/j.polymer.2016.08.108.

501 Rolph, M.S., Pitto-Barry, A., and O'Reilly, R.K. (2017). *Polym. Chem.* 8: 5060–5070. https://doi.org/10.1039/C7PY00219J.

502 Evans, C.M., Bridges, C.R., Sanoja, G.E. et al. (2016). *ACS Macro Lett.* 5: 925–930. https://doi.org/10.1021/acsmacrolett.6b00534.

503 Yamamoto, S., Miyashita, T., and Mitsuishi, M. (2017). *RSC Adv.* 7: 44954–44960. https://doi.org/10.1039/C7RA06788G.

504 Park, J., Kim, H., da Silveira, K.C. et al. (2019). *Fuel* 235: 1266–1274. https://doi.org/10.1016/j.fuel.2018.08.036.

505 Brisson, E.R.L., Griffith, J.C., Bhaskaran, A. et al. (2019). *J. Polym. Sci., Part A: Polym. Chem.* 57: 1964–1973. https://doi.org/10.1002/pola.29351.

506 Kwak, J., Mishra, A.K., Lee, J. et al. (2017). *Macromolecules* 50: 6813–6818. https://doi.org/10.1021/acs.macromol.7b00945.

507 Weber, C., Neuwirth, T., Kempe, K. et al. (2011). *Macromolecules* 45: 20–27. https://doi.org/10.1021/ma2021387.

508 Otsuka, C., Wakahara, Y., Okabe, K. et al. (2019). *Macromolecules* 52: 7646–7660. https://doi.org/10.1021/acs.macromol.9b00880.

509 Savage, A.M., Walck, S.D., Lambeth, R.H., and Beyer, F.L. (2018). *Macromolecules* 51: 1636–1643. https://doi.org/10.1021/acs.macromol.7b02536.

510 Tselepy, A., Schiller, T.L., Harrisson, S. et al. (2018). *Macromolecules* 51: 410–418. https://doi.org/10.1021/acs.macromol.7b02104.

511 Pavía-Sanders, A., Nissen, A., and O'Bryan, G. (2018). *Macromol. Mater. Eng.* 303: 1800278. https://doi.org/10.1002/mame.201800278.

512 Upadhyay, A.P., Sadhukhan, P., Roy, S. et al. (2014). *RSC Adv.* 4: 27135–27139. https://doi.org/10.1039/C4RA02734E.

513 Jacobs, J., Gathergood, N., and Heise, A. (2013). *Macromol. Rapid Commun.* 34: 1325–1329. https://doi.org/10.1002/marc.201300402.

514 Rieger, J., Antoun, T., Lee, S.-H. et al. (2012). *Chem. Eur. J.* 18: 3355–3361. https://doi.org/10.1002/chem.201101771.

515 Zhang, Z., Vanparijs, N., Vandewalle, S. et al. (2016). *Polym. Chem.* 7: 7242–7248. https://doi.org/10.1039/C6PY01438K.

516 Wallyn, S., Zhang, Z., Driessen, F. et al. (2014). *Macromol. Rapid Commun.* 35: 405–411. https://doi.org/10.1002/marc.201300690.

517 Huang, Z. and Xu, J. (2013). *Tetrahedron* 69: 10272–10278. https://doi.org/10.1016/j.tet.2013.10.031.

518 Kinnane, C.R., Such, G.K., and Caruso, F. (2011). *Macromolecules* 44: 1194–1202. https://doi.org/10.1021/ma102593k.

519 Nandy, K., Srivastava, A., Afgan, S. et al. (2020). *Eur. Polym. J.* 122: 109387. https://doi.org/10.1016/j.eurpolymj.2019.109387.

520 Yap, H.P., Hao, X., Tjipto, E. et al. (2008). *Langmuir* 24: 8981–8990. https://doi.org/10.1021/la8011074.

521 Ferreira, J., Syrett, J., Whittaker, M. et al. (2011). *Polym. Chem.* 2: 1671–1677. https://doi.org/10.1039/C1PY00102G.

522 Fu, C., Xu, J., Tao, L., and Boyer, C. (2014). *ACS Macro Lett.* 3: 633–638. https://doi.org/10.1021/mz500245k.

523 Zhang, K., Jia, Y.-G., Tsai, I.H. et al. (2017). *Biomacromolecules* 18: 778–786. https://doi.org/10.1021/acs.biomac.6b01640.

524 Kim, Y., Lee, J., Kwon, W. et al. (2019). *Polymer* 178: 121584. https://doi.org/10.1016/j.polymer.2019.121584.

525 Yhaya, F., Lim, J., Kim, Y. et al. (2011). *Macromolecules* 44: 8433–8445. https://doi.org/10.1021/ma2013964.

526 Glass, J.J., Li, Y., De Rose, R. et al. (2017). *ACS Appl. Mater. Interfaces* 9: 12182–12194. https://doi.org/10.1021/acsami.6b15942.

527 Wong, K.H., Davis, T.P., Barner-Kowollik, C., and Stenzel, M.H. (2007). *Polymer* 48: 4950–4965. https://doi.org/10.1016/j.polymer.2007.06.048.

528 Goldmann, A.S., Walther, A., Nebhani, L. et al. (2009). *Macromolecules* 42: 3707–3714. https://doi.org/10.1021/ma900332d.

529 Yhaya, F., Binauld, S., Kim, Y., and Stenzel, M.H. (2012). *Macromol. Rapid Commun.* 33: 1868–1874. https://doi.org/10.1002/marc.201200473.

530 Yamano, T., Higashi, N., and Koga, T. (2020). *Macromol. Rapid Commun.*: 1900550. https://doi.org/10.1002/marc.201900550.

531 Adharis, A., Vesper, D., Koning, N., and Loos, K. (2018). *Green Chem.* 20: 476–484. https://doi.org/10.1039/C7GC03023A.

532 Lan, T., Yang, W., Peng, J. et al. (2014). *Polym. Int.* 63: 1691–1698. https://doi.org/10.1002/pi.4693.

533 Köllisch, H., Barner-Kowollik, C., and Ritter, H. (2006). *Macromol. Rapid. Commun.* 27: 848–853. https://doi.org/10.1002/marc.200600067.

534 Barsbay, M., Guven, O., Davis, T.P. et al. (2009). *Polymer* 50: 973–982. https://doi.org/10.1016/j.polymer.2008.12.027.

535 Wallyn, S., Lammens, M., O'Reilly, R.K., and Prez, F.D. (2011). *J. Polym. Sci., Part A: Polym. Chem.* 49: 2878–2885. https://doi.org/10.1002/pola.24723.
536 Assem, Y., Chaffey-Millar, H., Barner-Kowollik, C. et al. (2007). *Macromolecules* 40: 3907–3913. https://doi.org/10.1021/ma0629079.
537 Kollisch, H.S., Barner-Kowollik, C., and Ritter, H. (2009). *Chem. Commun.*: 1097–1099. https://doi.org/10.1039/b818897a.
538 Jia, Y., Wang, S., Wang, W.-J. et al. (2019). *Macromolecules* 52: 7920–7928. https://doi.org/10.1021/acs.macromol.9b01556.
539 Li, Y., Beija, M., Laurent, S. et al. (2012). *Macromolecules* 45: 4196–4204. https://doi.org/10.1021/ma300521c.
540 Schweizerhof, S., Demco, D.E., Mourran, A. et al. (2017). *Macromol. Chem. Phys.* 218: 1600495. https://doi.org/10.1002/macp.201600495.
541 Zhu, Y., Batchelor, R., Lowe, A.B., and Roth, P.J. (2016). *Macromolecules* 49: 672–680. https://doi.org/10.1021/acs.macromol.5b02056.
542 Quek, J.Y., Zhu, Y., Roth, P.J. et al. (2013). *Macromolecules* 46: 7290–7302. https://doi.org/10.1021/ma4013187.
543 Zhu, Y., Quek, J.Y., Lowe, A.B., and Roth, P.J. (2013). *Macromolecules* 46: 6475–6484. https://doi.org/10.1021/ma401096r.
544 Bingham, N.M. and Roth, P.J. (2019). *Chem. Commun.* 55: 55–58. https://doi.org/10.1039/C8CC08287A.
545 Spick, M.P., Bingham, N.M., Li, Y. et al. (2020). *Macromolecules* 53: 539–547. https://doi.org/10.1021/acs.macromol.9b02497.
546 Zhang, Y., Guan, T., Han, G. et al. (2019). *Macromolecules* 52: 718–728. https://doi.org/10.1021/acs.macromol.8b02427.
547 Ishigaki, Y. and Mori, H. (2018). *Polymer* 140: 198–207. https://doi.org/10.1016/j.polymer.2018.02.025.
548 Huang, Z., Noble, B.B., Corrigan, N. et al. (2018). *J. Am. Chem. Soc.* 140: 13392–13406. https://doi.org/10.1021/jacs.8b08386.
549 Ting, S.R.S., Gregory, A.M., and Stenzel, M.H. (2009). *Biomacromolecules* 10: 342–352. https://doi.org/10.1021/bm801123b.
550 Cheng, S., Ting, S.R.S., Lucien, F.P., and Zetterlund, P.B. (2012). *Macromolecules* 45: 1803–1810. https://doi.org/10.1021/ma202744f.
551 Wong, E.H.H., Lam, S.J., Nam, E., and Qiao, G.G. (2014). *ACS Macro Lett.* 3: 524–528. https://doi.org/10.1021/mz500225p.
552 Nguyen, T.-K., Lam, S.J., Ho, K.K.K. et al. (2017). *ACS Infect. Dis.* 3: 237–248. https://doi.org/10.1021/acsinfecdis.6b00203.
553 Lang, X., Patrick, A.D., Hammouda, B., and Hore, M.J.A. (2018). *Polymer* 145: 137–147. https://doi.org/10.1016/j.polymer.2018.04.068.
554 You, Y., Hong, C., Wang, W. et al. (2004). *Macromolecules* 37: 9761–9767. https://doi.org/10.1021/ma048444t.
555 He, P. and He, L. (2009). *Biomacromolecules* 10: 1804–1809. https://doi.org/10.1021/bm9002283.
556 He, P., Zheng, W.M., Tucker, E.Z. et al. (2008). *Anal. Chem.* 80: 3633–3639. https://doi.org/10.1021/ac702608k.

557 Zhao, J., Zhou, Y., Zhou, Y. et al. (2016). *Polym. Chem.* 7: 1782–1791. https://doi.org/10.1039/C5PY01861G.

558 Lampley, M.W. and Harth, E. (2018). *ACS Macro Lett.* 7: 745–750. https://doi.org/10.1021/acsmacrolett.8b00290.

559 Grover, G.N., Lee, J., Matsumoto, N.M., and Maynard, H.D. (2012). *Macromolecules* 45: 4958–4965. https://doi.org/10.1021/ma300575e.

560 Lian, X., Jin, J., Tian, J., and Zhao, H. (2010). *ACS Appl. Mater. Interfaces* 2: 2261–2268. https://doi.org/10.1021/am1003156.

561 Jin, J., Tian, J., Lian, X. et al. (2011). *Soft Matter* 7: 11194–11202. https://doi.org/10.1039/C1SM06225E.

562 Cai, T., Yang, W.J., Zhang, Z. et al. (2012). *Soft Matter* 8: 5612–5620. https://doi.org/10.1039/C2SM25368B.

563 Zhang, T., Zheng, Z., Ding, X., and Peng, Y. (2008). *Macromol. Rapid Commun.* 29: 1716–1720.

564 Wang, L., Zeng, K., and Zheng, S. (2011). *ACS Appl. Mater. Interfaces* 3: 898–909. https://doi.org/10.1021/am101258k.

565 Wang, J., Kang, Z., Qi, B. et al. (2014). *RSC Adv.* 4: 51510–51518. https://doi.org/10.1039/C4RA07987F.

566 Jin, J., Zhang, M., Xiong, Q. et al. (2012). *Soft Matter* 8: 11809–11816. https://doi.org/10.1039/C2SM26362A.

567 St Thomas, C., Maldonado-Textle, H., Cabello-Romero, J.N. et al. (2014). *Polym. Chem.* 5: 3089–3097. https://doi.org/10.1039/C3PY01270K.

568 St Thomas, C., Cabello-Romero, J.N., Garcia-Valdez, O. et al. (2017). *J. Polym. Sci., Part A: Polym. Chem.* 55: 437–444. https://doi.org/10.1002/pola.28411.

569 von Kugelgen, S., Sifri, R., Bellone, D., and Fischer, F.R. (2017). *J. Am. Chem. Soc.* 139: 7577–7585. https://doi.org/10.1021/jacs.7b02225.

570 Mahanthappa, M.K., Bates, F.S., and Hillmyer, M.A. (2005). *Macromolecules* 38: 7890–7894. https://doi.org/10.1021/ma051535l.

571 Fu, C., Xu, J., Kokotovic, M., and Boyer, C. (2016). *ACS Macro Lett.* 5: 444–449. https://doi.org/10.1021/acsmacrolett.6b00121.

572 Fu, C., Xu, J., and Boyer, C. (2016). *Chem. Commun.* 52: 7126–7129. https://doi.org/10.1039/C6CC03084J.

573 Hales, M., Barner-Kowollik, C., Davis, T.P., and Stenzel, M.H. (2004). *Langmuir* 20: 10809–10817. https://doi.org/10.1021/la0484016.

574 Mukherjee, I., Ghosh, A., Bhadury, P., and De, P. (2018). *ACS Omega* 3: 769–780. https://doi.org/10.1021/acsomega.7b01674.

575 Eissa, A.M., Abdulkarim, A., Sharples, G.J., and Cameron, N.R. (2016). *Biomacromolecules* 17: 2672–2679. https://doi.org/10.1021/acs.biomac.6b00711.

576 Tsuji, S., Aso, Y., Ohara, H., and Tanaka, T. (2019). *Polym. J.* 51: 1015–1022. https://doi.org/10.1038/s41428-019-0221-4.

577 Tanaka, T. and Okamoto, M. (2018). *Polym. J.* 50: 523–531. https://doi.org/10.1038/s41428-018-0038-6.

578 Ganda, S., Jiang, Y., Thomas, D.S. et al. (2016). *Macromolecules* 49: 4136–4146. https://doi.org/10.1021/acs.macromol.6b00266.

579 Wang, J., Song, Y., Sun, P. et al. (2016). *Langmuir* 32: 2737–2749. https://doi.org/10.1021/acs.langmuir.6b00356.

580 Samarajeewa, S., Shrestha, R., Li, Y., and Wooley, K.L. (2012). *J. Am. Chem. Soc.* 134: 1235–1242. https://doi.org/10.1021/ja2095602.

581 Redondo, F.L., Ninago, M.D., de Freitas, A.G.O. et al. (2018). *Int. J. Polym. Sci.* 2018: 8252481 (15 pp pp). https://doi.org/10.1155/2018/8252481.

582 de Freitas, A.G.O., Trindade, S.G., Muraro, P.I.R. et al. (2013). *Macromol. Chem. Phys.* 214: 2336–2344. https://doi.org/10.1002/macp.201300416.

583 Jiang, Y., Wong, S., Chen, F. et al. (2017). *Bioconjugate Chem.* 28: 979–985. https://doi.org/10.1021/acs.bioconjchem.6b00698.

584 Saeed, A.O., Dey, S., Howdle, S.M. et al. (2009). *J. Mater. Chem.* 19: 4529–4535. https://doi.org/10.1039/B821736J.

585 Seo, M., Murphy, C.J., and Hillmyer, M.A. (2013). *ACS Macro Lett.* 2: 617–620. https://doi.org/10.1021/mz400192f.

586 Petzetakis, N., Dove, A.P., and O'Reilly, R.K. (2011). *Chem. Sci.* 2: 955–960. https://doi.org/10.1039/C0SC00596G.

587 Sun, L., Petzetakis, N., Pitto-Barry, A. et al. (2013). *Macromolecules* 46: 9074–9082. https://doi.org/10.1021/ma401634s.

588 Li, Z., Sun, L., Zhang, Y. et al. (2016). *ACS Macro Lett.* 5: 1059–1064. https://doi.org/10.1021/acsmacrolett.6b00419.

589 Li, Z., Zhang, Y., Wu, L. et al. (2019). *ACS Macro Lett.* 8: 596–602. https://doi.org/10.1021/acsmacrolett.9b00221.

590 Pflughaupt, R.L., Hopkins, S.A., Wright, P.M., and Dove, A.P. (2016). *J. Polym. Sci., Part A: Polym. Chem.* 54: 3326–3335. https://doi.org/10.1002/pola.28221.

591 Chen, T., Xu, Z., Zhou, L. et al. (2019). *Tetrahedron Lett.* 60: 419–422. https://doi.org/10.1016/j.tetlet.2018.12.051.

592 Larnaudie, S.C., Brendel, J.C., Jolliffe, K.A., and Perrier, S. (2016). *J. Polym. Sci., Part A: Polym. Chem.* 54: 1003–1011. https://doi.org/10.1002/pola.27937.

593 Chen, T., Xu, Z., Zhou, L. et al. (2019). *Mol. Catal.* 474: 110422. https://doi.org/10.1016/j.mcat.2019.110422.

594 Thankappan, H., Zelcak, A., Taykoz, D., and Bulmus, V. (2018). *Eur. Polym. J.* 103: 421–432. https://doi.org/10.1016/j.eurpolymj.2018.04.025.

595 Catrouillet, S., Brendel, J.C., Larnaudie, S. et al. (2016). *ACS Macro Lett.* 5: 1119–1123. https://doi.org/10.1021/acsmacrolett.6b00586.

596 Li, H., Yu, S.S., Miteva, M. et al. (2013). *Adv. Funct. Mater.* 23: 3040–3052. https://doi.org/10.1002/adfm.201202215.

597 Benoit, D.S.W., Srinivasan, S., Shubin, A.D., and Stayton, P.S. (2011). *Biomacromolecules* 12: 2708–2714. https://doi.org/10.1021/bm200485b.

598 Duvall, C.L., Convertine, A.J., Benoit, D.S.W. et al. (2010). *Mol. Pharm.* 7: 468–476. https://doi.org/10.1021/mp9002267.

599 Bagheri, A., Arandiyan, H., Adnan, N.N.M. et al. (2017). *Macromolecules* 50: 7137–7147. https://doi.org/10.1021/acs.macromol.7b01405.

600 Smith, A.A.A., Zuwala, K., Pilgram, O. et al. (2016). *ACS Macro Lett.* 5: 1089–1094. https://doi.org/10.1021/acsmacrolett.6b00544.

601 Oyeneye, O.O., Xu, W.Z., and Charpentier, P.A. (2015). *RSC Adv.* 5: 76919–76926. https://doi.org/10.1039/C5RA16193B.
602 Togashi, D., Otsuka, I., Borsali, R. et al. (2014). *Biomacromolecules* 15: 4509–4519. https://doi.org/10.1021/bm501314f.
603 Zammarelli, N., Luksin, M., Raschke, H. et al. (2013). *Langmuir* 29: 12834–12843. https://doi.org/10.1021/la402870p.
604 Jia, Z., Bobrin, V.A., Truong, N.P. et al. (2014). *J. Am. Chem. Soc.* 136: 5824–5827. https://doi.org/10.1021/ja500092m.
605 Han, D.H., Yang, L.P., Zhang, X.F., and Pan, C.Y. (2007). *Eur. Polym. J.* 43: 3873–3881. https://doi.org/10.1016/j.eurpolymj.2007.06.029.
606 Zhang, X., Li, J., Li, W., and Zhang, A. (2007). *Biomacromolecules* 8: 3557–3567. https://doi.org/10.1021/bm700729t.
607 Phillips, D.J., Prokes, I., Davies, G.-L., and Gibson, M.I. (2014). *ACS Macro Lett.* 3: 1225–1229. https://doi.org/10.1021/mz500686w.
608 Zong, W., Thingholm, B., Itel, F. et al. (2018). *Langmuir* 34: 6874–6886. https://doi.org/10.1021/acs.langmuir.8b01073.
609 Fan, F., Wang, W., Holt, A.P. et al. (2016). *Macromolecules* 49: 4557–4570. https://doi.org/10.1021/acs.macromol.6b00714.
610 Zhang, J., Chen, W., Yu, L. et al. (2018). *ACS Appl. Nano Mater.* 1: 1513–1521. https://doi.org/10.1021/acsanm.8b00017.
611 You, Y.-Z. and Oupický, D. (2007). *Biomacromolecules* 8: 98–105. https://doi.org/10.1021/bm060635b.
612 Lv, W., Liu, L., Luo, Y. et al. (2011). *J. Colloid Interface Sci.* 356: 16–23. https://doi.org/10.1016/j.jcis.2011.01.005.
613 Xing, T. and Yan, L. (2014). *RSC Adv.* 4: 28186–28194. https://doi.org/10.1039/C4RA04423A.
614 Huang, X., Wang, S., Zhu, M. et al. (2015). *Nanotechnology* 26: 15705. https://doi.org/10.1088/0957-4484/26/015705.
615 Montarnal, D., Delbosc, N., Chamignon, C. et al. (2015). *Angew. Chem. Int. Ed.* 54: 11117–11121. https://doi.org/10.1002/anie.201504838.
616 Wang, S., Huang, X., Wang, G. et al. (2015). *J. Phys. Chem. C* 119: 25307–25318. https://doi.org/10.1021/acs.jpcc.5b09066.
617 Oz, Y., Arslan, M., Gevrek, T.N. et al. (2016). *ACS Appl. Mater. Interfaces* 8: 19813–19826. https://doi.org/10.1021/acsami.6b04664.
618 Zhang, H., Chen, J., Zhang, X. et al. (2017). *Biomacromolecules* 18: 924–930. https://doi.org/10.1021/acs.biomac.6b01760.
619 Oyeneye, O.O., Xu, W.Z., and Charpentier, P.A. (2017). *J. Polym. Sci., Part A: Polym. Chem.* 55: 4062–4070. https://doi.org/10.1002/pola.28879.
620 Li, L., Zhang, T., Lü, J., and Lü, C. (2018). *Appl. Surf. Sci.* 454: 181–191. https://doi.org/10.1016/j.apsusc.2018.05.157.
621 Duan, H., Yang, Y., Lü, J., and Lü, C. (2018). *Nanoscale* 10: 12487–12496. https://doi.org/10.1039/C8NR02719F.
622 Li, B., Yuan, Z., Hung, H.-C. et al. (2018). *Angew. Chem. Int. Ed.* 57: 13873–13876. https://doi.org/10.1002/anie.201808615.

623 Erzina, M., Guselnikova, O., Postnikov, P. et al. (2018). *Adv. Mater. Interfaces* 5: 1801042. https://doi.org/10.1002/admi.201801042.

624 Vanparijs, N., Maji, S., Louage, B. et al. (2015). *Polym. Chem.* 6: 5602–5614. https://doi.org/10.1039/C4PY01224K.

625 Lueckerath, T., Strauch, T., Koynov, K. et al. (2019). *Biomacromolecules* 20: 212–221. https://doi.org/10.1021/acs.biomac.8b01328.

626 Vandewalle, S., Billiet, S., Driessen, F., and Du Prez, F.E. (2016). *ACS Macro Lett.* 5: 766–771. https://doi.org/10.1021/acsmacrolett.6b00342.

627 Koda, Y., Terashima, T., Sawamoto, M., and Maynard, H.D. (2015). *Polym. Chem.* 6: 240–247. https://doi.org/10.1039/C4PY01346H.

628 Godula, K., Rabuka, D., Nam, K.T., and Bertozzi, C.R. (2009). *Angew. Chem. Int. Ed.* 48: 4973–4976. https://doi.org/10.1002/anie.200805756.

629 Georgiou, P.G., Baker, A.N., Richards, S.-J. et al. (2020). *J. Mater. Chem. B* 8: 136–145. https://doi.org/10.1039/C9TB02004G.

630 Quan, W.-D., Pitto-Barry, A., Baker, L.A. et al. (2016). *Chem. Commun.* 52: 1938–1941. https://doi.org/10.1039/C5CC09095D.

631 Tomás, R.M.F., Martyn, B., Bailey, T.L., and Gibson, M.I. (2018). *ACS Macro Lett.* 7: 1289–1294. https://doi.org/10.1021/acsmacrolett.8b00675.

632 Otten, L., Vlachou, D., Richards, S.-J., and Gibson, M.I. (2016). *Analyst* 141: 4305–4312. https://doi.org/10.1039/C6AN00549G.

633 Richards, S.-J. and Gibson, M.I. (2014). *ACS Macro Lett.* 3: 1004–1008. https://doi.org/10.1021/mz5004882.

634 Mathias, F., Tahir, M.N., Tremel, W., and Zentel, R. (2014). *Macromol. Chem. Phys.* 215: 604–613. https://doi.org/10.1002/macp.201300759.

635 De Vrieze, J., Van Herck, S., Nuhn, L., and De, B.G. (2020). *Geest. Macromol. Rapid Commun.*: 2000034. https://doi.org/10.1002/marc.202000034.

636 Luo, X., Liu, J., Liu, G. et al. (2012). *J. Polym. Sci., Part A: Polym. Chem.* 50: 2786–2793. https://doi.org/10.1002/pola.26067.

637 Cui, L., Wang, R., Ji, X. et al. (2014). *Mater. Chem. Phys.* 148: 87–95. https://doi.org/10.1016/j.matchemphys.2014.07.016.

638 Huang, X., Appelhans, D., Formanek, P. et al. (2012). *ACS Nano* 6: 9718–9726. https://doi.org/10.1021/nn3031723.

639 Ho, H.T., Leroux, F., Pascual, S. et al. (2012). *Macromol. Rapid Commun.* 33: 1753–1758. https://doi.org/10.1002/marc.201200367.

640 Schauenburg, D., Divandari, M., Neumann, K. et al. (2020). *Angew. Chem. Int. Ed.* 59: 14656–14663. https://doi.org/10.1002/anie.202006273.

641 Mancini, R.J., Lee, J., and Maynard, H.D. (2012). *J. Am. Chem. Soc.* 134: 8474–8479. https://doi.org/10.1021/ja2120234.

642 Evgrafova, Z., Voigt, B., Baumann, M. et al. (2019). *ChemPhysChem* 20: 236–240. https://doi.org/10.1002/cphc.201800867.

643 Song, Q., Yang, J., Hall, S.C.L. et al. (2019). *ACS Macro Lett.* 8: 1347–1352. https://doi.org/10.1021/acsmacrolett.9b00538.

644 Heredia, K.L., Nguyen, T.H., Chang, C.W. et al. (2008). *Chem. Commun.*: 3245–3247. https://doi.org/10.1039/b804812f.

645 Liu, J., Bulmus, V., Barner-Kowollik, C. et al. (2007). *Macromol. Rapid Commun.* 28: 305–314. https://doi.org/10.1002/marc.200600693.
646 Mohammed, F., Ke, W., Mukerabigwi, J.F. et al. (2019). *ACS Appl. Mater. Interfaces* 11: 31681–31692. https://doi.org/10.1021/acsami.9b10950.
647 Zhao, Y., Houston, Z.H., Simpson, J.D. et al. (2017). *Mol. Pharm.* 14: 3539–3549. https://doi.org/10.1021/acs.molpharmaceut.7b00560.
648 Wang, K., Peng, H., Thurecht, K.J. et al. (2014). *Polym. Chem.* 5: 1760–1771. https://doi.org/10.1039/C3PY01311A.
649 Le Bohec, M., Piogé, S., Pascual, S., and Fontaine, L. (2017). *J. Polym. Sci., Part A: Polym. Chem.* 55: 3597–3606. https://doi.org/10.1002/pola.28742.
650 Xu, G., Neoh, K.G., Kang, E.-T., and Teo, S.L.-M. (2020). *ACS Sustain. Chem. Eng.* 8: 2586–2595. https://doi.org/10.1021/acssuschemeng.9b07836.
651 Ranjan, R. and Brittain, W.J. (2007). *Macromol. Rapid Commun.* 28: 2084–2089. https://doi.org/10.1002/marc.200700428.
652 Ranjan, R. and Brittain, W.J. (2008). *Macromol. Rapid Commun.* 29: 1104–1110. https://doi.org/10.1002/marc.200800085.
653 Li, S. and Gao, C. (2013). *Polym. Chem.* 4: 4450–4460. https://doi.org/10.1039/C3PY00546A.
654 John, J.V., Chung, C.-W., Johnson, R.P. et al. (2016). *Biomacromolecules* 17: 20–31. https://doi.org/10.1021/acs.biomac.5b01474.
655 Ma, W., Zhao, Y., Li, Y. et al. (2018). *Appl. Surf. Sci.* 435: 79–90. https://doi.org/10.1016/j.apsusc.2017.10.190.
656 Guo, Y., van Beek, J.D., Zhang, B. et al. (2009). *J. Am. Chem. Soc.* 131: 11841–11854. https://doi.org/10.1021/ja9032132.
657 Nasrullah, M.J., Vora, A., and Webster, D.C. (2011). *Macromol. Chem. Phys.* 212: 539–549. https://doi.org/10.1002/macp.201000628.
658 Ramesh, K., Anugrah, D.S.B., and Lim, K.T. (2018). *React. Funct. Polym.* 131: 12–21. https://doi.org/10.1016/j.reactfunctpolym.2018.06.011.
659 Huang, Y., Zhang, X.R., Ye, S. et al. (2019). *Nanoscale* 11: 13502–13510. https://doi.org/10.1039/C9NR04664J.
660 Joubert, F., Musa, O., Hodgson, D.R.W., and Cameron, N.R. (2015). *Polym. Chem.* 6: 1567–1575. https://doi.org/10.1039/C4PY01413H.
661 Inglis, A.J., Pierrat, P., Muller, T. et al. (2010). *Soft Matter* 6: 82–84.
662 Meereboer, N.L., Terzić, I., Mellema, H.H. et al. (2019). *Macromolecules* 52: 1567–1576. https://doi.org/10.1021/acs.macromol.8b02382.
663 Zhang, W. and Müller, A.H.E. (2010). *Polymer* 51: 2133–2139. https://doi.org/10.1016/j.polymer.2010.03.028.
664 Xie, Y., Peng, C., Gao, Y. et al. (2017). *J. Polym. Sci., Part A: Polym. Chem.* 55: 3908–3917. https://doi.org/10.1002/pola.28776.
665 Namvari, M., Biswas, C.S., Galluzzi, M. et al. (2017). *Sci. Rep.* 7: 44508. https://doi.org/10.1038/srep44508.
666 Zigmond, J.S., Letteri, R.A., and Wooley, K.L. (2016). *ACS Appl. Mater. Interfaces* 8: 33386–33393. https://doi.org/10.1021/acsami.6b11112.
667 Zigmond, J.S., Pavía-Sanders, A., Russell, J.D., and Wooley, K.L. (2016). *Chem. Mater.* 28: 5471–5479. https://doi.org/10.1021/acs.chemmater.6b02013.

668 Sudo, Y., Sakai, H., Nabae, Y. et al. (2015). *Polymer* 70: 307–314. https://doi.org/10.1016/j.polymer.2015.06.035.
669 Zhou, J. and Hu, B. (2015). *J. Appl. Polym. Sci.*: 132. https://doi.org/10.1002/app.42649.
670 Khor, S.Y., Hu, J., McLeod, V.M. et al. (2015). *Nanomed.: Nanotechnol. Biol. Med.* 11: 2099–2108. https://doi.org/10.1016/j.nano.2015.08.001.
671 Li, Y., Duong, H.T.T., Jones, M.W. et al. (2013). *ACS Macro Lett.* 2: 912–917. https://doi.org/10.1021/mz4004375.
672 Kakwere, H., Payne, R.J., Jolliffe, K.A., and Perrier, S. (2011). *Soft Matter* 7: 3754–3757. https://doi.org/10.1039/C0SM01237H.
673 Lim, J., Yang, H., Paek, K. et al. (2011). *J. Polym. Sci., Part A: Polym. Chem.* 49: 3464–3474. https://doi.org/10.1002/pola.24782.
674 Nölle, J.M., Primpke, S., Müllen, K. et al. (2016). *Polym. Chem.* 7: 4100–4105. https://doi.org/10.1039/C6PY00590J.
675 Soto-Cantu, E., Lokitz, B.S., Hinestrosa, J.P. et al. (2011). *Langmuir* 27: 5986–5996. https://doi.org/10.1021/la2000798.
676 Caciagli, A., Zupkauskas, M., Levin, A. et al. (2018). *Langmuir* 34: 10073–10080. https://doi.org/10.1021/acs.langmuir.8b01828.
677 Gondi, S.R., Vogt, A.P., and Sumerlin, B.S. (2007). *Macromolecules* 40: 474–481. https://doi.org/10.1021/ma061959v.
678 Bajj, D.N.F., Tran, M.V., Tsai, H.-Y. et al. (2019). *ACS Appl. Nano Mater.* 2: 898–909. https://doi.org/10.1021/acsanm.8b02149.
679 Willersinn, J., Bogomolova, A., Cabré, M.B., and Schmidt, B.V.K.J. (2017). *Polym. Chem.* 8: 1244–1254. https://doi.org/10.1039/C6PY02212J.
680 Li, S. and Schroeder, C.M. (2018). *ACS Macro Lett.* 7: 281–286. https://doi.org/10.1021/acsmacrolett.8b00016.
681 Wilks, T.R., Bath, J., de Vries, J.W. et al. (2013). *ACS Nano* 7: 8561–8572. https://doi.org/10.1021/nn402642a.
682 Terzic, I., Meereboer, N.L., Acuautla, M. et al. (2019). *Macromolecules* 52: 354–364. https://doi.org/10.1021/acs.macromol.8b02131.
683 Liu, Z., Lu, G., Li, Y. et al. (2014). *RSC Adv.* 4: 60920–60928. https://doi.org/10.1039/C4RA07825J.
684 Wu, L., Glebe, U., and Böker, A. (2017). *Adv. Mater. Interfaces* 4: 1700092. https://doi.org/10.1002/admi.201700092.
685 Reichstein, P.M., Brendel, J.C., Drechsler, M., and Thelakkat, M. (2019). *ACS Appl. Nano Mater.* 2: 2133–2143. https://doi.org/10.1021/acsanm.9b00108.
686 Qiao, R., Esser, L., Fu, C. et al. (2018). *Biomacromolecules* 19: 4423–4429. https://doi.org/10.1021/acs.biomac.8b01282.
687 Hua, Z., Keogh, R., Li, Z. et al. (2017). *Macromolecules* 50: 3662–3670. https://doi.org/10.1021/acs.macromol.7b00286.
688 Robin, M.P., Jones, M.W., Haddleton, D.M., and O'Reilly, R.K. (2011). *ACS Macro Lett.* 1: 222–226. https://doi.org/10.1021/mz200164x.
689 Robin, M.P., Wilson, P., Mabire, A.B. et al. (2013). *J. Am. Chem. Soc.* 135: 2875–2878. https://doi.org/10.1021/ja3105494.

690 Gody, G., Rossner, C., Moraes, J. et al. (2012). *J. Am. Chem. Soc.* 134: 12596–12603. https://doi.org/10.1021/ja3030643.

691 Suguri, T. and Olsen, B.D. (2019). *Polym. Chem.* 10: 1751–1761. https://doi.org/10.1039/C8PY01228H.

692 Chang, D., Lam, C.N., Tang, S., and Olsen, B.D. (2014). *Polym. Chem.* 5: 4884–4895. https://doi.org/10.1039/C4PY00448E.

693 Lam, C.N. and Olsen, B.D. (2013). *Soft Matter* 9: 2393–2402. https://doi.org/10.1039/C2SM27459K.

694 Thomas, C.S., Glassman, M.J., and Olsen, B.D. (2011). *ACS Nano* 5: 5697–5707. https://doi.org/10.1021/nn2013673.

695 Hirschbiel, A.F., Konrad, W., Schulze-Sünninghausen, D. et al. (2015). *ACS Macro Lett.* 4: 1062–1066. https://doi.org/10.1021/acsmacrolett.5b00485.

696 Li, X., Prukop, S.L., Biswal, S.L., and Verduzco, R. (2012). *Macromolecules* 45: 7118–7127. https://doi.org/10.1021/ma301046n.

697 Hufendiek, A., Barner-Kowollik, C., and Meier, M.A.R. (2015). *Polym. Chem.* 6: 2188–2191. https://doi.org/10.1039/C5PY00063G.

698 Mah, A.H., Afzali, P., Qi, L. et al. (2018). *Macromolecules* 51: 5665–5675. https://doi.org/10.1021/acs.macromol.8b00719.

699 Li, X., ShamsiJazeyi, H., Pesek, S.L. et al. (2014). *Soft Matter* 10: 2008–2015. https://doi.org/10.1039/C3SM52614C.

700 Wuest, K.N.R., Trouillet, V., Goldmann, A.S. et al. (2016). *Macromolecules* 49: 1712–1721. https://doi.org/10.1021/acs.macromol.5b02607.

701 Pesek, S.L., Li, X., Hammouda, B. et al. (2013). *Macromolecules* 46: 6998–7005. https://doi.org/10.1021/ma401246b.

702 Mitra, I., Li, X., Pesek, S.L. et al. (2014). *Macromolecules* 47: 5269–5276. https://doi.org/10.1021/ma501070w.

703 Teo, Y.C. and Xia, Y. (2015). *Macromolecules* 48: 5656–5662. https://doi.org/10.1021/acs.macromol.5b01176.

704 Brendel, J.C., Martin, L., Zhang, J., and Perrier, S. (2017). *Polym. Chem.* 8: 7475–7485. https://doi.org/10.1039/C7PY01636K.

705 Liu, W., Zhang, S., Liu, S. et al. (2019). *Macromol. Rapid Commun.* 40: 1900310. https://doi.org/10.1002/marc.201900310.

706 Liu, W., Dong, Y., Liu, S. et al. (2019). *Macromol. Rapid Commun.* 40: 1900379. https://doi.org/10.1002/marc.201900379.

707 Theriot, J.C., Miyake, G.M., and Boyer, C.A. (2018). *ACS Macro Lett.* 7: 662–666. https://doi.org/10.1021/acsmacrolett.8b00281.

708 Li, Z., Zhang, K., Ma, J. et al. (2009). *J. Polym. Sci., Part A: Polym. Chem.* 47: 5557–5563. https://doi.org/10.1002/pola.23626.

709 Dalsin, S.J., Rions-Maehren, T.G., Beam, M.D. et al. (2015). *ACS Nano* 9: 12233–12245. https://doi.org/10.1021/acsnano.5b05473.

710 Radzinski, S.C., Foster, J.C., Chapleski, R.C. et al. (2016). *J. Am. Chem. Soc.* 138: 6998–7004. https://doi.org/10.1021/jacs.5b13317.

711 Li, Z., Ma, J., Cheng, C. et al. (2010). *Macromolecules* 43: 1182–1184. https://doi.org/10.1021/ma902513n.

712 Yu, L., Martin, I.J., Kasi, R.M., and Wei, M. (2018). *ACS Appl. Mater. Interfaces* 10: 28440–28449. https://doi.org/10.1021/acsami.8b10234.
713 Alaboalirat, M., Qi, L., Arrington, K.J. et al. (2019). *Macromolecules* 52: 465–476. https://doi.org/10.1021/acs.macromol.8b02366.
714 Li, Z., Ma, J., Lee, N.S., and Wooley, K.L. (2011). *J. Am. Chem. Soc.* 133: 1228–1231. https://doi.org/10.1021/ja109191z.
715 Mah, A.H., Mei, H., Basu, P. et al. (2018). *Soft Matter* 14: 6728–6736. https://doi.org/10.1039/C8SM01127C.
716 Mei, H., Laws, T.S., Mahalik, J.P. et al. (2019). *Macromolecules* 52: 8910–8922. https://doi.org/10.1021/acs.macromol.9b01801.
717 Saito, K., Hirose, K., Okayasu, T. et al. (2013). *RSC Adv.* 3: 9752–9756. https://doi.org/10.1039/C3RA41823E.
718 Ohno, K., Ma, Y., Huang, Y. et al. (2011). *Macromolecules* 44: 8944–8953. https://doi.org/10.1021/ma202105y.
719 Sabouri, H., Huang, Y., Ohno, K., and Perrier, S. (2015). *Nanoscale* 7: 19036–19046. https://doi.org/10.1039/C5NR06400G.
720 Kim, K., Ahn, J., Park, M. et al. (2019). *Macromolecules* 52: 7448–7455. https://doi.org/10.1021/acs.macromol.9b01331.
721 Baratha, K.V., Nourry, A., and Pilard, J.-F. (2015). *Eur. Polym. J.* 70: 317–330. https://doi.org/10.1016/j.eurpolymj.2015.07.030.
722 Lopez-Oliva, A.P., Warren, N.J., Rajkumar, A. et al. (2015). *Macromolecules* 48: 3547–3555. https://doi.org/10.1021/acs.macromol.5b00576.
723 Rymaruk, M.J., Hunter, S.J., O'Brien, C.T. et al. (2019). *Macromolecules* 52: 2822–2832. https://doi.org/10.1021/acs.macromol.9b00129.
724 Duong, T.H., Margaillan, A., and Bressy, C. (2019). *Polym. Degrad. Stab.* 164: 136–144. https://doi.org/10.1016/j.polymdegradstab.2019.04.002.
725 Guazzelli, E., Galli, G., Martinelli, E. et al. (2020). *Polymer* 186: 121954. https://doi.org/10.1016/j.polymer.2019.121954.
726 Wadley, M.L. and Cavicchi, K.A. (2010). *J. Appl. Polym. Sci.* 115: 635–640. https://doi.org/10.1002/app.31106.
727 Zhao, W., Fonsny, P., FitzGerald, P. et al. (2013). *Polym. Chem.* 4: 2140–2150. https://doi.org/10.1039/C3PY21038C.
728 Guo, H., Liu, M., Xie, C. et al. (2020). *Chem. Eng. J.* 402: 126161. https://doi.org/10.1016/j.cej.2020.126161.
729 Chen, C., Richter, F., Guerrero-Sanchez, C. et al. (2020). *ACS Macro Lett.* 9: 260–265. https://doi.org/10.1021/acsmacrolett.9b00647.
730 Chen, C., Kong, F., Wei, X., and Thang, S.H. (2017). *Chem. Commun.* 53: 10776–10779. https://doi.org/10.1039/C7CC05316A.
731 Pribyl, J. and Benicewicz, B.C. (2022). Surface and particle modification via RAFT polymerization: an update. In: *RAFT Polymerization: Materials, Synthesis and Applications* (eds. G. Moad and E. Rizzardo). Weinheim: Wiley-VCH, 1017–1050.
732 Gauthier-Jaques, M., Mutlu, H., Gaballa, H., and Theato, P. (2021). Synthesis and application of reactive polymers via RAFT polymerization. In: *RAFT*

Polymerization: Materials, Synthesis and Applications (eds. G. Moad and E. Rizzardo). Weinheim: Wiley-VCH, 829–872.

733 Kazemi, M., Shiri, L., and Kohzadi, H. (2015). *Phosphorus, Sulfur Silicon Relat. Elem.* 190: 1398–1409. https://doi.org/10.1080/10426507.2014.993035.

734 Fallah-Mehrjardi, M. (2018). *Monatsh. Chem. Chem. Mon.* 149: 1931–1944. https://doi.org/10.1007/s00706-018-2256-1.

735 Yousefi, A. (2015). *J. Sulfur Chem.* 36: 672–677. https://doi.org/10.1080/17415993.2015.1079912.

736 Vestberg, R., Piekarski, A.M., Pressly, E.D. et al. (2009). *J. Polym. Sci., Part A: Polym. Chem.* 47: 1237–1258. https://doi.org/10.1002/pola.23186.

737 Tam, W.Y., Mak, C.S.K., Ng, A.M.C. et al. (2009). *Macromol. Rapid Commun.* 30: 622–626. https://doi.org/10.1002/marc.200800714.

738 Zhou, Y., Ahn, S.-k., Lakhman, R.K. et al. (2011). *Macromolecules* 44: 3924–3934. https://doi.org/10.1021/ma102922u.

739 Chandrawati, R., Städler, B., Postma, A. et al. (2009). *Biomaterials* 30: 5988–5998. https://doi.org/10.1016/j.biomaterials.2009.07.040.

740 Pavlov, G.M., Breul, A.M., Hager, M.D., and Schubert, U.S. (2012). *Macromol. Chem. Phys.* 213: 904–916. https://doi.org/10.1002/macp.201100653.

741 Sohn, H.-S., Cha, S.-H., Lee, W.-K. et al. (2011). *Macromol. Res.* 19: 722–728. https://doi.org/10.1007/s13233-011-0705-3.

742 Xu, X., Smith, A.E., and McCormick, C.L. (2009). *Aust. J. Chem.* 62: 1520–1527. https://doi.org/10.1071/CH09255.

743 Gody, G., Boullanger, P., Ladaviere, C. et al. (2008). *Macromol. Rapid Commun.* 29: 511–519. https://doi.org/10.1002/marc.200700768.

744 Zorn, M. and Zentel, R. (2008). *Macromol. Rapid Commun.* 29: 922–927. https://doi.org/10.1002/marc.200800165.

745 Chen, M., Haeussler, M., Moad, G., and Rizzardo, E. (2011). *Org. Biomol. Chem.* 9: 6111–6119. https://doi.org/10.1039/C1OB05276D.

746 Mao, J., Qi, X., Cao, X. et al. (2011). *Chem. Commun.* 47: 4228–4230. https://doi.org/10.1039/C1CC10610D.

747 Yu, B., Lowe, A.B., and Ishihara, K. (2009). *Biomacromolecules* 10: 950–958. https://doi.org/10.1021/bm8014945.

748 Campos, L.M., Killops, K.L., Sakai, R. et al. (2008). *Macromolecules* 41: 7063–7070. https://doi.org/10.1021/ma801630n.

749 Wang, J., Zhu, X.L., Cheng, Z.P. et al. (2007). *J. Polym. Sci., Part A: Polym. Chem.* 45: 3788–3797. https://doi.org/10.1002/pola.22105.

750 Xiao, N.-Y., Li, A.-L., Liang, H., and Lu, J. (2008). *Macromolecules* 41: 2374–2380. https://doi.org/10.1021/ma702510n.

751 Zhang, X., Lian, X., Liu, L. et al. (2008). *Macromolecules* 41: 7863–7869. https://doi.org/10.1021/ma801405j.

752 Quemener, D., Le Hellaye, M., Bissett, C. et al. (2008). *J. Polym. Sci., Part A: Polym. Chem.* 46: 155–173. https://doi.org/10.1002/pola.22367.

753 Cavalieri, F., Postma, A., Lee, L., and Caruso, F. (2009). *ACS Nano* 3: 234–240. https://doi.org/10.1021/nn800705m.

754 Such, G.K., Tjipto, E., Postma, A. et al. (2007). *Nano Lett.* 7: 1706–1710. https://doi.org/10.1021/nl070698f.
755 Such, G.K., Quinn, J.F., Quinn, A. et al. (2006). *J. Am. Chem. Soc.* 128: 9318–9319. https://doi.org/10.1021/ja063043+.
756 Yanjarappa, M.J., Gujraty, K.V., Joshi, A. et al. (2006). *Biomacromolecules* 7: 1665–1670. https://doi.org/10.1021/bm060098v.
757 Aamer, K.A. and Tew, G.N. (2007). *J. Polym. Sci., Part A: Polym. Chem.* 45: 5618–5625. https://doi.org/10.1002/pola.22309.
758 Yan, J.-J., Hong, C.-Y., and You, Y.-Z. (2011). *Macromolecules* 44: 1247–1251. https://doi.org/10.1021/ma102944k.
759 Chytil, P., Etrych, T., Kríz, J. et al. (2010). *Eur. J. Pharm. Sci.* 41: 473–482. https://doi.org/10.1016/j.ejps.2010.08.003.
760 Hwang, J.Y., Li, R.C., and Maynard, H.D. (2007). *J. Controlled Release* 122: 279–286. https://doi.org/10.1016/j.jconrel.2007.04.010.
761 Li, R.C., Hwang, J., and Maynard, H.D. (2007). *Chem. Commun.*: 3631–3633. https://doi.org/10.1039/b709304g.
762 Seo, M., Shin, S., Ku, S. et al. (2010). *J. Mater. Chem.* 20: 94–102. https://doi.org/10.1039/b914941d.
763 Hatton, F.L. (2020). *Polym. Chem.* https://doi.org/10.1039/C9PY01128E.
764 O'Reilly, R.K. (2010). *Polym. Int.* 59: 568–573. https://doi.org/10.1002/pi.2830.
765 Boyer, C., Bulmus, V., Davis, T.P. et al. (2009). *Chem. Rev.* 109: 5402–5436. https://doi.org/10.1021/cr9001403.
766 Ahmad, N.M., Charleux, B., Farcet, C. et al. (2009). *Macromol. Rapid Commun.* 30: 2002–2021. https://doi.org/10.1002/marc.200900450.
767 Ballard, N. and Asua, J.M. (2018). *Prog. Polym. Sci.* 79: 40–60. https://doi.org/10.1016/j.progpolymsci.2017.11.002.
768 Reyes, Y. and Asua, J.M. (2011). *Macromol. Rapid Commun.* 32: 63–67. https://doi.org/10.1002/marc.201000375.
769 Gaborieau, M., Koo, S.P.S., Castignolles, P. et al. (2010). *Macromolecules* 43: 5492–5495. https://doi.org/10.1021/ma100991c.
770 Liang, K., Hutchinson, R.A., Barth, J. et al. (2011). *Macromolecules* 44: 5843–5845. https://doi.org/10.1021/ma201391t.
771 Moad, G. (2017). *Polym. Int.* 66: 26–41. https://doi.org/10.1002/pi.5173.
772 Roth, P.J. and Theato, P. (2016). Polymer analogous reactions. In: *Reference Module in Materials Science and Materials Engineering*. Elsevier 26 pages. https://doi.org/10.1016/B978-0-12-803581-8.01420-X.
773 Roth, P.J. and Theato, P. (2011). *ACS Symp. Ser.* 1066: 23–37 (3 pp). https://doi.org/10.1021/bk-2011-1066.ch003.
774 Rzayev, J. (2009). *Macromolecules* 42: 2135–2141. https://doi.org/10.1021/ma802304y.
775 Destarac, M., Guinaudeau, A., Geagea, R. et al. (2010). *J. Polym. Sci., Part A: Polym. Chem.* 48: 5163–5171. https://doi.org/10.1002/pola.24314.
776 Simonova, Y.A., Topchiy, M.A., Filatova, M.P. et al. (2020). *Eur. Polym. J.* 122: 109363. https://doi.org/10.1016/j.eurpolymj.2019.109363.

777 Pasini, D. and Takeuchi, D. (2018). *Chem. Rev.* 118: 8983–9057. https://doi.org/10.1021/acs.chemrev.8b00286.

778 Pasini, D. and Nitti, A. (2020). *Eur. Polym. J.* 122: 109378. https://doi.org/10.1016/j.eurpolymj.2019.109378.

779 Paulusse, J.M.J., Amir, R.J., Evans, R.A., and Hawker, C.J. (2009). *J. Am. Chem. Soc.* 131: 9805–9812. https://doi.org/10.1021/ja903245p.

780 Ganda, S., Dulle, M., Drechsler, M. et al. (2017). *Macromolecules* 50: 8544–8553. https://doi.org/10.1021/acs.macromol.7b01453.

781 Jackson, A.W., Chennamaneni, L.R., and Thoniyot, P. (2020). *Eur. Polym. J.* 122: 109391. https://doi.org/10.1016/j.eurpolymj.2019.109391.

782 Allison-Logan, S., Karimi, F., Nothling, M.D., and Qiao, G.G. (2022). Star polymers by RAFT polymerization. In: *RAFT Polymerization: Materials, Synthesis and Applications* (eds. G. Moad and E. Rizzardo). Weinheim: Wiley-VCH.

783 Moad, G. (2015). *Polym. Int.* 64: 15–24. https://doi.org/10.1002/pi.4767.

784 Pérez-Salinas, P., López-Domínguez, P., Rosas-Aburto, A. et al. (2022). RAFT crosslinking polymerization. In: *RAFT Polymerization: Materials, Synthesis and Applications* (eds. G. Moad and E. Rizzardo). Weinheim: Wiley-VCH, 873–932.

785 Barlow, K.J., Bernabeu, V., Hao, X. et al. (2015). *React. Funct. Polym.* 96: 89–96. https://doi.org/10.1016/j.reactfunctpolym.2015.09.008.

786 Alfurhood, J.A., Bachler, P.R., and Sumerlin, B.S. (2016). *Polym. Chem.* 7: 3361–3369. https://doi.org/10.1039/C6PY00571C.

787 Wang, X. and Gao, H. (2017). *Polymers* 9: 188. https://doi.org/10.3390/polym9060188.

788 Wilson, J.T., Postma, A., Keller, S. et al. (2015). *AAPS J.* 17: 358–369. https://doi.org/10.1208/s12248-014-9697-1.

789 Wang, K., Peng, H., Thurecht, K.J. et al. (2015). *Biomacromolecules* 16: 2827–2839. https://doi.org/10.1021/acs.biomac.5b00800.

790 Chen, Y., Shi, Y., Liang, Y. et al. (2019). *ACS Appl. Energy Mater.* 2: 1608–1615. https://doi.org/10.1021/acsaem.8b02188.

791 Alfurhood, J.A., Sun, H., Bachler, P.R., and Sumerlin, B.S. (2016). *Polym. Chem.* 7: 2099–2104. https://doi.org/10.1039/C6PY00111D.

792 Zhang, C., Zhou, Y., Liu, Q. et al. (2011). *Macromolecules* 44: 2034–2049. https://doi.org/10.1021/ma1024736.

793 Zhao, J., Li, D., Han, H. et al. (2019). *Langmuir* 35: 2630–2638. https://doi.org/10.1021/acs.langmuir.8b03231.

794 Liu, Y., Zhou, J., Hou, J. et al. (2019). *ACS Appl. Polym. Mater.* 1: 76–82. https://doi.org/10.1021/acsapm.8b00058.

795 Zhuang, Y., Zhu, Q., Tu, C. et al. (2012). *J. Mater. Chem.* 22: 23852–23860. https://doi.org/10.1039/C2JM34306A.

796 Zhuang, Y., Su, Y., Peng, Y. et al. (2014). *Biomacromolecules* 15: 1408–1418. https://doi.org/10.1021/bm500018s.

797 Zhang, Y., Teo, B.M., Postma, A. et al. (2013). *J. Phys. Chem. B* 117: 10504–10512. https://doi.org/10.1021/jp407106z.

798 Ghosh Roy, S. and De, P. (2014). *Polym. Chem.* 5: 6365–6378. https://doi.org/10.1039/C4PY00766B.

799 Chen, X., Liu, X., Miao, C. et al. (2018). *Eur. Polym. J.* 107: 229–235. https://doi.org/10.1016/j.eurpolymj.2018.08.016.

800 Nicolaÿ, R., Kamada, J., Van Wassen, A., and Matyjaszewski, K. (2010). *Macromolecules* 43: 4355–4361. https://doi.org/10.1021/ma100378r.

801 Fenoli, C.R. and Bowman, C.N. (2014). *Polym. Chem.* 5: 62–68. https://doi.org/10.1039/C3PY00709J.

802 Yu, L.-X., Zhuo, D., and Ran, R. (2013). *Int. J. Polym. Mater. Polym. Biomater.* 62: 749–754. https://doi.org/10.1080/00914037.2013.769237.

803 Amamoto, Y., Kamada, J., Otsuka, H. et al. (2011). *Angew. Chem. Int. Ed.* 50: 1660–1663. https://doi.org/10.1002/anie.201003888.

804 Park, H.Y., Kloxin, C.J., Abuelyaman, A.S. et al. (2012). *Macromolecules* 45: 5640–5646. https://doi.org/10.1021/ma300228z.

805 Shanmugam, S., Cuthbert, J., Kowalewski, T. et al. (2018). *Macromolecules* 51: 7776–7784. https://doi.org/10.1021/acs.macromol.8b01708.

806 Fenoli, C.R., Wydra, J.W., and Bowman, C.N. (2014). *Macromolecules* 47: 907–915. https://doi.org/10.1021/ma402548e.

807 Xu, J. (2019). *Macromolecules* 52: 9068–9093. https://doi.org/10.1021/acs.macromol.9b01365.

808 Haven, J.J., Neve, J.D., and Junkers, T. (2022). Sequence-encoded RAFT oligomers and polymers. In: *RAFT Polymerization: Materials, Synthesis and Applications* (eds. G. Moad and E. Rizzardo). Weinheim: Wiley-VCH, 805–828.

809 Lin, S., Zhang, L., Huang, Z. et al. (2019). *Macromolecules* 52: 7157–7166. https://doi.org/10.1021/acs.macromol.9b01534.

810 Zhou, Y., Zhang, Z., Postma, A., and Moad, G. (2019). *Polym. Chem.* 10: 3284–3287. https://doi.org/10.1039/C9PY00507B.

811 Henry, S.M., Convertine, A.J., Benoit, D.S.W. et al. (2009). *Bioconjugate Chem.* 20: 1122–1128. https://doi.org/10.1021/bc800426d.

812 Isahak, N., Gody, G., Malins, L.R. et al. (2016). *Chem. Commun.* 52: 12952–12955. https://doi.org/10.1039/C6CC06010B.

813 Montagna, V., Haupt, K., and Gonzato, C. (2020). *Polym. Chem.* https://doi.org/10.1039/C9PY01629E.

814 Guo, X., Choi, B., Feng, A., and Thang, S.H. (2018). *Macromol. Rapid Commun.* 39: 1800479. https://doi.org/10.1002/marc.201800479.

815 Kermagoret, A. and Gigmes, D. (2016). *Tetrahedron* 72: 7672–7685. https://doi.org/10.1016/j.tet.2016.07.002.

816 Zhang, X., Oddon, M., Giani, O. et al. (2010). *Macromolecules* 43: 2654–2656. https://doi.org/10.1021/ma9025916.

817 Cheng, C., Khoshdel, E., and Wooley, K.L. (2007). *Macromolecules* 40: 2289–2292. https://doi.org/10.1021/ma0627525.

818 Li, L., Huang, J., and Zhang, Y. (2018). *Macromol. Chem. Phys.* 219: 1800217. https://doi.org/10.1002/macp.201800217.

819 Uchiyama, M. and Kamigaito, M. (2022). Cationic RAFT polymerization. In: *RAFT Polymerization: Materials, Synthesis and Applications* (eds. G. Moad, S.H. Thang and E. Rizzardo). Weinheim: Wiley-VCH, 1159–1182.

820 Zhang, Z., Xia, L., Zeng, T.-Y. et al. (2019). *Polym. Chem.* 10: 2117–2125. https://doi.org/10.1039/C9PY00230H.
821 Wang, C.-H., Fan, Y.-S., Zhang, Z. et al. (2019). *Appl. Surf. Sci.* 475: 639–644. https://doi.org/10.1016/j.apsusc.2019.01.033.
822 Favier, A., Luneau, B., Vinas, J. et al. (2009). *Macromolecules* 42: 5953–5964. https://doi.org/10.1021/ma9006939.
823 Bolton, J. and Rzayev, J. (2012). *ACS Macro Lett.* 1: 15–18. https://doi.org/10.1021/mz200003j.
824 Bolton, J. and Rzayev, J. (2014). *Macromolecules* 47: 2864–2874. https://doi.org/10.1021/ma500625k.
825 Cuthbert, J., Zhang, T., Biswas, S. et al. (2018). *Macromolecules* 51: 9184–9191. https://doi.org/10.1021/acs.macromol.8b01880.
826 Delduc, P., Tailhan, C., and Zard, S.Z. (1988). *J. Chem. Soc., Chem. Commun.*: 308–310. https://doi.org/10.1039/C39880000308.
827 McKenzie, T.G., Fu, Q., Uchiyama, M. et al. (2016). *Adv. Sci.* 3: 1500394. https://doi.org/10.1002/advs.201500394.
828 Shanmugam, S., Xu, J., and Boyer, C. (2017). *Macromol. Rapid Commun.* 38: 1700143. https://doi.org/10.1002/marc.201700143.
829 Xu, J., Shanmugam, S., Corrigan, N.A., and Boyer, C. (2015). Catalyst-free visible light-induced RAFT photopolymerization. In: *Controlled Radical Polymerization: Mechanisms*, ACS Symposium Series, vol. 1187 (eds. K. Matyjaszewski, B.S. Sumerlin, N.V. Tsarevsky and J. Chiefari), 247–267. American Chemical Society. https://doi.org/10.1021/bk-2015-1187.ch013.
830 Li, S., Han, G., and Zhang, W. (2020). *Polym. Chem.* https://doi.org/10.1039/D0PY00054J.
831 Strover, L.T., Cantalice, A., Lam, J.Y.L. et al. (2019). *Macro Lett.* 8: 1316–1322. https://doi.org/10.1021/acsmacrolett.9b00598.
832 Zhang, Z., Zhang, W., Zhu, X. et al. (2007). *J. Polym. Sci., Part A: Polym. Chem.* 45: 5722–5730. https://doi.org/10.1002/pola.22320.
833 Kwak, Y., Nicolay, R., and Matyjaszewski, K. (2008). *Macromolecules* 41: 6602–6604. https://doi.org/10.1021/ma801502s.
834 Nicolaÿ, R., Kwak, Y., and Matyjaszewski, K. (2010). *Angew. Chem. Int. Ed.* 49: 541–544. https://doi.org/10.1002/anie.200905340.
835 Nicolaÿ, R. and Kwak, Y. (2012). *Israel J. Chem.* 52: 288–305. https://doi.org/10.1002/ijch.201100124.
836 Pan, J., Miao, J., Zhang, L. et al. (2013). *Polym. Chem.* 4: 5664–5670. https://doi.org/10.1039/C3PY00671A.
837 Maximiano, P., Mendonça, P.V., Costa, J.R.C. et al. (2016). *Macromolecules* 49: 1597–1604. https://doi.org/10.1021/acs.macromol.5b02647.
838 Lorandi, F., Fantin, M., Shanmugam, S. et al. (2019). *Macromolecules* 52: 1479–1488. https://doi.org/10.1021/acs.macromol.9b00112.
839 Zhou, J., Yao, H., and Ma, J. (2018). *Polym. Chem.* 9: 2532–2561. https://doi.org/10.1039/C8PY00065D.
840 Eggers, S. and Abetz, V. (2017). *Polymers* 9: 668. https://doi.org/10.3390/polym9120668.

841 Rieger, J., Stoffelbach, F., Bui, C. et al. (2008). *Macromolecules* 41: 4065–4068. https://doi.org/10.1021/ma800544v.

842 Truong, N.P., Dussert, M.V., Whittaker, M.R. et al. (2015). *Polym. Chem.* 6: 3865–3874. https://doi.org/10.1039/C5PY00166H.

843 Truong, N.P., Quinn, J.F., Anastasaki, A. et al. (2017). *Polym. Chem.* 8: 1353–1363. https://doi.org/10.1039/C6PY02158A.

844 Penfold, N.J.W., Yeow, J., Boyer, C., and Armes, S.P. (2019). *ACS Macro Lett.* 8: 1029–1054. https://doi.org/10.1021/acsmacrolett.9b00464.

845 D'Agosto, F., Lansalot, M., and Rieger, J. (2022). RAFT-mediated polymerization-induced self-assembly (PISA). In: *RAFT Polymerization: Materials, Synthesis and Applications* (eds. G. Moad and E. Rizzardo). Weinheim: Wiley-VCH, 707–752.

846 Convertine, A.J., Lokitz, B.S., Lowe, A.B. et al. (2005). *Macromol. Rapid Commun.* 26: 791–795. https://doi.org/10.1002/marc.200500042.

847 Zhou, H., Liu, C., Gao, C. et al. (2016). *J. Polym. Sci., Part A: Polym. Chem.* 54: 1517–1525. https://doi.org/10.1002/pola.28002.

848 Guerrero-Sanchez, C., Keddie, D.J., Saubern, S., and Chiefari, J. (2012). *ACS Comb. Sci.* 14: 389–394. https://doi.org/10.1021/co300044w.

849 Wang, M., Zhang, J., Guerrero-Sanchez, C. et al. (2019). *ACS Comb. Sci.* 21: 643–649. https://doi.org/10.1021/acscombsci.9b00082.

850 Liu, Z., Lv, Y., and An, Z. (2017). *Angew. Chem. Int. Ed.* 56: 13852–13856. https://doi.org/10.1002/anie.201707993.

851 Gormley, A.J., Yeow, J., Ng, G. et al. (2018). *Angew. Chem. Int. Ed.* 57: 1557–1562. https://doi.org/10.1002/anie.201711044.

852 Ng, G., Yeow, J., Chapman, R. et al. (2018). *Macromolecules* 51: 7600–7607. https://doi.org/10.1021/acs.macromol.8b01600.

853 Judzewitsch, P.R., Corrigan, N., Trujillo, F. et al. (2020). *Macromolecules* 53: 631–639. https://doi.org/10.1021/acs.macromol.9b02207.

854 Willcock, H. and O'Reilly, R.K. (2010). *Polym. Chem.* 1: 149–157. https://doi.org/10.1039/b9py00340a.

855 Moad, G., Rizzardo, E., and Thang, S.H. (2011). *Polym. Int.* 60: 9–25. https://doi.org/10.1002/pi.2988.

856 Lowe, A.B. and Dallerba, E. (2022). RAFT functional end-groups: installation and transformation. In: *RAFT Polymerization: Materials, Synthesis and Applications* (eds. G. Moad and E. Rizzardo). Weinheim: Wiley-VCH, 753–804.

857 Lunn, D.J., Discekici, E.H., Read de Alaniz, J. et al. (2017). *J. Polym. Sci., Part A: Polym. Chem.* 55: 2903–2914. https://doi.org/10.1002/pola.28575.

858 Cornel, E.J., van Meurs, S., Smith, T. et al. (2018). *J. Am. Chem. Soc.* 140: 12980–12988. https://doi.org/10.1021/jacs.8b07953.

859 Karunakaran, R. and Kennedy, J.P. (2007). *J. Polym. Sci., Part A: Polym. Chem.* 45: 4284–4290. https://doi.org/10.1002/pola.22169.

860 Vo, C.-D., Rosselgong, J., Armes, S.P., and Tirelli, N. (2010). *J. Polym. Sci., Part A: Polym. Chem.* 48: 2032–2043. https://doi.org/10.1002/pola.23973.

861 Thurecht, K.J., Blakey, I., Peng, H. et al. (2010). *J. Am. Chem. Soc.* 132: 5336–5337. https://doi.org/10.1021/ja100252y.

862 Zhou, Y., Jiang, K., Song, Q., and Liu, S. (2007). *Langmuir* 23: 13076–13084. https://doi.org/10.1021/la702548h.

863 Alagi, P., Hadjichristidis, N., Gnanou, Y., and Feng, X. (2019). *ACS Macro Lett.* 8: 664–669. https://doi.org/10.1021/acsmacrolett.9b00357.

864 Carmean, R.N., Figg, C.A., Scheutz, G.M. et al. (2017). *ACS Macro Lett.* 6: 185–189. https://doi.org/10.1021/acsmacrolett.7b00038.

865 Mattson, K.M., Pester, C.W., Gutekunst, W.R. et al. (2016). *Macromolecules* 49: 8162–8166. https://doi.org/10.1021/acs.macromol.6b01894.

866 Destarac, M., Kalai, C., Wilczewska, A. et al. (2006). Various strategies for the chemical transformation of xanthate-functional chain termini in MADIX copolymers. In: *Controlled/Living Radical Polymerization. From Synthesis to Materials*, ACS Symposium Series, vol. 944 (ed. K. Matyjaszewski), 564–577. Washington, DC: American Chemical Society. https://doi.org/10.1021/bk-2006-0944.ch038.

867 Tong, Y.-Y., Dong, Y.-Q., Du, F.-S., and Li, Z.-C. (2009). *J. Polym. Sci., Part A: Polym. Chem.* 47: 1901–1910. https://doi.org/10.1002/pola.23288.

868 Le Neindre, M., Magny, B., and Nicolay, R. (2013). *Polym. Chem.* 4: 5577–5584. https://doi.org/10.1039/C3PY00754E.

869 Desmet, G.B., D'hooge, D.R., Sabbe, M.K. et al. (2016). *J. Org. Chem.* 81: 11626–11634. https://doi.org/10.1021/acs.joc.6b01844.

870 Kakwere, H. and Perrier, S.b. (2009). *J. Am. Chem. Soc.* 131: 1889–1895. https://doi.org/10.1021/ja8075499.

871 Zhang, X., Jiang, J., and Zhang, Y. (2016). *J. Appl. Polym. Sci.* 133: 43992. https://doi.org/10.1002/app.43992.

872 Altintas, O., Abbasi, M., Riazi, K. et al. (2014). *Polym. Chem.* 5: 5009–5019. https://doi.org/10.1039/C4PY00484A.

873 Altintas, O., Riazi, K., Lee, R. et al. (2013). *Macromolecules* 46: 8079–8091. https://doi.org/10.1021/ma401749h.

874 Jesson, C.P., Pearce, C.M., Simon, H. et al. (2017). *Macromolecules* 50: 182–191. https://doi.org/10.1021/acs.macromol.6b01963.

875 Zhang, T. and Palasz, P.D. (2017). Thiocarbonylthio-free RAFT polymers and the process of making the same. (Henkel), WO2017027557A1.

876 Pfukwa, R., Pound, G., and Klumperman, B. (2008). *Polym. Prepr. (Am. Chem. Soc., Div. Polym. Chem.)* 49: 117–118.

877 Vega-Rios, A. and Licea-Claverie, A. (2011). *J. Mex. Chem. Soc.* 55: 21–32. https://doi.org/10.29356/jmcs.v55i1.848.

878 Moad, G. (2022). Dithiocarbamates in RAFT polymerization. In: RAFT Polymerization: Materials, Synthesis and Applications (eds. G. Moad and E. Rizzardo). Weinheim: Wiley-VCH.

10

Xanthates in RAFT Polymerization

Mingxi Wang[1,2], Jean-Daniel Marty[1], and Mathias Destarac[1]

[1] IMRCP, UMR 5623, Université de Toulouse, 118, route de Narbonne, F-31062, Cedex 9, Toulouse, France
[2] College of Chemistry and Chemical Engineering, Shaanxi University of Science and Technology, Xi'an Weiyang University Park, Xi'an, Shaanxi Province, 710021, China

10.1 Introduction

Reversible addition–fragmentation chain transfer polymerization (RAFT) recently celebrated its 20th anniversary [1, 2]. In 1998, CSIRO disclosed the RAFT process in a first patent [3] followed soon after by their seminal *Macromolecules* paper [4]. Owing to their too low transfer constants, xanthates were not claimed in their original patent to be efficient RAFT agents [4]. Later the same year, Rhodia and CNRS published a patent where xanthates were central to mediating a reversible chain transfer process similar to RAFT [5]. They coined this process MADIX for Macromolecular Design by Interchange of Xanthates. The first paper came out in 2000 [6]. For the sake of clarity, we will use xanthate-mediated RAFT, or RAFT with xanthates, or just RAFT to describe MADIX throughout this document. Regardless of these historical considerations, xanthate RAFT agents gained increasing attention over the years and are today firmly established as best suited for the RAFT polymerization of non-conjugated monomers [7, 8]. A series of recent reviews address various aspects of xanthate-mediated RAFT [2, 9–11].

This chapter will highlight the most recent developments in this field since our chapter in the previous 2008 edition [12], covering areas such as xanthate synthesis, polymerization kinetics and reaction conditions, range of monomers, macromolecular architectures, xanthate end-group removal, and industrial applications.

10.2 Synthesis of RAFT/MADIX Agents

Synthetic methodologies to RAFT agents have been well reported and reviewed by different groups [13–15]. Here we outline three main methods for preparing a variety of xanthates (Table 10.1).

RAFT Polymerization: Methods, Synthesis and Applications, First Edition.
Edited by Graeme Moad and Ezio Rizzardo.

Table 10.1 Xanthates (ZOC(=S)SR) used as RAFT agents.

RAFT agent[a)]	Synthesis[a)]	Monomer[b)]
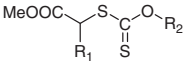	A [16–19]	CMS [20], *n*-BA [21], BDDA [22], EGDA [22], AA [17], AM [23], VAc [19, 24, 25], VTFAc [26, 27], VTFBu [28], CF_3VAc [29], vinyl sulfonate ester derivatives [18, 30], VDF [31–33], MDO [16, 34], DADMAC [35]
X0a: $R_1 = -CH_3$, $R_2 = -CH_2CH_3$		
X0b: $R_1 = -H$, $R_2 = -CH_2CH_3$	A [19, 25]	VAc [19, 25, 36, 37], ethylene [38]
X0c: $R_1 = -H$, $R_2 = -CH_3$	A [38]	VAc [36, 38, 39], ethylene [38]
X0d: $R_1 = -CH_3$, $R_2 = -CH(CH_3)_2$	A [16]	MDO [16]
X0e: $R_1 = -CH_3$, $R_2 = -C_4H_9$		
X0f: $R_1 = -CH_3$, $R_2 = -Ph-O-CH_3$		
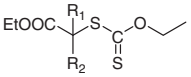	A [15, 34, 40–44] B [45]	St [45, 46], BDDA [22], EGDA [22], DMA [44, 47], NIPAM [48], MMA [45], VAc [15, 42, 43, 49–52], VBu [51], *S*-vinyl sulfide derivatives [53], NVP [54, 55], NVPiP [56], NVTri [41], NVPi [57], NVCbz [15, 54], *N*-vinylimidazolium salts [48]
X1a: $R_1 = -H$, $R_2 = -CH_3$		
X1b: $R_1 = -CH_3$, $R_2 = -CH_3$	A [40, 43, 49, 57]	VAc [43, 49], NVPi [57]
X1c: $R_1 = -H$, $R_2 = -H$	A [57]	NVPi [57]
X1d: $R_1 = -H$, $R_2 = -Ph$	A [55, 58]	VAc [59], NVP [55, 58, 59]
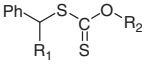	A [15, 18, 41, 48]	St [60], DMA [61], NIPAM [48, 61], VAc [15, 19], vinyl sulfonate ester derivatives [18, 30], *S*-vinyl sulfide derivatives [53], NVP [58], NVCL [62], NVPi [57], NVCbz [15], *N*-vinylimidazolium salts [48], *N*-vinylindole derivatives [63]
X2a: $R_1 = -CH_3$, $R_2 = CH_2CH_3$		
X2b: $R_1 = -H$, $R_2 = -CH_2CH_3$	A [15, 18, 41]	VAc [64, 65], NVCL [62], vinyl sulfonate ester derivatives [18, 30], *S*-vinyl sulfide derivatives [53], NVPi [57], *N*-vinylindole derivatives [63]

X2c: $R_1 = -H$, $R_2 = -CH(CH_3)_2$	A [15]	VAc [15, 16], NVCbz [15]
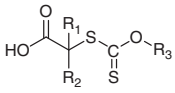	A [55, 66, 67]	MA [67], DMA [67], MMA [67], VAc [67], NVP [55], NVP-*b*-VAc [66], VPA [68–70]
X3a: $R_1 = -H$, $R_2 = -CH_3$, $R_3 = -CH_2CH_3$		
X3b: $R_1 = -H$, $R_2 = -H$, $R_3 = -CH_2CH_3$	A [71–73]	VAc [71, 73], DADMAC [72]
X3c: $R_1 = -H$, $R_2 = -CH_3$, $R_3 = -CH(CH_3)_2$	A [74]	*n*-BA-*b*-GMA [74]
X3d: $R_1 = -H$, $R_2 = -H$, $R_3 = -CH_3$	A [73]	VAc [73]
X3e: $R_1 = -H$, $R_2 = -H$, $R_3 = -CH(CH_3)_2$		
X3f: $R_1 = -H$, $R_2 = -H$, $R_3 = -(CH_2)_7CH_3$		
X3g: $R_1 = -H$, $R_2 = -H$, $R_3 = -C(CH_3)_3$	A [75]	
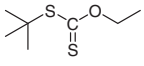 **X4**	C [58]	NVP [58]
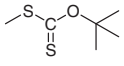 **X5**	A [75]	

(*continued*)

Table 10.1 (Continued)

RAFT agent[a)]	Synthesis[a)]	Monomer[b)]
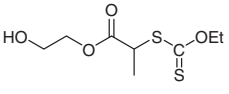 **X6**	A [76]	VC [76] NVP [77]
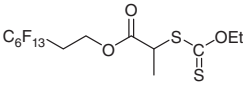 **X7**	A [78, 79]	VAc [76] VC [76, 78]
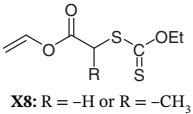 **X8:** R = –H or R = $-CH_3$	A [80, 81]	VAc [80, 81] MDO [34]
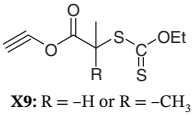 **X9:** R = –H or R = $-CH_3$	A [25, 82]	St [82] VAc [25, 82] NVP [82]
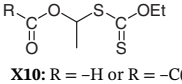 **X10:** R = –H or R = $-C(CH_3)_3$	A [19, 42]	VAc [42] VBz [42] VPi [42]

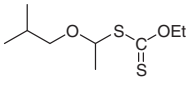 **X11**	A [83]	EVE [84]
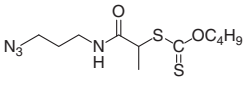 **X12**	A [85]	VAc [85, 86]
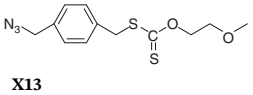 **X13**	A [87]	VAc [87]
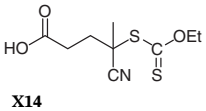 **X14**	B [55, 58]	NVP [55, 58]
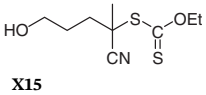 **X15**	B [55]	NVP [55]
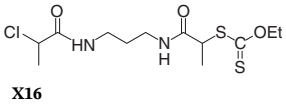 **X16**	A [88]	VAc [88]

(*continued*)

Table 10.1 (Continued)

RAFT agent[a)]	Synthesis[a)]	Monomer[b)]
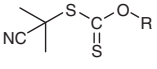 **X17a**: R = $-CH_2CH_3$ **X17b**: R = $-CH(CH_3)_2$ **X17c**: R = $-CH_2CF_3$	B [7, 58, 63, 89, 90]	VAc [7, 90, 91] NVP [7, 55, 58, 89] NVCbz [7] N-vinylindole derivatives [63] MMA [92]
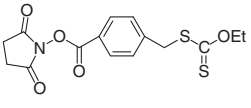 **X18**	A [93]	NVP [93]
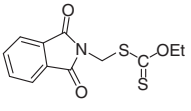 **X19**	A [94]	NVP [94]
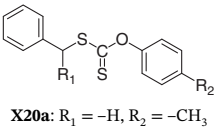 **X20a**: $R_1 = -H$, $R_2 = -CH_3$ **X20b**: $R_1 = -CH_3$, $R_2 = -H$	A [49]	VAc [49] NVP [95]

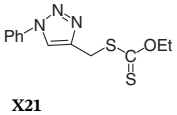 **X21**	C [96, 97]	VAc [96, 97] NVP [96]
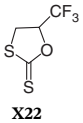 **X22**	A [98]	VDF [98]
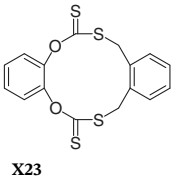 **X23**	A [99]	MA [99]
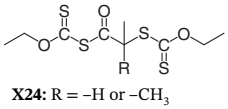 **X24:** R = –H or –CH_3	A [82]	NVP [82]
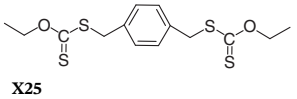 **X25**	A [100]	NVP [100, 101] NVCbz [102]

a) The letter indicates the synthetic method used.
b) Monomer abbreviations and structures are shown in Table 10.2.

10.2.1 Reaction of a Xanthate Salt with an Alkylating Agent

The synthesis of xanthates is most commonly achieved by treating a xanthate salt with an alkyl halide in conditions favourable to an S_N2 reaction. This method was mainly used for the efficient preparation of xanthates containing primary and secondary R groups, and yields were generally lower by substitution of tertiary halides (40–60%) [40, 49]. Commercially available potassium *O*-ethyl xanthate salt with structure $EtO(C{=}S)S^-K^+$ was by far the most considered [41, 42, 57]. Alternatively, xanthate salts can be produced by treatment of an alcohol precursor with carbon disulfide in the presence of a strong base such as sodium or potassium hydroxide [16, 40, 43, 49, 74, 103].

10.2.2 Reaction with Xanthogen Disulfides

Since xanthates bearing tertiary R leaving groups are more cumbersome to be prepared via nucleophilic substitution of tertiary halides, Zard and coworkers [104] and CSIRO [105] simultaneously reported the effective radical-induced decomposition of a xanthogen disulfide by R group radicals derived from azo-initiators such as AIBN. This method is now well established to produce S-tertiary xanthates in good yields [58, 63, 104, 105]. It is also possible to use this chemistry to generate xanthates in situ during polymerization [7, 89, 90].

Kwak et al. [45] reported a related atom transfer radical addition–fragmentation process to synthesize various RAFT agents including xanthates (Scheme 10.1). The process was accomplished using stoichiometric amounts of secondary or tertiary alkyl halides and *O*-ethyl xanthogen disulfide in the presence of an atom transfer radical polymerization (ATRP) catalyst and, optionally, Cu metal as a reducing agent. Xanthate yields were lower (43%) compared with dithioesters (82–92%) under similar conditions.

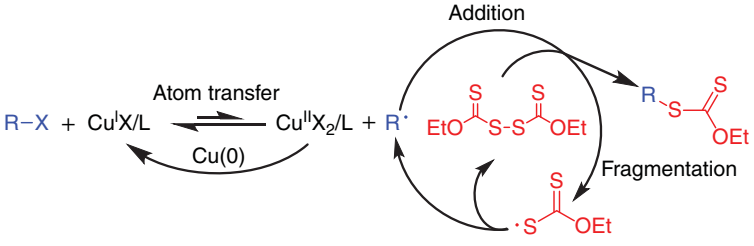

Scheme 10.1 Atom transfer radical addition–fragmentation for the synthesis of xanthate RAFT agents. Source: Adapted with permission from Kwak et al. [45]. Copyright 2009, John Wiley & Sons.

10.2.3 Xanthates Used as Precursors to Provide New Xanthates

Functional xanthates can be derivatized into a variety of other xanthates of interest. For instance, the Cu(I)-catalysed Huisgen 1,3-dipolar cycloaddition of *S*-propargyl *O*-ethyl xanthate with phenyl azide yielded the triazolinyl xanthate **X21** [96]. Owing to the aromaticity of the triazole ring, the triazolinyl leaving group exhibits a similar

Table 10.2 Monomers compatible with the RAFT/MADIX process.

Monomer	Abbreviations and structures			
Styrenics	St 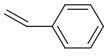		CMS 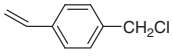	
Acrylates	MA 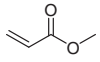	*n*-BA 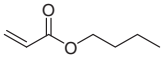	EGDA 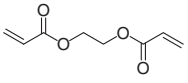	BDDA 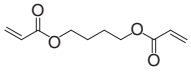
Acrylamides	AM 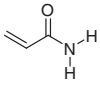	DMA 		NIPAM 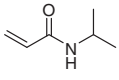
Methacrylates			MMA 	
Vinyl esters	VAc 	VBu 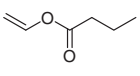	VBr 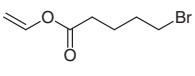	VPi 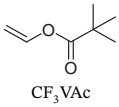
	VBz 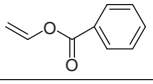	VTFAc 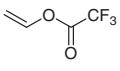	VTFBu 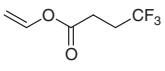	CF_3VAc 

(*continued*)

Table 10.2 (Continued)

Monomer	Abbreviations and structures			
S-Vinyl monomers	MES 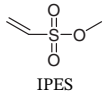	EES 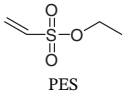	BES 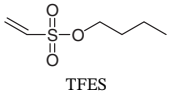	NES 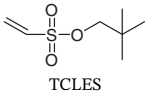
	IPES 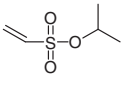	PES 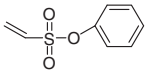	TFES 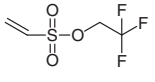	TCLES 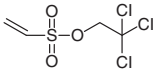
	PVS 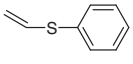	CPVS 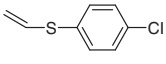	DCPVS 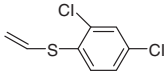	BPVS 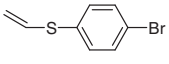
Vinyl phosphonic acid			VPA 	
N-Vinyl monomers	NVP 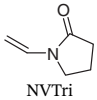	NVCL 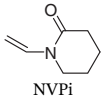	NVPiP 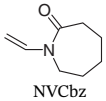	
	NVTri 	NVPi 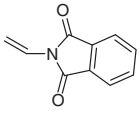	NVCbz 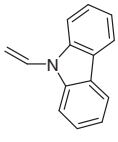	

	PVI-Br	EtOEVI-Br	EHVI-Br	
	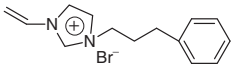	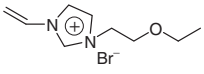	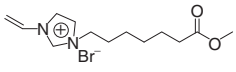	
	NVIn	2MNVIn	3MNVIn	
	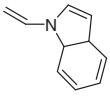	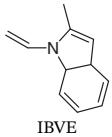	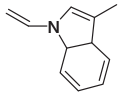	
Vinyl ethers	EVE	IBVE	HOVE	
		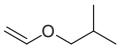	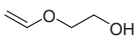	
Halo-olefins	VDF	PMVE	TFE	
		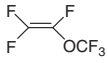		
	CTFE	HFP	VC	
				
Miscellaneous	Ethylene	MDO	BMDO	DADMAC
			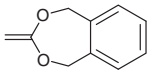	

St, styrene; CMS, 4-chloromethylstyrene or 4-vinylbenzyl chloride; MA, methyl acrylate;, *n*-BA, *n*-butyl acrylate; EGDA, ethylene glycol diacrylate; BDDA, 1,4-butanediol diacrylate; AM, acrylamide; DMA, *N,N*-dimethylacrylamide; NIPAM, *N*-isopropylacrylamide; MMA, methyl methacrylate; VAc, vinyl acetate; VBu, vinyl butyrate; VBr, vinyl bromobutanoate; VPi, vinyl pivalate; VBz, vinyl benzoate; VTFAc, vinyl trifluoroacetate; VTFBu, vinyl trifluorobutyrate; CF_3VAc, 1-(trifluoromethyl)vinyl acetate; MES, methyl ethenesulfonate; EES, ethyl ethenesulfonate; BES, 1-butyl ethenesulfonate; NES, neopentyl ethenesulfonate; IPES, isopropyl ethenesulfonate; PES, phenyl ethenesulfonate; TFES, 2,2,2-trifluoroethyl ethenesulfonate; TCLES, 2,2,2-trichloroethyl ethenesulfonate; PVS, phenyl vinyl sulfide; CPVS, 4-chlorophenyl vinyl sulfide; DCPVS, 2,4-dichlorophenyl vinyl sulfide; BPVS, 4-bromophenyl vinyl sulfide; VPA, vinylphosphonic acid; NVP, *N*-vinylpyrrolidone; NVCL, *N*-vinylcaprolactam; NVPiP, *N*-vinylpiperidone; NVTri, *N*-vinyl-1,2,4-triazole; NVPi, *N*-vinylphthalimide; NVCbz, *N*-vinylcarbazole; PNI-Br, 1-(3-phenylpropyl)-3-vinylimidazolium bromide; EtOEVI-Br, 1-(2-ethoxyethyl)-3-vinylimidazolium bromide; EHVI-Br, 1-(6-ethoxycarbonylhexyl)-3-vinylimidazolium bromide; NVIn, *N*-vinylindole; 2MNVIn, 2-methyl-*N*-vinylindole; 3MNVIn, 3-methyl-*N*-vinylindole; IBVE, isobutyl vinyl ether; EVE, ethyl vinyl ether; HOVE, 2-hydroxylethyl vinyl ether; VDF, vinylidene fluoride; PMVE, perfluoro(methyl vinyl ether); TFE, tetrafluoroethylene; CTFE, chlorotrifluoroethylene; HFP, hexafluoropropylene; VC, vinyl chloride; MDO, 2-methylene-1,3-dioxepane; BMDO, 5,6-benzo-2-methylene-1,3-dioxepane; DADMAC, diallyldimethylammonium chloride.

performance to that of a benzyl leaving group, and hence has been confirmed as an appropriate leaving group for RAFT polymerizations of *N*-vinylpyrrolidone (NVP) and VAc (see footnote of Table 10.2 for the complete list of monomer abbreviations) [96].

S-(*tert*-Butyl)-*O*-ethyl xanthate (**X4**) with high purity (>96%) and moderate yield (55%) has been synthesized by thiol exchange between a thioglycolic acid-based xanthate and *tert*-butyl thiol [58].

10.3 Experimental Conditions

In this section, an overview of recent reports on various modes of initiation and polymerization processes involving xanthate RAFT agents is proposed.

10.3.1 Initiation

As with other classes of RAFT agents, the commonly used methods to generate active radicals in RAFT polymerization with xanthates include (i) decomposition of thermal initiators, (ii) UV or visible light irradiation, (ii) ^{60}Co γ-ray irradiation, and (iv) redox initiation.

10.3.1.1 Thermal Initiators

The most common source of radicals for xanthate-mediated RAFT polymerization is azo-type initiators. AIBN and other commercially available azo initiators [16] have been selected according to their solubility and activation temperature.

Roy and Sumerlin [71] synthesized well-defined homopolymers and block copolymers of vinyl esters via xanthate-mediated RAFT with AIBN initiator under microwave heating. An unexplained enhancement of molecular weight controllability without significant inhibition or retardation was observed.

10.3.1.2 UV or Visible Light

An attractive alternative method to generate radicals uses UV or visible light to control the flux of radicals through simple 'ON/OFF' modulation of the light irradiation. A first approach consists in direct homolysis of the xanthate under irradiation, which plays a dual role of initiator and mediator. This strategy avoids the introduction of external radical sources and metal complexes into the polymerization, hence pushing back the limits in terms of molar mass control [50, 106–110]. Another approach involves photoinitiators. Successful RAFT polymerization of VAc has been demonstrated using **X0b** RAFT agent and bis(2,4,6-trimethylbenzoyl)phenylphosphine oxide as photoinitiator [111].

Boyer's group reported the first RAFT polymerization based on a photoinduced electron transfer (PET) process between a RAFT agent and the photoredox catalyst *fac*-[Ir(ppy)$_3$] under visible light irradiation [112, 113]. The proposed mechanism with xanthate RAFT agents for the so-called PET-RAFT polymerization is described in Scheme 10.2. Since then, a few xanthate/photoredox catalyst systems

such as **X0a**/ZnTPP [103] and **X3a**/Bi_2O_3 [67] have been applied to PET-RAFT polymerization. Conveniently, PET-RAFT polymerization is oxygen tolerant and can be carried out without the conventional degassing procedure [103].

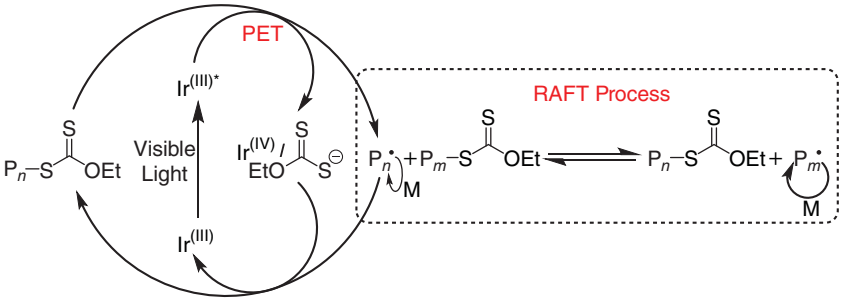

Scheme 10.2 Proposed mechanism for xanthate-mediated PET-RAFT polymerization. Source: Adapted with permission from Xu et al. [112]. Copyright 2014, John Wiley & Sons.

10.3.1.3 ^{60}Co γ-ray Irradiation

^{60}Co γ-ray irradiation as a source of active radicals has attracted increasing attention over the years, since the first γ-ray-initiated RAFT polymerization of methyl acrylate (MA) performed with five *S*-benzyl xanthates, including **X2b** [114]. Later, the same group reported the RAFT polymerization of the same monomer with a cyclic dixanthate (**X23**) at different temperatures (28, −30 and −76 °C) [99]. Polymers with well-controlled macromolecular characteristics were obtained. The lower the temperature is, the better the control of the polymerization. Yu et al. [52] investigated bulk RAFT polymerization of VAc with **X1a** at room temperature, and compared to AIBN initiation at 60 °C. Much lower dispersities and slightly better control of the polymer regioregularity were found with γ-ray initiation, presumably mainly due to differences in temperature. Segura et al. [91] reported miniemulsion polymerization of VAc with **X17a** at room temperature. Controlled M_n values with relatively high dispersities ($1.5 < Đ < 2.4$) were obtained, for a process yielding stable latexes produced with high rates and high conversions. Sütekin and Güven [17] also studied the γ-radiation-induced RAFT polymerization of AA in aqueous media and in ethanol, using xanthate **X0a**. PAAs with controlled M_n and dispersities in the range of 1.23–1.39 were synthesized. Wang et al. [115] investigated the xanthate-mediated living/controlled radical copolymerization of hexafluoropropylene (HFP) and butyl vinyl ether (BVE) at room temperature under ^{60}Co γ-ray irradiation. Xanthate **X1b** was used to control the synthesis of poly(HFP-*alt*-BVE) [115] with dispersities close to 1.3 up to M_n of 35 000 g mol^{-1}. After that, the xanthate terminal was oxidized to produce a fluoroalkyl sulfonic acid chain end.

10.3.1.4 Redox Initiation

Only one case of organosoluble redox initiating system (benzoyl peroxide/*N*,*N*-dimethylaniline) under high pressure (5 kbar) was reported, for VAc polymerization

with **X1a** [49]. In contrast, numerous examples of aqueous redox initiators were reported relatively recently. *tert*-Butylhydroperoxide (TBHP) in combination with ascorbic acid (AsAc) allowed the RAFT polymerization of *N*-vinylcaprolactam (NVCL) in water–ethanol mixtures with **X0a** [116] and that of NVP in pure water at room temperature with the same xanthate [117]. Using xanthate **X1a**, TBHP/AsAc initiated the polymerization-induced thermal self-assembly (PITSA) of *N*-isopropylacrylamide (NIPAM) and pentafluorophenyl acrylate (PFPA) [44]. In association with sodium sulfite Na_2SO_3 as reducing agent [118], TBHP initiated the controlled RAFT polymerization of NVP in water, by maintaining pH under basic conditions in order to avoid the formation of NVP hydration by-products. The ammonium persulfate (APS)/sodium formaldehyde sulfoxylate (NaFS) redox system was proved an excellent initiator for the aqueous polymerization of Am [23, 119] and derivatives [119] with **X0a** at room temperature, or for comonomer compositions comprising Am [120].

10.3.2 Polymerization Conditions

One of the major advantages of RAFT polymerizations is its compatibility with various reaction conditions, as it only requires the introduction of a CTA to an otherwise conventional-radical polymerization. In recent years, high-pressure polymerization and the RAFT PISA process have attracted the attention of researchers.

10.3.2.1 High-Pressure Polymerization

The use of high-pressure conditions (several kbar) for radical polymerization can increase the propagation rate coefficient k_p by several orders of magnitude and decrease the overall activation volumes [121]. Hence, high molecular weight polymers can be obtained with accessible industrial polymerization processes. Chen et al. [49] reported the use of high pressure (up to 5 kbar) for the synthesis of high molecular weight PVAc ($M_n = 123\,000\,\mathrm{g\,mol^{-1}}$, $Đ = 1.28$) via RAFT polymerization at 35 °C using **X1a**, **X1b,** and **X20a** CTAs. Under these conditions, the polymerization rate was significantly increased (15.2 times) in comparison with atmospheric pressure conditions. An induction period of four hours was observed, and polymerizations were kept below 40% conversion in order to maintain an acceptable level of control of M_n and $Đ$. A decrease of efficiency in the order of **X1a** > **X1b** > **X20a** was found.

10.3.2.2 Heterogeneous Polymerizations

Xanthate-mediated RAFT polymerization is compatible with all kinds of heterogeneous processes, in particular aqueous emulsion polymerization. Owing to their inherently low transfer constant for conjugated monomers and suitably limited solubility in water, xanthates were the first RAFT CTAs in early 2000s to circumvent issues associated with particle nucleation and allow controlled emulsion polymerization under *ab initio* conditions [122]. Since then, other strategies such as seeded emulsion, miniemulsion, and microemulsion polymerizations using xanthates have been successfully carried out and recently reviewed

[123, 124]. RAFT-mediated PISA is a recent and very powerful process for preparing block copolymer nanoparticles [125]. Recently, Binauld et al. [126] reported the xanthate-mediated RAFT emulsion PISA of VAc in the presence of PNVP, PEG, and poly(acryloylmorpholine) macro-CTAs, giving access to original surfactant-free PVAc latexes in water. Siirilä et al. [127] reported the aqueous emulsion PISA polymerization of NVCL with PEG-**X1a** above the thermal transition temperature of PNVCL, producing larger vesicular morphologies than the most commonly found spherical core–shell particles. In order to design waterborne physically crosslinked thermoresponsive particles, a successful approach of the xanthate-mediated RAFT PISA copolymerization of VAc and NVCL in emulsion with PEG-**X1a** was reported [128]. Zhang et al. [129] synthesized poly(ionic liquid) (PIL) nanoparticles through the aqueous RAFT PISA process of 3-*n*-dodecyl-1-vinylimidazolium bromide, using PEG-**X1a** as macro-CTA. Vakili et al. [44] recently reported the preparation of thermoresponsive crosslinked nanoobjects by aqueous PISA of PFPA starting from a monomer-in-water emulsion or NIPAm, using a PDMA-**X1a** reactive stabilizer and either redox or UV activation at room temperature. The synthesis of PVAc-*b*-PVDF block copolymers was investigated by RAFT PISA in dispersion in dimethylcarbonate [130]. The presence of PVAc and PVDF homopolymer contaminants was confirmed as a result of side reactions. New flake-like crystalline structures were obtained, with morphologies presumably governed by the crystallization of the PVDF block.

Two supercritical CO_2-($scCO_2$) soluble xanthate-terminated PVAc (PVAc-**X0b** and PVAc-**X0c**) were reported by Pham et al. [36] for RAFT homopolymerization of VAc and VPi in $scCO_2$. As expected for an efficient RAFT process, an increase in the initial loading of macroRAFT agent resulted in a decrease in both M_n and dispersities of PVAc, whereas the conversion was not affected (relatively low, <37%). Dispersities increased during polymerization for both VAc and VPi. The xanthate agent with an ethoxy group (**X0b**) showed better controllability (with lower $Đ$ value) than that with a methoxy group (**X0c**). The reported process could be referred to as a dispersion RAFT PISA in $scCO_2$ even though the authors did not address the nature of the reaction medium during polymerization. Howdle and coworkers developed **X1a**-RAFT PISA dispersion of NVP in $scCO_2$ using statistical copolymers of VAc with VBu [51] and VPi [131, 132] as macro-CTAs.

10.4 Kinetics

The different aspects of the kinetics of RAFT polymerization with xanthate CTAs, including their structure–reactivity relationship [133–135], initialization phenomenon [136], and computational studies of their addition–fragmentation pathways [137], have been largely reported in the 2000s. Owing to their strong σ-withdrawing character, alkoxy Z groups stabilize the intermediate RAFT radicals to a limited extent. Hence fragmentation is fast, and consequently xanthates have a very limited impact on the rate of polymerization in comparison with more reactive RAFT agents.

The reactivity of xanthate **X0a** has been largely explored over the whole range of monomers. Its chain transfer constant C_{tr} can vary by orders of magnitude depending on the monomer. For non-conjugated monomers such as vinyl esters [35], *N*-vinyl monomers [117, 138], *S*-vinyl monomers [18, 53], vinyl phosphonic acid (VPA) [68, 92], diallyldimethylammonium chloride (DADMAC) [35], and ethylene [38], a systematic good correlation between theoretical and experimental M_n in the early stages of polymerization reflected the high reactivity of **X0a** (C_{tr} typically >10). In a few cases such as for NVP and VAc, the selective formation of the *O*-ethyl xanthate/monomer 1 : 1 adduct prior to polymerization (so-called initialization period) was evidenced [136]. The interchain transfer constant C_{ex} can be quite high and result in narrowly dispersed polymers such as for *N*-vinyl lactams [138] and vinyl esters [35]. In contrast, relatively high dispersities for PVPA [92] and PDADMAC [35] were attributed to a slow reversible transfer of the *O*-ethyl xanthate end-group during polymerization. For conjugated monomers, the reactivity scale of xanthate **X0a** is as follows: acrylamides > acrylates > styrenics ≫ methacrylates. For substituted acrylamides (AMs), C_{tr} and C_{ex} are in the two to five range, which allows the formation of polyacrylamides with dispersities down to 1.2 in best cases [139]. Xanthates exhibit slightly lower reactivities for acrylate monomers; C_{tr} and C_{ex} are in the range of 1.5–2.0 for **X0a**, leading to dispersities generally between 1.5 and 1.8 [139]. *O*-Ethyl xanthates are poorly reactive for styrene and derivatives, with C_{tr} in the 0.65–0.80 range [46, 133, 139] and reported C_{ex} values of 0.65 [139] and 0.44 [46] for St. Polymerization of methacrylates with *O*-ethyl xanthates is uncontrolled, as illustrated by the very low C_{tr} values recently reported for this monomer (<0.1) [140].

10.5 Monomers

Xanthates RAFT agents can control a very broad range of monomers with highly disparate reactivities, typically from ethylene to methacrylates under specific conditions. A summary of compatible monomers is given in Table 10.2.

10.5.1 Styrenics

A limited number of recent studies deal with the use of xanthates in the polymerization of styrene and derivatives because of their poor transfer ability. Devlaminck et al. [46] recently reported a detailed study on **X1a**-mediated RAFT polymerization of St in bulk and solution conditions by successfully combining experimental and modelling analysis tools. Couture and Améduri [20] investigated the kinetics of RAFT polymerization of 4-chloromethyl styrene (CMS) initiated by AIBN at 80 °C in the presence of xanthate **X0a**. M_n decreased with constant high $Đ$ values (≈1.8) during the reaction, indicating that the polymerization is poorly controlled in a similar fashion with St.

10.5.2 Acrylates and Acrylamides

RAFT polymerizations of acrylates and acrylamides with xanthate CTAs have been widely studied. Mori and Tsukamoto [22] investigated RAFT polymerization of

diacrylate derivatives having different spacers under dilute conditions by using xanthates **X0a** and **X1a** and comparing with benzyl 1-pyrrolecarbodithioate of much higher reactivity. Owing to their moderate reactivity, xanthates led to comparatively faster polymerization rates, higher molecular weights, broader molecular weight distributions, and crosslinked products in some cases. Reports of polymerization of acrylamide monomers with xanthate RAFT agents include pioneering works on AM by Taton et al. using **X0a** and a difunctional xanthate in aqueous media [141], *N*,*N*-dimethylacrylamide (DMA) [47, 61, 67] and NIPAM [44, 61]. In all cases, polymerizations led to controlled M_n at high conversions and relatively narrow molecular weight distributions ($1.2 < Đ < 1.5$). Yuan et al. [61] reported the controlled synthesis of double hydrophilic block copolymers comprising either PNIPAM or PDMA as neutral first block and poly(1-vinylimidazolium) ionic liquid block using **X2a** CTA. Hakobyan et al. [67] and Carmean et al. [47] were interested in the aqueous polymerization of DMA via PET-RAFT process with Bi_2O_3 catalyst using **X3a**, and by direct activation by UV light with **X0a**, respectively.

One of the most striking advances of the last decade in the field of RAFT polymerization is the access to ultra-high molar molecular weight (UHMW, M_n of typically 10^6 g mol^{-1} and above) polyacrylamides by the so-called aqueous RAFT gel polymerization process first reported by our group [119]. It involves the use of minute amounts of redox initiator at low temperatures (10–25 °C) for monomer concentrations >10 wt.%. Under these reaction conditions, polymerizations reach completion within a few hours while a physical gel is formed. Low-dispersity polymers ($Đ < 1.2$) were obtained for controlled M_n up to ~10^6 g mol^{-1} for AM and DMA homopolymers, AM/AMPS statistical copolymers, and a PNIPAM-*b*-DMA copolymer [119]. Inspired by this work, Mejia et al. [142] developed an adiabatic gel process to perform polymerizations to a much higher volume and monomer concentration (from 2.0 to 3.47 M). They obtained controlled high molar mass P(AM-*stat*-AMPS) copolymers up to 3×10^6 g mol^{-1} over the whole range of composition. Adiabatic and conventional gel processes gave similar results. Alternatively, Sumerlin's group reported a photomediated-RAFT polymerization under conditions of gel polymerization with xanthate **X1a** as the single source of radicals [109]. By doing so, well-defined PDMAs were obtained using a UV light source. The molar masses reached 8.67×10^6 g mol^{-1} in less than five minutes of irradiation, and dispersities below 1.2 were achieved.

Thanks to well-defined polyacrylamides produced by RAFT gel polymerization with **X0a** [119] the outcome and kinetics of competitive adsorption between low and high molar mass chains of neutral PAM or partially hydrolyzed-PAM in aqueous solution at the surface of siliceous materials were better understood [143, 144].

10.5.3 Methacrylates

The reactivity of *O*-ethyl xanthates in methacrylate polymerization is very low (C_{tr} typically <0.1) [4, 92], hence no block copolymerization comprising a methacrylate sequence is possible under classical RAFT batch polymerization conditions. At best, a limited amount (up to ~20 mol%) of methacrylate comonomer can be statistically copolymerized in a controlled manner with a xanthate-compatible monomer, e.g. an acrylate. Recently, Destarac et al. [92] adapted a semi-batch RAFT

emulsion polymerization strategy reported for methacrylate polymerization with oligo(methacrylate) macromonomer CTAs [145] to fluorinated xanthate **X17c** of similar reactivity. By keeping very low instantaneous methyl methacrylate (MMA) concentrations, well-controlled PMMA latexes with controlled molar masses and low dispersities ($1.2 < Đ < 1.3$) were obtained prior to chain extension with VAc, leading to PMMA-*b*-PVAc copolymers.

10.5.4 Vinyl Esters

Xanthates are the most popular RAFT agents for controlling the polymerization of vinyl esters [9], among which VAc was by far the most studied. The reactivity of **X0a**-**X0c** [24, 25, 36–39], **X1a** [15, 42, 43, 49–52], **X1b** [43, 49], **X1d** [59], **X2a** [15], **X2c** [15, 16], **X3a** [67], **X3b** [71, 73], **X3d**-**X3f** [73], **X7**-**X10** [25, 42, 76, 80–82], **X12** [85, 86], **X13** [87], **X16** [88], **X17a** [7, 90, 91], **X20a** [49], and **X21** [96, 97] under different conditions of VAc polymerization was examined by different groups. The high reactivity of the propagating radical leads to a non-negligible fraction of side reactions such as 1–2% head-to-head addition [146] and chain transfer to solvent, monomer, and polymer, which explains limited RAFT control in terms of M_n (typically $<10^5$ g mol^{-1}) while maintaining low dispersities ($Đ < 1.2$). Other vinyl alkylates such as vinyl benzoate (VBz) [42], vinyl butyrate (VBu) [51], and vinyl pivalate (VPi) [42, 131, 132, 147, 148] were also successfully polymerized with xanthates (Table 10.2). Most of these studies aimed at improving the solubility of their copolymers with VAc in $scCO_2$.

Using RAFT agent **X0f**, Hedir et al. [149] synthesized a series of thermoresponsive poly(oligo(ethylene glycol) vinyl acetate)s (P(MeO_2VAc)s) with excellent control over their molecular properties. Moreover, the statistical copolymerization of MeO_2VAc with 2-methylene-1,3-dioxepane (MDO) cyclic ketene acetal (CKA) enabled to independently control the thermal properties and degradation behaviour of the resulting polymers.

Well-defined poly(fluorovinyl esters) from vinyl trifluoroacetate (VTFAc) [26, 27] and vinyl trifluorobutyrate (VTFBu) [28] were synthesized via RAFT polymerization using **X0a** as CTA. The solubility of PVTFBu and VTFAc/VAc statistical copolymers in $scCO_2$ was shown to be greatly enhanced compared to PVAc [26–28]. As PVTFAc is much more susceptible to hydrolysis than VAc, diblock copolymers of VAc and VTFAc allowed the preparation of PVAc-PVOH diblock copolymers by selective methanolysis. 1-(Trifluoromethyl)vinyl acetate (CF_3VAc) has been copolymerized with VAc by **X0a**-mediated RAFT polymerization with a strong tendency towards alternated microstructure [29]. By increasing the CF_3VAc molar fraction from 10% to 50% in the feed, an increase of dispersities ($1.2 < Đ < 1.7$) was observed although control over molecular weight was maintained ($M_n \sim 4000$ g mol^{-1}).

10.5.5 *S*-Vinyl Monomers

Mori and his colleagues focused on *S*-vinyl monomers, including eight vinyl sulfonate ester derivatives (in Table 10.2) [18, 30]: methyl ethenesulfonate (MES), ethyl

ethenesulfonate (EES), 1-butyl ethenesulfonate (BES), neopentyl ethenesulfonate (NES), 2,2,2-trifluoroethyl ethenesulfonate (TFES), 2,2,2-trichloroethyl ethenesulfonate (TCLES), isopropyl ethenesulfonate (IPES), phenyl ethenesulfonate (PES); and four *S*-vinyl sulfide derivatives (in Table 10.2) [53]: phenyl vinyl sulfide (PVS), 4-chlorophenyl vinyl sulfide (CPVS), 2,4-dichlorophenyl vinyl sulfide (DCPVS), 4-bromophenyl vinyl sulfide (BPVS). All the homopolymers exhibited relatively narrow molecular weight distributions ($1.3 < Đ < 1.7$) and pre-determined molecular weights when RAFT agent **X0a** was used. Block copolymerizations were also successfully conducted via RAFT polymerization using PNIPAM-**X0a** [30] or PNVCbz-**X0a** [18, 53] as macro-CTA, the synthesized block copolymers having distinct thermoresponsive property [18, 30] or optoelectronic functionalities [53].

10.5.6 Vinyl Phosphonic Acid

VPA is a monomer of great interest due to the multiple properties of the corresponding polymers associated with its strong diacid character. It had been a very challenging candidate for RDRP due to its vinyl nature and unprotected phosphonic acid character, until Blidi et al. [68] first reported the controlled aqueous RAFT polymerization of VPA using **X3a** under thermal initiation conditions. Using ^{31}P NMR spectroscopy the authors established that transfer to **X3a** is fast compared to propagation with early formation of xanthate-terminated oligomers. By means of a **X3a**/VPA 1 : 1 adduct, it was shown by SEC and ^{31}P NMR spectroscopy that chain growth proceeds with a relatively slow interchain transfer of the xanthate terminal group, resulting in relatively high dispersities [68]. Destarac's group tried to accelerate VPA polymerization by using microwave irradiation [70] or by adding metal alkali hydroxides [69]. Microwave heating with **X3a** caused a threefold increase of the initial rate of RAFT/MADIX aqueous polymerization compared with conventional heating, with no visible impact on the macromolecular parameters of PVPA. With metal alkali hydroxide additives, the use of 0.5 equiv NaOH relative to VPA led to the fastest polymerizations, while 0.5 equiv KOH and NH_4OH provided a moderate increase in rate coupled with a significant reduction in dispersity of the final polymers [69].

10.5.7 *N*-Vinyl Monomers

A wide range of xanthates, including **X1a**, **X1d**, **X2a**, **X3a**, **X4**, **X9**, **X14**, **X15**, **X17a**–**X19**, **X21**, **X24**, and **X25**, have been used for the polymerization of NVP [7, 54, 55, 58, 82, 89, 93, 94, 100, 101, 150] either in bulk or in organic solvent with thermal initiation. Pound et al. [55] evidenced several side reactions in RAFT polymerization of NVP, among which are hydration products of NVP at acidic pH and elimination of the xanthate from the polymer chain end. The main lessons learnt from this precious contribution was that control of pH when using aqueous media and the application of low temperatures should lead to a decrease of undesired reactions. Later, Guinaudeau et al. [117] reported successful aqueous RAFT polymerization of NVP under concentrated conditions at room temperature (pH = 6–7)

with TBHP/ascorbic acid as redox initiator. For the synthesis of NVP-based double hydrophilic block copolymers under more dilute conditions, sodium sulfite was used instead as reducing agent (pH ~ 9) [117]. Very recently, Wang et al. [95] reported RAFT polymerization of NVP under UV or visible light irradiation at room temperature with xanthate **X20b** and without extra initiator or catalyst. Wan et al. [62] and Beija et al. [138] reported the successful RAFT polymerization of NVCL, respectively with **X2a** and **X0a**. Well-controlled statistical copolymers of NVP and NVP of tunable LCST and hydrogel properties were effectively designed using **X0a** [151]. The polymerization of several other *N*-vinyl monomers, *N*-vinylpiperidone (NVPiP)/**X1a** [56], *N*-vinyl-1,2,4-triazole (NVTri)/**X1a** [41], *N*-vinylphthalimide (NVPi)/**X1b** [57], *N*-vinylcarbazole (NVCbz)/**X17a,** and **X25** [7, 108], was controlled by RAFT polymerization.

Mori et al. [48] reported the RAFT polymerizations of a series of four *N*-vinylimidazolium salts (Table 10.2) by using **X1a** and **X2a** as CTAs. The polymerizations proceeded in a controlled fashion. Maki et al. [63] examined the RAFT polymerization of three *N*-vinylindole derivatives: NVIn, 2MNVIn, and 3MNVIn (Table 10.2) with five different xanthates. Among them, **X2a** was the most efficient ($Đ = 1.20–1.40$).

10.5.8 Halo-olefins

Recent years have witnessed a growing interest in the development of xanthate-mediated RAFT to control the polymerization of vinylidene fluoride (VDF), perfluoro(methyl vinyl ether) (PMVE), tetrafluoroethylene (TFE), chlorotrifluoroethylene (CTFE), and hexafluoropropene (HFP) and prepare well-defined fluoropolymer-based architectures including end-functional [115, 152] and star [153] polymers, statistical [79, 154, 155], alternated [115, 156], and block copolymers [31, 83, 84, 98, 154, 157]. As VDF was the only fluoro-olefin of the series to be homopolymerized in a controlled fashion by RAFT [32, 33, 154, 157], it will be the only study described in this section. All the other works on various microstructures and architectures will be developed in dedicated sections.

Guerre et al. [32] carried out a thorough study of the RAFT polymerization of VDF using xanthate **X0a** in dimethylcarbonate. PVDF-**X0a** homopolymers with $DP_n < 50$ showed narrow molar mass distributions ($Đ < 1.5$), and were expected to be used as macro-CTAs for preparing novel fluorinated architectures. It was found that polymerizations suffer from several side reactions, among which are transfer to solvent and reverse additions during propagation. The latter effect is responsible for an accumulation of $–CH_2–X$ chain ends during polymerization until $–CF_2–X$ terminal groups completely disappear. The authors defined this stage as the end of RAFT control with conventional radical polymerization taking over, until they demonstrated by means of NMR and DFT calculations that the reverse xanthate adducts $–CF_2CH_2–X$ can actually be reactivated by a small fraction of $–CF_2CH_2\cdot$ radicals present in the system [33]. Transfer to solvent contributed to the loss of ~10% of xanthate terminal functionality with ~90% of chains remaining potentially reactive.

Solution and aqueous miniemulsion of RAFT polymerizations of VC mediated by fluorinated xanthate **X7** were successfully conducted by Huang et al. [78]. The miniemulsion polymerization exhibits higher rate and broader molecular weight distribution than solution polymerization. It was further reported that the **X7**-terminated PVC can be reinitiated and extended by VAc and NVP in solution; and the **X7**-terminated PVC can also be chain-extended by VAc in miniemulsion polymerization to obtain PVC-*b*-PVAc diblock copolymers. Very recently, Coelho and coworkers [158] reported the efficient low-temperature (30 °C) RAFT polymerization of VC in cyclopentyl methyl ether with xanthate **X0b**. Dispersities in the 1.2–1.3 range were obtained. Very small fractions of structural defects were revealed by NMR spectroscopy. Successful chain extensions were performed with VAc and NVCL to produce the corresponding diblock copolymers.

10.5.9 Ethylene

Dommanget et al. [38] reported the first example of RAFT polymerization of ethylene in the presence of xanthates **X0b** and **X0c** as CTAs in dimethylcarbonate under relatively mild conditions (70 °C, $P \leq 200$ bars). The livingness of the process was confirmed by the linear increase of predicted molar masses vs. conversion and by PE chain extension. A side fragmentation of the *O*-ethyl group was evidenced by ^{1}H NMR, which limited control to low M_n (~2 K). Semicrystalline copolymers of ethylene and vinyl acetate were further produced under mild conditions and exhibited low contents of the VAc unit (<10%). In a later report [159], the *O*-fragmentation was suppressed by the same group using aromatic xanthates **X0f**. The loss of living chain ends was nevertheless detected via a mechanism based on cross-termination. PEs with $Đ = 1.2$–1.3 were obtained for M_n up to 1000 g mol^{-1}.

10.5.10 Cyclic Ketene Acetals (CKAs)

Ring-opening polymerization of CKAs by radical polymerization has attracted increasing attention over the past years [160]. The widely studied MDO, a seven-membered ring CKA (Table 10.2) for which the corresponding polymer PMDO is identical to poly(ε-caprolactone), was successfully polymerized by RAFT using xanthates [16, 161, 162]. Bell et al. [16] reported the controlled homopolymerization of MDO in the presence of **X0a** and **X0d**–**X0f**. The *p*-methoxyphenyl xanthate **X0f** offers significantly enhanced control over molecular weight and dispersity compared to other xanthates. In-depth investigation showed loss of the xanthate functionality as a result of Z group fragmentation leading to the formation of carbonodithioate groups (Scheme 10.3). Then the authors applied **X0f** to the statistical copolymerization of VAc and MDO, all dispersities were within 1.3–1.5. Hedir et al. successfully synthesized linear degradable copolymers P(MDO-*co*-VAc) [162] and P(MDO-*co*-VBr) [161]. The bromine atom of the VBr units was converted to an azide for further derivatization by alkyne–azide click coupling.

Hydrolytically degradable statistical copolymers of 5,6-benzo-2-methylene-1,3-dioxepane (BMDO) (Table 10.2) with NVCL ($Đ = 1.4$–1.6) [163] and VAc ($Đ < 1.26$)

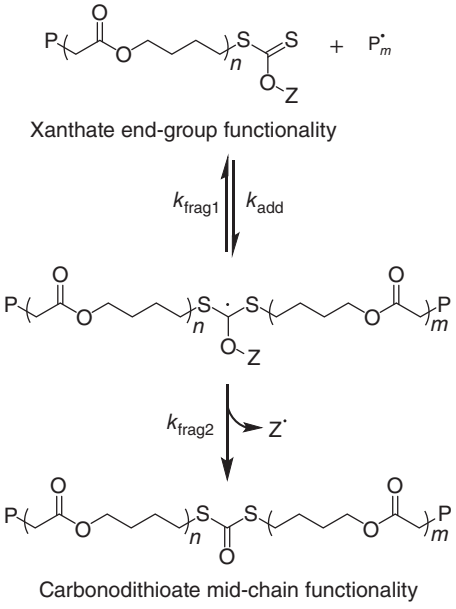

Scheme 10.3 Rearrangement and Z-group fragmentation occurring during the polymerization of MDO in the presence of a xanthate. Source: Bell et al. 2015 [16] and Xu et al. 2019 [34]. Adapted with permission of John Wiley & Sons. [16, 34].

[164] were achieved by RAFT polymerization with F_{BMDO} up to 0.5 using **X0b** and 0.4 with **X0a**, respectively. In both, BMDO was found to be much more reactive than its comonomer.

10.5.11 Diallyl Monomers

In the case of diallyl monomers, Assem et al. [72] first reported the RAFT/MADIX cyclopolymerization of DADMAC in aqueous medium via RAFT process with trithiocarbonates in 2007. Comparatively, the RAFT agent **X3b** was much less efficient to control M_n, despite unexpectedly giving low dispersities ($Đ \approx 1.12$).

Soon after, our group [35, 92] investigated the aqueous DADMAC polymerization at 50 °C using a **X0a**-terminated AM oligomer of $DP_n = 7$. Excellent control of M_n was observed with dispersities ($1.8 < Đ < 2.2$), which contradicted the works of Assem et al. [72]. Based on a kinetic study using the SEC-peak resolution method, it was concluded that C_{ex} was quite low (1.5), which supported the existence of broad molar mass distributions.

10.6 Macromolecular Architectures

Xanthate-mediated RAFT copolymerization is a versatile and powerful tool to design and synthesize controlled copolymers with 'complex' macromolecular architectures, including end-functional homopolymers/statistical copolymers, block copolymers,

gradient copolymers, cyclic polymers, graft/comb/brush copolymers, and star and hyperbranched polymers (HPs). This section reviews the recent achievements in macromolecular engineering with RAFT using xanthates.

10.6.1 End-Functional Homopolymers/Statistical Copolymers

Well-defined functional polymers can be obtained by using either a functionalized monomer or a xanthate agent. Recently, Jia et al. [165] demonstrated the first example of a lysine-based NVCL derivative and its RAFT copolymerization to afford a sustainable and amino-functionalized PNVCL with thermo and pH dual-stimuli responsiveness. Langlais et al. [166] designed two new thiolactone-based xanthates from a single hydroxy thiolactone (Scheme 10.4), which were further used in the RAFT polymerization of NVP, NVCL, VAc, and NIPAM. The efficiency of these xanthates was evidenced through the successful synthesis of related functional homopolymers of controlled M_n and low dispersities ($Đ < 1.22$), bearing α-terminal thiolactone groups. The thiolactone group at the end of the polymer chains was post-modified with an amine-thiol-thiosulfonate strategy.

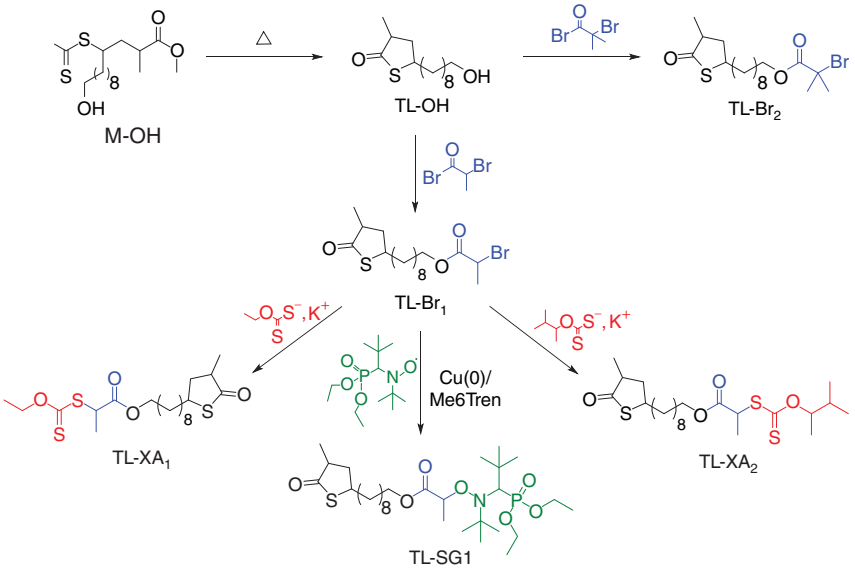

Scheme 10.4 Synthetic route to thiolactone-containing RDRP agents for controlled polymerizations. Source: Adapted with permission from Langlais et al. [166]. Copyright 2018, John Wiley & Sons.

Post-polymerization modification (PPM) of functional polymers has also gained the most attention these years. Chen et al. [167] have reported the synthesis of PVAc with fluorescence properties via a combination of RAFT polymerization and 'click' chemistry. They first used an azido-functional xanthate to mediate RAFT polymerization of VAc and give rise to azide-terminated PVAc. Then the resulting PVAc was 'clicked' with a fluorescent alkyne.

Etchenausia et al. [168] synthesized well-defined thermoresponsive amphiphilic statistical copolymers based on NVCL and VAc by polymerization mediated by **X1a** at 65 °C. Copolymers with controlled molar masses and low dispersities ($Đ < 1.3$) were produced over a wide range of monomer feed ratios. Reactivity ratio values demonstrated that NVCL and VAc units are distributed homogeneously along the copolymer chains.

Several types of statistical and alternated copolymers based on fluoro-olefins using RAFT polymerization have been recently reported using xanthate **X0a**, more precisely poly(VDF-*stat*-PMVE) [154], poly(VDF-*stat*-TCP) [79], poly(VDF-*stat*-MAF-TBE) [155], and low-dispersity ($Đ \sim 1.1$) poly(TFE-*alt*-iBuVE) of low molar mass [156]. Another example of end-functional fluoropolymer was reported by Guerre et al. [152] who synthesized a PVDF methacrylate macromonomer by **X0a**-mediated RAFT polymerization of VDF followed by a one-pot thio-Michael addition with 3-(acryloyl)-2-hydroxypropyl methacrylate.

10.6.2 Block Copolymers

Considerable strides were recently made in the synthesis of block copolymers through sequential monomer addition using xanthate RAFT agents, especially from some rarely reported monomers (e.g. VC [78], VDF [98, 154], VPA [72, 141], DADMAC [35, 92], vinyl sulfonates [18, 30]). In addition, xanthate-capped poly(ethylene oxide) [147, 169–178] and polysaccharides [179, 180] have been largely exploited by a variety of research groups as precursors for the synthesis of block copolymers.

Some researchers focused on the investigation of the self-assembly properties of amphiphilic [41, 54, 60, 181, 182] or double hydrophilic block copolymers [61, 173, 183]. For example, Peng et al. [60] synthesized well-defined ($Đ = 1.24$) amphiphilic PSt-*b*-PNVim block copolymers by sequential RAFT polymerization using **X2a** as CTA. The size and morphology of the copolymer aggregates were investigated by DLS and TEM. The copolymers assembled into uniform spheroidal micelles with PSt as the dense core and PNVim as the loose corona in water. Mori et al. [41] reported the controlled synthesis of amphiphilic PNVTri-*b*-PNVCbz block copolymers by RAFT polymerization using **X1a** as CTA. The block copolymers formed spherical micelles and inverse micelles depending on the nature of the solvents (Scheme 10.5). Huang et al. [54] synthesized the two PNVCbz-*b*-PNVP and PNVP-*b*-PNVCbz amphiphilic block copolymers via xanthate-mediated RAFT polymerization by changing the order of monomer addition. The particle size distributions of the prepared block copolymers were measured in several organic solvents with different polarities. Depending on their composition, block copolymer PNVCbz-*b*-PNVP formed micelles in methanol whereas PNVP-*b*-PNVCbz formed larger aggregates and precipitates. Our group reported the synthesis of PDMA-*b*-PVAc amphiphilic diblock copolymers and studied their solubility in $scCO_2$ using high-pressure IR spectroscopy [182]. The copolymer solubility was low and further decreased on increasing the weight fraction of the PDMA block and/or the total molecular weight of the polymer.

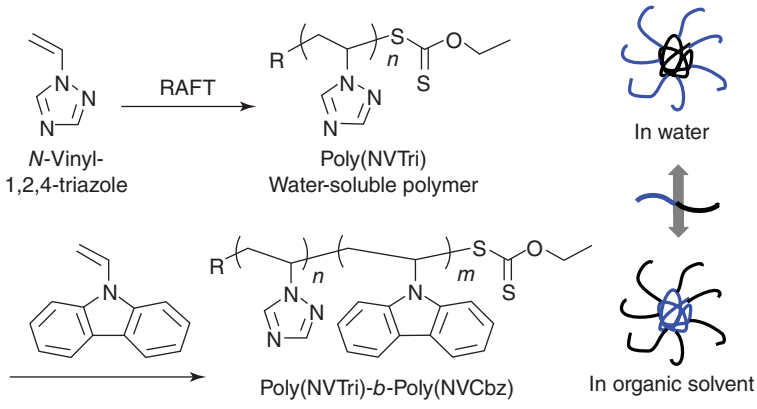

Scheme 10.5 Synthesis of amphiphilic block copolymer PNVTri-*b*-PNVCbz and their self-assembly behaviour in selective solvents. Source: Reproduced with permission from Mori et al. [41]. Copyright 2012, John Wiley & Sons.

Markiewicz et al. [173] reported the synthesis of PEO-*b*-PVPA diblock copolymer in water and their use to stabilize iron oxide nanoparticles formed in situ. Willersinn and Schmidt [180] studied the synthesis of pullulan-*b*-PNVP copolymer from xanthate-capped pullulan. The well-defined copolymers were self-assembled in water to form vesicles. After crosslinking with cystamine, vesicles became redox- and pH-cleavable.

The assembly behaviour of thermoresponsive double hydrophilic [56, 183] and amphiphilic [56, 184–187] block copolymers in aqueous media was also an important centre of focus. Nguyen et al. [187] reported the behaviour of thermoresponsive block copolymers of BA and *N*-alkylacrylamides in 1-ethyl-3-methylimidazolium bis(trifluoromethylsulfonyl)imide ($[C_2mim][NTf_2]$) ionic liquid. The polymers exhibited double thermoresponsiveness with both upper critical solution temperature (UCST) and lower critical solution temperature (LCST). For a given molar mass, these temperatures can be easily controlled by choosing the PBA to PNIPAM balance or by altering the polymer composition of the PNIPAM block by copolymerizing NIPAM with hydrophobic *N*-*tert*-butylacrylamide (NtBuA).

Yuan et al. [61] synthesized PNIPAM-*b*-PIL double hydrophilic block copolymers comprising a 1-vinylimidazolium-based poly(ionic liquid) segment via the RAFT process using xanthate CTAs. Copolymers showed dual-stimuli-responsive behaviour against changes in temperature and ionic strength in aqueous solution.

The combination of xanthate-mediated RAFT with other polymerization techniques, such as ATRP [88, 97, 188–191], ring-opening polymerization (ROP) [76, 77, 85, 192–196], living cationic polymerization [197], or click coupling reactions [85, 97, 181], are efficient approaches for the synthesis of block copolymers.

Kang et al. [77] synthesized well-defined PNVP-*b*-PCL amphiphilic block copolymers at 30 °C via the combination of ROP and RAFT polymerization in a one-pot procedure using the hydroxyl-functional xanthate **X6** as dual initiator. The copolymers showed narrow molecular weight distributions ($Đ < 1.2$) and predicted molar masses, indicating that the ROP and RAFT polymerization proceeded

independently in a controlled manner. The block copolymers could be labeled fluorescently through a reaction with rhodamine B isothiocyanate in the same pot.

Numerous examples of block copolymers comprising one poly(fluoro-olefin) sequence have emerged in recent literature. Guerre et al. [83] reported the first block copolymerization of ethyl vinyl ether (EVE) with VDF via sequential cationic and xanthate-mediated RAFT polymerization [84]. It was found that xanthate **X11** gave moderate control for cationic radical polymerization of EVE ($Đ \sim 1.5$) but efficient cross-over for VDF polymerization by radical RAFT polymerization. The same strategy was followed by the same authors who considered the combination of nearly equimolar amounts of CTFE and EVE monomers for an alternated radical RAFT polymerization step [83] (Scheme 10.6). It was demonstrated that block copolymerization was much better controlled by performing cationic RAFT polymerization of EVE as first block (Scheme 10.6). Cationic RAFT polymerization of EVE afforded PEVE macro-CTAs with high chain end fidelity and chain extension

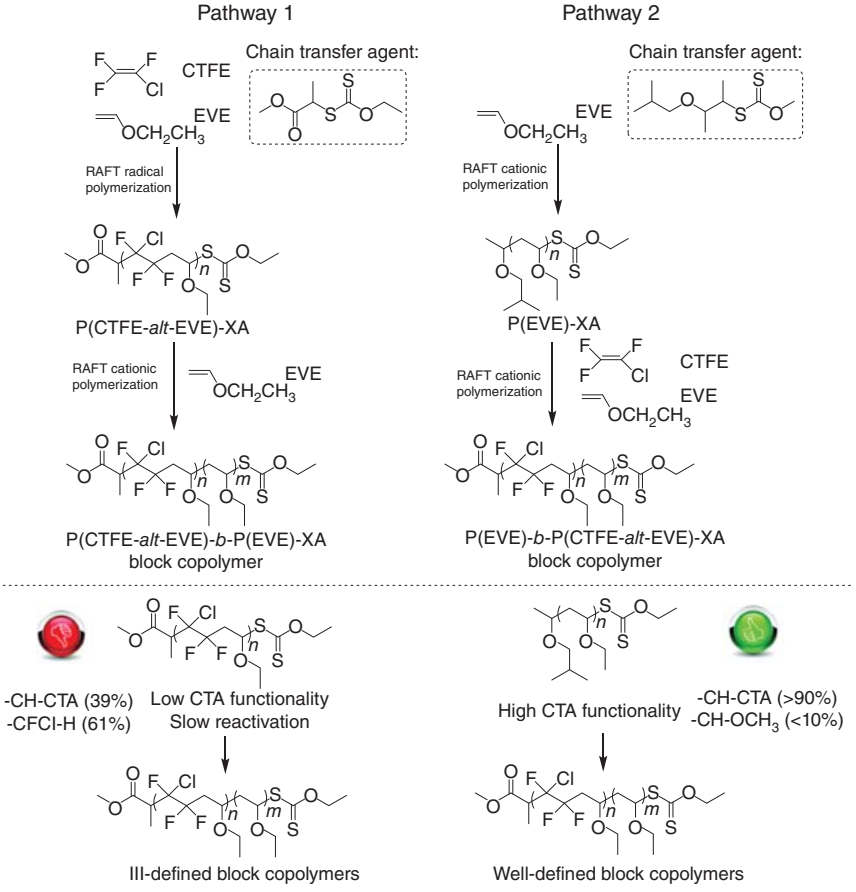

Scheme 10.6 Synthesis of P(CTFE-*alt*-EVE)-*b*-PEVE and PEVE-*b*-P(CTFE-*alt*-EVE) block copolymers. Source: Adapted with permission from Guerre et al. [83]. Copyright 2018, John Wiley & Sons.

reactions, resulting in well-defined PEVE-*b*-P(CTFE-*alt*-EVE) block copolymers with low dispersities ($Đ < 1.35$).

Through a kinetic study, chain extension experiments, and DFT calculations, Guerre et al. [157] demonstrated that PVDF-*b*-PVAc block copolymerization could be carried out with fast reactivation of the $-CH_2CF_2-$**X0a** normal terminal adducts and a slower but still possible activation of the $-CF_2CH_2-X$ reverse adducts [157]. For PVDF-*b*-PNVP, block copolymerization was much less efficient with slower activation of the normal PVDF-**X0a** chain ends, and no activation of the reverse ones [157]. Later in 2018, Li et al. [31] reported the synthesis of PVDF-*b*-PNVP copolymers and studied their self-assembly behaviour. Even though the block copolymers self-assembled in water, it is likely that the control of block copolymerization remained limited. PVDF-*b*-PVAc and PVDF-*b*-(PVAc-*alt*-MAF-TBE) (MAF-TBE = *tert*-butyl 2-trifluoromethacrylate) multiblock copolymers were successfully synthesized using fluorinated cyclic xanthate **X22** [98]. Amphiphilic PDMA-*b*-PDVF and PDMA-*b*-P(VDF-*stat*-PMVE) copolymers were also prepared using xanthate **X0a** [154].

10.6.3 Gradient Copolymers

Gradient copolymers are defined as containing at least one section of continuously varying monomer composition [198]. Xanthates are particularly well suited for the synthesis of spontaneous gradient copolymers, which can be formed in a one-pot procedure when copolymerizing monomers of disparate reactivities by any kind of controlled or living polymerization.

To date, only a few cases of spontaneous gradient copolymers have been reported using xanthate-mediated RAFT polymerization [199–201]. This approach can lead to 'block-like' structures with an initial region of nearly constant composition, a relatively steep transitional region, and a final segment of homopolymer [199, 201].

Spontaneous block-like gradient copolymers synthesized by RAFT polymerization with xanthates usually exhibit intriguing differences with block analogues. For instance, our group [201] investigated the synthesis and self-assembly behaviour of P(NIPAM-*grad*-VAc) amphiphilic gradient copolymers in water. ^{1}H NMR spectroscopy results suggested the formation of dynamic aggregates that respond rapidly to changes in solubility, in contrast to the kinetically frozen aggregates formed by block copolymers. Furthermore, they display a single, broad glass transition, as is typically found for gradient copolymers. We also reported **X0a**-mediated RAFT polymerization of spontaneous amphiphilic gradient terpolymers of DMA, VPi, and VAc [199]. The copolymers exhibited slightly lower cloud point pressures in $scCO_2$ than the corresponding diblock copolymers. Moreover, much more pronounced differences were established at the water/$scCO_2$ interface, with larger critical aggregation concentration (CAC), much faster adsorption kinetics and equilibration, and lower surface tension for gradient copolymers compared to their diblock counterparts.

10.6.4 Cyclic Copolymers

Cyclic polymers have markedly different physicochemical characteristics from their linear counterparts. In general, homo- or hetero-telechelic polymers are

synthesized by controlled/living polymerization, and click chemistry is then employed to ring-close the linear precursors and prepare the corresponding cyclic polymers. Tang et al. [202] and Li et al. [203] reported a strain-promoted azide–alkyne cycloaddition (SPAAC) reaction for the ring closure of telechelic polymers derived from xanthate-mediated RAFT polymerization of unconjugated monomers. As shown in Scheme 10.7 [202], a functional xanthate agent bearing the cyclopropenone-masked dibenzocyclooctyne and azide end-groups was designed to polymerize VAc and NVP. The resultant linear precursors were then directly used to prepare the corresponding cyclic polymers by the catalyst-free UV-induced SPAAC ring-closure reaction, in air at room temperature.

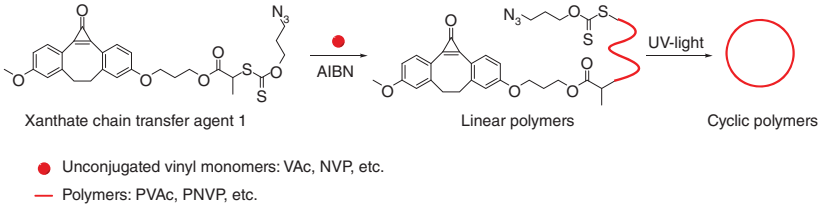

Scheme 10.7 Preparation of PVAc and PNVP cyclic polymers by RAFT polymerization and light-induced SPAAC reaction. Source: Adapted with permission from Tang et al. [202]. Copyright 2015, John Wiley & Sons.

10.6.5 Graft/Comb/Brush Copolymers

Graft copolymers are comb-shaped copolymers, which generally consist of a linear backbone of one composition and randomly distributed branches of another composition. Well-defined graft copolymers can be prepared via RAFT polymerization using xanthate CTAs by either a *grafting from* or a *grafting to* process.

In the 'grafting from' process, the macromolecular backbone is chemically modified in order to introduce xanthates. Atanase et al. [204] synthesized PVAc-*graft*-PNVP copolymers of low grafting density and with a PVAc backbone of constant length. In a first step, a series of P(VAc-*co*-VClAc) copolymers were prepared by RAFT, followed by their functionalization with xanthate groups. Then RAFT polymerization of NVP was performed from the xanthate-functional backbone to yield the graft copolymers. Kashio et al. [205] reported the xanthate-mediated RAFT graft polymerization of DMA, NIPAM, and acryloylmorpholine from a xanthate-modified polysilsesquioxane (PSQ) backbone. No crosslinked product was formed during polymerizations. Amphiphilic organic–inorganic hybrid polymers were achieved in this way, some of them showing some thermoresponsiveness. Li et al. [206] prepared a series of well-defined amphiphilic PAA-*graft*-PVAc copolymers according to a *grafting from* methodology. *tert*-Butyl 2-((2-bromopropanoyloxy)-methyl)acrylate (tBBPMA) was successfully polymerized via RAFT with a dithiobenzoate to obtain a well-defined homopolymer backbone with narrow molecular weight distribution ($Đ = 1.08$), which was subsequently converted into a xanthate-functional macro-CTA by substitution of the pendant bromide groups with an *O*-ethyl xanthate salt. Then, well-defined

PtBA-*graft*-PVAc copolymers with narrow molecular weight distributions ($Đ < 1.40$) were synthesized by RAFT polymerization of VAc. The final PAA-*graft*-PVAc amphiphilic copolymers were obtained by selective acidic hydrolysis of the PtBA backbone without affecting the PVAc side chains.

Dual ATRP/RAFT polymerization has also been applied to the preparation of brush copolymers with block copolymer side chains. Nese et al. [207] synthesized the well-defined PPXEM-*graft*-PVOAc linear molecular brushes using a combination of ATRP and RAFT polymerization. A macro-chain transfer agent poly(2-((2-ethylxanthatepropanoyl)oxy)ethyl methacrylate) (PPXEM) was prepared through the esterification of carboxy-functional **X3a** and –OH groups of poly(2-hydroxyethyl methacrylate) (PHEMA). PVAc side chains (DP = 50 and 60) were then grown from this macro-CTA to generate molecular brushes. It was found that the longer spacer separating the xanthate moiety from the backbone (7 vs. 3 atoms) was essential for the synthesis of the well-defined PVOAc side chains. Two years later, the same authors [208] synthesized well-defined molecular bottlebrushes with PNVP-*b*-PVAc block copolymer side chains using the same procedure. The structure of the bottlebrushes PPXEM-*graft*-(PNVP-*b*-PVAc) was confirmed by AFM where it was noted that relatively large amounts of linear polymer chains were formed due to transfer reactions and new chains generated by AIBN during the side chain growth.

The *grafting to* process has become a more efficient method for the preparation of graft copolymers with the development of various click chemistries. However, its combination with xanthate-mediated RAFT polymerization has been rarely reported in the literature. Quémener et al. [86] achieved well-defined comb copolymers of PVAc with low dispersities through the combination of RAFT polymerization and CuAAC click reaction. As shown in Scheme 10.8, propargyl methacrylate with its acetylene function protected with a silyl group was first polymerized via a RAFT process and subsequently deprotected to afford a polymer backbone where each repeated unit carries an alkyne functionality. In parallel, an azido functional xanthate **X12** was employed to prepare narrowly dispersed PVAc. PVAc chains were finally grafted to the polymer backbone by CuAAC reaction to afford comb-like graft copolymers with low dispersities ($1.12 < Đ < 1.18$). Using the same CuAAC click coupling, Joubert et al. [209] successfully prepared graft copolymers of hydroxyethyl cellulose (HEC) and a RAFT-derived polyacrylate ionic liquid. Well-defined PILs of different DP_n (10, 50, and 100) of relatively low dispersity ($Đ = 1.5$ for PIL_{100}) were first prepared via RAFT polymerization using an alkyne-functional xanthate as transfer agent. The PIL chains were then coupled to ^{15}N-labeled azido-functionalized HEC, forming graft copolymers of HEC-*graft*-PILs with different chain lengths and graft densities.

10.6.6 Star Polymers

In the context of RAFT polymerization, the two R-group and Z-group approaches, involving two different types of multifunctional xanthates (Scheme 10.9), can be employed for the synthesis of star-like polymers.

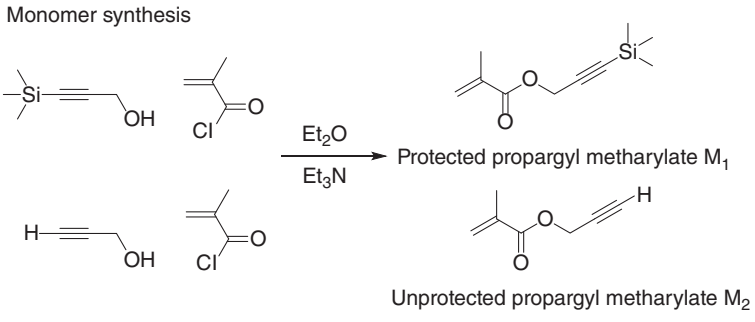

Scheme 10.8 Schematic representation of the general synthetic approach from monomer synthesis to the preparation of the final PVAc comb-like graft polymer. Source: Adapted with permission from Quémener et al. [86]. Copyright 2008, John Wiley & Sons.

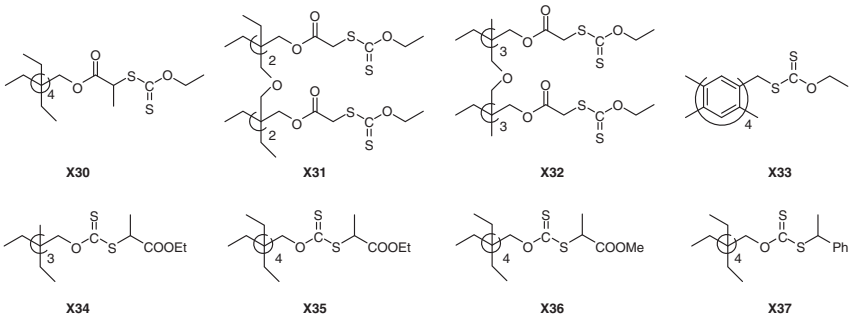

Scheme 10.9 Representative multifunctional xanthates used in RAFT polymerization for star polymer synthesis (R-group approach: **X30**-**X33**, Z-group approach: **X34**-**X37**).

A few examples of multifunctional xanthates (e.g. **X30**–**X33)** were designed to grow star polymers by the R-group approach. This method has been effectively used for AA [210], NVP [211, 212], NVCL [213], NVTri [214], NVCbz [215], and VEI-Br [216]. Following the Z-group approach, star-like polymers of VAc [217, 218] and NVCbz [215, 219] were synthesized using xanthates **X34–X37**. For an optimal design of the star polymers, a suitable choice of the approach and xanthate structure is required, depending on the nature of the monomer. For example, Mori et al. [215] synthesized PNVCbz star polymers via RAFT using three different xanthate-type CTAs: **X30** for the R-group approach and two xanthates **X36** and **X37** having different R leaving groups for the Z-group approach. The R-group approach was found to be the most efficient for the synthesis of the four-arm PNVCbz stars having a low dispersity ($Đ = 1.16$) and controlled molecular weights. In the case of Z-group approach, the results suggested that the R leaving group of xanthates had a clear effect on the polymerization kinetics involving an induction period and retardation, but had no significant influence on the controlled character of the polymerization. The controlled character was affected by the R-group or Z-group approach, and the polymerization kinetics was independent of the difference in the approach. Well-defined four-arm star PVDF was synthesized with tetrafunctional xanthate **X30** [153] and used as precursors for photo-crosslinked coatings. In addition to star homopolymers, some star-like copolymers (statistical, block, …) [213–216, 220] have also been achieved via RAFT polymerization mediated by different multifunctional xanthates.

Miktoarm star polymers [221–224] or the star polymers containing degradable chains [192, 224–226] are of interest because of their unique properties and potential application in many areas. However, their synthesis usually requires the combination of different polymerization or coupling methods, e.g. RAFT polymerization associated with ATRP, NMP, ROP, SET-LRP or click chemistry. For instance, Zhang et al. [222] synthesized the well-defined amphiphilic A_2B_2 miktoarm star-block copolymer $(PAA)_2(PVAc)_2$ via the combination of SET-LRP and RAFT/MADIX polymerization using xanthates. Hira et al. [225] prepared well-defined

four-arm star (PDLLA-*b*-PNVP)$_4$ amphiphilic block copolymer that consists of D,L-lactide (DLLA) via the combination of ROP and xanthate-mediated RAFT polymerization.

Alternatively, a 'coupling onto' approach is also a possibility to prepare star-like polymers, where a linear telechelic polymer is reacted with a preformed core molecule containing complementary functionality. This approach until recently had not received as much attention. For example, seven-armed star-like PNVP polymers with a lysozyme core were obtained by coupling succinimidyl-terminated PVP to the primary amine groups of the protein used as the core [93].

10.6.7 Hyperbranched Polymers/Polymer Gels

HPs [227] have attracted significant attention because of their characteristic topological structure associated with their unique physical properties compared with those of the corresponding linear polymers.

Poly et al. [228] reported the one-pot xanthate-mediated reversible crosslinking copolymerization (RCC) process for PVAc nanogels with controlled constitutive chain length using either a di- or a tri-functional crosslinker (divinyl adipate or 2,4,6-tris(allyloxy)-1,3,5-triazine, respectively). The use of xanthate **X0a** allowed for the incorporation of large amounts of crosslinker without macrogel formation. Significant intramolecular crosslinking (cyclization) favourably contributes to the formation of such nanogels. Reactivation of the multiple xanthate end-groups of the parent PVAc nanogels allowed for the synthesis of 'second generation' nanogels with core–shell structures. After this, Poly et al. applied their well-defined PVAc nanogels for the fabrication of patterned porous surfaces. Schmitt et al. [81] especially designed a polymerizable xanthate **X8** (R = –CH_3) for the one-step synthesis of well-defined branched PVAc by self-condensing vinyl polymerization (SCVP) based on a RAFT mechanism. The branching density as well as the length of the branches could be efficiently tuned by adjusting either the concentration of polymerizable functions C_0 or the $C_0/[\mathbf{X8}]_0$ ratio. Additionally, xanthate **X8** was also homopolymerized to afford hyperbranched oligomers, which were subsequently used as multifunctional CTA for the divergent synthesis of star-like PVAcs following a chain extension procedure. Similarly the same year, Zhou et al. [80] synthesized hyperbranched PVAc via the combination of SCVP and RAFT polymerization in the presence of unsaturated **X8** (R = –H). The average degree of branching and branch length were readily tuned by the reaction stoichiometry.

Cong et al. [100] employed xanthate-mediated RCC/RAFT process from PNIPAM-*b*-PNVP copolymers using xanthate **X29** and *N*,*N*′-methylenebisacrylamide (MBA) as the crosslinker. Zheng and Zheng [178] synthesized PEO-*b*-PNIPAM copolymers via RCC/RAFT polymerization using a xanthate-terminated PEO as macro-CTA and MBA as the crosslinking agent. Song et al. [89] prepared PNIPAM-*graft*-PNVP copolymer hydrogels in the presence of MBA as the crosslinking agent. In this RAFT polymerization, the xanthate CTA was formed in situ via the reaction of isopropylxanthic disulfide (DIP) with AIBN.

10.7 Methodologies for Xanthate End-Group Removal

Although RAFT/MADIX polymerization offers numerous advantages, in some circumstances, removal of the thiocarbonylthio terminal group is desirable. Concerns with the end-group are linked to colour, their inherent reactivity, and especially the thermal and chemical stability (which may generate low molar mass malodorous or potentially toxic sulfur-based by-products), depending on applications. Several methodologies to remove the thiocarbonylthio end-groups are reviewed by Willcock and O'Reilly [229], Harvison et al. [230], and Moad et al. [9, 231, 232]. In this section, we specifically refer to xanthates. Four main kinds of chemical modification of a xanthate group were reported in the literature: nucleophilic reaction, oxidation, thermolysis, and radical-induced reduction (Scheme 10.10).

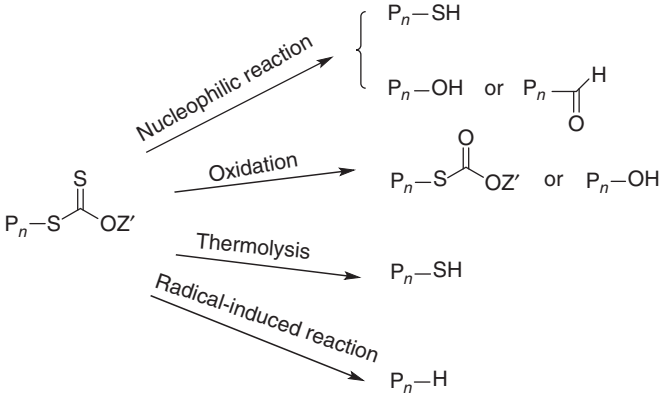

Scheme 10.10 Modification of the xanthate group: a summary.

10.7.1 Nucleophilic Reaction (Aminolysis/Hydrolysis/Ionic Reduction)

The reduction of thiocarbonylthio end-groups into thiols by aminolysis, hydrolysis, or reaction with ionic reducing agents (e.g. borohydrides) is one of the most commonly encountered end-group transformation of a RAFT polymer. In a recent patent, Holbein et al. [233] synthesized a copolymer containing a metal-chelating methacrylamido monomer and NVP via RAFT polymerization with xanthates as CTAs. They successfully modified the thiocarbonylthio terminal groups into thiol group using three separate methods, i.e. by aminolysis, by thermal treatment, and using sodium borohydride as a mild reducing agent. Shimoni et al. [94] treated the xanthate end-group of PNVP with hydrazine hydrate in methanol, and subsequently, by reduction with sodium borohydride. Ellman's reagent was allowed to react with the thiol functionality for treatment with dithiothreitol (DTT) and used in bioconjugation (Scheme 10.11).

Wu et al. [234] reported a 'universal' and effective approach for removing thiocarbonylthio end-groups of RAFT-made polymers by the utilization of sodium azide in

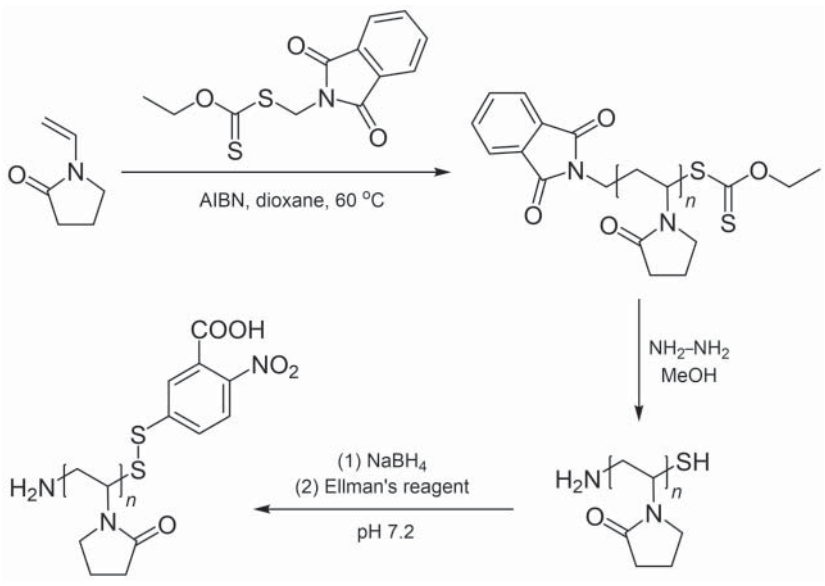

Scheme 10.11 RAFT/MADIX polymerization of PNVP and end-group transformation. Source: Adapted with permission from Shimoni et al. [94]. Copyright 2012, John Wiley & Sons.

an open system at ambient temperature without deoxygenation. Through the examination with three different RAFT agents (including a xanthate) and four polymers including PBA, PSt, PMMA and PVAc, it was concluded that the terminal thiocarbonylthio group was successfully converted to the thiol group by NaN_3 via a nucleophilic process (Scheme 10.12).

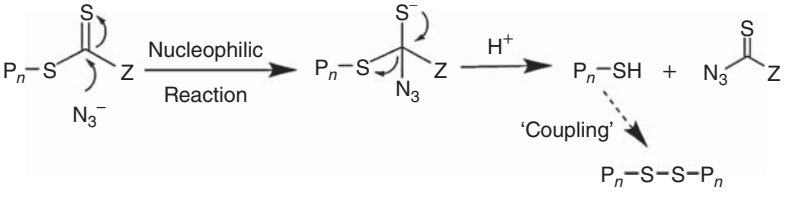

Scheme 10.12 Mechanism of the reaction by NaN_3 via a nucleophilic process. Source: Adapted with permission from Wu et al. [234]. Copyright 2014, John Wiley & Sons.

Pound et al. [235] reported that PNVP chain ends formed with xanthate RAFT agents are susceptible to hydrolysis and can be converted to hydroxyl and aldehyde end-groups under different conditions (Scheme 10.13) [235]. They took advantage of this feature for the preparation of ω-aldehyde functional PNVP, and then coupled the polymer to a model protein lysozyme via reductive amination.

10.7.2 Oxidation

Reaction with oxidizing agents, such as ozone (O_3) and hydrogen peroxide (H_2O_2), is also an effective process for removing the xanthate end-groups from

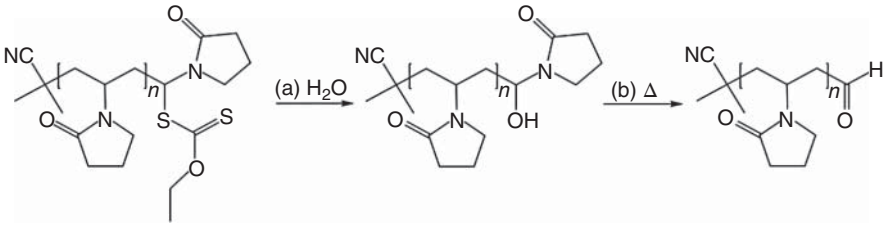

Scheme 10.13 Modification of PNVP xanthate chain ends into hydroxyl and aldehyde end-groups. Reagents and conditions: (a) distilled water (pH = 4–10), 40 °C, 16 hours; (b) 120 °C, 1 mbar, 20 hours. Source: Adapted with permission from Pound et al. [235]. Copyright 2008, John Wiley & Sons.

RAFT-synthesized polymers. For instance, two articles [236, 237] and a patent [238] reported the ozonolysis of a xanthate, quantitatively forming the corresponding polymer with a thionocarbonate end-group. The oxidation reaction was successfully performed not only in solution but also on a poly(*n*-butylacrylate) latex. It is the only reported effective technique for RAFT latexes without latex destabilization [237]. A possible mechanism has been proposed (Scheme 10.14) [236].

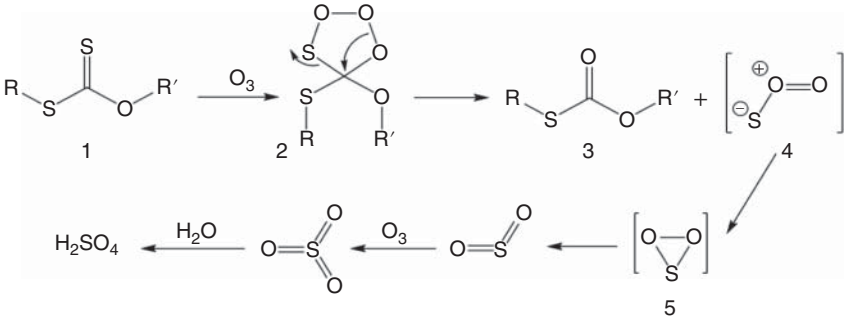

Scheme 10.14 A possible mechanism for the ozonolysis of xanthate. Source: Adapted with permission from Quiclet-Sire et al. [236]. Copyright 2010, John Wiley & Sons.

Pfukwa et al. [239] reported a facile method for directly transforming RAFT end-groups into hydroxyl end-groups by using H_2O_2 as the oxidizing agent. The process was applied to PNVP with xanthate chain ends, which involves heating the polymers in solution with H_2O_2 at 60 °C. The proposed mechanism is shown in Scheme 10.15. However, the xanthate-terminated PNVP showed a tendency to take part in side reactions during the end-group modification.

10.7.3 Thermolysis

If complete removal of the thiocarbonylthio group is required, the effective processes are either thermolysis [240, 241] or radical-induced reaction (see Section 10.7.4). Thermolysis, usually carried out at temperatures higher than 150 °C, is a simple and powerful method to cleave the thiocarbonylthio groups and introduce an alkene at the polymer chain end, but the dominant mechanism of reaction

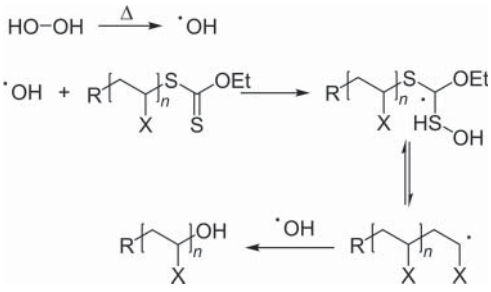

Scheme 10.15 The mechanism for RAFT end-group removal by H_2O_2. Source: Adapted with permission from Pfukwa et al. [239]. Copyright 2008, John Wiley & Sons.

depends on both the particular polymer and the type of thiocarbonylthio group. For example, the high-temperature (~ 180 °C) thermolysis of polymers terminated with *O*-alkyl xanthates possessing at least a β-hydrogen atom (e.g. *O*-isobutyl xanthate), known as the Chugaev elimination, provides 2-butene and polymers with a thiol end-group (Scheme 10.16) [240]. Applying this methodology, Langlais et al. [166] used thiolactone-based xanthates (TL-Xa) in RAFT polymerization of NIPAM, and the TL-PNIPAM-Xa polymers at the ω-end decomposed into TL-PNIPAM-SH under thermolysis conditions through Chugaev elimination. The terminal thiol group was unstable and led to thiolactonization with the penultimate NIPAM unit. Postma et al. [242] studied the thermolysis of PVAc synthesized with a phtalilimido xanthate. At 220 °C, discolouration of the polymer was observed with concomitant increase of the molar mass. It was concluded that thermal degradation may lead to homolysis of C—S bond followed by radical coupling or decay by backbiting followed by β-scission.

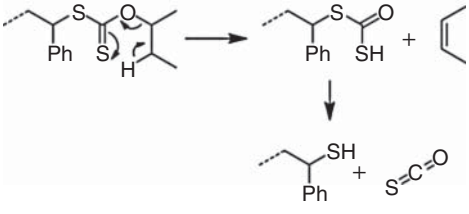

Scheme 10.16 Thermolysis of PSt with *O*-isobutyl xanthate end-group. Source: Adapted with permission from Destarac et al. [240]. Copyright 2006, John Wiley & Sons.

10.7.4 Radical-Induced Reduction

Radical-induced reduction also allows the thiocarbonylthio end-group of RAFT-synthesized polymers to be replaced with a hydrogen atom [243]. For instance, our group reported the transformation of TL-PVP-Xa [166], PNIPAM-**X0a** [244], and PVAc-**X0a** [182] into the corresponding hydrogen-terminated polymers by radical reduction with lauroyl peroxide (LPO) in propan-2-ol.

Hu et al. [172] used radical-induced reduction with tributylstannane (Bu_3SnH) as the most effective H-donor to remove the xanthate end-groups from the homopolymer PVNCbz.

Tong et al. [87] exposed the azido-functional PVAc with a xanthate end-group to stoichiometric amounts of LPO in refluxing 2-propanol/THF as H-donors, resulting in the complete replacement of the xanthate group by a hydrogen atom via radical-induced reduction (Scheme 10.17). This method is ecologically superior to the abovementioned using Bu_3SnH as the H-donor. And in this case, the peroxide initiator LPO appears generally more effective in radical-induced reduction than azo-type compounds such as AIBN, which is attributed to the peroxide-derived radicals being more effective in displacing the propagating radicals than the cyanoalkyl radical [243].

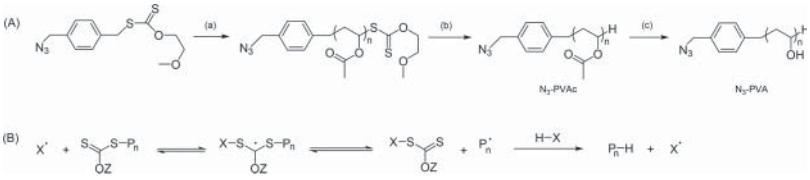

Scheme 10.17 (A) RAFT synthesis of N_3-PVAc and ω-xanthate group removal. Reagents and conditions: (a) VAc, AIBN, 80 °C; (b) LPO, 2-propanol/THF, 80 °C. Source: Adapted with permission from Tong et al [87]. Copyright 2009, John Wiley & Sons.), and (B) radical-induced reduction of xanthate end-groups. Source: Adapted with permission from Chong et al. [243]. Copyright 2007, John Wiley & Sons.

Carmean et al. [47] also reported a novel photo-induced end-group removal (PEGR) process, which provides a low temperature, initiator- and catalyst-free method to efficient end-group modification in the presence of *N*-ethylpiperidine hypophosphite (EPHP) as a H-donor. Under long-wave ultraviolet irradiation, polymers with thiocarbonylthio end-groups derived from acrylamido, acrylic, methacrylic, styrenic, and vinylpyrrolidone monomers undergo excitation and photolytic cleavage to reveal an active macro-radical capable of irreversible termination with a suitable hydrogen source. This straightforward method was successfully demonstrated by the removal of a range of end-groups that commonly result from RAFT agents including xanthates among other classes of thiocarbonylthio compounds. Under identical reaction conditions, PDMA-Xa showed complete end-group removal to PDMA-H in eight hours and exhibited a photolysis rate nearly six times more rapid than the PDMA analogue with trithiocarbonate-terminated chains [47].

10.8 Industrial Applications of RAFT/MADIX Polymerization

The industrial developments of reversible deactivation radical polymerization, and RAFT polymerization in particular, have been recently reviewed [10]. RAFT process

can be seen as a conventional radical polymerization in the presence of a reversible thiocarbonylthio chain transfer agent. Therefore, it can be implemented in classical industrial polymerization reactors, under normal conditions of temperature and pressure.

Rhodia Chimie (now part of Solvay) and the CNRS pioneered xanthate-mediated RAFT (coined MADIX), based on *O*-ethyl-*S*-(1-methoxycarbonylethyl)dithiocarbonate, which was registered under the trade name Rhodixan A1. They have joint ownership in intellectual property on RAFT agent design, xanthate end-group removal, and aqueous processes to produce ultra-high molar mass polymers or controlled architectures based on NVP. In the 2000s, the first commercial success with MADIX was Rhodibloc® RS, an amphiphilic block copolymer with improved stabilizing properties for inverse emulsions, especially under high shear conditions. Solvay's Rhodibloc® FL fluid loss block copolymer additives for cementing applications for the Oilfield market were developed during the 2010s. These products are effective in retaining water within slurries over a wide range of temperatures. Rhodibloc® GC is a gas migration control agent that is based on styrene–butadiene latex and a proprietary block copolymer surfactant. It is stable in cement slurries up to 150 °C. Over the last five years, Solvay Novecare developed MADIX micellar polymerization, a direct aqueous route to associative multiblock copolymers, by simply adding a xanthate to a conventional micellar polymerization medium comprising mainly hydrophilic monomers (most often a mixture of AM and AMPS), a small amount of hydrophobic monomer (e.g. *N*-laurylmethacrylamide or *t*-Bu styrene), and a surfactant. Thanks to an improved control of the copolymer microstructure, molar mass, and dispersity over conventional processes, the multiblock amphiphilic copolymers exhibit excellent rheological properties for extracting and fracturing fluids or suspending agents in oil recovery applications, in particular in very concentrated saline media.

The reactivity of Rhodixan A1 covers a very broad spectrum of monomers, nearly all of them, with the exception of 1,1-disubstituted monomers such as methacrylates. It is compatible with all kinds of reaction media, and based on the estimated cost of the raw materials used for its synthesis, the extra cost associated with the use of Rhodixan A1 in an industrial polymer should be much lower than for the other classes of commercially available RAFT agents. For all these reasons, Rhodixan A1 and *O*-ethyl xanthates in general hold a strong position for the development of future generations of complex polymer architectures at the industrial level.

10.9 Conclusion

Over the last decade, giant steps have been taken in the development of RAFT polymerization with xanthates with a vast amount of academic literature and an increasing number of industrial products. Today's breadth and depth of knowledge on xanthate RAFT agents is primarily due to their practicality: xanthates are easier to synthesize and generate little or no retardation of polymerization compared to the other classes of RAFT agents, and they are compatible with all kinds of polymerization media and monomer reactivities. In particular, they can control the polymerization of both conjugated and non-conjugated monomers, which

opens an infinite number of original options for block copolymer synthesis or more complex microstructures, e.g. spontaneous gradient copolymers. Xanthates are best known for their great ability to control RAFT polymerization of non-conjugated monomers. Since the last edition of this handbook in 2008, a strong focus on vinyl esters and *N*-vinyl monomers was observed and a great deal of important monomers complemented the range of xanthate-compatible monomers for RAFT polymerization, including VDF, vinyl sulfonates and sulfides, vinyl phosphonic acid, diallyl(dimethylammonium chloride), CKAs, and ethylene. Novel strategies for removal of the xanthate terminal group were proposed, such as UV light-induced radical reduction and ozonolysis. In parallel, significant progress has been accomplished in the industrial development of MADIX technology by Solvay (Rhodia) for aqueous formulation additives, using Rhodixan A1. Xanthates surely have some surprises left for the future.

References

1 Moad, G. and Rizzardo, E. (2019). A 20th anniversary perspective on the life of RAFT (RAFT coming of age). *Polym. Int.* https://doi.org/10.1002/pi.5944.

2 Perrier, S. (2017). 50th anniversary perspective: RAFT polymerization – a user guide. *Macromolecules* 50 (19): 7433–7447.

3 Le, T.P., Moad, G., Rizzardo, E. et al. (2001). Polymerization with living characteristics. WO Patent 1998001478A1, filed July 03, 1997 and issued December 12, 2001.

4 Chiefari, J., Chong, Y., Ercole, F. et al. (1998). Living free-radical polymerization by reversible addition-fragmentation chain transfer: the RAFT process. *Macromolecules* 31 (16): 5559–5562.

5 Corpart, P., Charmot, D., Biadatti, T. et al. (2007). Method for block polymer synthesis by controlled radical polymerisation. WO Patent 1998058971A1, filed June 23, 1998 and issued May 09, 2007.

6 Charmot, D., Corpart, P., Adam, H. et al. (2000). Controlled radical polymerization in dispersed media. *Macromol. Symp.* 150 (1): 23–32.

7 Yan, Y., Zhang, W., Qiu, Y. et al. (2010). Universal xanthate-mediated controlled free radical polymerizations of the "less activated" vinyl monomers. *J. Polym. Sci., Part A: Polym. Chem.* 48 (22): 5206–5214.

8 Nakabayashi, K. and Mori, H. (2013). Recent progress in controlled radical polymerization of *N*-vinyl monomers. *Eur. Polym. J.* 49 (10): 2808–2838.

9 Moad, G., Rizzardo, E., and Thang, S.H. (2012). Living radical polymerization by the RAFT process–a third update. *Aust. J. Chem.* 65 (8): 985–1076.

10 Destarac, M. (2018). Industrial development of reversible-deactivation radical polymerization: is the induction period over? *Polym. Chem.* 9 (40): 4947–4967.

11 Moad, G. (2015). RAFT polymerization – then and now. In: *Controlled Radical Polymerization: Mechanisms* (eds. K. Matyjaszewski, B.S. Sumerlin, N.V. Tsarevsky and J. Chiefari), 211–246. ACS Publications.

12 Taton, D., Destarac, M., and Zard, S.Z. (2008). Macromolecular design by interchange of xanthates: design, scope and applications. In: *Handbook of RAFT Polymerization*, 1e (ed. C. Barner-Kowollik), 373–421. Wiley-VCH.

13 Lai, J.T. and Shea, R. (2006). Controlled radical polymerization by carboxyl- and hydroxyl-terminated dithiocarbamates and xanthates. *J. Polym. Sci., Part A: Polym. Chem.* 44 (14): 4298–4316.

14 Keddie, D.J., Moad, G., Rizzardo, E. et al. (2012). RAFT agent design and synthesis. *Macromolecules* 45 (13): 5321–5342.

15 Skey, J. and O'Reilly, R.K. (2008). Facile one pot synthesis of a range of reversible addition-fragmentation chain transfer (RAFT) agents. *Chem. Commun.* (35): 4183–4185.

16 Bell, C.A., Hedir, G.G., O'Reilly, R.K. et al. (2015). Controlling the synthesis of degradable vinyl polymers by xanthate-mediated polymerization. *Polym. Chem.* 6 (42): 7447–7454.

17 Sütekin, S.D. and Güven, O. (2018). Radiation-induced controlled polymerization of acrylic acid by RAFT and RAFT-MADIX methods in protic solvents. *Radiat. Phys. Chem.* 142: 82–87.

18 Mori, H., Kudo, E., Saito, Y. et al. (2010). RAFT polymerization of vinyl sulfonate esters for the controlled synthesis of poly(lithium vinyl sulfonate) and sulfonated block copolymers. *Macromolecules* 43 (17): 7021–7032.

19 Tong, Y.-Y., Dong, Y.-Q., Du, F.-S. et al. (2008). Synthesis of well-defined poly(vinyl acetate)-*b*-polystyrene by combination of ATRP and RAFT polymerization. *Macromolecules* 41 (20): 7339–7346.

20 Couture, G. and Améduri, B. (2012). Kinetics of RAFT homopolymerisation of vinylbenzyl chloride in the presence of xanthate or trithiocarbonate. *Eur. Polym. J.* 48 (7): 1348–1356.

21 Sistach, S., Beija, M., Rahal, V. et al. (2010). Thermoresponsive amphiphilic diblock copolymers synthesized by MADIX/RAFT: properties in aqueous solutions and use for the preparation and stabilization of gold nanoparticles. *Chem. Mater.* 22 (12): 3712–3724.

22 Mori, H. and Tsukamoto, M. (2011). RAFT polymerization of diacrylate derivatives having different spacers in dilute conditions. *Polymer* 52 (3): 635–645.

23 Barthet, C., Wilson, J., Cadix, A. et al. (2018). Influence of sodium dodecyl sulfate on the kinetics and control of RAFT/MADIX polymerization of acrylamide. *J. Polym. Sci., Part A: Polym. Chem.* 56 (7): 760–765.

24 Wen, L., Wang, L., Fang, S. et al. (2018). Stabilization of CO_2-in-water emulsions with high internal phase volume using PVAc-*b*-PVP and PVP-*b*-PVAc-*b*-PVP as emulsifying agents. *J. Appl. Polym. Sci.* 135 (23): 46351.

25 Góis, J.R., Popov, A.V., Guliashvili, T. et al. (2015). Synthesis of functionalized poly(vinyl acetate) mediated by alkyne-terminated RAFT agents. *RSC Adv.* 5 (111): 91225–91234.

26 Girard, E., Liu, X., Marty, J.-D. et al. (2014). RAFT/MADIX (co)polymerization of vinyl trifluoroacetate: a means to many ends. *Polym. Chem.* 5 (3): 1013–1022.

27 Girard, E., Tassaing, T., Camy, S. et al. (2012). Enhancement of poly(vinyl ester) solubility in supercritical CO_2 by partial fluorination: the key role of polymer-polymer interactions. *J. Am. Chem. Soc.* 134 (29): 11920–11923.

28 Liu, X., Coutelier, O., Harrisson, S. et al. (2014). Enhanced solubility of polyvinyl esters in $scCO_2$ by means of vinyl trifluorobutyrate monomer. *ACS Macro Lett.* 4 (1): 89–93.

29 Girard, E., Tassaing, T., Ladavière, C. et al. (2012). Distinctive features of solubility of RAFT/MADIX-derived partially trifluoromethylated poly(vinyl acetate) in supercritical CO_2. *Macromolecules* 45 (24): 9674–9681.

30 Mori, H., Saito, Y., Takahashi, E. et al. (2012). Controlled synthesis of sulfonated block copolymers having thermoresponsive property by RAFT polymerization of vinyl sulfonate esters. *Polymer* 53 (18): 3861–3877.

31 Li, L., Li, J., and Zheng, S. (2018). Poly(vinylidene fluoride)-block-poly(*N*-vinylpyrrolidone) diblock copolymers: synthesis via sequential RAFT/MADIX polymerization and self-assembly behavior. *Polymer* 142: 61–71.

32 Guerre, M., Campagne, B., Gimello, O. et al. (2015). Deeper insight into the MADIX polymerization of vinylidene fluoride. *Macromolecules* 48 (21): 7810–7822.

33 Guerre, M., Rahaman, S.W., Améduri, B. et al. (2016). Limits of vinylidene fluoride RAFT polymerization. *Macromolecules* 49 (15): 5386–5396.

34 Xu, P., Huang, X., Pan, X. et al. (2019). Hyperbranched polycaprolactone through RAFT polymerization of 2-methylene-1,3-dioxepane. *Polymers* 11 (2): 318.

35 Destarac, M., Guinaudeau, A., Geagea, R. et al. (2010). Aqueous MADIX/RAFT polymerization of diallyldimethylammonium chloride: extension to the synthesis of poly (DADMAC)-based double hydrophilic block copolymers. *J. Polym. Sci., Part A: Polym. Chem.* 48 (22): 5163–5171.

36 Pham, Q.L., Haldorai, Y., Kang, C. et al. (2014). Reversible addition-fragmentation chain transfer polymerization of vinyl acetate and vinyl pivalate in supercritical carbon dioxide. *Korean J. Chem. Eng.* 31 (11): 2101–2107.

37 Dufils, P.E., David, G., Boutevin, B. et al. (2012). Phosphonate-terminated poly(vinyl acetate) synthesized by RAFT/MADIX polymerization. *J. Polym. Sci., Part A: Polym. Chem.* 50 (10): 1997–2007.

38 Dommanget, C., D'Agosto, F., and Monteil, V. (2014). Polymerization of ethylene through reversible addition–fragmentation chain transfer (RAFT). *Angew. Chem. Int. Ed.* 53 (26): 6683–6686.

39 Jiang, B., Zhang, Q.H., Zhan, X.L. et al. (2009). The reversible addition-fragmentation chain transfer (RAFT) miniemulsion polymerization of vinyl acetate mediated by xanthate. *Chin. Chem. Lett.* 20 (6): 733–737.

40 Patel, V.K., Mishra, A.K., Vishwakarma, N.K. et al. (2010). (S)-2-(ethyl propionate)-(*O*-ethyl xanthate) and (*S*)-2-(ethyl isobutyrate)-(*O*-ethyl xanthate)-mediated RAFT polymerization of *N*-vinylpyrrolidone. *Polym. Bull.* 65 (2): 97–110.

41 Mori, H., Ishikawa, K., Abiko, Y. et al. (2012). Synthesis of triazole-based amphiphilic block copolymers containing carbazole moiety by RAFT polymerization. *Macromol. Chem. Phys.* 213 (17): 1803–1814.

42 Lipscomb, C.E. and Mahanthappa, M.K. (2009). Poly(vinyl ester) block copolymers synthesized by reversible addition-fragmentation chain transfer polymerizations. *Macromolecules* 42 (13): 4571–4579.

43 Patel, V.K., Vishwakarma, N.K., Mishra, A.K. et al. (2012). (*S*)-2-(ethyl propionate)-(*O*-ethyl xanthate) and (*S*)-2-(ethyl isobutyrate)-(*O*-ethyl xanthate)-mediated RAFT polymerization of vinyl acetate. *J. Appl. Polym. Sci.* 125 (4): 2946–2955.

44 Vakili, M., Cunningham, V.J., Trebbin, M. et al. (2019). Polymerization-induced thermal self-assembly of functional and thermo-responsive diblock copolymer nano-objects via RAFT aqueous polymerization. *Macromol. Chem. Phys.* 220 (2): 1800370.

45 Kwak, Y., Nicolaÿ, R., and Matyjaszewski, K. (2009). A simple and efficient synthesis of RAFT chain transfer agents via atom transfer radical addition-fragmentation. *Macromolecules* 42 (11): 3738–3742.

46 Devlaminck, D.J., Van Steenberge, P.H., De Keer, L. et al. (2017). A detailed mechanistic study of bulk MADIX of styrene and its chain extension. *Polym. Chem.* 8 (45): 6948–6963.

47 Carmean, R.N., Figg, C.A., Scheutz, G.M. et al. (2017). Catalyst-free photoinduced end-group removal of thiocarbonylthio functionality. *ACS Macro Lett.* 6 (2): 185–189.

48 Mori, H., Yahagi, M., and Endo, T. (2009). RAFT polymerization of *N*-vinylimidazolium salts and synthesis of thermoresponsive ionic liquid block copolymers. *Macromolecules* 42 (21): 8082–8092.

49 Chen, J., Zhao, X., Zhang, L. et al. (2015). Reversible addition-fragmentation chain transfer polymerization of vinyl acetate under high pressure. *J. Polym. Sci., Part A: Polym. Chem.* 53 (12): 1430–1436.

50 Wang, J., Rivero, M., Muñoz-Bonilla, A. et al. (2016). Natural RAFT polymerization: recyclable-catalyst-aided, opened-to-air, and sunlight-photolyzed RAFT polymerizations. *ACS Macro Lett.* 5 (11): 1278–1282.

51 Lee, H., Terry, E., Zong, M. et al. (2008). Successful dispersion polymerization in supercritical CO_2 using polyvinylalkylate hydrocarbon surfactants synthesized and anchored via RAFT. *J. Am. Chem. Soc.* 130 (37): 12242–12243.

52 Yu, H., Chen, Q., Zhang, Z. et al. (2012). ^{60}Co γ-irradiation-initiated RAFT polymerization of VAc at room temperature. *React. Funct. Polym.* 72 (2): 153–159.

53 Nakabayashi, K., Abiko, Y., and Mori, H. (2013). RAFT polymerization of *S*-vinyl sulfide derivatives and synthesis of block copolymers having two distinct optoelectronic functionalities. *Macromolecules* 46 (15): 5998–6012.

54 Huang, C.-F., Yoon, J.A., and Matyjaszewski, K. (2010). Synthesis of *N*-vinylcarbazole-*N*-vinylpyrrolidone amphiphilic block copolymers by xanthate-mediated controlled radical polymerization. *Can. J. Chem.* 88 (3): 228–235.

55 Pound, G., Eksteen, Z., Pfukwa, R. et al. (2008). Unexpected reactions associated with the xanthate-mediated polymerization of *N*-vinylpyrrolidone. *J. Polym. Sci., Part A: Polym. Chem.* 46 (19): 6575–6593.

56 Ieong, N.S., Redhead, M., Bosquillon, C. et al. (2011). The missing lactam-thermoresponsive and biocompatible poly(*N*-vinylpiperidone) polymers by xanthate-mediated RAFT polymerization. *Macromolecules* 44 (4): 886–893.

57 Maki, Y., Mori, H., and Endo, T. (2007). Controlled RAFT polymerization of *N*-vinylphthalimide and its hydrazinolysis to poly(vinyl amine). *Macromol. Chem. Phys.* 208 (24): 2589–2599.

58 Klumperman, B. and Pound, G. (2009). Reversible addition fragmentation chain transfer (RAFT) mediated polymerization of *N*-vinylpyrrolidone: RAFT agent design. In: *Controlled/Living Radical Polymerization: Progress in RAFT, DT, NMP & OMRP* (ed. K. Matyjaszewski), 167–179. ACS Publications.

59 Pound, G., Aguesse, F., McLeary, J.B. et al. (2007). Xanthate-mediated copolymerization of vinyl monomers for amphiphilic and double-hydrophilic block copolymers with poly(ethylene glycol). *Macromolecules* 40 (25): 8861–8871.

60 Peng, C., Huang, K., Han, M. et al. (2013). Facile synthesis and catalytic activity of well-defined amphiphilic block copolymers based on *N*-vinylimidazolium. *Polym. Adv. Technol.* 24 (12): 1089–1093.

61 Yuan, J., Schlaad, H., Giordano, C. et al. (2011). Double hydrophilic diblock copolymers containing a poly (ionic liquid) segment: controlled synthesis, solution property, and application as carbon precursor. *Eur. Polym. J.* 47 (4): 772–781.

62 Wan, D., Zhou, Q., Pu, H. et al. (2008). Controlled radical polymerization of *N*-vinylcaprolactam mediated by xanthate or dithiocarbamate. *J. Polym. Sci., Part A: Polym. Chem.* 46 (11): 3756–3765.

63 Maki, Y., Mori, H., and Endo, T. (2007). Xanthate-mediated controlled radical polymerization of *N*-vinylindole derivatives. *Macromolecules* 40 (17): 6119–6130.

64 Congdon, T., Dean, B.T., Kasperczak-Wright, J. et al. (2015). Probing the biomimetic ice nucleation inhibition activity of poly(vinyl alcohol) and comparison to synthetic and biological polymers. *Biomacromolecules* 16 (9): 2820–2826.

65 Congdon, T., Shaw, P., and Gibson, M.I. (2015). Thermoresponsive, well-defined, poly(vinyl alcohol) co-polymers. *Polym. Chem.* 6 (26): 4749–4757.

66 Fandrich, N., Falkenhagen, J., Weidner, S.M. et al. (2010). Characterization of new amphiphilic block copolymers of *N*-vinyl pyrrolidone and vinyl acetate, 1–analysis of copolymer composition, end groups, molar masses and molar mass distributions. *Macromol. Chem. Phys.* 211 (8): 869–878.

67 Hakobyan, K., Gegenhuber, T., McErlean, C.S. et al. (2019). Visible-light-driven MADIX polymerisation via a reusable, low-cost, and non-toxic bismuth oxide photocatalyst. *Angew. Chem. Int. Ed.* 58 (6): 1828–1832.

68 Blidi, I., Geagea, R., Coutelier, O. et al. (2012). Aqueous RAFT/MADIX polymerisation of vinylphosphonic acid. *Polym. Chem.* 3 (3): 609–612.

69 Seiler, L., Loiseau, J., Leising, F. et al. (2017). Acceleration and improved control of aqueous RAFT/MADIX polymerization of vinylphosphonic acid in the presence of alkali hydroxides. *Polym. Chem.* 8 (25): 3825–3832.

70 Coutelier, O., Blidi, I., Reynaud, S. et al. (2015). Aqueous RAFT/MADIX polymerization of vinylphosphonic acid under microwave irradiation. In: *Controlled radical polymerization: Mechanisms* (eds. N.V. Tsarevsky, B.S. Sumerlin, K. Matyjaszewski and J. Chiefari), 283–294. ACS Publications.

71 Roy, D. and Sumerlin, B.S. (2011). Block copolymerization of vinyl ester monomers via RAFT/MADIX under microwave irradiation. *Polymer* 52 (14): 3038–3045.

72 Assem, Y., Chaffey-Millar, H., Barner-Kowollik, C. et al. (2007). Controlled/living ring-closing cyclopolymerization of diallyldimethylammonium chloride via the reversible addition fragmentation chain transfer process. *Macromolecules* 40 (11): 3907–3913.

73 Xiao, S., Xu, W.Z., and Charpentier, P.A. (2014). Bifunctional 2-(alkoxycarbonothioylthio) acetic acids for the synthesis of TiO_2-poly(vinyl acetate) nanocomposites via RAFT polymerization. *J. Polym. Sci., Part A: Polym. Chem.* 52 (5): 606–618.

74 Chambhare, S.U., Lokhande, G.P., and Jagtap, R.N. (2017). Effects of incorporated imine functionality and dispersed nano zinc oxide particles on antimicrobial activity synthesized by RAFT polymerization. *Polym. Bull.* 74 (5): 1421–1439.

75 Chibber, B.A. (2010). Efficient method for partial sequencing of peptide/protein using acid or base labile xanthates. US Patent 20100069252A1, filed October 30, 2006 and issued March 18, 2010.

76 Sun, Z., Choi, B., Feng, A. et al. (2019). Nonmigratory poly(vinyl chloride)-block-polycaprolactone plasticizers and compatibilizers prepared by sequential RAFT and ring-opening polymerization (RAFT-T-ROP). *Macromolecules* 52 (4): 1746–1756.

77 Kang, H.U., Yu, Y.C., Shin, S.J. et al. (2013). One-pot synthesis of poly(*N*-vinylpyrrolidone)-*b*-poly(ε-caprolactone) block copolymers using a dual initiator for RAFT polymerization and ROP. *Macromolecules* 46 (4): 1291–1295.

78 Huang, Z., Pan, P., and Bao, Y. (2016). Solution and aqueous miniemulsion polymerization of vinyl chloride mediated by a fluorinated xanthate. *J. Polym. Sci., Part A: Polym. Chem.* 54 (14): 2092–2101.

79 Kostov, G., Boschet, F., Buller, J. et al. (2011). First amphiphilic poly(vinylidene fluoride-*co*-3, 3, 3-trifluoropropene)-*b*-oligo(vinyl alcohol) block copolymers as potential nonpersistent fluorosurfactants from radical polymerization controlled by xanthate. *Macromolecules* 44 (7): 1841–1855.

80 Zhou, X., Zhu, J., Xing, M. et al. (2011). Synthesis and characters of hyperbranched poly(vinyl acetate) by RAFT polymeraztion. *Eur. Polym. J.* 47 (10): 1912–1922.

81 Schmitt, J., Blanchard, N., and Poly, J. (2011). Controlled synthesis of branched poly(vinyl acetate)s by xanthate-mediated RAFT self-condensing vinyl (co)polymerization. *Polym. Chem.* 2 (10): 2231–2238.

82 Patel, V.K., Vishwakarma, N.K., Mishra, A.K. et al. (2013). Synthesis of alkyne-terminated xanthate RAFT agents and their uses for the controlled

radical polymerization of *N*-vinylpyrrolidone and the synthesis of its block copolymer using click chemistry. *J. Appl. Polym. Sci.* 127 (6): 4305–4317.

83 Guerre, M., Uchiyama, M., Lopez, G. et al. (2018). Synthesis of PEPE-*b*-P(CTFE-alt-EVE) block copolymers by sequential cationic and radical RAFT polymerization. *Polym. Chem.* 9 (3): 352–361.

84 Guerre, M., Uchiyama, M., Folgado, E. et al. (2017). Combination of cationic and radical RAFT polymerizations: a versatile route to well-defined poly(ethyl vinyl ether)-block-poly(vinylidene fluoride) block copolymers. *ACS Macro Lett.* 6 (4): 393–398.

85 Mishra, A.K., Park, J., Joseph, K.V. et al. (2016). Synthesis and self-assembly of amphiphilic and biocompatible poly(vinyl alcohol)-block-poly(l-lactide) copolymer. *Polymer* 100: 28–36.

86 Quémener, D., Hellaye, M.L., Bissett, C. et al. (2008). Graft block copolymers of propargyl methacrylate and vinyl acetate via a combination of RAFT/MADIX and click chemistry: reaction analysis. *J. Polym. Sci., Part A: Polym. Chem.* 46 (1): 155–173.

87 Tong, Y.Y., Wang, R., Xu, N. et al. (2009). Synthesis of well-defined azide-terminated poly(vinyl alcohol) and their subsequent modification via click chemistry. *J. Polym. Sci., Part A: Polym. Chem.* 47 (18): 4494–4504.

88 Mishra, A.K., Choi, C., Maiti, S. et al. (2018). Sequential synthesis of well-defined poly(vinyl acetate)-block-polystyrene and poly(vinyl alcohol)-block-polystyrene copolymers using difunctional chloroamide-xanthate iniferter. *Polymer* 139: 68–75.

89 Song, J., Yu, R., Wang, L. et al. (2011). Poly(*N*-vinylpyrrolidone)-grafted poly(*N*-isopropylacrylamide) copolymers: synthesis, characterization and rapid deswelling and reswelling behavior of hydrogels. *Polymer* 52 (10): 2340–2350.

90 Gu, Y., He, J., Li, C. et al. (2010). Block copolymerization of vinyl acetate and vinyl neo-decanoate mediated by dithionodisulfide. *Macromolecules* 43 (10): 4500–4510.

91 Segura, T., Menes-Arzate, M., León, F. et al. (2016). Synthesis of narrow molecular weight distribution polyvinyl acetate by gamma-rays initiated RAFT/MADIX miniemulsion polymerization. *Polymer* 102: 183–191.

92 Destarac, M., Blidi, I., Coutelier, O. et al. (2012). Aqueous RAFT/MADIX polymerization: same monomers, new polymers? In: *Progress in Controlled Radical Polymerization: Mechanisms and Techniques* (eds. K. Matyjaszewski, B.S. Sumerlin and N.V. Tsarevsky), 259–275. ACS Publications.

93 McDowall, L., Chen, G., and Stenzel, M.H. (2008). Synthesis of seven-arm poly(vinyl pyrrolidone) star polymers with lysozyme core prepared by MADIX/RAFT polymerization. *Macromol. Rapid Commun.* 29 (20): 1666–1671.

94 Shimoni, O., Postma, A., Yan, Y. et al. (2012). Macromolecule functionalization of disulfide-bonded polymer hydrogel capsules and cancer cell targeting. *ACS Nano* 6 (2): 1463–1472.

95 Wang, Y.J., Wang, M.Q., Bai, L.J. et al. (2020). Facile synthesis of poly(*N*-vinyl pyrrolidone) block copolymers with “more-activated” monomers by using

photoinduced successive RAFT polymerization. *Polym. Chem.* https://doi.org/10.1039/c9py01763a.

96 Akeroyd, N., Pfukwa, R., and Klumperman, B. (2009). Triazole-based leaving group for RAFT-mediated polymerization synthesized via the Cu-mediated huisgen 1,3-dipolar cycloaddition reaction. *Macromolecules* 42 (8): 3014–3018.

97 Altintas, O., Speros, J.C., Bates, F.S. et al. (2018). Straightforward synthesis of model polystyrene-block-poly(vinyl alcohol) diblock polymers. *Polym. Chem.* 9 (31): 4243–4250.

98 Banerjee, S., Patil, Y., Gimello, O. et al. (2017). Well-defined multiblock poly(vinylidene fluoride) and block copolymers thereof: a missing piece of the architecture puzzle. *Chem. Commun.* 53 (79): 10910–10913.

99 Hua, D., Ge, X., Tang, J. et al. (2007). Low-temperature controlled free-radical polymerization of vinyl monomers in the presence of a novel cyclic dixanthate under γ-ray irradiation. *J. Polym. Sci., Part A: Polym. Chem.* 45 (14): 2847–2854.

100 Cong, H., Li, L., and Zheng, S. (2013). Poly(*N*-isopropylacrylamide)-block-poly(vinyl pyrrolidone) block copolymer networks: synthesis and rapid thermoresponse of hydrogels. *Polymer* 54 (4): 1370–1380.

101 Cong, H., Li, J., Li, L. et al. (2014). Thermoresponsive gelation behavior of poly(*N*-isopropylacrylamide)-block-poly(*N*-vinylpyrrolidone)-block-poly(*N*-isopropylacrylamide) triblock copolymers. *Eur. Polym. J.* 61: 23–32.

102 Xiang, Y., Cong, H., Li, L. et al. (2016). Poly(*N*-vinyl pyrrolidone)-block-poly(*N*-vinyl carbazole)-block-poly(*N*-vinyl pyrrolidone) triblock copolymers: synthesis via RAFT/MADIX process, self-assembly behavior, and photophysical properties. *J. Polym. Sci., Part A: Polym. Chem.* 54 (12): 1852–1863.

103 Shanmugam, S., Xu, J., and Boyer, C. (2015). Exploiting metalloporphyrins for selective living radical polymerization tunable over visible wavelengths. *J. Am. Chem. Soc.* 137 (28): 9174–9185.

104 Bouhadir, G., Legrand, N., Quiclet-Sire, B. et al. (1999). A new practical synthesis of tertiary *S*-alkyl dithiocarbonates and related derivatives. *Tetrahedron Lett.* 40 (2): 277–280.

105 Thang, S.H., Chong, Y.K., Mayadunne, R.T.A. et al. (1999). A novel synthesis of functional dithioesters, dithiocarbamates, xanthates and trithiocarbonates. *Tetrahedron Lett.* 40 (12): 2435–2438.

106 Khan, M.Y., Cho, M.-S., and Kwark, Y.-J. (2014). Dual roles of a xanthate as a radical source and chain transfer agent in the photoinitiated RAFT polymerization of vinyl acetate. *Macromolecules* 47 (6): 1929–1934.

107 Ding, C., Fan, C., Jiang, G. et al. (2015). Photocatalyst-free and blue light-induced RAFT polymerization of vinyl acetate at ambient temperature. *Macromol. Rapid Commun.* 36 (24): 2181–2185.

108 Poly, J., Cabannes-Boué, B., Hebinger, L. et al. (2015). Polymers synthesized by RAFT as versatile macrophotoinitiators. *Polym. Chem.* 6 (31): 5766–5772.

109 Carmean, R.N., Becker, T.E., Sims, M.B. et al. (2017). Ultra-high molecular weights via aqueous reversible-deactivation radical polymerization. *Chem* 2 (1): 93–101.

110 Uyar, Z., Turgut, F., Arslan, U. et al. (2019). Synthesis and characterization of well-defined end-chain functional macrophotoinitiators of polystyrene and polyacrylonitrile by RAFT/MADIX polymerization. *Eur. Polym. J.* 119: 102–113.

111 Ham, M.-k., HoYouk, J., Kwon, Y.-K. et al. (2012). Photoinitiated RAFT polymerization of vinyl acetate. *J. Polym. Sci., Part A: Polym. Chem.* 50 (12): 2389–2397.

112 Xu, J., Jung, K., Atme, A. et al. (2014). A robust and versatile photoinduced living polymerization of conjugated and unconjugated monomers and its oxygen tolerance. *J. Am. Chem. Soc.* 136 (14): 5508–5519.

113 Shanmugam, S., Xu, J., and Boyer, C. (2014). Photoinduced electron transfer-reversible addition-fragmentation chain transfer (PET-RAFT) polymerization of vinyl acetate and *N*-vinylpyrrolidinone: kinetic and oxygen tolerance study. *Macromolecules* 47 (15): 4930–4942.

114 Hua, D., Xiao, J., Bai, R. et al. (2004). Xanthate-mediated controlled/living free-radical polymerization under ^{60}Co γ-ray irradiation: structure effect of O-group. *Macromol. Chem. Phys.* 205 (13): 1793–1799.

115 Wang, P., Dai, J., Liu, L. et al. (2013). Xanthate-mediated living/controlled radical copolymerization of hexafluoropropylene and butyl vinyl ether under ^{60}Co γ-ray irradiation and preparation of fluorinated polymers end-capped with a fluoroalkyl sulfonic acid group. *Polym. Chem.* 4 (6): 1760–1764.

116 Van Nieuwenhove, I., Maji, S., Dash, M. et al. (2017). RAFT/MADIX polymerization of *N*-vinylcaprolactam in water-ethanol solvent mixtures. *Polym. Chem.* 8 (16): 2433–2437.

117 Guinaudeau, A., Mazières, S., Wilson, D.J. et al. (2012). Aqueous RAFT/MADIX polymerisation of *N*-vinyl pyrrolidone at ambient temperature. *Polym. Chem.* 3 (1): 81–84.

118 Guinaudeau, A., Coutelier, O., Sandeau, A. et al. (2013). Facile access to poly(*N*-vinylpyrrolidone)-based double hydrophilic block copolymers by aqueous ambient RAFT/MADIX polymerization. *Macromolecules* 47 (1): 41–50.

119 Read, E., Guinaudeau, A., James Wilson, D. et al. (2014). Low temperature RAFT/MADIX gel polymerisation: access to controlled ultra-high molar mass polyacrylamides. *Polym. Chem.* 5 (7): 2202–2207.

120 Zhao, J., Yang, B., Mao, J. et al. (2018). A novel hydrophobic associative polymer by RAFT-MADIX copolymerization for fracturing fluids with high thermal stability. *Energy Fuels* 32 (3): 3039–3051.

121 Rzayev, J. and Penelle, J. (2004). HP-RAFT: a free-radical polymerization technique for obtaining living polymers of ultrahigh molecular weights. *Angew. Chem.* 116 (13): 1723–1726.

122 Monteiro, M.J. and de Barbeyrac, J. (2001). Free-radical polymerization of styrene in emulsion using a reversible addition−fragmentation chain transfer agent with a low transfer constant: effect on rate, particle size, and molecular weight. *Macromolecules* 34 (13): 4416–4423.

123 Zetterlund, P.B., Kagawa, Y., and Okubo, M. (2008). Controlled/living radical polymerization in dispersed systems. *Chem. Rev.* 108 (9): 3747–3794.

124 Zetterlund, P.B., Thickett, S.C., Perrier, S. et al. (2015). Controlled/living radical polymerization in dispersed systems: An update. *Chem. Rev.* 115 (18): 9745–9800.

125 D'Agosto, F., Rieger, J., and Lansalot, M. (2019). RAFT-mediated polymerization-induced self-assembly. *Angew. Chem. Int. Ed.* https://doi.org/10.1002/anie.201911758.

126 Binauld, S., Delafresnaye, L., Charleux, B. et al. (2014). Emulsion polymerization of vinyl acetate in the presence of different hydrophilic polymers obtained by RAFT/MADIX. *Macromolecules* 47 (10): 3461–3472.

127 Siirilä, J., Häkkinen, S., and Tenhu, H. (2019). The emulsion polymerization induced self-assembly of a thermoresponsive polymer poly(*N*-vinylcaprolactam). *Polym. Chem.* 10 (6): 766–775.

128 Etchenausia, L., Khoukh, A., Lejeune, E.D. et al. (2017). RAFT/MADIX emulsion copolymerization of vinyl acetate and *N*-vinylcaprolactam: towards waterborne physically crosslinked thermoresponsive particles. *Polym. Chem.* 8 (14): 2244–2256.

129 Zhang, Q., Fu, M., Wang, C. et al. (2017). Preparation of poly(ionic liquid) nanoparticles through RAFT/MADIX polymerization-induced self-assembly. *Polym. Chem.* 8 (36): 5469–5473.

130 Guerre, M., Semsarilar, M., Godiard, F. et al. (2017). Polymerization-induced self-assembly of PVAc-b-PVDF block copolymers via RAFT dispersion polymerization of vinylidene fluoride in dimethyl carbonate. *Polym. Chem.* 8 (9): 1477–1487.

131 Birkin, N.A., Arrowsmith, N.J., Park, E.J. et al. (2011). Synthesis and application of new CO_2-soluble vinyl pivalate hydrocarbon stabilisers via RAFT polymerisation. *Polym. Chem.* 2 (6): 1293–1299.

132 Birkin, N.A., Wildig, O.J., and Howdle, S.M. (2013). Effects of poly(vinyl pivalate)-based stabiliser architecture on CO_2-solubility and stabilising ability in dispersion polymerisation of *N*-vinyl pyrrolidone. *Polym. Chem.* 4 (13): 3791–3799.

133 Destarac, M., Brochon, C., Catala, J.-M. et al. (2002). Macromolecular design via the interchange of xanthates (MADIX): polymerization of styrene with *O*-ethyl xanthates as controlling agents. *Macromol. Chem. Phys.* 203 (16): 2281–2289.

134 Destarac, M., Bzducha, W., Taton, D. et al. (2002). Xanthates as chain-transfer agents in controlled radical polymerization (MADIX): structural effect of the *O*-alkyl group. *Macromol. Rapid Commun.* 23 (17): 1049–1054.

135 Destarac, M., Taton, D., Zard, S.Z. et al. (2003). On the importance of xanthate substituents in the MADIX process. In: *Advances in Controlled/Living Radical Polymerization* (ed. K. Matyjaszewski), 536–550. ACS Publications.

136 Pound, G., McLeary, J.B., McKenzie, J.M. et al. (2006). In-situ NMR spectroscopy for probing the efficiency of RAFT/MADIX agents. *Macromolecules* 39 (23): 7796–7797.

137 Coote, M.L., Krenske, E.H., and Izgorodina, E.I. (2006). Computational studies of RAFT polymerization–mechanistic insights and practical applications. *Macromol. Rapid Commun.* 27 (7): 473–497.

138 Beija, M., Marty, J.-D., and Destarac, M. (2011). Thermoresponsive poly(*N*-vinyl caprolactam)-coated gold nanoparticles: sharp reversible response and easy tunability. *Chem. Commun.* 47 (10): 2826–2828.

139 Guinaudeau, A. (2010). Towards sustainability of RAFT/MADIX polymerization: low temperature initiation and environmentally friendly reaction media. PhD thesis. Université Toulouse III-Paul Sabatier.

140 Destarac, M., Matioszek, D., Vila, X. et al. (2018). How can xanthates control the RAFT polymerization of methacrylates? In: *Reversible Deactivation Radical Polymerization: Mechanisms and Synthetic Methodologies* (eds. K. Matyjaszewski, H. Gao, B.S. Sumerlin and N.V. Tsarevsky), 291–305. ACS Publications.

141 Taton, D., Wilczewska, A.Z., and Destarac, M. (2001). Direct synthesis of double hydrophilic statistical di- and triblock copolymers comprised of acrylamide and acrylic acid units via the MADIX process. *Macromol. Rapid Commun.* 22 (18): 1497–1503.

142 Mejia, A., Rodriguez, L., Schmitt, C. et al. (2019). Synthesis and viscosimetric behavior of poly(acrylamide-*co*-2-acrylamido-2-methylpropanesulfonate) obtained by conventional and adiabatic gel process via RAFT/MADIX polymerization. *ACS Omega* 4 (6): 11119–11125.

143 Bessaies-Bey, H., Fusier, J., Harrisson, S. et al. (2018). Impact of polyacrylamide adsorption on flow through porous siliceous materials: state of the art, discussion and industrial concern. *J. Colloid Interface Sci.* 531: 693–704.

144 Bessaies-Bey, H., Fusier, J., Hanafi, M. et al. (2019). Competitive adsorption of PAM and HPAM on siliceous material. *Colloids Surf., A* 579: 123673.

145 Krstina, J., Moad, G., Rizzardo, E. et al. (1995). Narrow polydispersity block copolymers by free-radical polymerization in the presence of macromonomers. *Macromolecules* 28 (15): 5381–5385.

146 Flory, P.J. and Leutner, F.S. (1948). Occurrence of head-to-head arrangements of structural units in polyvinyl alcohol. *J. Polym. Sci.* 3 (6): 880–890.

147 Lipscomb, C.E. and Mahanthappa, M.K. (2011). Microphase separation mode-dependent mechanical response in poly(vinyl ester)/PEO triblock copolymers. *Macromolecules* 44 (11): 4401–4409.

148 Matioszek, D., Brusylovets, O., Wilson, D.J. et al. (2013). Reversible addition-fragmentation chain-transfer polymerization of vinyl monomers with N,N-dimethyldiselenocarbamates. *J. Polym. Sci., Part A: Polym. Chem.* 51 (20): 4361–4368.

149 Hedir, G.G., Arno, M.C., Langlais, M. et al. (2017). Poly(oligo(ethylene glycol) vinyl acetate)s: a versatile class of thermoresponsive and biocompatible polymers. *Angew. Chem. Int. Ed.* 56 (31): 9178–9182.

150 Ilchev, A., Pfukwa, R., Hlalele, L. et al. (2015). Improved control through a semi-batch process in RAFT-mediated polymerization utilizing relatively poor leaving groups. *Polym. Chem.* 6 (46): 7945–7948.

151 Zhao, X.G., Coutelier, O., Nguyen, H.H. et al. (2015). Effect of copolymer composition of RAFT/MADIX-derived *N*-vinylcaprolactam/*N*-vinylpyrrolidone

statistical copolymers on their thermoresponsive behavior and hydrogel properties. *Polym. Chem.* 6 (29): 5233–5243.

152 Guerre, M., Ameduri, B., and Ladmiral, V. (2016). One-pot synthesis of poly(vinylidene fluoride) methacrylate macromonomers via thia-michael addition. *Polym. Chem.* 7 (2): 441–450.

153 Lopez, G., Guerre, M., Améduri, B. et al. (2017). Photocrosslinked PVDF-based star polymer coatings: an all-in-one alternative to PVDF/PMMA blends for outdoor applications. *Polym. Chem.* 8 (20): 3045–3049.

154 Girard, E., Marty, J.-D., Ameduri, B. et al. (2012). Direct synthesis of vinylidene fluoride-based amphiphilic diblock copolymers by RAFT/MADIX polymerization. *ACS Macro Lett.* 1 (2): 270–274.

155 Patil, Y. and Ameduri, B. (2013). First RAFT/MADIX radical copolymerization of tert-butyl 2-trifluoromethacrylate with vinylidene fluoride controlled by xanthate. *Polym. Chem.* 4 (9): 2783–2799.

156 Puts, G., Venner, V., Améduri, B. et al. (2018). Conventional and RAFT copolymerization of tetrafluoroethylene with isobutyl vinyl ether. *Macromolecules* 51 (17): 6724–6739.

157 Guerre, M., Wahidur Rahaman, S.M., Améduri, B. et al. (2016). RAFT synthesis of well-defined PVDF-b-PVAc block copolymers. *Polym. Chem.* 7 (45): 6918–6933.

158 Abreu, C.M.R., Rezende, T.C., Fonseca, A.C. et al. (2019). Polymerization of vinyl chloride at ambient temperature using macromolecular design via the interchange of xanthate: kinetic and computational studies. *Macromolecules* 53 (1): 190–202.

159 Wolpers, A., Bergerbit, C., Ebeling, B. et al. (2019). Aromatic xanthates and dithiocarbamates for the polymerization of ethylene through reversible addition-fragmentation chain transfer (RAFT). *Angew. Chem. Int. Ed.* 58 (40): 14295–14302.

160 Hill, M.R., Kubo, T., Goodrich, S.L. et al. (2018). Alternating radical ring-opening polymerization of cyclic ketene acetals: access to tunable and functional polyester copolymers. *Macromolecules* 51 (14): 5079–5084.

161 Hedir, G.G., Bell, C.A., O'Reilly, R.K. et al. (2015). Functional degradable polymers by radical ring-opening copolymerization of mdo and vinyl bromobutanoate: synthesis, degradability and post-polymerization modification. *Biomacromolecules* 16 (7): 2049–2058.

162 Hedir, G.G., Bell, C.A., Ieong, N.S. et al. (2014). Functional degradable polymers by xanthate-mediated polymerization. *Macromolecules* 47 (9): 2847–2852.

163 Andrei, M., Stănescu, P.O., Drăghici, C. et al. (2018). Synthesis and characterization of hydrolytically degradable poly(*N*-vinylcaprolactam) copolymers with in-chain ester groups. *Colloid. Polym. Sci.* 296 (11): 1905–1915.

164 d'Ayala, G.G., Malinconico, M., Laurienzo, P. et al. (2014). RAFT/MADIX copolymerization of vinyl acetate and 5,6-benzo-2-methylene-1,3-dioxepane. *J. Polym. Sci., Part A: Polym. Chem.* 52 (1): 104–111.

165 Jia, F., Wang, S., Zhang, X. et al. (2016). Amino-functionalized poly(*N*-vinylcaprolactam) derived from lysine: a sustainable polymer with thermo and pH dual stimuli response. *Polym. Chem.* 7 (46): 7101–7107.

166 Langlais, M., Coutelier, O., and Destarac, M. (2018). Thiolactone-functional reversible deactivation radical polymerization agents for advanced macromolecular engineering. *Macromolecules* 51 (11): 4315–4324.

167 Chen, F., Cheng, Z., Zhu, J. et al. (2008). Synthesis of poly(vinyl acetate) with fluorescence via a combination of RAFT/MADIX and "click" chemistry. *Eur. Polym. J.* 44 (6): 1789–1795.

168 Etchenausia, L., Rodrigues, A.M., Harrisson, S. et al. (2016). RAFT copolymerization of vinyl acetate and *N*-vinylcaprolactam: kinetics, control, copolymer composition, and thermoresponsive self-assembly. *Macromolecules* 49 (18): 6799–6809.

169 Besada, L.N., Peruzzo, P., Cortizo, A.M. et al. (2018). Preparation, characterization, and in vitro activity evaluation of triblock copolymer-based polymersomes for drugs delivery. *J. Nanopart. Res.* 20 (3): 67.

170 Chen, K., Grant, N., Liang, L. et al. (2010). Synthesis of CO_2-philic xanthate-oligo(vinyl acetate)-based hydrocarbon surfactants by RAFT polymerization and their applications on preparation of emulsion-templated materials. *Macromolecules* 43 (22): 9355–9364.

171 Pal, A. and Pal, S. (2018). Synthesis of triblock copolymeric micelle based on poly(ethylene glycol) and poly(vinyl acetate) through reversible addition-fragmentation chain transfer polymerization. *J. Colloid Interface Sci.* 524: 122–128.

172 Hu, N., Ji, W.-X., Tong, Y.-Y. et al. (2010). Synthesis of diblock copolymers containing poly(*N*-vinylcarbazole) by reversible addition-fragmentation chain transfer polymerization. *J. Polym. Sci., Part A: Polym. Chem.* 48 (20): 4621–4626.

173 Markiewicz, K.H., Seiler, L., Misztalewska, I. et al. (2016). Advantages of poly(vinyl phosphonic acid)-based double hydrophilic block copolymers for the stabilization of iron oxide nanoparticles. *Polym. Chem.* 7 (41): 6391–6399.

174 Willersinn, J., Drechsler, M., Antonietti, M. et al. (2016). Organized polymeric submicron particles via self-assembly and cross-linking of double hydrophilic poly(ethylene oxide)-*b*-poly(*N*-vinylpyrrolidone) in aqueous solution. *Macromolecules* 49 (15): 5331–5341.

175 Lee, S., Nam, J.H., Kim, Y.J. et al. (2011). Synthesis of PEO-based glucose-sensitive block copolymers and their application for preparation of superparamagnetic iron oxide nanoparticles. *Macromol. Res.* 19 (8): 827–834.

176 Jeon, H.J., Choi, S.-Y., Kim, K.M. et al. (2008). Synthesis of poly(ethylene oxide)-based thermoresponsive block copolymers by RAFT radical polymerization and their uses for preparation of gold nanoparticles. *Colloids Surf., A* 317 (1–3): 496–503.

177 Tong, Y.Y., Dong, Y.Q., Du, F.S. et al. (2009). Block copolymers of poly(ethylene oxide) and poly(vinyl alcohol) synthesized by the RAFT methodology. *J. Polym. Sci., Part A: Polym. Chem.* 47 (7): 1901–1910.

178 Zheng, Q. and Zheng, S. (2012). From poly(*N*-isopropylacrylamide)-block-poly (ethylene oxide)-block-poly(*N*-isopropylacrylamide) triblock copolymer to poly(*N*-isopropylacrylamide)-block-poly(ethylene oxide) hydrogels: synthesis and rapid deswelling and reswelling behavior of hydrogels. *J. Polym. Sci., Part A: Polym. Chem.* 50 (9): 1717–1727.

179 Lohmann, J., Houga, C., Driguez, H. et al. (2009). Hybrid block copolymers incorporating oligosasaccharides and d synthetic blocks grown by controlled radical polymerization. In: *Controlled/living radical polymerization: Progress in ATRP*, ACS Symposium Series (ed. K. Matyjaszewski), 231–240. American Chemical Society.

180 Willersinn, J. and Schmidt, B.V. (2018). Pure hydrophilic block copolymer vesicles with redox- and pH-cleavable crosslinks. *Polym. Chem.* 9 (13): 1626–1637.

181 Muller, J., Marchandeau, F., Prelot, B. et al. (2015). Self-organization in water of well-defined amphiphilic poly(vinyl acetate)-*b*-poly(vinyl alcohol) diblock copolymers. *Polym. Chem.* 6 (16): 3063–3073.

182 Girard, E., Tassaing, T., Marty, J.-D. et al. (2011). Influence of macromolecular characteristics of RAFT/MADIX poly(vinyl acetate)-based (co) polymers on their solubility in supercritical carbon dioxide. *Polym. Chem.* 2 (10): 2222–2230.

183 Liang, X., Kozlovskaya, V., Cox, C.P. et al. (2014). Synthesis and self-assembly of thermosensitive double-hydrophilic poly(*N*-vinylcaprolactam)-*b*-poly(*N*-vinyl-2-pyrrolidone) diblock copolymers. *J. Polym. Sci., Part A: Polym. Chem.* 52 (19): 2725–2737.

184 Özgüç, Ç., Helvacıoğlu, E., Nugay, N. et al. (2013). Synthesis and characterization of poly(*N*-isopropylacrylamide) and poly(vinyl acetate) diblock copolymers via MADIX process. *Macromol. Symp.* 323 (1): 18–25.

185 Zhu, Z. and Sukhishvili, S.A. (2009). Temperature-induced swelling and small molecule release with hydrogen-bonded multilayers of block copolymer micelles. *ACS Nano* 3 (11): 3595–3605.

186 Destarac, M., Papon, A., Van Gramberen, E. et al. (2009). MADIX thermoresponsive amphiphilic block copolymers as stimulable emulsion stabilizers. *Aust. J. Chem.* 62 (11): 1488–1491.

187 Nguyen, H.H., El Ezzi, M., Mingotaud, C. et al. (2016). Doubly thermo-responsive copolymers in ionic liquid. *Soft Matter* 12 (13): 3246–3251.

188 Huang, C.-F., Hsieh, Y.-A., Hsu, S.-C. et al. (2014). Synthesis of poly (*N*-vinyl carbazole)-based block copolymers by sequential polymerizations of RAFT-ATRP. *Polymer* 55 (23): 6051–6057.

189 Petruczok, C.D., Barlow, R.F., and Shipp, D.A. (2008). Synthesis of poly(tert-butyl acrylate-block-vinyl acetate) copolymers by combining ATRP and RAFT polymerizations. *J. Polym. Sci., Part A: Polym. Chem.* 46 (21): 7200–7206.

190 Zhang, S., Luo, W., Yan, W. et al. (2014). Synthesis of a CO_2-philic poly(vinyl acetate)-based cationic amphiphilic surfactant by RAFT/ATRP and its application in preparing monolithic materials. *Green Chem.* 16 (9): 4408–4416.

191 Bao, L., Fang, S., Hu, D. et al. (2018). Stabilization of CO_2-in-water emulsions by nonfluorinated surfactants with enhanced CO_2-philic tails. *J. Supercrit. Fluids* 133: 163–170.

192 Mishra, A.K., Ramesh, K., Paira, T.K. et al. (2013). Synthesis and self-assembly properties of well-defined four-arm star poly(ε-caprolactone)-*b*-poly(*N*-vinylpyrrolidone) amphiphilic block copolymers. *Polym. Bull.* 70 (11): 3201–3220.

193 Mishra, A.K., Patel, V.K., Vishwakarma, N.K. et al. (2011). Synthesis of well-defined amphiphilic poly(ε-caprolactone)-*b*-poly (*N*-vinylpyrrolidone) block copolymers via the combination of ROP and xanthate-mediated RAFT polymerization. *Macromolecules* 44 (8): 2465–2473.

194 Ramesh, K., Gundampati, R.K., Singh, S. et al. (2016). Self-assembly, doxorubicin-loading and antibacterial activity of well-defined ABA-type amphiphilic poly(*N*-vinylpyrrolidone)-*b*-poly(D, L-lactide)-*b*-poly (*N*-vinyl pyrrolidone) triblock copolymers. *RSC Adv.* 6 (31): 25864–25876.

195 Pal, A. and Pal, S. (2017). Effect of Fe_3O_4 NPs on micellization and release behavior of CBABC-type pentablock copolymer. *Polymer* 133: 184–194.

196 Yu, Y.C., Shin, S.J., Ko, K.D. et al. (2013). One-pot synthesis of poly(vinyl alcohol)-based biocompatible block copolymers using a dual initiator for ROP and RAFT polymerization. *Polymer* 54 (21): 5595–5600.

197 Ma'Radzi, A.H., Sugihara, S., Toida, T. et al. (2014). Synthesis of polyvinyl alcohol stereoblock copolymer via the combination of living cationic polymerization and RAFT/MADIX polymerization using xanthate with vinyl ether moiety. *Polymer* 55 (21): 5332–5345.

198 Zhang, J., Farias-Mancilla, B., Destarac, M. et al. (2018). Asymmetric copolymers: synthesis, properties, and applications of gradient and other partially segregated copolymers. *Macromol. Rapid Commun.* 39 (19): 1800357.

199 Liu, X., Wang, M., Harrisson, S. et al. (2017). Enhanced stabilization of water/$scCO_2$ interface by block-like spontaneous gradient copolymers. *ACS Sustainable Chem. Eng.* 5 (11): 9645–9650.

200 Guerrero-Sanchez, C., Harrisson, S., and Keddie, D.J. (2013). High-throughput method for RAFT kinetic investigations and estimation of reactivity ratios in copolymerization systems. In: *Macromolecular Symposia*, 38–46. Weinheim: Wiley-VCH.

201 Yañez-Macias, R., Kulai, I., Ulbrich, J. et al. (2017). Thermosensitive spontaneous gradient copolymers with block-and gradient-like features. *Polym. Chem.* 8 (34): 5023–5032.

202 Tang, Q., Chen, J., Zhao, Y. et al. (2015). A ring-closure method for preparing cyclic polymers from unconjugated vinyl monomers. *Polym. Chem.* 6 (37): 6659–6663.

203 Li, Z., Qu, L., Zhu, W. et al. (2018). Self-accelerating click reaction for preparing cyclic polymers from unconjugated vinyl monomers. *Polymer* 137: 54–62.

204 Atanase, L.I., Winninger, J., Delaite, C. et al. (2014). Reversible addition-fragmentation chain transfer synthesis and micellar characteristics of biocompatible amphiphilic poly(vinyl acetate)-graft-poly(*N*-vinyl-2-pyrrolidone) copolymers. *Eur. Polym. J.* 53: 109–117.

205 Kashio, M., Sugizaki, T., Miyasaka, Y. et al. (2012). Graft polymerization of acrylamide monomers from polysilsesquioxane containing xanthate groups. *Polym. J.* 44 (12): 1214.

206 Li, Y., Zhang, Y., Yang, D. et al. (2009). Well-defined amphiphilic graft copolymer consisting of hydrophilic poly(acrylic acid) backbone and hydrophobic poly(vinyl acetate) side chains. *J. Polym. Sci., Part A: Polym. Chem.* 47 (22): 6032–6043.

207 Nese, A., Kwak, Y., Nicolaÿ, R. et al. (2010). Synthesis of poly(vinyl acetate) molecular brushes by a combination of atom transfer radical polymerization (ATRP) and reversible addition- fragmentation chain transfer (RAFT) polymerization. *Macromolecules* 43 (9): 4016–4019.

208 Nese, A., Li, Y., Averick, S. et al. (2011). Synthesis of amphiphilic poly(*N*-vinylpyrrolidone)-*b*-poly(vinyl acetate) molecular bottlebrushes. *ACS Macro Lett.* 1 (1): 227–231.

209 Joubert, F., Yeo, R.P., Sharples, G.J. et al. (2015). Preparation of an antibacterial poly(ionic liquid) graft copolymer of hydroxyethyl cellulose. *Biomacromolecules* 16 (12): 3970–3979.

210 Duan, S., Cai, S., Xie, Y. et al. (2012). Synthesis and characterization of a multi-arm poly(acrylic acid) star polymer for application in sustained delivery of cisplatin and a nitric oxide prodrug. *J. Polym. Sci., Part A: Polym. Chem.* 50 (13): 2715–2724.

211 Johnson, I.J., Khosravi, E., Musa, O.M. et al. (2015). Xanthates designed for the preparation of *N*-vinyl pyrrolidone-based linear and star architectures via RAFT polymerization. *J. Polym. Sci., Part A: Polym. Chem.* 53 (6): 775–786.

212 Nguyen, T.L.U., Eagles, K., Davis, T.P. et al. (2006). Investigation of the influence of the architectures of poly(vinyl pyrrolidone) polymers made via the reversible addition-fragmentation chain transfer/macromolecular design via the interchange of xanthates mechanism on the stabilization of suspension polymerizations. *J. Polym. Sci., Part A: Polym. Chem.* 44 (15): 4372–4383.

213 Cortez-Lemus, N.A. and Licea-Claverie, A. (2017). Preparation of a mini-library of thermo-responsive star (NVCL/NVP-VAc) polymers with tailored properties using a hexafunctional xanthate RAFT agent. *Polymers* 10 (1): 20.

214 Mori, H., Ishikawa, K., Abiko, Y. et al. (2013). Water-soluble poly(*N*-vinyl-1,2,4-triazole) star and amphiphilic star block copolymers by RAFT polymerization. *Polymer* 54 (8): 2001–2010.

215 Mori, H., Ookuma, H., and Endo, T. (2008). Poly(*N*-vinylcarbazole) star polymers and amphiphilic star block copolymers by xanthate-mediated controlled radical polymerization. *Macromolecules* 41 (19): 6925–6934.

216 Mori, H., Ebina, Y., Kambara, R. et al. (2012). Temperature-responsive self-assembly of star block copolymers with poly(ionic liquid) segments. *Polym. J.* 44 (6): 550–560.

217 Fleet, R., McLeary, J.B., Grumel, V. et al. (2007). Preparation of new multiarmed RAFT agents for the mediation of vinyl acetate polymerization. *Macromol. Symp.* 255 (1): 8–19.

218 Zhang, S., Chen, K., Liang, L. et al. (2013). Synthesis of oligomer vinyl acetate with different topologies by RAFT/MADIX method and their phase behaviour in supercritical carbon dioxide. *Polymer* 54 (20): 5303–5309.

219 Mori, H., Ookuma, H., and Endo, T. (2007). Synthesis of star polymers based on xanthate-mediated controlled radical polymerization of N-vinylcarbazole. *Macromol. Symp.* 249–250 (1): 406–411.

220 Zheng, X., Ji, C., Liu, J. et al. (2018). Novel star polymers as chemically amplified positive-tone photoresists for KrF lithography applications. *Ind. Eng. Chem. Res.* 57 (19): 6790–6796.

221 Qiu, Y., Zhang, W., Yan, Y. et al. (2010). Preparation of miktoarm star-block copolymers PS_n-b-$PVAc_{4-n}$ via combination of ATRP and RAFT polymerization. *J. Polym. Sci., Part A: Polym. Chem.* 48 (22): 5180–5188.

222 Zhang, W., Zhang, W., Zhu, J. et al. (2009). Controlled synthesis of pH-responsive amphiphilic A_2B_2 miktoarm star block copolymer by combination of SET-LRP and RAFT polymerization. *J. Polym. Sci., Part A: Polym. Chem.* 47 (24): 6908–6918.

223 Zhang, W., Zhang, W., Zhang, Z. et al. (2010). Thermo-responsive fluorescent micelles from amphiphilic A_3B miktoarm star copolymers prepared via a combination of SET-LRP and RAFT polymerization. *J. Polym. Sci., Part A: Polym. Chem.* 48 (19): 4268–4278.

224 Ramesh, K., Thangagiri, B., Mishra, A.K. et al. (2018). AB_2-type miktoarm poly($_L$-lactide)-*b*-poly(*N*-acryloylmorpholine) amphiphilic star block copolymers as nanocarriers for drug delivery. *React. Funct. Polym.* 132: 112–119.

225 Hira, S.K., Ramesh, K., Gupta, U. et al. (2015). Methotrexate-loaded four-arm star amphiphilic block copolymer elicits CD^{8+} T cell response against a highly aggressive and metastatic experimental lymphoma. *ACS Appl. Mater. Interfaces* 7 (36): 20021–20033.

226 Xie, C., Zhang, P., Zhang, Z. et al. (2015). Drug-loaded pseudo-block copolymer micelles with a multi-armed star polymer as the micellar exterior. *Nanoscale* 7 (29): 12572–12580.

227 Zheng, Y., Li, S., Weng, Z. et al. (2015). Hyperbranched polymers: advances from synthesis to applications. *Chem. Soc. Rev.* 44 (12): 4091–4130.

228 Poly, J., Wilson, D.J., Destarac, M. et al. (2008). Synthesis of poly(vinyl acetate) nanogels by xanthate-mediated radical crosslinking copolymerization. *Macromol. Rapid Commun.* 29 (24): 1965–1972.

229 Willcock, H. and O'Reilly, R.K. (2010). End group removal and modification of RAFT polymers. *Polym. Chem.* 1 (2): 149–157.

230 Harvison, M.A., Roth, P.J., Davis, T.P. et al. (2011). End group reactions of RAFT-prepared (co)polymers. *Aust. J. Chem.* 64 (8): 992–1006.

231 Moad, G., Chong, Y., Postma, A. et al. (2005). Advances in RAFT polymerization: the synthesis of polymers with defined end-groups. *Polymer* 46 (19): 8458–8468.

232 Moad, G., Rizzardo, E., and Thang, S.H. (2011). End-functional polymers, thiocarbonylthio group removal/transformation and reversible

addition-fragmentation-chain transfer (RAFT) polymerization. *Polym. Int.* 60 (1): 9–25.

233 Holbein, B.E., Ang, M.T.C., Palaskar, D.V. et al. (2019). Polymeric metal chelating compositions and methods of preparing same for controlling growth and activities of living cells and organisms. US Patent 20190169126A1, filed August 26, 2016 and issued June 6, 2019.

234 Wu, Y., Zhou, Y., Zhu, J. et al. (2014). Fast conversion of terminal thiocarbonylthio groups of RAFT polymers to "clickable" thiol groups via versatile sodium azide. *Polym. Chem.* 5 (19): 5546–5550.

235 Pound, G., McKenzie, J.M., Lange, R.F. et al. (2008). Polymer-protein conjugates from ω-aldehyde endfunctional poly(*N*-vinylpyrrolidone) synthesised via xanthate-mediated living radical polymerisation. *Chem. Commun.* 27: 3193–3195.

236 Quiclet-Sire, B. and Zard, S.Z. (2010). A convenient, high yielding cleavage of the thiocarbonyl group in xanthates. *ChemInform* 31 (3): 543–544.

237 Matioszek, D., Dufils, P.E., Vinas, J. et al. (2015). Selective and quantitative oxidation of xanthate end-groups of RAFT poly(*N*-butyl acrylate) latexes by ozonolysis. *Macromol. Rapid Commun.* 36 (14): 1354–1361.

238 Zard, S., Sire, B., and Jost, P. (2009). Method for partial or total oxidation of one or several thiocarbonylthio ends of a polymer obtained by radical polymerisation controlled by reversible addition-fragmentation. US Patent 7473740B2, filed October 22, 2003 and issued January 6, 2009.

239 Pfukwa, R., Pound, G., and Klumperman, B. (2008). Facile end group modification of RAFT made polymers, by radical exchange with hydrogen peroxide. *Polym. Prepr.* 49 (2): 117.

240 Destarac, M., Kalai, C., Wilczewska, A. et al. (2006). Various strategies for the chemical transformation of xanthate-functional chain termini in MADIX copolymers. In: *Controlled/Living Radical Polymerization*, ACS Symposium Series, vol. 944 (ed. K. Matyjaszewski), 564–577. American Chemical Society.

241 Wilczewska, A.Z., Destarac, M., and Zard, S. et al. (2002). Method for synthesis of polymers with thiol functions. WO2002090424A1, Rhodia Chimie, Fr.

242 Postma, A., Davis, T.P., Li, G. et al. (2006). RAFT polymerization with phthalimidomethyl trithiocarbonates or xanthates. On the origin of bimodal molecular weight distributions in living radical polymerization. *Macromolecules* 39 (16): 5307–5318.

243 Chong, Y.K., Moad, G., Rizzardo, E., and Thang, S.H. (2007). Thiocarbonylthio end group removal from RAFT-synthesized polymers by radical-induced reduction. *Macromolecules* 40 (13): 4446–4455.

244 Glaria, A., Beija, M., Bordes, R. et al. (2013). Understanding the role of ω-end groups and molecular weight in the interaction of PNIPAM with gold surfaces. *Chem. Mater.* 25 (9): 1868–1876.

11

Dithiocarbamates in RAFT Polymerization

Graeme Moad

CSIRO Manufacturing, Research Way, Clayton, VIC 3168, Australia

11.1 Introduction

This review updates a review on the same topic that was originally published in *Journal of Polymer Science, Polymer Chemistry* in 2019 [1]. Much of the text and many of the figures and schemes are from that source [1].

Dithiocarbamates (Z′Z″NC(=S)SR, IUPAC recommended term is carbamodithioate) are versatile RAFT agents. Their activity as a class spans a continuum ranging from the most active to the least active of RAFT agents and depends strongly on the substituents R and NZ′Z″ (Figure 11.1). In the initial RAFT agent, R should be a good homolytic leaving group both in absolute terms and when considered in relation to the propagating species. It must also be an effective initiating radical for the monomers being polymerized. The substituents Z′, Z″ largely determine the reactivity of the thiocarbonyl double bond towards radical addition and the facility of intermediate fragmentation. Early work showed that depending on Z′, Z″, the attributes of good control (i.e. predicted molar mass, low dispersity ($Đ$), little retardation, high end-group fidelity) could be obtained in the polymerization of both more activated monomers (MAMs; (meth)acrylates, styrenes, acrylamides) and less activated monomers (LAMs; vinyl esters, vinylamides, allyl monomers).

Dithiocarbamates with Z′Z″NC(=S)S— appearing near the centre of Figure 11.1a show capacity for controlling the polymerization of both MAMs and LAMs. For this reason, they are said to have balanced activity. However, the activity of these RAFT agents with respect to one or both monomer classes is compromised to some extent [2–6] such that molar mass may be higher than predicted for low monomer conversions, higher $Đ$ (e.g. >1.3) is seen for 1,1-disubstituted MAMs (e.g. methyl methacrylate [MMA]), and some retardation is observed with LAMs (e.g. vinyl acetate) and intermediate activated monomers (IAMs) (e.g. *N*-vinylcarbazole [NVC]) [7].

Despite their versatility, dithiocarbamates have to date had limited impact as RAFT agents. The publication rate in both the patent and open literature on dithiocarbamate RAFT agents lags behind those relating to the use of xanthate RAFT agents (those currently most popular for controlling polymerization of

RAFT Polymerization: Methods, Synthesis and Applications, First Edition.
Edited by Graeme Moad and Ezio Rizzardo.

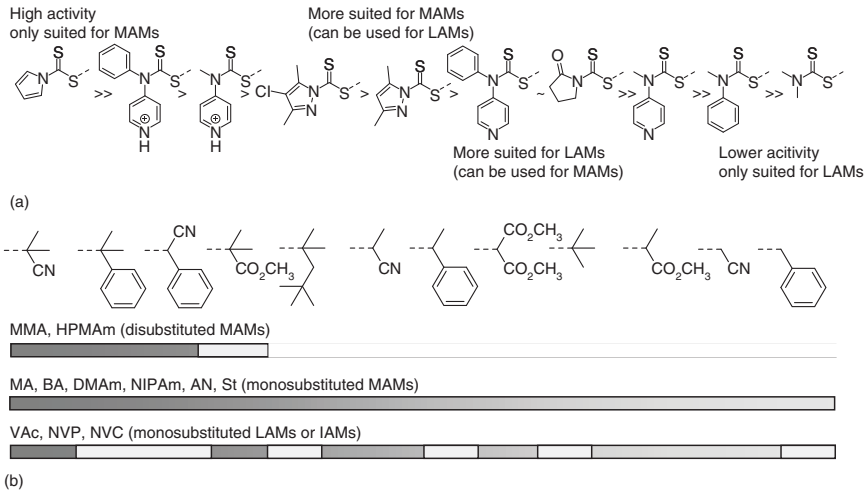

Figure 11.1 (a) Effect of Z′Z″NC(=S)-group and (b) R group on activity of dithiocarbamates Z′Z″NC(=S)SR in RAFT polymerization. Activity increases from right to left. MAM, more activated monomer; LAM, less activated monomer; IAM, intermediate activated monomer; AN, acrylonitrile; BA, butyl acrylate; DMAm, *N,N*-dimethylacrylamide; HPMAm, *N*-(2-hydroxypropyl)methacrylamide; MA, methyl acrylate; MMA, methyl methacrylate; NIPAm, *N*-isopropylacrylamide; NVC, *N*-vinylcarbazole; NVP, *N*-vinylpyrrolidone; St, styrene; VAc, vinyl acetate. Source: Moad [1]. © 2019, John Wiley and Sons.

LAMs – Figure 11.2) [8], and they lie substantially further behind those relating to the use of dithioesters [9] and trithiocarbonates (currently preferred for MAMs – Figure 11.2) [10]. This can in large part be attributed to the lack of commercial availability of dithiocarbamates with suitable activity for controlling the polymerization of MAMs, which has only recently been addressed.

RAFT polymerization with dithiocarbamate RAFT agents should be distinguished from radical polymerization performed with dithiocarbamate 'iniferters'. The carbon-sulfur bonds of *N,N*-dialkyldithiocarbamates and related compounds can undergo reversible homolysis under irradiation with light of appropriate wavelength to allow monomer insertion into the C—S bond. The *N,N*-dialkyldithiocarbamyl radical is considered persistent, reacting with most monomers very slowly if at all. Otsu developed this chemistry as a method of controlled polymerization. Their first experiments in the field were reported in 1956–1957 [11, 12]. The monomer insertion process with *N,N*-dialkyldithiocarbamates is, like nitroxide-mediated polymerization (NMP) [13–16], a form of stable radical-mediated polymerization (SRMP).

In 1982, Otsu et al. [17–19] proposed the concept of living radical polymerization, now termed reversible-deactivation radical polymerization (RDRP) [16, 20]. They recognized that radical polymerizations might display living attributes in the presence of reagents that are capable of reversibly deactivating active chains (propagating radicals, $P_n\cdot$) such that the majority of living chains are maintained in a dormant form (P_n–X). They also introduced the terms 'initer'

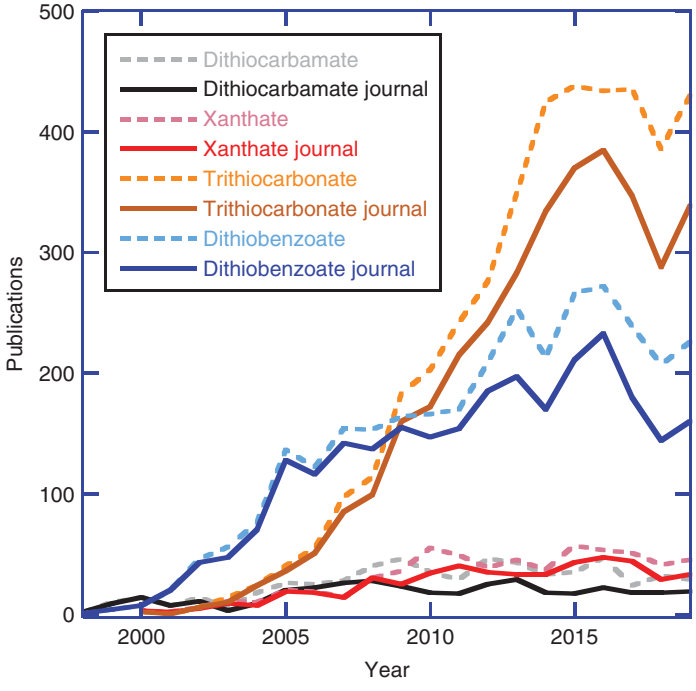

Figure 11.2 RAFT polymerization publication rate per annum. Includes both patent and open literature publications (dashed lines) or just journal publications (solid lines). Based on Scifinder™ Search carried out in May 2020 on the RAFT agent structures and the terms 'RAFT' or 'reversible addition–fragmentation chain transfer', and the term 'MADIX', in the case of xanthates, and the term 'iniferter', in the case of dithiocarbamates.

(for *ini*tiator-*ter*minator) and 'iniferter' (for *ini*tiator-trans*fer* agent-*ter*minator) to describe the reagents used. A similar terminology ('inifer' [for *ini*tiator-trans*fer* agent]) had already been used by Kennedy et al. [21, 22] in describing cationic polymerizations with reversible deactivation.

Otsu recognized that reversible chain transfer could contribute to living characteristics. However, they, and others [23], soon demonstrated that the *N,N*-dialkyldithiocarbamates they used had very low transfer constants in the polymerizations of MAMs. Thiuram disulfide 'iniferters' have higher transfer constants and are deserving of the name (C_{tr}(St, 60 °C) = 0.29) [24]. However, they are immediately transformed to less active *N,N*-dialkyldithiocarbamate end-groups when used in polymerization.

Sulfur-centred radical-mediated polymerization making use of *N,N*-dialkyldithiocarbamate photoiniferters or photoiniters has been reviewed by Sebenik [25], Otsu and Matsumoto [26], and Otsu [19] with respect to the literature through 2000, and more recently by Tasdelen and Yagci [27]. The 'photoiniferter' process as originally conceived, whether with simple alkyl *N,N*-dialkyldithiocarbamates or with thiuram disulfides, is not generally useful for the synthesis of well-defined polymers, though recent examples of block [28] and star polymer syntheses [29–31] can be found. The main current use of iniferter chemistry is in photoinitiated grafting from

particles or surfaces of various types with a significant number of publications from just 2016–2018 [32–44]. The process of surface-initiated photoiniferter-mediated polymerization (SI-PIMP) is compared with surface-initiated atom-transfer radical polymerization (SI-ATRP), surface-initiated reversible addition-fragmentation chain transfer polymerization (SI-RAFT), and surface-initiated nitroxide-mediated polymerization (SI-NMP) in a recent review [45].

This said, there has been a marked upsurge in interest in photoinitiated RAFT polymerization (mainly using trithiocarbonates or dithioesters) where radicals are generated by direct or photosensitized photolysis of the RAFT agent [46–52], by what can be recognized as Otsu's photoiniferter mechanism, or through a photo-redox process involving the RAFT agent. The last process, making use of a photosensitizer or a photo-redox catalyst, is known as (photoinduced electron/energy transfer) PET-RAFT [53–58].

Visible (blue) light-initiated RAFT polymerization with dithiocarbamates (where Z′Z″NC(=S)S– includes **126**, **127**, **128**, **149**, **150**) has been reported [59]. There has been debate about the relative importance of RAFT and the SRMP mechanisms in providing control over polymerization. However, it is likely in most, if not all, cases that when an effective (high transfer coefficient) RAFT agent is used, it is the RAFT process that is dominant in providing low dispersities and good control [46, 55]. On the other hand, when a poor RAFT agent for the monomer being polymerized is used the iniferter mechanism may dominate [60].

11.2 Dithiocarbamate Transfer Constants

The efficiency of RAFT can be measured in terms of two transfer coefficients, C_{tr} ($=k_{tr}/k_p$) and C_{-tr} ($=k_{-tr}/k_{-\beta}$), where k_{tr} and k_{-tr} are given by Eqs. (11.1) and (11.2), respectively. The value of k_{tr} depends on the rate of addition of the propagating radical ($P_n\cdot$) to the RAFT agent and a partition coefficient (ϕ) that describes the partitioning of intermediate radical between starting materials and products – refer to Scheme 11.1 for rate coefficient definitions.

For less active RAFT agents where $C_{tr} \leq 1$, transfer constants for RAFT agents may be determined with reasonable accuracy by the usual methods (e.g. the Mayo method [61], the log CLD method [62], or the Walling method [63]) [64].

However, these methods, which include an implicit assumption that C_{-tr} is zero, will typically underestimate the actual C_{tr} and the values so obtained should be called apparent transfer constants, ${C_{tr}}^{app}$. While values of ${C_{tr}}^{app}$ obtained are useful for ranking RAFT agents, it should be stressed that for more active RAFT agents, values of C_{tr} can be higher than ${C_{tr}}^{app}$ by several orders of magnitude [65, 66]. Further details on the methods for determining transfer coefficients in RAFT polymerization are provided in the Chapter by Quinn et al. [67].

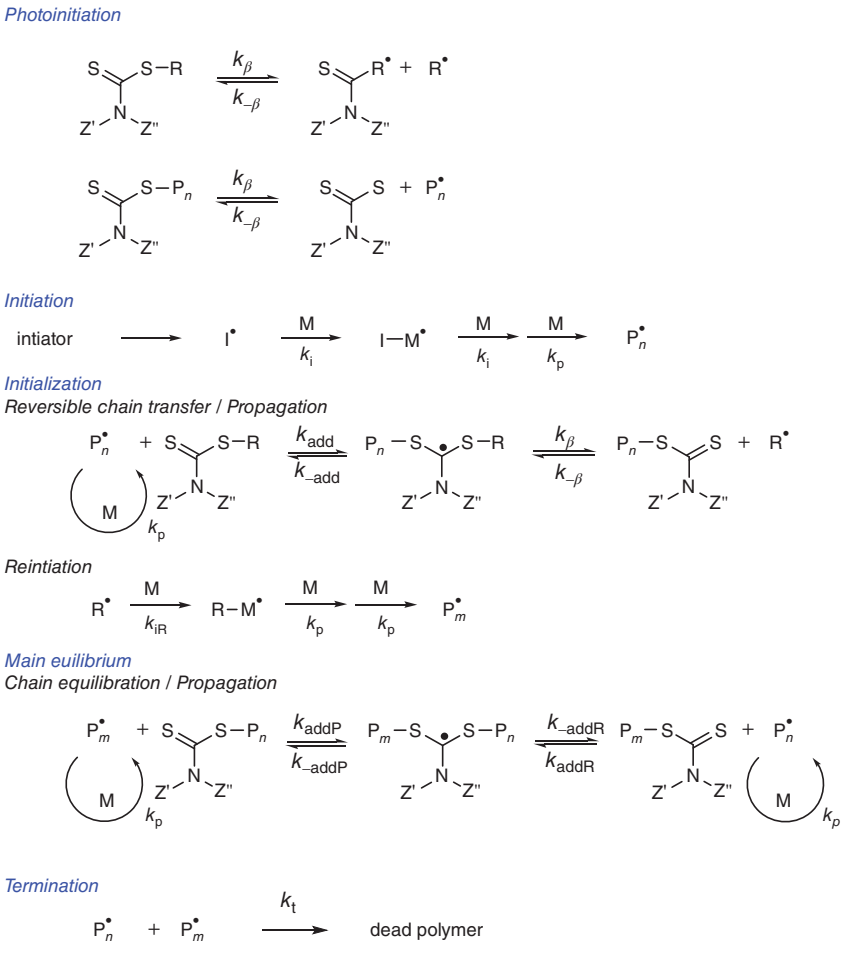

Scheme 11.1 Major pathways in the mechanism of RAFT polymerization with dithiocarbamates.

A listing of available transfer constants, C_{tr}^{app}, for dithiocarbamates is provided in Table 11.1 and values can be seen to span more than four orders of magnitude depending on the substituents Z′Z″NC(=S)S— and R.

$$k_{tr} = k_{add}\phi = k_{add}\left[\frac{k_\beta}{k_{-add} + k_\beta}\right] \tag{11.1}$$

$$k_{-tr} = k_{-\beta}(1-\phi) = k_{-\beta}\left[\frac{k_{-add}}{k_{-add} + k_\beta}\right] \tag{11.2}$$

Table 11.1 Estimates of apparent transfer coefficients (C_{tr}^{app}) for dithiocarbamates [Z′Z″NC(=S)S−R] in RAFT polymerization.

Z′ZNC(=S)S− [a]	R	Monomer [b]	T (°C)	C_{tr}^{app}	Method [c]	References
126	$\dot{C}(CH_3)_2CN$	St	110	>50	W	[65]
126	$\dot{C}H(CH_3)Ph$	St	85	81	M	[68]
126	$\dot{C}H_2Ph$	St	110	11	W	[65]
140	$\dot{C}H_2Ph$	St	110	1.6	W	[65]
156	$\dot{C}H_2Ph$	St	80	0.009	W	[65]
156	$\dot{C}H_2Ph$	St	60	0.0044	N	[24]
156	$\dot{C}H_2Ph$	St	30	0.07	N	[69]
156	$\dot{C}H_2Ph\dot{C}H_2$	St	60	0.011	N	[24]
127	$\dot{C}(CH_3)_2CO_2R^a$	MMA	60	2.6	M	[70, 71]
127	$\dot{C}(CH_3)_2CO_2Et$	MMA	60	1.1	M	[70, 71]
156	$\dot{C}H(CH_3)CO_2Bu$	BA	80	0.3	M	[72]
138-H$^+$	$\dot{C}H_2CN$	MA	70	12.5	W	[73]
137-H$^+$	$\dot{C}H_2CN$	MA	70	6.9	W	[73]
138	$\dot{C}H_2CN$	MA	70	2.9	W	[73]
137	$\dot{C}H_2CN$	MA	70	0.9	W	[73]
138	$\dot{C}H_2CN$	NVC	60	56.0	W	[73]
137	$\dot{C}H_2CN$	NVC	60	33.3	W	[73]
138	$\dot{C}H_2CN$	VAc	70	124	W	[73]
137	$\dot{C}H_2CN$	VAc	70	41.7	W	[73]

a) For Structures refer to Table 11.17.
b) Monomer: St, styrene; MMA, methyl methacrylate; BA, butyl acrylate; MA, methyl acrylate; NVC, *N*-vinylcarbazole; VAc, vinyl acetate.
c) Method used to determine transfer coefficient: M, Mayo method; [61, 64] N, not stated; W, Walling method [63, 64]. Refer to Quinn et al. [67] for further details on methods.
d) R = (4-phenylazo)phenyl.
Source: Updated from Moad [1]. Copyright 2019, John Wiley & Sons.

11.3 Dithiocarbamates and RAFT Polymerization

The factors that influence the choice of RAFT agent for a particular polymerization are detailed in previous reviews [74–78]. The effectiveness of a given RAFT agent depends on the monomer being polymerized and is determined by the properties of the free radical leaving group R and the activating group Z (NZ′Z″ in the case of dithiocarbamates). For effective RAFT polymerization (refer Scheme 11.1, Figure 11.3) the following conditions should be met:

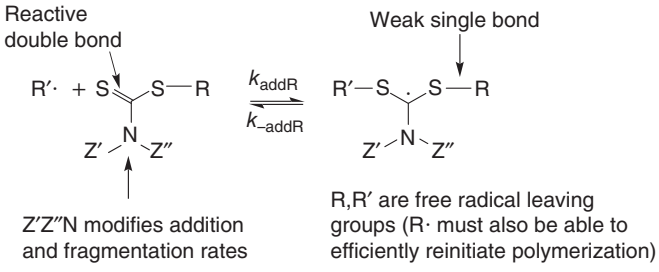

Figure 11.3 Structural features of dithiocarbamate RAFT agents and the intermediate formed by radical addition. Source: Moad [1]. Copyright 2019, John Wiley and Sons.

- The initial RAFT agents and the macroRAFT agent should have a suitably reactive C=S double bond (high k_{add}).
- The intermediate radicals should fragment rapidly and give no side reactions (high k_{β}, weak S—R bond in intermediate).
- The intermediate should partition in favour of products ($k_{\beta} \geq k_{-add}$).
- The expelled radicals (R·) must efficiently reinitiate polymerization ($k_i > k_p$).

RAFT polymerizations making use of the most commonly encountered dithiocarbamate RAFT agents are summarized in Table 11.2. Switchable RAFT agents are listed separately in Table 11.3. In the tables we indicate those dithiocarbamates that are commercially available from sources such as Boron Molecular [227], Merck (Sigma-Aldrich) [228, 229], or Strem Chemicals [230, 231].

11.4 Monomers for RAFT Polymerization

Polymer syntheses making use of dithiocarbamate RAFT agents are summarized in the tables above. The only systems that require separate comment are mentioned here or in the subsequent sections. Some of the more exotic monomers subjected to RAFT polymerization are included in the tables that follow. They include methacrylates and other 1,1-disubstituted MAMs, (Table 11.4), acrylates and acrylamides (Table 11.5), styrene derivatives (Table 11.6), and vinyl monomers and other LAMs (Table 11.7).

11.4.1 1,1-Disubstituted MAMs (Methacrylates)

RAFT polymerization with dithiocarbamate RAFT agents has been successfully applied to methacrylates, which include butyl methacrylate (BMA), *tert*-butyl methacrylate (tBMA), (diethylene glycol monomethyl ether) methacrylate (DEGMA), 2-(dimethylamino)ethyl methacrylate (DMAEMA), glycidyl methacrylate (GMA), MAA, MMA, (poly(ethylene glycol)monomethyl ether)methacrylate

(*sentence continued on p. 572*)

Table 11.2 RAFT polymerization with dithiocarbamate RAFT agents.

RAFT agent	Synthesis[a)]	Polymerizations[b)]
(a) *More active RAFT agents suitable for MAMs* (1*H*-pyrrole-1-carbodithioates, 9*H*-carbazole-9-carbodithioates)		
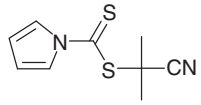 **1** 2-cyanopropan-2-yl 1*H*-pyrrole-1-carbodithioate	D [65]	*Methacrylates*: MMA [65, 79–81] *Styrenes*: PFS [82] St [65] **90** [83] *Others*: (**65**) [84]
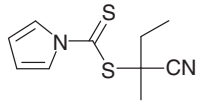 **2** 2-cyanobutan-2-yl 1*H*-pyrrole-1-carbodithioate	D [85]	*Methacrylates*: MMA [85]
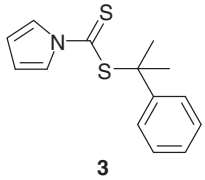 **3** 2-phenylpropan-2-yl 1*H*-pyrrole-1-carbodithioate	A [86] C [86, 87]	*Methacrylates*: GMA [87] *Acrylamides*: NIPAm [86, 88] *Styrenes*: St [87] *Copolymers*: tBMA/DEGMA [87] *Blocks*: tBMA/DEGMA-*b*-GMA [87]
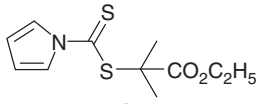 **4** ethyl 2-((1*H*-pyrrole-1-carbonothioyl) thio)-2-methylpropanoate	A [89]	*Styrenes*: St [89] *Blocks*: St-*b*-2VP [89] *ATRP*: St [90]
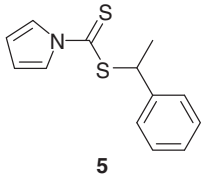 **5** 1-phenylethyl 1*H*-pyrrole-1-carbodithioate	A [91]	*Styrenes*: St [68, 92]

(*continued*)

Table 11.2 (Continued)

RAFT agent	Synthesis[a)]	Polymerizations[b)]
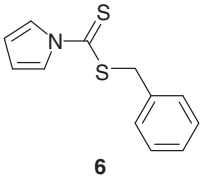 **6** benzyl 1*H*-pyrrole-1-carbodithioate	A [65] G (Merck)	*Methacrylates*: MMA[a)] [93] **60** [94] **61** [94] *Acrylates*: (AA) [95] MA [93, 96–98] *BA* [99] *EHA* [99] *Acrylamides*: NIPAm [88, 100] **70** [101] **71** [102, 103] **72** [104] **73** [104] **74** [105–107] **75** [107] **76** [102] **77** [108] **83** [107, 109] **84** [102, 105, 107] **78** [110] **79** [110] **80** [111] **81** [111] **85** [102] **86** [112] **89** [113] *Styrenes*: St [65, 98] (**94**) [114] **95** [115] *Dienes*: (*Cp*) [116] *Others*: (NES) [117] NVPI [108, 118] (**99**–**101**) [119] **107**–**106** [120] (**110**–**111**) [121] **112** [122] **103** [123] **104** [123] (NVC) [124] *Copolymers*: NIPAm/NVPI [125] NIPAm/**102** [126] (AA/ACE) [95] (DMAm/**102**) [126] (MA/**102**) [126] (MAH/**103**) [127] (NMMI/**103**) [127] (NPMI/**103**) [127] **94**/CMS [115] **94**/St [128] *Blocks*: MMA-*b*-St[c)] [93] MA-*b*-St[c)] [93] **71**-*b*-**92** [103] St-*b*-**74** [106] **76**-*b*-**74** [106] **76**-*b*-**83** [105] **76**-*b*-**84** [105] **83**-*b*-**84** [105] **83**-*b*-**78** [105] **83**-*b*-**79** [105] **86**-*b*-NIPAm [112] **103**-*b*-NIPAm [123] **104**-*b*-NIPAm [123] NVPI-*b*-**74** [108] NVPI-*b*-**77** [108]
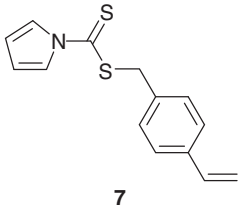 **7** 4-vinylbenzyl 1*H*-pyrrole-1-carbodithioate	A [129]	*Acrylamides*: NIPAm [95, 129–132]

(*continued*)

Table 11.2 (Continued)

RAFT agent	Synthesis[a)]	Polymerizations[b)]
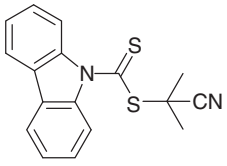 **8** 2-cyanopropan-2-yl 9*H*-carbazole-9-carbodithioate	D [133]	*Methacrylates*: BMA [134] EMA [134] MMA [133, 135] *Blocks*: BMA-*b*-MMA [134] EMA-*b*-MA [134]
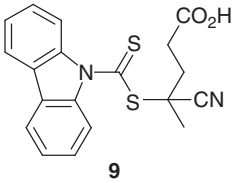 **9** 4-((9H-carbazole-9-carbonothioyl) thio)-4-cyanopentanoic acid	D [133]	*Methacrylates*: MMA [133]
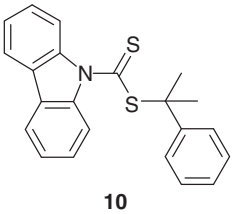 **10** 2-phenylpropan-2-yl 9*H*-carbazole-9-carbodithioate	A [136]	*Methacrylates*: MMA [136] *Styrenes*: St [136]
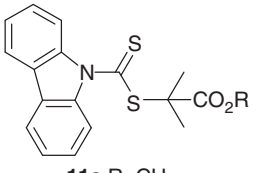 **11a** R=CH_3 **11b** R=C_2H_5 alkyl 2-((9*H*-carbazole-9-carbonothioyl) thio)-2-methylpropanoate	A [50, 137]	*Methacrylates*: MMA [50] (MMA) [137] *Acrylates*: BA [50] BA[a)] [50] MA [137, 138] *Styrenes*: St [50] *Vinyls*: NVC [50] *Blocks*: MA-*b*-St [137]
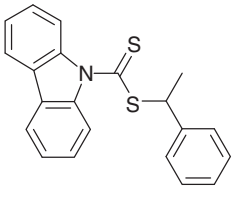 **12** 1-phenylethyl 9*H*-carbazole-9-carbodithioate	A [136]	*Methacrylates*: (MMA) [136] (*MMA*) [136, 139] *Styrenes*: St [136] (*St*) [139]

(*continued*)

Table 11.2 (Continued)

RAFT agent	Synthesis[a)]	Polymerizations[b)]
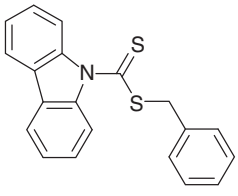 **13** benzyl 9*H*-carbazole-9-carbodithioate	A [136, 140–143] G	*Acrylates*: BA [134, 142] BzA [144] EA [134] EHA [134] MA [142, 143] PEGA [145] OA [142] *Methacrylates*: MMA[e)] [141] (MMA) [136] *Styrenes*: St [134, 136, 140, 142, 146] CMS [147] *Blocks*: BA-*b*-MA [134] BzA-*b*-MA [144] EA-*b*-MA [134] EHA-*b*-BA [134] PEGA-*b*-St [145] PEGA-*b*-St/DMAm [145] St-*b*-MA [134] St-*b*-PVK [146] St-*b*-PVK-*b*-AA [146] St-*b*-PVK-*b*-MA [146]
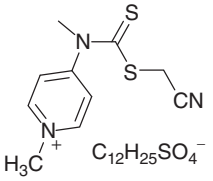 **14** 4-((((cyanomethyl)thio)carbonothioyl)(methyl)amino)-1-methylpyridin-1-ium dodecylsufonate	F [148]	St [148]

(b) *RAFT agents with balanced activity suitable for MAMs and LAMs*
(1*H*-pyrazole-1-carbodithioates, diphenylcarbamodithioates)

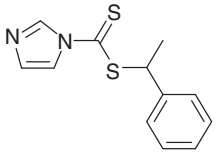 **15** 1-phenylethyl 1*H*-imidazole-1-carbodithioate	A [91] B [149]	*Acrylates*: (AA) [149]
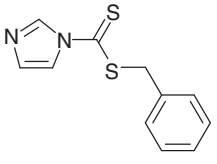 **16** benzyl 1*H*-imidazole-1-carbodithioate	A [150–152] B [153] G	*Methacrylates*: (MMA) [154] *Acrylates*: (AA) [149] MA [79, 97, 154–156] MA [59] **66** [157, 158] *Styrenes*: St [159, 160] **91** [154, 156, 160, 161] *Copolymers*: MA/**62** [161] St/**62** [161] MA/**91** [161] St/**91** [161] **96**/MA [156] **97**/MA [162] *Blocks*: **66**-*b*-St [158] St-*b*-**96**/MA [156, 159]

(*continued*)

Table 11.2 (Continued)

RAFT agent	Synthesis[a)]	Polymerizations[b)]
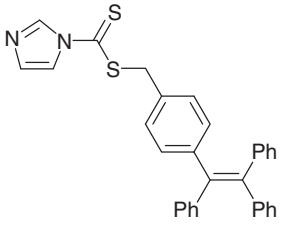 **18** 4-(1,2,2-triphenylvinyl)benzyl 1*H*-imidazole-1-carbodithioate	A [59]	*Acrylates*: MA [59]
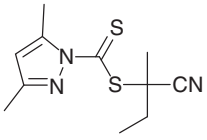 **19** 2-cyanobutan-2-yl 3,5-dimethyl-1*H*-pyrazole-1-carbodithioate	D [3] G	*Methacrylates*: (MMA) [3] *Acrylates*: MA [3] *Acrylamides*: DMAm [3] *Styrenes*: St [3, 163] *Vinyls*: VAc [3] *Copolymers*: BA/CHPMA [164] DMAm/VAc [164]
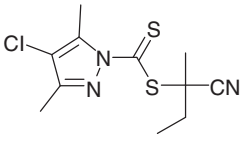 **20** 2-cyanobutan-2-yl 4-chloro-3,5-dimethyl-1*H*-pyrazole-1-carbodithioate	D [2] G	*Methacrylates*: MMA [2] *Acrylates*: MA [2] *Acrylamides*: DMAm [2] *Styrenes*: St [2] *Vinyls*: VAc [2]
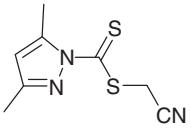 **21** cyanomethyl 3,5-dimethyl-1*H*-pyrazole-1-carbodithioate	A [3] G	*Methacrylates*: (MMA) [3] *Acrylates*: MA [3] *Acrylamides*: DMAm [3, 165] *Styrenes*: St [3] *Vinyls*: E [166] VAc [3] *Copolymers*: AA/BA [167] *Blocks*: (AA/BA-*b*-MA) [167] AA/BA-*b*-MA-b-*MA/EGDA* [167]

(*continued*)

Table 11.2 (Continued)

RAFT agent	Synthesis[a)]	Polymerizations[b)]
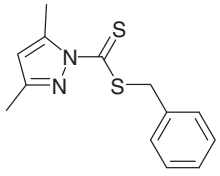 **22** benzyl 3,5-dimethyl-1*H*-pyrazole-1-carbodithioate	A [3] F [168] G	*Acrylates*: MA [3] *Acrylamides*: DMAm [3] *Styrenes*: St [163] *Vinyls*: VAc [3]
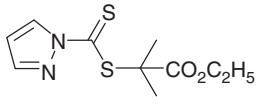 **23** ethyl 2-((1*H*-pyrazole-1-carbonothioyl) thio)-2-methylpropanoate	A [89]	*Styrenes*: St [89]
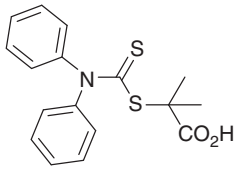 **24** 2-((diphenylcarbamothioyl)thio)-2-methylpropanoic acid	E [169] G	*Acrylates*: AA [169] BA [169] *Vinyls*: (NVCL) [170]
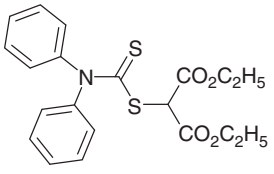 **25** diethyl 2-((diphenylcarbamothioyl) thio)malonate	A [4, 5]	*Acrylates*: EA [6] MA [5] *t*BA [5] *Styrenes*: (St) [4, 5] *Vinyls*: VAc [6] *Blocks*: St-*b*-VAc [4, 5]
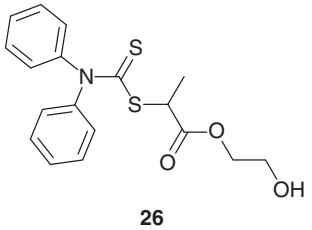 **26** 2-hydroxyethyl 2-((diphenylcarbamothioyl) thio)propanoate	A [171]	*Vinyls*: NVP [171]

(*continued*)

Table 11.2 (Continued)

RAFT agent	Synthesis[a)]	Polymerizations[b)]
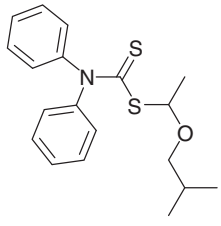 **27** 1-isobutoxyethyl diphenylcarbamodithioate	C [172]	*Vinyls*: EVE[f)] [173] iBVE[f)] [172] *Blocks*: EVE-*b*-(EVE-*alt*-CTFE) [173]
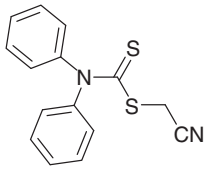 **28** cyanomethyl diphenylcarbamodithioate	G (Merck)	*Acrylates*: (MA) [174]
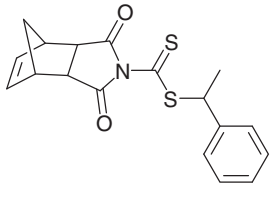 **29** 1-phenylethyl 1,3-dioxo-1,3,4,7-tetrahydro-2*H*-4,7-methanoisoindole-2-carbodithioate	A [175]	*Methacrylates*: (MMA) [175] *Acrylates*: MA [175] *Acrylamides*: NAM [175] *Styrenes*: St [175] *Vinyls*: (VAc) [175]
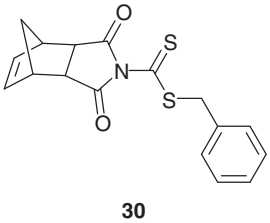 **30** benzyl 1,3-dioxo-1,3,4,7-tetrahydro-2*H*-4,7-methanoisoindole-2-carbodithioate	A [175, 176]	*Methacrylates*: (MMA) [175] *Acrylates*: BA [176] *Styrenes*: St [176] *Vinyls*: (VAc) [175] ROMP-*T*-RAFT [176, 177]

(*continued*)

Table 11.2 (Continued)

RAFT agent	Synthesis[a)]	Polymerizations[b)]
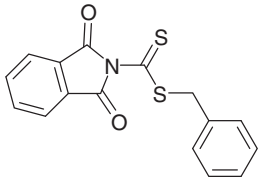 **31** benzyl 1,3-dioxoisoindoline-2-carbodithioate	A [153]	*Acrylates*: (MA) [153] *Styrenes*: St [153]
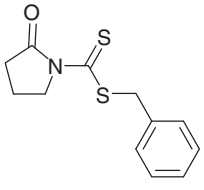 **32** benzyl 2-oxopyrrolidine-1-carbodithioate	A [65, 153]	*Acrylates*: MA [98, 153, 178] *Styrenes*: (St) [65, 153]
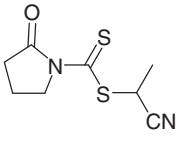 **33** 1-cyanoethyl 2-oxopyrrolidine-1-carbodithioate	A	*Acrylamides*: **82** [88] *Acrylates*: AA [88, 179] MA [178] *Others*: **64** [88] (**63**) [180] *Blocks*: AA-*b*-NIPAm [88, 179] AA-*b*-**64** [88]
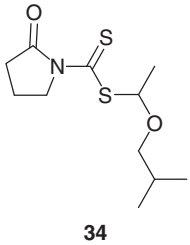 **34** 1-isobutoxyethyl 2-oxopyrrolidine-1-carbodithioate	C [181]	*Vinyls*: (*i*BVE)[f)] [172, 181] *Blocks*: EVE-*b*-(EVE/VAc) [181]

(*continued*)

Table 11.2 (Continued)

RAFT agent	Synthesis[a)]	Polymerizations[b)]
(c) *Less active RAFT agents suitable for LAMs* (alkyl(aryl)carbamodithioates, dialkylcarbamodithioates)		
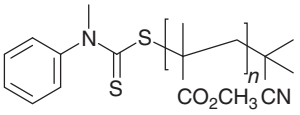 **35**	D [182]	*Vinyls*: VAc [182] E [182]
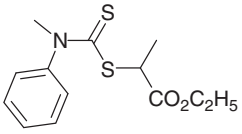 **36** ethyl 2-((methyl(phenyl)carbamothioyl) thio)propanoate	A [5]	*Vinyls*: VAc [5] NVP [183]
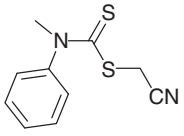 **37** cyanomethyl methyl(phenyl) carbamodithioate	A [184] G	*Acrylates*: (MA) [3] (MA) [174] *Dienes*: (Cp) [185] *Vinyls*: E [166] HEVE [186] NVP [186] VAc [2, 3, 53, 98, 186–191] VAc [189] (VAc)[e)][53] VC [190, 192] vinyl ethers [186] iBVE [193] MOVE [193] **98** [194] *Blocks*: (HEVE-*b*-VAc) [186] (HEVE-*b*-NVP) [186] VAc-*b*-HEVE [186] VAc-*b*-VC [190]
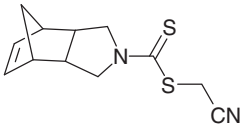 **38** cyanomethyl 1,3,3a,4,7, 7 a-hexahydro-2*H*-4, 7-methanoisoindole- 2-carbodithioate	A [175]	*Methacrylates*: (MMA) [175] *Acrylates*: (MA) [175] *Acrylamides*: (NAM) [175] *Styrenes*: (St) [175] *Vinyls*: VAc [175]
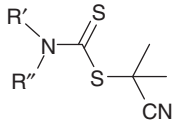 2-cyanopropan-2-yl dialkylcarbamodithioate **39a** R′ = R″ = CH_3 **39b** R′ = R″ = C_2H_5	D [195]	*Methacrylates*: (MMA) [79] *Vinyls*: (VAc) [28] *ATRP*: DMAEMA [196] MMA [195–198] PEGMA [196] BA [196] *t*BA [196] St [195–197, 199] VAc [196]

(*continued*)

Table 11.2 (Continued)

RAFT agent	Synthesis[a)]	Polymerizations[b)]
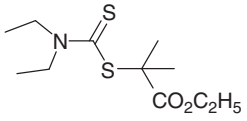 **40** ethyl 2-((diethylcarbamothioyl) thio)-2-methylpropanoate	A [195, 200] D [200] E [200]	*Vinyls*: VAc [28] *ATRP*: MMA [195, 197, 198, 201] St [195, 197, 199] *Photoiniferter*: HEMA[d)] [202] HEMA-*b*-MMA[d)] [202]
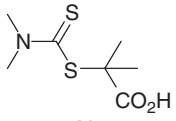 **41** 2-((dimethylcarbamothioyl) thio)-2-methylpropanoic acid	A [203] E [169]	*Acrylates*: (BA) [169] (EA) [169] *Styrenes*: (St) [169] *Vinyls*: (VAc) [169] NVCL [204] *Copolymers*: *BA/MAA/MMA/DAAm* [205]
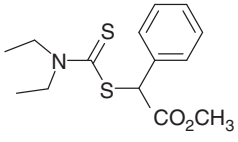 **42** methyl 2-((diethylcarbamothioyl) thio)-2-phenylacetate	A [195]	*ATRP*: MMA [195, 198]
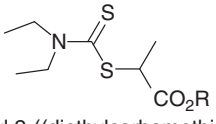 alkyl 2-((diethylcarbamothioyl) thio)propanoate **43a** R = CH_3 **43b** R = C_2H_5	A [206] B[g)] [207] D [208]	*Vinyls*: VAc [28] *VAc*[g)] [207] *Others*: VF2 [206]
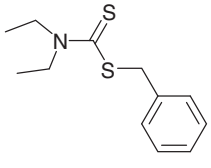 **44** benzyl diethylcarbamodithioate	A [65] G (Merck)	*Vinyls*: (*VAc*) [207] *Styrenes*: (St) [65, 79]

(*continued*)

Table 11.2 (Continued)

RAFT agent	Synthesis[a)]	Polymerizations[b)]
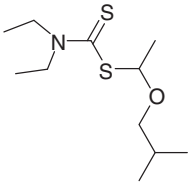 **45** 1-isobutoxyethyl diethylcarbamodithioate	C [172]	*Vinyls*: EVE[f)] [173, 206] iBVE[f)] [172][f)] HOSt[f)] [172] *Blocks*: EVE-*b*-(EVE-*alt*-CTFE) [173] EVE-*b*-VF2 [206]
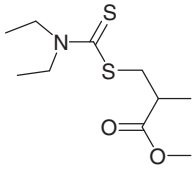 **46** methyl 3-((diethylcarbamothioyl)thio)-2-methylpropanoate	C [209]	*Other*: **113** [209]

a) Method of synthesis (the letters (A-G) correspond to the method of synthesis in Section 11.5).
b) Red – photoinitiated polymerization, italics – heterogeneous polymerization, (parentheses) – little or poor control (e.g. molar mass substantially higher than predicted, dispersity ≥1.4 and/or marked retardation). Refer to *Abbreviations* at the end of the chapter for a full list of abbreviations.
c) Microfuidic reactor.
d) Photoinitiated process – SRMP mechanism likely to be dominant.
e) Photoinitiated process – RAFT mechanism likely to be dominant.
f) Cationic RAFT polymerization.
g) Ethyl ester.

Table 11.3 RAFT polymerization with switchable dithiocarbamate RAFT agents.

RAFT agent	Synthesis[a)]	Polymerizations[b)c)]	Switched RAFT agent	Polymerizations[b)]
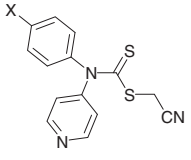 cyanomethyl aryl(pyridin-4-yl) carbamodithioate **47a** X = OCH_3 **b** X = H **c** X = F **d** X = CN cyanomethyl (4-chlorophenyl) (pyridin-4-yl)carbamodithioate **47d**	A [73]	(MA) [73] NVC [73] VAc [73] NVP [210] NIPAm-*b*-NVP [210] CTFE/EVE [211]	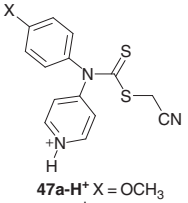 **47a-H⁺** X = OCH_3 **b-H⁺** X = H **c-H⁺** X = F **d-H⁺** X = CN cyanomethyl (4-chlorophenyl) (pyridin-4-yl) carbamodithioate	MA [73] NIPAm [210]
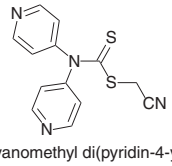 cyanomethyl di(pyridin-4-yl) carbamodithioate **48**	A [73]	(MA) [73] NVC [73] VAc [73] NVP [210]	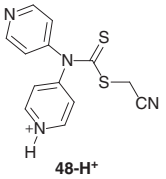 **48-H⁺**	MA [73]

(*continued*)

Table 11.3 (Continued)

RAFT agent	Synthesis[a)]	Polymerizations[b)c)]	Switched RAFT agent	Polymerizations[b)]
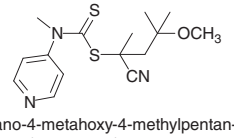 2-cyano-4-metahoxy-4-methylpentan-2-yl methyl(pyridin-4-yl)carbamodithioate **49**	D [184]	–	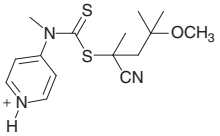 **49-H$^+$**	MMA [184]
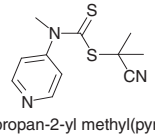 2-cyanopropan-2-yl methyl(pyridin-4-yl) carbamodithioate **50**	D [184] G	E [166] (VIm) [212] MMA-*b*-VAc [184, 213],[c] *i*BVE [193] MOVE [193] tBMA-*b*-NVP [214],[c] PFS-*b*-NVP [215] PFS-*b*-VAc [215] St-*b*-NVP [215] St-*b*-VAc [215]	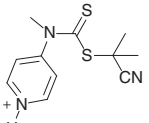 **50-H$^+$**	*BMA* [148] MMA [184, 213, 216] *MMA* [148] tBMA [214] PFS [215] St [215]
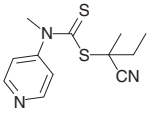 2-cyanobutan-2-yl methyl(pyridin-4-yl) carbamodithioate **51**	G[227, 229]			

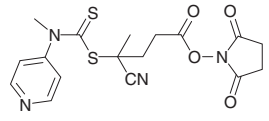 2,5-dioxopyrrolidin-1-yl 4-cyano-4-((methyl(pyridin-4-yl)carbamothioyl)thio)pentanoate **52**	G	NVP [217, 218]		
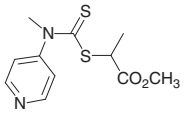 **53**	A [184] G	E [166] MA [184, 213] NVC [184, 213] NVP [184, 213] MA-*b*-NVC [213],[c] St-*b*-VAc [184, 219],[c] St-*b*-MA-*grad*-VAc [184, 219],[c]	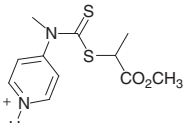 **53-H$^+$**	DMAm [220] St [184, 213, 219] (NVC) [184, 213] St-*b*-MA [184, 219]
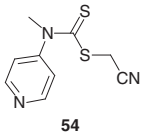 **54**	A [184] G	E [166] BA [184, 213] VAc [184, 213, 216] *VAc* [148] *VBz* [148] NVP [210, 216] MA/VAc [221] NVP/VAc [222] DMAm-*b*-NVC [220] DMAm-*b*-NVP [220] DMAm-*b*-VAc [220] Am/AN-*b*-NVP [223] DMAm-*b*-MMA [60]	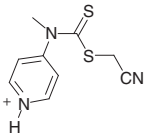 **54-H$^+$**	BA [184, 213] *BA* [148] DMAm [60, 220, 224] *St* [148] NIPAm [216] St [216] Am/AN [223]

(*continued*)

Table 11.3 (Continued)

RAFT agent	Synthesis[a)]	Polymerizations[b)c)]	Switched RAFT agent	Polymerizations[b)]
–	–	–	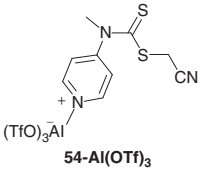 **54-Al(OTf)$_3$**	BA [184]
–	–	–	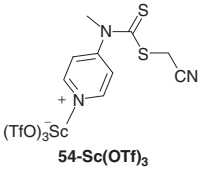 **54-Sc(OTf)$_3$**	MA/VAc [221]
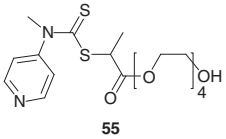 **55**	A [220]	(DMAm) [220]	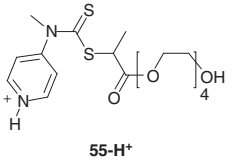 **55-H$^+$**	DMAm [220]

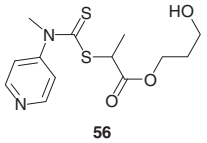 **56**	A [225]	NVP [225] VAc [225] ROP-*T*-RAFT [225]	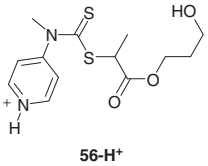 **56-H$^+$**	MA [225] DMAm [225] ROP-*T*-RAFT [225]
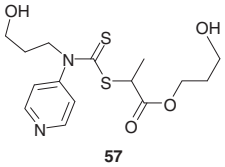 **57**	A [226]	NVC [226]	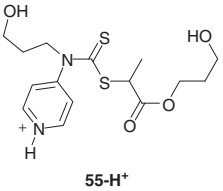 **55-H$^+$**	St [226]
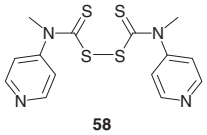 **58**	G [227]			

a) Reference to method of synthesis (the letters (A-G) correspond to the method of synthesis in Section 11.5).
b) Red – photoinitiated polymerization *italics* – heterogeneous polymerization, (parentheses) – little or poor control (e.g. molar mass substantially higher than predicted, dispersity ≥1.4 and/or marked retardation). Refer to *Abbreviations* at the end of the chapter for a full list of abbreviations.
c) For MAM-*b*-LAM, the RAFT agent was protonated for synthesis of MAM block and switched (neutralized) to make the LAM block.

Table 11.4 Methacrylate and other 1,1-disubstituted monomers subjected to RAFT polymerization with dithiocarbamate RAFT agents.

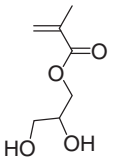

59
Glycerol monomethacrylate

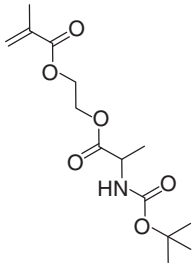

60 [94]

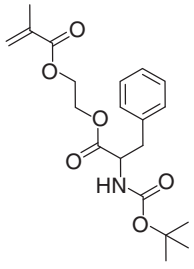

61 [94]

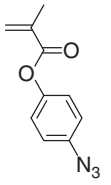

62 [161]

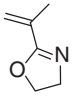

63

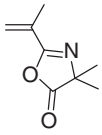

64 [88]

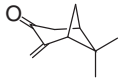

65 [84]

(PEGMA), and those listed in Table 11.4. Low dispersities require the use of a RAFT agent with a suitably high transfer constant, which in turn requires that the 'Z' group is suitable for MAMs and that the 'R' group is a good leaving group with respect to the methacrylate propagating radical. The most suitable dithiocarbamate RAFT agents in this context include those where Z is pyrrole (**127**), carbazole (**128**), or imidazole (**129**) and switchable dithiocarbamates in their more active switched or protonated form (**137-H$^+$** and **138-H$^+$**). The RAFT agents where Z is pyrazole (**134**–**136**) provide higher dispersities but still give reasonable control.

11.4.2 Monosubstituted MAMs (Acrylates, Acrylamides, Styrenes)

Attaining low dispersities with RAFT polymerization of acrylates, acrylamides, or styrenes requires a RAFT agent suitable for MAMs. Acrylates and acrylamides include methyl acrylate (MA), butyl acrylate (BA), DEGMA, hexyl acrylate (HA), Am, DMAm, NIPAm, *N*-acryloyl acrylamide (NAM), and those listed in Table 11.5, which include a range of amino acid-based acrylamides [239]. Styrenes include 4-(chloromethyl)styrene (CMS), HOSt, St, 2VP, 4VP, and those in Table 11.6.

11.4.3 LAMs, IAMs (Vinyl Monomers)

Vinyl monomers in the present context include the vinyl esters (e.g. VAc, VBz, VPv), the *N*-vinylamides (e.g. *N*-vinylcaprolactam [NVCL], *N*-vinylpyrrolidone [NVP]), the *N*-vinyl heteroaromatics (e.g. Vim, NVC), the halo-olefins (vinyl chloride [VC], VF2), the vinyl ethers, and the monomers in Table 11.7. Most of these monomers are LAMs or IAMs and good control over homopolymerization requires use a RAFT agent suited for that class of monomer, which is usually a xanthate or a less active dithiocarbamate. Note, however, that good control over copolymerization of LAMs

Table 11.5 Acrylate and acrylamide derivatives subjected to RAFT polymerization with dithiocarbamate RAFT agents.

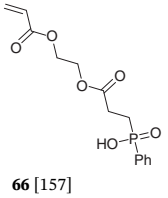 **66** [157]	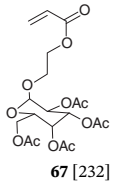 **67** [232]	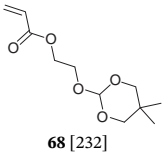 **68** [232]	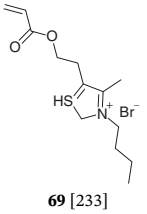 **69** [233]
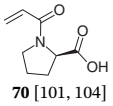 **70** [101, 104]	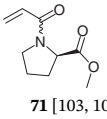 **71** [103, 104]	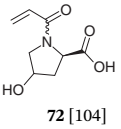 **72** [104]	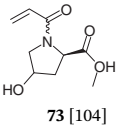 **73** [104]
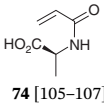 **74** [105–107]	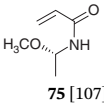 **75** [107]	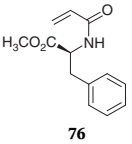 **76** [102, 105, 106, 234]	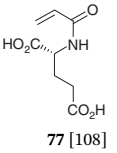 **77** [108]

(*continued*)

Table 11.5 (Continued)

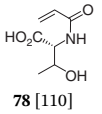 **78** [110]	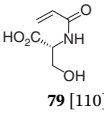 **79** [110]	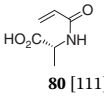 **80** [111]	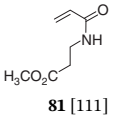 **81** [111]	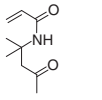 **82** [88]
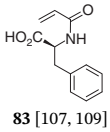 **83** [107, 109]	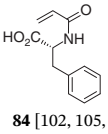 **84** [102, 105, 107]	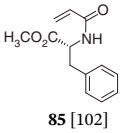 **85** [102]	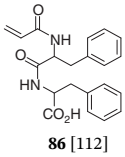 **86** [112]	
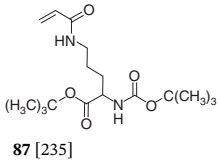 **87** [235]	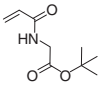 **88** [236]	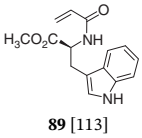 **89** [113]		

Table 11.6 Styrene derivatives subjected to RAFT polymerization with dithiocarbamate RAFT agents.

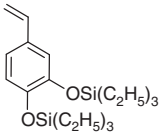

90 [83]

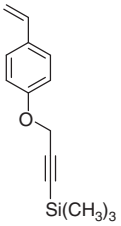

91 [237]

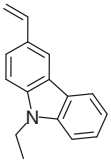

92 [103]

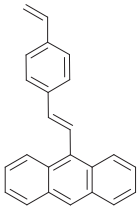

93 [238]

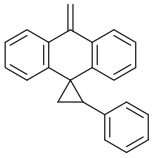

94
[114, 115, 128]

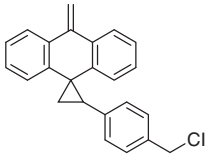

95 [115]

with MAMs can be obtained with more active RAFT agents suited to MAMs (e.g. NVPI/NIPAm with **6** [125]). Also included in this section is vinylene carbonate (1,3-dioxol-2-one, **113**).

The polymerization of NVP in aqueous media was reported as problematic due to the sensitivity of the macroRAFT agent with a terminal NVP unit to hydrolysis [210]. It has been shown for xanthate-mediated RAFT polymerization [240, 241] that this problem might be overcome by conducting the polymerization at ambient temperature with redox initiation. We have found that for trithiocarbonate-mediated RAFT, photoinitiation at 30 °C provides low dispersities [242]. These methods are also likely to be successful in dithiocarbamate-mediated RAFT polymerization of NVP.

11.5 Synthesis of Dithiocarbamate RAFT Agents

The methods most commonly exploited for the synthesis of dithiocarbamate RAFT agents are listed below. The letters A-G correspond to those indicated in the Synthesis columns of Tables 22.3 snf 22.3. The method of choice is dependent on the structure of the desired RAFT agent, the amount required, the toxicity and ease of handling of reagents, and other factors. A review of methods for RAFT agent synthesis covering the literature through 2012 provides further details [78].

11.5.1 Method A – Reaction of a Carbodithioate Anion with an Alkylating Agent

The preparation of RAFT agents, including dithiocarbamates, is most commonly achieved by reaction of a carbodithioate anion with an alkylating agent (RX) for

Table 11.7 Vinyl monomers subjected to RAFT polymerization.

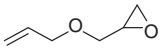 **96** [156, 159]	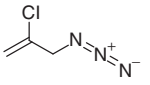 **97** [162]	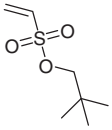 NES [117]	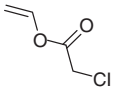 **98** [194]
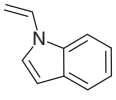 **99** [119]	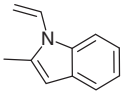 **100** [119]	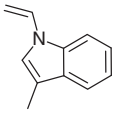 **101** [119]	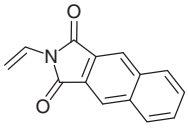 **102** [126]
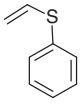 **103** [127]	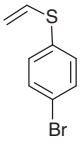 **104** [127]	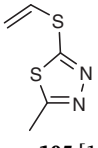 **105** [120]	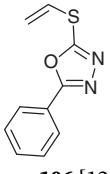 **106** [120]
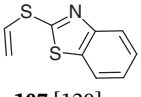 **107** [120]	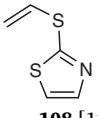 **108** [120]	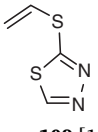 **109** [120]	
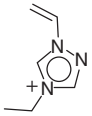 **110** [121]	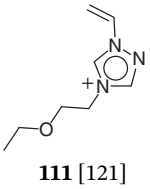 **111** [121]	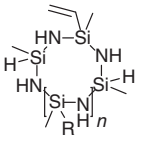 **112** vinylcyclosilazane, R = H or vinyl, $n \sim 20$ [122]	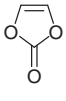 **113** [209]

NES, neopentyl ethenesulfonate.

which a general mechanism is shown in Scheme 11.2 (Table 11.8). Many variants of this technique have been reported. The method generally provides high yields for RAFT agents containing primary and secondary 'R' groups. However, RAFT agents with tertiary 'R' groups are more difficult to prepare as nucleophilic substitution on tertiary alkylating agents is relatively slow and elimination is often complicated.

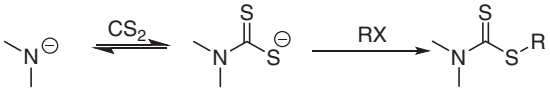

Scheme 11.2 Preparation of RAFT agents using carbodithioate salts.

The synthesis of dithiocarbamates often requires the use of a strong base, such as sodium hydroxide [245–247] or sodium hydride [248–251], to promote formation

Table 11.8 Examples of syntheses of dithiocarbamates by alkylation of a carbodithioate anion.

Entry	ZH	Base	Halide	Reaction conditions[a)]	Yield (%)	References
4	Pyrrole	NaH	$PhCH_2Br$	DMSO, 1 h	50	[65]
–	Pyrrole	NaOH	Polystyrene-Br[b)]	DMF, 24 h	(100)[c)]	[243]
–	Pyrazole	NaOH	Polystyrene-Br[b)]	DMF, 40 h	(100)[c)]	[244]
12	Carbazole	NaH	$PhCH(CH_3)Br$	H_2O, 2 h	93	[136]
13	Carbazole	NaH	$PhCH_2Br$	H_2O, 2 h	89	[136]
10	Carbazole	NaH	$PhC(CH_3)_2Br$	H_2O, 2 h	69	[136]
–	Carbazole	NaH	$(CH_3)_3CBr$	H_2O, 2 h	76	[136]
11a	Carbazole	NaOH	$(CH_3)C(CO_2CH_3)Br$	DMSO, 24 h	42	[50]

a) Conditions for halide displacement step. DMSO, dimethyl sulfoxide; DMF, *N,N*-dimethylformamide.
b) Bromine end-functional polystyrene.
c) Reaction assumed to be quantitative.

Table 11.9 Synthesis of 1-phenylethyl or benzyl dithiocarbamates.

Entry	ZH	Halide	Reaction conditions	Yield (%)
4	Imidazole	$(Ph)CH(CH_3)Br$	Acetone, K_3PO_4, 4 h	78
—	$(i\text{-}Pr)_2NH$	$PhCH_2Br$	Acetone, Cs_2CO_3, 10 min	61
—	$(Ph)(CH_3)NH$	$PhCH_2Br$	Ethanol, Cs_2CO_3 [252], 4 h	70

of the carbodithioate salt, although sodium *N*,*N*-diethyldithiocarbamate is commercially available. Skey and O'Reilly [91] published on the synthesis of various RAFT agents including dithiocarbamates. They found that the use of a non-nucleophilic base (phosphate or cesium carbonate) and, typically, acetone as solvent provided high yields. Dithiocarbamate examples are provided in Table 11.9.

Alkyl 1*H*-imidazole-1-carbodithioates can be prepared in high yield through the reaction of imidazole and carbon disulfide and an alkylating agent [151]. However, mixtures of the alkyl 1*H*-imidazole-1-carbodithioate and a symmetrical dialkyl trithiocarbonate may be obtained with the proportion of the two being dependent on the reaction conditions (cf. method B, Section 11.5.2) [152]. Anhydrous solvents favour the exclusive formation of the 1*H*-imidazole-1-carbodithioate.

11.5.2 Method B – Reaction of a Dithiochloroformate or a Thiocarbonyl-bis-imidazole with a Nucleophile

Benzyl [153] and 1-phenylethyl 1*H*-imidazole-1-carbodithioate [149] were prepared by reaction of the appropriate mercaptan with thiocarbonyl-bis-imidazole (Scheme 11.3). Perrier and coworkers [253] have shown that a range of trithiocarbonates, dithiocarbamates, and xanthates can be prepared in moderate to

high yield by reaction of the 1*H*-imidazole-1-carbodithioate with the appropriate thiol, amine, or thiol-derived nucleophile. A further example of this approach is the synthesis of **43b** (Scheme 11.3) [207].

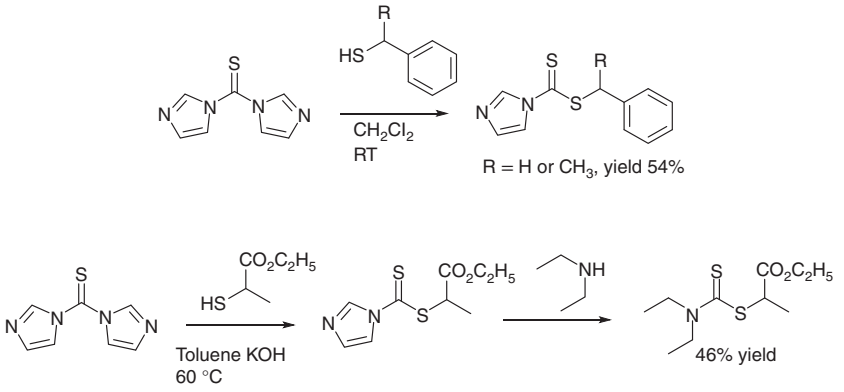

Scheme 11.3 Preparation of dithiocarbamates from 1,1′-thiocarbonyl diimidazole.

11.5.3 Method C – Addition of a Dithioic Acid Across an Olefinic Double Bond

The reaction of dithioic acids with a variety of electron-rich alkenes has been shown to provide very high yields of the required Markovnikov addition product [254]. The olefins successfully used in this context include St, AMS, VAc, vinyl ethers and vinyl sulfones. The process was used to synthesize cumyl 1*H*-pyrrole-1-carbodithioate (**3**) [86, 87], and **27** [172], **34** [181] and **45** [172], derived by addition of the dithiocarbamic acid across the double bond of isobutyl vinyl ether (iBVE). Note that dithioic acids, including dithiocarbamic acids [255], react with electron-deficient alkenes, such as acrylates, by Michael addition.

11.5.4 Method D – Radical-induced Decomposition of a Thiuram Disulfide

Radical-induced decomposition of thiuram disulfides by radicals derived from azo-initiators is arguably the most effective technique for the synthesis of functional tertiary RAFT agents (see Scheme 11.4 and Table 11.10, synthesis of dithiocarbamate RAFT agents by reaction of dialkyldiazenes (R—N=N—R) with bis(thioacyl)disulfides $[ZC(=S)S]_2\cdot$) [256, 257, 260]. The method has been applied

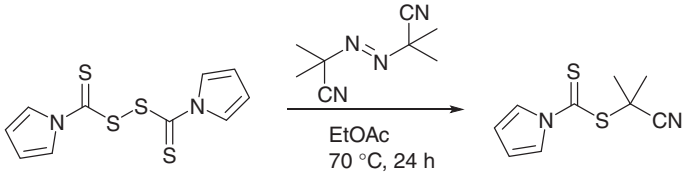

Scheme 11.4 Synthesis of a tertiary RAFT agent from a thiuram disulfide.

Table 11.10 Synthesis of dithiocarbamate RAFT agents by reaction of dialkyldiazenes (R−N=N−R) with bis(thioacyl) disulfides $[ZC(=S)S]_2$.

RAFT agent	Z	Initiator[a)]	Reaction conditions[b)]	Yield (%)[c)]	References
1	**126**	AIBN	A	61	[65, 85, 256]
2	**126**	AMBN	A	28	[85]
39a	**155**	AIBN	B	93 95	[256, 257]
—	**126**	ACPA	C	88	[258]
—	**127**	ACPA	C	94	[259]
19	**134**	AMBN	D	Not stated	[3]
20	**134**	AMBN	D	73	[2]

a) AIBN, azobis(isobutyronitrile) (2,2′-azobis(2-methylproionitrile)); AMBN, 2,2′-azobis(2-methylbutyronitrile); ACPA, 4,4′-azobis(4-cyanopentanoic acid).
b) Reaction conditions: A: degas, ethyl acetate, 70 °C, 24 hours; B: reflux, benzene, 24 hours; C: degas, ethyl acetate, 75 °C, 18 hours; D: ethyl acetate, reflux, 20 hours.
c) Isolated yield after purification.

to each of most forms of RAFT agents including dithiocarbamates. The usual radical source is an excess of an azo-compound initiator [256, 257, 260] and the main contaminants in the product are the by-products of azo-compound decomposition (e.g. tetramethylsuccinonitrile when azobis(isobutyronitrile) (2,2′-azobis(2-methylproionitrile)) (AIBN) is used).

The thiuram disulfide can be prepared by oxidation of the appropriate carbodithioate salt with molecular iodine, which generally proceeds in quantitative yield [260, 261]. Other methods that have been used with good effect include oxidation of the carbodithioate salt with potassium ferricyanide [135, 258], *p*-toluenesulfonyl chloride [262], or sodium chlorite [263].

Polymers with dithiocarbamate ends can be formed by radical polymerization in the presence of a thiuram disulphide. This enables the synthesis of polymers that might not be easily produced by RAFT polymerization. For example, the process was used to prepare PMMA as shown in Scheme 11.5.

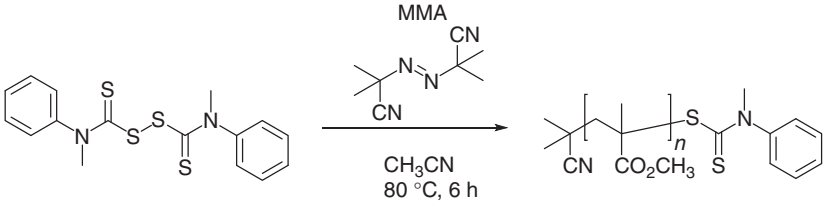

Scheme 11.5 Synthesis of a PMMA macroRAFT agent (**35**) from radical polymerization in the presence of a thiuram disulfide.

A related process has been reported by Wager et al. [264] and Kwak et al. [208] in which an atom-transfer radical polymerization (ATRP) initiator (a secondary or tertiary alkyl halide and a copper catalyst) is used as the radical source. The latter group termed the process atom-transfer radical addition–fragmentation (ATRAF) [208].

For dithioesters reported yields were generally high (82–92%) but significantly lower yields were observed for dithiocarbamate (65%) and xanthate (43%) examples [208].

11.5.5 Method E – Ketoform Reaction

Lai et al. adapted the ketoform reaction [265] to prepare trithiocarbonates [266], dithiocarbamates, and xanthates [169]. Their proposed mechanism involves ring opening of a dichloroepoxide intermediate with a carbodithioate salt [265, 266]. Subsequent hydrolysis of the acyl chloride formed provides the RAFT agent. Reaction of a secondary amine, carbon disulfide, chloroform, a ketone, and sodium hydroxide in the presence of a phase transfer catalyst (PTC) provides the dithiocarbamate in good to high yield (Scheme 11.6, Table 11.11).

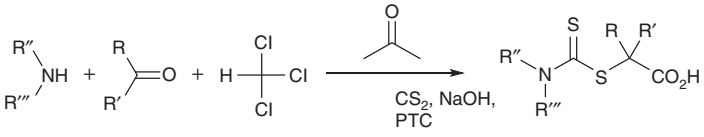

Scheme 11.6 Synthesis of tertiary carboxyl-functional dithiocarbamates via the ketoform reaction.

11.5.6 Method F – Other Methods

Some RAFT agents are prepared by modification of other dithiocarbamates. For example, the pyrazole RAFT agent **22** was prepared by a base catalysed condensation reaction between *S*-benzyl dithiocarbazate and 2,4-pentandione [168]. RAFT agent **14** was prepared from **54** by methylation and ion exchange (Scheme 11.7).

11.5.7 Method G – Commercially Available

A variety of dithiocarbamate RAFT agents are commercially available.

11.6 Activity of Dithiocarbamate RAFT Agents

The Z′Z″N– group of dithiocarbamates [Z′Z″NC(=S)SR] modifies both the rate of addition of propagating radicals ($P_n\cdot$) to the thiocarbonyl and the rate of fragmentation of the intermediate radical. The value of C_{tr}^{app} can be 'adjusted' over some 4 orders of magnitude through manipulation of Z′Z″N– (Table 11.1) [65].

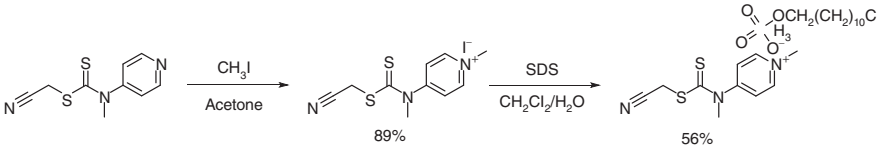

Scheme 11.7 Synthesis of dithiocarbamate **54** from **14** by methylation and ion exchange.

Table 11.11 Examples of syntheses of tertiary carboxyl-functional dithiocarbamates via the ketoform reaction [169].

Amine	Ketone	Product	Yield (%)
Dimethylamine	Acetone	—	100
Dimethylamine	2-Butanone	—	80
Dimethylamine	Cyclohexanone	—	85
Diethylamine	Acetone	**41**	85
Diethylamine	Cyclohexanone	—	78
Diethylamine	Acetophenone	—	35
Diphenylamine	Acetone	**24**	60
Diallylamine	Cyclohexanone	—	78
Diallylamine	Acetone	—	72
Morpholine	Acetone	—	85
Azepane	Acetone	—	85
Piperazine	Acetone	—	95
Piperazine	2-Butanone	—	83
Piperazine	2-Pentanone	—	65
1,4-Diazacycloheptane	Acetone	—	100

The most reactive RAFT agents include the dithioesters and trithiocarbonates which have carbon or sulfur adjacent to the thiocarbonylthio group.

N,N-Dialkyldithiocarbamates have a lone pair on nitrogen adjacent to the thiocarbonyl, which can dramatically lower reactivity towards radical addition. Lower rate coefficients for addition are predicted by molecular orbital calculations (vide infra) [2, 65, 267, 268] and can be qualitatively understood in terms of the importance of the zwitterionic canonical forms **114** and **115** (Figure 11.4). The interaction between the lone pair and the C=S double bond both reduces the double bond character of the thiocarbonyl group and stabilizes the RAFT agent relative to the intermediate radical [65, 248, 268, 269]. Dithiocarbamates where the nitrogen lone pair is not as available because it is part of an aromatic ring system, such as a pyrrole (in **117**) or carbazole, or where a carbonyl (in **120**) is α to the nitrogen lone pair (Figure 11.4), have reactivities closer to those of the dithioesters and trithiocarbonates [6, 65, 79]. In these cases, the importance of canonical forms such as **116** and **119** effectively reduces the contribution of **118** and **121** respectively (Figure 11.4).

Propagating radicals with a terminal MAM unit are less reactive in radical addition (lower k_p, lower k_{add}) and one of the more reactive RAFT agents is required for good control. The poly(MAM) propagating radicals are also relatively good homolytic leaving groups (higher k_β, k_{-add}), and therefore, retardation solely due to slow fragmentation is unlikely. The more active RAFT agents such as the dithioesters, trithiocarbonates, and aromatic dithiocarbamates allow the preparation of

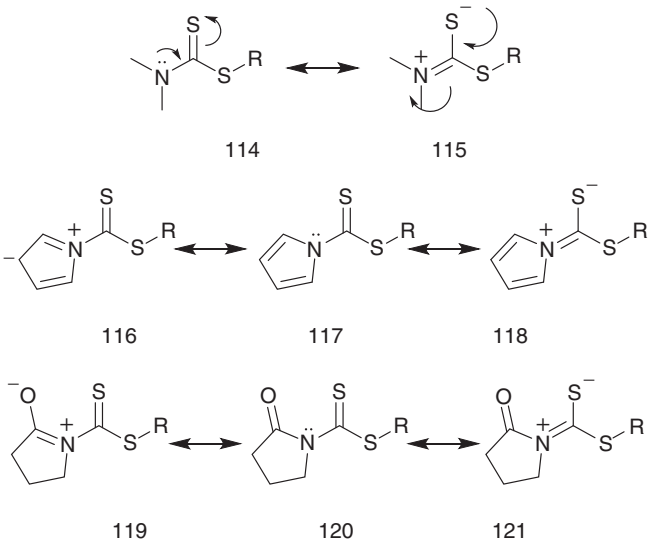

Figure 11.4 Canonical forms of dithiocarbamates.

low-dispersity polymers from MAMs whereas the *N*-alkyl-*N*-aryldithiocarbamates typically have lower transfer constants and provide poor control.

Propagating radicals with a terminal LAM unit are highly reactive in radical addition (higher k_p, higher k_{add}). Thus, the *N*-alkyl-*N*-aryldithiocarbamates have high transfer constants in LAM polymerization. However, the poly(LAM) propagating radicals are relatively poor homolytic leaving groups (lower k_{β}, lower k_{-add}) such that inhibition or retardation is likely with the more active RAFT agents, such as the pyrrolocarbodithioates (**117**).

11.6.1 Dithiocarbamate RAFT Agents with Balanced Activity

Some dithiocarbamates show capacity for controlling the polymerization of both MAMs and LAMs (see Table 11.2b and Figure 11.5). The activity of these intermediate activity RAFT agents with respect to one or both monomer classes is compromised [2–6] to the extent that while achieving control over molar mass for both MAMs and LAMs, they provide higher dispersities with MAMs (most noticeable, with methacrylates) and some retardation with LAMs (e.g. VAc). Nonetheless, these RAFT agents allow most polymerizations to be controlled, and may be the best choice when there is uncertainty about what to do. Their use can allow the formation of poly(MAM)-*block*-poly(LAM).

Early work from the Rhodia group [6] showed that dithiocarbamates **122** and **123** with Z′Z″N– as 5,5-dimethyloxazolidin-2-one (**142**) and an appropriate R group provided control (i.e., molecular weights consistent with prediction, $Đ < 1.2$) over the polymerization of MAMs (St, EA) and LAM (VAc). The Rhodia group also reported the *N*,*N*-diphenyldithiocarbamate **124,** which provided modest control

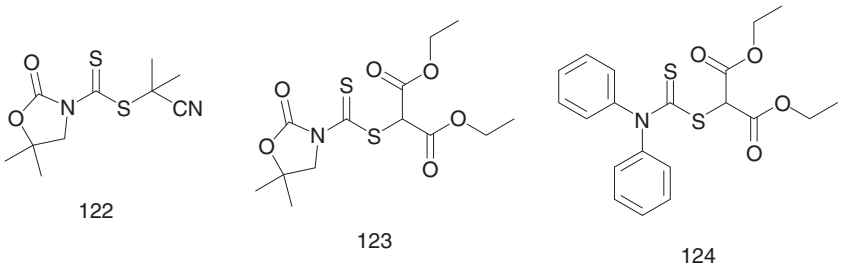

Figure 11.5 Further examples of RAFT agents with balanced activity.

($Đ \sim 1.4$, molecular weights consistent with prediction) over the polymerizations of both ethyl acrylate (EA) and VAc. Shipp and coworkers [4, 5] further explored the use of **124** in BA, VAc, NVP, and vinyl laurate polymerization obtaining $Đ \leq 1.4$ at higher conversions, and St, $Đ \leq 1.5$ at higher conversions. They also used **124** to synthesize poly(St)-*block*-poly(VAc) with $Đ \leq 1.4$ [4].

The use of 1*H*-pyrazole-1-carbodithioates (**133** refer Table 11.17) as RAFT agents for controlling the polymerization of monosubstituted MAMs was first reported in a series of patents issued to Symyx [270–276]. Subsequently, Babu and Dhamodharan [89] successfully used **133** (R = benzyl) in the polymerization of styrene and 2-vinylpyridine. However, the full utility of the 1*H*-pyrazole-1-carbodithioates as RAFT agents was not recognized until very recently when Gardiner et al. [2, 3] demonstrated the 3,5-dimethyl-1*H*-pyrazole-1-carbodithioates (**134**–**136**) in polymerizations of both MAMs and LAMs. Thus, the parent (**19** and **20**) and the 4-chloro-(**21**) and 4-bromo derivatives gave low-dispersity ($Đ \leq 1.2$) polymers with monosubstituted MAMs, St, MA, and DMAm. Dithiocarbamate **21** provided a poly(MMA) with the anticipated molar mass and $Đ$ as low as 1.3 at high monomer conversion [2]. Low dispersities ($Đ \leq 1.2$) and molar mass control were also achieved for homo- and copolymerizations of the LAM, VAc, albeit with some retardation [2, 3]. Low-dispersity poly(DMAm)-*block*-poly(VAc), a poly(MAM)-*block*-poly(LAM), was also prepared.

11.6.2 Switchable Dithiocarbamate RAFT Agents

Stimuli-responsive, switchable, RAFT agents [73, 184, 210, 213, 219, 220, 277] can be switched, potentially *in situ*, to allow good control over polymerization of either MAMs or LAMs depending on the state of the switch. The primary motivation for developing switchable RAFT agents was to provide a direct route to low-dispersity poly(MAM)-*block*-poly(LAM). The *N*-methyl-*N*-(4-pyridinyl)dithiocarbamates, like other *N*-aryl-*N*-alkyldithiocarbamates, control the polymerization of LAMs but are not effective in controlling the polymerization of MAMs. With addition of stoichiometric strong acid, the switched *N*-methyl-*N*-(4-pyridinium)dithiocarbamates provide excellent control over the polymerization of MAMs. Protonation reduces the importance of canonical forms**,** which contain two positive charges in proximity (Figure 11.6).

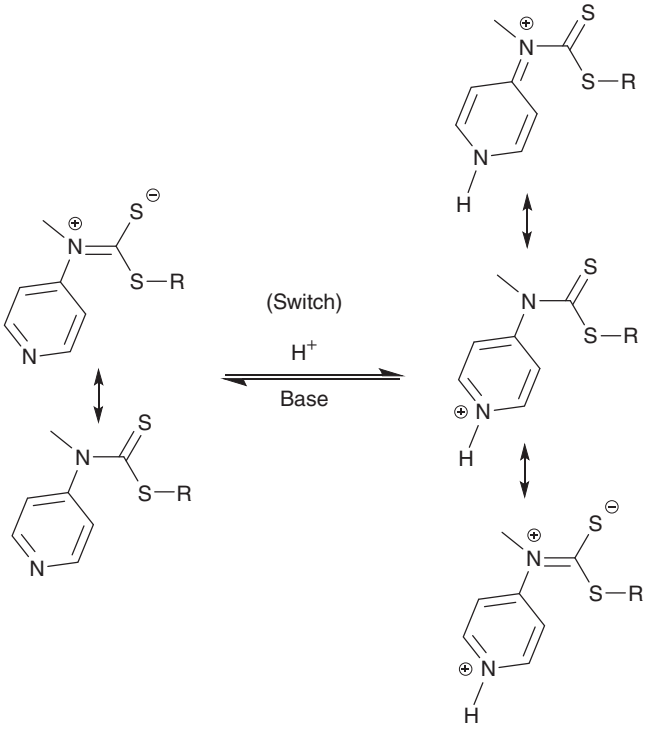

Figure 11.6 Canonical forms of *N*-(4-pyridinyl)-*N*-methyldithiocarbamate switchable RAFT agents.

Lewis acids, such as aluminium triflate [184, 213] or scandium triflate [221], can be used as switches with similar effect. These Lewis acids can be used to control RAFT (co)polymerization of VAc, whereas protic acids would rapidly hydrolyse macroRAFT agents with a terminal VAc unit to an aldehyde chain-end [221].

In applying such RAFT agents to prepare poly(MAM)-*block*-poly(LAM), the block comprising the MAM generally needs to be synthesized first. This is necessary because poly(LAM) propagating radicals are poor homolytic leaving groups with respect to poly(MAM) propagating radicals and, consequently, poly(LAM)-derived macroRAFT agents have very low transfer constants in MAM polymerization. For example, attempts to synthesize poly(St)-*block*-poly(VAc) or other poly(St)-*block*-poly(LAM) starting from a poly(St) macroRAFT agent gave no significant yield of polymer for an extended period (>4 hours) corresponding to the time needed to convert the initial macroRAFT agent [184, 219]. This was attributed to the very low rate of polystyrene propagating radicals adding to VAc, possibly compounded by the presence of trace amounts of styrene monomer in the polystyrene macroRAFT agent (styrene is an inhibitor of VAc polymerization). A solution to this difficulty involves forming an intermediate 'block' of poly(MA) [184, 219]. Polystyrene propagating radicals give facile addition to MA, and MA readily copolymerizes with VAc. The problems associated with 'wrong way' addition

may be circumvented through the use of starved-feed protocol (though this has not been demonstrated for dithiocarbamates) [269] or through the use of photoinitiation [60].

Switchable RAFT agents and their use in polymerization are summarized in Table 11.3.

11.6.3 Dithiocarbamates as Mediators of Cationic Polymerization

RAFT-mediated cationic polymerization of vinyl ethers (e.g. iBVE) has been described [172, 173, 181, 206]. Various RAFT agents were prepared. The best, as judged by the precision of molar mass control and the low dispersity ($Đ < 1.2$) of the polymers formed, were based on Z′Z″NC(=S)S— **156** or **159** [172]. Dithiocarbamate **140** gave broader dispersities ($Đ \sim 1.8$), which is attributed to the greater ability of the Z′Z″N– in **156** or **159** to stabilize a positive charge. Xanthates and dithiocarbonates were also effective mediators in cationic RAFT polymerization.

The mechanism of cationic RAFT polymerization was proposed to be analogous to that in radical RAFT polymerization. The RAFT end-groups are retained in the product polymer enabling block copolymer synthesis by sequential cationic and then radical RAFT polymerization.

Cationic RAFT polymerization is considered in more detail elsewhere in this volume [278].

11.6.4 Dithiocarbamate R Substituents

The R substituents of dithiocarbamates Z′Z″NC(=S)S—R need to be chosen for compatibility with the monomer(s) to be polymerized. The radical R· should be a good initiating radical for at least one of the monomers comprising the feed. The rate of addition of R· to the monomer should be greater than the rate of propagation such that initiation is not a rate-determining step. The radical R· should also be a good homolytic leaving group relative to the propagating radicals generated.

Guidelines to R group selection have been provided elsewhere [78, 279]. A summary is provided in Figure 11.1. The following are the points to note:

- Electron-rich benzyl and alkyl radicals add only slowly to most LAMs and RAFT agents where R is benzyl and can cause potentially lengthy inhibition periods.
- A similar situation can apply with tertiary cyanoalkyl radicals. They are good homolytic leaving groups, but their addition to the monomer may be rate determining in the initialization phase of polymerization where tertiary cyanoalkyl RAFT agents are used with certain monomers, including acrylates, acrylamides, and vinyl esters [280].
- One of the most versatile R substituents, being suited to most 1-substituted MAMs and LAMs, is the cyanomethyl group [7, 277].

11.6.5 Prediction of Dithiocarbamate Activity

Both *ab initio* and semi-empirical methods have been employed in attempts to explain or predict RAFT activity.

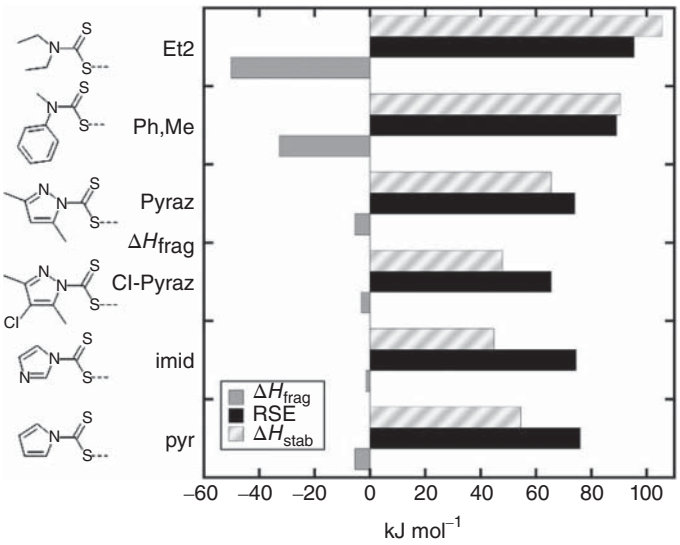

Figure 11.7 Values of ΔH_{frag}, ΔH_{stab}, and RSE for dithiocarbamates derived from *ab initio* calculations. Parameter values are taken from Gardiner et al. [2]. Source: Moad [1]. Copyright 2019, John Wiley & Sons.

Extensive studies on RAFT agent activity using *ab initio* methods have been performed by Coote and coworkers [2, 281, 282]. Calculated values of ΔH_{frag}, ΔH_{stab}, and the resonance stabilization energy (RSE) for dithiocarbamates [2] are shown in Figure 11.7. ΔH_{frag} provides a measure of the effect of the Z group on the enthalpy of the fragmentation reaction, relative to a reference compound with Z = H. The more exothermic the value, the more easily a given leaving group will fragment. Typical values for known RAFT agents span nearly 100 kJ mol^{-1} with the most exothermic values being associated with *O*-alkyl xanthates and *N,N*-dialkyldithiocarbamates. The most endothermic values are associated with RAFT agents containing π-acceptor Z groups such as phenyl, which retard fragmentation to the extent that they are only suitable when R is a very good homolytic leaving group, such as the propagating radicals in styrene or MMA polymerization.

The enthalpy of fragmentation for a fixed leaving group depends on how the Z group stabilizes the RAFT agent and the RAFT-adduct radical. Decoupling these two effects is important as it is the stabilization of the RAFT agent, rather than the adduct radical, that has the most dramatic impact on k_{add}. The value of ΔH_{stab} reflects the effect of the Z group on the stability of the RAFT agent C=S bond. The stability of the RAFT-adduct radical is measured using the standard RSE.

The data reported in Figure 11.7 [2] helps in understanding the difference in activity between *N*,*N*-dialkyl (**155**–**159**) or *N*-alkyl-*N*-aryl (**152**–**154**) and those where the nitrogen is part of an aromatic ring system (**126**–**136**). However, discrimination between the individual members of these classes or of these from those with intermediate activity (**137**–**140**) is less obvious.

11.7 Dithiocarbamates in RAFT Emulsion Polymerization

A process called vesicle-templated RAFT-based emulsion polymerization was examined by Rusli et al. [167]. The process made use of a P(AA-*co*-BA)-*b*-PMA-**133** macro RAFT agent.

Dithiocarbamates **156** would not be anticipated to provide good control, yet such a RAFT agent (with R = 2-cyanoethyl) was reported to successfully mediate miniemulsion polymerization of EHA [283].

11.8 Dithiocarbamates in Mechanism-Transformation Processes

Block, star, or graft copolymers comprising segments formed by RAFT and other mechanisms (including other RDRP) can be combined through the use of dual initiator-RAFT agents [284–286] or through the polymerization of reactively orthogonal monomers. The terminology RAFT-*𝓣*-process (RAFT first) or process-*𝓣*-RAFT (other process first) was coined [284] to describe these processes, where the I character is short for transformation. We do not consider transformation of end-functional polymers formed by non-RAFT mechanisms to install dithiocarbamate functionality or end linking of RAFT-synthesized polymers to other functional polymers in this section.

Le Neindre et al. [287] in a study of thiocarbonyl and thioesters as protecting groups for thiols found that a simple dithiocarbamate (**156** with *n*-propyl as R) inhibited the polymerization of acrylates and chain transfer was observed during styrene polymerization. The result appears at odds with the findings that dithiocarbamates **156** are essentially inert in polymerizations of MAMs [65].

11.8.1 Ring-Opening Polymerization (ROP)

Dithiocarbamates comprising a primary hydroxy substituent allow preparation of block copolymers by ROP-*𝓣*-RAFT. Examples of ring-opening polymerization (ROP) in this context are acid catalysed ROP of ε-caprolactone (CL) or trimethylenecarbonate (TMC) and base catalysed ROP of lactide (LA) making use of **26** [171] (Table 11.2) or the switchable dithiocarbamate **56** [225] (Table 11.3). Use of **56** allowed ROP-*𝓣*-RAFT of ROP monomers with both MAMs (MA and DMAm) and LAMs (VAc and NVP).

11.8.2 Ring-Opening Metathesis Polymerization (ROMP)

Many of the monomers for ring-opening metathesis polymerization (ROMP) appear essentially inert under the conditions used for RAFT polymerization. Thus, dithiocarbamates containing such functionality can be used as precursors

to 'ene' end-functional macro-dithiocarbamates and then of brush polymers in a RAFT-*T*-ROMP 'grafting-through' process. The ene functionality of the dithiocarbamates can also be polymerized by ROMP and brush copolymers formed in a 'grafting-from' process by ROMP-*T*-RAFT. Dithiocarbamates used in such RAFT-*T*-ROMP are **29**, **30**, and **38** (Table 11.2). Dithiocarbamate **30** has been used in ROMP-*T*-RAFT.

11.8.3 Atom-Transfer Radical Polymerization (ATRP)

It is possible to convert ATRP (halide) initiators and macro-initiators to dithiocarbamates by ATRAF (Method D (Section 11.5.4)) [208, 264]. Dithiocarbamates have been used a pseudohalide initiators in ATRP [288].

11.9 Dithiocarbamate Group Removal/Transformation

Most of the methods described for removal or transformation of thiocarbonylthio end-groups of RAFT-synthesized polymers [289, 290] are applicable to polymers with dithiocarbamate chain-ends. However, the *N*,*N*-dialkyldithiocarbamates (e.g. **156**) and *N*-aryl-*N*-alkyldithiocarbamates (e.g. **153**) have a significantly lower reactivity towards radical addition or nucleophilic attack than dithiocarbamates, such as the 1*H*-pyrrole-1-carbodithioates (**126**), and most other thiocarbonylthio-RAFT agents (the dithioesters and the trithiocarbonates).

11.9.1 Dithiocarbamate Group Removal by Radical-Induced Coupling

A method developed by Perrier et al. [291] involves heating a RAFT-synthesized polymer with a large excess of a radical initiator (e.g. 20 molar equiv), most often a dialkyldiazene. The method has been successfully applied to 1*H*-pyrrole-1-carbodithioates (**126**) [292]. Related chemistry, making use of organic peroxides, is described in the patent literature [293]. Another method, also described in the patent literature [273] that involves heating the RAFT-synthesized polymer with a mixture of an initiator and a non-propagating monomer (e.g. a maleimide) appears substantially more economical in initiator. For examples, see Table 11.12.

11.9.2 Dithiocarbamate Group Removal by Radical-Induced Disproportionation

A method for removing thiocarbonylthio groups by what might be considered as radical-induced disproportionation has been reported [191]. The process involves use of triethylborane (or another triakylborane) and oxygen to generate ethyl radicals that react with thiocarbonylthio groups to produce a propagating species by irreversible addition–fragmentation. This reacts with further ethyl radicals mainly by disproportionation with H-transfer to the propagating species. The process appears rapid and quantitative (for end-group removal). Smaller amounts of other

Table 11.12 End-group removal by radical-induced coupling.

RAFT end-group[a)]	Polymer[b)]	Initiator[b)]	Comment[b)]	References
126	NIPAm	ACPA	20×, 60 °C, DMF	[292]
129	St	AIBN	20×, 80 °C, toluene, 5 h	[294]
134	NLA/EADA/HADA	AIBMe/NPMI	4×, reflux, MEK, 2 h	[273]
133	BA	AIBN/NPMI	4×, reflux, MEK, 2 h	[273]
134	*t*BA	LPO	4×, reflux, toluene, 2 h	[293]

a) Refer Table 11.17.
b) ACPA, 4,4′-azobis(4-cyanopentanoic acid); NLA, 6-(5-hydroxynorbornane-2-carboxylic acid lactone)yl acrylate; EADA, 2-[2-ethyladamantyl]acrylate; HADA, 1-[13-hydroxyadamantyl]acrylate; DMF, *N*,*N*-dimethylformamide; MEK, butan-2-one; tBA, *tert*-butyl acrylate; NPMI, *N*-phenylmaleimide; LPO, dodecanoyl peroxide (lauroyl peroxide). Refer to *Abbreviations* at the end of the chapter for a full list of abbreviations.

Table 11.13 End-group removal by radical-induced disproportionation.

RAFT end-group[a)]	Polymer	Initiator[b)]	Comment	References
152	VAc	TEB/O_2	Product is PVAc-H (80%)[c)] plus some PVAc-Et[d)]	[191]

a) Refer Table 11.17.
b) TEB, triethylborane.
c) Disproportionation product.
d) Combination product.

chain-ends may also be formed. The application to removal of dithiocarbamate ends is shown in Table 11.13.

11.9.3 Dithiocarbamate Group Removal by Radical-Induced Reduction

Radical-induced reduction allows the thiocarbonylthio group of RAFT-synthesized polymers to be replaced with a hydrogen atom [261, 295, 296]. The process involves reaction of the radicals formed by RAFT with a hydrogen atom donor such as a stannane or a hypophosphite. Radical formation by heating the RAFT-synthesized polymer with an added initiator can be inefficient with the dithiocarbamates. Photogeneration of radicals directly from the RAFT agent offers an alternative, which also solves the issue of initiator-derived products [292] (for examples, see Table 11.14).

11.9.4 Dithiocarbamate Group Removal by Reaction with Nucleophiles

Dithiocarbamate chain-ends are substantially less susceptible to nucleophilic attack than most other RAFT end-groups (dithioesters, trithiocarbonates, xanthates) [287, 297], which most likely accounts for variable results (for Examples see Table 11.15). The theoretically estimated order of reactivity of RAFT end-groups towards primary amine nucleophiles is dithioate ≥ dithiobenzoate > xanthate ≥

Table 11.14 End-group removal by radical-induced reduction.

RAFT end-group[a)]	Polymer	Initiator	Reagent	References
156	St[b)]	$h\nu$	Bu_3SnH	[292]
126	**88**	AIBN	EPHP[c)]	[236]

a) Refer Table 11.17.
b) Polymer formed by ATRP.
c) EPHP, *N*-ethylpiperidine hypophosphate.

Table 11.15 End-group removal by reaction with nucleophiles.

RAFT end-group[a)]	Polymer	Reagent	Comment	References
127	MA	$EtNH_2$/Zn powder	Quantitative at 40 °C, 72 h	[143]
140	AA-*b*-NIPAm	NaOH/ MeOH – EDTA	Quantitative at ambient temperature, 3 days	[179]
[b)]	St	CH_3NH_2/H_2O	Quantitative at ambient temperature, 3 days	[176]
156	Model compound	nBuNH$_2$	No reaction at ambient temperature, <8 h	[287]

a) Refer Table 11.17.
b) Bottlebrush polymer formed by ring-opening metathesis polymerization (ROMP) [176].

trithiocarbonate ≫ dithiocarbamate [297], where the dithiocarbamate is an *N*,*N*-dimethyldithiocarbamate.

Partial end-group loss has been found to complicate aqueous size exclusion chromatography of RAFT-synthesized polymers (e.g. DMAm prepared with **21**). The issue has been shown to stem from reaction with the azide salt present in the eluent (0.2 M $NaNO_3$, 0.01 M Na_3PO_4, 200 ppm NaN_3, in water adjusted to pH 8). The reaction produces a polymer with a thiol end.

11.9.5 Dithiocarbamate Group Removal by Thermolysis

Studies with model compounds (RAFT agents) show that dithiocarbamates are more thermally stable than other RAFT agents, with *N*,*N*-dialkyldithiocarbamates being stable under conditions where facile end-group elimination is seen for analogous dithioesters, trithiocarbonate, and xanthates [298, 299]. Poly(MMA) formed with a thiuram disulfide as thermal iniferter appeared relatively stable to thermolysis with no mass loss to 300 °C [300].

A series of experiments with polymers, polystyrene, poly(MMA), poly(NIPAm), poly(NVP), and poly(VAc), prepared with a switchable, *N*-(4-pyridinyl)-*N*-methyl-dithiocarbamate RAFT agent demonstrated successful end-group removal by thermolysis for the polymers in either the switched (**137**) or the unswitched state (**137-H$^+$**) [216]. The nature of the chain-ends formed depends on the particular polymer and in some cases remains to be clarified. Polymers based on LAMs were stable relative to those based on MAMs. The non-protonated form of the end-group was stable relative to the protonated form.

11.9.6 Dithiocarbamate Group Removal by Oxidation

RAFT end-groups can be readily removed by reaction with hydrogen peroxide [301–305]. The process has been demonstrated for dithiobenzoates [302, 305], trithiocarbonates [303], and xanthates [304] and is also claimed to be effective with dithiocarbamate chain-ends **137** and **134** [303]. The processes are claimed to lead to the thiocarbonylthio group being replaced with a hydroxyl group [304]. Note that hydrogen peroxide can also be used as a component of a redox initiating system for RAFT polymerization [306–311], which must be understood in terms of the rate of reaction of hydrogen peroxide with a RAFT end-group being very much slower than that for reaction with a monomer under the reaction conditions.

11.9.7 Dithiocarbamate Group Removal by Other Methods

Thiocarbonylthio compounds have been shown to undergo copper-promoted cross-coupling reaction with aryl boronic acids, which leads to replacement of the thiocarbonylthio group with an aryl group (Scheme 11.8) [163]. The method is effective for polystyrene but leads to a complex mixture in the case of (meth)acrylates (Table 11.16).

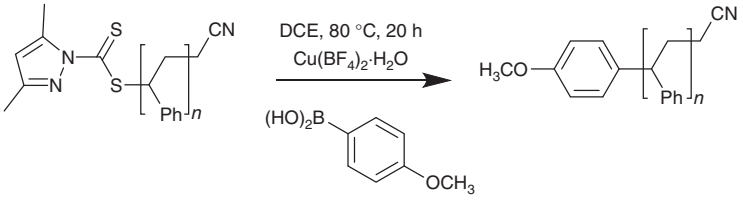

Scheme 11.8 End-group transformation by copper-promoted cross-coupling DCE – 1,2-dichloroethane.

11.10 Dithiocarbamate Z′Z″NC(=S)S groups

Table 11.17 provides a summary of Z′Z″NC(=S)S groups in reported dithiocarbamate RAFT agents. Not all are mentioned in this chapter. For additional details on those not mentioned, refer to our recent review [1].

Table 11.16 End-group removal by copper-promoted cross-coupling.

RAFT end-group[a)]	Polymer	Reagent	Comment	References
134	St		Complete end-group removal (Scheme 11.8)	[163]
134	MA		Decomposition	[163]

a) Refer Table 11.17.

Table 11.17 Dithiocarbamate RAFT agent Z′Z″NC(=S)S− groups.

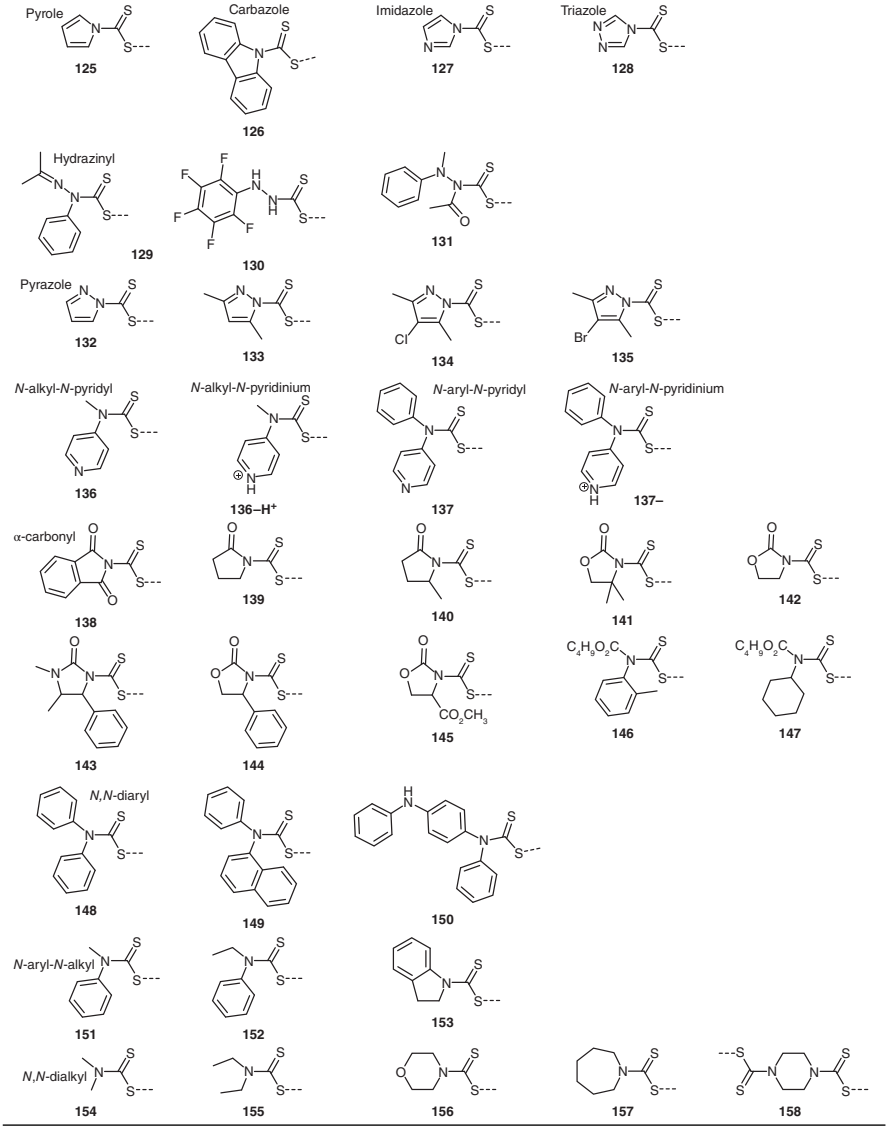

Source: Moad [1]. Copyright 2019, John Wiley and Sons.

11.11 Conclusions

The use of dithiocarbamates Z′Z″NC(=S)SR in RAFT polymerization has been reviewed. Dithiocarbamates are an extremely versatile class of RAFT agents. Through choice of substituents on nitrogen (Z′, Z″), the polymerization of most monomer types can be controlled. Historically, it has been necessary to choose one dithiocarbamate for controlling polymerization of MAMs (e.g. 1-pyrrolocarbodithioate) and another for LAMs, (e.g. *N*-alkyl-*N*-aryldithiocarbamate). It is now possible to have one dithiocarbamate that controls all monomer classes (MAMs, LAMs, IAMs). Depending on the degree of control required, this might be a RAFT agent with balanced activity (e.g. 1*H*-pyrazole-1-carbodithioates) or a switchable RAFT agent (e.g. *N*-methyl-*N*-(4-pyridinyl)dithiocarbamate).

Acknowledgements

This review borrows heavily from and updates a review on the same topic published in *Journal of Polymer Science, Polymer Chemistry* [1].

Abbreviations

Abbreviations are listed alphabetically by the abbreviated term. In general, abbreviations of methacrylates end with 'MA', methacrylamides end with 'MAm', acrylates end with an 'A'. acrylamides end with an 'Am' or begin with 'NA' (for *N*-acryloyl). Except as indicated below the suffix 'P' is an abbreviation for 'poly()'. Thus, poly(methyl methacrylate) is abbreviated as PMMA.

AA	acrylic acid
ACE	acenaphthylene
AIBN	azobis(isobutyronitrile) [2,2′-azobis(2-methylproionitrile)]
ACHN	1,1′-azobis(1-cyclohexanenitrile)
ACPA	4,4′-azobis(4-cyanopentanoic acid)
Am	acrylamide
AMS	α-methylstyrene [prop-1-en-2-ylbenzene]
AN	acrylonitrile
ATRP	atom-transfer radical polymerization
BA	butyl acrylate
BMA	butyl methacrylate
BPO	benzoyl peroxide
CEVE	2-chloroethyl vinyl ether
CL	ε-caprolactone
CMS	4-(chloromethyl)styrene
CMS	chloromethylstyrene
CTFE	chlorotrifluoroethylene

$Đ$	molar mass dispersity = ratio of mass average to number average molar mass [312]
DAAm	diacetone acrylamide
DCE	1,2-dichloroethane
DEGMA	(diethylene glycol monomethyl ether) methacrylate
DMAm	*N,N*-dimethylacrylamide
DMAEMA	2-(dimethylamino)ethyl methacrylate
E	ethylene
EA	ethyl acrylate
EDTA	ethylenediaminetetraacetic acid
EHA	2-ethylhexyl acrylate
EMA	ethyl methacrylate
EVE	ethyl vinyl ether
GMA	glycidyl methacrylate
HA	hexyl acrylate
HEA	2-hydroxyethyl acrylate
HEMA	2-hydroxyethyl methacrylate
HEVE	2-hydroxyethyl vinyl ether
HOSt	4-hydroxystyrene
HPMAm	*N*-(2-hydroxylpropyl)methacrylamide
*i*BVE	isobutyl vinyl ether
IAM	intermediate activated monomer (IAMs include NVC)
Ip	isoprene
LA	lactide
LAM	less activated monomer (LAMs include vinyl monomers such as VAc, VC, NVP)
Lim	limonene
LMA	lauryl methacrylate (dodecyl methacrylate)
LPO	dodecanoyl peroxide (lauroyl peroxide)
MA	methyl acrylate
MAA	methacrylic acid
MADIX	macromolecular design by interchange of xanthates
MAH	maleic anhydride
MAM	more activated monomer (MAMs include styrenes, (meth)acrylates, (meth)acrylamides)
MMA	methyl methacrylate
MOVE	2-methoxyethyl vinyl ether
NAM	*N*-acryloylacrylamide
NES	neopentyl ethenesulfonate
NIPAm	*N*-isopropylacrylamide
NMMI	*N*-methylmaleimide
NMP	aminoxyl- (nitroxide-)mediated polymerization
NPMI	*N*-phenylmaleimide
NVC	*N*-vinylcarbazole
NVCL	*N*-vinylcaprolactam
NVP	*N*-vinylpyrrolidone

NVPI	*N*-vinylphthalimide
PEGA	(poly(ethylene glycol) monomethyl ether) acrylate
PEGMA	(poly(ethylene glycol) monomethyl ether) methacrylate
PEO	poly(ethylene oxide)
PFS	2,3,4,5,6-pentafluorostyrene
PTC	phase transfer catalyst
PVK	phenyl vinyl ketone
RAFT	reversible addition-fragmentation chain transfer
RDRP	reversible-deactivation radical polymerization
SDS	sodium dodecyl sulfate
St	styrene
tBA	*tert*-butyl acrylate
tBMA	*tert*-butyl methacrylate
TMC	trimethylenecarbonate
VAc	vinyl acetate
VBz	vinyl benzoate
VC	vinyl chloride
VF2	vinylidene fluoride
Vim	4-vinylimidazole
VPv	vinyl pivalate
2VP	2-vinylypyridine
4VP	4-vinylpyridine

References

1 Moad, G. (2019). *J. Polym. Sci., Part A: Polym. Chem.* 57: 216–227. https://doi.org/10.1002/pola.29199.

2 Gardiner, J., Martinez-Botella, I., Kohl, T.M. et al. (2017). *Polym. Int.* 66: 1438–1447. https://doi.org/10.1002/pi.5423.

3 Gardiner, J., Martinez-Botella, I., Tsanaktsidis, J., and Moad, G. (2016). *Polym. Chem.* 7: 481–492. https://doi.org/10.1039/C5PY01382H.

4 Dayter, L.A., Murphy, K.A., and Shipp, D.A. (2013). *Aust. J. Chem.* 66: 1564–1569. https://doi.org/10.1071/CH13375.

5 Malepu, V., Petruczok, C.D., Tran, T. et al. (2009). RAFT polymerization of vinyl acetate, styrene and acrylates using N,N-dithiocarbamates. In: *Controlled/Living Radical Polymerization: Progress in RAFT, DT, NMP & OMRP*, ACS Symposium Series, vol. 1024 (ed. K. Matyjaszewski), 37–47. Washington, DC: American Chemical Society https://doi.org/10.1021/bk-2009-1024.ch003.

6 Destarac, M., Charmot, D., Franck, X., and Zard, S.Z. (2000). *Macromol. Rapid Commun.* 21: 1035–1039. https://doi.org/10.1002/1521-3927(20001001)21:15<1035::AID-MARC1035>3.0.CO;2-5.

7 Keddie, D.J., Guerrero-Sanchez, C., and Moad, G. (2013). *Polym. Chem.* 4: 3591–3601. https://doi.org/10.1039/c3py00487b.

8 Wang, M., Marty, J.-D., and Destarac, M. (2022). Xanthates in RAFT polymerization. In: *RAFT Polymerization: Materials, Synthesis and Applications* (eds. G. Moad and E. Rizzardo), 495–550. Weinheim: Wiley-VCH.

9 Moad, G. (2022). Dithioesters in RAFT polymerization. In: *RAFT Polymerization: Materials, Synthesis and Applications* (eds. G. Moad and E. Rizzardo), 272–370. Weinheim: Wiley-VCH.

10 Moad, G. (2022). Trithiocarbonates in RAFT polymerization. In: *RAFT Polymerization: Materials, Synthesis and Applications* (eds. G. Moad and E. Rizzardo), 371–494. Weinheim: Wiley-VCH.

11 Otsu, T. (1956). *J. Polym. Sci.* 21: 559–561. https://doi.org/10.1002/pol.1956.120219924.

12 Otsu, T. (1957). *J. Polym. Sci.* 26: 236–239. https://doi.org/10.1002/pol.1957.1202611313.

13 Hawker, C.J., Bosman, A.W., and Harth, E. (2001). *Chem. Rev.* 101: 3661–3688. https://doi.org/10.1021/cr990119u.

14 Moad, G. and Rizzardo, E. (2016). History of nitroxide-mediated polymerization. In: *Nitroxide Mediated Polymerization: From Fundamentals to Applications in Materials* (ed. D. Gigmes), 1–44. Cambridge: The Royal Society of Chemistry. https://doi.org/10.1039/9781782622635-00001.

15 Gigmes, D. (ed.) (2016). *Nitroxide Mediated Polymerization: From Fundamentals to Applications in Materials Science*. Cambridge: The Royal Society of Chemistry. https://doi.org/10.1039/9781782622635.

16 Moad, G., Rizzardo, E., and Thang, S.H. (2008). *Acc. Chem. Res.* 41: 1133–1142. https://doi.org/10.1021/ar800075n.

17 Otsu, T. and Yoshida, M. (1982). *Makromol. Chem. Rapid Commun.* 3: 127–132. https://doi.org/10.1002/marc.1982.030030209.

18 Otsu, T., Yoshida, M., and Kuriyama, A. (1982). *Polym. Bull.* 7: 45–50. https://doi.org/10.1007/BF00264156.

19 Otsu, T. (2000). *J. Polym. Sci., Part A: Polym. Chem.* 38: 2121–2136. https://doi.org/10.1002/(SICI)1099-0518(20000615)38:12<2121::AID-POLA10>3.0.CO;2-X.

20 Jenkins, A.D., Jones, R.I., and Moad, G. (2010). *Pure Appl. Chem.* 82: 483–491. https://doi.org/10.1351/PAC-REP-08-04-03.

21 Kennedy, J., Chang, V.C., Smith, R., and Iván, B. (1979). *Polym. Bull.* 1: 575–580. https://doi.org/10.1007/bf00254487.

22 Kennedy, J.P. and Smith, R.A. (1980). *J. Polym. Sci., Polym. Chem. Ed.* 18: 1523–1537. https://doi.org/10.1002/pol.1980.170180509.

23 Nair, C.P.R. and Clouet, G. (1991). *J. Macromol. Sci., Rev. Macromol. Chem. Phys.* C31: 311–340. https://doi.org/10.1080/15321799108021926.

24 Otsu, T., Matsunaga, T., Doi, T., and Matsumoto, A. (1995). *Eur. Polym. J.* 31: 67–78. https://doi.org/10.1016/0014-3057(94)00122-7.

25 Sebenik, A. (1998). *Prog. Polym. Sci.* 23: 875–917. https://doi.org/10.1016/S0079-6700(98)00001-X.

26 Otsu, T. and Matsumoto, A. (1998). Controlled synthesis of polymers using the iniferter technique: developments in living radical polymerization. In: *Microencapsulation Microgels Iniferters* (eds. S. DiMari, W. Funke, M.A. Haralson, et al.), 75–137. Berlin, Heidelberg: Springer-Verlag. https://doi.org/10.1007/3-540-69682-2_3.

27 Tasdelen, M.A. and Yagci, Y. (2013). Controlled/living radical polymerization in the presence of iniferters. In: *Fundamentals of Controlled/Living Radical Polymerization* (eds. N.V. Tsarevsky and B.S. Sumerlin), 78–111. Cambridge: The Royal Society of Chemistry. https://doi.org/10.1039/9781849737425-00078.

28 Wang, M., Jiang, X., Luo, Y. et al. (2017). *Polym. Chem.* 8: 5918–5923. https://doi.org/10.1039/C7PY01222E.

29 Yasuhide, N., Takeshi, M., Makoto, N. et al. (2005). *Curr. Drug Deliv.* 2: 53–57. https://doi.org/10.2174/1567201052772825.

30 Nemoto, Y., Borovkov, A., Zhou, Y.-M. et al. (2009). *Bioconjugate Chem.* 20: 2293–2299. https://doi.org/10.1021/bc900283h.

31 Nakayama, Y. (2012). *Acc. Chem. Res.* 45: 994–1004. https://doi.org/10.1021/ar200220t.

32 Gutiérrez-Climente, R., Gómez-Caballero, A., Halhalli, M. et al. (2016). *J. Mol. Recognit.* 29: 106–114. https://doi.org/10.1002/jmr.2443.

33 Bonomi, P., Attieh, M.D., Gonzato, C., and Haupt, K. (2016). *Chem. Eur. J.* 22: 10150–10154. https://doi.org/10.1002/chem.201600750.

34 Fukui, Y., Sakai, D., and Fujimoto, K. (2016). *Colloids Surf., B* 148: 503–510. https://doi.org/10.1016/j.colsurfb.2016.09.032.

35 Lv, Y.-K., Zhang, J., Li, M.-Z. et al. (2016). *Anal. Methods* 8: 3982–3989. https://doi.org/10.1039/C6AY00417B.

36 Jing, L., Zhang, Q., Wang, Y., and Wei, T. (2016). *Anal. Lett.* 49: 1696–1710. https://doi.org/10.1080/00032719.2015.1119838.

37 Gao, X., Hu, X., Guan, P. et al. (2016). *RSC Adv.* 6: 110019–110031. https://doi.org/10.1039/C6RA24518H.

38 Salmi-Mani, H., Ait-Touchente, Z., Lamouri, A. et al. (2016). *RSC Adv.* 6: 88126–88134. https://doi.org/10.1039/C6RA14713E.

39 Ayadi, H., Mekhalif, T., Salmi, Z. et al. (2016). *J. Appl. Polym. Sci.* 133 https://doi.org/10.1002/app.43694.

40 Wang, H., Wu, H., Lee, C.-J. et al. (2016). *Langmuir* 32: 6544–6550. https://doi.org/10.1021/acs.langmuir.6b01465.

41 Ding, S., Hu, X., Guan, P. et al. (2017). *J. Mater. Sci.* 52: 8027–8040. https://doi.org/10.1007/s10853-017-1005-x.

42 Gong, X., Tang, B., Liu, J.J. et al. (2017). *Biosens. Bioelectron.* 87: 858–864. https://doi.org/10.1016/j.bios.2016.09.027.

43 Prete, M.C., Dos Santos, D.M., Effting, L., and Tarley, C.R.T. (2019). *J. Chem. Eng. Data* https://doi.org/10.1021/acs.jced.8b01010.

44 García-Mutio, D., Gómez-Caballero, A., Gotiandia, A. et al. (2018). *Electrochim. Acta* 279: 57–65. https://doi.org/10.1016/j.electacta.2018.05.075.

45 Zoppe, J.O., Ataman, N.C., Mocny, P. et al. (2017). *Chem. Rev.* 117: 1105–1318. https://doi.org/10.1021/acs.chemrev.6b00314.

46 Quinn, J.F., Barner, L., Barner-Kowollik, C. et al. (2002). *Macromolecules* 35: 7620–7627. https://doi.org/10.1021/ma0204296.

47 Wang, H., Li, Q., Dai, J. et al. (2013). *Macromolecules* 46: 2576–2582. https://doi.org/10.1021/ma400208j.

48 McKenzie, T.G., Fu, Q., Wong, E.H.H. et al. (2015). *Macromolecules* 48: 3864–3872. https://doi.org/10.1021/acs.macromol.5b00965.

49 Xu, J., Shanmugam, S., Corrigan, N.A., and Boyer, C. (2015). Catalyst-free visible light-induced RAFT photopolymerization. In: *Controlled Radical Polymerization: Mechanisms*, ACS Symposium Series, vol. 1187 (eds. K. Matyjaszewski, B.S. Sumerlin, N.V. Tsarevsky and J. Chiefari), 247–267. American Chemical Society. https://doi.org/10.1021/bk-2015-1187.ch013.

50 Cabannes-Boue, B., Yang, Q., Lalevee, J. et al. (2017). *Polym. Chem.* 8: 1760–1770. https://doi.org/10.1039/C6PY02220K.

51 Fu, C., Huang, Z., Hawker, C.J. et al. (2017). *Polym. Chem.* 8: 4637–4643. https://doi.org/10.1039/C7PY00713B.

52 Aerts, A., Lewis, R.W., Zhou, Y. et al. (2018). *Macromol. Rapid. Commun.* 39: 1800240 (7 pp). https://doi.org/10.1002/marc.201800240.

53 Shanmugam, S., Xu, J., and Boyer, C. (2014). *Macromolecules* 47: 4930–4942. https://doi.org/10.1021/ma500842u.

54 Figg, C.A., Hickman, J.D., Scheutz, G.M. et al. (2018). *Macromolecules* 51: 1370–1376. https://doi.org/10.1021/acs.macromol.7b02533.

55 Xu, J., Fu, C., Shanmugam, S. et al. (2017). *Angew. Chem. Int. Ed.* 56: 8376–8383. https://doi.org/10.1002/anie.201610223.

56 Sivaprakash, S., Jiangtao, X., and Cyrille, B. (2016). *Angew. Chem. Int. Ed.* 55: 1036–1040. https://doi.org/10.1002/anie.201510037.

57 Seal, P., Xu, J., De Luca, S. et al. (2019). *Adv. Theory Simul.* 2: 1900038. https://doi.org/10.1002/adts.201900038.

58 Shanmugam, S., Xu, J., and Boyer, C. (2017). *Macromol. Rapid Commun.* 38: 1700143. https://doi.org/10.1002/marc.201700143.

59 Liu, S., Cheng, Y., Zhang, H. et al. (2018). *Angew. Chem. Int. Ed.* 57: 6274–6278. https://doi.org/10.1002/anie.201803268.

60 Easterling, C.P., Xia, Y., Zhao, J. et al. (2019). *ACS Macro Lett.* 8: 1461–1466. https://doi.org/10.1021/acsmacrolett.9b00716.

61 Mayo, F.R. (1948). *J. Am. Chem. Soc.* 70: 3689–3694. https://doi.org/10.1021/ja01191a044.

62 Moad, G. and Moad, C.L. (1996). *Macromolecules* 29: 7727–7733. https://doi.org/10.1021/ma960851k.

63 Walling, C. (1948). *J. Am. Chem. Soc.* 70: 2561–2564. https://doi.org/10.1021/ja01187a079.

64 Moad, G. and Solomon, D.H. (2006). Chain transfer. In: *The Chemistry of Radical Polymerization*, 279–331. Elsevier: Oxford. https://doi.org/10.1016/B978-008044288-4/50025-X.

65 Chiefari, J., Mayadunne, R.T.A., Moad, C.L. et al. (2003). *Macromolecules* 36: 2273–2283. https://doi.org/10.1021/ma020883+.

66 Chong, Y.K., Krstina, J., Le, T.P.T. et al. (2003). *Macromolecules* 36: 2256–2272. https://doi.org/10.1021/ma020882h.

67 Quinn, J.F., Moad, G., and Barner-Kowollik, C. (2022). RAFT polymerization: mechanistic considerations. In: *RAFT Polymerization: Materials, Synthesis and Applications* (eds. G. Moad and E. Rizzardo), 59–94. Weinheim: Wiley-VCH.

68 Altarawneh, I.S., Srour, M., and Gomes, V.G. (2007). *Polym. Plast. Technol. Eng.* 46: 1103–1115. https://doi.org/10.1080/03602550701557928.

69 Zaremskii, M.Y., Olenin, A.V., Garina, Y.S. et al. (1991). *Polym. Sci. U.S.S.R.* 33: 2036–2045. https://doi.org/10.1016/0032-3950(91)90104-X.

70 Wan, X., Zhang, Z., Zhu, X. et al. (2008). *e-Polymers* (1): 8. https://doi.org/10.1515/epoly.2008.8.1.1028.

71 Wan, X., Zhu, X., Zhu, J. et al. (2007). *J. Polym. Sci., Part A: Polym. Chem.* 45: 2886–2896. https://doi.org/10.1002/pola.22045.

72 Dika Manga, J., Tardi, M., Polton, A., and Sigwalt, P. (1998). *Polym. Int.* 45: 243–254. https://doi.org/10.1002/(SICI)1097-0126(199803)45:3<243::AID-PI913>3.0.CO;2-U.

73 Keddie, D.J., Guerrero-Sanchez, C., Moad, G. et al. (2012). *Macromolecules* 45: 4205–4215. https://doi.org/10.1021/ma300616g.

74 Moad, G., Rizzardo, E., and Thang, S.H. (2006). *Aust. J. Chem.* 59: 669–692. https://doi.org/10.1071/CH06250.

75 Moad, G., Rizzardo, E., and Thang, S.H. (2005). *Aust. J. Chem.* 58: 379–410. https://doi.org/10.1071/CH05072.

76 Moad, G., Rizzardo, E., and Thang, S.H. (2009). *Aust. J. Chem.* 62: 1402–1472. https://doi.org/10.1071/CH09311.

77 Moad, G., Rizzardo, E., and Thang, S.H. (2008). *Polymer* 49: 1079–1131. https://doi.org/10.1016/j.polymer.2007.11.020.

78 Keddie, D.J., Moad, G., Rizzardo, E., and Thang, S.H. (2012). *Macromolecules* 45: 5321–5342. https://doi.org/10.1021/ma300410v.

79 Mayadunne, R.T.A., Rizzardo, E., Chiefari, J. et al. (1999). *Macromolecules* 32: 6977–6980. https://doi.org/10.1021/ma9906837.

80 Chong, Y.K., Moad, G., Rizzardo, E. et al. (2007). *Macromolecules* 40: 9262–9271. https://doi.org/10.1021/ma071100t.

81 Zhang, M. and Ray, W.H. (2001). *Ind. Eng. Chem. Res.* 40: 4336–4352. https://doi.org/10.1021/ie0009482.

82 ten Brummelhuis, N. and Weck, M. (2014). *J. Polym. Sci., Part A: Polym. Chem.* 52: 1555–1559. https://doi.org/10.1002/pola.27148.

83 Takeshima, H., Satoh, K., and Kamigaito, M. (2017). *Macromolecules* 50: 4206–4216. https://doi.org/10.1021/acs.macromol.7b00970.

84 Miyaji, H., Satoh, K., and Kamigaito, M. (2016). *Angew. Chem. Int. Ed.* 55: 1372–1376. https://doi.org/10.1002/anie.201509379.

85 Chiefari, J., Mayadunne, R.T., Moad, G. et al. (2003). (du Pont/CSIRO), US6642318B1.

86 Schilli, C., Lanzendoerfer, M.G., and Mueller, A.H.E. (2002). *Macromolecules* 35: 6819–6827. https://doi.org/10.1021/ma0121159.

87 Merican, Z., Schiller, T.L., Hawker, C.J. et al. (2007). *Langmuir* 23: 10539–10545. https://doi.org/10.1021/la702218b.

88 Schilli, C.M., Muller, A.H.E., Rizzardo, E. et al. (2003). RAFT Polymers: novel precursors for polymer protein conjugates. In: *Advances in Controlled/Living Radical Polymerization*, ACS Symposium Series, vol. 854

(ed. K. Matyjaszewski), 603–618. Washington, DC: American Chemical Society https://doi.org/10.1021/bk-2003-0854.ch041.

89 Babu, R.P. and Dhamodharan, R. (2008). *Polym. Int.* 57: 365–371. https://doi.org/10.1002/pi.2363.

90 Harihara, S.S., Prakash, B.R., and Dhamodharan, R. (2008). *Macromolecules* 41: 262–265. https://doi.org/10.1021/ma7021056.

91 Skey, J. and O'Reilly, R.K. (2008). *Chem. Commun.*: 4183–4185. https://doi.org/10.1039/b804260h.

92 Altarawneh, I., Rawadieh, S., and Gomes, V.G. (2014). *Des. Monomers Polym.* 17: 430–437. https://doi.org/10.1080/15685551.2013.867566.

93 Hoang, P.H., Nguyen, C.T., Perumal, J., and Kim, D.-P. (2011). *Lab Chip* 11: 329–335. https://doi.org/10.1039/C0LC00321B.

94 Kumar, S., Roy, S.G., and De, P. (2012). *Polym. Chem.* 3: 1239–1248. https://doi.org/10.1039/C2PY00607C.

95 Swift, T., Lapworth, J., Swindells, K. et al. (2016). *RSC Adv.* 6: 71345–71350. https://doi.org/10.1039/C6RA13139E.

96 Luo, R. and Sen, A. (2007). *Macromolecules* 40: 154–156. https://doi.org/10.1021/ma062341o.

97 Hua, D., Bai, R., Lu, W., and Pan, C. (2004). *J. Polym. Sci., Part A: Polym. Chem.* 42: 5670–5677. https://doi.org/10.1002/pola.20394.

98 Rizzardo, E., Chiefari, J., Mayadunne, R.T.A. et al. (2000). Synthesis of defined polymers by reversible addition fragmentation chain transfer. In: *Controlled/Living Radical Polymerization*, ACS Symposium Series, vol. 768 (ed. K. Matyjaszewski), 278–296. Washington, DC: American Chemical Society. https://doi.org/10.1021/bk-2000-0768.ch020.

99 Ishigaki, Y. and Mori, H. (2018). *Polymer* 140: 198–207. https://doi.org/10.1016/j.polymer.2018.02.025.

100 Sun, X.-L., He, W.-D., Li, J. et al. (2008). *J. Polym. Sci., Part A: Polym. Chem.* 46: 6950–6960. https://doi.org/10.1002/pola.23004.

101 El-Newehy, M.H., Elsherbiny, A.S., and Mori, H. (2016). *RSC Adv.* 6: 72761–72767. https://doi.org/10.1039/C6RA14307E.

102 Mori, H., Sutoh, K., Iwaya, H. et al. (2006). Controlled synthesis of amino acid-based polymers by reversible addition fragmentation chain transfer polymerization. In: *Controlled/Living Radical Polymerization. From Synthesis to Materials*, Controlled/Living Radical Polymerization, vol. 944 (ed. K. Matyjaszewski), 533–546. Washington, DC: American Chemical Society. https://doi.org/10.1021/bk-2006-0944.ch036.

103 Mori, H. and Okabayashi, S. (2009). *React. Funct. Polym.* 69: 441–449. https://doi.org/10.1016/j.reactfunctpolym.2009.01.012.

104 Mori, H., Kato, I., Matsuyama, M., and Endo, T. (2008). *Macromolecules* 41: 5604–5615. https://doi.org/10.1021/ma800181h.

105 Mori, H., Matsuyama, M., and Endo, T. (2009). *Macromol. Chem. Phys.* 210: 217–229. https://doi.org/10.1002/macp.200800446.

106 Mori, H., Matsuyama, M., and Endo, T. (2008). *Macromol. Chem. Phys.* 209: 2100–2112. https://doi.org/10.1002/macp.200800254.

107 El-Newehy, M.H., Elsherbiny, A.S., and Mori, H. (2013). *J. Appl. Polym. Sci.* 127: 4918–4926. https://doi.org/10.1002/app.37611.
108 Koseki, T., Kanto, R., Yonenuma, R. et al. (2020). *React. Funct. Polym.* 150: 104540. https://doi.org/10.1016/j.reactfunctpolym.2020.104540.
109 Mori, H., Matsuyama, M., Sutoh, K., and Endo, T. (2006). *Macromolecules* 39: 4351–4360. https://doi.org/10.1021/ma052756u.
110 Shoji, K., Nakayama, M., Koseki, T. et al. (2016). *Polymer* 97: 20–30. https://doi.org/10.1016/j.polymer.2016.05.003.
111 Higashi, N., Sekine, D., and Koga, T. (2017). *J. Colloid Interface Sci.* 500: 341–348. https://doi.org/10.1016/j.jcis.2017.04.027.
112 Yonenuma, R., Ishizuki, A., Nakabayashi, K., and Mori, H. *J. Polym. Sci., Part A: Polym. Chem.* https://doi.org/10.1002/pola.29531.
113 Mori, H., Takahashi, E., Ishizuki, A., and Nakabayashi, K. (2013). *Macromolecules* 46: 6451–6465. https://doi.org/10.1021/ma400596r.
114 Mori, H., Masuda, S., and Endo, T. (2006). *Macromolecules* 39: 5976–5978. https://doi.org/10.1021/ma0612879.
115 Nakabayashi, K., Tsuda, A., Otani, H., and Mori, H. (2015). *React. Funct. Polym.* 86: 52–59. https://doi.org/10.1016/j.reactfunctpolym.2014.11.004.
116 Ishigaki, Y. and Mori, H. (2018). *J. Appl. Polym. Sci.* 135: 46008 (13pp pp). https://doi.org/10.1002/app.46008.
117 Mori, H., Kudo, E., Saito, Y. et al. (2010). *Macromolecules* 43: 7021–7032. https://doi.org/10.1021/ma100905w.
118 Maki, Y., Mori, H., and Endo, T. (2007). *Macromol. Chem. Phys.* 208: 2589–2599. https://doi.org/10.1002/macp.200700330.
119 Maki, Y., Mori, H., and Endo, T. (2007). *Macromolecules* 40: 6119–6130. https://doi.org/10.1021/ma062839q.
120 Nakabayashi, K., Matsumura, A., Abiko, Y., and Mori, H. (2016). *Macromolecules* 49: 1616–1629. https://doi.org/10.1021/acs.macromol.5b02573.
121 Nakabayashi, K., Umeda, A., Sato, Y., and Mori, H. (2016). *Polymer* 96: 81–93. https://doi.org/10.1016/j.polymer.2016.04.062.
122 Nguyen, C.T., Nghiem, Q.D., Kim, D.-P. et al. (2009). *Polymer* 50: 5037–5041. https://doi.org/10.1016/j.polymer.2009.08.035.
123 Abiko, Y., Matsumura, A., Nakabayashi, K., and Mori, H. (2014). *Polymer* 55: 6025–6035. https://doi.org/10.1016/j.polymer.2014.09.025.
124 Mori, H., Ookuma, H., Nakano, S., and Endo, T. (2006). *Macromol. Chem. Phys.* 207: 1005–1017. https://doi.org/10.1002/macp.200600070.
125 Maki, Y., Mori, H., and Endo, T. (2010). *Macromol. Chem. Phys.* 211: 1137–1147. https://doi.org/10.1002/macp.200900544.
126 Maki, Y., Mori, H., and Endo, T. (2008). *Macromolecules* 41: 8397–8404. https://doi.org/10.1021/ma801359y.
127 Abiko, Y., Matsumura, A., Nakabayashi, K., and Mori, H. (2015). *React. Funct. Polym.* 93: 170–177. https://doi.org/10.1016/j.reactfunctpolym.2015.06.014.
128 Mori, H., Masuda, S., and Endo, T. (2008). *Macromolecules* 41: 632–639. https://doi.org/10.1021/ma0714262.

129 Plenderleith, R., Swift, T., and Rimmer, S. (2014). *RSC Adv.* 4: 50932–50937. https://doi.org/10.1039/C4RA10076J.

130 Teratanatorn, P., Hoskins, R., Swift, T. et al. (2017). *Biomacromolecules* 18: 2887–2899. https://doi.org/10.1021/acs.biomac.7b00800.

131 Sarker, P., Shepherd, J., Swindells, K. et al. (2011). *Biomacromolecules* 12: 1–5. https://doi.org/10.1021/bm100922j.

132 Carter, S.R., England, R.M., Hunt, B.J., and Rimmer, S. (2007). *Macromol. Biosci.* 7: 975–986. https://doi.org/10.1002/mabi.200700108.

133 Ruiwei, G. and Jianhua, Z. (2010). *Acta Polym. Sin.* 010: 691. https://doi.org/10.3724/SP.J.1105.2010.09228.

134 Zhu, Y., Xue, Y., Li, X. et al. (2019). *Polym. Chem.* 10: 2073–2082. https://doi.org/10.1039/C9PY00120D.

135 Liu, B., Deng, L., Guo, C. et al. (2012). *J. Appl. Polym. Sci.* 126: 740–748. https://doi.org/10.1002/app.36859.

136 Zhang, J., Dong, A., Cao, T., and Guo, R. (2008). *Eur. Polym. J.* 44: 1071–1080. https://doi.org/10.1016/j.eurpolymj.2008.01.037.

137 Zhou, D., Zhu, X., Zhu, J. et al. (2007). *J. Appl. Polym. Sci.* 103: 982–988. https://doi.org/10.1002/app.25280.

138 Zhou, Y., Zhu, X., Cheng, Z., and Zhu, J. (2007). *J. Appl. Polym. Sci.* 103: 1769–1775. https://doi.org/10.1002/app.25357.

139 Butte, A., Storti, G., and Morbidelli, M. (2001). *Macromolecules* 34: 5885–5896. https://doi.org/10.1021/ma002130y.

140 Brown, S.L., Konkolewicz, D., Gray-Weale, A. et al. (2009). *Aust. J. Chem.* 62: 1533–1536. https://doi.org/10.1071/CH09242.

141 Lalevée, J., Blanchard, N., El-Roz, M. et al. (2008). *Macromolecules* 41: 2347–2352. https://doi.org/10.1021/ma702406b.

142 Zhou, D., Zhu, X., Zhu, J. et al. (2006). *e-Polymers* (059): 6. https://doi.org/10.1515/epoly.2006.6.1.755.

143 Guo, R., Wang, X., Guo, C. et al. (2012). *Macromol. Chem. Phys.* 213: 1851–1862. https://doi.org/10.1002/macp.201200258.

144 Guo, R., Yao, Y., Bai, S. et al. (2017). *Polym. Chem.* 8: 3560–3573. https://doi.org/10.1039/C7PY00720E.

145 Guo, R., Liu, Y., Zhang, Y. et al. (2013). *Macromol. Res.* 21: 1127–1137. https://doi.org/10.1007/s13233-013-1142-2.

146 Guo, R., Mei, P., Zhong, Q. et al. (2015). *RSC Adv.* 5: 31365–31374. https://doi.org/10.1039/C5RA02863A.

147 Guo, J., Zhou, Y., Qiu, L. et al. (2013). *Polym. Chem.* 4: 4004–4009. https://doi.org/10.1039/C3PY00460K.

148 Stace, S.J., Vanderspikken, J., Howard, S.C. et al. (2019). *Polym. Chem.* 10: 5044–5051. https://doi.org/10.1039/C9PY00893D.

149 Ladaviere, C., Dorr, N., and Claverie, J.P. (2001). *Macromolecules* 34: 5370–5372. https://doi.org/10.1021/ma010358v.

150 Brunhofer-Bolzer, G., Gabriel, M., Studenik, C.R., and Erker, T. (2015). *Bioorg. Med. Chem.* 23: 4710–4718. https://doi.org/10.1016/j.bmc.2015.05.049.

151 Wang, Y.-Q., Ge, Z.-M., Hou, X.-L. et al. (2004). *Synthesis* 675–678. https://doi.org/10.1055/s-2004-815972.

152 Soleiman-Beigi, M. and Taherinia, Z. (2014). *J. Sulfur Chem.* 35: 470–476. https://doi.org/10.1080/17415993.2014.919296.

153 Chiefari, J., Mayadunne, R.T., Moad, G., et al. (2004). Polymerization process with living characteristics and polymers made therefrom Polymerization process with living characteristics and polymers made therefrom (E.I. Du Pont De Nemours and Company, Commonwealth Scientific and Industrial Research Organization), US6747111.

154 Zheng, H., Bai, W., Hu, K. et al. (2008). *J. Polym. Sci., Part A: Polym. Chem.* 46: 2575–2580. https://doi.org/10.1002/pola.22590.

155 Hua, D., Cheng, K., Bai, R. et al. (2004). *Polym. Int.* 53: 821–823. https://doi.org/10.1002/pi.1525.

156 Yu, Q., Hua, D., Ge, X. et al. (2006). *Polymer* 47: 6575–6580. https://doi.org/10.1016/j.polymer.2006.07.049.

157 Hua, D., Tang, J., Jiang, J., and Zhu, X. (2009). *Polymer* 50: 5701–5707. https://doi.org/10.1016/j.polymer.2009.09.074.

158 Hua, D., Tang, J., Jiang, J. et al. (2009). *Macromolecules* 42: 8697–8701. https://doi.org/10.1021/ma9018334.

159 Yu, Q., Li, X., Tao, Y., and Cheng, G. (2012). *Adv. Mater. Res.* 356–360: 74–77. https://doi.org/10.4028/www.scientific.net/AMR.356-360.74.

160 Yu, Q. and Li, X. (2012). *Adv. Mater. Res. (Durnten-Zurich, Switz.)* 482–484: 1886–1889. https://doi.org/10.4028/www.scientific.net/AMR.482-484.1886.

161 Li, G., Zheng, H., and Bai, R. (2009). *Macromol. Rapid Commun.* 30: 442–447. https://doi.org/10.1002/marc.200800666.

162 Li, G., Wang, H., Zheng, H., and Bai, R. (2010). *J. Polym. Sci., Part A: Polym. Chem.* 48: 1348–1356. https://doi.org/10.1002/pola.23896.

163 Golf, H., O'Shea, R., Braybrook, C. et al. (2018). *Chem. Sci.* 9: 7370–7375. https://doi.org/10.1039/C8SC01862F.

164 Saubern, S., Nguyen, X., Nguyen, V. et al. (2017). *Macromol. React. Eng.* 11: 1600065. https://doi.org/10.1002/mren.201600065.

165 Lewis, R.W., Evans, R.A., Malic, N. et al. (2017). *Polym. Chem.* 8: 3702–3711. https://doi.org/10.1039/C7PY00682A.

166 Wolpers, A., Bergerbit, C., Ebeling, B. et al. (2019). *Angew. Chem. Int. Ed.* 58: 14295–14302. https://doi.org/10.1002/anie.201905629.

167 Rusli, W., Jackson, A.W., and Van Herk, A. (2018). *Polymers* 10: 774. https://doi.org/10.3390/polym10070774.

168 Tarafder, M.T.H., Miah, M.A.J., Howlader, M.B.H. et al. (1989). *J. Bangladesh Chem. Soc.* 2: 73–75.

169 Lai, J.T. and Shea, R. (2006). *J. Polym. Sci., Part A: Polym. Chem.* 44: 4298–4316. https://doi.org/10.1002/pola.21532.

170 Wan, D., Zhou, Q., Pu, H., and Yang, G. (2008). *J. Polym. Sci., Part A: Polym. Chem.* 46: 3756–3765. https://doi.org/10.1002/pola.22722.

171 Shin, S.J., Yu, Y.C., Seo, J.D. et al. (2014). *J. Polym. Sci., Part A: Polym. Chem.* 52: 1607–1613. https://doi.org/10.1002/pola.27160.

172 Uchiyama, M., Satoh, K., and Kamigaito, M. (2015). *Angew. Chem. Int. Ed.* 54: 1924–1928. https://doi.org/10.1002/anie.201410858.
173 Guerre, M., Uchiyama, M., Lopez, G. et al. (2018). *Polym. Chem.* 9: 352–361. https://doi.org/10.1039/C7PY01924F.
174 Christmann, J., Ibrahim, A., Charlot, V. et al. (2016). *ChemPhysChem* 17: 2309–2314. https://doi.org/10.1002/cphc.201600034.
175 Foster, J.C., Radzinski, S.C., Lewis, S.E. et al. (2015). *Polymer* 79: 205–211. https://doi.org/10.1016/j.polymer.2015.10.028.
176 Radzinski, S.C., Foster, J.C., and Matson, J.B. (2015). *Polym. Chem.* 6: 5643–5652. https://doi.org/10.1039/C4PY01567C.
177 Radzinski, S.C., Foster, J.C., Lewis, S.E. et al. (2017). *Polym. Chem.* 8: 1636–1643. https://doi.org/10.1039/C6PY01982J.
178 Moad, G., Mayadunne, R.T.A., Rizzardo, E. et al. (2003). Kinetics and mechanism of RAFT polymerization. In: *Advances in Controlled/Living Radical Polymerization*, ACS Symposium Series, vol. 854 (ed. K. Matyjaszewski), 520–535. Washington, DC: American Chemical Society https://doi.org/10.1021/bk-2003-0854.ch036.
179 Kulkarni, S., Schilli, C., Grin, B. et al. (2006). *Biomacromolecules* 7: 2736–2741. https://doi.org/10.1021/bm060186f.
180 Weber, C., Neuwirth, T., Kempe, K. et al. (2011). *Macromolecules* 45: 20–27. https://doi.org/10.1021/ma2021387.
181 Aoshima, H., Uchiyama, M., Satoh, K., and Kamigaito, M. (2014). *Angew. Chem. Int. Ed.* 53: 10932–10936. https://doi.org/10.1002/anie.201406590.
182 Bergerbit, C., Farías-Mancilla, B., Seiler, L. et al. (2019). *Polym. Chem.* 10: 6630–6640. https://doi.org/10.1039/C9PY01181A.
183 Ilchev, A., Pfukwa, R., Hlalele, L. et al. (2015). *Polym. Chem.* 6: 7945–7948. https://doi.org/10.1039/C5PY01293G.
184 Moad, G., Benaglia, M., Chen, M. et al. (2011). Block copolymer synthesis through the use of switchable RAFT agents. In: *Non-Conventional Functional Block Copolymers*, ACS Symposium Series, vol. 1066 (eds. P. Theato, A.F.M. Kilbinger and E.B. Coughlin), 81–102. Columbus, OH: American Chemical Society https://doi.org/10.1021/bk-2011-1066.ch007.
185 Pullan, N., Liu, M., and Topham, P.D. (2013). *Polym. Chem.* 4: 2272–2277. https://doi.org/10.1039/c3py21151g.
186 Sugihara, S., Kawamoto, Y., and Maeda, Y. (2016). *Macromolecules* 49: 1563–1574. https://doi.org/10.1021/acs.macromol.6b00145.
187 Hornung, C.H., Guerrero-Sanchez, C., Brasholz, M. et al. (2011). *Org. Process Res. Dev.* 15: 593–601. https://doi.org/10.1021/op1003314.
188 Hornung, C.H., Nguyen, X., Kyi, S. et al. (2013). *Aust. J. Chem.* 66: 192–198. https://doi.org/10.1071/CH12479.
189 Oliveira, M., Barbosa, B.S., Nele, M., and Pinto, J.C. (2014). *Macromol. React. Eng.* 8: 493–502. https://doi.org/10.1002/mren.201300175.
190 Abreu, C.M.R., Maximiano, P., Guliashvili, T. et al. (2016). *RSC Adv.* 6: 7495–7503. https://doi.org/10.1039/C5RA21975B.

191 Alagi, P., Hadjichristidis, N., Gnanou, Y., and Feng, X. (2019). *ACS Macro Lett.* 8: 664–669. https://doi.org/10.1021/acsmacrolett.9b00357.
192 Abreu, C.M.R., Mendonça, P.V., Serra, A.C. et al. (2012). *Macromolecules* 45: 2200–2208. https://doi.org/10.1021/ma300064j.
193 Sugihara, S., Yoshida, A., Kono, T.-a. et al. (2019). *J. Am. Chem. Soc.* 141: 13954–13961. https://doi.org/10.1021/jacs.9b06671.
194 Olijve, L.L.C., Hendrix, M.M.R.M., and Voets, I.K. (2016). *Macromol. Chem. Phys.* 217: 951–958. https://doi.org/10.1002/macp.201500497.
195 Kwak, Y. and Matyjaszewski, K. (2008). *Macromolecules* 41: 6627–6635. https://doi.org/10.1021/ma801231r.
196 Fan, L., Jiang, H., Zhang, L. et al. (2015). *RSC Adv.* 5: 31657–31663. https://doi.org/10.1039/C5RA03264D.
197 Zhang, Y., Schröder, K., Kwak, Y. et al. (2013). *Macromolecules* 46: 5512–5519. https://doi.org/10.1021/ma400539s.
198 Jiang, X., Wu, J., Zhang, L. et al. (2014). *Macromol. Rapid Commun.* 35: 1879–1885. https://doi.org/10.1002/marc.201400393.
199 Zhang, W., Zhu, X.L., Cheng, Z.P., and Zhu, J. (2007). *J. Appl. Polym. Sci.* 106: 230–237.
200 Guillaneuf, Y., Couturier, J.-L., Gigmes, D. et al. (2008). *J. Org. Chem.* 73: 4728–4731. https://doi.org/10.1021/jo800422a.
201 Kwak, Y. and Matyjaszewski, K. (2010). *Macromolecules* 43: 5180–5183. https://doi.org/10.1021/ma100850a.
202 Ishizu, K., Khan, R.A., Ohta, Y., and Furo, M. (2004). *J. Polym. Sci., Part A: Polym. Chem.* 42: 76–82. https://doi.org/10.1002/pola.10982.
203 Bertin, D., Couturier, J.L., Gigmes, D. et al. (2009). Method for preparing alkoxyamines by photolysis of dithiocarbamates (Arkema France), WO2006111637A1.
204 Shao, L., Hu, M., Chen, L. et al. (2012). *React. Funct. Polym.* 72: 407–413. https://doi.org/10.1016/j.reactfunctpolym.2012.04.002.
205 Lubnin, A., O'Malley, K., Hanshumaker, D., and Lai, J. (2010). *Eur. Polym. J.* 46: 1563–1575. https://doi.org/10.1016/j.eurpolymj.2010.04.005.
206 Guerre, M., Uchiyama, M., Folgado, E. et al. (2017). *ACS Macro Lett.* 6: 393–398. https://doi.org/10.1021/acsmacrolett.7b00150.
207 Nomura, N., Shinoda, K., Takasu, A. et al. (2013). *J. Polym. Sci., Part A: Polym. Chem.* 51: 534–545. https://doi.org/10.1002/pola.26424.
208 Kwak, Y., Nicolay, R., and Matyjaszewski, K. (2009). *Macromolecules* 42: 3738–3742. https://doi.org/10.1021/ma9005389.
209 Kumru, B. and Bicak, N. (2015). *RSC Adv.* 5: 30936–30942. https://doi.org/10.1039/C5RA02783G.
210 Stace, S.J., Moad, G., Fellows, C.M., and Keddie, D.J. (2015). *Polym. Chem.* 6: 7119–7126. https://doi.org/10.1039/C5PY01021G.
211 Jiang, K., Han, S., Ma, M. et al. (2020). *J. Am. Chem. Soc.* 142: 7108–7115. https://doi.org/10.1021/jacs.0c01016.
212 Skouta, R., Wei, S., and Breslow, R. (2009). *J. Am. Chem. Soc.* 131: 15604–15605. https://doi.org/10.1021/ja9072589.

213 Benaglia, M., Chiefari, J., Chong, Y.K. et al. (2009). *J. Am. Chem. Soc.* 131: 6914–6915. https://doi.org/10.1021/ja901955n.

214 Pan, X., Guo, X., Choi, B. et al. (2019). *Polym. Chem.* 10: 2083–2090. https://doi.org/10.1039/C9PY00110G.

215 Rajput, F., Colantuoni, A., Bayahya, S. et al. (2018). *J. Polym. Sci., Part A: Polym. Chem.* 56: 2445–2457. https://doi.org/10.1002/pola.29219.

216 Stace, S.J., Fellows, C.M., Moad, G., and Keddie, D.J. (2018). *Macromol. Rapid Commun.* 39: 1800228 (9 pp). https://doi.org/10.1002/marc.201800228.

217 Pan, G., Zu, B., Guo, X. et al. (2009). *Polymer* 50: 2819–2825. https://doi.org/10.1016/j.polymer.2009.04.053.

218 Zheng, J., Wang, L., Zeng, X. et al. (2016). *ACS Appl. Mater. Interfaces* 8: 18684–18692. https://doi.org/10.1021/acsami.6b04348.

219 Benaglia, M., Chen, M., Chong, Y.K. et al. (2009). *Macromolecules* 42: 9384–9386. https://doi.org/10.1021/ma9021086.

220 Keddie, D.J., Guerrero-Sanchez, C., Moad, G. et al. (2011). *Macromolecules* 44: 6738–6745. https://doi.org/10.1021/ma200760q.

221 Tselepy, A., Schiller, T.L., Harrisson, S. et al. (2018). *Macromolecules* 51: 410–418. https://doi.org/10.1021/acs.macromol.7b02104.

222 Kitov, P.I., Kotsuchibashi, Y., Paszkiewicz, E. et al. (2013). *Org. Lett.* 15: 5190–5193. https://doi.org/10.1021/ol402315n.

223 Palanisamy, A. and Sukhishvili, S.A. (2018). *Macromolecules* 51: 3467–3476. https://doi.org/10.1021/acs.macromol.8b00519.

224 Guerrero-Sanchez, C., Keddie, D.J., Saubern, S., and Chiefari, J. (2012). *ACS Comb. Sci.* 14: 389–394. https://doi.org/10.1021/co300044w.

225 Dong, H., Zhu, Y., Li, Z. et al. (2017). *Macromolecules* 90: 9295–9306. https://doi.org/10.1021/acs.macromol.7b01784.

226 Liu, X., Chen, J.-Q., Zhang, M. et al. (2019). *J. Polym. Sci., Part A: Polym. Chem.* 57: 1811–1820. https://doi.org/10.1002/pola.29452.

227 BoronMolecular. RAFT Agents. https://www.boronmolecular.com/polymers/raft-polymerisation-technology/ (accessed 6 December 2020).

228 Moad, G., Rizzardo, E., and Thang, S.H. (2010). *Mater. Matters* 5: 2–5.

229 Sigma-Aldrich. RAFT Agents. https://www.sigmaaldrich.com/materials-science/material-science-products.html?TablePage=103936134 (accessed 6 December 2020).

230 Moad, G., Rizzardo, E., and Thang, S.H. (2011). *Strem Chem.* 25: 2–10.

231 Strem Chemicals. RAFT Agent. https://www.strem.com/catalog/family/RAFT+Agent/ (accessed 6 December 2020).

232 An, J., Dai, X., Wu, Z. et al. (2015). *Biomacromolecules* 16: 2444–2454. https://doi.org/10.1021/acs.biomac.5b00693.

233 Dai, X., Chen, X., Zhao, Y. et al. (2018). *Biomacromolecules* 19: 141–149. https://doi.org/10.1021/acs.biomac.7b01316.

234 Mori, H., Sutoh, K., and Endo, T. (2005). *Macromolecules* 38: 9055–9065. https://doi.org/10.1021/ma0509558.

235 Hasegawa, U., van der Vlies, A.J., Simeoni, E. et al. (2010). *J. Am. Chem. Soc.* 132: 18273–18280. https://doi.org/10.1021/ja1075025.

236 Hasegawa, U. and van der Vlies, A.J. (2015). *MedChemComm* 6: 273–276. https://doi.org/10.1039/C4MD00373J.
237 Stadermann, J., Fleischmann, S., Messerschmidt, M. et al. (2009). *Macromol. Symp.* 275–276: 35–42. https://doi.org/10.1002/masy.200950104.
238 Mao, J., Qi, X., Cao, X. et al. (2011). *Chem. Commun.* 47: 4228–4230. https://doi.org/10.1039/C1CC10610D.
239 Mori, H. and Endo, T. (2012). *Macromol. Rapid Commun.* 33: 1090–1107. https://doi.org/10.1002/marc.201100887.
240 Destarac, M., Blidi, I., Coutelier, O. et al. (2012). *ACS Symp. Ser.* 1100: 259–275. https://doi.org/10.1021/bk-2012-1100.ch017.
241 Guinaudeau, A., Mazieres, S., Wilson, D.J., and Destarac, M. (2012). *Polym. Chem.* 3: 81–84. https://doi.org/10.1039/C1PY00373A.
242 Haven, J., Hendrikx, M., Danial, M. et al. (2021). *Polym. Chem.* (to be submitted).
243 Zhang, S., Yin, L., Zhang, W. et al. (2016). *Polym. Chem.* 7: 2112–2120. https://doi.org/10.1039/C6PY00012F.
244 Rajendran Prakash, B. and Raghavachari, D. (2012). *J. Polym. Sci., Part A: Polym. Chem.* 50: 4772–4782. https://doi.org/10.1002/pola.26301.
245 Hu, D. and Zheng, S. (2010). *Polymer* 51: 6346–6354. https://doi.org/10.1016/j.polymer.2010.10.047.
246 Xue, X., Zhu, J., Zhang, Z. et al. (2010). *Polymer* 51: 3083–3090. https://doi.org/10.1016/j.polymer.2010.04.052.
247 Chen, K., Grant, N., Liang, L. et al. (2010). *Macromolecules* 43: 9355–9364. https://doi.org/10.1021/ma101182f.
248 Destarac, M., Bzducha, W., Taton, D. et al. (2002). *Macromol. Rapid Commun.* 23: 1049–1054. https://doi.org/10.1002/marc.200290002.
249 Stamenović, M.M., Espeel, P., Camp, W.V., and Du Prez, F.E. (2011). *Macromolecules* 44: 5619–5630. https://doi.org/10.1021/ma200799b.
250 Nagai, A., Yoshii, R., Otsuka, T. et al. (2010). *Langmuir* 26: 15644–15649. https://doi.org/10.1021/la102597y.
251 Jana, S. and Parthiban, A. (2011). *Macromol. Chem. Phys.* 212: 790–798. https://doi.org/10.1002/macp.201000701.
252 Du, J., Willcock, H., Ieong, N.S., and O'Reilly, R.K. (2011). *Aust. J. Chem.* 64: 1041–1046. https://doi.org/10.1071/CH11131.
253 Wood, M.R., Duncalf, D.J., Rannard, S.P., and Perrier, S. (2006). *Org. Lett.* 8: 553–556. https://doi.org/10.1021/ol0525617.
254 Oae, S., Yagihara, T., and Okabe, T. (1972). *Tetrahedron* 28: 3203–3216. https://doi.org/10.1016/S0040-4020(01)93661-0.
255 Xia, S., Wang, X., Ge, Z.-m. et al. (2009). *Tetrahedron* 65: 1005–1009. https://doi.org/10.1016/j.tet.2008.11.084.
256 Thang, S.H., Chong, Y.K., Mayadunne, R.T.A. et al. (1999). *Tetrahedron Lett.* 40: 2435–2438. https://doi.org/10.1016/S0040-4039(99)00177-X.
257 Bouhadir, G., Legrand, N., Quiclet-Sire, B., and Zard, S.Z. (1999). *Tetrahedron Lett.* 40: 277–280. https://doi.org/10.1016/S0040-4039(98)02380-6.

258 Wang, L. and Benicewicz, B.C. (2017). Raft agents and their use in the development of polyvinylpyrrolidone grafted nanoparticles (University of South Carolina), US9732169B2.

259 Sha, Y., Zhu, Q., Wan, Y. et al. (2016). *J. Polym. Sci., Part A: Polym. Chem.* 54: 2413–2420. https://doi.org/10.1002/pola.28116.

260 Moad, G., Chong, Y.K., Rizzardo, E. et al. (2005). *Polymer* 46: 8458–8468. https://doi.org/10.1016/j.polymer.2004.12.061.

261 Chong, Y.K., Moad, G., Rizzardo, E., and Thang, S.H. (2007). *Macromolecules* 40: 4446–4455. https://doi.org/10.1021/ma062919u.

262 Weber, W.G., McLeary, J.B., and Sanderson, R.D. (2006). *Tetrahedron Lett.* 47: 4771–4774. https://doi.org/10.1016/j.tetlet.2006.04.031.

263 Ramadas, K. and Srinivasan, N. (1995). *Synth. Commun.* 25: 227–234. https://doi.org/10.1080/00397919508010811.

264 Wager, C.M., Haddleton, D.M., and Bon, S.A.F. (2004). *Eur. Polym. J.* 40: 641–645. https://doi.org/10.1016/j.eurpolymj.2003.10.025.

265 Lai, J.T. (2002). *Tetrahedron Lett.* 43: 1965–1967. https://doi.org/10.1016/S0040-4039(02)00159-4.

266 Lai, J.T., Filla, D., and Shea, R. (2002). *Macromolecules* 35: 6754–6756. https://doi.org/10.1021/ma020362m.

267 Coote, M.L. and Henry, D.J. (2005). *Macromolecules* 38: 1415–1433. https://doi.org/10.1021/ma047814a.

268 Coote, M.L., Krenske, E.H., and Izgorodina, E.I. (2008). Quantum-chemical studies of RAFT polymerization: methodology, structure-reactivity correlations and kinetic implications. In: *Handbook of RAFT Polymerization* (ed. C. Barner-Kowollik), 5–49. Weinheim: Wiley-VCH. https://doi.org/10.1002/9783527622757.ch2.

269 Moad, G., Chiefari, J., Krstina, J. et al. (2000). *Polym. Int.* 49: 993–1001. https://doi.org/10.1002/1097-0126(200009)49:9<993::AID-PI506>3.0.CO;2-6.

270 Charmot, D., Chang, H.T., and Li, Y. (2002). Compounds useful for living-type free radical polymerization (Symyx Technologies, Inc.), US6482909.

271 Charmot, D., Chang, H.T., and Huefner, P. (2002). Control agents for living-type free radical polymerization, methods of polymerizing and polymers with same (Symyx Technologies, Inc.), US6380335.

272 Chang, H.T., Charmot, D., and Li, Y. (2003). Compounds useful for living-type free radical polymerization (Symyx Technologies, Inc.), US6518448.

273 Charmot, D. and Piotti, M. (2005). Removal of the thiocarbonylthio or thiophosphorylthio end group of polymers and further functionalization thereof (Symyx Technologies, Inc.), US6919409.

274 Benoit, D., Safir, A., Chang, H.T. et al. (2008). Synthesis of photoresist polymers (Symyx Technologies, Inc.), US7399806.

275 Benoit, D., Safir, A., Chang, H.T. et al. (2007). Synthesis of photoresist polymers (Symyx Technologies, Inc.), US7250475.

276 Blokzijl, W., Carswell, R.J., Charmot, D. et al. (2007). Laundry treatment compositions comprising a polymer with a cationic and polydialkylsiloxane moiety (Unilever Home & Personal Care USA Division of Conopco, Inc.), US7179777.

277 Moad, G., Keddie, D., Guerrero-Sanchez, C. et al. (2015). *Macromol. Symp.* 350: 34–42. https://doi.org/10.1002/masy.201400022.

278 Uchiyama, M., Satoh, K., and Kamigaito, M. (2022). Cationic RAFT polymerization. In: *RAFT Polymerization: Materials, Synthesis and Applications* (eds. G. Moad and E. Rizzardo), 1077–1158. Weinheim: Wiley-VCH.

279 Moad, G., Rizzardo, E., and Thang San, H. (2013). Fundamentals of RAFT polymerization. In: *Fundamentals of Controlled/Living Radical Polymerization*, RSC Polymer Chemistry Series No. 4 (eds. N.V. Tsarevsky and B.S. Sumerlin), 205–249. Cambridge: Royal Society of Chemistry https://doi.org/10.1039/9781849737425-00205.

280 Moad, G. (2014). *Macromol. Chem. Phys.* 215: 9–26. https://doi.org/10.1002/macp.201300562.

281 Krenske, E.H., Izgorodina, E.I., and Coote, M.L. (2006). An ab initio guide to structure–reactivity trends in reversible addition fragmentation chain transfer polymerization. In: *Controlled/Living Radical Polymerization. From Synthesis to Materials*, ACS Symposium Series, vol. 944 (ed. K. Matyjaszewski), 406–420. Washington, DC: American Chemical Society. https://doi.org/10.1021/bk-2006-0944.ch028.

282 Coote, M.L., Krenske, E.H., and Izgorodina, E.I. (2006). *Macromol. Rapid Commun.* 27: 473–497. https://doi.org/10.1002/marc.200500832.

283 Ingale, R.P., Jagtap, R.N., and Adivarekar, R.V. (2016). *J. Adhes.* 92: 236–256. https://doi.org/10.1080/00218464.2015.1022649.

284 Guo, X., Choi, B., Feng, A., and Thang, S.H. (2018). *Macromol. Rapid. Commun.* 39: 1800479. https://doi.org/10.1002/marc.201800479.

285 Kermagoret, A. and Gigmes, D. (2016). *Tetrahedron* 72: 7672–7685. https://doi.org/10.1016/j.tet.2016.07.002.

286 Pearson, S., Thomas, C.S., Guerrero-Santos, R., and D'Agosto, F. (2017). *Polym. Chem.* 8: 4916–4946. https://doi.org/10.1039/C7PY00344G.

287 Le Neindre, M., Magny, B., and Nicolay, R. (2013). *Polym. Chem.* 4: 5577–5584. https://doi.org/10.1039/C3PY00754E.

288 Jiang, X., Liu, Y., Ding, M. et al. (2015). *Macromol. Chem. Phys.* 216: 1171–1179. https://doi.org/10.1002/macp.201500092.

289 Willcock, H. and O'Reilly, R.K. (2010). *Polym. Chem.* 1: 149–157. https://doi.org/10.1039/b9py00340a.

290 Moad, G., Rizzardo, E., and Thang, S.H. (2011). *Polym. Int.* 60: 9–25. https://doi.org/10.1002/pi.2988.

291 Perrier, S., Takolpuckdee, P., and Mars, C.A. (2005). *Macromolecules* 38: 2033–2036. https://doi.org/10.1021/ma047611m.

292 Carmean, R.N., Figg, C.A., Scheutz, G.M. et al. (2017). *ACS Macro Lett.* 6: 185–189. https://doi.org/10.1021/acsmacrolett.7b00038.

293 Charmot, D., Chang, H.T., Wang, W., and Piotti, M. (2006).Cleaving and replacing thio control agent moieties from polymers made by living-type free radical polymerization (Symyx Technologies, Inc.), US7012119B2.

294 Zhang, W., Yan, Y., Zhu, X. et al. (2010). *Macromol. React. Eng.* 4: 264–271. https://doi.org/10.1002/mren.200900056.

295 Destarac, M., Kalai, C., Wilczewska, A. et al. (2006). Various strategies for the chemical transformation of xanthate-functional chain termini in MADIX copolymers. In: *Controlled/Living Radical Polymerization. From Synthesis to Materials*, ACS Symposium Series, vol. 944 (ed. K. Matyjaszewski), 564–577. Washington, DC: American Chemical Society. https://doi.org/10.1021/bk-2006-0944.ch038.

296 Tong, Y.-Y., Dong, Y.-Q., Du, F.-S., and Li, Z.-C. (2009). *J. Polym. Sci., Part A: Polym. Chem.* 47: 1901–1910. https://doi.org/10.1002/pola.23288.

297 Desmet, G.B., D'hooge, D.R., Sabbe, M.K. et al. (2016). *J. Org. Chem.* 81: 11626–11634. https://doi.org/10.1021/acs.joc.6b01844.

298 Zhou, Y., He, J., Li, C. et al. (2011). *Macromolecules* 44: 8446–8457. https://doi.org/10.1021/ma201570f.

299 Legge, T.M., Slark, A.T., and Perrier, S. (2006). *J. Polym. Sci., Part A: Polym. Chem.* 44: 6980–6987. https://doi.org/10.1002/pola.21803.

300 Nair, C.P.R., Clouet, G., and Chaumont, P. (1989). *J. Polym. Sci., Part A: Polym. Chem.* 27: 1795–1809. https://doi.org/10.1002/pola.1989.080270601.

301 Chiefari, J., Chong, Y.K., Ercole, F. et al. (1998). *Macromolecules* 31: 5559–5562. https://doi.org/10.1021/ma9804951.

302 Jesson, C.P., Pearce, C.M., Simon, H. et al. (2017). *Macromolecules* 50: 182–191. https://doi.org/10.1021/acs.macromol.6b01963.

303 Zhang, T. and Palasz, P.D. (2017). Thiocarbonylthio-free RAFT polymers and the process of making the same (Henkel), WO2017027557A1.

304 Pfukwa, R., Pound, G., and Klumperman, B. (2008). *Polym. Prepr. (Am. Chem. Soc., Div. Polym. Chem.)* 49: 117–118.

305 Vega-Rios, A. and Licea-Claverie, A. (2011). *J. Mex. Chem. Soc.* 55: 21–32.

306 Danielson, A.P., Van Kuren, D.B., Lucius, M.E. et al. (2016). *Macromol. Rapid Commun.* 37: 362–367. https://doi.org/10.1002/marc.201500633.

307 Reyhani, A., McKenzie, T.G., Ranji-Burachaloo, H. et al. (2017). *Chem. Eur. J.* 23: 7221–7226. https://doi.org/10.1002/chem.201701410.

308 Zhang, B., Wang, X., Zhu, A. et al. (2015). *Macromolecules* 48: 7792–7802. https://doi.org/10.1021/acs.macromol.5b01893.

309 Shanmugam, S., Xu, J., and Boyer, C. (2017). *Macromolecules* 50: 1832–1846. https://doi.org/10.1021/acs.macromol.7b00192.

310 Nothling, M.D., McKenzie, T.G., Reyhani, A., and Qiao, G.G. (2018). *Macromol. Rapid Commun.* 39: 1800179. https://doi.org/10.1002/marc.201800179.

311 Wang, X.-H., Wu, M.-X., Jiang, W. et al. (2018). *Macromolecules* 51: 716–723. https://doi.org/10.1021/acs.macromol.7b02650.

312 Gilbert, R.G., Hess, M., Jenkins, A.D. et al. (2009). *Pure Appl. Chem.* 81: 351–353. https://doi.org/10.1351/PAC-REC-08-05-02.

12

PhotoRAFT Polymerization

Robert Chapman[1,2], Kenward Jung[3], and Cyrille Boyer[3]

[1] The University of Newcastle, Discipline of Chemistry, Callaghan, NSW 2308, Australia
[2] UNSW Sydney, School of Chemistry, Centre for Advanced Macromolecular Design (CAMD), Sydney, NSW 2052, Australia
[3] UNSW Sydney, School of Chemical Engineering, Centre for Advanced Macromolecular Design (CAMD) and the Australian Centre for Nanomedicine (ACN), Sydney, NSW 2052, Australia

12.1 Introduction

Light is a powerful stimulus providing users with the ability to control in real time when (temporal) and where (spatial) reactions may occur [1, 2]. This powerful capability comes hand in hand with surprising efficiency that is yet to be fully harnessed for chemical syntheses. The rekindling of interest in photochemistry in recent years, which could be attributed to the widespread proliferation of low-cost, narrow-emission light sources, has resulted in the development of a wide range of novel polymerization processes regulated by visible light [3]. By utilizing these less energetic wavelengths, reaction conditions have become even milder, offering new opportunities, particularly in the arena of bioapplications. Moreover, the increased spectral real estate available from the broadening of the usable electromagnetic spectrum holds the promise of realizing orthogonal reactions using light alone [4].

In addition to the intrinsic advantages of exerting spatio-temporal control, reversible addition–fragmentation chain transfer (RAFT) photopolymerizations have gained several interesting new capabilities. From the re-investigation of iniferter chemistry under visible light to the application of photoredox catalysis, the single biggest change is arguably the elimination of hazardous exogenous radical initiators. This change alone significantly increases the safety and atom efficiency of RAFT polymerizations. Additionally, the implementation of photoredox catalysis, when paired with the appropriate co-agents, enables the facile removal of oxygen in situ, thereby avoiding tedious and potentially costly deoxygenation procedures (Figure 12.1). This chapter aims to provide a broad overview on the current state of the art with regard to the use of light to mediate RAFT polymerizations.

RAFT Polymerization: Methods, Synthesis and Applications, First Edition.
Edited by Graeme Moad and Ezio Rizzardo.

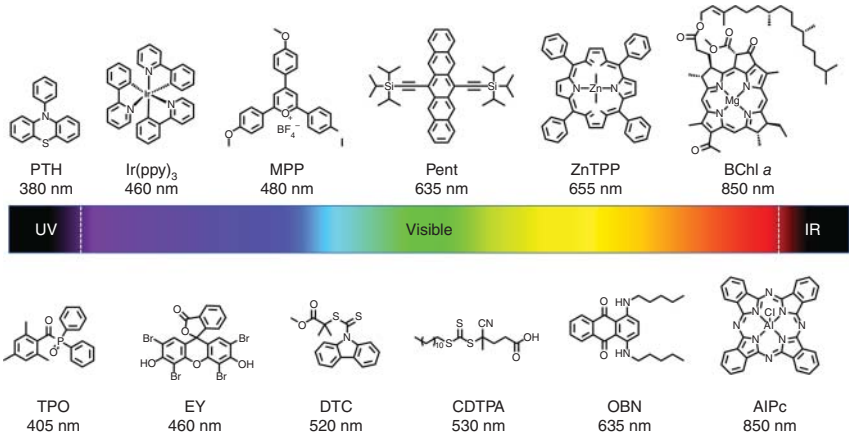

Figure 12.1 Representative chromophores used in light-regulated polymerizations. From left to right, top then bottom, PTH, 10-phenylphenothiazine; $Ir(ppy)_3$, tris[2-phenylpyridinato-C^2,*N*]iridium(III); MPP, 2,4,6-tris(*p*-methoxyphenyl)pyrylium tetrafluoroborate; Pent, 6,13-bis(triisopropylsilylethynyl)pentacene; ZnTPP, 5,10,15,20-tetraphenyl-21*H*,23*H*-porphine zinc; BChl *a*, bacteriochlorophyll *a*; TPO, (2,4,6-trimethylbenzoyl)diphenylphosphine oxide; EY, eosin Y; DTC, methyl 2-((9*H*-carbozole-9-carbonothioyl)thio)-2-methylpropanoate; CDTPA, 4-cyano-4-[(dodecylsulfanylthiocarbonyl)sulfanyl]pentanoic acid; OBN, oil blue N; AlPc, aluminium phthalocyanine. Source: Reproduced with permission from Corrigan et al. [3]. Copyright 2019, John Wiley & Sons.

12.2 Photoinitiation

Light can be used to drive RAFT polymerizations by the creation of a radical propagating centre through energy transfer to one of the chemical components in the system. The simplest mechanism involves creating the radical propagating centre from an initiator, which is external to the RAFT process. This is known as photoinitiation. Once the propagating centre is generated, the polymerization can be controlled by a chain transfer (or RAFT) agent, which is not in itself photo-active. Alternatively, the propagating centre can be formed from the RAFT agent itself, via cleavage of the sulfur–carbon bond between the thiocarbonylthio group and the 'R' group of the chain transfer agent. This second mechanism has come to be known as photoiniferter polymerization, because in these systems the same chemical species acts as both the *ini*tiator of polymerization and a chain trans*fer* agent (*ini-fer*) [5–7].

Photoinitiators have been adopted into RAFT systems from their widespread application in conventional free radical polymerizations, particularly in the field of 3D printing, where rapid polymerizations that can be triggered on demand at room temperature are desirable. Common photoinitiators can be based either on homolytic cleavage of an aromatic carbonyl compound such as benzoin ethers, benzoin ketals, aceto-phenones, or acyl-phosphine oxides (type I photoinitiators) or through bimolecular hydrogen abstraction of an aromatic ketone, benzophenone, or quinone (type II photoinitiators). Type II systems require a second species, typically an amine, to donate a proton to the excited photoinitiator. Most early type I

photoinitiators were only UV active, but the two-component type II systems enabled longer wavelengths in the visible region. Addition of a third component, typically an iodonium salt, to the photoinitiator and amine greatly enhances the speed of initiation [8, 9]. While the precise mechanisms that drive the rate enhancement are still debated in the literature, there is strong evidence that the iodonium salt is able to both oxidize dye radicals back to their ground state for reinitiation and participate itself in photolysis to generate a phenyl-based radical [9–11]. Regardless of the mechanism, three-component (type III) systems such as these do offer a great deal of versatility in the choice of dye, and therefore in the wavelengths of light that can be used. Dyes based on various ketone xanthene, thioxanthene, xanthone, thioxanthone, coumarin, ketocoumarin, thiazine, and merocyanine derivatives have been used in type III systems [8, 9].

Mechanistically, RAFT polymerization initiated by a photoinitiator is no different to one initiated by a thermal free radical initiator such as AIBN. The propagating centre is rapidly transferred across the chain transfer agent by conventional processes and is terminated by combination or disproportionation. As in any RAFT process, for a high degree of control it is important to ensure that the concentration of radicals is low relative to the chain transfer agent, and this can be tuned both by the intensity of the light and the concentration of the photoinitiator.

12.3 Photoiniferter Polymerizations

In contrast to photoinitiated systems, photoiniferter polymerizations generate a radical from the RAFT agent directly, through cleavage of the sulfur–carbon bond between the thioester and the 'R' group [12]. This can be done via direct energy transfer, in which the light causes photolysis of the bond without any additional sensitizer or photocatalyst (PC) (the so-called 'catalyst-free' photoiniferter systems; see Scheme 12.1a) [12–15]. Although typically performed using high-intensity UV, this approach has recently been reported in certain RAFT systems with visible light. Regardless of the wavelength used, such a system will only undergo propagation in the presence of light and will cease the moment the light is switched off. Alternatively, photoiniferter polymerization can be performed using a photocatalyst (PC) to transfer either an electron or energy to the chain transfer agent via an oxidative or reductive quenching cycle, promoting the photolysis of the RAFT agent (Scheme 12.1b,c). In the oxidative cycle (Scheme 12.1b), the excited photocatalyst PC^* is oxidized to $PC^{+\cdot}$ as the chain transfer agent is reduced to $(A–B)^{-\cdot}$. The $PC^{+\cdot}$ is returned to the ground state by re-oxidizing the chain transfer agent $(A–B)^{-\cdot}$ back to (A–B). In the reductive cycle (Scheme 12.1c), an electron donor (D) is added to the system, which transfers an electron to the exited photocatalyst (PC^*) to form $PC^{-\cdot}$, which then reduces the chain transfer agent to $(A–B)^{-\cdot}$ as it returns to its ground state (PC). Both metal-based and non-metallic photocatalysts have been explored for these processes and will be discussed in detail below.

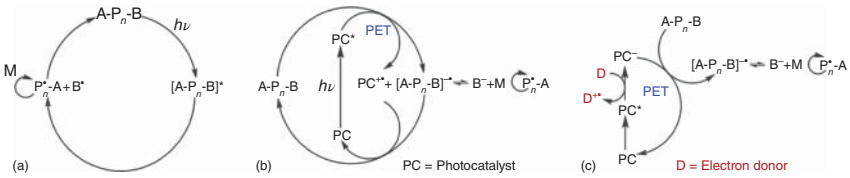

Scheme 12.1 Photomediated controlled/radical polymerization (photo-CRP). (a) Energy transfer to induce bond cleavage, (b) photoredox-catalyzed electron transfer through an oxidative cycle, and (c) photoredox-catalyzed electron transfer through a reductive cycle. Source: Reproduced with permission from Shanmugam et al. [13]. Copyright 2017, John Wiley & Sons.

12.3.1 Catalyst-Free Photoiniferter

There are a number of examples of dithiobenzoate [16], trithiocarbonate [17–23], dithiocarbamate [24–26], xanthate [27, 28], and disulfide [29] chain transfer agents that can be directly photolyzed using high-intensity UV light. This is possible due to the strong absorbance of the thiocarbonylthio group in the 250–350 nm region. Unfortunately, prolonged exposure to this high-energy source can lead to degradation of the chain transfer agent and undesirable side reactions, resulting in loss of control during the polymerization [16, 30–33]. The direct photolysis of trithiocarbonate RAFT agents using visible light was first reported by the Boyer group in 2015, who took advantage of a small amount of absorption in the spectrum of trithiocarbonates at 400–500 nm, corresponding to the spin-forbidden n to π^* transition [34]. Because the energy of the light is lower at this wavelength, less damage to the RAFT agent and fewer side reactions were observed, leading to significantly better control throughout the polymerization. In their original study, four different RAFT agents, 4-cyano-4-[(dodecylsulfanylthiocarbonyl)sulfanyl]pentanoic acid (CDTPA), 2-(dodecylthiocarbonothioylthio)-2-methylpropionic acid (DDMAT), 4-cyanopentanoic acid dithiobenzoate (CPADB), and 2-(*n*-butyltrithiocarbonate) propionic acid (BTPA) (Figure 12.2), were employed in the polymerization of methyl

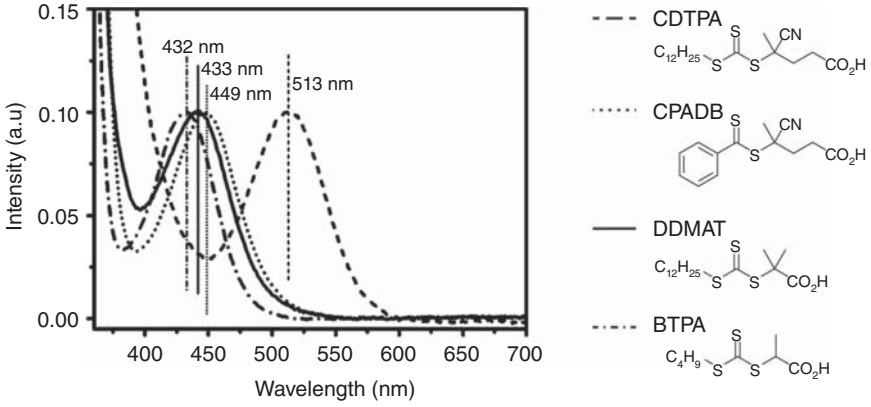

Figure 12.2 Absorption profiles of different RAFT agents in the visible spectrum. Source: Adapted with permission from Xu et al. [34]. Copyright 2015, American Chemical Society.

acrylate (MA) and MMA under blue ($\lambda_{max} = 461$ nm), green ($\lambda_{max} = 530$ nm), and red ($\lambda_{max} = 635$ nm) irradiation.

Both MA and MMA polymerizations were able to proceed under blue light using CDTPA and DDMAT, albeit after long inhibition periods. The polymerization kinetics showed a gradual increase in the concentration of the propagating radical with time, indicating that the photolysis of the carbon–sulfur bond is quite slow [34]. The long inhibition periods were presumed to be due to the time taken to establish the initial RAFT equilibrium, although later studies suggest that these are more likely due to the consumption of oxygen or other impurities in the system [35, 36]. The stability of the carbon–sulfur bond in the RAFT agent and in the macroRAFT agent (after addition of the first few monomer units) is crucial to the success of this approach. If the stability is too high, then polymerization will not proceed. For this reason, under green light irradiation (which has a lower energy than the blue light) only the MMA polymerizations with CDTPA, and not with DDMAT, were able to proceed due to the lower carbon–sulfur bond dissociation energy in CDTPA. Similarly, no conversion was observed in MA polymerizations conducted under green light, due to the higher stability of the carbon–sulfur bond in the MA macroRAFT agent after the first monomer insertion than in the MMA analogue. No polymerization was observed in any of the examples under red light, due to its low energy and the lack of any overlap of this wavelength light with the RAFT agent absorption spectra. The approach is reasonably indiscriminate to solvent or monomer functionality, and the polymerization of a range of methacrylates including glycidyl methacrylate (GMA), dimethylaminoethyl methacrylate (DMAEMA), and 2-hydroxyethyl methacrylate (HEMA) in solvents such as *N*,*N*-dimethylformamide (DMF), acetonitrile (MeCN), dioxane, and toluene has been shown for CDTPA under blue or green light [34]. The degradation of a similar set of trithiocarbonate RAFT agents under blue light ($\lambda_{max} = 460$ nm) was studied in closer detail by Qiao and coworkers, who followed the π to π^* transition of the thiocarbonyl at 305 nm during photolysis (Figure 12.3) [37]. RAFT agents with low fragmentation rates, in which the leaving 'R' group forms a shorter lived primary or secondary radical, were found to rapidly recombine. By contrast, RAFT agents with a tertiary R group and higher rates of fragmentation degraded in the UV–vis experiment. In the presence of monomer, photolysis of these tertiary RAFT agents can lead to a successful RAFT polymerization. The approach is not restricted to methacrylates, and Xiao and coworkers have shown that blue light irradiation of DDMAT with no other photocatalysts can be used to polymerize 2-vinylpyridine in solvents such as ethanol, acetic ether, acetone, methanol, and dimethyl sulfoxide (DMSO) [38]. Qiao and coworkers have extended the concept to polymerize acrylates and acrylamides including MA, 2-hydroxyethyl acrylate (HEA), oligo(ethyleneglycol) acrylate (OEGA), *tert*-butyl acrylate (*t*BA), and *N*-isopropyl acrylamide (NIPAAm) using blue light irradiation of trithiocarbonate RAFT agents [39, 40].

The absorption of the RAFT agent at 400–500 nm can be enhanced by the introduction of *N*-carbazole onto the Z group of the RAFT agent, as shown recently by Poly and coworkers (Figure 12.4a) [41]. This leads to significantly improved

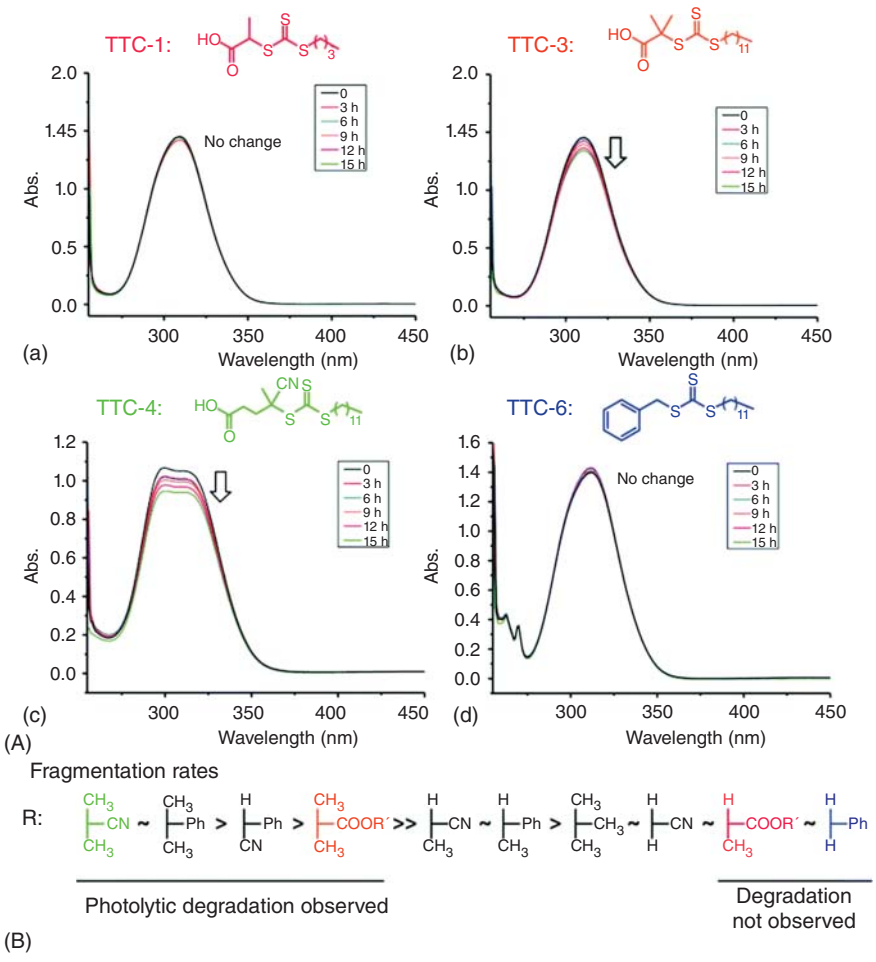

Figure 12.3 UV–vis experiment for degradation of thiocarbonylthio compounds (TTC) upon continuous irradiation (A) and fragmentation rates of RAFT agents (B). Source: Reproduced with permission from McKenzie et al. [37]. Copyright 2016, Royal Society of Chemistry.

kinetics and control over the photoiniferter polymerization in the visible region without the need for any photocatalyst. While they only showed the success of this approach on butyl acrylate, it could likely be extended to less active monomers such as methacrylates and styrenics. Zhu and coworkers have shown similar results using a xanthate ethyl 2-((phenoxycarbonothioyl)thio)propanoate, PXEP), under purple led emission (λ_{max} = 400 nm) for polymerization of butyl acrylate [42], and with a napthalate-bearing RAFT agent (2-cyanoprop-2-yl-1-dithionaphthalate, CPDN) for polymerization of MMA, MA, VAc, and NIPAAm under sunlight (see Figure 12.4b,c) [43]. Oxygen tolerance was achieved in this second system by the introduction of a $Zn_{0.64}Fe_{2.36}O_4$ semiconductor, which could be removed magnetically after polymerization.

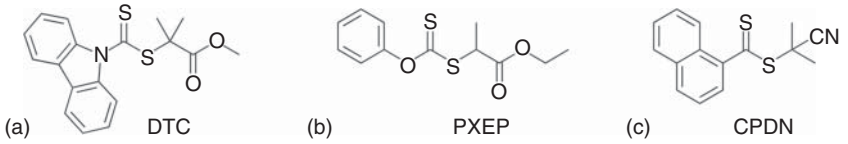

Figure 12.4 Structures of some visible light catalyst-free photoiniferter RAFT agents. (a) DTC [41], (b) PXEP [42], and (c) CPDN [43].

12.3.2 Photoredox Catalysis

The use of photoredox catalysis to drive RAFT polymerization, also known as photoinduced electron/energy transfer (PET)–RAFT polymerization, follows a similar iniferter mechanism to the catalyst-free approaches, through the formation of radicals from the R group of the RAFT agent [34, 44]. However, in a photoredox catalysis the processes of absorption (by the catalyst) and activation (of the RAFT agent) are decoupled. Because photoredox catalysts possess superior photophysical characteristics to the RAFT agent, more efficient RAFT activation yielding better control over the polymerization is possible [45]. Furthermore, judicious selection of the catalyst provides an avenue to extend the activation wavelength further away from the UV, which not only provides milder reaction conditions but also affords opportunities to incorporate latent chromophores, which would have been inevitably activated at more energetic wavelengths [46, 47]. Because many photoredox catalysts also generate singlet oxygen, addition of a singlet oxygen quencher to the reaction can afford the convenience of an oxygen-tolerant process [48].

An interesting discovery in the implementation of various photoredox catalysts for PET–RAFT polymerization has been the apparent existence of RAFT agent selectivity, as summarized in Table 12.1. The transition metal photoredox catalyst *fac*-Ir(ppy)$_3$ is capable of activating trithiocarbonates, dithiobenzoates, and xanthates. At the other end of the spectrum, the metalloporphyrin, 5,10,15,20-tetraphenyl-21*H*,23*H*-porphine zinc (ZnTPP), has presented high specificity towards trithiocarbonates, with poor or no activation of dithiobenzoates and xanthates, respectively [49]. This discovery, in tandem with the specificity of Pheophorbide *a* for a dithiobenzoate RAFT agent, enabled the preparation of complex architectures, which is not possible using conventional RAFT approaches [50]. While more instances of selectivity may exist, the narrow focus of many studies leads this to be an underexplored aspect of PET–RAFT polymerization.

The ease of implementation aided by the availability of light sources has fuelled the continued interest in the PET–RAFT process and new species are consistently added to the growing list of compatible photocatalysts. Just as the seminal work reported the implementation of *fac*-Ir(ppy)$_3$, which was first demonstrated for visible light atom transfer radical polymerization (ATRP), phenothiazine and phenazine organophotocatalysts have also been demonstrated as compatible with the PET–RAFT process [51–53]. Heterogeneous catalysis of the PET–RAFT processes appears to be increasing in frequency, attributable to the potential for facile recycling in comparison to homogeneous photocatalysts [54–59]. This section aims

Table 12.1 RAFT agent compatibility of representative photoredox catalysts for PET–RAFT polymerization.

	RAFT agent compatibility		
Photoredox catalyst	**Trithiocarbonate**	**Dithiobenzoate**	**Xanthate**
fac-Ir(ppy)$_3$[a)]	✓✓✓	✓✓✓	✓✓✓
Ru(bpy)$_3$Cl$_2$[b)]	✓✓✓	✓✓✓	✘
Eosin Y[c)]	✓✓✓	✓	✘
ZnTPP[d)]	✓✓✓	✘	✘

✓✓✓: Excellent activation; ✓: Poor activation; ✘: Inability to activate.
a) Tris[2-phenylpyridinato-C^2,*N*]iridium(III).
b) Tris(bipyridine)ruthenium(II) chloride.
c) 2′,4′,5′,7′-Tetrabromofluorescein.
d) 5,10,15,20-Tetraphenyl-21*H*,23*H*-porphine zinc.

to provide an overview of the major families of photoredox catalysts compatible with the PET–RAFT process with insight into their characteristic properties and capabilities.

12.3.2.1 PET–RAFT with Ir/Ru

Inspired by the work of Hawker and Fors [60], the Boyer group introduced the concept of PET–RAFT polymerization in 2014, using either *fac*-Ir(ppy)$_3$ or the water-soluble Ru(bpy)$_3$Cl$_2$ as photocatalysts to activate RAFT polymerizations [45, 61–63]. These catalysts were proposed to operate via an oxidative reduction cycle (Scheme 12.1b). When excited under blue light irradiation ($\lambda_{max} = 460$ nm) to either $Ir^{(III)*}$ or $Ru^{(III)*}$, both catalysts were able to reduce thiocarbonylthio RAFT agents via electron transfer, cleaving the carbon–sulfur bond to produce the radical leaving group ($P_n^{\cdot}$) and either $Ir^{(IV)}$ or $Ru^{(IV)}$ (Scheme 12.2a). The propagating centre can be deactivated back to the initial state by returning the electron to the $Ir^{(IV)}$ or $Ru^{(IV)}$ species. More recent studies suggest that an energy transfer process mediated by Dexter electron exchange was energetically more favourable when compared to the electron transfer mechanism (Scheme 12.2b) [65, 66]. The Ir(ppy)$_3$-catalyzed system was typified by the combination of fast rates and excellent control, which enable the synthesis of high molecular weight polymers of up to 2×10^6 Da, and multiblock copolymers (up to 10 blocks) by repeated chain extension reactions [45]. Furthermore, Ir(ppy)$_3$ was demonstrated to be compatible with the Lewis acid yttrium(III) trifluoromethanesulfonate (Y(OTf)$_3$) to exert stereotactic control over the polymerization without compromising the livingness [67]. High degrees of isotacticity (>80%) was afforded by the complexation of Y(OTf)$_3$ with *N*,*N*-dimethylacrylamide in mixtures of methanol and toluene.

Although similar in catalytic activity, Ru(bpy)$_3$Cl$_2$ presents additional advantages of lower cost and a broader solubility range. Arising from its water solubility, Ru(bpy)$_3$Cl$_2$ provides well-controlled aqueous polymerizations, including the

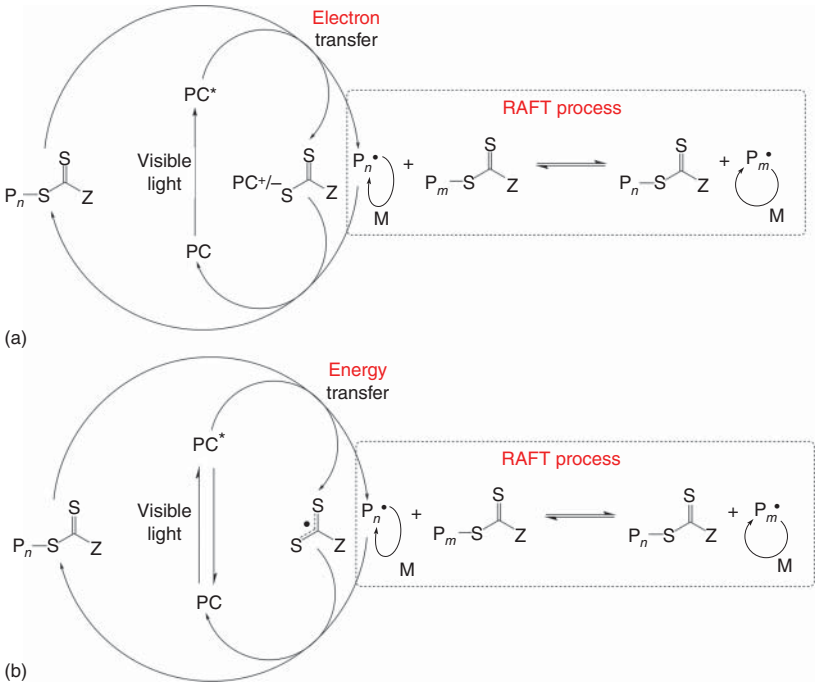

Scheme 12.2 Proposed mechanisms for photoinduced electron/energy transfer–reversible addition–fragmentation chain transfer (PET–RAFT) polymerization in the presence of photocatalyst: (a) electron transfer and (b) energy transfer mechanism. PC, photocatalyst. Source: Reproduced with permission from Corrigan et al. [64]. Copyright 2016, Royal Society of Chemistry.

ability to 'graft-from' bovine serum albumin with almost complete preservation of the esterase activity [63]. Notably, these early studies revealed the interesting and highly advantageous capability to perform polymerizations in the presence of air [45, 62]. Polymerizations mediated by $Ir(ppy)_3$ and $Ru(bpy)_3Cl_2$ in the presence of air differed from deoxygenated experiments only by the presence of an initial induction period wherein it was proposed that ground-state oxygen (O_2) was converted to superoxide ($O_2^{\cdot -}$). In hindsight, the oxygen-tolerant capabilities of these photocatalysts likely stems from the photosensitized conversion of ground-state oxygen to singlet oxygen ($^1O_2$) and subsequent trapping by the solvent DMSO [68].

12.3.2.2 PET–RAFT with Porphyrins

Following the successful implementation of the transition metal photoredox catalysts, $Ir(ppy)_3$ and $Ru(bpy)_3Cl_2$, a more economic species capable of operating under longer wavelengths was sought. Inspired by the photosynthetic capabilities of plants, chlorophyll was investigated for its ability to regulate the PET–RAFT process. Chlorophyll *a* (Chl *a*) extracted from spinach leaves was demonstrated as a capable photocatalyst enabling controlled polymerizations of (meth)acrylates and (meth)acrylamides under blue ($\lambda = 430$ nm) and red ($\lambda = 665$ nm) lights [69]. The crude extract of Chl *a* was also demonstrated as an equally capable photocatalyst

[70]. Except for a longer induction period in comparison to the purified Chl *a*, the crude extract provided similarly excellent control over the polymerization, with the additional advantage of degradation under prolonged light exposure. Further extension of the activation wavelength was achieved through the use of Bacteriochlorophyll *a* (Bachl *a*) [71]. Extracted from bacteria living in deep sea vents, the far-red ($\lambda = 780$ nm) and near-infrared (NIR) ($\lambda = 850$ nm) absorptions of Bachl *a* provided photo-regulated polymerizations at unprecedented wavelengths. Furthermore, the enhanced penetrative capabilities of NIR light enabled polymerizations to proceed through translucent paper barriers.

Upon identification of chlorophyll as a photocatalyst capable of regulating the PET–RAFT process, studies were initiated into the implementation of synthetic metalloporphyrins. From an initial screening of Zn, Ni, Co, and Fe(III) metallated tetraphenylporphyrins (TPPs), only ZnTPP was capable of activating trithiocarbonate RAFT agents [49]. Critically, the broad absorption spectra of ZnTPP enables polymerization under wavelengths that span from blue ($\lambda = 460$ nm) to red ($\lambda = 635$ nm), with the highest rates occurring under yellow ($\lambda = 570$ nm) light. In comparison to the abovementioned chlorophyll photocatalysts, the significantly superior photostability of ZnTPP, coupled with their superior singlet oxygen generation, permits polymerizations under open air conditions (Scheme 12.3).

Oxygen tolerance in PET–RAFT is facilitated by the photosensitized formation of $^1O_2$, which can be subsequently trapped by the solvent, DMSO (Scheme 12.3), or other singlet oxygen quenchers such as ascorbic acid, limonene, or 9,10-dimethylanthracene [48, 72]. The ability to eliminate oxygen in this way has enabled the relatively straightforward implementation of PET–RAFT in flow [68]. Flow systems not only provide enhanced light penetration due to narrower optical path lengths but also provide an avenue to facile scale up with the additional capability of tailoring molecular weight distributions [73, 74].

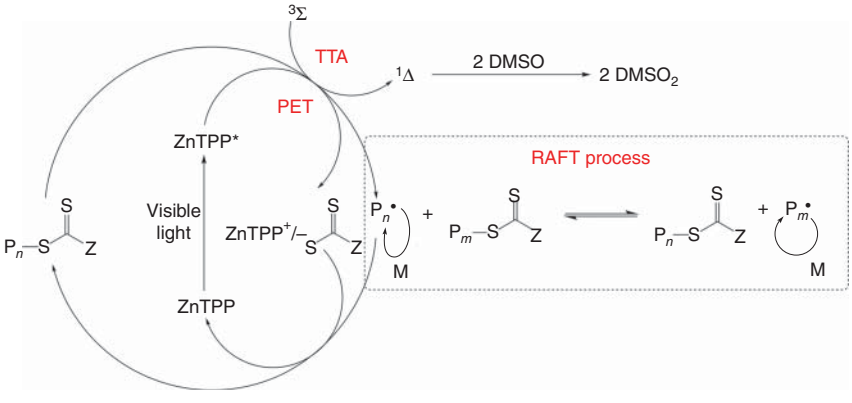

Scheme 12.3 Proposed mechanism for ZnTPP-mediated PET–RAFT polymerization in the presence of oxygen. $^3\Sigma$, ground state oxygen; $^1\Delta$, singlet oxygen; TTA, triplet–triplet annihilation; DMSO, dimethyl sulfoxide; $DMSO_2$, dimethyl sulfone. Source: Reproduced with permission from Corrigan et al. [68]. Copyright 2016, American Chemical Society.

As one of the most widely studied macrocycles, porphyrins as a class of photocatalysts possess abundant avenues to vary their photophysical characteristics. A donor–acceptor strategy was used to overcome the poor activation of PET–RAFT polymerization in the presence of metal-free TPP [15]. By conjugating a RAFT agent via the Z-group functionality to a mono-hydroxylate TPP, significantly faster polymerizations, in comparison to the use of free TPP, were observed under green (λ = 530 nm) and red (λ = 635 nm) lights. Aqueous polymerizations using a water-soluble zinc porphyrin have also been reported. Zn(II) *meso*-tetra(4-sulfonatophenyl) porphyrin ($ZnTPPS^{4-}$) was shown to provide well-controlled aqueous polymerizations under red (λ = 635 nm) light at pH 8.6 [75]. However, with decreasing pH, the rate was observed to slow down, with polymerization being suppressed at pH ~ 3. This capability was used to demonstrate a dual-gated activation system wherein polymerization could be reversibly paused by turning off the light or acidifying the reaction mixture. Conversely, reactivation of the polymerization required both resumption of irradiation and pH ~ 7–8. Aqueous PET–RAFT polymerizations utilizing $ZnTPPS^{4-}$ could also be made oxygen tolerant via the addition of ascorbic acid as a singlet oxygen quencher [76].

More recently, the Boyer group reported a peculiar porphyrin photocatalyst, which possessed the property of only facilitating polymerization in the presence of oxygen [77]. Zinc(II) (2,3,7,8,12,13,17,18-octaethyl-5,10,15,20-tetraphenylporphyrin) (ZnOETPP), by virtue of its dense functionalization, adopts a distorted conformation, enabling the absorption of lower energy wavelengths in the far-red (λ = 685 nm) region. Surprisingly, polymerization only proceeds in the presence of a tertiary amine species, such as triethylamine, and oxygen; polymerization was suppressed in inert gases such as nitrogen or carbon dioxide. Conversely, in the presence of pure oxygen, as opposed to air, the polymerization rate was observed to accelerate. This capability was used to demonstrate a gas-gated polymerization wherein the (de)activation could be readily switched by bubbling with the appropriate gas (Figure 12.5).

As synthetic analogues of porphyrins, phthalocyanines are another class of macrocycles that have been widely studied for their photoactive properties. In addition to their more straightforward synthesis in comparison to porphyrins, phthalocyanines are attractive for their strongly absorbing Q-band peak in the far-red (λ > 650 nm) region. However, due to their difficulty in forming π-cation radicals compared to porphyrins, phthalocyanines are unable to directly reduce the RAFT agent for PET–RAFT polymerization. Nevertheless, phthalocyanines are attractive chromophores for enabling polymerizations mediated by NIR wavelengths.

In an initial study, aluminium phthalocyanine (AlPc) was found to facilitate polymerizations in the presence of the solvent *N*-methyl-2-pyrrolidone under red and NIR (λ = 780 and 850 nm) lights [78]. Radical generation was proposed to occur via oxidation of axially ligated solvent molecules, which then propagated under RAFT control. The activation of peroxides to generate radicals was recently demonstrated to facilitate faster polymerizations under far-red (λ = 680 nm) and NIR (λ = 780 and 850 nm) lights using AlPc and aluminium napthalocyanine

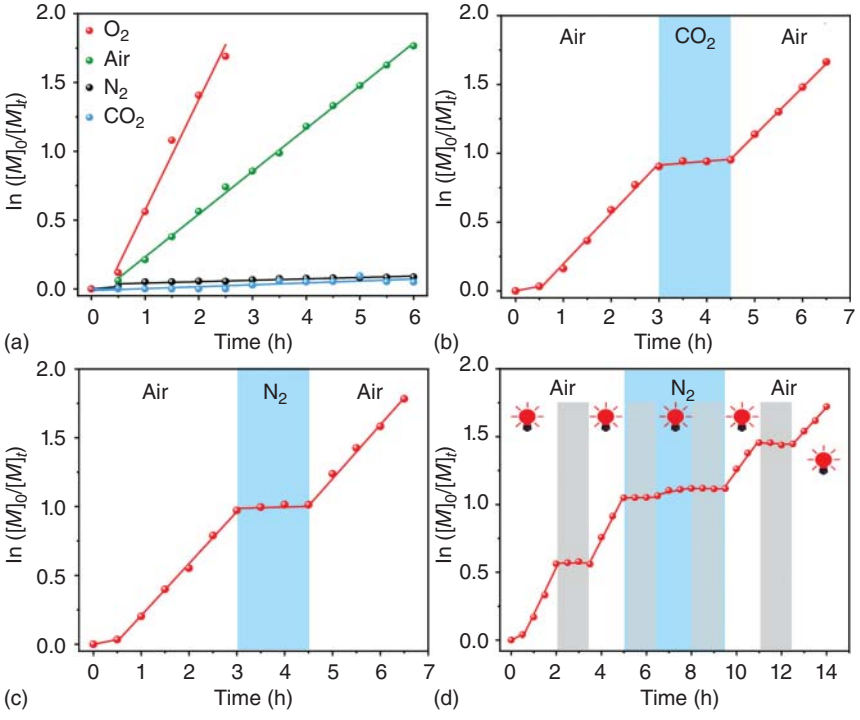

Figure 12.5 Gas-controlled temporal control of ZnOETPP-mediated PET–RAFT polymerization of methyl acrylate in DMSO. (a) Plot of $\ln([M]_0/[M]_t)$ in pure O_2, Air, N_2, and CO_2; ON/OFF control induced by injecting (b) CO_2 or (c) N_2; (d) demonstration of dual-gated temporal control induced by both injecting N_2 and switching the light ON/OFF. Source: Reproduced with permission from Zhang et al. [77]. Copyright 2019, John Wiley & Sons.

(AlNc) respectively [79]. Critically, the efficiency of this initiation system facilitated polymerizations through thick barriers such as paper (0.2 mm), chicken skin (1.0 mm), and pig skin (15.0 mm). Furthermore, owing to their narrow absorptions, these phthalocyanines could be combined with other photocatalysts possessing complementary absorptions to enable more efficient utilization of broadband emissions, such as sunlight, for concurrent macromolecule and organic synthesis in segregated vessels (Figure 12.6).

12.3.2.3 Metal-Free Photocatalysts

Since the inception of the PET–RAFT process, a major research focus has been the discovery and implementation of metal-free photocatalysts. Although undoubtedly effective, the high cost of transition metal catalysts, together with their potential toxicity, limits their wide-scale adoption or commercialization. To this end, a variety of organo-photocatalysts, including 10-phenylphenothiazine (PTH) [51, 52, 80], *N*,*N*-diaryl dihydrophenazines [53], bismuth oxide (Bi_2O_3) [58], zinc oxide (ZnO) [57], graphitic carbon nitride (g-C_3N_4) [54, 81], and carbon dots [55] have been successfully reported to mediate the PET–RAFT process. Most works pertaining to

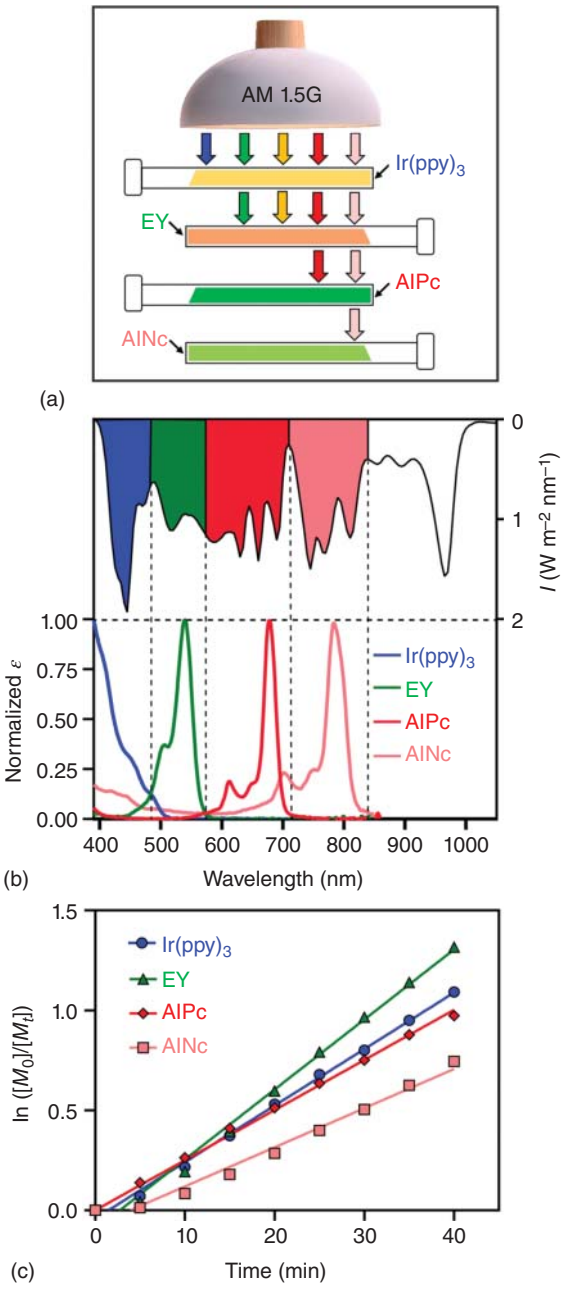

Figure 12.6 (a) Scheme depicting layered photocatalysts in the order (top to bottom) of *fac*-Ir(ppy)$_3$ (λ_{max} = 390 nm), eosin Y (λ_{max} = 540 nm), AlPc (λ_{max} = 678 nm), and AlNc (λ_{max} = 783 nm) irradiated by simulated sunlight (AM 1.5G). (b) Spectral comparison of broadband solar emission (AM 1.5G) and the normalized absorptions of the layered photocatalysts. (c) Comparison of layered photopolymerization kinetics mediated simultaneously under a broadband solar emission (AM 1.5G) by different photocatalysts. Source: Reproduced with permission from Wu et al. [79]. Copyright 2020, John Wiley & Sons.

metal-free PET–RAFT polymerizations have revolved around the use of xanthene dyes, which are widely accessible and possess strong absorptions that extend further into the visible spectrum in comparison to the aforementioned catalysts.

Of the xanthene dyes, Eosin Y (EY) has undoubtedly received the most attention with regard to facilitating PET–RAFT polymerization under metal-free conditions

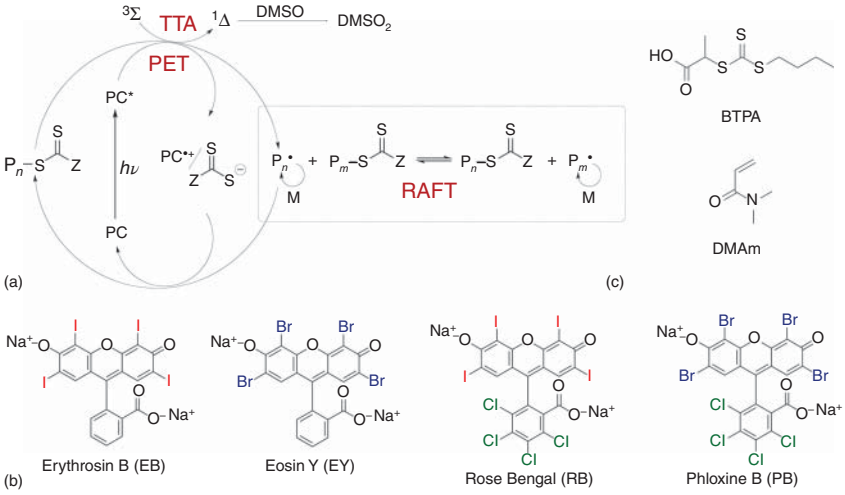

Scheme 12.4 (a) Proposed mechanism of oxygen-tolerant PET–RAFT polymerization mediated by (b) xanthene dyes and (c) the model RAFT agent (BTPA) and monomer (*N*,*N*-dimethylacrylamide). $^3\Sigma$, ground-state oxygen; $^1\Delta$, singlet oxygen; TTA, triplet–triplet annihilation; DMSO, dimethyl sulfoxide; $DMSO_2$, dimethyl sulfone. Source: Reproduced with permission from Wu et al. [82]. Copyright 2018, American Chemical Society.

(Scheme 12.4) [83]. Mediated by blue ($\lambda = 460$ nm) light, EY enabled activation of a dithiobenzoate for the polymerization of methacrylates via an oxidative quenching cycle. Critically, through the addition of a tertiary amine species, as a sacrificial electron donor, the process is transformed into a reductive quenching cycle with the ability to polymerize in the presence of oxygen. Further investigations into the mechanism of EY-mediated PET–RAFT revealed that the direct photolysis of trithiocarbonate RAFT agents can occur under blue light irradiation [84]. Control over molecular weight was best achieved through the use of an oxidative pathway under green light, which removed the potential activation of the trithiocarbonates via the iniferter pathway.

Oxygen tolerance in xanthene-mediated PET–RAFT can also be accessed via the addition of ascorbic acid. The use of EY or Rose Bengal in conjunction with ascorbic acid can promote dark polymerization, wherein oxygen contained in the reaction mixture is quickly converted into hydrogen peroxide during a short exposure period ($t = 5$–45 minutes) [85]. Thereafter, the slow reduction of hydrogen peroxide into hydroxyl radicals by ascorbic acid enables polymerization to occur even in the absence of sustained light exposure. The same photochemistry has also been exploited to enable controlled polymerizations at ultralow volumes under sustained irradiation [86].

The aqueous solubility of xanthene dyes is an advantage that has been exploited for the preparation of bioconjugates. Sumerlin and coworkers utilized EY in conjunction with a tertiary amine species to successfully graft water-soluble acrylates and acrylamides from trithiocarbonate-functionalized lysozyme under blue light [87]. Notably, fast polymerizations were observed even at high dilutions, signifying the efficiency of the polymerization mechanism. More recently, Weil and coworkers

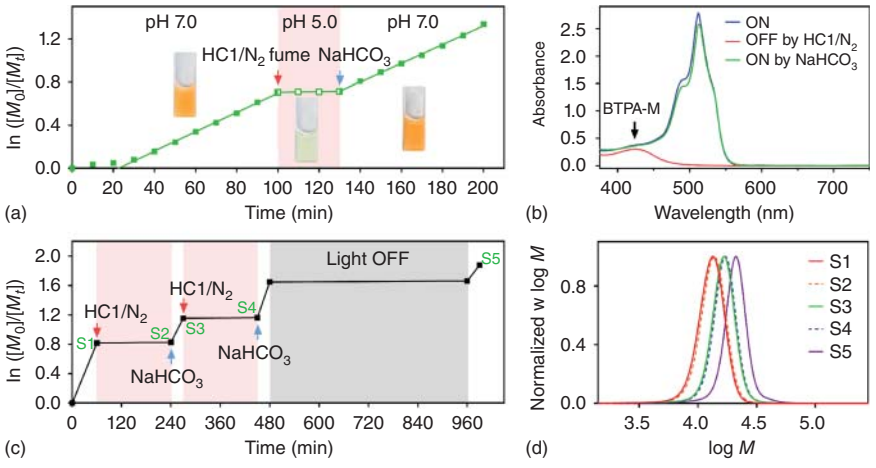

Figure 12.7 pH-controlled temporal control of tetrabrominated benzoic fluorescein (TBrFL)-mediated PET–RAFT polymerization of *N*,*N*-dimethylacrylamide in water and in the presence of oxygen under green light. (a) Plot of $\ln([M]_0/[M]_t)$ wherein acidification (HCl fumes) induces a colour-to-colourless transition to pause the polymerization. Reverting to neutral pH via the addition of base ($NaHCO_3$) reactivates the system by returning the colour of the TBrFL photocatalyst. (b) Corresponding UV–vis spectra of the different coloured/colourless states in (a). (c) Demonstration of temporal control exerted using both pH and light. (d) Molecular weight distributions of samples taken during the kinetic experiment presented in (c). Source: Adapted with permission from Wu et al. [89]. Copyright 2019, American Chemical Society.

reported DNA–polymer conjugates prepared by an approach that was mediated by EY in conjunction with ascorbic acid [88]. However, poor control was noted and was attributed to potential chain transfer reactions to the single-stranded DNA sequence.

With the successful application of EY, the effect of halogen substituents on the photophysical and electrochemical properties of xanthene dyes in the context of PET–RAFT polymerization was examined [82]. This theoretical framework paved the way for the discovery of a xanthene catalyst with an accessible pH-switch (Figure 12.7) [89]. Although commercially available xanthene dyes possess such transitions, they usually occur at prohibitively acidic conditions (pH < 2). Under neutral conditions (pH = 7) the 'new' photocatalyst retained its colour to enable polymerization to proceed. However, under slightly acidic conditions (pH = 5), the catalyst became colourless and therefore was unable to absorb the incident wavelength, resulting in cessation of polymerization.

12.4 Applications

12.4.1 Single Unit Monomer Insertion (SUMI)

One of the advantages of photoRAFT over other forms of controlled radical polymerization is the access it enables to new types of polymers. Light is a very versatile medium – it is possible to precisely control its delivery not only with respect to time

and space but also with respect to energy. Chemical processes can be selectively activated by light of different energies, enabling orthogonal reactions within a single system to be controlled.

One area where this might become important is in the field of sequence-controlled polymers. The ability to precisely define the monomer sequence in a polymer chain has long been a dream of polymer chemists. Except for carbohydrates, such control is present in all of nature's macromolecules – DNA, RNA, and proteins – and is critical to their folding and function. From a tiny set of monomeric building blocks (just 5 nucleobases and 20 canonical amino acids) comes the entire function of biology because of the precision with which their arrangement in the polymer chain can be defined. Even a single out of place amino acid or nucleobase can lead to dramatic changes to the conformational structure in solution. The complexity of protein synthesis is possible thanks to the ribosome. This machine uses DNA to template the position of amino acid monomers such that they react in the desired order to form the protein chain. By contrast, controlled radical polymers are built in solution by a stochastic process and even the most well-controlled systems show some dispersity of molecular weight and architecture. It is very difficult to imagine how we might build any molecular machinery that would mimic the ribosome in a radical polymerization given our current chemical toolkit.

A wide range of strategies for achieving sequence control in synthetic polymers have been proposed, although it would be fair to say that no approach has been completely successful to date [90]. Multiblock copolymers are one way to achieve a form of sequence control in controlled radical polymerization. In this case, polymerization is performed with a single monomer at a relatively low target degree of polymerization (perhaps 5–10 units) and driven to full monomer conversion before addition of the next monomer. Reinitiation of the polymerization causes chain extension with this monomer, and after repetition of the process enough times a polymer with a defined sequence of blocks can be obtained. Polymers with up to 21 blocks have been demonstrated by a variety of controlled radical polymerization techniques [91–98], including photoRAFT [99]. The order of units in the backbone comes from the sequence of monomer addition. However, in the absence of any templating, controlled radical polymerizations such as these will always be stochastic in nature, and so the length of each block will always have a distribution. Worse than this, as the length of each block is reduced, or the number of blocks increased, there will be a growing proportion of polymer chains with missing blocks. The maths, as demonstrated by Harrisson and coworkers, shows that even under ideal conditions 5% of chains in each chain extension reaction will fail to reinitiate if the targeted block length is equal to or less than 3, such that after 18 chain extensions the majority of chains will be missing at least one block [100]. If the targeted block length is doubled to 6, the situation is greatly improved, but 5% of chains will still be missing at least one block after 20 chain extensions. One way around this problem is to isolate the desired product from the stochastic mixture produced at each step, and although the groups of both Hawker and Junkers have shown very workable methodologies for this, the physical challenge of performing a purification at every step remains [101, 102]. Another alternative is to build up polymers by sequential click reactions,

rather than via a radical polymerization, but even these often require intermediate purification steps [103–106].

Even with only this brief background to the field, the power of single unit monomer insertion (SUMI) reactions should become evident. In the ideal case, such a reaction would cause the reinitiation of all chains but halt the reaction after the first monomer addition to each chain. This would eliminate all distribution in the system – every chain would have precisely one monomer unit attached and could be reinitiated with the next desired monomer. In RAFT, the character of the C—S bond on the R group side of the RAFT agent changes after addition of the first monomer. Before activation, the sulfur is connected to the carbon of the R group, and after addition of the first monomer it is connected to the monomer unit. This should result in slightly different bond strength. If we use light rather than a free radical initiator to activate this bond it should be possible to tune the energy of the light to cause cleavage in the case of the RAFT agent, but not after addition of the first monomer. This was first shown by the Boyer group in collaboration with Moad and Hawker's groups, using the PET–RAFT system (Figure 12.8).

Investigations were initiated by the discovery that the catalyst pheophorbide *a*, which selectively activated the dithiobenzoate RAFT agent, CPADB, could not facilitate the polymerizations of monomers that generated secondary propagating radicals [50]. Rather, polymers were only formed in the presence of methacrylic monomers, which generated tertiary propagating species. In the case of acrylate, acrylamido, and styrenic monomers, it was found that the single unit adduct of the RAFT agent could not be reactivated by the catalyst because of the change in C—S bond strength from a tertiary carbon to a secondary carbon.

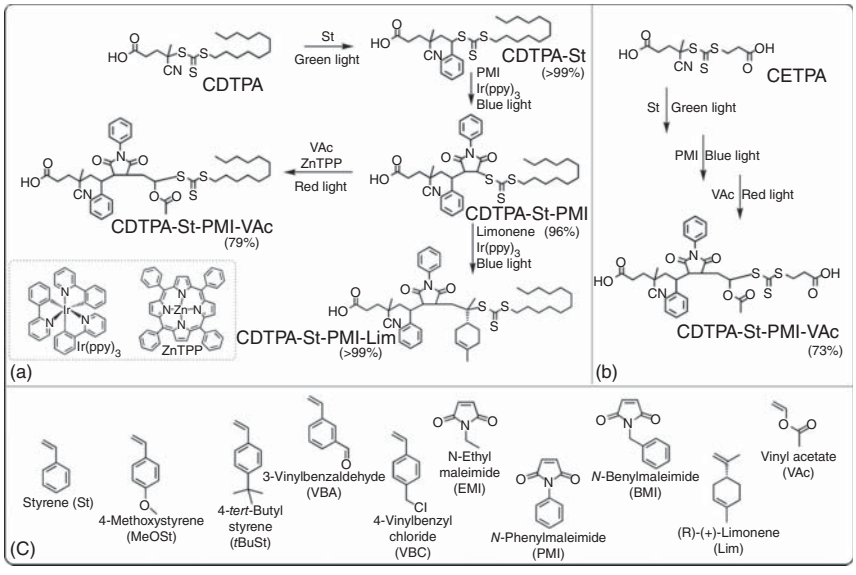

Figure 12.8 Synthetic strategy for the preparation of sequence-defined trimers. (a) Monofunctional trimer, (b) difunctional trimer, and (c) investigated monomers. Source: Reproduced with permission from Xu et al. [107]. Copyright 2017, John Wiley & Sons.

Advancement to the preparation of trimers was made possible by adapting this strategy to trithiocarbonate RAFT agents (Figure 12.8) [107]. The lability of the tertiary C—S bond in CDTPA under green light provided a single unit monomer adduct of styrenic monomers, which could not progress further due to the absence of catalyst and low propagation rate constant of the monomer at room temperature. Addition of the transition metal photoredox catalyst, *fac*-Ir(ppy)$_3$, could facilitate reactivation of the single unit monomer adduct and in the presence of maleimido monomers, which cannot homopolymerize, provided a dimeric species. Thereafter, the C—S bond was reactivated by the metalloporphyrin, ZnTPP, to insert either vinyl acetate or limonene as monomers that could not be polymerized by ZnTPP and trithiocarbonates. In this manner, sequence-defined trimers were successfully synthesized.

More recently, the reactivity of the radical generated from the PET process was exploited for the preparation of pentamers [108]. Indene and maleimido monomers incapable of homopolymerization were selected for an alternating insertion strategy. Critically, due to the electron-accepting qualities of maleimides, preparation of a maleimido mono-adduct required the starting trithiocarbonate RAFT agent to possess an electron-donating R group. Conversely, the electron-donating capabilities of indene necessitated a trithiocarbonate RAFT agent possessing an electron-accepting cyano-isopropyl R group. Successive PET-mediated cleavage by the metalloporphyrin ZnTPP facilitated alternating insertions of maleimido and indene monomers up to pentamers with the main limitation to achieving higher lengths being the purification of the products for each addition step. Interestingly, the insertion of the cyclic maleimido and indene monomers was found to be *trans* only resulting in oligomers that were both sequence controlled and stereospecific.

12.4.2 Wavelength Orthogonal Polymerization

The broad range of catalyst families demonstrated for the PET–RAFT enables the process to be activated by wavelengths along the entire visible electromagnetic spectrum and even into the NIR region. Arising from the narrow and distinct absorption spectra between different catalyst families and other chromophores, there is an opportunity to perform orthogonal reactions in a single pot by utilizing two different photocatalysts with distinct photophysical and photochemical characteristics.

One example is the photocatalyst pheophorbide *a* (PheoA), which has been shown to selectively activate the dithiobenzoate RAFT agent CPADB in the presence of trithiocarbonate BTPA during methacrylate PET–RAFT polymerizations under red light (λ_{max} = 690 nm) [50]. The selectivity arises from the secondary R-group of BTPA, which disfavours addition of the tertiary methacrylic propagating radical-facilitated selective polymerization. This selectivity was exploited to polymerize a trithiocarbonate-functionalized methacrylate monomer, BTPEMA (2-(2-(*n*-butyltrithiocarbonate)-propionate)ethyl methacrylate) and subsequently polymerize MA from the pendant trithiocarbonate functionalities under green light (λ_{max} = 530 nm) through ZnTPP, affording a graft copolymer (PMMA-*r*-BTPEMA)-*g*-PMA in a single reaction vessel (Scheme 12.5).

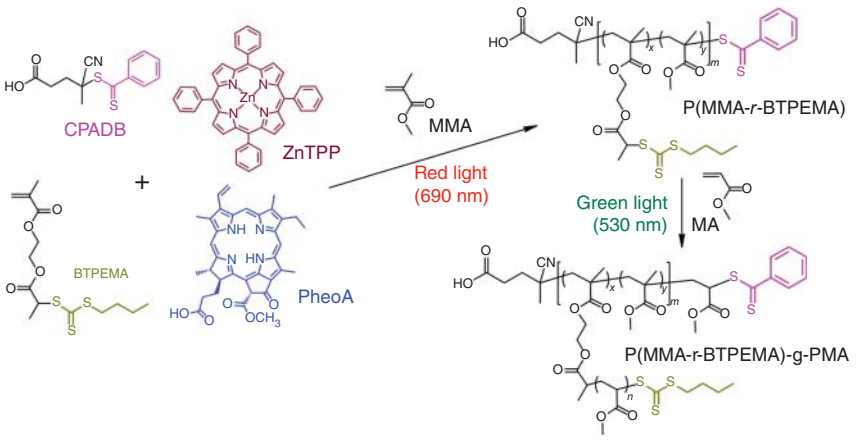

Scheme 12.5 Selective photoactivation of thiocarbonylthio compounds with SUMI reactions and PET–RAFT polymerization. Source: Reproduced with permission from Xu et al. [50]. Copyright 2016, American Chemical Society.

In another example, wavelength-orthogonal ring-opening polymerization (ROP) and PET–RAFT polymerization was achieved through the combination of a merocyanine-based photoacid and ZnTPP [109]. Specifically, merocyanine undergoes photoinduced cyclization under blue light ($\lambda = 460$ nm, 0.7 mW cm^{-2}) to release a proton capable of catalyzing the ROP of cyclic esters. Combining this blue light-mediated ROP with ZnTPP mediated PET–RAFT of acrylates enabled a one-pot orthogonal polymerization that was switchable between ROP (blue light) and PET–RAFT (red light).

The extended absorption and efficient photocatalysis of ZnTPP has invited further investigation of its use in conjunction with orthogonally absorbing chromophores. *o*-Nitrobenzyl functionalities are a common photo-protecting group that undergo photocleavage under UV irradiation (300–365 nm), which prohibits their usage in conjunction with most conventional photoinitiators. By employing yellow ($\lambda = 560$ nm) and red ($\lambda = 635$ nm) light, ZnTPP successfully mediated the PET–RAFT polymerization of *o*-nitrobenzyl methacrylate, enabling the facile preparation of UV-sensitive polymers [46]. More recently, the water-soluble ZnTPP analogue, zinc *meso*-tetra(*N*-methyl-4-pyridyl) porphine tetrachloride (ZnTPMPyP), afforded successful polymerization of a coumarin-functionalized methacrylamide under red light ($\lambda = 595$ nm)-mediated dispersion conditions [47]. Various morphologies such as micelles, worms, and vesicles were produced via polymerization-induced self-assembly (PISA); the coumarin moieties in the hydrophobic core enabled facile cross-linking under UV irradiation ($\lambda = 365$ nm) to fix the morphologies.

12.4.3 High-Throughput Polymer Libraries

In addition to enabling access to more complex polymers, photoRAFT techniques are usually very practical methods for obtaining regular controlled radical polymers.

They can be performed at room temperature, and the temporal control afforded by the light enables reactions to be turned off and on at will. Many of the photocatalytic systems discussed in this chapter enable polymerization in the presence of oxygen and in volumes as low as 10–20 μl. All these features make photoRAFT well suited to the preparation of high-throughput (HTP) polymer libraries. HTP techniques have been used extensively to map out structure–function relationships of small-molecule drug candidates in the pharmaceutical industry [110, 111]. The potential chemical landscape for a small-molecule scaffold is often too vast, and the biological interactions too complicated, to rationally design a drug from the ground up. Computational methods and in silico screening have improved library design in recent years, but this has been seen as a complement to, rather than a replacement for, experimental screening [112]. HTP techniques have also been widely applied to develop new materials, particularly in the fields of solar energy, batteries, inorganic materials, catalysis, and nanomaterials [113, 114]. Polymers are natural candidates for HTP techniques [115, 116]. HTP libraries of controlled radical polymers traditionally required glove box-bound automated synthesizers and dedicated degassed solvent lines, severely limiting widespread adoption and use [117–121]. By contrast, oxygen-tolerant polymerizations can be performed on multi-well plates in the open atmosphere, enabling library synthesis in low volume (<40 μl) with simple automated pipetting systems [122]. This dramatically simplifies the process and removes many of the technical barriers. PET–RAFT [123–126], eosin-Y [86], and a few other photoRAFT systems [42, 127] have been used to prepare polymer libraries on well plates without any degassing steps, and these have been applied to begin to map out structure–property relationships for lectin-binding polymers [123], antimicrobial polymers [125–127], haemotoxic polymers [127], and in PISA [86]. We anticipate that oxygen-tolerant photoRAFT techniques will be increasingly applied to investigate structure–property relationships for controlled radical polymers in a wide range of fields.

Take, for example, our own work studying lectin-binding polymers, which applied a porphyrin-catalyzed PET–RAFT system to the synthesis of star-shaped polymer libraries on 384 well plates [123]. By using zinc tetraphenyl porphyrin (ZnTPP) as the photocatalyst, very high tolerance to oxygen was achieved. This is because of the high quantum yield this catalyst has for the conversion of triplet to singlet oxygen, which is subsequently trapped by the solvent (DMSO) as $DMSO_2$. While a few previous reports had shown oxygen-tolerant controlled/radical polymerization (CRP) in water, none had worked in purely organic solvents [128–130]. Both of these features are highly advantageous. (i) The high oxygen tolerance enables polymerization at a wide range of DPs in very low volume and low concentrations without worrying about effects from oxygen, and (ii) by working in DMSO rather than water as a solvent we could prepare star-shaped polymers with reactive ester handles, which had not been previously accessible. By post-polymerization modification of these scaffolds bioactive functionality could be easily installed in a HTP manner. We applied this system to prepare star-polymers functionalized with mannose to probe the relationships between a polymers structure and its binding strength to the lectin *Concanavalin A* (*ConA*); see Figure 12.9. This class of carbohydrate-binding

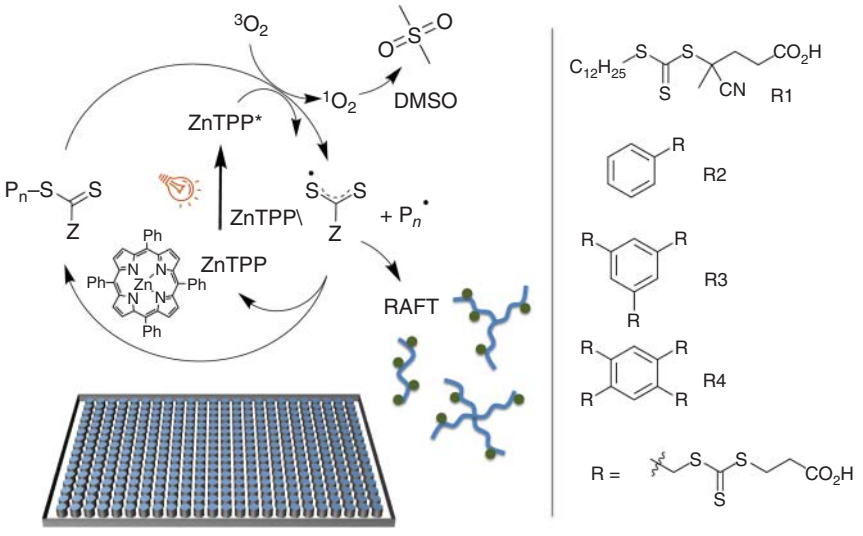

Figure 12.9 Representation showing the ZnTPP polymerization mechanism and RAFT agents used in the library design. Source: Reproduced with permission from Gormley Adam et al. [123]. Copyright 2018, John Wiley & Sons.

proteins are important recognition units in the body, controlling cellular communication pathways, the binding of bacteria and viruses, and uptake of nanoparticles. Our libraries showed that the polymer–protein binding affinity was the strongest for the three-arm star polymers. It was found to increase with size (DP) relative to polymer molarity, but relative to the total mannose concentration smaller polymers had the stronger affinity.

HTP polymer libraries have also been recently applied in the development of antimicrobial polymers. Such polymers are designed to break open the cell membrane in order to destroy the cell and take advantage of the fact that most bacterial membranes are more negatively charged than their mammalian equivalents for their selectivity. Because they disrupt the membranes via a physical process and not by blocking a receptor or the action of the ribosome, it is very difficult for bacteria to develop resistance. It is hoped that this might enable the design of a new class of drugs able to target multi-drug resistant strains. Most effective antimicrobial polymers contain some mixture of hydrophobicity (which aids insertion into the lipophilic membrane), some degree of positive charge (to target the negatively charged membrane surface), and some degree of hydrophilicity (to enable overall solubility in water). Their activity relies on the structural conformation they adopt in solution, but unlike the antimicrobial peptides they aim to mimic [125], the rules governing their conformational folding are not well understood.

In a recent work from the Boyer group, libraries of antimicrobial copolymers were prepared using a HTP PET–RAFT approach to study the effect of polymer architecture and composition on gram-negative *Pseudomonas aeruginosa*, *Acinetobacter baumannii*, and *Escherichia coli*; and gram-positive *Staphylococcus aureus*, as well as *Mycobacterium smegmatis* [125, 126]. Haemolysis was performed as a control to

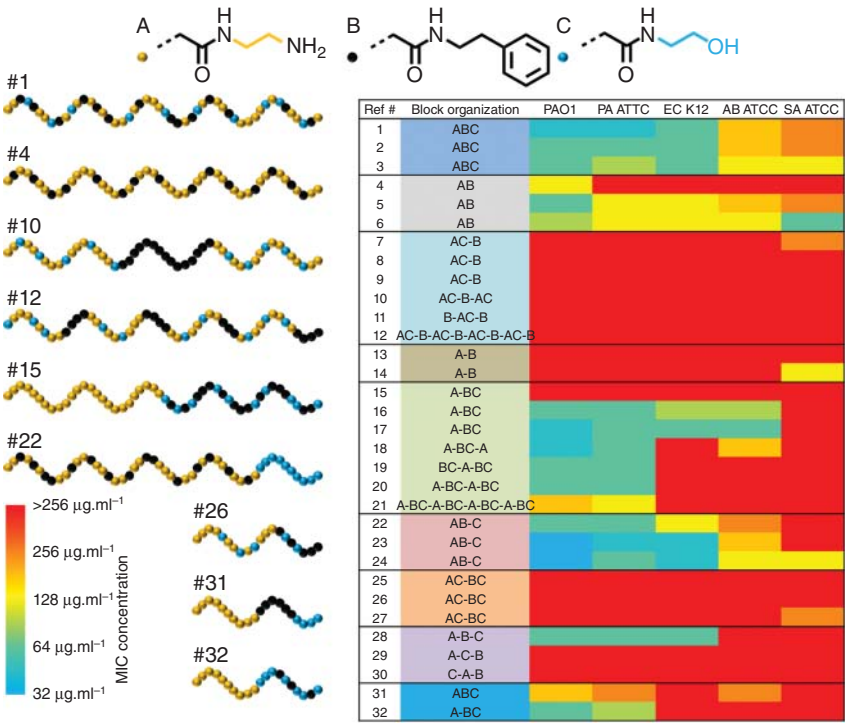

Figure 12.10 Heat map of MICs for all polymers synthesized in this study where the selection of polymer structures from each family is shown. The bacterial strains are *Pseudomonas aeruginosa* PAO1 and ATCC 27853 strains, *Escherichia coli* K12 strain, *Acinetobacter baumannii* ATCC 19606 strain, and *Staphylococcus aureus* ATCC 29213 strain. Source: Reproduced with permission from Judzewitsch et al. [125]. Copyright 2018, John Wiley & Sons.

determine the mammalian cell compatibility. In the first study, 32 polymers were prepared with the same overall monomer composition but different architectures (blocks vs. various mixtures of random copolymers) (Figure 12.10) [125]. Monomers based on the amino acids lysine, phenylalanine, and serine were chosen to impart cationic, hydrophobic, and hydrophilic character to the polymer respectively. Both the antimicrobial and haemolytic activity were found to be dependent on the distribution of monomers within blocks, and bacteria genus specificity could be tuned via polymer block order and to a lesser extent via combined modulation of polymer chain length. In the second study, the library was expanded to 120 polymers comparing three different amine functionalities across a range of compositional formulations [126]. Primary amines were found to work best against gram-negative *P. aeruginosa*, while quaternary ammonium provided better activity against *M. smegmatis*. Leveraging a slightly different photoRAFT system, originally developed by Qiao and coworkers [131], the Gibson group have performed similar studies towards the development of antimicrobial polymers [127]. Using a Gilson Pipetmax 268 liquid-handling robot, they were able to prepare a library of 108 cationic statistical copolymers from DMAEMA and eight different co-monomers

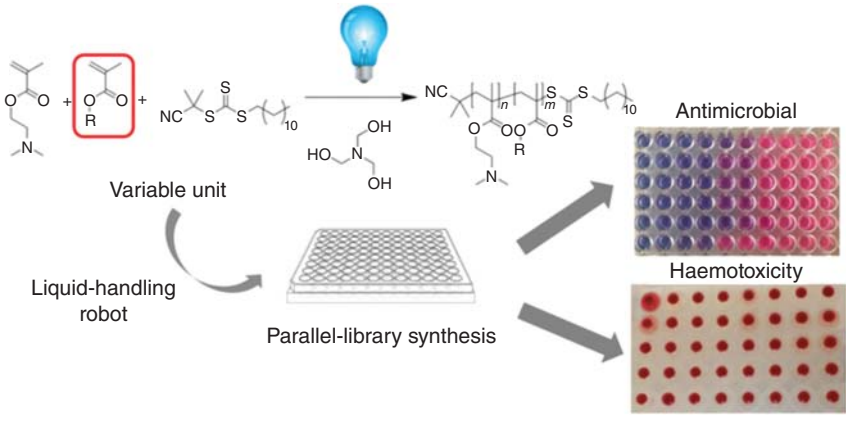

Figure 12.11 Schematic showing the HTP RAFT synthesis of amine-containing antimicrobial polymers in well-plates. Source: Reproduced with permission from Richards et al. [127]. Copyright 2018, John Wiley & Sons.

with four concentrations of either hydrophobic or hydrophilic substituents (5, 10, 15, 20 mol%) in 96 well plates (Figure 12.11). The polymers were then screened for antimicrobial and haemotoxic activity. Using automation and HTP size exclusion chromatography (for polymer characterization) significantly streamlines both the synthetic and analytical processes. A number of hits were identified, including one copolymer with propylene glycol side chains, which showed significantly enhanced antimicrobial activity.

These few examples give a taste for the power of HTP polymer chemistry, which is only just beginning to be leveraged. Lessons learnt from combinatorial work in the small-molecule space will be valuable moving forward. Even with HTP polymer synthesis techniques it is impossible to sample the entirety of the available chemical space, and so these need to be paired with some form of rational experimental design. However, where structure–property relationships are not well defined they should be very helpful in mapping out the key parameters.

12.4.4 Hydrogels and 3D Printing

Light is a very widely used medium for curing both hydrogels and 3D printed materials. It is typically used either to photoinitiate a free radical polymerization in the presence of a vinylic crosslinker or to catalyze click reactions between two pre-prepared polymers, such as between a polyethylene glycol (PEG) dithiol and multi-armed PEG-maleimide or PEG-norbornene. Compared to other sources of initiation, light affords excellent spatial resolution, so polymerization can be driven only in the desired voxels. It can trigger the rapid generation of large quantities of radicals, enabling rapid curing times. In addition, because the wavelength can be so finely tuned, orthogonal functionality can be very easily polymerized into the material. For these reasons many 3D printers, whether extrusion or stereolithographic in design, are already designed to be cured using light. Many researchers have

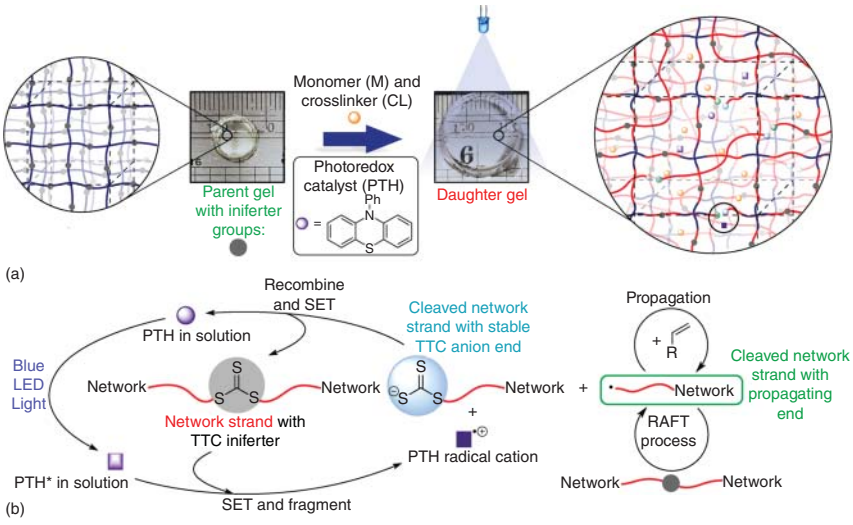

Figure 12.12 Polymer network structure from PRCG via photoredox catalysis using PTH under blue light irradiation [132]. (a) Photoredox catalyzed growth (PRCG) of polymer gels, (b) PRCG mechanism. Source: Reproduced with permission from Chen et al. [132]. Copyright 2017, American Chemical Society.

taken advantage of this to 3D print controlled polymer scaffolds using photoRAFT systems, giving them access to highly functional and adaptable materials.

Johnson and coworkers were among the first to use a photoredox catalyst to produce a 'living' hydrogel [132]. They prepared 'parent' hydrogels using well-established strain-promoted azide–alkyne cycloaddition (SPAAC) chemistry, from a four arm PEG-dibenzocyclooctyne (tetra-DBCO-PEG) and a bis-azide RAFT agent (bis-N_3-thiocarbonylthio compound [TTC]). Because of the inclusion of the RAFT agent within the network, when these parent gels were swollen with monomer and the redox photocatalyst PTH [51, 133], the PTH could be used to catalyze the controlled radical chain extension at the RAFT agent junctions to expand the hydrogel network (Figure 12.12). By introducing additional crosslinker monomers in this chain extension step the stiffness of the daughter hydrogel could be modulated. The group were able to perform this chain extension using a range of monomers including NIPAAm, OEGMA, and *n*BA. Daughter gels could also be welded together through polymerization to afford self-healing gels, and gels with spatially heterogeneous chemistries.

12.4.5 Live Cell Graft Polymerizations

The mild conditions provided by visible light-mediated RAFT polymerizations have been attractive for the preparation of polymer-modified biomaterials. In particular, the modification of proteins with polymers via a grafting-from PET–RAFT approach has been investigated in the works of Boyer and coworkers [63], Sumerlin and coworkers [87], and Averick and coworkers [134]. More recently, the use of

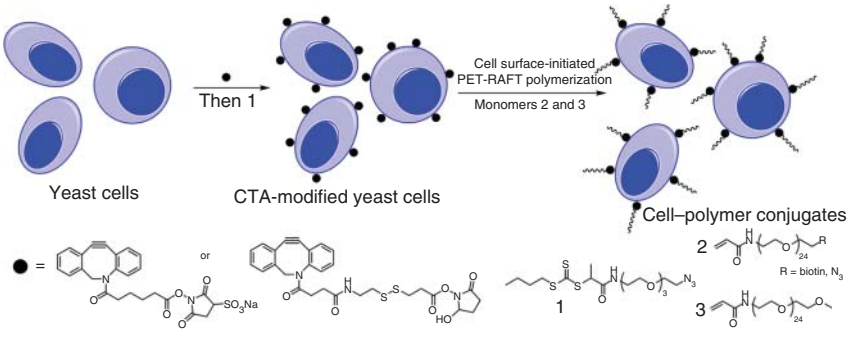

Figure 12.13 PET–RAFT mediated polymerization initiated from the surface of yeast cells. Source: Reproduced with permission from Messina et al. [137]. Copyright 2020, Elsevier.

PET–RAFT was extended to the preparation of DNA–polymer conjugates and bioactive peptide brush polymers [88, 135]. Save for the initial report by Boyer, which utilized the transition metal catalyst $Ru(bpy)_3Cl_2$, the common thread among these works has been the use of the xanthene dye, EY, as the photoredox catalyst. Its water solubility, low cost, and availability make it an accessible photocatalyst that has been proved to be effective for the preparation of biomaterials with preserved activities.

Perhaps the greatest demonstration of biocompatibility of EY-mediated PET–RAFT was the modification of live cell surfaces by Soh and coworkers [136]. PEG-based acrylamides were grafted-from *Saccharomyces cerevisiae* (Baker's yeast) cells using optimized conditions to generate polymer-grafted yeast cells in under five minutes of blue LED ($\lambda = 465\,nm$, $5.0\,mW\,cm^{-2}$) irradiation. Cleavage of the attached polymers confirmed the controlled nature of the process. More importantly, high viability of the modified yeast cells was confirmed by flow cytometry together with an unchanged growth curve when compared to wild-type cells. Following confirmation of the process's remarkable biocompatibility, polymer modification was extended to human Jurkat cells. Poor cell viability, which was reasoned to occur from covalent modification, was rectified by utilizing a lipid-modified RAFT agent that was inserted into the cell membrane and led to polymer-modified mammalian cells with approximately 90% of the cells confirmed as being metabolically active (Figure 12.13).

12.5 Conclusions and Outlook

The visible light-mediated regulation of RAFT processes has undoubtedly created exciting new opportunities. The accessibility of low-cost and narrow-emission light sources has inextricably fuelled its development and this availability will continue to increase the proliferation of these techniques. The ability to stop and start reactions at will in combination with easy access to oxygen tolerance no doubt makes for an attractive proposition for non-specialists. In this vein, a critical area of investigation is in the effective scale up of these light-mediated processes. Indeed, the longer

optical path lengths demanded by larger volumes result in inhomogeneities in irradiation intensity, leading to broad molecular weight distributions and other undesirable effects. The narrow optical path lengths offered by flow chemistry is a potential answer to this problem and has the added benefit of enabling continuous operation. Photoredox catalysis has emerged as an effective tool in regulating many polymerizations. An ongoing area of research is undoubtedly the development of more effective photocatalysts. Increasing the accessibility through decreased costs and broader capabilities needs to be addressed for wide-scale proliferation of this technology. Additionally, a route to facile catalyst recycling is another area that must also be addressed. At the other end of the spectrum, photoredox catalysis has unveiled the potential to exert more selective control over photopolymerizations, enabling the realization of sequence control through SUMI reactions and the potential for implementing orthogonal polymerizations in single pot by simply switching between different wavelengths. In a relatively short period, a broad range of catalysts with exciting properties have been discovered and hints at the potential of what remains unseen. Considering these potential gains, the future is bright for photopolymerizations.

References

1 Jung, K., Corrigan, N., Ciftci, M. et al. (2020). Designing with light: advanced 2D, 3D, and 4D materials. *Adv. Mater.* 32 (18): 1903850.

2 Chatani, S., Kloxin, C.J., and Bowman, C.N. (2014). The power of light in polymer science: photochemical processes to manipulate polymer formation, structure, and properties. *Polym. Chem.* 5 (7): 2187–2201.

3 Corrigan, N., Yeow, J., Judzewitsch, P. et al. (2019). Seeing the light: advancing materials chemistry through photopolymerization. *Angew. Chem.* 131 (16): 5224–5243.

4 Corrigan, N., Ciftci, M., Jung, K., and Boyer, C.A.J.M. (2019). Mediating reaction orthogonality in polymer and materials science. *Angew. Chem. Int. Ed.* 59: 2–36.

5 Chen, M., Zhong, M., and Johnson, J.A. (2016). Light-controlled radical polymerization: mechanisms, methods, and applications. *Chem. Rev.* 116 (17): 10167–10211.

6 Zivic, N., Bouzrati-Zerelli, M., Kermagoret, A. et al. (2016). Photocatalysts in polymerization reactions. *ChemCatChem* 8 (9): 1617–1631.

7 Dadashi-Silab, S., Doran, S., and Yagci, Y. (2016). Photoinduced electron transfer reactions for macromolecular syntheses. *Chem. Rev.* 116 (17): 10212–10275.

8 Padon, K.S. and Scranton, A.B. (2000). A mechanistic investigation of a three-component radical photoinitiator system comprising methylene blue, *N*-methyldiethanolamine, and diphenyliodonium chloride. *J. Polym. Sci., Part A: Polym. Chem.* 38 (11): 2057–2066.

9 Shao, J., Huang, Y., and Fan, Q. (2014). Visible light initiating systems for photopolymerization: status, development and challenges. *Polym. Chem.* 5 (14): 4195–4210. https://doi.org/10.1039/C4PY00072B.

10 Cook, W.D. and Chen, F. (2015). Polymer chemistry dimethacrylates with the three component system. *Polym. Chem.* 6: 1325–1338.

11 Mousawi, A.A., Garra, P., Sallenave, X. et al. (2018). π-Conjugated dithienophosphole derivatives as high performance photoinitiators for 3D printing resins. *Macromolecules* 51 (5): 1811–1821.

12 Allegrezza, M.L., DeMartini, Z.M., Kloster, A.J. et al. (2016). Visible and sunlight driven RAFT photopolymerization accelerated by amines: kinetics and mechanism. *Polym. Chem.* 7 (43): 6626–6636.

13 Shanmugam, S., Xu, J., and Boyer, C. (2017). Photocontrolled living polymerization systems with reversible deactivations through electron and energy transfer. *Macromol. Rapid Commun.* 38 (13, SI): 1700143.

14 Skrabania, K., Miasnikova, A., Bivigou-Koumba, A.M. et al. (2011). Examining the UV–vis absorption of RAFT chain transfer agents and their use for polymer analysis. *Polym. Chem.* 2 (9): 2074–2083.

15 Xu, J., Shanmugam, S., and Boyer, C. (2015). Organic electron donor–acceptor photoredox catalysts: enhanced catalytic efficiency toward controlled radical polymerization. *ACS Macro Lett.* 4 (9): 926–932.

16 Quinn, J.F., Barner, L., Barner-Kowollik, C. et al. (2002). Reversible addition–fragmentation chain transfer polymerization initiated with ultraviolet radiation. *Macromolecules* 35 (20): 7620–7627.

17 Ran, R., Wan, T., Gao, T. et al. (2008). Controlled free radical photopolymerization of styrene initiated by trithiocarbonate. *Polym. Int.* 57 (1): 28–34.

18 Zhou, H. and Johnson, J.A. (2013). Photo-controlled growth of telechelic polymers and end-linked polymer gels. *Angew. Chem. Int. Ed.* 52 (8): 2235–2238.

19 Lu, L., Yang, N., and Cai, Y. (2005). Well-controlled reversible addition–fragmentation chain transfer radical polymerisation under ultraviolet radiation at ambient temperature. *Chem. Commun.* 42: 5287–5288.

20 Carmean, R.N., Becker, T.E., Sims, M.B., and Sumerlin, B.S. (2017). Ultra-high molecular weights via aqueous reversible-deactivation radical polymerization. *Chem* 2 (1): 93–101.

21 Singh, A., Kuksenok, O., Johnson, J.A., and Balazs, A.C. (2016). Tailoring the structure of polymer networks with iniferter-mediated photo-growth. *Polym. Chem.* 7 (17): 2955–2964.

22 Muthukrishnan, S., Pan, E.H., Stenzel, M.H. et al. (2007). Ambient temperature RAFT polymerization of acrylic acid initiated with ultraviolet radiation in aqueous solution. *Macromolecules* 40 (9): 2978–2980.

23 You, Y.-Z., Hong, C.-Y., Bai, R.-K. et al. (2002). Photo-initiated living free radical polymerization in the presence of dibenzyl trithiocarbonate. *Macromol. Chem. Phys.* 203 (3): 477–483.

24 Lalevée, J., Blanchard, N., El-Roz, M. et al. (2008). New photoiniferters: respective role of the initiating and persistent radicals. *Macromolecules* 41 (7): 2347–2352.

25 Yasutake, M., Andou, Y., Hiki, S. et al. (2004). Controlled radical polymerization of vaporized vinyl monomers on solid surfaces under UV irradiation. *Macromol. Chem. Phys.* 205 (4): 492–499.

26 Kwak, Y. and Matyjaszewski, K. (2010). Photoirradiated atom transfer radical polymerization with an alkyl dithiocarbamate at ambient temperature. *Macromolecules* 43 (12): 5180–5183.

27 Khan, M.Y., Cho, M.-S., and Kwark, Y.-J. (2014). Dual roles of a xanthate as a radical source and chain transfer agent in the photoinitiated RAFT polymerization of vinyl acetate. *Macromolecules* 47 (6): 1929–1934.

28 Ham, M.-k., HoYouk, J., Kwon, Y.-K., and Kwark, Y.-J. (2012). Photoinitiated RAFT polymerization of vinyl acetate. *J. Polym. Sci., Part A: Polym. Chem.* 50 (12): 2389–2397.

29 Lalevée, J., El-Roz, M., Allonas, X., and Fouassier, J.P. (2007). Controlled photopolymerization reactions: the reactivity of new photoiniferters. *J. Polym. Sci., Part A: Polym. Chem.* 45 (12): 2436–2442.

30 Moad, G. and Barner-Kowollik, C. (2008). The mechanism and kinetics of the RAFT process: overview, rates, stabilities, side reactions, product spectrum and outstanding challenges. In: *Handbook of RAFT Polymerization* (ed. C. Barner-Kowollik), 51–104. Wiley-VCH Verlag GmbH & Co. KGaA.

31 Zhang, H., Deng, J., Lu, L., and Cai, Y. (2007). Ambient-temperature RAFT polymerization of styrene and its functional derivatives under mild long-wave UV–vis radiation. *Macromolecules* 40 (26): 9252–9261.

32 Wang, H., Li, Q., Dai, J. et al. (2013). Real-time and in situ investigation of "living"/controlled photopolymerization in the presence of a trithiocarbonate. *Macromolecules* 46 (7): 2576–2582.

33 Lu, L., Zhang, H., Yang, N., and Cai, Y. (2006). Toward rapid and well-controlled ambient temperature RAFT polymerization under UV–vis radiation: effect of radiation wave range. *Macromolecules* 39 (11): 3770–3776.

34 Xu, J., Shanmugam, S., Corrigan, N.A., and Boyer, C. (2015). Catalyst-free visible light-induced RAFT photopolymerization. In: *Controlled Radical Polymerization: Mechanisms*, *ACS Symposium Series*, vol. 1187 (eds. K. Matyjaszewski, B.S. Sumerlin, N.V. Tsarevsky and J. Chiefari), 247–267. American Chemical Society.

35 McLeary, J.B., Calitz, F.M., McKenzie, J.M. et al. (2005). A 1H NMR investigation of reversible addition–fragmentation chain transfer polymerization kinetics and mechanisms. Initialization with different initiating and leaving groups. *Macromolecules* 38 (8): 3151–3161.

36 McLeary, J.B., Calitz, F.M., McKenzie, J.M. et al. (2004). Beyond inhibition: a 1H NMR investigation of the early kinetics of RAFT-mediated polymerization with the same initiating and leaving groups. *Macromolecules* 37 (7): 2383–2394.

37 McKenzie, T.G., Costa, L.P.d.M., Fu, Q. et al. (2016). Investigation into the photolytic stability of RAFT agents and the implications for photopolymerization reactions. *Polym. Chem.* 7 (25): 4246–4253.

38 Luo, J., Li, M., Xin, M. et al. (2016). Visible light induced RAFT polymerization of 2-vinylpyridine without exogenous initiators or photocatalysts. *Macromol. Chem. Phys.* 217 (16): 1777–1784.

39 McKenzie, T.G., Fu, Q., Wong, E.H.H. et al. (2015). Visible light mediated controlled radical polymerization in the absence of exogenous radical sources or catalysts. *Macromolecules* 48 (12): 3864–3872.

40 da M. Costa, L.P., McKenzie, T.G., Schwarz, K.N. et al. (2016). Observed photoenhancement of RAFT polymerizations under fume hood lighting. *ACS Macro Lett.* 5 (11): 1287–1292.

41 Cabannes-Boue, B., Yang, Q., Lalevee, J. et al. (2017). Investigation into the mechanism of photo-mediated RAFT polymerization involving the reversible photolysis of the chain-transfer agent. *Polym. Chem.* 8: 1760–1770.

42 Li, J., Ding, C., Zhang, Z. et al. (2016). Visible light-induced living radical polymerization of butyl acrylate: photocatalyst-free, ultrafast, and oxygen tolerance. *Macromol. Rapid Commun.* 38 (13): 1600482.

43 Wang, J., Rivero, M., Muñoz Bonilla, A. et al. (2016). Natural RAFT polymerization: recyclable-catalyst-aided, opened-to-air, and sunlight-photolyzed RAFT polymerizations. *ACS Macro Lett.* 5 (11): 1278–1282.

44 Otsu, T. (2000). Iniferter concept and living radical polymerization. *J. Polym. Sci., Part A: Polym. Chem.* 38 (12): 2121–2136.

45 Xu, J., Jung, K., Atme, A. et al. (2014). A robust and versatile photoinduced living polymerization of conjugated and unconjugated monomers and its oxygen tolerance. *J. Am. Chem. Soc.* 136 (14): 5508–5519.

46 Bagheri, A., Yeow, J., Arandiyan, H. et al. (2016). Polymerization of a photocleavable monomer using visible light. *Macromol. Rapid Commun.* 37 (11): 905–910.

47 Xu, S., Yeow, J., and Boyer, C. (2018). Exploiting wavelength orthogonality for successive photoinduced polymerization-induced self-assembly and photo-crosslinking. *ACS Macro Lett.* 7 (11): 1376–1382.

48 Ng, G., Yeow, J., Xu, J., and Boyer, C. (2017). Application of oxygen tolerant PET-RAFT to polymerization-induced self-assembly. *Polym. Chem.* 8 (18): 2841–2851.

49 Shanmugam, S., Xu, J., and Boyer, C. (2015). Exploiting metalloporphyrins for selective living radical polymerization tunable over visible wavelengths. *J. Am. Chem. Soc.* 137 (28): 9174–9185.

50 Xu, J., Shanmugam, S., Fu, C. et al. (2016). Selective photoactivation: from a single unit monomer insertion reaction to controlled polymer architectures. *J. Am. Chem. Soc.* 138 (9): 3094–3106.

51 Chen, M., MacLeod, M.J., and Johnson, J.A. (2015). Visible-light-controlled living radical polymerization from a trithiocarbonate iniferter mediated by an organic photoredox catalyst. *ACS Macro Lett.* 4 (5): 566–569.

52 Gong, H., Zhao, Y., Shen, X. et al. (2018). Organocatalyzed photocontrolled radical polymerization of semifluorinated (meth)acrylates driven by visible light. *Angew. Chem. Int. Ed.* 57 (1): 333–337.

53 Theriot, J.C., Miyake, G.M., and Boyer, C.A. (2018). *N*,*N*-Diaryl dihydrophenazines as photoredox catalysts for PET-RAFT and sequential PET-RAFT/O-ATRP. *ACS Macro Lett.* 7 (6): 662–666.

54 Fu, Q., Ruan, Q., McKenzie, T.G. et al. (2017). Development of a robust PET-RAFT polymerization using graphitic carbon nitride (g-C_3N_4). *Macromolecules* 50 (19): 7509–7516.

55 Jiang, J., Ye, G., Wang, Z. et al. (2018). Heteroatom-doped carbon dots (CDs) as a class of metal-free photocatalysts for PET-RAFT polymerization under visible light and sunlight. *Angew. Chem. Int. Ed.* 57 (37): 12037–12042.

56 Li, X., Li, J.L., Huang, W.G. et al. (2018). Metalloporphyrin-bound Janus nanocomposites with dual stimuli responsiveness for nanocatalysis in living radical polymerization. *Nanoscale* 10 (41): 19254–19261.

57 Liang, E., Liu, M.-s., He, B., and Wang, G.-X. (2018). ZnO as photocatalyst for photoinduced electron transfer–reversible addition–fragmentation chain transfer of methyl methacrylate. *Adv. Polym. Technol.* 37 (8): 2879–2884.

58 Hakobyan, K., Gegenhuber, T., McErlean, C.S.P., and Müllner, M. (2019). Visible-light-driven MADIX polymerisation via a reusable, low-cost, and non-toxic bismuth oxide photocatalyst. *Angew. Chem. Int. Ed.* 58 (6): 1828–1832.

59 Zhu, Y. and Egap, E. (2020). PET-RAFT polymerization catalyzed by cadmium selenide quantum dots (QDs): grafting-from QDs photocatalysts to make polymer nanocomposites. *Polym. Chem.* 11: 1018–1024.

60 Fors, B.P. and Hawker, C.J. (2012). Control of a living radical polymerization of methacrylates by light. *Angew. Chem. Int. Ed.* 51 (35): 8850–8853.

61 Shanmugam, S., Xu, J., and Boyer, C. (2014). Photoinduced electron transfer–reversible addition–fragmentation chain transfer (PET-RAFT) polymerization of vinyl acetate and *N*-vinylpyrrolidinone: kinetic and oxygen tolerance study. *Macromolecules* 47 (15): 4930–4942.

62 Xu, J., Jung, K., and Boyer, C. (2014). Oxygen tolerance study of photoinduced electron transfer–reversible addition–fragmentation chain transfer (PET-RAFT) polymerization mediated by $Ru(Bpy)_3Cl_2$. *Macromolecules* 47 (13): 4217–4229.

63 Xu, J., Jung, K., Corrigan, N.A., and Boyer, C. (2014). Aqueous photoinduced living/controlled polymerization: tailoring for bioconjugation. *Chem. Sci.* 5 (9): 3568–3575.

64 Corrigan, N., Shanmugam, S., Xu, J., and Boyer, C. (2016). Photocatalysis in organic and polymer synthesis. *Chem. Soc. Rev.* 45 (22): 6165–6212.

65 Christmann, J., Ibrahim, A., Charlot, V. et al. (2016). Elucidation of the key role of $[Ru(Bpy)_3]^{2+}$ in photocatalyzed RAFT polymerization. *ChemPhysChem* 17 (15): 2309–2314.

66 Corrigan, N., Xu, J., Boyer, C., and Allonas, X. (2019). Exploration of the PET-RAFT initiation mechanism for two commonly used photocatalysts. *ChemPhotoChem* 3 (11): 1193–1199.

67 Shanmugam, S. and Boyer, C. (2015). Stereo-, temporal and chemical control through photoactivation of living radical polymerization: synthesis of block and gradient copolymers. *J. Am. Chem. Soc.* 137 (31): 9988–9999.

68 Corrigan, N., Rosli, D., Jones, J.W.J. et al. (2016). Oxygen tolerance in living radical polymerization: investigation of mechanism and implementation in continuous flow polymerization. *Macromolecules* 49 (18): 6779–6789.

69 Shanmugam, S., Xu, J., and Boyer, C. (2015). Utilizing the electron transfer mechanism of chlorophyll a under light for controlled radical polymerization. *Chem. Sci.* 6 (2): 1341–1349.

70 Wu, C., Shanmugam, S., Xu, J. et al. (2017). Chlorophyll a crude extract: efficient photo-degradable photocatalyst for PET-RAFT polymerization. *Chem. Commun.* 53 (93): 12560–12563.
71 Shanmugam, S., Xu, J., and Boyer, C. (2016). Light-regulated polymerization under near-infrared/far-red irradiation catalyzed by bacteriochlorophyll a. *Angew. Chem. Int. Ed.* 55 (3): 1036–1040.
72 Niu, J., Page, Z.A., Dolinski, N.D. et al. (2017). Rapid visible light-mediated controlled aqueous polymerization with in situ monitoring. *ACS Macro Lett.* 6 (10): 1109–1113.
73 Corrigan, N., Almasri, A., Taillades, W. et al. (2017). Controlling molecular weight distributions through photoinduced flow polymerization. *Macromolecules* 50 (21): 8438–8448.
74 Corrigan, N., Manahan, R., Lew, Z.T. et al. (2018). Copolymers with controlled molecular weight distributions and compositional gradients through flow polymerization. *Macromolecules* 51 (12): 4553–4563.
75 Shanmugam, S., Xu, J., and Boyer, C. (2016). A logic gate for external regulation of photopolymerization. *Polym. Chem.* 7 (42): 6437–6449.
76 Shanmugam, S., Xu, J., and Boyer, C. (2016). Aqueous RAFT photopolymerization with oxygen tolerance. *Macromolecules* 49 (24): 9345–9357.
77 Zhang, L., Wu, C., Jung, K. et al. (2019). An oxygen paradox: catalytic use of oxygen in radical photopolymerization. *Angew. Chem. Int. Ed.* 58 (47): 16811–16814.
78 Corrigan, N., Xu, J., and Boyer, C. (2016). A photoinitiation system for conventional and controlled radical polymerization at visible and NIR wavelengths. *Macromolecules* 49 (9): 3274–3285.
79 Wu, Z., Jung, K., and Boyer, C.A.J.M. (2020). Effective utilization of NIR wavelengths for photo-controlled polymerization – penetration through thick barriers and parallel solar syntheses. *Angew. Chem. Int. Ed.* 59 (5): 2013–2017.
80 Mattson, K.M., Pester, C.W., Gutekunst, W.R. et al. (2016). Metal-free removal of polymer chain ends using light. *Macromolecules* 49 (21): 8162–8166.
81 Zhang, L., Ye, G., Huo, X. et al. (2019). Structural engineering of graphitic carbon nitrides for enhanced metal-free PET-RAFT polymerizations in heterogeneous and homogeneous systems. *ACS Omega* 4 (14): 16247–16255.
82 Wu, C., Corrigan, N., Lim, C.-H. et al. (2019). Guiding the design of organic photocatalyst for PET-RAFT polymerization: halogenated xanthene dyes. *Macromolecules* 52 (1): 236–248.
83 Xu, J., Shanmugam, S., Duong, H.T., and Boyer, C. (2015). Organo-photocatalysts for photoinduced electron transfer-reversible addition–fragmentation chain transfer (PET-RAFT) polymerization. *Polym. Chem.* 6 (31): 5615–5624.
84 Figg, C.A., Hickman, J.D., Scheutz, G.M. et al. (2018). Color-coding visible light polymerizations to elucidate the activation of trithiocarbonates using eosin Y. *Macromolecules* 51 (4): 1370–1376.
85 Shanmugam, S., Xu, J., and Boyer, C. (2017). Photoinduced oxygen reduction for dark polymerization. *Macromolecules* 50 (5): 1832–1846.

86 Yeow, J., Chapman, R., Xu, J., and Boyer, C. (2017). Oxygen tolerant photopolymerization for ultralow volumes. *Polym. Chem.* 8 (34): 5012–5022.

87 Tucker, B.S., Coughlin, M.L., Figg, C.A., and Sumerlin, B.S. (2017). Grafting-from proteins using metal-free PET–RAFT polymerizations under mild visible-light irradiation. *ACS Macro Lett.* 6 (4): 452–457.

88 Lueckerath, T., Strauch, T., Koynov, K. et al. (2019). DNA–polymer conjugates by photoinduced RAFT polymerization. *Biomacromolecules* 20 (1): 212–221.

89 Wu, C., Chen, H., Corrigan, N. et al. (2019). Computer-guided discovery of a pH-responsive organic photocatalyst and application for pH and light dual-gated polymerization. *J. Am. Chem. Soc.* 141 (20): 8207–8220.

90 Lutz, J.-F.F., Ouchi, M., Liu, D.R., and Sawamoto, M. (2013). Sequence controlled polymers. *Science* 341 (6146): –1238149.

91 Carroll, D.R., Constantinou, A.P., Stingelin, N., and Georgiou, T.K. (2018). Scalable syntheses of well-defined pentadecablock bipolymer and quintopolymer. *Polym. Chem.* 9 (25): 3450–3454.

92 Clothier, G.K.K., Guimarães, T.R., Khan, M. et al. (2019). Exploitation of the nanoreactor concept for efficient synthesis of multiblock copolymers via macroraft-mediated emulsion polymerization. *ACS Macro Lett.* 8 (8): 989–995.

93 Engelis, N.G., Anastasaki, A., Nurumbetov, G. et al. (2017). Sequence-controlled methacrylic multiblock copolymers via sulfur-free RAFT emulsion polymerization. *Nat. Chem.* 9 (2): 171–178.

94 Gody, G., Barbey, R., Danial, M., and Perrier, S. (2015). Ultrafast RAFT polymerization: multiblock copolymers within minutes. *Polym. Chem.* 6: 1502–1511.

95 Gody, G., Maschmeyer, T., Zetterlund, P.B., and Perrier, S. (2013). Rapid and quantitative one-pot synthesis of sequence-controlled polymers by radical polymerization. *Nat. Commun.* 4: 1–9.

96 Gody, G., Maschmeyer, T., Zetterlund, P.B., and Perrier, S. (2014). Pushing the limit of the RAFT process: multiblock copolymers by one-pot rapid multiple chain extensions at full monomer conversion. *Macromolecules* 47 (10): 3451–3460.

97 Soeriyadi, A.H., Boyer, C., Nyström, F. et al. (2011). High-order multiblock copolymers via iterative Cu(0)-mediated radical polymerizations (SET-LRP): toward biological precision. *J. Am. Chem. Soc.* 133 (29): 11128–11131.

98 Anastasaki, A., Oschmann, B., Willenbacher, J. et al. (2017). One-pot synthesis of ABCDE multiblock copolymers with hydrophobic, hydrophilic, and semi-fluorinated segments. *Angew. Chem. Int. Ed.* 56 (46): 14483–14487.

99 Ng, G., Yeow, J., Chapman, R. et al. (2018). Pushing the limits of high throughput PET-RAFT polymerization. *Macromolecules* 51 (19): 7600–7607.

100 Gody, G., Zetterlund, P.B., Perrier, S., and Harrisson, S. (2016). The limits of precision monomer placement in chain growth polymerization. *Nat. Commun.* 7: 10514–10514.

101 Haven, J.J., De Neve, J.A., and Junkers, T. (2017). Versatile approach for the synthesis of sequence-defined monodisperse 18- and 20-Mer oligoacrylates. *ACS Macro Lett.* 6 (7): 743–747.

102 Lawrence, J., Lee, S.H., Abdilla, A. et al. (2016). A versatile and scalable strategy to discrete oligomers. *J. Am. Chem. Soc.* 138 (19): 6306–6310.
103 Barnes, J.C., Ehrlich, D.J.C., Gao, A.X. et al. (2015). Iterative exponential growth of stereo- and sequence-controlled polymers. *Nat. Chem.* 7 (10): 810–815.
104 Jiang, Y., Golder, M.R., Nguyen, H.V.T. et al. (2016). Iterative exponential growth synthesis and assembly of uniform diblock copolymers. *J. Am. Chem. Soc.* 138 (30): 9369–9372.
105 Espeel, P., Carrette, L.L.G., Bury, K. et al. (2013). Multifunctionalized sequence-defined oligomers from a single building block. *Angew. Chem. Int. Ed.* 52 (50): 13261–13264.
106 Martens, S., Van Den Begin, J., Madder, A. et al. (2016). Automated synthesis of monodisperse oligomers, featuring sequence control and tailored functionalization. *J. Am. Chem. Soc.* 138 (43): 14182–14185.
107 Xu, J., Fu, C., Shanmugam, S. et al. (2017). Synthesis of discrete oligomers by sequential PET-RAFT single-unit monomer insertion. *Angew. Chem. Int. Ed.* 56 (29): 8376–8383.
108 Huang, Z., Noble, B.B., Corrigan, N. et al. (2018). Discrete and stereospecific oligomers prepared by sequential and alternating single unit monomer insertion. *J. Am. Chem. Soc.* 140 (41): 13392–13406.
109 Fu, C., Xu, J., and Boyer, C. (2016). Photoacid-mediated ring opening polymerization driven by visible light. *Chem. Commun.* 52 (44): 7126–7129.
110 Kodadek, T. (2011). The rise, fall and reinvention of combinatorial chemistry. *Chem. Commun.* 47 (35): 9757–9763.
111 Schneider, G. (2018). Automating drug discovery. *Nat. Rev. Drug Discovery* 17 (February): 97–113.
112 Curtarolo, S., Hart, G.L.W., Nardelli, M.B. et al. (2013). The high-throughput highway to computational materials design. *Nat. Mater.* 12 (3): 191–201.
113 Potyrailo, R., Rajan, K., Stoewe, K. et al. (2011). Combinatorial and high-throughput screening of materials libraries: review of state of the art. *ACS Comb. Sci.* 13 (6): 579–633.
114 Hook, A.L., Anderson, D.G., Langer, R. et al. (2010). High throughput methods applied in biomaterial development and discovery. *Biomaterials* 31 (2): 187–198.
115 Audus, D.J. and De Pablo, J.J. (2017). Polymer informatics: opportunities and challenges. *ACS Macro Lett.* 6 (10): 1078–1082.
116 Oliver, S., Zhao, L., Gormley, A.J. et al. (2019). Living in the fast lane – high throughput controlled/living radical polymerization. *Macromolecules* 52 (1): 3–23.
117 Hoogenboom, R., Meier Michael, A.R., and Schubert Ulrich, S. (2003). Combinatorial methods, automated synthesis and high-throughput screening in polymer research: past and present. *Macromol. Rapid Commun.* 24 (1): 15–32.
118 Hoogenboom, R. and Schubert Ulrich, S. (2003). The fast and the curious: high-throughput experimentation in synthetic polymer chemistry. *J. Polym. Sci., Part A: Polym. Chem.* 41 (16): 2425–2434.

119 Hoogenboom, R. and Schubert, U.S. (2005). High-throughput synthesis equipment applied to polymer research. *Rev. Sci. Instrum.* 76 (6): 062202.

120 Huiqi, Z., Richard, H., Michael, A.R.M., and Ulrich, S.S. (2005). Combinatorial and high-throughput approaches in polymer science. *Meas. Sci. Technol.* 16 (1): 203.

121 Stefan, S., Meier, M.A.R., and Schubert, U.S. (2003). Instrumentation for combinatorial and high-throughput polymer research: a short overview. *Macromol. Rapid Commun.* 24 (1): 33–46.

122 Yeow, J., Chapman, R., Gormley, A.J., and Boyer, C. (2018). Up in the air: oxygen tolerance in controlled/living radical polymerisation. *Chem. Soc. Rev.* 47 (12): 4357–4387.

123 Gormley Adam, J., Yeow, J., Ng, G. et al. (2018). An oxygen-tolerant PET-RAFT polymerization for screening structure–activity relationships. *Angew. Chem.* 130 (6): 1573–1578.

124 Yeow, J., Joshi, S., Chapman, R., and Boyer, C. (2018). A self-reporting photocatalyst for online fluorescence monitoring of high throughput RAFT polymerization. *Angew. Chem. Int. Ed.* 57 (32): 10102–10106.

125 Judzewitsch, P.R., Nguyen, T.-K., Shanmugam, S. et al. (2020). Towards sequence-controlled antimicrobial polymers: effect of polymer block order on antimicrobial activity. *Angew. Chem. Int. Ed.* 59 (17): 4559–4564.

126 Judzewitsch, P.R., Zhao, L., Wong, E.H.H., and Boyer, C. (2019). High-throughput synthesis of antimicrobial copolymers and rapid evaluation of their bioactivity. *Macromolecules* 52 (11): 3975–3986.

127 Richards, S.-J., Jones, A., Thomás, R.M.F., and Gibson, M.I. (2018). Photochemical 'in-air' combinatorial discovery of antimicrobial copolymers. *Chem. Eur. J.* 42 (52): 13758–13761.

128 Chapman, R., Gormley, A.J., Herpoldt, K.-l., and Stevens, M.M. (2014). Highly controlled open vessel RAFT polymerizations by enzyme degassing. *Macromolecules* 47 (24): 8541–8547.

129 Chapman, R., Gormley, A.J., Stenzel, M.H., and Stevens, M.M. (2016). Combinatorial low-volume synthesis of well-defined polymers by enzyme degassing. *Angew. Chem. Int. Ed.* 128 (14): 4576–4579.

130 Liu, Z., Lv, Y., and An, Z. (2017). Enzymatic cascade catalysis for the synthesis of multiblock and ultrahigh-molecular-weight polymers with oxygen tolerance. *Angew. Chem. Int. Ed.* 56 (54): 13852–13856.

131 Fu, Q., Xie, K., McKenzie, T.G., and Qiao, G.G. (2017). Trithiocarbonates as intrinsic photoredox catalysts and RAFT agents for oxygen tolerant controlled radical polymerization. *Polym. Chem.* 8 (9): 1519–1526.

132 Chen, M., Gu, Y., Singh, A. et al. (2017). Living additive manufacturing: transformation of parent gels into diversely functionalized daughter gels made possible by visible light photoredox catalysis. *ACS Cent. Sci.* 3 (2): 124–134.

133 Tumbleston, J.R., Shirvanyants, D., Ermoshkin, N. et al. (2015). Additive manufacturing. Continuous liquid interface production of 3D objects. *Science* 347 (6228): 1349–1352.

134 Kovaliov, M., Allegrezza, M.L., Richter, B. et al. (2018). Synthesis of lipase polymer hybrids with retained or enhanced activity using the grafting-from strategy. *Polymer* 137: 338–345.

135 Sun, H., Choi, W., Zang, N. et al. (2019). Bioactive peptide brush polymers via photoinduced reversible-deactivation radical polymerization. *Angew. Chem. Int. Ed.* 58 (48): 17359–17364.

136 Niu, J., Lunn, D.J., Pusuluri, A. et al. (2017). Engineering live cell surfaces with functional polymers via cytocompatible controlled radical polymerization. *Nat. Chem.* 9 (6): 537–545.

137 Messina, M.S., Messina, K.M.M., Bhattacharya, A. et al. (2020). Preparation of biomolecule-polymer conjugates by grafting-from using ATRP, RAFT, or ROMP. *Prog. Polym. Sci.* 100: 101186.

13

Redox-Initiated RAFT Polymerization and (Electro)chemical Activation of RAFT Agents

Francesca Lorandi, Marco Fantin, and Krzysztof Matyjaszewski

Carnegie Mellon University, Department of Chemistry, 4400 Fifth Avenue, Pittsburgh, PA 15213, USA

13.1 Introduction

Reversible addition–fragmentation chain transfer (RAFT) polymerization is one of the leading techniques for the preparation of polymeric materials with precisely controlled and complex architectures [1]. Typically, the polymerization control is enabled via a degenerate transfer between propagating radicals and dormant species, regulated by a chain transfer agent (CTA or RAFT agent). A distinct feature of RAFT polymerization among other reversible deactivation radical polymerization (RDRP) methods is the presence of sulfur-containing moieties as chain end-groups.

RAFT polymerizations are generally thermally initiated by conventional radical initiators such as azobisisobutyronitrile (AIBN). Importantly, the use of thermal initiator causes the continuous generation of new chains throughout the polymerization, which could lead to polymers with larger dispersity and lower functionality, hampering the preparation of pure block copolymers.

The careful selection of the RAFT agent in correlation to the monomer activity and polymerization conditions can minimize the formation of new chains, so that block copolymers and polymers with more complex architectures can be accessed [2]. Moreover, novel initiation systems that can minimize (or eliminate) the formation of new chains have been developed in the past decade [1c, f, 3]. These systems employ (i) external molecules and/or stimuli that can generate radicals at ambient temperature or (ii) direct activation of the RAFT agent to form radicals to start the polymerization.

The latter approach has been vastly employed recently because of the increasing interest in photo-induced polymerizations. Indeed, light can promote the dissociation of a CTA either directly, through a photoiniferter approach, or in the presence of a photoredox catalyst, as in a photoinduced electron/energy transfer (PET)–RAFT polymerization [4].

This chapter is focused on the chemical and electrochemical approaches towards radical generation in RAFT systems. Chemical approaches such as the use of redox initiators to generate radicals at low temperature [5], and the use of transition metal

RAFT Polymerization: Methods, Synthesis and Applications, First Edition.
Edited by Graeme Moad and Ezio Rizzardo.

complexes to directly activate CTAs [6], were first reported a decade ago. Recently, these methods were extended to a Fenton–RAFT polymerization [7]. Moreover, electrochemical stimuli have been applied to RAFT systems to electrochemically reduce conventional radical initiators or RAFT agents, thus developing an electrochemically mediated reversible addition–fragmentation chain transfer (*e*RAFT) polymerization [8c, d].

13.2 Redox Initiation

The most relevant redox pairs used for initiating RAFT polymerizations are summarized in Scheme 13.1, together with some monomers employed for the various redox-initiated RAFT polymerizations.

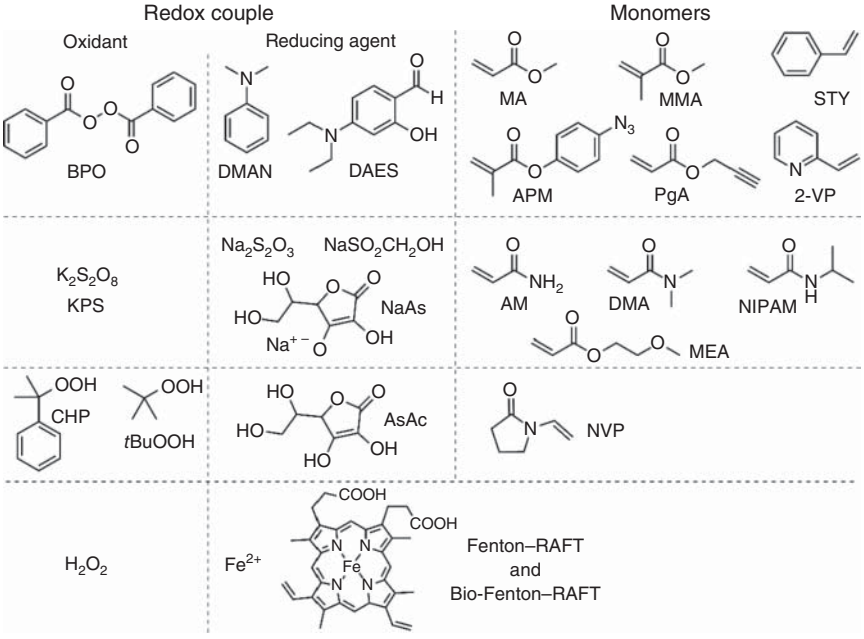

Scheme 13.1 Redox couples employed to initiate RAFT polymerizations at room temperature (or lower) and examples of monomers polymerized via redox-initiated RAFT polymerization.

Room temperature RAFT polymerization of methyl acrylate (MA), methyl methacrylate (MMA), and styrene (STY) was reported by Pan and coworkers by exploiting a redox initiation system based on benzoyl peroxide (BPO) and *N*,*N*′-dimethylaniline (DMAN) [5]. The BPO/amine redox couple has been extensively used to initiate free radical polymerizations [9]. Mechanistic studies showed that amine-based radicals, benzoate anions, and benzoyloxy radicals are generated as a consequence of a nucleophilic displacement on BPO by the amine [9b]. Then,

benzoyloxy radicals initiate the polymerizations, but amine radical cations can also contribute to initiating polymer chains.

The RAFT polymerization of MA initiated by an equimolar amount of BPO and DMAN at $T = 25\,^{\circ}C$ and with a target degree of polymerization (DP) 200 gave polymers with molecular weight (MW) matching theoretical values and low dispersities ($Đ < 1.1$), both in bulk or in tetrahydrofuran (THF) as a solvent, and using a dithiobenzoate (DB) or trithiocarbonate CTA. Short induction periods were attributed to the slow fragmentation of the chain-CTA adduct. The redox-initiated RAFT polymerization of MMA under similar conditions gave polymers with low dispersity but with MW values higher than expected. In the case of STY, the reaction temperature was raised to 35 °C in bulk polymerizations to reach c. 50% conversion in two to three days, with overall good control. Finally, a PSTY-*b*-PMA block copolymer was prepared with no visible tailing in the gel permeation chromatography (GPC) traces, confirming the livingness of the process and the negligible generation of new chains during the polymerization.

The BPO/DMAN redox initiation system was also used for the RAFT polymerization of the azide-containing monomer 4-azidophenyl methacrylate (APM) [10]. At room temperature, the redox-initiated RAFT polymerization of APM in bulk, under similar conditions to the above described systems, reached c. 50% conversion in 24 hours, giving a polymer with MW matching the theoretical value and $Đ = 1.19$. The copolymerization of equimolar amounts of MA and APM reached 56% conversion in 2.5 hours, yielding a low-dispersity statistical copolymer containing about 30 mol% APM. Although azido groups are known to undergo a cycloaddition reaction to the C=C double bond of acrylates [11], this undesired reaction was not observed at room temperature, thus highlighting the benefits of the redox initiation. Therefore, the same strategy was used to prepare block copolymers of MA and 2-chloroallyl azide, which were further extended with a semi-fluorinated acrylate monomer and then reacted with an alkyne-capped poly(ethylene glycol) via 'click' chemistry [12]. Similar procedures were adopted to fabricate, among others, hydrophobic glass surfaces [12] and superhydrophobic cotton fibres [13].

Monomers containing acetylenic moieties are also prone to side reactions during radical polymerizations. Therefore, the BPO/DMAN redox initiators have been employed to prepare a MMA/propargyl acrylate (PgA) copolymer via RAFT copolymerization at $T = 25\,^{\circ}C$ [14]. Well-defined P(MMA-*co*-PgA) copolymers were then converted into intrachain cross-linked nanoparticles via 'click' reaction under diluted conditions at room temperature.

Redox-initiated RAFT polymerization of 2-vinylpyridine (2-VP) at $T = 25\,^{\circ}C$ was reported by using BPO but in the absence of an added reducing agent [15]. The proposed interaction of BPO with the amine-containing monomer 2-VP led to the formation of an intermediate adduct, followed by proton transfer and generation of radicals. Furthermore, surface-initiated RAFT polymerization was successfully paired to a redox initiation system, by using BPO together with 4-(diethylamino) salicylaldehyde (DEAS) as a reducing agent. The latter was first attached onto the surface of a nanoclay attapulgite (ATP). The functionalized ATP was subsequently placed in a solution with BPO, MMA, and a dithiobenzoate CTA. Polymerization

conditions were tuned as to increase the grafting ratio of PMMA relative to hybrids, which reached 47 wt%. The ATP@PMMA showed better solubility in organic solvents compared to naked ATP [16].

A redox initiation system for room temperature aqueous RAFT polymerization was developed by Bai et al. by using the redox couple potassium persulfate ($K_2S_2O_8$, KPS) – sodium thiosulfate ($Na_2S_2O_3$) [17]. These species generate radicals according to the reactions in Eqs. (13.1) and (13.2); moreover, for relatively high concentrations of $S_2O_3^{\cdot-}$, hydroxyl radicals are also generated (Eq. (13.3)), which initiate the polymerization [9a].

$$S_2O_8^{2-} \rightarrow 2SO_4^{\cdot-} \tag{13.1}$$

$$S_2O_8^{2-} + S_2O_3^{2-} \rightarrow 2SO_4^{\cdot-} + S_2O_3^{\cdot-} + SO_4^{2-} \tag{13.2}$$

$$SO_4^{\cdot-} + H_2O \rightarrow HSO_4^{-} + HO^{\cdot} \tag{13.3}$$

The redox-initiated RAFT polymerization of acrylamide (AM) and *N*-isopropylacrylamide (NIPAM) was conducted in triple-distilled water in the presence of a water-soluble trithiocarbonate CTA [17]. In the case of AM, a phosphate buffer was employed to prevent hydrolysis of monomer and CTA. A control experiment proved that the $K_2S_2O_8$–$Na_2S_2O_3$ redox system was not able to oxidize the CTA at room temperature. Almost quantitative conversion of NIPAM was obtained in six hours, giving a polymer with $M_n = 4 \times 10^4$ g mol^{-1}, in agreement with the theoretical value, and $Đ = 1.05$. The chain extension of a PNIPAM macro(CTA) confirmed the preservation of chain end functionalities. The redox-initiated RAFT polymerization of AM was slower (88% conversion in 20 hours) but well controlled. By increasing the temperature to 45 °C, 80% conversion was reached in two hours, while retaining the polymerization control.

Destarac and coworkers reported the redox-initiated aqueous RAFT/macromolecular design by interchange of xanthate (RAFT/MADIX) polymerization of various acrylamides with a xanthate CTA at 10 °C [18]. The redox initiator pair was composed of ammonium persulfate as an oxidant and sodium formaldehyde sulfoxylate dihydrate as a reducing agent. Homopolymers and block copolymers with M_n up to 10^6 g mol^{-1} and $Đ < 1.32$ were obtained, and quantitative monomer conversion was observed within two hours, by using relatively high concentrations of monomers and a very small amount of CTA (Figure 13.1).

Various aqueous dispersion RAFT polymerizations were carried out with redox initiation systems based on persulfates, combined with a bisulfite or ascorbate salt as a reducing agent [19]. By using a low concentration (0.02 mol% relative to monomer) of KPS and sodium ascorbate (NaAs) in equimolar amount, RAFT dispersion polymerization of 2-methoxyethylacrylate (MEA) was carried out at $T = 30$ or 40 °C with a poly(ethylene glycol) methyl ether methacrylate (PPEGMA) as macro(CTA) [19b]. The dispersion polymerization was faster than a corresponding RAFT polymerization in dimethylformamide (DMF) at $T = 70$ °C with a conventional thermal initiator. PPEGMA-*b*-PMEA copolymers prepared in dispersed media showed lower

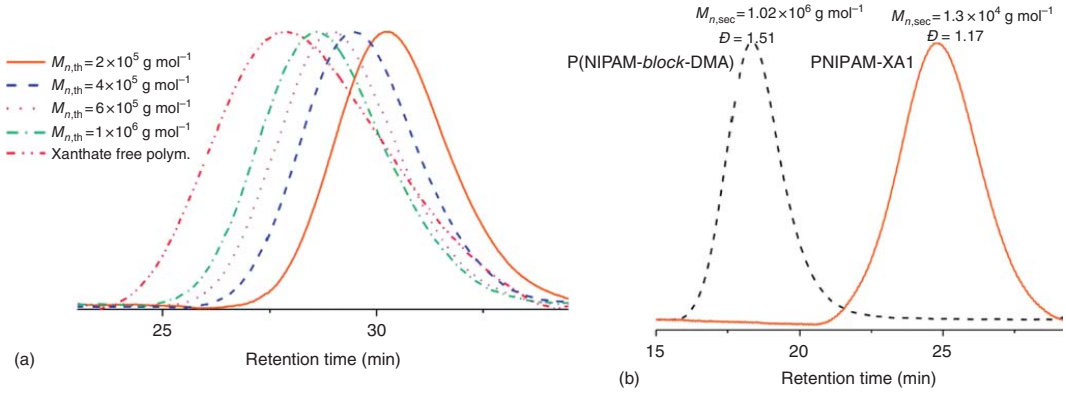

Figure 13.1 GPC traces of (a) PAM synthesized via redox-initiated RAFT/MADIX polymerization at $T = 10\,°C$ and (b) PNIPAM-*b*-PDMA. Source: Adapted with permission from Read et al. [18]. Copyright 2014, Royal society of chemistry.

dispersity compared to the one prepared in solution, likely because of the decreased chain transfer to polymer at low temperatures.

The KPS/NaAs redox initiator system was also used for aqueous RAFT cryopolymerizations, in which the polymerization mixture was cooled at a temperature lower than its freezing point, thus forming a heterogeneous system composed of an ice phase and a monomer-containing liquid microphase [20]. Well-defined homopolymers and copolymers of *N*,*N*-dimethylacrylamide (DMA) and NIPAM were synthesized with a water-soluble trithiocarbonate CTA at −15 °C. Cryogels were also prepared by exploiting the porogenic effect of ice crystals in the polymerization medium and using a disulfide crosslinker to allow for a subsequent chemical degradation. Redox-initiated RAFT cryopolymerization was extended to organic solvents by using cumene hydroperoxide (CHP) and ascorbic acid (AsAc) as redox initiators [21]. Well-controlled homo- and copolymerizations of several acrylates and acrylamides have been reported in frozen 1,4-dioxane at −5 °C.

The combination of organic hydroperoxides as oxidants and ascorbic acid as a reducing agent has been used to initiate aqueous RAFT polymerization under various conditions. The RAFT/MADIX polymerization of *N*-vinyl pyrrolidone (NVP) was reported in water at $T = 25\,^{\circ}\mathrm{C}$ using *tert*-butyl hydroperoxide (*t*BuOOH) and AsAc [22]. This redox couple enabled polymerization at a pH = 6.5, which decreased the extent of side reactions between NVP and water compared to more acidic conditions. At ambient temperature, the hydrolysis of terminal groups was successfully prevented [23], thus obtaining PVP and PAM-*b*-PVP block copolymer with M_n up to $1.2 \times 10^4\ \mathrm{g\,mol^{-1}}$ and $Đ < 1.3$. Perrier and coworkers used *t*BuOOH/AsAc redox-initiated aqueous RAFT polymerization to synthesize multiblock copolymers via a one-pot sequential monomer addition approach, without intermediate purifications [24]. Despite relatively high amounts of *t*BuOOH being used with monomers owing to relatively low propagation rate constants, well-defined multiblock copolymers (with 4–10 blocks) were prepared with different combinations of acrylates, acrylamides, and acidic monomers. Minimal polymer branching and hydrolysis of chain ends were observed by working at room temperature.

More recently, a Fenton reaction was exploited by Qiao and coworkers to develop a catalytic redox initiation system for RAFT polymerization, which provided high polymerization rates [7]. Typical Fenton's reagents are ferrous ions (Fe^{2+}) and H_2O_2, which in water generate oxidizing hydroxyl radicals through the reactions shown in Eqs. (13.4) and (13.5) [7, 25]:

$$Fe^{2+} + H_2O_2 \longrightarrow Fe^{3+} + OH^{\cdot} + OH^{-} \tag{13.4}$$

$$Fe^{3+} + H_2O_2 \longrightarrow Fe^{2+} + OH_2^{\cdot} + H^{+} \tag{13.5}$$

$OH^{\cdot}$ is a non-specific highly reactive radical, which can therefore cause several undesired reactions, particularly at high concentration of H_2O_2 and Fe^{2+}.

The relative concentration of these two species was first optimized for the Fenton–RAFT polymerization of DMA in water in the presence of a water-soluble trithiocarbonate CTA. The optimal ratio of 3 : 1 $[H_2O_2]$:$[Fe^{2+}]$ gave 85% monomer conversion in only five minutes, yielding PDMA with MW matching the theoretical

value and $Đ = 1.04$. Importantly, oxidation of Fe^{2+} to Fe^{3+} by oxygen or impurities was carefully avoided because Fe^{3+} can inhibit the polymerization.

Control experiments in the absence of the Fenton's reagents or the CTA, either gave no monomer conversion or resulted in gelation, respectively. The target DP was successfully increased from 50 to 400 by changing the molar ratio between monomer and RAFT agent and increasing the amount of Fe^{2+} for higher DPs. A chain extension experiment and the aminolysis of the final polymer confirmed that the RAFT end-group was not hydrolyzed by H_2O_2 [26].

Poly(*N*-acryloylmorpholine) and poly(2-hydroxyethyl acrylate) with $Đ < 1.1$ were also prepared via Fenton–RAFT, reaching >60% conversion in one minute [7]. Furthermore, the Fenton–RAFT polymerization could be performed without traditional degassing: it was proposed that the Fenton reagents promoted the scavenging of residual O_2 through generation of singlet oxygen. Sequential additions of H_2O_2 allowed for chemically degassing and temporally controlling the polymerization, which stopped when all H_2O_2 was consumed and restarted when a new batch was added into the solution (Figure 13.2).

Nevertheless, because of their high and indiscriminate reactivity, the hydroxyl radicals were rapidly consumed by many side reactions, often preventing to achieve full monomer conversion. Therefore, a metered addition strategy was subsequently developed, in which H_2O_2 was fed into the system through a syringe pump, in

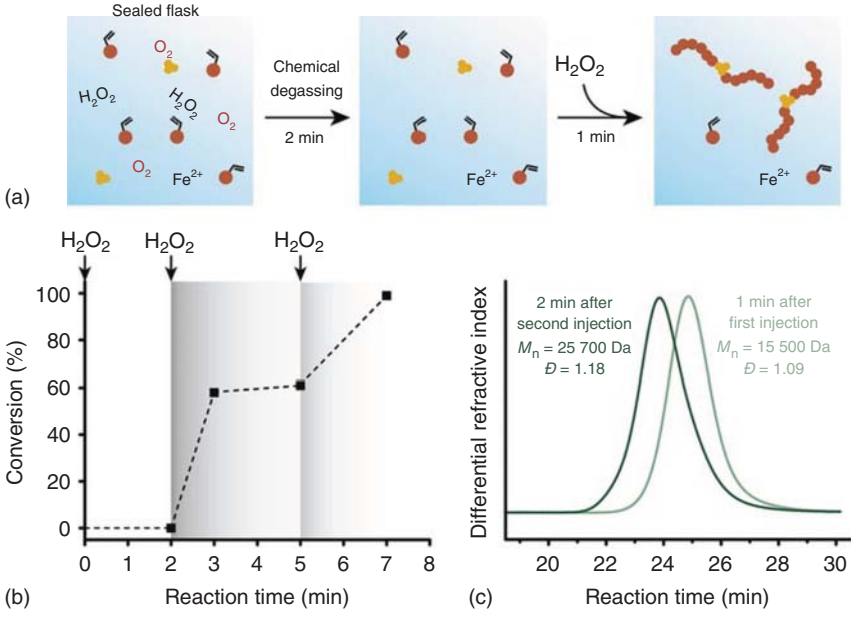

Figure 13.2 (a) Schematic of a Fenton–RAFT without traditional degassing: first, chemical degassing by H_2O_2, followed by injection of new H_2O_2 to start the polymerization; (b) monomer conversions measured during sequential addition of H_2O_2; (c) GPC chromatograms at total reaction times of three and seven minutes (with c. 60% and >99% conversion, respectively). Source: Reproduced with permission from Reyhani et al. [7]. Copyright 2017, John Wiley & Sons.

order to control the radical concentration profile [27]. By using the Fenton–RAFT of DMA with a water-soluble trithiocarbonate CTA as a model system, quantitative and fast polymerization was obtained with relatively high concentrations of Fenton's reagents (e.g. [DMA]:[CTA]:[Fe^{2+}]:[H_2O_2] = 200 : 1 : 1 : 3). Decreasing the concentrations of Fenton's reagents and increasing the feeding time reduced the polymerization rate but provided improved control. Induction periods observed for relatively low doses of H_2O_2 suggested that a threshold amount of H_2O_2 was needed to start the polymerization.

The control over MW, MW distribution, and dispersity did not depend on the feeding strategy: indeed, the continuous supply of radicals served to reactivate the chains trapped by the CTA, which was primarily responsible for the polymerization control. Moreover, the polymer properties only slightly changed with a non-linear H_2O_2 feeding profile, suggesting that the radical concentration was approximately constant because both the radical flux and the extent of side reactions increased with increasing dosing rate.

Following these reports on Fenton–RAFT polymerization, a 'solvent-initiated' RAFT was proposed, in which 'non-fresh' THF and 1,4-dioxane were used as both solvents and initiators for the RAFT polymerization of DMA and *N*-acryloylpyrrolidine [28]. The authors proposed that a Fenton-like process was occurring because of the presence of metal traces in the solvents, together with the hydroperoxides that typically form over time by autoxidation reaction in cyclic ether-based solvents. This process formed oxygen-centred radicals that could abstract a hydrogen from another ether molecule, generating a carbon-centred radical that could attack the C—S double bond of the CTA. Homo- and block copolymers were obtained with acceptable control, when the estimated hydroperoxide content was <100 ppm. End-group analysis confirmed the presence of a few chains initiated by ether-based radicals.

A Bio-Fenton–RAFT polymerization was reported by using haemoglobin (Hb) as a source of iron and glucose oxidase (GOx) to enzymatically produce H_2O_2 in situ by catalyzing the reaction between O_2 and glucose [29]. The Bio-Fenton–RAFT polymerization of DMA with a trithiocarbonate CTA in a non-degassed flask was slower than a Fenton–RAFT (i.e. with a Fe^{2+} salt) under otherwise similar conditions. However, almost quantitative conversion was obtained in <8 hours, with MW matching the theoretical value and $Đ < 1.1$. Similar results were obtained with different target DPs and acrylates or other acrylamides, paired with suitable CTAs. Both commercial bovine Hb and bovine blood were successfully used as a Fe source, with the polymerization rate depending on the actual concentration of red blood cells.

A colorimetric assay showed that radicals were steadily, albeit relatively slowly, generated after a short induction period. Therefore, the slow radical generation by Hb was further exploited to prepare ultra-high molecular weight (UHMW) PDMA by simply adjusting the [DMA]:[CTA] ratio [30]. Indeed, the synthesis of UHMW polymers is based on enhancing the ratio between the rate of propagation and termination [31]. The very low concentration of radicals in the Bio-Fenton–RAFT of DMA drastically suppressed the termination reactions, thus enabling to obtain

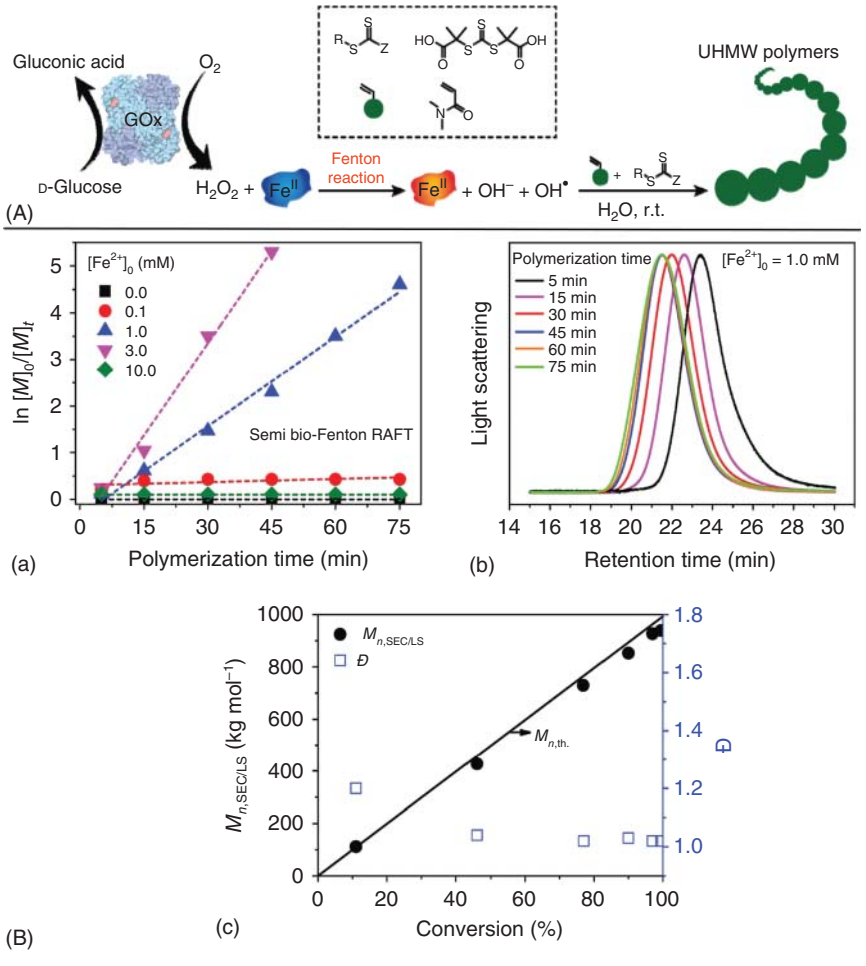

Figure 13.3 (A) Mechanism of semi-bio-Fenton RAFT polymerization. (B) (a) Semi-logarithmic kinetic plot of semi-bio-Fenton RAFT polymerization of DMA with different $[Fe^{2+}]$ and (b) GPC traces and (c) MW and dispersity evolution for the DMA polymerization with $[Fe^{2+}] = 10^{-3}$ M. Other conditions: [GOx] = 250 nM, [D-glucose] = 0.1 M, open-to-air vessel. Source: Adapted with permission from Reyhan et al. [30]. Copyright 2019, John Wiley & Sons.

PDMA with MW between 8.9×10^5 and 1.2×10^7 g mol^{-1} (M_w values from static light scattering measurements), in good agreement with theoretical values, in 48 hours.

Aiming to reduce the polymerization time, Hb was replaced with ammonium ferrous sulfate (Semi Bio-Fenton RAFT, Figure 13.3). The concentration of Fe^{2+} was adjusted to reach almost quantitative conversion in two hours (Figure 13.3a). Relatively high concentrations of Fe^{2+} led to precipitation of $Fe(OH)_3$ and consequently halting the polymerization because of the lack of Fe^{2+} in solution. The livingness of the process was confirmed by two consecutive chain extensions of a PDMA–macro(CTA) with DMA, providing a semi-triblock copolymer

with $M_w = 2.2 \times 10^6\,\mathrm{g\,mol^{-1}}$. The upper limit observed in the final M_w (about $2 \times 10^7\,\mathrm{g\,mol^{-1}}$) was attributed to the very low concentration of RAFT agent to ensure the control when targeting DP > 200 000. Finally, the GOx/glucose system was replaced with feeding H_2O_2 through a syringe pump. By adjusting the feeding rate to match the rate of radical generation in the enzymatic system, similar control over the polymerization was achieved in a regularly degassed flask.

The enzymatic degassing by GOx was also combined with a redox initiation by introducing in solution AsAc as a reducing agent for the H_2O_2 generated by consumption of the solubilized O_2. The redox couple initiated aqueous RAFT polymerizations of DMA in open air [32]. The use of enzymes as deoxygenating agents and biocatalysts for RDRPs is gaining increasing attention [33]. Enzymatic cascades were effectively used to initiate RAFT polymerizations under bio-relevant conditions; however, discussion of enzyme-initiated RAFT polymerization is beyond the scope of the present chapter.

13.3 Chemical Activation of RAFT Agents

Atom transfer radical polymerization (ATRP) is another powerful and versatile RDRP technique [34, 35]. In ATRP, the dynamic equilibrium between propagating radicals and dormant species is regulated by a transition metal catalyst, typically a Cu complex with a polydentate amine ligand (L). The active catalyst, $Cu^{I}L^{+}$, reductively cleaves the carbon–halogen (C—X) bond in the initiator or dormant species, thus generating propagating radicals and the deactivator $XCu^{II}L^{+}$, which reverts the radicals back to dormant species.

Because ATRP is based on a reversible deactivation mechanism, no external source of radicals is required to initiate the polymerization, and thus no new chains are generated. This raised the question whether ATRP catalysts could activate alkyl pseudohalides (i.e. RAFT agents) and how this reaction will affect the polymerization mechanism. As a consequence, traditional ATRP catalysts have been combined with CTAs both in the absence and presence of ATRP initiators, with the purpose of avoiding the need of external radical sources, thus preventing the generation of new chains during polymerizations [6]. Moreover, the synergistic interaction between ATRP and RAFT can lead to improved control because of the deactivation/exchange by both Cu(II) species and CTAs [36].

Several ATRP catalysts were initially used for the polymerization of STY and MMA in the presence of various alkyl diethyldithiocarbamate (DC) species, which served as RAFT agents and ATRP initiators as alkyl pseudohalides. Mechanistic studies and end-group analysis showed that the process was a conventional ATRP where the DC species acted as an alkyl pseudohalide initiator, and thus, DC-capped chains were obtained (Scheme 13.2a) [37]. The trend in catalyst activity towards DCs was different than towards conventional alkyl halide ATRP initiators. In general, CuX/*N*,*N*,*N*′,*N*″,*N*″-pentamethyldiethylenetriamine (PMDETA) allowed for better controlled polymerizations. Well-defined polymers were obtained in <3 hours, at elevated temperatures and with an equimolar amount of Cu catalyst

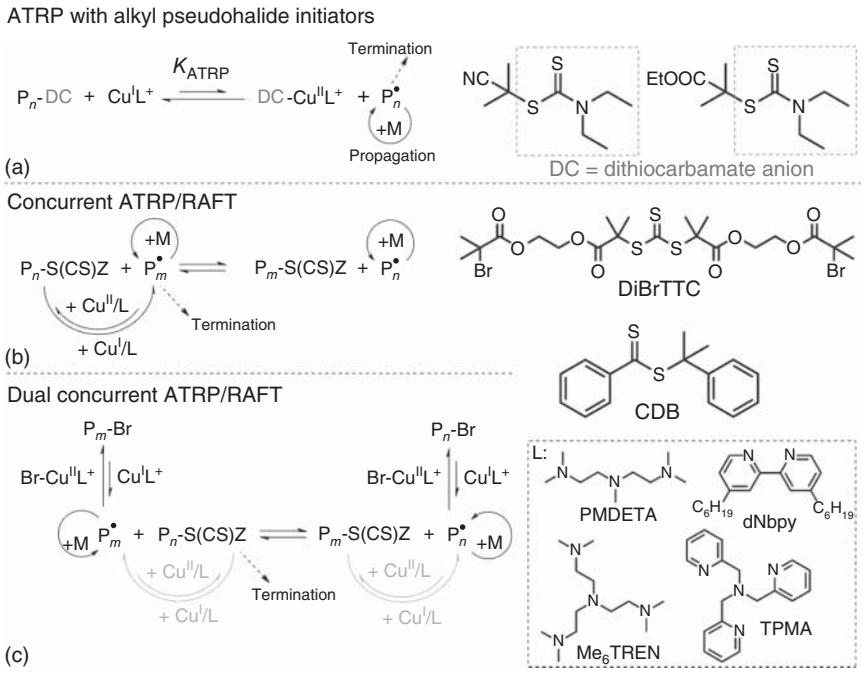

Scheme 13.2 Mechanism of (a) ATRP with dithiocarbamates as alkyl pseudohalides; (b) concurrent ATRP/RAFT; and (c) dual concurrent ATRP/RAFT (equilibria in grey marginally contribute to the polymerization). On the right: examples of CTAs used in these processes. Dashed square: structures of commonly used ATRP ligands.

and DC initiator. Electrochemical characterization showed that Cu/L complexes with a coordinated DC group were reduced at more negative potentials than in the case of coordinated Br^- or Cl^- ions. Thus, DC anions have strong affinity for $Cu^{II}L^{2+}$ and form more reducing Cu complexes. Because higher reducing power typically results in higher ATRP activity, $Cu^{II}L^{2+}$ complexes with DC anions could result in faster polymerization; however, the strong interaction between DC^- and $Cu^{II}L^{2+}$ could decrease the deactivation efficiency [38]. The combination of these two aspects likely caused the different trend in polymerization control compared to conventional ATRP with halide ions.

A first concurrent ATRP/RAFT was developed by using a dibromotrithiocarbonate (DiBrTTC) initiator (Scheme 13.2b), CuBr/PMDETA, or CuBr/4,4′-dinonyl-2,2′-bipyridine (dNbpy) as a catalyst and *n*-butyl acrylate (BA), MMA, and STY as monomers under various conditions [39]. After polymerizations, aminolysis and methanolysis of the polymers confirmed that chain growth occurred both through the bromine chain end and the TTC moiety. However, because DiBrTTC was an inefficient CTA in the RAFT polymerization of MMA, this result proved that the Cu complexes could activate the TTC chain end similar to the case of dithiocarbamates.

Dithioester CTAs could also be activated by Cu complexes [40]. Indeed, the concurrent ATRP/RAFT of STY and MMA was reported by using cumyl dithiobenzoate (CDB, Scheme 13.2) as alkyl pseudohalide. Well-defined PMMA, PSTY, and PMMA-*b*-PSTY block copolymers were prepared in anisole at 80–100 °C with CuBr/PMDETA and CuBr/tris[2-(dimethylamino)ethyl]amine (Me_6TREN). Polymerization rates increased when Cu(0) was added to regenerate the Cu(I) activator from the accumulated Cu(II) species. High MW PMMA was prepared by adjusting the [MMA]:[CDB] ratio and decreasing the amount of Cu catalyst (0.1 equiv relative to CDB) in the presence of Cu(0) as a reducing agent, as in activators regenerated by electron transfer (ARGET)–ATRP conditions. PMMA with $M_n > 10^6$ g mol^{-1} and $Đ < 1.3$ was synthesized under similar conditions with CuBr/tris(2-pyridylmethyl)amine (TPMA), Cu(0), and CDB [41]. Moreover, the PMMA-*b*-PSTY block copolymer synthesized by concurrent ATRP/RAFT exhibited higher retention of chain end functionality as compared to the same copolymer prepared by RAFT polymerization with thermal initiation (Figure 13.4).

In order to better exploit the degree of control offered by the fast chain transfer between propagating radicals and (macro)CTA, the concurrent ATRP/RAFT of STY and MMA was also carried out with Cu complexes that are inefficient ATRP catalysts [42]. Indeed, Cu(II) complexes with macrocyclic and anionic ligands are poor deactivators in ATRP [38]. However, when combined with CDB, well-controlled concurrent ATRP/RAFT was observed under ARGET or conventional ATRP conditions.

The controlled polymerization of acrylate monomers required the development of a dual concurrent ARGET–ATRP/RAFT (Scheme 13.2c), in which a conventional

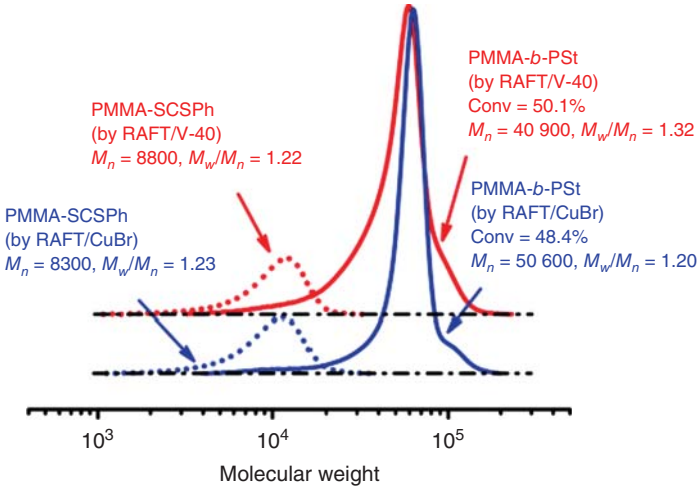

Figure 13.4 GPC traces of PMMA-S-C(S)-Ph macroinitiators (broken lines) and PMMA-*b*-PSTY (right side, solid lines) synthesized via conventional RAFT polymerization (red) and concurrent ATRP/RAFT (blue). Conditions: 50% STY in anisole, $T = 80$ °C. [STY]:[macroinitiator]:[V-40] = 1000 : 1 : 2 (RAFT), [STY]:[macroinitiator]:[$CuBr_2$]:[PMDETA]:[Cu(0)] = 1000 : 1 : 20 : 30 : 10 (concurrent ATRP/RAFT). Source: Reproduced with permission from Kwak et al. [40]. Copyright 2008, American chemical society.

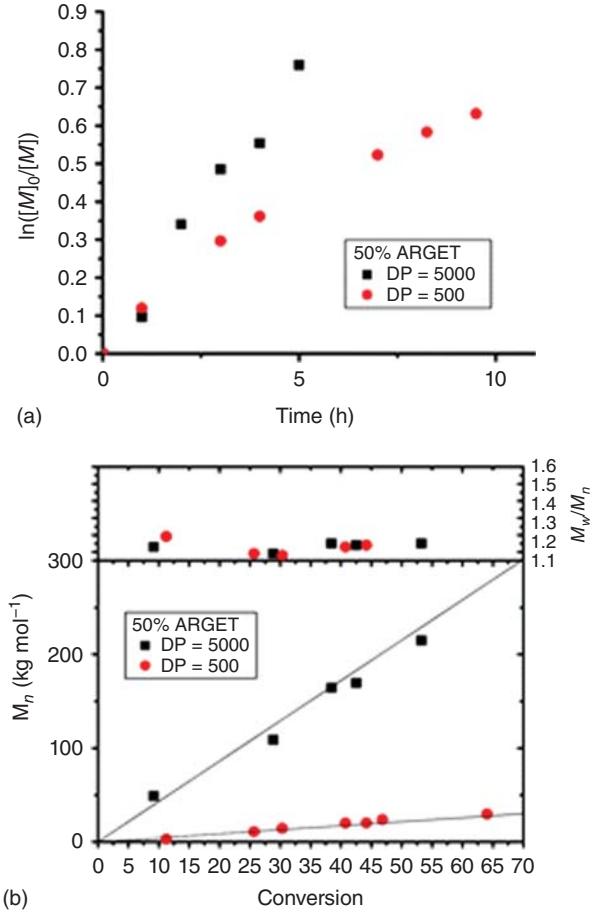

Figure 13.5 (a) Semi-logarithmic kinetic plots and (b) MW and dispersity evolution with conversion of dual concurrent ATRP/RAFT at targeted DP = 5000 (black) and DP = 500 (red). Conditions: 50 vol% MA in anisole, $T = 50\,°C$, [EBiB]:[CDB] = 1, [TPMA]:[$CuBr_2$] = 3, and Cu(0) wire ($L = 20$ cm, $d = 1$ mm). Source: Reproduced with permission from Elsen et al. [43]. Copyright 2011, American chemical society.

alkyl halide ATRP initiator was used together with a Cu catalyst, Cu(0), and a CTA [43]. Well-defined PMA was obtained at both target DP 50 and 5000 (Figure 13.5). Interestingly, by varying the molar ratio between ATRP initiator and CTA, it was observed that higher amounts of CTA afforded slower polymerizations, but the prepared polymers had lower dispersity, particularly at the early stage of the process. Afterwards, it was reported that a dual concurrent ATRP/RAFT polymerization of PEGMA in water was faster than in the absence of an ATRP initiator (i.e. concurrent ATRP/RAFT) [44]. This trend was observed at different temperatures ($T = 30$ and 90 °C), with a 1 : 2 ratio between alkyl halide and CTA, and $Fe^{III}Cl_3 \cdot H_2O/PPh_3$ as a catalyst.

A similar system composed of an alkyl halide and a dithiobenzoate CTA was used in the presence of Cu wire and an amine ligand [36, 45]. Dimethylsulfoxide (DMSO)

was typically used as a solvent, and well-controlled room temperature polymerizations of STY, *N*-vinylcarbazole, and various methacrylates were demonstrated [46]. Noticeably, when the ratio between alkyl halide and CTA was decreased, polymerizations were slower and better controlled, similar to the dual concurrent system.

A transition-metal-free activation of RAFT agents was developed by employing sodium sulfite salts, mainly sodium dithionite ($Na_2S_2O_4$) [47]. The proposed reaction mechanism (Scheme 13.3) involved (i) the thermal dissociation of dithionite anions to SO_2^{-}, (ii) the injection of one electron from SO_2^{-} to the CTA, and (iii) the dissociative electron transfer (DET) of the RAFT agent, which was reduced to a radical anion that fragmented into a propagating radical and an anion. The latter reaction was supported by density functional theory (DFT) computation of energy states. The process was therefore called DET–RAFT polymerization.

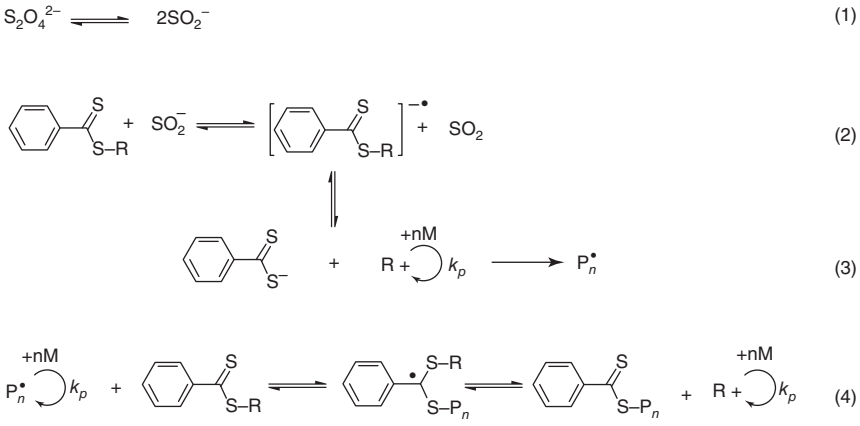

Scheme 13.3 Proposed mechanism of DET—RAFT polymerization using a dithiobenzoate CTA and a dithionite salt.

Control experiments showed that $Na_2S_2O_4$ could initiate the polymerization of MMA in the absence of a CTA, but the process was extremely slow, and therefore, its contribution in the presence of a CTA was neglected. In the DET–RAFT polymerizations of MMA using a dithiobenzoate CTA, the reaction rate was observed to increase with increasing $[Na_2S_2O_4]$, but the match between theoretical and experimental MW was poorly controlled. Several other methacrylates, as well as MA and STY, were polymerized with good control, but the reactions required 3–10 days to reach 36–53% monomer conversion.

13.4 Electrochemical Activation of RAFT Agents

Electrochemically triggered controlled polymerizations benefit from easily tunable parameters, 'green' character, and in situ monitoring of polymerization systems [48]. In electrochemically mediated atom transfer radical polymerization (*e*ATRP), electrochemical stimuli (i.e. applied current or potential) are used to reduce the ATRP deactivator, $XCu^{II}L^{+}$, to the active catalyst $Cu^{I}L^{+}$, which reductively cleaves the

dormant species to generate propagating radicals [49]. However, by modifying the stimulus (i.e. by applying an oxidative current/potential), all Cu species can be converted to the $XCu^{II}L^{+}$ deactivator, thus stopping the polymerization on-demand.

Electrochemical oxidation of a CTA in the presence of a mediator has been recently used to trigger controlled cationic polymerization of vinyl ethers [50]. In addition, electrochemical reduction of CTAs or external radical initiators was explored as an approach towards an electrochemically mediated RAFT polymerization.

13.4.1 Electrochemistry of RAFT Agents

The development of electrochemical methods to initiate and trigger RAFT polymerizations required a careful analysis of the redox properties of RAFT agents. The library of available RAFT agents is vast, as well as the mechanistic information about the performances of CTAs under polymerization conditions [1f]. Conversely, the electrochemical properties of these species are nearly unexplored. The advent of PET–RAFT has raised interest in measuring the redox potentials of RAFT agents in order to pair them with suitable photoredox catalysts [4]. However, this brief analysis concerned only a few RAFT agents.

More extensive electrochemical characterizations of some dithiobenzoates and trithiocarbonates can be found in the literature of organic electrochemistry. Lund and coworker and Savèant and coworkers conducted bulk electrolysis and voltammetric analysis of various thiocarbonylthio compounds, aiming to define the mechanism and the products of the electro-reduction of these species [51].

The dithiobenzoates analyzed by Lund and coworker had C_6H_5-C(S)-SR structure with R = C_6H_5, 4-ClC_6H_4, $C_6H_5CH_2$, $(CH_3)_3C$, CH_3 [51b]. In cyclic voltammetry (CV), all these compounds exhibited a reduction signal with cathodic peak potential $E_{pc} < -1$ V vs. saturated calomel electrode (SCE) because of the reduction to the corresponding radical anions $[C_6H_5CSSR]^{\cdot -}$. The CVs were conducted in DMF on a platinum electrode. The cathodic peak was irreversible at a scan rate below 0.2 V s^{-1}, likely because of a rapid subsequent dimerization of the electro-generated $[C_6H_5CSSR]^{\cdot -}$. The dimerization reaction was supported by the observation of a negative shift of the E_{pc} values when increasing the compounds' concentration ($dE_{pc}/d \log C = -0.02$ V $decade^{-1}$). It should be noted that such a negative shift was not observed for most commonly used RAFT agents in more recent analyses [8b, d]. Constant potential electrolysis followed by chromatographic analysis yielded diphenylacetylene and thiolates as most abundant products [51].

Similarly, the CVs of analyzed trithiocarbonates (RS-C(S)-SR with R = CH_3, C_2H_5, and $(CH_3)_2CH$) exhibited a cathodic peak because of the formation of $[RSCSSR]^{\cdot -}$ [51a, c]. The peak was irreversible at a scan rate <1 V s^{-1} on a mercury drop electrode in DMF. The analysis of reduction products after constant potential electrolysis showed that the initial compounds were further reacting with some products, in overall complicated reduction mechanisms.

Although the compounds analyzed by Lund et al. were different from traditionally used RAFT agents, their study suggests that (i) the electro-reduction of dithiobenzoates and trithiocarbonates generates their corresponding radical anions

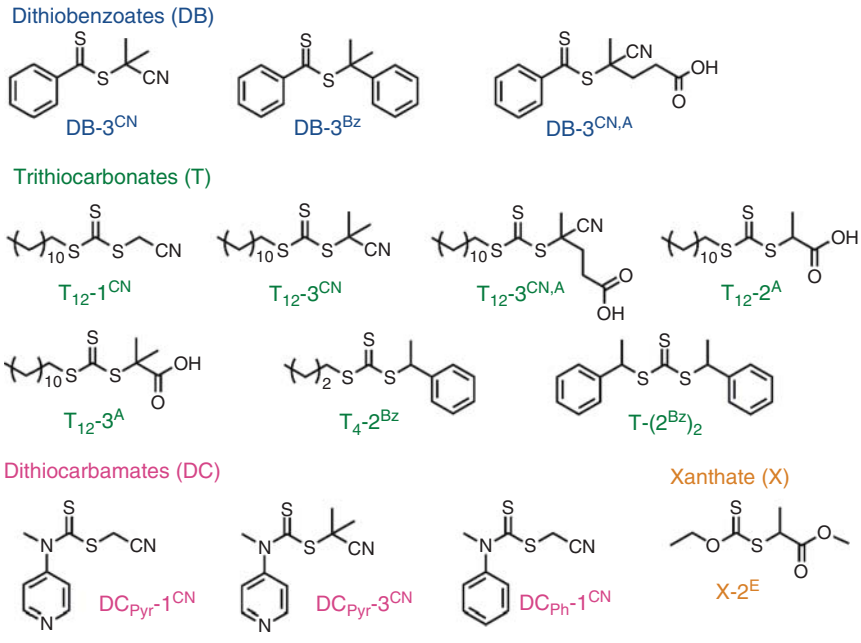

Figure 13.6 Molecular structures of electrochemically characterized RAFT agents. Source: Adapted with permission from Lorandi et al. [8b]. Copyright 2019, American chemical society.

and (ii) the radical anions are unstable and involved in subsequent chemical reactions.

Aiming to investigate compounds more relevant to RAFT polymerizations, we recently performed a voltammetric analysis of the RAFT agents in Figure 13.6 [8b]. In order to facilitate the identification of structure–reactivity relationships, a unified nomenclature is proposed to identify the CTAs. Considering their general structure as Z-C(S)-SR (or Z(CS)SR), the RAFT agents were coded with a first group of characters identifying the Z group, followed by a dash, followed by a second group of characters identifying the R group (i.e. Z–R). The Z groups were subdivided into four categories, namely, dithiobenzoates (DBs), trithiocarbonates (T), dithiocarbamates (DC), and xanthates (X). For trithiocarbonates, the subscripts T_4 and T_{12} indicated a Z group with a butyl or a dodecyl alkyl chain, respectively. For dithiocarbamates, DC_{Pyr} and DC_{Ph} indicated the presence of a pyridyl or a phenyl ring, respectively. Concerning the R group, the numbers 1, 2, and, 3 identified primary, secondary, and tertiary structures. Then, a superscript abbreviation indicated the nature of functional groups present in the R fragment: CN = cyano, Bz = benzyl, A = acidic carboxyl group, and E = ester.

The CVs of the RAFT agents were conducted on a glassy carbon (GC) electrode in DMF, and the general recorded pattern is shown in Figure 13.7. In agreement with the observations of Lund et al., the cathodic peak in region A was attributed to the generation of the radical anion $[Z(CS)SR]^{\cdot -}$. When the scan was extended

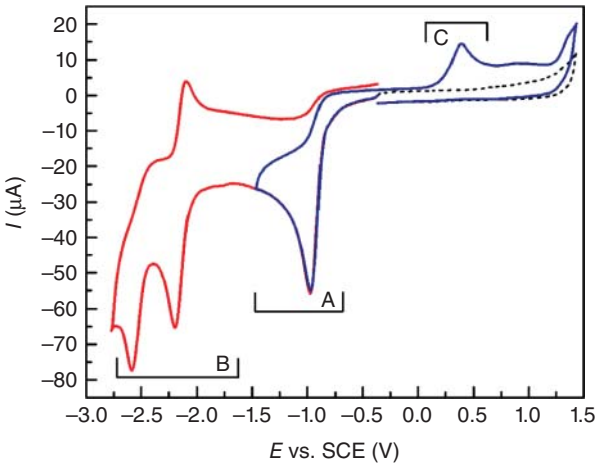

Figure 13.7 Cyclic voltammetry of 2×10^{-3} M DB-$3^{CN,A}$ in DMF + 0.1 M Et_4NBF_4 recorded on a GC disk at scan rate = 0.2 V s^{-1} and $T = 25$ °C. The letters A, B, and C denote regions common to all RAFT agents in Figure 13.6. The dashed line represents an oxidative scan not preceded by the reduction of the CTA, i.e. with initial potential −0.5 V vs. SCE. Source: Reprinted with permission from Lorandi et al. [8b]. Copyright 2019, American chemical society.

to more negative potentials, several peaks were recorded (region B), indicating that the overall reduction process involved various reactions and products. Finally, when reversing the scan, an anodic irreversible peak was observed in the potential range 0.3–0.5 V vs. SCE (region C). The peak was proposed to derive from the oxidation of some thiolates (RS^-) to disulfides because RS^- was observed as a reduction product by Lund et al. and the oxidation of RS^- was previously reported to occur at a similar potential range.

All compounds, with the exception of T_{12}-2^A and T_{12}-3^A, exhibited one irreversible reduction peak at any tested scan rate (0.02–20 V s^{-1}). This indicates that the electro-generated $[Z(CS)SR]^{\cdot -}$ was rapidly involved in one or more chemical reactions, which prevented the observation of the oxidation signal for $[Z(CS)SR]^{\cdot -}$ when the scan direction was reversed. T_{12}-2^A and T_{12}-3^A exhibited two irreversible reduction peaks, likely because of a 'father–son' interaction (i.e. the reaction of an electro-generated product with the initial compound). Indeed, it was postulated that the electro-generated $[Z(CS)SR]^{\cdot -}$ was rapidly protonated by the carboxylic group of the initial CTA molecule, and the resulting radical was further reduced at the electrode (i.e. self-protonation reaction).

The onset potential (E_{onset}) of the reduction of analyzed RAFT agents and the corresponding E_{pc} are listed in Table 13.1. E_{pc} values decreased in the order: dithiobenzoates > trithiocarbonates > dithiocarbamates ≈ xanthates. For each Z group, E_{pc} depended on the nature of the R group, with more positive values observed for tertiary R groups, followed by secondary, then primary R groups. Moreover, electron-withdrawing substituents in the R group shifted E_{pc} to more positive values because of the increased stability of the corresponding radicals. The

Table 13.1 Onset potential values for the reduction of electrochemically characterized RAFT agents in DMF on a GC electrode, at $T = 25\,°C$.[a)]

	RAFT agent	E_{onset} (V vs. SCE)	E_{pc} (V vs. SCE)
Dithiobenzoates	DB-3^{CN}	−0.887	−1.000
	DB-3^{Bz}	−1.044	−1.150
	DB-$3^{CN,A}$	−0.826	−0.940
Trithiocarbonates	T_{12}-1^{CN}	−0.987	−1.220
	T_{12}-3^{CN}	−1.118	−1.092
	T_{12}-$3^{CN,1}$	−1.101	−1.050
	T_{12}-2^{A}	−0.927	−1.338 (−1.691)
	T_{12}-3^{A}	−1.216	−1.228 (−1.556)
	T_{4}-2^{Bz}	−1.377	−1.500
	T-$(2^{Bz})_2$	−1.286	−1.437
Dithiocarbamates	DC_{Pyr}-1^{CN}	−1.378	−1.513
	DC_{Pyr}-3^{CN}	−1.285	−1.455
	DC_{Ph}-1^{CN}	−1.716	−1.898
Xanthate	X-2^{E}	−1.652	−1.812

a) 0.1 M Et_4NBF_4 was used as a supporting electrolyte. 2×10^{-3} M CTA, scan rate = 0.2 V s^{-1}. E_{onset} was measured as the intersection between the tangent to the baseline and the tangent to the reduction peak. The quasi-reference electrode used in the study was composed of Ag|AgI| (0.1 M *n*-Bu_4NBI in DMF). Ferrocene was used as an internal standard to refer the potential values to SCE, according to the conversion factors in the literature [52].

Source: Lorandi et al. [8b]. © 2019, American chemical society.

observed trends were further confirmed by electrochemical characterizations of a larger pool of RAFT agents [8d].

The solvent nature and electrode materials affected the voltammetric response of the RAFT agents. In CH_3CN, the measured E_{pc} values were generally 20–200 mV more negative than in DMF. Electrode materials other than GC were partially passivated during the reduction process, thus resulting in the E_{pc} values shifting to more negative potentials and poor reproducibility among consecutive potential cycles. Indeed, different potential values and even reversible voltammetric signals were previously reported for a few RAFT agents in different reports [4a, 53], likely because of the poor reproducibility of this measurement on Pt electrodes. Therefore, GC electrodes are recommended for electrochemical analysis of RAFT agents.

Bulk electrolysis of some RAFT agents performed at an applied potential $E_{app} = E_{pc}$ in the absence and presence of excess acid showed that (i) the C—S bond between the Z(CS)S unit and the R group was reductively cleaved in accordance with DFT analysis and (ii) reduction products reacted with initial compounds (father–son and grandfather–grandson interactions) in a multistep reduction process [8b, 54].

13.4.2 Direct and Mediated Electro-reduction of RAFT Agents

Common RAFT agents were observed to form short-lived radical anions upon electrochemical reduction [8]. This means that the initial RAFT agent is irreversibly lost after being electro-reduced. As a consequence, an *e*RAFT process in which radicals are generated by directly reducing the RAFT agent at the electrode surface (Scheme 13.4a) appears unlikely because the RAFT agent is invariably consumed, thus challenging the polymerization control.

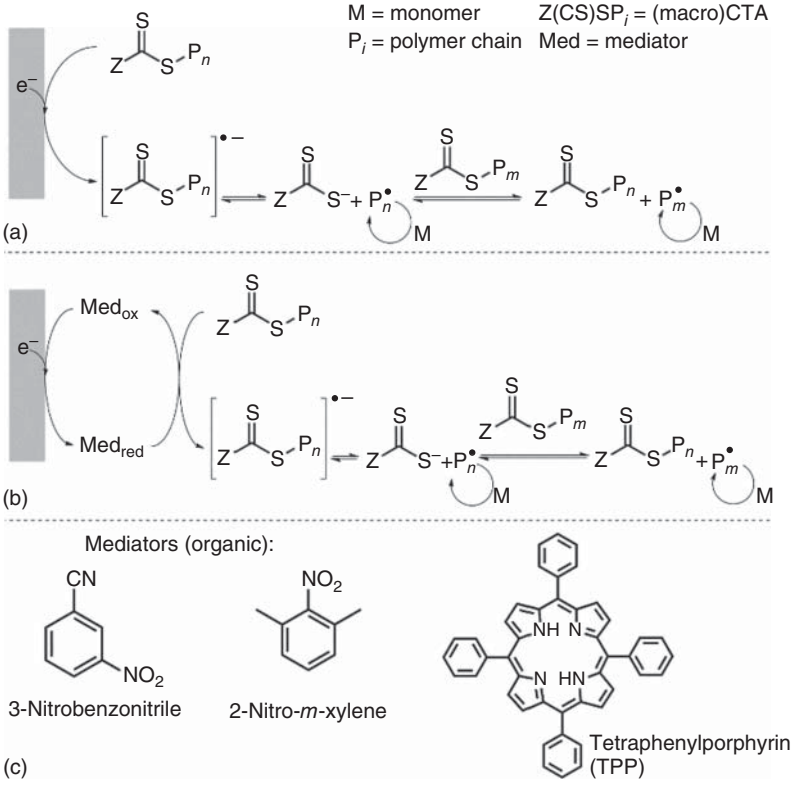

Scheme 13.4 Envisioned mechanisms of electrochemically mediated RAFT polymerization via direct (a) and mediated (b) electrolysis of a CTA. (c) Organic molecules tested as mediators for *e*RAFT polymerizations. Source: Adapted with permission from Lorandi et al. [8b]. Copyright 2019, American chemical society.

The rather negative cathodic peak potentials of RAFT agents made necessary to investigate the stability of other species in a RAFT system under the application of such reducing potential values. CV of commonly employed monomers in RDRPs showed that their reduction typically occurs at potential values more negative than −1.7 V vs. SCE (in DMF, Table 13.2). Therefore, most monomers will be electrochemically stable during the reduction of the vast majority of analyzed RAFT agents.

However, the direct electro-reduction of RAFT agents can produce a locally high concentration of radicals in the proximity of the electrode surface. It was previously

Table 13.2 Cathodic peak and onset potential value for the reduction of common monomers and standard reduction potentials of the corresponding radicals to carbanions measured in DMF at $T = 25\,°C$.[a)]

Monomer	$E^{\theta}_{radical}$ (V)[b)]	E_{pc} (V)[c)]	E_{onset} (V)[d)]
n-Butyl acrylate	−0.63[e)]	−2.18	−1.74
Methyl methacrylate	−0.91	−2.28	−1.97
Styrene	−1.53	−2.57	−2.23

a) 0.1 M Et_4NBF_4 was used as supporting electrolyte, scan rate = 0.2 V s^{-1}. All potentials are referred to SCE.
b) From [55].
c) Measured with 10 mM monomer.
d) Measured for 50 vol% monomer as the potential at the intersection between the tangent to the baseline and the tangent to the reduction signal.
e) For methyl acrylate radical.

reported that the propagating radicals of common monomers are reduced to carbanions at potentials more positive than the E_{pc} of many RAFT agents [56]. In particular, MA, MMA, and acrylonitrile radicals had standard reduction potentials (E^{θ}) between −0.63 and −0.91 V vs. SCE (Table 13.2). Consequently, if an *e*RAFT polymerization of one of these monomers is attempted by applying a potential $E_{app} = E_{pc}(CTA)$, the propagating radicals formed near to the electrode surface will be rapidly reduced to carbanions.

Radicals generated from similar monomers are expected to display similar reduction potentials. Only STY radicals ($E^{\theta} = -1.53$ V vs. SCE) can be preserved during the electro-reduction of dithiobenzoates or trithiocarbonates (i.e. the styryl radical is reduced at more negative potentials than the CTAs). Nevertheless, a few *e*RAFT polymerizations of STY via direct electro-reduction of dithiobenzoate or trithiocarbonate CTAs at various applied potentials resulted in slow reactions and polymers with high dispersity [8b]. Voltammetric analysis before and after the polymerizations confirmed the consumption of the RAFT agents.

In brief, an *e*RAFT polymerization is hampered by (i) the very short lifetime of $[Z\text{-}C(S)\text{-}SR]^{\cdot -}$ and their involvement in side reactions and (ii) the reduction of propagating radicals to carbanions occurring at similar or more positive potentials than the reduction of many RAFT agents (Scheme 13.5).

Therefore, it appeared necessary to develop an alternative pathway towards *e*RAFT polymerization. The use of a redox active mediator is a common strategy to convert a heterogeneous electron transfer (ET) between the electrode and the substrate of interest to a homogeneous ET occurring in solution (Scheme 13.4b). In order to efficiently shuttle electrons from the electrode to the solution, (i) the reduction potential of the mediator (E^{θ}_{Med}) should be more positive, but relatively close to the one of the substrate, (ii) the ET between the electrode and mediator and between the mediator and substrate must be fast, and (iii) the reduced mediator should not participate in side reactions (e.g. coupling with radicals, reduction of radicals to carbanions) [57].

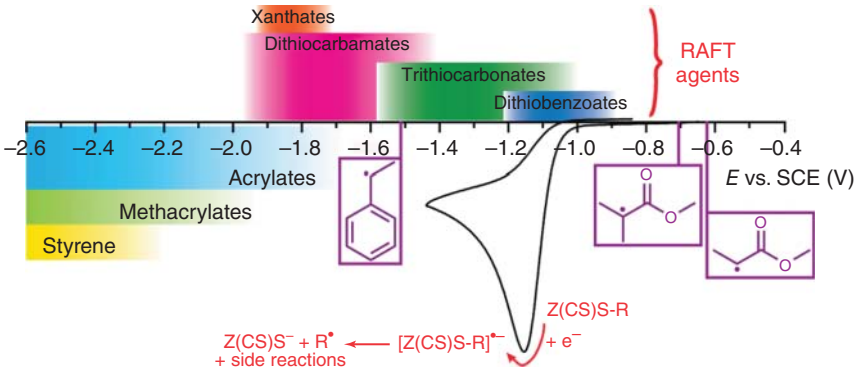

Scheme 13.5 Reduction potential range of typical RAFT agents, monomers, and propagating radicals measured by cyclic voltammetry in DMF at $T = 25$ °C. Source: Reprinted with permission from Lorandi et al. [8b]. Copyright 2019, American chemical society.

Typical mediators for electro-reduction reactions are aromatic hydrocarbons or transition metal complexes. A few compounds from both these classes were tested as mediators for *e*RAFT polymerizations.

13.4.2.1 Organic Mediators for *e*RAFT Polymerizations

Small-molecule aromatic hydrocarbons such as 3-nitrobenzonitrile and 2-nitro-*m*-xylene (Scheme 13.4c) were tested as mediators for the *e*RAFT polymerization of STY [8b]. The CV of these mediators showed reversible signals that were modified after the addition of the RAFT agents DB-3^{Bz} or T_4-2^{Bz}. Indeed, the cathodic currents of mediators' signals increased in intensity while the anodic currents decreased, indicating that mediators catalytically reduced the RAFT agents. However, negligible conversion or poor control were observed in the polymerization of STY, at $E_{app} \approx E^{\theta}_{Med}$.

This result was attributed to a coupling reaction between the radicals in solution and the radical anions derived from the small-molecule mediators. Therefore, tetraphenylporphyrin (TPP, Scheme 13.4c) was tested as a mediator because of a more bulky and conjugated structure. The *e*RAFT polymerization of acrylates in the presence of TPP as a mediator and T_{12}-2^{A} or T_{12}-3^{A} RAFT agents at room temperature gave polymers with pre-determined molecular weight and low dispersity. The mediator loading could be decreased to 0.01 mol% relative to the CTA. However, the polymerizations were relatively slow (<20% conversion in six hours) and voltammetric analysis showed that the CTA was partially lost. Anthraquinone (AQ) was subsequently tested as mediator for *e*RAFT polymerization, owing to its reversible redox chemistry and efficient electron transfer to several RAFT agents [8c]. *e*RAFT polymerizations of MMA in DMSO mediated by AQ reached > 60% conversions in 24 h at room temperature. The polymerization rate strongly decreased when targeting high DP (200-400). Nevertheless, PMMA with low dispersity was obtained, indicating that the identification of suitable mediators and reaction consitions can broaden the scope of *e*RAFT polymerizations.

A mediated electrolysis of RAFT agents was exploited for electro-RAFT polymerization catalyzed by a redox-active coenzyme, the nicotinamide adenine dinucleotide (NADH) [53]. The electro-reduction of NAD^+ to NADH promoted the reaction of the latter with a CTA, which could generate radicals to start the polymerization. However, repeated attempts to reproduce this system by our group gave no monomer conversion, possibly because the NADH molecule is not sufficiently hindered to prevent coupling with generated radicals.

In summary, *e*RAFT polymerizations could be conducted through a mediated electro-reduction of RAFT agents, in which suitable mediators were employed to transfer electrons from the electrode surface to the CTA in solutions, thus preventing the direct electro-reduction of the CTA and a high local concentration of radicals at the electrode. Nevertheless, efforts should be devoted to find mediators that efficiently and rapidly exchange electrons with the CTA, without being involved in side reactions.

13.4.2.2 Activation of RAFT Agents via Electro-reduction of ATRP Catalysts

Transition metal complexes and particularly traditional ATRP catalysts can activate RAFT agents, as described in Section 13.3 [6]. Because the active form of the catalysts is the Cu(I) species, electrochemistry can be used to reduce an air-stable Cu(II) precursor to the active Cu(I) [49], which can further reduce the CTA. As a result, the Cu complex is a mediator for the electro-reduction of the RAFT agent.

The use of electrochemical stimuli to trigger ATRP with alkyl DC initiators and (dual) concurrent ATRP/RAFT polymerization should provide several benefits for these processes, as in the case of *e*ATRP. In situ regeneration of the active Cu(I) species, no need of chemical reducing agents and consequently no by-products, diminished catalyst loadings, and facile temporal control are among these advantages [48, 58].

Electrochemical tools have been successfully applied to reduce a Cu(II) complex in the presence of a dithiocarbamate, thus developing an *e*ATRP of MMA with an alkyl pseudohalide initiator [59]. Preliminary CV showed that the reversible signal of $Cu^{II}(DC)_2$/2,2′-bipyridine (bpy) became catalytic after the addition of the RAFT agent 1-cyano-1-methylethyl diethyldithiocarbamate (MANDC, Figure 13.8a). This analysis proved that the Cu complexes could catalytically activate MANDC and guided the selection of the E_{app} values to be applied during the electrolysis. The reduction potential of the Cu catalyst was 1.5 V more positive than the reduction of MANDC, which therefore was not directly reduced during the electrolysis.

*e*ATRPs of MMA with alkyl pseudohalides at $T = 80\,^{\circ}C$ were well-controlled giving polymers with expected MWs and $Đ < 1.4$. The polymerization rate increased with decreasing E_{app}, as generally observed in *e*ATRP. The Cu loading was successfully diminished to 500 ppm, while different DPs were targeted, showing an increase in the polymerization rate with decreasing the target DP, as expected for an ATRP process. Control experiments conducted in the dark and in the absence of a Cu catalyst allowed to exclude that the polymerization proceeded through a photoiniferter or a traditional RAFT mechanism, respectively. Finally, the retention of chain end functionality was demonstrated by chain extending a PMMA–DC block with *n*-butyl methacrylate (BMA) and STY. A clean shift towards higher MWs was observed in the GPC traces (Figure 13.9).

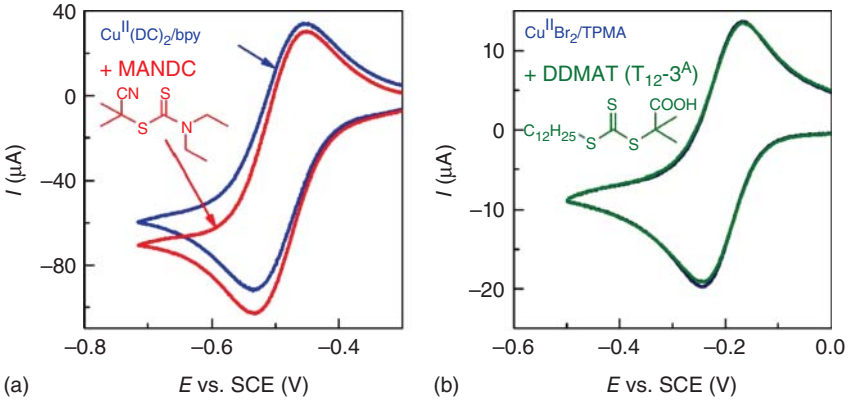

Figure 13.8 (a) CV of 4.7×10^{-3} M $Cu^{II}(DC)_2$/bpy in the absence and presence of 2.3×10^{-2} M MANDC in 50 vol% MMA in DMF + 0.1 M n-Bu_4NClO_4, $T = 80\,°C$. Source: Adapted with permission from Wang et al. [59]. Copyright 2019, John Wiley & Sons. (b) CV of 1.1×10^{-3} M $Cu^{II}Br_2$/TPMA in the absence and presence of 3.5×10^{-3} M DDMAT (T_{12}-3^A), in 50 vol% BA in DMF + 0.1 M Et_4NBF_4, $T = 50\,°C$. Source: Adapted with permission from Wang et al. [60]. Copyright 2018, John Wiley and Sons.

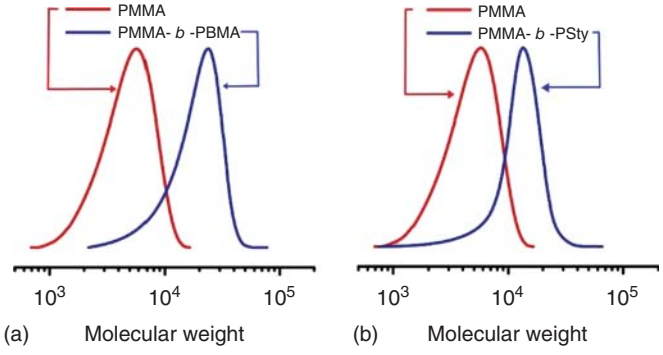

Figure 13.9 Chain extension from PMMA macroinitiators via (a) *e*ATRP of BMA. [BMA]:[PMMA-DC]:[$Cu(DC)_2$]:[bpy] = 150 : 1 : 0.2 : 0.2, 50 vol% BMA in DMF + 0.1 M n-Bu_4NClO_4, $T = 80\,°C$, $E_{app} = E_{pc,Cu}$, and (b) normal ATRP of STY. [STY]:[PMMA-DC]:[CuBr]:[PMDETA] = 200 : 1 : 1 : 1, 50 vol% STY in DMF, $T = 120\,°C$. Source: Adapted with permission from Wang et al. [59]. Copyright 2019, John Wiley & Sons.

A dual concurrent electrochemically mediated ATRP/RAFT was recently proposed aiming to combine the ATRP/RAFT synergy with the electrochemical triggering [60]. 2-(Dodecylthiocarbonothioylthio)-2-methylpropionic acid (DDMAT or T_{12}-3^A) was selected as a CTA for the polymerization of BA at $T = 50\,°C$. The CV of a typical ATRP catalyst, $CuBr_2$/TPMA, was not modified in the presence of T_{12}-3^A (Figure 13.8b), suggesting that the Cu complex could not activate the CTA, thus excluding the possibility of an *e*ATRP with T_{12}-3^A as alkyl pseudohalide. Therefore, a conventional ATRP initiator, ethyl α-bromoisobutyrate (EBiB), was used to generate radicals, which were subsequently deactivated by both reacting

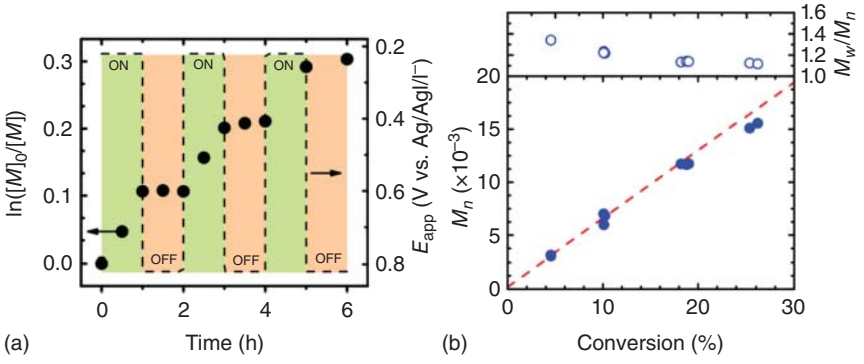

Figure 13.10 Temporal control in dual concurrent *e*ATRP/RAFT polymerization of BA. (a) Polymerization kinetics and (b) MW and $Đ$ evolution with conversion. Conditions: 50 vol% BA in DMF + 0.1 M Et_4NBF_4, $T = 50\,°C$. [BA]:[T_{12}-3^A]:[EBiB]:[$CuBr_2$]:[TPMA] = 500 : 0.5 : 0.5 : 0.015 : 0.03, 'ON' $E_{app} = E_{pc,Cu}$, 'OFF' $E_{app} = E_{pc,Cu} + 0.6\,V$. Source: Reproduced with permission from Wang et al. [60]. Copyright 2018, John Wiley & Sons.

with the ATRP deactivator $BrCu^{II}TPMA^+$ and by degeneratively exchanging with the CTA. Indeed, a control experiment in the absence of T_{12}-3^A gave a four times faster polymerization than with a 1/1 ratio of T_{12}-3^A/EBiB. This indicates that T_{12}-3^A caused rate retardation in the polymerization, likely because of the slow fragmentation of the macro(CTA) and in agreement with previous reports [43, 44].

The dual concurrent *e*ATRP/RAFT gave PBA with MW matching the theoretical values and $Đ < 1.20$. By decreasing the T_{12}-3^A/EBiB ratio, the polymerization rate increased because of the smaller rate of retardation, as well as the higher radical concentration. Interestingly, well-controlled polymerizations could be obtained with as low as 10 ppm of Cu catalyst and 1% or 2% T_{12}-3^A relative to EBiB, whereas in the absence of T_{12}-3^A, such a small amount of Cu complex was not enough to ensure an efficient deactivation.

Finally, temporal control over the polymerization of BA was achieved by simply tuning the applied potential (Figure 13.10). Indeed, the polymerization was effectively switched off by applying a potential much more positive than the reduction of the catalyst ($E_{pc,Cu} + 0.6\,V$) and then restarted by applying $E_{app} = E_{pc,Cu}$.

13.5 Electro-reduction of Radical Initiators

Another way to obviate the direct electro-reduction of a CTA at the electrode surface is to electro-reduce a conventional radical initiator, such as to generate radicals at room temperature. The electro-generated radicals can initiate the polymerization in solution. Importantly, the reduction of the radical initiator must occur at a more positive potential than the reduction of the RAFT agent, which otherwise will be irreversibly consumed. This approach is similar to the redox-initiated RAFT polymerization described in Section 13.2, with replacing the chemical redox process with an electrochemical stimulus.

Two radical initiators, BPO and the diazonium salt 4-bromobenzenediazonium tetrafluoroborate ($BrPhN_2^+$), were tested for the *e*RAFT polymerization of BA and MMA (50 vol% monomer in DMF) [8a]. The reduction of BPO was investigated by CV, showing an irreversible reduction peak with $E_{pc,BPO} = -0.83$ V vs. SCE in DMF. Two electrons are required for the reduction of a molecule of BPO, according to the following equations [61]:

$$(RO)_2 + e^- \rightleftharpoons RO^{\cdot} + RO^- \tag{13.6}$$

$$RO^{\cdot} + e^- \rightleftharpoons RO^- \tag{13.7}$$

The electro-generated radicals were stable enough to initiate a free radical polymerization of MMA in the absence of any RAFT agents. However, the voltammetric signal of BPO strongly overlapped with the reduction signal of 4-cyano-4-(phenylcarbonothioylthio)pentanoic acid (CPAD or DB-$3^{CN,A}$, $E_{pc,DB\text{-}3CN,A} = -1$ V vs. SCE in DMF), which was selected as suitable CTA for the polymerization of methacrylates. As a consequence, when the applied potential was $E_{app} = E_{pc,BPO} - 0.17$ V, CPAD was also partially electro-reduced and MMA radicals formed in the vicinity of the electrode were further reduced to carbanions. Indeed, <5% conversion was obtained in 20 hours. Conversely, when $E_{app} = E_{pc,BPO} + 0.34$ V, the reduction of BPO was inefficient and negligible conversion was observed after 20 hours. Finally, $E_{app} = E_{pc,BPO}$ allowed to obtain PMMA with $Đ = 1.17$, but the process was relatively slow (22% conversion in 20 hours). The MW of PMMA was 30% lower than expected, indicating that new chains were generated by the electro-reduced BPO. Similar results were obtained for BA and T_{12}-3^A as CTA ($E_{pc,T12\text{-}3A} = -1.25$ V vs. SCE in DMF).

The CV of the diazonium salt $BrPhN_2^+$ gave a reduction peak with $E_{pc,BrPhN_2^+} = -0.1$ V vs. SCE, about 1 V more positive than DB-$3^{CN,A}$ (Figure 13.11a), thus removing any limitations on the E_{app} value. The reduction of $BrPhN_2^+$ gives highly reactive bromophenyl radicals, which can quickly graft onto the electrode surface. A free radical polymerization of BA was tested by reducing the diazonium salt ($E_{app} = E_{pc,BrPhN_2^+}$) in the absence of a RAFT agent. A 75% conversion was reached in 16 hours, proving that some BrPh· could initiate the polymerization in the solution instead of grafting onto the electrode.

The effect of the $[T_{12}\text{-}3^A]$:$[BrPhN_2^+]$ ratio was analyzed for the *e*RAFT polymerization of MMA conducted at $E_{app} = E_{pc,BrPhN_2^+}$. A large amount of $BrPhN_2^+$ (10 equiv relative to T_{12}-3^A) generated a high concentration of radicals; therefore, the polymerization was relatively fast but the control was limited. In contrast, when using $[T_{12}\text{-}3^A]$:$[BrPhN_2^+] = 1:1$, the system reached 48% conversion in 20 hours, giving PBA with MW matching the theoretical value and $Đ = 1.27$. However, the rate was strongly reduced after five hours, likely because initiating radicals grafted onto the electrode surface, preventing the further reduction of the diazonium salt, as supported by the recorded current rapidly decaying to zero.

The 'passivation' of the electrode surface was overcome by working under galvanostatic conditions, i.e. by applying a constant current to electro-reduce $BrPhN_2^+$. A galvanostatic approach requires a simpler electrochemical apparatus because

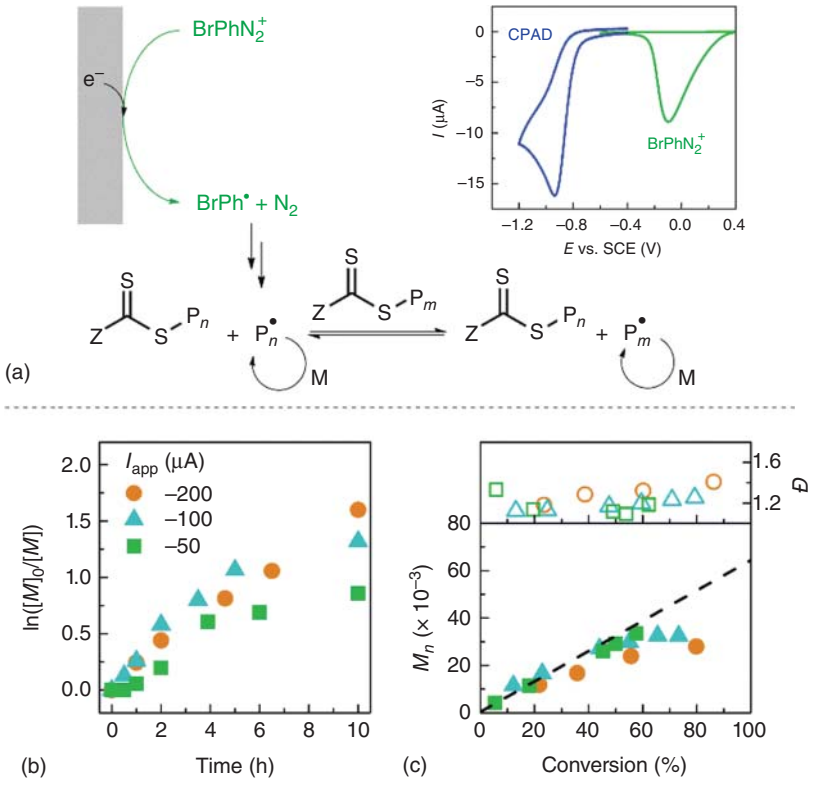

Figure 13.11 (a) Mechanism of *e*RAFT via electro-reduction of the diazonium salt $BrPhN_2^+$ and CV of 10^{-3} M CPAD (DB-$3^{CN,A}$) + 10^{-3} M $BrPhN_2^+$ in DMF + 0.1 M Et_4NPF_6, $T = 25\,°C$, scan rate = 0.1 V s^{-1}. (b) Semi-logarithmic kinetic plot and (c) MW and dispersity evolution with monomer conversion during the galvanostatic *e*RAFT of 50 vol% BA in DMF + 0.1 M Et_4NPF_6, [BA]:[T_{12}-3^A]:[$BrPhN_2^+$] = 500 : 1 : 1, $T = 25\,°C$. Source: Adapted with permission from Wang et al. [8a]. Copyright 2017, American chemical society.

a common current generator and two electrodes can replace the conventional potentiostat with a three-electrode set-up [48, 58]. Different applied current values were tested ($I_{app} = -50$, -100, and -200 mA). Faster polymerization was observed with the highest I_{app} (Figure 13.11b,c). However, the lowest current provided better control, particularly a better match between theoretical and measured MW of PBA because fewer new chains were generated during the *e*RAFT polymerization. This method was also used to prepare a PBA-macro(CTA) that was successfully extended with *tert*-butyl acrylate, yielding a well-defined block copolymer.

This redox initiation technique based on the electro-reduction of $BrPhN_2^+$ was recently applied to a surface-initiated *e*RAFT polymerization (SI-*e*RAFT) in order to prepare a biosensor for the electrochemical detection of protein kinase (PK) activity [62]. It should be noted that a combination of electropolymerization on a surface and RAFT agents was previously reported, where the presence of RAFT agents was proved to promote the growth of a more uniform PNIPAM film [63]. The fabrication of the biosensor via SI-*e*RAFT required the following

steps: (i) self-assembly of substrate peptides on the surface of an Au electrode, (ii) site-specific phosphorylation of substrate peptides by PKs, (iii) anchoring a CTA containing a –COOH group to the phosphorylated sites, and (iv) SI-*e*RAFT of ferrocenyl methacrylate (FcMMA) initiated by $BrPhN_2^+$. The effective grafting of several ferrocenyl units allowed for strongly amplifying the detection signal of PK.

The biosensors tested with a model target showed a low detection limit by 1–2 orders of magnitude lower as compared to other detection methods. Indeed, the latter are typically based on the (photoelectro)chemical detection of stoichiometric reaction between phosphorylated sites and electroactive tags. Therefore, the *e*RAFT polymerization served as a powerful amplification strategy. Moreover, the proposed biosensor exhibited strong specificity for the model target, high reproducibility, and long-term stability.

13.6 Conclusions and Perspectives

The development of novel initiation methods has brought several advantages to RAFT polymerizations. Redox-initiated RAFT polymerizations, including Fenton–RAFT and *e*RAFT via electro-reduction of radical generators, allow for the preparation of (co)polymers at low temperatures, thus diminishing the extent of side reactions and enabling to work under biological conditions. *e*RAFT polymerization via electro-reduction of CTAs remains challenging because of the very negative reduction potential of typical RAFT agents, which can be more negative than the reduction potential of vinyl monomers. Thus, an effective *e*RAFT requires the development of new efficient mediators. Chemical and electrochemical activation of RAFT agents eliminate the issue of new chains generation during polymerizations. Moreover, both ATRP and RAFT polymerization can benefit from the synergistic interaction between the two processes. Therefore, these techniques can give access to new functional and biocompatible materials.

Acknowledgement

The support from NSF (CHE 1707490) is gratefully acknowledged.

References

1 (a) Chiefari, J., Chong, Y.K., Ercole, F. et al. (1998). *Macromolecules* 31: 5559–5562. https://doi.org/10.1021/ma9804951. (b) Barner-Kowollik, C. (2008). *Handbook of RAFT Polymerization*. Wiley. (c) Semsarilar, M. and Perrier, S. (2010). *Nat. Chem.* 2: 811–820. https://doi.org/10.1038/Nchem.853. (d) Moad, G., Rizzardo, E., and Thang, S.H. (2012). *Aust. J. Chem.* 65: 985–1076. https://doi.org/10.1071/CH12295. (e) Hill, M.R., Carmean, R.N., and Sumerlin, B.S. (2015). *Macromolecules* 48: 5459–5469. https://doi.org/10.1021/acs.macromol.5b00342.

(f) Perrier, S. (2017). *Macromolecules* 50: 7433–7447. https://doi.org/10.1021/acs.macromol.7b00767.

2 Destarac, M. (2011). *Polym. Rev.* 51: 163–187. https://doi.org/10.1080/15583724.2011.568130.

3 McKenzie, T.G., Fu, Q., Uchiyama, M. et al. (2016). *Adv. Sci.* 3: 1500394. https://doi.org/10.1002/advs.201500394.

4 (a) Xu, J., Jung, K., Atme, A. et al. (2014). *J. Am. Chem. Soc.* 136: 5508–5519. https://doi.org/10.1021/ja501745g. (b) Xu, J., Shanmugam, S., Duong, H.T., and Boyer, C. (2015). *Polym. Chem.* 6: 5615–5624. https://doi.org/10.1039/C4PY01317D.

5 Zheng, H.T., Bai, W., Hu, K.L. et al. (2008). *J. Polym. Sci., Part A: Polym. Chem.* 46: 2575–2580. https://doi.org/10.1002/pola.22590.

6 Kwak, Y., Nicolay, R., and Matyjaszewski, K. (2009). *Aust. J. Chem.* 62: 1384–1401. https://doi.org/10.1071/Ch09230.

7 Reyhani, A., McKenzie, T.G., Ranji-Burachaloo, H. et al. (2017). *Chem. Eur. J.* 23: 7221–7226. https://doi.org/10.1002/chem.201701410.

8 (a) Wang, Y., Fantin, M., Park, S. et al. (2017). *Macromolecules* 50: 7872–7879. https://doi.org/10.1021/acs.macromol.7b02005. (b) Lorandi, F., Fantin, M., Shanmugam, S. et al. (2019). *Macromolecules* 52: 1479–1488. https://doi.org/10.1021/acs.macromol.9b00112. (c) Strover, L.T., Postma, A., Horne, M.D. and Moad, G. (2020). *Macromolecules.* 53: 10315–10322. https://doi.org/10.1021/acs.macromol.0c02392. (d) Strover, L.T., Cantalice, A., Lam, J.Y.L. et al. (2019). *ACS Macro Lett.* 8: 1316–1322. https://doi.org/10.1021/acsmacrolett.9b00598.

9 (a) Sarac, A.S. (1999). *Prog. Polym. Sci.* 24: 1149–1204. https://doi.org/10.1016/S0079-6700(99)00026-X. (b) Sideridou, I.D., Achilias, D.S., and Karava, O. (2006). *Macromolecules* 39: 2072–2080. https://doi.org/10.1021/ma0521351.

10 Li, G., Zheng, H., and Bai, R. (2009). *Macromol. Rapid Commun.* 30: 442–447. https://doi.org/10.1002/marc.200800666.

11 Li, Y., Yang, J.W., and Benicewicz, B.C. (2007). *J. Polym. Sci. Pol. Chem.* 45: 4300–4308. https://doi.org/10.1002/pola.22172.

12 Li, G., Wang, H., Zheng, H., and Bai, R. (2010). *J. Polym. Sci., Part A: Polym. Chem.* 48: 1348–1356. https://doi.org/10.1002/pola.23896.

13 Zheng, H.T., Ye, X.D., Wang, H. et al. (2011). *Soft Matter* 7: 3956–3962. https://doi.org/10.1039/c0sm01132k.

14 Sanchez-Sanchez, A., Asenjo-Sanz, I., Buruaga, L., and Pomposo, J.A. (2012). *Macromol. Rapid Commun.* 33: 1262–1267. https://doi.org/10.1002/marc.201200180.

15 Luo, J.X., Li, M.C., Xin, M.H., and Sun, W.F. (2015). *Macromol. Chem. Phys.* 216: 1646–1652. https://doi.org/10.1002/macp.201500156.

16 Yang, H., Xue, S., Pan, J. et al. (2016). *RSC Adv.* 6: 14120–14127. https://doi.org/10.1039/C5RA25078A.

17 Bai, W., Zhang, L., Bai, R., and Zhang, G. (2008). *Macromol. Rapid Commun.* 29: 562–566. https://doi.org/10.1002/marc.200700823.

18 Read, E., Guinaudeau, A., Wilson, D.J. et al. (2014). *Polym. Chem.* 5: 2202–2207. https://doi.org/10.1039/c3py01750h.

19 (a) Dos Santos, A.M., Le Bris, T., Graillat, C. et al. (2009). *Macromolecules* 42: 946–956. https://doi.org/10.1021/ma802117h. (b) Liu, G.Y., Qiu, Q., Shen, W.Q., and An, Z.S. (2011). *Macromolecules* 44: 5237–5245. https://doi.org/10.1021/ma200984h.

20 Sun, X.L., He, W.D., Li, J. et al. (2009). *J. Polym. Sci., Part A: Polym. Chem.* 47: 6863–6872. https://doi.org/10.1002/pola.23725.

21 Sun, X.L., He, W.D., Pan, T.T. et al. (2010). *Polymer* 51: 110–114. https://doi.org/10.1016/j.polymer.2009.11.014.

22 Guinaudeau, A., Mazieres, S., Wilson, D.J., and Destarac, M. (2012). *Polym. Chem.* 3: 81–84. https://doi.org/10.1039/c1py00373a.

23 Pound, G., Eksteen, Z., Pfukwa, R. et al. (2008). *J. Polym. Sci., Part A: Polym. Chem.* 46: 6575–6593. https://doi.org/10.1002/pola.22968.

24 Martin, L., Gody, G., and Perrier, S. (2015). *Polym. Chem.* 6: 4875–4886. https://doi.org/10.1039/c5py00478k.

25 McKenzie, T.G., Reyhani, A., Nothling, M.D., and Qiao, G.G. (2018). Hydroxyl radical activated RAFT polymerization. In: *Reversible Deactivation Radical Polymerization: Mechanisms and Synthetic Methodologies* (eds. K. Matyjaszewski, H. Gao, B.S. Sumerlin and N.V. Tsarevsky), 307–321. American Chemical Society.

26 Jesson, C.P., Pearce, C.M., Simon, H. et al. (2016). *Macromolecules* 50: 182–191. https://doi.org/10.1021/acs.macromol.6b01963.

27 Nothling, M.D., McKenzie, T.G., Reyhani, A., and Qiao, G.G. (2018). *Macromol. Rapid Commun.* 39: e1800179. https://doi.org/10.1002/marc.201800179.

28 Eggers, S. and Abetz, V. (2018). *Macromol. Rapid Commun.* 39: 1700683. https://doi.org/10.1002/marc.201700683.

29 Reyhani, A., Nothling, M.D., Ranji-Burachaloo, H. et al. (2018). *Angew. Chem. Int. Ed.* 57: 10288–10292. https://doi.org/10.1002/anie.201802544.

30 Reyhani, A., Allison-Logan, S., Ranji-Burachaloo, H. et al. (2019). *J. Polym. Sci., Part A: Polym. Chem.* 57: 1922–1930. https://doi.org/10.1002/pola.29318.

31 Carmean, R.N., Becker, T.E., Sims, M.B., and Sumerlin, B.S. (2017). *Chem* 2: 93–101. https://doi.org/10.1016/j.chempr.2016.12.007.

32 Lv, Y., Liu, Z., Zhu, A., and An, Z. (2017). *J. Polym. Sci., Part A: Polym. Chem.* 55: 164–174. https://doi.org/10.1002/pola.28380.

33 (a) Zhang, B., Wang, X., Zhu, A. et al. (2015). *Macromolecules* 48: 7792–7802. https://doi.org/10.1021/acs.macromol.5b01893. (b) Liu, Z., Lv, Y., and An, Z. (2017). *Angew. Chem. Int. Ed.* 56: 13852–13856. https://doi.org/10.1002/anie.201707993. (c) Enciso, A.E., Fu, L., Russell, A.J., and Matyjaszewski, K. (2018). *Angew. Chem. Int. Ed.* 57: 933–936. https://doi.org/10.1002/anie.201711105. (d) Enciso, A.E., Fu, L., Lathwal, S. et al. (2018). *Angew. Chem. Int. Ed.* 57: 16157–16161. https://doi.org/10.1002/anie.201809018.

34 Matyjaszewski, K. (2012). *Macromolecules* 45: 4015–4039. https://doi.org/10.1021/ma3001719.

35 (a) Matyjaszewski, K. (2018). *Adv. Mater.* 30: e1706441. https://doi.org/10.1002/adma.201706441. (b) Matyjaszewski, K. and Tsarevsky, N.V. (2014). *J. Am. Chem. Soc.* 136: 6513–6533. https://doi.org/10.1021/ja408069v.

36 Harihara Subramanian, S., Prakash Babu, R., and Dhamodharan, R. (2008). *Macromolecules* 41: 262–265. https://doi.org/10.1021/ma7021056.

37 Kwak, Y. and Matyjaszewski, K. (2008). *Macromolecules* 41: 6627–6635. https://doi.org/10.1021/ma801231r.

38 Ribelli, T.G., Lorandi, F., Fantin, M., and Matyjaszewski, K. (2019). *Macromol. Rapid Commun.* 40: e1800616. https://doi.org/10.1002/marc.201800616.

39 Nicolay, R., Kwak, Y., and Matyjaszewski, K. (2008). *Macromolecules* 41: 4585–4596. https://doi.org/10.1021/ma800539v.

40 Kwak, Y., Nicolay, R., and Matyjaszewski, K. (2008). *Macromolecules* 41: 6602–6604. https://doi.org/10.1021/ma801502s.

41 Nicolaÿ, R., Kwak, Y., and Matyjaszewski, K. (2010). *Angew. Chem. Int. Ed.* 122: 551–554. https://doi.org/10.1002/anie.200905340.

42 Kwak, Y., Yamamura, Y., and Matyjaszewski, K. (2010). *Macromol. Chem. Phys.* 211: 493–500. https://doi.org/10.1002/macp.200900509.

43 Elsen, A.M., Nicolay, R., and Matyjaszewski, K. (2011). *Macromolecules* 44: 1752–1754. https://doi.org/10.1021/ma200263w.

44 Pan, J., Miao, J., Zhang, L. et al. (2013). *Polym. Chem.* 4: 5664–5670. https://doi.org/10.1039/C3PY00671A.

45 (a) Zhang, W., Zhang, W., Zhang, Z. et al. (2010). *Macromol. Rapid Commun.* 31: 1354–1358. https://doi.org/10.1002/marc.201000008. (b) Haridharan, N., Ponnusamy, K., and Dhamodharan, R. (2010). *J. Polym. Sci., Part A: Polym. Chem.* 48: 5329–5338. https://doi.org/10.1002/pola.24333.

46 (a) Haridharan, N. and Dhamodharan, R. (2011). *J. Polym. Sci., Part A: Polym. Chem.* 49: 1021–1032. https://doi.org/10.1002/pola.24518. (b) Shen, Q., Zhang, J., Zhang, S. et al. (2012). *J. Polym. Sci., Part A: Polym. Chem.* 50: 1120–1126. https://doi.org/10.1002/pola.25868.

47 Maximiano, P., Mendonça, P.V., Costa, J.R.C. et al. (2016). *Macromolecules* 49: 1597–1604. https://doi.org/10.1021/acs.macromol.5b02647.

48 Lorandi, F., Fantin, M., Isse, A.A., and Gennaro, A. (2018). *Curr. Opin. Electrochem.* 8: 1–7. https://doi.org/10.1016/j.coelec.2017.11.004.

49 Magenau, A.J., Strandwitz, N.C., Gennaro, A., and Matyjaszewski, K. (2011). *Science* 332: 81–84. https://doi.org/10.1126/science.1202357.

50 Peterson, B.M., Lin, S., and Fors, B.P. (2018). *J. Am. Chem. Soc.* 140: 2076–2079. https://doi.org/10.1021/jacs.8b00173.

51 (a) Falsig, M. and Lund, H. (1980). *Acta Chem. Scand. Ser. B* 34: 545–549. https://doi.org/10.3891/acta.chem.scand.34b-0545. (b) Falsig, M. and Lund, H. (1980). *Acta Chem. Scand. Ser. B* 34: 585–590. https://doi.org/10.3891/acta.chem.scand.34b-0585. (c) Falsig, M., Lund, H., Nadjo, L., and Saveant, J.M. (1980). *Acta Chem. Scand. Ser. B* 34: 685–691. https://doi.org/10.3891/acta.chem.scand.34b-0685.

52 Falciola, L., Gennaro, A., Isse, A.A. et al. (2006). *J. Electroanal. Chem.* 593: 47–56. https://doi.org/10.1016/j.jelechem.2006.02.003.

53 Sang, W., Xu, M.M., and Yan, Q. (2017). *ACS Macro Lett.* 6: 1337–1341. https://doi.org/10.1021/acsmacrolett.7b00886.

54 Arévalo, M.C., Farnia, G., Severin, M.G., and Vianello, E. (1987). *J. Electroanal. Chem. Interfacial Electrochem.* 220: 201–211. https://doi.org/10.1016/0022-0728(87)85108-2.

55 Tang, W., Kwak, Y., Braunecker, W. et al. (2008). *J. Am. Chem. Soc.* 130: 10702–10713. https://doi.org/10.1021/ja802290a.

56 Bortolamei, N., Isse, A.A., and Gennaro, A. (2010). *Electrochim. Acta* 55: 8312–8318. https://doi.org/10.1016/j.electacta.2010.02.099.

57 Francke, R. and Little, R.D. (2014). *Chem. Soc. Rev.* 43: 2492–2521. https://doi.org/10.1039/c3cs60464k.

58 Chmielarz, P., Fantin, M., Park, S. et al. (2017). *Prog. Polym. Sci.* 69: 47–78. https://doi.org/10.1016/j.progpolymsci.2017.02.005.

59 Wang, Y., Fantin, M., and Matyjaszewski, K. (2019). *J. Polym. Sci., Part A: Polym. Chem.* 57: 376–381. https://doi.org/10.1002/pola.29197.

60 Wang, Y., Fantin, M., and Matyjaszewski, K. (2018). *Macromol. Rapid Commun.* 39: e1800221. https://doi.org/10.1002/marc.201800221.

61 Antonello, S., Musumeci, M., Wayner, D.D., and Maran, F. (1997). *J. Am. Chem. Soc.* 119: 9541–9549. https://doi.org/10.1021/ja971416o.

62 Hu, Q., Kong, J., Han, D. et al. (2019). *Anal. Chem.* 91: 1936–1943. https://doi.org/10.1021/acs.analchem.8b04221.

63 Bünsow, J., Mänz, M., Vana, P., and Johannsmann, D. (2010). *Macromol. Chem. Phys.* 211: 761–767. https://doi.org/10.1002/macp.200900596.

14

Considerations for and Applications of Aqueous RAFT Polymerization

Alexander W. Fortenberry[1], *Charles L. McCormick*[2], *and Adam E. Smith*[1]

[1] *The University of Mississippi, Department of Chemical Engineering, University, MS 38677, USA*
[2] *The University of Southern Mississippi, School of Polymer Science and Engineering, Hattiesburg, MS 39406, USA*

14.1 Introduction

Aqueous reversible addition–fragmentation chain transfer (aRAFT) polymerization appeared in the original report detailing the reversible addition–fragmentation chain transfer (RAFT) process in 1998 by Moad, Rizzardo, Thang, and coworkers [1]. As part of their seminal work, the authors reported the RAFT polymerization of sodium 4-styrenesulfonate (SS) directly in water using the water-soluble chain transfer agent (CTA) 4-cyanopentanoic acid dithiobenzoate (CTP). Inspired by this work, the McCormick group reported the first AB diblock copolymers directly in water in 2001 [2]. Since these initial reports, aRAFT has been utilized to polymerize a wide array of water-soluble monomers directly in aqueous media [3]. This chapter will focus on considerations that must be taken into account in order to perform well-controlled RAFT polymerizations directly in aqueous media, including hydrolysis and aminolysis of CTAs in aqueous media, the types of initiation systems utilized for aRAFT, and efforts to perform oxygen-tolerant aRAFT polymerizations. The chapter will also discuss two applications of aRAFT, polymerization-induced self-assembly (PISA), and the synthesis of protein–polymer and DNA–polymer conjugates using 'grafting from' strategies.

14.2 Chain Transfer Agents

In the generally accepted RAFT mechanism (Scheme 14.1), the CTA reacts with a growing polymer chain, $P_n\cdot$, and fragments to release the R· radical, which is responsible for the reinitiation of polymerization. Once the polymerization proceeds past the pre-equilibrium, the polymerization enters the main equilibrium involving the degenerative chain transfer of the thiocarbonylthio end group between propagating chains. The exchange between active and dormant chains is established by the rapid

RAFT Polymerization: Methods, Synthesis and Applications, First Edition.
Edited by Graeme Moad and Ezio Rizzardo.

fragmentation of the intermediate radical in both directions, allowing for the controlled, intermittent addition of monomer to each growing polymer chain ($P_m\cdot$ and $P_n\cdot$) with equal probability.

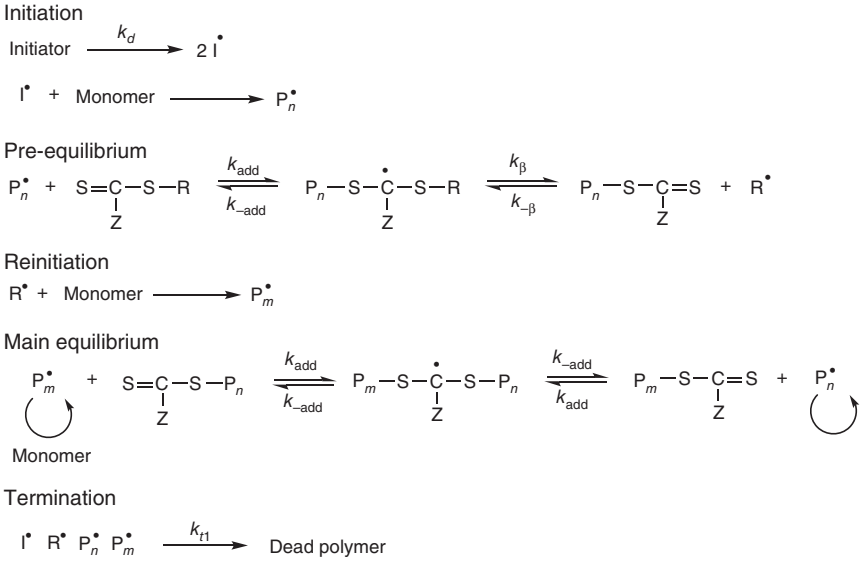

Scheme 14.1 The generally accepted RAFT polymerization mechanism.

A wide range of polymers and block copolymers have been prepared directly in aqueous media utilizing water-soluble CTAs, some common examples of which are shown in Figure 14.1. In addition to these small-molecule CTAs, water-soluble macroCTAs can be chain extended with subsequent monomers to produce block copolymers by aRAFT. One benefit of utilizing a macroCTA with regard to aRAFT polymerization is that a macroCTA may have higher water solubility than the small-molecule CTA based on the hydrophilicity of the polymer chain. In order to take advantage of the economic and environmental benefits of utilizing aRAFT, special attention must be paid to competing reactions such as hydrolysis and aminolysis of the CTA that can affect the ability to produce well-defined polymers.

14.2.1 Hydrolysis of the CTA

Because thiocarbonylthio compounds are sulfur analogues of esters, it is not surprising that they are susceptible to hydrolysis. In 2000, Levesque et al. examined the effect of pH and temperature on thiocarbonylthio compounds [4]. In the study, they varied the temperature from 20 to 35 °C and the pH from 7.5 to 8.5 and found that the rate of hydrolysis of the compounds increases with both increasing temperature and increasing pH. Building on this work, the McCormick group performed the first examination of the effects of hydrolysis and aminolysis of CTAs on aRAFT polymerization [5]. They examined the effects of temperature and pH on CTP and two

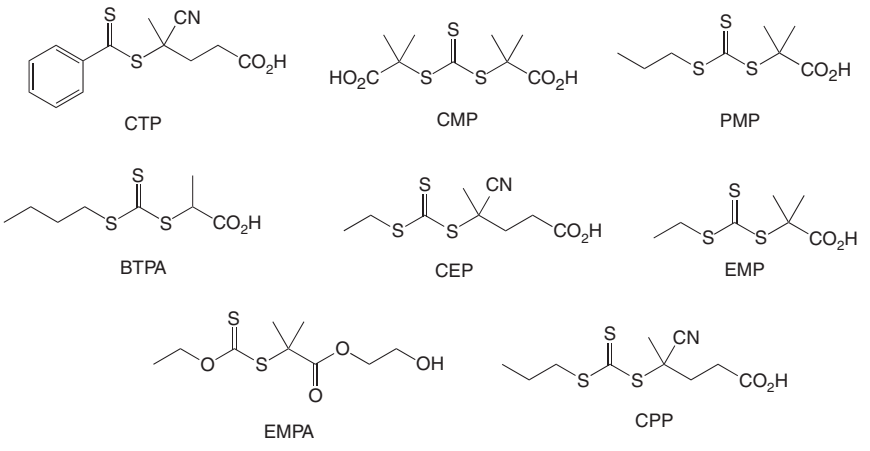

Figure 14.1 Common CTAs utilized to enable the synthesis of well-defined polymers and block copolymers using aRAFT polymerization. The acronym for each is shown below the structure.

sodium 2-acrylamido-2-methylpropanesulfonate (AMPS) macroCTAs in water. The hydrolysis of the CTA can be assumed to be zero order with respect to water because water is present in large excess. The rate of CTA hydrolysis can be expressed in terms of the apparent rate constant, k_{hyd}, and the CTA concentration as shown in Eq. (14.1).

$$-\frac{d\,[\mathrm{CTA}]}{dt} = k_{\mathrm{hyd}}\,[\mathrm{CTA}] \tag{14.1}$$

Figure 14.2 shows the pseudo-first-order rate plots for the hydrolysis of CTP and the two AMPS macroCTAs made using CTP [5]. It is evident from these plots that the rates of hydrolysis of CTP and the two macroCTAs increase with increasing pH, which is consistent with the findings of Levesque et al. [4]. Additionally, it is important to note the sharp decrease in the rates of hydrolysis of the two macroCTAs compared to CTP with the larger of the macroCTAs ($AMPS_{38}$) having the lowest rate of hydrolysis of all three CTAs. Thomas et al. attributed this to the effect of steric hindrance on the attack of water molecules on the dithioester moiety, which is analogous to the well-known steric effects observed for carboxylic ester hydrolysis [5].

14.2.2 Aminolysis

Thiocarbonylthio species are also susceptible to aminolysis by primary and secondary amines present in solution. Levesque et al. studied the reaction of thiocarbonylthio compounds with primary and secondary amines and found that the reaction is first order with respect to the concentration of thiocarbonylthio compounds and displays a second-order dependence with the amine concentration [4, 6]. In their report, the McCormick group also examined the effect of aminolysis on the stability of CTAs by exposing CTP to ammonia in buffered aqueous solutions [5]. They analyzed the fraction of CTP remaining over a period of eight hours at solution pH values of 5.5 and 7, where both hydrolysis and aminolysis may play

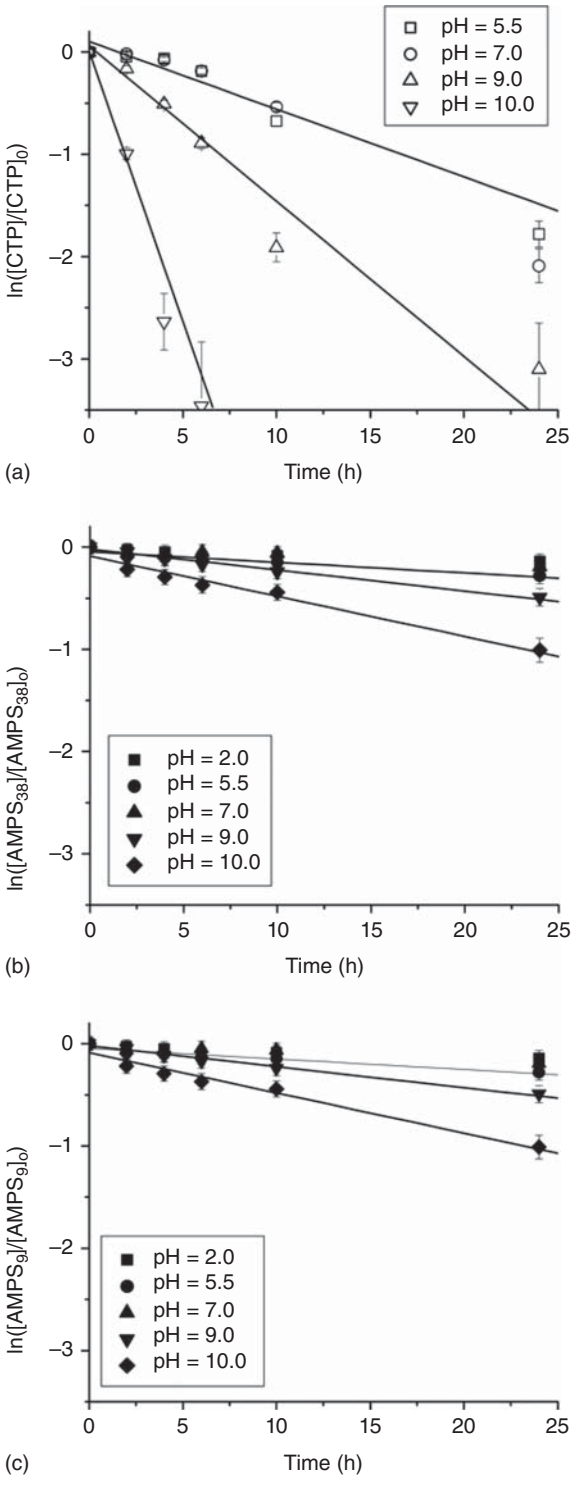

Figure 14.2 Pseudo-first-order rate plots for the hydrolysis of (a) CTP, (b) $AMPS_{38}$, and (c) $AMPS_9$ at 70 °C. Source: Reprinted with permission from Thomas et al. [5]. © 2004, American Chemical Society.

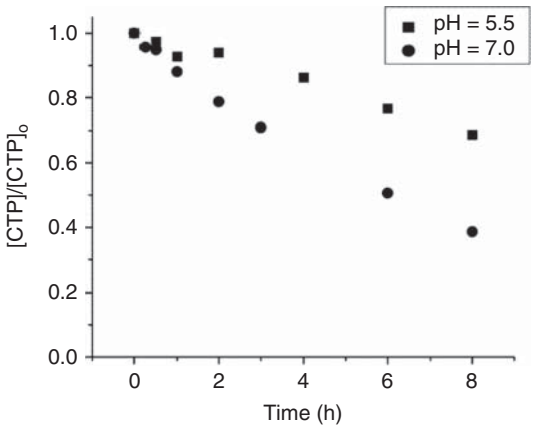

Figure 14.3 Fraction of CTP remaining in solution over time under conditions, where both hydrolysis and aminolysis may lead to the disappearance of the thiocarbonylthio moiety. Source: Reprinted with permission from Thomas et al. [5]. © 2004, American Chemical Society.

a role in the disappearance of the thiocarbonylthio moiety of CTP. As can be seen from Figure 14.3, the CTP concentration decreases more rapidly at pH 7 than at a pH of 5.5. The authors attributed this to the fact that at pH 5.5, only hydrolysis plays a major role in the disappearance of the CTA moiety, while at pH 7, aminolysis also leads to the disappearance of the CTA. The authors developed an expression to model the CTA concentration over time as a function of hydrolysis and aminolysis, Eq. (14.2).

$$-\frac{d\,[\mathrm{CTA}]}{dt} = k_{\mathrm{hyd}}\,[\mathrm{CTA}] + k_a\,[\mathrm{CTA}]\left[\mathrm{NH_3}\right]^2 \tag{14.2}$$

where k_a is the aminolysis rate constant and $[NH_3]$ is the concentration of ammonia in solution. Taking the rates of CTA hydrolysis and aminolysis into account, Eq. (14.3) was developed to determine the theoretical molecular weight under conditions where hydrolysis and aminolysis are occurring.

$$[M]_n\,(t) = \frac{M_{\mathrm{MW}}\left([M]_0 - \left[M_0 e^{-k_p^*\left(t-t_{\mathrm{ind}}\right)}\right]\right)}{\mathrm{CTA}_{\mathrm{ind}} e^{-\left(k_{\mathrm{hyd,macro}} + k_{a,\mathrm{macro}}\left[\mathrm{NH_3}\right]^2\right)\left(t-t_{\mathrm{ind}}\right)}} \tag{14.3}$$

Because of the possible contribution of aminolysis in the destruction of the CTA moiety, monomers containing primary and secondary amines were initially thought to be precluded from direct polymerization by RAFT. However, Levesque et al. demonstrated that the aminolysis of thiocarbonylthio compounds can be significantly reduced by lowering the pH of the reaction media, thereby protonating the amine-containing compounds [4, 6]. The McCormick group subsequently demonstrated the ability to polymerize the primary amine containing monomer *N*-(3-aminopropyl)methacrylamide (APMA) in a water/dioxane mix at a pH between 4 and 5 using CTP [7] and from a poly(ethylene oxide) (PEO)-based macroCTA directly in water (pH 4–5) with subsequent chain extension with 2-(diisopropylamino)ethyl methacrylate (DPAEMA) [8]. In both cases, good control of the molecular weight and low dispersities were demonstrated.

In addition to the susceptibility of CTAs to hydrolysis via attack from water molecules, certain monomers can also undergo hydrolysis and produce primary

and secondary amines, which can then react with the CTAs. Given the high monomer-to-CTA ratio, the hydrolysis of even a few percent of this type of monomer can result in complete loss of the thiocarbonylthio end groups and hence loss of control of the polymerization. Thomas et al. examined the effect of hydrolysis of acrylamide (AM) on the loss of CTA and found that by conducting the polymerization under acidic conditions, the hydrolysis of AM could be minimized sufficiently to allow for a well-controlled polymerization [5, 9].

14.3 Initiation

Because radicals are neither generated nor consumed in the main equilibrium of the RAFT mechanism, RAFT polymerizations must be initiated by a source of radicals [10]. Because RAFT polymerization is essentially a conventional radical polymerization conducted in the presence of a CTA, initiation systems commonly employed in radical polymerizations can also be employed in RAFT polymerizations. Common examples include azo initiators, UV and γ irradiation, and redox initiation [3, 10, 11]. In RAFT polymerization, the initiators serve two purposes, to react with the CTA and liberate the R· to initiate chain growth and to replenish radicals lost to side reactions. In order to maintain control of the polymerization, the CTA:initiator concentration in most RAFT polymerizations is maintained at >10 because every pair of radicals generated from the initiating species leads to a pair of radicals terminating to produce dead polymer impurities. In a well-designed RAFT polymerization, the fraction of initiator derived chains will be less than 5% [3, 10].

14.3.1 Initiation via Azo-containing Species

Most early reports of RAFT polymerization utilize the homolytic cleavage of azo compounds to initiate polymerization. In the early days of aRAFT polymerization, initiation was almost exclusively done by the cleavage of azo-containing species at elevated temperatures [1, 2, 12–16]. Examples of the water-soluble initiators used for early reports of aRAFT are 4,4′-Azobis(4-cyanopentanoic acid) (V-501) [1, 2, 12–14, 16] and 2,2′-azobis[2-methyl-*N*-(2-hydroxyethyl)propionamide] (VA-086) [15].

In 2005, Convertine et al. [17] were the first to report room temperature aRAFT polymerization utilizing 2,2′-Azobis(4-methoxy-2,4-dimethylpentanenitrile) (V-70) as the thermal initiator. In this work, they employed 2-(1-carboxyl-1- methylethyl-sulfanylthiocarbonylsulfanyl)-2-methylpropionic acid (CMP) as the CTA in acidic solution and synthesized AM and *N*,*N*-dimethylacrylamide (DMA) homopolymers at 25, 50, and 70 °C. The polymerizations at 50 °C were initiated by 2,2′-azobis(*N*-(2-carboxyethyl)-2-methylpropionamidine) (VA-057) and the polymerizations at 70 °C were initiated by V-501. They found that at temperatures up to 50 °C, the trithiocarbonate functionality is stable and that above 50 °C, CTA hydrolysis becomes significant. They followed this work by synthesizing thermally responsive AB and ABA block copolymers based on DMA and NIPAM in water at room temperature utilizing 4,4′-azobis[2-(imidazolin-2-yl)propane] dihydrochloride

(VA-044) as the thermal initiator and CMP and *S*-ethyl-*S*′-(α,α′-dimethyl-α″-acetic acid)-trithiocarbonate (EMP) as the CTAs [18].

Because of the increased rate of hydrolysis of the CTAs as described by Thomas et al. [5], it is advantageous to conduct aRAFT polymerization at temperatures below 50 °C to obtain better control over the polymerization. Performing the polymerizations at such temperatures also opens the door for potential in situ functionalization of biological molecules under reaction conditions that do not lead to denaturing. Because of these considerations, much work has been devoted to investigating aRAFT photopolymerization at room temperature as discussed in more detail in Section 14.3.2.

14.3.2 Photochemical Initiation

Visible light is an attractive initiation source in contrast to γ radiation (where sources are not commonly available) and UV radiation (which can cause the photolysis of CTA moieties leading to premature termination [19]). Visible light is also a low energy irradiation source that minimizes damage to biomolecules and often does not require high temperatures for polymerizations, which can reduce the rate of CTA hydrolysis. These factors make visible light-mediated aRAFT polymerization appealing for the synthesis of macromolecules for biological applications, and most of the reports of aRAFT photopolymerization have been visible light mediated. As Figg and Sumerlin described in their review on the topic [20], visible light mediated aRAFT photopolymerization can be divided into roughly three categories: externally catalyzed, catalyst-free, and photoinduced electron/energy transfer (PET)-RAFT.

14.3.2.1 Externally Initiated aRAFT Photopolymerization

Because aRAFT polymerization is another type of free radical polymerization, it can be initiated photochemically via externally initiating species that absorb light, fragment, and initiate RAFT polymerization. To our knowledge, the first report of aRAFT photopolymerization appeared in 2009 when Shi et al. utilized (2,4,6-trimethylbenzoyl) diphenylphosphine oxide (TPO) as the photoinitiator for the EMP-mediated RAFT polymerization of poly(ethylene glycol) methyl ether acrylate (PEGA) at 25 °C in water [21]. They then chain extended PEGA macroCTAs with 2-hydroxyethyl acrylate (HEA) in water to illustrate the living character of the polymerization. They subsequently demonstrated the ability to copolymerize acrylate-based monomers (*N*-(2-acryloyloxyethyl) pyrrolidone [NAP] and HEA) in water under similar conditions [22]. The polymerizations exhibited a negligible thermoactivating effect (the kinetic character of the polymerization did not change much when performing the reaction at 7 °C vs. 25 °C) and periodic exposure to visible light led to a corresponding repeatable periodic polymerization.

Much of the externally catalyzed aRAFT photopolymerization has been performed utilizing sodium phenyl-2,4,6-trimethylbenzoyl phosphinate (SPTP) as the water-soluble photoinitiator [23–29]. SPTP decomposes rapidly upon exposure to UV or visible light irradiation, making it a useful initiator in such systems [23]. Much of this work was reported by the Tan and Zhang groups in their studies

of the room temperature photoinitiated polymerization-induced self-assembly (photo-PISA) of *N*-(2-hydroxypropyl)methacrylamide (HPMA) with water-soluble macroCTAs [23–26]. They reported the rapid formation of nanoparticles with complex morphologies (i.e. spheres, worms, and vesicles) via aqueous dispersion polymerization when exposed to sunlight or visible light and that the polymerizations could be controlled by turning on or off the light source [23–25]. They subsequently performed kinetic studies to compare the rate of polymerization of photoinitiated PISA to PISA initiated by V-501 at 70 °C [26]. Figure 14.4 shows the comparison of the photopolymerization of HPMA at 25 °C and the V-501-initiated polymerization of HPMA at 70 °C using a water-soluble glycerol monomethacrylate (GMA) macroCTA. They found that the rate of polymerization is much faster for the photopolymerization because of the short half-life of SPTP under photolytic conditions [26]. In addition, visible light-mediated room temperature aRAFT polymerization utilizing SPTP as the photoinitiator has been utilized to synthesize zwitterionic polyelectrolytes for their potential benefit in emerging biological applications [27] and for the synthesis of stimuli-responsive cylindrical vesicular nanotubes formed via hydrogen-bond driven PISA [28].

14.3.2.2 Initiator-Free aRAFT Photopolymerization

Most thiocarbonylthio compounds are able to initiate polymerization because of a photoiniferter mechanism as they absorb light in the visible region between 380 and 525 nm because of the $n \rightarrow \pi^*$ transition of the C=S bond [30]. As depicted in Figure 14.5, initiation occurs via a homolytic C—S bond cleavage to generate a carbon-centred radical that is capable of adding monomer and a thiocarbonylthio radical that is capable of deactivating growing chains via reversible termination [20]. This mechanism is attractive because it produces polymer chains with homogeneous end groups, unlike externally initiated RAFT polymerization, which produces polymers with heterogeneous end groups due to some initiator-derived chains.

The first instance of a initiator-free aRAFT photopolymerization was reported in 2015 by McKenzie et al. in which they polymerized *N*-isopropylacrylamide (NIPAM) under visible light irradiation at an intensity of 4.8 W in a 4 : 1 water:dioxane mixture, where the dioxane was included only to help the CTA, 2-(((butylthio)carbonothioyl)thio)propanoic acid (BTPA), dissolve [31]. Because of the low irradiation intensity, the polymerization took ~20 hours to reach high monomer conversion (>99%). Lewis et al. experimented with increasing the light intensity for the polymerization of AM and DMA and reported that increasing the light-emitting diode (LED) power from 6 to 208 W at $\lambda = 402$ nm led to a decrease in reaction time to reach >85% conversion from 12 hours to 11 minutes for AM without a significant loss in the control of the polymerization [32]. A similar conversion was also shown for DMA. Polymerizations under high irradiation powers, where the temperatures were not controlled, often led to solution temperatures of up to 80 °C because of both the exothermic nature of the polymerizations and the intense irradiation. They noted some loss in control of the DMA polymerization at higher irradiation intensities, probably because of the increased hydrolysis rate of the CTA

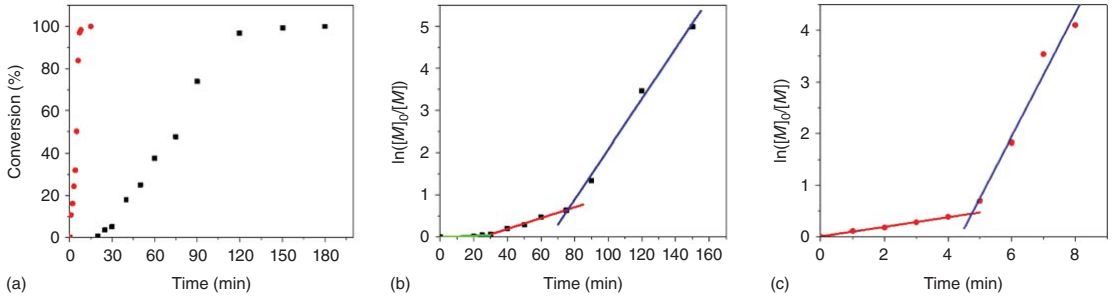

Figure 14.4 (a) Polymerization kinetics for V-501-initiated polymerization at 70 °C (squares) and photoinitiated polymerization of HPMA at 25 °C (circles) in water using a GMA macroCTA, (b) plots of $\ln([M]_0/[M])$ vs. reaction time for V-501 initiated, and (c) for photoinitiated PISA of HPMA in water using a GMA macroCTA. Source: Reproduced with permission from Tan et al. [26]. © 2004, The Royal Society of Chemistry.

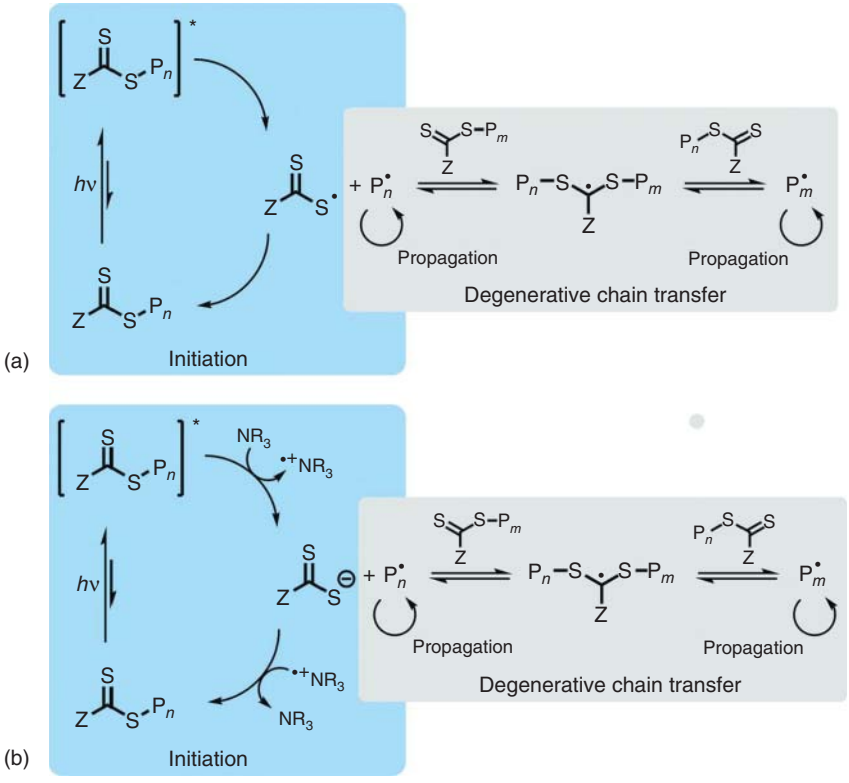

Figure 14.5 (a) Initiator-free photopolymerizations where initiation occurs via carbon-sulfur bond photolysis and subsequent addition to monomer to achieve a degenerative chain transfer equilibrium between propagating chains and reversible termination with the stable sulfur-centred radical. (b) The polymerization rate can be increased using a tertiary amine (NR_3) that is proposed to undergo a redox reaction with the excited-state thiocarbonylthio moiety. Source: Reprinted with permission from Figg et al. [20]. © 2018, American Chemical Society.

at elevated temperatures [32]. Therefore, taking necessary measures to maintain moderate temperatures is essential for RAFT photopolymerizations in water.

As noted by Figg and Sumerlin [20] in their review on visible light-mediated aRAFT polymerization, an alternative way to increase the rate of polymerization for such a system is via the addition of a tertiary amine [33], which has been hypothesized to undergo a redox reaction with the excited-state thiocarbonylthio to yield the thiocarbonylthio anion and a carbon-centred radical for initiation/propagation (Figure 14.5b). The disadvantage to this route is that high stoichiometric amounts of amine to CTA are often required.

14.3.2.3 PET-RAFT Photopolymerizations

In addition to externally initiated and initiator-free reactions, RAFT polymerization can also be mediated by PET photocatalysts (PCs). PET catalysts are commonly used

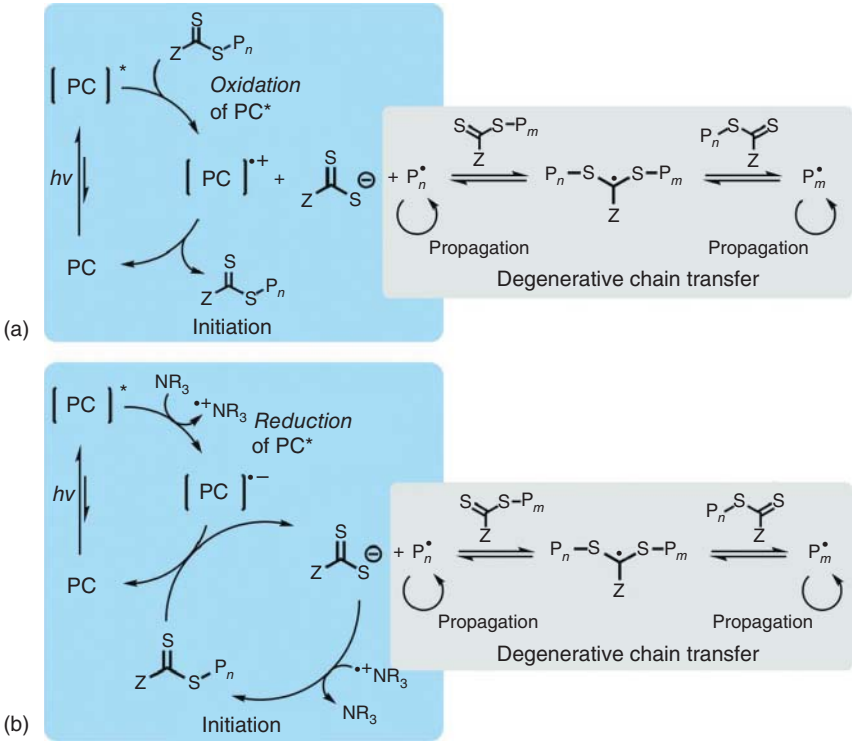

Figure 14.6 Photo-induced electron transfer RAFT polymerization using a photocatalyst (PC) via either (a) an oxidative catalyst pathway or (b) a reductive catalyst pathway (NR_3 can also be ascorbic acid). Source: Reprinted with permission from Figg et al. [20]. © 2018, American Chemical Society.

in organic syntheses to conduct single-electron redox reactions [34]. PCs can mediate RAFT polymerization through a redox reaction with the CTA to generate a radical that can initiate polymerization [35]. Thus in these systems, the CTA acts as both an initiator and a CTA. As displayed in Figure 14.6, PET-RAFT polymerizations can occur in two distinct pathways, either an oxidative catalyst pathway (Figure 14.6a) or a reductive catalyst pathway in the presence of a reducing agent like ascorbic acid or a tertiary amine (Figure 14.6b).

Boyer and coworkers were the first to report aqueous PET-RAFT polymerization by employing tris(2,2′-bipyridyl)ruthenium(II) chloride ($Ru[bpy]_3Cl_2$) to polymerize DMA in water at low catalyst loadings relative to CTA (CTA/$[Ru(bpy)_3Cl_2]$ = 1/0.0002) to form polymers with low dispersities [36]. Utilizing the inexpensive zinc porphyrin (Zn(II) meso-tetra(4-sulfonatophenyl)porphyrin) as the catalyst, they reported the aqueous PET-RAFT polymerization of DMA and demonstrated that the performance of the catalyst could be affected by the pH of the polymerization media with faster polymerization occurring in near-neutral and basic environments [37].

In addition to metallic compounds, certain water-soluble organic compounds can act as catalysts for aRAFT photopolymerization. An example of this is the organic dye eosin Y (EY), which absorbs blue and green light with the absorbance attributed

to the dimer and monomer, respectively [38]. Another example is the water-soluble version of vitamin B_2 (riboflavin)-riboflavin 5′-mononucleotide (FMN) [39]. FMN is an intriguing example because it is a naturally occurring biomolecule and opens the door for potential bioapplications of photo-RAFT polymerization. One of the first examples of the aRAFT photopolymerization utilizing EY was reported in 2017 by Hawker and coworkers in which they performed a grafting from approach to graft polymer chains onto yeast and mammalian cells in room temperature aqueous solution by attaching BTPA to the surface of the cells and then polymerized PEGA by exposing the solution to visible light irradiation for five minutes [40]. To provide insights into the use of EY for RAFT polymerization, the Sumerlin group reported mechanistic studies of EY under blue and green light irradiation using both oxidative and reductive PET mechanisms [41]. Because thiocarbonylthio compounds such as CTAs can absorb blue light and undergo photolysis to initiate polymerization, they found that the best way to prepare precise polymers with predictable molecular weights utilizing EY as a PET catalyst is under an oxidative mechanism during green light irradiation. The authors also found that a reduced solution pH resulted in slower polymerization rates, which they attributed to the partial protonation/deactivation of the tertiary amine reducing agent or catalyst.

14.4 Deoxygenation Methods

One key limitation of RAFT polymerizations is the sensitivity of the technique to the presence of oxygen. Unlike conventional radical polymerization where low concentrations of oxygen can be overcome by increasing the concentration of the initiating species, RAFT typically requires stringent deoxygenation procedures such as freeze–pump–thaw cycles or purging with an inert gas before polymerization because the maintenance of the CTA end group is dependent on the ratio of the CTA to initiator [3, 10]. In order to synthesize well-defined polymers and block copolymers, the concentration of the initiating species must be kept low compared to the CTA concentration, often precluding the ability to add sacrificial initiator to overcome the presence of oxygen [42].

14.4.1 PET-RAFT

PET-RAFT polymerization can achieve oxygen tolerance in water via a reductive catalyst pathway if a secondary catalyst (usually a tertiary amine or ascorbic acid) is included in the system in addition to the PC (Figure 14.6b). In their studies of EY, the Sumerlin group demonstrated that oxidative catalyst pathways can yield polymers with molecular weights closer to their predicted molecular weights [41], although reductive catalyst pathways are commonly reported. Subsequently, Niu et al. [43] reported the polymerization of DMA using BTPA as the CTA without prior deoxygenation and $Ru(bpy)_3Cl_2$ in the presence of ascorbic acid as a reducing agent, which induced a reductive quenching mechanism of the excited state (Figure 14.6b). They reported monomer conversions of >90% in

30 minutes. Boyer and coworkers [44] showed that like the $Ru(bpy)_3Cl_2$ systems, systems employing a Zn(II) meso-tetra(4-sulfonatophenyl)porphyrin ($ZnTPPS^{4-}$) photocatalyst can achieve oxygen tolerance by the addition of ascorbic acid to the system and polymerization in the presence of air could be achieved after a short inhibition period. They also investigated the formation of nanoparticles with complex morphologies (i.e. spheres, worms, and vesicles) via PET-RAFT dispersion polymerization of HPMA with water-soluble macroCTAs by utilizing zinc meso-tetra(*N*-methyl-4-pyridyl porphine tetrachloride (ZnTMPyP) as a catalyst and biotin (vitamin B7) as a singlet oxygen quencher and reported that the addition of a photoresponsive monomer 7-[4-(trifluoromethyl)coumarin] methacrylamide could be used to crosslink the polymers under UV irradiation, so the nanoparticles could retain their morphologies in organic solvents [45]. Boyer and coworkers also reported that EY and FMN in conjunction with ascorbic acid as a reducing agent can initiate aRAFT polymerization of various monomer families, including AMs, acrylates, and methacrylates, for the synthesis of homo- and block copolymers without prior deoxygenation in volumes ranging from 20 to 4400 μl [39].

Zaquen et al. performed oxygen-tolerant PET-RAFT in continuous flow tubular reactors using EY in the presence of amine-based reducing agents to synthesize various AM and acrylate diblock and triblock copolymers with high end group fidelity [46]. They were able to obtain high levels of control over the polymerizations by manipulating flow rates and light intensity. By coupling multiple flow reactors, they were able to synthesize triblock copolymers without the need for intermediate purification.

14.4.2 Enzyme-Catalyzed Deoxygenation

14.4.2.1 Initiation by Thermal Initiation

Recently, the Stevens group demonstrated the ability to utilize glucose oxidase (GOx) to deoxygenate the VA-044-initiated RAFT polymerization of HEA, methacrylic acid (MA), DMA, and HPMA in aqueous phosphate-buffered saline (PBS) solutions of methanol or dioxane in the presence of CTA 2-(propylthiocarbonothioylthio)-2-methylpropionoic acid (PMP) in reaction vessels open to the air [47]. GOx consumes oxygen and produces hydrogen peroxide through the oxidation of glucose into D-glucono-δ-lactone. Initial kinetic experiments compared the use of GOx to deoxygenate the thermally initiated polymerization of HEA in both a closed vessel and an open vessel and compared those polymerizations to one utilizing a conventional argon degassing procedure (Figure 14.7). The GOx-deoxygenated polymerization kinetics in both the closed vessel and the open vessel were found to be similar to those of the polymerization degassed with argon. Although the GOx-catalyzed oxidation of glucose into D-glucono-δ-lactone produces hydrogen peroxide, which can generate hydroxyl radicals, no appreciable monomer conversion was measured in polymerizations without the exogenous initiator VA-044 added (Figure 14.7a, open circles). The polymerizations exhibited linear growth of molecular weight with increasing conversion, $Đ < 1.2$, and monotonic shifts in the chromatograms with no low molecular weight tailing at both target degrees

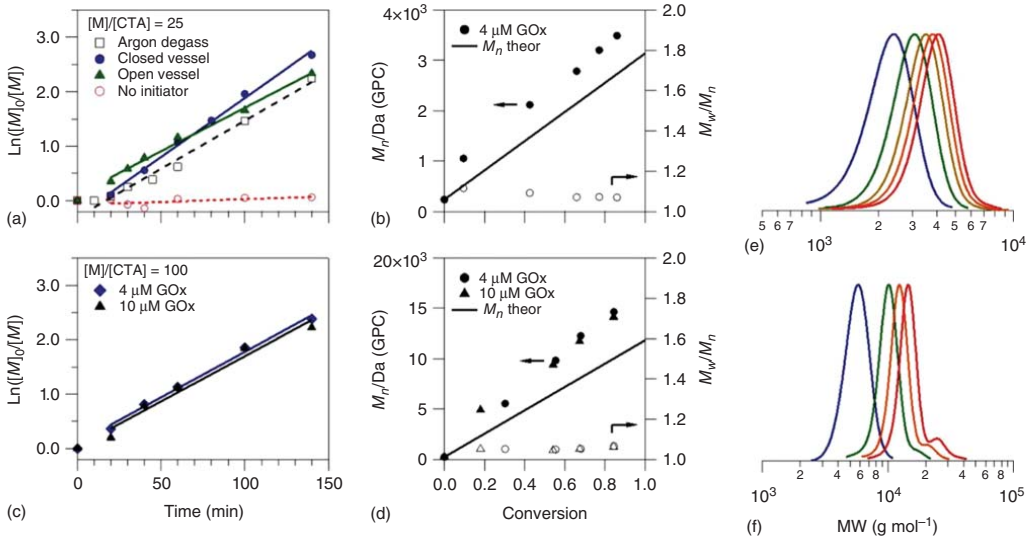

Figure 14.7 Kinetics of 2 M HEA polymerizations in 20% methanol/PBS degassed by GOx and stirred at 45 °C. (a, b) Pseudo-first-order kinetic plots with (closed symbols) and without (open symbols) GOx and VA-044 (a) [*M*]/[CTA] = 25 and (b) [*M*]/[CTA] = 100. (c, d) M_n (closed symbols) and *Đ* (open symbols) vs. conversion for GOx degassed polymerizations in closed vessels (c) [*M*]/[CTA] = 25, [GOx] = 4 μM; (d) [*M*]/[CTA] = 100. (e, f) Corresponding SEC-normalized refractive index (RI) traces for the kinetics in (c) and (d), respectively, showing a shift in molecular weight with conversion. Source: Reprinted with permission from Chapman et al. [47]. © 2014, American Chemical Society.

of polymerization (DPs) of 25 (Figure 14.7c,e) and 100 (Figure 14.7d,f). The high molecular weight shoulders in the chromatograms for the polymerization with a target DP of 100 that appear at higher conversions were attributed to bimolecular termination because of increased viscosity and not the presence of GOx because similar peaks are not seen in the DP 25 chromatograms at high conversion.

The Stevens group later utilized GOx deoxygenation to enable a combinatorial approach to produce a library of highly controlled homo and block copolymers from DMA, HPMA, *N*-acryloylmorpholine (NAM), HEA, 2-hydroxyethyl methacrylate (HEMA), and poly(ethylene glycol) methyl ether methacrylate (PEGMA) via open-to-air RAFT polymerizations in 40 μl mixtures of PBS buffer and methanol or *t*-butanol using the CTA 4-cyano-4-(propylthiocarbonothioylthio)pentanoic acid (CPP) [48]. With the use of the GOx, very low concentrations of initiator were able to be used, allowing high monomer conversion at high target DPs (400 for acrylates and AMs and 200 for methacrylates and methacrylamides). Additionally, block copolymers were prepared by the simple addition of a subsequent monomer to the same well after completion of the previous polymerization.

The Rowan group recently demonstrated the ability of the GOx deoxygenation system to work for RAFT polymerizations of HEA conducted using PMP as the CTA and the thermal initiator VA-044 in a variety of complex aqueous solutions including beer, wine, liquor, and fermentation broth [49]. The RAFT polymerization of HEA in all the studied mixtures resulted in $Đ > 1.2$. Interestingly, the pH of the solution played an important role in the RAFT polymerizations in the complex solutions, with low pH solutions resulting in lower conversion. The lower conversions at low pHs were attributed to a decrease in the stability of GOx at lower pH values, thus impacting its ability to deoxygenate the polymerization mixture.

14.4.2.2 Enzymatic Initiation Systems

Enzymes have also been studied as a means of initiating RAFT polymerizations. In 2015, the An group utilized horseradish peroxidase (HRP) to catalyze the oxidation of acetylacetone (ACAC) by hydrogen peroxide to generate ACAC radicals to initiate the RAFT polymerization in PBS (pH 7) of the 'more activated monomers' DMA, PEGA, HEA, and PEGMA using 4-cyano-4-(ethylsulfanylthiocarbonyl)sulfanylpentanoic acid (CEP) and the 'less-activated monomer' *N*-vinyl-2-pyrrolidone (NVP) using the xanthate 2-ethoxythiocarbonylsulfanyl-2-methyl-propionic acid 2-hydroxy-ethyl ester (EMPA) after degassing with nitrogen and injecting hydrogen peroxide to initiate polymerization [50]. All of the HRP-initiated RAFT polymerizations exhibited pseudo-first-order kinetics, linear increases in molecular weight with conversion, and monotonic shifts in size exclusion chromatography (SEC) chromatograms. Figure 14.8 shows the result of the HRP-initiated RAFT polymerization of DMA in PBS (pH 7). The An group also investigated coupling GOx deoxygenation to produce hydrogen peroxide reported by the Stevens group [47] with the HRP initiation system where they dubbed RAFT polymerization initiated by enzymatic cascade catalysis. In this novel system, hydrogen peroxide produced by the oxidation of glucose and consumption of oxygen is used to generate ACAC radicals as the

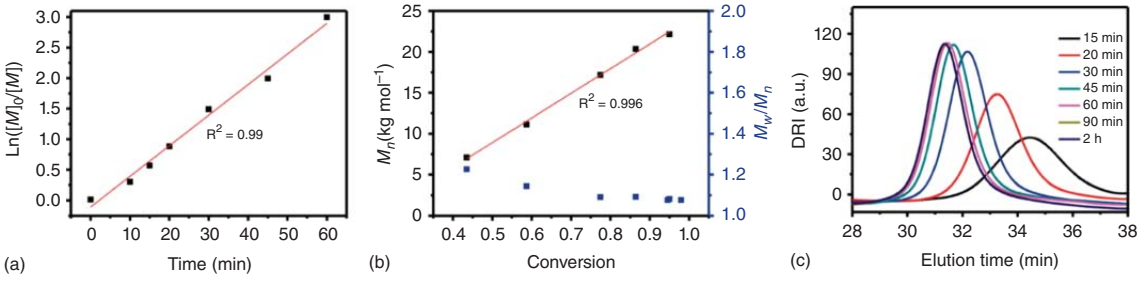

Figure 14.8 (a) Pseudo-first-order kinetics, (b) dependence of molecular weight and dispersity on conversion, and (c) evolution of GPC traces over polymerization time for HRP-initiated aRAFT polymerization of DMA. Source: Reprinted with permission from Zhang et al. [50]. © 2015, American Chemical Society.

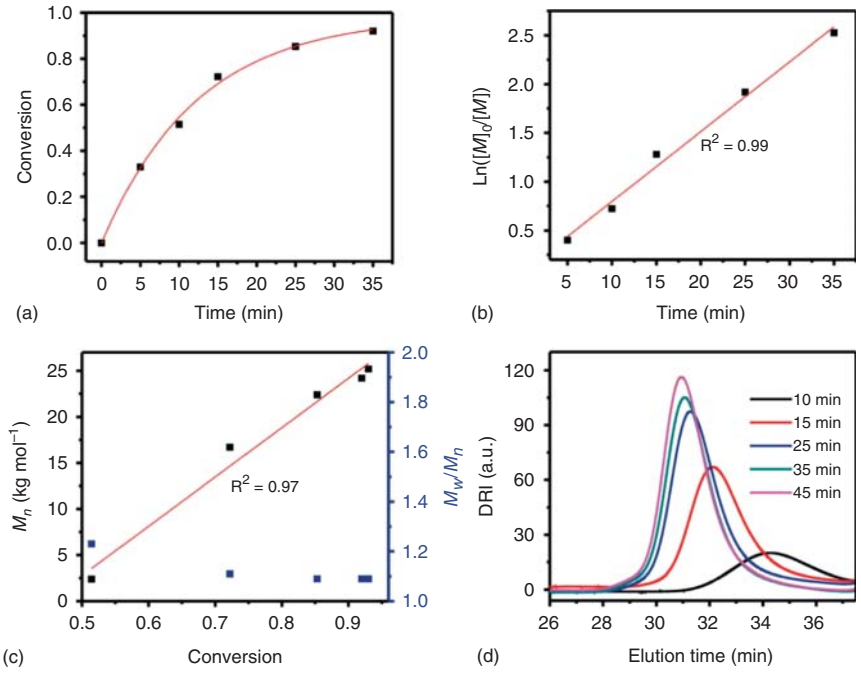

Figure 14.9 (a) Plot of monomer conversion over polymerization time, (b) pseudo-first-order kinetics, (c) dependence of molecular weight and dispersity on conversion, and (d) evolution of GPC traces over polymerization time for the aRAFT polymerization of DMA initiated by GOx–HRP cascade catalysis in air. Source: Reprinted with permission from Zhang et al. [50]. © 2015, American Chemical Society.

initiating species for the RAFT polymerization of DMA in a reaction vessel open to air. As shown in Figure 14.9, the RAFT polymerization of DMA initiated by the enzymatic cascade catalysis exhibits all the hallmarks of controlled radical polymerization, linear pseudo-first-order kinetics, linear increase in molecular weight with conversion, low $Đ$, and monotonic shifts in the SEC chromatograms.

Subsequently, An and coworkers investigated utilizing vitamin C (ascorbic acid) in the GOx deoxygenation-redox initiation cascade to efficiently generate hydroxyl radicals to initiate the RAFT polymerization of DMA in PBS (pH 7) using CEP as the CTA in open and sealed reaction vessels exposed to air [51]. In their kinetics study, the polymerizations conducted in open and sealed vessels have similar polymerization rates, but the final conversion in the sealed vessel (70%) was lower than that of the open vessel (80%). The similar kinetics suggests that the radical concentration was similar in the two vessels, which is reasonable given that both polymerizations had the same 10 minutes pre-polymerization incubation in which hydrogen peroxide was generated by the GOx before the injection of ascorbic acid. The difference in the final conversion was suggested to be due to the slightly higher hydrogen peroxide concentration generated in the open vessel during the later stages of the polymerization because of a higher oxygen diffusion rate due to the vessel being open to air. Later, Tan, Zhang, et al. reported that photopolymerizations initiated with SPTP

could become oxygen tolerant, and capable of occurring in open vessels, while in the presence of the oxygen scavenging enzyme GOx and glucose [52].

In an effort to eliminate the restrictions associated with employing natural enzyme-based catalytic initiation systems, Qiao and coworkers utilized a glycine-modified metal–organic framework (MOF), MIL-53(FE), composite as a peroxidase mimic for the generation of hydroxyl radicals to be used to initiate the RAFT polymerization of DMA, *N*-hydroxyethyl acrylamide (NHEA), methyl acrylate (MeA), and 2-(dimethylamino)ethyl methacrylate (DMAEMA) [53]. Qiao and coworkers utilized both argon purging and the GOx oxidation of glucose for the deoxygenation of the polymerization solutions. Hydrogen peroxide was injected in the polymerizations purged with argon while hydrogen peroxide was formed in situ in the GOx-catalyzed oxidation of glucose. Although both methods demonstrated characteristic-controlled radical polymerization, it is notable that the GOx-deoxygenated systems were capable of achieving ultrahigh molecular weight polymers ($M_n > 1$ MDa) with low $Đ$. The enzyme mimicking glycine-modified MIL-53(FE) presents several advantages over natural occurring enzymes for the initiation of RAFT polymerizations including catalytic activity over a wider range of experimental conditions (solvent, temperature, and monomer) and simple post-polymerization catalyst removal.

14.5 Polymerization-Induced Self-assembly

Over the past decade, considerable attention has been devoted to investigating the formation of nano-objects in solution by PISA via aRAFT polymerization. In a typical process, a water-soluble macroCTA homopolymer of monomer A is chain extended in water with a monomer B that gradually becomes insoluble as the chain grows. This drives the in situ self-assembly to form AB diblock copolymer nano-objects. The polyA macroCTA serves as a steric stabilizer and can either be formed in water via solution polymerization or in a suitable organic solvent, then isolated, and added to water. As Warren and Armes explained in their review on PISA [54], the B block is usually synthesized via dispersion polymerization of a monomer like HPMA, NIPAM, *N*,*N*′-diethylacrylamide (DEA), and 2-methoxyethylacrylate (MEA). HPMA is a commonly reported monomer in the aqueous PISA literature [23–26, 45, 47, 52] and, in its monomeric form, is water soluble, but forms water-insoluble polymers at high degrees of polymerization. There are also a few examples of PISA consisting of the emulsion polymerization of hydrophobic monomers like styrene [55–57]. Aqueous PISA offers a couple of advantages over typical emulsion polymerization because it can form nanoparticles below 100 nm and it does not require the use of added surfactants, which could contaminate the final products. One characteristic of PISA is the acceleration of polymerization that begins early in the process upon micellar nucleation as shown in Figure 14.10. This occurs when micelles begin to form and monomer B diffuses into the micellar core to solvate the growing hydrophobic block, which leads to a higher local monomer concentration, thus increasing the rate of polymerization.

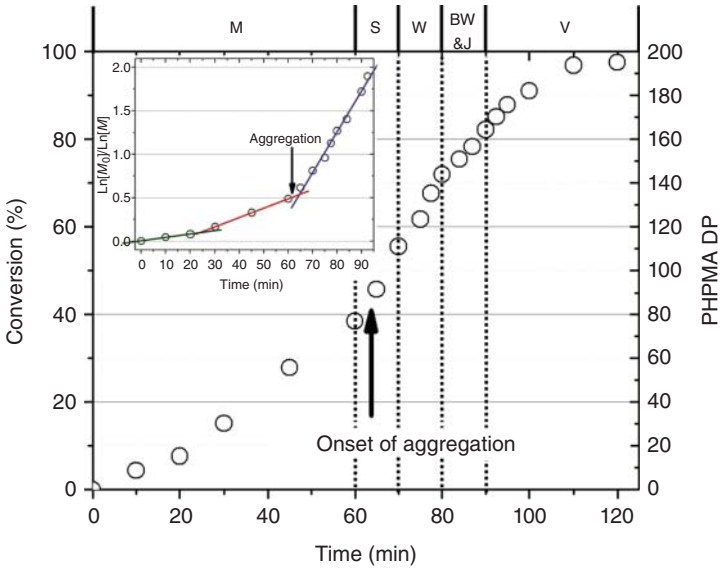

Figure 14.10 HPMA polymerization kinetics obtained for the targeted poly(GMA_{47}-*b*-$HPMA_{200}$) diblock copolymer prepared via aRAFT dispersion polymerization at 70 °C and the corresponding morphologies found via transmission electron microscopy (TEM): molecularly dispersed copolymer chains (M), spherical micelles (S), wormlike micelles (W), branched wormlike micelles, jellyfish (BW & J), and vesicles (V). Source: Reprinted with permission from Blanazs et al. [58]. © 2011, American Chemical Society.

This effect can also be seen in the inset in Figure 14.10. The first regime corresponds to an induction period, which is common to RAFT polymerization, the second regime corresponds to the formation of diblock copolymer chains, and the last regime corresponds to an acceleration of the heterogeneous polymerization because the HPMA monomers partitioning into the micelle core and solvating the hydrophobic polyHPMA chains, resulting in a high monomer concentration.

PISA can be conducted with relatively high solid content (≥10% w/w) [24–26]. Various nano-object morphologies have been reported in the literature [25, 59–64], including spheres, worms, and vesicles. Depending on several factors such as temperature, block molecular weight, composition, concentration, and charge, these nano-objects can possess kinetically trapped morphologies or can undergo transitions to form different morphologies [65]. An example of the latter was reported by Ma et al. in which they demonstrated the temperature-induced vesicle-to-lamellae or vesicle-to-worm morphological transitions of temperature-responsive nano-objects formed via aRAFT dispersion polymerization [29]. Obtaining consistent morphologies from a given PISA synthesis often requires the construction of a detailed phase diagrams [25, 59–64]. An example is from the work of Blanazs et al. who synthesized various nano-objects via RAFT dispersion polymerization of HPMA with GMA macroCTAs of various lengths [60]. As can be observed from Figures 14.11 and 14.12, the morphologies of the resulting nano-objects were dependent on three parameters:

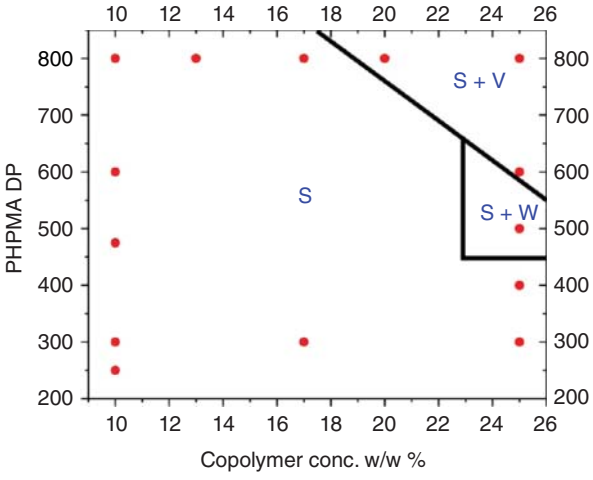

Figure 14.11 Phase diagram for poly(GMA_{78}-*b*-$HPMA_X$) copolymers synthesized via aqueous RAFT dispersion polymerization at various concentrations ranging between 10 and 25% w/w. S = spherical micelles, W = worms, and V = vesicles. Source: Reprinted with permission from Blanazs et al. [60]. © 2012, American Chemical Society.

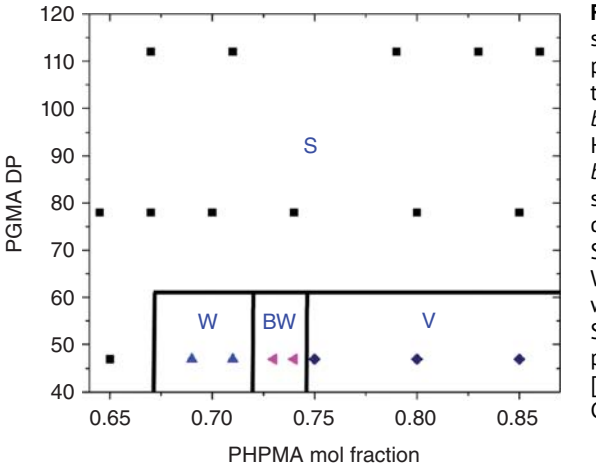

Figure 14.12 Phase diagram summarizing the various morphologies observed for the three series of poly(GMA_{112}-*b*-$HMPA_X$), poly(GMA_{78}-*b*-$HMPA_X$), and poly(GMA_{47}-*b*-$HMPA_X$) diblock copolymers synthesized by aRAFT dispersion polymerization. S = spherical micelles, W = worms, BW = branched worms, and V = vesicles. Source: Reprinted with permission from Blanazs et al. [60]. © 2012, American Chemical Society.

the mean DP of the GMA stabilizing block, the mean DP of the HPMA core forming block, and the total concentration of copolymer in solution.

PISA-formed nano-objects can be endowed with stimuli responsiveness by the appropriate choice of macroCTA. Some of the common stimuli include pH [66, 67] and temperature [24, 25, 61, 64, 68]. Penfold et al. synthesized a morpholine-functionalized GMA macroCTA and then chain extended it with HPMA via dispersion polymerization [64]. Lowering the solution pH resulted in the protonation of the morpholine end groups, which increased the hydrophilic character of the GMA stabilizing block. Guragain and Perez-Mercader synthesized pH-responsive nano-objects via a one-pot synthesis by utilizing a PEG-*b*-polyDMAEMA diblock copolymer macroCTA and chain extending it with HPMA to form triblock copolymers via PET-RAFT aqueous dispersion polymerization [67]. Because of the pH-sensitive DMAEMA block, the morphologies of the nano-objects could be manipulated by changing the solution pH. Blanazs

et al. synthesized biocompatible thermoresponsive poly(GMA-*b*-HPMA) diblock copolymer nano-objects that form worm-like particles at ambient temperature and display reversible worm-to-sphere transitions upon cooling to 4 °C [68]. The Tan and Zhang groups synthesized temperature-responsive nano-objects by utilizing a temperature-responsive stabilizer block and chain extending it with HPMA in water via dispersion polymerization [24, 25]. They also synthesized poly(PEGMA-*b*-HPMA) nanoparticles that demonstrated irreversible morphological changes from worms-to-spheres upon cooling from 25 to 4 °C. They attributed this irreversible nature to the effective steric stabilization effect of the PEGMA stabilizing block, which may have prevented the sphere-to-worm transition because of an increase in the interfacial surface energy of the spheres. Penfold et al. synthesized PEG-*b*-polyHPMA diblock copolymers that demonstrated irreversible morphological changes from worms-to-spheres upon cooling from 25 to 4 °C [64]. However, after constructing phase diagrams, they were able to identify a single diblock copolymer composition, which could undergo reversible worm-to-sphere changes upon a temperature cycle. Doncom et al. synthesized nanoparticles via PISA by chain extending a [2-(methacryloyloxy)-ethyl] dimethyl(3-sulfopropyl) ammonium hydroxide (SBMA)-based macroCTA with HPMA [61]. The SBMA stabilizer block endowed the particles with temperature responsiveness and also salt tolerance.

14.6 Grafting from Biomolecules

aRAFT polymerization also offers the unique ability to produce well-defined protein–polymer conjugates by polymerizing from the surface of a protein under conditions that will not denature the protein. Two different methods have been reported in the literature for grafting a polymer from the surface of a protein using RAFT polymerization, by attaching a CTA to the protein via the Z group or by attaching the CTA via the R group (Scheme 14.2; [69]). The Z group approach, while not strictly a 'grafting from' polymerization process, offers the benefit of only dormant 'living' chains are attached to the protein because all the terminated polymer chains remain in solution. Additionally, the polymer can be easily cleaved from the protein by reducing the thiocarbonylthio moiety. Alternatively, the R group approach leads to the thiocarbonylthio moiety being distal to the protein, allowing monomer to be easily added to the growing polymer chain end without the growing polymer having to diffuse back to the surface of the protein to undergo chain transfer as is required in the Z group approach. Additionally, the distal location of the thiocarbonylthio group leads to conjugates that are more stable and allows for better chain extension to form synthetic block copolymers immobilized on the protein surface [69].

The Davis and Bulmus groups were the first to report the Z group approach by attaching a CTA to bovine serum albumin (BSA) using a thiol–disulfide exchange reaction [70, 71]. In their first report, the BSA macroCTA was utilized to mediate the γ ray initiated polymerization of oligo(ethylene glycol) acrylate (OEGA) in

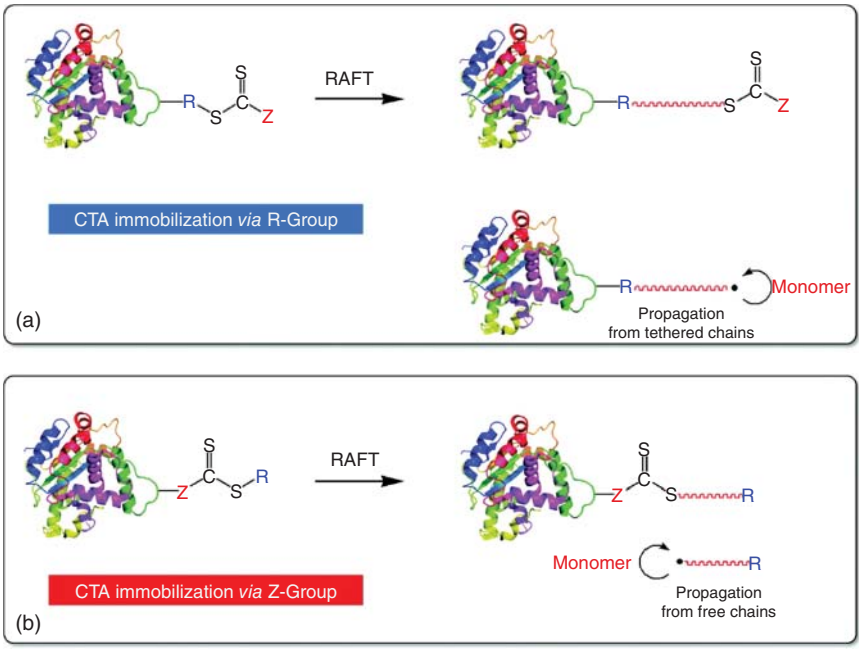

Scheme 14.2 R-group (a) and Z-group (b) strategies for preparing polymer–protein conjugates by reversible addition–fragmentation chain transfer (RAFT) polymerization. Source: Reprinted with permission from Sumerlin et al. [69]. © 2012, American Chemical Society.

a 9 : 1 water:DMF (dimethylformamide) mixture at room temperature [70]. The polymerizations exhibited linear molecular weight increases with monomer conversion, indicating that the in situ polymerizations were controlled. The authors published a subsequent study in which they polymerized NIPAM and HEA from the BSA macroCTA in aqueous media at 25 °C and characterized using SEC, ^{1}H nuclear magnetic resonance (NMR) spectroscopy, matrix assisted laser desorption ionization-time of flight mass spectrometry (MALDI-TOF), and polyacrylamide gel electrophoresis (PAGE) [71]. Notably, the authors demonstrated that the polymerization process did not prevent the conformation-related esterase activity of BSA.

The Sumerlin group was the first to report the use of the R group approach to graft polymers from the surface of a protein using aRAFT polymerization [72]. The authors reacted a maleimide-functionalized CTA, 2-dodecylsulfanylthiocarbonylsulfanyl-2-methylpropionic acid maleimido ethoxyethyl ester, with a free sulfhydryl cysteine residue of BSA and subsequently utilized the BSA macroCTA to polymerize NIPAM in phosphate buffer (pH 6). The molecular weight of the formed poly(NIPAM) was 239 000 g mol^{-1} (theoretical M_n of 234 000 g mol^{-1}) with a $Đ$ of 1.38. Additionally, the authors demonstrated the ability of the temperature-responsive nature of poly(NIPAM) to allow the thermal regulation of the BSA's activity without thermally denaturing the protein after multiple heating/cooling cycles. The Sumerlin group followed their initial work by publishing

reports on the synthesis of block copolymer protein conjugates using BSA [73] and lysozyme (LYS) [74] macroCTAs to perform aRAFT polymerization of NIPAM and DMA. The block copolymer conjugates maintained the thermoresponsive behavior of the NIPAM block, while the DMA block provided sufficient colloidal stability to prevent precipitation of the conjugates. Subsequently, the Sumerlin group utilized metal-free PET-RAFT polymerization using a LYS macroCTA to synthesize a library of AM, acrylic, and styrenic homo- and block copolymers conjugated to LYS [75].

In addition to the work done to graft synthetic polymers from proteins, there have also been some reports on using aRAFT polymerization to graft polymers from nucleic acids. The He group first reported the aRAFT polymerization of oligo(ethylene glycol) methacrylate (OEGMA) from surface-anchored DNA strands for biosensing applications [76]. In order to perform the polymerizations, they attached the CTA CMP to the 5′ end of a single-stranded DNA (ssDNA). The CMP-functionalized ssDNA was hybridized to the complimentary oligonucleotide anchored on the surface of a gold nanoparticle. Because CMP is a difunctional, symmetric trithiocarbonate, the polymerization takes place both on the surface and on solution. In a later report, the He group reported the surface-initiated aRAFT polymerization of OEGMA and HEMA using a similar immobilization scheme as in their previous report [77]. Their results demonstrated an increase in the polymerization kinetics using the DNA-conjugated CMP compared to CMP conjugated to the surface using a small-molecule linker. The authors speculated that the increase in kinetics is a result of the presence of highly charged DNA backbones and purine/pyrimidine moieties surrounding the reaction sites. Subsequently, Lueckerath et al. reported the aqueous solution-based photoRAFT of three monomer families (methacrylates, acrylates, and AMs) from ssDNA via a grafting from approach using two conjugated CTAs, BTPA, and CTP and initiated by the combinations of EY and ascorbic acid [78].

References

1 Chiefari, J., Chong, Y.K., Ercole, F. et al. (1998). *Macromolecules* 31 (16): 5559–5562. https://doi.org/10.1021/ma9804951.

2 Mitsukami, Y., Donovan, M.S., Lowe, A.B., and McCormick, C.L. (2001). *Macromolecules* 34 (7): 2248–2256. https://doi.org/10.1021/ma0018087.

3 Smith, A.E., Xu, X., and McCormick, C.L. (2010). *Prog. Polym. Sci.* 35 (1–2): 45–93. https://doi.org/10.1016/j.progpolymsci.2009.11.005.

4 Levesque, G., Arsène, P., Fanneau-Bellenger, V., and Pham, T.N. (2000). *Biomacromolecules* 1 (3): 400–406. https://doi.org/10.1021/bm000037b.

5 Thomas, D.B., Convertine, A.J., Hester, R.D. et al. (2004). *Macromolecules* 37 (5): 1735–1741. https://doi.org/10.1021/ma035572t.

6 Levesque, G., Arsène, P., Fanneau-Bellenger, V., and Pham, T.N. (2000). *Biomacromolecules* 1 (3): 387–399. https://doi.org/10.1021/bm000288k.

7 Li, Y., Lokitz, B.S., and McCormick, C.L. (2006). *Angew. Chem. Int. Ed.* 45 (35): 5792–5795. https://doi.org/10.1002/anie.200602168.

8 Xu, X., Smith, A.E., Kirkland, S.E., and McCormick, C.L. (2008). *Macromolecules* 41 (22): 8429–8435. https://doi.org/10.1021/ma801725w.

9 Thomas, D.B., Convertine, A.J., Myrick, L.J. et al. (2004). *Macromolecules* 37 (24): 8941–8950. https://doi.org/10.1021/ma048199d.

10 Moad, G., Rizzardo, E., and Thang, S.H. (2005). *Aust. J. Chem.* 58 (6): 379–410. https://doi.org/10.1071/CH05072.

11 Lowe, A.B. and McCormick, C.L. (2008). *Handbook of RAFT Polymerization*, 235–284. Wiley https://doi.org/10.1002/9783527622757.ch7.

12 Sumerlin, B.S., Donovan, M.S., Mitsukami, Y. et al. (2001). *Macromolecules* 34 (19): 6561–6564. https://doi.org/10.1021/ma011288v.

13 Donovan, M.S., Sanford, T.A., Lowe, A.B. et al. (2002). *Macromolecules* 35 (12): 4570–4572. https://doi.org/10.1021/ma020191l.

14 Lai, J.T., Filla, D., and Shea, R. (2002). *Macromolecules* 35 (18): 6754–6756. https://doi.org/10.1021/ma020362m.

15 Thomas, D.B., Sumerlin, B.S., Lowe, A.B., and McCormick, C.L. (2003). *Macromolecules* 36: 1436–1439. https://doi.org/10.1021/ma025960f.

16 Vasilieva, Y.A., Thomas, D.B., Scales, C.W., and McCormick, C.L. (2004). *Macromolecules* 37 (8): 2728–2737. https://doi.org/10.1021/ma035574d.

17 Convertine, A.J., Lokitz, B.S., Lowe, A.B. et al. (2005). *Macromol. Rapid Commun.* 26 (10): 791–795. https://doi.org/10.1002/marc.200500042.

18 Convertine, A.J., Lokitz, B.S., Vasileva, Y. et al. (2006). *Macromolecules* 39 (5): 1724–1730. https://doi.org/10.1021/ma0523419.

19 Quinn, J.F., Barner, L., Barner-Kowollik, C. et al. (2002). *Macromolecules* 35 (20): 7620–7627. https://doi.org/10.1021/ma0204296.

20 Figg, C.A. and Sumerlin, B.S. (2018), ACS Symposium Series, vol. 1285, 43–56. https://doi.org/10.1021/bk-2018-1285.ch003.

21 Shi, Y., Gao, H., Lu, L., and Cai, Y. (2009). *Chem. Commun.* 45 (11): 1368–1370. https://doi.org/10.1039/b821486g.

22 Shi, Y., Liu, G., Gao, H. et al. (2009). *Macromolecules* 42 (12): 3917–3926. https://doi.org/10.1021/ma9000513.

23 Tan, J., Sun, H., Yu, M. et al. (2015). *ACS Macro Lett.* 4 (11): 1249–1253. https://doi.org/10.1021/acsmacrolett.5b00748.

24 Tan, J., Bai, Y., Zhang, X. et al. (2016). *Macromol. Rapid Commun.* 37 (17): 1434–1440. https://doi.org/10.1002/marc.201600299.

25 Tan, J., Bai, Y., Zhang, X., and Zhang, L. (2016). *Polym. Chem.* 7 (13): 2372–2380. https://doi.org/10.1039/c6py00022c.

26 Tan, J., Liu, D., Bai, Y. et al. (2017). *Polym. Chem.* 8 (8): 1315–1327. https://doi.org/10.1039/c6py02135b.

27 Li, G., Xu, N., Yu, Q. et al. (2014). *Macromol. Rapid Commun.* 35 (16): 1430–1435. https://doi.org/10.1002/marc.201400153.

28 Gao, P., Cao, H., Ding, Y. et al. (2016). *ACS Macro Lett.* 5 (12): 1327–1331. https://doi.org/10.1021/acsmacrolett.6b00796.

29 Ma, Y., Gao, P., Ding, Y. et al. (2019). *Macromolecules* 52 (3): 1033–1041. https://doi.org/10.1021/acs.macromol.8b02490.

30 Otsu, T. (2000). *J. Polym. Sci., Part A: Polym. Chem.* 38 (12): 2121–2136. https://doi.org/10.1002/(SICI)1099-0518(20000615)38:12<2121::AID-POLA10>3.0.CO;2-X.

31 McKenzie, T.G., Fu, Q., Wong, E.H.H. et al. (2015). *Macromolecules* 48 (12): 3864–3872. https://doi.org/10.1021/acs.macromol.5b00965.

32 Lewis, R.W., Evans, R.A., Malic, N. et al. (2018). *Polym. Chem.* 9 (1): 60–68. https://doi.org/10.1039/c7py01752a.

33 Fu, Q., McKenzie, T.G., Tan, S. et al. (2015). *Polym. Chem.* 6 (30): 5362–5368. https://doi.org/10.1039/c5py00840a.

34 Prier, C.K., Rankic, D.A., and MacMillan, D.W.C. (2013). *Chem. Rev.* 113 (7): 5322–5363. https://doi.org/10.1021/cr300503r.

35 Xu, J., Jung, K., Atme, A. et al. (2014). *J. Am. Chem. Soc.* 136 (14): 5508–5519. https://doi.org/10.1021/ja501745g.

36 Xu, J., Jung, K., Corrigan, N.A., and Boyer, C. (2014). *Chem. Sci.* 5 (9): 3568–3575. https://doi.org/10.1039/c4sc01309c.

37 Shanmugam, S., Xu, J., and Boyer, C. (2016). *Polym. Chem.* 7 (42): 6437–6449. https://doi.org/10.1039/c6py01361a.

38 Chakraborty, M. and Panda, A.K. (2011). *Spectrochim. Acta, Part A* 81 (1): 458–465. https://doi.org/10.1016/j.saa.2011.06.038.

39 Yeow, J., Chapman, R., Xu, J., and Boyer, C. (2017). *Polym. Chem.* 8 (34): 5012–5022. https://doi.org/10.1039/c7py00007c.

40 Niu, J., Lunn, D.J., Pusuluri, A. et al. (2017). *Nat. Chem.* 9 (6): 537–545. https://doi.org/10.1038/nchem.2713.

41 Figg, C.A., Hickman, J.D., Scheutz, G.M. et al. (2018). *Macromolecules* 51 (4): 1370–1376. https://doi.org/10.1021/acs.macromol.7b02533.

42 Hill, M.R., Carmean, R.N., and Sumerlin, B.S. (2015). *Macromolecules* 48 (16): 5459–5469. https://doi.org/10.1021/acs.macromol.5b00342.

43 Niu, J., Page, Z.A., Dolinski, N.D. et al. (2017). *ACS Macro Lett.* 6 (10): 1109–1113. https://doi.org/10.1021/acsmacrolett.7b00587.

44 Shanmugam, S., Xu, J., and Boyer, C. (2016). *Macromolecules* 49 (24): 9345–9357. https://doi.org/10.1021/acs.macromol.6b02060.

45 Xu, S., Yeow, J., and Boyer, C. (2018). *ACS Macro Lett.* 7 (11): 1376–1382. https://doi.org/10.1021/acsmacrolett.8b00741.

46 Zaquen, N., Kadir, A.M.N.B. et al. (2019). *Macromolecules* 52 (4): 1609–1619. https://doi.org/10.1021/acs.macromol.8b02628.

47 Chapman, R., Gormley, A.J., Herpoldt, K.L., and Stevens, M.M. (2014). *Macromolecules* 47 (24): 8541–8547. https://doi.org/10.1021/ma5021209.

48 Chapman, R., Gormley, A.J., Stenzel, M.H., and Stevens, M.M. (2016). *Angew. Chem. Int. Ed.* 55 (14): 4500–4503. https://doi.org/10.1002/anie.201600112.

49 Schneiderman, D.K., Ting, J.M., Purchel, A.A. et al. (2018). *ACS Macro Lett.* 7 (4): 406–411. https://doi.org/10.1021/acsmacrolett.8b00069.

50 Zhang, B., Wang, X., Zhu, A. et al. (2015). *Macromolecules* 48 (21): 7792–7802. https://doi.org/10.1021/acs.macromol.5b01893.

51 Lv, Y., Liu, Z., Zhu, A., and An, Z. (2017). *J. Polym. Sci., Part A: Polym. Chem.* 55 (1): 164–174. https://doi.org/10.1002/pola.28380.

52 Tan, J., Liu, D., Bai, Y. et al. (2017). *Macromolecules* 50 (15): 5798–5806. https://doi.org/10.1021/acs.macromol.7b01219.

53 Fu, Q., Ranji-Burachaloo, H., Liu, M. et al. (2018). *Polym. Chem.* 9 (35): 4448–4454. https://doi.org/10.1039/c8py00832a.

54 Warren, N.J. and Armes, S.P. (2014). *J. Am. Chem. Soc.* 136 (29): 10174–10185. https://doi.org/10.1021/ja502843f.

55 Zhang, X., Boissé, S., Zhang, W. et al. (2011). *Macromolecules* 44 (11): 4149–4158. https://doi.org/10.1021/ma2005926.

56 Gurnani, P., Bray, C.P., Richardson, R.A.E. et al. (2019). *Macromol. Rapid Commun.* 40 (2): 1800314 (1 of 7)–1800314 (7 of 7). https://doi.org/10.1002/marc.201800314.

57 Ebeling, B., Belal, K., Stoffelbach, F. et al. (2019). *Macromol. Rapid Commun.* 40 (2): 1800455 (1 of 5)–1800455 (5 of 5). https://doi.org/10.1002/marc.201800455.

58 Blanazs, A., Madsen, J., Battaglia, G. et al. (2011). *J. Am. Chem. Soc.* 133 (41): 16581–16587. https://doi.org/10.1021/ja206301a.

59 Sugihara, S., Blanazs, A., Armes, S.P. et al. (2011). *J. Am. Chem. Soc.* 133 (39): 15707–15713. https://doi.org/10.1021/ja205887v.

60 Blanazs, A., Ryan, A.J., and Armes, S.P. (2012). *Macromolecules* 45 (12): 5099–5107. https://doi.org/10.1021/ma301059r.

61 Doncom, K.E.B., Warren, N.J., and Armes, S.P. (2015). *Polym. Chem.* 6 (41): 7264–7273. https://doi.org/10.1039/c5py00396b.

62 Byard, S.J., Williams, M., McKenzie, B.E. et al. (2017). *Macromolecules* 50 (4): 1482–1493. https://doi.org/10.1021/acs.macromol.6b02643.

63 Varlas, S., Georgiou, P.G., Bilalis, P. et al. (2018). *Biomacromolecules* 19 (11): 4453–4462. https://doi.org/10.1021/acs.biomac.8b01326.

64 Penfold, N.J.W., Whatley, J.R., and Armes, S.P. (2019). *Macromolecules* 52 (4): 1653–1662. https://doi.org/10.1021/acs.macromol.8b02491.

65 Williams, M., Penfold, N.J.W., Lovett, J.R. et al. (2016). *Polym. Chem.* 7 (23): 3864–3873. https://doi.org/10.1039/c6py00696e.

66 Penfold, N.J.W., Lovett, J.R., Warren, N.J. et al. (2016). *Polym. Chem.* 7 (1): 79–88. https://doi.org/10.1039/c5py01510c.

67 Guragain, S. and Perez-Mercader, J. (2018). *Polym. Chem.* 9 (29): 4000–4006. https://doi.org/10.1039/c8py00775f.

68 Blanazs, A., Verber, R., Mykhaylyk, O.O. et al. (2012). *J. Am. Chem. Soc.* 134 (23): 9741–9748. https://doi.org/10.1021/ja3024059.

69 Sumerlin, B.S. (2012). *ACS Macro Lett.* 1 (1): 141–145. https://doi.org/10.1021/mz200176g.

70 Liu, J., Bulmus, V., Herlambang, D.L. et al. (2007). *Angew. Chem. Int. Ed.* 46 (17): 3099–3103. https://doi.org/10.1002/anie.200604922.

71 Boyer, C., Bulmus, V., Liu, J. et al. (2007). *J. Am. Chem. Soc.* 129 (22): 7145–7154. https://doi.org/10.1021/ja070956a.

72 De, P., Li, M., Gondi, S.R., and Sumerlin, B.S. (2008). *J. Am. Chem. Soc.* 130 (34): 11288–11289. https://doi.org/10.1021/ja804495v.

73 Li, M., Li, H., De, P., and Sumerlin, B.S. (2011). *Macromol. Rapid Commun.* 32 (4): 354–359. https://doi.org/10.1002/marc.201000619.

74 Li, H., Li, M., Yu, X. et al. (2011). *Polym. Chem.* 2 (7): 1531–1535. https://doi.org/10.1039/c1py00031d.

75 Tucker, B.S., Coughlin, M.L., Figg, C.A., and Sumerlin, B.S. (2017). *ACS Macro Lett.* 6 (4): 452–457. https://doi.org/10.1021/acsmacrolett.7b00140.

76 He, P., Zheng, W., Tucker, E.Z. et al. (2008). *Anal. Chem.* 80 (10): 3633–3639. https://doi.org/10.1021/ac702608k.

77 He, P. and He, L. (2009). *Biomacromolecules* 10 (7): 1804–1809. https://doi.org/10.1021/bm9002283.

78 Lueckerath, T., Strauch, T., Koynov, K. et al. (2019). *Biomacromolecules* 20 (1): 212–221. https://doi.org/10.1021/acs.biomac.8b01328.

15

RAFT-Mediated Polymerization-Induced Self-Assembly (PISA)†

Franck D'Agosto[1], Muriel Lansalot[1], and Jutta Rieger[2]

[1] Université de Lyon, Université Claude Bernard Lyon 1, CPE Lyon, CNRS, UMR 5128, Catalysis, Polymerization Processes and Materials (CP2M), 43 Bd du 11 Novembre 1918, Villeurbanne 69616, France
[2] Sorbonne Université and CNRS, UMR 8232, Institut Parisien de Chimie Moléculaire (IPCM), Polymer Chemistry Team (ECP), 4 Place Jussieu, Paris 75005, France

15.1 Introduction

There is no doubt that among the available reversible deactivation radical polymerization (RDRP) techniques, reversible addition–fragmentation chain transfer (RAFT) is the most versatile and powerful way to combine the tolerance of a radical process with a controlled chain growth for the production of well-defined polymers [2]. Since the edition of the first handbook on RAFT edited by Wiley in 2008 [3], RAFT has been confirming its fame and great potential over the existing RDRP techniques. This is attested by its ever-growing interest since the first report on RAFT polymerization in the open literature in 1998 [4] and by constantly improving the control on molar mass while expanding the range of controllable monomers [5–7]. In addition, the development of RAFT in heterogeneous media has provided new tools to design macromolecular objects, contributing to the development of new and original applications [8].

As we will see in this chapter, polymerization-induced self-assembly (PISA) is probably the best example of this evolution. Indeed, the myriad of macromolecular architectures that have been obtained through the use of RDRP techniques lies in the fact that the formed chains can be further extended for the generation of a second block. Although this feature was extensively used for the production of block copolymers in solution or bulk polymerizations [9, 10], PISA makes the most of polymerizations in dispersed media by chain extending a solvophilic polymer obtained by RDRP with a solvophobic block and inducing, concomitantly to the growth of a second solvophobic block, the self-assembly of the resulting block copolymers. This is made possible by the choice of a dispersing phase that is a selective solvent of the first block. As a result, PISA is not only an extremely valuable tool to efficiently produce block copolymers, generally including amphiphilic ones, but has

† D'Agosto et al. [1].

RAFT Polymerization: Methods, Synthesis and Applications, First Edition.
Edited by Graeme Moad and Ezio Rizzardo.

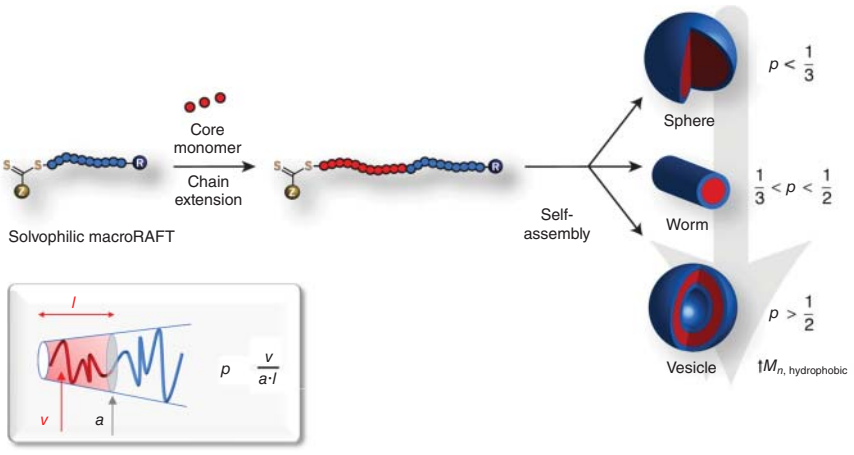

Figure 15.1 RAFT-mediated polymerization-induced self-assembly and illustration of the packing parameter p (by analogy to surfactants, a is the area of the hydrophilic segment and v and l are the volume and length of the hydrophobic segment, respectively) and the impact of the solvophobic block molar mass on the packing parameter/morphology [13–15].

also rapidly reached interest as a technique of choice to form nano-objects [11, 12] that can exhibit various morphologies (Figure 15.1) [13–15].

Theoretically, any RDRP technique or living polymerization technique can be selected to produce these block copolymer nano-objects by PISA. Indeed, nitroxide-mediated polymerization (NMP) [13, 16–19], atom transfer radical polymerization (ATRP) [20–25] or Cu-mediated controlled polymerization [26], iodine transfer polymerization (ITP) [27], organotellurium-mediated radical polymerization (TERP) [28–30], Co-mediated radical polymerization [31], ring-opening metathesis polymerization (ROMP) [32–35], or reversible complexation-mediated polymerization (RCMP) [36] have been successfully implemented. However, RAFT-mediated PISA remains the most employed strategy. In the above-mentioned first book edition in 2008, the pioneering works of Ferguson et al. [37] on chain extension of preformed poly(acrylic acid) (PAA) macromolecular RAFT agent (macroRAFT) in water with a slow feed of *n*-butyl acrylate (BA) were the only mention to this strategy, not yet called PISA. Since then, there has been ca. 4000 citations to papers related to PISA (source: Web of Science June 2019; keywords: PISA – polymer science), among which more than 90% are based on RAFT polymerization, which confirms the general adoption of this fast maturing sub-discipline. It is worth mentioning that a process that probably strongly inspired RAFT inventors and called addition-fragmentation chain transfer [38–42] (AFCT) exploits the reactivity of radicals towards vinyl moiety such as methacrylates to form an adduct radical that is known to proceed mainly via fragmentation, with a minimal contribution of copolymerization. Although the level of control is not comparable to RAFT carried out in the presence of thiocarbonylthio compounds, it allows the production of low dispersity block copolymers if the methacrylate controlling agent is carried by a macromolecular chain. Early work on so-called macromonomer or

sulfur-free RAFT polymerization, including its use to form self-stabilized latices by PISA, is mentioned in Chapter 24 [44–46]. More recent studies have appeared [43] but will not be the focus of the present review.

To date, more than 20 reviews have already been published on PISA, mainly on RAFT-mediated PISA, covering the general concepts of the strategy [11, 12, 47–59], the corresponding design of reactive nano-objects [60], and their biomedical applications [61–64]. The aim of this chapter is thus not to be an additional contribution of this type but rather to provide the reader, both incomers to the field and experts, with a general overview of the topic. For a detailed account of specific features of RAFT-mediated PISA, the reader should thus be referred to these reviews. After a brief history that positions PISA in the field of polymer chemistry, this chapter will cover the fundamentals of the PISA mechanism and review some features and limitations of RAFT-mediated PISA in terms of the choice of the components involved, the nature of the nano-objects that is achievable, the morphologies that are accessible and how they can be controlled, and some potential applications.

15.2 History/Origin of PISA

Block copolymers are very attractive materials that have gained attention in many high-performance applications. These polymers are particularly interesting when the chemical nature of both blocks is such that the corresponding properties are not compatible with each other (polar/apolar, attractive/repulsive, and hydrophilic/hydrophobic). The resulting materials generally exhibit a unique behaviour originating from hybrid properties. However, the synthesis of A–B diblock copolymers with such properties is often tricky. In the particular field of amphiphilic block copolymers, the conditions for the preparation of each block are sometimes incompatible and the synthesis of the block copolymer then requires two (or more) steps. The main strategies are (i) the synthesis of one block, followed by the initiation of the second block, (ii) the selective post-modification of a preformed diblock copolymer composed of compatible blocks, or (iii) a polymer–polymer coupling reaction. In any case, the choice of the solvent for an efficient chemistry is narrowed by the nature of the monomers involved or the targeted polymers.

PISA can find its origin in different fields of polymer science. Polymer chemists will see in PISA a very original strategy to produce (amphiphilic) block copolymers. Indeed, PISA that can be in essence defined as the self-assembly of (amphiphilic) block copolymers during polymerization is a way to alleviate the problems mentioned above. Works published by polymer chemists almost 25 years ago, exploiting the livingness of poly(*t*-butyl styryl)-lithium chains to initiate the anionic dispersion polymerization of styrene (St) [65] or divinylbenzene (DVB) [66] in *n*-hexane, did indeed probably pioneer the concept of what is called today a PISA process. More recently, Yamauchi et al. [67] observed what they named a polymerization reaction-induced molecular self-assembling process when simultaneously polymerizing isoprene and St in deuterated benzene by living anionic polymerization initiated by *sec*-butyllithium. Indeed, the reactivity ratios are such

that a polyisoprene-*b*-polystyrene block copolymer is formed, and the authors set up experiments by means of time-resolved small angle neutron scattering (SANS) measurements to visualize the self-assembly upon the growth of the polystyrene (PS) block from the polyisoprene first block.

For the emulsion polymer chemists, however, PISA is the result of constant efforts from researchers in the field of latex synthesis, particularly for coating applications. These efforts were concentrated on both finding appropriate ways to get rid of molecular surfactants and transposing all the features of homogeneous RDRP (solution or bulk) to polymerization in dispersed media [68, 69]. As already mentioned, the pioneering works on RAFT-mediated PISA from Hawkett, Gilbert, and coworkers [37] consisted in the starve-feed addition of BA to an aqueous solution of a PAA macroRAFT. The low solubility of BA in water was sufficient to induce chain extension of PAA and form a PBA block. The resulting PAA-*b*-PBA amphiphilic block copolymers then self-assembled into micellar aggregates that could swell with BA. The polymerization thus quickly switched from the aqueous phase to the particle core with a constant feed of radicals coming from water. These seminal works launched a series of important patents from the University of Sydney related to coating applications [70, 71]. It is worth mentioning here that, very soon after the discoveries of RAFT by CSIRO/DuPont [72] and macromolecular interchange of xanthate (MADIX) [73, 74] by Rhodia Chimie, and two years before the works patented and published by Hawkett, Gilbert, and coworkers [37], Rhodia Chimie patented the use of hydrophilic macroxanthates for particle surface functionalization using, however, some molecular surfactants in emulsion polymerization [2, 75]. These last works clearly did not aim at producing well-defined block copolymers but targeted the formation of latex particles (formed through conventional emulsion polymerization) stabilized by the in situ formation of a fraction of block copolymers, which concomitantly allowed the surface modification of the particles by the hydrophilic macroxanthate structure.

As mentioned in Section 15.1, these works performed on aqueous emulsion polymerization were the first PISA systems based on RAFT and more generally speaking on a RDRP technique. RAFT-mediated PISA was then quickly transposed to aqueous [11, 12, 49] and organic dispersion polymerization [47, 51].

15.3 PISA Process

15.3.1 Emulsion, Dispersion, and Precipitation Polymerizations: The Reference Processes

As already mentioned, PISA proceeds by polymerization in dispersed media, by the chain extension of a solvophilic polymer obtained by RDRP with a monomer for which the corresponding polymer is not soluble. Emulsion, dispersion, and precipitation polymerizations are the three relevant processes to produce polymers in dispersed media and they are briefly depicted in Sections 15.3.1.1–15.3.1.3.

- Emulsion Polymerization

The main ingredients of an emulsion polymerization are water, a water-soluble initiator, a surfactant, and a hydrophobic monomer, mostly located in micrometric droplets and in nanometric surfactant micelles, with however a slight solubility in water. The decomposition of the initiator in water generates hydrosoluble radicals that start to add monomer units in the aqueous phase and produce oligoradicals. Beyond a critical degree of polymerization, the growing oligomeric species become insoluble and migrate into the monomer-swollen surfactant micelles that then become nucleated particles, where the polymerization continues. This is called micellar nucleation. In the absence of micelles, homogeneous nucleation takes place and consists in the precipitation of these oligomers, generating nuclei that are stabilized by the surfactant. Regardless of the nucleation, the growing particles are swollen with monomer diffusing from large monomer droplets through the aqueous phase, and the polymerization continues until full monomer consumption. The stability of the final particles is thus achieved by a key component in the process: the surfactant

- Dispersion Polymerization

In a dispersion polymerization, the situation is different because the monomer is soluble in the continuous phase, which can be aqueous or organic. However, the corresponding polymer is not. The stability of the nuclei formed upon polymerization is generally ensured by the in situ formation of grafted macromolecular stabilizers resulting from chain transfer reactions occurring along solvophilic polymer chains or protective colloids used in the formulation.

- Precipitation Polymerization

Precipitation polymerization is a particular case of dispersion polymerization for which the monomer does not or poorly swell its polymer. This is, for example, the case for *N*-isopropylacrylamide (NIPAM) in water for which the polymerization can be conducted above the lower critical solubility temperature (LCST) of PNIPAM in the absence of the surfactant [76, 77].

Replacing the surfactant or stabilizer by a solvophilic chain prepared by RAFT has led to successful PISA under both emulsion and dispersion polymerization conditions to generate block copolymer particles in a few hours at a similar high solid content (up to 50 wt% [78]) and under the same undemanding conditions as in emulsion or dispersion polymerization. This is in striking contrast to the strategies used so far to obtain the same nano-objects, such as the co-solvent method used to self-assemble the preformed block copolymers that requires extended periods of time and results in very low polymer concentrations (<2 wt%) [79].

Regardless of the polymerization process, most of the studies dealing with PISA employ a preformed, well-defined solvophilic macroRAFT agent. However, several examples showed that this macroRAFT could be synthesized in the same reactor as the solvophobic block. This led to the development of the so-called one-pot processes either starting with a hydrophilic monomer such as acrylic acid (AA) or methacrylic acid (MAA) in water for emulsion [57, 80, 81], or after hydrolysis of a monomer

such as glycidyl methacrylate (GlyMA), followed by the RAFT polymerization of the formed glycerol methacrylate (GMA) and dispersion polymerization of hydroxypropyl methacrylate (HPMA) [82], or using a monomer soluble in mineral oil, such as lauryl methacrylate (LMA), in dispersion polymerization [78].

In addition, the simultaneous in situ formation and self-assembly in water of amphiphilic block copolymers should give rise to the formation of morphologies that have already been observed when self-assembling preformed block copolymers in a selective solvent of one of the two blocks [79]. The full range of expected morphologies (spheres, worms, fibres, vesicles, and lamellae) was indeed obtained by RAFT-PISA by varying the nature and molar mass of the solvophilic macroRAFT and the solvophobic block and/or the solid content. So far, the vast majority of the non-spherical morphologies have been obtained in dispersion polymerization. The monomer-swollen spherical block copolymer particles initially formed during the process fuse together according to a polymerization-induced reorganization mechanism [48], as visualized in transmission electron microscopy (TEM) studies by Armes and coworkers [83]. Although the same process could take place in emulsion polymerization [84–89], kinetically trapped spheres are obtained most of the time [90–93] (see Section 15.5).

15.3.2 Main Parameters at Play for a Successful PISA at a Glance

15.3.2.1 MacroRAFT Type

Regardless of the polymerization process (emulsion, dispersion, and precipitation), the vast majority of the solvophilic macroRAFT employed is based on dithioesters or trithiocarbonates (TTCs). A slight preference goes to TTCs when water is used as the dispersing phase because these compounds have been shown to be less sensitive to hydrolysis. As a result, almost all the papers published on RAFT-mediated PISA deal with the formation of solvophobic blocks from more activated monomers. Indeed, as far as we know, only five papers depict the use of solvophilic macro-RAFT carrying a dithiocarbonate chain end for the formation of block copolymer particles based on less-activated monomers such as vinyl acetate (VAc) [94–96] or *N*-vinylcaprolactam [96–98].

15.3.2.2 Initiation in RAFT-PISA

Contrary to other RDRP techniques such as NMP or ATRP for instance, RAFT generally requires an external source of radicals usually provided through the decomposition of organic molecules under thermal-, redox-, or photo-activation. The initiating step in RAFT is complex and the control partly depends on the fine-tuning of the relative amounts of the initiator and chain transfer agent. This is a disadvantage compared to other techniques, particularly when considering block copolymer syntheses and particularly PISA. Indeed, the formation of the second block will be unavoidably accompanied by the formation of its homopolymer as a side product, which may impact the efficiency of the self-assembly. In emulsion polymerization for example, the desired block copolymer self-assembly may thus

compete with homogeneous nucleation, leading to precipitation of solvophobic oligomers. This situation is indeed also favoured when the chain transfer efficiency to the solvophilic macroRAFT is too low [86]. This is however not the case for the vast majority of RAFT-mediated PISA studies. Regardless of whether PISA is performed in emulsion or dispersion, the initiator concentration is generally optimized as in conventional RAFT to minimize the quantity of the homopolymer produced. As demonstrated by the successful polymerization-induced cooperative assembly (PICA) process (detailed below) for which the formation of the homopolymer is exacerbated, this low proportion of the homopolymer probably helps in the nucleation of the block copolymer particles. It is worth mentioning here that promoting the formation of homopolymer to the detriment of block copolymer is not without interest as it may boost up the development of surfactant-free emulsion polymerization based on PISA [57], as discussed in Section 15.3.4.

In conclusion, most of the conventional initiators employed to conduct conventional emulsion or dispersion polymerization such as azo-initiators or photoactive molecules can be employed to perform RAFT-PISA. When the dispersing phase is water, ionic azo-initiators or persulfates are preferred.

Photoinitiators can also be used in PISA [56] under appropriate irradiation conditions using UV [99] or visible light [100]. Original and efficient photoinitiating systems based on horseradish peroxidase have also been successfully developed in combination with hydrogen peroxide and ascorbic acid [101]. A way to get around the additional use of radical initiator can be the recourse to photoinitiated systems in the absence of molecular photoinitiators. Indeed, the photosensitivity of the thio-thiocarbonyl chain ends of the solvophilic macroRAFT can also be exploited, circumventing the undesired formation of homopolymer when targeting block copolymers. In this case, visible light is preferred over UV to maintain the integrity of the RAFT end all along the PISA process [102, 103].

15.3.2.3 Chemical Nature of the Blocks

The solvophilic macroRAFT can be obtained by post-modification of a preformed polymer as observed when poly(ethylene glycol) (PEG) or polydimethylsiloxane is employed, for example. It is however generally obtained by RAFT polymerization of the corresponding solvophilic monomer either performed in organic solution, purified and redissolved in the continuous phase, or directly in water. As mentioned above, a one-pot strategy, for which the whole PISA process is performed in the same solvent and reactor, is thus possible [78, 80–82]. The solvophobic core monomer is selected with respect to the nature of the thiothiocarbonyl chain end of the solvophilic macroRAFT to ensure a good blocking efficiency [9, 10] and thus a fast reinitiation (fast consumption of the starting macroRAFT) that often favours the homogeneity of the resulting block copolymer particle size and morphology.

The rest of the present chapter will provide the reader with a representative range of solvophilic monomers and macroRAFT, solvophobic monomers, and solvents to perform RAFT-PISA.

15.3.3 PITSA, PICA, PIESA, and PIHSA: Different Acronyms However All Boiling Down to PISA

The vast majority of the RAFT-PISA systems are operating according to the process explained above, i.e. chain extension of a preformed solvophilic macroRAFT with a solvophobic block either by emulsion or dispersion polymerization. However, considering the tremendous amount of systems and operating conditions used to conduct RAFT-PISA, the researchers sometimes observed that peculiar behaviours and different acronyms related to PISA can be found in the literature.

Polymerization-induced thermal self-assembly (PITSA) was coined by Figg et al. [104] but developed for the first time by An et al. [105] Starting from a poly(*N,N*-dimethyl acrylamide) (PDMAAm) macroRAFT, NIPAM was polymerized under precipitation conditions in the presence of a crosslinker in water at 70 °C. The chain extension, performed above LCST of PNIPAM, led to the self-assembly of the resulting PDMAAm-*b*-PNIPAM triggered both by the growth of the hydrophobic PNIPAM block and the polymerization temperature. Compared to particles formed by PISA, PITSA results in amphiphilic block copolymer assemblies that disassemble by cooling the resulting nano-object dispersion and thus require crosslinking during the formation of block copolymer particles to maintain their integrity at room temperature.

PICA was recently coined by Zhu et al. [106] and contemporaneously reported by Tan et al. [107, 108]. It consists in performing RAFT-PISA in the presence of both a macroRAFT and a molecular RAFT agent (Figure 15.2). Consequently, amphiphilic block copolymers form simultaneously to a solvophobic homopolymer, and particles are generated from homopolymer-based nuclei stabilized by amphiphilic block copolymers. The additional presence of homopolymer can to some extent help the transition from the spherical morphology to higher order morphologies as explained in Section 15.5.3.

PIESA stands for polymerization-induced electrostatic self-assembly. It consists in synthesizing a double hydrophilic block copolymer by RAFT in water in which the second block is a polyelectrolyte. The self-assembly is then induced by in situ polyion complexation either by the presence of a preformed polyelectrolyte homopolymer

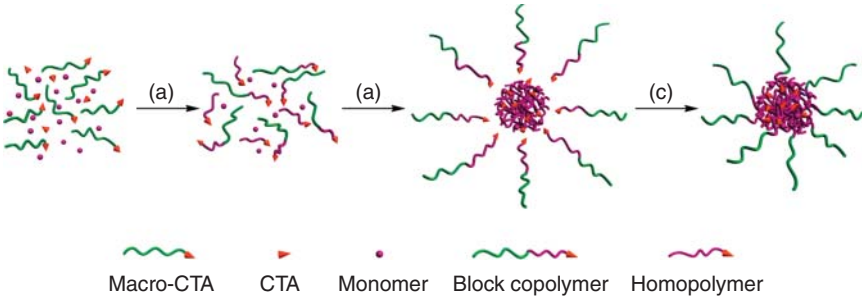

Figure 15.2 Polymerization-induced cooperative assembly (PICA). CTA stands for chain transfer agent. Source: Reprinted with permission from Zhu et al. [106]. Copyright 2017, American chemical society.

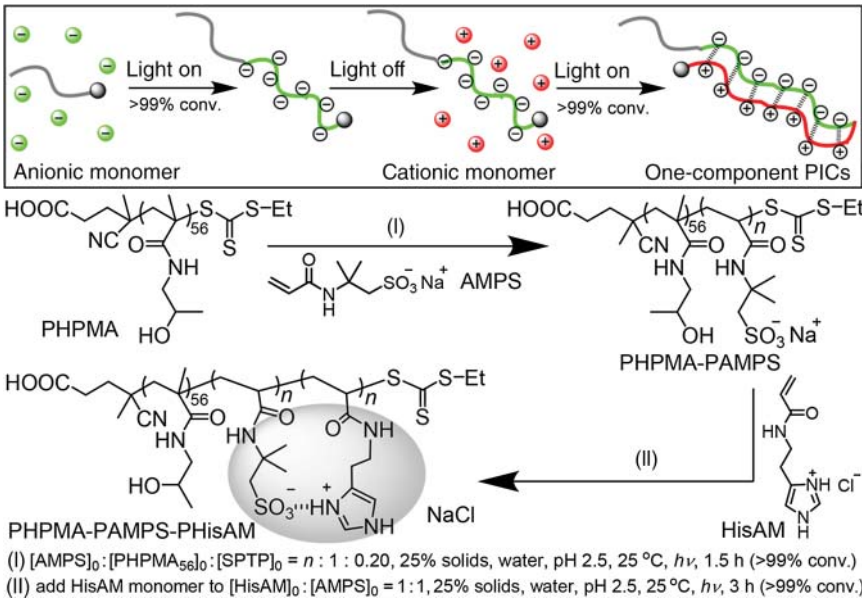

Figure 15.3 Polymerization-induced electrostatic self-assembly (PIESA). Source: Reprinted with permission from Cai et al. [111]. Copyright 2018, American chemical society.

during PISA [109, 110] and the growth of a polyelectrolyte block of opposite charge from the macroRAFT, or by the chain extension of the resulting soluble diblock copolymer with a monomer of opposite charge [111]. In the last case, this leads to the formation of a third block strongly interacting upon its growth with the second block through electrostatic interactions inducing the self-assembly (Figure 15.3).

Eventually, polymerization-induced hierarchical self-assembly (PIHSA) [112] was performed in ethanol by chain extending a poly(methacrylic acid) (PMAA) macroRAFT with a monomer containing an azobenzene side group. While the formed block copolymers self-assemble as a result of solvophobicity of the second block, the liquid crystalline property of the azobenzene group allows the core block to self-organize at the same time. This system not only consists in hierarchical self-assembly, leading to the formation of unconventional morphologies and their transitions (cuboids, short belts, and ellipsoidal vesicles), but also produces light-sensitive nano-objects thanks to the configuration switch of the azobenzene group (see Section 15.3.3).

15.3.4 PISA-Inspired Synthesis of Surfactant-Free Latexes

In the first works reporting the use of macroRAFTs to mediate polymerization in dispersed media, the main motivation was to introduce a reactive stabilizer, which was covalently anchored to the final latex particles, or to functionalize the particle surface (a molecular surfactant being still present) with less emphasis placed on their ability to control the polymerization of the core-forming block. With this in mind, PISA has been used for the synthesis of PS particles

using macroRAFT of polysoaps [113], poly(2-diethylaminoethyl methacrylate) (PDEAEMA) [114], poly(ethylene glycol) (PEG), poly(2-dimethylaminoethyl methacrylte) (PDMAEMA) and PEG-*b*-PDMAEMA [115], or PMAA [116]. PVAc particles using a dextran-based macroxanthate [94] or PBA particles from a galactopyranose-functionalized poly(*N*-acryloylmorpholine) (PNAM) macroRAFT [117] have also been reported. These latter systems involved low amount of macroRAFT, high amount of initiator, and/or the use of macroRAFT with a poor reinitiation efficiency.

The PISA process can thus also provide a valuable pathway for performing surfactant-free emulsion polymerization, expanding the range of strategies based on the use of reactive surfactants that have been investigated for many years [118]. It is worth mentioning here that most of the PISA systems reported in the literature require important amount of solvophilic species, typically 3–15 wt% with respect to the core-forming polymer. Considering the restrictions on the use of low molar mass surfactants, using low amount of macroRAFT consists in an interesting and economically viable approach to synthesize high solid content surfactant-free latexes. So far, little attention has been paid to produce such industrially relevant colloidal formulations. For instance, Lansalot, D'Agosto, and coworkers recently demonstrated that different kinds of latex particles (40 wt% solids, based on poly(vinylidene chloride) [119, 120], poly(vinylidene fluoride) (PVDF) [121], and acrylic latexes [122–125]), incorporating less than 2 wt% of hydrophilic PEG, PAA, PMAA, or poly(sodium 4-styrene sulfonate) (PSSNa), could be produced using this strategy. In the latter case, it was also demonstrated that the strategy was compatible with well-established film crosslinking strategies (namely, 2-(acetoacetoxy)ethyl methacrylate [AAEM]/hexamethylenediamine, and diacetone acrylamide [DAAm]/adipic acid dihydrazide [ADH]) and that water barrier properties of the resulting films could be improved with regard to the use of low molar mass surfactants. Using a similar low quantity of stabilizer, Rieger and coworkers had prepared PAA-*b*-PBA latex nanoparticles [126] to create soft films [127] possessing a percolating network of PAA, which allowed to combine high stiffness with extensibility in addition to water and solvent resistance [128].

15.4 Reactive/Functional Nano-objects

As demonstrated in the previous sections, the focus of PISA was initially the control of the macromolecular architecture via heterogeneous polymerization processes, progressively associated with the control of particle morphology. The robustness of the PISA process has now opened up many possibilities to provide the nano-objects with reactivity and/or functionality, which can be introduced at various stages of the process: in the initial RAFT agent, in the macroRAFT, and/or in the particle core. Regardless of the chosen strategy, the aim is either the introduction of a specific function for a specific goal or a targeted application, or the incorporation of reactive groups, allowing post-synthesis modification of the particles by further coupling or crosslinking reactions. Both options can also be combined. In addition, many studies

report the introduction of functional groups able to induce morphological transitions and these examples are discussed in Section 15.5. Moreover, potential applications of the formed nano-objects are sometimes mentioned in the present section, even if those developed for very specific applications (e.g. catalysis and bioimaging) are presented in more detail in Section 15.6.

As mentioned in Section 15.1, PISA is a rapidly expanding field, and the literature is regularly enriched with new studies. Our aim is not to provide an exhaustive list of all the functional particles already prepared by PISA but rather to provide the reader with some specific examples illustrating the different synthetic strategies. A thorough review on the synthesis of reactive and functional nano-objects has recently been published by Delaittre and coworkers [60].

The examples detailed below rely on either dispersion or emulsion polymerization. However, for the sake of simplicity, the process used in each case is not systematically indicated.

15.4.1 Via the RAFT Agent: Functionalization of the α-End of the Shell Polymer

An easy way to produce particles with a functional shell is to use a RAFT agent with a functional R reinitiating group, producing solvophilic polymers with functional α-ends. In most cases, the goal is to functionalize the particle surface. One of the very first works reporting the synthesis of surface-functional particles relying on this strategy was made by An et al. [129], who used an azido-functionalized RAFT agent to prepare PDMAAm polymers, which were then used for the aqueous microwave-assisted polymerization of NIPAM in the presence of *N*,*N*′-methylene bisacrylamide as a crosslinker. The surface reactivity of the obtained nanogels (size < 100 nm) was demonstrated via copper-catalyzed azide–alkyne cycloaddition with a dansyl probe, leading to the production of fluorescent particles. Later on, alkoxyamine-functionalized particles were prepared by St Thomas et al. starting from a symmetrical TTC holding two alkoxyamine moieties [130]. The PAA macroRAFT prepared from this RAFT agent was used for the synthesis of triblock copolymer nanoparticles of either PS or PBA in water. The NMP of either St or SSNa was then triggered from the particle surface, leading to morphological changes under certain conditions. Aiming at the synthesis of building blocks for larger supramolecular structures, Ebeling et al. [131] have recently reported the synthesis of PS particles carrying naphthalene units initially present at the α-chain end of the macroRAFT agent. They overcame the challenge to localize an intrinsically hydrophobic moiety at the surface of particles dispersed in water, by using charged PAA as a stabilizer. Similarly, György et al. [132] aimed at inserting one reactive epoxy group per chain on average in the shell of poly(benzyl methacrylate) (PBzMA) nanospheres, either with an epoxy-functional RAFT agent or through a stepwise copolymerization strategy using GlyMA as a comonomer. They demonstrated that the epoxy function was much more resistant towards hydrolysis when it was inserted within the polymer chain than when it was exposed at the α-chain end.

Amine or carboxylic acid functionalities were then introduced via reaction of the epoxy groups with various thiols.

15.4.2 Via the Solvophilic Block: Functionalization Along the Shell Polymer

Unlike the previous approach that allows functionalization of the α-end of the solvophilic block only, the use of functional monomers leads to the introduction of reactive/functional groups distributed along the solvophilic block, increasing the density of functional groups on the particle surface. It also broadens the range of accessible functionalities. Again, the aim is to design shell-functionalized nano-objects, which are sometimes further crosslinked to freeze their morphology or to design nano-objects for specific applications.

15.4.2.1 A Variety of Functions

Two strategies were developed by Warren et al. to introduce disulfide groups at the surface of PGMA-*b*-PHPMA diblock copolymer worms, thus allowing the introduction of a latent thiol functionality (Figure 15.4) [133]. In the first route, a disulfide dimethacrylate (DSDMA) was copolymerized with GMA, while the second one involved the use of a bifunctional disulfide-based RAFT agent (DSDB). Each of these macroRAFT was used in varying proportions with a non-functional PGMA macroRAFT for HPMA dispersion polymerization, leading to different disulfide-functionalized worm gels. For both kinds of formulation, it was shown that higher disulfide contents led to stronger gels, presumably as a result of inter-worm covalent bond formation via disulfide/thiol exchange. The gels produced by the DSDMA strategy are promising materials to prepare thermoreversible 3D matrix for sheet-based cell cultures [134]. DSDMA was also used to produce thiol-functionalized vesicles [135]. Indeed, the reductive cleavage of the disulfide bonds generates thiol groups that readily react with an acrylate containing a quaternary ammonium to produce cationic vesicles, or with a rhodamine B isothiocyanate reagent to produce fluorescent vesicles. In the former case, drug delivery applications were targeted because enhanced muco-adhesion was anticipated for these cationic vesicles. Core-crosslinked thiol-functional vesicles were also readily prepared by the addition of ethylene glycol dimethacrylate at the end of the polymerization of HPMA.

Targeting a cheaper and more straightforward synthetic strategy, the Armes group developed another approach to introduce disulfide groups at the outer surface of worms. Ratcliffe et al. [136] prepared epoxy-functionalized worm particles of P(GMA-*co*-GlyMA)-*b*-PHPMA that were reacted with cystamine allowing the introduction of disulfide groups in the worm shell. The simultaneous formation of secondary amine groups conferred a cationic character to the nano-objects in water. Depending on the cystamine/epoxy molar ratio, either covalently crosslinked disulfide-bridged worm gels (stoichiometric amount) or linear primary amine-functionalized worm gels (large excess of cystamine) were obtained. Again, such amine-functional hydrogels are expected to offer enhanced mucoadhesive properties.

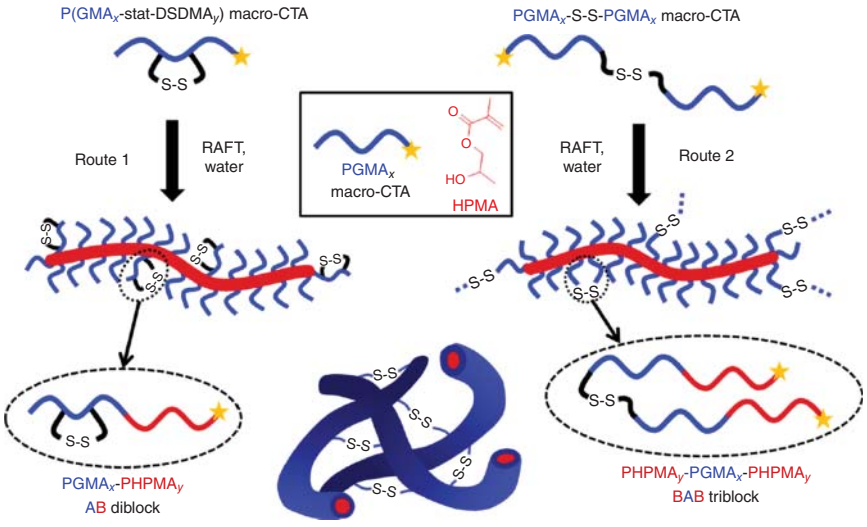

Figure 15.4 Incorporation of disulfide functionality into PGMA-*b*-PHPMA worm gels using either a disulfide-based methacrylate (DSDMA) or a disulfide-based RAFT agent (DSDB). Source: Reprinted with permission from Warren et al. [133]. Copyright 2015, American chemical society.

Yao et al. [137] used a similar approach to form vesicles of P(GMA-*co*-GlyMA)-*b*-PHPMA, however, decorated with β-cyclodextrin (β-CD) via reaction of the epoxy groups with amine-functionalized β-CD. Taking advantage of the host–guest chemistry operating between β-CD and azobenzene groups, azobenzene-functionalized PEG chains were attached to the vesicle surface, inducing morphological transition to worms and/or spheres.

Thiol–ene chemistry was also investigated. Oleic acid decorated nano-objects of various morphologies were first synthesized using a macroRAFT of poly(2-(methacryloyloxy)ethyl oleate) for BzMA dispersion polymerization in *n*-heptane [138]. Alkyl, carboxyl, hydroxyl, and protected amine functionalities could then be introduced onto the particle surface via reaction of the corresponding thiols with the pendant double bond of the stabilizer.

Core–shell particles with an organic photosensitizer incorporated in the shell were recently prepared by Save, Lacombe, and coworkers [139]. Indeed, a photoreactive monomer, 2-Rose Bengal ethyl acrylate, was successfully incorporated in the PAA shell of PBA particles, which were then used to produce photoactive films exhibiting photo-oxidation activity.

Finally, a last example worth mentioning reports the possibility to produce shell-crosslinked spheres using DAAm as the shell constituting monomer [140]. Polymerization of *tert*-BA led to the formation of various particle morphologies, the shell of which could be crosslinked via a ketone–amine reaction.

15.4.2.2 Surface Functionalization by Sugar Moieties and Amino Acids

PISA has also been shown to be a powerful tool to produce particles stabilized by various polysaccharides or glycopolymers. Ting et al. [141] prepared a macroRAFT from

a glucopyranose-based methacrylamide, which was subsequently used for the synthesis of PS particles prepared with a degradable disulfide crosslinker, thus enabling eventual degradation to the corresponding linear glycopolymers by a reductant for drug release applications. Both effective degradation of the particles by a thiol reagent and successful binding of lectins to the glucose moieties were demonstrated. Ladmiral et al. [142] later used a similar approach with a galactose-based methacrylate for the shell and HPMA for the core to form particles of various morphologies. The availability of the galactose moieties on the particle surface was confirmed by effective interaction with galectins, and the vesicles proved to be biocompatible and allowed intracellular delivery of encapsulated rhodamine B. Another variety of carbohydrate-functional PS nanoparticles was successfully obtained from glycuronan macromonomers derived from alginates [88]. The synthesis of xyloglucan (XG)-functionalized poly(methyl methacrylate) (PMMA) particles, a natural hemicellulose, was also recently reported [143]. In this case, XG was functionalized with a dithioester chain end and used for MMA emulsion polymerization. Relying on the known affinity of XG for cellulose, XG-PMMA particles were adsorbed on various cellulosic substrates.

Another class of functional particles of interest are the one decorated with amino acids. In the first system studied by Ladmiral et al. [144], cysteine (Cys) or glutathione (GSH)-based solvophilic macroRAFT were prepared from the corresponding methacrylic monomers. They were then chain extended with a PHPMA block to produce nano-objects of various morphologies. The obtained worm aqueous dispersions formed soft free-standing thermoresponsive gels that underwent degelation on cooling, resulting from worm to sphere transition. In the second system developed by Bauri et al. [145], a side-chain L-alanine containing macroRAFT was used to form PBzMA particles of various morphologies. One of their formulations led to pure worms, forming a free-standing gel, but in this case, degelation occurred upon heating. Besides, the molecular chirality coming from the L-alanine groups was maintained in the polymer, and the hydrogen bonding interactions between these side-chain chiral amino acids in the fibres led to the formation of one-handed helical ropes through the hierarchical self-assembly of the block copolymers' nanofibres. Finally, films made from such diblock copolymers formed a wrinkle surface where the fibres were twisted and weaved together. Such nanostructured materials could, for instance, be applied in adhesive materials or to create platforms for tissue engineering and enhanced cell growth.

15.4.2.3 Fluorinated Shells

A few groups also worked on the introduction of fluorinated moieties in the particle shell. For instance, Pei et al. prepared particles with pentafluorophenyl (PFP) shell units [146]. Passerini reaction-derived methacrylates containing PFP groups were first copolymerized with DMAEMA. The use of the obtained macroRAFT for dispersion polymerization of 3-phenylpropyl methacrylate resulted in the formation of different particle morphologies. Reaction of the PFP residues with various functional thiols allowed the preparation of surface-modified nanoparticles. The same group also described the synthesis of pentafluorophenyl methacrylate

(PFPMA)-decorated particles and their shell functionalization using various primary amines [147]. In the study from Shen et al. [148], fluoro moieties were introduced both in the shell and the core of different particles. In all cases, the core was composed of poly(heptadecafluorodecyl methacrylate) (PHDFDMA), which is a semi-fluorinated liquid crystalline (SFLC) polymer. Dispersion polymerization to form the particles was performed in various solvents using various macroRAFT, i.e. PEG, PDMAEMA, PMMA, poly(stearyl methacrylate) (PSMA), and finally poly(2,2,2-trifluoroethyl methacrylate) (PTFEMA). Thus, depending on the molar mass of the blocks, PTFEMA-*b*-PHDFDMA ellipsoidal nanoparticles and vesicles comprising two different semi-fluorinated blocks (respectively amorphous and crystalline) could be obtained through dispersion polymerizations performed in DMF. Finally, an interesting study reported the formation of particles with a fluorinated shell for imaging purposes [149].

15.4.2.4 PISA and CO_2

Supercritical carbon dioxide ($scCO_2$) is an attractive alternative solvent for dispersion polymerization. Fluorinated stabilizers have shown their ability to provide efficient steric stabilization to prevent particle aggregation in $scCO_2$, and of course, the use of fluorinated macroRAFT was investigated in PISA. The very first report was made by Zong et al. [150] who used a poly(1*H*,1*H*,2*H*,2*H*-perfluorooctyl methacrylate) (PFOMA) macroRAFT to mediate MMA dispersion polymerization in $scCO_2$. Micrometric spherical particles with a broad size distribution and stabilized by a fluoro-shell were obtained. The presence of fluorine inside the particles was also shown, indicating that $scCO_2$ acted as a compatibilizer between the PFOMA and PMMA phases. More recently, Xu et al. also reported MMA dispersion polymerization in $scCO_2$, but using a poly(dodecafluoroheptyl methacrylate) macroRAFT [151]. The influence of the molar mass of both blocks as well as the pressure was studied, and nanoparticles with low size distribution were formed in the best cases, with particle sizes ranging from 80 to 260 nm depending on the block copolymer composition.

CO_2 has also been used to tune particle morphology. A macroRAFT of poly(4-vinylpyridine) (P4VP) was used to mediate styrene dispersion polymerization in isopropanol, without CO_2 or with a low pressure of CO_2 (8.0 MPa, i.e. 80 bar) [152]. The presence of CO_2 had a strong effect on the particle morphology. Indeed, the properties of the continuous phase are altered by generating a gas-expanded liquid in the presence of CO_2, and the formation of nano-objects with a high interfacial core/corona curvature was favoured relative to the corresponding system without CO_2, e.g. rods are formed (with CO_2) under conditions where vesicles (no CO_2) would otherwise form. In a latter work, the same team used a CO_2-responsive macroRAFT (namely, a statistical copolymer comprising *N,N*-diethylaminoethyl methacrylate (DEAEMA) and poly(ethylene glycol) methyl ether methacrylate (M_n = 475 g mol^{-1}) for dispersion polymerization of 2-hydroxypropyl methacrylate in water and water/MeOH [153]. Pressurization with CO_2 led to protonation of DEAEMA units, thereby offering a means of adjusting the charge density of the stabilizing layer. The authors demonstrated that a wide

range of tunable particle morphologies were accessible by simply varying the CO_2 pressure during polymerization in the range of 10–45 bar.

CO_2 use was also valued in a different way by the preparation of CO_2-responsive particles. Among other approaches, PISA has been used for the synthesis of CO_2 switchable latexes. The team of Cunningham [154] used a PDEAEMA macroRAFT for the synthesis of PS or PMMA particles, with a shell that was both pH and CO_2 responsive, which are actually related properties. The tertiary amine groups of the DEAEMA units can be protonated by introducing CO_2 and reversibly deprotonated by CO_2 removal allowing particle coagulation/redispersion cycles.

15.4.3 Via the Solvophobic Block: Core Functionalization

Most of the reported works dealing with core functionalization aim at introducing specific functional groups inside the particle core and/or provide enhanced particle stabilization by core-crosslinking. In essence, the thiocarbonylthio chain end of the polymer chains is buried inside the particles formed by PISA. One of the most straightforward ways to introduce functionality inside the particle core thus consists in converting this chain end into a thiol. An et al. used this strategy to functionalize the PNIPAM-core-crosslinked/PDMAAm-shell particles discussed in Section 15.4.1 [129]. Before surface functionalization with dansyl probes, the core was functionalized with fluorescein groups by one-pot aminolysis (with 2-hydroxyethylamine)/Michael addition (with fluorescein *o*-acrylate). In most cases though, functionalization comes from the use of a functional comonomer in the core formation step, allowing access to a broad range of nano-objects.

15.4.3.1 Fluoroparticles

A significant amount of work has been dedicated to the synthesis of fluorine-core containing particles, one of the main goals being the preparation of (super)hydrophobic surfaces (SHS). In the study from Shen et al. described above for shell functionalization [148], fluoro moieties were present in the core of different PHDFDMA particles prepared from macroRAFT of PEG, PDMAEMA, PMMA, PSMA, and PTFEMA. Depending on the macroRAFT, particles with different properties could be obtained. Indeed, the core was in all cases crystalline, whereas the shells could be either amorphous (PDMAEMA, PMMA, and PTFEMA) or crystalline (PEG and PSMA). The liquid crystalline nature of the core-forming PHDFDMA was responsible for the general formation of non-spherical morphologies. The PHDFDMA containing nanoparticles were demonstrated to be robust Pickering emulsifiers, leading to the formation of several types of stable oil-in-water or oil-in-oil emulsions.

PTFEMA can also be used as a core-forming block [92]. The aim of the study was to design particles with a high core mass density to determine the effective particle density and the thickness of the PGMA stabilizer layer using both small angle X-ray scattering (SAXS) and disk centrifuge photosedimentometry. The same core polymer was used for the formation of PMAA-*b*-PTEFMA [155] and PMAA-*b*-PBzMA-*b*-PTFEMA [156] particles. PTFEMA was also selected to prepare

SHS [157]. A copolymer of 4-vinyl pyridine (4VP) and vinyl triethoxysilane (VTES) in which the 4VP units were quaternized was used for the emulsion polymerization of TFEMA. The particles were thus not only core functionalized but also possessed shell-reactive groups. Indeed, the VTES units allowed further grafting of silica nanoparticles onto the particles. The film formed from these hybrid latexes exhibited a nanostructured surface and modification with fluorinated trichlorosilane led to SHS. Such coatings were also prepared from spin coating of a mixture of PMAA-*b*-PBA-*b*-P(BA-*co*-FDA) nanoparticles and silica beads (with FDA: 1*H*,1*H*,2*H*,2*H*-perfluorodecyl acrylate) [158]. In the study of Qiao et al., a symmetrical RAFT agent was used to prepare triblock copolymer nanoparticles of poly(acrylic acid)-*b*-poly(2,2,3,3,4,4,4-hexafluorobutyl acrylate)-*b*-poly(acrylic acid) [159]. Transparent films with elastomer properties were obtained from these latexes, and further thermal annealing provided hydrophobic coatings.

Another very interesting fluoropolymer is PVDF. The only attempt to perform PISA starting from VDF was recently reported by Guerre et al. [160] PVAc-*b*-PVDF block copolymers were formed in dimethyl carbonate (DMC). The occurrence of head-to-head additions for both VAc and VDF homopolymerization, combined with transfer to DMC in the case of VDF, however led to the concomitant formation of PVAc and PVDF homopolymers. Nevertheless, original micrometric (1–5 μm) ovoidal flake morphologies, able to stack on each other, were observed, likely driven by PVDF crystallization.

Finally, two recent studies describe the synthesis of reactive fluorinated core-crosslinked block copolymer particles. Couturaud et al. [161] proposed the use of a linear PEG macroRAFT for the polymerization of PFPMA as a core monomer yielding spherical particles. Similar to the work of Pei et al. discussed above for shell functionalization [147], the particles could be crosslinked after polymerization by reaction of the PFP groups with diamines and thus remained stable in water. In particular, the use of cystamine allowed the formation of redox-responsive particles, which could be disassembled by the addition of GSH. These core-crosslinked micelles also demonstrated cytocompatibility. Alternatively, Busatto et al. [162] reported the dispersion polymerization of 2,3,4,5,6-pentafluorobenzyl methacrylate mediated by a poly[poly(ethylene glycol) methyl ether methacrylate] (PPEGMA) macroRAFT. Depending on the respective molar mass of both blocks, the particles exhibited spherical, worm-like, or vesicular morphologies. Thermoreversible morphological changes were observed, notably worm-to-sphere transitions. The morphology could however be locked by crosslinking reaction through thiol–*para*-fluoro substitution reactions using dithiols, enabling the morphology to be maintained across a temperature range and in non-selective solvents.

15.4.3.2 Core-crosslinking

One of the very first examples reporting core-crosslinking, where the aim was to freeze the particle morphology, was published by Zheng and Pan [163]. A PS macroRAFT was used for the dispersion copolymerization of 4VP and DVB in cyclohexane. Since then, and as mentioned above, crosslinking has been the focus of many studies dealing with core functionalization. While in the previous section GlyMA was used

in many instances to introduce reactive epoxy groups in the particle shell, GlyMA can also be used for core functionalization. This was the case in the work of Lovett et al. [164] who prepared PGMA-shell/P(HPMA-*co*-GlyMA)-core worms. The epoxy groups could be ring-opened using 3-aminopropyltriethoxysilane (APTES) in order to prepare core-crosslinked worms via hydrolysis condensation with siloxane groups and/or hydroxyl groups on the HPMA residues. The ring-opening and crosslinking reactions occurred on similar timescales. Crosslinking led to stiffer worm gels, which remained intact when exposed to methanol or an anionic surfactant. In addition, the worm aspect ratio could be tuned by the temperature at which APTES was added, and the cross-linked worms were evaluated as emulsifiers for the stabilization of *n*-dodecane-in-water emulsions [165]. A similar study was conducted with vesicles crosslinked by addition of various diamines [166]. More recently, the Armes group was able to produce PGMA-*b*-PGlyMA block copolymer nanoparticles by emulsion polymerization, preserving most of the epoxy groups from hydrolysis [93]. A third PBMA block could also be attached to the PGlyMA one. For PGMA-*b*-PGlyMA, reaction with NaN_3 provided azide-functional nanoparticles, and the possibility to crosslink the particle core by the addition of diamines was evidenced. Interestingly, using a shorter PGMA block led to the formation of worms, a morphology that is not very often obtained by emulsion polymerization [167]. Subsequent reaction with 4-amino-2,2,6,6-tetramethylpiperidin-1-oxyl produced crosslinked worms bearing a high local concentration of stable nitroxide groups within the worm cores. Such anisotropic nanoparticles could offer potential applications for charge storage and transport. In all of these studies, some residual pendent amine groups could be protonated to provide cationic nano-objects. In the work of Tan et al. [168], particles of pure PGlyMA were also prepared through photoinitiated dispersion polymerization using a linear PEG macroRAFT. Different morphologies were obtained, and worms and vesicles were crosslinked by addition of ethylene diamine. Residual amine groups could be used to complex Ag salts, then reduced to form vesicles loaded with silver nanoparticles. Their catalytic activity was demonstrated by reduction of methyl blue.

An and coworkers used AAEM, another interesting monomer employed in Section 15.3.4, as a comonomer to induce crosslinking with amines, however employed here as core-forming monomer to form nanospheres and vesicles stabilized by PPEGMA chains [169]. These nano-objects could be further functionalized or crosslinked via keto-alkoxylamine chemistry. In situ formation of silver nanoparticles by metal complexation and reduction was also demonstrated. The same team reported the synthesis of ketone-functionalized particles [170]. Using a PDMAAm macroRAFT, both spheres and vesicles composed of a PDMAAm core were prepared by dispersion polymerization of DAAm. The nano-objects could be functionalized using oxime (addition of *O*-allyl hydroxylamine) or hydrazine (fluorescein-based semicarbazide) chemistry. They also formed crosslinked vesicles by copolymerization of allyl acrylamide and DAAm, crosslinking being delayed to the late stage of the polymerization (when morphology transition was completed), because of the different reactivities of the two vinyl groups [171]. Byard et al. prepared PDMAAm-*b*-PDAAm particles, but in addition to spheres and vesicles, worms could

also be obtained [172]. Addition of ADH led to crosslinked nano-objects. An interesting class of reactive particles was reported by Jiang et al. who prepared nanospheres by chain extension of a poly(2-hydroxypropyl methacrylamide) macroRAFT with DAAm and an ammonium-based *N*-2-aminoethyl acrylamide hydrochloride [100]. Conjugation with pyridine-2,6-dicarboxaldehyde led to core-crosslinking forming tridendate ligands able to coordinate Zn(II) species. Using the same copolymer, the same group also reported the formation of pore-switchable nanotubes (or long cylindrical vesicles) driven by hydrogen bondings [173].

As mentioned above, PS particles decorated with glucopyranose units could be crosslinked by copolymerization with a degradable disulfide diacrylate crosslinker [141]. Addition of 1,4-dithiothreitol as a reductant led to particle degradation into the corresponding linear chains, demonstrating potential use as drug carriers.

Another way of inducing core-crosslinking is the use of light. This was achieved by Huang et al. who prepared particles of poly(2-((3-(4-(diethylamino)phenyl)acryloyl) oxy)ethyl methacrylate) in the presence of PHPMA macroRAFT [174]. Crosslinking occurred upon UV irradiation by photoinduced [2+2] cycloaddition of the cinnamate groups. The crosslinked nano-objects were used as templates for in situ formation of gold nanoparticles. An original crosslinking strategy was reported by the same team [175]. Different particle morphologies were obtained by dispersion polymerization of 3-formyl-4-hydroxybenzyl methacrylate (FHMA) mediated by a PHPMA macroRAFT. Reaction of dihydrazine with the salicylaldehyde groups of PFHMA not only formed salicylaldazine crosslinks but also conferred fluorescence properties by aggregation-induced emission.

15.4.3.3 Adding a Function Allowing Degradation of the Particle Core

As illustrated in the previous examples, core-crosslinking can provide particles with additional properties. However, dissolution of the particle core could also be a powerful tool. In that vein, an original work reporting the synthesis of degradable block copolymer nanoparticles was recently published by Guégain et al. [176]. Radical ring-opening copolymerization-induced self-assembly (rROPISA) was performed by copolymerizing BzMA and cyclic ketene acetals (CKA), such as 2-methylene-4-phenyl-1,3-dioxolane or 5,6-benzo-2-methylene-1,3-dioxepane, in heptane from a poly(lauryl methacrylate) macroRAFT, leading to spherical particles regardless of the copolymer compositions investigated. The amount of CKA in the copolymers ranged from 4 to about 40 mol%, leading to nearly complete degradation for CKA contents above about 15 mol%. Such degradable vinyl polymer nanoparticles may find applications in the biomedical field or for environmental protection.

15.4.3.4 CO_2-sensitive Particles

Finally, as mentioned in the previous section, CO_2-responsive particles can present interesting properties. In the work of Tan et al. [177], the CO_2-sensitive units were located in the core of P(HPMA-*co*-DMAEMA) particles prepared from a PPEGMA macroRAFT. The responsive properties of the particles were illustrated by the CO_2-triggered release of bovine serum albumin (BSA) used as a model protein.

15.5 Control over the Particle Morphology

The main objective of this section is to establish and explain the fundamental principles that control particle morphology in PISA, where the term 'morphology' refers to the particle shape or morphological structure, typically spheres, worms, or vesicles. Again, we will not provide an exhaustive list of all examples reported in the literature but rather illustrate the different parameters that determine morphology by citing both pioneering works and most recent studies.

15.5.1 From Spherical to Anisotropic Block Copolymer Particles

As mentioned in Section 15.1, at the start of RAFT-mediated PISA, independently of the polymerization mechanism, only *spherical* particles were reported. In some cases, the size of the particles increased with increasing degree of polymerization (DP_n) of the solvophobic block [178–180], but in other reports, no correlation was observed. It rapidly appeared that the particle formation mechanism in PISA was rather complex and strongly dependent on the studied system. It generally includes the aggregation of primary particles and their fusion to larger particles [181]. The first examples of *non-spherical* particles were described in 2009 by the groups of Charleux and C.Y. Pan, reporting a NMP polymerization system in water [13] and a RAFT-mediated dispersion polymerization in methanol [14, 15, 182], respectively. Shortly after, Armes group reported for the first time the formation of vesicles in water, also obtained in RAFT dispersion polymerization conditions [183]. These morphologies were composed of PGMA-*b*-PHPMA copolymers. Continuous monitoring of the polymerizations by ^{1}H-NMR, size exclusion chromatography (SEC), TEM, cryo-TEM, dynamic light scattering (DLS), static light scattering (SLS), and SAXS provided important insights into the formation mechanism of the different morphologies [50, 184]. The first nanostructures to form are always spherical micelles. As the polymerization continues within the particles (increase of DP_n), non-spherical morphologies can form. It is now well-established that worm-like particles are formed through fusion of spherical particles following inelastic particle collisions. In the course of the polymerization, these 1D structures become branched and the resulting flat octopi-like morphologies reorganize to form vesicles. Such morphological transitions during polymerization are driven by the increase of the hydrophobic volume fraction (see Section 15.5.2). Morphological transitions during polymerization require a reorganization of the macromolecular chains within the assembly. As such, it has been shown that particles swelling by the monomer plasticizes the core chains increasing their mobility and promoting chain reorganization.

Today, a myriad of solvophilic macroRAFT and solvophobic polymers have been successfully used to form higher order morphologies under RAFT *dispersion polymerization* conditions. In *water*, however, the number of suitable solvophobic polymers is very limited. The most frequently studied solvophobic polymers are PHPMA [54, 184] and PDMAAm [170, 172, 185], but poly(2-methoxyethyl acrylate) (PMEA) [186], PNIPAM [104], and poly(α-hydroxymethyl acrylates) [187] have also successfully been used to prepare non-spherical morphologies. Recently, Foster

et al. reported an in silico method based on octanol–water partition coefficients to predict additional suitable monomers for the use in PISA in aqueous dispersion. Although the predicted monomers were less common and not all commercially available, this method might be a valuable tool not only to predict new monomers but also to predict their self-assembly behaviour, that is, morphologies [188].

Although the choice of monomers for aqueous dispersion polymerizations remains restricted, all kinds of stabilizer blocks, neutral, ionic, or functionalized polymers (e.g. PGMA [183], PEG [189], PPEGMA [190], poly(2-(methacryloyloxy)ethylphosphorylcholine) [83], poly(2-(methacryloyloxy)ethyl dimethyl(3-sulfopropyl) ammonium hydroxide) [191], poly(2-ethyl-2-oxazoline) [192], dextran [193], etc.), have successfully been used to obtain particles of various morphologies. However, particle fusion and consequently the formation of higher order morphologies can be hampered by a too strong particle repulsion [50], typically by using charged polymers as stabilizers, for instance, using weak polyacids or polybases (e.g. PAA) [91, 194], cationic stabilizers [195], or high molar mass stabilizing blocks [196].

In *emulsion polymerization* conditions, the monomer forms a separate reservoir phase and the formed diblock copolymer particles are swollen by the monomer. The first description of non-spherical particles dates back to 2010 [194], reporting the emulsion polymerization of styrene using graft copolymers based on AA and poly(ethylene glycol) acrylate (PEGA), namely, P(AA-*co*-PEGA), as macroRAFT. By adjusting the targeted DP_n of the PS block, worm-like micelles and small vesicles were obtained. Moreover, a transition from spheres to fibres was observed with increasing monomer conversion, i.e. with an increase in the DP_n of the PS block. Again, these changes in morphologies directly relate to the relative hydrophilic/hydrophobic block volume fractions. Interestingly, higher order non-spherical morphologies were only obtained with the graft copolymer, while linear PAA or PEG homopolymers used as macroRAFT yielded only spherical particles. In addition, the morphologies were very sensitive to changes in pH or ionic strength of the polymerization medium. The authors postulated that the particular structure of the macroRAFT, composed of AA and EO units capable of forming hydrophobic complexes, was the key element for the formation of non-spherical particles.

Since then, additional systems have been described where non-spherical particles could be obtained in emulsion polymerization conditions, but the number of examples remains limited compared to the booming development of higher order morphologies via dispersion/precipitation polymerization. In terms of hydrophobic monomers, mainly styrene has been studied [84, 85, 87, 89–91, 178, 179, 194], but it was shown that MMA [86], *t*-BA [197], and the more water-soluble monomers 2-hydroxybutyl methacrylate (HBMA) [198] and GlyMA [167] could also provide non-spherical morphologies. It should be mentioned that – except for the last two monomers – for all other examples, graft copolymers comprising PEG(M)A macromonomers were used as stabilizers (copolymers of PEG(M)A with either (M)AA [84, 85, 179, 194, 199], NAM [87], or hydroxyethyl acrylamide [HEAAm]) [89]. There are a few other reports of higher order morphologies by RAFT aqueous emulsion polymerization, but these routes typically required small quantities of either a surfactant and/or a plasticizer [200–203].

15.5.2 Main Parameters that Impact the Particle Morphology

It is nowadays well established that the particle morphology obtained by PISA depends on various parameters, notably factors that influence the packing parameter P, such as the type of polymers used, the solvent, and the molar mass and architecture of the polymers. These factors have been widely studied for block copolymer assemblies prepared by traditional post-polymerization assembly methods [79]. In contrast to these latter methods, in PISA, the assembly forms while the solvophobic block grows, indicating that not only the properties of the polymer change during the process but also the solvent properties evolve constantly during polymerization (as the monomer is consumed). While at the beginning of the polymerization thermodynamic assemblies might be formed, kinetically frozen assemblies are often obtained at the end of the polymerization. Morphology prediction in PISA remains thus difficult. Actually, in addition to intrinsic changes in the chemical nature of the polymer and the solvent, in PISA, the experimental polymerization conditions, for instance, stirring, temperature, initiating system, and monomer concentration and conversion, also play a role. As mentioned above, particle fusion following inelastic collisions and chain reorganization are prerequisites for the formation of higher order morphologies. As such, the impact of stirring speed on morphology has been clearly evidenced in a PISA emulsion polymerization system [204]. In dispersion polymerization formulations, more and more authors decrease the volume of the experimental set-ups (<1 ml NMR tubes [188] or microtitre scales such as in 96-well microtitre plates [205]) and monitor PISA in situ by NMR or SAXS in unstirred set-ups, but it is questionable whether such unstirred PISA provides 'valuable' results on morphologies.

Another important parameter, which determines the morphology in PISA, is the monomer concentration. As mentioned above, a higher monomer concentration promotes the formation of higher order morphologies through plasticizing of the core chains and an increased number of particles per volume unit in the reaction medium [186, 189, 206]. The polymerization temperature is another parameter to be taken into account. Indeed, modification of the polymerization temperature affects the polymer/polymer and polymer/solvent interaction parameters and may result in morphological changes through the alteration of the packing parameter (see also Section 15.5.4). In addition, the temperature also has an effect on the particle formation mechanism through changes in the propagation rate coefficient k_p or on the polymerization control through alteration in radical flux (in the case of thermal initiation) [86]. Furthermore, an impact of the initiator concentration [89, 207] or the type of the initiating system (thermal PISA vs. photo-PISA) has also been reported [208].

The self-assembly of diblock copolymers has been rationalized by the packing parameter p (Figure 15.1) [209], a concept which was initially developed for small amphiphilic molecules (surfactants). p is defined as $v/(al)$, where a is the area of the surfactant head group, and v and l are the volume and length of the surfactant tail, respectively. The self-assembly and the resulting morphology are essentially a balance between the degree of stretching of the core-forming chains, the interfacial tension between the solvophobic core and its external environment, and repulsive

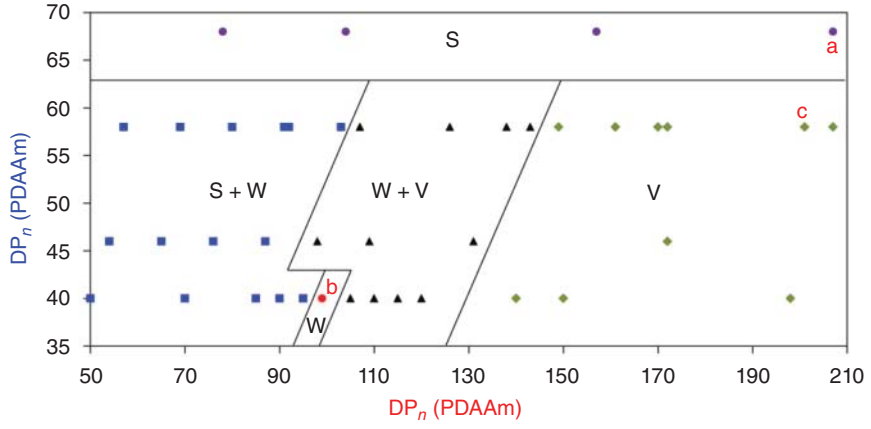

Figure 15.5 Phase diagram constructed for a series of PDMAAm-*b*-PDMAAm diblock copolymer nano-objects. S = spheres, S + W = mixed spheres and worms, W = worms, W + V = mixed worms and vesicles, and V = vesicles. Source: Reprinted with permission from Byard et al. [172]. Copyright 2017, American chemical society.

interactions between shell chains [79]. In essence, the morphology changes with the increasing volume ratio between the solvophilic and solvophobic segments from spheres ($p \leq 1/3$) to cylinders ($1/3 \leq p \leq 1/2$) to vesicles ($1/2 \leq p \leq 1$) (Figure 15.1). Strictly speaking, this concept holds only for morphologies at thermodynamic equilibrium. With the discovery of higher order morphologies by PISA, the concept was however rapidly applied to PISA-derived assemblies – which are not necessarily at equilibrium – by varying a certain number of features that are listed below.

15.5.2.1 Varying the Molar Mass

A direct way to control the morphology is thus to tune the volume fraction of the solvophobic and solvophilic segments through the adjustment of the molar mass of each block. For a given solvophilic block, by increasing the *molar mass* of the solvophobic block, the morphology can thus be transformed from spheres towards worms to vesicles – provided that a morphological transition is possible [12, 50, 52, 85, 196]. This has been widely explored in the literature, and many, rather complete, pseudo-phase diagrams have been constructed. As the packing parameter is the result of the interplay of polymer/polymer and solvent/polymer interactions, the absolute molar mass of the block segments depends on the polymer type and the solvent used for the polymerization. The packing parameter and thus the morphology are very sensitive to small changes in molar mass [210], and generally, the pure worms are typically accessible in a very narrow window of composition (Figure 15.5).

15.5.2.2 Varying the Chemical Nature of the Solvophobic Block

As mentioned above, Mathers, O'Reilly, and coworkers have shown a correlation between the chemical nature of the monomers to be polymerized and the particle morphology by comparing the aqueous dispersion polymerization of increasingly

hydrophobic monomers using an in silico method. In identical experimental conditions, the morphologies changed from spherical particles to worms and vesicles with increasing hydrophobicity of the monomers [188]. An and coworkers synthesized a series of alkyl α-hydroxymethyl acrylates of tunable water solubility to study systematically the impact of the monomer solubility on morphology [189]. They have notably observed that the less water-soluble monomers, *ethyl*- and *isopropyl* α-hydroxymethyl acrylate in particular, promoted the formation of higher order morphologies at lower DP_ns of the solvophobic block.

The former systems were based on monomers with relatively high water solubility, so that the polymerization mechanism was essentially that of a dispersion polymerization formulation. As mentioned above, monomers classically used in aqueous *emulsion* polymerization formulations often lead to kinetically trapped spheres – unless stabilizers comprising PEG grafts were used. It should be noted that the effect of the monomer water solubility on morphology has also been assessed for monomers that possess a lower solubility in water, which are polymerized at a much higher concentration. For instance, replacing BzMA (aqueous solubility = $0.4\,g\,l^{-1}$ at 70 °C) by HBMA (aqueous solubility = $20\,g\,l^{-1}$ at 70 °C) [198] (using a PMAA macroRAFT at pH 5) allowed to form unusual so-called 'monkey nut' morphologies, whereas spheres were obtained with the less-soluble BzMA. Such an effect of the monomer solubility had already been reported before comparing the emulsion polymerization of MMA with that of styrene (aqueous solubility of MMA = $15\,g\,l^{-1}$ at 30 °C, of styrene = $0.3\,g\,l^{-1}$ at 20 °C) [86]. It seemed that the formation of higher order morphologies was favoured in the case of more soluble monomer MMA, but an influence of the differences in rate coefficient was also postulated.

An interesting alternative to selecting suitable monomers or designing new monomers to tune morphology is the incorporation of solvophilic monomer units in the solvophobic block. Since 2015, this concept has been reported by several authors. For instance, 4VP [211] or MMA [212] were added as a comonomer to the dispersion polymerization of styrene. It was possible to tune the morphology by the molar ratio of 4VP/styrene in the monomer feed, in addition to adjusting the ratio of monomer/RAFT ratio (DP_n). Besides, while for styrene alone, only spherical micelles were generated, the insertion of 25 mol% of MMA into the solvophobic block enhanced its mobility promoting morphological transitions and the formation of worms and vesicles. Both examples showed that the incorporation of a more solvophilic monomer was beneficial for the formation of high-order morphologies. More recently, the same concept has also been explored by Figg et al. in the aqueous dispersion polymerization of DAAm with DMAAm demonstrating the general validity of this concept [213]. Based on SLS analysis, the authors suggested that the insertion of a hydrophilic monomer alters the thermodynamics of the aggregation, promoting morphological reorganization.

15.5.2.3 Varying the Topology of the Shell or the Core

As mentioned above, in emulsion polymerization formulations, non-spherical morphologies are scarce. They had exclusively been observed for formulations using graft copolymers as macroRAFT obtained by copolymerization of PEG

macromonomers. In 2016, the group of Lansalot and D'Agosto has shown that the topology of the stabilizer composed of PNAM, to which an average of three PEGA units as pendant chains were incorporated, had a critical impact on the particle morphology obtained in the successive emulsion polymerization of styrene [87]. Depending on the presence or absence and the position of the pendant PEG chains (at the beginning, randomly distributed, or at the end of the chain), different morphologies, notably spheres, nanometric vesicles, or large vesicles, were obtained. Again, only spherical particles were obtained for the linear, non-branched polymer, i.e. PNAM homopolymer.

Instead of tuning the topology of the solvophilic macroRAFT agent, Yuan group inserted bulky and solvophobic comonomers, namely, stearyl acrylate [214] and 2-(perfluorooctyl)ethyl methacrylate [215], in the solvophobic block. They showed that the vesicle size could be tuned by the molar fraction of the comonomer.

15.5.2.4 Varying the Solvent Quality

Instead of varying the monomer, others have studied the effect of the solvent on the morphological phase diagram. In one of the first reports, it was shown that the addition of organic co-solvents (ethanol or dioxane) to the aqueous emulsion polymerization of BzMA was beneficial for morphological transitions and the formation of higher order morphologies. It was also shown that the morphologies strongly depended on the co-solvent properties: although small amounts of 1,4-dioxane led to huge morphological changes, much higher amounts of ethanol were necessary to tune the morphology [199]. More recently, the introduction of non-reactive PEG in the polymerization medium as a means to alter morphology and to promote in particular the formation of complex membrane morphologies [216] and the production of vesicles of uniform size was also described [217]. A particular case is the combination of specific monomers (styrene/*N*-phenylmaleimide) with the mixture of specific solvents (ethanol/methyl ethyl ketone), allowing the formation of complex morphologies, such as micrometric particles comprising inverse bicontinuous phases [218].

Instead of co-solvents, additives have also been added to traditional PISA formulations in order to alter the solubility of the monomers. As such, cyclodextrin (CD) has been added to aid dissolution of a water-immiscible monomer (styrene), allowing for its aqueous dispersion polymerization thanks to host–guest complex formation [219]. Performing PISA of the CD–styrene complexes in the presence of a PEG macroRAFT gave access to the direct synthesis of various kinetically trapped PS-based nanostructures in water, in particular hollow nanotubes.

15.5.2.5 PISA in Aqueous Media: Varying pH and/or Ionic Strength

One should not forget the possibility to greatly tune the solvent properties of water by addition of salts or by changing the pH, which is of greatest importance whenever weak polyacids or polybases are used as macroRAFT. For instance, the effect of pH on morphology had been largely studied for the aqueous emulsion polymerization of styrene using P[(M)AA-*co*-PEG(M)A] macroRAFT as stabilizers [85, 194]. In addition to being sensitive to changes in pH, a strong impact of the ionic strength

and the salt type was evidenced, both in emulsion [194, 204] and dispersion polymerization formulations [220]. The presence of salts may directly alter the packing parameter through changes in interaction parameters, which may explain the observed changes in morphology. In addition, salts diminish the electrostatic repulsion between individual particles, thereby promoting particle fusion.

Although these former examples demonstrate the pH and salt sensitivity of PISA when weak polyacids or polybases were used, the surprising effect of a single charged moiety present in non-ionic macroRAFT agents has also been demonstrated. Several articles report indeed a great impact of pH on nanoparticles stabilized by a neutral polymer and terminated by a single weak acid group or a charged unit, but in the majority of cases, the morphological transitions were induced through pH variation post-synthesis (cf. Section 15.5.4) [221–223]. To demonstrate the importance of such an α-end-group during PISA, Khor et al. had compared the aqueous emulsion polymerization of styrene using two types of P(HEAm-*co*-PEGA) macroRAFT agents, the first one bearing a carboxylic acid α-end-group while the second one was the methyl ester [89]. Their study revealed a great effect of the end group on the morphologies over a large range of pH.

15.5.2.6 Varying the Block Copolymer Architecture via the RAFT Agent

Although the impact of the respective molar masses, polymer nature, and solvent has been extensively studied, much less attention has been paid on the macromolecular architecture. In most of the studies, monofunctional RAFT agents are used, generating linear copolymers, mostly AB diblock copolymers (A is the solvophilic block synthesized in the first step and B is the solvophobic block synthesized in the second step), but ABC triblock copolymers have also been reported. Virtually from the start of PISA, bifunctional symmetrical RAFT agents producing ABA structures have also been implemented successfully [224–227], but more recently, trifunctional [228] or tetrafunctional RAFT agents [229] – leading to the formation of tri-arm or tetra-arm star polymers – have also been used. These articles show that the structure of the RAFT agent, i.e. the number of functionality (mono-, bi-, or multifunctional), the inversion of the Z and R groups leading to BAB [185, 230–232], or $(BA)_n$ stars [229, 233, 234] has a crucial impact not only on the polymerization mechanism and control but also on the resulting particle morphology. Although it was not always

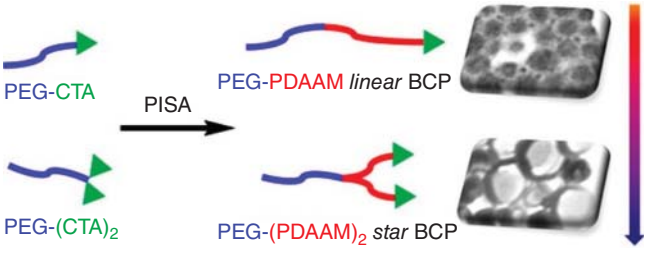

Figure 15.6 $A(B)_2$ star architecture promoting the formation of complex morphologies compared to linear diblock copolymers. Source: Reprinted with permission from Wang et al. [235]. Copyright 2017, American chemical society.

straightforward to correlate macromolecular architecture and morphology in the former examples [228, 230], An's group [235] has proposed an elegant approach to rationally increase the packing parameter via macromolecular architecture design. They synthesized a bifunctional asymmetric RAFT agent to which a PEG chain was coupled through an additional functional group at the symmetry point of the RAFT agent (Figure 15.6). Compared to linear AB architectures, the resulting $A(B)_2$ tri-arm star copolymers clearly promoted the formation of vesicles as expected for copolymers with bulky hydrophobic segments, considering the packing parameter theory (Figure 15.1).

15.5.3 Strategies to Stir Specific Morphologies

Apart from studying systematically different parameters and assessing their impact on particle morphology, recently, several strategies have been devised to control the morphology instead of suffering from it. In the previous section, we have reported that the formation of higher order morphologies can be promoted by increasing the volume fraction of the hydrophobic block through the rational design of the RAFT agents [235].

Besides from increasing the hydrophobic volume to increase the packing parameter promoting the formation of vesicles/lamellae, other strategies aimed at synthesizing a targeted particle morphology in *robust synthesis conditions* and to obtain it as a pure phase, which is not mixed with other morphologies as often observed in PISA. As an example, the worm morphology is generally obtained in a narrow experimental window [54, 172] (Figure 15.5), and in view of the possible applications, it would be of great interest to find means to enlarge the experimental window in which worms can be obtained. In addition, other research projects aim at producing complex particle morphologies that are not observed in simple PISA formulations, for instance, cuboids or ellipsoids.

15.5.3.1 Using PICA

As mentioned in Section 15.3.3, Zhu et al. used binary mixtures of macroRAFT and the parent molecular RAFT agent to promote the formation of higher order morphologies through the concomitant formation of solvophobic homopolymer in a derived-PISA system called PICA [106]. It should be mentioned that this concept of mixing a macroRAFT with a molecular RAFT agent has also been explored by the group of Tan and Zhang using a PEG macroRAFT instead of a PDMAEMA one [107, 108]. Finally, Zhang group who has worked a lot on inverted RAFT agent structures, has shown that the mixture of monofunctional PEG TTC macroRAFT with its bifunctional analogue TTC-PEG-TTC promoted the formation of compartmentalized vesicles [231].

15.5.3.2 Using Mesogenic Monomers (PIHSA)

In order to form anisotropic nanoparticles, such as cylinders [236], cuboids [112], or ellipsoids [148, 237], a known strategy in post-synthesis block copolymer self-assembly relies on the use of polymers that are able to organize within the

core into (semi)crystalline or liquid crystalline domains [238, 239]. In this respect, mesogenic monomers, containing cholesteryl [236], azobenzene [112], or long (semi)fluorinated chains [148, 237], have been used, generally in non-aqueous dispersion polymerization formulations. Particles with unusual shapes were obtained in all examples, which were attributed to the internal liquid crystalline (mostly smectic phases) organization as determined by SAXS. As discussed in Section 15.3.3, the formation of such anisotropic nanoparticles by PISA containing liquid crystalline mesogens in their core has also been termed as PIHSA [112].

15.5.3.3 Using Ionic Complexes (PIESA) and Hydrogen-Bonding Units

Other authors have shown that using particular monomers that can undergo supramolecular interactions, such as H-bonding or the formation of polymeric ionic complexes (PIC), is also a means to tune morphology in PISA and to produce rather exotic morphologies (Section 15.3.3). For instance, acrylamides such as DAAm [173] or nucleobase-based monomers [240, 241] are capable of forming H-bondings with themselves or with mediator molecules leading to specific structures, while charged monomers can generate PICs with polyelectrolytes added to PISA [110] or formed through chain extension of double-hydrophilic AB block copolymers with a third block of opposite charge [109]. This latter strategy is PIESA, as discussed in Section 15.3.3.

The previous examples show that there is a current trend to combine supramolecular chemistry and PISA. Although the latter examples were based on supramolecular interactions between monomer units of the core chains, Rieger, Stoffelbach, and coworkers have very recently devised a templating strategy based on interactions between a single sticker unit placed at the ω-end of each chain. They actually designed macroRAFTs functionalized by a hydrogen-bonded bisurea sticker [242] in order to drive PISA towards the nanofibre morphology, via one-dimensional, directed assembly of the sticker units, which is reinforced by the creation of hydrophobic domains during PISA (Figure 15.7). This concept was tested in the synthesis of poly(*N*,*N*-dimethylacrylamide)-*b*-poly(2-methoxyethyl acrylate) diblock copolymers prepared by dispersion polymerization in water. The results clearly showed that the developed strategy promotes the formation of nanofibres in a large experimental window [243].

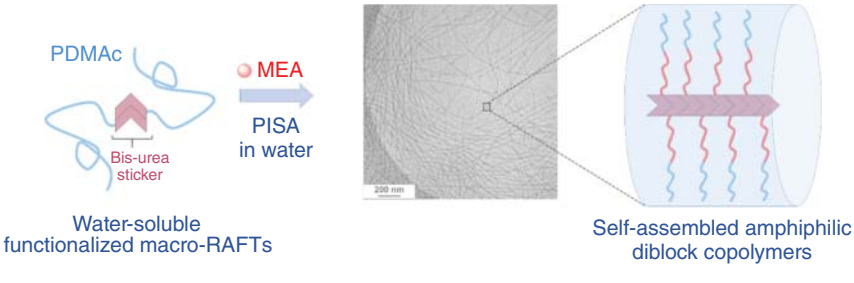

Figure 15.7 Using bis-urea functional macroRAFT agent for 'templated PISA' in water. Source: Reprinted with permission from Mellot et al. [243]. Copyright 2019, Wiley.

15.5.3.4 Hierarchical Assembly Between Particles

Finally, one should also mention the possibility to construct complex hierarchical assemblies from primary nanoparticles (obtained by PISA) through supramolecular interparticle interactions. As an example, raspberry-like nanoparticles have been produced by controlled heterocoagulation of PEG-stabilized and PAA-stabilized nanoparticles via hydrogen bonding interactions between PAA and PEG chains [244]. More recently, the possibility to functionalize the surface of PS particles by naphthalene units, present at the α-chain end of the PAA macroRAFT, was also demonstrated [131]. The latter particles should be useful as building blocks to construct larger supramolecular structures through host–guest interactions.

15.5.4 Post-polymerization Morphological Transitions/Chain Reorganization

It is well known that amphiphilic block copolymer assemblies prepared by traditional assembly methods (such as nanoprecipitation or solvent displacement) can undergo morphological transitions if one of the blocks is responsive to external stimuli – such as pH or temperature in the simplest case. The result is either the dissociation of the assembly (also called 'order-disorder transition') or a change in morphology (termed 'order-order transition' or 'morphological transition'). Although the former case has been largely explored, the latter case was actually rarely reported for such conventional block copolymer assemblies. In contrast, post-polymerization morphological order-order transitions play nowadays a major role in PISA, probably because of the large variety of systems explored and the possibility to synthesize highly concentrated dispersions, which pave the way to new properties and applications. Firstly, simply observed, such transitions are now understood (they are mainly the result of changes in the packing parameter) and have also found applications. It should be mentioned that they are not always desired and that chain crosslinking is a means to prevent them by freezing the assembly (cf. Sections 15.4.2 and 15.4.3). On the other hand, the dynamics of the assembly must be favourable to the transition. In other words, a kinetically frozen assembly will not be able to rearrange chains, resulting in a change of morphology (in reasonable timescales).

Several reviews have summarized and commented order-order transitions (among other aspects of PISA) [50, 52, 54, 60] or even dedicated the whole review to this subject [55]. We will thus only briefly summarize the most important stimuli that have been reported to induce post-polymerization morphological transitions in PISA and illustrate them by some representative examples. Some of the examples will be detailed in Section 15.6.

15.5.4.1 Temperature

Temperature-induced morphological transitions (TIMTs) in water have first been reported for diblock copolymers possessing PHPMA as a core block [245]. It was shown that such PGMA-*b*-PHPMA block copolymer worms transformed into spherical micelles, when the solution was cooled from room temperature to 4 °C. The

morphological transition resulted in a change in bulk properties: although entangled worms form free-standing gels, the corresponding sphere dispersion is a liquid of low viscosity. A possible application of such thermoresponsive gels is their use as sterilizable gels. Since then, other types of core polymers (generally rather 'hydrophilic' polymers prepared through dispersion polymerization formulations) have also been reported, for instance, using PDMAAm [172, 246]. These post-polymerization transitions have been termed temperature-induced morphological transitions (TIMTs) by Wang et al. [246], and they are usually explained by a change in surface plasticization, leading to a change in the packing parameter. The transition temperature is generally very sensitive to the molar mass of the polymers and can thus be tuned by the DP_n [210] or by copolymerization. For instance, Warren, Plamper, and coworkers copolymerized NIPAM with *tert*-butyl acrylamide (*t*BuAAm) to afford PDMAAm-*b*-P(NIPAM-*co*-*t*BuAAm) assemblies for which morphological transitions could be induced by both temperature and hydrostatic pressure [206].

TIMT have not only been reported in water but also in non-aqueous media, such as in *n*-dodecane [247] or in mineral oil [248]. In the latter case, PSMA-*b*-PBzMA diblock copolymer assemblies were synthesized through a dispersion polymerization formulation. DP_n of the polymers was tuned in order to obtain vesicles, which underwent a vesicle-to-worm transition upon heating above a critical gelation temperature (at 135 °C, as the non-interacting vesicles are converted into weakly interacting worms). This concept provides a new mechanism for the high-temperature thickening of oils.

15.5.4.2 pH

As mentioned above (Section 15.5.2), morphological transitions can be triggered by a change of pH, in case the nano-objects are stabilized by a weak polyelectrolyte shell, or even by a neutral polymer possessing a single ionizable functional group (such as a carboxylic acid group [221, 222] or a morpholine end group [223]). In the case of a PGMA-*b*-PHPMA diblock copolymer synthesized from a carboxylic acid functional RAFT agent, worm-to-sphere [221] or vesicle-to-worm (or sphere) transitions [222] could be induced by a pH increase. The ionization of the terminal carboxylic acid group should increase the volume of the hydrophilic segment, triggering the observed slow morphological transitions. Instead of triggering morphological transitions, it was also possible to trigger the inversion of the core and shell of spherical diblock copolymer micelles, possessing two pH-responsive blocks, in the example a polyamine and a hydrophobic polyacid block, prepared by PISA. Such pH-responsive spherical micelles are called 'schizophrenic' micelles, and they offer the possibility to incorporate and release a payload on demand [249]. In addition to pH-responsive diblock copolymer self-assemblies, the concept was also reported for ABC triblock copolymers, where morphological transitions could be induced by the protonation of a polyamine middle block [250].

15.5.4.3 'Reactive' Groups

As already mentioned in Section 15.4, 'reactive groups' that are able to interact or react in a larger sense may also induce morphological transitions.

- *Degradation*. As reported above, morphology is related to the packing parameter and thus in the simplest case to the DP_n of the hydrophilic and hydrophobic blocks. So finally, a means to alter morphology after polymerization is thus to alter the DP_n of the core block. An elegant while slow strategy to induce order-order morphological transitions was thus the design of a degradable core block by copolymerizing 3-methylidene-1,9-dioxa-5,12,13-trithiacyclopentadecane-2,8-dione (MTC), a disulfide-based cyclic monomer, yielding copolymers with degradable disulfide bonds in the main chain. The authors validated their concept and showed that worm could be transformed into sphere thanks to the chemical degradation of the hydrophobic P(HPMA-*co*-MTC) block [251].
- *Initiators*. A particular type of reactive groups are initiators, i.e. groups that are capable of initiating the growth of a new polymer chain. As such, in the work of St Thomas et al., alkoxyamine-functionalized latex nanoparticles were synthesized by RAFT-PISA and depicted in Section 15.4.1. They were used in a second polymerization step performed at higher temperature (130 °C) to form of a double hydrophilic corona (PAA-*b*-PSSNa), which went along with a switch in morphology [130].
- *Dynamic covalent bonds and supramolecular interactions*. A completely different type of reactive group is the supramolecular interacting group that may bind to a specific molecule by complexation. The Armes group showed in 2017 how dynamic covalent chemistry can drive order-order morphological transitions in aqueous dispersions of PGMA-*b*-PHPMA diblock copolymer vesicles in order to release nanoparticle payloads from the vesicles [252, 253]. In the first example [252], the addition of 3-aminophenylboronic acid (APBA) to such vesicles at pH ~ 10 resulted in specific binding of this reagent to some of the pendent *cis*-diol groups of the hydrophilic PGMA chains to form phenylboronate ester bonds. This led to a subtle increase in the effective volume fraction of this stabilizer block, which in turn caused a reduction in the packing parameter and hence induced a vesicle-to-worm (or vesicle-to-sphere) morphological transition, and eventually the release of silica particles. In the same year, the same group also explored host–guest chemistry, another subclass of supramolecular chemistry, to modify the morphological transition of preformed diblock copolymer assemblies [137]. CD (host)–azobenzene (guest) interactions were exploited to tune, in particular, the rate of thermally induced morphological transitions for β-CD-functionalized vesicles constituted of P(GMA-*co*-GlyMA)-*b*-PHPMA diblock copolymers. Addition of azobenzene–methoxypoly(ethylene glycol) to such vesicles resulted in the formation of an inclusion complex with the β-CD groups present at the hydrophilic P(GMA-*co*-GlyMA) chains and led to a significantly faster change in copolymer morphology compared to the β-CD-functionalized vesicles alone.

15.5.4.4 Light

In addition to being hydrophobic mesogenic moieties, which can arrange in a liquid crystalline order (see Sections 15.3.3 and 15.4.2), and their ability to interact with CD, azobenzenes are also known to be light responsive. Triggered by changes in

wavelength, they can undergo a reversible trans–cis isomerization, which results in a change in hydrophobicity. Already largely explored for assemblies prepared from preformed polymers, copolymers possessing pendant azobenzene groups in their core have also been synthesized by PISA. The UV-light-induced morphological transformations were again rationalized by the volume change of the hydrophobic block caused by the isomerization of the azobenzene moieties [112, 254]. Bagheri et al. proposed another strategy to use light as a trigger to change morphology. They incorporated 1-pyrenemethyl methacrylate as a comonomer in the solvophobic block of photoactive nanoparticles, as a means to photochemically trigger particle dissociation by cleavage of pyrene moieties, leading to a solvophobic–solvophilic transition of the core polymer [255].

15.5.4.5 Oxygen

To finish with, the same group has also prepared nano-objects possessing core polymers sensitive to reactive oxygen species, namely, poly(2-(methylthio)ethyl methacrylate), by a PISA process. In this work, particle disassembly rather than morphological transitions were observed through a hydrophobic–hydrophilic change in the block copolymer properties because of the oxidation of the thioether groups [256]. Similarly, Sobotta et al. demonstrate that the cyclic thioether *N*-acryloyl thiomorpholine can be used in PISA to afford a hydrophobic block, which can be transformed upon oxidation into a highly water-soluble sulfoxide, leading again to the disassembly of the particles [257].

15.6 Applications

As mentioned in previous sections, the possibility to produce nano-objects of various shapes in high amount and concentration opens the door towards their application in various fields. Although standard applications of micellar objects/nanoparticles – such as their use as drug delivery vehicles – have been explored, original applications related to the possibility to synthesize them at high solid contents have also been reported. In the latter case, the bulk properties of these concentrated dispersions have been explored, typically in the case of worm dispersions that may form free-standing gels and for which the rational design of the copolymer allowed to make them thermoresponsive. The following part summarizes the main applications of PISA-derived nanoparticles that have been explored. For each application, some representative examples are provided.

To date, the most explored field of application for PISA certainly concerns ***biomedical applications***. Indeed, PISA allows the synthesis of core–shell nanoparticles directly in aqueous media without using co-solvents, combined with the possibility to encapsulate any kind of payload in situ, i.e. during polymerization. All main morphologies accessible by PISA have been explored for the encapsulation and delivery of drugs [64]. Although spherical and worm-like morphologies have been used to encapsulate hydrophobic drugs, vesicles (also termed polymersomes in the biomedical field) allow the encapsulation of both hydrophobic (in the bilayer membrane) and

hydrophilic drugs (in the cavity) or other bio-relevant agents (such as enzymes). A related biomedical application concerns the encapsulation of any type of molecules or materials useful for imaging purposes. As such, fluorescent dyes, magnetic particles [258], or alternatively ^{19}F-containing fluorinated monomers [149, 258] have been incorporated. Some papers reported the synthesis of model stimuli-responsive vesicles by PISA able to release various species such as silica nanoparticles [252, 259, 260], BSA [177, 259], rhodamine B [261], Nile red [262], or enzymes [263].

Worm dispersions that form free-standing gels at room temperature (or physiological temperature) and that are less viscous at low temperature (because of reversible morphological worm-sphere transitions, see Section 15.5.4) have also found interest for biomedical applications as they are sterilizable by filtration at low temperature [134, 245]. Their potential use as drug delivery systems, for tissue engineering or for cell storage, has been considered [264]. In contrast, vesicles have also found interest as mimicking systems for living cells [63, 265]. For instance, enzymes have successfully been encapsulated in vesicles and their permeability has been modulated, for instance, by the incorporation of pores [266]. In addition to mimicking living cells, another aspect of such bio-hybrids is their use as enzymatic nanoreactors [263, 267]. For more details on biomedical applications of PISA-derived nano-objects, the reader can refer to recent reviews, which provide an excellent overview on the existing systems [60, 62, 64].

Another application of particles produced by PISA is ***catalysis***. PISA was employed to nanostructure the particle cores in order to generate catalytic nanoreactors dispersed in water. This was achieved by the use of hydrophobic monomers carrying triphenylphosphine ligands and a crosslinker introduced either at the beginning of the emulsion polymerization or at a later stage. After complexation of Ru, the resulting catalytic nanoreactors proved to be useful for hydroformylation of octene [268–271]. Metallic Pd(0) nanoparticles have also been introduced, for instance, into nanogels obtained by PISA, and showed a remarkable stability in the solid state and in solution. This feature allowed their successful application as catalysts for the Mizoroki–Heck reaction between *n*-BA and a series of bromo- and iodo-arenes [272]. In addition to the examples cited above, a large variety of metal-hybrid nanocatalysts (most of the incorporating metal particles) have now been synthesized using PISA, but their detailed description is out of the scope of this review.

An expanding application of PISA-derived particles is their use for the stabilization of liquid–liquid interfaces to form the so-called ***Pickering emulsions*** [273]. Block copolymer nanoparticles of various morphologies, mainly spheres and worms [165, 274, 275], but also vesicles [274] have been investigated. Furthermore, the utility of thermoresponsive particles that undergo worm-to-sphere morphological transitions in the field of Pickering emulsions has also been demonstrated [276]. The different studies revealed that not only the type of shell and core (crosslinked or not) polymer but also the particle morphology play a crucial role in their efficiency to stabilize emulsions. Eventually, one may note that worm-like particles have also been used successfully to stabilize high internal phase emulsions (HIPEs) [277].

The main particle morphologies have also all been used as ***templating agents*** to produce hollow inorganic nanoparticles, porous materials, or nanocomposites.

One of the first examples was the use of nanoworms as soft templates to produce hollow silica nanotubes through calcination of the hybrid nanoworms prepared in a previous synthesis step [278]. More recently, spherical nanoparticles possessing a soft poly(hydroxyethyl acrylate) core have been used to prepare uniform mesoporous carbon materials [103]. Another type of inorganic material used in combination with nanoparticles made by PISA is calcite ($CaCO_3$) [279, 280].

Other applications of PISA nanoparticles concern their ***use as additives*** in complex formulations. Anisotropic particles or particles that undergo morphological transitions are of particular interest for these applications. Aqueous dispersions of long fibres can be used as rheomodifiers to adjust the rheology of complex formulations [281], whereas thermoresponsive vesicles that exhibit a heat-induced vesicle-to-worm morphological transition in mineral oil have a potential interest as lubricants for oils, as heat thickening is an unusual and desired rheological feature [248]. Another application is in the field of coatings, with the use of hollow particles (vesicles [282] or bicontinuous microparticles [218]) as opacifiers for paint films. Besides, the utility of high T_g PISA nanofibres as mechanically reinforcing fillers for soft films has also been demonstrated [283], while highly asymmetric diblock copolymer nanoparticles composed of a large soft PBA core block and a short hard PAA shell can be used to prepare nanostructured films with enhanced properties [127, 128].

Although most of the previous applications concern the individual nanoparticle itself or the bulk properties of a particle dispersion, other applications concern the films that can be produced after drying or processing the dispersions. For instance, ***thin nanostructured films*** of PISA nanoparticles (pure polymer particles [284, 285] or hybrids [286]) have been spin-coated as thin films to construct membranes for water ultrafiltration purposes.

As mentioned in Section 15.1, PISA was initially developed for emulsion polymerization formulations to produce ***surfactant-free latexes***. The presence of free surfactants is still an important issue in the coating industry, and the current expiration of the RAFT patents is expecting to further boost the industrial demands for developing PISA for coating applications, hopefully with the aid of academic collaborations.

15.7 Conclusions

As shown in the previous sections, PISA is a very simple and efficient tool to produce amphiphilic block copolymers in high concentrations and a way to self-assemble these block copolymers into nano-structured aggregates during their formation. PISA is attracting a broad range of interests from polymer chemists and physico-chemists to biologists and, as a direct consequence, PISA is generating a broad range of hopes for various applications. We believe that the reading of this overview on RAFT-mediated PISA will easily allow the reader to comprehend the vast potential of this technique. The transposition of new processes or technologies to industry is a challenge because it always faces the robustness of, and the experience gained on, the existing systems. PISA will perform even better in the

near future with the development of process parameters, e.g. continuous processes [287–289] and will undoubtedly benefit from the well-established industrial field of polymerization in dispersed media.

Acknowledgements

Drs Bastian Ebeling and Arne Wolpers (C2P2) are gratefully acknowledged for helpful discussions.

Abbreviations

(M)AA	(meth)acrylic acid
AAEM	2-(acetoacetoxy)ethyl methacrylate
ADH	adipic acid dihydrazide
BA	*n*-butyl acrylate
CD	cyclodextrin
BzMA	benzyl methacrylate
DAAm	diacetone acrylamide
DEAAm	*N,N*-diethyl acrylamide
DEAEMA	2-diethylaminoethyl methacrylate
DLS	dynamic light scattering
DMAAm	*N,N*-dimethyl acrylamide
DMAEMA	2-dimethylaminoethyl methacrylate
DP_n	number-average degree of polymerization
DVB	divinylbenzene
GMA	glycerol methacrylate
GlyMA	glycidyl methacrylate
HBMA	2-hydroxybutyl methacrylate
HDFDMA	heptadecafluorodecyl methacrylate
HEAAm	hydroxyethyl acrylamide
HPMA	2-hydroxypropyl methacrylate
NMR	nuclear magnetic resonance
LCST	lower critical solution temperature
macroRAFT	macromolecular RAFT agent
MMA	methyl methacrylate
NAM	*N*-acryloylmorpholine
NIPAM	*N*-isopropylacrylamide
p	packing parameter
PEG	poly(ethylene glycol)
PEG(M)A	poly(ethylene glycol) methyl ether (meth)acrylate
PFPMA	pentafluorophenyl methacrylate
PISA	polymerization-induced self-assembly
RAFT	reversible addition-fragmentation chain transfer
RDRP	reversible-activation radical polymerization

SANS	samll angle neutron scattering
SAXS	small angle x-ray diffraction
SLS	static light scattering
$^{sc}CO_2$	supercritical carbon dioxide
SEC	size exclusion chromatography
SMA	stearyl methacrylate
St	styrene
SSNa	sodium 4-styrene sulfonate
(cryo)TEM	(cryogenic)transmission electron microscopy
TFEMA	2,2,2-trifluoroethyl methacrylate
TIMT	temperature-induced morphological transitions
VAc	vinyl acetate
VDF	vinylidene fluoride
4VP	4-vinyl pyridine

References

1 D'Agosto, F., Rieger, J., and Lansalot, M. (2020). RAFT-Mediated Polymerization-Induced Self-Assemply. *Angew. Chem. Int. Ed.* 59: 8368. https://doi.org/10.1002/anie.201911758.
2 Destarac, M. (2018). *Polym. Chem.* 9: 4947.
3 Barner-Kowollik, C. (ed.) (2008). *Handbook of RAFT Polymerization*. Weinheim: Wiley-VCH.
4 Chiefari, J., Chong, B.Y.K., Ercole, F. et al. (1998). *Macromolecules* 31: 5559.
5 Dommanget, C., D'Agosto, F., and Monteil, V. (2014). *Angew. Chem. Int. Ed.* 53: 6683.
6 Guerre, M., Rahaman, S.M.W., Améduri, B. et al. (2016). *Macromolecules* 49: 5386.
7 Abreu, C.M.R., Mendonça, P.V., Serra, A.C. et al. (2012). *Macromolecules* 45: 2200.
8 Perrier, S. (2017). *Macromolecules* 50: 7433.
9 Jennings, J., He, G., Howdle, S.M., and Zetterlund, P.B. (2016). *Chem. Soc. Rev.* 45: 5055.
10 Keddie, D.J. (2014). *Chem. Soc. Rev.* 43: 496.
11 Charleux, B., D'Agosto, F., and Delaittre, G. (2010). *Adv. Polym. Sci.* 233: 125.
12 Charleux, B., Delaittre, G., Rieger, J., and D'Agosto, F. (2012). *Macromolecules* 45: 6753.
13 Delaittre, G., Dire, C., Rieger, J. et al. (2009). *Chem. Commun.*: 2887.
14 Wan, W.-M., Hong, C.-Y., and Pan, C.-Y. (2009). *Chem. Commun.*: 5883.
15 Wan, W.-M., Sun, X.-L., and Pan, C.-Y. (2009). *Macromolecules* 42: 4950.
16 Delaittre, G., Nicolas, J., Lefay, C. et al. (2005). *Chem. Commun.*: 614.
17 Brusseau, S., D'Agosto, F., Magnet, S. et al. (2011). *Macromolecules* 44: 5590.
18 Groison, E., Brusseau, S., D'Agosto, F. et al. (2012). *ACS Macro Lett.* 1: 47.

19 Qiao, X.G., Lansalot, M., Bourgeat-Lami, E., and Charleux, B. (2013). *Macromolecules* 46: 4285.
20 Wan, W.-M. and Pan, C.-Y. (2007). *Macromolecules* 40: 8897.
21 Sugihara, S., Sugihara, K., Armes, S.P. et al. (2010). *Macromolecules* 43: 6321.
22 Wang, G., Schmitt, M., Wang, Z. et al. (2016). *Macromolecules* 49: 8605.
23 Wang, Y., Han, G., Duan, W., and Zhang, W. (2019). *Macromol. Rapid Commun.* 40: 1800140.
24 Wang, J., Wu, Z., Wang, G., and Matyjaszewski, K. (2019). *Macromol. Rapid Commun.* 40: 1800332.
25 Alzahrani, A., Zhou, D., Kuchel, R.P. et al. (2019). *Polym. Chem.* 10: 2658–2665.
26 Kapishon, V., Whitney, R.A., Champagne, P. et al. (2015). *Biomacromolecules* 16: 2040.
27 Sue-eng, S., Boonchuwong, T., Chaiyasat, P. et al. (2017). *Polymer* 110: 124.
28 Okubo, M., Sugihara, Y., Kitayama, Y. et al. (2009). *Macromolecules* 42: 1979.
29 Kitayama, Y., Chaiyasat, A., Minami, H., and Okubo, M. (2010). *Macromolecules* 43: 7465.
30 Kitayama, Y., Moribe, H., Kishida, K., and Okubo, M. (2012). *Polym. Chem.* 3: 1555.
31 Cordella, D., Debuigne, A., Jérôme, C. et al. (2016). *Macromol. Rapid Commun.* 37: 1181.
32 Wright, D.B., Touve, M.A., Adamiak, L., and Gianneschi, N.C. (2017). *ACS Macro Lett.* 6: 925.
33 Foster, J.C., Varlas, S., Blackman, L.D. et al. (2018). *Angew. Chem. Int. Ed.* 57: 10672.
34 Torres-Rocha, O.L., Wu, X., Zhu, C. et al. (2019). *Macromol. Rapid Commun.* 40: 1800326.
35 Le, D., Dilger, M., Pertici, V. et al. (2019). *Angew. Chem. Int. Ed.* 58: 4725.
36 Sarkar, J., Xiao, L., Jackson, A.W. et al. (2018). *Polym. Chem.* 9: 4900.
37 Ferguson, C.J., Hughes, R.J., Pham, B.T.T. et al. (2002). *Macromolecules* 35: 9243.
38 Meijs, G.F. and Rizzardo, E. (1988). *Macromol. Chem. Rapid Commun.* 9: 547.
39 Yamada, B. and Kobatake, S. (1994). *Prog. Polym. Sci.* 19: 1089.
40 Rizzardo, E., Meijs, G.F., and Thang, S.H. (1995). *Macromol. Symp.* 98: 101.
41 Colombani, D. and Chaumont, P. (1996). *Prog. Polym. Sci.* 21: 439.
42 Moad, G., Rizzardo, E., and Thang, S.H. (2008). *Polymer* 49: 1079–1131.
43 Moad, G. (2022). An industrial pistory of RAFT Polymerization. In *RAFT Polymerization: Materials, Synthesis and Applications* (eds. Moad, G., Rizzardo, E.), Weinheim: Wiley-VCH.
44 Zhou, D., Kuchel, R.P., and Zetterlund, P.B. (2017). *Polym. Chem.* 8: 4177.
45 Lotierzo, A., Schofield, R.M., and Bon, S.A.F. (2017). *ACS Macro Lett.* 6: 1438.
46 Schreur-Piet, Heuts, J.P.A. (2017). *Polym. Chem.* 8: 6654.
47 Sun, J.-T., Hong, C.-Y., and Pan, C.-Y. (2012). *Soft Matter* 8: 7753.
48 Sun, J.-T., Hong, C.-Y., and Pan, C.-Y. (2013). *Polym. Chem.* 4: 873.
49 Warren, N.J. and Armes, S.P. (2014). *J. Am. Chem. Soc.* 136: 10174.
50 Rieger, J. (2015). *Macromol. Rapid Commun.* 36: 1458.

51 Derry, M.J., Fielding, L.A., and Armes, S.P. (2016). *Prog. Polym. Sci.* 52: 1.

52 Lansalot, M., Rieger, J., and D'Agosto, F. (2016). Polymerization-induced self-assembly: the contribution of controlled radical polymerization to the formation of self-stabilized polymer particles of various morphologies. In: *Macromolecular Self-assembly* (eds. L. Billon and O. Bourisov), 33. Wiley.

53 Lowe, A.B. (2016). *Polymer* 106: 161.

54 Canning, S.L., Smith, G.N., and Armes, S.P. (2016). *Macromolecules* 49: 1985.

55 Pei, Y., Lowe, A.B., and Roth, P.J. (2017). *Macromol. Rapid Commun.* 38: 1600528.

56 Yeow, J. and Boyer, C. (2017). *Adv. Sci.* 4: 1700137.

57 Zhou, J., Yao, H., and Ma, J. (2018). *Polym. Chem.* 9: 2532.

58 Six, J.-L. and Ferji, K. (2019). *Polym. Chem.* 10: 45.

59 Wang, X. and An, Z. (2019). *Macromol. Rapid Commun.* 40: 1800325.

60 Le, D., Keller, D., and Delaittre, G. (2019). *Macromol. Rapid Commun.* 40: 1800551.

61 Truong, N.P., Quinn, J.F., Whittaker, M.R., and Davis, T.P. (2016). *Polym. Chem.* 7: 4295.

62 Khor, S.Y., Quinn, J.F., Whittaker, M.R. et al. (2019). *Macromol. Rapid Commun.* 40: 1800438.

63 Cheng, G. and Pérez-Mercader, J. (2019). *Macromol. Rapid Commun.* 40: 1800513.

64 Zhang, W.J., Hong, C.Y., and Pan, C.Y. (2019). *Macromol. Rapid Commun.* 40: 1800279.

65 Kim, J., Jeong, S.Y., Kim, K.U. et al. (1996). *J. Polym. Sci., Part A: Polym. Chem.* 34: 3277.

66 Okay, O. and Funke, W. (1990). *Macromolecules* 23: 2623.

67 Yamauchi, K., Hasegawa, H., Hashimoto, T. et al. (2006). *Macromolecules* 39: 4531.

68 Monteiro, M.J. and Cunningham, M.F. (2012). *Macromolecules* 45: 4939.

69 Zetterlund, P.B., Thickett, S.C., Perrier, S. et al. (2015). *Chem. Rev.* 115: 9745.

70 Such, C.H., Rizzardo, E., Serelis, A.K., et al. (2003). Aqueous dispersions of polymer particles. WO2003055919A1, filed 20 December 2002 and issued 10 July 2003. University of Sydney, Australia.

71 Hawkett, B.S., Such, C.H., Nguyen, D.N., et al. (2006). Surface polymerisation process and polymer product using raft agent. WO2006037161A1, filed 04 October 2005 and issued 13 April 2006. The University of Sydney, Australia.

72 Le, T.P., Moad, G., Rizzardo, E., and Thang, S.H. (1998). WO9801478A1, filed 03 July 1997 and issued 15 January 1998. E. I. Du Pont de Nemours & Co., USA.

73 Corpart, P., Charmot, D., Biadatti, T., et al. (1998). Method for block polymer synthesis by controlled radical polymerisation. WO9858974A1, filed 23 June 1998 and issued 30 December 1998. Rhodia Chimie, Fr. invs.

74 Charmot, D., Corpart, P., Adam, H. et al. (2000). *Macromol. Symp.* 150: 23.

75 Bett, W., Castaing, J.-C., and D'Allest, J.-F. (2001). Surface chemistry modified latex and resdispersible powders, production and use thereof.

WO2001042325A1, filed 08 December 2000 and issued 14 June 2001. Rhodia Chimie, Fr., invs.
76 Meunier, F., Elaïssari, A., and Pichot, C. (1995). *Polym. Adv. Technol.* 6: 489.
77 Chan, K., Pelton, R., and Zhang, J. (1999). *Langmuir* 15: 4018.
78 Derry, M.J., Fielding, L.A., and Armes, S.P. (2015). *Polym. Chem.* 6: 3054.
79 Mai, Y. and Eisenberg, A. (2012). *Chem. Soc. Rev.* 41: 5969.
80 Ferguson, C.J., Hughes, R.J., Nguyen, D. et al. (2005). *Macromolecules* 38: 2191.
81 Chaduc, I., Zhang, W., Rieger, J. et al. (2011). *Macromol. Rapid Commun.* 32: 1270.
82 Ratcliffe, L.P.D., Ryan, A.J., and Armes, S.P. (2013). *Macromolecules* 46: 769.
83 Sugihara, S., Blanazs, A., Armes, S.P. et al. (2011). *J. Am. Chem. Soc.* 133: 15707.
84 Zhang, X., Boissé, S., Zhang, W. et al. (2011). *Macromolecules* 44: 4149.
85 Zhang, W., D'Agosto, F., Boyron, O. et al. (2012). *Macromolecules* 45: 4075.
86 Zhang, W., D'Agosto, F., Dugas, P.-Y. et al. (2013). *Polymer* 54: 2011.
87 Lesage de la Haye, J., Zhang, X., Chaduc, I. et al. (2016). *Angew. Chem. Int. Ed.* 55: 3739.
88 Chaduc, I., Reynaud, E., Dumas, L. et al. (2016). *Polymer* 106: 218.
89 Khor, S.Y., Truong, N.P., Quinn, J.F. et al. (2017). *ACS Macro Lett.* 6: 1013.
90 Chaduc, I., Girod, M., Antoine, R. et al. (2012). *Macromolecules* 45: 5881.
91 Chaduc, I., Crepet, A., Boyron, O. et al. (2013). *Macromolecules* 46: 6013.
92 Akpinar, B., Fielding, L.A., Cunningham, V.J. et al. (2016). *Macromolecules* 49: 5160.
93 Hatton, F.L., Lovett, J.R., and Armes, S.P. (2017). *Polym. Chem.* 8: 4856.
94 Bernard, J., Save, M., Arathoon, B., and Charleux, B. (2008). *J. Polym. Sci., Part A: Polym. Chem.* 46: 2845.
95 Binauld, S., Delafresnaye, L., Charleux, B. et al. (2014). *Macromolecules* 47: 3461.
96 Etchenausia, L., Khoukh, A., Deniau Lejeune, E., and Save, M. (2017). *Polym. Chem.* 8: 2244.
97 Etchenausia, L., Deniau, E., Brûlet, A. et al. (2018). *Macromolecules* 51: 2551.
98 Siirilä, J., Häkkinen, S., and Tenhu, H. (2019). *Polym. Chem.* 10: 766.
99 Liu, Z., Zhang, G., Lu, W. et al. (2015). *Polym. Chem.* 6: 6129.
100 Jiang, Y., Xu, N., Han, J. et al. (2015). *Polym. Chem.* 6: 4955.
101 Tan, J., Xu, Q., Li, X. et al. (2018). *Macromol. Rapid Commun.* 39: 1700871.
102 Yeow, J., Sugita, O.R., and Boyer, C. (2016). *ACS Macro Lett.* 5: 558.
103 Tkachenko, V., Matei Ghimbeu, C., Vaulot, C. et al. (2019). *Polym. Chem.* 10: 2316.
104 Figg, C.A., Simula, A., Gebre, K.A. et al. (2015). *Chem. Sci.* 6: 1230.
105 An, Z., Shi, Q., Tang, W. et al. (2007). *J. Am. Chem. Soc.* 129: 14493.
106 Zhu, A., Lv, X., Shen, L. et al. (2017). *ACS Macro Lett.* 6: 304.
107 Tan, J., Huang, C., Liu, D. et al. (2017). *ACS Macro Lett.* 6: 298.
108 Tan, J., Xu, Q., Zhang, Y. et al. (2018). *Macromolecules* 51: 7396.
109 Yu, Q., Ding, Y., Cao, H. et al. (2015). *ACS Macro Lett.* 4: 1293.
110 Ding, Y., Cai, M., Cui, Z. et al. (2018). *Angew. Chem. Int. Ed.* 57: 1053.

111 Cai, M., Ding, Y., Wang, L. et al. (2018). *ACS Macro Lett.* 7: 208.
112 Guan, S., Zhang, C., Wen, W. et al. (2018). *ACS Macro Lett.* 7: 358.
113 Tichagwa, L., Götz, C., Tonge, M. et al. (2003). *Macromol. Symp.* 193: 251.
114 Manguian, M., Save, M., and Charleux, B. (2006). *Macromol. Rapid Commun.* 27: 399.
115 Dos Santos, A.M., Pohn, J., Lansalot, M., and D'Agosto, F. (2007). *Macromol. Rapid Commun.* 28: 1325.
116 Wi, Y., Lee, K., Lee, B.H., and Choe, S. (2008). *Polymer* 49: 5626.
117 Bathfield, M., D'Agosto, F., Spitz, R. et al. (2007). *Macromol. Rapid Commun.* 28: 1540.
118 Guyot, A. (2004). *Adv. Colloid Interface Sci.* 108–109: 3.
119 Vinas, J., Velasquez, E., Dufils, P.-E., et al. (2013). Process for the preparation of a vinylidene chloride polymer. WO2013092587A1, filed 18 December 2012 and issued 27 June 2013.
120 Velasquez, E., Rieger, J., Stoffelbach, F. et al. (2016). *Polymer* 106: 275.
121 Devisme, S., Kahn, A., Fuentes-Exposito, M., et al. (2019). Synthesis of surfactant-free poly(vinylidene fluoride) latexes via raft emulsion polymerization. WO2019063445, filed 21 September 2018 and issued 04 April 2019.
122 Lesage de la Haye, J., Martin-Fabiani, I., Schulz, M. et al. (2017). *Macromolecules* 50: 9315.
123 Martín-Fabiani, I., Lesage de la Haye, J., Schulz, M. et al. (2018). *ACS Appl. Mater. Interfaces* 10: 11221.
124 Martín-Fabiani, I., Makepeace, D.K., Richardson, P.G. et al. (2019). *Langmuir* 35: 3822.
125 Dehan, V., Bourgeat-Lami, E., D'Agosto, F. et al. (2017). *Steel Constr.* 10: 254.
126 Chenal, M., Bouteiller, L., and Rieger, J. (2013). *Polym. Chem.* 4: 752.
127 Chenal, M., Rieger, J., Véchambre, C. et al. (2013). *Macromol. Rapid Commun.* 4: 1524.
128 Chenal, M., Véchambre, C., Chenal, J.-M. et al. (2017). *Polymer* 109: 187.
129 An, Z., Tang, W., Wu, M. et al. (2008). *Chem. Commun.*: 6501.
130 St Thomas, C., Guerrero-Santos, R., and D'Agosto, F. (2015). *Polym. Chem.* 6: 5405.
131 Ebeling, B., Belal, K., Stoffelbach, F. et al. (2019). *Macromol. Rapid Commun.* 40: 1800455.
132 György, C., Lovett, J.R., Penfold, N.J.W., and Armes, S.P. (2019). *Macromol. Rapid Commun.* 40: 1800289.
133 Warren, N.J., Rosselgong, J., Madsen, J., and Armes, S.P. (2015). *Biomacromolecules* 16: 2514.
134 Simon, K.A., Warren, N.J., Mosadegh, B. et al. (2015). *Biomacromolecules* 16: 3952.
135 Rosselgong, J., Blanazs, A., Chambon, P. et al. (2012). *ACS Macro Lett.* 1: 1041.
136 Ratcliffe, L., Bentley, K., Wehr, R. et al. (2017). *Polym. Chem.* 8: 5962.
137 Yao, H., Ning, Y., Jesson, C.P. et al. (2017). *ACS Macro Lett.* 6: 1379.
138 Maiti, B., Bauri, K., Nandi, M., and De, P. (2017). *J. Polym. Sci., Part A: Polym. Chem.* 55: 263.

139 Boussiron, C., Le Bechec, M., Petrizza, L. et al. (2019). *Macromol. Rapid Commun.* 40: 1800329.

140 He, J., Xu, Q., Tan, J., and Zhang, L. (2019). *Macromol. Rapid Commun.* 40: 1800296.

141 Ting, S.R.S., Min, E.H., Zetterlund, P.B., and Stenzel, M.H. (2010). *Macromolecules* 43: 5211.

142 Ladmiral, V., Semsarilar, M., Canton, I., and Armes, S.P. (2013). *J. Am. Chem. Soc.* 135: 13574.

143 Hatton, F.L., Ruda, M., Lansalot, M. et al. (2016). *Biomacromolecules* 17: 1414.

144 Ladmiral, V., Charlot, A., Semsarilar, M., and Armes, S.P. (2015). *Polym. Chem.* 6: 1805.

145 Bauri, K., Narayanan, A., Haldar, U., and De, P. (2015). *Polym. Chem.* 6: 6152.

146 Pei, Y., Noy, J.-M., Roth, P.J., and Lowe, A.B. (2015). *Polym. Chem.* 6: 1928.

147 Pei, Y., Noy, J.-M., Roth, P.J., and Lowe, A.B. (2015). *J. Polym. Sci., Part A: Polym. Chem.* 53: 2326.

148 Shen, L., Guo, H., Zheng, J. et al. (2018). *ACS Macro Lett.* 7: 287.

149 Zhao, W., Ta, H.T., Zhang, C., and Whittaker, A.K. (2017). *Biomacromolecules* 18: 1145.

150 Zong, M., Thurecht, K.J., and Howdle, S.M. (2008). *Chem. Commun.*: 5942.

151 Xu, A., Lu, Q., Huo, Z. et al. (2017). *RSC Adv.* 7: 51612.

152 Dong, S., Zhao, W., Lucien, F.P. et al. (2015). *Polym. Chem.* 6: 2249–2254.

153 Zhou, D., Kuchel, R.P., Dong, S. et al. (2019). *Macromol. Rapid Commun.*

154 Shirin-Abadi, A.R., Jessop, P.G., and Cunningham, M.F. (2017). *Macromol. React. Eng.* 11: 1600035.

155 Guo, L., Jiang, Y., Qiu, T. et al. (2014). *Polymer* 55: 4601.

156 Semsarilar, M., Jones, E.R., and Armes, S.P. (2014). *Polym. Chem.* 5: 195.

157 Chakrabarty, A., Ponnupandian, S., Kang, N.G. et al. (2018). *J. Polym. Sci., Part A: Polym. Chem.* 56: 266.

158 Ouhib, F., Dirani, A., Aqil, A. et al. (2016). *Polym. Chem.* 7: 3998.

159 Qiao, Z., Qiu, T., Liu, W. et al. (2016). *Polym. Chem.* 7: 3993.

160 Guerre, M., Semsarilar, M., Godiard, F. et al. (2017). *Polym. Chem.* 8: 1477.

161 Couturaud, B., Georgiou, P.G., Varlas, S. et al. (2019). *Macromol. Rapid Commun.* 40: 1800460.

162 Busatto, N., Stolojan, V., Shaw, M. et al. (2019). *Macromol. Rapid Commun.*: 1800346.

163 Zheng, G. and Pan, C. (2006). *Macromolecules* 39: 95.

164 Lovett, J.R., Ratcliffe, L.P.D., Warren, N.J. et al. (2016). *Macromolecules* 49: 2928.

165 Hunter, S.J., Thompson, K.L., Lovett, J.R. et al. (2019). *Langmuir* 35: 254.

166 Chambon, P., Blanazs, A., Battaglia, G., and Armes, S.P. (2012). *Langmuir* 28: 1196.

167 Hatton, F.L., Park, A.M., Zhang, Y. et al. (2019). *Polym. Chem.* 10: 194.

168 Tan, J., Liu, D., Huang, C. et al. (2017). *Macromol. Rapid Commun.* 38: 1700195.

169 Zhou, W., Qu, Q., Yu, W., and An, Z. (2014). *ACS Macro Lett.* 3: 1220.

170 Zhou, W., Qu, Q., Xu, Y., and An, Z. (2015). *ACS Macro Lett.* 4: 495.

171 Qu, Q., Liu, G., Lv, X. et al. (2016). *ACS Macro Lett.* 5: 316.
172 Byard, S.J., Williams, M., McKenzie, B.E. et al. (2017). *Macromolecules* 50: 1482.
173 Gao, P., Cao, H., Ding, Y. et al. (2016). *ACS Macro Lett.* 5: 1327.
174 Huang, J., Li, D., Liang, H., and Lu, J. (2017). *Macromol. Rapid Commun.* 38: 1700202.
175 Huang, J., Zhu, H., Liang, H., and Lu, J. (2016). *Polym. Chem.* 7: 4761.
176 Guégain, E., Zhu, C., Giovanardi, E., and Nicolas, J. (2019). *Macromolecules* 52: 3612.
177 Tan, J., Zhang, X., Liu, D. et al. (2017). *Macromol. Rapid Commun.* 38: 1600508.
178 Rieger, J., Stoffelbach, F., Bui, C. et al. (2008). *Macromolecules* 41: 4065.
179 Zhang, W., D'Agosto, F., Boyron, O. et al. (2011). *Macromolecules* 44: 7584.
180 Fielding, L.A., Derry, M.J., Ladmiral, V. et al. (2013). *Chem. Sci.* 4: 2081.
181 Grazon, C., Rieger, J., Sanson, N., and Charleux, B. (2011). *Soft Matter* 7: 3482.
182 Wan, W.M., Sun, X.L., and Pan, C.Y. (2010). *Macromol. Rapid Commun.* 31: 399.
183 Li, Y. and Armes, S.P. (2010). *Angew. Chem. Int. Ed.* 49: 4042.
184 Blanazs, A., Madsen, J., Battaglia, G. et al. (2011). *J. Am. Chem. Soc.* 133: 16581.
185 Biais, P., Beaunier, P., Stoffelbach, F., and Rieger, J. (2018). *Polym. Chem.* 9: 4483.
186 Sugihara, S., Ma'Radzi, A.H., Ida, S. et al. (2015). *Polymer* 76: 17.
187 Wang, X., Man, S., Zheng, J., and An, Z. (2018). *ACS Macro Lett.* 7: 1461.
188 Foster, J.C., Varlas, S., Couturaud, B. et al. (2018). *Angew. Chem. Int. Ed.* 57: 15733.
189 Warren, N.J., Mykhaylyk, O.O., Mahmood, D. et al. (2014). *J. Am. Chem. Soc.* 136: 1023.
190 Tan, J., Bai, Y., Zhang, X., and Zhang, L. (2016). *Polym. Chem.* 7: 2372.
191 Doncom, K.E.B., Warren, N.J., and Armes, S.P. (2015). *Polym. Chem.* 6: 7264.
192 Le, D., Wagner, F., Takamiya, M. et al. (2019). *Chem. Commun.* 55: 3741.
193 Ferji, K., Venturini, P., Cleymand, F. et al. (2018). *Polym. Chem.* 9: 2868.
194 Boissé, S., Rieger, J., Belal, K. et al. (2010). *Chem. Commun.* 46: 1950.
195 Semsarilar, M., Ladmiral, V., Blanazs, A., and Armes, S.P. (2013). *Langmuir* 29: 7416.
196 Blanazs, A., Ryan, A.J., and Armes, S.P. (2012). *Macromolecules* 45: 5099.
197 Tan, J., Dai, X., Zhang, Y. et al. (2019). *ACS Macro Lett.* 8: 205.
198 Cockram, A.A., Neal, T.J., Derry, M.J. et al. (2017). *Macromolecules* 50: 796.
199 Zhang, X., Rieger, J., and Charleux, B. (2012). *Polym. Chem.* 3: 1502.
200 Jia, Z., Bobrin, V.A., Truong, N.P. et al. (2014). *J. Am. Chem. Soc.* 136: 5824.
201 Truong, N.P., Whittaker, M.R., Anastasaki, A. et al. (2016). *Polym. Chem.* 7: 430.
202 Truong, N.P., Quinn, J.F., Anastasaki, A. et al. (2016). *Chem. Commun.* 52: 4497.
203 Truong, N.P., Quinn, J.F., Anastasaki, A. et al. (2017). *Polym. Chem.* 8: 1353.
204 Boissé, S., Rieger, J., Pembouong, G. et al. (2011). *J. Polym. Sci., Part A: Polym. Chem.* 49: 3346.
205 Yeow, J., Chapman, R., Xu, J., and Boyer, C. (2017). *Polym. Chem.* 8: 5012.
206 Steinschulte, A.A., Scotti, A., Rahimi, K. et al. (2017). *Adv. Mater.* 29: 1703495.

207 Wan, W.-M. and Pan, C.-Y. (2010). *Macromolecules* 43: 2672.
208 Blackman, L.D., Doncom, K.E.B., Gibson, M.I., and O'Reilly, R.K. (2017). *Polym. Chem.* 8: 2860.
209 Israelachvili, J. (2011). *Intermolecular and Surface Forces*, *3*e. London: Academic Press.
210 Warren, N.J., Derry, M.J., Mykhaylyk, O.O. et al. (2018). *Macromolecules* 51: 8357.
211 Shi, P., Zhou, H., Gao, C. et al. (2015). *Polym. Chem.* 6: 4911.
212 Zhou, J., Zhang, W., Hong, C., and Pan, C. (2016). *Polym. Chem.* 7: 3259.
213 Figg, C.A., Carmean, R.N., Bentz, K.C. et al. (2017). *Macromolecules* 50: 935.
214 Huo, M., Xu, Z., Zeng, M. et al. (2017). *Macromolecules* 50: 9750.
215 Huo, M., Zeng, M., Wu, D. et al. (2018). *Polym. Chem.* 9: 912.
216 Zhang, Y., Han, G., Cao, M. et al. (2018). *Macromolecules* 51: 4397.
217 Wu, Y., Tan, M., Su, Z. et al. (2018). *New J. Chem.* 42: 19353.
218 Yang, P., Ning, Y., Neal, T.J. et al. (2019). *Chem. Sci.* 10: 4200.
219 Chen, X., Liu, L., Huo, M. et al. (2017). *Angew. Chem. Int. Ed.* 56: 16541.
220 Zhou, D., Dong, S., Kuchel, R.P. et al. (2017). *Polym. Chem.* 8: 3082.
221 Lovett, J.R., Warren, N.J., Ratcliffe, L.P.D. et al. (2015). *Angew. Chem. Int. Ed.* 54: 1279.
222 Lovett, J.R., Warren, N.J., Armes, S.P. et al. (2016). *Macromolecules* 49: 1016.
223 Penfold, N.J.W., Lovett, J.R., Warren, N.J. et al. (2016). *Polym. Chem.* 7: 79.
224 Rieger, J., Zhang, W., Stoffelbach, F., and Charleux, B. (2010). *Macromolecules* 43: 6302.
225 Qiao, Z., Qiu, T., Liu, W. et al. (2017). *Polym. Chem.* 8: 3013.
226 Chernikova, E.V., Serkhacheva, N.S., Smirnov, O.I. et al. (2016). *Polym. Sci. Ser. B Polym. Chem.* 58: 629.
227 Serkhacheva, N.S., Smirnov, O.I., Tolkachev, A.V. et al. (2017). *RSC Adv.* 7: 24522.
228 Mellot, G., Beaunier, P., Guigner, J.-M. et al. (2019). *Macromol. Rapid Commun.* 40: 1800315.
229 Cao, M., Nie, H., Hou, Y. et al. (2019). *Polym. Chem.* 10: 403.
230 Gao, C., Li, S., Li, Q. et al. (2014). *Polym. Chem.* 5: 6957.
231 Gao, C., Wu, J., Zhou, H. et al. (2016). *Macromolecules* 49: 4490.
232 Qu, Y., Wang, S., Khan, H. et al. (2016). *Polym. Chem.* 7: 1953.
233 Zhang, Y., Cao, M., Han, G. et al. (2018). *Macromolecules* 51: 5440.
234 Zhang, Y., Guan, T., Han, G. et al. (2019). *Macromolecules* 52: 718.
235 Wang, X., Figg, C.A., Lv, X. et al. (2017). *ACS Macro Lett.* 6: 337.
236 Zhang, X., Boissé, S., Bui, C. et al. (2012). *Soft Matter* 8: 1130.
237 Huo, M., Song, G., Zhang, J. et al. (2018). *ACS Macro Lett.* 7: 956.
238 Tritschler, U., Pearce, S., Gwyther, J. et al. (2017). *Macromolecules* 50: 3439.
239 Boissé, S., Rieger, J., Di-Cicco, A. et al. (2009). *Macromolecules* 42: 8688.
240 Kang, Y., Pitto-Barry, A., Maitland, A., and O'Reilly, R.K. (2015). *Polym. Chem.* 6: 4984.
241 Kang, Y., Pitto-Barry, A., Willcock, H. et al. (2015). *Polym. Chem.* 6: 106.
242 Mellot, G., Guigner, J.-M., Jestin, J. et al. (2018). *Macromolecules* 51: 10214.

243 Mellot, G., Guigner, J.-M., Bouteiller, L. et al. (2019). *Angew. Chem. Int. Ed.* 58: 3173.
244 Chenal, M., Rieger, J., Philippe, A., and Bouteiller, L. (2014). *Polymer* 55: 3516.
245 Blanazs, A., Verber, R., Mykhaylyk, O.O. et al. (2012). *J. Am. Chem. Soc.* 134: 9741.
246 Wang, X., Zhou, J., Lv, X. et al. (2017). *Macromolecules* 50: 7222.
247 Fielding, L.A., Lane, J.A., Derry, M.J. et al. (2014). *J. Am. Chem. Soc.* 136: 5790.
248 Derry, M.J., Mykhaylyk, O.O., and Armes, S.P. (2017). *Angew. Chem. Int. Ed.* 56: 1746.
249 Canning, S.L., Neal, T.J., and Armes, S.P. (2017). *Macromolecules* 50: 6108.
250 Guragain, S. and Perez-Mercader, J. (2018). *Polym. Chem.* 9: 4000.
251 Ratcliffe, L.P.D., Couchon, C., Armes, S.P., and Paulusse, J.M.J. (2016). *Biomacromolecules* 17: 2277.
252 Deng, R., Derry, M.J., Mable, C.J. et al. (2017). *J. Am. Chem. Soc.* 139: 7616.
253 Deng, R., Ning, Y., Jones, E.R. et al. (2017). *Polym. Chem.* 8: 5374.
254 Ye, Q., Huo, M., Zeng, M. et al. (2018). *Macromolecules* 51: 3308.
255 Bagheri, A., Boyer, C., and Lim, M. (2019). *Macromol. Rapid Commun.* 40: 1800510.
256 Xu, S., Ng, G., Xu, J. et al. (2017). *ACS Macro Lett.* 6: 1237.
257 Sobotta, F.H., Hausig, F., Harz, D.O. et al. (2018). *Polym. Chem.* 9: 1593.
258 Karagoz, B., Yeow, J., Esser, L. et al. (2014). *Langmuir* 30: 10493.
259 Tan, J., Sun, H., Yu, M. et al. (2015). *ACS Macro Lett.* 4: 1249.
260 Mable, C.J., Gibson, R.R., Prevost, S. et al. (2015). *J. Am. Chem. Soc.* 137: 16098.
261 Xu, X.-F., Pan, C.-Y., Zhang, W.-J., and Hong, C.-Y. (2019). *Macromolecules* 52: 1965.
262 Karagoz, B., Boyer, C., and Davis, T.P. (2014). *Macromol. Rapid Commun.* 35: 417.
263 Blackman, L.D., Varlas, S., Arno, M.C. et al. (2017). *ACS Macro Lett.* 6: 1263.
264 Canton, I., Warren, N.J., Chahal, A. et al. (2016). *ACS Cent. Sci.* 2: 65.
265 Garni, M., Wehr, R., Avsar, S.Y. et al. (2019). *Eur. Polym. J.* 112: 346.
266 Varlas, S., Blackman, L.D., Findlay, H.E. et al. (2018). *Macromolecules* 51: 6190.
267 Blackman, L.D., Varlas, S., Arno, M.C. et al. (2018). *ACS Cent. Sci.* 4: 718.
268 Zhang, X., Cardozo, A.F., Chen, S. et al. (2014). *Chem. Eur. J.* 20: 15505.
269 Cardozo, A.F., Julcour, C., Barthe, L. et al. (2015). *J. Catal.* 324: 1.
270 Chen, S., Cardozo, A.F., Julcour, C. et al. (2015). *Polymer* 72: 327.
271 Lobry, E., Cardozo, A.F., Barthe, L. et al. (2016). *J. Catal.* 342: 164.
272 Pontes da Costa, A., Nunes, D.R., Tharaud, M. et al. (2017). *ChemCatChem* 9: 2167.
273 Wang, F., Tang, J., Liu, H. et al. (2019). *Mater. Chem. Front.* 3: 356.
274 Thompson, K.L., Chambon, P., Verber, R., and Armes, S.P. (2012). *J. Am. Chem. Soc.* 134: 12450.
275 Thompson, K.L., Mable, C.J., Cockram, A. et al. (2014). *Soft Matter* 10: 8615.
276 Thompson, K.L., Fielding, L.A., Mykhaylyk, O.O. et al. (2015). *Chem. Sci.* 6: 4207.
277 Zhang, Q., Wang, C., Fu, M. et al. (2017). *Polym. Chem.* 8: 5474.

278 Zhang, W.-J., Hong, C.-Y., and Pan, C.-Y. (2014). *J. Mater. Chem. A* 2: 7819.
279 Ning, Y., Whitaker, D.J., Mable, C.J. et al. (2018). *Chem. Sci.* 9: 8396.
280 Ning, Y., Han, L., Derry, M.J. et al. (2019). *J. Am. Chem. Soc.* 141: 2557.
281 Charleux, B., D'Agosto, F., Inoubli, R., and Magnet, S. (2015). Viscosifiant a base de particules polymeriques filamenteuses. WO2015011412A1, filed 23 July 2014 and issued 29 January 2015. Universite Claude Bernard Lyon 1, Centre National de la Recherche Scientifique. Arkema France, Fr.
282 Pham, B.T.T., Nguyen, D., Huynh, V.T. et al. (2018). *Langmuir* 34: 4255.
283 Albiges, R., Klein, P., Roi, S. et al. (2017). *Polym. Chem.* 8: 4992.
284 Upadhyaya, L., Semsarilar, M., Fernandez-Pacheco, R. et al. (2016). *Polym. Chem.* 7: 1899.
285 Luppi, L., Babut, T., Petit, E. et al. (2019). *Polym. Chem.* 10: 336.
286 Upadhyaya, L., Egbosimba, C., Qian, X. et al. (2019). *Macromol. Rapid Commun.* 40: 1800333.
287 Cockram, A.A., Bradley, R.D., Lynch, S.A. et al. (2018). *React. Chem. Eng.* 3: 645.
288 Zaquen, N., Azizi, W.A.A.W., Yeow, J. et al. (2019). *Polym. Chem.* 10: 2406.
289 Zaquen, N., Yeow, J., Junkers, T. et al. (2018). *Macromolecules* 51: 5165.

16

RAFT-Functional End Groups: Installation and Transformation

Andrew B. Lowe and Elena Dallerba

Curtin University, School of Molecular and Life Sciences (MLS), Kent Street, Bentley, Perth, Western Australia 6102, Australia

16.1 Introduction

As detailed in previous chapters, reversible addition–fragmentation chain transfer (RAFT) [1–4] is a robust and versatile example of a reversible deactivation radical polymerization (RDRP) that operates on the principle of degenerative chain transfer mediated by certain thiocarbonylthio compounds. Such thiocarbonylthio compounds are referred to as RAFT agents or more simply as chain transfer agents (CTAs). The most common examples of such RAFT agent families are dithioesters (a) (typically dithiobenzoates), trithiocarbonates (b), xanthates (c), and dithiocarbamates (d) (Figure 16.1).

The relevant structural features of these mediating agents are the so-called R- and Z-groups. The former is the initiating fragment while the latter controls the bulk reactivity of a RAFT agent – it essentially determines to which of the above four general species a particular RAFT agent belongs. We will not discuss the design, synthesis, and activity of the many reported RAFT agents in this chapter as this is highlighted in detail elsewhere [5]. However, we note two important features, one of which is pertinent in the context of this chapter: (i) dithioesters (a) and trithiocarbonates (b) are the most versatile and widely employed families of RAFT agents, while in general, the use of xanthates (c) and dithiocarbamates (d) is commonly limited to particular monomer classes and especially vinyl esters and vinyl amides and (ii) RAFT agents are often intensely coloured – red, orange, purple, and yellow are common for dithioesters and trithiocarbonates. This colour, a result of the C=S bond, is conferred on the resulting (co)polymer as a result of the underlying RAFT mechanism, vide infra.

From a practical viewpoint, a RAFT (co)polymerization is no more challenging to conduct than a traditional radical (co)polymerization. In its basic form, a RAFT (co)polymerization is merely a conventional radical polymerization performed in the presence of an added thiocarbonylthio compound. As such, the RAFT mechanism involves the same initiation, propagation, and termination steps as a

RAFT Polymerization: Methods, Synthesis and Applications, First Edition.
Edited by Graeme Moad and Ezio Rizzardo.

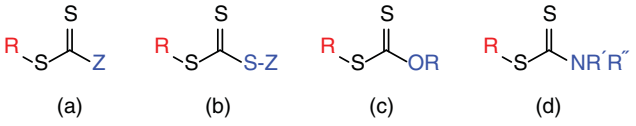

Figure 16.1 General chemical structure of the four main classes of RAFT agent. (a) Dithioesters, (b) trithiocarbonates, (c) xanthates, and (d) dithiocarbamates.

conventional radical (co)polymerization but with degenerative chain transfer steps involving radicals and the RAFT agent superimposed on the underlying chain mechanism (Scheme 16.1). The finer details associated with the RAFT mechanism are discussed elsewhere in this book.

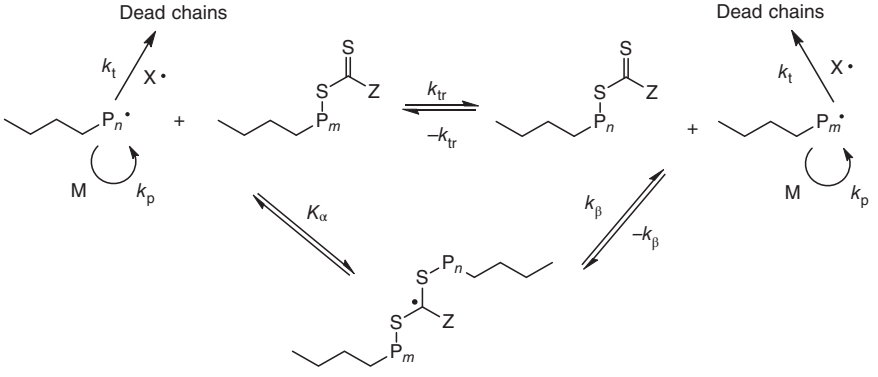

Scheme 16.1 The RAFT process operating in the main equilibrium stage highlighting the transfer of thiocarbonylthio groups between the propagating chain ends.

The product of a RAFT (co)polymerization, Scheme 16.2 (as with all RDRP processes), contains very specific α and ω end groups, the exact nature of which is determined by the choice of RAFT-mediating agent employed in the (co)polymer synthesis. The produced (co)polymer, in a typical synthesis, will, at the α chain end, contain initiating groups whose structure is R, assuming that the R-group of the CTA initiates the majority of polymer chains and not primary radicals formed from the decomposition of added initiator (I). In the case where the primary radicals formed from I have the same structure as R, for example, when 2,2′-azobis(2-methylpropionitrile) (AIBN) is used in conjunction with a CTA such as 2-cyanopropan-2-yl benzodithioate, then all polymer chains should have

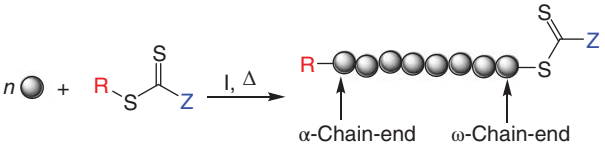

Scheme 16.2 RAFT polymerization highlighting the presence of functionality at the α and ω termini.

identical initiating groups. For the ω chain end, assuming there are no undesirable side reactions, each (co)polymer chain will contain a thiocarbonylthio-Z-functional group. In essence, under ideal conditions, a small-molecule RAFT CTA is converted to a macromolecular RAFT agent by what amounts to monomer insertion between the C—S bond.

Several factors motivated the historical development of end group chemistries on RAFT-prepared (co)polymers. The first open literature report of RAFT came in late 1998 [6]; the 1990s and early 2000s were an exciting time in synthetic chemistry and not just polymer chemistry. In 2001, Kolb et al. published their seminal paper detailing 'click' chemistry as a means of preparing new compounds with a high degree of reliability and selectivity from readily available and cheap reagents employing a handful of well-developed highly efficient reactions [7]. While arguably aimed, at least initially, at researchers working on the synthesis of highly complex molecules such as natural products or in the field of drug discovery and development, the general 'click' approach to synthesis was quickly adopted, and developed, by the polymer chemistry community. It was recognized early in the history of modern 'click' chemistry that the reactions detailed by Kolb et al. could help address a long-standing problem in polymer science and specifically the issue of non-quantitative chemical modification of preformed (co)polymers. Although this may not seem like a particularly important issue on first inspection, it is worth remembering that all synthetic polymers possess a molecular weight distribution and, in the case of copolymers, a superimposed compositional distribution. Non-quantitative modification of a pre-prepared (co)polymer superimposes a second, or third, functionality distribution. In effect, the 'product' is highly heterogeneous.

Before the late 1980s, prior to the development and application of RDRP processes such as stable radical polymerization (SRP), best exemplified by nitroxide-mediated polymerization (NMP), and atom transfer radical polymerization (ATRP) in the early 1990s, the issue of specific functional group incorporation into (co)polymers could be tackled via the application of protecting group chemistry (especially in the case of (co)polymers prepared by more traditional 'living' processes such as anionic polymerization or group transfer polymerization [GTP]) or by the copolymerization of an appropriately functionalized monomer if compatible with the polymerization process. However, protecting group chemistry still suffers from limitations in the context of synthetic polymer chemistry, and at that time, many functional monomers were simply incompatible with controlled polymerization processes of the day and thus were only generally amenable to radical (co)polymerization. The development of the RDRP processes, first NMP, then ATRP, and later RAFT, largely eliminated the functional group compatibility issue while still facilitating the preparation of (co)polymers with well-defined molecular characteristics. However, while the RDRP processes are highly functional group tolerant, direct (co)polymerization as a route to instil specific functional groups commonly still requires the synthesis of a functional monomer. 'Click' chemistry, it seemed, offered the opportunity synthetic polymer chemists had long searched for – the ability to generate libraries of novel materials from one reactive parent

material, containing a specific functionality, employing highly efficient reactions. The disclosure of RAFT in late 1998 coupled with the 'click' approach to chemical synthesis in 2001 led to a renaissance in synthetic polymer chemistry. As a result, the archetypal 'click' reaction, the Cu(I)-catalyzed coupling between an alkyne and an azide [8–10], was quickly applied in synthetic polymer chemistry and especially in the field of RAFT (co)polymerization, vide infra. The demonstrated utility of this chemistry subsequently motivated other polymer chemists to examine and develop additional 'click' reactions specifically for the chemical modification of (co)polymers, and today, there is an impressive, and ever-growing, toolbox of 'click', or 'click'-like, reactions that have become a near-ubiquitous feature in modern synthetic (polymer) chemistry.

As noted above, (co)polymers prepared by RAFT can be viewed as polymeric RAFT agents. From an application perspective, this may be an undesirable structural feature. This is because (co)polymers prepared by RAFT are inherently coloured due to the presence of the C=S bond, albeit typically not as intensely as the corresponding small-molecule RAFT agents. The highly reactive nature of the terminal thiocarbonylthio group can likewise be perceived to be problematic because it can result in the undesirable release of sulfur-containing compounds, which can be highly malodorous. Both these aspects were, in the early days of RAFT polymerization, viewed by many as clear disadvantages of the technique and features that would likely limit its large-scale commercial adoption and almost certainly its use in bio-applications. Not surprisingly, these two features prompted researchers to explore methods for efficiently removing the thiocarbonylthio group at the ω chain end in RAFT-prepared polymers and thus the colour and any potential degradation products. While initially motivated by the perceived disadvantages noted above, research in this area of RAFT end group cleavage/removal unwittingly led to the subsequent development of a range of approaches for not just removing the end groups but for the further modification and application of RAFT (co)polymers in novel (bio-)applications.

If we revisit the generic structure of a RAFT-prepared (co)polymer shown in Scheme 16.2, it is evident that in the context of end group transformations, we have three options. We can exploit specific functional groups incorporated as part of the R-group, i.e. the initiating fragment at the α terminus; we can utilize chemical transformations of the thiocarbonylthio ω end group, or we can use both. In Sections 16.2 and 16.3, we will highlight how researchers have employed both α and ω end group chemistries as a means of generating new and interesting materials, although we state at the outset that transformations/modifications at the ω chain end are currently the preferred approach given the broader range of chemistries available. This chapter is not intended to be an exhaustive review of the field of RAFT end group modification; many excellent reviews are available that deal with this topic in more detail [11–15]. However, hopefully, this chapter will aid those new to the field, as well as current practitioners, to gain an appreciation for the historical development of certain aspects of RAFT (co)polymerization and the range of chemistries that are available for the introduction of specific terminal functional groups by pre- and post-polymerization approaches.

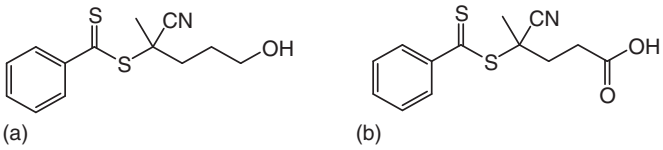

Figure 16.2 Chemical structures of (a) 2-cyano-5-hydroxypentan-2-yl benzodithioate (CHPB) and (b) 4-cyano-4-((phenylcarbonothioyl)thio)pentanoic acid (CPTP).

16.2 Functionalization and Transformation of RAFT Polymers via the R-group

The potential to exploit functional groups within the R-group fragment of RAFT CTAs, and thus at the α chain end of (co)polymers, was evident in the first literature report concerning RAFT, although not explicitly stated [6]. Of the eight dithioesters described in this original paper, two (Figure 16.2) contained functional groups with the potential to serve as reactive handles for further modification.

These two examples were, presumably, included to highlight not only the broader functional group tolerance of the RAFT process but to demonstrate the impressive range of conditions under which RAFT polymerization could be performed. For example, the sodium salt of 4-cyano-4-((phenylcarbonothioyl)thio)pentanoic acid (CPTP), CPTP-Na, was reported to facilitate the homogeneous aqueous polymerization of sodium styrenesulfonate in a controlled manner. It is fair to state that from a historical perspective, this single example inspired an extensive research program focused around homogeneous aqueous RAFT with significant contributions coming from the groups of McCormick [16–30] and others [31–39]. It is also likely the reason that of all the functional groups that can be built into RAFT agents, those containing $-CO_2H$ groups, have attracted particular attention, especially in the 2000s [5, 11, 40–48]. The key point here, however, is that one clear, and often straightforward, approach for the introduction of specific functional groups at the α terminus is via the application of an R-group-functionalized CTA [49–55]. The only criteria are that the target functional group be compatible firstly with the CTA, and more specifically the thiocarbonylthio functional group, and secondly be inert under RAFT polymerization conditions. This does, of course, preclude certain functional groups, thiols, and 1° and 2° amines, for example, but for the most part, desirable functionality can be built directly into the R-group structure [1–5].

As noted earlier, the interest in RAFT in the late 1990s and early 2000s was spurred, in part, by the introduction of the concept of the 'click' chemistry approach to synthesis. Many groups globally quickly explored opportunities for combining RAFT polymerization with the gold standard 'click' reaction, the Cu(I)-catalyzed reaction between an alkyne and an azide [10, 56, 57] (Scheme 16.3).

The main approach adopted by research groups involved the incorporation of azide or yne functionality into the R-group of RAFT CTAs. Recalling that provided the desirable functionality is compatible with the overall process of CTA synthesis and polymerization, then this represents a very powerful, and direct, route for instilling functionality specifically at the α chain end. The azide functionality is

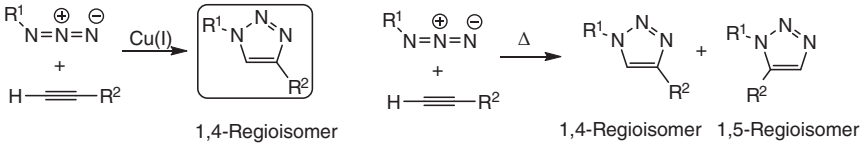

Scheme 16.3 The regioselective Cu(I)-catalyzed reaction of an azide with an alkyne and the non-selective thermal 1,3-dipolar cycloaddition products.

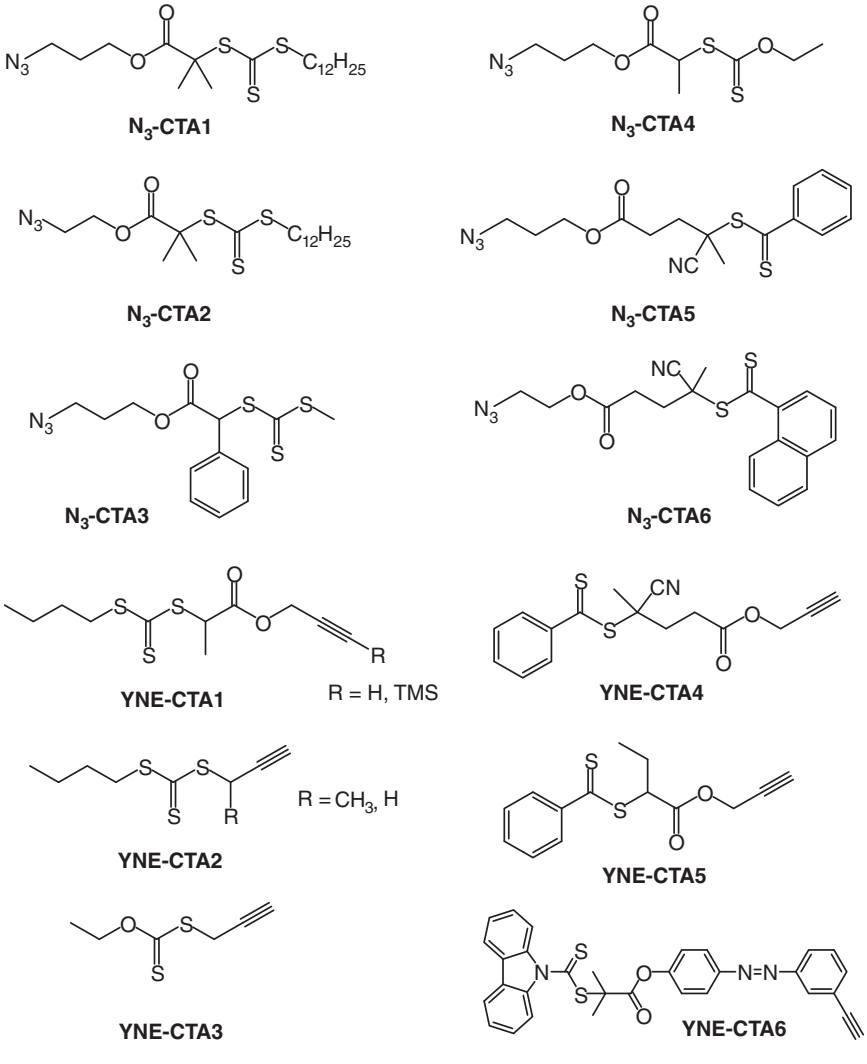

Figure 16.3 Representative examples of RAFT CTAs in which the R-group fragment contains alkyne or azide functionality.

compatible (note: care should be taken when handling organic azides [58]), the yne slightly less so given its susceptibility to radical addition but providing care is taken can be readily incorporated directly via a functional CTA. Figure 16.3 shows examples of R-group-functionalized azide and alkyne RAFT CTAs, including trithiocarbonates (**N_3-CTA1**, **N_3-CTA2**, **N_3-CTA3**, **YNE-CTA1**, and **YNE-CTA2**), dithioesters (**N_3-CTA5**, **N_3-CTA6**, **YNE-CTA4**, and **YNE-CTA5**), xanthates (**N_3-CTA4** and **YNE-CTA3**), and dithiocarbamates (**YNE-CTA6**) [14]. It is needless to state, that with such RAFT agents available, the synthetic opportunities are extensive. For example, each of the compounds shown in Figure 16.3 can be further modified by *pre-polymerization* to generate new functional RAFT agents or exploited *post-polymerization* to prepare a range of new species.

For example, Akeroyd et al. [59] reported the synthesis and application of novel triazole-functional trithiocarbonates and xanthates prepared from precursor yne-functional CTAs, including **YNE-CTA2** and **YNE-CTA3** (Figure 16.3). All RAFT agents were reported to be effective in mediating the controlled polymerization of monomers, including styrene, *n*-butyl acrylate, vinyl acetate, and *N*-vinylpyrrolidone. The general synthetic approach adopted is shown in Figure 16.4 and examples of prepared RAFT agents are given below. A similar pre-polymerization approach was reported by Puttick et al. [60] in which a yne-functional trithiocarbonate was reacted with an azido alkyl imidazolium bromide, yielding a novel room temperature ionic liquid CTA.

Cu(I)-mediated alkyne-azide coupling is not the only 'click' process that has been employed in the post-polymerization modification of RAFT polymer R-groups. Stamenović et al. [61] reported the synthesis, application, and modification of norbornenyl-functional xanthate, dithiobenzoate, and trithiocarbonate RAFT agents (Figure 16.5). The polymerization of styrene, methyl acrylate, 1-ethoxyethyl

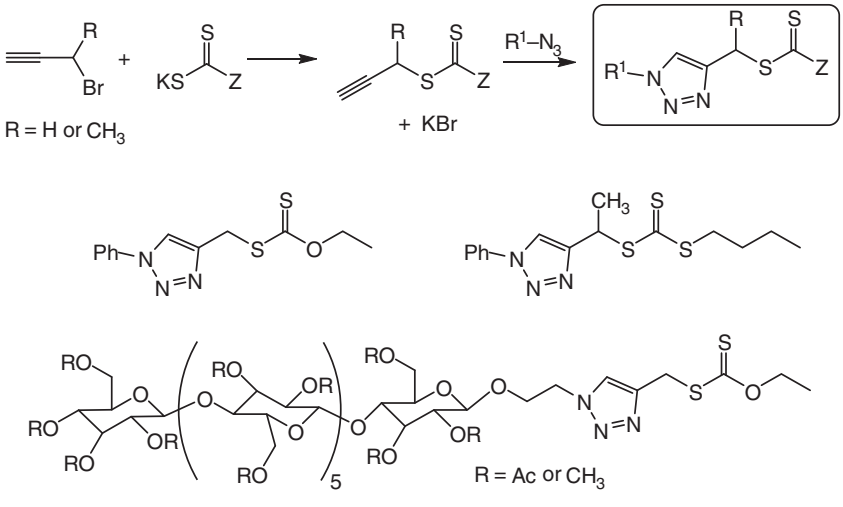

Figure 16.4 The synthesis of triazole functional RAFT agents from precursor yne-functional RAFT CTAs and representative examples of CTAs reported.

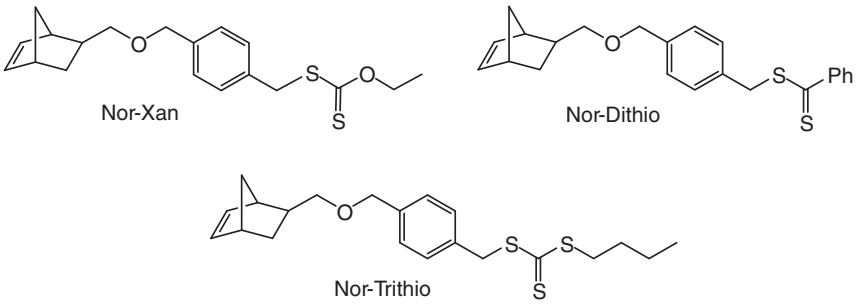

Figure 16.5 Chemical structures of norbornenyl-functional RAFT agents.

acrylate, and vinyl acetate proceeded in a controlled manner, provided that monomer conversions were limited to avoid interference from the norbornenyl group. The motivation for introducing a norbornenyl reactive species at the α terminus is based on the well-known, unusually high, reactivity of such groups in radical thiol–ene reactions [62–64].

For example, polystyrene prepared with **Nor-Trithio** was reacted with 3-mercaptopropionic acid, benzyl mercaptan, and dodecanethiol (1–5 equiv based on terminal ene groups) in the presence of 2,2-dimethoxy-2-phenylacetophenone as a UV-active photoinitiator. In all cases, the terminal groups could be quantitatively modified within 15 minutes as judged by NMR spectroscopy. Given the large number of commercially available thiols coupled with the ability to introduce alternative ene species in the R-group fragment, it is evident that this approach is highly versatile as a route to α-functional materials. In a complementary approach employing thiol–yne chemistry, Fontaine and coworkers [65] reported the synthesis of α,ω-functionalized poly(*N*-isopropylacrylamide) via the sequential approach outlined in Scheme 16.4. Homopolymerization of *N*-isopropylacrylamide with the yne-functional trithiocarbonate 2-cyano-5-oxo-5-(prop-2-yn-1-ylamino)pentan-2-yl dodecyltrithiocarbonate yielded a well-defined polymer with unimodal molecular weight distributions provided conversions were limited. Treatment of the poly(*N*-isopropylacrylamide) homopolymer with an excess of AIBN [66] resulted in the removal of the trithiocarbonate end group, with it being replaced by a

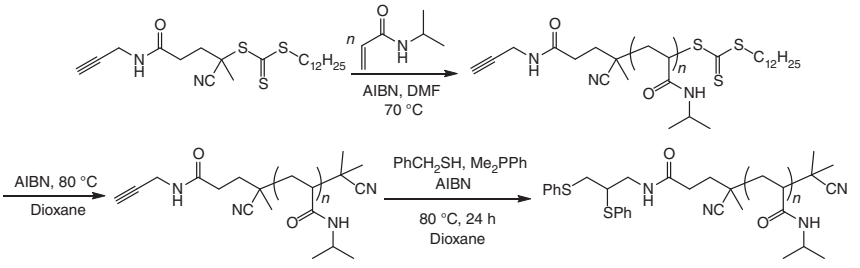

Scheme 16.4 The synthesis of α,ω-end-functionalized poly(*N*-isopropylacrylamide) via sequential AIBN-mediated trithiocarbonate end group removal, followed by radical-mediated thiol–yne modification of the α-yne group.

cyanoisopropyl group. In the second step, the ω-modified polymer was treated with benzyl mercaptan, in the presence of AIBN, under conditions to affect a radical-mediated double hydrothiolation of the α-yne group yielding the dithioether product. The authors noted that while the first step was essentially quantitative, the second, thiol–yne, reaction gave, at best, 40% conversion. Although not discussed, it seems that a number of yne groups could very well have been lost during the first step. The same product was also reported to be accessible in a one-pot process.

One particularly powerful and versatile method for the functionalization of the R-group fragment involves the use of activated ester chemistry and, in particular, the use of pentafluorophenylesters [67, 68], although *N*-hydroxysuccinimide derivatives have also been employed [69, 70]. Such chemistries have been used to prepare intermediate RAFT agents that are subsequently modified with an appropriate amine-containing species, including proteins [71], employed directly as polymerization mediators and modified post-polymerization [72, 73], or used in conjunction with other facile conjugation chemistries or both [74–78].

Du Prez and coworkers have worked extensively with the thiolactone-functional species in various applications in monomer/polymer synthesis and modification [79–82]. Within this body of work, Stamenović et al. [83] reported the synthesis and application of a thiolactone R-group-functionalized RAFT CTA that was demonstrated to be useful for the synthesis of cyclic polymers via intramolecular disulfide formation between the α- and ω-thiol groups (Scheme 16.5).

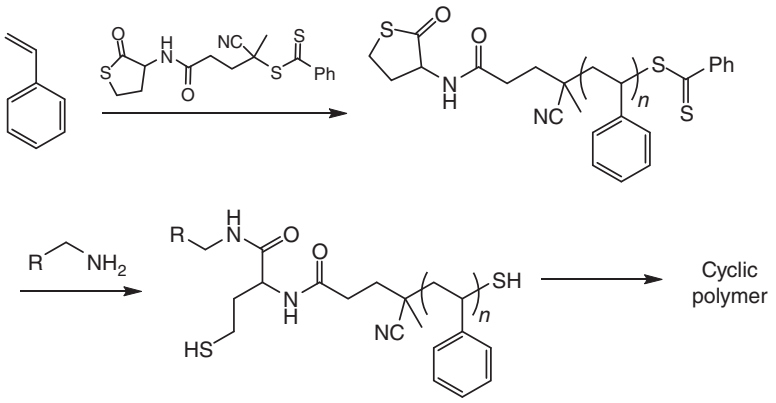

Scheme 16.5 The synthesis of cyclic polystyrene via intramolecular disulfide formation via one-pot aminolysis of α-thiolactone groups and ω-thiocarbonylthio species.

Later in the chapter, we will highlight the routes available for end group functionalization employing disulfide chemistry involving thiols derived from cleaved thiocarbonylthio groups. However, such disulfide chemistry can also be employed as part of functional R-groups in RAFT CTAs [84–86]. For example, Evgrafova et al. reported the synthesis of protein/thermoresponsive polymer conjugates employing a thiol exchange reaction between a pyridyl disulfide group at the α-terminus (derived from the disulfide-functional R-group) in diethylene glycol acrylate and the parathyroid peptide hormone (PTH) (Scheme 16.6) [85].

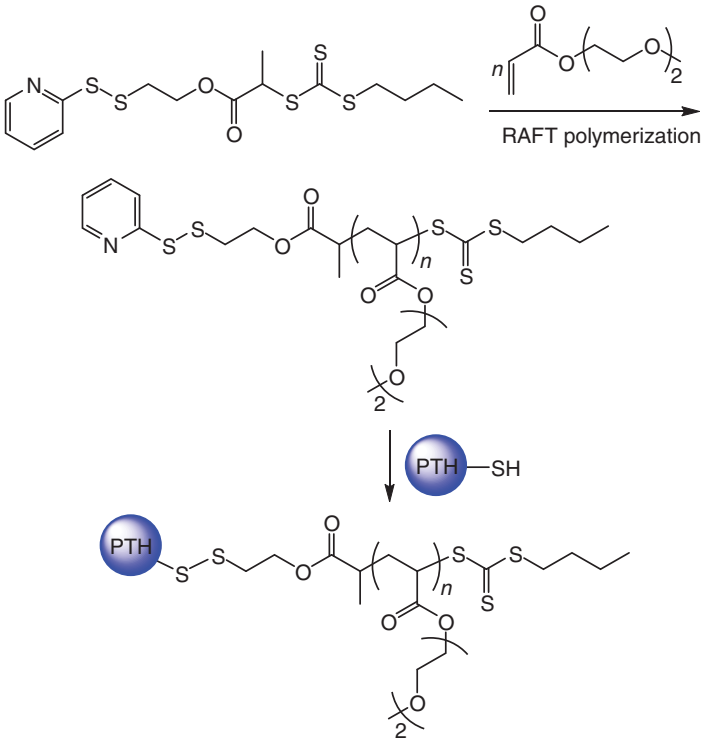

Scheme 16.6 Conjugation of the parathyroid peptide hormone at the α-terminus of a RAFT-prepared polymer via a disulfide exchange reaction on a functional RAFT CTA R-group containing pyridyl disulfide.

16.3 Thiocarbonylthio End Group Removal and Transformation

As noted in Section 16.1, under certain circumstances, it may be necessary, or at least desirable, to remove the thiocarbonylthio end group in RAFT-prepared (co)polymers. The main reasons for this are to remove the colour inherently associated with the products of a RAFT polymerization, elimination of possible sulfur-based degradation products, which may be toxic or malodorous, or to negate the inherent high reactivity of thiocarbonylthio groups for specific applications and especially those that are bio-based. When we present examples in which the thiocarbonylthio group is located at the ω chain terminus, we note that these groups are not necessarily always located at a chain end. However, the chemistries we will highlight are equally applicable to those materials in which the thiocarbonylthio groups may be present mid-chain in linear (co)polymers or, for example, in the core of certain star (co)polymers.

There are many available approaches for the removal or modification of thiocarbonylthio groups in RAFT-prepared polymers. All of the known methods have their roots in small-molecule organic chemistry and as such are, for the most part, well

understood and developed. At the top level, we can classify two general approaches for modifying RAFT thiocarbonylthio end groups:

1) Complete desulfurization. Such an approach removes the thiocarbonylthio group in its entirety and is accomplished via one of several radical-based modification pathways.
2) Chemical modification of the thiocarbonylthio group in which the 'problematic' end group is cleaved to yield a macromolecular thiol or converted to a different S-based species. In the case of end group cleavage, the resulting macromolecular thiol (or thiolate) is commonly captured by one of a variety of available chemistries. This is arguably the most versatile and widely reported approach and can yield many different types of new end-functional materials.

16.3.1 Desulfurization of RAFT (Co)Polymers

16.3.1.1 Thermolysis

The total removal of S-containing species from RAFT polymers can be accomplished by several radical-based routes (Figure 16.6). Executionally, the easiest method involves thermolysis – simply heating the (co)polymer. This can be performed on isolated materials or via a flow process [87]. However, the extent, purity of the product, and mechanism by which end group removal occurs are dependent on the monomer and the nature of the thiocarbonylthio species. This was evident

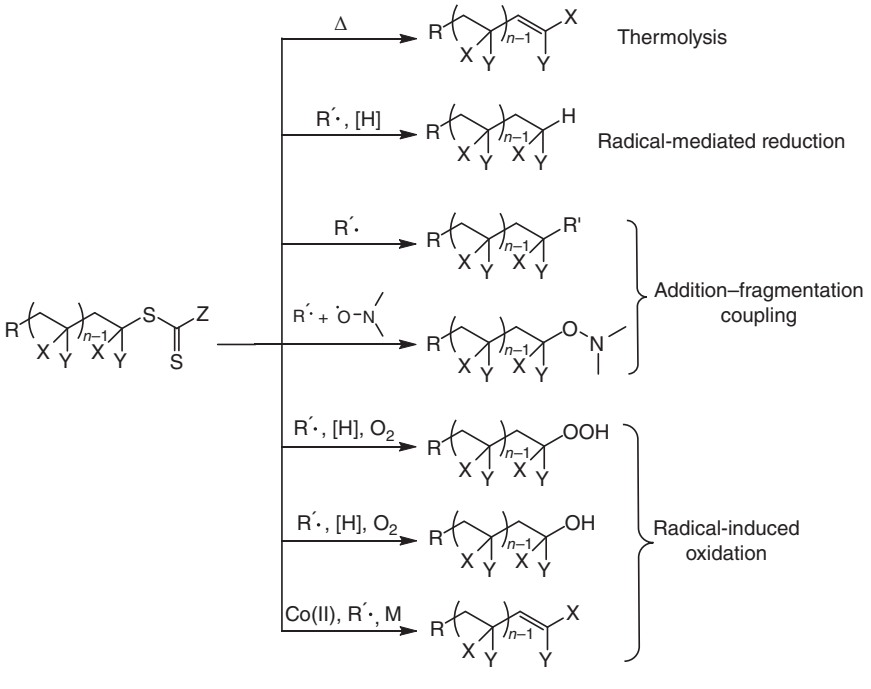

Figure 16.6 General approaches for the desulfurization of RAFT thiocarbonylthio end groups.

even in the earliest reports from Postma et al. in their studies on trithiocarbonate and xanthate end group removal in polymers prepared with phthalimidomethyl R-group-functional CTAs [88, 89]. Researchers from the same group have also reported on the thermolysis of RAFT-prepared poly(methyl methacrylate) (PMMA) [90]. The products obtained were highly dependent on the RAFT agent employed in polymer synthesis. For PMMA prepared with a trithiocarbonate CTA (2-cyanoprop-2-yl methyl trithiocarbonate), end group removal was proposed to occur via homolytic cleavage of the PMMA—S bond, followed by depolymerization, a process that continued until radical annihilation (Scheme 16.7a).

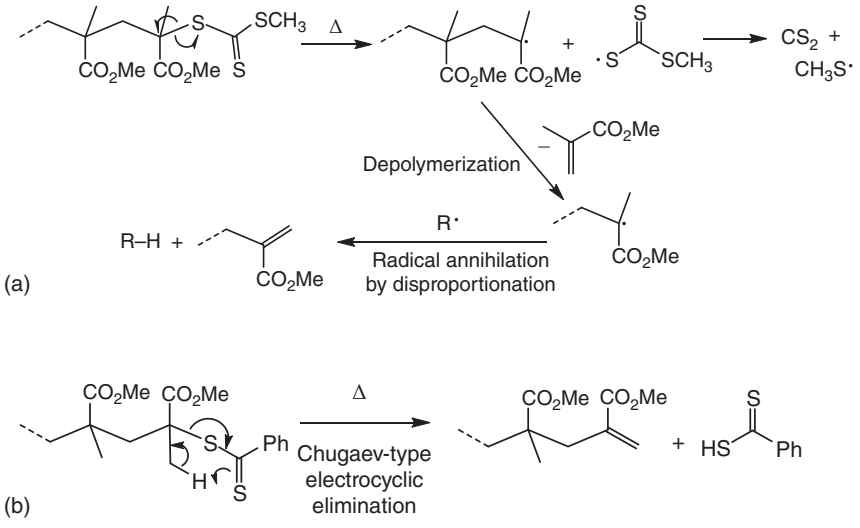

Scheme 16.7 Desulfurization pathways in poly(methyl methacrylate) prepared with a trithiocarbonate CTA (a) and with a dithioester (b).

For PMMA prepared with a dithiobenzoate CTA, elimination was proposed to proceed by a concerted intramolecular process analogous to the Chugaev reaction [91] (Scheme 16.7b). In general, thermolysis of dithiobenzoate-prepared (co)polymers is cleaner and yields macromonomer products whose molecular weight and molecular weight distribution are comparable to the parent polymer, whereas degradation products are also observed with PMMA prepared with a trithiocarbonate. Similar findings were reported by Bressy et al. with silylated methacrylic homopolymers [92]. More recently, Stace et al. [93] examined the effect of the Z-group and nature of the macro-R-group in 'switchable' RAFT agents and thermal desulfurization. Although differences were observed between various MAMs (more activated monomers), the principle finding in this study related to the significantly higher thermolysis temperatures required for polymers derived from LAMs (less-activated monomers) such as vinyl acetate vs. those derived from MAMs. Finally, we note that the thermal stability of a range of small-molecule RAFT agents has also been examined by Zhou et al. [94].

16.3.1.2 Radical-Mediated Reduction

Complete desulfurization of RAFT polymers can be achieved by radical-mediated reduction. Inspired by the Barton–McCombie reaction for the deoxygenation of secondary alcohols [95], such radical-mediated reduction has been applied to other thiocarbonylthio species including RAFT agents [96]; not surprisingly, the general approach has also been successfully applied to the complete removal of thiocarbonylthio end groups in RAFT-prepared (co)polymers [11, 97].

The general process is based on the fundamental RAFT addition–fragmentation mechanism (Scheme 16.8). The reaction involves the addition of a radical (X·) to the thiocarbonyl group of the RAFT-prepared (co)polymer (**1**) generating an intermediate (**2**), which fragments to provide a new thiocarbonylthio compound (**3**) and the propagating radical (**4**). Reaction of the propagating radical (**4**) with a H atom donor gives the final product, P_n–H, with the thiocarbonylthio group being replaced with hydrogen.

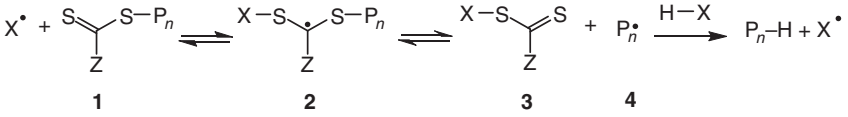

Scheme 16.8 General mechanism for the radical-mediated reduction of a RAFT thiocarbonylthio end group.

Various side reactions can occur, including 'normal' termination reactions. The intermediate (**2**) and the propagating radical (**4**) can react with other radical species such as initiator-derived radicals, transfer agent-derived radicals, and propagating radicals.

Tributylstannane, Bu_3SnH, has been employed extensively as a H-donor source in radical-mediated reductions on RAFT-prepared (co)polymers [98–100]. However, because of the toxicity of stannane and stannane-derived by-products, alternative H-donors have also been investigated. For example, Chong et al. [97] investigated the influence of H-donor on polymers with dithiobenzoate and trithiocarbonate end groups. They reported that the use of toluene and toluene/2-propanol as H-donors in conjunction with dibenzoyl peroxide or lauroyl peroxide as initiators resulted in complete end group removal, but bimodal molecular weight distributions of poly(*n*-butyl acrylate) and polystyrene were observed. This was attributed to the coupling of propagating radicals (**4**) or to termination reactions involving intermediate (**2**).

Silanes have also been investigated as H-donors in radical-mediated reduction reactions [101]. Chong et al. reported that a bimodal molecular weight distribution was observed when tris(trimethylsilyl)silane was employed as a H-donor in radical-mediated reduction of polystyrene terminated with dodecyltrithiocarbonate chain ends [97]. They concluded that radical-mediated reduction of RAFT end groups is more effective with more active H-donor species, with the most effective being tributylstannane, followed by *N*-ethylpiperidine hypophosphite (EPHP) and tris(trimethylsilyl)silanes, followed by 2-propanol, and the least effective being toluene.

Although not as effective as Bu_3SnH, hypophosphite salts, such as EPHP, do serve as convenient alternatives to both stannanes and silanes given their reduced toxicity and aqueous solubility that can aid significantly in work-up. In fact, EPHP has been shown to be effective for the removal of dithioester, trithiocarbonate, and dithiocarbamate end groups on different RAFT-prepared (co)polymers [102–105]. A further indication of the advantages of using EPHP is the fact that it is commonly employed to reduce end groups in polymers specifically targeted for bioapplications [106–108].

More recently, there has been interest in photo-induced RAFT end group reduction [109–111]. For example, Carmean and coworkers described the efficient, catalyst-free, UV-mediated removal of thiocarbonylthio groups of all four major RAFT agent families from a range of polymers including poly(*N*,*N*-dimethylacrylamide), PMMA, poly(*N*-vinylpyrrolidone), polystyrene, and poly(methyl acrylate). The general approach, with poly(*N*,*N*-dimethylacrylamide) highlighted, is shown in Scheme 16.9. Simple UV irradiation of the parent RAFT polymer results in homolytic cleavage of the terminal C—S bond liberating, what is in essence, a propagating poly(*N*,*N*-dimethylacrylamide) radical. This immediately abstracts H from the donor source, EPHP in this instance, yielding the H-terminated polymer. The use of EPHP was efficient for all the above noted polymers with the exception of polystyrene. In this instance, incomplete end group conversion was observed with EPHP; however, switching the H-donor source to Bu_3SnH did yield full H-terminated polystyrene without any evidence of undesirable coupled products.

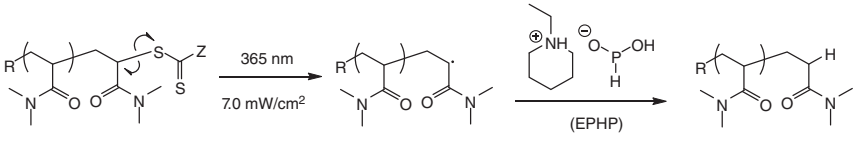

Scheme 16.9 UV-initiated photolysis, followed by H abstraction from EPHP as a facile route to H-terminated poly(*N*,*N*-dimethylacrylamide).

16.3.1.3 Addition–Fragmentation Coupling

In a related process, the reaction of thiocarbonylthio end-terminated (co)polymers with an excess of an added azo species can be employed to substitute RAFT end groups with radical fragments originating from the thermal decomposition of the added azo compound [15]. The general process, highlighting the use of AIBN as the azo compound, is shown in Scheme 16.10.

AIBN decomposes to form two cyanoisopropyl radicals, which react at the C=S bond of the thiocarbonylthio group, forming the intermediate carbon-centred radical, just as expected in a typical RAFT reaction. This intermediate can either fragment back into the original attacking radical or free the polymeric leaving group. Assuming that fragmentation occurs in the direction liberating the polymeric radical, $P_n\cdot$, then this species is formed in the absence of monomer but in

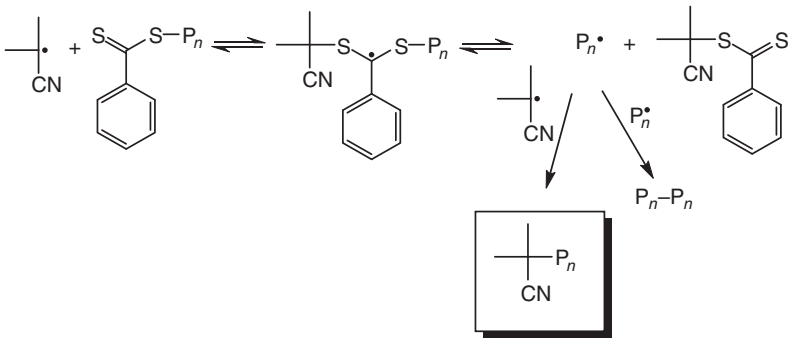

Scheme 16.10 Desulfurization of RAFT-prepared polymer via the reaction with an excess of AIBN.

the presence of a potentially very high concentration of cyanoisopropyl radicals. This species can, of course, self-terminate but under the right conditions will react with a cyanoisopropyl radical, yielding the target end-capped polymer. Perrier et al. [112] were the first to describe such addition–fragmentation coupling reactions, highlighting not just the ability to use this chemistry as a means for end group modification but also as a potential route for recovering CTA. They successfully applied this approach to a variety of dithiobenzoate/thiocarbonylthio end group methacrylic, acrylic, acrylamido, and styrenic polymers with various azo initiators. Chen et al. [113] also examined the removal of thiocarbonylthio end groups in RAFT-prepared polymers with AIBN. These authors found that while end group transformation was successful with methacrylic polymers, it was less effective with acrylic and styrenic polymers. In contrast, the use of lauroyl peroxide did result in the complete removal of end groups in acrylic and styrenic polymers, but it was not a clean process and yielded a significant amount of polymer–polymer coupled products. Interestingly, the amount of polymer–polymer coupled species could be minimized if a combination of lauroyl peroxide (2 equiv) with AIBN (20 equiv) was employed.

As with many of the end group transformation chemistries developed during the preceding two decades, many are now used routinely in many areas of RAFT chemistry and often feature only as an intermediary step en route to a specific desired functionality or application. For example, Sarapas et al. [114] employed such azo coupling chemistry to modify methacrylic and styrenic polymer end groups in guanidinium-functional species, while Bohec et al. [65] used AIBN to modify the trithiocarbonate end groups in alkyne-R-group-functionalized poly(*N*-isopropylacrylamide). Zhang et al. [66] likewise employed AIBN to cleave trithiocarbonate end groups in poly(*N*-isopropylacrylamide) containing a Boc-protected primary amine in the R fragment before removing the protecting group and using the polymeric amine to initiate the ring-opening polymerization of γ-benzyl-L-glutamate *N*-carboxyanhydride (NCA). Kinoshita et al. [115] successfully synthesized telechelic hydroxyl copolymers by using a dithiobenzoate-type CTA bearing hydroxyl groups, followed by further reaction with VA-086 to cleave

the dithiobenzoate end group and instil a second −OH-functional group. Further examples of telechelic polymers obtained by such radical addition–fragmentation coupling have been reported in the literature [74, 116].

An alternative approach to achieve a radical-induced end group modification, to replace the thiocarbonylthio moiety, is the use of alkoxyamines as a radical source. Alkoxyamines are, of course, well known in nitroxide-mediated radical polymerization [117]. Although not technically involving RAFT, the potential to exchange nitroxide end groups with thiocarbonylthio species was demonstrated by Beyou et al. in the reaction between nitroxide-terminated polymers and thiuram disulfides (Scheme 16.11), a process that was demonstrated to proceed quantitatively [118].

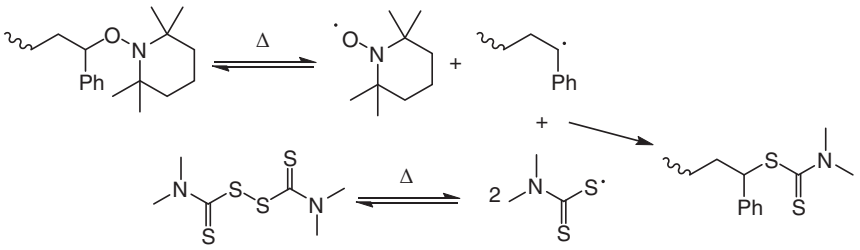

Scheme 16.11 Conversion of a nitroxide end-terminated polystyrene to a dithiocarbamate end-functional polymer.

The first reaction between an alkoxyamine and an RAFT agent was carried out by Ao et al. [119] as part of a study of the kinetics of the RAFT process, while the exchange of nitroxides with RAFT agents, essentially via an identical route as shown in Scheme 16.11, was reported by Favier et al. [120]. The efficacy of the process was reported to be dependent on the nature of both the (macro)alkoxyamine and the (macro)RAFT agent such that the resulting (macro)alkoxyamine should be more stable than the starting species.

16.3.1.4 Radical-Induced Oxidation

End group modification of RAFT-synthesized (co)polymers can occur upon reaction with oxidizing species. Cleavage of the thiocarbonylthio end group and substitution with a hydroxide group can be achieved through radical-induced oxidation. It has, for example, been observed that the storage of RAFT CTAs and RAFT-prepared polymers in cyclic ethers such as tetrahydrofuran (THF) and 1,4-dioxane can lead to the formation of hydroperoxides end groups through a radical autoxidation process with molecular oxygen [121]. It is possible to control the reaction by heating a RAFT-synthesized (co)polymer at 60 °C with an azo initiator (typically AIBN) in ambient air. This first step produces hydroperoxide end-terminated (co)polymers, and subsequent reduction to hydroxyl-functional (co)polymers is achieved by using triphenylphosphine (Scheme 16.12) [122, 123].

The mechanism involves a radical oxidation cycle with an intermediate chain transfer step, analogous to the radical autoxidation of ethers [124].

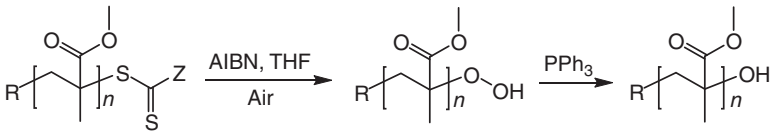

Scheme 16.12 Formation of hydroxy-terminated poly(methyl methacrylate).

Dietrich et al. [122] reported that the radical-induced oxidation of poly(acrylate)s with trithiocarbonate end groups resulted in the quantitative formation of hydroperoxyl- and hydroxyl-terminated analogues, whereas dithioester-terminated polymers gave additional products such as sulfines. In related work, Li et al. [125] studied the kinetics of radical-induced oxidation of RAFT agents with respect to the effect of molecular structure. They found that, according to chain transfer ability, the stability of thiocarbonylthio compounds towards oxidation depends on both Z and R-groups: electron-deficient Z-groups or bulky R-substituents lead to a decreased stability, while electron-donating groups in Z-substituents lead to an increase in stability. As such, trithiocarbonates and xanthates were found to have higher stability than dithioesters towards oxidation.

Recently, Jesson et al. [126] noted the use of hydrogen peroxide in water as a convenient route to remove the thiocarbonylthio end groups in methacrylic block copolymers prepared by polymerization-induced self-assembly.

16.3.2 Heteroatom Diels–Alder Chemistry

One of the 'click' chemistries initially noted by Kolb et al. was the Diels–Alder (DA) reaction [7]. In the classic [4+2] cycloaddition reaction, a hydrocarbon ene (the dienophile) reacts with a diene via a concerted process to give a cyclohexene product. Although the synthetic versatility of the DA reaction is undeniable, traditional reactions can often require high temperatures (>100 °C) and long reaction times (>24 hours). Of course, the reactivity of the diene and dienophile can be tuned. The presence of electron-withdrawing groups on the dienophile, in conjunction with electron-donating groups on the diene, significantly enhances reactivity (normal electron demand DA reactions), as does the use of a diene that is locked in the *s-cis* conformation such as cyclopentadiene or furan, for example. Similarly, reactivity can be controlled via inverse electron demand in which electron-donating groups are attached to the dienophile and electron-withdrawing groups to the diene. Intimately related to the normal DA reactions are those in which the dienophile or diene, or both, contains heteroatoms (most commonly the heteroatoms are O, N, or S); such processes are generally referred to as hetero Diels–Alder (HDA) reactions.

Conveniently, the thiocarbonyl-functional group, C=S, serves as an efficient dienophile in HDA reactions, provided it is 'activated' by the presence of an electron-withdrawing group bonded to C. The general reaction is shown in Scheme 16.13. Examples of suitable RAFT agents that have been employed are benzyl (diethoxyphosphoryl)methanedithioate (DEPMD) and benzyl pyridine-2-carbodithioate (BPCD) (Figure 16.7).

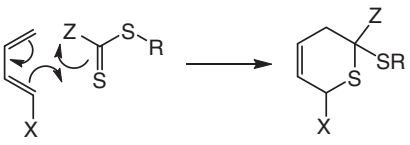

Scheme 16.13 The hetero Diels–Alder reaction between a diene and dithioesters.

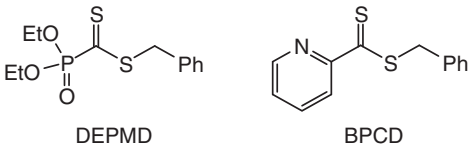

Figure 16.7 Chemical structures of benzyl (diethoxyphosphoryl) methanedithioate (DEPMD) and benzyl pyridine-2-carbodithioate (BPCD).

Interestingly, such HDA chemistries have been most commonly employed in modular approaches to block or star copolymers [127–131] (with the individual blocks often prepared by two different polymerization processes) or as a means of surface modification [132, 133]. For example, Sinnwell et al. described the modular synthesis of AB diblock copolymers of polystyrene with poly(ε-caprolactone) (Scheme 16.14) [127]. Styrene was homopolymerized under standard RAFT conditions with benzyl (diethoxyphosphoryl)methanedithioate (DEPMA) or BPCD to give low molecular weight species with $M_n \sim 2$ and 3 kg mol^{-1} and corresponding $Đ$ of 1.11 and 1.14, respectively. The poly(ε-caprolactone) was prepared with *trans*,*trans*-2,4-hexadien-1-ol as the initiator under enzymatic conditions, yielding a homopolymer with a M_n of ~2.5 kg mol^{-1} and $Đ$ of 1.37. HDA coupling between the polystyrene homopolymers and poly(ε-caprolactone) were conducted at 50 °C in $CHCl_3$. In the presence of $ZnCl_2$ as a catalyst, effective coupling was achieved, although there was clearly residual polystyrene homopolymer even after 24 hours.

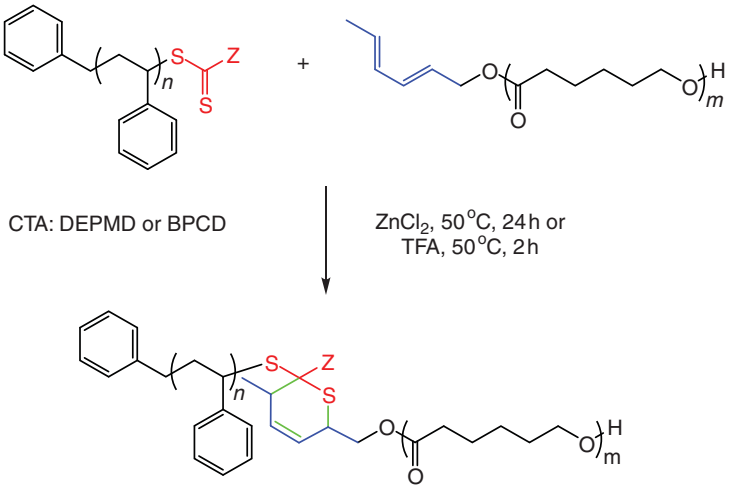

Scheme 16.14 A modular approach to AB diblock copolymers of styrene with poly(ε-caprolactone) prepared via HDA coupling. Source: Modified from Sinnwell et al. [127].

In contrast, when the HDA reaction was catalyzed by trifluoroacetic acid, essentially complete conversion was realized after only two hours.

Multiarm star polymers are accessible under the same conditions using the same catalysts (Scheme 16.15) [128]. High yields of the target star polymers were obtained (although none were quantitatively formed) with those formed from **BPCD**-terminated polystyrene being generated faster and in higher yield (Scheme 16.15). Given the specific usefulness of this particular HDA reaction as a tool for the modular synthesis of block copolymers and (co)polymers of higher architecture, it is perhaps not surprising that others have explored HDA chemistry as a coupling tool for the 'clicking' together of homopolymers prepared by RAFT. Several strategies have been reported including the tetrazine-norbornene inverse electron demanding DA reaction by Hansell et al. [135]. Although efficient, this is perhaps limited by the lack of ready availability of the required tetrazine starting material. However, the application of tetrazines as ligation tools in chemical biology still attracts significant attention [136–139].

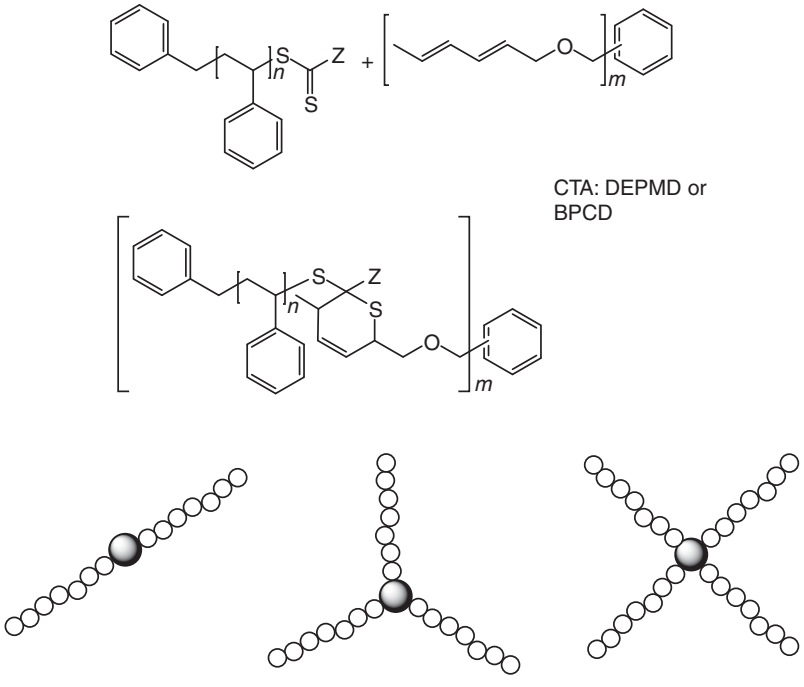

Scheme 16.15 Synthesis of 2-, 3-, and 4-arm star polymers via convergent HDA coupling of polystyrene homopolymers to a multifunctional diene 'core' molecule.

Du Prez and coworkers [140–147], and others [148–153], have reported extensively on applications of the 1,2,4-triazoline-3,5-dione (TAD)-based reaction with examples of normal DA and ene-type reactions known (Scheme 16.16), and readers are directed to these, and other, references for a more detailed description of various TAD-based applications. Indeed, TAD chemistry is extremely well established;

however, in the context of this chapter, we note that there remain few examples in which it has been applied as a tool for modifying RAFT polymer end groups.

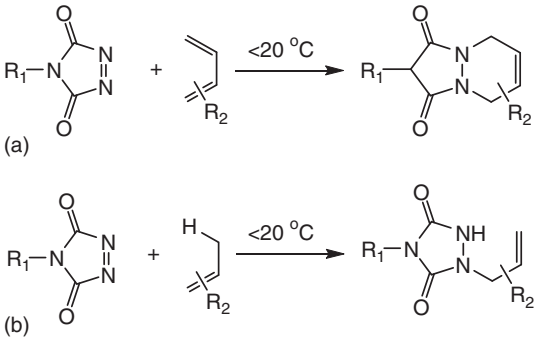

Scheme 16.16 The triazolinedione-diene normal DA reaction (a) and the triazolinedione Alder-ene reaction (b).

Vandewalle et al. [154] detailed an approach for the introduction of TAD groups at the α-terminus of RAFT-prepared poly(*n*-butyl acrylate) via the use of a pro-TAD-functional trithiocarbonate shown in Figure 16.8. Employing a precursor urazole derivative is actually common practice, given the well-documented and extensive chemistry associated with TAD; this approach avoids undesirable side reactions during initial polymer synthesis. The urazole-functional trithiocarbonate (URZ-TTC) was readily prepared and isolated on a multigram scale.

URZ-TTC was demonstrated to be an effective CTA and readily mediated the controlled polymerization of *n*-butyl acrylate, *N*,*N*-dimethylacrylamide, and styrene under standard RAFT conditions. The authors focused their discussion on poly(*n*-butyl acrylate) homopolymers, for which polymerizations were halted at <70% conversion in order to maximize end group fidelity while also keeping the molecular weights low. To facilitate conjugation, the urazole functionality was first converted to the 3*H*-1,2,4-triazole-3,5(4*H*)-dione (Scheme 16.17). This was accomplished via mild oxidation with 1,4-diazabicyclo[2.2.2]octane and bromine (DABCO-Br). Removal of the dispersed oxidizing agent by simple filtration, followed by immediate reaction with hexa-2,4-dien-1-ol, resulted in formation of the target species within a few seconds.

16.3.3 Generation and Application of Macromolecular Thiols

Perhaps the most common, and certainly the most versatile, approach for modifying thiocarbonylthio groups involves nucleophilic cleavage, followed by trapping

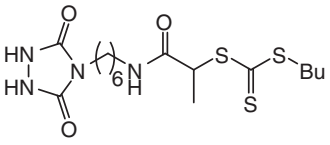

Figure 16.8 Chemical structure of a urazole-functional trithiocarbonate: butyl (1-((6-(3,5-dioxo-1,2,4-triazolidin-4-yl)hexyl)amino)-1-oxopropan-2-yl) carbonotrithioate (URZ-TTC).

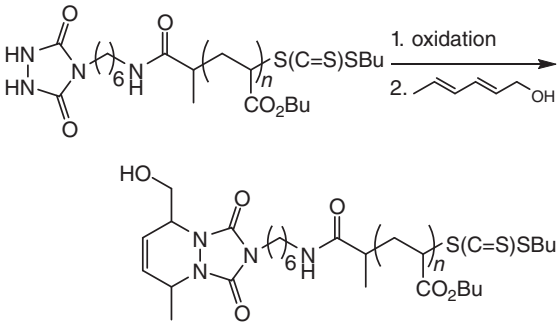

Scheme 16.17 Synthesis of α-end-functionalized poly(*n*-butyl acrylate) by oxidation of a terminal urazole-functional group, followed by an HDA reaction with hexa-2,4-dien-1-ol.

of the resulting macromolecular thiol, or thiolate, by one of the numerous available routes [155] (Figure 16.9). Suitable nucleophiles include 1° and 2° amines (and hydrazine hydrate) [54, 134, 156–166], hydroxides [86, 167], azide [168], and hydride reagents such as $NaBH_4$ [169–173] or $LiBEt_3H$ [174]. In general, all the nucleophilic cleavage reactions are reasonably rapid and give the corresponding macromolecular thiol quantitatively. We do, however, note one precaution that is commonly adopted in such cleavage reactions – it is typical to perform these reactions under oxygen free conditions and in the presence of a reducing agent such as tributylphosphine (PBu_3) or tris(2-carboxyethyl)phosphine (TCEP) [175] in order to negate any appreciable build-up of corresponding macromolecular disulfide (Scheme 16.18). This is even advisable when using reagents such as hydrazine hydrate, which is able to serve as a cleavage agent and anti-oxidant because disulfide formation has been detected in polymers cleaved with this reagent even under deoxygenated conditions [163]. While we have noted the one-pot approach to clean macromolecular thiol, it is also possible, if desirable, to conduct a two-step process involving initial cleavage without taking any precautions against disulfide formation, followed by a second step in which the product mixture is treated with a reducing agent to obtain pure macromolecular thiol.

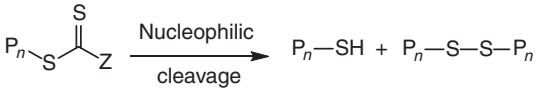

Scheme 16.18 Nucleophilic cleavage of RAFT thiocarbonylthio end group yielding the corresponding macromolecular thiol and polymeric disulfide.

Oxidative coupling yielding polymeric disulfides is not the only potential side reaction that can occur during cleavage of thiocarbonylthio end groups. The nature of the polymer repeat units, i.e. styrenic vs. methacrylate, can also influence the outcome of such reactions and must be considered when the goal is to prepare pristine polymeric thiol. As a representative example, in an early study, Xu et al. [156] compared the products from the aminolysis, employing cyclohexylamine,

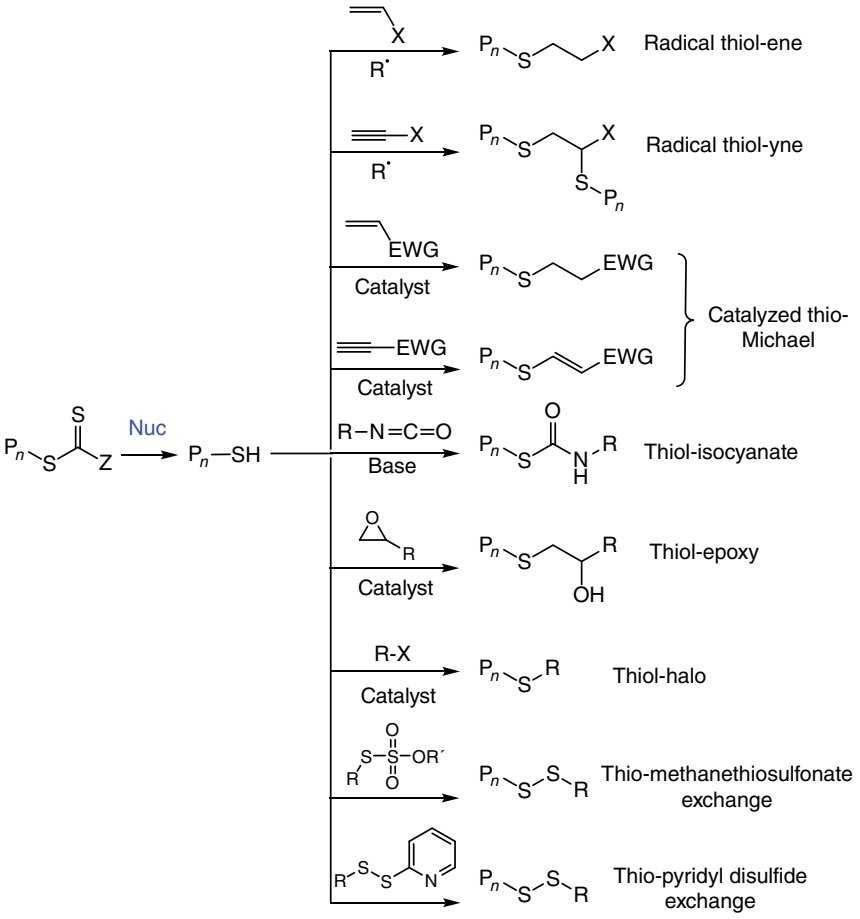

Figure 16.9 Thiol-X reactions potentially suitable for the modification of macromolecular thiols derived from RAFT-prepared (co)polymers.

of low molecular weight polystyrene and PMMA-containing dithiobenzoate ω end groups. In the case of polystyrene, following the reaction for 24 hours, the major product was the polymeric disulfide formed by oxidative coupling, the concentration of which increased steadily over the 24 hours reaction time frame. In the case of PMMA, initially, it appears that disulfide formation did occur; however, the concentration of this species gradually decreased, ultimately giving a product with nearly the same molecular weight as the starting material. Using a combination of size exclusion chromatography (SEC), NMR spectroscopy, matrix-assisted laser desorption/ionization time of flight (MALDI-TOF) mass spectrometry, and elemental analysis, the authors established that the main product from the aminolysis of PMMA was a species containing a terminal thiolactone-functional group formed via a 'backbiting' reaction of thiol on the penultimate MMA repeat unit. Similar results were obtained for poly(2-(dimethylamino)ethyl methacrylate) and poly(lauryl methacrylate). While the formation of polymers with thiolactone end

groups may be undesirable, it is noted that these early studies on the synthetic utility of thiolactones in polymer chemistry has been greatly advanced and today represents one of many functionalities with proven broad utility [79, 176, 177], including in the general field of RAFT polymerization [178–180].

As a general statement, the occurrence of side reactions during cleavage of thiocarbonylthio end groups can largely be avoided if the resulting macromolecular thiol is immediately 'captured', often by a reactive species present in situ during the cleavage process. In fact, and as noted above, while historically end group cleavage reactions were developed to address the perceived deleterious effect of the thiocarbonylthio groups in RAFT-prepared (co)polymers, they actually played a major role in the advancement and application of thiol-based 'click' chemistries in synthetic polymer chemistry [181]. With a macromolecular thiol in hand, it is possible to access the wide range of the so-called thiol-X chemistries in end group modification (Figure 16.9), although not all of these reactions are equally applicable to polymeric thiols.

16.3.3.1 Radical Thiol–Ene Reaction

The radical-mediated hydrothiolation of a C=C bond, with anti-Markovnikov orientation, the thiol–ene reaction, is perhaps the most studied of all the common thiol-X chemistries and has an extremely broad synthetic utility [62–64, 182, 183]. However, it is quite rare for an RAFT-derived macromolecular thiol to be employed directly in a radical thiol–ene reaction. While the synthetic utility of the thiol–ene reaction is unquestionable, if there is a limitation of the chemistry, then it is the fact that 2° and 3° macromolecular thiols derived from RAFT polymer thiocarbonylthio end groups exhibit very low reactivity in radical thiol–ene processes especially at stoichiometric ratios of thiol:ene. This low reactivity is typically attributed to the effective low concentration of thiol groups, especially when attempting polymer–polymer conjugation reactions [184]. The lower reactivity of 2° and 3° thiols in small-molecule thiol–ene chemistry has also been noted. However, there are examples in which the direct reaction of macromolecular thiols with enes, under radical conditions, has been reported. For example, as part of a broader report regarding the limitations of radical thiol–ene chemistry for polymer–polymer conjugation, Koo et al. [185] detailed the reactions of thiol-terminated polystyrene (prepared by trithiocarbonate-mediated RAFT, followed by aminolysis with propylamine) with several small-molecule enes such as dodecyl vinyl ether, allyl ether, and undecanoic acid, under photoinitiated radical conditions. As a general observation, yields were typically high (c. 90%), except for undecanoic acid (30%), under a range of conditions and reaction stoichiometries.

However, this is not to say that the radical thiol–ene reaction has not been more widely employed in the field of RAFT chemistry, indeed in polymer and materials science in general, vide infra [181]. We have already highlighted the ability to introduce functionality at the α-terminus via this chemistry in RAFT polymers prepared with norbornenyl-functionalized RAFT agents [61]. In addition, while a detailed discussion is beyond the scope of this chapter, we note that the radical thiol–ene

reaction has been adopted by numerous groups to modify main chain pendent ene groups in a range of RAFT-prepared (co)polymers [183].

16.3.3.2 Radical Thiol–Yne Reaction

The radical thiol–yne reaction can be viewed as a sister reaction to the radical thiol–ene process [186–190]. As such, it possesses similar advantages and limitations. In the radical thiol–yne reaction, we assume that 2 equiv of thiol will add across the C≡C bond, in a terminal alkyne, which is formally sequential thiol–yne/thiol–ene processes; the product is the 1,2-dihydrothiolation species, B in Scheme 16.19. It is beyond the purview of this chapter to discuss the mechanistic features of the thiol–yne reaction in detail, but we will note that it can be performed with both activated and non-activated ynes and that the nature of the product can be tuned based on reaction conditions. In fact, there are *six* possible products from the reaction of an yne with thiols, all of which are accessible under appropriate conditions [190].

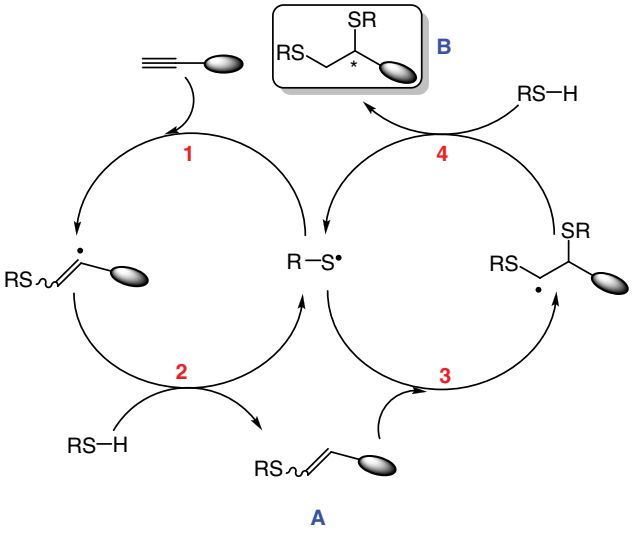

Scheme 16.19 General mechanism of the radical-mediated double hydrothiolation of a C≡C bond, the thiol–yne process.

As with the thiol–ene reaction, the thiol–yne process has been adopted widely in various areas of synthetic chemistry [190]. In the context of polymer chemistry, the development of the so-called thiol–yne click copolymerization, characterized by the single addition of a thiol to an yne (to give poly(vinyl sulfide)s), represents an emerging but ever-growing field of research [191–194]. By analogy with the thiol–ene reaction, the direct use of polymeric thiols derived from RAFT polymers is uncommon. However, combining yne-functional RAFT polymers (both as R-groups and as pendent groups) with small-molecule thiols in the radical thiol–yne process is known, as highlighted earlier in the work of Le Bohec et al. [65]. The thiol–yne reaction has

also been employed in sequential modification reactions. For example, Kumar et al. [195] reported the combination of RAFT polymer HDA functionalization, followed by radical thiol–yne double hydrothiolation of ω-terminal groups in poly(*tert*-butyl acrylate) polymers (Scheme 16.20).

The synthesis of low molecular weight poly(*tert*-butyl acrylate) was accomplished in toluene with **BPCD** (Figure 16.7). Subsequent selective reaction of the diene/yne-functional diester, (2*E*,4*E*)-hexa-2,4-dien-1-yl prop-2-yn-1-yl succinate, with the poly(*tert*-butyl acrylate) polymers yielded the HDA adducts containing terminal yne-functional groups. Radical-mediated thiol–yne reaction with thioglycerol, in the presence of a small amount of photoinitiator, gave the four-functional OH-ω-terminal products. The authors also studies the effect of double hydrothiolation with thioglucose, yielding materials capable of binding lectins. This is not the only example in which sequential 'click' reactions have been adopted as a means of modifying RAFT polymer end groups and additional examples are given below.

16.3.3.3 Catalyzed Thiol-Michael Additions

The catalyzed addition of a thiol to an activated substrate, the thiol-Michael reaction [196], is, arguably, the most commonly employed reaction in the modification of thiocarbonylthio end groups, and many examples have been reported in which the reaction has been utilized to directly instil functional end groups, generate new materials, or simply as a means of trapping a polymeric thiol to yield an inert end group [134, 159, 197, 198].

The thiol-Michael reaction can be performed under base- or nucleophile-mediated conditions; the two different mechanisms are shown in Figure 16.10. A detailed description of the process is not given here, and readers are directed to several reviews and papers where it is discussed in more detail [199, 200]. Briefly, and regardless of the conditions adopted, the thiol, or thiolate, in all instances is derived from the RAFT-prepared (co)polymer. As such, it is clear that many different types of macromolecular thiols can be generated simply by varying the (co)monomer and architecture. The structure of the Michael acceptor can, likewise, be one of many different species. In fact, it is the wide choice of both donor and acceptor that makes this chemistry so powerful and popular. In the context of modifying polymeric thiols prepared by RAFT, suitable families of Michael acceptors that have been utilized include acrylates [201–209], methacrylates [205], acrylamides [49, 210–213], maleimides [175, 214–223], vinyl sulfones [224], octavinyl-polyhedral oligomeric silsesquioxane (POSS) [225], vinyl azlactone [226], and multi-functional variants of these [221, 224, 227, 228]. Typically, such conjugate additions are performed in one-pot process, i.e. the RAFT polymer thiocarbonylthio end groups are cleaved in the presence of the Michael acceptor to effectively trap the thiol as soon as it is formed. Although it is not possible to discuss all of these examples, below we will highlight several literature reports involving sequential 'click' reactions for end group modification.

Yu et al. [205] reported the synthesis of ω-functionalized poly(*N*-isopropylacrylamide) employing sequential thiol-Michael reactions with radical thiol–ene

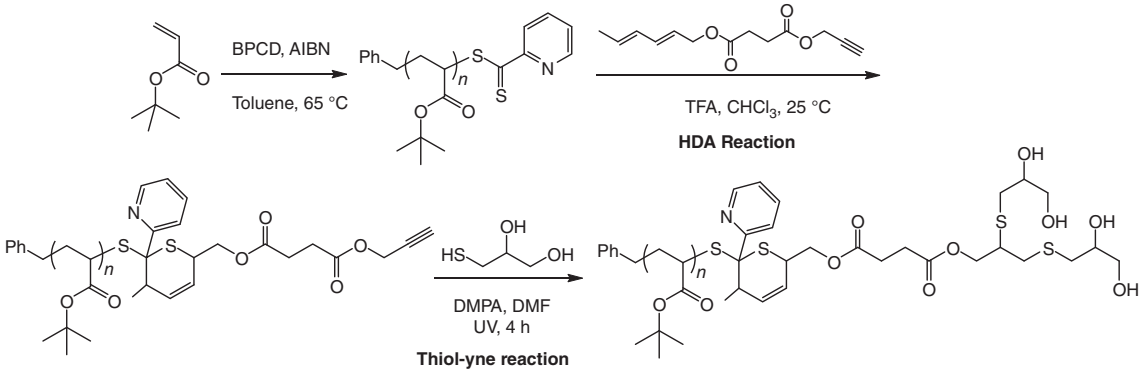

Scheme 16.20 Sequential HDA and thiol–yne reactions as a route to ω-functionalized poly(*tert*-butyl acrylate).

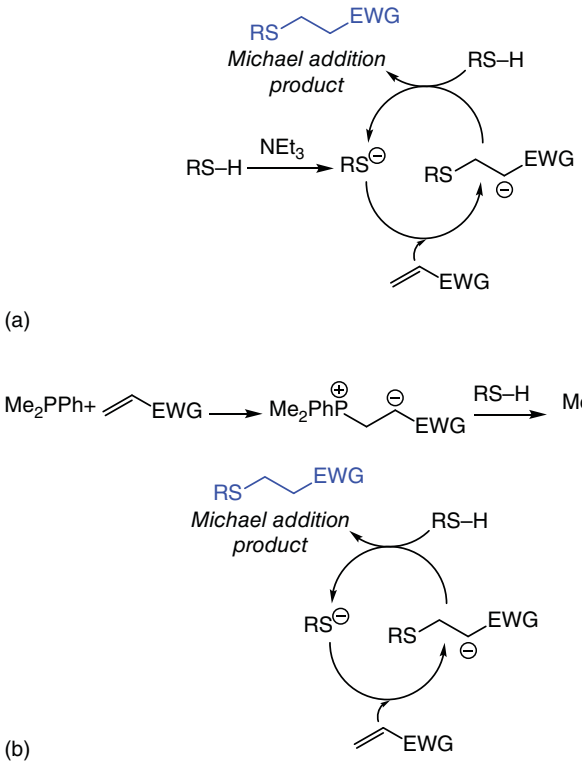

Figure 16.10 The general mechanism of the base-catalyzed thiol-Michael reaction (a) and the nucleophile (phosphine)-catalyzed mechanism (b).

and thiol–yne chemistries. Scheme 16.21 highlights the thiol-Michael/thiol–yne modification route.

Poly(*N*-isopropylacrylamide), prepared in the presence of 2-cyanopropan-2-yl benzodithioate, was treated with octylamine (to cleave the dithioesters to the corresponding thiols) and propargyl acrylate (the Michael acceptor) in the presence of dimethylphenylphosphine (a potent catalyst for thiol-Michael addition reactions [196]) yielding the yne end-functionalized poly(*N*-isopropylacrylamide). The ω-yne-functional polymer was subsequently reacted with 6-mercapto-1-hexanol, 1-hexanethiol, and 3-mercaptopropyl polyhedral oligomeric silsesquioxane (100% excess based on yne-functional groups) in the presence of Irgacure 651 (benzil dimethyl ketal) as a photoinitiator. This resulted in the quantitative formation, as judged by ^{1}H NMR spectroscopy, of the corresponding bis-ω-thioether adducts. Likewise, if the Michael addition reaction is conducted with allyl methacrylate rather than propargyl acrylate, it provides access to an allyl-end-functionalized polymer that can be modified by a radical thiol–ene reaction.

In a related example, also with poly(*N*-isopropylacrylamide), Li et al. [229] reported sequential trithiocarbonate end group cleavage with 2-ethanolamine in the presence of PBu_3, followed by base-mediated thiol-Michael addition to an added

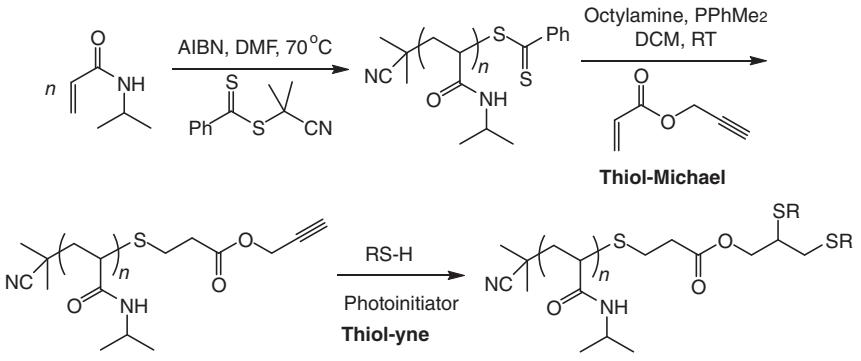

Scheme 16.21 Sequential end group cleavage/Michael addition with propargyl acrylate, followed by radical thiol–yne reaction with the ω-yne-functional group.

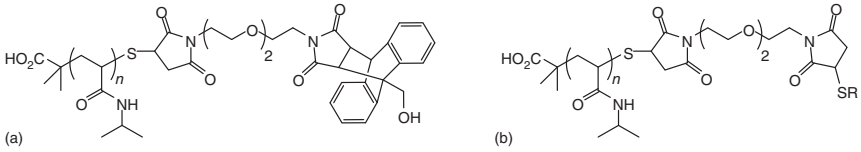

Figure 16.11 Structures of poly(*N*-isopropylacrylamide)s formed by sequential thiol–maleimide/Diels–Alder reactions (a) and thiol–maleimide/thiol–maleimide reactions (b).

excess of bis-maleimidodiethyleneglycol, yielding the corresponding maleimide end-functionalized polymer. This was then used to effect further functionalization via a HDA reaction with anthracen-9-ylmethanol or by reaction with thiols to give the species shown in Figure 16.11.

In an interesting example of an intra-molecular thiol-Michael reaction, Lu et al. [230] detailed the synthesis of alkyne-functionalized cyclic polymers from precursor linear polymers with the key cyclization step being accomplished via a thiol-Michael process (Scheme 16.22). For example, polystyrene was prepared utilizing the yne-OH-functional trithiocarbonate RAFT CTA 3-hydroxy-2-methyl-2-((prop-2-yn-1-yloxy)methyl)propyl 2-(((butylthio)carbonothioyl)thio)-2-methylpropanoate. The –OH group in the R fragment of the polystyrene polymer was then acylated with acryloyl chloride, yielding the acrylic-functional species. The final cyclization step involved a one-pot aminolysis/thiol-Michael reaction in which hexylamine cleaved the ω-terminal trithiocarbonate and served as the catalyst for the Michael addition of the resulting macromolecular thiol to the R-group acrylate functionality giving the cyclic species in ~80% yield. The same synthetic procedure was applied to homopolymers of *tert*-butyl acrylate, *N*-isopropylacrylamide, and *N*,*N*-dimethylacrylamide.

16.3.3.4 Thiol-Isocyanate Modification

The reaction between thiols and isocyanates is an example of a non-Aldol carbonyl reaction highlighted by Finn et al. as a member of the general 'click' family of

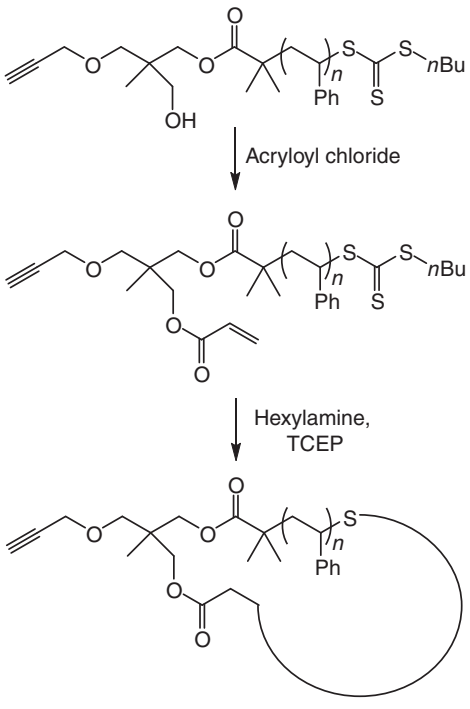

Scheme 16.22 Synthesis of alkyne-functionalized cyclic polystyrene via an intramolecular thiol-Michael addition process.

reactions. Intimately related to the more common alcohol–isocyanate reaction, the thiol-based variant does not suffer from the same side reactions seen in the alcohol reaction. The product of a thiol–isocyanate reaction, an *S*-thiocarbamate (or thiourethane), can generally be obtained quantitatively within a few seconds. In fact, thiol–isocyanate coupling is one of, if not the, fastest of the thiol-based coupling chemistries. As with many of these thiol-based chemistries, the thiol-isocyanate reaction is widely employed in synthetic chemistry and materials science [231–237].

Not surprisingly, this chemistry has been utilized in conjunction with RAFT-prepared polymers. However, even though the chemistry is facile, quantitative, and generally extremely rapid, there are few reports regarding end group modification via thiol–isocyanate coupling, and more emphasis has been placed on side chain modification of RAFT-synthesized (co)polymers with pendent isocyanate groups [238, 239]. The first report detailing RAFT end group modification via thiol–isocyanate coupling came from Li et al. (Scheme 16.23) [240].

Poly(*N*,*N*-diethylacrylamide) with a mean degree of polymerization of 30 (M_n ca. 2540 g mol^{-1}), prepared via dithiobenzoate-mediated RAFT, was first treated with CH_3NH_2 to cleave the thiocarbonylthio end group. The product was subsequently treated with TCEP, a mild reducing agent, to convert any polymeric disulfide to the pristine macromolecular thiol. End group cleavage and disulfide reduction was confirmed by a combination of SEC and UV–vis spectroscopy. The polymeric

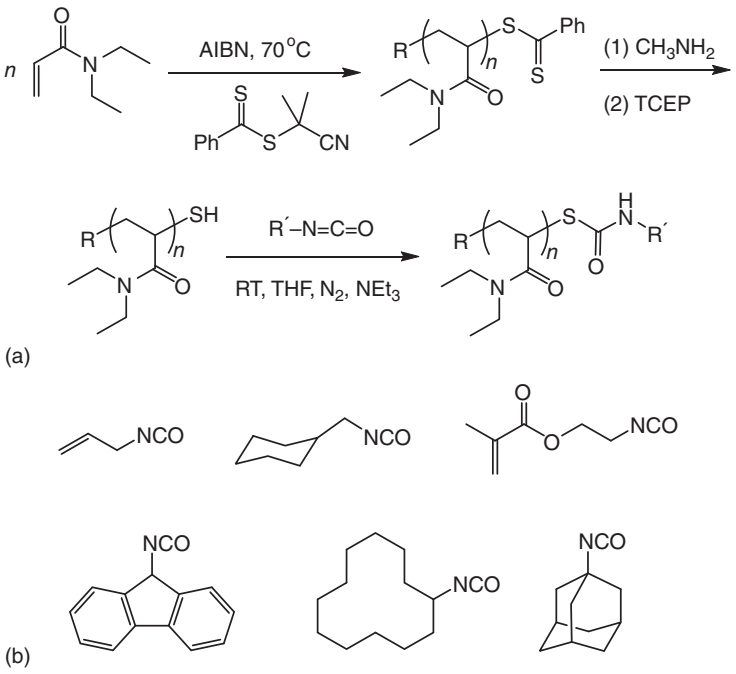

Scheme 16.23 (a) General scheme for the preparation of thiocarbamate end-functionalized poly(*N,N*-diethylacrylamide) and (b) representative examples of small-molecule isocyanates employed in end group modification.

thiol was subsequently reacted with 14 different small-molecule hydrophobic isocyanates, examples of which are also shown in Scheme 16.23. As a representative example, employing real-time FTIR spectroscopy, the authors demonstrated that the reaction between poly(*N*,*N*-diethylacrylamide)-SH and hexyl isocyanate was rapid, attaining ~95% conversion within 15 minutes. In all instances, the modified polymer retained its narrow molecular weight distribution with no evidence of any coupled disulfide species, attesting to the clean nature of this chemistry. More recently, Boursier et al. [241] employed the same approach to prepare methacrylic poly(*N*-acryloylmorpholine) macromonomers. RAFT-synthesized poly(*N*-acryloylmorpholine) was treated with hydrazine hydrate, followed by NEt_3-mediated coupling with 2-isocyanatoethyl methacrylate. Formation of the macromonomer was confirmed by a combination of ^{1}H NMR spectroscopy and SEC. The authors demonstrated the ability to copolymerize the macromonomer with methacrylic acid via normal radical polymerization, yielding novel graft copolymers with potential application as plasticizers in concrete formulations.

16.3.3.5 Thiol-Epoxy Ring Opening

Nucleophilic ring opening of strained heterocycles, such as epoxides, is another example of a 'click' process [7]. The general high reactivity of epoxides has naturally resulted in their use in a wide range of applications in polymer and materials science [242–245]. However, as with some of the former chemistries highlighted, the direct

use of a RAFT-derived polymeric thiol in such nucleophilic ring-opening reactions is rare. Harvison et al. [171] detailed the thiolysis of a series of small-molecule oxiranes with polystyrene and poly(*N*,*N*-diethylacrylamide) under base-mediated conditions and in the presence of the Lewis acid $ZnCl_2$. In the case of polystyrene, the thiocarbonylthio end groups were cleaved with hydrazine hydrate and the macromolecular thiol isolated and characterized. In reactions with monofunctional epoxides and $ZnCl_2$, high conversions were attained, although none were quantitative with the highest degree of modification being 88%. Under base-mediated conditions, the degree of end group modification was similar but suffered from the formation of macromolecular disulfide as an impurity. In contrast, in a one-pot approach with poly(*N*,*N*-diethylacrylamide) employing $NaBH_4$ as the end group cleaving agent, and Me_2PPh as a reducing agent in the presence of a small-molecule epoxide, reactions proceeded smoothly giving essentially quantitative formation of the ring-opened product as determined by NMR spectroscopy.

16.3.3.6 Thiol-Halo Substitution

Nucleophilic substitution, S_N, reactions with alkyl and aryl halides proceed, under appropriate conditions, with 'click' or 'click'-like characteristics. With respect to thiol-based reactions, the two most prominent in the literature are the thiol-bromo/iodo [246, 247] and thiol-*para*-fluoro [248, 249] reactions.

Nakayama and Okano detailed the one-pot aminolysis/thiol–iodo reaction between amphiphilic block copolymers prepared by RAFT and 2-iodoethanol [250] as part of their study on the effect of end groups on the thermoresponsive behaviour of block copolymers of poly(*N*-isopropylacrylamide-*co*-*N*,*N*-dimethylacrylamide)-*block*-poly(benzyl methacrylate), and Segui et al. [251] likewise adopted the thiol–iodo reaction in the synthesis of α,ω-dicholesteryl and α,ω-dipyrenyl poly(*N*-isopropylacrylamide)s employing a difunctional RAFT agent (Scheme 16.24). The analogous difunctional cholesteryl derivative was obtained under the same conditions by substituting 1-(4-iodobutyl)pyrene with cholest-5-en-3β-yl 6-iodohexyl ether.

Xu et al. reported the thiol–bromo reaction as a convenient method for end group modification of RAFT polymers and also for the preparation of multiblock and hyperbranched polymers [252]. For example, the one-pot treatment of RAFT-synthesized poly(methyl acrylate) with hexylamine (end group cleavage agent), triethylamine (base), and 2-bromopropanoate yielded the ester-end-functionalized polymer quantitatively within 30 minutes.

Reaction with methyl 2-bromo-2-propanoate, a 3° halide, was also successful as was analogous modification on poly(*N*-isopropylacrylamide). In the same work, it was demonstrated that use of the R-group bis-bromo-ester-functional RAFT CTA (Figure 16.12) facilitates the synthesis of polymers which, after aminolysis of the thiocarbonylthio end groups, are able to undergo inter/intra-molecular thiol–bromo reactions yielding hyperbranched materials.

In a related work, Chen et al. [253] reported the one-pot synthesis and assembly of supramolecular dendritic polymers from X-Y_2-type polymeric precursors [254]. Figure 16.13 shows the two precursor building blocks.

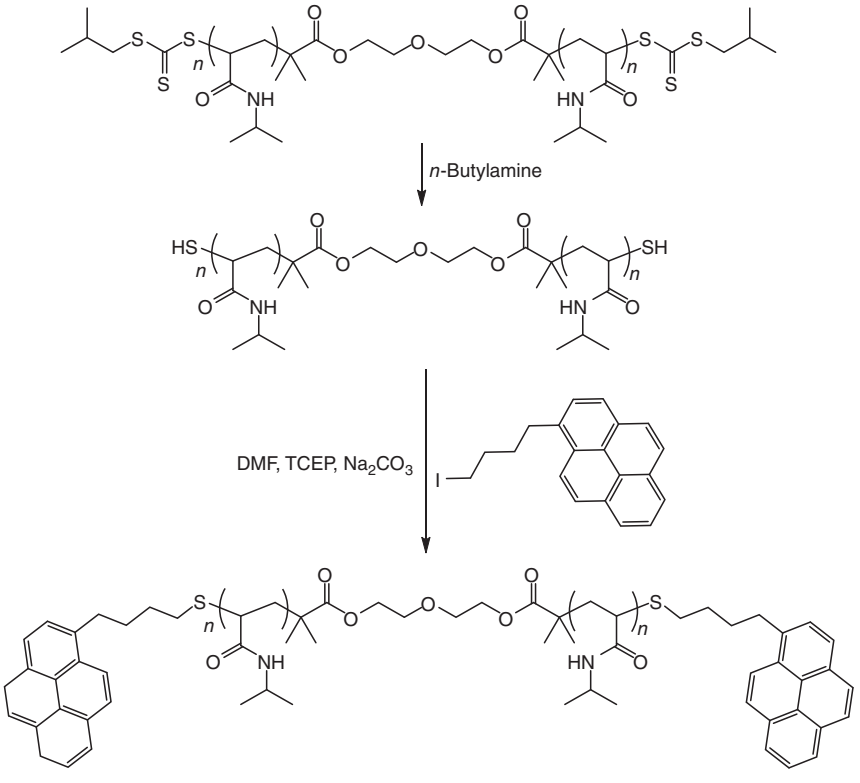

Scheme 16.24 The synthesis of α,ω-pyrene difunctionalized poly(*N*-isopropylacrylamide).

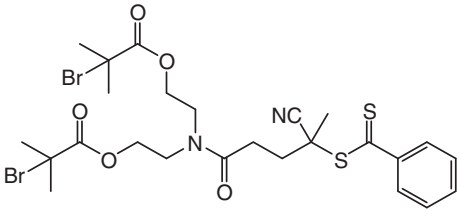

Figure 16.12 Chemical structure of ({4-cyano-4-[(phenylcarbonothioyl)thio] pentanoyl} azanediyl)bis(ethane-2,1-diyl)bis (2-bromo-2-methylpropanoate).

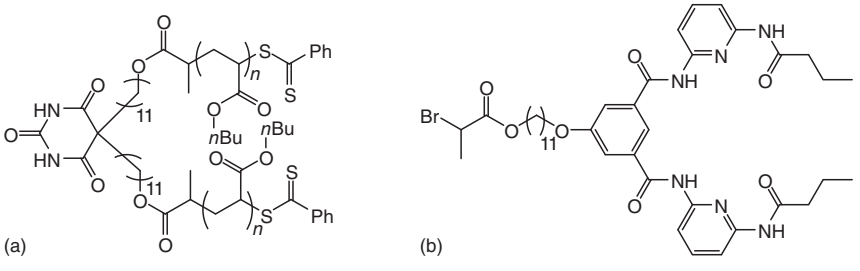

Figure 16.13 Barbiturate-linked poly(*n*-butyl acrylate) (a) and bromo-functional bipyridyl building blocks (b).

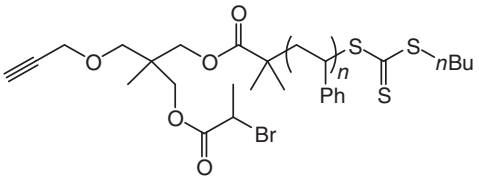

Figure 16.14 Chemical structure of an α-yne/bromide-functional polystyrene.

In a one-pot, two-step process, the α,ω-dithiobenzoate terminal groups in poly(*n*-butyl acrylate), containing a central pyrimidine-2,4,6(1*H*,3*H*,5*H*)-trione, unit were cleaved with hexylamine. Performed in the presence of (3,5-bis((6-butyramidopyridin-2-yl)carbamoyl)phenoxy)methyl 2-bromopropanoate (Figure 16.13b), and following a thiol-bromo reaction, the target X-Y_2 species was isolated. The isolation of the target X-Y_2 species was confirmed via a combination of NMR spectroscopy, MALDI-TOF mass spectrometry (MS), and liquid chromatography at critical conditions. These wedge-like species were shown to undergo supramolecular self-assembly into disc-like structures as evidenced by NMR and atomic force microscopies.

In Scheme 16.22, we highlighted the work of Lu et al. and the synthesis of cyclic polymers from RAFT-prepared linear precursors via an intramolecular thiol-Michael reaction pathway. In the same report, the authors also described attempts to obtain the same functional cyclic polymers employing thiol–bromo chemistry in the cyclization step. With reference to Scheme 16.22, acylation of the α-located −OH group with 2-bromopropionyl bromide, rather than acryloyl chloride, yielded the α-yne/Br-functional species (Figure 16.14). One-pot aminolysis/thiol–bromo reactions gave cyclic species, although yields were significantly reduced compared to the thiol-Michael approach with <24% of the cyclic species formed. Perhaps not surprisingly, the lower yields were due to competing reaction of the added hexylamine with the 2° bromide.

In a recent example of the thiol–bromo reaction, Döhler et al. [255] reported the chain end functionalization of three-arm star polymers of poly(*n*-butyl acrylate) and polystyrene with barbiturate and imidazolium-functional species. Figure 16.15 shows the poly(*n*-butyl acrylate) derivatives. The poly(*n*-butyl acrylate) stars were prepared with a novel trifunctional RAFT agent in which the R-group fragment was part of the trifunctional core. Star polymer formation was readily accomplished under standard RAFT conditions yielding materials with M_n (as

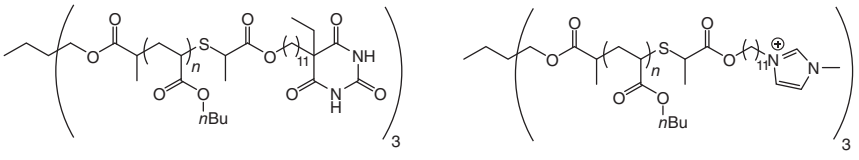

Figure 16.15 Chemical structures of barbiturate and imidazolium end-functionalized poly(*n*-butyl acrylate) three-arm star polymers formed by a thiol–bromo 'click' reaction.

determined by ^{1}H NMR spectroscopy) between ~5500 and 14 300 g mol^{-1} and correspond $Đ$ of 1.27 and 1.26. Subsequent methylamine-mediated aminolysis, followed by reaction of the resulting thiol-terminated star polymers with (5-ethyl-2,4,6-trioxohexahydropyrimidin-5-yl)methyl 2-bromopropanoate or 3-(((2-bromopropanoyl)oxy)methyl)-1-methyl-1*H*-imidazol-3-ium, yielded the target materials in Figure 16.15 with >95% functionality.

While gaining in popularity, the thiol-*para*-fluorophenyl reaction is one of the least examined in the toolbox of thiol-X chemistries. Although it has been employed in the modification of pendent pentafluorophenyl and pentafluorobenzyl functional [256, 257] groups, its use in RAFT ω chain end functionalization remains largely unexplored.

Zhu and coworkers [258, 259] reported the synthesis and application of diselenocarbonyl compounds as mediators for the controlled radical polymerization of activated and non-activated monomers, the so-called Se-RAFT process. These Se-analogues of thiol-based RAFT agents have much in common. They can be prepared via the same general synthetic routes, they are assumed to mediate radical polymerization via the same addition–fragmentation mechanistic pathway as thiocarbonylthio compounds, and they are able to undergo many of the same types of chemistries as reported herein, including selenol–Michael addition, selenol–epoxy, selenol–bromo, and selenol–isocyanate coupling. Interestingly, selenolcarbonylselenol end-functional polystyrenes have been modified by all of these chemistries as well as by nucleophilic aromatic substitution with pentafluorostyrene (Scheme 16.25) [259].

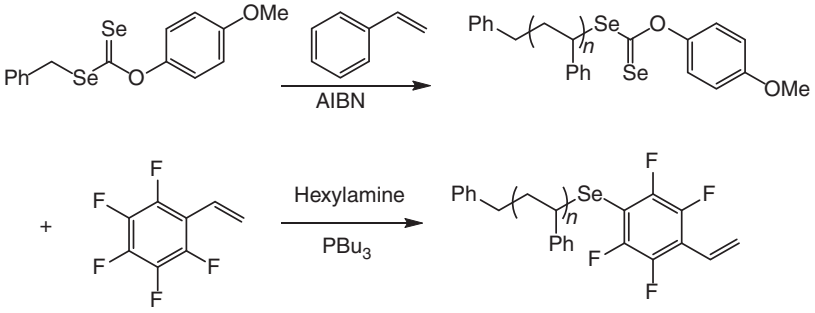

Scheme 16.25 Preparation of polystyrene macromonomers via a combination of Se-RAFT, aminolysis, and *para*-fluoro aromatic nucleophilic substitution.

Homopolymerization of styrene in the presence of Se-benzyl *O*-(4-methoxyphenyl) carbonodiselenoate and AIBN yielded the expected polymeric species with an SEC-measured M_n of 4300 g mol^{-1} and $Đ$ of 1.22 (at c. 40% monomer conversion). Employing typical conditions for thiocarbonylthio end group removal, the polystyrene–Se(C=Se)Z analogue was reacted with hexylamine in the presence of pentafluorostyrene and PBu_3 yielding the target styrenic-based macromonomer.

16.3.3.7 Disulfide Reactions

Earlier in this chapter, we noted that in accessing polymeric thiols from RAFT-prepared (co)polymers, it is common practice to perform the end group cleavage reaction in the presence of a reducing agent to avoid polymer–polymer coupling via disulfide formation. However, it is possible to exploit such facile, and reversible, disulfide formation in the preparation of higher ordered materials as well as effecting simple end group modification.

Recently, Dao et al. [165] reported the synthesis of ultra-high molecular weight ABA triblock copolymers employing RAFT. The key to obtaining the target materials was the aminolysis of trithiocarbonate end groups in precursor AB diblock copolymers, under oxidizing conditions, to intentionally promote polymer–polymer disulfide bond formation. Scheme 16.26 shows an example for ABA triblock copolymers of poly(acrylic acid-*b*-acrylamide-*b*-acrylic acid). The authors prepared eight different examples of such triblocks and obtained materials whose final SEC-measured M_n were $\geq 1 \times 10^6$ g mol^{-1}. The same general approach has been employed by Whittaker et al. [260] in the reversible formation of linear and cyclic polymers from α,ω-dithiol-functional polystyrene (HS–polystyrene–SH); by Gho et al. [261] in the preparation of monocyclic, linear multiblock, bicyclic, and crosslinked networks based on polystyrene three-arm stars with arms terminated by SH groups; and by Vogt and Sumerlin [262] and the preparation of redox-responsive

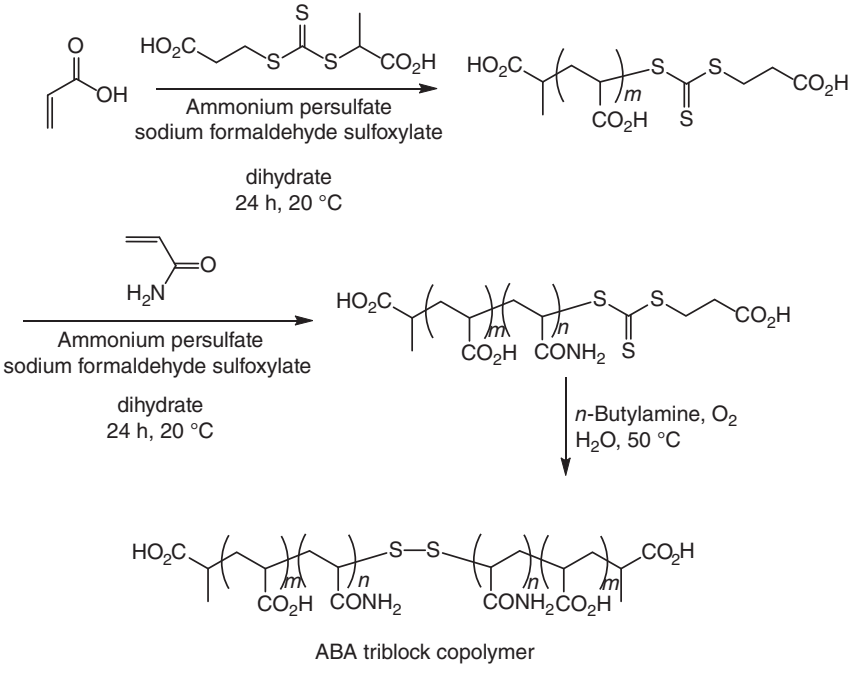

Scheme 16.26 Synthesis of ABA triblock copolymers of acrylic acid and acrylamide formed by disulfide coupling of precursor AB diblock copolymers.

hydrogels based on ABA RAFT-prepared triblocks, with gel formation occurring after aminolysis/oxidation of the trithiocarbonate groups in self-assembled micelles.

Because disulfides are stable in the absence of a reducing agent or a strong nucleophile, disulfide formation may be employed as a route to incorporate functional, or reactive, groups into (co)polymers via disulfide exchange reactions. This is readily achieved in the reaction of RAFT-derived polymeric thiols with reagents containing an electrophilic sulfur atom [263]. Suitable reagents include pyridyl disulfide [84, 264–266] or methane thiosulfonates [267–270]. The general reactions are shown in Scheme 16.27.

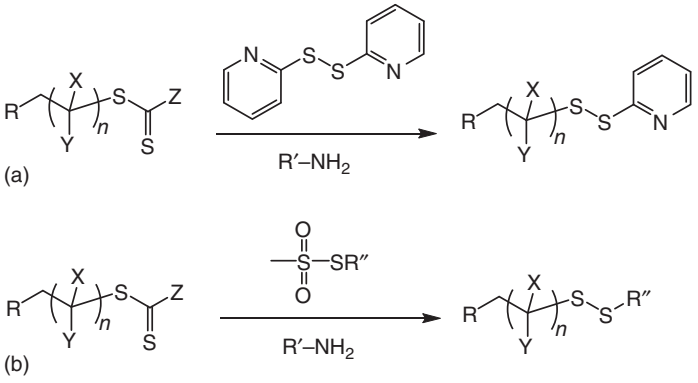

Scheme 16.27 The general thiol–pyridyl disulfide (a) and thiol–methanethiosulfonate exchange reactions (b).

Additionally, and in keeping with many of the other chemistries highlighted herein, such disulfide exchange reactions are also applicable as a route for modifying pendent groups in (co)polymers [271–273].

Although it may be desirable to simply isolate and use a pyridyl disulfide end-terminated polymer, the versatility of this approach lies in the fact that it is possible to perform thiol exchange reactions on such end-functional materials. An elegant example of such chemistry was reported by Yu et al. in the preparation of materials capable of releasing H_2S (Scheme 16.28) [274]. Dithiobenzoate-terminated poly[(oligoethylene glycol methyl ether) methacrylate]

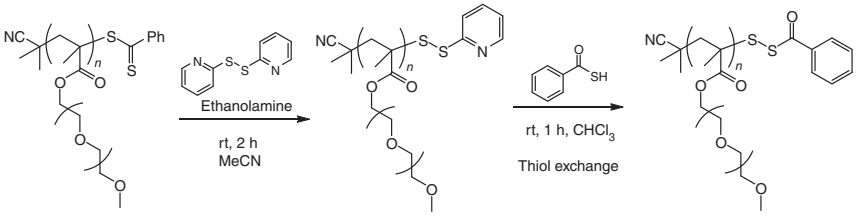

Scheme 16.28 The synthesis of an H_2S-releasing polymer via sequential modification of dithiobenzoate end groups involving cleavage and capture by pyridyl disulfide, followed by thiol exchange with benzothioic *S*-acid.

was treated with ethanolamine in the presence of dipyridyl disulfide, yielding the corresponding pyridyl disulfide end-functional polymer. Subsequent treatment with benzothioic *S*-acid gave the acyl-protected perthiol-terminated polymer. Treatment of the acyl-protected polymer with cysteine, in the presence of a chemoselective H_2S-responsive fluorescence probe, immediately resulted in a strong fluorescence at 520 nm indicative of the presence of free H_2S. This proof of concept was extended to copolymers with advanced architectures, including those capable of pH-induced self-assembly giving H_2S-releasing micelles.

A real advantage of the thiol–methanethiosulfonate reaction is the ease with which such reagents are prepared and a broad range of functionalities that can be introduced, i.e. the nature of R″. Two examples based on the introduction of bio-related functionality should serve to highlight this particular advantage. Roth et al. [275] detailed a two-step approach to α,ω-functionalized poly(diethylene glycol monomethyl ether methacrylate) with thyroxin, **II** in Figure 16.16, at the α terminus and biotin at the ω-terminus. Key to success was the use of a pentafluorophenylester-functionalized R-group dithiobenzoate as the RAFT agent, **I** and a biotin-functionalized methanethiosulfonate, **III** Figure 16.16. Following homopolymerization, the polymer was first reacted with thyroxin in a regioselective manner at the pentafluorophenylester, instilling thyroxin at the α-terminus. Even though this reaction involves a primary amine, the dithiobenzoate ω-terminal groups remain unaffected during this step. Such regioselectivity is one of the many advantages associated with pentafluorophenylester chemistry. In the second step, the dithiobenzoate end group is cleaved with propylamine in the presence of **III**, resulting in polymeric thiol formation, followed by exchange yielding the α,ω-functional homopolymer.

α,ω-Modification was confirmed via a combination of ^{1}H, ^{13}C, and ^{19}F NMR; UV–vis and IR spectroscopies; and SEC. The thyroxin transport protein prealbumin

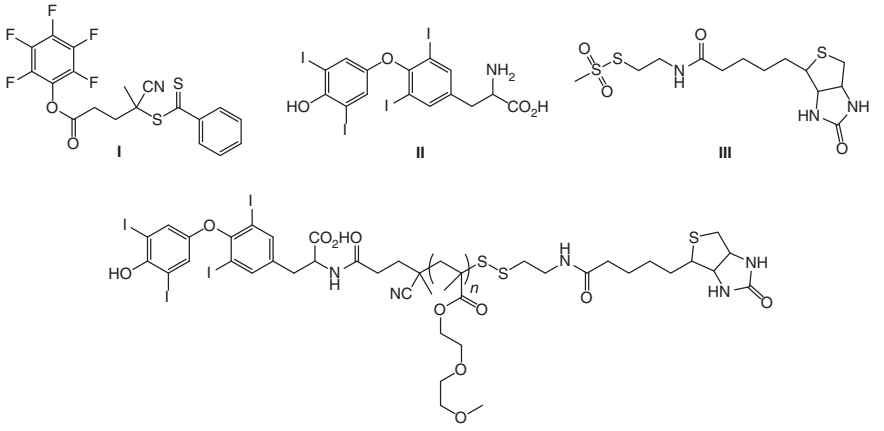

Figure 16.16 Chemical structures of a pentafluorophenylester-functional R-group dithiobenzoate RAFT CTA, **I**, thyroxin, **II**, a biotin-functional methanethiosulfonate, **III**, and a α,ω-difunctional poly(diethylene glycol monomethyl ether methacrylate) obtained via sequential nucleophilic substitution and sulfur exchange reactions.

(with two binding sites) and streptavidin (with four biotin binding sites) was conjugated to the α,ω-functional polymer, resulting in protein–polymer network formation.

Wang and Ling [276] detailed the synthesis of well-defined block copolymers of polystyrene with poly(γ-benzyl L-glutamate) via a combination of RAFT and NCA polymerization. The overall approach is shown in Scheme 16.29.

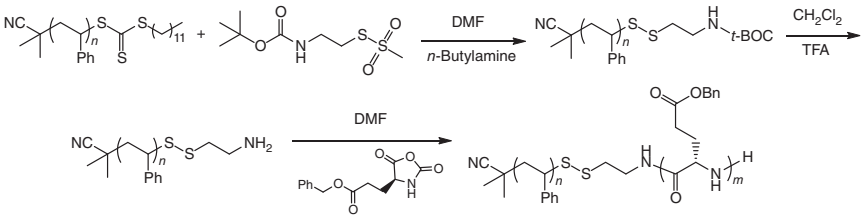

Scheme 16.29 End group modification via aminolysis/sulfur exchange with a protected amine methanethiolsulfonate, followed by removal of the *t*-Boc-protecting group and primary amine-initiated *N*-carboxyanhydride ring-opening polymerization.

Treatment of trithiocarbonate-terminated polystyrene with *n*-butylamine in the presence of *S*-(2-((*tert*-butoxycarbonyl)amino)ethyl) methanesulfonothioate yields the corresponding disulfide end-functional homopolymer; acid-mediated removal of the *t*-Boc protecting group gives the primary amine end-functional polystyrene. The macromolecular primary amine is able to serve as an initiating species in the ring-opening polymerization of benzyl L-glutamate NCA. Following block copolymerization, the benzyl group is removed by treatment with NaOH, yielding the target polystyrene–polypeptide copolymeric material. It should be noted, however, that while disulfide formation was successful, conversion of the *t*-Boc-protected macroinitiator to the free amine analogue was only 50% successful. Fortunately, polystyrene homopolymer impurity (containing the *t*-Boc-protected end group) was readily removed at the end of the ring-opening polymerization by selective precipitation.

16.3.3.8 Miscellaneous Examples of End Group Transformation and Applications

As noted earlier in this chapter, researchers continue to develop approaches for the facile synthesis and modification of (co)polymers; this includes new methods for modifying end groups in RAFT-prepared (co)polymers, in many cases for very specific, or targeted, applications. For example, Yu et al. [163] described an approach for converting dithiobenzoate end groups in RAFT-prepared poly[(oligoethyleneglycol methyl ether) methacrylate] to the corresponding *S*-nitrosothiol species, an important class of nitric oxide donor. Reaction of the parent RAFT polymer with hydrazine hydrate, followed by purification by dialysis yielded the corresponding macromolecular thiol, as verified by UV–vis spectrophotometry, albeit with c. 15% polymeric disulfide. Subsequent reaction of the macromolecular thiol, POEGMA-SH, with nitrous acid ($H_2SO_4 + NaNO_2$, 1 : 2) yielded the polymeric

S-nitrosothiol, POEGMA-SNO, as confirmed by UV–vis spectrophotometry. It is important to carefully control the stoichiometry in this modification and use a 1 : 1 polymer-SH:nitrous acid ratio. The use of excess nitrous acid results in either lower yields of the target *S*-nitrosothiol or in the case of >4 equiv of nitrous acid, no formation. The authors extended this approach to chain end modification of pH-responsive copolymer.

Recently, Lee et al. described a process for the conversion of thiocarbonylthiol end groups in RAFT polymers to the corresponding Br-terminated species [160]. Inspired by the facile and quantitative conversion of low molecular thiols such as 1-dodecanethiol and 1-adamantanethiol to the corresponding bromides using PPh_3Br_2, the authors examined the same chemistry for the modification of polystyrene thiocarbonylthio end groups prepared by RAFT. Unfortunately, the conditions that proved successful for small molecules proved inefficient for the polystyrene-SH (obtained via aminolysis of the parent homopolymer) yielding a mixture of polystyrene-SH, polystyrene-Br, and polystyrene-alkene. Following optimization, the authors did report the successful preparation of polystyrene-Br, but it required the addition of PPh_3 and Br_2 separately with careful control of the stoichiometry. Despite being a promising approach for effecting RAFT-to-ATRP crossover polymerizations, the general route has not currently been optimized.

The use of hydride reagents such as $NaBH_4$ for the cleavage of RAFT end groups was first reported in the context of generating polymers capable of stabilizing gold nanoparticles [169]. In other words, the nanoparticles serve as the 'capture' agents for the in situ-generated polymeric thiolates [277]. This is an extremely facile and rapid route to polymer–gold conjugates and has also been reported for the modification of planar gold surfaces [170] and gold nanorods [278]. The general approach has been extended to other metallic species including Fe_3O_4 [279].

Zhang et al. [280] described the application of the squaric ester 3,4-diethoxycyclobut-3-ene-1,2-dione as a hydrolysis-resistant substrate, facilitating polymer–protein ligation. Several routes were presented in this report, and here, we highlight the incorporation of the squaric ester species into the R-group of a RAFT CTA and its subsequent use. Scheme 16.30 outlines the approach adopted.

A two-step process involving substitution, followed by carbodiimide coupling yielded the squaric ester-functional trithiocarbonate, **A** (Scheme 16.30). This was shown to be an effective RAFT agent for the controlled polymerization of *N*,*N*-dimethylacrylamide. Importantly, following polymerization the α-located squaric ester/amide was demonstrated to be available for a second coupling with lysozyme. The application of the squaric ester species for protein conjugation was compared to a similar α-*N*-hydroxysuccinimide (NHS)-functional polymer with the squaric ester derivative, exhibiting significantly enhanced hydrolytic stability that facilitated the formation of the protein–polymer conjugate in a higher yield.

Golf et al. [281] reported an approach for the total removal of RAFT thiocarbonylthio end groups based on a Cu(II)-mediated cross-coupling with boronic acids. The advantages of this particular route are that it allows for the incorporation of highly functional end groups connected by a C—C bond, and it works quantitatively with low-to-medium molecular weight polymers. The drawback of this chemistry

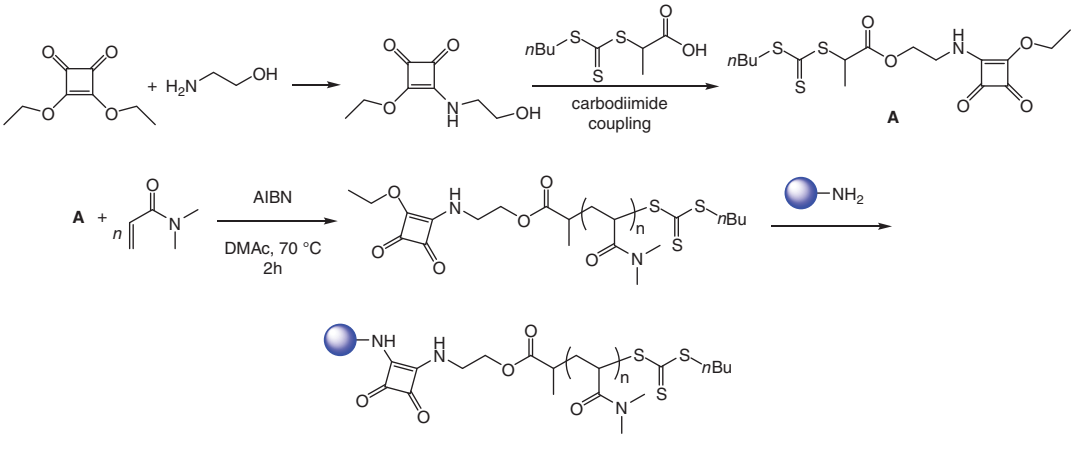

Scheme 16.30 Synthesis of a squaric ester R-group-functional trithiocarbonate, its use as a mediator for the polymerization of *N*,*N*-dimethylacrylamide, and as an amine-reactive site for conjugation post-polymerization.

is that it requires a benzylic species at the α-carbon. As such, it works well for polystyrene but is ineffective for acrylates, for example. However, the authors noted that it was possible to overcome this limitation by a single monomer insertion strategy (Scheme 16.31).

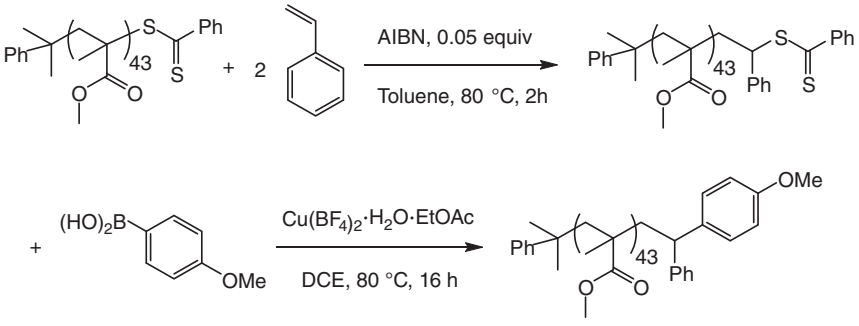

Scheme 16.31 Single styrene monomer insertion in a poly(methyl methacrylate) homopolymer followed by Cu-mediated coupling with (4-methoxyphenyl)boronic acid as a route to ω-functional polymers.

Matioszek et al. [282] developed a methodology to quantitatively transform xanthate groups on acrylic polymers into less-reactive thiocarbonate functions, by using ozone as the oxidizing agent, transforming the C=S group to a carbonyl [283] (Scheme 16.32).

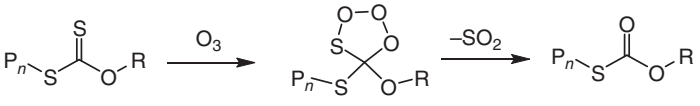

Scheme 16.32 Proposed mechanism for the ozonolysis of xanthates.

In a final example, we note that Soeriyadi et al. detailed the combination of cobalt-mediated catalytic chain transfer polymerization (CCTP) and RAFT, resulting in the removal of the thiocarbonylthtio end groups in PMMA, yielding the corresponding sulfur-free macromonomers [254].

16.4 Summary

In this chapter, we have highlighted the various chemistries that have been developed, many now routinely employed, to functionalize RAFT-prepared (co)polymers at the α-terminus, ω-terminus, or both. We hope that this overview has aided those new to the field of RAFT end group modification, as well as more experienced researchers, in the continued development and investigation of novel routes to ever-more functional materials.

References

1 Moad, G., Rizzardo, E., and Thang, S.H. (2005). *Aust. J. Chem.* 58: 379–410.
2 Moad, G., Rizzardo, E., and Thang, S.H. (2006). *Aust. J. Chem.* 59: 669–692.
3 Moad, G., Rizzardo, E., and Thang, S.H. (2009). *Aust. J. Chem.* 62: 1402–1472.
4 Moad, G., Rizzardo, E., and Thang, S.H. (2012). *Aust. J. Chem.* 65: 985–1076.
5 Keddie, D.J., Moad, G., Rizzardo, E., and Thang, S.H. (2012). *Macromolecules* 45: 5321–5342.
6 Chiefari, J., Chong, Y.K.B., Ercole, F. et al. (1998). *Macromolecules* 31: 5559–5562.
7 Kolb, H.C., Finn, M.G., and Sharpless, K.B. (2001). *Angew. Chem. Int. Ed.* 40: 2004–2021.
8 Iha, R.K., Wooley, K.L., Nyström, A.M. et al. (2009). *Chem. Rev.* 109: 5620–5686.
9 Tasdelen, M.A., Kiskan, B., and Yagci, Y. (2016). *Prog. Polym. Sci.* 52: 19–78.
10 Binder, W.H. and Sachsenhofer, R. (2007). *Macromol. Rapid Commun.* 28: 15–54.
11 Moad, G., Chong, Y.K., Postma, A. et al. (2005). *Polymer* 46: 8458–8468.
12 Willcock, H. and O'Reilly, R.K. (2010). *Polym. Chem.* 1: 149–157.
13 Moad, G., Rizzardo, E., and Thang, S.H. (2011). *Polym. Int.* 60: 9–25.
14 Harvison, M.A. and Lowe, A.B. (2011). *Macromol. Rapid Commun.* 32: 779–800.
15 Harvison, M.A., Roth, P.J., Davis, T.P., and Lowe, A.B. (2011). *Aust. J. Chem.* 64: 992–1006.
16 Mitsukami, Y., Donovan, M.S., Lowe, A.B., and McCormick, C.L. (2001). *Macromolecules* 34: 2248–2256.
17 Sumerlin, B.S., Donovan, M.S., Mitsukami, Y. et al. (2001). *Macromolecules* 34: 6561–6564.
18 Donovan, M.S., Sanford, T.A., Lowe, A.B. et al. (2002). *Macromolecules* 35: 4570–4572.
19 Donovan, M.S., Sumerlin, B.S., Lowe, A.B., and McCormick, C.L. (2002). *Macromolecules* 35: 8663–8666.
20 Thomas, D.B., Sumerlin, B.S., Lowe, A.B., and McCormick, C.L. (2003). *Macromolecules* 36: 1436–1439.
21 Donovan, M.S., Lowe, A.B., Sanford, T.A., and McCormick, C.L. (2003). *J. Polym. Sci., Part A: Polym. Chem.* 41: 1262–1281.
22 Sumerlin, B.S., Lowe, A.B., Thomas, D.B., and McCormick, C.L. (2003). *Macromolecules* 36: 5982–5987.
23 Sumerlin, B.S., Lowe, A.B., Thomas, D.B. et al. (2004). *J. Polym. Sci., Part A: Polym. Chem.* 42: 1724–1734.
24 Thomas, D.B., Convertine, A.J., Hester, R.D. et al. (2004). *Macromolecules* 37: 1735–1741.
25 Thomas, D.B., Convertine, A.J., Myrick, L.J. et al. (2004). *Macromolecules* 37: 8941–8950.
26 Convertine, A.J., Lokitz, B.S., Lowe, A.B. et al. (2005). *Macromol. Rapid Commun.* 26: 791–795.

27 Vasilieva, Y.A., Scales, C.W., Thomas, D.B. et al. (2005). *J. Polym. Sci., Part A: Polym. Chem.* 43: 3141–3152.

28 Scales, C.W., Vasilieva, Y.A., Convertine, A.J. et al. (2005). *Biomacromolecules* 6: 1846–1850.

29 Convertine, A.J., Lokitz, B.S., Vasilieva, Y. et al. (2006). *Macromolecules* 39: 1724–1730.

30 Mitsukami, Y., Hashidzume, A., Yusa, S.-i. et al. (2006). *Polymer* 47: 4330–4340.

31 Lowe, A.B., Sumerlin, B.S., and McCormick, C.L. (2003). *Polymer* 44: 6761–6765.

32 Wang, R. and Lowe, A.B. (2007). *J. Polym. Sci., Part A: Polym. Chem.* 45: 2468–2483.

33 Lowe, A.B., Wang, R., Tiriveedhi, V. et al. (2007). *Macromol. Chem. Phys.* 208: 2339–2347.

34 Yu, B., Lowe, A.B., and Ishihara, K. (2009). *Biomacromolecules* 10: 950–958.

35 Obata, M., Kobori, T., Hirohara, S., and Tanihara, M. (2015). *Polym. Chem.* 6: 1793–1804.

36 Hoff, E.A., Abel, B.A., Tretbar, C.A. et al. (2017). *Polym. Chem.* 8: 4978–4982.

37 McKenzie, T.G., Colombo, E., Fu, Q. et al. (2017). *Angew. Chem. Int. Ed.* 56: 12302–12306.

38 Keddie, D.J., Guerrero-Sanche, C., Moad, G. et al. (2011). *Macromolecules* 44: 6738–6745.

39 Muthukrishnan, S., Pan, E.H., Stenzel, M.H. et al. (2007). *Macromolecules* 40: 2978–2980.

40 Quek, J.Y., Liu, X., Davis, T.P. et al. (2015). *Polym. Chem.* 6: 118–127.

41 Wang, R., McCormick, C.L., and Lowe, A.B. (2005). *Macromolecules* 38: 9518–9525.

42 Ferguson, C.J., Hughes, R.J., Pham, B.T.T. et al. (2002). *Macromolecules* 35: 9243–9245.

43 Krieg, A., Pietsch, C., Baumgaertel, A. et al. (2010). *Polym. Chem.* 1: 1669–1676.

44 Harrisson, S. and Wooley, K.L. (2005). *Chem. Commun.*: 3259–3261.

45 Skrabania, K., Laschewsky, A., Berlepsch, H.v., and Bottcher, C. (2009). *Langmuir* 25: 7594–7601.

46 Skrabania, K., Miasnikov, A., Bivigou-Koumb, A.M. et al. (2011). *Polym. Chem.* 2: 2074–2083.

47 Lai, J.T. and Shea, R. (2006). *J. Polym. Sci., Part A: Polym. Chem.* 44: 4298–4316.

48 Shi, L., Chapman, T.M., and Beckman, E.J. (2003). *Macromolecules* 36: 2563–2567.

49 Roth, P.J., Davis, T.P., and Lowe, A.B. (2014). *Macromol. Rapid Commun.* 35: 813–820.

50 Van Herck, S., Hassannia, B., Louage, B. et al. (2019). *Eur. Polym. J.* 110: 313–318.

51 Tucker, B.S., Coughlin, M.L., Figg, C.A., and Sumerlin, B.S. (2017). *ACS Macro Lett.* 6: 452–457.

52 Jiang, D., Zhu, H., Yang, W. et al. (2017). *Sens. Actuators, B: Chem.* 239: 193–202.

53 Louage, B., van Steenbergen, M.J., Nuhn, L. et al. (2017). *ACS Macro Lett.* 6: 272–276.

54 Duret, D., Haftek-Terreau, Z., Carretier, M. et al. (2017). *Polym. Chem.* 8: 1611–1615.

55 Lueckerath, T., Strauch, T., Koynov, K. et al. (2019). *Biomacromolecules* 20: 212–221.

56 Meldal, M. and Tornøe, C.W. (2008). *Chem. Rev.* 108: 2952–3015.

57 Hein, J.E. and Fokin, V.V. (2010). *Chem. Soc. Rev.* 39: 1302–1315.

58 Brase, S., Gil, C., Knepper, K., and Zimmermann, V. (2005). *Angew. Chem. Int. Ed.* 44: 5188–5240.

59 Akeroyd, N., Pfukwa, R., and Klumperman, B. (2009). *Macromolecules* 42: 3014–3018.

60 Puttick, S., Irvine, D.J., Licence, P., and Thurecht, K.J. (2009). *J. Mater. Chem.* 19: 2679–2682.

61 Stamenović, M.M., Espeel, P., Camp, W.V., and Du Prez, F.E. (2011). *Macromolecules* 44: 5619–5630.

62 Hoyle, C.E., Lee, T.Y., and Roper, T. (2004). *J. Polym. Sci., Part A: Polym. Chem.* 42: 5301–5338.

63 Hoyle, C.E. and Bowman, C.N. (2010). *Angew. Chem. Int. Ed.* 49: 1540–1573.

64 Hoyle, C.E., Lowe, A.B., and Bowman, C.N. (2010). *Chem. Soc. Rev.* 39: 1355–1387.

65 Bohec, M.e.L., Pioge, S., Pascual, S., and Fontaine, L. (2017). *J. Polym. Sci., Part A: Polym. Chem.* 55: 3597–3606.

66 Zhang, X., Li, J., Li, W., and Zhang, A. (2007). *Biomacromolecules* 8: 3557–3567.

67 Theato, P. (2008). *J. Polym. Sci., Part A: Polym. Chem.* 46: 6677–6687.

68 Nilles, K. and Theato, P. (2010). *J. Polym. Sci., Part A: Polym. Chem.* 48: 3683–3692.

69 Aamer, K.A. and Tew, G.N. (2007). *J. Polym. Sci., Part A: Polym. Chem.* 45: 5618–5625.

70 Vanparijs, N., Maji, S., Louage, B. et al. (2015). *Polym. Chem.* 6: 5602–5614.

71 Vanparijs, N., Coen, R.D., Laplace, D. et al. (2015). *Chem. Commun.* 51: 13972–13975.

72 Wiss, K.T. and Theato, P. (2010). *J. Polym. Sci., Part A: Polym. Chem.* 48: 4758–4767.

73 Wilkins, L.E., Hasan, M., Fayter, A.E.R. et al. (2019). *Polym. Chem.* https://doi.org/10.1039/c1038py01719k.

74 Roth, P.J., Wiss, K.T., Zentel, R., and Theato, P. (2008). *Macromolecules* 41: 8513–8519.

75 Wiss, K.T., Krishna, O.D., Roth, P.J. et al. (2009). *Macromolecules* 42: 3860–3863.

76 Roth, P.J., Jochum, F.D., Forst, F.R. et al. (2010). *Macromolecules* 43: 4638–4645.

77 Roth, P.J., Haase, M., Basché, T. et al. (2010). *Macromolecules* 43: 895–902.

78 Roth, P.J., Jochum, F.D., and Theato, P. (2011). *Soft Matter* 7: 2484–2492.

79 Driessen, F., Martens, S., Meyer, B.D. et al. (2016). *Macromol. Rapid Commun.* 37: 947–951.

80 Frank, D., Espeel, P., Badi, N., and Du Prez, F.E. (2018). *Eur. Polym. J.* 98: 246–253.

81 Lysebetten, D.V., Felissati, S., Antonatou, E. et al. (2018). *ChemBioChem* 19: 641–646.

82 Celasun, S., Remmler, D., Schwaar, T. et al. (2019). *Angew. Chem. Int. Ed.* 58: 1960–1964.

83 Stamenović, M.M., Espeel, P., Baba, E. et al. (2013). *Polym. Chem.* 4: 184–193.

84 Liu, J., Bulmus, V., Barner-Kowollik, C. et al. (2007). *Macromol. Rapid Commun.* 28: 305–314.

85 Evgrafova, Z., Voigt, B., Baumann, M. et al. (2019). *ChemPhysChem* 20: 236–240.

86 Decker, C.G. and Maynard, H.D. (2015). *Eur. Polym. J.* 65: 305–312.

87 Hornung, C.H., Postma, A., Saubern, S., and Chiefari, J. (2014). *Polymer* 55: 1427–1435.

88 Postma, A., Davis, T.P., Moad, G., and O'Shea, M.S. (2005). *Macromolecules* 38: 5371–5374.

89 Postma, A., Davis, T.P., Li, G. et al. (2006). *Macromolecules* 39: 5307–5318.

90 Chong, B., Moad, G., Rizzardo, E. et al. (2006). *Aust. J. Chem.* 59: 755–762.

91 DePuy, C.H. and King, R.W. (1960). *Chem. Rev.* 60: 431–457.

92 Bressy, C., Ngo, V.G., and Margaillan, A. (2013). *Polym. Degrad. Stab.* 98: 115–121.

93 Stace, S.J., Fellows, C.M., Moad, G., and Keddie, D.J. (2018). *Macromol. Rapid Commun.* 39: 1800228.

94 Zhou, Y., He, J., Li, C. et al. (2011). *Macromolecules* 44: 8446–8457.

95 Barton, D.H.R. and McCombie, S.W. (1975). *J. Chem. Soc., Perkin Trans. 1*: 1574–1585.

96 Crich, D. and Quintero, L. (1989). *Chem. Rev.* 89: 1413–1432.

97 Chong, Y.K., Moad, G., Rizzardo, E., and Thang, S.H. (2007). *Macromolecules* 40: 4446–4455.

98 Chen, M., Ghiggino, K.P., Rizzardo, E. et al. (2008). *Chem. Commun.*: 1112–1114.

99 Tilley, A.J., Chen, M., Danczak, S.M. et al. (2012). *Polym. Chem.* 3: 892–899.

100 Hu, N., Ji, W.-X., Tong, Y.-Y. et al. (2010). *J. Polym. Sci., Part A: Polym. Chem.* 48: 4621–4626.

101 Postma, A., Davis, T.P., Evans, R.A. et al. (2006). *Macromolecules* 39: 5293–5306.

102 Moughton, A.O., Stubenrauch, K., and O'Reilly, R.K. (2009). *Soft Matter* 5: 2361–2370.

103 Hasegawa, U., van der Vlies, A.J., Simeoni, E. et al. (2010). *J. Am. Chem. Soc.* 132: 18273–18280.

104 Hornung, C.H., Postma, A., Saubern, S., and Chiefari, J. (2012). *Macromol. React. Eng.* 6: 246–251.

105 Sykes, K.J., Harrisson, S., and Keddie, D.J. (2016). *Macromol. Chem. Phys.* 217: 2310–2320.

106 Xia, Y., Tang, S., and Olsen, B.D. (2013). *Chem. Commun.* 49: 2566–2568.

107 Michl, T.D., Locock, K.E.S., Stevens, N.E. et al. (2014). *Polym. Chem.* 5: 5813–5822.
108 Chong, J.Y.T., Keddie, D.J., Postma, A. et al. (2015). *Colloids Surf., A* 470: 60–69.
109 Mattson, K.M., Pester, C.W., Gutekunst, W.R. et al. (2016). *Macromolecules* 49: 8162–8166.
110 Discekici, E.H., Shankel, S.L., Anastasaki, A. et al. (2017). *Chem. Commun.* 53: 1888–1891.
111 Carmean, R.N., Figg, C.A., Scheutz, G.M. et al. (2017). *ACS Macro Lett.* 6: 185–189.
112 Perrier, S., Takolpuckdee, P., and Mars, C.A. (2005). *Macromolecules* 38: 2033–2036.
113 Chen, M., Moad, G., and Rizzardo, E. (2009). *J. Polym. Sci., Part A: Polym. Chem.* 47: 6704–6714.
114 Sarapas, J.M., Backlund, C.M., deRonde, B.M. et al. (2017). *Chem. Eur. J.* 23: 6858–6863.
115 Kinoshita, K., Takami, T., Mori, Y. et al. (2017). *J. Polym. Sci., Part A: Polym. Chem.* 55: 8513–8519.
116 Heredia, K.L., Grover, G.N., Tao, L., and Maynard, H.D. (2009). *Macromolecules* 42: 2360–2367.
117 Nicolas, J., Guillaneuf, Y., Lefay, C. et al. (2013). *Prog. Polym. Sci.* 38: 63–235.
118 Beyou, E., Chaumont, P., Chauvin, F. et al. (1998). *Macromolecules* 31: 6828–6835.
119 Ao, Y., He, J., Han, X. et al. (2007). *J. Polym. Sci., Part A: Polym. Chem.* 45: 374–387.
120 Favier, A., Luneau, B., Vinas, J. et al. (2009). *Macromolecules* 42: 5953–5964.
121 Gruendling, T., Pickford, R., Guilhaus, M., and Barner-Kowollik, C. (2008). *J. Polym. Sci., Part A: Polym. Chem.* 46: 7447–7461.
122 Dietrich, M., Glassner, M., Gruendling, T. et al. (2010). *Polym. Chem.* 1: 634–644.
123 Gruendling, T., Dietrich, M., and Barner-Kowollik, C. (2009). *Aust. J. Chem.* 62: 806–812.
124 Howard, J.A. and Ingold, K.U. (1969). *Can. J. Chem.* 47: 3809–3815.
125 Li, C., He, J., Zhou, Y. et al. (2011). *J. Polym. Sci., Part A: Polym. Chem.* 49: 1351–1360.
126 Jesson, C.P., Pearce, C.M., Simon, H. et al. (2017). *Macromolecules* 50: 182–191.
127 Sinnwell, S., Inglis, A.J., Davis, T.P. et al. (2008). *Chem. Commun.*: 2052–2054.
128 Inglis, A.J., Sinnwell, S., Davis, T.P. et al. (2008). *Macromolecules* 41: 4120–4126.
129 Sinnwell, S., Lammens, M., Stenzel, M.H. et al. (2009). *J. Polym. Sci., Part A: Polym. Chem.* 47: 2207–2213.
130 Inglis, A.J., Sinnwell, S., Stenzel, M.H., and Barner-Kowollik, C. (2009). *Angew. Chem. Int. Ed.* 48: 2411–2414.
131 Langer, M., Mueller, J.O., Goldmann, A.S. et al. (2016). *ACS Macro Lett.* 5: 597–601.
132 Nebhani, L., Sinnwell, S., Inglis, A.J. et al. (2008). *Macromol. Rapid Commun.* 29: 1431–1437.

133 Goldmann, A.S., Tischer, T., Barner, L. et al. (2011). *Biomacromolecules* 12: 1137–1145.

134 Qiu, X.-P. and Winnik, F.M. (2006). *Macromol. Rapid Commun.* 27: 1648–1653.

135 Hansell, C.F., Espeel, P., Stamenović, M.M. et al. (2011). *J. Am. Chem. Soc.* 133: 13828–13831.

136 Oliveira, B.L., Guo, Z., and Bernardes, G.J.L. (2017). *Chem. Soc. Rev.* 46: 4895–4950.

137 Carthew, J., Frith, J.E., Forsythe, J.S., and Truong, V.X. (2018). *J. Mater. Chem. B.* 6: 1394–1401.

138 Koshy, S.T., Zhang, D.K.Y., Grolman, J.M. et al. (2018). *Acta Biomaterialia* 65: 36–43.

139 Wu, Y., Hu, J., Sun, C. et al. (2018). *Bioconjugate Chem.* 29: 2287–2295.

140 Houck, H.A., Bruycker, K.D., Billiet, S. et al. (2017). *Chem. Sci.* 8: 3098–3108.

141 Becker, G., Vlaminck, L., Velencoso, M.M. et al. (2017). *Polym. Chem.* 8: 4074–4078.

142 Baroni, A., Vlaminck, L., Mespouille, L. et al. (2019). *Macromol. Rapid Commun.* 40: 1800743.

143 Vonhören, B., Roling, O., Bruycker, K.D. et al. (2015). *ACS Macro Lett.* 4: 331–334.

144 Houck, H.A., Bruycker, K.D., Barner-Kowollik, C. et al. (2018). *Macromolecules* 51: 3156–3164.

145 Malgorzata, B., Melania, B., Laetitia, V. et al. (2017). *Eur. Polym. J.* 89: 230–240.

146 Herck, N.V. and Du Prez, F.E. (2018). *Macromolecules* 51: 3405–3414.

147 Bruycker, K.D., Billiet, S., Houck, H.A. et al. (2016). *Chem. Rev.* 116: 3919–3974.

148 Xiao, L., Chen, Y., and Zhang, K. (2016). *Macromolecules* 49: 4452–4461.

149 Mondal, P., Behera, P.K., and Singha, N.K. (2017). *Chem. Commun.* 53: 8715–8718.

150 Zhao, Y., Chen, J., Zhu, W., and Zhang, K. (2015). *Polymer* 74: 16–20.

151 Chen, J., Sun, R., Liao, X. et al. (2018). *Macromolecules* 51: 10202–10213.

152 Huang, J., Zhang, L., Tang, Z. et al. (2017). *Macromol. Rapid Commun.* 38: 1600678.

153 Hanay, S.B., Brougham, D.F., Dias, A.A., and Heise, A. (2017). *Polym. Chem.* 8: 6594–6597.

154 Vandewalle, S., Billiet, S., Driessen, F., and Du Prez, F.E. (2016). *ACS Macro Lett.* 5: 766–771.

155 Lowe, A.B. (2013). End-group functionalization of RAFT-prepared polymers using thiol-X chemistries. In: *Thiol-X Chemistries in Polymer and Materials Science*, Chapter 2 (eds. A.B. Lowe and C.N. Bowman), 28–58. RSC Publishing.

156 Xu, J., He, J., Fan, D. et al. (2006). *Macromolecules* 39: 8616–8624.

157 Mayadunne, R.T.A., Rizzardo, E., Chiefari, J. et al. (2000). *Macromolecules* 33: 243–245.

158 Mayadunne, R.T.A., Jeffery, J., Moad, G., and Rizzardo, E. (2003). *Macromolecules* 36: 1505–1513.

159 Zhang, Q., Voorhaar, L., Geest, B.G.D., and Hoogenboom, R. (2015). *Macromol. Rapid Commun.* 36: 1177–1183.

160 Lee, I.-H., Discekici, E.H., Shankel, S.L. et al. (2017). *Polym. Chem.* 8: 7188–7194.
161 Shen, W., Qiu, Q., Wang, Y. et al. (2010). *Macromol. Rapid Commun.* 31: 1444–1448.
162 Lee, C.-U., Roy, D., Sumerlin, B.S., and Dadmun, M.D. (2010). *Polymer* 51: 1244–1251.
163 Yu, S.H., Hu, J., Ercole, F. et al. (2015). *ACS Macro Lett.* 4: 1278–1282.
164 Glaria, A., Beija, M., Bordes, R. et al. (2013). *Chem. Mater.* 25: 1868–1867.
165 Dao, V.H., Cameron, N.R., and Saito, K. (2017). *Polym. Chem.* 8: 6834–6843.
166 Fan, K.W. and Granville, A.M. (2016). *Polymers* 8: 81–93.
167 Llauro, M.-F., Loiseau, J., Boisson, F. et al. (2004). *J. Polym. Sci., Part A: Polym. Chem.* 42: 5439–5462.
168 Wu, Y., Zhou, Y., Zhu, J. et al. (2014). *Polym. Chem.* 5: 5546–5550.
169 Lowe, A.B., Sumerlin, B.S., Donovan, M.S., and McCormick, C.L. (2002). *J. Am. Chem. Soc.* 124: 11562–11563.
170 Sumerlin, B.S., Lowe, A.B., Stroud, P.A. et al. (2003). *Langmuir* 19: 5559–5562.
171 Harvison, M.A., Davis, T.P., and Lowe, A.B. (2011). *Polym. Chem.* 2: 1347–1354.
172 Levit, M., Zashikhina, N., Dobrodumov, A. et al. (2018). *Eur. Polym. J.* 105: 26–37.
173 Litmanovich, E.A., Bekanova, M.Z., Shanddryuk, G.A. et al. (2018). *Polymer* 142: 1–10.
174 Shan, J., Nuopponen, M., Jiang, H. et al. (2003). *Macromolecules* 36: 4526–4533.
175 Scales, C.W., Convertine, A.J., and McCormick, C.L. (2006). *Biomacromolecules* 7: 1389–1392.
176 Espeel, P. and Du Prez, F.E. (2015). *Eur. Polym. J.* 62: 247–272.
177 Espeel, P., Goethals, F., and Du Prez, F.E. (2011). *J. Am. Chem. Soc.* 133: 1678–1681.
178 Martens, S., Driessen, F., Wallyn, S. et al. (2016). *ACS Macro Lett.* 5: 942–945.
179 Langlais, M., Coutelier, O., and Destarac, M. (2018). *Macromolecules* 51: 4315–4324.
180 Rudolph, T., Espeel, P., Du Prez, F.E., and Schacher, F.H. (2015). *Polym. Chem.* 6: 4240–4251.
181 Lowe, A.B. and Bowman, C.N. (eds.) (2013). *Thiol-X Chemistries in Polymer and Materials Science*. Cambridge: RSC Publishing.
182 Lowe, A.B. (2010). *Polym. Chem.* 1: 17–36.
183 Lowe, A.B. (2014). *Polym. Chem.* 5: 4820–4870.
184 Fairbanks, B.D., Love, D.M., and Bowman, C.N. (2017). *Macromol. Chem. Phys.* 218: 1700073.
185 Koo, S.P.S., Stamenovic, M.M., Prasath, R.A. et al. (2010). *J. Polym. Sci., Part A: Polym. Chem.* 48: 1699–1713.
186 Chan, J.W., Zhou, H., Hoyle, C.E., and Lowe, A.B. (2009). *Chem. Mater.* 21: 1579–1585.
187 Chan, J.W., Hoyle, C.E., and Lowe, A.B. (2009). *J. Am. Chem. Soc.* 131: 5751–5753.

188 Lowe, A.B., Hoyle, C.E., and Bowman, C.N. (2010). *J. Mater. Chem.* 20: 4745–4750.

189 Chan, J.W., Shin, J., Hoyle, C.E. et al. (2010). *Macromolecules* 43: 4937–4942.

190 Lowe, A.B. (2014). *Polymer* 55: 5517–5549.

191 Liu, J., Lam, J.W.Y., Jim, C.K.W. et al. (2011). *Macromolecules* 44: 68–79.

192 Yao, B., Mei, J., Li, J. et al. (2014). *Macromolecules* 47: 1325–1333.

193 Huang, D., Liu, Y., Guo, S. et al. (2019). *Polym. Chem.* https://doi.org/10.1039/c1039py00161a.

194 Alameddine, B., Baig, N., Shetty, S. et al. (2018). *Polymer* 154: 233–240.

195 Kumar, J., Bousquet, A., and Stenzel, M.H. (2011). *Macromol. Rapid Commun.* 32: 1620–1626.

196 Chan, J.W., Hoyle, C.E., Lowe, A.B., and Bowman, M. (2010). *Macromolecules* 43: 6381–6388.

197 Boyer, C., Granville, A., Davis, T.P., and Bulmus, V. (2009). *J. Polym. Sci., Part A: Polym. Chem.* 47: 3773–3794.

198 Ida, S., Yamawaki, M., Maruta, T., and Hirokawa, Y. (2018). *Trans. Mater. Res. Soc. Jpn.* 43: 71–74.

199 Xi, W., Wang, C., Kloxin, C.J., and Bowman, C.N. (2012). *ACS Macro Lett.* 1: 811–814.

200 Nair, D.P., Podgórski, M., Chatani, S. et al. (2014). *Chem. Mater.* 26: 724–744.

201 Yin, L., Dalsin, M.C., Sizovs, A. et al. (2012). *Macromolecules* 45: 4322–4332.

202 Bian, Q., Xiao, Y., and Lang, M. (2012). *Polymer* 53: 1684–1693.

203 Neindre, M. and Nicolay, R. (2013). *Polym. Int.* 63: 887–893.

204 Spruell, J.M., Levy, B.A., Sutherland, A. et al. (2009). *J. Polym. Sci., Part A: Polym. Chem.* 47: 346–356.

205 Yu, B., Chan, J.W., Hoyle, C.E., and Lowe, A.B. (2009). *J. Polym. Sci., Part A: Polym. Chem.* 47: 3544–3557.

206 Zhu, Y., Batchelor, R., Lowe, A.B., and Roth, P.J. (2016). *Macromolecules* 49: 672–680.

207 Wang, Y., Zheng, Z., Huang, Z., and Ling, J. (2017). *Polym. Chem.* 8: 2659–2665.

208 Duret, D., Haftek-Terreau, Z., Carretier, M. et al. (2018). *Polym. Chem.* 9: 1857–1868.

209 Messina, M.S., Graefe, C.T., Chong, P. et al. (2019). *Polym. Chem.* 10: 1660–1667.

210 Roth, P.J., Davis, T.P., and Lowe, A.B. (2012). *Macromolecules* 45: 3221–3230.

211 Roth, P.J., Davis, T.P., and Lowe, A.B. (2012). *Polym. Chem.* 3: 2228–2235.

212 Zhu, Y., Quek, J.Y., Lowe, A.B., and Roth, P.J. (2013). *Macromolecules* 46: 6475–6484.

213 Zhu, Y., Lowe, A.B., and Roth, P.J. (2014). *Polymer* 55: 4425–4431.

214 Ho, H.T., Levere, M.E., Pascual, S. et al. (2012). *J. Polym. Sci., Part A: Polym. Chem.* 50: 1657–1661.

215 Delaittre, G., Pauloehrl, T., Bastmeyer, M., and Barner-Kowollik, C. (2012). *Macromolecules* 45: 1792–1802.

216 Li, M., De, P., Li, H., and Sumerlin, B.S. (2010). *Polym. Chem.* 1: 854–859.

217 Huang, X., Boyer, C., Davis, T.P., and Bulmus, V. (2011). *Polym. Chem.* 2: 1505–1512.
218 Espeel, P., Goethals, F., Stamenović, M.M. et al. (2012). *Polym. Chem.* 3: 1007–1015.
219 Abel, B.A. and McCormick, C.L. (2016). *Macromolecules* 49: 6193–6202.
220 Zhao, J., Zhou, Y., Zhou, Y. et al. (2016). *Polym. Chem.* 7: 1782–1791.
221 Chakma, P., Digby, Z.A., Via, J. et al. (2018). *Polym. Chem.* 9: 4744–4756.
222 Battistella, C., Yang, Y., Chen, J., and Klok, H.-A. (2018). *ACS Omega* 3: 9710–9721.
223 Hiruta, Y., Nagumo, Y., Miki, A. et al. (2015). *RSC Adv.* 5: 73217–73224.
224 Grover, G.N., Alconcel, S.N.S., Matsumoto, N.M., and Maynard, H.D. (2009). *Macromolecules* 42: 7675–7663.
225 Yang, Z., Fu, K., Yu, J., and Liu, X. (2019). *J. Inorg. Organomet. Polym. Mater.* 29: 59–65.
226 Ho, H.T., Levere, M.E., Soutif, J.-C. et al. (2011). *Polym. Chem.* 2: 1258–1260.
227 Chan, J.W., Yu, B., Hoyle, C.E., and Lowe, A.B. (2008). *Chem. Commun.*: 4959–4961.
228 Chan, J.W., Yu, B., Hoyle, C.E., and Lowe, A.B. (2009). *Polymer* 50: 3158–3168.
229 Li, M., De, P., Gondi, S.R., and Sumerlin, B.S. (2008). *J. Polym. Sci., Part A: Polym. Chem.* 46: 5093–5100.
230 Lu, D., Jia, Z., and Monteiro, M.J. (2013). *Polym. Chem.* 4: 2080–2089.
231 Shin, J., Lee, J., and Jeong, H.M. (2018). *J. Appl. Polym. Sci.* 135: 46070.
232 Tan, J., Li, C., Dan, S. et al. (2016). *Chem. Eng. J.* 304: 461–468.
233 Gamardella, F., Ramis, X., De la Flor, S., and Serra, A. (2019). *React. Funct. Polym.* 134: 174–182.
234 Shin, J., Matsushima, H., Comer, C.M. et al. (2010). *Chem. Mater.* 22: 2616–2625.
235 Zou, F., Yue, P., Zheng, X. et al. (2016). *J. Mater. Chem. A* 4: 10801–10805.
236 Hensarling, R.M., Rahane, S.B., LeBlanc, A.P. et al. (2011). *Polym. Chem.* 2: 88–90.
237 Hensarling, R.M., Hoff, E.A., LeBlanc, A.P. et al. (2013). *J. Polym. Sci., Part A: Polym. Chem.* 51: 1079–1090.
238 Flores, J.D., Shin, J., Hoyle, C.E., and McCormick, C.L. (2010). *Polym. Chem.* 1: 213–220.
239 Hoff, E.A., Abel, B.A., Tretbar, C.A. et al. (2016). *Macromolecules* 49: 554–563.
240 Li, H., Yu, B., Matsushima, H. et al. (2009). *Macromolecules* 42: 6537–6542.
241 Boursier, T., Georges, S., Mosquet, M. et al. (2016). *Polym. Chem.* 7: 917–925.
242 Stuparu, M.C. and Khan, A. (2016). *J. Polym. Sci., Part A: Polym. Chem.* 54: 3057–3070.
243 De, S. and Khan, A. (2012). *Chem. Commun.* 48: 3130–3132.
244 Muzammil, E.M., Khan, A., and Stuparu, M.C. (2017). *RSC Adv.* 7: 55874–55884.
245 McLeod, D.C. and Tsarevsky, N.V. (2016). *Macromolecules* 49: 1135–1142.
246 Rosen, B.M., Lligadas, G., Hahn, C., and Percec, V. (2009). *J. Polym. Sci., Part A: Polym. Chem.* 47: 3931–3939.

247 Rosen, B.M., Lligadas, G., Hahn, C., and Percec, V. (2009). *J. Polym. Sci., Part A: Polym. Chem.* 47: 3940–3948.
248 Agar, S., Baysak, E., Hizal, G. et al. (2018). *J. Polym. Sci., Part A: Polym. Chem.* 56: 1181–1198.
249 Bhebhe, M.N., De Eulate, E.A., Pei, Y. et al. (2017). *Macromol. Rapid Commun.* 38: 1600450.
250 Nakayama, M. and Okano, T. (2005). *Biomacromolecules* 6: 2320–2327.
251 Segui, F., Qiu, X.-P., and Winnik, F.M. (2008). *J. Polym. Sci., Part A: Polym. Chem.* 46: 314–326.
252 Xu, J., Tao, L., Boyer, C. et al. (2010). *Macromolecules* 43: 20–24.
253 Chen, S., Schulz, M., Lechner, B.-D. et al. (2015). *Polym. Chem.* 6: 7988–7994.
254 Soeriyadi, A.H., Boyer, C., Burns, J. et al. (2010). *Chem. Commun.* 46: 6338–6340.
255 Döhler, D., Kaiser, J., and Binder, W.H. (2017). *Polymer* 133: 148–158.
256 Noy, J.-M., Friedrich, A.-K., Batten, K. et al. (2017). *Macromolecules* 50: 7028–7040.
257 Noy, J.-M., Koldevitz, M., and Roth, P.J. (2015). *Polym. Chem.* 6: 436–447.
258 Zeng, J., Zhu, J., Pan, X. et al. (2013). *Polym. Chem.* 4: 3453–3457.
259 Lu, W., An, X., Gao, F. et al. (2017). *Macromol. Chem. Phys.* 218: 1600485.
260 Whittaker, M.R., Goh, Y.-K., Gemici, H. et al. (2009). *Macromolecules* 39: 9028–9034.
261 Goh, Y.-K., Whittaker, A.K., and Monteiro, M.J. (2007). *J. Polym. Sci., Part A: Polym. Chem.* 45: 4150–4153.
262 Vogt, A.P. and Sumerlin, B.S. (2009). *Soft Matter* 5: 2347–2351.
263 Schäfer, O. and Barz, M. (2018). *Chem. Eur. J.* 24: 12131–12142.
264 Boyer, C., Liu, J., Bulmus, V., and Davis, T.P. (2009). *Aust. J. Chem.* 62: 830–847.
265 Grover, G.N., Lee, J., Matsumoto, N.M., and Maynard, H.D. (2012). *Macromolecules* 45: 4958–4965.
266 Urquhart, M.C., Ercole, F., Whittaker, M.R. et al. (2018). *Polym. Chem.* 9: 4431–4439.
267 Chua, G.B.H., Roth, P.J., Duong, H.T.T. et al. (2012). *Macromolecules* 45: 1362–1374.
268 Quek, J.Y., Roth, P.J., Evans, R.A. et al. (2013). *J. Polym. Sci., Part A: Polym. Chem.* 51: 394–404.
269 Quek, J.Y., Zhu, Y., Roth, P.J. et al. (2013). *Macromolecules* 46: 7290–7302.
270 Roth, P.J., Kessler, D., Zentel, R., and Theato, P. (2009). *J. Polym. Sci., Part A: Polym. Chem.* 47: 3118–3130.
271 Gevrek, T.N., Cosar, M., Aydin, D. et al. (2018). *ACS Appl. Mater. Interfaces* 10: 14399–14409.
272 Peng, H., Rübsam, K., Huang, X. et al. (2016). *Macromolecules* 49: 7141–7154.
273 Ji, X., Liu, J., Liu, L., and Zhao, H. (2016). *Colloids Surf., B* 148: 41–48.
274 Yu, S.H., Ercole, F., Veldhuis, N.A. et al. (2017). *Polym. Chem.* 8: 6362–6367.
275 Roth, P.J., Jochum, F.D., Zentel, R., and Theato, P. (2010). *Biomacromolecules* 11: 238–244.
276 Wang, Y. and Ling, J. (2015). *RSC Adv.* 5: 18546–18553.

277 Pereira, S.O., Barros-Timmons, A., and Trindade, T. (2018). *Polymers* 10: 198–215.
278 Hotchkiss, J.W., Lowe, A.B., and Boyes, S.G. (2007). *Chem. Mater.* 19: 6–13.
279 Wua, Y., Yang, H., Lin, Y. et al. (2016). *Mater. Lett.* 169: 218–222.
280 Zhang, Z., Vanparijs, N., Vandewalle, S. et al. (2016). *Polym. Chem.* 7: 7242–7248.
281 Golf, H., O'Shea, R., Braybrook, C. et al. (2018). *Chem. Sci.* 9: 7370–7375.
282 Matioszek, D., Dufils, P.-E., Vinas, J., and Destarac, M. (2015). *Macromol. Rapid Commun.* 36: 1354–1361.
283 Quiclet-Sire, B. and Zard, S.Z. (2010). *Bull. Korean Chem. Soc.* 31: 543–544.

17

Sequence-Encoded RAFT Oligomers and Polymers

Joris J. Haven, Jeroen De Neve, and Tanja Junkers

Monash University, School of Chemistry, Polymer Reaction Design Group, 19 Rainforest Walk, Clayton, VIC 3800, Australia

Reversible deactivation radical polymerization (RDRP) techniques such as reversible addition fragmentation chain transfer (RAFT) polymerization provide an unprecedented level of control over molecular weight (distributions), compositions, and architectures [1–3]. Compared to natural polymers, such as DNA, proteins, or complex carbohydrates, radical chain growth copolymerization always results in statistical distributions of chain lengths and monomers (determined by the monomer reactivity ratios) [4]. Products are inherently of a disperse nature (dispersity [$Đ$] > 1). Dispersity is typically defined for describing the non-uniformity with respect to molecular weight but can also be used to describe monomer distributions, or, for example, branches within a chain. Nonetheless, absolute control over monomer sequence, with precision as achieved by nature in protein or polynucleotide biosynthesis, was thoroughly explored in the last decennia [5]. These materials have enormous potential for application in, e.g. catalysis (artificial enzymes), molecular recognition, or data storage [6]. The field has advanced significantly, with RAFT polymerization playing an important role as a tool to deliver such materials. Most research has been devoted to the development of materials with encoded sequence information. Information is thereby stored in a macromolecule by the order of comonomers in a multiblock copolymer. The more blocks are added to a chain, the more information is saved. The advances of RAFT polymerization in terms of polymerization efficiency and foremost improvements in livingness of polymerizations have enabled the synthesis of multiblock copolymers with a significant number of blocks. Although the standard of synthesis was tri- or tetrablock copolymers just a few years ago [7], materials with more than 20 blocks are nowadays available with high precision from both RAFT polymerization and cobalt- or copper-mediated radical polymerizations [5]. If RAFT polymers are sequentially chain extended in this way, one refers to the so-called sequence-controlled (SC) polymers. SC polymers generally require a high livingness of polymerizations. Fast polymerizations are useful to achieve significant sequence lengths in a given period of time but are not strictly necessary. Still, most SC polymers are built from

RAFT Polymerization: Methods, Synthesis and Applications, First Edition.
Edited by Graeme Moad and Ezio Rizzardo.

acrylates or acrylamides. High livingness can be achieved by improving process control [8–10] and by rational choice of initiator concentrations [11, 12]. Perrier and coworkers had demonstrated that if initiator concentrations are kept significantly low, full monomer conversions are still achievable for 99% livingness of the process [11]. In this way, the number of blocks in a polymer becomes virtually infinite. Yet, the longest reported SC chain for RAFT polymerization consists of 20 blocks [11], with the overall record being held by Haddleton and coworkers with a polymer consisting of 24 blocks (made from addition fragmentation radical polymerization using macromonomers) [13]. Limitations in the number of blocks are given by several factors. For one, any exogenous production of radicals inevitably creates new chains during each block extension, diluting the actual multiblock copolymers. Alongside with some accumulated dead polymer chains, this can lead to significant amounts of materials already after several block extension steps [14]. Further, the dispersity of each block increases with each successive extension even if the overall dispersity remains low [15]. In this way, the sequence information is 'smeared out' and becomes prone to errors. Likewise, the dispersity per block needs to be taken into account as a lower limit for each block extension, in order to ensure that every chain in the mixture actually contains all blocks [4]. Yet – despite these limitations – an impressive realm of materials is opened up by SC polymers, and the study of the physical properties of these materials is still in its infancy.

In this chapter, the focus will be on the so-called sequence-defined (SD), discrete polymers ($Đ = 1$) obtained via RAFT or macromolecular design via the interchange of xanthates (MADIX) polymerization. SD oligomers are a subclass of SC polymers where single monomers rather than full (higher dispersity) blocks are inserted into a chain [16]. Various strategies towards the synthesis of SD materials have to date been proposed, with the majority of them relying on click chemistry-type coupling reactions [17–25]. These methods are reviewed here [5, 6, 26–29]. RDRP techniques including RAFT constitute interesting alternatives to these methods. Because RAFT (or any other RDRP technique) is inherently governed by statistical addition of monomers to growing chain ends, a stepwise addition of single-monomer units must rely on either overcoming the statistical nature by selective insertion of single units into the initiator or control agent or on the separation of mixtures of oligomers obtained after polymerization.

Zard took a first step towards achieving this via xanthate transfer chemistry [30]. Selective insertion of a single-monomer unit of less-activated monomers (LAMs) such as vinyl esters, vinyl amides, and allyl monomers was performed in 20–70% isolated yields [31–35]. In the same study, it was also analysed that single-unit monomer insertion (SUMI) into xanthates was not possible with more activated monomers (MAMs). Scheme 17.1 illustrates the radical exchange process of thiocarbonylthio derivatives for addition of xanthates to LAMs. Radicals, generated by an external radical source, can add to the starting xanthate to form a stabilized adduct radical, which is sterically too hindered to terminate (path A). Therefore, it can only undergo fragmentation (path B or C). Path B is highly unlikely because of the generation of a high energy ethyl radical; therefore, favouring path C that simply leads to the starting xanthate making this reaction path reversible and degenerate.

Therefore, the lifetime of a radical increases significantly, making addition to LAMs (e.g. non-activated alkenes) possible. In the case of addition to a LAM (path D), a new radical (**4**) is generated, which in turn can react reversibly with the starting xanthate (**5**). Analogous to path C, fragmentation of the intermediate radical (**5**) yields the final SUMI product (**6**) and the initial radical. The presence of xanthate in the SUMI product, by intermolecular radical addition, was used to introduce various functional groups, and complex structures could be rapidly assembled. This novel radical exchange process proved a powerful asset for further modifications via both radical and non-radical pathways.

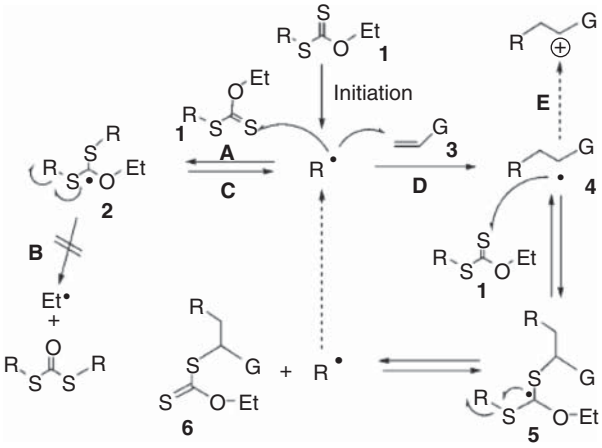

Scheme 17.1 Reaction scheme for the addition of xanthates to less-activated monomers (LAMs), in this case olefins. Source: Reproduced with permission from Quiclet-Sire and Zard [31]. Copyright 2006, John Wiley & Sons.

SUMI of MAMs was reported for the first time by Chen et al. [36]. They used such an approach for the synthesis of functionalized RAFT agents for light harvesting polymers. A method was proposed to introduce suitable chromophores into a dithiobenzoate RAFT agent to synthesize light harvesting polymers of acenaphthylene, containing a coumarin terminal energy trap (coumarin SUMI, followed by polymerization of acenaphthylene). Acenaphthyl and coumarin chromophores were selected as the energy donor and acceptor, respectively, as they fulfil the spectral overlap requirements for radiationless energy transfer. A conventional RAFT polymerization of coumarin was performed; however, an equimolar monomer to RAFT agent ratio was employed (instead of a large excess of monomer), initiated by a small amount (1–2% molar equiv) of free radical initiator. As a result, a new dithiobenzoate macro-RAFT agent was synthesized in 85% isolated yield via a selective SUMI of a styrene derivative (coumarin) into an initial dithiobenzoate RAFT agent. This methodology was extended to more complex examples of SUMI via RAFT polymerization (see example in Scheme 17.2) [38, 39].

Multiple research groups described strategies to synthesize end-functionalized polymers and junction-functionalized diblock copolymers via SUMI of maleic

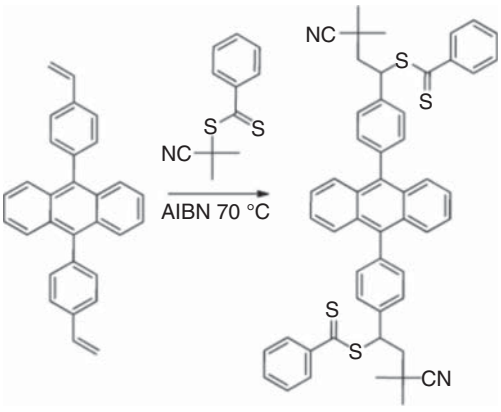

Scheme 17.2 Example of a more complex SUMI for the synthesis of dithiobenzoate macro-RAFT agents. Source: Reproduced with permission from Houshyar et al. [37]. Copyright 2012, Royal Society of Chemistry.

anhydride (MAH) [40, 41] or maleimide [42] into macro-RAFT agents. Both monomers do not readily homopolymerize; as a consequence, they could be used in large excess with respect to the macro-RAFT agent to yield the SUMI product.

Klumperman and coworkers investigated the processes that occur during the early stages (the first few monomer insertion steps) of a RAFT polymerization. Polymerization species formed over time were monitored via online (*in situ*) ^{1}H nuclear magnetic resonance spectroscopy (^{1}H-NMR). In a first report, an AIBN-initiated RAFT polymerization of styrene, mediated by the RAFT agent cyanoisopropyl dithiobenzoate at various temperatures and RAFT agent concentrations, and a low monomer to RAFT agent ratio (first few monomer insertions), was monitored as a function of time [43]. They found that RAFT polymers with a degree of polymerization (DP) greater than one were formed only after complete conversion of the initial dithiobenzoate RAFT agent to a dithiobenzoate macro-RAFT agent with one styrene monomer inserted. This phenomenon was called selective initialization, with almost no production of RAFT polymers with a DP > 1 until all of the cyanoisopropyl dithiobenzoate was converted to a single-monomer insertion macro-RAFT agent. This selective behaviour was explained by the selective fragmentation in the RAFT pre-equilibrium towards tertiary radicals and the addition of propagating radicals (of at least DP = 1) to the dithiobenzoate RAFT agent that is much faster than to the monomer (propagation). Figure 17.1 shows the concentration of dithiobenzoate species for the RAFT polymerization described above as a function of time, monitored via online ^{1}H-NMR. Fast depletion of the initial dithiobenzoate RAFT agent (AD) and rapid formation of the SUMI product (ASD) were observed. After complete depletion of the dithiobenzoate RAFT agent (AD, 50 minutes), the ASD SUMI product was formed quantitatively, and higher insertion products were identified. However, no similar behaviour was observed for subsequent monomer additions.

This observed selective initialization behaviour of RAFT-mediated polymerization was studied in more depth for a range of different RAFT/MADIX agents and monomers (including styrene, methyl acrylate, *N*-vinylpyrrolidone, vinyl acetate,

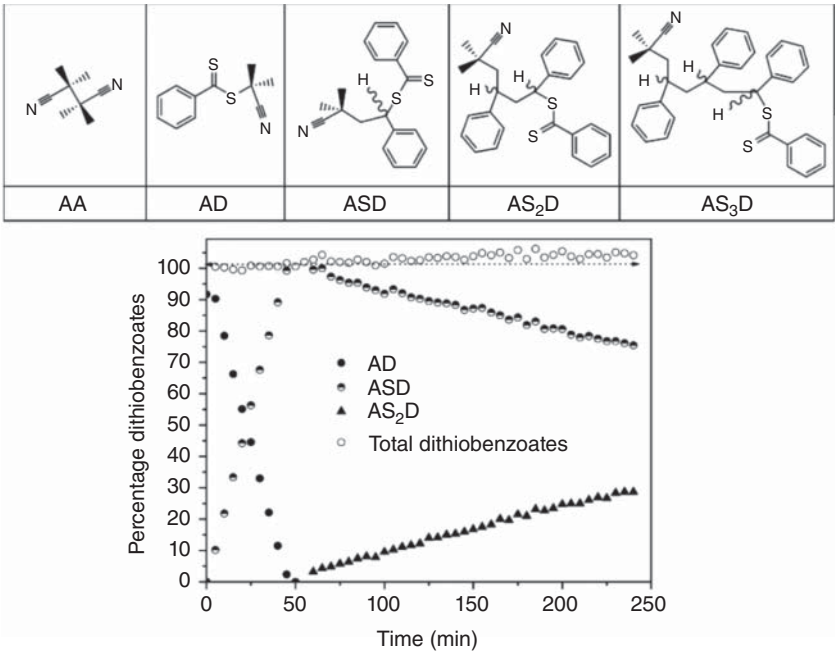

Figure 17.1 Online ^{1}H-NMR monitoring of dithiobenzoate species as a function of time during the free radical polymerization of styrene at 70 °C mediated by a cyanoisopropyl dithiobenzoate RAFT agent using AIBN as a thermal initiator. Source: Reprinted with permission from McLeary et al. [43]. Copyright 2004, American Chemical Society.

and MAH) [43–49]. It was argued by Moad and coworkers that such a selective initialization process should be observed only if (i) addition of the radical R to monomer is rapid (efficient reinitiation) with respect to monomer propagation ($k_{p(0)} \gg k_{p(1)}$) and (ii) the RAFT agent has a high transfer constant so that less than one monomer unit is inserted per activation cycle ($k_{tr} \gg k_p$, transfer constant depends on relative rate of addition to the RAFT agent and fragmentation of the intermediate radical). Bearing this in mind, the system (choice of RAFT agent and monomers) can be tuned to obtain high yields (>95%) for the SUMI process [50, 51]. In general, this means that xanthates and dithiocarbamates are preferred RAFT agents for SUMI of LAMs (vinyl monomers) and dithiobenzoates and trithiocarbonates for MAMs (styrenic and acrylic monomers). Switchable RAFT agents could be suitable for both MAMs and LAMs [52, 53].

The first sequence-defined dimers were synthesized by Quiclet-Sire et al. by xanthate transfer chemistry [34]. This was achieved by a SUMI of the electron-poor vinyl phthalimide, followed by an electron-rich LAM. Moad and coworkers extended the range of SUMI processes with MAMs into dithiobenzoate and trithiocarbonate RAFT agents and showed that a wide range of MAMs can be inserted when certain criteria were met (high transfer constant of RAFT agent and rapid addition of radical to monomer) [37]. The synthesis of new macro-RAFT agents was explored by two sequential SUMI of MAMs 'one at a time' into an initial trithiocarbonate RAFT

agent [37, 54, 55]. The reaction of the initial RAFT agent, 2-cyanopropan-2-yl decyl trithiocarbonate, with styrene monomer and AIBN as the thermal initiator, resulted in the formation of the SUMI product in an isolated yield of 85% (see Scheme 17.3). Oligomers were not detected, and the main side products were a small amount of initial RAFT agent and the expected by-products from AIBN decomposition. The same procedure was applied to a SUMI of *N*-isopropylacrylamide (NIPAm) with a slightly higher yield (90%, Scheme 17.3). In a next step, both macro-RAFT SUMI products were subjected to a similar SUMI process. NIPAm was inserted into the earlier synthesized styrene SUMI (**3**) and the styrene-NIPAm dimer (**4**) was obtained in 35% isolated yield. The reaction rate was relatively slow (because of fragmentation of the intermediate macro-RAFT radical in favour of the starting materials, for more details see literature [37]), and the reaction was stopped because of exhaustion of the thermal initiator. Again, no higher oligomers were detected. A SUMI of styrene in the NIPAm SUMI product for the synthesis of a NIPAm-styrene dimer was unsuccessful.

More in depth analysis of the process was performed via online ^{1}H-NMR of similar SUMI reactions and the kinetics of the system were simulated to consider the advantages and limitations of the process. In another contribution by Moad et al. [54], SUMI into a dithioester RAFT agent (2-cyanopropan-2-yl dithiobenzoate) was explored. AIBN was used as a thermal radical source to avoid initiator-derived insertion products in the first SUMI step. As expected, styrene and NIPAm were successfully inserted into the RAFT agent in high yields. Attempts with other monomers were less successful. SUMI of methyl methacrylate (MMA) formed oligomeric products (because of low transfer constant of dithiobenzoates in MMA polymerization). Low yields were observed in the SUMI process of MAH (because of the low reactivity of MAH towards AIBN and reinitiating 2-cyanopropan-2-yl radicals). Also dimers of styrene –X (with X = MAH, styrene, and NIPAm) were targeted via SUMI of X in the styrene macro-RAFT agent. SUMI with styrene and NIPAm was slow, which could be explained by the poor leaving group ability of the propagating species. SUMI of MAH into the styrene macro-RAFT agent proved to be fast and efficient. Furthermore, RAFT SUMI of various acrylamides was explored in aqueous media [55]. It seems, however, very crucial to carefully select the RAFT agent, monomer, initiator, and reaction parameters to optimize the yield of the desired products.

Although SUMI reactions can be carried out with very high efficiency, it is problematic to use the above strategy to create longer sequences, as monomer reactivities and RAFT agents must be carefully tuned, thereby limiting the available choice of monomers. When inserting monomers of the same family, oligomerization becomes unavoidable after the first SUMI step. Thus, the group of Junkers and coworkers developed a procedure for the synthesis of SD oligo(acrylate)s with up to four monomer insertions (consisting of *n*-butyl acrylate (*n*BA), *tert*-butyl acrylate (*t*BA), and 2-ethylhexyl acrylate (EHA)) via RAFT polymerization based on oligomer separation [56]. The RAFT agent 2-cyano-2-propyl dodecyl trithiocarbonate (CPD-TTC) was used in very short reactions of only 10 minutes, with NMR and electrospray ionization mass spectrometry (ESI-MS) analysis showing >99% RAFT end group retention. This method is independent of the specific acrylate monomer applied, and as such, a free selection of the preferable sequence order

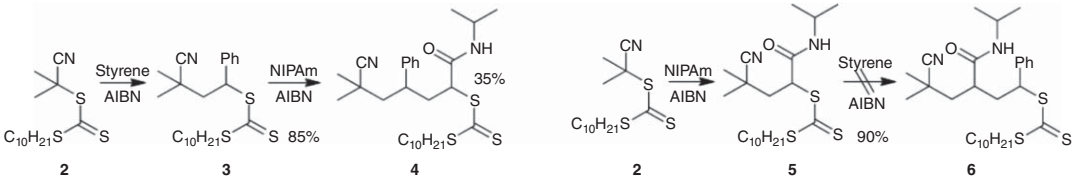

Scheme 17.3 Schematic representation of the single-unit monomer insertion (SUMI) process for styrene-NIPAm and NIPAm-styrene macro-RAFT agents (dimers). Source: Reproduced with permission from Houshyar et al. [37]. Copyright 2012, Royal Society of Chemistry.

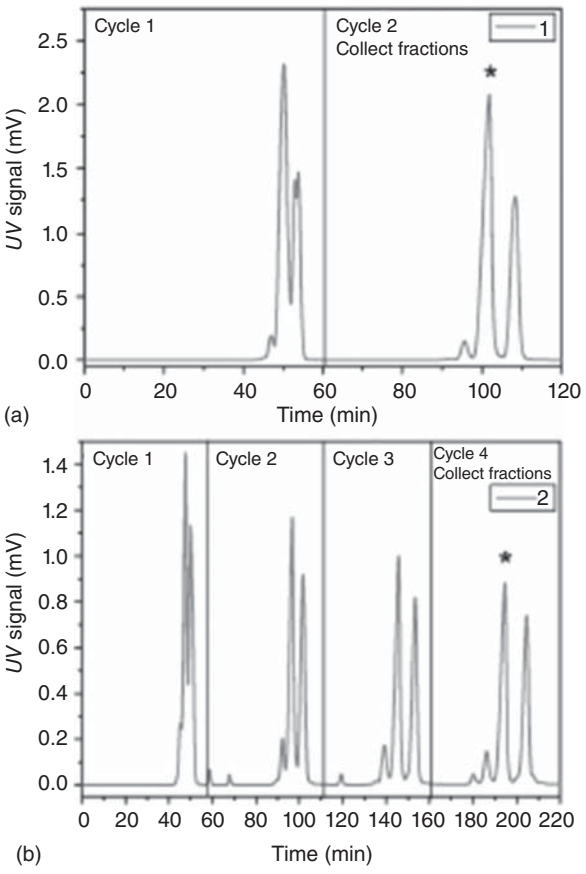

Figure 17.2 Recycling SEC trace recorded during consecutive purification cycles of (a) *n*BA oligo-RAFT agent and (b) *n*BA-EHA macro-RAFT agent. The desired oligomer is marked with an asterisk. Source: Vandenbergh et al. [56]. © 2013, Royal Society of Chemistry.

could be synthesized. To cope with the statistical nature of a radical polymerization reaction, a purification step after each insertion was always performed. Instead of laborious manual column chromatography, preparative recycling size exclusion chromatography (SEC) was found to allow facile and automated purification of mixed samples to obtain uniform SD materials (Figure 17.2). The setup operated by returning the elution flow of a column bank back to the column entry until molecules with a different size were separated, monitored via both UV and RI detection. Separation via recycling SEC gets more difficult the more monomer units are added to the growing oligomer chain because the hydrodynamic volume, being the separating factor of SEC, does not scale linearly with chain length. Where the first monomer insertion still resulted in a respectable yield of 55% (also relatively low because of the statistical nature of radical polymerization), the final reaction step and subsequent purification reached a yield of only around 15%.

A further optimization of the SUMI process could be established by continuous online monitoring and rapid kinetic screening of the reaction via an ESI-MS microreactor coupling [57]. In this respect, ESI-MS is unmatched in its ability to determine specific product patterns, with the possibility for accelerated optimization of SUMI

reactions. In this specific case, the SUMI of EHA into a CPD-TTC macro-RAFT agent already containing one acrylate monomer insertion was investigated. Insertions of up to three EHA units were identified and yields for the single-insertion product were optimized through tuning of reaction temperature, residence time, and reagent ratios. Only trace amounts of material and minimal time were required because a single experimental setup affords all experimental data. The so-optimized reaction conditions of five minutes residence time and a fivefold ratio of EHA to macro-RAFT agent at 100 °C were easily transferable to the upscaled synthesis (100×) from a micro- to milliflow reactor process, with a resulting isolated yield of almost 45% for the EHA-SUMI product.

Subsequently, kinetic modelling was employed to investigate the parameters that had a positive influence on SUMI reaction efficiencies via RAFT polymerization [58]. Factors such as radical flux, termination, and RAFT addition rate coefficients or monomer concentration (at a fixed ratio) were shown to have a negligible effect on the outcome of the simulations. However, it was the propagation rate that exhibited a strong chain length dependency with a resulting decrease of individual reaction yields, especially for the first few insertion steps. From these insights, several recommendations for reaction optimization could be formulated. Monomer and RAFT agent concentration can be chosen freely. Reaction temperature and initiator concentration can be picked according to the desired reaction time unless extreme conditions are considered that would favour the creation of side products. To increase the overall polymerization rate, higher monomer equivalents are advised, while insertion of multiple units does not have a significant effect when the monomer to RAFT agent ratio is kept below 10 : 1. The observed product distributions in the simulations are an immediate effect of the individual rate coefficients rather than the employed control methodology, and thus, similar results are to be expected from other RDRP techniques [59]. It could further be shown that after initialization of the RAFT process – once the main equilibrium is reached – a maximum yield of 50% can be expected per SUMI reaction, thus limiting the efficiency of the process even for perfect oligomer separation conditions.

These insights enabled the synthesis of a uniform decamer by relying on the fact that chain growth is not limited to one unit at a time in RDRP reactions [60]. In other words, well-defined structures could be produced directly via multiple unit monomer insertion (MUMI) resembling the perfectly defined repeating sequences often found in biological SD materials. Employing this power of RAFT polymerizations, SUMI and MUMI reactions were combined with four different acrylic monomers. The targeted discrete oligomers were isolated by automated flash column chromatography, which was significantly faster than recycling SEC with isolation of a decamer taking roughly one hour (Figure 17.3). Flash chromatography as an oligomer separation method had been introduced by Hawker and coworkers and provides surprisingly easy access to chain length separations at low DP [61]. This approach also made it possible to separate longer sequence lengths than recycling SEC. Isolated yields could be maximized because of the baseline separation of the various insertion products, hence considerably limiting product losses. The RAFT end groups were then used to couple two telechelic discrete

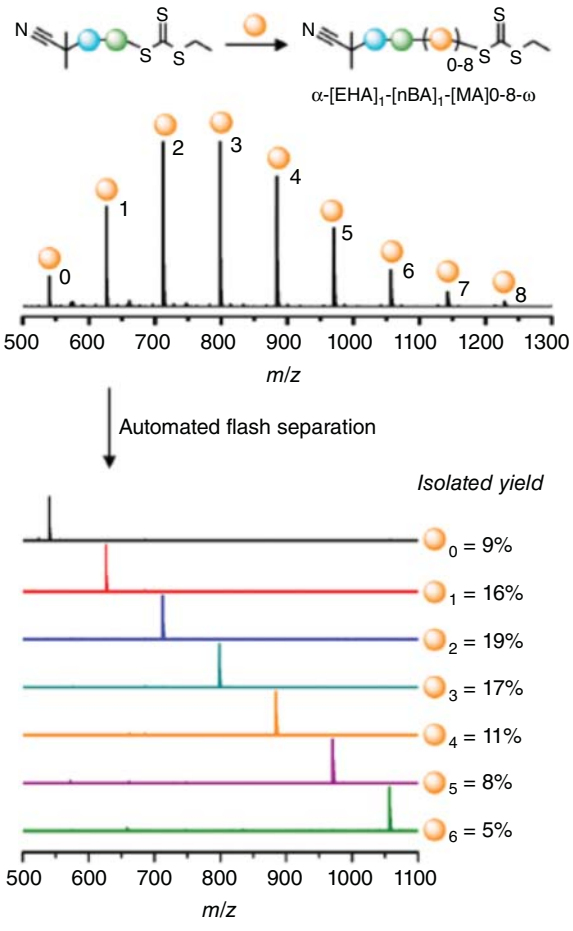

Figure 17.3 Flash column chromatography purification of the oligomer chain extension with six methyl acrylate units for the synthesis of octamers (8-mers). Source: Reprinted with permission from Haven et al. [60]. Copyright 2017, American Chemical Society.

decamers together. Apart from increasing the attainable chain length, this approach also showcased the plethora of further functionalization possibilities available for the SUMI and MUMI products by RDRP techniques.

Sawamoto, Ouchi, and coworkers introduced sequence definition via a selective single-monomer addition process in RDRP via metal-catalyzed living radical polymerization (LRP) [62, 63]. Although not RAFT polymerization, a brief overview of this work is highlighted herein because of the high importance in the field of sequence control via radical polymerization. Also, the strategies used are in principle transferable to RAFT reactions. Their work was inspired by nature, which utilizes templates to control the order of propagating monomer sequence for biopolymers (e.g. DNA and peptides) via an accurately controlled production process. Radical polymerization would be appropriate for the design of template chemistry because of the wide range of monomers that could be used. Metal-catalyzed LRP proved highly suitable for the construction of template systems towards sequence definition. In a first attempt to design SD oligomers, two methacrylate monomers were polymerized where control of selectivity in the

radical addition of the monomers was demonstrated via a halide initiator that carried a recognition site (template) for one of the monomers via ionic interactions [64]. The competitive radical addition of methacrylic acid (MAA) over MMA by a factor of 10 (because of the specific interaction between the template amine and the acid in MAA) permits the predominant synthesis of alternating adducts of both monomers. In an attempt to optimize the template-assisted system, a crown ether functionality was introduced, which allowed the recognition of cationic monomers according to their size [65]. Selective insertion of a sodium methacrylate over a much more bulky ammonium cation derivative could in this way be achieved. This concept is illustrated in Scheme 17.4. However, the concept was not appropriate for iterative processes (oligomers/polymers with full selectivity were still out of reach) to synthesize SD oligomers unless some recognition sites for different comonomers could be incorporated. Although both methods showcase selective insertion of a monomer unit, further development towards longer and more complex structures still seemed out of reach.

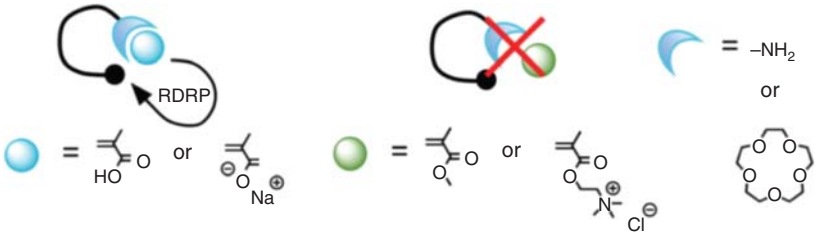

Scheme 17.4 Schematic representation of a template-assisted selective monomer addition. Selective addition of a monomer through recognition of the template moiety via metal-catalyzed LRP resulting in 1 : 1 adducts. Source: Reproduced with permission from De Neve et al. [5]. Copyright 2018, Royal Society of Chemistry.

In this template-assisted concept, the monomer addition can be regarded as a cyclization, controlled via reversible activation under dilute conditions. To gain more control over the primary oligomer structure (monomer sequence), a new concept was proposed by Sawamoto and coworkers based on the repetition of cyclization by introducing two types of orthogonally cleavable and renewable covalent bonds [66]. The initiator-monomer (inimer) molecule in this process carries both a radical-generating site and an alkene, leading to a repetitive cyclization, bond cleavage, and regeneration. A schematic representation of this concept is illustrated in Scheme 17.5. The halide initiator for atom transfer radical polymerization (ATRP) was connected with a methacrylate-based monomer via two orthogonally cleavable and renewable bonds, *N*-hydroxysuccinimide (NHS) ester and 2-pyridyl disulfide (for detailed reaction schemes of the process, see literature) [66]. The metal catalyst needed to be carefully selected, and dilute reaction conditions are required for selective radical formation and cyclization without further chain growth. Furthermore, for every additional ring closure, the reaction solvent, temperature, and catalyst amount had to be carefully tuned, which makes the application potential of the process rather limited. However, an iterative method for the template-assisted

synthesis of SD oligomers through radical addition of a single-monomer unit was designed. High conversion (>90%) was reached for the synthesis of a SD trimer, thus for a total of two radical additions into the starting inimer molecule.

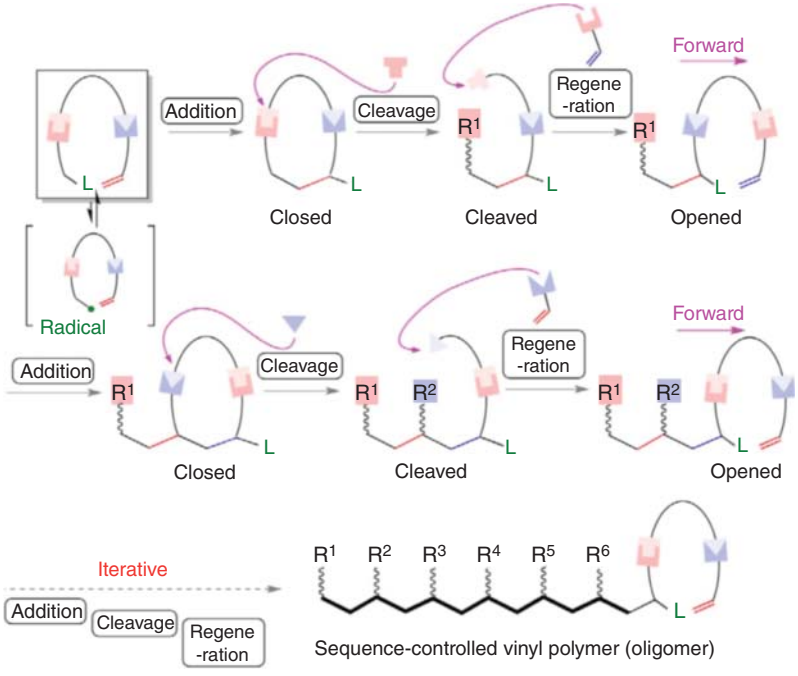

Scheme 17.5 Schematic representation of the iterative cyclization and the molecular structure of inimer carrying two types of cleavable/renewable bonds (NHS-ester and 2-pyridyl disulfide). SUMI was controlled via cyclization. To repeat the cyclization, one of the cleavable/renewable bonds was cleaved; this was followed by regeneration of the bond carrying the next vinyl group. Source: Hibi et al. [66]. Licensed under CC by 4.0.

The same group introduced another concept towards the synthesis of SD oligomers; in this approach, the monomer sequence was controlled by using methacrylate-based monomers that carry exceptional bulky (adamantyl and isopropyl-based) and convertible pendant groups [67, 68]. Because of the bulky pendant group, the monomer is unlikely to homopolymerize because of the steric hindrance and low ceiling temperature (T_c). The bulky pendant groups could be easily transformed into any less bulky substituents to reactivate the chain via selective acidolysis and subsequent esterification reactions (Scheme 17.6). Three iterative cycles of methacrylate-based monomers were demonstrated to yield a SD trimer. As mentioned above, the approaches by Sawamoto and Ouchi did not rely on RAFT reactions per se but are to a large degree transferrable in their concepts to RAFT SUMI reactions. A fusion of the approaches in the future appears to be promising.

Returning to RAFT reactions, two significant issues come with sequential RAFT-SUMI using thermal initiating systems being (i) initiator-derived by-products such as cage products and, in particular, the by-products formed by the

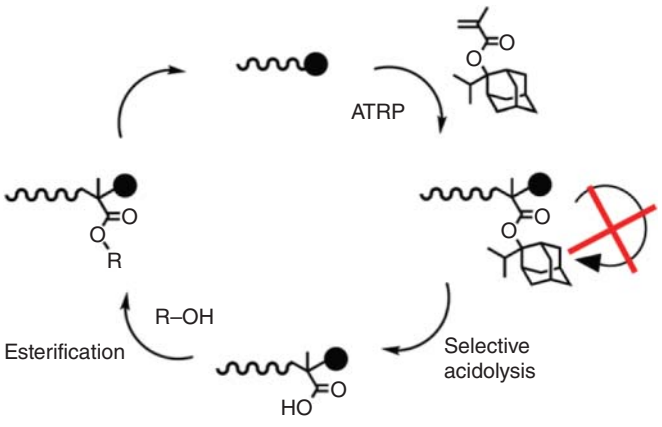

Scheme 17.6 Schematic representation of the SUMI process via bulky and convertible pendant group. Subsequent additions become available via post-modification steps (acidolysis and subsequent esterification). Source: Reproduced with permission from De Neve et al. [5]. Copyright 2018, Royal Society of Chemistry.

initiator-derived radicals adding to the monomer (especially when initiator-derived radicals are different from the initial RAFT leaving or reinitiating group) and (ii) the low initiator efficiency [14]. These by-products may be avoided by generating initiating radicals directly from the RAFT agent by photolysis, a process introduced by Gruendling et al. [69] very similar to the photoiniferter process first described by Otsu [70]. Recently, these photoinitiating (either directly or with the use of a photoredox catalyst) processes were investigated in the context of SUMI by a visible light-mediated radical chain process (photoRAFT) to synthesize discrete ($Đ = 1$) oligomers [71]. For the first time, discrete trimers were successfully synthesized by successive SUMI in high yield under mild reaction conditions. To avoid oligomerization (multiple monomer units added to an active radical), it is important that the transfer constant of the RAFT agent is high and addition of reinitiating radical to the monomer is fast ($k_{p(1)} \gg k_{p(n)}$) as discussed earlier. Moreover, it is preferred that the product macro-RAFT agent formed by SUMI is less active as a photoiniferter than the initial RAFT agent. The first styrene-like monomer was introduced via a direct photoRAFT process with green light in very high yield. As a second monomer, N-substituted maleimides were selected because of their high reactivity towards styrene-like propagating radicals (first monomer), while homopolymerization of maleimides is slow. The SUMI step was performed via photoinduced electron/energy transfer PET-RAFT polymerization with a photoredox catalyst under blue light irradiation. Complete conversion was achieved in 48 hours. As a third monomer, vinyl acetate (VAc) was inserted via PET-RAFT SUMI using a photocatalyst under red light irradiation. RAFT polymerization of VAc using trithiocarbonate RAFT agents with thermal initiation is known to be strongly inhibited (because of slow fragmentation of the intermediate radical) [72]. In the case of SUMI, processes that disfavour propagation following a single-unit insertion are highly preferable. Figure 17.4 shows gel permeation chromatography

(GPC) and ESI-MS analysis of the corresponding photoRAFT SUMI products (discrete oligomers).

The proposed mechanism of photoRAFT-SUMI is shown in Scheme 17.7. Photolysis of the RAFT agent causes reversible dissociation of the C—S bond (iniferter process). The radical (R·) formed can add monomer (or RAFT agent, which is a degenerate process). The radical formed by addition of monomer (R–M·) can combine with a thiocarbonylthio radical to form the SUMI product. It can react with RAFT agent by addition fragmentation, also to form the SUMI product. It may also add further monomer, which is slow. The relative concentrations of the reacting species dictate that RAFT should be the dominant process.

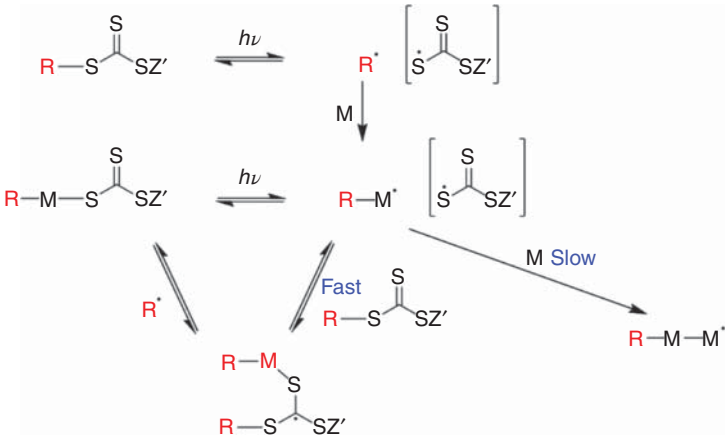

Scheme 17.7 Mechanism of photoRAFT-SUMI with a trithiocarbonate RAFT agent. Source: Reprinted with permission from Haven et al. [55]. Copyright 2018, American Chemical Society.

In another approach, a new protocol was proposed for incorporating a broad range of functionalities via available vinyl monomers (acrylates, acrylamides, and styrene) via catalyst-free photoRAFT-SUMI (green light) [73]. The success of this strategy relies on successive aminolysis, thiol–ene, and esterification steps to transform the secondary trithiocarbonate end group photo-SUMI into a more active tertiary cyanoalkyl trithiocarbonate. Yields were mostly limited by the efficiency of the isolation step. Discrete oligomers, up to five vinyl monomer repeat units, were synthesized. In the case of the pentamers, three consecutive SUMI reactions and two intermediate esterification and thiol–ene steps were performed (Scheme 17.8).

Very recently, Moad and coworkers studied visible light-initiated SUMI of *N*,*N*-dimethylacrylamide (DMAm) into trithiocarbonates in aqueous solution [74]. They concluded that very selective photoSUMI was achieved upon using a high monomer concentration (up to 1 M solutions) with equimolar RAFT agent/DMAm ratio and the irradiation wavelength was of high importance for the formation of SUMI over higher oligomers (or other by-products). For this particular system (DMAm and 4-((((2-carboxyethyl)thio)carbonothioyl)thio)-4-cyanopentanoic acid

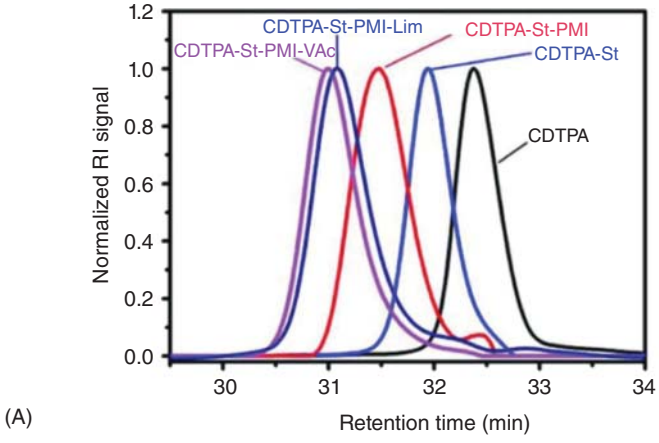

(A)

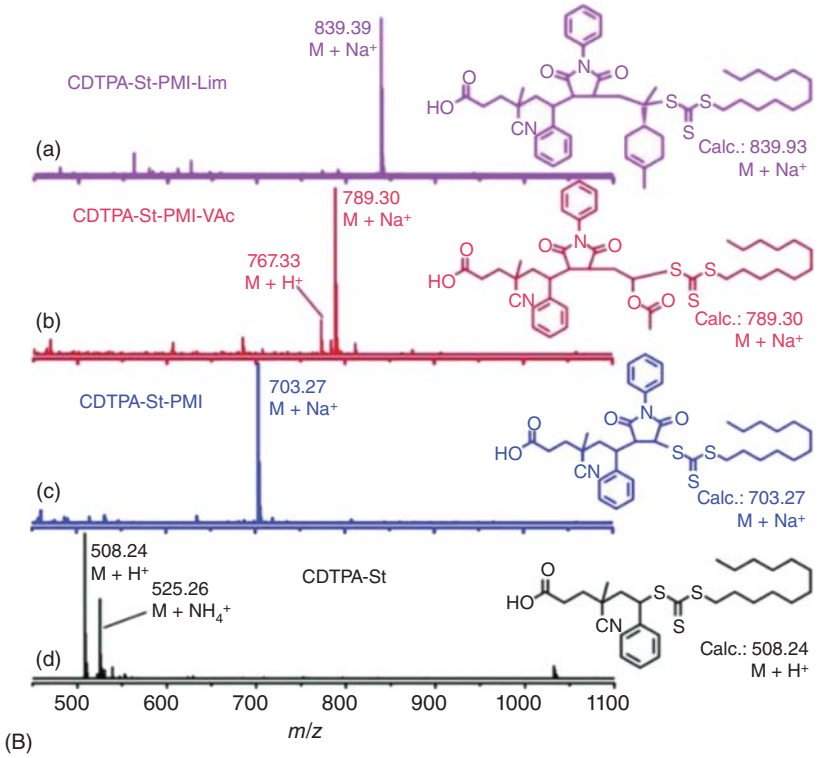

(B)

Figure 17.4 GPC traces for the products from sequential PET-RAFT-SUMI into 4-cyano-4-[(dodecylsulfanylthiocarbonyl)sulfanyl]pentanoic acid (CDTPA) (A) and ESI-MS spectra for the products from sequential PET-RAFT-SUMI (B) into a trithiocarbonate RAFT agent. Source: Reprinted with permission from Haven et al. [55]. Copyright 2018, American Chemical Society.

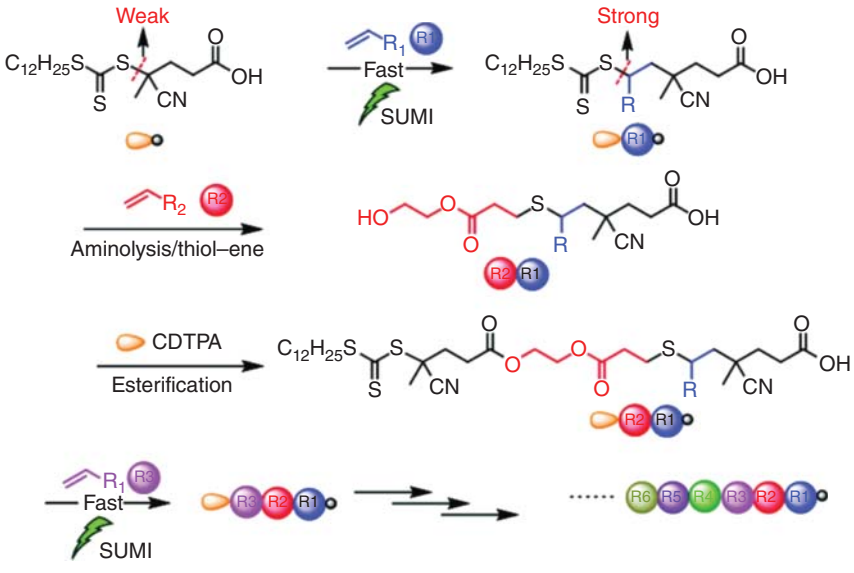

Scheme 17.8 Schematic representation for the synthesis of discrete pentamers by SUMI, aminolysis, thiol-ene, and esterification steps. Source: Reprinted with permission from Haven et al. [55]. Copyright 2018, American Chemical Society.

RAFT agent), red light (633 nm) provided for selective excitation of the initial RAFT agent in the presence of DMAm with high-purity SUMI product and high monomer conversion (>80%). Shorter irradiation wavelengths such as deep blue (402 nm), blue (451 nm), or green (512 nm) light gave a conversion plateau at 60–70% monomer conversion. Also, a preferred linear pseudo-first-order kinetic profile to high (>80%) conversion was observed with red light initiation, but these conditions also showed the slowest reaction rate. The rate of DMAm-RAFT formation decreased in the series 402 nm (deep blue) > 512 nm (green) > 451 nm (blue) > 633 nm (red). Furthermore, the use of higher reaction temperatures for the photoSUMI reaction (65 °C vs. ambient temperature) resulted in a higher reaction rate and more selective SUMI process (reduction of oligomer formation).

Challenges remaining in the synthesis of SD polymers or oligomers (sequential SUMI processes) are scalability limitations such as low reaction yields and long reaction times. Recently, these scalability challenges were addressed by a PET-RAFT-SUMI protocol through sequential and alternating SUMI of *N*-phenyl maleimide (PMI) and indene (Ind) – both non-homopolymerizable monomers – into a trithiocarbonate RAFT agent under mild reaction conditions in batch and hand-made flow reactors (Scheme 17.9) [75]. A series of discrete SD polymers up to pentamers (five sequential SUMI reactions) were synthesized. Purification after each monomer insertion step was performed by automated flash chromatography [61]. Pentamers on a gram scale with an overall isolated yield of 56% were obtained in short production times (<1 week). The authors also studied oxygen tolerance during the PET-RAFT SUMI process and suggested that the presence of oxygen had negligible effects on both the activation of the RAFT agent and formation of

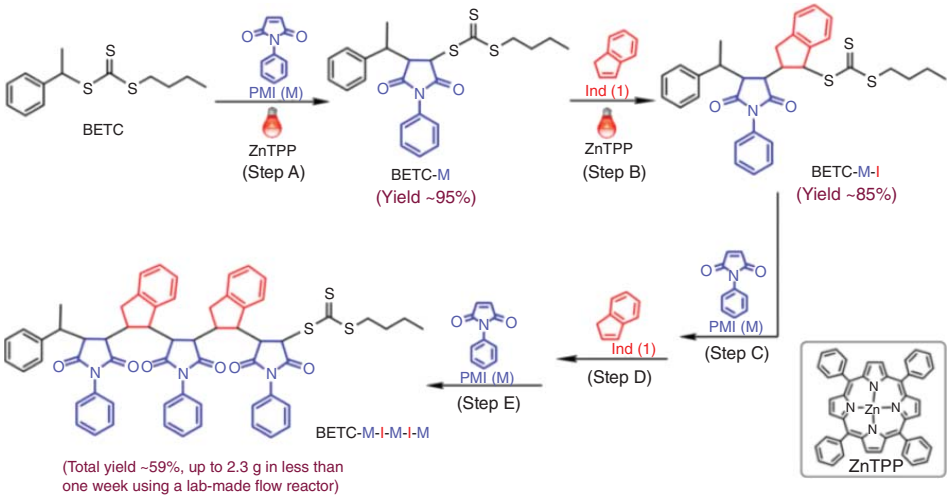

Scheme 17.9 Schematic representation for the PET-RAFT SUMI process for the synthesis of pentamers of *N*-phenyl maleimide and indenes. Source: Reproduced with permission from Huang et al. [75]. Copyright 2019, John Wiley & Sons.

the SUMI adduct under the investigated reaction conditions (on product purity and yield). This facilitated the upscaling process; however, limitations of the process were running cost and amount of reagents. By implementation of SUMI processes in flow, theoretically, kilogram scales could be targeted and the production time could be reduced by increasing the length of the flow reactor (by keeping the same dimensions of the tubing), light strip, and the volume capacity of the syringes.

With such marked advances in the synthesis of SD polymers and oligomers via RAFT, interest has started shifting towards the application of these materials in, for example, biomimetics. Functional precision polymers open up a wide array of opportunities that rely on sequence-specific interactions as observed in biosystems. Recently, SD N-substituted oligo(acrylamide)s were synthesized that originated from a direct translation of the side chain functionalities of a well-studied peptide sequence (Scheme 17.10) [76]. The uniform N-substituted oligo(acrylamide) pentamers were obtained via RAFT polymerization, following the SUMI protocol and flash column chromatography separation with isolated yields between 16% and 37% for individual reaction steps. The parent peptide sequence was known to solubilize *meta*-tetra(hydroxyphenyl)-chlorin (*m*-THPC), a photosensitizer for photodynamic cancer therapy, by drug structure-specific hosting. Translation of the active sequence towards synthetic precision polymers showed that the resulting peptide-mimetic macromolecule retained the drug solubilization and release kinetics of the parent peptide. Furthermore, these characteristics could be influenced by varying the side chain on position three with various N-substituted oligo(acrylamide)s and thereby even allowed for 40% higher payloads and 27 times faster initial drug release than the natural peptide sequence counterpart.

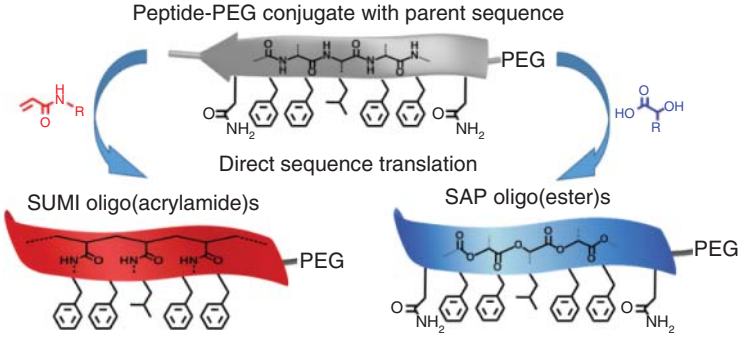

Scheme 17.10 Schematic representation of the sequence transfer strategy from a peptide-PEG conjugate to PEG-conjugated precision sequences. Source: Reproduced with permission from Maron et al. [76]. Copyright 2019, John Wiley & Sons.

Moving one step closer to biological precision, the concept of stereoregularity was introduced into synthetic SD SUMI polymers by Xu and coworkers using alternating radical chain growth via sequential photoRAFT-SUMI [77]. Two monomer families, being indenes and maleimides, showing little or no tendency

for homopolymerization were inserted. The pool of available monomers could also be broadened by adjusting the functionalities carried by the selected monomer families. Insertion of these cyclic monomers into a trithiocarbonate RAFT agent occurred in a stereospecific manner irrespective of reaction conditions or monomer functionalities and resulted in trans-linkages along the backbone because of steric hindrance and the restricted rotation of cyclic monomers during radical addition. This selectivity was not observed for analogous acyclic monomers, which gave mixed cis- and trans-insertions. The selection criteria for the monomer and RAFT agent to ensure successful SUMI reaction were identical to the ones already highlighted before. Additionally, indenes are electron donating, whereas maleimides act as electron acceptors, thereby forming a charge transfer complex and leading to high reaction rates in an alternating copolymerization.

Recently, Junkers and coworkers studied the physical properties of discrete oligo(methyl acrylates)s with a degree of polymerization between 1 and 22 (molecular weight range 432–2261 g mol^{-1}) [78]. The aforementioned library was created by deconstructing an oligomer distribution, obtained via RAFT polymerization, into its uniform components. Because of the applied synthesis methodology, the discrete oligomers closely resembled disperse synthetic polymers with a hydrocarbon backbone as used in the industry. Properties such as diffusivity, glass transition temperature, and viscosity were systematically examined and compared to the existing knowledge on disperse higher molecular weight polymers. As could be expected, marked differences were observed for these discrete oligomers with glass transition temperatures and intrinsic viscosities well below what is known for higher dispersity polymers, whereas the inverse was perceived for diffusion constants. Furthermore, the discrete library offered the opportunity to create new oligomer distributions on demand (Figure 17.5), hence making it, in principle, possible to directly target material properties purely by mixing the correct discrete building blocks together. The artificial oligomer distributions that were established this way highlighted the limitations associated with molecular weight analysis via SEC. Understanding the deceptive feature of molecular weight distribution dispersity is crucial, especially when more and more research aims to create SD precision polymers.

Within the field of synthesis of sequence-defined materials, RDRP and RAFT in particular take a special role. Most SD synthesis methods rely on click-like chemistry in order to build up sequences in a step-wise manner, conceptually not unlike classical peptide synthesis. In consequence, solid-supported synthesis is available for these methods. RDRP SUMI does not allow for the same strategy and appear thus to be more tedious to carry out. Although the maximum chain length is limited, synthesis can, however, be carried out relatively fast. Purification steps are required, yet the same is often true for alternative methods. Chain lengths of up to 10 units are currently possible, and promising results have been obtained by various research groups, showing that this range can still be extended further. Overall, RDRP-based SD materials feature the advantage of a stable carbon–carbon backbone. Also, spacers between two functional R groups on the oligomers are relatively small, allowing for a high information density, and potentially advantageous

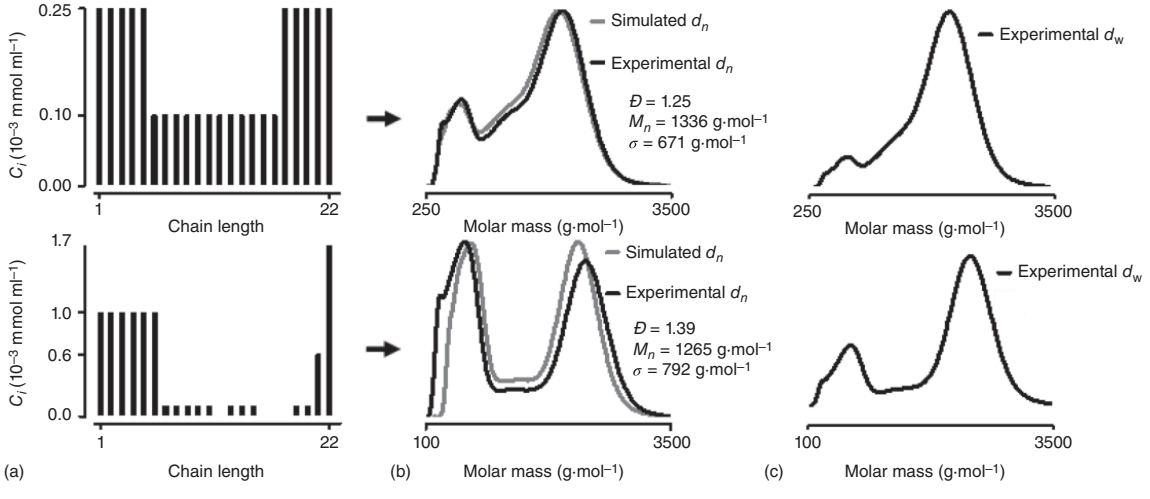

Figure 17.5 Schematic representation of the on-demand oligomer distributions with (a) concentrations of each oligomer chain length that were mixed together, (b) resulting number distributions (simulated and experimental), and (c) resulting double-weighted distributions. Source: Reproduced with permission from De Neve et al. [78]. Copyright 2019, John Wiley & Sons.

interaction with biological polymers that feature similarly densely spaced chemical information. First endeavours into biomedical applications have shown that RAFT-derived oligo(acrylamide)s are able to fulfil the same function as classical peptides. This proposes an interesting peptidomimetic route to functional bioactive materials. The future of these materials is certainly bright, and more application examples can be expected to be found soon.

References

1 Chiefari, J., Chong, Y.K., Ercole, F. et al. (1998). *Macromolecules* 31: 5559–5562.
2 Moad, G., Rizzardo, E., and Thang, S.H. (2005). *Aust. J. Chem.* 58: 379–410.
3 Perrier, S. (2017). *Macromolecules* 50: 7433–7447.
4 Gody, G., Zetterlund, P.B., Perrier, S., and Harrisson, S. (2016). *Nat. Commun.* 7: 10514.
5 De Neve, J., Haven, J.J., Maes, L., and Junkers, T. (2018). *Polym. Chem.* 9: 4692–4705.
6 Lutz, J.-F., Lehn, J.-M., Meijer, E.W., and Matyjaszewski, K. (2016). *Nat. Rev. Mater.* 1: 16024.
7 Haven, J.J., Guerrero-Sanchez, C., Keddie, D.J. et al. (2014). *Polym. Chem.* 5: 5236–5246.
8 Vandenbergh, J., de Moraes Ogawa, T., and Junkers, T. (2013). *J. Polym. Sci. A: Polym. Chem.* 51: 2366–2374.
9 Baeten, E., Haven, J.J., and Junkers, T. (2017). *Polym. Chem.* 8: 3815–3824.
10 Derboven, P., Van Steenberge, P.H.M., Vandenbergh, J. et al. (2015). *Macromol. Rapid Commun.* 36: 2149–2155.
11 Gody, G., Maschmeyer, T., Zetterlund, P.B., and Perrier, S. (2013). *Nat. Commun.* 4: 2505.
12 Gody, G., Maschmeyer, T., Zetterlund, P.B., and Perrier, S. (2014). *Macromolecules* 47: 639–649.
13 Engelis, N.G., Anastasaki, A., Nurumbetov, G. et al. (2017). *Nat. Chem.* 9: 171–178.
14 Vandenbergh, J. and Junkers, T. (2014). *Macromolecules* 47: 5051–5059.
15 Harrisson, S. (2018). *Polym. Chem.* 9: 1366–1370.
16 Lutz, J.-F. (2010). *Polym. Chem.* 1: 55–62.
17 Hartmann, L. (2011). *Macromol. Chem. Phys.* 212: 8–13.
18 Martens, S., Landuyt, A., Espeel, P. et al. (2018). *Nat. Commun.* 9: 4451.
19 Al Ouahabi, A., Kotera, M., Charles, L., and Lutz, J.-F. (2015). *ACS Macro Lett.* 4: 1077–1080.
20 Gunay, U.S., Petit, B.E., Karamessini, D. et al. (2016). *Chem* 1: 114–126.
21 Takizawa, K., Tang, C., and Hawker, C.J. (2008). *J. Am. Chem.* 130: 1718–1726.
22 Solleder, S.C., Zengel, D., Wetzel, K.S., and Meier, M.A.R. (2016). *Angew. Chem. Int. Ed.* 55: 1204–1207.
23 Zydziak, N., Konrad, W., Feist, F. et al. (2016). *Nat. Commun.* 7: 13672.
24 Milnes, P.J., McKee, M.L., Bath, J. et al. (2012). *Chem. Commun.* 48: 5614–5616.

25 Porel, M., Thornlow, D.N., Phan, N.N., and Alabi, C.A. (2016). *Nat. Chem.* 8: 590–596.

26 ten Brummelhuis, N. (2015). *Polym. Chem.* 6: 654–667.

27 Solleder, S.C., Schneider, R.V., Wetzel, K.S. et al. (2017). *Macromol. Rapid Commun.* 38: 1600711. https://doi.org/10.1002/marc.201600711.

28 Badi, N. and Lutz, J.-F. (2009). *Chem. Soc. Rev.* 38: 3383–3390.

29 Lutz, J.-F., Ouchi, M., Liu, D.R., and Sawamoto, M. (2013). *Science* 341: 628.

30 Zard, S.Z. (1997). *Angew. Chem. Int. Ed.* 36: 672–685.

31 Quiclet-Sire, B. and Zard, S.Z. (2006). *Chemistry* 12: 6002–6016.

32 Quiclet-Sire, B. and Zard, S.Z. (2008). *Org. Lett.* 10: 3279–3282.

33 Lebreux, F., Quiclet-Sire, B., and Zard, S.Z. (2009). *Org. Lett.* 11: 2844–2847.

34 Quiclet-Sire, B., Revol, G., and Zard, S.Z. (2010). *Tetrahedron* 66: 6656–6666.

35 Zard, S. and Quiclet-Sire, B. (2016). *Synlett* 27: 680–701.

36 Chen, M., Ghiggino, K.P., Mau, A.W.H. et al. (2004). *Macromolecules* 37: 5479–5481.

37 Houshyar, S., Keddie, D.J., Moad, G. et al. (2012). *Polym. Chem.* 3: 1879–1889.

38 Chen, M., Ghiggino, K.P., Rizzardo, E. et al. (2008). *Chem. Commun.*: 1112–1114. https://doi.org/10.1039/b716471h.

39 Chen, M., Haussler, M., Moad, G., and Rizzardo, E. (2011). *Org. Biomol. Chem.* 9: 6111–6119.

40 Feng, X.-S. and Pan, C.-Y. (2002). *Macromolecules* 35: 4888–4893.

41 Sasso, B., Dobinson, M., Hodge, P., and Wear, T. (2010). *Macromolecules* 43: 7453–7464.

42 Henry, S.M., Convertine, A.J., Benoit, D.S. et al. (2009). *Bioconjug. Chem.* 20: 1122–1128.

43 McLeary, J.B., Calitz, F.M., McKenzie, J.M. et al. (2004). *Macromolecules* 37: 2383–2394.

44 McLeary, J.B., McKenzie, J.M., Tonge, M.P. et al. (2004). *Chem. Commun.*: 1950–1951. https://doi.org/10.1039/b404857a.

45 McLeary, J.B., Calitz, F.M., McKenzie, J.M. et al. (2005). *Macromolecules* 38: 3151–3161.

46 Pound, G., McLeary, J.B., McKenzie, J.M. et al. (2006). *Macromolecules* 39: 7796–7797.

47 McLeary, J.B., Tonge, M.P., and Klumperman, B. (2006). *Macromol. Rapid Commun.* 27: 1233–1240.

48 van den Dungen, E.T.A., Rinquest, J., Pretorius, N.O. et al. (2006). *Aust. J. Chem.* 59: 742–748.

49 van den Dungen, E.T.A., Matahwa, H., McLeary, J.B. et al. (2008). *J. Polym. Sci. A: Polym. Chem.* 46: 2500–2509.

50 Moad, G., Chiefari, J., Chong, Y.K. et al. (2000). *Polym. Int.* 49: 993–1001.

51 Chiefari, J., Mayadunne, R.T.A., Moad, C.L. et al. (2003). *Macromolecules* 36: 2273–2283.

52 Benaglia, M., Chiefari, J., Chong, Y.K. et al. (2009). *J. Am. Chem. Soc.* 131: 6914–6915.

53 Moad, G., Keddie, D., Guerrero-Sanchez, C. et al. (2015). *Macromol. Symp.* 350: 34–42.

54 Moad, G., Guerrero-Sanchez, C., Haven, J.J. et al. (2014). RAFT for the control of monomer sequence distribution – single unit monomer insertion (SUMI) into dithiobenzoate RAFT agents. In: *Sequence-Controlled Polymers: Synthesis, Self-Assembly, and Properties* ACS Symposium Series, vol. 1170, ch. 9 (eds. J.-F. Lutz, T.Y. Meyer, M. Ouchi and M. Sawamoto), 133–147. American Chemical Society.

55 Haven, J.J., Hendrikx, M., Junkers, T. et al. (2018). RAFT 20 years later: RAFT-synthesis of uniform, sequence-defined (Co)polymers. In: *Reversible Deactivation Radical Polymerization: Mechanisms and Synthetic Methodologies*, ACS Symposium Series, vol. 1284, ch. 4 (eds. K. Matyjaszewski, H. Gao, B.S. Sumerlin and N.V. Tsarevsky), 77–103. American Chemical Society.

56 Vandenbergh, J., Reekmans, G., Adriaensens, P., and Junkers, T. (2013). *Chem. Commun.* 49: 10358–10360.

57 Haven, J.J., Vandenbergh, J., and Junkers, T. (2015). *Chem. Commun.* 51: 4611–4614.

58 Haven, J.J., Vandenbergh, J., Kurita, R. et al. (2015). *Poly. Chem.* 6: 5752–5765.

59 Vandenbergh, J., Reekmans, G., Adriaensens, P., and Junkers, T. (2015). *Chem. Sci.* 6: 5753–5761.

60 Haven, J.J., De Neve, J.A., and Junkers, T. (2017). *ACS Macro Lett.* 6: 743–747.

61 Lawrence, J., Lee, S.H., Abdilla, A. et al. (2016). *J. Am. Chem. Soc.* 138: 6306–6310.

62 Kato, M., Kamigaito, M., Sawamoto, M., and Higashimura, T. (1995). *Macromolecules* 28: 1721–1723.

63 Ouchi, M. and Sawamoto, M. (2017). *Poly. J.* 50: 83–94.

64 Ida, S., Terashima, T., Ouchi, M., and Sawamoto, M. (2009). *J. Am. Chem. Soc.* 131: 10808–10809.

65 Ida, S., Ouchi, M., and Sawamoto, M. (2010). *J. Am. Chem. Soc.* 132: 14748–14750.

66 Hibi, Y., Ouchi, M., and Sawamoto, M. (2016). *Nat. Commun.* 7: 11064.

67 Oh, D., Ouchi, M., Nakanishi, T. et al. (2016). *ACS Macro Lett.* 5: 745–749.

68 Oh, D., Sawamoto, M., and Ouchi, M. (2019). *Poly. Chem.* 10: 1998–2003.

69 Gruendling, T., Kaupp, M., Blinco, J.P., and Barner-Kowollik, C. (2011). *Macromolecules* 44: 166–174.

70 Otsu, T. (2000). *J. Polym. Sci. A: Polym. Chem.* 38: 2121–2136.

71 Xu, J., Fu, C., Shanmugam, S. et al. (2016). *Angew. Chem.* 129 https://doi.org/10.1002/ange.201610223.

72 Postma, A., Davis, T.P., Li, G. et al. (2006). *Macromolecules* 39: 5307–5318.

73 Xu, J., Fu, C., Shanmugam, S. et al. (2017). *Angew. Chem. Int. Ed. Engl.* 56: 8376–8383.

74 Aerts, A., Lewis, R.W., Zhou, Y. et al. (2018). *Macromol. Rapid Commun.* 39: 1800240.

75 Huang, Z., Corrigan, N., Lin, S. et al. (2019). *J. Polym. Sci. A: Polym. Chem.* 57: 1947–1955.

76 Maron, E., Swisher, J.H., Haven, J. et al. *Angew. Chem. Int. Ed. Engl.* 58: 10747–10751.

77 Huang, Z., Noble, B.B., Corrigan, N. et al. (2018). *J. Am. Chem. Soc.* 140: 13392–13406.

78 De Neve, J., Haven, J.J., Harrisson, S., and Junkers, T. (2019). *Angew. Chem. Int. Ed.* 131: 14007–14011.

18

Synthesis and Application of Reactive Polymers via RAFT Polymerization

Martin Gauthier-Jaques[1], Hatice Mutlu[2], Heba Gaballa[3], and Patrick Theato[1,2]

[1] Institute for Chemical Technology and Polymer Chemistry (ITCP), Karlsruhe Institute of Technology (KIT), Engesserstraße 18, D-76131 Karlsruhe, Germany
[2] Soft Matter Synthesis Laboratory, Institute for Biological Interfaces 3 (IBG-3), Karlsruhe Institute of Technology (KIT), Hermann-von-Helmholtz-Platz 1, D-76344 Eggenstein-Leopoldshafen, Germany
[3] Institute of Technical and Macromolecular Chemistry, University of Hamburg, Bundesstr. 45, D-20146 Hamburg, Germany

18.1 Introduction

In this chapter, we will review synthetic methods that will allow for an efficient chemical functionalization of polymers, which have been synthesized via a reversible addition fragmentation chain transfer (RAFT) polymerization. Post-polymerization modifications have undoubtedly contributed enormously to the synthesis of functional macromolecules. Particularly, the intensive exploitation of polymers bearing reactive side group moieties that are obtained by reversible deactivation radical polymerization (RDRP) techniques of the respective reactive monomers have enabled the synthetic access to polymers with highly defined functionality and architecture. This chemical transformation has become possible because of the readily available diverse orthogonal organic reactions. Indeed, the synthetic pool of reactive groups amendable for post-polymerization modifications has increased considerably in recent years. However, before addressing these recent advances, it is essential to note and consider some of the pioneering studies, particularly applicable to the synthesis of these well-defined polymers. For this purpose, the reader is encouraged to refer to the following recent reviews and monographs present in the area of post-polymerization modifications [1–6].

In the following, we will first discuss the most common reactive groups (Scheme 18.1) and the respective monomers thereof, which have been employed jointly with RAFT polymerization and have been intensively investigated in past and recent years. They are organized by functional group, which will allow the reader to easily read only selected paragraphs if desired. Next, we will highlight selected examples of applications with a biological context, which rely on the efficient use and interplay of RAFT polymerization and post-polymerization modification. It shall be noted that the selection of examples was made in order to

RAFT Polymerization: Methods, Synthesis and Applications, First Edition.
Edited by Graeme Moad and Ezio Rizzardo.

stimulate the reader in regard to what is synthetically possible and hence makes no claim to be complete.

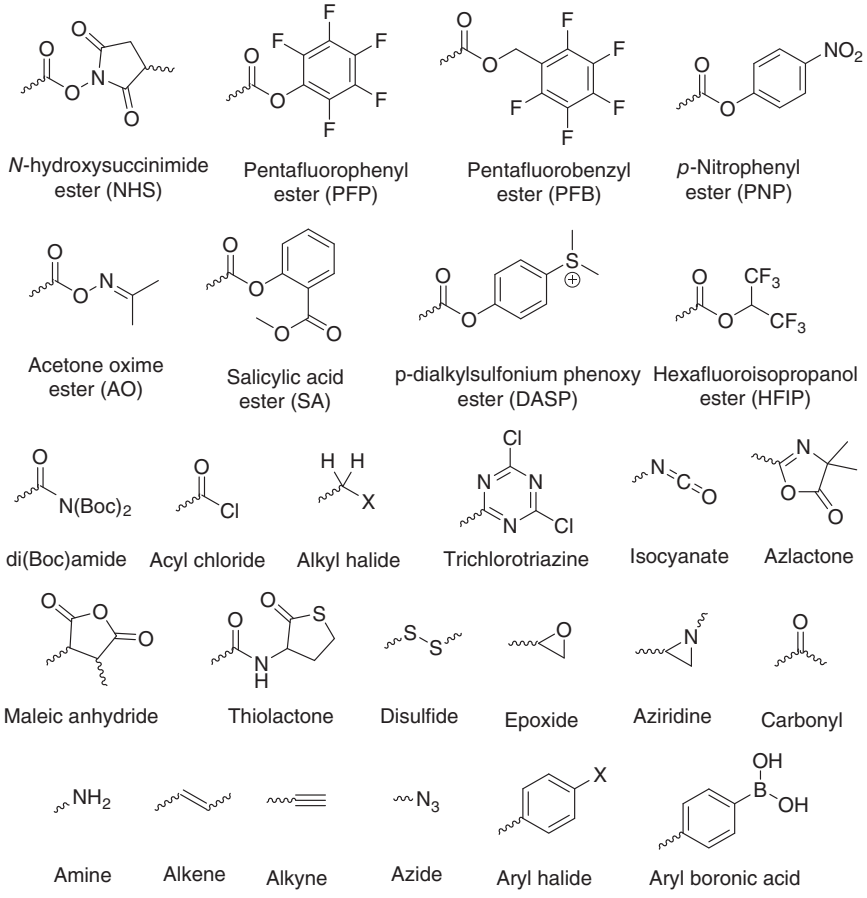

Scheme 18.1 Overview of the principal reactive groups suitable for post-polymerization modification that will be discussed thereafter.

18.2 N-Hydroxysuccinimide (NHS)

The *N*-hydroxysuccinimide (NHS) active ester is a valuable handle to (bio)conjugate manifold amine-containing compounds onto diverse (co)polymers. Indeed, the development and utilization of NHS dates back to 1970s when Ringsdorf [7] and Feré [8] independently reported for the first time the radical polymerization of a methacrylate derivative of NHS (NHSMA, Scheme 18.2). On the other hand, initial attempts to polymerize NHSMA through RAFT polymerization using various dithiocarbamates and dithiobenzoates as chain transfer agent (CTA) in *N,N′*-dimethyl formamide (DMF) have been less successful [9]. The resulting

polymers had unacceptably broad molecular weight distributions ($Đ > 1.5$), which was particularly due to its susceptibility to nucleophilic reaction. Also, utilizing high concentrations of CTA did not improve the limited control over the polymerization rate. Subsequently, random and block copolymers of NHSMA with diverse vinyl monomers were prepared and thoroughly characterized in order to tackle the above-mentioned issue. For instance, Kane and coworkers have shown that RAFT copolymerization of NHSMA with *N*-(2-hydroxypropyl)methacrylamide yielded copolymers with M_n as high as 50 000 g mol^{-1} and narrow molecular weight distributions ($1.1 < Đ < 1.3$), also disclosing potential applications of these materials in polymeric therapeutics [10]. In a similar manner, the statistical copolymerization of NHSA, the acrylate analogue of NHSMA (Scheme 18.2), with *N*,*N*-diethylacrylamide was successful under RAFT conditions with a very good control of molecular weight ($5000 < M_n < 130\,000$ g mol^{-1}) for copolymers of different microstructures.

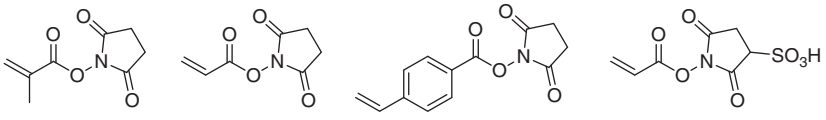

Scheme 18.2 Some of the most common NHS monomers.

Although most of the research activities focused on NHS-active ester based monomers utilize acrylates or methacrylates, the homopolymerization of the NHS-activated ester of 4-vinyl benzoic acid (NHS4VB) was evaluated by Aamer and Tew in order to expand the toolbox of polymeric NHS-activated esters synthesized by RAFT [11]. Interestingly, the polymerization was conducted with a CTA based on 4-cyano, 4-(thiobenzoylthio)-*N*-succinimide valerate, i.e. a CTA that contains the same activated ester as in the monomer. Nonetheless, this CTA was demonstrated to provide unimodal polymers with control over M_n ($44\,000 < M_n < 61\,000$ g mol^{-1}) and dispersity ($1.03 < Đ < 1.07$).

The NHS-active esters of acrylic acid and methacrylic acid provide access to polyacrylamides and polymethacrylamides that typically cannot be prepared via direct polymerization of their corresponding acrylamide monomers. However, the substitution of these activated esters with amine-containing compounds is often restricted to organic solvents such as DMSO and DMF. Therefore, to overcome this limitation, Hawker and coworkers [12] have introduced a novel water-soluble NHS-based monomer, i.e. *N*-hydroxysulfosuccimidyl acrylate (sulfoNHSA), which was subjected to a rapid photoelectron transfer RAFT polymerization in water at ambient temperature. The consequent conjugation with amine-containing compounds was performed in situ because the sulfoNHSA monomer and its respective polymer were unstable (the half-life of sulfoNHSA is ~60 minutes), as evidenced by ^{1}H NMR spectroscopy. This instability occurs because the sulfoNHSA functional group is prone to rapid hydrolysis in water. Inspired by this work, Tanaka and coworkers developed

a novel monomer in which the vinyl group and a sulfoNHS-active ester group were spaced with an alkyl chain linker in order to tune the hydrolytic stability [13]. The sulfoNHSA was subsequently subjected to RAFT polymerization in DMSO using a trithiocarbonate derivative, 2-(benzylsulfanylthiocarbonylsulfanyl)ethanol (BTSE), at 35 °C to deliver polymers with M_n ($37\,000 < M_n < 62\,000\,\mathrm{g\,mol^{-1}}$) and acceptable dispersities ($1.34 < Đ < 1.52$). Eventually, a post-polymerization modification with an amine-containing saccharide derivative revealed that the hydrolytic stability of the sulfoNHS ester groups on these polymers was higher than that of the previously reported sulfoNHS acrylate monomer.

Although a variety of homo- and copolymers based on the above-mentioned NHS-activated ester derivatives have been successfully prepared in a controlled fashion by RAFT, two significant side reactions accompany the post-polymerization reaction of NHS-activated ester-based acrylate and methacrylate (co)polymers: (i) ring-opening of NHS moieties and (ii) formation of backbone glutarimides by attack of initially formed methacrylamides on adjacent NHS esters, which limits their specific implementation as tailor-made polymers.

18.3 Pentafluorophenyl (PFP) Ester and Its Derivatives

The pentafluorophenyl (PFP) ester is a particularly appealing alternative to NHS esters because of the facts that the PFP functional group is stable during a (radical) polymerization, not prone to undesired hydrolysis or alcoholysis, and has better solubility in most common organic solvents. Intriguingly, the first reports on the activity of the PFP moiety as an active ester functional group date back to the same time when NHS active ester monomers were recognized [14]. Nevertheless, it took more than three decades until PFP esters were exploited as a versatile tool for synthetic polymer functionalization. Subsequently, after the seminal report on acrylate/methacrylate [15], RAFT polymerization of pentafluorophenyl methacrylate (PFPMA) was explored in the presence of cumyldithiobenzoate and 4-cyano-4-((thiobenzoyl)sulfanyl)pentanoic acid, respectively, as CTAs. The isolated macromolecules exhibited the expected features of well-defined polymers with M_n up to $17\,000\,\mathrm{g\,mol^{-1}}$ ($Đ < 1.20$). The compatibility of these PPFPMAs as macromolecular RAFT agents was further tested for the copolymerization of PFPMA with MMA, *N*-acryloylmorpholine (NAM), and *N,N*-diethylacrylamide (DEAM). Based on this work, Klok and coworkers [16] applied RAFT polymerization to synthesize well-defined PPFPMA, which was further reacted with a manifold functional primary amine to yield water-soluble macromolecules with identical degrees of polymerization and molecular weight distributions. As a continuation, Boyer and Davis expanded the horizon of PFP active esters by the polymerization of an acrylate derivative of PFP, i.e. PFPA [17]. In this pioneering work, 3-(benzylsulfanylthiocarbonylsulfanyl)propionic acid was selected as a CTA to synthesize polymers with a well-defined structure (M_n in the range of $16\,000\,\mathrm{g\,mol^{-1}}$ and $Đ$ of 1.20). A subsequent quantitative post-polymerization modification of PPFPA with glucosamine and galactosamine opened the possibility

of synthesizing functionalized glycopolymers in one pot. In addition, star-shaped polymers ($5000 < M_n < 15\,000\ \mathrm{g\,mol^{-1}}$, $Đ < 1.20$) with predesigned chemical functionality were synthesized by employing the copolymerization of PFPAs with difunctional diamine monomers used as cross-linkers [18]. In order to broaden the synthetic portfolio, a styrenic derivative of PFP active ester was designed, namely, pentafluorophenyl 4-vinylbenzoate (PFP4VB, Scheme 18.3) [19]. The respective polymers ($4200 < M_n < 28\,200\ \mathrm{g\,mol^{-1}}$, $1.07 < Đ < 1.41$) were synthesized by employing various dithiobenzoates as the CTAs and AIBN as the radical initiator. The PFP4VB functional moieties were found to be distinguishably more reactive than their acrylate and methacrylate counterparts to the extent that they could be quantitatively modified with even aromatic amines. As a result of the latter, the variation of the chemical nature of the backbone by combining both PFPMA and PFP4VB as monomers made it feasible to obtain statistical copolymers that allow for a sequential conversion of both groups (i.e. with just one specific reactive group) in an orthogonal-like manner with different amines [20]. In other words, the PFP4VB repeat units of the copolymers were selectively modified first with aromatic amines, then modification of PFPMA units with aliphatic amine imparted fully functionalized statistical copolymers. In addition, block copolymerization with extreme precision of diverse styrenic derivatives was accomplished by virtue of a macro-CTA based on the PFP4VB monomer motif [18].

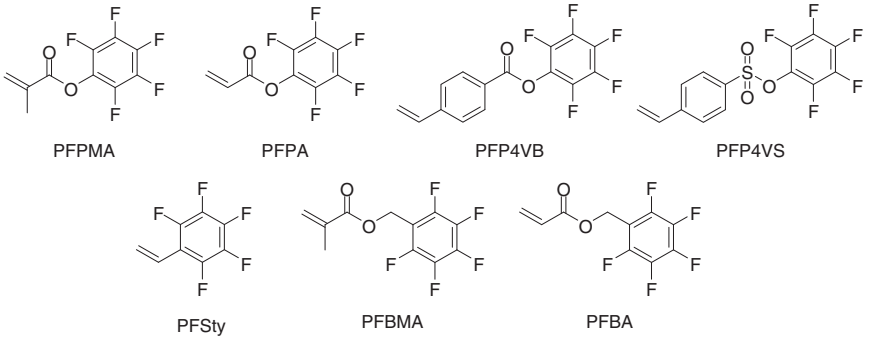

Scheme 18.3 Most common PFP monomers and some of their derivatives.

Apart from acrylate, methacrylate, and styrenic PFP-activated ester derivatives, the synthesis of polymers that utilize activated esters of sulfonic acid (e.g. PFP4VS in Scheme 18.3) as reactive groups has been investigated. Accordingly, the respective sulfonic acid ester polymers were reacted with an excess amount of amine under ambient conditions in order to obtain polymeric sulfonamides. Even though the sulfonic acid ester is significantly slower than the carboxylic acid ester analogue, it opened the route to a second functionalization using alcohols via a Mitsunobu reaction.

Another divergent reaction in the realm of PFP active esters is the regioselective nucleophilic aromatic substitution of the labile para-fluoro substituent of the PFP-group by nucleophiles (such as thiols, amines, etc.). Indeed, quite

recent contributions [21, 22] are comprehensively summarizing and discussing not only the applications but also the potential of this versatile reaction in the context of synthesis and modification of polymers and materials made thereof. Hence, we intend to underpin only some paramount studies in this field of relevance to the RAFT polymerization. In fact, initially, the para-fluoro substitution reaction (PFTR) had been exploited exclusively for the modification of pentafluorostyrene (PFSty)-based homo- and copolymers, which have been synthesized under RAFT polymerization conditions, explicitly with AIBN as an initiator and 2-(dodecylthiocarbonothioylthio)-2-methylpropionic acid (DDMAT) as a CTA at 70 °C in anisole or DMF [23]. The polymer-analogous reaction was carried out quantitatively under ambient conditions using a well-defined PPFSy homopolymer as well as block copolymers in the presence of primary thiol derivatives and commercially available base (i.e. triethylamine (Et_3N)). Although the PFSty homopolymer represents a suitable precursor for post-polymerization functionalization with thiol derivatives, bearing perfluorinated side groups induced limited solubility in more polar solvents [24]. Furthermore, as a styrene analogue, PFSty is also not readily suitable for copolymerization with the different methacrylate-based monomers, hence limiting its versatility. Nonetheless, PFTR studies on a block copolymer containing PFSty and PFPMA moieties, which was synthesized by RAFT polymerization with precise control over the molar mass, dispersity, and functional group incorporation, revealed that PFPMA motif was not inert to PFTR conditions [25]. Indeed, under optimized reaction conditions (1 equiv base, i.e. 1,8-diazabicyclo[5.4.0]undec-7-ene (DBU), and 5 equiv thiol) used for the PFTR, the PFPMA units of the above-mentioned block copolymer were more susceptible to thiol substitution compared to PFSty units. It was also observed that, in addition to the para position, both meta positions of PFPMA are also reactive towards thiols.

A highly interesting class of acrylic and methacrylic PFP monomers, which are synthesized by the virtue of multicomponent Passerini three-component reactions [26], have been recently reported by Roth and coworkers [27]. Subsequently, a series of well-defined homopolymers ($9700 < M_n < 41\,800\ \mathrm{g\,mol^{-1}}$, $1.12 < Đ < 1.19$) and copolymers of the resulting monomers were prepared by RAFT polymerization. PFTR of the pendent PFP moieties was efficiently performed with a range of aromatic, glycosidic, and primary, secondary, and tertiary aliphatic thiols within 3–80 minutes, hence resulting in well-defined functional products in the absence of any observable side reactions. The efficiency of the PFTR was dependent on the nature of both thiols and base. In other words, in the presence of a weak base such as Et_3N, acidic thiol derivatives (e.g. thiophenol) are quantitatively undergoing PFTR in 69 minutes, while utilization of strong base drives the PFTR to completion within three minutes for less acidic thiol derivates (e.g. 1-octanethiol).

Alternatively, the group of Roth synthesized a novel methacrylic monomer, namely, pentafluorobenzyl methacrylate (PFBMA, Scheme 18.3), which was for the first time polymerized via RAFT and further employed in PFTR [28]. In fact, PPFBMA homopolymers ($8600 < M_n < 19\,800\ \mathrm{g\,mol^{-1}}$, $1.14 < Đ < 1.29$) reacted quantitatively through para-fluoro substitution with a range of thiols (typically 1.1 equiv of thiol) in the presence of base (DBU or Et_3N) within one hour under

ambient conditions. Interestingly, no ester cleavage or substitution of *ortho*- or *meta*-fluorides was observed implying a functional group tolerance and the regioselectivity of the PFTR, respectively. Furthermore, in order to introduce structural diversity, the PFBMA unit was reacted with arguably the most important class of nucleophiles for polymer modification, i.e. amines. Contrary to the PFPMA and PFPA analogues, reactions of PFBMA with various amines did not result in an ester cleavage via amidation. Indeed, although with less efficiency, a selective and quantitative substitution of the *para*-fluoride with amines took place, even if the reactions were conducted at higher temperatures (i.e. 60 °C) and utilizing an excess of amines (2.5 equiv). Unfortunately, primary amines delivered products with di-substitution and slightly increased dispersity ($Đ = 1.27$), hence indicating that the efficiency of the post-polymerization functionalization of the polymer-tethered PFB groups is largely restricted by the availability of functional thiols. Comprehensively, the group of Roth expanded the toolbox of efficient chemistries that utilize the *para*-fluoride of PFBMA and the related Passerini ester–amide methacrylate derivatives, by introducing the quantitative azide–*para*-fluoro substitution reaction [29]. The above-mentioned monomers were polymerized under RAFT conditions and reacted with sodium azide in DMF at 80 °C within 60–90 minutes. The respective azide-modified polymer can undergo three different sequential post-polymerization modifications, i.e. prototypical click reaction, azide–thioacid reaction, and azide reduction to amine. Although the prototypical click reaction was the least efficient, requiring heating overnight and a relatively high amount of Cu(I) catalyst, the azide–thioacid reaction proceeded under click-like conditions with full conversion within 15 minutes at ambient temperature. Nevertheless, the poor commercial availability of the thioacid starting materials may restrict the widespread use of this chemistry. On the other hand, the azide reduction utilizing DL-dithiothreitol paved the way towards primary amine-functional polymers, which were successfully acylated in a third successive post-polymerization modification. Hence, it can be concluded that the azide-based chemistries could be adopted as a valuable tool for the (sequential) modification of polymers and the preparation of well-defined multi-functional materials.

18.4 *p*-Nitrophenyl Esters and Their Derivatives

In comparison to the growing popularity of the RAFT polymerization of monomers possessing the NHS and PFP active ester groups, *p*-nitrophenyl (PNP) active ester derivatives (Scheme 18.4), which are known for the last 50 years [30], are considerably less recognized in the field of RAFT polymerization. Although the advantages of the PNP monomeric derivatives arise from the UV/Vis spectroscopically observable *p*-nitrophenyl phenol via aminolysis, the control over the polymerization of PNP bearing monomers is slightly challenging because of their inherent properties as inhibitors/retardators in radical polymerizations and their susceptibility to produce radicals when heated. Nonetheless, Hu and coworkers reported for the very first time the synthesis of well-defined PNP-functionalized

polymers based on poly(*p*-nitrophenyl acrylate) (PPNPA) by RAFT polymerization [31]. Interestingly, the polymerization was performed in bulk in the presence of 1-(ethoxy carbonyl)prop-1-yl dithiobenzoate (EPDTB) as the CTA and yielded well-defined PPNPAs ($2500 < M_n < 11\,000\,\mathrm{g\,mol^{-1}}$, $1.02 < Đ < 1.18$). The latter were further utilized as macro-CTAs for the synthesis of block copolymers with Sty. The block copolymer PPNPA-*b*-PS ($Đ = 1.13$) was self-assembled in nitromethane and subsequently cross-linked with ethylenediamine at ambient temperature to afford stable nanoparticles. The methacrylate analogue of PNP (i.e. PNPMA, Scheme 18.4) was polymerized in DMSO using cumyl dithiobenzoate as the RAFT agent by Maynard et al. [32], and well-defined PPNPMAs ($7700 < M_n < 19\,400\,\mathrm{g\,mol^{-1}}$) with slightly broader molecular weight distributions ($1.15 < Đ < 1.29$) were obtained in comparison to PPNPA reported by Hu and coworkers. Nevertheless, the PPNPMA homopolymer showed considerably high reactivity with amine derivatives (86% conversion with 10-fold excess) in the presence of Et_3N as a base.

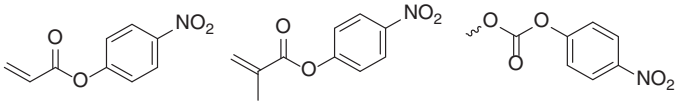

Scheme 18.4 Some of the most common PNP monomers and their carbonate general structure derivatives.

Another successful attempt to polymerize a PNP active ester was accomplished by the virtue of its carbonate analogue (PNPC, Scheme 18.4) [33]. Accordingly, a monomer with a functionality of PNPC connected to the methacrylate via a spacer composed of a disulfide linkage and self-immolative linker was copolymerized via RAFT. Unfortunately, the conversions of the polymerization were rather low (18–46%), particularly because of the small release of PNP, which inhibits the polymerization. Regardless, the active PNP carbonate ester groups within the copolymer were reacted with an amine derivative of an anticancer drug to obtain a water-soluble prodrug with a molecular weight in the range of $6000 < M_n < 13\,000\,\mathrm{g\,mol^{-1}}$ with $Đ < 1.30$.

18.5 Miscellaneous Activated Ester Functional Group Transformations

In the following discussion, we will focus on examples of polymers featuring less popular activated ester groups, which are considerably limited compared to the vast literature available on NHS, PFP (PFB), and PNP active ester-based polymers.

18.6 Acetone Oxime (AO)

The acetone oxime (AO) moiety, which exhibits good solubility in various organic solvents, was introduced as a new class of activated ester derivatives polymerizable

under conventional and photo-induced RAFT conditions [34]. Polymers of the acrylate derivative of AO (AOA, Scheme 18.5) were obtained with well-defined structure with an apparent number-average molecular weights in the range of $4700 < M_n < 51\,200\ \mathrm{g\,mol^{-1}}$ ($1.19 < Đ < 1.31$). The outstanding advantage of these polyacrylate active esters is their high efficacy to transform themselves into poly(*N*-isopropylacrylamides) (PNIPAM) simply by the polymer analogous reaction with isopropylamine.

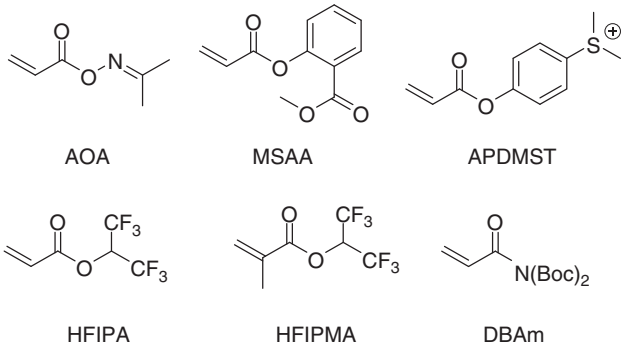

Scheme 18.5 Selection of some less common activated ester monomers.

18.7 Salicylic Acid (SA)

Among the manifold activated ester building blocks, the ones based on salicylic acid (SA) are of great interest, especially in the field of biological applications, because of their broad availability, cheap prices, and inherent low cytotoxicity. Therefore, RAFT polymerization of the methyl ester derivative of SA acrylate (MSAA, Scheme 18.5) [35] was performed in the presence of DDMAT as a CTA in dioxane at 65 °C to deliver homopolymers in the range of $4400 < M_n < 15\,900\ \mathrm{g\,mol^{-1}}$ ($1.19 < Đ < 1.25$). Kinetic studies showed that PMSAA has a lower reactivity towards primary and secondary amines during the post-functionalization reaction when compared with PPFPMA.

18.8 *p*-Dialkylsulfonium Phenoxy Ester (DASPE)

In order to induce an external stimuli triggered reactivity switching via polymer analogous reactions, Kakuchi et al. [36] developed a novel monomer, featuring *para*-dialkylsulfonium phenoxy ester moieties, namely, 4-acryloxyphenyldimethylsulfonium triflate (APDMST, Scheme 18.5), which is further readily reactive under RAFT polymerization conditions in the presence of pentafluorophenyl-(4-phenylthiocarbonylthio-4-cyanovalerate) as a CTA. Although the reactive PAPDMST reacted selectively with amines, demonstrating typical activated ester behaviour, PAPDMST was also successfully converted to its deactivated ester state by

thermo-triggered demethylation. As anticipated, the nonreactive polymer did not afford a conversion with amines, hence featuring a "switched off" reactivity.

18.9 1,1,1,3,3,3-Hexafluoroisopropanol (HFIP)

Although the reactivity of 1,1,1,3,3,3-hexafluoroisopropanol (HFIP) derivatives is considered to be lower than, e.g., their *p*-nitrophenyl derivatives, HFIP esters avoid facile side reactions even at elevated temperatures and prevent amino acid racemization. Attempts to polymerize acrylate- and methacrylate-based HFIP esters (e.g. HFIPA and HFIPMA, Scheme 18.5) under controlled conditions via RAFT mediated by 4-cyano-4-(phenylcarbonothioylthio)pentanoic acid were only successful for HFIPMA and resulted in homopolymers and block copolymers with adjustable molecular weight ($16\,400 < M_n < 37\,900\,\mathrm{g\,mol^{-1}}$) and narrow molecular weight distributions ($1.15 < Đ < 1.30$) [37]. Indeed, HFIP esters enabled a quantitative polymer analogous reaction with various water-soluble amines. The only restriction of the reactions is the formation of the non-acidic volatile by-product, i.e. HFIP, which on the other hand tolerates manifold functional groups and promotes the straightforward polymer of the water-soluble methacrylamide polymers. Nevertheless, because of the toxic nature of the HFIP, the utilization of these polymers is still controversial.

18.10 Di(Boc)-Acrylamide (DBAm)

Although the field of active ester derivatives is broad, the activation of amide moieties is less investigated largely because of their inherently lower susceptibility toward nucleophilic substitution. Surprisingly, the activation of amide derivatives through the introduction of π-electron-withdrawing groups (such as tosylate or *tert*-butyloxycarbamate, Boc) on the amide nitrogen rendered more electrophilic character to the carbonyl and also enhanced the susceptibility of the amides towards nucleophilic substitution [38]. Accordingly, a new activated acrylamide monomer, di(Boc)-acrylamide (DBAm, Scheme 18.5), possessing the above-mentioned properties, was developed [39]. DBAm was subjected to RAFT polymerization utilizing a trithiocarbonate derivative as CTA. Subsequently, the obtained well-defined homopolymers with M_n up to $11\,000\,\mathrm{g\,mol^{-1}}$ ($Đ = 1.27$) were modified via nucleophilic substitution reaction in the presence of both amines and alcohols to yield the corresponding polyacrylamides and polyacrylates, respectively. Even though less nucleophilic secondary amines and alcohols required slightly harsher conditions, the isolated post-modified polymers remained intact during the modification. However, the final polymers also contained a putative cyclic imide repeating unit, likely as a result of base-promoted cyclization of adjacent DBAm units. Despite this, these results expanded the potential of the DBAm active moiety within the field of advanced macromolecular engineering.

18.11 Acyl Chloride

Another group of activated ester substitutes, the acyl chloride monomers, are an old class and well-known activated carboxylic acid derivatives that can be subsequently modified by a broad range of alcohols and amines in order to quantitatively obtain the related esters and amides. Such monomers are the best choice for post-polymerization modification at preparative/industrial scale, as the acyl chloride monomers are themselves produced at industrial scale, the produced chloride salt does not necessitate a heavy work-up, and as the reactions allow fast and quantitative conversion of the reactant to a large scope of products with a satisfying atom economy. Acyl chloride monomers also play an important precursor role for the synthesis of functionalized monomers. Nevertheless, the main drawbacks of such acyl chloride monomers remain in their incompatibility with nucleophilic functional groups as well as their high sensitivity to moisture and to nucleophilic impurities. RAFT copolymerization of acyl chloride monomers (Scheme 18.6) such as acryloyl chloride (AC), methacryloyl chloride (MAC), or vinylbenzoyl chloride (VBzC) in styrene were reported to form their respective statistical copolymers [40].

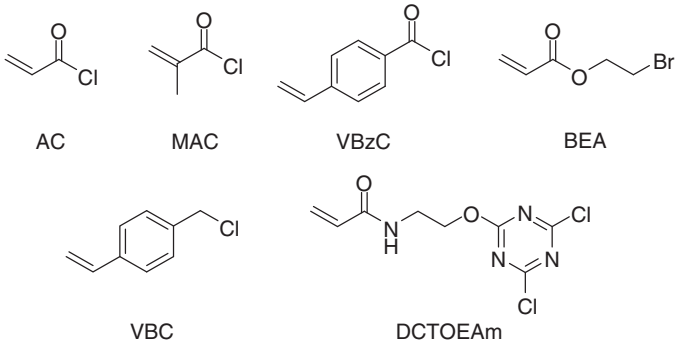

Scheme 18.6 Selection of reactive acyl, alkyl, and aryl halide monomers.

18.12 Alkyl Halide

Alternatively, the halide substitution scope can be extended to the alkyl halide. Such post-polymerization modifications of alkyl halides preserve the good atom economy of the acyl chloride but also broaden the range of the nucleophiles, which can be efficiently used at a price of a reduced reactivity. Because of the undesired reactivity of alkyl halides with radical species, the polymerization control is usually disadvantaged by the use of monomers bearing alkyl halides. However, the polymerization of monomers such as vinyl benzyl chloride (VBC, Scheme 18.6) was successfully investigated and even used as a linear precursor for the synthesis of polymer brushes by modification of the PVBC precursor with the *n*-alkyl trithiocarbonate anion, leading to a 'grafting from' copolymerization with styrene poly(St-*graft*-VBC))

[41]. Moreover, the library of monomers bearing a primary halide was broadened in recent years. An example of such a monomer is bromoethyl acrylate (BEA, Scheme 18.6) which was successfully polymerized to poly(bromoethyl acrylate) by RAFT polymerization. Such alkyl halide polymers are predisposed to post-polymerization modification by reaction with a large variety of nucleophiles such as amines, alcohols, thiols, phosphites, sulfites, or azide anions [42].

18.13 Trichlorotriazine (TCT)

Related to the post-polymerization modification by the substitution of halide, trichlorotriazine (TCT) chemistry offers interesting outcomes for the generation of amphiphilic monomers and more generally for the homo- and heterodifunctionalization of monomers as amphiphilic monomers are globally difficult to handle or to obtain by standard post-polymerization modification. Nevertheless, heterodifunctionalization from a single monomer precursor may constitute a good approach to the synthesis of amphiphilic homopolymers. For this purpose, an acrylamide monomer bearing one cyanuric chloride ring (2,4,6-trichloro-1,3,5-triazine, TCT) with two remaining reactive sites (DCTOEAm, Scheme 18.6) was prepared and polymerized by RAFT polymerization. Subsequent post-polymerization modification by nucleophilic aromatic substitution with various amines and thiols led to the desired homodifunctionalization [43] and heterodifunctionalization [44].

18.14 Isocyanate (NCO)

The isocyanate (NCO)-containing monomers constitute a class of reactive monomers that exhibit great tolerance for the CTA over the polymerization. Their reactivity towards thiols, amines, and alcohols allows selective, fast, and quantitative post-polymerization modifications without by-product formation. As the organic isocyanates are industrially produced by the condensation of primary amine and phosgene, isocyanates are commercially available in large scales. The versatility of the post-polymerization modification of isocyanates was recently highlighted by the RAFT polymerization of 2-(acryloyloxy)ethylisocyanate (AOI, Scheme 18.7) and its subsequent modification with various amines and thiols, yielding the respective urea and thiourethane derivatives. Weaker nucleophiles such as alcohols were also reported to be converted quantitatively into urethane in the presence of a catalytic amount of dibutyltin dilaurate [45]. A second recent publication investigated the functionalization of polymers with isocyanate small molecules. For this purpose, poly(*N*,*N*-dimethylacrylamide)-*block*-poly(*N*-(2-hydroxyethyl)acrylamide) ((PDMAm-*block*-PHEAm) was first prepared before further modification of the alcohol groups of the PHEAm block with allylisocyanate or AOI, allowing a second phase of modification by the Michael addition of a broad range of thiols in the case of the acrylate or by the thiol-ene reaction in the case of the allyl [46]. A similar strategy was later applied with the polymerization of *N*-(2-hydroxypropyl)methacrylamide

(HPMA) by RAFT to poly[*N*-(2-hydroxypropyl)methacrylamide], which is promising in biomedical applications. Allylisocyanate was one again used in order to obtain partial conversion of the alcohol into urethane bearing a terminal allyl for subsequent thiol-ene chemistry with different dyes, sugars, and biological triggers [47].

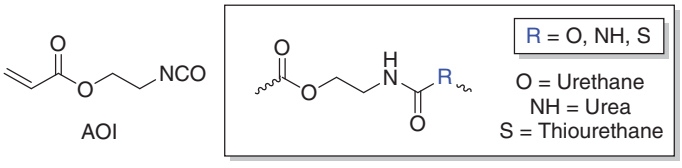

Scheme 18.7 Overview of the post-polymerization modification available from NCO bearing monomers.

The use of activated urea as a protected isocyanate was investigated in recent years. For this purpose, 2-isocyanatoethyl methacrylate was protected with 3,5-dimethyl pyrazole, imidazole, and 1,2,4-triazole in order to form three respective azole-*N*-carboxamide methacrylates as protected isocyanates: (3,5-dimethylpyrazole-*N*-carboxamide methacrylate (NCOP), imidazole-*N*-carboxamide methacrylate (NCOI), and 1,2,4-triazole-*N*-carboxamide methacrylate (NCOT) (Scheme 18.8). The three *N*-heterocycles showed varying reactivity in the presence of thiols and amines, i.e. reactivity order: pyrazole < imidazole < triazole), which could allow for selective post-polymerization modification of NCOT, NCOP, and NCOI block copolymers. The exact mechanism is not known yet; however,

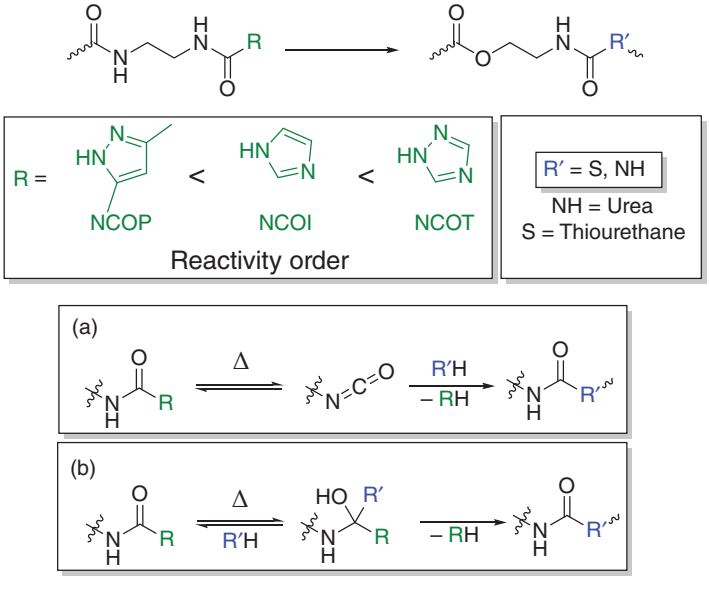

Scheme 18.8 Key aspects of the use of activated urea as protected isocyanate. (a) Elimination–addition and (b) addition–elimination.

the elimination–addition and the addition–elimination mechanisms are both acceptable candidates [48].

18.15 Azlactone

The azlactone group within monomers shares many advantages with the isocyanate chemistry discussed above, as it allows a quantitative and quick conversion of amines, thiols, and alcohols without by-product formation. In order to illustrate the azlactone post-polymerization chemistry, poly(2-vinyl-4,4-dimethylazlactone) was prepared from 2-vinyl-4,4-dimethylazlactone (VDMA, Scheme 18.9) by RAFT polymerization and subsequently modified by ring opening by a broad range of amines and alcohols, yielding the functionalized poly(2-acrylamido isobutyrate)s and poly(2-acrylamido isobutyramide)s [49]. Furthermore, because of the reactivity gap between the azlactone and the pentafluorophenyl acrylate in the presence of nucleophiles, block PVDM-*b*-PPFPA and statistical poly(VDM-*stat*-PFPA) copolymers were sequentially functionalized by two different nucleophiles, yielding functionalized polymers bearing two functionalities dispatched with a high degree of precision [50]. 2-vinyl-4,4-dimethylazlactone (VDMA) was also reported for the post-polymerization functionalization of PVDMA with amino-pyrene derivative and "grafted to" PS side chains [51].

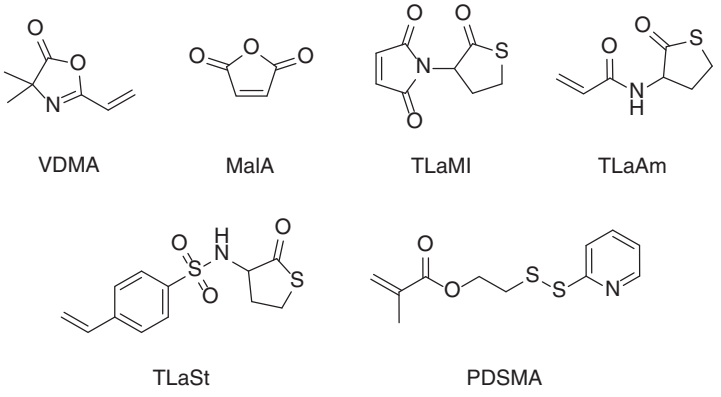

Scheme 18.9 Selection of common azlactone, anhydride, thiolactone, and disulfide bearing monomers.

18.16 Anhydride

Another example of post-polymerization modification by ring-opening reaction is illustrated by maleic anhydride (MalA, Scheme 18.9), which can directly be incorporated in the polymer backbone by copolymerization with a wide range of styrene derivative monomers [52]. Moreover, alternative copolymerizations of the electron poor maleic anhydride with the electron-rich vinyl acetate (VAc) or isopropenyl acetate (IPAc) were also reported [53]. The key benefit of the introduction of such

anhydride directly in the polymer backbone consist in the post-polymerization formation of zwitterionic pH-responsive copolymers by the anhydride ring-opening reaction with various nucleophiles such as ethanolamine derivatives.

18.17 Thiolactone

The key advantage of thiolactones over other cyclic monomers is their capacity to yield a stoichiometric amount of thiol directly from the initial post-polymerization ring-opening reaction. The newly formed thiol can be subsequently reacted with various olefins by Michael addition and thiol–ene chemistries. For example, RAFT copolymerization of thiolactone-functionalized styrenic monomer (TLaSt, Scheme 18.9) with styrene yielded poly[St-*co*-(TLaSt)]. The ring opening of the thiolactone by several primary amines was reported and subsequent thiol–ene reactions from the freshly formed thiols were achieved [54]. In a similar way, RAFT copolymerization of thiolactone-functionalized acrylamide monomers (TLaAm, Scheme 18.9) and *N*-isopropylacrylamide (NIPAM) yielded to poly[(NIPAM)-*co*-(TLaAm)]. Ring opening was once again achieved with different primary amines and the formed thiol reacted this time by Michael addition to the relative acrylate esters [55]. Finally, the RAFT copolymerization of thiolactone-functionalized maleimide (TLaMI, Scheme 18.9) with *N*-isopropylacrylamide (NIPAM) or styrene were also reported and yielded the expected poly[(NIPAM)-*co*-(TLaMI)] and poly[(St)-*co*-(TLaMI)] copolymers. The expected ring-opening of the thiolactone with several primary amines followed by Michael addition was also reported [56].

18.18 Thiol Exchange (Disulphide)/Michael Addition/Thiol–Ene

Concerning the thiol–disulfide exchange chemistry, the RAFT copolymerization of pyridyl disulfide ethyl methacrylate (PDSMA, Scheme 18.9) and poly(ethylene glycol) methacrylate (PEG-MA) yielded poly[(PDSMA)-*co*-(PEG-MA)]. Post-polymerization modification by thiol–disulfide exchange yielded a random copolymer with chemically, physically, and biologically responsive properties [57]. A key aspect to highlight in the thiol–disulfide exchange, the thiol–ene, and the Michael addition post-polymerization modification is their incompatibility as first modification methods as the thiol and the alkene are not well tolerated during RAFT polymerization or more generally during radical polymerization.

18.19 Epoxide

Epoxide (oxirane) chemistry is widely employed at an industrial scale for the production of cross-linked resins and adhesives. Indeed, in the presence of a

catalytic amount of Lewis acid/base in an aprotic medium, cross-linking by ring-opening polymerization (CROP/AROP) is favoured. However, by varying the post-polymerization modification conditions, the ring-opening chemistry of oxiranes can yield new outcomes. By changing the reaction conditions with an excess of nucleophile in a protic medium, the polymerization can be totally avoided and a quantitative functionalization of the initial polymer with α-substituted-β-hydroxy groups can be achieved. For this purpose, RAFT block copolymerization of glycidyl methacrylate (GMA, Scheme 18.10) with pentafluorostyrene (PFSty), styrene, methyl acrylate, or butyl acrylate yielded the respective PGMA block copolymers. Subsequent hydrolysation of the epoxides into diol resulted in an amphiphilic block copolymer in the case of the PGMA-*b*-PPFSty copolymer [58]. The post-polymerization modification by a selection of nucleophiles including amines, thiols, phenol, and azide was also investigated [59]. Furthermore, the RAFT block copolymerization of 4-vinylphenyloxirane (VPO, Scheme 18.10) with styrene was also reported and the subsequent CBr_4- and BF_3-catalysed ring-opening reactions of the epoxides were investigated for a large choice of alcohols [60]. As the last example, employment of unsaturated fatty acid has been reported. The RAFT polymerization of a methacrylate-functionalized oleic acid, 2-(methacryloyloxy)ethyl oleate (MAEO, Scheme 18.10) was reported and the olefinic group of PMAEO was subsequently modified by thiol–ene chemistry or by mCPBA epoxidation, followed by the ring opening of the epoxide with diamine as a cross-linker [61]. Unlike the oxirane, the ring-opening reactivity of the aziridine can be greatly moderated by the third substituent present on the nitrogen as the presence of electron-withdrawing groups (EWGs) and aromatic substituents will lead to an increase in reactivity and electron-donating groups (EDG) to a decrease. Furthermore, the post-polymerization modification of the α-substituted-β-amino groups also allows great versatility in the functionality of the aziridine polymers. Finally, the RAFT polymerization of a methanesulfonyl-protected aziridine *N*-mesyl-2-(4-vinylphenyl)aziridine (NMVPA, Scheme 18.10) yielded PNMVPA in a controlled fashion [62].

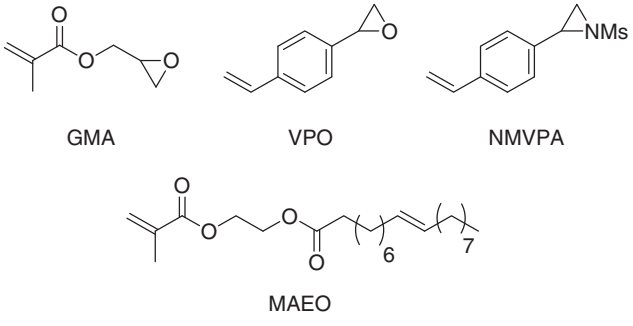

Scheme 18.10 Selection of epoxide, epoxide precursor, and aziridine monomers.

18.20 Diels–Alder Cycloaddition

The Diels–Alder [2+4] cycloaddition was widely employed during the last century in chemistry and in the last decades in the end-functionalization of polymers. Considering the temperature-driven nature of the equilibrium reaction, thermally triggered self-healing of Diels–Alder cross-linked polymers was investigated. In this topic, the RAFT polymerization of furfuryl methacrylate (FMA, Scheme 18.11) and its post-polymerization cross-linking by addition of bismaleimides derivatives was achieved [63].

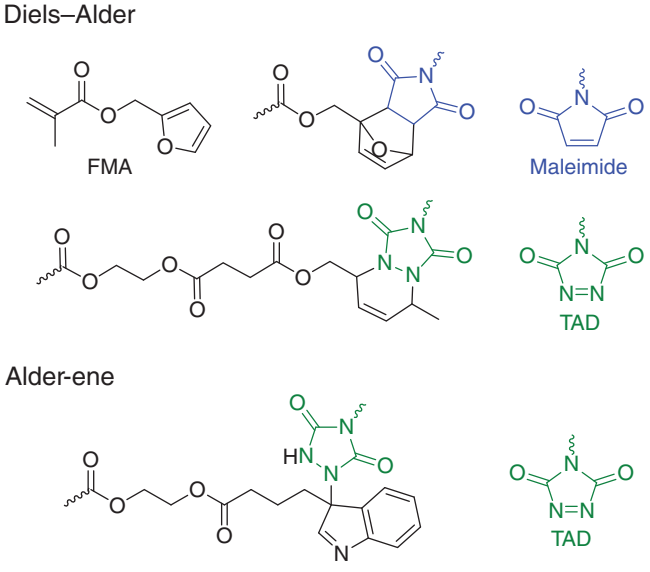

Scheme 18.11 Similarities between Diels–Alder and Alder–Ene reactions.

18.21 Triazolinedione

In a similar way, the highly electron-deficient double bond of the triazolinedione (TAD) functional groups allows for an ultrafast Diels–Alder [2+4] cycloaddition at room temperature. RAFT polymerization of 2-hydroethyl acrylate (HEA) yielded PHEA. Post-polymerization modification by reaction with hexa-2,4-dienyl ester succinic anhydride yielded the desired poly(HEA-diene). TAD-terminated poly(methyl methacrylate) (PMMA), poly(*tert*-butyl acrylate) (P*t*BA), or PS addition yielded in a one minute timescale the expected PHEA-*g*-PMMA], PHEA-*g*-P*t*BA], and PHEA-*gt*-PS] [64]. Similarly, to the TAD-diene Diels–Alder chemistry, the retro Alder–Ene reaction is available at high temperature. Indeed,

the presence of indole with TAD allows an ultrafast Alder–Ene reaction at room temperature. For example, RAFT copolymerization of 2-hydroxyethyl methacrylate (HEMA) and methyl methacrylate (MMA) yielded poly[HEMA-*co*-MMA]. The post-polymerization incorporation of the indole groups via Steglich esterification was successfully followed by an ultra-fast Alder–Ene reaction with a bifunctional 1,2,4-triazoline-3,5-dione (TAD) cross-linker [65].

18.22 Carbonyl Groups and their Derivatives

The pH-dependent condensation equilibrium taking place between a primary amine and a carbonyl to an imine groups is well known, and its use in the polymer field is well documented. For example, a pH-responsive RAFT triblock copolymer (mPEO-*b*-PAPMAm-*b*-PNIPAM) was synthesized from an initial mPEO-CTA with *N*-(3-aminopropyl)methacrylamide (APMAm, Scheme 18.12) and *N*-isopropylacrylamide (NIPAm) as second and third block monomers. The pH-dependent cross-linking of the central PAPMAm block with terephthaldicarboxaldehyde (TDA) yielded shell cross-linked (SCL) micelles, which could be subsequently used as pH-triggered drug release carriers [66]. Nevertheless, the scope of post-polymerization condensation of carbonyl groups is not restricted toimine chemistry, as the more stable hydrazone, oxime, and thiooxime by their respective condensation with hydrazine, hydroxylamine, and thiohydroxylamine were successfully reported. In order to illustrate the versatility of condensation products, the RAFT block polymerization of 2-(4-formylbenzoyloxy)ethyl methacrylate (FBEMA, Scheme 18.12) with MMA yielded (PFBEMA)-*b*-PMMA. Post-polymerization modification by the condensation of the aldehyde with *tert*-butylhydrazide, *O*-benzylhydroxylamine, or *S*-aroylthiohydroxylamine yielded the related hydrazone, oxime, and thiooxime, respectively. Such thiooximes were reported to degrade in presence of thiol at neutral pH with the formation of H_2S [67]. Finally, the acid-catalysed dynamic equilibrium of β-ketoesters and enaminones

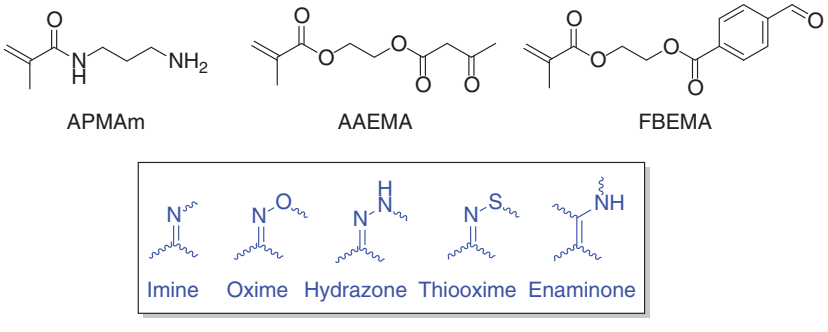

Scheme 18.12 Overview of the carbonyl post-polymerization modifications and some related examples of monomers.

in the presence of primary amine can also be highlighted. RAFT polymerization of 2-(acetoacetoxy)ethyl methacrylate (AAEMA, Scheme 18.12) yielded PAAEMA. Statistical and block copolymerization with poly(ethylene glycol) 500 methacrylate (PEG-500-MA) or MMA yielded the expected copolymers. Post-polymerization modification of the β-ketoesters by TsOH-catalysed condensation reactions with primary amines was achieved [68].

18.23 Copper-Catalysed Azide–Alkyne Cycloaddition (CuAAC)

In the click chemistry realm, copper-catalysed azide–alkyne cycloaddition (CuAAC) is known to be one of the most versatile and tolerant orthogonal reactions, and its application in the polymer field has been widely investigated since its initial report by Sharpless et al. [69] Nevertheless, both azide and alkyne groups may suffer from side reactions in the presence of radical species, which can negatively affect polymerization outcomes. Indeed, side reactions between the RAFT CTA and the azide may occur when spatially close. Furthermore, any electron-withdrawing groups should be avoided next to the alkyne group to avoid any incorporation of the alkyne into the polymer backbone. As an example, a one-pot RAFT polymerization of a common alkyne monomer, propargyl methacrylate (PgMA, Scheme 18.13), in tandem with a CuAAC reaction with azide-functionalized galactose, yielded the desired glycopolymer. Subsequent end-group modification by aminolysis of the CTA yielded a thiol, which was thereafter employed for the functionalization of a gold surface [70]. In the case of the presence of azido groups within the polymer backbone, a RAFT copolymerization of HPMA and *N*-(3-azidopropyl) methacrylamide (AzMA, Scheme 18.13) yielded poly[(HPMA)-*stat*-(AzMA)]. Post-polymerization modification by CuAAC with propargyl dye, propargyl PEG, and biosensor (prop-2-yn-phosphocholine (PPhCh)) yielded the desired polyfunctionalized copolymers [71].

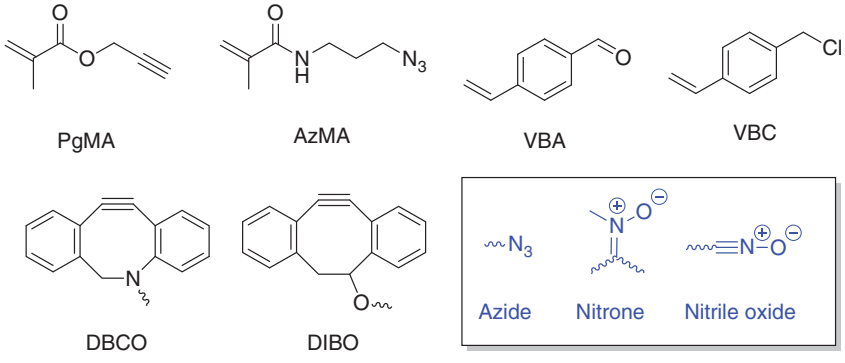

Scheme 18.13 Selection of CuAAC-, SPAAC-, SPANOC-, and SPANC-related structures.

18.24 Strain-Promoted Azide–Alkyne Cycloaddition (SPAAC)

A related catalyst-free azide–alkyne reaction, the strain-promoted azide–alkyne cycloaddition (SPAAC), can also be highlighted. In order to favour the [2+3] cycloaddition, the enthalpy gain during the reaction is highly increased by the high strain energy contained in the cyclooctyne ring. An example of such chemistry was investigated with the RAFT polymerization of PFPMA and the post-polymerization substitution of PFP by dibenzocyclooctyne-amine (DBCO-NH_2, Scheme 18.13) and ethanolamine, followed by the SPAAC click reaction with azido-modified mannose and galactose, yielding the desired homogeneous and heterogeneous glycopolymers [72].

18.25 Nitrone– and Nitrile Oxide–Alkyne Cycloadditions (SPANOC/SPANC)

Next to the SPAAC chemistry, two similar [2 + 3] dipolar cycloadditions promoted by the high strain enthalpy of cyclooctyne rings were also published. By substituting the azido group by a nitrone or a nitrile oxide group, strain-promoted alkyne–nitrone cycloadditions (SPANC) and strain-promoted alkyne–nitrile oxide cycloadditions (SPANOC) were successfully reported. RAFT copolymerization of VBC (Scheme 18.13) and styrene, followed by chain extension with 4-vinylbenzaldehyde (VBA) and styrene, yielded the expected P(VBC-*co*-St)-*b*-P(VBA-*co*-St). Azide and oxime functionalities were then introduced at the VBC and VBA units, respectively. Post-polymerization modification at the azide (SPAAC) and oxime (oxidized with (diacetoxyiodo)benzene [BAIB] followed by SPANOC) moieties yielded orthogonal bifunctionalization with a selection of several dibenzocyclooctynol (DIBO) derivatives. A similar route was used to post-functionalize polymers with nitrone groups for DIBO-functionalization via SPANC [73].

18.26 Cross-coupling Reactions

Among the post-polymerization modification methods, the formation of C—C bonds is mainly achieved by cross-coupling reaction. As such Suzuki, Buchwald-Hartwig, and Sonogashira cross-couplings were successfully reported for the post-polymerization modification of RAFT polymers. RAFT polymerization of *N*-[2-(4-bromophenyl)ethyl]acrylamide (BPEAm, Scheme 18.14) yielded PBPEAm. Chain extension was achieved by block copolymerization with NIPAM, yielding the expected PBPEAm-*b*-PNIPAM], from which Suzuki cross-couplings with a range of aromatic boronic acid were achieved [74]. RAFT block copolymerization of 4-bromophenyl vinyl sulfide (BPVS, Scheme 18.14) and NIPAM yielded PBPVS-*b*-PNIPAM. RAFT copolymerization of trimethylsilyl propargyl methacrylate (TMS-PgMA, Scheme 18.14) and MMA yielded the desired

poly[(TMS-PgMA)-*co*-MMA]. Post-polymerization deprotection of the terminal alkyne and subsequent cross-linking by a Sonogashira cross-coupling reaction with *para*-diiodo benzene as a cross-linking agent was achieved [75].

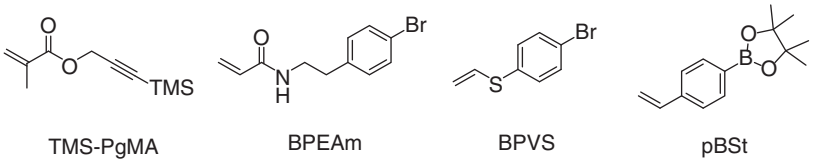

Scheme 18.14 Selection of monomers for cross-coupling and boronic acid/diol condensation.

18.27 Boronic Acid/Diol Condensation

Aromatic boronic acids present in Suzuki cross-coupling were reported to achieve quantitative condensation in the appropriate basic pH range with diol-rich molecules such as sugars. In the recent literature, a pinacol-protected boronic acid monomer, 4-pinacolatoborylstyrene (pBSt, Scheme 18.14), was reported to be efficiently block RAFT copolymerized with *N*,*N*-dimethylacrylamide (DMA), yielding PpBSt-*b*-PDMA. Efficient post-polymerization deprotection by trifluoroacetic acid addition yielded a polymer bearing boronic acid functional groups [76]. Furthermore, the boronic acid polymer was also obtained by an alternative pathway from PFPA (Scheme 18.3) via post-polymerization substitution. RAFT block copolymerization of *N*-acryloylmorpholine (AcM) and PFPA yielded PAcM-*b*-PPFPA. Substitution of the PFP by (3-aminomethyl) phenyl boronic acid and glycine were achieved to form glucose delivery pH-responsive materials [77].

18.28 Multicomponent Reactions (MCR)

The so-called multicomponent reactions (MCR) consist of a series of efficient and versatile one-pot reactions involving three or more molecules reacting to form a single product. For example, post-polymerization modifications by Biginelli reactions were recently investigated several times. The RAFT polymerization of 2-(acetoacetoxy)ethyl methacrylate (AAEMA, Scheme 18.15) yielded poly[2-(acetoacetoxy)ethyl methacrylate] (PAEMA). Post-polymerization modification by Biginelli reaction with urea and benzaldehyde in the presence of catalysts was achieved [78]. Secondly, the six possible RAFT triblock polymers consisting of 2-(acetoacetoxy)ethylacrylamide (AAEAm), *N*,*N*-dimethylacrylamide (DMAm), and 4-acryloylmorpholine (AMPL) were synthetized. Five different benzaldehyde derivatives with urea or thiourea were used in order to form a $6 \times 5 \times 2$ combinational block copolymer library including post-polymerization modification by Biginelli chemistry [79]. Thirdly, an example of post-polymerization

modification involving the Kabachnik–Fields reaction was also reported in recent years with the RAFT polymerization of *N*-(3-aminopropyl)methacrylamide (APMA, Scheme 18.15). Post-polymerization modification by the Kabachnik–Fields reaction was achieved with diethylphosphite and a range of aromatic and aliphatic aldehydes to form the expected poly(aminophosphonate) (polyAPP) polymers. A one-pot approach was also successfully investigated [80].

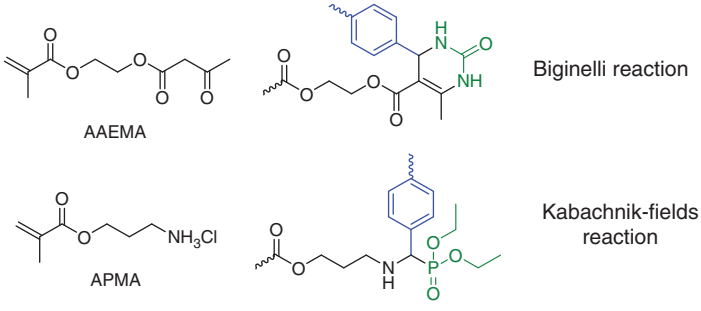

Scheme 18.15 Overview of the Biginelli and the Kabachnik–Fields reactions from the corresponding monomer examples.

18.29 Metal–Ligand Coordination

Beside the classical post-polymerization reactions via the modification of a covalent bond, the creation of ligand–metal bonds results in the incorporation of a metal complex directly in the polymer structure. Such polymers containing active metal complexes may play an interesting role in catalysis. In this regard, the RAFT polymerization of various ligand bearing monomers has been published in the recent years. Statistical copolymerization of MMA with bipyridine-MA and/or triphenylphosphine-MA was achieved. Post-polymerization modification by metal incorporation (Pt, Pd, and Au) was investigated (Scheme 18.16) [81]. In a different approach, a Zn(II) phthalocyanine cross-linked polymer was obtained from the RAFT polymerization of 2-methyl-acrylic acid 6-(3,4-dicyano-phenoxy)-hexyl ester and its post-polymerization modification by the formation of polymeric Zn(II) phthalocyanine at high temperature [82].

18.30 Bioapplications of Reactive Polymers

In the following paragraphs, selected examples of applications of reactive polymers in a biological context will be presented. Noteworthy, reactive polymers prepared via RAFT polymerization also find application in other areas but will be omitted within the present chapter.

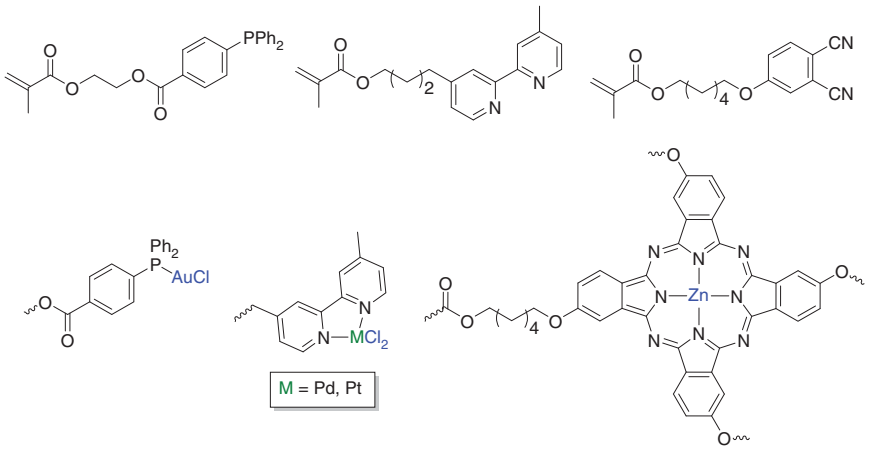

Scheme 18.16 Selection of monomers sharing the capacity to coordinate metal cations.

18.31 Drug Delivery

Amphiphilic block copolymers (ABCs) are widely investigated for biomedical and pharmaceutical applications owing to their self-assembly into nanostructured morphologies depending on the solvent properties. Self-assembled amphiphilic macromolecules, for example, with a hydrophilic shell and a hydrophobic core, have become some of the most attractive vehicles for insoluble drugs and biomolecules because of their advantageous stability, biocompatibility, and triggered drug release. The combination of RDRP techniques and post-polymerization modification has been extensively employed in engineering functional block copolymers for various applications. In this regard, the preparation of well-defined amphiphilic block copolymers was mainly achieved by RAFT polymerization of reactive monomers. Stenzel et al. reported the synthesis of amphiphilic block copolymers based on poly(*N*-(2-hydroxypropyl)methacrylamide (PHPMA) and the reactive PFPMA via RAFT polymerization, obtaining a macroRAFT stabilizer (Scheme 18.17) [83]. A successive cross-linking by chain extension of the block copolymer in the presence of divinyl cross-linkers generated cross-linked nanocapsules. This allowed for the encapsulation of a hydrophilic cancer drug such as Gemcitabine inside these polymeric nanocapsules, which was achieved in a one-pot process via the inverse mini-emulsion periphery RAFT polymerization (IMEPP) approach, stabilized by the prepared block copolymers. Because of the presence of highly reactive PFP moieties, a functional biocompatible glucosamine was then introduced via post-polymerization modification yielding glycopolymer nanocapsules. Exposure to glutathione led to the degradation of the cross-links of the loaded nanocapsules in water and hence their disintegration. These biocompatible glycopolymer nanocapsules showed potential against pancreatic cancer cells, offering a new drug delivery carrier of cancer drugs.

Similarly, Zentel et al. proposed a synthetic approach to prepare multifunctional PHPMA-based copolymers by RAFT polymerization and subsequent

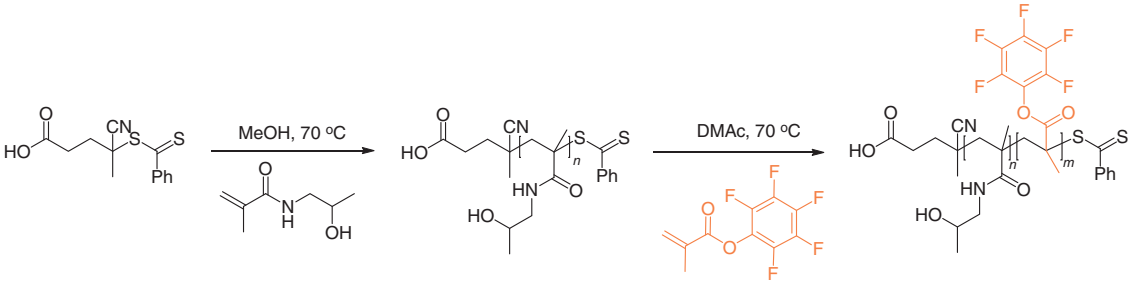

Scheme 18.17 The synthesis of functional block copolymer featuring PFP-active ester via RAFT (macroRAFT stabilizer).

post-polymerization modification of activated ester precursor polymers via aminolysis [84]. PFPMA and lauryl methacrylate (LMA) precursor polymers offered a platform to prepare homo-, statistical, and block copolymers of PHPMA by subsequent polymer-analogous reaction as represented in Figure 18.1. These libraries of novel amphiphilic HPMA-LMA copolymers that self-assemble into nano-sized objects have unique properties for in vitro and in vivo applications. The multi-functional HPMA-LMA copolymers prepared by the reactive ester chemistry have high potential as drug carriers in the field of tumour immunotherapy.

Further, Theato and coworkers have utilized active ester chemistry to prepare glucose-responsive block copolymers and glycopolymers from a single reactive prepolymer made by RAFT polymerization containing polyPFPA as a hydrophobic block [85]. 3-Aminophenylboronic acid, 3-amino-1,2-propanediol, and *D*-glucosamine were easily incorporated within the polymer by post-polymerization modification under mild conditions. Of note, the reactive polyPFPA-based precursor provided a straightforward synthetic approach for the preparation of boronic acid containing polymers that are otherwise incompatible with direct controlled polymerization. All polymers obtained showed an identical degree of polymerization and low dispersities. The self-assembly behaviour of these polymers could be adjusted by boronic acid and diol complexation, forming cross-linked micelles with diameters in the 100 nm range. Upon the addition of glucose, the disintegration of the polymeric micelles occurred under neutral conditions depending on glucose concentration. Finally, a controlled release of insulin from the cross-linked micelles was achieved under diabetic glucose concentrations, offering a very promising candidate for self-regulated insulin delivery.

The synergy of RAFT polymerization associated with post-polymerization modification techniques allows the synthesis of a broad range of complex structures and architectures for drug delivery applications. A similar synthesis involving the incorporation of multiple functional groups in the polymer structure without post-polymerization modifications is otherwise very limited. For example, Sanyal et al. reported the synthesis of multi-functional copolymers based on PEG, a furan-protected maleimide-containing methacrylate (FuMaMA) monomer, and a hydroxyl group containing methacrylate (HEMA) monomer using RAFT polymerization (Figure 18.2) [86]. The thermo-responsive self-assembly of these copolymers and subsequent cross-linking via thiol-maleimide click reaction between a dithiol-based cross-linker and maleimide reactive groups on the copolymers resulted in multi-functionalized nanogels. The cross-linked nanogels were successfully conjugated to an amine-containing anti-cancer drug (i.e. doxorubicin) through acid-labile carbamate linkages. Additionally, the reactive maleimide groups were modified by thiol-containing peptides and thiol groups from the cross-linker were utilized to install a maleimide-containing fluorescent dye. The fabrication strategy offered an interesting platform to allow the multi-functionalization of polymers for targeted applications in drug delivery.

Dhara and coworkers synthesized a dual-responsive PNIPAM-*b*-PAA copolymer by RAFT polymerization and magnetic iron oxide nanoparticles by aqueous coprecipitation of 3-aminopropyl-triethoxysilane [87]. PNIPAM-*b*-PAA copolymers and

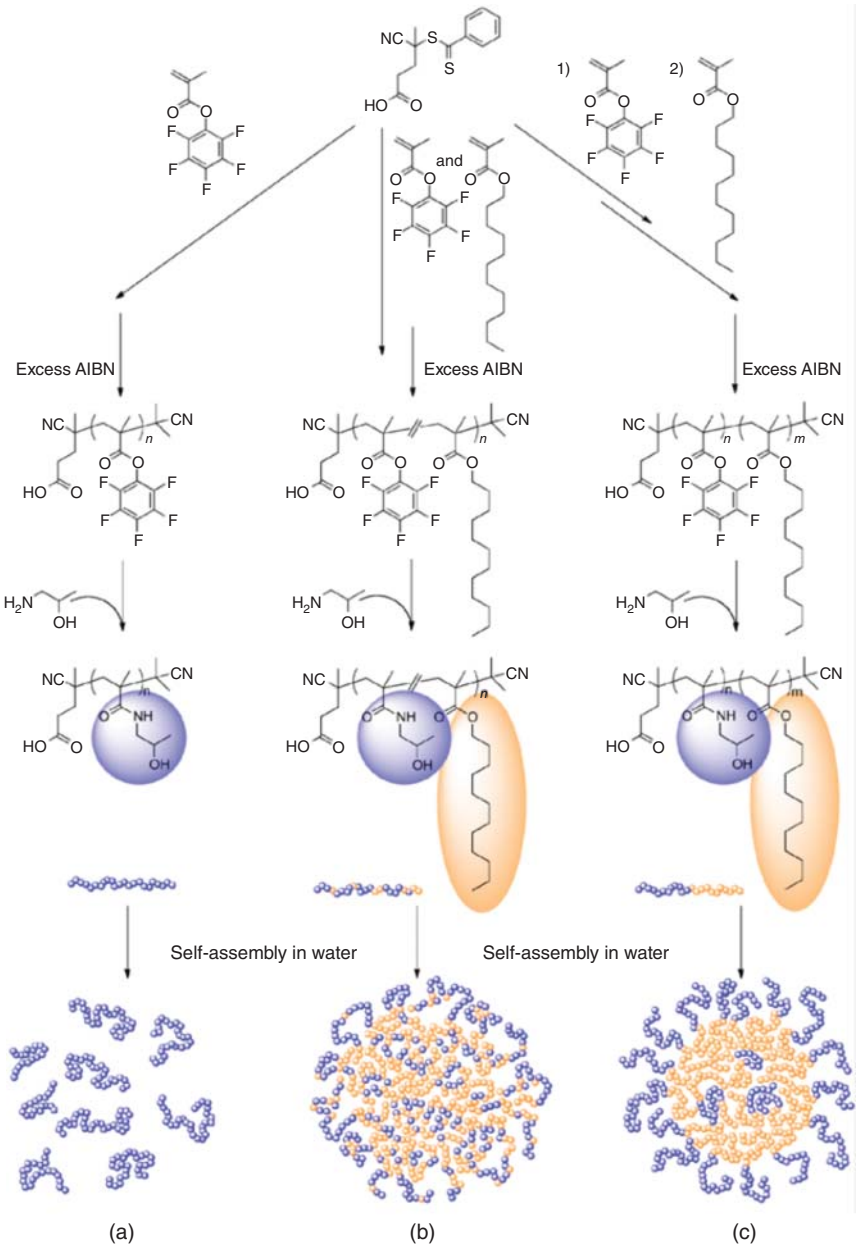

Figure 18.1 Synthetic concept of HPMA-based copolymers derived by post-polymerization modification – RAFT-copolymerized precursor polymers of pentafluorophenyl methacrylate and LMA can selectively be aminolysed by 2-aminopropanol affording HPMA homo, statistical, or block copolymers. While (a) HPMA homopolymers are highly water-soluble, the amphiphilic HPMA-LMA statistical or block copolymers self-assemble into (b) multicompartment or (c) compound micelles in water. Source: Reprinted with permission from Nuhn et al. [84]. © 2014, John Wiley & Sons.

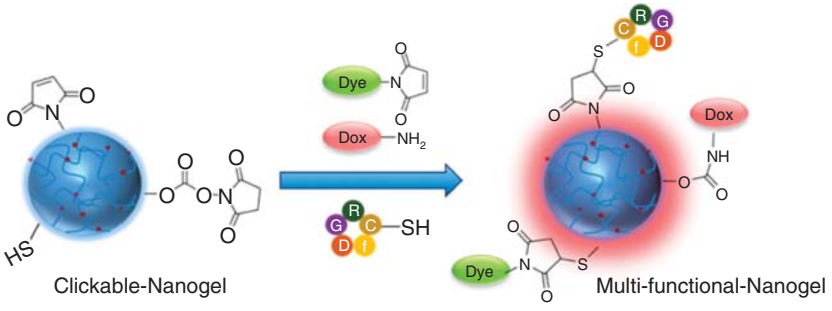

Figure 18.2 Schematic illustration of nanogels multi-functionalization. Source: Reprinted with permission from Chambre et al. [86]. © 2018, American Chemical Society.

folic acid were then modified by the aminated iron oxide nanoparticles (NH_2-MNPs) via EDC/NHS chemistry, yielding modified magnetic nanoparticles (Poly-MNPs) and folic acid tethered polymer-modified magnetic nanoparticles (FA-MNPs). For cellular imaging, rhodamine B isothiocyanate was conjugated to FA-MNPs and doxorubicin (DOX) was loaded into Poly-MNPs and its release in vitro was achieved under lysosomal conditions. The multi-functional magnetic nanoparticles have the potential to be used in magnet-guided drug delivery applications and cellular imaging.

18.32 Bio-conjugation

NHS-based polymers have drawn considerable interest in biomedical sciences because of their fast bioconjugation with biomolecules featuring amino groups such as proteins, peptides, or carbohydrates. Pich and coworkers copolymerized cyclic *N*-vinylamides (*N*-vinylcaprolactam, *N*-vinylpiperidine, and *N*-vinylpyrrolidone) with methacrylic acid *N*-hydroxysuccinimide ester via RAFT polymerization at varied temperatures and in a range of solvents, obtaining copolymers with variable chemical composition, controlled molecular weight, and narrow dispersity *Đ*. The obtained water-soluble reactive copolymers with NHS-ester groups showed fast cross-linking with proteins containing lysine linkages, such as enhanced green fluorescent protein (EGFP) and cellulase (CelA2_M2), in water-in-oil (W/O) emulsion, resulting in fascinating biohybrid nanogels. These conjugated nanogels were proven to be promising candidates for protein imaging and good colloidal catalysts for depolymerization of cellulose [88]. Interestingly, the same group later also described a controlled synthesis of pyridyl disulfide (PDS)-functionalized poly(vinyl lactams), such as statistical reactive copolymers of poly(*N*-vinylpyrrolidone-*co*-pyridyl disulfide ethyl methacrylate) (PVPD), poly(*N*-vinylpiperidone-*co*-pyridyl disulfide ethyl methacrylate) (PVPID), and poly(*N*-vinylcaprolactam-*co*-pyridyl disulfide ethyl methacrylate) (PVD), via RAFT polymerization at 60 °C in anisole with methyl 2-(ethoxycarbonothioylthio)-propanoate as a chain transfer agent (Figure 18.3) [89]. Because of the highly reactive PDS group towards thiol

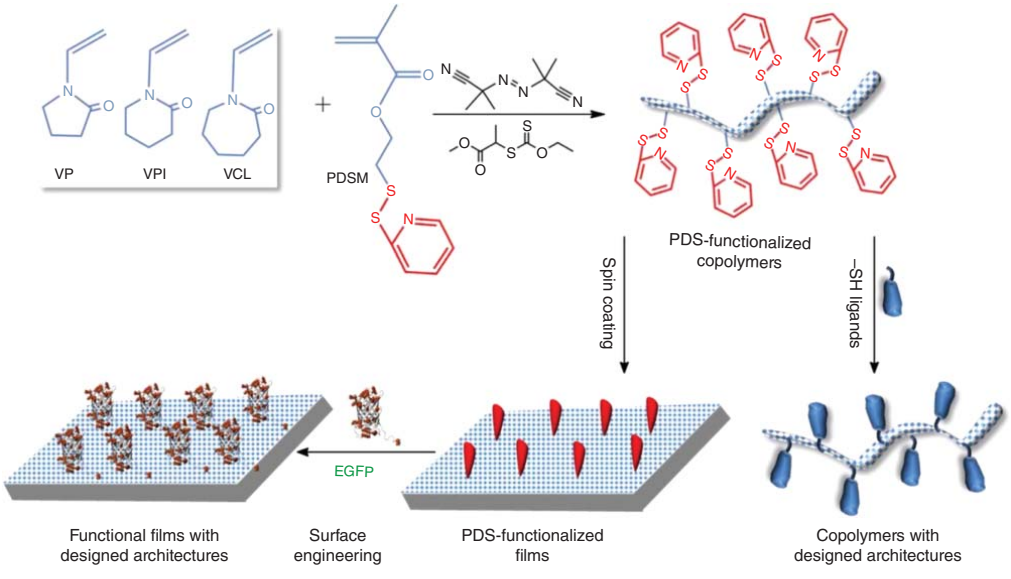

Figure 18.3 Synthesis of reactive copolymers based on *N*-vinyl lactams with pyridyl disulfide side groups via RAFT polymerization and post-modification via thiol–disulfide exchange reaction. Source: Reprinted with permission from Peng et al. [89]. © 2016, American Chemical Society.

groups via a specific thiol–disulfide exchange, the PDS-functionalized reactive polymers were post-modified with a variety of thiol-containing functional groups including 2-phenylethanethiol (2P), 3-mercaptopropionic acid (3M), methyl 3-mercaptopropionate (M3), 2-mercaptoethanol (2M), 2-aminoethanethiol (2A), poly(ethylene glycol) methyl ether thiol (PEG-SH), and EGFP under extremely mild conditions to control cell attachment and growth activity on modified polymer films. Owing to the high potential cell adhesion and growth, surface engineering of biocompatible PDS-functionalized copolymers with thiol-containing ligands offered great potential in tissue engineering, medical implants, and diagnostic molecular biology.

Li and coworkers synthesized a well-defined protected glycopolymer poly(2-(2,3,4,6-tetra-*O*-acetyl-β-*D*-glucosyloxy)ethyl methacrylate) (PAcGlcEMA) by RAFT polymerization with end thiol-reactive PDS group [90]. After deprotection, pendent glucose units were attached to polymer backbone to yield a hydrophilic glycopolymer poly(2-β-*D*-glucosyloxy)ethyl methacrylate) (PGlcEMA) with high binding affinity for protein Concanavalin A (Con A). Reduced *L*-glutathione (GSH) is an endogenous antioxidant that was conjugated to the reactive thiol end by thiol–disulfide exchange reaction to generate peptide–glycopolymer bioconjugates employed for the delivery of antioxidants. O'Reilly's group reported decorated thermo-responsive poly[(oligo ethylene glycol) methyl ether methacrylate] (PEGMA) polymers with superfolder green fluorescent protein (sfGFP) in three steps (Figure 18.4) [91]. First, PEGMA with an alkyne-functional end group was prepared via RAFT polymerization targeting different molecular weights. Second, the fluorescent protein (sfGFP) was functionalized with non-canonical azide-functional amino acid residues at different positions. And third, the reactive azide moieties of sfGFP were conjugated with the alkyne-functional end group of PEGMA using copper-catalysed alkyne–azide cycloaddition (CuAAC). The self-assembled structures of these polymer–protein conjugates were found to be dependent on temperature and on the site of conjugation.

Functionalized CTAs also allow a flexible installation of functional groups, either prior to or after the polymerization, to the end group of polymers, thus enabling enhanced delivery characteristics [10]. For example, NHS-folate-functionalized CTAs were synthesized to prepare a diblock copolymer consisting of a dimethylaminoethyl methacrylate block and a dimethylaminoethyl methacrylate, butyl methacrylate, propylacrylic acid copolymer block (poly(DMAEMA)-*b*-poly(DMAEMA-*co*-BMA-*co*-PAA)) for targeted siRNA delivery (Figure 18.5). The folate-functionalized CTA was not only found to be suitable for the synthesis of a well-defined multi-functional diblock copolymer with narrow dispersities but also allows for complexation and protection of siRNA and hence demonstrates an efficient, specific cellular folate receptor interaction and in vitro gene knockdown [92]. Narumi and coworkers prepared maltopentaose-conjugated (Mal_5-CTA)-conjugated chain transfer agent bearing NHS-activated ester moieties for RAFT polymerization [93]. The use of Mal_5-CTAs enabled the installation of maltopentaose into the α-chain end of the polymer chain by direct RAFT polymerizations of styrene (S) and MMA to yield Mal_5-PS and Mal_5-PMMA, respectively, resulting in Mal_n-hybrid

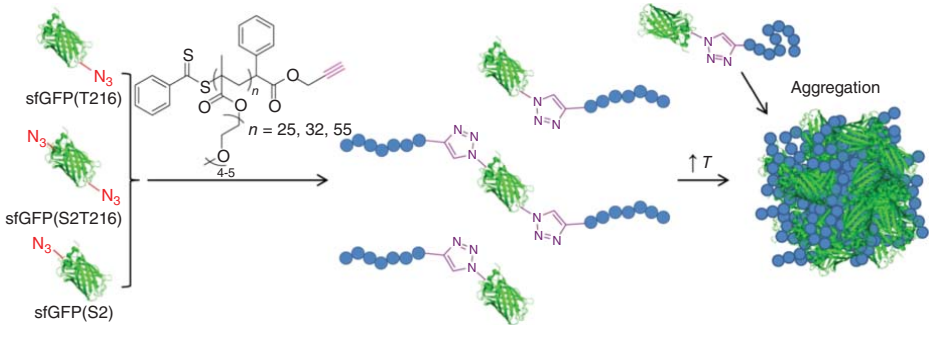

Figure 18.4 Strategy followed for the synthesis of sfGFP-PEGMA bioconjugates via the engineering of three sfGFP analogues with T216, S2T216, and S2 site modification with *p*AzF before the CuAAc of alkyne-functional PEGMA. Source: Reprinted with permission from Moatsou et al. [91]. © 2015, American Chemical Society.

amphiphilic block copolymers (BCPs) with well-defined structures as materials for the next generation of sustainable nanostructured bioresource-block copolymer lithography.

Recently, Sanyal and coworkers synthesized copolymers containing a masked maleimide group and dopamine via RAFT polymerization featuring surface anchoring units [94]. Polymeric precursors were coated on a titanium surface and subjected to a retro-Diels–Alder reaction using a simple thermal treatment. Antimicrobial peptide E6, successfully conjugated to such polymer coated layers through a Michael addition, showed antifouling and antimicrobial properties against both Gram-positive and Gram-negative bacteria.

18.33 Surface/Particle Modification

Char and Li described the synthesis of poly(PFPA) polymer brushes grafted on silica particle surfaces via surface-initiated (SI)-RAFT polymerization [95]. The reactive poly(PFPA) polymer brushes were then modified with amine-containing antibodies followed by amino-terminated PEG yielding silica particles with both PEG and antibody immobilized on the surface. This study demonstrates that poly(PFPA)-grafted SiPs can be an effective alternative for providing clean protein purification and can also be a suitable material platform for antibody immobilization (Figure 18.6).

Perrier et al. exploited the potential of 4-vinylbenzyl chloride as a functional halogenated monomer for the introduction of chemical functionalities under RAFT conditions [96]. They described the synthesis of uniform silica–polymer core–shell nanoparticles via SI-RAFT utilizing a silica-supported RAFT agent in DMF and post-polymerization modification of the pVBC-grafted silica particles with pyren-1-ylmethyl acrylate and TEA-quaternized particles (Figure 18.7). The incorporation of a charged group and a fluorescent moiety resulted in hybrid nanoparticles that are sterically stable in biologically relevant conditions with promising bio-applications. The hybrid nanoparticles are promising for cell imaging owing to their ability to be endocytosed into human colon cancer cells.

Gopalan et al. synthesized a well-defined block copolymer poly(styrene)-*block*-poly(2-vinyl-4,4-dimethylazlactone) (PS-*b*-PVDMA) by RAFT polymerization in two steps [97]. The resulting block copolymers not only contain the amine-reactive azlactone functional group but can also self-assemble into thin films with a hexagonally ordered cylindrical morphology with ~12 nm scale. Interestingly, the self-assembly of cylinder-forming PS-*b*-PVDMA BCP thin films prepared by solvent annealing with toluene revealed defect-free morphologies over large areas. The resulting parallel and perpendicularly oriented morphologies containing reactive azlactone functionality were post-fabricated with infused trimethylaluminium (TMA) vapour and subsequently yielded arrays of aluminium oxide (ALO) nanowires or nanodots. The self-assembled PS-*b*-PVDMA thin films containing azlactone functional groups provide new platforms for the development of nanometre-sized hard masks for potential applications in advanced lithography (Figure 18.8).

Gibson and coworkers demonstrated an interesting possibility to combine the benefits of thiol coating on gold surface with the utility of a glass slide using

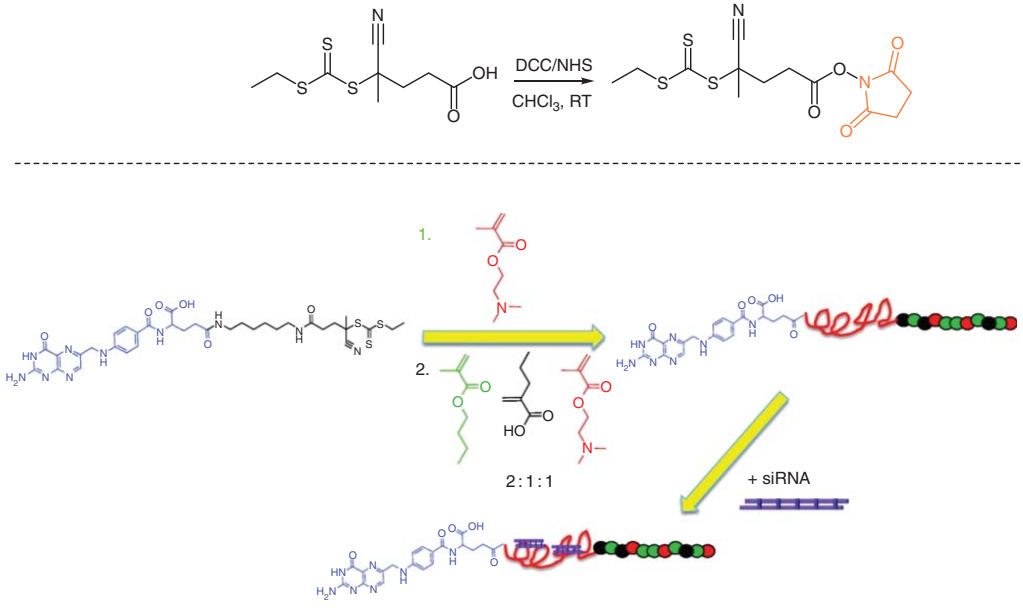

Figure 18.5 Synthesis of folate-CTA for polymerization of folate-functionalized diblock copolymers for siRNA delivery. Source: Adapted with permission from Benoit et al. [92]. © 2011, American Chemical Society.

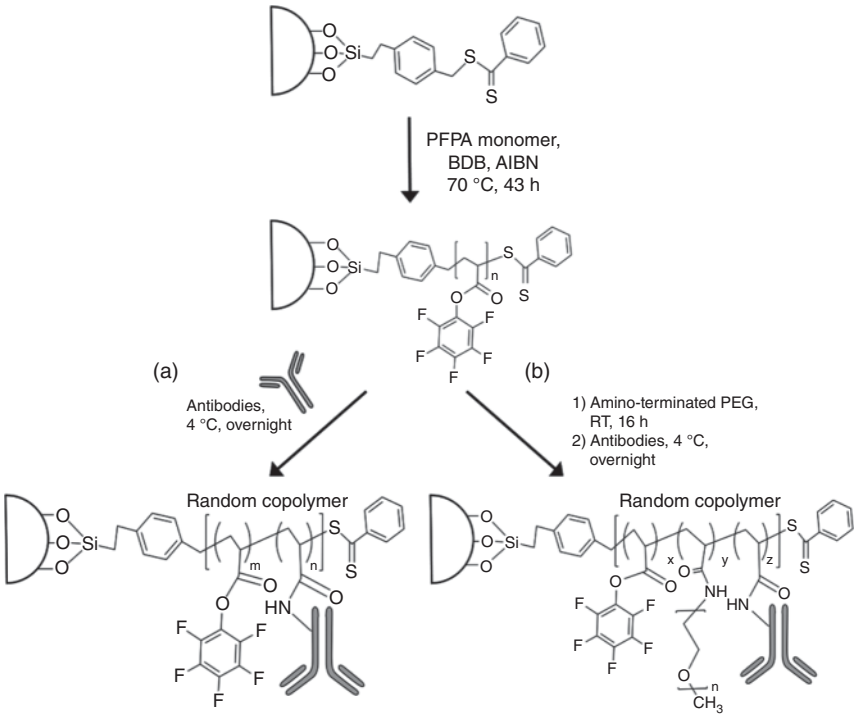

Figure 18.6 Schematic for the preparation of poly(PFPA) brush via SI-RAFT polymerization and (a) subsequent post-modification to immobilize antibody and (b) partial substitution with amino-PEG, followed by antibody immobilization. Source: Reprinted with permission from Son et al. [95]. © 2018, American Chemical Society.

thio–ene chemistry in tandem with RAFT polymerization [98]. They prepared two representative thermo-responsive polymers of poly[oligo(ethylene glycol) methyl ether methacrylate] (POEGMA) and PNIPAM functionalized with thiol at the ω-chain ends, providing an anchor points for surface modification by a grafting-to approach. Polymers prepared by RAFT polymerization with a thiol-end functionality were then grafted onto acrylated glass and silicon substrates by a 'thiol–ene click' (Michael addition) (Figure 18.9). The installation of hydrophilic polymers on surfaces is commonly limited in terms of controlled radical polymerization and the chemical space for attachment chemistry. This 'grafting-to' approach gives an easy and a straightforward approach to prepare grafted polymers and the characterizations confirmed that the PNIPAMs resulted in much higher grafting densities than the POEGMAs. However, both POEGMA and PNIPAM resulted in a significant decrease in protein binding because of their hydrophilicity. The polymer-coated glass slides with their nonfouling characteristics will find application in array applications, particularly for glycomics.

In summary, reactive polymers prepared by RAFT polymerization of various reactive monomers provide a versatile synthetic platform for numerous applications. The advantage to not only introduce functionality along the macromolecular

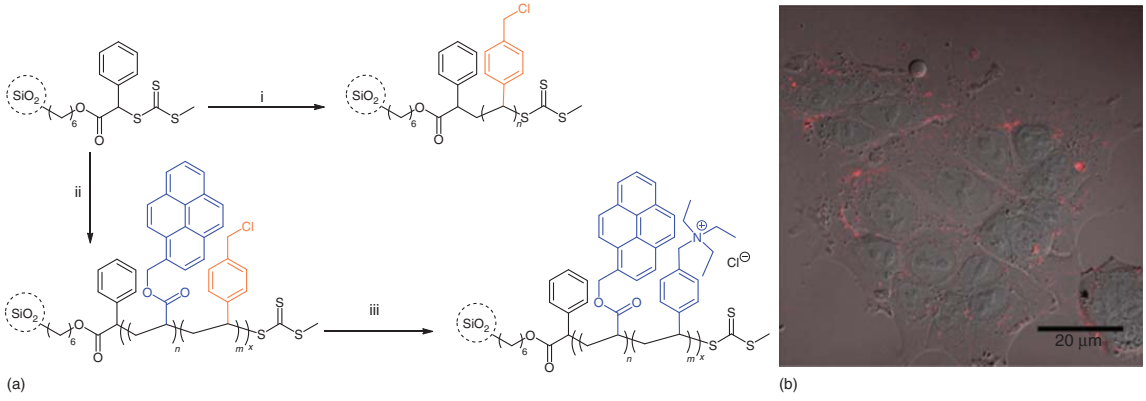

Figure 18.7 (a) Synthetic scheme of silica-supported RAFT polymerization of 4-vinylbenzyl chloride and post-polymerization modification of the resultant core–shell nanoparticles and (b) confocal microscopy image of human colon cancer cells after two hours of incubation with TEA-quaternized SiP-p(VBC-*co*-PyAc) particles. Source: Adapted with permission from Moraes et al. [96]. Copyright 2013, American Chemical Society.

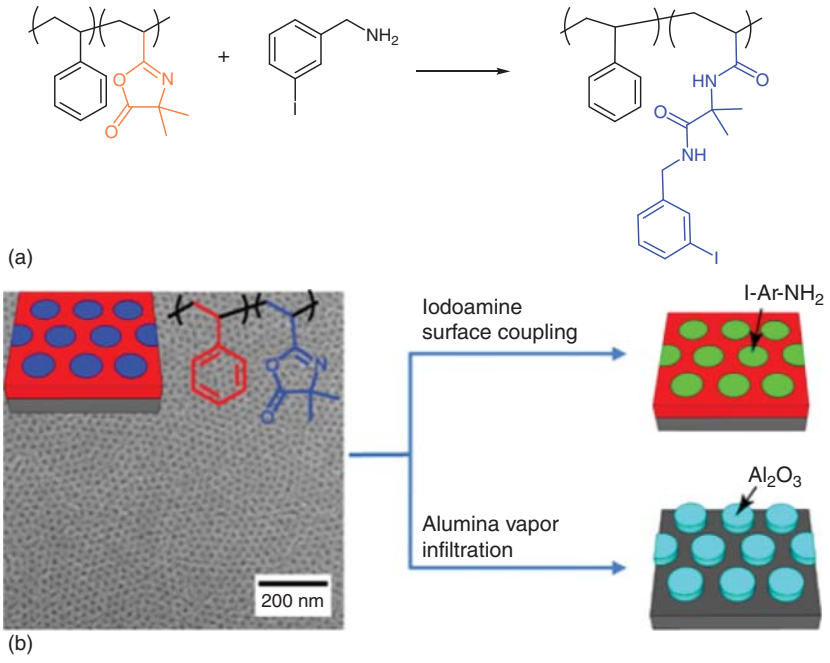

Figure 18.8 (a) Scheme showing the ring opening of azlactone groups in the PVDMA block of PS-*b*-PVDMA by iodobenzylamine. (b) The post-modification of reactive azlactone and the resultant morphologies. Source: Adapted with permission from Choi et al. [97]. Copyright 2016, American Chemical Society.

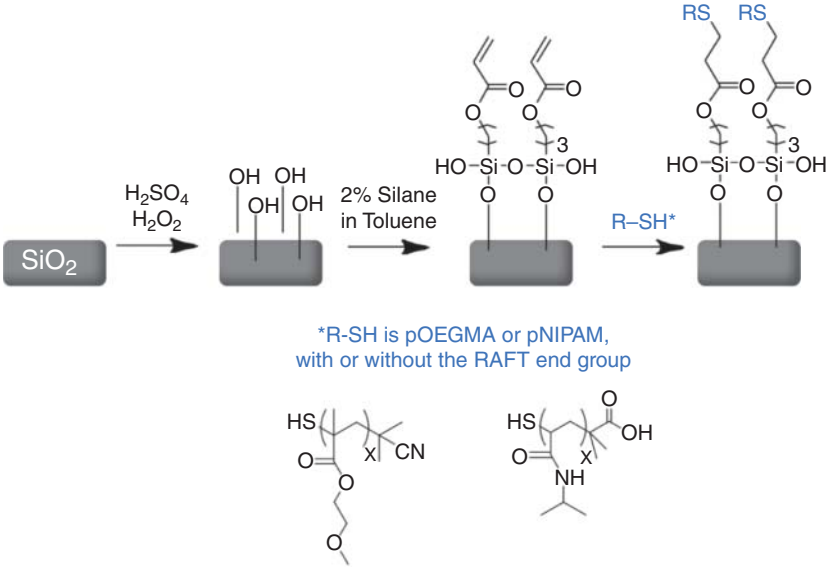

Figure 18.9 Schematic representation of the immobilization of polymers onto acrylate silane-functionalized glass and silicon surfaces. Source: Reprinted with permission from Biggs et al. [98]. Copyright 2016, American Chemical Society. Licensed under CCBY 4.0.

chain but also easily at the chain ends provides the synthetic basis for polymers in numerous applications.

18.34 Conclusion and Outlook

The recent years have witnessed an enormous development of new chemistries suitable for efficient post-polymerization modifications, especially of polymers that have been prepared by RAFT polymerization but also other RDRP techniques. In most cases, this has led to unprecedented synthetic access to polymers with highly defined functionality and architecture. Clearly, the development of new efficient chemical ligation techniques that are compatible with RAFT polymerization will continue. In this regard, multi-component and sequential reactions will play an important role as much as externally triggered reactions, such as photo-reactions. In the future, we will also likely see increased development and application of orthogonal chemistries within the area of post-polymerization modifications, enabling not only the synthetic access to ever more diversely functionalized polymers, but also digitalization in polymer synthesis, because of the plethora of applicable orthogonal reactions, which could be fully automated.

References

1 Theato, P. (2008). Synthesis of well-defined polymeric activated esters. *J. Polym. Sci. A Polym. Chem.* 46 (20): 6677–6687.

2 Günay, K.A., Theato, P., and Klok, H.A. (2013). History of post-polymerization modification. In: *Functional Polymers by Post-Polymerization Modification* (eds. P. Theato and H.-A. Klok), 1–44. Weinheim: Wiley-VCH.

3 Günay, K.A., Theato, P., and Klok, H.A. (2013). Standing on the shoulders of Hermann Staudinger: post-polymerization modification from past to present. *J. Polym. Sci. A Polym. Chem.* 51 (1): 1–28.

4 Das, A. and Theato, P. (2015). Activated ester containing polymers: opportunities and challenges for the design of functional macromolecules. *Chem. Rev.* 116 (3): 1434–1495.

5 Blasco, E., Sims, M.B., Goldmann, A.S. et al. (2017). 50th anniversary perspective: polymer functionalization. *Macromolecules* 50 (14): 5215–5252.

6 Theato, P. and Klok, H.A. (eds.) (2013). *Functional Polymers by Post-Polymerization Modification: Concepts, Guidelines and Applications*. Weinheim: Wiley-VCH.

7 Batz, H.G., Franzmann, G., and Ringsdorf, H. (1972). Model reactions for synthesis of pharmacologically active polymers by way of monomeric and polymeric reactive esters. *Angew. Chem. Int. Ed. Engl.* 11 (12): 1103–1104.

8 Ferruti, P., Bettelli, A., and Fere, A. (1972). High polymers of acrylic and methacrylic esters of *N*-hydroxysuccinimide as polyacrylamide and polymethacrylamide precursors. *Polymer* 13 (10): 462–464.

9 Schilli, C., Müller, A.H., Thang, S.H. et al. (2002). Controlled radical polymerization of *N*-isopropylacrylamide and of activated esters for the synthesis of polymer-protein and polymer-drug conjugates. *Polym. Prepr.* 43 (2): 687–688.

10 Yanjarappa, M.J., Gujraty, K.V., Joshi, A. et al. (2006). Synthesis of copolymers containing an active ester of methacrylic acid by RAFT: controlled molecular weight scaffolds for biofunctionalization. *Biomacromolecules* 7 (5): 1665–1670.

11 Aamer, K.A. and Tew, G.N. (2007). RAFT polymerization of a novel activated ester monomer and conversion to a terpyridine-containing homopolymer. *J. Polym. Sci. A Polym. Chem.* 45 (23): 5618–5625.

12 Niu, J., Page, Z.A., Dolinski, N.D. et al. (2017). Rapid visible light-mediated controlled aqueous polymerization with in situ monitoring. *ACS Macro Lett.* 6 (10): 1109–1113.

13 Tsuji, S., Aso, Y., Ohara, H., and Tanaka, T. (2019). Polymeric water-soluble activated esters: synthesis of polymer backbones with pendant *N*-hydoxysulfosuccinimide esters for post-polymerization modification in water. *Polym. J.*

14 Kisfaludy, L., Löw, M., Nyéki, O. et al. (1973). Die Verwendung von Pentafluorphenylestern bei Peptidsynthesen. *Justus Liebigs Ann. Chem.* 1973 (9): 1421–1429.

15 Eberhardt, M., Mruk, R., Zentel, R., and Théato, P. (2005). Synthesis of pentafluorophenyl (meth) acrylate polymers: new precursor polymers for the synthesis of multifunctional materials. *Eur. Polym. J.* 41 (7): 1569–1575.

16 Gibson, M.I., Fröhlich, E., and Klok, H.A. (2009). Postpolymerization modification of poly (pentafluorophenyl methacrylate): synthesis of a diverse water-soluble polymer library. *J. Polym. Sci. A Polym. Chem.* 47 (17): 4332–4345.

17 Boyer, C. and Davis, T.P. (2009). One-pot synthesis and biofunctionalization of glycopolymers via RAFT polymerization and thiol–ene reactions. *ChemComm* 40: 6029–6031.

18 Boyer, C., Whittaker, M., and Davis, T.P. (2011). Synthesis and postfunctionalization of well-defined star polymers via "double" click chemistry. *J. Polym. Sci. A Polym. Chem.* 49 (24): 5245–5256.

19 Nilles, K. and Theato, P. (2009). RAFT polymerization of activated 4-vinylbenzoates. *J. Polym. Sci. A Polym. Chem.* 47 (6): 1696–1705.

20 Nilles, K. and Theato, P. (2010). Sequential conversion of orthogonally functionalized diblock copolymers based on pentafluorophenyl esters. *J. Polym. Sci. A Polym. Chem.* 48 (16): 3683–3692.

21 Agar, S., Baysak, E., Hizal, G. et al. (2018). An emerging post-polymerization modification technique: the promise of thiol-Para-fluoro click reaction. *J. Polym. Sci. A Polym. Chem.* 56 (12): 1181–1198.

22 Delaittre, G. and Barner, L. (2018). The Para-fluoro-thiol reaction as an efficient tool in polymer chemistry. *Polym. Chem.* 9 (20): 2679–2684.

23 Riedel, M., Stadermann, J., Komber, H. et al. (2011). Synthesis, post-modification and self-assembled thin films of pentafluorostyrene containing block copolymers. *Eur. Polym. J.* 47 (4): 675–684.

24 Pryor, W.A. and Huang, T.L. (1969). The kinetics of the polymerization of pentafluorostyrene. *Macromolecules* 2 (1): 70–77.

25 Varadharajan, D. and Delaittre, G. (2016). Accessing libraries of bifunctional block copolymers using two distinct pentafluorophenyl moieties. *Polym. Chem.* 7 (48): 7488–7499.

26 Dömling, A. and Ugi, I. (2000). Multicomponent reactions with isocyanides. *Angew. Chem. Int. Ed.* 39 (18): 3168–3210.

27 Noy, J.M., Koldevitz, M., and Roth, P.J. (2015). Thiol-reactive functional poly (meth) acrylates: multicomponent monomer synthesis, RAFT (co) polymerization and highly efficient thiol–Para-fluoro postpolymerization modification. *Polym. Chem.* 6 (3): 436–447.

28 Noy, J.M., Friedrich, A.K., Batten, K. et al. (2017). Para-fluoro postpolymerization chemistry of poly (pentafluorobenzyl methacrylate): modification with amines, thiols, and carbonylthiolates. *Macromolecules* 50 (18): 7028–7040.

29 Noy, J.M., Li, Y., Smolan, W., and Roth, P.J. (2019). Azide–Para-fluoro substitution on polymers: multipurpose precursors for efficient sequential postpolymerization modification. *Macromolecules* 52 (8): 3083–3091.

30 Bodanszky, M. (1955). Synthesis of peptides by aminolysis of nitrophenyl esters. *Nature* 175 (4459): 685.

31 Hu, Y.C., Liu, Y., and Pan, C.Y. (2004). Reversible addition–fragmentation transfer polymerization of *p*-nitrophenyl acrylate and synthesis of diblock copolymers poly (*p*-nitrophenyl acrylate)-*b*-polystyrene. *J. Polym. Sci. A Polym. Chem.* 42 (19): 4862–4872.

32 Hwang, J., Li, R.C., and Maynard, H.D. (2007). Well-defined polymers with activated ester and protected aldehyde side chains for bio-functionalization. *J. Control. Release* 122 (3): 279–286.

33 Zuwala, K., Smith, A.A., Tolstrup, M., and Zelikin, A.N. (2016). HIV anti-latency treatment mediated by macromolecular prodrugs of histone deacetylase inhibitor, panobinostat. *Chem. Sci.* 7 (3): 2353–2358.

34 Metz, N. and Theato, P. (2007). Controlled synthesis of poly (acetone oxime acrylate) as a new reactive polymer: stimuli-responsive reactive copolymers. *Eur. Polym. J.* 43 (4): 1202–1209.

35 He, L., Shang, J., and Theato, P. (2015). Preparation of dual stimuli-responsive block copolymers based on different activated esters with distinct reactivities. *Eur. Polym. J.* 69: 523–531.

36 Kakuchi, R. and Theato, P. (2012). Changing the reactivity of polymeric activated esters by temperature: on–off switching of the reactivity of poly(4-acryloxyphenyldimethylsulfonium triflate). *Macromolecules* 45 (3): 1331–1338.

37 Nuhn, L., Overhoff, I., Sperner, M. et al. (2014). RAFT-polymerized poly(hexafluoroisopropyl methacrylate)s as precursors for functional water-soluble polymers. *Polym. Chem.* 5 (7): 2484–2495.

38 Szostak, R., Shi, S., Meng, G. et al. (2016). Ground-state distortion in *N*-acyl-tert-butyl-carbamates (Boc) and *N*-acyl-tosylamides (Ts): twisted amides of relevance to amide N–C cross-coupling. *J. Org. Chem.* 81 (17): 8091–8094.

39 Larsen, M.B., Herzog, S.E., Quilter, H.C., and Hillmyer, M.A. (2018). Activated polyacrylamides as versatile substrates for postpolymerization modification. *ACS Macro Lett.* 7 (1): 122–126.

40 Seo, M. and Hillmyer, M.A. (2014). RAFT copolymerization of acid chloride-containing monomers. *Polym. Chem.* 5 (1): 213–219.

41 Zheng, Z., Ling, J., and Müller, A.H. (2014). Revival of the R-group approach: a "CTA-shuttled" grafting from approach for well-defined cylindrical polymer brushes via RAFT polymerization. *Macromol. Rapid Commun.* 35 (2): 234–241.

42 Barlow, T.R., Brendel, J.C., and Perrier, S. (2016). Poly (bromoethyl acrylate): a reactive precursor for the synthesis of functional RAFT materials. *Macromolecules* 49 (17): 6203–6212.

43 Kubo, T., Figg, C.A., Swartz, J.L. et al. (2016). Multifunctional homopolymers: postpolymerization modification via sequential nucleophilic aromatic substitution. *Macromolecules* 49 (6): 2077–2084.

44 AdrianáFigg, C. (2017). Modular and rapid access to amphiphilic homopolymers via successive chemoselective post-polymerization modification. *Polym. Chem.* 8 (39): 6028–6032.

45 Flores, J.D., Shin, J., Hoyle, C.E., and McCormick, C.L. (2010). Direct RAFT polymerization of an unprotected isocyanate-containing monomer and subsequent structopendant functionalization using "click"-type reactions. *Polym. Chem.* 1 (2): 213–220.

46 Flores, J.D., Treat, N.J., York, A.W., and McCormick, C.L. (2011). Facile, modular transformations of RAFT block copolymers via sequential isocyanate and thiol-ene reactions. *Polym. Chem.* 2 (9): 1976–1985.

47 Francini, N., Purdie, L., Alexander, C. et al. (2015). Multifunctional poly[*N*-(2-hydroxypropyl) methacrylamide] copolymers via postpolymerization modification and sequential thiol–ene chemistry. *Macromolecules* 48 (9): 2857–2863.

48 Hoff, E.A., Abel, B.A., Tretbar, C.A. et al. (2016). RAFT polymerization of "splitters" and "Cryptos": exploiting azole-*N*-carboxamides as blocked isocyanates for ambient temperature postpolymerization modification. *Macromolecules* 49 (2): 554–563.

49 Zhu, Y., Quek, J.Y., Lowe, A.B., and Roth, P.J. (2013). Thermoresponsive (co) polymers through postpolymerization modification of poly(2-vinyl-4, 4-dimethylazlactone). *Macromolecules* 46 (16): 6475–6484.

50 Li, Y., Duong, H.T., Jones, M.W. et al. (2013). Selective postmodification of copolymer backbones bearing different activated esters with disparate reactivities. *ACS Macro Lett.* 2 (10): 912–917.

51 Kanimozhi, C., Shea, M.J., Ko, J. et al. (2019). Removable nonconjugated polymers to debundle and disperse carbon nanotubes. *Macromolecules* 52 (11): 4278–4286.

52 Davies, M.C., Dawkins, J.V., and Hourston, D.J. (2005). Radical copolymerization of maleic anhydride and substituted styrenes by reversible

addition-fragmentation chain transfer (RAFT) polymerization. *Polymer* 46 (6): 1739–1753.

53 Stubbs, C., Lipecki, J., and Gibson, M.I. (2016). Regioregular alternating polyampholytes have enhanced biomimetic ice recrystallization activity compared to random copolymers and the role of side chain versus main chain hydrophobicity. *Biomacromolecules* 18 (1): 295–302.

54 Espeel, P., Goethals, F., Stamenović, M.M. et al. (2012). Double modular modification of thiolactone-containing polymers: towards polythiols and derived structures. *Polym. Chem.* 3 (4): 1007–1015.

55 Reinicke, S., Espeel, P., Stamenović, M.M., and Du Prez, F.E. (2013). One-pot double modification of p (NIPAAm): a tool for designing tailor-made multiresponsive polymers. *ACS Macro Lett.* 2 (6): 539–543.

56 Rudolph, T., Espeel, P., Du Prez, F.E., and Schacher, F.H. (2015). Poly (thiolactone) homo-and copolymers from maleimide thiolactone: synthesis and functionalization. *Polym. Chem.* 6 (23): 4240–4251.

57 Liu, X., Hu, D., Jiang, Z. et al. (2016). Multi-stimuli-responsive amphiphilic assemblies through simple postpolymerization modifications. *Macromolecules* 49 (17): 6186–6192.

58 Gudipati, C.S., Tan, M.B., Hussain, H. et al. (2008). Synthesis of poly (glycidyl methacrylate)-block-poly (pentafluorostyrene) by RAFT: precursor to novel amphiphilic poly(glyceryl methacrylate)-block-poly(pentafluorostyrene). *Macromol. Rapid Commun.* 29 (23): 1902–1907.

59 Benaglia, M., Alberti, A., Giorgini, L. et al. (2013). Poly (glycidyl methacrylate): a highly versatile polymeric building block for post-polymerization modifications. *Polym. Chem.* 4 (1): 124–132.

60 McLeod, D.C. and Tsarevsky, N.V. (2016). Well-defined epoxide-containing styrenic polymers and their functionalization with alcohols. *J. Polym. Sci. A Polym. Chem.* 54 (8): 1132–1144.

61 Maiti, B., Kumar, S., and De, P. (2014). Controlled RAFT synthesis of side-chain oleic acid containing polymers and their post-polymerization functionalization. *RSC Adv.* 4 (99): 56415–56423.

62 McLeod, D.C. and Tsarevsky, N.V. (2016). Reversible deactivation radical polymerization of monomers containing activated aziridine groups. *Macromol. Rapid Commun.* 37 (20): 1694–1700.

63 Pramanik, N.B., Bag, D.S., Alam, S. et al. (2013). Thermally amendable tailor-made functional polymer by RAFT polymerization and "click reaction". *J. Polym. Sci. A Polym. Chem.* 51 (16): 3365–3374.

64 Xiao, L., Chen, Y., and Zhang, K. (2016). Efficient metal-free "grafting onto" method for bottlebrush polymers by combining RAFT and triazolinedione–diene click reaction. *Macromolecules* 49 (12): 4452–4461.

65 Mondal, P., Raut, S.K., and Singha, N.K. (2018). Thermally amendable tailor-made acrylate copolymers via RAFT polymerization and ultrafast alder-ene "click" chemistry. *J. Polym. Sci. A Polym. Chem.* 56 (20): 2310–2318.

66 Xu, X., Flores, J.D., and McCormick, C.L. (2011). Reversible imine shell cross-linked micelles from aqueous RAFT-synthesized thermoresponsive triblock copolymers as potential nanocarriers for "pH-triggered" drug release. *Macromolecules* 44 (6): 1327–1334.

67 Foster, J.C. and Matson, J.B. (2014). Functionalization of methacrylate polymers with thiooximes: a robust postpolymerization modification reaction and a method for the preparation of H_2S-releasing polymers. *Macromolecules* 47 (15): 5089–5095.

68 Sims, M.B., Lessard, J.J., Bai, L., and Sumerlin, B.S. (2018). Functional diversification of polymethacrylates by dynamic β-ketoester modification. *Macromolecules* 51 (16): 6380–6386.

69 Himo, F., Lovell, T., Hilgraf, R. et al. (2005). Copper (I)-catalyzed synthesis of azoles. DFT study predicts unprecedented reactivity and intermediates. *J. Am. Chem. Soc.* 127 (1): 210–216.

70 Lu, J., Zhang, W., Richards, S.J. et al. (2014). Glycopolymer-coated gold nanorods synthesised by a one pot copper (0) catalyzed tandem RAFT/click reaction. *Polym. Chem.* 5 (7): 2326–2332.

71 Ebbesen, M.F., Schaffert, D.H., Crowley, M.L. et al. (2013). Synthesis of click-reactive HPMA copolymers using RAFT polymerization for drug delivery applications. *J. Polym. Sci. A Polym. Chem.* 51 (23): 5091–5099.

72 Martyn, B., Biggs, C.I., and Gibson, M.I. (2019). Comparison of systematically functionalized heterogeneous and homogenous glycopolymers as toxin inhibitors. *J. Polym. Sci. A Polym. Chem.* 57 (1): 40–47.

73 Ledin, P.A., Kolishetti, N., and Boons, G.J. (2013). Multifunctionalization of polymers by strain-promoted cycloadditions. *Macromolecules* 46 (19): 7759–7768.

74 Howe, D.H., McDaniel, R.M., and Magenau, A.J. (2017). From click chemistry to cross-coupling: designer polymers from one efficient reaction. *Macromolecules* 50 (20): 8010–8018.

75 Prasher, A., Loynd, C.M., Tuten, B.T. et al. (2016). Efficient fabrication of polymer nanoparticles via sonogashira cross-linking of linear polymers in dilute solution. *J. Polym. Sci. A Polym. Chem.* 54 (1): 209–217.

76 Cambre, J.N., Roy, D., Gondi, S.R., and Sumerlin, B.S. (2007). Facile strategy to well-defined water-soluble boronic acid (co) polymers. *J. Am. Chem. Soc.* 129 (34): 10348–10349.

77 Gaballa, H., Shang, J., Meier, S., and Theato, P. (2019). The glucose-responsive behavior of a block copolymer featuring boronic acid and glycine. *J. Polym. Sci. A Polym. Chem.* 57 (3): 422–431.

78 Zhu, C., Yang, B., Zhao, Y. et al. (2013). A new insight into the Biginelli reaction: the dawn of multicomponent click chemistry? *Polym. Chem.* 4 (21): 5395–5400.

79 Wu, H., Yang, L., and Tao, L. (2017). Polymer synthesis by mimicking nature's strategy: the combination of ultra-fast RAFT and the Biginelli reaction. *Polym. Chem.* 8 (37): 5679–5687.

80 Zhang, Y., Zhao, Y., Yang, B. et al. (2014). One pot'synthesis of well-defined poly (aminophosphonate) s: time for the Kabachnik–fields reaction on the stage of polymer chemistry. *Polym. Chem.* 5 (6): 1857–1862.

81 Müller, R., Feuerstein, T.J., Trouillet, V. et al. (2018). Spatially-resolved multiple metallopolymer surfaces by photolithography. *Chem. Eur. J.* 24 (71): 18933–18943.

82 Zhang, J., Wang, L., Li, C. et al. (2014). Preparation and characterization of solution processable phthalocyanine-containing polymers via a combination of RAFT polymerization and post-polymerization modification techniques. *J. Polym. Sci. A Polym. Chem.* 52 (5): 691–698.

83 Utama, R.H., Jiang, Y., Zetterlund, P.B., and Stenzel, M.H. (2015). Biocompatible glycopolymer nanocapsules via inverse miniemulsion periphery RAFT polymerization for the delivery of gemcitabine. *Biomacromolecules* 16 (7): 2144–2156.

84 Nuhn, L., Barz, M., and Zentel, R. (2014). New perspectives of HPMA-based copolymers derived by post-polymerization modification. *Macromol. Biosci.* 14 (5): 607–618.

85 Gaballa, H. and Theato, P. (2019). Glucose-responsive polymeric micelles via Boronic acid–diol complexation for insulin delivery at neutral pH. *Biomacromolecules* 20 (2): 871–881.

86 Chambre, L., Degirmenci, A., Sanyal, R., and Sanyal, A. (2018). Multi-functional nanogels as theranostic platforms: exploiting reversible and nonreversible linkages for targeting, imaging, and drug delivery. *Bioconjug. Chem.* 29 (6): 1885–1896.

87 Sahoo, B., Devi, K.S.P., Banerjee, R. et al. (2013). Thermal and pH responsive polymer-tethered multifunctional magnetic nanoparticles for targeted delivery of anticancer drug. *ACS Appl. Mater. Inter.* 5 (9): 3884–3893.

88 Peng, H., Kather, M., Rübsam, K. et al. (2015). Water-soluble reactive copolymers based on cyclic N-vinylamides with succinimide side groups for bioconjugation with proteins. *Macromolecules* 48 (13): 4256–4268.

89 Peng, H., Rübsam, K., Huang, X. et al. (2016). Reactive copolymers based on N-vinyl lactams with pyridyl disulfide side groups via RAFT polymerization and postmodification via thiol–disulfide exchange reaction. *Macromolecules* 49 (19): 7141–7154.

90 Shi, H., Liu, L., Wang, X., and Li, J. (2012). Glycopolymer–peptide bioconjugates with antioxidant activity via RAFT polymerization. *Polym. Chem.* 3 (5): 1182–1188.

91 Moatsou, D., Li, J., Ranji, A. et al. (2015). Self-assembly of temperature-responsive protein–polymer bioconjugates. *Bioconjug. Chem.* 26 (9): 1890–1899.

92 Benoit, D.S., Srinivasan, S., Shubin, A.D., and Stayton, P.S. (2011). Synthesis of folate-functionalized RAFT polymers for targeted siRNA delivery. *Biomacromolecules* 12 (7): 2708–2714.

93 Togashi, D., Otsuka, I., Borsali, R. et al. (2014). Maltopentaose-conjugated CTA for RAFT polymerization generating nanostructured bioresource-block copolymer. *Biomacromolecules* 15 (12): 4509–4519.

94 Gevrek, T.N., Yu, K., Kizhakkedathu, J.N., and Sanyal, A. (2019). Thiol-reactive polymers for titanium interfaces: fabrication of antimicrobial coatings. *ACS Appl. Polym. Mater.* 1 (6): 1308–1316.

95 Son, H., Ku, J., Kim, Y. et al. (2018). Amine-reactive poly(pentafluorophenyl acrylate) brush platforms for cleaner protein purification. *Biomacromolecules* 19 (3): 951–961.

96 Moraes, J., Ohno, K., Maschmeyer, T., and Perrier, S. (2013). Monodisperse, charge-stabilized, core–shell particles via silica-supported reversible addition–fragmentation chain transfer polymerization for cell imaging. *Chem. Mater.* 25 (17): 3522–3527.

97 Choi, J.W., Carter, M.C., Wei, W. et al. (2016). Self-assembly and post-fabrication functionalization of microphase separated thin films of a reactive azlactone-containing block copolymer. *Macromolecules* 49 (21): 8177–8186.

98 Biggs, C.I., Walker, M., and Gibson, M.I. (2016). "Grafting to" of RAFTed responsive polymers to glass substrates by thiol–ene and critical comparison to thiol–gold coupling. *Biomacromolecules* 17 (8): 2626–2633.

19

RAFT Crosslinking Polymerization

Patricia Pérez-Salinas[1], Porfirio López-Domínguez[1], Alberto Rosas-Aburto[1], Julio César Hernández-Ortiz[2], and Eduardo Vivaldo-Lima[1]

[1] Universidad Nacional Autónoma de México, Facultad de Química, Departamento de Ingeniería Química, Ciudad Universitaria, Circuito Exterior S/N, Coyoacán, Ciudad de México 04510, México
[2] Amcor Flexibles Gent, Film Extrusion, Ottergemsesteenweg-ZUID 801 B-9000, Ghent, Belgium

19.1 Introduction

Crosslinked polymers are materials of great interest in research and industrial fields. If synthesized beyond the gelation point, these materials possess a three-dimensional network structure. Crosslinking in polymer synthesis by step growth polymerization may result from the polymerization of monomers with functionality greater than two. Branching promoting functional groups such as pendent double bonds (PDB) or labile atoms can also promote crosslinking in chain growth polymerization. Polymer networks can be defined as highly crosslinked macromolecules in which essentially all the units are connected to each other in some way, by covalent chemical bonds or physical associations [1, 2].

Polymer networks, gels, and hydrogels are materials designed to swell under the action of a solvent, which is contained or trapped within the network structure. Chemical substances can thus be loaded and released, giving rise to a good number of applications in diverse fields such as catalysis [3]; controlled release of drugs [4–8], proteins [9], and human cells [10]; synthesis of structured polymers (hierarchical porous polymers, HPP) [11]; energy storage [11, 12]; water desalinization [13]; advanced materials [14], such as self-healing polymers [15–18]; and other applications [19]. One of the most important routes to synthesize polymer networks, represented in Figure 19.1, is the conventional radical copolymerization (RP) of vinyl monomers and multivinyl crosslinker comonomers [20–24].

One disadvantage of polymer networks synthesized by conventional RP of divinyl or multivinyl monomers with vinyl monomers is that their crosslink density distribution is intrinsically very heterogeneous [2]. One way to reduce the heterogeneity of polymer networks synthesized by RP is to introduce a chemical compound that acts

RAFT Polymerization: Methods, Synthesis and Applications, First Edition.
Edited by Graeme Moad and Ezio Rizzardo.

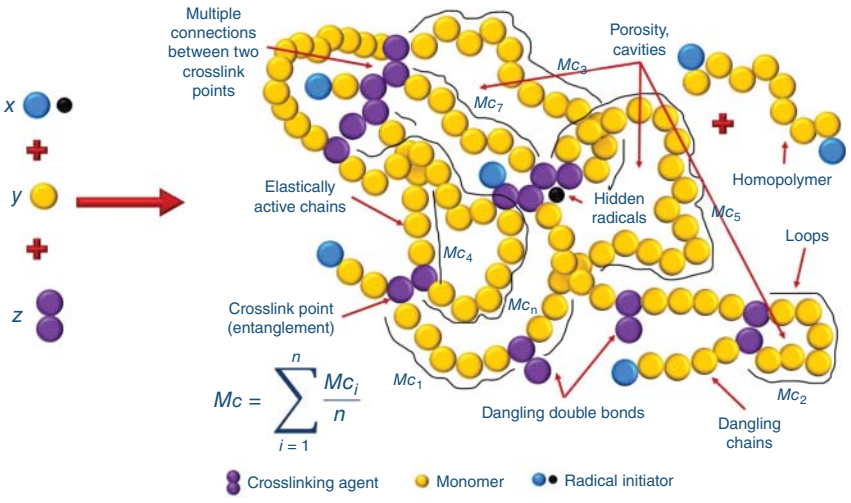

Figure 19.1 Schematic representation of synthesis of polymer networks by RP, representation of the structures within the network structure, and the concept of molecular weight between entanglements (M_c). Source: Adapted with permission from Saldívar-Guerra and Vivaldo-Lima [2]. Copyright 2013, John Wiley & Sons.

as a controller in reversible deactivation radical polymerization (RDRP) techniques into the reacting formulation [2, 25–28]. As evident from the companion chapters of this handbook, reversible addition fragmentation chain transfer (RAFT) polymerization is one of the most employed RDRP techniques [29].

Although there is a debate in the literature regarding the effect on polymer network homogeneity of adding a RDRP controller in the recipe, with some authors claiming that more homogeneous polymer networks are obtained [30, 31], whereas others claim that no changes are observed [32, 33], the effect in the case of RAFT synthesis of polymer networks seems to be the production of less heterogeneous polymer networks [34].

The scope of this chapter includes surveying the plurality of applications found in the literature related to the synthesis of polymer networks (gels, hydrogels, and smart polymer networks) by RAFT (co)polymerization with crosslinking of multi-olefinic monomers. Our starting point is the review by Moad on the RAFT crosslinking copolymerization of multi-olefinic monomers to form polymer networks [25]. In that sense, our chapter can be viewed as an update of Moad's review. However, our survey of the literature also includes reversible polymer networks based on ionic bonds, as well as the syntheses of materials described as nanogels, microgels, core-crosslinked stars, thermo- or pH- responsive materials, self-healing polymer networks, 'arm-first' stars, or hyperbranched polymers that can be formed by RAFT (co)polymerization of similar components under different reaction conditions before gelation. Another distinctive characteristic of our chapter is that it includes a survey on the modelling of polymer network formation by RAFT (co)polymerization of vinyl/divinyl monomers.

19.2 Structure and Characteristics of Polymer Networks

RP can be carried out in the presence or absence of solvents. When solvents are used for the synthesis of polymer networks, the growing polymer chains are in a relaxed state at the early stages of the polymerization. They are therefore able to move freely during the pre-gelation period. On the other hand, the growing polymer molecules curl, exposing as little as possible of their surface, when the polymer network synthesis proceeds in the absence of solvents. The final structure, properties, and characteristics, such as mechanical properties of the produced polymer network, are therefore influenced by the presence or absence of solvent during the polymerization [2, 35]. Calculation of polymer network properties such as diffusion coefficients of loaded chemical compounds [36], molecular weight between entanglements [35, 37], swelling [38], and theta temperature [39] depends on the way the synthesis proceeded.

As stated earlier, the synthesis of polymer networks by RP of vinyl/multi-vinyl monomers leads to heterogeneous structures. Different substructures within the polymer network are generated by that process, as observed in Figure 19.1 [2]. From all these substructures, only elastically active chains can generate porosity and are responsible for the swelling properties of the polymer network (see Figure 19.1). The study of swelling is fundamental for the understanding and estimation of properties and performance of polymer networks. Two theories are available for the calculation and analysis of swelling. Both are related to large elastic (reversible) deformation of solids but explained under thermodynamic and mechanical perspectives, respectively [35, 40–45]. Molecular weight between entanglements and average crosslink density are important parameters for the study of polymer networks. They can be estimated from swelling measurements. The thermodynamic description of swelling leads to the Flory–Rehner equation, given by Eqs. (19.1) and (19.2) for polymer networks synthesized in the absence and presence of solvent, respectively [40, 41].

$$\left(\frac{1}{M_c}\right) = \frac{2}{M_n} - \frac{\rho_{\text{polymer}}\left(\ln\left(1-\upsilon_{2,s}\right)+\upsilon_{2,s}+\chi_1\upsilon_{2,s}\right)}{V_{\text{solvent}}\left(\left(\upsilon_{2,s}\right)^{1/3}-\left(\frac{\upsilon_{2,s}}{2}\right)\right)} \tag{19.1}$$

$$\left(\frac{1}{M_c^{\circ}}\right) = \frac{2}{M_n} - \frac{\rho_{\text{polymer}}\left(\ln\left(1-\upsilon_{2,s}\right)+\upsilon_{2,s}+\chi_1\upsilon_{2,s}\right)}{\upsilon_{2,r}\,V_{\text{solvent}}\left(\left(\frac{\upsilon_{2,s}}{\upsilon_{2,r}}\right)^{1/3}-\left(\frac{\upsilon_{2,s}}{2\,\upsilon_{2,r}}\right)\right)} \tag{19.2}$$

M_c and $M_c{}^0$ are molecular weights between entanglements for polymer networks synthesized in the absence and presence of solvent, respectively (g mol^{-1}); M_n is the number-average molecular weight of primary molecules, polymer population resulting if all crosslinks were broken (g mol^{-1}); V_{solvent} is the solvent or swelling agent molar volume (cm^3 g^{-1} mol^{-1}); ρ_{polymer} is the polymer-specific volume (cm^3 g^{-1}); χ_1 is the Flory polymer solvent interaction parameter (dimensionless); $\upsilon_{2,s}$ is the polymer volume fraction in the gel, which can be estimated as inverse experimentally measured swelling index, S_{index}, (dimensionless); and $\upsilon_{2,r}$ is the polymer volume fraction during the pre-gelation period (dimensionless).

The mechanical description of swelling, in terms of M_c, is given by the Mooney–Rivlin model, given by Eq. (19.3), where σ is the first normal stress difference (J); R is the universal gas constant (8.3145 J mol^{-1} K^{-1}); T is the temperature (K); λ is the solid material deformation (length/characteristic length); and Q is a material constant (dimensionless) that takes the value of 0.4 for soft materials (elastomers and gels) and 0.5 for more rigid materials (polyolefin and polyacrylate rubbers, as well as other networks) [40, 41]. M_c should be calculated using Eqs. (19.1) or (19.2), depending on the absence or presence of solvent, respectively.

$$\sigma_{\text{Mooney}} = \left(\frac{R\,T}{M_c\,\rho_{\text{polymer}}} \right) \left[1 - \frac{1}{Q\,\lambda} + \frac{1}{\lambda} \right] \tag{19.3}$$

Crosslink density distribution, which can be related to the distribution of M_c, determines the size of chemicals that can be loaded into the polymer network, its release rate, and its mechanical properties. Nowadays, polymer networks have extended their fields of application. As a result, some issues related to polymer network formation, such as the type of monomers, their structures and architectures, their construction sequences and the operating mechanisms of polymer networks under the action of solvents, chemical compounds, or other stimuli (e.g. temperature, mechanical deformation, light, pH, and so on), have gained importance [44, 46–55].

19.3 RAFT Crosslinking Polymerization

It is possible to control the extent of crosslinking and the occurrence of the gelation point in RP of vinyl/multivinyl monomers in the presence of solvents [56–58] or chain transfer agents [59]. However, process control strategies in the synthesis of polymer networks by conventional RP cannot reduce heterogeneity (reduction of variance of the crosslink density distribution) of the produced materials. That is why, RDRP methods for synthesis of polymer networks, including RAFT copolymerization of vinyl/multi-divinyl monomers, have been proposed and analysed [26–28]. The idea is that controlled growth of polymer branches from PDBs will result in less heterogeneous polymer networks.

The most widely used RAFT controllers are those based on thiocarbonylthio compounds. Their general chemical structure is shown in Figure 19.2 [60]. It is observed in Figure 19.2 that two main groups, Z and R, are attached to the thiocarbonylthio structure. ‘Z’ modifies both the rate of addition to thiocarbonyl groups of propagating radicals and the rate of fragmentation of intermediate radicals. The kinetic rate constant for the addition reaction can change by several orders of magnitude by manipulation of the Z group [60]. The nature of R determines the fragmentation rate. ‘R’ must be a good homolytic leaving group with respect to the propagating radicals if adequate control is desired. Criteria for adequate selection of RAFT agents, based on groups R and Z, are available in the literature [25, 29, 60, 61].

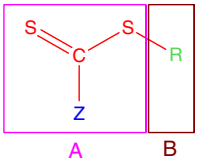

Figure 19.2 Chemical structure representation of a thiocarbonylthio RAFT agent split in two segments, denoted as A and B.

19.3.1 Synthesis Pathways to Obtain Polymer Networks

The synthesis of polymer networks using RAFT controllers is focused on obtaining different network architectures, properties, or characteristics. Different synthesis pathways, sequences, or strategies to assemble the desired material have been proposed. These strategies can be classified in terms of the following categories:

(1) *One-step polymerization*. In this synthetic route, initiator(s), RAFT agent, monomer(s), and crosslinking agent are added to the reactor at the same time at the beginning of the polymerization. Most of these (co)polymerizations are carried out in batch or semi-batch reactors in the presence of solvents or dispersing media. As explained earlier, the presence (or absence) of solvent(s) or dispersing media affects the average value of M_c obtained, and the heterogeneity of the polymer network. The literature related to this type of polymerization is focused on kinetic studies, performance of selected RAFT controllers, kinetic and molecular weight development simulations studies, and characterization/performance of the synthesized polymer networks under different synthesis conditions [8, 62–72].

(2) *Multistep polymerization including RAFT block (co)polymerization of linear segments followed by crosslinking*. This route for the synthesis of polymer networks using RAFT controllers has received significant attention in the literature [25, 73, 74]. It consists of the RAFT synthesis of one or more linear polymer segments (blocks), followed by crosslinking using different techniques, as illustrated in Figure 19.3. Crosslinking routes can be classified according to the following categories:

   (a) *Synthesis of linear polymer molecules by RAFT polymerization, followed by crosslinking*. Linear polymer molecules with narrow molecular weight distributions are synthesized by RAFT polymerization. These linear chains are then placed into a reactor where crosslinker molecules have been charged [3, 7, 16, 73–76].

   (b) *Synthesis of linear precursors by sequential RAFT block copolymerization, followed by crosslinking*. In this category, a first polymer block is built by RAFT polymerization of one of the monomers. After consumption or

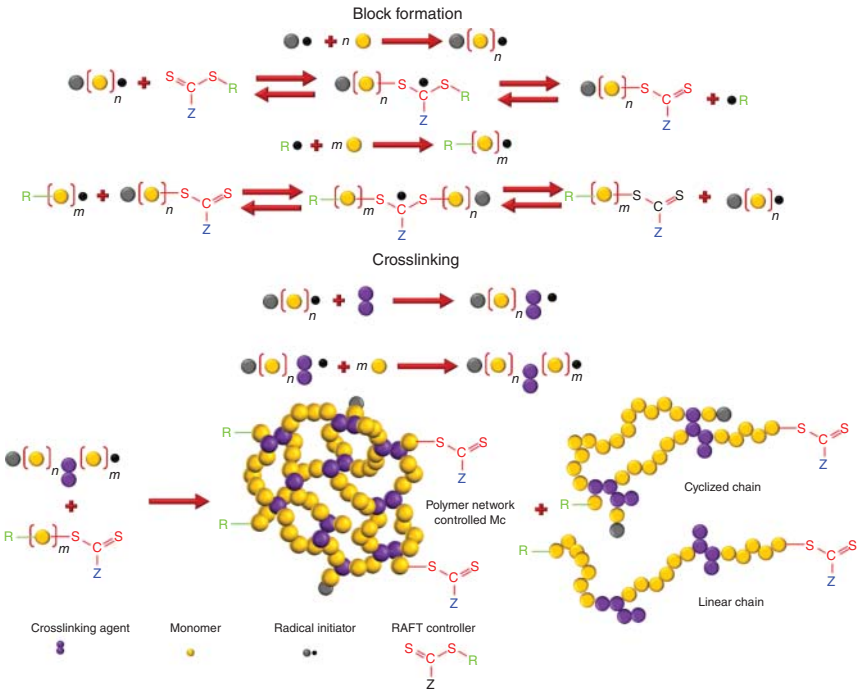

Figure 19.3 Schematic representation of multistep polymerizations including a RAFT block (co)polymerization stage and further crosslinking processes. Source: Adapted with permission from Moad [25]. Copyright 2014, Society of Chemical Industry.

the first monomer, the second monomer is added, and a second block is then produced. If multiblock copolymers are desired, sequential blocks can be added in the same way. At the end, these multi-block polymer molecules are crosslinked by adding a crosslinker. In some cases, the crosslinking process takes place at intermediate stages and not at the end [6, 8, 10, 11, 13, 17–19, 74, 77–84].

(3) *Multistep polymerization using a RAFT macro-controller, followed by crosslinking*. This type of synthesis has gained importance because of its versatility. RAFT controllers containing carboxylic acid groups (RAFT-COOH) can be chemically bonded to almost any type of macromolecule containing hydroxyl groups (e.g. polymer molecules, ceramics, or fibres). It is based on Steglich esterification using *N,N′*-dicyclohexylcarbodiimide (DCC). As observed in Figure 19.4, an anhydride is produced from DCC and the acid group of a RAFT controller. This anhydride is made to react in situ with the desire surface. 4-Dimethylaminopyridine (DMAP) is used as a catalyst, although other procedures can be used. The resulting product is a macro-RAFT controller or macro-controller [4, 5, 9, 12, 14, 15, 83, 85–89].

(4) *Polymer network synthesis using bifunctional RAFT controllers*. Symmetric bifunctional RAFT agents are used in this synthetic route. Under adequate reaction conditions, these molecules react at both ends, leading to crosslinked structures. As observed in Figure 19.5, two types of bifunctional RAFT controllers have been used [25, 90–97].

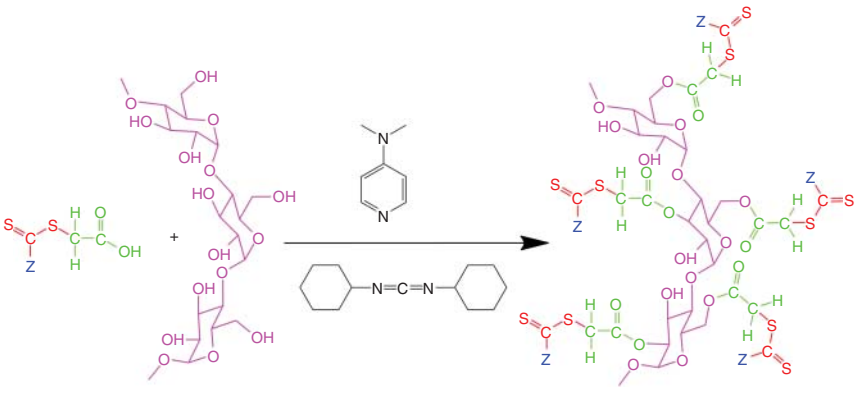

Figure 19.4 Schematic representation of the synthesis of a RAFT macro-controller using Steglich esterification.

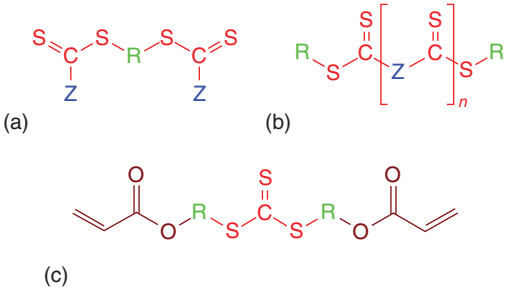

Figure 19.5 Chemical structure representation of different bifunctional RAFT agents. (a) 'R'-connected bis-macro-RAFT agents; (b) 'Z'-connected bis-RAFT agents (symmetrical trithiocarbonates); and (c) diolefinic RAFT agents.

(a) Symmetrical structures containing more than one thiocarbonylthio group, known as 'R'-connected bis-macro-RAFT agents (see Figure 19.5a).
(b) Symmetrical trithiocarbonates, known as 'Z'-connected bis-RAFT agents (see Figure 19.5b). The size of the Z or R groups will determine the size of pores or cavities within the polymer network structure.

Specific cases of 'Z'-connected bis-RAFT agents result when the ending groups are olefinic (double bond), as observed in Figure 19.5c. These diolefinic RAFT agents work as crosslinking agents with controlled molecular weight between entanglements [98–102].

19.3.2 RAFT Controllers Used in the Synthesis of Polymer Networks

Several issues need to be considered when selecting a RAFT agent for a specific situation. Not only must the chemical structures of the desired material to be synthesized and polymerization rates be taken into account but also the availability or ease of synthesis of candidate RAFT agents. As an attempt to gather and straighten the information related to the state of art on RAFT agents used for synthesis of polymer networks, we centred our analysis on RAFT agents used for such a purpose. The information was organized into three tables. In Table 19.1, the acronyms or abbreviations used in Tables 19.2 and 19.3 are defined. Table 19.2 summarizes the RAFT agents used in the synthesis of polymer networks. The case of polymer networks synthesized using multifunctional RAFT agents is addressed in Table 19.3.

Table 19.1 Abbreviations employed for monomers and chemical compounds.

AIBN	Azobis(isobutyronitrile)
Am	Acrylamide
AcAc	Acrylic acid
AMA	Allyl methacrylate
AdAMA	2-(2-[Adenine-9-yl]acetoxyl) ethyl methacrylate
AN	Acrylonitrile
BA	Butyl acrylate
tBA	*tert*-Butyl acrylate
BAC	*N,N′*-bis(acryloyl) cystamine
BDDA	Butane-1,4-diyl diacrylate
BisEMA	Bisphenol A ethoxylate dimethacrylate
BisGMA	Bisphenol A glycidyl methacrylate
BMA	Butyl methacrylate
BzMA	Benzyl methacrylate
CPDTC	2-Cyanopropan-2-yl dodecyl trithiocarbonate
CDMA	β-Cyclodextrin methacrylate
DAAM	*N*-(1,1-dimethyl-3-oxobutyl)-acrylamide (diacetone acrylamide)
DAAmEP	Diethyl-2-(acrylamido) ethylphosphonate
DEGDMA	Diethylene glycol dimethacrylate
DEGMA	(Diethylene glycol) monomethyl ether methacrylate [2-(2-methoxyethoxy)ethyl methacrylate]
DMAEMA	Dimethyl aminoethyl methacrylate
DMAPM	*N*-[3-(dimethylamine)-propyl]methacrylamide
DMAm	*N,N*-dimethylacrylamide
DPEHA	Dipentaerythritol hexaacrylate
DSDMA	Bis(2-methacryloyloxyethyl) disulfide (disulfide dimethacrylate)
DIPMDGP	1,2:3,4-Di-*O*-isopropylidene-6-*O*-methacryloyl-*a*-D-galactopyranose
DVTPhPy	4′-(4,4″-Divinyl-[1,1′:3′,1″-terphenyl]-5′-yl)-2,2′:6′,2″-terpyridine
DVB	Divinylbenzene
DBVBC	3,6-Dibromo-9-(4-vinylbenzyl)-9*H*-carbazole
EGDMA	Ethylene glycol dimethacrylate
FMA	Furfuryl methacrylate
HAD	1,6-Hexanediol diacrylate
HEA	Hydroxy ethyl acrylate
HPMAm	*N*-(2-hydroxypropyl) methacrylamide
IBA	Isobornyl acrylate
LauMA	Lauryl methacrylate
MA	Methyl acrylate

(*continued*)

Table 19.1 (Continued)

MAnh	Maleic Anhydride
MAA	Methacrylic acid
MMA	Methyl methacrylate
MEMA	2-*N*-morpholinoethyl methacrylate
MBAm	*N,N′*-methylenbisacrylamide
MPh	4-methoxyphenol
MRhB	Methacryloxyethyl thiocarbamoyl rhodamine B
MTAC	2-(Methacryloyloxy)ethyltrimethyl ammonium chloride
NAM	*N*-acryloylmorpholine
NAS	*N*-acryloxysuccinimide
NVC	*N*-vinylcarbazole
NVP	*N*-vinylpyrrolidone
NIPAM	*N*-isopropylacrylamide
OEGDMA	Oligo(ethylene glycol) dimethacrylate
OEGMEMA	Oligo(ethylene glycol) monomethyl ether methacrylate
PDMA	Poly(*N,N′*-dimethylacrylamide)
PEGDA	Poly(ethylene glycol) diacrylate
PEGDMA	Poly(ethylene glycol) dimethacrylate
PEGMA	Poly(ethylene glycol) methacrylate
PEGMEM	Poly(ethylene glycol) methyl ether methacrylate
PDMAEMA	Poly (2-[dimethylamino]ethyl methacrylate)
PFPA	Perfluorophenyl azide
PPEGMA	Poly(poly(ethylene glycol) methyl ether methacrylate)
PDSEMA	Pyridyl disulfide ethyl methacrylate
POSS-NH_2	Amino isobutyl polyhedral oligomeric silsesquioxane
PVA	Polyvinyl alcohol
PDMS	Bis(hydroxyethyloxypropyl) polydimethylsiloxane
pSS	Sodium 4-vinylbenzenesulfonate
Ph-TAD	Phenyl-1,2,4-triazoline-3,5-dione
TEGDMA	Triethylene glycol dimethacrylate
STY	Styrene
TFEMA	2,2,2-trifluoroethyl methacrylate
TMSPM	3-(trimethoxysilyl)propyl methacrylate
VPy	4-Vinyl Pyridine
VAc	Vinyl acetate
VBA	4-Vinylbenzoic acid
VBzCl	4-Vinylbenzyl chloride
VDM	2-Vinyl-4,4-dimethylazlactone

Table 19.2 RAFT agents used in the synthesis of polymer networks.

Chemical structure	References	Monomer	Crosslinking agent	Application
	[78]	PEGMEM $M_n = 300$	TMSPM	Interfacial crosslinking Nanoparticle dispersions
	[103]	DEGDMA copolymers	DEGDMA	Hydrogel
	[104]	DEGMA	DEGDMA	Hydrogel
	[105]	DEGMA	DEGDMA	Hydrogel
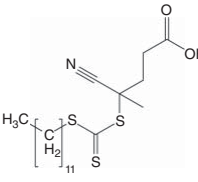	[10]	BMA, MAA, PEGMA, NAS	MRhB	Effective macrophage delivery nanogels
	[106]	PPEGMA, PDMAEMA, PDMA	BAC	Core crosslinked star (CCS)
4-cyano-4-[(dodecylsulfanylthiocarbonyl) sulfanyl] pentanoic acid CAS 870196–80-8 $C_{19}H_{33}NO_2S_3$ 403.67 g mol^{-1} Elemental analysis (%): C, 56.53; H, 8.24; N, 3.47; O, 7.93; S, 23.83	[49, 50]	HEMA, BMA	PEGDMA	Structurally tailored and engineered macromolecular (STEM) gels
	[51]	FMA DMAPM	1–3 Propane Sultone	Phototriggered zwitterionic hydrogel Ionic crosslinking
	[48]	HEMA, MMA, BMA	Ph-TAD	Healable thermoreversible polymer networks
	[17]	FMA, pSS, MTAC	pSS/MTAC ions acts as crosslinking agents	Dual responsive self-healable hydrogels. Ionic crosslink
	[8]	HEMA, DMAEMA	PEGDA	Controlled release of drugs

	[77]	PDSEMA, DIPMDGP	Glutathione	Controlled release of drugs
	[107]	PEGMA	DEGDMA, POSS-NH_2	Thermo-responsive hydrogel with improved mechanical strength
	[108]	NIPAM	MBAm	Hydrogel
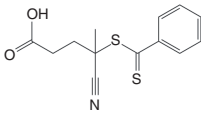	[109]	DMAEMA AcAc MPhc	PVA	Surface modification of PVA
	[55]	DBVBC STY Bromobenzene	DVTPhPy (Heck Reaction)	Responsive fluorescence chemosensory crosslinked polymer
4-cyano-4-(phenylcarbonothioylthio) pentanoic acid CAS 201611–92-9 $C_{13}H_{13}NO_2S_2$ 279.38 g mol^{-1} Elemental analysis (%): C, 55.89; H, 4.69; N, 5.01; O, 11.45; S, 22.95	[86]	MEMA	CDMA	RAFT Macro-controller of amine-terminated silicon wafer Crosslinked-polymer brushes Improved diagnostic tools and bioseparation
	[110]	PEGMA+Hexyl amine MTAC	Gold Nanoparticles	Medical application. Gold coating enhances X-ray imaging microcapsules
	[111]	MAnh, AN	Hydrolysis of MAnh leading to acid. Interactions with pendent AN groups	Electrospinning polymerization

(*continued*)

Table 19.2 (Continued)

Chemical structure	References	Monomer	Crosslinking agent	Application
	[112]	STY VBA STY-imidazole derivates	STY-imidazole derivates	Reversible ionically crosslinked single-chain nanoparticles for catalysis
	[6]	NIPAM DMAm tBA	pH and Temperature	pH- and thermo-responsive crosslinked polymer. Controlled release of drugs
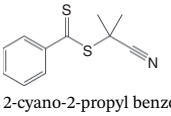 2-cyano-2-propyl benzodithioate CAS 201611–85-0 $C_{11}H_{11}NS_2$ 221.34 g mol^{-1} Elemental analysis (%): C, 59.69; H, 5.01; N, 6.33; S, 28.97	[113]	DMAEMA LauMA	EGDMA	pH-Responsive dual networks, RP and RAFT synthesis
	[114]	NIPAM tBA VPy	pH and temperature	pH- and thermo-responsive crosslinked polymer
	[115]	PEGMA DMAEMA STY	4-Azidomethyl styrene	Stimuli-responsive amphiphilic network. Nanogel formation through core crosslinking and macrogelation
	[116]	DMAEMA BA	1,2-bis-(2-iodothoxy) ethane	Amphiphilic polymer networks with tunable and predictable mechanical response
	[117]	HEMA PFPA	Glass substrate Concanavalin A	Photoactive substrate based on Steglich esterification

	[118]	—	PEGDMA	Photopolymerization kinetics
	[13]	AcAc, NIPAM	MBAm	Hydrogel. Water desalinization
	[11]	VBzCl, STY	DVB	Hierarchically porous polymer Porosity control
	[18]	DAAM Am	Hexanedihydrazide	pH-responsive self-healable hydrogel of covalent bonds
	[119]	PDMS, DMAm, AMA	Pentaerythritol tetra (3-mercaptopropionate)	Amphiphilic co-networks Biomaterial
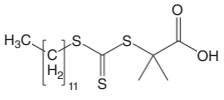 2-(dodecyl thiocarbonothioylthio)-2-methylpropionic acid CAS 461642–78-4 $C_{17}H_{32}O_2S_3$ 364.63 g mol^{-1} Elemental analysis (%): C, 56.00; H, 8.85; O, 8.78; S, 26.38	[120]	PEO VDM	3-aminopropyl triethoxysilane-grafted magnetic nanoparticles	Controlled release of antibodies
	[121]	PEGMEM	Graphene oxide	Graphene oxide macro-controller obtained by Stenglich esterification Improved mechanical properties
	[122]	NIPAM	Organoplatinum(II) metallacycles	Thermo-sensitive self-healing hydrogel
	[123]	Sulfur chain with diisopropyl benzene	RAFT agent	Electroactive sulfur networks for Li ion batteries
	[124]	tBA, PEGMEM, DMAEMA	1,2-bis(2-iodoethoxy) ethane	Zwitterionic shell-crosslinked micelles

(*continued*)

Table 19.2 (Continued)

Chemical structure	References	Monomer	Crosslinking agent	Application
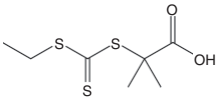 2-(([ethylthio]carbonothioyl)thio) 2-methylpropanoic acid CAS 881037–62-3 $C_7H_{12}O_2S_3$ 224.36 g mol^{-1} Elemental analysis (%): C, 37.47; H, 5.39; O, 14.26; S, 42.87	[125]	DMAm NIPAM AcAc	Ethylenediamine	Thermal-self-assembly nanocrosslinked particles
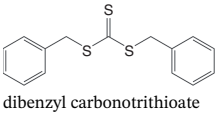 dibenzyl carbonotrithioate CAS 26504–29-0 $C_{15}H_{14}S_3$ 290.47 g mol^{-1} Elemental analysis (%): C, 62.02; H, 4.86; S, 33.12	[126]	STY p-Chloromethyl styrene	Sodium borohydride Silver nanoparticles	Crosslinked core/shell silver nanoparticles with improved thermal stability for nanoelectronics
	[127, 128]	MMA	EGDMA	Molecular imprinted monolith [25][a)]
	[129]	EHMA	EGDMA	Chromatographic monolith [25][a)]

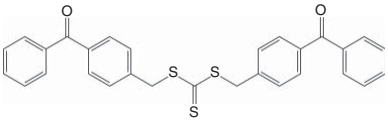 bis(4-benzoylbenzyl) carbonotrithioate $C_{29}H_{22}O_2S_3$ 498.68 g mol^{-1} Elemental analysis(%): C, 69.85; H, 4.45; O, 6.42; S, 19.29	[130]	MMA HEA	RAFT Agent	Self-healing polymers based on a photoactive RAFT polymerization
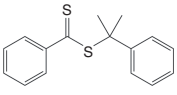 2-phenylpropan-2-yl benzodithioate CAS 201611–77-0 $C_{16}H_{16}S_2$ 272.43 g mol^{-1} Elemental analysis (%): C, 70.54; H, 5.92; S, 23.54	[131]	MMA	DSDMA	Polymerization kinetics and quantification of cycle formation
	[132]	STY	DVB	Polymer kinetics

(*continued*)

Table 19.2 (Continued)

Chemical structure	References	Monomer	Crosslinking agent	Application
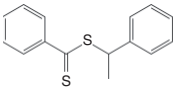 1-phenylethyl benzodithioate CAS 37912–25-7 $C_{15}H_{14}S_2$ 258.40 g mol^{-1} Elemental analysis (%): C, 69.72; H, 5.46; S, 24.82	[133]	—	OEGDMA	Polymerization kinetics [25][a)]
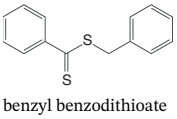 benzyl benzodithioate CAS 27249–90-7 benzyl benzodithioate $C_{14}H_{12}S_2$ 244.38 g mol^{-1} Elemental analysis (%): C, 68.81; H, 4.95; S, 26.24	[134, 135]	OEGMEMA	OEGMEMA	Polymerization kinetics [25][a)]

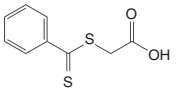 2-([phenylcarbonothioyl]thio) acetic acid CAS 942–91-6 $C_9H_8O_2S_2$ 212.29 g mol^{-1} Elemental analysis (%): C, 50.92; H, 3.80; O, 15.07; S, 30.21	[65]	MMA	EGDMA	Polymerization kinetics. Polymerization in supercritical CO_2 [25][a)]
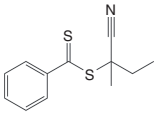 2-cyanobutan-2-yl benzodithioate $C_{12}H_{13}NS_2$ 235.37 g mol^{-1} Elemental analysis (%): C, 61.24; H, 5.57; N, 5.95; S, 27.25	[136, 137]	BzMA	DPEHA	Photoembossing application

(*continued*)

Table 19.2 (Continued)

Chemical structure	References	Monomer	Crosslinking agent	Application
	[98, 102]	MMA	Diolefinic RAFT agent	Self-healing polymer
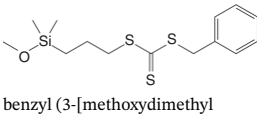 benzyl (3-[methoxydimethyl silyl]propyl) carbonotrithioate	[138]	BA	Silica Nanoparticles	RAFT agents immobilized on silica nanoparticles via monofunctional, bifunctional, and trifunctional anchor groups
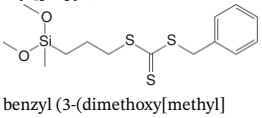 benzyl (3-(dimethoxy[methyl] silyl)propyl) carbonotrithioate				
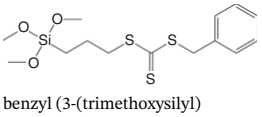 benzyl (3-(trimethoxysilyl) propyl) carbonotrithioate				

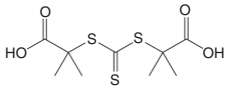 2,2′-(thiocarbonylbis [sulfanediyl])bis(2-methyl propanoic acid) CAS 355120–40-0 $C_9H_{14}O_4S_3$ 282.40 g mol^{-1} Elemental analysis (%): C, 38.28; H, 5.00; O, 22.66; S, 34.06	[139]	—	BisEMA BisGMA TEGDMA	Stress relief mechanism
	[16]	STY VPy	Chlorinated with oxalyl chloride and esterification with 2-bromoethanol	Self-healable ionic crosslinked polystyrene and poly(4-vinyl pyridine)
	[140]	STY	HDA	Nematic liquid crystal composite. Macro-RAFT agent prepared in first step
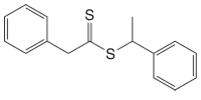 1-phenylethyl 2-phenylethanedithioate $C_{16}H_{16}S_2$ 272.43 g mol^{-1} Elemental analysis (%): C, 70.54; H, 5.92; S, 23.54	[141] (synthesis of macro-controller), [142] (polymer network synthesis)	Macro-controller: STY MAnh Polymer Network: STY BA	EGDMA	Core poly(butyl acrylate) and polystyrene – shell polystyrene-*alt*-maleic acid particles

(*continued*)

Table 19.2 (Continued)

Chemical structure	References	Monomer	Crosslinking agent	Application
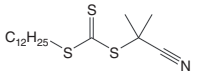 2-cyanopropan-2-yl dodecyl carbonotrithioate CAS 870196–83-1 $C_{17}H_{31}NS_3$ 345.63 g mol^{-1} Elemental analysis (%): C, 59.08; H, 9.04; N, 4.05; S, 27.83	[143]	STY	DVB	Porous monolith preparation. Modification post-network formation
	[144]	DAAmEP	Phosphate groups	Synthesis of polymer network based on phosphorous groups
	[145]	MMA AdAMA OEGMA	Dangling groups with Nitrogen	Synthesis of nucleobase-containing polymers by RAFT polymerization and RAFT dispersion polymerization. Self-assembly behaviour of nucleobase polymers
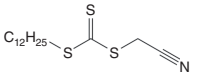 cyanomethyl dodecyl carbonotrithioate CAS 796045–97-1 $C_{15}H_{27}NS_3$ 317.58 g mol^{-1} Elemental analysis (%): C, 56.73; H, 8.57; N, 4.41; S, 30.29	[67]	STY	DVB	Polymerization kinetics

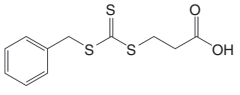 3-(([benzylthio]carbonothioyl)thio) propanoic acid CAS 497931–76-7 $C_{11}H_{12}O_2S_3$ 272.41 g mol^{-1} Elemental analysis (%): C, 48.50; H, 4.44; O, 11.75; S, 35.31	[146]	Am	MBAm	Hydrogel
	[147]	BA	EGDMA	Controlled release
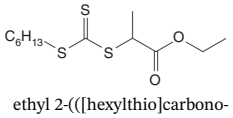 ethyl 2-(([hexylthio]carbono-thioyl)thio)propanoate $C_{12}H_{22}O_2S_3$ 294.50 g mol^{-1} Elemental analysis (%): C, 48.94; H, 7.53; O, 10.87; S, 32.66	[148]	BA	BDDA	Photo-initiated preparation of crosslinked film

(*continued*)

Table 19.2 (Continued)

Chemical structure	References	Monomer	Crosslinking agent	Application
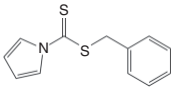 benzyl 1H-pyrrole-1-carbodithioate CAS 60795–38-2 $C_{12}H_{11}NS_2$ 233.35 g mol^{-1} Elemental analysis (%): C, 61.76; H, 4.75; N, 6.00; S, 27.48	[149]	—	BDDA PEGDA	Dilute solution hyperbranched polymer synthesis
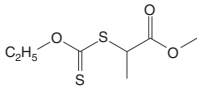 methyl 2-([ethoxycarbonothioyl] thio)propanoate	[149]	—	BDDA	Dilute solution hyperbranched polymer synthesis [3][a)]
$C_7H_{12}O_3S_2$ 208.30 g mol^{-1}	[98]	STY	Di-olefinic RAFT agent	Self-healing polymer
Elemental analysis (%): C, 40.36; H, 5.81; O, 23.04; S, 30.79	[99, 100]	BA	Di-olefinic RAFT agent	Stress-relief mechanism

a) Poor RAFT control.

Source: Adapted with permission from Moad [25]. Copyright 2014, Society of Chemical Industry.

Table 19.3 Multifunctional RAFT agents used in the synthesis of polymer networks.

Chemical structure	References	Monomer	Crosslinking agent	Application
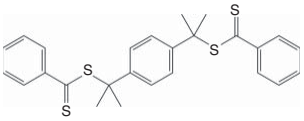 1,4-phenylenebis(propane-2,2-diyl) dibenzodithioate $C_{26}H_{26}S_4$ 466.74 g mol^{-1} Elemental analysis (%): C, 66.91; H, 5.61; S, 27.48	[90]	BMA DMAEMA	EGDMA	Model (co)networks. Bis-macro-RAFT agent prepared in first step
	[91]	BA, BMA, DMAEMA, STY	EGDMA	Model (co)networks. Bis-macro-RAFT agent prepared in first step
	[92]	TFEMA, DMAEMA	EGDMA	Model (co)networks. Bis-macro-RAFT agent prepared in first step
	[93]	DMAEMA, MAA	EGDMA	Model (co)networks. Bis-macro-RAFT agent prepared in first step
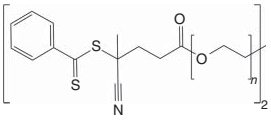	[94]	MMA BA STY	EGDMA EGDA	Model (co)networks. Bis-macro-RAFT agent prepared in first step
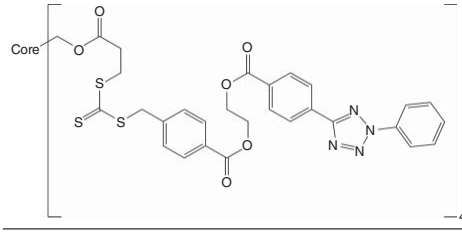	[150]	—	—	Wavelength-selective polymer network.

(*continued*)

Table 19.3 (Continued)

Chemical structure	References	Monomer	Crosslinking agent	Application
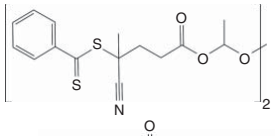	[95]	DMAEMA, MMA	EGDMA	Model(co)networks with hydrolytically degradable crosslinks. Bis-macro-RAFT agent prepared in first step.
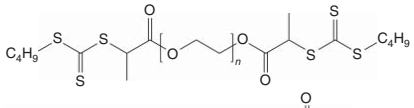	[25, 97]	NAM	PEGDA	Hydrogel with photodegradable crosslinks. Bis-macro-RAFT agent.
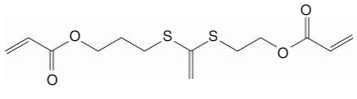	[151]	Pentaerythritol tetrakis(3-mercaptopropionate)	Tetra(ethylene glycol) diacrylate	Light-stimulated reconfiguration crosslinked polymer microparticles.
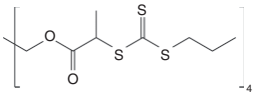	[152]	NIPA	RAFT agent Cyclodextrins	Thermo-responsive hydrogels.
STAR-CTA 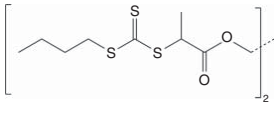	[153]	NAM IBA	Physical crosslinked hydrogel	Self-healing physically crosslinked hydrogels

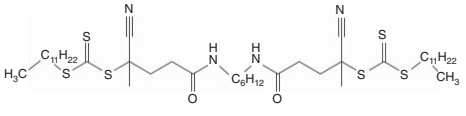	[154]	BA Adenine acrylate Thymine acrylate	Adenine and thymine dangling groups	Supramolecular blends.
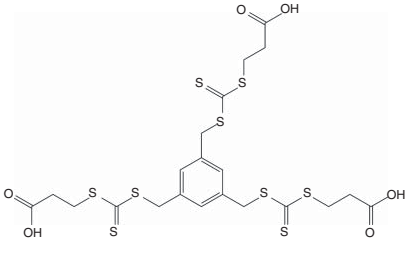	[155]	1-[2-(2-hydroxyethoxy) ethoxy]-5-[2-(2-methoxy ethoxy) ethoxy]-naphthalene	RAFT Agent	Elaboration of well-defined telechelic 3-arm star polymer.

Source: Adapted with permission from Moad [25]. Copyright 2014, Society of Chemical Industry.

The information provided in Tables 19.2 and 19.3 includes basic information about RAFT agents (structure, name, CAS number if available, molecular weight, etc.), monomers and crosslinkers used, applications or comments related to each RAFT agent, and cited references. The main RAFT agents used in the synthesis of polymer networks, based on literature citations, are 2-cyano-2-propyl benzodithioate, 4-cyano-4-[(dodecylsulfanylthiocarbonyl)sulfanyl] pentanoic acid, and 2-(dodecyl thiocarbonothioylthio)-2-methylpropionic acid. As observed in Tables 19.2 and 19.3, the application fields for these polymer networks are diverse.

19.4 Synthesis of Polymer Networks by RAFT Copolymerization of Vinyl/Multivinyl Monomers in Supercritical Carbon Dioxide as Green Solvent

As explained earlier, RAFT agents and other types of RDRP controllers have been used in the copolymerization of vinyl/multivinyl monomers, with or without solvent, aiming at producing polymer networks of reduced heterogeneity [156, 157]. When the synthesis proceeds in the presence of solvents [56–58] or chain transfer agents [59], which help in controlling M_c, solvent selection and removal are important issues to be considered. Supercritical carbon dioxide ($scCO_2$) has been used as a solvent in polymerization processes, including RDRP [158, 159]. Some of the advantages of using $scCO_2$ as a solvent include its innocuousness, its ease of removal and recovery, and the fact that it is inexpensive and easy to acquire. On the other hand, the disadvantages for its use include the initial high cost of investment in equipment because reactors and other process vessels should withstand moderate to high pressures and moderate to high temperatures [160].

The design and operation of polymerization processes carried out in $scCO_2$ require an understanding of the thermodynamic behaviour of the reacting mixture (e.g. the vapour–liquid equilibrium, VLE, region in a pressure vs. temperature chart, as shown Figure 19.6). Solubilities of chemical species in compressed fluids such as $scCO_2$ are usually not known with precision [161]. Estimation of such values from thermodynamic equations requires knowing or estimating parameters such as Hildebrand solubility parameters (δ) [162] or Flory interaction parameters. [40] A novel process for the synthesis of polymer networks of reduced heterogeneity by RAFT copolymerization of vinyl/divinyl monomers in $scCO_2$ was developed in our group [163]. Polymerizations in $scCO_2$ usually proceeded in two or more phases as a dispersion polymerization process. As observed in Figure 19.7, differentiated characteristics of the obtained polymer networks are obtained when the polymerization proceeds in more than one phase.

Because of severe solubility limitations of many polymers in $scCO_2$, heterogeneous polymerizations are carried out by precipitation, dispersion, or emulsion processes. The specific type of heterogeneous process will depend on the solubility of the monomers and initiators in $scCO_2$. Most of the polymeric materials obtained in $scCO_2$ are produced by heterogeneous processes [164–166]. One way to envision a dispersion polymerization process is to consider that it starts as a

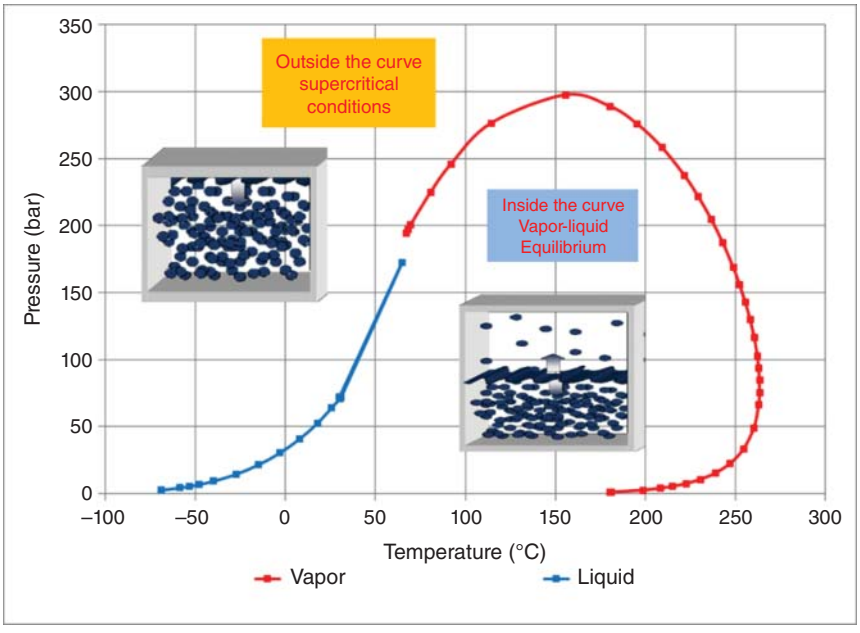

Figure 19.6 Schematic representation of a pressure (P) vs. temperature (T) curve for a mixture containing monomers and carbon dioxide. Source: Adapted with permission from Pérez-Salinas et al. [34]. Licensed under CC by 4.0.

Figure 19.7 Image of a poly(HEMA-*co*-EGDMA) polymer network synthesized in $scCO_2$. Two distinguishable materials were obtained because of separation of the reaction mixture during the synthesis in two phases: (i) a hard and brittle polymer network of hemispherical shape, which corresponds to the shape of the bottom of the reactor vessel, and (ii) a soft fluffy powder polymer network polymerized in the upper section of the reactor.

homogeneous process (solution polymerization, stage 1), followed by formation of a dispersed phase by precipitation of polymer molecules that exceed a critical size (stage 2) where the polymerization takes place in both phases, and concluding in stage 3 where monomer is present only in the dispersed phase [166]. Even though a dispersed phase will be formed in stage 2, it is important for process operation and reduction of heterogeneity purposes that the reacting mixture is indeed homogeneous during stage 1. That requires adequate determination of the

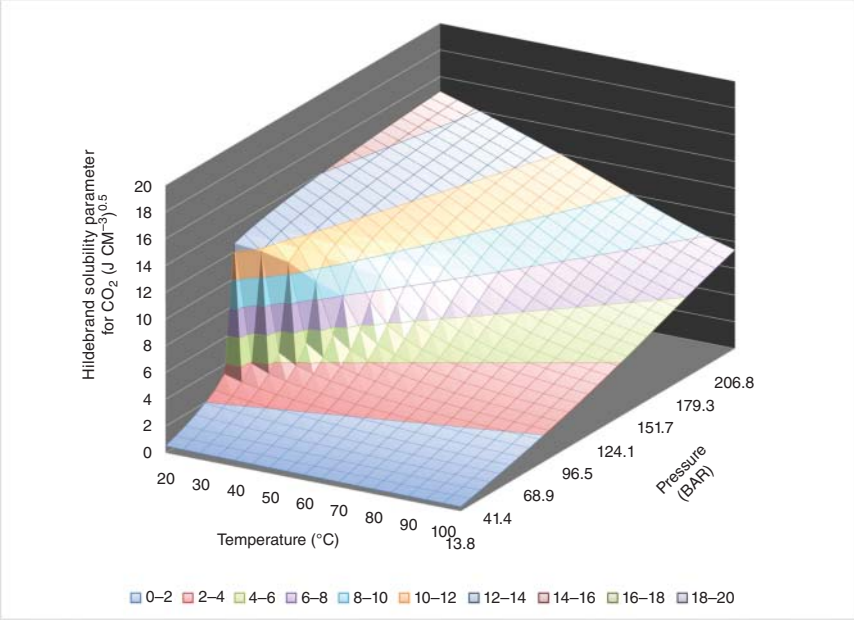

Figure 19.8 Hildebrand solubility parameter for CO_2 around subcritical and supercritical conditions.

initial operating conditions, and how they change during polymerization before the formation of the dispersed phase (Figure 19.6) [166]. Estimation of component solubilities for the reacting mixture (monomer(s), initiator, RAFT agent, etc.) at initial conditions can be obtained from Hildebrand solubility parameters (δ) or Flory interaction parameters (χ) [40]. Solubility of solute in solvent is expected to occur if $\delta_{CO_2\ (T,P)} \approx \delta_{\text{solute}\,(T,P)}$. A polymer solute will be soluble in CO_2 at the given T and P if $\chi < 0.84$.

Calculation of δ_{CO_2} at temperatures and pressures typical of dispersion polymerization processes using a procedure described in the literature [162] is summarized in Figure 19.8. Calculated values of the Flory interaction parameter (using the methods described in Ref. [162]) between a polymer network based on HEMA (95% weight) and EGDMA (5% weight) and CO_2, system studied experimentally by our group [34], are shown in Figure 19.9. Finally, the calculated values of χ for a 2-hydroxyethyl methacrylate (HEMA) and $scCO_2$ system are summarized in a 3-D plot in Figure 19.10.

It is well known that stabilizers are needed in dispersion polymerization processes to obtain particles of small and controlled sizes [164, 165, 167, 168]. One easily available commercial stabilizer used in the synthesis of polymers by RP in $scCO_2$ is Krytox, a carboxylic acid end-capped perfluorinated polyether from DuPont® [34, 169]. Krytox was used as a stabilizer in the pioneering studies on the synthesis of polymer networks in $scCO_2$ by RAFT copolymerization of STY/DVB [65], MMA/EGDMA [170], and HEMA/EDGMA, where experimental conditions are described in Table 19.4 [34].

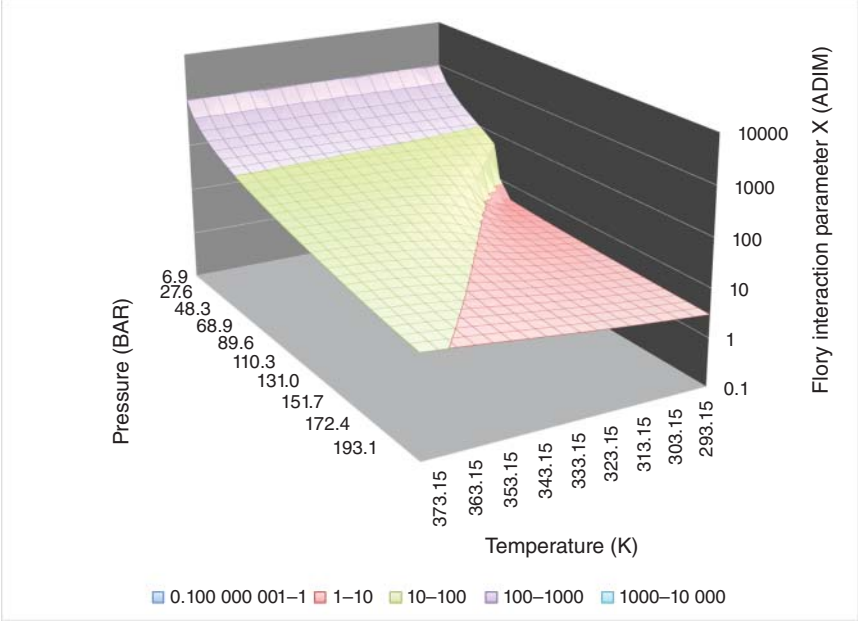

Figure 19.9 Calculated values of χ between a polymer network based on HEMA (95% weight) and EGDMA (5% weight), and CO_2 at operating conditions typical of dispersion polymerization processes. δ_{solute} in the calculations was estimated using Fedor's method.

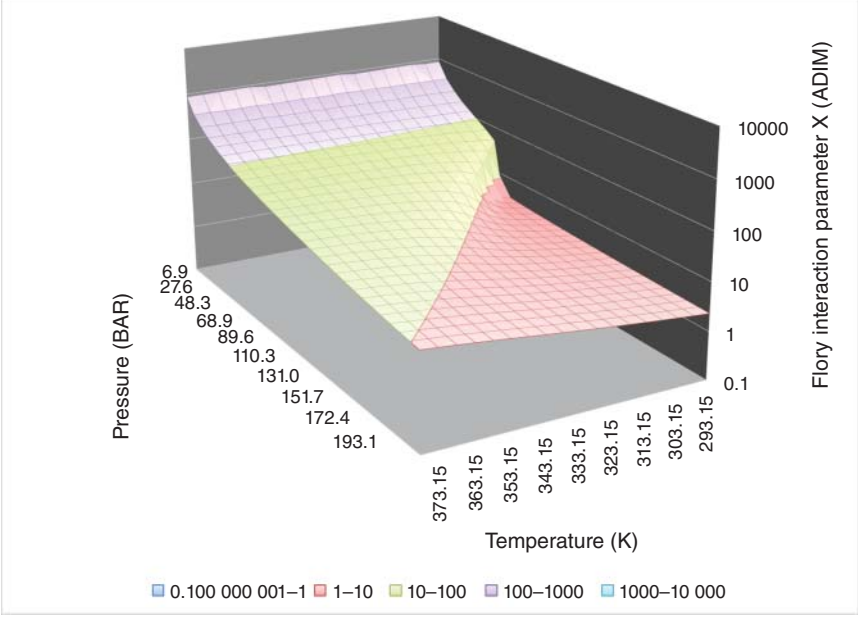

Figure 19.10 Calculated values of χ between HEMA and CO_2.

Table 19.4 Swelling index (SI) and M_c results for conventional RP and RAFT copolymerization of HEMA and EDGMA in $scCO_2$.

	Sample	HEMA (mmol)	EGDMA (mmol)	AIBN (mmol)	RAFT agent (mmol)	Krytox (Wt% wrt HEMA)	SI	M_c experimental (g mol^{-1})
RP	G311	25	1.25	0.1	0	5	8.3	7681
	G312	25	1.25	0.1	0	0	9.5	10 541
	G313	25	1.25	0.1	0	5	6.6	4407
RAFT	G314	25	1.25	0.1	0	0	7.6	6221
	G315	25	1.25	0.1	0.05	5	5.9	3329
	G316	25	1.25	0.1	0.05	0	7.1	5274
	G317	25	1.25	0.1	0.05	5	5.1	2289
	G318	25	1.25	0.1	0.05	0	5.3	2530

Conditions: $T = 65\,^{\circ}C$, $P = 173$ bar, $t = 24$ hours, 22% w/v CO_2.
Source: Adapted with permission from Pérez-Salinas et al. [34]. Licensed under CC by 4.0.

However, a comparison of scanning electron microscopy (SEM) microphotographs for a case of RAFT copolymerization of HEMA/EDGMA in $scCO_2$ with no Krytox included in the formulation, and a case where Krytox was present in the reacting system, resulted in no significant differences being noticed (see Figure 19.11). As a matter of fact, larger particles were obtained in the case where Krytox was included in the formulation.

This unexpected result may be explained by the inefficient mixing provided by the magnetic stirrer bar placed in the interior of the high-pressure cell used as a reactor. A description of the reacting system used for the experiments with HEMA/EDGMA [34] is provided in García-Morán et al. [171].

Another possible explanation for this result may be that the appearance of the dispersed phase may take place from the very beginning of the polymerization if the initial operating conditions are contained in the two-phase zone of a pressure–temperature diagram, as the one shown in Figure 19.6 for the case of RAFT copolymerization of HEMA/EDGMA in $scCO_2$ [34]. That is why, our operating procedure for the synthesis of polymer networks by RAFT copolymerization of vinyl/divinyl monomers in $scCO_2$ starts with creating a pressure (P) vs. temperature (T) diagram using the software ASPEN for the actual formulation used in the copolymerization. The P–T diagram for the system studied by Pérez-Salinas et al. [34] is shown in Figure 19.6. Temperature is set to a value where the initiator works properly (above 60 °C). Pressure is then set at a value where the reacting mixture is at supercritical conditions. By following this procedure, it is assured that the initial conditions are within the supercritical region of the mixture (which can differ from the supercritical region for pure $scCO_2$).

Pressure and RAFT agent content are two important variables for control of polymer network homogeneity, particle size, and morphology. The effects of pressure and the presence or absence of RAFT agent (4-cyano-4-[(dodecylsulfanylthiocarbonyl)

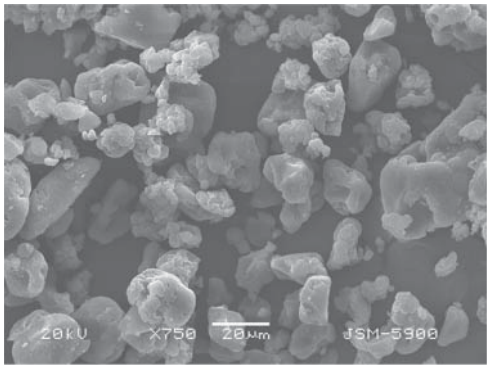

(a)

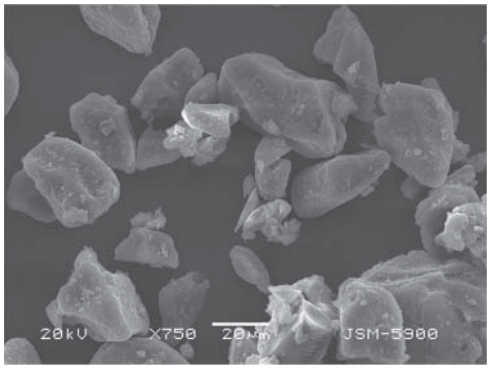

(b)

Figure 19.11 SEM images of poly(HEMA-*co*-EGDMA) synthesized by RAFT copolymerization in $scCO_2$: (a) synthesis in the absence of Krytox and (b) synthesis in the presence of Krytox. Reaction conditions summarized in Table 19.4.

sulfanyl] pentanoic acid) on the textural characteristics of poly(HEMA-*co*-EDGMA) synthesized in $scCO_2$ is shown are Figure 19.12 [172]. Synthesis conditions are detailed in Figure 19.12 [172]. In summary, higher pressures seem to improve the homogeneity of the produced polymer network. The presence of RAFT controller dramatically improves the texture of the polymer network at higher pressures. Detailed characterization results and further discussion are offered in Pérez-Salinas [172].

Characterization by SEM, nitrogen physisorption, differential scanning calorimetry (DSC), dynamic mechanical analysis (DMA), Fourier transform infrared spectroscopy (FTIR), as well as performance evaluation in loading and release of ciprofloxacin and vitamin B_{12} (see Figure 19.13), of the poly(HEMA-*co*-EDGMA) polymer networks synthesized in our group [163], in the presence or absence of RAFT agent (4-cyano-4-[(dodecylsulfanylthiocarbonyl)sulfanyl] pentanoic acid), was carried out [63, 163]. Significant structural and morphological differences were observed. Polymer network particles synthesized by RAFT copolymerization of HEMA and EDGMA in $scCO_2$ were much more porous than the ones synthesized in the absence of RAFT agent. They were able to retain higher amounts of vitamin B_{12} within their structures. These combined results (including DSC and DMA) suggest that the polymer network particles synthesized by RAFT copolymerization are significantly less heterogeneous (nodes more evenly distributed within the

Reaction Pressure	Conventional RP	RAFT
~1500-1700 psi	  Two different particle size populations, implying presence of at least two phases.	 Monolith with two different textures, also implying at least two phases.
~4600-4800 psi	  Two different textures: a hard, compact hydrogel, and particulate granules, which suggest presence of two or more phases.	 Homogeneous, fine, fluffy powder.

Figure 19.12 Comparison of textural characteristics of poly(HEMA-*co*-EGDMA) synthesized in $scCO_2$ at different pressures in the presence and absence of RAFT agents.

polymer network structure) than the ones synthesized in the absence of a RAFT controller [163].

19.5 Modelling of Polymer Network Formation

Our companion chapter in this book entitled 'Mathematical Modeling of RAFT Polymerization', is focused on the modelling of RAFT polymerization processes where

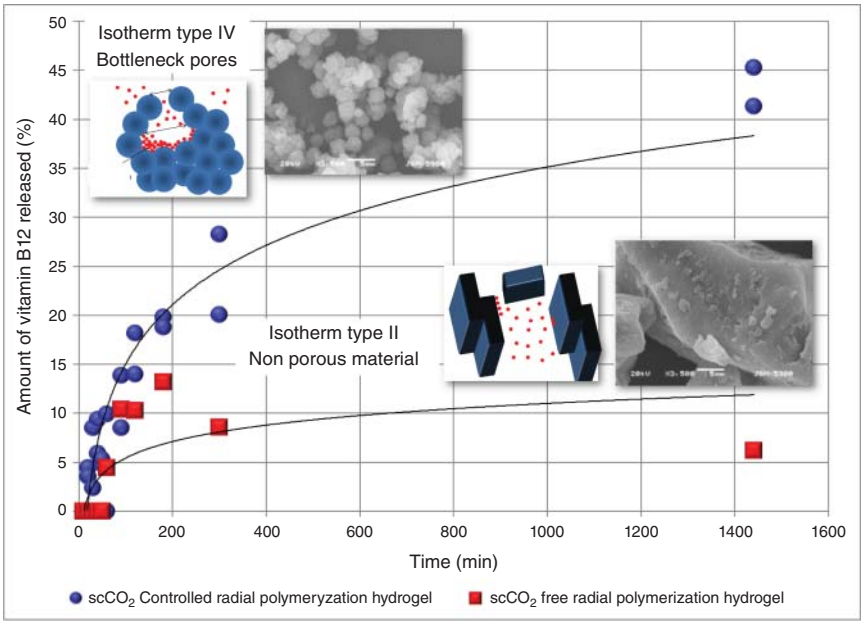

Figure 19.13 Vitamin B_{12} release profiles, morphology, and interpretation of nitrogen physisorption results for RAFT (blue circles) and conventional RP (red squares) polymer networks. Source: Adapted with permission from Pérez-Salinas et al. [63]. Copyright 2016, John Wiley & Sons.

crosslinking and gelation are not an issue. The polymer reaction engineering (PRE) tools for analysis of polymerization processes, including the use of different modelling techniques for calculation of molecular weight distributions or other polymer structural characteristics, focused on 'simple' polymerization systems using RAFT chemistry, are described in Chapter 7. This section is focused on the use or extension of those techniques to the modelling of polymerization kinetics, molecular weight development, as well as evolution of gel fraction and crosslinking density for systems where polymer networks are produced.

Two of the pioneering works related to the synthesis of polymer networks by RDRP are those from Ide and Fukuda [30, 31]. They studied the copolymerization of vinyl and divinyl monomers in the presence of nitroxide controllers by nitroxide-mediated radical polymerization (NMP). They concluded that polymer networks synthesized by NMP are less heterogeneous than those synthesized by conventional RP. Since then, numerous studies focused on the synthesis of polymer networks using RDRP methodologies have been conducted, including NMP [173, 174], atom transfer radical polymerization (ATRP) [175], and RAFT [25, 176] polymerization. This topic has been reviewed previously [25, 173]. The versatility of RAFT polymerization is exemplified by its use in the production of polymer networks with unprecedented capabilities [7, 46, 177]. It is desirable that these techniques allow the synthesis of homogeneous structures with narrow molar mass distributions (MMDs).

The prediction of polymer network properties, which affect product end-use performance, including copolymer composition, crosslinking density, and swelling

index, can be achieved by implementation of numerical methods. This section is focused exclusively on polymer networks synthesized by mechanisms that involve RAFT chemistry.

19.5.1 Background on Modelling of Crosslinking and RAFT

Polymer molecules synthesized by RAFT copolymerization with crosslinking of vinyl/divinyl/multivinyl monomers contain several functional groups produced through conventional and activation/deactivation reactions. The polymerization scheme includes, as in conventional RP, the following chemical reactions: chemical initiation, dimerization, thermal self-initiation, first propagation, chain transfer to small molecules (monomer, solvent, and chain transfer agent), cyclization, crosslinking, and termination by both combination and disproportionation [173]. Crosslinking occurs when active polymer molecules react with polymer molecules with available PDB, as shown in Figure 19.14. Crosslinking leads to increasing or even diverging weight average molecular weight (or weight-average chain length $\overline{P_w}$).

Divinyl monomers are often used as crosslinkers (e.g., DVB and EGDMA) yielding 'bridges' between two polymer molecules. In the case of conventional RP, several numerical approaches, such as the method of moments [178], Monte Carlo (MC) [179–184], numerical fractionation technique (NFT) [179, 180, 185–188], generating functions (GF) method [180, 189], and the software Predici® [181, 183, 187] have been used to study polymer network formation.

Recently, the copolymerizations of STY and EDGMA, as well as STY and TEGDMA at 95 °C, in toluene, were studied using NFT [185]. Model predictions and experimental data of monomer conversion, consumed PDBs, copolymer composition, and gelation time agreed well.

Lazzari et al. [180] compared calculated profiles of weight-average chain length ($\overline{P_w}$), gel fraction (w_g), and crosslink density obtained from four modeling approaches: NFT, kinetic MC, a hybrid statistic/kinetic Flory/Tobita model (FT), and the GF method [180]. It was found that NFT and FT are fast and reliable when focusing on average properties, while kinetic MC and GF allow calculation of more detailed properties, such as chain length distribution (CLD), at the expense of larger computational times. Kinetic MC has also been used to study the copolymerization of STY and DVB with different amounts of DVB [181]. The model yielded the same results as the corresponding polymerization scheme implemented in the Predici software during the pre-gelation period.

On the other hand, if a RAFT agent, whose structure and representation are shown in Figure 19.2, is added to the reacting mixture, it will react with active polymer radicals, $R_m^{\cdot}$, to produce one-arm adduct polymer molecules, R_mA˙B,

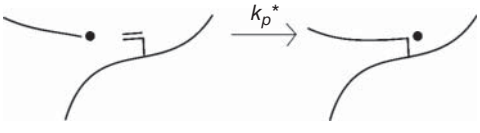

Figure 19.14 Crosslinking reaction, where k_p^* is the crosslinking kinetic rate constant.

Table 19.5 Systems properties.

Property	Equations
Total monomer conversion	$x = \frac{M_{10} + M_{20} - M_1 - M_2}{M_{10} + M_{20}}$
Unreacted monomer composition	$\frac{df_i}{dt} = \frac{f_i - F_i}{1 - x}\frac{dx}{dt}$
Instantaneous copolymer composition	$F_j = \frac{\sum_{i=1}^{2} k_{pij}\varphi_i^{\cdot} f_j}{k_p}$
Accumulated copolymer composition	$\overline{F}_i = \frac{f_{i0} - f_i(1 - x)}{x}$

which undergo fragmentation to yield R_mA capped/dormant polymer molecules. This reaction with the RAFT agent (AB molecule) is known as the pre-equilibrium step. In the main equilibrium reaction, active polymer radicals and dormant polymer molecules react to produce two-arm adduct polymer molecules, which upon fragmentation produce dormant and living polymer molecules of exchanged sizes. Additionally, $R_m\text{A}^{\cdot}R_n$ molecules can undergo termination with active polymer radicals generating three-arm dead polymer molecules [190]. Polymerization and product properties for the copolymerization of vinyl monomer M_1 and crosslinker M_2 can be calculated using the equations summarized in Table 19.5.

19.5.2 Trifunctional Polymer Molecule Modelling Approach

In this approach, the main equilibrium between active polymer radicals and dormant polymer molecules is simplified as a direct chain transfer reaction between the two polymeric species (no polymer adducts produced), as shown in row 4 of Table 19.6. The model is based on the pseudo-kinetic rate constant method [191]. The elementary reactions of the polymerization scheme considered in this model, expressed in terms of a single type of polymer molecule denoted as $R_{m,r,p}$, where m, r, and p refer to total number of monomer units, radicals and 'A' RAFT capped/dormant units (see Figure 19.15), respectively, are summarized in Table 19.6. The trifunctional modelling approach has been used to study several important copolymerizations with crosslinking systems, such as the batch and semi-batch RAFT copolymerization of AM and *N,N'*-methylenebis(acrylamide) (BisAM) using 3-benzyltrithiocarbonyl propionic acid (BCPA) and ammonium persulfate (APS), at 60 °C [146]. The same total amount of a BisAM solution was continuously added to the reacting mixture at a constant rate from 0 (batch) to 2, 3, and 4.5 hours to investigate the effect of semi-batch operation on MMD and branching structure. It was found that higher instantaneous BisAM concentrations were obtained when shorter feeding periods were used, which resulted in higher molar masses and branching densities; the model agreed well with the available experimental data. Gelation took place only when the process was operated in batch

Table 19.6 Polymerization scheme for the trifunctional approach.

Reaction	Equations	Kinetic rate constant
Initiation	$I \rightarrow 2\,R_{0,1,0}$	f, k_d
First propagation	$R_{0,1,0} + M \rightarrow R_{1,1,0}$	k_i
Propagation	$R_{m,r,p} + M \rightarrow R_{m+1,r,p}$	$(r)k_p$
Chain transfer to dormant polymer	$R_{m,r,p} + R_{n,s,q} \rightarrow R_{m,r-1,p+1} + R_{n,s+1,q-1}$	$(r)(q)k_p$
Intermolecular crosslinking	$R_{m,r,p} + R_{n,s,q} \rightarrow R_{m+n,r+s,p+q}$	$(r)\,(n)\,k_p^*$
Cyclization	$R_{m,r,p,} \rightarrow R_{m,r,p}$	$(r)(m)k_{\mathrm{cyc}}$
Termination by disproportionation	$R_{m,r,p} + R_{n,s,q} \rightarrow R_{m,r-1,p} + R_{n,s-1,q}$	$(r)(s)k_{\mathrm{td}}$
Termination by combination	$R_{m,r,p} + R_{n,s,q} \rightarrow R_{m+n,r+s-2,p+q}$	$(r)(s)k_{\mathrm{tc}}$

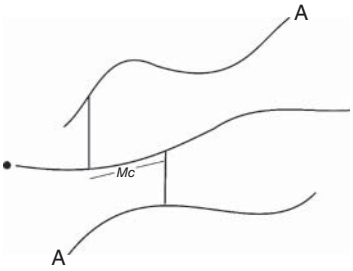

Figure 19.15 Schematic representation of the trifunctional polymer molecule approach.

mode. Semi-batch operation resulted in molar masses of up to 1.5×10^6 g mol^{-1} (hyperbranched polymer) without gelation taking place.

The trifunctional model has also been used to study the RAFT miniemulsion copolymerization of STY and triethylene glycol dimethacrylate (Tri-EGDMA) using BCPA and sodium dodecyl sulfate (SDS), at 70 °C [192]. It was observed that higher Tri-EGDMA and lower RAFT agent concentrations resulted in higher values of polymerization rate, weight-average molar mass ($\overline{M}_w$), molar mass dispersity ($Đ$), cyclization density (CD), and average number of propagating radicals per particle ($\overline{n}$). Furthermore, two cases conducted in semi-batch mode (continuous addition of STY) yielded branched polymer molecules with uniform branching density (BD) distributions.

The RAFT copolymerization of MMA and bis(2-methacryloyl)oxyethyl disulfide (BMAODS, a cleavable monomer) using 2-cyano-2-propyldodecyl trithiocarbonate (CPDTTC) and azobis(isobutyronitrile) (AIBN) in toluene, at 70 °C, was investigated with the purpose of obtaining information on the branching mechanism [193]. After the formation of branched copolymer molecules, the presence of tributylphosphine (Bu_3P) promoted the degradation of BMAODS disulfide crosslinkages, resulting in the production of primary chains. The MMDs before and after disulfide bond degradation were measured by gel permeation chromatography (GPC). The GPC traces of the primary chains showed narrow MMDs and $\overline{M}_n$ increased linearly

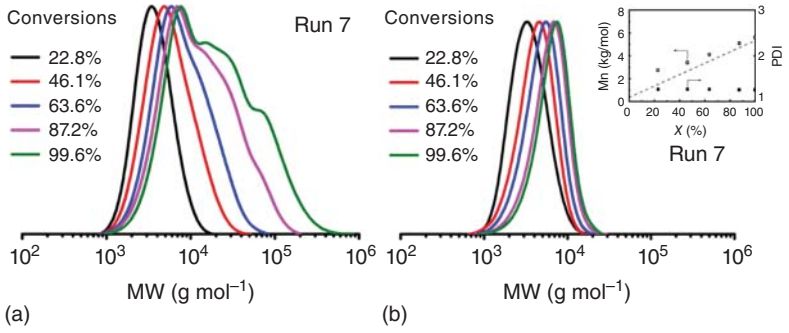

Figure 19.16 GPC traces of samples collected at different conversions for the RAFT copolymerization of MMA and BMAODS using $[MMA]_0/[BMAODS]_0 = [MMA]_0/[CPDTTC]_0 = 50$ and $[MMA]_0/[AIBN]_0 = 50/0.2$ in toluene (55 wt%) at 70 °C: (a) before and (b) after disulfide bond degradation. Source: Reproduced with permission from Liang et al. [193]. Copyright 2016, American Chemical Society.

with conversion suggesting living behavior of the copolymerization as observed in Figure 19.16. The trifunctional molecule approach was used to study the effect of the amounts of divinyl monomer, RAFT agent, and monomer on the evolution with conversion of $\overline{M}_n$, BD, and CD. The weight fraction of the copolymer containing i-primary chains $\omega(i)$, estimated from the GPC traces agreed well with Zhu's equation [194] (see Eqs. (19.4), (19.5), and Figure 19.17), where λ_p is the average

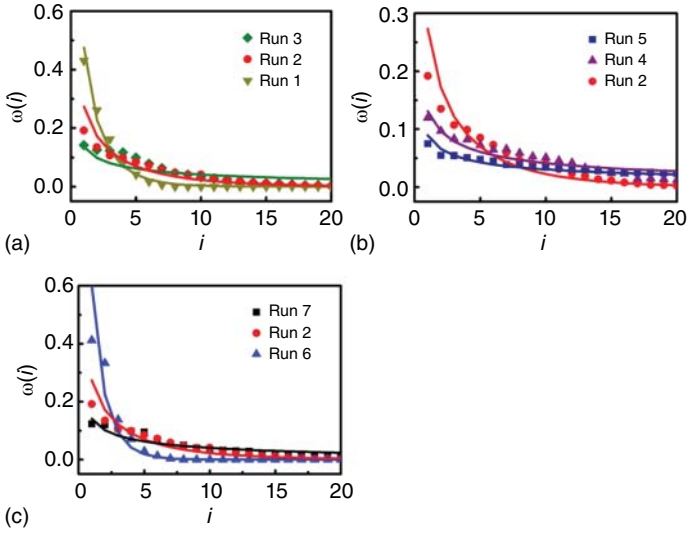

Figure 19.17 Evolution of weight fraction of polymers containing i-primary chains synthesized by RAFT copolymerization of MMA (1) and BMAODS (2) at (a) various $[M_1]_0/[M_2]_0$(run 1 = 50/0.5, run 2 = 50/1, and run 3 = 50/1.5); (b) various primary chain lengths by controlling $[AB]_0/[M_1]_0$ at 1/50 (run 2), 1/75 (run 4), and 1/100 (run 5); and (c) various initial monomer concentrations of 15 (run 6), 30 (run 2), and 45 wt% (run 7). Source: Reproduced with permission from Liang et al. [193]. Copyright 2016, American Chemical Society.

number of branching points per primary molecule and $Đ_p$ is the molar mass dispersity of the primary molecule, thus providing support to the random branching mechanism that takes place in the RAFT copolymerization of vinyl/divinyl monomers.

$$\omega(i) = \frac{\left[\left(\sigma_Z + 1\right) i - 1\right]!}{\left(\sigma_Z i\right)!\,(i-1)!}\left(\frac{\sigma_Z}{\sigma_Z + \lambda_p}\right)^{\sigma_Z i}\left(\frac{\lambda_p}{\sigma_Z + \lambda_p}\right)^{i-1} \tag{19.4}$$

$$Đ_p = \frac{\sigma_Z + 1}{\sigma_Z} \tag{19.5}$$

19.5.3 Multifunctional Polymer Molecule Modelling Approach

In the multifunctional polymer molecule modelling approach, a single polymer population with several functionalities is assumed to be present in the system. This multifunctional polymer molecule is represented as $R_{m,r,p,x,f,\psi}$, where m, r, p, x, f, and ψ refer to the number of monomer units, active radicals, 'A' capped/dormant units attached to the polymer molecule, 'A' groups attached to two segments of the polymer network, '*AB' groups, and the reacting phase, respectively. The main difference with the trifunctional model is that in the multifunctional model reactions with intermediate radicals $R_m\text{A}^{\cdot}\text{B}$ and $R_m\text{A}^{\cdot}\text{R}_n$ as well as termination between $R_m^{\cdot}$ with $R_m\text{A}^{\cdot}\text{R}_n$ are considered in the polymerization scheme and model equations [195]. The polymerization scheme for the RAFT copolymerization with crosslinking of vinyl and divinyl monomers, represented in terms of multifunctional molecules (schematic representation shown in Figure 19.18**)**, is summarized in Table 19.7).

A direct solution for $R_{m,r,p,x,f,\psi}$ implies the solution of a set of $m \times r \times p \times x \times f \times \psi$ stiff non-linear ordinary differential equations (ODEs). Because m could reach up to 10^6 or higher values, this results in prohibitive computational costs. The reduction of such a set of ODEs can be achieved by using the method of moments, as defined in Eq. (19.6).

$$Y_{i,j,u,v,w,\psi} = \sum_{m=1}^{\infty} m^i \sum_{r=0}^{\infty} r^j \sum_{p=0}^{\infty} p^u \sum_{x=0}^{\infty} x^v \sum_{f=0}^{\infty} f^w \left[R_{m,r,p,x,f,\psi}\right] \tag{19.6}$$

The multifunctional modelling approach has been used to analyse the effect of polymerization conditions on the formation of linear and crosslinked polymer molecules by RAFT copolymerizations of vinyl/divinyl monomers [195]. The performance of the multifunctional model has been compared to that of the

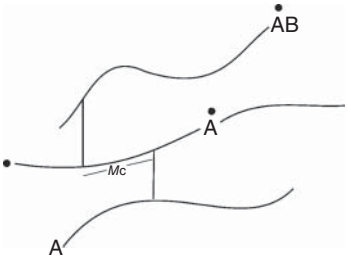

Figure 19.18 Schematic representation of the multifunctional polymer molecule approach.

Table 19.7 Polymerization scheme for the RAFT copolymerization with crosslinking of vinyl/divinyl monomers in terms of multifunctional polymer molecules, in phase ψ.

Reaction	Equations	Kinetic rate constant
Initiation	$I_\psi \rightarrow 2\,R^{\bullet}_{\mathrm{in},\psi}$	$f, k_{d,\psi}$
Dimerization	$2M_\psi \rightarrow D_\psi$	$k_{\mathrm{dim},\psi}$
Thermal self-initiation	$D_\psi + M_\psi \rightarrow D^{\bullet}_\psi + R_{1,1,0,0,0,\psi}$	$k_{\mathrm{thi},\psi}$
First propagation: (a) primary radicals	$R^{\bullet}_{\mathrm{in},\psi} + M_\psi \rightarrow R_{1,1,0,0,0,\psi}$	$k_{i,\psi}$
(b) radicals from RAFT leaving group	$B^{\bullet}_\psi + M_\psi \rightarrow R_{1,1,0,0,0,\psi}$	$k_{i,\psi}$
(c) dimeric radicals	$D^{\bullet}_\psi + M_\psi \rightarrow R_{1,1,0,0,0,\psi}$	$k_{i,\psi}$
Propagation	$R_{m,r,p,x,f,\psi} + M_\psi \rightarrow R_{m+1,r,p,x,f,\psi}$	$(r)k_{p,\psi}$
Reversible chain transfer to the RAFT agent (pre-equilibrium)	$R_{m,r,p,x,f,\psi} + AB_\psi \leftrightarrow R_{m,r-1,p,x,f+1,\psi} \leftrightarrow R_{m,r-1,p+1,x,f,\psi} + B^{\bullet}_\psi$	$(r)k_{add,\psi}, (f+1)k_{\_add,\psi}$; $(f+1)k_{bd,\psi}$, $(p+1)k_{\_bd,\psi}$
Chain equilibration (main equilibrium)	$R_{m,r,p,x,f,\psi} + R_{n,s,q,y,g,\psi} \leftrightarrow R_{m+n,r+s-1,p+q-1,x+y+1,f+g,\psi} \leftrightarrow R_{m,r-1,p+1,x,f,\psi} + R_{n,s+1,q-1,y,g,\psi}$	$(r)(q)k_{a,\psi}$, $(x+y+1)k_{\_a,\psi}$; $(x+y+1)k_{b,\psi}$, $(p+1)(s+1)k_{\_b,\psi}$
Intermediate radical termination	$R_{m,r,p,x,f,\psi} + R_{n,s,q,y,g,\psi} \rightarrow R_{m+n,r+s-1,p+q,x+y-1,f+g,\psi}$	$(r)(y)k_{\mathrm{tir},\psi}$
Intermolecular crosslinking (propagation through pendant double bonds)	$R_{m,r,p,x,f,\psi} + R_{n,s,q,y,g,\psi} \rightarrow R_{m+n,r+s,p+q,x+y,f+g,\psi}$	$(r)\,(n)\,k^{*}_{p,\psi}$
Cyclization	$R_{m,r,p,x,f,\psi} \rightarrow R_{m,r,p,x,f,\psi}$	$(r)(m)k_{\mathrm{cyc},\psi}$
Termination by disproportionation	$R_{m,r,p,x,f,\psi} + R_{n,s,q,y,g,\psi} \rightarrow R_{m,r-1,p,x,f,\psi} + R_{n,s-1,q,y,g,\psi}$	$(r)(s)k_{\mathrm{td},\psi}$
Termination by combination	$R_{m,r,p,x,f,\psi} + R_{n,s,q,y,g,\psi} \rightarrow R_{m+n,r+s-2,p+q,x+y,f+g,\psi}$	$(r)(s)k_{\mathrm{tc},\psi}$

monofunctional model [196] for the RAFT homopolymerization of styrene using 2-cyano-prop-2-yl 1-dithionaftalate (CPDN) and AIBN at 60 and 72 °C [195]. Both models generated the same results for monomer conversion vs. time and $\overline{M}_n$ vs. conversion, as well as concentrations of polymeric species [195]. The RAFT copolymerization with crosslinking of STY and DVB using benzoyl peroxide (BPO) and *S*-thiobenzoyl thioglycolic acid (TBTGA) at 80 °C was also addressed. The model captured well the effect of RAFT agent concentration on the onset of gelation and gel content in the polymer.

The multifunctional polymer molecule modelling approach was also used to study the RAFT homo- and copolymerization (with crosslinking) of HEMA

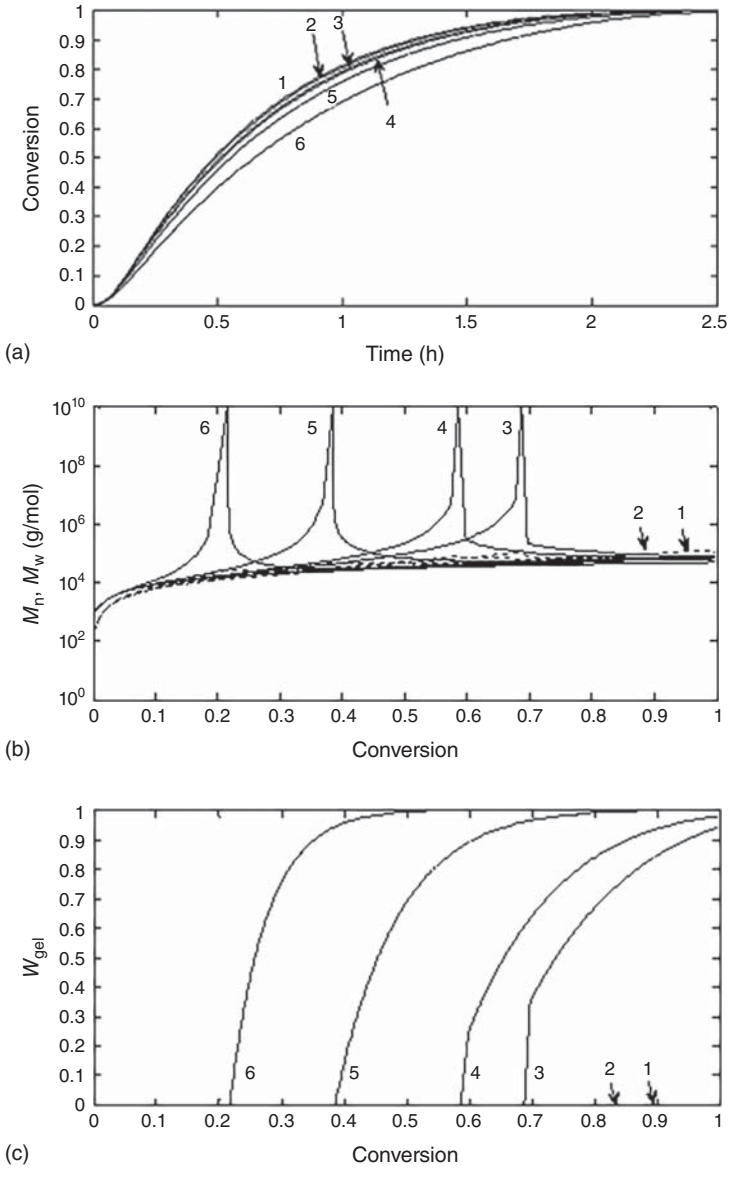

Figure 19.19 Effect of crosslinker content on (a) conversion vs. time, (b) molecular weight development, and (c) gel fraction evolution in the RAFT copolymerization of HEMA/EGDMA in p-dioxane. Simulated profiles: (1) $f_{20} = 0.001$; (2) $f_{20} = 0.003$; (3) $f_{20} = 0.008$; (4) $f_{20} = 0.01$; (5) $f_{20} = 0.02$; and (6) $f_{20} = 0.05$. Source: Reproduced with permission from Espinosa-Pérez et al. [64]. Copyright 2014, John Wiley & Sons.

(and a crosslinker). The crosslinkers used were EGDMA and DEGMA [64]. Model predictions and experimental profiles of conversion vs. time agreed well for the homopolymerization of HEMA using AIBN and cumyl dithiobenzoate (CDB) in dimethylformamide (DMF) at 60 °C. In the case of copolymerization of HEMA/DEGMA using CDB and AIBN, it was found that increasing the amount of crosslinker (5–10 wt%) or decreasing the RAFT/initiator ratio (7 to 5) yielded polymer networks with higher crosslink densities ($\overline{\rho}$). It was also found that gelation occurred sooner while gel fraction (w_g) increased gradually with conversion. The copolymerization of HEMA and EGDMA using 4-cyano-4-(dodecylsulfanylthiocarbonyl)sulfanyl pentanoic acid in *p*-dioxane and in $scCO_2$ was also investigated [64]. It was found for the copolymerization in *p*-dioxane that an increase in the amount of crosslinker resulted in lower polymerization rates because the propagation rate (k_p) for EGDMA was lower that k_p for HEMA. However, the gelation point occurred sooner for the cases with higher amounts of divinyl comonomer, as shown in Figure 19.19. The model could also describe the case in $scCO_2$ where 93% monomer conversion was reached in 16 hours for a polymerization carried out at 65 °C.

Polymer monoliths are porous solid materials synthesized by RP of vinyl/divinyl monomers with a high content of the divinyl monomer (crosslinker) in an unstirred mould or vessel to obtain a single piece of material. RAFT agents can be used to introduce functional groups into the polymer monolith. The copolymerization of STY and DVB using AIBN and 2-cyano-2-propyl dodecyl trithiocarbonate (CPDTC) at 60 °C in dodecanol (45 vol%) and benzene (5 vol%) aimed at producing monolith structures was investigated by researchers from CSIRO [143] and modelled by our group [197]. Eight cases were addressed: conventional RP (Case A); RAFT polymerization with $[AB]_0/[I]_0$=2 (Case B); conventional RP with $f_{20} = 0.28$ (Case C); and RAFT copolymerization with $f_{20} = 0.28$ and $[AB]_0/[I]_0$= 0.4, 1, 2, and 10 (Cases D–G) [143, 197]. As observed in Figure 19.20, typical profiles of $\ln[M]/[M]_0$ vs. time and $\overline{M}_n$, $\overline{M}_w$ vs. conversion for Cases A and B were obtained. On the other hand,

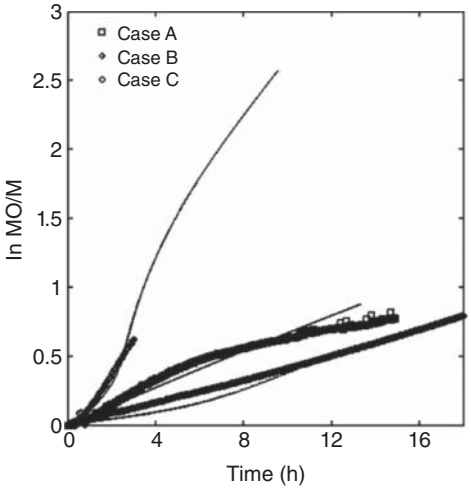

Figure 19.20 Comparison of conventional homopolymerization of styrene (Case A) with RAFT homopolymerization of styrene (Case B) and conventional copolymerization of styrene-DVB (Case C). Source: Reproduced with permission from López-Domínguez et al. [197]. Copyright 2014, John Wiley & Sons.

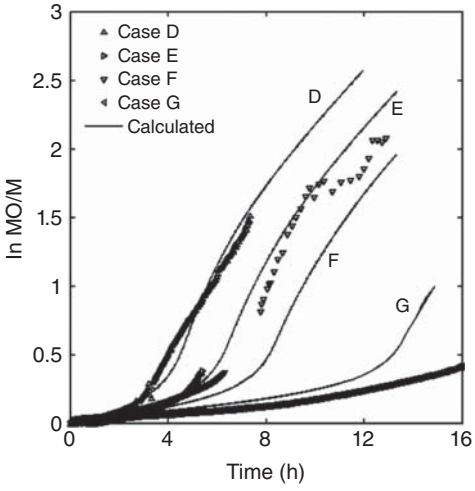

Figure 19.21 Effect of concentration of the RAFT agent on polymerization rate expressed as $\ln M_0/M$ vs. time. $[RAFT]_0$=0.0111, 0.0277, 0.0556, and 0.277 M for cases D, E, F, and G, respectively. Source: Reproduced with permission from López-Domínguez et al. [197]. Copyright 2014, John Wiley & Sons.

strong auto-acceleration effects are observed in Figure 19.21 for Cases C–G (bulk systems). Diffusion-controlled effects (DCE) were accounted for using free volume theory, as shown in Eq. (19.7). Unusually high values for the β_i parameters, up to one order of magnitude higher than those used for systems with low crosslinker content, were required to fit the experimental data. These unusually high values accounted for non-isothermal effects during the polymerization, an effect not included in the model [197]. As expected, it was observed that the increase of RAFT agent delayed the gelation point, increased compositional drift in the low conversion region, and increased $\overline{\rho}$, which suggested that less heterogeneous polymer networks were produced. Regarding the concentration of polymeric species, living polymer increased as a consequence of the auto-acceleration effect, while dormant polymer was the dominant species and remained constant throughout the polymerization.

$$k_i = k_i^0 \exp\left[-\beta_i\left(\frac{1}{V_f} - \frac{1}{V_{f0}}\right)\right] \tag{19.7}$$

The multifunctional polymer molecule modelling approach was extended to two-phase polymerization [62]. The polymerization was assumed to proceed in three stages. The partition of components between the two phases was calculated using semi-empirical equations. Formation of polymer network molecules was assumed to proceed in the dispersed phase only. DCEs were assumed to take place only in this phase. The system studied was the copolymerization of STY and DVB (crosslinker constant remained constant at $f_{20} = 0.01$) using BPO and TBTGA at 80 °C and 300 bars. Four cases were analysed. Case 1 corresponded to a conventional RP system (absence of RAFT agent), which was modelled using a monofunctional approach reported earlier. As shown in Figure 19.22, RAFT agent content varied in Cases 2–4 ($[AB]_0/[I]_0 = 0.7$, 1, and 1.5). As expected, in Case 1, the gelation point occurred early during the polymerization and it was delayed in Cases 1–4; the more RAFT agent included in the formulation, the longer it took for gelation to occur. However, the agreement between experimental data and model predictions was only fair.

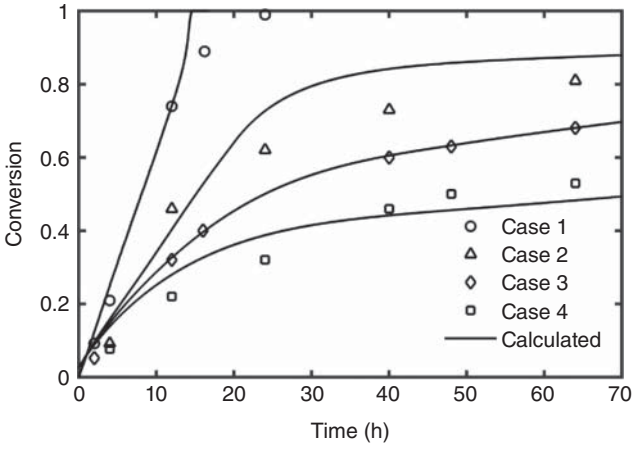

Figure 19.22 Comparison of calculated and experimental profiles of conversion vs. time for Cases 1–4. Source: Reproduced with permission from López-Domínguez et al. [62]. Copyright 2017, John Wiley & Sons.

The multifunctional molecule modelling approach developed in our group has also been used by Oliveira et al. [198] to model the copolymerization of HEMA and EGDMA using 4-cyano-4-(phenylcarbonothioylthio)pentanoic acid (CPA), as well as the copolymerization of MMA and EGDMA using 2-cyano-2-propyl benzodithiobenzoate (CYDB) at 60 °C. The model was contrasted against experimental data of monomer conversion and gel fraction.

19.5.4 Kinetic Random Branching Theory (KRBT)

The development of the structure properties in solution of branched polymers synthesized by RDRP methods can be followed by using kinetic random branching theory (KRBT). [199]. KRBT is based on random branching theory (RBT), which considers that branched polymers are built up by random assembly of simple units (oligomeric chains or cluster of linear chains) [200, 201]. If these simple units are linear chains produced by RDRP methods, their molar masses should follow a Gaussian-like distribution. Linear chains synthesized by conventional methods should follow an exponential distribution.

The structure of polymer molecules is determined by five parameters: mean size of the simple unit ($\overline{\sigma}$ (nm)), average number of random steps in the simple unit (γ), persistence number (τ), and maximum density of simple units (ρ_0).

Several experiments were carried out to test the relationship between size-mass scaling (radius of gyration (r_g(nm)) vs. molar mass ($\overline{M}_w$) predicted by the theory. It was found that copolymers of MMA/EGDMA $\left(\frac{[M]_o}{[AB]_o} = 200\right)$, MMA/DVB $\left(\frac{[M]_o}{[AB]_o} = 20\right)$, alternating maleic anhydride (MAnh)/Sty with DVB $\left(\frac{[DVB]_o}{[AB]_o} = 0.8 \text{ and } \frac{[DVB]_o}{[AB]_o} = 1\right)$, DVB $\left(\frac{[DVB]_o}{[AB]_o} = 1 \text{ and } \frac{[DVB]_o}{[AB]_o} = 20\right)$, and DVB/MAnh $\left(\frac{[DVB]_o}{[AB]_o} = 1\right)$ agreed well with the theory, suggesting that the polymers can be

Table 19.8 List of parameters used in model equations.

Parameter	Representation
Branching density	BD (Dimensionless)
Cyclization density	CD (Dimensionless)
Molar mass dispersity	$Đ$ (Dimensionless)
Molar mass dispersity of the primary molecule	$Đ_p$ (Dimensionless)
Unreacted monomer fraction	f_i (Dimensionless)
Instantaneous copolymer composition	F_j (Dimensionless)
Accumulated copolymer composition	$\overline{F}_i$ (Dimensionless)
Second-order intrinsic kinetic rate constant for reaction i	k_i^0 (l mol^{-1} s^{-1})
Kinetic rate constant for propagation of radical type i with monomer unit j	k_{pij}(l mol^{-1} s^{-1})
Pseudo-kinetic rate constant for the forward and reverse addition step of the chain equilibration reaction	k_a(l mol^{-1} s^{-1}), $k_{\_a}$(s^{-1})
Pseudo-kinetic rate constant for the forward and reverse addition step of the reversible chain transfer to RAFT agent reaction	k_{add}(l mol^{-1} s^{-1}), $k_{\_\text{add}}$(s^{-1})
Pseudo-kinetic rate constant for the forward and reverse fragmentation step of the chain equilibration reaction	k_b(s^{-1}), k_{-b}(l mol^{-1} s^{-1})
Kinetic rate constant for the forward and reverse fragmentation step of the reversible chain transfer to RAFT agent	k_{bd}(s^{-1}), k_{-bd}(l mol^{-1} s^{-1})
Pseudo-kinetic rate constant for effective intramolecular propagation through pendant double bonds	k_{cyc}(s^{-1})
Initiator decomposition kinetic rate constant	k_d(s^{-1})
Initiator decomposition kinetic rate constant	k_{dim}(l mol^{-1} s^{-1})
Kinetic rate constant for the first propagation step	k_i(l mol^{-1} s^{-1})
Pseudo-kinetic rate constant for propagation	k_p(l mol^{-1} s^{-1})
Termination by combination kinetic rate constant	k_{tc}(l mol^{-1} s^{-1})
Termination by disproportionation kinetic rate constant	k_{td}(l mol^{-1} s^{-1})
Kinetic rate constant for thermal self-initiation	k_{thi}(l mol^{-1} s^{-1})
kinetic rate constant for intermediate termination	k_{tir}(l mol^{-1} s^{-1})
Monomer j	M_j (mol)
Molar mass between crosslinking points in absence and presence of solvent	M_c, M_c^0 (g mol^{-1})
Number and weight molar mass	$\overline{M}_n$ (g mol^{-1})
Average number of propagating radicals per particle	$\overline{n}$ (Dimensionless)
Number- and weight-average chain length	$\overline{P_n}$, $\overline{P_w}$ (Dimensionless)

(*continued*)

Table 19.8 (Continued)

Parameter	Representation
Material constant	Q (Dimensionless)
Radius of gyration	r_g (nm)
Universal gas constant	R (J mol^{-1} K^{-1})
Trifuncional polymer molecule	$R_{m,r,p}$ (mol)
Multifunctional polymer molecule	$R_{m,r,p,x,f}$ (mol)
Polymer radical of size m	$R_m^{\bullet}$
One-arm adduct of size m	$R_mA^{\bullet}B$
Dormant polymer of size m	R_mA
Two-arm adduct (macro-RAFT radical) of size $m+n$	$R_mA^{\bullet}R_n$
Polymer volume fraction in the gel	$\upsilon_{2,s}$ (Dimensionless)
Polymer volume fraction during the pre-gelation period	$\upsilon_{2,r}$ (Dimensionless)
Free volume	V_f (l)
Solvent molar volume	V_{solvent} (l mol^{-1})
Swelling index	S_{index} (Dimensionless)
Monomer conversion	x (Dimensionless)
Gel fraction	w_g (Dimensionless)
Diffusion-controlled parameter	β_i (Dimensionless)
Hildebrand solubility parameter	δ (Dimensionless)
Polymer density	ρ_{polymer} (g cm^{-3})
Solvent density	ρ_s (g cm^{-3})
Crosslinking density	$\overline{\rho}$ (Dimensionless)
Maximum density of simple units	ρ_0 (Dimensionless)
Average number of random steps in the simple unit	γ (Dimensionless)
Flory polymer solvent interaction parameter	χ_1 (Dimensionless)
Parameter used in KBT	κ (Dimensionless)
Solid material deformation	λ (Dimensionless)
Average number of branching points per primary molecule	λ_p (Dimensionless)
Persistent number	τ (Dimensionless)
Normal stress difference	σ_{Mooney} (J)
Constant used in Zhu's equation	σ_Z (Dimensionless)
Mean size of the simple unit	$\overline{\sigma}$ (nm)
Weight fraction of the copolymer containing i-primary chains	$\omega(i)$ (Dimensionless)
Phase	ψ (Dimensionless)

considered as randomly branched simple units. The evolution of $\overline{\sigma}$ and r_g with time was also studied for copolymer MMA/DVB ($\frac{[M]_o}{[AB]_o} = 20$). In addition, by assuming an exponential distribution of monomers in the simple unit, it was shown that increasing dimensionless parameter $\kappa = \rho_0 \overline{\sigma}^3$ or decreasing parameter γ changes the relationship between radius of gyration and molar mass from $r_g \sim \log \overline{M}_w$ to $r_g^2 \sim \log \overline{M}_w$. The parameters used throughout the text are listed in Table 19.8.

19.6 Closing Remarks

An overview on the use of RAFT chemistry for the synthesis of polymer networks was presented. Our chapter updates the review on the topic by Moad [25] and expands it to topics of polymer chemistry not originally covered by him (e.g. reversible polymer networks based on ionic bonds; syntheses of materials described as nanogels, microgels, core-crosslinked stars, thermo- or pH- responsive materials, self-healing polymer networks, and 'arm-first' stars or hyperbranched polymers that can be formed by RAFT (co)polymerization of similar components under different reaction conditions before gelation).

Two very important topics included in our chapter that were not considered in Ref. [25] are the synthesis of polymer networks by RAFT copolymerization of vinyl/divinyl monomers in $scCO_2$ and the mathematical modelling of polymer network formation by copolymerization with crosslinking of vinyl/divinyl monomers.

Acknowledgements

Financial support from the following sources is gratefully acknowledged: (a) Consejo Nacional de Ciencia y Tecnología (CONACYT, México), PhD scholarships granted to P.P.-S. and P.L.-D.; (b) DGAPA-UNAM, Projects PAPIIT IG100718, IV100119, TA100818, and TA102120, as well as PASPA sabbatical support (U. of Waterloo, Canada) to E.V.-L.; (c) Facultad de Química-UNAM, research funds granted to E. V.-L. and A.R.-A. (PAIP 5000-9078 and 5000-9167, respectively); and (d) University of Waterloo, Department of Chemical Engineering, partial sabbatical support to E.V.-L.

References

1 Bhattacharya, A. and Ray, P. (2009). Introduction. In: *Polymer Grafting and Crosslinking* (eds. A. Bhattacharya, J.W. Rawlins and P. Ray), 1–5. Hoboken, NJ: Wiley.

2 Hernández-Ortiz, J.C. and Vivaldo-Lima, E. (2013). Crosslinking. In: *Handbook of Polymer Synthesis, Characterization, and Processing* (eds. E. Saldívar-Guerra and E. Vivaldo-Lima), 187–204. Hoboken, NJ: Wiley.

3 Li, X., Wang, S., Wang, K. et al. (2018). Polymer ionic liquid network: a highly effective reusable catalyst for one-pot synthesis of heterocyclic compounds. *RSC Adv.* 8 (74): 42292–42299.

4 Yang, Z., Kangyu, F., Yu, J. et al. (2018). "pH-triggered" drug release using shell cross-linked micelles from aqueous RAFT-synthesized PAPMA-*b*-PNIPAM copolymers. *J. Polym. Res.* 25 (8): 164.

5 Yildirim, E. and Caykara, T. (2018). Ibuprofen-imprinted ultrathin poly[*N*-(2-hydroxypropyl) methacrylamide] films. *J. Appl. Polym. Sci.* 135 (4): 45707.

6 Chen, Y., Gao, Y., and Lucília P. Silva, et al. (2018). A thermo-/pH-responsive hydrogel (PNIPAM-PDMA-PAA) with diverse nanostructures and gel behaviors as a general drug carrier for drug release. *Polym. Chem.* 9 (29): 4063–4072.

7 Peng, H., Huang, X., Melle, A. et al. (2019). Redox-responsive degradable prodrug nanogels for intracellular drug delivery by crosslinking of amine-functionalized poly(*N*-vinylpyrrolidone) copolymers. *J. Colloid Interface Sci.* 540: 612–622.

8 Roointan, A., Farzanfar, J., Mohammadi-Samani, S. et al. (2018). Smart pH responsive drug delivery system based on poly(HEMA-*co*-DMAEMA) nanohydrogel. *Int. J. Pharm.* 552 (2): 301–311.

9 Liu, S., Tian, L., Mao, H. et al. (2018). Micellization and sol-gel transition of novel thermo- and pH-responsive ABC triblock copolymer synthesized by RAFT. *J. Polym. Res.* 25 (12): 264.

10 Montgomery, K.S., Davidson, R.W.M., Cao, B. et al. (2018). Effective macrophage delivery using RAFT copolymer derived nanoparticles. *Polym. Chem.* 9 (1): 131–137.

11 Kim, S. and Seo, M. (2018). Control of porosity in hierarchically porous polymers derived from hyper-crosslinked block polymer precursors. *J. Polym. Sci. A Polym. Chem.* 56 (8): 900–913.

12 Shin, I., Nam, J., Lee, K. et al. (2018). Poly(ethylene glycol) (PEG)-crosslinked poly(vinyl pyridine)–PEG–poly(vinyl pyridine)-based triblock copolymers prepared by RAFT polymerization as novel gel polymer electrolytes. *Polym. Chem.* 9 (42): 5190–5199.

13 Ali, W., Gebert, B., Altinpinar, S. et al. (2018). On the potential of using dual-function hydrogels for brackish water desalination. *Polymers* 10 (6): 567.

14 Chen, M., Li, J.-W., Zhang, W.-J. et al. (2019). pH- and reductant-responsive polymeric vesicles with robust membrane-cross-linked structures: in situ cross-linking in polymerization-induced self-assembly. *Macromolecules* 52 (3): 1140–1149.

15 Banerjee, S.L., Hoskins, R., Swift, T. et al. (2018). A self-healable fluorescence active hydrogel based on ionic block copolymers prepared via ring opening polymerization and xanthate mediated RAFT polymerization. *Polym. Chem.* 9: 1190–1205.

16 Dong, P., Cui, K., Xu, F. et al. (2018). Synthesis of new ionic crosslinked polymer hydrogel combining polystyrene and poly(4-vinyl pyridine) and its self-healing through a reshuffling reaction of the trithiocarbonate moiety under irradiation of ultraviolet light. *Polym. Int.* 67 (7): 868–873.

17 Banerjee, S.L. and Singha, N.K. (2017). A new class of dual responsive self-healable hydrogels based on a core crosslinked ionic block copolymer micelle prepared via RAFT polymerization and Diels–Alder "click" chemistry. *Soft Matter* 13 (47): 9024–9035.

18 Guo, Z., Ma, W., Hongjian, G. et al. (2017). pH-switchable and self-healable hydrogels based on ketone type acylhydrazone dynamic covalent bonds. *Soft Matter* 13 (40): 7371–7380.

19 Chen, Y., Wang, W., Wu, D. et al. (2018). Injectable self-healing zwitterionic hydrogels based on dynamic Benzoxaborole–sugar interactions with tunable mechanical properties. *Biomacromolecules* 19 (2): 596–605.

20 Flory, P.J. (1953). Molecular weight distributions in nonlinear polymers and the theory of gelation. In: *Principles of Polymer Chemistry*, 386–395. Ithaca, NY: Cornell University Press.

21 Stockmayer, W.H. (1943). Theory of molecular size distribution and gel formation in branched-chain polymers. *J. Chem. Phys.* 11 (2): 45–55.

22 Stockmayer, W.H. (1944). Theory of molecular size distribution and gel formation in branched polymers II. General cross linking. *J. Chem. Phys.* 12 (4): 125–131.

23 Walling, C. (1945). Gel formation in addition polymerization. *J. Am. Chem. Soc.* 67 (3): 441–447.

24 Storey, B.T. (1965). Copolymerization of styrene and *p*-divinylbenzene. Initial rates and gel points. *J. Polym. Sci. A: Gen. Papers* 3 (1): 265–282.

25 Moad, G. (2015). RAFT (reversible addition–fragmentation chain transfer) crosslinking (co)polymerization of multi-olefinic monomers to form polymer networks. *Polym. Int.* 64 (1): 15–24.

26 Solomon D. H., Qiao G. G. and Abrol S. (1999). Process for microgel preparation. Patent WO9958588A1.

27 Berge C. T., Fryd M., Johnson J. W., et al. (2000). Microgels and process for their preparation. Patent WO2000002939A1.

28 Moad, G., Mayadunne, R.T.A., Rizzardo, E. et al. (2003). Synthesis of novel architectures by radical polymerization with reversible addition fragmentation chain transfer (RAFT polymerization). *Macromol. Symp.* 192 (1): 1–12.

29 Moad, G., Rizzardo, E., and Thang, S.H. (2008). Radical addition–fragmentation chemistry in polymer synthesis. *Polymer* 49 (5): 1079–1131.

30 Ide, N. and Fukuda, T. (1997). Nitroxide-controlled free-radical copolymerization of vinyl and divinyl monomers. Evaluation of pendant-vinyl reactivity. *Macromolecules* 30 (15): 4268–4271.

31 Ide, N. and Fukuda, T. (1999). Nitroxide-controlled free-radical copolymerization of vinyl and divinyl monomers. 2. Gelation. *Macromolecules* 32 (1): 95–99.

32 Scott, A.J., Nabifar, A., and Penlidis, A. (2014). Branched and crosslinked polymers synthesized through NMRP: quantitative indicators for network homogeneity? *Macromol. React. Eng.* 8: 639–657.

33 Ward, J.H. and Peppas, N.A. (2000). Kinetic gelation modeling of controlled radical polymerizations. *Macromolecules* 33 (14): 5137–5142.

34 Pérez-Salinas, P., Jaramillo-Soto, G., Rosas-Aburto, A. et al. (2017). Comparison of polymer networks synthesized by conventional free radical and RAFT copolymerization processes in supercritical carbon dioxide. *Processes* 5 (2): 26.

35 Yui, N., Mrsny, R.J., Park, K. et al. (2004). *Reflexive Polymers and Hydrogels. Understanding and Designing Fast Responsive Polymeric Systems*. Boca Raton, FL (chapter 7): CRC Press LLC.

36 Amsden, B. (1998). Solute diffusion within hydrogels. Mechanisms and models. *Macromolecules* 31 (23): 8382–8395.

37 Bell, C.L. and Peppas, N.A. (1996). Equilibrium and dynamic swelling of polyacrylates. *Polym. Eng. Sci.* 36 (14): 1856–1861.

38 Chuang, W.-Y., Young, T.-H., Wang, D.-M. et al. (2000). Swelling behavior of hydrophobic polymers in water/ethanol mixtures. *Polymer* 41 (23): 8339–8347.

39 Lopez, C.G. and Richtering, W. (2017). Does Flory–Rehner theory quantitatively describe the swelling of thermoresponsive microgels? *Soft Matter* 13 (44): 8271–8280.

40 Van Krevelen, D.W. and te Nijenhuis, K. (2009). Mechanical properties of solid polymers. In: *Properties of Polymers. Their Correlation with Chemical Structure; their Numerical Estimation and Prediction from Additive Group Contributions*, 4e, 402–405. Amsterdam, the Netherlands: Elsevier.

41 Hamed, G.R. (2012). Materials and compounds. In: *Engineering with Rubber. How to Desing Rubber Components*, 3e (ed. A.N. Gent), 11–36. Cincinnati, OH: Hanser Publications.

42 Sperling, L.H. (2006). Crosslinked polymers and rubber elasticity. In: *Introduction To Physical Polymer Science*, 4e, 427–505. Hoboken, NJ: Wiley.

43 Armando Ortiz Prado, Juan Armando Ortiz Valera, Osvaldo Ruiz Cervantes. (2013). Introducción a la Mecánica del Medio Contínuo, Universidad Nacional Autónoma de México, Facultad de Ingeniería, Ciudad Universitaria, México, pp. 199–324.

44 Chakma, P., Digby, Z.A., Via, J. et al. (2018). Tuning thermoresponsive network materials through macromolecular architecture and dynamic thiol-Michael chemistry. *Polym. Chem.* 9 (38): 4744–4756.

45 Mark, J.E. and Erman, B. (2007). Swelling of networks and volume phase transitions. In: *Rubberlike Elasticity. A Molecular Primer*, 2e, 71–77. Cambridge, UK: Cambridge University Press.

46 Yuan, B., Ding, M., Duan, W. et al. (2018). Thermoresponsive hydrogels with high elasticity and rapid response synthesized by RAFT polymerization via special crosslinking. *Polymer* 159: 1–5.

47 Yang, Z., Abbas, Z.M., Sarkar, A. et al. (2018). Surface-initiated reversible addition-fragmentation chain transfer polymerization of chloroprene and mechanical properties of matrix-free polychloroprene nanocomposites. *Polymer* 135: 193–199.

48 Mondal, P., Raut, S.K., and Singha, N.K. (2018). Thermally amendable tailor-made acrylate copolymers via RAFT polymerization and ultrafast alder-ene "click" chemistry. *J. Polym. Sci. A Polym. Chem.* 56 (20): 2310–2318.

49 Cuthbert, J., Zhang, T., Biswas, S. et al. (2018). Structurally tailored and engineered macromolecular (STEM) gels as soft elastomers and hard/soft interfaces. *Macromolecules* 51 (22): 9184–9191.

50 Cuthbert, J., Beziau, A., Gottlieb, E. et al. (2018). Transformable materials: structurally tailored and engineered macromolecular (STEM) gels by controlled radical polymerization. *Macromolecules* 51 (10): 3808–3817.

51 Banerjee, S.L., Bhattacharya, K., Samanta, S. et al. (2018). Self-healable antifouling zwitterionic hydrogel based on synergistic phototriggered dynamic disulfide metathesis reaction and ionic interaction. *ACS Appl. Mater. Interfaces* 10 (32): 27391–27406.

52 Li, H., Luo, Y., and Gao, X. (2017). Core–shell nano-latex blending method to prepare multi-shape memory polymers. *Soft Matter* 13 (31): 5324–5331.

53 Xu, Q., Sigen, A., Gao, Y. et al. (2018). A hybrid injectable hydrogel from hyperbranched PEG macromer as a stem cell delivery and retention platform for diabetic wound healing. *Acta Biomater.* 75: 63–74.

54 Li, L., Jiang, R., Chen, J. et al. (2017). In situ synthesis and self-reinforcement of polymeric composite hydrogel based on particulate macro-RAFT agents. *RSC Adv.* 7 (3): 1513–1519.

55 Yang, P.-C., Li, S.-Q., Chien, Y.-H. et al. (2017). Synthesis, chemosensory properties, and self-assembly of terpyridine-containing conjugated polycarbazole through RAFT polymerization and heck coupling reaction. *Polymers* 9 (9): 427.

56 Antonietti, M. and Rosenauer, C. (1991). Properties of fractal divinylbenzene microgels. *Macromolecules* 24 (11): 3434–3442.

57 Zhu, S. and Hamielec, A. (1992). Kinetics of polymeric network synthesis via free-radical mechanisms – polymerization and polymer modification. *Macromol. Symp.* 63 (1): 135–182.

58 Tobita, H. and Zhu, S. (1996). Polyradical distribution in free radical crosslinking of polymer chains. *J. Polym. Sci. Part B Polym. Phys.* 34 (12): 2099–2104.

59 O'Brien, N., McKee, A., Sherrington, D.C. et al. (2000). Facile, versatile and cost effective route to branched vinyl polymers. *Polymer* 41 (15): 6027–6031.

60 Keddie, D.J., Moad, G., Rizzardo, E. et al. (2012). RAFT agent design and synthesis. *Macromolecules* 45 (13): 5321–5342.

61 Moad, G., Rizzardo, E., and Thang, S.H. (2012). Living radical polymerization by the RAFT process – a third update. *Aust. J. Chem.* 65 (8): 985–1076.

62 López-Domínguez, P., Hernández-Ortiz, J.C., and Vivaldo-Lima, E. (2018). Modeling of RAFT copolymerization with crosslinking of styrene/divinylbenzene in supercritical carbon dioxide. *Macromol. Theo. Simul.* 27 (1): 1700064.

63 Pérez-Salinas, P., Rosas-Aburto, A., Antonio-Hernández, C.H. et al. (2016). Controlled release of vitamin B-12 using hydrogels synthesized by free radical and RAFT copolymerization in $scCO_2$. *Macromol. Symp.* 360 (1): 69–77.

64 Espinosa-Pérez, L., Hernández-Ortiz, J.C., López-Domínguez, P. et al. (2014). Modeling of the production of hydrogels from hydroxyethyl methacrylate and (Di)ethylene glycol dimethacrylate in the presence of RAFT agents. *Macromol. React. Eng.* 8 (8): 564–579.

65 Jaramillo-Soto, G. and Vivaldo-Lima, E. (2012). RAFT copolymerization of styrene/divinylbenzene in supercritical carbon dioxide. *Aust. J. Chem.* 65 (8): 1177–1185.

66 Gonçalves, M.A.D., Pinto, V.D., Costa, R.A.S. et al. (2013). Stimuli-responsive hydrogels synthesis using free radical and RAFT polymerization. *Macromol. Symp.* 333 (1): 41–54.

67 Gonçalves, M.A.D., Pinto, V.D., Dias, R.C.S. et al. (2013). Dynamics of network formation in aqueous suspension RAFT styrene/divinylbenzene copolymerization. *Macromol. Symp.* 333 (1): 273–285.

68 Liu, Q., Wen, X., Xu, S. et al. (2015). Synthesis and properties of the antibacterial hydrogels with enhanced mechanical strengths. *Colloid Polym. Sci.* 293 (6): 1705–1712.

69 Apostolides, D.E., Hadjicosta, A., and Patrickios, C.S. (2015). Enamine-based hydrophilic dynamic covalent polymer networks: effects of pH, and copolymer composition and concentration on the aqueous swelling degrees and the gel formation times. *Macromol. Symp.* 358 (1): 21–27.

70 Pal, S., Hill, M.R., and Sumerlin, B.S. (2015). Doubly-responsive hyperbranched polymers and core-crosslinked star polymers with tunable reversibility. *Polym. Chem.* 6 (45): 7871–7880.

71 Zhao, X., Coutelier, O., Nguyen, H.H. et al. (2015). Effect of copolymer composition of RAFT/MADIX-derived N-vinylcaprolactam/*N*-vinylpyrrolidone statistical copolymers on their thermoresponsive behavior and hydrogel properties. *Polym. Chem.* 6 (29): 5233–5243.

72 Hu, W.-t., Yang, H., He, C. et al. (2017). Morphology evolution of polystyrene-core/poly(*N*-isopropylacrylamide)-shell microgel synthesized by one-pot polymerization. *Chin. J. Polym. Sci.* 35 (9): 1156–1164.

73 Stenzel, M.H. (2008). RAFT polymerization: an avenue to functional polymeric micelles for drug delivery. *Chem. Commun.* 30 (30): 3486–3503.

74 Stenzel, M.H. (2009). Hairy core–shell nanoparticles via RAFT: where are the opportunities and where are the problems and challenges? *Macromol. Rapid Commun.* 30 (19): 1603–1624.

75 Wang, J.-Y., Wang, K., Xi, G. et al. (2016). Polymerization of hydrogel network on microfiber surface: synthesis of hybrid water-absorbing matrices for biomedical applications. *ACS Biomater Sci. Eng.* 2 (6): 887–892.

76 Sheng, W., Liu, T., Liu, S. et al. (2015). Temperature and pH responsive hydrogels based on polyethylene glycol analogues and poly(methacrylic acid) via click chemistry. *Polym. Int.* 64 (10): 1415–1424.

77 Zhao, J., Yan, C., Chen, Z. et al. (2018). Synthesis and self-assembly properties of intracellular redox bioresponsive block copolymers with hepatoma-targeting groups. *Chem. J. Chin. Univ.* 39 (7): 1592–1601.

78 Teo, G.H., Zetterlund, P.B., and Thickett, S.C. (2019). Interfacial crosslinking of self-assembled triblock copolymer nanoparticles via alkoxysilane hydrolysis and condensation. *J. Polym. Sci. A Polym. Chem.* 57 (18): 1897–1907.

79 McMahon, S., Kennedy, R., Duffy, P. et al. (2016). Poly(ethylene glycol)-based Hyperbranched polymer from RAFT and its application as a

silver-sulfadiazine-loaded antibacterial hydrogel in wound care. *ACS Appl. Mater. Interfaces* 8 (40): 26648–26656.

80 Tan, V.T.G., Nguyen, D.H.T., Utama, R.H. et al. (2017). Modular photo-induced RAFT polymerised hydrogels via thiol–ene click chemistry for 3D cell culturing. *Polym. Chem.* 8 (39): 6123–6133.

81 Zhao, J., Lu, H., Wong, S. et al. (2017). Influence of nanoparticle shapes on cellular uptake of paclitaxel loaded nanoparticles in 2D and 3D cancer models. *Polym. Chem.* 8 (21): 3317–3326.

82 Sun, X.-L., He, W.-D., Li, J. et al. (2009). RAFT cryopolymerizations of *N*,*N*-dimethylacrylamide and *N*-isopropylacrylamide in moderately frozen aqueous solution. *J. Polym. Sci. A Polym. Chem.* 47 (24): 6863–6872.

83 An, Z., Qiu, Q., and Liu, G. (2011). Synthesis of architecturally well-defined nanogels viaRAFT polymerization for potential bioapplications. *Chem. Commun.* 47 (46): 12424–12440.

84 Zhao, T., Sellers, D.L., Cheng, Y. et al. (2017). Tunable, injectable hydrogels based on peptide-cross-linked, cyclized polymer nanoparticles for neural progenitor cell delivery. *Biomacromolecules* 18 (9): 2723–2731.

85 Derry, M.J., Fielding, L.A., and Armes, S.P. (2016). Polymerization-induced self-assembly of block copolymer nanoparticles via RAFT non-aqueous dispersion polymerization. *Prog. Polym. Sci.* 52 (1): 1–18.

86 Demirci, S. (2018). Crosslinked-polymer brushes with switchable capture and release capabilities. *Polymers* 10 (9): 956.

87 Zhu, M., Zhang, M., Chen, Q. et al. (2017). Synthesis of midblock-quaternized triblock copolystyrenes as highly conductive and alkaline-stable anion-exchange membranes. *Polym. Chem.* 8 (13): 2074–2086.

88 Namvari, M., Biswas, C.S., Wang, Q. et al. (2017). Crosslinking hydroxylated reduced graphene oxide with RAFT-CTA: a nano-initiator for preparation of well-defined amino acid-based polymer nanohybrids. *J. Colloid Interface Sci.* 504: 731–740.

89 Ribeiro, T., Coutinho, E., Rodrigues, A.S. et al. (2017). Hybrid mesoporous silica nanocarriers with thermovalve-regulated controlled release. *Nanoscale* 9 (36): 13485–13494.

90 Krasia, T.C. and Patrickios, C.S. (2006). Amphiphilic polymethacrylate model co-networks: synthesis by RAFT radical polymerization and characterization of the swelling behavior. *Macromolecules* 39 (7): 2467–2473.

91 Achilleos, M., Krasia-Christoforou, T., and Patrickios, C.S. (2007). Amphiphilic model conetworks based on combinations of methacrylate, acrylate, and styrenic units: synthesis by RAFT radical polymerization and characterization of the swelling behavior. *Macromolecules* 40 (15): 5575–5581.

92 Pafiti, K.S., Loizou, E., Patrickios, C.S. et al. (2010). End-linked semifluorinated amphiphilic polymer conetworks: synthesis by sequential reversible addition–fragmentation chain transfer polymerization and characterization. *Macromolecules* 43 (12): 5195–5204.

93 Pafiti, K.S., Philippou, Z., Loizou, E. et al. (2011). End-linked poly[2-(dimethylamino)ethyl methacrylate]–poly(methacrylic acid) polyampholyte conetworks:

synthesis by sequential RAFT polymerization and swelling and sans characterization. *Macromolecules* 44 (13): 5352–5362.

94 Achilleos, M., Legge, T.M., Perrier, S. et al. (2008). Poly(ethylene glycol)-based amphiphilic model conetworks: synthesis by RAFT polymerization and characterization. *J. Polym. Sci. Part A: Polym. Chem.* 46 (22): 7556–7565.

95 Rikkou-Kalourkoti, M. and Patrickios, C.S. (2012). Synthesis and characterization of end-linked amphiphilic copolymer conetworks based on a novel bifunctional cleavable chain transfer agent. *Macromolecules* 45 (19): 7890–7899.

96 Patrickios, C.S. and Georgiou, T.K. (2003). Covalent amphiphilic polymer networks. *Curr. Opin. Colloid Interface Sci.* 8 (1): 76–85.

97 Ercole, F., Thissen, H., Tsang, K. et al. (2012). Photodegradable hydrogels made via RAFT. *Macromolecules* 45 (20): 8387–8400.

98 Nicolaÿ, R., Kamada, J., Van Wassen, A. et al. (2010). Responsive gels based on a dynamic covalent trithiocarbonate cross-linker. *Macromolecules* 43 (9): 4355–4361.

99 Amamoto, Y., Kamada, J., Otsuka, H. et al. (2011). Repeatable photoinduced self-healing of covalently cross-linked polymers through reshuffling of trithiocarbonate units. *Angew. Chem. Int. Ed. Engl.* 50 (7): 1660–1663.

100 Amamoto, Y., Otsuka, H., Takahara, A. et al. (2012). Changes in network structure of chemical gels controlled by solvent quality through photoinduced radical reshuffling reactions of trithiocarbonate units. *ACS Macro Lett.* 1 (4): 478–481.

101 Fenoli, C.R., Wydra, J.W., and Bowman, C.N. (2014). Controllable reversible addition–fragmentation termination monomers for advances in photochemically controlled covalent adaptable networks. *Macromolecules* 47 (3): 907–915.

102 Yu, L.-X., Zhuo, D., and Ran, R. (2013). Repeatable self-healing of gels based on a dynamic covalent trithiocarbonate cross-linker under microwave irradiation. *Int. J. Polym. Mater. Polym. Biomater.* 62 (14): 749–754.

103 Roy, S.G., Haldar, U., and De, P. (2014). Remarkable swelling capability of amino acid based cross-linked polymer networks in organic and aqueous medium. *ACS Appl. Mater. Interfaces* 6 (6): 4233–4241.

104 Patil, N., Soni, J., Ghosh, N. et al. (2012). Swelling-induced optical anisotropy of thermoresponsive hydrogels based on poly(2-(2-methoxyethoxy)ethyl methacrylate): deswelling kinetics probed by quantitative mueller matrix polarimetry. *J. Phys. Chem. B* 116 (47): 13913–13921.

105 Patil, N., Roy, S.G., Haldar, U. et al. (2013). CdS quantum dots doped tuning of deswelling kinetics of thermoresponsive hydrogels based on poly(2-(2-methoxyethoxy)ethyl methacrylate). *J. Phys. Chem. B* 117 (50): 16292–16302.

106 Chen, Q., Han, F., Lin, C. et al. (2018). Synthesis of bioreducible core crosslinked star polymers with *N*,*N*′-bis(acryloyl)cystamine crosslinker via aqueous ethanol dispersion RAFT polymerization. *Polymer* 146: 378–385.

107 Haldar, U., Nandi, M., Maiti, B. et al. (2015). POSS-induced enhancement of mechanical strength in RAFT-made thermoresponsive hydrogels. *Polym. Chem.* 6 (28): 5077–5085.

108 Liu, Q.F., Zhang, P., Qing, A.X. et al. (2006). Poly(*N*-isopropylacrylamide) hydrogels with improved shrinking kinetics by RAFT polymerization. *Polymer* 47 (7): 2330–2336.

109 Lin, Y., Wang, L., Zhou, J. et al. (2019). Surface modification of PVA hydrogel membranes with carboxybetaine methacrylate via PET-RAFT for anti-fouling. *Polymer* 162: 80–90.

110 Qie, F., Astolfo, A., Wickramaratna, M. et al. (2015). Self-assembled gold coating enhances X-ray imaging of alginate microcapsules. *Nanoscale* 7 (6): 2480–2488.

111 Niu, S., Ding, M., Chen, M. et al. (2013). Synthesis of well-defined copolymer of acrylonitrile and maleic anhydride via RAFT polymerization. *J. Polym. Sci. A Polym. Chem.* 51 (24): 5263–5269.

112 Garmendia, S., Dove, A.P., Taton, D. et al. (2018). Reversible ionically-crosslinked single chain nanoparticles as bioinspired and recyclable nanoreactors for *N*-heterocyclic carbene organocatalysis. *Polym. Chem.* 9 (43): 5286–5294.

113 Kitiri, E.N., Patrickios, C.S., Voutouri, C. et al. (2017). Double-networks based on pH-responsive, amphiphilic "core-first" star first polymer conetworks prepared by sequential RAFT polymerization. *Polym. Chem.* 8 (1): 245–259.

114 Yong, P., Yang, Y., Wang, Z. et al. (2016). Diverse nanostructures and gel behaviours contained in a thermo- and dual-pH-sensitive ABC(PNIPAM–PAA–P4VP) terpolymer in an aqueous solution. *RSC Adv.* 6 (91): 88306–88314.

115 Liu, J.C., Uhlir, C., and Parag K. Shah, et al. (2016). Controlled nanogel and macrogel structures from self-assembly of a stimuli-responsive amphiphilic block copolymer. *RSC Adv.* 6 (69): 64791–64798.

116 Achilleos, M., Mpekris, F., Stylianopoulos, T. et al. (2016). Structurally-defined semi-interpenetrating amphiphilic polymer networks with tunable and predictable mechanical response. *RSC Adv.* 6 (49): 43278–43283.

117 Sundhoro, M., Wang, H., Boiko, S.T. et al. (2016). Fabrication of carbohydrate microarrays on a poly(2-hydroxyethyl methacrylate)-based photoactive substrate. *Org. Biomol. Chem.* 14 (3): 1124–1130.

118 Zhuo, D., Ruan, Y., Zhao, X. et al. (2011). Kinetics of UV-initiated RAFT crosslinking polymerization of dimethacrylates. *J. Appl. Polym. Sci.* 121 (2): 660–665.

119 Zhang, L., Zhang, C., Peng, X. et al. (2016). A clean synthesis approach to biocompatible amphiphilic conetworks via reversible addition–fragmentation chain transfer polymerization and thiol–ene chemistry. *RSC Adv.* 6 (21): 17228–17238.

120 Prai-in, Y., Boonthip, C., Rutnakornpituk, B. et al. (2016). Recyclable magnetic nanocluster crosslinked with poly(ethylene oxide)-block-poly(2-vinyl-4,4-dimethylazlactone) copolymer for adsorption with antibody. *Mater. Sci. Eng. C* 67: 285–293.

121 Mangadlao, J.D., Huang, R., Foster, E.L. et al. (2016). Graphene oxide–poly(ethylene glycol) methyl ether methacrylate nanocomposite hydrogels. *Macromol. Chem. Phys.* 217 (1): 101–107.

122 Zheng, W., Chen, L.-J., Yang, G. et al. (2016). Construction of smart supramolecular polymeric hydrogels crosslinked by discrete organoplatinum(II)

metallacycles via post-assembly polymerization. *J. Am. Chem. Soc.* 138 (14): 4927–4937.

123 Almeida, C., Costa, H., Kadhirvel, P. et al. (2016). Electrochemical activity of sulfur networks synthesized through RAFT polymerization. *J. Appl. Polym. Sci.* 133 (39): 43993.

124 Ding, Z.-L., Tao, W.-D.H.J., Jiang, W.-X. et al. (2011). Zwitterionic shell-crosslinked micelles from block-comb copolymer of PtBA-b-P(PEGMEMA-co-DMAEMA). *J. Polym. Sci. A Polym. Chem.* 49 (13): 2783–2789.

125 Adrian Figg, C., Simula, A., Gebre, K.A. et al. (2015). Polymerization-induced thermal self-assembly (PITSA). *Chem. Sci.* 6 (2): 1230–1236.

126 Li, A., Zhang, G., Zhu, L. et al. (2015). Facile synthesis of crosslinked core/shell silver nanoparticles with significantly improved thermal stability. *Eur. Polym. J.* 68: 379–384.

127 Liu, H., Zhuang, X., Turson, M. et al. (2008). Enrofloxacin-imprinted monolithic columns synthesized using reversible addition-fragmentation chain transfer polymerization. *J. Sep. Sci.* 31 (10): 1694–1701.

128 Turson, M., Zhuang, X.L., Liu, H.N. et al. (2009). Evaluation of the clenbuterol imprinted monolithic column prepared by reversible addition-fragmentation chain transfer polymerization. *Chin. Chem. Lett.* 20 (9): 1136–1140.

129 Turson, M., Zhou, M., Jiang, P. et al. (2011). Monolithic poly(ethylhexyl methacrylate-co-ethylene dimethacrylate) column with restricted access layers prepared via reversible addition-fragmentation chain transfer polymerization. *J. Sep. Sci.* 34 (2): 127–134.

130 Cheng, C., Bai, X., Xu, Z. et al. (2015). Self-healing polymers based on a photo-active reversible addition-fragmentation chain transfer (RAFT) agent. *J. Polym. Res.* 22: 46.

131 Rosselgong, J. and Armes, S.P. (2012). Quantification of intramolecular cyclization in branched copolymers by 1H NMR spectroscopy. *Macromolecules* 45 (6): 2731–2737.

132 Norisuye, T., Morinaga, T., Tran-Cong-Miyata, Q. et al. (2005). Comparison of the gelation dynamics for polystyrenes prepared by conventional and living radical polymerizations: a time-resolved dynamic light scattering study. *Polymer* 46 (6): 1982–1994.

133 Yu, Q., Zhu, Y., Ding, Y. et al. (2008). Reaction behavior and network development in RAFT radical polymerization of dimethacrylates. *Macromol. Chem. Phys.* 209 (5): 551–556.

134 Yu, Q., Xu, S., Zhang, H. et al. (2009). Comparison of reaction kinetics and gelation behaviors in atom transfer, reversible addition–fragmentation chain transfer and conventional free radical copolymerization of oligo(ethylene glycol) methyl ether methacrylate and oligo(ethylene glycol) dimethacrylate. *Polymer* 50 (15): 3488–3494.

135 Yu, Q., Gan, Q., Zhang, H. et al. (2009). Gelation kinetics of RAFT radical copolymerization of methacrylate and dimethacrylate. *ACS Symp. Ser.* 1024: 181–193.

136 Perelaer, J., Hermans, K., Bastiaansen, C.W.M. et al. (2008). Photo-embossed surface relief structures with an increased aspect ratios by addition of a

reversible addition-fragmentation chain transfer Agent. *Adv. Mater.* 20 (16): 3117–3121.

137 Perelaer, J., Hermans, K., Bastiaansen, C.W.M. et al. (2009). Photo-embossed surface relief structures with an increased aspect ratio by addition of kinetic interfering compounds. *J. Photopolym. Sci. Technol.* 22 (5): 667–670.

138 Huebner, D., Koch, V., Ebeling, B. et al. (2015). Comparison of monomethoxy-, dimethoxy-, and trimethoxysilane anchor groups for surface-initiated RAFT polymerization from silica surfaces. *J. Polym. Sci. A Polym. Chem.* 53 (1): 103–113.

139 Leung, D. and Bowman, C.N. (2012). Reducing shrinkage stress of dimethacrylate networks by reversible addition–fragmentation chain transfer. *Macromol. Chem. Phys.* 213 (2): 198–204.

140 He, J., Yan, B., Yu, B.Y. et al. (2008). Fine adjustment of network in polymer network liquid crystal film employing RAFT polymerization. *J. Polym. Sci. A Polym. Chem.* 46 (9): 3140–3144.

141 Zhan, X., He, R., Zhang, Q. et al. (2014). Microstructure and mechanical properties of amphiphilic tetrablock copolymer elastomers via RAFT miniemulsion polymerization: influence of poly[styrene-alt-(maleic anhydride)] segments. *RSC Adv.* 4 (93): 51201–51207.

142 He, R., Zhan, X., Zhang, Q. et al. (2016). Toughening of an epoxy thermoset with poly [styrene-alt-(maleic acid)]-block-polystyreneblock-poly(*n*-butyl acrylate) reactive core–shell particles. *RSC Adv.* 6 (42): 35621–35627.

143 Barlow, K.J., Hao, X., Hughes, T.C. et al. (2014). Porous, functional, poly(styrene-*co*-divinylbenzene) monoliths by RAFT polymerization. *Polym. Chem.* 5 (3): 722–732.

144 Graillot, A., Monge, S., Faur, C. et al. (2013). Synthesis by RAFT of innovative well-defined (co)polymers from a novel phosphorus-based acrylamide monomer. *Polym. Chem.* 4 (3): 795–803.

145 Yan Kang. (2015). Synthesis and self-assembly of nucleobase-containing polymers by RAFT techniques. PhD Thesis. The University of Warwick.

146 Wang, D., Li, X., Wang, W.-J. et al. (2012). Kinetics and modeling of semi-batch RAFT copolymerization with hyperbranching. *Macromolecules* 45 (1): 28–38.

147 Huang, J., Wang, W.J., Li, B.G. et al. (2013). Design and synthesis of poly(butyl acrylate) networks through RAFT polymerization with crosslinking for controlled-release applications. *Macromol. Mater. Eng.* 298 (4): 391–399.

148 Henkel, R. and Vana, P. (2014). The influence of RAFT on the microstructure and the mechanical properties of photopolymerized poly(butyl acrylate) networks. *Macromol. Chem. Phys.* 215 (2): 182–189.

149 Mori, H. and Tsukamoto, M. (2011). RAFT polymerization of diacrylate derivatives having different spacers in dilute conditions. *Polymer* 52 (3): 635–645.

150 Kaupp, M., Hiltebrandt, K., Trouillet, V. et al. (2016). Wavelength selective polymer network formation of end-functional star polymers. *Chem. Commun.* 52 (9): 1975–1978.

151 Cox, L.M., Sun, X., Wang, C. et al. (2017). Light-stimulated permanent shape reconfiguration in cross-linked polymer microparticles. *ACS Appl. Mater. Interfaces* 9 (16): 14422–14428.

152 Wang, J., Zhu, Z., Jin, X. et al. (2016). Preparation of well-defined propargyl-terminated tetra-arm poly(*N*-isopropylacrylamide)s and their click hydrogels crosslinked with β-cyclodextrin. *Polymers* 8 (4): 93.

153 Voorhaar, L., De Meyer, B., Du Prez, F. et al. (2016). One-pot automated synthesis of quasi triblock copolymers for self-healing physically crosslinked hydrogels. *Macromol. Rapid Commun.* 37: 1682–1688.

154 Zhang, K., Aiba, M., Fahs, G.B. et al. (2015). Nucleobase-functionalized acrylic ABA triblock copolymers and supramolecular blends. *Polym. Chem.* 6 (13): 2434–2444.

155 Belal, K., Poitras-Jolicoeur, S., Lyskawa, J. et al. (2016). A triple carboxylic acid-functionalized RAFT agent platform for the elaboration of well-defined telechelic 3-arm star PDMAc. *Chem. Commun.* 52 (9): 1847–1850.

156 Scherf, R., Müller, L.S., Grosch, D. et al. (2015). Investigation on the homogeneity of PMMA gels synthesized via RAFT polymerization. *Polymer* 58: 36–42.

157 Matyjaszewski, K. (2016). Atom transfer radical polymerization (ATRP): current status and future perspectives. *Macromolecules* 45 (10): 4015–4039.

158 Kiran, E. (2016). Supercritical fluids and polymers—the year in review—2014. *J. Supercrit. Fluids* 110: 126–153.

159 Boyère, C., Jérôme, C., and Debuigne, A. (2014). Input of supercritical carbon dioxide to polymer synthesis: an overview. *Eur. Polym. J.* 61: 45–63.

160 Sadowski, G. (2005). Phase behavior of polymer systems in high-pressure carbon dioxide. In: *Supercritical Carbon Dioxide in Polymer Reaction Engineering*, 1e (eds. M.F. Kemmere and T. Meyer), 15–34. Weinheim, Germany: Wiley-VCH Verlag GmbH & Co.

161 Gupta, R.B. and Shim, J.J. (2007). Introduction. In: *Solubility in Supercritical Carbon Dioxide*, 1e, 1–18. Boca Raton, FL: CRC Press, Taylor & Francis Group.

162 Bush, D. (2005). *Equation of State for Windows 95*. Software, version 1.0.14. Atlanta, GA: Georgia Institute of Technology.

163 E. Vivaldo-Lima, M. J. Bernad-Bernad, A. Licea-Claverie, et al. (2013). Polymers with a low-density network structure and method for producing same by means of reversible-deactivation radical polymerisation in compressed fluids. Patent Application MX/a/2013/009053 2013.

164 Kendall, J.L., Canelas, D.A., Young, J.L., and DeSimone, J.M. (1999). Polymerizations in supercritical carbon dioxide. *Chem. Rev.* 99 (2): 543–563.

165 Canelas, D.A. and DeSimone, J.M. (1997). Polymerizations in liquid and supercritical carbon dioxide. *Adv. Polym. Sci.* 133: 103–140.

166 Quintero-Ortega, I.A., Vivaldo-Lima, E., Luna-Barcenas, G. et al. (2005). Modeling of the free-radical copolymerization kinetics with cross linking of vinyl/divinyl monomers in supercritical carbon dioxide. *Ind. Eng. Chem. Res.* 44 (8): 2823–2844.

167 Canelas, D.A. and DeSimone, J.M. (1997). Dispersion polymerizations of styrene in carbon dioxide stabilized with poly(styrene-*b*-dimethylsiloxane). *Macromolecules* 30 (19): 5673–5682.

168 Jaramillo-Soto, G., Garcıa-Moran, P.R., Enrıquez-Medrano, F.J. et al. (2009). Effect of stabilizer concentration and controller structure and composition on polymerization rate and molecular weight development in RAFT polymerization of styrene in supercritical carbon dioxide. *Polymer* 50 (21): 5024–5030.

169 Temtem, M., Teresa, C., Gil Santos, A. et al. (2007). Molecular interactions and CO_2-philicity in supercritical CO_2. A high-pressure NMR and molecular modeling study of a perfluorinated polymer in $scCO_2$. *J. Phys. Chem. B* 111 (6): 1318–1326.

170 Jaramillo-Soto, G., Villa-Ávila, C.M., and Vivaldo-Lima, E. (2013). RAFT copolymerization with crosslinking of methyl methacrylate and ethylene glycol Dimethacrylate in supercritical carbon dioxide. *J. Macromol. Sci., A: Pure Appl. Chem.* 50 (3): 281–286.

171 García-Morán, P.R., Jaramillo-Soto, G., Albores-Velasco, M.E., and Vivaldo-Lima, E. (2009). An experimental study on the free-radical copolymerization kinetics with crosslinking of styrene and divinylbenzene in supercritical carbon dioxide. *Macromol. React. Eng.* 3 (1): 58–70.

172 Patricia Pérez-Salinas. (2019). Síntesis y caracterización de redes poliméricas con heterogeneidad reducida usando copolimerización RAFT de metacrilato de hidroxietilo (HEMA) y dimetacrilato de etilén glicol (EGDMA) en dióxido de carbono supercrítico ($scCO_2$), Ph.D. Thesis, Materials Science and Engineering Graduate Program (PCeIM), Instituto de Investigaciones en Materiales (IIM), Universidad Nacional Autónoma de México (UNAM), Mexico City, México.

173 Vivaldo-Lima, E., Jaramillo-Soto, G., and Penlidis, A. (2016). Nitroxide-mediated polymerization. In: *Encyclopedia of Polymer Science and Technology* (ed. H.F. Mark), 1–48. Wiley.

174 Scott, A.J., Nabifar, A., Hernández-Ortiz, J.C. et al. (2014). Crosslinking nitroxide-mediated radical copolymerization of styrene with divinylbenzene. *Eur. Polym. J.* 51: 87–111.

175 Lyu, J., Gao, Y., Zhang, Z. et al. (2018). Monte Carlo simulations of atom transfer radical (Homo)polymerization of divinyl monomers: applicability of Flory–Stockmayer theory. *Macromolecules* 51 (17): 6673–6681.

176 Poly, J., Wilson, D.J., Destarac, M. et al. (2009). A comprehensive investigation into "controlled/living" chain growth crosslinking copolymerization including a back to basics modeling. *J. Polym. Sci., Part A: Polym. Chem.* 47 (20): 5313–5327.

177 Satheeshkumar, C. and Seo, M. (2018). Creation of micropores by RAFT copolymerization of conjugated multi-vinyl cross-linkers. *Polym. Chem.* 9 (48): 5680–5689.

178 Bachmann, R., Melchiors, M., and Avtomonov, E. (2016). Modelling and optimization of nonlinear polymerization processes. *Macromol. Symp.* 370 (1): 135–143.

179 Lattuada, M., Del Gado, E., Abete, T. et al. (2013). Kinetics of free-radical cross-linking polymerization: comparative experimental and numerical study. *Macromolecules* 46 (15): 5831–5841.

180 Lazzari, S., Hamzehlou, S., Reyes, Y. et al. (2014). Bulk crosslinking copolymerization: comparison of different modeling approaches. *Macromol. React. Eng.* 8 (10): 678–695.

181 Hamzehlou, S., Reyes, Y., and Leiza, J.R. (2013). A new insight into the formation of polymer networks: a kinetic Monte Carlo simulation of the cross-linking polymerization of S/DVB. *Macromolecules* 46 (22): 9064–9073.

182 Tripathi, A.K., Tsavalas, J.G., and Sundberg, D.C. (2015). Monte Carlo simulations of free radical polymerizations with divinyl cross-linker: pre- and postgel simulations of reaction kinetics and molecular structure. *Macromolecules* 48 (1): 184–197.

183 Kryven, I., Berkenbos, A., Melo, P. et al. (2013). Modeling crosslinking polymerization in batch and continuous reactors. *Macromol. React. Eng.* 7 (5): 205–220.

184 Lyu, J., Gao, Y., Zhang, Z. et al. (2018). Can Flory-Stockmayer theory be applied to predict conventional free radical polymerization of multivinyl monomers? A study via Monte Carlo simulations. *Sci. China Chem.* 61 (3): 319–327.

185 Aguiar, L.G. (2016). Styrene–dimethacrylate copolymerization kinetic modeling. *Polym. Int.* 65 (1): 142–151.

186 Lazzari, S. and Storti, G. (2014). Modeling multiradicals in crosslinking MMA/EGDMA bulk copolymerization. *Macromol. Theory Simul.* 23 (1): 15–35.

187 Nikitin, A.N., Wulkow, M., and Schütte, C. (2013). Modeling of free radical styrene/divinylbenzene copolymerization with the numerical fractionation technique. *Macromol. Theory Simul.* 22 (9): 475–489.

188 Aguiar, L.G. (2015). A cross-linking copolymerization mathematical model including phase separation and cyclization kinetics. *Macromol. Theory Simul.* 24 (3): 176–180.

189 Gonçalves, M.A.D., Pinto, V.D., Dias, R.C.S. et al. (2011). Modeling studies on the synthesis of superabsorbent hydrogels using population balance equations. *Macromol. Symp.* 306–307 (1): 107–125.

190 Monteiro, M.J. and De Brouwer, H. (2001). Intermediate radical termination as the mechanism for retardation in reversible addition-fragmentation chain transfer polymerization. *Macromolecules* 34 (3): 349–352.

191 Wang, R., Luo, Y., Li, B.-G. et al. (2009). Modeling of branching and gelation in RAFT copolymerization of vinyl/divinyl systems. *Macromolecules* 42 (1): 85–94.

192 Li, X., Wang, W.-J., Li, B.-G. et al. (2015). Branching in RAFT miniemulsion copolymerization of styrene/triethylene glycol dimethacrylate and control of branching density distribution. *Macromol. React. Eng.* 9 (2): 90–99.

193 Liang, S., Li, X., Wang, W.-J. et al. (2016). Toward understanding of branching in RAFT copolymerization of methyl methacrylate through a cleavable dimethacrylate. *Macromolecules* 49 (3): 752–759.

194 Zhu, S. (1998). Analytical functions for molecular weight and branching distributions in star-, comb-, and random-branched polymers. *Macromolecules* 31 (21): 7519–7527.

195 Hernández-Ortiz, J.C., Vivaldo-Lima, E., Dubé, M.A. et al. (2014). Modeling of network formation in reversible addition-fragmentation transfer (RAFT) copolymerization of vinyl/divinyl monomers using a multifunctional polymer molecule approach. *Macromol. Theory Simul.* 23 (3): 147–169.

196 Pallares, J., Jaramillo-Soto, G., Flores Cataño, C. et al. (2006). A comparison of reaction mechanisms for reversible addition - fragmentation chain transfer polymerization using Modeling tools. *J. Macromol. Sci., Part A: Pure Appl. Chem.* 43 (9): 1293–1322.

197 López-Domínguez, P., Hernández-Ortiz, J.C., Barlow, K.J. et al. (2014). Modeling the kinetics of monolith formation by RAFT copolymerization of styrene and divinylbenzene. *Macromol. React. Eng.* 8 (10): 706–722.

198 Oliveira, D., Dias, R.C.S., and Costa, M.R.P.F.N. (2016). Modeling RAFT gelation and grafting of polymer brushes for the production of molecularly imprinted functional particles. *Macromol. Symp.* 370 (1): 52–65.

199 Konkolewicz, D., Gray-Weale, A., and Perrier, S. (2010). The structure of randomly branched polymers synthesized by living radical methods. *Polym. Chem.* 1 (7): 1067–1077.

200 Konkolewicz, D., Gilbert, R.G., and Gray-Weale, A. (2007). Randomly hyperbranched polymers. *Phys. Rev. Lett.* 98 (23): 238301.

201 Konkolewicz, D., Gray-Weale, A., and Perrier, S. (2010). Describing the structure of a randomly hyperbranched polymer. *Macromol. Theory Simul.* 19 (5): 219–227.

20

Complex Polymeric Architectures Synthesized through RAFT Polymerization

Thomas G. Floyd[1], Satu Häkkinen[1], Matthias Hartlieb[2], Andrew Kerr[1], and Sébastien Perrier[1,3,4]

[1] *University of Warwick, Department of Chemistry, Gibbet Hill Road, Coventry CV4 7AL, UK*
[2] *University of Potsdam, Institute of Chemistry, Karl-Liebknecht-Straße 24-25, Potsdam 14476, Germany*
[3] *University of Warwick, Warwick Medical School, Gibbet Hill Road, Coventry CV4 7AL, UK*
[4] *Monash University, Faculty of Pharmacy and Pharmaceutical Sciences, 381 Royal Parade, Parkville, VIC 3052, Australia*

20.1 Introduction

As reversible addition-fragmentation chain transfer (RAFT) polymerization has grown into a versatile and widely used technique, it has paved the way to the design of a broad range of polymeric architectures. Chapter 20 describes the various polymeric structures that can be obtained by RAFT (Figure 20.1), either as unique materials that can only be obtained by the RAFT process or more traditional polymeric architectures, whose synthesis is made easily accessible. This chapter provides an overview of the various architectures obtained by RAFT to date, with a comment on best practice and general guidelines.

20.2 RAFT Synthesis of Block Copolymers

One of the most advantageous features of RAFT polymerization over radical polymerization is the maintenance of chain end fidelity with a 'living' chain transfer agent (CTA) end group, which facilitates the synthesis of block copolymers. Broadly speaking, there are three main approaches to block copolymer synthesis via RAFT polymerization – multiple sequential polymerization steps, pre-modification of a CTA with a polymer to yield a macroCTA followed by chain extension, or the coupling of two polymeric species using the CTA-derived end group (either R or Z) functionalities (Figure 20.2). There are yet further variations including assembling blocks through supramolecular interactions or combining multiple polymerization techniques in various orders.

RAFT Polymerization: Methods, Synthesis and Applications, First Edition.
Edited by Graeme Moad and Ezio Rizzardo.

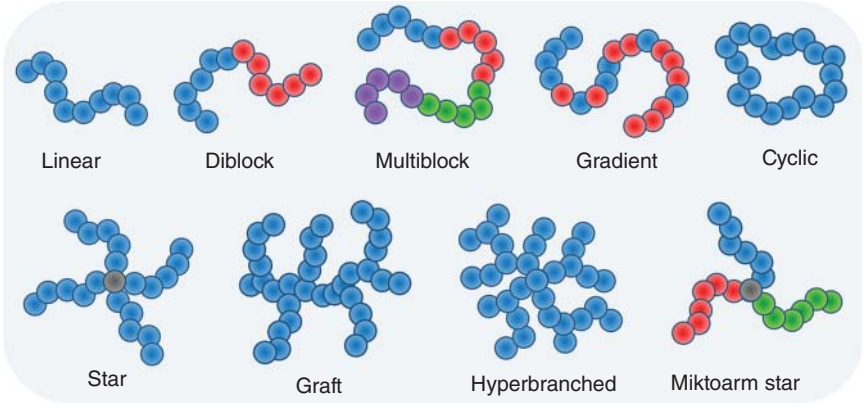

Figure 20.1 Schematic of the various architectures described in this chapter.

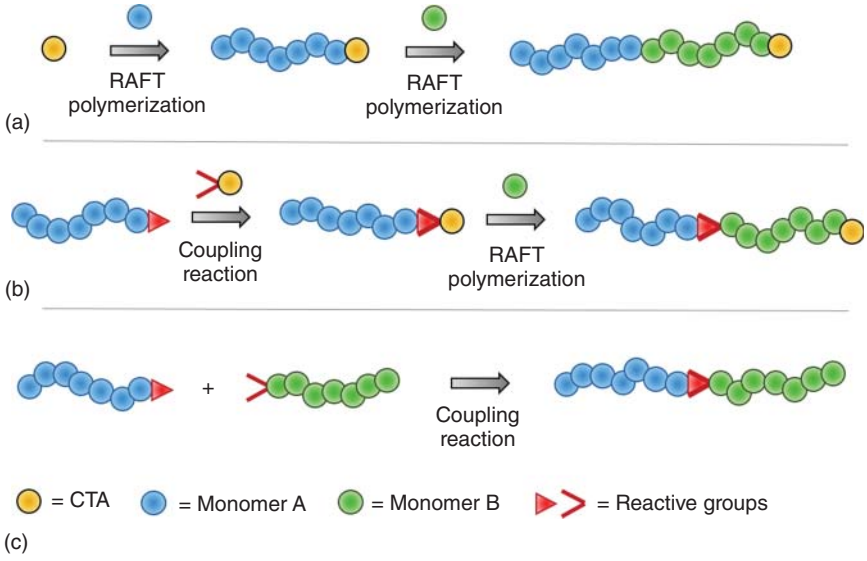

Figure 20.2 (a) Preparation of block copolymers by sequential RAFT polymerizations, (b) block copolymer synthesis by preparation of a macroCTA and subsequent chain extension, and (c) block copolymer synthesis by conjugation of two polymeric species.

20.2.1 Block Copolymer by Sequential Polymerization Steps

Of these options, accessing block copolymers through the sequential polymerization approach is arguably the simplest and most accessible as it can yield diblocks in two standard polymerization processes starting from the respective monomers and CTA, in appropriate quantities for the desired molecular weight. For large-scale processes, this is the most appealing and simplest procedure, similar to standard radical polymerization, to access diblock materials. The RAFT process has excellent tolerance of reaction conditions and functional groups, with the versatility to polymerize a wide range of monomers among the so-called 'more activated monomer' (MAM)

and 'less activated monomer' (LAM) groups. As a res1ult of these advantages, there have been a huge number of publications utilizing RAFT technology to access block architectures to yield materials for a plethora of applications [1]. There are a number of considerations for successful block copolymer synthesis though this technique – the choice of CTA, order of blocks, chain end livingness, polymer solubility, monomer conversion, and potential side reactions, which will be discussed in sections 20.2.1.1–20.2.1.6.

20.2.1.1 Choice of CTA

Firstly, as per a standard RAFT homopolymerization, a CTA of suitable reactivity must be selected to control the monomers of choice in the block polymerization (see Figure 20.3 for typical examples of CTAs). For the first block, the R and Z groups play an important role in this; however, for the second block, only the Z group is pertinent in controlling the polymerization, and therefore, the Z group must provide control for both monomer species. In the simplest case of block copolymers of two monomers from the same family (e.g. acrylates), this is trivial; however, if a block of MAM-LAM were desired, a CTA providing good control of the MAM such as a trithiocarbonate will retard or entirely inhibit the polymerization rate for the LAM. The development of switchable RAFT agents has provided a route to controlling this combination of highly different monomer reactivities.

Dithiobenzoates provide excellent control of meth(acrylates/acrylamides) and styrene, therefore are highly effective for production of block copolymers from these monomer families. For block combinations of meth(acrylates/acrylamides) with acrylates/acrylamides, the use of a trithiocarbonate is generally preferable, as the dithiobenzoates commonly induce substantial rate retardation for the polymerization of acrylates/acrylamides because of slow fragmentation of the highly stabilized intermediate radical with respect to propagation [2, 3]. Narrow dispersities (~1.1–1.2) can still be obtained for the use of trithiocarbonate with methacrylates [4], so they are generally a more versatile choice of RAFT agent for block copolymer synthesis of MAMs. For LAMs, the use of either xanthates or dithiocarbamates is recommended [5]; however, these CTAs possess low chain transfer constants for MAMs, so diblocks with these monomers are not well

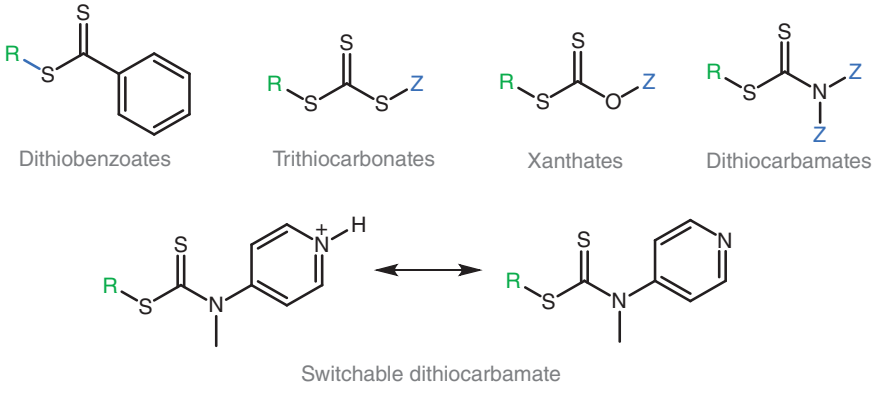

Figure 20.3 General chemical structures of some of the most commonly used RAFT agents.

controlled. For these architectures, the aforementioned switchable RAFT agents provide uniquely effective control [6–8]. This class of dithiocarbamate compounds contain a pH-responsive pyridyl functionality on the Z group, while in its unprotonated form, it possesses a low chain transfer constant, suitable for LAMs, but upon protonation, the intermediate radical is much more effectively stabilized, thus enabling improved control of MAM polymerizations. One-pot conditions can therefore be used by the addition of acid to modify the pH and reversibly switch the CTA from controlling LAMs to MAMs. The use of xanthates for control of ethylene has also been established by the use of specialized reaction conditions at high pressures (70 °C, >200 bar) [9]. It is also worth noting the usage of 'sulphur-free' RAFT agents, consisting of macromonomers derived from catalytic chain transfer polymerization, has been reported for the synthesis of multiblock structures of hydrophobic methacrylate monomers [10]. While such CTAs possess a very low chain transfer constant and thus perform poorly in solution polymerization [11], the usage of emulsion conditions with monomer feeding was able to compensate for this and enable excellent control of block copolymerizations.

Recent advancements in RAFT have also established its use for the control of cationic polymerizations, enabling the controlled synthesis of poly(vinyl ethers), which cannot be accessed through radical mechanisms [12, 13]. Trithiocarbonates, xanthates, and dithiocarbamates with a vinyl ether R group can be used, also allowing for chain extension through a radical process (e.g. vinyl acetate) to yield novel diblock copolymer structures [14]. This technique therefore allows the direct synthesis of block combinations of radically and cationically polymerizable monomers, which would otherwise be challenging to access [15, 16].

Difunctional CTAs offer a facile route to higher order block copolymers in fewer polymerization steps, however are limited to symmetrical structures as a result of chain extension occurring in both directions (Figure 20.4) [17]. They are particularly useful for the synthesis of ABA block copolymers in two reactions steps as opposed to the three required for a mono-functional CTA. Linkage of the CTA groups can be performed through either the Z or R group of the RAFT agent – in the case of Z-group, a thiocarbonylthio functionality will be incorporated into the centre of the polymer, which may be prone to degradation. The polymerization of the exterior block is performed first and chain extensions will occur within the centre of the

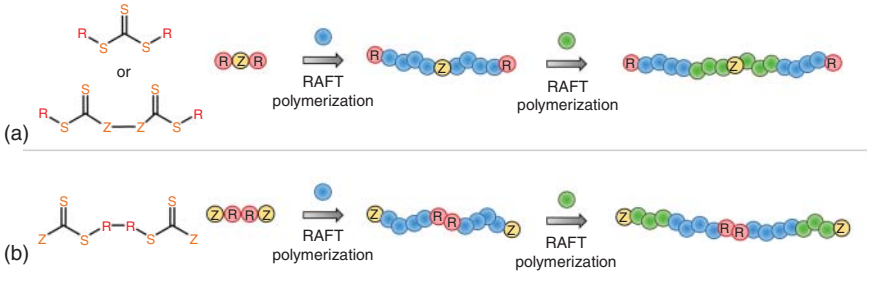

Figure 20.4 (a) Scheme outlining the structure of difunctional CTAs linked by the Z group and order of monomer incorporation upon polymerization. (b) Scheme of difunctional CTAs linked by the R groups.

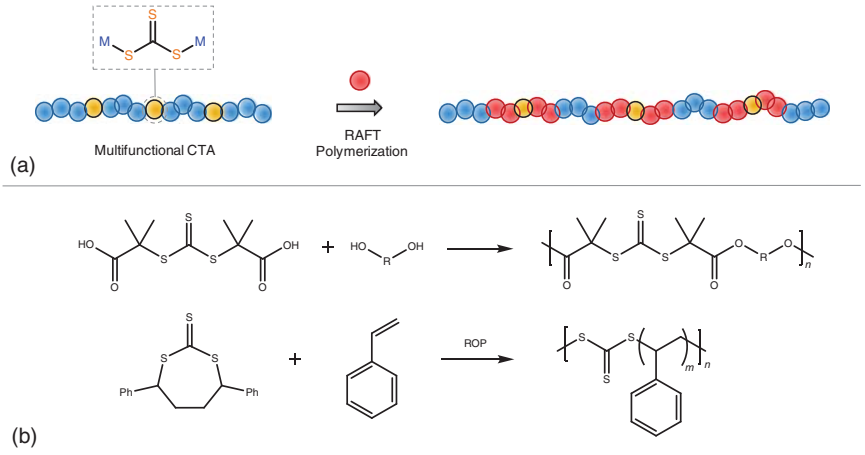

Figure 20.5 (A) Scheme showing chain extension of a multifunctional polymeric CTA to form a mulitblock copolymer. (B) (a) Preparation of the multifunctional CTA by a condensation reaction. (b) Preparation by ring-opening radical copolymerization of a cyclic trithiocarbonate with styrene monomer.

polymer to insert the core block. Alternatively by coupling two R groups to make a difunctional CTA, the composition of central segment will be determined by the chemical linkage used and thus can be designed for superior stability, while the block orders must be performed in the opposite order to the Z-group linkage to yield the same polymeric structure.

Multifunctional CTAs, consisting of a polymer with multiple thiocarbonylthio moieties placed along the backbone, are another option that allow for the synthesis of higher order multiblocks in just two reaction steps, although the exact number of blocks per chain will not be controlled. Polymeric CTAs of this nature can be prepared by coupling reactions of telechelic RAFT agents [18, 19], or alternatively by the polymerization of cyclic CTA structures through a ring-opening mechanism (Figure 20.5) [20, 21]. Because the multifunctional polymer has a distribution of molecular weights, the number of CTA groups per chain varies significantly; therefore, upon chain extension, there will also be a broad distribution of the number of block segments in the resulting structure. Furthermore, the RAFT mechanism entails fragmentation events across the CTAs of the backbone, leading to a scrambling of the block orders and the creation of initiator-derived chains of decreased block quantity. As a result of this, the dispersity of the multiblock copolymer product is often high (PDI > 2) – this technique does not provide precise control of polymeric architecture. The individual block segments, however, are of narrow dispersity with molecular weight controlled by the RAFT process, which can be confirmed by cleavage of the thiocarbonylthio groups and subsequent size exclusion chromatography (SEC) analysis of the resulting low molecular weight species [20].

20.2.1.2 Block Order

For the synthesis of block copolymers incorporating two different monomer families, the order of the polymerization steps is a vital consideration for assuring

effective control. After the first step of the polymerization effectively, a 'macroCTA' is synthesized, where the R group is now the polymeric unit. The ability of the macroCTA to efficiently chain extend polymerization of the second block will be related to the nature of the macro 'R' group of the CTA with respect to the propagating monomer of the second block. It must be an effective leaving group, possessing a good chain transfer constant, and also be capable of reinitiating polymerization of the second monomer. According to the RAFT mechanism, an initial propagating oligomeric radical will add to the CTA to form an intermediate radical situated on the CTA. This can then fragment either towards the initial propagating species or towards the macro 'R-group', and for successful block copolymer synthesis, the latter fragmentation must occur. For this to be favourable, the macro R group should form a more stable radical than the propagating monomer of the second block. As a general rule, therefore, in RAFT, the MAM should be polymerized first to ensure efficient chain extension.

As a result of this requirement, monomers that create stabilized tertiary radicals such as meth(acrylates/acrylamides) must be polymerized as the first block, followed by chain extension with monomers that produce secondary radicals (styrenes/acrylamides/acrylates) and then finally by LAMs. Attempting to polymerize the blocks in the opposite order will often lead to inefficient reinitiation from the macroCTA and thus lead to multimodal distributions and increased dispersities. Combinations of possible blocks are thus restricted by these synthetic requirements. Early work in RAFT has demonstrated for effective synthesis of a poly(styrene)-poly(methyl methacrylate) diblock copolymer, that the PMMA block must be synthesized first as a result of the difference in reactivity. This concept has been established for a variety of monomer systems, although there will be variations depending on the exact structure of monomer and thus it is often necessary to try alternative block orders.

A scheme summarizing these guidelines is shown (Figure 20.6), with the suggested order of polymerization of a monomer going from left to right. The selected CTAs are merely examples of suitable choices and a large range of many other RAFT agents have been reported in the literature that may be better suited to a specific circumstance.

20.2.1.3 Polymer Livingness

During the RAFT process, the use of an external radical initiator source leads to the formation of initiator-derived chains and ultimately terminated polymers lacking the CTA end group. In the case of block copolymer synthesis, the presence of defected chains devoid of the CTA is detrimental to high-fidelity materials and leads to the formation of 'dead' homopolymers of the first block unable to undergo chain extension, often apparent as a low molecular tail in SEC analysis. Every radical species introduced into the system will inevitably terminate and those that initiated polymerization will lead to the formation of a dead polymer product. Therefore, the livingness (percentage of polymers with the 'living' CTA end group) can be defined as the ratio of moles of CTA to the moles of CTA plus initiated radicals. A further consideration is the predominant nature of termination – through a disproportionation mechanism, two separate 'dead' chains would be produced,

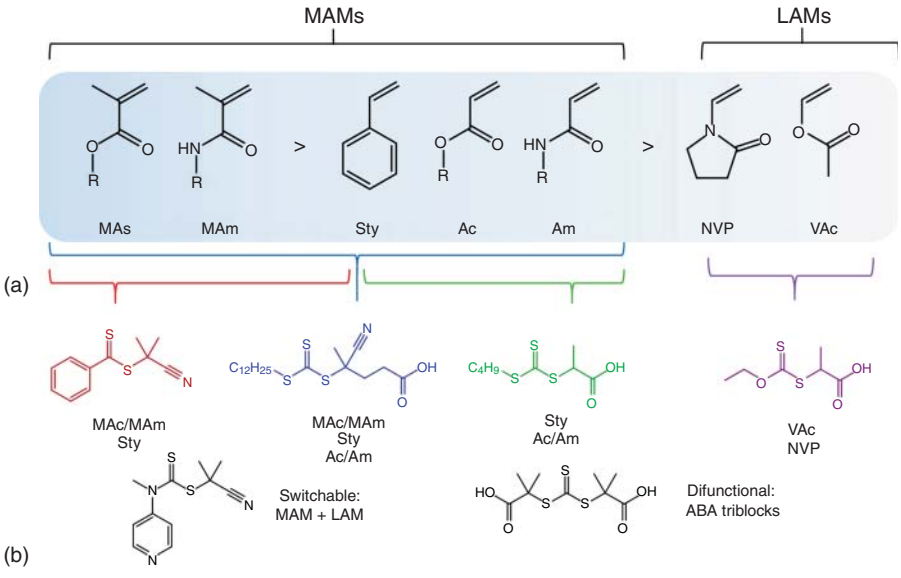

Figure 20.6 (a) Monomers that fall under the categories of MAMs and LAMs. Blocks should be prepared starting from left to right. (b) Small selection of suitable CTAs for the polymerization of the respective monomer families.

whereas recombination would result in one 'dead' chain of higher molecular weight; thus, the ratio of moles of dead to living chains would be affected. Written as an equation, taking into account the initiator decomposition rate and initiating efficiency (typically 50% for azoinitiators) gives:

$$L\,(\%) = \frac{[\mathrm{CTA}]}{[\mathrm{CTA}] + 2f \times [I]_0 \times \left(1 - e^{-k_d \times t}\right) \times \left(1 - \frac{f_c}{2}\right)} \tag{20.1}$$

where [CTA] is the initial concentration of CTA, f is the initiation efficiency (typically assumed to be 50%), $[I]_0$ is the initial initiator concentration, k_d is the rate coefficient of decomposition, t is the time, and f_c is the coupling factor referring to whether the terminations occur by combination ($f_c = 1$) or disproportionation ($f_c = 0$).

An implication of this is that there will always be a number of living chains according to the moles of CTA, despite the number of terminations that occur. Thus, some percentage of chains will always be able to undergo chain extension (assuming effective consumption of macroCTA), unlike in other reversible deactivation radical polymerizations (RDRPs), such as atom transfer radical polymerization (ATRP) and nitroxide-mediated polymerization (NMP), in which excessive terminations could result in complete removal of all active end groups. In these alternative techniques, an external source of initiator is not required, so the number of termination is not 'guaranteed' in the same manner as RAFT, so this is not to say RAFT is necessarily superior in terms of livingness.

In order to obtain low-dispersity block copolymers, it is paramount to maintain a high livingness, which in practice is achieved by modifying the polymerization conditions, in particular, the moles of initiating species ideally to as low a value as

feasible for the polymerization. The CTA/I ratio is a commonly reported parameter to give a handle on the expected livingness – a CTA/I ratio > 10 is generally recommended for diblock copolymer synthesis to ensure that at least 90% of chains can chain extend to successfully create a diblock. In actuality for the purposes of estimating livingness, the ratio of importance is that of CTA to the initiator *consumed* and thus will be highly dependent on the reaction time and temperature, which alters the degree of decomposition of the initiating species. Under equivalent reaction conditions, monomers with slower propagation rates, such as styrene and methacrylates, will require higher initiator concentrations than monomers with higher k_p values, and therefore, for some systems, there will be greater limitations in how much the initiator concentration can be lowered. Additionally, targeting larger degrees of polymerization of each block will decrease chain end livingness – with equivalent initiator concentrations, a higher molecular weight polymerization will have a lowered CTA concentration and thus CTA/I ratio, indicating that a larger proportion of chains will be terminated. This reflects the inherent limit of RAFT where it theoretically will depress the maximal achievable molecular weight with respect to a comparable radical process. All else being equal targeting lower molecular weights of each block will therefore be easier to control.

It is also worth noting that, as a result of the RAFT mechanism, a number of other possible terminated species will occur (Figure 20.7). During the polymerization of the first block, initiator-derived chains will introduce an initiator fragment end group as opposed to the R group from the RAFT agent, and terminations (either by recombination or by disproportionation) will lead to polymers devoid of the CTA end group. For the second block chain extension, the possibilities increase further, as now the initiator-derived chains will lead to the formation of a 'B' homopolymer, which will remain in the final reaction mixture, and additionally, radical terminations could occur between various species, leading to ABA triblock copolymers. Through these processes, the synthesis of a diblock by sequential polymerization steps can lead to the formation of homopolymers of both 'A' and 'B' monomers, in

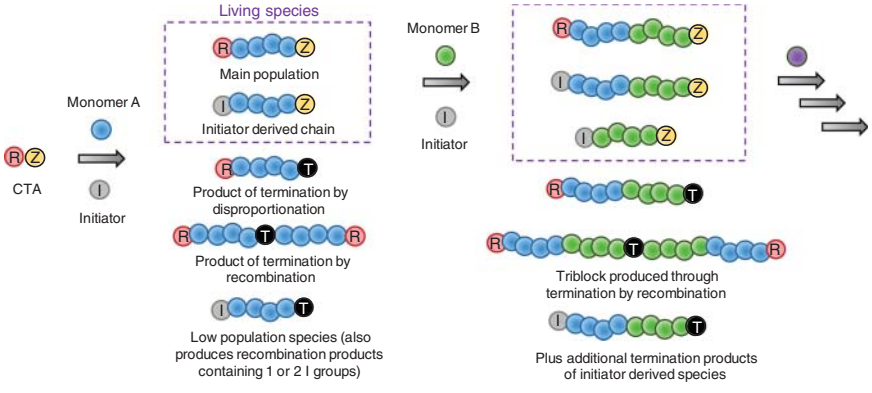

Figure 20.7 Potential polymeric structures formed during a standard RAFT diblock polymerization initiated by an external source of radicals from an initiator species.

addition to chain ends differing from that of the R and Z from the CTA – the quantity of these defect chains should again be equivalent to the number of radicals and thus can be mitigated by the usage of low initiator concentrations. In the case of a difunctional CTA linked by the R groups, the types of terminations increases yet further, leading to a complex variety of possibilities including some terminations, which would not lead to a chain deficient in CTA end groups.

An important consideration when selecting an initiator concentration (and accordingly the polymer livingness) is the extent of monomer conversion obtained, which will affect the experimental procedure possible. For quantitative monomer consumptions, a one-pot procedure can be used where after synthesis of the first block, a batch of the second monomer can be directly added to the reaction mixture. If full conversions of the first block are not achievable, however, the reaction mixture must be purified (often by dialysis or precipitation) before chain extension, leading to additional experimental steps. Residual quantities of the first monomer would lead to a gradient-like architecture in the final product if they are not removed from the reaction mixture before the second step. It is therefore desirable to use the simpler one-pot procedure, although there can be limitations in terms of livingness for this approach. RAFT follows standard radical polymerization kinetics with a first-order relationship to monomer concentrations and accordingly the reaction rate drops off over the course of the polymerization – this makes the final period going from 89 to 99% monomer conversion particularly long compared to a 10% change at lower conversions. Assuming a constant decomposition rate of initiator for the duration of the polymerization, the longer a reaction time, the more radical production occurs and thus livingness of the polymer is reduced. Therefore, to achieve maximal livingness, it would be theoretically preferable to quench polymerizations at moderate conversions (e.g. 70%) rather than drive the polymerization to completion as substantially more initiating radicals would be required to achieve this. In practice, however, one-pot procedures reaching almost complete conversion with very high chain end fidelity have been established for block copolymers of a range of monomer families. Despite this, some monomers may display unusual polymerization behaviour and be difficult to polymerize to high conversions, necessitating purification steps.

20.2.1.4 Initiation System

In addition to the traditional thermally decomposing initiators (e.g. azo initiators and peroxide compounds), there are a number of other options, such as redox pair initiators [22, 23]. These are useful for polymerizations at room temperature; however, their mechanism of decomposition is less well understood and thus calculations of livingness through the number of radicals produced may not be accurate. Initiators that decompose to produce radicals upon exposure to light irradiation can also be used at varying temperatures and behave in a similar manner to the thermally decomposing systems. There has also been substantial focus in literature on the use of 'photo-RAFT', either through an iniferter mechanism by direct activation of the CTA compound itself [24–26] or with the usage of a photocatalyst (PET-RAFT) [27, 28]. Both have been established as effective methods for the synthesis of block

copolymers and complex architectures [29, 30]. In these systems, an external initiator source is not required; therefore, the number of radicals produced is not precisely known and thus the livingness equations do not apply here, while the potential defect species arising from initiator-derived chains will also not be present.

20.2.1.5 Further Considerations

Ensuring the solubility of both polymer blocks and monomer throughout the course of the reaction is an important factor for maintaining control of the polymerization and accessing the desired molecular weights. It is generally suggested that a good solvent for all components ([macro]RAFT agent, monomer, and resulting block copolymer) should be used, although in the case of amphiphilic diblocks, for example, this can be particularly challenging. For some syntheses, it may be preferable to carry out the first block polymerization in one solvent, purify the macroRAFT agent and then perform chain extended in a different solvent system. In some cases, a difference in solubility can be exploited for emulsion or polymerization-induced self-assembly (PISA) processes, where a solvent selective for one block can be utilized to undergo polymerization in a heterogeneous reaction mixture. Although these approaches can be advantageous, they often entail additional complications when compared to a standard solution polymerization.

Finally, the CTA end group could be lost through side reactions of the end group functionality – in the case of block polymerization, it is particularly pertinent to prevent this from occurring in order to retain a suitably high chain end fidelity. Dithiobenzoates and trithiocarbonates are reactive towards nucleophiles, in particular, amines that will reduce the end group to a thiol and thus prevent further chain extension – therefore, for the synthesis of amine-containing polymers, they must be non-nucleophilic (tertiary of quaternized) or utilize monomers with a protected amine group during polymerization, followed by a deprotection step post-polymerization. Additionally, CTA groups, particularly dithiobenzaotes, can be susceptible to hydrolysis in basic aqueous conditions [31] – for aqueous polymerization at elevated temperatures, such as for the monomer hydroxypropylmethacylamide, the use of acidic buffer solutions is recommended to reduce RAFT agent degradation [32]. Other conditions such as excessive heat (typically >120 °C) [33], UV irradiation [26], and oxidation [34] are also known to induce degradation of the CTA end group and therefore should be avoided.

20.2.1.6 Multiblock Copolymers

Increasing the number of blocks in the target polymeric architecture is inherently challenging because of the accumulation of dead chains throughout each block extension process. For ease of experimental synthesis, as is important in the case of multiblocks of high block orders, a one-pot procedure reaching full monomer conversion is preferred as otherwise time consuming purifications would be required for each step. The limitation of reaching full monomer conversion is concomitant with reduction of the polymer livingness as a result of the increased initiator quantity required. Despite these issues, fairly recent developments in RAFT synthesis have led to reports of as high as 20 block copolymer structures

with short overall reaction times [35]. These have been most commonly reported for the acrylamide family of monomers, which have been exploited as a result of their very high propagation rates, especially in aqueous conditions [36] to enable polymerization to full monomer conversion with very low concentrations of initiators and conveniently short reaction times [23, 37]. To achieve fast reactions rates, the equation for the rate of propagation can be considered, where it is evident that this can be increased by three parameters – usage of a monomer with high k_p, (increased by temperature), a high $[M]$, and a high radical flux:

$$R_p = k_p\,[\mathrm{M}]\left[\mathrm{R}^*\right] = k_p\,[\mathrm{M}]\sqrt{\frac{f k_d [\mathrm{I}]_0 e^{-k_d t}}{k_t}} \tag{20.2}$$

where R_p = rate of propagation, k_p = rate constant of propagation, [M] = monomer concentration, [R*] = radical concentration, f = initiation efficiency, k_d = rate constant of initiator decomposition, $[\mathrm{I}]_0$ = initial initiator concentration, and t = time, k_t = rate constant of termination.

By adopting a rapidly decomposing initiator system, for example, VA-044 at 70 °C (10 hour half-life temperature = 44 °C), effectively full consumption of initiator can be reached in under two hours, which facilitates rapid propagation and is convenient for calculation of the initiator concentration as unreacted reagent is not accumulated between block extensions. Usage of high monomer concentrations also increases polymerization rates and is an important factor, although too high concentration will lead to experimental issues in terms of excessively high viscosities, making the mixing of subsequent monomer aliquots ineffectual. While a ratio of CTA/I = 10 is typically adequate for control of diblock architectures, this would lead to a very low livingness (~38%) for a dodecablock ($n = 10$) architecture; therefore, the use of very low initiation concentrations (often CTA/I > 100) and targeting of relatively short degrees of polymerization are prerequisite for optimal multiblock synthesis. This approach has also been utilized in continuous flow reactors for the preparation of acrylate-based multiblock copolymers on scales up to 150 g within 26 hours of reaction time [38, 39].

20.2.2 Block Copolymers by Chain Extension of a Pre-functionalized MacroCTA

Alternatively to performing sequential RAFT polymerizations, instead the modification of the starting CTA with a polymeric group through a coupling reaction offers another route to block copolymers (Figure 20.8). One significant advantage is the ability to incorporate polymers that cannot be polymerized through RAFT, while also requiring less dependence on developing suitable polymerization conditions for all blocks. The polymer can be conjugated through either the Z or R group of the CTA; in either case, this should not significantly impact the activity of the CTA in terms of its ability to control the polymerization of a second monomer. Therefore, potential issues with chain extension of the macroCTA due to differences in monomer reactivity are avoided by this approach, making the synthesis of various diblocks facile. Performing the initial conjugation through the Z group, however,

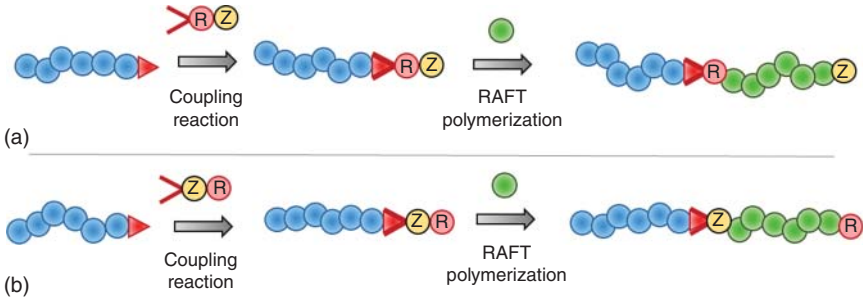

Figure 20.8 Scheme showing the preparation of a macroRAFT agent and subsequent chain extension for (a) connection through the R group and (b) connection through the Z group. This choice will affect the position of the respective groups in the final block copolymer.

will upon chain extension yield a diblock containing the thiocarboylthio group in the centre of the polymer, which may be more prone to degradation.

This approach is most conveniently applied with the conjugation of commercial polymers, although this can be somewhat restrictive in the selection of available molecular weights. The use of a polymer of high chain end fidelity is also essential to ensure efficient macroCTA synthesis through the coupling reaction of the end group – if functionalization is incomplete, residual homopolymer side products will remain after the chain extension. A common example is the conjugation of poly(ethylene glycol) containing a terminal alcohol/amine functionality with a carboxylic acid containing CTA [40, 41], which has been used extensively for the synthesis of amphiphilic block copolymers by chain extension with a hydrophobic monomer. Other frequently studied macroCTAs include poly(dimethylsiloxanes) [42, 43] and poly(lactides) [44], among other examples such as poly(isoprene) [45] and poly(thiophenes) [46]. Click chemistry has also been used to access a poly(isobutylene) macroCTA, which was then chain extended with *N*-isopropylacrylamide to synthesize novel diblocks [47].

20.2.3 Block Copolymers by Conjugation of Two Polymeric Chains

A third method of block polymer synthesis is the coupling of two already formed polymers, as opposed to the previous example of attaching a polymer to a small-molecule RAFT agent. In this case, two polymeric materials containing complementary end group functionalities are reacted together to covalently bind the two blocks. This approach is particularly appealing as in principle essentially any two polymer substrates can be reacted to yield a diblock, without the restraints of sequential polymerizations, thus broadening the possibilities of polymeric structures. A number of challenges are associated with this technique – the low concentration of reactive end group when placed on a high molecular weight polymer and steric hindrance effects reduce the rate of reaction substantially, often yielding sub-quantitative conversion. For ease of purification, the use of equimolar quantities of each polymer would be preferable; however, inaccuracies in the determination of polymer molecular weight (MW) make this difficult to achieve

precisely, and even if done so, the slow reaction rate of the two macromolecules could lead to incomplete conjugation. Any residual excess of one of the polymer reactants, either as a result of difference in molarities or incomplete conjugation, must then be purified to obtain the desired diblock, which depending on the nature of the substrates may be challenging. For successful implementation of this approach, it is most commonly combined with Click Chemistries, defined by their high conversions and lack of side products, facilitating high yield couplings with minimal purification requirements [48, 49].

20.2.3.1 Block Copolymer Synthesis Through Click Chemistry

As the most established click chemistry reaction, the copper-catalysed azide–alkyne cycloaddition has been utilized for a range of RAFT-derived polymeric coupling approaches (Figure 20.9). Through the use of a dithiobenzoate containing a protected alkyne moiety and an azide functional xanthate, polymers of 6-*O*-methacryloyl mannose and vinyl acetate could be prepared, respectively, with the end groups then coupled via 'click' to yield a diblock copolymer [50]. This combination of methacrylate and vinyl acetate polymers would otherwise be quite challenging to access through sequential polymerizations and demonstrates the increased versatility of the conjugation approach. There are a number of other examples of this chemistry being utilized with RAFT [51–53]. While usage of a trimethyl silyl-protected alkyne group appears recommended to ensure that no side reactions occur during the radical polymerization [54], there have been successful reports of unprotected alkyne groups being used [55, 56]. One limitation of the azide–alkyne reaction is the requirement of exogenous copper catalyst, which can be problematic for the synthesis of polymers intended for biomedical applications as residual copper contaminant is often present even after purification. As a result, alternative 'additive-free' click chemistries have been explored for diblock copolymer synthesis. These include the inverse electron demand Diels–Alder between tetrazine and polymeric norbornene end group [57], and the Diels-alder of a triazolinedione moiety with a diene [58]. Other click type reactions such as the sulfur fluoride exchange (SuFEx) chemistry has been identified as orthogonal to RAFT radical polymerization and applied to block copolymer synthesis [59, 60].

Specific to the use of RAFT, the CTA end group itself can also be directly utilized for coupling reactions such as with hetero-Diels–Alder (HDA) reaction. The C=S double bond of electron-deficient dithioester compounds is known to undergo [4+2]-cycloaddition with dienes and therefore by using a CTA with a suitable Z group functionality, the cycloaddition can be performed post-polymerization with a diene functional macromolecule. This atom-efficient approach was first demonstrated by the synthesis of diblocks of poly(styrene)-*b*-poly(caprolactam) [61], and since then, further improvements to the reaction were obtained by the use of a cyclopentadienyl end group in which rapid reaction times (<10 minutes) for high molecular weight polymers (up to 100 000 g mol^{-1}) were observed [62]. In further combination with photoenol chemistry by the usage of a dual functional CTA, a triblock copolymer of poly(isoprene-co-styrene)-*b*-(poly(ethyl

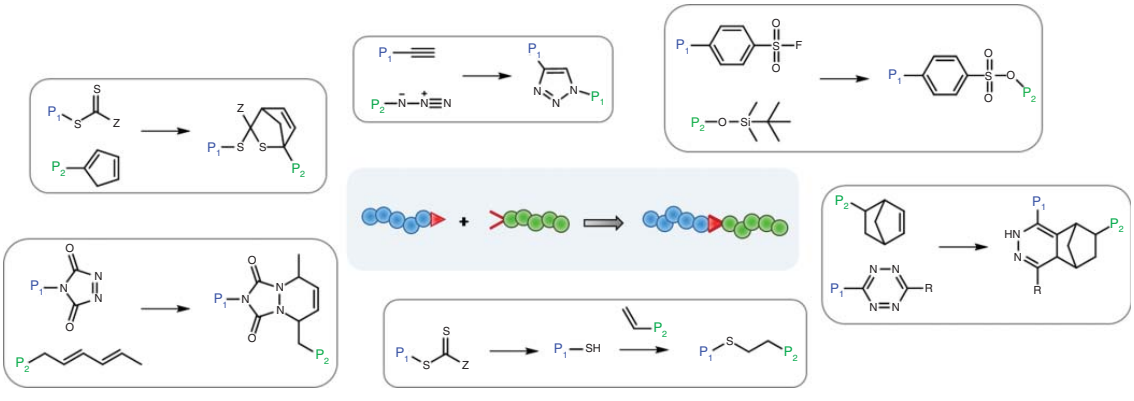

Figure 20.9 A selection of reported 'click' reactions for preparation of RAFT-derived block copolymers.

acrylate)-*b*-(poly(ethylene oxide) was synthesized by sequential polymer coupling onto one chain end through thermally induced HDA and secondly to the other chain end through photo-induced ligation [63].

Additionally, the thiocarbonylthio moiety can be considered a masked thiol functionality, which can then be used for a range of chemistries [64]. Treatment of a RAFT polymer with nucleophiles such as primary/secondary amines or hydrides such as $NaBH_4$ can be performed to reveal the reactive thiol polymeric chain end. Care must be taken, however, to prevent thiol oxidation into disulfides which leads to formation of high molecular weight species, and therefore, the addition of a phosphine reducing agent can be advantageous. This process can also be inefficient for poly(meth)acrylates where the thiol end group is susceptible to a backbiting side reaction to yield a thiolactone [65]. Once deprotected, the thiol can then be used for conjugation to another polymer with a complementary end group, most frequently via a Michael addition onto an electron-deficient alkene such as a poly(ethylene glycol) (PEG) functional acrylate [66], or sequential conjugations to a bismaleimide linker [67]. Radical thiol-ene additions can also be performed for polymer–polymer coupling but generally result in poorer yields [68].

In comparison to the other two approaches of block copolymer synthesis, the conjugation of two polymeric reagents is arguably the most synthetically challenging and is generally most effective for relatively low molecular weight polymers in which chain end fidelity and reaction rates are higher. While the click chemistry techniques are a very powerful tool, especially for accessing more exotic polymer structures and block orders, the previous two techniques are often more appropriate for block copolymer synthesis particularly for large-scale processes or targeting of high molecular weights.

20.2.3.2 Supramolecular Block Copolymers

In a conceptually similar manner, rather than coupling two polymer chains through a covalent bond, instead supramolecular chemistry can be used to attach the chains through reversible interactions. There are numerous examples of RAFT-derived materials using these approaches for block copolymer assembly such as hydrogen bonding [69], metal complexation [70], or host–guest chemistry [71]. Such an approach can endow the material with self-healing properties because of the dynamic nature of supramolecular interactions. The use of a functional CTA compound containing the supramolecular bonding moiety is a common approach to synthesize telechelic assembling block copolymers. For example, poly(styrene) and poly(methyl methacrylate) were synthesized by RAFT using two different CTAs containing complementary binding units, which then interacted to form a supramolecular diblock. This could then undergo self-assembly in bulk to yield highly order phase separated morphologies, which upon exposure to polar solvents, the hydrogen bonding interactions were disrupted allowing one block to be removed, forming a nanoporous membrane [72]. Through a similar approach with the use of Hamilton receptor and barbiturate functional CTAs, ABCD tetrablocks could be created through the selective binding affinity of the two end groups [73],

and in further work with difunctional CTAs of the same chemistry, it was possible to access higher order multiblock architectures [74].

20.2.4 General Guidelines

Through the outlined approaches, there are often multiple routes to synthesize a desired block copolymer architecture. In general, the preparation by sequential polymerizations is the most recommended as it is suitable for a broad range of monomer classes, allows for precise control of the molecular weights of each block, and can be used for a high number of block extensions with appropriate reaction conditions. Alternatively, the usage of a pre-functionalized macroCTA can be a highly efficient approach, although less versatile in terms of MW control and selection of monomers. It is particularly useful for synthesis of architectures such as amphiphilic diblocks involving chain extension from a PEG macroCTA, for example. Finally, the use of conjugation reactions between polymeric chains, because of their low yield and limitation in molecular weights, is generally only recommended if the desired architecture is not accessible through the previously described means.

20.3 Gradient Copolymers

Perhaps the simplest and most easily accessed variation in polymeric architecture are gradient copolymers, which display an asymmetric distribution of two or more monomer species across a polymeric chain, offering alternative properties to that of block or statistical structures [75, 76]. For a radical polymerization of two monomers of different reactivity ratios, the unequal rate of consumption of each monomer will lead to a compositional drift of the polymeric product over the course of the reaction because the lifetime of an individual radical is very short with respect to the total polymerization time (Figure 20.10). In the case of RAFT, on the other hand, all polymer chains can effectively be considered to grow at the same rate and remain 'living' throughout the polymerization, thereby yielding polymer products of approximately equal composition. Rather than between the separate chains, the compositional drift will rather be observed across each individual chain, leading to a gradient copolymer architecture. RAFT, or other RDRP techniques, therefore provides a route to access alternative gradient copolymer architectures by prevention of compositional drift. There are two main experimental approaches to synthesize gradient copolymers: first, the spontaneous approach involving the copolymerization of two monomers of different reactivity ratios, or secondly, the 'forced' approach, whereby one or both monomers are fed into the reaction mixture at a specific rate. With the latter methodology, the composition of the gradient can be much more finely tuned as it is no longer limited by the reactivity ratios, however, requires experimental optimization and detailed theoretical understanding to yield the desired composition [77].

The use of xanthate CTAs enables good control of vinyl acetate monomers and acceptable control of acrylates/acrylamides – because the monomer families possess significantly different reactivity ratios, they can therefore be copolymerized to

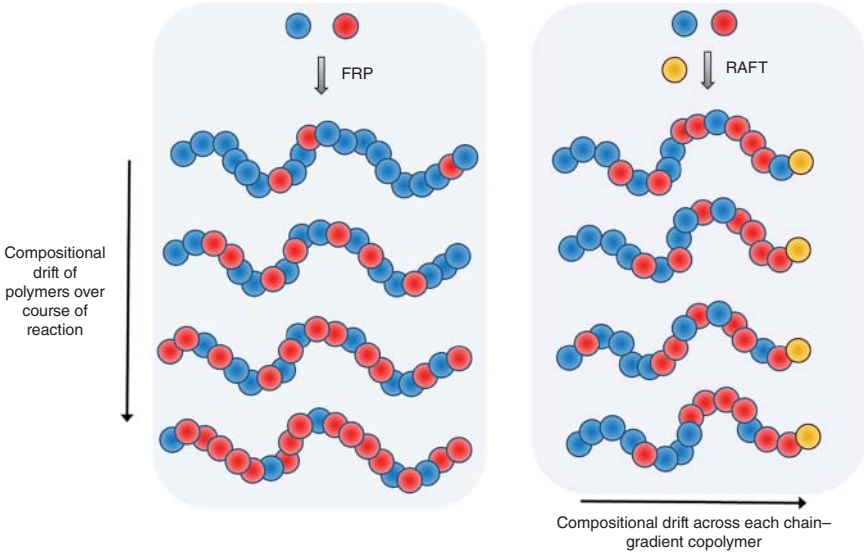

Figure 20.10 Copolymerization of two monomers of differing reactivity ratio by (a) – radical polymerization leads to compositional drift, whereas with (b) – RAFT, gradient copolymers are formed.

access spontaneous gradient copolymers, as has been demonstrated by copolymerzations of VAc/*N*-isopropylacrylamide NIPAM [78] and VAc/MA [79]. As an additional route to gradient copolymers, RAFT was used for radical polymerization with concomitant reaction of monomers with an enzyme, thus changing the monomer feed ratio over the course of the polymerization to yield a gradient copolymer [80]. For this approach to be successful, the chemical transformation should occur on the monomer but not on polymeric units and must also be orthogonal to the required polymerization conditions, which limits the scope in terms of potential substrates.

20.4 Cyclic Polymers

Cyclic polymers represent an interesting class of polymeric architecture because of their lack of end groups, which can play a significant role in physical properties. Ring closure reactions of polymeric end groups is the most commonly reported methodology to access cyclic RAFT-derived polymers, either using reactions involving the CTA end group directly such as Diels–Alder [81] and disulfide [82, 83] approaches or click chemistries such as the azide/alkyne cycloaddition [84] (see section 20.2.3.1 for more details on these reactions). The usage of a CTA with appropriate functionalities on the Z and R groups is the simplest approach to realize this. After radical polymerization, the end groups can then be cyclized by a coupling reaction under very dilute conditions, which is necessary to prevent intermolecular conjugations. As a result of the low concentrations required, the coupling reactions tend to proceed slowly and are thus limited to relatively low molecular of polymers (typically $<30\,000\ \mathrm{g\,mol^{-1}}$).

Cyclic polymers are therefore a synthetically challenging polymeric architecture and while they have received a fair amount of research focus, they are generally less well studied than the other architectures outlined in this chapter.

20.5 Star-Shaped Polymers

A further polymer architecture that can be achieved using RAFT polymerization are star-shaped or star (co)polymers. Here, linear polymers (arms) radiate from a central unit (core) and the properties of such structures can be, similarly to hyperbranched or bottlebrush copolymers, quite different to the linear building block. Star polymers can be classified in two main ways: by their composition or by their synthetic origin. As the focus of this chapter is on synthetic strategies leading to complex polymer architectures, the latter approach will be thoroughly examined, whereas compositional differences in star polymers, such as stars including block copolymers or miktoarm stars will only be discussed briefly.

20.5.1 Methods to Produce Star-Shaped Copolymers

In general, two major strategies to from star-shaped polymers are known: (i) divergent (also described as core-first method) and (ii) convergent (or arm-first method). Both are subdivided in different methodologies, which will be discussed here. It should be mentioned that we restrict the described systems to star polymers that have been polymerized solely by RAFT polymerization, excluding the use of other polymerization techniques.

20.5.1.1 Divergent Synthesis of Star (Co)Polymers

Using this principle, the star-shaped polymer is produced by using a multi-functional core molecule, that is able to initiate a polymerization reaction. In the case of a RAFT polymerization, CTA molecules are immobilized on the core molecule and polymeric arms are subsequently grown from this central multifunctional molecule.

A large variety of structures have been used as core molecules for RAFT-based star polymers including four-armed stars based on aromatic cores or pentaerythritol as initial structural motifs [85], cyclodextrins [86], porphyrins [87], and other molecules (Scheme 20.1) with numbers of arms usually ranging between three and seven [88]. Dendritic or hyperbranched core molecules can be used as well providing an even higher number of initiation sites per core molecule [89]. A comprehensive overview can be found in recent review articles [88, 90]. By attachment of different types of CTA motifs such as trithiocarbonates, dithiobenzoates, or xanthates, and by utilizing different R-groups, various monomer classes can be controlled and incorporated into the shell of the star polymer, ranging from styrenes, (meth)acrylates, (meth)acrylamides, and vinyl esters.

A general advantage of a divergent process compared to a convergent route is the improved control over the number of arms of the final structure, as this variable is

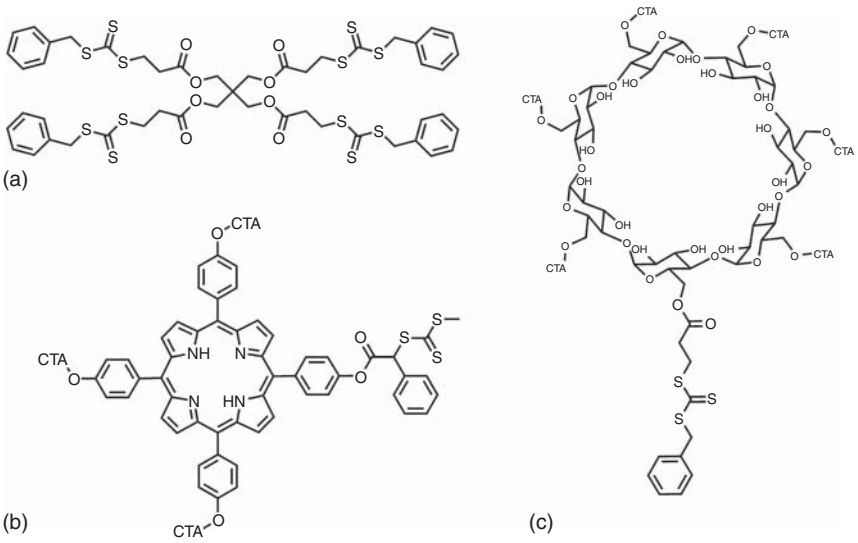

Scheme 20.1 Examples of core molecules carrying different CTAs as basis for the synthesis of star-shaped polymers: (a) pentaerythritol-based CTA [85], (b) porphyrin-based CTA [87], and (c) cyclodextrin-based CTA [86].

predefined by the substitution of the core molecule. Also, the production of linear chains that are not coupled to the core and have to be removed after synthesis is a less drastic problem when using a divergent approach, as linear polymers do not detach from the core during propagation. However, because of the mechanism of the RAFT process, a certain amount of initiator-derived linear chains will still be produced. Disadvantages are that single arms cannot be analysed without detachment from the star polymer after its synthesis, and, that the synthesis of miktoarm stars using solely RAFT-polymerization is not possible.

Using the RAFT methodology and a divergent synthesis approach of star-shaped copolymers, a further variable has to be considered: whether the CTA molecule is attached to the core via its R-group or via the Z-group. Both scenarios lead to different mechanisms during the polymerization process and have different advantages and disadvantages (Figure 20.11).

Using the R-group approach, the leaving group of the CTA, which after fragmentation carries the active radical, is connected to the core molecule. As a result, polymers grow directly from the core outwards and radicals are always centred at the growing polymer star. Using the Z-group approach, the activating group of the CTA is coupled to the core and fragmentation during polymerization will lead to a detachment of the growing chain from its initial core molecule. The polymer chains will subsequently grow in solution and are immobilized again by reaction with core-bound Z-group during the RAFT equilibrium.

A major disadvantage of the R-group approach is the localization of the active radical near the core during chain propagation. This can lead to termination reactions with other star molecules or linear chains, resulting in the loss of an active arm and

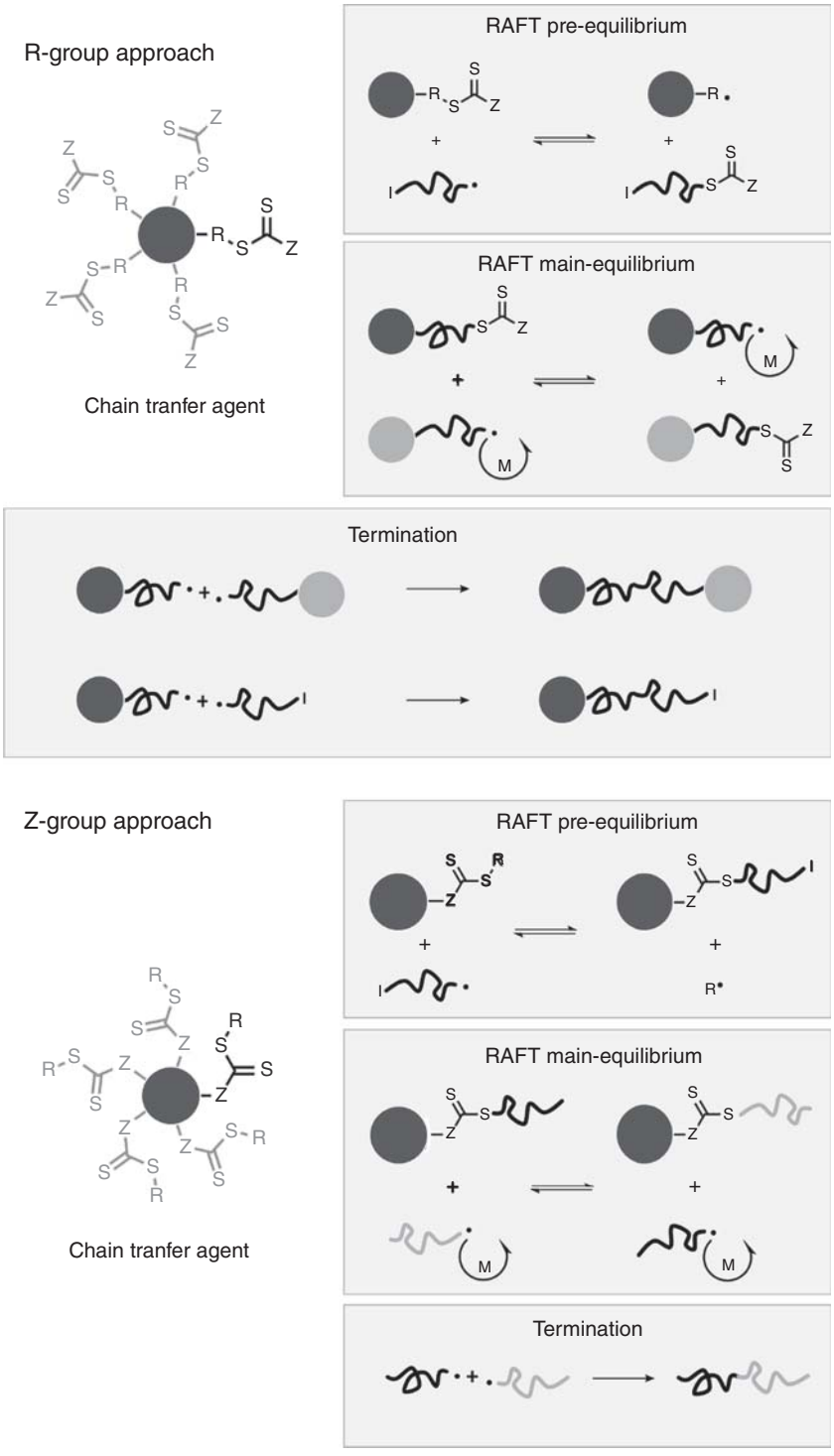

Figure 20.11 Schematic representation of R and Z-group approach in the synthesis of star-shaped polymers using RAFT polymerization.

deviation from the theoretical molecular weight. In particular, star–star coupling can lead to bimodal molecular weight distributions, a problem which increases with concentration and conversion, as well as with the number of arms per core [91]. A general countermeasure to prevent this type of bimolecular coupling is to keep the concentration of radicals as low as possible, which can be ensured by a high ratio of CTA to initiator, or by the use of monomers with a fast propagation rate [91].

Using a Z-group approach, the propagating polymer chains are detached form the core and termination usually leads to the formation of small linear side products, which are easier to remove form the final product.

Thus, relatively high molecular weights can be targeted without a significant broadening of the distribution [92]. A main disadvantage of this method is the necessity of the diffusion of growing chains to the core molecule. Especially when polymer arms have a high degree of polymerization, the radical end group might not be able to access the sterically crowded area near the core molecule, which is further shielded by already attached polymer arms. This effect leads to an increased amount of termination as radicals are not able to participate in the RAFT equilibrium because of steric hindrance of other polymeric arms [93]. In addition, when core molecules with a low number of attached CTAs are used, the side product resulting from bimolecular termination of two linear chains is difficult or even impossible to remove and appears as a shoulder in the molecular weight distribution, increasing the dispersity.

A further point to consider is the stability of the final star copolymer. Using the Z-group approach, polymer arms are connected to the core via the thiocarbonylthio group of the CTA. These molecules are susceptible to degradation by aminolysis, thermolysis, or mechanical stress [94]. Whether this is considered a feature or a flaw is strongly dependent on the envisioned application for the produced star-shaped copolymer.

20.5.1.2 Convergent Synthesis of Star Polymers by RAFT Polymerization

The second major strategy to produce star polymers is the convergent or arm-first method. As the name suggests, the linear polymer arms are produced first and are used to from a star architecture in a second reaction step. One obvious advantage over a divergent approach is the possibility to analyse single arms before incorporation into the final architecture. However, there is usually a broader distribution of the number of arms when compared to a divergent strategy, as multiple linear polymers with non-negligible steric impact have to be coupled to a small-molecule core. Thus, the reactions used for star formation have to be very efficient and, even then, the presence of residual linear polymers can usually not be excluded and the isolation of the final product from the mixture can make this strategy difficult.

In general, one can distinguish between two ways to produce star polymers in a convergent process based on the connection of arms to the core molecule. (i) A second polymerization step can (after initial arm synthesis) be used to connect multiple polymers to a star-like object and (ii) polymers can be reacted onto a multifunctional core molecule by a polymer analogue reaction.

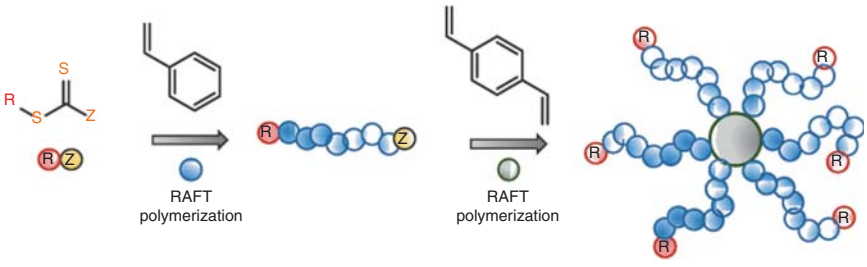

Figure 20.12 Star polymer synthesis by chain extension using a multifunctional monomer to form a cross-linked core – example of styrene and divinyl benzene.

When using RAFT polymerization, the first strategy offers an easy access to star-shaped copolymers as the CTA end groups, located at the chain end of linear arms, can be utilized for star formation, usually using a bis-functional monomer (Figure 20.12). Polymerization in the presence of arms will result in the formation of a highly cross-linked core structure connecting multiple polymers [95]. Compared to divergent methods, the core compartment will be much bigger and it is much harder to control the number of arms. While in general the definition is lower using this convergent strategy, there are many factors influencing the process and careful optimization can lead to the formation of well-defined star copolymers.

One essential parameter is the ratio of crosslinker to CTA. The size of the core, as well as the number of arms, scales with the amount of crosslinker. Low crosslinker/CTA ratios will lead to small star polymer, with a low number of arms and a low yield of the final structure. With increasing crosslinker amount, the core will become bigger and the number of arms will consequently increase [96]. However, above a certain ratio, star–star coupling and eventually gelation will occur [97]. Optimal ratios are often described to be around 10 [96, 98]. The solubility of the crosslinker molecule seems to play an important role as a low solubility in the polymerization medium leads to a preformation of the core by phase segregation, which aids in the synthesis of star polymers and increases the definition of the final product [96]. This can be improved by the application of heterogeneous reaction conditions where linear precursors and crosslinkers are part of a dispersion [97]. This is reported to decrease reaction times drastically while also improving the definition of star copolymers. The core of such systems is however much bigger than in previous examples, resembling a core cross-linked micelle. Also, the length of the polymeric arms plays an important role in this context, which is mainly associated with steric factors. Longer polymer arms are harder to incorporate into a central core and thus the yield of star polymer, as well as the number of incorporated arms decreases with increasing molecular weight of the linear precursor [97, 99]. An interesting example of the arm-first synthetic approach is the Asteric™ viscosity modifier developed by Lubrizol, which is a methacrylate-based star-shaped polymer [100]. Superior shear stability was observed for these additives as a result of the star architecture when compared to standard linear polymeric materials. The multi-ton scale synthesis of this commercial product demonstrates the suitability of the RAFT process in industrial applications for the preparation of complex architectures.

A second convergent strategy to from star-shaped polymers is the use of functional end groups to connect linear polymer arms to a central core molecule. The RAFT methodology is perfectly suited for such an approach as a large variety of functional groups are tolerated by the polymerization, enabling a range of chemistries to be used for the connections. Usually, the R-group of the CTA is used for this type of reaction as it often possesses a functional handle. To ensure a high conversion of core functionalities, highly efficient reactions have to be used and usually, an excess of linear precursor is necessary, which has to be removed afterwards. Still the number of arms is limited as the steric impact of already coupled arms will decrease the probability of further attachment. A few reactions suitable to synthesize star-shaped polymers by this method will briefly be described here.

One example is the use of copper-mediated azide alkyne cycloaddition, which was used to form four-armed star polymers based on an azide functional core and polymers with an alkyne end group, which was introduced by the R-group of the CTA [101]. Another strategy, particularly suited for polymers made by a RAFT process, is the direct use of the dithio-ester function in a hetero hetero-Diels–Alder reaction with a multifunctional diene. As the CTA can be used directly, no further functional group has to be installed on the polymer or the CTA [102]. A further method making direct use of the CTA is the reduction of the thiocarbonylthio end group to the thiol under mild conditions. Thiol end groups can in turn be reached to a multifunctional core, carrying activated double bonds, in a thiol-ene reaction [103]. A special case within this frame is the use of a cross-linkable block instead of a single end group functionality in order to create a star copolymer. This route was for instance followed by functionalization of one block of a diblock copolymer with furan functionalities, followed by the addition of bis-functional maleimides, forming a core structure in a Diels–Alder reaction [104].

20.5.2 Classification by Composition

While so far star polymers have been classified by their origin, a second way to distinguish between them is by their architecture. The majority of star-shaped copolymer discussed so far had only one polymeric component constituting the polymer arm. However, the use of different homopolymers to form the shell or even the use of block copolymers offers new perspective for the design of functional nanomaterials.

One main category is miktoarm stars, which have a mixed shell consisting of different linear polymeric arms. There are only a few ways to produce such structures entirely using RAFT polymerization and the most straight forward method is the mixing of different precursors, followed by star formation by formation of a cross-linked core (Figure 20.13).

Using such a method, the hydrophobicity of different arms plays an important role. Indeed, the amphiphilic balance of linear precursors has a significant impact on the definition of the final star polymer [105]. In this context also, the medium used for the cross-linking reaction and the respective solubilities of the components have to be considered. It has been shown that combinatorial chemistry can be used to create a multitude of different star-shaped copolymers by synthesizing different arms

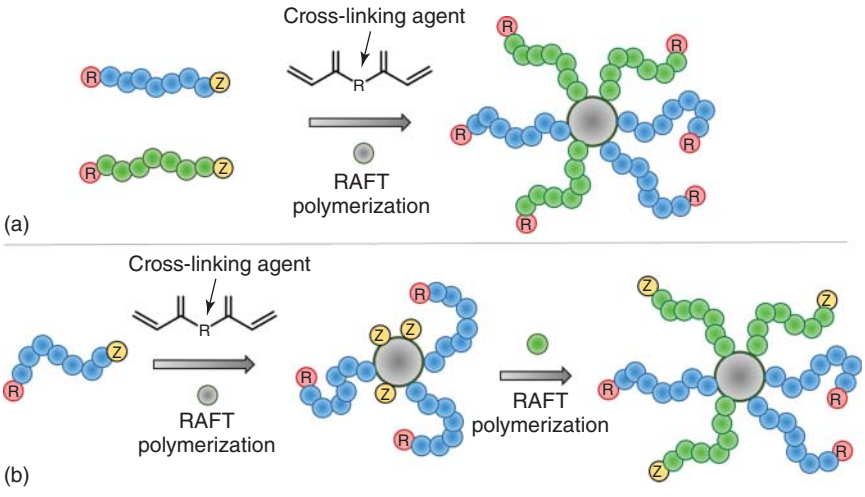

Figure 20.13 Methods to produce miktoarm star copolymer using RAFT polymerization using a convergent approach: (a) mixing of different arms before cross-linking and (b) 'in-out.'

and mixing them in various ratios before cross-linking [106]. Thus, a large number of different structures are accessible and can be screened for various applications. One problem using this method is that different linear precursors might have different probabilities to be incorporated into the star copolymer, based on their steric hindrance or solubility.

A method to create miktoarm stars with a predefined composition is the so-called 'in-out' method. Here, the thiocarbonylthio end groups located in the core of the star polymer after polymerization of a bis-functional monomer are utilized to grow a further linear arm from the cross-linked centre. Here also, the hydrophobicity of the two monomers used can be different without jeopardizing the definition of the final structure [107]. This approach can also be performed combining core formation and growth of the second population of arms in one step. Using the alternating copolymerization of styrene and maleimide (as crosslinker) in the presence of an excess of styrene, which will form homopolymeric arms after the maleimide component is consumed leads to the formation of miktoarm stars [108].

Finally, (multi)block copolymers can be used to create the shell of star-shaped copolymers using the methods as described before in the section on block copolymer synthesis by sequential polymerization steps [98].

20.6 Graft Polymers

Graft polymers are macromolecules composed of a long, linear backbone and polymeric branches attached to the main chain. When the grafts are of uniform length, such structures are often referred to as bottlebrush or comb polymers. The topology of the polymer can range from a comb-like structure to a bottlebrush-like structure

with increasing grafting density, i.e. number of side chains per backbone. High grafting density and long side chains promote extended conformations in both backbone and side chain directions, whereas low grafting densities and short side chains result in Gaussian conformations [109] Moreover, if the relative length of the backbone to the side chain is small, the polymer will appear more star-like [110]. Bottlebrush polymers typically exhibit high intramolecular and intermolecular steric repulsion, resulting in unique intrinsic properties. The architecture has gained a fair amount of attention and has been extensively reviewed in recent literature [111–119]. The structural complexity of the bottlebrush architecture has also been taken a step further by designing bottlebrush polymers into star-like structures [120, 121], networks [109, 122], and dendronized architectures [123].

Three general synthetic strategies are known for bottlebrush synthesis: grafting through, grafting from, and grafting onto (Figure 20.14). RAFT polymerization can be used in all three approaches to yield well-controlled structures. Each approach offers a good control over some structural parameters while setting limitations to others; these include the backbone length, side chain length, and grafting density. For the best results, the aforementioned parameters should be prioritized in order to select the most appropriate approach. The strategies can also be combined to overcome challenges associated with a single technique – that is, grafting from can, for example, be used to complement the grafting through method [124]. The benefits and limitations of each, as well as some practical and mechanistic considerations, are discussed in detail below.

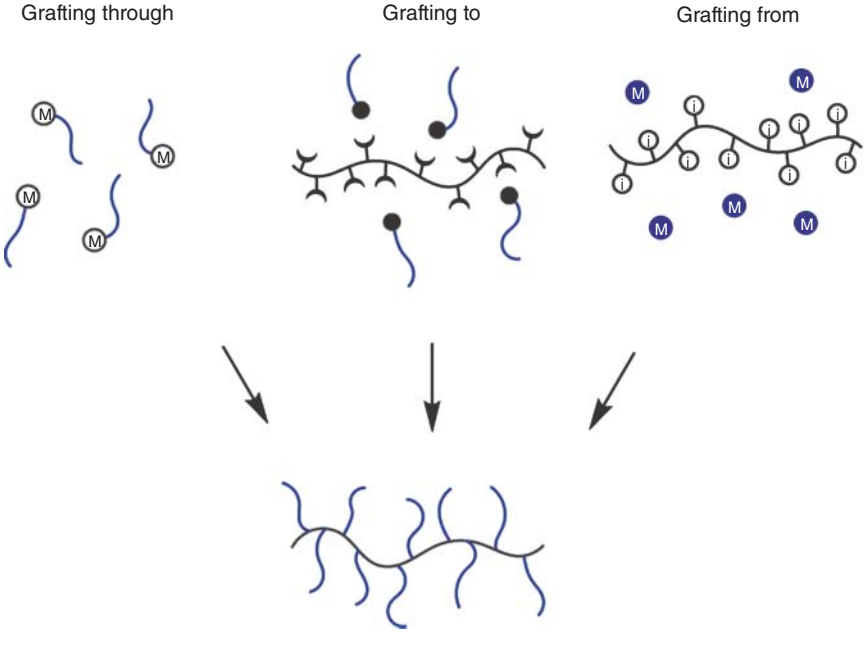

Figure 20.14 Three synthetic pathways used for bottlebrush polymer synthesis.

A popular pathway to bottlebrush synthesis is to use two or more living polymerization techniques to yield the bottlebrush structure. Typically, one is used for the polymerization of the backbone and another for polymerizing the side chains; however, complementary techniques can also be used to yield multiblock and heterograft structures. Various highlighted examples combine RAFT with other living polymerization techniques, such as ATRP and ring-opening metathesis polymerization (ROMP). In doing so, the complex architecture can in some cases be accessed through sequential or even simultaneous monomer addition in one pot using initiator-functionalized monomers. Other strategies for dual polymerizations include the use of post-polymerization methods to functionalize a polymer chain end with a new polymerizable group, and functionalizing polymer side groups with initiator motifs; such polymers can be used to carry out grafting through and grafting from polymerizations, respectively [125]. A combination of polymerization techniques allows the use of a greater variety of monomers than one alone can cover. Moreover, options for one-pot synthesis are more varied.

20.6.1 Grafting Through

In the grafting through approach, a macromonomer is polymerized to yield a bottlebrush-like structure where the side chain length is determined by the size of the macromonomer. Such polymerizations result in bottlebrushes where every repeating unit along the backbone is guaranteed to have a side chain attached to it; the method is thus effective for synthesizing high-density bottlebrushes. A co-monomer can be incorporated in the structure to yield a heterograft bottlebrush or to act as a spacer between the side chains to reduce the density. In such cases, the reactivity ratios of the co-monomers should be carefully considered, as different reactivities may result in gradient polymers. Heterograft block copolymer bottlebrushes are more easily accessible via the grafting through approach than with the other two approaches. The use of a RAFT agent in a grafting through polymerization acts as a means to control the backbone length and yields a bottlebrush with a CTA terminus, available for further chain extensions [126, 127] or post-modification [128]. The grafting through strategy can also be advantageous when thorough characterization of the side chains is required, as this can be carried out before the polymerization step.

A significant advantage of the grafting through approach is its simplicity: when commercially available macromonomers can be used, only one step is required for bottlebrush synthesis. Typical examples of commercial macromonomers used for the RAFT polymerization of bottlebrush-like polymers include acryloyl and methacryloyl-functionalized poly(ethylene glycols) [129, 130] and poly(dimethylsiloxanes) [129, 131], as well as acrylates and methacrylates carrying long aliphatic side groups [132]. Although commercial macromonomers offer the most effortless route to making bottlebrush polymers, only few suitable macromonomers are currently commercially available, and thus, macromonomer synthesis is often required. Macromonomer synthesis can be carried out either by functionalizing a polymer with a polymerizable end group [133] or by employing a monomer-functionalized initiator in the macromonomer polymerization

[134–138]. It is important to note that when RAFT is used in the macromonomer synthesis, a practical upper limit is set for the conversion of the macromonomer into polymer that can be reached in the grafting through step. This is due to some polymer chains inevitably lacking the functionality needed for further polymerization: initiator-derived chains have no R-group functionality at the α-end and terminated chains lack the thiocarbonylthio functionality at the ω-end [139].

The use of two polymerization techniques for grafting through synthesis has proven rather popular: typically, one is used to prepare the macromonomer and another for polymerizing the backbone. A considerable amount of grafting through literature making use of RAFT combines it with ROMP to give an easy access to long backbones with narrow dispersities; however, other polymerization techniques have also been employed [133–138]. By careful consideration of the macromonomer and backbone polymerizations, the two can in some instances be carried out sequentially in one pot, yet such reports are rare [136, 140]. The tolerance of RAFT towards impurities and functional groups makes it a promising candidate for the second step of a one-pot grafting through synthesis; however, polymerization of macromonomers with RAFT can be more challenging than with other living polymerization techniques because of mechanistic reasons.

When the grafting through synthesis of bottlebrush polymers is carried out using RAFT, the main limitations of the method are typical to any RAFT polymerization [141]. In order to have a good control over the reaction, the monomer-to-CTA ratio must remain low enough to limit the time a growing chain spends as a propagating radical. Thus, the method is best used for preparing bottlebrushes with relatively short backbones. The use of a macromonomer instead of a low molecular weight monomer effectively dilutes down the concentration of polymerizable groups in the reaction mixture; this sets a practical upper limit for the initial monomer concentration and therefore for the rate of polymerization. As a result, the concentration of polymerizable groups will be extremely low at high conversions, and the reaction can be difficult to push to completion. Moreover, low initiator concentrations further complicate the polymerization of a slow propagating macromonomer. For the synthesis of long brushes, special reaction conditions – such as feeding – may prove helpful. Overall, RAFT polymerization of macromonomers appears less popular than with other techniques, and the macromonomers tend to be of moderate size. Some of this could be attributed to unfavourable steric factors, as the RAFT mechanism requires a propagating bottlebrush to approach the end group of another. Typical reaction conditions such as low initiator concentration can further render the synthesis challenging. It is also worth noting that RAFT polymers of vinyl macromonomers have been shown to exhibit an equilibrium between the rate of propagation and the rate of depolymerization when heated in the absence of initiator [129].

20.6.2 Grafting Onto

Grafting onto (also known as grafting to) is a modular approach in which the backbone and the side chains of the resulting bottlebrush are prepared separately;

side chains are then attached to the backbone by employing complementary functionalities. The strategy is especially useful for preparing bottlebrush polymers containing functionalities that are not compatible with the desired polymerization techniques. The grafting onto method is suitable for preparing bottlebrushes with long backbones; however, coupling high molecular weight side chains onto the backbone can prove challenging because of steric effects, especially when targeted grafting densities are high. RAFT polymerization of the building blocks opens up possibilities for the preparation of block copolymer and other complex structures, as well as for end-group modification through functionalities in the R- or the Z-group of the CTA [128]. The tolerance of RAFT towards a wide range of functionalities [142] makes it an ideal candidate to be used in the grafting onto strategy. Functional groups needed for the coupling step can, however, limit the functionalities carried by the backbone and side chain monomers.

The most significant challenge in the grafting onto approach is the coupling step, the efficiency of which determines the grafting density of the resulting bottlebrush. Each attachment of a side chain increases shielding effects near the neighbouring reacting sites, and the attachment of subsequent side chains becomes sterically more challenging. The effect is more pronounced with long grafts; thus, side chain length sets a practical upper limit for the grafting density [143]. Despite the challenges, high grafting densities have been reported. A typical synthetic route involves the use of nucleophilic substitution reactions [144, 145] or click chemistry, such as copper-catalysed azide–alkyne [146–149] or Diels–Alder [150] cycloadditions. Catalytic reactions can potentially benefit from the proximity of the subsequent reacting group, as demonstrated by Gan et al. [146]

Steric hindrance near the reacting site can be reduced by employing a backbone monomer with a relatively long side group; the side group will act as a spacer between the backbone and the reacting group, and thus neighbouring reactive sites will be more spread out. Crowdedness near the reacting site can also be reduced by introducing a comonomer, thus making a bottlebrush with a reduced grafting density. Similar to the grafting through strategy, an incomplete coupling step can complicate purification, as the unconjugated side chains must be separated from the bottlebrush. Typically, an excess of side chains is used to drive the coupling step to high conversions. Efficient coupling chemistries result in less linear polymer in the product.

20.6.3 Grafting From

In the grafting from approach, the bottlebrush is synthesized by first preparing a backbone with pendent initiator functionalities that can then be used to polymerize the side chains. When RAFT polymerization is used for polymerizing the side chains, these functionalities are CTA moieties that can be tethered to the backbone either by the R- or Z-group. This strategy can be seen as complementary to the grafting through approach in that it provides an excellent control over the backbone composition in exchange for reduced control of the side chains. The approach is useful for making high-density bottlebrush polymers with long backbones and side

chains – a combination that can be difficult to achieve through other strategies. The backbone composition can be constructed in the same manner as any linear polymer prepared through RAFT polymerization, and the side chains can be further chain-extended multiple times after the initial bottlebrush has been prepared. This allows for an immense level of structural complexity to be achieved through sequential monomer additions. To demonstrate this, Kerr et al. reported the three-step synthesis of a bottlebrush polymer comprising 29 separate domains across the backbone and side chain regions [151]. Furthermore, heterograft structures can be achieved by carrying out multiple grafting steps with different polymerization techniques, as reported by Bolton and Rzayev [152]. The terminal CTA units in the grafts can also act as reacting sites for further functionalization. Low-density bottlebrushes can be easily made by incorporating a co-monomer in the backbone from which no side chains will be grown.

Whether the CTA is attached to the backbone via the Z- or the R-group makes a considerable difference in the dynamics of the side chain polymerization (Figure 20.15). When the CTA is attached via the Z-group (Z-group approach; also known as transfer to [153]), the side chain detaches from the backbone to propagate. Thus, the approach is mechanistically similar to the grafting onto technique. As side chains grow longer, shielding effects near the thiocarbonylthio group grow greater, making the addition of a propagating chain back to the CTA on the main chain more challenging. This can result in a reduced grafting density, a broad size distribution of the grafts, and a secondary linear side product – in addition to initiator-derived chains [137]. In the Z-group approach, intermolecular brush–brush coupling and

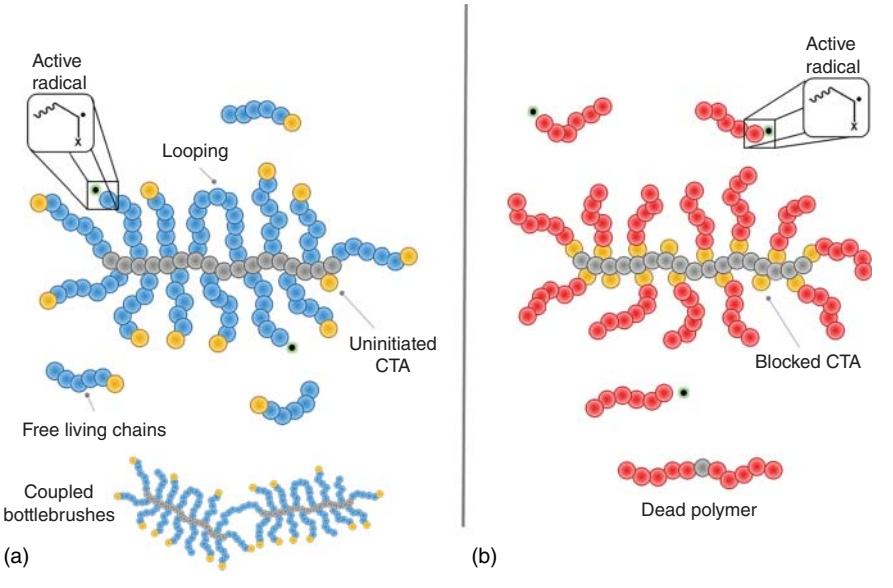

Figure 20.15 Comparison of the grafting from R- and Z-group approaches. (a) The R-group grafting from approach. (b) The Z-group grafting from approach.

intramolecular side chain coupling reactions encountered in the R-group approach are absent for mechanistic reasons.

When the CTA is tethered to the backbone via the R-group (R-group approach), the propagating chain stays attached to the backbone. The radical can transfer intramolecularly to an adjacent CTA or intermolecularly to a CTA of another molecule, allowing for better control over chain growth than in the Z-group approach. The R-group approach can, however, suffer from bi-radical brush–brush coupling reactions, manifested as a high molecular weight species or gelation of the product. The problem is especially pronounced in the preparation of high-density bottlebrushes and when high backbone concentrations are used, and the effect typically escalates at high monomer conversions. Furthermore, if the intermolecular transfer of active radicals is sparse, the bottlebrushes with more active radicals will grow faster, leading to broad molecular weight distributions. The addition of a small amount of free CTA, or shuttle-CTA, in the system has been shown to enhance radical transfer between growing bottlebrushes, as well as suppress brush–brush coupling [151, 154]. The effect is a result of an increased probability of radicals getting transferred from a bottlebrush to another with the assistance of small molecular weight linear chains. In doing so, a linear CTA-derived side product will be found in the product; however, it can be removed by selective precipitation methods. Of all the synthetic strategies discussed above, the grafting from R-group approach is superior for making bottlebrushes with long side chains.

For the preparation of a CTA-decorated bottlebrush backbone, the coupling of CTA onto the monomer can be carried out either before [155, 156] or after [151, 154, 157, 158] the backbone polymerization. Coupling onto a polymer chain can typically be expected to be more challenging than coupling reactions between two small molecules; the same applies for the characterization and purification of the resulting product. Here, thorough purification is of high importance as traces of uncoupled CTA result in a shuttle CTA effect, yielding a linear side product during the grafting step. In order to achieve a bottlebrush structure by using a CTA-functionalized monomer, the monomer should not add to the coupled CTA during the backbone polymerization; addition of functionalized monomer to itself results in hyperbranched structures (see section 20.7.1). It follows that when RAFT is used to polymerize both the backbone and the side chains, coupling onto the backbone is the standard approach; polymerization of a CTA-functionalized monomer requires a special strategies. Orthogonality can be achieved by combining RAFT with other polymerization techniques, such as ROMP, ATRP, NMP, or cationic polymerization [159–163]. RAFT polymerization in both the backbone and the side chain direction using a CTA-functionalized monomer in one pot was recently reported using selective photoactivation of the backbone and side chain CTAs [155, 156].

In the grafting from approach characterization of the side chains is more challenging than in the other two strategies. The investigation of the initiation efficiency of the pendant CTAs and a closer look at the side chains requires their cleavage off the backbone. Moreover, any initiated CTAs cause deviation between the targeted and

resulting side chain degree of polymerizations (DPs). Studies of side chain cleavage can be found in the literature [137, 151, 164]. The Z-group approach can potentially provide an easier route for removing the grafts through aminolysis or other degradation of the thiocarbonyl thio-group, whereas for the R-group approach, harsher reaction conditions are often required. Determination of the final grafting density can prove difficult, as it arises from an interplay between the initial CTA density on the backbone, reinitiation efficiency, and termination events – and in the Z-group approach, steric shielding effects.

20.6.4 General Guidelines

RAFT polymerization of graft polymers can yield highly complex structures. The successful preparation of well-defined polymers requires the selection of an appropriate synthetic pathway, as each of the three general approaches has its strengths and limitations.

The simplest route for making bottlebrush polymers using RAFT polymerization is to use the grafting through approach with commercial macromonomers. RAFT polymerization can also be utilized in the macromonomer synthesis. It is the only approach where every repeating unit along the main chain is guaranteed to have a side chain attached to it, making it a viable option for the preparation of high-density bottlebrushes. However, only moderate backbone DPs can be achieved whilst retaining low dispersity of the resulting polymer because of the limited concentration of reactive groups in the reaction mixture. The problem of low concentration can potentially be overcome by monomer feeding. The side chains of the resulting bottlebrush are as well defined as the macromonomer and can be characterized separately from the bottlebrush without the need for their detachment. Low monomer conversions can lead to tedious purification processes of the product.

For the preparation of bottlebrush polymers with long backbones, the grafting onto and grafting from approaches are more suitable. Both methods allow for the backbone to be as long as any linear polymer made by RAFT polymerization. If long side chains are also required, the grafting from approach is more appropriate than the grafting onto approach, as the coupling step of the grafting onto approach can suffer from steric shielding effects near the reacting site. In the grafting onto synthesis, an excess of side chains may be required to achieve high grafting densities, and any uncoupled side chains require their removal to yield an isolated bottlebrush product. Using this modular approach, both the backbone and the side chains can be characterized separately before the coupling step.

While the grafting from the R-group approach is the superior method for making bottlebrush polymers with long backbones, long side chains, and high grafting densities, careful consideration of reaction conditions is needed to minimize brush–brush coupling. The coupling reactions can be suppressed through the addition of a low molecular weight shuttle-CTA into the side chain polymerization, and by quenching, the reaction before full monomer conversion is reached. The use of a free CTA in the polymerization results in a linear side product. Characterization of the side

chains requires their cleavage off the backbone. Moreover, the grafting from the synthesis of bottlebrush polymers requires a large amount of CTA to be used and yields a product with high CTA content, which can potentially be an undesirable property for certain applications.

20.7 Hyperbranched Polymers

Hyperbranched polymers are an attractive class of polymeric architecture because of their highly branched and globular, three-dimensional structure. From drug and gene delivery [165] to oil additives, these materials have found a use in a wide range of fields. The history of hyperbranched polymers is one as long as synthetic polymerization itself, with the first reported hyperbranched structure originating at the end of the nineteenth century, 20 years before Staudinger's report 'Über Polymerization' [166]. Step growth polymerization of AB_n ($n \geq 2$) monomers has been the focus of a significant portion of the studies into the preparation of hyperbranched polymers. Whilst this is a facile method for the synthesis of this polymer class, radical polymerization offers a scalable and efficient route towards highly functional polymers. Combining this with controlled radical polymerization (CRP) techniques such as RAFT or ATRP, the ability to finely tune the architecture of the resulting hyperbranched polymers can be realized.

One common challenge in the preparation of hyperbranched polymers is the avoidance of macroscopic gelation. This can be readily overcome by employing CRP and in particular RAFT polymerization because of the low concentration of radicals at a time. Whilst CTAs are generally used to control the polymerization and reduce dispersity, when applied to hyperbranched systems, their function is to primarily hinder gelation. Employment of CTAs has the added benefit of introducing functional handles to the surface of the polymer and allowing for degradable bonds to be positioned within the polymeric structure.

20.7.1 Self-condensing Vinyl Polymerization

First described by Fréchet et al. [167], SCVP is a method for synthesizing dendritic polymers by the polymerization of a vinyl monomer containing a pendent group capable of initiating further polymerization. These *inimers* can either be homopolymerized or copolymerized with other vinyl monomers to form highly branched polymeric structures. Defined as AB* monomers, upon activation, the B group is transformed to initiate further polymerization and branching. This is traditionally achieved by using a monomer containing a vinyl group and an alkyl halide bond. However, CRP was readily applied to the system by replacement of alkyl halides with CTAs such as nitroxides (NMP) or thiocarbonylthiols (RAFT/MADIX) [168]. Employing the use of CTAs offers several advantages: reduction of radical concentration – disfavouring macroscopic gel formation, control over the location and density of branching points, and post-polymerization modification by end group removal [128].

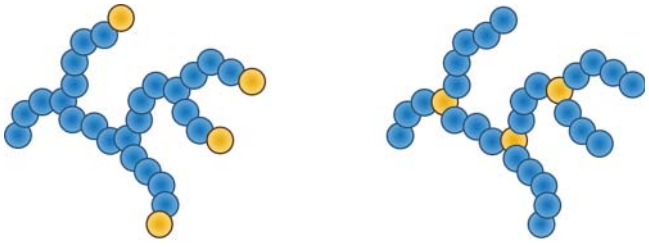

Figure 20.16 Positioning of the thiocarbonylthio group in a polymeric architecture obtained by SCVP depending on the polymer being prepared via (a) the R- or (b) the Z-group approach.

For RAFT-SCVP, an *inimer* is formed by modification of a RAFT agent to include a vinyl group capable of polymerization. The vinyl group can be attached via the R- or Z-group of the RAFT agent, with the site of attachment leading to structural differences (Figure 20.16). As with traditional RAFT polymerization, the choice of R- and Z-groups dictates the monomer families able to be polymerized in a controlled fashion. Trithiocarbonates, xanthates, and even selenium-based RAFT agents have all been transformed to *inimers* for RAFT-SCVP and copolymerized with an exhaustive list of monomers [168]. The vast majority of *inimers* reported in the literature focused on the modification of the R-group, with only a few reporting Z-group modification. One could postulate that this is due to the ease of R-group modification, especially for carboxylic acid containing RAFT agents, with esterification being a common and facile route. However, this disparity could be due to the structural differences between the resulting polymers. Modification of the R-group results in the thiocarbonylthio positioned at the polymer chain end, whereas Z-group modification leads to positioning of this functionality at the branching points within the polymer. Because of the susceptibility of this motif to degradation (i.e. aminolysis or reduction), this could be seen as an advantage or disadvantage, depending on the required properties.

Polymer growth is mediated by two pathways in RAFT-SCVP: propagation of the vinyl group and chain transfer to the thiocarbonylthio moiety. Backbone formation is governed by vinyl group propagation of the *inimer* and, if present, comonomer, whereas branching is introduced by chain transfer to the thiocarbonylthio groups incorporated into the backbone, followed by re-initiation and further propagation. Copolymerization of *inimers* with monovinyl monomers allows for control over the branching density and is also used for the introduction of functionality into the polymer. The relative reactivity of the *inimer* and monomer requires consideration as differences in reactivity can heavily influence the distribution and location of the branching points.

Because of the versatility of the RAFT process, a wide range of comonomers have been applied to RAFT-SCVP. Monomers such as NIPAM have been commonly incorporated to introduce temperature responsiveness to the polymer [169, 170].

pH [171, 172], redox [173], and enzyme [172] responsive systems have all been applied to RAFT-SCVP by copolymerization of appropriate monomers.

Functionality can also be introduced into the *inimer* structure. Wei et al. reported the synthesis and use of an enzyme-responsive *inimer* for mediating the polymerization of *N*-(2-hydroxypropyl)methacrylamide [172]. In the presence of the enzyme papain, these hyperbranched polymers were degraded into smaller polymeric units.

For a detailed overview of RAFT-SCVP and the applications of the resulting polymers, please refer to the following reviews [168, 174].

20.7.2 Copolymerization of Multifunctional Monomers

The synthesis of hyperbranched polymers can also be achieved by copolymerization of a monovinyl monomer with a multivinyl monomer. In a radical copolymerization, macroscopic gel formation will occur when the number of divinyl monomers per chain exceeds one.[165] Use of a CTA allows for an increase in divinyl monomer incorporation whilst avoiding macroscopic gel formation. This was first reported by Sherrington in what is now known as the 'Strathclyde route'. [175] It was demonstrated that by addition of 1-dodecanthiol (DDT) to the polymerization mixture, macroscopic gel formation could be avoided, whereas in the absence of DDT, gel formation was observed.

Because of the high availability of multifunctional monomers and the avoidance of *inimer* synthesis, the preparation of hyperbranched polymers via this method is straightforward and accessible. It also readily allows for the introduction of stimuli-responsive crosslinkers, allowing for the preparation of a wide range of responsive materials.

With the Strathclyde route using irreversible chain transfer, Perrier and coworkers were the first to employ the use of a RAFT agent to control the copolymerization of multifunctional monomers [176]. Initially focusing on the copolymerization of methyl methacrylate (MMA) and ethylene glycol dimethacrylate (EGDMA), variation of the CTA/EGDMA ratio was studied. Because of the lower radical concentration in RAFT polymerization, an increase in cross-linking density is able to be achieved without macroscopic gelation. A CTA/EGDMA ratio of 1 exhibited no macroscopic gel formation, even at 100% monomer conversion. However, by increasing the CTA/EGDMA ratio to 2, beyond the theoretical limit determined by Flory, gel formation was observed, although only at high monomer conversion (>95%).

Following on from their initial study, Perrier and coworkers conducted a series of reactions to investigate the influence of reaction parameters on the obtained hyperbranched polymers [177]. By increasing the ratio of crosslinker to CTA, higher MW polymers were obtained; however, one has to be careful when increasing the crosslinker concentration as to avoid gelation. If the ratio of crosslinker to CTA is kept constant, but the comonomer concentration is increased, then the observed MW also increases. This parallels traditional RAFT as the $[M]_0 : [\mathrm{CTA}]_0$ determines the chain length, and subsequently, the MW. Kinetic studies reveal that whilst the crosslinker is statistically incorporated into the polymer throughout the

polymerization, the physical cross-linking tends to take place at high monomer conversion. This is evidenced by an initial linear evolution in MW, followed by a rapid increase towards high conversions, and can be explained by the relative concentrations of vinyl bonds. The concentration of pendent vinyl bonds capable of cross-linking the polymer chains is low compared to that of the comonomer, which will therefore preferentially react first. As the reaction proceeds, the relative concentration increases, thereby increasing the likelihood of cross-linking. By increasing the ratio of a crosslinker relative to comonomer, the cross-linking will take place at lower concentrations.

The solubility of the crosslinker can also affect the resulting hyperbranched structure. Use of a hydrophobic crosslinker and hydrophilic monomer in an aqueous system results in 'star-like' polymers with a cross-linked core (See section 20.5.1.2).

Copolymerization of a degradable crosslinker by Pal et al. gave useful insights into the controlled nature of the RAFT-mediated copolymerization of multifunctional monomers [178]. Basic degradation of a dilactone crosslinker and subsequent analysis of the resulting chains revealed that the hyperbranched polymers were composed of linear chains with narrow dispersities. This was further confirmed by Rosselgong et al. who carried out a similar study with a disulfide cross-linked polymer [179]. Reduction of the disulfides and subsequent analysis of the polymer chains revealed well-controlled linear chains, analogous to those synthesized in the absence of a crosslinker.

From these studies, one can assume that hyperbranched polymers consist of primary chains with dispersity and molecular weight equal to those obtained from the polymerization in the absence of a crosslinker. Therefore, it is possible to calculate the number of branching units incorporated, n_b, using Eq. (20.3) [180].

$$n_b = \frac{M_{n,b}}{M_{n,l}} - 1 \tag{20.3}$$

$M_{n,b}$ is the number-average molecular weight of the branched polymer and $M_{n,l}$ is the number-average molecular weight of the primary linear chain.

RAFT polymerization has also been applied to the homopolymerization of multifunctional monomers such as divinylbenzene (DVB) [181]. In conventional radical polymerization of DVB, gelation is observed at 15% monomer conversion; however, by addition of a RAFT agent, this can be delayed to 68%. Linear chains consisting of pendent vinyl bonds are initially formed, before cross-linking to form a highly branched network. The same phenomenon was observed when using a poly(methyl acrylate) macroRAFT agent; however, the point of gelation occurred earlier, at 37% monomer conversion.

20.7.3 Alternative Methods of Hyperbranched Synthesis

As discussed above, classically hyperbranched polymers were synthesized via the step growth polymerization of AB_n-type ($n \geq 2$) monomers. Thiocarbonylthios can be considered to be masked thiols; therefore, with simple deprotection (i.e. aminolysis), a polymer prepared by RAFT polymerization can be transformed into

an AB_2-type monomer. Introduction of a B_2 functionality to the R-group is straightforward, with the introduction of di-bromide [182], 2,2′-dipyridyl disulfide [183], or alkynes [184] being reported in the literature. Preparation of hyperbranched polymers via this convergent method allows for greater control over the linear polymer between the branching points, with the chain length determined before cross-linking. It would also enable the introduction of greater structural variation into the hyperbranched polymer, for example, by use of multiblock copolymers.

20.7.4 General Guidelines

If one is attempting to synthesize hyperbranched polymers, the best method developed so far is that of multifunctional monomer copolymerization. Hyperbranched polymers can be readily achieved through the copolymerization of commercially available monomers, removing the synthetic steps required in the other methods described, e.g. *inimer* synthesis. However, this method does not offer the best control over the backbone of the hyperbranched polymer. If fine structural control is required, then modification of a RAFT agent to include AB_n-functionality is preferred. Ultimately, the choice of synthetic route comes down to the required properties of the resulting hyperbranched polymer.

20.8 Conclusion

RAFT polymerization has developed as one of the most versatile techniques to generate polymeric architectures, whose complexity spans from diblock copolymers to multifunctional macromolecules such as graft, star, and hyperbranched copolymers. Its popularity among chemists not only comes from its versatility in the materials it generates but also from the simplicity of the process, which can be relatively easily scaled up, as illustrated by the few examples of large-scale industrial productions. The field continues to expand, through contribution on the one hand from polymer chemists aiming at developing new synthetic methodologies, complex architectures, and simpler process for product scale up and on the other hand from scientists seeking specific architecture for a given application, being in the medical field, materials science, and so on. Its simple setup and the commercial availability of all reactants that make RAFT the technique of choice for scientists of any background to obtain complex architectures that until now were only reachable by skilled chemists.

Acknowledgements

The Royal Society Wolfson Merit Award (WM130055; S.P.), Monash-Warwick Alliance (S.P.), the German Research Foundation (DFG, GZ: HA 7725/1-1; M.H.), and Lubrizol (S.H., A.K.) are acknowledged for financial support.

References

1 Moad, G., Rizzardo, E., and Thang, S.H. (2013). RAFT polymerization and some of its applications. *Chem–An Asian J.* 8 (8): 1634–1644.

2 Perrier, S., Barner-Kowollik, C., Quinn, J.F. et al. (2002). Origin of inhibition effects in the reversible addition fragmentation chain transfer (RAFT) polymerization of methyl acrylate. *Macromolecules* 35 (22): 8300–8306.

3 McLeary, J., McKenzie, J., Tonge, M. et al. (2004). Initialisation in RAFT-mediated polymerisation of methyl acrylate. *Chem. Commun.* 17: 1950–1951.

4 Moad, G., Chong, Y., Postma, A. et al. (2005). Advances in RAFT polymerization: the synthesis of polymers with defined end-groups. *Polymer* 46 (19): 8458–8468.

5 Destarac, M., Charmot, D., Franck, X., and Zard, S. (2000). Dithiocarbamates as universal reversible addition-fragmentation chain transfer agents. *Macromol. Rapid Commun.* 21 (15): 1035–1039.

6 Benaglia, M., Chiefari, J., Chong, Y.K. et al. (2009). Universal (switchable) RAFT agents. *J. Am. Chem. Soc.* 131 (20): 6914–6915.

7 Keddie, D.J., Guerrero-Sanchez, C., Moad, G. et al. (2011). Switchable reversible addition–fragmentation chain transfer (RAFT) polymerization in aqueous solution, *N*,*N*-dimethylacrylamide. *Macromolecules* 44 (17): 6738–6745.

8 Keddie, D.J., Guerrero-Sanchez, C., Moad, G. et al. (2012). Chain transfer kinetics of acid/base switchable *N*-aryl-*N*-pyridyl dithiocarbamate RAFT agents in methyl acrylate, *N*-vinylcarbazole and vinyl acetate polymerization. *Macromolecules* 45 (10): 4205–4215.

9 Dommanget, C., D'Agosto, F., and Monteil, V. (2014). Polymerization of ethylene through reversible addition–fragmentation chain transfer (RAFT). *Angew. Chem. Int. Ed.* 53 (26): 6683–6686.

10 Engelis, N.G., Anastasaki, A., Nurumbetov, G. et al. (2017). Sequence-controlled methacrylic multiblock copolymers via sulfur-free RAFT emulsion polymerization. *Nat. Chem.* 9 (2): 171.

11 Krstina, J., Moad, G., Rizzardo, E. et al. (1995). Narrow polydispersity block copolymers by free-radical polymerization in the presence of macromonomers. *Macromolecules* 28 (15): 5381–5385.

12 Uchiyama, M., Satoh, K., and Kamigaito, M. (2015). Cationic RAFT polymerization using ppm concentrations of organic acid. *Angew. Chem. Int. Ed.* 54 (6): 1924–1928.

13 Sugihara, S., Konegawa, N., and Maeda, Y. (2015). HCl· Et_2O-catalyzed metal-free RAFT cationic polymerization: one-pot transformation from metal-free living cationic polymerization to RAFT radical polymerization. *Macromolecules* 48 (15): 5120–5131.

14 Guerre, M., Uchiyama, M., Folgado, E. et al. (2017). Combination of cationic and radical RAFT polymerizations: a versatile route to well-defined poly (ethyl vinyl ether)-block-poly (vinylidene fluoride) block copolymers. *ACS Macro Lett.* 6 (4): 393–398.

15 Kottisch, V., Michaudel, Q., and Fors, B.P. (2016). Cationic polymerization of vinyl ethers controlled by visible light. *J. Am. Chem. Soc.* 138 (48): 15535–15538.

16 Peterson, B.M., Kottisch, V., Supej, M.J., and Fors, B.P. (2018). On demand switching of polymerization mechanism and monomer selectivity with orthogonal stimuli. *ACS Central Sci.* 4 (9): 1228–1234.

17 Mayadunne, R.T., Rizzardo, E., Chiefari, J. et al. (2000). Living polymers by the use of trithiocarbonates as reversible addition–fragmentation chain transfer (RAFT) agents: ABA triblock copolymers by radical polymerization in two steps. *Macromolecules* 33 (2): 243–245.

18 Liu, Y. and Cavicchi, K.A. (2009). Reversible addition fragmentation chain transfer (RAFT) polymerization with a polymeric RAFT agent containing multiple trithiocarbonate groups. *Macromol. Chem. Phys.* 210 (19): 1647–1653.

19 Ebeling, B. and Vana, P. (2011). Multiblock copolymers of styrene and butyl acrylate via polytrithiocarbonate-mediated RAFT polymerization. *Polymers* 3 (2): 719–739.

20 Hong, J., Wang, Q., and Fan, Z. (2006). Synthesis of multiblock polymer containing narrow polydispersity blocks. *Macromol. Rapid Commun.* 27 (1): 57–62.

21 Wu, Y. and Wang, Q. (2010). One-pot synthesis of well-defined multiblock polymer: combination of ATRP and RAFT polymerization involving cyclic trithiocarbonate. *J. Polym. Sci., Part A: Polym. Chem.* 48 (11): 2425–2429.

22 Bai, W., Zhang, L., Bai, R., and Zhang, G. (2008). A very useful redox initiator for aqueous RAFT polymerization of *N*-isopropylacrylamide and acrylamide at room temperature. *Macromol. Rapid Commun.* 29 (7): 562–566.

23 Martin, L., Gody, G., and Perrier, S. (2015). Preparation of complex multiblock copolymers via aqueous RAFT polymerization at room temperature. *Polym. Chem.* 6 (27): 4875–4886.

24 Ran, R., Yu, Y., and Wan, T. (2007). Photoinitiated RAFT polymerization in the presence of trithiocarbonate. *J. Appl. Polym. Sci.* 105 (2): 398–404.

25 Otsu, T., Matsunaga, T., Kuriyama, A., and Yoshioka, M. (1989). Living radical polymerization through the use of iniferters: controlled synthesis of polymers. *Eur. Polym. J.* 25 (7-8): 643–650.

26 Wang, H., Li, Q., Dai, J. et al. (2013). Real-time and in situ investigation of "living"/controlled photopolymerization in the presence of a trithiocarbonate. *Macromolecules* 46 (7): 2576–2582.

27 Xu, J., Shanmugam, S., Duong, H.T., and Boyer, C. (2015). Organo-photocatalysts for photoinduced electron transfer-reversible addition–fragmentation chain transfer (PET-RAFT) polymerization. *Polym. Chem.* 6 (31): 5615–5624.

28 Xu, J., Jung, K., Atme, A. et al. (2014). A robust and versatile photoinduced living polymerization of conjugated and unconjugated monomers and its oxygen tolerance. *J. Am. Chem. Soc.* 136 (14): 5508–5519.

29 McKenzie, T.G., Fu, Q., Wong, E.H. et al. (2015). Visible light mediated controlled radical polymerization in the absence of exogenous radical sources or catalysts. *Macromolecules* 48 (12): 3864–3872.

30 Fu, C., Xu, J., Tao, L., and Boyer, C. (2014). Combining enzymatic monomer transformation with photoinduced electron transfer – reversible addition-fragmentation chain transfer for the synthesis of complex multiblock copolymers. *ACS Macro Lett.* 3 (7): 633–638.

31 Thomas, D.B., Convertine, A.J., Hester, R.D. et al. (2004). Hydrolytic susceptibility of dithioester chain transfer agents and implications in aqueous RAFT polymerizations. *Macromolecules* 37 (5): 1735–1741.

32 Scales, C.W., Vasilieva, Y.A., Convertine, A.J. et al. (2005). Direct, controlled synthesis of the nonimmunogenic, hydrophilic polymer, poly(*N*-(2-hydroxypropyl) methacrylamide) via RAFT in aqueous media. *Biomacromolecules* 6 (4): 1846–1850.

33 Chong, B., Moad, G., Rizzardo, E. et al. (2006). Thermolysis of RAFT-synthesized poly(methyl methacrylate). *Aust. J. Chem.* 59 (10): 755–762.

34 Vana, P., Albertin, L., Barner, L. et al. (2002). Reversible addition–fragmentation chain-transfer polymerization: unambiguous end-group assignment via electrospray ionization mass spectrometry. *J. Polym. Sci., Part A: Polym. Chem.* 40 (22): 4032–4037.

35 Gody, G., Maschmeyer, T., Zetterlund, P.B., and Perrier, S. (2013). Rapid and quantitative one-pot synthesis of sequence-controlled polymers by radical polymerization. *Nat. Commun.* 4: 2505.

36 Valdebenito, A. and Encinas, M.V. (2010). Effect of solvent on the free radical polymerization of *N*,*N*-dimethylacrylamide. *Polym. Int.* 59 (9): 1246–1251.

37 Gody, G., Maschmeyer, T., Zetterlund, P.B., and Perrier, S. (2014). Pushing the limit of the RAFT process: multiblock copolymers by one-pot rapid multiple chain extensions at full monomer conversion. *Macromolecules* 47 (10): 3451–3460.

38 Vandenbergh, J., de Moraes Ogawa, T., and Junkers, T. (2013). Precision synthesis of acrylate multiblock copolymers from consecutive microreactor RAFT polymerizations. *J. Polym. Sci., Part A: Polym. Chem.* 51 (11): 2366–2374.

39 Baeten, E., Haven, J.J., and Junkers, T. (2017). RAFT multiblock reactor telescoping: from monomers to tetrablock copolymers in a continuous multistage reactor cascade. *Polym. Chem.* 8 (25): 3815–3824.

40 Bartels, J.W., Cauët, S.I., Billings, P.L. et al. (2010). Evaluation of isoprene chain extension from PEO macromolecular chain transfer agents for the preparation of dual, invertible block copolymer nanoassemblies. *Macromolecules* 43 (17): 7128–7138.

41 Warren, N.J., Mykhaylyk, O.O., Mahmood, D. et al. (2014). RAFT aqueous dispersion polymerization yields poly (ethylene glycol)-based diblock copolymer nano-objects with predictable single phase morphologies. *J. Am. Chem. Soc.* 136 (3): 1023–1033.

42 Pai, T.S., Barner-Kowollik, C., Davis, T.P., and Stenzel, M.H. (2004). Synthesis of amphiphilic block copolymers based on poly (dimethylsiloxane) via fragmentation chain transfer (RAFT) polymerization. *Polymer* 45 (13): 4383–4389.

43 Duong, T.H., Bressy, C., and Margaillan, A. (2014). Well-defined diblock copolymers of poly(*tert*-butyldimethylsilyl methacrylate) and poly(dimethylsiloxane) synthesized by RAFT polymerization. *Polymer* 55 (1): 39–47.

44 Crossland, E.J., Cunha, P., Scroggins, S. et al. (2010). Soft-etch mesoporous hole-conducting block copolymer templates. *ACS Nano* 4 (2): 962–966.

45 Saetung, N., Campistron, I., Pascual, S. et al. (2011). Synthesis of natural rubber-based telechelic *cis*-1,4-polyisoprenes and their use to prepare block copolymers via RAFT polymerization. *Eur. Polym. J.* 47 (5): 1151–1159.

46 Chen, M., Häussler, M., Moad, G., and Rizzardo, E. (2011). Block copolymers containing organic semiconductor segments by RAFT polymerization. *Org. Biomol. Chem.* 9 (17): 6111–6119.

47 Magenau, A.J., Martinez-Castro, N., Savin, D.A., and Storey, R.F. (2009). Polyisobutylene RAFT CTA by a click chemistry site transformation approach: synthesis of poly (isobutylene-*b*-*N*-isopropylacrylamide). *Macromolecules* 42 (21): 8044–8051.

48 Espeel, P. and Du Prez, F.E. (2014). "Click"-inspired chemistry in macromolecular science: matching recent progress and user expectations. *Macromolecules* 48 (1): 2–14.

49 Harvison, M.A. and Lowe, A.B. (2011). Combining RAFT radical polymerization and click/highly efficient coupling chemistries: a powerful strategy for the preparation of novel materials. *Macromol. Rapid Commun.* 32 (11): 779–800.

50 Ting, S.S., Granville, A.M., Quémener, D. et al. (2007). RAFT chemistry and Huisgen 1,3-dipolar cycloaddition: a route to block copolymers of vinyl acetate and 6-*O*-methacryloyl mannose? *Aust. J. Chem.* 60 (6): 405–409.

51 Huang, Y., Hou, T., Cao, X. et al. (2010). Synthesis of silica-polymer hybrids by combination of RAFT polymerization and azide-alkyne cycloaddition 'click' reactions. *Polym. Chem.* 1 (10): 1615–1623.

52 Xue, X., Zhu, J., Zhang, Z. et al. (2010). Synthesis and characterization of azobenzene-functionalized poly (styrene)-*b*-poly (vinyl acetate) via the combination of RAFT and "click" chemistry. *Polymer* 51 (14): 3083–3090.

53 Zhao, G., Zhang, P., Zhang, C., and Zhao, Y. (2012). Facile synthesis of highly pure block copolymers by combination of RAFT polymerization, click reaction and de-grafting process. *Polym. Chem.* 3 (7): 1803–1812.

54 Quémener, D., Davis, T.P., Barner-Kowollik, C., and Stenzel, M.H. (2006). RAFT and click chemistry: a versatile approach to well-defined block copolymers. *Chem. Commun.* 48: 5051–5053.

55 O'Reilly, R.K., Joralemon, M.J., Hawker, C.J., and Wooley, K.L. (2006). Facile syntheses of surface-functionalized micelles and shell cross-linked nanoparticles. *J. Polym. Sci., Part A: Polym. Chem.* 44 (17): 5203–5217.

56 Zhang, T., Zheng, Z., Ding, X., and Peng, Y. (2008). Smart surface of gold nanoparticles fabricated by combination of RAFT and click chemistry. *Macromol. Rapid Commun.* 29 (21): 1716–1720.

57 Hansell, C.F., Espeel, P., Stamenovic, M.M. et al. (2011). Additive-free clicking for polymer functionalization and coupling by tetrazine–norbornene chemistry. *J. Am. Chem. Soc.* 133 (35): 13828–13831.

58 Vandewalle, S., Billiet, S., Driessen, F., and Du Prez, F.E. (2016). Macromolecular coupling in seconds of triazolinedione end-functionalized polymers prepared by RAFT polymerization. *ACS Macro Lett.* 5 (6): 766–771.

59 Brendel, J.C., Martin, L., Zhang, J., and Perrier, S. (2017). SuFEx–a selectively triggered chemistry for fast, efficient and equimolar polymer–polymer coupling reactions. *Polym. Chem.* 8 (48): 7475–7485.

60 Wang, P., Dong, Y., Lu, X. et al. (2018). Combining click sulfur (VI)-fluoride exchange with photoiniferters: a facile, fast, and efficient strategy for postpolymerization modification. *Macromol. Rapid Commun.* 39 (3): 1700523.

61 Sinnwell, S., Inglis, A.J., Davis, T.P. et al. (2008). An atom-efficient conjugation approach to well-defined block copolymers using RAFT chemistry and hetero Diels–Alder cycloaddition. *Chem. Commun.* 17: 2052–2054.

62 Inglis, A.J., Stenzel, M.H., and Barner-Kowollik, C. (2009). Ultra-fast RAFT-HDA click conjugation: an efficient route to high molecular weight block copolymers. *Macromol. Rapid Commun.* 30 (21): 1792–1798.

63 Langer, M., Mueller, J.O., Goldmann, A.S. et al. (2016). α,ω-reactive building blocks based on a dual functional RAFT agent for thermal and light-induced ligation. *ACS Macro Lett.* 5 (5): 597–601.

64 Roth, P.J., Boyer, C., Lowe, A.B., and Davis, T.P. (2011). RAFT polymerization and thiol chemistry: a complementary pairing for implementing modern macromolecular design. *Macromol. Rapid Commun.* 32 (15): 1123–1143.

65 Roth, P.J., Kessler, D., Zentel, R., and Theato, P. (2008). A method for obtaining defined end groups of polymethacrylates prepared by the RAFT process during aminolysis. *Macromolecules* 41 (22): 8316–8319.

66 Spruell, J.M., Levy, B.A., Sutherland, A. et al. (2009). Facile postpolymerization end-modification of RAFT polymers. *J. Polym. Sci., Part A: Polym. Chem.* 47 (2): 346–356.

67 Li, M., De, P., Gondi, S.R., and Sumerlin, B.S. (2008). End group transformations of RAFT-generated polymers with bismaleimides: functional telechelics and modular block copolymers. *J. Polym. Sci., Part A: Polym. Chem.* 46 (15): 5093–5100.

68 Koo, S.P., Stamenović, M.M., Prasath, R.A. et al. (2010). Limitations of radical thiol-ene reactions for polymer–polymer conjugation. *J. Polym. Sci., Part A: Polym. Chem.* 48 (8): 1699–1713.

69 Bertrand, A., Chen, S., Souharce, G. et al. (2011). Straightforward preparation of telechelic H-bonding polymers from difunctional trithiocarbonates and supramolecular block copolymers thereof. *Macromolecules* 44 (10): 3694–3704.

70 Moughton, A.O., Stubenrauch, K., and O'Reilly, R.K. (2009). Hollow nanostructures from self-assembled supramolecular metallo-triblock copolymers. *Soft Matter.* 5 (12): 2361–2370.

71 Schmidt, B.V. and Barner-Kowollik, C. (2014). Supramolecular X-and H-shaped star block copolymers via cyclodextrin-driven supramolecular self-assembly. *Polym. Chem.* 5 (7): 2461–2472.

72 Montarnal, D., Delbosc, N., Chamignon, C. et al. (2015). Highly ordered nanoporous films from supramolecular diblock copolymers with hydrogen-bonding junctions. *Angew. Chem. Int. Ed.* 54 (38): 11117–11121.
73 Chen, S., Rocher, M., Ladaviere, C. et al. (2012). AB/ABC/ABCD supramolecular block copolymers from Hamilton wedge and barbiturate-functionalized RAFT agents. *Polym. Chem.* 3 (11): 3157–3165.
74 Chen, S., Deng, Y., Chang, X. et al. (2014). Facile preparation of supramolecular (ABAC) *n* multiblock copolymers from Hamilton wedge and barbiturate-functionalized RAFT agents. *Polym. Chem.* 5 (8): 2891–2900.
75 Beginn, U. (2008). Gradient copolymers. *Colloid. Polym. Sci.* 286 (13): 1465–1474.
76 Zhang, J., Farias-Mancilla, B., Destarac, M. et al. (2018). Asymmetric copolymers: synthesis, properties, and applications of gradient and other partially segregated copolymers. *Macromol. Rapid Commun.* 39 (19): 1800357.
77 Sun, X., Luo, Y., Wang, R. et al. (2008). Semibatch RAFT polymerization for producing ST/BA copolymers with controlled gradient composition profiles. *AlChE J.* 54 (4): 1073–1087.
78 Yañez-Macias, R., Kulai, I., Ulbrich, J. et al. (2017). Thermosensitive spontaneous gradient copolymers with block-and gradient-like features. *Polym. Chem.* 8 (34): 5023–5032.
79 Guerrero-Sanchez, C., Harrisson, S., and Keddie, D.J. (2013). High-throughput method for RAFT kinetic investigations and estimation of reactivity ratios in copolymerization systems. *Macromol. Symp.* 325 (1): 38–46.
80 Fu, C., Yang, B., Zhu, C. et al. (2013). Synthesis of gradient copolymers by concurrent enzymatic monomer transformation and RAFT polymerization. *Polym. Chem.* 4 (24): 5720–5725.
81 Tang, Q., Wu, Y., Sun, P. et al. (2014). Powerful ring-closure method for preparing varied cyclic polymers. *Macromolecules* 47 (12): 3775–3781.
82 Stamenović, M.M., Espeel, P., Baba, E. et al. (2013). Straightforward synthesis of functionalized cyclic polymers in high yield via RAFT and thiolactone–disulfide chemistry. *Polym. Chem.* 4 (1): 184–193.
83 Whittaker, M.R., Goh, Y.-K., Gemici, H. et al. (2006). Synthesis of monocyclic and linear polystyrene using the reversible coupling/cleavage of thiol/disulfide groups. *Macromolecules* 39 (26): 9028–9034.
84 Goldmann, A.S., Quémener, D., Millard, P.-E. et al. (2008). Access to cyclic polystyrenes via a combination of reversible addition fragmentation chain transfer (RAFT) polymerization and click chemistry. *Polymer* 49 (9): 2274–2281.
85 Skey, J., Willcock, H., Lammens, M. et al. (2010). Synthesis and self-assembly of amphiphilic chiral poly(amino acid) star polymers. *Macromolecules* 43 (14): 5949–5955.
86 Zhang, L. and Stenzel, M.H. (2009). Spherical glycopolymer architectures using RAFT: from stars with a – cyclodextrin Core to thermoresponsive CoreShell particles. *Aust. J. Chem.* 62 (8): 813–822.

87 Yusa, S.-I., Endo, T., and Ito, M. (2009). Synthesis of thermo-responsive 4-arm star-shaped porphyrin-centered poly(*N*,*N*-diethylacrylamide) via reversible addition-fragmentation chain transfer radical polymerization. *J. Polym. Sci., Part A: Polym. Chem.* 47 (24): 6827–6838.

88 Ren, J.M., McKenzie, T.G., Fu, Q. et al. (2016). Star polymers. *Chem. Rev.* 116 (12): 6743–6836.

89 Zhang, C., Zhou, Y., Liu, Q. et al. (2011). Facile synthesis of hyperbranched and star-shaped polymers by RAFT polymerization based on a polymerizable trithiocarbonate. *Macromolecules* 44 (7): 2034–2049.

90 Hu, J., Qiao, R., Whittaker, M.R. et al. (2017). Synthesis of star polymers by RAFT polymerization as versatile nanoparticles for biomedical applications. *Aust. J. Chem.* 70 (11): 1161–1170.

91 Chaffey-Millar, H., Stenzel, M.H., Davis, T.P. et al. (2006). Design criteria for star polymer formation processes via living free radical polymerization. *Macromolecules* 39 (19): 6406–6419.

92 Boschmann, D. and Vana, P. (2007). Z-RAFT star polymerizations of acrylates: star coupling via intermolecular chain transfer to polymer. *Macromolecules* 40 (8): 2683–2693.

93 Stenzel, M.H. and Davis, T.P. (2002). Star polymer synthesis using trithiocarbonate functional β-cyclodextrin cores (reversible addition–fragmentation chain-transfer polymerization). *J. Polym. Sci., Part A: Polym. Chem.* 40 (24): 4498–4512.

94 Altintas, O., Abbasi, M., Riazi, K. et al. (2014). Stability of star-shaped RAFT polystyrenes under mechanical and thermal stress. *Polym. Chem.* 5 (17): 5009–5019.

95 Zhang, L. and Chen, Y. (2006). Allyl functionalized telechelic linear polymer and star polymer via RAFT polymerization. *Polymer* 47 (15): 5259–5266.

96 Ferreira, J., Syrett, J., Whittaker, M. et al. (2011). Optimizing the generation of narrow polydispersity 'arm-first' star polymers made using RAFT polymerization. *Polym. Chem.* 2 (8): 1671–1677.

97 Tucker, B.S., Getchell, S.G., Hill, M.R., and Sumerlin, B.S. (2015). Facile synthesis of drug-conjugated PHPMA core-cross-linked star polymers. *Polym. Chem.* 6 (23): 4258–4263.

98 Bray, C., Peltier, R., Kim, H. et al. (2017). Anionic multiblock core cross-linked star copolymers via RAFT polymerization. *Polym. Chem.* 8 (36): 5513–5524.

99 Dong, Z.-M., Liu, X.-H., Liu, H.-W., and Li, Y.-S. (2010). Synthesis of novel star polymers with vinyl-functionalized hyperbranched core via "arm-first" strategy. *Macromolecules* 43 (19): 7985–7992.

100 Brzytwa, A.J. and Johnston, J. (2011). Scaled production of RAFT CTA – a star performer. *Polym. Prepr.* 52: 533–534.

101 Roberts, D.A., Crossley, M.J., and Perrier, S. (2014). Fluorescent bowl-shaped nanoparticles from 'clicked' porphyrin–polymer conjugates. *Polym. Chem.* 5 (13): 4016–4021.

102 Inglis, A.J., Sinnwell, S., Davis, T.P. et al. (2008). Reversible addition fragmentation chain transfer (RAFT) and hetero-Diels–Alder chemistry as a convenient

conjugation tool for access to complex macromolecular designs. *Macromolecules* 41 (12): 4120–4126.

103 Chan, J.W., Yu, B., Hoyle, C.E., and Lowe, A.B. (2008). Convergent synthesis of 3-arm star polymers from RAFT-prepared poly(*N*,*N*-diethylacrylamide) via a thiol–ene click reaction. *Chem. Commun.* 40: 4959–4961.

104 Bapat, A.P., Ray, J.G., Savin, D.A. et al. (2012). Dynamic-covalent nanostructures prepared by Diels–Alder reactions of styrene-maleic anhydride-derived copolymers obtained by one-step cascade block copolymerization. *Polym. Chem.* 3 (11): 3112–3120.

105 Wei, X., Moad, G., Muir, B.W. et al. (2014). An arm-first approach to cleavable Mikto-arm star polymers by RAFT polymerization. *Macromol. Rapid Commun.* 35 (8): 840–845.

106 Cosson, S., Danial, M., Saint-Amans, J.R., and Cooper-White, J.J. (2017). Accelerated combinatorial high throughput star polymer synthesis via a rapid one-pot sequential aqueous RAFT (rosa-RAFT) polymerization scheme. *Macromol. Rapid Commun.* 38 (8): 1600780.

107 Kitiri, E.N., Varnava, C.K., Patrickios, C.S. et al. (2018). Double-networks based on interconnected amphiphilic "in–out" star first polymer conetworks prepared by RAFT polymerization. *J. Polym. Sci., Part A: Polym. Chem.* 56 (19): 2161–2174.

108 Ahn, N.Y. and Seo, M. (2016). Heteroarm core cross-linked star polymers via RAFT copolymerization of styrene and bismaleimide. *RSC Adv.* 6 (53): 47715–47722.

109 Daniel, W.F.M., Burdyńska, J., Vatankhah-Varnoosfaderani, M. et al. (2015). Solvent-free, supersoft and superelastic bottlebrush melts and networks. *Nat. Mater.* 15: 183.

110 Levi, A.E., Lequieu, J., Horne, J.D. et al. (2019). Miktoarm stars via grafting-through copolymerization: self-assembly and the star-to-bottlebrush transition. *Macromolecules* 52 (4): 1794–1802.

111 Sheiko, S.S., Sumerlin, B.S., and Matyjaszewski, K. (2008). Cylindrical molecular brushes: synthesis, characterization, and properties. *Prog. Polym. Sci.* 33 (7): 759–785.

112 Lee, H.-I., Pietrasik, J., Sheiko, S.S., and Matyjaszewski, K. (2010). Stimuli-responsive molecular brushes. *Prog. Polym. Sci.* 35 (1): 24–44.

113 Feng, C., Li, Y., Yang, D. et al. (2011). Well-defined graft copolymers: from controlled synthesis to multipurpose applications. *Chem. Soc. Rev.* 40 (3): 1282–1295.

114 Rzayev, J. (2012). Molecular bottlebrushes: new opportunities in nanomaterials fabrication. *ACS Macro Lett.* 1 (9): 1146–1149.

115 Verduzco, R., Li, X., Pesek, S.L., and Stein, G.E. (2015). Structure, function, self-assembly, and applications of bottlebrush copolymers. *Chem. Soc. Rev.* 44 (8): 2405–2420.

116 Müllner, M. and Müller, A.H.E. (2016). Cylindrical polymer brushes – anisotropic building blocks, unimolecular templates and particulate nanocarriers. *Polymer* 98: 389–401.

117 Foster, J.C., Varlas, S., Couturaud, B. et al. (2019). Getting into shape: reflections on a new generation of cylindrical nanostructures' self-assembly using polymer building blocks. *J. Am. Chem. Soc.* 141 (7): 2742–2753.

118 Xie, G., Martinez, M.R., Olszewski, M. et al. (2019). Molecular bottlebrushes as novel materials. *Biomacromolecules* 20 (1): 27–54.

119 Abbasi, M., Faust, L., and Wilhelm, M. (2019). Comb and bottlebrush polymers with superior rheological and mechanical properties. *Adv. Mater.* 31 (26): 1806484.

120 Altay, E. and Rzayev, J. (2016). Synthesis of star-brush polymer architectures from end-reactive molecular bottlebrushes. *Polymer* 98: 487–494.

121 Cao, X., Zhang, C., Wu, S., and An, Z. (2014). A highly efficient macromonomer approach to core cross-linked star (CCS) polymers via one-step RAFT emulsion polymerization. *Polym. Chem.* 5 (14): 4277–4284.

122 Vatankhah-Varnosfaderani, M., Keith, A.N., Cong, Y. et al. (2018). Chameleon-like elastomers with molecularly encoded strain-adaptive stiffening and coloration. *Science* 359 (6383): 1509–1513.

123 Schlüter, A.D., Halperin, A., Kröger, M. et al. (2014). Dendronized polymers: molecular objects between conventional linear polymers and colloidal particles. *ACS Macro Lett.* 3 (10): 991–998.

124 Shen, D., Xu, B., Huang, X. et al. (2018). (PtBA-*co*-PPEGMEMA-*co*-PDOMA)-g-PPFA polymer brushes synthesized by sequential RAFT polymerization and ATRP. *Polym. Chem.* 9 (20): 2821–2829.

125 Lee, D.C., Lamm, R.J., Prossnitz, A.N. et al. (2019). Dual polymerizations: untapped potential for biomaterials. *Adv. Healthc. Mater.* 8 (6): 1800861.

126 Minoda, M., Shimizu, T., Miki, S., and Motoyanagi, J. (2013). Thermoresponsive NIPAM block copolymers containing densely grafted poly(vinyl ether) brushes synthesized by a combination of living cationic polymerization and RAFT polymerization. *J. Polym. Sci., Part A: Polym. Chem.* 51 (4): 786–792.

127 Tanaka, J., Moriceau, G., Cook, A. et al. (2019). Tuning the structure, stability, and responsivity of polymeric arsenical nanoparticles using polythiol cross-linkers. *Macromolecules* 52 (3): 992–1003.

128 Willcock, H. and O'Reilly, R.K. (2010). End group removal and modification of RAFT polymers. *Polym. Chem.* 1 (2): 149–157.

129 Flanders, M.J. and Gramlich, W.M. (2018). Reversible-addition fragmentation chain transfer (RAFT) mediated depolymerization of brush polymers. *Polym. Chem.* 9 (17): 2328–2335.

130 Rossi, N.A.A., Zou, Y., Scott, M.D., and Kizhakkedathu, J.N. (2008). RAFT synthesis of acrylic copolymers containing poly(ethylene glycol) and dioxolane functional groups: toward well-defined aldehyde containing copolymers for bioconjugation. *Macromolecules* 41 (14): 5272–5282.

131 Lejars, M., Margaillan, A., and Bressy, C. (2013). Well-defined graft copolymers of tert-butyldimethylsilyl methacrylate and poly(dimethylsiloxane) macromonomers synthesized by RAFT polymerization. *Polym. Chem.* 4 (11): 3282–3292.

132 Chong, J.Y.T., Keddie, D.J., Postma, A. et al. (2015). RAFT preparation and the aqueous self-assembly of amphiphilic poly(octadecyl acrylate)-block-poly(polyethylene glycol methyl ether acrylate) copolymers. *Colloids Surf., A* 470: 60–69.

133 Boursier, T., Georges, S., Mosquet, M. et al. (2016). Synthesis of poly(N-acryloylmorpholine) macromonomers using RAFT and their copolymerization with methacrylic acid for the design of graft copolymer additives for concrete. *Polym. Chem.* 7 (4): 917–925.

134 Maher, M.J., Schibur, H.J., and Bates, F.S. (2017). When convergent syntheses of graft block copolymers diverge: the treachery of chemical images. *J. Polym. Sci., Part A: Polym. Chem.* 55 (18): 3097–3104.

135 Patton, D.L. and Advincula, R.C. (2006). A versatile synthetic route to macromonomers via RAFT polymerization. *Macromolecules* 39 (25): 8674–8683.

136 Li, A., Ma, J., Sun, G. et al. (2012). One-pot, facile synthesis of well-defined molecular brush copolymers by a tandem RAFT and ROMP, "grafting-through" strategy. *J. Polym. Sci., Part A: Polym. Chem.* 50 (9): 1681–1688.

137 Radzinski, S.C., Foster, J.C., and Matson, J.B. (2015). Synthesis of bottlebrush polymers via transfer-to and grafting-through approaches using a RAFT chain transfer agent with a ROMP-active Z-group. *Polym. Chem.* 6 (31): 5643–5652.

138 Pesek, S.L., Li, X., Hammouda, B. et al. (2013). Small-angle neutron scattering analysis of bottlebrush polymers prepared via grafting-through polymerization. *Macromolecules* 46 (17): 6998–7005.

139 Vandenbergh, J. and Junkers, T. (2014). Alpha and omega: importance of the nonliving chain end in RAFT multiblock copolymerization. *Macromolecules* 47 (15): 5051–5059.

140 Radzinski, S.C., Foster, J.C., and Matson, J.B. (2016). Preparation of bottlebrush polymers via a one-pot ring-opening polymerization (ROP) and ring-opening metathesis polymerization (ROMP) grafting-through strategy. *Macromol. Rapid Commun.* 37 (7): 616–621.

141 Perrier, S. (2017). 50th anniversary perspective: RAFT polymerization—a user guide. *Macromolecules* 50 (19): 7433–7447.

142 Moad, G. (2017). RAFT polymerization to form stimuli-responsive polymers. *Polym. Chem.* 8 (1): 177–219.

143 Michalek, L., Mundsinger, K., Barner-Kowollik, C., and Barner, L. (2019). The long and the short of polymer grafting. *Polym. Chem.* 10 (1): 54–59.

144 Lanson, D., Schappacher, M., Borsali, R., and Deffieux, A. (2007). Synthesis of (poly[chloroethyl vinyl ether]-g-polystyrene)comb-b-(poly[chloropyran ethoxy vinyl ether]-g-polyisoprene)comb copolymers and study of hyper-branched micelle formation in dilute solutions. *Macromolecules* 40 (15): 5559–5565.

145 Moriceau, G., Tanaka, J., Lester, D. et al. (2019). Influence of grafting density and distribution on material properties using well-defined alkyl functional poly(styrene-co-maleic anhydride) architectures synthesized by RAFT. *Macromolecules* 52 (4): 1469–1478.

146 Gan, W., Shi, Y., Jing, B. et al. (2017). Produce molecular brushes with ultrahigh grafting density using accelerated CuAAC grafting-onto strategy. *Macromolecules* 50 (1): 215–222.

147 Chu, Y., Li, H., Huang, H. et al. (2018). Uni-molecular nanoparticles of poly(2-oxazoline) showing tunable thermoresponsive behaviors. *J. Polym. Sci., Part A: Polym. Chem.* 56 (2): 174–183.

148 Wu, Y., Tang, Q., Zhang, M. et al. (2018). Synthesis of bottlebrush polymers with v-shaped side chains. *Polymer* 143: 190–199.

149 Quémener, D., Hellaye, M.L., Bissett, C. et al. (2008). Graft block copolymers of propargyl methacrylate and vinyl acetate via a combination of RAFT/MADIX and click chemistry: reaction analysis. *J. Polym. Sci., Part A: Polym. Chem.* 46 (1): 155–173.

150 Xiao, L., Chen, Y., and Zhang, K. (2016). Efficient metal-free "grafting onto" method for bottlebrush polymers by combining RAFT and triazolinedione–diene click reaction. *Macromolecules* 49 (12): 4452–4461.

151 Kerr, A., Hartlieb, M., Sanchis, J. et al. (2017). Complex multiblock bottle-brush architectures by RAFT polymerization. *Chem. Commun.* 53 (87): 11901–11904.

152 Bolton, J. and Rzayev, J. (2014). Synthesis and melt self-assembly of PS–PMMA–PLA triblock bottlebrush copolymers. *Macromolecules* 47 (9): 2864–2874.

153 Foster, J.C., Radzinski, S.C., and Matson, J.B. (2017). Graft polymer synthesis by RAFT transfer-to. *J. Polym. Sci., Part A: Polym. Chem.* 55 (18): 2865–2876.

154 Zheng, Z., Ling, J., and Müller, A.H.E. (2014). Revival of the R-group approach: a "CTA-shuttled" grafting from approach for well-defined cylindrical polymer brushes via RAFT polymerization. *Macromol. Rapid Commun.* 35 (2): 234–241.

155 Xu, J., Shanmugam, S., Fu, C. et al. (2016). Selective photoactivation: from a single unit monomer insertion reaction to controlled polymer architectures. *J. Am. Chem. Soc.* 138 (9): 3094–3106.

156 Shanmugam, S., Cuthbert, J., Kowalewski, T. et al. (2018). Catalyst-free selective photoactivation of RAFT polymerization: a facile route for preparation of comb-like and bottlebrush polymers. *Macromolecules* 51 (19): 7776–7784.

157 Xiong, L., Zhang, H., Zhong, A. et al. (2014). Acid- and base-functionalized core-confined bottlebrush copolymer catalysts for one-pot cascade reactions. *Chem. Commun.* 50 (94): 14778–14781.

158 Wang, Y., Ren, R., Ling, J. et al. (2018). One-pot "grafting-from" synthesis of amphiphilic bottlebrush block copolymers containing PLA and PVP side chains via tandem ROP and RAFT polymerization. *Polymer* 138: 378–386.

159 Wu, W., Dai, W., Zhao, X. et al. (2018). Synthesis, self-assembly and drug release behaviors of reduction-labile multi-responsive block miktobrush quater-polymers with linear and V-shaped grafts. *Polym. Chem.* 9 (15): 1947–1960.

160 Nese, A., Li, Y., Averick, S. et al. (2012). Synthesis of amphiphilic poly(N-vinylpyrrolidone)-b-poly(vinyl acetate) molecular bottlebrushes. *ACS Macro Lett.* 1 (1): 227–231.

161 Zehm, D., Laschewsky, A., Liang, H., and Rabe, J.P. (2011). Straightforward access to amphiphilic dual bottle brushes by combining RAFT, ATRP, and NMP polymerization in one sequence. *Macromolecules* 44 (24): 9635–9641.

162 Fenyves, R., Schmutz, M., Horner, I.J. et al. (2014). Aqueous self-assembly of Giant bottlebrush block copolymer surfactants as shape-tunable building blocks. *J. Am. Chem. Soc.* 136 (21): 7762–7770.

163 Ma'Radzi, A.H., Sugihara, S., Miura, S. et al. (2014). Synthesis of thermoresponsive block and graft copolymers via the combination of living cationic polymerization and RAFT polymerization using a vinyl ether-type RAFT agent. *Polymer* 55 (8): 1920–1930.

164 Sumerlin, B.S., Neugebauer, D., and Matyjaszewski, K. (2005). Initiation efficiency in the synthesis of molecular brushes by grafting from via atom transfer radical polymerization. *Macromolecules* 38 (3): 702–708.

165 Cook, A.B. and Perrier, S. (2019). Branched and dendritic polymer architectures: functional nanomaterials for therapeutic delivery. *Adv. Funct. Mater.* 30 (2): 1901001. https://doi.org/10.1002/adfm.201901001.

166 Kienle, R.H. and Hovey, A.G. (1929). The polyhydric alcohol-polybasic acid reaction. I. Glycerol-phthalic anhydride. *J. Am. Chem. Soc.* 51 (2): 509–519.

167 Fréchet, J.M.J., Henmi, M., Gitsov, I. et al. (1995). Self-condensing vinyl polymerization: an approach to dendritic materials. *Science* 269 (5227): 1080–1083.

168 Alfurhood, J.A., Bachler, P.R., and Sumerlin, B.S. (2016). Hyperbranched polymers via RAFT self-condensing vinyl polymerization. *Polym. Chem.* 7 (20): 3361–3369.

169 Vogt, A.P., Gondi, S.R., and Sumerlin, B.S. (2007). Hyperbranched polymers via RAFT copolymerization of an acryloyl trithiocarbonate. *Aust. J. Chem.* 60 (6): 396–399.

170 Carter, S., Rimmer, S., Sturdy, A., and Webb, M. (2005). Highly branched stimuli responsive poly[(N-isopropyl acrylamide)-co-(1,2-propandiol-3-methacrylate)]s with protein binding functionality. *Macromol. Biosci.* 5 (5): 373–378.

171 Ghosh Roy, S. and De, P. (2014). Facile RAFT synthesis of side-chain amino acids containing pH-responsive hyperbranched and star architectures. *Polym. Chem.* 5 (21): 6365–6378.

172 Wei, X., Luo, Q., Sun, L. et al. (2016). Enzyme- and pH-sensitive branched polymer–doxorubicin conjugate-based nanoscale drug delivery system for cancer therapy. *ACS Appl. Mater. Interfaces* 8 (18): 11765–11778.

173 Zheng, L., Wang, Y., Zhang, X. et al. (2018). Fabrication of hyperbranched block-statistical copolymer-based prodrug with dual sensitivities for controlled release. *Bioconjugate Chem.* 29 (1): 190–202.

174 Wang, X. and Gao, H. (2017). Recent Progress on Hyperbranched Polymers Synthesized via Radical-Based Self-Condensing Vinyl Polymerization. *Polymers* 9 (6): 188. https://doi.org/10.3390/polym9060188.

175 O'Brien, N., McKee, A., Sherrington, D.C. et al. (2000). Facile, versatile and cost effective route to branched vinyl polymers. *Polymer* 41 (15): 6027–6031.

176 Liu, B., Kazlauciunas, A., Guthrie, J.T., and Perrier, S. (2005). One-pot hyperbranched polymer synthesis mediated by reversible addition fragmentation chain transfer (RAFT) polymerization. *Macromolecules* 38 (6): 2131–2136.

177 Liu, B., Kazlauciunas, A., Guthrie, J.T., and Perrier, S. (2005). Influence of reaction parameters on the synthesis of hyperbranched polymers via reversible addition fragmentation chain transfer (RAFT) polymerization. *Polymer* 46 (17): 6293–6299.

178 Pal, S., Brooks, W.L.A., Dobbins, D.J., and Sumerlin, B.S. (2016). Employing a sugar-derived dimethacrylate to evaluate controlled branch growth during polymerization with multiolefinic compounds. *Macromolecules* 49 (24): 9396–9405.

179 Rosselgong, J., Armes, S.P., Barton, W.R.S., and Price, D. (2010). Synthesis of branched methacrylic copolymers: comparison between RAFT and ATRP and effect of varying the monomer concentration. *Macromolecules* 43 (5): 2145–2156.

180 Bannister, I., Billingham, N.C., Armes, S.P. et al. (2006). Development of branching in living radical copolymerization of vinyl and divinyl monomers. *Macromolecules* 39 (22): 7483–7492.

181 Koh, M.L., Konkolewicz, D., and Perrier, S. (2011). A simple route to functional highly branched structures: RAFT homopolymerization of divinylbenzene. *Macromolecules* 44 (8): 2715–2724.

182 Xu, J., Tao, L., Boyer, C. et al. (2010). Combining thio–bromo "click" chemistry and RAFT polymerization: a powerful tool for preparing functionalized multiblock and hyperbranched polymers. *Macromolecules* 43 (1): 20–24.

183 Xu, J., Tao, L., Liu, J. et al. (2009). Synthesis of functionalized and biodegradable hyperbranched polymers from novel AB2 macromonomers prepared by RAFT polymerization. *Macromolecules* 42 (18): 6893–6901.

184 Konkolewicz, D., Poon, C.K., Gray-Weale, A., and Perrier, S. (2011). Hyperbranched alternating block copolymers using thiol–yne chemistry: materials with tuneable properties. *Chem. Commun.* 47 (1): 239–241.

21

Star Polymers by RAFT Polymerization

Stephanie Allison-Logan, Fatemeh Karimi, Mitchell D. Nothling, and Greg G. Qiao

University of Melbourne, Department of Chemical Engineering, Polymer Science Group, Parkville, Victoria 3010, Australia

21.1 Star Polymers

Star polymers are a class of branched polymers in which three or more linear arms extend outwards from a central core. The dense, compact nature of star polymers can result in unique chemical, thermal, and rheological properties compared with their linear counterparts. In addition, the unique architecture of star polymers results in distinct core, arm, and peripheral regions that offer great versatility for customized structures [1]. As shown in Figure 21.1, each region of the star can be altered and optimized, enabling endless possibilities.

Star polymers can be synthesized using numerous polymerization techniques with the most common being ring-opening polymerization (ROP), ring-opening metathesis polymerization (ROMP), and the controlled radical polymerization (CRP) methods atom transfer radical polymerization (ATRP), single electron transfer living radical polymerization (SET-LRP), nitroxide-mediated living radical polymerization (NMP), and reversible addition fragmentation deactivation chain transfer (RAFT) polymerization.

ROP involves the ring opening of cyclic monomers such as cyclic esters and *O*- and *N*-carboxyanhydrides (OCA and NCA, respectively) resulting in poly(esters) from cyclic ester and OCA monomers and poly(amides) from NCA monomers. Because of the biodegradable nature of the resulting polymers, ROP techniques are frequently used to synthesize polymers for biomedical applications. ROP typically requires the use of organic acids/bases or organometallic complexes to achieve fast reaction times and/or low dispersities. Unlike CRP, ROP is not sensitive to oxygen scavengers; however, protic contaminants such as water can initiate polymerization and induce side reactions and even terminate reactions during NCA and OCA ROP. In addition, incorporation of compatible side chain functionality is more difficult and the number of commercially available monomers more limited than for CRP. ROMP also proceeds via ring opening of cyclic monomers and results in well-defined polymers with readily modified end groups. The development of novel

RAFT Polymerization: Methods, Synthesis and Applications, First Edition.
Edited by Graeme Moad and Ezio Rizzardo.

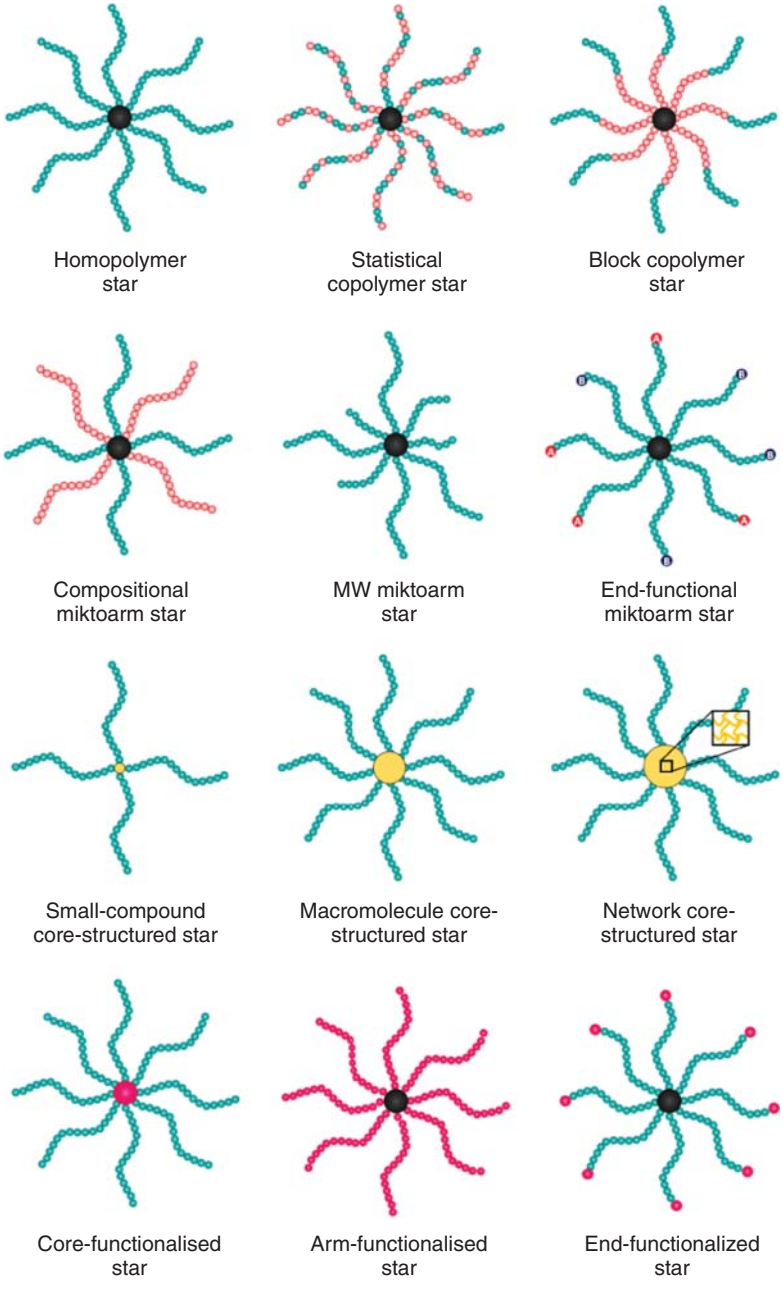

Figure 21.1 An illustration of potential star polymer structures including stars with varied composition and sequence of arm polymer, possible miktoarm and core structures, and different regions of functionalization.

ruthenium and molybdenum catalysts has led to a wider pool of monomers with a greater range of functionalities; however, the presence of transition metals is often undesirable.

CRP techniques maintain high chain-end fidelity, which ensures high conversions and low dispersities; however, stringent oxygen-free environments are generally required. NMP was the first type of CRP developed, however is less frequently used because of the developments of ATRP and RAFT due to high reaction temperatures, poor control over methacrylate and methacrylamide monomers, and comparatively lower chain-end fidelity. Transition metal-mediated CRP including ATRP and SET-LRP has been widely used for the synthesis of star polymers using both the arm-first and core-first approaches. Although compatible of with a large array of vinylic monomers and capable of conversions greater than 95%, the use of a transition metal is required and not ideal for certain applications.

RAFT polymerization readily lends itself to the synthesis of star polymers. Compatible with an enormous range of monomers and multiple possible synthetic approaches, RAFT is a leading approach for star polymer synthesis. In addition, the development of photo-mediated RAFT has eradicated the necessity of additional initiators or catalysts. Although requiring further optimization, recent investigations into the use of xanthates to control radical ROP demonstrate that RAFT polymerization may also be used to synthesize degradable polymers.

21.2 Synthesis of Star Polymers via RAFT Polymerization

RAFT polymerization offers exceptional control over polymer molecular weights, dispersities, and is compatible with a wide range of monomers, making it an efficient and widely used method for the synthesis of star polymers. The two approaches to star polymer synthesis via RAFT polymerization are known as the core-first and arm-first approach. The advantages, disadvantages, and major developments for both approaches will be thoroughly discussed.

21.2.1 Core-first Approach

The core-first approach requires a multifunctional initiator from which arms can be polymerized. Any molecule that can be functionalized with three or more RAFT agents can serve as a core, enabling the use of a wide array of compounds and a great amount of freedom. Cores as varied as cyclodextrins, [3] porphyrins, [4] hyperbranched polymers, [5] metal–organic polyhedrons (MOPs), [6] metal–organic macrocycles (MOMs), [7], and quantum dots [8] have been used for the synthesis of star polymers, with benzene- and pentaerythritol-based cores among the most commonly used.

When using the core-first approach, the number of arms is equal to the number of initiating sites and is therefore known before polymerization (assuming 100% initiation). This varies greatly from the arm-first approach, where the number of arms

cannot be known until after polymerization and is not easily controlled. To achieve star polymers with low molecular weight dispersities, all initiating sites must have equal reactivity and 100% initiation efficiency. It is also important that the rate of initiation is greater than the rate of propagation and that either no or minimal chain termination occurs, both of which result in arms that contain different numbers of repeat units. The primary advantages of the core-first approach are high yields and facile purification, as low molecular weight monomers are easily separated from the resulting star polymers [1].

The core-first approach does suffer from some limitations. Star arms cannot be directly analyzed unless cleaved from the core. The synthesis of star polymers containing more than one type of arm, known as miktoarm stars, is difficult as different initiating groups are required, although it has been demonstrated [9, 10]. Star polymers synthesized via the core-first approach generally have a smaller core domain and lower number of arms than star polymers synthesized using the arm-first approach; however, the use of hyperbranched cores such as dendrimers has somewhat alleviated these limitations.

Perhaps the most challenging aspect of the core-first approach is the synthesis of the multifunctional core. Cores should have the same number of initiating sites to ensure that the resulting star polymers have the same number of arms, arm molecular weight, and total molecular weight, any of which could impact the star properties. Purification is generally required after synthesis of the core, inhibiting one-pot star polymer synthesis. Although the synthesis of cores is more commonly performed through conjugation chemistries, RAFT polymerization has been employed as a facile method of core synthesis.

Zhang et al. reported the use of self-condensing vinyl polymerization (SCVP)-RAFT to synthesize a core using a polymerizable RAFT agent, followed by polymerization from these RAFT agents to synthesize the star arms (Figure 21.2) [2]. To form the hyperbranched macro-chain transfer agent (CTA) core, a RAFT agent containing a styryl group was copolymerized with methyl acrylate or styrene. Branching points occurred when both the styryl and trithiocarbonate groups in one molecule participated in RAFT polymerization. A wide range of conditions were investigated and the authors concluded that the degree of branching, end group composition, and CTA functionality could be adjusted by altering the RAFT monomer and comonomer ratios and reaction time. Although initial macroCTA cores had dispersities greater than two, the authors were able to adjust conditions to achieve cores with dispersities as low as 1.16.

Hyperbranched macroCTA cores with approximately 7, 13, or 56 functional RAFT agents were subsequently used to polymerize styrene or *tert*-butyl acrylate to form star polymers. Theoretical and observed molecular weights were similar and dispersities ranged from 1.21 to 1.88, indicating that controlled star polymers could be achieved using this approach. Subsequent works using RAFT to synthesize hyperbranched cores and subsequent polymerization of arms has further shown the versatility and ease of core-first star polymerization performed using RAFT [11–13].

Although the core-first approach to star polymer synthesis is compatible with a wide range of polymerization techniques, star polymer synthesis via RAFT

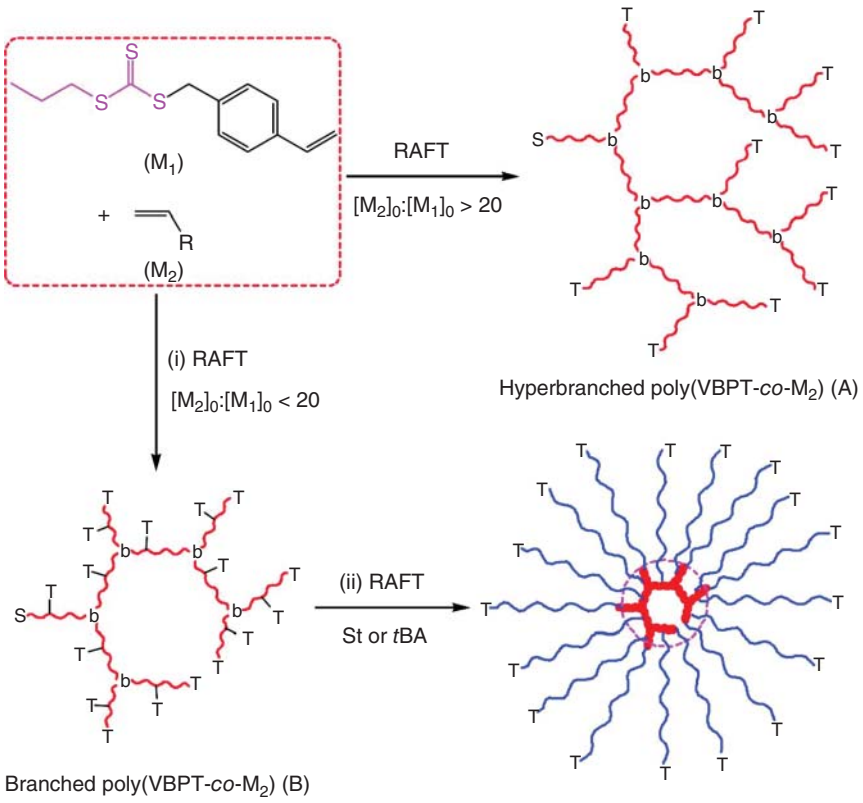

Where M_2 = MMA, MA, *t*BA, St; S = Styryl group; b = Polymerized S group; T- = Remaining unreacted CTA functionality in VBPT unit; T = Terminal propyltrithiocarbonate group.

Figure 21.2 Synthesis of hyperbranched cores using a styryl-RAFT monomer (M_1) and styrene or methyl acrylate (M_2). Once the core synthesis was optimized, subsequent polymerization from the core via RAFT resulted in well-defined star polymers. Source: Reprinted with permission from Zhang et al. [2]. Copyright 2011, American Chemical Society.

polymerization is unique because of the asymmetrical nature of RAFT agents, which contain a Z- and R-group (Figure 21.3). Which group is conjugated to the core has important implications for the synthesis and functionality of the star polymer and should be considered before synthesis of the multifunctional core. Both approaches have advantages and disadvantages, which have been extensively studied and will be discussed [1, 14, 15].

21.2.1.1 Z-group Approach

The Z-group approach is used when the Z-group of the RAFT agent is conjugated to the core. The R-group remains at the periphery of the star polymer while the thiocarbonylthio moiety remains at the core. As polymerization proceeds, a linear macroradical is formed away from the star polymer core. Because the propagating radical is not attached to the star core, star–star coupling is prevented. This avoidance of

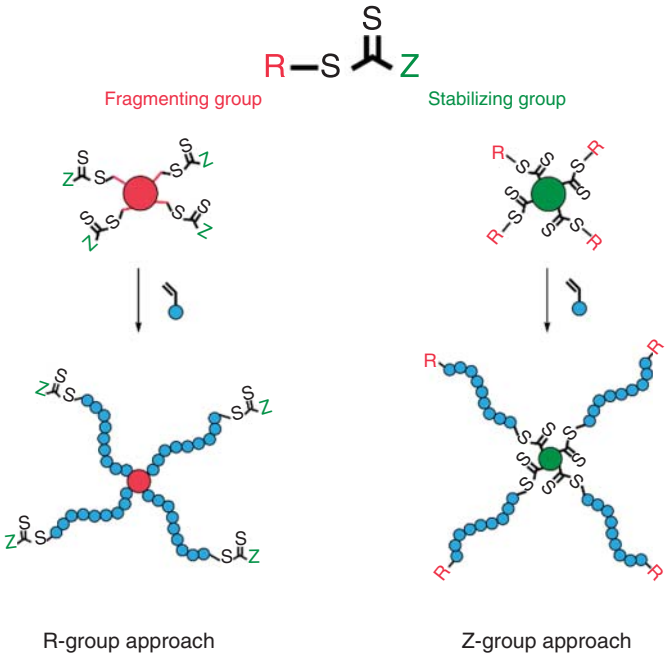

Figure 21.3 RAFT polymerization of star polymers using the core-first R- and Z-group approaches.

star–star coupling initially made the Z-group approach the preferred method of star polymer synthesis via the core-first approach. Termination events can still occur when two macroradicals react, producing a low molecular weight linear byproduct and resulting in the loss of at least one living arm from a star. However, this linear byproduct is much easier to purify from the desired star polymer than the high molecular weight byproducts resulting from star–star coupling. The mechanism of polymerization via the Z-group core-first approach is illustrated in Figure 21.4.

The mechanism of polymerization does lead to certain limitations. Macroradical arms must reattach to the core, which becomes more difficult as the molecular weight of the arms and the number of arms is increased [3, 5]. The location of the thiocarbonylthio group in the star core must also be carefully considered. The thiocarbonylthio group is sensitive to nucleophiles and radicals, both of which can cause destruction of the RAFT agent. With the RAFT agent located at the core, this means that the destruction of a RAFT agent will lead to the loss of an arm. This could be intentionally exploited if a degradable star is desired or to analyse the arms following star polymer synthesis [16, 17]. It is important to consider before synthesis if exposure to nucleophiles and radicals is likely during the intended application of the star polymer.

21.2.1.2 R-group Approach

The R-group approach is used when the R-group of the RAFT agent is conjugated to the core. Because of the orientation of the RAFT agent, the thiocarbonylthio group is

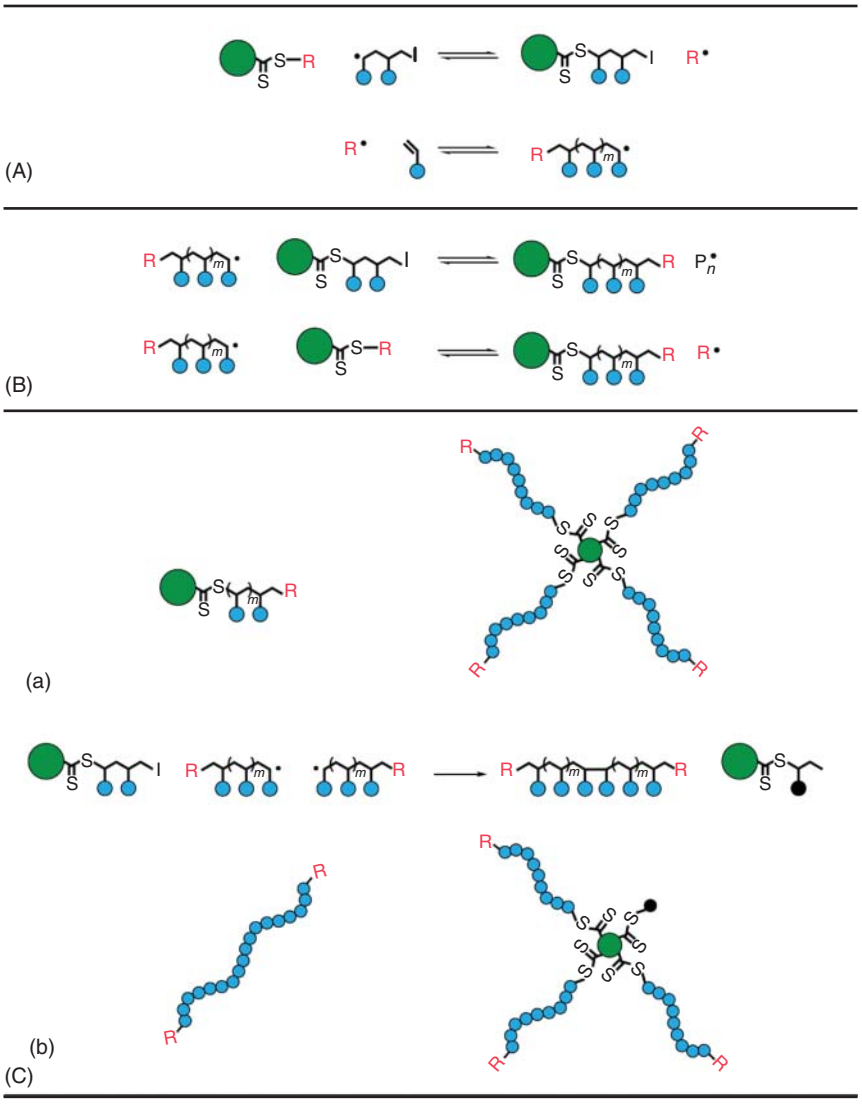

Figure 21.4 RAFT polymerization of star polymers using the Z-group core-first approach. Using this approach, the thiocarbonylthio moiety remains attached to the core while the macroradical arms propagate away from the core, then reattach. The polymerization proceeds in three phases: (A) initiation, (B) propagation, and (C) termination, and can result in both (a) desired product and (b) products of undesired termination. Unwanted termination can occur when macroradical arms react with each other, resulting in a linear byproduct and stars that have dead chain ends (black circle).

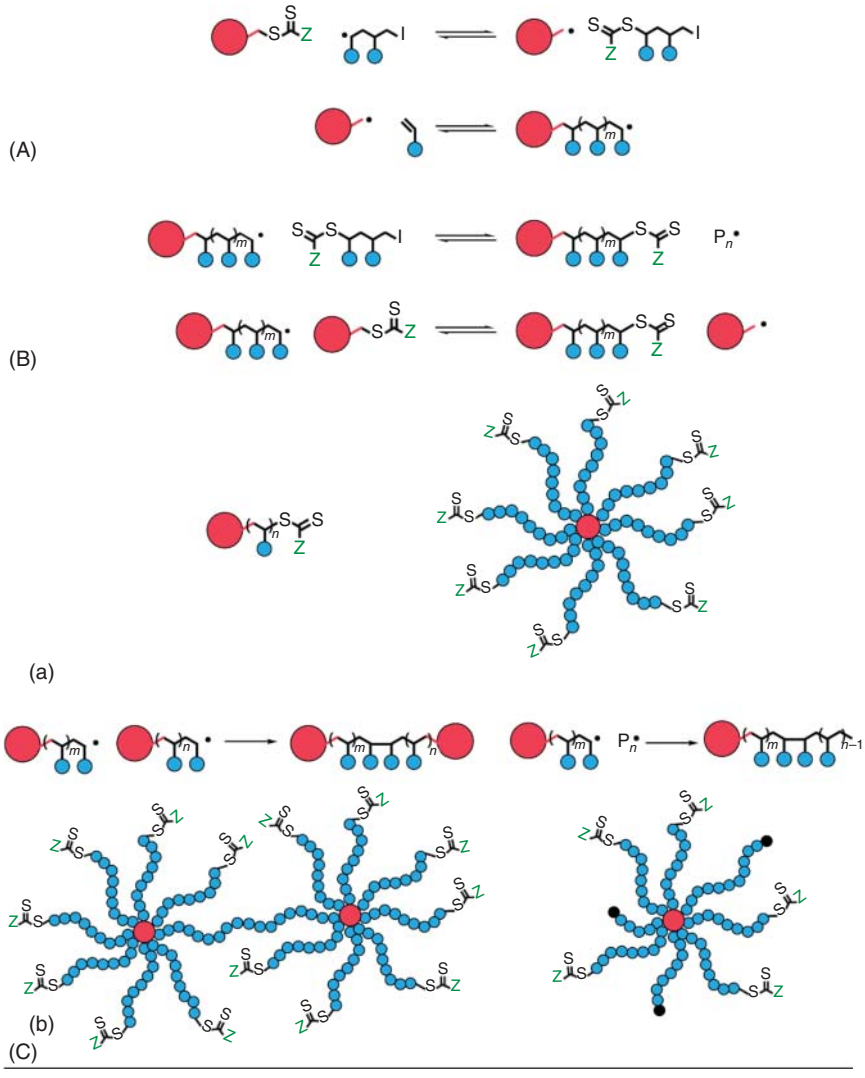

Figure 21.5 RAFT polymerization of star polymers using the R-group core-first approach. In this approach, the propagating radical remains at the star periphery. The polymerization proceeds in three phases: (A) initiation, (B) propagation, and (C) termination, and can result in both (a) desired product and (b) products of undesired termination. Unwanted termination reactions can result in star–star coupling and dead polymer arms that no longer contain the thiocarbonylthio moiety.

situated at the periphery of the star and the propagating radical moves outwards as polymerization progresses (Figure 21.5). This has important implications for possible side and termination reactions throughout the polymerization. Because the propagating radical is at the star periphery, termination reactions between the growing arms can result in intra-star termination causing two dead arms, or inter-star

termination, also known as star–star coupling. Both inter- and intra-star termination reactions will lead to high dispersities; however, inter-star termination results in a high molecular weight product up to twice the intended molecular weight that can be difficult to remove.

The primary advantage of the R-group approach is that the thiocarbonylthio group remains at the periphery of the star. RAFT agents are often coloured, resulting in coloured products, which is often undesired. The location of the RAFT agent at the exterior enables destruction of the RAFT agent to remove colour or to introduce additional functionality. The conversion of RAFT agents to functional groups has been extensively reviewed, with conversion to groups that can participate in click reactions being the most appealing [18–20].

The Maynard group exploited the terminal RAFT groups resulting from the R-group core-first approach to synthesize star poly(*N*-isopropylacrylamide) (PNIPAAm)-lysozyme conjugates [21]. The polymerization of four-arm PNIPAAm stars was stopped at 52% conversion to limit star–star coupling and ensure retention of the RAFT end group. Using a mechanism previously reported by Perrier et al. [22], the RAFT agents were reacted with a symmetrical azo-initiator containing furan-protected maleimide groups to achieve star polymers with terminal protected maleimide groups. Once deprotected, the enzyme lysozyme was conjugated to the star polymer via thiol-maleimide click chemistry [21]. More recently, Wang et al. synthesized four-arm PNIPAAm stars and converted the RAFT group to an alkyne via one-pot aminolysis and subsequent Michael addition of propargyl acrylate (Figure 21.6) [23]. The four-arm PNIPAAm star was then reacted with azide-functionalized β-cyclodextrin, forming a temperature-responsive PNIPAAm hydrogel. These examples highlight the ease with which star polymers synthesized using the R-group approach can undergo end-group functionalization.

21.2.1.3 Developments in Synthesis

Although the R- and Z-group approaches for core-first star polymers have been well studied, there have been few developments that have altered the way the RAFT core-first approach is conducted since its inception. Most reactions are still carried out using thermal initiators such as 2,2′-azobis(2-methylpropionitrile) (AIBN) and 2,2′-azobis[2-(2-imidazolin-2-yl)propane] dihydrochloride (VA-044). Therefore, the recent usage of photo-mediated RAFT polymerization for the synthesis of star polymers using the core-first approach has been a welcome and exciting development. One mechanism for photoinduced electron or energy transfer (PET)-RAFT polymerization involves a photoredox reaction between the thiocarbonylthio group and a photoredox catalyst [24]. The use of a photoredox catalyst provides temporal control over the polymerization, meaning that reactions can be stopped and restarted at will. In addition, PET-RAFT can proceed in the presence of air, thereby eliminating the need for degassing and stringent oxygen-free conditions typically required for RAFT polymerizations.

The Boyer group reported the use of PET-RAFT to synthesize three- and four-armed stars with photocatalyst zinc tetraphenylporphyrin (ZnTPP) [25]. The star polymers were reasonably well controlled with dispersities ranging from 1.1 to 1.5 and used for screening structure–activity relationships. More recently, the

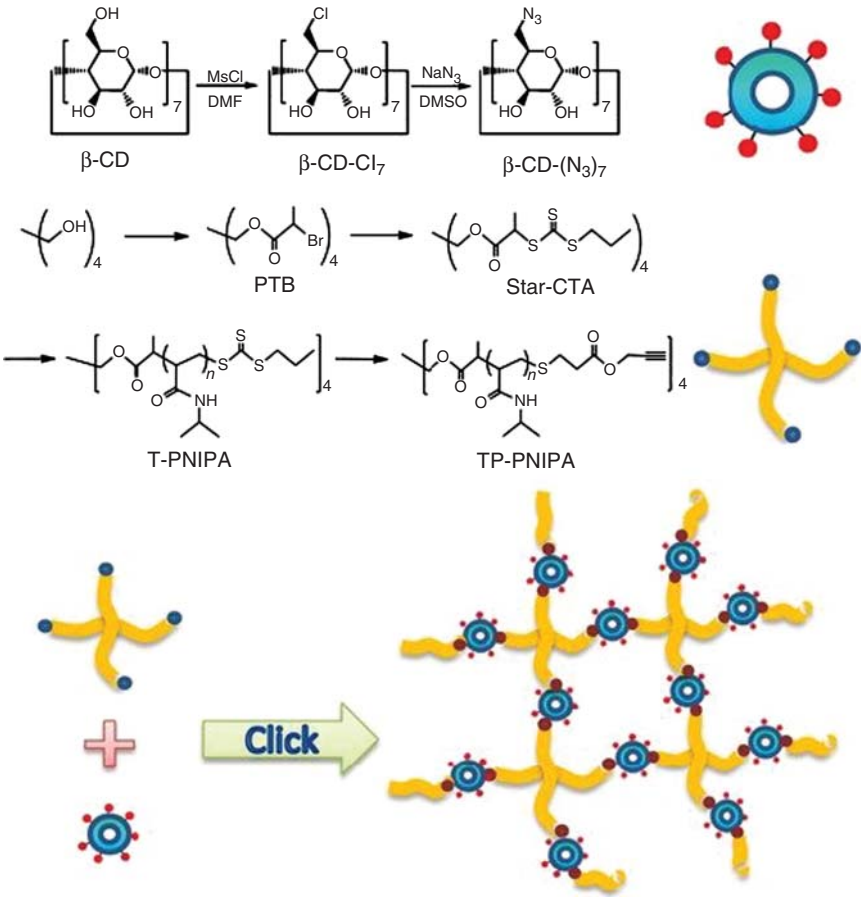

Figure 21.6 Synthesis of star polymers via R-group core-first approach using RAFT polymerization. Terminal thiocarbonylthio groups were converted to alkynes, facilitating hydrogel synthesis through click chemistry. Source: Reprinted with permission from Wang et al. [23]. Licensed under CC by 4.0.

Boyer and Lim groups used PET-RAFT to modify lanthanide-doped upconversion nanoparticles (UCNPs), which have unique photoluminescent properties with potential biomedical applications [26]. UCNPs were coated with silica and functionalized with RAFT agent, from which poly(oligoethylene glycol methyl ether methacrylate) (POEGMA) was polymerized. The addition of the POEGMA shell rendered the UNCPs water soluble without affecting the upconversion emission spectrum of the particles.

Photo-mediated RAFT polymerization can also be performed via direct photolysis of the RAFT agent, a method known as photoiniferter RAFT polymerization. Linear polymers synthesized via photoiniferter RAFT polymerization have been shown to exhibit exceptional chain-end fidelity, leading to monomer conversions greater than 95% as well as multiblock and ultra-high molecular weight (UHMW) polymers [27, 28]. Exploiting the high chain-end fidelity resulting from photoinferter RAFT

polymerization, the Qiao group synthesized UHMW star polymers with molecular weights in excess of 20 MDa using the R-group core-first approach [29]. The authors first demonstrated the controlled synthesis of poly(dimethylacrylamide) (PDMA) star polymers from tetrafunctional trithiocarbonate (4-TTC) and xanthate (4-XAN) cores under blue and purple light, respectively. Further experiments with the 4-XAN core resulted in star polymers with molecular weights of 3.8 MDa, equivalent to 0.96 MDa per arm, using both purple and UV light. Finally, a modified β-cyclodextrin core containing 21 RAFT agents was synthesized. A molecular weight of 23 MDa was targeted, with 96% conversion achieved after 18 hours of UV irradiation for a theoretical molecular weight of 21.9 MDa. This finding was corroborated by static light scattering as well as gel-permeation chromatography (GPC) analysis of the star polymer arms following their cleavage from the core. The authors reported difficulties synthesizing star polymers when molecular weights greater than 1 MDa per arm were targeted and attributed these difficulties to the extreme dilution of the CTA. A summary of the UHMW PDMA star polymers synthesized is shown in Table 21.1.

The synthesis of UHMW diblock star polymers was reported in 2019 by Dao et al. [30]. Using a tetrafunctional CTA, the authors synthesized star polymers containing a neutral poly(acrylamide) inner block and a negatively charged poly(acrylic acid) outer block via the Z-group core-first approach. Size exclusion chromatograms of the star polymers showed bimodal distributions following polymerization of the first block and multimodal distributions following polymerization of the second block, indicating a loss of control and termination events. Despite the large dispersities and multimodal distributions observed, the synthesis of UHMW block star

Table 21.1 Summary of UHMW PDMA star polymers synthesized via photoiniferter RAFT polymerization using the R-group, core-first approach.

Number of arms	DP per arm	Target MW (MDa)	$[M]_0$ (M)	Time (h)	Conversion (%)[a]	$M_{n(\text{theo})}$ (MDa)[b]	$M_{W\,(\text{SLS})}$ (MDa)[c]	R_G (nm)[c]
4	10 100	4	1	6	96	3.8	2.5	71.1
4[d]	10 100	4	1	102	96	3.8	3.8	74.7
4	20 200	8	3	6	94	7.5	6.3	124.1
21	1 900	4	1	3.5	95	3.8	5.3	105.7
21	**11 000**	**23**	**0.5**	**18**	**96**	**21.9**	**20.4**	**205.1**
21	22 000	46	0.5	18	94	43.3	3.2	79.6

a) Conversion was determined using ^{1}H NMR spectroscopy.
b) Theoretical molecular weights ($M_{n,(\text{theo})}$) were determined via monomer conversion values.
c) $M_{W\,(\text{SLS})}$ and R_G were determined by static light scattering.
d) This polymerization was performed using purple light irradiation, while all others were irradiated with ultraviolet light. The largest reported RDRP star polymer, with $M_{W\,(\text{SLS})}$ of 20.4 MDa, is highlighted in bold text.

Source: Adapted with permission from Allison-Logan et al. [29]. Copyright 2019, American Chemical Society.

polymers is an exciting development in the field of polymer chemistry. In addition, the block star polymers showed promise as polymeric flocculants, highlighting potential applications of UHMW star polymers.

21.2.2 Arm-first Approach

The arm-first approach to star polymer synthesis requires the crosslinking of linear arms using di- or multi-functional crosslinking or coupling agents. Unlike the core-first approach, where the molecular weight of the core is often negligible, the arm-first approach results in a core that is a crosslinked network and typically represents approximately 30% of the star polymer's total molecular weight. Stars synthesized using the arm-first approach are often referred to as core-crosslinked stars (CCS), distinguishing them from stars synthesized using the core-first or grafting-onto approaches [1].

The arm-first approach offers several advantages over the core-first approach. Most importantly, the arm-first approach does not require synthesis of a multi-functional core, enabling one-pot synthesis. Unlike the core-first approach, the polymer arms are easily characterized before crosslinking. The unique nature of the core resulting from the arm-first approach lends itself to further functionalization, including the loading of functional compounds. In addition, miktoarm star polymers are more easily synthesized using the arm-first approach. There are however some disadvantages. Although a greater number of arms can be achieved with the arm-first approach, the number of arms can only be determined after synthesis and controlling the number of arms and star molecular weight is difficult. Star polymers can also be difficult to purify if not all arms are incorporated into the star polymer because the arms are of a high molecular weight and have similar properties to the star. Star–star coupling can also occur if the growing cores of separate stars come into contact.

The arm-first approach via RAFT polymerization can be further divided into the macroRAFT and macromonomer routes (Figure 21.7). The macroRAFT method, also referred to as the macro-chain transfer agent (macroCTA) method, is most common. Following RAFT polymerization of the arm, the incorporated RAFT agent then acts as the CTA during the crosslinking polymerization step. This method is dependent on the presence of living RAFT agents in the polymer and achieving near complete monomer conversion. Any dead chains will not be crosslinked and therefore not incorporated into the star polymer, so maintaining livingness of the RAFT end group is essential. Following arm synthesis, crosslinker can be added directly to the reaction mixture enabling a facile, one-pot approach to obtain well-defined star polymers. The macroRAFT approach can also be used with arms synthesized through alternative polymerization techniques provided a RAFT agent is incorporated into the arms before crosslinking, allowing RAFT star polymerization of arms synthesized using other polymerization techniques.

The macromonomer route was first demonstrated by the Matyjaszewski group using ATRP and requires an arm with a polymerizable vinyl end group [31]. A small-molecule RAFT agent is used and the arm is incorporated into the star as

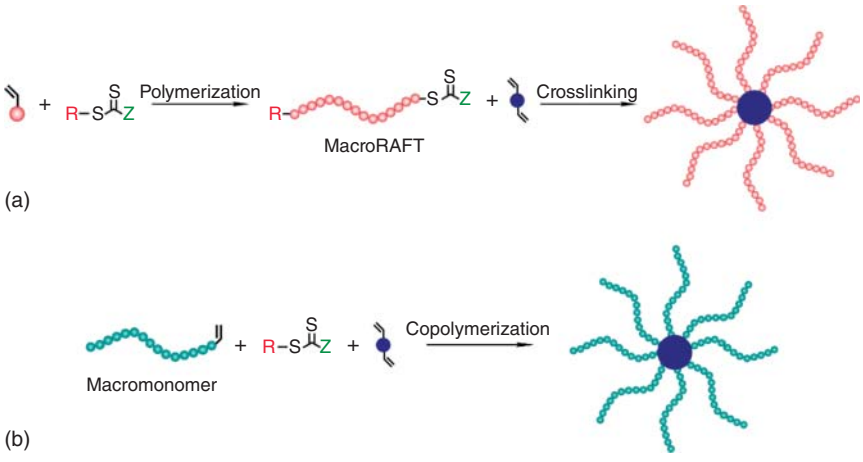

Figure 21.7 Synthesis of star polymers using the arm-first approach via RAFT polymerization can be performed using the (a) macroRAFT and (b) macromonomer approaches.

a macromonomer during polymerization. The macromonomer route allows for a lower number of initiating sites than the macroinitiator approach, reducing the likelihood of star–star coupling [31].

The An group used commercially available 2 kDa poly(ethylene glycol) methacrylate (PEGMA), highlighting that synthesis of a macroRAFT agent either through RAFT polymerization of the arm or conjugation of RAFT agent to the arm was not required for this approach [32]. The PEGMA arm, RAFT agent, and radical initiator were soluble in phosphate buffer pH 7, while the crosslinker and optional comonomer formed oil droplets. As polymerization proceeded, a random copolymer of the macromonomer arm, crosslinker, and spacer comonomer (if used) was produced. This is in contrast to the macroRAFT approach where polymerization results in a block copolymer. The resulting amphiphilic copolymers then self-assembled with the hydrophobic portions forming the core while the PEGMA chains radiated outwards. The authors investigated each component of the system, varying the concentration of phosphate buffer and macromonomer, ratio of crosslinker, presence of comonomer, and molecular weight of the macromonomer. Most star polymers formed showed greater than 90% arm incorporation, narrow size distributions, and dispersities below 1.2. However, poor star formation was observed when the molecular weight of the arm was increased to 4 kDa [32].

This method is ideally suited for the crosslinking of arms that were synthesized using polymerization techniques other than RAFT. The Heise group synthesized poly(glutamic acid) (PGA) via NCA ROP initiated by 4-vinylbenzylamine, ensuring that all polymer chains contained a vinyl end group [33]. Initial star polymers formed via RAFT polymerization were well defined with a dispersity of 1.2, although arm incorporation was only 14%. The authors found that arm incorporation could be increased by periodically adding more crosslinker to the reaction, although this also led to an increase in dispersity. Despite the low arm incorporation, this work

demonstrated the versatility of RAFT polymerization for the crosslinking of star polymers, even when the arms were prepared using other techniques.

21.2.2.1 Developments in Synthesis

The synthesis of star polymers via the arm-first approach has undergone a number of developments in the past decade that have led to improved polymers. During the early days of RAFT polymerization, the arm-first approach was plagued by low arm incorporation into the star, resulting in high dispersities. Low incorporation of arms was thought to be due to 'dead' chain ends that could not participate in further polymerization. However, major developments by the Boyer, Davis, An, and Qiao groups have made the arm-first approach the new method of choice.

In a seminal paper by Boyer and Davis, the synthesis of well-defined star polymers with low molecular weight dispersities and high arm incorporation were reported using the arm-first approach by selecting poorly soluble crosslinkers [34]. Star polymers with POEGA arms and *N*,*N*′-bis(acryloyl)cystamine or 1,6-hexanediol diacrylate as a crosslinker were synthesized using *N*,*N*-dimethylformamide (DMF), acetonitrile, and toluene as a solvent to investigate the effect of crosslinker solubility on star formation (Figure 21.8a). 1,6-Hexanediol diacrylate is soluble in all three solvents, while *N*,*N*′-bis(acryloyl)cystamine is soluble in DMF and acetonitrile but only partially soluble in toluene. POEGA arms crosslinked with *N*,*N*′-bis(acryloyl)cystamine in toluene resulted in well-defined star polymers with a dispersity of 1.12 and greater than 90% arm incorporation, a dramatic improvement over previously reported star polymers. All other reactions resulted in dispersities greater than 1.5, demonstrating the importance of crosslinker and solvent choice (Figure 21.8b–e). The authors hypothesized that the improved star formation using *N*,*N*′-bis(acryloyl)cystamine in toluene was a result of nanophase separation that induced compartmentalization of the crosslinking. Further experiments demonstrated that high arm incorporation and low dispersity could be achieved using arms of varying composition and molecular weight as well as other poorly soluble crosslinkers [34].

Applying a similar concept, the An group has developed and thoroughly investigated the use of heterogeneous RAFT polymerization systems to develop well-defined star polymers by emulsion and dispersion RAFT [32, 35–42]. First reported in 2011, the An group demonstrated the synthesis of CCS polymers in water with a solid content of 10% w/v via emulsion and dispersion polymerization and that these star polymers stabilized emulsions during particle synthesis [35]. The versatility of the method was shown using poly(*N*,*N*′-dimethylacrylamide) (PDMA), poly(poly(ethylene glycol) methyl ether methacrylate) (PPEGMA), and poly(2-methoxyethyl acrylate-*co*-poly(ethylene glycol) methyl ether acrylate) (P(MEA-*co*-PEGA) arms. The emulsion system was conducted with spacing monomer butyl acrylate and crosslinker poly(ethylene glycol) diacrylate (PEGDA), while the dispersion system contained *N*-isopropylacrylamide (NIPAAm) and methylene bisacrylamide (MBA) as the spacing monomer and the cross-linker, respectively (Figure 21.9a). In all cases, a high degree of arm incorporation and dispersities of 1.12 and below were observed from GPC analysis. Interestingly,

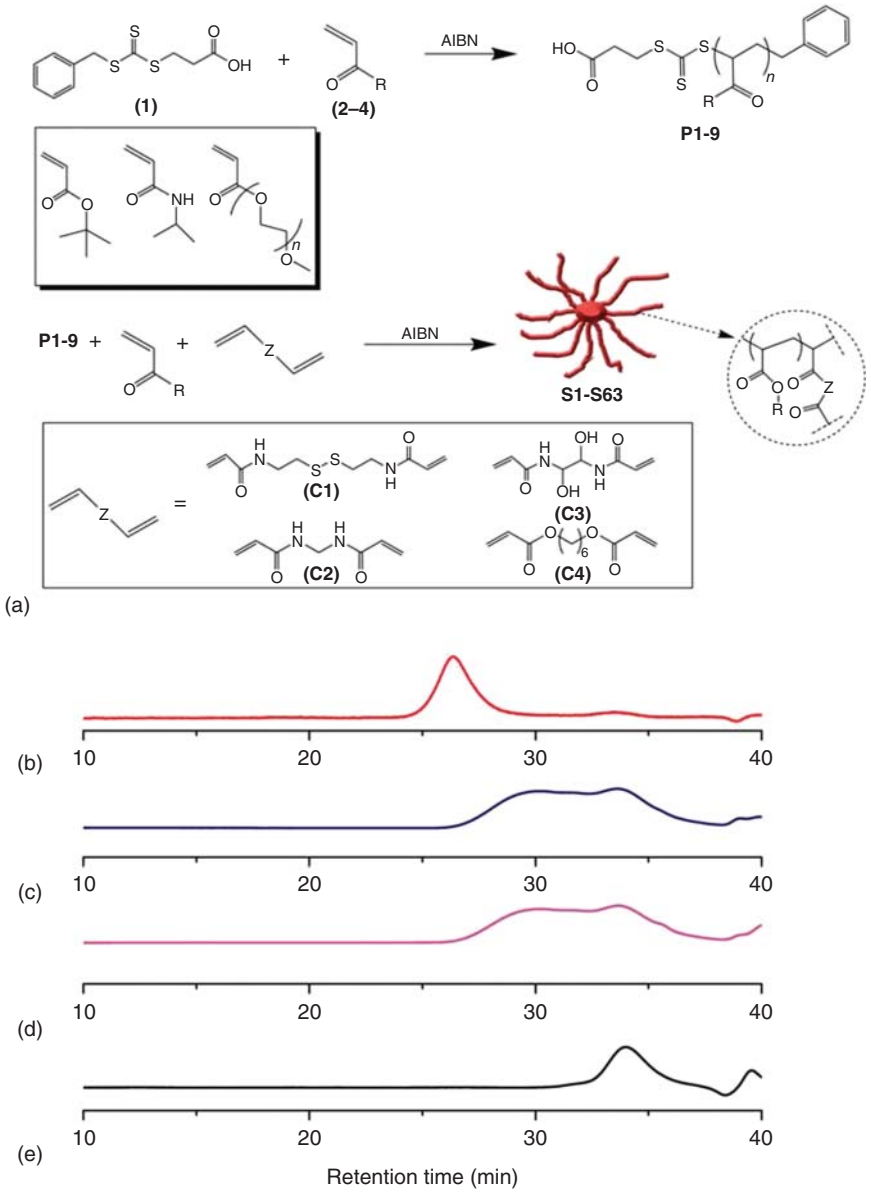

Figure 21.8 (a) Synthesis of star polymers with varying arm compositions and crosslinkers in a range of solvents to investigate the impact of crosslinker solubility on star formation. GPC traces of star polymers obtained by RAFT, using *N*,*N*′-bis(acryloyl)cystamine (BAC) as the crosslinker, in (b) toluene, (c) DMF, (d) acetonitrile, and (e) arm polymer used in this study before crosslinking. BAC is poorly soluble in toluene, leading to well-defined stars and is soluble in DMF and acetonitrile where limited star formation was observed [34]. Source: Adapted with permission from Ferreira et al. [34]. Copyright 2011, Royal Society of Chemistry.

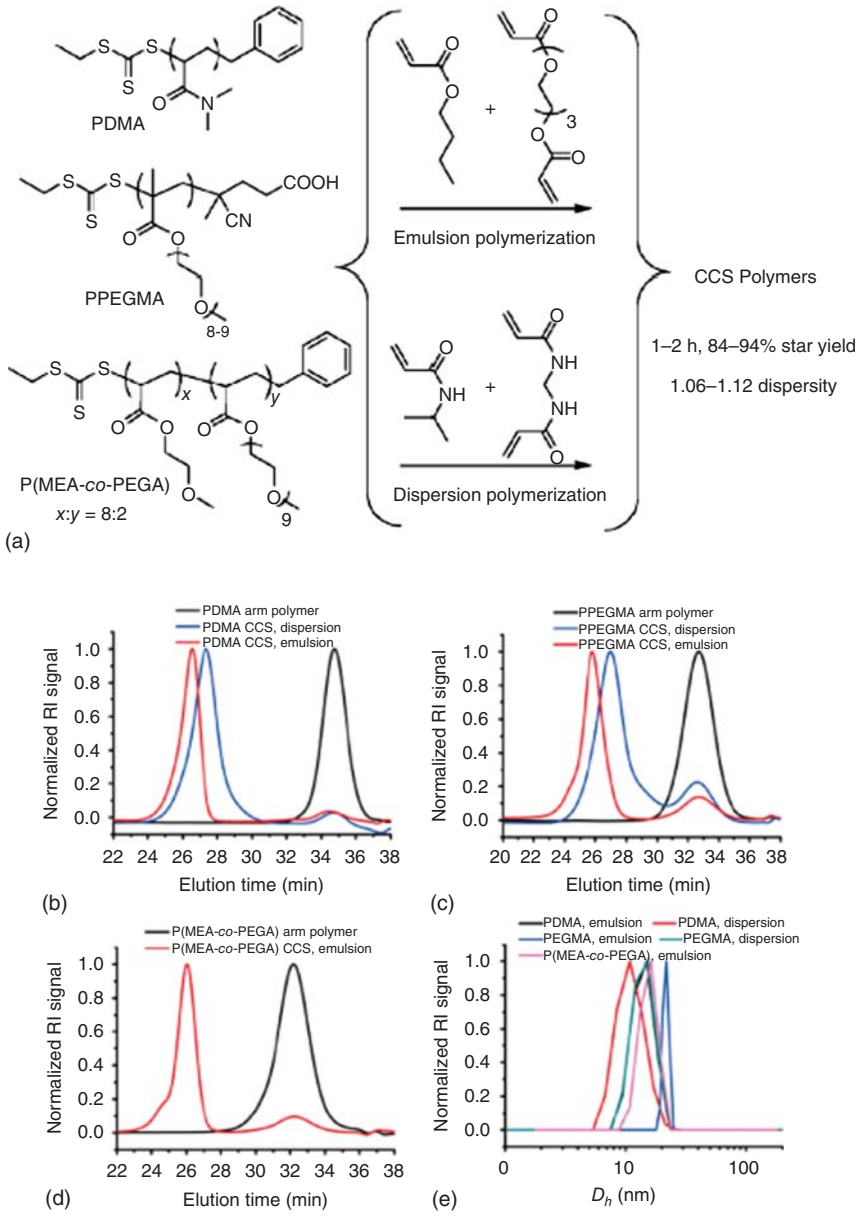

Figure 21.9 Core-crosslinked stars synthesized using emulsion and dispersion RAFT polymerization. (a) Monomers and crosslinkers used for emulsion and dispersion polymerization. GPC chromatograms of (b) PDMA, (c) PPEGMA, and (d) P(MEA-*co*-PEGA) arm and star polymers. (e) Dynamic light scattering chromatogram showing the hydrodynamic radius of star polymers synthesized used emulsion and dispersion polymerization [35]. Source: Adapted with permission from Qiu et al. [35]. Copyright 2011, Royal Society of Chemistry.

emulsion polymerization led to greater arm incorporation, higher molecular weight, and lower dispersity than dispersion polymerization (Figure 21.9b–e).

The next major development was reported by the Qiao group when they used photoiniferter RAFT polymerization in the synthesis of star polymers via the arm-first approach [43]. The synthesis of linear polymers via visible light-mediated RAFT without the use of exogenous radical sources or catalysts was first reported in 2015 and resulted in improved livingness at monomer conversions greater than 90%, demonstrated using matrix-assisted laser desorption/ionization (MALDI)-ToF and the one-pot synthesis of a pseudohexablock copolymer [27]. Irradiation with blue light was shown to directly activate trithiocarbonates, eliminating the need for additional radical sources. The improved livingness is likely due to the significantly lower concentration of radicals present in the reaction mixture, resulting in less termination reactions.

The highly living nature of polymers synthesized via photoiniferter RAFT made them excellent candidates for the synthesis of star polymers. Using a two-step, one-pot approach, McKenzie et al. synthesized linear poly(methyl acrylate) (PMA), which was then crosslinked using ethylene glycol diacrylate (EGDA) (Figure 21.10a). The ratio of crosslinker to arm was investigated with a ratio of 10 : 1 resulting in the best star formation. A ratio of 5 : 1 resulted in incomplete star formation while a ratio of 15 : 1 led to a broader size distribution. The degree of polymerization (DP) of the arm was also important in the synthesis of star polymers. The crosslinker to arm ratio was held at 10 : 1 while PMA arms with DPs of 60, 80, and 120 were crosslinked. GPC analysis of the stars formed from PMA DP 60 was bimodal, with the higher molecular weight product likely the result of coupling between two star cores because of the small arm length. A DP of 80 resulted in well-defined star polymers with a dispersity of 1.41 and arm incorporation of 94%. The largest arms, with DP 120, also result in well-defined stars, albeit with a slightly higher dispersity and only 89% arm conversion. The lower conversion of DP 120 arms into the star is thought to be caused by reduced access to the core due to the greater arm length [43].

Importantly, the RAFT chain ends were shown to be still living following star polymerization. An in/out star was synthesized, with monomer added to the already formed stars. Further irradiation with blue light resulted in the polymerization of new arms from the star core (Figure 21.10b). The number of arms in the initial star was calculated to be 31 and the number of arms following the in/out polymerization was found to be 60. The kinetics of monomer conversion during the in/out chain extension were compared to a control synthesis of linear PMA, with the apparent rate constant, indicating that the efficiency of polymerization from the core was 95% and that the functionality of most RAFT agents was maintained [43].

In 2017, the Qiao and Kamigaito groups demonstrated the synthesis of novel star polymers using a mechanistic transformation from cationic RAFT polymerization to radical RAFT polymerization [44]. Cationic RAFT was first reported by Kamigaito and coworkers, who demonstrated polymerization of electron-rich vinyl ether monomers that are not readily polymerized via radical RAFT polymerization to obtain linear polymers with dispersities below 1.1 [45]. Synthesis of

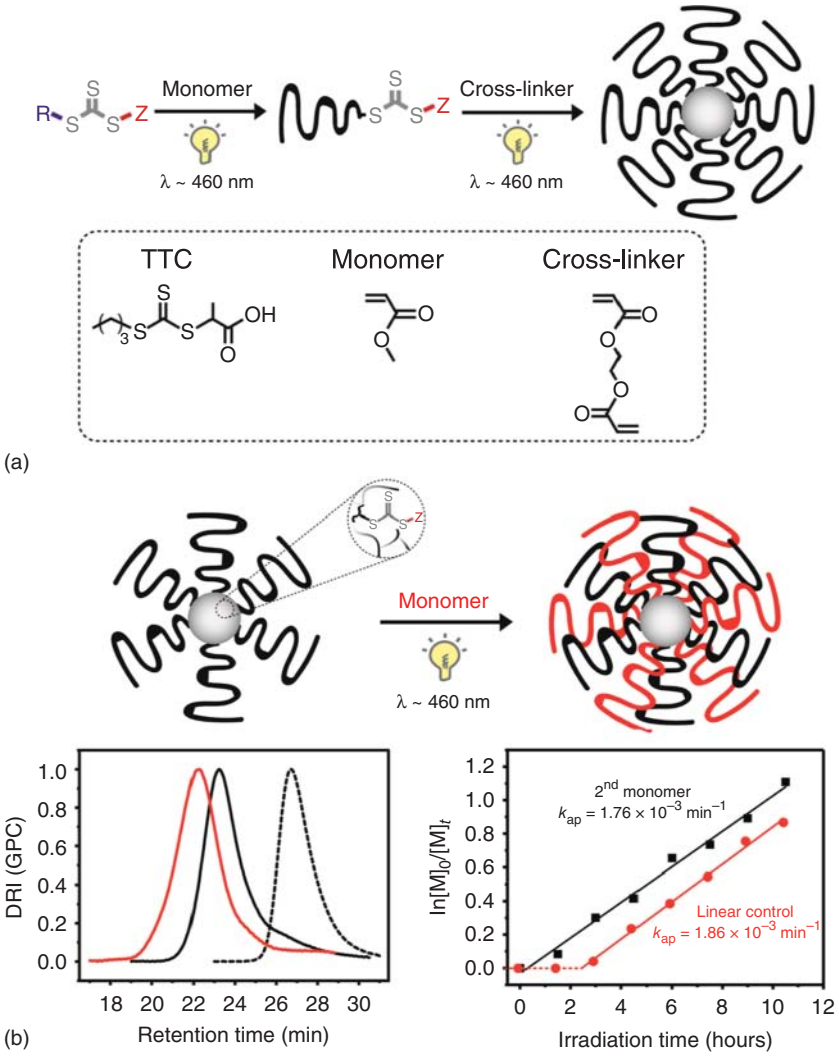

Figure 21.10 Photo-mediated RAFT polymerization for the synthesis of star polymers via the (a) arm-first approach and (b) from the resulting star core using the in/out technique. GPC chromatograms show the RI trace of the arm, CCS polymer, and star polymer following the in/out reaction. The apparent rate of polymerization of the second monomer compared to the linear control indicated the efficiency of polymerization from the core was 95%. Source: Adapted with permission from McKenzie et al. [43]. Copyright 2015, American Chemical Society.

star polymers via cationic RAFT was demonstrated in a one-pot approach, with linear poly(isobutyl vinyl ether) (PIBVE) prepared and then crosslinked using a divinyl ether crosslinker. A mechanistic transformation to radical RAFT was also possible with PIBVE arms being crosslinked using a diacrylate crosslinker. Finally, the authors showed that a block copolymer of PIBVE and a heterobifunctional monomer with structure vinyl ether-*R*-acrylate (e.g. 2-(vinyloxy)ethyl acrylate)

could be synthesized via cationic polymerization of the vinyl ether groups and then crosslinked to form a star polymer through radical RAFT polymerization of the pendant acrylate groups. This mechanistic switch enables the synthesis of star polymers containing monomers not easily synthesized by cationic or radical RAFT polymerization alone and resulted in the synthesis of well-defined star polymers with high arm incorporation and dispersities as low as 1.18 [45].

The development of simple, rapid, high-throughput techniques to synthesize well-defined polymers of all architectures has been an important area in recent years. In 2017, the Cooper-White group reported the development of rapid one-pot sequential aqueous RAFT (rosa-RAFT) for the high-throughput synthesis of star polymers (Figure 21.11) [46]. Polymerizations of acrylate and acrylamide monomers were performed in a water/dioxane mixture (80/20 v/v) using water-soluble thermal

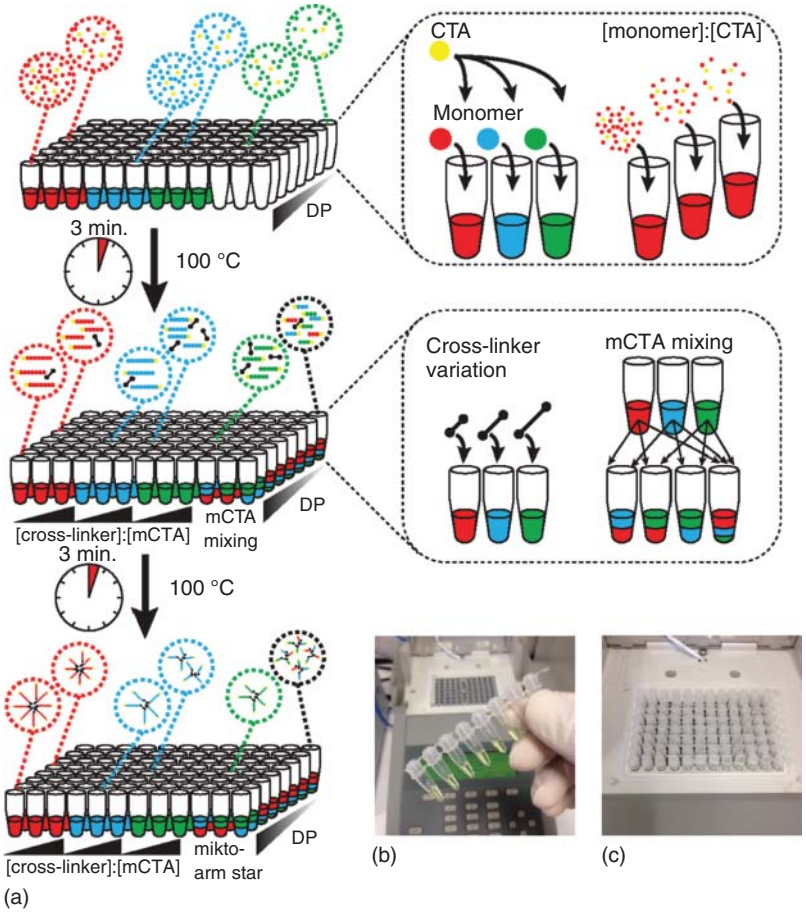

Figure 21.11 (a) Synthesis of homopolymer and mikto-arm star polymers via high-throughput rosa-RAFT. (b) Reactions were performed in air in 50 μL volumes (c) utilizing a thermocycler to control each reaction step. Source: Reprinted with permission from Cosson et al. [46]. Copyright 2017, John Wiley & Sons.

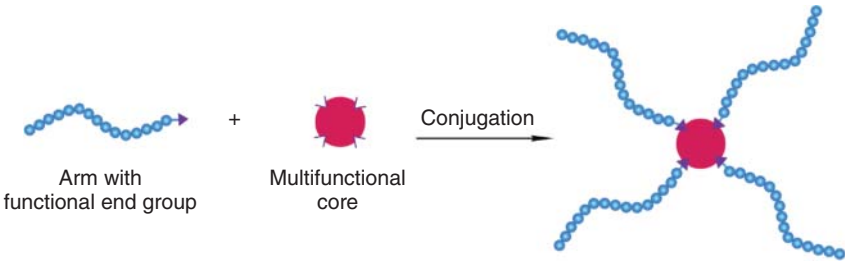

Figure 21.12 The grafting-to approach requires the conjugation of arms with a functional end group to a multifunctional core.

radical initiator VA-044. Crucially, these polymerizations did not require degassing. Arm polymerization and crosslinking steps only required three minutes each at 100 °C in a thermocycler. The high-throughput technique enabled the rapid synthesis of a library of star polymers using different crosslinkers, crosslinking ratios, and mixing of macroRAFT arms to synthesis miktoarm star polymers, marking an important development in the synthesis of star polymers.

21.2.3 Grafting-to Approach

A third method of star polymer synthesis is known as the grafting-to approach and involves the conjugation of arms onto a functional core (Figure 21.12). This approach allows for excellent characterization as both the core and arm can be analyzed before conjugation. It is important to note that although the linear arms can be synthesized via RAFT polymerization, the actual formation of the star is a result of chemical conjugation. Similar to end group functionalization of star polymers synthesized by the R-group core-first approach, RAFT agents can be readily modified to functional groups that can participate in coupling reactions.

Like the core-first approach, the number of possible arms is pre-determined. However, ensuring 100% conjugation can be difficult. Achieving quantitative conjugation becomes more difficult as the number of arms and the molecular weight of arms increases due to congestion at the core.

21.3 Application of Star polymers

The ease with which RAFT polymerization affords the preparation of various star sizes, compositions, and functionalities has seen the development of a broad array of RAFT-mediated star polymers for targeted applications. The unimolecular structure of star polymers ensures that they maintain their structure and are not susceptible to shear or disassembly under fluctuating or extreme conditions. The combined tolerance of RAFT polymerization to many functional groups and the distinct regions of star polymers facilitates the generation of core-, arm-, or end-functionalized star polymers [1, 47]. By leveraging the unique property of star

architectures, star polymers prepared via RAFT have found application in diverse fields, including as drug delivery and imaging contrast agents, viscosity modifiers, emulsion stabilization, and in advanced material synthesis.

21.3.1 Star Polymers in Biomedical Applications

Controlled delivery of therapeutics is one of the most common applications for star polymers synthesized by RAFT polymerization. Star polymers have several advantages that enable them to safely transport therapeutic agents to the appropriate site and control the rate of release. Star polymers are generally between 10 and 100 nm in diameter, which is often considered the ideal size of nanoparticles for cancer therapy. Particles greater than 10 nm avoid the removal from circulation by the renal system experienced by smaller particles, while nanoparticles smaller than 100 nm are thought to passively accumulate in tumours because of the irregular blood vessel structure in tumours that results from abnormal gene expression and rapid growth. The core–shell structure of star polymers can shield loaded therapeutics or imaging agents from unwanted degradation and uptake by the body's immune system, resulting in increased delivery efficiency while also facilitating functionalization of the star surface with specific targeting moieties such as peptides, antibodies, and sugars, thus improving delivery to the target site or tissue. In addition, intelligent design of star polymers can result in therapeutic release over a desired timescale or upon exposure to a particular stimulus. Because of their advantages and versatility, star polymers synthesized by RAFT polymerization are promising candidates for delivery of drug, gene, biomolecule, protein, and imaging agents. As with all materials designed for biomedical applications, it is essential to ensure the star polymers and their possible degradation products do not induce inflammatory response or toxicity before, during, or after delivery [1, 48–50].

The Whittaker and Davis groups designed and synthesized star polymers by RAFT polymerization for biomedical applications including the delivery of chemotherapeutic agents, genes, imaging agents, protein inhibitors, and signalling molecules [50]. In order to prepare star polymers which are soluble in water and the biological environment, hydrophilic monomers such as poly(oligo(ethylene glycol) methyl ether acrylate/methacrylate) (POEGA/MA) are most commonly used to form the star polymer arms. Star polymers comprising POEGA/MA arms have demonstrated reduced protein adsorption and also provide stability to star polymers during circulation as they are not susceptible to dissociation in the same way as self-assembled structures [51–53]. In vivo and in vitro studies have shown that the POEGA star polymers with different molecular weights (49, 64, and 94 kDa), and therefore hydrodynamic volumes, exhibit different pharmacokinetics and tumour disposition behaviours, with the largest star polymers (94 kDa) displaying longer plasma exposure and improved uptake into solid tumours [52]. The star polymers may include stimuli-responsive functionalities such as thermoresponsive monomer NIPAAm [54] and pH-responsive monomer 2-(dimethylamino)ethyl methacrylate (DMAEMA) [53, 55], which were used in the arm or as a secondary monomer in the

core. These star polymers change their size when exposed to changing temperature or pH and stimulate the release of the drug at the target site.

Star polymers for biomedical applications should be large enough to avoid removal by the renal system, leading to improved circulation half-lives. However, star degradation is desirable after cell internalization to improve therapeutic delivery or after delivery to prevent bioaccumulation. To achieve this end, degradable crosslinkers such as acid-labile crosslinkers [56, 57] and reduction-sensitive disulfide crosslinkers are utilized in core structure [53, 58, 59]. These crosslinkers are readily hydrolyzed in the acidic environment of tumour tissue or reduced by glutathione upon exposure to the glutathione-rich intracellular environment, resulting in degradation of the core and therefore the star polymer.

The unique structure of star polymers facilitates the functionalization of the core, arm, or peripheral regions and can be accomplished by incorporating functional groups into the crosslinkers, monomers, and RAFT agents used. Common functionalities include therapeutic molecules, imaging agents, and dyes. *N*-hydroxysuccinimide (NHS)-functionalized RAFT agents have been used to prepare end-functionalized star polymers [60]. Arm-functionalized star polymers were synthesized by incorporating activated ester-based monomers such as pentafluorophenyl acrylate (PFPA) [60, 61] and 4-vinylbenzyl chloride (VBC) [62] into the arms. PFPA [60, 63] and vinyl benzaldehyde (VBA) [51, 64] have been incorporated into cores as secondary monomers during crosslinking to generate core-functionalized star polymers. It has also been shown that two types of functional groups could be incorporated into star polymers to functionalize them with both chemotherapeutic drug and magnetic resonance imaging (MRI) contrast agent. Star polymers were synthesized by incorporating aldehyde-functional monomer VBA into the core and activated-ester monomer PFPA in the arm (Figure 21.13). The VBA and PFPA monomers were subsequently modified with chemotherapeutic drug doxorubicin and an MRI contrast agent based on disparate reactivities of VBA and PFPA [61].

For gene delivery applications, cationic monomers or cationizable monomers such as 2-(dimethylamino)ethyl acrylate/methacrylate (DMAEA/MA) were incorporated into star polymers [65–68]. These monomers form electrostatic interactions with negatively charged genetic molecules such as DNA or RNA, resulting in complexes called polyplexes. This electrostatic complexation protects genes from enzymatic degradation during circulation and ensures the necessary compaction to enter to the target cells. In addition, star polymers synthesized by RAFT polymerization have been used for micelle and vesicle formation for drug delivery and imaging [69, 70], bone regeneration, [71] cell sheet engineering, [72] lectin binding [72], delivery of nitric oxide to prevent biofilm formation [72], and targeting primary human immune cell subsets [73], demonstrating their versatility in biomedical applications.

21.3.2 Star Polymers in Other Applications

The unique properties of star polymers allow tunable interactions with other species in solution. The compact nature of star polymers leads to significantly different

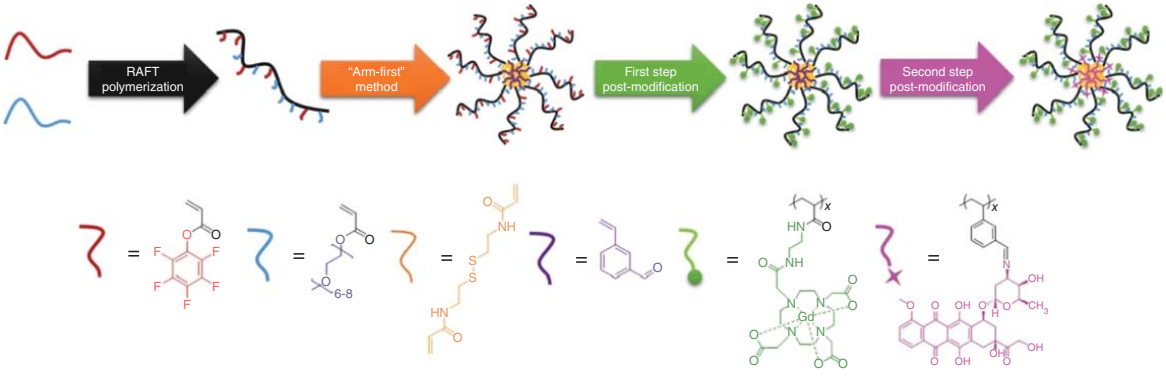

Figure 21.13 Schematic illustration of the synthesis of multifunctional core cross-linked star polymers functionalized with MRI contrast agent and chemotherapeutic drug [61]. Source: Reprinted with permission from Li et al. [61]. Copyright 2015, John Wiley & Sons.

properties than linear polymers of the same molecular weight, while their flexible arms lead to different behaviours than particles of the same size. Such interactions can be leveraged for controlling the reactivity of these other species, leading to altered chemical pathways and affording the preparation of advanced materials. This section will present a selection of applications in which star polymers were essential for improved performance.

21.3.2.1 Emulsion Stabilization

Since reporting the synthesis of core-crosslinked star (CCS) polymers via emulsion and dispersion polymerization in 2011 [35], An and coworkers have pioneered the use of CCS polymers as emulsion stabilizers [39, 40, 42, 74, 75]. Emulsion systems have wide industrial relevance, including in food, cosmetics, pharmaceuticals, coatings, oil recovery, and chemical processing. Qiu et al. demonstrated the use of a fluorescein-tagged PDMA CCS that adsorbed to the interface of a toluene/water emulsion with excess PDMA stars remaining the aqueous phase, shown in Figure 21.14a, and Nile red-stained toluene droplets shown in Figure 21.14b. Stabilized emulsions were used as templates for the synthesis of spherical polystyrene particles inside the oil droplets. Following solvent evaporation, aggregation of PDMA stars around the particles (Figure 21.14c) and Nile red-stained poly(styrene) particles were observed (Figure 21.14d).

Exploiting the versatility of RAFT polymerization, the An group developed reversible emulsification/demulsification systems readily triggered by external stimuli, including heat/salt/pH through targeted interactions between stars and between star arms and solvents (Figure 21.15) [39, 40, 42, 74]. While previous work had been carried out using amphiphilic star polymers to stabilize emulsions by having them act as surfactants, An and coworkers focused on CCS polymers with entirely hydrophilic arms and the structural properties of star polymers that may cause this stabilizing behaviour. Star polymers are similar in size to particulate

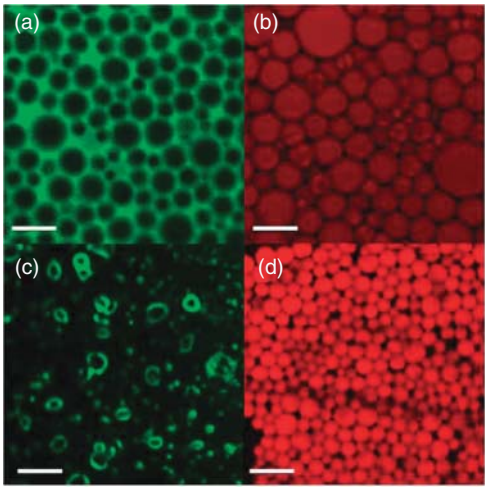

Figure 21.14 Confocal images of water/toluene (60/40 v/v%) emulsions containing (a) 0.2 wt% fluorescein-tagged PDMA stars and (b) Nile red stained toluene demonstrating the emulsion stabilizing activity of the PDMA stars. Following solvent evaporation, (c) PDMA stars at particle surface and (d) particles synthesized using emulsion templating. Scale bar is 20 μm [35]. Source: Adapted with permission from Qiu et al. [35]. Copyright 2011, the Royal Society of Chemistry.

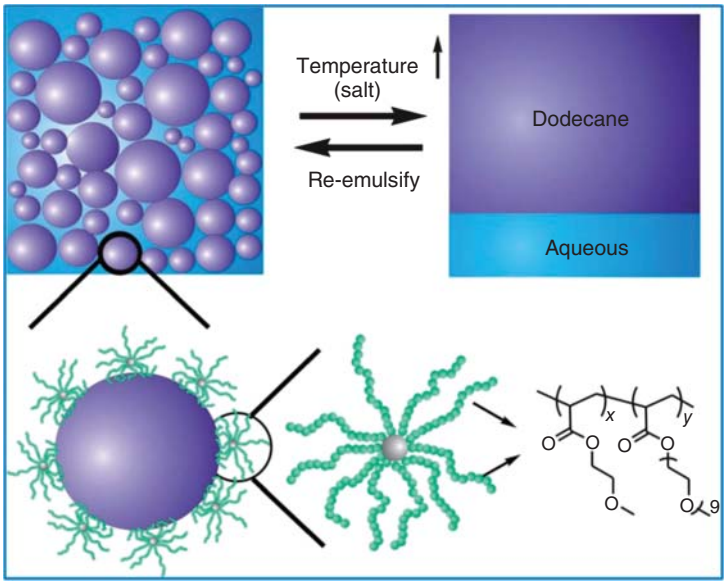

Figure 21.15 High internal phase emulsion (HIPE) stabilized by poly(MEA$_x$-*co*-PEGA$_y$) star co-polymers exhibit on-demand demulsification triggered by salt and temperature [42]. Source: Adapted with permission from Chen et al. [42]. Copyright 2014, Royal Society of Chemistry.

emulsifiers but display greater flexibility, which Chen et al. hypothesized would allow the CCS polymers to adopt favourable configurations once adsorbed onto the surface and aid their residence at the surface [39].

Star polymers have also been recently used as dispersants of multiwalled carbon nanotubes (MWNTs) in aqueous and acetone solutions [76]. Gao et al. reported the synthesis of an amphiphilic 'octopus' star polymer with a RAFT agent-functionalized silsesquioxane cage using the core-first approach. Star polymers were shown to produce more stable MWNT dispersions than linear polymers, which the authors suggested was due to hydrophobic core anchoring to the nanotube surface while the hydrophilic arms extended outwards and reduced the hydrophobic area of the MWNT surface (Figure 21.16) [76].

21.3.2.2 Advanced Materials

Numerous applications have been reported in which use of star polymers resulted in improved properties in comparison to linear polymers. Hendrich and Vana synthesized linear and star-shaped polymers that underwent redistribution of copolymer blocks because of the incorporation of bifunctional RAFT agents [77]. Tensile testing demonstrated that inclusion of as little as 5 mol% star polymer led to higher ultimate strength and material toughness compared to films of pure linear multiblock polymers. Zheng et al. reported improved resolution using a novel star polymer photoresist for krypton fluoride (KrF) photolithography [78]. Star copolymers were synthesized from a tetra-RAFT functionalized pentaerythritol core

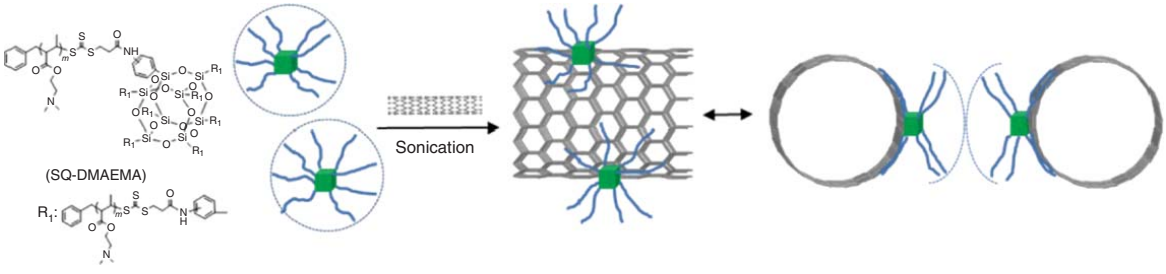

Figure 21.16 Star polymers with POSS core and hydrophilic arms stabilized MWNTs in aqueous solvent [76]. Source: Adapted with permission from Gao et al. [76]. Copyright 2016, Royal Society of Chemistry.

using *tert*-butyl acrylate and *p*-acetoxystyrene as monomers. Use of star copolymers results in a pattern resolution of 200 nm, demonstrating greater resolution than analogous linear photoresists.

Star polymers have also shown superior properties as single-ion conduction polymer electrolytes (SCPE), which are valued for their potential use in energy storage applications [10]. Miktoarm star polymers were composed of a polyhedral oligomeric silsesquioxane (POSS) core and poly(ethylene glycol) (PEG) and lithium poly([styrene-4-sulfonyltrifluoromethyl-sulfonyl] imide) (PSTF-Li) arms. The lithium-ion conducting stars demonstrated high thermal stability and tunable dc-conductivity. The improved thermal stability of the star polymer in comparison to a linear analogue was thought to be a result of the restricted motion of the star polymer, which is less sensitive to heat. PEG-*b*-PSTF linear copolymers were found to have greater dc-conductivity than the star polymer because of the star's higher T_g value; however, the addition of more PEG arms led to significantly increased conductivity, highlighting the tunability of star polymer composition and performance [10].

Star polymers can also be used in situations where the use of linear polymers is not possible. Lin and coworkers synthesized degradable star polymers through a combination of ROP and RAFT polymerization [79]. ROP of ε-caprolactone was performed from a β-cyclodextrin core and R-group of RAFT agents were conjugated to the resulting terminal alcohol groups. RAFT polymerization of 4-chloromethylstyrene was performed, followed by azide-functionalization by reacting sodium azide with the chlorine groups. The star polymers were irradiated with UV under dilute conditions to crosslink the azide groups, resulting in uniform nanoparticles with a crosslinked shell (Figure 21.17). The authors were able to tailor the nanoparticle size

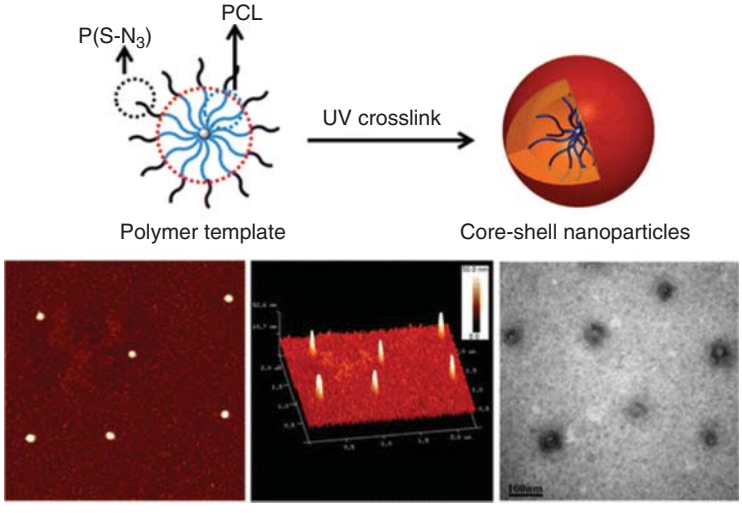

Figure 21.17 Star polymers with degradable inner block and crosslinkable shell were synthesized using ROP and subsequent RAFT polymerization. Crosslinking of outer block and degradation of polyester block resulted in the formation of hollow nanoparticles. Source: Reprinted with permission from Feng et al. [76]. Copyright 2014, American Chemical Society.

and shell thickness by altering the size of each block and could control the density of shell crosslinking by varying the duration of UV irradiation. Finally, degradation of the poly(caprolactone) core was possible under acidic conditions [79].

21.4 Conclusion

Star polymers are highly valued because of their unique architecture and physical properties. Although star polymers can be synthesized using a variety of polymerization techniques, RAFT polymerization provides excellent control and a greater degree of tunability and functionalization than most. The multiple synthetic approaches available facilitate the facile synthesis of star polymers, with varied arm and core compositions readily produced.

Continued development of RAFT polymerization, in particular novel mechanisms of initiation and RAFT agents offering improved control over a wider range of monomers, will result in more controlled and more complex star polymers opening up new materials and applications. As greater spatial and temporal control develops along with reduced dependence on oxygen-free environments, the application of star polymers synthesized via RAFT polymerization will continue to expand and transition towards industrial use.

References

1 Ren, J.M., McKenzie, T.G., Fu, Q. et al. (2016). Star polymers. *Chem. Rev.* 116 (12): 6743–6836.

2 Zhang, C., Zhou, Y., Liu, Q. et al. (2011). Facile synthesis of hyperbranched and star-shaped polymers by RAFT polymerization based on a polymerizable trithiocarbonate. *Macromolecules* 44 (7): 2034–2049.

3 Stenzel, M.H. and Davis, T.P. (2002). Star polymer synthesis using trithiocarbonate functional ?-cyclodextrin cores (reversible addition-fragmentation chain-transfer polymerization). *J. Polym. Sci. A Polym. Chem.* 40 (24): 4498–4512.

4 Rodriguez, K.J., Hanlon, A.M., Lyon, C.K. et al. (2016). Porphyrin-cored polymer nanoparticles: macromolecular models for Heme iron coordination. *Inorg. Chem.* 55 (19): 9493–9496.

5 Huang, J., Wan, D., and Huang, J. (2006). Polymerization of ethyl acrylate using hyperbranched polyglycerol with multi-RAFT groups as chain transfer agent. *J. Appl. Polym. Sci.* 100 (3): 2203–2209.

6 Hosono, N., Gochomori, M., Matsuda, R. et al. (2016). Metal–organic polyhedral core as a versatile scaffold for divergent and convergent star polymer synthesis. *J. Am. Chem. Soc.* 138 (20): 6525–6531.

7 Ji, T., Xia, L., Zheng, W. et al. (2019). Porphyrin-functionalized coordination star polymers and their potential applications in photodynamic therapy. *Polym. Chem.* 10 (45): 6116–6121.

8 Dilag, J., Kobus, H., and Ellis, A.V. (2013). CdS/polymer nanocomposites synthesized via surface initiated RAFT polymerization for the fluorescent detection of latent fingermarks. *Forensic Sci. Int.* 228 (1–3): 105–114.

9 Ranganathan, K., Deng, R., Kainthan, R.K. et al. (2008). Synthesis of thermoresponsive mixed arm star polymers by combination of RAFT and ATRP from a multifunctional core and its self-assembly in water. *Macromolecules* 41 (12): 4226–4234.

10 Cao, P.-F., Wojnarowska, Z., Hong, T. et al. (2017). A star-shaped single lithium-ion conducting copolymer by grafting a POSS nanoparticle. *Polymer* 124: 117–127.

11 Kitiri, E.N., Patrickios, C.S., Voutouri, C. et al. (2017). Double-networks based on pH-responsive, amphiphilic "core-first" star first polymer conetworks prepared by sequential RAFT polymerization. *Polym. Chem.* 8 (1): 245–259.

12 Haldar, U., Roy, S.G., and De, P. (2016). POSS tethered hybrid "inimer" derived hyperbranched and star-shaped polymers via SCVP-RAFT technique. *Polymer* 97: 113–121.

13 Roy, S.G. and De, P. (2014). Facile RAFT synthesis of side-chain amino acids containing pH-responsive hyperbranched and star architectures. *Polym. Chem.* 5 (21): 6365–6378.

14 Barner-Kowollik, C., Davis, T.P., and Stenzel, M.H. (2006). Synthesis of star polymers using RAFT polymerization: what is possible? *Aust. J. Chem.* 59 (10): 719–727.

15 Mayadunne, R.T., Jeffery, J., Moad, G., and Rizzardo, E. (2003). Living free radical polymerization with reversible addition–fragmentation chain transfer (RAFT polymerization): approaches to star polymers. *Macromolecules* 36 (5): 1505–1513.

16 Boschmann, D., Edam, R., Schoenmakers, P.J., and Vana, P. (2009). Characterization of Z-RAFT star polymerization of butyl acrylate by size-exclusion chromatography. *Macromol. Symp.* 275-276 (1): 184–196.

17 Wan, D., Yang, Z., Pu, H. et al. (2009). Xanthate-mediated polymerization of styrene on hyperbranched polyethylenimine: synthesis, characterization, and guest-encapsulating property. *J. Appl. Polym. Sci.* 113 (6): 3702–3709.

18 Moad, G., Rizzardo, E., and Thang, S.H. (2011). End-functional polymers, thiocarbonylthio group removal/transformation and reversible addition–fragmentation–chain transfer (RAFT) polymerization. *Polym. Int.* 60 (1): 9–25.

19 Harvison, M.A. and Lowe, A.B. (2011). Combining RAFT radical polymerization and click/highly efficient coupling chemistries: a powerful strategy for the preparation of novel materials. *Macromol. Rapid Commun.* 32 (11): 779–800.

20 Roth, P.J., Boyer, C., Lowe, A.B., and Davis, T.P. (2011). RAFT polymerization and thiol chemistry: a complementary pairing for implementing modern macromolecular design. *Macromol. Rapid Commun.* 32 (15): 1123–1143.

21 Tao, L., Kaddis, C.S., Loo, R.R. et al. (2009). Synthesis of Maleimide-end functionalized star polymers and multimeric protein-polymer conjugates. *Macromolecules* 42 (21): 8028–8033.

22 Perrier, S., Takolpuckdee, P., and Mars, C.A. (2005). Reversible addition–fragmentation chain transfer polymerization: end group modification for

functionalized polymers and chain transfer agent recovery. *Macromolecules* 38 (6): 2033–2036.

23 Wang, J., Zhu, Z., Jin, X. et al. (2016). Preparation of well-defined propargyl-terminated tetra-arm poly(*N*-isopropylacrylamide)s and their click hydrogels crosslinked with β-cyclodextrin. *Polymers* 8 (4): 93.

24 Xu, J., Jung, K., Atme, A. et al. (2014). A robust and versatile photoinduced living polymerization of conjugated and unconjugated monomers and its oxygen tolerance. *J. Am. Chem. Soc.* 136 (14): 5508–5519.

25 Gormley, A.J., Yeow, J., Ng, G. et al. (2018). An oxygen-tolerant PET-RAFT polymerization for screening structure-activity relationships. *Angew. Chem. Int. Ed.* 57 (6): 1557–1562.

26 Bagheri, A., Arandiyan, H., Adnan, N.N.M. et al. (2017). Controlled direct growth of polymer shell on upconversion nanoparticle surface via visible light regulated polymerization. *Macromolecules* 50 (18): 7137–7147.

27 McKenzie, T.G., Fu, Q., Wong, E.H. et al. (2015). Visible light mediated controlled radical polymerization in the absence of exogenous radical sources or catalysts. *Macromolecules* 48 (12): 3864–3872.

28 Carmean, R.N., Becker, T.E., Sims, M.B., and Sumerlin, B.S. (2017). Ultra-high molecular weights via aqueous reversible-deactivation radical polymerization. *Chem* 2 (1): 93–101.

29 Allison-Logan, S., Karimi, F., Sun, Y. et al. (2019). Highly living stars via Core-first photo-RAFT polymerization: exploitation for ultra-high molecular weight star synthesis. *ACS Macro Lett.* 8 (10): 1291–1295.

30 Dao, V.H., Cameron, N.R., and Saito, K. (2019). Synthesis of UHMW star-shaped AB block copolymers and their flocculation efficiency in high-ionic-strength environments. *Macromolecules* 52 (20): 7613–7624.

31 Gao, H., Ohno, S., and Matyjaszewski, K. (2006). Low polydispersity star polymers via cross-linking macromonomers by ATRP. *J. Am. Chem. Soc.* 128 (47): 15111–15113.

32 Cao, X., Zhang, C., Wu, S., and An, Z. (2014). A highly efficient macromonomer approach to core cross-linked star (CCS) polymers via one-step RAFT emulsion polymerization. *Polym. Chem.* 5 (14).

33 Audouin, F., Knoop, R.J.I., Huang, J., and Heise, A. (2010). Star polymers by cross-linking of linear poly(benzyl-*L*-glutamate) macromonomers via free-radical and RAFT polymerization. A simple route toward peptide-stabilized nanoparticles. *J. Polym. Sci. A Polym. Chem.* 48 (20): 4602–4610.

34 Ferreira, J., Syrett, J., Whittaker, M. et al. (2011). Optimizing the generation of narrow polydispersity 'arm-first' star polymers made using RAFT polymerization. *Polym. Chem.* 2 (8).

35 Qiu, Q., Liu, G., and An, Z. (2011). Efficient and versatile synthesis of star polymers in water and their use as emulsifiers. *ChemComm* 47 (47): 12685–12687.

36 Shen, W., Chang, Y., Liu, G. et al. (2011). Biocompatible, antifouling, and Thermosensitive Core–Shell Nanogels synthesized by RAFT aqueous dispersion polymerization. *Macromolecules* 44 (8): 2524–2530.

37 Shi, X., Zhou, W., Qiu, Q., and An, Z. (2012). Amphiphilic heteroarm star polymer synthesized by RAFT dispersion polymerization in water/ethanol solution. *ChemComm* 48 (59).

38 Zhang, C., Miao, M., Cao, X., and An, Z. (2012). One-pot RAFT synthesis of core cross-linked star polymers of polyPEGMA in water by sequential homogeneous and heterogeneous polymerizations. *Polym. Chem.* 3 (9).

39 Chen, Q., Cao, X., Liu, H. et al. (2013). pH-responsive high internal phase emulsions stabilized by core cross-linked star (CCS) polymers. *Polym. Chem.* 4 (15).

40 Shi, X., Miao, M., and An, Z. (2013). Core cross-linked star (CCS) polymers with tunable polarity: synthesis by RAFT dispersion polymerization, self-assembly and emulsification. *Polym. Chem.* 4 (6).

41 Zhou, W., Yu, W., and An, Z. (2013). RAFT emulsion polymerization of styrene mediated by core cross-linked star (CCS) polymers. *Polym. Chem.* 4 (6).

42 Chen, Q., Xu, Y., Cao, X. et al. (2014). Core cross-linked star (CCS) polymers with temperature and salt dual responsiveness: synthesis, formation of high internal phase emulsions (HIPEs) and triggered demulsification. *Polym. Chem.* 5 (1): 175–185.

43 McKenzie, T.G., Wong, E.H.H., Fu, Q. et al. (2015). Controlled formation of star polymer nanoparticles via visible light photopolymerization. *ACS Macro Lett.* 4 (9): 1012–1016.

44 Uchiyama, M., Satoh, K., McKenzie, T.G. et al. (2017). Diverse approaches to star polymers via cationic and radical RAFT cross-linking reactions using mechanistic transformation. *Polym. Chem.* 8 (38): 5972–5981.

45 Uchiyama, M., Satoh, K., and Kamigaito, M. (2015). Cationic RAFT polymerization using ppm concentrations of organic acid. *Angew. Chem. Int. Ed.* 54 (6): 1924–1928.

46 Cosson, S., Danial, M., Saint-Amans, J.R., and Cooper-White, J.J. (2017). Accelerated combinatorial high throughput star polymer synthesis via a rapid one-pot sequential aqueous RAFT (rosa-RAFT) polymerization scheme. *Macromol. Rapid Commun.* 38 (8).

47 Förster, N., Schmidt, S., and Vana, P. (2015). Tailoring confinement: nano-carrier synthesis via Z-RAFT star polymerization. *Polymers* 7 (4): 695–716.

48 Uhrich, K.E., Cannizzaro, S.M., Langer, R.S., and Shakesheff, K.M. (1999). Polymeric systems for controlled drug release. *Chem. Rev.* 99 (11): 3181–3198.

49 Moad, G., Rizzardo, E., and Thang, S.H. (2013). RAFT polymerization and some of its applications. *Chem. Asian J.* 8 (8): 1634–1644.

50 Chung, J.J., Fujita, Y., Li, S. et al. (2017). Biodegradable inorganic-organic hybrids of methacrylate star polymers for bone regeneration. *Acta Biomater.* 54: 411–418.

51 Liu, J., Duong, H., Whittaker, M.R. et al. (2012). Synthesis of functional core, star polymers via RAFT polymerization for drug delivery applications. *Macromol. Rapid Commun.* 33 (9): 760–766.

52 Khor, S.Y., Hu, J., McLeod, V.M. et al. (2015). Molecular weight (hydrodynamic volume) dictates the systemic pharmacokinetics and tumour disposition of PolyPEG star polymers. *Nanomedicine* 11 (8): 2099–2108.

53 Wang, K., Peng, H., Thurecht, K.J. et al. (2014). Biodegradable core crosslinked star polymer nanoparticles as 19 F MRI contrast agents for selective imaging. *Polym. Chem.* 5 (5): 1760–1771.

54 Ghamkhari, A., Sarvari, R., Ghorbani, M., and Hamishehkar, H. (2018). Novel thermoresponsive star-liked nanomicelles for targeting of anticancer agent. *Eur. Polym. J.* 107: 143–154.

55 Wang, K., Peng, H., Thurecht, K.J. et al. (2013). pH-responsive star polymer nanoparticles: potential 19 F MRI contrast agents for tumour-selective imaging. *Polym. Chem.* 4 (16): 4480–4489.

56 Wiltshire, J.T. and Qiao, G.G. (2007). Recent advances in star polymer design: degradability and the potential for drug delivery. *Aust. J. Chem.* 60 (10): 699–705.

57 Gibson, T.J., Smyth, P., Semsarilar, M. et al. (2020). Star polymers with acid-labile diacetal-based cores synthesized by aqueous RAFT polymerization for intracellular DNA delivery. *Polym. Chem.* 11 (2): 344–357.

58 Wei, X., Gunatillake, P.A., Moad, G. et al. (2014). Synthesis of cleavable multi-functional mikto-arm star polymer by RAFT polymerization: example of an anti-cancer drug 7-ethyl-10-hydroxycamptothecin (SN-38) as functional moiety. *Sci. China Chem.* 57 (7): 995–1001.

59 Chen, C., Guo, X., Du, J. et al. (2019). Synthesis of multifunctional miktoarm star polymers via an RGD peptide-based RAFT agent. *Polym. Chem.* 10 (2): 228–234.

60 Li, Y., Laurent, S., Esser, L. et al. (2014). The precise molecular location of gadolinium atoms has a significant influence on the efficacy of nanoparticulate MRI positive contrast agents. *Polym. Chem.* 5 (7): 2592–2601.

61 Li, Y., Duong, H.T., Laurent, S. et al. (2015). Nanoparticles based on star polymers as theranostic vectors: endosomal-triggered drug release combined with MRI sensitivity. *Adv. Healthc. Mater.* 4 (1): 148–156.

62 Esser, L., Lengkeek, N.A., Moffat, B.A. et al. (2018). A tunable one-pot three-component synthesis of an 125 I and Gd-labelled star polymer nanoparticle for hybrid imaging with MRI and nuclear medicine. *Polym. Chem.* 9 (25): 3528–3535.

63 Li, Y., Beija, M., Laurent, S. et al. (2012). Macromolecular ligands for gadolinium MRI contrast agents. *Macromolecules* 45 (10): 4196–4204.

64 Kim, S.J., Ramsey, D.M., Boyer, C. et al. (2013). Effectively delivering a unique Hsp90 inhibitor using star polymers. *ACS Med. Chem. Lett.* 4 (10): 915–920.

65 Boyer, C., Teo, J., Phillips, P. et al. (2013). Effective delivery of siRNA into cancer cells and tumors using well-defined biodegradable cationic star polymers. *Mol. Pharm.* 10 (6): 2435–2444.

66 Dearnley, M., Reynolds, N.P., Cass, P. et al. (2016). Comparing gene silencing and physiochemical properties in siRNA bound cationic star-polymer complexes. *Biomacromolecules* 17 (11): 3532–3546.

67 Teo, J., McCarroll, J.A., Boyer, C. et al. (2016). A rationally optimized nanoparticle system for the delivery of RNA interference therapeutics into pancreatic tumors in vivo. *Biomacromolecules* 17 (7): 2337–2351.

68 Liao, X., Walden, G., Falcon, N.D. et al. (2017). A direct comparison of linear and star-shaped poly(dimethylaminoethyl acrylate) polymers for polyplexation with DNA and cytotoxicity in cultured cell lines. *Eur. Polym. J.* 87: 458–467.

69 Hira, S.K., Ramesh, K., Gupta, U. et al. (2015). Methotrexate-loaded four-arm star amphiphilic block copolymer elicits CD8+ T cell response against a highly aggressive and metastatic experimental lymphoma. *ACS Appl. Mater. Interfaces* 7 (36): 20021–20033.

70 Pei, D., Li, Y., Huang, Q. et al. (2015). Quantum dots encapsulated glycopolymer vesicles: synthesis, lectin recognition and photoluminescent properties. *Colloid. Surface. B* 127: 130–136.

71 Chung, J.J., Li, S., Stevens, M.M. et al. (2016). Tailoring mechanical properties of sol–gel hybrids for bone regeneration through polymer structure. *Chem. Mater.* 28 (17): 6127–6135.

72 Sudo, Y., Kawai, R., Sakai, H. et al. (2018). Star-shaped thermoresponsive polymers with various functional groups for cell sheet engineering. *Langmuir* 34 (2): 653–662.

73 Glass, J.J., Li, Y., De Rose, R. et al. (2017). Thiol-reactive star polymers display enhanced association with distinct human blood components. *ACS Appl. Mater. Interfaces* 9 (14): 12182–12194.

74 Chen, Q., Deng, X., and An, Z. (2014). pH-induced inversion of water-in-oil emulsions to oil-in-water high internal phase emulsions (HIPEs) using Core cross-linked star (CCS) polymer as interfacial stabilizer. *Macromol. Rapid Commun.* 35 (12): 1148–1152.

75 Ma, K. and An, Z. (2016). Enzymatically crosslinked emulsion gels using star-polymer stabilizers. *Macromol. Rapid Commun.* 37 (19): 1593–1597.

76 Gao, S., Yu, Z., Xu, K. et al. (2016). Silsesquioxane-cored star amphiphilic polymer as an efficient dispersant for multi-walled carbon nanotubes. *RSC Adv.* 6 (36): 30401–30404.

77 Hendrich, M. and Vana, P. (2017). Tuning the mechanical properties of multiblock copolymers generated by Polyfunctional RAFT agents. *Macromol. Mater. Eng.* 302 (6): 1700018.

78 Zheng, X., Ji, C., Liu, J. et al. (2018). Novel star polymers as chemically amplified positive-tone photoresists for KrF lithography applications. *Ind. Eng. Chem.* 57 (19): 6790–6796.

79 Feng, C., Pang, X., He, Y. et al. (2014). Robust route to unimolecular core–shell and hollow polymer nanoparticles. *Chem. Mater.* 26 (20): 6058–6067.

22

Surface and Particle Modification via RAFT Polymerization: An Update

Julia Pribyl[1,2] *and Brian C. Benicewicz*[1]

[1] *University of South Carolina, Department of Chemistry and Biochemistry, Columbia, SC, 29201, USA*
[2] *United States Naval Academy, Chemistry Department, Annapolis, MD 21402, USA*

22.1 Introduction

The past decade has seen tremendous utility of reversible addition-fragmentation chain transfer (RAFT) polymerization to synthesize populations of polymers attached to surfaces (informally termed 'brushes'). To date, many common RAFT agents are commercially available or easily synthesized, leading to their ubiquity in the synthesis of polymer brushes. The resulting polymer-grafted hybrid materials exhibit unique properties and are often prepared with exquisite molecular-scale control. Conveniently, RAFT agents often absorb strongly in the UV-visible region, making spectroscopic characterization of RAFT agent content simple in many cases. Ease of characterization and the versatility of RAFT as a polymerization technique have led to rich development of polymer-grafted surfaces made using RAFT chemistry.

The physical properties of polymer-grafted surfaces are fundamentally dictated by the surface density of grafted chains (graft density, σ). On flat surfaces, brush regimes range from 'pancake' conformation at low graft densities to a dense 'brush' at high graft densities (Figure 22.1) [2]. Early simulation work done by Alexander [3] and de Gennes [4] predicted that low to intermediate brush densities on a flat surface adhered to a linear dependence of brush height as a function of degree of polymerization (N) for low to intermediate brush densities. Somewhat richer behaviour was predicted and experimentally measured for brushes grafted from a curved surface [1]. In short, dilute and semi-dilute polymer brushes (SDPBs) adopt a coiled 'mushroom' conformation, but as the graft density increases, steric repulsions between chains force chain stretching at the surface. For polymers of sufficient N, a transition to a more coiled SDPB occurs because of the increased volume at a farther radial distance from the particle surface. The ability to control these brush parameters (σ,N) is crucial for obtaining the desired properties of polymer-grafted materials. RAFT chemistry offers the control needed to obtain predictable N, and various grafting strategies discussed below allow for control of graft density.

RAFT Polymerization: Methods, Synthesis and Applications, First Edition.
Edited by Graeme Moad and Ezio Rizzardo.

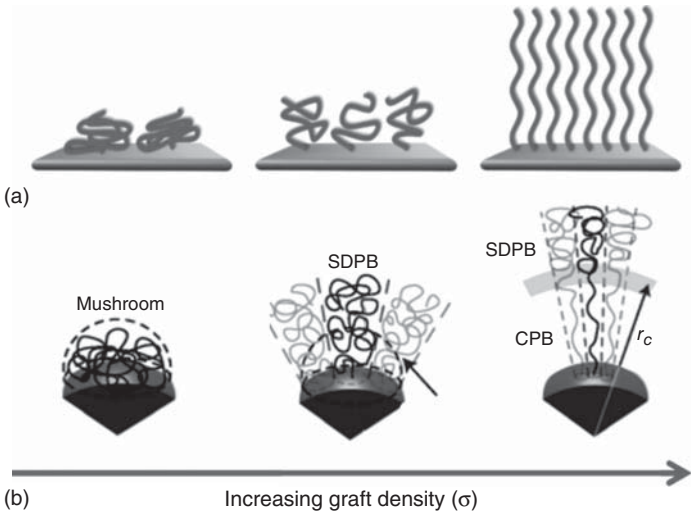

Figure 22.1 Brush regimes on flat surfaces (a); Brush conformations on curved surfaces (b) (SDPD = semi-dilute polymer brush, CPB = concentrated polymer brush). Source: Reprinted with permission from Dukes et al. [1]. Copyright 2010, American Chemical Society.

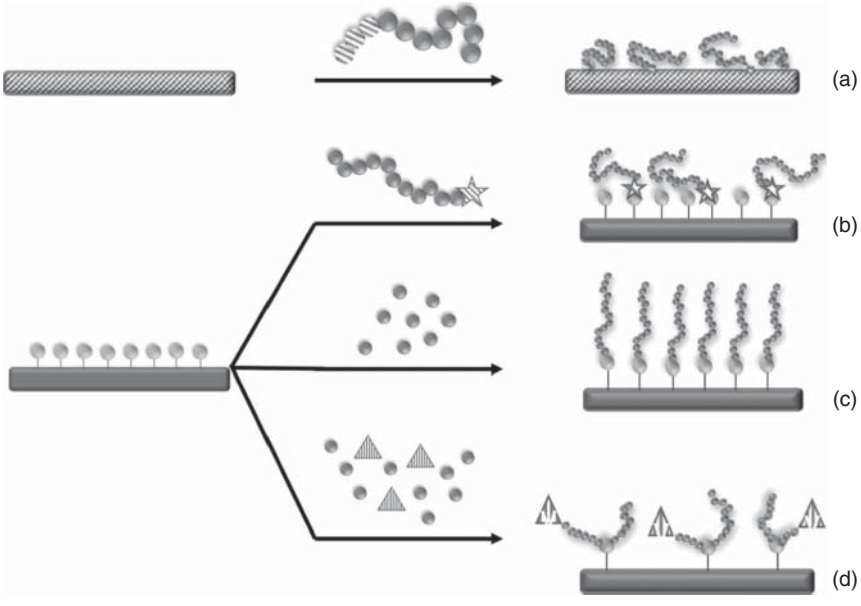

Scheme 22.1 Common polymer grafting strategies: (a) physisorption, (b) grafting-to, (c) grafting-from, and (d) grafting-through.

The method of polymer attachment largely dictates the resulting brush density. Scheme 22.1 illustrates the four most commonly used polymer attachment methods, each having its own benefits and drawbacks. Physisorption is achieved through an attractive (non-covalent) physical association between a portion of a polymer

chain and a surface (Scheme 22.1a). Grafting-to is similar in that a polymer chain must diffuse to a surface, but it is then attached through a covalent chemical linkage (Scheme 22.1a). Both these grafting strategies have the advantage of achieving a polymer brush in as little as one synthetic step, but physisorbed chains easily desorb from the surface. Only low graft densities can be achieved with these methods because surface-associated chains sterically limit additional polymer chains from diffusing to the surface. Higher graft densities can be achieved using a grafting-from approach (Scheme 22.1c), where polymer chains are grown from a tethered initiating group. In grafting-through approach (Scheme 22.1d), the polymerization is not initiated at the surface, but polymerizable functional groups on the surface are quickly incorporated into the growing polymer, resulting in a tethered chain (although not always at the chain end). In surface-initiated RAFT (SI-RAFT) systems, grafting-from is the dominant approach because of the degree of control and broader range of graft densities that can be obtained.

In 'grafting-from' SI-RAFT syntheses, three specific attachment chemistries exist, of which generalized structures are shown in Figure 22.2. By simply attaching a radical initiator to the surface (Figure 22.2a) [5], polymer chains are initiated from the surface and mediated by a RAFT agent (also termed chain transfer agent, CTA) in solution. Although it is simple to control the molecular weight (MW) of the grafted chains by varying the [monomer] : [RAFT] ratio, this approach results in a relatively high fraction of ungrafted chains. More commonly, the RAFT agent is attached to the surface from either the R-group (Figure 22.2b) [6] or the radical-stabilizing Z-group (Figure 22.2c) [7]. In these instances, a small amount of free initiator in solution starts the polymerization, and the surface-tethered RAFT agent mediates the growing chains from the surface. In general, the majority of polymer chains end up grafted to the surface using an R- or Z-RAFT attachment, often the desired result when preparing polymer-grafted surfaces. R-attachment is the most popular technique because it is more convenient to perform post-polymerization modifications with the chain transfer functionality at the chain end rather than near the surface.

The general synthetic strategies to prepare polymer-grafted surfaces using RAFT polymerization have been laid out here in a general form to to facilitate the discussion in this chapter. Excellent and comprehensive reviews of specific synthetic SI-RAFT methods have been discussed by authors of previous reviews [2, 8–10], so they will not be discussed in-depth here. Rather, the focus of this chapter will be to highlight unique and advanced polymer-grafted materials developed over approximately the past decade made possible by the versatility and macromolecular control exhibited by RAFT chemistry.

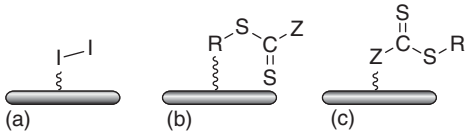

Figure 22.2 RAFT attachment strategies: (a) surface-tethered radical initiator, (b) R-group attachment, and (c) Z-group attachment.

22.2 Complex Brush Architectures

Almost immediately after the first examples of well-controlled functionalization of surfaces with polymer brushes via RAFT polymerization and other methods were published, attempts to model and experimentally create complex brush architectures and spatially patterned surfaces were commenced. Glotzer and coworkers developed some of the first theoretical models of shaped particles with attractive polymer patches assembling to form colloidal crystals, and many other interestingly shaped particles with patches of grafted polymer were proposed [11, 12]. Many of the proposed structures are still inaccessible with 'bottom-up' synthetic techniques either because of the challenge of creating the shaped nanoparticles or designing robust attachment chemistry that is spatially controlled. Many advances in preparing complex brushes on flat or particle surfaces are owed to the control and versatility offered by RAFT chemistry.

Figure 22.3 summarizes some of the advanced brush architectures that have been synthesized using SI-RAFT. Bimodal brush particles (Figure 22.3a,b) were born from the discovery that thermodynamically stable dispersion of nanoparticles in a high MW polymer matrix was not generally achievable with small-molecule ligands nor a monomodal brush of polymer. In a monomodal system, a large volume fraction of the grafted polymer is in a stretched conformation, and only the polymer chain ends, which exist in the semi-dilute polymer regime, have the conformational freedom to entangle with the free chains in a surrounding polymer matrix. Generally, this leads to a phenomenon known as autophobic dewetting, which is discussed in further detail in Section 22.4.

Alternatively, a sparsely grafted brush gives the grafted chains the necessary conformational freedom. However, at low densities, enough of the particle surface (which is presumably immiscible with the matrix) is exposed to be a driving force

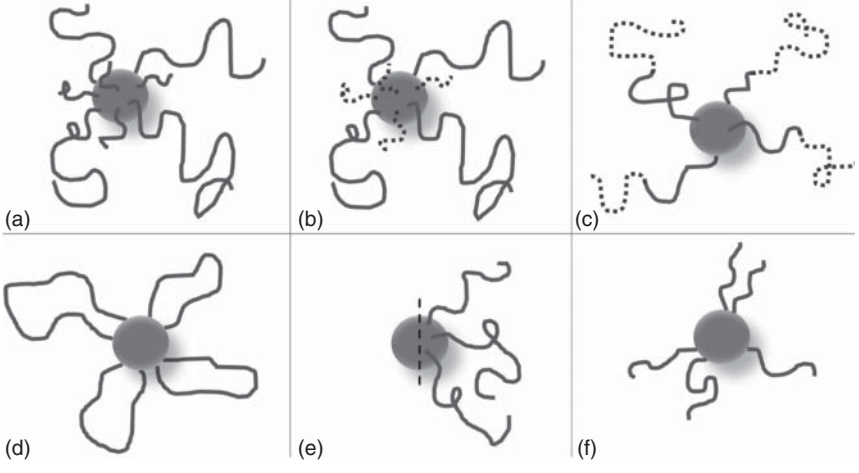

Figure 22.3 Some complex brush architectures prepared via SI-RAFT: (a) bimodal (mixed MW), (b) mixed bimodal (mixed chemistry), (c) surface-anchored block copolymer, (d) looped polymer brush, (e) Janus particle, and (f) 'patchy' particle.

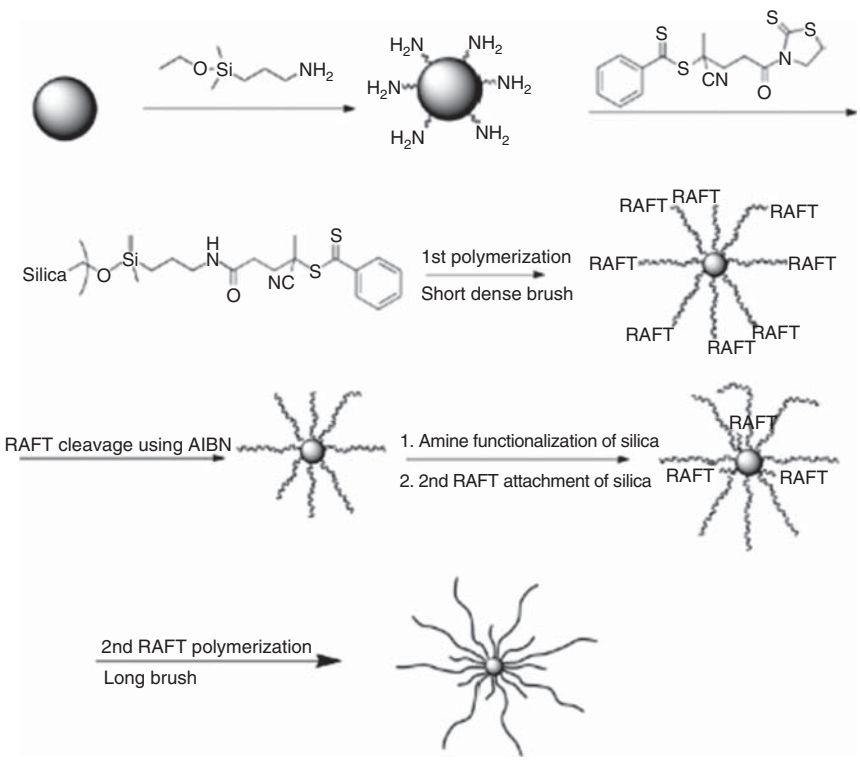

Scheme 22.2 Synthetic strategy to prepare bimodal brush-grafted silica nanoparticles via SI-RAFT. Source: Reprinted with permission from Rungta et al. [13]. Copyright 2012, American Chemical Society.

for phase separation. The idea of grafting a dense and low MW short brush to screen the attractive van der Waals forces between nanoparticles and then adding a sparsely grafted high MW brush with the conformational freedom to entangle with the polymer matrix was achieved using an iterative 'grafting-from' SI-RAFT strategy (Scheme 22.2) first employed by Rungta et al. [13] Two discrete populations of polymers could be attached with elegant control of graft density and graft MW of each population. Graft density of a mercaptothiazoline-activated RAFT agent on spherical silica nanoparticles was controlled by varying the feed ratio of aminopropyldimethylethoxy silane to silica particles, and excellent control of either grafted polystyrene (PS) or poly(methyl methacrylate) was demonstrated. Treating the polymer-grafted particles with a large excess of azobis(isobutyronitrile) (AIBN, 2,2′-azobis(2-methylpropionitrile)) cleaved the RAFT agent from the chain ends, and a second (generally less dense) population of RAFT agent was attached using the same procedure. This second population of tethered RAFT agent was used to grow a second population of grafted chains. Notably, the second population of polymer could differ from the first brush based on MW (bimodal, Figure 22.3a), or it could consist of a different polymer, even a polymer that is immiscible with the first brush to form a mixed-bimodal brush (Figure 22.3b). The ability to decouple the

entropic and enthalpic aspects of particle dispersion led to enhanced mechanical and thermal properties in the resulting nanocomposites compared to monomodal nanocomposites in a similar dispersion state. These enhanced thermomechanical properties were attributed to the increased interfacial binding between graft and matrix polymer chains [14].

Grafted block copolymers (Figure 22.3c) are generally prepared by first attaching the RAFT agent, then growing the first block, isolating the grafted particles, and then chain-extending with a second monomer to form a grafted block copolymer [15]. Looped graft polymers (Figure 22.3d) have been prepared according to Scheme 22.3 through the use of a RAFT agent, which is bound to the particle on both ends [16]. RAFT attachment via the R-group is shown, but double attachment via the Z-groups was also demonstrated.

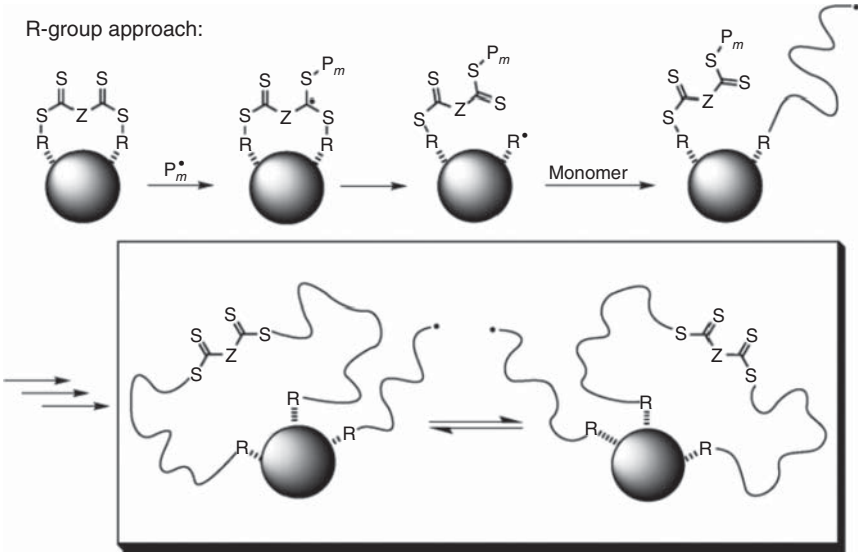

Scheme 22.3 Proposed mechanism for the formation of polymer loops via doubly R-anchored RAFT agents. Source: Reprinted with permission from Rotzoll et al. [16]. Copyright 2008, John Wiley & Sons.

The complex brush architectures described so far have largely been applied homogeneously to the surfaces of interest. There is great interest in building anisotropically functionalized particles known as patchy particles [17]. The simplest of these patchy particles are those which contain only two regions, which are chemically or physically disparate, Janus particles (Figure 22.3e). These anisotropic particles have the potential to assemble into complex supracolloidal structures [18], act as single-particle surfactants [19], or lock and key colloids, which mimic nature's enzyme/receptor system [20, 21], etc. Generally, the chemically disparate sides are prepared by controlling the surface distribution of small ligands; modifying the particles with a polymer brush is more challenging. Early work creating Janus nanoparticles focused on physically limiting access to one side of isotropic colloids by either masking, deposition, or modification at the surface of an emulsion [22, 23]. Most of these techniques were limited to modification of large particles.

In an attempt to create small Janus nanoparticles, the Huisgen 1,3-dipolar cycloaddition, commonly known as the copper 'click' reaction, was used to attach small (15 nm diameter) alkyne-functionalized silica nanoparticles to the surface of 100 nm silica nanoparticles (Figure 22.4a) [24]. Azido-terminated poly(methyl methacrylate) prepared via RAFT polymerization was then grafted to the exposed side of the alkyne-functionalized small silica nanoparticles. The small nanoparticles were then successfully released by ultrasonication, which cleaved the mechanically labile triazole ring that tethered them to the larger nanoparticle. Micelles comprising the freed Janus particles in THF were observed, indicating that these might make good particle-based surfactants.

An approach to prepare polymeric Janus nanosheets (PJS) using a clever particle templating technique was published by Liu et al. [25] A self-assembled monolayer of RAFT agent was formed on the surface of $CaCO_3$ template particles, then a bilayer of poly(*N*-isopropylacrylamide) (PNIPAM), followed by PS was grown from the surface of the particle (outline of this scheme shown in Figure 22.4d). By virtue of the RAFT process, the ratios of PS/PNIPAM were highly tunable. The $CaCO_3$ template particle could then be digested with acid, and the Janus nanosheets comprising the polymer bilayer were separated using ultrasonication. The PNIPAM/PS nanosheets were shown to be flexible and thermoresponsive (Figure 22.4e). Dually responsive PJS were prepared from a similarly constructed poly(acrylic acid) (PAA)/PNIPAM system.

Recently, syntheses to create patchy particles have transitioned to more scalable routes. Using template particles, particle deposition, other means of 'masking', or other bottom-up approaches generally yield very little material to study. Top-down approaches generally offer better scalability. An excellent top-down approach to prepare particles with tunable size and number of 'patches' was recently published by Lotierzo and coworkers [26]. Nanogels of ω-end unsaturated poly(methyl methacrylate-*co*-methacrylic acid)-*block*-poly(butyl methacrylate) (P(MMA/MAA)-*b*-PBMA) were prepared via sulfur-free RAFT polymerization. Upon addition of base, micelles formed and were core-crosslinked using a trifunctional methacrylate. The prepared nanogels were then used as a stabilizer in the emulsion polymerization of styrene. By controlling the pH of the emulsion polymerization before initiation, the number of nanogel lobes, which decorated the PS latex particles, was elegantly controlled, ranging from a single lobe per latex particle at high pH, to many lobes per particle at lower pH values (Figure 22.5a–d).

Preparing flat surfaces that are functionalized with a spatially or chemically patterned polymer brush is ostensibly more straightforward than doing the same on small particle surfaces. There are two general approaches to preparing patterned surfaces, bottom-up in which the CTA is patterned onto the surface, then SI-RAFT results in a spatially patterned brush. Top-down approaches tend to be simpler and more scalable; an unpatterned brush is grown from the surface and is then patterned post-polymerization. A simple way to create a complex brush pattern that leveraged the UV sensitivity of dithiobenzoate-type RAFT agents was investigated by Choi et al. [27] First, an unpatterned layer of dithiobenzoic acid benzyl-(4-ethyltrimethoxysilyl) ester was condensed onto the surface of a silicon

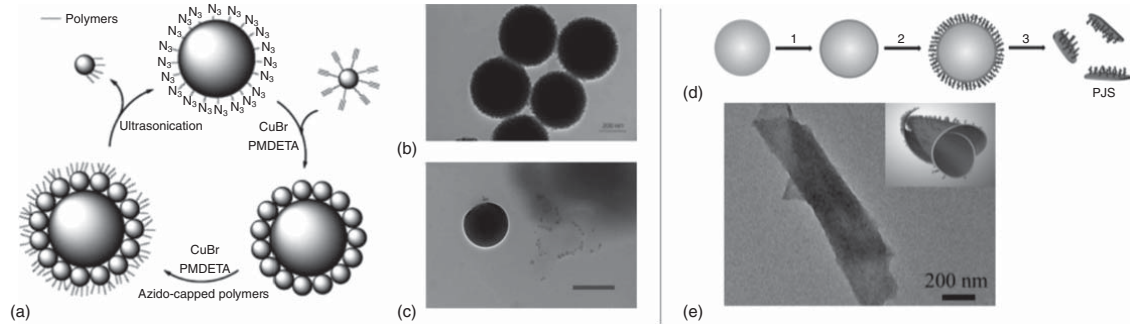

Figure 22.4 (a) Synthetic route to prepare small (15 nm diameter) Janus nanoparticles, (b) transmission electron microscopy (TEM) image of 15 nm silica particles attached to larger silica nanoparticles via the copper 'click' reaction, (c) Janus particle micelle observed after ultrasonication cleavage of triazole-linked nanoparticles (scale bars in (b) and (c) = 200 nm). Source: (a) Adapted with permission from Li et al. [24]. Copyright 2013, American Chemical Society, (b, c) Adapted with permission from Li et al. [24]. Copyright 2011, American Chemical Society (d) synthetic scheme of Janus nanosheet formation: 1 = RAFT monolayer formation, 2 = growth of polymer bilayer, and 3 = particle digestion/sonication to form discrete PJS; and (e) TEM image of 'scrolled' PJS (Scale bar = 200 nm). Source: (d) Adapted with permission from Liu et al. [25]. Copyright 2017, American Chemical Society, (e) Adapted with permission from Liu et al. [25]. Copyright 2017, American Chemical Society.

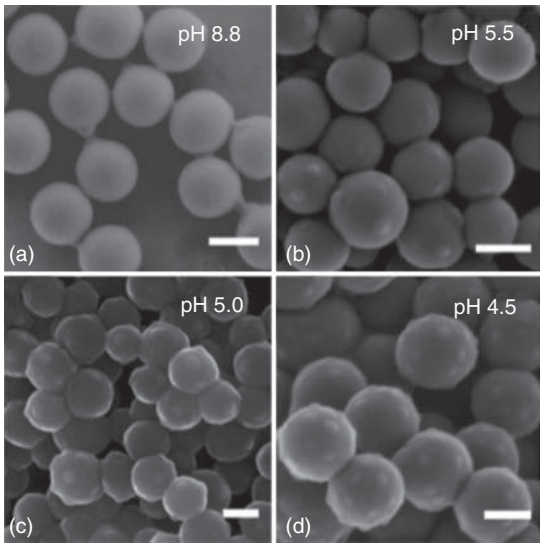

Figure 22.5 Scanning electron microscopy (SEM) images of styrene latex particles prepared via emulsion polymerization using a nanogel stabilizer at 2.8 wt% with respect to monomer in which the pH was adjusted to 8.8 (a), 5.5 (b), 5.0 (c), and 4.5 (d) before polymerization. Scale bars = 100 nm. Source: Adapted with permission from Lotierzo et al. [26] 2019, American Chemical Society.

wafer. A TEM grid was used as a photomask as the CTA-functionalized wafer was exposed to UV light, degrading the CTA in regions where the wafer surface was exposed. Subsequent SI-RAFT polymerization yielded patterned brushes of poly(pentafluorophenyl acrylate) (PFPA). The PFPA brush was then post-modified with a fluorescent dye, 5((2-aminoethyl) amino) naphthalene-1-sulfonic acid (EDANS). Imaging of the dye-functionalized patterned brush with confocal laser scanning microscopy (CLSM) showed confinement of the dye molecules to the regions in which the CTA was not photodegraded, and the static water contact angle for the patterned brushes decreased from 96° in PFPA brush to 23° for the EDANS-modified brush. It is important to note that UV exposure with a TEM grid as the photomask does not represent the lower limit of pattern feature sizes that can be achieved.

Photopatterned attachment of RAFT agents was also investigated by Barner-Kowollik and coworkers, which is illustrated in Figure 22.6 [28]. Silicon wafers were coated with (3-aminopropyl)triethoxysilane and were subsequently reacted with 4-amidobutyroyl chloride to create a maleimide-coated surface. A photomask was applied to the surface, and a photoenol-tagged CTA was reacted with the surface-tethered maleimide groups upon irradiation with 320 nm light. SI-RAFT from the patterned regions of styrenic imidazolium monomers resulted in highly patterned ionic polymer brushes. Salt metathesis of the ionic polymer brush with $KMnO_4$ immediately resulted in a bright purple indication of where the brush was successfully patterned.

The flexibility of RAFT as a polymer synthesis strategy has enabled the elegant syntheses of materials with excellent control of grafted polymer architecture on the molecular scale. Clever combination of RAFT polymerization with other chemistries has also enabled the development of materials with polymer brushes that are spatially resolved on particle or flat surfaces and can have a high degree

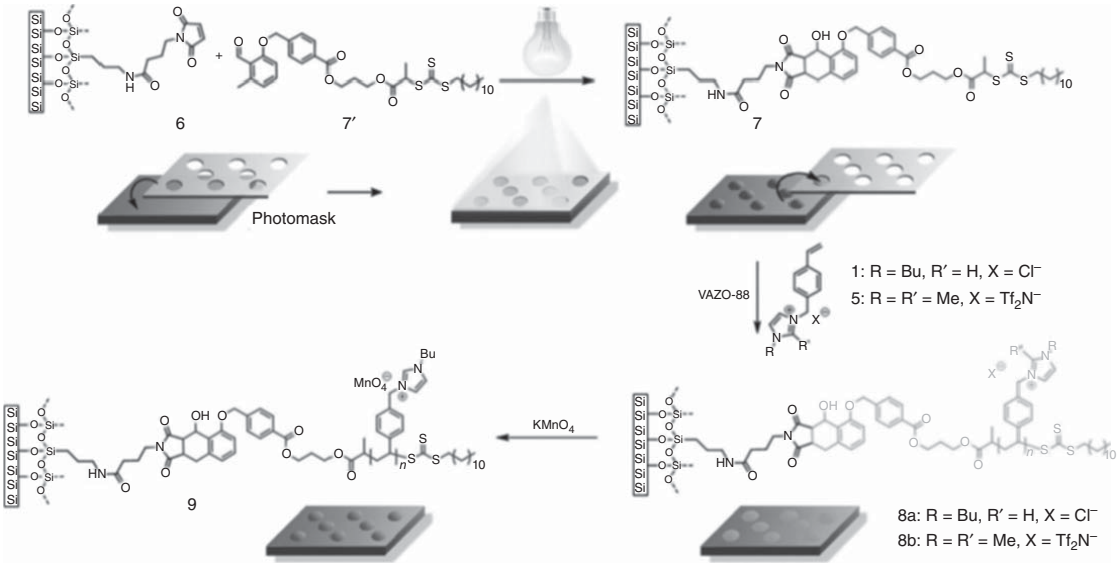

Figure 22.6 Illustration of CTA photopatterning via a light-activated photoenol reaction and SI-RAFT polymerization of styrenic imidazolium monomers. Visualization of the patterned ionic polymer brush was achieved by salt metathesis with $KMnO_4$. Source: Reproduced with permission from Steinkoenig et al. [28]. Licensed under CCBY 3.0 unported.

of incorporated functionality. These combinatorial strategies were first adopted primarily for the synthesis of materials in this section but were quickly adopted for biomaterials and advanced composites, which are discussed in Sections 22.3–22.5.

22.3 Bioconjugation and Stimuli-responsive Polymer Brushes

Grafting polymers from proteins is important for improving their solubility and processability, but the chemical transformations necessary to attach the polymer are at risk of harming the native folded conformation of the protein [29]. In addition to these challenges, much of the work done on protein conjugation has employed a grafting-to method, which results in many complications including low reaction conversion (especially when the polymer or protein has high MW) and the challenge of separating ungrafted proteins [30]. RAFT polymerization is well suited for grafting polymers from proteins because it can adhere to the mild conditions needed to preserve protein structure and functionality. Recently, Tucker and co-workers employed photoinduced electron/energy transfer–reversible addition–fragmentation chain transfer (PET–RAFT) to graft a variety of monomers from a lysozyme-conjugated CTA [31]. The authors chose to use this light-initiated RAFT variant to allow for fast polymerization even under dilute monomer conditions. Efficient polymerization of *N*,*N*-dimethylacrylamide (DMAM) was observed using 2 mol% of eosin Y as an organo-photocatalyst. As anticipated, the MWs of the conjugate increased linearly with conversion, and polymerization could be cycled on or off with light irradiation (Figure 22.7). Importantly, it was demonstrated that chain extending from the conjugated CTA with NIPAM was done with high blocking efficiency, indicating that the trithiocarbonate end groups did not undergo significant degradation. The authors noted that there was a distribution of the number of CTAs attached to the proteins as this conjugation approach was not site specific.

A site-specific conjugation strategy was employed by Li and coworkers [32]. To prepare proteins with just one CTA per protein, site-directed mutagenesis was used to substitute a cysteine residue for the Lys148 site present in *Escherichia coli* inorganic pyrophosphatase (PPase). Although the Cys-substituted PPase contains two other Cys residues, they are buried within the folded protein structure and are not thought to be accessible for modification. The exposed Cys residue was reacted with a maleimide-bearing trithiocarbonate CTA, and light-induced RAFT polymerization of PNIPAM proceeded with good control. The resulting conjugates had a lower critical solution temperature (LCST) of 35 °C (slightly higher than the LCST of pure PNIPAM), and the LCST behaviour was used to tune the activity of PPase. Natively, PPase catalyzes the hydrolysis of inorganic pyrophosphase to inorganic phosphate. Below the LCST, the PPase activity was significantly decreased compared to that of the unmodified protein. Above the LCST of the conjugate, the activity increased, thus demonstrating the ability of the conjugated PNIPAM to 'switch' the function of the protein on or off depending on temperature.

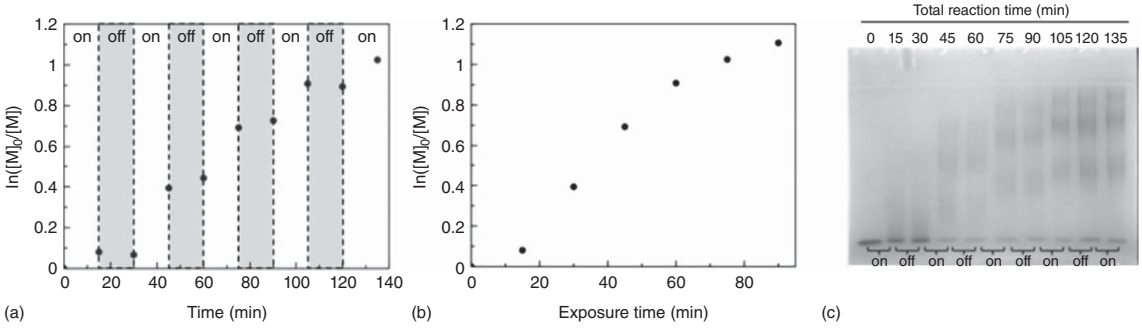

Figure 22.7 (a) Pseudo-first-order kinetics plot showing each on-and-off cycle vs. total reaction time, (b) pseudo-first-order kinetics plot of total light exposure time, and (c) sodium dodecyl sulphate-polyacrylamide gel electrophoresis (SDS–PAGE) results showing MW growth only in the presence of light for each cycle. Source: (a, b) Reprinted with permission from Tucker et al. [31]. Copyright 2017, American Chemical Society, (c) Reprinted with permission Tucker et al. [31]. Copyright 2017, American Chemical Society.

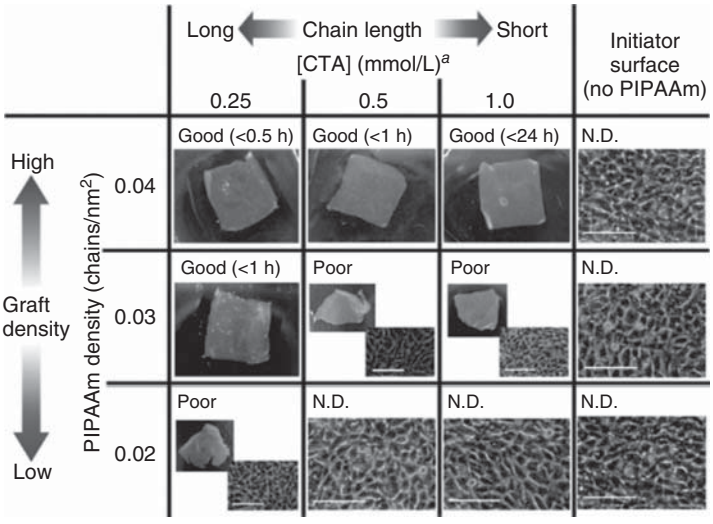

Figure 22.8 Cell sheets recovered from grafted PNIPAM brush surfaces by reducing the temperature to 20 °C. Results are described either as 'Good', 'Poor', or 'N.D.' (not detached). Scale bars = 100 μm; here, PIPAAm refers to poly(*N*-isopropylacrylamide). Source: Reprinted with permission from Takahashi et al. [33]. © 2010, American Chemical Society.

Brushes of PNIPAM as a thermoresponsive polymer are also useful for modulating cell adhesion. Takahashi et al. used a tethered azo-initiator to graft PNIPAM via RAFT polymerization from glass slides [33]. By simply changing the temperature, adhesion or detachment behaviour of a sheet of bovine carotid artery endothelial cells was manipulated (Figure 22.8). In general, the best detachment of a single sheet of cells was achieved with the highest tested graft density and graft MW below the LCST of the PNIPAM brush. The proposed mechanism for good cell sheet detachment was that the interaction between the PNIPAM brush and adsorbed cells was decreased below the LCST, facilitating easy release of the cell sheets from the surface.

A dually responsive drug nanocarrier was synthesized and tested by Zhang and coworkers [34]. SI-RAFT was used to grow a block copolymer composed of poly(methacrylic acid)-*block*-poly(*N*-isopropylacrylamide) from silica nanoparticles (PMAA-*b*-PNIPAM-*g*-SiO_2). At neutral pH and ambient temperature, doxorubicin (DOX, pK_a = 8.6) is protonated and thus strongly interacts with the negatively charged PMAA block and the drug-loaded nanoparticles are individually dispersed in an aqueous medium (Figure 22.9, bottom left). In principle, when the pH is decreased from seven to five, PMAA becomes protonated and the DOX is released from the inner block. When the DOX release was tested at 25 °C at pH = 5, approximately 50% of the drug was released after 50 hours. The release of DOX was amplified by leveraging the thermoresponsiveness of the PNIPAM block above the LCST temperature. At pH = 5 and 40 °C, the interaction between PMAA and DOX is weakened and the PNIPAM blocks collapses, causing the particles to aggregate in solution. The authors asserted that this combination of responses improved the DOX release by 'squeezing' the drug out of the assembly (Figure 22.9, top right).

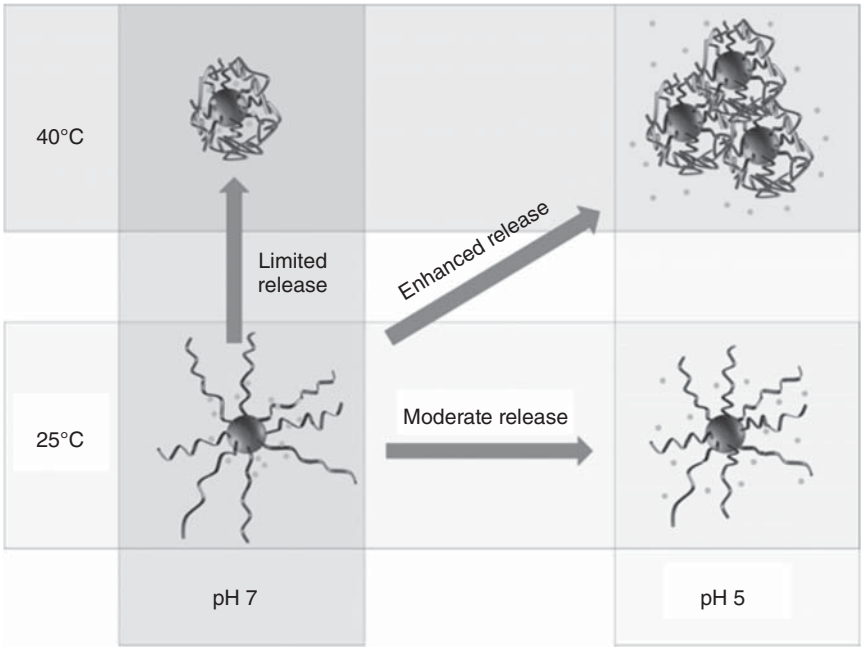

Figure 22.9 Proposed mechanism for dually responsive DOX release from PMAA-*b*-PNIPAM-*g*-SiO_2 nanocarriers. Source: Reprinted with permission from Zheng et al. [34]. Copyright 2017, American Chemical Society.

After 30 hours, approximately 80% of the loaded DOX was released. These DOX nanocarriers were found to be highly effective against Hela cells and exceeded the efficacy of free DOX in an equivalent dose. The synergistic effect of increasing the local concentration by loading drugs or other antibacterial properties within nanocarriers has been noted in other work [35, 36].

22.4 Advanced Composites

Perhaps the most mature area of materials prepared by SI-RAFT lies in the field of composites and polymer-grafted nanoparticles. In this discovery space, much fundamental work has been conducted on understanding the relationship between graft density/MW and composite microstructure and properties but also the attachment chemistry to achieve robust polymer attachment to a large variety of particle substrates. To date, SI-RAFT has been applied to a diverse array of substrates including silica [37–41], gold [42, 43], TiO_2 [44, 45], $BaTiO_3$ [46–48], iron oxide [49–51], silica-coated iron oxide [52], quantum dots [53, 54], montmorillonite [55], halloysite nanotubes [56], cellulose [57], indium tin oxide [58], carbon substrates including graphene oxide [59] and carbon nanotubes [60], polymeric foams [61, 62], and other polymer substrates [63, 64]. Often, when the substrate is a small particle (micro- or nano-sized), the intent is to incorporate the particles into a homopolymer

to form a composite material with properties greater than the sum of its parts. When homogeneously incorporated into the polymer matrix, sub-micron-sized fillers generate a large interfacial volume with the surrounding polymer matrix where load transfer (thermal, mechanical, etc.) from the matrix to the filler occurs. This large interfacial volume between matrix and filler amplifies the property enhancement bestowed by the filler much beyond what can be achieved using an identical filler of larger dimension [65]. Sometimes, the nano-sized filler also has innately superior properties than a chemically similar filler of a larger dimension. A classic example of this dimension-based property disparity is the comparison between graphite and carbon nanotubes. Although chemically identical, Young's modulus of the nanotubes is nearly an order of magnitude greater than graphitic carbon fibres [66]. In this section, the use of SI-RAFT polymerization to understand nanofiller behaviour and to prepare advanced composites and hybrid materials will be discussed.

Predictable and controlled dispersion of nanofiller within a polymer matrix in which the bare filler is presumably immiscible is dependent on precise control of the MW and graft density of the polymer brush that compatibilizes the filler with the matrix. Intuitively, it seems that simply coating a nanofiller with a brush of polymer with matching chemistry and similar MW to the desired matrix polymer should lead to thermodynamically favourable homogeneous mixing of the nanofiller and matrix. However, the story is much more complicated. Early nanocomposite work showed that when $N_{\text{graft}} \gg N_{\text{matrix}}$ and $\sigma^2 N_{\text{matrix}} \gg 1$ (where N is the chain length and σ is the brush graft density), the matrix polymer chains cannot wet the brush interface [67]. The consequence is macroscopic phase separation of two phases containing chemically identical polymer. This phenomenon (autophobic dewetting) is caused by a high osmotic pressure penalty for high MW polymers to penetrate into a dense polymer brush. SI-RAFT offers the flexibility to independently tailor the graft density and MW so that this effect is overcome. Not only can wetting behaviour be tuned but the parameters can be systematically tuned to achieve a variety of isotropic and anisotropic filler morphologies.

Systematic manipulation of graft density and grafted chain MW with respect to matrix MW was studied, and a morphology diagram from these experiments was constructed (Figure 22.10) [68]. PS-grafted nanoparticles (PS-*g*-SiO_2) prepared via SI-RAFT at a series of carefully controlled graft densities and MWs and were each mixed with a PS matrix (MW = 142 kg mol^{-1}). At low graft density and low MW with respect to the matrix polymer (0.01 ch nm^{-2}, 25 kg mol^{-1}), small spherical aggregates were observed. As graft density and graft MW were independently increased, a number of morphologies were observed, both isotropic and anisotropic in nature. The ability to predict and reproducibly achieve a variety of thermodynamically stable nanoparticle arrangements represented an exciting advance in the understanding of how to control nanofiller dispersion. The anisotropic structures (strings or elongated sheets) are fundamentally interesting, and the ability to predict and target nanofiller dispersion states had important implications for nanocomposite processing and ultimately the nanocomposite properties.

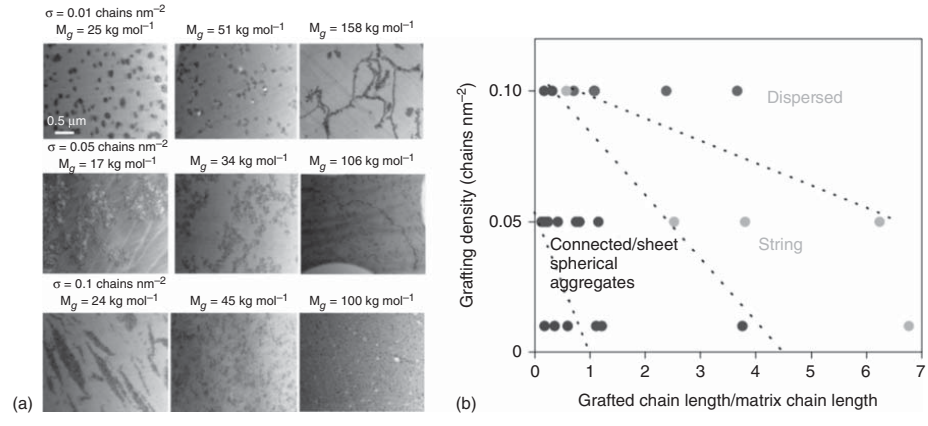

Figure 22.10 Experimentally determined morphology diagram of PS-*g*-SiO_2 in the PS matrix (b) and transmission electron micrographs (a) of PS-*g*-SiO_2 of varying MW and σ in the PS matrix (MW = 142 kg mol^{-1}). Source: Reprinted with permission from Akcora et al. [68]. Copyright 2009, Springer Nature.

Precise control of the nanofiller dispersion state led to significant investigation into the effect of different dispersion states on nanocomposite properties. There used to be some debate about the mechanism by which nanofillers improved properties compared to bulk polymers. On one end of the spectrum, it was thought that large aggregates of particles in the matrix were the source of reinforcement by acting as a pathway through the polymer on which stress could propagate [69, 70]. On the other end of the spectrum, other proposed mechanisms included chain immobilization around a polymer-grafted nanoparticle and reinforcement is a result of the percolation of particle-bound glassy layers [71] or that the matrix chains and polymer-grafted particles form a network with polymer bridges connecting them [72–74]. These arguments were settled after SI-RAFT allowed for the control of graft density and MW needed to systematically prepare nanocomposites with either large agglomerates or smaller dispersed particles. It was unequivocally shown that the grafted chains on adjacent particles could entangle forming a percolating network throughout the material [75]. This work supported the hypothesis that a network mechanism was the source of polymer reinforcement. This knowledge also allowed for the development of high-performance materials where the maximum material reinforcement could be targeted, and the interfacial volume where load transfer and property enhancement occurs is maximized.

The concept of using the nanofiller interface to incorporate properties other than mechanical reinforcement is pronounced in dielectric nanocomposites. Bell and coworkers independently investigated the effect of filler dispersion as well as the effect of several π-conjugated electroactive surface ligands [76]. Briefly, 15 nm silica nanoparticles were first functionalized with a dense coating (between 0.22 and 0.44 ch nm^{-2}) of either anthracene, thiophene, or terthiophene. A relatively sparse brush of poly(glycidyl methacrylate) (PGMA) (between 0.04 and 0.15 ch nm^{-2}) was grafted via SI-RAFT to selected samples as a matrix-compatibilizing brush. As expected, the best improvements in dielectric breakdown strength were observed for nanocomposites with good (homogeneous) particle dispersion. Good dispersion of nanoparticles, in this case, where the average interparticle distance was 200 nm or less, creates the largest interfacial area between the nanoparticles. The greatest dielectric breakdown enhancement was observed for well-dispersed PGMA-*g*-SiO_2 (σ = 0.1 ch nm^{-2}) with 0.22 ch nm^{-2} terthiophene as the surface-tethered electron trapping ligand. This study is an excellent demonstration of using two surface-tethered functionalities not only to allow for particle dispersion but also to enhance a property somewhat decoupled from matrix compatibilization – in this case, improved dielectric breakdown strength.

Early work on polymer nanocomposites prepared via SI-RAFT focused on materials that were obviously compatible with the classes of monomers typically polymerized by RAFT polymerization (styrenics, acrylates, methacrylates, etc.). Processing and studying nanocomposites made from these materials are generally straightforward as they are generally highly amorphous, have high glass transition temperatures, etc. However, many commodity plastics of interest including polyolefins (polyethylene, polypropylene, etc.) and rubbery polymers are not conventionally compatible with these classes of monomers. However, there are a few

recent examples of nanoparticles modified via SI-RAFT polymerization to prepare nanomaterials compatible with some of these popular commodity materials.

In principle, reinforcing rubbery materials with nanofillers is straightforward – tires have been filled with various fillers, chiefly carbon black and silica, for decades. However, incorporating nano-sized fillers into rubbery materials is not as deeply explored. Employing an SI-RAFT strategy to prepare small silica particles, for example, would provide the ability to tune the compatibility of the nanofiller with a rubbery matrix. Khani and coworkers investigated a high-temperature SI-RAFT polymerization of isoprene from the surface of silica nanoparticles [77]. A high-temperature stable trithiocarbonate RAFT agent was chosen, (dodecylthio)carbonothioyl)thio)propanoic acid (DoPAT), based on the reports of high-temperature bulk polymerization of isoprene [78, 79]. The surface-initiated polymerization was shown to be well-controlled, having predictable MW with monomer conversion although done in solvent conditions to maintain dispersion of the silica nanoparticles (Figure 22.11b). Interestingly, the SI-RAFT polymerization was faster than the free isoprene polymerization in solution, and there was also a dependence of the polymerization rate on graft density (Figure 22.11a). The higher graft density was notably faster than the lower graft density. This is similar to the trend observed for SI-RAFT of PS but the opposite of the trend observed for SI-RAFT of poly(methyl methacrylate) [80]. To date, no concrete theory exists in the literature explaining the phenomenon of why the SI-RAFT polymerization of some monomers is faster than the free polymerization, and sometimes, the SI-RAFT system is slower. The polyisoprene (PI)-grafted silica nanoparticles showed reasonably good dispersion in a PI matrix, demonstrating one of the first examples of a rubbery nanocomposite prepared via SI-RAFT.

Matrix-free polychloroprene-grafted silica nanocomposites (PCP-*g*-SiO_2) were prepared using a similar trithiocarbonate SI-RAFT system to the PI work described above [81]. In this case, 2-methyl-2-[(dodecylsulfanylthiocarbonyl) sulfanyl]propanoic acid (MDSS) was the RAFT agent used. The as-synthesized PCP-*g*-SiO_2 was crosslinked with MgO and ZnO forming vulcanized rubber sheets with excellent nanoparticle dispersion. The vulcanized nanocomposites exhibited tensile strengths up to ~13 MPa attributed to the good nanoparticle dispersion in the matrix-free composite. The authors noted that normally silica-reinforced rubbery composites exhibit decreased tensile strain because of the defects introduced by particle aggregate defects [82], but that effect was avoided here.

The most abundantly produced class of polymers, polyolefins, represents a significant challenge for obtaining homogeneous dispersion of nano-sized fillers because of the high degree of crystallinity, which makes it difficult for polymers of a lesser degree of crystallinity to mix, even if they are chemically identical. For example, low-density polyethylene (highly branched) is not miscible with high-density polyethylene (HDPE, completely linear). This challenge was addressed using SI-RAFT of poly(alkyl methacrylates) [83]. Silica nanoparticles were grafted with poly(hexyl methacrylate) (PHMA), poly(lauryl methacrylate) (PLMA), or poly(stearyl methacrylate) (PSMA). The prepared grafted nanoparticles were processed into nanocomposites with linear low-density polyethylene as the matrix.

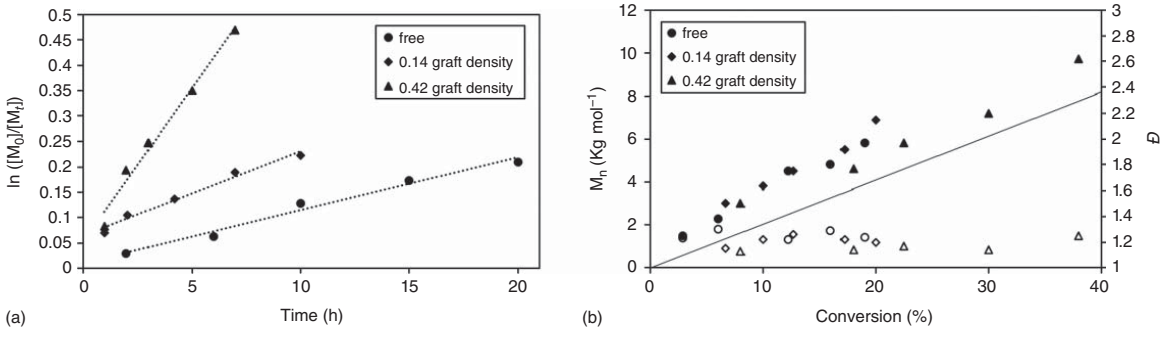

Figure 22.11 (a) First-order kinetic plots and (b) dependence of molecular weight (solid line, M_n, theory) on the conversion for the SI-RAFT polymerization of PI-*g*-SiO_2 high surface density (triangle, 100 mmol g^{-1}, 0.42 ch nm^{-2}), low surface density (diamond, 32 mmol g^{-1}, 0.14 ch nm^{-2}), free DoPAT (circle). All polymerizations were conducted under identical conditions with the ratio of [monomer]:[CTA]:[initiator] 5300 :1: 0.1. Source: Reproduced with permission from Khani et al. [77]. Copyright 2017, John Wiley & Sons.

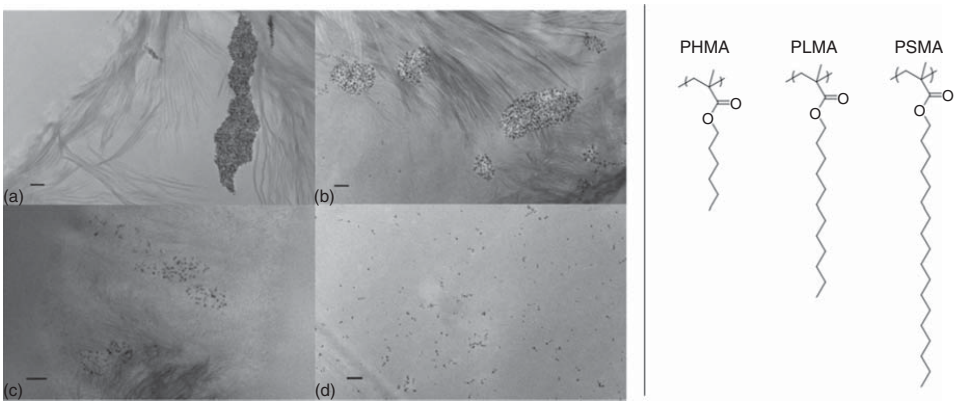

Figure 22.12 TEM images of LLDPE nanocomposites each filled with 4 wt% silica loading of (a) bare silica, (b) PHMA-*g*-SiO_2, (c) PLMA-*g*-SiO_2, and (d) PSMA-*g*-SiO_2. Grafted samples all had a graft density of 0.16 ch nm^{-2}. Scale bars = 200 nm. PHMA, poly(hexyl methacrylate); PLMA, poly(lauryl methacrylate); PSMA, poly(stearyl methacrylate). Chemical structures of grafted polymers (right). Source: Reproduced with permission from Khani et al. [83]. Copyright 2017, Elsevier.

The dispersion states of the prepared nanocomposites and polymer chemical structures are shown in Figure 22.12. As the length of the alkyl pendant group increased, the nanoparticle dispersion in linear low density polyethylene (LLDPE) improved, with the best dispersion exhibited by PSMA-*g*-SiO_2. Notably, just the alkyl pendant groups both allow for matrix-compatibility and shield the polar methacrylic backbone from the non-polar matrix.

The narrow dispersity of grafted polymer chains afforded by SI-RAFT polymerization was leveraged to tune the free volume in matrix-free nanocomposites which were then evaluated for gas separations [84]. In this work, thin films of nanoparticles grafted with poly(methyl acrylate) or poly(methyl methacrylate) were prepared via SI-RAFT at varying graft densities and chain lengths. Specifically, for the PMA-*g*-SiO_2 system with $\sigma = 0.43\,\text{ch}\,\text{nm}^{-2}$, as the chain length increased, the permeability of CO_2, N_2, and CH_4 through the film increased gradually, all reaching a maximum 'volcano' point at the same graft length, followed by a sharp decrease in permeability. Computer simulations of these systems suggest that at certain chain lengths, the polymer layer must deform to accommodate ideal nanoparticle packing, and this deformation results in lower polymer density in periodic regions of the film (Figure 22.13a). As a result, improved separation of a gaseous mixture of CH_4 and CO_2 which approached the Robeson upper bound (an empirical model of the best possible membranes for this gas separation), is shown in Figure 22.13b. This promising membrane performance enhancement was attributed to this tunable free volume.

An exciting advance that used the miscibility of PMMA-*g*-SiO_2 nanoparticles prepared by SI-RAFT with poly(ethylene oxide) (PEO, a semi-crystalline polymer) to study the effects of matrix crystallization on the nanofiller was recently published [85]. As the authors mention, approximately 75% of commodity plastics are semi-crystalline but are generally of little use as engineering materials because

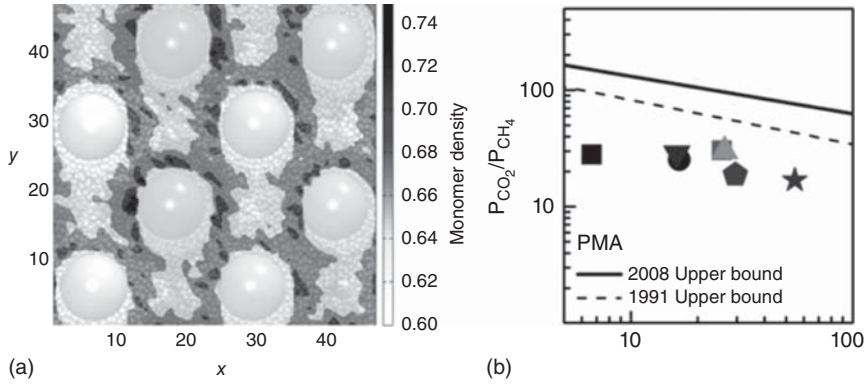

Figure 22.13 (a) Computer-simulated 'heatmap' of monomer density in NPs (diameter = 10) grafted with polymer chains (monomer diameter = 1, chain length = 10 200 chains per particle, averaged over 500 simulations). (b) Robeson plots comparing the permeabilities of CO_2 and CH_4 PMA composites with graft lengths of (●) 27 kDa, (▼) 38 kDa, (□) 52 kDa, (♦) 62 kDa, (★) 92 kDa, and (▲) 132 kDa compared with (♦) neat PMA. Source: Reproduced with permission Bilchak et al. [84]. © 2017, American Chemical Society.

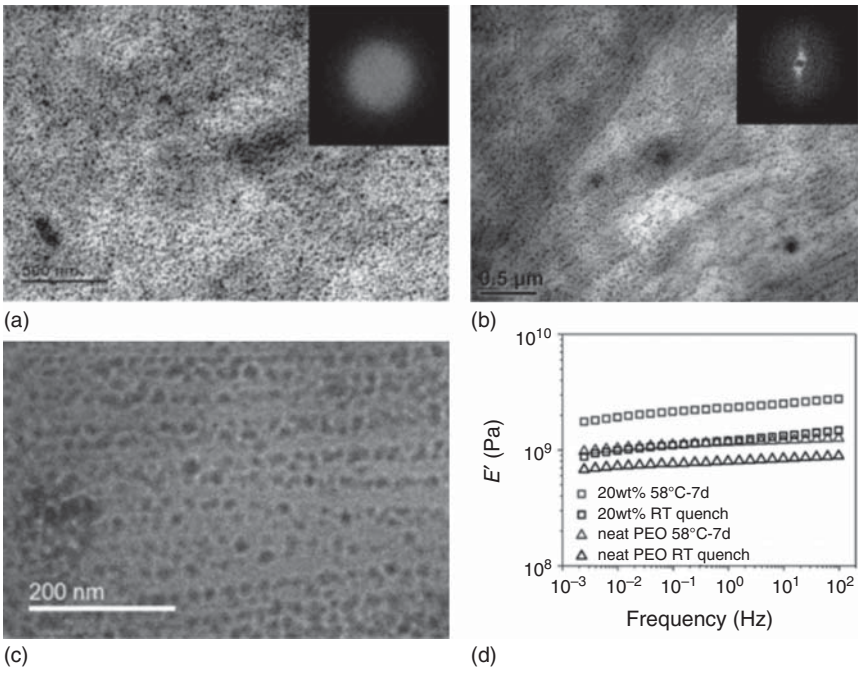

Figure 22.14 (a) 20 wt% PMMA-*g*-SiO_2 in 100 kg mol^{-1} PEO quenched at room temperature, (b) 20 wt% PMMA-*g*-SiO_2 in 100 kg mol^{-1} PEO isothermally crystallized at 58 °C for seven days, and (c) high-magnification TEM image for 40 wt% PMA-*g*-SiO_2 in 100 kg mol^{-1} PEO isothermally crystallized at 58 °C for seven days. (d) Storage modulus (E') at room temperature for samples either quenched at room temperature (RT quench) or crystallized at 58 °C for seven days. Source: Reprinted with permission from Zhao et al. [85]. Copyright 2017, American Chemical Society.

of low mechanical moduli and low glass transition temperatures. These property deficiencies were addressed by leveraging the crystallization behaviour of PEO to template the multi-scale assembly of nanoparticles within the composite. Figure 22.14a shows the TEM micrograph of the PMMA-g-SiO_2/PEO nanocomposite simply quenched at room temperature with no particle organization. Figure 22.14c shows the same composite (same silica loading) after isothermal crystallization at 58 °C for seven days. The long-range ordering after crystallization is clearly seen and agrees with molecular dynamics simulations that the particles can be driven into one of three hierarchical domains during crystallization. From smallest to largest domain, the regions are (i) engulfed within the PEO crystals (ii) in the interlamellar regions, or (iii) in the interfibrillar regions. There was an appreciable increase (nearly an order of magnitude) in the storage modulus (E') between the quenched composite and the hierarchically assembled composite with the same silica loading (Figure 22.14d). This improvement in E' was attributed to the nanoscale 'brick and mortar' structure templated by the PEO crystallization. Importantly, this work begins to fill out some untouched discovery space in the nanomaterials community by using an influence other than control of nanofiller

molecular parameters (σ and MW) to direct the assembly of nanofiller in a way that improves the nanocomposite properties.

The past decade has seen tremendous growth in the field of advanced composites owed to the molecular-scale control afforded by SI-RAFT. A staggering array of substrates been used as fillers in composites for a variety of applications. Perhaps the most significant new direction of nanocomposites stems from the discovery of self-assembled anisotropic structures made possible by tuning graft density and MW of grafted chains. This line of thinking has led to using top-down strategies to assemble nanofillers, leading to once innocuous materials having new-found potential.

22.5 Shaped Polymer-Grafted Particles

As mentioned at the beginning of Section 22.2, shaped polymer-grafted nanomaterials (PGNMs) are interesting because of their theorized properties. However, in-depth study of such materials remains quite underexplored because of the synthetic challenge of making shaped PGNMs with a high degree of control. Early work in this field relied on the self-assembly of block copolymers containing a reactive group, which would be self-assembled in bulk and the discontinuous phase would then be stabilized by various chemistries including gelation of silicates [86–88], 1–3 ring-opening of epoxy groups [89], UV initiation of vinyl groups [90], etc. Generally, after crosslinking, the block copolymer assembly may be exposed to a solvent good for the continuous phase to disperse the stabilized nanoobjects. This dispersion step is conducted with varying degrees of success. For example, lamellae that form polymer-grafted plates after solubilization can be particularly difficult to separate into single sheets, for example. However, this type of approach is robust in that the domain sizes and desired morphology is easily tuned by simply manipulating the length of each block within the copolymer – whose RAFT chemistry easily enables.

A simpler method of generating shaped nanoobjects with tunable domain sizes and orthogonally tunable morphology shape was investigated by Ruan and coworkers [91]. RAFT polymerization was used to prepare poly(3-(triethoxysilyl)propyl) methacrylate-*block*-polystyrene (PTEPM-*b*-PS). Once assembled in the bulk, the triethoxysilyl groups can be crosslinked upon exposure to acid, forming a silicate. The authors demonstrated that by starting with only a few different versions of the PTEPM-*b*-PS block copolymer and small homopolymers of each PTEPM and PS, the core shape, core size, and brush length could be independently tuned. Their elegant approach is summarized in Figure 22.15. For example, if starting with a PTEPM-*b*-PS with block lengths such that the bulk morphology is lamellar, adding sufficient PS homopolymer to the assembly changes the bulk morphology to PTEPM spheres in a PS continuous phase. Excitingly, it was also demonstrated that the brush length and core domain size were independently tunable. If simply using a block copolymer to change morphology or domain size, and a larger core domain is desired, there is the risk that changing the volume fraction of the PTEPM block would result in morphological change. By adding small homopolymers to the block copolymer system, the morphology can remain unchanged and core or brush length

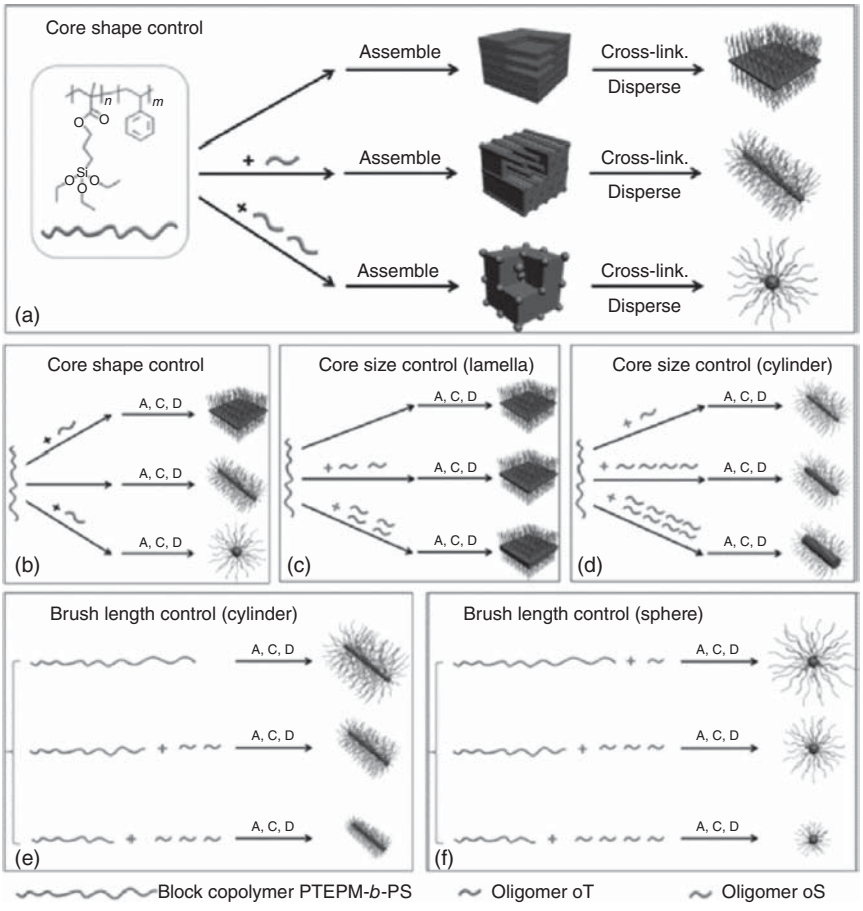

Figure 22.15 Illustrations of PGNP preparation of various structures by 'assembly–crosslink–dispersion method'. (a), (b) PGNPs with different core shapes; (c) lamellar PGNPs with different core thicknesses; (d) cylindrical PGNPs with different core diameters; (e) cylindrical PGNPs with different polymer brush lengths; and (f) spherical PGNPs with different polymer brush lengths. A: Assembly of block copolymer and oligomers. C: Crosslinking of PTEPM domains. D: Dispersion of bulk materials. Source: Reprinted with permission from Ruan et al. [91]. © 2015, American Chemical Society.

can be independently tuned. After crosslinking the core, the nanoobjects could then be dispersed in a good solvent for the PS block. This work represents a significant advance in top-down preparation of tunable polymer-grafted nanoobjects.

Perhaps more pervasive in the past half-decade of literature is the concept of polymerization-induced self-assembly (PISA) to prepare tunable nanostructures. In essence, PISA is the result of chain extending from a macro-CTA with a monomer that becomes insoluble in the reaction medium as a polymer [92]. As a result of chain extension, the insoluble polymer aggregates in solution, forming nanostructures whose shape is a function of the ratio between solvophilic and solvophobic regions of the block copolymer. RAFT is a flexible platform for this technique,

which is generally performed in water or highly polar media. The most common nano-shapes accessible by PISA are spherical micelles, worms, and vesicles. In principle, the nanoobjects can then be stabilized by crosslinking the continuous domain. Karagoz et al. explored this idea of preparing stabilized structures via PISA by chain extending from a dithiobenzoate-functionalized poly(oligo(ethylene glycol)methacrylate with a mixture of styrene and 4-vinylbenzaldehyde [93]. The incorporated aldehyde groups in the assembled structure were sites for crosslinking with 1,3-diaminopropane or conjugation with doxorubicin. When release of the doxorubicin was studied, the shape of the drug-loaded assemblies had a pronounced effect on cellular uptake. Worm and rod-like assemblies had much lower IC_{50} values compared to micelles and vesicles, although no significant difference in the drug release rate between the different assemblies was observed.

Further fine-tuning of PISA as a technique to prepare well-defined polymeric particles was explored by Zhou and coworkers [94]. Often, the goal of preparing highly functional nanostructures is to approximate nature's elegant structural control of macromolecules and their assemblies. In this work, low-dispersity nanospheres and vesicles were prepared via PISA formation of poly(*N*,*N*-dimethylacrylamide)-*block*-poly(diacetone acrylamide) (PDMAM-*b*-PDAAM) (diacetone acrylamide (DAAM) is *N*-(2-methyl-4-oxopentan-2-yl)acrylamide). By lowering the polymerization temperature and concentration of radical initiator compared to conventional PISA systems, the dispersity of the assembled structures was significantly decreased. Likely, both measures reduced the rate of polymerization, allowing the assembling structure time to reorganize and resulting in improved uniformity. The highly keto-rich core block was then available for post-modification. Although not used for crosslinking in this work, a highly functional core domain presents opportunities for incorporating multi-functionality – approaching the molecular-scale control necessary to mimic and manipulate biological systems.

Dynamic polymeric nanoobjects were prepared via RAFT-mediated PISA, representing a further enhancement of nanoscale structural control [95]. PISA of poly(glycerol monomethacrylate)-*block*-poly(2-hydroxypropyl methacrylate) (PGlyMA-*b*-PHPMA) (glycerol monomethacrylate (GlyMA) is 2,3-dihydroxypropyl methacrylate) was conducted starting with a $PGlyMA_{56}$ macro-CTA. At room temperature, the dominant morphology was worms, but upon cooling to 5 °C, a worm-to-sphere transition was observed (Figure 22.16). In this work, this temperature-induced morphology transition was used as a wholly synthetic biomimetic alternative to hydroxyethyl starch (HES), commonly used as a cryoprotectant in blood preservation. The addition of a small amount of poly(vinyl alcohol) to the PGlyMA-*b*-PHPMA worms resulted in a red blood cell recovery level indistinguishable from the system currently employed for cellular cryopreservation.

To summarize, at the beginning of this decade, there were a few scarce and rudimentary methods for creating shaped PGNMs, some with fair control of the particle shape but fewer with control of particle size or grafted polymer length. Now, bulk assembly of block copolymers or PISA have evolved as the dominant routes to preparing nanoobjects with excellent control of shape and dispersity of size in some cases.

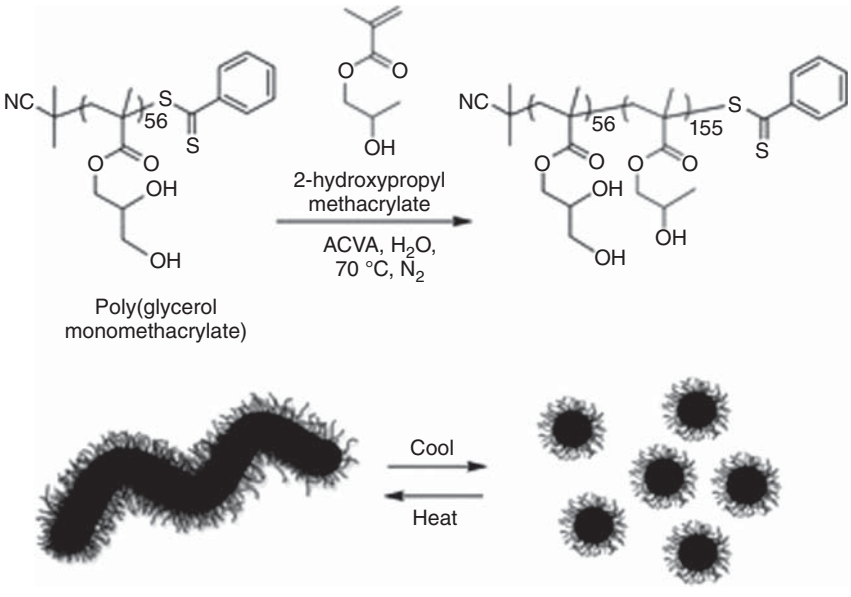

Figure 22.16 PISA synthesis of PGlyMA-*b*-PHPMA diblock copolymer worms and illustration of reversible worm-to-sphere transition upon cooling below 12 °C. Source: Reproduced with permission from Mitchell et al. [95]. © 2016, John Wiley & Sons. ACVA is 4,4′-azobis(4-cyanopentanoic acid) (ACPA).

22.6 Conclusion

The past decade has seen incredible growth in the field of polymer-grafted surfaces and nanomaterials. Much of the progress and success is owed to RAFT chemistry. Unparalleled in its chemical compatibility, mild conditions, and general versatility, RAFT polymerization has been applied liberally in every area of nanoscience. The result is materials that are stronger, more durable, biomimetic, smarter, and advanced in every sense. When SI-RAFT is combined with materials made already great by nature, the result is greater than the sum of its parts.

Happily, the last few years are rich with development in RAFT methodology. The work conducted on polymer-grafted surfaces described in this chapter focused solely on RAFT as a controlled radical polymerization, largely in conventional organic solvent as a polymerization medium. Advances such as aqueous RAFT [96], light-activated RAFT [97], temperature-programmed RAFT [98], cationic RAFT [99, 100], switchable RAFT [101, 102], etc., are sure to begin infiltrating the topics mentioned here. With these new methodologies, the outlook is bright for the next decade of advanced materials made possible by the ever-increasing versatility of RAFT as a polymerization technique.

Acknowledgements

This work was supported by the U.S. Department of Energy, Office of Science, Basic Energy Sciences (BES) under award no. DE-SC0018135.

References

1 Dukes, D., Li, Y., Lewis, S. et al. (2010). Conformational transitions of spherical polymer brushes: synthesis, characterization, and theory. *Macromolecules* 43: 1564–1570.

2 Zoppe, J.O., Ataman, N.C., Mocny, P. et al. (2017). Surface-initiated controlled radical polymerization: state-of-the-art, opportunities, and challenges in surface and interface engineering with polymer brushes. *Chem. Rev.* 117: 1185–1318.

3 Alexander, S. (1977). Adsorption of chain molecules with a polar head a scaling description. *J. Phys. (Paris)* 38: 983–987.

4 de Gennes, P. (1980). Conformations of polymers attached to an interface. *Macromolecules* 13: 1069–1075.

5 Pirri, G., Chiari, M., Damin, F., and Meo, A. (2006). Microarray glass slides coated with block copolymer brushes obtained by reversible addition chain-transfer polymerization. *Anal. Chem.* 78: 3118–3124.

6 Li, C. and Benicewicz, B.C. (2005). Synthesis of well-defined polymer brushes grafted onto silica nanoparticles via surface reversible addition fragmentation chain transfer polymerization. *Macromolecules* 38: 5929–5936.

7 Stenzel, M.H., Zhang, L., and Huck, W.T.S. (2006). Temperature-responsive glycopolymer brushes synthesized via RAFT polymerization using the Z-group approach. *Macromol. Rapid Commun.* 27: 1121–1126.

8 Barbey, R., Lavanant, L., Paripovic, D. et al. (2009). Polymer brushes via surface-initiated controlled radical polymerization: synthesis, characterization, properties, and applications. *Chem. Rev.* 109: 5437–5527.

9 Kumar, S.K., Jouault, N., Benicewicz, B.C., and Neely, T. (2013). Nanocomposites with grafted nanoparticles. *Macromolecules* 46: 3199–3214.

10 Perrier, S. (2017). 50th Anniversary perspective: RAFT polymerization – a user guide. *Macromolecules* 50: 7433–7447.

11 Zhang, Z., Keys, A.S., Chen, T., and Glotzer, S.C. (2005). Self-assembly of patchy particles into diamond structures through molecular mimicry. *Langmuir* 21: 11547–11551.

12 Glotzer, S.C. and Solomon, M.J. (2007). Anisotropy of building blocks and their assembly into complex structures. *Nat. Mater.* 6: 557–562.

13 Rungta, A., Natarajan, B., Neely, T. et al. (2012). Grafting bimodal polymer brushes on nanoparticles using controlled radical polymerization. *Macromolecules* 45: 9303–9311.

14 Natarajan, B., Neely, T., Rungta, A. et al. (2013). Thermomechanical properties of bimodal brush modified nanoparticle composites. *Macromolecules* 46: 4909–4918.

15 Huang, Y., Zheng, Y., Sarkar, A. et al. (2017). Matrix-free polymer nanocomposite thermoplastic elastomers. *Macromolecules* 50: 4742–4753.

16 Rotzoll, R. and Vana, P. (2008). Synthesis of poly(methyl acrylate) loops grafted onto silica nanoparticles via reversible addition-fragmentation chain transfer polymerization. *J. Polym. Sci. A. Polym. Chem.* 46: 7656–7666.

17 Zhang, J., Grzybowski, B.A., and Granick, S. (2017). Janus particle synthesis, assembly, and application. *Langmuir* 33: 6964–6977.

18 Kraft, D.J., Ni, R., Smallenburg, F. et al. (2012). Surface roughness directed self-assembly of patchy particles into colloidal Micelles. *Proc. Natl. Acad. Sci. U. S. A.* 109: 10787–10792.

19 Chen, Q., Whitmer, J.K., Jiang, S. et al. (2011). Supracolloidal reaction kinetics of Janus spheres. *Science* 331: 199–202.

20 Sacanna, S., Irvine, W.T.M., Chaikin, P.M., and Pine, D.J. (2010). Lock and key colloids. *Nature* 464: 575–578.

21 Wang, Y., Wang, Y., Zheng, X. et al. (2014). Three-dimensional lock and key colloids. *J. Am. Chem. Soc.* 136: 6866–6869.

22 Jiang, S., Schultz, M.J., Chen, Q. et al. (2008). Solvent-free synthesis of Janus colloidal particles. *Langmuir* 24: 10073–10077.

23 Zhang, G., Wang, D.Y., and Mohwald, H. (2005). Patterning microsphere surfaces by templating colloidal crystals. *Nano Lett.* 5: 143–146.

24 Li, J., Wang, L., and Benicewicz, B.C. (2013). Synthesis of Janus nanoparticles via combination of reversible click reaction and "Grafting-to" strategies. *Langmuir* 29: 11547–11553.

25 Liu, Y., Xu, X., Liang, F., and Yang, Z. (2017). Polymeric Janus nanosheets by template RAFT polymerization. *Macromolecules* 50: 9042–9047.

26 Lotierzo, A., Longbottom, B.W., Lee, W.H., and Bon, S.A.F. (2019). Synthesis of Janus and patchy particles using nanogels as stabilizers in emulsion polymerization. *ACS Nano* 13: 399–407.

27 Choi, J., Schattling, P., Jochum, F.D. et al. (2012). Functionalization and patterning of reactive polymer brushes based on surface reversible addition and fragmentation chain transfer polymerization. *J. Polym. Sci. A Polym. Chem.* 50: 4010–4018.

28 Steinkoenig, J., Bloesser, F.R., Huber, B. et al. (2016). Controlled radical polymerization and in-depth mass-spectrometric characterization of poly(ionic liquid)s and their photopatterning on surfaces. *Polym. Chem.* 7: 451–461.

29 Alconcel, S.N.S., Baas, A.S., and Maynard, H.D. (2011). FDA-approved poly(ethylene glycol) – protein conjugate drugs. *Polym. Chem.* 2: 1442–1448.

30 Wallat, J.D., Rose, K.A., and Pokorski, J.K. (2014). Proteins as substrates for controlled radical polymerization. *Polym. Chem.* 5: 1545–1558.

31 Tucker, B.S., Coughlin, M.L., Figg, C.A., and Sumerlin, B.S. (2017). Grafting-from proteins using metal-free PET–RAFT polymerizations under mild visible-light irradiation. *ACS Macro Lett.* 6: 452–457.

32 Li, X., Wang, L., Chen, G. et al. (2014). Visible light induced fast synthesis of protein-polymer conjugates: controllable polymerization and protein activity. *Chem. Commun.* 50: 6506–6508.

33 Takahashi, H., Nakayama, M., Yamato, M., and Okano, T. (2010). Controlled chain length and graft density of thermoresponsive polymer brushes for optimizing cell sheet harvest. *Biomacromolecules* 11: 1991–1999.

34 Zheng, Y., Wang, L., Lu, L. et al. (2017). pH and thermal dual-responsive nanoparticles for controlled drug delivery with high loading content. *ACS Omega* 2: 3399–3405.

35 Wang, L., Chen, Y.P., Miller, K.P. et al. (2014). Functionalized nanoparticles complexed with antibiotic efficiently kill MRSA and other bacteria. *Chem. Commun.* 50: 12030–12033.

36 Inam, M., Foster, J.C., Gao, J. et al. (2019). Size and shape affects the antimicrobial activity of quaternized nanoparticles. *J. Polym. Sci. Part A: Polym. Chem.* 57: 255–259.

37 Giovino, M., Pribyl, J., Benicewicz, B.C. et al. (2017). Linear rheology of polymer nanocomposites with polymer-grafted nanoparticles. *Polymer* 131: 104–110.

38 Guenay, K.A., Schuewer, N., and Klok, H.-A. (2012). Synthesis and postpolymerization modification of poly(pentafluorophenyl methacrylate) brushes. *Polym. Chem.* 3: 2186–2192.

39 Liu, J., Zhang, L., Shi, S. et al. (2010). A novel and universal route to SiO_2-supported organic/inorganic hybrid noble metal nanomaterials via surface RAFT polymerization. *Langmuir* 26: 14806–14813.

40 Moraes, J., Ohno, K., Maschmeyer, T., and Perrier, S. (2013). Monodisperse, charge-stabilized, core-shell particles via silica supported reversible addition-fragmentation chain transfer polymerization for cell imaging. *Chem. Mater.* 25: 3522–3527.

41 Li, Q., Zhang, L., Bai, L. et al. (2011). Multistimuli-responsive hybrid nanoparticles with magnetic core and thermoresponsive fluorescence-labeled shell via surface-initiated RAFT polymerization. *Soft Matter* 7: 6958–6966.

42 Grande, C.D., Tria, M.C., Jiang, G. et al. (2011). Grafting of polymers from electrodeposited macro-RAFT initiators on conducting surfaces. *React. Funct. Polym.* 71: 938–942.

43 Zengin, A. and Caykara, T. (2012). RAFT-mediated synthesis of poly(oligoethylene glycol) methyl ether acrylate brushes for biological functions. *J. Polym. Sci., Part A: Polym. Chem.* 50: 4443–4450.

44 Hojjati, B. and Charpentier, P.A. (2010). Synthesis of TiO_2-polymer nanocomposite in supercritical CO_2 via RAFT polymerization. *Polymer* 51: 5345–5351.

45 Tao, P., Li, Y., Rungta, A. et al. (2011). TiO_2 nanocomposites with high refractive index and transparency. *Journal of Materials Chemistry* 21: 18623–18629.

46 Yang, K., Huang, X., Huang, Y. et al. (2013). FluoroPolymer@$BaTiO_3$ hybrid nanoparticles prepared via RAFT polymerization: toward ferroelectric polymer nanocomposites with high dielectric constant and low dielectric loss for energy storage application. *Chem. Mater.* 25: 2327–2338.

47 Qiao, Y., Islam, M.S., Wang, L. et al. (2014). Thiophene polymer-grafted barium titanate nanoparticles toward nanodielectric composites. *Chem. Mater.* 26: 5319–5326.

48 Qiao, Y., Yin, X., Wang, L. et al. (2015). Bimodal polymer brush core–shell barium titanate nanoparticles: a strategy for high-permittivity polymer nanocomposites. *Macromolecules* 48: 8998–9006.

49 Xiao, Z.-P., Yang, K.-M., Liang, H., and Lu, J. (2010). Synthesis of magnetic, reactive, and thermoresponsive Fe_3O_4 nanoparticles via surface-initiated RAFT copolymerization of *N*-isopropylacrylamide and acrolein. *J. Polym. Sci., Part A: Polym. Chem.* 48: 542–550.

50 Niu, S., Zhang, L., Wang, N. et al. (2013). Fabrication of magnetic nanofibers via surface-initiated RAFT polymerization and coaxial electrospinning. *React. Funct. Polym.* 73: 1447–1454.

51 Wang, H., Luo, W., and Chen, J. (2012). Fabrication and characterization of thermoresponsive Fe_3O_4@PNIPAM hybrid nanomaterials by surface-initiated RAFT polymerization. *J. Mater. Sci.* 47: 5918–5925.

52 Wang, L., Cole, M., Li, J. et al. (2015). Polymer grafted recyclable magnetic nanoparticles. *Polym. Chem.* 6: 248–255.

53 Dilag, J., Kobus, H., and Ellis, A.V. (2013). CdS/polymer nanocomposites synthesized via surface initiated RAFT polymerization for the fluorescent detection of latent fingermarks. *Forensic Sci. Int.* 228: 105–114.

54 Matsuno, R., Goto, Y., Konno, T. et al. (2009). Controllable nanostructured surface modification on quantum dot for biomedical application in aqueous medium. *J. Nanosci. Nanotechnol.* 9: 358–365.

55 Rzayev, Z.M.O. and Soylemez, A.E. (2011). Functional copolymer/organo-MMT nanoarchitectures. VI. Synthesis and characterization of novel nanocomposites by Interlamellar controlled/living radical copolymerization via preintercalated RAFT-agent/organoclay complexes. *J. Nanosci. Nanotechnol.* 11: 3523–3532.

56 Hou, Y., Jiang, J., Li, K. et al. (2014). Grafting amphiphilic brushes onto halloysite nanotubes via a living RAFT polymerization and their pickering emulsification behavior. *J. Phys. Chem. B* 118: 1962–1967.

57 Boujemaoui, A., Mazieres, S., Malmstrom, E. et al. (2016). SI-RAFT/MADIX polymerization of vinyl acetate on cellulose nanocrystals for nanocomposite applications. *Polymer* 99: 240–249.

58 Grande, C.D., Tria, M.C., Jiang, G.Q. et al. (2011). Surface-grafted polymers from electropolymerized polythiophene RAFT agent. *Macromolecules* 44: 966–975.

59 Yeole, N., Kutcherlapati, S.N.R., and Jana, T. (2015). Polystyrene–graphene oxide (GO) nanocomposite synthesized by interfacial interactions between RAFT modified GO and core–shell polymeric nanoparticles. *J. Colloid Interface Sci.* 443: 137–142.

60 Macdonald, T., Gibson, C.T., Constantopoulos, K. et al. (2012). Functionalization of vertically aligned carbon nanotubes with polystyrene via surface initiated reversible addition fragmentation chain transfer polymerization. *Appl. Surf. Sci.* 258: 2836–2843.

61 Audouin, F. and Heise, A. (2013). Surface-initiated RAFT polymerization of NIPAM from monolithic macroporous polyHIPE. *Eur. Polym. J.* 49: 1073–1079.

62 Barlow, K.J., Hao, X., Hughes, T.C. et al. (2014). Porous, functional, poly(styrene-*co*-divinylbenzene) monoliths by RAFT polymerization. *Polym. Chem.* 5: 722–732.

63 Pan, G., Ma, Y., Zhang, Y. et al. (2011). Controlled synthesis of water-compatible molecularly imprinted polymer microspheres with ultrathin hydrophilic polymer shells via surface-initiated reversible addition-fragmentation chain transfer polymerization. *Soft Matter* 7: 8428–8439.

64 Yu, H.-Y., Li, W., Zhou, J. et al. (2009). Thermo- and pH-responsive polypropylene microporous membrane prepared by the photoinduced RAFT-mediated graft copolymerization. *J. Membr. Sci.* 343: 82–89.

65 Schadler, L.S., Kumar, S.K., Benicewicz, B.C. et al. (2007). Designed interfaces in polymer nanocomposites: a fundamental viewpoint. *MRS Bull.* 32: 335–340.

66 Treacy, M.M.J., Ebbesen, T.W., and Gibson, J.M. (1996). Exceptionally high Young's modulus observed for individual carbon nanotubes. *Nature* 381: 678–680.

67 Bansal, A., Yang, H., Li, C. et al. (2006). Controlling the thermomechanical properties of polymer nanocomposites by tailoring the polymer-particle interface. *J. Polym. Sci. B Polym. Phys.* 44: 2944–2950.

68 Akcora, P., Liu, H., Kumar, S.K. et al. (2009). Anisotropic self-assembly of spherical polymer-grafted nanoparticles. *Nature Mater.* 8: 354–359.

69 Heinrich, G. and Kluppel, M. (2002). Recent advances in the theory of filler networking in elastomers. *Adv. Polym. Sci.* 160: 1–44.

70 Gusev, A.A. (2006). Micromechanical mechanism of reinforcement and losses in filled rubbers. *Macromolecules* 39: 5960–5962.

71 Long, D. and Sotta, P. (2007). Stress relaxation of large amplitudes and long timescales in soft thermoplastic and filled elastomers. *Rheol. Acta* 46: 1029–1044.

72 Maier, P.G. and Goritz, D. (1996). Molecular interpretation of the Payne effect. *Kautsch. Gummi Kunstst.* 49: 18–21.

73 Zhu, Z.Y., Thompson, T., Wang, S.Q. et al. (2005). Investigating linear and nonlinear viscoelastic behavior using model silica-particle-filled polybutadiene. *Macromolecules* 38: 8816–8824.

74 Zhu, A.J. and Sternstein, S.S. (2003). Nonlinear viscoelasticity of nanofilled polymers: interfaces, chain statistics and properties recovery kinetics. *Compos. Sci. Technol.* 63: 1113–1126.

75 Moll, J.F., Akcora, P., Rungta, A. et al. (2011). Mechanical reinforcement in polymer melts filled with polymer grafted nanoparticles. *Macromolecules* 44: 7473–7477.

76 Bell, M., Krentz, T., Nelson, J.K. et al. (2017). Investigation of dielectric breakdown in silica-epoxy nanocomposites using designed interfaces. *J. Colloid Interface Sci.* 495: 130–139.

77 Khani, M.M., Abbas, Z.M., and Benicewicz, B.C. (2017). Well-defined polyisoprene-grafted silica nanoparticles via the RAFT process. *J. Polym. Sci. Part A: Polym. Chem.* 55: 1493–1501.

78 Jitchum, V. and Perrier, S. (2007). Living radical polymerization of isoprene via the RAFT process. *Macromolecules* 40: 1408–1412.

79 Germack, D.S. and Wooley, K.L. (2007). Isoprene polymerization via reversible addition fragmentation chain transfer polymerization. *Polym. Sci. Part A: Polym. Chem.* 45: 4100–4108.

80 Li, C., Han, J., Ryu, C.Y., and Benicewicz, B.C. (2006). A versatile method to prepare RAFT agent anchored substrates and the preparation of PMMA grafted nanoparticles. *Macromolecules* 39: 3175–3183.

81 Zheng, Y., Abbas, Z.M., Sarkar, A. et al. (2018). Surface-initiated reversible addition-fragmentation chain transfer polymerization of chloroprene and mechanical properties of matrix-free polychloroprene nanocomposites. *Polymer* 135: 193–199.

82 Qu, L., Wang, L., Xie, X. et al. (2014). Contribution of silica-rubber interactions on the viscoelastic behaviors of modified solution polymerized styrene butadiene rubbers (M–S–SBRs) filled with silica. *RSC Advances* 4: 64354–64363.

83 Khani, M.M., Woo, D., Mumpower, E.L., and Benicewicz, B.C. (2017). Poly(alkyl methacrylate)-grafted silica nanoparticles in polyethylene nanocomposites. *Polymer* 109: 339–348.

84 Bilchak, C.R., Buenning, E., Asai, M. et al. (2017). Polymer-grafted nanoparticle membranes with controllable free volume. *Macromolecules* 50: 7111–7120.

85 Zhao, D., Gimenez-Pinto, V., Jimenez, A.M. et al. (2017). Tunable multiscale nanoparticle ordering by polymer crystallization. *ACS Cent. Sci.* 3: 751–758.

86 Zhang, K., Gao, L., and Chen, Y. (2007). Organic-inorganic hybrid materials by self-gelation of block copolymer assembly and nanoobjects with controlled shapes therof. *Macromolecules* 40: 5916–5922.

87 Zhang, K., Gao, L., and Chen, Y. (2008). Smart organic/inorganic hybrid nanoobjects with controlled shapes by self-assembly of gelable block copolymers. *Macromolecules* 41: 1800–1807.

88 Gao, L., Zhang, K., and Chen, Y. (2011). Functionalization of shaped polymeric nanoobjects via bulk co-self assembling gelable block copolymers with silane coupling agents. *Polymer* 52: 3681–3686.

89 Qin, J., Jiang, X., Gao, L., and Chen, Y. (2010). Functional polymeric nanoobjects by cross-linking bulk self-assemblies of poly(*tert*-butyl acrylate)-block-poly(glycidyl methacrylate). *Macromolecules* 43: 8094–8100.

90 Hoppenbrouwers, E., Li, Z., and Liu, G. (2003). Triblock nanospheres with amphiphilic coronal chains. *Macromolecules* 36: 876–881.

91 Ruan, Y., Gao, L., Yao, D. et al. (2015). Polymer-grafted nanoparticles with precisely controlled structures. *ACS Macro Lett.* 4: 1067–1071.

92 Charleux, B., Delaittre, G., Rieger, J., and D'Agosto, F. (2012). Polymerization-induced self-assembly: from soluble macromolecules to block copolymer nano-objects in one step. *Macromolecules* 45: 6753–6765.

93 Karagoz, B., Esser, L., Duong, H.T. et al. (2014). Polymerization-induced self-assembly (PISA) – control over the morphology of nanoparticles for drug delivery applications. *Polym. Chem.* 5: 350–355.

94 Zhou, W., Qu, Q., Xu, Y., and An, Z. (2015). Aqueous polymerization-induced selfassembly for the synthesis of ketone-functionalized nano-objects with low polydispersity. *ACS Macro. Lett.* 4: 495–499.

95 Mitchell, D.E., Lovett, J.R., Armes, S.P., and Gibson, M.I. (2016). Combining biomimetic block copolymer worms with an ice-inhibiting polymer for the solvent-free cryopreservation of red blood cells. *Angew. Chem. Int. Ed. Engl.* 55: 2801–2804.

96 Carmean, R.N., Becker, T.E., Sims, M.B., and Sumerlin, B.S. (2017). Ultra-high molecular weights via aqueous reversible-deactivation radical polymerization. *Chem* 2: 93–101.

97 Figg, C.A., Hickman, J.D., Scheutz, G.M. et al. (2018). Color-coding visible light polymerizations to elucidate the activation of trithiocarbonates using Eosin Y. *Macromolecules* 51: 1370–1376.

98 Li, N., Ding, D., Pan, X. et al. (2017). Temperature programed photo-induced RAFT polymerization of stereo-block copolymers of poly(vinyl acetate). *Polym. Chem.* 8: 6024–6027.

99 Uchiyama, M., Satoh, K., and Kamigaito, M. (2016). A phosphonium intermediate for cationic RAFT polymerization. *Polym. Chem.* 7: 1387–1396.

100 Michaudel, Q., Chauvire, T., Kottisch, V. et al. (2017). Mechanistic insight into the photocontrolled cationic polymerization of vinyl ethers. *J. Am. Chem. Soc.* 139: 15530–15538.

101 Guerre, M., Uchiyama, M., Folgado, E. et al. (2017). Combination of cationic and radical RAFT polymerizations: a versatile route to well-defined poly(ethyl vinyl ether)-block-poly(vinyl fluoride) block copolymers. *ACS Macro Lett.* 6: 393–398.

102 Kottisch, V., Michaudel, Q., and Fors, B.P. (2017). Photocontrolled interconversion of cationic and radical polymerizations. *J. Am. Chem. Soc.* 139: 10665–10668.

23

High-Throughput/High-Output Experimentation in RAFT Polymer Synthesis

Carlos Guerrero-Sanchez[1,2], Roberto Yañez-Macias[3], Miguel Rosales-Guzmán[4], Marco A. De Jesus-Tellez[5], Claudia Piñon-Balderrama[6], Joris J. Haven[7], Graeme Moad[8], Tanja Junkers[7], and Ulrich S. Schubert[1,2]

[1] *Friedrich Schiller University Jena, Laboratory of Organic and Macromolecular Chemistry (IOMC), Humboldtstrasse 10, Jena 07743, Germany*
[2] *Friedrich Schiller University Jena, Jena Center for Soft Matter (JCSM), Philosophenweg 7, Jena 07743, Germany*
[3] *Centro de Investigación en Química Aplicada (CIQA), Blvd. Enrique Reyna H. 140, Saltillo, Coahuila 25100, México*
[4] *Universidad Tecnológica de Saltillo, Calle Nogal s/n, Ejido la Providencia, Saltillo, Coahuila 25300, México*
[5] *Centro de Investigación y de Estudios Avanzados (CINVESTAV) Unidad Mérida, A.P. 73, Cordemex, Mérida, Yucatán 97310, México*
[6] *Centro de Investigación en Materiales Avanzados S. C. (CIMAV-Unidad Monterrey), Advanced Functional Materials & Nanotechnology Group, Polymer Science & Nanotechnology Lab., Av. Alianza Norte 202, Autopista Monterrey-Aeropuerto Km 10, PIIT, Apodaca, Nuevo León C.P.66628, México*
[7] *Monash University, School of Chemistry, Polymer Reaction Design Group, 19 Rainforest, Walk Clayton, VIC 3800, Australia*
[8] *CSIRO Manufacturing, Research Way, Clayton, VIC 3168, Australia*

23.1 Introduction

High-throughput/high-output experimentation (HT/HO-E), introduced in polymer research laboratories around the globe over the past two decades, has proven to be a powerful technique for synthesis, characterization, and screening of polymers. The main goal has been to expedite the discovery process for new materials by making it both more efficient and cost-effective [1–12]. The versatility of HT/HO-E has allowed the study of a diverse range of reversible addition fragmentation chain transfer (RAFT) polymerization processes, for instance, in homogeneous or heterogeneous media, [13–17] or at ambient or high pressure (e.g. suitable techniques for polymerizing low boiling point monomers) [18]. In addition, both on- and off-line techniques have also been developed for monitoring the progress of polymerization reactions [19–24] as well as HT/HO-E techniques for measuring properties of generated polymer libraries [1, 2, 5–12]. Thus, HT/HO-E has led to the efficient identification of suitable polymers for applications such as industrial coatings, sensors, and biomaterials [6, 7, 9, 11, 25–28].

This contribution analyses the state of the art and utility of HT/HO-E applied in RAFT synthesis, characterization, and screening of polymer materials. Emphasis is

RAFT Polymerization: Methods, Synthesis and Applications, First Edition.
Edited by Graeme Moad and Ezio Rizzardo.

placed on fundamental aspects and experimental 'bottlenecks', which are normally not addressed in detail in the existing literature. Some of these bottlenecks include achieving precision and reproducibility in synthetic and product purification methods. The utilization of HT/HO-E in the field of RAFT polymerization to screen reagents, evaluate reaction conditions (i.e. the so-called kinetic investigations), and generate comprehensive and systematic polymer libraries is also discussed. Next, the importance of screening RAFT polymer libraries generated by HT/HO-E is illustrated with selected applications in the biomedicine field. Finally, some recommendations and future perspectives for HT/HO-E for RAFT polymer research are provided.

23.2 Fundamental Experimentation and Limitations of HT/HO-E in RAFT Polymer Synthesis

Perhaps the most crucial aspect of utilizing HT/HO-E relates to the generation of reliable experimental data and, therefore, meaningful conclusions derived thereof. Often, this aspect is partly overlooked. The sometimes over-enthusiastic descriptions of the technological features incorporated in available HT/HO-E platforms can give rise to the perception that they are all-purpose machines. However, while they have been validated for several experimental protocols, HT/HO-E platforms must not be regarded as 'black boxes' where all generated data and results are necessarily precise and reliable. Thus, it is 'a must' for any experimentalist to, first of all, verify the reproducibility and accuracy of the HT/HO-E methods for specific research tasks.

A particular example of this situation relates to air-sensitive polymerizations (i.e. moisture and/or oxygen intolerant systems), where suitable pre-conditioning procedures for reaction vessels and the various components involved in these reactions must be developed and applied before synthesis (e.g. ionic polymerizations). This is also true for RAFT synthesis as propagating polymer chains are prone to react with oxygen at diffusion-controlled rates. In this regard, suitable degassing processes to eliminate oxygen from reaction media in conventional lab-scale reactors have been reported, including refluxing of reaction media, inert gas sparging, ultrasonic agitation, and freeze–evacuate–thaw protocols [29]. Implementation of these pre-conditioning processes might negatively impact on the number of reactions that can be performed in a determined period of time and, therefore, on the productivity and cost of a project. To minimize this drawback, different degassing methods have been successfully adapted to HT/HO-E platforms. For instance, many HO-E platforms designed for automated parallel synthesis can maintain an inert atmosphere within parallel reactors to avoid the exposure of polymerization media to atmospheric oxygen [30]. Furthermore, parallel reactors can also be placed inside of a hood or glove box containing an inert atmosphere to allow handling reagents under these conditions throughout the course of the synthesis [30]. Under these set-ups, the parallel reactors of a given automated parallel synthesizer would first be heated and subjected to several evacuate – 'fill with inert gas' cycles to eliminate

oxygen and create an appropriate inert atmosphere for the polymerizations [31–33]. Other alternative oxygen-tolerant synthetic techniques and degassing methods have also been successfully implemented to perform RAFT polymerizations, for instance, in microwell plates open to air using simple robotics [34] or manual preparation of the reaction mixtures, [23, 35–39] and an automated parallel freeze–evacuate procedure [40]. This latter example demonstrated that RAFT polymerizations carried out in a commercially available automated parallel synthesizer can be very similar to those performed utilizing a high vacuum freeze–evacuate–thaw protocol in individual flame-sealed glass ampoules. Other degassing experimental procedures to eliminate oxygen from polymerization reactions have also been discussed in the literature [41–43].

23.3 HT/HO-E Kinetic Investigations

Fundamental understanding of reaction mechanisms and kinetics is essential for designing polymer materials and optimizing chemical processes [13, 20, 44–50] For instance, the estimation of reactivity ratios for a comonomer pair is a crucial quantitative aspect in efficiently designing copolymer materials. In this regard, experimental data obtained through HT/HO-E, available kinetic models, and computer programs [51] are valuable tools for the estimation of such parameters. For example, Rosales-Guzmán et al. reported a HO-E protocol (suitable for low boiling point monomers) to perform RAFT parallel copolymerizations of glycidyl methacrylate (GMA) and isoprene (IP) at different reaction conditions (i.e. relatively high pressure and high temperature) and used the obtained kinetic data to estimate the reactivity ratios of this comonomer system [18]. Guerrero-Sanchez et al. reported a detailed kinetic study on the RAFT copolymerization of methyl acrylate (MA) and vinyl acetate (VAc) over a broad interval of comonomer feed compositions, where the obtained comprehensive experimental data allowed for reliable estimation of the reactivity ratios for this copolymerization system [20].

Other kinetic investigations are the contributions reported by Keddie et al. [13, 47, 50] on the use of acid/base switchable RAFT agents for the copolymerization of more- and less-activated monomers. For example, the effect of acids of different strengths and stoichiometries with respect to RAFT agent on the polymerization of *N,N*-dimethylacrylamide (DMAm) was investigated taking advantage of automated pH measurements and nuclear magnetic resonance (NMR) sampling incorporated in a commercially available parallel synthesizer (Figure 23.1) [13]. The results showed the effect of pK_a and acid concentration on the dispersity ($Đ$), molar mass, and end groups of the synthesized polymers and demonstrated that switchable RAFT polymerization is most effectively carried out in the presence of strong acids in equimolar amounts (i.e. not exceeding the RAFT agent concentration). On neutralizing the RAFT end group, it was also possible to form a second block with the less-activated monomers, VAc and *N*-vinylpyrrolidone (NVP), and the intermediate-activated monomer *N*-vinylcarbazole (NVC), thereby demonstrating

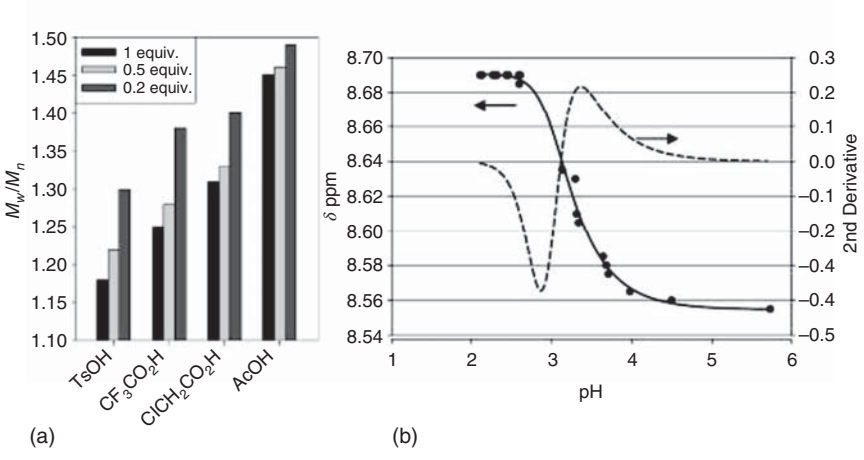

Figure 23.1 (a) Relationship between acid strength or concentration on the polymer dispersity (*Đ*) and (b) a proton nuclear magnetic resonance (^{1}H NMR) titration curve of a switchable RAFT agent with an acid; experiments were performed in an automated parallel synthesizer. Source: Keddie et al. [13]. © 2011, American Chemical Society.

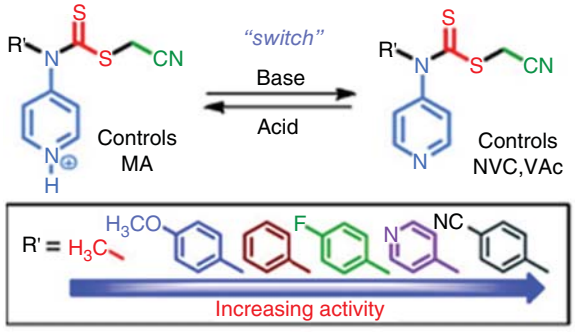

Figure 23.2 Schematic representation of acid/base switchable RAFT agents for the polymerization of MA, VAc, and NVC screened with the aid HO–E techniques. Source: Reproduced with permission from Keddie et al. [47]. © 2012, American Chemical Society.

the utility of the switchable RAFT procedure for the synthesis of block copolymers comprising segments of more- and less-active monomers.

In a second contribution, the RAFT polymerization of MA, NVC, and VAc was investigated by screening a series of acid/base switchable RAFT agents with *N*-aryl substituents (Figure 23.2) [47]. The outcome of these HO-E investigations [13, 47, 50] allowed optimal conditions for the preparation of low *Đ* NVC-containing block copolymers to be established and provided a better understanding of the kinetics of acid/base switchable RAFT polymerization reactions of MA, VAc, and NVC. The status of NVC as an intermediate-activated monomer was also established.

In another approach, Voorhaar et al. [46] discussed the preparation of ABA amphiphilic *quasi*-triblock copolymers with self-healing properties, where the middle hydrophilic block contained *N*-acryloylmorpholine (NAM) units, while the outer hydrophobic *quasi*-blocks were formed with isobornyl acrylate (IBA). Firstly, a HO-E kinetic study was performed to determine conditions for an acceptable rate

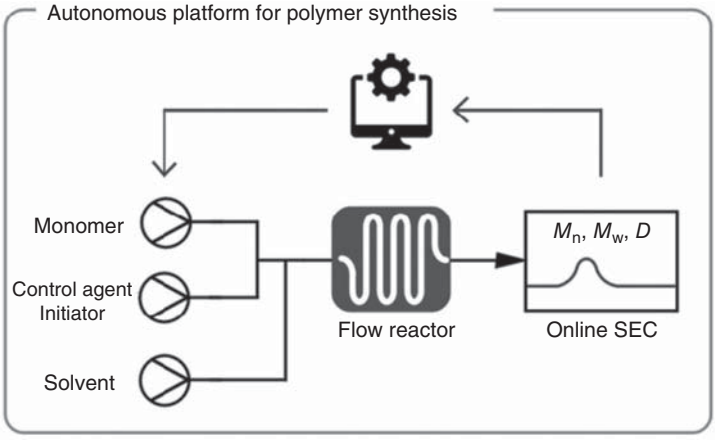

Figure 23.3 Schematic representation of the system for the self-optimization of RAFT polymerizations described by Rubens et al. The product stream is injected into an on-line SEC system, subsequently analyzed and processed by an optimization algorithm. Source: Rubens et al. [48]. © 2019, John Wiley & Sons.

of the RAFT polymerization of NAM. The use of an appropriate bifunctional RAFT agent ensured that IBA was incorporated on both sides of the NAM segment to provide ABA triblock copolymers.

A relatively new RAFT polymerization technique known as photoinduced energy or electron transfer polymerization (PET-RAFT) has also been reported, which under certain conditions can be performed under the presence of oxygen [52, 53]. Kinetic investigations of this technique have been carried out using parallel polymerizations in micro-well plates [23, 38, 54]. For example, Yeow et al. [23] carried out the HT/HO-E PET-RAFT synthesis of poly(*N*,*N*-dimethylacrylamide) (PDMAm) using 5,10,15,20-tetraphenylporphine zinc (ZnTPP) as a photocatalyst, where a spectroscopic technique was utilized to estimate monomer conversion. Ng et al. [38] also utilized PET-RAFT to study polymerization kinetics of acrylamides, (meth-)acrylates, and styrenics utilizing ZnTPP as a photocatalyst activated under yellow light; these systems exhibited an oxygen tolerance as well as a good control over architecture and molar mass of the obtained polymers.

Continuous flow systems can also be used as HT/HO-E tools for the optimization of reaction conditions [48, 55–57]. Rubens et al. introduced an autonomous platform system for polymer reactions that comprises a continuous flow reactor coupled with a size exclusion chromatography (SEC) equipment for online measurements (Figure 23.3) [48]. The system is controlled by a self-learning algorithm able to self-optimize reaction conditions by modifying reaction time, monomer concentration, and RAFT agent/initiator ratio to produce polymers of targeted molar mass with high precision and reproducibility (<2.5% deviation from pre-selected goal). As model reactions, the thermal and photo-induced RAFT polymerization of (meth-)acrylates was reported.

23.4 Utilization of HT/HO-E for the RAFT Synthesis of Polymer Libraries

The synthesis and accessibility of polymer libraries have opened straightforward opportunities for the elucidation of structure–property–function relationships of polymers, a better understanding of any potential impediments to research and/or the development of new applications. Several HT/HO-E approaches to access such libraries have been reviewed in the literature [12]. These polymer libraries, in combination with different robotic platforms, allow for a fast and efficient optimization of material properties and materials design [6, 7, 9, 23, 38, 45, 50, 58–60].

A relatively recent trend has revolved around the development of 'one-pot' synthetic strategies that produce the so-called *quasi*-block copolymers [45, 46, 61–63]. The strategy can be considered as a variant of spontaneous gradient copolymers [20, 64]. These 'one-pot' RAFT syntheses have driven efficient HT/HO-E workflows by eliminating time-consuming intermediate purification steps from complex multi-step reaction protocols and thereby increased research productivity. Additionally, premature hydrolytic cleavage was achieved in copolymerization reactions employing monomers that possess esters and amides as a side group; the prepared polymer libraries could be used in applications such as surface modification or drug delivery systems [65].

Guerrero-Sanchez et al. [61] prepared a 15-member *quasi*-diblock copolymer library of poly(butyl methacrylate-*quasi-block*-methyl methacrylate) (P(BMA-*qb*-MMA)). Three poly(butyl methacrylate) (PBMA) macroRAFT agents were prepared and aliquots distributed into three sets of five reactors each with the aid of a liquid handling system of an automated parallel synthesizer. Next, different amounts of methyl methacrylate (MMA) monomer were added into each reactor of each series, respectively, and allowed polymerizations continued. Figure 23.4 shows a schematic representation of one of these series (i.e. 5 *quasi*-diblock copolymers). This synthetic approach yields *quasi*-diblock copolymers rather than pure diblock copolymers. Nonetheless, it was demonstrated by differential scanning calorimetry (DSC) that the properties of these materials strongly resemble those expected for the pure diblock copolymers in that two well-defined glass transition temperatures characteristic of PBMA and poly(methyl methacrylate) (PMMA) were observed.

In a similar fashion, Haven et al. [45] reported the synthesis of a comprehensive *quasi*-diblock copolymer library of butyl methacrylate (BMA) with MMA. In this approach, PBMA was first synthesized as a macroRAFT agent in high, but not complete, monomer conversion. Thereafter, without any intermediate purification procedure, predetermined amounts of MMA (second monomer), additional initiator, and solvent were sequentially added into the same reaction pot for proceeding with the synthesis of a series of the *quasi*-block copolymer materials or, more accurately, PBMA-*block*-P(BMA-*stat*-MMA). Different temperature profiles were also tested in optimizing the reaction parameters. In a single experiment, 23 *quasi*-diblock copolymers (corresponding to time intervals for sampling of one hour) were obtained by simply taking aliquots from the reactor with the automated liquid handling system of the parallel synthesizer. This procedure provided valuable

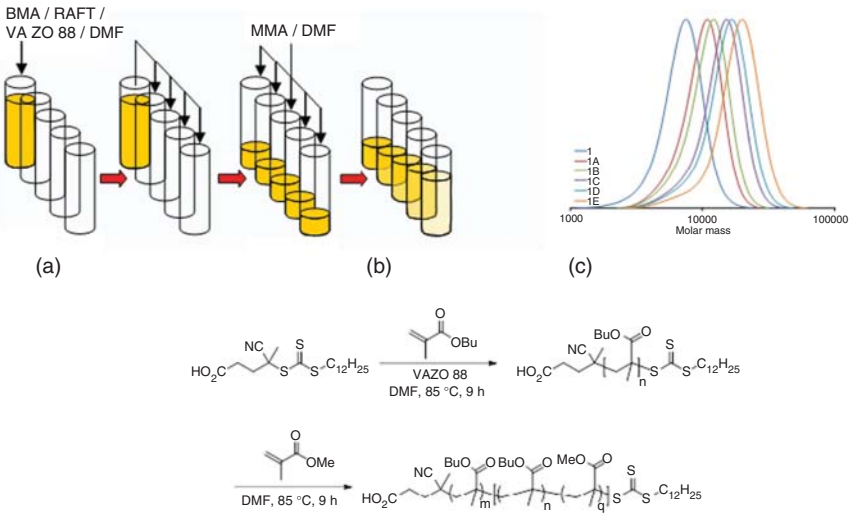

Figure 23.4 Schematic representation of the automated parallel synthesis of a *quasi*-diblock copolymer library via sequential RAFT polymerization (a). SEC traces of some of the obtained *quasi*-diblock copolymers illustrating a successful chain extension process or block formation (b). Reaction scheme of the utilized sequential RAFT polymerization process (c). Source: Adapted with permission from Guerrero-Sanchez et al. [61]. © 2013, Royal Society of Chemistry.

and detailed information about the evolution of the molar mass distribution and the rate of incorporation of MMA and the BMA 'impurity' into the *quasi*-block and, thus, the monomer sequence distribution. From the kinetic plots, it was concluded that the sequential RAFT polymerization reaction was well controlled throughout the entire process. Haven et al. [62] also applied these sequential RAFT polymerization techniques to prepare a higher order *quasi*-block copolymer library comprising 71 different *quasi*-diblock, -triblock, -tetrablock, and -pentablock copolymers in an automated parallel synthesizer. A mono-functional RAFT agent was utilized for the synthesis of ABC and ABCD copolymers while a bi-functional RAFT agent allowed preparation of BAB and CBABC sequences. In these examples A, B, C, and D represent BMA, MMA, di(ethylene glycol) methyl ether methacrylate (DEGMA), and benzyl methacrylate (BzMA), respectively.

While conventional RAFT polymerizations require an inert atmosphere and the elimination or minimization of oxygen in the reaction media, the implementation of RAFT polymerization in the presence of oxygen has also been reported with the subsequent synthesis of polymer libraries [23, 34, 36–38, 60, 63, 66]. For example, Chapman et al. [37] reported a manual combinatorial approach for the low-temperature (up to 50 °C) RAFT synthesis of homo and copolymers based on DMAm, NAM, 2-hydroxyethyl methacrylate (HEMA), 2-hydroxyethyl acrylate (HEA), poly(ethylene glycol) methyl ether methacrylate (PEGMA), and *N*-(2-hydroxypropyl)methacrylamide (HPMAm) using glucose oxidase (GOx) as the deoxygenating agent. Later, Wang et al. [67] also reported the use of GOx to deplete oxygen in the RAFT polymerization of HEA in an automated and unattended

parallel synthesizer. The reactions were performed in open vessel systems to probe the effectiveness GOx. The results of the enzyme-degassed reactions were compared to those observed in reactions using a conventional degassing technique (i.e. sparging nitrogen gas followed by a closed vessel to maintain an inert atmosphere). At the investigated conditions, the results revealed that GOx retains sufficient activity towards oxygen to carry out RAFT polymerizations in different aqueous media offering a good control on the molar mass of the synthesized polymers and low $Đ$ (< 1.10). Cosson et al. [63] also reported the RAFT synthesis of star polymers in PCR tubes in a conventional heating block, leading to a library of 60 polymers based on *N,N*-diethylacrylamide (DEAm), *N*-hydroxyethylacrylamide (HEAm), *N*-(3-methoxypropyl)acrylamide (MPAm), NAM, and *N*-ethylacrylamide (NEAm).

Nanoparticle libraries derived from block copolymer libraries with predictable highly ordered morphologies (i.e. spherical and worm-like micelles, vesicles, etc.) can also be produced by a simultaneous RAFT copolymerization/self-assembly using the technique known as polymerization-induced self-assembly (PISA) [68–71] in combination with HT/HO-E methods [59, 72, 73]. For example, Tan et al. [73] developed a photoinitiated oxygen-tolerant method to prepare well-defined nano-objects from the self-assembly of diblock and triblock copolymers in multi-well plates open to air and at room temperature. A wide range of morphologies such as sphere, worms, jellyfish, and vesicles were obtained by this one-pot approach (Figure 23.5).

Piñón-Balderrama et al. [74] also used a HT/HO-E approach for the sulfonation of the styrenic segment in a PMMA-PS library in order to introduce the functionality of proton conductivity in this diblock copolymer system. Sulfonated polymers were deposited on silicon wafers in the form of thin films to evaluate different self-assembled morphologies. Block copolymers at moderate sulfonation level (<50%) revealed the formation of lamellar and cylindric morphologies, while highly sulfonated thin films (~90%) showed a variety of morphologies such as a bicontinuous structure, micelles, worm-like, and a combination of worm-like and micelles structures after being exposed to different solvent vapours or to thermal annealing procedures.

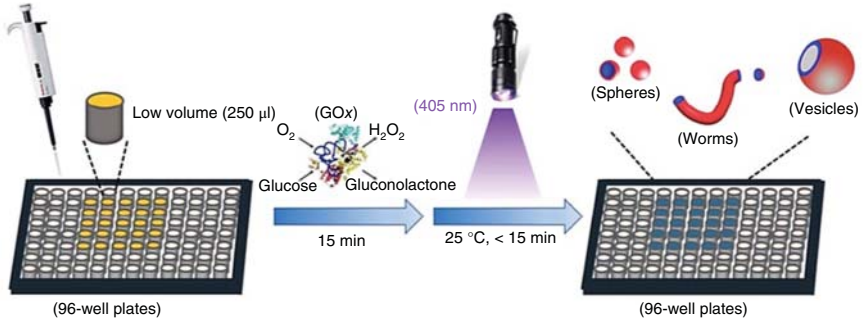

Figure 23.5 Schematic representation of enzymatically degassed photo-PISA-RAFT polymerizations in 96-well plates. Source: Reproduced with permission from Tan et al. [73]. © 2017, American Chemical Society.

A different strategy for modifying solvophobic behaviour and introducing amphiphilic features in different substances was proposed by Estrada et al. [75]. They used a series of poly(alkylmethacrylates) (i.e. poly(hexyl methacrylate), poly(lauryl methacrylate), and poly(stearyl methacrylate)) to encapsulate methylaluminoxane (MAO). The proposed encapsulation procedure induces the formation of self-assembled nanostructures (inverse micellar like) in the presence of organic solvents such as *n*-hexane and/or *n*-heptane. Subsequently, the inverse micellar solution containing encapsulated MAO was treated with a metallocene ($(n\text{-Bu-Cp})_2ZrCl_2$) to produce different catalytic systems of PnAMAs/MAO/$(n\text{-Bu-Cp})_2ZrCl_2$ that were tested in the polymerization of ethylene. The results revealed that these micellar-like systems are able to function as 'nanoreactors' to favour the coordination polymerization of ethylene by improving the stabilization of the metallocene system.

23.5 Applications of RAFT Polymer Libraries in Nanomedicine and Drug Delivery Systems

Research in drug delivery systems is a very active field whose main purpose is to reach the precise control over the release process and the amount of drugs delivered in a specific location for any particular disease in order to increase drug efficacy and the safety of the patient. In this regard, bioactives, including small organic bioactive molecules and biomacromolecules (i.e. (ribonucleic acid) RNA, deoxyribonucleic acid (DNA), proteins, and peptides), and materials with amphiphilic, biodegradable, or stimuli-responsive (pH and temperature) properties, are intensively studied compounds for this purpose [76–79]. RAFT copolymers represent a promising alternative for drug delivery systems because they can be readily synthesized containing important properties for fulfilling the requirements of these applications. In this regard, molar mass, macromolecular architecture, functionality, and composition of (co-)polymers all play an important role in determining the effectiveness of a certain drug delivery vehicle. Because structure–property–function relationships cannot be easily predicted, it is often necessary to synthesize polymer libraries covering a broad range of properties in order to identify suitable candidates that show an optimal performance in a particular application. HT/HO-E approaches offer advantages over conventional experimental methods by allowing the accelerated synthesis of comprehensive and systematic polymer libraries with improved accuracy and reproducibility.

In this context, researchers have efficiently utilized HT/HO-E approaches for the preparation of RAFT polymer libraries to screen different materials for applications in nanomedicine. Selected examples in this direction are briefly discussed below.

Hinton et al. [27], synthesized a set of ABA *quasi*-triblock copolymers by sequential RAFT polymerization using an automated parallel synthesizer to investigate the effect of polymer composition on cell viability, siRNA uptake, serum stability, and gene silencing. These copolymers were based on oligo(ethylene glycol) methyl

ether methacrylate (OEGMA) and quaternized *N,N*-dimethylaminoethyl methacrylate (DMAEMA) (cationic block). The ABA *quasi*-triblock copolymer series was synthesized with different chain lengths of DMAEMA (38–192 monomer units) and OEGMA (7–37 monomer units) blocks to determine 'optimal' values for copolymer composition and molar mass to deliver active siRNA while retaining serum stability and minimal toxicity. The copolymers were prepared in a one-pot synthesis without removing unreacted DMAEMA from the reaction mixture after the first polymerization step. The results of this screening suggested that cell viability and gene silencing efficiency were strongly correlated with the chain length of the cationic block with 110–120 monomer units being 'optimal'. The ABA block copolymer architecture also proved to be a critical aspect because the outer hydrophilic blocks inhibit particle aggregation and contribute to serum stability and overall efficiency.

Poly(*N,N*-dimethylaminoethyl methacrylate) (PDMAEMA) is the basis of a promising system for designing advanced biomaterials for gene transfection [80]. In this regard, HT/HO-E has been a very useful approach to systematically modify and optimize copolymers containing this monomer. Adjustment of parameters, such as molar mass, comonomer composition, degree of quaternization, allow fine tuning properties such as solubility and cloud point of derived aqueous solutions [81]. In this context, Perevyazko et al. [82] investigated a PDMAEMA library and their corresponding quaternized versions (i.e. poly[2-(methacryloyloxy) ethyl] trimethyl-ammonium iodide]s (PQDMAEMAs)) to evaluate fundamental macromolecular characteristics of these polymers in solution such as the molecular hydrodynamics – size, molar mass, shape, and conformation of the polymer chains. The effect of electrostatic interactions between and within the quaternized polymer chains and the solvents was studied by evaluating different properties such as viscosity, sedimentation velocity, density, diffusivity, and absolute molar mass. The obtained results allowed establishing structure–property relationships of the quaternized polymers in solution. For example, it was observed that, even at low concentrations of heavy iodine ions in the quaternized polymer chains, their rigidity and molecular volume in solution was increased. In contrast, the partial specific volume showed lower values as compared to the non-quaternized PDMAEMA precursors, which arose the discussion whether iodine ions may be bound to the macromolecules or fully dissociated in the solution. Lechuga et al. [83] have also employed a HT/HO-E strategy to access a library of *quasi*-block copolymers based on PDMAEMA and quaternized PDMAEMA (PDMAEMA-*qb*-P(DMAEMA-*co*-QDMAEMA)), which have a modified hydrophilic nature and thermo-induced self-assembly properties in aqueous solution. The one-pot synthetic strategy in combination with the proposed chemical modification yielded a variety of nanostructures as a function of temperature. Morphological transitions of the PDMAEMA-*qb*-P(DMAEMA-*co*-QDMAEMA) were assessed by atomic force microscopy (AFM), revealing the formation of metastable nanostructures in aqueous solution, where the associative and cationic interactions of the quaternized moieties present in the polymer chains allows the stabilization of the formed nanostructures.

A promising approach to improve drug delivery processes is to covalently attach bioactive moieties into the backbone of polymer chains to yield the so-called macromolecular prodrugs (MPs) [84]. Zelikin's group has explored HT/HO-E polymer synthesis to obtain antiviral RAFT polymer libraries. This effort has resulted in several valuable contributions focused on the synthesis of MPs [85–87]. One of these contributions described two different ribavirin (RBV)-containing polymer libraries and demonstrated the therapeutic benefit of these compounds as broad-spectrum antiviral agents [87]. RBV is a nucleoside analogue that acts as an antiviral, but it has a limited efficacy because it can produce side effects (i.e. accumulation in the red blood cells) linked to the development of anaemia [88]. To address this dose limiting side effect and facilitate an efficient delivery of RBV, the synthesis and screening of MP libraries with systematic variations in molar mass and RBV content was performed [87]. These polymer libraries were based on RBV (meth-)acrylate derivatives that were copolymerized with either acrylic or methacrylic acid (MAA) using the RAFT technique to achieve a good control over the RBV loading onto the polymer chains as well as of the molar mass. The materials were prepared in a commercially available automated parallel synthesizer and consisted of a total of 48 copolymers divided in one library of 23 poly(acrylate)s and another one of 25 poly(methacrylate)s. Figure 23.6 graphically shows the obtained experimental values of the number-average molar mass (M_n), $Đ$, and RBV content. The therapeutic effect of these two MP libraries was assessed by measuring the inhibition of production of nitric oxide (NO) in cultured macrophages. The results showed that copolymers with M_n greater than 20 kDa were ineffective in delivering RBV, whereas acrylate-based polymers within the range of $M_n \approx 5$–10 kDa showed the most effectiveness to suppress the production

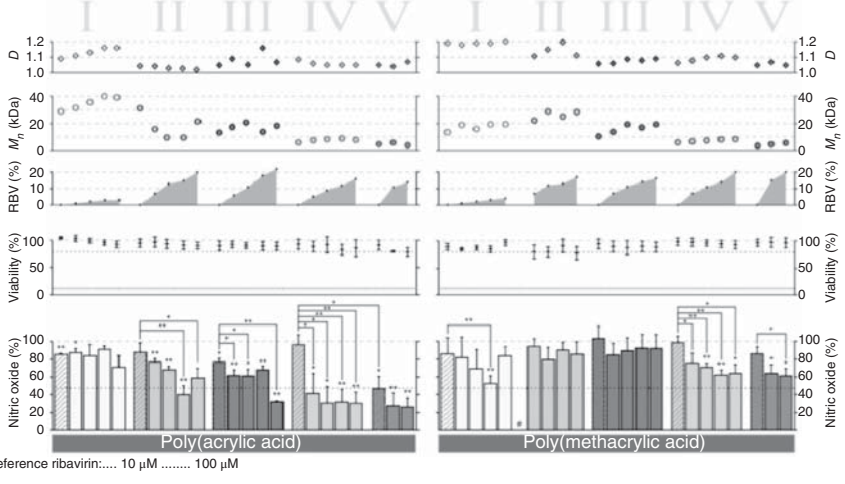

Figure 23.6 Graphic representation of the macromolecular characteristics of an MP library synthesized by RAFT (from top to bottom: $Đ$, M_n, and drug loading (mol% of RBV (meth-)acrylate)), as well as viability of cultured macrophages and levels of NO produced. Source: Reproduced with permission from Smith et al. [87]. © 2014, John Wiley & Sons.

of NO and matched the effect achieved by pristine RBV. In each series, an increase in RBV content resulted in an enhancement of the therapeutic activity. Another important observation was that poly(acrylic acid)-based polymers without a RBV load (especially in the low molar mass range) exhibited low production levels of NO, suggesting that RBV and polymer carrier both contributed to the overall therapeutic effect. It is important to highlight that this was the first contribution that used HT/HO-E for the accelerated synthesis, screening, optimization, and establishment of structure–property–function relationships of antiviral MPs.

In another contribution, the same research group further exploited the bioactivity of RBV and the advantages of HT/HO-E by designing, synthesizing, and evaluating a MP library with a dual activity for fighting human immunodeficiency virus (HIV) and alleviating hepatitis (liver inflammation) [89]. For this, a RBV methacrylate derivative was copolymerized with HPMAm, a monomer that has been widely used in the synthesis of biocompatible polymers that act as carriers of drugs [86]. HT/HO-E was used to perform RAFT polymerizations to obtain a MP library comprising 17 unique compositions. The RAFT technique allowed the synthesis of materials with well-defined macromolecular characteristics including low $Đ$, which is an important property for establishing reliable structure–property–function relationships. The dual bioactivity of this MP library was evaluated using cell culture models of relevance to the viral hepatitis and anti-HIV research. Because of toxic side effects of RBV, the hemocompatibility of the polymers was also evaluated in parallel through a quantitative analysis of their association with red blood cells, hemolysis, and agglutination. The results were very promising because these MPs resulted in being blood-safe, equally active, as compared to the pristine drug, in preventing infectivity of HIV and as efficacious as the pristine drug in the inflammation read-out.

A third example in this field described effective and non-toxic MPs with therapeutic effect against the HIV [85]. To accomplish this, Zelikin and coworkers synthesized a methacrylate derivative of a well-established anti-HIV drug, azidothymidine (AZT), and obtained copolymer libraries with systematic variation of molar mass and AZT content. These polymer libraries were based on MAA and HPMAm monomers and were synthesized with different degrees of polymerization (50, 25, 250) and AZT load (from 0 up to 15 mol%) using RAFT polymerization and HT/HO-E techniques. The polymers had low $Đ$ and molar mass in good agreement with theoretical values consistent with a good control over the polymerization reaction. After analysing the antiviral activity of these polymer libraries by various quantitative and qualitative methods, it was concluded that pristine HPMAm polymers showed no intrinsic antiviral activity. In contrast, treatments with AZT/HPMAm-containing copolymers showed an improved degree of inhibition of viral infection as the AZT content increased regardless of molar mass. For MAA-based MPs, remarkable results were achieved with pristine polymers, which were highly efficient in preventing viral replication, for example, a 20 kDa poly(methacrylic acid) (PMAA) homopolymer afforded an inhibition of the viral replication to a non-detectable level, whereas a 10 kDa polymer decreased viral replication by *ca*. 70%. This antiviral activity was improved by incorporating AZT

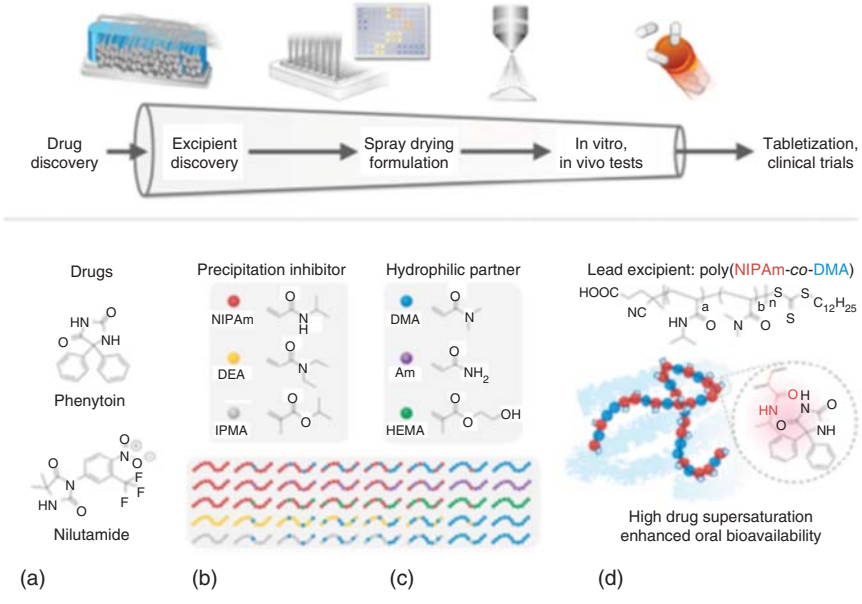

Figure 23.7 Design of polymer carriers to tailor solubilization for highly hydrophobic drugs of interest. (a) High-throughput controlled polymer synthesis and screening tools. In this scheme, (b) the cyclic imide groups of phenytoin and nilutamide motivated the (c) synthon approach to construct excipients combinatorially with precipitation inhibitor and hydrophilic units. (d) For spray-dried dispersions with the leading excipient, the NIPAm inhibitor units adsorbed onto amorphized phenytoin to increase the apparent drug solubility by over an order of magnitude. Source: Reproduced with permission from Ting et al. [91]. © 2016, American Chemical Society.

even at low levels. This information suggested that PMAA and AZT might act synergistically against HIV.

Because many active pharmaceutical ingredients used in drug formulations are highly hydrophobic, external inactive agents, known as excipients, are often used in order to improve stability and bioavailability [90]. These compounds are frequently polymer biomaterials that act as solubilizers of amorphous drug molecules by suppressing their re-crystallization and by maintaining supersaturation in corresponding dissolutions. This overcomes poor water solubility in gastrointestinal tract and thereby increasing the therapeutic efficacy and safety. In this regard, Reineke's group developed valuable HT/HO-E methods to perform controlled polymerizations and screenings for the systematic design of tailored polymer carriers in terms of solubilization of highly hydrophobic drugs (i.e. phenytoin and nilutamide) (Figure 23.7) [91]. RAFT polymerizations were carried out in a semi-continuous parallel pressure reactor (ScPPR) to generate over 60 well-defined polymers with molar masses ranging from 20 to 60 kDa. As depicted in Figure 23.7c, *N*-isopropylacrylamide (NIPAm), DEAm, and isopropyl methacrylate (IPMAm) monomers acted as precipitation inhibitors, while DMAm, acrylamide (Am), and HEMA increased hydrophilicity of the system. With this HT/HO-E approach, it was possible to determine an optimal balance between inhibitory and hydrophilic

co-monomers for maximizing drug solubility. In the case of phenytoin, the highest solubilization was obtained with a poly(NIPAm-*co*-DMAm) containing 70 mol% NIPAm.

The use of polymer nanoparticles for cellular delivery of bioactive agents has also gained great research interest, with targets ranging from tumour cells to inflamed tissues. These vehicles enable the delivery of pharmaceutical compounds in a specific and controlled manner. HT/HO-E approaches have allowed the preparation of block copolymer libraries, which can subsequently be utilized for self-assembling nanoparticles. The potential benefit of using HT/HO-E approaches in the field of RAFT copolymer-derived nanoparticles for cellular delivery was demonstrated by Montgomery et al. [72], who reported the formation of polymer nanoparticles (from 16 to 143 nm) from a library of RAFT *quasi*-block copolymers of poly(butyl methacrylate-*co*-methacrylic acid) (P(BMA-*co*-MAA)) hydrophobic block and a poly[poly(ethylene glycol) methyl ether methacrylate (475)] (P(PEGMA-475)) hydrophilic block, and their ability to act as delivery vehicles into macrophages. Yildirim et al. [77] reported a dual responsiveness (pH and ultrasound) of polymer nanoparticles based on a series of statistical RAFT copolymers derived from 3,4-dihydro-2*H*-pyran-protected HEMA 2-((tetrahydro-2*H*-pyran-2-yl)oxy)ethyl methacrylate as hydrophobic moiety and DMAEMA as hydrophilic moiety with varying content of DMAEMA. In further evaluations of this copolymer system, Nile red was encapsulated into the nanoparticles and its release profile was investigated under ultrasound and acidic media exposures.

All in all, the contributions summarized above are clear examples of the benefits and potential of HT/HO-E for the rapid development of efficient drug delivery systems based on RAFT polymers.

23.5.1 Applications of RAFT Polymer Libraries as Antimicrobial Agents

HT/HO-E platforms have also been utilized for the RAFT synthesis of polymer materials with antimicrobial properties. This has facilitated the understanding of the interactions of different polymer materials with bacteria as different variables, such as monomer nature, molar mass, macromolecular architecture, among others, can be more systematically investigated. In the past decade, several groups have developed antimicrobial materials based on cationic polymers prepared via RAFT polymerization with conventional synthetic approaches [92–95]. Further understanding of the antimicrobial mechanisms of action and optimization of these drug-like polymers has also been achieved by combining HT/HO-E and the PET-RAFT polymerization synthetic technique. For example, Richards et al. studied a set of 108 antimicrobial copolymers based on DMAEMA (Figure 23.8) [34]. In this contribution, copolymers with propylene glycol units with outstanding antimicrobial activity were investigated and mechanistic studies demonstrated the ability of these materials to inhibit growth of bacteria while minimizing the perturbation of the cell membranes, suggesting an alternative antimicrobial mechanism of action. Likewise, Boyer group studied the sequence effect of blocks of linear block copolymers on antimicrobial and hemolytic activity [96]. Specifically, a library of 32

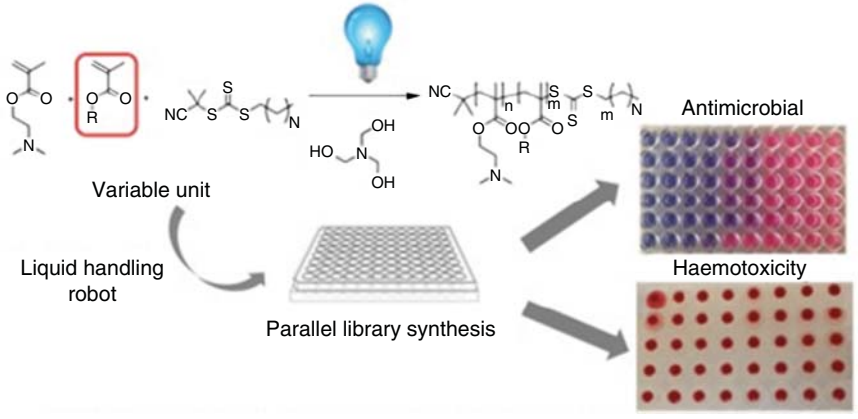

Figure 23.8 Schematic representation of a HT/HO-E workflow for the discovery of antimicrobial polymers prepared by PET-RAFT. Source: Reproduced with permission from Richards et al. [34]. © 2018, John Wiley & Sons.

well-defined multiblock copolymers with the same global composition comprising hydrophobic, hydrophilic, and cationic monomeric units was synthesized in order to mimic the structural features and function of phenylalanine, serine, and lysine, respectively. With the rapid spread of antibiotic-resistant bacterial infections next to a decline in the availability of new antibiotic drugs, the utilization of RAFT polymerization in combination with HT/HO-E methods will be powerful tools in the near future to produce optimized and effective antimicrobial polymers by allowing fine-tuning different macromolecular parameters. Similarly, this research approach might provide the required experimental evidence for a deeper understanding of antimicrobial mechanisms as well as for establishing better structure–property–function relationships.

23.6 Conclusions

The application of HT/HO-E methods has already provided significant progress in the study of diverse RAFT polymers. While a substantial outlay of infrastructure is required to implement HT/HO-E, traditional one-at-a-time methodologies are very time consuming and therefore ultimately are of high cost with respect to HT/HO-E in a long-term approach. Automated parallel synthesizers are now recognized to be of high value for providing fundamental understanding of reaction mechanisms and kinetics, essential for the design and optimization of RAFT polymerization processes (Figure 23.9). HT/HO-E has made the synthesis of systematic polymer libraries more accessible, which, in turn, offer more straightforward opportunities for the elucidation of structure–property–function relationships. For example, HT/HO-E synthesis and screening of polymer libraries has led to several advances in nanomedicine. Although, the use of HT/HO-E has allowed continuous progress in different areas of polymer chemistry, it has still limitations and various challenges

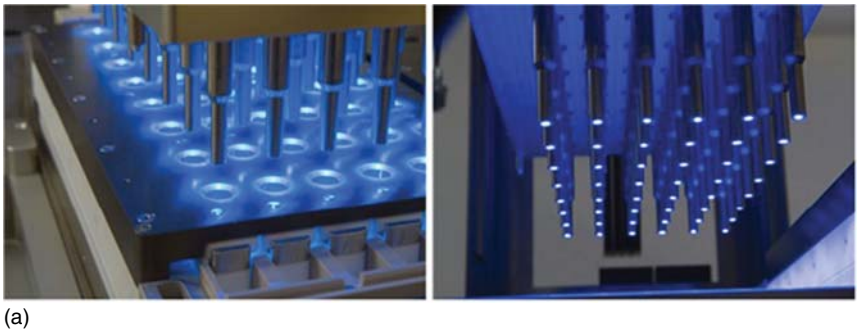

(a)

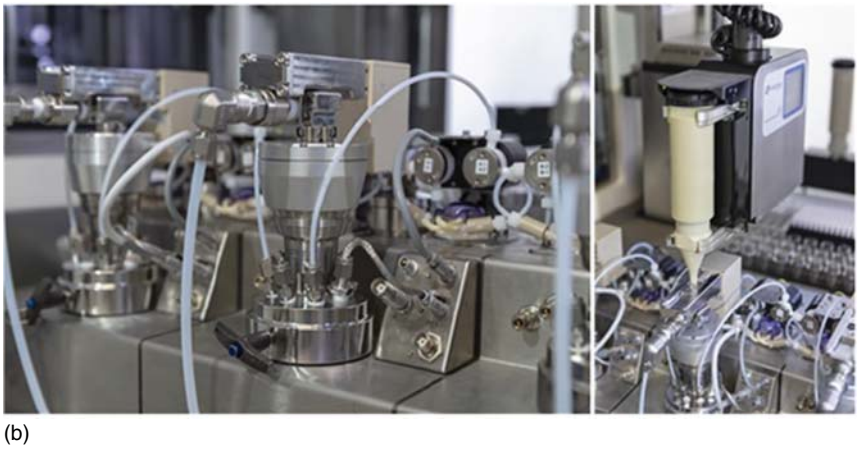

(b)

(c)

Figure 23.9 Images of commercially available HO-E tools for photo-assisted parallel RAFT polymerizations (a), for process research and development with multiple feeding pumps and automated gravimetric solid dispensing for PISA-RAFT polymerizations, (b) and high-pressure parallel MTP/well-plate screening reactor blocks for small-scale RAFT synthesis (c). Source: Images were kindly provided by Chemspeed Technologies AG (Switzerland).

that have to be addressed to further increase its efficiency and output. First of all, researchers must verify the reproducibility and accuracy of utilized HT/HO-E methodologies to draw reliable research conclusions. An important example, in this regard, relates to air-sensitive polymerizations, such as RAFT, where the utilization of suitable degassing protocols or methods for eliminating oxygen is a mandatory aspect for trustworthy HT/HO-E workflows. Furthermore, the development of reliable and more efficient automated and parallel purification procedures as well as the integration of on-line characterization methods is still largely unsolved issues preventing the widespread exploitation and potential of HT/HO-E in the polymer field. In relation to this, the HT/HO-E methods for the development of novel synthetic approaches, such as the synthesis of *quasi*-block copolymers summarized herein, offer ingenious but still perfectible solutions for the generation of systematic and comprehensive advanced polymer libraries. Nevertheless, HT/HO-E approaches to obtain strictly 'pure' block copolymer libraries must be still established for some polymerization methods such as RAFT, which need to include automated, fast, and/or parallel polymer purification methods. Furthermore, one-pot approaches may not always be fully suitable for the preparation of block copolymers because of the intrinsic limitations of different reaction systems such as solubility of the reagents, monomer reactivity ratios, tolerance to impurities, etc. All in all, and even with these mentioned limitations, it can be concluded that HT/HO-E is a facile, versatile, and cost-efficient method for the RAFT synthesis and screening of polymer materials, as well as for the development and optimization of RAFT polymerization processes. In the years to come, HT/HO-E is an experimental methodology that will continue evolving and improving, in particular with the advent of machine learning and artificial intelligence era, [21, 23, 24] to deliver new and advanced polymer materials for the development of novel applications in diverse areas of science and technology.

Abbreviations

Am	acrylamide
AMA	alkyl methacrylates
APMAm	*N*-(3-aminopropyl)methacrylamide
AZT	azidothymidine
BMA	*n*-butyl methacrylate
BzMA	benzyl methacrylate
DEAm	*N,N*-diethylacrylamide
DEGMA	di(ethylene glycol) methyl ether methacrylate
DMAm	*N,N*-dimethylacrylamide
DMAEMA	*N,N*-dimethylaminoethyl methacrylate
DMAPMAm	*N*-[3-(dimethylamino)propyl]methacrylamide
DNA	deoxyribonucleic acid
DSC	differential scanning calorimetry
$Đ$	dispersity

GMA	glycidyl methacrylate
GOx	glucose oxidase
HO-E	high-output experimentation
HT/HO-E	high-throughput and high-output experimentation
HIV	human immunodeficiency virus
HEA	hydroxyethyl acrylate
HEAm	*N*-(2-hydroxyethyl)acrylamide
HEMA	2-hydroxyethyl methacrylate
HPMAm	*N*-(2-hydroxypropyl)methacrylamide
IBA	isobornyl acrylate
IP	Isoprene
IPMA	isopropyl methacrylate
MA	methyl acrylate
MAA	methacrylic acid
MAO	methylaluminoxane
MMA	methyl methacrylate
M_n	number average molar mass
MPs	macromolecular prodrugs
MPAm	*N*-(3-methoxypropyl)acrylamide
NAM	*N*-acryloylmorpholine
NEAm	*N*-ethylacrylamide
NIPAm	*N*-isopropylacrylamide
NMR	nuclear magnetic resonance
NO	nitric oxide
OEGMA	oligo(ethylene glycol) methyl ether methacrylate
PET-RAFT	photo-induced electron/energy transfer-reversible addition fragmentation chain transfer
PBMA	poly(butyl methacrylate)
P(BMA-*co*-MAA)	poly(butyl methacrylate-*co*-methacrylic acid)
P(BMA-*qb*-MMA)	poly(butyl methacrylate-*quasi-block*-methyl methacrylate)
PDMAm	poly(*N,N*-dimethylacrylamide)
P(PEGMA-475)	Poly[poly(ethylene glycol) methyl ether methacrylate (475)]
PDMAEMA	poly(*N,N*-dimethylaminoethyl methacrylate)
PEGMA	poly(ethylene glycol) methyl ether methacrylate
PMAA	poly(methacrylic acid)
PMMA	poly(methyl methacrylate)
^{1}H NMR	proton nuclear magnetic resonance
-qb-	*-quasi-block-*
RAFT	reversible addition fragmentation chain transfer
RBV	Ribavirin
RDRP	reversible deactivation radical polymerizations
RNA	ribonucleic acid
ScPPR	semi-continuous parallel pressure reactor

SEC	size exclusion chromatography
VAc	vinyl acetate
NVC	*N*-vinylcarbazole
NVP	*N*-vinylpyrrolidone
ZnTPP	5,10,15,20-tetraphenylporphine zinc

Acknowledgements

R.Y.M thanks the support from CONACYT (Consejo Nacional de Ciencia y Tecnologia, Mexico) through the research grant 299092 (LANIAUTO). M.R.G. acknowledges the support provided by Universidad Autónoma de Saltillo. M.A.J.T acknowledges the financial support from CONACyT through project CB-2015/253303.

C.G.S and U.S.S. thank the Center for Excellence "PolyTarget" (SFB 1278, projects B02 and Z01) of the Deutsche Forschungsgemeinschaft (DFG, Germany) for financial support.

J.J.H. kindly acknowledges funding from Monash University.

References

1 Davies, M.C., Alexander, M.R., Hook, A.L. et al. (2010). High throughput surface characterization: a review of a new tool for screening prospective biomedical material arrays. *J. Drug Targeting* 18: 741–751. https://doi.org/10.3109/1061186X.2010.521941.

2 Kranenburg, J.M., Tweedie, C.A., van Vliet, K.J., and Schubert, U.S. (2009). Challenges and progress in high-throughput screening of polymer mechanical properties by indentation. *Adv. Mater.* 21: 3551–3561. https://doi.org/10.1002/adma.200803538.

3 Guerrero-Sanchez, C., Zhang, J., Vitz, J., and Schubert, U.S. (2018). High-throughput synthesis of polymers. *Encycl. Polym. Sci. Technol.* 6: 1–21. https://doi.org/10.1002/0471440264.pst668.

4 Oliver, S., Zhao, L., Gormley, A.J. et al. (2019). Living in the fast lane – high throughput controlled/living radical polymerization. *Macromolecules* 52: 3–23. https://doi.org/10.1021/acs.macromol.8b01864.

5 Hook, A.L., Anderson, D.G., Langer, R. et al. (2010). High throughput methods applied in biomaterial development and discovery. *Biomaterials* 31: 187–198. http://dx.doi.org/10.1016/j.biomaterials.2009.09.037.

6 Potyrailo, R., Rajan, K., Stoewe, K. et al. (2011). Combinatorial and high-throughput screening of materials libraries: review of state of the art. *ACS Comb. Sci.* 13: 579–633. https://doi.org/10.1021/co200007w.

7 De Boer, J. and Van Blitterswijk, C.A. (2013). *Materiomics: High-Throughput Screening of Biomaterial Properties*. Cambridge University Press.

8 Schubert, U.S. and Kniep, C.S. (2003). High-throughput and combinatorial methods in polymer research: their time has come. *Macromol. Rapid Commun.* 24: 13–14. https://doi.org/10.1002/marc.200390009.

9 Algahtani, M.S., Scurr, D.J., Hook, A.L. et al. (2014). High throughput screening for biomaterials discovery. *J. Controlled Release* 190: 115–126. http://dx.doi.org/10.1016/j.jconrel.2014.06.045.

10 Schubert, U.S. and Amis, E.J. (2004). Combinatorial and high-throughput approaches in polymer and materials science: hype or real paradigm shift? *Macromol. Rapid Commun.* 25: 19. https://doi.org/10.1002/marc.200390106.

11 Grunlan, J.C. and Mehrabi, A.R. (2005). Introduction: combinatorial instruments and techniques. *Rev. Sci. Instrum.* 76: 62101. https://doi.org/10.1063/1.1921587.

12 Webster, D.C. and Meier, M.A.R. (2010). *Polymer Libraries: Preparation and Applications BT – Polymer Libraries*, 1–15. Berlin, Heidelberg: Springer Berlin Heidelberg https://doi.org/10.1007/12_2009_15.

13 Keddie, D.J., Guerrero-Sanchez, C., Moad, G. et al. (2011). Switchable reversible addition–fragmentation chain transfer (RAFT) polymerization in aqueous solution, *N*,*N*-dimethylacrylamide. *Macromolecules* 44: 6738–6745. https://doi.org/10.1021/ma200760q.

14 Vandenbergh, J., de Moraes Ogawa, T., and Junkers, T. (2013). Precision synthesis of acrylate multiblock copolymers from consecutive microreactor RAFT polymerizations. *J. Polym. Sci. Part A Polym. Chem.* 51: 2366–2374. https://doi.org/10.1002/pola.26593.

15 Guerrero-Sanchez, C., Paulus, R.M., Fijten, M.W.M. et al. (2006). High-throughput experimentation in synthetic polymer chemistry: from RAFT and anionic polymerizations to process development. *Appl. Surf. Sci.* 252: 2555–2561. https://doi.org/10.1016/j.apsusc.2005.05.088.

16 Fijten, M.W.M., Meier, M.A.R., Hoogenboom, R., and Schubert, U.S. (2004). Automated parallel investigations/optimizations of the reversible addition-fragmentation chain transfer polymerization of methyl methacrylate. *J. Polym. Sci. Part A Polym. Chem.* 42: 5775–5783. https://doi.org/10.1002/pola.20346.

17 Stace, S.J., Vanderspikken, J., Howard, S.C. et al. (2019). *Polym. Chem.* 10: 5044–5051. https://doi.org/10.1039/C9PY00893D.

18 Rosales-Guzmán, M., Pérez-Camacho, O., Guerrero-Sánchez, C. et al. (2019). Semiautomated parallel RAFT copolymerization of isoprene with glycidyl methacrylate. *ACS Comb. Sci.* 21: 771–781. https://doi.org/10.1021/acscombsci.9b00110.

19 Meier, M.A.R. and Schubert, U.S. (2005). Integration of MALDI-TOFMS as high-throughput screening tool into the workflow of combinatorial polymer research. *Rev. Sci. Instrum.* 76: 62211. https://doi.org/10.1063/1.1906123.

20 Guerrero-Sanchez, C., Harrisson, S., and Keddie, D.J. (2013). High-throughput method for RAFT kinetic investigations and estimation of reactivity ratios in copolymerization systems. *Macromol. Symp.* 325–326: 38–46. https://doi.org/10.1002/masy.201200038.

21 Haven, J.J., Vandenbergh, J., and Junkers, T. (2015). Watching polymers grow: real time monitoring of polymerizations via an on-line ESI-MS/microreactor coupling. *Chem. Commun.* 51: 4611–4614. https://doi.org/10.1039/C4CC10426A.

22 Potyrailo, R.A., Wroczynski, R.J., Lemmon, J.P. et al. (2003). Fluorescence spectroscopy and multivariate spectral descriptor analysis for high-throughput multiparameter optimization of polymerization conditions of combinatorial 96-microreactor arrays. *J. Comb. Chem.* 5: 8–17. https://doi.org/10.1021/cc020062g.

23 Yeow, J., Joshi, S., Chapman, R., and Boyer, C. (2018). A self-reporting photocatalyst for online fluorescence monitoring of high throughput RAFT polymerization. *Angew. Chem. Int. Ed.* 57: 10102–10106. https://doi.org/10.1002/anie.201802992.

24 Liu, S., Cheng, Y., Zhang, H. et al. (2018). In Situ monitoring of RAFT polymerization by tetraphenylethylene-containing agents with aggregation-induced emission characteristics. *Angew. Chem. Int. Ed.* 57: 6274–6278. https://doi.org/10.1002/anie.201803268.

25 Schubert, U.S. and Kniep, C.S. (2003). No title. *Macromol. Rapid Commun. (Special Issue Guest Eds.).* 24: 3–142.

26 Schubert, U.S. and Amis, E.J. (2004). Combinatorial material research and high-throughput experimentation in polymer and material research. *Macromol. Rapid Commun. (Special Issue Guest Eds.).* 25: 3–386.

27 Hinton, T.M., Guerrero-Sanchez, C., Graham, J.E. et al. (2012). The effect of RAFT-derived cationic block copolymer structure on gene silencing efficiency. *Biomaterials* 33: 7631–7642. http://dx.doi.org/10.1016/j.biomaterials.2012.06.090.

28 Russell, A.J., Baker, S.L., Colina, C.M. et al. (2018). Next generation protein-polymer conjugates. *AlChE J.* 64: 3230–3245. https://doi.org/10.1002/aic.16338.

29 Brown, J.N., Hewins, M., Van Der Linden, J.H.M., and Lynch, R.J. (1981). Solvent degassing and other factors affecting liquid chromatographic detector stability. *J. Chromatogr. A.* 204: 115–122. http://dx.doi.org/10.1016/S0021-9673(00)81646-5.

30 Schmatloch, S., Meier, M.A.R., and Schubert, U.S. (2003). Instrumentation for combinatorial and high-throughput polymer research: a short overview. *Macromol. Rapid Commun.* 24: 33–46. https://doi.org/10.1002/marc.200390018.

31 Hoogenboom, R., Fijten, M.W.M., Paulus, R.M., and Schubert, U.S. (2006). Tailor-made copolymers via reversible addition fragmentation chain transfer the fast way. In: *Controlled Radical Polymerization* (ed. K. Matyjaszewski), 32–473. American Chemical Society https://doi.org/10.1021/bk-2006-0944.ch032.

32 Paulus, R.M., Fijten, M.W.M., de la Mar, M.J. et al. (2005). Reversible addition-fragmentation chain transfer polymerization on different synthesizer platforms. *QSAR Comb. Sci.* 24: 863–867. https://doi.org/10.1002/qsar.200520122.

33 Hoogenboom, R. and Schubert, U.S. (2003). The fast and the curious: High-throughput experimentation in synthetic polymer chemistry. *J. Polym. Sci. Part A Polym. Chem.* 41: 2425–2434. https://doi.org/10.1002/pola.10788.

34 Richards, S.-J., Jones, A., Tomás, R.M.F., and Gibson, M.I. (2018). Photochemical "In-Air" combinatorial discovery of antimicrobial co-polymers. *Chem. A Eur. J.* 24: 13758–13761. https://doi.org/10.1002/chem.201802594.

35 Yeow, J., Chapman, R., Xu, J., and Boyer, C. (2017). Oxygen tolerant photopolymerization for ultralow volumes. *Polym. Chem.* 8: 5012–5022. https://doi.org/10.1039/C7PY00007C.

36 Lv, C., He, C., and Pan, X. (2018). Oxygen-initiated and regulated controlled radical polymerization under ambient conditions. *Angew. Chem. Int. Ed.* 57: 9430–9433. https://doi.org/10.1002/anie.201805212.

37 Chapman, R., Gormley, A.J., Stenzel, M.H., and Stevens, M.M. (2016). Combinatorial low-volume synthesis of well-defined polymers by enzyme degassing. *Angew. Chemie.* 128: 4576–4579. https://doi.org/10.1002/ange.201600112.

38 Ng, G., Yeow, J., Chapman, R. et al. (2018). Pushing the limits of high throughput PET-RAFT polymerization. *Macromolecules* 51: 7600–7607. https://doi.org/10.1021/acs.macromol.8b01600.

39 Fu, Q., Xie, K., McKenzie, T.G., and Qiao, G.G. (2017). Trithiocarbonates as intrinsic photoredox catalysts and RAFT agents for oxygen tolerant controlled radical polymerization. *Polym. Chem.* 8: 1519–1526. https://doi.org/10.1039/C6PY01994C.

40 Guerrero-Sanchez, C., Keddie, D.J., Saubern, S., and Chiefari, J. (2012). Automated parallel freeze–evacuate–thaw degassing method for oxygen-sensitive reactions: RAFT polymerization. *ACS Comb. Sci.* 14: 389–394. https://doi.org/10.1021/co300044w.

41 Becer, C.R., Groth, A.M., Hoogenboom, R. et al. (2008). Protocol for automated kinetic investigation/optimization of the RAFT polymerization of various monomers. *QSAR Comb. Sci.* 27: 977–983. https://doi.org/10.1002/qsar.200720159.

42 Rojas, R., Harris, N.K., Piotrowska, K., and Kohn, J. (2009). Evaluation of automated synthesis for chain and step-growth polymerizations: can robots replace the chemists? *J. Polym. Sci. Part A Polym. Chem.* 47: 49–58. https://doi.org/10.1002/pola.23119.

43 Chapon, P., Mignaud, C., Lizarraga, G., and Destarac, M. (2003). Automated parallel synthesis of MADIX (co)polymers. *Macromol. Rapid Commun.* 24: 87–91. https://doi.org/10.1002/marc.200390016.

44 Zheng, Y., Luo, Y., Feng, K. et al. (2019). High throughput screening of glycopolymers: balance between cytotoxicity and antibacterial property. *ACS Macro Lett.* 8: 326–330. https://doi.org/10.1021/acsmacrolett.9b00091.

45 Haven, J.J., Guerrero-Sanchez, C., Keddie, D.J., and Moad, G. (2014). Rapid and systematic access to quasi-diblock copolymer libraries covering a comprehensive composition range by sequential RAFT polymerization in an automated synthesizer. *Macromol. Rapid Commun.* 35: 492–497. https://doi.org/10.1002/marc.201300459.

46 Voorhaar, L., De Meyer, B., Du Prez, F., and Hoogenboom, R. (2016). One-Pot automated synthesis of quasi triblock copolymers for self-healing physically

crosslinked hydrogels. *Macromol. Rapid Commun.* 37: 1682–1688. https://doi.org/10.1002/marc.201600380.

47 Keddie, D.J., Guerrero-Sanchez, C., Moad, G. et al. (2012). Chain transfer kinetics of acid/base switchable *N*-Aryl-*N*-Pyridyl dithiocarbamate RAFT agents in methyl acrylate, *N*-vinylcarbazole and vinyl acetate polymerization. *Macromolecules* 45: 4205–4215. https://doi.org/10.1021/ma300616g.

48 Rubens, M., Vrijsen, J.H., Laun, J., and Junkers, T. (2019). Precise polymer synthesis by autonomous self-optimizing flow reactors. *Angew. Chem. Int. Ed.* 58: 3183–3187. https://doi.org/10.1002/anie.201810384.

49 Ting, J.M., Wu, H., Herzog-Arbeitman, A. et al. (2018). Synthesis and assembly of designer styrenic diblock polyelectrolytes. *ACS Macro Lett.* 7: 726–733. https://doi.org/10.1021/acsmacrolett.8b00346.

50 Tselepy, A., Schiller, T.L., Harrisson, S. et al. (2018). Effect of scandium triflate on the RAFT copolymerization of methyl acrylate and vinyl acetate controlled by an acid/base "Switchable" chain transfer agent. *Macromolecules* 51: 410–418. https://doi.org/10.1021/acs.macromol.7b02104.

51 Van Den Brink, M., Van Herk, A.M., and German, A.L. (1999). Nonlinear regression by visualization of the sum of residual space applied to the integrated copolymerization equation with errors in all variables. I. Introduction of the model, simulations and design of experiments. *J. Polym. Sci. Part A Polym. Chem.* 37: 3793–3803. https://doi.org/10.1002/(sici)1099-0518(19991015)37:20<3793::aid-pola8>3.0.co;2-q.

52 Xu, J., Jung, K., Atme, A. et al. (2014). A robust and versatile photoinduced living polymerization of conjugated and unconjugated monomers and its oxygen tolerance. *J. Am. Chem. Soc.* 136: 5508–5519. https://doi.org/10.1021/ja501745g.

53 Xu, J., Shanmugam, S., Duong, H.T., and Boyer, C. (2015). Organo-photocatalysts for photoinduced electron transfer-reversible addition–fragmentation chain transfer (PET-RAFT) polymerization. *Polym. Chem.* 6: 5615–5624. https://doi.org/10.1039/C4PY01317D.

54 Gormley, A.J., Yeow, J., Ng, G. et al. (2018). An oxygen-tolerant PET-RAFT polymerization for screening structure-activity relationships. *Angew. Chem. Int. Ed.* 57: 1557–1562. https://doi.org/10.1002/anie.201711044.

55 Corrigan, N., Rosli, D., Jones, J.W.J. et al. (2016). Oxygen tolerance in living radical polymerization: investigation of mechanism and implementation in continuous flow polymerization. *Macromolecules* 49: 6779–6789. https://doi.org/10.1021/acs.macromol.6b01306.

56 Hornung, C.H., Guerrero-Sanchez, C., Brasholz, M. et al. (2011). Controlled RAFT polymerization in a continuous flow microreactor. *Org. Process Res. Dev.* 15: 593–601. https://doi.org/10.1021/op1003314.

57 Hornung, C.H., von Känel, K., Martinez-Botella, I. et al. (2014). Continuous flow aminolysis of RAFT polymers using multistep processing and inline analysis. *Macromolecules* 47: 8203–8213. https://doi.org/10.1021/ma501628f.

58 Becer, C.R., Hahn, S., Fijten, M.W.M. et al. (2008). Libraries of methacrylic acid and oligo(ethylene glycol) methacrylate copolymers with LCST behavior.

J. Polym. Sci. Part A Polym. Chem. 46: 7138–7147. https://doi.org/10.1002/pola.23018.

59 Cockram, A.A., Bradley, R.D., Lynch, S.A. et al. (2018). Optimization of the high-throughput synthesis of multiblock copolymer nanoparticles in aqueous media via polymerization-induced self-assembly. *React. Chem. Eng.* 3: 645–657. https://doi.org/10.1039/C8RE00066B.

60 Judzewitsch, P.R., Zhao, L., Wong, E.H.H., and Boyer, C. (2019). High-throughput synthesis of antimicrobial copolymers and rapid evaluation of their bioactivity. *Macromolecules* 52: 3975–3986. https://doi.org/10.1021/acs.macromol.9b00290.

61 Guerrero-Sanchez, C., O'Brien, L., Brackley, C. et al. (2013). Quasi-block copolymer libraries on demand via sequential RAFT polymerization in an automated parallel synthesizer. *Polym. Chem.* 4: 1857–1862. https://doi.org/10.1039/C3PY21135E.

62 Haven, J.J., Guerrero-Sanchez, C., Keddie, D.J. et al. (2014). One pot synthesis of higher order quasi-block copolymer libraries via sequential RAFT polymerization in an automated synthesizer. *Polym. Chem.* 5: 5236–5246. https://doi.org/10.1039/C4PY00496E.

63 Cosson, S., Danial, M., Saint-Amans, J.R., and Cooper-White, J.J. (2017). Accelerated combinatorial high throughput star polymer synthesis via a rapid one-pot sequential aqueous RAFT (rosa-RAFT) polymerization scheme, macromol. *Rapid Commun.* 38 (8): 1600780. https://doi.org/10.1002/marc.201600780.

64 Yañez-Macias, R., Kulai, I., Ulbrich, J. et al. (2017). Thermosensitive spontaneous gradient copolymers with block- and gradient-like features. *Polym. Chem.* 8 (34): 5023–5032. https://doi.org/10.1039/C7PY00495H.

65 Heraud, C., Basuki, J., Hughes, T.C., and Mueller, M. (2019). Copolymerization of pentafluorophenylmethacrylate with hydrophilic methacrylamide monomers induces premature hydrolytic cleavage. *Macromol. Rapid Commun.* 40: 1900278. https://doi.org/10.1002/marc.201900278.

66 Chapman, R., Gormley, A.J., Herpoldt, K.-L., and Stevens, M.M. (2014). Highly controlled open vessel RAFT polymerizations by enzyme degassing. *Macromolecules* 47: 8541–8547. https://doi.org/10.1021/ma5021209.

67 Wang, M., Zhang, J., Guerrero-Sanchez, C. et al. (2019). Enzyme degassing for oxygen-sensitive reactions in open vessels of an automated parallel synthesizer: RAFT polymerizations. *ACS Comb. Sci.* 21: 643–649. https://doi.org/10.1021/acscombsci.9b00082.

68 Karagoz, B., Boyer, C., and Davis, T.P. (2014). Simultaneous polymerization-induced self-assembly (PISA) and guest molecule encapsulation. *Macromol. Rapid Commun.* 35: 417–421. https://doi.org/10.1002/marc.201300730.

69 Warren, N.J. and Armes, S.P. (2014). Polymerization-induced self-assembly of block copolymer nano-objects via RAFT aqueous dispersion polymerization. *J. Am. Chem. Soc.* 136: 10174–10185. https://doi.org/10.1021/ja502843f.

70 Pei, Y. and Lowe, A.B. (2014). Polymerization-induced self-assembly: ethanolic RAFT dispersion polymerization of 2-phenylethyl methacrylate. *Polym. Chem.* 5: 2342–2351. https://doi.org/10.1039/C3PY01719B.

71 Ng, G., Yeow, J., Xu, J., and Boyer, C. (2017). Application of oxygen tolerant PET-RAFT to polymerization-induced self-assembly. *Polym. Chem.* 8: 2841–2851. https://doi.org/10.1039/C7PY00442G.

72 Montgomery, K.S., Davidson, R.W.M., Cao, B. et al. (2018). Effective macrophage delivery using RAFT copolymer derived nanoparticles. *Polym. Chem.* 9: 131–137. https://doi.org/10.1039/C7PY01363A.

73 Tan, J., Liu, D., Bai, Y. et al. (2017). Enzyme-assisted photoinitiated polymerization-induced self-assembly: an oxygen-tolerant method for preparing block copolymer nano-objects in open vessels and multiwell plates. *Macromolecules* 50: 5798–5806. https://doi.org/10.1021/acs.macromol.7b01219.

74 Piñón-Balderrama, C., Leyva-Porras, C., Olayo-Valles, R. et al. (2019). Self-assembly investigations of sulfonated poly(methyl methacrylate-*block*-styrene) diblock copolymer thin films. *Adv. Polym. Tech.* 2019: 4375838. https://doi.org/10.1155/2019/4375838.

75 Estrada-Ramirez, A.N., Ventura-Hunter, C., Vitz, J. et al. (2019). Poly(*n*-alkyl methacrylate)s as metallocene catalyst supports in nonpolar media. *Macromol. Chem. Phys.* 220: 1970037. https://doi.org/10.1002/macp.201970037.

76 Stenzel, M.H. (2008). RAFT polymerization: an avenue to functional polymeric micelles for drug delivery. *Chem. Commun.* 2008 (30): 3486–3503. https://doi.org/10.1039/B805464A.

77 Yildirim, T., Yildirim, I., Yañez-Macias, R. et al. (2017). Dual pH and ultrasound responsive nanoparticles with pH triggered surface charge-conversional properties. *Polym. Chem.* 8: 1328–1340. https://doi.org/10.1039/C6PY01927G.

78 York, A.W., Kirkland, S.E., and McCormick, C.L. (2008). Advances in the synthesis of amphiphilic block copolymers via RAFT polymerization: Stimuli-responsive drug and gene delivery. *Adv. Drug Delivery Rev.* 60: 1018–1036. http://dx.doi.org/10.1016/j.addr.2008.02.006.

79 Fairbanks, B.D., Gunatillake, P.A., and Meagher, L. (2015). Biomedical applications of polymers derived by reversible addition – fragmentation chain-transfer (RAFT). *Adv. Drug Delivery Rev.* 91: 141–152. http://dx.doi.org/10.1016/j.addr.2015.05.016.

80 Agarwal, S., Zhang, Y., Maji, S., and Greiner, A. (2012). PDMAEMA based gene delivery materials. *Mater. Today* 15: 388–393. https://doi.org/10.1016/S1369-7021(12)70165-7.

81 Yañez-Macias, R., Alvarez-Moises, I., Perevyazko, I. et al. (2017). Effect of the degree of quaternization and molar mass on the cloud point of poly[2-(dimethylamino)ethyl methacrylate] aqueous solutions: a systematic investigation. *Macromol. Chem. Phys.* 218: 1700065. https://doi.org/10.1002/macp.201700065.

82 Perevyazko, I., Lezov, A., Gubarev, A.S. et al. (2019). Structure-property relationships via complementary hydrodynamic approaches: poly(2-(dimethylamino)ethyl methacrylate)s. *Polymer (Guildf).* 182: 121828. https://doi.org/10.1016/j.polymer.2019.121828.

83 Lechuga-Islas, V.D., Festag, G., Rosales-Guzmán, M. et al. (2020). Quasi-block copolymer design of quaternized derivatives of poly(2-(dimethylamino)ethyl

methacrylate): investigations on thermo-induced self-assembly. *Eur. Polym. J.* 124: 109457. https://doi.org/10.1016/j.eurpolymj.2019.109457.

84 Zovko, M., Zorc, B., Novak, P. et al. (2004). Macromolecular prodrugs: XI. Synthesis and characterization of polymer–estradiol conjugate. *Int. J. Pharm.* 285: 35–41. http://dx.doi.org/10.1016/j.ijpharm.2004.07.013.

85 Zuwala, K., Smith, A.A.A., Postma, A. et al. (2015). Polymers fight HIV: potent (pro)drugs identified through parallel automated synthesis. *Adv. Healthc. Mater.* 4: 46–50. https://doi.org/10.1002/adhm.201400148.

86 Smith, A.A.A., Zuwala, K., Kryger, M.B.L. et al. (2015). Macromolecular prodrugs of ribavirin: towards a treatment for co-infection with HIV and HCV. *Chem. Sci.* 6: 264–269. https://doi.org/10.1039/C4SC02754J.

87 Smith, A.A.A., Wohl, B.M., Kryger, M.B.L. et al. (2014). Macromolecular prodrugs of ribavirin: concerted efforts of the carrier and the drug. *Adv. Healthc. Mater.* 3: 1404–1407. https://doi.org/10.1002/adhm.201300637.

88 Soota, K. and Maliakkal, B. (2014). Ribavirin induced hemolysis: a novel mechanism of action against chronic hepatitis C virus infection. *World J. Gastroenterol.* 20: 16184–16190.

89 Kryger, M.B.L., Smith, A.A.A., Wohl, B.M., and Zelikin, A.N. (2014). Macromolecular prodrugs for controlled delivery of ribavirin. *Macromol. Biosci.* 14: 173–185. https://doi.org/10.1002/mabi.201300244.

90 Ting, J.M., Navale, T.S., Jones, S.D. et al. (2015). Deconstructing HPMCAS: excipient design to Tailor polymer–drug interactions for oral drug delivery. *ACS Biomater. Sci. Eng.* 1: 978–990. https://doi.org/10.1021/acsbiomaterials.5b00234.

91 Ting, J.M., Tale, S., Purchel, A.A. et al. (2016). High-throughput excipient discovery enables oral delivery of poorly soluble pharmaceuticals. *ACS Cent. Sci.* 2: 748–755. https://doi.org/10.1021/acscentsci.6b00268.

92 Paslay, L.C., Abel, B.A., Brown, T.D. et al. (2012). Antimicrobial poly(methacrylamide) derivatives prepared via aqueous RAFT polymerization exhibit biocidal efficiency dependent upon cation structure. *Biomacromolecules* 13: 2472–2482. https://doi.org/10.1021/bm3007083.

93 Chen, Y., Wilbon, P.A., Chen, Y.P. et al. (2012). Amphipathic antibacterial agents using cationic methacrylic polymers with natural rosin as pendant group. *RSC Adv.* 2: 10275–10282. https://doi.org/10.1039/c2ra21675b.

94 Treat, N.J., Smith, D., Teng, C. et al. (2012). Guanidine-containing methacrylamide (co)polymers via aRAFT: toward a cell-penetrating peptide mimic. *ACS Macro Lett.* 1: 100–104. https://doi.org/10.1021/mz200012p.

95 Michl, T.D., Locock, K.E.S., Stevens, N.E. et al. (2014). RAFT-derived antimicrobial polymethacrylates: elucidating the impact of end-groups on activity and cytotoxicity. *Polym. Chem.* 5: 5813–5822. https://doi.org/10.1039/C4PY00652F.

96 Judzewitsch, P.R., Nguyen, T.-K., Shanmugam, S. et al. (2018). Towards sequence-controlled antimicrobial polymers: effect of polymer block order on antimicrobial activity. *Angew. Chem. Int. Ed.* 57: 4559–4564. https://doi.org/10.1002/anie.201713036.

24

An Industrial History of RAFT Polymerization

Graeme Moad

CSIRO Manufacturing, Research Way, Clayton VIC 3168, Australia

24.1 Introduction

This chapter describes the history of radical polymerization with reversible addition–fragmentation chain transfer (RAFT) and the rapid evolution in applications of that technique mainly through reference to the patent literature. To limit the scope of this document, the tables are populated mainly by examples that have proceeded to granted US patents.

In their 2008 *Handbook of RAFT Polymerization* chapter '*Toward New Materials Prepared via the RAFT Process: From Drug Delivery to Optoelectronics?*' (note the question mark), Favier et al. [1] surveyed the potential for RAFT polymerization in various areas and commented that the industrial impact would depend on the versatility and applicability, and on the extra cost for the final product. In 2010, Destarac came to a similar conclusion [2].

Ten years later, in 2018, the industrial uptake of RAFT and commercial successes of the various processes for reversible deactivation radical polymerization (RDRP), including RAFT with thiocarbonylthio compounds, were again considered by Destarac [3], who asked whether the induction period was over. He comments that, while the RDRP methods are firmly established as a powerful means for the development of next-generation polymer products, there must still be improvements in their cost/benefit ratio to bring about a broader adoption by industry. Despite this challenge, the literature, including the patent literature, has seen extremely rapid growth over the last 20 years.

24.2 Macromonomer RAFT Polymerization

The development of RAFT polymerization using thiocarbonylthio compounds within the CSIRO–DuPont Engineered Resins Strategic Alliance has its origins in the earlier developments of macromonomer RAFT polymerization and with the earlier developments of catalytic chain transfer (CCT) and (not necessarily reversible) addition–fragmentation chain transfer.

RAFT Polymerization: Methods, Synthesis and Applications, First Edition.
Edited by Graeme Moad and Ezio Rizzardo.

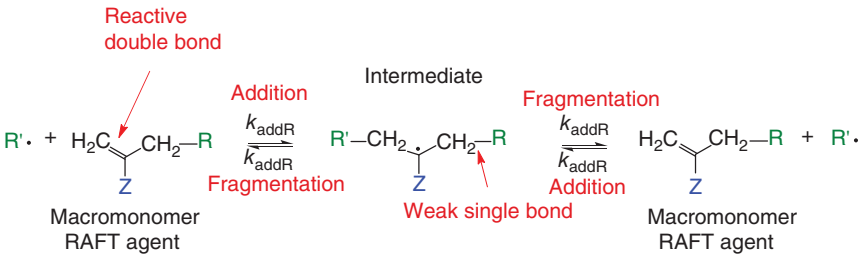

Figure 24.1 Structural features of macromonomer RAFT agents and the intermediate formed by addition of a radical R′·. R, R′ are homolytic leaving groups (R· must also be able to efficiently reinitiate polymerization). The activating group Z modifies addition and fragmentation rates and is typically ester (**1**), nitrile (**2**), or aryl (**3**). Compare with Scheme 2.1 in Chapter 2 (Terminology) [4].

Table 24.1 Macromonomer RAFT agent α-methylvinyl end groups, $ZC(=CH_2)CH_2^-$.

Methacrylate	Methacrylonitrile	α-Methylstyrene
1 R=H, alkyl, substituted alkyl	**2**	**3**

The use of the macromonomers (**1**-**3**, Figure 24.1, Table 24.1) as addition–fragmentation transfer agents dates from the 1980s [5]. However, the first publication relating explicitly to block copolymer synthesis using macromonomers was published in 1994 (Table 24.2, entry 2). There are earlier patents on the use of macromonomers in copolymerization of acrylates and methacrylates for the production of graft copolymers (e.g. Table 24.2, entry 1). Based on the polymerization conditions used, it is likely that RAFT complicated these polymer syntheses. The first patent on the use of the macromonomer RAFT process to impart the characteristics of living polymerization (low molar mass dispersity, ability to chain extend, retained end-group functionality) to radical polymerization appeared in 1996 (Table 24.2, entry 4). The patent was filed only shortly before the first papers on the topic [27, 28]. Other patents covering the use of RAFT-crosslinking polymerization to synthesize arm-first stars (Table 24.2; entry 9) and the synthesis of core- or shell-crosslinked micelles based on RAFT-synthesized amphiphilic block copolymers followed sometime later (Table 24.2; entry 12).

Patents relating to the synthesis of macromonomers with an α-methylvinyl end group published subsequent to 1995 are likely to indicate block copolymer synthesis as a potential application. Very recently, there has been a resurgence of interest in macromonomer RAFT with various groups examining the properties of macromonomer-based non-aqueous dispersions (NADs) [29, 30] and what is now called 'sulfur-free' RAFT polymerization [31–33]. This has not yet been reflected in new patent activity.

Table 24.2 Patents relating to macromonomer RAFT polymerization.

	Number	Priority[a)]	Date[b)]	Assignee	Title	Brief description	ZC(=CH_2)CH_2 –[c)]
1.	US5010140A [6]	1989	1991	DuPont	Process for preparing stabilized polymer dispersion	CCT used to prepare stabilized non-aqueous dispersions	**1**
2.	US5362826A US5371151A WO1993022351A1 [7]	1992	1994 1994 1993	DuPont	Method of preparing macromonomer compositions	CCT used to prepare macromonomers, which can be used to make blocks, etc.	**1**
3.	US5310807A [8] WO1995021205A1	1992	1994	DuPont	Star polymers made from macromonomers made by cobalt chain transfer process	CCT used to prepare macromonomers, which can be used to make stars	
4.	WO199615157A1 [9] US6291620B1	1994	1996 2001	DuPont–CSIRO	Polymer synthesis	Low-dispersity polymers and block polymers by macromonomer RAFT polymerization	**1 3**
5.	US5955532A WO199903937A1 [10]	1997	1999 1999	DuPont	Aqueous coating composition of a self-stabilized crosslinked latex	Coatings based on use of macromonomers to form self-stabilized latex by RAFT-crosslinking polymerization	
6.	US5587431A WO1996033224A1 [11]	1995	1996 1996	DuPont	Synthesis of terminally unsaturated oligomers	Block synthesis in the presence of cobalt catalyst	

(*continued*)

Table 24.2 (Continued)

	Number	Priority[a)]	Date[b)]	Assignee	Title	Brief description	ZC(=CH_2)CH_2–[c)]
7.	US6117921A EP826751A2 [12]	1996	2000 1998	DuPont	Process for making printed images using pigmented ink jet compositions	Blocks/grafts as dispersants in ink-jet ink	
8.	WO199731030A1 [13] US6624261B1 US7148297B2 US7109282B2 US7144963B2	1997	1997 2003 2006 2006 2006	DuPont–CSIRO	Catalytic polymerization process	Hyperbranched polymer synthesis	
9.	WO2000002939 US6653407B2 [14][d)]	1998	2000 2003	DuPont–CSIRO	Microgels and process for their preparation	Star microgels by arm-first method	**1**
10.	US6262152B1 WO2000020520A1 [15]	1998	2001 2000	DuPont	Particles dispersed w/polymer dispersant having liquid soluble and cross-linkable insoluble segments	Blocks/grafts as dispersants in ink-jet ink	**1**
11.	US6306994B1 [16]	1999	2001	DuPont	Inks with enhanced substrate binding characteristics	Block copolymer pigment dispersants	**1**
12.	WO2001077198A1 [17][e)] US7064151B1	2000	2001 2006	DuPont–CSIRO	Process of microgel synthesis and products produced therefrom	Microgels from self-assembly of RAFT-made block copolymers followed by crosslinking	**1**
13.	US6503975B1 EP1138730A2 [18]	2000	2003	DuPont Axalta Coating Systems	Surfactant free aqueous emulsions	Emulsion polymerization with macromonomers as polymerizable surfactants	**1**

14.	WO2006138312A1 US20060287437A1 [19] US8937129B2	2005	2006 2015	DuPont Axalta Coating Systems	Rapid drying lacquers containing triblock copolymer for rheology control	Rheology control agents for coatings	**1**
15.	WO2008080579A1 [20] US8153731B2	2006	2008 2012	Byk Chemie	Comb (block) copolymers	Comb polymers based on poly(styrene-*co*-maleic anhydride) AMS dimer RAFT agent	**3**
16.	WO2009098025A1 [21] US8097076B2	2008	2009 2012	Byk Chemie	Wetting and dispersing agent	Dispersing agents for paints. AMS dimer RAFT agent	**3**
17.	US20100081769A1 [22]	2008	2010	DuPont Axalta Coating Systems	Process for producing block copolymer pigment dispersants	Block copolymer pigment dispersants	**1**
18.	WO2010036867A1 [23] US20110144263A1 [24]	2008	2010 2011	DuPont Axalta Coating Systems	Block copolymer pigment dispersants	Block copolymer pigment dispersants	**1**
19.	WO2014074427A1 [25] US9410030B2	2012	2014 2016	3M	Addition-fragmentation agents	Allyl sulfide and macromonomer transfer agents described	**1**
20.	WO2016133668A1 [26] US10479848B2	2015	2019	3M	Addition-fragmentation oligomers	Stress-reducing crosslinking oligomers	**1**

a) Priority date.
b) Date published.
c) $ZC(=CH_2)CH_2-$ groups exemplified (Table 24.1).
d) Other US divisionals cover other forms of RDRP.
e) Also covers thiocarbonylthio-RAFT.

Abbreviations: AMS, α-methylstyrene; AMS dimer, 2,4-dimethylpentene; CCT, catalytic chain transfer.

The CSIRO invention of macromonomer RAFT polymerization as a process for RDRP can be traced to experiments making use of CCT in semi-batch (starved monomer feed) emulsion polymerization that often provided polymers, which were thought to have unusually low molar mass dispersity ($Đ < 1.4$). The use of CCT for macromonomer synthesis with some reference to the patent literature and applications of macromonomers has been reviewed by Gridnev and Ittel [34], Heuts and Smeets [35], and more recently by Slavin et al. [36] and Demarteau et al. [37] Relevant patents on CCT are summarized in Table 24.3.

There is indication of commercial exploitation of the technology in the literature [32, 33], although the scale of this effort is difficult to establish. Various application patents (Table 24.2) were filed by DuPont Performance Coatings, and later DuPont Electronics or Axalta Coatings Systems, covering products such as coatings compositions, dye or pigment dispersants for inks and coatings, and rheology control agents (Table 24.2).

Several other methods for forming macromonomers with an α-methylvinyl end group make use of addition–fragmentation chain transfer. This chemistry has been reviewed by Rizzardo et al. [51], Moad et al. [52, 53], and Colombani et al. [54, 55]. Some of the patents filed in this area are summarized in Table 24.4. Another method for producing macromonomers involves polymerization of monosubstituted monomers under high-temperature/high-dilution conditions, where the α-methylvinyl end group is formed by backbiting β-scission – see Table 24.5.

24.3 Thiocarbonylthio-RAFT Polymerization

If the term RAFT agent is used unqualified, it can usually be understood to refer to a thiocarbonylthio-RAFT agent, most often a dithioester, trithiocarbonate, xanthate, or dithiocarbamate. In this section, we mainly consider thiocarbonylthio-RAFT agents.

The number of patents **or** patent applications issued per year on thiocarbonylthio-RAFT polymerization using the main classes of RAFT agent for the period 1998–2019 is shown in Figure 24.2a. The analysis is based on a Scifinder™ substructure search carried out in April 2020 on the RAFT agent structures combined with the terms ('RAFT polymerization' or 'radical polymerization') then refined by document type = patent. Some patents may refer to more than one class of RAFT agent. In this case, it will only contribute once to the total number. Scifinder groups patents and patent applications that share a priority document. These patent families will only contribute once to the total.

The substructure search is used to generate Figure 24.2, rather than simply a search for RAFT polymerization, as there are a large number of patents that mention RAFT polymerization in passing without any actual use of the technique.

In Figure 24.2b, the breakdown of patents or patent applications according to language is shown. The number of Chinese language patents or patent applications is approximately half the total. However, most Chinese applications do not proceed to grant or to applications in other countries. In the tabulations that follow we have,

Table 24.3 Patents relating to forming macromonomers by catalytic chain transfer polymerization (CCT).

	Number	Priority[a)]	Date[b)]	Assignee	Title	Brief description	ZC(=CH_2)CH_2–[c)]
21.	SU664434A1 [38]	1977	1980	USSR	Method of preparing polymers, iminomers and oligomers (Molecular weight control of methacrylic polymers)	CCT using Co porphyrin catalysts	**1**
22.	US4526945A [39]	1984	1985	SCM Corp	Low molecular weight polymers and copolymers	CCT using Co(II) glyoxime complexes	**1**
23.	US4680354A [40]	1986	1987	Glidden	Low molecular weight polymers and copolymers	CCT using Co(II) complexes	**1**
24.	US4694054A [41]	1985	1987	DuPont	Cobalt(II) chelates as chain transfer agents in free radical polymerizations	CCT using Co(II) complexes	**1 2**
25.	US4722984A EP229481A2 [42]	1985	1988 1987	DuPont	Pentacyanocobaltate(II) catalytic chain transfer agents for molecular weight control in free radical polymerization	CCT using Co(II) complexes	**1**
26.	US4886861A [43]	1985	1989	DuPont	Molecular weight control in free radical polymerizations	CCT using Co(II) complexes with coordinated Lewis base	**1**
27.	US4746713A [44]	1985	1988	DuPont	Bimetallic catalytic chain transfer agents for molecular weight control in free radical polymerization	CCT using bimetallic complexes of W, Cr, Ru, Mo, Fe, Os	

(*continued*)

Table 24.3 (Continued)

	Number	Priority[a)]	Date[b)]	Assignee	Title	Brief description	ZC(=CH_2)CH_2–[c)]
28.	US5028677A [45]	1986	1991	DuPont	Novel macromonomer compositions	Macromonomers formed by CCT	
29.	WO1987003605A1 [46] US5324879A	1985	1987 1994	CSIRO	Oligomerization process	CCT using Co(III) complexes	**1**
30.	WO199517435A1 [47] US5770665A	1993	1995 1998	Zeneca	Free radical polymerization process	CCT using Co(II) or Co(III) diarylglyoxime complexes	
31.	WO1996013527A1 [48] US5962609A	1994	1996 1999	Zeneca	Free radical polymerization process	CCT using Co(II) or Co(III) diarylglyoxime complexes	
32.	WO9941218A1 [49] US6294708B1 US6388153B2	1999	1999 2001 2002	DuPont	Alpha-methylstyrene dimer derivatives	AMS dimer synthesis by CCT	**3**
33.	US20020087006A1 [50] US6559327B2 US6713427B2 US6740618B2 US6858745B2	2001	2002 2003 2004 2004 2005	DuPont Axalta Coating Systems	Alkyl cobalt (III) dioximates and process for forming the same	CCT using Co(III) complexes	—

a) Priority date.
b) Date published.
c) ZC(=CH_2)CH_2– groups exemplified (Table 24.1).
Abbreviations: CCT, catalytic chain transfer.

Table 24.4 Patents relating to forming macromonomers by addition–fragmentation chain transfer polymerization.

	Number	Priority[a)]	Date[b)]	Assignee	Title	Brief description	ZC(=CH_2)CH_2–[c)]
34.	WO1988004304A1 [56] US5385996A US5874511A US5932675A [57]	1986	1988 1995 1999	CSIRO	Control of molecular weight and end-group functionality of polymers	Allyl transfer agents	
35.	WO9512568A1 [58] US5773543A US5977278A	1993	1995 1998 1999	CSIRO/DuPont	Polymers formed from allylic chain transfer agents	Allyl malonate Transfer agents	
36.	WO1997013792A1 [59] US6235857B1	1995	1997 2001	CSIRO/DuPont	Control of molecular weight and end-group functionality in polymers	Allyl (Cl, Br, alkyl-, or arylsulfonyl) transfer agents	
37.	WO2000011041A1 [60] US6576684B1	1998	2003	BASF Ciba Spec Chem	Thermal- and photoinitiated radical polymerization in the presence of an addition fragmentation agent	Allyl (ammonium, sulfonium, phosphonium) transfer agents	
38.	WO 2007110882A1 [61] US7875659B2	2006	2007 2009	Council of Scientific and Industrial Research, India	Water-soluble macromonomers containing terminal unsaturation and a process for the preparation thereof	AMS dimer inclusion complex with methylated cyclodextrin	**3**

a) Priority date.
b) Date published.
c) ZC(=CH_2)CH_2– groups exemplified (Table 24.1).
Abbreviations: AMS, α-methylstyrene; AMS dimer, 2,4-dimethylpentene.

Table 24.5 Patents relating to forming macromonomers **1-3** by other methods.

	Number	Priority[a)]	Date[b)]	Assignee	Title	Brief description	ZC(=CH_2)CH_2–[c)]
39.	WO9847927A1 [62] US6376626B1	1997	1998 2002	DuPont/ CSIRO	Method of macro-monomer synthesis	Macromonomer synthesis by polymerization of monosubsti-tuted monomers with backbiting β-scission	**1 2 3**

a) Priority date.
b) Date published.
c) ZC(=CH_2)CH_2– groups exemplified (Table 24.1).

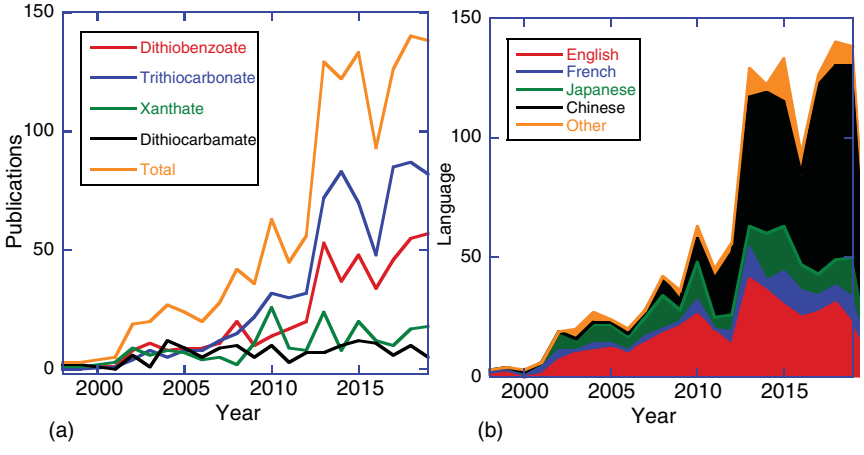

Figure 24.2 Number of patents or patent applications issued per year on thiocarbonylthio-RAFT polymerization, (a) using different classes of RAFT agent and (b) for different languages, for the period 1998–2019. Based on a Scifinder™ substructure search carried out in April 2020 on the RAFT agent structures and the terms 'RAFT polymerization' or 'radical polymerization'. Some patents may refer to more than one class of RAFT agent. In this case, it will only contribute one to the total. Patents that do not specify a RAFT agent structure will not contribute. Patent families will only contribute once to the total.

with a few exceptions, limited the scope to patents, which have progressed to being granted in the US and which have a working example making use of RAFT.

24.3.1 Development of RAFT Polymerization

In this section, we describe that part of the history of RAFT polymerization that relates to design and synthesis of thiocarbonylthio-RAFT agents (Table 24.6) and to the development of the method for the synthesis of low-dispersity, block and end-functional polymers.

Table 24.6 Thiocarbonylthio-RAFT agent ZC(=S)S– groups described in the patent literature.

Dithioester

Dithiobenzoate 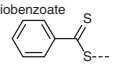 **4**

Aryl dithioester 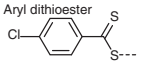 **5**

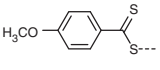 **6**

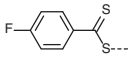 **7**

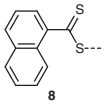 **8**

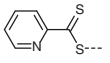 **9**

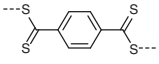 **10**

Trifluorodithioacetate  **11**

Phenyldithioacetate 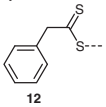 **12**

Dithioacetate  **13**

Alkenyldithioacetate 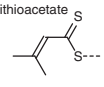 **14**

Vinylogous dithoester 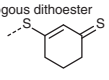 **15**

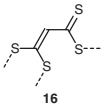 **16**

Trithiocarbonates

Symmetrical  **17**

Methanesulfanyl 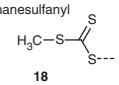 **18**

Ethanesulfanyl 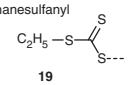 **19**

Propanesulfanyl 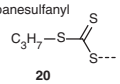 **20**

Butanesulfanyl 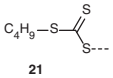 **21**

Hexanesulfanyl 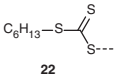 **22**

Dodecanesulfanyl 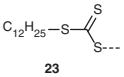 **23**

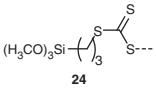 **24**

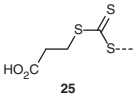 **25**

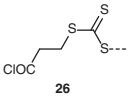 **26**

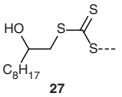 **27**

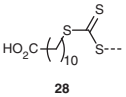 **28**

Xanthate

O-alkyl 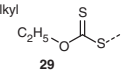 **29**

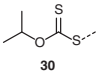 **30**

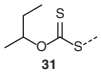 **31**

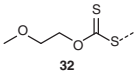 **32**

O-fluoroalkyl 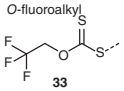 **33**

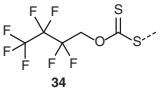 **34**

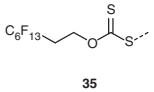 **35**

O-perfluorophenyl 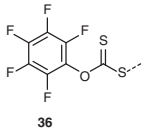 **36**

O-phenyl xanthate 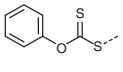 **37**

O-(1-(diethoxyphosphaneyl)ethyl 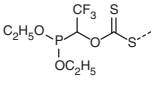 **38**

O-(1-(diethoxyphosphaneyl)ethyl 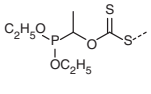 **39**

(*continued*)

Table 24.6 (Continued)

Dithiocarbamate			
Pyrole 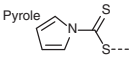 **40**	Carbazole 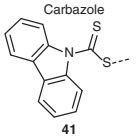 **41**	Imidazole 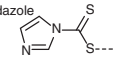 **42**	Triazole 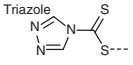 **43**
Hydrazinyl 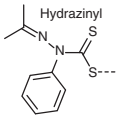 **44**	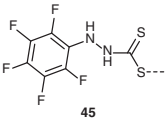 **45**	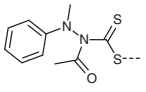 **46**	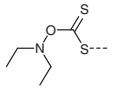 **47**
Pyrazole 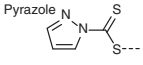 **48**	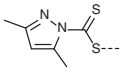 **49**	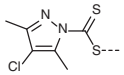 **50**	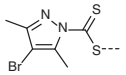 **51**
N-alkyl-*N*-pyridyl 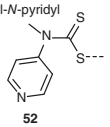 **52**	*N*-alkyl-*N*-pyridinium 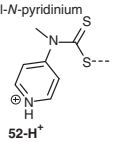 **52-H$^+$**		
α-carbonyl 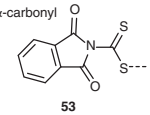 **53**	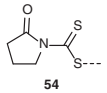 **54**	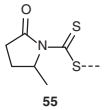 **55**	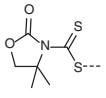 **56**	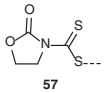 **57**
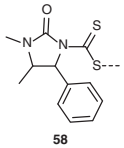 **58**	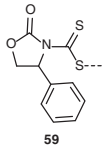 **59**	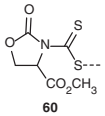 **60**	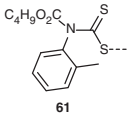 **61**	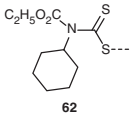 **62**
N,*N*-diaryl 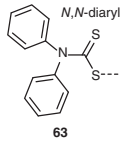 **63**	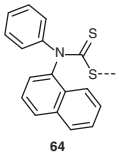 **64**	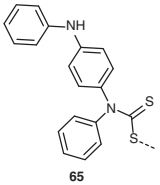 **65**		
N-aryl-*N*-alkyl 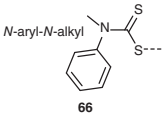 **66**	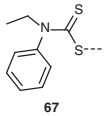 **67**	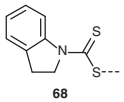 **68**		
N,*N*-dialkyl  **69**	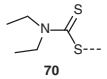 **70**	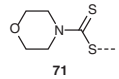 **71**	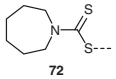 **72**	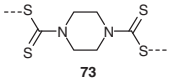 **73**

(*continued*)

Table 24.6 (Continued)

Phosphorous-containing RAFT agents		
Diethoxyphosphanecarbodithioate	Tertrathiophosphate	
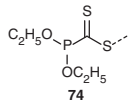	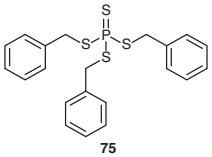	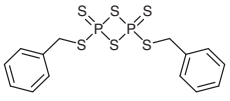
74	75	76
Others		
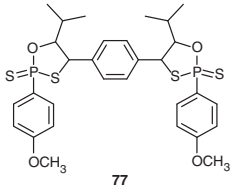	Sulfine	Bis(allyl sulfide)
77	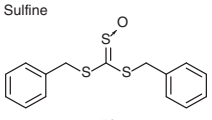	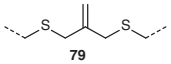
	78	79

The first patents on RAFT polymerization making use of thiocarbonylthio-RAFT agents were published in 1998 (Table 24.7, entry 1). The CSIRO/DuPont provisional on thiocarbonylthio-RAFT polymerization filed in 1996 embraced all major classes of RAFT agents, namely, dithiocarbamates, xanthates, trithiocarbonates, and dithioesters. However, in filing the first patent (Table 24.7, entry 1) [63] based on this provisional, only material relating to dithioesters and trithiocarbonates was included to avoid potential confusion with the earlier iniferter chemistry [144].

The first Rhodia patent application related to RAFT polymerization (Table 24.7, entry 3) [75] was also published in 1998 and had claims that pertained to the use of xanthate and trithiocarbonate RAFT agents, though only xanthates were exemplified. The Rhodia patent was based on a French provisional that broadly described a wider range of RAFT agents.

A subsequent CSIRO/DuPont filing in 1997 (Table 24.7, entry 6) [83], (published in 1999), still largely based on the 1996 provisional, broadly claimed xanthate, dithiocarbamate, and vinylogous dithioester RAFT agents. Rhodia filings based on their original 1997 French provisional claimed dithiocarbamates (Table 24.7, entry 5) [80] and vinylogous dithioesters (Table 24.7, entry 4).

The overlap in scope of the various CSIRO/DuPont and Rhodia patent filings ultimately led to an arrangement whereby going forward the exploitation of RAFT at Rhodia focused largely on xanthates (in a process they termed MADIX – macromolecular design by interchange of xanthate), while CSIRO/DuPont concentrated on dithioesters, trithiocarbonates, and dithiocarbamates. This division was in line with the commercial interests of both groups at the time.

Other early patents related to the synthesis of specific RAFT agents. The second CSIRO patent on thiocarbonylthio-RAFT disclosed the synthesis of RAFT agents, where R is a tertiary radical by radical-induced decomposition of bis(thioacyl) disulfides (Table 24.7, entry 2). This process allowed the synthesis of RAFT agents most suited to mediating the polymerization of methacrylates. This patent also claimed the in situ generation of RAFT agents during radical polymerization by

Table 24.7 Patents relating to the development of thiocarbonylthio-RAFT polymerization

	Number	Priority[a)]	Date[b)]	Assignee	Title[c)]	Brief description	ZC(=S)S–[d)]
1.	WO9801478A1 [63] US7250479B2 [64] US7662986B2 [65] US7666962B2 [66] US7714075B1 [67] pub [68–71]	1996	1998 2007 2010 2010 2010	DuPont/CSIRO	Polymerization with living characteristics	Original CSIRO/DuPont RAFT patent. Focus on RAFT process with dithioesters, trithiocarbonates. Low $Đ$ polymers. Block and star polymers	**4 5 10 8 13 17 74**
2.	WO199905099A1 [72] US6512081B1 [73] pub [74]	1997	1999 2003	DuPont/CSIRO	Synthesis of dithioester chain transfer agents and use of bis(thioacyl) disulfides or dithioesters as chain transfer agents	Functional RAFT agent synthesis. In situ generation of RAFT agents or macroRAFT agents	**4**
3.	WO1998058974A1 [75] US6153705A [76] pub [77, 78]	1997	2000	Rhodia Chimie	Method for block polymer synthesis by controlled radical polymerisation	Block copolymers syntheses with xanthate RAFT agents	**29 30**
4.	WO1999035178A1 US6545098B1 [79]	1997	1999 2003	Rhodia Chimie	Synthesis method for block polymers by controlled radical polymerization from dithioester compounds	Block copolymers with dithioester RAFT agents. Dithioesters Z–C(=S)S–R with Z = alkene. Examples are the narrow polydispersity ethyl acrylate (EA) and styrene homopolymers, and block copolymer of EA and styrene	**14** + others not listed
5.	WO1999035177A1 [80] US6812291B1 [81] pub [82]	1997	1999 2004	Rhodia Chimie	Method for block polymer synthesis by controlled radical polymerization from dithiocarbamate compounds	Polymers formed by RAFT polymerization with dithiocarbamates	**41 43 66 54 53** (**69**) (**70**)

6.	WO9931144A1 [83] US6642318B1 [84] US6747111B2 [85] pub [86]	1997	1999 2003 2004	DuPont/CSIRO	Polymerization process with living characteristics and polymers made therefrom	RAFT process with xanthates, dithiocarbamates, and vinylogous dithioesters. Polymers with low dispersity	**15 16 37 38 29 41 43 54 53 66** (**69**) (**70**)
7.	WO2000002939 US6355718B1 [87] US6462114B2 [88] US6646055B2 [89] US6653407B2 [14] US6822056B2 [90]	1998	2000 2002 2002 2003 2003 2004	DuPont/CSIRO	Microgels and process for their preparation	Microgels by arm-first method	**4**
8.	US7049373B2 [91]	1997	2006	Carnegie Mellon University	Process for preparation of graft polymers	Synthesis of graft copolymers by copolymerization of macromonomers	**4**
9.	WO2000075207A1 US6777513B1 [92]	1999	2000 2004	Rhodia Chimie	Synthesis method for polymers by controlled radical polymerisation using halogenated xanthates	Polymers made with halogenated xanthates RAFT	**33 34 35**
10.	WO2001042312A1 US6809164B2 [93] US7285610B2 [94]	1999	2000 2004 2007	Rhodia Chimie	Synthesis method for polymers by controlled radical polymerisation with xanthates	Use of phosphorylated xanthate esters as RAFT agents	**39 40**
11.	WO 2001042325A1 [95] US7012114B2	1999	2001 2006	Rhodia Chimie	Surface chemistry modified latex and redispersible powders, production and use thereof	RAFT emulsion polymerization for block copolymers	**29**
12.	WO2001077198A1 [17] US7064151B1 [96]	2000	2001 2006	DuPont/CSIRO	Process of microgel synthesis and products produced therefrom	Microgels from self-assembly of RAFT-made block copolymers followed by crosslinking	**4**

(*continued*)

Table 24.7 (Continued)

	Number	Priority[a)]	Date[b)]	Assignee	Title[c)]	Brief description	ZC(=S)S–[d)]
13.	WO2002094887A1 US6395850B1 [97]	2000	2002 2002	Symyx	Heterocycle containing control agents for living-type free radical polymerization	Hydrazine-based dithiocarbamate RAFT agents. Hydrazine part of heterocycle (1,2 imidazoline). Polymerization process	**48**
14.	WO2002026836A2 US6380335B1 [98] US6482909B2 [99] US6518448B2 [100] US6569969B2 [101] US6841624B2 [102] US6844407B2 [103]	2000	2002 2002 2002 2003 2003 2005 2005	Symyx	Control agents for living-type free radical polymerization, methods of polymerizing and polymers with same	Hydrazine-based dithiocarbamate RAFT agents. Polymerization process in forming block copolymer, or star or hyper-branched polymer	**45 48 46 47**
15.	WO2002022688A2 US6916884B2 [104]	2000	2002 2005	Rhodia Chimie	Method for block polymer synthesis by controlled radical polymerization in the presence of a disulphide compound	Polymerization in the presence of a RAFT agent or a disulfide RAFT agent. Very broad RAFT agent definition. Examples are xanthates and xanthogen disulfides	**29 33**
16.	WO2002036640A1 [105] US6890980B2	2000	2002 2005	Rhodia Chimie	Synthesis of block polymers obtained by controlled free radical polymerization	Use of tetrathiophosphate RAFT agents	**76**
17.	WO2002010223A2 US7247688B2 [106]	2000	2002 2007	Rhodia Chimie	Method for synthesis of block polymers by controlled free radical polymerization	Dithiophosphoroester $Z^1Z^2P(=S)S–R$ compound as RAFT agent	**75**

18.	WO2001060792A1 US6596899B1 [107] US6962961B2 [108] US7279591B2 [109] US7495128B2 [110] US7659345B2 [111] pub [112]	2000	2001 2003 2005 2007 2009	Noveon Lubrizol	S,S′-bis-(α,α′-disubstituted-α″-acetic acid)-trithiocarbonates and derivatives as initiator-chain transfer agent-terminator for controlled radical polymerizations and the process for making the same	Synthesis and use of trithiocarbonate RAFT agents prepared by the ketoform reaction	**17 23**
19.	WO2004037780A1 US7335788B2 [113] US7851582B2 [114] pub [115]	2002	2004 2008	Lubrizol	S-(α,α′-disubstituted-α″-acetic acid) substituted dithiocarbonate derivatives for controlled radical polymerizations, process and polymers made therefrom	Synthesis and use of dithiocarbamate RAFT agents prepared by the ketoform reaction	**63 61 62 72 71 73 64 65**
20.	US7205368B2 [116] US7498456B2 [117]	2000	2007 2009 2010	Lubrizol	S-(α,α′-disubstituted-α″-acetic acid) substituted dithiocarbonate derivatives for controlled radical polymerization, process and polymers made therefrom	Synthesis and use of xanthate RAFT agents prepared by the ketoform reaction	**29**
21.	US6518364B2 [118]	2001	2003	Symyx	Emulsion living-type free radical polymerization, methods and products of same	Hydrazine-based dithiocarbamate RAFT agents. Emulsion polymerization	**45**
22.	US7214751B2 [119]	2001	2007	Rhodia Chimie	Radical polymerization method performed in the presence of disulfide compounds	Radical polymerization in presence of Z^1-C(=S)–S–S–C(=S)–Z^2. In situ formation of RAFT agents. The method is used in the preparation of block copolymers containing especially a methacrylic block	**29**

(*continued*)

Table 24.7 (Continued)

	Number	Priority[a)]	Date[b)]	Assignee	Title[c)]	Brief description	ZC(=S)S–[d)]
23.	US7317050B2 [120]	2001	2008	Rhodia Chimie	Controlled mini-emulsion free radical polymerization	Controlled mini-emulsion radical polymerization in presence of a RAFT agent	**21 29**
24.	WO2003055919A1 US7745553B2 [121]	2001	2003 2010	University of Sydney	Aqueous dispersions of polymer particles	RAFT in emulsion. Amphiphilic macroRAFT agents	**12 17 21** **23 25**
25.	WO2003031480A2 US7064166B2 [122]	2001	2003 2006	Carnegie Mellon University	Process for monomer sequence control in polymerizations	RAFT (and other RDRP) in presence of Lewis acids. An example is cumyl dithiobenzoate	**4**
26.	WO2003066685A2 US6855840B2 [123] US7179872B2 [124] US7186786B2 [125] US7402690B2 [126]	2002	2003 2005 2007 2007 2008	University of Southern Mississippi	Chain transfer agents for RAFT polymerization in aqueous media	Dithioesters for use in aqueous polymerization. Examples are dithiobenzoates with hydrophilic R	**4 12 29**
27.	WO2004108770A1 US7332552B2 [127]	2003	2004 2008	Rensselaer Polytechnic Institute	Low odor chain transfer agents for controlled radical polymerization	RAFT agents ZC(=S)S–CH(CN)R. with R aryl	**4 6 7 29 66**
28.	WO2005116097A1 US20080114128A1 [128]	2004	2005 2008	Rhodia Chimie	Synthesis of Copolymers in the Form of a Mikto Star by Controlled Radical Polymerization	Arm-first stars and mikto-arm stars	**29**
29.	US7632966B2 [129]	2004	2009	DuPont	Synthesis of trithiocarbonate RAFT agents and intermediates thereof	Improved trithiocarbonate synthesis from disulfide	**23**

30.	WO2007071591A1 [130] US8163100B2	2005	2007 2012	Rhodia Chimie	Synthetic microgel polymer compositions for treating and/or modifying hard surfaces	Core-first and arm-first stars	**29**
31.	WO2008078055A2 US8389643B2 [131]	2006	2008 2013	Arkema	Copolymers based on methacrylate units, preparation method thereof and use of same	Use of comonomer (styrene acrylate) to facilitate control over RAFT polymerization of methacrylates	**17**
32.	WO2009153162A1 US8912273B2 [132]	2008	2009 2014	BASF SE	Process for the preparation of an aqueous polymer dispersion	Hydrophilic macroRAFT agent prepared and used for styrene polymerization in aqueous emulsion	**17 21 25**
33.	WO2009111725A1 US8445610B2 [133]	2008	2009 2013	Carnegie Mellon University	Controlled radical polymerization processes	RAFT agents used for ATRP initiation. RAFT used to control ATRP. Dual ATRP initiator/RAFT agents. Macro RAFT agent synthesis	**4 17 29 70**
34.	WO2011075156A1 US8815971B2 [134] US9012528B2 [135] US9518136B2	2008	2011 2014 2015 2016	ATRP Solutions Pilot Polymer Technologies	Control over controlled radical polymerization processes	Feed addition of initiator or reducing agent during polymerization. No RAFT example. US9518136B2 relates specifically to RAFT	—
35.	WO2012078716A1 US8822610B2 [136] US9856331B2	2008	2012 2014 2018	ATRP Solutions	Control over controlled radical polymerization processes	Feed addition of initiator or reducing agent during polymerization. No RAFT example	—
36.	WO2010083569A1 US9340498B2 [137]	2009	2010 2016	CSIRO	RAFT polymerisation	Switchable RAFT agents	**52**

(*continued*)

Table 24.7 (Continued)

	Number	Priority[a)]	Date[b)]	Assignee	Title[c)]	Brief description	ZC(=S)S−[d)]
37.	WO2010019563A1 [138] US8883912B2	2008	2009 2011	University of Akron	Synthesis of arborescent polymers via controlled inimer-type reversible addition-fragmentation chain transfer (RAFT) polymerization	RAFT self-condensing vinyl polymerization	**4**
38.	WO2012037596A1 US8946360B2 [139]	2010	2012 2015	CSIRO	Continuous flow polymerisation process	RAFT solution polymerization in tubular reactor	**23 66**
39.	WO2016054689A1 [140]	2014	2016	CSIRO	All-purpose RAFT agent for polymerization	3,5-Dimethylpyrazole RAFT agent. R = cyanomethyl	**49**
40.	US9156921B2 [141]	2013	2015	California Institute of Technology	Organocatalyzed photoredox mediated polymerization using visible light	PET-RAFT making use of organic catalysts claimed. No RAFT examples	—
41.	WO2015113114A1 [142] US20160340463A1	2014	2015 2016	NewSouth Innovations	Process for preparing a polymer	PET-RAFT process using either organic or organometallic photoredox catalysts	**4 21 23 25 29**
42.	WO2016197187A1 [143]	2016	2016	CSIRO	Versatile RAFT agent	4-Subsituted-3,5-dimethyl-pyrazole RAFT agents. R = cyanoisobutyl	**49 50 51**

a) Priority date.
b) Date published.
c) Title of the patent as published.
d) ZC(=S)S– groups exemplified (Table 24.6).
Abbreviations: RDRP, reversible deactivation radical polymerization; PET-RAFT, photo energy or electron transfer-RAFT.

radical-induced decomposition of a bis(thioacyl) disulfide. Similar chemistry with reference to the use of xanthates was also claimed in two Rhodia patents (Table 24.7, entries 15, 22). The CSIRO patent also covered other processes that generate a RAFT agent *in situ* such as radical addition to a ketene dithioacetal.

Rhodia also filed on more active xanthates with electron-withdrawing groups on oxygen as RAFT agents. Symyx filed on dithiocarbamate RAFT agents where the dithiocarbamate nitrogen was contained in a hydrazinyl group (Table 24.7, entries 13, 14, and 21). This class includes the 1*H*-pyrazole-1-carbodithioates **48** and **49**. Examples of **49** with R = cyanoalkyl were more recently the subject of a CSIRO patent (Table 24.7, entry 39).

A series of patents filed by Noveon (now Lubrizol) relate to the synthesis of trithiocarbonate, xanthate, and dithiocarbamate RAFT agents using the ketoform process (Table 24.7, entries 18–20). The trithiocarbonates prepared by this process are currently amongst the most used RAFT agents for mediating the polymerization of more activated monomers (MAMs, see chapter on trithiocarbonates) [145]. The synthesis of RAFT agents by this process has been successfully produced on industrial scale and exploited in the production of rheology modifiers for oil [146].

Switchable RAFT agents can be 'switched', typically by protonation, to be highly effective with either MAMs and less activated monomers (LAMs) (e.g. **52**, **52-H**$^+$, Table 24.7, entry 36). RAFT agents with balanced activity are those that show effectiveness with both LAMs and MAMs even though the quality of control may be to some extent compromised. This class includes various dithiocarbamates and xanthates described in the Rhodia and Symyx patents (Table 24.7). CSIRO patented specific 3,5-dimethyl-1*H*-pyrazole-1-carbodithioates (**49** and **50**) in this context (Table 24.7, entries 39 and 42).

24.3.2 RAFT Emulsion Polymerization

Successful semi-batch RAFT emulsion polymerizations to form low-dispersity polymers and block copolymers were described in the earliest CSIRO/DuPont patents (Table 24.7, entries 1 and 6). The starved feed strategy that had been found successful in improving living characteristics in macromonomer RAFT polymerization in emulsion was also successful in minimizing retardation and achieving colloidal stability in thiocarbonylthio-RAFT emulsion polymerization with the more active thiocarbonylthio-RAFT agents. Examples of RAFT emulsion polymerization with xanthates appear in the first Rhodia patents (Table 24.7, entry 2, see also entries 12 and 25).

The use of amphiphilic macroRAFT agents in thiocarbonylthio-RAFT polymerization was pioneered by University of Sydney (Table 24.7, entry 25, see also Table 24.8, entries 240–244). This form of RAFT emulsion polymerization was exploited on a commercial scale by Dulux in Australia in acrylic surface–coatings applications and for pigment encapsulation/dispersion. There was also a substantial effort at Goodyear focused on diene-based polymers (Table 24.9, entries 74–85).

Later patents that deal specifically with emulsion or miniemulsion polymerization are shaded blue in Tables 24.7 and 24.9.

Table 24.8 RAFT agents that have been produced/used on a large scale by industry.

Trade name(s)	IUPAC name/structure	CAS no	EC no[a)]	PubChem CID no
Rhodixan A1™	Methyl 2-((ethoxycarbonothioyl)thio)propanoate 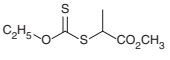 **80**	351491-23-1	435-410-2	16720359
BlocBuilder DB™ DBTTC BM1361	Dibenzyl carbonotrithioate 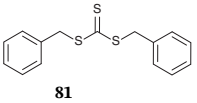 **81**	26504-29-0	460-390-7	233929
DOPAT BM1430	2-(((dodecylthio)carbonothioyl)thio)propanoic acid 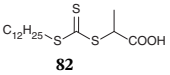 **82**	558484-21-2	695-614-4	59347140
DDMAT CTA-acid	2-(((dodecylthio)carbonothioyl)thio)-2-methylpropanoic acid 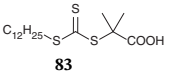 **83**	461642-78-4	663-505-0	11473994
CTA1 CTA-ester	Butyl 2-(((dodecylthio)carbonothioyl)thio)-2-methylpropanoate 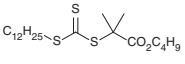 **84**	1034630-38-0	924-887-7	—

CPDTTC	2-Cyanopropan-2-yl dodecyl carbonotrithioate 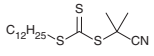 **85**	870196-83-1	—	71310910
CDTPA BM1432	4-Cyano-4-(((dodecylthio)carbonothioyl)thio)pentanoic acid 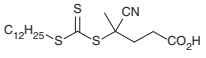 **86**	870196-80-8	687-390-1	57354956
CPDB	2-Cyanopropan-2-yl benzodithioate 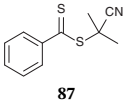 **87**	201611-85-0	687-395-9	9964525
	4-Cyano-4-((phenylcarbonothioyl)thio)pentanoic acid 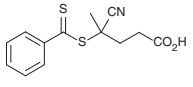 **88**	201611-92-9	687-398-5	9921763
	2-((phenylcarbonothioyl)thio)acetic acid 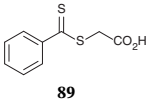 **89**	942-91-6	213-393-0	70336

a) European Chemical Agency.

Table 24.9 Patents relating to applications of thiocarbonylthio-RAFT polymerization.

Number	Priority[a]	Date[b]	Assignee	Title[c]	Brief description	ZC(=S)S–[d]
1. WO2004099275A1 US6762257B1 [147]	2003	2004 2004	3M	Azlactone chain transfer agents for radical polymerization	Chain transfer agents for controlled radical polymerization (RAFT) are described. The chain transfer agents have an azlactone or ring-opened azlactone to provide telechelic (co)polymers	**29**
2. US6747104B1 [148] US6818716B2	2003	2004	3M	Azlactone photoiniferters for radical polymerization	Dithiocarbamate photoinitiators	**70**
3. WO2007050532A1 US7439000B2 [149]	2005	2007 2008	3M	High clarity cholesteric liquid crystal films	Polymers made by RAFT polymerization. 4-Cyanobiphenyl benzoate ethyl acrylate. Conventional chain transfer also used	**23**
4. WO2007050433A1 US7652736B2 [150]	2005	2007 2010	3M	Infrared light reflecting film	Acrylate polymer with liquid crystalline pendants made by RAFT polymerization with trithiocarbonate	**23**
5. WO2013028397A2 [151] US9907733B2	2012	2013 2018	3M	Dental compositions comprising addition-fragmentation agents	Graft to silica particles. Also relates to macromonomer RAFT	**24**
6. WO2015057413A1 [152] US9758478B2	2013	2015 2017	3M	Allyl disulfide-containing addition-fragmentation oligomers	Dynamic covalent polymers	**79**
7. WO2010131628A1 [153] US20120059137A1	2009	2010 2012	AGC Seimi Chemical Ltd	Monodisperse chloromethylstyrene polymer and producing method thereof	Higher M_n poly(chloromethylstyrene) made by RAFT	**4**

8.	US7674843B2 [154] US7678845 [155]	2005	2010 2010	Agfa Graphics	Stable pigment dispersions	Dispersions containing RAFT-synthesized block copolymer dispersants	**4**
9.	WO2006111637A1 [156] US20090221850A1	2005	2006 2009	Arkema	Method for preparing alkoxyamines by photolysis of dithiocarbamates	Alkoxyamines prepared by photolysis of a dithiocarbamate in the presence of a nitroxide	**70**
10.	WO2012004480A1 [157]	2010	2012	Arkema	Compositions with improved odour comprising a raft agent or a polymer obtained using one of these agents	Masking odour of RAFT agents, including BlocBuilder DB	**17**
11.	US7713508B2 [158]	2005	2010	Arrowhead Center	Thiation of carbon nanotubes and composite formation	RAFT agent functionality formed on carbon nanotubes	—
12.	WO2012089352A1 WO2012089602A1 US8426554B2 [159] US8802773B2 [160] US9198947B2 US9301990B2 US9968647B2	2010	2012 2012 2013 2014 2015 2016 2017	Arrowhead Madison Hoffmann La Roche	In vivo polynucleotide delivery conjugates having enzyme sensitive linkages	SiRNA delivery. Example 16 of US8426554B2 is made by RAFT	**4**
13.	WO2013032829A1 US8932572B2 [161] US9089611B2 [162]	2011	2013 2015	Arrowhead Madison	Poly(vinyl ester) polymers for in vivo nucleic acid delivery	RAFT-synthesized vinyl ester copolymers	**63**
14.	WO2013158141A1 US8933047B2 [163]	2012	2013 2015	Arrowhead Madison	Poly(acrylate) polymers for in vivo nucleic acid delivery	Poly(meth)acrylate. Amine functional polymers made via tBOC protected monomers	**4**
15.	WO2016149313A1 US10047361B2	2015	2016 2018	Arrowhead Pharma-ceuticals Corp	Disulfide-containing alkyne linking agents	Cyclooctyne-alkyl disulfide compound as reagent for making conjugates	**4**

(*continued*)

Table 24.9 (Continued)

	Number	Priority[a)]	Date[b)]	Assignee	Title[c)]	Brief description	ZC(=S)S−[d)]
18.	WO2010147876A2 US8083348B2 [167]	2009	2011 2011	Bausch & Lomb	Biomedical devices	Contact lenses	**23 29**
19.	WO2010147875A2 US8133960B2 [168]	2009	2010 2012	Bausch & Lomb	Biomedical devices	Biomedical devices	**23 29**
20.	WO2010147874A1 US8337551B2 [169]	2009	2012	Bausch & Lomb	Biomedical devices, polymeric materials and contact lenses comprising same	Silicone diblock copolymer hydrogels	**17 23 29**
21.	US7169937B2 [170] US7825193B2 [171] US7977431B2 [172]	2002 2002 2002	2007 2010 2011	Bayer Lanxess Lanxess	Dithiocarbamic esters	Dithiocarbamate RAFT agents with R = haloalkenyl. Main application is RAFT emulsion polymerization of chloroprene	**30 41 43 (67)**
22.	WO2011032832A1 [173] US9023914B2	2009	2011 2015	Lanxess	Nitrile rubbers and production thereof in organic solvents	NBR by RAFT in solution	**4 17 23**
23.	WO2004055060A1 US7205362B2 [174]	2002	2007	BioMérieux	Method for controlled radical polymerization	RAFT process to form high M_n polymer in relatively short reaction time with control of radical flux	**4**
24.	WO2007003781A1 US8133411B2 [175]	2005	2007 2012	Biomerieux, CNRS	Fluorescent polymers soluble in an aqueous solution and a method for the production thereof	Fluorescent RAFT-synthesized polymer for medical diagnostics or therapeutics	**4**
25.	WO2014165530A1 [176] US9123541B2	2013	2014 2015	Brewer Science Inc.	Highly etch-resistant polymer block for use in block copolymers for directed self-assembly	RAFT used for resists to be used in block copolymer self-assembly	**25**

26.	US7230051B2 [177]	2002	2007	BYK-Chemie GmbH	Use of polyacrylate-modified polysiloxanes as levelling agents in coating compositions	Block copolymers (polysiloxane pre-polymer) as levelling agents (examples made by RAFT) for surface-coating compositions	**29**
27.	WO2004014963A2 [178] US7019082B2	2002	2004 2004	Carnegie Mellon University	Polymers, supersoft elastomers and methods for preparing the same	Crosslinked brush polymer as elastomer	**4**
28.	WO2005087818A1 [179] US7795355B2	2005	2010	Carnegie Mellon University	Preparation of functional polymers	RAFT in combination with 'click' chemistry	**4**
29.	WO2002070571A1 US7345121B2 [180]	2001	2002 2008	Coatex SAS	Method of controlled free radical polymerisation of acrylic acid and its salts thereof, resulting low-polydispersity polymers, and their uses	Poly(acrylic acid) synthesis by RAFT	**4 17 29 32 38 43**
30.	WO2004014967A2 US7462676B2 [181]	2002	2004 2008	Coatex SAS	Method for the controlled radical polymerisation of acrylic acid and the salts thereof, polymers thus obtained and applications thereof	Poly(acrylic acid) synthesis by RAFT	**29**
31.	WO2005095466A1 US7956211B2 [182] US8227633B2 [183] US8470750B2 [184]	2004 2002	2005 2011 2012 2013	Coatex SAS	Trithiocarbonate derivatives and the use thereof in the form of transfer agents for acrylic acid controlled radical polymerisation	Trithiocarbonates used for RAFT AA polymerization in water	**17**
32.	WO2006024706A1 US8053497B2 [185]	2004	2006 2011	Coatex SAS.	Polymers produced by using sulphur compounds in the form of transfer agents for controlled radical polymerisation of acrylic acid and the use thereof	Poly(AA) by RAFT polymerization in water	**17 29**

(*continued*)

Table 24.9 (Continued)

	Number	Priority[a]	Date[b]	Assignee	Title[c]	Brief description	ZC(=S)S–[d]
33.	WO2008084298A1 US8110130B2 [186]	2007	2012	Coatex SAS	Use of a rheological additive in the manufacture of concrete by vibrocompaction	Additive can be made by RAFT. No RAFT examples	—
34.	US7851572B2 [187]	2004	2010	Coatex SAS	Polymers produced by using sulphur compounds in the form of transfer agents for controlled radical polymerisation of acrylic acid and the use thereof	Low-dispersity AA copolymers by RAFT polymerization	**17 29**
35.	WO2014022365A1 [188] US9758606B2 US10385150B2	2012	2014 2017 2019	Columbia University of New York	Cyclopropenium polymers and methods for making the same	Monomers containing cyclopropenium ions polymerized by RAFT	**4**
36.	WO2010096464A1 US8968705B2 [189]	2008	2010 2015	Colorado School of Mines	Gold/lanthanide nanoparticle conjugates and uses thereof	Nanoparticle-bound RAFT polymers. Biomedical imaging applications	**23**
37.	WO2008064972A1 US7960479B2 [190]	2006	2008 2011	Unilever Conopco, Inc	Brush copolymers	Brush copolymers made by ROMP/RAFT	**23**
38.	WO2012069403A2 US8912267B2 [191]	2010	2012 2014	Continental Reifen	Process for producing polymer-functionalized filler particles	Surface-initiated RAFT polymerization from silica particles or carbon black	**17 20**
39.	WO2016180805A1 [192] US10442877B2	2015	2015 2018	Continental Reifen	Raft agent, polymerization method, polymer, rubber mixture, and use thereof	Tyre compositions	**23**
40.	EP3109064B1 [193]	2016	2018	Continental Reifen	Method for co-polymerization, co-polymer and rubber composition and their use	Preparation of butadiene-*b*-VAc and related copolymers	**52**
41.	US7811555B2 [194]	2005	2010	Cordis Corporation	Tri-branched biologically active copolymer	Tri-branched copolymers. Biomedical applications. No actual examples	**4**

42.	US7411053B2 [195]	2006	2008	(Clark University, Atlanta)	Ligand-functionalized/azo compounds and methods of use	Metallopolymers. Ligand functional chain ends	**4**
43.	WO2017029412A1 US10005900B2 US10329414B2 [196]	2015	2017 2018 2020	CNRS, Ecole Superieure de Physique et Chimie Industrielles de Ville Paris	Boronic polymer crosslinking	Dynamic covalent polymers. MMA copolymer with pendant boronic ester functionality prepared	**4**
44.	WO2017029311A1 WO2017029315A1 US9994651B2 US10584190B2 [197]	2015 2015	2017 2017 2018 2020	Ecole Superieure de Physique et Chimie Industrielles de Ville Paris	Composition comprising a cross-linked polymer network, prepared by radical copolymerisation, comprising pending links and cross-links exchangeable by aldehyde-imine exchange reactions and/or by imine-imine exchange reactions, preparation process and use	Dynamic covalent polymers. MMA copolymer with pendant aldehyde functionality prepared	**4**
45.	WO2015099913A1 [198] US10189985B2 US10647844B2	2013	2019	Cytec Industries Inc	Polyacrylonitrile (PAN) polymers with low polydispersity index (PDI) and carbon fibres made therefrom	Acrylonitrile copolymer for carbon fibre	**4 17 23**
46.	WO2010147011A1 [199]	2009	2010	Denka	Polychloroprene, process for production of same, and adhesives containing same	RAFT emulsion polymerization of chloroprene	4 41 42
47.	WO2005031461A1 US7696292B2 [200]	2003	2005 2010	DuPont	Low-polydispersity photoimageable acrylic polymers, photoresists and processes for microlithography	Resist polymers made by RAFT	**25**

(*continued*)

Table 24.9 (Continued)

	Number	Priority[a]	Date[b]	Assignee	Title[c]	Brief description	ZC(=S)S−[d]
48.	WO2005031462A1 US7408013B2 [201]	2004	2005 2008	DuPont CSIRO	Low-polydispersity photoimageable polymers and photoresists and processes for microlithography	Photoresist polymers by RAFT	**25**
49.	US8034534B2 [202]	2006	2011	DuPont	Fluorinated polymers for use in immersion lithography	Resist polymers made by RAFT	**25**
50.	WO2008019450A1 US8124188B2 [203] US8795782B2 [204]	2006	2008 2012 2014	CSIRO	Polymeric coatings and methods for forming them	Surface-initiated polymerization to form biocompatible surfaces	**19 70**
51.	WO2009155657A1 US8501889B2 [205] US8993697B2 [206]	2009 2008 2008	2013 2015	CSIRO	Conducting and semiconducting organic materials	Synthesis of block copolymers comprising a semiconductor segment by RAFT. Divisional covers macroRAFT agents	**4 18 21**
52.	WO2014138807A1 US9458263B2 US9777081B2 [207]	2013	2014 2016 2017	CSIRO	Polymer derived from acrylonitrile	High-molecular-weight polyacrylonitrile and copolymers for carbon fibre	**4**
53.	US7468415B2 [208]	2007	2008	DuPont	Method for preparing glycidyloxystyrene monomers and polymers thereof	Monomer is polymerized by RAFT in the examples	**25**
54.	US8304572B2 [209]	2007	2012	DuPont	Synthesis of fluoroalcohol-substituted (meth)acrylate esters and polymers derived therefrom	Monomer synthesis based on fluorinated epoxide. Tetrapolymer example made by RAFT	**25**
55.	US8734898B2 [210]	2012	2014	DuPont	Method for producing encapsulated nanoparticles	Styrene/acrylic acid/butyl acrylate copolymer made by RAFT	—

56.	US9815947B2 [211]	2015	2017	DuPont	Substantially symmetrical 3-arm star block copolymers	Star comprising central core and outer blocks RAFT agent prepared from acid functional trithiocarbonate and tris(4-hydroxy-phenyl)ethane	**25**
57.	WO2010096422A1 US8497356B2 [212]	2009	2010 2013	Duke Univer-sity	Biomolecule polymer conjugates and methods for making the same	RAFT polymerization from protein-bound RAFT agents	**4**
58.	WO2009090252A1 [213] US9567476B2	2008	2009 2017	DSM	Water-borne crosslinkable block copolymers obtained using RAFT	Crosslinkable copolymer coatings. Block copolymer dispersant made by RAFT	**29**
59.	WO2008122576A1 [214] US9340699B2	2007	2008 2016	DSM	Aqueous oligomer/polymer emulsion with cationic functionality	Anti-microbial coatings. Quaternary amine functional polymers	**29**
60.	WO2010000725A1 [215]	2008	2010	DSM	Adhesion to metal surfaces with block copolymers obtained using RAFT	Anti-corrosive coatings	**29**
61.	WO2009121911A1 [216] US9255211B2	2008	2009 2016	DSM	Adhesion to plastic with block copolymers obtained using RAFT	Coatings for plastics. Block copolymer dispersant made by RAFT	**29**
62.	WO2009138493A1 [217]	2008	2009	DSM	Block copolymers obtained using raft	Blocks made by RAFT emulsion polymerization	**29**
63.	WO2019121782A1 [218]	2018	2019	DSM	Waterborne crosslinkable dispersions	Blocks made by RAFT emulsion polymerization for coatings applications	**13 18 22**

(*continued*)

Table 24.9 (Continued)

	Number	Priority[a)]	Date[b)]	Assignee	Title[c)]	Brief description	ZC(=S)S–[d)]
64.	US6756457B2 [219]	2002	2004	Eastman Kodak	Polymerization process	Onium salt plus an organic sulfur compound (e.g. sulfide, disulfide, RAFT agents) gives living polymerization initiator	**70**
65.	US9428649B2 [220] US9732231B2 [221]	2010 2010	2016 2017	E Ink California	Electrophoretic dispersion Method of making electrophoretic dispersion	Polymer-grafted pigment particles made by surface-initiated RAFT	**4**
66.	WO2017046652A1 [222] US10046056B2	2014	2018	Ecole Polytechnique Federale de Lausanne	Glycotargeting therapeutics	Glycopolymer–antigen conjugates	**4**
67.	WO2004083169A1 [223] US6841695B2	2003	2004 2005	Rohmax Evonik	Process for preparing dithioesters	Dithiobenzoate synthesis	**4**
68.	WO2004087850A1 [224] US8288327B2	2003	2004 2012	Rohmax Evonik	Lubricating oil composition with good frictional properties	Lubricating oil composition	**4**
69.	WO2011101176A1 [225] US8916635B2	2010	2011 2014	Evonik	Functional materials with reversible crosslinking	Hetero-Diels–Alder process for chain linking to thiocarbonylthio compound	**9**
70.	WO2013013873A1 [226] US8981010B2	2011	2013 2015	Evonik	Polymer powder for producing three-dimensional objects	Hetero-Diels–Alder process. No RAFT examples	—
71.	WO2013017349A1 [227] US10030105B2	2011	2013 2018	Evonik	Low molecular weight products and use thereof as reversible or permanent low-temperature crosslinking agent in Diels-Alder reactions	Hetero-Diels–Alder process for chain linking to thiocarbonylthio compound	**74**
72.	US10308748B2 [228]	2015	2019	Florida State University	Lignin-containing polymers	RAFT-click chemistry used	**23**

73.	WO2007137418A1 [229] US9012239B2 US9296838B2 US10072104B2	2006	2007 2015 2016 2018	Fluidigm Canada Inc	Polymer backbone element tags	DMAm/NAS copolymer, NAS converted to metal-ligating pendant group	**4**
74.	US6369158B1 [230]	1999	2002	Goodyear	Dibenzyltrithio-carbonate molecular weight regulator for emulsion polymerization	RAFT copolymerization in emulsion. Dibenzyl trithiocarbonate used for SBR. Poor control	(**17**)
75.	WO2004060928A1 US7592409B2 [231]	2002	2004 2009	Goodyear	Styrene acrylonitrile isoprene triblock copolymer	Triblock made by RAFT emulsion polymerization	**17**
76.	WO2004060928A1 US7767775B2 [232]	2002	2004 2010	Goodyear	Controlled Polymerization	Preparation of poly(St)-*b*-(diene-*co*-MAN) and other MAN blocks by RAFT emulsion polymerization	**17**
77.	US6992156B2 [233] US7098280B2 [234]	2003	2006 2006	Goodyear	Controlled polymerization	RAFT emulsion polymerization. Emulsifier prepared in situ	**17**
78.	US7528204B2 [235]	2004	2009	Goodyear	Hydrogenation and epoxidation of polymers made by controlled polymerization	RAFT emulsion polymerization followed by other processes	**17**
79.	US7462674B2 [236] US7345186B2 [237] US7488786B2 [238]	2005	2008 2008 2009	Goodyear	Oxathiazaphospholidine free radical control agent	Potential RAFT agent	**77**
80.	US7625985B1 [239]	2005	2009	Goodyear	Water-based process for the preparation of polymer-clay nanocomposites	Poly(4-vinylpyridine) block copolymers used in water as dispersants/exfoliants for clay nanocomposites	**17 23 27**

(*continued*)

Table 24.9 (Continued)

Number	Priority[a]	Date[b]	Assignee	Title[c]	Brief description	ZC(=S)S–[d]
81. US7230063B1 [240]	2006	2007	Goodyear	Functional trithiocarbonate RAFT agents	Trithiocarbonates of general structure for emulsion polymerization ZS–C(=S)S–Y, where Z group is a functional alkyl (contains COOH, OH); Y group is capable of activating a vinylic carbon towards free-radical addition	**17 23 27 28**
82. US7671152B2 [241]	2006	2010	Goodyear	Surfactantless synthesis of amphiphilic cationic block copolymers	Poly(4-vinylpyridine) macro-RAFT agent-derived block copolymers. RAFT emulsion	**17 23 27**
83. US7335714B1 [242]	2007	2008	Goodyear	Sulfine control agents for synthesizing polymers	Sulfines claimed to give RDRP possibly by RAFT	**78**
84. US7812108B2 [243]	2007	2010	Goodyear	Hydrogenation and epoxidation of polymers made by controlled polymerization	Hydrogenation of RAFT-synthesized polymers with hydrazine	**17**
85. US8178637B2 [244]	2007	2012	Goodyear	Controlled Polymerization	Preparation of poly(St)-*b*-(diene-*co*-AN) by RAFT and other RDRP in emulsion	**17**
86. US8415432B1 [245]	2011	2013	Goodyear	Rubber composition and pneumatic tire	PNIPAm-bisthiol (made by RAFT) used in vulcanization of poly styrene-butadiene rubber	**23**
87. US8759451B2 [246]	2011	2013	Goodyear	Method of making a graft copolymer	Graft copolymers to diene polymers by RAFT	**23**

88.	US8563656B1 [247]	2012	2013	Goodyear	Method to improve green strength in elastomers	Thiol functional poly(NIPAm) made by RAFT use as blend component	**23**
89.	US8883884B2 [248]	2012	2014	Goodyear	Pneumatic tire	Thiol functional poly(NIPAm) made by RAFT use as blend component	**23**
90.	US8309630B2 [249]	2010	2012	Hewlett-Packard	Polymer-encapsulated pigment	Example use RAFT. RAFT pigment dispersants	**4**
91.	US7521090B1 [250] US7989026B2 [251]	2008 2008	2009 2011	IBM	Method of use of epoxy-containing cycloaliphatic acrylic polymers as orientation control layers for block copolymer thin films	Block copolymer lithography. poly(St)-*b*-poly(MMA) used in process was made by RAFT	**4**
92.	WO2016066586A1 [252] US9815916B2 US10208142B2 US10577439B2	2014	2016 2017 2019 2019	Illumina Cambridge Ltd	Polymers and DNA copolymer coatings	Coatings with grafted DNA	**4 23**
93.	US10093758B2 [253]	2013	2018	Iowa State University Research Foundation	Thermoplastic elastomers via reversible addition-fragmentation chain transfer polymerization of triglycerides	Block copolymers based on monomers derived from triglycerides	**4 17**
94.	US6720429B2 [254]	2002	2004	ITRI	Thiocarbonylthio compound and living free radical polymerization using the same	RAFT agents Z–C(=S)S–R with R = imidomethyl	**4 6**
95.	US7632959B2 US7968743B2 [255]	2003	2011	ITRI	Thiocarbonylthio compound and free radical polymerization employing the same	RAFT agents with Z = CF_3 or 4-methoxyphenyl	**6 11**

(*continued*)

Table 24.9 (Continued)

Number	Priority[a]	Date[b]	Assignee	Title[c]	Brief description	ZC(=S)S–[d]
96. WO2005038734A2 US7799568B2 [256]	2003	2005 2010	Johns Hopkins University	Authentication of products using molecularly imprinted polymers	Molecularly imprinted polymers	**4**
97. WO2005103655A1 US7678870B2 [257]	2004	2005 2010	Johns Hopkins University	Processable molecularly imprinted polymers	Molecularly imprinted polymers	**4**
98. US8241575B2 [258]	2008	2012	Johns Hopkins Univer-sity	Molecularly imprinted polymer sensor device	RAFT-made polymers used to make sensor	**4**
99. WO2005003198A1 US7510817B2 [259]	2003	2005 2009	JSR	Photoresist polymer compositions	Photoresists based on bulky methacrylates	**48 49**
100. WO2005000924A1 US7517634B2 [260]	2003	2005 2009	JSR	Photoresist polymers	Photoresists based on bulky methacrylates	**48 49**
101. WO2002098944A1 US6992138B2 [261]	2001	2002 2006	Kaneka	Polyurethane polymer	Polyurethanes prepared from bis-thiols made by RAFT end-group aminolysis	**4**
102. WO2002098929A1 US6914110B2	2001	2002 2005	Kaneka	Process for producing polymer having crosslinkable silyl group and curable composition	Silyl-functional isocyanate used	**4**
103. WO2003008474A1 US7094833B2 [262]	2001	2003 2006	Kaneka	Block copolymer	Acrylonitrile or methacrylonitrile containing block copolymers made by RAFT	**4**
104. WO2002081561A1 US7211625B2 [263]	2001	2002 2007	Kaneka	Thermoplastic resin composition and elastomer composition	Thermoplastic elastomers (acrylic block copolymers) made by RAFT	**4**
105. WO2016112883A2 [264] US10302632B2	2015	2019	Karlova Univer-sity	Macromolecular conjugates for visualization and separation of proteins and cells	Protein bioconjugates comprising an imaging probe	**4**

106.	WO2009012202A1 US7875213B2 [265]	2007	2009 2011	Kemira Oyj	Mineral dispersants and methods for preparing mineral slurries using the same	RAFT-made acrylic polyelectrolyte dispersants for processing mineral slurries	**17**
107.	US8518497B2 [266]	2009	2013	Korea Advanced Institute of Science and Technology	Methods for the preparation of coil-comb block copolymers and their nanostructures	Concurrent RAFT and ATRP	**4**
108.	WO2009107987A2 US8420771B2 [267]	2008	2009 2013	Kyung Hee University	pH-sensitive polyethylene oxide co-polymer and synthetic method thereof	PEO macro-RAFT agent used to make pH-responsive block copolymer	**29**
109.	US20050238594A1 [268]	2003	2005	L'Oreal	Block ethylenic copolymers comprising a vinyllactam block, cosmetic or pharmaceutical compositions comprising them and cosmetic use of these copolymers	Block copolymers made by RAFT	**29 63**
110.	US7585922B2 [269] US7816464B2 [270]	2005	2009	L'Oreal	Polymer particle dispersion, cosmetic compositions comprising it and cosmetic process using it	Block copolymers containing a segment based on methacrylates with silane functionality made by RAFT	**4**
111.	WO2006097529A1 [271] US20080233077A1	2005	2006 2008	L'Oreal	Cosmetic Use of a Particular Copolymer as Skin Tensor in a Cosmetic Composition	Block copolymers made by RAFT	**29**
112.	WO2010046229A1 [272] US10745582B2	2008	2010 2020	L'Oreal	Dispersion of soft polymer particles, cosmetic composition comprising it and cosmetic treatment method	Block copolymers made by RAFT	**12**

(*continued*)

Table 24.9 (Continued)

Number	Priority[a)]	Date[b)]	Assignee	Title[c)]	Brief description	ZC(=S)S– [d)]
113. WO2009101113A2 [273] US10925815B2	2008	2009 2011	L'Oreal	Oil-in-water emulsion comprising an amphiphilic polymer	Block copolymers made by RAFT emulsion polymer	**29**
114. WO2012156630A1 [274] US20140105838A1	2011	2012 2014	L'Oreal	Block polymer including isobutyl acrylate and acrylic acid, cosmetic composition and treatment method	Block copolymers made by RAFT	**23**
115. US7115683B2 [275]	2002	2006	LG Chem	Organic-inorganic nanocomposite and preparation thereof	Nanocomposite prepared from layered silicate salt made by adding a cationic initiator and a cationic RAFT agent to a layered silicate	**4**
116. US6888020B2 [276]	2003	2005	LG Chem	Water-soluble dithioesters and method for polymerization thereof	RAFT agents with quaternary ammonium substituent on R and use for polymerization in aqueous media	**4 41**
117. US8911537B2 [277]	2010	2014	LG Chem, ICUF Hanyang University	Adsorbent of volatile organic compounds and adsorption method using thereof	Acrylamide-based macroporous polymer prepared by RAFT	**4**
118. WO2012057443A2 US9109063B2	2010	2012 2015	LG Chem	Acrylamide-based mesoporous polymer and preparation method thereof		**4 23**
119. WO2012144735A2 [278] US9493588B2	2011	2012 2016	LG Chem	Diblock copolymer, preparation method thereof, and method of forming nano pattern using the same	Polymers for block copolymer lithography	**4**

120.	WO2016053014A1 [279] US10287430B2	2014	2016 2019	LG Chem	Method of manufacturing patterned substrate	Block copolymer lithography process	**4**
121.	WO2016053005A1 [280] US10310378B2 US10532546B2	2014	2016 2019 2020	LG Chem	Block copolymer	Block copolymers for self-assembly. Block copolymer lithography	**4**
122.	WO2001060792A1 US6894116B2 [281]	2002	2005	Noveon	S,S′-bis-(α,α′-disubstituted-α″-acetic acid)-trithiocarbonates and polymers thereof for toughening thermosetting resins	RAFT-made polymers as toughening agents in, e.g. adhesive, composite, coatings, sealants, caulks, potting resins, or laminates	**12 23**
123.	WO2006023691A2 US7495050B2 [282]	2004	2006 2009	Lubrizol	Associative thickeners for aqueous systems	Rheology modifiers prepared by RAFT	**12 23 73**
124.	US8137754B2 [283]	2004	2012	Lubrizol	Hydroxyl-terminated thiocarbonate containing compounds, polymers, and copolymers, and polyurethanes and urethane acrylics made therefrom	Synthesis of hydroxyl-functional telechelics for use in polyurethanes	**69 73**
125.	WO2006020281A1 US8709543B2 [284]	2004	2006 2014	Lubrizol	Hydroxyl-terminated thiocarbonate containing compounds, polymers, and copolymers, and polyurethanes and urethane acrylics made therefrom	Polyurethanes prepared from RAFT-synthesized hydroxy-functional polymers	**17 29 69 73**
126.	WO2006047393A1 [285] US8513172B2 US9809780B2	2005	2006 2013 2017	Lubrizol	Process for preparing polymers and compositions thereof	RAFT polymer synthesis includes blocks and stars	**4 23**

(*continued*)

Table 24.9 (Continued)

Number	Priority[a)]	Date[b)]	Assignee	Title[c)]	Brief description	ZC(=S)S–[d)]
127. WO2008058108A2 US8012917B2 [286]	2006	2008 2011	Lubrizol	Crosslinked polymer	Star microgel oil additives	**4**
128. WO2007127661A1 US9006159B2 [287]	2006	2007 2015	Lubrizol	Star polymer lubricating composition	Star microgel oil additives	**23**
129. WO2007127660A1 [288] US9359577B2 US9410104B2	2006	2013	Lubrizol	Star polymer lubricating composition	Star polymer additive	**4 23**
130. WO2008145613A1 US8268925B2 [289]	2007	2008 2012	Lubrizol	Graft copolymer and compositions thereof	Graft copolymers as pigment dispersants	-
131. US8507422B2 [290]	2007	2013	Lubrizol	Antiwear polymer and lubricating composition thereof	Star microgel anti-wear additives	**23**
132. WO2012030616A1 US8937035B2 [291]	2010	2012 2015	Lubrizol	Star polymer and lubricating composition thereof	Microgel star-block copolymers	**23**
133. WO2011031659A1 [292] US9528072B2	2010	2011 2012	Lubrizol	Farm tractor lubricating composition with good water tolerance	Amphiphilic block copolymer additive	**23**
134. WO2014031154A1 [293] US20150183915A1 US20180208696A1	2013	2014 2015 2018	Lubrizol	Loose core star polymers and lubricating composition thereof	Star polymers by crosslinking polymerization	—
135. WO2016182711A1 [294] US10280101B2	2015	2019	Lubrizol	Water soluble chain transfer agents	Salts of carboxyl-functional RAFT agents	**23**
136. WO2012048009A2 US8916683B2 [295]	2010	2012 2014	Massachusetts Institute of Technology	Nanostructured physically-associating hydrogels for injectable, responsive, and tough biomaterials	Example is peptide conjugate to RAFT poly(NIPAm) via maleimide	**19**
137. WO2014161031A1 [296] US10251958B2	2013	2014 2019	NewSouth Innovations	Nanoparticles for drug delivery comprising albumin having a polymer chain coupled thereto	Drug-delivery vehicle based on albumin conjugate	**4**

138.	WO 2010133680A1 US8383744B2 [297]	2009	2010 2013	Novartis AG	Actinically-crosslinkable siloxane-containing copolymers	Crosslinkable prepolymer made by RAFT. Contact lens application	**4**
139.	US6858309B2 [298]	2001	2005	Polymerat	Methods of polymerization	Living/controlled polymerization on polymeric solid supports	**4 12**
140.	WO2004078785A1 US7837899B2 [299]	2003	2004 2010	Polymers Australia	Dispersing agents in nanocomposites	Copolymer dispersants prepared by controlled radical polymerization (ATRP, RAFT, NMP) for clay in polymer nanocomposites	**23**
141.	WO2004113436A1 US7288585B2 [300]	2003	2004 2007	Ciba Specialty Chemicals, Polymers Australia, CSIRO	Acrylic dispersing agents in nanocomposites	Copolymer dispersants made by RAFT used in polyolefin nanocomposites	**21 23 37**
142.	WO2007039435A1 US8110626B2 [301]	2005	2012	Advanced Polymerik	Dispersing agents in composites	Dispersants as in US7837899 for talc (and other particles) in polymers	-
143.	WO2010015599A1 US8544658B2 [302]	2008	2010 2013	Polymers CRC	Functionalized thin film polyamide membranes	RAFT functional membrane used for surface-initiated polymerization	**18 26**
144.	US8658149B2 [303] US9095618B2 [304]	2008	2014	Ramot At Tel-Aviv Univer-sity	Conjugates of a polymer, a bisphosphonate and an anti-angiogenesis agent and uses thereof in the treatment and monitoring of bone related diseases	HPMA-based (amongst other) copolymers comprising segments with attached anti-angiogenesis agent and segments with bisphosphonate bone-targeting agent	**17**

(*continued*)

Table 24.9 (Continued)

Number	Priority[a)]	Date[b)]	Assignee	Title[c)]	Brief description	ZC(=S)S– [d)]
145. US6765076B2 [305]	2001	2004	Rensselaer Polytechnic Institute	Transition metal superoxides	The transition metal superoxide is effectively used as heterogeneous initiator for living or controlled free-radical polymerization. Dibenzyl trithiocarbonate used	**4 12**
146. US6458968B2 [306]	2000	2002	Rensselaer Polytechnic Institute	Dithiocarboxylic ester synthetic process	Dithioester synthesis by reacting a carboxylic acid compound, an alcohol or a thiol, and phosphorous pentasulfide	**4**
147. US8518473B2 [307]	2010	2013	Rensselaer Polytechnic Institute	Nanofilled polymeric nanocomposites with tunable index of refraction	TiO_2 nanocomposites. Titania-bound RAFT agent	**4**
148. WO2012148631A1 US8796372B2 [308]	2011	2012 2014	Rensselaer Polytechnic Institute	Self-healing electrical insulation	6-Azidohexyl methacrylate–grafted nanoparticles	**4**
149. WO2001016187A1 US6506837B2 [309]	1999	2001 2003	Rhodia Chimie	Gelled aqueous composition comprising a block copolymer containing at least one water-soluble block and one hydrophobic block	Viscoelastic gels from amphiphilic block copolymers	**29**
150. WO2001094263A2 US6500871B1 [310]	2000	2001 2002	Rhodia Chimie	Process for preparing colloids of particles coming from the hydrolysis of a salt of a metal cation	Preparation of mineral colloids of defined size in aqueous dispersion using block surfactants	**29**
151. WO2002008307A1 US6858696B2 [311]	2000	2002 2005	Rhodia Chimie	Method for synthesis of hybrid silicon and organic copolymers by controlled free radical polymerization	Preparation of hybrid silicone–organic block copolymers containing siloxane segments by RAFT	**29**

152.	WO2001095034A1 US6953649B2 [312]	2000	2001 2005	Rhodia Chimie	Photosensitive composition for photoresist manufacture	Styrenic block copolymer photoresists made by RAFT	**14 39**
153.	WO2003050195A2 US7473730B2 [313]	2001	2009	Rhodia	Method for depositing a polymer onto a surface by applying a composition onto said surface	Block copolymer containing ionic block for cosmetic applications	**29**
154.	WO2003050185A1 US7531597B2 [314]	2001	2009	Rhodia	Formulation comprising an ionic compound, a polyionic polymer, and a block copolymer	Block copolymer containing ionic block for cosmetic applications. Formulation for stable dispersion	**29**
155.	WO2002068486A2 US6437040B2 [315]	2001	2002 2002	Rhodia Chimie	Water-soluble block copolymers comprising a hydrophilic block and a hydrophobic block	Water-soluble hydrophilic–hydrophobic blocks. Use as adhesion promoter in paint or as wetting agent	**29**
156.	WO2003006549A1 US6559233B2 [316]	2001	2003 2003	Rhodia Chimie	Composition comprising a copolymer at least two charged blocks and type of opposite charge	Aqueous gel from block copolymer. Charged block copolymers. The aqueous composition is used as thickeners, in exploitation of petroleum or gas deposits; in detergents and cosmetics; and for metal treatment	**29**
157.	WO2002070861A1 US6579947B2 [317]	2001	2002 2003	Rhodia Chimie	Hydraulic fracturing fluid comprising a block copolymer containing at least one water-soluble block and one hydrophobic block	Hydraulic fluids based on block copolymers	**29**

(*continued*)

Table 24.9 (Continued)

Number	Priority[a)]	Date[b)]	Assignee	Title[c)]	Brief description	ZC(=S)S− [d)]
158. WO2003050195A2 US6906128B2 [318]	2001	2003 2005	Rhodia Chimie	Method for depositing a polymer onto a surface by applying a composition onto said surface	Water-borne hair/skin coatings	**29**
159. WO2003050185A1 US6933340B2 [319]	2001	2003 2005	Rhodia Chimie	Formulation comprising an ionic compound, a polyionic polymer, and a block copolymer	Block copolymer synthesized by RAFT used in cosmetics application	**29**
160. WO2003050184A1 US7235231B2 [320]	2001	2003 2007	Rhodia Chimie	Cosmetic composition comprising a block copolymer	The use of diblock copolymer as a modifier of properties of cosmetic compositions, copolymer comprises two blocks, block A and block B, wherein block A is a polycationic block and block B is a neutral block	**29**
161. WO2002090392A1 US6825290B2 [321]	2001	2002 2004	Rhodia Inc.	Process for the preparation of latices using block copolymers as surfactants	Hydrophilic–hydrophobic blocks as surfactants in making latex paints	**29**
162. WO2004044114A1 US7378033B2 [322]	2002	2004 2008	Rhodia Chemie	Crease-resistant composition comprising a copolymer of controlled architecture, for articles made of textile fibres	Block copolymer application	**29**
163. US7423161B2 [323] US7820831B2 [324]	2002 2002	2008 2010	Rhodia Chimie	Compounds comprising a thiocarbonyl-sulfanyl group, which can be used for the radical synthesis of-α-perfluoroalkylamines	LPO-initiated SUMI of functional xanthates	**29**

164.	WO2003076531A1 US7439292B2 [325]	2002	2003 2008	Rhodia Chimie	Use of block copolymers bearing phosphate and/or phosphonate functions as adhesion promoters or as protecting agents against the corrosion of a metallic surface	Block copolymers containing, e.g. 2-(methacryloyloxy)ethyl phosphate	**29**
165.	WO2005074631A2 US7468413B2 [326]	2004	2005 2008	Rhodia Inc.	Rare earth aggregate formulation using di-block copolymers	Block copolymers are made by RAFT and used in extracting, dispersing rare-earth metals, and forming nanoparticles	—
166.	WO2006097641A1 US8207273B2 [327]	2005	2006 2012	Rhodia Chimie	Block copolymers useful as tensioning agents	Styrene-*co*-MAA acrylate blocks made with xanthate RAFT agents	**29**
167.	WO2010046342A1 US8791058B2	2008	2010 2014	Rhodia Operations	Composition for household care containing a cationic nanogel	AM/MBA-based microgels	**29**
168.	WO2013113750A1 [328] US9487598B2	2012	2013 2016	Rhodia Operations	Live poly(*N*-vinyl lactam) reactive stabilizers for dispersed phase polymerization	NVP-based blocks	**29**
169.	WO2013113752A1 [329] US9255163B2	2012	2013 2016	Rhodia Operations	Dispersed phase polymerization of halogenated vinyl monomers in the presence of life reactive stabilizers	NVP-based blocks used as stabilizers for dispersion polymerization	**29**
170.	WO2014167056A1 [330] US10323175B2	2013	2014 2019	Rhodia Operations	Fracturing fluids based on associative polymers and on labile surfactants	High molar mass AM/AMPS/LMA as associative polymer	**29**

(*continued*)

Table 24.9 (Continued)

Number	Priority[a)]	Date[b)]	Assignee	Title[c)]	Brief description	ZC(=S)S− [d)]
171. WO2013060741A1 [331] US9580535B2	2011	2013 2017	Rhodia Operations	Preparation of amphiphilic block polymers by controlled radical micellar polymerisation	RAFT emulsion polymerization. Initial formation of a hydrophilic block. Rheology control agents. Oil recovery	**29**
172. WO2013132108A1 [332] US10160821B2	2012	2013 2018	Rhodia Operations	Controlled radical polymerization in water-in-water dispersion	Aqueous dispersion polymerization	**29**
173. WO2015144475A1 [333] US10450397B2	2014	2015 2019	Rhodia Operations	Amphiphilic multiblock polymers	RAFT emulsion polymerization. Initial formation of a hydrophilic block	**29**
174. US8829133B2 [334]	2012	2014	Ricoh, University of Hyogo	ABA triblock copolymer, thickener, and aqueous composition	Poly(11-acrylamidoundecanoic acid)-*block*-poly(DMAm)-*block*-poly(11-acrylamidoundecanoic acid) as thickener	**17**
175. US6841695B2 [335]	2003	2005	RohMax	Process for preparing dithioesters	Preparation of dithioester from dithioacid and olefin or dithiocarboxylic salt with alkyl halide by phase- transfer chemistry	**4**
176. WO2006105926A1 US8101559B2 [336] US8722601B2 [337]	2005	2006 2012 2014	Rohmax Additives Evonik	Polyalkyl (meth)acrylate copolymers having outstanding properties	Anti-friction oil additive	**4**
177. WO2007108867 A1US7498398B2 [338]	2001	2007 2009	SABIC Innovative Plastics	Thermoplastic composition, method of making, and articles formed therefrom	Polycarbonates, including acrylate blocks	**17**
178. US8757264B2 [339]	2010	2014	Schlumberger Technology Corporation	Viscous wellbore fluids	Amphiphilic copolymers comprising cucurbituril 8	**23**

179.	WO2004011505A1 [340]	2002	2004	Stichting Dutch Polymer Institute	Process for the copolymerization of a-olefins with vinyl monomers	RAFT copolymerization of α-olefins with acrylates	**4 17**
180.	WO2016005288A1 [341] WO2016012219A2 [342]	2104	2016	Smith & Nephew	Improvements in and relating to devices	Sensor comprising a hyperbranched PNIPAm	**41**
181.	WO2017029630A1 [343]	2015	2017	Stellenbosch University	3-methylene-2-pyrrolidone based polymers	RAFT (co)polymerization of NVP. Also other RDRP	**4 20**
182.	WO2016024240A1 [344] US10479854B2	2014	2016 2019	Stellenbosch University	Conjugate for treating malaria	PNVP biopolymer conjugate	**29**
183.	US6716948B1 [345] US7259217B2 [346]	1999	2004 2007	Symyx	Controlled-architecture polymers and use thereof as separation media	Star, branched, grafted, or hyper-branched polymers soluble or dispersible in aqueous media, useful for electrophoresis. Examples are alkoxyamines. RAFT agents claimed	—
184.	WO2001002452A1 US6692914B1 [347] US6833276B2 [348]	2000	2001 2004 2004	Symyx	Polymer brushes for immobilizing molecules to a surface or substrate, where the polymers have water-soluble or water-dispersible segments and probes bonded thereto	Biosensors for detecting the presence and concentration of bio-molecules in a biological sample. Silica surface–bound dithiocarbamates (or nitroxide)	**70**
185.	WO2002028932A2 US7067586B2 [349]	2000	2006	Symyx	Methods of making ABA-type block copolymers having a random block of hydrophobic and hydrophilic monomers	Bis-RAFT agents used for making ABA triblocks	**41**
186.	US6667376B2 [350]	2002	2003	Symyx	Control agents for living-type free radical polymerization and methods of polymerizing	RAFT agents Z–C(=S)S–R, where Z is –O–N(R^1)(R^2)	**36**

(*continued*)

Table 24.9 (Continued)

Number	Priority[a)]	Date[b)]	Assignee	Title[c)]	Brief description	ZC(=S)S–[d)]
187. US6803410B2 [351]	2003	2004	Symyx	Cellulose copolymers that modify fibres and surfaces	Grafts to cellulose using RAFT. The cellulosic backbone polymers allow for the modification of fibres or surfaces, preferably in presence of water to provide a desired effect	**29 41**
188. WO2005003192A1 US7250475B2 [352] US7399806B2 [353]	2003	2005 2007 2008	Symyx	Synthesis of photoresist polymers	Photoresists based on bulky methacrylates made by RAFT. Pyrazoline RAFT agent	**48 49**
189. WO2001098383A1 US6765078B2 [354]	2000	2001 2004	Tesa AG	Method for producing polyacrylates	Pressure-sensitive adhesives made by RAFT. Claim focuses on reaction conditions. Step claimed to be novel is late addition of a peroxide initiator to drive polymerization to high conversion and possibly introduce branching	**4 17**
190. US6703441B2 [355]	2001	2004	Tesa AG	Oriented acrylic block copolymers	Pressure-sensitive adhesives based on triblock copolymers. Bis(phenylethyl) trithiocarbonate) used in examples	**17**
191. US6720399B2 [356]	2001	2004	Tesa AG	UV-crosslinkable acrylic hotmelt PSAs with narrow molecular weight distribution	Acrylic triblocks made by RAFT as UV-curable pressure-sensitive adhesives	**17**

192. WO2003000794A1 US6723407B2 [357]	2001	2003 2004	Tesa AG	Strippable systems based on acrylic block copolymers	Polyacrylate-based block copolymers as pressure-sensitive adhesives with improved adhesive properties (especially adhesive strength)	**17**
193. US6723786B2 [358]	2001	2004	Tesa AG	Pressure sensitive adhesive, particularly for apolar surfaces	Acrylic triblocks made with trithiocarbonates as pressure-sensitive adhesives	**17**
194. WO2003046030A1 US7271203B2 [359]	2001	2003 2007	Tesa AG	Crosslinking of photoinitiator-initialized polyacrylates	A process for increasing the molecular weight of polyacrylates, where polyacrylates are functionalized at least on one part of their chain ends by photoinitiator groups X are exposed to UV radiation, so that a direct linking reaction of the polyacrylates takes place	**17**
195. WO2002010309 A1US7307115B2 [360]	2001	2002 2007	Tesa AG	Adhesive material based on block copolymers having a p(a)-p(b)-p(a) structure	Block copolymers of P(A)–P(B)–P(A) as pressure-sensitive adhesives made with RAFT, where P(A) has a glass transition temperature of 0 °C or below, P(B) has a glass transition temperature of 20 °C or above, and P(A) and P(B) are immiscible.	**17**
196. WO2003046031A1 US7402632B2 [361]	2001	2008	Tesa AG	2-Component crosslink of end-functionalized polyacrylates	A process for increasing the molecular weight of polyacrylates, wherein polyacrylates functionalized at least on some of their chain ends by functional groups X are prepared by the RAFT process using thiocarbonates	**17**

(*continued*)

Table 24.9 (Continued)

Number	Priority[a)]	Date[b)]	Assignee	Title[c)]	Brief description	ZC(=S)S−[d)]
197. WO2003000794A1 WO2003000819A1 US8129470B2 [362]	2001	2003 2003 2012	Tesa AG	Adhesive masses based on block copolymers of structure P(A)-P(B)-P(A) and P(B)-P(A)-P(B)	Triblock polymers made by RAFT in adhesive compositions	**17**
198. WO2004018582A1 US7514515B2 [363]	2002	2004 2009	Tesa AG	Method for the production of acrylate adhesive materials using metal-sulphur compounds	Pressure-sensitive adhesives. Contains metal complexes	**17**
199. WO2004015020A1 US7758933B2 [364]	2002	2004 2010	Tesa AG	Adhesive materials having a high refractive index based on acrylate block copolymers	Pressure-sensitive adhesive comprising an acrylate block copolymer with high refractive index	**17**
200. US7459499B2 [365]	2003	2008	Tesa AG	Pressure-sensitive adhesive based on acrylate block copolymers	Pressure-sensitive adhesive comprising an acrylate block copolymer having at least two chemically distinguishable, covalently interlinked acrylate polymer blocks P in microphase-separated regions and each having a softening temperature between −125 and +20 °C.	**17**
201. US7432326B2 [366]	2004	2008	Tesa AG	Pressure-sensitive adhesive based on acrylate block copolymers	The invention provides an acrylate-based pressure-sensitive adhesive comprising a polymer blend	**17**
202. WO2006027385A1 WO2006027386A1 US7605212B2 [367]	2004	2006 2006 2009	Tesa AG	Method for producing contact adhesive masses containing acrylic	Contact adhesives made by RAFT. Dibenzyl trithiocarbonate used	**17**
203. US8822130B2 [368]	2012	2014	Texas A&M University, Rohm and Haas Electronics Materials	Self-assembled structures, method of manufacture thereof and articles comprising the same	Photoresists based on graft-block copolymers	**4**

204.	WO2003010268A1 EP1409627B1 [369]	2001	2003 2005	Unilever	Use of compounds in products for laundry applications	Polysaccharide-based graft polymers. Isocyanate functional RAFT agents	**29 41**
205.	WO2004056952A1 US7179777B2 [370]	2002	2004 2007	Unilever Henkel	Laundry treatment compositions comprising a polymer with a cationic and polydialkylsiloxane moiety	A laundry treatment–based PDMS-*block*-(cationic polymer) that can be made by RAFT	On
206.	WO2009147338A1 US8598289B2 [371]	2008	2009 2013	Universite Pierre Et Marie Curie, CNRS, Univer-site De Liege	Amphiphilic block copolymer and method for preparing same	Amphiphilic PEO-based macroRAFT agents in emulsion	**4 23**
207.	US10023700B2 [372]	2016	2018	University of Alberta	Hydrogel	Hydrogel based on NIPAm/dopamine acrylamide copolymer segment for drug delivery	**23**
208.	US9158200B2 [373]	2013	2015	University of California	Compositions for controlled assembly and improved ordering of silicon-containing block copolymers	Silicon-containing blocks for lithographic applications. 4VP blocks by RAFT	**4**
209.	US8211996B2 [374]	2008	2012	University of Cali-fornia	Well-defined donor-acceptor rod-coil diblock copolymer based on P3HT containing C60	RAFT-made block copolymer	**26**
210.	US8153729B2 [375]	2008	2012	University of California Mitsubishi Chemical	Highly efficient agents for dispersion of nanoparticles in matrix materials	RAFT-synthesized hyperbranched polymers as dispersants	**4**

(*continued*)

Table 24.9 (Continued)

	Number	Priority[a)]	Date[b)]	Assignee	Title[c)]	Brief description	ZC(=S)S−[d)]
211.	US9676888B2 [376] US9452978B2 [377]	2010 2010	2017 2016	Mitsubishi Chemical	Chain transfer agent and emulsion polymerization using the same	Amphiphilic RAFT agents for emulsion polymerization. Aryl dithioester or trithiocarbonate where Z is hydrophilic group	Not listed
212.	WO 2013082196 [378] US 9925270B2 US10039807B2	2011	2013 2018 2018	University of California	bFGF-polymer conjugates, methods for making the same and applications thereof	Heparin-mimicking polymer and conjugates	**19**
213.	WO2016025668A1 [379] US10273333B2	2014	2016 2019	University of California	Substituted polyesters by thiol-ene modification: rapid diversification for therapeutic protein stabilization	Conjugates. Formation of trehalose co-polymers. Polyesters formed by RAFT ROP of BMDO	**19**
214.	WO2013112897A1 [380] US9901648B2 US10543280B2	2012	2013 2018 2020	University of California	Stabilization of biomolecules using sugar polymers	Glycopolymer conjugates for stabilization of biomolecules	**19**
215.	WO2006086646A2 US7943680B2 [381] US8404758B2 [382]	2005 2005	2006 2011 2013	University of Colorado	Stress relief for crosslinked polymers for dental materials	Use of a RAFT process to control stress in crosslinking polymerization. Dynamic covalent polymers	**17 79**
216.	US8877830B2 [383]	2005	2014	University of Colorado	Stress relief for crosslinked polymers	Dental application of polymer containing trithiocarbonate functionality. Dynamic covalent polymers	**17 79**

217. US9193682B2 [384]	2013	2016	University of Colorado	Synthesis of trithiocarbonates and allyl sulfides and their application into advances in covalent adaptable networks	Dynamic covalent polymers	**17 79**
218. US9758597B2 [385]	2011	2017	University of Colorado	Reducing polymerization-induced shrinkage stress by reversible addition-fragmentation chain transfer	Symmetrical RAFT agents used in crosslinking formulations	**17**
219. WO2019183140A1 [386]	2018	2019	University of Colorado	Tough, healable composites displaying stress relaxation at the resin-filler interface	Self-healing materials. Dynamic covalent polymers	**79**
220. US10512607B2 [387]	2015	2019	University of Florida Vanderbilt University	Polymeric particles, method for cytosolic delivery of cargo, methods of making the particles	Propacrylic acid–based polymer used in drug delivery	**23**
221. US8669335B2 [388]	2010	2014	University of Houston	Knotty polymers via supramolecularly templated macroinitiators and living polymerization and methods for making and using same	Macrocyclic structures. Various dithioesters and trithiocarbonates used	—
222. US8802235B2 [389]	2012	2014	University of Kansas	Drug and imaging agent delivery compositions and methods	Star polymers from multi-xanthate RAFT agent	**29**
223. US7687600B2 [390]	2004	2010	University of Massachusetts	Invertible amphiphilic polymers	Invertible micelles for drug delivery from block copolymers made by RAFT	**4**

(*continued*)

Table 24.9 (Continued)

Number	Priority[a]	Date[b]	Assignee	Title[c]	Brief description	ZC(=S)S–[d]
224. US8198368B2 [391] US8546488B2 [392]	2007 2007	2012 2013	University of Massachusetts	Cleavable block copolymers, functionalized nanoporous thin films and related methods of preparation	Thiol-terminated polymer converted to macroRAFT agent and used to make blocks	**4**
225. WO2009023158A2 US8969026B2 [393]	2007	2009 2015	University of Massachusetts	Polymeric reverse micelles as selective extraction agents and related methods of MALDI-MS analysis	Amphiphilic polymeric micelles	**4**
226. WO2012162307A2 [394] US9592302B2 US10358531B2	2011	2013 2017 2019	University of Massachusetts	Crosslinked polymer nano-assemblies and uses thereof	Encapsulated therapeutics	**4 23**
227. US10562901B2 [395]	2017	2020	University of Massachusetts	Temozolomide compounds, polymers prepared therefrom, and method of treating a disease	Polymer therapeutic containing temozolomide	**4**
228. US8496997B2 [396]	2010	2013	University of Melbourne	Process for the preparation of a cross-linked multilayer film	Layer-by-layer assembly and crosslinking process. RAFT used amongst other methods	**4**
229. US7999020B2 [397]	2007	2011	University of Minnesota	Ion gels and electronic devices utilizing ion gels	An ion gel, including an ionic liquid and a block copolymer	**23**
230. US8420704B2 [398]	2007	2013	University of Minnesota	Nano-structured polymer composites and process for preparing same	Crosslinked polymer monoliths with degradable block. RAFT agent not specified	—

231. US8840339B2 [399]	2008	2014	University of Queensland	Soil remediation process	Polymers containing groups with bind metals	**29**
232. WO2014152451A2 [400] US9949950B2 US10195284B2	2013	2014 2018 2019	University of Rochester	Compositions and methods for controlled localized delivery of bone forming therapeutic agents	Therapeutic delivery to bone	**19**
233. US8592539B2 [401]	2010	2013	University of South Carolina	Preparation of cobaltocenium-containing monomers and their polymers	No RAFT examples	—
234. US8865796B2 [402] US9109070B2 [403] US9475922B2	2011	2014	University of South Carolina	Nanoparticles with multiple attached polymer assemblies and use thereof in polymer composites	Surface-initiated RAFT polymerization multiple functionalization–polymerization–deactivation steps	**4**
235. US9725544B2 [404]	2013	2017	University of South Carolina	Preparation of conjugated aromatic/heteroaromatic oligomer-containing dielectric polymers and their applications	RAFT polymerization of macromonomers containing conjugated oligomeric (e.g. oligothiophene) segments	**4**
236. US9732169B2 [405] US10494461B2	2014	2017	University of South Carolina	Raft agents and their use in the development of polyvinyl-pyrrolidone grafted nanoparticles	Grafting from RAFT-functionalized silica nanoparticles	**41**
237. US10556980B2	2014	2020	University of South Carolina	Poly alkyl (meth)acrylates grafted nanoparticles and their methods of manufacture and use	Surface-initiated RAFT polymerization from particles	**4**

(*continued*)

Table 24.9 (Continued)

	Number	Priority[a]	Date[b]	Assignee	Title[c]	Brief description	ZC(=S)S–[d]
238.	US7138468B2 [406] US7417096B2 [407] US8084558B2 [408]	2002 2002 2002	2006 2008 2011	University of Southern Missis-sippi	Preparation of transition metal nanoparticles and surfaces modified with (co)polymers synthesized by RAFT	Gold and other nanoparticles from RAFT-made polymers, useful in optics, medicine, electronics, biochips, high-throughput screening, and biological transfer agents	**4**
239.	US7718432B2 [409]	2006	2010	University of Southern Missis-sippi	Non-immunogenic, hydrophilic/cationic block copolymers and uses thereof	HPMAm block copolymer for controlled-release applications	**4**
240.	WO2006037161A1 [410] US9731321B2	2004	2006 2017	University of Sydney	Polymerisation process and polymer product	RAFT in emulsion. Amphiphilic macroRAFT agents. TiO_2 particle encapsulation	**17 21**
241.	WO2007112503A1 US8796359B2 [411] US8779029B2 [411]	2006	2007 2014 2014	University of Sydney	Polymer product and interfacial polymerisation process using RAFT agent	Polymer-encapsulated particles made by RAFT emulsion polymerization	**21**
242.	WO2009137889A1 US8765183B2 [412]	2008	2009 2014	University of Sydney	Polymer microgel beads	Polymer-encapsulated magnetic nanoparticles made by RAFT emulsion polymerization	**21**
243.	WO2009137888A1 US8852641B2 [413]	2008	2009 2014	University of Sydney	Polymer microgel beads and preparative method thereof	Polymer-encapsulated magnetic nanoparticles made by RAFT emulsion polymerization	**21 22**

244.	WO2009137890A1 US8709486B2 [414]	2008	2009 2014	University of Sydney	Administrable compositions	Drug-delivery particles made by RAFT emulsion polymerization	**21**
245.	WO2011066608A1 [415] US9255198B2	2009	2010 2016	University of Sydney	Water swellable polymer materials comprising particulate core and water swellable RAFT polymer shell	Polymer-encapsulated particulate material (e.g. TiO_2) prepared by RAFT emulsionpolymerization	**17 21**
246.	WO2012142669A1 [416] US10376589B2 [417]	2011	2012 2019	University of Sydney	Method for the treatment of a solid tumour	Iron oxide nanoparticles formed by emulsion polymerization	**21**
247.	US7718193B2 [418]	2007	2010	University of Washington	Temperature- and pH-responsive polymer compositions	Block copolymers	**23**
248.	US7981688B2 [419] US8507283B2 [420]	2007 2007	2011 2013	University of Washington	Stimuli-responsive magnetic nanoparticles and related methods	Stimuli-responsive magnetic nanoparticles	**23**
249.	WO2011159721A2 US8426214B2 [421]	2009	2013	University of Washington	System and method for magnetically concentrating and detecting biomarkers	PNIPAm-based magnetic nanoparticles	**23**
250.	WO2009140427A2 [422] US9476063B2 US9862792B2	2008	2009 2016 2018	University of Washington, Genevant Sciences	Diblock copolymers and polynucleotide complexes thereof for delivery into cells	Block copolymers for therapeutic delivery of polynucleotides	**19**

(*continued*)

Table 24.9 (Continued)

Number	Priority[a)]	Date[b)]	Assignee	Title[c)]	Brief description	ZC(=S)S−[d)]
251. WO2009140421A2 [423] US9006193B2	2008	2009 2015	University of Washington, Genevant Sciences	Polymeric carrier	Block copolymers for therapeutic delivery	**19**
252. WO2010077678A2 [424] US9593169B2 US10066043B2	2008	2010 2017 2018	University of Washington, Genevant Sciences	ω-functionalized polymers, junction-functionalized block copolymers, polymer bioconjugates, and radical chain extension polymerization	Polymer conjugates with different architectures	**19**
253. WO2011062965A2 [425] US9415113B2	2009	2011 2016	University of Washington, Genevant Sciences	Targeting monomers and polymers having targeting blocks	Polymerization of monomer derivatives of folate	**19**
254. WO2009140429A2 [426] US9339558B2 US9662403B2 US10420790B2	2009	2010 2016 2017 2017	University of Washington, Genevant Sciences	Micellic assemblies comprising a plurality of copolymers	Therapeutic delivery	**19**
255. WO2018165194A1 [427] WO2018165198A1 [428]	2017	2018	University of Washington, CSIRO	Cell-based methods and compositions for therapeutic agent delivery and treatments using same	Therapeutic delivery	**19**
256. WO2019160983A1 [429]	2018	2019	University of Washington, CSIRO	Radiant star nanoparticle prodrugs and related methods	Stars with hyperbranched core made by RAFT used for therapeutic delivery	**19**
257. US9533006B2 [430] US10544312B2	2007	2017 2020	University of Washington	Marine coatings based on cationic polymers	Anti-fouling coatings based on copolymers containing betaines	**4**

258.	US9181432B2 [431] US10494485B2	2012	2013 2019	US Secretary of Army	Branched additives for polymer toughening	Thiol-functional polymer grafted to SBS by thiol-ene process. Other grafting processes also mentioned	**23**
259.	WO2017156250A2 [432] US10472450B2	2016	2019	US Secretary of Navy	Acute care cover for severe injuries	Wound dressings	**23**
260.	WO2014066912 [433] US10172956B2	2012	2014 2019	Vanderbilt Univer-sity	Polymeric nanoparticles	Library of PEG block copolymers synthesized	**19**
261.	US8197847B2 [434]	2006	2012	Warwick Effect Polymers	Process for making polymers and supports comprising pendant sugar side groups	Polymers with pendant azide or alkyne groups. Used for glycopolymer synthesis. No RAFT examples	—
262.	WO2016138528A1 [435] US10596300B2	2015	2016	Wayne State Uni-versity	Methods and compositions relating to biocompatible implants	Block copolymer used in hydrogel coating for implants	**17**
263.	WO2011140318A1 [436] US9815979B2 [437] US10301465B2	2010	2017	Johnson & Johnson Vision Care	Non-reactive, hydrophilic polymers having terminal siloxanes and methods for making and using the same	Polymers comprising a hydrophilic segment and a siloxane segment. Made by copolymerization of hydrophilic monomers using a siloxane-based RAFT agent (PNVP with xanthate, PDMAm with trithiocarbonate)	**22 29**
264.	WO2012151135A1 [438] US9170349B2 US9599751B2 US10386545B2	2011	2012 2015 2017 2019	Johnson & Johnson Vision Care	Medical devices having homogeneous charge density and methods for making same	Ionic silicone hydrogels as contact lens material	**22**

(*continued*)

Table 24.9 (Continued)

Number	Priority[a)]	Date[b)]	Assignee	Title[c)]	Brief description	ZC(=S)S–[d)]
265. WO2013176886A2 WO2013177506A2 [439] WO2013177523A2 [440] US9244196B2 US9297929B2 US9625617B2 US9726906B2 US10073192B2 US10502978B2 US10502867B2	2012	2013 2013 2013 2016 2016 2017 2017 2018 2019 2019	Johnson & Johnson Vision Care	Polymers and nanogel materials and methods for making and using the same	Contact lens material	**22**
266. US9428649B2 [220] US9732231B2 [221]	2010 2010	2016 2017	E Ink California	Electrophoretic dispersion Method of making electrophoretic dispersion	Polymer-grafted pigment particles made by surface-initiated RAFT	**4**

a) Priority date.
b) Date published.
c) Spelling of Title reflects that used on the patent document.
d) ZC(=S)S– groups exemplified (refer Table 24.6).

24.3.3 Synthesis of Stars and Nano- or Microgels by RAFT Polymerization

Star synthesis making use of multi-RAFT agents is described in the first RAFT patents (Table 24.7, entry 1). The arm-first method for synthesis of stars (also called microgels) involves a RAFT crosslinking copolymerization mediated by a macroRAFT agent (Table 24.7, entry 7). Use of a mixture of macroRAFT agents, in principle, provides a mikto-arm polymer (Table 24.7, entry 30). The core-first approach involves a RAFT crosslinking copolymerization to which arms are grafted by a subsequent RAFT polymerization step (Table 24.7, entries 30 and 32). These arm-first and core-first strategies can be combined in the so-called in–out method.

Other processes for star or microgel synthesis by RAFT polymerization involve the self-assembly of amphiphilic block copolymer followed by core or shell crosslinking (Table 24.7, entry 12) and self-condensing vinyl polymerization (Table 24.7, entry 36).

24.3.4 RAFT Applications

There are many patents that describe applications of RAFT polymerization. In the tabulation below we have, for the most part, limited the scope to patents that have progressed to being granted in the US and that have a working example making use of RAFT polymerization. We also indicate the type of RAFT agent used in those examples. Often a larger range of RAFT agents and sometimes RDRP methods is claimed.

This survey is not comprehensive but does serve to illustrate the potential applications of RAFT in an industrial/commercial context. Various bioapplications (therapeutic, cosmetic, ophthalmic) are highlighted in green. Patents relating to RAFT emulsion polymerization are shaded blue. Electronics applications (resists, polymer semiconductors) are shaded yellow.

Some open literature publications on the industrial application of RAFT polymerization have appeared [441–443]. The development of RAFT applications has been facilitated by the availability of RAFT agents in quantities suitable for research by Strem [444], Merck (Sigma Aldrich) [445, 446], and Boron Molecular under license from CSIRO. Recent years have seen the large-scale (multi-kg or, in a few cases, multi-ton) production of Rhodixan A1™ (**80**) by Rhodia (Solvay), Blocbuilder DB™ (**81**) by Arkema [447], CTA-1 (**84**) by Lubrizol [146], DOPAT (**82**) by Dulux, and CDTPA (**86**) by DuPont (Table 24.7, entry 30) [448] mainly for internal use within the respective companies. Those known to be listed on the European Chemical Agency C&L inventory are shown in Table 24.8. Only **80**, **81**, and **89** appear to be registered for REACH in Europe. RAFT agents **81** and **82** are registered under NICNAS in Australia. A wider range of thiocarbonylthio-RAFT agents, including **81**, **85**, and **86**, is available on scale for industry from Boron Molecular [449].

24.3.5 RAFT Thiocarbonylthio-End-Group Removal/Transformation

A significant amount of patent activity has concerned RAFT end-group removal (Table 24.10). In these patents, the methods are typically only exemplified for a very limited selection of RAFT agents and for a narrow range of polymers with those end groups. However, broad applicability for the various methods is usually claimed.

Table 24.10 Patents disclosing methods for RAFT end-group removal/transformation.

	Number	Priority[a)]	Date[b)]	Assignee	Title[c)]	Brief description	ZC(=S)S–[d)]
1.	WO2002072642A1 US7009004B2 [450] US7081503B2 [451]	2001	2002 2006 2006	Kaneka	Process producing vinyl polymer having alkenyl group at end, vinyl polymer, and curable composition	Alkene-terminated polymers made by RAFT end-group aminolysis and reaction thiol end polymer with allyl-isocyanate	**4**
2.	WO2002090397A1 US7109276B2 [452]	2001	2002 2006	Rhodia Chimie	Method for free radical reduction of dithiocarbonylated or dithiophosphorylated functions borne by a polymer	A method of removing thiocarbonylthio and dithiophosphoryl terminal groups by contacting it with a source of free radicals and an organic compound with a labile hydrogen atom.	**29**
3.	WO2002090424A1 US7396901B2 [453]	2001	2002 2008	Rhodia Chimie	Method for synthesis of polymers with thiol functions	Isobutyl xanthate end-group thermolysis	**31**
4.	WO2003070780A1 US6794486B2 [454]	2002	2003 2004	Rhodia Chimie	Process for removing a dithiocarbonyl group at the end of a polymer chain	Removal of thiocarbonylthio group by treatment with amine not triethanolamine in an organic solvent. Only example is aqueous ammonium hydroxide.	**29**

5.	WO2004089994A1 [455] US7012119B2	2001	2004 2006	Symyx	Cleaving and replacing thio-control agent moieties from polymers made by living-type free radical polymerization	End-group removal by heating with peroxide (LPO). Optional presence of addition–fragmentation transfer agents (AMS dimer) is mentioned.	**49**
6.	US20040266953A1 US6919409B2 [456]	2003	2004 2005	Symyx	Removal of the thiocarbonylthio or thiophosphorylthio end group of polymers and further functionalization thereof	RAFT end-group removal by chain transfer with a radical source. At least 50% of the thio-groups are replaced with a group of interest other than hydrogen.	**48 49**
7.	WO2005061555A1 [457] US20070299221A1 US20090215965A1 US20100160574A1	2003	2005 2007 2009 2010	University of Leeds	Polymerisation using chain transfer agents	RAFT end-group removal by radical-induced coupling. Solid-supported RAFT polymerization.	**4 25**
8.	WO2005040233A1 US7473740B2 [458] pub [459]	2003	2005 2009	Rhodia Chimie	Method for partial or total oxidation of one or several thiocarbonylthio ends of a polymer obtained by radical polymerisation controlled by reversible addition-fragmentation	Ozonolysis of RAFT end groups.	**29**
9.	WO2005113612A1 US7807755B2 [460]	2004	2005 2010	CSIRO	Method for removing sulfur-containing end-groups	End-group removal with radical-induced reduction with hypophosphite	**4 23**

(*continued*)

Table 24.10 (Continued)

	Number	Priority[a)]	Date[b)]	Assignee	Title[c)]	Brief description	ZC(=S)S–[d)]
10.	WO2013086585A1 [461] US9650450B2	2011	2013 2017	CSIRO	RAFT polymers	End-group removal in continuous flow by thermolysis, radical-induced reduction, or aminolysis	**4 18 23 25**
11.	US8283436B2 [462]	2006	2012	CSIRO	Process for synthesizing thiol terminated polymers	Use of functional reagent in end-group removal	**4 23**
12.	WO2013062789A1 [463]	2012	2013	DuPont	Processes for removing sulfur-containing end groups from polymers	Improved procedure for end-group removal with hypophosphite	**23**
13.	WO2017027557A1 [464] US20180155463A1	2015	2017	Henkel	Thiocarbonylthio-free RAFT polymers and the process of making the same	End-group removal with hydrogen peroxide	**23**
14.	WO2018017478A1 [465]	2016	2018	University of California	Catalytic functional group removal from a polymer	End-group removal with use of photoredox catalyst and H-atom donor	**23**
15.	WO2020100086A1 [466]	2018	2020	KAUST	Removal of thiocarbonylthio end groups from polymers synthesized by reversible addition-fragmentation chain transfer polymerization	End-group removal with trialkylborane plus oxygen.	**4 23 29 66**

a) Priority date.
b) Date published.
c) Spelling of Title reflects that used on the patent document.
d) ZC(=S)S– groups exemplified (refer Table 24.6).

Table 24.10 is not a comprehensive list of patents disclosing methods for end-group removal. It contains most patents where end-group removal is a primary focus. Detailed discussion on end-group removal/transformation can be found in the chapter by Lowe and Dallerba [467] and is given some coverage in the chapters on the individual classes of RAFT agents (i.e. dithioesters [468], trithiocarbonates [145], xanthates [469], dithiocarbamates [470]).

Abbreviations

AA	acrylic acid
ATRP	atom-transfer radical polymerization
BMDO	5,6-benzo-2-methylene-1,3-dioxepane
CCT	catalytic chain transfer
DMAm	*N,N*-dimethylacrylamide
HPMAm	*N*-(2-hydroypropyl)methacrylamide
LAM	less activated monomer
LPO	lauroyl peroxide
MAM	more activated monomer
MMA	methyl methacrylate
NIPAm	*N*-isopropylacrylamide
NMP	nitroxide-mediated polymerization
NVP	*N*-vinyl pyrrolidone
PDMS	poly(dimethylsiloxane)
PEG	poly(ethylene glycol)
PEO	poly(ethylene oxide)
RDRP	reversible-deactivation radical polymerization
ROMP	ring-opening metathesis polymerization
ROP	ring-opening polymerization
SUMI	single-unit monomer insertion
VAc	vinyl acetate
4VP	4-vinylpyridine

References

1 Favier, A., de Lambert, B., and Charreyre, M.-T. (2008). Toward new materials prepared via the RAFT process: from drug delivery to optoelectronics? In: *Handbook of RAFT Polymerization* (ed. C. Barner-Kowollik), 483–535. Weinheim: Wiley-VCH. doi: 10.1002/9783527622757.ch13.

2 Destarac, M. (2010). Controlled radical polymerization: industrial stakes, obstacles and achievements. *Macromol. React. Eng.* 4: 165–179. doi: 10.1002/mren.200900087.

3 Destarac, M. (2018). Industrial development of reversible-deactivation radical polymerization: is the induction period over? *Polym. Chem.* 9: 4947–4967. doi: 10.1039/C8PY00970H.

4 Moad, G. (2022). Terminology in reversible deactivation radical polymerization (RDRP) and reversible addition-fragmentation chain transfer (RAFT) polymerization. In: *RAFT Polymerization: Materials, Synthesis and Applications* (eds. G. Moad, E. Rizzardo), 15–24. Weinheim: Wiley-VCH.

5 Cacioli, P., Hawthorne, D.G., Laslett, R.L. et al. (1986). Copolymerization of w-unsaturated oligo(methyl methacrylate): new macromonomers. *J. Macromol. Sci., Chem.* A23: 839–852. doi: 10.1080/00222338608069476.

6 Antonelli, J.A., Scopazzi, C., and Doherty, M.M. (1991). Process for preparing stabilized polymer dispersion. US5010140A. du Pont de Nemours, E. I., and Co.

7 Darmon, M.J., Berge, C.T., and Antonelli, J.A. (1993). Process of polymerization in an aqueous system. WO9322351A1. du Pont de Nemours, E. I., and Co.

8 Antonelli, J.A. and Scopazzi, C. (1994). Star polymers made from macromonomers made by cobalt chain transfer process. US5310807A. du Pont de Nemours, E. I., and Co.

9 Moad, G., Moad, C.L., Krstina, J. et al. (1996). Preparation of block copolymer with low dispersity by radical polymerization. WO9615157A1. Du Pont/CSIRO.

10 Chang, D.C.K. and Fryd, M. (1999). Water-thinned coatings compositions containing self-stabilized crosslinked latexes. WO9903937A1. E. I. Du Pont de Nemours & Co.

11 Gridnev, A.A. and Ittel, S.D. (1996). Synthesis of terminally unsaturated oligomers. WO9633224A1. E. I. Du Pont de Nemours & Co.

12 Ma, S.-H. and Fryd, M. (1998). Aqueous dispersions containing graft copolymers as the dispersants. EP826751A2. E. I. Du Pont de Nemours & Co.

13 Moad, G., Rizzardo, E., Moad, C.L. et al. (1997). Catalytic polymerization process and the resulting polymers with terminal unsaturation. WO9731030A1. E. I. Du Pont de Nemours & Co., USA; Commonwealth Scientific & Industrial Research Organization; Moad, G., Rizzardo, E., Moad, C.L., Ittel, S.D., Wilczek, L., Gridnev, A.A.

14 Berge, C.T., Fryd, M., Johnson, J.W. et al. (2003). Process for preparing star shaped microgels from macromonomers with terminal ethylenic unsaturation. US6653407B2. duPont/CSIRO/University of Melburne.

15 Fryd, M. and Visscher, K.B. (2000). Dispersions having improved stability using polymer dispersant for encapsulating pigment. WO2000020520A1. E. I. Du Pont de Nemours & Co.

16 Donald, D.S., Hertler, W.R., and Ma, S.-H. (2001). Block copolymer dispersing agents for inks with enhanced substrate binding characteristics. US6306994B1. E. I. Du Pont de Nemours & Co.

17 Berge, C.T., Chiefari, J., Johnson, J.W. et al. (2001). Microgel synthesis and products produced therefrom. WO2001077198A1. E. I. Du Pont de Nemours & Co; Commonwealth Scientific and Industrial Research Organization.

18 Huybrechts, J. (2001). Aqueous polymer emulsions for coatings. EP1138730A2. E. I. Dupont De Nemours and Co.

19 Ma, S.-H. and Kelly, R.J. (2006). Rapid drying lacquers containing triblock copolymer for rheology control. US20060287437A1. E. I. du Pont de Nemours and Co., USA.

20 Goebelt, B., Omeis, J., Orth, U. et al. (2008). Graft (block)copolymers for wetting agents or dispersants for powders. WO2008080579A1. BYK-Chemie G.M.b.H., Germany.

21 Goebelt, B., Nagel, C., Omeis, J. et al. (2009). Wetting and dispersing agent. WO2009098025A1. BYK-Chemie GmbH, Germany.

22 Ma, S.-H. (2010). Producing block copolymer pigment dispersants. US20100081769A1. E. I. Du Pont de Nemours and Company, USA.

23 Ma, S.-H. (2010). Block copolymer pigment dispersants. WO2010036867A1. E. I. Du Pont de Nemours and Company, USA.

24 Ma, S.-H. (2011). Block copolymer pigment dispersants. US20110144263A1. E. I. Du Pont De Nemours and Company, USA.

25 Joly, G.D., Abuelyaman, A.S., Fornof, A.R. et al. (2014). Addition-fragmentation agents used in dental compositions. WO2014074427A1. 3M Innovative Properties Company, USA.

26 Moser, W.H., Fornof, A.R., Joly, G.D. et al. (2016). Addition-fragmentation process for preparation of stress-reducing crosslinked oligomers and dental applications. WO2016133668A1. 3M Innovative Properties Company, USA.

27 Krstina, J., Moad, G., Rizzardo, E. et al. (1995). Narrow polydispersity block copolymers by free-radical polymerization in the presence of macromonomers. *Macromolecules* 28: 5381–5385. doi: 10.1021/ma00119a034.

28 Krstina, J., Moad, C.L., Moad, G. et al. (1996). A new form of controlled growth free radical polymerization. *Macromol. Symp.* 111: 13–23. doi: 10.1002/masy.19961110104.

29 Zhang, M. and Hutchinson, R.A. (2018). Synthesis and utilization of low dispersity acrylic macromonomer as dispersant for nonaqueous dispersion polymerization. *Macromolecules* 51: 6267–6275. doi: 10.1021/acs.macromol.8b01169.

30 Yang, W. and Hutchinson, R.A. (2016). Investigating the effectiveness of reactive dispersants in non-aqueous dispersion polymerization. *Macromol. React. Eng.* 10: 71–81. doi: 10.1002/mren.201500028.

31 Shegiwal, A., Wemyss, A.M., Schellekens, M.A.J. et al. (2019). Exploiting catalytic chain transfer polymerization for the synthesis of carboxylated latexes via sulfur-free RAFT. *J. Polym. Sci., Part A: Polym. Chem.* 57: E1–E9. doi: 10.1002/pola.29302.

32 Engelis, N.G., Anastasaki, A., Whitfield, R. et al. (2018). Sequence-controlled methacrylic multiblock copolymers: expanding the scope of sulfur-free RAFT. *Macromolecules* 51: 336–342. doi: 10.1021/acs.macromol.7b01987.

33 Engelis, N.G., Anastasaki, A., Nurumbetov, G. et al. (2016). Sequence-controlled methacrylic multiblock copolymers via sulfur-free RAFT emulsion polymerization. *Nat. Chem.* 9: 171–178. doi: 10.1038/nchem.2634.

34 Gridnev, A.A. and Ittel, S.D. (2001). Catalytic chain transfer in free-radical polymerizations. *Chem. Rev.* 101: 3611–3660. doi: 10.1021/cr9901236.

35 Heuts, J.P.A. and Smeets, N.M.B. (2011). Catalytic chain transfer and its derived macromonomers. *Polym. Chem.* 2: 2407–2423. doi: 10.1039/C1PY00224D.

36 Slavin, S., McEwan, K., and Haddleton, D.M. (2012). Cobalt-catalyzed chain transfer polymerization: a review. *Polymer Science: A Comprehensive Reference* (eds. K. Matyjaszewski and M. Möller), 249–275. Amsterdam: Elsevier. doi: 10.1016/B978-0-444-53349-4.00068-6.

37 Demarteau, J., Debuigne, A., and Detrembleur, C. (2019). Organocobalt complexes as sources of carbon-centered radicals for organic and polymer chemistries. *Chem. Rev.* 119: 6906–6955. doi: 10.1021/acs.chemrev.8b00715.

38 Enikolopov, N.S., Korolev, G.V., Marchenko, A.P. et al. (1980). Molecular weight control of methacrylic polymers. SU664434A1. Institute of Chemical Physics, Chernogolovka, USSR; Siberian Institute of Petroleum Chemistry.

39 Carlson, G.M. and Abbey, K.J. (1985). Low-molecular-weight polymers and copolymers. US4526945A. SCM Corp.

40 Lin, J.C. and Abbey, K.J. (1987). Low molecular weight polymers and copolymers. US4680354A. Glidden Co., USA.

41 Melby, L.R., Janowicz, A.H., and Ittel, S.D. (1986). Cobalt(II) chelates as chain-transfer agents in free-radical polymerizations. EP199436A1. du Pont de Nemours, E. I., and Co.

42 Janowicz, A.H. (1987). Pentacyanocobaltate (II) catalytic chain transfer agents for molecular weight control in free radical polymerization. EP229481A2. du Pont de Nemours, E. I., and Co.

43 Janowicz, A.H. (1989). Process and agents for molecular weight control in free-radical polymerization reactions of acrylic and/or styrene monomers. US4886861A. du Pont de Nemours, E. I., and Co.

44 Janowicz, A.H. (1988). Bimetallic catalytic chain transfer agents for molecular weight control in free radical polymerization. US4746713A. du Pont de Nemours, E. I., and Co.

45 Janowicz, A.H. (1991). Catalytic chain-transfer agents for macromer preparation. US5028677A. du Pont de Nemours, E. I., and Co.

46 Hawthorne, D.G. (1987). Oligomerization process. WO8703605A1. Commonwealth Scientific and Industrial Research Organization, Australia.

47 Haddleton, D.M., Muir, A.V.G., and Leeming, S.W. (1995). Free radical polymerization process. WO9517435A1. Zeneca Ltd.

48 Haddleton, D.M., Muir, A.V.G., Leeming, S.W. et al. (1996). Cobalt complex preparation and use for molecular weight control in oligomerization. WO199613527A1. Zeneca Limited.

49 Gridnev, A.A. (1999). Process and cobalt coordination complex catalysts for the preparation of dimers from α-methylstyrenes. WO9941218A1. E. I. Du Pont de Nemours & Co.

50 Gridnev, A.A. and Nikiforov, G.A. (2002). Preparation of alkylcobalt(III) dioximates as polymerization catalysts. US20020087006A1. E. I. Du Pont de Nemours and Company.

51 Rizzardo, E., Meijs, G.F., and Thang, S.H. (1995). Chain transfer by radical addition-fragmentation mechanisms: synthesis of macromonomers and end functional oligomers. *Macromol. Symp.* 98: 101–123. doi: 10.1002/masy.19950980109.

52 Moad, G., Rizzardo, E., and Thang, S.H. (2008). Radical addition-fragmentation chemistry in polymer synthesis. *Polymer* 49: 1079–1131. doi: 10.1016/j.polymer.2007.11.020.

53 Moad, G., Rizzardo, E., and Thang, S.H. (2012). Radical addition-fragmentation chemistry and RAFT polymerization. *Polymer Science: A Comprehensive Reference*, vol. 3 (eds. K. Matyjaszewski and M. Möller), 181–226. Amsterdam: Elsevier. doi: 10.1016/B978-0-444-53349-4.00066-2.

54 Colombani, D. and Chaumont, P. (1996). Addition-fragmentation processes in free radical polymerization. *Prog. Polym. Sci.* 21: 439–503. doi: 10.1016/0079-6700(95)00024-0.

55 Colombani, D. (1999). Driving forces in free radical addition-fragmentation processes. *Prog. Polym. Sci.* 24: 425–480.

56 Rizzardo, E., Meijs, G.F., and Thang, S.H. (1988). Control of molecular weight and end group functionality of polymers. WO8804304A1. Commonwealth Scientific and Industrial Research Organization, Australia.

57 Rizzardo, E., Meijs, G.F., and Thang, S.H. (1999). Free-radical chain transfer polymerization process. US5932675A. Commonwealth Scientific and Industrial Research Organisation, Australia.

58 Rizzardo, E., Thang, S.H., Moad, G., and Berge, C.T. (1995). Allylic chain transfer agents. WO9512568A1. Commonwealth Scientific and Industrial Research Organisation, Australia.

59 Rizzardo, E., Thang, S.H., Moad, G., and Chong, Y.K. (1997). Control of molecular weight and end-group functionality in addition polymers. WO9713792A1. Commonwealth Scientific and Industrial Research Organisation, Australia; E. I. Du Pont de Nemours & Co.; Rizzardo, E., Thang, S.H., Moad, G., Chong, Y.K.

60 Desobry, V., Murer, P., and Schuwey, A. (2000). Thermal- and photoinitiated radical polymerization in the presence of an addition fragmentation agent. WO2000011041A1. Ciba Specialty Chemicals Holding.

61 Kulkarni, M.G. and Patil, P.M. (2007). Water-soluble macromonomers containing terminal unsaturation and their preparation. WO2007110882A1. Council of Scientific & Industrial Research, India.

62 Chiefari, J., Moad, G., Rizzardo, E., and Gridnev, A.A. (1998). Method of macromonomer synthesis. WO9847927A1. DuPont/CSIRO.

63 Le, T.P., Moad, G., Rizzardo, E., and Thang, S.H. (1998). Polymerization with living characteristics. WO9801478A1. DuPont/CSIRO.

64 Le, T.P., Moad, G., Rizzardo, E., and Thang, S.H. (2007). Polymerization with living characteristics. US7250479B2. CSIRO.

65 Le, T.P., Moad, G., Rizzardo, E., and Thang, S.H. (2010). Polymerization with living characteristics. US7662986B2. CSIRO.

66 Le, T.P., Moad, G., Rizzardo, E., and Thang, S.H. (2010). Polymerization with living characteristics. US7666962B2. CSIRO.

67 Le, T.P., Moad, G., Rizzardo, E., and Thang, S.H. (2010). Polymerization with living characteristics. US7714075B1. CSIRO.

68 Chiefari, J., Chong, Y.K., Ercole, F. et al. (1998). Living free-radical polymerization by reversible addition-fragmentation chain transfer – the RAFT process. *Macromolecules* 31: 5559–5562. doi: 10.1021/ma9804951.

69 Chong, Y.K., Le, T.P.T., Moad, G. et al. (1999). A more versatile route to block copolymers and other polymers of complex architecture by living radical polymerization – the RAFT process. *Macromolecules* 32: 2071–2074. doi: 10.1021/ma981472p.

70 Moad, G., Chiefari, J., Krstina, J. et al. (2000). Living free radical polymerization with reversible addition fragmentation chain transfer (the life of RAFT). *Polym. Int.* 49: 993–1001. doi: 10.1002/1097-0126(200009)49:9<993::AID-PI506>3.0.CO;2-6.

71 Rizzardo, E., Chiefari, J., Mayadunne, R.T.A. et al. (2000). Synthesis of defined polymers by reversible addition fragmentation chain transfer. In *Controlled/Living Radical Polymerization*, ACS Symposium Series 768 (ed. K. Matyjaszewski), 278–296. Washington, DC: American Chemical Society. doi: 10.1021/bk-2000-0768.ch020.

72 Rizzardo, E., Thang, S.H., and Moad, G. (2003). Synthesis of dithioester chain transfer agents and use of bis(thioacyl) disulfides or dithioesters as chain transfer agents. WO1999005099A1. CSIRO/DuPont.

73 Rizzardo, E., Thang, S.H., and Moad, G. (2003). Synthesis of dithioester chain transfer agents and use of bis(thioacyl) disulfides or dithioesters as chain transfer agents. US6512081B1. CSIRO/DuPont.

74 Thang, S.H., Chong, Y.K., Mayadunne, R.T.A. et al. (1999). A novel synthesis of functional dithioesters, dithiocarbamates, xanthates and trthicarbonates. *Tetrahedron Lett.* 40: 2435–2438. doi: 10.1016/S0040-4039(99)00177-X.

75 Corpart, P., Charmot, D., Zard, S.Z. et al. (1998). Method for block polymer synthesis by controlled radical polymerisation. WO1998058974A1. Rhodia Chimie.

76 Corpart, P., Charmot, D., Zard, S.Z. et al. (2000). Method for block polymer synthesis by controlled radical polymerisation. US6153705A. Rhodia Chimie.

77 Charmot, D., Corpart, P., Adam, H. et al. (2000). Controlled radical polymerization in dispersed media. *Macromol. Symp.* 150: 23–32. doi: 10.1002/1521-3900(200002)150:1<23::AID-MASY23>3.0.CO;2-E.

78 Taton, D., Wilczewska, A.Z., and Destarac, M. (2001). Direct synthesis of double hydrophilic statistical di- and triblock copolymers comprised of acrylamide and acrylic acid units via the MADIX process. *Macromol. Rapid Commun.* 22: 1497–1503. doi: 10.1002/1521-3927(20011201)22:18<1497::AID-MARC1497>3.0.CO;2-M.

79 Bouhadir, G., Charmot, D., Corpart, P., and Zard, S. (2003). Synthesis method for block polymers by controlled radical polymerization from dithioester compounds. US6545098B1. Rhodia Chimie.

80 Corpart, P., Charmot, D., Zard, S. et al. (1999). Method for block polymer synthesis by controlled radical polymerization from dithiocarbamate compounds. WO1999035177A1. Rhodia Chimie.

81 Corpart, P., Charmot, D., Zard, S. et al. (2004). Method for block polymer synthesis by controlled radical polymerization from dithiocarbamate compounds. US6812291B1. Rhodia Chimie.

82 Destarac, M., Charmot, D., Franck, X., and Zard, S.Z. (2000). Dithiocarbamates as universal reversible addition-fragmentation chain transfer

agents. *Macromol. Rapid Commun.* 21: 1035–1039. doi: 10.1002/1521-3927(20001001)21:15<1035::AID-MARC1035>3.0.CO;2-5.

83 Chiefari, J., Mayadunne, R.T., Moad, G. et al. (1999). Polymerization with living characteristics with controlled dispersity using chain transfer agents. WO9931144A1. E. I. Du Pont De Nemours and Company, USA; Commonwealth Scientific and Industrial Research Organization.

84 Chiefari, J., Mayadunne, R.T., Moad, G. et al. (2003). Polymerization process with living characteristics and polymers made therefrom. US6642318B1. du Pont/CSIRO.

85 Chiefari, J., Mayadunne, R.T., Moad, G. et al. (2004). Polymerization process with living characteristics and polymers made therefrom. US6747111B2. du Pont/CSIRO.

86 Mayadunne, R.T.A., Rizzardo, E., Chiefari, J. et al. (1999). Living radical polymerization with reversible addition-fragmentation chain transfer (RAFT polymerization) using dithiocarbamates as chain transfer agents. *Macromolecules* 32: 6977–6980. doi: 10.1021/ma9906837.

87 Berge, C.T., Fryd, M., Johnson, J.W. et al. (2002). Microgels and process for their preparation. US6355718B1. duPont/CSIRO.

88 Berge, C.T., Fryd, M., Johnson, J.W. et al. (2002). Microgels and process for their preparation. US6462114B2. duPont.

89 Berge, C.T., Fryd, M., Johnson, J.W. et al. (2003). Microgels and process for their preparation. US6646055B2. duPont/CSIRO.

90 Berge, C.T., Fryd, M., Johnson, J.W. et al. (2004). Microgels and process for their preparation. US6822056B2. duPont/CSIRO.

91 Matyjaszewski, K., Lutz, J.-f., and Shinoda, H. (2006). Process for preparation of graft polymers. US7049373B2. Carnegie Mellon University, USA.

92 Destarac, M., Charmot, D., Zard, S., and Franck, X. (2004). Synthesis method for polymers by controlled radical polymerisation using halogenated xanthates. US6777513B1. Rhodia Chimie.

93 Destarac, M., Charmot, D., Zard, S., and Gauthier-Gillaizeau, I. (2004). Synthesis method for polymers by controlled radical polymerisation with xanthates. US6809164B2. Rhodia Chimie.

94 Destarac, M., Charmot, D., Zard, S., and Gauthier-Gillaizeau, I. (2007). Synthesis method for polymers by controlled radical polymerisation with xanthates. US7285610B2. Rhodia Chimie.

95 Bett, W., Castaing, J.-c., and D'Allest, J.-f. (2001). Surface chemistry modified latex and redispersible powders, production and use thereof. WO2001042325A1. Rhodia Chimie.

96 Berge, C.T., Chiefari, J., Johnson, J.W. et al. (2006). Process of microgel synthesis and products produced therefrom. US7064151B1. duPont/CSIRO.

97 Charmot, D. and Chang, H.T. (2002). Heterocycle containing control agents for living-type free radical polymerization. US6395850B1. Symyx Technologies, Inc.

98 Charmot, D., Chang, H.T., and Huefner, P. (2002). Control agents for living-type free radical polymerization, methods of polymerizing and polymers with same. US6380335B1. Symyx Technologies, Inc.

99 Charmot, D., Chang, H.T., and Li, Y. (2002). Compounds useful for control agents for living-type free radical polymerization. US6482909B2. Symyx Technologies, Inc.

100 Chang, H.T., Charmot, D., and Li, Y. (2003). Compounds useful for control agents for living-type free radical polymerization. US6518448B2. Symyx Technologies, Inc.

101 Charmot, D. and Chang, H.T. (2003). Control agents for living-type free radical polymerization, methods of polymerizing and polymers with same. US6569969B2. Symyx Technologies, Inc.

102 Charmot, D., Chang, H.T., Li, Y., and Huefner, P. (2005). Control agents for living-type free radical polymerization, methods of polymerizing and polymers with same. US6841624B2. Symyx Technologies, Inc.

103 Charmot, D., Chang, H.T., and Wang, W. (2005). Control agents for living-type free radical polymerization, methods of polymerizing and polymers with same. US6844407B2. Symyx Technologies, Inc.

104 Destarac, M. (2005). Method for block polymer synthesis by controlled radical polymerization in the presence of a disulphide compound. US6916884B2. Rhodia Chimie.

105 Destarac, M., Leising, F., Dureault, A. et al. (2002). Synthesis of block polymers obtained by controlled free radical polymerization. WO2002036640A1. Rhodia Chimie.

106 Destarac, M., Leising, F., Gnanou, Y. et al. (2007). Method for synthesis of block polymers by controlled free radical polymerization. US7247688B2. Rhodia Chimie.

107 Lai, J.T. (2003). S,S′-bis-(α,α-disubstituted-α″-acetic acid)-trithiocarbonates and derivatives as initiator-chain transfer agent-terminator for controlled radical polymerizations and the process for making the same. 6596899. Noveon.

108 Lai, J.T. (2005). S,S′-bis-(α,α-disubstituted-α″-acetic acid)-trithiocarbonates and derivatives as initiator-chain transfer agent-terminator for controlled radical polymerizations and the process for making the same. US6962961B2. Noveon.

109 Lai, J.T. (2007). S,S′-bis-(α,α-disubstituted-α″-acetic acid)-trithiocarbonates and derivatives as initiator-chain transfer agent-terminator for controlled radical polymerizations and the process for making the same. US7279591B2. Noveon.

110 Lai, J.T.-Y. (2009). S-S′-bis-(α,α′-Disubstituted-α″-acetic acid) – trithiocarbonates and derivatives as initiator-chain transfer agent-terminator for controlled radical polymerizations and the process for making the same. US7495128. Lubrizol.

111 Lai, J.T.-Y. (2010). S,S′-bis-(α,α′-Disubstituted-α″-acetic acid) – trithiocarbonates and derivatives as initiator-chain transfer agent-terminator for controlled radical polymerizations and the process for making the same. US7659345B2. Lubrizol.

112 Lai, J.T., Filla, D., and Shea, R. (2002). Functional polymers from novel carboxyl-terminated trithiocarbonates as highly efficient RAFT agents. *Macromolecules* 35: 6754–6756. doi: 10.1021/ma020362m.

113 Lai, J.T.-Y. (2008). S-(α,α′-disubstituted-α″-acetic acid) substituted dithiocarbonate derivatives for controlled radical polymerizations, process and polymers made therefrom. US7335788B2. Lubrizol Advanced Materials, Inc.

114 Lai, J.T.-Y. (2010). S-(α,α′-disubstituted-α″-acetic acid) – substituted dithiocarbonate derivatives for controlled radical polymerizations, process and polymers made therefrom. US7851582. Lubrizol.

115 Lai, J.T. and Shea, R. (2006). Controlled radical polymerization by carboxyl- and hydroxyl-terminated dithiocarbamates and xanthates. *J. Polym. Sci., Part A: Polym. Chem.* 44: 4298–4316. doi: 10.1002/pola.21532.

116 Lai, J.T.-Y. (2007). S,S′-bis-(α,α-disubstituted-α″-acetic acid)-substituted dithiocarbonate derivatives for controlled radical polymerizations, process and polymers made therefrom. US7205368B2. Noveon, Inc.

117 Lai, J.T.-Y. (2009). S-(α,α′-disubstituted-α″-acetic acid) substituted dithiocarbonate derivatives for controlled radical polymerization, process and polymers made therefrom. US7498456. Lubrizol

118 Charmot, D., Chang, H.T., Huefner, P., and Li, Y. (2003). Emulsion living-type free radical polymerization, methods and products of same. US6518364B2. Symyx Technologies, Inc.

119 Catala, J.-M. (2007). Radical polymerization method performed in the presence of disulfide compounds. US7214751B2. Rhodia Chimie.

120 Destarac, M. and Bzducha, W. (2008). Controlled mini-emulsion free radical polymerization. US7317050B2. Rhodia Chimie.

121 Such, C.H., Rizzardo, E., Serelis, A.K. et al. (2010). Aqueous dispersions of polymer particles. US7745553B2. University of Sydney.

122 Matyjaszewski, K., Kirci, B., Lutz, J.F., and Pintauer, T. (2006). Process for monomer sequence control in polymerizations. US7064166B2. Carnegie Mellon University.

123 McCormick, C.L., Donovan, M.S., Lowe, A.B. et al. (2005). Chain transfer agents for raft polymerization in aqueous media. US6855840B2. University of Southern Mississippi.

124 McCormick, C.L., Donovan, M.S., Lowe, A.B. et al. (2007). Chain transfer agents for RAFT polymerization in aqueous media. US7179872B2. University of Southern Mississippi.

125 McCormick, C.L., Donovan, M.S., Lowe, A.B. et al. (2007). Chain transfer agents for RAFT polymerization in aqueous media. US7186786B2. University of Southern Mississippi.

126 McCormick, C.L., Donovan, M.S., Lowe, A.B. et al. (2008). Chain transfer agents for RAFT polymerization in aqueous media. US7402690B2. University of Southern Mississippi.

127 Benicewicz, B. and Li, C. (2008). Low odor chain transfer agents for controlled radical polymerization. US7332552B2. Rensselaer Polytechnic Institute.

128 Pitois, C., Destarac, M., and Taton, D. (2008). Synthesis of mikto-star copolymers by controlled radical polymerization. US20080114128A1. Rhodia Chimie.

129 Farnham, W.B. (2009). Synthesis of trithiocarbonate raft agents and intermediates thereof. US7632966B2. du Pont.

130 Pitois, C. and Karagianni, K. (2007). Composition for treating and/or modifying hard surfaces, containing a synthetic polymer. WO2007071591A1. Rhodia Operations.

131 Couvreur, L. and Magnet, S. (2013). Copolymers based on methacrylate units, preparation method thereof and use of same. US8389643B2. Arkema.

132 Venkatesh, R. and Raman, V.I. (2014). Process for the preparation of an aqueous polymer dispersion. US8912273B2. BASF SE.

133 Kwak, Y., Nicolay, R., and Matyjaszewski, K. (2013). Controlled radical polymerization processes. US8445610B2. Carnegie Mellon University.

134 Jakubowski, W. and Spanswick, J. (2014). Control over controlled radical polymerization processes. US8815971B2. ATRP Solutions.

135 Jakubowski, W. and Spanswick, J. (2015). Control over controlled radical polymerization processes. US9012528B2. ATRP Solutions.

136 Jakubowski, W. and Spanswick, J. (2014). Control over controlled radical polymerization processes. US8822610B2. ATRP Solutions.

137 Rizzardo, E., Chiefari, J., Benaglia, M. et al. (2016). RAFT polymerisation. US9340498B2. CSIRO.

138 Puskas, J.E. and Heidenreich, A.J. (2010). Synthesis of arborescent polymers via controlled inimer-type reversible addition-fragmentation chain transfer (RAFT) polymerization. WO2010019563A1. The University of Akron, USA.

139 Chiefari, J., Hornung, C., and Saubern, S. (2015). Continuous flow polymerisation process. US8946360B2. CSIRO.

140 Tsanaktsidis, J. and Gardiner, J. (2016). All purpose RAFT agent for polymerization. WO2016054689A1. CSIRO.

141 Miyake, G.M. (2015). Organocatalyzed photoredox mediated polymerization using visible light. US9156921B2. California Institute Of Technology.

142 Xu, J. and Boyer, C.A.J.-M. (2015). Manufacture of polymers by photopolymerization. WO2015113114A1. NewSouth Innovations Pty. Limited, Australia.

143 Gardiner, J. and Tsanaktsidis, J. (2016). Versatile RAFT agent, polymers prepared using the RAFT agent, and method of preparing polymer using the RAFT agent. WO2016197187A1. Commonwealth Scientific and Industrial Research Organisation, Australia.

144 Otsu, T. (2000). Iniferter concept and living radical polymerization. *J. Polym. Sci., Part A: Polym. Chem.* 38: 2121–2136. doi: 10.1002/(SICI)1099-0518(20000615)38:12<2121::AID-POLA10>3.0.CO;2-X.

145 Moad, G. (2022). Trithiocarbonates in RAFT polymerization. In: *RAFT Polymerization: Materials, Synthesis and Applications* (eds. G. Moad and E. Rizzardo), 371–494. Weinheim: Wiley-VCH.

146 Brzytwa, A.J. and Johnson, J. (2011). *Polym. Prepr. (Am. Chem. Soc., Div. Polym. Chem.)* 52: 533–534.

147 Lewandowski, K.M., Fansler, D.D., Wendland, M.S. et al. (2004). Azlactone chain transfer agents for radical polymerization. US6762257B1. 3M Innovative Properties Company.

148 Wendland, M.S., Lewandowski, K.M., Fansler, D.D. et al. (2004). Azlactone photoiniferters for radical polymerization. US6747104B1. 3M Innovative Properties.

149 Bai, F., Radcliffe, M.D., Montello, A.D. et al. (2008). High clarity cholesteric liquid crystal films. US7439000B2. 3M.

150 Padiyath, R., Radcliffe, M.D., Thomas, C.U. et al. (2010). Infrared light reflecting film. US7652736. 3M.
151 Joly, G.D., Abuelyaman, A.S., Craig, B.D. et al. (2013). Dental compositions comprising addition-fragmentation agents. WO2013028397A2. 3M Innovative Properties Company.
152 Fornof, A.R., Moser, W.H., Abuelyaman, A.S. et al. (2015). Allyl disulfide-containing addition-fragmentation oligomers. WO2015057413A1. 3M Innovative Properties Company.
153 Kambara, R., Mori, H., Endo, T., and Yonemori, S. (2010). Monodisperse chloromethylstyrene polymers and their manufacture. WO2010131628A1. AGC Seimi Chemical, Japan.
154 Louwet, F., Deroover, G., Groenendaal, B. et al. (2010). Stable pigment dispersions. US7674843. Agfa Graphics.
155 Louwet, F., Deroover, G., Groenendaal, B. et al. (2006). Stable pigment dispersions comprising a block copolymer consisting of ionic aromatic monomers. US7678845B2. Agfa-Gevaert, Belg.
156 Bertin, D., Couturier, J.L., Gigmes, D. et al. (2009). Method for preparing alkoxyamines by photolysis of dithiocarbamates. WO2006111637A1. Arkema France.
157 Couvreur, L. (2012). Compositions with improved odor comprising a RAFT agent or a polymer obtained using one of these agents. WO2012004480A1. Arkema France.
158 Curran, S.A. and Ellis, A.V. (2010). Thiation of carbon nanotubes and composite formation. US7713508B2. Arrowhead Center.
159 Rozema, D.B., Wakefield, D.H., Lewis, D.L. et al. (2013). In vivo polynucleotide delivery conjugates having enzyme sensitive linkages. US8426554B2. Arrowhead Madison.
160 Rozema, D.B., Lewis, D.L., Wakefield, D.H. et al. (2014). In vivo polynucleotide delivery conjugates having enzyme sensitive linkages. US8802773B2. Arrowhead Madison.
161 Wakefield, D.H., Rossi, N., and Sheik, D. (2015). Poly(vinyl ester) polymers for in vivo nucleic acid delivery. US8932572B2. Arrowhead Madison.
162 Wakefield, D.H., Rossi, N.A., and Sheik, D. (2015). Poly(vinyl ester) polymers for in vivo nucleic acid delivery. US9089611B2. Arrowhead Madison Inc.
163 Wakefield, D.H., Rozema, D.B., Rossi, N. et al. (2015). Poly(acrylate) polymers for in vivo nucleic acid delivery. US8933047B2. Arrowhead Madison.
164 Linhardt, J.G., Shipp, D.A., and Kunzler, J.F. (2011). Coating solutions comprising segmented reactive block copolymers. US7942929B2. Bausch & Lomb.
165 Linhardt, J.G., Shipp, D.A., Kunzler, J.F., and Vanderbilt, D.P. (2012). Coating solutions comprising segmented interactive block copolymers. US8100528B2. Bausch & Lomb.
166 Linhardt, J.G., Nunez, I.M., McGee, J.A. et al. (2011). Biomedical devices. US8043369B2. Bausch & Lomb.
167 Linhardt, J.G., Kunzler, J.F., and Shipp, D.A. (2011). Biomedical devices. US8083348B2. Bausch & Lomb.

168 Linhardt, J.G., McGee, J.A., and Nunez, I.M. (2012). Biomedical devices. US8133960B2. Bausch & Lomb.

169 Linhardt, J.G., Nunez, I.M., McGee, J.A. et al. (2012). Biomedical devices. US8337551B2. Bausch & Lomb.

170 Achten, D., Klimpel, M., Barriau, E. et al. (2007). Dithiocarbamic esters. US7169937B2. Bayer Aktiengesellschaft.

171 Achten, D., Klimpel, M., Barriau, E. et al. (2010). Dithiocarbamic esters. US7825193B2. Lanxess.

172 Achten, D., Klimpel, M., Barriau, E. et al. (2011). Dithiocarbamic esters. US7977431B2. Lanxess.

173 Klimpel, M., Brandau, S., Westeppe, U. et al. (2011). Nitrile rubbers and production of same in organic solvents. WO2011032832A1. LANXESS Deutschland.

174 Favier, A. and Charreyre, M.-T. (2007). Method for controlled radical polymerization. US7205362B2. bioMérieux.

175 Charreyre, M.-T., Mandrand, B., Martinho, J.M.G. et al. (2012). Fluorescent polymers soluble in an aqueous solution and a method for the production thereof. US8133411B2. Biomerieux, CNRS.

176 Xu, K., Hockey, M.A., and Guerrero, D. (2014). Highly etch-resistant polymer block for use in block copolymers for directed self-assembly. WO2014165530A1. Brewer Science Inc., USA.

177 Gobelt, B., Bubat, A., Frank, A., and Haubennestel, K. (2007). Use of polyacrylate-modified polysiloxanes as levelling agents in coating compositions. US7230051B2. BYK-Chemie GmbH.

178 Pakula, T. and Matyjaszewski, K. (2004). Polymers, supersoft elastomers and methods for preparing the same. WO2004014963A2. Carnegie Mellon University, USA.

179 Matyjaszewski, K., Sumerlin, B.S., Tsarevsky, N., and Spanswick, J. (2005). Preparation of tetrazole polymers with controlled functionality for pharmaceutical use. WO2005087818A1. Carnegie Mellon University.

180 Suau, J.M., Egraz, J.B., Claverie, J., and Ladaviere, C. (2008). Method of controlled free radical polymerisation of acrylic acid and its salts thereof, resulting low-polydispersity polymers, and their uses. US7345121B2. Coatex S.A.S.

181 Suau, J.M. and Egraz, J.B. (2008). Method for the controlled radical polymerisation of acrylic acid and the salts thereof, polymers thus obtained and applications thereof. US7462676B2. Coatex S.A.S.

182 Suau, J.-M. and Jacquemet, C. (2011). Trithiocarbonate derivatives and the use thereof in the form of transfer agents for acrylic acid controlled radical polymerisation. US7956211B2. Coatex.

183 Suau, J.M. and Jacquemet, C. (2012). Trithiocarbonate derivatives and the use thereof in the form of transfer agents for acrylic acid controlled radical polymerisation. US8227633B2. Coatex S.A.S.

184 Suau, J.M. and Jacquemet, C. (2013). Trithiocarbonate derivatives and the use thereof in the form of transfer agents for acrylic acid controlled radical polymerisation. US8470750B2. Coatex S.A.S.

185 Suau, J.-M. and Jacquemet, C. (2011). Polymers produced by using sulphur compounds in the form of transfer agents for controlled radical polymerisation of acrylic acid and the use thereof. US8053497B2. Coatex.

186 Kensicher, Y. and Platel, D. (2012). Use of a rheological additive in the manufacture by vibrocompaction of a water and hydraulic binder based formulation, formulation obtained. US8110130B2. Coatex.

187 Suau, J.-M. and Jacquemet, C. (2010). Polymers produced by using sulphur compounds in the form of transfer agents for controlled radical polymerisation of acrylic acid and the use thereof. US7851572B2. Coatex.

188 Lambert, T.H., Campos, L.M., and Bandar, J. (2014). Manufacturing of stable cyclopropenium cation-containing branched, dendritic, cross-linked and block polymeric systems. WO2014022365A1. Columbia University New York, USA.

189 Boyes, S.G. and Rowe, M.D. (2015). Gold/lanthanide nanoparticle conjugates and uses thereof. US8968705B2. Colorado School Of Mines.

190 Cheng, C., Khoshdel, E., and Wooley, K.L. (2011). Brush copolymers. US7960479B2. Conopco.

191 Herzog, K., Vana, P., Mueller, L. et al. (2014). Process for producing polymer-functionalized filler particles. US8912267B2. Continental Reifen Deutschland.

192 Herzog, K., Mueller, L., Recker, C. et al. (2016). RAFT agent, polymerization method, polymer, rubber mixture, and use thereof. WO2016180805A1. Continental Reifen Deutschland.

193 Herzog, K., Mueller, L., Recker, C. et al. (2016). Method for co-polymerization, co-polymer and rubber composition and their use. EP3109064A1. Continental Reifen.

194 Zhao, J.Z. (2010). Tri-branched biologically active copolymer. US7811555B2. Cordis.

195 Harruna, I.I. and Zhou, G. (2008). Ligand-functionalized/azo compounds and methods of use thereof. US7411053B2 (inventors).

196 Leibler, L., Nicolay, R., and Rottger, M. (2020). Boronic polymer crosslinking. US10329414B2. CNRS, Ecole Superieure de Physique de Chimie Industrielles de la Ville de Paris.

197 Leibler, L., Nicolay, R., and Rottger, M. (2020). Crosslinked polymers comprising exchangeable bonds and crosslinks via aldehyde-imine and imine-imine exchange reactions. WO2017029311A1. Ecole Superieure de Physique et de Chimie Industrielles de la Ville de Paris, Fr.

198 Tang, L., Thomas, A.D., and Harmon, B.D. (2015). Polyacrylonitrile with low polydispersity index for carbon fibers. WO2015099913A1. Cytec Industries.

199 Tamai, H., Otsu, T., and Mori, H. (2010). Polychloroprenes with narrow polydispersibility, their manufacture and their adhesives. WO2010147011A1. Denki Kagaku Kogyo Kabushiki Kaisha.

200 Farnham, W.B., Fryd, M., and Schadt, F.L. III (2010). Low-polydispersity photoimageable acrylic polymers, photoresists and processes for microlithography. US7696292B2. CSIRO.

201 Feiring, A.E., Fryd, M., and Schadt, F.L. (2008). Low-polydispersity photoimageable polymers and photoresists and processes for microlithography. US7408013B2. CSIRO.
202 Farnham, W.B. and Moudgil, S. (2011). Fluorinated polymers for use in immersion lithography. US8034534B2. du Pont.
203 Meagher, L., Thissen, H., Pasic, P. et al. (2012). Polymeric coatings and methods for forming them. US8124188B2. CSIRO.
204 Meagher, L., Thissen, H., Pasic, P. et al. (2014). Polymeric coatings and methods for forming them. US8795782B2. CSIRO.
205 Chen, M., Moad, G., Rizzardo, E. et al. (2013). Conducting and semiconducting organic materials. US8501889B2. CSIRO.
206 Chen, M., Moad, G., Rizzardo, E. et al. (2015). Conducting and semiconducting organic materials. US8993697B2. CSIRO.
207 Cai, J.Y. (2017). Polymer derived from acrylonitrile. US9777081B2. CSIRO.
208 Kunitsky, K., Shah, M.C., Shuey, S.W., and Wagman, M.E. (2008). Method for preparing glycidyloxystyrene monomers and polymers thereof. US7468415B2. duPont.
209 Farnham, W.B. (2012). Synthesis of fluoroalcohol-substituted (meth)acrylate esters and polymers derived therefrom. US8304572B2. duPont.
210 Meth, J.S. (2014). Method for producing encapsulated nanoparticles. US8734898B2. duPont.
211 Farnham, W.B., Sheehan, M.T., Tran, H.V., and Zhang, D. (2017). Substantially symmetrical 3-arm star block copolymers. US9815947B2. duPont.
212 Chilkoti, A. and Gao, W. (2013). Biomolecule polymer conjugates and methods for making the same. US8497356B2. Duke University.
213 Schellekens, M.A.J., Nabuurs, T., Geurts, J., and Overbeek, G.C. (2009). Water borne crosslinkable block copolymers obtained using RAFT polymn. WO2009090252A1. DSM IP Assets.
214 Schellekens, M.A.J., Geurts, J., Nabuurs, T., and Overbeek, G.C. (2008). Aqueous oligomer/polymer emulsion with cationic functionality. WO2008122576A1. DSM IP Assets B.V., Neth.
215 Schellekens, M.A.J., Nabuurs, T., Geurts, J., and Overbeek, G.C. (2010). RAFT block copolymer-containing coating compositions with improved adhesion to metal surfaces. WO2010000725A1. DSM IP Assets.
216 Schellekens, M.A.J., Overbeek, G.C., Nabuurs, T., and Geurts, J. (2009). Adhesion to plastic with block copolymers obtained using RAFT. WO2009121911A1. DSM IP Assets.
217 Schellekens, M.A.J., Nabuurs, T., Geurts, J., and Overbeek, G.C. (2009). Block copolymers obtained using raft. WO2009138493A1. DSM IP Assets.
218 Schellekens, M.A.J., De Bont, J.H., Barbosa, J. et al. (2019). Waterborne crosslinkable dispersions. WO2019121782A1. DSM IP Assets.
219 Wang, J.-S. (2004). Polymerization process. US6756457B2. Eastman Kodak Company.
220 Li, Y., Du, H., Liu, Y. et al. (2016). Electrophoretic dispersion. US9428649B2. E Ink California.

221 Li, Y., Du, H., Liu, Y. et al. (2017). Method of making electrophoretic dispersion. US9732231B2. E Ink California.
222 Hubbell, J.A. and Wilson, D.S. (2017). Glycotargeting therapeutics. WO2017046652A1. Ecole Polytechnique Federale de Lausanne.
223 Bollinger, J.M. and Wang, J.-L. (2004). Process for preparing dithioesters in a biphasic system. WO2004083169A1. Rohmax Additives.
224 Dardin, A., Mueller, M., and Eisenberg, B. (2004). Lubricating oil composition with good friction characteristics. WO2004087850A1. Rohmax Additives.
225 Schmidt, F.G., Krause, S., Hennig, A. et al. (2011). Function materials with reversible crosslinking. WO2011101176A1. Evonik Roehm.
226 Schmidt, F.G., Hilf, S., Zhou, J. et al. (2013). Polymer powder for producing three-dimensional objects. WO2013013873A1. Evonik Roehm.
227 Schmidt, F.G., Hilf, S., Spyrou, E. et al. (2013). Low molecular products, and their use as reversible or permanent low-temperature crosslinking agents by Diels–Alder reactions. WO2013017349A1. Evonik Degussa.
228 Chung, H. (2016). Lignin-containing polymers and their preparation and self-healing polymers. US20160222151A1. Florida State University Research Foundation, Inc., USA.
229 Winnik, M.A., Nitz, M., Baranov, V., and Lou, X. (2007). Polymer backbone element tags in form of metal-polymer conjugates for ICP-MS linked immunoassays. WO2007137418A1. Can.
230 Senyek, M.L., Kulig, J.J., and Parker, D.K. (2002). Dibenzyltrithiocarbonate molecular weight regulator for emulsion polymerization. US6369158B1. The Goodyear Tire & Rubber Company.
231 Parker, D.K., Feher, F.J., and Mahadevan, V. (2009). Styrene acrylonitrile isoprene triblock copolymer. US7592409. Goodyear.
232 Parker, D.K., Feher, F.J., and Mahadevan, V. (2010). Controlled polymerization. US7767775. Goodyear.
233 Parker, D.K., Feher, F.J., and Mahadevan, V. (2006). Controlled polymerization. US6992156B2. The Goodyear Tire & Rubber Company.
234 Parker, D.K., Feher, F.J., and Mahadevan, V. (2006). Controlled polymerization. US7098280B2. The Goodyear Tire & Rubber Company.
235 Parker, D.K., Feher, F.J., and Mahadevan, V. (2009). Hydrogenation and epoxidation of polymers made by controlled polymerization. US7528204B2. Goodyear.
236 Parker, D.K. (2008). Oxathiazaphospholidine free radical control agent. US7462674B2. Goodyear.
237 Parker, D.K. (2008). Oxathiazaphospholidine free radical control agent. US7345186B2. Goodyear.
238 Parker, D.K. (2009). Oxathiazaphospholidine free radical control agent. US7488786B2. Goodyear.
239 Parker, D.K. and Yang, X. (2009). Water-based process for the preparation of polymer-clay nanocomposites. US7625985B1. Goodyear.
240 Parker, D.K. (2007). Functional trithiocarbonate RAFT agents. US7230063B1. The Goodyear Tire & Rubber Company.

241 Parker, D.K. and Kulig, J.J. (2010). Surfactantless synthesis of amphiphilic cationic block copolymers. US7671152B2. Goodyear.
242 Feher, F.J., Mahadevan, V., and Parker, D.K. (2008). Sulfine control agents for synthesizing polymers. US7335714B1. The Goodyear Tire & Rubber Company.
243 Parker, D.K., Feher, F.J., and Mahadevan, V. (2010). Hydrogenation and epoxidation of polymers made by controlled polymerization. US7812108B2. Goodyear.
244 Parker, D.K., Feher, F.J., and Mahadevan, V. (2012). Controlled polymerization. US8178637. Goodyear.
245 Mruk, R., Schmitz, F., Roskamp, R.F. et al. (2013). Rubber composition and pneumatic tire. US8415432B1. Goodyear.
246 Mruk, R., Schmitz, F., Roskamp, R.F. et al. (2014). Method of making a graft copolymer. US8759451B2. Goodyear.
247 Ma, L., Mruk, R., and Hahn, B.R. (2013). Method to improve green strength in elastomers. US8563656B1. Goodyear.
248 Ma, L., Roskamp, R.F., Mruk, R. et al. (2014). Pneumatic tire. US8883884B2. Goodyear.
249 Chun, D.P.Y. and Ng, H.T. (2012). Polymer-encapsulated pigment. US8309630B2. Hewlett-Packard.
250 Cheng, J., Kim, H., Rettner, C.T. et al. (2009). Method of use of epoxy-containing cycloaliphatic acrylic polymers as orientation control layers for block copolymer thin films. US7521090B1. IBM.
251 Cheng, J., Kim, H.-C., Rettner, C.T. et al. (2011). Method of use of epoxy-containing cycloaliphatic acrylic polymers as orientation control layers for block copolymer thin films. US7989026B2. IBM.
252 Brown, A.A., George, W.N., Richez, A. et al. (2016). Novel polymers for surface functionalization and immobilization of DNA for high-throughput DNA sequencing by synthesis. US20160122816A1. Illumina Cambridge Limited, UK.
253 Cochran, E.W., Williams, R.C., Hernandez, N., and Cascione, A. (2014). Thermoplastic elastomers via reversible addition-fragmentation chain transfer polymerization of triglycerides. US20140343192A1. Iowa State University Research Foundation, Inc., USA.
254 Mathew, L. and Shih, K.-C. (2004). Thiocarbonylthio compound and living free radical polymerization using the same. US6720429B2. Industrial Technology Research Institute.
255 Shih, K.C., Chung, P.W., and Wang, M.H. (2011). Thiocarbonylthio compound and free radical polymerization employing the same. US7968743B2. ITRI.
256 Charles, J.H.K. and Murray, G.M. (2010). Authentication of products using molecularly imprinted polymers. US7799568B2. Johns Hopkins University.
257 Southard, G.E. and Murray, G.M. (2010). Processable molecularly imprinted polymers. US7678870B2. Johns Hopkins University.
258 Murray, G.M., Mason, A.F., and Ott, E.W. (2012). Molecularly imprinted polymer sensor device. US8241575B2. Johns Hopkins University.
259 Benoit, D., Safir, A., Chang, H.-T. et al. (2009). Photoresist polymer compositions. US7510817B2. JSR.

260 Benoit, D., Safir, A., Chang, H.-T. et al. (2009). Photoresist polymers. US7517634B2. JSR.
261 Tsuji, R. and Hiiro, T. (2006). Polyurethane polymer. US6992138B2. Kaneka Corporation.
262 Tsuji, R. and Hiiro, T. (2006). Block copolymer. US7094833B2. Kaneka Corporation.
263 Tsuji, R. and Hiiro, T. (2007). Thermoplastic resin composition and elastomer composition. US7211625B2. Kaneka Corporation.
264 Sacha, P., Konvalinka, J., Schimer, J. et al. (2016). Macromolecular conjugates for visualization and separation of proteins and cells. WO2016112883A2. Ustav Organicke Chemie a Biochemie Av Cr, V.V.I., Czech Rep.; Ustav Makromolekularni Chemie Av Cr, V.V.I.; Univerzita Karlova v Praze, Prirodovedecka Fakulta.
265 Lynch, T.J. (2011). Mineral dispersants and methods for preparing mineral slurries using the same. US7875213B2. Kemira.
266 Kim, S.Y. and Seo, M. (2013). Methods for the preparation of coil-comb block copolymers and their nanostructures. US8518497B2. Korea Advanced Institute Of Science And Technology.
267 Kim, J.A. and Yoo, H. (2013). PH-sensitive polyethylene oxide co-polymer and synthetic method thereof. US8420771B2 (inventors).
268 Mougin, N. (2005). Block copolymer comprising a vinyllactam block for cosmetics and pharmaceuticals. EP1514884A1. L'Oreal.
269 Farcet, C. (2009). Polymer particle dispersion, cosmetic compositions comprising it and cosmetic process using it. US7585922B2. L'Oreal.
270 Farcet, C. (2010). Polymer particle dispersion, cosmetic composition comprising it and cosmetic process using it. US7816464B2. L'Oreal.
271 Cassin, G. (2006). Cosmetic use of a particular copolymer as skin tensor in a cosmetic composition. WO2006097529A1. L'Oreal.
272 Farcet, C., Houillot, L., Save, M., and Charleux, B. (2010). Cosmetic composition comprising a dispersion of soft polymer particles. WO2010046229A1. L'Oreal.
273 Simonnet, J.-T., L'Alloret, F., Bressy, L., and Moujahed, Z. (2009). Oil-in-water emulsion comprising an amphiphilic polymer. WO2009101113A2. L'Oreal.
274 Farcet, C. and Lion, B. (2012). Cosmetic compositions comprising isobutyl acrylate and acrylic acid diblock copolymers. WO2012156630A1. L'Oreal.
275 Kim, H.-J. and Kim, D.-R. (2006). Organic-inorganic nanocomposite and preparation thereof. US7115683B2. LG Chem, Ltd.
276 Kim, H.-J. and Kim, D.-R. (2005). Water-soluble dithioesters and method for polymerization thereof. US6888020B2. LG Chem, Ltd.
277 Han, Y.K., Lee, J.G., and Kim, S.H. (2014). Adsorbent of volatile organic compounds and adsorption method using thereof. US8911537B2. LG Chem, Industry-University Cooperation Foundation Hanyang University.
278 Han, Y.-K., Lee, J.-G., and Kim, S.-H. (2012). Acrylate-acrylamide diblock copolymers and methods of producing diblock copolymers and forming nanopatterns. WO2012144735A2. LG Chem.

279 Ku, S.J., Lee, M.S., Ryu, H.J. et al. (2016). Method for producing patterned substrate using self-assembly of block copolymers. WO2016053014A1. LG Chem.
280 Choi, E.Y., Park, N.J., Kim, J.K. et al. (2016). Production of diblock copolymer with self-assembly characteristic using RAFT polymerization. WO2016053005A1. LG Chem.
281 Lai, J.T.-Y., Lepilleur, C.A., Weber, C.D. et al. (2005). S,S′-bis-(α,α-disubstituted-α″-acetic acid) – trithiocarbonates and polymers thereof for toughening thermosetting resins. US6894116B2. Noveon.
282 Lai, J.T.-Y. and Hsu, S.-J.R. (2009). Associative thickeners for aqueous systems. US7495050B2. Lubrizol.
283 Lai, J.T.-Y., Pajerski, A.D., and Shea, R.P. (2012). Hydroxyl-terminated thiocarbonate containing compounds, polymers, and copolymers, and polyurethanes and urethane acrylics made therefrom. US8137754B2. Lubrizol.
284 Lai, J.T.Y., Pajerski, A.D., and Shea, R.P. (2014). Hydroxyl-terminated thiocarbonate containing compounds, polymers, and copolymers, and polyurethanes and urethane acrylics made therefrom. US8709543B2. Lubrizol Advanced Materials.
285 Baum, M., Schober, B., Davies, M., and Visger, D. (2006). Process for preparing star polymers by controlled radical polymerization and compositions thereof. WO2006047393A1. The Lubrizol Corporation.
286 Johnson, J.R., Visger, D.C., Baum, M. et al. (2011). Crosslinked polymer. US8012917B2. Lubrizol.
287 Schober, B.J., Davies, M.C., Sutton, M.R. et al. (2015). Star polymer lubricating composition. US9006159B2. Lubrizol.
288 Baker, M.R., Baum, M., and Schober, B.J. (2007). Star polymer lubricating composition. WO2007127660A1. The Lubrizol Corporation.
289 Richards, S.N. and Shooter, A.J. (2012). Graft copolymer and compositions thereof. US8268925B2. Lubrizol.
290 Price, D., Mosier, P.E., Vilardo, J.S., and Baum, M. (2013). Antiwear polymer and lubricating composition thereof. US8507422B2. Lubrizol.
291 Qin, H., Baum, M., and Johnson, J.R. (2015). Star polymer and lubricating composition thereof. US8937035B2. Lubrizol.
292 Abraham, W.D., Baum, M., Qin, H., and Wang, Y. (2011). Farm tractor lubricating oil composition with good water tolerance. WO2011031659A1. The Lubrizol Corporation.
293 Johnson, J.R. and Schober, B.J. (2014). Loose core star polymers and lubricating composition thereof. WO2014031154A1. The Lubrizol Corporation.
294 Miller, C.G. and Kim, H. (2016). Water-soluble chain transfer agents for preparing water-soluble polymers by Reversible Addition Fragmentation Chain Transfer polymerization. WO2016182711A1. The Lubrizol Corporation.
295 Olsen, B.D., Glassman, M.J., and Chan, J. (2014). Nanostructured physically-associating hydrogels for injectable, responsive, and tough biomaterials. US8916683B2. Massachusetts Institute Of Technology.
296 Stenzel, M.H., Scarano, W., Svejkar, D., and Liang, M. (2014). Nanoparticles for drug delivery comprising albumin and antisense DNA having a polymer chain

of acrylic polymers, polyesters and polyethers. WO2014161031A1. NewSouth Innovations.

297 Justynska, J. and Seiferling, B. (2013). Actinically-crosslinkable siloxane-containing copolymers. US8383744B2. Novartis AG.

298 Kambouris, P., Whittaker, M., Davis, T. et al. (2005). Methods of polymerization. US6858309B2. Polymerat Pty. Ltd.

299 Moad, G., Simon, G.P., Dean, K.M. et al. (2010). Dispersing agents in nanocomposites. US7837899B2. Polymers Australia.

300 Moad, G., Simon, G.P., Dean, K.M. et al. (2007). Acrylic dispersing agents in nanocomposites. US7288585B2. Ciba Specialty Chemicals Corp.

301 Moad, G., Li, G., Campbell, J.A. et al. (2012). Dispersing agents in composites. US8110626B2. Advanced Polymerik.

302 Stenzel, M.H., Godoy-Lopez, R., Harrisson, S., and Rizzardo, E. (2013). Functionalized thin film polyamide membranes. US8544658B2. Polymers CRC.

303 Satchi-Fainaro, R., Miller, K., Shabat, D., and Erez, R. (2014). Conjugates of a polymer, a bisphosphonate and an anti-angiogenesis agent and uses thereof in the treatment and monitoring of bone related diseases. Ramot At Tel-Aviv University.

304 Satchi-Fainaro, R., Miller, K., Shabat, D., and Erez, R. (2015). Conjugates of a polymer, a bisphosphonate and an anti-angiogenesis agent and uses thereof in the treatment and monitoring of bone related diseases. US9095618B2. Ramot At Tel-Aviv University.

305 Benicewicz, B.C., Kanagasabapathy, S., and Sudalai, A. (2004). Transition metal superoxides. US6765076B2. Rensselaer Polytechnic Institute.

306 Benicewicz, B.C., Kanagasabapathy, S., and Sudalai, A. (2002). Dithiocarboxylic ester synthetic process. US6458968B2. Rensselaer Polytechnic Institute.

307 Tao, P., Li, Y., Benicewicz, B. et al. (2013). Nanofilled polymeric nanocomposites with tunable index of refraction. US8518473B2. Rensselaer Polytechnic Institute.

308 Nelson, J.K., Benicewicz, B., Rungta, A., and Schadler, L.S. (2014). Self-healing electrical insulation. US8796372B2. Rensselaer Polytechnic Institute.

309 Destarac, M., Joanicot, M., and Reeb, R. (2003). Gelled aqueous composition comprising a block copolymer containing at least one water-soluble block and one hydrophobic block. US6506837B2. Rhodia Chimie.

310 Gerardin, C., Anthony, O., Chane-Ching, J.-Y., and Destarac, M. (2002). Process for preparing colloids of particles coming from the hydrolysis of a salt of a metal cation. US6500871B1. Rhodia Chimie.

311 Destarac, M., Mignani, G., Zard, S. et al. (2005). Method for synthesis of hybrid silicon and organic copolymers by controlled free radical polymerization. US6858696B2. Rhodia Chimie.

312 Prat, E. and Destarac, M. (2005). Photosensitive composition for photoresist manufacture. US6953649B2. Rhodia Chimie.

313 Cadena, N., Destarac, M., Herve, P., and Wilczewska, A.Z. (2009). Method for depositing a polymer onto a surface by applying a composition onto said surface. US7473730B2. Rhodia.

314 Herve, P., Destarac, M., Anthony, O. et al. (2009). Formulation comprising an ionic compound, a polyionic polymer, and a block copolymer. US7531597B2. Rhodia.

315 Anthony, O., Bonnet-Gonnet, C., Destarac, M. et al. (2002). Water-soluble block copolymers comprising a hydrophilic block and a hydrophobic block. US6437040B2. Rhodia Chimie.

316 Bavouzet, B., Destarac, M., Herve, P., and Taton, D. (2003). Composition comprising a copolymer at least two charged blocks and type of opposite charge. US6559233B2. Rhodia Chimie.

317 Heitz, C., Joanicot, M., and Tillotson, R.J. (2003). Hydraulic fracturing fluid comprising a block copolymer containing at least one water-soluble block and one hydrophobic block. US6579947B2. Rhodia Chimie.

318 Cadena, N., Destarac, M., Herve, P., and Wilczewska, A.Z. (2005). Method for depositing a polymer onto a surface by applying a composition onto said surface. US6906128B2. Rhodia Chimie.

319 Herve, P., Destarac, M., Anthony, O. et al. (2005). Formulation comprising an ionic compound, a polyionic polymer, and a block copolymer. US6933340B2. Rhodia Chimie.

320 Bavouzet, B., Destarac, M., Herve, P., and Wilczewska, A.Z. (2007). Cosmetic composition comprising a block copolymer. US7235231B2. Rhodia Chimie.

321 Adam, H. and Liu, W.-L. (2004). Process for the preparation of latices using block copolymers as surfactants. US6825290B2. Rhodia Inc.

322 Harrison, I., Destarac, M., and Geffroy, C. (2008). Crease-resistant composition comprising a copolymer of controlled architecture, for articles made of textile fibers. US7378033B2. Rhodia.

323 Zard, S., Gagosz, F., and Tournier, L. (2008). Compounds comprising a thiocarbonyl-sulfanyl group, which can be used for the radical synthesis of-α-perfluoroalkylamines. US7423161B2. Rhodia.

324 Zard, S., Gagosz, F., and Tournier, L. (2010). Compounds comprising a thiocarbonyl-sulfanyl group which can be used for the radical synthesis of α-perfluoroalkylamine compounds. US7820831B2. Rhodia.

325 Destarac, M., Bonnet-Gonnet, C., and Cadix, A. (2008). Use of block copolymers bearing phosphate and/or phosphonate functions as adhesion promoters or as protecting agents against the corrosion of a metallic surface. US7439292B2. Rhodia.

326 Yokota, K., Berret, J.F., Tolla, B., and Morvan, M. (2008). Rare earth aggregate formulation using di-block copolmers. US7468413B2. Rhodia.

327 Bzducha, W. (2012). Block copolymers useful as tensioning agents. US8207273B2. Rhodia.

328 Destarac, M. and Wilson, J. (2013). Living poly(N-vinyllactam) reactive stabilizers for dispersed phase polymerization. WO2013113750A1. Rhodia Operations.

329 Destarac, M. and Wilson, J. (2013). Dispersed phase polymerization of halogenated vinyl monomers in the presence of life reactive stabilizers. WO2013113752A1. Rhodia Operations.

330 Cadix, A. and Wilson, J. (2014). Fracturing fluids based on associative polymers and displaceable surfactants. WO2014167056A1. Rhodia Operations.
331 Wilson, J., Destarac, M., and Cadix, A. (2013). Preparation of amphiphilic block polymers by controlled radical micellar polymerization. WO2013060741A1. Rhodia Operations.
332 Destarac, M. and Wilson, J.D. (2013). Controlled radical polymerization in a water-in-water dispersion. WO2013132108A1. Rhodia Operations.
333 Harrisson, S. and Wilson, J. (2015). Amphiphilic multiblock polymers. WO2015144475A1. Rhodia Operations.
334 Usui, Y. and Yusa, S. (2014). ABA triblock copolymer, thickener, and aqueous composition. US8829133B2. Ricoh, University Of Hyogo.
335 Bollinger, J.M. and Wang, J.-L. (2005). Process for preparing dithioesters. US6841695B2. Rohmax Additives GmbH.
336 Mueller, M., Stoehr, T., and Eisenberg, B. (2012). Polyalkyl (meth)acrylate copolymers having outstanding properties. US8101559B2. Rohmax Additives.
337 Mueller, M., Stoehr, T., and Eisenberg, B. (2014). Polyalkyl (meth)acrylate copolymers having outstanding properties. US8722601B2. Rohmax Additives.
338 Di, J., Mullen, B., and Sybert, P.D. (2009). Thermoplastic composition, method of making, and articles formed therefrom. US7498398B2. Sabic Innovative Plastics.
339 Scherman, O.A., Appel, E., and Hughes, T. (2014). Viscous wellbore fluids. US8757264B2. Schlumberger Technology Corporation.
340 Venkatesh, R. and Klumperman, L. (2004). Process for copolymerization of α-olefins with vinyl monomers using thiocarbonylthio compounds as chain transfer agents. EP1384729A1. Dutch Polymer Institute, Neth.
341 Hicks, J.K., Rimmer, S., McCulloch, D., and Hoskins, R. (2016). Improvements in and relating to polymer materials. WO2016005288A1. Smith & Nephew.
342 Hicks, J.K., Rimmer, S., Hoskins, R., and McCulloch, D. (2016). Improvements in and relating to devices. WO2016012219A2. Smith & Nephew.
343 Klumperman, L., Pfukwa, R., and Heyns, I.M. (2017). Synthesis of 3-methylene-2-pyrrolidone based polymers. WO2017029630A1. Stellenbosch University, S. Afr.
344 Klumperman, L., Reader, P.W., and Rautenbach, M. (2016). Conjugate for treating malaria. WO2016024240A1. Stellenbosch University, S. Afr.
345 Klaerner, G., Petro, M., Charmot, D., and Benoit, D. (2004). Controlled-architecture polymers and use thereof as separation media. US6716948B1. Symyx Technologies, Inc.
346 Klaerner, G., Petro, M., Charmot, D., and Benoit, D. (2007). Controlled-architecture polymers and use thereof as separation media. US7259217B2. Symyx Technologies, Inc.
347 Klaerner, G., Nielsen, R.B., Mansky, P. et al. (2004). Polymer brushes for immobilizing molecules to a surface or substrate, where the polymers have water-soluble or water-dispersible segments and probes bonded thereto. US6692914B1. Symyx Technologies, Inc.

348 Klaerner, G., Nielsen, R.B., Mansky, P. et al. (2004). Polymer brushes for immobilizing molecules to a surface and having water-soluble or water-dispersible segments therein and probes bonded thereto. US6833276B2. Symyx Technologies, Inc.

349 Liu, M., Hajduk, D., Frechet, J.M.J. et al. (2006). Methods of making ABA-type block copolymers having a random block of hydrophobic and hydrophilic monomers. US7067586B2. Symyx Technologies, Inc.

350 Charmot, D., Chang, H.-T., Jayaraman, M., and Nava-Salgado, V. (2003). Control agents for living-type free radical polymerization and methods of polymerizing. US6667376B2B2. Symyx Technologies, Inc.

351 Charmot, D., Jayaraman, M., Chang, H.T. et al. (2004). Cellulose copolymers that modify fibers and surfaces. 6803410. Symyx Technologies, Inc.

352 Benoit, D., Safir, A., Chang, H.-T. et al. (2007). Synthesis of photoresist polymers. US7250475B2. Symyx Technologies, Inc.

353 Benoit, D., Safir, A., Chang, H.T. et al. (2008). Synthesis of photoresist polymers. US7399806B2B2. Symyx.

354 Husemann, M., Zollner, S., and Losch, M. (2004). Method for producing polyacrylates. US6765078B2. Tesa AG.

355 Husemann, M. and Dollase, T. (2004). Oriented acrylic block copolymers. US6703441B2. Tesa Aktiengesellschaft.

356 Husemann, M. and Zollner, S. (2004). UV-crosslinkable acrylic hotmelt PSAs with narrow molecular weight distribution. US6720399B2. Tesa AG.

357 Dollase, T., Husemann, M., and Luhmann, B. (2004). Strippable systems based on acrylic block copolymers. US6723407B2. Tesa AG.

358 Husemann, M. and Zollner, S. (2004). Pressure sensitive adhesive, particularly for apolar surfaces. US6723786B2. Tesa AG.

359 Husemann, M. and Zöllner, S. (2007). Crosslinking of photoiniator-initialized polyacrylates. US7271203B2. tesa Aktiengesellschaft.

360 Husemann, M. and Zöllner, S. (2007). Adhesive material based on block copolymers having a P(A)-P(B)-P(A) structure. US7307115B2. tesa AG.

361 Husemann, M. and Zöllner, S. (2008). 2-Component crosslink of end-functionalized polyacrylates. US7402632B2. Tesa AG.

362 Dollase, T., Husemann, M., and Luhmann, B. (2012). Adhesive masses based on block copolymers of structure P(A)-P(B)-P(A) and P(B)-P(A)-P(B). US8129470B2. Tesa.

363 Husemann, M. and Zollner, S. (2009). Method for the production of acrylate adhesive materials using metal-sulphur compounds. US7514515B2. Tesa.

364 Dollase, T. and Husemann, M. (2010). Adhesive materials having a high refractive index based on acrylate block copolymers. US7758933B2. Tesa.

365 Husemann, M., Dollase, T., and Luhmann, B. (2008). Pressure-sensitive adhesive based on acrylate block copolymers. US7459499B2. Tesa AG.

366 Husemann, M., Dollase, T., and Lühmann, B. (2008). Pressure-sensitive adhesive based on acrylate block copolymers. US7432326B2. Tesa AG.

367 Dollase, T. and Koop, M. (2009). Method for producing contact adhesive masses containing acrylic. US7605212B2. Tesa.

368 Cho, S., Sun, G., Wooley, K.L. et al. (2014). Self-assembled structures, method of manufacture thereof and articles comprising the same. US8822130B2. Texas A&M University, Rohm And Haas Electronics Materials.

369 Charmot, D., Jayaraman, M., Chang, H. et al. (2005). Use of compounds in products for laundry applications. EP1409627B1. Unilever Research.

370 Blokzijl, W., Carswell, R.J., Charmot, D. et al. (2007). Laundry treatment compositions comprising a polymer with a cationic and polydialkylsiloxane moiety. US7179777B2. Unilever Home & Personal Care USA Division of Conopco, Inc.

371 Charleux, B., Rieger, J., and Stoffelbach, F. (2013). Amphiphilic block copolymer and method for preparing same. US8598289B2. Universite Pierre Et Marie Curie, CNRS, Universite De Liege.

372 Zeng, H., Li, L., and Yan, B. (2018). A mussel-inspired injectable hydrogel with self-healing and anti-biofouling capabilities. US10023700B2. The Governors of the University of Alberta, Can.

373 Montarnal, D., Hawker, C.J., Kramer, E.J., and Fredrickson, G.H. (2015). Compositions for controlled assembly and improved ordering of silicon-containing block copolymers. US9158200B2. University of California.

374 Yang, C. and Wudl, F. (2012). Well-defined donor-acceptor rod-coil diblock copolymer based on P3HT containing C_{60}. US8211996B2. University of California.

375 Hawker, C.J., Vestberg, R., and Ueno, N. (2012). Highly efficient agents for dispersion of nanoparticles in matrix materials. US8153729B2. University of California, Mitsubishi Chemical.

376 Noda, T., Nakaya, F., Sakashita, K. et al. (2012). Novel chain transfer agent and emulsion polymerization using the same. US9676888B2. Mitsubishi Chemical.

377 Noda, T., Nakaya, F., Sakashita, K. et al. (2016). Chain transfer agent and emulsion polymerization using the same. US9452978B2. Mitsubishi Rayon.

378 Maynard, H.D. and Nguyen, T. (2013). Basic fibroblast growth factor (bFGF)-polymer conjugates as heparin mimicking polymers. WO2013082196A1. University of California, USA.

379 Maynard, H.D. (2016). Biodegradable trehalose glycopolymers, structures and methods of making biodegradable trehalose co-polymers. WO2016025668A1. University of California, USA.

380 Maynard, H.D., Mancini, R.J., Lee, J., and Lin, E.-W. (2013). Stabilization of biomolecules using sugar polymers. WO2013112897A1. University of California, USA.

381 Bowman, C.N. and Scott, T.F. (2011). Stress relaxation in crosslinked polymers. US7943680B2. University of Colorado.

382 Bowman, C.N. and Scott, T.F. (2013). Stress relaxation in crosslinked polymers. US8404758B2. University Of Colorado.

383 Bowman, C.N., Kloxin, C., Park, H.Y., and Leung, D. (2014). Stress relief for crosslinked polymers. US8877830B2. University Of Colorado.

384 Fenoli, C.R. and Bowman, C.N. (2015). Synthesis of trithiocarbonates and allyl sulfides and their application into advances in covalent adaptable networks. US9193682B2, USA.

385 Bowman, C. and Leung, D. (2017). Reducing polymerization-induced shrinkage stress by reversible addition-fragmentation chain transfer. US9758597B2. University of Colorado, USA.

386 Bowman, C.N., Sowan, N., and Cox, L.M. (2019). Tough, healable composites displaying stress relaxation at the resin-filler interface. WO2019183140A1. The Regents of the University of Colorado, USA.

387 Keselowsky, B.G., Lewis, J., Fernando, L.P. et al. (2017). Polymeric particles, method for cytosolic delivery of cargo, methods of making the particles. US10512607B2. Vanderbilt University, USA; University of Florida Research Foundation, Inc.

388 Advincula, R (2011). Knotty polymers via supramolecularly templated macroinitiators and living polymerization and methods for making and using same. US8669335B2. University Of Houston.

389 Forrest, M.L., Duan, S., Cai, S. et al. (2014). Drug and imaging agent delivery compositions and methods. US8802235B2. University Of Kansas.

390 Thayumanavan, S. (2010). Invertible amphiphilic polymers. US7687600B2. University of Massachusetts.

391 Thayumanavan, S., Klaikherd, A., and Ghosh, S. (2012). Cleavable block copolymers, functionalized nanoporous thin films and related methods of preparation. US8198368B2. University of Massachusetts.

392 Thayumanavan, S., Klaikherd, A., and Ghosh, S. (2013). Cleavable block copolymers, functionalized nanoporous thin films and related methods of preparation. US8546488B2. University Of Massachusetts.

393 Thayumanavan, S., Vachet, R., Savariar, E.N., and Combariza, M.Y. (2015). Polymeric reverse micelles as selective extraction agents and related methods of MALDI-MS analysis. US8969026B2. University Of Massachusetts.

394 Thayumanavan, S. (2012). Crosslinked polymer nanoassemblies for drug delivery and diagnostic agents. WO2012162307A2. University of Massachusetts, USA.

395 Emrick, T., Skinner, M., Ward, S.M., and Saha, B. (2018). Temozolomide compounds, polymers prepared therefrom, and method of treating a disease. US10562901B2. The University of Massachusetts, USA.

396 Caruso, F., Qiao, G.G., Blencowe, A.R. et al. (2013). Process for the preparation of a cross-linked multilayer film. US8496997B2. University Of Melbourne.

397 Frisbie, C.D. and Lodge, T.P. (2011). Ion gels and electronic devices utilizing ion gels. US7999020B2. University of Minnesota.

398 Hillmyer, M. and Chen, L. (2013). Nano-structured polymer composites and process for preparing same. US8420704B2. University Of Minnesota.

399 Rossato, L.S.R., Monteiro, M., Whittaker, M. et al. (2014). Soil remediation process. US8840339B2. University Of Queensland.

400 Benoit, D. and Puzas, J.E. (2014). Compositions and methods for controlled localized delivery of bone forming therapeutic agents. WO2014152451A2. University of Rochester, USA.

401 Tang, C. and Ren, L. (2013). Preparation of cobaltocenium-containing monomers and their polymers. US8592539B2. University Of South Carolina.

402 Benicewicz, B.C., Rungta, A., Viswanath, A. et al. (2014). Nanoparticles with multiple attached polymer assemblies and use thereof in polymer composites. US8865796B2. University Of South Carolina.

403 Benicewicz, B.C., Rungta, A., Viswanath, A. et al. (2015). Nanoparticles with multiple attached polymer assemblies and use thereof in polymer composites. US9109070B2. University of South Carolina.

404 Tang, C., Qiao, Y., Ploehn, H.J., and Islam, M.D.S. (2017). Preparation of conjugated aromatic/heteroaromatic oligomer-containing dielectric polymers and their applications. US9725544B2. University of South Carolina.

405 Wang, L. and Benicewicz, B.C. (2017). Raft agents and their use in the development of polyvinylpyrrolidone grafted nanoparticles. US9732169B2. University Of South Carolina.

406 McCormick, C.L. III Lowe, A.B., and Sumerlin, B.S. (2006). Preparation of transition metal nanoparticles and surfaces modified with (CO)polymers synthesized by RAFT. US7138468B2. University of Southern Mississippi.

407 McCormick, C.L., Lowe, A.B., and Sumerlin, B.S. (2008). Preparation of transition metal nanoparticles and surfaces modified with (CO) polymers synthesized by RAFT. US7417096B2. University Of Southern Mississippi.

408 McCormick, C.L. III Lowe, A.B., and Sumerlin, B.S. (2011). Preparation of transition metal nanoparticles and surfaces modified with (co)polymers synthesized by RAFT. US8084558B2. University of Southern Mississippi.

409 Scales, C.W., Huang, F., and McCormick, C.L. (2010). Non-immunogenic, hydrophilic/cationic block copolymers and uses thereof. US7718432B2. University of Southern Mississippi.

410 Hawkett, B.S., Such, C.H., Nguyen, D.N. et al. (2006). Surface polymerization process using RAFT agents for manufacture of polymer-encapsulated particulates. WO2006037161A1. The University of Sydney, Australia.

411 Hawkett, B.S., Such, C.H., and Nguyen, N. (2014). Polymer product and interfacial polymerisation process using RAFT agent. US8796359B2. University of Sydney.

412 Hawkett, B.S. and Jain, N. (2014). Polymer microgel beads. US8765183B2. University of Sydney.

413 Hawkett, B.S. and Jain, N. (2014). Polymer microgel beads and preparative method thereof. US8852641B2. University of Sydney.

414 Hawkett, B.S., Jain, N., Pham, T.T.B. et al. (2014). Administrable compositions. US8709486B2. University of Sydney.

415 Baker, M.P., Davey, T.W., Hawkett, B.S. et al. (2011). Water-swellable polymer-encapsulated materials. WO2011066608A1. The University of Sydney, Australia.

416 Hawkett, B.S., Hambley, T.W., Bryce, N.S. et al. (2012). Treatment of a solid tumour comprising co-administration of polymeric steric stabilized particulate material and cellular toxin. WO2012142669A1. The University of Sydney, Australia.

417 Hawkett, B.S., Hambley, T.W., Bryce, N.S. et al. (2015). Method for the treatment of a solid tumour. US10376589B2. The University of Sydney, Australia.

418 Stayton, P.S., Hoffman, A.S., Yin, X. et al. (2010). Temperature- and pH-responsive polymer compositions. US7718193B2. University of Washington.
419 Stayton, P.S., Hoffman, A.S., Lai, J.-i. et al. (2011). Stimuli-responsive magnetic nanoparticles and related methods. US7981688B2. University of Washington.
420 Stayton, P.S., Hoffman, A.S., Lai, J. et al. (2013). Stimuli-responsive magnetic nanoparticles and related methods. US8507283B2. University of Washington.
421 Stayton, P.S., Nash, M., and Lai, J. (2013). System and method for magnetically concentrating and detecting biomarkers. US8426214B2. University of Washington.
422 Stayton, P.S., Hoffman, A.S., Convertine, A.J. et al. (2009). Diblock copolymers and polynucleotide complexes thereof for delivery into cells. WO2009140427A2. University of Washington, USA; PhaseRx.
423 Stayton, P.S., Hoffman, A.S., Convertine, A.J. et al. (2009). Polymeric carrier for the delivery of polynucleotides into a living cell. WO2009140421A2. University of Washington, USA; PhaseRx, Inc.
424 Stayton, P.S., Hoffman, A.S., Convertine, A.J. et al. (2010). Omega-functionalized polymers, junction-functionalized block copolymers, polymer bioconjugates, and radical chain extension polymerization. WO2010077678A2. University of Washington, USA; PhaseRx, Inc.
425 Monahan, S.D., Johnson, P.H., Declue, M.S. et al. (2011). Targeting monomers and polymers having targeting blocks. WO2011062965A2. University of Washington, USA; Phaserx, Inc.
426 Stayton, P.S., Hoffman, A.S., Convertine, A.J. et al. (2009). Micellic assemblies comprising a plurality of copolymers. WO2009140429A2. University of Washington, USA; PhaseRx.
427 Stayton, P.S., Montgomery, K., Crane, C. et al. (2018). Engineered cells and agent compositions for therapeutic agent delivery and treatments using same. WO2018165194A1. University of Washington, USA; Seattle Children's Research Institute; Commonwealth Scientific and Industrial Research Organisation.
428 Stayton, P.S., Convertine, A., Das, D. et al. (2018). Cell-based methods and compositions for therapeutic agent delivery and treatments using same. WO2018165198A1. University of Washington, USA; Seattle Children's Research Institute; Commonwealth Scientific and Industrial Research Organisation.
429 Convertine, A.J., Postma, A., Ratner, D.M. et al. (2019). Radiant star nanoparticle prodrugs and related methods. WO2019160983A1. University of Washington, USA; Commonwealth Scientific and Industrial Research Organisation.
430 Jiang, S., Xu, X., Li, Y. et al. (2009). Marine coatings. US9533006B2. University of Washington, USA.
431 Mrozek, R.A., Lenhart, J.L., Lambeth, R.H., and Andzelm, J.W. (2013). Branched additives for polymer toughening. US20130303712A1. United States Dept. of the Army, USA.
432 Wynne, J.H., Lundin, J.G., McGann, C.L. et al. (2017). Acute care cover for severe injuries. WO2017156250A2. United States Dept. of the Navy, USA.
433 Duvall, C.L., Nelson, C.E., Kintzing, J. et al. (2014). Polymeric nanoparticles comprising PEG-methacrylate block copolymers. WO2014066912A1. Vanderbilt University, USA.

434 Haddleton, D.M., Mantovani, G., and Ladmiral, V. (2012). Process for making polymers and supports comprising pendant sugar side groups. US8197847B2. Warwick Effect Polymers.

435 Cao, Z., Wang, W., and Yue, Z. (2016). Methods and compositions relating to biocompatible implants and a biocompatible hydrogel-encapsulated therapeutic agent. WO2016138528A1. Wayne State University, USA.

436 Scales, C., Venkatasubban, K., Mahadevan, S. et al. (2011). Non-reactive, hydrophilic polymers having terminal siloxanes and uses of the same. WO2011140318A1. Johnson & Johnson Vision Care, Inc., USA.

437 Scales, C., Venkatasubban, K., Mahadevan, S. et al. (2017). Non-reactive, hydrophilic polymers having terminal siloxanes and methods for making and using the same. US9815979B2. Johnson & Johnson Vision Care.

438 George, E., Mahadevan, S., Venkatasubban, K. et al. (2012). Medical devices having homogeneous charge density and methods for making same. WO2012151135A1. Johnson & Johnson Vision Care, Inc., USA.

439 Scales, C.W., McCabe, K.P., and Healy, B.M. (2013). Polymers and nanogel materials and methods for making and using the same. WO2013177506A2. Johnson & Johnson Vision Care, Inc., USA.

440 Scales, C.W., McCabe, K.P., and Healy, B.M. (2013). Polymers and nanogel materials and methods for making and using the same. WO2013177523A2. Johnson & Johnson Vision Care, Inc., USA.

441 Lai, J., Egan, D., Hsu, R. et al. (2006). Applications of telechelic reversible addition fragmentation chain transfer polymers. In: *ACS Symposium Series*. 944 (ed. K. Matyjaszewski), 547–563. https://doi.org/10.1021/bk-2006-0944.ch037.

442 Lubnin, A., Lenhard, S., and Lai, J. (2006). RAFT emulsions, microemulsions and dispersions. *Surf. Coat. Int., Part B: Coat. Trans.* 89: 293–304. doi: 10.1007/BF02765581.

443 Lubnin, A., O'Malley, K., Hanshumaker, D., and Lai, J. (2010). Waterborne RAFT polymers. *Eur. Polym. J.* 46: 1563–1575. doi: 10.1016/j.eurpolymj.2010.04.005.

444 Moad, G., Rizzardo, E., and Thang, S.H. (2011). A RAFT tutorial. *Strem Chem.* 25: 2–10.

445 Grajales, S. (ed.) (2012). *Controlled Radical Polymerization Guide*. St. Louis, MO: Sigma-Aldrich.

446 Moad, G., Rizzardo, E., and Thang, S.H. (2010). Reversible addition fragmentation chain transfer (RAFT) polymerization. *Mater. Matters* 5: 2–5.

447 Couvreur, L., Guerret, O., Laffitte, J.-A., and Magnet, S. (2005). *Polym. Prepr. (Am. Chem. Soc., Div. Polym. Chem.)* 46: 219–220.

448 Sheehan, M.T., Farnham, W.B., Okazaki, H. et al. (2008). RAFT technology for the production of advanced photoresist polymers. *Proc. SPIE* 6923: 69232E/69231–69232E/69239. doi: 10.1117/12.772115.

449 Postma, A. and Skidmore, M. (2022). How to do a RAFT polymerisation. In: *RAFT Polymerization: Materials, Synthesis and Applications* (eds. G. Moad and E. Rizzardo), 24–58. Weinheim: Wiley-VCH.

450 Tsuji, R. and Hiiro, T. (2006). Process producing vinyl polymer having alkenyl group at end, vinyl polymer, and curable composition. US7009004B2. Kaneka Corporation.

451 Tsuji, R. and Hiiro, T. (2006). Process producing vinyl polymer having alkenyl group at end, vinyl polymer, and curable composition. US7081503B2. Kaneka Corporation.

452 Wilczewska, Z.A., Destarac, M., Zard, S. et al. (2006). Method for free radical reduction of dithiocarbonylated or dithiophosphorylated functions borne by a polymer. US7109276B2. Rhodia Chimie.

453 Wilczewska, Z.A., Destarac, M., Adam, H. et al. (2008). Method for synthesis of polymers with thiol functions. US7396901B2. Rhodia Chimie.

454 Adam, H. and Liu, W.-L. (2004). Process for removing a dithiocarbonyl group at the end of a polymer chain. US6794486B2. Chimie, Rhodia.

455 Charmot, D., Chang, H.-t., Wang, W., and Piotti, M. (2004). Removal of thiocarbonyl end groups of polymers. WO2004089994A1. Symyx Technologies, Inc., USA.

456 Charmot, D. and Piotti, M. (2005). Removal of the thiocarbonylthio or thiophosphorylthio end group of polymers and further functionalization thereof. US6919409B2. Symyx Technologies, Inc.

457 Perrier, S. (2005). Polymerisation using chain transfer agents. WO2005061555A1. The University of Leeds, UK.

458 Zard, S., Sire, B., and Jost, P. (2005). Process for partial or total oxidizing one or several thiocarbonylthio ends of a polymer arising from radical polymerization controlled by reversible addition-fragmentation. US7473740B2. Rhodia Chimie, Fr.

459 Matioszek, D., Dufils, P.-E., Vinas, J., and Destarac, M. (2015). Selective and quantitative oxidation of xanthate end-groups of RAFT poly(*n*-butyl acrylate) latexes by ozonolysis. *Macromol. Rapid Commun.* 36: 1354–1361. doi: 10.1002/marc.201500115.

460 Farnham, W.B., Moad, G., Thang, S.H. et al. (2010). Method for removing sulfur-containing end groups. US7807755B2. CSIRO.

461 Chiefari, J., Hornung, C., Postma, A., and Saubern, S. (2013). Removal of thiocarbonylthio groups from RAFT polymers. WO2013086585A1. Commonwealth Scientific and Industrial Research Organisation, Australia.

462 Moad, G., Rizzardo, E., and Thang, S.H. (2012). Process for synthesizing thiol terminated polymers. US8283436B2. CSIRO.

463 Farnham, W.B., Fryd, M., and Sheehan, M.T. (2013). Methods for removing sulfur-containing end groups from polymers. WO2013062789A1. E. I. du Pont de Nemours and Company, USA.

464 Zhang, T. and Palasz, P.D. (2017). Thiocarbonylthio-free RAFT polymers and the process of making the same. WO2017027557A1. Henkel.

465 Mattson, K.M., Hawker, C.J., Pester, C.W. et al. (2018). Catalytic functional group removal from a polymer. WO2018017478A1. The Regents of University of California, USA.

466 Feng, X., Alagi, P., Gnanou, Y., and Hadjichristidis, N. (2020). Removal of thiocarbonylthio end groups from polymers synthesized by reversible addition-fragmentation chain transfer polymerization. WO2020100086A1. King Abdullah University of Science and Technology, Saudi Arabia.

467 Lowe, A.B. and Dallerba, E. (2022). RAFT functional end-groups: installation and transformation. In: *RAFT Polymerization: Materials, Synthesis and Applications* (eds. G. Moad and E. Rizzardo), 753–804. Weinheim: Wiley-VCH.

468 Moad, G. (2022). Dithioesters in RAFT polymerization. In: *RAFT Polymerization: Materials, Synthesis and Applications* (G. Moad and E. Rizzardo), 223–270. Weinheim: Wiley-VCH.

469 Wang, M., Marty, J.-D., and Destarac, M. (2022). Xanthates in RAFT polymerization. In: *RAFT Polymerization: Materials, Synthesis and Applications* (eds. G. Moad and E. Rizzardo), 495–550. Weinheim: Wiley-VCH.

470 Moad, G. (2022). Dithicarbamates in RAFT polymerization. In: *RAFT Polymerization: Materials, Synthesis and Applications* (eds. G. Moad and E. Rizzardo), 551–610. Weinheim: Wiley-VCH.

25

Cationic RAFT Polymerization

Mineto Uchiyama, Kotaro Satoh, and Masami Kamigaito

Nagoya University, Graduate School of Engineering, Department of Molecular and Macromolecular Chemistry, Furo-cho, Chikusa-ku, Nagoya 464-8603, Japan

25.1 Introduction

Reversible addition fragmentation chain transfer (RAFT) polymerizations refer to radical polymerizations involving a RAFT process mainly using a thiocarbonylthio compound, and the term was coined to describe such polymerizations by Rizzardo et al. in 1998 [1]. As described in this book, radical RAFT polymerizations based on sulfur compounds are among the most widely used living/controlled or reversible deactivation radical polymerizations for precision polymer synthesis [2]. However, the term RAFT, which is an acronym for reversible addition fragmentation chain transfer, is not limited to polymerizations proceeding via radical processes using thiocarbonylthio compounds and can be used more generally for describing any reaction proceeding via a similar RAFT chain transfer mechanism. Furthermore, RAFT polymerizations are categorized as degenerative chain transfer (DT) polymerizations, proceeding via similar reversible chain transfers between propagating and dormant polymer chain ends, which allows the effective control of not only radical polymerizations but also other chain growth polymerizations using appropriate chain transfer agents [3, 4].

This chapter focuses on RAFT or DT polymerizations that specifically proceed via a cationic intermediate, namely, cationic RAFT or DT polymerizations, in contrast to many chapters, which mainly address radical RAFT polymerizations. Therefore, this chapter first presents the background and provides an overview of cationic RAFT polymerizations and then presents details in terms of effective RAFT or DT agents; cationic initiators, cationogens, or catalysts; monomers; and the design of well-defined polymers such as end-functionalized, block, and star polymers.

RAFT Polymerization: Methods, Synthesis and Applications, First Edition.
Edited by Graeme Moad and Ezio Rizzardo.

25.2 Background and Overview of Cationic RAFT Polymerizations

25.2.1 Living Cationic Polymerization and Mechanism

Living cationic polymerization was achieved with isobutyl vinyl ether (IBVE) using hydrogen iodide (HI) as an initiator and iodine (I_2) as an activator by Higashimura, Sawamoto, and Miyamoto in 1984 [5] and with isobutylene (IB) using cumyl acetate and BCl_3 by Faust and Kennedy in 1986 [6]. Since then, many living cationic polymerizations have been developed with various monomers using a broad range of compounds; however, except for a few examples, they are mostly based on the Lewis acid-catalyzed processes [7–11].

The Lewis acid-catalyzed living cationic polymerizations proceed via carbocationic species generated through the reversible activation of a covalent carbon–halogen or carbon–oxygen ester bond by a metal halide, where the propagating cationic species can be stabilized by nucleophilic counter-anions derived from the halide or carboxylate and Lewis acid catalyst (Figure 25.1a). In view of kinetic treatments [12], this type of living cationic polymerization can be categorized into the same family as that of metal-catalysed living radial polymerizations [13] or atom transfer radical polymerizations [14] because the reversible generation of the propagating species relies on the catalyst-induced activation of the dormant species.

In addition to the Lewis acid-catalyzed mechanisms, another type of living cationic polymerization without using Lewis acid catalysts was reported by Webster et al. in 1990 [15]. Living cationic polymerization is achieved using

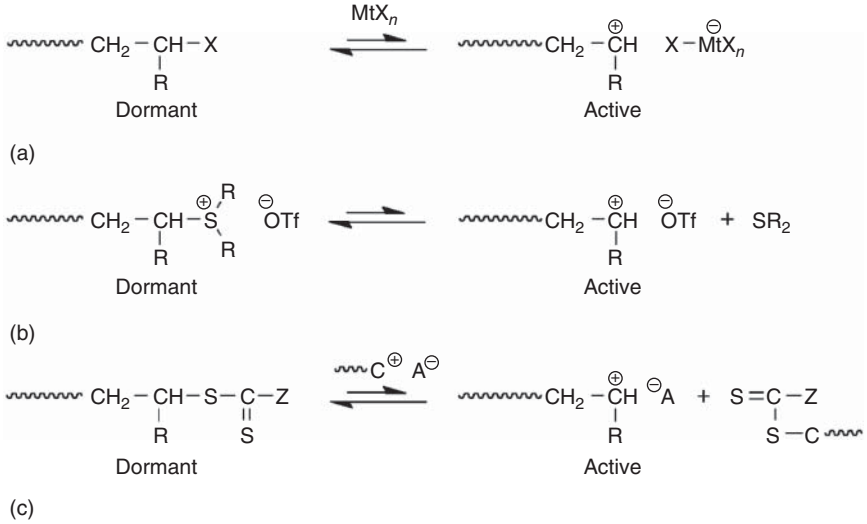

Figure 25.1 Three general mechanisms for living cationic polymerization. (a) Lewis acid-catalyzed living cationic polymerization, (b) sulfide-mediated living cationic polymerization, and (c) cationic RAFT polymerization.

trifluoromethanesulfonic or triflic acid (TfOH) as the initiator in the presence of a large amount of dialkyl sulfide, such as Me_2S or tetrahydrothiophene, which forms a stable sulfonium polymer chain end via interactions with the propagating carbocationic species derived from TfOH and vinyl ether (Figure 25.1b). The sulfonium terminal serves as the dormant species and automatically and reversibly generates the propagating cationic species to induce living cationic polymerization. This living cationic polymerization can be grouped in the same category as nitroxide-mediated radial polymerizations [16] because the propagating species reversibly forms without a catalyst based on a dissociation–combination mechanism.

Despite such similarities in the mechanisms of living cationic and radical polymerizations, no distinct RAFT or DT processes were reported until 2015 [17]. In 1996, a DT process for a living cationic polymerization was suggested by Müller et al. [18], who kinetically analysed the cationic polymerization of isobutylene with dicumyl dichloride (DiCumCl) and BCl_3 originally developed by Kennedy, Smith, and Ivan in the 1980s [19, 20]. Although Kennedy and coworkers only mentioned the contribution of the *irreversible* chain transfer of the polyisobutylene cation to DiCumCl in the polymerization, in which DiCumCl was named *inifer*, other researchers evaluated and discussed the possibility of a *reversible* chain transfer process between the carbocationic species and the dormant C–Cl terminal later on [18, 21, 22]. A reversible chain transfer process has also been suggested by Cramail, Deffieux, and Nuyken in the living cationic polymerization of vinyl ethers using the HI adduct of IBVE (HI–IBVE) as an initiator without Lewis acid catalysts but in the presence of an ammonium salt [23, 24]. The contribution of the DT process is indirectly supported by the result that the HCl adduct of IBVE (HCl–IBVE), which does not initiate the polymerization of IBVE in the presence of nBu$_4$NClO$_4$, can participate in the initiation in the presence of HI–IBVE and nBu$_4$NClO$_4$. This result suggests that the carbocationic species, which is generated from the C—I bond of HI–IBVE and nBu$_4$NClO$_4$, abstracts a chloride anion from the C—Cl bond of HCl–IBVE to generate an additional initiating carbocationic species and that similar activations of the C—I and C—Cl bonds by the carbocationic species also occur even during the cationic polymerization. Then, in 2015, a distinct cationic RAFT polymerization of vinyl ether was reported using a similar thiocarbonylthio compound in the presence of a cationic initiator such as TfOH (Figure 25.1c) [17].

25.2.2 Overview of Cationic RAFT Polymerizations and Comparison to Radical RAFT Polymerizations

As in radical RAFT polymerizations, the cationic RAFT polymerizations proceed via a similar RAFT mechanism but via a cationic intermediate. In the first example of a cationic RAFT polymerization (Figure 25.2), the carbocationic species, which is generated from a cationic initiator such as TfOH, adds to the C=S bond of a thiocarbonylthio compound as a chain transfer agent to generate the cationic intermediate stabilized by the sulfur atoms, which is quite typical of such reactions. The cationic intermediate then undergoes fragmentation to generate the carbocationic species that originates from the chain transfer agent along with a dormant species with a

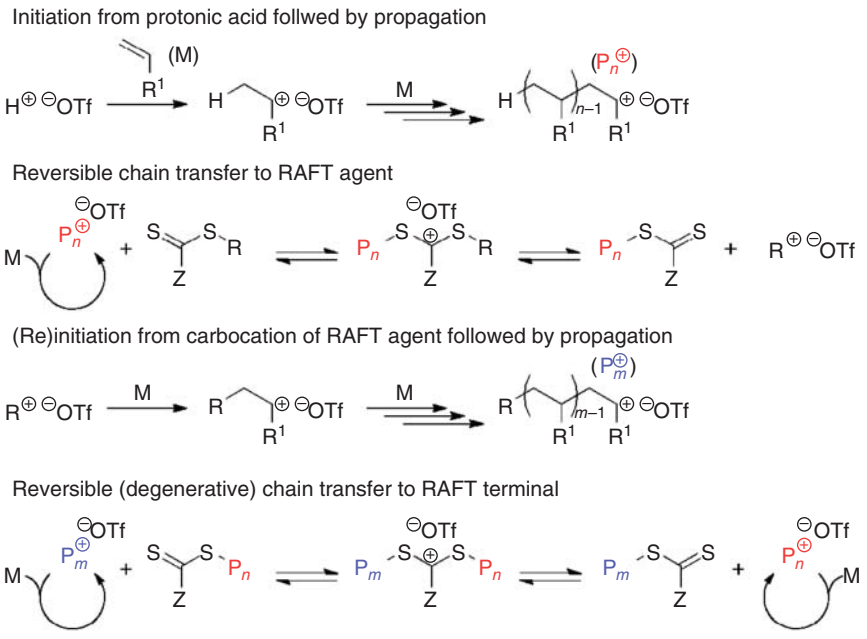

Figure 25.2 General scheme for cationic RAFT polymerization using RSC(S)Z and TfOH.

thiocarbonylthio terminal. The resulting carbocationic species originating from the RAFT agent adds to the monomer to form the cationic propagating species, and the resulting thiocarbonylthio chain end undergoes a similar addition fragmentation process with another propagating carbocationic chain end to generate a new carbocationic propagating species via the RAFT mechanism.

As expected from the cationic RAFT mechanism, compared with its radical RAFT counterpart, it offers some similar and some different features. (i) The molecular weight distribution (MWD) should become narrower as the RAFT process becomes faster than the propagation. (ii) The R and Z groups of the thiocarbonylthio compound (R–SC(S)Z) should be selected such that the RAFT process is faster. (iii) The R group should promptly form the cationic species via fragmentation once the addition to the C=S group occurs. (iv) The Z group should be more or less electron donating such that it can stabilize the intermediate to facilitate the RAFT process. (v) The RAFT or DT agents may not be limited to thiocarbonylthio compounds and can be varied as long as they mediate a fast and reversible chain transfer process (Figure 25.3). (vi) The cationic RAFT process requires a cationic initiator, cationogen, or catalyst that can generate the propagating carbocationic species. (vii) The molecular weight can be generally controlled by the feed ratio of monomer to RAFT agent when the amount of initiator is very low compared with the RAFT agent. (viii) The counter-anion, which typically originates from the initiator, should affect the cationic propagation in terms of the rate and stereochemistry, unlike in radical RAFT polymerizations, where no such counterpart exists. (ix) Cationic RAFT polymerizations using a thiocarbonylthio RAFT agent may be compatible with radical

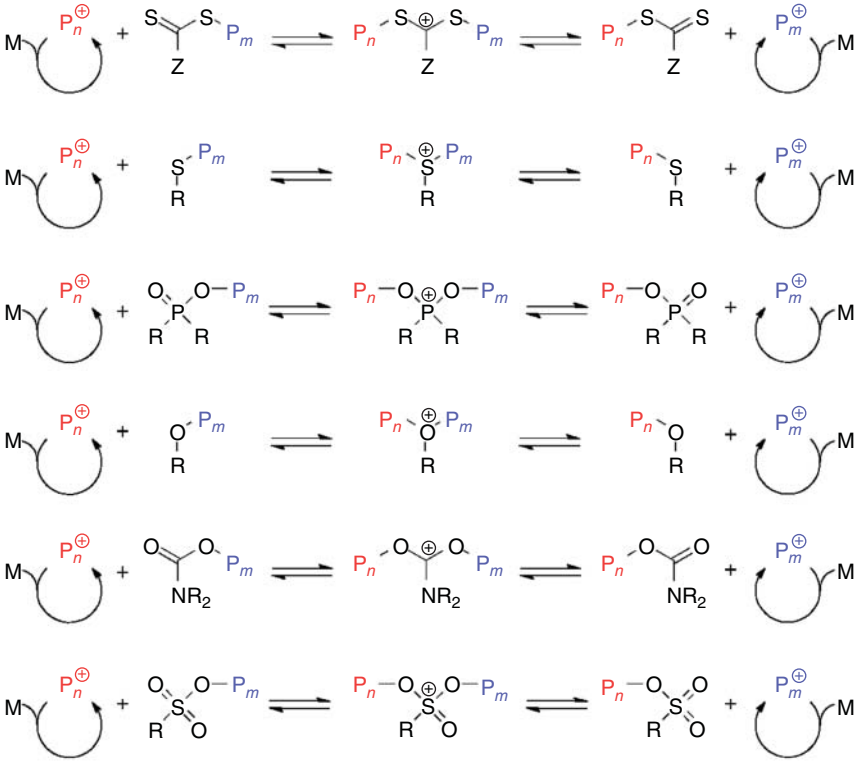

Figure 25.3 Intermediates in cationic RAFT or DT polymerization.

RAFT polymerizations and can be utilized for the synthesis of novel well-defined copolymers consisting of cationically and radically polymerizable monomers.

These features are important not only for designing cationic RAFT or DT polymerizations but also for creating novel well-defined polymers with unique properties and functions, as described below.

25.3 Design of Cationic RAFT or DT Polymerizations

The components of cationic RAFT or DT polymerizations are (i) the chain transfer agents, which efficiently induce fast and reversible chain transfer reactions via a cationic intermediate; (ii) initiators, cationogens, or catalysts, which generate cationic initiating species; and (iii) cationically polymerizable monomers. This section summarizes the design of cationic RAFT or DT polymerizations in terms of these components.

25.3.1 RAFT or DT Agents for Cationic Polymerizations

Various compounds, which are formally adducts of a protonic acid and a cationically polymerizable monomer such as vinyl ethers and *p*-methoxystyrene (pMOS),

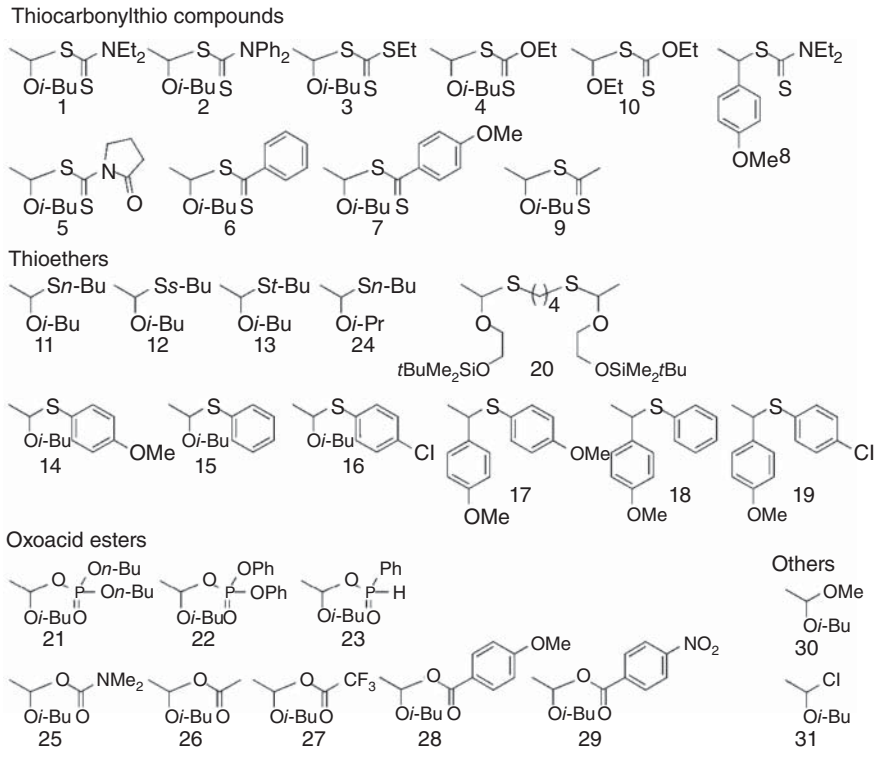

Figure 25.4 Various cationic RAFT or DT agents.

have been employed as possible chain transfer agents in cationic polymerizations (Figure 25.4). Cationic RAFT polymerizations were first reported for IBVE using a series of thiocarbonylthio compounds (R–SC(S)Z) (**1**–**5**), which may generate carbocations (R^+) with the same structure as those derived from IBVE, with various Z groups, such as dithiocarbamates, trithiocarbonates, and xanthates, in the presence of a small amount of TfOH as the initiator or cationogen [17]. The MWDs of the resulting polymers are highly dependent on the Z group. Dithiocarbamates with alkyl and phenyl groups (**1** and **2**) give the narrowest MWDs ($M_w/M_n < 1.1$), whereas pyrrolidinone dithiocarbamate (**5**) with an adjacent electron-withdrawing carbonyl moiety results in a broader MWD ($M_w/M_n = 1.8$). Furthermore, trithiocarbonate (**3**) also effectively provides polymers with narrow MWDs ($M_w/M_n = 1.1$–1.2) with high molecular weights ($M_n \sim 10^5$), while xanthate (**4**) results in slightly broader MWDs ($M_w/M_n = 1.5$–1.6). An electron-donating substituent thus stabilizes the cationic intermediate, enhancing the reversible chain transfer process and enabling good molecular weight control.

Some of these thiocarbonylthio compounds (**1** and **3**–**5**) and additional compounds (**6** and **7**) have been used for the cationic polymerizations of various alkyl vinyl ethers, including IBVE, using photoredox catalysts (see Section 25.3.2), which produces cationic propagating species directly from the RAFT agents [25–27]. Similarly, dithiocarbamate (**1**) and trithiocarbonate (**3**) can serve as efficient cationic

RAFT agents to provide polymers with narrow MWDs (M_w/M_n = 1.1–1.2) [26]. In addition, xanthate (**4**), pyrrolidinone dithiocarbamate (**5**), and dithiobenzoate (**6**) give polymers with M_ns close to the calculated values but with broader MWDs (M_w/M_n = 1.9–2.2) because of the slower RAFT process [27]. A similar electronic effect through resonance, which narrows the MWD (M_w/M_n = 1.5), is observed with an electron-donating *p*-methoxy substituent on dithiobenzoate (**7**). The dithiocarbamate that can generate the carbocation of pMOS (**8**) is not efficient as a RAFT agent for vinyl ethers because fragmentation into the pMOS carbocation hardly occurs in comparison to the formation of the more stable vinyl ether cation.

Other thiocarbonylthio compounds (dithioacetate [**9**] and xanthate [**10**]) and trithiocarbonate (**3**), which can generate vinyl ether carbocations, have been employed for the cationic polymerization of vinyl ethers and pMOS in the presence of HCl with Et_2O to produce polymers with controlled molecular weights and narrow MWDs [28–30].

In contrast to radical RAFT polymerizations, compounds other than thiocarbonylthio can be used as cationic RAFT or DT agents, as they can react with the propagating carbocationic species and induce fast, reversible chain transfer reactions via a stable cationic intermediate. Another series of efficient cationic chain transfer agents is thioether. In particular, thioacetal (**11**), which can be easily prepared from IBVE and *n*-butanethiol in the presence of a catalytic amount of methanesulfonic acid (CH_3SO_3H), is effective for controlling the cationic polymerization of IBVE in the presence of a small amount of TfOH to give polymers with controlled molecular weights and narrow MWDs (M_w/M_n = 1.1–1.2) [31]. The polymerization is supposed to proceed via a cationic DT mechanism, in which the sulfonium intermediate forms via the attack of the dormant thioether terminal by the propagating cationic species. In addition to the similar electronic effects of thioethers, steric effects are observed. By increasing the bulkiness around the thioether using secondary (**12**) and tertiary butanethiol (**13**) derivatives, the MWDs become broader (M_w/M_n = 1.6 and 1.8) because of the slower DT process, which is significantly affected by the adjacent substituents. Electronic effects are observed when using thioethers derived from substituted thiophenols (**14**–**16**), and the MWDs gradually become broader (M_w/M_n = 1.52, 1.90, and 1.93). While thioacetal such as **11** completely inhibit the cationic polymerization of pMOS, thioethers, such as adducts of pMOS and thiophenols (**17**–**19**), are more efficient cationic DT agents. A slight electronic effect is observed on the MWDs. A notable feature of the thioether-based system is the high stability of not only the adduct but also the dormant polymer terminal, even during the work-up process under air. Based on these characteristics, a thioether derived from a functionalized vinyl ether and butanedithiol (**20**) can serve as a bifunctional reversible chain transfer agent to give α,ω-functionalized telechelic polymers linked by stable thioacetal linkages in the middle of the polymer chains [31].

Oxoacid esters can also serve as RAFT agents in cationic polymerizations. Especially, adducts of IBVE and phosphorous-based acids, such as phosphoric and phosphinic acids (**21**–**23**), are efficient reversible chain transfer agents for producing poly(IBVE) with controlled molecular weights up to 10^5 and narrow

MWDs (M_w/M_n = 1.1–1.2), where the phosphonium intermediate contributes to the RAFT process, as suggested by ^{31}P NMR analysis [32]. The phosphorous-based RAFT agents and the obtained polymers are colourless and odourless, although the quenching of the polymerization with methanol results in complete removal of the phosphorous group from the dormant terminal. Interestingly, mixtures of phosphoric acid- (**21**) and thiol-based (**24**) chain transfer agents give polymers not only with controlled molecular weights and narrow MWDs but also with mixtures of α- and ω-termini, indicating nearly equivalent crossover reactions between the two reversible chain transfer agents during propagation.

Carboxylic acid esters (**25**–**29**) are less efficient as reversible chain transfer agents for the cationic polymerization of IBVE. However, some electronic effects are observed. Among them, a carbamic acid ester with an electron-donating nitrogen atom (**25**) results in polymers with M_ns close to the calculated values but with a slightly broadened MWD (M_w/M_n = 1.6). In contrast, carboxylic acid esters with electron-withdrawing substituents such as CF_3– and NO_2– moieties, as in **27** and **29**, are much less effective, resulting in much higher molecular weights than those achieved with CH_3- and MeO-moieties, as in **26** and **28**, respectively.

Table 25.1 summarizes the M_n and M_w/M_n values of polymers obtained via cationic polymerizations of IBVE under similar conditions [31, 32] and chain transfer constants (C_{tr}) calculated using M_n, M_w, monomer conversions, and concentrations of each component according to the equations describing their relationships [33]. The effective chain transfer agents with high C_{tr} values for vinyl ethers thus include dithiocarbamates, phosphoric or phosphinic acid esters, trithiocarbonates, and thioethers. An acetal (**30**) was less efficient than thioacetal. In addition, HCl–IBVE (**31**), which is one of the best initiators for Lewis acid-catalyzed living cationic polymerizations of vinyl ethers, is not suitable as a reversible chain transfer agent.

Although RAFT or DT agents can generally be synthesized before the polymerization, preparation and isolation are not necessary for producing polymers with controlled molecular weights and narrow MWDs [32, 34]. The addition of mixtures of phosphoric acid dibutyl ester ($(n\text{-BuO})_2PO_2H$) and a trace amount of TfOH to a solution of IBVE provides polymers with a level of control similar to that obtained using the isolated adducts. 1-Octanethiol ($n\text{-}C_8H_{17}SH$) can be used in place of $(n\text{-BuO})_2PO_2H$. In these polymerizations, the corresponding adduct, which works as a chain transfer agent, is formed in situ before the cationic polymerization. This method is very simple and easy to handle and does not require the preparation of a chain transfer agent. In addition, methanesulfonic acid (CH_3SO_3H), whose adduct is difficult to isolate because of its instability, is also effective in the presence of a small amount of TfOH, indicating that sulfoxonium ions can also work as intermediates for cationic RAFT polymerizations [34].

Simple alcohols, such as methanol, ethanol, and isopropanol, have been used as precursors of chain transfer agents for the cationic polymerization of pMOS in the presence of photoredox catalysts to afford polymers with controlled molecular weights and narrow MWDs (M_w/M_n = 1.1–1.2) (see Section 25.3.2) [35]. The contribution of the oxonium intermediate via the DT mechanism has been suggested.

Table 25.1 M_n, M_w/M_n, chain transfer constants (C_{tr}) obtained in cationic RAFT or DT polymerization of IBVE under similar conditions.[a)]

Entry	Compound	–X	Conv. (%)[b)]	M_n[c)]	M_n (Calcd)[d)]	M_w/M_n[c)]	C_{tr}[e)]
1	**1**	$-SC(S)NEt_2$	96	5100	5000	1.08	150
2	**2**	$-SC(S)NPh_2$	95	5900	5100	1.08	150
3	**20**	$-OP(O)(OnBu)_2$	97	4900	5000	1.09	60
4	**22**	–OP(O)PhH	94	5100	4800	1.08	37
5	**21**	$-OP(O)(OPh)_2$	93	4900	4800	1.16	18
6	**3**	–SC(S)SEt	90	5000	4700	1.18	12
7	**11**	–S*n*-Bu	92	5600	4900	1.19	8.5
8	**4**	–SC(S)OEt	94	4700	4900	1.59	2.0
9[f)]	**24**	$-OC(O)NMe_2$	96	4900	5000	1.62	1.7
10	**29**	$-OCH_3$	89	5800	4800	1.82	1.6
11	**5**	–SC(S)pyrrolidone	92	4900	4900	1.88	1.3
12	**25**	$-OC(O)CH_3$	92	8700	4900	3.41	0.22
13	**27**	$-OC(O)C_6H_4OCH_3$	97	8000	5000	5.33	0.20
14	**30**	–Cl	94	27700	4800	2.72	0.07
15	**28**	$-OC(O)C_6H_4NO_2$	96	29500	5000	3.23	0.05
16	**26**	$-OC(O)CF_3$	91	37200	4700	2.84	0.05

a) Polymerization condition: $[M]_0/[\text{chain transfer agent}]_0/[TfOH]_0 = 500/10/0.05$ mM in *n*-hexane/CH_2Cl_2/Et_2O (80/10/10) at –40 °C.
b) Determined by ^1H NMR.
c) The M_n and M_w/M_n were determined by SEC.
d) $M_n(\text{Calcd}) = \text{MW(IBVE)} \times [M]_0/[\text{chain transfer agent}] \times \text{Conv.} + \text{MW (chain transfer agent)}$.
e) Chain transfer constant.
f) $[TfOH]_0 = 0.50$ mM.
Modified from tables in [31, 32].

25.3.2 Initiators, Cationogens, or Catalysts for Cationic RAFT or DT Polymerizations

For cationic RAFT or DT polymerization, initiators, cationogens, cation sources, or catalysts that can generate propagating carbocationic species must be used (Figure 25.5) in addition to chain transfer agents.

As conventional radical initiators are employed in radical RAFT polymerization, as typical cationic initiators, strong protonic acids such as TfOH have been employed for cationic RAFT polymerizations [17]. In contrast to radical initiators, such as 4,4′-azobisisobutyronitrile (AIBN) that gradually decomposes to generate radical species, all TfOH molecules can immediately initiate cationic polymerizations. Therefore, the molecular weights are influenced not only by the concentration of RAFT agent but also by that of TfOH, where the M_n value

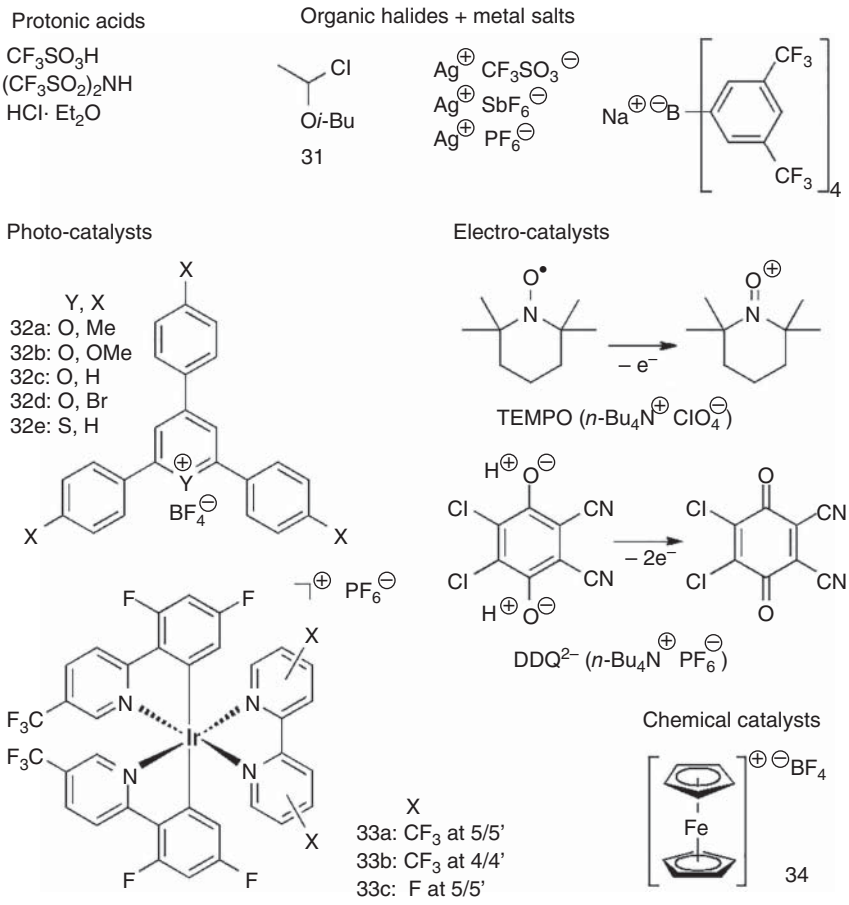

Figure 25.5 Initiators, cationogens, and catalysts for cationic RAFT or DT polymerization.

is theoretically determined by the feed ratio of the monomer to the sum of the RAFT agent and TfOH ($M_n \propto [M]_0/([\text{RAFT agent}]_0 + [\text{TfOH}]_0)$). This relationship has been confirmed in cationic RAFT polymerizations of IBVE using **3** and TfOH [17]. However, the effects of TfOH on the molecular weight of the resulting polymers can be negligible when the concentration of TfOH is sufficiently low. Indeed, a trace amount of TfOH ($[\text{TfOH}]_0 = 0.05$ mM or 8 ppm in the solution; $[\text{TfOH}]_0/[M]_0 = 10^{-4}$; $[\text{TfOH}]_0/[\mathbf{3}]_0 = 5 \times 10^{-3}$) is enough to induce the cationic RAFT polymerization of IBVE, while the molecular weight of the polymer is substantially determined by the feed ratio of IBVE to **3**.

Other strong protonic acids, such as trifluoromethanesulfonic imide or triflimide ($(CF_3SO_2)_2NH$: Tf_2NH), can be used to induce very fast polymerization [17]. However, weaker protonic acids, such as CH_3SO_3H and CF_3CO_2H, do not produce polymers, most likely because they form an adduct of IBVE with its more nucleophilic counter-anion. An interesting but curious result has been obtained using an HCl solution of Et_2O as an initiator in conjunction with **9** or an acetic acid

adduct of 2-methoxyethyl vinyl ether as a chain transfer agent [28]. The cationic polymerization of IBVE gives polymers with narrow MWDs. Because acetate is not a good chain transfer agent for cationic RAFT polymerizations of vinyl ethers (Table 25.1) but is a good initiator for Lewis acid-catalyzed cationic polymerizations [11], a small amount of HCl, which may remain due to the slow initiation in the presence of Lewis basic Et_2O, can act as a Lewis acid catalyst for the activation of the thioester and oxygen ester terminals.

Another method to form cationic species is to use mixtures of an organic halide and a metal salt with a counter-anion with low nucleophilicity. In particular, equimolar mixtures of HCl–IBVE (**31**) and silver salts (Ag^+) of triflate (TfO^-), hexafluoroantimonate (SbF_6^-), or hexaflurophosphate (PF_6^-) result in cationic species with various counter-anions and insoluble silver chloride to induce the cationic RAFT polymerization of IBVE in the presence of **1** as a RAFT agent, affording polymers with controlled molecular weights and narrow MWDs ($M_w/M_n \leq 1.1$) [36]. A sodium salt with a non-nucleophilic counter-anion ($Na^+B[3,5\text{-}(CF_3)_2Ph]_4^-$ or Na^+BArF^-) can also be used upon mixing with **31** in the presence of **3** at −78 °C to achieve almost atactic poly(IBVE) ($r : m = 48 : 52$) with narrow MWDs ($M_w/M_n \leq 1.1$) because the tacticity is determined by the non-nucleophilic counter-anion and the molecular weight is controlled by the RAFT process. This result suggests the possibility of simultaneously controlling the molecular weight and tacticity with the RAFT agent and counter-anion, respectively; simultaneously controlling these parameters in Lewis acid-catalyzed living cationic polymerizations is quite difficult because the counter-anion plays both roles.

As in the case of photoredox radical RAFT polymerizations [4], photoredox catalysts are similarly effective for generating cationic species directly from chain transfer agents to induce cationic RAFT polymerizations. However, in cationic RAFT polymerizations, photoredox catalysts should oxidize the RAFT agent to produce the carbocationic species and a radical fragment, in contrast to the photoredox radical RAFT polymerization in which the photoredox catalysts reduce the RAFT agent to produce the radical and an anionic fragment. The first process has been reported in the cationic polymerization of pMOS using 2,4,6-tri(*p*-tolyl)pyrylium tetrafluoroborate (**32a**) under blue LED irradiation (450 nm) in the presence of MeOH as a precursor of the chain transfer agent, where an initiation mechanism involving the single-electron oxidation of pMOS is proposed [35]. Furthermore, a series of 2,4,6-triarylpyrylium salts (**32a**–**32e**) have been employed in conjunction with various thiocarbonylthio compounds for the cationic polymerization of various vinyl ethers under blue LED irradiation (450 nm) [26, 27]. All these photoredox catalysts afford poly(IBVE) with controlled molecular weights and narrow MWDs ($M_w/M_n = 1.1$–1.2), although the polymerization rates depend on the substituents of the pyrylium salts, which affect the activities and redox potentials of the photoredox catalysts. The temporal control of the polymerization was achieved by switching the irradiation on and off, and the controllability is also dependent on the photoredox catalysts. The temporal control can be improved by using more stable polypyridyl iridium complexes (**33a**–**33c**), as both the excited- and ground-state redox potentials of the catalysts are important [37].

Electroredox catalysts can also be used to generate cationic propagating species from vinyl ethers and the thiocarbonylthio moiety of the RAFT agents upon exposure to an electric current. As a precursor of the oxidizing agent, (2,2,6,6-tetramethylpiperidin-1-yl)oxyl (TEMPO) has been used in the presence of **1** and n-Bu_4NClO_4, which serves as an electrolyte as well as a counter-anion, for the cationic polymerization of IBVE [38]. When an oxidizing current is applied, TEMPO is oxidized at the anode to generate the TEMPO cation, which oxidizes **1** to generate the carbocation and a thiyl radical via the mesolytic cleavage of the C—S bond. This electrochemical system is effective not only for vinyl ethers but also for pMOS, which cannot be polymerized by photochemical processes with thiocarbonylthio compounds, and provides polymers with controlled molecular weights. Temporal control is achieved by switching the electrical stimulus between oxidizing and reducing currents. Alternatively, 2,3-dichloro-5,6-dicyanodipehnol (DDHQ) has been employed in conjunction with **3** and n-Bu_4NPF_6 in the polymerization of IBVE to afford polymers with controlled molecular weights under an oxidizing potential, which oxidized DDQ^{2-} to DDQ [39]. The system is also effective for other vinyl ethers, pMOS, and *p*-hydroxystyrene (pHS). Temporal control can also be achieved by switching the applied potential on and off.

As a chemical single-electron oxidizing catalyst, ferrocenium tetrafluoroborate ($FcBF_4$) effectively provides well-controlled polymers with narrow MWDs from vinyl ethers and pMOS in conjunction with **1**, which is oxidized by $FcBF_4$ [40, 41]. The temporal control of the polymerization can be achieved through the addition of a dithiocarbamate anion with sodium salt as the reducing agent.

25.3.3 Monomers for Cationic RAFT or DT Polymerizations

Monomers that can be polymerized in a controlled manner using cationic RAFT or DT polymerizations include vinyl ethers and relatively highly cationically polymerizable styrenes with electron-donating substituents, such as *p*-alkoxystyrenes, pHS, and α-methylstyrene (αMS) (Figure 25.6).

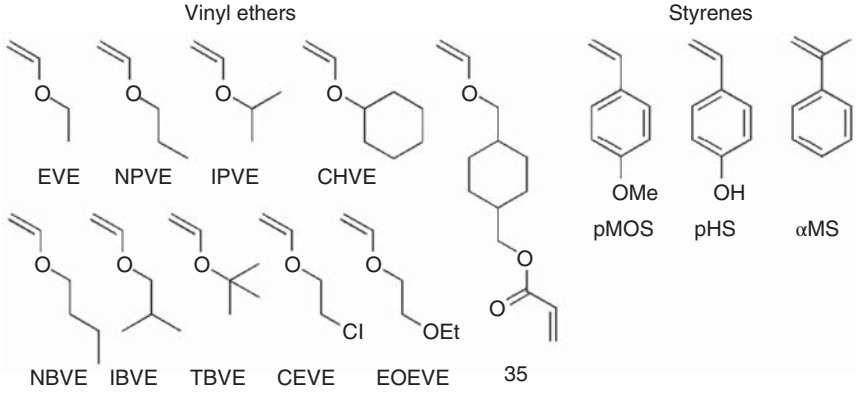

Figure 25.6 Monomers for cationic RAFT or DT polymerization.

The cationic RAFT or DT polymerizations based on not only thiocarbonylthio compounds but also thioethers and phosphoric acid esters are generally effective for polymerizing various alkyl vinyl ethers, including IBVE [17, 26–28, 30–32, 34, 36–42], ethyl vinyl ether (EVE) [24, 26, 27, 31, 36, 38, 40, 43, 44], *n*-propyl vinyl ether (NPVE) [26, 28, 39, 40], isopropyl vinyl ether (IPVE) [30], *n*-butyl vinyl ether (NBVE) [26, 27, 30, 38–40], *tert*-butyl vinyl ether (TBVE) [30], and cyclohexyl vinyl ether (CHVE) [31, 40], as are the Lewis acid-catalyzed living cationic polymerizations [7–11]. The RAFT or DT agents should be designed to generate a vinyl ether-type cation, which is similar to the propagating species in cationic polymerizations of vinyl ethers to induce smooth chain transfer reactions. For vinyl ethers, all the cationogens (protonic acids and organic halides with metal salts) and catalysts (oxidizing photo-, electro-, and chemical redox catalysts) already shown in Figure 25.5 are available. Interestingly, alkyl vinyl ethers, such as IPVE, TBVE, and CHVE, which have a branch on the carbon adjacent to the ether oxygen, are the most reactive monomers in cationic polymerizations and can be polymerized in a controlled manner using the same RAFT cationic systems; however, slightly broader MWDs are observed in some cases [31, 40]. Cationic RAFT polymerizations are thus more universal than Lewis acid-catalyzed polymerizations, in which an initiator, a Lewis acid catalyst, and/or an additive are more judiciously selected depending on the reactivity of the monomer.

Functionalized vinyl ethers, such as 2-chloroethyl vinyl ether (CEVE) [17, 26, 38–40] and 2-ethoxyethyl vinyl ether (EOEVE) [28], are also polymerized in a controlled fashion via a cationic RAFT mechanism, in which the polar groups in the side chains are not involved in the polymerization. In addition, a vinyl ether (**35**) with an acrylate unit in the side chain can be polymerized in a controlled manner to give linear polymers with the acrylate moiety in the side chains, which can be subsequently used for crosslinking reactions to generate star polymers as described in Section 25.4 [41].

As for styrenic monomers, pMOS, one of the most cationically reactive styrenic monomers due to the electron-donating methoxy substituent at the four position of the phenyl group, has been successfully polymerized using thiocarbonylthio compounds, thioethers, and methanol as chain transfer agents in the presence of TfOH, organic halides with metal salts, and photo-, electro-, and chemical redox catalysts [17, 29, 31, 35, 36, 38–40]. Effective chain transfer agents for styrenic monomers include not only **3**, which generates a more stable vinyl ether-type cation and can induce efficient chain transfer, but also **17**, which results in pMOS-type carbocationic species similar to the propagating carbocation in the cationic polymerization of pMOS. Although photoredox catalysts are not effective for inducing the cationic polymerization of pMOS when combined with thiocarbonylthio compounds, combinations with electro- and chemical redox catalysts are more efficient due to their stronger oxidizing potentials [38–40].

A phenolic monomer, pHS, can also be polymerized in a controlled manner without using any protecting groups, which are usually used for cationic polymerizations of pHS because phenols can react with Lewis acids to deactivate the catalyst. Cationic RAFT polymerizations can be metal-catalyst free and thus effective for

direct polymerizations resulting in polymers with controlled molecular weights and narrow MWDs [17, 39].

Another cationically reactive styrenic monomer, αMS, can be polymerized in a controlled manner in the presence of thioether **18** using a mixture of **30** and metal salts with PF_6^-, SbF_6^-, or $BArF^-$ as a cationogen, although the MWDs are relatively broad (M_w/M_n = 1.3–1.6) in comparison to those of vinyl ethers and pMOS [36]. The selection of the counter-anion is also important as triflate anion results in only low molecular weight oligomers because of irreversible chain transfer via β-proton elimination from the α-methyl group induced by triflate anion.

Although cationic RAFT or DT polymerizations are thus effective for vinyl ethers and highly cationically polymerizable styrenes such as pMOS, there have been no successful results for less-activated monomers such as styrene and isobutylene, which result in less stable carbocations. These could be more challenging targets in terms of metal-free controlled/living cationic polymerizations of common vinyl monomers.

25.4 Design of Well-Defined Polymers by Cationic RAFT or DT Polymerizations

Cationic RAFT or DT polymerizations are effective for the synthesis of various well-defined polymers with controlled structures including (i) end-functionalized, (ii) block, and (iii) star polymers. These polymers may be obtained not only via a cationic mechanism but also by combining the cationic and radical RAFT processes based on the similarity between the two systems. This section describes the design and synthesis of well-defined polymers using cationic RAFT and DT polymerizations.

25.4.1 End-Functionalized Polymers

As there are generally two methods, i.e. functionalized initiator and end-capping methods, for the synthesis of end-functionalized polymers in controlled/living polymerizations, both methods are also effective in cationic RAFT or DT polymerizations (Figure 25.7).

As for the functionalized initiator method, a bifunctional DT agent (**20**) has been prepared from *tert*-butyldimethylsilyl-protected 2-hydroxyethyl vinyl ether and 1,4-butanedithiol and used for the cationic DT polymerization of IBVE in the presence of trance TfOH [31]. Even after quenching the polymerization with methanol followed by deprotection of the silyl group, the thioacetal linkage in the middle of the polymer chains is intact and retains the telechelic structure because of the presence of hydroxyl groups at both chain ends. This telechelic polymer can undergo chain extension with diisocyanate via the formation of urethane linkages to afford higher molecular weight polymers with multiblock polyurethane structures.

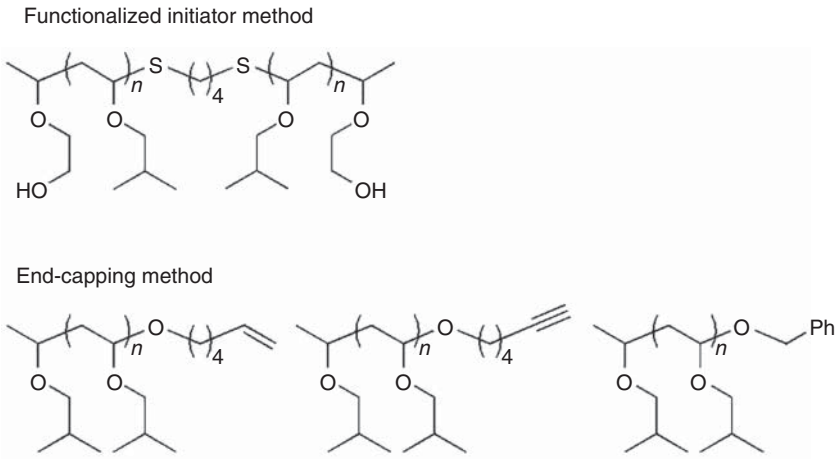

Figure 25.7 End-functionalized polymers via cationic RAFT or DT polymerization.

An efficient one-pot end-capping reaction of poly(IBVE), which is prepared from **3** in the presence of an Ir-based photoredox catalyst (**33a**) under blue LED irradiation, is attained by using a series of functionalized alcohols upon further addition of the photocatalyst and 2,6-di-*tert*-butylpyridine as a proton trap to yield the end-functionalized polymers with alkene, alkyne, and benzene units via the formation of acetal linkages [37]. In contrast, no acetal formation is observed when using other photoredox pyrylium catalysts, such as **32b**.

25.4.2 Block Copolymers

Because cationic RAFT or DT polymerizations yield well-controlled polymers of vinyl ethers and pMOS with high chain end fidelity, their block copolymers have been prepared by the addition of a second monomer to the polymerization mixture upon nearly complete consumption of the first monomer; this process is similar to what is used in Lewis acid-catalyzed living cationic polymerizations.

In addition to successful results in monomer addition experiments for the cationic RAFT or DT polymerizations of vinyl ethers using thiocarbonylthio compounds, thioethers, and phosphoric acid esters in the presence of trace TfOH [17, 31, 32], block copolymers of IBVE and EVE can be synthesized via cationic RAFT polymerizations using **1** and **3** in the presence of photoredox (**32b**), electroredox (TEMPO), and chemical redox (**34**) catalysts [26, 38, 40] (Figure 25.8). The formation of undesired homopolymers of the second monomer can be suppressed in cationic RAFT polymerization because all the TfOH molecules initiate the polymerization instantaneously. This is in sharp contrast to what is observed in radical RAFT polymerizations, in which radical initiators such as AIBN gradually decompose and constantly generate new chains even during block copolymerizations.

The sequential addition of a vinyl ether with an acryloyl group (**35**) to a cationic RAFT polymerization of IBVE with **3** in the presence of trace TfOH results in block copolymers possessing acryloyl moieties in the side chains of the second

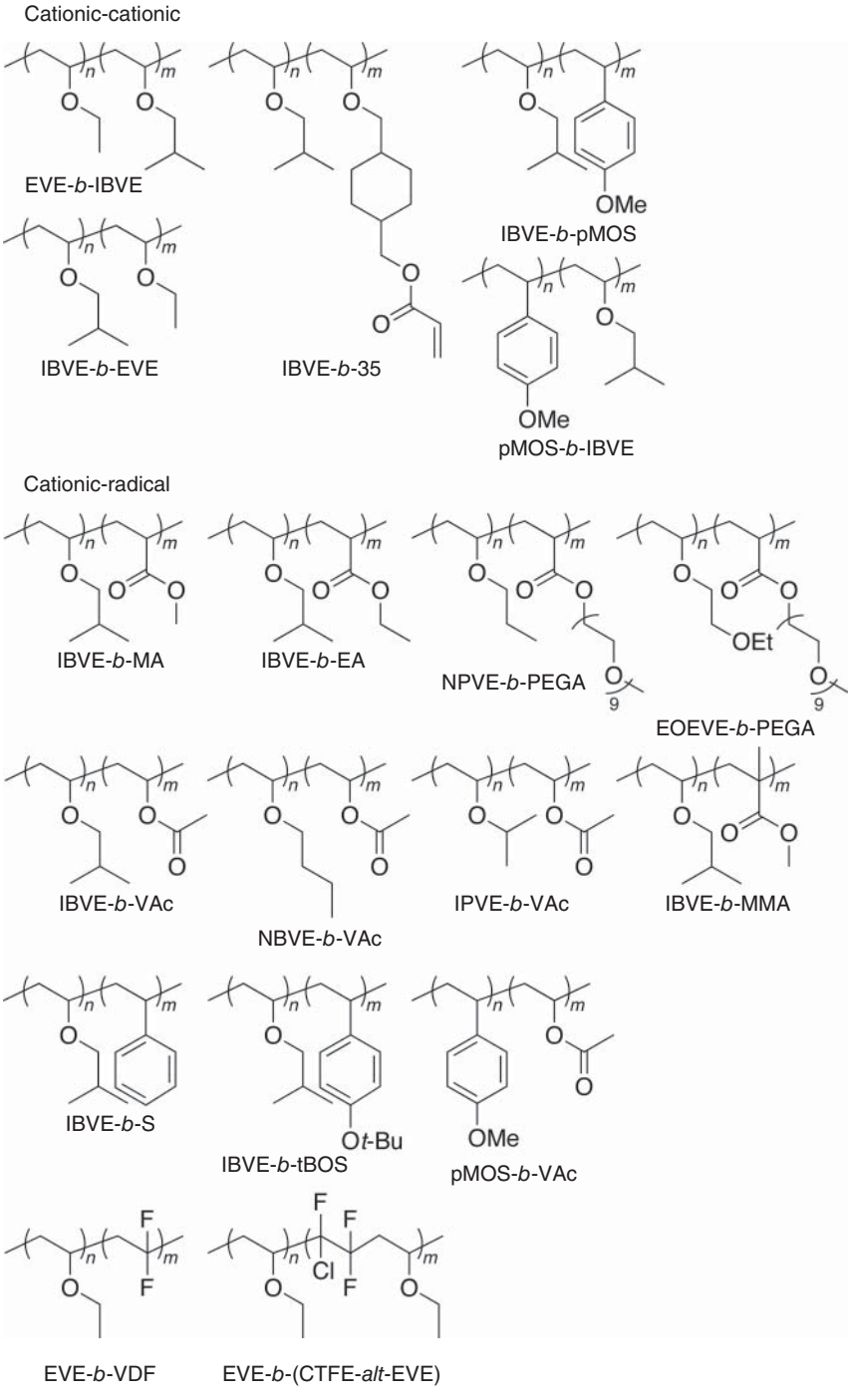

Figure 25.8 Block copolymers via cationic RAFT or DT polymerization.

block, which can be used for the synthesis of star polymers by subsequent radical crosslinking reaction as described below [45].

Block copolymers of IBVE and pMOS have also been prepared by adding pMOS to poly(IBVE) prepared from **3** in the presence of an electroredox catalyst (DDQ) [39]. The block copolymer with the opposite order of pMOS and IBVE has also been reported using a sequential addition method, where IBVE is added to poly(pMOS) obtained from **4** in the presence of HCl and Et_2O, although this order may not be appropriate for block copolymer synthesis as the RAFT terminus of the second monomer is more likely to undergo fragmentation rather than the first block [29].

One of the most notable features of cationic RAFT polymerizations using thiocarbonylthio compounds is in the terminal structure, which can be directly utilized for subsequent radical RAFT polymerizations without any modification reactions for the synthesis of block copolymers consisting of cationically and radically polymerizable monomers. Vinyl ethers and pMOS are used as the cationically polymerizable monomers, whereas the radically polymerizable monomers are various conjugated and unconjugated vinyl monomers, including acrylates, methacrylates, vinyl acetate (VAc), styrenes, vinylidene fluoride (VDF), and chlorotrifluoroethylene (CTFE). In most of these syntheses, the first block is prepared by a cationic RAFT polymerization followed by precipitation, and this block is used as a macroRAFT agent for the radical RAFT polymerization of the second monomer to result in the block copolymers, in which the block segments are directly linked via stable carbon–carbon single bonds originating from the vinyl groups through a mechanistic switch from cationic to radical RAFT polymerizations. The thiocarbonylthio compounds should be selected primarily based on the second monomer because the structures of the RAFT agents that are suitable for conjugated monomers are different from those suitable for unconjugated monomers.

Block copolymers of EVE and methyl acrylate (MA) have been prepared using trithiocarbonate (**3**) as the RAFT agent for the cationic polymerization of EVE in the presence of TfOH, followed by the radical polymerization of MA using isolated poly(EVE) as the macroRAFT agent in the presence of AIBN [17]. The synthesis of a series of block copolymers of various vinyl ethers (IBVE, NPVE, and EOEVE) and acrylates with ethyl (EA) and poly(ethylene glycol) methyl ether (PEGA) substituents has been achieved using dithioacetate (**9**) in the presence of HCl and Et_2O for the first block and AIBN for the second block [28]. One-pot direct block copolymerization is possible without isolation of the first block for the synthesis of the IBVE-*b*-EA block copolymer. For block copolymers containing other conjugated vinyl monomers in the second block, methyl methacrylate (MMA), styrene, and *tert*-butoxystyrene (tBOS) have been employed as radically polymerizable monomers for the radical RAFT polymerization using poly(IBVE) prepared from **9** as the macroRAFT agent [28].

Xanthate or dithiocarbamate should be used for the synthesis of diblock copolymers of unconjugated monomers such as VAc because they are more suitable for the second RAFT radical polymerization. Block copolymers of IBVE and VAc have thus been prepared using xanthate (**4**) for the cationic polymerization of IBVE in the presence of TfOH, followed by the radical polymerization of VAc using isolated

poly(IBVE) with the xanthate terminal as the macroRAFT agent in the presence of AIBN [17]. The acetyl groups of the VAc units are removed by saponification to afford the amphiphilic block copolymers of alkyl vinyl ether and vinyl alcohol. Similarly, a series of block copolymers of other alkyl vinyl ethers (NBVE and IPVE) or pMOS with VAc have been prepared using another xanthate (**10**) in the presence of HCl and Et_2O for the first block and AIBN for the second block [30]. The saponification also results in amphiphilic block copolymers, which form micelles in water.

Fluoroalkenes such as VDF and CTFE have been used as the second monomer for the preparation of block copolymers containing vinyl ether as the first block [43, 44]. Since these fluoroalkenes are unconjugated monomers, xanthate (**4**) and dithiocarbamate (**1**, **2**) were selected for the synthesis of the first block (the poly(EVE) segment) in the presence of TfOH. The isolated poly(EVE) was then employed as the macroRAFT agent for the radical polymerization of VDF in the presence of *tert*-amyl peroxy-2ethylhexanoate (Trigonox 121) as a radical initiator to afford block copolymers having incompatible block segments with a low glass transition temperature (T_g = −35 °C) of poly(EVE) and a high melting temperature (T_m = 160–170 °C) of poly(VDF). Similarly, the same isolated poly(EVE) has been used as a macroRAFT agent for the alternating radical copolymerization of CTFE and EVE in the presence of Trigonox 121 to afford an EVE-*b*-(CTFE-*alt*-EVE) block copolymer. Another approach with the block order reversed using poly(CTFE-*alt*-EVE) as the macroRAFT agent for the second cationic RAFT polymerization of EVE was not successful because the electron-withdrawing CTFE unit adversely affects the RAFT process in cationic RAFT polymerizations.

The thiocarbonylthio terminal resulting from vinyl ether can also be cleaved to afford the cationic species using a metal halide as a Lewis acid catalyst for the living cationic polymerization of vinyl ethers [46]. However, the contribution of the cationic RAFT mechanism is negligible under these conditions. The block copolymers of MA and IBVE have thus been prepared by radical RAFT polymerizations of MA followed by a Lewis acid-catalyzed living cationic polymerization of IBVE. The combination of radical RAFT polymerization and Lewis acid-catalyzed living cationic polymerization for mixtures of vinyl ethers and radically polymerizable monomers, such as MA and VAc, enables the synthesis of multiblock copolymers via in situ reversible switching between radical and cationic polymerization [47–49].

Such interconvertible cationic and radical polymerizations via concurrent activation of the dormant thioester bond also proceed via both cationic and radical RAFT mechanisms. Photocontrolled interconvertible polymerizations have been reported for IBVE and MA using **3** as a common RAFT agent in the presence of photo-oxidizing (**32b**) and photo-reducing ($Ir(ppy)_3$; ppy = 2-phenylpyridine) catalysts, which generate the cationic and radical propagating species, respectively, to result in multiblock copolymers under blue LED irradiation [42]. Alternatively, the combination of two orthogonal stimuli, such as the photo-reducing catalyst ($Ir(ppy)_3$) and a chemical oxidizing catalyst (**34**), enables the production of similar multiblock copolymers in which the block segment lengths can be tuned by the two stimuli [40].

25.4.3 Star Polymers

Among the various methods for synthesizing star or star-shaped polymers using controlled/living polymerizations, the linking reactions of linear polymers with divinyl compounds are the most efficient for the large-scale synthesis of star polymers with a relatively large number of arms (>10) and a statistical distribution of the numbers of arms.

This method has been used in the cationic RAFT polymerization of IBVE with **3** and TfOH in conjunction with divinyl ethers, such as **36** and **37**, which forms a microgel core via simultaneous block polymerization and crosslinking reactions (Figure 25.9) [45]. In particular, **37**, which has a relatively rigid cyclohexane-based linker, results in star polymers with controlled molecular weights ($M_w = 3–7 \times 10^5$), narrow MWDs (M_w/M_n = 1.1–1.2), and controlled arm numbers (N_{arm} = 20–50) and sizes (D_n = 20–28 nm, D_w/D_n = 1.03–1.05) in high yields (>90%). Although another approach using diacrylates, such as **38** and **39**, for simultaneous block

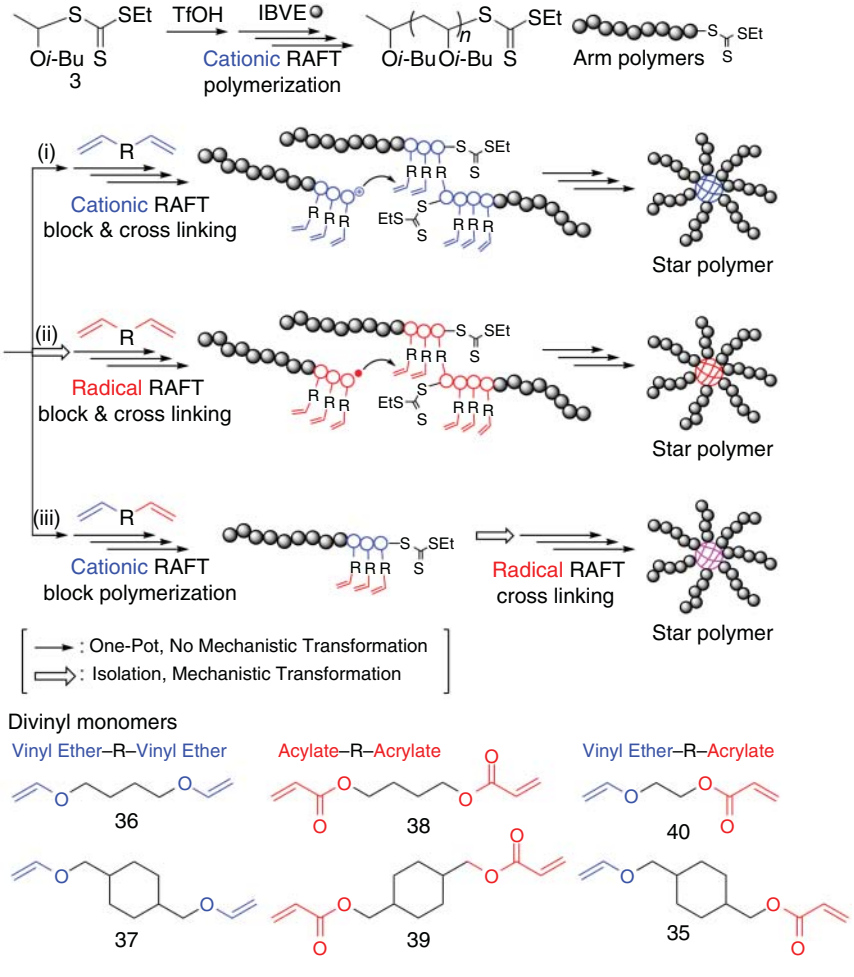

Figure 25.9 Star polymers via cationic RAFT or DT polymerization.

polymerization and crosslinking reactions of isolated poly(IBVE) with a trithiocarbonate terminal via a radical RAFT mechanism is less efficient in terms of the yield of star polymer, and hetero divinyl monomers (**35**, **40**) with a vinyl ether and acrylate unit are more efficient for the radical crosslinking reaction. Furthermore, a block copolymer of IBVE and **35** prepared by a cationic RAFT polymerization via the sequential addition of **35** has been isolated, and the pendent acrylate units of the polymer were subjected to radical crosslinking in the presence of V-70 (2,2′-azobis(4-methoxy-2,4-dimethylvaleronitrile)) to afford star polymers with controlled molecular weights ($M_w = 2.7 \times 10^5$), narrow MWDs ($M_w/M_n = 1.18$), and controlled arm numbers ($N_{arm} = 16$) and sizes ($D_n = 19$ nm, $D_w/D_n = 1.04$) in high yields (89%). The combination of cationic and radical RAFT processes thus allows access to diverse star polymers and their synthetic methods.

25.5 Summary and Outlook for Cationic RAFT or DT Polymerizations

The field of cationic RAFT polymerizations, which began with the use of thiocarbonylthio compounds by analogy to radical RAFT polymerizations, has grown in terms of the available chain transfer agents, initiators or catalysts, monomers, and controlled polymer structures. The RAFT and DT mechanisms have thus created a new branch of controlled/living cationic polymerizations. The cationic RAFT and DT polymerizations can be metal-free and operationally simpler than Lewis acid-catalyzed living cationic polymerizations. The similarity and good compatibility with radical RAFT polymerizations not only enables the direct synthesis of block copolymers of cationically and radically polymerizable monomers but also allows the preparation of copolymers with novel sequences via interconvertible radical and cationic polymerizations.

Because cationic RAFT or DT polymerizations are still developing, a few challenges remain. Styrene and isobutylene are important targets because they are more common but less reactive in cationic polymerizations. A system that works at higher temperatures may also be another challenge. The development and combination of stereocontrolled cationic polymerizations, which enable the simultaneous control of the molecular weight and structure of the resulting polymers, are attractive in view of the new polymeric materials developed based on cationic polymerizations. Further combinations of other controlled/living polymerizations, including radical RAFT polymerizations, widen the scope of accessible, novel, and well-defined polymer structures. In addition, products obtained via metal-free cationic RAFT or DT polymerizations will contribute to the development of novel materials, such as biomaterials and electronic materials.

Abbreviations

αMS	α-methylstyrene
AIBN	4,4′-azobisisobutyronitile

CEVE	2-chloroethyl vinyl ether
CHVE	cyclohexyl vinyl ether.
CTFE	chlorotrifluoroethylene
DDHQ	2,3-dichloro-5,6-dicyanodipehnol
DDQ	2,3-dichloro-5,6-dicyano-*p*-benzoquinone
DiCumCl	dicumyl dichloride
DT	degenerative chain transfer
EOEVE	2-ethoxyethyl vinyl ether
EVE	ethyl vinyl ether
IB	isobutene
IBVE	isobutyl vinyl ether
MA	methyl acrylate
MMA	methyl methacrylate
MWD	molecular weight distribution
NBVE	*n*-butyl vinyl ether
NPVE	*n*-propyl vinyl ether
PEGA	poly(ethylene glycol) methyl ether acrylate
pHS	*p*-hydroxystyrene
pMOS	*p*-methoxystyrene
RAFT	reversible addition fragmentation chain transfer
tBOS	*tert*-butoxystyrene
TBVE	*tert*-butyl vinyl ether
TEMPO	(2,2,6,6-tetramethylpiperidin-1-yl)oxyl
Tf_2NH	trifluoromethanesulfonic imide
TfOH	trifluoromethanesulfonic acid
VAc	vinyl acetate
VDF	vinylidene fluoride
V-70	2,2′-azobis(4-methoxy-2,4-dimethylvaleronitrile)

References

1 Chiefari, J., Chong, Y.K., Ercole, F. et al. (1998). Living free-radical polymerization by reversible addition–fragmentation chain transfer: the RAFT process. *Macromolecules* 31: 5559–5562.

2 Moad, G. and Solomon, D.H. (2006). *The Chemistry of Radical Polymerization: Second Fully Revised Edition*. Oxford: Elsevier.

3 Kamigaito, M., Satoh, K., and Uchiyama, M. (2019). Degenerative chain-transfer process: controlling all chain-growth polymerizations and enabling novel monomer sequences. *J. Polym. Sci., Part A: Polym. Chem.* 57: 243–254.

4 McKenzie, T.G., Fu, Q., Uchiyama, M. et al. (2016). Beyond traditional RAFT: alternative activation of thiocarbonylthio compounds for controlled polymerization. *Adv. Sci.* 3: 1500394.

5 Miyamoto, M., Sawamoto, M., and Higashimura, T. (1984). Living polymerization of isobutyl vinyl ether with the hydrogen iodide/iodine initiating system. *Macromolecules* 17: 265–268.

6 Faust, R. and Kennedy, J.P. (1986). Living carbocationic polymerization. *Polym. Bull.* 15: 317–323.

7 Sawamoto, M. (1991). Modern cationic vinyl polymerization. *Prog. Polym. Sci.* 16: 111–172.

8 Matyjaszewski, K. (ed.) (1996). *Cationic Polymerizations*. New York: Marcel Dekker.

9 Puskas, J.E. and Kaszas, G. (2000). Living cationic polymerization of resonance-stabilized monomers. *Prog. Polym. Sci.* 25: 403–452.

10 Goethals, E.J. and Du Prez, F. (2007). Carbocationic polymerizations. *Prog. Polym. Sci.* 32: 220–246.

11 Aoshima, S. and Kanaoka, S. (2009). A renaissance in living cationic polymerization. *Chem. Rev.* 109: 5245–5287.

12 Goto, A. and Fukuda, T. (2004). Kinetics in living radical polymerization. *Prog. Polym. Sci.* 29: 329–385.

13 Kamigaito, M., Ando, T., and Sawamoto, M. (2001). Metal-catalyzed living radical polymerization. *Chem. Rev.* 101: 3689–3745.

14 Matyjazsewski, K. and Xia, J. (2001). Atom transfer radical polymerization. *Chem. Rev.* 101: 2921–2990.

15 Cho, C.G., Feit, B.A., and Webster, O.W. (1990). Cationic polymerization of isobutyl vinyl ether: livingness enhancement by dialkyl sufides. *Macromolecules* 23: 1918–1923.

16 Hawker, C.J., Bosman, A.W., and Harth, E. (2001). New polymer synthesis by nitroxide mediated living radical polymerizations. *Chem. Rev.* 101: 3661–3688.

17 Uchiyama, M., Satoh, K., and Kamigaito, M. (2015). Cationic RAFT polymerization using ppm concentrations of organic acid. *Angew. Chem. Int. Ed.* 54: 1924–1928.

18 Müller, A.H.E., Yan, D., and Litvinenko, G. (1996). Kinetic analysis of "living" polymerization systems exhibiting slow equilibria. 4. "Degenerative" mechanism of group transfer polymerization and generation of free ions in cationic polymerization. *Macromolecules* 29: 2346–2353.

19 Kennedy, J.P. and Smith, R.M. (1980). New telechelic polymers and sequential copolymers by polyfunctional *ini*tiator-trans*fer* agents (inifers). II. Synthesis and characterization of α,ω-di(*tert*-chloro)polyisobutylenes. *J. Polym. Sci., Polym. Chem. Ed.* 18: 1523–1537.

20 Iván, B. and Kennedy, J.P. (1990). Living carbocationic polymerization. 31. A comprehensive view of the inifer and living mechanisms in isobutylene polymerization. *Macromolecules* 23: 2880–2885.

21 Mayr, H. and Shade, C. (1988). The role of chain transfer process in inifer/boron trichloride initiated polymerizations of isobutene. *Makromol. Chem., Rapid Commun.* 9: 483–488.

22 Matyjaszewski, K. (1997). Comparison of controlled living carbocationic and radical polymerizations. *ACS Symp. Ser.* 665: 12–24.

23 Cramail, H., Deffieux, A., and Nuyken, O. (1993). Polymerization of isobutyl vinyl ether in the presence of mixed α-chloro- and α-iodo ethers with tetrabutylammonium perchlorate. *Makromol. Chem., Rapid Commun.* 14: 17–27.

24 Cramail, H. and Deffieux, A. (1994). Kinetic study of the "living" cationic polymerization of cyclohexyl vinyl ether initiated by hydrogen iodide in the presence of ammonium salts. *Macromolecules* 27: 1401–1406.

25 Michaudel, Q., Kottisch, V., and Fors, B.P. (2017). Cationic polymerization: from photoinitiation to photocontrol. *Angew. Chem. Int. Ed.* 56: 9670–9679.

26 Kottisch, V., Michaudel, Q., and Fors, B.P. (2016). Cationic polymerization of vinyl ethers controlled by visible light. *J. Am. Chem. Soc.* 138: 15535–15538.

27 Michaudel, Q., Chauviré, T., Kottisch, V. et al. (2017). Mechanistic insight into the photocontrolled cationic polymerization of vinyl ethers. *J. Am. Chem. Soc.* 139: 15530–15538.

28 Sugihara, S., Konegawa, N., and Maeda, Y. (2015). $HCl{\cdot}Et_2O$-catalyzed metal-free RAFT cationic polymerization: one-pot transformation from metal-free living cationic polymerization to RAFT radical polymerization. *Macromolecules* 48: 5120–5131.

29 Sugihara, S., Okubo, S., and Maeda, Y. (2016). Metal-free RAFT cationic polymerization of *p*-methoxystyrene with $HCl{\cdot}Et_2O$ using a xanthate-type RAFT cationogen. *Polym. Chem.* 7: 6854–6863.

30 Sugihara, S., Sakamoto, Y., Nakayama, M. et al. (2018). Transformation from xanthate-type cationogen mediated metal-free RAFT cationic polymerization with "$HCl{\cdot}Et_2O$" into RAFT radical polymerization to form poly(alkyl vinyl ether)-*b*-polyvinyl alcohol amphiphiles. *Polymer* 154: 153–163.

31 Uchiyama, M., Satoh, K., and Kamigaito, M. (2015). Thioether-mediated degenerative chain-transfer cationic polymerization: a simple metal-free system for living cationic polymerization. *Macromolecules* 48: 5533–5542.

32 Uchiyama, M., Satoh, K., and Kamigaito, M. (2016). A phosphonium intermediate for cationic RAFT polymerization. *Polym. Chem.* 7: 1387–1396.

33 Müller, A.H.E., Yan, D., Litvinenko, G. et al. (1995). Kinetic analysis of "living" polymerization systems exhibiting slow equilibria. 2. Molecular weight distribution for degenerative chain transfer (direct actively exchange between active and "dormant" species) at constant monomer concentration. *Macromolecules* 28: 7335–7338.

34 Uchiyama, M., Sakaguchi, M., Satoh, K., and Kamigaito, M. (2019). A user-friendly living cationic polymerization: degenerative chain-transfer polymerization of vinyl ethers by simply using mixtures of weak and superstrong protonic acids. *Chinese J. Polym. Sci.* 37: 851–857.

35 Perkowski, A.J., You, W., and Nicewicz, D.A. (2015). Visible light photoinitiated metal-free living cationic polymerization of 4-methoxytstyrene. *J. Am. Chem. Soc.* 137: 7580–7583.

36 Uchiyama, M., Satoh, K., and Kamigaito, M. (2016). Diversifying cationic RAFT polymerization with various counteranions: Generation of cationic species from organic halides and various metal salts. *ACS Macro Lett.* 5: 1157–1161.

37 Kottisch, V., Supej, M.J., and Fors, B.P. (2018). Enhancing temporal control and enabling chain-end modification in photoregulated cationic polymerizations by using iridium-based catalysts. *Angew. Chem. Int. Ed.* 57: 8260–8264.

38 Peterson, B.M., Lin, S., and Fors, B.P. (2018). Electrochemically controlled cationic polymerization of vinyl ethers. *J. Am. Chem. Soc.* 140: 2076–2079.

39 Sang, W. and Yan, Q. (2018). Electro-controlled living cationic polymerization. *Angew. Chem. Int. Ed.* 57: 4907–4911.

40 Peterson, B.M., Kottisch, V., Supej, M.J., and Fors, B.P. (2018). On demand switching of polymerization mechanism and monomer selectivity with orthogonal stimuli. *ACS Cent. Sci.* 4: 1228–1234.

41 Discekici, E.H. and de Alaniz, J.R. (2018). Next-generation materials via orthogonal stimuli. *ACS Cent. Sci.* 4: 1087–1088.

42 Kottisch, V., Michaudel, Q., and Fors, B.P. (2017). Photocontrolled interconversion of cationic and radical polymerizations. *J. Am. Chem. Soc.* 139: 10665–10668.

43 Guerre, M., Uchiyama, M., Folgado, E. et al. (2017). Combination of cationic and radical RAFT polymerizations: a versatile route to well-defined poly(ethyl vinyl ether)-*block*-poly(vinyliene fluoride) block copolymers. *ACS Macro Lett.* 6: 393–398.

44 Guerre, M., Uchiyama, M., Lopez, G. et al. (2018). Synthesis of PEVE-*b*-P(CTFE-*alt*-EVE) block copolymers by sequential cationic and radical RAFT polymerization. *Polym. Chem.* 9: 352–361.

45 Uchiyama, M., Satoh, K., McKenzie, T.G. et al. (2017). Diverse approaches to star polymers *via* cationic and radical RAFT cross-linking reactions using mechanistic transformation. *Polym. Chem.* 8: 5972–5981.

46 Kumagai, S., Nagai, K., Satoh, K., and Kamigaito, M. (2010). In-situ direct mechanistic transformation form RAFT to living cationic polymerization for (meth)acrylate–vinyl ether block copolymers. *Macromolecules* 43: 7523–7531.

47 Aoshima, H., Uchiyama, M., Satoh, K., and Kamigaito, M. (2014). Interconvertible living radical and cationic polymerization through reversible activation of dormant species with dual activity. *Angew. Chem. Int. Ed.* 53: 10932–10936.

48 Satoh, K., Hashimoto, H., Kumagai, S. et al. (2017). One-shot controlled/living copolymerization for various comonomer sequence distributions *via* dual radical and cationic active species from RAFT terminals. *Polym. Chem.* 8: 5002–5011.

49 Satoh, K., Fujiki, Y., Uchiyama, M., and Kamigaito, M. (2018). Vinyl ether/vinyl ester copolymerization by cationic and radical interconvertible simultaneous polymerization. *ACS Symp. Ser.* 1284: 323–334.

Index

RAFT Polymerization: Methods, Synthesis and Applications, First Edition.
Edited by Graeme Moad and Ezio Rizzardo.

b

d

e

f

g

h

i

j

k

n

S

t

x

y

z